

The background of the cover is a collage of overlapping circular shapes representing microbial cells. The top half features cells in shades of green and yellow-green, while the bottom half features cells in shades of blue and cyan. The cells have a textured, watercolor-like appearance.

# MICROBIAL ECOTOXICOLOGY

EDITED BY: Stéphane Pesce, Fabrice Martin-Laurent, Ed Topp and  
Ghiglione Jean-Francois  
PUBLISHED IN: Frontiers in Microbiology



# frontiers

## Frontiers eBook Copyright Statement

The copyright in the text of individual articles in this eBook is the property of their respective authors or their respective institutions or funders. The copyright in graphics and images within each article may be subject to copyright of other parties. In both cases this is subject to a license granted to Frontiers.

The compilation of articles constituting this eBook is the property of Frontiers.

Each article within this eBook, and the eBook itself, are published under the most recent version of the Creative Commons CC-BY licence.

The version current at the date of publication of this eBook is CC-BY 4.0. If the CC-BY licence is updated, the licence granted by Frontiers is automatically updated to the new version.

When exercising any right under the CC-BY licence, Frontiers must be attributed as the original publisher of the article or eBook, as applicable.

Authors have the responsibility of ensuring that any graphics or other materials which are the property of others may be included in the CC-BY licence, but this should be checked before relying on the CC-BY licence to reproduce those materials. Any copyright notices relating to those materials must be complied with.

Copyright and source acknowledgement notices may not be removed and must be displayed in any copy, derivative work or partial copy which includes the elements in question.

All copyright, and all rights therein, are protected by national and international copyright laws. The above represents a summary only. For further information please read Frontiers' Conditions for Website Use and Copyright Statement, and the applicable CC-BY licence.

ISSN 1664-8714

ISBN 978-2-88963-881-9

DOI 10.3389/978-2-88963-881-9

## About Frontiers

Frontiers is more than just an open-access publisher of scholarly articles: it is a pioneering approach to the world of academia, radically improving the way scholarly research is managed. The grand vision of Frontiers is a world where all people have an equal opportunity to seek, share and generate knowledge. Frontiers provides immediate and permanent online open access to all its publications, but this alone is not enough to realize our grand goals.

## Frontiers Journal Series

The Frontiers Journal Series is a multi-tier and interdisciplinary set of open-access, online journals, promising a paradigm shift from the current review, selection and dissemination processes in academic publishing. All Frontiers journals are driven by researchers for researchers; therefore, they constitute a service to the scholarly community. At the same time, the Frontiers Journal Series operates on a revolutionary invention, the tiered publishing system, initially addressing specific communities of scholars, and gradually climbing up to broader public understanding, thus serving the interests of the lay society, too.

## Dedication to Quality

Each Frontiers article is a landmark of the highest quality, thanks to genuinely collaborative interactions between authors and review editors, who include some of the world's best academicians. Research must be certified by peers before entering a stream of knowledge that may eventually reach the public - and shape society; therefore, Frontiers only applies the most rigorous and unbiased reviews. Frontiers revolutionizes research publishing by freely delivering the most outstanding research, evaluated with no bias from both the academic and social point of view. By applying the most advanced information technologies, Frontiers is catapulting scholarly publishing into a new generation.

## What are Frontiers Research Topics?

Frontiers Research Topics are very popular trademarks of the Frontiers Journals Series: they are collections of at least ten articles, all centered on a particular subject. With their unique mix of varied contributions from Original Research to Review Articles, Frontiers Research Topics unify the most influential researchers, the latest key findings and historical advances in a hot research area! Find out more on how to host your own Frontiers Research Topic or contribute to one as an author by contacting the Frontiers Editorial Office: [researchtopics@frontiersin.org](mailto:researchtopics@frontiersin.org)

# MICROBIAL ECOTOXICOLOGY

Topic Editors:

**Stéphane Pesce**, INRAE Clermont-Auvergne-Rhône-Alpes, France

**Fabrice Martin-Laurent**, Institut National de la Recherche Agronomique (INRA), France

**Ed Topp**, Agriculture and Agri-Food Canada (AAFC), Canada

**Ghiglione Jean-Francois**, Centre National de la Recherche Scientifique (CNRS), France

**Citation:** Pesce, S., Martin-Laurent, F., Topp, E., Jean-Francois, G., eds. (2020). Microbial Ecotoxicology. Lausanne: Frontiers Media SA. doi: 10.3389/978-2-88963-881-9

# Table of Contents

- 07 Editorial: Microbial Ecotoxicology**  
Stéphane Pesce, Jean-François Ghiglione, Edward Topp and Fabrice Martin-Laurent
- 13 Cloning, Expression, Isotope Labeling, and Purification of Transmembrane Protein MerF From Mercury Resistant Enterobacter sp. AZ-15 for NMR Studies**  
Aatif Amin and Zakia Latif
- 24 Fungal Unspecific Peroxygenases Oxidize the Majority of Organic EPA Priority Pollutants**  
Alexander Karich, René Ullrich, Katrin Scheibner and Martin Hofrichter
- 39 Salinity-Based Toxicity of CuO Nanoparticles, CuO-Bulk and Cu Ion to Vibrio anguillarum**  
Alice Rotini, Andrea Tornambè, Riccardo Cossi, Franco Iamunno, Giovanna Benvenuto, Maria T. Berducci, Chiara Maggi, Maria C. Thaller, Anna M. Cicero, Loredana Manfra and Luciana Migliore
- 50 Microbial Community Structure and Function Indicate the Severity of Chromium Contamination of the Yellow River**  
Yaxin Pei, Zhengsheng Yu, Jing Ji, Aman Khan and Xiangkai Li
- 62 Multiple Modes of Nematode Control by Volatiles of Pseudomonas putida 1A00316 From Antarctic Soil against Meloidogyne incognita**  
Yile Zhai, Zongze Shao, Minmin Cai, Longyu Zheng, Guangyu Li, Dian Huang, Wanli Cheng, Linda S. Thomashow, David M. Weller, Ziniu Yu and Jibin Zhang
- 73 Vancomycin and/or Multidrug-Resistant Citrobacter Freundii Altered the Metabolic Pattern of Soil Microbial Community**  
Mariusz Cycoń, Kamila Orlewska, Anna Markowicz, Agnieszka Żmijowska, Joanna Smoleń-Dzirba, Jolanta Bratosiewicz-Wąsik, Tomasz J. Wąsik and Zofia Piotrowska-Seget
- 90 Metal-Adapted Bacteria Isolated From Wastewaters Produce Biofilms by Expressing Proteinaceous Curli Fimbriae and Cellulose Nanofibers**  
M. K. Mosharaf, M. Z. H. Tanvir, M. M. Haque, M. A. Haque, M. A. A. Khan, A. H. Molla, Mohammad Z. Alam, M. S. Islam and M. R. Talukder
- 107 Use of the PCR-DGGE Method for the Analysis of the Bacterial Community Structure in Soil Treated With the Cephalosporin Antibiotic Cefuroxime and/or Inoculated With a Multidrug-Resistant Pseudomonas putida Strain MC1**  
Kamila Orlewska, Zofia Piotrowska-Seget and Mariusz Cycoń
- 120 Experimental Warming Differentially Influences the Vulnerability of Phototrophic and Heterotrophic Periphytic Communities to Copper Toxicity**  
Stéphane Pesce, Anne-Sophie Lambert, Soizic Morin, Arnaud Foulquier, Marina Coquery and Aymeric Dabrin

- 134** *Fullerenes Influence the Toxicity of Organic Micro-Contaminants to River Biofilms*  
Anna Freixa, Vicenç Acuña, Marina Gutierrez, Josep Sanchís, Lúcia H. M. L. M. Santos, Sara Rodriguez-Mozaz, Marinella Farré, Damià Barceló and Sergi Sabater
- 146** *Plant Species and Heavy Metals Affect Biodiversity of Microbial Communities Associated With Metal-Tolerant Plants in Metalliferous Soils*  
Sławomir Borymski, Mariusz Cycoń, Manfred Beckmann, Luis A. J. Mur and Zofia Piotrowska-Seget
- 164** *Colonization of Non-biodegradable and Biodegradable Plastics by Marine Microorganisms*  
Claire Dussud, Cindy Hudec, Matthieu George, Pascale Fabre, Perry Higgs, Stéphane Bruzard, Anne-Marie Delort, Boris Eyheraguibel, Anne-Leïla Meistertzheim, Justine Jacquin, Jingguang Cheng, Nolwenn Callac, Charlène Odobel, Sophie Rabouille and Jean-François Ghiglione
- 177** *Plant and Microbial Responses to Repeated Cu(OH)<sub>2</sub> Nanopesticide Exposures Under Different Fertilization Levels in an Agro-Ecosystem*  
Marie Simonin, Benjamin P. Colman, Weiyi Tang, Jonathan D. Judy, Steven M. Anderson, Christina M. Bergemann, Jennifer D. Rocca, Jason M. Unrine, Nicolas Cassar and Emily S. Bernhardt
- 191** *Environmental Concentrations of Copper, Alone or in Mixture With Arsenic, Can Impact River Sediment Microbial Community Structure and Functions*  
Ayanleh Mahamoud Ahmed, Emilie Lyautey, Chloé Bonnineau, Aymeric Dabrin and Stéphane Pesce
- 204** *Toward Integrative Bacterial Monitoring of Metolachlor Toxicity in Groundwater*  
Gwenaël Imfeld, Ludovic Besaury, Bruno Maucourt, Stéphanie Donadello, Nicole Baran and Stéphane Vuilleumier
- 218** *Interactive Effects of Pesticides and Nutrients on Microbial Communities Responsible of Litter Decomposition in Streams*  
Florent Rossi, Stéphane Pesce, Clarisse Mallet, Christelle Margoum, Arnaud Chaumot, Matthieu Masson and Joan Artigas
- 231** *Molecular and Microbiological Insights on the Enrichment Procedures for the Isolation of Petroleum Degrading Bacteria and Fungi*  
Giulia Spini, Federica Spina, Anna Poli, Anne-Laure Blieux, Tiffanie Regnier, Carla Gramellini, Giovanna C. Varese and Edoardo Puglisi
- 250** *A Time-Dose Response Model to Assess Diuron-Induced Photosynthesis Inhibition in Freshwater Biofilms*  
Soizic Morin, Betty Chaumet and Nicolas Mazzella
- 259** *Evaluation of Phototrophic Stream Biofilms Under Stress: Comparing Traditional and Novel Ecotoxicological Endpoints After Exposure to Diuron*  
Linn Sgier, Renata Behra, René Schönenberger, Alexandra Kroll and Anze Zupanic
- 270** *Soil Particles and Phenanthrene Interact in Defining the Metabolic Profile of Pseudomonas putida G7: A Vibrational Spectroscopy Approach*  
Andrea Fanasi, Asfaw Zegeye, Christian Mustin and Aurélie Cébron

- 284** *Hydrodynamics Alter the Tolerance of Autotrophic Biofilm Communities Toward Herbicides*  
Bastian H. Polst, Christine Anlanger, Ute Risse-Buhl, Floriane Larras, Thomas Hein, Markus Weitere and Mechthild Schmitt-Jansen
- 296** *Negative Effects of Copper Oxide Nanoparticles on Carbon and Nitrogen Cycle Microbial Activities in Contrasting Agricultural Soils and in Presence of Plants*  
Marie Simonin, Amélie A. M. Cantarel, Armelle Crouzet, Jonathan Gervaix, Jean M. F. Martins and Agnès Richaume
- 307** *Effect of Acidic Industrial Effluent Release on Microbial Diversity and Trace Metal Dynamics During Resuspension of Coastal Sediment*  
Hana Zouch, Léa Cabrol, Sandrine Chifflet, Marc Tedetti, Fatma Karray, Hatem Zaghden, Sami Sayadi and Marianne Quéméneur
- 321** *Nicosulfuron Degradation by an Ascomycete Fungus Isolated From Submerged Alnus Leaf Litter*  
Louis Carles, Florent Rossi, Pascale Besse-Hoggan, Christelle Blavignac, Martin Leremboure, Joan Artigas and Isabelle Batisson
- 334** *Dynamics of Bacterial Communities Mediating the Treatment of an As-Rich Acid Mine Drainage in a Field Pilot*  
Elia Laroche, Corinne Casiot, Lidia Fernandez-Rojo, Angélique Desoeuvre, Vincent Tardy, Odile Bruneel, Fabienne Battaglia-Brunet, Catherine Joulian and Marina Héry
- 347** *Volatolomics in Bacterial Ecotoxicology, A Novel Method for Detecting Signatures of Pesticide Exposure?*  
Kevin Hidalgo, Jeremy Ratel, Frederic Mercier, Benedicte Gauriat, Philippe Bouchard and Erwan Engel
- 358** *Copper Affects Composition and Functioning of Microbial Communities in Marine Biofilms at Environmentally Relevant Concentrations*  
Natàlia Corcoll, Jianghua Yang, Thomas Backhaus, Xiaowei Zhang and Karl Martin Eriksson
- 373** *AgNPs Change Microbial Community Structures of Wastewater*  
Yuting Guo, Nicolas Cichocki, Florian Schattenberg, Robert Geffers, Hauke Harms and Susann Müller
- 385** *The Microbiome Stress Project: Toward a Global Meta-Analysis of Environmental Stressors and Their Effects on Microbial Communities*  
Jennifer D. Rocca, Marie Simonin, Joanna R. Blaszczak, Jessica G. Ernakovich, Sean M. Gibbons, Firas S. Midani and Alex D. Washburne
- 399** *Novel Mechanism for Surface Layer Shedding and Regenerating in Bacteria Exposed to Metal-Contaminated Conditions*  
Archjana Chandramohan, Elodie Duprat, Laurent Remusat, Severine Zirah, Carine Lombard and Adrienne Kish
- 409** *Mangrove Facies Drives Resistance and Resilience of Sediment Microbes Exposed to Anthropogenic Disturbance*  
Cécile Capdeville, Thomas Pommier, Jonathan Gervaix, François Fromard, Jean-Luc Rols and Joséphine Leflaive

- 426** *Functional Genes and Bacterial Communities During Organohalide Respiration of Chloroethenes in Microcosms of Multi-Contaminated Groundwater*  
Louis Hermon, Jennifer Hellal, Jérémie Denonfoux, Stéphane Vuilleumier, Gwenaél Imfeld, Charlotte Urien, Stéphanie Ferreira and Catherine Jouliau
- 442** *Changes in Bacterioplankton Communities Resulting From Direct and Indirect Interactions With Trace Metal Gradients in an Urbanized Marine Coastal Area*  
Clément Coclet, Cédric Garnier, Gaël Durrieu, Dario Omanović, Sébastien D'Onofrio, Christophe Le Poupon, Jean-Ulrich Mullot, Jean-François Briand and Benjamin Misson
- 456** *Shift in Natural Groundwater Bacterial Community Structure Due to Zero-Valent Iron Nanoparticles (nZVI)*  
Marc Crampon, Catherine Jouliau, Patrick Ollivier, Mickaël Charron and Jennifer Hellal
- 470** *Benthic Diatom Communities in an Alpine River Impacted by Waste Water Treatment Effluents as Revealed Using DNA Metabarcoding*  
Teofana Chonova, Rainer Kurmayer, Frédéric Rimet, Jérôme Labanowski, Valentin Vasselon, François Keck, Paul Illmer and Agnès Bouchez
- 487** *Global Metabolomic Characterizations of Microcystis spp. Highlights Clonal Diversity in Natural Bloom-Forming Populations and Expands Metabolite Structural Diversity*  
Séverine Le Manach, Charlotte Duval, Arul Marie, Chakib Djediat, Arnaud Catherine, Marc Edery, Cécile Bernard and Benjamin Marie
- 503** *Interactive Impacts of Silver and Phosphorus on Autotrophic Biofilm Elemental and Biochemical Quality for a Macroinvertebrate Consumer*  
Clément Crenier, Kévin Sanchez-Thirion, Alexandre Bec, Vincent Felten, Jessica Ferriol, Aridane G. González, Joséphine Leflaive, Fanny Perrière, Loïc Ten-Hage and Michael Danger
- 517** *Microbial Ecotoxicology of Marine Plastic Debris: A Review on Colonization and Biodegradation by the "Plastisphere"*  
Justine Jacquin, Jinguang Cheng, Charlène Odobel, Caroline Pandin, Pascal Conan, Mireille Pujo-Pay, Valérie Barbe, Anne-Leila Meistertzheim and Jean-François Ghiglione
- 533** *Impact of Leptospermone, a Natural  $\beta$ -Triketone Herbicide, on the Fungal Composition and Diversity of Two Arable Soils*  
Clarisse Mallet, Sana Romdhane, Camille Loiseau, Jérémie Béguet, Fabrice Martin-Laurent, Christophe Calvayrac and Lise Barthelmebs
- 542** *Soil Photosynthetic Microbial Communities Mediate Aggregate Stability: Influence of Cropping Systems and Herbicide Use in an Agricultural Soil*  
Olivier Crouzet, Laurent Consentino, Jean-Pierre Pétraud, Christelle Marraud, Jean-Pierre Aguer, Sylvie Bureau, Carine Le Bourvellec, Line Touloumet and Annette Bérard
- 557** *Earthworms Mitigate Pesticide Effects on Soil Microbial Activities*  
Sylvain Bart, Céline Pelosi, Alexandre Barraud, Alexandre R. R. Péry, Nathalie Cheviron, Virginie Grondin, Christian Mougin and Olivier Crouzet



# Editorial: Microbial Ecotoxicology

Stéphane Pesce<sup>1\*</sup>, Jean-François Ghiglione<sup>2</sup>, Edward Topp<sup>3</sup> and Fabrice Martin-Laurent<sup>4</sup>

<sup>1</sup> INRAE, UR RiverLy, Villeurbanne, France, <sup>2</sup> CNRS, UMR 7621 Laboratoire d'Océanographie Microbienne, Sorbonne Université, Observatoire Océanologique de Banyuls-sur-Mer, Banyuls-sur-Mer, France, <sup>3</sup> Agriculture and Agri-Food Canada, University of Western Ontario, London, ON, Canada, <sup>4</sup> AgroSup Dijon, INRAE, Univ. Bourgogne, Univ. Bourgogne Franche-Comté, Agroécologie, Dijon, France

**Keywords:** biodegradation, biodiversity, bioindicator, communities, ecosystem functions, pollutants, risk assessment

## Editorial on the Research Topic

### Microbial Ecotoxicology

In the age of the Anthropocene, the world is facing unprecedented environmental challenges that have multifactorial and interlinked causes including population growth, pollution, and climate change. The “One Health” and “EcoHealth” paradigms emphasize the urgent need to protect ecosystem health in order to ensure human well-being and food security (Naeem et al., 2016; Destoumieux-Garzón et al., 2018). It is noteworthy that the majority of the 17 United Nations Sustainable Development Goals (UN-SDGs) fundamentally link environmental health to human health and well-being (Blicharska et al., 2019).

Within this context, mitigating anthropogenic impacts on ecosystem functions and services is a paramount challenge. Perhaps because they are not visible, microorganisms that provide or support key ecosystem services have generally been neglected as endpoints of concern in environmental risk assessment frameworks (Brandt et al., 2015). This, in spite of the fact that microbial communities deliver ecological processes and ecosystem services that are essential to life on earth (Cavicchioli et al., 2019). Exposure to inorganic or organic chemical pollutants, sometimes at very low concentrations, has the potential to kill or inhibit sensitive environmental microorganisms, or disrupt their activities. As with all biology on earth, microorganisms are subject to multiple physical and chemical stressors, including mixtures of commercial chemicals, pharmaceuticals, pesticides, and other agents that reach the environment either by design or in waste streams. Setting acceptable standards for chemical pollution on the basis of microbial impacts remains a significant challenge (Rockström et al., 2009).

Over the last few decades, a wide range of studies has investigated the interactions between microorganisms and pollutants at different biological scales ranging from the molecular to community levels. These studies have contributed to the emergence and the development of a new Research Topic designated “microbial ecotoxicology” (Ghiglione et al., 2016), built on key concepts from both microbial ecology and “classical” ecotoxicology. This Research Topic has recently benefited from tremendous technological improvements in several related fields, including environmental chemistry, microbiology, and microbial ecology as well as molecular and so called “omics ecology” (Marco and Abram, 2019). Indeed, a wide range of tools are now available to characterize microbial responses at different biological levels following exposure to a large variety of pollutants and their transformation products. Those concern so-called “legacy pollutants” (e.g., metals and metalloids, pesticides, chlorinated solvents or polycyclic aromatic hydrocarbons, PAHs), but also pollutants of emerging concern (e.g., pharmaceuticals, nanoparticles, plastic debris, biopesticides, or cyanotoxins). These responses are very complex and include reciprocal interactions because of the capacity of microorganisms to modify the bioavailability of pollutants and to transform or degrade many of them. Microbially biodegradable pollutants include

## OPEN ACCESS

### Edited and reviewed by:

Eric Altermann,  
AgResearch Ltd, New Zealand

### \*Correspondence:

Stéphane Pesce  
stephane.pesce@inrae.fr

### Specialty section:

This article was submitted to  
Microbiotechnology,  
a section of the journal  
Frontiers in Microbiology

**Received:** 28 April 2020

**Accepted:** 26 May 2020

**Published:** 26 June 2020

### Citation:

Pesce S, Ghiglione J-F, Topp E and  
Martin-Laurent F (2020) Editorial:  
Microbial Ecotoxicology.  
*Front. Microbiol.* 11:1342.  
doi: 10.3389/fmicb.2020.01342

substances that were initially specifically designed to inhibit microbial activities, such as some antibiotics (Cycon et al., 2019). Therefore, and as nicely illustrated in the present Research Topic bringing together 41 articles co-authored by 308 investigators, microbial ecotoxicology is a growing Research Topic that overcomes disciplinary approaches and compartment boundaries within ecosystems to assess the interactions between both prokaryotic and eukaryotic microorganisms and a wide range of pollutants with the final objective of tackling urgent environmental and societal challenges.

## **MICROBIAL EVOLUTION AND ADAPTATION TO POLLUTANTS: RESULTING ENVIRONMENTAL BENEFITS AND ASSOCIATED ECOLOGICAL COSTS**

Mechanistic and evolutionary approaches are still needed to characterize and understand how microorganisms adapt to pollutants, not only to tolerate, resist or transform them, but also in some cases to take benefit from them as energy sources for metabolism and growth. Research in microbial ecotoxicology continuously contributes to identify and characterize undescribed mechanisms involved in detoxification and/or degradation of pollutants by different kinds of microorganisms. Bacterial membranes (Amin and Latif), surface layers (Chandramohan et al.), and external components such as extracellular polymeric substances constituting biofilm matrix (Mosharaf et al.) provide a barrier protecting microorganisms against diverse pollutants. This was nicely illustrated by Amin and Latif who coupled heteronuclear single-quantum coherence nuclear magnetic resonance (HSQC NMR) and scanning electron microscopy (SEM) to study and visualize the accumulation of mercury (Hg) on the cell surface of the Hg-resistant strain *Enterobacter* sp. AZ-15. Microbial detoxification systems involving pollutant sequestration are potentially useful to remove these substances from contaminated environments, such as wastewater (Mosharaf et al.). Extracellular enzymes can also be liberated in the surrounding environment to protect microorganisms through detoxification. Therefore, Karich et al. showed that two fungal unspecific peroxygenases from the basidiomycetous *Agrocybe aegerita* and *Marasmius rotula* were able to transform most of the compounds listed as priority pollutants by the United States Environmental Protection Agency (EPA). The fungal role in pollutant biodegradation was also highlighted by Carles et al. who described the cometabolic degradation of the herbicide nicosulfuron by *Plectosphaerella cucumerina* ARI isolated from *Alnus* leaf litter submerged in freshwater.

Evolution of microbial catabolic capabilities enhances the self-purifying capacity of contaminated environments, an important ecosystem service in both terrestrial and aquatic systems. However, studying and understanding the mechanisms that mediate biodegradation activity of recalcitrant pollutants remains necessary to better estimate the efficiency of such microbial processes and the resulting effects on pollutant fate and

persistence in the different environmental compartments. For instance, Fanesi et al. demonstrated through the use of innovative vibrational spectroscopy techniques that soil content in organic matter and mineral particles is a strong driver of the metabolic profile of a PAH-degrading bacterium, *Pseudomonas putida* G7. Such knowledge is of particular interest to develop, improve, and implement innovative and successful bioremediation strategies for polluted soils and surface or ground waters (Donati et al., 2019; Hermon et al.; Laroche et al.; Spini et al.). As an example, a critical review of the role of marine microorganisms in the biodegradation of plastic debris and on the relevance of current standard tests for plastic biodegradability in seawater ecosystems is provided in the present Research Topic (Jacquin et al.). This review is complemented by an original study that described the successive phases of colonization, growing, and maturation phases of marine biofilms on non-biodegradable and biodegradable plastics (Dussud et al.).

Besides potential environmental benefits due to the development of biodegradation capacities, adaptation to pollutants is, on a one hand, a key process that confers resistance and resilience in exposed microbial communities supporting the ecological functioning of contaminated ecosystems (Pesce et al., 2017; Capdeville et al.). On the other hand, mechanisms and processes driving microbial adaptation to pollutants at individual level can represent a genetic burden decreasing the fitness of adapted populations when the selection pressure by the pollutant is released (Changey et al., 2011). Adaptive responses to pollutants, including notably the acquisition of tolerance, can be studied at the microbial community level. The emergence, at the end of the twentieth century, of the concept of pollution induced community tolerance (PICT; Blanck et al., 1988), is one of the best illustrations of this kind of approach, which is still currently used in microbial ecotoxicology to assess the causal relationship between pollutant exposure and microbial responses (e.g., Brandt et al., 2015; Tlili et al., 2016). However, there is evidence that PICT is generally associated with a decrease in diversity and the associated ecological functions (Mahamoud Ahmed et al., 2020) in line with the paradigm that biodiversity serves as ecological insurance (Yachi and Loreau, 1999). These resulting costs of tolerance can be viewed as ecological costs of adaptation (Clements and Rohr, 2009). Indeed, loss of diversity in microbial communities following pollutant exposure may not only alter the functions they support but also increase their vulnerability to further environmental disturbances. Conversely, environmental stressors (such as warming; Lambert et al., 2017 or hydrodynamics; Polst et al.) can influence microbial diversity and modify the capacity of microbial communities to tolerate pollutant toxicity. The development of pollutant-resistant species can also modify community functional pattern and alter some metabolic capacities (Cycon et al.). Moreover, within the One Health framework, the development or acquisition of resistance to antibiotics by environmental microorganisms is contributing to the emergence of multi-drug-resistant human and animal pathogens thus endangering livestock production and the efficacy of medicines to treat infections (Smalla et al., 2016; Topp et al., 2018).

## POLLUTANT EFFECTS ON MICROBIAL COMMUNITIES THREATEN ECOSYSTEM BIODIVERSITY AND FUNCTIONS IN ALL ENVIRONMENTAL COMPARTMENTS

Since the early 2000s, ecotoxicological studies (including “microbial ecotoxicology”) have progressively moved toward experimental designs that better assess and predict the ecological risks of a given chemical stressor under realistic environmental conditions. Several articles of this Research Topic highlight the potential effects of a wide range of pollutants on microbial structure, diversity and functions in contaminated soils (Borymski et al.; Cycon et al.; Mallet et al.; Simonin, Colman et al.; Simonin, Cantarel et al.), wastewaters (Guo et al.), continental (Chonova et al.; Freixa et al.; Pei et al.) and coastal surface water (Coclet et al.; Corcoll et al.; Zouch et al.), groundwater (Crampon et al.; Imfeld et al.), and sediments (Mahamoud Ahmed et al.). Such effects on microbial communities can threaten important ecosystem functions and services such as agricultural soil aggregation (Crouzet et al.), wastewater treatment (Guo et al.), primary production (Corcoll et al.), organic matter decomposition and nutrient cycling (Mahamoud Ahmed et al.; Rossi et al.; Simonin, Colman et al.), or energy transfer among trophic levels (Crenier et al.). Unsurprisingly, a large proportion of the above-mentioned studies concerns metal pollutants that are ubiquitously found in the environment due to the combination of natural and anthropogenic sources. Therefore, this Research Topic provides further evidence that metals are one of the major drivers of microbial community structure and diversity, affecting both bacteria, archaea and algae and the functions they ensure within ecosystems (Borymski et al.; Pei et al.; Coclet et al.; Corcoll et al.; Zouch et al.; Mahamoud Ahmed et al.). However, metals are also present in the environment as nanoparticles due to their high production and use for numerous applications. Simonin, Colman et al. and Simonin, Cantarel et al. showed that copper-based nanopesticides used as a fungicide and bactericide can impact microbial processes involved in soil carbon and phosphorus cycling after chronic exposure, revealing that short-term studies may underestimate the ecotoxicological risks of these new generation of metallic pesticides on soil microbial communities and ecosystem functioning. Other metal nanoparticles, such as zero-valent iron nanoparticles that are used for remediation of different kinds of pollutants (Crampon et al.) or silver nanoparticles that are used for antimicrobial treatment (Guo et al.), were also shown to present risks for bacterial community structure and metabolic potential. As nanopesticides, biobased pesticides are often viewed as a safe alternative to synthetic organic pesticides in agriculture to achieve the agroecology transition (Seiber et al., 2014). However, ecotoxicological risks and effects of these natural active substances are still under documented (Amichot et al., 2018). The study of Mallet et al. provides evidence that natural  $\beta$ -triketone herbicide leptospermone can impact the composition and diversity of fungal communities in arable soils. All these results underline the need of incorporating microbial endpoints for environmental risk assessment and homologation processes

of novel agrochemicals such as nanopesticides or biobased pesticides. Those are viewed as pollutants of emerging concerns, such as pharmaceuticals or plastics, which are also taken into consideration in this Research Topic (Chonova et al.; Cycon et al.; Dussud et al.; Freixa et al.; Jacquin et al.; Orlewska et al.). Cyanotoxins are also sometimes cited as pollutants of emerging concerns (Snow et al., 2017) that can be harmful to both environmental and human health. Using a metabolomics approach, Le Manach et al. reported the production of a wide set of metabolites by 24 *Microcystis* strains, including different classes of cyanotoxins together with a large set of unknown molecules.

However, assessing and predicting the consequences of legacy pollutants or pollutants of emerging concerns on ecosystem functions and services remains a challenge because multiple stressors proceed simultaneously on complex interconnected biological communities. For a better understanding of the chain of causality starting from pollutant exposure to microbial community responses and then mediated ecosystem alteration, microbial ecotoxicological approaches and indicators that take into account the possible interactions between multiple pollutants are needed (Freixa et al.; Mahamoud Ahmed et al.). Therefore, Freixa et al. showed that carbon nanoparticles (fullerenes  $C_{60}$ ) can modulate the effects of organic pollutants on aquatic biofilm communities. However, they observed that both the magnitude and the direction of the interaction following joint exposure varied regarding the kind of organic pollutant, being sometimes antagonistic (e.g., fullerenes  $C_{60}$ /diuron), synergistic (fullerenes  $C_{60}$ /triclosan), or neutral (fullerenes  $C_{60}$ /venlafaxine) (Freixa et al.). Effect interactions can also vary according to the microbial endpoint considered. For instance, Mahamoud Ahmed et al. observed that arsenic and copper had an additive or synergetic negative impact on sediment denitrification while no interaction was recorded when considering other functions such as respiration or several extracellular enzymatic activities.

Moreover, interactions between pollutants and other environmental abiotic and biotic stressors must also be considered since they can modulate both the exposure and the sensitivity of microbial communities to toxicants. These parameters can be both physical, such as temperature (Pesce et al.) or hydrodynamic (Polst et al.), chemical, such as nutrients (Crenier et al.; Rossi et al.; Simonin, Cantarel et al.) or salinity (Rotini et al.), or biological (Bart et al.). More frequent studies evaluating the impact of combined or cumulative exposure to multiple chemical and non-chemical stressors on microbial communities in controlled conditions or along environmental gradients are being published (see above examples). Nevertheless, it is still difficult to go beyond these case-by-case studies and to generalize concepts that can be deployed widely in environmental risk assessment procedures. Large-scale initiatives (i.e., meta-studies) such as the “Microbiome Stress Project” proposed by Rocca et al. to leverage existing metagenomic studies assessing the response of microbial communities to various environmental stressors are timely. The crucial issue of data-sharing has recently been pinpointed by Eckert et al. (2020) who claimed that at least 20% of published metagenomic data are not generally accessible for other scientists, and lack robust metadata.

## RESEARCH IN MICROBIAL ECOTOXICOLOGY SHOULD IMPROVE POLLUTANT RISK ASSESSMENT AND ECOSYSTEM QUALITY MONITORING BUT LACKS ROBUST TRANSFER TO STAKEHOLDERS AND ENVIRONMENTAL MANAGERS

Microbial ecotoxicology is a growing Research Topic that contributes to improve knowledge on the microbial responses to pollutants under variable exposure scenarios. Furthermore, innovative methods and approaches are being developed including novel ecotoxicological endpoints (Sgier et al.), new types of bioassays (Morin et al.) and next generation methods, such as volatolomics to detect signatures of pollutant exposure (Hidalgo et al.). Efforts have also been made to develop and test bioindicator approaches to assess biological exposure to pollutants and/or resulting effects on ecological quality in contaminated ecosystems through the study of microbial communities naturally present in the different environmental compartments (Imfeld et al.; Pei et al.; Pesce et al., 2017). However, despite strong evidence of the relevance of developed methods and approaches, these remain case studies that do not entirely respond to the needs of environmental regulators and managers. Operational and generalizable procedures have not been examined so far, from sampling strategies to data analysis, including tests for robust interpretation methodologies with reference baselines and quality levels. Accordingly, changes in microbial assemblages are still not well taken into account for pollutant risk assessment and ecosystem quality monitoring, as regularly pointed out, for example, by the European Food Safety Authority (EFSA PPR Panel, 2013, 2017; EFSA Scientific Committee, 2016). As an example, potential impacts on microbial communities are completely ignored in the development of Environmental Quality Standards (EQS) in the EU water framework directive (WFD) that is the most significant European water legislation to date. These EQS mandate concentration thresholds that should not be exceeded for a range of selected pollutants to preserve ecological integrity in aquatic ecosystems. Only diatom biodiversity is used to assess the biological quality of water bodies within the WFD.

In 2016, Bengtsson-Palme and Larsson (2016) also underlined the need for considering the risks of antibiotic resistance development associated with antibiotic pollution and subsequent dissemination to human pathogens. They determined “predicted no effect concentrations” (PNECs) for 11 selected antibiotics based on available minimum inhibitory concentrations (MICs). Most of the PNECs were below available PNECs for ecotoxicological effects, suggesting that current environmental guidelines are not protective enough for environmental and human health (Tell et al., 2019).

## KEY CHALLENGES AND FUTURE PERSPECTIVES

Knowledge about the interactions between pollutants and microbial communities is continuously increasing. The following challenges, which are far from being exhaustive, underline the necessity (i) to reinforce disciplinary knowledge to better characterize microbial responses to pollutants at the species, population, and community levels but also (ii) to develop multi-disciplinary approaches combining among others microbial ecotoxicology, ecology, microbiology, toxicology, environmental chemistry and physics, big data science, modeling, as well as animal and human health sciences to better explore and predict the consequences of these responses on ecosystem and human health and well-being, in line with the “One Health” paradigm.

A major challenge is to go beyond the community level, which is commonly considered in microbial ecotoxicology (Ghiglione et al., 2016) in order to translate the microbial response to ecosystem scale. This is the policy-relevant scale to which prevention and mitigation strategies need to be deployed. This crucial and non-trivial issue goes beyond the sole scope of microbial ecotoxicology and needs the inclusion of the latest advances and concepts in microbial ecology (Graham et al., 2016) but also in general ecology to take into account the interactions between micro- and macro-organisms. The short- and long-term ecological costs of microbial adaptation processes (at both the species and community levels), as well as community and ecosystem resistance and resilience capacities that guarantee the preservation and/or the recovery of ecosystem biodiversity and functioning under pollutant exposure, need to be characterized. This cannot be done without taking into account the fact that microbial communities are generally chronically exposed to complex mixtures of pollutants and are otherwise subjected to a wide range of additional chemical, physical, and/or biological stressors. This is conceptually and technically challenging since the enormous diversity of pollutants and possible environmental stressors preclude the testing of every possible binary and multiple combinations. To face this gap, initiatives aiming to facilitate data sharing from multistress studies and their meta-analysis are greatly encouraged. Together with studies developing mechanistic models of interaction at different levels, these initiatives will be needed to produce robust and generalizable predictive models for the purposes of improving the *a priori* and *a posteriori* risk assessment of pollutants in the context of global change.

Another main challenge concerns the urgent need of extending our knowledge on the environmental factors (including pollutants) and the microbial mechanisms that contribute to the development, the proliferation and the dispersal of pathogenic microorganisms, microbial resistance to pharmaceuticals and microbial toxins in various environmental compartments. Managing microorganisms of human or animal health concern requires consideration of the environmental dimension of the One Health Continuum.

Finally, future research in microbial ecotoxicology should also gain in transferability to end-users, including policy-makers and environmental managers, to develop more effective policies and efficient regulations aiming at preserving our environment and health from the adverse effects of pollutants. We mentioned above the need of better considering microbial communities, their functional diversity and their role in the evolution and spreading of antibiotic-resistant pathogens in the elaboration of Environmental Quality Standards (EQS) and in homologation procedures (including those of nanopesticides or biobased pesticides). Given how rapidly research in microbial ecotoxicology and related methods are developing, it is a challenge to identify, standardize, and normalize the most relevant protocols for operational and regulatory applications. Indeed, standards are required (Philippot et al., 2012; Römbke et al., 2018) and large-scale studies are needed to perform meta-analyses and inform models to establish reference baselines, such as “normal operating ranges” of microbial functions (EFSA Scientific Committee, 2016). Moreover, one may not exclude the fact that the microbial world, which is most often invisible to the human eye, remains largely unknown to the general public and, even more worryingly, to a wide range of stakeholders and deciders. Among others, this is probably one of the main

reasons why knowledge transfer from science to end-users and other stakeholders is particularly poor and has to be improved. It is thus important to have a dialogue between the research community, regulators, industry and broader society in order to share a common understanding making possible the achievement of a societal consensus defining the acceptable effect of pollutants on microbial communities and supported ecosystem services.

## AUTHOR CONTRIBUTIONS

All authors listed have made a substantial, direct and intellectual contribution to the work, and approved it for publication.

## ACKNOWLEDGMENTS

This Research Topic was promoted by the International Network on Microbial Ecotoxicology – EcotoxicoMic (<https://ecotoxicomic.org/>). We thank all participating authors and reviewers for having made this Research Topic a success. We are also grateful to Dr. Philippe Garrigues for his support and help since the early stages of development of the EcotoxicoMic Network.

## REFERENCES

- Amichot, M., Joly, P., Martin-Laurent, F., Siauxat, D., and Lavoit, A.-V. (2018). Biocontrol, new questions for Ecotoxicology? *Environ. Sci. Pollut. Res.* 25, 33895–33900. doi: 10.1007/s11356-018-3356-5
- Bengtsson-Palme, J., and Larsson, D. G. (2016). Concentrations of antibiotics predicted to select for resistant bacteria: proposed limits for environmental regulation. *Environ. Int.* 86, 140–149. doi: 10.1016/j.envint.2015.10.015
- Blanck, H., Wängberg, S.-A., and Molander, S. (1988). “Pollution induced community tolerance - a new ecotoxicological tool,” in: *Functional Testing of Aquatic Biota for Estimating Hazards of Chemicals*, eds J. Cairns Jr and J.R. Pratt (Philadelphia, PA: ASTM STP 988), 219–230. doi: 10.1520/STP26265S
- Blicharska, M., Smithers, R. J., Mikusinski, G., Rönnbäck, P., Harrison, P. A., Nilsson, M., et al. (2019). Biodiversity’s contributions to sustainable development. *Nat. Sustain.* 2, 1083–1093. doi: 10.1038/s41893-019-0417-9
- Brandt, K. K., Amézquita, A., Backhaus, T., Boxall, A., Coors, A., Heberer, T., et al. (2015). Ecotoxicological assessment of antibiotics: a call for improved consideration of microorganisms. *Environ. Int.* 85, 189–205. doi: 10.1016/j.envint.2015.09.013
- Cavicchioli, R., Ripple, W. J., Timmis, K. N., Azam, F., Bakken, L. R., Baylis, M., et al. (2019). Scientists’ warning to humanity: microorganisms and climate change. *Nat. Rev. Microbiol.* 17, 247–260. doi: 10.1038/s41579-019-0222-5
- Changey, F., Devers-Lamrani, M., Rouard, N., and Martin-Laurent, F. (2011). *In vitro* evolution of an atrazine-degrading population under cyanuric acid selection pressure: evidence for selective loss of a 47 kb region on the plasmid pADP1 containing the atzA, B and C genes. *Gene* 490, 18–25. doi: 10.1016/j.gene.2011.09.005
- Clements, W. H., and Rohr, J. R. (2009). Community responses to contaminants: using basic ecological principles to predict ecotoxicological effects. *Environ. Toxicol. Chem.* 28, 1789–1800. doi: 10.1897/09-140.1
- Cycon, M., Mroczek, A., and Piotrowska-Seget, Z. (2019). Antibiotics in the soil environment -degradation and their impact on microbial activity and diversity. *Front. Microbiol.* 10:338. doi: 10.3389/fmicb.2019.00338
- Destoumieux-Garzón, D., Mavingui, P., Boetsch, G., Boissier, J., Darriet, F., Duboz, P., et al. (2018). The one health concept: 10 years old and a long road ahead. *Front. Vet. Sci.* 5:14. doi: 10.3389/fvets.2018.00014
- Donati, E. R., Sani, R. K., Goh, K. M., and Chan, K.-G. (2019). Editorial: recent advances in bioremediation/biodegradation by extreme microorganisms. *Front. Microbiol.* 10:1851. doi: 10.3389/fmicb.2019.01851
- Eckert, E. M., Di Cesare, A., Fontaneto, D., Berendonk, T. U., Bürgmann, H., Cytryn, E., et al. (2020). Every fifth published metagenome is not available to science. *PLoS Biol.* 18:e3000698. doi: 10.1371/journal.pbio.3000698
- EFSA PPR Panel (EFSA Panel on Plant Protection Products and their Residues) (2013). Guidance on tiered risk assessment for plant protection products for aquatic organisms in edge-of-field surface waters. *EFSA J.* 11, 3290. doi: 10.2903/j.efsa.2013.3290
- EFSA PPR Panel (EFSA Panel on Plant Protection Products and their Residues) (2017). Scientific Opinion addressing the state of the science on risk assessment of plant protection products for in-soil organisms. *EFSA J.* 15:4690. doi: 10.2903/j.efsa.2017.4690
- EFSA Scientific Committee (2016). Scientific opinion on recovery in environmental risk assessments at EFSA. *EFSA J.* 14:4313. doi: 10.2903/j.efsa.2016.4313
- Ghiglione, J., Martin-Laurent, F., and Pesce, S. (2016). Microbial ecotoxicology: an emerging discipline facing contemporary environmental threats. *Environ. Sci. Pollut. Res.* 23, 3981–3983. doi: 10.1007/s11356-015-5763-1
- Graham, E. B., Knelman, J. E., Schindlbacher, A., Siciliano, S., Breulmann, M., Yannarell, A., et al. (2016). Microbes as engines of ecosystem function: when does community structure enhance predictions of ecosystem processes? *Front. Microbiol.* 7:214. doi: 10.3389/fmicb.2016.00214
- Lambert, A. S., Dabrin, A., Foulquier, A., Morin, S., Rosy, C., Coquery, M., et al. (2017). Influence of temperature in pollution-induced community tolerance approaches used to assess effects of copper on freshwater phototrophic periphyton. *Sci. Total Environ.* 607–608, 1018–1025. doi: 10.1016/j.scitotenv.2017.07.035
- Mahamoud Ahmed, A., Tardy, V., Bonnineau, C., Billard, P., Pesce, S., and Lyautey, E. (2020). Changes in sediment microbial diversity following chronic copper-exposure induce community copper-tolerance without increasing sensitivity to arsenic. *J. Hazard. Mater.* 391:122197. doi: 10.1016/j.jhazmat.2020.122197
- Marco, D. E., and Abram, F. (2019). Editorial: Using genomics, metagenomics and other “omics” to assess valuable microbial ecosystem services

- and novel biotechnological applications. *Front. Microbiol.* 10:151. doi: 10.3389/fmicb.2019.00151
- Naeem, S., Chazdon, R., Duffy, J. E., Prager, C., and Worm, B. (2016). Biodiversity and human well-being: An essential link for sustainable development. *Proc. Biol. Sci.* 283:20162091. doi: 10.1098/rspb.2016.2091
- Pesce, S., Ghiglione, J. F., and Martin-Laurent, F. (2017). "Microbial communities as ecological indicators of ecosystem recovery following chemical pollution," in *Microbial Ecotoxicology*, eds C. Cravo-Laureau, C. Cagnon, B. Lauga, and R. Duran (Cham: Springer), 227–250. doi: 10.1007/978-3-319-61795-4\_10
- Philippot, L., Ritz, K., Pandard, P., Hallin, S., and Martin-Laurent, F. (2012). Standardisation of methods in soil microbiology: progress and challenges. *FEMS Microbiol. Ecol.* 82, 1–10. doi: 10.1111/j.1574-6941.2012.01436.x
- Rockström, J., Steffen, W., Noone, K., Persson, Å., Chapin, F. S. III., Lambin, E., et al. (2009). A safe operating space for humanity. *Nature* 461, 472–475. doi: 10.1038/461472a
- Römbke, J., Bernard, J., and Martin-Laurent, F. (2018). Standard methods for the assessment of structural and functional diversity of soil organisms: a review. *Integr. Environ. Assess. Manage.* 14, 463–479. doi: 10.1002/ieam.4046
- Seiber, J. N., Coats, J., Duke, S. O., and Gross, A. D. (2014). Biopesticides: State of the art and future opportunities. *J. Agric. Food Chem.* 62, 11613–11619. doi: 10.1021/jf504252n
- Smalla, K., Simonet, P., Tiedje, J., and Topp, E. (2016). Editorial: Special section of FEMS microbiology ecology on the environmental dimension of antibiotic resistance. *FEMS Microbiol. Ecol.* 94:fix185. doi: 10.1093/femsec/fiw172
- Snow, D. D., Cassada, D. A., Larsen, M. L., Mware, N. A., Li, X., D'Alessio, M., et al. (2017). Detection, occurrence and fate of emerging contaminants in agricultural environments. *Water Environ. Res.* 89, 897–920. doi: 10.2175/106143017X15023776270160
- Tell, J., Caldwell, D. J., Haner, A., Hellstern, J., Hoeger, B., Journal, R., et al. (2019). Science-based targets for antibiotics in receiving waters from pharmaceutical manufacturing operations. *Integr. Environ. Assess. Manage.* 15, 312–319. doi: 10.1002/ieam.4141
- Tlili, A., Bérard, A., Blanck, H., Bouchez, A., Cássio, F., Eriksson, K. M., et al. (2016). Pollution-induced community tolerance (PICT): towards an ecologically relevant risk assessment of chemicals in aquatic systems. *Freshw. Biol.* 61, 2141–2151. doi: 10.1111/fwb.12558
- Topp, E., Larsson, D. G. J., Miller, D. N., Van den Eede, C., and Virta, M. P. J. (2018). Antimicrobial resistance and the environment: assessment of advances, gaps and recommendations for agriculture, aquaculture and pharmaceutical manufacturing. *FEMS Microbiol. Ecol.* 92:fiw172. doi: 10.1093/femsec/fix185
- Yachi, S., and Loreau, M. (1999). Biodiversity and ecosystem productivity in a fluctuating environment: the insurance hypothesis. *Proc. Nat. Acad. Sci. U. S. A.* 96, 1463–1468. doi: 10.1073/pnas.96.4.1463

**Conflict of Interest:** The authors declare that the research was conducted in the absence of any commercial or financial relationships that could be construed as a potential conflict of interest.

Copyright © 2020 Pesce, Ghiglione, Topp and Martin-Laurent. This is an open-access article distributed under the terms of the Creative Commons Attribution License (CC BY). The use, distribution or reproduction in other forums is permitted, provided the original author(s) and the copyright owner(s) are credited and that the original publication in this journal is cited, in accordance with accepted academic practice. No use, distribution or reproduction is permitted which does not comply with these terms.



# Cloning, Expression, Isotope Labeling, and Purification of Transmembrane Protein MerF from Mercury Resistant *Enterobacter* sp. AZ-15 for NMR Studies

Aatif Amin\* and Zakia Latif

Department of Microbiology and Molecular Genetics, University of the Punjab, Lahore, Pakistan

## OPEN ACCESS

### Edited by:

Stéphane Pesce,  
National Research Institute of Science  
and Technology for Environment and  
Agriculture, France

### Reviewed by:

Willem J. H. Van Berkel,  
Wageningen University and Research,  
Netherlands  
Weimin Ma,  
Shanghai Normal University, China

### \*Correspondence:

Aatif Amin  
aatifamin93@gmail.com

### Specialty section:

This article was submitted to  
Microbiotechnology, Ecotoxicology  
and Bioremediation,  
a section of the journal  
Frontiers in Microbiology

Received: 28 April 2017

Accepted: 21 June 2017

Published: 07 July 2017

### Citation:

Amin A and Latif Z (2017) Cloning,  
Expression, Isotope Labeling, and  
Purification of Transmembrane Protein  
MerF from Mercury Resistant  
*Enterobacter* sp. AZ-15 for NMR  
Studies. *Front. Microbiol.* 8:1250.  
doi: 10.3389/fmicb.2017.01250

Mercury resistant (Hg<sup>R</sup>) *Enterobacter* sp. AZ-15 was isolated from heavy metal polluted industrial wastewater samples near to districts Kasur and Sheikhpura, Pakistan. 16S rDNA ribotyping and phylogenetic analysis showed 98% homology with already reported *Enterobacter* species. The *merF* gene encoding transmembrane protein-MerF was amplified from genomic DNA and ligated into pET31b+ vector using restriction endonucleases, *SphI* and *XhoI*. The genetic codons of *merF* gene encoding cysteine residues were mutated into codons, translating into serine residues by site-directed mutagenesis. Ketosteroid isomerase (KSI), a fusion tag which is present in pET31b+ vector, was used in the expression of *merFm* gene. KSI was used to drive the target peptide (MerFm) into inclusion bodies so that the peptide yield and purity were increased. The stable plasmid pET31b+:*merFm* was transformed into C43(DE3) *E. coli* cells. The high expression of uniformly <sup>15</sup>N isotopically labeled-MerFm protein was induced with 1 mM IPTG. The purification of <sup>15</sup>N-MerFm recombinant protein by Ni-NTA and size exclusion chromatography involved an unfolding/refolding procedure. The two-dimensional HSQC NMR spectra of MerFm protein showed the purity and correct number of resonances for each amide. <sup>1</sup>H-<sup>15</sup>N HSQC NMR experiment also confirmed that no modification of the tryptophan residue occurred during cyanogen bromide cleavage. A small scale reservoir of Luria Bertani (LB) medium supplemented with 20 μg/ml of HgCl<sub>2</sub> showed 90% detoxification of Hg by *Enterobacter* sp. AZ-15. The accumulation of Hg on the cell surface of this strain was visualized by scanning electron microscopy (SEM) which confirmed its potential use in Hg-bioremediation.

**Keywords:** *Enterobacter* sp. AZ-15, pET31b+, MerF, Size exclusion chromatography, <sup>1</sup>H-<sup>15</sup>N heteronuclear single quantum coherence, Hg-detoxification, scanning electron microscopy (SEM)

## INTRODUCTION

Mercury toxicity is a worldwide problem to both human and animals. The level of mercury pollution in the environment is being increased day by day due to anthropogenic sources and activities like the discharge of industrial effluent from chlor-alkali industries, mining of metal and incineration of coal (Steenhuisen and Wilson, 2015). It is obvious that both forms of mercury

(inorganic and organic) cause cytotoxic and neurotoxic effects to humans and animals (WHO, 2000).

Bacterial detoxification systems have spawned much interest in recent times for their potential usefulness in the bioremediation of environmental contaminants (Silver, 1992). Heavy metals are just one of a variety of contaminants that have appeared in our environment, and quite a few natural resistances to them have already been documented. Plasmid-born resistances to a wide variety of heavy metals have been explored and the genes encoding their resistances have been sequenced (Silver, 1992). The best characterized of these systems is the bacterial mercury detoxification system, the *mer* operon, and in particular those on transposons Tn21, Tn501, and Tn5053 (Gilbert and Summers, 1988; Dahlberg and Hermansson, 1995).

Bacteria can be used for bioremediation because they take up mercury *via* membrane potential-dependent sequence-diverged members of the mercuric ion (Mer) superfamily, i.e., a periplasmic Hg-scavenging protein (MerP) and one or more inner membrane-spanning proteins (MerC, MerE, MerF, and MerT), which transport Hg<sup>2+</sup> into the cytoplasm (Barkay et al., 2003). All the *mer* operons have *merT* and *merP*, however, some operons, such as transposon Tn21, have *merC*. The *merF* is also part of *mer* operons of Gram negative bacteria and is absent in the *mer* operons of Gram positive bacteria. The additional *merC* gene is located between *merP* and *merA*. However, it seems not to be essential for Hg<sup>2+</sup> resistance since it is absent from Tn501, which confers identical Hg<sup>2+</sup> resistance levels (Summers, 1986).

The enzymatic mercury detoxification system is one of the most remarkable because of its level of sophistication. Mercury is toxic at very low levels, as Hg<sup>2+</sup> with no known biological benefit. Its toxicity is related to nonspecific reactivity with sulfhydryl groups in proteins and high permeability through biological membranes. Expression of proteins encoding mercury resistance is governed by an operator/promoter region, which interacts with a divergently transcribed MerR biosensor protein. The roles of the gene products designated T (116 amino acids), P (72 amino acids), C (143 amino acids), and A have been worked out using gene deletion studies (Hamlett et al., 1992; Wilson et al., 2000). In detoxification mechanism, the toxic Hg<sup>2+</sup> atoms are 'handed off' from MerP to MerT, which transports Hg<sup>2+</sup> to the reductase, MerA (Ghosh et al., 1999). More recently, a homolog of MerT, designated MerF (81 residues), has been sequenced from *Alcaligenes* and *Pseudomonas* genera posited to have the same function (Yeo et al., 1998; Sone et al., 2013).

Integral to this transport system are several pairs of cysteine residues, which are known to bind Hg<sup>2+</sup> in a linear bicoordinate manner. In particular, the motifs -CC-, -CXC-, -CXXC-, and -CXXXXXC- are found in MerT/MerF, MerE, MerP, and MerC, respectively (DeSilva et al., 2002). Mutagenesis of the cysteine residues suggests that only one of the cysteine residues in MerP, Cl7, is important, and only the first -CC- pair in MerT and MerF is important (Powlowski and Sahlman, 1999). In MerT mutation of a cysteine residue in the -CXXXXXC- pair is only slightly detrimental to its transport function, while mutation in the vicinal -CC- residues in either MerT or MerF is detrimental in the transportation (Hobman and Brown, 1997).

MerF is predicted to have two membrane-spanning segments. It has been shown definitively to function as a transporter of mercuric ions into the cell by possession of two vicinal pairs of cysteine residues which are involved in the transport of Hg<sup>2+</sup> across the membrane and are exposed to the cytoplasm. More importantly, MerF alone is sufficient for the transport of Hg<sup>2+</sup> across the cell membrane. NMR studies of integral membrane domain and full length MerF from *Escherichia coli* (C41 and C43 cells) have been investigated (Das et al., 2012; Lu et al., 2013; Tian et al., 2014).

Inoculation of contaminated sites with selected or engineered bacteria has often not been satisfactory, partly because the introduced metabolic potential was not the limiting factor for pollutant degradation (Cases and de Lorenzo, 2005). This applies also to mercury resistance, which is ubiquitous in soil and water, even in the Arctic (Barkay and Poulain, 2007; Møller et al., 2011). For the treatment of mercury-contaminated groundwater, pilot experiments have been carried out with the aim to establish bio-barriers in the groundwater where sulfate reducing bacteria (SRB) could adsorb mercury and precipitate it as insoluble cinnabar (Wagner-Döbler et al., 2000; Dash and Das, 2012; He et al., 2015).

In the present study, a major transporter protein of bacterial Hg-detoxification system, MerF isolated from Hg-resistant *Enterobacter* sp. AZ-15 was first time studied and then the potential of selected bacterial strain AZ-15 in the detoxification of Hg (II) was evaluated. These objectives were achieved by (1) the screening of mercury resistant bacteria from polluted natural environment and their 16S rDNA phylogenetic analysis (2) designing the gene construct and expression of mutated *merF* (*merFm*) gene (3) purification of MerFm protein by Ni-NTA and size exclusion chromatography (4) NMR studies of <sup>15</sup>N isotopically labeled-MerFm protein (5) the analysis of Hg-detoxification potential at lab scale and SEM of selected bacterial cells.

## MATERIALS

Enzymes were purchased from New England Biolabs (www.neb.com) unless otherwise noted, and the oligonucleotides were synthesized by Integrated DNA Technologies (www.idtdna.com). GeneJET genomic DNA purification kit and MAX efficiency<sup>®</sup> DH5 $\alpha$ <sup>™</sup> competent *E. coli* cells were purchased from Thermo Fisher<sup>®</sup> (www.thermofisher.com). Rapid DNA Dephos & ligation kit was obtained from Life Sciences<sup>®</sup> (www.lifescience.roche.com). Gel extraction kit, miniprep kit for small-scale plasmid preparations and His-tag nickel affinity resin (Ni-NTA) were purchased from Qiagen<sup>®</sup> (www.qiagen.com). QuikChange lightning site-directed mutagenesis kit was from Agilent Technologies<sup>®</sup> (www.genomics.agilent.com). Plasmid DNA of pET-31b(+) and bacterial strain OverExpress<sup>™</sup> C43(DE3) were purchased from Lucigen<sup>®</sup> (www.lucigen.com). <sup>15</sup>N-ammonium sulfate and d<sub>25</sub>-sodium dodecyl sulfate were obtained from Cambridge isotope laboratories (www.isotope.com). FPLC Sephacryl S-200 was obtained from Pharmacia LKB (Piscataway, NJ).

## Methods—Bacterial Isolates and Growth Conditions

Industrial water samples from different geological areas of districts Kasur and Sheikhpura, Punjab, Pakistan were collected in sterilized polythene bags. All samples were brought to laboratory and different physico-chemical parameters were analyzed within 24–48 h. Bacterial load of the samples was determined by making serial dilutions of  $10^{-1}$  to  $10^{-4}$  from 1% initial water sample. In order to isolate the individual colonies, 100  $\mu$ l of the  $10^{-3}$  and  $10^{-4}$  dilutions were spread on LB agar plates containing different concentrations of  $\text{HgCl}_2$  ranging from 1 to 20  $\mu$ g/ml. The plates were incubated at 37°C for 24 h. The single isolated and  $\text{HgCl}_2$  resistant colonies were selected and re-streaked on new LB agar plates without  $\text{HgCl}_2$  to get purified colonies. All  $\text{Hg}$ -resistant and purified bacterial cultures were stored as glycerol stocks (30%) at  $-80^\circ\text{C}$ .

## Biochemical and Molecular Characterization

Highly  $\text{Hg}$ -resistant isolate AZ-15 was biochemically characterized by different tests *viz.*, Gram staining, shape, motility, spore formation, catalase, oxidase, oxygen requirement, MacConkey agar growth, indole production, methyl red, Voges-Proskauer, citrate (Simmon) agar growth, and  $\text{H}_2\text{S}$  production by following the protocols of Cappuccino and Sherman (2008). The bacterial genomic DNA of AZ-15 was extracted by genomic DNA purification kit. The universal primers were used for the amplification of 16S rRNA gene using BIOER XP-thermal cycler (Normand, 1995). The amplification conditions for both genes were set as: 5 min at 95°C, 35 cycles of 1 min at 95°C, 1 min at 55°C, and 2 min at 72°C, with a final 5 min chain elongation at 72°C. The sequence results obtained from MacroGen sequencing core facility, Korea were checked through nucleotide blast and submitted to NCBI GenBank.

## Cloning of *merF* Gene into pET31b(+) Vector

The *merF* gene (wild type) of highly mercury resistant *Enterobacter* sp. AZ-15 was amplified using the primers given in Table 1. The amplified product of 246 bp was digested with the restriction enzymes *XhoI* and *SphI*, and purified by gel extraction kit. The digested *merF* gene was ligated with the *XhoI*-*SphI*-cleaved expression vector pET31b(+) (Kuliopulos et al., 1987). The genetic codons encoding cysteine residues in the native sequence of *merF* gene were mutated into codons encoding serine residues using site directed mutagenesis kit by designing two sets of primers (Table 1). Both sequences of *merF* gene (*merF* wild type and mutated *merF*) along with translated peptide sequences were submitted to the NCBI database ([www.ncbi.nlm.nih.gov/](http://www.ncbi.nlm.nih.gov/)) and obtained accession numbers as MF185183 and MF185184, respectively. The designed recombinant plasmid containing mutated *merF* (*merFm*) gene was transformed into DH5 $\alpha$  competent cells and identified by using same restriction enzymes on agarose gel. The nucleotide sequence of recombinant pET31b(+) containing *merFm* gene was confirmed by DNA sequencing facility provided marketplace, University

**TABLE 1** | Oligonucleotides for the amplification of 16S rRNA, wild type *merF* and mutated *merF* (*merFm*) genes.

Gene	Primer pair	Primer sequence
16S rRNA	16S-F	5'AGAGTTTGATCCTGGCTCAG3'
	16S-R	5'AAGGAGGTGATCCAGCCGCA3'
<i>merF</i>	<i>merF</i> -F	5'ATCTAT <b>GCATGC</b> ATGAAAGACCCGAAGACTGC TGC GGGT CAGC3'
	<i>merF</i> -R	5'ATATAT <b>CTCGAG</b> TCATTTTTTACTCCATTGAATTT CGGGG3'
<i>merFm</i>	<i>merFm</i> -1	5'GTGGCGCTCAGTTCGTTCCACCCCTGTTCTGG3'
	<i>merFm</i> -1	5'CCAGAACAGGGGTGAACGAAGTGAAGCCAC3'
	<i>merFm</i> -2	5'CAAGCCGATGCTCGTCCACCCGAAATTCAT3'
	<i>merFm</i> -2	5'ATTGAATTCGGGGTGGACGAGGCATCGGCTTG3'

*Bold sequences are restriction sites of specific enzymes.*

of California, San Diego (USA). Then the recombinant plasmid pET31b(+) was transformed into C43(DE3) competent *E. coli* cells. After transformation, stable C43(DE3): pET31b+*merFm* clones were screened and stored as glycerol stocks (20% of glycerol) at  $-80^\circ\text{C}$ .

## Production of $^{15}\text{N}$ -Labeled Recombinant MerFm

The expression of recombinant *merFm* gene was optimized in LB medium and unlabeled M9 medium supplemented with different concentrations (0.2, 0.5, and 1 mM) of isopropyl- $\beta$ -D-thiogalactoside (IPTG) at different time intervals (2, 4, 6, 7 h, and overnight) of incubation. For expression of isotopically labeled MerFm protein, 5 ml of LB medium with final concentration of 50 mg/l of carbenicillin was inoculated with 5  $\mu$ l of clone C43(DE3): pET31b+*merFm* glycerol stock. After 5 h incubation at 37°C, 1 ml of starter culture was used to inoculate 50 ml of M9 minimal medium (per liter) containing  $\text{Na}_2\text{HPO}_4$  7.0 g,  $\text{KH}_2\text{PO}_4$  3.0 g, NaCl 0.5g,  $\text{CaCl}_2$  0.1 mM,  $\text{MgSO}_4$  1 mM, thiamin 50 mg, d-glucose 10 g, and  $^{15}\text{N}$ - $(\text{NH}_4)_2\text{SO}_4$  1 g containing 50 mg/l of carbenicillin. The culture was kept at 300 rpm at 37°C for overnight and 50 ml culture was poured into 450 ml of same  $^{15}\text{N}$  labeled-M9 medium. The cells were allowed to grow at 37°C in shaking incubator until the optical density (O.D<sub>600</sub>) of 0.6 was achieved. The expression of recombinant plasmid (KSI\_MerFm\_His-tag) was achieved by adding 1 mM of IPTG as a final concentration and kept on shaking for another 7 h on same conditions. The pellet of C43(DE3) cells containing recombinant protein was obtained by subsequent harvesting at 7,000 rpm for 30 min at 4°C.

## Purification of the Recombinant Protein by Ni-NTA Chromatography

The cell pellets were resuspended in 30 ml lysis buffer (50 mM Tris hydrochloride, 15% glycerol (v/v), 1 mM  $\text{NaN}_3$ , pH 8.0). After 10 min of incubation at room temperature, cell lysate was sonicated by a probe sonicator ([www.fishersci.com](http://www.fishersci.com)) for 5 min (cycles: 5 s on/10 s off) on ice and then centrifuged at

17,000 rpm for 30 min at 4°C. The pellet at this stage contains purified inclusion bodies containing more than 90% of MerFm fusion protein. The pellet containing inclusion bodies was then resuspended in the nickel column binding buffer (20 mM Tris hydrochloride, 500 mM NaCl, 6 M guanidinium hydrochloride (GndCl), 5 mM imidazole, pH 8.0) by tip sonication, and centrifuged again at 19,000 rpm for 1 h to remove remaining protein, lipids, and lipid-associated debris. The supernatant was loaded onto a Ni-NTA His-Bind Resin column, pre-equilibrated with binding buffer. The column was then washed with washing buffer (20 mM Tris hydrochloride, 500 mM NaCl, 6 M guanidinium hydrochloride (GndCl), 50 mM imidazole, pH 8.0). The fusion protein was eluted with elution buffer (20 mM Tris hydrochloride, 500 mM NaCl, 6 M GndCl, 500 mM imidazole, pH 8.0) and concentrated to 30 ml using an Amicon stirred concentrator cell with YM10 filter membrane and dialyzed against ddH<sub>2</sub>O in a 10,000 kDa MWCO dialysis membrane with four water changes until the protein precipitates out of solution. The precipitated protein was then lyophilized.

## Cyanogen Bromide Cleavage of the Fusion Protein

The lyophilized protein was dissolved in 70% formic acid solution and cleaved by addition of a three-fold excess of cyanogen bromide (CNBr) for 3–5 h in the absence of light. The cleavage reaction was stopped by adding double volume of 1M NaOH. The cleaved polypeptide was dialyzed by using 3,500 kDa MWCO dialysis membrane against water and then lyophilized.

## Purification of MerFm by FPLC

Cleaved protein was re-dissolved in 4 ml phosphate SDS buffer (100 mM Na<sub>2</sub>HPO<sub>4</sub>, 4 mM SDS, 1 mM EDTA, 1mM NaN<sub>3</sub>, pH 8.2) and 1 ml 1 N NaOH. Size-Exclusion gel chromatography using a Sephacryl S-200 column equilibrated with phosphate-SDS buffer on a Pharmacia FPLC system used to separate the KSI fusion partner from the pure MerFm protein. Fractions containing MerFm were pooled and concentrated down to 30 ml using an Amicon Stirred cell with a 3,500 MWCO membrane. The pure protein was then dialyzed against ddH<sub>2</sub>O (with 40 mM β-mercaptoethanol for native MerFm) to remove SDS for six times with time interval of 12 h until the protein precipitates. Each time the protein was centrifuged out of solution, quickly lyophilized, and stored at –20°C for further use, Yields of MerFm were approximately 2–3 mg/l of cell culture. SDS-PAGE was run to monitor the purification, with the final native MerFm protein.

## NMR Spectroscopy of MerFm

All NMR samples were prepared by resolubilizing the lyophilized protein in NMR buffer (10 mM Na<sub>2</sub>HPO<sub>4</sub>, 500 mM d<sub>25</sub>-SDS, 1mM NaN<sub>3</sub>, pH 6.0). The protein was then incubated at 40°C for 30 min with intermittent bath sonication and centrifuged at 13,000 rpm for 15 min to remove undissolved protein and other debris. The labeled peptide samples were prepared in different concentrations 10, 40, and 75% of D<sub>2</sub>O. Two-dimensional heteronuclear single quantum coherence (HSQC) spectra of uniformly <sup>15</sup>N-labeled MerFm were recorded on Bruker DMX

600 spectrometer equipped with a triple resonance probe, three-axis pulsed field gradients, a deuterium lock channel and operated at a <sup>1</sup>H NMR frequency of 600 MHz with total recording time 7 h. The other parameters for obtaining <sup>15</sup>N–<sup>1</sup>H fast Heteronuclear Single Quantum Coherence (fHSQC) spectra include pulse sequence with 1,024 points in t<sub>2</sub> and 256 points in t<sub>1</sub> and 50°C using a 1.5 s recycle delay. The spectra were processed by using Sparky 3 [Goddard and Kneller, University of California San Francisco (UCSF), USA].

## Detoxification of Hg<sup>2+</sup> by Bacteria and SEM Analysis

An experiment was designed to check the detoxification potential of *Enterobacter* sp. at a lab scale. Mercury resistant (Hg<sup>R</sup>) bacterial strain AZ-15 and mercury sensitive strain (Hg<sup>S</sup>) *Enterobacter cloacae* ZA-15 (KJ728671) with equal number of cells (cfu/ml) were inoculated separately in flasks containing 30 mL of LB medium, supplemented each flask with 20 µl/ml of HgCl<sub>2</sub> to determine the detoxification efficiency of mercury. The flasks were incubated at 37°C for up to 8 h with 2 h of time intervals at 120 rpm of agitation in triplicates. After incubation, cultures were spun down at 14,000 rpm for 15 min and detoxification of Hg<sup>2+</sup> was estimated by dithizone method (Elly, 1973; Khan et al., 2006). For scanning electron microscopy (SEM), one drop of 48 h culture was diluted into 15 ml of ddH<sub>2</sub>O and dried on carbon surface slide. The topographical, morphological and crystallographic information of bacterial cell membrane was monitored using Scanning Electron Microscope (SEM) (JEOL-JSM-6480).

## Statistical Analysis

The phylogenetic analysis of *Enterobacter* sp. AZ-15 with already reported bacteria on the basis of 16S rRNA gene was done by Mega 6.0 software (Tamura et al., 2013). The results of lab scale mercury detoxification experiment were subjected to mean, standard deviation, analysis of variance (ANOVA) by using SPSS V.20 software (IBM, 2011). The hydrophathy plot predicting membrane spanning regions was built by SWISS-MODEL homology ([www.expasy.org](http://www.expasy.org)).

## RESULTS

### Screening of Hg-Resistant Bacteria

Industrial water samples collected from different geological sites (tanneries) of district Kasur and Itehad chemicals limited, district Sheikhpura, Lahore were checked for physico-chemical properties such as temperature, pH, Hg<sup>2+</sup> concentration, bacterial load in the presence of metal stress of HgCl<sub>2</sub>. Data indicate the level of pH in water sample falls in the range of 6.47–7.65. All samples (100%) were within the pH ranges of WHO drinking water guidelines (WHO, 2004) but the value of HgCl<sub>2</sub> which range from 5 to 17 µg/ml has crossed limit described by WHO (1 µg/ml) (Javendra, 1995). The bacterial count in these samples is also variable, ranging from 2.1 × 10<sup>2</sup> to 2.9 × 10<sup>5</sup> as presented in **Table 2**. A total 30 bacterial strains including Gram positive and Gram negative were screened on the basis of showing resistance against different concentrations of HgCl<sub>2</sub>.

**TABLE 2** | Level of physico-chemical parameters and bacterial load in industrial water samples.

Samples	Temperature	pH	Bacterial load	Hg <sup>2+</sup> (μg/ml)
Officers colony	28.5	6.47	3.02 × 10 <sup>3</sup>	1
Gullberg Town	30.5	7.45	2.90 × 10 <sup>5</sup>	5
Civil Hospital	29	7.23	3.00 × 10 <sup>4</sup>	8
Nafees colony	33.5	7.65	2.90 × 10 <sup>4</sup>	1
Itehad chemicals	34	7.25	2.1 × 10 <sup>2</sup>	2
<b>WHO guidelines for drinking water quality</b>				
	.....	6.5–8.5	.....	1

**TABLE 3** | Results of biochemical tests of bacterial isolate AZ-15.

Biochemical tests	Results
Gram staining	Gram-ve
Shape	Rods
Motility	Motile
Spore formation	Non-spore forming
Catalase	Positive
Oxidase	Negative
Oxygen requirement	Facultative anaerobe
MacConkey growth	Positive
Indole production	Negative
Methyl red	Negative
Voges-Proskauer	Positive
Citrate (Simmon)	Positive
H <sub>2</sub> S production	Negative
AZ-15	<i>Enterobacter</i> sp.

## Biochemical and 16S rDNA Identification

The most highly Hg-resistant bacterial isolate AZ-15 showing growth at 20 μg/ml of HgCl<sub>2</sub>, was characterized on the basis of colony morphology and biochemical tests. The results are shown in **Table 3**. Mercury resistant bacterial isolate was identified by 16S rDNA sequencing (≈1.5 kb) as *Enterobacter* sp. with accession number KU558920. Other close matches to *Enterobacter* sp. AZ-15 (KU558920) includes *E. cloacae* strain E717 (EF059865), *Enterobacter* sp. BSRA3 (FJ868807), *E. cloacae* strain NBRC 13535 (NR113615), *E. cloacae* strain DSM 30054 (NR117679), *E. cloacae* strain RPR-CCFL3 (KR611993) and *Enterobacter* sp. Wy2-D9 (JN986806). *Enterobacter* sp. GJ1-11 (EU139848), *Enterobacter* sp. BAB-3140 (KF984440), and *Enterobacter* sp. STJ12 (KC833508) represent as an out group in this phylogenetic analysis (Supplementary Figure 1).

## Plasmid Construction

As shown in **Figure 1A**, the gene construct *merFm* was designed by ligation of wild type *merF* gene in pET31b(+) vector. The deduced amino acid sequence of *merF* gene showed two cysteine residues at the positions 71 and 72. The cysteine residues were mutated into serine residues in *merFm* gene by site-directed mutagenesis which results no cysteine residue in the final *merFm*

gene construct as shown in **Figure 1B**. The salient features of construct include T7 promoter, ketosteroid isomerase (KSI) fusion partner, 5' overhanging sequences compatible with *SphI* and *XhoI* restriction enzyme sites, within restriction sites; a transcription initiation codon (ATG) of *merFm* followed by encoding region of respective protein and a termination codon and a region encoding a hexahistidine amino acid tag and T7 terminator. His-tag sequence is for ease of purification and the KSI peptide sequence is designed to form inclusion bodies. After the transformation of recombinant plasmid into competent DH5α *E. coli* cells, the plasmid DNA was purified at concentration of 45 mg/ml. The plasmid was then transformed into *E. coli* C43(DE3) cells for expressing high concentration of MerFm recombinant protein and is thus protected from proteolysis. The fusion protein is non-toxic to the *E. coli* host cell, and is expressed at levels up to 20% of total cellular protein in *E. coli* strain C43(DE3). This approach to the production of MerFm in *E. coli* may be generally applicable to other membrane proteins. We have used it successfully with several other small membrane proteins.

## Expression and Purification of <sup>15</sup>N-Labeled MerFm Protein

For optimization of recombinant protein MerFm, three different concentrations, 0.2, 0.5, and 1 mM of IPTG were used at different post-induction time (h) viz., 2, 4, 6, 7, and overnight. The high expression of recombinant protein MerFm was achieved with 1 mM of IPTG and 7 h of post-induction time as shown in lane 12 of Supplementary Figure 2. The same conditions were maintained for expression of <sup>15</sup>N-labeled MerFm fusion protein. After expression, the separation and purification of <sup>15</sup>N-MerFm were performed by following the procedure described in detail in the methodology section. Briefly, the recombinant/fusion protein formed as inclusion bodies was separated from the total cell lysate by centrifugation. The fusion protein was partially purified by nickel affinity chromatography. The data in Supplementary Figure 3, illustrate the expression and isolation of inclusion bodies of full-length MerFm by Ni-NTA column. Lane 1 is showing Mark12™ unstained protein ladder (www.lamdabio.com). After the post-induction period of 7 h, the cells were lysed by sonication and centrifuged. After centrifugation, the supernatant was discarded which contained the total cellular proteins except inclusion bodies is shown in lane 2 of a 12% SDS-PAGE. Lane 3 contains the inclusion bodies solubilized in binding buffer and lanes 4 and 5 show the soluble fraction (flow through) and washing of other proteins with washing buffer, respectively except the targeted fusion protein. The lanes 6–10 show that the insoluble fractions (inclusion bodies) containing primarily the targeted fusion protein. After elution from the nickel column, the KSI fusion partner was cleaved from the MerFm polypeptide in the presence of CNBr at methionine for obtaining purified native MerFm. The lane 2 in **Figure 2A** shows the cleavage of fusion protein and the lane 3 contains the little bit impurity of KSI fusion partner while lanes 4–8 show the purified fractions <sup>15</sup>N-MerFm after size-exclusion chromatography (FPLC). **Figure 2B** shows the peaks of <sup>15</sup>N-MerFm and KSI in FPLC.



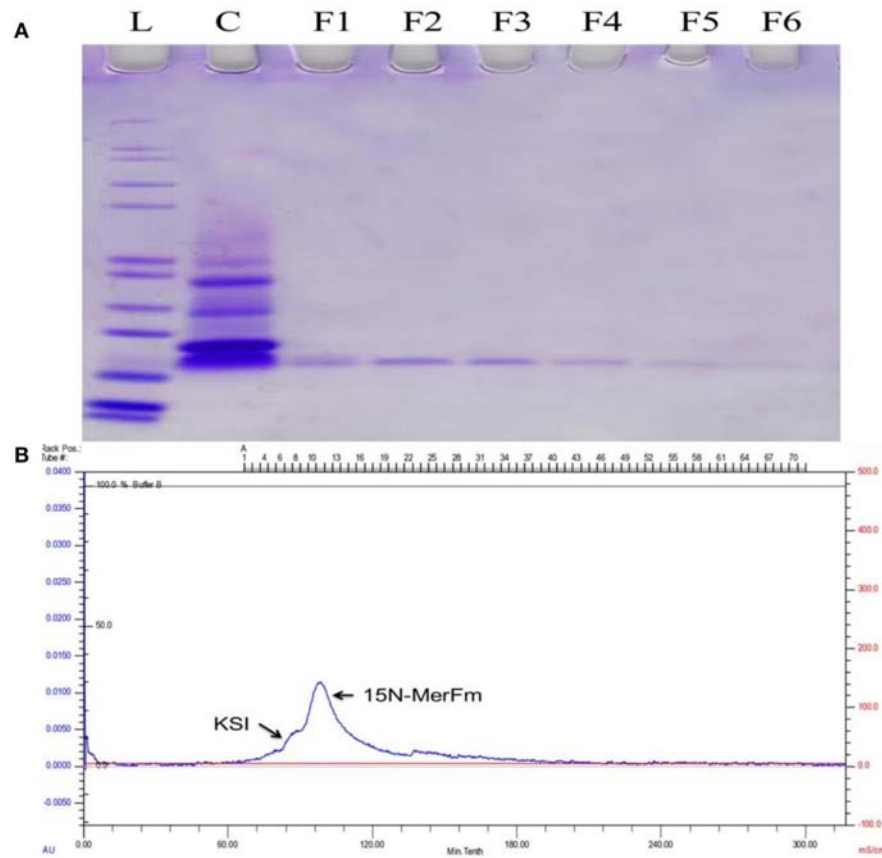


**FIGURE 2 | (A)** L: Molecular weight (kDa) ladder. C: cleavage of fusion protein. F1–F5: Purified fractions of MerFm from FPLC column. **(B)** FPLC chromatogram showing peaks of native MerFm and fusion partner KSI.

organomercurials. Among these tools, the transportation of mercury through microbial membranes plays a crucial role in the bacterial mercury detoxification system (Barkay et al., 2003; Parks et al., 2013).

Four families of integral membrane proteins (IMPs) have been identified in the characterized *mer* operons, ranging from 2 to 4 predicted transmembrane elements: MerE, MerF, MerT, and MerC. Across the *mer* operons, MerT, a tri-spanning, 116 residue protein, is considered to be the principal mercury transporter and has been shown to be an essential component in most *mer* operons capable of bestowing mercuric resistance. The extent to which the other IMPs, MerF and MerE, are capable of functioning independently of MerT has not yet been conclusively determined (Mok et al., 2012).

In previous studies, the full length and truncated structures of MerF have been deeply studied by NMR spectroscopy found in *E. coli* and in plasmid pMER327/419 of *Pseudomonas fluorescens* between *merP* and *merA* (Veglia and Opella, 2000; Wilson et al., 2000). This is the first study to analyze the gene construction, expression and purification of mutated MerF (MerFm) amplified from *Enterobacter* sp. AZ-15. The bacterium, *Enterobacter* sp. AZ-15 isolated from mercury

contaminated industrial effluent samples, could resist  $Hg^{2+}$  upto 20  $\mu g/ml$ . In other reports, the potential of *Enterobacter* sp. to tolerate  $Hg^{2+}$  varied (Table 4). Phylogenetic analysis of this bacterium AZ-15 showed 98% similarity to already reported *Enterobacter* species (Supplementary Figure 1). A gene construct of mutated *merF* was designed and expressed with 1 mM IPTG and 7 h post-induction at 37°C. The cysteine residues in wild type MerF sequence induce aggregation due to disulfide bonds which makes the protein difficult to purify.

Moreover, the MerFm was purified by fast protein liquid chromatography (FPLC) but Lu and Opella (2014) used high performance liquid chromatography (HPLC) for purification of wild type and truncated MerF. The high quality spectra of  $^1H$ - $^{15}N$  HSQC confirmed full expression of the native sequence of MerFm and each amino acid (with the exception of proline) contains one  $^1H$ - $^{15}N$  unit in the backbone. The hydropathy plot (Supplementary Figure 4) suggests that MerF has two hydrophobic trans-membrane helices, although the N-terminal portion of the plot is somewhat atypical. Wild-type MerF has two pairs of vicinal Cys residues (replaced by serines in MerFm), which is unusual, and contrasts with the -CXXC- sequences

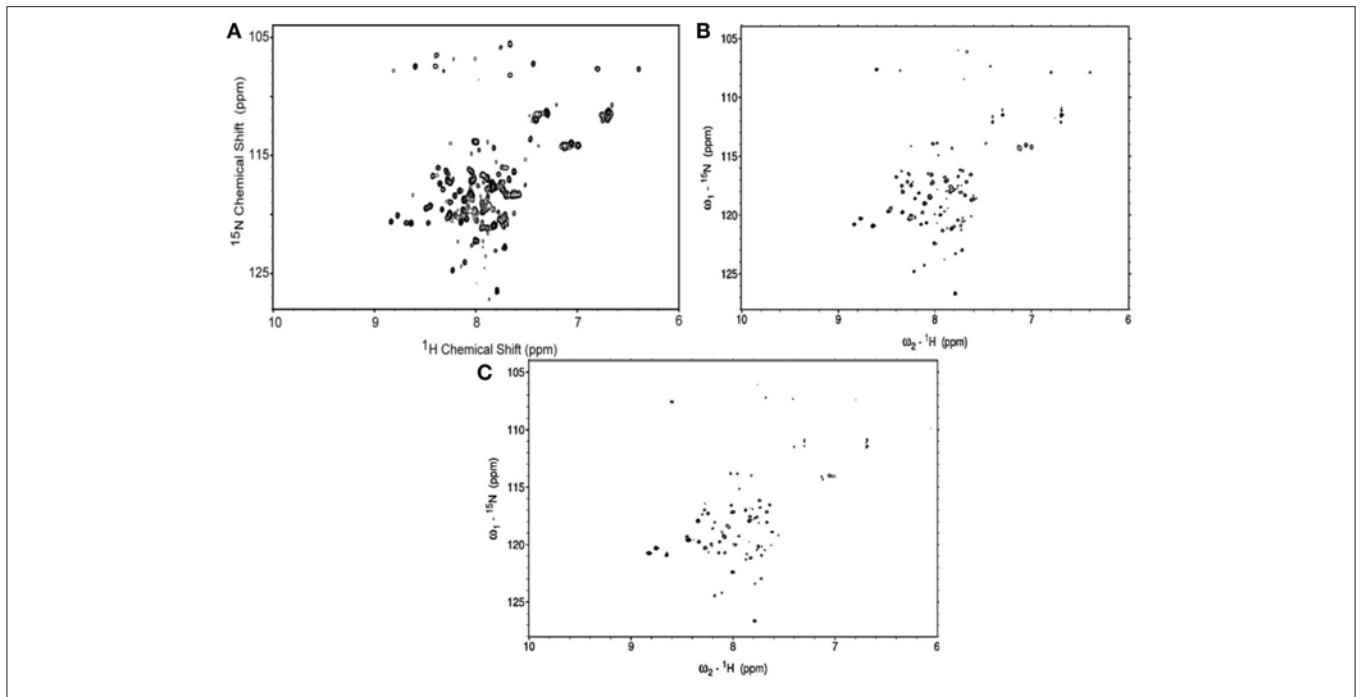


**FIGURE 3 |**  $^1\text{H}$ - $^{15}\text{N}$  HSQC spectra of uniformly- $^{15}\text{N}$ -labeled MerFm in SDS micelles with different concentrations of  $\text{D}_2\text{O}$  (A) 10% (B) 40%, and (C) 75%.

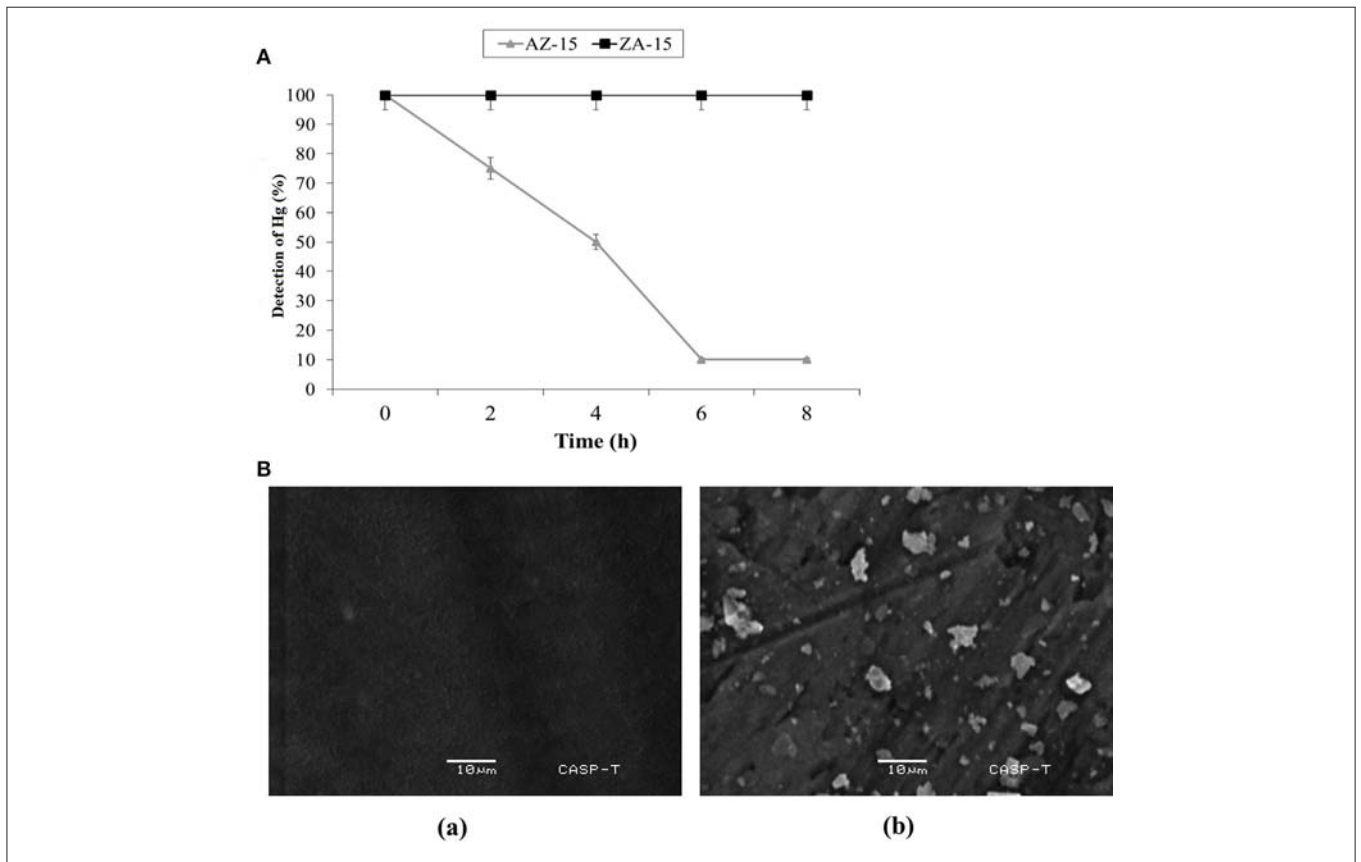


**FIGURE 4 | (A)** Detoxification of Hg in LB medium. X-axis shows the given incubation time (h) and Y-axis shows the % of Hg detected at different time intervals **Ba**, SEM analysis of Hg-resistant *Enterobacter* sp. AZ-15 **Bb**, Hg-sensitive *Enterobacter cloacae* ZA-15.

**TABLE 4** | Mercury resistant bacteria and their patterns of resistance to different concentrations of Hg<sup>2+</sup> in different media.

Bacteria	MIC	Media used	References
<i>Pseudomonas putida</i> SPI3	NR	LB	Von Canstein et al., 1999
<i>Psychrobacter</i> sp. ORHg1	100 μM (20.06 μg/ml)	NEM	Pepi et al., 2011
<i>Pseudomonas putida</i> SP1	300 μM (60 μg/ml)	2216E	Zhang et al., 2012
<i>Bacillus cereus</i>	30 μM (6 μg/ml)	LB	François et al., 2012
	15 μM (3 μg/ml)	PB	
<i>Lysinibacillus</i> sp.	60 μM (12 μg/ml)	LB	François et al., 2012
	15 μM (3 μg/ml)	PB	
<i>Kocuria rosa</i>	20 μM (4 μg/ml)	LB	François et al., 2012
	30 μM (6 μg/ml)	PB	
<i>Microbacterium oxydans</i>	100 μM (20 μg/ml)	LB	François et al., 2012
	30 μM (6 μg/ml)	PB	
<i>Serratia marcescens</i>	60 μM (12 μg/ml)	LB	François et al., 2012
	30 μM (6 μg/ml)		
<i>Ochrobactrum</i> sp.	60 μM (12 μg/ml)	LB	François et al., 2012
	30 μM (6 μg/ml)		
<i>Ensifer medicae</i>	6 μM (1.2 μg/ml)	YEM	Ruiz-Diez et al., 2012
<i>Rhizobium leguminosarum</i>	12.5 μM (2.5 μg/ml)	YEM	Ruiz-Diez et al., 2012
<i>Rhizobium radiobacter</i>	30 μM (6 μg/ml)	YEM	Ruiz-Diez et al., 2012
<i>Bradyrhizobium canariense</i>	12.5 μM (2.5 μg/ml)	YEM	Ruiz-Diez et al., 2012
<i>Providencia alcalifaciens</i>	9.2 μM (1.84 μg/ml)	LB	Cabral et al., 2013
<i>Pseudomonas putida</i>	11.5 μM (2.3 μg/ml)	LB	Cabral et al., 2013
<i>Enterobacter</i> sp. AZ-15	100 μM (20 μg/ml)	LB	This study
<i>Sphingobium</i> sp. SA2	25.43 μM (5.1 μg/ml)	LP	Mahbub et al., 2016
	220 μM (44.15 μg/ml)	NB	
<i>Enterobacter</i> sp. A25B	400 μM (80 μg/ml)	LB	Giovanella et al., 2016
<i>Enterobacter</i> sp. B50C	250 μM (50 μg/ml)		
<i>Bacillus</i> sp. AZ-1	100 μM (20 μg mL <sup>-1</sup> )	LB	Amin and Latif, 2016
<i>Bacillus cereus</i> AZ-2	100 μM (20 μg mL <sup>-1</sup> )		
<i>Enterobacter cloacae</i> AZ-3	50 μM (10 μg mL <sup>-1</sup> )		

typically found in proteins that bind mercury and other heavy metals (Opella et al., 2002). The vicinal arrangements of the cysteines have profound consequences for their metal-binding properties and the selectivity for Hg<sup>2+</sup> over other metals (DeSilva et al., 2002). With both metal transfer and transport activities, the structural biology of MerF is too elaborate to be explained simply by Hg<sup>2+</sup> binding to pairs of cysteines. Therefore, it is essential to determine its three-dimensional structure in phospholipid bilayers, where it executes its functions. Experiments are underway to explore further structural properties of MerFm having natural origin.

The capability of different bacterial species to detoxify Hg<sup>2+</sup> varies in different Hg supplemented enriched media as shown in Table 4. The present study also determined that the merF gene in *Enterobacter* sp. AZ-15 encodes a polypeptide sequence capable of proper folding, NMR studies and also ensures the presence of mer operon. The favorable thermodynamic and spectral characteristics of the recombinant protein will allow the detailed description of this natural protein. During the investigation of Hg-detoxification capability, *Enterobacter* sp. AZ-15 showed 90% detoxification potential of

Hg<sup>2+</sup> from HgCl<sub>2</sub> supplemented LB medium. The crystalline structures of deposited Hg were visualized by SEM. Sathyavathi et al. (2013) and Mahbub et al. (2016) have previously reported the SEM analysis of same crystalline structures of detoxified Hg.

In conclusion, the expression and purification of <sup>15</sup>N-labeled MerFm from mercury resistant *Enterobacter* sp. AZ-15 (MIC-20 μg/ml), was first time successfully achieved. <sup>1</sup>H-<sup>15</sup>N HSQC NMR spectra confirmed the expression of exact number of all residues of MerFm by producing one cross peak for each <sup>1</sup>H-<sup>15</sup>N pair in a protein. In lab scale experiment, *Enterobacter* sp. AZ-15 showed 90% bioremediation of Hg from Hg-supplemented LB medium. On the basis of these characteristics, mercury resistant *Enterobacter* sp. AZ-15 could be used as a potential candidate to deteriorate the toxic effects of Hg<sup>2+</sup> from the environment.

## AUTHOR CONTRIBUTIONS

AA conducted the experiments and wrote the paper while ZL proofread and overall supervised the project.

## ACKNOWLEDGMENTS

This project was financially supported by Higher Education Commission, Pakistan (Pin No. 112-23128-2BM1-164) and University of the Punjab (Grant No. D/5719/Est.1). The authors are thankful to Prof. Stanley Opella, University of California, San Diego, USA for providing laboratory facilities to conduct research work on MerF protein, Prof. Simon Silver, University of Illinois, USA, and Prof. Ginro Endo, Tohoku Gakuin University,

Japan for providing *B. megaterium* MB1 strain isolated from the sediments of Minamata Bay, as a positive control for Hg-resistance.

## SUPPLEMENTARY MATERIAL

The Supplementary Material for this article can be found online at: <http://journal.frontiersin.org/article/10.3389/fmicb.2017.01250/full#supplementary-material>

## REFERENCES

- Amin, A., and Latif, Z. (2016). Screening of mercury-resistant and indole-3-acetic acid producing bacterial-consortium for growth promotion of *Cicer arietinum* L. *J. Basic Microbiol.* 57, 204–217. doi: 10.1002/jobm.2016.00352
- Barkay, T., Miller, S. M., and Summers, A. O. (2003). Bacterial mercury resistance from atoms to ecosystems. *FEMS Microbiol. Rev.* 27, 355–384. doi: 10.1016/S0168-6445(03)00046-9
- Barkay, T., and Poulain, A. J. (2007). Mercury (micro) biogeochemistry in polar environments. *FEMS Microbiol. Ecol.* 59, 232–241. doi: 10.1111/j.1574-6941.2006.00246.x
- Cabral, L., Giovanella, P., Gianello, C., Bento, F. M., Andrezza, R., and Camargo, F. A. O. (2013). Isolation and characterization of bacteria from mercury contaminated sites in Rio Grande do Sul, Brazil, and assessment of methylmercury removal capability of a *Pseudomonas putida* V1 strain. *Biodegradation* 24, 319–331. doi: 10.1007/s10532-012-9588-z
- Cappuccino, J. G., and Sherman, N. (2008). *Microbiology: A Laboratory Manual*. San Francisco, CA: Pearson/Benjamin Cummings.
- Cases, I., and de Lorenzo, V. (2005). Genetically modified organisms for the environment: stories of success and failure and what we have learned from them. *Int. Microbiol.* 8, 213–222.
- Dahlberg, C., and Hermansson, M. (1995). Abundance of Tn3, Tn21, and Tn501 transposase (tnpA) sequences in bacterial community DNA from marine environments. *Appl. Environ. Microbiol.* 61, 3051–3056.
- Das, B. B., Nothnagel, H. J., Lu, G. J., Son, W. S., Tian, Y., Marassi, F. M., et al. (2012). Structure determination of a membrane protein in proteoliposomes. *J. Am. Chem. Soc.* 134, 2047–2056. doi: 10.1021/ja209464f
- Dash, H. R., and Das, S. (2012). Bioremediation of mercury and the importance of bacterial mer genes. *Int. Biodeterior. Biodegrad.* 75, 207–213. doi: 10.1016/j.ibiod.2012.07.023
- DeSilva, T. M., Veglia, G., Porcelli, F., Prantner, A. M., and Opella, S. J. (2002). Selectivity in heavy metal-binding to peptides and proteins. *Biopolymers* 64, 189–197. doi: 10.1002/bip.10149
- Elly, C. T. (1973). Dithizone procedure for mercury analysis. *J. Water Pollut. Control Fed.* 45, 940–945.
- François, F., Lombard, C., Guigner, J.-M., Soreau, P., Brian-Jaisson, F., Martino, G., et al. (2012). Isolation and characterization of environmental bacteria capable of extracellular biosorption of mercury. *Appl. Environ. Microbiol.* 78, 1097–1106. doi: 10.1128/AEM.06522-11
- Ghosh, S., Sadhukhan, P., Chaudhuri, J., Ghosh, D., and Mandal, A. (1999). Purification and properties of mercuric reductase from *Azotobacter chroococcum*. *J. Appl. Microbiol.* 86, 7–12. doi: 10.1046/j.1365-2672.1999.00605.x
- Gilbert, M. P., and Summers, A. O. (1988). The distribution and divergence of DNA sequences related to the Tn21 and Tn501 mer operons. *Plasmid* 20, 127–136. doi: 10.1016/0147-619X(88)90015-7
- Giovanella, P., Cabral, L., Bento, F. M., Gianello, C., and Camargo, F. A. O. (2016). Mercury (II) removal by resistant bacterial isolates and mercuric (II) reductase activity in a new strain of *Pseudomonas* sp. B50A. *New Biotechnol.* 33, 216–223. doi: 10.1016/j.nbt.2015.05.006
- Hamlett, N., Landale, E., Davis, B., and Summers, A. (1992). Roles of the Tn21 merT, merP, and merC gene products in mercury resistance and mercury binding. *J. Bacteriol.* 174, 6377–6385. doi: 10.1128/jb.174.20.6377-6385.1992
- He, F., Gao, J., Pierce, E., Strong, P., Wang, H., and Liang, L. (2015). *In situ* remediation technologies for mercury-contaminated soil. *Environ. Sci. Pollut. Res.* 22, 8124–8147. doi: 10.1007/s11356-015-4316-y
- Hobman, J., and Brown, N. (1997). Bacterial mercury-resistance genes. *Met. Ions Biol. Syst.* 34, 527.
- IBM, C. (2011). *IBM SPSS Statistics for Windows*.
- Javendra, S. (1995). *Water Pollution Management*. New Delhi: Venus Publishing House.
- Khan, H., Ahmed, M. J., and Bhangar, M. I. (2006). A simple spectrophotometric method for the determination of trace level lead in biological samples in the presence of aqueous micellar solutions. *J. Spectrosc.* 20, 285–297. doi: 10.1155/2006/269568
- Kuliopulos, A., Shortle, D., and Talalay, P. (1987). Isolation and sequencing of the gene encoding delta 5-3-ketosteroid isomerase of *Pseudomonas testosteroni*: overexpression of the protein. *Proc. Natl. Acad. Sci. U.S.A.* 84, 8893–8897. doi: 10.1073/pnas.84.24.8893
- Lu, G. J., and Opella, S. J. (2014). Resonance assignments of a membrane protein in phospholipid bilayers by combining multiple strategies of oriented sample solid-state NMR. *J. Biomol. NMR* 58, 69–81. doi: 10.1007/s10858-013-9806-y
- Lu, G. J., Tian, Y., Vora, N., Marassi, F. M., and Opella, S. J. (2013). The structure of the mercury transporter MerF in phospholipid bilayers: a large conformational rearrangement results from N-terminal truncation. *J. Am. Chem. Soc.* 135, 9299–9302. doi: 10.1021/ja4042115
- Mahbub, K. R., Krishnan, K., Megharaj, M., and Naidu, R. (2016). Bioremediation potential of a highly mercury resistant bacterial strain *Sphingobium* SA2 isolated from contaminated soil. *Chemosphere* 144, 330–337. doi: 10.1016/j.chemosphere.2015.08.061
- Mok, T., Chen, J. S., Shlykov, M. A., and Saier, M. H. Jr. (2012). Bioinformatic analyses of bacterial mercury ion (Hg<sup>2+</sup>) transporters. *Water Air Soil Pollut.* 223, 4443–4457. doi: 10.1007/s11270-012-1208-3
- Møller, A. K., Barkay, T., Al-Soud, W. A., Sørensen, S. J., Skov, H., and Kroer, N. (2011). Diversity and characterization of mercury-resistant bacteria in snow, freshwater and sea-ice brine from the High Arctic. *FEMS Microbiol. Ecol.* 75, 390–401. doi: 10.1111/j.1574-6941.2010.01016.x
- Normand, P. (1995). Utilisation des séquences 16S pour le positionnement phylétique d'un organisme inconnu. *Oceanis* 21, 31–56.
- Opella, S. J., DeSilva, T. M., and Veglia, G. (2002). Structural biology of metal-binding sequences. *Curr. Opin. Chem. Biol.* 6, 217–223. doi: 10.1016/S1367-5931(02)00314-9
- Parks, J. M., Johs, A., Podar, M., Bridou, R., Hurt, R. A., Smith, S. D., et al. (2013). The genetic basis for bacterial mercury methylation. *Science* 339, 1332–1335. doi: 10.1126/science.1230667
- Pepi, M., Gaggi, C., Bernardini, E., Focardi, S., Lobianco, A., Ruta, M., et al. (2011). Mercury-resistant bacterial strains *Pseudomonas* and *Psychrobacter* spp. isolated from sediments of Orbetello Lagoon (Italy) and their possible use in bioremediation processes. *Int. Biodeterior. Biodegrad.* 65, 85–91. doi: 10.1016/j.ibiod.2010.09.006
- Powlowski, J., and Sahlman, L. (1999). Reactivity of the two essential cysteine residues of the periplasmic mercuric ion-binding protein, MerP. *J. Biol. Chem.* 274, 33320–33326. doi: 10.1074/jbc.274.47.33320
- Ruiz-Díez, B., Qui-ones, M. A., Fajardo, S., López, M. A., Higuera, P., and Fernández-Pascual, M. (2012). Mercury-resistant rhizobial bacteria isolated from nodules of leguminous plants growing in high Hg-contaminated soils. *Appl. Microbiol. Biotechnol.* 96, 543–554. doi: 10.1007/s00253-011-3832-z

- Sathyavathi, S., Manjula, A., Rajendhran, J., and Gunasekaran, P. (2013). Biosynthesis and characterization of mercury sulphide nanoparticles produced by *Bacillus cereus* MRS-1. *Indian J. Exp. Biol.* 51, 973–978.
- Silver, S. (1992). “Bacterial heavy metal detoxification and resistance systems,” in *Biotechnology and Environmental Science: Molecular Approaches*, eds. S. Mongkolsuk, P. S. Lovett and J. E. Trempy. (Boston, MA: Springer US), 109–129. doi: 10.1007/978-0-585-32386-2\_14
- Sone, Y., Nakamura, R., Pan-Hou, H., Itoh, T., and Kiyono, M. (2013). Role of MerC, MerE, MerF, MerT, and/or MerP in resistance to mercurials and the transport of mercurials in *Escherichia coli*. *Biol. Pharm. Bull.* 36, 1835–1841. doi: 10.1248/bpb.b13-00554
- Steenhuisen, F., and Wilson, S. J. (2015). Identifying and characterizing major emission point sources as a basis for geospatial distribution of mercury emissions inventories. *Atmos. Environ.* 112, 167–177. doi: 10.1016/j.atmosenv.2015.04.045
- Summers, A. O. (1986). Organization, expression, and evolution of genes for mercury resistance. *Annu. Rev. Microbiol.* 40, 607–634. doi: 10.1146/annurev.mi.40.100186.003135
- Tamura, K., Stecher, G., Peterson, D., Filipinski, A., and Kumar, S. (2013). MEGA6: molecular evolutionary genetics analysis version 6.0. *Mol. Biol. Evol.* 30, 2725–2729. doi: 10.1093/molbev/mst197
- Tian, Y., Lu, G. J., Marassi, F. M., and Opella, S. J. (2014). Structure of the membrane protein MerF, a bacterial mercury transporter, improved by the inclusion of chemical shift anisotropy constraints. *J. Biomol. NMR* 60, 67–71. doi: 10.1007/s10858-014-9852-0
- Veglia, G., and Opella, S. J. (2000). Lanthanide ion binding to adventitious sites aligns membrane proteins in micelles for solution NMR spectroscopy. *J. Am. Chem. Soc.* 122, 11733–11734. doi: 10.1021/ja002119d
- Von Canstein, H., Li, Y., Timmis, K., Deckwer, W.-D., and Wagner-Döbler, I. (1999). Removal of mercury from chloralkali electrolysis wastewater by a mercury-resistant *Pseudomonas putida* strain. *Appl. Environ. Microbiol.* 65, 5279–5284.
- Wagner-Döbler, I., Von Canstein, H., Li, Y., Timmis, K. N., and Deckwer, W.-D. (2000). Removal of mercury from chemical wastewater by microorganisms in technical scale. *Environ. Sci. Technol.* 34, 4628–4634. doi: 10.1021/es0000652
- WHO (2000). *Air Quality Guidelines for Europe*. WHO Regional Publication, European Series Copenhagen: Regional Office for Europe, WHO.
- WHO (2004). *Guidelines for Drinking-Water Quality: Recommendations*. World Health Organization.
- Wilson, J. R., Leang, C., Morby, A. P., Hobman, J. L., and Brown, N. L. (2000). MerF is a mercury transport protein: different structures but a common mechanism for mercuric ion transporters? *FEBS Lett.* 472, 78–82. doi: 10.1016/s0014-5793(00)01430-7
- Yeo, C. C., Tham, J. M., Kwong, S. M., Yiin, S., and Poh, C. L. (1998). Tn5563, a transposon encoding putative mercuric ion transport proteins located on plasmid pRA2 of *Pseudomonas alcaligenes*. *FEMS Microbiol. Lett.* 165, 253–260. doi: 10.1111/j.1574-6968.1998.tb13154.x
- Zhang, W., Chen, L., and Liu, D. (2012). Characterization of a marine-isolated mercury-resistant *Pseudomonas putida* strain SP1 and its potential application in marine mercury reduction. *Appl. Microbiol. Biotechnol.* 93, 1305–1314. doi: 10.1007/s00253-011-3454-5

**Conflict of Interest Statement:** The authors declare that the research was conducted in the absence of any commercial or financial relationships that could be construed as a potential conflict of interest.

Copyright © 2017 Amin and Latif. This is an open-access article distributed under the terms of the Creative Commons Attribution License (CC BY). The use, distribution or reproduction in other forums is permitted, provided the original author(s) or licensor are credited and that the original publication in this journal is cited, in accordance with accepted academic practice. No use, distribution or reproduction is permitted which does not comply with these terms.



# Fungal Unspecific Peroxygenases Oxidize the Majority of Organic EPA Priority Pollutants

Alexander Karich<sup>1\*</sup>, René Ullrich<sup>1</sup>, Katrin Scheibner<sup>2</sup> and Martin Hofrichter<sup>1</sup>

<sup>1</sup> Department of Bio- and Environmental Sciences, Technische Universität Dresden–International Institute Zittau, Zittau, Germany, <sup>2</sup> Enzyme Technology Unit, Brandenburg University of Technology, Cottbus, Germany

## OPEN ACCESS

### Edited by:

Fabrice Martin-Laurent,  
Institut National de la Recherche  
Agronomique (INRA), France

### Reviewed by:

Lígia O. Martins,  
Universidade Nova de Lisboa,  
Portugal  
Yonghong Bi,  
Institute of Hydrobiology (CAS), China

### \*Correspondence:

Alexander Karich  
alexander.karich@tu-dresden.de

### Specialty section:

This article was submitted to  
Microbiotechnology, Ecotoxicology  
and Bioremediation,  
a section of the journal  
Frontiers in Microbiology

Received: 16 June 2017

Accepted: 20 July 2017

Published: 09 August 2017

### Citation:

Karich A, Ullrich R, Scheibner K and  
Hofrichter M (2017) Fungal Unspecific  
Peroxygenases Oxidize the Majority of  
Organic EPA Priority Pollutants.  
*Front. Microbiol.* 8:1463.  
doi: 10.3389/fmicb.2017.01463

Unspecific peroxygenases (UPOs) are secreted fungal enzymes with promiscuity for oxygen transfer and oxidation reactions. Functionally, they represent hybrids of P450 monooxygenases and heme peroxidases; phylogenetically they belong to the family of heme-thiolate peroxidases. Two UPOs from the basidiomycetous fungi *Agrocybe aegerita* (AaeUPO) and *Marasmius rotula* (MroUPO) converted 35 out of 40 compounds listed as EPA priority pollutants, including chlorinated benzenes and their derivatives, halogenated biphenyl ethers, nitroaromatic compounds, polycyclic aromatic hydrocarbons (PAHs) and phthalic acid derivatives. These oxygenations and oxidations resulted in diverse products and—if at all—were limited for three reasons: (i) steric hindrance caused by multiple substitutions or bulkiness of the compound as such (e.g., hexachlorobenzene or large PAHs), (ii) strong inactivation of aromatic rings (e.g., nitrobenzene), and (iii) low water solubility (e.g., complex arenes). The general outcome of our study is that UPOs can be considered as extracellular counterparts of intracellular monooxygenases, both with respect to catalyzed reactions and catalytic versatility. Therefore, they should be taken into consideration as a relevant biocatalytic detoxification and biodegradation tool used by fungi when confronted with toxins, xenobiotics and pollutants in their natural environments.

**Keywords:** EC 1.11.2.1, peroxidase, xenobiotics, chlorobenzene, nitroaromatics, polycyclic aromatic hydrocarbons, fungi

## INTRODUCTION

The most important classes of organic pollutants in the environment are mineral oil constituents as well as halogenated and nitrated products of petrochemicals. Enzymatic transformation and degradation of such recalcitrant compounds, many of them xenobiotics *in sensu stricto*, generally proceeds via two modes: reductive and oxidative attack (Spain, 1995; Durán and Esposito, 2000; Ye et al., 2004). Oxidoreductases, (e.g., dehydrogenases and oxygenases/[per]oxidases, respectively) play key roles in both degradative strategies and have been well studied (Durán and Esposito, 2000). Oxidases, oxygenases and peroxidases (POX) can be classified according to their co-substrates; the most important of them—involved in the aerobic degradation of numerous organic pollutants—are shortly discussed below.

Polyphenol oxidases, i.e., laccase (LAC) and tyrosinase (TYR), are copper containing enzymes that catalyze the oxidation of phenolic compounds with dioxygen (O<sub>2</sub>) as electron acceptor and without the need of additional co-enzymes, such as NAD(P)H. They are found in almost all

domains of aerobic life and fulfill diverse metabolic functions (Ullrich and Hofrichter, 2007). Whereas, LAC does not directly incorporate oxygen into substrates, TYR can do so along with phenol/catechol oxidation (Jergil et al., 1983; Majcherczyk et al., 1998). Nevertheless, also LAC may indirectly oxyfunctionalize molecules, for example, polycyclic aromatic hydrocarbons (PAHs) or phenols, via one-electron oxidation followed by disproportionation and water addition (Majcherczyk et al., 1998; Wu et al., 2008).

Oxidases using O<sub>2</sub> and reduced co-enzymes (e.g., NAD(P)H or FADH<sub>2</sub>) as oxygen donor (electron acceptor) and electron donor, respectively, are usually referred to as oxygenases (Guengerich, 2001). In dependence on the number of oxygen atoms introduced into the substrate molecule, monooxygenases, and dioxygenases are distinguished. Cytochrome-P450 monooxygenases (P450s) are heme-thiolate proteins where a porphyrin moiety (iron protoporphyrin IX; heme) is ligated via a cysteine residue to the polypeptide chain ( $\alpha$ -helix) of the apo-enzyme (Munro et al., 2012). The protein superfamily of P450s is highly diverse and comprises versatile intracellular biocatalysts found in all domains of life (Anzenbacher and Anzenbacherová, 2001; Meunier et al., 2004; Munro et al., 2012), and even virally encoded P450s have been described (Lamb et al., 2009). P450s usually utilize NAD(P)H as electron-delivering co-substrate but some of them can also catalyze monooxygenations with peroxides as oxygen donor via the so-called shunt pathway (Munro et al., 2012). While some P450s play specific anabolic roles, e.g., in sterol biosynthesis (Lepesheva and Waterman, 2004), others are rather unspecific and involved in the metabolism of xenobiotics, toxins and drugs (Anzenbacher and Anzenbacherová, 2001; Guengerich, 2001).

Multicomponent monooxygenases (BMMs) represent another family of versatile biocatalysts transferring oxygen to various substrates (Leahy et al., 2003). Thus, toluene 4-monooxygenase and methane monooxygenase are capable of oxygenating—in addition to their eponymous substrates—diverse alkenes and arenes including hardly reactive benzene (Whited and Gibson, 1991; Sazinsky et al., 2004). BMMs have only been found (and characterized) in bacteria and archaea so far (Notomista et al., 2003). Other non-heme monooxygenases contain flavin as prosthetic group (FMOs) (van Berkel et al., 2006; Huijbers et al., 2014). They activate O<sub>2</sub> with a reduced flavin cofactor to form a peroxyflavin that attacks the substrate (van Berkel et al., 2006). As P450s, FMOs are found in bacteria and eukaryotes (van Berkel et al., 2006).

Oxygenases that catalyze the incorporation of the entire O<sub>2</sub> molecule are called dioxygenases (DIOXs). Most DIOXs are iron containing enzymes, e.g., Rieske-type DIOXs (also referred to as arene DIOXs) (Bugg and Ramaswamy, 2008). Rieske-type

DIOXs contain a [2Fe-2S] cluster and preferably catalyze the formation of *cis*-dihydroxylated metabolites (Ferraro et al., 2005). Arene DIOXs are capable of oxidizing inactivated arenes, such as toluene, benzene and even nitrobenzene (Lessner et al., 2002; Bagn eris et al., 2005).

All types of oxygenases can be involved in the detoxification and biodegradation of organic pollutants and xenobiotics by microorganisms and often they initiate catabolic pathways resulting in the utilization of these compounds as sole carbon and energy sources (Fewson, 1988; Copley, 2000). In this context, the incorporation of oxygen does not only activate the molecules but also increases the compounds' water solubility and hence their bioavailability. That way, many compounds listed as EPA priority pollutants, such as benzene and its derivatives, become accessible to enzymatic attack by other enzymes (e.g., ring-fission enzymes, POX or LAC) upon hydroxylation.

Secreted peroxidases, such as fungal lignin peroxidase (LIP), manganese peroxidase (MNP), and versatile peroxidase (VP), plant horseradish peroxidase (HRP), animal dehaloperoxidase and lactoperoxidase as well as bacterial and fungal dye-decolorizing peroxidases (DYPs), are typical degradative and detoxifying biocatalysts that utilize hydrogen peroxide as electron acceptor (Camarero et al., 1999; Piontek et al., 2001; Hofrichter, 2002; Osborne et al., 2009; Strittmatter et al., 2011). They all contain heme as prosthetic group that is linked via a proximal histidine to the polypeptide chain (heme-imidazole POX) (Ullrich and Hofrichter, 2007). Heme peroxidases are known from all kingdoms of life (Vlasits et al., 2010). Because of the involvement of some of them in lignin biodegradation (MNP, LIP, and VP), which opens an eco-physiological niche for specialized fungi (basidiomycetous white-rotters and litter-decomposers) and is of general interest for the pulp and paper sector, they have been intensely studied over the last three decades (Kirk and Farrell, 1987; Hofrichter, 2002; Mart nez et al., 2009). Interestingly, it has recently been proposed that the appearance of fungal ligninolytic peroxidases led to the end of the carboniferous period (Floudas et al., 2012). In addition to lignin, these enzymes were found to efficiently oxidize diverse organic pollutants as well and hence were proposed to be part of unspecific bioremediation/bioattenuation systems in nature (Pointing, 2001; Hammel and Cullen, 2008; Qayyum et al., 2009; Harms et al., 2011).

Unlike the ligninolytic heme peroxidases, the heme iron of chloroperoxidase (CPO) from the ascomycete *Caldariomyces (Leptoxyphium) fumago* (Dawson, 1988) is linked to a cysteine (heme-thiolate peroxidase-HTP), as in the case of P450s. In 2004, a new HTP type was discovered, which is presently known as unspecific peroxygenase (UPO) (Ullrich et al., 2004; Ullrich and Hofrichter, 2005; Hofrichter and Ullrich, 2006) representing a functional hybrid of peroxidases and P450s (Hofrichter and Ullrich, 2006; Hofrichter et al., 2015). Besides prototypical peroxidase reactions like one electron oxidations, UPO transfers hydrogen peroxide-borne oxygen and catalyze various hydroxylations, e.g., of aromatic and aliphatic hydrocarbons (Kluge et al., 2009, 2012; Aranda et al., 2010; Kinne et al., 2010; Peter et al., 2011; Karich et al., 2013). Moreover, epoxidation, sulfoxidation, heterocyclic *N*-oxidation, and ether

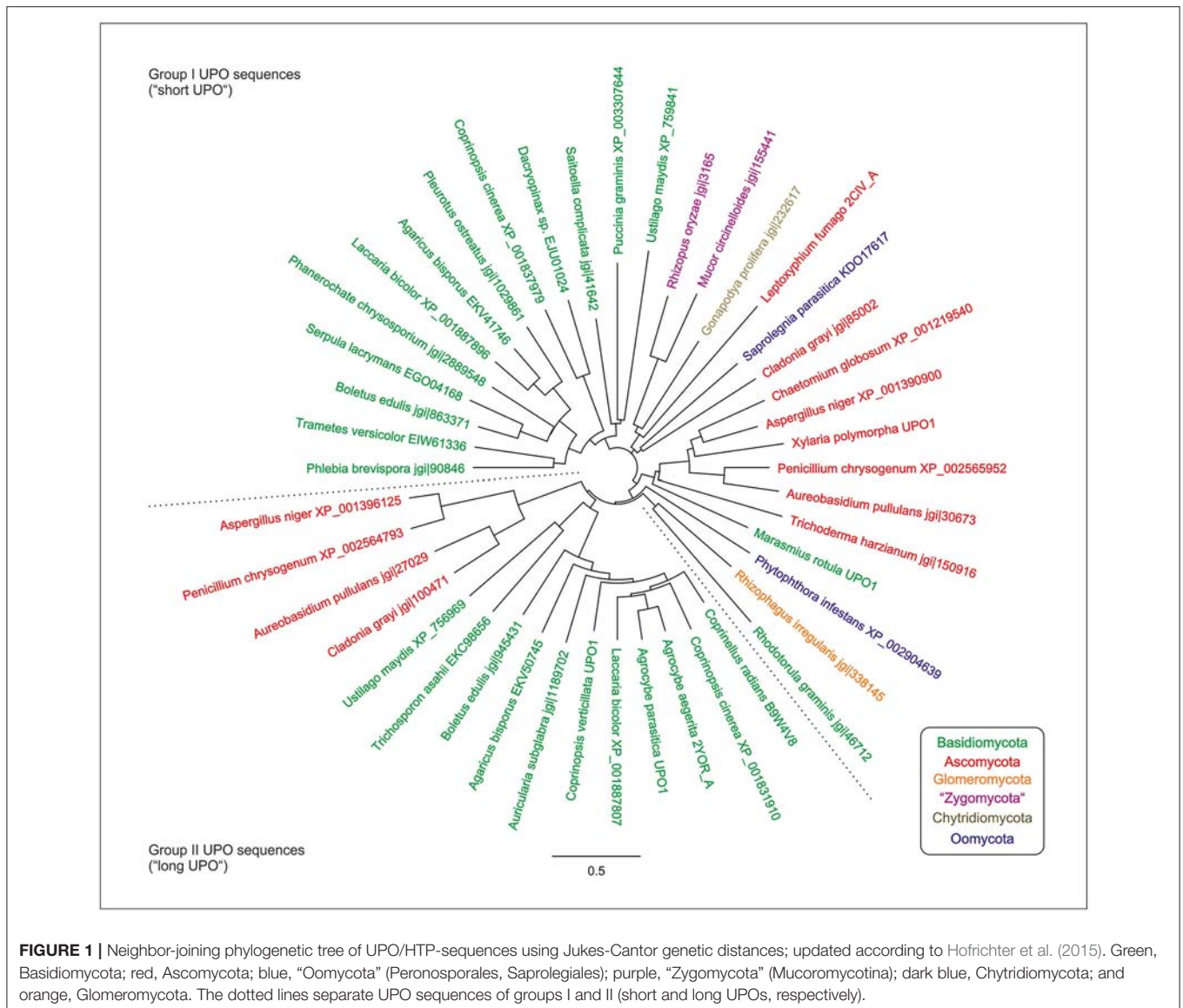
**Abbreviations:** UPO, unspecific peroxygenase; *Aae*, *Agrocybe aegerita*; *Mro*, *Marasmius rotula*; POX, peroxidases; LAC, laccase; TYR, tyrosinase; PAH, polycyclic aromatic hydrocarbons; P450, cytochrome-P450 monooxygenase; BMM, Multicomponent monooxygenase; TMO, toluene 4-monooxygenase; DIOX, dioxygenase; LIP, lignin peroxidase; MNP, manganese peroxidase; VP, versatile peroxidase; HRP, horseradish peroxidase; DYP, dye-decolorizing peroxidase; CPO, chloroperoxidase; HCB, hexachlorobenzene; PCP, pentachlorophenol; PE, phthalate esters; IP, ionization potential.

cleavage (*O*-dealkylation) have been reported (Ullrich et al., 2008; Aranda et al., 2009; Kinne et al., 2009b; Kluge et al., 2012), and moreover, UPO has catalase and haloperoxidase activities (Hofrichter et al., 2015). Thus, UPO combines features of LAC/POX (one-electron oxidation), monooxygenases (incorporation of one oxygen atom into the substrate) and POX/catalase (H<sub>2</sub>O<sub>2</sub> as co-substrate) and hence represents a multifunctional type of oxidoreductase with almost catalytic promiscuity (Pandya et al., 2014; Hofrichter et al., 2015).

UPO genes are ubiquitous in the fungal kingdom (Eumycota) and beyond that, have only been found in the (super) phylum of heteroconta (e.g., in fungus-like Peronosporales belonging to the former class of oomycetes and in a few diatoms) (Pecyna, 2016). Horizontal gene transfer from ascomycetes was proposed to be the most probable explanation for the occurrence of UPO genes in the latter organisms, leading to the conclusion that they are an autapomorphic feature in the kingdom of fungi (Pecyna, 2016).

Phylogenetically, Unspecific peroxygenases (UPOs) can be classified into two large groups/families, which differ, among others, in molecular size: (i) group I, the short UPOs with an average mass of 29 kDa and (ii) group II, the long UPOs with an average mass of 44 kDa (compare **Figure 1**; Hofrichter et al., 2015). The latter are exclusively found in ascomycetes and basidiomycetes, while the former are distributed among all fungal phyla (compare **Figure 1**; Hofrichter et al., 2015). The herein studied UPOs of *Agrocybe aegerita* (*Aae*UPO) and *Marasmius rotula* (*Mro*UPO) belong to the long and short basidiomycetous UPOs, respectively. Interestingly, the above-mentioned CPO, which had been an “orphan” among the heme peroxidases for decades, can now be classified into group I of UPOs/HTPs as well.

Against the background of widespread occurrence of UPOs in the fungal kingdom and their catalytic versatility, it is worth to study the conversion of a representative number of organic pollutants by these enzymes. So we have tested here



44 substrates, of which 40 are listed as EPA priority pollutants including chlorinated benzenes, halogenated biphenyl ethers, nitroaromatics, PAHs and phthalates (USEPA, 1979).

## MATERIALS AND METHODS

### Enzyme Preparation and Chemicals

*AaeUPO* and *MroUPO* were prepared as described by Ullrich et al. (2004) and Gröbe et al. (2011), respectively. Final enzyme preparations had specific activities of 98 and 28 U/mg for *AaeUPO* and *MroUPO*, respectively. Chemicals used were purchased from Sigma Aldrich-Germany (Munich, Germany) with the highest purity available.

### Enzyme Assay and Reaction Setup

Enzymatic activity of UPOs was routinely assayed by following the oxidation of veratryl alcohol to veratraldehyde at 310 nm ( $\epsilon_{310} = 9,300 \text{ M}^{-1} \text{ cm}^{-1}$ ) in a buffered reaction mixture (pH 7.0) according to Ullrich et al. (2004). Photometric measurements were performed using a Cary Bio 50 spectrophotometer (Varian Inc., Walnut Creek, CA, USA).

Enzymatic reactions were performed in triplicate in 1.5-mL HPLC vials containing 50 mM potassium phosphate buffer (pH 7) and acetonitrile at concentrations between 5 and 30% vol/vol. The substrate concentration ranged from 0.1 to 1 mM, e.g., in the case of large PAHs and phenolic compounds, respectively. The total reaction volume varied between 0.5 and 1 mL. Reactions were started by addition of  $\text{H}_2\text{O}_2$  (final concentration 0.5–2 mM).  $\text{H}_2\text{O}_2$  was added via syringe pumps over 30 min or, in the case of large PAHs, over 2 h. In additional reaction setups, ascorbic acid (4 mM) was added to the reaction mixtures to prevent polymerization starting from intermediate phenoxy radicals formed by one-electron oxidation (Kinne et al., 2009a). The final enzyme activity (*AaeUPO* and *MroUPO*) in the reaction mixtures ranged between 0.5 and 1 U/mL (veratryl alcohol units measured at pH 7). Controls for each reaction setup were run without enzyme. Detailed information on the reaction setups, analytical methods and some specific results (e.g., HPLC elution profiles) are given in the Supplementary section.

### Sample Preparation

Samples from the reaction mixtures were collected 30 min after the reaction had started and stopped by injection into an HPLC system or by addition of 1 mM sodium azide. To ensure dissolving, in a few cases, the reaction mixtures were diluted with acetonitrile (e.g., for the analysis of phthalic acid derivatives or small PAHs, such as acenaphthene) or acetone (e.g., for large PAHs, such as benzo[a]pyrene or benz[a]anthracene) prior to injection.

### HPLC Analyses

Reaction products were analyzed by HPLC with MS and/or UV-Vis detection using an Agilent Series 1,200 instrument equipped with a diode array detector (Agilent Technologies Deutschland GmbH, Böblingen, Germany). The HPLC system was generally equipped with reversed phase columns; i.e., Luna C18(2), Synergi polar, Kinetex C18 and Kinetex PFP

(each supplied by Phenomenex, Aschaffenburg, Germany). An electrospray ionization mass spectrometer (6310 IonTrap, Agilent Technologies Germany GmbH), in negative and positive mode, was used to determine mass-to-charge ratios of substrates tested and metabolites formed in the course of UPO reactions.

Oxidation products were identified by comparing their retention times, mass and spectral data with authentic standards (so far available) and with literature data. In the absence of standards or reference data, metabolites were tentatively assigned according to their mass and UV-Vis spectra.

## RESULTS AND DISCUSSION

The main outcome of the enzymatic oxidation tests with two fungal UPOs and diverse EPA organopollutants is summarized in **Table 1**. This includes the respective type of substrate functionalization (incorporation of oxygen, release of functional groups, one-electron oxidation, etc.), the relative conversion of the tested compounds in semi-quantitative form (five levels of conversion) and the products formed. Polymerization products were observed in all cases, in which phenolic groups were present in the substrates or emerged in the course of the reaction as intermediates (with the exception of 2,4-dinitrophenol).

### Chlorobenzene and Its Derivatives

Chlorobenzene (**1**) was oxygenated by *AaeUPO* to give 2-chlorophenol (**2**) and 4-chlorophenol (**3**) as major products; oxygenation at the *meta* position of **1** and thus formation of 3-chlorophenol (**4**) was not observed. Further oxidation of **2** led to 3-chlorocatechol (**5**) and chlorohydroquinone (**6**), whereas oxidation of **3** gave 4-chlorocatechol (**7**); **5**, **6**, and **7** are direct oxygenation products of **2**, **3**, or **4**, respectively (**Figures 2A,B**). *p*-Benzoquinone (**8**) was detected (**Figure 2A**) when ascorbic acid was omitted from the reaction mixture of **3**; *vice versa*, **8** was not observed in the presence of ascorbic acid. Hence **8** must be a product deriving from two consecutive or parallel enzymatic one-electron oxidations, which represents a type of oxidative dehalogenation known from LAC and POX (Hammel and Tardone, 1988; Osborne et al., 2007; Kordon et al., 2010). Hydrogen abstraction at the phenolic function of **3** would give a phenoxy radical. Two of the latter can disproportionate to **3** and an arene cation (Ullrich and Hofrichter, 2007). A nucleophile, e.g., water, may add to the aromatic cation and subsequent elimination of hydrochloric acid leaves **8** behind, analogously to the Ritter reaction (Krimen and Cota, 2004). The pathway described resembles the enzymatic dehalogenation of **3** described for dehaloperoxidases (Osborne et al., 2009). Masses of triple hydroxylated products arising from **5** to **7** were detected in low amounts; however, their unambiguous identification was not possible, due to the lacking of authentic standards.

Oxygenation of three dichlorobenzenes was indicated by the detection of the corresponding dichlorophenols in the reaction mixture. In the case of 1,3-dichlorophenol, dehalogenation occurred in a second step upon oxygenation giving rise to chlorohydroquinone. The reaction cascade is assumed to proceed analogously to the dehalogenation of **3**. Dehalogenation

**TABLE 1** | EPA priority pollutants (and a few other recalcitrant compounds) tested with respect to their conversion by UPOs, including references to literature data of other oxidoreductases.

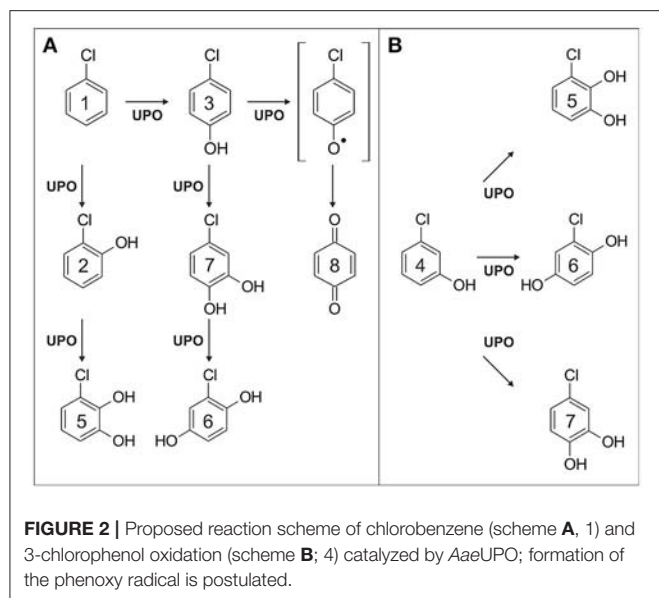
Compound	Functional groups introduced and/or released*	Relative conversion		Oxidases	References
		AaeUPO	MroUPO		
Chlorobenzene	-OH (1x, 2x)	+	nt	P450; DIOx	de Bont et al., 1986; Nedelcheva et al., 1998
2-Chlorophenol	-OH (1x, 2x)	+++	nt	LAC; HRP; CPO; LIP; MNP; TYR; VP	Wada et al., 1995; Durán and Esposito, 2000; Zhang et al., 2008; Hibi et al., 2012
1,2-Dichlorobenzene	-OH	+	nt	P450; DIOx	Nedelcheva et al., 1998; Jones et al., 2001; Montferran et al., 2007
1,3-Dichlorobenzene	-OH; -Cl	++	nt	P450; DIOx	de Bont et al., 1986; Jones et al., 2001
1,4-Dichlorobenzene	-OH	+	nt	P450; DIOx	de Bont et al., 1986; Spiess et al., 1995; Nedelcheva et al., 1998; Jones et al., 2001; Montferran et al., 2007
2,4-Dichlorophenol	-OH	+	+++	LAC; HRP; LIP; DYP; VP; MNP; P450 FMO	Beadle and Smith, 1982; Valli and Gold, 1991; Schomburg and Stephan, 1994; Yee and Wood, 1997; Xu and Bhandari, 2003; Zhang et al., 2008; Fodili et al., 2011; Hibi et al., 2012
1,2,4-Trichlorobenzene	-OH	++	nt	P450; DIOx	van der Meer et al., 1991; Marco-Urrea et al., 2009
2,4,6-Trichlorophenol	-OH; -Cl	+++	nt	LAC; VP; LIP; MNP; DYP; FMO	Wieser et al., 1997; Reddy et al., 1998; Leontievsky et al., 2001; Fodili et al., 2011; Hibi et al., 2012
Pentachlorophenol	-	0	0	P450; LAC; LIP; MNP; TYR; DYP; VP; FMO	Reddy and Gold, 2000; Thakur et al., 2002; Montiel et al., 2004; Davila-Vazquez et al., 2005; Crawford et al., 2007; Jeon et al., 2008; Fodili et al., 2011
Hexachlorobenzene	-	0	0	P450	Jones et al., 2001
para-Chloro-meta-cresol	-OH; -Cl	+++	nt	LAC; TYR	Bollag et al., 1988; Freire et al., 2003
2-Chloronaphthalene	-OH (1x, 2x)	+++	nt	P450	Mori et al., 2003
3,3-dichlorobenzidine	-OH	++	nt	P450; FMO	Iba and Thomas, 1988; Imaoka et al., 1997
4-Chlorophenyl phenyl ether	-OH (1x, 2x)	++	nt	P450	Hundt et al., 1999; Hiratsuka et al., 2001
4-Bromophenyl phenyl ether	-OH (1x, 2x)	++	nt	P450	Hundt et al., 1999
3-Chlorophenol**	-OH (1x, 2x)	+++	nt	LAC; HRP; CPO; LIP; MNP; TYR; VP	Wada et al., 1995; Durán and Esposito, 2000; Hibi et al., 2012
4-Chlorophenol**	-OH (1x, 2x); -Cl	+++	nt	LAC; HRP; CPO; LIP; MNP; TYR; DYP; VP	Wada et al., 1995; Durán and Esposito, 2000; Freire et al., 2003; Zhang et al., 2008; Fodili et al., 2011; Hibi et al., 2012; Liers et al., 2014
Nitrobenzene	-	0	nt	BMM; DIOx	Spain, 1995; Lessner et al., 2002; Fishman et al., 2004; Ye et al., 2004
2-Nitrophenol	-OH	+	nt	BMM; FMO; DYP	Ye et al., 2004; Vardar and Wood, 2005; Xiao et al., 2007; Büttner et al., 2015
4-Nitrophenol	-OH	++	nt	BMM; FMO; P450; DYP	Spain, 1995; Amato et al., 1998; Kadiyala and Spain, 1998; Fishman et al., 2004; Ye et al., 2004; Büttner et al., 2015
2,4-Dinitrophenol	-	0	nt	FMO	Cassidy et al., 1999
2,4-Dinitrotoluene	=O	t	nt	DIOx	Spain, 1995; Johnson et al., 2002; Ye et al., 2004
2,6-Dinitrotoluene	-	t	nt	DIOx	Nishino et al., 2000; Ye et al., 2004
4,6-Dinitro-o-cresol	-OH	t	nt	FMO	Cassidy et al., 1999
Benzidine	-OH	t	+	P450; CPO; HRP; LPO; LAC	Phillips and Leonard, 1976; Yamazoe et al., 1988; Lakshmi et al., 1996

(Continued)

TABLE 1 | Continued

Compound	Functional groups introduced and/or released*	Relative conversion		Oxidases	References
		AaeUPO	MroUPO		
1,2-Diphenylhydrazine	-OH	++	nt		
bis(2-Ethylhexyl) phthalate	-	0	0	P450	Wittassek and Angerer, 2008
Butyl benzyl phthalate	-OH; =O	+	t		
Di-n-butyl phthalate	-OH; =O	+	+	DIOX	Eaton and Ribbons, 1982
Di-n-octyl phthalate	-OH; =O	t	t		
Diethyl phthalate	-	0	0		
Dimethyl phthalate	-	0	0		
Acenaphthylene	-OH (1x, 2x); =O	++	++	LAC; DIOx; P450	Majcherzyk et al., 1998; Pinyakong et al., 2004; Shimada et al., 2015
Acenaphthene	-OH (1x, 2x); =O	++	++	LIP; LAC; DIOx; P450	Vazquez-Duhalt et al., 1994; Majcherzyk et al., 1998; Pinyakong et al., 2004; Shimada et al., 2015
Benzo[a]pyrene	-OH (1x, 2x)	+	++	MNP, LAC; LIP; DIOx; P450	Haemmerli et al., 1986; Warshawsky et al., 1988; Bogan and Lamar, 1995; Sack et al., 1997; Kim et al., 1998; Dodor et al., 2004
Benzo[a]anthracene	-OH (1x, 2x)	++	+	MNP, LAC; LIP; P450	Wood et al., 1976; Bogan and Lamar, 1995; Sack et al., 1997; Majcherzyk et al., 1998
Indeno[1,2,3-cd]pyrene	-OH (1x, 2x)	t	t	LAC	Wu et al., 2008
Benzo[b]fluoranthene	-OH	0	t	LAC; LIP	Bogan and Lamar, 1995; Majcherzyk et al., 1998
Benzo[k]fluoranthene	-OH; (1x, 2x)	t	t	LAC; LIP	Bogan and Lamar, 1995; Majcherzyk et al., 1998
Dibenz[a,h]anthracene		0	0	LAC	Wu et al., 2008
Benzo[g,h,i]perylene		0	0	LAC; LIP	Bogan and Lamar, 1995; Wu et al., 2008
Perylene**	-OH; (1x, 2x)	t	+	LAC	Majcherzyk et al., 1998
9,10-Dihydrophenanthrene**	-OH; (1x, 2x)	t	+		
2,4-Dimethylphenol	-OH; =O	+++	nt	FMO; LAC; HRP	Kilbanov et al., 1980; Arengi et al., 2001; Ghosh et al., 2008
Benzene		+		UPO	Karich et al., 2013
Naphthalene		++		UPO	Kluge et al., 2009
Phenol		+++		UPO	Karich et al., 2013
Anisole		+++		UPO	Kinne, 2010
Toluene		+++		UPO	Kinne et al., 2010
Ethylbenzene		+++		UPO	Kluge et al., 2012
Anthracene				UPO	Aranda et al., 2010
Fluorene		+		UPO	Aranda et al., 2010
Phenanthrene		+		UPO	Aranda et al., 2010
Pyrene		+		UPO	Aranda et al., 2010

Evaluation of relative conversion was done according to the following pattern: no conversion ("0"), little conversion—well detectable products, decrease of substrate <20% ("+"), moderate conversion—decrease of substrate <50% ("++"), good conversion—decrease of substrate >50% ("+++"); \*introduced (green) and released functional group (red); \*\*not in the EPA priority pollutants list; "nt" not tested"; P450, cytochrome P-450 monooxygenase; DIOx, Rieske-type dioxygenase; LAC, laccase; TYR, tyrosinase; LIP, lignin peroxidase; MNP, manganese peroxidase; VP, versatile peroxidase; HRP, horseradish peroxidase; CPO, chloroperoxidase; DYP, dye-decolorizing peroxidase; LPO, lactoperoxidase; BMM, bacterial multicomponent monooxygenase; FMO, flavin-dependent monooxygenase (flavo-protein monooxygenase).



products were also observed when *p*-chloro-*m*-cresol and 2,4,6-trichlorophenol were applied as UPO substrates.

Interestingly, the conversion of chlorinated benzenes did not follow the expected reaction sequence; thus the introduction of chlorine substituents usually decreases the charge density of the aromatic system and hence inactivates the latter. However, all three dichlorobenzenes and 1,2,3-trichlorobenzene were more effectively oxidized by *AaeUPO* than **1**. A possible explanation for that finding could be the “steric fixation” of the substrate molecule inside the heme pocket, positively affected by two or more chlorine substituents, resulting in a closer distance to the enzyme’s reactive compound I and/or less motion within the heme pocket. To our best knowledge, only P450s and DIOX have been reported to oxygenate mono- and dichlorinated benzenes (de Bont et al., 1986; Spiess et al., 1995; Nedelcheva et al., 1998; Jones et al., 2001; Monferran et al., 2007).

All three tested chlorophenols were oxygenated by *AaeUPO*. This was most evident when ascorbic acid was present in the reaction mixtures, which prevented polymerizing side activities. Chlorocatechols (i.e., **5** and **7** and not chlorohydroquinones) were the major products deriving from the oxygenation of **3** and **4**. This is an interesting fact, since chlorocatechols are the substrates of ring-cleaving DIOX within intracellular degradation pathways of chlorinated arenes (Kaschabek et al., 1998; Moiseeva et al., 2002). Thus, we can consider UPOs being involved in fungal catabolic routes of chloroaromatics, with the advantage that toxic chlorophenols will not have to be taken up into the hyphae (Mars et al., 1997). Chlorophenols and chlorocatechols can additionally serve as substrates for one-electron oxidations and thus, besides oxygenases (Beadle and Smith, 1982; Xu and Bhandari, 2003), several POX and phenol oxidases (LAC, TYR) were found to oxidize chlorinated phenols and their derivatives to reactive phenoxy radicals (Xu and Bhandari, 2003; Zhang et al., 2008; Hibi et al., 2012).

Neither oxygenation nor one-electron oxidation was observed when hexachlorobenzene (HCB) and pentachlorophenol (PCP)

were applied as substrates for *AaeUPO* and *MroUPO*. They are the only halogenated compounds tested here that were not converted. Chlorine substituents in higher number may protect the arene C-atoms from attack by UPO’s compound I via steric hindrance and/or the impossibility to find a suitable point of attack. On the other hand, some P450s were found to be able to oxygenate both HCB and PCP (Jones et al., 2001; Crawford et al., 2007), and the phenolic functionality of PCP makes it susceptible to one-electron oxidation catalyzed by phenol oxidases and POX (Reddy and Gold, 2000; Montiel et al., 2004; Jeon et al., 2008; Fodil et al., 2011). All other tested halogenated compounds (compare **Table 1**) served also as substrates for UPOs, but are not explicitly discussed here; more pieces of information are given in the Supplementary section.

Benzoquinones and polymerization products emerged in all reaction setups where ascorbic acid was omitted. The latter acted as radical scavenger that reduced chlorinated phenoxy radicals formed via one-electron oxidation (peroxidative activity of UPO) and prevented that way radical coupling (Niki, 1991).

## Nitroarenes

The charge density at the aromatic ring is reduced by nitro substituents; thus, with regard to electrophilic attack, nitroarenes are strongly deactivated compounds (McDaniel and Brown, 1958; Spain, 1995). This property is reflected by the low reactivity of UPOs toward nitroaromatic compounds (compare **Table 1**) and consequently, oxygenation of nitrobenzene was not observed. On the other hand, 2-nitrophenol and 4-nitrophenol served as substrates and were oxidized into the corresponding dihydroxylated nitrobenzenes, which in turn underwent one-electron oxidation resulting in the formation of coupling products. A second nitro group (e.g., 2,4-dinitrophenol), however, made an enzymatic attack by UPOs impossible. Trace amounts of oxidation products were found when 2,4-dinitrotoluene (**9**) and 4,6-dinitro-*o*-cresol were applied as substrates. Since the electron density at the aromatic ring of **9** is lower than in 2,4-dinitrophenol, it is assumed that hydroxylation took place at toluene’s methyl group, which in case of 2,6-dinitrotoluene is shielded by two flanking nitro groups preventing attack by UPO compound I. A second indication for the oxidation at the benzylic carbon of **9** is the mass shift of “+14” for one of the products detected, which cannot be explained by aromatic ring hydroxylation. In consequence, we conclude that **9** was attacked by two consecutive two-electron oxidations (compare **Figure 3**) resulting in the formation of 2,4-dinitrobenzaldehyde via the corresponding benzyl alcohol and *gem*-diol (aldehyde hydrate) intermediates. This finding confirms similar observations previously made for 4-nitrotoluene oxidation by *AaeUPO* (Kinne et al., 2010).

Overall, these results are not surprising when considering literature data of other enzymes. Only a few oxidoreductases are able to oxidize nitrobenzene, e.g., a few DIOXs and BMMs (Spain, 1995; Fishman et al., 2004). The latter was also found to oxidize nitrophenols (Fishman et al., 2004). Furthermore, oxygenation of nitrophenols was reported for some P450s and FMOs (Cassidy et al., 1999; Ye et al., 2004), whereas one-electron oxidation of nitrophenols can be realized by high-redox potential POX, e.g.,

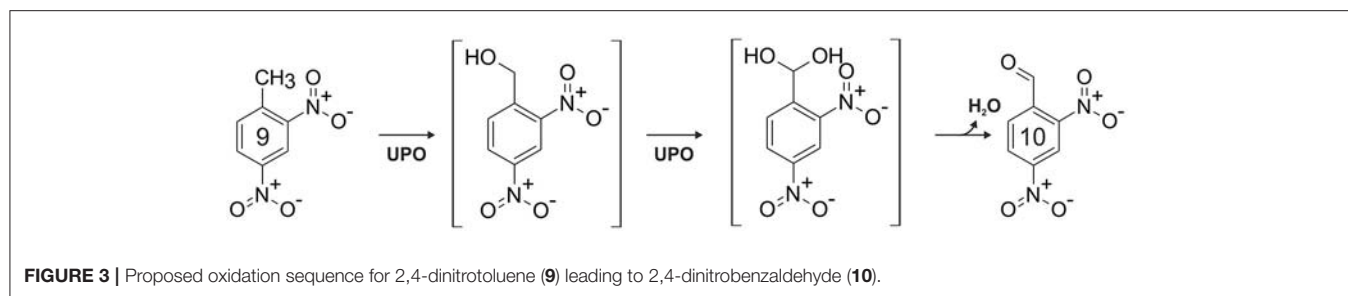


**FIGURE 3** | Proposed oxidation sequence for 2,4-dinitrotoluene (9) leading to 2,4-dinitrobenzaldehyde (10).

DYP (Büttner et al., 2015). In contrast, reductive pathways for nitroaromatics are widely distributed in nature and have been well summarized in previous reviews (Spain, 1995; Ye et al., 2004).

### Phthalate Esters

In the course of a screening, six phthalate esters (PEs) were tested for oxygenation by *Aae*UPO and *Mro*UPO and three of them were converted: butyl benzyl phthalate, di-*n*-butyl and di-*n*-octyl phthalate. In case of the latter, only trace amounts of products could be detected. Analogously to 2,4-dinitrotoluene, the “+14” mass shift of products rules out that the oxygen insertion occurred at the aromatic ring and thus oxygenation at the  $\beta$ -position of the alkyl moieties (i.e., butyl or octyl) is most plausible (Peter et al., 2011). No conversion was observed for *bis*(2-ethyl-hexyl) phthalate and the short chain PEs, such as dimethyl phthalate and diethyl phthalate.

Most studies dealing with the degradation of PE have used whole cells (bacterial or fungal pure or mixed cultures). Hydrolysis of the ester bond by esterases was the typical reaction observed (Wang et al., 1995, 2003; Staples et al., 1997). The ring of phthalic acid can be oxidized by a specific bacterial DIOX resulting in the formation the corresponding catechol (Eaton and Ribbons, 1982); side chain oxidation of PEs was also reported for human PE metabolism probably realized by liver P450s (Wittassek and Angerer, 2008). Wittassek and Angerer (2008) reported the oxidation of long chain PE, e.g., di(2-ethyl-hexyl) phthalate, by a P450 and emphasized that short chain PEs, (e.g., dimethyl and diethyl) phthalate, were not oxidized by this enzyme; an observation that corresponds with our findings here.

### Polycyclic Aromatic Hydrocarbons

Eleven PAHs were tested for the conversion by *Aae*UPO and *Mro*UPO. The majority of them was in fact oxygenated and oxidized by both UPOs with the exception of bulky dibenz[a,h]anthracene and benzo[g,h,i]perylene; benzo[b]fluoranthene was a substrate for *Mro*UPO only. In dependence on the particular PAH, the extent of product formation reached from trace amounts (e.g., benzo[k]fluoranthene) to substantial amounts (e.g., acenaphthylene).

From all PAHs tested, acenaphthylene (14) was oxidized to the highest extent by both UPOs. The major product detected was a monohydroxylated metabolite ( $m/z$  +16) with a UV-Vis spectrum resembling that of 1-naphthol (Kluge et al., 2009)

(data in supplement). Hence, we assume that oxygenation of 14 proceeded via a 4,5-epoxy acenaphthylene intermediate to give 5-hydroxy acenaphthylene, analogously to naphthalene oxygenation catalyzed by UPO (Kluge et al., 2009). Another interesting finding was the detection of acenaphthenone (13) in the reaction setup of 14. Oxygenation of 14 led to 1-hydroxy-acenaphthylene (15) that is the enolic form of 13. Again, an epoxide intermediate can be postulated, i.e., 1,2-epoxy acenaphthene (compare Figure 4).

Thirteen (13) was also a product deriving from acenaphthene (11) that was next to 14 the best PAH substrate. Oxygenation of a  $sp^3$ -carbon (aliphatic carbon) may give 1-acenaphthol (12); via a second attack at the same carbon (i.e., at C1 position), a geminal diol intermediate (*gem*-diol, carbonyl hydrate) may be formed that is in equilibrium via spontaneous dehydration with the corresponding ketone (13, Figure 4). Similar to 14, oxygenation at the aromatic system of 11 was observed as well. However, in contrast to the reaction setup of 14, two oxygenation products were detected with UV-Vis spectra resembling those of 1-naphthol and 2-naphthol (Kluge et al., 2009). The reported oxidation pathway of P450s for 11 and 14 is rather similar to the reaction sequences proposed herein, including the proof of 1,2-epoxy-acenaphthene formation (only the formation of 13 was not ascertained for P450s) (Shimada et al., 2015). Conversion of all other (positively) tested PAHs was evident by detection of products with mass shifts of +16 or +32, representing mono- and dihydroxylated products, respectively.

Water solubility and thus bioavailability decreases with increasing size of PAHs and this fact was reflected by their decreasing relative conversion by UPOs the bigger they were (compare Table 2). It has to be noted that the two UPOs tested accomplished the formation of different PAH products and patterns; thus, *Mro*UPO was capable of hydroxylating more bulky PAHs than *Aae*UPO. This can be explained by the wider heme channel of *Mro*UPOs (11 Å) compared to the relatively narrow channel of *Aae*UPO (7 Å) (Poraj-Kobielska, 2013; Piontek et al., 2017), which limits *Aae*UPO to oxidize PAHs that are larger than 6 Å in diameter (e.g., dibenz[a,h]anthracene or benzo[g,h,i]perylene). The results of the UPO-catalyzed conversion of selected PAHs in relation to some physicochemical properties are summarized in Table 2. Aranda and coworkers had already reported about the successful conversion of several PAHs and related compounds by *Aae*UPO in 2010 (Aranda et al., 2010); four of these PAHs are also listed in Table 2, namely anthracene, fluorene, phenanthrene, and pyrene.

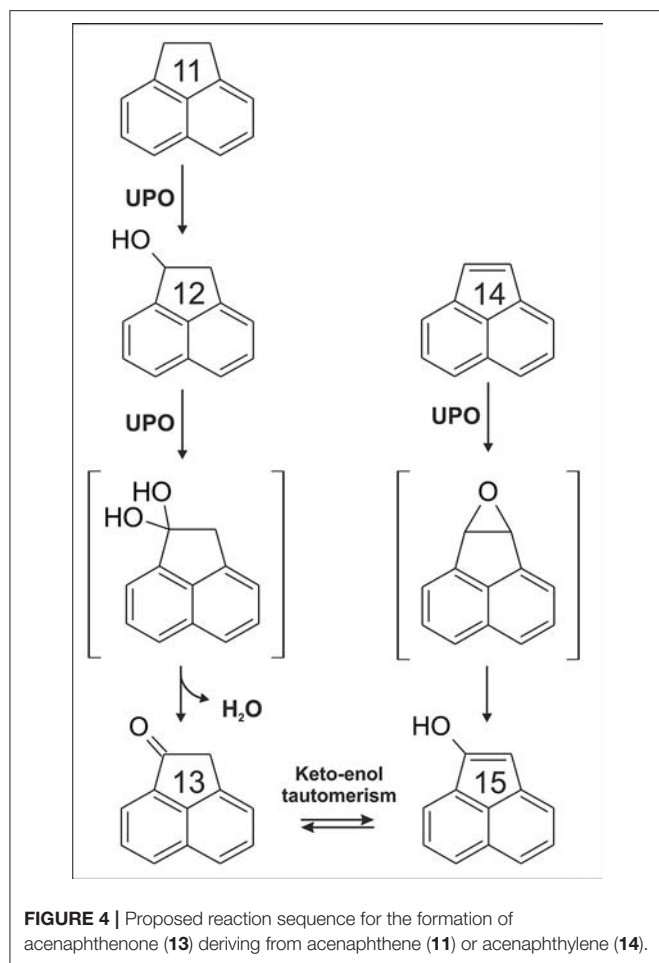


**FIGURE 4** | Proposed reaction sequence for the formation of acenaphthenone (13) deriving from acenaphthene (11) or acenaphthylene (14).

Typical enzymes capable of catalyzing the oxygenation of PAHs are P450s and DIOX (Shimada et al., 1989; Pinyakong et al., 2004). Among fungi, especially P450s were shown to directly oxygenate PAHs (van Gorcom et al., 1998). However, PAHs can be also attacked by enzymes catalyzing one-electron oxidations, such as different POX and LAC, whereat their oxidizability will depend on the ionization potential (IP) and the presence of suitable redox mediators (Sack et al., 1997; Majcherczyk et al., 1998; Johannes and Majcherczyk, 2000; Haritash and Kaushik, 2009). The reaction of these enzymes leads, via instable aryl cations and water addition, to the formation of PAH quinones, in particular in the case of 4-ring and 5-ring PAHs with IP <7.7 eV (Hammel, 1995; Steffen et al., 2003). Quinoid products (whose formation would have been indicated by a mass shift of  $m/z +28$ ), however, were not detected in our study and the main reaction products of 4- and 5-ring PAHs oxidized by UPOs were mono-hydroxylated products. Thus, substantial one-electron oxidation can be ruled out and hence, the oxyfunctionalizations observed had to be the result of true oxygen transfers (and not of water addition) (Hammel et al., 1986). This finding is largely consistent with the data presented by Aranda et al. (2010) for smaller PAHs, although quinones (e.g., anthraquinone) were observed as minor products. When the data presented herein

are being compared with literature data, it becomes evident that quinones are detectable in decreasing order beginning with benzene>naphthalene>anthracene>4- and 5-ring PAHs (e.g., benz[a]anthracene and perylene, respectively); hence the formation of quinoid products from arenes, catalyzed by UPOs, is inversely proportional to the size of the aromatic system (Kluge et al., 2007; Aranda et al., 2010; Karich et al., 2013).

Oxidation of PAHs by ligninolytic peroxidases (e.g., MNP, LIP) and LAC is strictly dependent on the substrates' IP and high-molecular mass PAHs, e.g., benzo[g,h,i]perylene or benzo[a]pyrene, were found to be faster oxidized than smaller PAHs, some of which cannot be oxidized at all (e.g., phenanthrene and fluoranthene) (Steffen et al., 2003). In contrast, UPOs favor low-molecular mass PAHs over high-molecular ones as oxygen acceptor and the substrate IP seems to be of minor relevance for the extent of conversion (Table 2).

### Other Substrates

Benzidine (18), 1,2-diphenylhydrazine (16) and 2,4-dimethylphenol do not really fit into the above classification of potential UPO substrates; therefore, we deal with them herein separately. Treatment of 18 samples with *Aae*UPO and *Mro*UPO mainly resulted in the formation of coupling products. However, in the case of *Mro*UPO, an oxygenation product of 18 was detectable as well. Again, the larger heme channel of *Mro*UPO (compared to *Aae*UPO) may explain that fact. We assume that 3-hydroxybenzidine (19) was the product formed, which is most plausible to proceed via a lateral oxidative attack on 18. Azo derivatives based on 18 have been widely used as textile dyes and some of them are known to be carcinogenic (Lowry et al., 1980). Thus, 18 has been subject of various (eco)toxicological studies with focus on its carcinogenicity. In this context, oxygenation/hydroxylation of 18 by P450s as well as its POX-catalyzed oxidation to benzidine diimine ensuing binding to DNA were described (Yamazoe et al., 1988; Lakshmi et al., 1996). To supplement this, we have shown here that UPOs are capable of catalyzing these reactions as well.

Studying 16-conversion turned out to be rather difficult for several reasons. The compound instantaneously autoxidizes in aqueous solution to *cis*- and *trans*-azobenzene (17) (Riggin and Howard, 1979) or it rearranges to 18 and diphenylene (Hammond and Shine, 1950; Ghigo et al., 2011); the latter reaction, however, is acid-dependent and was therefore not observed under the conditions applied here. Furthermore, authentic standards of potential 16 products are commercially not available and it was impossible to ionize 16 in a way to get a quality mass spectrum. Nevertheless, one product with a mass spectrum shift of "+32" in relation to 16 was detected and might be the result of two hydroxylations at the benzene rings of 16. Two products most probably deriving from the oxygenation of spontaneously formed 17 were additionally detected. The first product's mass spectrum shifted by  $m/z+16$  in relation to 17 (and by  $m/z+14$  compared to 16). The latter mass (+14) could hypothetically stand for a single keto function, which is, however, impossible to emerge at the aromatic rings of 16. Therefore, it may rather represent an oxygenation product of 17 (a hydroxy-azobenzene, 20). Logically, the second product (mass shift  $m/z+32$  compared to

**TABLE 2** | Conversion of selected PAHs by *AaeUPO* and *MroUPO* with reference to their water solubility and molecular size.

Substrate	Water solubility [mg L <sup>-1</sup> ] (ref.)	Carbon atoms [C <sub>n</sub> ]	Minimum and maximum width [Å]*	Relative conversion by <i>AaeUPO</i> # (Ref.)	Relative conversion by <i>MroUPO</i>	Ionization potential [eV] (Ref.)
Acenaphthylene	16.1 (Tegge, 1983)	12	4.0/4.6	++	++	8.22 (Majcherzyk et al., 1998)
Acenaphthene	3.93 (Mackay and Shiu, 1977)	12	4.0/4.6	++	++	7.86 (Majcherzyk et al., 1998)
Fluorene	1.98 (Mackay and Shiu, 1977)	13	3.07.4	+++ (Aranda et al., 2010)	n.t	7.89 (Majcherzyk et al., 1998)
Phenanthrene	1.29 (Mackay and Shiu, 1977)	14	4.07.6	++ (Aranda et al., 2010)	n.t	7.91 (Majcherzyk et al., 1998)
Anthracene	0.073 (Mackay and Shiu, 1977)	14	3.07.9	++ (Aranda et al., 2010)	n.t	7.43 (Majcherzyk et al., 1998)
Pyrene	0.135 (Mackay and Shiu, 1977)	16	5.27.6	++ (Aranda et al., 2010)	n.t	7.43 (Majcherzyk et al., 1998)
Benzoflanthracene	0.014 (Mackay and Shiu, 1977)	18	4.88.1	++	+	7.44 (Majcherzyk et al., 1998)
Benzoflapyren	0.0038 (Tegge, 1983)	20	4.88.1	+	++	7.12 (Majcherzyk et al., 1998)
Perylene	0.0004 (Mackay and Shiu, 1977)	20	4.6/6.6	t	+	6.97 (Majcherzyk et al., 1998)
Indeno[1,2,3-c]pyrene	0.062 (Tegge, 1983)	22	5.88.4	t	t	-
Benzofluoranthene	0.0012 (Tegge, 1983)	20	4.8/9.6	0	t	7.70 (Majcherzyk et al., 1998)
Benzokjfluoranthene	0.00055 (Tegge, 1983)	20	4.6/10.1	t	t	7.48 (Majcherzyk et al., 1998)
Dibenz[a,h]anthracene	0.0005 (Tegge, 1983)	22	6.9/10.6	0	0	7.38 (Dabestani and Ivanov, 1999)
Benzofl,h]perylene	0.00026 (Mackay and Shiu, 1977)	22	6.7/6.9	0	0	7.16 (Simonsick and Hites, 1984)

# 0, no conversion; t, trace amounts of products detected; +, little conversion; ++, moderate conversion; + + +, good conversion (for more explanations, compare legend of Table 1). \*Calculated with PyMOL 1.3 (<https://www.pymol.org>).

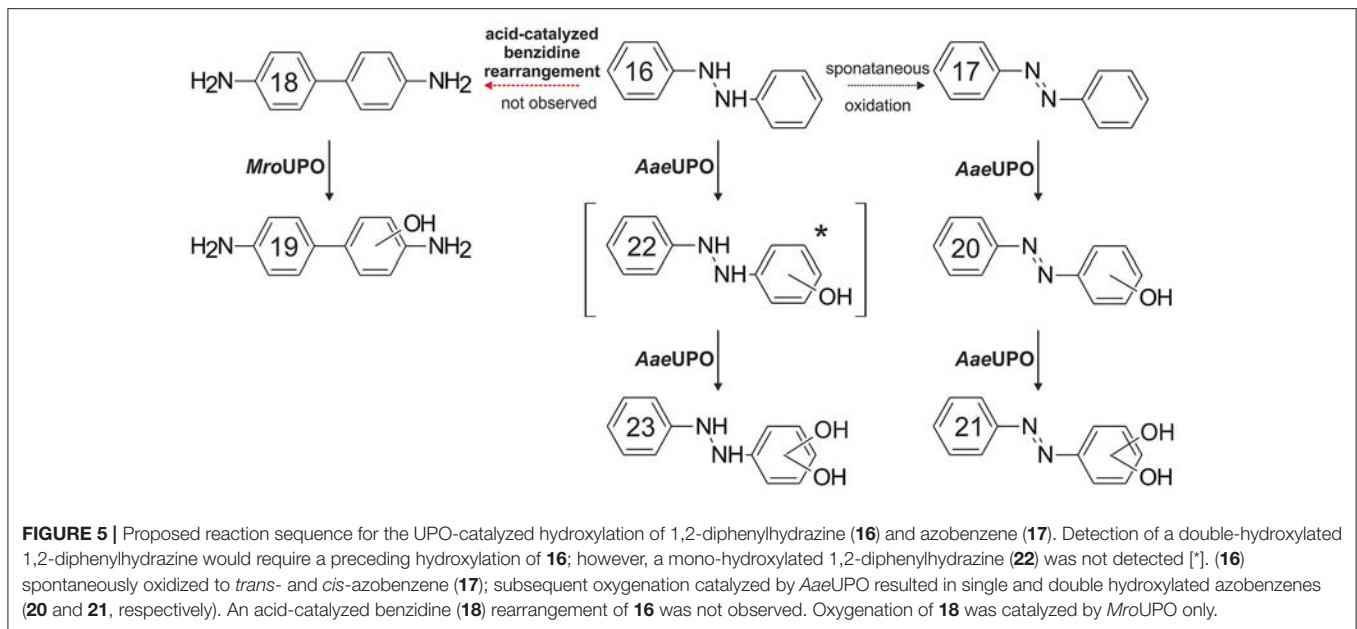
17) presumably resulted from a second hydroxylation of 17 (or it may represent a quinone of a double hydroxylated 16). However, whether *cis*- or *trans*-17 served as initial substrate, could not be exactly found out but the decrease of *trans*-17 in samples containing *AaeUPO* (compare Supplementary Material) implies the latter. A proposed pathway for spontaneous and UPO-catalyzed hydroxylation of 16 is given in Figure 5. Mammalian metabolism of 17 and derivatives usually proceeds via reductive pathways and 16 typically rearranges to 18 (Walker, 1970; Levine, 1991). Hydroxylation of 17 or 16 by mammalian P450 was not observed (Bray et al., 1951).

In the reaction setup of 2,4-dimethylphenol with *AaeUPO*, polymerization products, oxygenation products and combinations of both were found. This finding is not surprising, since methylphenols (cresols) are well-known substrates both for one-electron oxidations by POX (or LAC) (Klibanov et al., 1980; Ghosh et al., 2008) and for oxyfunctionalizations by P450s (Yan et al., 2005) and other monooxygenases (Arengi et al., 2001). Thus, our results fit well to these reports and supplement an own previous study dealing with benzene oxidation by *AaeUPO*, in the course of which phenol emerged as an intermediate that was rapidly further converted (Karich et al., 2013).

### Concluding Remarks

The majority of organopollutants tested here (i.e., 35 out of 44 substances, compare Table 1)—including xenobiotics, such as chlorinated benzenes and their derivatives, halogenated biphenyl ethers, nitroaromatic compounds, polycyclic aromatics and phthalates—were oxidatively converted by two fungal model UPOs. UPO-catalyzed oxidations were limited for three main reasons: (i) steric hindrance caused by the number of substituents or general bulkiness of the compound, e.g., hexachlorobenzene or large PAHs, such as benzo[g,h,i]perylene; (ii) strong inactivation of the aromatic ring by electron-withdrawing groups, e.g., nitrobenzene, and (iii) low bioavailability (water solubility) of the potential substrate.

Currently, 41 EPA priority pollutants have been reported to be oxidized by UPOs including the herein tested compounds and several other substances investigated in previous studies. Intensely investigated *AaeUPO* was found to oxygenate and oxidize numerous substance classes (Aranda et al., 2009, 2010; Kluge et al., 2009, 2012; Kinne et al., 2010; Peter et al., 2011; Poraj-Kobielska et al., 2011; Karich et al., 2013; Poraj-Kobielska, 2013) and at present, as much as 300 aromatic, heterocyclic, aliphatic and alicyclic compounds have been identified to serve as substrates for this enzyme (Hofrichter et al., 2015). This fact points out that UPOs are highly versatile oxidoreductases with an exceptional broad substrate spectrum. Besides UPOs, only P450s realize a comparable catalytic promiscuity for oxyfunctionalization reactions (compare Table 1). In fact, UPOs share with P450s the heme-thiolate as prosthetic group as well as highly reactive compound-I and protonated compound-II intermediates in the catalytic cycle (Yosca et al., 2017). On the other hand, UPOs and P450s do not share any sequence homology and act in different micro-environments (extracellularly vs. intracellularly). Maybe the catalytic systems of P450s and UPOs complement each other in a suitable way



by eliminating similar, often toxic compounds inside and outside of fungal cells, respectively. Thus, UPOs are secretory enzymes using the rather simple co-substrate ( $H_2O_2$ ) that can be generated outside the fungal hyphae, while P450s—as membrane-bound or cytosolic enzymes—use a complex accessory machinery, which allows their precise action in different hyphal compartments. In other words, UPOs can directly interact with the fungus' micro-environment and do rather "dirty catalytic jobs," whereas P450s are responsible for the fine-tuning of similar reactions in the cells. UPOs may represent an extracellular equivalent to intracellular P450s, in which they function as a universal fungal detoxification system ("extracellular fungal liver") that can oxidize plant ingredients, microbial metabolites and xenobiotics. The high number of putative UPO genes distributed among rather different ecological and phylogenetic groups of fungi (compare **Figure 1**) may strongly support this assumption.

Until now, all substrate conversion studies regarding UPOs have been carried out in cell-free systems with isolated enzyme preparations and it is still unclear, under which circumstances UPOs are induced and expressed in fungi under natural conditions. So it is rather difficult to appraise, which roles (others than detoxification) these enzymes may still play. Whilst the actual physiological functions of UPOs in individual fungi will still have to be elucidated, the wealth of catalyzed reactions is without doubt and in any case, interesting from the environmental and biotechnological points of view. Notably, UPOs do not only complement P450 activities but they may also support the action of extracellular fungal enzyme systems catalyzing one-electron oxidations, as needed for lignin and humus decomposition (i.e., POX and LAC reactions).

Future studies on UPOs will have to focus, amongst others, on the conditions, under which the production and secretion of

UPOs are induced and how their activities can be stimulated in different ecological and phylogenetic groups of fungi. Because UPO genes are widely distributed in the whole fungal kingdom and fungi indeed permeate the living scene, a powerful tool may become available to foster bioattenuation processes, such as the self-cleaning function of soils.

## AUTHOR CONTRIBUTIONS

Conceived and designed the experiments: AK, RU, and MH. Performed the experiments: AK. Wrote the manuscript, supervised, and discussed the experiments and data: AK, RU, KS, and MH.

## FUNDING

This research was supported by the EU projects INDOX (KBBE-2013-7-613549) and ENZO2 (H2020-BBI-PPP-2015-2-1-720297). The funders did not influence the study design, data collection and analysis, the decision to publish, or preparation of the manuscript.

## ACKNOWLEDGMENTS

We thank Henrik Lund† (in memoriam) for numberless scientific discussions and his strong commitment to peroxygenases.

## SUPPLEMENTARY MATERIAL

The Supplementary Material for this article can be found online at: <http://journal.frontiersin.org/article/10.3389/fmicb.2017.01463/full#supplementary-material>

## REFERENCES

- Amato, G., Longo, V., Mazzaccaro, A., and Gervasi, P. G. (1998). Chlorzoxazone 6-hydroxylase and p-nitrophenol Hhydroxylase as the most suitable activities for assaying cytochrome P450 2E1 in cynomolgus monkey liver. *Drug Metab. Dispos.* 26, 483–489.
- Anzenbacher, P., and Anzenbacherová, E. (2001). Cytochromes P450 and metabolism of xenobiotics. *Cell. Mol. Life Sci.* 58, 737–747. doi: 10.1007/PL00000897
- Aranda, E., Kinne, M., Kluge, M., Ullrich, R., and Hofrichter, M. (2009). Conversion of dibenzothiophene by the mushrooms *Agrocybe aegerita* and *Coprinellus radians* and their extracellular peroxygenases. *Appl. Microbiol. Biotechnol.* 82, 1057–1066. doi: 10.1007/s00253-008-1778-6
- Aranda, E., Ullrich, R., and Hofrichter, M. (2010). Conversion of polycyclic aromatic hydrocarbons, methyl naphthalenes and dibenzofuran by two fungal peroxygenases. *Biodegradation* 21, 267–281. doi: 10.1007/s10532-009-9299-2
- Arengi, F. L. G., Berlanda, D., Galli, E., Sello, G., and Barbieri, P. (2001). Organization and regulation of meta cleavage pathway genes for toluene and o-xylene derivative degradation in *Pseudomonas stutzeri* OX1. *Appl. Environ. Microbiol.* 67, 3304–3308. doi: 10.1128/AEM.67.7.3304-3308.2001
- Bagnéris, C., Cammack, R., and Mason, J. R. (2005). Subtle difference between benzene and toluene dioxygenases of *Pseudomonas putida*. *Appl. Environ. Microbiol.* 71, 1570–1580. doi: 10.1128/AEM.71.3.1570-1580.2005
- Beadle, C. A., and Smith, A. R. W. (1982). The purification and properties of 2,4-dichlorophenol hydroxylase from a strain of *Acinetobacter* species. *Eur. J. Biochem.* 123, 323–332. doi: 10.1111/j.1432-1033.1982.tb19771.x
- Bogan, B. W., and Lamar, R. T. (1995). One-electron oxidation in the degradation of creosote polycyclic aromatic hydrocarbons by *Phanerochaete chrysosporium*. *Appl. Environ. Microbiol.* 61, 2631–2635.
- Bollag, J. M., Shuttleworth, K. L., and Anderson, D. H. (1988). Laccase-mediated detoxification of phenolic compounds. *Appl. Environ. Microbiol.* 54, 3086–3091.
- Bray, H., Clowes, R., and Thorpe, W. (1951). The metabolism of azobenzene and p-hydroxyazobenzene in the rabbit. *Biochem. J.* 49:lxv.
- Bugg, T. D. H., and Ramaswamy, S. (2008). Non-heme iron-dependent dioxygenases: unravelling catalytic mechanisms for complex enzymatic oxidations. *Curr. Opin. Chem. Biol.* 12, 134–140. doi: 10.1016/j.cbpa.2007.12.007
- Büttner, E., Ullrich, R., Strittmatter, E., Piontek, K., Plattner, D. A., Hofrichter, M., et al. (2015). Oxidation and nitration of mononitrophenols by a DyP-type peroxidase. *Arch. Biochem. Biophys.* 574, 86–92. doi: 10.1016/j.abb.2015.03.003
- Camarero, S., Sarkar, S., Ruiz-Dueñas, F. J., Martínez, M. A. J., and Martínez, Á.T. (1999). Description of a versatile peroxidase involved in the natural degradation of lignin that has both manganese peroxidase and lignin peroxidase substrate interaction sites. *J. Biol. Chem.* 274, 10324–10330. doi: 10.1074/jbc.274.15.10324
- Cassidy, M. B., Lee, H., Trevors, J. T., and Zablotowicz, R. B. (1999). Chlorophenol and nitrophenol metabolism by *Sphingomonas* sp UG30. *J. Ind. Microbiol. Biotechnol.* 23, 232–241. doi: 10.1038/sj.jim.2900749
- Copley, S. D. (2000). Evolution of a metabolic pathway for degradation of a toxic xenobiotic: the patchwork approach. *Trends Biochem. Sci.* 25, 261–265. doi: 10.1016/S0968-0004(00)01562-0
- Crawford, R., Jung, C., and Strap, J. (2007). The recent evolution of pentachlorophenol (PCP)-4-monoxygenase (PcpB) and associated pathways for bacterial degradation of PCP. *Biodegradation* 18, 525–539. doi: 10.1007/s10532-006-9090-6
- Dabestani, R., and Ivanov, I. N. (1999). A compilation of physical, spectroscopic and photophysical properties of polycyclic aromatic hydrocarbons. *Photochem. Photobiol.* 70, 10–34.
- Davila-Vazquez, G., Tinoco, R., Pickard, M. A., and Vazquez-Duhalt, R. (2005). Transformation of halogenated pesticides by versatile peroxidase from *Bjerkandera adusta*. *Enzyme Microbial Technol.* 36, 223–231. doi: 10.1016/j.enzmictec.2004.07.015
- Dawson, J. (1988). Probing structure-function relations in heme-containing oxygenases and peroxidases. *Science* 240, 433–439. doi: 10.1126/science.3358128
- de Bont, J. A., Vorage, M. J., Hartmans, S., and van den Tweel, W. J. (1986). Microbial degradation of 1,3-dichlorobenzene. *Appl. Environ. Microbiol.* 52, 677–680.
- Dodor, D. E., Hwang, H.-M., and Ekunwe, S. I. N. (2004). Oxidation of anthracene and benzo[a]pyrene by immobilized laccase from *Trametes versicolor*. *Enzyme Microbial Technol.* 35, 210–217. doi: 10.1016/j.enzmictec.2004.04.007
- Durán, N., and Esposito, E. (2000). Potential applications of oxidative enzymes and phenoloxidase-like compounds in wastewater and soil treatment: a review. *Appl. Catal. B Environ.* 28, 83–99. doi: 10.1016/S0926-3373(00)00168-5
- Eaton, R. W., and Ribbons, D. W. (1982). Metabolism of dibutylphthalate and phthalate by *Micrococcus* sp. strain 12B. *J. Bacteriol.* 151, 48–57.
- Ferraro, D. J., Gakhar, L., and Ramaswamy, S. (2005). Rieseke business: structure-function of rieske non-heme oxygenases. *Biochem. Biophys. Res. Commun.* 338, 175–190. doi: 10.1016/j.bbrc.2005.08.222
- Fewson, C. A. (1988). Biodegradation of xenobiotic and other persistent compounds: the causes of recalcitrance. *Trends Biotechnol.* 6, 148–153. doi: 10.1016/0167-7799(88)90084-4
- Fishman, A., Tao, Y., Bentley, W. E., and Wood, T. K. (2004). Protein engineering of toluene 4-monoxygenase of *Pseudomonas mendocina* KR1 for synthesizing 4-nitrocatechol from nitrobenzene. *Biotechnol. Bioeng.* 87, 779–790. doi: 10.1002/bit.20185
- Floudas, D., Binder, M., Riley, R., Barry, K., Blanchette, R. A., Henrissat, B., et al. (2012). The paleozoic origin of enzymatic lignin decomposition reconstructed from 31 fungal genomes. *Science* 336, 1715–1719. doi: 10.1126/science.1221748
- Fodil, D., Badis, A., Jaouadi, B., Zarái, N., Ferradji, F. Z., and Boutoumi, H. (2011). Purification and characterization of two extracellular peroxidases from *Streptomyces* sp. strain AM2, a decolorizing actinomycetes responsible for the biodegradation of natural humic acids. *Int. Biodeterior. Biodegradation* 65, 470–478. doi: 10.1016/j.ibiod.2011.01.009
- Freire, R. S., Ferreira, M. M. C., Durán, N., and Kubota, L. T. (2003). Dual amperometric biosensor device for analysis of binary mixtures of phenols by multivariate calibration using partial least squares. *Anal. Chim. Acta* 485, 263–269. doi: 10.1016/S0003-2670(03)00414-8
- Ghigo, G., Osella, S., Maranzana, A., and Tonachini, G. (2011). The mechanism of the acid-catalyzed benzidine rearrangement of hydrazobenzene: a theoretical study. *European J. Org. Chem.* 2011, 2326–2333. doi: 10.1002/ejoc.201001636
- Ghosh, J. P., Taylor, K. E., Bewtra, J. K., and Biswas, N. (2008). Laccase-catalyzed removal of 2,4-dimethylphenol from synthetic wastewater: effect of polyethylene glycol and dissolved oxygen. *Chemosphere* 71, 1709–1717. doi: 10.1016/j.chemosphere.2008.01.002
- Gröbe, G., Ullrich, R., Pecyna, M., Kapturska, D., Friedrich, S., Hofrichter, M., et al. (2011). High-yield production of aromatic peroxygenase by the agaric fungus *Marasmius rotula*. *AMB Express* 1:31. doi: 10.1186/2191-0855-1-31
- Guengerich, F. P. (2001). Common and uncommon cytochrome P450 reactions related to metabolism and chemical toxicity. *Chem. Res. Toxicol.* 14, 611–650. doi: 10.1021/tx0002583
- Haemmerli, S. D., Leisola, M. S., Sanglard, D., and Fiechter, A. (1986). Oxidation of benzo(a)pyrene by extracellular ligninases of *Phanerochaete chrysosporium*. Veratryl alcohol and stability of ligninase. *J. Biol. Chem.* 261, 6900–6903.
- Hammel, K. E. (1995). Mechanisms for polycyclic aromatic hydrocarbon degradation by ligninolytic fungi. *Environ. Health Perspect.* 103(Suppl. 5), 41–43. doi: 10.1289/ehp.95103s441
- Hammel, K. E., and Cullen, D. (2008). Role of fungal peroxidases in biological ligninolysis. *Curr. Opin. Plant Biol.* 11, 349–355. doi: 10.1016/j.pbi.2008.02.003
- Hammel, K. E., Kalyanaraman, B., and Kirk, T. K. (1986). Oxidation of polycyclic aromatic hydrocarbons and dibenzo[p]-dioxins by *Phanerochaete chrysosporium* ligninase. *J. Biol. Chem.* 261, 16948–16952.
- Hammel, K. E., and Tardone, P. J. (1988). The oxidative 4-dechlorination of polychlorinated phenols is catalyzed by extracellular fungal lignin peroxidases. *Biochemistry* 27, 6563–6568. doi: 10.1021/bi00417a055
- Hammond, G. S., and Shine, H. J. (1950). The mechanism of the benzidine rearrangement. i. the effect of acid concentration on rate. *J. Am. Chem. Soc.* 72, 220–221. doi: 10.1021/ja01157a062
- Haritash, A. K., and Kaushik, C. P. (2009). Biodegradation aspects of Polycyclic Aromatic Hydrocarbons (PAHs): a review. *J. Hazard. Mater.* 169, 1–15. doi: 10.1016/j.jhazmat.2009.03.137

- Harms, H., Schlosser, D., and Wick, L. Y. (2011). Untapped potential: exploiting fungi in bioremediation of hazardous chemicals. *Nat Rev Micro* 9, 177–192. doi: 10.1038/nrmicro2519
- Hibi, M., Hatahira, S., Nakatani, M., Yokozeki, K., Shimizu, S., and Ogawa, J. (2012). Extracellular oxidases of *Cerrena* sp. complementarily functioning in artificial dye decolorization including laccase, manganese peroxidase, and novel versatile peroxidases. *Biocatal. Agric. Biotechnol.* 1, 220–225. doi: 10.1016/j.bcab.2012.03.003
- Hiratsuka, N., Wariishi, H., and Tanaka, H. (2001). Degradation of diphenyl ether herbicides by the lignin-degrading basidiomycete *Coriolus versicolor*. *Appl. Microbiol. Biotechnol.* 57, 563–571. doi: 10.1007/s002530100789
- Hofrichter, M. (2002). Review: lignin conversion by manganese peroxidase (MnP). *Enzyme Microb. Technol.* 30, 454–466. doi: 10.1016/S0141-0229(01)00528-2
- Hofrichter, M., Kellner, H., Pecyna, M. J., and Ullrich, R. (2015). Fungal unspecific peroxidases: heme-thiolate proteins that combine preoxidase and cytochrome p450 properties. *Adv. Exp. Med. Biol.* 851, 341–368. doi: 10.1007/978-3-319-16009-2\_13
- Hofrichter, M., and Ullrich, R. (2006). Heme-thiolate haloperoxidases: versatile biocatalysts with biotechnological and environmental significance. *Appl. Microbiol. Biotechnol.* 71, 276–288. doi: 10.1007/s00253-006-0417-3
- Huijbers, M. M. E., Montersino, S., Westphal, A. H., Tischler, D., and van Berkel, W. J. H. (2014). Flavin dependent monooxygenases. *Arch. Biochem. Biophys.* 544, 2–17. doi: 10.1016/j.abb.2013.12.005
- Hundt, K., Jonas, U., Hammer, E., and Schauer, F. (1999). Transformation of diphenyl ethers by *Trametes versicolor* and characterization of ring cleavage products. *Biodegradation* 10, 279–286. doi: 10.1023/A:1008384019897
- Iba, M. M., and Thomas, P. E. (1988). Activation of 3,3'-dichlorobenzidine in rat liver microsomes to mutagens: involvement of cytochrome P-450. *Carcinogenesis* 9, 717–723. doi: 10.1093/carcin/9.5.717
- Imaoka, S., Yoneda, Y., Matsuda, T., Degawa, M., Fukushima, S., and Funae, Y. (1997). Mutagenic activation of urinary bladder carcinogens by CYP4B1 and the presence of CYP4B1 in bladder mucosa. *Biochem. Pharmacol.* 54, 677–683. doi: 10.1016/S0006-2952(97)00216-5
- Jeon, J.-R., Murugesan, K., Kim, Y.-M., Kim, E.-J., and Chang, Y.-S. (2008). Synergistic effect of laccase mediators on pentachlorophenol removal by *Ganoderma lucidum* laccase. *Appl. Microbiol. Biotechnol.* 81, 783–790. doi: 10.1007/s00253-008-1753-2
- Jergil, B., Lindbladh, C., Rorsman, H., and Rosengren, E. (1983). Dopa oxidation and tyrosine oxygenation by human melanoma tyrosinase. *Acta Derm. Venereol.* 63, 468–475.
- Johannes, C., and Majcherczyk, A. (2000). Natural mediators in the oxidation of polycyclic aromatic hydrocarbons by laccase mediator systems. *Appl. Environ. Microbiol.* 66, 524–528. doi: 10.1128/AEM.66.2.524-528.2000
- Johnson, G. R., Jain, R. K., and Spain, J. C. (2002). Origins of the 2,4-dinitrotoluene pathway. *J. Bacteriol.* 184, 4219–4232. doi: 10.1128/JB.184.15.4219-4232.2002
- Jones, J. P., O'Hare, E. J., and Wong, L.-L. (2001). Oxidation of polychlorinated benzenes by genetically engineered CYP101 (cytochrome P450cam). *Eur. J. Biochem.* 268, 1460–1467. doi: 10.1046/j.1432-1327.2001.02018.x
- Kadiyala, V., and Spain, J. C. (1998). A two-component monooxygenase catalyzes both the hydroxylation of p-nitrophenol and the oxidative release of nitrite from 4-nitrocatechol in *Bacillus sphaericus* JS905. *Appl. Environ. Microbiol.* 64, 2479–2484.
- Karich, A., Kluge, M., Ullrich, R., and Hofrichter, M. (2013). Benzene oxygenation and oxidation by the peroxxygenase of *Agrocybe aegerita*. *AMB Express* 3:5. doi: 10.1186/2191-0855-3-5
- Kaschabek, S. R., Kasberg, T., Müller, D., Mars, A. E., Janssen, D. B., and Reineke, W. (1998). Degradation of chloroaromatics: purification and characterization of a novel type of chlorocatechol 2,3-dioxygenase of *Pseudomonas putida* GJ31. *J. Bacteriol.* 180, 296–302.
- Kim, J. H., Stansbury, K. H., Walker, N. J., Trush, M. A., Strickland, P. T., and Sutter, T. R. (1998). Metabolism of benzo[a]pyrene and benzo[a]pyrene-7,8-diol by human cytochrome P450 1B1. *Carcinogenesis* 19, 1847–1853. doi: 10.1093/carcin/19.10.1847
- Kinne, M. (2010). *The Extracellular Peroxygenase of the Agaric Fungus Agrocybe aegerita: Catalytic Properties and Physiological Background with Particular Emphasis on Ether Cleavage*. IHI Zittau.
- Kinne, M., Poraj-Kobielska, M., Aranda, E., Ullrich, R., Hammel, K. E., Scheibner, K., et al. (2009a). Regioselective preparation of 5-hydroxypropranolol and 4'-hydroxydiclofenac with a fungal peroxxygenase. *Bioorg. Med. Chem. Lett.* 19, 3085–3087. doi: 10.1016/j.bmcl.2009.04.015
- Kinne, M., Poraj-Kobielska, M., Ralph, S. A., Ullrich, R., Hofrichter, M., and Hammel, K. E. (2009b). Oxidative cleavage of diverse ethers by an extracellular fungal peroxxygenase. *J. Biol. Chem.* 284, 29343–29349. doi: 10.1074/jbc.M109.040857
- Kinne, M., Zeisig, C., Ullrich, R., Kayser, G., Hammel, K. E., and Hofrichter, M. (2010). Stepwise oxygenations of toluene and 4-nitrotoluene by a fungal peroxxygenase. *Biochem. Biophys. Res. Commun.* 397, 18–21. doi: 10.1016/j.bbrc.2010.05.036
- Kirk, T. K., and Farrell, R. L. (1987). Enzymatic "Combustion": the microbial degradation of lignin. *Annu. Rev. Microbiol.* 41, 465–501. doi: 10.1146/annurev.mi.41.100187.002341
- Klibanov, A. M., Alberti, B. N., Morris, E. D., and Felshin, L. M. (1980). Enzymatic removal of toxic phenols and anilines from waste waters. *J. Appl. Biochem.* 2:5, 414–421.
- Kluge, M., Ullrich, R., Dolge, C., Scheibner, K., and Hofrichter, M. (2009). Hydroxylation of naphthalene by aromatic peroxxygenase from *Agrocybe aegerita* proceeds via oxygen transfer from and intermediary epoxidation. *Appl. Microbiol. Biotechnol.* 81, 1071–1076. doi: 10.1007/s00253-008-1704-y
- Kluge, M., Ullrich, R., Scheibner, K., and Hofrichter, M. (2007). Spectrophotometric assay for detection of aromatic hydroxylation catalyzed by fungal haloperoxidase-peroxxygenase. *Appl. Microbiol. Biotechnol.* 75, 1473–1478. doi: 10.1007/s00253-007-0942-8
- Kluge, M., Ullrich, R., Scheibner, K., and Hofrichter, M. (2012). Stereoselective benzylic hydroxylation of alkylbenzenes and epoxidation of styrene derivatives catalyzed by the peroxxygenase of *Agrocybe aegerita*. *Green Chem.* 14, 440–446. doi: 10.1039/C1GC16173C
- Kordon, K., Mikolasch, A., and Schauer, F. (2010). Oxidative dehalogenation of chlorinated hydroxybiphenyls by laccases of white-rot fungi. *Int. Biodeterior. Biodegradation* 64, 203–209. doi: 10.1016/j.ibiod.2009.10.010
- Krimer, L. I., and Cota, D. J. (2004). "The Ritter Reaction," in *Organic Reactions*. ed S. E. Denmark (Chichester: John Wiley & Sons, Inc.) doi: 10.1002/0471264180.or017.03
- Lakshmi, V. M., Zenser, N. T., Hsu, F. F., Mattammal, M. B., Zenser, T. V., and Davis, B. B. (1996). NADPH-dependent oxidation of benzidine by rat liver. *Carcinogenesis* 17, 1941–1947. doi: 10.1093/carcin/17.9.1941
- Lamb, D. C., Lei, L., Warrilow, A. G. S., Lepesheva, G. I., Mullins, J. G. L., Waterman, M. R., et al. (2009). The first virally encoded cytochrome P450. *J. Virol.* 83, 8266–8269. doi: 10.1128/JVI.00289-09
- Leahy, J. G., Batchelor, P. J., and Morcomb, S. M. (2003). Evolution of the soluble diiron monooxygenases. *FEMS Microbiol. Rev.* 27, 449–479. doi: 10.1016/S0168-6445(03)00023-8
- Leontievsky, A., Myasoedova, N., Baskunov, B., Golovleva, L., Bucke, C., and Evans, C. (2001). Transformation of 2,4,6-trichlorophenol by free and immobilized fungal laccase. *Appl. Microbiol. Biotechnol.* 57, 85–91. doi: 10.1007/s002530100756
- Lepesheva, G. I., and Waterman, M. R. (2004). CYP51—the omnipotent P450. *Mol. Cell. Endocrinol.* 215, 165–170. doi: 10.1016/j.mce.2003.11.016
- Lessner, D. J., Johnson, G. R., Parales, R. E., Spain, J. C., and Gibson, D. T. (2002). Molecular characterization and substrate specificity of nitrobenzene dioxygenase from *Comamonas* sp. strain JS765. *Appl. Environ. Microbiol.* 68, 634–641. doi: 10.1128/AEM.68.2.634-641.2002
- Levine, W. G. (1991). Metabolism of AZO dyes: implication for detoxication and activation. *Drug Metab. Rev.* 23, 253–309. doi: 10.3109/03602539109029761
- Liers, C., Aranda, E., Strittmatter, E., Piontek, K., Plattner, D. A., Zorn, H., et al. (2014). Phenol oxidation by DyP-type peroxidases in comparison to fungal and plant peroxidases. *J. Mol. Catal. B Enzymatic* 103, 41–46. doi: 10.1016/j.molcatb.2013.09.025
- Lowry, L. K., Tolos, W. P., Boeniger, M. F., Nony, C. R., and Bowman, M. C. (1980). Chemical monitoring of urine from workers potentially exposed to benzidine-derived azo dyes. *Toxicol. Lett.* 7, 29–36. doi: 10.1016/0378-4274(80)90081-8
- Mackay, D., and Shiu, W. Y. (1977). Aqueous solubility of polynuclear aromatic hydrocarbons. *J. Chem. Eng. Data* 22, 399–402. doi: 10.1021/jc60075a012

- Majcherczyk, A., Johannes, C., and Hüttermann, A. (1998). Oxidation of polycyclic aromatic hydrocarbons (PAH) by laccase of *Trametes versicolor*. *Enzyme Microb. Technol.* 22, 335–341. doi: 10.1016/S0141-0229(97)00199-3
- Marco-Urrea, E., Pérez-Trujillo, M., Caminal, G., and Vicent, T. (2009). Dechlorination of 1,2,3- and 1,2,4-trichlorobenzene by the white-rot fungus *Trametes versicolor*. *J. Hazard. Mater.* 166, 1141–1147. doi: 10.1016/j.jhazmat.2008.12.076
- Mars, A. E., Kasberg, T., Kaschabek, S. R., van Agteren, M. H., Janssen, D. B., and Reineke, W. (1997). Microbial degradation of chloroaromatics: use of the meta-cleavage pathway for mineralization of chlorobenzene. *J. Bacteriol.* 179, 4530–4537. doi: 10.1128/jb.179.14.4530-4537.1997
- Martínez, Á. T., Ruiz-Dueñas, F. J., Martínez, M. J., del Río, J. C., and Gutiérrez, A. (2009). Enzymatic delignification of plant cell wall: from nature to mill. *Curr. Opin. Biotechnol.* 20, 348–357. doi: 10.1016/j.copbio.2009.05.002
- McDaniel, D. H., and Brown, H. C. (1958). An extended table of hammett substituent constants based on the ionization of substituted benzoic acids. *J. Org. Chem.* 23, 420–427. doi: 10.1021/jo01097a026
- Meunier, B., de Visser, S. P., and Shaik, S. (2004). Mechanism of oxidation reactions catalyzed by cytochrome P450 enzymes. *Chem. Rev.* 104, 3947–3980. doi: 10.1021/cr020443g
- Moiseeva, O. V., Solyanikova, I. P., Kaschabek, S. R., Gröning, J., Thiel, M., Golovleva, L. A., et al. (2002). A new modified ortho cleavage pathway of 3-chlorocatechol degradation by rhodococcus opacus 1CP: genetic and biochemical evidence. *J. Bacteriol.* 184, 5282–5292. doi: 10.1128/JB.184.19.5282-5292.2002
- Monferran, M. V., Wunderlin, D. A., Nimptsch, J., and Pflugmacher, S. (2007). Biotransformation and antioxidant response in *Ceratophyllum demersum* experimentally exposed to 1,2- and 1,4-dichlorobenzene. *Chemosphere* 68, 2073–2079. doi: 10.1016/j.chemosphere.2007.02.016
- Montiel, A. M., Fernández, F. J., Marcial, J., Soriano, J., Barrios-González, J., and Tomasini, A. (2004). A fungal phenoloxidase (tyrosinase) involved in pentachlorophenol degradation. *Biotechnol. Lett.* 26, 1353–1357. doi: 10.1023/B:BILE.0000045632.36401.86
- Mori, T., Kitano, S., and Kondo, R. (2003). Biodegradation of chloronaphthalenes and polycyclic aromatic hydrocarbons by the white-rot fungus *Phlebia lindtneri*. *Appl. Microbiol. Biotechnol.* 61, 380–383. doi: 10.1007/s00253-003-1253-3
- Munro, A. W., Girvan, H. M., Mason, A. E., Dunford, A. J., and McLean, K. J. (2012). What makes a P450 tick? *Trends Biochem. Sci.* 38, 140–150. doi: 10.1016/j.tibs.2012.11.006
- Nedelcheva, V., Gut, I., Souček, P., and Frantik, E. (1998). Cytochrome P450 catalyzed oxidation of monochlorobenzene, 1,2- and 1,4-dichlorobenzene in rat, mouse, and human liver microsomes. *Chem. Biol. Interact.* 115, 53–70. doi: 10.1016/S0009-2797(98)00058-1
- Niki, E. (1991). Action of ascorbic acid as a scavenger of active and stable oxygen radicals. *Am. J. Clin. Nutr.* 54, 1119S–1124S.
- Nishino, S. F., Paoli, G. C., and Spain, J. C. (2000). Aerobic degradation of dinitrotoluenes and pathway for bacterial degradation of 2,6-dinitrotoluene. *Appl. Environ. Microbiol.* 66, 2139–2147. doi: 10.1128/AEM.66.5.2139-2147.2000
- Notomista, E., Lahm, A., Di Donato, A., and Tramontano, A. (2003). Evolution of bacterial and archaeal multicomponent monooxygenases. *J. Mol. Evol.* 56, 435–445. doi: 10.1007/s00239-002-2414-1
- Osborne, R. L., Coggins, M. K., Raner, G. M., Walla, M., and Dawson, J. H. (2009). The mechanism of oxidative halophenol dehalogenation by amphitrite ornata dehaloperoxidase is initiated by H<sub>2</sub>O<sub>2</sub> binding and involves two consecutive one-electron steps: role of ferryl intermediates. *Biochemistry* 48, 4231–4238. doi: 10.1021/bi900367e
- Osborne, R. L., Coggins, M. K., Ternier, J., and Dawson, J. H. (2007). Caldariomyces fumago chloroperoxidase catalyzes the oxidative dehalogenation of chlorophenols by a mechanism involving two one-electron steps. *J. Am. Chem. Soc.* 129, 14838–14839. doi: 10.1021/ja0746969
- Pandya, C., Farelli, J. D., Dunaway-Mariano, D., and Allen, K. N. (2014). Enzyme promiscuity: engine of evolutionary innovation. *J. Biol. Chem.* 289, 30229–30236. doi: 10.1074/jbc.R114.572990
- Pecyna, M. (2016). *Molekularbiologische Charakterisierung von Häm-thiolat- und DYP-type-Peroxidasen ausgewählter Basidiomyceten*. PhD PhD, TU-Dresden.
- Peter, S., Kinne, M., Wang, X., Ullrich, R., Kayser, G., Groves, J. T., et al. (2011). Selective hydroxylation of alkanes by an extracellular fungal peroxxygenase. *FEBS J.* 278, 3667–3675. doi: 10.1111/j.1742-4658.2011.08285.x
- Phillips, L. E., and Leonard, T. J. (1976). Benzidine as a substrate for measuring phenoloxidase activity in crude cell-free extracts of *Schizophyllum commune*. *Mycologia* 68, 277–285. doi: 10.2307/3758999
- Pinyakong, O., Habe, H., Kouzuma, A., Nojiri, H., Yamane, H., and Omori, T. (2004). Isolation and characterization of genes encoding polycyclic aromatic hydrocarbon dioxygenase from acenaphthene and acenaphthylene degrading *Shingomonas* sp. strain A4. *FEMS Microbiol. Lett.* 238, 297–305. doi: 10.1111/j.1574-6968.2004.tb09770.x
- Piontek, K., Smith, A. T., and Blodig, W. (2001). Lignin peroxidase structure and function. *Biochem. Soc. Trans.* 29, 111–116. doi: 10.1042/bst0290111
- Piontek, K., Strittmatter, E., Dimitrova, E., Zámocký, M., Kiebišt, J., Ullrich, R., et al. (2017). Extensive substrate palette – exclusive products: crystal structure of a dimeric peroxxygenase from *Marasmius rotula*. *J Biol Chem.*
- Pointing, S. (2001). Feasibility of bioremediation by white-rot fungi. *Appl. Microbiol. Biotechnol.* 57, 20–33. doi: 10.1007/s002530100745
- Poraj-Kobielska, M. (2013). *Conversion of Pharmaceuticals and Other Drugs by Fungal Peroxygenases: Umsetzung von Pharmazeutika und Psychoaktiven Substanzen mit Pilzlichen Peroxygenasen*. Dissertation, Technical University Dresden. Available online at: [http://www.qucosa.de/recherche/frontdoor/?tx\\_slubopus4frontend\[id\]=11333](http://www.qucosa.de/recherche/frontdoor/?tx_slubopus4frontend[id]=11333)
- Poraj-Kobielska, M., Kinne, M., Ullrich, R., Scheibner, K., Kayser, G., Hammel, K. E., et al. (2011). Preparation of human drug metabolites using fungal peroxxygenases. *Biochem. Pharmacol.* 82, 789–796. doi: 10.1016/j.bcp.2011.06.020
- Qayyum, H., Maroof, H., and Yasha, K. (2009). Remediation and treatment of organopollutants mediated by peroxidases: a review. *Crit. Rev. Biotechnol.* 29, 94–119. doi: 10.1080/07388550802685306
- Reddy, G. V. B., and Gold, M. H. (2000). Degradation of pentachlorophenol by *Phanerochaete chrysosporium*: intermediates and reactions involved. *Microbiology* 146, 405–413. doi: 10.1099/00221287-146-2-405
- Reddy, G. V. B., Sollewijn Gelpke, M. D., and Gold, M. H. (1998). Degradation of 2,4,6-trichlorophenol by *Phanerochaete chrysosporium*: involvement of reductive dechlorination. *J. Bacteriol.* 180, 5159–5164.
- Riggin, R. M., and Howard, C. C. (1979). Determination of benzidine, dichlorobenzidine, and diphenylhydrazine in aqueous media by high performance liquid chromatography. *Anal. Chem.* 51, 210–214. doi: 10.1021/ac50038a014
- Sack, U., Hofrichter, M., and Fritsche, W. (1997). Degradation of polycyclic aromatic hydrocarbons by manganese peroxidase of *Nematoloma frowardii*. *FEMS Microbiol. Lett.* 152, 227–234. doi: 10.1111/j.1574-6968.1997.tb10432.x
- Sazinsky, M. H., Bard, J., Di Donato, A., and Lippard, S. J. (2004). Crystal structure of the toluene/o-xylene monooxygenase hydroxylase from *Pseudomonas stutzeri* OX1: insight into the substrate specificity, substrate channeling, and active site tuning of multicomponent monooxygenases. *J. Biol. Chem.* 279, 30600–30610. doi: 10.1074/jbc.M400710200
- Schomburg, D., and Stephan, D. (1994). “2,4-Dichlorophenol 6-monooxygenase,” in *Enzyme Handbook*, eds D. Schomburg and D. Stephan (Berlin; Heidelberg: Springer), 481–485.
- Shimada, T., Martin, M. V., Pruess-Schwartz, D., Marnett, L. J., and Guengerich, F. P. (1989). Roles of individual human cytochrome P-450 enzymes in the bioactivation of benzo(a)pyrene, 7,8-dihydroxy-7,8-dihydrobenzo(a)pyrene, and other dihydrodiol derivatives of polycyclic aromatic hydrocarbons. *Cancer Res.* 49, 6304–6312.
- Shimada, T., Takenaka, S., Murayama, N., Yamazaki, H., Kim, J.-H., Kim, D., et al. (2015). Oxidation of acenaphthene and acenaphthylene by human cytochrome P450 enzymes. *Chem. Res. Toxicol.* 28, 268–278. doi: 10.1021/tx500505y
- Simonsick, W. J. Jr., and Hites, R. A. (1984). Analysis of isomeric polycyclic aromatic hydrocarbons by charge-exchange chemical ionization mass spectrometry. *Anal. Chem.* 56, 2749–2754. doi: 10.1021/ac00278a028
- Spain, J. C. (1995). Biodegradation of nitroaromatic compounds. *Annu. Rev. Microbiol.* 49, 523–555. doi: 10.1146/annurev.mi.49.100195.002515
- Spies, E., Sommer, C., and Görisch, H. (1995). Degradation of 1,4-dichlorobenzene by *Xanthobacter flavus* 14p1. *Appl. Environ. Microbiol.* 61, 3884–3888.

- Staples, C. A., Peterson, D. R., Parkerton, T. F., and Adams, W. J. (1997). The environmental fate of phthalate esters: a literature review. *Chemosphere* 35, 667–749. doi: 10.1016/S0045-6535(97)00195-1
- Steffen, K. T., Hatakka, A., and Hofrichter, M. (2003). Degradation of benzo[a]pyrene by the litter-decomposing basidiomycete *Stropharia coronilla*: role of manganese peroxidase. *Appl. Environ. Microbiol.* 69, 3957–3964. doi: 10.1128/AEM.69.7.3957-3964.2003
- Strittmatter, E., Plattner, D. A., and Piontek, K. (2011). “Dye-Decolorizing Peroxidase (DyP),” in *Encyclopedia of Inorganic and Bioinorganic Chemistry*, ed R. A. Scott (Chichester: John Wiley & Sons, Ltd). doi: 10.1002/9781119951438.eibc2276
- Tege, G. (1983). “Biotechnology, A comprehensive treatise in 8 volumes,” in *Biomass, Microorganisms for Special Applications, Microbial Products I, Energy from Renewable Resources*. Vol. 3, eds H. J. Rehm, G. Reed and H. Dellweg (Weinheim: Verlag Chemie; Deerfield Beach–Basel Starch-Stärke), 367.
- Thakur, I. S., Verma, P., and Upadhayaya, K. (2002). Molecular cloning and characterization of pentachlorophenol-degrading monooxygenase genes of *Pseudomonas* sp. from the chemostat. *Biochem. Biophys. Res. Commun.* 290, 770–774. doi: 10.1006/bbrc.2001.6239
- Ullrich, R., Dolge, C., Kluge, M., and Hofrichter, M. (2008). Pyridine as novel substrate for regioselective oxygenation with aromatic peroxygenase from *Agrocybe aegerita*. *FEBS Lett.* 582, 4100–4106. doi: 10.1016/j.febslet.2008.11.006
- Ullrich, R., and Hofrichter, M. (2005). The haloperoxidase of the agaric fungus *Agrocybe aegerita* hydroxylates toluene and naphthalene. *FEBS Lett.* 579, 6247–6250. doi: 10.1016/j.febslet.2005.10.014
- Ullrich, R., and Hofrichter, M. (2007). Enzymatic hydroxylation of aromatic compounds. *Cell. Mol. Life Sci.* 64, 271–293. doi: 10.1007/s00018-007-6362-1
- Ullrich, R., Nüske, J., Scheibner, K., Spantzel, J., and Hofrichter, M. (2004). Novel haloperoxidase from the agaric basidiomycete *Agrocybe aegerita* oxidizes aryl alcohols and aldehydes. *Appl. Environ. Microbiol.* 70, 4575–4581. doi: 10.1128/AEM.70.8.4575-4581.2004
- USEPA (1979). *Priority Pollutant List [Online]*. Washington, DC: United States Environmental Protection Agency. Available online at: <https://www.epa.gov/sites/production/files/2015-09/documents/priority-pollutant-list-epa.pdf> (Accessed 07.13. 2016).
- Valli, K., and Gold, M. H. (1991). Degradation of 2,4-dichlorophenol by the lignin-degrading fungus *Phanerochaete chrysosporium*. *J. Bacteriol.* 173, 345–352. doi: 10.1128/jb.173.1.345-352.1991
- van Berkel, W. J. H., Kamerbeek, N. M., and Fraaije, M. W. (2006). Flavoprotein monooxygenases, a diverse class of oxidative biocatalysts. *J. Biotechnol.* 124, 670–689. doi: 10.1016/j.jbiotec.2006.03.044
- van der Meer, J. R., van Neerven, A. R., de Vries, E. J., de Vos, W. M., and Zehnder, A. J. (1991). Cloning and characterization of plasmid-encoded genes for the degradation of 1,2-dichloro-, 1,4-dichloro-, and 1,2,4-trichlorobenzene of *Pseudomonas* sp. strain P51. *J. Bacteriol.* 173, 6–15. doi: 10.1128/jb.173.1.6-15.1991
- van Gorcom, R. F., van den Hondel, C. A., and Punt, P. J. (1998). Cytochrome P450 enzyme systems in fungi. *Fungal Genet. Biol.* 23, 1–17. doi: 10.1006/fgbi.1997.1021
- Vardar, G., and Wood, T. K. (2005). Alpha-subunit positions methionine 180 and glutamate 214 of *Pseudomonas stutzeri* OX1 toluene-o-xylylene monooxygenase influence catalysis. *J. Bacteriol.* 187, 1511–1514. doi: 10.1128/JB.187.4.1511-1514.2005
- Vazquez-Duhalt, R., Westlake, D. W. S., and Fedorak, P. M. (1994). Lignin peroxidase oxidation of aromatic compounds in systems containing organic solvents. *Appl. Environ. Microbiol.* 60, 459–466.
- Vlasits, J., Jakopitsch, C., Bernroither, M., Zamocky, M., Furtmüller, P. G., and Obinger, C. (2010). Mechanisms of catalase activity of heme peroxidases. *Arch. Biochem. Biophys.* 500, 74–81. doi: 10.1016/j.abb.2010.04.018
- Wada, S., Ichikawa, H., and Tatum, K. (1995). Removal of phenols and aromatic amines from wastewater by a combination treatment with tyrosinase and a coagulant. *Biotechnol. Bioeng.* 45, 304–309. doi: 10.1002/bit.260450404
- Walker, R. (1970). The metabolism of azo compounds: a review of the literature. *Food Cosmet. Toxicol.* 8, 659–676. doi: 10.1016/S0015-6264(70)80455-2
- Wang, J., Liu, P., and Qian, Y. (1995). Microbial degradation of di-n-butyl phthalate. *Chemosphere* 31, 4051–4056. doi: 10.1016/0045-6535(95)00282-D
- Wang, Y., Fan, Y., and Gu, J.-D. (2003). Aerobic degradation of phthalic acid by *Comamonas acidovorans* Fy-1 and dimethyl phthalate ester by two reconstituted consortia from sewage sludge at high concentrations. *World J. Microbiol. Biotechnol.* 19, 811–815. doi: 10.1023/A:1026201424385
- Warshawsky, D., Radike, M., Jayasimhulu, K., and Cody, T. (1988). Metabolism of benzo(A)pyrene by a dioxygenase enzyme system of the freshwater green alga *Selenastrum capricornutum*. *Biochem. Biophys. Res. Commun.* 152, 540–544. doi: 10.1016/S0006-291X(88)80071-8
- Whited, G. M., and Gibson, D. T. (1991). Toluene-4-monooxygenase, a three-component enzyme system that catalyzes the oxidation of toluene to p-cresol in *Pseudomonas mendocina* KR1. *J. Bacteriol.* 173, 3010–3016. doi: 10.1128/jb.173.9.3010-3016.1991
- Wieser, M., Wagner, B., Eberspächer, J., and Lingens, F. (1997). Purification and characterization of 2,4,6-trichlorophenol-4-monooxygenase, a dehalogenating enzyme from *Azotobacter* sp. strain GP1. *J. Bacteriol.* 179, 202–208. doi: 10.1128/jb.179.1.202-208.1997
- Wittassek, M., and Angerer, J. (2008). Phthalates: metabolism and exposure. *Int. J. Androl.* 31, 131–138. doi: 10.1111/j.1365-2605.2007.00837.x
- Wood, A. W., Levin, W., Lu, A. Y. H., Ryan, D., West, S. B., Lehr, R. E., et al. (1976). Mutagenicity of metabolically activated benzo[a]anthracene 3,4-dihydrodiol: evidence for bay region activation of carcinogenic polycyclic hydrocarbons. *Biochem. Biophys. Res. Commun.* 72, 680–686. doi: 10.1016/S0006-291X(76)80093-9
- Wu, Y., Teng, Y., Li, Z., Liao, X., and Luo, Y. (2008). Potential role of polycyclic aromatic hydrocarbons (PAHs) oxidation by fungal laccase in the remediation of an aged contaminated soil. *Soil Biol. Biochem.* 40, 789–796. doi: 10.1016/j.soilbio.2007.10.013
- Xiao, Y., Zhang, J.-J., Liu, H., and Zhou, N.-Y. (2007). Molecular characterization of a novel ortho-nitrophenol catabolic gene cluster in *Alcaligenes* sp. strain NyZ215. *J. Bacteriol.* 189, 6587–6593. doi: 10.1128/JB.00654-07
- Xu, F., and Bhandari, A. (2003). Retention and extractability of phenol, cresol, and dichlorophenol exposed to two surface soils in the presence of horseradish peroxidase enzyme. *J. Agric. Food Chem.* 51, 183–188. doi: 10.1021/jf025852s
- Yamazoe, Y., Zenser, T. V., Miller, D. W., and Kadlubar, F. F. (1988). Mechanism of formation and structural characterization of DNA adducts derived from peroxidative activation of benzidine. *Carcinogenesis* 9, 1635–1641. doi: 10.1093/carcin/9.9.1635
- Yan, Z., Zhong, H. M., Maher, N., Torres, R., Leo, G. C., Caldwell, G. W., et al. (2005). Bioactivation of 4-methylphenol (p-cresol) via cytochrome p450-mediated aromatic oxidation in human liver microsomes. *Drug Metabol. Disposition* 33, 1867–1876. doi: 10.1124/dmd.105.006387
- Ye, J., Singh, A., and Ward, O. (2004). Biodegradation of nitroaromatics and other nitrogen-containing xenobiotics. *World J. Microbiol. Biotechnol.* 20, 117–135. doi: 10.1023/B:WIBI.0000021720.03712.12
- Yee, D. C., and Wood, T. K. (1997). 2,4-Dichlorophenol degradation using *Streptomyces viridosporus* T7A lignin peroxidase. *Biotechnol. Prog.* 13, 53–59. doi: 10.1021/bp960091x
- Yosca, T. H., Ledray, A. P., Ngo, J., and Green, M. T. (2017). A new look at the role of thiolate ligation in cytochrome P450. *J. Biol. Inorganic Chem.* 22, 209–220. doi: 10.1007/s00775-016-1430-3
- Zhang, J., Liu, X., Xu, Z., Chen, H., and Yang, Y. (2008). Degradation of chlorophenols catalyzed by laccase. *Int. Biodeterior. Biodegradation* 61, 351–356. doi: 10.1016/j.ibiod.2007.06.015

**Conflict of Interest Statement:** The authors declare that the research was conducted in the absence of any commercial or financial relationships that could be construed as a potential conflict of interest.

Copyright © 2017 Karich, Ullrich, Scheibner and Hofrichter. This is an open-access article distributed under the terms of the Creative Commons Attribution License (CC BY). The use, distribution or reproduction in other forums is permitted, provided the original author(s) or licensor are credited and that the original publication in this journal is cited, in accordance with accepted academic practice. No use, distribution or reproduction is permitted which does not comply with these terms.



# Salinity-Based Toxicity of CuO Nanoparticles, CuO-Bulk and Cu Ion to *Vibrio anguillarum*

Alice Rotini<sup>1,2</sup>, Andrea Tornambè<sup>2</sup>, Riccardo Cossi<sup>3</sup>, Franco Iamunno<sup>4</sup>, Giovanna Benvenuto<sup>4</sup>, Maria T. Berducci<sup>2</sup>, Chiara Maggi<sup>2</sup>, Maria C. Thaller<sup>1</sup>, Anna M. Cicero<sup>2</sup>, Loredana Manfra<sup>2,5\*†</sup> and Luciana Migliore<sup>1†</sup>

<sup>1</sup> Department of Biology, University of Rome Tor Vergata, Rome, Italy, <sup>2</sup> Institute for Environmental Protection and Research (ISPRA) Rome, Italy, <sup>3</sup> Qi Technologies Pomezia, Rome, Italy, <sup>4</sup> Research Infrastructures for Marine Biological Resources, Stazione Zoologica Anton Dohrn, Naples, Italy, <sup>5</sup> Department of Biology and Evolution of Marine Organisms, Stazione Zoologica Anton Dohrn, Naples, Italy

## OPEN ACCESS

### Edited by:

Stéphane Pesce,  
National Research Institute of Science  
and Technology for Environment and  
Agriculture, France

### Reviewed by:

Uwe Strotmann,  
Westfälische Hochschule, Germany  
Xiaoke Hu,  
Yantai Institute of Coastal Zone  
Research (CAS), China

### \*Correspondence:

Loredana Manfra  
loredana.manfra@isprambiente.it

<sup>†</sup>These authors have contributed  
equally to this work

### Specialty section:

This article was submitted to  
Microbiotechnology, Ecotoxicology  
and Bioremediation,  
a section of the journal  
Frontiers in Microbiology

Received: 20 June 2017

Accepted: 10 October 2017

Published: 25 October 2017

### Citation:

Rotini A, Tornambè A, Cossi R,  
Iamunno F, Benvenuto G,  
Berducci MT, Maggi C, Thaller MC,  
Cicero AM, Manfra L and Migliore L  
(2017) Salinity-Based Toxicity of CuO  
Nanoparticles, CuO-Bulk and Cu Ion  
to *Vibrio anguillarum*.  
*Front. Microbiol.* 8:2076.  
doi: 10.3389/fmicb.2017.02076

Bacteria are used in ecotoxicology for their important role in marine ecosystems and their quick, reproducible responses. Here we applied a recently proposed method to assess the ecotoxicity of nanomaterials on the ubiquitous marine bacterium *Vibrio anguillarum*, as representative of brackish and marine ecosystems. The test allows the determination of 6-h EC<sub>50</sub> in a wide range of salinity, by assessing the reduction of bacteria actively replicating and forming colonies. The toxicity of copper oxide nanoparticles (CuO NPs) at different salinities (5–20–35 ‰) was evaluated. CuSO<sub>4</sub> 5H<sub>2</sub>O and CuO bulk were used as reference toxicants (solubility and size control, respectively). Aggregation and stability of CuO NP in final testing dispersions were characterized; Cu<sup>2+</sup> dissolution and the physical interactions between *Vibrio* and CuO NPs were also investigated. All the chemical forms of copper showed a clear dose-response relationship, although their toxicity was different. The order of decreasing toxicity was: CuSO<sub>4</sub> 5H<sub>2</sub>O > CuO NP > CuO bulk. As expected, the size of CuO NP aggregates increased with salinity and, concurrently, their toxicity decreased. Results confirmed the intrinsic toxicity of CuO NPs, showing modest Cu<sup>2+</sup> dissolution and no evidence of CuO NP internalization or induction of bacterial morphological alterations. This study showed the *V. anguillarum* bioassay as an effective tool for the risk assessment of nanomaterials in marine and brackish environments.

**Keywords:** metal oxide, marine bacteria, bioassay, nanoparticle behavior, copper dissolution, salinity influence

## INTRODUCTION

The metal nanoparticles, including metal oxides, represent one of the major classes of commercial nanomaterials, which are manufactured on a large scale for both industrial and household applications (Chang et al., 2012). Copper (II) oxide nanoparticles (CuO NPs) are increasingly used in several products (Huang et al., 2010; Chang et al., 2012; Rossetto et al., 2014). The wide variety of applications entails the risk of environmental contamination, as a consequence of the environmental release of CuO NP during their production, use and disposal (Weinberg et al., 2011; Sanchis et al., 2013; Fan et al., 2014). This kind of contamination could bias both organisms and

ecosystems (Gambardella et al., 2013), as CuO NPs can exert toxic effects but also antimicrobial activity on (environmental) microbes (Bondarenko et al., 2013; Rossetto et al., 2014); hence, they could seriously affect estuarine and coastal environments, considered the ultimate sink for different kinds of NPs (Canesi et al., 2012). Accordingly, the investigation on CuO NP effects in the brackish/marine ecosystems has become a very important issue, and must include information on NP fate, transport and toxicity (Lowry et al., 2012).

Nevertheless, ecotoxicity of CuO NPs, particularly to marine organisms, is still little explored and the available data are often inconsistent, due to different and no standardized experimental approaches that highlighted some procedural limitations, mainly related to the stability of nanomaterials during the test exposure (reviewed by Minetto et al., 2016). The great majority of the studies evaluated endpoints as oxidative stress, genotoxicity, bioaccumulation and behavioral impairments (Bondarenko et al., 2013; Ivask et al., 2013; Minetto et al., 2016; Gonçalves et al., 2017) or soil toxicity (Urine et al., 2010; Amorim and Scott-Fordsmand, 2012; Amorim et al., 2012; Gomes et al., 2012; Gomes S. I. et al., 2015; Gomes S. I. L. et al., 2015; Gonçalves et al., 2017), with few  $EC_{50}$  identifications, although it is mandatory to define the hazard of CuO NPs in environment and human health and enhance their safe use.

Bacteria are an important component of brackish/marine ecosystems and alterations of the microbial communities could have significant effects on biogeochemical cycling and other critical ecosystem services. Toxicity tests based on microorganisms are gaining popularity even because they are relatively quick, reproducible, cheap and do not imply ethical issues (Parvez et al., 2006). Among bacterial bioassays, *V. fischeri* luminescence inhibition test, based on the enzymatic activity of the bacterial luciferase, is the most common and well-standardized one (Azur Environmental, 1995). However, this bioassay has some constraints even for conventional contaminants: for example, it cannot be utilized with samples at salinities exceeding a quite narrow range (APAT IRSA-CNR, 2003), or with colored and turbid samples, due to possible interferences with luminescence measurements. As regard other bioassays with bacterial species (*B. subtilis*, *E. coli*, *L. brevis* and *S. aureus*), most of them are based on the same endpoint, i.e., the inhibition of replication rate of the bacterial culture, but they use different and no standardized protocols (Baek and An, 2011; Kaweteerawat et al., 2015; Bondarenko et al., 2016). These methods present some criticisms that can influence the NP toxicity assessment and affect the repeatability of the bioassay. For instance, the possible interactions between NPs and organic matter in the exposure medium, the excessively reduced test volumes, without any mixing during the exposure, or the need of correction factors for colored/turbid samples.

In order to provide a useful tool for NP toxicity assessments in marine environments, we recently developed a new bioassay with the marine bacterium *Vibrio anguillarum* and demonstrated its effectiveness in evaluating the toxicity of a reference toxicant (Rotini et al., 2017). The model organism *V. anguillarum* is a Gram-negative, short curve-shaped rod bacterium with a polar flagellum. It was chosen because of its intrinsic characteristics: it

is halotolerant, ubiquitous and plays important ecological roles in marine/brackish ecosystems (Thompson et al., 2004). The bioassay allows to assess the decrease of bacterial culturability and to determine the  $EC_{50}$  (i.e., the concentration causing the 50% reduction of bacteria actively replicating and forming colonies, after 6-h exposure).

In this study, the suitability of this bioassay in evaluating NP toxicity has been checked. To this end, the study evaluated and compared the ecotoxicity of CuO NPs, CuO-bulk and  $Cu^{2+}$  ion ( $CuSO_4 \cdot 5H_2O$ ) in a wide range of salinity (5–35‰), by using the recently proposed test on the marine bacterium *V. anguillarum*. To deepen the CuO NP behavior during the test and relate it to toxicity, the physicochemical characterization of NPs in the exposure medium was carried out and the size distribution, sedimentation rates and  $Cu^{2+}$  dissolution from NPs were analyzed. These data allow a better understanding of NP aggregation dynamics and stability at the different salinities. Furthermore, to provide the most accurate picture, even CuO NP internalization or morphological alterations were evaluated in bacteria at the end of the test exposure.

## MATERIALS AND METHODS

### Reagents and Solutions

0.5–2–3.5% NaCl solutions were prepared as exposure media by dissolving NaCl (Sigma-Aldrich, pure grade) in deionized water. Tryptic Soy Agar (TSA, Liofilchem, 40 g/L) and Tryptic Soy Broth (TSB, Liofilchem, 30 g/L) growth media for bacteria were prepared in deionized water adding the appropriate amount of NaCl to obtain the same salinity of the exposure medium. NaCl solutions, TSA and TSB media were sterilized (121°C, 15'). CuO NPs (25–55 nm size) were purchased by US Research Nanomaterials, Inc. shipped as ultrapure water dispersion (20% w/v, purity of 99.95%). CuO NP stock dispersion (1 g/l) was prepared in 0.22  $\mu$ m filtered milli-Q water (mQW) from the 20% dispersion after 15 min of sonication (1210E-MT Branson ultrasonic bath) at 60 w and 47 kHz. CuO NP stock dispersion was sonicated for 15 min, stored in the dark at 4 °C and used for preparation of all the final testing dispersions. CuO NP final dispersions were prepared from the stock dispersion, previously sonicated for 15 min.  $CuSO_4 \cdot 5H_2O$  (Sigma-Aldrich, purity  $\geq$  98%) was used as positive and solubility control;  $CuSO_4 \cdot 5H_2O$  stock solution (400 mg/l) was prepared in deionized water and the necessary aliquots were sterilized by using a 0.22  $\mu$ m syringe filter. CuO-bulk (micrometric particles of CuO) was purchased by US Research Nanomaterials Inc. to be used as size control (Schultz et al., 2014); CuO-bulk stock (8 g/l) and final dispersions were prepared following the same procedure described above for CuO NPs.

For ICP-MS measurements, stock Cu standard solution (1,000  $\mu$ g/l) and  $HNO_3$  Ultrapur were purchased from Romil. Calibration standards were prepared within a linear range (2.5–40  $\mu$ g/l) from the stock Cu standard solution in 0.5 M  $HNO_3$ . Standard solutions were freshly prepared and standard calibration curves with  $R^2 = 0.99998$  were achieved daily.

## CuO NP Characterization

The CuO NP stock dispersion (1 g/l), in milli-Q water, was analyzed via SEM to characterize particle sizes and shapes. The stock dispersion was diluted 1/100, placed on a membrane filter of 0.2  $\mu\text{m}$ -pore size and platinum sputter coated (Polaron SC7640, Quo-rum Technologies Ltd., Ashford, UK). Stubs were observed with a Field Emission Scanning Electron Microscope JSM6700F (JEOL, Ltd, Tokyo, Japan).

Two different characterization techniques were used to estimate the particle size distributions and stability in the final testing dispersions at different salinities: Analytical Centrifugation (LUMISizer, L.U.M. GmbH, Berlin) and DLS (NICOMP 380 DLS Particle Size Analyzer, PSS, FL USA). The size distribution of the CuO NPs in the saline solutions (0.5-2.0-3.5% NaCl) and in the reference medium (mQW), was measured by DLS, with a 658 nm wavelength 30 Mw laser and a 90° scattered light Avalanche Photo Detector. Two readings of 5 min per sample were acquired and data processed following the NICOMP algorithm that automatically selects the best fitting distribution and recognizes from one to three particle size populations. The dimensional analyses for each population calculated the volume-weighted diameters ( $\pm$  standard deviation) and the relative percentages. Zeta ( $\zeta$ -) potential of the CuO NPs in the saline solutions (0.5-2.0-3.5% NaCl) and in the reference medium (mQW) was also measured by DLS. Measurements were carried out in triplicate, each consisting in 7 runs. The average particle sedimentation velocity as well as the particle size distribution (PSD) were also investigated (according to ISO 13318-2, 2007) by the Dispersion Analyser LUMiSizer. This instrument consists of an analytical centrifuge with an optoelectronic sensor system. It measures variations in the transmitted near infra-red radiations along horizontally inserted sample tubes, due to the sedimentation of suspended material. The integration of transmission profiles, sedimentation rates and particle size distributions were calculated by using the LUMiSizer software, SEPView 6.3.

The amount of metal dissolution from the CuO NPs into the exposure medium has been investigated. A CuO NP final dispersion (40 mg/l), at different salinities (0.5-1.5-2.0-3.5% NaCl), was centrifuged at  $4,000 \times g$  (centrifuge PK121R, ALC International S.r.l., Italy) for 60 min to remove the non-soluble fraction of CuO. The concentration of Cu ions was quantified by inductively-coupled plasma mass spectrometry (ICP-MS 7900 Agilent) according to USEPA 6020b (2014). Control and centrifuged samples were analyzed in triplicate after acidification with  $\text{HNO}_3$  s.p. (0.5% v/v).

## Ecotoxicity Test

*Vibrio anguillarum* (strain AL 102, serotype O1; from NOFIMA collection) was exposed to five concentrations of three Cu forms (CuO NP, CuO bulk and  $\text{CuSO}_4 \cdot 5\text{H}_2\text{O}$ ) in saline solution (no growth medium), to evaluate the reduction of the bacterial culturability (i.e., the capability to replicate and form colonies) after 6-h exposure, according to the protocol shown in Rotini et al. (2017). A liquid fresh culture of *V. anguillarum* was used to obtain the bacterial inoculum. After the overnight incubation (12–18 h, 25 °C) the bacterial concentration of

the inoculum was estimated spectrophotometrically (UV/Visible Spectrophotometer Beckmann 473) at 600 nm and diluted to an OD value of 0.14 (corresponding to the 0.5 point of McFarland nephelometric standard). The diluted inoculum was then centrifuged for 10 min at 3,000 g. The bacterial pellet was resuspended in 1 ml of exposure medium (saline solution) and 150  $\mu\text{l}$  were added to each test tube, including the control, in a final volume of 5 ml. Control and test dispersions were incubated for 6 h at 25°C, in the dark with continuous shaking (120 rpm), to avoid sedimentation. At the beginning ( $T_0$ ) and the end ( $T_6$ ) of the exposure time, bacterial counts in all the CuO NP dispersions and control were evaluated, by using the liquid-to-plate micro-counting method (Migliore et al., 2013; Rotini et al., 2017). Briefly, it consists in preparing serial dilutions of each exposed bacterial suspension, applying a ten-fold dilution factor (up to  $10^{87225}$ ). A small aliquot (10  $\mu\text{l}$ ) of dilutions is plated on TSA Petri dishes, then incubated at 25°C for 48 h. Colonies grown on petri dishes were counted and results were used to estimate the number of Colonies Forming Units per ml (CFU/ml). The counting from three replicate plates for each toxicant concentration and control were used to evaluate the mean number of bacteria actively replicating and forming colonies. Three independent tests, (using a freshly prepared bacterial inoculum for each test) at each of the three different salinities (0.5-2-3.5% NaCl) were performed on and five concentrations of each chemical (CuO NPs: 10-20-40-80-160, CuO bulk: 80-160-320-640-1280,  $\text{CuSO}_4 \cdot 5\text{H}_2\text{O}$ : 0.625-1.25-2.5-5-10, mg/l), i.e., 9 tests each time, as a total of 27 tests. The concentrations were chosen as a result of preliminary tests. In these tests the toxicants showed very different toxicity, hence, for each toxicant, the final testing concentrations were chosen to allow the calculation of the Effect Concentration ( $\text{EC}_{50}$ ).

The  $\text{EC}_{50}$ , i.e., the Effect Concentration of toxicant that reduces of 50% the number of bacteria actively replicating and forming colonies, after 6-h exposure, was calculated by non-linear regression (Log-Normal model) of the mean number of CFU/ml for each concentration, by using R software, drc package (Ritz and Streibig, 2005). Significant differences among treatments were evaluated by using one-way analysis of variance (ANOVA) followed by *post-hoc* pairwise *t*-tests (R software, stats package).

## Scanning Electron Microscope (SEM) Analysis

After exposure, bacteria were centrifuged at 3,000 g for 10 min and fixed in 2% glutaraldehyde in 2% NaCl solution. After 24 h, fixed bacteria were rinsed three times with PBS 1X and post-fixed with 1% osmium tetroxide, at 4°C for 1 h. After three washes with bi-distilled water, bacteria were placed on a membrane filter of 0.4  $\mu\text{m}$ -pore size in a Swinnex filter holder (Millipore, Billerica, Massachusetts, USA). Samples were then washed with 10 mL of bi-distilled water for approximately 30 min and dehydrated in a graded ethanol series. The sample was critical point dried, platinum sputter coated (Polaron SC7640, Quo-rum Technologies Ltd., Ashford, UK) and observed by a field emission SEM, JEOL JSM 6700F (JEOL Ltd, Tokyo, Japan).

## Transmission Electron Microscope (TEM) Analysis

After exposure, bacteria were centrifuged at 3,000 g for 10 min and fixed in 2% glutaraldehyde in 2% NaCl. After 24 h, fixed bacteria were rinsed three times with PBS1X and post-fixed with 1% osmium tetroxide, at 4°C for 1 h, rinsed five times with bi-distilled water, dehydrated in a graded ethanol series, further substituted by propylene oxide, embedded in Epon 812 (TAAB, TAAB Laboratories Equipment Ltd, Berkshire, UK) and kept at room temperature for 1 day and then polymerized at 60°C for 2 days. Resin blocks were sectioned with an Ultracut UCT ultramicrotome (Leica, Vienna, Austria). Ultrathin sections (50–60 nm) were placed on nickel grids, contrasted with 4% aqueous uranyl acetate for 30 min, rinsed once with a mix of methanol and bi-distilled water (1:1), twice with bi-distilled water and observed by a TEM Zeiss LEO 912AB (Zeiss, Oberkochen, Germany).

## RESULTS

### CuO NP Characterization

The CuO NP stock dispersion, in milli-Q water, has been characterized by SEM (Figure 1). Nanoscale spherical particles (about 50 nm) were present, confirming particle sizes provided by the manufacturer; microscale aggregates with diameters ranging from about 100 to 500 nm were also observed.

The Zeta ( $\zeta$ -) potential and average volume-weighted diameters (Table 1) of the CuO NP dispersions were measured by DLS in the reference medium (mQW) and the saline solutions (0.5–2.0–3.5% NaCl) used as exposure media (see Figure S1).

The average sedimentation rate of CuO NP agglomerates in the reference medium (mQW) was comparable to that measured in the 0.5% saline solution: 0.34 mm/h and 0.81 mm/h, respectively (see Figure S2). While, the average sedimentation rates of CuO NP agglomerates in 2.0 and 3.5% saline solutions were 2.52 and 2.85 mm/h, respectively. These high values account for the big sizes of agglomerates at the highest salinities. The particle size distribution in the exposure and reference media, returned by the LUMISizer analysis, is shown in Figure 2.

The Cu<sup>2+</sup> concentration dissolved in the solution was limited, assuming a reduced release of ions from the CuO NP. The dissolved Cu<sup>2+</sup> content slightly decreased with increasing salinity (see Table S1).

### Ecotoxicity Tests

The results obtained from the exposure of *V. anguillarum* to the CuO NPs showed a clear dose-response relationship, although the toxicity changed according to both the concentration of CuO NPs and the salinity of the medium. In fact, all the tests showed inhibition of bacterial culturability, i.e., the capability to replicate and form colonies (measured as number of CFU/ml), at increasing NP concentration. However, a progressively reduced inhibition was found as salinity increases (Figure 3). Consequently, the average EC<sub>50</sub> of CuO NPs increased with salinity (Table 2).

The results obtained from the exposure of *V. anguillarum* to the solubility and size controls also showed a clear dose-response relationship. The solubility/positive control (CuSO<sub>4</sub> 5H<sub>2</sub>O)

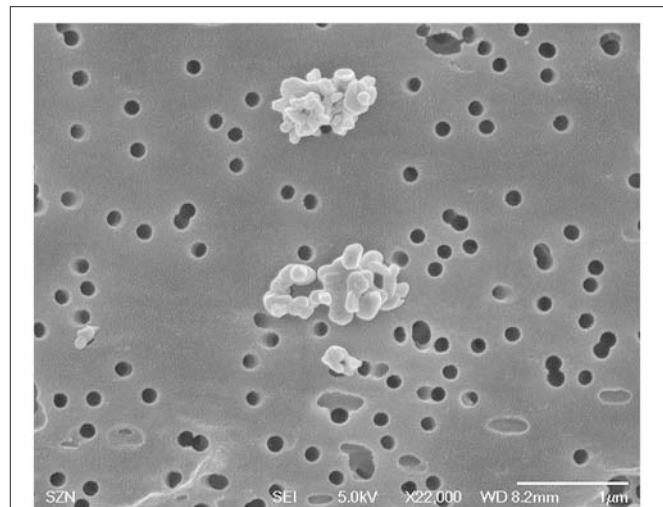


**FIGURE 1** | Characterization of CuO NPs used in this study in reference medium (milli-Q water) by SEM analysis.

**TABLE 1** | Characterization of CuO NP dispersions in milli-Q water (mQW, T = 25°C) and three saline solutions used as exposure media (T = 25°C, 0.5–2.0–3.5% NaCl) using DLS analysis.

	Peak 1 - D (nm)	%	Peak 2 - D (nm)	%	$\zeta$ -potential (mV)
mQW	78.7 ± 26.9	41.28	191.9 ± 44.2	58.72	-15.2 ± 2.0
0.5% NaCl	74.6 ± 16.0	68.57	247.8 ± 48.7	31.43	-2.5 ± 0.3
2.0% NaCl	211.7 ± 34.8	100	–	–	-1.4 ± 0.2
3.5% NaCl	313.1 ± 56.5	100	–	–	-1.7 ± 0.5

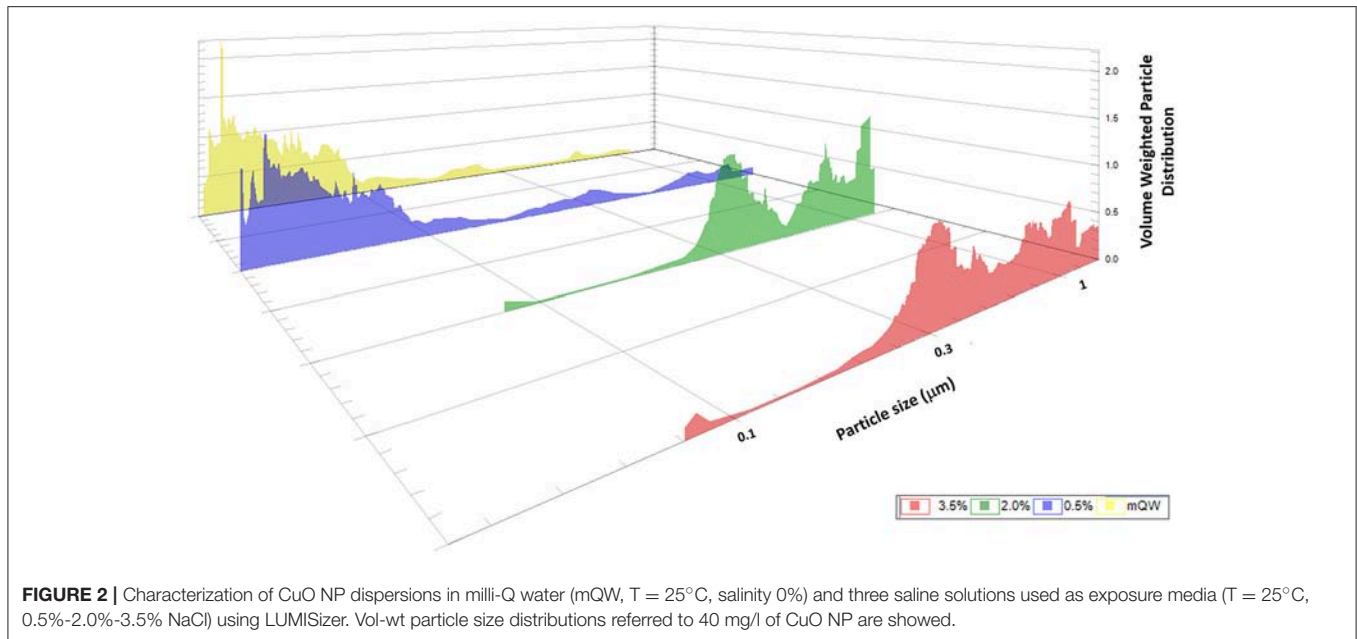
Vol-wt diameters (D), relative percentage of each peak (%) and Zeta ( $\zeta$ ) potential are reported. Data are referred to 40 mg/l of CuO NP and values are average ± standard deviation of 3 measurements.

showed a significant and progressive reduction of culturability, at increasing concentration of the toxicant (ANOVA,  $p < 0.001$ ; see Figure S3). The number of CFU/ml is significantly reduced at 1.25 mg/l (*post hoc t*-test,  $p < 0.01$ ), compared with control, regardless the medium salinity. Similarly, the size control (CuO bulk) showed a significant decrease of culturability with increasing concentration of the toxicant (ANOVA,  $p < 0.001$ ) (see Figure S4). The number of CFU/ml is significantly reduced always at 320 mg/l (*post hoc t*-test,  $p < 0.01$ ), compared with control and regardless the medium salinity. The average EC<sub>50</sub> of solubility and size controls remained quite constant at different salinities (see Table 2).

### Microscopy Analyses

The Scanning Electron Microscope (SEM) analysis (Figure 4) did not highlight morphological differences between control and CuO NPs exposed bacteria. In both batches, blebs of different size and fibrils can be observed on the surface of the microbial cells.

The Transmission Electron Microscope (TEM) analysis (Figure 5) again did not highlight morphological differences between control and CuO NPs exposed bacteria. No evidence



of internalization or adsorption were found. Some opaque very small particles are present on the biological material.

## DISCUSSION

The bioassay with *V. anguillarum* allowed to assess the CuO NP toxicity and highlighted a significant variation of the toxic effect with salinity, depending on a different aggregation state of NPs.

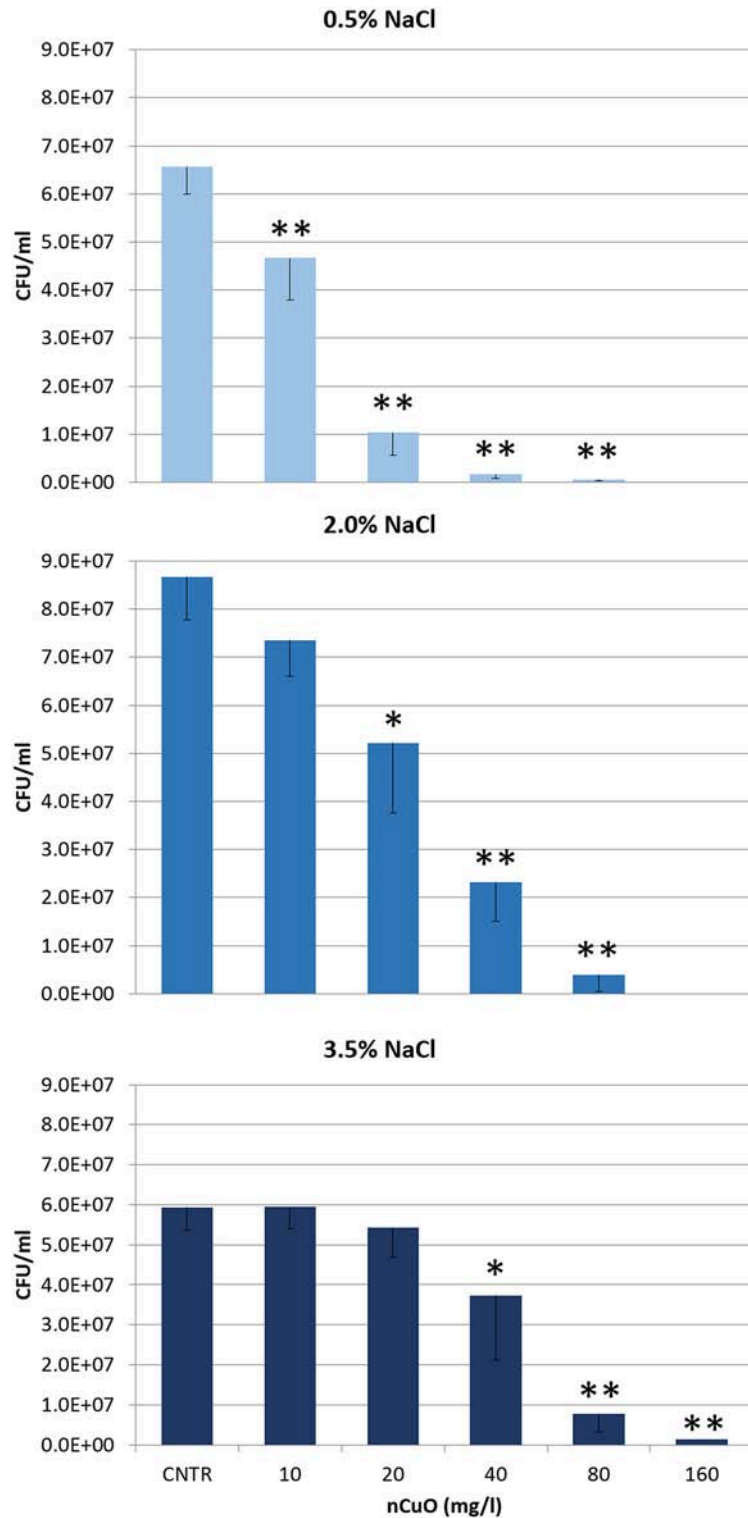
According to the OECD guidelines (OECD, 2014), the CuO NP behavior in the control and exposure media has been accurately investigated, to link characterization data with ecotoxicological results; this allowed a correct interpretation of the response. In our study, through the analyses by DLS and LUMISizer, the aggregation and stability of the CuO NPs were verified at three different salinities of the exposure media. The DLS analysis (see **Table 1** and Figure S1) highlighted a bimodal particle size distribution, with nanoscale (about 80 nm) and microscale (about 200 nm) aggregates, in both mQW and 0.5% saline solution; while, the dispersions in 2.0 and 3.5% saline solutions showed a single size population of microscale aggregates (250–300 nm). The low  $\zeta$ -potential absolute values also confirmed the aggregation state and instability of the CuO NPs. Although Zeta ( $\zeta$ -) potential is commonly considered a key parameter to describe the NP behavior in complex environmental media, it is worth to note that the high ionic strength of saline exposure medium, may shield electric charge of NPs, lowering the measured  $\zeta$ -potential.

The LUMISizer analysis (see **Figure 2**) confirmed the characterization by DLS and provided an even more accurate representation of the particle size distribution in the exposure media. In fact, LUMISizer better characterized the big size nanoparticle populations: the presence of nano- and micro-scale aggregates in mQW and 0.5% saline solution was confirmed, and also the microscale aggregates in 2.0 and 3.5% saline solutions

up to a size of about 1,000 nm were detected. Furthermore, the LUMISizer analysis allowed to quantify the sedimentation rates of CuO NP aggregates in the exposure media (see Figure S2). Only a negligible sedimentation of the CuO NPs as aggregates occurred during the exposure time (6 h), even at the highest salinity. This result was obtained with some dedicated features of the bioassay (i.e., test tube size, exposure volume and continuous agitation), designed to limit the NP sedimentation. Being inversely correlated with NP toxicity (Buffet et al., 2011; Villareal et al., 2014), the NP sedimentation rate represents a relevant parameter to describe the NP behavior in environmental media, particularly for salt water matrix. However, only few studies address the NP sedimentation rate and, at our best knowledge, this study is the only one that measured the sedimentation rates in seawater.

The particle diameter and sedimentation rate increased at increasing salt concentrations, due to the effect of ionic strength. Low salinity (mQW and 0.5% NaCl) allowed optimal and stable dispersion of CuO NPs, without differences between the two media. While, at high salinity (2.0–3.5% NaCl) agglomeration was promoted by the presence of salt ions, which shield the NP charge reducing the repulsive effect among NPs.

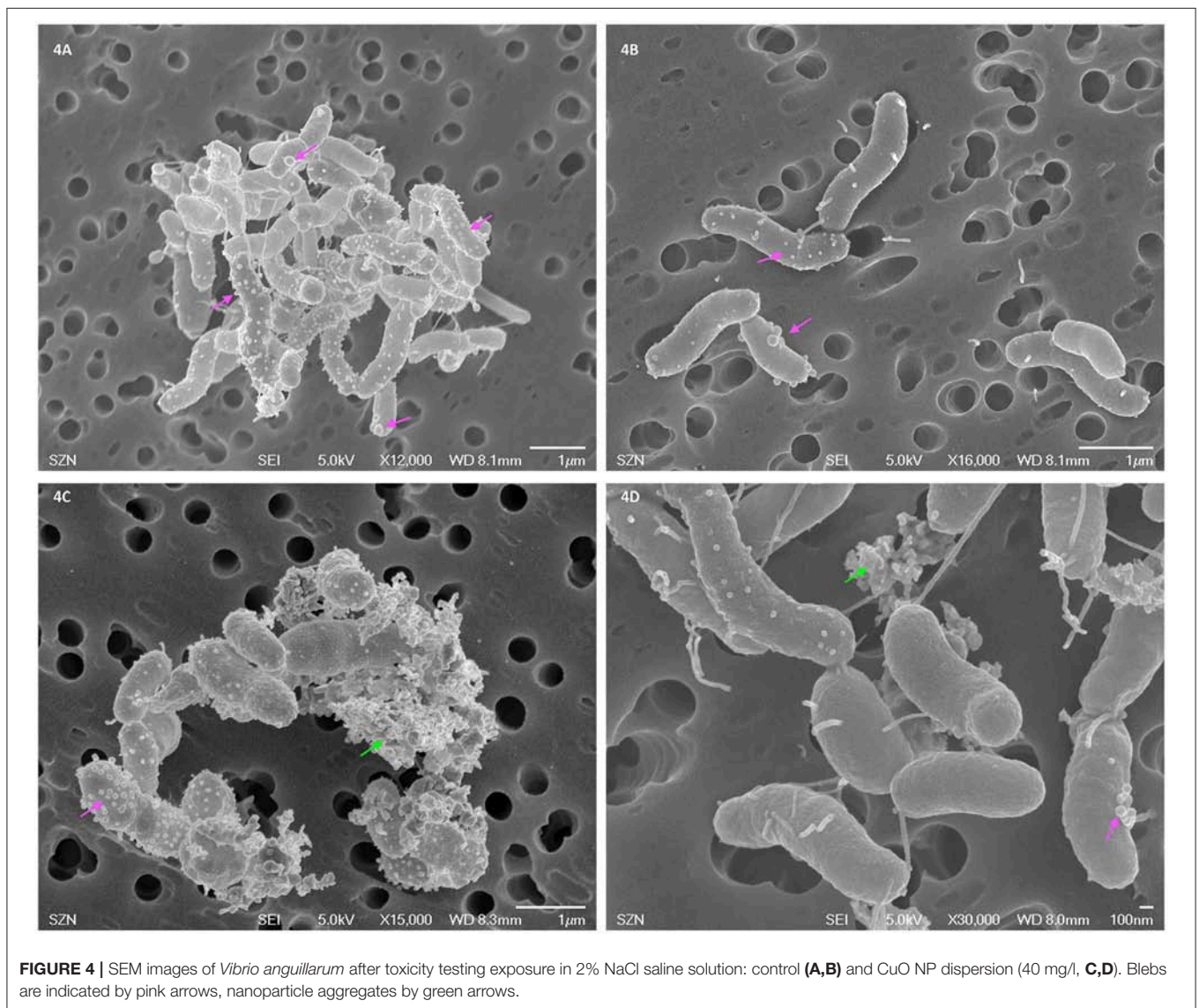
The increased particle size at high salinity determines a decrease of the total surface area; this implies a decrease of the superficial reactivity of NPs (because of agglomeration) which, in turn, produces a reduction of the toxic effects. The results obtained with this bioassay confirm that agglomeration and stability of CuO NPs are inversely related to their toxicity. At the lowest salinity (0.5% NaCl), when CuO NP agglomeration was the least and stability of dispersions was optimal, high toxicity ( $EC_{50} = 12.6$  mg/l) was recorded, suggesting a particularly relevant hazard for these NPs when released in brackish habitats. At the highest salinity, typical of marine environments, the occurring aggregation and sedimentation suggest that Cu NPs



**FIGURE 3 |** Mean number of CFU/ml (CFU=Colony Forming Unit) of *Vibrio anguillarum* after 6-h exposure to different concentrations of CuO NPs in exposure medium at three different salinities ( $T = 25^{\circ}\text{C}$ , 0.5-2.0-3.5% NaCl). Values represent the mean of three independent trials; error bars represent standard deviation. Significant reduction of CFU/ml compared to control, based on *post hoc t*-test, are indicated with asterisks (\* $p < 0.05$ ; \*\* $p < 0.01$ ).

**TABLE 2** | Mean effect concentration (EC<sub>50</sub>) (mg/l) and 95% Confidence Limits of CuO NP, CuSO<sub>4</sub> 5 H<sub>2</sub>O and CuO bulk calculated from three tests at three different salinities (*T* = 25°C, 0.5-2.0-3.5% NaCl).

	%NaCl	Test 1	Test 2	Test 3	Geometric mean
CuO NP	0.5	11.7 (10.4–13.0)	12.4 (11.7–13.1)	13.7 (12.8–14.7)	12.6 (11.6–13.6)
	2.0	24.3 (20.0–28.5)	26.3 (22.6–30.1)	20.5 (17.5–23.6)	23.6 (19.9–27.2)
	3.5	55.0 (41.6–68.3)	40.9 (36.9–44.8)	37.7 (29.8–45.6)	43.9 (35.7–51.9)
	0.5	1.2 (1.1–1.3)	1.2 (1.1–1.3)	1.3 (1.1–1.5)	1.2 (1.1–1.4)
CuSO <sub>4</sub>	2.0	1.0 (0.8–1.1)	1.0 (0.8–1.1)	0.8 (0.7–0.9)	0.9 (0.8–1.0)
	3.5	1.6 (1.4–1.8)	1.4 (1.2–1.7)	1.2 (1.0–1.4)	1.4 (1.3–1.8)
	0.5	241.0 (206.7–275.3)	223.1 (193.5–252.7)	231.8 (210.6–253.0)	231.9 (200.0–263.8)
CuO bulk	2.0	194.1 (177.4–210.8)	248.9 (238.0–259.8)	175.4 (130.9–219.9)	203.9 (176.8–229.2)
	3.5	182.0 (164.1–199.8)	222.1 (200.4–243.8)	184.1 (97.6–270.7)	195.2 (147.5–236.2)



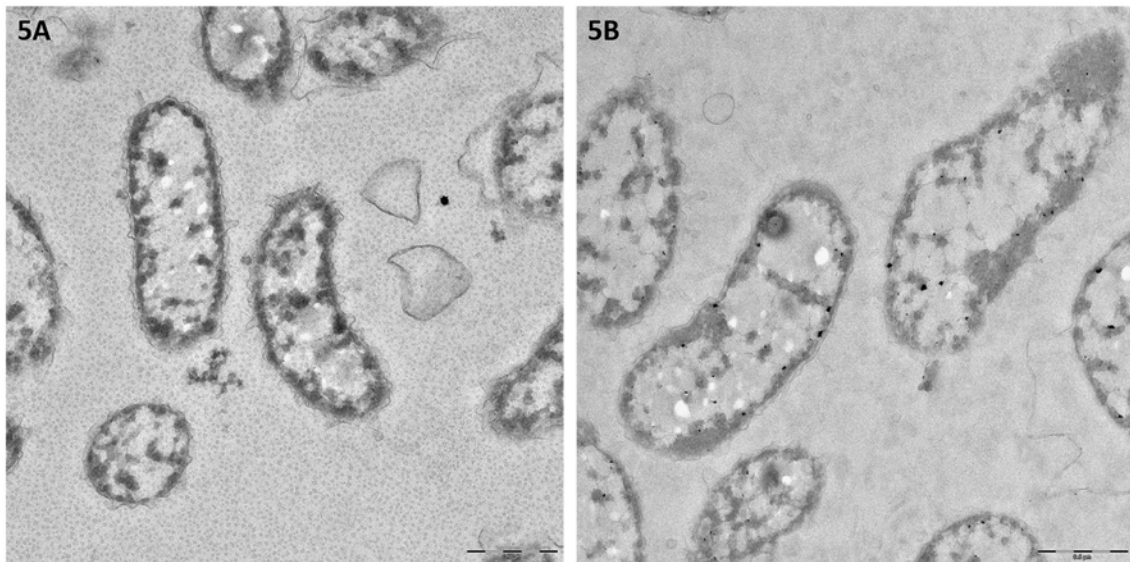


**FIGURE 5** | TEM images of *Vibrio anguillarum* after toxicity testing exposure in 2% NaCl saline solution: control (A) and CuO NP dispersion (40 mg/l, B).

may accumulate in sediments (Buffet et al., 2013) and therefore, benthic organisms are supposed to be the most exposed to NPs. However, the fate and bioavailability of NPs in sediments can be highly variable and depend on several abiotic and biotic factors, including ionic strength of water, amount of suspended natural organic matter (Keller et al., 2010), light intensity or temperature (Zhou et al., 2012) and biogenic transformation processes (decomposition, bioturbation, or digestion; Farré et al., 2009).

**Table 3** summarizes the studies on CuO NP toxic effects on bacterial species; they show highly variable values of the Effect Concentrations, even in test on the same bacterial species/strain. This depends on the type of nanoparticles and on the experimental conditions (Bondarenko et al., 2013). This variability confirms the difficulty to compare the ecotoxicological assessments of nanomaterials, even among standardized bioassays, and highlights the need of highly reliable and reproducible tests.

The bioassay with *V. anguillarum* clearly showed a significant decrease of bacterial culturability, at increasing concentration of  $\text{CuSO}_4 \cdot 5\text{H}_2\text{O}$  and CuO bulk, used in this study as solubility and size controls, respectively. Unlike CuO NPs, size and solubility controls did not elicit different toxicities at different salinities. As expected, a clearly different toxicity was observed among the three copper forms; according with the  $\text{EC}_{50}$  values, toxicity ranking is as follows:  $\text{CuSO}_4 \cdot 5\text{H}_2\text{O} > \text{CuO NP} > \text{CuO bulk}$ . CuO NPs toxicity is an order of magnitude lower than  $\text{CuSO}_4 \cdot 5\text{H}_2\text{O}$  but higher than CuO bulk. Importantly, the  $\text{EC}_{50}$  values for  $\text{CuSO}_4 \cdot 5\text{H}_2\text{O}$  are comparable with those obtained by acute tests on other marine species (Adams and Stauber, 2004; Manfra et al., 2015; Rotini et al., 2018) including bacteria (see **Table 3**); this demonstrates the good sensitivity of our recently proposed bioassay for both conventional contaminants and NPs.

It is generally accepted that CuO NP toxicity is higher than CuO-bulk, depending on size, surface characteristics, dissolution, and exposure routes (reviewed by Chang et al., 2012), on the contrary, the contribution of dissolved  $\text{Cu}^{2+}$  ions to the observed toxicity of CuO NPs is still under discussion (Ivask et al., 2013; Gonçalves et al., 2017). Several studies ascribe primarily to the  $\text{Cu}^{2+}$  ion dissolution the CuO NP toxicity in biological systems (Heinlaan et al., 2008; Aruoja et al., 2009; Kahru and Dubourguier, 2010; Mortimer et al., 2010; Bondarenko et al., 2012; Kasemets et al., 2013). A solubility-dependent toxicity of CuO NPs has been observed in *Daphnia magna* (Heinlaan et al., 2008; Blinova et al., 2010; Fan et al., 2012; Jo et al., 2012), *Cyprinus carpio* (Zhao et al., 2011) and zebrafish embryos (Lin et al., 2015). On the contrary, just as many other studies found that the toxic effects of CuO NPs do not depend from the ion dissolution (Heinlaan et al., 2008; Jiang et al., 2009; Baek and An, 2011; Isani et al., 2013). Agreeing with this last group, our results indicate a modest  $\text{Cu}^{2+}$  dissolution with an inverse salinity-dependence; as a consequence, the toxic effects observed for CuO NPs might be due to intrinsic toxicity mechanisms related to the nano-form as, for instance, aggregation plays a key role. This was already suggested by other authors (Buffet et al., 2013; Gonçalves et al., 2017), although the issue deserves further investigations. Both SEM and TEM analyses did not evidenced morphological differences between control and CuO NPs exposed bacteria. Interestingly, the SEM images (see **Figure 1**) showed two surface structures present on both control and exposed bacteria: outer membrane vesicles (*a.k.a.* blebs), known to be unique for *Vibrio* strains, and fibrils. Blebs and fibrils are signature of starvation and are produced by the bacterial cells in response to the growth arrest (Östling et al., 1993). This response was expected because during the test bacteria are exposed to the toxicant in the absence of nutrients. The TEM images again do not suggest CuO

**TABLE 3** | Comparison of EC<sub>50</sub> and/or main results obtained for short- and long-term exposures to copper oxide nanoparticles (CuO NPs) on different bacterial species.

Species	Exposure medium	Exposure time	Endpoint (inhibition of)	CuO NP size (nm) <sup>a</sup>	CuO NP EC <sub>50</sub> (mg/l)	EC <sub>50</sub> controls CuSO <sub>4</sub> , (CuObulk) (mg/l)	References
<i>Bacillus subtilis</i>	LB agar	24 h	Growth	20–30 <sup>a</sup>	61.1	–	Baek and An, 2011
<i>Bacillus subtilis</i>	LB	4 h	Growth	24.5 ± 2.3 <sup>c</sup> 152 ± 2 <sup>b</sup>	>100	>100	Bondarenko et al., 2016
<i>Escherichia coli</i>	LB agar	24 h	Growth	20–30 <sup>a</sup>	28.6	–	Baek and An, 2011
<i>Escherichia coli</i>	LB	4 h	Growth	24.5 ± 2.3 <sup>c</sup> 152 ± 2 <sup>b</sup>	>100	>100	Bondarenko et al., 2016
<i>Escherichia coli</i>	MMD	24h	Growth (OD) <sup>5</sup>	20–100 <sup>c</sup> 300 ± 2 <sup>b</sup>	160	140 (>250)	Kaweeteerawat et al., 2015
<i>Escherichia coli</i> **	HMM	8h	Bioluminescence (ROS induction/SS DNA breaks)	30 <sup>a</sup> 385 <sup>b</sup>	6*	0.6 (600)	Bondarenko et al., 2012
<i>Lactobacillus brevis</i>	MRS	24 h	Growth (OD) <sup>5</sup>	20–100 <sup>c</sup> 470 ± 4 <sup>b</sup>	3.6	24 (>250)	Kaweeteerawat et al., 2015
<i>Pseudomonas aeruginosa</i>	LB	4 h	Growth	24.5 ± 2.3 <sup>c</sup> 152 ± 2 <sup>b</sup>	>100	>100	Bondarenko et al., 2016
<i>Pseudomonasputida</i>	LB	4 h	Growth	24.5 ± 2.3 <sup>c</sup> 152 ± 2 <sup>b</sup>	>100	>100	Bondarenko et al., 2016
<i>Staphylococcus aureus</i>	LB agar	24 h	Growth	20–30 <sup>a</sup>	65.9	–	Baek and An, 2011
<i>Staphylococcus aureus</i>	LB	4 h	Growth	24.5 ± 2.3 <sup>c</sup> 152 ± 2 <sup>b</sup>	>100	>100	Bondarenko et al., 2016
<i>Vibrio fischeri</i>	2% NaCl	30 min	Bioluminescence (Flash test)	24.5 ± 2.3 <sup>c</sup> 152 ± 2 <sup>b</sup>	4.3	0.3	Bondarenko et al., 2016
<i>Vibrio fischeri</i>	2% NaCl	30 min	Bioluminescence	30 <sup>a</sup>	79	1.6 (3,811)	Heinlaan et al., 2008
<i>Vibrio fischeri</i>	2% NaCl	30 min	Bioluminescence (Flash test)	30 <sup>a</sup>	68.1 (cuve) 204 (plate)	2.0 (3,894)	Mortimer et al., 2008
<i>Vibrio fischeri</i>	2% NaCl	30 min	Bioluminescence	30–40 <sup>a</sup> 302 ± 31.37 <sup>b</sup>	257 mg/L	(1,472)	Rossetto et al., 2014

<sup>a</sup>Declared.

<sup>b</sup>Measured in test solution (hydrodynamic diameter).

<sup>c</sup>Primary size (TEM).

\*mg Cu/l \*\*Recombinant strains, bioassays performed in 96 well-microplate.

NP internalization into or intimate adhesion to bacteria. Some opaque particles seem to be included into the bacterial cells, but their small size and shape does not support their identification as the NPs used in this study. Hence, our results do not chime with the evidence by Kaweeteerawat et al. (2015), which found nano Cu species strongly bound to or internalized within *E. coli* cells and stated that both nano Cu and nano CuO can be internalized into the bacterial cell. Probably the different findings can be ascribed to the size of NPs and their aggregates that, in our study, are not compatible with internalization into a *Vibrio* bacterial cell.

The bioassay with *V. anguillarum* benefits from several procedural points in assessing the NP toxicity. As a first point, it assesses culturability, *i.e.* the bacterial capability to actively replicate and form colonies after the exposure to NPs in a saline medium. The endpoint culturability allows an easier comparison of results with those from the most common ecotoxicological bioassays for marine environments, which often have survival/mortality as endpoint; this will facilitate its introduction in test batteries. Furthermore, it is interesting to highlight that the reduction of bacterial culturability can be also due to the reversible VBNC (Viable But NonCulturable) state which is known to be induced/triggered by a variety of stressors such as out range of growth temperature, oxygen concentrations, heavy metals, etc. (Oliver, 2005, 2009), hence increasing the sensitivity of the test. Moreover, the exposure is carried out in simple saline solution, avoiding any possible interferences of nutrients with the NPs, known to modify the reproducibility of results by increasing or reducing NP bioavailability (Ivask et al., 2013; Kasemets et al., 2013). Again, the short time of exposure (6 h) is long enough to observe and evaluate acute effects on

the bacterial population and short enough to limit sedimentation and aggregation of metal NPs in salt water, ensuring repeatability of the exposure conditions. Last but not least, this bioassay has no limitations for colored/turbid samples, and is applicable on a wider range of salinities, common limitations of the existing methods with microorganisms. This feature of the bioassay gives the possibility to carry out contemporary assays in a wide range of salinity (0.5–3.5%), which is known to affect NP behavior and toxicity (Corsi et al., 2014).

## CONCLUSION

In this study, a recently designed bioassay with the marine bacterium *V. anguillarum* allowed to assess the toxic effects of CuO NPs, showing a clear dose-response relationships and a crucial role of salinity and particle aggregation in the observed toxicity. Results highlighted the high toxicity of CuO NPs, particularly at low salinity, and pointed out a relevant hazard for these NPs in brackish environments. While, at salinities typical of marine environments the high aggregation and sedimentation rate of these NPs suggest a possible accumulation in sediments, increasing the risk of exposure for benthic organisms. The influence of salinity on the NP toxicity is a hitherto little explored issue and further ecotoxicity assessments, including different NPs and bioassays are particularly needed. Moreover, our results demonstrated the effectiveness of *V. anguillarum* bioassay as a promising tool for the risk assessment of nanomaterials and confirmed its useful application on conventional contaminants too.

## AUTHOR CONTRIBUTIONS

LM, AR, MT, and LoM conceived and designed the study. AR, AT, and LoM performed ecotoxicological analyses. MB, CM, and RC performed chemical analyses. FI and GB performed microscopy. MT choose the suitable *Vibrio* strain and the cultural conditions. AR, AT, and LoM wrote the manuscript; all authors contributed to the discussion and approved the final manuscript.

## FUNDING

This work was financed by the research project: “NanoBioTech ambiente e salute. Progetto 2: Ambiente. Strumenti e metodi per il monitoraggio ecotossicologico delle Nanoparticelle” (Nano-BioTechnology: environment and health. Project 2: Environment. Tools and methods for ecotoxicological monitoring of nanoparticles)” granted to LM from Regione Lazio-Consortio Hypatia. AR was funded by a Postdoctoral grant from the University of Tor Vergata/Regione Lazio-Consortio Hypatia under the framework of the over-cited project.

## REFERENCES

- Adams, M. S., and Stauber, J. L. (2004). Development of a whole-sediment toxicity test using a benthic marine microalgae. *Environ. Toxicol. Chem.* 23, 1957–1968. doi: 10.1897/03-232
- Amorim, M. J. B., Gomes, S. I. L., Soares, A. M. V. M., and Scott-Fordsmand, J. J. (2012). Energy basal levels and allocation among lipids, proteins, and carbohydrates in *Enchytraeus albidus*: changes related to exposure to Cu salt and Cu nanoparticles. *Water Air Soil Poll.* 223, 477–482. doi: 10.1007/s11270-011-0867-9
- Amorim, M. J. B., and Scott-Fordsmand, J. J. (2012). Toxicity of copper nanoparticles and CuCl<sub>2</sub> salt to *Enchytraeus albidus* worms: survival, reproduction and avoidance responses. *Environ. Pollut.* 164, 164–168. doi: 10.1016/j.envpol.2012.01.015
- APAT IRSA-CNR (2003). “Metodo 8060,” in *Metodi Analitici Per le Acque. Manuali e Linee Guida*, 29/2003, Vol. Terzo (Roma), 1043–1049.
- Aruoja, V., Dubourguier, H. C., Kasemets, K., and Kahru, A. (2009). Toxicity of nanoparticles of CuO, ZnO and TiO<sub>2</sub> to microalgae *Pseudokirchneriella subcapitata*. *Sci. Total Environ.* 407, 1461–1468. doi: 10.1016/j.scitotenv.2008.10.053
- Azur Environmental (1995). *Microtox™ Acute Toxicity Basic Test Procedures*. Carlsbad, CA: AZUR Environmental LTD.
- Baek, Y. W., and An, Y. J. (2011). Microbial toxicity of metal oxide nanoparticles (CuO, NiO, ZnO, and Sb<sub>2</sub>O<sub>3</sub>) to *Escherichia coli*, *Bacillus subtilis*, and *Streptococcus aureus*. *Sci. Total Environ.* 409, 1603–1608. doi: 10.1016/j.scitotenv.2011.01.014
- Blinova, I., Ivask, A., Heinlaan, M., Mortimer, M., and Kahru, A. (2010). Ecotoxicity of nanoparticles of CuO and ZnO in natural water. *Environ. Pollut.* 158, 41–47. doi: 10.1016/j.envpol.2009.08.017
- Bondarenko, O., Heinlaan, M., Sihtmäe, M., Ivask, A., Kurvet, I., Joonas, E., et al. (2016). Multilaboratory evaluation of 15 bioassays for (eco)toxicity screening and hazard ranking of engineered nanomaterials: FP7 project NANOVALID. *Nanotoxicology* 10, 1229–1242. doi: 10.1080/17435390.2016.1196251
- Bondarenko, O., Ivask, A., Käkänen, A., and Kahru, A. (2012). Sub-toxic effects of CuO nanoparticles on bacteria: kinetics, role of Cu ions and possible mechanisms of action. *Environ. Pollut.* 169, 81–89. doi: 10.1016/j.envpol.2012.05.009
- Bondarenko, O., Juganson, K., Ivask, A., Kasemets, K., Mortimer, M., and Kahru, A. (2013). Toxicity of Ag, CuO and ZnO nanoparticles to selected environmentally relevant test organisms and mammalian cells *in vitro*: a critical review. *Arch. Toxicol.* 84, 1181–1200. doi: 10.1007/s00204-013-1079-4
- Buffet, P. E., Richard, M., Caupos, F., Vergnoux, A., Perrein-Ettajani, H., Luna-Acosta, A., et al. (2013). A mesocosm study of fate and effects of

An agreement ISPRA-Tor Vergata University (N. 2015/52857) and the scientific association of LoMa to SZN allowed the mutual use of facilities and exchange of researchers.

## ACKNOWLEDGMENTS

The authors gratefully acknowledge for the technical assistance Enrica Terranova and Giorgia Matteucci within Tor Vergata University laboratories, Valerio Fabrizi within the ISPRA laboratory of inorganic chemistry and Rita Graziano and Giampiero Lanzotti for technical assistance within the SZN Research Infrastructures for Marine Biological Resources. *Vibrio anguillarum* strain was kindly provided by Prof. Henning Sørum, Norwegian University of Life Science.

## SUPPLEMENTARY MATERIAL

The Supplementary Material for this article can be found online at: <https://www.frontiersin.org/articles/10.3389/fmicb.2017.02076/full#supplementary-material>

- CuO nanoparticles on endobenthic species (*Scrobicularia plana*, *Hediste diversicolor*). *Environ. Sci. Technol.* 47, 1620–1628. doi: 10.1021/es303513r
- Buffet, P. E., Tankoua, O. F., Pan, J. F., Berhanu, D., Herrenknecht, C., Poirier, L., et al. (2011). Behavioural and biochemical responses of two marine invertebrates *Scrobicularia plana* and *Hediste diversicolor* to copper oxide nanoparticles. *Chemosphere* 84, 166–174. doi: 10.1016/j.chemosphere.2011.02.003
- Canesi, L., Ciacci, C., Fabbri, R., Marcomini, A., Pojana, G., and Gallo, G. (2012). Bivalve molluscs as a unique target group for nanoparticle toxicity. *Mar. Environ. Res.* 76, 16–21. doi: 10.1016/j.marenvres.2011.06.005
- Chang, Y., Zhang, M., Xia, L., Zhang, J., and Xing, G. (2012). The toxic effects and mechanisms of CuO and ZnO nanoparticles. *Materials* 5, 2850–2871. doi: 10.3390/ma5122850
- Corsi, I., Cherr, G. N., Lenihan, H. S., Labille, J., Hasselov, M., Canesi, L., et al. (2014). Common strategies and technologies for the ecosafety assessment and design of nanomaterials entering the marine environment. *ACS Nano* 8, 9694–9709. doi: 10.1021/nn504684k
- Fan, R., Huang, Y. C., Grusak, M. A., Huang, C. P., and Sherrier, D. J. (2014). Effects of nano-TiO<sub>2</sub> on the agronomically-relevant *Rhizobium-legume* symbiosis. *Sci. Total Environ.* 466–467, 503–512. doi: 10.1016/j.scitotenv.2013.07.032
- Fan, W. H., Shi, Z. W., Yang, X. P., Cui, M. M., Wang, X. L., and Zhang, D. F. (2012). Bioaccumulation and biomarker responses of cubic and octahedral Cu<sub>2</sub>O micro/nanocrystals in *Daphnia magna*. *Water Res.* 46, 5981–5988. doi: 10.1016/j.watres.2012.08.019
- Farré, M., Gajda-Schrantz, K., Kantiani, L., and Barceló, D. (2009). Ecotoxicity and analysis of nanomaterials in the aquatic environment. *Anal. Bioanal. Chem.* 393, 81–95. doi: 10.1007/s00216-008-2458-1
- Gambardella, C., Aluigi, M. G., Ferrando, S., Gallus, L., Ramoino, P., Gatti, A. M., et al. (2013). Developmental abnormalities and changes in cholinesterase activity in sea urchin embryos and larvae from sperm exposed to engineered nanoparticles. *Aquat. Toxicol.* 130–131, 77–85. doi: 10.1016/j.aquatox.2012.12.025
- Gomes, S. I. L., Scott-Fordsmand, J. J., and Amorim, M. J. B. (2015). Cellular energy allocation to assess the impact of nanomaterials on soil invertebrates (Enchytraeids): the effect of Cu and Ag. *Int. J. Environ. Res. Public Health* 12, 6858–6878. doi: 10.3390/ijerph120606858
- Gomes, S. I., Murphy, M., Nielsen, M. T., Kristiansen, S. M., Amorim, M. J., and Scott-Fordsmand, J. J. (2015). Cu-nanoparticles ecotoxicity-explored and explained? *Chemosphere* 139, 240–245. doi: 10.1016/j.chemosphere.2015.06.045
- Gomes, S. I., Novais, S. C., Gravato, C., Guilhermino, L., Scott-Fordsmand, J. J., Soares, A. M., et al. (2012). Effect of Cu-nanoparticles versus one Cu-salt: analysis of stress and neuromuscular biomarkers response

- in *Enchytraeus albidus* (Oligochaeta). *Nanotoxicology* 6, 134–143. doi: 10.3109/17435390.2011.562327
- Gonçalves, M. F. M., Gomes, S. I. L., Scott-Fordsmand, J. J., and Amorim, M. J. B. (2017). Shorter lifetime of a soil invertebrate species when exposed to copper oxide nanoparticles in a full lifespan exposure test. *Sci. Rep.* 7:1355. doi: 10.1038/s41598-017-01507-8
- Heinlaan, M., Ivask, A., Blinova, I., Dubourguier, H. C., and Kahru, A. (2008). Toxicity of nanosized and bulk ZnO, CuO and TiO<sub>2</sub> to bacteria *Vibrio fischeri* and crustaceans *Daphnia magna* and *Thamnocephalus platyurus*. *Chemosphere* 71, 1308–1316. doi: 10.1016/j.chemosphere.2007.11.047
- Huang, Y., Wu, C., and Aronstam, R. S. (2010). Toxicity of transition metal oxide nanoparticles: recent insights from *in vitro* studies. *Materials* 3, 4842–4859. doi: 10.3390/ma3104842
- Isani, G., Falcioni, M. L., Barucca, G., Sekar, D., Andreani, G., Carpenè E., et al. (2013). Comparative toxicity of CuO nanoparticles and CuSO<sub>4</sub> in rainbow trout. *Ecotox. Environ. Saf.* 97, 40–46. doi: 10.1016/j.ecoenv.2013.07.001
- ISO 13318-2 (2007). *Determination of Particle Size Distribution by Centrifugal Liquid Sedimentation Methods – Part 2: Photocentrifuge Method*. Brussels.
- Ivask, A., Juganson, K., Bondarenko, O., Mortimer, M., Aruoja, V., Kasemets, K., et al. (2013). Mechanisms of toxic action of Ag, ZnO and CuO nanoparticles to selected ecotoxicological test organisms and mammalian cells *in vitro*: a comparative review. *Nanotoxicology* 8, 57–71. doi: 10.3109/17435390.2013.855831.
- Östling, J., Holmquist, L., Flårdh, K., Svenblad, B., Jøuper-Jaan, Å., and Kjelleberg, S. (1993). “Starvation and recovery of *Vibrio*,” in *Starvation in Bacteria*, ed S. Kjelleberg (New York, NY: Springer Science+Business Media), 103–127.
- Jiang, W., Mashayekhi, H., and Xing, B. (2009). Bacterial toxicity comparison between nano- and micro-scaled oxide particles. *Environ. Pollut.* 157, 1619–1625. doi: 10.1016/j.envpol.2008.12.025
- Jo, H. J., Choi, J. W., Lee, S. H., and Hong, S. W. (2012). Acute toxicity of Ag and CuO nanoparticle suspensions against *Daphnia magna*: the importance of their dissolved fraction varying with preparation methods. *J. Hazard. Mater.* 227, 301–308. doi: 10.1016/j.jhazmat.2012.05.066
- Kahru, A., and Dubourguier, H. C. (2010). From ecotoxicology to nanoecotoxicology. *Toxicology* 269, 105–119. doi: 10.1016/j.tox.2009.08.016
- Kasemets, K., Suppi, S., Kunis-Beres, K., and Kahru, A. (2013). Toxicity of CuO nanoparticles to yeast *Saccharomyces cerevisiae* BY4741 wild-type and its nine isogenic single-gene deletion mutants. *Chem. Res. Toxicol.* 26, 356–367. doi: 10.1021/tx300467d
- Kaweteerawat, C., Chang, C. H., Roy, K. R., Liu, R., Li, R., Toso, D., et al. (2015). Cu nanoparticles have different impacts in *Escherichia coli* and *Lactobacillus brevis* than their micro-sized and ionic analogues. *ACS Nano* 9, 7215–7225. doi: 10.1021/acsnano.5b02021
- Keller, A. A., Wang, H. T., Zhou, D. X., Lenihan, H. S., Cherr, G., Cardinale, B. J., et al. (2010). Stability and aggregation of metal oxide nanoparticles in natural aqueous matrices. *Environ. Sci. Technol.* 44, 1962–1967. doi: 10.1021/es902987d
- Lin, S., Taylor, A. A., Ji, Z., Chang, C. H., Kinsinger, N. M., Ueng, W., et al. (2015). Understanding the transformation, speciation, and hazard potential of copper particles in a model septic tank system using zebrafish to monitor the effluent. *ACS Nano* 9, 2038–2048. doi: 10.1021/nn507216f
- Lowry, G. V., Gregory, K. B., Apte, S. C., and Lead, J. R. (2012). Transformations of nanomaterials in the environment. *Environ. Sci. Technol.* 46, 6893–6899. doi: 10.1021/es300839e
- Manfra, L., Tornambè, A., Savorelli, F., Rotini, A., Canepa, S., Mannozi, M., et al. (2015). Ecotoxicity of diethylene glycol and risk assessment for marine environment. *J. Hazard. Mater.* 284, 130–135. doi: 10.1016/j.jhazmat.2014.11.008
- Migliore, L., Rotini, A., and Thaller, M. C. (2013). Low doses of tetracycline trigger the *E. coli* growth: a case of hormetic response. *Dose Response* 11, 550–557. doi: 10.2203/dose-response.13-002.Migliore
- Minetto, D., Volpi Ghirardini, A., and Libralato, G. (2016). Saltwater ecotoxicology of Ag, Au, CuO, TiO<sub>2</sub>, ZnO and C60 engineered nanoparticles: an overview. *Environ. Int.* 92–93, 189–201. doi: 10.1016/j.envint.2016.03.041
- Mortimer, M., Kasemets, K., Heinlaan, M., Kurvet, I., and Kahru, A. (2008). High throughput kinetic *Vibrio fischeri* bioluminescence inhibition assay for study of toxic effects of nanoparticles. *Toxicol. In Vitro* 22, 1412–1417. doi: 10.1016/j.tiv.2008.02.011
- Mortimer, M., Kasemets, K., and Kahru, A. (2010). Toxicity of ZnO and CuO nanoparticles to ciliated protozoa *Tetrahymena thermophila*. *Toxicology* 269, 182–189. doi: 10.1016/j.tox.2009.07.007
- OECD (2014). “Ecotoxicology and environmental fate of manufactured nanomaterials: test guidelines” in *Expert Meeting Report. Series on the Safety of Manufactured Nanomaterials No. 40. ENV/JM/MONO(2014)1* (Paris).
- Oliver, J. D. (2005). The viable but nonculturable state in bacteria. *J. Microbiol.* 43, 93–100.
- Oliver, J. D. (2009). Recent findings on the viable but non culturable state in pathogenic bacteria. *FEMS Microbiol. Rev.* 34, 415–425. doi: 10.1574-6976.2009.00200.x1111/j.
- Parvez, S., Venkataraman, C., and Mukherji, S. (2006). A review on advantages of implementing luminescence inhibition test (*Vibrio fischeri*) for acute toxicity prediction of chemicals. *Environ. Int.* 32, 256–268. doi: 10.1016/j.envint.2005.08.022
- Ritz, C., and Streibig, J. C. (2005). Bioassay analysis using R. *J. Stat. Softw.* 12, 1–22. doi: 10.18637/jss.v012.i05
- Rossetto, A. L. D. O.F., Melegari, S. P., Ouriques, L. C., and Matias, W. G. (2014). Comparative evaluation of acute and chronic toxicities of CuO nanoparticles and bulk using *Daphnia magna* and *Vibrio fischeri*. *Sci. Total. Environ.* 490, 807–814. doi: 10.1016/j.scitotenv.2014.05.056
- Rotini, A., Gallo, A., Parlapiano, I., Berducci, M. T., Boni, F., Tosti, E., et al. (2018). Insights into the CuO nanoparticles ecotoxicity with suitable marine model species. *Ecotox. Environ. Saf.* 147, 852–860. doi: 10.1016/j.ecoenv.2017.09.053
- Rotini, A., Manfra, L., Spanu, F., Pisapia, M., Cicero, A. M., Migliore, L. (2017). Ecotoxicological method with the marine bacteria *Vibrio anguillarum* to evaluate the acute toxicity of environmental contaminants. *J. Vis. Exp.* 123:e55211. doi: 10.3791/55211
- Sanchis, J., Božović, D., Al-Harbi, N. A., Silva, L. F., Farré, M., and Barceló, D. (2013). Quantitative trace analysis of fullerenes in river sediment from Spain and soils from Saudi Arabia. *Anal. Bioanal. Chem.* 405, 5915–5923. doi: 10.1007/s00216-013-6924-z
- Schultz, A. G., Boyle, D., Chamot, D., Ong, K. J., Wilkinson, K. J., McGeer, J. C., et al. (2014). Aquatic toxicity of manufactured nanomaterials: challenges and recommendations for future toxicity testing. *Environ. Chem.* 11, 207–226. doi: 10.1071/EN13221
- Thompson, F., Iida, T., and Swings, J. (2004). Biodiversity of *Vibrios*. *Microbiol. Mol. Biol. Rev.* 68, 403–431. doi: 10.1128/MMBR.68.3.403-431.2004
- Unrine, J. M., Tsyusko, O. V., Hunyadi, S. E., Judy, J. D., and Bertsch, P. M. (2010). Effects of particle size on chemical speciation and bioavailability of copper to earthworms (*Eisenia fetida*) exposed to copper nanoparticles. *J. Environ. Qual.* 39, 1942–1953. doi: 10.2134/jeq2009.0387
- USEPA (2014). *Method 6020b Inductively Coupled Plasma—Mass Spectrometry*. Washington, DC.
- Villareal, F. D., Das, G. K., Abid, A., Kennedy, I. M., and Kültz, I. (2014). Sublethal effects of CuO nanoparticles on mozambique tilapia (*Oreochromis mossambicus*) are modulated by environmental salinity. *PLoS ONE* 9:e88723. doi: 10.1371/journal.pone.0088723
- Weinberg, H., Galyean, A., and Leopold, M. (2011). Evaluating engineered nanoparticles in natural waters. *Anal. Chem.* 30, 72–83. doi: 10.1016/j.trac.2010.09.006
- Zhao, J., Wang, Z., Liu, X., Xie, X., Zhang, K., and Xing, B. (2011). Distribution of CuO nanoparticles in juvenile carp (*Cyprinus carpio*) and their potential toxicity. *J. Hazard. Mater.* 197, 304–310. doi: 10.1016/j.jhazmat.2011.09.094
- Zhou, D., Bennett, S. W., and Keller, A. A. (2012). Increased mobility of metal oxide nanoparticles due to photo and thermal induced disagglomeration. *PLoS ONE* 7:e37363. doi: 10.1371/journal.pone.0037363

**Conflict of Interest Statement:** The authors declare that the research was conducted in the absence of any commercial or financial relationships that could be construed as a potential conflict of interest.

Copyright © 2017 Rotini, Tornambè, Cossi, Iamunno, Benvenuto, Berducci, Maggi, Thaller, Cicero, Manfra and Migliore. This is an open-access article distributed under the terms of the Creative Commons Attribution License (CC BY). The use, distribution or reproduction in other forums is permitted, provided the original author(s) or licensor are credited and that the original publication in this journal is cited, in accordance with accepted academic practice. No use, distribution or reproduction is permitted which does not comply with these terms.



# Microbial Community Structure and Function Indicate the Severity of Chromium Contamination of the Yellow River

Yaxin Pei<sup>†</sup>, Zhengsheng Yu<sup>†</sup>, Jing Ji, Aman Khan and Xiangkai Li\*

Ministry of Education Key Laboratory of Cell Activities and Stress Adaptations, School of Life Sciences, Lanzhou University, Lanzhou, China

## OPEN ACCESS

### Edited by:

Stéphane Pesce,  
National Research Institute of Science  
and Technology for Environment  
and Agriculture, France

### Reviewed by:

Olivier Crouzet,  
Institut National de la Recherche  
Agronomique (INRA), France  
Wenli Chen,  
Huazhong Agricultural University,  
China

### \*Correspondence:

Xiangkai Li  
xkli@lzu.edu.cn

<sup>†</sup>These authors have contributed  
equally to this work.

### Specialty section:

This article was submitted to  
Microbiotechnology, Ecotoxicology  
and Bioremediation,  
a section of the journal  
Frontiers in Microbiology

Received: 27 June 2017

Accepted: 09 January 2018

Published: 25 January 2018

### Citation:

Pei Y, Yu Z, Ji J, Khan A and Li X  
(2018) Microbial Community Structure  
and Function Indicate the Severity  
of Chromium Contamination of the  
Yellow River. *Front. Microbiol.* 9:38.  
doi: 10.3389/fmicb.2018.00038

The Yellow River is the most important water resource in northern China. In the recent past, heavy metal contamination has become severe due to industrial processes and other anthropogenic activities. In this study, riparian soil samples with varying levels of chromium (Cr) pollution severity were collected along the Gansu industrial reach of the Yellow River, including samples from uncontaminated sites (XC, XGU), slightly contaminated sites (LJX, XGD), and heavily contaminated sites (CG, XG). The Cr concentrations of these samples varied from 83.83 mg·kg<sup>-1</sup> (XGU) to 506.58 mg·kg<sup>-1</sup> (XG). The chromate [Cr (VI)] reducing ability in the soils collected in this study followed the sequence of the heavily contaminated > slightly contaminated > the un-contaminated. Common Cr remediation genes *chrA* and *yieF* were detected in the XG and CG samples. qRT-PCR results showed that the expression of *chrA* was up-regulated four and threefold in XG and CG samples, respectively, whereas the expression of *yieF* was up-regulated 66- and 7-fold in the same samples after 30 min treatment with Cr (VI). The copy numbers of *chrA* and *yieF* didn't change after 35 days incubation with Cr (VI). The microbial communities in the Cr contaminated sampling sites were different from those in the uncontaminated samples. Especially, the relative abundances of *Firmicutes* and *Bacteroidetes* were higher while *Actinobacteria* was lower in the contaminated group than uncontaminated group. Further, potential indicator species, related to Cr such as Cr-remediation genera (*Geobacter*, *PSB-M-3*, *Flavobacterium*, and *Methanosarcina*); the Cr-sensitive genera (*Skermanella*, *lamia*, *Arthrobacter*, and *Candidatus Nitrososphaera*) were also identified. These data revealed that Cr shifted microbial composition and function. Further, Cr (VI) reducing ability could be related with the expression of Cr remediation genes.

**Keywords:** the Yellow River, Cr, microbial indicator species, MiSeq sequencing, qRT-PCR, Cr (VI) reduction test

## INTRODUCTION

River contaminants, especially heavy metals, because of their high toxicity, abundance, and persistent properties, can damage aquatic ecosystems (Varol, 2011; Liao et al., 2016). The Yellow River, the second largest river in China and the sixth largest river in the world, irrigates 15% of the agricultural land, supports a population of 107 million, and contributes 9% to China's GDP (Hu et al., 2015). The Yellow River is an important water source in arid northern China and suffers

the continually increasing environmental pressures from large amounts of pollutants, especially heavy metals, since it receives billions of tons of sewage annually resulting from anthropogenic activities (Yuan et al., 2012; Liu et al., 2015). A large number of water-intensive industries such as petrochemical industries, mining, and animal husbandry are located in cities along the Gansu industrial reach of the Yellow River and are strongly dependent on the Yellow River for their water demands (Ma et al., 2016). However, studies about heavy metals toxicity, mobility, and bioavailability along Gansu industrial reach of the Yellow River are still scarce.

Several studies have shown riparian soils, due to a variety of processes such as adsorption, biological uptake, and sedimentation to reflect the heavy metal contamination conditions of aquatic ecosystems. For example, heavy metal contamination conditions were evaluated for the Pearl River estuary by collecting riparian soil samples (Bai et al., 2011b). In another study, the effects of heavy metals on microbial communities were assessed using riparian soils around a settling pond for mine drainage treatment (Fan et al., 2016). Numerous studies have revealed that microbes are much more sensitive to heavy metals than plants in the same area (Giller et al., 2009; Sun et al., 2012). Thus, microbial community structure could also be a good indicator for revealing the severity of heavy metal contamination. For instance, *Firmicutes* and *Bacteroidetes* are the main phyla in the Cr contaminated environments (Miao et al., 2015; Zhang et al., 2017), whereas another study showed that influent zones, which possess higher heavy metal concentrations, contained more *Firmicutes*, *Bacteroidetes*, and *Actinobacteria* in comparison to upstream, downstream, and effluent zones did (Fan et al., 2016). Microorganisms exposed to strong selective pressures from heavy metal contaminated environments can process corresponding function for the ecosystem (Epelde et al., 2015). This has resulted in the evolution of heavy metal resistance mechanisms, including not only the structural changes of microbial communities (Fan et al., 2016), but also transfer of heavy metal resistance genes to other community members by transposons or plasmids and expression level changes of such genes (He et al., 2011; Epelde et al., 2015). Thus, the phenotype of microbial communities can also reflect the severity of the pollution. However, studies about the correlation between phenotypic function and composition of microbial community have not been reported along Gansu industrial reach of the Yellow River.

Chromium is a common pollutant in the river (Zhang et al., 2009; Bai et al., 2011a). Cr (VI) and Cr (III) are the stable forms of Cr commonly found in nature. Highly toxic Cr (VI) can be reduced to Cr (III) by microbes (Pradhan et al., 2016). Cr concentration in the sediments of Xigu area and the isolated Cr-remediation bacteria have been reported (Liu et al., 2009; Huang et al., 2016). Thus, this study is focused on the Cr contamination in Gansu industrial reach of the Yellow River. In this study, riparian soil samples were collected from six sites along Gansu industrial reach of the Yellow River with a contamination gradient of Cr pollution. The main objectives of this study were: (1) to study the effect of environmental factors on the microbial diversity and composition along the Gansu industrial reach of

the Yellow River; (2) to understand the functional genes of the microbial communities involved in the Cr (VI) remediating process; and (3) to determine which microbial taxa can be used as indicators for revealing the Cr contamination level in Gansu industrial reach of the Yellow River aquatic ecosystem.

## MATERIALS AND METHODS

### Study Sites and Sampling

Riparian soil samples were collected from six different sites along the Gansu industrial reach of the Yellow River in August of 2014 (Figure 1). The Xigu district (XG) in Lanzhou, because of its industrial prosperity, has long been reported as contaminated by heavy metals such as Cu, Zn, Pb, and Cr (Yu et al., 2016). The Chengguan district (CG) has also been polluted for over 50 years as a consequence of the discharge of domestic sewage discharge (Luo et al., 2011). The Liujiaxia reservoir (LJX) was found to be at a middle level of contamination in 2012 from analyzing the characteristics of algal communities (Sang et al., 2012). The downstream of Xigu district (XGD) sample was collected downstream of XG. It was polluted, but not as severely as the XG sample and the pollution could be a result of the recent industrial expansion. Moreover, no contamination was reported in Xincheng district (XC) and upstream of Xigu district (XGU) because of the fewer factories and population. Five spatially independent subsamples (2 cm in diameter, 0–15 cm in depth) were collected from each site along the bank of the Yellow River (10 m intervals) and combined to act as one sample. Three of these combined riparian soil samples were collected independently at each sampling site. The riparian soil samples were transferred to the lab on ice and then each sample was weighed and divided into three subsamples: the first set of subsamples was used for RNA extraction and immediately incubation with Cr (VI); the second was kept at room temperature for determining physicochemical properties; and the third was kept at  $-80^{\circ}\text{C}$  for DNA extraction and downstream analyses.

### Physicochemical Detection of Riparian Soils

Soils were air-dried until their weights were stable and then sieved ( $<1$  mm) for the following processes. Soil moisture was measured with thermo-gravimetric method (Al-Kayssi, 2002). The pH was measured with a pH meter after incubating a 1:5 mixture of riparian soil to 1 M KCL for 2 h (Wu et al., 2010). N, P, soil organic matter (SOM), the total concentration of metals (K, Cu, Zn, Cr, and Mn), and the salt extractable fractions (SK, SCu, SZn, SCr, and SMn) of metals were measured as previously described (Havlin and Westfall, 1985; Akcay et al., 2003; Sitters et al., 2013; Yu et al., 2016). Heavy metal concentrations that exceeded the natural background values were regarded as polluted sites (Bao et al., 2009).

### Illumina MiSeq Sequencing of 16S rDNA

DNA was extracted using a soil DNA Extraction Kit (MO BIO, United States, 12888-50). Each site was processed in

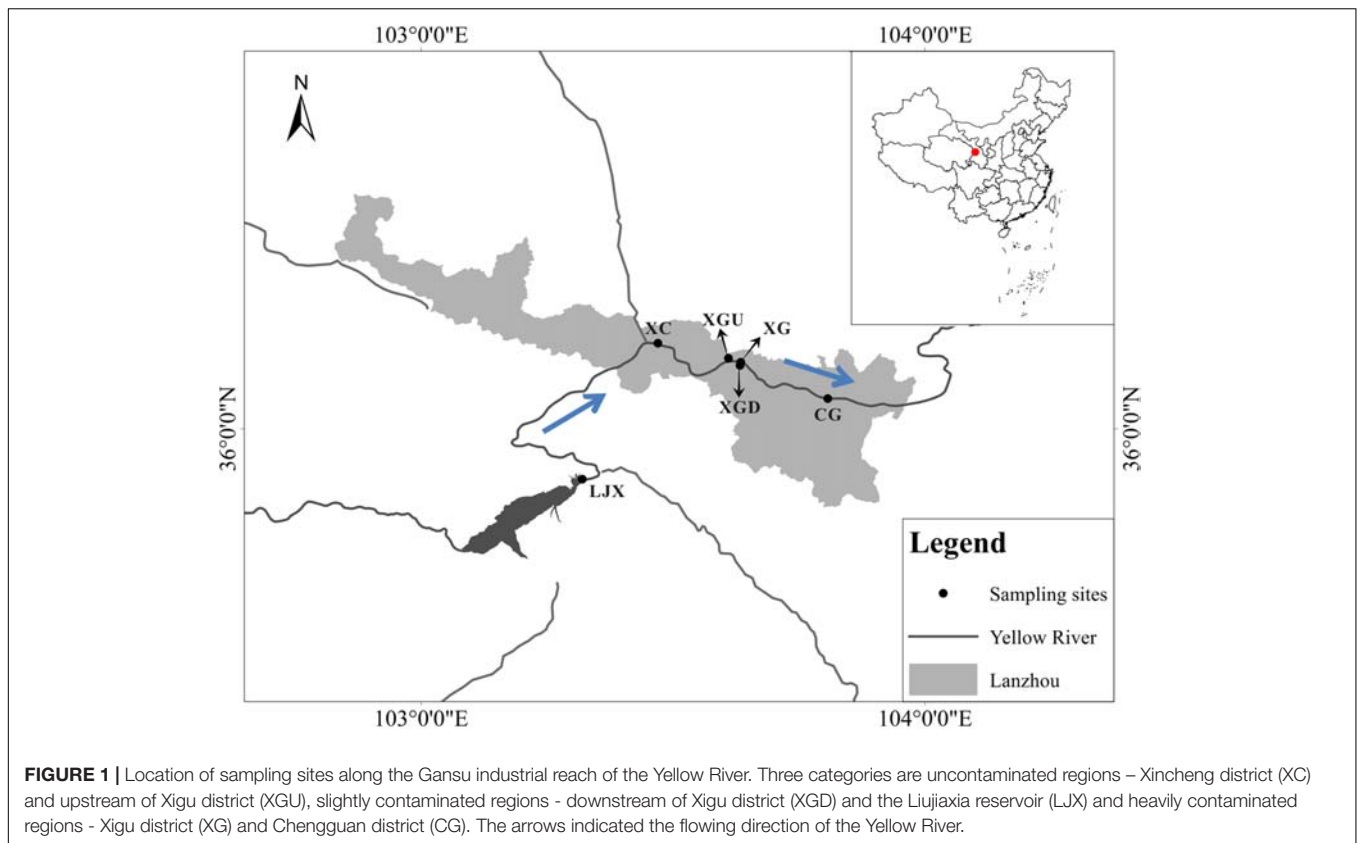


**FIGURE 1** | Location of sampling sites along the Gansu industrial reach of the Yellow River. Three categories are uncontaminated regions – Xincheng district (XC) and upstream of Xigu district (XGU), slightly contaminated regions – downstream of Xigu district (XGD) and the Liujiaxia reservoir (LJX) and heavily contaminated regions - Xigu district (XG) and Chengguan district (CG). The arrows indicated the flowing direction of the Yellow River.

triplicate. DNA concentration and quality were determined using a NanoDrop2000 Spectrophotometer (Thermo Scientific, United States). Totally, 18 extracted genomic DNA samples were sent to the Chengdu Institute of Biology for high-throughput sequencing using primers of 16s rRNA gene [515F (5'-GTGCCAGCMGCCGCGGTAA-3') and 909R (5'-CCC CGYCAATTCMTTTRAGT-3')] (Wu et al., 2016). The original pyrosequencing data are available from the MG-RAST database (accession no. 4750235.3 – 4750252.3).

## Cr (VI) Reduction Test of the Soil Microbial Community

To detect the Cr (VI) reduction ability of the microbial community in different riparian soil samples, for each fresh riparian soil sample, 10 g of the sample was added to a 50 mL plastic tube spiked with 20 mL 0.85% NaCl. An additional tube for each sample was autoclaved (110 kPa, 121°C, 1 h) for complete sterilization and regarded as a control because a previous study reported that the Cr (VI) reduction ability of soil samples was not affected by autoclave sterilization but the microbes in the soil were (Xiao et al., 2014).  $K_2Cr_2O_7$  was added to the tubes for a final concentration of 0.05 mM. The sterile and non-sterile riparian soil samples were incubated at 37°C for 35 days. Additionally, more  $K_2Cr_2O_7$  was added to the initial concentration once the yellow color of the initial  $K_2Cr_2O_7$  solution faded completely in riparian soil samples. Riparian soil moisture was maintained at a constant level by periodic watering.

Each sample was processed in triplicate. Finally, detection of Cr (VI) concentrations was carried out via spectrophotometry using the Cr (VI)-specified reagent *S*-diphenylcarbazide (DPC) (Pattanapitpaisal et al., 2001). Cr (VI) reduction ability was evaluated using the following formula:

$$\text{Cr (VI) reduction ability (\%)} = \frac{[(Cr_A - Cr_B) / Cr_A] \times 100}{}$$

where  $Cr_A$  is the total Cr consumption amount in the non-sterile group, including reduced and adsorbed Cr (VI) amount; and  $Cr_B$  is the total adsorbed Cr (VI) amount in the sterile group.

## Real-Time Quantitative RT-PCR (qRT-PCR)

Two Cr remediation related genes, *chrA* (chromate transporter) and *yieF* (chromate reductase) were detected using genomic DNA as the template in PCR with Ex Taq<sup>TM</sup> (TaKaRa, Japan, RR001A) following the manufacturer's instructions. Riparian soil samples were treated with 0.85% NaCl containing 0.5 mM  $K_2Cr_2O_7$  or 0.85% NaCl only for 30 min. Subsequently, total RNA was extracted from the riparian soil samples above using an RNA PowerSoil<sup>®</sup> Total RNA Isolation Kit (MO BIO, United States, 12866-25). Any remaining genomic DNA was removed via an RTS DNase<sup>TM</sup> Kit (MO BIO, United States, 15200-50). Then, first-strand cDNA synthesis was completed using a PrimeScript<sup>TM</sup> RT Reagent Kit (TaKaRa, Japan, RR047A) according to the manufacturer's protocols. Expression levels

of *chrA* and *yieF* after 30 min Cr (VI) treatment, copy numbers changes of *chrA* and *yieF* after 35 days of chromate incubation, and microbial biomass were assessed via real-time PCR. Reactions were performed on CFX96™ Real-Time PCR Detection System (Bio-Rad) according to the manufacturer's instructions (Wu et al., 2014). All genes were analyzed in triplicate. The primer sequences of the target genes and the 16S rRNA gene are listed in Supplementary Table S1.

## Statistical Analysis

Data were expressed as the mean  $\pm$  SD. Soil physicochemical properties, microbial diversity indices, Cr (VI) reduction abilities, and RT-PCR results were examined by Tukey's test. We used Spearman's rank correlation coefficient to determine whether there was a significant correlation between different environmental variables or between the relative abundances of dominant microbes and the environmental variables. The statistical analyses were performed in SPSS 16.0 for Windows. Principal coordinate analysis (PCoA), Canonical correspondence analysis (CCA), and Variation partition analysis (VPA) were performed using R version 2.15.2 as described before (R Core Team, 2015; Yu et al., 2016).

## RESULTS

### Riparian Soil Physicochemical Properties

The physicochemical properties of the soil samples collected from the six sites were measured. These included soil texture (Supplementary Figure S1), pH, water content, the concentrations of N, P, K, Cu, Zn, Cr, and Mn; and SOM (Table 1). The pH values of the soil samples varied slightly, from 7.64 to 8.28. The XG samples contain higher amount of N and K, while the P content was almost the same across all site samples. The Cr concentrations ranged from 83.83 to 506.58 mg kg<sup>-1</sup>. Based on the Cr contamination states, the six sites were divided into three different categories: (i) uncontaminated regions, including XC and XGU, where the Cr concentration was less than the natural background (90 mg kg<sup>-1</sup>); (ii) slightly contaminated regions where the Cr concentration is greater than the natural background (90 mg kg<sup>-1</sup>), but less than the limited standard of Chinese Soil Quality Criterion (250 mg kg<sup>-1</sup>). These included regions such as XGD and the LJX; and (iii) heavily contaminated regions, including XG and CG, where the Cr concentration exceed the limited standard of Chinese Soil Quality Criterion (250 mg kg<sup>-1</sup>) (Table 1). On the other hand, the pollution conditions for Cu, Zn, and Mn were not as severe as Cr and only showed contamination at the XG site. The salt extractable fraction of metals like K, Cu, Zn, and Cr were detected in higher concentrations in XG samples in comparison to other sites the concentration of Mn was higher in CG samples.

### Cr (VI) Reduction Test of the Soil Microbial Community

To evaluate the severity of Cr in Gansu industrial reach of the Yellow River, the Cr (VI) reduction abilities of the riparian soil

microbial communities from different samples were measured (Figure 2A). No Cr (VI) reduction was observed for the XC and XGU samples which may be due to the low Cr stress in these sites. The heavily contaminated group (XG, CG) exhibited the highest Cr (VI) reduction ability, whereas the slightly contaminated group (LJX, XGD) had moderate Cr (VI) reduction ability. The Cr (VI) reduction ability of the uncontaminated, slightly contaminated, and heavily contaminated groups are probably associated with the severity of Cr contamination. Additionally, Spearman's correlation analysis showed that Cr (VI) reduction ability did increase with Cr concentrations (Supplementary Table S3). Therefore, microbial function could indicate the severity of Cr contamination.

### *chrA* and *yieF* Related to Cr (VI) Remediation

Two common Cr remediation genes *chrA* (chromate transporter) and *yieF* (chromate reductase) were chosen to explain the different Cr (VI) reduction abilities among the samples. After treatment with Cr (VI) for 30 min, RNA was extracted from the riparian soil samples and the qRT-PCR results showed that the expression of *chrA* was up-regulated four and threefold in XG and CG samples, respectively, whereas the expression of *yieF* was up-regulated 66- and 7-fold in the same samples (Figure 2B). Further, copies of *chrA* and *yieF* did not change after being incubated with Cr (VI) in lab for 35 days (Figures 2C,D). *chrA* and *yieF* were not detected in uncontaminated and slightly contaminated groups because Cr (VI) contamination of those sites was not as severe as that of CG and XG sites (Figures 2B–D). This result not only indicated that the Cr (VI) reduction ability of the CG and XG soil samples might be related to the expression of Cr (VI) remediation genes but also further implied that Cr may only influenced the microbial community functions at the transcriptional level nor copy numbers of genes.

### Microbial Community Grouping Based on the Contamination Situations

MiSeq sequencing data of the 16S rRNA gene showed that 9080 qualified reads were obtained from each sample and 18,097 operational taxonomic units were obtained based on 3% dissimilarity (Supplementary Figure S2). Microbial diversity indices of each sample were in close range except for slightly lower richness and diversity of the LJX samples (Supplementary Table S2).

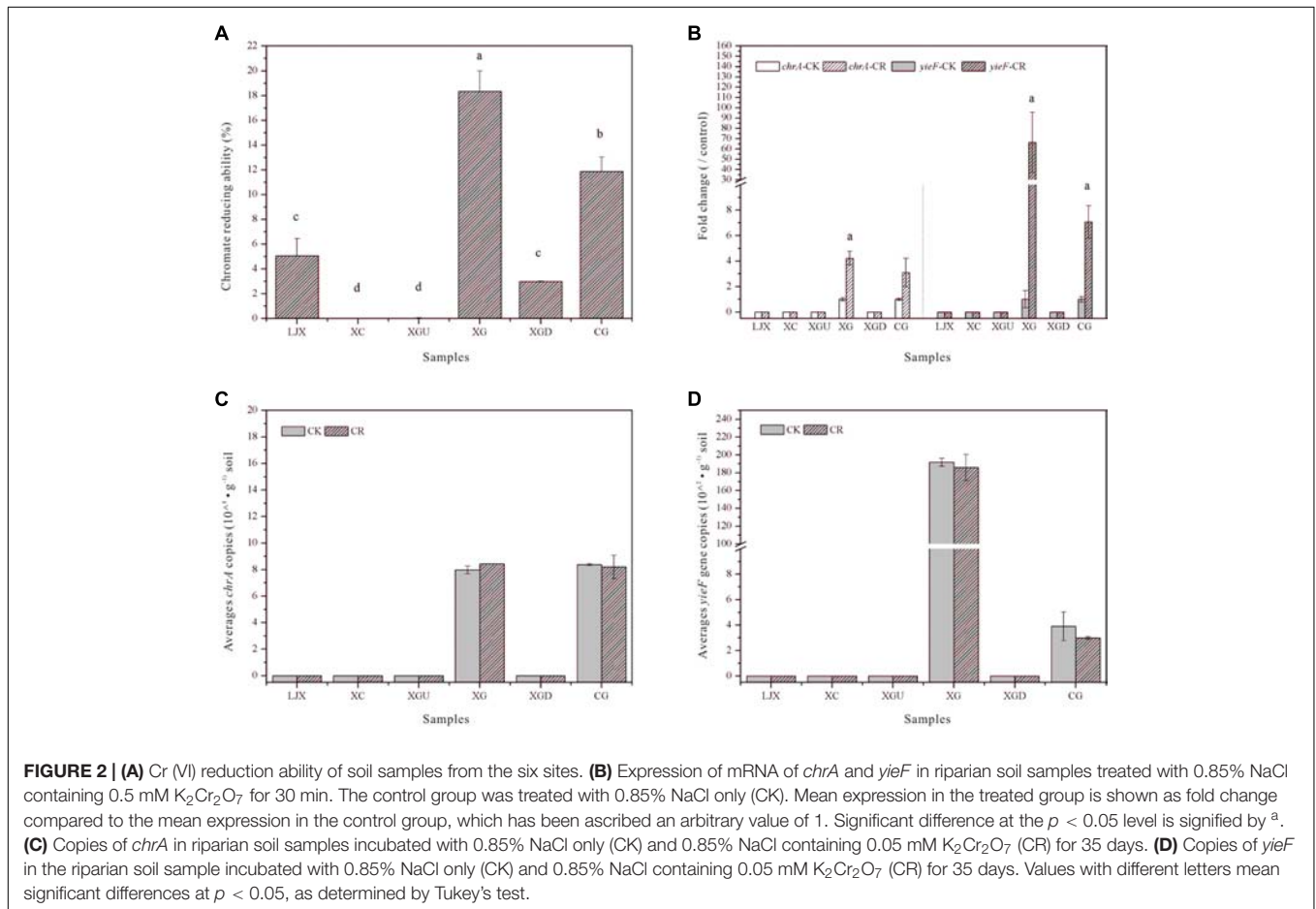
For these sites, 66 different phyla were observed. At least 87% of total reads were affiliated with bacterial phyla and 4.48% of total reads were assigned to archaeal phyla. *Proteobacteria* (33.03–49.99%) was the most abundant phylum for all six sites, followed by *Bacteroidetes* (7.07–25.73%), *Actinobacteria* (1.59–19.89%), *Chloroflexi* (2.14–9.69%), *Firmicutes* (0.58–21.85%), and *Acidobacteria* (0.57–6.25%). In this study, these six phyla accounted for more than 67% of the total bacteria. The archaea *Crenarchaeota* (0.23–8.98%) and *Euryarchaeota* (1.05–8.73%) were also dominant (Figure 3A).

The distributions of each phylum at the six riparian sites (Figure 3A) imply that the dominant species of the

**TABLE 1** | Physicochemical properties of the sites' soil samples.

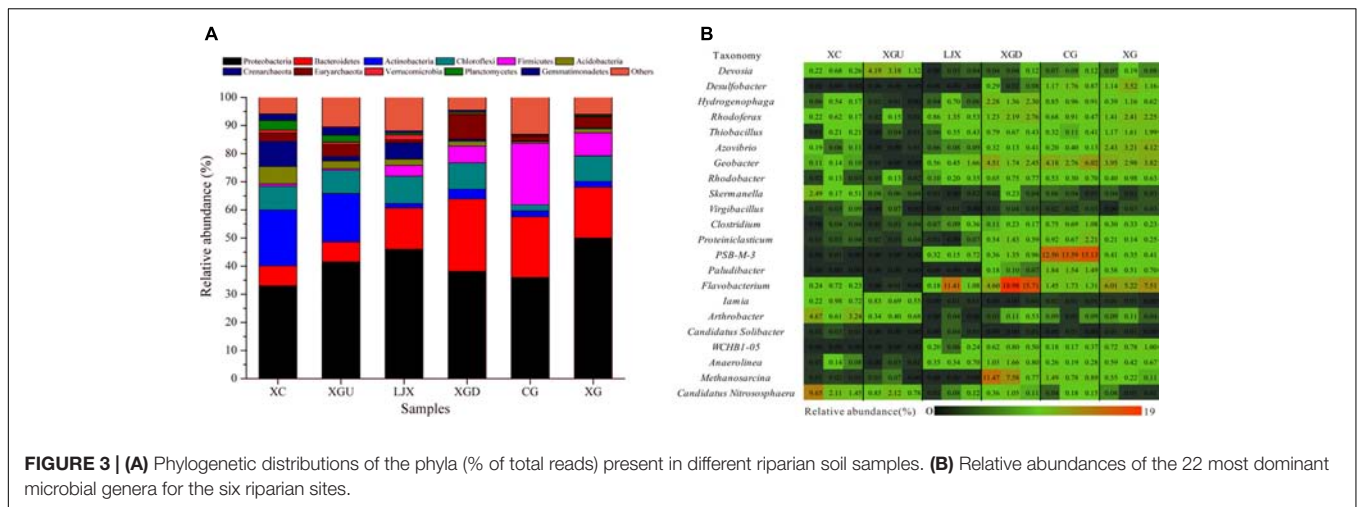
Variables	Different sites' soil samples					
	XC	XGU	LJX	XGD	CG	XG
pH	8.03 ± 0.05 <sup>bc</sup>	7.64 ± 0.05 <sup>e</sup>	8.28 ± 0.03 <sup>a</sup>	7.90 ± 0.01 <sup>d</sup>	8.15 ± 0.06 <sup>b</sup>	7.98 ± 0.06 <sup>cd</sup>
Water content (%)	9.46 ± 0.46 <sup>d</sup>	9.75 ± 0.86 <sup>d</sup>	25.38 ± 0.90 <sup>c</sup>	30.27 ± 0.65 <sup>b</sup>	33.98 ± 1.30 <sup>ab</sup>	37.61 ± 3.88 <sup>a</sup>
N (mg · kg <sup>-1</sup> )	7296.23 ± 326.87 <sup>bcd</sup>	9723.15 ± 1859.78 <sup>b</sup>	5957.70 ± 1206.44 <sup>cd</sup>	5383.55 ± 325.96 <sup>d</sup>	9033.46 ± 330.46 <sup>bc</sup>	14397.08 ± 1525.51 <sup>a</sup>
P (mg · kg <sup>-1</sup> )	879.18 ± 62.79 <sup>a</sup>	688.24 ± 87.27 <sup>a</sup>	746.06 ± 82.46 <sup>a</sup>	685.86 ± 30.15 <sup>a</sup>	1081.08 ± 285.85 <sup>a</sup>	885.68 ± 178.13 <sup>a</sup>
K (mg · kg <sup>-1</sup> )	8235.00 ± 103.76 <sup>bc</sup>	8006.33 ± 177.43 <sup>c</sup>	8442.00 ± 55.68 <sup>bc</sup>	8676.67 ± 227.73 <sup>b</sup>	8222.00 ± 166.44 <sup>bc</sup>	18220.67 ± 258.81 <sup>a</sup>
Cu (mg · kg <sup>-1</sup> )	3.63 ± 0.53 <sup>c</sup>	9.19 ± 0.68 <sup>b</sup>	8.69 ± 0.34 <sup>b</sup>	8.12 ± 0.62 <sup>bc</sup>	10.50 ± 0.55 <sup>b</sup>	28.58 ± 3.83 <sup>a</sup>
Zn (mg · kg <sup>-1</sup> )	66.57 ± 9.27 <sup>b</sup>	57.64 ± 6.95 <sup>b</sup>	65.17 ± 0.55 <sup>b</sup>	66.08 ± 4.77 <sup>b</sup>	62.28 ± 6.95 <sup>b</sup>	342.55 ± 4.68 <sup>a</sup>
Cr (mg · kg <sup>-1</sup> )	87.35 ± 27.08 <sup>c</sup>	83.83 ± 6.02 <sup>c</sup>	116.37 ± 13.75 <sup>c</sup>	135.08 ± 12.47 <sup>c</sup>	239.02 ± 34.93 <sup>b</sup>	506.58 ± 13.79 <sup>a</sup>
Mn (mg · kg <sup>-1</sup> )	5685.67 ± 230.53 <sup>bc</sup>	5056.67 ± 246.58 <sup>d</sup>	5456.00 ± 35.51 <sup>c</sup>	5756.00 ± 26.85 <sup>bc</sup>	5895.33 ± 14.50 <sup>b</sup>	10753.33 ± 45.09 <sup>a</sup>
SK (mg · kg <sup>-1</sup> )	37.06 ± 0.47 <sup>d</sup>	40.03 ± 0.89 <sup>ab</sup>	37.99 ± 0.25 <sup>cd</sup>	39.91 ± 1.05 <sup>bc</sup>	38.64 ± 0.78 <sup>bcd</sup>	41.91 ± 0.60 <sup>a</sup>
SCu (mg · kg <sup>-1</sup> )	0.02 ± 0.00 <sup>d</sup>	0.05 ± 0.00 <sup>bc</sup>	0.04 ± 0.00 <sup>bc</sup>	0.04 ± 0.00 <sup>c</sup>	0.05 ± 0.00 <sup>b</sup>	0.07 ± 0.01 <sup>a</sup>
SZn (mg · kg <sup>-1</sup> )	0.30 ± 0.04 <sup>b</sup>	0.29 ± 0.03 <sup>b</sup>	0.29 ± 0.00 <sup>b</sup>	0.30 ± 0.02 <sup>b</sup>	0.29 ± 0.03 <sup>b</sup>	0.79 ± 0.01 <sup>a</sup>
SCr (mg · kg <sup>-1</sup> )	0.39 ± 0.01 <sup>d</sup>	0.43 ± 0.02 <sup>d</sup>	0.52 ± 0.01 <sup>c</sup>	0.62 ± 0.02 <sup>b</sup>	1.12 ± 0.02 <sup>a</sup>	1.18 ± 0.06 <sup>a</sup>
SMn (mg · kg <sup>-1</sup> )	25.59 ± 1.04 <sup>bc</sup>	25.28 ± 1.23 <sup>bc</sup>	24.55 ± 0.16 <sup>c</sup>	26.48 ± 0.12 <sup>ab</sup>	27.71 ± 0.07 <sup>a</sup>	24.73 ± 0.10 <sup>bc</sup>
SOM (mg · g <sup>-1</sup> )	1.68 ± 0.16 <sup>b</sup>	1.56 ± 0.17 <sup>b</sup>	2.76 ± 0.10 <sup>b</sup>	3.32 ± 0.26 <sup>b</sup>	5.36 ± 0.65 <sup>b</sup>	29.57 ± 6.13 <sup>a</sup>

All data are presented as mean ± standard deviation (n = 3). Values with different letters in a row mean significant differences at  $p < 0.05$  as determined by Turkey's test.



uncontaminated group (XC and XGU) were remarkably different from that of the contaminated group (LJX, XGD, CG, and XG). The most abundant phyla associated with

the contaminated group (LJX, XGD, CG, and XG) were *Proteobacteria*, *Bacteroidetes*, and *Firmicutes*. In comparison, *Firmicutes* and *Bacteroidetes* content in the contaminated



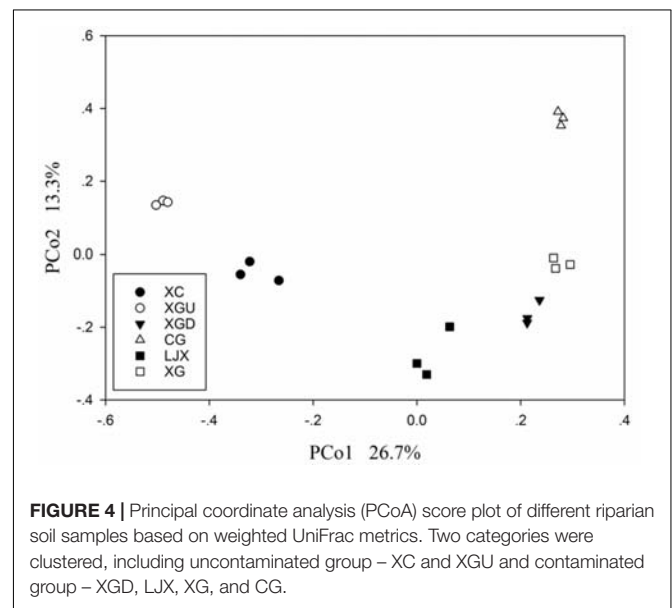
group was higher than those in the uncontaminated group, whereas *Proteobacteria* did not differ much between the two groups. In contrast, *Actinobacteria* was more prevalent in the uncontaminated group than in the contaminated group. Almost all samples contained similar amounts of *Chloroflexi* except for the CG site.

Analysis of microbial composition at the genus level provided additional information on microbial adaptation in response to environmental variations. Among all riparian soil samples, 1469 genera were detected and 22 of the most dominant genera showed differences among samples (Figure 3B). In the contaminated group (LJX, XGD, CG, and XG), the microbial communities were dominated by *Desulfobacter*, *Hydrogenophaga*, *Rhodoferax*, *Thiobacillus*, *Azovibrio*, *Geobacter*, *Clostridium*, *Proteiniclasticum*, *PSB-M-3*, *Flavobacterium*, *WCHB1-05* and *Anaerolinea*, and *Methanosarcina*. All these genera belong to *Proteobacteria*, *Firmicutes*, *Bacteroidetes*, and *Chloroflexi* which were the most abundant phyla in the contaminated group (Figure 3B). In contrast, the uncontaminated group consisted of completely different dominant bacteria including *Skermanella*, *Iamia*, *Arthrobacter*, and *Candidatus Nitrososphaera* which are affiliated to the *Proteobacteria*, *Actinobacteria*, and *Crenarchaeota*.

Principal coordinate analysis was conducted to investigate the dissimilarities among the six sites. The first axis explained 26.7% variance of species and 13.3% was explained by the second axis (Figure 4). All samples formed two clusters as follows: uncontaminated group containing the XC and XGU samples and the contaminated group including both slightly contaminated and heavily contaminated samples. This result is consistent with the Cr pollution condition indicating that Cr may be the main factor altering microbial community structure.

### Correlation between the Microbial Communities and Environmental Variables

Soil organic matter and water content exhibited positive correlations with K, Cu, Cr, and Mn ( $p < 0.01$ ) while K, Cu,



Zn, and Cr showed positive correlations with Mn ( $p < 0.05$ ). Additionally, Cr was significantly and positively correlated with K and Cu (Table 2). In general, the salt extractable part of heavy metals showed significant and high positive correlations with the total heavy metal concentrations ( $p < 0.01$ , Supplementary Table S3). This result indicated that S<sub>Cr</sub> could reflect the total Cr contamination condition. Although Cr (VI) reduction ability presented significantly positive correlations with S<sub>Cu</sub>, S<sub>Cr</sub>, and microbial biomass ( $p < 0.01$ ), the correlation coefficient with S<sub>Cr</sub> was the highest, reaching up to 0.889. Microbial biomass also presented significant correlations with S<sub>K</sub>, S<sub>Cu</sub>, and S<sub>Cr</sub> ( $p < 0.05$ , Supplementary Table S3).

Canonical correspondence analysis and VPA were performed to evaluate the relative contributions of different environmental variables to changes in the microbial community structure. Physicochemical characteristics of the riparian soils, including heavy metals (HM: S<sub>Cu</sub>, S<sub>Zn</sub>, S<sub>Cr</sub>, S<sub>Mn</sub>), soil physical properties

**TABLE 2** | Spearman's correlation coefficients between environmental variables.

	SOM	Water content	pH	Mn	Cr	Zn	Cu	K	P
N	0.383	0.386	-0.155	0.436	0.347	0.208	0.743**	-0.056	0.483*
P	0.341	0.301	0.481*	0.442	0.297	0.024	0.258	-0.132	
K	0.647**	0.606**	0.146	0.560*	0.641*	0.585*	0.238		
Cu	0.664**	0.746**	0.035	0.480*	0.651**	0.255			
Zn	0.439	0.424	0.093	0.608**	0.408				
Cr	0.928**	0.928**	0.266	0.725**					
Mn	0.839**	0.732**	0.167						
pH	0.255	0.207							
Water content	0.926**								

\*\*Means the correlation is significant at the  $p < 0.01$  level. \*Means the correlation is significant at the  $p < 0.05$  level.

(SPP: pH, water content), and soil nutrient (SN: SK, N, P, and SOM) were considered as the environmental parameters (**Figure 5A**). As illustrated from the results from CCA ( $p = 0.001$ ), the two axes explained 18.97 and 13.57% of the microbial community differentiation, respectively. The CCA results showed that pH and water content largely shaped the microbial community even though pH values varied little among the different sites. As indicated, SCr, SCu, SZn, and SOM were also strongly linked to the microbial community correspondingly to the length of the vector. SMn, SK, P, and N had lower contribution to the structure of microbial communities. VPA was performed to further discern the possible relationship between microbial communities and environmental variables. The results of VPA showed that 69.49% of the variance in the microbial community structure could be explained by three major types of variables, i.e., HM, SPP, and SN, leaving 30.51% of the variation unexplained (ANOVA  $p = 0.001$ ). SN alone only explained 20.42% of the variation and half of its contribution was shared with HM (9.66%). HM alone explained 19.30% of the variation, among which SCr, as the single factor, accounted for 5.80%. This result indicates that Cr contamination contributed a lot to the differences of microbial communities among those samples. SPP alone explained 10.34% of the variation. Moreover, significant

interactive effects among the rest of the factors including interaction of SN with SPP (6.90%) and SPP with HM (5.27%) were observed, while no significant interaction of those three factors (0.00%) was shown in this study (**Figure 5B**).

Spearman's correlation analysis at the phylum level (**Table 3**) showed that *Firmicutes* and *Bacteroidetes* displayed the highest positive correlation coefficients with SCr, whereas *Actinobacteria*, *Acidobacteria*, and *Crenarchaeota* presented negative correlations ( $p < 0.01$ ). The correlation of SOM and water content with the relative abundances of dominant microbial communities was similar to that of SCr. SCu was negatively correlated with *Actinobacteria* and *Acidobacteria*. Unexpectedly, *Chloroflexi* had a positive correlation with SZn. In addition, *Actinobacteria* and *Euryarchaeota* exhibited negative correlations with pH ( $p < 0.05$ ) although the pH value range varied little among the six sites.

The relative abundances of 20 different microbial genera correlated with SCr, water content or SOM significantly ( $p < 0.01$ ) and 18 of them, such as *Desulfobacter*, *Azovibrio*, and *Geobacter*, showed significant correlation with both SCr, water content, and SOM simultaneously. However, *Skermanella* was the only genus which was significantly correlated with SCr not with SOM or water content. This result implied that SCr, water content and SOM have comprehensive impacts on the microbial

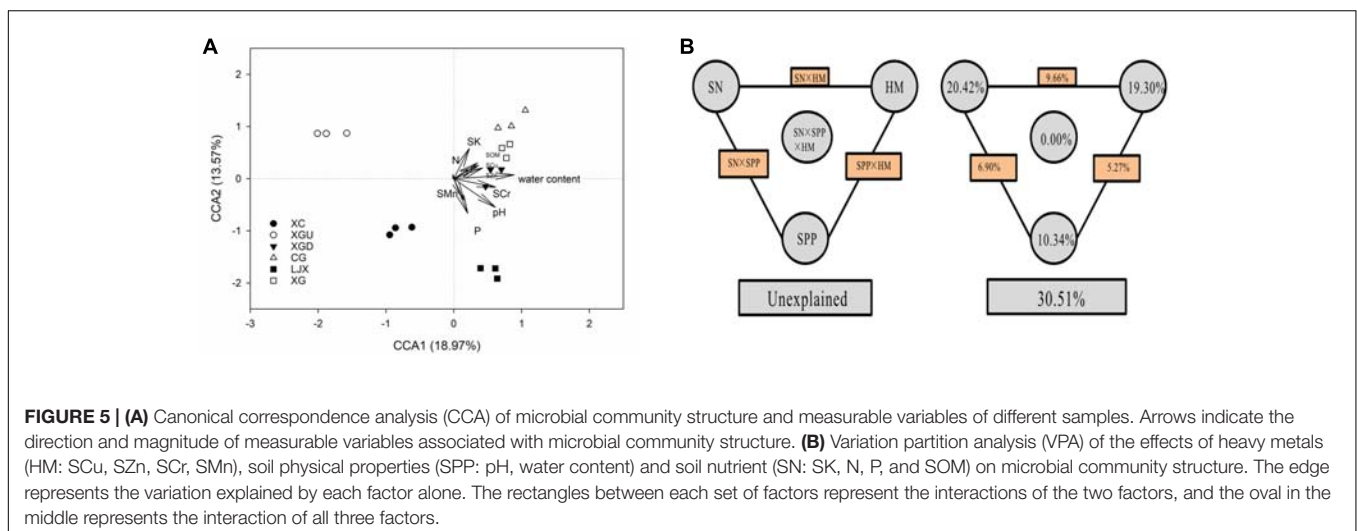


**TABLE 3** | Spearman's correlation coefficients between the relative abundance of the dominant microbes (at phylum and genus level, respectively) and environmental variables.

	N	P	SK	SCu	SZn	SCr	SMn	pH	Water content	SOM
<b>Proteobacteria</b>	0.344	-0.158	0.482*	0.333	0.154	0.207	-0.311	-0.211	0.143	0.214
<i>Devosia</i>	0.413	0.142	0.056	0.002	0.021	-0.433	0.010	-0.560*	-0.440	-0.470*
<i>Desulfobacter</i>	0.494*	0.382	0.488*	0.665**	0.343	0.910**	0.488*	0.073	0.905**	0.903**
<i>Hydrogenophaga</i>	-0.207	0.085	0.199	0.042	0.169	0.593**	0.568*	0.091	0.647**	0.643**
<i>Rhodoferrax</i>	-0.076	-0.104	0.437	0.199	0.453	0.669**	0.162	0.119	0.736**	0.759**
<i>Thiobacillus</i>	0.068	-0.010	0.459	0.317	0.497*	0.706**	0.033	0.068	0.718**	0.766**
<i>Azovibrio</i>	0.252	0.297	0.387	0.376	0.318	0.757**	0.222	0.141	0.781**	0.856**
<i>Geobacter</i>	0.211	0.343	0.291	0.448	0.173	0.832**	0.480*	0.290	0.818**	0.888**
<i>Rhodobacter</i>	0.056	0.067	0.482*	0.320	0.347	0.764*	0.417	0.004	0.790**	0.792**
<i>Skermanella</i>	-0.020	0.061	-0.300	-0.380	0.160	-0.489*	0.162	-0.415	-0.454	-0.462
<b>Firmicutes</b>	0.202	0.353	0.247	0.362	0.129	0.791**	0.432	0.416	0.769**	0.820**
<i>Virgibacillus</i>	-0.022	0.129	-0.067	-0.257	0.290	-0.074	0.332	-0.237	0.099	0.045
<i>Clostridium</i>	0.207	0.349	0.247	0.487*	0.166	0.859**	0.330	0.447	0.801**	0.808**
<i>Proteinclasticum</i>	0.133	0.199	0.340	0.312	0.113	0.696**	0.566*	-0.028	0.637**	0.644**
<i>PSB-M-3</i>	0.020	0.228	0.217	0.323	0.083	0.767**	0.525*	0.361	0.748**	0.753**
<b>Bacteroidetes</b>	-0.250	-0.211	0.364	0.183	0.046	0.635**	0.364	0.083	0.620**	0.604**
<i>Paludibacter</i>	0.443	0.373	0.405	0.627**	0.257	0.875**	0.588*	0.108	0.859**	0.859**
<i>Flavobacterium</i>	-0.206	-0.154	0.380	0.137	0.394	0.638**	0.215	0.102	0.699**	0.689**
<b>Actinobacteria</b>	-0.099	-0.086	-0.160	-0.474*	-0.090	-0.706**	-0.086	-0.575*	-0.645**	-0.668**
<i>Iamia</i>	0.190	0.193	-0.359	-0.207	0.016	-0.570*	-0.060	-0.229	-0.624**	-0.638**
<i>Arthrobacter</i>	0.026	0.004	-0.068	-0.416	0.016	-0.530*	-0.080	-0.526*	-0.528*	-0.477*
<b>Acidobacteria</b>	-0.379	-0.361	-0.297	-0.634**	-0.065	-0.765**	-0.366	-0.349	-0.752**	-0.695**
<i>Candidatus</i>	-0.266	0.193	-0.316	-0.298	0.163	-0.095	-0.232	0.421	-0.047	-0.024
<i>Solibacter</i>										
<b>Chloroflexi</b>	-0.265	-0.541*	0.162	-0.216	0.521*	-0.208	-0.236	-0.367	-0.102	-0.156
<i>WCHB1-05</i>	0.110	-0.037	0.591**	0.404	0.368	0.774**	0.125	0.045	0.803**	0.828**
<i>Anaerolinea</i>	-0.309	-0.233	0.328	0.063	0.237	0.573*	0.075	0.118	0.579*	0.622**
<b>Euryarchaeota</b>	-0.069	-0.154	0.057	-0.028	0.036	-0.128	-0.003	-0.549*	-0.242	-0.282
<i>Methanosarcina</i>	0.168	0.194	0.338	0.333	0.220	0.604**	0.793**	-0.264	0.634**	0.590*
<b>Crenarchaeota</b>	-0.160	0.072	-0.342	-0.416	-0.100	-0.617**	-0.152	-0.269	-0.596**	-0.577*
<i>Candidatus</i>	-0.270	-0.025	-0.401	-0.517*	-0.269	-0.736**	0.124	-0.414	-0.674**	-0.717**
<i>Nitrososphaera</i>										

\*\*Means the correlation is significant at the  $p < 0.01$  level. \*Means the correlation is significant at the  $p < 0.05$  level.

communities rather than individual impacts. SCu and SMn were significantly ( $p < 0.05$ ) correlated with four and seven genera, respectively. In addition, pH was only significantly correlated with two genera at  $p < 0.05$ . In general, only a few genera showed significant correlation with N, P, SK, and SZn. This result indicates that N, P, SK, SCu, SZn, SMn, and pH have minor influence on the abundances of microbial communities as compared to the influences of water content, SCr, and SOM.

## DISCUSSION

The Yellow River as one of the most important water resources for agriculture, industry, and population in northern China and its heavy metal contamination condition is a complex phenomenon (Yu et al., 2009). Previous studies have shown that the heavy metal concentrations (in  $\text{mg kg}^{-1}$  dry weight) in 2008 ranged from 89.80–201.88 (Zn), 41.49–128.30 (Cr), 29.72–102.22 (Cu), and 773.23–1459.699 (Mn) (Liu et al., 2009). However, in our study, only Zn, Cr, and Mn showed higher contamination

concentration (in  $\text{mg kg}^{-1}$  dry weight) and ranged from 57.64–342.55 (Zn), 83.83–506.58 (Cr), and 5056.67–10753.33 (Mn) while Cu showed a lower concentration, reaching up to 3.63–25.58  $\text{mg kg}^{-1}$ . Since Cu concentration in both researches was low, it implied that Cu is not the main pollutant in this area. Previous studies have shown that Cr contamination is severe in the Pearl River estuary, South China, varying from 91.42 to 125.21  $\text{mg kg}^{-1}$ , whereas Cr concentration in surface sediment from 59 stations ranged from 36.9 to 173  $\text{mg kg}^{-1}$  in Yangtze River (Zhang et al., 2009; Bai et al., 2011b). This indicated that Cr is a common pollutant in the river and Cr concentration in Gansu industrial reach of the Yellow River is much higher than other aquatic systems reported in China. Thus, this study focused on the Cr contamination.

The qRT-PCR results showed that the expression of the Cr (VI) remediation genes *chrA* and *yieF* of the XG and CG samples, was significantly ( $p < 0.05$ ) up-regulated after 30 min Cr (VI) treatment. Induction of the two genes by Cr was always the case in Cr reducing bacteria such as *Lysinibacillus fusiformis* ZC1 (He et al., 2011). Further, copies of *chrA* and

*yieF* did not change after incubation with Cr (VI) in the lab for 35 days (Figures 2C,D). This result indicated that the adaptation of microbial community may only depend on the expression level changes of heavy metal resistance genes. Thus, analysis of the function of microbial community should be focused on the both DNA and RNA of microbes in the environment. Metagenomic sequencing data also showed that the microbial community in ground water contaminated long-term with heavy metals possessed heavy metal resistance genes such as *chrAB* chromate efflux, *CzcABC* efflux, and *mer* operon (Yu et al., 2016). Although metagenomic sequencing provided a comprehensive way to understand microbial community function, it has a very limited function in revealing microbially expressed functions or microbial community activities (Wang W.-L et al., 2015). Therefore, compared to high-throughput metagenomic methods, the phenotype test is a straightforward way to evaluate heavy metal contamination conditions. Microbial Cr (VI) remediation ability is related to Cr remediation related genes and proteins in microorganisms (Pradhan et al., 2016). Although *chrA* and *yieF* were not found in the XGD and LJX samples, the microbial communities of these three sites also exhibited Cr (VI) reduction ability. This may be due to the function of other Cr (VI) reductases, such as SOD, catalase, Nema, and LpDH (Thatoi et al., 2014; Pradhan et al., 2016). Although the riparian soil samples were incubated in the laboratory, the copies of *chrA* and *yieF* did not change after incubation. This result indicated that microbial community function was not affected in our lab incubation conditions.

Spearman's correlation analysis showed that SOM exhibited a positive correlation with K, Cu, Cr, and Mn ( $p < 0.01$ ) (Table 2) which is consistent with previous studies that highlight that SOM can act as a major sink for heavy metals due to its strong complexing capacity (Zayre et al., 2006). Previous reports also showed that SOM can keep Cu mobility low in soil by chemisorptions and accelerated the reduction of toxic and mobile Cr (VI) to stable Cr (III) (Bai et al., 2011b). However, Zn did not significantly correlate with SOM suggesting that the SOM might be mainly imported by Cu, Cr, and Mn in the study area. A previous study has also depicted that heavy metals might not always be immobilized by SOM under certain conditions of high inputs of anthropogenic interfere (Kumpiene et al., 2008). K, Cu, Cr, and Mn also showed significant correlations with water content which also correlated with heavy metals significantly (Table 2). This result is in agreement with previous studies that soil water capacity increased with SOM content (Hudson, 1994) and thus, metals exhibit a correlation with water content. Significantly positive relationship between Mn and K, Cu, Zn, or Cr was identified which indicates that these metals may come from the same source or similar transportation mechanisms and get accumulated in the soils (Qiu, 2010). Additionally, the salt exchangeable part of metals was measured to analyze the correlation with microbes since the bioavailability of total metals can be strongly influenced by other environmental factors such as pH (Zhu et al., 2013). The salt extractable parts of SCu, SZn, and SCr exhibited high significant correlations with the total concentrations of Cu, Zn, and Cr ( $p < 0.01$ , Supplementary Table S3) which indicated that the analysis of the salt extractable

part of these heavy metals with microbes could reflect the relationship between their total heavy metal condition and the microbial community. Additionally, the total Cr concentrations did show significant and high positive correlations with the Cr (VI) reduction ability of microbial community ( $p < 0.01$ , Supplementary Table S3) which implicated that Cr (VI) reduction ability of the microbial community could reflect the total Cr concentration condition in this area. Moreover, Cr (VI) reduction ability presented significantly positive correlations with microbial biomass ( $p < 0.01$ ) which indicated that there may be some microbes in soil could be indicators of Cr. Thus, we speculate that Cr might have a great effect on microbial community structure and function in this area.

Although the function of microbial communities could also separate contaminated samples from uncontaminated samples, microbial community structure analysis is necessary for revealing the instant microbial compositions and Cr indicators. PCoA showed microbial communities in the six sites were divided into two groups, the uncontaminated group and the contaminated group. This is similar with a previous study in that PCoA of microbial community structure in sediments collected from four sites revealed different levels of heavy metal contamination along the Xiangjiang River (Zhu et al., 2013).

MiSeq sequencing and Spearman's correlation analysis were performed to analyze the structure of the microbial community in the riparian soil samples of the six sites. Previous reports state that *Proteobacteria* was the most abundant phylum, both in highly Cr-contaminated soil samples and uncontaminated soil samples of a tributary of the Alviela River, reaching 66 and 47%, respectively (Desai et al., 2009). This is consistent with our study where *Proteobacteria* was the most abundant phylum in samples from all six sites and did not show significant correlation with Cr (Figure 2A and Table 3). *Firmicutes* and *Bacteroidetes* in the contaminated group were richer than in the uncontaminated group and positively correlated with SCr (Figure 3A and Table 3). Numerous studies have confirmed that *Firmicutes* and *Bacteroidetes* are the main phyla in the Cr contaminated environment (Miao et al., 2015; Zhang et al., 2017). The relative abundance of *Actinobacteria* ranged from 1.59 to 19.89% for the six sites, showing a negative correlation with SCr (Figure 3A and Table 3). This is not consistent with a previous study which reported that after 28 days of Cr (VI) incubation, based on the DGGE analysis, *Actinobacteria* became one of the most abundant phyla in agricultural soils collected from the Mediterranean area of Santa Bàrbara, Tarragona (Branco et al., 2005). The difference in *Actinobacteria* relative abundance may be due to the diverse methods used. Further, *Iamia* and *Arthrobacter*, as the most abundant genera of *Actinobacteria*, were sensitive to Cr in our study which are in line with a previous study where *Arthrobacter* was correlated with heavy metals (Ellis et al., 2003). Almost all samples contained similar amounts of *Chloroflexi* except for the CG site as *Chloroflexi* is a common phyla in aquatic ecosystems (Yamada and Sekiguchi, 2009). MiSeq sequencing data showed that the percentages of *Desulfobacter*, *Hydrogenophaga*, *Rhodoferrax*, *Thiobacillus*, *Azovibrio*, *Geobacter*, *Rhodobacter*, *Clostridium*, *Proteiniclasticum*, *PSB-M-3*, *Paludibacter*, *Flavobacterium*, *WCHB1-05*, *Anaerolinea*, and

*Methanosarcina* in the contaminated group were higher than those in the uncontaminated group (Figure 3B). These 15 genera showed a positive correlation with SCr (Table 3) which indicated they may have Cr remediation potential under diverse Cr pressure and could be regarded as indicators for Cr pollution. This result is in agreement with previous studies. *Desulfobacter*, *Hydrogenophaga*, and *Rhodobacter* were found to be correlated with trace heavy metals (Martins et al., 2009; Bier et al., 2015). As revealed by genome sequencing, *Rhodoferrax* was reported as a well-adapted bacteria that could deal with many environmental assaults including heavy metals, organic contamination, and oxidative stress (Risso et al., 2009). *Thiobacillus* could remove 100% of the Cr from tannery sludge after 8 days via bioleaching technology (Zhou et al., 2004). *Geobacter* and *Clostridium* are known to be involved in multiple metal reduction processes including Cr (VI), U (VI), and Fe (III) and perform *in situ* bioremediation at high levels of Cr contamination (Yu et al., 2016). *Proteiniclasticum* (6.66%) is one of the most abundant genera in the sediments of the Xiangjiang River, China, where Cr concentrations are 591–805 times of the national standard value (Zhu et al., 2013). *Anaerolinea* and *Methanosarcina* have also been reported in Cr contaminated environment (Somenahally et al., 2013; Yu et al., 2016). Although *Azovibri*, *PSB-M-3*, *Flavobacterium*, and *WCHB1-05* have not been reported in Cr-contaminated environments, they have been found under the pressure of other contaminants such as linear alkylbenzenesulfonate, nonylphenol, Cd, and petroleum (Allen et al., 2007; Kuffner et al., 2008; Rajbanshi, 2009; Macedo et al., 2015; Wang Z. et al., 2015). In contrast, the uncontaminated group contained different dominant bacteria such as *Skermanella*, *Iamia*, *Arthrobacter*, and *Candidatus Nitrososphaera* which were negatively correlated with Cr (Table 3). The microbial community structures in the riparian soil samples of these six sites are generally shaped by the severity of Cr contamination and some of the details from the microbial community data could be Cr indicators in the Gansu industrial reach of the Yellow River.

In this study, the combined analysis of microbial community structure and function provided a comprehensive insight into evaluating the severity of heavy metal contamination situations. Although the severity of Cr contamination could be assessed depending on microbial community function alone, microbial

community structure analysis is also indispensable. Through the analysis of microbial community structure, not only the instant microbial composition was revealed but also the Cr indicators could be identified. In conclusion, combined microbial community composition and phenotypic function identification are potentially valuable for evaluating the severity of Cr contamination in the Gansu industrial reach of the Yellow River. Although bioinformatics analysis and functional verification showed Cr remediating microbes in this study, their molecular mechanisms should be clarified. Thus, further research should be aimed at the genera positively correlated with Cr and elucidation of their mechanisms related to genes which adapted to Cr contamination via metagenomic and metatranscriptomic approaches.

## AUTHOR CONTRIBUTIONS

YP did most of the experiments, analyzed data, and contributed to writing and revising the manuscript. ZY extracted DNA of soil samples and contributed to analyzing data, and revising the manuscript. JJ helped with detecting physicochemical properties of soils. AK contributed to revising the manuscript. XL provided overall directions and contributed to revising the manuscript. All authors approved submission of this manuscript to *Frontiers in Microbiology*.

## ACKNOWLEDGMENTS

The present study was supported by the National Natural Science Foundation (Nos. 31470224 and 31400430); MOST International Cooperation (No. 2014DFA91340) and Gansu Provincial International Cooperation (No. 1504WKCA089-2).

## SUPPLEMENTARY MATERIAL

The Supplementary Material for this article can be found online at: <https://www.frontiersin.org/articles/10.3389/fmicb.2018.00038/full#supplementary-material>

## REFERENCES

- Akçay, H., Oğuz, A., and Karapire, C. (2003). Study of heavy metal pollution and speciation in Buyak Menderes and Gediz river sediments. *Water Res.* 37, 813–822. doi: 10.1016/S0043-1354(02)00392-5
- Al-Kayssi, A. (2002). Spatial variability of soil temperature under greenhouse conditions. *Renew. Energy* 27, 453–462. doi: 10.1016/S0960-1481(01)00132-X
- Allen, J. P., Atekwana, E. A., Atekwana, E. A., Duris, J. W., Werkema, D. D., and Rossbach, S. (2007). The microbial community structure in petroleum-contaminated sediments corresponds to geophysical signatures. *Appl. Environ. Microbiol.* 73, 2860–2870. doi: 10.1128/AEM.01752-06
- Bai, J., Huang, L., Yan, D., Wang, Q., Gao, H., Xiao, R., et al. (2011a). Contamination characteristics of heavy metals in wetland soils along a tidal ditch of the Yellow River Estuary, China. *Stoch. Environ. Res. Risk Assess.* 25, 671–676. doi: 10.1007/s00477-011-0475-7
- Bai, J., Xiao, R., Cui, B., Zhang, K., Wang, Q., Liu, X., et al. (2011b). Assessment of heavy metal pollution in wetland soils from the young and old reclaimed regions in the Pearl River Estuary, South China. *Environ. Pollut.* 159, 817–824. doi: 10.1016/j.envpol.2010.11.004
- Bao, Q.-S., Lu, C.-Y., Song, H., Wang, M., Ling, W., Chen, W.-Q., et al. (2009). Behavioural development of school-aged children who live around a multi-metal sulphide mine in Guangdong province, China: a cross-sectional study. *BMC Public Health* 9:217. doi: 10.1186/1471-2458-9-217
- Bier, R. L., Voss, K. A., and Bernhardt, E. S. (2015). Bacterial community responses to a gradient of alkaline mountaintop mine drainage in Central Appalachian streams. *ISME J.* 9, 1378–1390. doi: 10.1038/ismej.2014.222
- Branco, R., Chung, A.-P., Verissimo, A., and Morais, P. V. (2005). Impact of chromium-contaminated wastewaters on the microbial community of a river. *FEMS Microbiol. Ecol.* 54, 35–46. doi: 10.1016/j.femsec.2005.02.014
- Desai, C., Parikh, R. Y., Vaishnav, T., Shouche, Y. S., and Madamwar, D. (2009). Tracking the influence of long-term chromium pollution on soil bacterial

- community structures by comparative analyses of 16S rRNA gene phylotypes. *Res. Microbiol.* 160, 1–9. doi: 10.1016/j.resmic.2008.10.003
- Ellis, R. J., Morgan, P., Weightman, A. J., and Fry, J. C. (2003). Cultivation-dependent and-independent approaches for determining bacterial diversity in heavy-metal-contaminated soil. *Appl. Environ. Microbiol.* 69, 3223–3230. doi: 10.1128/AEM.69.6.3223-3230.2003
- Epelde, L., Lanzen, A., Blanco, F., Urlich, T., and Garbisu, C. (2015). Adaptation of soil microbial community structure and function to chronic metal contamination at an abandoned Pb-Zn mine. *FEMS Microbiol. Ecol.* 91, 1–11. doi: 10.1093/femsec/fiu007
- Fan, M., Lin, Y., Huo, H., Liu, Y., Zhao, L., Wang, E., et al. (2016). Microbial communities in riparian soils of a settling pond for mine drainage treatment. *Water Res.* 96, 198–207. doi: 10.1016/j.watres.2016.03.061
- Giller, K. E., Witter, E., and Mcgrath, S. P. (2009). Heavy metals and soil microbes. *Soil Biol. Biochem.* 41, 2031–2037. doi: 10.1016/j.soilbio.2009.04.026
- Havlin, J. L., and Westfall, D. G. (1985). Potassium release kinetics and plant response in calcareous soils. *Soil Sci. Soc. Am. J.* 49, 366–370. doi: 10.2136/sssaj1985.03615995004900020019x
- He, M., Li, X., Liu, H., Müller, S. J., Wang, G., and Rensing, C. (2011). Characterization and genomic analysis of a highly chromate resistant and reducing bacterial strain *Lysinibacillus fusiformis* ZC1. *J. Hazard. Mater.* 185, 682–688. doi: 10.1016/j.jhazmat.2010.09.072
- Hu, B., Li, J., Bi, N., Wang, H., Yang, J., Wei, H., et al. (2015). Seasonal variability and flux of particulate trace elements from the Yellow River: impacts of the anthropogenic flood event. *Mar. Pollut. Bull.* 91, 35–44. doi: 10.1016/j.marpolbul.2014.12.030
- Huang, H., Wu, K., Khan, A., Jiang, Y., Ling, Z., Liu, P., et al. (2016). A novel *Pseudomonas gessardii* strain LZ-E simultaneously degrades naphthalene and reduces hexavalent chromium. *Bioresour. Technol.* 207, 370–378. doi: 10.1016/j.biortech.2016.02.015
- Hudson, B. D. (1994). Soil organic matter and available water capacity. *J. Soil Water Conserv.* 49, 189–194.
- Kuffner, M., Puschenreiter, M., Wieshammer, G., Gorfer, M., and Sessitsch, A. (2008). Rhizosphere bacteria affect growth and metal uptake of heavy metal accumulating willows. *Plant Soil* 304, 35–44. doi: 10.1007/s11104-007-9517-9
- Kumpiene, J., Lagerkvist, A., and Maurice, C. (2008). Stabilization of As, Cr, Cu, Pb and Zn in soil using amendments—a review. *Waste Manage.* 28, 215–225. doi: 10.1016/j.wasman.2006.12.012
- Liao, J., Wen, Z., Ru, X., Chen, J., Wu, H., and Wei, C. (2016). Distribution and migration of heavy metals in soil and crops affected by acid mine drainage: public health implications in Guangdong Province, China. *Ecotoxicol. Environ. Saf.* 124, 460–469. doi: 10.1016/j.ecoenv.2015.11.023
- Liu, C., Dong, X., and Liu, Y. (2015). Changes of NPP and their relationship to climate factors based on the transformation of different scales in Gansu, China. *CATENA* 125(Suppl. C), 190–199. doi: 10.1016/j.catena.2014.10.027
- Liu, C., Xu, J., Liu, C., Zhang, P., and Dai, M. (2009). Heavy metals in the surface sediments in Lanzhou Reach of Yellow River, China. *Bull. Environ. Contam. Toxicol.* 82, 26–30. doi: 10.1007/s00128-008-9563-x
- Luo, Y.-Q., Chen, Y.-P., Tao, L., Li, Y.-Q., and Wang, X.-M. (2011). Investigation and evaluation on heavy metals pollution in farmland soil in Lanzhou City. *J. Gansu Agric. Univ.* 46, 98–104.
- Ma, X., Zuo, H., Tian, M., Zhang, L., Meng, J., Zhou, X., et al. (2016). Assessment of heavy metals contamination in sediments from three adjacent regions of the Yellow River using metal chemical fractions and multivariate analysis techniques. *Chemosphere* 144, 264–272. doi: 10.1016/j.chemosphere.2015.08.026
- Macedo, T. Z., Okada, D. Y., Delforno, T. P., Braga, J. K., Silva, E. L., and Varesche, M. B. (2015). The comparative advantages of ethanol and sucrose as co-substrates in the degradation of an anionic surfactant: microbial community selection. *Bioprocess Biosyst. Eng.* 38, 1835–1844. doi: 10.1007/s00449-015-1424-5
- Martins, M., Faleiro, M. L., Barros, R. J., Verissimo, A. R., Barreiros, M. A., and Costa, M. C. (2009). Characterization and activity studies of highly heavy metal resistant sulphate-reducing bacteria to be used in acid mine drainage decontamination. *J. Hazard. Mater.* 166, 706–713. doi: 10.1016/j.jhazmat.2008.11.088
- Miao, Y., Liao, R., Zhang, X.-X., Wang, Y., Wang, Z., Shi, P., et al. (2015). Metagenomic insights into Cr (VI) effect on microbial communities and functional genes of an expanded granular sludge bed reactor treating high-nitrate wastewater. *Water Res.* 76, 43–52. doi: 10.1016/j.watres.2015.02.042
- Pattanapitpaisal, P., Brown, N., and Macaskie, L. (2001). Chromate reduction and 16S rRNA identification of bacteria isolated from a Cr (VI)-contaminated site. *Appl. Microbiol. Biotechnol.* 57, 257–261. doi: 10.1007/s002530100758
- Pradhan, S. K., Singh, N. R., Rath, B. P., and Thatoi, H. (2016). Bacterial chromate reduction: a review of important genomic, proteomic, and bioinformatic analysis. *Crit. Rev. Environ. Sci. Technol.* 46, 1659–1703. doi: 10.1080/10643389.2016.1258912
- Qiu, H. (2010). Studies on the potential ecological risk and homology correlation of heavy metal in the surface soil. *J. Agric. Sci.* 2, 194–201. doi: 10.5539/jas.v2n2p194
- R Core Team (2015). *R: A Language and Environment for Statistical Computing*. Vienna: R Foundation for Statistical Computing.
- Rajbanshi, A. (2009). Study on heavy metal resistant bacteria in Guheswori sewage treatment plant. *Our Nat.* 6, 52–57. doi: 10.3126/on.v6i1.1655
- Risso, C., Sun, J., Zhuang, K., Mahadevan, R., DeBoy, R., Ismail, W., et al. (2009). Genome-scale comparison and constraint-based metabolic reconstruction of the facultative anaerobic Fe (III)-reducer *Rhodospirillum rubrum*. *BMC Genomics* 10:447. doi: 10.1186/1471-2164-10-447
- Sang, B., Jie, Q., and Zheng-xue, M. (2012). Relationship between characteristics of algal community and water quality in Liujiaxia reservoir. *Adm. Tech. Environ. Monit.* 6:10.
- Sitters, J., Edwards, P. J., and Olde Venterink, H. (2013). Increases of soil C, N, and P pools along an acacia tree density gradient and their effects on trees and grasses. *Ecosystems* 16, 347–357. doi: 10.1007/s10021-012-9621-4
- Somenahally, A. C., Mosher, J. J., Yuan, T., Podar, M., Phelps, T. J., Brown, S. D., et al. (2013). Influence of hexavalent chromium on lactate-enriched Hanford groundwater microbial communities. *PLOS ONE* 8:e83909. doi: 10.1371/journal.pone.0083909
- Sun, M. Y., Dafforn, K. A., Brown, M. V., and Johnston, E. L. (2012). Bacterial communities are sensitive indicators of contaminant stress. *Mar. Pollut. Bull.* 64, 1029–1038. doi: 10.1016/j.marpolbul.2012.01.035
- Thatoi, H., Das, S., Mishra, J., Rath, B. P., and Das, N. (2014). Bacterial chromate reductase, a potential enzyme for bioremediation of hexavalent chromium: a review. *J. Environ. Manage.* 146, 383–399. doi: 10.1016/j.jenvman.2014.07.014
- Varol, M. (2011). Assessment of heavy metal contamination in sediments of the Tigris River (Turkey) using pollution indices and multivariate statistical techniques. *J. Hazard. Mater.* 195, 355–364. doi: 10.1016/j.jhazmat.2011.08.051
- Wang, W.-L., Xu, S.-Y., Ren, Z.-G., Tao, L., Jiang, J.-W., and Zheng, S.-S. (2015). Application of metagenomics in the human gut microbiome. *World J. Gastroenterol.* 21, 803–814. doi: 10.3748/wjg.v21.i3.803
- Wang, Z., Yang, Y., Dai, Y., and Xie, S. (2015). Anaerobic biodegradation of nonylphenol in river sediment under nitrate-or sulfate-reducing conditions and associated bacterial community. *J. Hazard. Mater.* 286, 306–314. doi: 10.1016/j.jhazmat.2014.12.057
- Wu, F., Dong, M., Liu, Y., Ma, X., An, L., Young, J. P. W., et al. (2010). Effects of long-term fertilization on AM fungal community structure and Glomalin-related soil protein in the Loess Plateau of China. *Plant Soil* 342, 233–247. doi: 10.1007/s11104-010-0688-4
- Wu, G., Sun, M., Liu, P., Zhang, X., Yu, Z., Zheng, Z., et al. (2014). *Enterococcus faecalis* strain LZ-11 isolated from Lanzhou reach of the Yellow River is able to resist and absorb cadmium. *J. Appl. Microbiol.* 116, 1172–1180. doi: 10.1111/jam.12460
- Wu, W., Chen, Y., Faisal, S., Khan, A., Chen, Z., Ling, Z., et al. (2016). Improving methane production in cow dung and corn straw co-fermentation systems via enhanced degradation of cellulose by cabbage addition. *Sci. Rep.* 6:33628. doi: 10.1038/srep33628
- Xiao, W., Yang, X., He, Z., and Li, T. (2014). Chromium-resistant bacteria promote the reduction of hexavalent chromium in soils. *J. Environ. Qual.* 43, 507–516. doi: 10.2134/jeq2013.07.0267

- Yamada, T., and Sekiguchi, Y. (2009). Cultivation of uncultured chloroflexi subphyla: significance and ecophysiology of formerly uncultured chloroflexi 'subphylum i' with natural and biotechnological relevance. *Microbes Environ.* 24, 205–216. doi: 10.1264/jsm2.ME09151S
- Yu, Y., Xu, J., Wang, P., Sun, H., and Dai, S. (2009). Sediment-porewater partition of polycyclic aromatic hydrocarbons (PAHs) from Lanzhou Reach of Yellow River, China. *J. Hazard. Mater.* 165, 494–500. doi: 10.1016/j.jhazmat.2008.10.042
- Yu, Z., He, Z., Tao, X., Zhou, J., Yang, Y., Zhao, M., et al. (2016). The shifts of sediment microbial community phylogenetic and functional structures during chromium (VI) reduction. *Ecotoxicology* 25, 1759–1770. doi: 10.1007/s10646-016-1719-6
- Yuan, H., Song, J., Li, X., Li, N., and Duan, L. (2012). Distribution and contamination of heavy metals in surface sediments of the South Yellow Sea. *Mar. Pollut. Bull.* 64, 2151–2159. doi: 10.1016/j.marpolbul.2012.07.040
- Zayre, I. G. A., Krachler, M., And, A. K. C., and Shotyk, W. (2006). Spatial distribution of natural enrichments of arsenic, selenium, and uranium in a minerotrophic peatland, Gola di Lago, Canton Ticino, Switzerland. *Environ. Sci. Technol.* 40, 6568–6574. doi: 10.1021/es061080v
- Zhang, W., Feng, H., Chang, J., Qu, J., Xie, H., and Yu, L. (2009). Heavy metal contamination in surface sediments of Yangtze River intertidal zone: an assessment from different indexes. *Environ. Pollut.* 157, 1533–1543. doi: 10.1016/j.envpol.2009.01.007
- Zhang, Y., Li, H., Gong, L., Dong, G., Shen, L., Wang, Y., et al. (2017). Nano-sized Fe<sub>2</sub>O<sub>3</sub>/Fe<sub>3</sub>O<sub>4</sub> facilitate anaerobic transformation of hexavalent chromium in soil–water systems. *J. Environ. Sci.* 57, 329–337. doi: 10.1016/j.jes.2017.01.007
- Zhou, L., Fang, D., Zhou, S., Wang, D., and Wang, S. (2004). Removal of Cr from tannery sludge by acidophilic Thiobacilli. *Huan Jing Ke Xue* 25, 62–66.
- Zhu, J., Zhang, J., Li, Q., Han, T., Xie, J., Hu, Y., et al. (2013). Phylogenetic analysis of bacterial community composition in sediment contaminated with multiple heavy metals from the Xiangjiang River in China. *Mar. Pollut. Bull.* 70, 134–139. doi: 10.1016/j.marpolbul.2013.02.023

**Conflict of Interest Statement:** The authors declare that the research was conducted in the absence of any commercial or financial relationships that could be construed as a potential conflict of interest.

Copyright © 2018 Pei, Yu, Ji, Khan and Li. This is an open-access article distributed under the terms of the Creative Commons Attribution License (CC BY). The use, distribution or reproduction in other forums is permitted, provided the original author(s) or licensor are credited and that the original publication in this journal is cited, in accordance with accepted academic practice. No use, distribution or reproduction is permitted which does not comply with these terms.



# Multiple Modes of Nematode Control by Volatiles of *Pseudomonas putida* 1A00316 from Antarctic Soil against *Meloidogyne incognita*

Yile Zhai<sup>1</sup>, Zongze Shao<sup>2</sup>, Minmin Cai<sup>1</sup>, Longyu Zheng<sup>1</sup>, Guangyu Li<sup>2</sup>, Dian Huang<sup>1</sup>, Wanli Cheng<sup>1</sup>, Linda S. Thomashow<sup>3</sup>, David M. Weller<sup>3</sup>, Ziniu Yu<sup>1</sup> and Jibin Zhang<sup>1\*</sup>

<sup>1</sup> State Key Laboratory of Agricultural Microbiology and National Engineering Research Center of Microbe Pesticides, College of Life Science and Technology, Huazhong Agricultural University, Wuhan, China, <sup>2</sup> Key Laboratory of Marine Biogenetic Resources, Third Institute of Oceanography, State Oceanic Administration, Xiamen, China, <sup>3</sup> Wheat Health, Genetics and Quality Research Unit, Agricultural Research Service, United States Department of Agriculture, Pullman, WA, United States

## OPEN ACCESS

### Edited by:

Ghiglione Jean-Francois,  
Centre National de la Recherche  
Scientifique (CNRS), France

### Reviewed by:

Birinchi Kumar Sarma,  
Banaras Hindu University, India  
Raquel Campos-Herrera,  
University of the Algarve, Portugal

### \*Correspondence:

Jibin Zhang  
zhangjb@mail.hzau.edu.cn

### Specialty section:

This article was submitted to  
Microbiotechnology, Ecotoxicology  
and Bioremediation,  
a section of the journal  
Frontiers in Microbiology

Received: 06 October 2017

Accepted: 31 January 2018

Published: 23 February 2018

### Citation:

Zhai Y, Shao Z, Cai M, Zheng L,  
Li G, Huang D, Cheng W,  
Thomashow LS, Weller DM, Yu Z  
and Zhang J (2018) Multiple Modes  
of Nematode Control by Volatiles  
of *Pseudomonas putida* 1A00316  
from Antarctic Soil against  
*Meloidogyne incognita*.  
*Front. Microbiol.* 9:253.  
doi: 10.3389/fmicb.2018.00253

*Pseudomonas putida* 1A00316 isolated from Antarctic soil showed nematicidal potential for biological control of *Meloidogyne incognita*; however, little was known about whether strain 1A00316 could produce volatile organic compounds (VOCs), and if they had potential for use in biological control against *M. incognita*. In this study, VOCs produced by a culture filtrate of *P. putida* 1A00316 were evaluated by *in vitro* experiments in three-compartment Petri dishes and 96-well culture plates. Our results showed that *M. incognita* juveniles gradually reduced their movement within 24–48 h of incubation with mortality ranging from 6.49 to 86.19%, and mostly stopped action after 72 h. Moreover, egg hatching in culture filtrates of strain 1A00316 was much reduced compared to that in sterile distilled water or culture medium. Volatiles from *P. putida* 1A00316 analysis carried out by solid-phase micro-extraction gas chromatography–mass spectrometry (SPME-GC/MS) included dimethyl-disulfide, 1-undecene, 2-nonanone, 2-octanone, (Z)-hexen-1-ol acetate, 2-undecanone, and 1-(ethenylloxy)-octadecane. Of these, dimethyl-disulfide, 2-nonanone, 2-octanone, (Z)-hexen-1-ol acetate, and 2-undecanone had strong nematicidal activity against *M. incognita* J2 larvae by direct-contact in 96-well culture plates, and only 2-undecanone acted as a fumigant. In addition, the seven VOCs inhibited egg hatching of *M. incognita* both by direct-contact and by fumigation. All of the seven VOCs repelled *M. incognita* J2 juveniles in 2% water agar Petri plates. These results show that VOCs from strain 1A00316 act on different stages in the development of *M. incognita* via nematicidal, fumigant, and repellent activities and have potential for development as agents with multiple modes of control of root-knot nematodes.

**Keywords:** *Pseudomonas putida* 1A00316, *Meloidogyne incognita*, chemotaxis, egg hatching, volatile organic compound, nematode control

## INTRODUCTION

Plant parasitic nematodes (PPNs) cause serious damage to a wide range of crops worldwide (Li et al., 2015). To date, more than 4100 species of PPNs have been described (Kyndt et al., 2014). Among these, the root-knot nematode (*Meloidogyne* spp.), found all over the world in tropical, subtropical, and temperate regions, is the most economically important plant nematode (Jones et al., 2013). The destruction caused by PPNs has been assessed to be more than 100–150 billion US dollars per year, of which more than half are due to *Meloidogyne* spp. (Nicol et al., 2011; Li et al., 2015; Kim et al., 2016). Among the *Meloidogyne* spp., *Meloidogyne incognita* is the most destructive because of its wide host range, including most flowering plants, as well as its short generation time, high reproduction rate, and ability to form complex diseases with other soil-borne pathogens such as fungi (Vos et al., 2013). *M. incognita* can infect the roots of over 2000 plant species and interferes with normal plant uptake of nutrients and water. Moreover, it causes physiological plant disorders (Jang et al., 2014), making it perhaps the most damaging of all crop pathogens (Trudgill and Blok, 2001). At present, the main method of controlling plant nematodes involves using chemical nematicides. However, these chemicals are toxic, have side effects against other organisms, and can adversely affect human health and the environment (Riga, 2011). The rotation and resistance of crop varieties are complementary strategies to control PPNs, but their effectiveness is limited (Jones et al., 2013). Therefore, new economical, effective, and environmentally friendly PPN controls are urgently needed.

Biological control is one such way to reduce pest losses, but more investigation on novel microorganisms in the environment is needed to speed the development of new agents for controlling root-knot nematodes (Li et al., 2016). These pathogens inhabit the soil and typically are infected with indigenous bacteria and fungi, suggesting the possibility of using microorganisms to control PPNs (Zhang et al., 2015). In fact, there are specific microorganisms in soil, such as nematophagous bacteria and fungi, which have complex strategies for capturing, killing, and digesting PPNs, and they often target a specific stage of the nematode life cycle (Li et al., 2015). Many secondary metabolites of microorganisms have nematicidal activity (NA) and therefore could become substitutes for highly toxic chemical nematicides. Through comparative genomic studies, isolation and purification, the nematicidal compounds alkaline metalloproteinase AprA and two metabolites, hydrogen cyanide and cyclo(L-Pro-L-Ile), were previously identified from *Pseudomonas putida* strain 1A00316 and shown to have good NA against *M. incognita* (Guo et al., 2016). *Bacillus cereus* strain S2 produced sphingosine and showed high NA against *M. incognita* (Gao et al., 2016). Moreover, *Purpureocillium lilacinum*, with the adjuvant avermectin, has been used effectively to control PPNs (Fisher, 1990; Kiewnick and Sikora, 2006).

*Pseudomonas* species are ubiquitous in nature and produce many secondary metabolites active against important plant pathogens (Giles et al., 2014). Members of the genus are physiologically and metabolically multifunctional, readily colonizing terrestrial and aquatic habitats such as soil, plants,

and water (Troxler et al., 2012). Among the species of this genus, *P. putida* has been isolated from many niches and survives in soil containing organic pollutants and heavy metals. For example, *P. putida* JMQS1 isolated from detergent-contaminated soil exhibited quorum sensing along with its ability to degrade phenol (Antony and Jayachandran, 2016). Some strains of *P. putida* inhabit the rhizosphere or are endophytes that promote plant growth, making them ideal for biocontrol. The nematicidal effects of *P. putida* against *M. incognita* were noted previously; strain 1A00316 isolated from Antarctic soil showed good inhibition of *M. incognita* *in vitro* and in pot experiments, with biocontrol efficiency of nematodes as high as 71.67%. In addition, strain 1A00316 itself could induce systematic resistance in tomato by increasing the activity of three defense enzymes: phenylalanine ammonia lyase, polyphenol oxidase, and peroxidase in tomato plants (Tang et al., 2014). Hydrogen cyanide and cyclo(L-Pro-L-Ile) also were identified from strain 1A00316 and exhibited NA against *M. incognita* (Guo et al., 2016), but little is known about whether volatile organic compounds (VOCs) are produced by the strain, or if they have potential for use in biological control against *M. incognita*.

Compared to solid nematicides, the greatest advantages of volatile nematicidal compounds are their good dispersibility and penetration in the soil. In the past, fumigants such as methyl bromide, which was used as nematicide, have been identified as contributing to the reduction of the ozone layer and overall poor air quality, so it is important to search for new green soil fumigation agents. Accordingly, this investigation focused on the identification and evaluation of VOCs from strain 1A00316. In the present study, we report (i) the identification the volatile compounds in the fermentation broth of *P. putida* 1A00316; and (ii) evaluation of their nematicidal, fumigation, and chemotaxis activities against *M. incognita*.

## MATERIALS AND METHODS

### Chemical Compounds

Dimethyl-disulfide and 2-nonanone were purchased from TCI (Shanghai, China) with a purity >98%. 1-undecene (>99.5%), 2-octanone (>99%), (Z)-hexen-1-ol acetate (99%), and 1-(ethenyloxy)-octadecane (90%) were purchased from Yuan Ye (Shanghai, China). 2-undecanone was purchased from Sigma Aldrich (Shanghai, China) with a purity >99%. Methanol, Tween-20 and activated charcoal were purchased from Sinopharm Chemical Reagent Company (Shanghai, China).

### Collection of *M. incognita* Eggs and Second-Stage Juveniles and Propagation of *Caenorhabditis elegans*

*Meloidogyne incognita* eggs were collected from the roots of infested tomato plants (*Solanum lycopersicum* L.), which were previously infected with the nematodes in the greenhouse at 23–26°C, and relative humidity 40–60%. The tomato plants were watered manually once a day. After 45 days, the plants were uprooted, the roots were rinsed free of soil with tap water, and

the egg masses were picked into a bottle with a dissecting needle (Lee et al., 2014). After shaking the egg mass with 1% NaOCl (sodium hypochlorite) solution by hand in the bottle for 3 min, the solution was passed in turn through a series of filters with pore sizes of 74, 45, and 25  $\mu\text{m}$ , and the sterilized eggs were collected from the 25- $\mu\text{m}$  filter by spraying with sterile distilled water (SDW; Seo et al., 2013). Second-stage juveniles of *M. incognita* were obtained by using a modified Baermann funnel method under sterile conditions (Barker et al., 1985; Southey, 1986). *Caenorhabditis elegans* N2 (Bristol, wild type), was purchased from the Caenorhabditis Genetics Center (CGC). *C. elegans* was maintained at 20°C on nematode growth medium plates seeded with *Escherichia coli* OP50.

### Preparation of Fermentation Broth of Strain *P. putida* 1A00316

Strain 1A00316 was isolated from Antarctic soil and identified as *P. putida* by sequence homology of the 16S rDNA and physiological and biochemical characteristics (Tang et al., 2014). The strain was cultured in 30-mL flasks containing 15 mL of 2216E broth (Morisaki et al., 1999) prepared from 10 g peptone, 5 g yeast powder, 1 g beef extract, 0.1 g ferric citrate, 1 g sodium acetate, 19.45 g NaCl, 0.75 g MgCl<sub>2</sub>, 0.75 g MgSO<sub>4</sub>, 1 g CaCl<sub>2</sub>, 0.55 g KCl, 0.16 g NaHCO<sub>3</sub>, 0.08 g KBr, 34 mg SrCl<sub>2</sub>, 22 mg H<sub>3</sub>BO<sub>3</sub>, 4 mg Na<sub>2</sub>SiO<sub>3</sub>, 2.4 mg NaF, 8 mg Na<sub>2</sub>HPO<sub>4</sub>, 0.5 mg MnCl<sub>2</sub>, 0.5 mg CuSO<sub>4</sub>, and 10 mg ZnSO<sub>4</sub> and adjusted to a pH value of 7.6–7.8. A seed culture was incubated at 28°C, shaken at 180 rpm, and 1% seed liquid (2.5 mL) was transferred after 18 h, to 500-mL flasks containing 250 mL of 2216E medium. The cultures were shaken as above for 48 h and then centrifuged at 4225  $\times g$  for 10 min at 4°C to obtain the supernatant, which was passed through a 0.22- $\mu\text{m}$  filter to remove bacterial cells. The filtrates were used at the original concentration and diluted 1/3, 1/5, 1/10, 1/15, and 1/20 with SDW.

### Nematicidal Activity of Volatiles

A three-compartment Petri plate (Figure 1A; 85 mm diameter; Fernando et al., 2005) was used to study the NA of bacterial VOCs. Three milliliters of the original culture filtrate was added into one compartment and 200 nematodes of either *M. incognita* or *C. elegans* were introduced onto the surface of layers of 2% water agar (WA) in the other two compartments. Control plates contained uninoculated 2216E medium in place of the culture filtrate. Plate lids were immediately sealed with Parafilm (Bemis) to avoid escape of the volatiles, and the plates were incubated at 28°C in the dark. There were three replicates for each treatment and the experiments were repeated twice. After 24, 48, and 72 h, the numbers of mobile and immobile nematodes were counted under a dissecting microscope (Jiang Nan JS25B).

In order to confirm the NA of bacterial VOCs produced by strain 1A00316, activated charcoal was introduced into one of the three compartments and culture supernatant and nematodes were added to each of the other two compartments of the Petri plate (Figure 1B; Gu et al., 2007). The activated charcoal can adsorb volatiles, blocking their activity and resulting in no loss of nematode viability. At the same time, 100 eggs

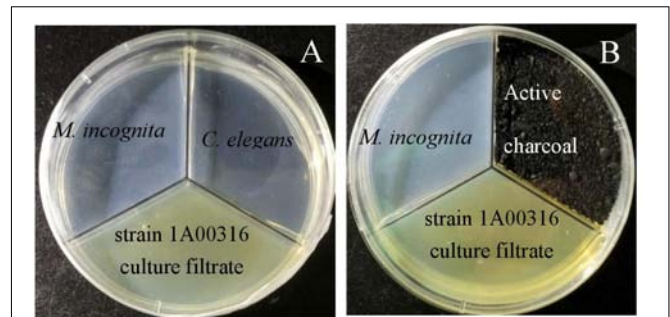


FIGURE 1 | Nematicidal activity of *P. putida* strain 1A00316 in Petri plates (A,B).

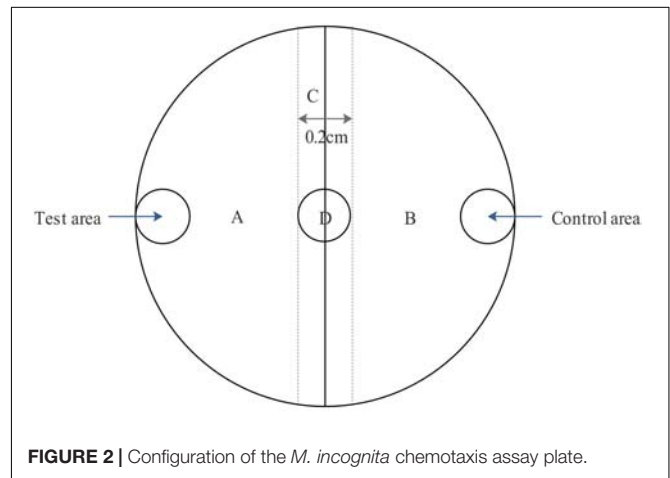
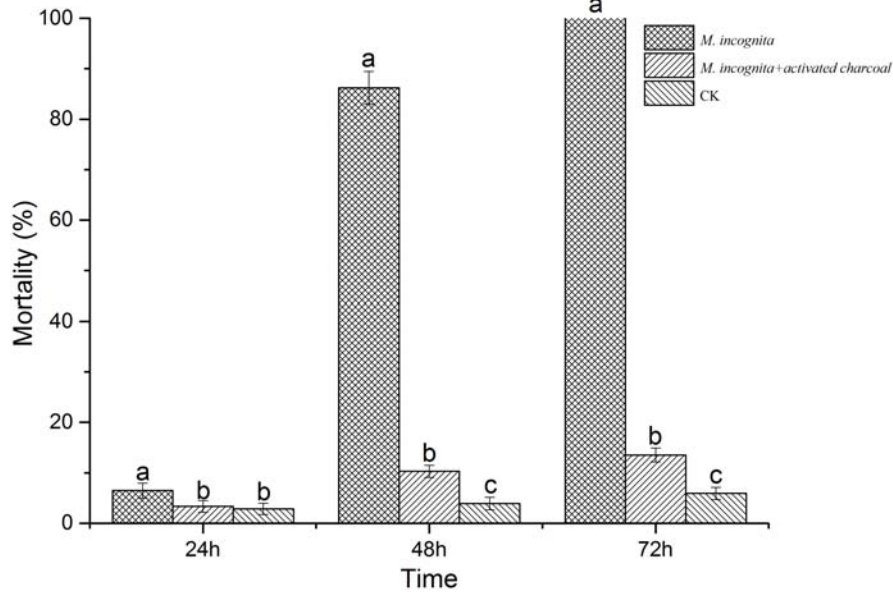


FIGURE 2 | Configuration of the *M. incognita* chemotaxis assay plate.

of *M. incognita* were immersed in 100  $\mu\text{L}$  of SDW in wells of 96-well tissue culture plates surrounded by four adjacent wells containing culture filtrate of strain 1A00316. SDW and 2216E media in the surrounding wells served as controls. The experiment was repeated three times. The numbers of eggs hatching were counted after 2, 4, 6, 8, and 10 days of exposure with an inverted microscope (XDS-1B COIC, Chongqing Mike Photoelectric Instrument Limited Company, China).

### Identification of Volatiles from Strain 1A00316

Strain 1A00316 was cultured for 48 h as described above, and volatiles were collected and analyzed by using SPME-GC/MS (Azenha and Vasconcelos, 2002; Diaz et al., 2004). Fiber (65  $\mu\text{m}$  PDMS/DVB fiber, Supelco, Bellefonte, PA, United States) used for SPME was first preconditioned with helium at 250°C for 20 min. The extractions were performed in 20-mL headspace vials (22.5 mm  $\times$  75.5 mm) filled with 9 mL fermentation broth and a magnetic stirring bar. The vials were fixed inside a thermostatic water bath and samples were equilibrated at 60°C for 1 h. The VOCs from 9 mL 2216E medium were used as controls. After the extraction, the fiber was inserted into the injection port of a gas chromatograph [Hewlett-Packard (HP) 7890A] coupled with a mass spectrometer (HP 5975C, Agilent Technologies,



**FIGURE 3** | Nematicidal effects of strain 1A00316 VOCs against *M. incognita* in a three-compartment Petri plate. Values with the same lowercase letters do not differ from each other at  $P < 0.05$ ; bars indicate the standard error of the means ( $n = 3$ ).

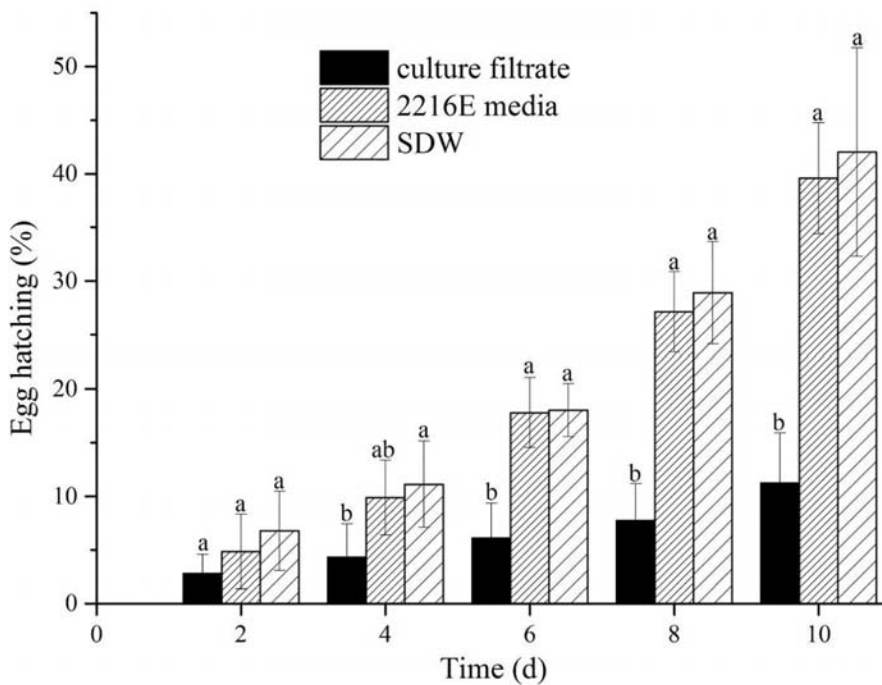
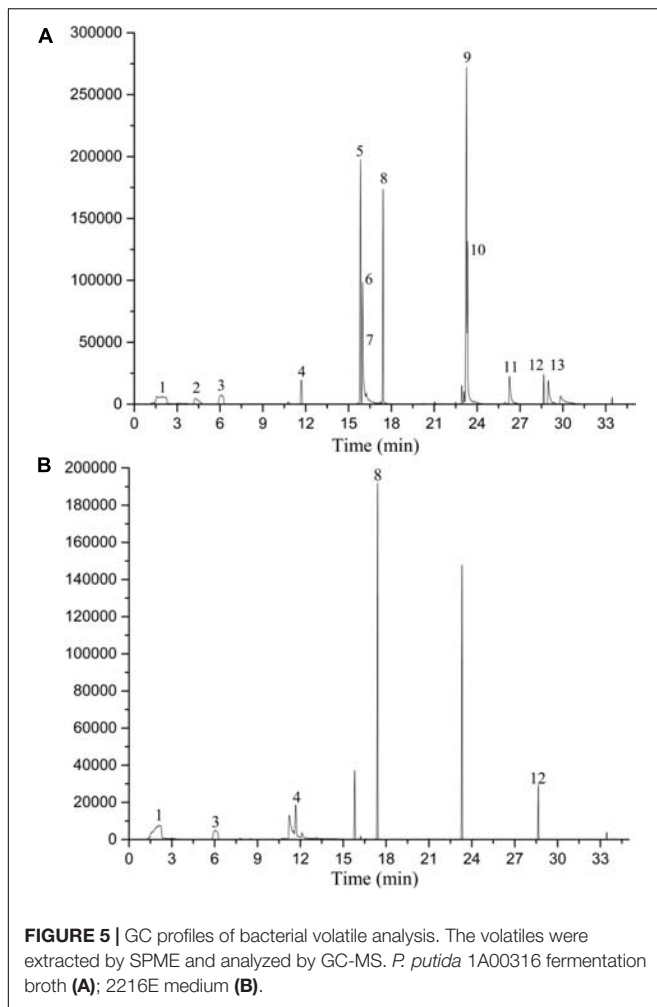


**FIGURE 4** | Fumigation effects of original culture filtrates on egg hatching of *M. incognita* after 2, 4, 6, 8, and 10 days of incubation. Values with the same lowercase letters do not differ from each other at  $P < 0.05$ ; bars indicate the standard error of the means ( $n = 4$ ).

United States) and desorbed for 5 min at 250°C (Gu et al., 2007). The chromatographic separation was performed on a HP-5MS (30 m × 0.25 mm) × 0.25 μL column and helium was used as the carrier gas at a constant flow of 1 mL/min. The column was held at 40°C for 2 min, then increased to 180°C at a rate of 4°C/min,

held for 0 min, then increased to 240°C at a rate of 5°C/min, and held for 6 min. The MS detector was programmed as follows: EI ion source operating at 70 eV, acquisition range between  $m/z$  35 and 550. The temperature of the transfer line and iron trap were 250 and 300°C, respectively. The identification of a volatile



compound was based on a comparison of the substance with GC/MS system data banks (NIST 08 Library). Each sample was tested twice.

## Nematicidal Activity of Commercial VOCs

The NA of commercial VOCs was tested against *M. incognita* J2 larvae at a dose range of 10–1000 mg/L, and the 50% lethal concentration (LC<sub>50</sub>) values were calculated. Stock solutions of pure compounds were prepared in methanol to overcome insolubility, whereas aqueous Tween-20 (0.3% v/v) was used for further dilution. Test solutions (200 μL) at various concentrations were added to detachable 96-well tissue culture plates and a suspension of 40–50 J2 juveniles was added to each well. SDW and a mixture of methanol and Tween-20 served as controls (Aissani et al., 2013). Plate lids were sealed with Parafilm to avoid evaporation and plates were kept at 20°C in the dark. Juveniles in solutions of VOCs were observed with the aid of an inverted microscope after 24, 48, and 72 h and were categorized as either motile or immotile/paralyzed. The experiments were performed three times, and every treatment was replicated three times.

## Fumigant Activity of VOCs against J2

The various commercial VOCs were introduced into one well in 96-well tissue culture plates surrounded by four wells containing 50 nematode J2 juveniles suspended in distilled water. SDW and a mixture of methanol and Tween-20 served as controls. Percentages of nematode death were recorded in response to the fumigant activity of the VOCs in the adjacent wells. Assessments were made at 24, 48, and 72 h (Ntalli et al., 2011). The experiments were performed three times, and every treatment was replicated three times.

## Effect of VOCs on Egg Hatching

Whether VOCs could inhibit egg hatching of *M. incognita* was tested over a dose range of 20–1000 mg/L. One hundred eggs of *M. incognita* suspended in 10 μL SDW were introduced into detachable 96-well tissue culture plates and combined with 200 μL of a range of concentrations of commercial VOCs. SDW as well as a mixture of methanol and Tween-20 served as controls. Each treatment had three replicates and the experiments were repeated twice.

At the same time, 100 eggs of *M. incognita* in 100 μL SDW were introduced into wells of 96-well tissue culture plates and surrounded by four wells containing 200 μL of one of the VOCs at 1000 μg/mL. SDW and 2216E media served as controls. Plate lids were sealed with Parafilm and plates were incubated in the dark at 20°C. The numbers of J2 hatchings were counted after 2, 4, 6, 8, and 10 days of exposure under the inverted microscope and hatch rate was measured. Each treatment had four replicates and the experiments were repeated twice.

## Chemotaxis of J2 Nematodes to Culture Filtrate and VOCs

Chemotaxis was assessed on Petri plates containing 2% WA (Tajima et al., 2001). A 5 mm filter paper disc immersed in various concentrations of culture filtrate or solutions of volatile substances was placed on the test area (A) of 35 mm Petri dishes, while a filter paper immersed in 2216E medium or a mixture of methanol and Tween-20 was added to the opposite side of the plate (area B) as a control (Figure 2). Subsequently, 150 J2 juveniles of *M. incognita* were added to the center (area D) of the Petri dish, and the dish was incubated in a dark cabinet at 20°C for 8 h (Hu et al., 2012). The numbers of J2s in areas A and B

**TABLE 1** | GC/MS analysis of *P. putida* 1A00316 fermentation broth.

Compound	RT (min)	Relative (%)	Mw	Peak number
Dimethyl-disulfide	4.3677	1.2082	94.20	2
1-Undecene	15.8418	17.5697	154.29	5
2-Nonanone	15.9762	11.7213	142.24	6
2-Octanone	16.2363	1.0448	128.21	7
(Z)-Hexen-1-ol acetate	22.9257	1.2278	325.29	9
2-Undecanone	23.2595	26.8984	170.29	10
1-(Ethenyloxy)-octadecane	26.2596	3.5459	296.53	11
(Z)-3-decen-1-ol acetate	28.9821	3.4962	198.30	13

were then counted under a dissecting microscope to calculate the chemotaxis index (C.I.; Saeki et al., 2001), calculated after 8 h as.

$$\text{C.I.} = \frac{(\text{the number of nematodes in test area} - \text{the number of nematodes in control area})}{(\text{the number of nematodes in test area} + \text{the number of nematodes in control area})}$$

For  $0 < \text{C.I.} < 1$ , *M. incognita* was attracted to the tested sample; if  $-1 < \text{C.I.} < 0$ , the tested sample repelled *M. incognita*; and if  $\text{C.I.} = 0$ , the sample had no effect on the nematode. Experiments were performed in triplicate, and treatments were replicated three times.

## Data Analysis and Statistics

Mortality values for *in vitro* bioassays against *M. incognita* were corrected by Abbott's formula (Abbott, 1925). The  $\text{LC}_{50}$  was calculated by Probit analysis. Data from the chemotaxis assay were analyzed using a homogeneity test of variance. If the variance was homogeneous ( $P \leq 0.05$ ), a paired Student's *t*-test was chosen; otherwise, the Wilcoxon rank sum test was used. Data from all assays except the chemotaxis assay were analyzed by one-way variance with SPSS 20. Means among treatments were compared by Fisher's least significant difference (LSD) test at the  $P = 0.05$  level.

## RESULTS

### Nematicidal Effects of Strain 1A00316 VOCs

We evaluated effects of VOCs produced by culture filtrate on *M. incognita* J2s by the three-compartment Petri plate method. Juveniles of *M. incognita* gradually reduced movement within 24–48 h and mostly were immobile after 72 h of incubation, with mortality ranging from 6 to 100% (Figure 3). We also found that strain 1A00316 had strong NA ( $\geq 80\%$ ) against *M. incognita* J2 juveniles, but not to *C. elegans* (Supplementary Table S1), indicating that *C. elegans* was not sensitive to these VOCs. Moreover, most of the VOCs were adsorbed in the plates containing activated charcoal, and NA values decreased from 86% to less than 10%. In addition, neither culture filtrate nor 2216E medium affected egg hatching after 2 and 4 days, although hatching slowly declined after 6 days, and reached

11.24% at 10 days, a value significantly less than control values in SDW or 2216E medium (Figure 4). These results suggest that the culture filtrate of strain 1A00316 contains VOCs that kill nematodes and inhibit egg hatching, and they are consistent with the hypothesis that VOCs from strain 1A00316 are responsible for the NA.

### Nematicidal Activity of Commercial VOCs against J2 Nematodes

According to GC-MS analysis (Figure 5), eight VOCs (peak area  $>1\%$ ) from strain 1A00316 fermentation broth accounted for 66.71% of the total area and were identified by SPME-GC/MS as dimethyl-disulfide, 1-undecene, 2-nonanone, 2-octanone, (Z)-hexen-1-ol acetate, 2-undecanone, 1-(ethenylloxy)-octadecane, and (Z)-3-decen-1-ol acetate (Table 1). Commercially available VOCs with similarity index  $>850$  from the database search were chosen to test NA.

With the aim of exploring the potency of seven of these VOCs [(Z)-3-decen-1-ol acetate was not commercially available], their NA was tested on juveniles of *M. incognita in vitro*. 2-Octanone, (Z)-hexen-1-ol acetate, and 2-undecanone were the most active, showing  $\text{LC}_{50}$  values at 24 and 48 h of 23.714 and 22.712 mg/L, 33.922 and 32.351 mg/L, and 27.810 and 22.872 mg/L, respectively. The results of dimethyl-disulfide and 2-nonanone were 139.082 and 134.330 mg/L and 70.977 and 63.320 mg/L, respectively. 1-Undecene and 1-(ethenylloxy)-octadecane were not active at the tested concentration (Table 2). Interestingly, only 2-undecanone had fumigation activity against *M. incognita*, with an  $\text{LC}_{50}$  value at 48 h of 185.298 mg/L and an  $\text{LC}_{90}$  of 672.244 mg/L. Other identified VOCs had no fumigation activity against *M. incognita* even at 2000 mg/L (Supplementary Table S2).

### Effect of Commercial VOCs on Egg Hatching of *M. incognita*

The effect of the seven commercial organic compounds was measured *in vitro* by direct-contact. The results of the tested concentrations suggested that all seven VOCs had adverse effects on egg hatching of *M. incognita* (see Supplementary Tables S3–S9). (Z)-hexen-1-ol acetate at concentrations from

**TABLE 2** |  $\text{LC}_{50}$  and FL values of commercial nematicidal compounds against *M. incognita*.

Compound	24 h		48 h	
	$\text{LC}_{50}$ (mg/L)	FL (mg/L)	$\text{LC}_{50}$ (mg/L)	FL (mg/L)
Dimethyl-disulfide	139.082	No	134.330	No
1-Undecene	$>1000$		$>1000$	
2-Nonanone	70.977	59.638–81.071	63.320	53.249–72.183
2-Octanone	23.714	1.134–39.489	22.712	19.852–25.280
(Z)-Hexen-1-ol acetate	33.922	28.875–39.180	32.351	28.021–36.826
2-Undecanone	27.810	24.887–31.022	22.872	20.078–25.678
1-(Ethenylloxy)-octadecane	$>1000$		$>1000$	
(Z)-3-decen-1-ol acetate	ND		ND	

FL, fiduciary limits; ND, not determined.

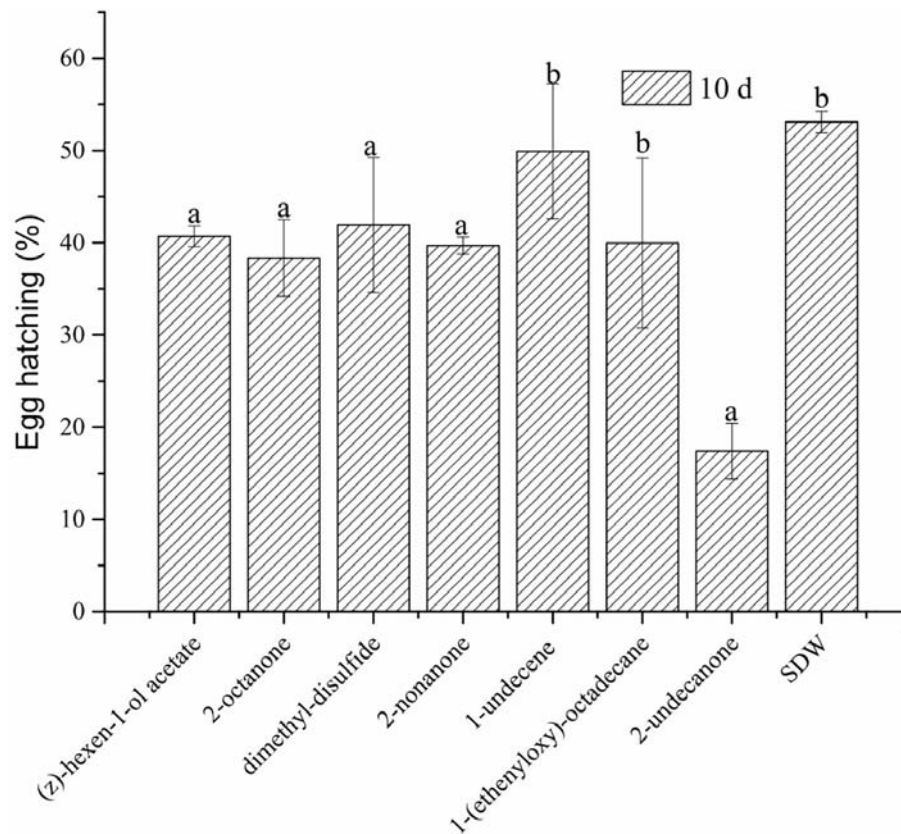


**FIGURE 6 |** Effects of seven VOCs on egg hatching of *M. incognita* after 10 days in direct-contact (Z)-hexen-1-ol acetate, 2-octanone, dimethyl-disulfide and 2-nonanone at 200 mg/L, 1-undecene and 1-(ethenyl-oxy)-octadecane at 250 mg/L, 2-undecanone at 40 mg/L. Values with the same lowercase letters do not differ from each other at  $P < 0.05$ ; bars indicate the standard error of the means ( $n = 3$ ).

100 to 200 mg/L, 2-octanone at 200 mg/L, and dimethyl-disulfide and 2-nonanone from 50 to 200 mg/L slightly but significantly inhibited egg hatching, and 1-undecene at from 500 to 1000 mg/L and 1-(ethenyl-oxy)-octadecane at 1000 mg/L also inhibited egg hatching (Supplementary Tables S3–S9). Compared to SDW (Figure 6), (Z)-hexen-1-ol acetate, 2-octanone, dimethyl-disulfide, and 2-nonanone at 200 mg/L showed good inhibition of egg hatching, but 1-undecene and 1-(ethenyl-oxy)-octadecane at 200 mg/L showed no significant difference. Conversely, 2-undecanone at 40 mg/L was strongly inhibitory to egg hatching. We also determined whether the seven VOCs had volatile activity against egg hatching of *M. incognita*. Compared to SDW, the seven VOCs did not inhibit egg hatching after 2, 4, and 6 days of exposure, but egg hatching slowly declined after 8 days, consistent with slight ability to inhibit the egg hatching of *M. incognita* (Figure 7).

### Chemotaxis of Culture Filtrates and VOCs by J2 Juveniles of *M. incognita*

Chemotaxis of culture filtrates from strain 1A00316 is presented in Figure 8. The results show that the higher concentrations of culture filtrates (original concentration and 1/3 original

concentration) immobilized J2 nematodes ( $-1 < \text{C.I.} < 0$ ) and acted as an attractant ( $0 < \text{C.I.} < 1$ ) at from 1/5 to 1/20 original concentration. Interestingly, many nematodes were found in the test area (A), and the seven VOCs at concentrations of 1–10,000 mg/L showed C.I. ranging from  $-1$  to  $0$  (Table 3). These results indicated that the seven VOCs repelled *M. incognita* J2 juveniles. Among them, the C.I. of different concentrations of (Z)-hexen-1-ol acetate, dimethyl-disulfide, and 2-nonanone showed no significant difference from the control. However, with the increase of concentration of 2-octanone, 1-undecene, 1-(ethenyl-oxy)-octadecane, and 2-undecanone, the absolute value of the C.I. gradually increased and the four VOCs had greater ability to repel nematodes. Comparing the C.I. of all seven VOCs at different concentrations, we found that 2-undecanone showed the greatest effect, with a C.I. value of  $-0.725$  at 10,000  $\mu\text{g/mL}$ .

### DISCUSSION

In a preliminary experiment, different concentrations of culture filtrate from strain 1A00316 were added to 96- or 24-well tissue culture plates to test NA against eggs or J2 juveniles of *M. incognita*. This work showed effects

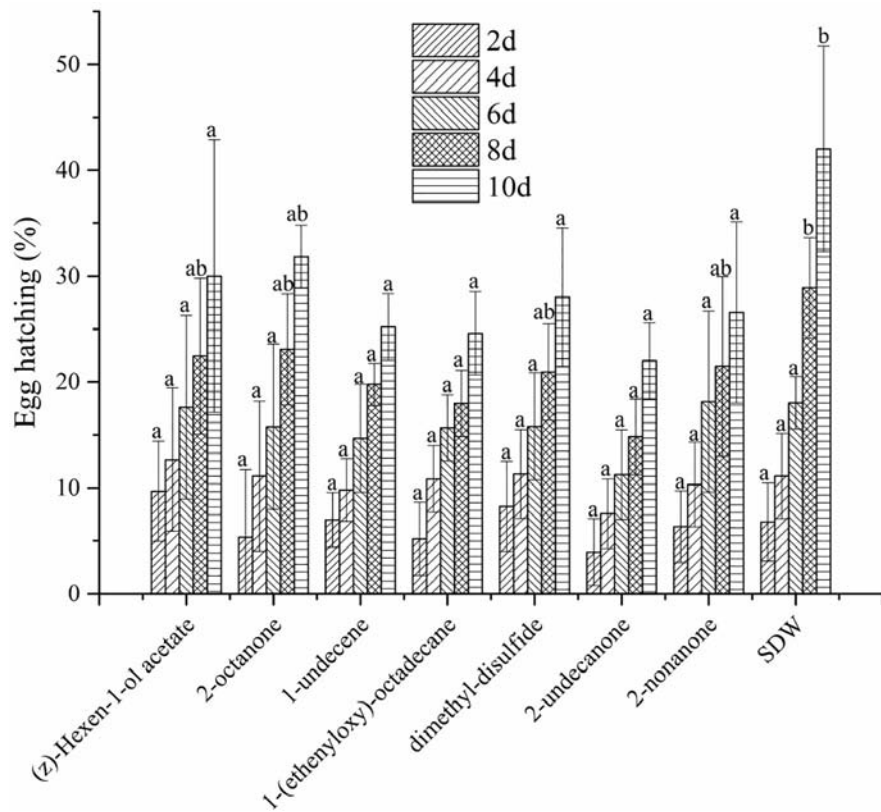


**FIGURE 7 |** Fumigation by seven VOCs at 1000 mg/L on egg hatching of *M. incognita* after 2, 4, 6, 8, and 10 days of incubation. Values with the same lowercase letters do not differ from each other at  $P < 0.05$ ; bars indicate the standard error of the means ( $n = 4$ ).

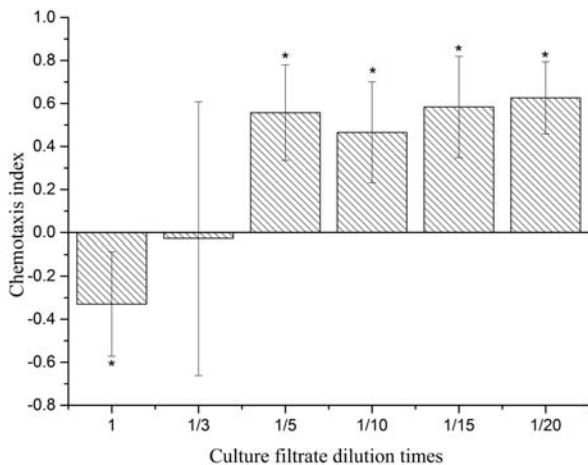


**FIGURE 8 |** Chemotaxis of *M. incognita* J2 to 1A00316 culture filtrates. Values with the \* do not differ from each other at  $P < 0.05$ , they means the side of the number of attracting or avoiding nematodes is significantly different from another side; bars indicate the standard error of the means ( $n = 3$ ).

The egg hatching in different 24-well plates containing 150 eggs, with SDW coexisting with different concentrations of culture filtrate in other wells, had significantly different inhibition effects on egg hatching after 10 days (Supplementary Figure S1). These results suggested that VOCs could contribute to the decrease in egg hatching in culture filtrates of strain 1A00316.

Based on the above experiment, we hypothesized that strain 1A00316 may produce volatiles to kill *M. incognita* J2 juveniles and inhibit egg hatching, and that there may be multiple modes of nematode control of *M. incognita*.

Subsequently, we identified eight VOCs with SPME-GC/MS analysis: dimethyl-disulfide, 2-nonanone, 2-undecanone, 2-octanone, 1-undecene, 1-(ethenyloxy)-octadecane, and (Z)-hexen-1-ol acetate. Dimethyl-disulfide, 2-nonanone, and 2-undecanone exhibited strong NA (NAs > 80%) against both juveniles and eggs at a concentration of 0.5 mmol by fumigation after 7 days of exposure (Huang et al., 2010). In another study, dimethyl-disulfide had the strongest NA ( $LC_{90} = 0.162$  mmol/L) against *Bursaphelenchus xylophilus* exposed for 24 h in direct-contact (Yu et al., 2015). 2-Nonanone and 2-undecanone were reported to induce paralysis in *M. incognita* and *M. javanica* by direct-contact (Ntalli et al., 2011). However, to our knowledge, no NA has been reported for 2-octanone, 1-undecene, 1-(ethenyloxy)-octadecane, and (Z)-hexen-1-ol acetate against

greater than 90% killing of *M. incognita* J2 juveniles in the control group situated near culture filtrates, leading us to test SDW and culture filtrates in separate plates.

**TABLE 3** | Chemotaxis index values of commercial VOCs toward *M. incognita*.

Compound	Chemotaxis index (C.I.)				
	1 mg/L	10 mg/L	100 mg/L	1000 mg/L	10,000 mg/L
(Z)-hexen-1-ol acetate	-0.42 ± 0.06a, B	-0.47 ± 0.05a, AB	-0.42 ± 0.13a, A	-0.53 ± 0.15a, A	-0.58 ± 0.20a, AB
2-Octanone	-0.41 ± 0.13a, B	-0.43 ± 0.08ab, AB	-0.44 ± 0.14ab, A	-0.55 ± 0.05ab, A	-0.56 ± 0.11b, AB
1-Undecene	-0.36 ± 0.15a, AB	-0.33 ± 0.12a, A	-0.32 ± 0.20a, A	-0.34 ± 0.09a, A	-0.56 ± 0.05b, AB
1-(Ethenyloxy)-octadecane	-0.23 ± 0.10a, A	-0.42 ± 0.12ab, AB	-0.45 ± 0.20b, A	-0.48 ± 0.16b, A	-0.49 ± 0.18b, A
Dimethyl-disulfide	-0.45 ± 0.10a, B	-0.43 ± 0.15a, AB	-0.48 ± 0.05a, A	-0.54 ± 0.07a, A	-0.54 ± 0.06a, A
2-Undecanone	-0.50 ± 0.08a, B	-0.53 ± 0.03a, B	-0.49 ± 0.15a, A	-0.54 ± 0.03a, A	-0.73 ± 0.12b, B
2-Nonanone	-0.42 ± 0.13a, B	-0.43 ± 0.11a, AB	-0.42 ± 0.15a, A	-0.46 ± 0.28a, A	-0.48 ± 0.10a, A

Each value represents the average ( $\pm$ SE) of three replicates. Different lowercase letters indicate significant differences among different concentrations of the same VOC (LSD test,  $P < 0.05$ ). Different uppercase letters indicate significant differences among different VOCs of the same concentration (LSD test,  $P < 0.05$ ).

*M. incognita*. In our study, we found the strongest direct contact NA by dimethyl-disulfide, 2-nonanone, 2-octanone, (Z)-hexen-1-ol acetate, and 2-undecanone, but only 2-undecanone had fumigant activity against J2 juveniles. In addition, the seven VOCs had the ability to inhibit egg hatching of *M. incognita* both by direct-contact and as a fumigant.

Our further analysis focused on chemotaxis by J2 juveniles of *M. incognita*, and we found that they were repelled by higher concentrations of culture filtrate and attracted to lower concentrations. In recent years, there has been a proliferation of research on the chemotaxis of nematocidal VOCs. Hu et al. (2012) reported that *Chaetomium globosum* NK102 repelled *M. incognita* chemotaxis, but in that study the whole colony was regarded as a research object and the authors did not explore which factors acted as repellants of the nematode. In our study, all of the identified VOCs had a phobotactic effect on the nematodes, which explains the repellent activity of higher concentrations of the culture filtrates against *M. incognita*. In nature, VOCs can also exhibit an attractant effect: for example, the bacterium *Bacillus nematocida* B16 lures the nematode by emitting six potent VOCs, of which benzyl benzoate, benzaldehyde, 2-heptanone, and acetophenone were potent attractants, with the bacteria then entering the nematode intestine and causing death (Niu et al., 2010). These examples demonstrate the diversity and complexity of the VOCs against nematodes.

In summary, the results of our experiments using three-compartment Petri dishes and identification by GC/MS were consistent with the hypothesis that strain 1A00316 may produce VOCs with multiple modes of nematode control. We identified eight VOCs from strain 1A00316. Among them, dimethyl-disulfide, 2-nonanone, 2-octanone, (Z)-hexen-1-ol acetate, and 2-undecanone had strong NA in direct contact with *M. incognita* J2 juveniles, but only 2-undecanone had fumigant activity. In addition, the seven VOCs inhibited egg hatching both by direct-contact and as a fumigant. All of the seven VOCs repelled *M. incognita*. Our results showed that the VOCs from strain 1A00316 have at least three modes

by which to control *M. incognita*: NA, fumigant activity, and repellent activity. The VOCs also acted on different stages in the nematode life cycle including J2 juveniles and eggs. The multiple modes of action of the VOCs produced from *P. putida* 1A00316 are consistent with the potential of the strain to be an effective biocontrol agent against *M. incognita* in the greenhouse. Further investigation is needed to understand the molecular mechanisms responsible for the NA of the VOC compounds produced by strain 1A00316.

## AUTHOR CONTRIBUTIONS

YZ conceived and designed the work that led to the submission, acquired data, and played an important role in interpreting the results. ZS and GL provided the strain *Pseudomonas putida* 1A00316. MC and LZ provided the suggestions and helped to perform the analysis with constructive discussions. DH and WC helped to perform the analysis with constructive discussions. LT and DW drafted and revised the manuscript. ZY provided a platform for the experiments. JZ drafted and revised the manuscript and approved the final version.

## FUNDING

This work was supported by the Fundamental Research Funds for the Central Universities, China (grant no. 2662016PY110) and grants (2013CB127504 and 2015CB150506) from the National Basic Research Program of China (973).

## SUPPLEMENTARY MATERIAL

The Supplementary Material for this article can be found online at: <https://www.frontiersin.org/articles/10.3389/fmicb.2018.00253/full#supplementary-material>

## REFERENCES

- Abbott, W. S. (1925). A method of computing the effectiveness of an insecticide. *J. Econ. Entomol.* 18, 265–267. doi: 10.1093/jee/18.2.265a
- Aissani, N., Tedeschi, P., Maietti, A., Brandolini, V., Garau, V. L., and Caboni, P. (2013). Nematicidal activity of allylisothiocyanate from horseradish (*Armoracia rusticana*) roots against *Meloidogyne incognita*. *J. Agric. Food Chem.* 61, 4723–4727. doi: 10.1021/jf4008949
- Antony, M., and Jayachandran, K. (2016). Regulation of acyl homoserine lactone synthesis in *Pseudomonas putida* jMQS1 under phenol stress. *Water Air Soil Pollut.* 227:338. doi: 10.1007/s11270-016-3018-5
- Azenha, M., and Vasconcelos, M. T. (2002). Headspace solid-phase micro-extraction gas chromatography–mass detection method for the determination of butyltin compounds in wines. *Anal. Chim. Acta* 458, 231–239. doi: 10.1016/S0003-2670(01)01620-8
- Barker, K. R., Carter, C. C., and Sasser, J. N. (1985). *An Advanced Treatise on Meloidogyne: Methodology*, Vol. II. Washington, DC: United States Agency for International Development.
- Diaz, A., Vázquez, L., Ventura, F., and Galceran, M. T. (2004). Estimation of measurement uncertainty for the determination of nonylphenol in water using solid-phase extraction and solid-phase microextraction procedures. *Anal. Chim. Acta* 506, 71–80. doi: 10.1016/j.aca.2003.10.083
- Fernando, W. D., Ramarathnam, R., Krishnamoorthy, A. S., and Savchuk, S. C. (2005). Identification and use of potential bacterial organic antifungal volatiles in biocontrol. *Soil Biol. Biochem.* 37, 955–964. doi: 10.1016/j.soilbio.2004.10.021
- Fisher, M. H. (1990). Recent advances in avermectin research. *Pure Appl. Chem.* 62, 1231–1240. doi: 10.1351/pac199062071231
- Gao, H., Qi, G., Yin, R., Zhang, H., Li, C., and Zhao, X. (2016). *Bacillus cereus* strain S2 shows high nematicidal activity against *Meloidogyne incognita* by producing sphingosine. *Sci. Rep.* 6:28756. doi: 10.1038/srep28756
- Giles, C. D., Hsu, P. C. L., Richardson, A. E., Hurst, M. R., and Hill, J. E. (2014). Plant assimilation of phosphorus from an insoluble organic form is improved by addition of an organic anion producing *Pseudomonas* sp. *Soil Biol. Biochem.* 68, 263–269. doi: 10.1016/j.soilbio.2013.09.026
- Gu, Y. Q., Mo, M. H., Zhou, J. P., Zou, C. S., and Zhang, K. Q. (2007). Evaluation and identification of potential organic nematicidal volatiles from soil bacteria. *Soil Biol. Biochem.* 39, 2567–2575. doi: 10.1016/j.soilbio.2007.05.011
- Guo, J., Jing, X., Peng, W. L., Nie, Q., Zhai, Y., Shao, Z., et al. (2016). Comparative genomic and functional analyses: unearthing the diversity and specificity of nematicidal factors in *Pseudomonas putida* strain 1A00316. *Sci. Rep.* 6:29211. doi: 10.1038/srep29211
- Hu, Y., Zhang, W., Zhang, P., Ruan, W., and Zhu, X. (2012). Nematicidal activity of chaetoglobosin A produced by *Chaetomium globosum* NK102 against *Meloidogyne incognita*. *J. Agric. Food Chem.* 61, 41–46. doi: 10.1021/jf304314g
- Huang, Y., Xu, C., Ma, L., Zhang, K., Duan, C., and Mo, M. (2010). Characterisation of volatiles produced from *Bacillus megaterium* YFM 3.25 and their nematicidal activity against *Meloidogyne incognita*. *Eur. J. Plant Pathol.* 126, 417–422. doi: 10.1007/s10658-009-9550-z
- Jang, J. Y., Le Dang, Q., Choi, Y. H., Choi, G. J., Jang, K. S., Cha, B., et al. (2014). Nematicidal activities of 4-quinolone alkaloids isolated from the aerial part of *Triumfetta grandidens* against *Meloidogyne incognita*. *J. Agric. Food Chem.* 63, 68–74. doi: 10.1021/jf504572h
- Jones, J. T., Haegeman, A., Danchin, E. G., Gaur, H. S., Helder, J., Jones, M. G., et al. (2013). Top 10 plant-parasitic nematodes in molecular plant pathology. *Mol. Plant Pathol.* 14, 946–961. doi: 10.1111/mpp.12057
- Kiewnick, S., and Sikora, R. A. (2006). Biological control of the root-knot nematode *Meloidogyne incognita* by *Paecilomyces lilacinus* strain 251. *Biol. Control* 38, 179–187. doi: 10.1016/j.biocontrol.2005.12.006
- Kim, T. Y., Jang, J. Y., Jeon, S. J., Lee, H. W., Bae, C. H., Yeo, J. H., et al. (2016). Nematicidal activity of kojic acid produced by *Aspergillus oryzae* against *Meloidogyne incognita*. *J. Microbiol. Biotechnol.* 26, 1383–1391. doi: 10.4014/jmb.1603.03040
- Kyndt, T., Fernandez, D., and Gheysen, G. (2014). Plant-parasitic nematode infections in rice: molecular and cellular insights. *Annu. Rev. Phytopathol.* 52, 135–153. doi: 10.1146/annurev-phyto-102313-050111
- Lee, Y. S., Naning, K. W., Nguyen, X. H., Kim, S. B., Moon, J. H., and Kim, K. Y. (2014). Ovicidal activity of lactic acid produced by *Lysobacter capsici* YS1215 on eggs of root-knot nematode, *Meloidogyne incognita*. *J. Microbiol. Biotechnol.* 24, 1510–1515. doi: 10.4014/jmb.1405.05014
- Li, J., Zou, C., Xu, J., Ji, X., Niu, X., Yang, J., et al. (2015). Molecular mechanisms of nematode-nematophagous microbe interactions: basis for biological control of plant-parasitic nematodes. *Annu. Rev. Phytopathol.* 53, 67–95. doi: 10.1146/annurev-phyto-080614-120336
- Li, N., Pan, F. J., Han, X. Z., and Zhang, B. (2016). Development of soil food web of microbes and nematodes under different agricultural practices during the early stage of pedogenesis of a Mollisol. *Soil Biol. Biochem.* 98, 208–216. doi: 10.1016/j.soilbio.2016.04.011
- Morisaki, H., Nagai, S., Ohshima, H., Ikemoto, E., and Kogure, K. (1999). The effect of motility and cell-surface polymers on bacterial attachment. *Microbiology* 145, 2797–2802. doi: 10.1099/00221287-145-10-2797
- Nicol, J. M., Turner, S. J., Coyne, D. L., Nijs, L., Hockland, S., and Maafi, Z. T. (2011). “Current nematode threats to world agriculture,” in *Genomics and Molecular Genetics of Plant-Nematode Interactions*, eds J. Jones, G. Gheysen, and C. Fenoll (Dordrecht: Springer).
- Niu, Q., Huang, X., Zhang, L., Xu, J., Yang, D., Wei, K., et al. (2010). A Trojan horse mechanism of bacterial pathogenesis against nematodes. *Proc. Natl. Acad. Sci. U.S.A.* 107, 16631–16636. doi: 10.1073/pnas.1007276107
- Ntalli, N. G., Manconi, F., Leonti, M., Maxia, A., and Caboni, P. (2011). Aliphatic ketones from *Ruta chalepensis* (Rutaceae) induce paralysis on root knot nematodes. *J. Agric. Food Chem.* 59, 7098–7103. doi: 10.1021/jf2013474
- Riga, E. (2011). The effects of Brassica green manures on plant parasitic and free living nematodes used in combination with reduced rates of synthetic nematicides. *J. Nematol.* 43, 119–121.
- Saeki, S., Yamamoto, M., and Iino, Y. (2001). Plasticity of chemotaxis revealed by paired presentation of a chemoattractant and starvation in the nematode *Caenorhabditis elegans*. *J. Exp. Biol.* 204, 1757–1764.
- Seo, D. J., Kim, K. Y., Park, R. D., Kim, D. H., Han, Y. S., Kim, T. H., et al. (2013). Nematicidal activity of 3, 4-dihydroxybenzoic acid purified from *Terminalia nigrovenulosa* bark against *Meloidogyne incognita*. *Microb. Pathog.* 59, 52–59. doi: 10.1016/j.micpath.2013.04.005
- Southey, J. F. (1986). In *Laboratory Methods for Work with Plant and Soil Nematodes*, 6th Edn. London: Ministry of Agriculture, Fisheries and Food, 202.
- Tajima, T., Watanabe, N., Kogawa, Y., Takiguchi, N., Kato, J., Ikeda, T., et al. (2001). Chemotaxis of the nematode *Caenorhabditis elegans* toward cycloheximide and quinine hydrochloride. *J. Biosci. Bioeng.* 91, 322–324. doi: 10.1016/S1389-1723(01)80144-4
- Tang, J. P., Zhang, Z., Jing, X., Yu, Z., Zhang, J., Shao, Z., et al. (2014). Mechanism of antagonistic bacteria *Pseudomonas putida* 1A00316 from the South Pole soil against *Meloidogyne incognita*. *Chin. J. Appl. Environ. Biol.* 20, 1046–1051. doi: 10.3724/SP.J.1145.2014.05009
- Troxler, J., Svercel, M., Natsch, A., Zala, M., Keel, C., Moëgne-Loccoz, Y., et al. (2012). Persistence of a biocontrol *Pseudomonas* inoculant as high populations of culturable and non-culturable cells in 200-cm-deep soil profiles. *Soil Biol. Biochem.* 44, 122–129. doi: 10.1016/j.soilbio.2011.09.020
- Trudgill, D. L., and Blok, V. C. (2001). Apomictic, polyphagous root-knot nematodes: exceptionally successful and damaging biotrophic root pathogens. *Annu. Rev. Phytopathol.* 39, 53–77. doi: 10.1146/annurev.phyto.39.1.53
- Vos, C., Schouteden, N., Van Tuinen, D., Chatagnier, O., Elsen, A., De Waele, D., et al. (2013). Mycorrhiza-induced resistance against the root-knot nematode *Meloidogyne incognita* involves priming of defense gene

- responses in tomato. *Soil Biol. Biochem.* 60, 45–54. doi: 10.1016/j.soilbio.2013.01.013
- Yu, J., Du, G., Li, R., Li, L., Li, Z., Zhou, C., et al. (2015). Nematicidal activities of bacterial volatiles and components from two marine bacteria, *Pseudoalteromonas marina* strain H-42 and *Vibrio atlanticus* strain S-16, against the pine wood nematode, *Bursaphelenchus xylophilus*. *Nematology* 17, 1011–1025. doi: 10.1163/15685411-00002920
- Zhang, X., Guan, P., Wang, Y., Li, Q., Zhang, S., Zhang, Z., et al. (2015). Community composition, diversity and metabolic footprints of soil nematodes in differently-aged temperate forests. *Soil Biol. Biochem.* 80, 118–126. doi: 10.1016/j.soilbio.2014.10.003

**Conflict of Interest Statement:** The authors declare that the research was conducted in the absence of any commercial or financial relationships that could be construed as a potential conflict of interest.

Copyright © 2018 Zhai, Shao, Cai, Zheng, Li, Huang, Cheng, Thomashow, Weller, Yu and Zhang. This is an open-access article distributed under the terms of the Creative Commons Attribution License (CC BY). The use, distribution or reproduction in other forums is permitted, provided the original author(s) and the copyright owner are credited and that the original publication in this journal is cited, in accordance with accepted academic practice. No use, distribution or reproduction is permitted which does not comply with these terms.



# Vancomycin and/or Multidrug-Resistant *Citrobacter Freundii* Altered the Metabolic Pattern of Soil Microbial Community

Mariusz Cycoń<sup>1\*</sup>, Kamila Orlewska<sup>1</sup>, Anna Markowicz<sup>2</sup>, Agnieszka Żmijowska<sup>3</sup>, Joanna Smoleń-Dzirba<sup>1</sup>, Jolanta Bratosiewicz-Wąsik<sup>1</sup>, Tomasz J. Wąsik<sup>1</sup> and Zofia Piotrowska-Seget<sup>2</sup>

<sup>1</sup> Department of Microbiology and Virology, School of Pharmacy with the Division of Laboratory Medicine, Medical University of Silesia, Sosnowiec, Poland, <sup>2</sup> Department of Microbiology, University of Silesia, Katowice, Poland, <sup>3</sup> Department of Ecotoxicology, Institute of Industrial Organic Chemistry, Pszczyna, Poland

## OPEN ACCESS

### Edited by:

Ed Topp,  
Agriculture and Agri-Food Canada  
(AAFC), Canada

### Reviewed by:

Marc Didier Auffret,  
Scotland's Rural College,  
United Kingdom  
Lori Ann Phillips,  
Agriculture and Agri-Food Canada  
(AAFC), Canada  
Ahmed Askora,  
Zagazig University, Egypt

### \*Correspondence:

Mariusz Cycoń  
mcycon@sum.edu.pl

### Specialty section:

This article was submitted to  
Microbiotechnology, Ecotoxicology  
and Bioremediation,  
a section of the journal  
Frontiers in Microbiology

Received: 01 January 2018

Accepted: 02 May 2018

Published: 23 May 2018

### Citation:

Cycoń M, Orlewska K, Markowicz A,  
Żmijowska A, Smoleń-Dzirba J,  
Bratosiewicz-Wąsik J, Wąsik TJ and  
Piotrowska-Seget Z (2018)  
Vancomycin and/or  
Multidrug-Resistant *Citrobacter  
Freundii* Altered the Metabolic Pattern  
of Soil Microbial Community.  
*Front. Microbiol.* 9:1047.  
doi: 10.3389/fmicb.2018.01047

Despite many studies, our knowledge on the impact of antibiotics and antibiotic-resistant bacteria on the metabolic activity of soil microbial communities is still limited. To ascertain this impact, the community level physiological profiles (CLPPs) and the activity of selected enzymes (dehydrogenase, urease, and phosphatases) in soils treated with vancomycin (VA) and/or multidrug resistant *Citrobacter freundii* were determined during a 90-day experiment. A multivariate analysis and the resistance (RS)/resilience (RL) concept were used to assess the potential of native microorganisms to maintain their catabolic activity under exposure of VA and/or a high level of *C. freundii*. In addition, the dissipation rate of VA was evaluated in non-sterile (nsS) and sterile (sS) soils. The results revealed a negative impact of VA on the metabolic activity of soil microorganisms on days 1, 15, and 30 as was showed by a decrease in the values of the CLPP indices (10–69%) and the enzyme activities (6–32%) for treated soils as compared to the control. These observations suggested a low initial resistance of soil microorganisms to VA and/or *C. freundii* but they were resilient in the long term. Considering the mean values of the RS index, the resistance of measured parameters was categorized in the following order: alkaline phosphatase (0.919) > acid phosphatase (0.899) > dehydrogenase (0.853) > the evenness index (0.840) > urease (0.833) > the Shannon-Wiener index (0.735) > substrate richness (0.485) > the AWCD (0.301). The dissipation process of VA was relatively fast and independent of the concentration used. The DT50 values for VA applied at both concentrations were about 16 days. In addition, the dissipation of VA in nsS was three times faster compared to the dissipation of antibiotic in sS. In conclusion, both CLPP and enzyme activities assays appeared to be useful tool for the determination of disturbances within soil microbial communities and used together may be helpful to understand the changes in their catabolic features. The entry of large quantities of VA and/or *C. freundii* into soil may temporarily change microbial activity thus pose a potential risk for soil functioning.

**Keywords:** vancomycin, multidrug-resistant bacteria, Biolog EcoPlates, enzyme activities, antibiotic dissipation, soil

## INTRODUCTION

Antibiotics and antibiotic-resistant microorganisms are primarily introduced into soil through the manure, municipal wastewater, or sewage sludge application (Kümmerer, 2003; Chee-Sanford et al., 2009; Li and Zhang, 2010). Moreover, several antibiotics are used and overused in agriculture practices (Chang and Ren, 2015). Due to their potential ecotoxicological effects and persistence in soil, antibiotics represent a durable contamination (Brandt et al., 2015). The presence of antibiotics in soil poses a prospective risk to ecosystem health because of the selective pressure that is exerted on soil microbial communities. Many studies have revealed that antibiotics affect the number of different groups of microorganisms (Pinna et al., 2012; Akimenko et al., 2015; Xu et al., 2016), the structural and genetic diversity of microorganisms and the overall microbial activity (Demoling et al., 2009; Cui et al., 2013; Liu et al., 2014; Reichel et al., 2014a,b; Cycoń et al., 2016a; Xu et al., 2016). Moreover, the impact of antibiotics on the enzyme activities, carbon mineralization, and nitrogen cycling has been proven (Liu et al., 2009; Kotzerke et al., 2011; Rosendahl et al., 2012; Chen et al., 2013; Ma et al., 2016).

The potential disturbances/alterations within soil microorganisms caused by various stress factors may be assessed using the resistance (RS)/resilience (RL) concept (Orwin and Wardle, 2004; Griffiths and Philippot, 2013). Resistance means the ability of a microbial community to maintain the population structure and function under a toxicity stress, whereas resilience is defined as the ability of community to recover from a perturbation or disturbance to its original or new stable composition and functionality (Allison and Martiny, 2008; Shade et al., 2012; Hodgson et al., 2015; Song et al., 2015). Soil microorganisms are faced with both abiotic (e.g., pollutants, physico-chemical factors) and biotic (e.g., bacteriophages, competition with other organisms) stressors. Although multiple stress factors typically co-occur in soil system, studies on their impact on microbial communities are limited. It has been reported that the resilience of polluted soils against further stress is different than those observed in non-contaminated soils (Schaeffer et al., 2016). An understanding of the reaction of soil microbial communities to biotic and abiotic stressors acting simultaneously is currently lacking.

Vancomycin (VA) is a glycopeptide antibiotic that inhibits the cell wall synthesis by affecting the peptidoglycan assembly. This mechanism leads to the inhibition of bacterial cell division (Courvalin, 2006; Gupta et al., 2011). VA has increasingly been used against different infections caused by Gram-positive bacteria in recent decades and has been detected in hospital effluents worldwide (Qiu et al., 2016; Quoc Tuc et al., 2017). Since conventional wastewater treatment processes have a limited efficiency in VA dissipation, this antibiotic may enter the environment via the final release of effluents and the application of sewage sludge into soil (Quoc Tuc et al., 2017). Moreover, multidrug-resistant strains in soil may have the same origin. In consequence, the presence of VA or other antibiotics in soil may favor the growth and spread of resistant microorganisms.

Multidrug-resistant strains of species such as *Citrobacter freundii* that are a part of the indigenous soil microbial communities have an advantage (Riber et al., 2014). Because *C. freundii* is also known to be an opportunistic pathogen, it is important to understand the impact of VA and/or multidrug-resistant *C. freundii* on the functional and structural diversity of natural soil microorganisms. Based on the denaturing gradient gel electrophoresis (DGGE) and phospholipid fatty acid (PLFA) approaches, we revealed that VA and/or multidrug-resistant *C. freundii* changed the structure and genetic biodiversity of a soil microbial community (Cycoń et al., 2016a).

Since the basic soil functions such as biomass production and nutrient turnover, biogeochemical cycling and soil formation are mainly provided by microorganisms, it is important to learn the resistance/resilience of soil activity to application of the antibiotic and a high number of antibiotic-resistant bacteria. In order to obtain knowledge about the metabolic potential of soil microorganisms, referred to as the community-level physiological profile (CLPP), the Biolog method and EcoPlates™ that contain 31 various carbon sources can be used (Garland, 1997; Floch et al., 2011). The CLPP approach has often been used to determine the microbial catabolic activity and functional diversity in soil that has been contaminated with different antibiotics and other chemicals (Mijangos et al., 2009; Liu W. et al., 2012; Cycoń et al., 2013a; Chessa et al., 2016; Fang et al., 2016). However, some authors stated that the effects of contamination can be better evaluated by measuring the activity of some soil enzymes rather than use of Biolog EcoPlates (Floch et al., 2011; Cycoń et al., 2013b). This conclusion may be due to the fact that the Biolog technique does not take into account the activity of catabolically inactive microorganisms that exist in a dormant state or non-culturable microorganisms. Moreover, mainly fast growing microorganisms are involved in this analysis (Floch et al., 2011). Many studies have indicated that dehydrogenase, phosphatase and urease activities are sensitive indicators of the microbial response to stress that is caused by antibiotics in the soil environment (Yang et al., 2009; Akimenko et al., 2015; Xu et al., 2016). However, interactions between the antibiotic and/or multidrug-resistant strain and the soil microbial biochemical potential are still little known. In this context, the application of VA and/or antibiotic-resistant bacteria into soil may change the biochemical potential of a soil microbial community. In this study we hypothesized that the introduction of VA and/or multidrug-resistant *C. freundii* into soil could shift the metabolic activity of a microbial community and the presence of a high number of antibiotic-resistant bacteria could change the response of indigenous microorganisms to VA. To check the above assumptions, the CLPP and enzyme activities, i.e., dehydrogenase (DHA), acid phosphatase (PHOS-H), alkaline phosphatase (PHOS-OH), and urease (URE) were determined. A multivariate analysis and the resistance (RS)/resilience (RL) concept were used to assess the potential of native microorganisms to maintain their catabolic activity under exposure of VA and/or a high level of *C. freundii*. In addition, an analysis of the VA dissipation in soil was also performed.

## MATERIALS AND METHODS

### Bacterial Strain

A raw sewage was used to isolate a bacterial strain. Growth of isolate was performed using a TSA medium in the presence of paper discs impregnated with VA. It was identified as *C. freundii* using the API 20E biochemical test (bioMérieux Inc., France) and 16S rRNA gene analysis with the universal primer pair 27f and 1492r. The *C. freundii* strain expressed a resistance to vancomycin, clindamycin and erythromycin. Isolated strain has been deposited in the culture collection of the Department of Microbiology and Virology, Medical University of Silesia, Poland. The standard biosecurity and institutional safety procedures for this bacterial strain have been carried out. Detailed information related to procedures of bacteria isolation and identification were described in a previous paper (Cycoń et al., 2016a).

### Design of Experiment

A loamy sand soil was used in the experiment. The properties of the soil were shown in a previous paper (Cycoń et al., 2016a) and determined according to suitable methods (Cycoń et al., 2010). The experiment with the non-sterile soil (nsS) had three replications of each treatment, i.e., C (non-sterile control), VA1 (nsS + 1 mg VA/kg soil), VA10 (nsS + 10 mg VA/kg soil), Cit (nsS + *C. freundii*), VA1+Cit (nsS + 1 mg VA/kg soil + *C. freundii*), and VA10+Cit (nsS + 10 mg VA/kg soil + *C. freundii*) for each sampling time. A suspension of a bacterial strain was introduced into the soil treatments at a concentration of  $1.6 \times 10^7$  cells/g soil (Cycoń et al., 2016a). Soil samples were stored at the temperature of  $22 \pm 1^\circ\text{C}$  and periodically removed from the test system to evaluate the metabolic pattern and physiological diversity of a bacterial community (on days 1, 15, 30, 60, and 90) and the concentration of VA (on days 0, 1, 8, 15, 23, 30, 60, and 90). Sterile soil (sS) for VA or VA with *C. freundii* was used to determine the dissipation of VA under abiotic conditions and the degradation potential of the bacterial strain, respectively. The same experimental conditions were used for both sterile and non-sterile soils. Detailed information related to the design of experiment are presented in Supplementary Materials.

### Analysis of the Community-Level Physiological Profile (CLPP)

The CLPP in the soil samples were obtained using the Biolog<sup>®</sup> EcoPlate<sup>™</sup> system (Biolog Inc., CA, USA) (Insam, 1997) and the method described in a previous paper (Cycoń et al., 2013b). Detailed information related to the determination of the CLPP are presented in Supplementary Materials.

### Determination of Enzyme Activities

The activities of DHA, PHOSs, and URE were determined by methods of Alef (1995), Tabatabai and Bremner (1969), and Gianfreda et al. (1994), respectively, and were described in a previous paper (Cycoń et al., 2016b). Detailed information related to the determination of the enzyme activities are presented in Supplementary Materials.

### Determination of the Vancomycin Concentration in Soil

In order to determine the VA concentration, 10 g soil samples were extracted with 10 mL of a mixture of deionized water/methanol/formic acid (90/10/0.1, v/v) for 5 min. and sonicated for 10 min. Samples were centrifuged and filtered through filter paper. Next, 5 mL of the extraction mixture were added to the soil once again. The procedure of shaking, sonication, centrifugation and filtration was repeated. Finally, 20  $\mu\text{L}$  of the combined extracts were introduced into a chromatographic column. The concentration of VA was determined by high performance liquid chromatography (HPLC) using a Shimadzu Prominence-*i* System LC-2030C 3D (Shimadzu, Inc., Japan) equipped with a DAD detector and a column [Kinetex C18 100A (150  $\times$  4.6  $\times$  5  $\mu\text{m}$ )]. A mixture of acetonitrile/0.05% ortho-phosphoric acid (10/90 v/v) was used as a mobile phase. The detection of VA was performed at a wavelength of 221 nm. The obtained data were analyzed using LabSolution Software LC-2030C 3D. The mean time of retention for VA was 6.1 min.

### Analysis and Interpretation of Results

Metabolic pattern of a soil microbial community expressed as the average well-color development (AWCD), substrate richness ( $R_s$ ), evenness (E), and the Shannon-Wiener index (H) was determined according to the equations described by Garland (1997). Indices adopted from Orwin and Wardle (2004) were used to evaluate the resistance (RS) and resilience (RL) of measured activities to disturbances caused by antibiotic and/or bacterial strain. Based on the analysis of the kinetics of VA dissipation in soil, its disappearance rate was fitted to a zero-order kinetic model. The DT50 values and rate constant ( $k$ ) were calculated by the equation adopted from Cycoń et al. (2013b).

The obtained data were evaluated by applying an analysis of variance (ANOVA) and the least significant differences (LSD) test ( $P < 0.05$ ). A principal component analyses (PCAs) were performed using the data for the CLPP indices, the AWCD data for the six groups in which the 31 carbon substrates of Biolog EcoPlates<sup>™</sup> were grouped and the data of enzyme activities. In addition, the analyses of the PC scores using the three-way and two-way MANOVA were also performed. All of the statistical analyses were performed using the Statistica 12.0 PL software package. Detailed information related to the analysis and interpretation of results are presented in Supplementary Materials.

## RESULTS

### Community-Level Physiological Profile (CLPP)

The obtained CLPPs showed that there were significant differences in the values of the AWCD (**Figure 1A**),  $R_s$  (**Figure 1B**), H (**Figure 1C**), and E (**Figure 1D**) indices between the soil treated with VA and/or *C. freundii* and the control soil during the 90-day incubation. A significant decrease ( $P < 0.05$ ) in the AWCD values in a response to VA and/or *C. freundii*

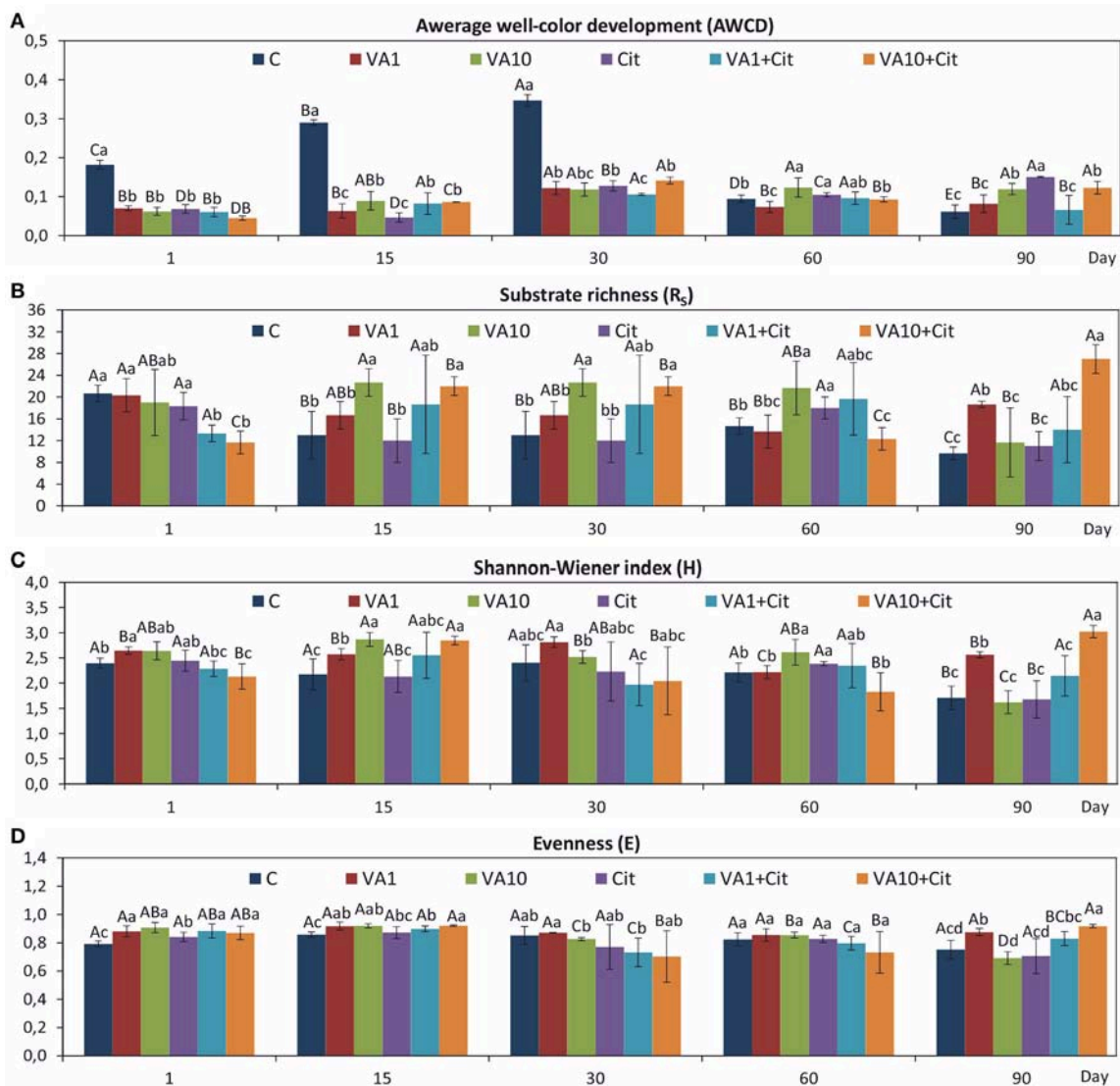


**FIGURE 1** | Values of the CLPP indices: AWCD (A),  $R_S$  (B), H (C), and E (D) for the soil with VA and/or *C. freundii* obtained during the experimental period. C, control; VA1, 1 mg VA/kg soil; VA10, 10 mg VA/kg soil; Cit, *C. freundii*; VA1+Cit, 1 mg VA/kg soil + *C. freundii*; VA10+Cit, 10 mg VA/kg soil + *C. freundii*. The data are the means with standard deviations ( $n = 3$ ). Different lowercase and uppercase letters within the values of each index indicate significant differences between treatments at the same sampling time and between sampling times within the same treatment (LSD *post hoc* test;  $P < 0.05$ ), respectively.

introduction was observed on days 1, 15, and 30 of the experiment. In turn, at the end of the incubation (day 90), a significant increase in the AWCD values was observed for the vancomycin (VA1 and VA1+Cit)- and *C. freundii*-treated soils, and these values were almost 2- and 2.5-fold higher as compared to the value for the non-treated control, respectively (Figure 1A). The ANOVA revealed that the dosage of VA, *C. freundii*, the time of incubation and the interaction between the factors tested had a significant impact ( $P < 0.001$ ) on the AWCD value (Table S1). The study revealed that the  $R_S$  value was only affected by the VA treatment (Table S1) and, that in general, its increase was found as compared to the non-treated control during the experiment. However, a higher

dose of VA (VA10+Cit) negatively affected the  $R_S$  value at the beginning of the experiment (day 1) (Figure 1B). In turn, the H index (Figure 1C) was affected by all of the factors tested (Table S1).

Evaluation of the resistance of the CLPP indices to VA and/or *C. freundii* showed that these factors affected the values of the RS index during the experimental period (Table 1). In general, the ANOVA revealed that the treatment, time, and interaction between the factors tested had a significant impact ( $P < 0.001$ ) on the resistance of the CLPP indices (Table S2). The highest reduction in the values of the RS index was observed in the case of the AWCD (Table 1). However, on day 90, this decrease was related to the stimulatory effect of

**TABLE 1** | Values of the resistance (RS) index for measured parameters obtained for each day of the experiment.

Parameter	Day	Treatment					$\bar{x}$
		VA1	VA10	Cit	VA1+Cit	VA10+Cit	
AWCD (average)	1	0.239 <sup>Ba</sup>	0.206 <sup>Ba</sup>	0.231 <sup>Ba</sup>	0.199 <sup>Ca</sup>	0.140 <sup>Ba</sup>	0.203 <sup>B</sup>
	15	0.123 <sup>Ba</sup>	0.182 <sup>Ba</sup>	0.087 <sup>Ba</sup>	0.166 <sup>Ca</sup>	0.175 <sup>Ba</sup>	0.147 <sup>B</sup>
	30	0.213 <sup>Ba</sup>	0.205 <sup>Ba</sup>	0.226 <sup>Ba</sup>	0.180 <sup>Ca</sup>	0.256 <sup>Ba</sup>	0.216 <sup>B</sup>
	60	0.634 <sup>Ac</sup>	0.553 <sup>Ac</sup>	0.800 <sup>Ab</sup>	0.814 <sup>Ab</sup>	0.951 <sup>Aa</sup>	0.750 <sup>A</sup>
	90	0.504 <sup>Aa</sup>	0.020 <sup>Cb</sup>	-0.187 <sup>Cc</sup>	0.623 <sup>Ba</sup>	-0.008 <sup>Bb</sup>	0.191 <sup>B</sup>
Substrate richness (R <sub>S</sub> )	1	0.896 <sup>Aa</sup>	0.710 <sup>Aab</sup>	0.796 <sup>Aa</sup>	0.475 <sup>Ab</sup>	0.392 <sup>Bb</sup>	0.654 <sup>A</sup>
	15	0.530 <sup>Bab</sup>	0.128 <sup>Bc</sup>	0.858 <sup>Aa</sup>	0.479 <sup>Abc</sup>	0.166 <sup>Bc</sup>	0.432 <sup>AB</sup>
	30	0.530 <sup>Bab</sup>	0.128 <sup>Bc</sup>	0.858 <sup>Aa</sup>	0.479 <sup>Abc</sup>	0.166 <sup>Bc</sup>	0.432 <sup>AB</sup>
	60	0.829 <sup>ABa</sup>	0.381 <sup>ABb</sup>	0.630 <sup>Aa</sup>	0.567 <sup>Aa</sup>	0.722 <sup>Aa</sup>	0.626 <sup>A</sup>
	90	0.034 <sup>Cb</sup>	0.437 <sup>ABa</sup>	0.769 <sup>Aa</sup>	0.443 <sup>Aa</sup>	-0.285 <sup>Cb</sup>	0.280 <sup>B</sup>
Shannon-Wiener index (H)	1	0.810 <sup>ABa</sup>	0.818 <sup>ABa</sup>	0.930 <sup>Aa</sup>	0.911 <sup>Aa</sup>	0.803 <sup>Aa</sup>	0.854 <sup>A</sup>
	15	0.686 <sup>Bbc</sup>	0.512 <sup>Cc</sup>	0.961 <sup>Aa</sup>	0.711 <sup>ABCb</sup>	0.524 <sup>Ac</sup>	0.679 <sup>BC</sup>
	30	0.704 <sup>Ba</sup>	0.847 <sup>ABa</sup>	0.832 <sup>Aa</sup>	0.691 <sup>BCa</sup>	0.738 <sup>Aa</sup>	0.762 <sup>AB</sup>
	60	0.964 <sup>Aa</sup>	0.696 <sup>BCb</sup>	0.853 <sup>Ab</sup>	0.831 <sup>ABab</sup>	0.705 <sup>Ab</sup>	0.810 <sup>AB</sup>
	90	0.331 <sup>Cc</sup>	0.904 <sup>Aa</sup>	0.888 <sup>Aa</sup>	0.603 <sup>Cb</sup>	0.127 <sup>Bd</sup>	0.571 <sup>C</sup>
Evenness (E)	1	0.797 <sup>Aa</sup>	0.744 <sup>Ba</sup>	0.881 <sup>ABa</sup>	0.792 <sup>Ba</sup>	0.823 <sup>ABa</sup>	0.808 <sup>B</sup>
	15	0.870 <sup>Aa</sup>	0.866 <sup>ABa</sup>	0.959 <sup>Aa</sup>	0.908 <sup>ABa</sup>	0.863 <sup>Aa</sup>	0.893 <sup>A</sup>
	30	0.894 <sup>Aab</sup>	0.906 <sup>Aa</sup>	0.810 <sup>Babc</sup>	0.753 <sup>Bbc</sup>	0.712 <sup>BCc</sup>	0.815 <sup>B</sup>
	60	0.927 <sup>Aab</sup>	0.930 <sup>Aab</sup>	0.964 <sup>Aa</sup>	0.935 <sup>Aab</sup>	0.794 <sup>Bb</sup>	0.910 <sup>A</sup>
	90	0.716 <sup>Bb</sup>	0.853 <sup>ABab</sup>	0.861 <sup>ABa</sup>	0.812 <sup>ABab</sup>	0.637 <sup>Cb</sup>	0.776 <sup>B</sup>
AWCD-amines	1	0.757 <sup>Aa</sup>	0.281 <sup>Ab</sup>	0.414 <sup>Ab</sup>	0.282 <sup>Ab</sup>	0.224 <sup>Ab</sup>	0.392 <sup>A</sup>
	15	0.065 <sup>Bcb</sup>	0.422 <sup>Aa</sup>	0.143 <sup>Aab</sup>	0.230 <sup>Aab</sup>	0.272 <sup>Aab</sup>	0.226 <sup>AB</sup>
	30	0.249 <sup>Bb</sup>	0.251 <sup>ABb</sup>	0.212 <sup>Ab</sup>	0.179 <sup>Ab</sup>	0.647 <sup>Aa</sup>	0.308 <sup>A</sup>
	60	-0.004 <sup>BCbc</sup>	-0.015 <sup>BCbc</sup>	-0.325 <sup>Bc</sup>	0.185 <sup>Aab</sup>	0.368 <sup>Aa</sup>	0.042 <sup>BC</sup>
	90	-0.148 <sup>Ca</sup>	-0.067 <sup>Ca</sup>	0.105 <sup>Aa</sup>	0.077 <sup>Aa</sup>	-0.535 <sup>Bb</sup>	-0.114 <sup>C</sup>
AWCD-amino acids	1	0.382 <sup>ABb</sup>	0.870 <sup>Aa</sup>	0.291 <sup>ABbc</sup>	0.245 <sup>ABbc</sup>	0.024 <sup>Bc</sup>	0.362 <sup>A</sup>
	15	0.181 <sup>ABa</sup>	0.137 <sup>Ca</sup>	0.054 <sup>Ba</sup>	0.089 <sup>Ba</sup>	0.147 <sup>Ba</sup>	0.120 <sup>B</sup>
	30	0.101 <sup>Ba</sup>	0.036 <sup>Ca</sup>	0.250 <sup>ABa</sup>	0.059 <sup>Ba</sup>	0.042 <sup>Ba</sup>	0.097 <sup>B</sup>
	60	0.489 <sup>Aa</sup>	0.071 <sup>Cb</sup>	0.582 <sup>Aa</sup>	0.537 <sup>Aa</sup>	0.543 <sup>Aa</sup>	0.444 <sup>A</sup>
	90	-0.553 <sup>Cc</sup>	0.480 <sup>Ba</sup>	-0.885 <sup>Cc</sup>	-0.121 <sup>Cb</sup>	-0.757 <sup>Cc</sup>	-0.367 <sup>C</sup>
AWCD-carbohydrates	1	0.570 <sup>Aa</sup>	0.810 <sup>Aa</sup>	0.513 <sup>Aa</sup>	0.792 <sup>Aa</sup>	0.698 <sup>Aa</sup>	0.676 <sup>A</sup>
	15	0.202 <sup>ABa</sup>	0.220 <sup>Ba</sup>	0.102 <sup>Ba</sup>	0.252 <sup>Ba</sup>	0.232 <sup>Ba</sup>	0.202 <sup>B</sup>
	30	0.117 <sup>Ba</sup>	0.095 <sup>Ba</sup>	0.051 <sup>Ba</sup>	0.050 <sup>Ba</sup>	0.064 <sup>BCa</sup>	0.075 <sup>BC</sup>
	60	0.274 <sup>ABa</sup>	-0.371 <sup>Cc</sup>	-0.119 <sup>Cab</sup>	-0.418 <sup>Cc</sup>	-0.256 <sup>Cbc</sup>	-0.178 <sup>C</sup>
	90	-0.222 <sup>Ca</sup>	0.040 <sup>Ba</sup>	0.014 <sup>Ba</sup>	-0.120 <sup>Ba</sup>	-0.526 <sup>Cb</sup>	-0.163 <sup>C</sup>
AWCD-carboxylic acids	1	0.305 <sup>Aa</sup>	0.300 <sup>Ba</sup>	0.344 <sup>ABa</sup>	0.143 <sup>Ba</sup>	0.162 <sup>Aa</sup>	0.251 <sup>B</sup>
	15	0.180 <sup>Aa</sup>	0.225 <sup>Ba</sup>	0.053 <sup>Ba</sup>	0.237 <sup>Ba</sup>	0.175 <sup>Aa</sup>	0.174 <sup>B</sup>
	30	0.309 <sup>Aab</sup>	0.179 <sup>Bb</sup>	0.215 <sup>Bb</sup>	0.602 <sup>Aa</sup>	0.128 <sup>Bb</sup>	0.286 <sup>B</sup>
	60	0.396 <sup>Abc</sup>	0.646 <sup>Aab</sup>	0.572 <sup>Aab</sup>	0.739 <sup>Aa</sup>	0.165 <sup>Ac</sup>	0.504 <sup>A</sup>
	90	-0.636 <sup>Bb</sup>	-0.566 <sup>Cb</sup>	-0.734 <sup>Cb</sup>	-0.230 <sup>Ca</sup>	-0.799 <sup>Bb</sup>	-0.593 <sup>C</sup>
AWCD-miscellaneous	1	0.091 <sup>Ba</sup>	0.095 <sup>Ba</sup>	0.255 <sup>Ba</sup>	0.193 <sup>Ba</sup>	0.100 <sup>Da</sup>	0.146 <sup>B</sup>
	15	0.119 <sup>Ba</sup>	0.145 <sup>Ba</sup>	0.160 <sup>Ba</sup>	0.222 <sup>Ba</sup>	0.172 <sup>Ca</sup>	0.164 <sup>B</sup>
	30	0.583 <sup>Ab</sup>	0.676 <sup>Aab</sup>	0.814 <sup>Aa</sup>	0.550 <sup>Ab</sup>	0.319 <sup>BCc</sup>	0.588 <sup>A</sup>
	60	0.583 <sup>Ab</sup>	0.574 <sup>Ab</sup>	0.814 <sup>Aa</sup>	0.639 <sup>Aab</sup>	0.518 <sup>Bb</sup>	0.626 <sup>A</sup>
	90	0.576 <sup>Ab</sup>	0.569 <sup>Ab</sup>	0.894 <sup>Aa</sup>	0.630 <sup>Aab</sup>	0.824 <sup>Aa</sup>	0.699 <sup>A</sup>

(Continued)

TABLE 1 | Continued

Parameter	Day	Treatment					$\bar{x}$
		VA1	VA10	Cit	VA1+Cit	VA10+Cit	
AWCD-polymers	1	0.107 <sup>Ba</sup>	0.137 <sup>Ba</sup>	0.068 <sup>Ba</sup>	0.081 <sup>Aa</sup>	0.084 <sup>Ca</sup>	0.096 <sup>B</sup>
	15	0.052 <sup>Ba</sup>	0.064 <sup>Ba</sup>	0.002 <sup>Ba</sup>	0.042 <sup>Aa</sup>	0.100 <sup>Ca</sup>	0.052 <sup>B</sup>
	30	0.099 <sup>Bb</sup>	0.170 <sup>Bb</sup>	0.063 <sup>Bb</sup>	0.059 <sup>Ab</sup>	0.501 <sup>Aa</sup>	0.178 <sup>AB</sup>
	60	0.184 <sup>Bb</sup>	0.717 <sup>Aa</sup>	0.425 <sup>Ab</sup>	0.205 <sup>Ab</sup>	0.202 <sup>BCb</sup>	0.346 <sup>A</sup>
	90	0.458 <sup>Ab</sup>	-0.516 <sup>Ca</sup>	-0.650 <sup>Ca</sup>	0.227 <sup>Ab</sup>	0.423 <sup>ABb</sup>	-0.011 <sup>B</sup>
DHA activity	1	0.800 <sup>Ba</sup>	0.650 <sup>Db</sup>	0.817 <sup>Ba</sup>	0.685 <sup>Bb</sup>	0.517 <sup>Dc</sup>	0.694 <sup>D</sup>
	15	0.972 <sup>Aa</sup>	0.794 <sup>Cb</sup>	0.812 <sup>Bb</sup>	0.970 <sup>Aa</sup>	0.655 <sup>Cc</sup>	0.841 <sup>C</sup>
	30	0.967 <sup>Aa</sup>	0.858 <sup>Bb</sup>	0.786 <sup>Bc</sup>	0.936 <sup>Aa</sup>	0.740 <sup>Bc</sup>	0.857 <sup>BC</sup>
	60	0.969 <sup>Aa</sup>	0.943 <sup>Aa</sup>	0.955 <sup>Aa</sup>	0.958 <sup>Aa</sup>	0.783 <sup>Bb</sup>	0.922 <sup>AB</sup>
	90	0.954 <sup>Aa</sup>	0.934 <sup>Aa</sup>	0.940 <sup>Aa</sup>	0.951 <sup>Aa</sup>	0.975 <sup>Aa</sup>	0.951 <sup>A</sup>
PHOS-H activity	1	0.921 <sup>Aa</sup>	0.780 <sup>Cc</sup>	0.944 <sup>Ba</sup>	0.844 <sup>Bb</sup>	0.728 <sup>Dd</sup>	0.843 <sup>C</sup>
	15	0.992 <sup>Aa</sup>	0.867 <sup>Bb</sup>	0.971 <sup>Aa</sup>	0.866 <sup>Bb</sup>	0.888 <sup>Bb</sup>	0.917 <sup>AB</sup>
	30	0.975 <sup>Aa</sup>	0.786 <sup>Cc</sup>	0.931 <sup>BCb</sup>	0.981 <sup>Aa</sup>	0.679 <sup>Ed</sup>	0.870 <sup>BC</sup>
	60	0.993 <sup>Aa</sup>	0.811 <sup>Cb</sup>	0.991 <sup>Aa</sup>	0.987 <sup>Aa</sup>	0.794 <sup>Cb</sup>	0.917 <sup>AB</sup>
	90	0.964 <sup>Aa</sup>	0.949 <sup>Ab</sup>	0.904 <sup>Cc</sup>	0.982 <sup>Aa</sup>	0.942 <sup>Ab</sup>	0.948 <sup>A</sup>
PHOS-OH activity	1	0.983 <sup>Aa</sup>	0.860 <sup>Bc</sup>	0.911 <sup>Abc</sup>	0.979 <sup>Ba</sup>	0.887 <sup>Bc</sup>	0.924 <sup>AB</sup>
	15	0.965 <sup>Aa</sup>	0.855 <sup>Bb</sup>	0.978 <sup>Aa</sup>	0.943 <sup>Ba</sup>	0.824 <sup>BCb</sup>	0.913 <sup>B</sup>
	30	0.957 <sup>Aa</sup>	0.845 <sup>Bb</sup>	0.977 <sup>Aa</sup>	0.957 <sup>Ba</sup>	0.819 <sup>Cb</sup>	0.911 <sup>B</sup>
	60	0.960 <sup>Aa</sup>	0.751 <sup>Cb</sup>	0.966 <sup>Aa</sup>	0.993 <sup>Aa</sup>	0.710 <sup>Dc</sup>	0.876 <sup>B</sup>
	90	0.963 <sup>Aa</sup>	0.978 <sup>Aa</sup>	0.946 <sup>Aa</sup>	0.966 <sup>ABa</sup>	0.997 <sup>Aa</sup>	0.971 <sup>A</sup>
URE activity	1	0.806 <sup>Ab</sup>	0.632 <sup>Cc</sup>	0.822 <sup>Ca</sup>	0.774 <sup>Bb</sup>	0.582 <sup>Dd</sup>	0.723 <sup>C</sup>
	15	0.981 <sup>Aa</sup>	0.568 <sup>Db</sup>	0.972 <sup>ABa</sup>	0.952 <sup>Aa</sup>	0.521 <sup>Eb</sup>	0.799 <sup>BC</sup>
	30	0.956 <sup>Aa</sup>	0.625 <sup>Cc</sup>	0.936 <sup>BCa</sup>	0.951 <sup>Aa</sup>	0.671 <sup>Cb</sup>	0.828 <sup>B</sup>
	60	0.955 <sup>Aa</sup>	0.688 <sup>Bc</sup>	0.983 <sup>Aa</sup>	0.946 <sup>Aa</sup>	0.738 <sup>Bb</sup>	0.862 <sup>AB</sup>
	90	0.984 <sup>Aa</sup>	0.948 <sup>Ab</sup>	0.939 <sup>ABb</sup>	0.937 <sup>Ab</sup>	0.958 <sup>ABb</sup>	0.953 <sup>A</sup>

The data are the means ( $n = 3$ ). Different lowercase and uppercase letters within the values of each parameter indicate significant differences between treatments at the same sampling time and between sampling times within the same treatment (LSD post hoc test;  $P < 0.05$ ), respectively. The values marked in gray or green indicate a significant inhibition or stimulation in relation to the non-treated soil, respectively. The explanation of the treatment abbreviations is given in **Figure 1**.

VA and/or *C. freundii* on AWCD (**Figure 1A**). In the case of the remaining CLPP indices, a decrease in the values of the RS index, which was observed for some soil treatments (**Table 1**), was generally associated with the stimulatory effect of antibiotic and/or *C. freundii* during the experimental period (**Figure 1**). Calculation of the RL index at the end of the experiment (day 90) revealed that its value was different for each CLPP index. The positive values of the RL index for all of the soil treatments were obtained in relation to the AWCD (**Table 2**).

The PCA plot obtained for the CLPPs (based on the AWCD,  $R_S$ , H, and E values) for all of the sampling days revealed that samples were mainly scattered along the PC1 axis (**Figure S1**) and the pattern of variability depended on the bacterial strain, VA dosage and time (**Table S3**). The PCA plots obtained for each sampling day (**Figure 2**) showed a significant impact of the VA concentration and/or *C. freundii* on the CLPPs and it was evident on days 1, 15, 30, and 90 of the experiment (**Table S4**).

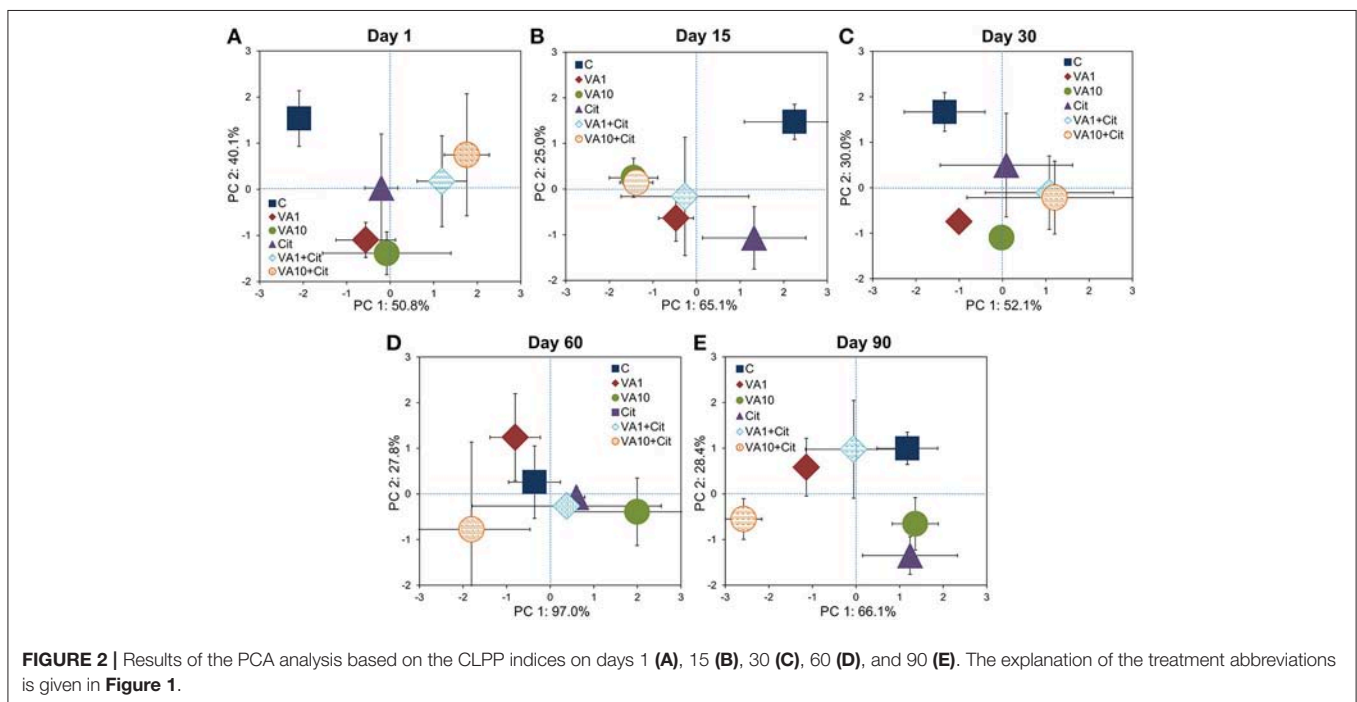
## Pattern of the Utilization of Carbon Substrate Groups

Analysis of the AWCD values for the six groups of 31 carbon substrates of the Biolog EcoPlates<sup>TM</sup> showed differences between the samples with VA and/or *C. freundii* and the non-treated soil (**Figure 3**). The obtained results generally indicated that all of the soil treatments contributed to a significant decrease ( $P < 0.05$ ) in the AWCD values for the utilization of amines, miscellaneous and polymers in the first 30 days of the incubation. The AWCD values for the utilization of amino acids, carbohydrates and carboxylic acids were similar to those that were calculated for the non-treated soil on day 1. However, a negative effect of all of the soil treatments on the utilization of these carbon substrates groups was detected on days 15 and 30. At the next sampling times (days 60 and 90), all of the substrate usage patterns had recovered and, in many cases were higher (up to 1.3-17-fold) than those found in the control (**Figure 3**). A multivariate analysis showed that the utilization pattern

**TABLE 2** | Values of the resilience (RL) index for measured parameters obtained at the end of the experiment.

Parameter	Treatment					$\bar{x}$
	VA1	VA10	Cit	VA1+Cit	VA10+Cit	
AWCD (average)	0.696 <sup>a</sup>	0.351 <sup>b</sup>	0.122 <sup>c</sup>	0.788 <sup>a</sup>	0.385 <sup>b</sup>	0.468
Substrate richness (R <sub>S</sub> )	-0.785 <sup>b</sup>	-0.066 <sup>ab</sup>	0.276 <sup>a</sup>	0.330 <sup>a</sup>	-0.315 <sup>ab</sup>	-0.112
Shannon-Wiener index (H)	-0.542 <sup>c</sup>	0.460 <sup>a</sup>	-0.003 <sup>b</sup>	-0.556 <sup>c</sup>	-0.681 <sup>c</sup>	-0.264
Evenness (E)	-0.140 <sup>ab</sup>	0.328 <sup>a</sup>	0.072 <sup>ab</sup>	0.077 <sup>ab</sup>	-0.341 <sup>b</sup>	-0.001
AWCD-amines	-0.429 <sup>b</sup>	0.305 <sup>a</sup>	0.313 <sup>a</sup>	0.396 <sup>a</sup>	-0.158 <sup>b</sup>	0.085
AWCD-amino acids	-0.067 <sup>b</sup>	0.165 <sup>ab</sup>	-0.647 <sup>c</sup>	0.479 <sup>a</sup>	-0.065 <sup>b</sup>	-0.027
AWCD-carbohydrates	-0.114 <sup>bc</sup>	0.133 <sup>ab</sup>	0.537 <sup>a</sup>	-0.337 <sup>bc</sup>	-0.622 <sup>c</sup>	-0.081
AWCD-carboxylic acids	-0.096 <sup>ab</sup>	0.043 <sup>ab</sup>	-0.329 <sup>b</sup>	0.481 <sup>a</sup>	-0.300 <sup>b</sup>	-0.040
AWCD-miscellaneous	0.715 <sup>a</sup>	0.717 <sup>a</sup>	0.887 <sup>a</sup>	0.708 <sup>a</sup>	0.889 <sup>a</sup>	0.783
AWCD-polymers	0.877 <sup>a</sup>	0.117 <sup>b</sup>	-0.044 <sup>c</sup>	0.774 <sup>a</sup>	0.857 <sup>a</sup>	0.516
DHA activity	0.723 <sup>a</sup>	0.773 <sup>a</sup>	0.621 <sup>a</sup>	0.812 <sup>a</sup>	0.940 <sup>a</sup>	0.774
PHOS-H activity	0.497 <sup>a</sup>	0.715 <sup>a</sup>	-0.110 <sup>b</sup>	0.851 <sup>a</sup>	0.736 <sup>a</sup>	0.538
PHOS-OH activity	-0.235 <sup>b</sup>	0.788 <sup>a</sup>	0.387 <sup>ab</sup>	-0.041 <sup>b</sup>	0.995 <sup>a</sup>	0.380
URE activity	0.875 <sup>a</sup>	0.815 <sup>a</sup>	0.607 <sup>a</sup>	0.623 <sup>a</sup>	0.868 <sup>a</sup>	0.757

The data are the means ( $n = 3$ ). Different letters within the values of each parameter indicate significant differences between treatments (LSD post hoc test;  $P < 0.05$ ). The explanation of the treatment abbreviations is given in **Figure 1**.



of each substrate group was affected by the concentration of VA, the *C. freundii* strain and the time of incubation (Table S5).

Mean values of the RS index calculated for all of the soil treatments demonstrated that among the substrates, the highest resistance was observed for miscellaneous (0.445) while the lowest for carboxylic acids (0.124) (Table 1). In addition, the two-way ANOVA analysis generally revealed that VA and/or *C. freundii* significantly affected the values of the RS index for the

utilization of carbon substrate groups during the experimental period (Table S2). Determination of the RL index at the end of the experiment (day 90) revealed that its value was different for the AWCD for each substrate group (Table 2). The positive values of the RL index for most of the soil treatments were obtained in relation to the AWCD for amines, miscellaneous, and polymers. In contrast, the RL index was found to be negative in the case of the AWCD for amino acids, carbohydrates and carboxylic acids (Table 2).

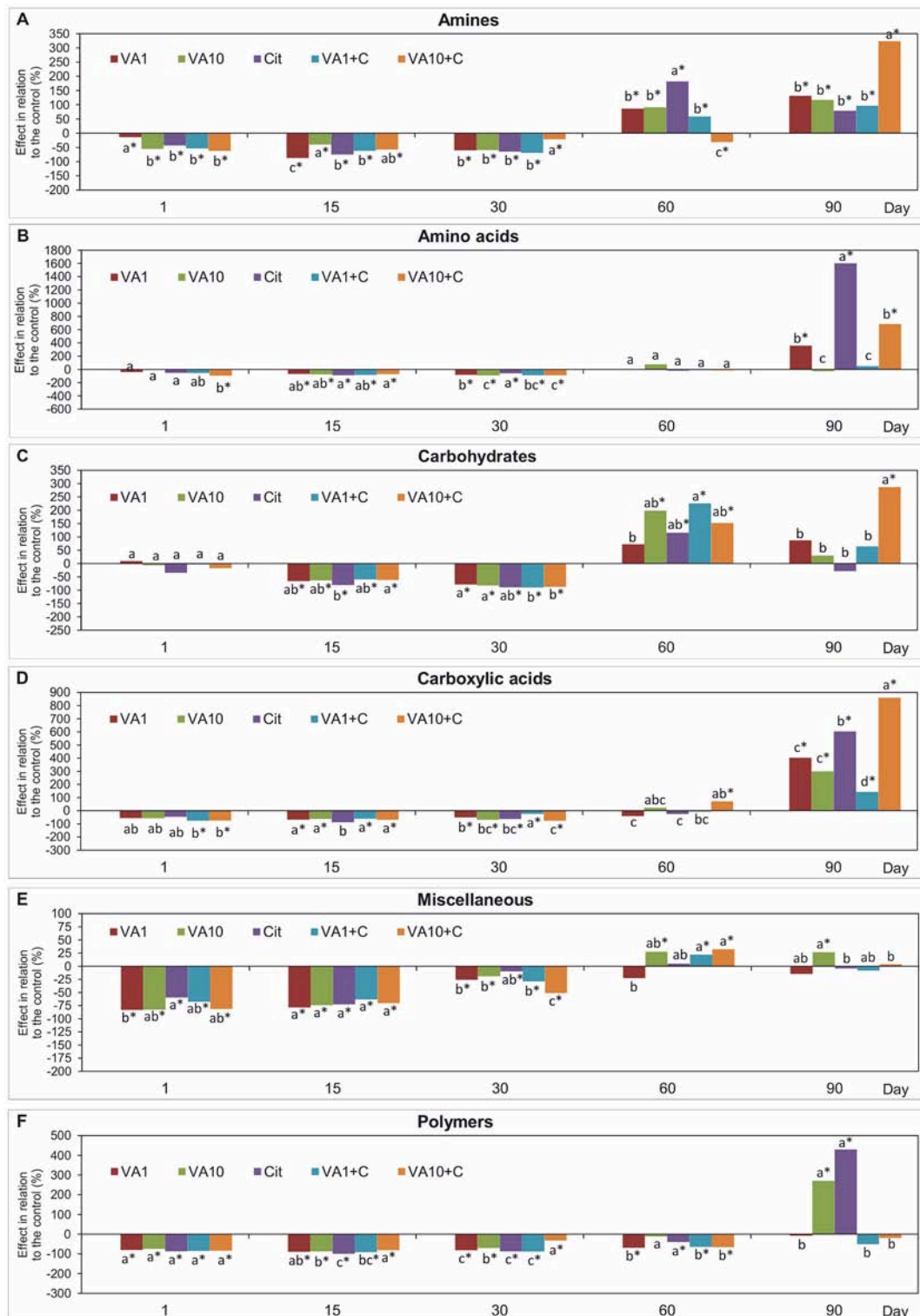


**FIGURE 3 |** Effect of VA and/or *C. freudii* on the AWCD of the carbon substrate groups: amines (A), amino acids (B), carbohydrates (C), carboxylic acids (D), miscellaneous (E), and polymers (F) during the experimental period. The data are the means ( $n = 3$ ) and expressed as a percentage of the inhibition or stimulation in relation to the control soil. Different letters and asterisks within the values of each substrate indicate significant differences between treatments, and between treatments and control at the same sampling time (LSD *post hoc* test;  $P < 0.05$ ), respectively. The explanation of the treatment abbreviations is given in Figure 1.

The PCA plots obtained from the AWCD values for the six groups of substrates for all of the sampling days (Figure S2) and for individual sampling days (Figure 4) revealed a pattern of variability depended on the bacterial strain, VA dosage and time (Table S6), and the bacterial strain and VA dosage (Table S7), respectively. Generally, a significant impact was evident on days 1, 15, and 30 of the experiment and, the carbon substrate utilization patterns for the treated soil samples separated from those obtained for the control soil (Figure 4 and Figure S2).

## Activity of Enzymes

Analysis of the activity of enzymes showed differences between the samples with VA and/or *C. freundii* and the non-treated soil (Figure 5). The obtained results generally indicated that the higher soil treatments contributed to a significant decrease ( $P < 0.05$ ) in the activity of DHA and PHOS-H, and PHOS-OH in the first 15 days and on day 1, respectively. In turn, a positive effect was detected on days 30 and 60. In the case of URE, an addition of the higher dose of VA and *C. freundii* stimulated its activity from day 1 up to day 60. On day 90, no

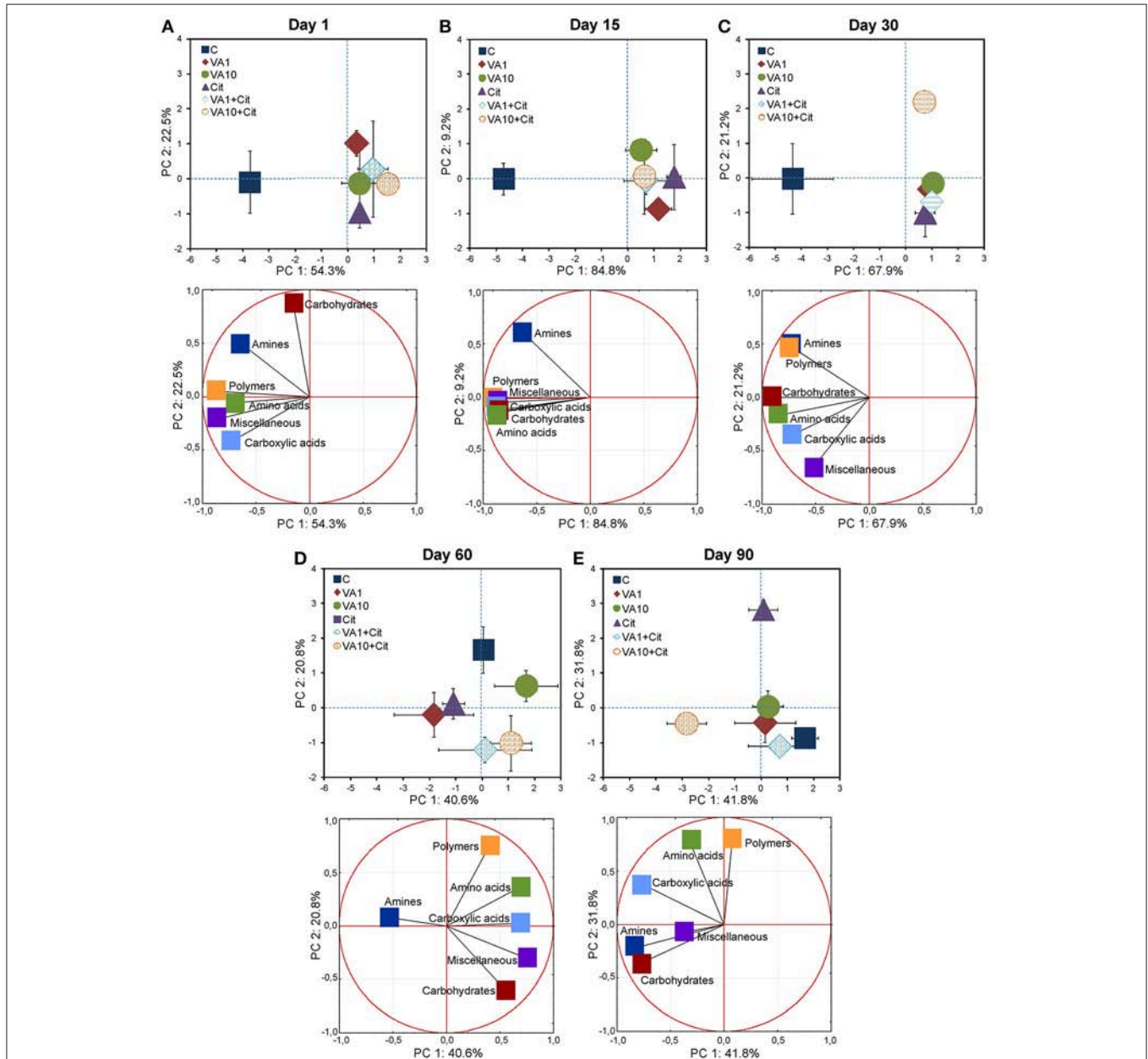


**FIGURE 4** | Results of the PCA analysis based on the data of the carbon substrate groups on days 1 (A), 15 (B), 30 (C), 60 (D), and 90 (E). The explanation of the treatment abbreviations is given in Figure 1.

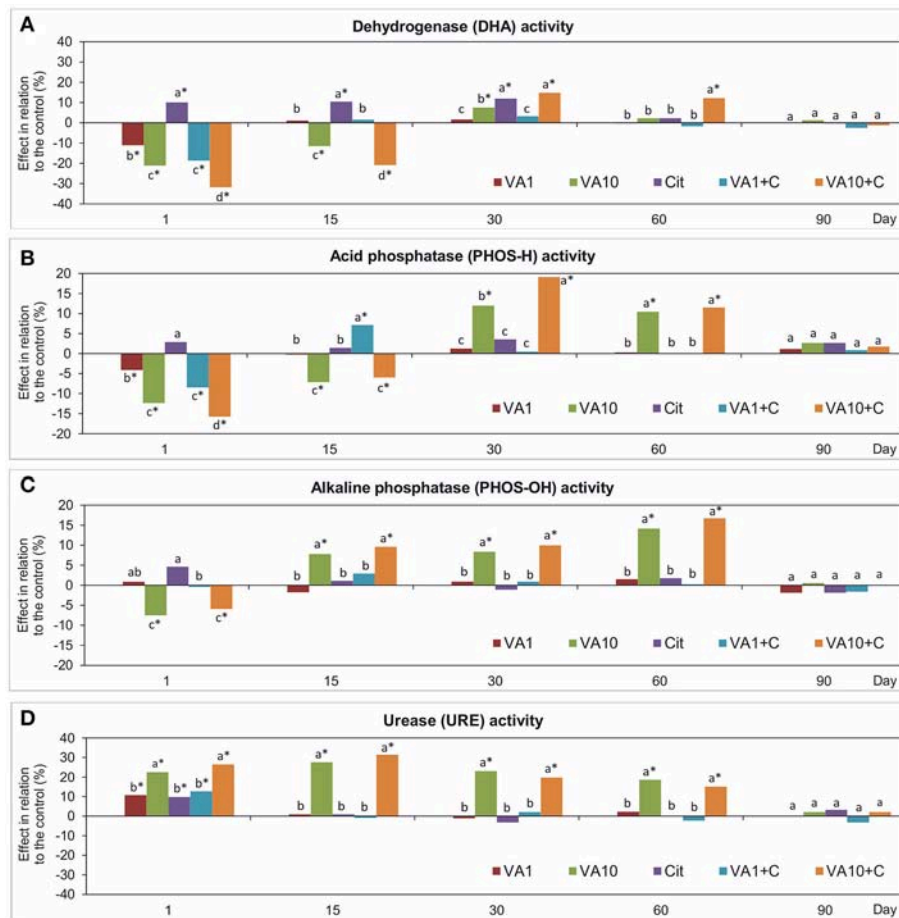


**FIGURE 5 |** Effect of VA and/or *C. freundii* on the DHA (A), PHOS-H (B), PHOS-OH (C), and URE (D) activity during the experimental period. The data are the means ( $n = 3$ ) and expressed as a percentage of the inhibition or stimulation in relation to the control soil. Different letters and asterisks within the values of each enzyme indicate significant differences between treatments, and between treatments and control at the same sampling time (LSD *post hoc* test;  $P < 0.05$ ), respectively. The explanation of the treatment abbreviations is given in **Figure 1**.

effect was noticed in the soil samples with both doses of VA and/or *C. freundii* bacterial strain and the activity of all of the enzymes was similar to those determined for the non-treated soil (**Figure 5**). The three-way ANOVA revealed that different factors significantly influenced the activity of enzymes tested (Table S8).

The mean values of the RS index calculated for all of the soil treatments demonstrated that among the enzymes tested, the highest resistance was observed for PHOS-OH (0.919) while the lowest for URE (0.833) (Table 1). In addition, the two-way ANOVA analysis generally revealed that VA and/or *C. freundii* significantly affected the values of the RS index for the activity of enzymes during the experimental period (Table S2). Determination of the RL index at the end of the experiment (day 90) revealed that its mean value was found to be positive and reached the values of 0.774, 0.538, 0.380, and 0.757 for DHA, PHOS-H, PHOS-OH, and URE, respectively (Table 2).

The PCA plots obtained from the enzyme activities for all of the sampling days (Figure S3) and for individual sampling days (**Figure 6**) revealed a pattern of variability depended on the

bacterial strain, VA dosage and time (Table S9), and the bacterial strain and VA dosage (Table S10), respectively. Generally, a significant impact was evident up to day 60 of the experiment and, the enzyme activity patterns for the treated soil samples separated from those obtained for the control soil (**Figure 6** and Figure S3).

## Dissipation of Vancomycin in Soil

Based on the validation studies, the calibration curve was linear within a range of 0.005–20.0  $\mu\text{g/mL}$  with  $R^2 = 0.9997$  (Figure S4). The limits of quantification (LOQ) and detection (LOD) as well as recoveries for VA were 0.01 mg/kg soil, 0.1 mg/kg soil and 87.2–102%, respectively (Table S11). Chromatograms for the VA standard, control and vancomycin-treated soil samples obtained during the validation studies are presented in Figures S5, S6. The results of the dissipation experiment of VA are presented in **Figure 7**. Our study showed that the dissipation of the antibiotic in VA1-, VA10-, VA1+Cit-, and VA10+Cit-treated nsS was relatively fast. Almost 100% of VA applied at both concentrations

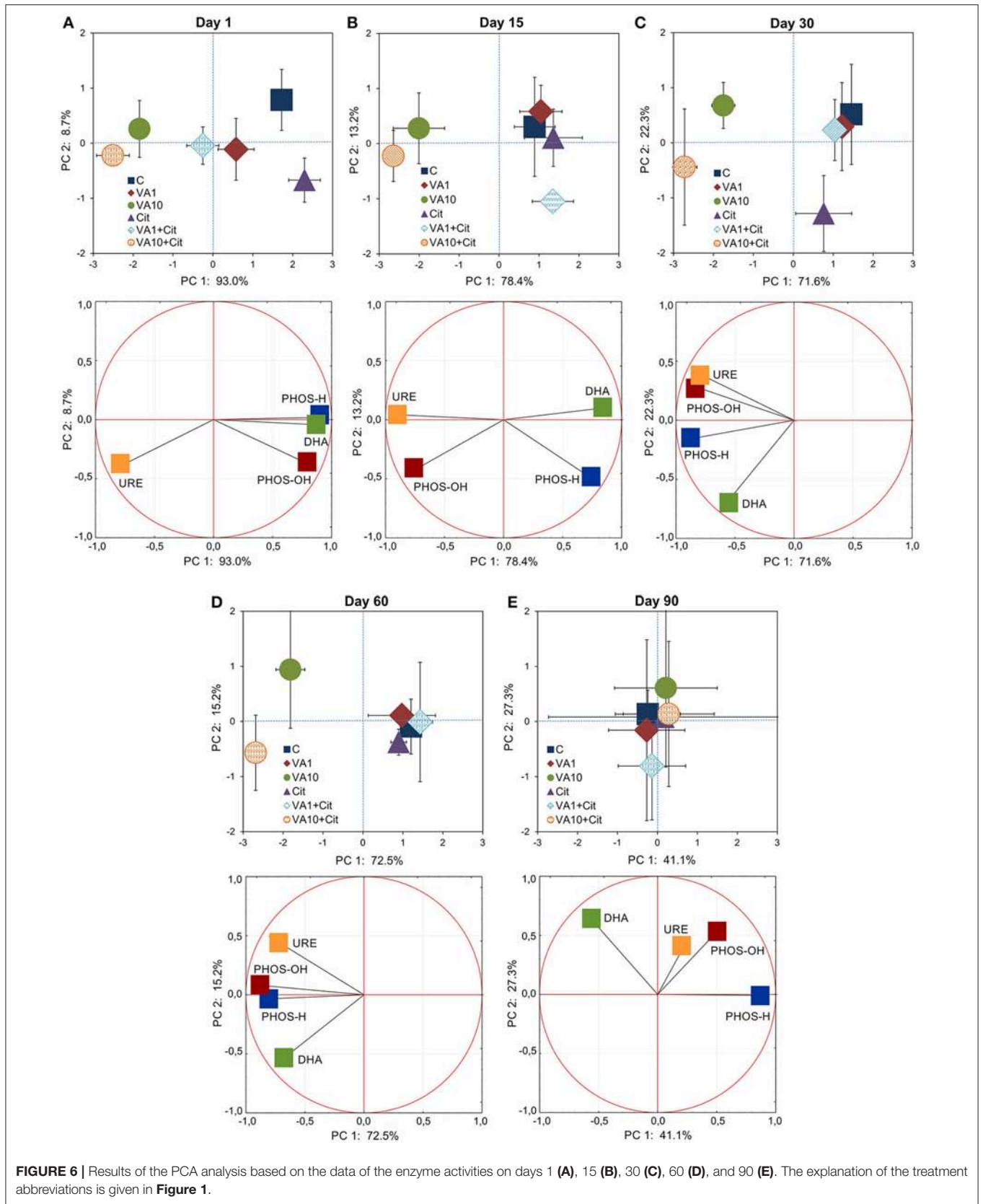


**FIGURE 6 |** Results of the PCA analysis based on the data of the enzyme activities on days 1 (A), 15 (B), 30 (C), 60 (D), and 90 (E). The explanation of the treatment abbreviations is given in Figure 1.

was degraded within 30 days of the experiment. There were no differences in the values of the DT50 of vancomycin between the treatments. The kinetic data indicated that the dissipation process followed zero-order kinetics and the calculated DT50 values were about 16 days for all of the non-sterile treatments (Table 3). The dissipation of VA in sS+VA and sS+VA10 was three times slower compared to the dissipation of the antibiotic in nsS. Both dosages of VA were almost completely degraded within 90 days and the DT50 values were 47.33 and 49.84 days, respectively (Table 3). Our study also showed that *C. freundii* had the potential to degrade VA and was able to degrade VA. In sS that had been inoculated with the *C. freundii* strain, the antibiotic was almost completely degraded within 60 days and the DT50 reached the values of 32.82 and 32.74 days for sS+VA+Cit and sS+VA10+Cit, respectively.

The obtained results indicated that the dissipation of the antibiotic was independent of the concentration that had been used. This was confirmed by an ANOVA analysis, which revealed that the DT50 value was only affected by the type of soil ( $P < 0.001$ ) and the *C. freundii* strain ( $P < 0.001$ ; Table S12). The type of soil explained up to 83.1% of the variability. The concentration of VA had no effect ( $P = 0.801$ ) on the DT50 value. A multivariate analysis also revealed that the DT50 value was

only affected by the interaction between the type of soil and the *C. freundii* strain ( $P < 0.001$ ) and that it explained 8.1% of the variability (Table S12).

## DISCUSSION

Studies on the metabolic activity of microorganisms are of great significance as they show the biochemical potential of soils. Any toxicant application into soils that might affect the soil microorganism and their metabolic potential may generate changes in the productivity of soils (Badiane et al., 2001; Gil-Sotres et al., 2005; Liu et al., 2015; Cycoń et al., 2016b). In our previous study, using the DGGE and PLFA profiling, we found that application of VA and VA+*C. freundii* significantly altered the genetic and structural diversity of soil microbial communities (Cycoń et al., 2016a). Surprisingly, we observed that the biomass of PLFAs characteristic for Gram-positive bacteria in the VA-treated soils was higher in comparison with the control. These data suggest that a large fraction of Gram-positive inhabiting tested soils was resistant to VA and reached a high biomass probably due to use of VA as the source of carbon. A high number of active metabolically Gram-positive bacteria allowed them to successfully competed with Gram-negative bacteria, for which a

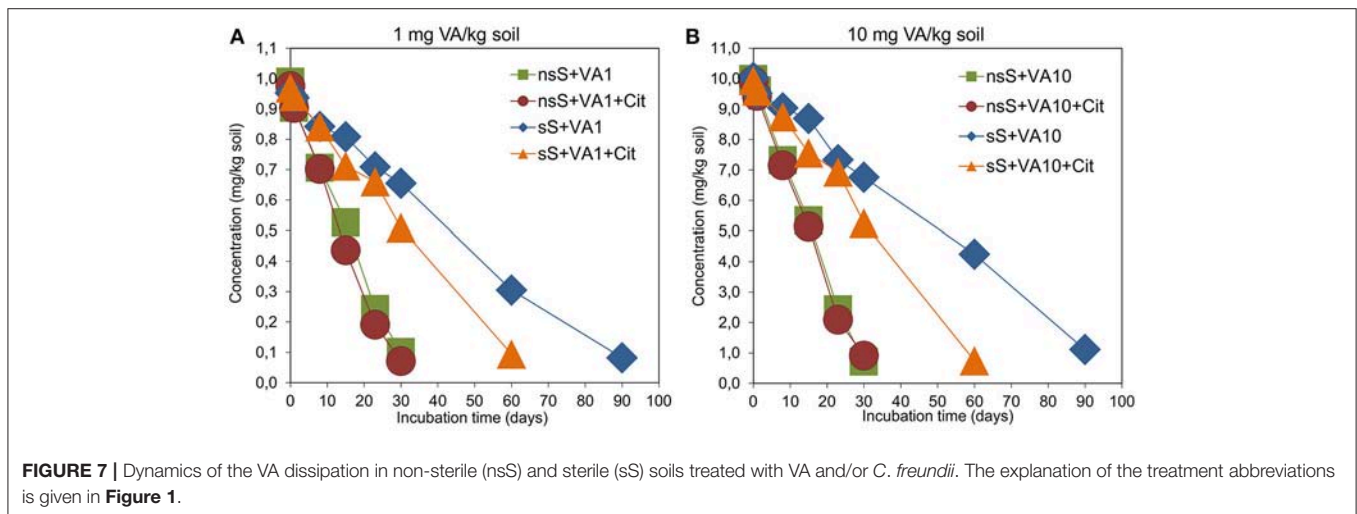


**TABLE 3 |** The kinetic data of the disappearance of vancomycin in the soil.

Treatment	Regression equation	$R^2$	$k$ (day)	DT <sub>50</sub> (days)
nsS+VA1	$C_t - C_0 = -0.0294t - 0.0349$	0.9934	$0.0296 \pm 0.0023$	$15.64 \pm 1.16^b$
nsS+VA10	$C_t - C_0 = -0.3132t - 0.0690$	0.9980	$0.3093 \pm 0.0084$	$15.73 \pm 0.72^b$
nsS+VA1+Cit	$C_t - C_0 = -0.0308t - 0.0338$	0.9889	$0.0301 \pm 0.0043$	$14.73 \pm 1.21^b$
nsS+VA10+Cit	$C_t - C_0 = -0.3085t - 0.1935$	0.9923	$0.3005 \pm 0.0068$	$15.46 \pm 0.92^b$
sS+VA1	$C_t - C_0 = -0.0098t - 0.0123$	0.9946	$0.0097 \pm 0.0012$	$47.33 \pm 1.46^a$
sS+VA10	$C_t - C_0 = -0.0963t - 0.2188$	0.9949	$0.0992 \pm 0.0223$	$49.84 \pm 1.76^a$
sS+VA1+Cit	$C_t - C_0 = -0.0144t - 0.0115$	0.9956	$0.0146 \pm 0.0063$	$32.82 \pm 0.58^c$
sS+VA10+Cit	$C_t - C_0 = -0.1516t - 0.0072$	0.9949	$0.1533 \pm 0.0440$	$32.74 \pm 0.89^c$

sS, sterile soil; nsS, non-sterile soil; VA1, vancomycin (1 mg/kg soil); VA10, vancomycin (10 mg/kg soil); Cit, *C. freundii*. The data are the means with standard deviations ( $n = 3$ ). Different letters within the DT<sub>50</sub> values indicate significant differences between treatments (LSD post hoc test;  $P < 0.05$ ).

substantial decrease in the PLFA biomass was observed. However, the effect of VA on qualitative and quantitative changes within indigenous microbial communities was transient.

Results of this study demonstrated that alterations in the structure of soil bacterial assemblages were reflected in changes of the total microbial activity. We found that the AWCD values for samples treated with VA and/or *C. freundii* were significantly lower as compared to the control, however this effect was observed only during 30 days of the experiment. A short-lasting effect of various antibiotics on soil microbial activity was also observed by other authors. For example, Fang et al. (2014, 2016) reported that chlortetracycline applied at 1 and 10 mg/kg soil decreased the values of the AWCD for 35 days. From this day, irrespective of the frequency of antibiotic application, the AWCD values gradually recovered to the control level. A short-term detrimental effect of tetracycline on the community level physiological profiles was also observed by Chessa et al. (2016). The CLPP data showed that tested soil were susceptible to tetracycline applied at the concentration of 500 mg/kg for only 7 days. In contrast, Toth et al. (2011) showed that the application of chlortetracycline and sulfadimethoxine did not significantly change the CLPP parameters, whereas monensin slightly increased the value of the H index. In our study, alterations in the preferential degradation of some of the substrates in Eco-plates by microorganisms from VA- and VA+C. *freundii*-treated soil samples were found. VA impacts microorganisms by changing their ability to utilize different carbon sources, thus affecting the metabolic diversity of soil microbial communities. Similarly, Xu et al. (2016) found that a high level of sulfadiazine decreased the utilization rates of carbohydrate, carboxylic acid, amino acid, and aromatic acid. Also, sulfamethoxazole applied at concentrations of 100 and 1,000 mg/kg decreased the degradation of all substrates with the exception of the polymers (Pino-Otín et al., 2017). A significant decrease in the utilization of some substrates (carbohydrates and miscellaneous) was also observed in soils treated with sulfamethoxazole (Liu F. et al., 2012). However, this short-term effect was only observed 7 days after the antibiotic application and on day 21, the utilization of the substrates increased compared to the first sampling day. In addition, Kong et al. (2006) observed that the substrate utilization pattern changed significantly with increasing concentrations of oxytetracycline. In contrast, doxycycline application had a general positive effect on the utilization of substrates (Wang et al., 2016).

Changes in the activity of soil microbial communities pointed by Biolog method were also proved by measuring the activities of selected enzymes. The application of VA (at a higher concentration) and/or *C. freundii* significantly shifted the pattern of the enzyme activities. A short-term negative effect of VA manifested toward the activity of DHA, PHOS-H, and PHOS-OH. Similar to our results, a temporary decrease in DHA in soil treated with oxytetracycline or lincomycin (both at 50 and 200 mg/kg soil) was observed by Unger et al. (2013). The same effect was found in soil treated with manure containing sulfamethazine (Pinna et al., 2012). An inhibition of DHA activity along the gradient of the oxytetracycline concentration over the entire experimental period was found by

and Chen et al. (2013). In another study, the activity of DHA in chlortetracycline-treated soils (1, 10 and 100 mg/kg) increased on the first day but then significantly decreased for up to 45 days (Liu et al., 2015). In our study, VA and VA+C. *freundii* increased the activity of all the enzymes on days 30 and 60 in comparison with the control. However, lower activities of both phosphatases were observed in VA-treatments at the beginning of the experiment. Similarly, six different antibiotics, i.e., chlortetracycline, tetracycline, tylosin, sulfamethoxazole, sulfamethazine and trimethoprim when applied at dosages of 1–300 mg/kg soil inhibited the PHOS-H activity during the experiment, although this effect was slight (Liu et al., 2009, 2015). The study by Yang et al. (2009) revealed that among the PHOSs tested, only PHOS-OH was sensitive to the application of oxytetracycline with a 41.3% decline in the activity of enzyme at a dosage of 10 mg/kg soil and, a further decrease of 64.3–80.8% when concentration of the antibiotic exceeded 30 mg/kg. In contrast, Ma et al. (2016) found that oxytetracycline had no effect on the soil neutral PHOS activity over a 120-day incubation period even when large amounts of the antibiotic were applied (up to 30 mg/kg). An analysis of URE activity in soil that had been treated with vancomycin and/or *C. freundii* showed stimulated stimulation of this enzyme for up to 60 days. In contrast, in oxytetracycline- and tetracycline-treated soils, the URE activity was significantly inhibited along the gradient of concentrations of the antibiotics (Wei et al., 2009; Chen et al., 2013). In other studies, the URE activity in the soil was slightly affected by sulfadiazine (Hammesfahr et al., 2011) or was affected for a short time by sulfamethazine (Pinna et al., 2012). Our results indicated that among the enzymes tested, DHA was the most sensitive to the application of the antibiotic. The low activity of DHA in the soils that had been treated with VA at the beginning of the experiment may be related with the death or inhibition of some microorganism that is sensitive to antibiotics and that is responsible for the production of enzymes. In addition, the DHAs that are released from dead microorganisms do not accumulate in soils since they are rapidly degraded (Alef, 1995). In turn, PHOSs and URE are more stable in soils because they are immobilized by various soil compounds (Gianfreda et al., 1994).

In addition to a higher activity of enzymes in higher VA dosage-treated soils (especially between 30 and 60 days), an increase of the AWCD values was observed, suggesting enhancement of the total catabolic potential of soil. This effect might be result from the ability of microorganisms to use an antibiotic as the additional compounds for their growth. This explanation might be supported by the fast disappearance of VA in soil used in our study. Moreover, the most of the inoculants do not survive for a long time in the bioaugmented soil, and nutrients released from dead cell provide an additional source of carbon and energy. The pool of nutrients might be also extended by compounds originated from sensitive bacteria killed by antibiotic applied into the soil (Pinna et al., 2012; Ding et al., 2014; Chessa et al., 2016). A consequence of these above phenomena may be the increase in the microbial biomass and enzyme production (Westergaard et al., 2001; Hammesfahr et al., 2011). In general, a multivariate analysis revealed that the inoculation of *C. freundii* had no significant effect on the

metabolic potential of soil microbial communities with the exception of the short-term stimulation of DHA, PHOSs and URE. This showed that inoculants, in contrast to VA, did not exert a stressful condition for indigenous microorganisms. Moreover, introduced bacteria did not modify the action of VA. The lack of changes might also be related to the competition with autochthonic microorganisms. In addition, the inhibition *via* compounds that are synthesized by these organisms may also be taken into consideration. Moreover, the introduction of inoculants into soil is stressful resulting in the necessity of their adaptation to the new soil conditions (Karpouzias et al., 2000; Singh et al., 2006).

The short-term changes in the soil metabolic diversity in the response to VA and/or *C. freundii* application may be also related to the resilience and resistance of tested microbial communities. The RS and RL indices enable to check if microbial communities exposed to various stressors can remain stable and/or achieve the origin level of metabolic activity (Orwin and Wardle, 2004). Significant changes in the RS value were observed up to 60 days of the experiment for soil treated with a higher dose of VA (irrespective of *C. freundii* inoculation). URE and DHA were more sensitive to VA in comparison with phosphatases. A similar phenomenon was also previously demonstrated for soil that had been contaminated with pesticides (Baćmaga et al., 2015). However, in our study, there were no differences in the values of the RS and RL indices between the soil treatments on day 90 of the experiment. These results showed that intrinsic properties of soil microbial communities are a key mechanism driving functional stability of soil ecosystem (Song et al., 2015). Even if microbial populations are sensitive to perturbation, the entire community may be resilient and have the ability to return to its original activity (Allison and Martiny, 2008). Second, microorganisms in a new community may act differentially but the final metabolic outcome is similar to those observed in the non-disturbed community. Moreover, the resilience potential reflects the multifunctionality of the soil microorganisms (Ludwig et al., 2017). It has been thought that two mechanisms are responsible for the lack of changes in the ecosystem processes rate despite the alteration in the biochemical microbial diversity. First, a new community may contain microorganisms that are functionally redundant with microorganism that were affected by stressors. Second, microorganism in a new community may act differentially but the final level of biological processes is similar to those observed in non-disturbed community (Allison and Martiny, 2008).

The obtained results revealed that the dissipation of VA in nsS was relatively fast and independent of the antibiotic concentration. Based on the kinetic model, the DT50 values for the dissipation of VA at 1 and 10 mg/kg soil were 15.64 and 15.73 days. As proposed by Crane et al. (2010), antibiotics that are characterized by DT50 values of 5–22 days belong to the group of high degradability chemicals in soils. In this context, VA with a DT50 of about 16 days may be classified as a compound with a low persistence in soil. The relatively short-term persistence of VA in soil might also be related to its solubility in water and its low affinity to

adsorption by various components of the soil (Thiele-Bruhn, 2003). Antibiotics are subjected to various processes in the soil such as volatilization, transformation or degradation, sorption-desorption, uptake by plants and transport into groundwater and surface waters (Accinelli et al., 2007; Lin and Gan, 2011; Yang et al., 2012; Manzetti and Ghisi, 2014; Awad et al., 2016; Pan and Chu, 2016; Topp et al., 2016). However, many factors such as the chemical structure, properties and concentration of an antibiotic, the physico-chemical properties of the soil, the microbial population and the incubation conditions play a major role in the degradation of antibiotics in soil. Antibiotics differ in their susceptibility to degradation in soil as was evidenced by the large range of the DT50 or half-life values between <1 and 3,466 days (Crane et al., 2010; Walters et al., 2010; Hammesfahr et al., 2011; Braschi et al., 2013; Awad et al., 2016).

Our study showed that the dissipation of VA in nsS was three times faster compared to the dissipation of antibiotics in sS as was indicated by the DT50 values. These results suggest that in addition to abiotic processes, degradation by microorganisms was the main mechanisms of VA disappearance in soil. Moreover, Pan and Chu (2016) showed that erythromycin (0.1 mg/kg soil) applied into clay loamy soil was degraded faster in nsS compared to sS with a DT50 of 6.4 and 40.8 days, respectively. Accinelli et al. (2007) reported that sulfachloropyridazine (10 mg/kg soil) was degraded almost three times faster in soils with autochthonous microorganisms (half-life 20–26 days) compared to sterile soils (half-life 68–71 days). (Zhang W. et al., 2017; Zhang Y. et al., 2017) also showed that microbial activity contributes in the biotransformation of sulfadiazine in soil, for which the calculated DT50 reached values of 8.48, 8.97, and 10.22 days (non-sterile soil) and 30.09, 26.55, and 21.21 days (sterile soil) for 4, 10, and 20 mg/kg, respectively. This phenomenon has also been found for other antibiotics (Lin and Gan, 2011; Srinivasan and Sarmah, 2014; Pan and Chu, 2016).

Our study also showed that *C. freundii* was characterized by a degradation potential in relation to the VA as showed by the disappearance of VA in sterile soil inoculated with this strain. In contrast, we did not observe an acceleration of VA dissipation in non-sterile soil by *C. freundii* and the DT50 values for VA were similar to those obtained for non-sterile soil without the strain. A lack of changes in the degradation rate of VA after the inoculation of *C. freundii* into the soil might be related to the ability of the inoculated strain to survive and its competition with autochthonic soil microorganisms or inhibition *via* compounds produced by these organisms (Karpouzias et al., 2000; Cycón et al., 2014), which were not observed in sS. In turn, the study by Topp et al. (2016) revealed that the bioremediation potential of *Microbacterium* sp. increased the mineralization of sulfamethazine by 44–57% in an agricultural soil. Other studies have confirmed that several bacteria isolated from antibiotic-contaminated sources (i.e., patients, soil, sediments, and sludge) belonging to different genera were capable of degrading antibiotics in liquid cultures (Xin et al., 2012; Topp et al., 2013; Leng et al., 2016; Mulla et al., 2018; Wen et al., 2018).

## CONCLUSIONS

The decrease in the activity of soil microorganisms found in this study was consistent with results of our previous experiments dealing with changes in the structural and genetic diversity of a microbial community in a response to the application of VA and/or *C. freundii*. As was shown by the degradation data, VA was almost completely degraded in nsS within 30 days. At that time, we also observed a decrease in the metabolic activity of soil microorganism as was indicated by the data from CLPP and enzyme activities. On the next sampling days, no effects or stimulation of microbial activity were found. These results suggest that as long as VA was present in the soil, it negatively affected microbial activity. Regardless if VA was applied alone or with *C. freundii* it altered the catabolic potential of soil thus created the stressful conditions for autochthonic microbes. In turn, *C. freundii* introduced into soil alone did not pose a threat for metabolic activity of microbial communities. An analysis of the RS and RL indices showed that there were differences in the resistance and resilience of measured activities to disturbances caused by antibiotic and/or *C. freundii*. The loss of the ability of microbial communities to degrade some substrates and the decreasing activity of soil enzymes in VA-treated soil may be connected with the inhibition of some microorganisms, which are responsible for the production of certain enzymes. However, the processes of the selection and adaptation of microorganisms to antibiotics as well their functional redundancy are responsible

for the recovery of microbial communities from disturbances that are caused by vancomycin. Although the negative effect of VA on the metabolic pattern of soil microorganism was transient, the application of VA into soil may temporarily pose a potential risk for soil functioning. It seems that deeper understanding of mechanisms involved in the response of soil microorganisms to disturbances is crucial for the assessment of the impact of stressors on the soil function.

## AUTHOR CONTRIBUTIONS

KO and MC Conceived and designed experiments. KO, MC, AM, AZ, JS-D, and JB-W Contributed reagents and materials, performed experiments. KO, MC, AM, AZ, TW, and ZP-S Analyzed results. KO, MC, and ZP-S Wrote the paper.

## ACKNOWLEDGMENTS

This work was carried out as part of the grant, which was financed by the National Science Centre, Poland (No. DEC-2014/15B/NZ9/04414).

## SUPPLEMENTARY MATERIAL

The Supplementary Material for this article can be found online at: <https://www.frontiersin.org/articles/10.3389/fmicb.2018.01047/full#supplementary-material>

## REFERENCES

- Accinelli, C., Koskinen, W. C., Becker, J. M., and Sadowsky, M. J. (2007). Environmental fate of two sulfonamide antimicrobial agents in soil. *J. Agric. Food Chem.* 55, 2677–2682. doi: 10.1021/jf063709j
- Akimenko, Y. V., Kazeev, K. S., and Kolesnikov, S. I. (2015). Impact assessment of soil contamination with antibiotics (For example, an ordinary chernozem). *Am. J. Appl. Sci.* 12, 80–88. doi: 10.3844/ajassp.2015.80.88
- Alef, K. (1995). “Dehydrogenase activity,” in *Methods in Applied Soil Microbiology and Biochemistry*, eds K. Alef and P. Nannipieri (London: Academic), 228–231.
- Allison, S. D., and Martiny, J. B. H. (2008). Resistance, resilience, and redundancy in microbial communities. *Proc. Natl. Acad. Sci. U.S.A.* 105, 11512–11519. doi: 10.1073/pnas.0801925105
- Awad, Y. M., Ok, Y. S., Igalavithana, A. D., Lee, Y. H., Sonn, Y.-K., Usman, A. R. A., et al. (2016). Sulphamethazine in poultry manure changes carbon and nitrogen mineralisation in soils. *Chem. Ecol.* 32, 899–918. doi: 10.1080/02757540.2016.1216104
- Baćmaga, M., Kucharski, J., and Wyszowska, J. (2015). Microbial and enzymatic activity of soil contaminated with azoxystrobin. *Environ. Monit. Assess.* 187, 615. doi: 10.1007/s10661-015-4827-5
- Badiane, N. N. Y., Chotte, J. L., Pate, E., Masse, D., and Rouland, C. (2001). Use of soil enzyme activities to monitor soil quality in natural and improved fallows in semi-arid tropical regions. *Appl. Soil Ecol.* 18, 229–238. doi: 10.1016/S0929-1393(01)00159-7
- Brandt, K. K., Amézquita, A., Backhaus, T., Boxall, A., Coors, A., Heberer, T., et al. (2015). Ecotoxicological assessment of antibiotics: a call for improved consideration of microorganisms. *Environ. Int.* 85, 189–205. doi: 10.1016/j.envint.2015.09.013
- Braschi, I., Blasioli, S., Fellet, C., Lorenzini, R., Garelli, A., Pori, M., et al. (2013). Persistence and degradation of new  $\beta$ -lactam antibiotics in the soil and water environment. *Chemosphere* 93, 152–159. doi: 10.1016/j.chemosphere.2013.05.016
- Chang, B.-V., and Ren, Y.-L. (2015). Biodegradation of three tetracyclines in river sediment. *Ecol. Eng.* 75, 272–277. doi: 10.1016/j.ecoleng.2014.11.039
- Chee-Sanford, J. C., Mackie, R. I., Koike, S., Krapac, I. G., Lin, Y.-F., Yannarell, A. C., et al. (2009). Fate and transport of antibiotic residues and antibiotic resistance genes following land application of manure waste. *J. Environ. Qual.* 38, 1086–1108. doi: 10.2134/jeq2008.0128
- Chen, W., Liu, W., Pan, N., Jiao, W., and Wang, M. (2013). Oxytetracycline on functions and structure of soil microbial community. *J. Soil Sci. Plant Nutr.* 13, 967–975. doi: 10.4067/S0718-95162013005000076
- Chessa, L., Pusino, A., Garau, G., Mangia, N. P., and Pinna, M. V. (2016). Soil microbial response to tetracycline in two different soils amended with cow manure. *Environ. Sci. Pollut. Res.* 23, 5807–5817. doi: 10.1007/s11356-015-5789-4
- Courvalin, P. (2006). Vancomycin resistance in gram-positive cocci. *Clin. Infect. Dis.* 42, 25–34. doi: 10.1086/491711
- Crane, M., Boxall, A. B. A., and Barret, K. (2010). *Veterinary Medicines in the Environment*. Boca Raton, FL: CRC Press. 240.
- Cui, H., Wang, S.-P., Jia, S.-G., Zhang, N., and Zhou, Z.-Q. (2013). Influence of ciprofloxacin on the microbial catabolic diversity in soil. *J. Environ. Sci. Health B Pestic. Food Contam. Agric. Wastes* 48, 869–877. doi: 10.1080/03601234.2013.796826
- Cycóń, M., Borymski, S., Zolnierczyk, B., and Piotrowska-Seget, Z. (2016b). Variable effects of non-steroidal anti-inflammatory drugs (NSAIDs) on selected biochemical processes mediated by soil microorganisms. *Front. Microbiol.* 7:1969. doi: 10.3389/fmicb.2016.01969
- Cycóń, M., Borymski, S., Orlewska, K., Wasik, T. J., and Piotrowska-Seget, Z. (2016a). An analysis of the effects of vancomycin and/or vancomycin-resistant *Citrobacter freundii* exposure on the microbial community structure in soil. *Front. Microbiol.* 7:1015. doi: 10.3389/fmicb.2016.01015

- Cycoń, M., Markowicz, A., Borymski, S., Wójcik, M., and Piotrowska-Seget, Z. (2013b). Imidacloprid induces changes in the structure, genetic diversity and catabolic activity of soil microbial communities. *J. Environ. Manage.* 131, 55–65. doi: 10.1016/j.jenvman.2013.09.041
- Cycoń, M., Markowicz, A., and Piotrowska-Seget, Z. (2013a). Structural and functional diversity of bacterial community in soil treated with the herbicide napropamide estimated by the DGGE, CLPP and r/K-strategy approaches. *Appl. Soil Ecol.* 72, 242–250. doi: 10.1016/j.apsoil.2013.07.015
- Cycoń, M., Piotrowska-Seget, Z., and Kozdrój, J. (2010). Linuron effects on microbiological characteristics of sandy soils as determined in a pot study. *Ann. Microbiol.* 60, 439–449. doi: 10.1007/s13213-010-0061-0
- Cycoń, M., Zmijowska, A., and Piotrowska-Seget, Z. (2014). Enhancement of deltamethrin degradation by soil bioaugmentation with two different strains of *Serratia marcescens*. *Int. J. Environ. Sci. Technol.* 11, 1305–1316. doi: 10.1007/s13762-013-0322-0
- Demoling, L. A., Bååth, E., Greve, G., Wouterse, M., and Schmitt, H. (2009). Effects of sulfamethoxazole on soil microbial communities after adding substrate. *Soil Biol. Biochem.* 41, 840–848. doi: 10.1016/j.soilbio.2009.02.001
- Ding, G. C., Radl, V., Schloter-Hai, B., Jechalke, S., Heuer, H., Smalla, K., et al. (2014). Dynamics of soil bacterial communities in response to repeated application of manure containing sulfadiazine. *PLoS ONE* 9:e92958. doi: 10.1371/journal.pone.0092958
- Fang, H., Han, L., Cui, Y., Xue, Y., Cai, L., and Yu, Y. (2016). Changes in soil microbial community structure and function associated with degradation and resistance of carbendazim and chlortetracycline during repeated treatments. *Sci. Total Environ.* 572, 1203–1212. doi: 10.1016/j.scitotenv.2016.08.038
- Fang, H., Han, Y., Yin, Y., Pan, X., and Yu, Y. (2014). Variations in dissipation rate, microbial function and antibiotic resistance due to repeated introductions of manure containing sulfadiazine and chlortetracycline to soil. *Chemosphere* 96, 51–56. doi: 10.1016/j.chemosphere.2013.07.016
- Floch, C., Chevremont, A.-C., Joanico, K., Capowicz, Y., and Criquet, S. (2011). Indicators of pesticide contamination: soil enzyme compared to functional diversity of bacterial communities via Biolog® Ecoplates. *Eur. J. Soil Biol.* 47, 256–263. doi: 10.1016/j.ejsobi.2011.05.007
- Garland, J. L. (1997). Analysis and interpretation of community-level physiological profiles in microbial ecology. *FEMS Microbiol. Ecol.* 24, 289–300. doi: 10.1111/j.1574-6941.1997.tb00446.x
- Gianfreda, L., Sannino, F., Ortega, N., and Nannipieri, P. (1994). Activity of free and immobilized urease in soil: effects of pesticides. *Soil Biol. Biochem.* 26, 777–784. doi: 10.1016/0038-0717(94)90273-9
- Gil-Sotres, F., Trasar-Cepeda, C., Leirós, M. C., and Seoane, S. (2005). Different approaches to evaluating soil quality using biochemical properties. *Soil Biol. Biochem.* 37, 877–887. doi: 10.1016/j.soilbio.2004.10.003
- Griffiths, B. S., and Philippot, L. (2013). Insights into the resistance and resilience of the soil microbial community. *FEMS Microbiol. Rev.* 37, 112–129. doi: 10.1111/j.1574-6976.2012.00343.x
- Gupta, A., Biyani, M., and Khaira, A. (2011). Vancomycin nephrotoxicity: myths and facts. *Neth. J. Med.* 69, 379–383.
- Hammesfahr, U., Bierl, R., and Thiele-Bruhn, S. (2011). Combined effects of the antibiotic sulfadiazine and liquid manure on the soil microbial community structure and functions. *J. Plant Nutr. Soil Sci.* 174, 614–623. doi: 10.1002/jpln.201000322
- Hodgson, D., McDonald, J. L., and Hosken, D. J. (2015). What do you mean, “resilient”? *Trends Ecol. Evol.* 30, 503–506. doi: 10.1016/j.tree.2015.06.010
- Insam, H. (1997). “A new set of substrates proposed for community characterization in environmental samples,” in *Microbial Communities: Functional Versus Structural Approaches*, eds H. Insam and A. Rangger (Berlin: Springer-Verlag), 259–260.
- Karpouzas, D. G., Morgan, J. A. W., and Walker, A. (2000). Isolation and characterisation of ethoprophos-degrading bacteria. *FEMS Microbiol. Ecol.* 33, 209–218. doi: 10.1111/j.1574-6941.2000.tb00743.x
- Kong, W.-D., Zhu, Y.-G., Fu, B.-J., Marschner, P., and He, J.-Z. (2006). The veterinary antibiotic oxytetracycline and Cu influence functional diversity of the soil microbial community. *Environ. Pollut.* 143, 129–137. doi: 10.1016/j.envpol.2005.11.003
- Kotzerke, A., Hammesfahr, U., Kleineidam, K., Lamshöft, M., Thiele-Bruhn, S., Schloter, M., et al. (2011). Influence of difloxacin-contaminated manure on microbial community structure and function in soils. *Biol. Fertil. Soils* 47, 177–186. doi: 10.1007/s00374-010-0517-1
- Kümmerer, K. (2003). Significance of antibiotics in the environment. *J. Antimicrob. Chemother.* 52, 5–7. doi: 10.1093/jac/dkg293
- Leng, Y., Bao, J., Chang, G., Zheng, H., Li, X., Du, J., et al. (2016). Biotransformation of tetracycline by a novel bacterial strain *Stenotrophomonas maltophilia* DT1. *J. Hazard. Mater.* 318, 125–133. doi: 10.1016/j.jhazmat.2016.06.053
- Li, B., and Zhang, T. (2010). Biodegradation and adsorption of antibiotics in the activated sludge process. *Environ. Sci. Technol.* 44, 3468–3473. doi: 10.1021/es903490h
- Lin, K., and Gan, J. (2011). Sorption and degradation of wastewater-associated non-steroidal anti-inflammatory drugs and antibiotics in soils. *Chemosphere* 83, 240–246. doi: 10.1016/j.chemosphere.2010.12.083
- Liu, B., Li, Y., Zhang, X., Wang, J., and Gao, M. (2014). Combined effects of chlortetracycline and dissolved organic matter extracted from pig manure on the functional diversity of soil microbial community. *Soil Biol. Biochem.* 74, 148–155. doi: 10.1016/j.soilbio.2014.03.005
- Liu, B., Li, Y., Zhang, X., Wang, J., and Gao, M. (2015). Effects of chlortetracycline on soil microbial communities: comparisons of enzyme activities to the functional diversity via Biolog EcoPlates™. *Eur. J. Soil Biol.* 68, 69–76. doi: 10.1016/j.ejsobi.2015.01.002
- Liu, F., Wu, J., Ying, G.-G., Luo, Z., and Feng, H. (2012). Changes in functional diversity of soil microbial community with addition of antibiotics sulfamethoxazole and chlortetracycline. *Appl. Microbiol. Biotechnol.* 95, 1615–1623. doi: 10.1007/s00253-011-3831-0
- Liu, F., Ying, G.-G., Tao, R., Zhao, J.-L., Yang, J.-F., and Zhao, L.-F. (2009). Effects of six selected antibiotics on plant growth and soil microbial and enzymatic activities. *Environ. Pollut.* 157, 1636–1642. doi: 10.1016/j.envpol.2008.12.021
- Liu, W., Pan, N., Chen, W., Jiao, W., and Wang, M. (2012). Effect of veterinary oxytetracycline on functional diversity of soil microbial community. *Plant Soil Environ.* 58, 295–301. doi: 10.17221/430/2011-PSE
- Ludwig, M., Wilmes, P., and Schrader, S. (2017). Measuring soil sustainability via soil resilience. *Sci. Total Environ.* 626, 1484–1493. doi: 10.1016/j.scitotenv.2017.10.043
- Ma, T., Pan, X., Chen, L., Liu, W., Christie, P., Luo, Y., et al. (2016). Effects of different concentrations and application frequencies of oxytetracycline on soil enzyme activities and microbial community diversity. *Eur. J. Soil Biol.* 76, 53–60. doi: 10.1016/j.ejsobi.2016.07.004
- Manzetti, S., and Ghisi, R. (2014). The environmental release and fate of antibiotics. *Mar. Pollut. Bull.* 79, 7–15. doi: 10.1016/j.marpolbul.2014.01.005
- Mijangos, I., Becerril, J. M., Albizu, I., Epelde, L., and Garbisu, C. (2009). Effects of glyphosate on rhizosphere soil microbial communities under two different plant compositions by cultivation-dependent and independent methodologies. *Soil Biol. Biochem.* 41, 505–513. doi: 10.1016/j.soilbio.2008.12.009
- Mulla, S. I., Hu, A., Sun, Q., Li, J., Suanon, F., Ashfaq, M., et al. (2018). Biodegradation of sulfamethoxazole in bacteria from three different origins. *J. Environ. Manage.* 206, 93–102. doi: 10.1016/j.jenvman.2017.10.029
- Orwin, K. H., and Wardle, D. A. (2004). New indices for quantifying the resistance and resilience of soil biota to exogenous disturbances. *Soil Biol. Biochem.* 36, 1907–1912. doi: 10.1016/j.soilbio.2004.04.036
- Pan, M., and Chu, L. M. (2016). Adsorption and degradation of five selected antibiotics in agricultural soil. *Sci. Total Environ.* 545–546, 48–56. doi: 10.1016/j.scitotenv.2015.12.040
- Pinna, M. V., Castaldi, P., Deiana, P., Pusino, A., and Garau, G. (2012). Sorption behavior of sulfamethazine on unamended and manure-amended soils and short-term impact on soil microbial community. *Ecotoxicol. Environ. Saf.* 84, 234–242. doi: 10.1016/j.ecoenv.2012.07.006
- Pino-Otín, M. R., Muñoz, S., Val, J., and Navarro, E. (2017). Effects of 18 pharmaceuticals on the physiological diversity of edaphic microorganisms. *Sci. Total Environ.* 595, 441–450. doi: 10.1016/j.scitotenv.2017.04.002
- Qiu, P., Guo, X., Zhang, Y., Chen, X., and Wang, N. (2016). Occurrence, fate, and risk assessment of vancomycin in two typical pharmaceutical wastewater treatment plants in Eastern China. *Environ. Sci. Pollut. Res.* 23, 16513–11523. doi: 10.1007/s11356-016-6676-3
- Quoc Tuc, D., Elodie, M.-G., Pierre, L., Fabrice, A., Marie-Jeanne, T., Martine, B., et al. (2017). Fate of antibiotics from hospital and domestic sources in a sewage network. *Sci. Total Environ.* 575, 758–766. doi: 10.1016/j.scitotenv.2016.09.118

- Reichel, R., Patzelt, D., Barleben, C., Rosendahl, I., Ellerbrock, R. H., and Thiele-Bruhn, S. (2014a). Soil microbial community responses to sulfadiazine-contaminated manure in different soil microhabitats. *Appl. Soil Ecol.* 80, 15–25. doi: 10.1016/j.apsoil.2014.03.010
- Reichel, R., Radl, V., Rosendahl, I., Albert, A., Amelung, W., Schloter, M., et al. (2014b). Soil microbial community responses to antibiotic-contaminated manure under different soil moisture regimes. *Appl. Microbiol. Biotechnol.* 98, 6487–6495. doi: 10.1007/s00253-014-5717-4
- Riber, L., Poulsen, P. H. B., Al-Soud, W. A., Skov Hansen, L. B., Bergmark, L., Brejnrod, A., et al. (2014). Exploring the immediate and long-term impact on bacterial communities in soil amended with animal and urban organic waste fertilizers using pyrosequencing and screening for horizontal transfer of antibiotic resistance. *FEMS Microbiol. Ecol.* 90, 206–224. doi: 10.1111/1574-6941.12403
- Rosendahl, I., Siemens, J., Kindler, R., Groeneweg, J., Zimmermann, J., Czerwinski, S., et al. (2012). Persistence of the fluoroquinolone antibiotic difloxacin in soil and lacking effects on nitrogen turnover. *J. Environ. Qual.* 41, 1275–1283. doi: 10.2134/jeq2011.0459
- Schaeffer, A., Amelung, W., Hollert, H., Kaestner, M., Kandeler, E., Kruse, J., et al. (2016). The impact of chemical pollution on the resilience of soils under multiple stresses: a conceptual framework for future research. *Sci. Total Environ.* 568, 1076–1085. doi: 10.1016/j.scitotenv.2016.06.161
- Shade, A., Peter, H., Allison, S. D., Baho, D. L., Berga, M., Bürgmann, H., et al. (2012). Fundamentals of microbial community resistance and resilience. *Front. Microbiol.* 3:417. doi: 10.3389/fmicb.2012.00417
- Singh, B. K., Walker, A., and Wright, D. J. (2006). Bioremediation potential of fenamiphos and chlorpyrifos degrading isolates: influence of different environmental conditions. *Soil Biol. Biochem.* 38, 2682–2693. doi: 10.1016/j.soilbio.2006.04.019
- Song, H.-S., Renslow, R. S., Fredrickson, J. K., and Lindemann, S. R. (2015). Integrating ecological and engineering concepts of resilience in microbial communities. *Front. Microbiol.* 6:1298. doi: 10.3389/fmicb.2015.01298
- Srinivasan, P., and Sarmah, A. K. (2014). Dissipation of sulfamethoxazole in pasture soils as affected by soil and environmental factors. *Sci. Total Environ.* 479–480, 284–291. doi: 10.1016/j.scitotenv.2014.02.014
- Tabatabai, M. A., and Bremner, J. M. (1969). Use of p-nitrophenyl phosphate for assay of soil phosphatase activity. *Soil Biol. Biochem.* 1, 301–307. doi: 10.1016/0038-0717(69)90012-1
- Thiele-Bruhn, S. (2003). Pharmaceutical antibiotic compounds in soils -A review. *J. Plant Nutr. Soil Sci.* 166, 145–167. doi: 10.1002/jpln.200390023
- Topp, E., Chapman, R., Devers-Lamrani, M., Hartmann, A., Marti, R., Martin-Laurent, F., et al. (2013). Accelerated biodegradation of veterinary antibiotics in agricultural soil following long-term exposure, and isolation of a sulfamethazine-degrading *Microbacterium* sp. *J. Environ. Qual.* 42, 173–178. doi: 10.2134/jeq2012.0162
- Topp, E., Renaud, J., Sumarah, M., and Sabourin, L. (2016). Reduced persistence of the macrolide antibiotics erythromycin, clarithromycin and azithromycin in agricultural soil following several years of exposure in the field. *Sci. Total Environ.* 562, 136–144. doi: 10.1016/j.scitotenv.2016.03.210
- Toth, J. D., Feng, Y., and Dou, Z. (2011). Veterinary antibiotics at environmentally relevant concentrations inhibit soil iron reduction and nitrification. *Soil Biol. Biochem.* 43, 2470–2472. doi: 10.1016/j.soilbio.2011.09.004
- Unger, I. M., Goynes, K. W., Kennedy, A. C., Kremer, R. J., McLain, J. E. T., and Williams, C. F. (2013). Antibiotic effects on microbial community characteristics in soils under conservation management practices. *Soil Sci. Soc. Am. J.* 77, 100–112. doi: 10.2136/sssaj2012.0099
- Walters, E., McClellan, K., and Halden, R. U. (2010). Occurrence and loss over three years of 72 pharmaceuticals and personal care products from biosolids-soil mixtures in outdoor mesocosms. *Water Res.* 44, 6011–6020. doi: 10.1016/j.watres.2010.07.051
- Wang, J., Lin, H., Sun, W., Xia, Y., Ma, J., Fu, J., et al. (2016). Variations in the fate and biological effects of sulfamethoxazole, norfloxacin and doxycycline in different vegetable-soil systems following manure application. *J. Hazard. Mater.* 304, 49–57. doi: 10.1016/j.jhazmat.2015.10.038
- Wei, X., Wu, S. C., Nie, X. P., Yediler, A., and Wong, M. H. (2009). The effects of residual tetracycline on soil enzymatic activities and plant growth. *J. Environ. Sci. Health B* 44, 461–471. doi: 10.1080/03601230902935139
- Wen, X., Wang, Y., Zou, Y., Ma, B., and Wu, Y. (2018). No evidential correlation between veterinary antibiotic degradation ability and resistance genes in microorganisms during the biodegradation of doxycycline. *Ecotoxicol. Environ. Saf.* 147, 759–766. doi: 10.1016/j.ecoenv.2017.09.025
- Westergaard, K., Müller, A. K., Christensen, S., Bloem, J., and Sørensen, S. J. (2001). Effects of tylosin as a disturbance on the soil microbial community. *Soil Biol. Biochem.* 33, 2061–2071. doi: 10.1016/S0038-0717(01)00134-1
- Xin, Z., Fengwei, T., Gang, W., Xiaoming, L., Qiuxiang, Z., Hao, Z., et al. (2012). Isolation, identification and characterization of human intestinal bacteria with the ability to utilize chloramphenicol as the sole source of carbon and energy. *FEMS Microbiol. Ecol.* 82, 703–712. doi: 10.1111/j.1574-6941.2012.01440.x
- Xu, Y., Yu, W., Ma, Q., Wang, J., Zhou, H., and Jiang, C. (2016). The combined effect of sulfadiazine and copper on soil microbial activity and community structure. *Ecotoxicol. Environ. Saf.* 134, 43–52. doi: 10.1016/j.ecoenv.2016.06.041
- Yang, J.-F., Ying, G.-G., Liu, S., Zhou, L.-J., Zhao, J.-L., Tao, R., et al. (2012). Biological degradation and microbial function effect of norfloxacin in a soil under different conditions. *J. Environ. Sci. Health B* 47, 288–295. doi: 10.1080/03601234.2012.638886
- Yang, Q., Zhang, J., Zhu, K., and Zhang, H. (2009). Influence of oxytetracycline on the structure and activity of microbial community in wheat rhizosphere soil. *J. Environ. Sci.* 21, 954–959. doi: 10.1016/S1001-0742(08)62367-0
- Zhang, W., Qiu, L., Gong, A., and Yuan, X. (2017). Isolation and characterization of a high-efficiency erythromycin A-degrading *Ochrobactrum* sp strain. *Mar. Pollut. Bull.* 114, 896–902. doi: 10.1016/j.marpolbul.2016.10.076
- Zhang, Y., Hu, S., Zhang, H., Shen, G., Yuan, Z., and Zhang, W. (2017). Degradation kinetics and mechanism of sulfadiazine and sulfamethoxazole in an agricultural soil system with manure application. *Sci. Total Environ.* 607–608, 1348–1356. doi: 10.1016/j.scitotenv.2017.07.083

**Conflict of Interest Statement:** The authors declare that the research was conducted in the absence of any commercial or financial relationships that could be construed as a potential conflict of interest.

The reviewer LAP and handling Editor declared their shared affiliation.

Copyright © 2018 Cycóń, Orlewska, Markowicz, Żmijowska, Smoleń-Dzirba, Bratosiewicz-Wąsik, Wąsik and Piotrowska-Seget. This is an open-access article distributed under the terms of the Creative Commons Attribution License (CC BY). The use, distribution or reproduction in other forums is permitted, provided the original author(s) and the copyright owner are credited and that the original publication in this journal is cited, in accordance with accepted academic practice. No use, distribution or reproduction is permitted which does not comply with these terms.



# Metal-Adapted Bacteria Isolated From Wastewaters Produce Biofilms by Expressing Proteinaceous Curli Fimbriae and Cellulose Nanofibers

M. K. Mosharaf<sup>1†</sup>, M. Z. H. Tanvir<sup>1†</sup>, M. M. Haque<sup>1\*†</sup>, M. A. Haque<sup>2</sup>, M. A. A. Khan<sup>3</sup>, A. H. Molla<sup>1</sup>, Mohammad Z. Alam<sup>1</sup>, M. S. Islam<sup>4</sup> and M. R. Talukder<sup>1</sup>

## OPEN ACCESS

### Edited by:

Stéphane Pesce,  
Institut National de Recherche en  
Sciences et Technologies pour  
l'Environnement et l'Agriculture  
(IRSTEA), France

### Reviewed by:

M. Oves,  
King Abdulaziz University,  
Saudi Arabia  
Santosh Kr Karn,  
Sardar Bhagwan Singh Post  
Graduate Institute of Biomedical  
Sciences & Research, India

### \*Correspondence:

M. M. Haque  
haque\_bes@bsmrau.edu.bd

† These authors have contributed  
equally to this work.

### Specialty section:

This article was submitted to  
Microbiotechnology, Ecotoxicology  
and Bioremediation,  
a section of the journal  
Frontiers in Microbiology

Received: 18 February 2018

Accepted: 31 May 2018

Published: 25 June 2018

### Citation:

Mosharaf MK, Tanvir MZH,  
Haque MM, Haque MA, Khan MAA,  
Molla AH, Alam MZ, Islam MS and  
Talukder MR (2018) Metal-Adapted  
Bacteria Isolated From Wastewaters  
Produce Biofilms by Expressing  
Proteinaceous Curli Fimbriae  
and Cellulose Nanofibers.  
Front. Microbiol. 9:1334.  
doi: 10.3389/fmicb.2018.01334

<sup>1</sup> Department of Environmental Science, Faculty of Agriculture, Bangabandhu Sheikh Mujibur Rahman Agricultural University, Gazipur, Bangladesh, <sup>2</sup> Department of Agro-Processing, Faculty of Agriculture, Bangabandhu Sheikh Mujibur Rahman Agricultural University, Gazipur, Bangladesh, <sup>3</sup> Department of Plant Pathology, Faculty of Agriculture, Bangabandhu Sheikh Mujibur Rahman Agricultural University, Gazipur, Bangladesh, <sup>4</sup> Bangladesh Jute Research Institute, Dhaka, Bangladesh

Bacterial biofilm plays a pivotal role in bioremediation of heavy metals from wastewaters. In this study, we isolated and identified different biofilm producing bacteria from wastewaters. We also characterized the biofilm matrix [i.e., extracellular polymeric substances (EPS)] produced by different bacteria. Out of 40 isolates from different wastewaters, only 11 (27.5%) isolates (static condition at 28°C) and 9 (22.5%) isolates (agitate and static conditions at 28 and 37°C) produced air-liquid (AL) and solid-air-liquid (SAL) biofilms, respectively, only on salt-optimized broth plus 2% glycerol (SOBG) but not in other media tested. Biomass biofilms and bacteria coupled with AL biofilms were significantly ( $P \leq 0.001$ ) varied in these isolates. *Escherichia coli* (isolate ENSD101 and ENST501), *Enterobacter asburiae* (ENSD102), *Enterobacter ludwigii* (ENSH201), *Pseudomonas fluorescens* (ENSH202 and ENSG304), uncultured *Vitreoscilla* sp. (ENSG301 and ENSG305), *Acinetobacter lwoffii* (ENSG302), *Klebsiella pneumoniae* (ENSG303), and *Bacillus thuringiensis* (ENSW401) were identified based on 16S rRNA gene sequencing. Scanning electron microscope (SEM) images revealed that biofilm matrix produced by *E. asburiae* ENSD102, uncultured *Vitreoscilla* sp. ENSG301, *A. lwoffii* ENSG302, and *K. pneumoniae* ENSG303 are highly fibrous, compact, and nicely interlinked as compared to the biofilm developed by *E. ludwigii* ENSH201 and *B. thuringiensis* ENSW401. X-ray diffraction (XRD) results indicated that biofilm matrix produced by *E. asburiae* ENSD102, uncultured *Vitreoscilla* sp. ENSG301, and *A. lwoffii* ENSG302 are non-crystalline amorphous nature. Fourier transform infrared (FTIR) spectroscopy showed that proteins and polysaccharides are the main components of the biofilms. Congo red binding results suggested that all these bacteria produced proteinaceous curli fimbriae and cellulose-rich polysaccharide. Production of cellulose was also confirmed by Calcofluor binding- and spectrophotometric assays. *E. asburiae* ENSD102, *Vitreoscilla* sp. ENSG301, and *A. lwoffii* ENSG302 were tested for their abilities to form the biofilms exposure to 0 to 2000 mg/L of copper sulfate (for Cu), zinc

sulfate (for Zn), lead nitrate (for Pb), nickel chloride (for Ni), and potassium dichromate (for Cr), several concentrations of these metals activated the biofilm formation. The polysaccharides is known to sequester the heavy metals thus, these bacteria might be applied to remove the heavy metals from wastewater.

**Keywords:** wastewater, biofilm, extracellular polymeric substance, cellulose, curli fimbriae, heavy metal

## INTRODUCTION

Discharge of untreated wastewater into the rivers, canals, lakes, and ponds is one of the major causes of water pollution. Generally, wastewater contains toxic heavy metals, synthetic dyes, and other hazardous substances (Jin et al., 2007; Das et al., 2011; Islam et al., 2011; Saratale et al., 2011; Sheikh et al., 2017), which pose threat to human health, fish, crops, and overall biodiversity (Islam et al., 2014, 2015; Naser et al., 2014; Ahmed et al., 2016; Alam et al., 2017). All around the world, numerous physico-chemical methods (e.g., chemical precipitation, oxidation, reduction, activated carbon, ion-exchange, reverse osmosis, membrane filtration, and evaporation) are being practiced to treat the wastewater. However, most of these methods are expensive, ineffective, and required high energy and produced large amount of sludge with hazardous by-products (Ahluwalia and Goyal, 2007; Dixit et al., 2015). By contrast, microbial-based techniques are eco-friendly, economic, and effectively detoxify the persistent organic pollutants (POPs), petroleum products, explosives, dyes, and metals from wastewater (Singh et al., 2006; Saratale et al., 2011; Edwards and Kjellerup, 2013; Elekwachi et al., 2014; Dixit et al., 2015; Mitra and Mukhopadhyay, 2016).

Biofilms are structured, surface-adherent, multicellular, microbial communities. Biofilms consist mainly of cells embedded in a self-produced extracellular polymeric substances [EPS (Costerton et al., 1999; Donlan and Costerton, 2002; Flemming and Wingender, 2010)]. EPS comprises polysaccharides, including cellulose nanofibers (Zogaj et al., 2001; Solano et al., 2002; Haque et al., 2009; Römmling and Galperin, 2015) and sucrose-derived glucans and fructans (Wingender et al., 2001), proteins, such as lectins, Bap-like proteins (Lasa and Penadé, 2006), and proteinaceous appendages mainly curli fimbriae (Prigent-Combaret et al., 2000; White et al., 2003; Zogaj et al., 2003), extracellular DNA (Whitchurch et al., 2002; Liang et al., 2010), lipids (e.g., surfactin, viscosin, and emulsan) (Conrad et al., 2003), surfactants (e.g., rhamnolipids) (Davey et al., 2003), and other biopolymers, including humic substances (Martín-Cereceda et al., 2001). The specific contents of the EPS controls biofilm morphology and stability (Flemming and Wingender, 2010). However, composition of the EPS vary between biofilms, species, surface on which biofilms are formed and environmental conditions, including availability of the nutrients, temperature, and oxygen tension (Prouty and Gunn, 2003; Haque et al., 2012; Koechler et al., 2015).

Bacterial biofilm matrix, i.e., EPS play significant roles compared with their free-living planktonic counterparts, including protection of the cells from adverse environmental stresses (e.g., high concentration of toxic chemicals, changes

in pH, temperature, salt concentration, and water content), ability to communicate through expression of signal molecules, exchange genetic materials, and persistence in different metabolic states (Teitzel and Parsek, 2003; Hall-Stoodley et al., 2004; Kaplan, 2010; McDougald et al., 2012; Koechler et al., 2015; Mitra and Mukhopadhyay, 2016; Haque et al., 2017). Among the contents of the EPS, specifically the polysaccharide binds to heavy metals (Ferris et al., 1989; Teitzel and Parsek, 2003; van Hullebusch et al., 2003; Li and Yu, 2014). Despite these advantages, bacterial biofilms have been appreciated and applied to remove xenobiotic compounds (Seo et al., 2009; Payne et al., 2011; Edwards and Kjellerup, 2013) and heavy metal ions (Huang et al., 2000; Labrenz et al., 2000; Chang et al., 2006; Muñoz et al., 2006; Singh et al., 2006; Pal and Paul, 2008; Yamaga et al., 2010; Das et al., 2012; Fida et al., 2012). Cellulose nanofibers have been shown to use as a scaffold for tissue engineering (Klemm et al., 2001; Maneerung et al., 2007).

Only a few bacterial biofilms, including *Acinetobacter calcoaceticus*, *Bacillus subtilis*, *B. cereus*, *Escherichia coli*, *Pseudomonas putida*, *P. aeruginosa*, and *Rhodococcus* sp. have been found to remove the toxic heavy metals (Wagner-Döbler et al., 2000; Al-Awadhi et al., 2003; Pal and Paul, 2008; Cristina et al., 2009; Fang et al., 2011; Sundar et al., 2011). More diverse biofilms is more efficient for bioremediation of heavy metals (von Canstein et al., 2002; Edwards and Kjellerup, 2013). The objective of this study was to isolate and identify the biofilm producing bacteria from dyeing, composite (mixture of household and different industries), garments, washing plant, and tannery wastewater of Bangladesh. In this study, we also characterized the matrix of the biofilms (i.e., EPS) produced by different bacteria by means of scanning electron microscope (SEM), Fourier transform infrared (FTIR) spectroscopy, X-ray diffraction (XRD), different binding (e.g., Congo red and Calcufluor binding assays) and spectrophotometric assays. The effect of bacterial biofilms in resistance to toxic heavy metals is well documented (Teitzel and Parsek, 2003; Harrison et al., 2005). However, information regarding the role of toxic heavy metals on biofilm formation is only poorly understood (Koechler et al., 2015). Therefore, it is aims to quantify the effect of different concentrations (0, 500, 750, 1000, 1250, 1500, 1750, and 2000 mg/L) of copper sulfate (for Cu), zinc sulfate (for Zn), lead nitrate (for Pb), nickel chloride (for Ni), and potassium dichromate (for Cr) on bacterial growth in agitate condition and biofilm formation in static condition in some selected bacteria. This study will contribute toward understanding the potential of different bacterial biofilms in bioremediation of toxic heavy metals presence in contaminated wastewaters.

## MATERIALS AND METHODS

### Sampling and Physico-Chemical Properties of the Wastewaters

Dyeing, composite (household plus different industrial wastewaters), garments, washing plant's wastewaters were collected from Gazipur city areas of Bangladesh, while tannery wastewater was collected from Hazaribagh of Dhaka city, Bangladesh. The samples were collected in cleaned and sterilized screw cap bottles, and cold chain was maintained during transportation to the laboratory. Collected samples were stored at 4°C before analysis. Color and odor of the samples were noted. Total dissolve solid (TDS), salinity, and electrical conductivity (EC) were measured by Conductivity meter (Model: DDSJ-308A). Water pH was determined by the digital pH meter (model: HI 8424, HANNA). Water temperature and dissolved oxygen (DO) were measured during sample collection with the help of digital thermometer and digital DO meter (Model: HI 8424, HANNA), respectively. Copper (Cu), zinc (Zn), lead (Pb), chromium (Cr), and nickel (Ni) in different wastewater samples were determined by atomic absorption spectrophotometer (Model- AA-7000, Shimadzu, Japan) followed by procedures of American Public Health Association [APHA] (1998). Physico-chemical characteristics of various wastewaters are presented in Supplementary Table S1.

### Isolation and Purification of Bacteria

Each wastewater sample was serially diluted with sterile distilled water then streaked on yeast extract peptone (YP) (1% of peptone, 0.5% of yeast extract, pH 6.8) agar (1.5%) plates. The plates were incubated at 28°C. After 24 h incubation, morphologically distinct (e.g., color, size, and shape) eight colonies from each sample were transferred to the fresh YP agar plate by the sterile toothpicks. Pure culture of each isolate was made by repeated streaking method and used for further studies.

### Screening of Biofilm Producing Isolates

Initially a single colony of each isolate was grown in YP broth at 28°C in shaking condition (180 rpm) overnight and diluted [1:100 (ca.  $10^6$  colony forming unit (CFU)/mL)]. Then 50  $\mu$ L diluted culture were inoculated in glass test tubes (Pyrex, flat bottom, Glassco, United Kingdom) containing 5 mL of salt-optimized broth (SOB) plus glycerol (SOBG) broth (per liter, 20 g of tryptone, 5 g of yeast extract, 0.5 g of NaCl, 2.4 g of  $MgSO_4 \cdot 7H_2O$ , 0.186 g of KCl, and 50 ml of 40% glycerol), YP, Luria Bertani (LB), King's B (KB), yeast peptone dextrose adenine (YPDA), and M63 glycerol minimal medium (per liter, 2.5 g of NaCl, 3 g of  $KH_2PO_4$ , 7 g of  $K_2HPO_4$ , 2 g of  $(NH_4)_2SO_4$ , 0.5 mg of  $FeSO_4$ , 2 g of thiamine hydrochloride, and 2 g of glycerol). Then each test tube was incubated at two different temperatures (28 or 37°C) in static or agitate (150 rpm) condition. After 72 h incubation, solid-air-liquid (SAL) and air-liquid (AL) biofilm producing isolates were identified visually.

### Quantification of AL Biofilms

Biomass of the rigid AL biofilms was extracted from the liquid medium and quantified as described in Haque et al. (2012) with a few modifications. In brief, each biofilm was gently removed from the glass test tube and washed two to three times with sterile distilled water. Then 1.5 mL sterile distilled water and 20 glass beads (3 mm) were added to each glass test tube. Each biofilm was detached by vortexing (50 s) at the highest speed. Then optical density (OD) was measured by reading the absorbance at 600 nm with an UV spectrophotometer (Ultrospec 3000, Pharmacia Biotech, Cambridge, United Kingdom). Biomass of the fragile AL biofilms was extracted/detached from the liquid and quantified as follows: after 72 h of incubation in static condition, 1 mL of planktonic culture, i.e., the culture beneath the AL biofilms was carefully collected by inserting the pipette tips, and OD ( $OD_{600}$ ) was determined by the UV spectrophotometer. Then each fragile AL biofilms was vigorously vortexed with 1 mL planktonic culture and 20 glass beads (3 mm), and  $OD_{600}$  was measured. Afterward, the  $OD_{600}$  of planktonic culture was subtracted from  $OD_{600}$  of biomass of fragile AL biofilm plus planktonic culture. This would provide the amount of fragile biomass present in the AL biofilm.

### Quantification of SAL Biofilms

After 72 h of incubation at 180 rpm at 28°C, 5.5 mL of 0.05% (w/v) crystal violet (CV) solution was added to each glass test tube then incubated for 45 min. Each test tube was rinsed with three times with sterile distilled water, and CV was eluted using 95% ethanol. The SAL biofilm was quantified by measuring the absorbance at 570 nm using UV spectrophotometer (Ultrospec 3000, Pharmacia, Biotech, Cambridge, United Kingdom).

### Enumeration of Cells Coupled With Biofilms

The rigid AL biofilms were carefully transferred from the broth, washed with sterile distilled water (twice), and then placed in sterile glass test tubes containing 3 mL of YP broth and 40 glass beads. The biofilms were disrupted for 1 min by vortexing, serially diluted, spread on YP agar plates, and incubated at 28°C. After 32 h, the cells were enumerated. The bacterial cells coupled with fragile AL biofilms were counted as follows: first, 1 mL of planktonic culture was gently removed, diluted, then spread on YP agar plates. Second, the fragile AL biofilms were mixed with 3 mL of planktonic culture by vortexing (without glass beads), diluted, and spread on YP agar plates. After 32 h incubation at 28°C, the CFU were counted. Afterward, CFU of the planktonic culture was subtracted from CFU of fragile AL biofilm plus planktonic culture. This would provide the cells present in the fragile AL biofilm.

### Identification of Biofilm Producing Bacterial Strains Using 16S rRNA Gene Sequencing

Extraction of genomic DNAs and gel electrophoresis was done as described in Sambrook et al. (1989). 16S rRNA genes were amplified by polymerase chain reaction (PCR)

using the universal bacterial 16S rRNA gene primers 27F (5'-AGAGTTTGATCMTGGCTCAG-3') and 1492R (5'-GGTTACCTTGTTACGACTT-3'). The PCR amplification conditions were as follows: initial DNA denaturation at 94°C for 5 min followed by 35 cycles of denaturation at 94°C for 30 s, annealing at 57°C for 45 s, and elongation at 72°C for 1.5 min, which was followed by a final extension at 72°C for 10 min. The PCR products were purified with QIAquick® Gel extraction kit (Qiagen), essentially according to the manufacturer's instructions. Nucleotide sequences were determined from the purified products by using 3500 Genetic Analyzer (Applied Bio-system). Two forward primers 27F (5'-AGAGTTTGATCMTGGCTCAG-3') and 533F (5'-GTGCCAGCAGCCGCG GTAA-3') and one reverse primer 1492R (5'-GGTTACCTTGTTACGACTT-3') were used for the sequencing. The gene sequences of different biofilm-producing bacterial strains were compared using the bioinformatics tool BLASTN (Basic Local Alignment Search for Nucleotide) against the sequences of bacteria available in National Center for Biotechnology Information (NCBI) data banks<sup>1</sup>.

### Construction of Phylogenetic Tree

All sequences were aligned with MUSCLE (Edgar, 2004). Alignments were pruned with G blocks (Castresana, 2000). The evolutionary history was inferred by using the Maximum Likelihood method based on the JTT matrix-based model (Jones et al., 1992). Evolutionary analyses were conducted in MEGA6 (Tamura et al., 2013).

### Scanning Electron Microscopy

A scanning electron microscopy (SEM) (SUI510, Hitachi, Japan) operated at 5.0 KV was used to image biofilm samples after centrifugation (10,000 rpm for 10 min) followed by drying (12 h) at 40°C. Each sample was coated with carbon using a vacuum sputter-coater to improve the conductivity of the sample.

### Acquiring and Analysis of the IR Spectra

The IR spectra of the biofilms were acquired through Perkin Elmer FTIR (Spectrum-2) instrument operated by CPU32M software. Biofilms were removed carefully from SOBGM broth after 72 h incubation by pouring the culture into the tube and centrifuged at 13,000 rpm for 20 min. The precipitates after centrifugation were directly used as samples for FTIR scanning; within 450 to 4000 cm<sup>-1</sup> using triglycine sulfate (TGS) detector. A total of 16 scans at 4 cm<sup>-1</sup>; resolution were accumulated at 0.2 cm/s scanning speed. The supernatant of the SOBGM broth was also scanned. The spectrum of the supernatant was subtracted from the sample spectra to present the result. The baseline subtracted biofilms spectra were analyzed by using Perkin Elmer's proprietary software (Version 10.05.03).

### X-Ray Diffraction Analysis

This study was carried out on a BRUKER D8 X-ray diffractometer with CuK $\alpha$ 1 radiation ( $\lambda = 1.54056$ ). A continuous scan type diffractograms were recorded between 5.01° and 74.99° (2 $\theta$ ) at

a rate of 0.3 s/step with a step size of 0.02° (2 $\theta$ ). A fixed-type anti-scatter slit of 0.10 mm and 1° divergence and receiving slits were used. The measurement temperature was recorded as 25°C.

### Congo Red Binding Assays

Congo red binding assays were done as described by Haque et al. (2017) with a few modifications. In brief, initially each biofilm producing bacteria was grown in YP broth overnight at 28°C in shaking condition (180 rpm). Then 1 mL of culture of each biofilm-producing bacterial strain was collected and centrifuged. The pellet was then diluted 1:100 (ca. 10<sup>5</sup> CFU/mL). Then 2  $\mu$ L diluted culture were spotted (five spot in each plate) onto SOBGM agar plates containing 40  $\mu$ g/mL of Congo red (Santa Cruz Biotechnology, United States). The plates were incubated at 28°C in still condition for 48 h, then photographs were taken.

### Calcofluor Binding Assays

Calcofluor binding assays were carried out as described in Haque et al. (2009) with a few modifications. In brief, each biofilm producing bacteria was grown in YP broth overnight at 28°C in agitate condition (180 rpm) and diluted 1:100 (ca. 10<sup>5</sup> CFU/mL). Then 2  $\mu$ L of diluted culture of each biofilm-producing bacterial strain were spotted (five spot in each plate) onto SOBGM agar plates containing 200  $\mu$ g/mL of Calcofluor white (Thomas Scientific, Fluka, United States). The plates were incubated at 28°C before being checked under UV light (366 nm). The photographs were taken after 48 h.

### Quantification of Cellulose From Biofilm Producing Bacteria

Cellulose production was quantified from different biofilm producing bacteria as the method described by Haque et al. (2017) with a few modifications. In brief, 2  $\mu$ L of diluted (overnight grown) culture (ca. 10<sup>5</sup> CFU/mL) were spotted (15 spots in each plate) onto SOBGM Calcofluor agar plates then incubated at 28°C in stationary condition. After 48 h incubation, approximately 3 g of cells from each bacterium were collected in 50-mL polystyrene conical tubes, covered then lyophilized. The lyophilized dry masses were mixed with 5 mL of 8:2:1 acetic acid: nitric acid: distilled water and boiled for 30 min then centrifuged at 15,000 rpm. The cell pellet was transferred to the Corex centrifuged bottles, washed two to three times with sterile distilled water and dried aseptically. The dried pellet was mixed with 200  $\mu$ L of concentrated H<sub>2</sub>SO<sub>4</sub> with gentle shaking (50 rpm) for 1.5 h at room temperature. The amount of cellulose was determined (OD<sub>620</sub>) using 800  $\mu$ L anthrone (Sigma-Aldrich, St. Louis, MO, United States) reagent (0.2 g in 100 mL H<sub>2</sub>SO<sub>4</sub>). The Avicel cellulose (Sigma-Aldrich, St. Louis, MO, United States) was used as standard.

### Heavy Metal Stress on Biofilm Formation

In order to study the effect of heavy metal stress on biofilm formation, 50  $\mu$ L of cultures were inoculated in 5 mL of magnesium-deprived SOBGM broth with different concentrations (0, 500, 750, 1000, 1250, 1500, 1750, and 2000 mg/L) of copper sulfate (CuSO<sub>4</sub>.5H<sub>2</sub>O for Cu), zinc sulfate (ZnSO<sub>4</sub>.7H<sub>2</sub>O for Zn),

<sup>1</sup><http://www.ncbi.nlm.nih.gov/>

lead nitrate [ $\text{Pb}(\text{NO}_3)_2$  for Pb], nickel chloride ( $\text{NiCl}_2$  for Ni), and potassium dichromate ( $\text{K}_2\text{Cr}_2\text{O}_7$  for Cr). The test tubes were incubated at  $28^\circ\text{C}$  in still condition. After 72 h incubation, the photographs were taken. The biomass biofilms were quantified after 72 h incubation as stated above.

## Statistical Analysis

All the experiments were laid out in a complete randomized design with four replications and repeated at least two times. Analysis of variance and comparison of means were calculated with the statistical package “agricolae” of R software version 3.3.3. The means were compared by using Fisher’s least significance difference (LSD) test ( $P < 0.001$ ).

## RESULTS

### Screening of Biofilm Producing Bacterial Isolates

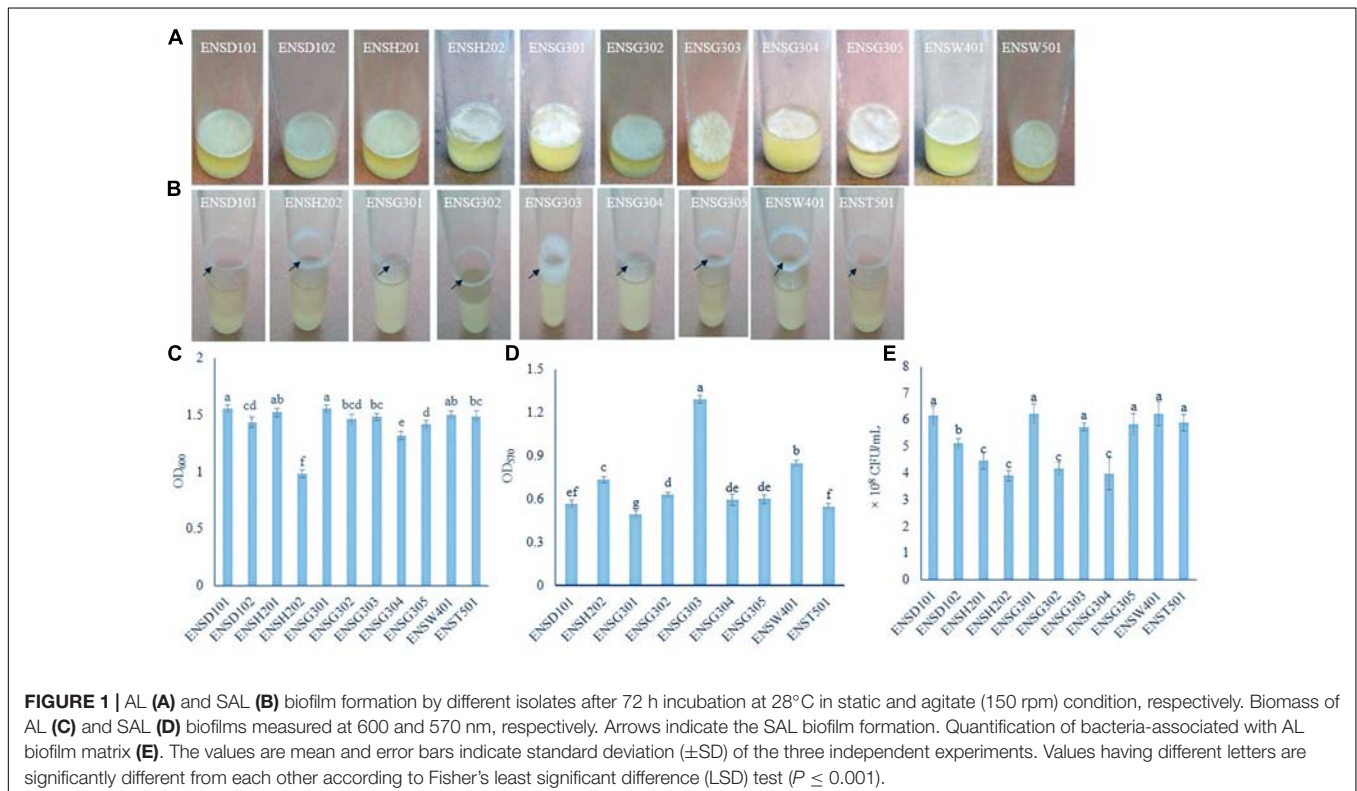
In order to isolate biofilm producing bacteria from different wastewaters, a total of 40 isolates (8 isolates/sample) were screened. In static condition, 11 (27.5%) isolates, such as ENSD101, ENSD102, ENSH201, ENSH202, ENSG301, ENSG302, ENSG303, ENSG304, ENSG305, ENSW401, and ENST501 were found to produce fragile to rigid AL biofilms at the air–liquid interface (also known as pellicle) in the glass test tubes containing 5 mL of SOBGM (Figure 1A) after 72 h incubation at  $28^\circ\text{C}$  but not in YP, LB, KB, YPDA, and M63 glycerol minimal media (data not shown). AL biofilms developed by ENSD101,

ENSD102, ENSH201, ENSG302, ENSG304, ENSW401, and ENST501 had a smooth surface, robust, and cells were not dispersed when the aggregates were agitated. Conversely, AL biofilms produced by ENSH202, ENSG301, ENSG303, and ENSG305 had a rough surface, fragile, and easily dispersed when disturbed. Conversely, at  $37^\circ\text{C}$ , all the AL biofilm-forming isolates produced the SAL biofilms on SOBGM broth but not in YP, LB, KB, YPDA, and M63 glycerol minimal media after 72 h incubation (data not shown).

In shaking (150 rpm) condition, only nine (22.5%) isolates, including ENSD101, ENSH202, ENSG301, ENSG302, ENSG303, ENSG304, ENSG305, ENSW401, and ENST501 were found to form the SAL biofilms as a ring at the solid–air–liquid interface in the glass test tubes containing 5 mL of SOBGM (Figure 1B) only but not in YP, LB, KB, YPDA, and M63 glycerol minimal media (data not shown) after 24 h incubation at  $28^\circ\text{C}$ . Isolate ENSG303 built a wide and thick SAL biofilm ring than the other isolates. Therefore, SOBGM broth was chosen to screen the biofilm producing bacteria from wastewaters. Furthermore, none of the biofilm producing bacterial isolate was found to be impaired in growth rate in SOBGM broth and M63 glycerol minimal medium in shaking condition (data not shown).

### Biomass of Biofilms Produced by Different Isolates

AL biomass of biofilm was found to be significantly ( $P \leq 0.001$ ) differed in these isolates (Figure 1C). The isolates of ENSD101 and ENSG301 produced significantly ( $P < 0.001$ ) more AL biomass biofilms ( $\text{OD}_{600}$  at 1.55) followed by ENSH201 ( $\text{OD}_{600}$



at 1.52) and ENSW401 (OD<sub>600</sub> at 1.50). However, the moderate biomass biofilms (OD<sub>600</sub> at 1.48) was generated by the ENSG303 and ENST501 followed by ENSG302 (OD<sub>600</sub> at 1.46), ENSD102 (OD<sub>600</sub> at 1.43), and ENSG305 (OD<sub>600</sub> at 1.41). Significantly the lowest biomass biofilm (OD<sub>600</sub> at 0.98) was produced by ENSH202. Like AL biomass biofilm, SAL biomass biofilm was also significantly ( $P \leq 0.001$ ) differed in these isolates (Figure 1D). The isolate ENSG303 produced more SAL biomass biofilm (OD<sub>570</sub> at 1.29) than the other isolates. The lowest SAL biomass biofilm (OD<sub>570</sub> at 0.49) was developed by the isolate ENSG301.

## Bacterial Cells Coupled With AL Biofilm Matrix

Bacterial cells coupled with AL biofilm matrix were counted by a serial dilution plating method (Figure 1E). The CFU was significantly ( $P \leq 0.001$ ) higher in the matrix produced by ENSG301 ( $6.23 \times 10^8$ ) and ENSW401 ( $6.23 \times 10^8$ ), which were statistically similar with ENSD101 ( $6.17 \times 10^8$ ), ENSG303 ( $5.73 \times 10^8$ ), ENSG305 ( $5.8 \times 10^8$ ), and ENST501 ( $5.9 \times 10^8$ ). However, the moderate CFU was recorded in the matrix produced by ENSD102. The lowest CFU was detected in the matrix created by ENSH202 ( $3.90 \times 10^8$ ), which was statistically similar with ENSH201 ( $4.47 \times 10^8$ ), ENSG302 ( $4.17 \times 10^8$ ), and ENSG304 ( $3.97 \times 10^8$ ).

## Identification of Biofilm Producing Bacteria

The 16S rRNA gene from biofilm producing isolates was sequenced, aligned, and the closest match was detected using BLASTN (Table 1). However, the isolates of ENSD101 and ENST501 were 99% homologous to *E. coli* (KJ803895.1) with maximum score (score of single best aligned sequence) 2545, ENSG301 and ENSG305 were 98% homologous to uncultured *Vitreoscilla* sp. (LN870312.1) with maximum score 2567, ENSH202 and ENSG304 were 99% homologous to *Pseudomonas fluorescens* (KP126776.1) with maximum score 2615, the isolates of ENSD102, ENSH201, ENSG302, and ENSG303 were 99%

homologous to *Enterobacter asburiae* (CP014993.1), *Enterobacter ludwigii* (KM077046.1), *Acinetobacter lwoffii* (KF993657.1), and *Klebsiella pneumoniae* (KF192506.1) with maximum score 2654, 2573, 2468, and 2675, respectively. Conversely the isolate of ENSW401 was 100% homologous to *Bacillus thuringiensis* (JX283457.1) with maximum score 2601. The 16S rRNA gene sequence data were submitted to the NCBI GenBank, and the assigned accession number for uncultured *Vitreoscilla* sp. ENSG301, *A. lwoffii* ENSG302, *E. ludwigii* ENSH201, *B. thuringiensis* ENSW401, *E. coli* ENSD101, *E. asburiae* ENSD102, *K. pneumoniae* ENSG303, and *P. fluorescens* ENSG304 were KU254758, KU254759, KU254760, KU254761, KU254762, KU254763, KU254764, and KU254765, respectively.

## Phylogenetic Tree

Phylogenetic tree revealed that there were at least seven major clades where each species belonged to a clade representing its genus with species (Supplementary Figure S1). ENSD101 and ENST501 belonged to the same clade as *E. coli*, ENSG301 and ENSG305 formed the same clade as uncultured *Vitreoscilla* sp., ENSH202 and ENSG304 into the same clade as *P. fluorescens*, and ENSD102 and ENSH201 formed another clade as *E. asburiae* and *E. ludwigii*. However, rest of the isolates, ENSG302, ENSG303, and ENSW401 formed individual clade as *A. lwoffii*, *K. pneumoniae*, and *B. thuringiensis*, respectively.

## Scanning Electron Microscopy

Scanning electron microscopy images of the biofilm matrix are shown in Figure 2. Biofilm matrix produced by *E. asburiae* ENSD101 (Figure 2A), uncultured *Vitreoscilla* sp. ENSG301 (Figure 2B), *A. lwoffii* ENSG302, and *K. pneumoniae* ENSG303 were highly fibrous, compact, and nicely interlinked as compared to the biofilm developed by *E. coli* ENSD101 and *B. thuringiensis* ENSW401 in resolution of 2.0 k. The images were clearer in high resolution of 6.5 k. Cracks were easily visible in the biofilm matrix generated by *E. ludwigii* ENSH201 and *P. fluorescens* ENSG304 leading to form an indented surface morphology. It may be due to the effect of drying and/or centrifugation. In this study, we were unable to measuring the size of interwoven mesh of microfibrils.

TABLE 1 | Identification of biofilm forming bacteria.

Strains	Source	Top hit against colony isolate	Accession no.	Maximum score	Maximum identity (%)
ENSD101	Dyeing industry	<i>Escherichia coli</i>	KJ803895.1	2545	99
ENSD102		<i>Enterobacter asburiae</i>	CP014993.1	2654	99
ENSH201	Composite (household plus different industrial wastewaters)	<i>Enterobacter ludwigii</i>	KM077046.1	2573	99
ENSH202		<i>Pseudomonas fluorescens</i>	KP126776.1	2615	99
ENSG301	Garments industry	Uncultured <i>Vitreoscilla</i> sp.	LN870312.1	2567	98
ENSG302		<i>Acinetobacter lwoffii</i>	KF993657.1	2468	99
ENSG303		<i>Klebsiella pneumoniae</i>	KF192506.1	2675	99
ENSG304		<i>P. fluorescens</i>	KP126776.1	2615	99
ENSG305		Uncultured <i>Vitreoscilla</i> sp.	LN870312.1	2567	98
ENSW401	Washing plant industry	<i>Bacillus thuringiensis</i>	JX283457.1	2601	100
ENST501	Tannery industry	<i>E. coli</i>	KJ803895.1	2545	99

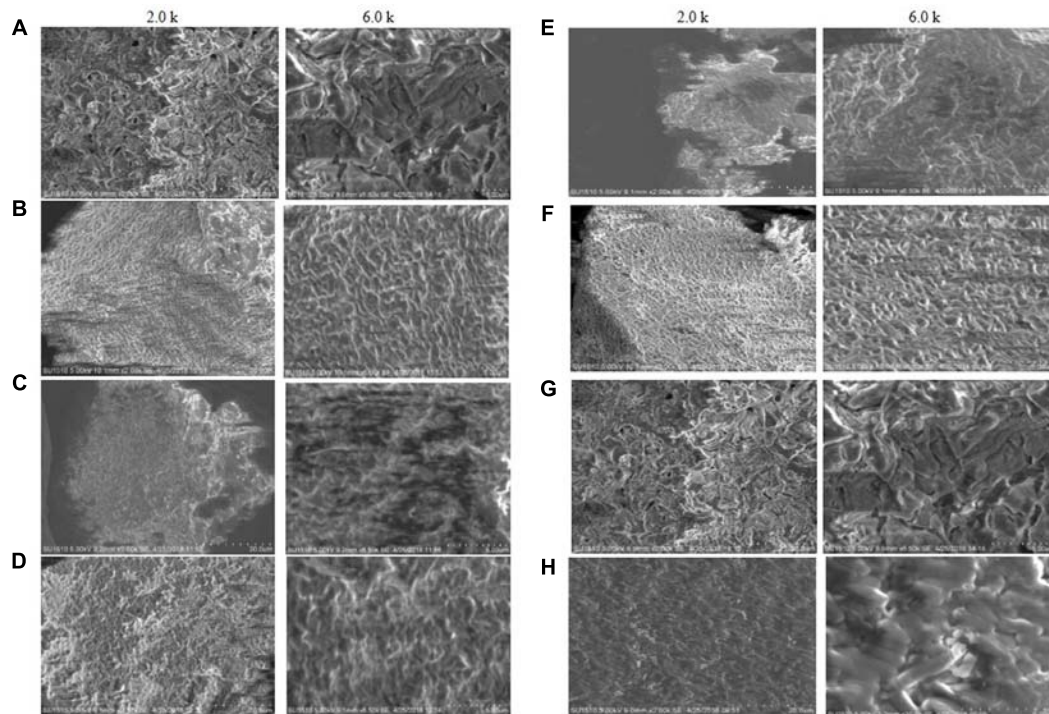


**FIGURE 2** | SEM images of the matrix produced by (A) *E. coli* ENSD101, (B) *E. asburiae* ENSD102, (C) *E. ludwigii* ENSH201, (D) uncultured *Vitreoscilla* sp. ENSG301, (E) *A. lwoffii* ENSG302, (F) *K. pneumoniae* ENSG303, (G) *P. fluorescens* ENSG304, and (H) *B. thuringiensis* ENSW401 with 2.0 and 6.0 k magnifications.

## Fourier Transform Infrared Spectroscopy and X-Ray Diffraction Analysis

The FTIR spectra of the EPS of different biofilms are presented in **Figure 3**. It was observed that all the bacterial EPS were dominant with protein contents producing peaks at amide I ( $1600\text{--}1700\text{ cm}^{-1}$ ), amide II ( $1500\text{--}1600\text{ cm}^{-1}$ ), and amide III ( $1200\text{--}1350\text{ cm}^{-1}$ ) regions. The EPS were also consisted of high content of polysaccharide which produced intense peaks near  $900\text{--}1150\text{ cm}^{-1}$ . The  $2800\text{--}2970\text{ cm}^{-1}$  domain indicates the presence of small amount of lipids in the EPS. The XRD analyses of the dried biofilm masses were carried out to assess the crystalline/amorphous nature. The XRD of *E. asburiae* ENSD102, uncultured *Vitreoscilla* sp. ENSG301, and *A. lwoffii* ENSG302 biofilms are presented in **Figure 4**. All the XRD patterns exhibit the non-crystalline amorphous nature with producing an extremely broad peak near at around  $15\text{--}25^\circ$  ( $2\theta$ ).

## Detection of Curli Fimbriae and Cellulose Nanofibers by Congo Red Binding Assays

Expression of curli fimbriae (a major proteinaceous component of the EPS) and cellulose nanofibers (a major polysaccharide component of the EPS) triggers the red, dry, and rough (rdar) morphotype/phenotype on Congo red agar plates (Römling, 2005; Milanov et al., 2015). However, sole expression of cellulose nanofibers leads the pink, dry and rough (pdar) or pink and

smooth (pas) morphotype, while sole expression of curli fimbriae creates the brown, dry and rough (bdar) morphotype (Zogaj et al., 2003). In the present study, we observed that all the biofilm producing bacteria produced the rdar morphotype (**Figure 5A**), associated with curli fimbriae and cellulose production. However, intensity of red color, dryness, and roughness of the surfaces were greatly varied in these bacteria (**Figure 5A**). Thus, amount of cellulose and/or curli fimbriae production might be differed in these bacteria.

## Detection of Cellulose by Calcofluor Binding Assays

Because rdar expressing bacteria binds to the cellulose specific dye Calcofluor (Zogaj et al., 2001; Solano et al., 2002; Römling, 2005; Uhlich et al., 2006; Milanov et al., 2015), we therefore evaluated these bacterial strains by spotting the cultures (ca.  $10^5$  CFU/mL) on Calcofluor ( $200\text{ }\mu\text{g/mL}$ ) agar plates and incubated at  $28^\circ\text{C}$ . After 48 h incubation, Calcofluor agar plates were examined under UV ( $366\text{ nm}$ ) light. However, the fluorescence intensity and pattern were varied greatly in these bacteria (**Figure 5B**). *E. coli* ENSD101 weakly fluoresced only at the side of the colonies, while *E. asburiae* ENSD102, *E. ludwigii* ENSH201, uncultured *Vitreoscilla* sp. ENSG301, *K. pneumoniae* ENSG303, and *P. fluorescens* ENSG304 strongly fluoresced all the spreading zones of the colonies. *A. lwoffii* ENSG302 also strongly fluoresced but covering only 85% of the spreading zones of the colonies, while *B. thuringiensis* ENSW401 fluoresced in a banding pattern. The results of the

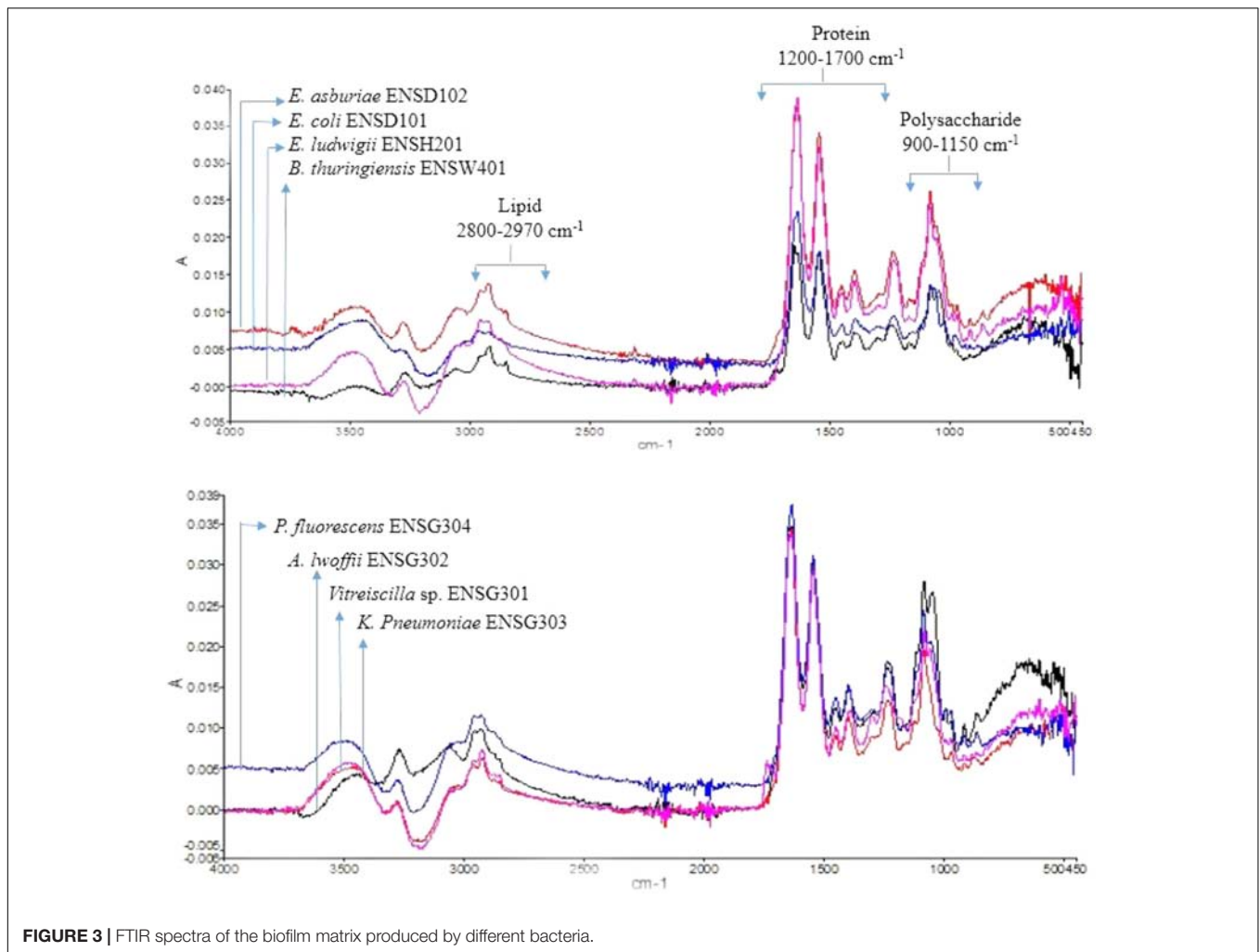


**FIGURE 3** | FTIR spectra of the biofilm matrix produced by different bacteria.

study confirmed that all these bacteria produced the cellulose-rich polysaccharide.

### Cellulose Production by Different Biofilm Producing Bacteria

Amount of cellulose production and intensity of fluorescence were correlated in bacteria (Haque et al., 2017), we, therefore, quantified cellulose production in different biofilm producing bacteria grown in Calcofluor agar plates after 48 h incubation at 28°C in static condition. Amount of cellulose production was found to be significantly ( $P \leq 0.001$ ) varied in these bacteria (Figure 6). *B. thuringiensis* ENSW401 produced significantly ( $P \leq 0.001$ ) more cellulose (153.36 ng), which was followed by *K. pneumoniae* ENSG303 (149.53). The second highest cellulose (133.9 ng) was produced by uncultured *Vitreoscilla* sp. ENSG301. However, cellulose production was statistically similar in *E. asburiae* ENSD102 (105.3 ng) and *P. fluorescens* ENSG304 (103.5 ng). Among the bacteria, *E. coli* ENSD101 produced the lowest amount of cellulose (65.2 ng). Thus, the increase of cellulose production seemed to have been reflected in the increase of Calcofluor binding.

### Bacterial Growth in Response to Different Concentrations of Cu, Zn, Pb, Ni, and Cr

Three novel bacteria, such as *E. asburiae* ENSD102, uncultured *Vitreoscilla* sp. ENSG301, and *A. lwoffii* ENSG302 were tested to ascertain the effect of different concentrations (0, 500, 750, 1000, 1250, 1500, 1750, and 2000 mg/L) of Cu, Zn, Pb, Ni, and Cr on cell growth in shaking condition (Figure 7). All the tested bacterial strains grew rapidly in the absence of any heavy metals in SOBGM broth. In general, as the concentrations increased, the growth rate was decreased in all the bacteria tested. Among the heavy metals, Pb severely affected the growth. These bacterial strains were incapable to recover their growth exposure to 1750 and 2000 mg/L of Pb and Cr, while they grew only slightly in response to 1750 and 2000 mg/L of Cu and Zn. Thus, specific metals and concentration of the metal might be important for the growth of these bacteria. Interestingly, when 50  $\mu$ L biofilm cells ( $10^7$  CFU/mL) of these bacteria (72-h old, biofilm formed on magnesium-deprived SOBGM broth containing 500 mg/L of Cu, Zn, Pb, and Cr) were transformed into the glass test tubes containing 5 mL of magnesium-deprived SOBGM broth with 1750

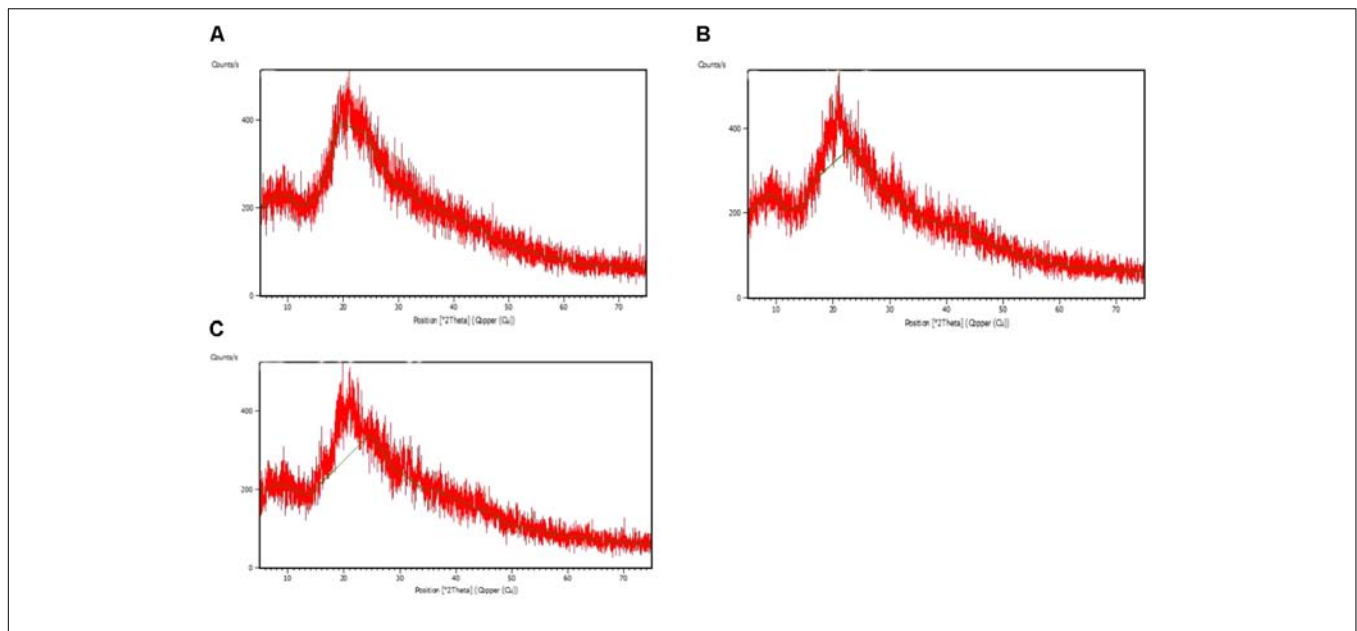


**FIGURE 4** | X ray diffraction (XRD) patterns of the matrix of the biofilms produced by *E. asburiae* ENSD102 (A), uncultured *Vitreoscilla* sp. ENSG301 (B), and *A. lwoffii* ENSG302 (C).

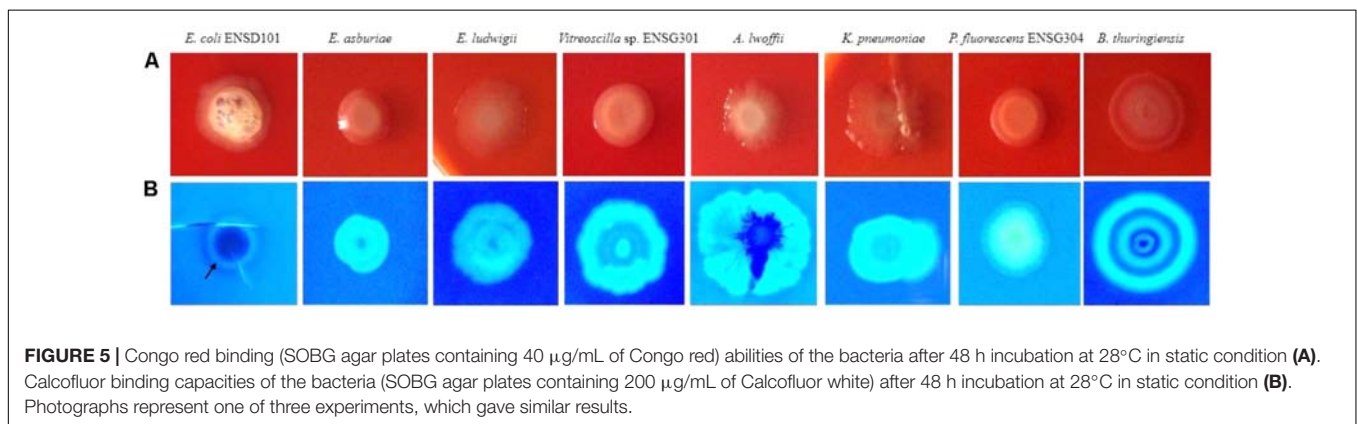


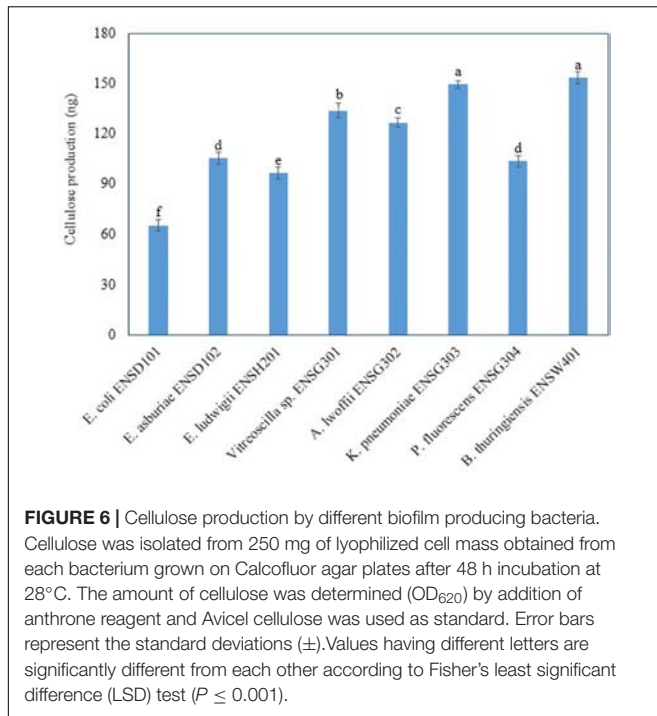
**FIGURE 5** | Congo red binding (SOBG agar plates containing 40  $\mu\text{g/mL}$  of Congo red) abilities of the bacteria after 48 h incubation at 28°C in static condition (A). Calcofluor binding capacities of the bacteria (SOBG agar plates containing 200  $\mu\text{g/mL}$  of Calcofluor white) after 48 h incubation at 28°C in static condition (B). Photographs represent one of three experiments, which gave similar results.

and 2000 mg/L of Cu, Zn, Pb, and Cr, the growth was increased in these bacteria in the presence of these metals (data not shown).

### Several Concentrations of Cu, Zn, Pb, Ni, and Cr Stimulates Biofilm Formation

Biofilm formation by *E. asburiae* ENSD102, uncultured *Vitreoscilla* sp. ENSG301, and *A. lwoffii* ENSG302 exposure to different concentrations of Cu, Zn, Pb, Ni, and Cr were not studied by any other contemporary researchers yet. *E. asburiae* ENSD102 produced the dense, robust, and smooth AL biofilms in response to 500, 750, and 1250 mg/L of Cu, while they developed the skinny and delicate AL biofilms responding to 1500 and 1750 mg/L of Cu (Figure 8A). This bacterium created a faint AL biofilm exposed to 2000 mg/L of Cu (Figure 8A). Uncultured *Vitreoscilla* sp. ENSG301 developed a thick, stout, and smooth AL biofilm responding to 500 mg/L of Cu (Figure 8B), but they constructed a tinny and uneven AL biofilms responding

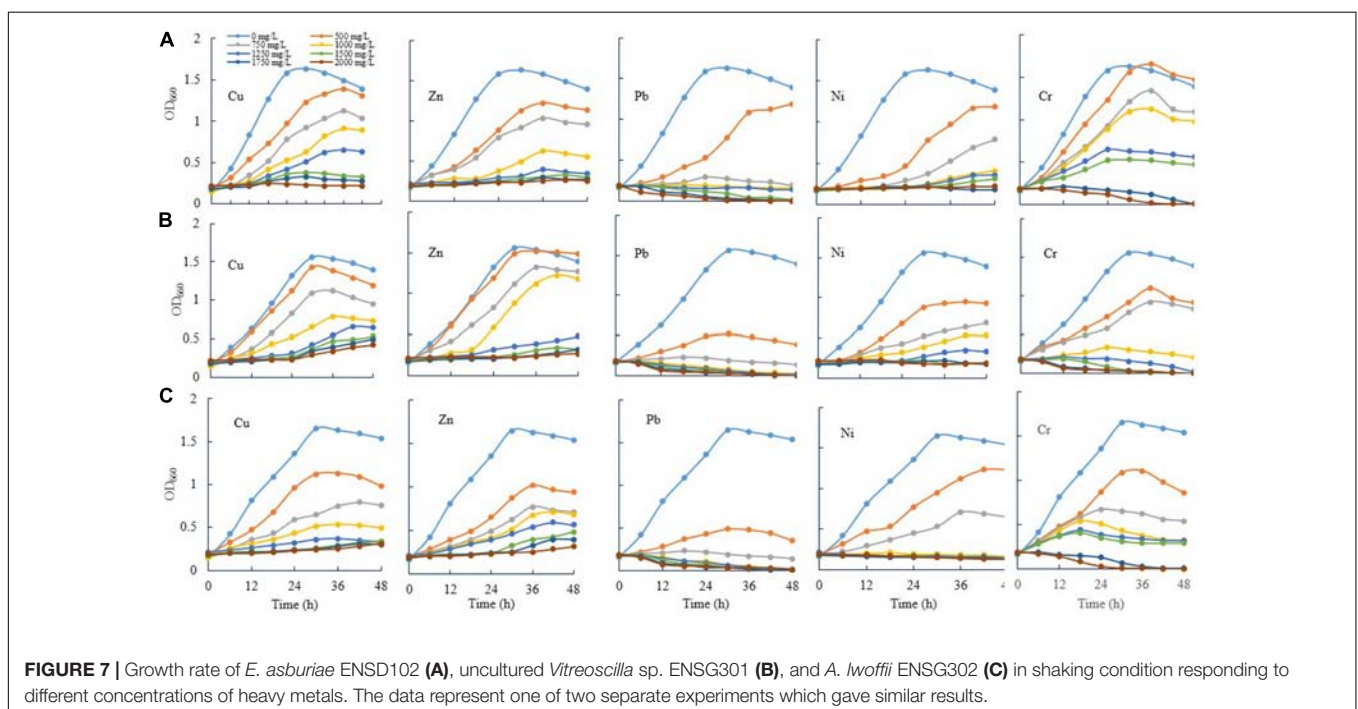
to 750, 1000, and 1250 mg/L of Cu (Figure 8B). Conversely, they generated the weak SAL biofilms in response to 1500 and 1750 mg/L of Cu (Figure 8B). Increasing the Cu concentration from 1750 to 2000 mg/L, completely inhibited the biofilm formation in uncultured *Vitreoscilla* sp. ENSG301 (Figure 8B). A profuse, firm, and smooth AL biofilm was generated by *A. lwoffii* ENSG302 increasing the Cu concentration from 0 to 500 mg/L (Figure 8C), while they developed a thin and fragile AL biofilm in response to 750 mg/L Cu (Figure 8C). Conversely, 1000 and 1250 mg/L of Cu triggered the SAL biofilm formation (Figure 8C), while 1500 mg/L of Cu prevented the biofilm formation in *A. lwoffii* ENSG302. Nevertheless, the minimal biofilm Cu inhibitory concentration (mg/L) for *E. asburiae* ENSD102, uncultured *Vitreoscilla* sp. ENSG301, and *A. lwoffii* ENSG302 was 2100, 2000, and 1500, respectively. When quantified (Figure 8D), compared to the absence of Cu, *E. asburiae* ENSD102 produced 3.39-, 4.61-, 5.4-, 7.53-, 3.38-, 3.37-, and 2.07-fold more biomass biofilms responding to 500,



750, 1000, 1250, 1500, 1750, and 2000 mg/L of Cu, respectively, while uncultured *Vitreoscilla* sp. ENSG301 developed 3.46-, 3.07-, 3.06-, 2.95-, 1.78-, and 1.57-fold higher biomass biofilms responding to 500, 750, 1000, 1250, 1500, and 1750 mg/L of Cu, respectively, and *A. lwoffii* ENSG302 generated 3.47-, 2.62-, 2.03-, and 1.46-fold increase biomass biofilms in response to 500, 750, 1000, and 1250 mg/L of Cu, respectively.

Different concentrations of Zn also influenced the biofilm formation (**Figure 9**). *E. asburiae* ENSD102 produced the profuse and rough AL biofilms exposure to 500, 750, 1000, 1250, and 1500 mg/L of Zn (**Figure 9A**), while uncultured *Vitreoscilla* sp. ENSG301 (**Figure 9B**) and *A. lwoffii* ENSG302 (**Figure 9C**) developed the prolific and uneven AL biofilms responding to 500, 750, 1000, and 1250 mg/L of Zn. However, biofilm formation of *E. asburiae* ENSD102 and *A. lwoffii* ENSG302 was prevented by 2000 mg/L of Zn (**Figures 9A,C**), while 1750 mg/L of Zn inhibited the biofilm formation of uncultured *Vitreoscilla* sp. ENSG301 (**Figure 9B**). The minimal biofilm Zn inhibitory concentration (mg/L) for *E. asburiae* ENSD102, uncultured *Vitreoscilla* sp. ENSG301 and *A. lwoffii* ENSG302 was detected at 2000, 2000, and 1750 mg/L, respectively.

Increasing the Pb concentration from 0 to 500 mg/L triggered an intense SAL biofilm formation by *E. asburiae* ENSD102 and *E. ludwigii* ENSG302, while uncultured *Vitreoscilla* sp. ENSG301 produced a faint SAL biofilm in this concentration (**Figure 10**). *E. asburiae* ENSD102 also induced AL biofilms responding up to 750 mg/L of Ni, while this bacterium generated the weak to strong SAL biofilms increasing the Ni concentration up to 1500 mg/L (**Figure 10**). A stout and thick AL biofilm developed by uncultured *Vitreoscilla* sp. ENSG301 responding to 500 mg/L of Ni, while *A. lwoffii* ENSG302 formed a fragile and thin AL biofilm at this concentration (**Figure 7**). All these bacterial strains also produced a lighter and fragile AL biofilms increasing the Cr concentration up to 750 mg/L (**Figure 10**). Thus, biofilm formation might be dependent on particular metal, concentration of the metal, and bacterial strain. All these bacteria produced the cellulose-rich polysaccharide (**Figures 3, 4**) responsible for biofilm formation. Polysaccharides were shown to bind with the metals (Ferris et al., 1989; Teitzel and Parsek, 2003;



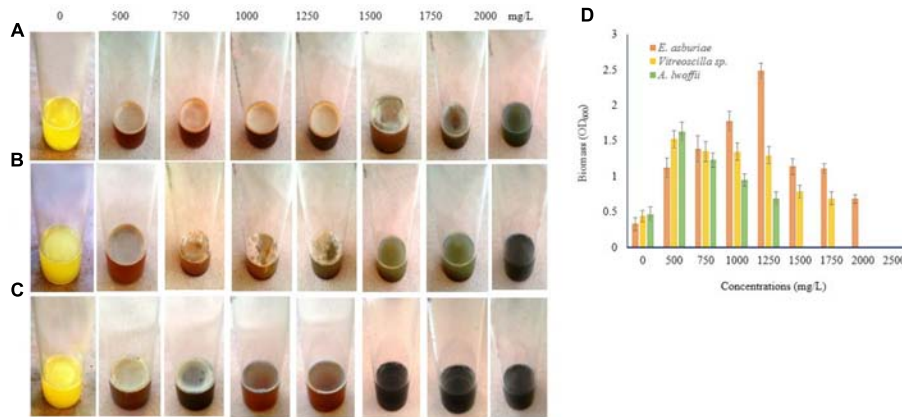


**FIGURE 8** | Several concentrations of copper sulfate (for Cu) stimulates biofilm formation in *E. asburiae* ENSD102 (A), uncultured *Vitreoscilla* sp. ENSG301 (B), and *A. Iwoffii* ENSG302 (C) after 72 h incubation at 28°C in static condition. Biomass of biofilms measured at 600 nm (D). The values are mean and error bars indicate standard deviation ( $\pm$ SD) of the three independent experiments.

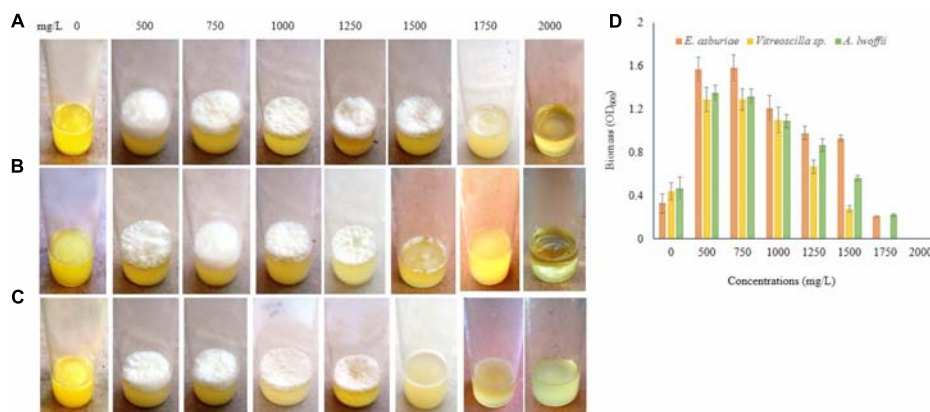


**FIGURE 9** | Certain concentrations of zinc sulfate (for Zn) activates biofilm formation in *E. asburiae* ENSD102 (A), uncultured *Vitreoscilla* sp. ENSG301 (B), and *A. Iwoffii* ENSG302 (C) in static condition after 72 h incubation at 28°C. Biomass of biofilms measured at 600 nm (D). The values are mean and error bars indicate standard deviation ( $\pm$ SD) of the three independent experiments.

van Hullebusch et al., 2003; Li and Yu, 2014). Thus, these biofilm producing bacterial strains might be an attractive biotechnological tool to remove the toxic heavy metals from wastewaters.

## DISCUSSION

Biofilm formation is an important colonization strategy for adaptation and survival in adverse environmental cues in bacteria. In nature, more than 99% bacteria exists as biofilms (Costerton et al., 1987). Ude et al. (2006) shown that 76% *Pseudomonas* isolates from diverse environmental origins develops AL biofilms on KB broth at 20–22°C within 15 days of incubation in stationary condition in the laboratory. Another survey conducted by Solano et al. (2002), 71% *Salmonella enterica* serovar Enteritidis isolates from environment, food, animals, and clinical origins were found to develop the AL biofilms on

Luria-Bertani broth at room temperature in static condition. In this study, only 27.5% (in static condition at 28 and 37°C) and 22.5% (in shaking condition at 28°C) isolates formed the AL and SAL biofilms, respectively, in the glass test tubes containing SOBG broth after 72 h incubation (Figures 1A,B) but not in YP, LB, KB, YPDA, and M63 glycerol minimal media (data not shown). SOBG broth was also found as a best biofilm inducing medium by other researchers (Yap et al., 2005; Jahn et al., 2008; Zou et al., 2012; Haque et al., 2009, 2017). Bacterial strains, chemical composition of the surface, nutritional (e.g., media composition, carbon sources, and divalent cations including, magnesium, calcium, and iron), and environmental conditions (e.g., temperature, oxygen tension, osmolarity, pH, and chemotaxis) are important to form the biofilms in the laboratory (Yap et al., 2005; Hossain and Tsuyumu, 2006; Liang et al., 2010; Haque et al., 2012, 2017). Thus, failure to develop the biofilms by several isolates of this study might be due to incongruous nutritional and environmental conditions.

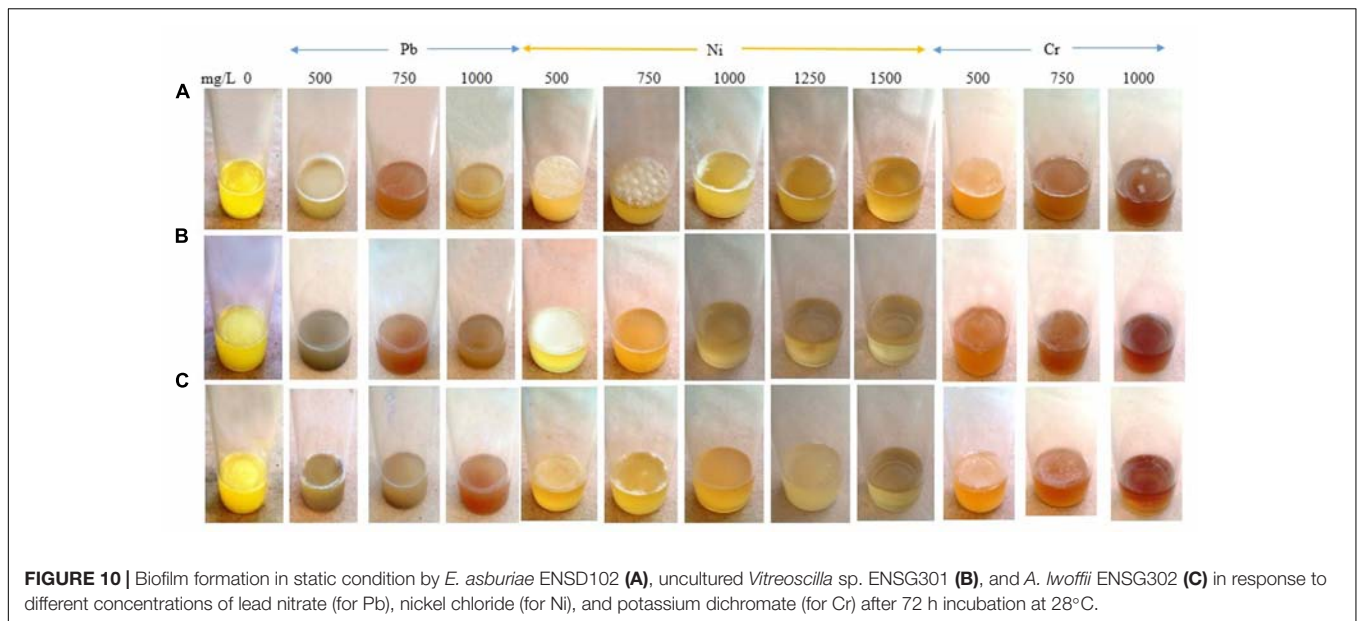


**FIGURE 10** | Biofilm formation in static condition by *E. asburiae* ENSD102 (A), uncultured *Vitreoscilla* sp. ENSG301 (B), and *A. lwoffii* ENSG302 (C) in response to different concentrations of lead nitrate (for Pb), nickel chloride (for Ni), and potassium dichromate (for Cr) after 72 h incubation at 28°C.

Bacterial biofilm formation depends on production and quantity of EPS (Sutherland, 2001). Concentration and composition of the EPS, hydrodynamic conditions, availability of nutrients, materials of the surface, motility, and intercellular communication system have been shown to regulate biofilm morphology (e.g., smooth and flat, rough, fluffy or filamentous, pillar, and mushroom) in bacteria (Zogaj et al., 2001; Solano et al., 2002; Hall-Stoodley et al., 2004; Flemming and Wingender, 2010). However, in the present study, the isolates of ENSD101, ENSD102, ENSH201, ENSG302, ENSG304, ENSW401, and ENST501 produced the smooth surface AL biofilms, while ENSH202, ENSG301, ENSG303, and ENSG305 developed the rough surface AL biofilms. Thus, biofilm morphology might depend on bacterial isolates/strains too.

Based on 16S rRNA gene sequencing, *E. coli* (ENSD101 and ENST501), *E. asburiae* (ENSD102), *E. ludwigii* (ENSH201), *P. fluorescens* (ENSH202 and ENSG304), uncultured *Vitreoscilla* sp. (ENSG301 and ENSG305), *A. lwoffii* (ENSG302), *K. pneumoniae* (ENSG303), and *B. thuringiensis* (ENSW401) were identified (Table 1). Except uncultured *Vitreoscilla* sp., all these bacteria have been isolated from different wastewaters (Zabłocka-Godłowska et al., 2012; Singh et al., 2015; Khan et al., 2015; Zhi et al., 2016; Radwan et al., 2017; Maintinguer et al., 2017). Importantly, the ability of these bacteria to produce the biofilms in the glass test tubes with SOBGM broth was not examined yet. Definitely, certain strains of *E. coli* (Weiss-Muszkat et al., 2010; Hung et al., 2013), *P. fluorescens* (Spiers et al., 2003; Koza et al., 2009), *K. pneumoniae* (Wang et al., 2016), *A. lwoffii* (Martí et al., 2011), and *B. thuringiensis* (El-Khoury et al., 2016) from other than wastewater origins have been reported to form the AL biofilms in defined laboratory systems. In this study, *E. asburiae* ENSD102 (from dyeing wastewater), uncultured *Vitreoscilla* sp. ENSG301 (from garments wastewater) and *E. ludwigii* ENSG302 (from garments wastewater) were identified as novel biofilm producing bacteria.

SEM images results revealed that several matrix of the biofilms produced highly fibrous ribbon-like microfibrils (Figure 2), popularly known as cellulose fibrils or nanofibers (Jahn et al., 2011; Hu et al., 2013). XRD data indicated that matrix produced by *E. asburiae* ENSD102, uncultured *Vitreoscilla* sp. ENSG301, and *A. lwoffii* ENSG302 are non-crystalline amorphous in nature (Figure 4). These results agree with the previously reported findings (Dogan et al., 2015). The results also came to an agreement that the absence of any ordered crystalline peak is due to the fact that the produced biofilms principally consisted of organic substances without forming any inorganic deposits (Hu et al., 2013). Besides, the literature suggests that presence of protein even in small amount can prevent the crystallization of sugar or sugar-protein mixture (Surewicz and Mantsch, 1988; Sharma and Kalonia, 2004; Haque M.A. et al., 2015). FTIR spectra (Figure 3) as well as Congo red binding (Figure 5A) results has confirmed that biofilm matrix produced by these bacteria are composed of proteins and cellulose-rich polysaccharides. The component of the matrix in the biofilms of *E. asburiae* ENSD102, uncultured *Vitreoscilla* sp. ENSG301, *A. lwoffii* ENSG302, and *B. thuringiensis* ENSW402 was not reported by any other contemporary researches.

Numerous species from *Enterobacteriaceae* [including certain strains of *E. coli* (Bokranz et al., 2005), some serovars of *Salmonella* (Steenackers et al., 2012), *Enterobacter* sp. (Zogaj et al., 2003; Hungund and Gupta, 2010), *A. baumannii* (Nucleo et al., 2009), *K. pneumoniae* (Zogaj et al., 2003; Wang et al., 2016), and *Pectobacterium carotovorum* subsp. *carotovorum* (Haque et al., 2017)] and *Pseudomonadaceae* [including several species of *Pseudomonas* (Spiers et al., 2003; Ude et al., 2006; Hinsia and O'Toole, 2006)] have been reported to produce the cellulose nanofibers and curli fimbriae, the major fraction of the EPS matrix. It was reported that expression of cellulose nanofibers and/or curli fimbriae depend on bacterial species/strains, chemical composition of the surfaces, growth,

and environmental conditions (Prouty and Gunn, 2003; Gerstel and Römling, 2003; García et al., 2004; Yap et al., 2005; Haque et al., 2012, 2017; Haque M.M. et al., 2015). EPS not only contains cellulose nanofibers and curli fimbriae but also contain extracellular DNA (Whitchurch et al., 2002; Liang et al., 2010). In this study, when we added up to 1000 U/mL of DNase I to SOBGM broth during biofilm formation process by these bacteria and incubated the culture at 28°C in static condition, all these bacteria produced the AL biofilms after 72 h incubation (data not shown). Thus, EPS of these bacterial strains might not be contained the extracellular DNA.

Bacterial biofilms are resistant to toxic metal ions (Teitzel and Parsek, 2003; Harrison et al., 2005; Koechler et al., 2015). Certain metal ions, such as  $\text{Ca}^{2+}$ ,  $\text{Mg}^{2+}$ ,  $\text{Fe}^{2+}$ ,  $\text{Fe}^{3+}$ ,  $\text{Ba}^{2+}$ ,  $\text{Cu}^{2+}$ , and  $\text{Zn}^{2+}$  induced the biofilm formation in bacteria (Turakhia and Characklis, 1989; Rinaudi et al., 2006; Song and Leff, 2006; Liang et al., 2010; Haque et al., 2012). Not only metals but their concentrations also played an important role in biofilm formation in bacteria. For example, increasing the  $\text{Cu}^{2+}$  concentration from 50 to 100  $\mu\text{M}$  increased the biofilm formation in *Xylella fastidiosa* strain Temecula, while higher concentrations (>200  $\mu\text{M}$ ) prevented the biofilm formation (Cobine et al., 2013). *X. fastidiosa* also increased the biofilm formation when PD2 amended with 400  $\mu\text{M}$   $\text{ZnSO}_4$  under flow conditions and with constant bacterial feeding (Navarrete and De La Fuente, 2014). *E. coli* K-12 produced twofold more biofilm biomass in the presence of 100  $\mu\text{M}$  of nickel compared to the biofilm grown in the absence of this metal (Perrin et al., 2009). We observed that several concentrations of Cu, Zn, Pb, Ni, and Cr stimulated the biofilm formation (Figures 8–10). We do not know exactly why several concentrations of these metals increased the biofilm formation in *E. asburiae* ENSD102, uncultured *Vitreoscilla* sp. ENSG301, and *A. lwoffii* ENSG302. Current study showed that all these bacteria produced both proteinaceous curli fimbriae and cellulose-rich polysaccharide (Figures 4, 5). The protein units reportedly gave the characteristics IR band through C = O stretching at amide I region, N–H bending and C–N stretching at amide II region and C–N bending and N–H stretching at amide III region (Liaqat et al., 2009; Haque et al., 2014). On the other hand, band region for polysaccharide principally resulted by stretching vibration of C–C and C–O bonds and deformation of C–O–H and C–O–C bonds (Naumann, 2000; Grube et al., 2002). It was reported that the positively charged metal bound with negatively charged functional groups present on the bacteria (Teitzel and Parsek, 2003; van Hullebusch et al., 2003). Thus, protein and/or polysaccharide produced by *E. asburiae* ENSD102, uncultured *Vitreoscilla* sp. ENSG301, and *A. lwoffii* ENSG302 in response to different concentrations of Cu, Zn, Pb, Ni, and Cr could sequester the toxic metal ions, giving to the bacteria the time required for adaptation thus driving to the physiological or metabolic changes necessary for eliminating the toxic effect of these metals, i.e., expression of enzymes and transporters for pumping out the metal or metal-binding proteins (Letelier et al., 2010; Mindlin et al., 2016; Nocelli et al., 2016; Karn et al., 2017). Thus, these bacterial strains might be an attractive biotechnological tool for bioremediation of toxic heavy metals from wastewaters.

Recently, several researchers have been shown that heavy metal resistant bacteria were also multidrug resistant (Bhagat et al., 2016; Aransiola et al., 2017; Andrade et al., 2018). Therefore, future studies should focus on study the virulence factor of these bacteria before used in bioremediation of heavy metals.

## CONCLUSION

Eleven biofilm producing bacterial strains were isolated and identified from diverse wastewaters of Bangladesh using 16S rRNA gene sequencing. All these bacteria produced proteinaceous curli fimbriae and cellulose—the two major components of the EPS. Cellulose has a wide variety of biomedical applications (e.g., wound dressing and blood vessels) as well as tissue engineering fields. Bacterial growth rate was decreased with the increase of the concentrations of the Cu, Zn, Pb, Ni, and Cr. Several concentrations of these heavy metals significantly enhanced the biofilm formation in *E. asburiae* ENSD102, uncultured *Vitreoscilla* sp. ENSG301, and *A. lwoffii* ENSG302. Biofilm/EPS matrix act as molecular sieve, e.g., sequestering metal ions, these bacterial strains might be an attractive biotechnological tool for bioremediation of Cu, Zn, Cr, Ni, and Pb from wastewaters.

## AUTHOR CONTRIBUTIONS

MM, ZHT, and MMH conducted the experiments. MMH conceived the idea, wrote the manuscript, and collected the research fund. MK, AM, MA, and MRT characterized the isolates and analyzed the data. MI identified the bacteria based on 16S rRNA gene sequencing. MAH conducted the FTIR analysis of the matrix of the biofilms produced by different bacteria. All the authors read the manuscript and approved for the submission.

## FUNDING

This research was supported by Research Management Committee (RMC) of Bangabandhu Sheikh Mujibur Rahman Agricultural University and Ministry of Science and Technology, Bangladesh to MMH.

## ACKNOWLEDGMENTS

We would like to thank Rajnee Hasan, Nasima Aktar, Rasel Ahmed, and Md. Sabbir Hossain, Bangladesh Jute Research Institute, Bangladesh for helping 16S rRNA gene sequencing. Professor Shah Mohammad Masum, University of Dhaka, Bangladesh for facilitating X-ray diffraction study.

## SUPPLEMENTARY MATERIAL

The Supplementary Material for this article can be found online at: <https://www.frontiersin.org/articles/10.3389/fmicb.2018.01334/full#supplementary-material>

## REFERENCES

- Ahluwalia, S. S., and Goyal, D. (2007). Microbial and plant derived biomass for removal of heavy metals from wastewater. *Bioresour. Technol.* 98, 2243–2257. doi: 10.1016/j.biortech.2005.12.006
- Ahmed, M. K., Baki, M. A., Kundu, G. K., Islam, M. S., Islam, M. M., and Hossain, M. M. (2016). Human health risks from heavy metals in fish of Buriganga river, Bangladesh. *Springer Plus* 5:1697. doi: 10.1186/s40064-016-3357-0
- Alam, M. Z., Carpenter-Boggs, L., Rahman, A., Haque, M. M., Miah, M. R. U., Moniruzzaman, M., et al. (2017). Water quality and resident perceptions of declining ecosystem services at Shitalakka wetland in Narayanganj city. *Sustain. Water Qual. Ecol.* 9–10, 53–66. doi: 10.1016/j.swa.2017.03.002
- Al-Adwahi, H., Al-Hasan, R. H., Sorkhoh, N. A., Salamah, S., and Radwan, S. S. (2003). Establishing oil-degrading biofilms on gravel particles and glass plates. *Int. Biodeterior. Biodegradation* 51, 181–185. doi: 10.1016/S0964-8305(02)00140-3
- American Public Health Association [APHA] (1998). *Standard Methods for the Examination of Water and Wastewater*, 20th Edn. Washington, DC: American Public Health Association.
- Andrade, L. N., Siqueira, T. E. S., Martinez, R., and Darini, A. L. C. (2018). Multidrug-resistant CTX-M-(15, 9, 2)- and KPC-2-producing *Enterobacter hormaechei* and *Enterobacter asburiae* isolates possessed a set of acquired heavy metal tolerance genes including a chromosomal *sil* operon (for acquired silver resistance). *Front. Microbiol.* 9:539. doi: 10.3389/fmicb.2018.00539
- Aransiola, E. F., Ige, O. A., Ehinmitola, E. O., and Layokun, S. K. (2017). Heavy metals bioremediation potential of *Klebsiella* species isolated from diesel polluted soil. *Afr. J. Biotechnol.* 16, 1098–1105. doi: 10.5897/AJB2016.15823
- Bhagat, N., Vermani, M., and Bajwa, H. S. (2016). Characterization of heavy metal (cadmium and nickel) tolerant Gram negative enteric bacteria from polluted Yamuna River, Delhi. *Afr. J. Microbiol. Res.* 10, 127–137. doi: 10.5897/AJMR2015.7769
- Bokranz, W., Wang, X., Tschape, H., and Romling, U. (2005). Expression of cellulose and curli fimbriae by *Escherichia coli* isolated from the gastrointestinal tract. *J. Med. Microbiol.* 54, 1171–1182. doi: 10.1099/jmm.0.46064-0
- Castresana, J. (2000). Selection of conserved blocks from multiple alignments for their use in phylogenetic analysis. *Mol. Biol. Evol.* 17, 540–552. doi: 10.1093/oxfordjournals.molbev.a026334
- Chang, W. C., Hsu, G. S., Chiang, S. M., and Su, M. C. (2006). Heavy metal removal from aqueous solution by wasted biomass from a combined AS-biofilm process. *Bioresour. Technol.* 97, 1503–1508. doi: 10.1016/j.biortech.2005.06.011
- Cobine, P. A., Cruz, L. F., Navarrete, F., Duncan, D., Tygart, M., and De Le Fuente, L. (2013). *Xyloella fastidiosa* differentially accumulates mineral elements in biofilm and planktonic cells. *PLoS One* 8:e54936. doi: 10.1371/journal.pone.0054936
- Conrad, A., Suutari, M. K., Keinänen, M. M., Cadoret, A., Faure, P., Mansuy-Huault, L., et al. (2003). Fatty acid lipid fractions in extracellular polymeric substances of activated sludge flocs. *Lipids* 38, 1093–1105. doi: 10.1007/s11745-006-1165-y
- Costerton, J. W., Cheng, K. J., Geesey, G. G., Ladd, T. I., Nickel, J. C., Dasgupta, M., et al. (1987). Bacterial biofilms in nature and disease. *Annu. Rev. Microbiol.* 41, 435–464. doi: 10.1146/annurev.mi.41.100187.002251
- Costerton, J. W., Stewart, P. S., and Greenberg, E. P. (1999). Bacterial biofilms: a common cause of persistent infections. *Science* 284, 1318–1322. doi: 10.1126/science.284.5418.1318
- Cristina, Q., Zelia, R., Bruna, F., Hugo, F., and Teresa, T. (2009). Biosorptive performance of an *Escherichia coli* biofilm supported on zeolite NaY for the removal of Cr(VI), Cd(II), Fe(III) and Ni(II). *Chem. Eng. J.* 152, 110–115. doi: 10.1016/j.cej.2009.03.039
- Das, N., Basak, L. V. G., Salam, J. A., and Abigail, M. E. A. (2012). Application of biofilms on remediation of pollutants – an overview. *J. Microbiol. Biotechnol. Res.* 2, 783–790. doi: 10.1007/s00253-013-5216-z
- Das, P., Aziz, S., and Obbard, J. (2011). Two phase microalgae growth in the open system for enhanced lipid productivity. *Renew. Energy* 36, 2524–2528. doi: 10.1016/j.renene.2011.02.002
- Davey, M. E., Cajazza, N. C., and O'Toole, G. A. (2003). Rhamnolipid surfactant production affects biofilm architecture in *Pseudomonas aeruginosa* PAO1. *J. Bacteriol.* 185, 1027–1036. doi: 10.1128/JB.185.3.1027-1036.2003
- Dixit, R., Wasiulla, M. D., Pandiyan, K., Singh, U. B., Sanu, A., et al. (2015). Bioremediation of heavy metals from soil and aquatic environment: an overview of principles and criteria of fundamental processes. *Sustainability* 7, 2189–2212. doi: 10.3390/su7022189
- Dogan, N. M., Doganli, G. A., Dogan, G., and Bozkaya, O. (2015). Characterization of extracellular polysaccharide (EPS) produced by thermal *Bacillus* and determination of environmental conditions affecting exopolysaccharide production. *Int. J. Environ. Res.* 9, 1107–1116. doi: 10.22059/IJER.2015.998
- Donlan, R. M., and Costerton, J. W. (2002). Biofilms: survival mechanisms of clinically relevant microorganisms. *Clin. Microbiol. Rev.* 15, 167–193. doi: 10.1128/CMR.15.2.167-193.2002
- Edgar, R. C. (2004). MUSCLE: multiple sequence alignment with high accuracy and high throughput. *Nucleic Acids Res.* 32, 1792–1797. doi: 10.1093/nar/gkh340
- Edwards, S. J., and Kjellerup, B. V. (2013). Applications of biofilms in bioremediation and biotransformation of persistent organic pollutants, pharmaceutical/personal care products, and heavy metals. *Appl. Microbiol. Biotechnol.* 97, 9909–9921. doi: 10.1007/s00253-013-5216-z
- Elekwachi, C. O., Andresen, J., and Hodgman, T. C. (2014). Global use of bioremediation technologies for decontamination of ecosystems. *J. Bioremediat. Biodegrad.* 5, 1–9. doi: 10.4172/2155-6199.1000225
- El-Khoury, N., Majed, R., Perchat, S., Kallassy, M., Lereclus, D., and Gohar, M. (2016). Spatio-temporal evolution of sporulation in *Bacillus thuringiensis* biofilm. *Front. Microbiol.* 7:1222. doi: 10.3389/fmicb.2016.01222
- Fang, L., Wei, X., Cai, P., Huang, Q., Chen, H., Liang, W., et al. (2011). Role of extracellular polymeric substances in Cu(II) adsorption on *Bacillus subtilis* and *Pseudomonas putida*. *Bioresour. Technol.* 102, 1137–1141. doi: 10.1016/j.biortech.2010.09.006
- Ferris, F. G., Schultze, S., Witten, T. C., Fyfe, W. S., and Beveridge, T. J. (1989). Metal interactions with microbial biofilms in acidic and neutral pH environments. *Appl. Environ. Microbiol.* 55, 1249–1257.
- Fida, T. T., Breugelmans, P., Lavigne, R., Coronado, E., Johnson, D. R., vander Meer, J. R., et al. (2012). Exposure to solute stress affects genome-wide expression but not the poly-cyclic aromatic hydrocarbon-degrading activity of *Sphingomonas* sp. strain LH128 in biofilms. *Appl. Environ. Microbiol.* 78, 8311–8320. doi: 10.1128/AEM.02516-12
- Flemming, H. C., and Wingender, J. (2010). The biofilm matrix. *Nat. Rev. Microbiol.* 8, 623–633. doi: 10.1038/nrmicro2415
- García, B., Latasa, C., Solano, C., García-del Portillo, F., Gamazo, C., and Lasa, I. (2004). Role of the GGDEF protein family in *Salmonella* cellulose biosynthesis and biofilm formation. *Mol. Microbiol.* 54, 264–277. doi: 10.1111/j.1365-2958.2004.04269.x
- Gerstel, U., and Römling, U. (2003). The *csgD* promoter, a control unit for biofilm formation in *Salmonella typhimurium*. *Res. Microbiol.* 154, 659–667. doi: 10.1016/j.resmic.2003.08.005
- Grube, M., Bekers, M., Upite, D., and Kaminska, E. (2002). Infrared spectra of some fructans. *Spectroscopy* 16, 289–296. doi: 10.1155/2002/637587
- Hall-Stoodley, L., Costerton, J. W., and Stoodley, P. (2004). Bacterial biofilms: from the natural environment to infectious diseases. *Nat. Rev. Microbiol.* 2, 95–108. doi: 10.1038/nrmicro821
- Haque, M. A., Aldred, P., Chen, J., and Adhikari, B. (2015). Denaturation and physical characteristics of spray dried whey protein isolate powders produced in the presence and absence of lactose, trehalose and polysorbate- 80. *Drying Technol.* 33, 1243–1254. doi: 10.1080/07373937.2015.1023311
- Haque, M. A., Aldred, P., Chen, J., Barrow, C. J., and Adhikari, B. (2014). Drying and denaturation characteristics of  $\alpha$ -lactalbumin,  $\beta$ -lactoglobulin and bovine serum albumin in convective drying process. *J. Agric. Food Chem.* 62, 4695–4706. doi: 10.1021/jf405603c
- Haque, M. M., Hirata, H., and Tsuyumu, S. (2012). Role of PhoP-PhoQ two-component system in pellicle formation, virulence and survival in harsh environments of *Dickeya dadantii* 3937. *J. Gen. Plant Pathol.* 78, 176–189. doi: 10.1007/s10327-012-0372-z
- Haque, M. M., Hirata, H., and Tsuyumu, S. (2015). SlyA regulates *motA* and *motB*, virulence and stress-related genes under conditions induced by the PhoP-PhoQ system in *Dickeya dadantii* 3937. *Res. Microbiol.* 166, 467–475. doi: 10.1016/j.resmic.2015.05.004
- Haque, M. M., Kabir, M. S., Aini, L. Q., Hirata, H., and Tsuyumu, S. (2009). SlyA, a MarR family transcriptional regulator, is essential for virulence in *Dickeya dadantii* 3937. *J. Bacteriol.* 191, 5409–5419. doi: 10.1128/JB.00240-09

- Haque, M. M., Oliver, M. M. H., Nahar, K., Alam, M. Z., Hirata, H., and Tsuyumu, S. (2017). CytR homolog of *Pectobacterium carotovorum* subsp. *carotovorum* controls air-liquid biofilm formation by regulating multiple genes involved in cellulose production, c-di-GMP signaling, motility, and type III secretion system in response to nutritional and environmental signals. *Front. Microbiol.* 8:972. doi: 10.3389/fmicb.2017.00972
- Harrison, J. J., Turner, R. J., and Ceri, H. (2005). Persister cells, the biofilm matrix and tolerance to metal cations in biofilm and planktonic *Pseudomonas aeruginosa*. *Environ. Microbiol.* 7, 981–994. doi: 10.1111/j.1462-2920.2005.00777.x
- Hinsa, S. M., and O'Toole, G. A. (2006). Biofilm formation by *Pseudomonas fluorescens* WCS365: a role for LapD. *Microbiology* 152, 1375–1383. doi: 10.1099/mic.0.28696-0
- Hossain, M. M., and Tsuyumu, S. (2006). Flagella-mediated motility is required for biofilm formation by *Erwinia carotovora* subsp. *carotovora*. *J. Gen. Plant Pathol.* 72, 34–39. doi: 10.1007/s10327-005-0246-8
- Hu, X.-B., Xu, K., Wang, Z., Ding, L.-L., and Ren, H.-Q. (2013). Characteristics of biofilm attaching to carriers in moving bed biofilm reactor used to treat vitamin C wastewater. *Scanning* 35, 283–291. doi: 10.1002/sca.21064
- Huang, Y.-B., Wang, W.-H., and Peng, A. (2000). Accumulation of Cu(II) and Pb(II) by biofilms grown on particulate in aquatic systems. *J. Environ. Sci. Health Part A Environ. Sci. Eng.* 35, 575–592. doi: 10.1080/10934520009376987
- Hung, C., Zhou, Y., Pinkner, J. S., Dodson, K. W., Crowley, J. R., Heuser, J., et al. (2013). *Escherichia coli* biofilms have an organized and complex extracellular matrix structure. *mBio* 4:e00645-13. doi: 10.1128/mBio.00645-13
- Hungund, B. S., and Gupta, S. G. (2010). Improved production of bacterial cellulose from *Gluconacetobacter persimmonis* GH-2. *J. Microb. Biochem. Technol.* 2, 127–133. doi: 10.4172/1948-5948.1000037
- Islam, M. M., Mahmud, K., Faruk, O., and Billah, M. S. (2011). Textile dyeing industries in Bangladesh for sustainable development. *Int. J. Environ. Sci. Dev.* 2, 428–436. doi: 10.7763/IJESD.2011.V2.164
- Islam, M. S., Ahmed, M. K., and Habibullah-Al-Mamun, M. (2014). Determination of heavy metals in fish and vegetables in Bangladesh and health implications. *Hum. Ecol. Risk Assess. Int. J.* 21, 986–1006. doi: 10.1080/10807039.2014.950172
- Islam, M. S., Ahmed, M. K., Raknuzzaman, M., Habibullah-Al-Mamun, M., and Masunaga, S. (2015). Metal speciation in sediment and their bioaccumulation in fish species of three urban rivers in Bangladesh. *Arch. Environ. Contam. Toxicol.* 68, 92–106. doi: 10.1007/s00244-014-0079-6
- Jahn, C. E., Selimi, D. A., Barak, J. D., and Charkowski, A. O. (2011). The *Dickeya dadantii* biofilm matrix consists of cellulose nanofibres, and is an emergent property dependent upon the type III secretion system and the cellulose synthesis operon. *Microbiology* 157, 2733–2744. doi: 10.1099/mic.0.051003-0
- Jahn, C. E., Willis, D. K., and Charkowski, A. O. (2008). The flagellar sigma factor FliA is required for *Dickeya dadantii* virulence. *Mol. Plant Microbe Interact.* 11, 1431–1442. doi: 10.1094/MPMI-21-11-1431
- Jin, H., Liu, G., and Tao, W. (2007). Decolorization of a dye industry effluent by *Aspergillus fumigatus* XC6. *Appl. Microbiol. Biotechnol.* 74, 239–243. doi: 10.1007/s00253-006-0658-1
- Jones, D. T., Taylor, W. R., and Thornton, J. M. (1992). The rapid generation of mutation data matrices for protein sequences. *Comput. Appl. Biosci.* 8, 275–282. doi: 10.1093/bioinformatics/8.3.275
- Kaplan, J. B. (2010). Biofilm dispersal: mechanisms, clinical implications, and potential therapeutic uses. *J. Dent. Res.* 89, 205–218. doi: 10.1177/0022034509359403
- Karn, S. K., Fang, G., and Duan, J. (2017). *Bacillus* sp. acting as dual role for corrosion induction and corrosion inhibition with carbon steel (CS). *Front. Microbiol.* 8:2038. doi: 10.3389/fmicb.2017.02038
- Khan, Z., Hussain, S. Z., Rehman, A., Zulfikar, S., and Shakoori, A. R. (2015). Evaluation of cadmium resistant bacterium, *Klebsiella pneumoniae*, isolated from industrial wastewater for its potential use to bioremediate environmental cadmium. *Pak. J. Zool.* 47, 1533–1543.
- Klemm, D., Schumann, D., Udhardt, U., and Marsch, S. (2001). Bacterial synthesized cellulose-artificial blood vessels for microsurgery. *Prog. Polym. Sci.* 26, 1561–1603. doi: 10.1016/S0079-6700(01)00021-1
- Koehler, S., Farasin, J., Cleiss-Arnold, J., and Arsène-Ploetze, F. (2015). Toxic metal resistance in biofilms: diversity of microbial responses and their evolution. *Res. Microbiol.* 10, 764–773. doi: 10.1016/j.resmic.2015.03.008
- Koza, A., Hallett, P. D., Moon, C. D., and Spiers, A. J. (2009). Characterization of a novel air-liquid interface biofilm of *Pseudomonas fluorescens* SBW25. *Microbiology* 155, 1397–1406. doi: 10.1099/mic.0.025064-0
- Labrenz, M., Druschel, G. K., Thomsen-Ebert, T., Gilbert, B., Welch, S. A., Kemner, K. M., et al. (2000). Formation of sphalerite (ZnS) deposits in natural biofilms of surface-reducing bacteria. *Science* 290, 1744–1747. doi: 10.1126/science.290.5497.1744
- Lasa, I., and Penadé, J. R. (2006). Bap: a family of surface proteins involved in biofilm formation. *Res. Microbiol.* 157, 99–107. doi: 10.1016/j.resmic.2005.11.003
- Letelier, M. E., Sebastian, S. J., Liliana, P. S., Cortés-Troncoso, J., and Aracena-Parks, P. (2010). Mechanisms underlying iron and copper ions toxicity in biological systems: pro-oxidant activity and protein-binding effects. *Chem. Biol. Interact.* 188, 220–227. doi: 10.1016/j.cbi.2010.06.013
- Li, W.-W., and Yu, H.-Q. (2014). Insight into the roles of microbial extracellular polymer substances in metal biosorption. *Bioresour. Technol.* 160, 15–23. doi: 10.1016/j.biortech.2013.11.074
- Liang, Y., Gao, H., Chen, J., Dong, Y., Wu, L., He, Z., et al. (2010). Pellicle formation in *Shewanella oneidensis*. *BMC Microbiol.* 10:291. doi: 10.1186/1471-2180-10-291
- Liaquat, I., Sumbal, F., and Sabri, A. N. (2009). Tetracycline and chloramphenicol efficiency against selected biofilm forming bacteria. *Curr. Microbiol.* 59, 212–220. doi: 10.1007/s00284-009-9424-9
- Maintinguer, S. I., Lazaro, C. Z., Pachiega, R., Varesche, M. B. A., Sequinel, R., and Oliveira, J. E. (2017). Hydrogen bioproduction with *Enterobacter* sp. isolated from brewery wastewater. *Int. J. Hydrogen Energy* 42, 152–160. doi: 10.1016/j.ijhydene.2016.11.104
- Maneering, T., Tokura, S., and Rujiravanit, R. (2007). Impregnation of silver nanoparticles into bacterial cellulose for antimicrobial wound dressing. *Carbohydr. Polym.* 72, 43–51. doi: 10.1016/j.carbpol.2007.07.025
- Martí, S., Rodríguez-Baño, J., Catel-Ferreira, M., Jouenne, T., Vila, J., Seifert, H., et al. (2011). Biofilm formation at the solid-liquid and air-liquid interfaces by *Acinetobacter* species. *BMC Short Notes* 4:5. doi: 10.1186/1756-0500-4-5
- Martín-Cereceda, M., Jorand, F., Guinea, A., and Block, J. C. (2001). Characterization of extracellular polymeric substances in rotating biological contactors and activated sludge flocs. *J. Environ. Technol.* 22, 951–959. doi: 10.1080/09593332208618231
- McDougald, D., Rice, S. A., Barraud, N., Steinberg, P. D., and Kjelleberg, S. (2012). Should we stay or should we go: mechanisms and ecological consequences for biofilm dispersal. *Nat. Rev. Microbiol.* 10, 39–50. doi: 10.1038/nrmicro2695
- Milanov, D. S., Prunic, B. Z., Velhner, M. J., Pajic, M. L., and Cabarkapa, I. S. (2015). Rdar morphotype- a resting stage of some *Enterobacteriaceae*. *Food Feed Res.* 42, 43–50. doi: 10.5937/FFR1501043M
- Mindlin, S., Petrenko, A., Kurakov, A., Beletsky, A., Mardanov, A., and Petrova, M. (2016). Resistance of permafrost and modern *Acinetobacter lwoffii* strains to heavy metals and arsenic revealed by genome analysis. *BioMed Res. Int.* 2016:3970831. doi: 10.1155/2016/3970831
- Mitra, A., and Mukhopadhyay, S. (2016). Biofilm mediated decontamination of pollutants from the environment. *AIMS Bioeng.* 3, 44–59. doi: 10.3934/bioeng.2016.1.44
- Muñoz, R., Alvarez, M. T., Muñoz, A., Terrazas, E., Guieysse, B., and Mattiasson, B. (2006). Sequential removal of heavy metals ions and organic pollutants using an algal680 bacterial consortium. *Chemosphere* 63, 903–911. doi: 10.1016/j.chemosphere.2005.09.062
- Naser, H. M., Sultana, S., Haque, M. M., Akhter, S., and Begum, R. A. (2014). Lead, cadmium and nickel accumulation in some common spice grown in industrial areas of Bangladesh. *Agriculturists* 12, 122–130. doi: 10.3329/agric.v12i1.19867
- Naumann, D. (2000). “FT-Infrared and FT-Raman spectroscopy in biomedical research,” in *Infrared and Raman Spectroscopy of Biological Materials*, eds H. U. Gremlich and B. Yan (Basel: Marcel Dekker, Inc.), 323–377. doi: 10.1021/ja004845m
- Navarrete, F., and De La Fuente, L. (2014). Response of *Xylella fastidiosa* to zinc: decreased culturability, increased exopolysaccharide production, and formation of resilient biofilms under flow conditions. *Appl. Environ. Microbiol.* 80, 1097–1107. doi: 10.1128/AEM.02998-13
- Nocelli, N., Bogino, P. C., Banchio, E., and Giordano, W. (2016). Roles of extracellular polysaccharides and biofilm formation in heavy metal resistance of rhizobia. *Materials* 9:418. doi: 10.3390/ma9060418

- Nucleo, E., Steffanoni, L., Fugazza, G., Migliavacca, R., Giacobone, E., Navarra, A., et al. (2009). Growth in glucose-based medium and exposure to subinhibitory concentrations of imipenem induce biofilm formation in a multidrug-resistant clinical isolate of *Acinetobacter baumannii*. *BMC Microbiol.* 9:270. doi: 10.1186/1471-2180-9-270
- Pal, A., and Paul, A. K. (2008). Microbial extracellular polymeric substances: central elements in heavy metal bioremediation. *Indian J. Microbiol.* 48, 49–64. doi: 10.1007/s12088-008-0006-5
- Payne, R. B., May, H. D., and Sowers, K. B. (2011). Enhanced reductive dechlorination of polychlorinated biphenyl impacted sediment by bioaugmentation with a dehalorespiring bacterium. *Environ. Sci. Technol.* 45, 8772–8779. doi: 10.1021/es201553c
- Perrin, C., Briandet, R., Jubelin, G., Lejeune, P., Mandrand-Berthelot, M. A., Rodrigue, A., et al. (2009). Nickel promotes biofilm formation by *Escherichia coli* K-12 strains that produce curli. *Appl. Environ. Microbiol.* 75, 1723–1733. doi: 10.1128/AEM.02171-08
- Prigent-Combaret, C., Prensier, G., Le Thi, T. T., Vidal, O., Lejeune, P., and Dorel, C. (2000). Development pathway for biofilm formation in curli-producing *Escherichia coli* strains: roles for flagella, curli and colonic acid. *Environ. Microbiol.* 2, 450–464. doi: 10.1046/j.1462-2920.2000.00128.x
- Prouty, A. M., and Gunn, J. S. (2003). Comparative analysis of *Salmonella enterica* serovar Typhimurium biofilm formation on gallstones and glass. *Infect. Immun.* 71, 7154–7158. doi: 10.1128/IAI.71.12.7154-7158.2003
- Radwan, T. E. E., Reyad, A. M. M., and Essa, A. M. M. (2017). Bioremediation of the nematicide oxamyl by *Enterobacter ludwigii* isolated from agricultural wastewater. *Egypt. J. Exp. Biol.* 13, 19–30. doi: 10.5455/egyjeb.20170131064321
- Rinaudi, L., Fujishige, N. A., Hirsch, A. M., Banchio, E., Zorreguieta, A., and Giordano, W. (2006). Effects of nutritional and environmental conditions on *Sinorhizobium meliloti* biofilm formation. *Res. Microbiol.* 15, 867–875. doi: 10.1016/j.resmic.2006.06.002
- Römling, U. (2005). Characterization of the rdar morphotype, a multicellular behavior in *Enterobacteriaceae*. *Cell Mol. Life Sci.* 62, 1234–1246. doi: 10.1007/s00018-005-4557-x
- Römling, U., and Galperin, M. (2015). Bacterial cellulose biosynthesis: diversity, of operons, subunits, products and functions. *Trends Microbiol.* 23, 545–557. doi: 10.1016/j.tim.2015.05.005
- Sambrook, J., Fritsch, E. F., and Maniatis, T. (1989). *Molecular Cloning*, 2nd Edn. Cold Spring Harbor, NY: Cold Spring Harbor Laboratory Press.
- Saratale, R. G., Saratale, G. D., Chang, J. S., and Govindwar, S. P. (2011). Bacterial decolorization and degradation of azo dyes: a review. *J. Taiwan Inst. Chem. Eng.* 42, 138–157. doi: 10.1016/j.jtice.2010.06.006
- Seo, Y., Lee, W. H., Sorial, G., and Bishop, P. L. (2009). The application of a mulch biofilm barrier for surfactant enhanced polycyclic aromatic hydrocarbon bioremediation. *Environ. Pollut.* 157, 95–101. doi: 10.1016/j.envpol.2008.07.022
- Sharma, V. K., and Kalonia, D. S. (2004). Effect of vacuum drying on protein-mannitol interactions: the physical state of mannitol and protein structure in the dried state. *AAPS PharmSciTech* 5, 1–12. doi: 10.1208/pt050110
- Sheikh, A. H., Molla, A. H., Haque, M. M., Hoque, M. Z., and Alam, M. Z. (2017). Evaluation of water quality and biodiversity of natural freshwater wetlands discharged by industrial effluent. *Acad. J. Environ. Sci.* 5, 52–64. doi: 10.15413/ajes.2017.0123
- Singh, A. L., Chaudhary, S., Kayastha, A. M., and Yadav, A. (2015). Decolorization and degradation of textile effluent with the help of *Enterobacter asburiae*. *Indian J. Biotechnol.* 14, 101–106.
- Singh, R., Paul, D., and Jain, R. K. (2006). Biofilms: implications in bioremediation. *Trends Microbiol.* 14, 389–397. doi: 10.1016/j.tim.2006.07.001
- Solano, C., García, B., Valle, J., Berasain, C., Ghigo, J. M., Gamazo, C., et al. (2002). Genetic analysis of *Salmonella enteritidis* biofilm formation: critical role of cellulose. *Mol. Microbiol.* 43, 793–808. doi: 10.1046/j.1365-2958.2002.02802.x
- Song, B., and Leff, L. G. (2006). Influence of magnesium ions on biofilm formation by *Pseudomonas fluorescens*. *Microbiol. Res.* 161, 355–361. doi: 10.1016/j.micres.2006.01.004
- Spiers, A. J., Bohannon, J., Gehrig, S. M., and Rainey, P. B. (2003). Biofilm formation at the air-liquid interface by the *Pseudomonas fluorescens* SBW25 wrinkly spreader requires an acetylated form of cellulose. *Mol. Microbiol.* 50, 15–27. doi: 10.1046/j.1365-2958.2003.03670.x
- Steenackers, H., Hermans, K., Vanderleyden, J., and Keersmaecker, D. (2012). *Salmonella* biofilms: an overview on occurrence, structure, regulation and eradication. *Food Res. Int.* 45, 502–531. doi: 10.1016/j.foodres.2011.01.038
- Sundar, K., Sadiq, M., Mukherjee, A., and Chandrasekaran, N. (2011). Bioremoval of trivalent chromium using *Bacillus* biofilms through continuous flow reactor. *J. Hazard. Mater.* 741, 44–51. doi: 10.1016/j.jhazmat.2011.08.066
- Surewicz, W. K., and Mantsch, H. H. (1988). New insight into protein secondary structure from resolution-enhanced infrared spectra. *Biochim. Biophys. Acta* 952, 115–130. doi: 10.1016/0167-4838(88)90107-0
- Sutherland, I. W. (2001). The biofilm matrix – an immobilized but dynamic microbial environment. *Trends Microbiol.* 9, 222–227. doi: 10.1016/S0966-842X(01)02012-1
- Tamura, K., Stecher, G., Peterson, D., Filipiński, A., and Kumar, S. (2013). MEGA6: molecular evolutionary genetics analysis version 6.0. *Mol. Biol. Evol.* 30, 2725–2729. doi: 10.1093/molbev/mst197
- Teitzel, G. M., and Parsek, M. R. (2003). Heavy metal resistance of biofilm and planktonic *Pseudomonas aeruginosa*. *Appl. Environ. Microbiol.* 69, 2313–2320. doi: 10.1128/AEM.69.4.2313-2320.2003
- Turakhia, M. H., and Characklis, W. G. (1989). Activity of *Pseudomonas aeruginosa* in biofilms-effect of calcium. *Biotechnol. Bioeng.* 33, 406–414. doi: 10.1002/bit.260330405
- Ude, S., Arnold, D. L., Moon, C. D., Timms-Wilson, T., and Spiers, A. J. (2006). Biofilm formation and cellulose expression among diverse environmental *Pseudomonas* isolates. *Environ. Microbiol.* 8, 1997–2011. doi: 10.1111/j.1462-2920.2006.01080.x
- Uhlich, G. A., Cooke, P. H., and Solomon, E. B. (2006). Analyses of the red-dry-rough phenotype of an *Escherichia coli* O157:H7 strain and its role in biofilm formation and resistance to antimicrobial agents. *Appl. Environ. Microbiol.* 72, 2564–2572. doi: 10.1128/AEM.72.4.2564-2572.2006
- van Hullebusch, E. D., Zandvoor, M. H., and Lens, P. N. L. (2003). Metal immobilization by biofilms: mechanisms and analytical tools. *Rev. Environ. Sci. Biotechnol.* 2, 9–33. doi: 10.1023/B:RESB.0000022995.48330.55
- von Canstein, H., Kelly, S., Li, Y., and Wagner-Döbler, I. (2002). Species diversity improves the efficiency of mercury-reducing biofilms under changing environmental conditions. *Appl. Environ. Microbiol.* 68, 2829–2837. doi: 10.1128/AEM.68.6.2829-2837.2002
- Wagner-Döbler, I., Lünsdorf, H., Lübbenhüsen, T., von Canstein, H. F., and Li, Y. (2000). Structure and species composition of mercury-reducing biofilms. *Appl. Environ. Microbiol.* 66, 4559–4563. doi: 10.1128/AEM.66.10.4559-4563.2000
- Wang, H., Yan, Y., Rong, D., Wang, J., Wang, H., Liu, Z., et al. (2016). Increased biofilm formation ability in *Klebsiella pneumoniae* after short-term exposure to a simulated microgravity environment. *Microbiologyopen* 5, 793–801. doi: 10.1002/mbo3.370
- Weiss-Muszkat, M., Shakh, D., Zhou, Y., Pinto, R., Belausov, E., Chapman, M. R., et al. (2010). Biofilm by and multicellular behavior of *Escherichia coli* O55:H7, an atypical enteropathogenic strain. *Appl. Environ. Microbiol.* 7, 1545–1554. doi: 10.1128/AEM.01395-09
- Whitchurch, C. B., Tolker-Nielsen, T., Ragas, P. C., and Mattick, J. S. (2002). Extracellular DNA required for bacterial biofilm formation. *Science* 295:1487. doi: 10.1126/science.295.5559.1487
- White, A., Gibson, D. L., Collinson, S. K., Banser, P. A., and Kay, W. W. (2003). Extracellular polysaccharides associated with thin aggregative fimbriae of *Salmonella enterica* serovar Enteritidis. *J. Bacteriol.* 185, 5398–5407. doi: 10.1128/JB.185.18.5398-5407.2003
- Wingender, J., Strathmann, M., Rode, A., Leis, A., and Flemming, H.-C. (2001). Isolation and biochemical characterization of extracellular polymeric substances from *Pseudomonas aeruginosa*. *Methods Enzymol.* 336, 302–314. doi: 10.1016/S0076-6879(01)36597-7
- Yamaga, F., Washio, K., and Morikawa, M. (2010). Sustainable biodegradation of phenol by *Acinetobacter calcoaceticus* P23 isolated from the rhizosphere of duckweed *Lemna aoukikusa*. *Environ. Sci. Technol.* 44, 6470–6474. doi: 10.1021/es1007017
- Yap, M.-N., Yang, C.-H., Barak, J. D., Jahn, C. E., and Charkowski, A. O. (2005). The *Erwinia chrysanthemi* type III secretion system is required for multicellular behavior. *J. Bacteriol.* 187, 639–648. doi: 10.1128/jb.187.2.639-648.2005

- Zabłocka-Godlewska, E., Przystaś, W., and Grabińska-Sota, E. (2012). Decolourization of diazo evans blue by two strains of *Pseudomonas fluorescens* isolated from different wastewater treatment plants. *Water Air Soil Pollut.* 223, 5259–5266. doi: 10.1007/s11270-012-1276-4
- Zhi, S., Banting, G., Li, Q., Edge, T. A., Topp, E., Sokurenko, M., et al. (2016). Evidence of naturalized stress-tolerant strains of *Escherichia coli* in municipal wastewater treatment plants. *Appl. Environ. Microbiol.* 82, 5505–5518. doi: 10.1128/AEM.00143-16
- Zogaj, X., Bokranz, W., Nimtz, M., and Römling, U. (2003). Production of cellulose and curli fimbriae by members of the family *Enterobacteriaceae* isolated from the human gastrointestinal tract. *Infect. Immun.* 71, 4151–4158. doi: 10.1128/IAI.71.7.4151-4158.2003
- Zogaj, X., Nimtz, M., Rohde, M., Bokranz, W., and Römling, U. (2001). The multicellular morphotypes of *Salmonella typhimurium* and *Escherichia coli* produce cellulose as the second compound of the extracellular matrix. *Mol. Microbiol.* 39, 1452–1463. doi: 10.1046/j.1365-2958.2001.02337.x
- Zou, L., Zeng, Q., Lin, H., Gyaneshwar, P., Chen, G., and Yang, C.-H. (2012). SlyA regulates type III secretion system (T3SS) genes in parallel with the T3SS master regulator HrpL in *Dickeya dadantii* 3937. *Appl. Environ. Microbiol.* 78, 2888–2895. doi: 10.1128/AEM.07021-11

**Conflict of Interest Statement:** The authors declare that the research was conducted in the absence of any commercial or financial relationships that could be construed as a potential conflict of interest.

Copyright © 2018 Mosharaf, Tanvir, Haque, Haque, Khan, Molla, Alam, Islam and Talukder. This is an open-access article distributed under the terms of the Creative Commons Attribution License (CC BY). The use, distribution or reproduction in other forums is permitted, provided the original author(s) and the copyright owner are credited and that the original publication in this journal is cited, in accordance with accepted academic practice. No use, distribution or reproduction is permitted which does not comply with these terms.



# Use of the PCR-DGGE Method for the Analysis of the Bacterial Community Structure in Soil Treated With the Cephalosporin Antibiotic Cefuroxime and/or Inoculated With a Multidrug-Resistant *Pseudomonas putida* Strain MC1

## OPEN ACCESS

### Edited by:

Stéphane Pesce,  
Institut National de Recherche en  
Sciences et Technologies Pour  
l'Environnement et l'Agriculture  
(IRSTEA), France

### Reviewed by:

Max Maurin,  
Université Grenoble Alpes, France  
Ramprasad E.V.V.,  
University of Hyderabad, India

### \*Correspondence:

Mariusz Cycoń  
mcycon@sum.edu.pl

### Specialty section:

This article was submitted to  
Microbiotechnology, Ecotoxicology  
and Bioremediation,  
a section of the journal  
Frontiers in Microbiology

**Received:** 06 February 2018

**Accepted:** 06 June 2018

**Published:** 26 June 2018

### Citation:

Orlewska K, Piotrowska-Seget Z and  
Cycoń M (2018) Use of the  
PCR-DGGE Method for the Analysis  
of the Bacterial Community Structure  
in Soil Treated With the Cephalosporin  
Antibiotic Cefuroxime and/or  
Inoculated With a Multidrug-Resistant  
*Pseudomonas putida* Strain MC1.  
*Front. Microbiol.* 9:1387.  
doi: 10.3389/fmicb.2018.01387

Kamila Orlewska<sup>1</sup>, Zofia Piotrowska-Seget<sup>2</sup> and Mariusz Cycoń<sup>1\*</sup>

<sup>1</sup> Department of Microbiology and Virology, School of Pharmacy with the Division of Laboratory Medicine, Medical University of Silesia, Sosnowiec, Poland, <sup>2</sup> Department of Microbiology, University of Silesia, Katowice, Poland

The widespread use of cefuroxime (XM) has resulted in the increase in its concentration in hospital and domestic wastewaters. Due to the limited removal of antibiotics and antibiotic-resistant genes in conventional systems, the drugs enter the surface water and soils. Moreover, the introduction of XM and/or XM-resistant bacteria into soil may cause a significant modification of the biodiversity of soil bacterial communities. Therefore, the goal of this research was to assess the genetic diversity of a bacterial community in the cefuroxime (XM1 – 1 mg/kg and XM10 – 10 mg/kg) and/or antibiotic-resistant *Pseudomonas putida* strain MC1 (Ps –  $1.6 \times 10^7$  cells/g)-treated soils as determined by the DGGE (denaturing gradient gel electrophoresis) method. The obtained data were also evaluated using a multivariate analysis and the resistance (RS)/resilience (RL) concept. Strain MC1 was isolated from raw sewage in the presence of XM and was resistant not only to this antibiotic but also to vancomycin, clindamycin and erythromycin. The DGGE patterns revealed that the XM10 and XM10+Ps treatments modified the composition of the bacterial community by the alteration of the DGGE profiles as well as a decline in the DGGE indices, in particular on days 30, 60, and 90. In turn, the XM1 and XM1+Ps or Ps treatments did not affect the values of richness and diversity of the soil bacteria members. A principal component analysis (PCA) also indicated that XM markedly changed the diversity of bacterial assemblages in the second part of the experiment. Moreover, there were differences in the RS/RL of the DGGE indices to the disturbances caused by XM and/or Ps. Considering the mean values of the RS index, the resistance was categorized in the following order: diversity (0.997) > evenness (0.993) > richness (0.970). The soil RL

index was found to be negative, thus reflecting the progressing detrimental impact of XM on the genetic biodiversity of bacteria within the experiment. These results indicate that the introduction of XM at higher dosages into the soil environment may exert a potential risk for functioning of microorganism.

**Keywords:** cefuroxime, multidrug resistance, *Pseudomonas putida*, DGGE, microbial diversity, soil, multivariate analysis

## INTRODUCTION

Antibiotics and antibiotic-resistant genes are thought to be emerging contaminants that attract considerable public attention due to their potential to harmful effect on the environment and increased risks to human health. They are primarily introduced into soil with sewage sludge, municipal wastewater or animal manures (Kümmerer, 2003; Xia et al., 2005; Chee-Sanford et al., 2009). Recent works have suggested that antibiotics also represent a significant pollution of sediments and soils (Tamtam et al., 2011; de La Torre et al., 2012). This group of pharmaceuticals may enter the fauna, plants and microorganisms, exhibiting a risk to soil organisms and favoring the spread of resistance to antibiotics (Fatta-Kassinos et al., 2011; Gullberg et al., 2011; Brandt et al., 2015).

The second-generation cephalosporins (CPs), active against a wide group of microorganisms, are the most frequently used antibiotics in 20 European countries and represent about 70% of the total outpatient cephalosporin consumption (Versporten et al., 2011). Among this group, cefuroxime (XM) is the most frequently prescribed and, its consumption in Poland and many other European countries constituted more than 50% of the total cephalosporin administration (Coenen et al., 2006; Versporten et al., 2011; Iatrou et al., 2014). Such a high consumption of XM is related to its broad spectrum of antibacterial activity, the resistance to  $\beta$ -lactamase from *Moraxella catarrhalis* and *Haemophilus influenzae*, and the activity against *Streptococcus pneumoniae* strains susceptible and resistant to penicillin. XM blocks the synthesis of bacterial cell wall, similarly to antibiotics belonging to the group of  $\beta$ -lactams. It binds with the proteins binding penicillin participated in the synthesis of the peptidoglycan bacterial cell wall causing the lysis of bacteria (Ishibiki et al., 1990; Cheng et al., 2012; Bhattacharya et al., 2015). In the human body, XM is quickly eliminated from the blood and, in unchanged form is nearly completely removed via urine system within 1–3 days (Ishibiki et al., 1990).

The CPs have been found in wastewater and surface water all over the world; however, their highest concentrations were detected in the effluents from hospitals and pharmaceutical industry (Saravanane and Sundararaman, 2009; Oguz and Mihçioğur, 2014; Yu et al., 2016). The concentration of CPs in urban wastewater usually does not exceed 10  $\mu\text{g/L}$ , while their mean concentration in wastewater influent and effluent of CPs producing wastewater is in the range of about 13–142 and 0.1–24  $\mu\text{g/L}$ , respectively. The highest noted

concentrations of XM in wastewater influent and effluent reached the values of 210 and 35  $\mu\text{g/L}$ , respectively (Yu et al., 2016). Due to the fact that conventional wastewater treatment plants remove XM from wastewater partially, this antibiotic is introduced into soils through the agricultural usage of sewage sludge. Unfortunately, there is no published data on XM concentrations in soils. However, it may be expected that the introduction of XM into soil may select XM-resistant bacteria and spread the resistance to XM to the bacteria in the environment (Rahube et al., 2014; Luczkiewicz et al., 2015; Kittinger et al., 2016; Devarajan et al., 2017).

Among the many bacteria resistant to antibiotics, some strains of *Pseudomonas putida* have been recognized as increasingly important human pathogens over the last 30 years (Carpenter et al., 2008; Bhattacharya et al., 2015; Fernández et al., 2015; Sun et al., 2016). This opportunistic pathogen is responsible for nosocomial infections, mainly in immunocompromised patients (Yoshino et al., 2011). Outbreaks of the bloodstream infections associated with contaminated fluids have also been observed (Erol et al., 2014; Liu et al., 2014a). *P. putida* is a gram-negative and aerobic bacterium commonly presents in soils. Strains of *P. putida* characterize a broad spectrum of biochemical activities related to the ability to degrade various natural and synthetic compounds (Rojas et al., 2001; Espinosa-Urgel et al., 2002; Nelson et al., 2002). In the environment, antibiotic-resistant *P. putida* strains may be participated in the spread of antibiotic-resistant genes among other pathogens (Molina et al., 2014; Sun et al., 2016).

Previously published papers revealed that antibiotics selected antibiotic-resistant bacteria and had an impact on the abundance of soil microorganisms and their activities (Chen et al., 2013; Cui et al., 2013; Liu et al., 2014b; Xu et al., 2016). Moreover, the impact of antibiotics on the genetic diversity and structure of soil microbial communities were reported using the DGGE (Zielezny et al., 2006; Reichel et al., 2013; Cleary et al., 2016; Orlewska et al., 2018) and the phospholipid fatty acid analysis (PLFA) (Demoling et al., 2009; Reichel et al., 2014; Cycon et al., 2016; Xu et al., 2016), respectively. Based on the results related to the activity of other antibiotics, the entry of XM and/or antibiotic-resistant bacteria into soil may also affect the soil bacterial communities. Findings concerning the effect of XM on the genetic diversity of soil bacteria are limited, and therefore, the goal of this research was to check the influence of XM and/or an antibiotic-resistant *Pseudomonas putida* strain on the bacterial community using the DGGE approach and the resistance (RS)/resilience (RL) concept.

## MATERIALS AND METHODS

### Isolation and Characterization of the Bacterial Strain

The strain designated as MC1 was isolated from raw sewage on a TSA medium (Tryptone-Soya Agar) with addition of 30  $\mu\text{g}$  XM (**Figure 1**) (Cycon et al., 2016). Strain MC1 was identified using the 16S rRNA gene analysis with the primers 27f and 1492r (Cycon et al., 2016) and additionally the API 20 NE biochemical test (Cycon et al., 2011). The sequence of strain MC1 was compared to other known sequences of 16S rRNA gene using the BLAST server (NCBI; <http://www.ncbi.nlm.nih.gov/>). Phylogenetic analysis was performed by the neighbor-joining method using the MEGA ver. 7.0 software. The sensitivity of strain MC1 to XM, clindamycin (CM), ciprofloxacin (CI), erythromycin (EM), vancomycin (VA), tetracycline (TC) or streptomycin (SM) (**Table 1**) was determined with the use of the disc diffusion and the *E*-test methods (Cycon et al., 2016).

### Design of the Soil Experiment

Soil collected from an experimental plot located near the town of Zywiec, Poland and, with the defined characteristics determined with the use of methods described in the ISO standards (Cycon et al., 2010), was used in this experiment. The soil was classified as loamy sand (sand 67%, silt 24%, and clay 9%) with the following main features: pH 6.9, density 1.4  $\text{g}/\text{cm}^3$ , water-holding capacity

43%, cation exchange capacity 10  $\text{cmol}^+/\text{kg}$ , microbial biomass 932  $\text{mg}/\text{kg}$ ,  $C_{\text{org}}$  1.6% and  $N_{\text{tot}}$  0.2%.

The experiment included three replications of the following treatments: C (control), XM1 – 1 mg XM/kg soil, XM10 – 10 mg XM/kg soil, Ps – *P. putida* MC1, XM1+Ps – 1 mg XM/kg soil + *P. putida* MC1 and XM10+Ps – 10 mg XM/kg soil + *P. putida* MC1. Strain MC1 was introduced into soil at  $1.6 \times 10^7$  cells/g soil and, the preparation of its suspension was made with the use of a previously described method (Cycon et al., 2016). Samples of soil were incubated at  $22 \pm 1^\circ\text{C}$  and randomly collected during the experimental period for the DGGE analysis.

### Analysis of Microbial Community Structure

The genetic diversity of soil bacteria was analyzed using the amplification of the 16S RNA gene fragment with the primers (GC-clamp)-F338 and R518 (Muyzer et al., 1993) with the use of a previously described method (Cycon et al., 2013). The electrophoresis was run in polyacrylamide gel (8% w/v, 37.5:1 acrylamide:bis-acrylamide) with a linear gradient of denaturant urea (40%–70) using a DCode Mutation Detection System (Bio-Rad, USA). The patterns of the DGGE bands were visualized using a G BOX F3 System (Syngene, UK) (Cycon et al., 2016).

### Data Analysis

The patterns of the DGGE bands were evaluated using BioNumerics software ver. 7.5 (Applied Math, Belgium), while the phylogenetic trees were prepared with the use of the unweighted pair-group method and the arithmetic averages (UPGMA) (Cycon et al., 2016). The DGGE indices, i.e., Shannon-Wiener index (*H*), richness (*S*) and evenness (*E*) were calculated using appropriate equations (Cycon et al., 2013). The three-way and two-way ANOVA analyses and the least significant differences (LSD) test ( $P < 0.05$ ) were used to evaluate the obtained results. The data for the DGGE indices were subjected to PCA, and additionally, the PC scores were also evaluated by applying the three-way and two-way MANOVA. Indices adopted from Orwin and Wardle (2004) were applied to assess the resistance (RS) and resilience (RL) of the determined indices to the disturbances caused by the antibiotic and/or bacterial strain. All details of statistical analyzes were presented in a previously published paper (Cycon et al., 2016).

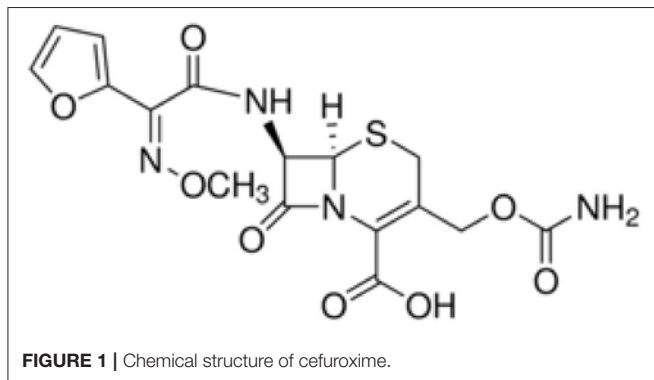


**TABLE 1** | Results of the sensitivity assays to selected antibiotics for strain MC1.

Antibiotic	Disc-diffusion method		<i>E</i> -test method	
	Concentration ( $\mu\text{g}$ )	Growth inhibition (mm)	Range of concentrations ( $\mu\text{g}/\text{mL}$ )	MIC ( $\mu\text{g}/\text{mL}$ )
CI	5	28	0.002–32	0.094
CM	2	–	0.016–256	>256
EM	15	–	0.016–256	>256
SM	300	34	0.064–1024	8
TC	30	22	0.016–256	6
VA	30	–	0.016–256	>256
XM	30	–	0.016–256	>256

CI, ciprofloxacin; CM, clindamycin; EM, erythromycin; SM, streptomycin; TC, tetracycline; VA, vancomycin; XM, cefuroxime; –, no inhibition zone; MIC, minimum inhibitory concentration.

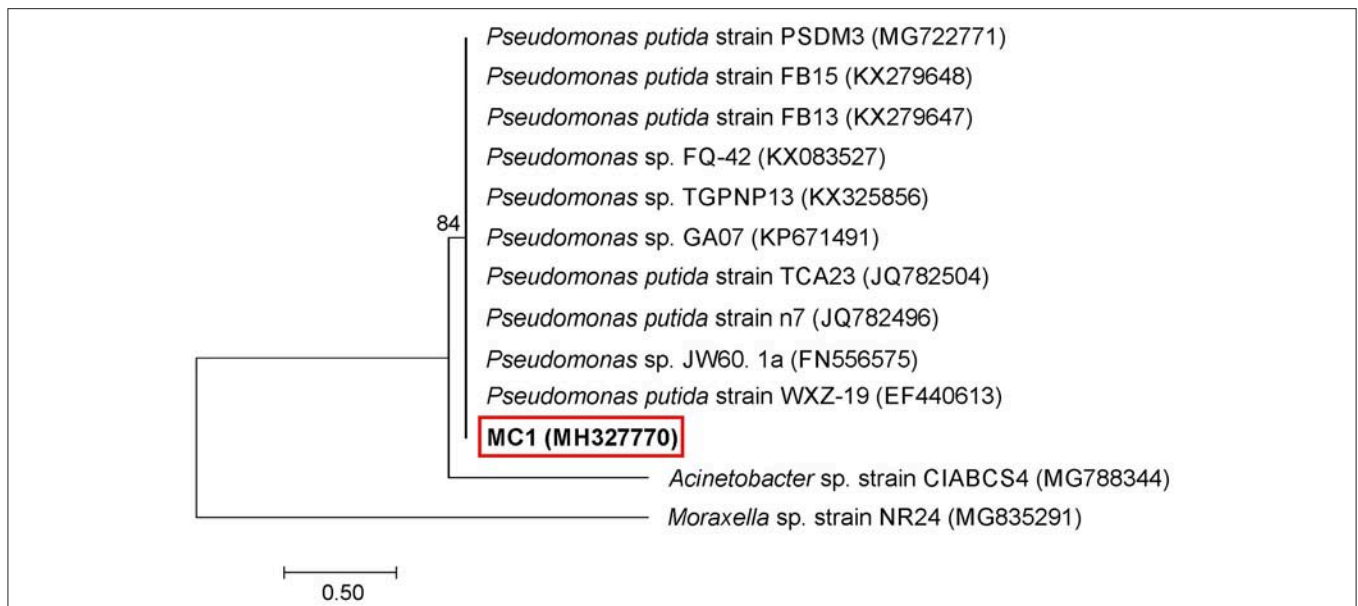


**FIGURE 2** | Phylogenetic tree of a multidrug-resistant strain MC1 based on the neighbor-joining method. Bootstrap values from 1,000 replications are indicated at the branches. GenBank accession numbers are given in parentheses.

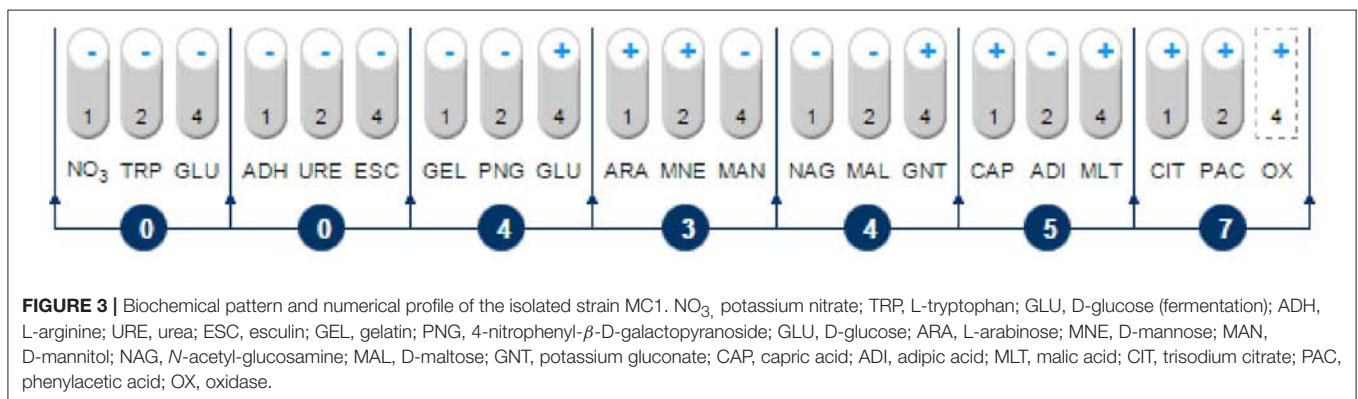


**FIGURE 3** | Biochemical pattern and numerical profile of the isolated strain MC1. NO<sub>3</sub>, potassium nitrate; TRP, L-tryptophan; GLU, D-glucose (fermentation); ADH, L-arginine; URE, urea; ESC, esculin; GEL, gelatin; PNG, 4-nitrophenyl- $\beta$ -D-galactopyranoside; GLU, D-glucose; ARA, L-arabinose; MNE, D-mannose; MAN, D-mannitol; NAG, *N*-acetyl-glucosamine; MAL, D-maltose; GNT, potassium gluconate; CAP, capric acid; ADI, adipic acid; MLT, malic acid; CIT, trisodium citrate; PAC, phenylacetic acid; OX, oxidase.

## RESULTS

### Characteristics of the Isolate

An analysis of the 16S rRNA gene sequence showed that strain MC1 is a member of the genus *Pseudomonas* with a high similarity to the species *Pseudomonas putida* (Figure 2). The sequence of strain MC1 was submitted to the GenBank under accession number MC327770. An additional analysis using a biochemical test (Figure 3) also confirmed (98.6% identity) the membership of strain MC1 to the species *P. putida* (numerical profile 0043457). The obtained resistance pattern of strain MC1 to antibiotics showed its resistance to XM, CM, EM and VA as was shown by the MIC values greater than 256  $\mu$ g/mL (Table 1). In turn, the highest sensitivity of *P. putida* MC1 was noted for SM, TC, and CI, with the MIC values of 8, 6 and 0.094  $\mu$ g/ml, respectively (Table 1).

### DGGE Analysis

The obtained results showed that XM affected the composition of the bacterial members in soil microbial community (Figures 4A–E). The DGGE profiles from XM-treated and non-treated soils differed with regards to the absence and density of the bands, in particular on days 30 (Figure 4C), 60 (Figure 4D), and 90 (Figure 4E) of the experiment. The results also revealed that XM at 10 mg/kg (XM10 and XM10+Ps) changed the overall richness (Figure 5A) and diversity (Figure 5B) of the member of bacterial community on days 30, 60, and 90. In contrast, no differences in the S and H values were observed between the lower XM and/or strain MC1 treatments (XM1 and XM1+Ps or Ps) and the non-exposed soil during 90 days. Also, the E<sub>H</sub> values were generally similar for both treated and non-treated soils on each sampling day (Figure 5C).

The ANOVA revealed that the S-value was significantly ( $P < 0.001$ ) affected by the time, the XM dose and the interaction

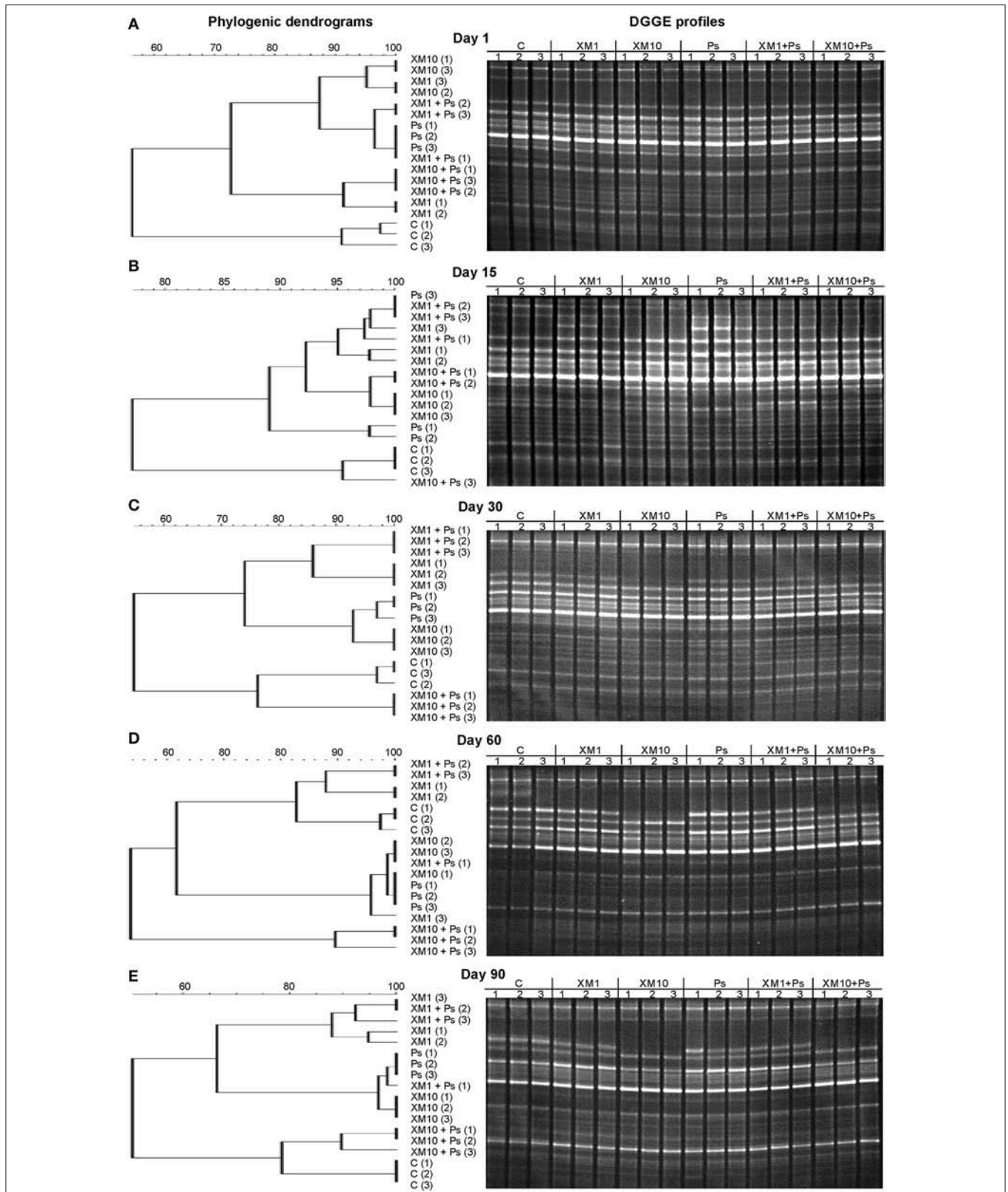


**FIGURE 4 |** Phylogenetic dendrograms based on the DGGE profiles for the soil treated with cefuroxime and/or strain MC1 on days 1 **(A)**, 15 **(B)**, 30 **(C)**, 60 **(D)**, and 90 **(E)**. C, non-exposed soil; XM1, cefuroxime at 1 mg/kg soil; XM10, cefuroxime at 10 mg/kg soil; Ps, *P. putida* MC1; XM1+Ps, cefuroxime at 1 mg/kg soil + *P. putida* MC1; XM10+Ps, cefuroxime at 10 mg/kg soil + *P. putida* MC1.

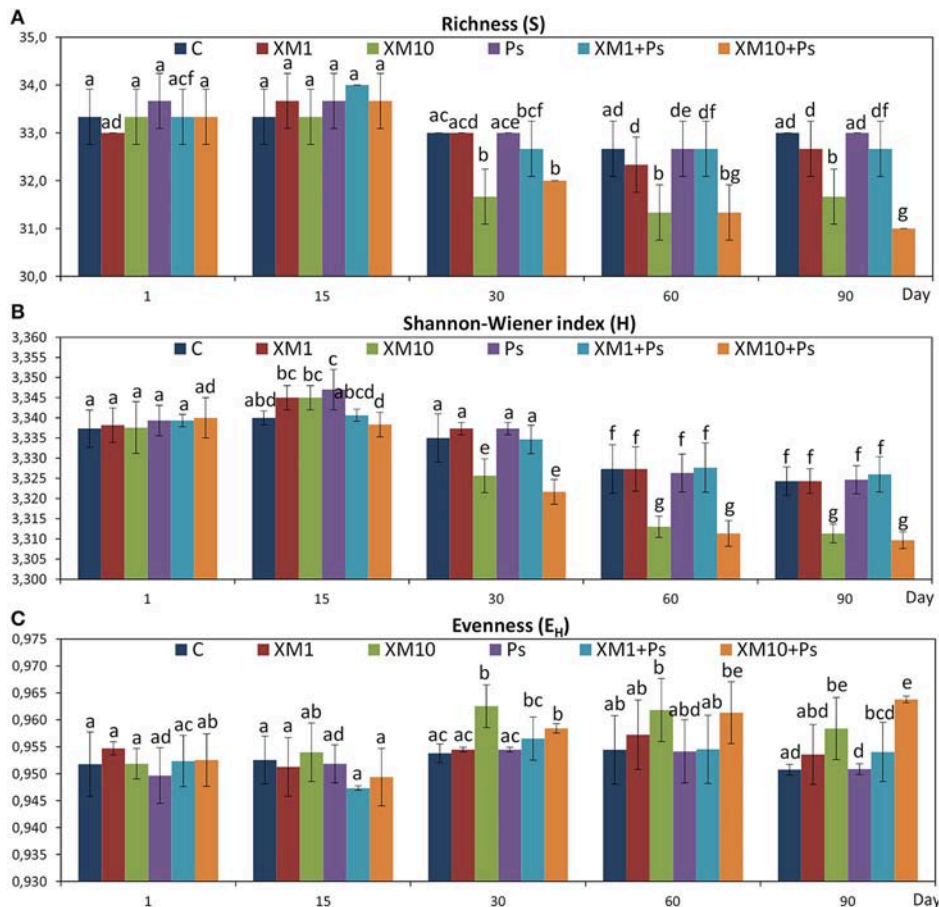


**FIGURE 5 |** Values of the richness (A), Shannon-Wiener (B), and evenness (C) indices for the cefuroxime (XM)- and/or *Pseudomonas putida* MC1 (Ps)-treated soils obtained during the experimental period. The data are the means ( $n = 3$ ) with standard deviations. Different letters within the values of each index indicate significant differences considering the effects of the dose of XM, strain MC1 and incubation time (LSD *post-hoc* test;  $P < 0.05$ ). The explanation of the treatment abbreviations is given in **Figure 4**.

**TABLE 2 |** Analysis of variance (the three-way ANOVA) for the DGGE indices: richness (S), Shannon-Wiener (H) and evenness ( $E_H$ ) as affected by the bacterial strain (S), concentration (C), time (T) and their interactions.

SV	S		H		$E_H$	
	VE	P	VE	P	VE	P
S	<1	0.386	<1	0.701	<1	0.400
C	20	<0.001***	14	<0.001***	16	<0.001***
T	44	<0.001***	67	<0.001***	21	<0.001***
S × C	<1	0.827	<1	0.093	<1	0.929
S × T	1	0.481	<1	0.711	2	0.554
C × T	12	<0.001***	8	<0.001***	11	0.087
S × C × T	1	0.860	1	0.413	3	0.840

SV, source of variance; VE, variance explained (%). Asterisks represent the significance level according to the ANOVA (\*\* $P < 0.001$ ).

between both factors. The time effect contributed to most of the observed variability (44%) (Table 2). The H index was primarily influenced by the time of incubation ( $P < 0.001$ ),

which explained most of the variability (67%) (Table 2). The ANOVA also showed that the concentration of XM and the incubation time were the factors influenced ( $P < 0.01$ ) the  $E_H$  index within 90 days and contributed to 16 and 21% of the variability, respectively. All details related to the results of the three-way ANOVA are presented in Table 2.

### Resistance (RS) and Resilience (RL) Indices

An evaluation of the resistance of the DGGE indices to XM and/or *P. putida* MC1 showed that these factors affected the values of the RS index within 90 days (Table 3). In general, the ANOVA revealed that the tested factors had a significant impact ( $P < 0.001$ ) on the resistance of the DGGE indices. The time effect contributed most to the variability in the case of the H index (42%), whereas this effect explained the least of the variability in relation to the  $E_H$  index (18%) (Table 4). The greatest decrease in the values of the RS index was observed for richness and the mean values of this index for all of the soil treatments were found to be 0.967, 0.965, and 0.950 on days 30, 60, and 90, respectively

**TABLE 3** | Values of the resistance (RS) index for measured parameters obtained for each day of the experiment.

Parameter	Day	Treatment					$\bar{x}$
		XM1	XM10	Ps	XM1+Ps	XM10+Ps	
Richness (S)	1	0.971 <sup>a</sup>	1.000 <sup>b</sup>	0.980 <sup>abf</sup>	1.000 <sup>b</sup>	1.000 <sup>b</sup>	0.990 <sup>A</sup>
	15	0.980 <sup>ac</sup>	1.000 <sup>ab</sup>	0.980 <sup>acf</sup>	0.961 <sup>ce</sup>	0.980 <sup>bc</sup>	0.980 <sup>AB</sup>
	30	1.000 <sup>c</sup>	0.923 <sup>d</sup>	1.000 <sup>acf</sup>	0.971 <sup>e</sup>	0.941 <sup>d</sup>	0.967 <sup>ABC</sup>
	60	0.980 <sup>ac</sup>	0.922 <sup>d</sup>	1.000 <sup>af</sup>	1.000 <sup>ab</sup>	0.922 <sup>d</sup>	0.965 <sup>BC</sup>
	90	0.971 <sup>ae</sup>	0.923 <sup>d</sup>	1.000 <sup>f</sup>	0.971 <sup>e</sup>	0.886 <sup>g</sup>	0.950 <sup>C</sup>
Shannon-Wiener index (H)	1	0.999 <sup>a</sup>	0.999 <sup>a</sup>	0.999 <sup>af</sup>	0.998 <sup>a</sup>	0.998 <sup>a</sup>	0.999 <sup>A</sup>
	15	0.997 <sup>b</sup>	0.997 <sup>b</sup>	0.996 <sup>b</sup>	1.000 <sup>a</sup>	0.999 <sup>a</sup>	0.998 <sup>AB</sup>
	30	0.998 <sup>b</sup>	0.994 <sup>c</sup>	0.998 <sup>ab</sup>	0.999 <sup>ab</sup>	0.992 <sup>d</sup>	0.996 <sup>B</sup>
	60	1.000 <sup>a</sup>	0.991 <sup>e</sup>	0.999 <sup>af</sup>	1.000 <sup>a</sup>	0.990 <sup>de</sup>	0.996 <sup>B</sup>
	90	1.000 <sup>af</sup>	0.992 <sup>e</sup>	1.000 <sup>f</sup>	0.999 <sup>af</sup>	0.991 <sup>de</sup>	0.996 <sup>B</sup>
Evenness (E <sub>H</sub> )	1	0.992 <sup>a</sup>	0.995 <sup>a</sup>	0.997 <sup>ae</sup>	0.998 <sup>af</sup>	0.998 <sup>a</sup>	0.996 <sup>A</sup>
	15	0.998 <sup>a</sup>	0.997 <sup>a</sup>	0.998 <sup>ae</sup>	0.989 <sup>bf</sup>	0.994 <sup>ab</sup>	0.995 <sup>A</sup>
	30	0.998 <sup>a</sup>	0.982 <sup>c</sup>	0.998 <sup>ae</sup>	0.994 <sup>abf</sup>	0.991 <sup>bd</sup>	0.993 <sup>AB</sup>
	60	0.994 <sup>a</sup>	0.985 <sup>c</sup>	0.999 <sup>ae</sup>	1.000 <sup>a</sup>	0.986 <sup>cd</sup>	0.993 <sup>AB</sup>
	90	0.992 <sup>af</sup>	0.985 <sup>c</sup>	1.000 <sup>e</sup>	0.992 <sup>f</sup>	0.974 <sup>g</sup>	0.988 <sup>B</sup>

Significant differences ( $P < 0.05$ , LSD test) within the mean values ( $n = 3$ ) of each parameter, considering the effects of the treatment and incubation time, are indicated by different lowercase letters. Significant differences ( $P < 0.05$ , LSD test) within the values of all of the treatments for each parameter considering the effect of the incubation time are indicated by different uppercase letters. The values marked in gray or green indicate a significant inhibition or stimulation in relation to the non-treated soil, respectively. The explanation of the treatment abbreviations is given in **Figure 4**.

**TABLE 4** | Analysis of variance (the two-way ANOVA) for the RS indices as affected by the treatment (Tr), time (T) and their interactions.

SV	S		H		E <sub>H</sub>	
	VE	P	VE	P	VE	P
Tr	27	<0.001***	42	<0.001***	18	<0.001***
T	16	<0.001***	11	<0.001***	8	<0.001***
Tr × T	14	<0.001***	40	<0.001***	6	<0.001***

SV, source of variance; VE, variance explained (%). Asterisks represent the significance level according to the ANOVA (\*\*\* $P < 0.001$ ).

(**Table 3**). This decrease was related to the inhibitory effect of XM and/or strain MC1 on the S index (**Figure 5A**). A similar trend was observed for the H index (**Table 3** and **Figure 5B**). In the case of the E<sub>H</sub> index, a decrease in the values of the RS index observed for some soil treatments (**Table 3**) was generally associated with the stimulatory effect of XM and/or strain MC1 during the experimental period (**Figure 5C**). Taking into account the mean values of the RS index that were calculated for all of the soil treatments during the experimental period, the resistance of the DGGE indices was categorized in the following order: diversity (0.997) > evenness (0.993) > richness (0.970). A calculation of the RL index at the end of the experiment (day 90) revealed that although its value was different for each DGGE index, negative mean values were obtained for all of the soil treatments (**Table 5**).

## PCA of the DGGE Pattern

Based on the PCA of the DGGE indices it was revealed that the introduction of XM and/or *P. putida* MC1 altered the

pattern of bacterial diversity. The PCA plot created for all days indicated that the treatments were scattered along the PC1 and PC2 axes, which explained 80 and 20% of the total variability, respectively (**Figure 6**). Also, a three-way MANOVA analysis confirmed this result. The time explained 48 and 28% of the total variance for PC1 and PC2, respectively (**Table 6**). In turn, the XM concentration explained 20% of the total variance only along PC1. Strain MC1 did not affect the pattern of bacterial biodiversity; it contributed to <1% of the total variance in the PCA plot. All details related to the results of the three-way MANOVA are presented in **Table 6**.

The PCA plots created for each sampling day revealed a meaningful impact of the concentration of XM on the bacterial diversity in the second part of the experiment (**Figure 7**). The effect of the dose explained 77, 65, and 85% of the variability only along PC1 on days 30, 60, and 90, respectively. On the contrary, no effect of *P. putida* MC1 along PC1 and PC2 was observed on any sampling day. All details related to the results of the three-way MANOVA are presented in **Table 7**.

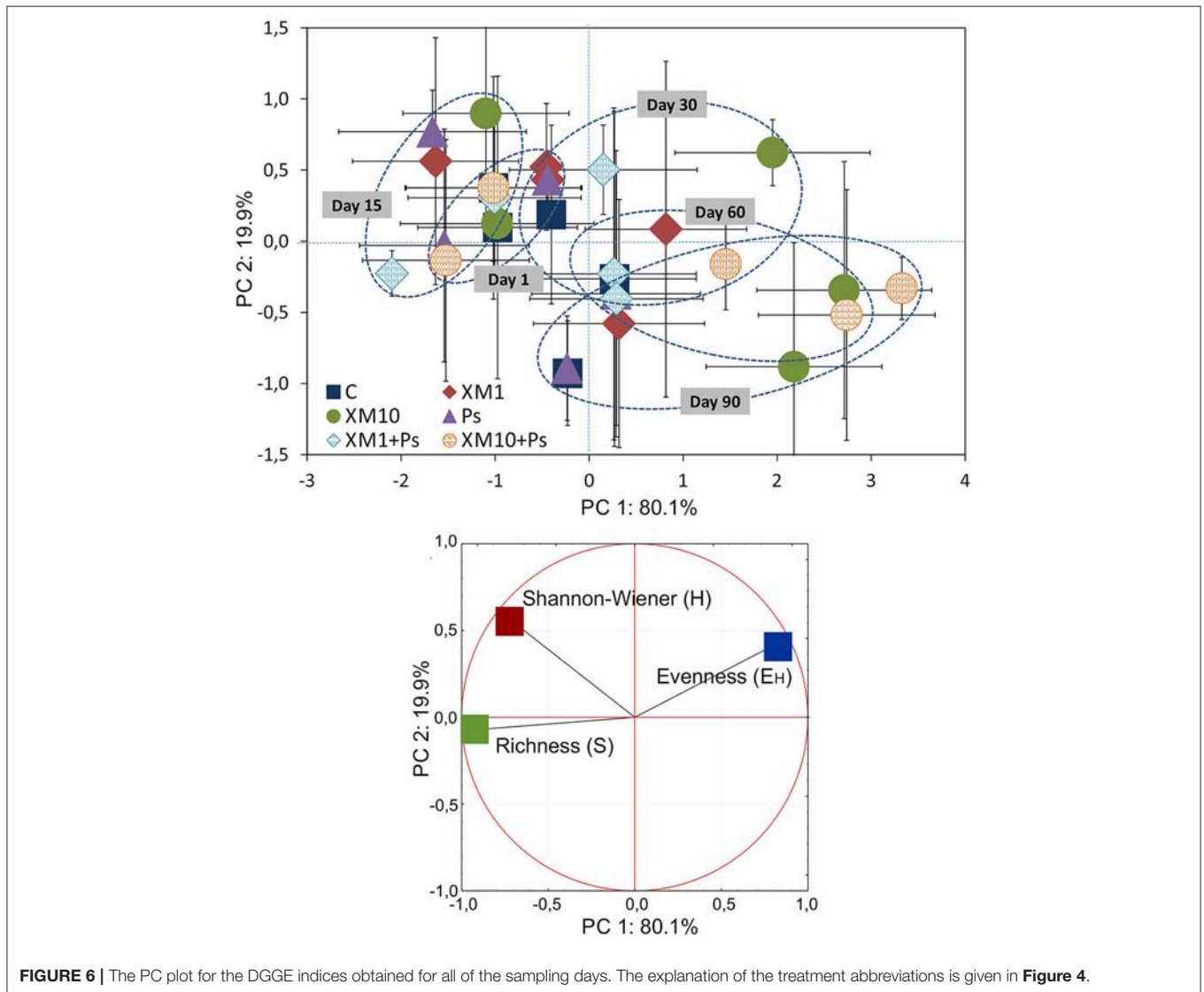
## DISCUSSION

Strain MC1 identified as *Pseudomonas putida* was isolated in this study. *P. putida* was considered as bacteria with low pathogenicity and generally sensitive to antibiotics belonging to different classes (Luczkiewicz et al., 2015; Devarajan et al., 2017). The highest sensitivity of *P. putida* MC1 was determined for CI, SM, and TC. The sensitivity assays to selected antibiotics also showed that the isolated strain MC1 had a multidrug-resistant ability. The disc diffusion and E-test methods revealed that this strain was characterized by a resistance not only to XM but

**TABLE 5** | Values of the resilience (RL) index for the measured parameters obtained at the end of the experiment.

Parameter	Treatment					$\bar{x}$
	XM1	XM10	Ps	XM1+Ps	XM10+Ps	
Richness (S)	0.000 <sup>a</sup>	-1.000 <sup>b</sup>	1.000 <sup>c</sup>	-1.000 <sup>b</sup>	-1.000 <sup>b</sup>	-0.400
Shannon-Wiener index (H)	0.471 <sup>a</sup>	-0.823 <sup>b</sup>	0.715 <sup>a</sup>	0.139 <sup>a</sup>	-0.693 <sup>b</sup>	-0.038
Evenness (E <sub>H</sub> )	-0.017 <sup>a</sup>	-0.466 <sup>bc</sup>	1.000 <sup>b</sup>	-0.428 <sup>ac</sup>	-0.858 <sup>c</sup>	-0.154

The data are the means ( $n = 3$ ). Significant differences ( $P < 0.05$ , LSD test) within the values of each parameter are indicated by different letters. The explanation of the treatment abbreviations is given in **Figure 4**.



also to CM, EM, and VA as was shown by the MIC values greater than 256  $\mu\text{g/ml}$ . Antibiotic-resistant strains of *P. putida* are frequently found in the environment; however, a multidrug-resistant *P. putida* has only been isolated from patients in recent years (Lombardi et al., 2002; Bhattacharya et al., 2015; Fernández et al., 2015; Kittinger et al., 2016). The presence of XM in soil may significantly increase the pool of genes responsible

for resistance to XM among soil microorganisms. Bacteria can develop resistance to XM and other CPs by producing extended-spectrum lactamases (ESBL), taking up of genes encoding ESBL from soil bacteria, and a high expression of lactamase (*bla*) genes located on chromosome (Pfeifer et al., 2010). The spreading of XM resistance genes may also result from the introduction of XM-resistant bacteria into soil. There is a potential risk that

**TABLE 6** | Multivariate analysis of variance (the three-way MANOVA) for the PC1 and PC2 based on the data of the DGGE indices for all of the sampling days as affected by the bacterial strain (S), concentration (C), time (T) and their interactions.

SV	PC1		PC2	
	VE	P	VE	P
S	<1	0.409	<1	0.429
C	20	<0.001***	<1	0.661
T	48	<0.001***	28	<0.001***
S × C	<1	0.739	1	0.624
S × T	1	0.462	2	0.661
C × T	13	<0.001***	3	0.922
S × C × T	1	0.832	5	0.758

SV, source of variance; VE, variance explained (%). Asterisks represent the significance level according to the ANOVA (\*\*\*P < 0.001).

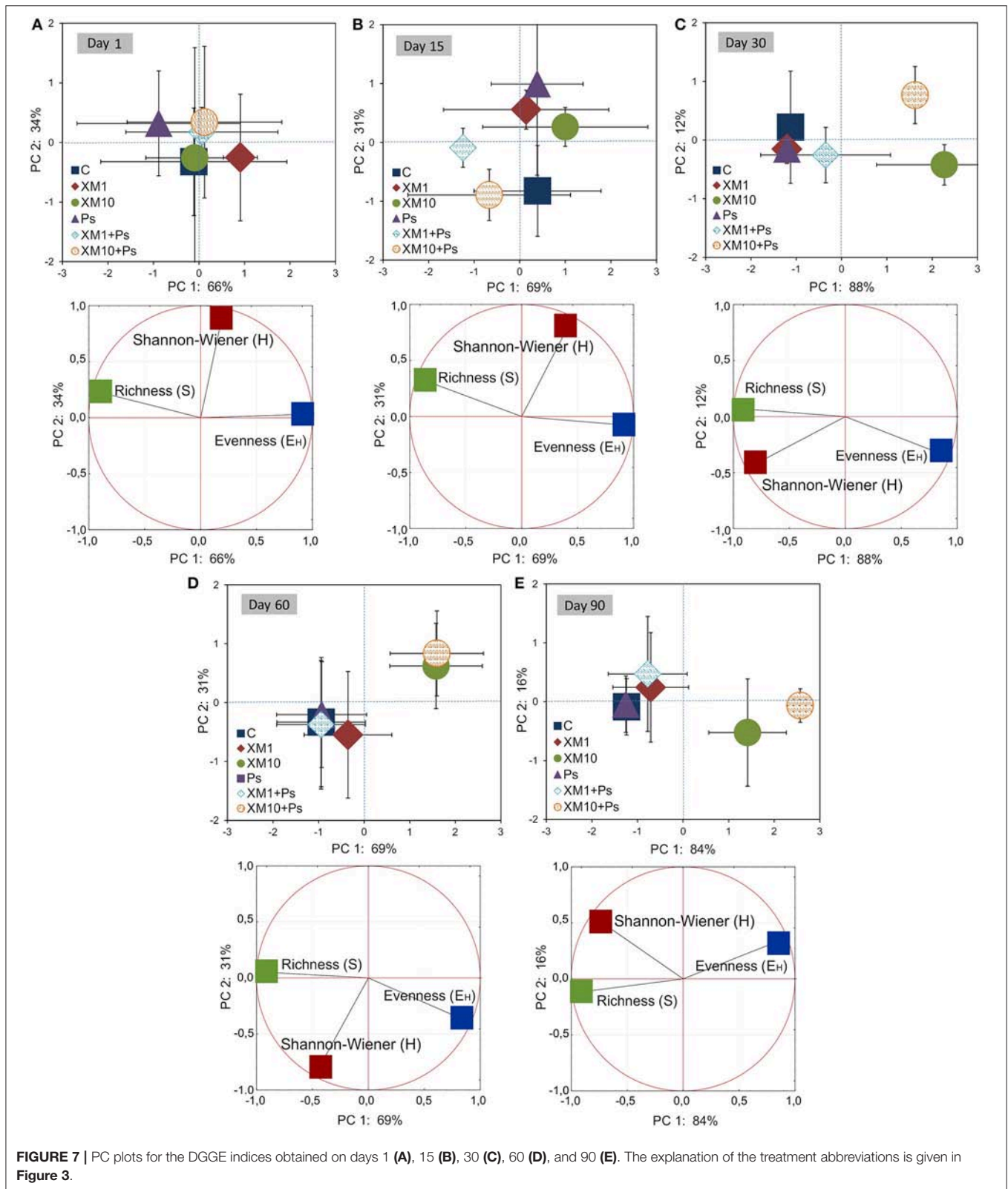
genes responsible for the resistance to XM located on both chromosomes and plasmids may be transferred between mobile genetic elements and spread through horizontal gene transfer (HGT) to autochthonous bacteria. Due to well adaptation of these bacteria to soil conditions, they might be participated in the long-term maintenance of antibiotic resistance genes in soils. HGT may also facilitate the transfer of antibiotic resistance genes from environmental to clinical strains (Pfeifer et al., 2010; Marti et al., 2013).

The application of bacteria resistant to antibiotics into soil may also produce significant changes within the soil microbial assemblages. However, in our study introduction of *P. putida* MC1 did not affect the genetic diversity of the autochthonous microbial communities. This effect might result from the competition between the introduced strain and indigenous microorganisms. Furthermore, many compounds produced by autochthonous microorganisms may limit the growth of inoculants (Karpouzias et al., 2000). The lack of any significant changes exerted by strain MC1 in the bacterial diversity may also be connected with the survival of inoculants in the soil environment. Strain MC1 was originated from raw sewage and it probably did not have the capability to adapt to soil conditions and compete with residential microorganisms. In turn, the obtained results indicated that XM may contribute to the modification of the soil microbial diversity. The DGGE band patterns of the soil samples treated with XM differed from the control what resulted from a disappearance of some of the bands in a response to the antibiotic presence, especially on days 30, 60, and 90 of the experiment. Moreover, a decline in the DGGE indices for soils treated with XM was found. There is no reported data concerning the impact of XM and/or *P. putida* on soil microbial diversity and therefore we cannot compare our results with those reported by other authors. However, some previously described results also showed alterations within bacterial communities expressed by the alterations in the number and intensity of bands in a response to the antibiotic application. Shifts in the DGGE band patterns obtained for soil treated with tylosin (TYL) were also noted by Westergaard et al. (2001). The authors revealed that the application of TYL at 2,000 µg/g soil altered

the bacterial structure in comparison with the control soil. A lower number of bands in the TYL-exposed soils as compared to the non-treated soil was noted after 2 and 3 weeks of the experiment, however the small changes were seen to the end of the experiment (Westergaard et al., 2001). Additionally, Cycon et al. (2016) revealed that the glycopeptide antibiotic vancomycin (VA) and/or the introduction of VA-resistant *Citrobacter freundii* exerted a selective pressure leading to alterations in the genetic diversity of soil bacterial communities within 90 days. Contrary, Zielesny et al. (2006) noted that the antibiotic sulfadiazine (SDZ) applied at different concentrations (1–50 mg/kg soil) did not affect the bacterial diversity as determined using the PCR-DGGE approach. The authors also revealed that chlortetracycline applied at the same concentrations as sulfadiazine did not change the microbial community structure.

The effect of antibiotics on soil autochthonous bacteria may also be connected with the resilience and resistance of tested microbial communities. The values of the RS and RL indices show whether microbial communities exposed to various stress factors can remain stable and/or achieve the original community structure (Orwin and Wardle, 2004; Orwin et al., 2006). Our experiment showed that the values of the RS index calculated for the DGGE indices for the soils with a higher dosage of XM (XM10, XM10+Ps) were significantly lower than those obtained for the XM1-treated soil. The negative effect of XM applied at a higher concentration on microbial diversity was also proven by the values of the RL index, which were found to be negative, thereby reflecting the progressing detrimental effect of XM on the genetic diversity of bacterial communities during the 90-day experiment. These results showed that in the soils that had been treated with a lower dose of XM and bacteria inoculants, the intrinsic properties of the soil microbial communities were protected the stability of soil ecosystem (Song et al., 2015). Even if some microbial populations were sensitive to the stressor, the whole community was resilient and had the ability to return to its original state (Allison and Martiny, 2008). Such an ability of microbial communities was not found in the XM10-treated soils. The high concentration of XM probably killed a significant part of the microbial population.

Our results showed that the negative effect of XM applied at a higher dosage (XM10 and XM10+Ps) was observed in the second part of the experiment. Although the reason for this phenomenon was not investigated in our study, a harmful effect of XM on a sensitive bacterial population might be connected with the stability and bioavailability of XM in soil and/or intermediates of XM degradation pathways that might also be characterized by antimicrobial properties. The stability of CPs and their susceptibility to degradation strongly depends on environmental conditions and, many biodegradation experiments conducted in various water systems showed that the effectiveness of CP removal varied significantly (Alexy et al., 2004; Gartiser et al., 2007; Jiang et al., 2010). For example, Gartiser et al. (2007) studying the inherent biodegradability of antibiotics using the CO<sub>2</sub> evolution test found that XM was degraded in activated sludge up to 10% of the initial dosage within 28 days. The middle persistence of XM was also observed in the closed bottle test, in which about 23% of XM remained in the system after 28 days



of the experiment (Alexy et al., 2004). The removal rate of about 30% of the initial XM concentration was also observed by Yu et al. (2016) at 25°C during the 144-h experiment. The authors also

reported that the persistence of XM was much higher than other tested CPs, i.e., ceftriaxone, cafelexin, and cephalosolin. In a study by Jiang et al. (2010), up to 80% of XM was degraded in the lake

**TABLE 7** | Multivariate analysis of variance (the two-way MANOVA) for the PC1 and PC2 based on the data of the DGGE indices for each sampling day (1, 15, 30, 60 and 90) as affected by the bacterial strain (S), concentration (C), time (T) and their interaction (S × C).

PC	SV	1		15		30		60		90	
		VE	P	VE	P	VE	P	VE	P	VE	P
PC1	S	3	0.532	13	0.163	<1	0.917	<1	0.693	1	0.235
	C	9	0.561	8	0.525	77	<0.001***	65	0.002**	85	<0.001***
	S × C	3	0.807	7	0.587	4	0.337	1	0.832	3	0.186
PC2	S	8	0.325	<1	0.990	4	0.349	1	0.708	3	0.492
	C	0	0.993	6	0.463	7	0.468	31	0.107	16	0.325
	S × C	0	0.985	49	0.012*	35	0.050	<1	0.997	2	0.887

PC, principal component; SV, source of variance; VE, variance explained (%). Asterisks represent the significance level according to the ANOVA (\* $P < 0.05$ , \*\* $P < 0.01$ , \*\*\* $P < 0.001$ ).

water and sediments within 168 h. Their results proved that the biodegradation is the main process responsible for the removal of CPs from sediments. Cefuroxime is slowly eliminated from soils and 42.8–80% of the initial dose was degraded within 64 days under aerobic conditions. Other studies also confirmed that the soil properties and additional compounds, such as slurry, manure or sewage, have a significant effect on the bioavailable fraction and degradation of antibiotics in different soils (Hammesfahr et al., 2008; Pan and Chu, 2016; Wang et al., 2016).

Because XM is characterized by a wide-spectrum activity against many bacteria, some of members of a bacterial assemblage in the XM-treated soil were negatively affected. Microorganisms that are sensitive to antibiotics are killed or their number decreases significantly, which results in increased numbers of bacteria resistant to antibiotics. Ding et al. (2014) observed a high disturbance and a low stability of soil bacterial communities in soil contaminated with SDZ (100 mg/kg soil) and manure compared to bacterial communities from soil treated with manure without SDZ. Moreover, numerous taxa such as *Gemmatimonas*, *Leifsonia*, *Devosia*, *Clostridium*, *Shinella*, and *Peptostreptococcus* containing also human pathogens dominated in the SDZ-amended soil while in the soil with SDZ and manure, the high number of the bacteria from the genera *Hydrogenophaga*, *Lysobacter*, *Pseudomonas*, and *Adhaeribacter* that typically are involved in the maintenance of high soil quality were found (Ding et al., 2014). In another study, SDZ (10 and 100 µg/g soil) applied into soil with manure also altered the bacterial diversity (Hammesfahr et al., 2008). Although the DGGE profiles proved the impact of SDZ+manure on soil bacterial communities on days 32 and 61 after the antibiotic introduction, these effects were not clearly visible for pseudomonads and  $\beta$ -Proteobacteria and may be explained by the resistance of many strains to sulfonamides (Hammesfahr et al., 2008). Genetic changes within the  $\beta$ -Proteobacteria and *Pseudomonas* group in manure and SDZ-amended soils were also reported by Reichel et al. (2014). Additionally, the presence of XM in soil might cause an overgrowth of fungi that are not susceptible to XM. Such phenomenon was earlier observed for soil treated with sulfadiazine (Hammesfahr et al., 2008), tetracycline (Yang et al., 2009) and oxytetracycline (Chessa et al., 2016).

## CONCLUSIONS

The results of our study indicated that the antibiotic-resistant *Pseudomonas putida* MC1 that was introduced into soil did not affect the genetic diversity of the autochthonous microbial communities. In turn, the obtained results showed that XM may cause alterations in the diversity of the soil bacteria. The DGGE patterns from the XM-treated soils differed from the patterns for non-treated control via the dissipation of some bands in a response to the XM application, especially on days 30, 60, and 90 of the experiment as was also evidenced by the decline in the S and H values. Because XM is active against different bacteria, some of members of bacterial communities in the XM-treated soil were negatively affected. The negative effect of XM observed in the second part of the experiment might be related to the stability/bioavailability of XM in the soil and/or more probably from the XM metabolites that are formed, which might also be characterized by antimicrobial properties. Moreover, differences in the resistance and resilience of the DGGE indices to disturbances caused by XM and/or strain MC1 have been demonstrated. The soil RL index was found to be negative, thereby reflecting the progressing detrimental impact of XM on the genetic diversity of soil bacteria within 90 days. These results that the introduction of XM at higher dosages into the soil may exert a potential risk for functioning of microorganism and further disturbances in the soil activity.

## AUTHOR CONTRIBUTIONS

KO and MC conceived and designed the experiments. KO contributed the reagents and materials. KO and MC performed the experiments. KO, MC, and ZP-S analyzed the results. KO, MC, and ZP-S wrote the paper.

## ACKNOWLEDGMENTS

This work was carried out as part of a grant that was financed by the National Science Centre, Poland (No. DEC-2014/15B/NZ9/04414).

## REFERENCES

- Alexy, R., Kämpel, T., and Kümmerer, K. (2004). Assessment of degradation of 18 antibiotics in the Closed Bottle Test. *Chemosphere* 57, 505–512. doi: 10.1016/j.chemosphere.2004.06.024
- Allison, S. D., and Martiny, J. B. H. (2008). Resistance, resilience and redundancy in microbial communities. *Proc. Natl. Acad. Sci. U.S.A.* 105, 11512–11519. doi: 10.1073/pnas.0801925105
- Bhattacharya, D., Dey, S., Kadam, S., Kalal, S., Jali, S., Koley, H., et al. (2015). Isolation of NDM-1-producing multidrug-resistant *Pseudomonas putida* from a pediatric case of acute gastroenteritis, India. *New Microbes New Infect.* 5, 5–9. doi: 10.1016/j.nmni.2015.02.002
- Brandt, K. K., Amézquita, A., Backhaus, T., Boxall, A., Coors, A., Heberer, T., et al. (2015). Ecotoxicological assessment of antibiotics: a call for improved consideration of microorganisms. *Environ. Int.* 85, 189–205. doi: 10.1016/j.envint.2015.09.013
- Carpenter, R. J., Hartzell, J. D., Forsberg, J. A., Babel, B. S., and Ganesan, A. (2008). *Pseudomonas putida* war wound infection in a US marine: a case report and review of the literature. *J. Infect.* 56, 234–240. doi: 10.1016/j.jinf.2008.01.004
- Chee-Sanford, J. C., Mackie, R. I., Koike, S., Krapac, I. G., Lin, Y.-F., Yannarell, A. C., et al. (2009). Fate and transport of antibiotic residues and antibiotic resistance genes following land application of manure waste. *J. Environ. Qual.* 38, 1086–1108. doi: 10.2134/jeq2008.0128
- Chen, W., Liu, W., Pan, N., Jiao, W., and Wang, M. (2013). Oxytetracycline on functions and structure of soil microbial community. *J. Soil Sci. Plant Nutr.* 13, 967–975. doi: 10.4067/S0718-95162013005000076
- Cheng, G., Hu, Y., Yin, Y., Yang, X., Xiang, C., Wang, B., et al. (2012). Functional screening of antibiotic resistance genes from human gut microbiota reveals a novel gene fusion. *FEMS Microbiol. Lett.* 336, 11–16. doi: 10.1111/j.1574-6968.2012.02647.x
- Chessa, L., Pusino, A., Garau, G., Mangia, N. P., and Pinna, M. V. (2016). Soil microbial response to tetracycline in two different soils amended with cow manure. *Environ. Sci. Pollut. Res.* 23, 5807–5817. doi: 10.1007/s11356-015-5789-4
- Cleary, D. W., Bishop, A. H., Zhang, L., Topp, E., Wellington, E. M. H., and Gaze, W. H. (2016). Long-term antibiotic exposure in soil is associated with changes in microbial community structure and prevalence of class 1 integrons. *FEMS Microbiol. Ecol.* 92:fw159. doi: 10.1093/femsec/fw159
- Coenen, S., Ferech, M., Dvorakova, K., Hendrickx, E., Suetens, C., and Goossens, H. (2006). European Surveillance of Antimicrobial Consumption (ESAC): outpatient cephalosporin use in Europe. *J. Antimicrob. Chemother.* 58, 413–417. doi: 10.1093/jac/dkl185
- Cui, H., Wang, S.-P., Jia, S.-G., Zhang, N., and Zhou, Z.-Q. (2013). Influence of ciprofloxacin on the microbial catabolic diversity in soil. *J. Environ. Sci. Heal. Part B Pestic. Food Contam. Agric. Wastes* 48, 869–877. doi: 10.1080/03601234.2013.796826
- Cycon, M., Borymski, S., Orlewska, K., Wasik, T. J., and Piotrowska-Seget, Z. (2016). An analysis of the effects of vancomycin and/or vancomycin-resistant *Citrobacter freundii* exposure on the microbial community structure in soil. *Front. Microbiol.* 7:1015. doi: 10.3389/fmicb.2016.01015
- Cycon, M., Markowicz, A., and Piotrowska-Seget, Z. (2013). Structural and functional diversity of bacterial community in soil treated with the herbicide napropamide estimated by the DGGE, CLPP and r/K-strategy approaches. *Agric. Ecosyst. Environ. Appl. Soil Ecol.* 72, 242–250. doi: 10.1016/j.apsoil.2013.07.015
- Cycon, M., Piotrowska-Seget, Z., and Kozdrój, J. (2010). Linuron effects on microbiological characteristics of sandy soils as determined in a pot study. *Ann. Microbiol.* 60, 439–449. doi: 10.1007/s13213-010-0061-0
- Cycon, M., Zmijowska, A., and Piotrowska-Seget, Z. (2011). Biodegradation kinetics of 2,4-D by bacterial strains isolated from soil. *Cent. Eur. J. Biol.* 6, 188–198. doi: 10.2478/s11535-011-0005-0
- de La Torre, A., Iglesias, I., Carballo, M., Ramirez, P., and Muñoz, M. J. (2012). An approach for mapping the vulnerability of European Union soils to antibiotic contamination. *Sci. Total Environ.* 414, 672–679. doi: 10.1016/j.scitotenv.2011.10.032
- Demoling, L. A., Bååth, E., Greve, G., Wouterse, M., and Schmitt, H. (2009). Effects of sulfamethoxazole on soil microbial communities after adding substrate. *Soil Biol. Biochem.* 41, 840–848. doi: 10.1016/j.soilbio.2009.02.001
- Devarajan, N., Köhler, T., Sivalingam, P., van Delden, C., Mulaji, C. K., Mpiana, P. T., et al. (2017). Antibiotic resistant *Pseudomonas* spp. in the aquatic environment: a prevalence study under tropical and temperate climate conditions. *Water Res.* 115, 256–265. doi: 10.1016/j.watres.2017.02.058
- Ding, G. C., Radl, V., Schloter-Hai, B., Jechalke, S., Heuer, H., Smalla, K., et al. (2014). Dynamics of soil bacterial communities in response to repeated application of manure containing sulfadiazine. *PLoS ONE* 9:e92958. doi: 10.1371/journal.pone.0092958
- Erol, S., Zenciroglu, A., Dilli, D., Okumus, N., Aydin, M., Gol, N., et al. (2014). Evaluation of nosocomial blood stream infections caused by *Pseudomonas* species in newborns. *Clin. Lab.* 60, 615–620. doi: 10.7754/Clin.Lab.2013.130325
- Espinosa-Urgel, M., Kolter, R., and Ramos, J.-L. (2002). Root colonization by *Pseudomonas putida*: love at first sight. *Microbiology* 148, 341–343. doi: 10.1099/00221287-148-2-341
- Fatta-Kassinos, D., Kalavrouziotis, I. K., Koukoulakis, P. H., and Vasquez, M. I. (2011). The risks associated with wastewater reuse and xenobiotics in the agroecological environment. *Sci. Total Environ.* 409, 3555–3563. doi: 10.1016/j.scitotenv.2010.03.036
- Fernández, M., Porcel, M., de la Torre, J., Molina-Henares, M. A., Daddaoua, A., Llamas, M. A., et al. (2015). Analysis of the pathogenic potential of nosocomial *Pseudomonas putida* strains. *Front. Microbiol.* 6:871. doi: 10.3389/fmicb.2015.00871
- Gartiser, S., Ulrich, E., Alexy, R., and Kümmerer, K. (2007). Ultimate biodegradation and elimination of antibiotics in inherent tests. *Chemosphere* 67, 604–613. doi: 10.1016/j.chemosphere.2006.08.038
- Gullberg, E., Cao, S., Berg, O. G., Ilbäck, C., Sandegren, L., Hughes, D., et al. (2011). Selection of resistant bacteria at very low antibiotic concentrations. *PLoS Pathog.* 7:e1002158. doi: 10.1371/journal.ppat.1002158
- Hammesfahr, U., Heuer, H., Manzke, B., Smalla, K., and Thiele-Bruhn, S. (2008). Impact of the antibiotic sulfadiazine and pig manure on the microbial community structure in agricultural soils. *Soil Biol. Biochem.* 40, 1583–1591. doi: 10.1016/j.soilbio.2008.01.010
- Iatrou, E. I., Stasinakis, A. S., and Thomaidis, N. S. (2014). Consumption-based approach for predicting environmental risk in Greece due to the presence of antimicrobials in domestic wastewater. *Environ. Sci. Pollut. Res.* 21, 12941–12950. doi: 10.1007/s11356-014-3243-7
- Ishibiki, K., Inoue, S., Suzuki, F., Okumura, K., Takeda, K., and Toshimitsu, Y. (1990). Investigation of adsorption, metabolism and excretion of cefuroxime axetil in volunteers of gastrectomized patients. *Jpn. J. Antibiot.* 43, 337–344
- Jiang, M., Wang, L., and Ji, R. (2010). Biotic and abiotic degradation of four cephalosporin antibiotics in a lake surface water and sediment. *Chemosphere* 80, 1399–1405. doi: 10.1016/j.chemosphere.2010.05.048
- Karpouzias, D. G., Morgan, J. A. W., and Walker, A. (2000). Isolation and characterisation of ethoprophos-degrading bacteria. *FEMS Microbiol. Ecol.* 33, 209–218. doi: 10.1111/j.1574-6941.2000.tb00743.x
- Kittinger, C., Lipp, M., Baumert, R., Folli, B., Koraimann, G., Toplitsch, D., et al. (2016). Antibiotic resistance patterns of *Pseudomonas* spp. isolated from the river Danube. *Front. Microbiol.* 7:586. doi: 10.3389/fmicb.2016.00586
- Kümmerer, K. (2003). Significance of antibiotics in the environment. *J. Antimicrob. Chemother.* 52, 5–7. doi: 10.1093/jac/dkg293
- Liu, B., Li, Y., Zhang, X., Wang, J., and Gao, M. (2014b). Combined effects of chlortetracycline and dissolved organic matter extracted from pig manure on the functional diversity of soil microbial community. *Soil Biol. Biochem.* 74, 148–155. doi: 10.1016/j.soilbio.2014.03.005
- Liu, H., Zhao, J., Xing, Y., Li, M., Du, M., Suo, J., et al. (2014a). Nosocomial infection in adult admissions with hematological malignancies originating from different lineages: a prospective observational study. *PLoS ONE* 9:e113506. doi: 10.1371/journal.pone.0113506
- Lombardi, G., Luzzaro, F., Docquier, J.-D., Riccio, M. L., Perilli, M., Coli, A., et al. (2002). Nosocomial infections caused by multidrug-resistant isolates of *Pseudomonas putida* producing VIM-1 metallo- $\beta$ -lactamase. *J. Clin. Microbiol.* 40, 4051–4055. doi: 10.1128/JCM.40.11.4051-4055.2002
- Luczkiwicz, A., Kotlarska, E., Artichowicz, W., Tarasewicz, K., and Fudala-Ksiazek, S. (2015). Antimicrobial resistance of *Pseudomonas* spp. isolated from wastewater and wastewater-impacted marine coastal zone. *Environ. Sci. Pollut. Res.* 22, 19823–19834. doi: 10.1007/s11356-015-5098-y

- Marti, R., Scott, A., Tien, Y.-C., Murray, R., Sabourin, L., Zhang, Y., et al. (2013). Impact of manure fertilization on the abundance of antibiotic-resistant bacteria and frequency of detection of antibiotic resistance genes in soil and on vegetables at harvest. *Appl. Environ. Microbiol.* 79, 5701–5709. doi: 10.1128/AEM.01682-13
- Molina, L., Udaondo, Z., Duque, E., Fernández, M., Molina-Santiago, C., Roca, A., et al. (2014). Antibiotic resistance determinants in a *Pseudomonas putida* strain isolated from a hospital. *PLoS ONE* 9:e81604. doi: 10.1371/journal.pone.0081604
- Muyzer, G., De Waal, E. C., and Uitterlinden, A. G. (1993). Profiling of complex microbial populations by denaturing gradient gel electrophoresis analysis of polymerase chain reaction-amplified genes coding for 16S rRNA. *Appl. Environ. Microbiol.* 59, 695–700.
- Nelson, K. E., Weinel, C., Paulsen, I. T., Dodson, R. J., Hilbert, H., Martins dos Santos, V. A. P., et al. (2002). Complete genome sequence and comparative analysis of the metabolically versatile *Pseudomonas putida* KT2440. *Environ. Microbiol.* 4, 799–808. doi: 10.1046/j.1462-2920.2002.00366.x
- Oguz, M., and Mihçioğru, H. (2014). Environmental risk assessment of selected pharmaceuticals in Turkey. *Environ. Toxicol. Pharmacol.* 38, 79–83. doi: 10.1016/j.etap.2014.05.012
- Orlewska, K., Piotrowska-Seget, Z., Bratosiewicz-Wasik, J., and Cycoń, M. (2018). Characterization of bacterial diversity in soil contaminated with the macrolide erythromycin and/or inoculated with a multidrug-resistant *Raoultella* sp. strain using the PCR-DGGE approach. *Appl. Soil Ecol.* 126, 57–64. doi: 10.1016/j.apsoil.2018.02.019
- Orwin, K. H., and Wardle, D. A. (2004). New indices for quantifying the resistance and resilience of soil biota to exogenous disturbances. *Soil Biol. Biochem.* 36, 1907–1912. doi: 10.1016/j.soilbio.2004.04.036
- Orwin, K. H., Wardle, D. A., and Greenfield, L. G. (2006). Context-dependent changes in the resistance and resilience of soil microbes to an experimental disturbance for three primary plant chronosequences. *Oikos* 112, 196–208. doi: 10.1111/j.0030-1299.2006.13813.x
- Pan, M., and Chu, L. M. (2016). Adsorption and degradation of five selected antibiotics in agricultural soil. *Sci. Total Environ.* 545–546, 48–56. doi: 10.1016/j.scitotenv.2015.12.040
- Pfeifer, Y., Cullik, A., and Witte, W. (2010). Resistance to cephalosporins and carbapenems in Gram-negative bacterial pathogens. *Int. J. Med. Microbiol.* 300, 371–379. doi: 10.1016/j.ijmm.2010.04.005
- Rahube, T. O., Marti, R., Scott, A., Tien, Y.-C., Murray, R., Sabourin, L., et al. (2014). Impact of fertilizing with raw or anaerobically digested sewage sludge on the abundance of antibiotic-resistant coliforms, antibiotic resistance genes, and pathogenic bacteria in soil and on vegetables at harvest. *Appl. Environ. Microbiol.* 80, 6898–6907. doi: 10.1128/AEM.02389-14
- Reichel, R., Radl, V., Rosendahl, I., Albert, A., Amelung, W., Schloter, M., et al. (2014). Soil microbial community responses to antibiotic-contaminated manure under different soil moisture regimes. *Appl. Microbiol. Biotechnol.* 98, 6487–6495. doi: 10.1007/s00253-014-5717-4
- Reichel, R., Rosendahl, I., Peeters, E. T. H. M., Focks, A., Groeneweg, J., Bierl, R., et al. (2013). Effects of slurry from sulfadiazine- (SDZ) and difloxacin- (DIF) medicated pigs on the structural diversity of microorganisms in bulk and rhizosphere soil. *Soil Biol. Biochem.* 62, 82–91. doi: 10.1016/j.soilbio.2013.03.007
- Rojas, A., Duque, E., Mosqueda, G., Golden, G., Hurtado, A., Ramos, J. L., et al. (2001). Three efflux pumps are required to provide efficient tolerance to toluene in *Pseudomonas putida* DOT-T1E. *J. Bacteriol.* 183, 3967–3973. doi: 10.1128/JB.183.13.3967-3973.2001
- Saravanane, R., and Sundararaman, S. (2009). Effect of loading rate and HRT on the removal of cephalosporin and their intermediates during the operation of a membrane bioreactor treating pharmaceutical wastewater. *Environ. Technol.* 30, 1017–1022. doi: 10.1080/09593330903032865
- Song, H.-S., Renslow, R. S., Fredrickson, J. K., and Lindemann, S. R. (2015). Integrating ecological and engineering concepts of resilience in microbial communities. *Front. Microbiol.* 6:1298. doi: 10.3389/fmicb.2015.01298
- Sun, F., Zhou, D., Wang, Q., Feng, J., Feng, W., Luo, W., et al. (2016). Genetic characterization of a novel blaDIM-2-carrying megaplasmid p12969-DIM from clinical *Pseudomonas putida*. *J. Antimicrob. Chemother.* 71, 909–912. doi: 10.1093/jac/dkv426
- Tamtam, F., van Oort, F., Le Bot, B., Dinh, T., Mompelat, S., Chevreuil, M., et al. (2011). Assessing the fate of antibiotic contaminants in metal contaminated soils four years after cessation of long-term waste water irrigation. *Sci. Total Environ.* 409, 540–547. doi: 10.1016/j.scitotenv.2010.10.033
- Versporten, A., Coenen, S., Adriaenssens, N., Muller, A., Minalu, G., Faes, C., et al. (2011). European Surveillance of Antimicrobial Consumption (ESAC): outpatient cephalosporin use in Europe (1997–2009). *J. Antimicrob. Chemother.* 66, 25–35. doi: 10.1093/jac/dkr455
- Wang, J., Lin, H., Sun, W., Xia, Y., Ma, J., Fu, J., et al. (2016). Variations in the fate and biological effects of sulfamethoxazole, norfloxacin and doxycycline in different vegetable-soil systems following manure application. *J. Hazard. Mater.* 304, 49–57. doi: 10.1016/j.jhazmat.2015.10.038
- Westergaard, K., Müller, A. K., Christensen, S., Bloem, J., and Sørensen, S. J. (2001). Effects of tylosin as a disturbance on the soil microbial community. *Soil Biol. Biochem.* 33, 2061–2071. doi: 10.1016/S0038-0717(01)00134-1
- Xia, K., Bhandari, A., Das, K., and Pillar, G. (2005). Occurrence and fate of pharmaceuticals and personal care products (PPCPs) in biosolids. *J. Environ. Qual.* 34, 91–104. doi: 10.2134/jeq2005.0091
- Xu, Y., Yu, W., Ma, Q., Wang, J., Zhou, H., and Jiang, C. (2016). The combined effect of sulfadiazine and copper on soil microbial activity and community structure. *Ecotoxicol. Environ. Saf.* 134, 43–52. doi: 10.1016/j.ecoenv.2016.06.041
- Yang, J.-F., Ying, G.-G., Zhou, L.-J., Liu, S., and Zhao, J.-L. (2009). Dissipation of oxytetracycline in soils under different redox conditions. *Environ. Pollut.* 157, 2704–2709. doi: 10.1016/j.envpol.2009.04.031
- Yoshino, Y., Kitazawa, T., Kamimura, M., Tatsuno, K., Ota, Y., and Yotsuyanagi, H. (2011). *Pseudomonas putida* bacteremia in adult patients: five case reports and a review of the literature. *J. Infect. Chemother.* 17, 278–282. doi: 10.1007/s10156-010-0114-0
- Yu, X., Tang, X., Zuo, J., Zhang, M., Chen, L., and Li, Z. (2016). Distribution and persistence of cephalosporins in cephalosporin producing wastewater using SPE and UPLC-MS/MS method. *Sci. Total Environ.* 569–570, 23–30. doi: 10.1016/j.scitotenv.2016.06.113
- Zielezny, Y., Groeneweg, J., Vereecken, H., and Tappe, W. (2006). Impact of sulfadiazine and chlorotetracycline on soil bacterial community structure and respiratory activity. *Soil Biol. Biochem.* 38, 2372–2380. doi: 10.1016/j.soilbio.2006.01.031

**Conflict of Interest Statement:** The authors declare that the research was conducted in the absence of any commercial or financial relationships that could be construed as a potential conflict of interest.

Copyright © 2018 Orlewska, Piotrowska-Seget and Cycoń. This is an open-access article distributed under the terms of the Creative Commons Attribution License (CC BY). The use, distribution or reproduction in other forums is permitted, provided the original author(s) and the copyright owner are credited and that the original publication in this journal is cited, in accordance with accepted academic practice. No use, distribution or reproduction is permitted which does not comply with these terms.



# Experimental Warming Differentially Influences the Vulnerability of Phototrophic and Heterotrophic Periphytic Communities to Copper Toxicity

Stéphane Pesce<sup>1\*†</sup>, Anne-Sophie Lambert<sup>1†</sup>, Soizic Morin<sup>2</sup>, Arnaud Foulquier<sup>1,3</sup>, Marina Coquery<sup>1</sup> and Aymeric Dabrin<sup>1</sup>

<sup>1</sup> Irstea, UR RiverLy, Centre de Lyon-Villeurbanne, Villeurbanne, France, <sup>2</sup> Irstea, UR EABX, Centre de Bordeaux, Gazinet-Cestas, France, <sup>3</sup> UMR CNRS 5553, Laboratoire d'Écologie Alpine, Université Grenoble Alpes, Grenoble, France

## OPEN ACCESS

### Edited by:

Jean Armengaud,  
Commissariat à l'Énergie Atomique et  
aux Énergies Alternatives (CEA),  
France

### Reviewed by:

Rafael Bosch,  
Universidad de les Illes Balears, Spain  
Xianhua Liu,  
Tianjin University, China

### \*Correspondence:

Stéphane Pesce  
stephane.pesce@irstea.fr

<sup>†</sup>These authors have contributed  
equally to this work.

### Specialty section:

This article was submitted to  
Microbiotechnology, Ecotoxicology  
and Bioremediation,  
a section of the journal  
Frontiers in Microbiology

**Received:** 30 March 2018

**Accepted:** 11 June 2018

**Published:** 02 July 2018

### Citation:

Pesce S, Lambert A-S, Morin S,  
Foulquier A, Coquery M and  
Dabrin A (2018) Experimental  
Warming Differentially Influences  
the Vulnerability of Phototrophic  
and Heterotrophic Periphytic  
Communities to Copper Toxicity.  
*Front. Microbiol.* 9:1424.  
doi: 10.3389/fmicb.2018.01424

Aquatic ecosystems are generally subjected to multiple perturbations due to simultaneous or successive combinations of various natural and anthropogenic environmental pressures. To better assess and predict the resulting ecological consequences, increasing attention should be given to the accumulation of stresses on freshwater ecosystems and its effects on the vulnerability of aquatic organisms, including microbial communities, which play crucial functional roles. Here we used a microcosm study to assess the influence of an experimental warming on the vulnerability of phototrophic and heterotrophic periphytic communities to acute and chronic copper (Cu) toxicity. Natural periphytic communities were submitted for 4 weeks to three different temperatures (18, 23, and 28°C) in microcosms contaminated (at about 15 µg L<sup>-1</sup>) or not with Cu. The vulnerability of both phototrophic and heterotrophic microbial communities to subsequent acute Cu stress was then assessed by measuring their levels of sensitivity to Cu from bioassays targeting phototrophic (photosynthetic activity) and heterotrophic (β-glucosidase and leucine aminopeptidase extracellular enzymatic activities) microbial functions. We postulated that both the increase in temperature and the chronic Cu exposure would modify microbial community structure, thus leading to changes in the capacity of phototrophic and heterotrophic communities to tolerate subsequent acute exposure to Cu. Our results demonstrated that the influence of temperature on the vulnerability of phototrophic and heterotrophic microbial communities to Cu toxicity can vary greatly according to function studied. These findings emphasize the importance of considering different functional compartments and different functional descriptors to better assess the vulnerability of periphyton to multiple stresses and predict the risks induced by multiple stressors for ecosystem balance and functioning.

**Keywords:** bioaccumulation, biofilms, extracellular enzymatic activities, freshwater, microbial ecotoxicology, multi-stress, photosynthesis, pollution-induced community tolerance (PICT)

## INTRODUCTION

Metals are ubiquitously present in freshwater ecosystems, whether occurring naturally (Bradl, 2005) or anthropogenically due to releases from agriculture, urbanization, mining, and industry (Ancion et al., 2013). Copper (Cu) is well representative of the widespread metal pollution of surface waters including rivers and streams in agricultural areas, where it has been widely used as a fungicide and weed-killer in both conventional and organic agriculture (Serra and Guasch, 2009; Provenzano et al., 2010). Cu is an essential element for organisms, serving as a cofactor in many enzymatic pathways that catalyze a wide variety of functions including several redox reactions as well as photosynthetic and mitochondrial electron transport (Ladomersky and Petris, 2015; Adams et al., 2016). However, high concentrations of Cu are toxic to aquatic life, and thus pose ecotoxicological risks in freshwater ecosystems. There is a large ecotoxicological dataset on the effects of Cu on aquatic macroorganisms, especially fish and invertebrates (e.g., US EPA, 2010). Aquatic microbial communities, which are composed of phototrophic and heterotrophic microorganisms (including microalgae, bacteria, fungi, and heterotrophic protists) can also be impacted by Cu toxicity, which can generate excess reactive oxygen species (Okamoto et al., 2001; Sabatini et al., 2009), induce lipid peroxidation (Rijstenbil et al., 1994), increase membrane permeability (Cid et al., 1995), inhibit growth (Prasad et al., 1998), and reduce chlorophyll or accessory pigment contents (Rijstenbil et al., 1994).

In lotic ecosystems including agricultural streams, benthic microbial assemblages such as periphytic communities (also called “biofilms”) provide key ecological functions, like primary production and nutrient recycling (Battin et al., 2003). These microbial communities, which are embedded in a polysaccharide–protein matrix, quickly interact with dissolved chemicals (Sabater et al., 2007), including Cu. Chronic exposure to Cu can functionally impact phototrophic and heterotrophic periphytic communities by reducing photosynthesis (Lambert et al., 2012), extracellular enzymatic activities such as  $\beta$ -glucosidase activity (Lambert et al., 2012) and substrate-induced respiration (Tlili et al., 2011). It can also modify community structure following changes in microbial biomasses, distribution of algal classes, taxonomic composition of diatom communities (Serra and Guasch, 2009; Morin et al., 2017), and bacterial diversity (Tlili et al., 2010). Microorganisms have nevertheless developed several defense mechanisms to cope with Cu toxicity (see Nies, 1999; Bruins et al., 2000 for details). The main mechanisms of Cu resistance include efflux ATPase pumps able to throw out Cu ions, chemo-osmotic Cu extrusion systems such as the *cus* system encoding especially for the *CusA* protein belonging to the resistance, nodulation, and cell division family responsible for metal export, and the periplasmic *pco* system unique to plasmids (Besaury et al., 2013). The polysaccharide–protein matrix, which plays a crucial structural role in biofilms, also serves as a protective layer protect against environmental stress such as metallic contamination due to its high metal ion adsorption capacity, which can prevent their diffusion to deeper layers of the periphyton, thus reducing microbial community

exposure (Rose and Cushing, 1970; Loaec et al., 1997; Lau et al., 2005).

The combination of structural changes (which are generally substantially attributable to the loss of sensitive species and/or the development of more tolerant ones) and microbial adaptation at individual level following chronic exposure to Cu can increase the potential of both phototrophic and heterotrophic periphytic microbial communities to tolerate Cu (Soldo and Behra, 2000; Tlili et al., 2010; Lambert et al., 2012), as postulated by the concept of pollution-induced community tolerance (PICT) first introduced by Blanck et al. (1988). Indeed, such adaptation processes partly condition the resilience and resistance capacities of microbial communities following acute or chronic exposure to Cu, thus defining their vulnerability to this toxicant.

Given the fact that aquatic microbial communities are generally subjected to multiple natural and anthropogenic environmental stressors due to simultaneous or successive combinations of various pressures (e.g., pollution, physical stresses, competition, and predation), it is necessary to better assess and predict how communities respond to multiple stressors rather than just a single compound (Clements and Rohr, 2009; Holmstrup et al., 2010). Accordingly, research needs to focus more attention on the accumulation of stresses on freshwater ecosystems and its resulting effects on the vulnerability of aquatic communities, including microbial ones (Morin et al., 2015).

Due to global warming, many freshwater ecosystems are increasingly subjected to extreme climate events including prolonged high-temperature periods (Easterling et al., 2000; Wreford and Adger, 2010). The resulting acute increase in water temperature can represent a heat stress that can interact with the toxicant effects induced by Cu exposure. Indeed, communities already sensitized by a temperature rise would likely be impoverished in terms of species and/or functionalities and consequently lose some capacity to cope with an additional stress such as toxicant exposure (e.g., Morin et al., 2015). While most of the studies dealing with the combined effects of heat stress and metal exposure on aquatic populations have concerned macroorganisms (for a review, see Holmstrup et al., 2010), there is increasing evidence that temperature conditions influence periphytic microbial community response to Cu toxicity (Boivin et al., 2005; Lambert et al., 2016, 2017; Morin et al., 2017). For instance, experimental warming (+5 to +15°C) was shown to significantly influence the chronic and acute ecotoxicological impact of Cu on phototrophic periphytic communities by reducing Cu bioavailability and bioaccumulation in periphyton (Lambert et al., 2016), inducing changes in diatom communities (Lambert et al., 2016; Morin et al., 2017), and decreasing both the basal and Cu-induced tolerance of phototrophic communities to acute Cu exposure (Lambert et al., 2017; Morin et al., 2017). Focusing on bacterial communities, Boivin et al. (2005) also highlighted the potential effect of temperature on PICT processes. However, and contrary to Lambert et al. (2017) and Morin et al. (2017), they showed a gradual increase in Cu-induced community tolerance when temperature increased from 10 to 20°C (Boivin et al., 2005). Interestingly, this experimental observation was consistent with the findings of a field survey by Faburé et al. (2015) who showed that heterotrophic periphytic

communities collected in winter were less Cu-tolerant than those collected in warmer seasons.

Taken together, these studies reveal that temperature can greatly influence the vulnerability of phototrophic and heterotrophic periphytic communities to Cu toxicity. However, results were quite divergent among studies, suggesting that the magnitude and direction of this influence depend on several parameters, such as magnitude of both Cu and temperature stresses and initial community composition which condition the sensitivity to Cu of the most thermotolerant species (Lambert et al., 2016), and the kind of microbial communities involved (i.e., phototrophic or heterotrophic). Moreover, until now, the combined effects of temperature and Cu on both the phototrophic and heterotrophic components of periphytic communities have not been simultaneously investigated.

In this context, research is still needed to better understand the mechanisms that drive the influence of temperature on the vulnerability of phototrophic and heterotrophic periphytic communities to acute and chronic Cu toxicity. To address this issue, we used a microcosm study where natural periphytic communities were submitted for 4 weeks to three different temperatures (18, 23, and 28°C) in microcosms contaminated (at about 15  $\mu\text{g L}^{-1}$ ) or not with Cu. For each treatment, we assessed the vulnerability of both phototrophic and heterotrophic microbial communities to subsequent acute Cu stress by measuring their levels of sensitivity to Cu via bioassays targeting phototrophic (photosynthetic activity) and heterotrophic (extracellular enzymatic activities) microbial functions. Given the potential influence of temperature on Cu bioavailability and accumulation in periphytic assemblages (Lambert et al., 2016) and the important protective role of the polysaccharide-protein matrix to Cu exposure, we also focused effort on measuring Cu concentrations in (i) the colloidal, (ii) the capsular fractions of the extracellular polymeric substances (EPS), and (iii) in the intracellular fraction of periphyton. In addition, we assessed structural changes in periphyton by measuring algal biomass and photosynthetic efficiency and by performing diatom taxonomic analysis.

Besides the simultaneous study of phototrophic and heterotrophic communities, the main originality of the study lies in the fact that we considered Cu and temperature stress levels representative of point-in-time contaminations and thermal conditions observed in the downstream section of the river where the periphytic communities were initially collected. We postulated that both the increase in temperature and the chronic Cu exposure would modify microbial community structure, thus leading to changes in the capacity of phototrophic and heterotrophic communities to tolerate subsequent acute exposure to Cu. In line with the PICT concept, our first hypothesis was that chronic exposure to Cu would have made both phototrophic and heterotrophic communities more tolerant to acute Cu toxicity. Based on the literature cited above, our second hypothesis was that the increase in temperature would have increased the vulnerability of phototrophic communities and decreased the vulnerability of heterotrophic communities to acute Cu toxicity, whatever their history of chronic Cu exposure.

## MATERIALS AND METHODS

### Experimental Setup

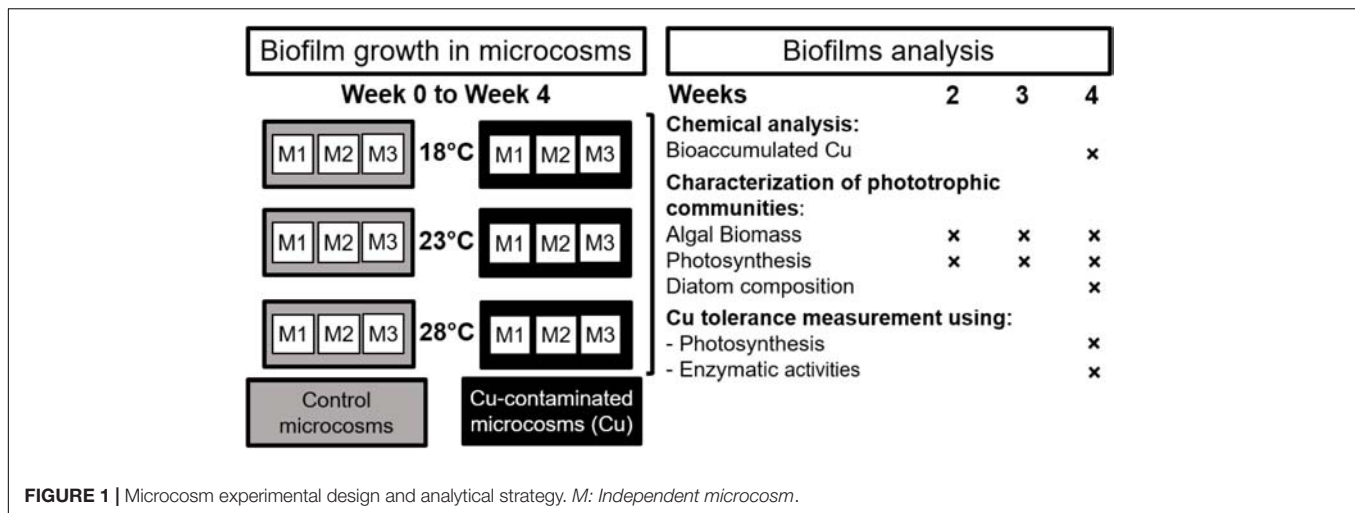
The experiment was carried out using a natural biofilm inoculum collected from the Morcille river (Beaujolais, Eastern France) in September 2014. Stones were collected at the upstream reference site of the Morcille River (see Rabiet et al., 2015 for details). The periphyton was scraped and suspended in the river water in order to obtain a periphytic inoculum, which was homogenized before being added at the start of the experiment (week 0) for colonization of glass slides vertically immersed a few centimeters below the water surface in the microcosms. The microcosms consisted in 18 independent glass aquariums (40 × 20 × 25 cm) incubated in three polyethylene tanks (250 L, 121 × 81 × 33 cm) containing water thermoregulated at 18°C (i.e., close to the average seasonal temperature of Morcille river water during the periphyton sampling), 23 and 28°C, respectively (**Figure 1**). This experimental warming can be considered as a realistic worst-case scenario, as recorded in the Morcille river in summer 2015 (e.g., 26.9°C recorded on July 21, 2015, at 6:00 p.m. on the downstream section of the river, unpublished data).

In each tank, six microcosms were filled with reconstituted water consisting of 3:1 (v/v) distilled water:groundwater, supplemented with nutrients in order to adjust conductivity (i.e., about 180  $\mu\text{S cm}^{-1}$ ) and nutrient concentrations (i.e., 15  $\text{mg L}^{-1}$  of silica; 8  $\text{mg L}^{-1}$  of nitrates; 0.2  $\text{mg L}^{-1}$  of orthophosphates) to the characteristics of the river water at the periphyton sampling site (**Table 1**). Water mixing, oxygenation, and lighting were operated as previously described in Lambert et al. (2015). Three microcosms were used as Control microcosms (“Control,” without Cu addition) and three Cu-exposed microcosms (“Cu”) were supplemented with  $\text{CuSO}_4 \cdot 5\text{H}_2\text{O}$  to obtain a Cu concentration close to the highest concentrations recorded in the downstream section of Morcille River (i.e., about 15  $\mu\text{g Cu L}^{-1}$ ; Montuelle et al., 2010; Rabiet et al., 2015). To avoid Cu adsorption by the experimental equipment during the exposure period, Cu microcosms (including glass slides and pumps) were saturated using the same Cu concentration for 24 h before start of the experiment.

This study was conducted for 4 weeks. After 1 week, the water level of each aquarium was adjusted to its initial value, and nutrients were added to maintain the initial trophic conditions. Then, water was renewed weekly to maintain Cu exposure and avoid nutrient depletion.

### Main Physico-Chemical Analyses

The main physical-chemical parameters of the water were measured in each microcosm before and 2 h after each water renewal. Conductivity, pH, and dissolved oxygen concentration were measured using portable meters (WTW). Water samples were collected at the same time for subsequent laboratory analyses. Standard operating procedures were followed to determine the concentrations of orthophosphates ( $\text{PO}_4$ ), nitrates ( $\text{NO}_3$ ), nitrites ( $\text{NO}_2$ ), ammonium ( $\text{NH}_4$ ), silicon dioxide



(SiO<sub>2</sub>), and dissolved organic carbon (DOC), as described in Lambert et al. (2017). Temperature was recorded every hour with dataloggers (HOBO® Pendant Temperature/Light, ProSensor).

## Copper Analysis in Water and in Periphyton

Total dissolved Cu concentrations were measured before and after each water renewal. Channel water (30 mL) was sampled, filtered [0.45 μm polyvinylidene difluoride (PVDF), Whatman], acidified to 0.5% (v/v) with nitric acid (14 M Suprapur, Merck), and stored at 4°C until analysis.

Cu concentrations in periphyton were measured at week 4 following a protocol adapted from Aguilera et al. (2008) to determine the concentrations of Cu in (i) the colloidal and (ii) the capsular fraction of the biofilm EPS as well as in (iii) the intracellular fraction of periphyton. Periphyton was scraped from glass substrates and suspended in the reconstituted water used to fill the microcosms. After homogenization, 30 mL of

the obtained biofilm suspension was lyophilized. Demineralized water (10 mL) was then added to obtain a suspension, which was gently shaken during 20 min at ambient temperature and centrifuged (4000 g, 15 min) to retrieve the supernatant containing the colloidal EPS fraction. Then, the pellet was incubated with EDTA (final concentration 4 mM) during 3 h under shaking at ambient temperature, and centrifuged (14,000 g, 20 min) to retrieve the supernatant containing the capsular EPS fraction. Both colloidal and capsular EPS fractions were acidified with 0.5% (v/v) nitric acid (14 M Suprapur, Merck) and stored at 4°C until analysis. The final pellet was dried and mineralized with nitric acid (14 M) in a microwave oven (CEM, Mars-5) to extract the intracellular Cu fraction.

Total dissolved Cu samples were analyzed by inductively coupled plasma-atomic emission spectroscopy (ICP-AES, Agilent 720-ES) and inductively coupled plasma-mass spectrometry (ICP-MS Series II, Thermo Electron). Periphyton extracts were analyzed by ICP-MS. Limits of quantification (LQ) were 1 μg L<sup>-1</sup> in water samples and 3 μg g<sup>-1</sup> dry weight (dw)

**TABLE 1** | Physico-chemical characteristics of water in the six tested conditions before (conditions after 1 week) and 2 h after (initial conditions) each water renewal during 4 weeks (mean values of weekly samples ± SD; *n* = 3).

	Initial conditions (after water renewal)		Conditions after 1 week (before water renewal)				
	All aquariums ( <i>n</i> = 18)	Control ( <i>n</i> = 3)	18°C		23°C		28°C
			Control ( <i>n</i> = 3)	Cu ( <i>n</i> = 3)	Control ( <i>n</i> = 3)	Cu ( <i>n</i> = 3)	Control ( <i>n</i> = 3)
pH	9.0 ± 0.1	8.9 ± 0.4	9.4 ± 0.4	9.0 ± 0.4	9.0 ± 0.7	8.9 ± 0.3	8.9 ± 0.4
Conductivity (μS cm <sup>-1</sup> )	130 ± 6	118 ± 17	110 ± 17	113 ± 12	122 ± 23	118 ± 13	120 ± 22
Dissolved O <sub>2</sub> (mg L <sup>-1</sup> )	9.25 ± 0.69	10.65 ± 0.30	11.04 ± 0.62	9.84 ± 0.40	10.24 ± 0.85	9.39 ± 0.38	9.83 ± 0.81
Dissolved Organic C (mg L <sup>-1</sup> )	0.58 ± 0.24	2.22 ± 0.41	1.89 ± 0.37	2.08 ± 0.50	1.88 ± 0.50	2.13 ± 0.47	1.73 ± 0.46
NO <sub>3</sub> (mg L <sup>-1</sup> )	5.81 ± 0.45	1.28 ± 0.43	1.10 ± 0.20	1.30 ± 0.51	2.01 ± 1.57	1.57 ± 0.87	1.66 ± 1.61
NO <sub>2</sub> (mg L <sup>-1</sup> )	<0.05	<0.05	<0.05	0.06 ± 0.01	0.14 ± 0.14	0.06 ± 0.02	0.14 ± 0.16
NH <sub>4</sub> (mg L <sup>-1</sup> )	0.03 ± 0.04	0.05 ± 0.10	<0.02	<0.02	<0.02	<0.02	<0.02
PO <sub>4</sub> (mg L <sup>-1</sup> )	0.15 ± 0.05	<0.10	<0.10	<0.10	<0.10	<0.10	<0.10
SiO <sub>2</sub> (mg L <sup>-1</sup> )	5.53 ± 0.33	0.64 ± 0.55	2.27 ± 1.75	0.91 ± 0.67	1.89 ± 1.52	1.47 ± 1.00	4.11 ± 2.25

in biofilms for ICP-AES, and  $0.050 \mu\text{g L}^{-1}$  and  $1.5 \mu\text{g g}^{-1}$  dw for ICP-MS. Routine quality Control checks used a certified reference material (River water, TM 27.3; plankton, BCR-414).

## Periphyton Characterization

After 14, 21, and 28 days in the microcosms, periphyton was carefully scraped from the slides with a plastic spatula and suspended in 1:1 (v/v) demineralized:mineral water (Volvic) before being homogenized and aliquoted to further measure the following parameters. Total chlorophyll *a* (chl *a*) and photosynthetic efficiency (derived from the maximal PSII quantum yield) were estimated weekly by multi-wavelength pulse-amplitude-modulated (PAM) fluorometry using a Phyto-PAM system (H. Walz GmbH) as described in Lambert et al. (2017). Diatom identification was performed on the inoculum and at week 4 as described in Morin et al. (2017).

## Tolerance Assessment of Phototrophic and Heterotrophic Communities to Copper (PICT Measurement)

A semi-logarithmic series of Cu concentrations was freshly prepared in 1:1 (v/v) demineralized:mineral water (Volvic) to obtain seven different Cu concentrations ranging from 0.32 to 320 mg/L for phototrophic tolerance assessment and from 0.032 to 32 mg/L for heterotrophic tolerance assessment. Cu concentrations in each dilution were checked by ICP-MS (ICP-MS X Series II, Thermo Electron) as described above.

Phototrophic and heterotrophic periphyton community tolerance to Cu was assessed at week 4 using photosynthetic efficiency, based on the measurement of maximal quantum yield ( $Y_{II}$ ), as endpoint for phototrophs and  $\beta$ -glucosidase ( $\beta$ -Glu), leucine aminopeptidase (Lap), and phosphatase (Pase) activities as endpoints for heterotrophs.

Given the influence of periphyton biomass on PICT measurement (Lambert et al., 2015), the initial periphyton suspension was diluted with the demineralized:mineral water mixture before toxicity tests. Based on the assumption that phototrophic biomass (estimated from chl *a* concentrations measured with the Phyto-PAM fluorometer) can be viewed as a proxy of total biomass of phototrophic biofilms (Lambert et al., 2015), periphyton suspensions were diluted to a standardized chl *a* concentration for further assessment of phototrophic and heterotrophic tolerance levels.

To assess phototrophic community tolerance, diluted periphyton suspensions (1.8 mL, at about  $2000 \mu\text{g chl } a/\text{L}$ ) were exposed to increasing concentrations of Cu (0.9 mL) in a climate chamber (MLR-350 Versatile Environmental Test Chamber, Sanyo) at the intermediate temperature of  $23^\circ\text{C}$  (Lambert et al., 2017) under artificial light (1400 lux). Samples were then kept for 30 min in a dark chamber, and PSII quantum yield (665 nm) was determined as stated above.

For heterotrophic communities,  $\beta$ -Glu, Lap, and Pase activities were measured using fluorescent-linked substrates [4-methylumbelliferyl- $\beta$ -D-glucopyranoside (MUF-GLU),

L-leucine-7-amido-4-methylcoumarin hydrochloride (MCA-Lap) and 4-methylumbelliferyl phosphatase (MUF-P); Sigma-Aldrich]. First, diluted periphyton suspensions (1.7 mL, at about  $5000 \mu\text{g chl } a/\text{L}$ ) were exposed to increasing concentrations of Cu (0.3 mL) in the dark, at  $23^\circ\text{C}$ , under gentle shaking, for 1 h. Then, periphyton suspensions were incubated with 1 mL of MUF-GLU, MCA-Lap, or MUF-P at saturating concentrations ( $750 \mu\text{M}$  for MUF-Glu and MCA-Lap and  $3000 \mu\text{M}$  for MUF-P), in the dark, at  $23^\circ\text{C}$ , under gentle shaking, for 1h40 ( $\beta$ -Glu), 1h (Lap), or 1h30 (Pase). Then, 300  $\mu\text{L}$  of glycine buffer (pH 10.4; glycine 0.05 M,  $\text{NH}_4\text{OH}$  0.2 M) was added to stop the enzymatic reaction. Fluorescence of MUF and MCA was measured promptly following centrifugation (5000 g, 10 min) using a Biotek SynergyHT fluorometer at 360/460 nm excitation/emission. For each sample replicate, four blanks and two analytical replicates were analyzed for each concentration.

## Data Processing

Variations in dissolved Cu among thermal conditions and sampling dates and variations in water physico-chemical characteristics among thermal and treatment conditions were tested using two-way repeated measures ANOVA followed by a *post hoc* Tukey test in R version 2.15.0 (R Development Core Team, 2012). Data were log-transformed before statistical analysis to satisfy the assumption of normality and homogeneity of variances. Variations in Cu bioaccumulation (colloidal, capsular, and intracellular fractions) in the Cu-exposed biofilms among thermal conditions were tested using one-way repeated measures ANOVA followed by a *post hoc* Tukey test.

PICT bioassay results were analyzed using functions from the “drc” package (Ritz and Streibig, 2005) in R version 2.15.0 (R Development Core Team, 2012). Dose–response curves were fitted to the data using the four-parameter log-logistic model given by the formula:

$$\text{response} = c + \frac{d - c}{1 + \exp \{b \times (\log(\text{Dose}) - \log(e))\}}$$

where *b* is the slope of the curve around *e*, parameters *c* and *d* are the lower and upper limits of the curve, respectively, and *e* is  $\text{EC}_{50}$ , i.e., the dose producing a response half-way between the upper and the lower limit.  $\text{EC}_{50}$  variations among thermal and treatment conditions were then tested using two-way repeated measures ANOVA followed by a *post hoc* Tukey test. Significance for all statistical tests was set at  $p < 0.05$ .

## RESULTS

### Physico-Chemical Data

Water temperatures measured every hour in each microcosm were close to target temperatures with mean values of  $18.3^\circ\text{C}$  ( $\pm 0.2$ ),  $23.5^\circ\text{C}$  ( $\pm 0.3$ ), and  $28.0^\circ\text{C}$  ( $\pm 0.2$ ), respectively, without significant difference between Control and Cu microcosms ( $p > 0.05$ ). **Table 1** reports the mean values of the main physical–chemical variables measured in the microcosms before and after each water renewal. In both Control and Cu-exposed microcosms, dissolved oxygen concentrations decreased

significantly from 10.6 to 9.8 mg L<sup>-1</sup> between 18 and 28°C ( $p < 0.05$ ). Silica concentrations decreased over time, but to a lower extent with higher temperatures ( $p > 0.05$ ). Silica concentrations were higher in Cu microcosms for each temperature tested, and the difference was significant at 28°C ( $p < 0.05$ ). In contrast, DOC concentrations slightly decreased in Cu-exposed microcosms compared to Control microcosms ( $p > 0.05$ ).

## Dissolved Copper Concentrations

In Control microcosms (i.e., without Cu addition), dissolved Cu concentrations remained below the limit of detection throughout the experiment. In all Cu-exposed microcosms, mean dissolved Cu concentrations measured 2 h after water renewal were  $10.2 \pm 0.4 \mu\text{g L}^{-1}$  at week 2 and  $8.3 \pm 0.2 \mu\text{g L}^{-1}$  at week 3, without significant difference between temperatures, whatever the sampling time ( $p > 0.05$ ; data not shown). Dissolved Cu concentrations were relatively stable in the microcosms between each water renewal ( $p > 0.05$ ) without a significant effect of temperature on Cu concentrations recorded one week after water renewal ( $p > 0.05$ ).

## Copper Bioaccumulation

After 4 weeks of exposure, total Cu concentration in periphyton growing in Cu-exposed microcosms was  $211 \pm 11 \mu\text{g g}^{-1}$  dw at 18°C,  $192 \pm 2 \mu\text{g g}^{-1}$  dw at 23°C, and  $168 \pm 25 \mu\text{g g}^{-1}$  dw at 28°C, with no significant difference between temperatures ( $p > 0.05$ ), despite a tendency of Cu accumulated to decrease with increasing temperatures (Figure 2). This tendency was mainly due to a decrease in externalized Cu concentrations, represented by colloidal and capsular fractions. In contrast, internalized Cu concentrations, represented by the intracellular fraction, were relatively stable, with mean values close to  $80 \mu\text{g g}^{-1}$  dw, whatever the temperature.

## Periphyton Characterization

### Algal Biomass and Photosynthetic Efficiency

Applied individually, each stress (i.e., warming or chronic Cu exposure) had a limited effect on chl *a* concentrations (Figure 3A). In Control microcosms (i.e., without Cu stress), chl *a* concentrations gradually increased during the 4 weeks, without significant difference between temperatures ( $p > 0.05$ ; Figure 3A). At 18°C (i.e., without warming stress), chronic Cu exposure had only a transient negative effect at week 2 ( $p < 0.05$ ). The combined effects of warming and Cu were more pronounced and led to a significant decrease ( $p < 0.05$ ) in chl *a* at week 3 (23°C–Cu and 28°C–Cu) and week 4 (23°C–Cu) compared to 18°C–Control microcosms.

The warming stress alone had no effect on photosynthetic efficiency, which remained stable during 4 weeks in Control microcosms ( $0.58 \pm 0.03$ ) without significant difference between temperatures ( $p > 0.05$ ; Figure 3B). Throughout the experiment and for each temperature tested, photosynthetic efficiency was slightly higher in Cu-exposed communities ( $0.63 \pm 0.02$ ), although the difference only reached significance after 4 weeks at

18°C ( $p < 0.05$ ). The combined effect of warming and Cu led to a significant, but only transient, increase of photosynthetic efficiency at week 2 in both 23°C–Cu and 28°C–Cu microcosms ( $p < 0.05$ ) compared to 18°C–Control microcosms.

## Diatom Assemblage Structure

The initial diatom assemblage (i.e., inoculum) sampled in the Morcille River was characterized by a higher specific richness ( $31 \pm 3$ ) than those sampled in the microcosms after a 4-week growing period (7 to 20 species according to temperature and Cu exposure). The 17 dominant diatom species (occurring at more than 3% relative abundance in at least one sample, including initial inoculum) are listed in Table 2. The initial diatom assemblage was dominated by three main species (i.e., *Cocconeis pseudolineata*, *Cocconeis placentula*, *Rhoicosphenia abbreviata*), which each represented >10% of total diatom assemblage.

Applied individually, the warming stress led to a significant decrease in specific richness but only at 28°C. In Control microcosms, species richness was similar between 18 and 23°C ( $20 \pm 0$ ) but was threefold lower at 28°C ( $7 \pm 1$ ). After 4 weeks at 18°C, Control communities were dominated by *Fragilaria gracilis* (FGRA) and *Nitzschia palea* (NPAL), which represented about 33 and 26%, respectively, of total relative diatom abundance. Under warming stress alone, the proportion of NPAL and FGRA was modified, with a gradual increase in proportion of FGRA which became strongly dominant at 23°C ( $63.9 \pm 2.3\%$ ) and especially at 28°C ( $97.0 \pm 2.5\%$ ), while NPAL followed a reverse trend, accounting for less than 3% of total diatoms at 28°C.

Cu stress alone exerted the opposite effect, inducing an increase in proportion of NPAL and a decrease in proportion of FGRA, which represented about 76 and 6%, respectively, of total relative diatom abundance at week 4. Under Cu exposure, no drastic change was observed with increasing temperature, as illustrated by both the relative abundance of these two dominant diatom species and specific richness ( $14 \pm 3$ ) which were relatively similar at the three temperatures tested.

The proportion of *Achnanthyidium minutissimum* (ADMI), which was well represented at 18°C in the Control communities ( $17.7 \pm 5.3\%$ ), significantly decreased under the two kinds of stresses, both alone and in combination.

## Tolerance Assessment

### Phototrophic communities

Applied individually, the warming stress had no significant effect on the levels of phototrophic community tolerance to Cu, as illustrated by the lack of significant difference ( $p > 0.05$ ) between EC<sub>50</sub> values obtained from toxicity tests on the photosynthetic efficiency of Control communities growing at 18, 23, and 28°C (Figure 4A). Whatever the tested temperature, the tolerance levels measured in Cu microcosms were higher than those measured in Control communities. However, significant differences ( $p < 0.05$ ) were only detected at 23°C, due to a very high EC<sub>50</sub> value obtained with Cu-exposed communities ( $283.8 \pm 27.0 \text{ mg L}^{-1}$ )

### Heterotrophic communities

The Cu tolerance assessment for heterotrophic communities was based on three extra-enzymatic activities (β-Glu, Lap, Pase). The

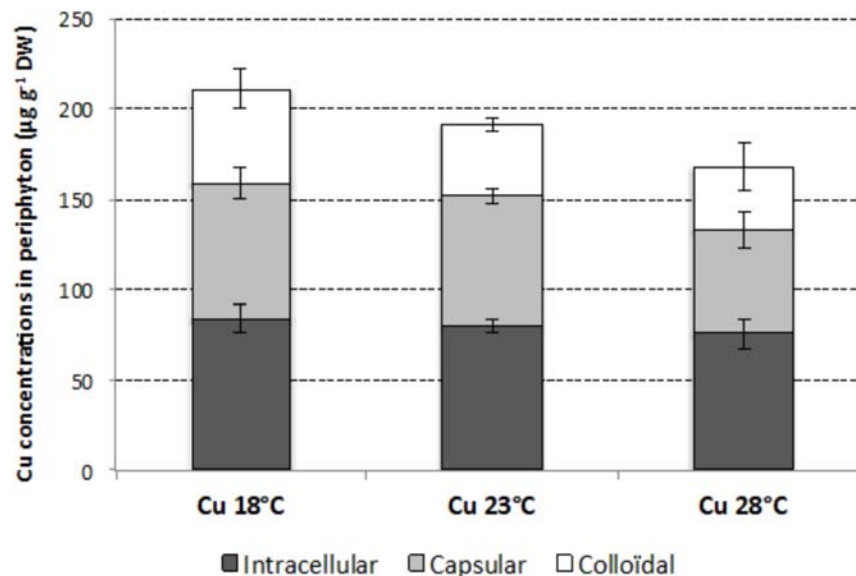


**FIGURE 2** | Mean ( $\pm$ SD;  $n = 3$ ) intracellular, capsular, and colloidal concentrations of Cu in periphyton ( $\mu\text{g g}^{-1}$  dry weight) at week 4, in the Cu-exposed microcosms incubated at 18, 23, and 28°C.

short-term toxicity tests performed using Pase activity revealed no acute effect of Cu on this parameter in our experimental conditions (data not shown). Accordingly, no  $\text{EC}_{50}$  values were determined.

Applied individually, the warming stress had a significant influence ( $p < 0.05$ ) on the tolerance levels estimated from toxicity tests on both  $\beta$ -Glu (**Figure 4B**) and Lap (**Figure 4C**) activities. However, the direction of temperature effects was reversed according to activity investigated. Results from the toxicity tests on  $\beta$ -Glu (**Figure 4B**) and Lap (**Figure 4C**) activities showed a gradual increase and a gradual decrease, respectively, in the tolerance of Control communities to acute Cu exposure when temperature increased, with significant differences between 18 and 28°C in both cases ( $p < 0.05$ ).

Cu stress alone only had a significant effect on the tolerance estimated with  $\beta$ -Glu activity (**Figure 4B**,  $p < 0.05$ ), leading to a 20-fold increase in  $\text{EC}_{50}$  values of Cu-exposed communities ( $1.02 \pm 0.55 \text{ mg L}^{-1}$ ) compared to Control communities ( $0.05 \pm 0.03 \text{ mg L}^{-1}$ ) under 18°C conditions. In contrast, Lap activity showed no significant difference at 18°C between Control ( $1.75 \pm 0.19 \text{ mg L}^{-1}$ ) and Cu-exposed ( $2.20 \pm 0.12 \text{ mg L}^{-1}$ ) communities, which were nevertheless slightly more tolerant to these metals (**Figure 4C**,  $p > 0.05$ ).

The combined effect of warming and Cu on tolerance levels was also variable according to activity measured. There was no effect of temperature on  $\text{EC}_{50}$  values of Cu-exposed communities based on  $\beta$ -Glu activity measurements (**Figure 4B**,  $p > 0.05$ ). Consequently, and due to the warming-induced increase in tolerance levels of Control communities based on  $\beta$ -Glu activity, there was no significant difference ( $p > 0.05$ ) between Control and Cu-exposed communities at 28°C (in contrast to 18 and 23°C). Based on Lap activity, tolerance levels of Cu-exposed communities decreased with

temperature, leading to a significant difference between 18 and 28°C (**Figure 4C**,  $p < 0.05$ ) as observed with Control communities. However, this decrease was less pronounced in Cu-exposed communities (Lap  $\text{EC}_{50} = 1.44 \pm 0.35 \text{ mg L}^{-1}$  at 28°C) than in Control communities ( $0.64 \pm 0.18 \text{ mg L}^{-1}$  at 28°C). Consequently, there was a significant difference ( $p < 0.05$ ) between tolerance levels of Control and Cu-exposed communities at 28°C (in contrast to 18 and 23°C).

## DISCUSSION

### Influence of Experimental Warming on the Vulnerability of Phototrophic Communities to Cu Toxicity

In accordance with our first hypothesis, temperature had significant effects on the structure of diatom assemblages of Control communities. Taxonomic analysis revealed a shift in diatom assemblage composition with increasing temperature, as previously shown by Morin et al. (2017), thus leading to a strong decrease in diversity after 4-week growth at 28°C. This result was consistent with Larras et al. (2013) who also observed a decrease in diatom diversity in periphyton communities between 18 and 28°C. In our study, increasing temperatures selected *Fragilaria gracilis* (FGRA), which accounted for more than 95% of total diatoms at 28°C at the end of the experiment (week 4), suggesting that this species was particularly adapted to the temperature increase. Despite this marked shift in diatom assemblages, and contrary to Lambert et al. (2017), we found no significant effect of temperature on total algal biomass nor on photosynthetic efficiency.

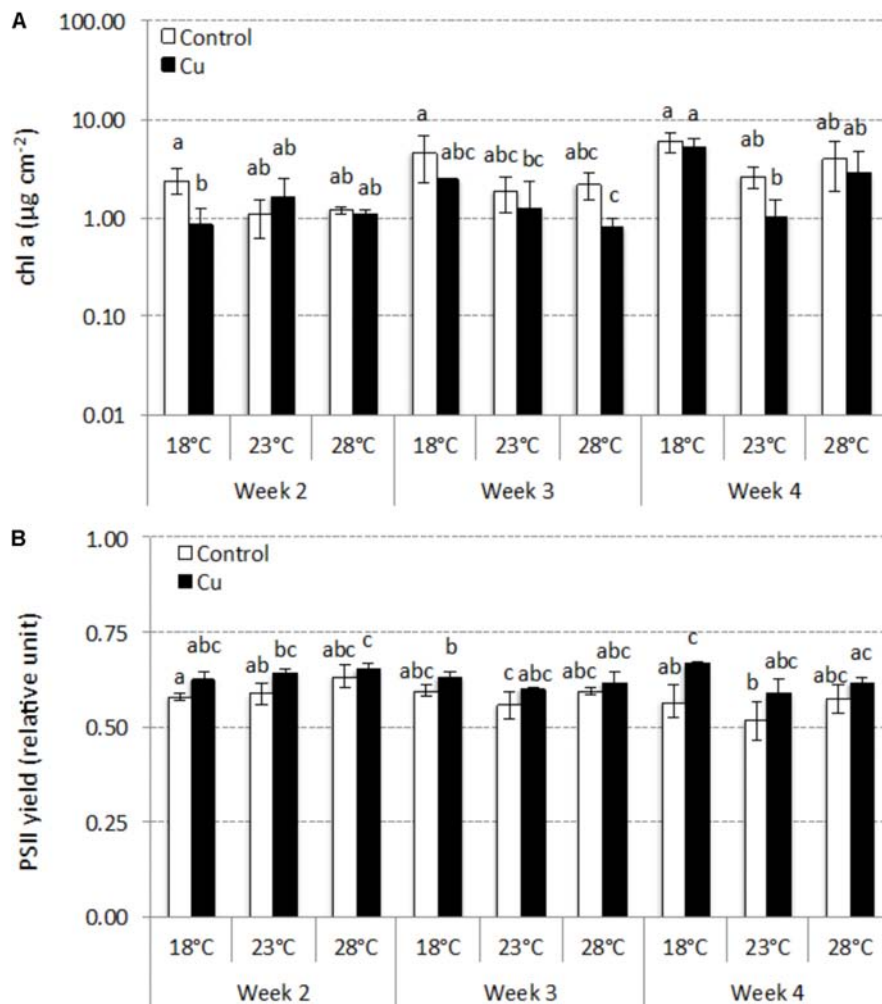


**FIGURE 3** | Time-course of concentrations of chlorophyll a (mean  $\pm$  SD,  $\mu\text{g cm}^{-2}$ ;  $n = 3$ ) **(A)** and PSII yield (mean  $\pm$  SD, relative units;  $n = 3$ ) **(B)** between week 2 and week 4 in Control and Cu-exposed microcosms incubated at 18, 23, and 28°C. Different letters indicate significant differences between treatments (thermal and exposure context) at a given sampling time (ANOVA,  $p < 0.05$ ).

This was consistent with the findings of Pesce et al. (2009), who reported that effects of environmental stressors on microbial diversity (i.e., algal and bacterial composition) are not always detectable with community-level endpoints such as algal biomass and microbial activities, according to the concept of functional redundancy (Lawton and Brown, 1993).

Even more surprisingly, we did not find significant difference in the tolerance level of Control phototrophic microbial communities to Cu (based on  $EC_{50}$  estimated from photosynthetic yield measurement) after a 4-week growing period at 18, 23, and 28°C. These results diverge from Lambert et al. (2017) and Morin et al. (2017), who previously observed that experimental warming (from 18 to 28°C and from 8 to 23°C, respectively) significantly decreased the basal tolerance of phototrophic periphyton to acute Cu exposure. In these previous studies, changes in basal tolerance were potentially attributable to changes in phototrophic community

structure as well as to a physiological stress induced by the temperature increase, which decreased photosynthetic activity and weakened the communities exposed to experimental warming. Here, the lack of significant effect of temperature on the photosynthetic efficiency of Control phototrophic communities suggests that the experimental warming did not drastically affect their physiological state. Moreover, the observed changes in structure of the Control phototrophic communities did not modify their vulnerability to acute Cu toxicity. This suggests that the temperature-induced species succession led to the replacement of the most temperature-sensitive species by species that are less temperature-sensitive but relatively similarly Cu-sensitive. Since the experimental warming mainly led to an increase in proportion of FGRA, which became strongly dominant at 23 and 28°C, to the expense of *Nitzschia palea* (NPAL) and *Achnanthydium minutissimum* (ADMI), it could be hypothesized that these three species exhibit comparable sensitivity to Cu. Both ADMI

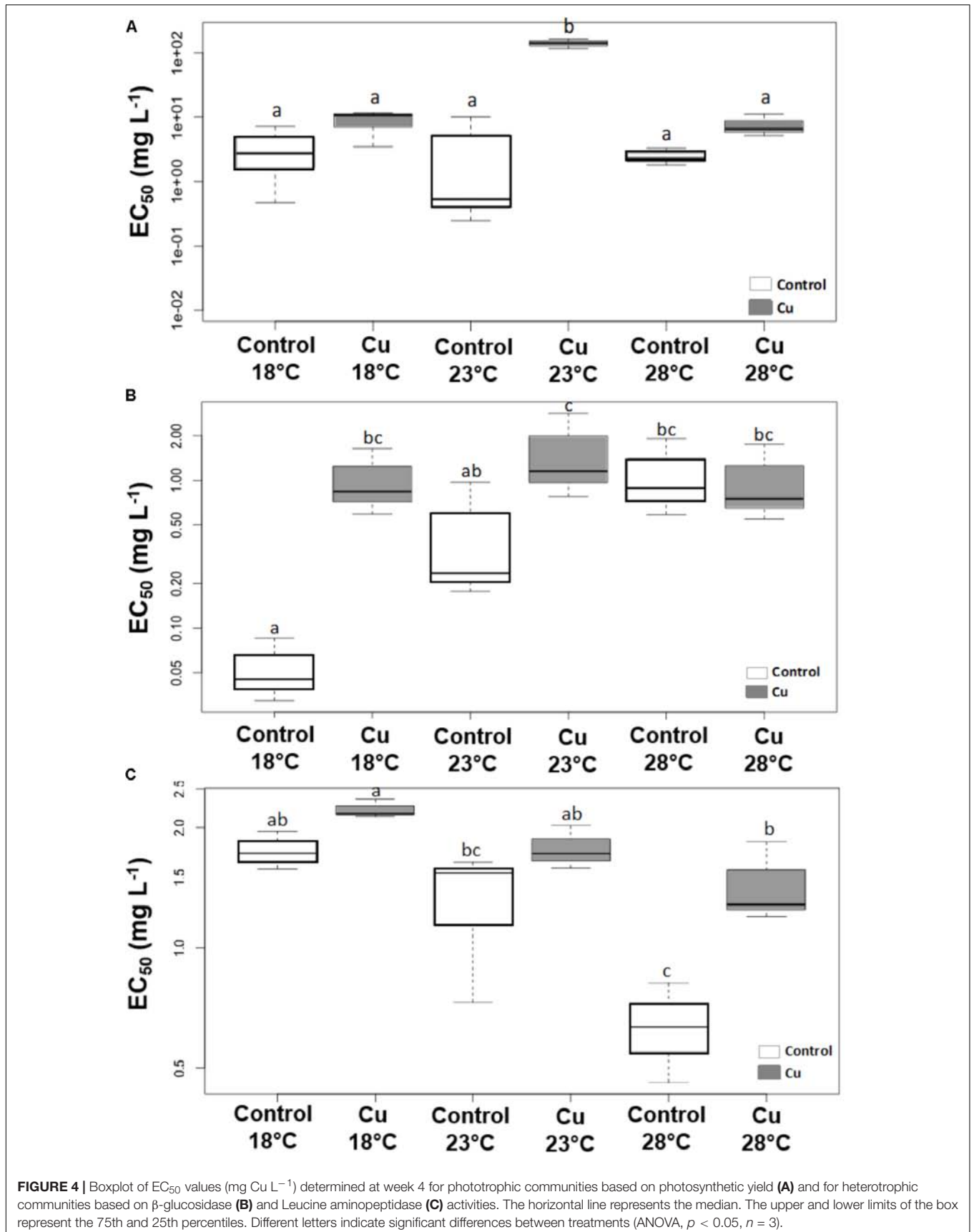
and FGRA (Morin et al., 2012a,b) were previously reported to be tolerant to metals. The tolerance of FGRA to Cu was confirmed here, since this species was well represented in Cu microcosms with mean proportions varying between 5.7 and 11.6% according to temperature tested. In addition, chronic Cu exposure mainly selected for NPAL, which was highly predominant in Cu-exposed communities whatever the temperature. Roussel et al. (2007) and Tien (2004) already highlighted that NPAL tends to be abundant in periphyton growing in metal-polluted waters. All these elements suggest that 4-week Control communities were mainly composed of relatively Cu-tolerant diatom species, whatever the temperature conditions. This could explain why EC<sub>50</sub> values obtained in Control communities at the three tested temperatures (i.e., mean value higher than 3.0 mg L<sup>-1</sup>) were relatively high compared to EC<sub>50</sub> values (i.e., 0.2–3.0 mg L<sup>-1</sup>) measured previously using the same toxicity test protocol with Control communities sourced from the same sampling site and grown for 3 weeks in the same experimental conditions (Lambert et al., 2017). Comparison of our results against Lambert et al. (2017) and Morin et al. (2017) finds that the influence of warming on the basal tolerance of phototrophic biofilm communities to Cu is strongly conditioned by the initial intrinsic characteristics of the community, especially initial distribution of temperature-sensitive (and temperature-tolerant) and/or Cu-sensitive (and Cu-tolerant) species and the temperature-induced succession.

Without temperature stress (i.e., at 18°C), the chronic Cu exposure delayed algal growth. Chl a concentrations were significantly lower in Cu-exposed than Control communities at week 2. Guasch et al. (2002) also observed growth inhibition with periphyton grown for 16 days at 16°C under comparable

Cu exposure conditions (i.e., 10–17 µg L<sup>-1</sup>). At 18°C, Cu exposure also had significant effects on algal structure, with a shift in diatom assemblage composition, as shown in other studies (Serra et al., 2009; Morin et al., 2012b). At week 4, Cu exposure mainly selected for NPAL, which was about threefold more represented in Cu-exposed communities (i.e., 76%) than Control communities at 18°C. However, and despite the selection of this Cu-tolerant species at 18°C, no Cu-induced tolerance was found at phototrophic community level. Indeed, no difference in EC<sub>50</sub> values based on photosynthetic yield was observed between Control and Cu-exposed communities at week 4, even if Cu-exposed communities appeared slightly more tolerant to acute Cu exposure. This lack of significant difference could be explained in the relatively high tolerance level observed in Control communities (see earlier) and by the moderate tolerance level of Cu-exposed communities (i.e., EC<sub>50</sub> close to 5 mg L<sup>-1</sup>) which was far lower than EC<sub>50</sub> values observed in previous studies (e.g., about 45 mg L<sup>-1</sup> in Lambert et al., 2017). The lack of gain in Cu tolerance suggests a limited exposure of periphytic phototrophic microorganisms to Cu. This hypothesis is supported by the observation of a slight stimulation of the photosynthetic efficiency of Cu-exposed communities, at 18°C, over the study (with a significant difference compared to Control communities at week 4), which could reflect a hormesis effect (i.e., favorable biological response to low exposure to stressor), in contrast to previous studies where Cu exposure reduced biofilm photosynthesis efficiency (e.g., Serra and Guasch, 2009; Lambert et al., 2012). Cu analysis in periphyton also argues for this hypothesis, as periphyton communities were characterized by low Cu bioaccumulation, with total Cu concentrations reaching only 168–211 µg Cu g<sup>-1</sup> dw, in contrast to Lambert et al. (2016) who found mean total Cu

**TABLE 2** | Mean relative abundances (±SD; *n* = 3) of the 17 dominant diatom species (i.e., representing more than 3% relative abundances in at least one sample) for the inoculum and the six thermal and exposure contexts at week 4.

	Inoculum	18°C		23°C		28°C	
		Control	Cu	Control	Cu	Control	Cu
<i>Achnanthes minutissimum</i>	8.6 ± 2.3	17.7 ± 5.3	3.2 ± 1.0	1.4 ± 0.5	0.5 ± 0.5	0.5 ± 0.3	0.6 ± 0.3
<i>Amphora inariensis</i>	7.4 ± 1.8	0.0 ± 0.0	0.1 ± 0.2	0.0 ± 0.0	0.0 ± 0.0	0.1 ± 0.2	0.0 ± 0.0
<i>Amphora pediculu</i>	5.4 ± 1.3	0.2 ± 0.3	0.1 ± 0.2	0.0 ± 0.0	0.0 ± 0.0	0.0 ± 0.0	0.0 ± 0.0
<i>Cyclotella comensis</i>	0.0 ± 0.0	1.8 ± 0.5	0.0 ± 0.0	1.3 ± 0.2	0.1 ± 0.2	0.0 ± 0.0	0.0 ± 0.0
<i>Cyclotella sp.</i>	0.0 ± 0.0	4.2 ± 2.1	0.2 ± 0.1	3.3 ± 0.0	0.0 ± 0.0	0.3 ± 0.4	0.0 ± 0.0
<i>Cocconeis pseudolineata</i>	15.6 ± 5.3	0.1 ± 0.1	0.0 ± 0.0	0.1 ± 0.3	0.2 ± 0.3	0.0 ± 0.0	0.1 ± 0.2
<i>Cocconeis placentula var. lineata</i>	11.4 ± 1.8	0.8 ± 1.0	1.0 ± 0.8	0.5 ± 0.4	1.1 ± 0.4	0.1 ± 0.1	0.1 ± 0.2
<i>Eolima minima</i>	5.7 ± 2.3	1.2 ± 0.6	2.4 ± 0.7	1.6 ± 0.1	0.9 ± 0.1	0.1 ± 0.2	2.3 ± 0.9
<i>Fragilaria gracilis</i>	0.5 ± 0.5	32.7 ± 15.1	5.7 ± 3.3	63.9 ± 2.2	7.8 ± 2.2	97.0 ± 2.5	11.6 ± 7.4
<i>Gomphonema exilissimum</i>	0.0 ± 0.0	3.4 ± 4.0	0.0 ± 0.0	3.4 ± 0.3	0.3 ± 0.3	0.0 ± 0.0	0.0 ± 0.0
<i>Mayamaea permissis</i>	0.4 ± 0.3	5.5 ± 3.6	0.9 ± 1.3	1.3 ± 0.1	0.2 ± 0.1	0.0 ± 0.0	0.0 ± 0.0
<i>Navicula gregaria</i>	2.2 ± 1.0	0.0 ± 0.0	0.0 ± 0.0	0.0 ± 0.0	0.0 ± 0.0	0.2 ± 0.2	0.0 ± 0.0
<i>Nitzschia linearis</i>	0.0 ± 0.0	0.5 ± 0.2	1.8 ± 1.3	0.5 ± 1.2	2.7 ± 1.2	0.0 ± 0.0	0.5 ± 0.6
<i>Nitzschia palea</i>	1.8 ± 0.4	26.4 ± 12.5	75.6 ± 10.1	15.3 ± 4.3	83.1 ± 4.3	0.8 ± 1.4	80.9 ± 8.4
<i>Planothidium frequentissimum</i>	3.2 ± 0.8	0.2 ± 0.1	0.3 ± 0.3	0.2 ± 0.2	0.1 ± 0.2	0.0 ± 0.0	0.2 ± 0.2
<i>Planothidium lanceolatum</i>	7.7 ± 1.6	1.1 ± 0.4	5.1 ± 3.5	1.3 ± 0.8	1.2 ± 0.8	0.0 ± 0.0	0.0 ± 0.0
<i>Rhoicosphenia abbreviata</i>	11.9 ± 1.9	0.0 ± 0.0	0.0 ± 0.0	0.2 ± 0.0	0.0 ± 0.0	0.2 ± 0.2	0.0 ± 0.0



concentrations of  $1580 \mu\text{g Cu g}^{-1} \text{ dw}$  under similar temperatures (i.e., 18 and  $23^\circ\text{C}$ ) and comparable dissolved Cu concentrations (i.e.,  $3\text{--}20 \mu\text{g L}^{-1}$ ). Moreover, Cu concentrations measured here in the intracellular and capsular fractions were almost fourfold lower than those in the corresponding fraction (i.e., so-called “internalized”) measured, at 18 and  $23^\circ\text{C}$ , in Lambert et al. (2016). The low Cu uptake by periphyton was in line with stable dissolved Cu concentrations measured in microcosms after each water renewal, contrary to previous microcosm studies showing a decrease in dissolved Cu concentrations due to high Cu uptake rates by periphyton (Knauer et al., 1997; Boivin et al., 2007; Lambert et al., 2012, 2016). Nevertheless, the lack of decreasing dissolved concentrations must be viewed with caution, since water sampling was performed 2 h after the addition of dissolved Cu. Indeed, Levy et al. (2007) reported that 1 h of Cu exposure was sufficient to ensure equilibrium between Cu in solution and Cu in marine algal cells. Accordingly, we cannot exclude that a decrease in Cu dissolved concentrations could have occurred immediately after Cu addition in the channels. The observed low Cu bioaccumulation could be explained by (i) high pH values (ranging between 8.3 and 9.7 during the experiment) which could induce a decrease in Cu bioavailability by favoring precipitated forms of Cu and/or by (ii) a strong biodilution of Cu in the periphyton biomass. This last hypothesis was supported by the fact that the periphyton biomass measured here at  $18^\circ\text{C}$  was a 1000-fold higher than measured at the same temperature by Lambert et al. (2016). Furthermore, this high periphyton biomass could have accelerated Cu adsorption, and prevented Cu internalization, due to an increase in the number of fixation sites in the EPS matrix.

Cu bioaccumulation, while being statistically non-significant, nevertheless tended to decrease with increasing temperature, as previously shown (Lambert et al., 2016) mainly because of a decrease in externalized Cu concentrations represented by colloidal and capsular fractions. It suggests that communities growing at 23 and  $28^\circ\text{C}$  under chronic Cu exposure were less exposed than those growing at  $18^\circ\text{C}$ . Nevertheless, and as observed with Control communities, temperature had no effect on photosynthetic efficiency of Cu-exposed communities. Furthermore, temperature combined with Cu had no effect on the structure of diatom assemblages, in contrast to Control communities, which suggests that Cu exposure was the main factor controlling the evolution of Control diatom assemblages. NPAL remained dominant whatever the temperature tested, showing that this species, which was favored by Cu exposure, was also particularly adapted to the temperature increase. In accordance with the observed stability in diatom assemblage structure, the tolerance levels of phototrophic Cu-exposed communities measured at week 4 were very similar at 18 and  $28^\circ\text{C}$ . However, and surprisingly, a strong increase in  $\text{EC}_{50}$  values was observed at  $23^\circ\text{C}$ . Based on our data, we cannot explain why this jump in tolerance occurred at this temperature. Note, however, that this jump occurred simultaneously with strong algal growth inhibition in Cu-exposed communities at  $23^\circ\text{C}$ , which could reflect a functional cost of adaptation (i.e., tolerance increase), as suggested by Navarro et al. (2008) who observed

a reduction in chlorophyll a concentrations in biofilms which increased their tolerance to ultraviolet radiation.

## Influence of Experimental Warming on the Vulnerability of Heterotrophic Communities to Cu Toxicity

PICT analysis was performed on heterotrophic communities using three enzymatic activities, i.e.,  $\beta$ -Glu, Lap, and Pase. The results obtained and the resulting interpretations varied greatly according to activity considered. As mentioned above, Cu had no acute toxicity on Pase activity, thus precluding any conclusions based on this heterotrophic parameter. Conversely, acute exposure to Cu strongly inhibited  $\beta$ -Glu and Lap activities. Analysis of the dose–response curves obtained with those enzymatic activities showed a strong influence of temperature on the sensitivity to Cu of Control heterotrophic communities. When considering  $\beta$ -Glu activity, we observed an increase in tolerance levels of Control communities with increasing temperatures, as proposed in our second hypothesis, which was based on the study of Boivin et al. (2005). Thus, based on this enzymatic activity, Control communities growing at 23 and  $28^\circ\text{C}$  appeared to be respectively about 8- and 18-fold more Cu-tolerant than those growing at  $18^\circ\text{C}$ . This suggests that the experimental warming increased the basal tolerance of heterotrophic periphyton to acute exposure to Cu, thus decreasing their vulnerability toward this toxic stress. This is in line with a field study by Faburé et al. (2015) who observed that Cu tolerance of natural biofilms (estimated from toxicity tests on the  $\beta$ -Glu activity) tended to increase during warm seasons.

Without temperature stress (i.e., at  $18^\circ\text{C}$ ), and despite the limited Cu bioaccumulation in periphyton discussed above, heterotrophic communities chronically exposed to Cu exhibited significantly higher Cu tolerance levels than Control communities when bioassays were based on  $\beta$ -Glu activity measurements. This enzymatic activity has previously been successfully used to show an increase in Cu tolerance in PICT approaches in both experimental (Fechner et al., 2010; Tlili et al., 2010; Lambert et al., 2012) and *in situ* approaches (Fechner et al., 2012; Faburé et al., 2015). Contrary to the observation made with Control communities, the experimental warming had no influence on the tolerance levels of Cu-exposed communities obtained from the  $\beta$ -Glu activity. Accordingly, and given the fact that this tolerance level gradually increased with increasing temperature in Control communities, there was no difference in  $\beta$ -Glu  $\text{EC}_{50}$  values obtained at  $28^\circ\text{C}$  between Control and Cu-exposed communities. These results suggest that the chronic Cu exposure as well as the experimental warming led to a selection of heterotrophic microorganisms, which were more tolerant to Cu, revealing in this case a possible co-tolerance process.

Surprisingly, results obtained with the PICT approach using Lap activity came to the opposite conclusion. Indeed, in this case, the tolerance levels of Control communities strongly decreased with increasing temperatures, and were almost threefold lower at  $28^\circ\text{C}$  than at  $18^\circ\text{C}$ . The same trend was observed in Cu-exposed communities, even if the decrease in tolerance was more moderate, with an about 1.5-fold lower tolerance level at

28°C than at 18°C. Accordingly, it appeared from the PICT approach performed using Lap activity that the experimental warming increased the vulnerability of periphyton heterotrophic communities to acute Cu toxicity, whatever the previous exposure history to this metal.

In line with the PICT concept, chronic Cu exposure was also an important driver of the vulnerability of the Lap activity to subsequent acute exposure to Cu. Indeed, whatever the temperature tested and despite a lack of statistical difference at 18°C, the tolerance levels measured from Lap analysis were higher with Cu-exposed communities than with Control ones. Contrary to  $\beta$ -Glu activity, increasing temperature increased the difference in sensitivity to acute Cu toxicity between Control and Cu-exposed communities, revealing a lack of any co-tolerance process based on the Lap activity.

In summary, we demonstrated using three functional parameters (photosynthesis, Lap, and  $\beta$ -Glu) that the influence of temperature on the vulnerability of phototrophic and heterotrophic microbial communities to Cu toxicity can vary greatly according to function considered. A similar conclusion was previously reached by Tlili et al. (2010) who found that the relative influence of chronic exposure to Cu and phosphorus, respectively, on functional vulnerability of microbial communities to subsequent Cu exposure depended on the function studied (i.e., photosynthesis, substrate-induced respiration, Lap, and  $\beta$ -Glu). Taken together, these results argue that it is crucial to consider different functional compartments and different functional descriptors in order to better assess the vulnerability of periphyton to multiple stressors. From an ecotoxicological standpoint, it should be interesting to explore whether our findings are specific of Cu or whether they are applicable to other metals. Tlili et al. (2011) observed that phototrophic and heterotrophic biofilm communities exposed to Cu were more tolerant to zinc (Zn) and *vice versa* (with Cu being more toxic than Zn). It reflects a positive co-tolerance between these metals, which was attributed by the authors to similar modes of action and/or detoxification. Accordingly, we should expect that the influence of temperature on the vulnerability

of communities to Cu and Zn (or others metals with similar modes of action and/or detoxification) toxicity would have been quite similar. In contrast, this hypothesis is probably not applicable with metals exhibiting a different mode of action or involving different detoxification pathways, such as arsenic (As). From an ecological standpoint, and given the fact that the functions studied are related to different biogeochemical cycles (i.e., photosynthesis and  $\beta$ -Glu: carbon cycle; Lap: nitrogen cycle), this kind of multi-function approach could allow to better assess and predict the risks of multiple stressors for ecosystem balance and functioning. Moreover it should be important to validate *in situ* the hypotheses derived from such experimental studies by performing field-based studies at large geographical and/or temporal scale.

## AUTHOR CONTRIBUTIONS

SP, A-SL, MC, and AD conceived and designed the study. A-SL performed the experiments and samplings. A-SL, AF, SM, and AD analyzed the samples and all co-authors analyzed and interpreted the data. SP and A-SL drafted the article. AF, SM, MC, and AD critically revised the article. All co-authors approved the final submitted version of the manuscript.

## FUNDING

This work was supported by the Long-Term Ecological Research (LTER) project 'Zone Atelier du Bassin du Rhône' (ZABR).

## ACKNOWLEDGMENTS

The authors thank Bernard Motte, Christophe Rosy, Bernadette Volat, the staff of the Water Chemistry Laboratory (LAMA), and especially Josiane Gahou for providing technical support, and ATT for language-proofing the manuscript.

## REFERENCES

- Adams, M. S., Dillon, C. T., Vogt, S., Lai, B., Stauber, J. L., and Jolley, D. F. (2016). Copper uptake, intracellular localization, and speciation in marine microalgae measured by synchrotron radiation X-ray fluorescence and absorption microspectroscopy. *Environ. Sci. Technol.* 50, 8827–8839. doi: 10.1021/acs.est.6b00861
- Aguilera, A., Souza-Egipsy, V., San Martín-Uriz, P., and Amils, R. (2008). Extraction of extracellular polymeric substances from extreme acidic microbial biofilms. *Appl. Microbiol. Biotechnol.* 78, 1079–1088. doi: 10.1007/s00253-008-1390-9
- Ancion, P. Y., Lear, G., Dopheide, A., and Lewis, G. D. (2013). Metal concentrations in stream biofilm and sediments and their potential to explain biofilm microbial community structure. *Environ. Pollut.* 173, 117–124. doi: 10.1016/j.envpol.2012.10.012
- Battin, T. J., Kaplan, L. A., Newbold, J. D., and Hansen, C. M. (2003). Contributions of microbial biofilms to ecosystem processes in stream mesocosms. *Nature* 426, 439–442. doi: 10.1038/nature02152
- Besaury, L., Bodilis, J., Delgas, F., Andrade, S., De la Iglesia, R., Ouddane, B., et al. (2013). Abundance and diversity of copper resistance genes *cusA* and *copA* in microbial communities in relation to the impact of copper on Chilean marine sediments. *Mar. Pollut. Bull.* 67, 16–25. doi: 10.1016/j.marpolbul.2012.12.007
- Blanck, H., Wänkberg, S. -Å., and Molander, S. (1988). "Pollution-induced community tolerance - a new ecotoxicological tool," in *Functional Testing of Aquatic Biota for Estimating Hazards of Chemicals*, eds J. Cairns Jr. and J. R. Pratt (Philadelphia, PA: ASTM STP), 219–230. doi: 10.1520/STP26265S
- Boivin, M. E. Y., Greve, G. D., Garcia-Meza, J. V., Massieux, B., Sprenger, W., Kraak, M. H. S., et al. (2007). Algal-bacterial interactions in metal contaminated floodplain sediments. *Environ. Pollut.* 145, 884–894. doi: 10.1016/j.envpol.2006.05.003
- Boivin, M. E. Y., Massieux, B., Breure, A. M., van den Ende, F. P., Greve, G. D., Rutgers, M., et al. (2005). Effects of copper and temperature on aquatic bacterial communities. *Aquat. Toxicol.* 71, 345–356. doi: 10.1016/j.aquatox.2004.12.004
- Bradl, H. B. (2005). "Sources and origins of heavy metals," in *Heavy Metals in the Environment: Origin, Interaction and Remediation*, ed. H. B. Bradl (London: Elsevier), 1–27.
- Bruins, M. R., Kapil, S., and Oehme, F. W. (2000). Microbial resistance to metals in the environment. *Ecotoxicol. Environ. Saf.* 45, 198–207. doi: 10.1006/eesa.1999.1860

- Cid, A., Herrero, C., Torres, E., and Abalde, J. (1995). Copper toxicity on the marine microalga *Phaeodactylum tricoratum*: effects on photosynthesis and related parameters. *Aquat. Toxicol.* 31, 165–174. doi: 10.1016/0166-445X(94)00071-W
- Clements, W. H., and Rohr, J. R. (2009). Community responses to contaminants: using basic ecological principles to predict ecotoxicological effects. *Environ. Toxicol. Chem.* 28, 1789–1800. doi: 10.1897/09-140.1
- Easterling, D. R., Meehl, G. A., Parmesan, C., Changnon, S. A., Karl, T. R., and Mearns, L. O. (2000). Climate extremes: observations, modeling, and impacts. *Science* 289, 2068–2074. doi: 10.1126/science.289.5487.2068
- Faburé, J., Dufour, M., Autret, A., Uher, E., and Fechner, L. C. (2015). Impact of an urban multi-metal contamination gradient: metal bioaccumulation and tolerance of river biofilms collected in different seasons. *Aquat. Toxicol.* 159, 276–289. doi: 10.1016/j.aquatox.2014.12.014
- Fechner, L. C., Gourlay-Francé, C., Uher, E., and Tusseau-Vuillemin, M. H. (2010). Adapting an enzymatic toxicity test to allow comparative evaluation of natural freshwater biofilms' tolerance to metals. *Ecotoxicology* 19, 1302–1311. doi: 10.1007/s10646-010-0517-9
- Fechner, L. C., Versace, F., Gourlay-Francé, C. T., and Usseau-Vuillemin, M.-H. (2012). Adaptation of copper community tolerance levels after biofilm transplantation in an urban river. *Aquat. Toxicol.* 106–107, 32–41. doi: 10.1016/j.aquatox.2011.09.019
- Guasch, H., Paulsson, M., and Sabater, S. (2002). Effect of copper on algal communities from oligotrophic calcareous streams. *J. Phycol.* 38, 241–248. doi: 10.1046/j.1529-8817.2002.01114.x
- Holmstrup, M., Bindesbol, A. M., Oostingh, G. J., Duschl, A., Scheil, V., Kohler, H. R., et al. (2010). Interactions between effects of environmental chemicals and natural stressors: a review. *Sci. Total Environ.* 408, 3746–3762. doi: 10.1016/j.scitotenv.2009.10.067
- Knauer, K., Behra, R., and Sigg, L. (1997). Effects of free Cu<sup>2+</sup> and Zn<sup>2+</sup> ions on growth and metal accumulation in freshwater algae. *Environ. Toxicol. Chem.* 16, 220–229. doi: 10.1002/etc.5620160218
- Ladomersky, E., and Petris, M. J. (2015). Copper tolerance and virulence in bacteria. *Metalomics* 7, 957–964. doi: 10.1039/c4mt00327f
- Lambert, A. S., Dabrin, A., Foulquier, A., Morin, S., Rosy, C., Coquery, M., et al. (2017). Influence of temperature in pollution-induced community tolerance approaches used to assess effects of copper on freshwater phototrophic periphyton. *Sci. Total Environ.* 607–608, 1018–1025. doi: 10.1016/j.scitotenv.2017.07.035
- Lambert, A. S., Dabrin, A., Morin, S., Gahou, J., Foulquier, A., Coquery, M., et al. (2016). Temperature modulates phototrophic periphyton response to chronic copper exposure. *Environ. Pollut.* 208, 821–829. doi: 10.1016/j.envpol.2015.11.004
- Lambert, A. S., Morin, S., Artigas, J., Volat, B., Coquery, M., Neyra, M., et al. (2012). Structural and functional recovery of microbial periphyton after a decrease in copper exposure: influence of the presence of pristine communities. *Aquat. Toxicol.* 109, 118–126. doi: 10.1016/j.aquatox.2011.12.006
- Lambert, A. S., Pesce, S., Foulquier, A., Gahou, J., Coquery, M., and Dabrin, A. (2015). Improved short-term toxicity test protocol to assess metal tolerance in phototrophic periphyton: toward standardization of PICT approaches. *Environ. Sci. Pollut. Res.* 22, 4037–4045. doi: 10.1007/s11356-014-3505-4
- Larras, F., Lambert, A. S., Pesce, S., Rimet, F., Bouchez, A., and Montuelle, B. (2013). The effect of temperature and a herbicide mixture on freshwater periphytic algae. *Ecotoxicol. Environ. Saf.* 98, 162–170. doi: 10.1016/j.ecoenv.2013.09.007
- Lau, T. C., Wu, X. A., Chua, H., Qian, P. Y., and Wong, P. K. (2005). Effect of exopolysaccharides on the adsorption of metal ions by *Pseudomonas* sp. CU-1. *Water Sci. Technol.* 52, 63–68. doi: 10.2166/wst.2005.0182
- Lawton, J. H., and Brown, V. K. (1993). “Redundancy in ecosystems,” in *Biodiversity and Ecosystem Function*, eds E.-D. Schulze and H. A. Mooney (Berlin: Springer), 255–270.
- Levy, J. L., Stauber, J. L., and Jolley, D. F. (2007). Sensitivity of marine microalgae to copper: the effect of biotic factors on copper adsorption and toxicity. *Sci. Total Environ.* 387, 141–154. doi: 10.1016/j.scitotenv.2007.07.016
- Loaec, M., Olier, R., and Guezennec, J. (1997). Uptake of lead, cadmium and zinc by a novel bacterial exopolysaccharide. *Water Res.* 31, 1171–1179. doi: 10.1016/S0043-1354(96)00375-2
- Montuelle, B., Dorigo, U., Bérard, A., Volat, B., Bouchez, A., Tlili, A., et al. (2010). The periphyton as a multimetric bioindicator for assessing the impact of land use on rivers: an overview of the Ardères-Morcille experimental watershed (France). *Hydrobiologia* 657, 123–141. doi: 10.1007/s10750-010-0105-2
- Morin, M., Bonet, B., Corcoll, N., Guasch, H., Bottin, M., and Coste, M. (2015). Cumulative stressors trigger increased vulnerability of diatom communities to additional disturbances. *Microb. Ecol.* 70, 585–595. doi: 10.1007/s00248-015-0602-y
- Morin, S., Cordonier, A., Lavoie, I., Arini, A., Blanco, S., Duong, T. T., et al. (2012a). “Consistency in diatom response to metal-contaminated environments,” in *Emerging and Priority Pollutants in Rivers*, eds H. Guasch, A. Ginebreda, and A. Geiszinger (Berlin: Springer), 117–146. doi: 10.1007/978-3-642-25722-3\_5
- Morin, S., Lambert, A. S., Artigas, J., Coquery, M., and Pesce, S. (2012b). Diatom immigration drives biofilm recovery after chronic copper exposure. *Freshwat. Biol.* 57, 1658–1666. doi: 10.1111/j.1365-2427.2012.02827.x
- Morin, S., Lambert, A. S., Planes Rodriguez, E., Dabrin, A., Coquery, M., and Pesce, S. (2017). Changes in copper toxicity towards diatom communities with experimental warming. *J. Hazard. Mater.* 334, 223–232. doi: 10.1016/j.jhazmat.2017.04.016
- Navarro, E., Robinson, C. T., and Behra, R. (2008). Increased tolerance to ultraviolet radiation (UVR) and cotolerance to cadmium in UVR-acclimatized freshwater periphyton. *Limnol. Oceanogr.* 53, 1149–1158. doi: 10.4319/lo.2008.53.3.1149
- Nies, D. H. (1999). Microbial heavy-metal resistance. *Appl. Microbiol. Biotechnol.* 51, 730–750. doi: 10.1007/s002530051457
- Okamoto, O. K., Pinto, E., Latorre, L. R., Bechara, E. J. H., and Colepicolo, P. (2001). Antioxidant modulation in response to metal-induced oxidative stress in algal chloroplasts. *Arch. Environ. Contam. Toxicol.* 40, 18–24. doi: 10.1007/s002440010144
- Pesce, S., Batisson, I., Bardot, C., Fajon, C., Portelli, C., Montuelle, B., et al. (2009). Response of spring and summer riverine microbial communities following glyphosate exposure. *Ecotoxicol. Environ. Saf.* 72, 1905–1912. doi: 10.1016/j.ecoenv.2009.07.004
- Prasad, N. M., Drej, K., Skawinska, A., and Stratka, K. (1998). Toxicity of cadmium and copper in *Chlamydomonas reinhardtii* wild-type (wt 2137) and cell wall deficient mutant strain (cw 15). *Bull. Environ. Contam. Toxicol.* 60, 306–311. doi: 10.1007/s001289900626
- Provenzano, M. R., El Bilali, H., Simeone, V., Baser, N., Mondelli, D., and Cesari, G. (2010). Copper contents in grapes and wines from a Mediterranean organic vineyard. *Food Chem.* 122, 1338–1343. doi: 10.1016/j.foodchem.2010.03.103
- R Development Core Team (2012). *R: A Language and Environment for Statistical Computing*. Vienna: R Foundation for Statistical Computing.
- Rabiet, M., Coquery, M., Carluet, N., Gahou, J., and Gouy, V. (2015). Transfer of metal(loid)s in a small vineyard catchment: contribution of dissolved and particulate fractions in river for contrasted hydrological conditions. *Environ. Sci. Pollut. Res.* 22, 19224–19239. doi: 10.1007/s11356-015-5079-1
- Rijstenbil, J. W., Derksen, J. W. M., Gerringa, L. J. A., Poortvliet, T. C. W., Sandee, A., Van den Berg, M., et al. (1994). Oxidative stress induced by copper: defense and damage in the marine planktonic diatom *Ditylum brightwellii* (Grunow) West, grown in continuous cultures with high and low zinc levels. *Mar. Biol.* 119, 583–590. doi: 10.1007/BF00354321
- Ritz, C., and Streibig, J. C. (2005). Bioassay analysis using R. *J. Stat. Softw.* 12, 1–22. doi: 10.18637/jss.v012.i05
- Rose, F. L., and Cushing, C. E. (1970). Periphyton: autoradiography of zinc-65 adsorption. *Science* 168, 576–577. doi: 10.1126/science.168.3931.576
- Roussel, H., Ten-Hage, L., Joachim, S., Le Cohu, R., Gauthier, L., and Bonzom, J. M. (2007). A long-term copper exposure on freshwater ecosystem using lotic mesocosms: primary producer community responses. *Aquat. Toxicol.* 81, 168–182. doi: 10.1016/j.aquatox.2006.12.006
- Sabater, S., Guasch, H., Ricart, M., Romani, A., Vidal, G., Klunder, C., et al. (2007). Monitoring the effect of chemicals on biological communities. The periphyton as an interface. *Anal. Bioanal. Chem.* 387, 1425–1434. doi: 10.1007/s00216-006-1051-8
- Sabatini, S. E., Juarez, A. B., Eppis, M. R., Bianchi, L., Luquet, C. M., and Molina, M. C. R. (2009). Oxidative stress and antioxidant defenses in two green microalgae exposed to copper. *Ecotoxicol. Environ. Saf.* 72, 1200–1206. doi: 10.1016/j.ecoenv.2009.01.003

- Serra, A., Corcoll, N., and Guasch, H. (2009). Copper accumulation and toxicity in fluvial periphyton: the influence of exposure history. *Chemosphere* 74, 633–641. doi: 10.1016/j.chemosphere.2008.10.036
- Serra, A., and Guasch, H. (2009). Effects of chronic copper exposure on fluvial systems: linking structural and physiological changes of fluvial biofilms with the instream copper retention. *Sci. Total Environ.* 407, 5274–5282. doi: 10.1016/j.scitotenv.2009.06.008
- Soldo, D., and Behra, R. (2000). Long-term effects of copper on the structure of freshwater periphyton communities and their tolerance to copper, zinc, nickel and silver. *Aquat. Toxicol.* 47, 181–189. doi: 10.1016/S0166-445X(99)00020-X
- Tien, C. J. (2004). Some aspects of water quality in a polluted lowland river in relation to the intracellular chemical levels in planktonic and epilithic diatoms. *Water Res.* 38, 1779–1790. doi: 10.1016/j.watres.2003.12.043
- Tlili, A., Bérard, A., Roulier, J. L., Volat, B., and Montuelle, B. (2010). PO43- dependence of the tolerance of autotrophic and heterotrophic biofilm communities to copper and diuron. *Aquat. Toxicol.* 98, 165–177. doi: 10.1016/j.aquatox.2010.02.008
- Tlili, A., Maréchal, M., Bérard, A., Volat, B., and Montuelle, B. (2011). Enhanced cotolerance and co-sensitivity from long-term metal exposures of heterotrophic and autotrophic components of fluvial biofilms. *Sci. Total Environ.* 409, 4335–4343. doi: 10.1016/j.scitotenv.2011.07.026
- US EPA (2010). *ECOTOX Database*. United States Environmental Protection Agency. Available at: <http://cfpub.epa.gov/ecotox/>
- Wreford, A., and Adger, W. N. (2010). Adaptation in agriculture: historic effects of heat waves and droughts on UK agriculture. *Int. J. Agric. Sustain.* 8, 278–289. doi: 10.3763/ijas.2010.0482
- Conflict of Interest Statement:** The authors declare that the research was conducted in the absence of any commercial or financial relationships that could be construed as a potential conflict of interest.

Copyright © 2018 Pesce, Lambert, Morin, Foulquier, Coquery and Dabrin. This is an open-access article distributed under the terms of the Creative Commons Attribution License (CC BY). The use, distribution or reproduction in other forums is permitted, provided the original author(s) and the copyright owner(s) are credited and that the original publication in this journal is cited, in accordance with accepted academic practice. No use, distribution or reproduction is permitted which does not comply with these terms.



# Fullerenes Influence the Toxicity of Organic Micro-Contaminants to River Biofilms

Anna Freixa<sup>1\*</sup>, Vicenç Acuña<sup>1</sup>, Marina Gutierrez<sup>1</sup>, Josep Sanchís<sup>2</sup>,  
Lúcia H. M. L. M. Santos<sup>1</sup>, Sara Rodriguez-Mozaz<sup>1</sup>, Marinella Farré<sup>2</sup>, Damià Barceló<sup>1,2</sup>  
and Sergi Sabater<sup>1,3</sup>

<sup>1</sup> Catalan Institute for Water Research, Girona, Spain, <sup>2</sup> Water and Soil Quality Research Group, Institute of Environmental Assessment and Water Research, Spanish National Research Council, Barcelona, Spain, <sup>3</sup> Research Group on Ecology of Inland Waters, Institute of Aquatic Ecology, University of Girona, Girona, Spain

## OPEN ACCESS

### Edited by:

Stéphane Pesce,  
Institut National de Recherche en  
Sciences et Technologies pour  
l'Environnement et l'Agriculture  
(IRSTEA), France

### Reviewed by:

Francesca Cappitelli,  
Università degli Studi di Milano, Italy  
Chloe Bonneau,  
IRSTEA Centre de Lyon-Villeurbanne,  
France

### \*Correspondence:

Anna Freixa  
afreixa@icra.cat

### Specialty section:

This article was submitted to  
Microbiotechnology, Ecotoxicology  
and Bioremediation,  
a section of the journal  
Frontiers in Microbiology

**Received:** 13 February 2018

**Accepted:** 11 June 2018

**Published:** 03 July 2018

### Citation:

Freixa A, Acuña V, Gutierrez M,  
Sanchís J, Santos LHMLM,  
Rodríguez-Mozaz S, Farré M,  
Barceló D and Sabater S (2018)  
Fullerenes Influence the Toxicity  
of Organic Micro-Contaminants  
to River Biofilms.  
*Front. Microbiol.* 9:1426.  
doi: 10.3389/fmicb.2018.01426

Organic micro-contaminants (OMCs) enter in freshwaters and interact with other contaminants such as carbon nanoparticles, becoming a problem of unknown consequences for river ecosystems. Carbon nanoparticles (as fullerenes C<sub>60</sub>) are good adsorbents of organic contaminants and their interaction can potentially affect their toxicity to river biofilms. We tested the C<sub>60</sub> interactions with selected OMCs and their effects on river biofilms in different short-term experiments. In these, river biofilms were exposed to C<sub>60</sub> and three OMCs (triclosan, diuron, or venlafaxine) and their respective mixtures with fullerenes (C<sub>60</sub> + each OMC). The effects were evaluated on structural, molecular, and functional descriptors of river biofilms. Our results showed that C<sub>60</sub> did not cause toxic effects in river biofilms, whereas diuron and triclosan significantly affected the heterotrophic and phototrophic components of biofilms and venlafaxine affected only the phototrophic component. The joint exposure of C<sub>60</sub> with venlafaxine was not producing differences with respect to the former response of the toxicant, but the overall response was antagonistic (i.e., decreased toxicity) with diuron, and synergistic (i.e., increased toxicity) with triclosan. We suggest that differences in the toxic responses could be related to the respective molecular structure of each OMC, to the concentration proportion between OMC and C<sub>60</sub>, and to the possible competition between C<sub>60</sub> pollutants on blocking the receptors of the biological cell membranes. We conclude that the presence of C<sub>60</sub> at low concentrations modified the toxicity of OMC to river biofilms. These interactions should therefore be considered when predicting toxicity of OMC in river ecosystems.

**Keywords:** carbon nanoparticles, pollutants, microbial ecotoxicology, mixtures, periphyton, diuron, triclosan, venlafaxine

## INTRODUCTION

Organic micro-contaminants (OMCs) and carbon nanoparticles enter in freshwater ecosystems *via* point (e.g., sewage discharge) and diffuse sources (e.g., run-off events) as well as from atmospheric depositions. The widespread use of carbon nanomaterials, in particular fullerenes (such as C<sub>60</sub>), has prompted the arrival of these nanomaterials to rivers. Concentrations of up to ng L<sup>-1</sup> have been

observed in effluents of wastewater treatment plants (Farré et al., 2010; Wang et al., 2010). C<sub>60</sub> are molecules with 60 atoms of carbon forming fused hexagons and pentagons, and their unique properties (i.e., proportionately very large surface area) led to several uses in nanotechnology industry such as water treatment, medical applications, microelectronics, photovoltaic devices, and cosmetics (Bakry et al., 2007; Benn et al., 2011; Farré et al., 2011). When reaching freshwater systems, these nanomaterials may undergo transformations such as oxidation, or photo- and biological degradation. In addition, they can easily aggregate and participate in sorption processes with OMCs, organic matter, and aquatic organisms (Bundschuh et al., 2016).

Although environmental concentrations of C<sub>60</sub> do not pose a direct threat on aquatic organisms, the co-occurrence of these materials with OMC can potentially modify their original availability (i.e., the degree of accessibility of every compound to the organisms) and their toxicity to river organisms (Freixa et al., 2018). The toxicity of OMC to them has been widely analyzed (Kuzmanović, 2015), and it is our assumption that C<sub>60</sub> can interact with OMC both as carriers and enhancers of the toxicity of contaminants and as blinding their action and reducing their toxic effect. This variety of responses may produce additive, synergistic, or antagonistic interactions (Folt et al., 1999; Crain et al., 2008; Côté, et al., 2016). Some previous studies have reported either synergistic or antagonistic effects to bacteria, daphnids, or fish (Yang et al., 2010; Ferreira et al., 2014; Hu et al., 2015; Sanchís et al., 2016). Specifically, Baun et al. (2008) showed that the toxicity may vary depending on the toxicant, and observed that the toxicity to phenanthrene in the planktonic alga *Pseudokirchneriella subcapitata* increased in the presence of C<sub>60</sub>, but that of pentachlorophenol decreased. However, the patterns of toxicity responses to biofilm communities produced by conjoint C<sub>60</sub> and OMC are still unclear and deserve detailed analysis.

Biofilms are complex communities of algae, bacteria, and fungi, all embedded within a polysaccharide matrix which contributes to the stability and protection of microorganisms (Gerbersdorf et al., 2008; Flemming and Wingender, 2010). Biofilms dominate the river microbial life and are particularly relevant as nutrient and organic matter recyclers (Battin et al., 2016). Biofilms as well are the early receivers and responders to the presence of OMC, mainly because of their position as interfaces between water and the sediments (Sabater et al., 2007). Most previous studies on the ecotoxicity of carbon nanomaterials

(Freixa et al., 2018) mainly derive from single-species analyses, and only a few (e.g., Lawrence et al., 2016) approach the response of such a complex consortium of microorganisms as those constituted by biofilms.

In this paper, we aim to ascertain the interactive effects of fullerenes on the toxicity of selected OMCs to river biofilms. We designed different short-term experiments using biofilms exposed to single and combined effects of C<sub>60</sub> and three different OMC. Specifically, the organic contaminants were selected for their different chemical structure, specific mode-of-action, widespread occurrence in rivers, capacity to bioaccumulate in biofilms and their known toxic effects in freshwater organisms *per se* (Table 1) (Kuzmanović, 2015; Huerta et al., 2016). The selected OMC were a pharmaceutical (venlafaxine), a personal care product (triclosan), and a pesticide (diuron), with specific mode-of-actions and different potential toxic effects. We hypothesized that the toxic effects of these OMC on biofilms, when mixed up with fullerenes, would not be homogeneous, but either synergic or antagonistic according to their different chemical structures.

## MATERIALS AND METHODS

### Experimental Design

Three different experiments were performed consecutively using 5-week-old epilithic biofilms. All the experiments consisted in a 72-h exposure of biofilms to the respective contaminants. So forth, we tested the toxicity of biofilm to each contaminant, first separately [fullerenes, venlafaxine (VEN); diuron (DIU); triclosan (TCS)], and second of the respective mixtures of each OMC with fullerenes. Each experiment was performed using 12 glass mesocosms, with 4 different treatments and 3 replicates per treatment. These were (1) a control with biofilms and without OMC or fullerenes (Control); (2) a treatment with biofilms exposed to fullerenes (C<sub>60</sub>); (3) a treatment with biofilms exposed to each OMC (VEN, DIU, or TCS); (4) a treatment with the corresponding mixture of fullerenes and the respective organic contaminant (VENC<sub>60</sub>, DIUC<sub>60</sub>, and TCSC<sub>60</sub>) (Supplementary Figure 1).

The mesocosms were 25 cm in diameter and 15 cm high and hold a central glass cylinder to define an area of 450 cm<sup>2</sup>. Each mesocosm was filled with 4.5 L of rainwater, and water level was kept constant by means of constant water addition (rate 4.5 mL day<sup>-1</sup>) through a peristaltic pump (Ismatec, MCP,

**TABLE 1** | Chemical and toxic characteristics of the organic micro-contaminants used in this experiment.

Compound		Formula	Molar mass (g/mol)	Log kow*	Log D8*	Major species at pH 8	pKa	EC <sub>50</sub>
Venlafaxine	Psychiatric drug	C <sub>17</sub> H <sub>27</sub> NO <sub>2</sub>	277.40	2.74	1.78	Cation	10.09	EC <sub>50</sub> 72 h algae = 11,000 μg L <sup>-1</sup> (Bastos et al., 2017)
Triclosan	Antibacterial	C <sub>12</sub> H <sub>7</sub> O <sub>2</sub> Cl <sub>3</sub>	289.54	4.98	4.50	Anion	7.9	EC <sub>50</sub> 48 h bacteria = 43.8 μg L <sup>-1</sup> (Ricart et al., 2010)
Diuron	Herbicide	C <sub>9</sub> H <sub>10</sub> Cl <sub>2</sub> N <sub>2</sub> O	233.09	2.53	2.53	Neutra	13.18	EC <sub>50</sub> 24 h algae = 13.3 μg L <sup>-1</sup> (Ricart et al., 2009)

\*Ref: ChemAxon (<https://chemicalize.com/> accessed in 12/01/2018).

150 W). A glass blade incorporated to a rotor (12 V, 2.2 W, 60 rpm, Philips) constantly moved the water at a constant velocity of  $3.4 \text{ cm s}^{-1}$  and forced a homogenous flow circulation in the mesocosms. The mesocosms were operated at  $20^\circ\text{C}$  temperature and a constant day–night cycle (12-h light/12-h darkness) using LED lamps (Lumina Led 62, 48 W).

The mesocosms were bottom-covered by glass tiles ( $1.5 \text{ cm} \times 1.5 \text{ cm}$  each) colonized with biofilms. The biofilms on the substrata were 5 weeks old and were separately grown in artificial stream channels (2 m long, 10 cm wide, 7.5 cm deep) located besides the mesocosms. The artificial streams received a constant flow of  $60 \text{ mL s}^{-1}$  of nutrient-poor water and daily cycles of also 12-h light and 12-h darkness. The original biofilm inoculum was obtained from an oligotrophic pristine stream close to the laboratory. Up to 20 glass tiles of colonized biofilms were moved from the artificial streams to each of the mesocosms 12 h before each experiment started.

## Chemicals Preparation

The analytical standards used were diuron (>98%, CAS: 330-54-1, Sigma-Aldrich), venlafaxine hydrochloride ( $\geq 98\%$ , CAS: 99300-78-4, Sigma-Aldrich), and triclosan ( $\geq 97\%$ , CAS: 3380-34-5, Sigma-Aldrich) (Table 1). Stock solutions of  $1000 \text{ mg L}^{-1}$  for each compound were previously prepared in methanol. The final concentration of methanol in the mesocosms was 0.001%. Nominal concentrations used in the experiments were  $10 \mu\text{g L}^{-1}$  for diuron and triclosan and  $50 \mu\text{g L}^{-1}$  for venlafaxine. The concentrations of each compound were selected following the EC<sub>50</sub> values reported in literature for diuron and triclosan. The added concentrations of venlafaxine were lower than those predicted by the available EC<sub>50</sub> values (Table 1).

Aqueous stock solution of  $100 \text{ mg L}^{-1}$  of C<sub>60</sub> (99.5% Sigma-Aldrich) was prepared using filtered rainwater (0.2- $\mu\text{m}$  pore size) and long-time stirring during 2 months, at constant temperature ( $20^\circ\text{C}$ ) and in absence of organic solvents (Sanchís et al., 2016). Particle size of C<sub>60</sub> suspension was characterized by transmission electron microscopy (TEM) (Zeiss EM 910). A subsample of stock solution was diluted 10 times with filtered rainwater, sonicated for 1 min, and placed onto 200-mesh grid Formvar membrane. The grid was air-dried and the sample was observed at 60 kV. TEM images (recorded using digital CCD Gatan Orius 200 camera) indicated that the stock solution of C<sub>60</sub> contained round-shaped aggregates with sizes between 100 and 200 nm, and the particles were clearly dispersed homogeneously after long-time stirring (Figure 1).

## Sample Collection

Water samples for nutrient and dissolved organic carbon (DOC) determination were collected at the end of each experiment (after 72 h). Samples were filtered (precombusted 0.45- $\mu\text{m}$  glass microfiber; and 0.2- $\mu\text{m}$  nylon pore size filters, Whatman, respectively) and kept at  $-20^\circ\text{C}$  until analysis. For quantification of C<sub>60</sub> and OMC, water samples were collected after 1 h of the initial spiking and at the end of each experiment (time 0 and 72 h). For the analysis of fullerenes, 150 mL of water were filtered by 0.7  $\mu\text{m}$  (glass microfiber filters, Whatman) and then by 0.45  $\mu\text{m}$  (nylon filters, Millipore), the filters were kept  $-20^\circ\text{C}$

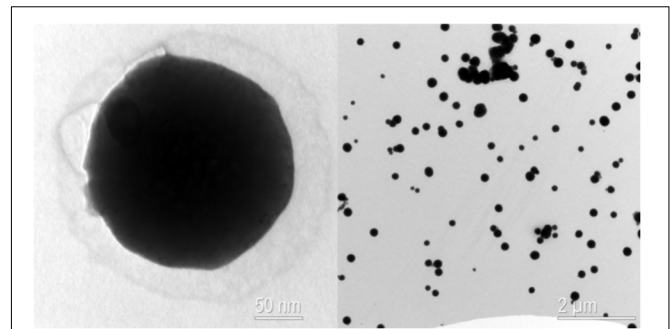


**FIGURE 1** | Transmission electron microscopy (TEM) image of fullerene C<sub>60</sub> from the suspension used in the experiments. The nano-C<sub>60</sub> aggregates were formed after 2 months stirring in water.

until analysis. For the analysis of the OMC, 10 mL of water were collected in amber glass vials in each mesocosms and kept at  $-20^\circ\text{C}$  until analysis.

Biofilms were randomly sampled at the end of exposure (72 h) in each of the mesocosms. Triplicate glass tiles were collected from each mesocosm in order to measure organic matter content, extracellular polymeric substances (EPSs), chlorophyll-*a* (chl-*a*) content, photosynthetic parameters (basal fluorescence and photosynthetic efficiency), extracellular enzyme activities, respiration, and absolute quantification of the expression of 16S and 18S rRNA genes. Chl-*a* content was also measured before any experiment started (time 0 h). Biofilm samples for chl-*a*, EPS, and gene expression were kept at  $-20^\circ\text{C}$  and  $-80^\circ\text{C}$  until analysis. The others endpoints were analyzed in fresh during the same day of experiment.

## Water Analysis

Physical variables (pH, oxygen, conductivity, and temperature) were measured using portable hand-held probes (WTW, Weilheim in Oberbayern, Germany) in each mesocosms at the end of each experiment. NO<sub>2</sub>, NO<sub>3</sub><sup>-</sup>, and NH<sub>4</sub><sup>+</sup> were analyzed by ionic chromatography (Dionex, ICS 5000) and PO<sub>4</sub><sup>3-</sup> was analyzed spectrophotometrically by the ascorbate-reduced molybdenum blue method. DOC was quantified using a total organic carbon analyzer (Shimadzu TOC-V CSH).

For the analysis of venlafaxine and diuron, 1 mL of water sample was centrifuged (7500 rpm, 10 min,  $4^\circ\text{C}$ ), then 0.9 mL of supernatant was transferred in a vial, and 0.1 mL of methanol was added. 10  $\mu\text{L}$  of a  $1 \text{ ng } \mu\text{L}^{-1}$  mixture of isotopically labeled standards solution (VLF-d<sub>6</sub> and DIU-d<sub>3</sub>) was added before the analysis by liquid chromatography coupled with a hybrid mass spectrometry detector (UPLC-QqLIT) (Gros et al., 2012). For the analysis of triclosan, 1.35 mL of water was mixed with 0.15 mL of methanol. Then, it was centrifuged (7500 rpm, 10 min,  $4^\circ\text{C}$ ) and 1 mL of supernatant was transferred in a vial. 50  $\mu\text{L}$  of a  $1 \text{ ng } \mu\text{L}^{-1}$  standard solution of TCS-d<sub>3</sub> was added before the analysis by UPLC-MS/MS using a methodology adapted from Gorga et al. (2013).

The concentration of fullerenes in water was analyzed using the method thoroughly described in Sanchís et al. (2015).

Briefly, fullerenes were extracted from filters by ultrasound-assisted extraction with toluene. The extracts were concentrated to 1.00 mL and analyzed by liquid chromatography coupled to high resolution mass spectrometry. The chromatographic separation was achieved with a Buckyprep column and a non-aqueous mobile phase, composed by toluene-methanol (90–10), in isocratic mode; the ionization was carried out with an atmospheric pressure photoionization source (APPI), working in negative polarity; and the acquisition was performed in full scan mode with a Q Exactive (Thermo Fisher Scientific, San Jose, CA, United States).

## Structural and Functional Biofilm Endpoints

Algal biomass was estimated by extracting *chl-a* with 90% acetone overnight at 4°C in the dark. Biomass was determined spectrophotometrically (Agilent technologies 8453) after filtration of the extract (GF/F, Whatman) by measuring absorbance at 430 and 665 nm (Jeffrey and Humphrey, 1975). Organic matter content was estimated after drying (70°C) during 72 h and then burnt using a muffle furnace (AAF 110, carbolite) for 4 h at 450°C to obtain the ash-free dry weight.

Extracellular polymeric substance was extracted using conditioned cation-exchange resin (Dowex Marathon C, Na<sup>+</sup> form, strongly acid, Sigma-Aldrich) following the method described in Romani et al. (2008). The polysaccharide content of biofilm was quantified by the phenol-sulfuric acid assay (Dubois et al., 1956) and measuring the absorbance at 485 nm using a spectrophotometer (Agilent technologies 8453). Glucose standards were also prepared (0–150 µg mL<sup>-1</sup>), and the results were given as glucose equivalents per cm<sup>2</sup> of biofilm.

*In vivo* *chl-a* fluorescence was used to estimate basal *chl-a* fluorescence ( $F_0$ ) and PSII photochemical efficiency of the *chl-a* fluorescence ( $Y_{\text{eff}}$ ) (Kumar et al., 2014). These parameters were measured randomly at five different glass tiles with a portable pulse amplitude modulate fluorometer (Diving PAM, Walz, Germany). Measurements were done for each microcosm at light-adapted state at the same day hour.

Extracellular enzyme activities were determined using artificial fluorescent substrates 4-methylumbelliferone (MUF)-β-D-glucoside, MUF phosphate, and L-leucine-4-7-methylcoumarylamide (AMC), for β-glucosidase (GLU), phosphatase (PHO), and Leu-aminopeptidase (LEU) activities, respectively. One glass tile was incubated at saturating conditions (i.e., 0.3 mM final substrate concentration) for each experiment and mesocosms, in agitation, for 1 h in the dark with filtered mesocosms water (0.2-µm pore size, nylon, Whatman). At the end of the incubation, glycine buffer (1/1, vol/vol) was added to each vial to stop the reaction. The fluorescence of the supernatant was measured into 96-well black microplates at 365/455 nm (excitation/emission) for MUF and 364/465 nm (excitation/emission) for AMC using a fluorometer (Hitachi, F-7000).

We used the MicroResp method for measuring the respiration of biofilm suspensions following the procedure described by Tlili et al. (2011). Briefly, 500 µL of biofilm suspension obtained

by scraping two glass tiles with 15 mL of 0.2-µm filtered water from each mesocosms was added to each well (96-well micro-plate). A detection microplate was previously prepared (indicator solution set in a 1% gel of agar, 1:2 ratio) following the manufacturer's instructions. The two micro-plates (detection plate and biofilm plate) were sealed and incubated in the dark at 20°C in constant agitation (150 rpm) during 24 h. Absorbance was measured at 570 nm (Epoch microplate reader, Biotek Instruments) immediately before sealing and after the 24 h of incubation. The CO<sub>2</sub> quantities were calculated using a calibration curve of absorbance values versus CO<sub>2</sub> quantity measured by gas chromatography. Results were expressed as µg of CO<sub>2</sub> production rate per gram of ash-free dry weight (AFDW<sup>-1</sup> h<sup>-1</sup>).

## Molecular Analysis

RNA was extracted after scraping one glass tile per mesocosms using the Power Biofilm RNA isolation Kit (Mo Bio Laboratories, Inc.) according to the manufacturer's instructions. Aliquots of 50 µL of extracted RNA were purified using a commercial kit TURBO DNA-free TM specifically designed to remove contaminating DNA. Then, SuperScript III for RT-PCR (Invitrogen) was used to synthesize cDNA using 1/2 diluted RNA and 50 ng µL<sup>-1</sup> random hexamers following the manufacturer's instructions. RNA and cDNA concentration was measured using Qubit 2.0 fluorometer (Life Technologies).

The genes for 16S ribosomal RNA (rRNA) and 18S rRNA were amplified by real-time PCR (qPCR) using cDNA samples. The primers used for quantification of 16S rRNA were F1048 and R1194 and for 18S rRNA were euk345F and euk499R. All qPCR assays were conducted on an Mx3005P system (Agilent Technologies). All reactions were performed in triplicate and contained a total volume of 30 µL, including 1 µL of cDNA, 1 µL of each specific primer (10 mM), 15 µL of SYBR-Green mix (Brilliant III Ultra-Fast SYBR-Green QPCR Master Mix, Agilent Technologies), and 12 µL of DEPC-treated water. For negative controls, cDNA was replaced by DEPC-treated water. The cycling protocol consisted in initial cycle of 95°C for 3 min, followed by 35 cycles at 95°C for 20 s and 60°C for 60 s for 16S rRNA and 50 cycles at 95°C for 15 s and 60°C for 60 s for 18S rRNA. Standard curves were used to known quantities of cloned target genes, obtained by a series of dilutions following the protocol previous described in Romero et al. (2018). A dissociation curve was constructed to verify the specificity of amplified products obtained during a gradual heating of the PCR products from 60 to 95°C. Results were expressed as number of copy of each gene per ng of cDNA<sup>-1</sup>.

## Data Treatment

Normality of all variables was checked prior to all the analyses by means of Shapiro-Wilk test and Levene's test for homogeneity of variance, after a log<sub>10</sub> transformation. A *t*-test was performed to compare the concentrations of nutrients and OMCs between treatments for each experiment. A generalized linear model (GLM) test was used to detect the individual and main effects (Crain et al., 2008) between C<sub>60</sub>, OMC, and their interactions. The main effects compare the net effect of a stressor (either

the C<sub>60</sub> or a given OMC) in the presence and absence of a second stressor (any contaminant different from the previous, and the control). Individual effects (the response in the presence of a stressor alone vs. the control) were used to calculate the effect size (Crain et al., 2008), from which it derived whether a significant interaction effect occurred against the null model of additively (i.e., the interaction could be resolved as the sum of the individual effects of C<sub>60</sub> and the respective OMC). When the interactions between C<sub>60</sub> and each of the OMC pointed to a response significantly different to that additive, the interactive effects were classified as (i) antagonism (A) when the combined effect of C<sub>60</sub> and the OMCs on a given variable was less than that predicted additively or (ii) synergism (S) when the combined effect of C<sub>60</sub> and the OMCs on a given variable was more pronounced than that predicted additively. These analyses were conducted in R software version 3.3.0 (R Core Team, 2017) using the *glm* and *t.test* functions.

Principal coordinates analysis (PCoA) based on Bray–Curtis distance matrices was performed including all the functional and structural endpoints. The PCoA is an unconstrained ordination approach aimed to visualize the differences between treatments. Data were used after their previous logarithmic transformation and later fitted to the PCoA plot using Spearman correlations (Blanchet et al., 2008). Finally, an analysis of similarity (ANOSIM) was used to determine statistical differences between each treatment for each experiment separately. These analyses were performed using PRIMER v6 software (PRIMER-E, Ltd., United Kingdom).

## RESULTS

### Water Analysis

The water chemical characteristics remained steady throughout the experiments. Conductivity ranged between 155.4 and 201  $\mu\text{S cm}^{-1}$ , pH averaged  $8.1 \pm 0.2$ , dissolved oxygen

$10.2 \pm 1.1 \text{ mg L}^{-1}$ , and water temperature  $19.4 \pm 0.1^\circ\text{C}$  (mean  $\pm$  SD;  $n = 36$ ). The average values for nutrients and DOC concentrations experienced some changes (Table 2). While differences between treatments were minor in the case of inorganic nutrients N-NO<sub>2</sub>, N-NO<sub>3</sub><sup>-</sup>, N-NH<sub>4</sub><sup>+</sup>, and P-PO<sub>4</sub><sup>3-</sup> (except in a few cases, Table 2), DOC largely increased at the treatments with venlafaxine (VEN and VENC60) and diuron (DIU and DIUC60) with respect to the Control and the C60 (*t*-test, Table 2), and showed a slightly increase in the experiments with triclosan (*t*-test, Table 2).

The concentrations of OMC in water decreased after 72 h of exposure (Table 3). In the absence of C<sub>60</sub>, the concentrations of venlafaxine significantly decreased by 9%, concentrations of diuron by 13% and concentrations of triclosan by 40% (*t*-test, Table 3). In the presence of C<sub>60</sub>, the concentration of diuron decreased by a 4.3 and 12% for venlafaxine (*t*-test, ns), but triclosan concentration decreased significantly by 50% (*t*-test,  $p < 0.01$ ) (Table 3). The mean concentration of C<sub>60</sub> after 72 h was  $1.0 \pm 0.4 \mu\text{g L}^{-1}$  ( $n = 18$ ), implying that fullerenes reduced by 64% (mean value) of the initial concentration (Table 3). However, the reduction of C<sub>60</sub> after 72 h was only significant in the TCS treatments (*t*-test, Table 3). The occurrence of very low concentrations of C<sub>60</sub> in the control of TCS and treatment of DIU could be due to air contamination between the mesocosms.

### Structural Endpoints

No significant differences in chl-*a* content occurred among treatments at time 0 h (data not shown) neither after 72 h of exposition in the three experiments (Table 4). EPS content significantly decreased in the TCS treatment with respect to the control (Figure 2A). The GLM analysis reported significant individual effects on EPS for TCS, but the interaction between TCS and C<sub>60</sub> did not differ from the additive response (Table 4). *In situ* basal chlorophyll fluorescence (*F*<sub>0</sub>) was responsive to OMC and C60 treatments (Figure 2C). *F*<sub>0</sub> was significantly

**TABLE 2 |** Nutrients and DOC concentrations for each treatment and experiment (1; venlafaxine, 2; diuron, 3; triclosan).

		DOC mgL <sup>-1</sup>	N-NO <sub>2</sub> μgL <sup>-1</sup>	N-NO <sub>3</sub> <sup>-</sup> mgL <sup>-1</sup>	N-NH <sub>4</sub> <sup>+</sup> μgL <sup>-1</sup>	P-PO <sub>4</sub> <sup>3-</sup> μgL <sup>-1</sup>
Experiment 1	Control	2.62 ± 0.18	18.55 ± 1.03	1.58 ± 0.07	3.87 ± 0.01	3.75 ± 0.01
	C60	2.38 ± 0.25	16.76 ± 2.30	1.59 ± 0.03	3.87 ± 0.01	4.16 ± 1.38
	VEN	7.41 ± 0.27**	23.86 ± 2.15**	1.56 ± 0.11	3.76 ± 0.28	2.77 ± 0.01
	VENC60	7.18 ± 0.43**	24.46 ± 0.58**	1.54 ± 0.09	<LOQ	3.75 ± 0.23
Experiment 2	Control	3.66 ± 0.37	22.41 ± 3.31	1.40 ± 0.09	4.13 ± 0.01	<LOQ
	C60	4.10 ± 0.54	28.77 ± 0.24*	1.32 ± 0.09	3.53 ± 0.01*	3.86 ± 0.90*
	DIU	8.99 ± 1.07**	29.07 ± 1.18*	1.50 ± 0.03*	7.28 ± 2.15	5.49 ± 1.97*
	DIUC60	7.76 ± 1.26*	28.40 ± 2.62	1.67 ± 0.01	<LOQ	4.73 ± 0.01
Experiment 3	Control	3.63 ± 0.13	26.47 ± 5.58	1.32 ± 0.07	7.54 ± 2.53	5.60 ± 1.96
	C60	4.52 ± 1.65	27.60 ± 4.95	1.24 ± 0.10	3.94 ± 0.29	3.26 ± 0.01*
	TCS	4.21 ± 0.18*	28.21 ± 6.91	1.21 ± 0.02	<LOQ**	3.26 ± 0.12*
	TCS60	4.23 ± 0.04**	25.52 ± 7.66	1.31 ± 0.08	<LOQ**	3.75 ± 0.01

Values are means  $\pm$  standard deviation ( $n = 3$ ). The asterisks indicate the significance (*t*-test, \* $p < 0.05$ ; \*\* $p < 0.001$ ) for the difference of the treatment values with respect to the control.

<Below limit of quantification (LOQ): N-NH<sub>4</sub><sup>+</sup>: 0.004 mg L<sup>-1</sup>; P-PO<sub>4</sub><sup>3-</sup>: 0.003 mg L<sup>-1</sup>.

**TABLE 3** | Fullerenes (C<sub>60</sub>) and organic micro-contaminants (OMCs) concentration, expressed as  $\mu\text{g L}^{-1}$ , at time 0 h and after 72 h of exposure for each experiment (1; venlafaxine, 2; diuron, 3; triclosan) and treatments.

		C(C60)		C(OMC)	
		t = 0 h	t = 72 h	t = 0 h	t = 72 h
Experiment 1	Control	<LOD	<LOD	<LOD	<LOD
	C60	3.08 ± 0.25	1.30 ± 0.07	<LOD	<LOD
	VEN	<LOD	<LOD	56.30 ± 2.13	51.01 ± 1.34*
	VENC60	3.02 ± 0.12	1.07 ± 0.04	49.90 ± 2.83	43.86 ± 1.01
Experiment 2	Control	<LOD	<LOD	<LOD	<LOD
	C60	2.50 ± 0.25	1.20 ± 0.39	<LOD	<LOD
	DIU	<LOD	0.002 ± 0.001	10.29 ± 0.25	8.95 ± 0.15**
	DIUC60	2.57 ± 0.04	1.04 ± 0.14	9.72 ± 0.33	9.31 ± 0.96
Experiment 3	Control	<LOD	0.016 ± 0.022	<LOD	<LOD
	C60	1.35 ± 0.03	0.30 ± 0.07*	<LOD	<LOD
	TCS	0.018 ± 0.005	0.017 ± 0.025	8.24 ± 0.95	4.87 ± 0.17
	TCSC60	1.25 ± 0.04	0.37 ± 0.04*	6.80 ± 0.87	3.39 ± 0.30*

Values are means ± standard deviation (n = 3). The asterisks indicate the significance (t-test, \*p < 0.05; \*\*p < 0.001) for the difference between time 72 h against time 0 h.

<Below limit of detection (LOD): venlafaxine (0.009  $\mu\text{g L}^{-1}$ ); diuron (0.019  $\mu\text{g L}^{-1}$ ); triclosan (0.012  $\mu\text{g L}^{-1}$ ); C60 (0.001  $\mu\text{g L}^{-1}$ ).

**TABLE 4** | Results of the generalized linear model (GLM) for the analyzed endpoints for each experiment and treatment.

Endpoints	Experiment 1 Venlafaxine			Experiment 2 Diuron			Experiment 3 Triclosan		
	C60	VEN	VENC60	C60	DIU	DIUC60	C60	TCS	TCSC60
Chl-a	ns	ns	ns	ns	ns	ns	ns	ns	ns
EPS	ns	ns	ns	ns	ns	ns	ns	0.002	ns
F <sub>0</sub>	0.015	0.006	0.017	0.002	<0.001	0.005	0.017	0.024	ns
Y <sub>eff</sub>	ns	ns	ns	ns	<0.001	0.047	ns	ns	ns
RESP	ns	ns	ns	ns	<0.001	0.005	ns	ns	0.020
GLU	ns	ns	ns	ns	ns	ns	ns	ns	ns
PHO	ns	ns	ns	ns	0.047	ns	ns	ns	ns
LEU	ns	ns	ns	ns	ns	ns	ns	ns	ns
16S rRNA	ns	ns	ns	ns	0.016	ns	ns	ns	ns
18S rRNA	ns	0.002	ns	ns	ns	ns	ns	ns	ns

Chl-a, chlorophyll-a; EPSs, extracellular polymeric substances; F<sub>0</sub>, basal fluorescence; Y<sub>eff</sub>, photosynthetic efficiency; RESP, respiration; GLU,  $\beta$ -glucosidase; PHO, phosphatase; LEU, Leu-aminopeptidase activities; ns, no significant effect.

decreased by C<sub>60</sub> in all the experiments (Table 4). The exposure to OMC decreased the F<sub>0</sub> in VEN and TCS and increased it in the DIU experiment (Figure 2C). Significant antagonistic effects in the F<sub>0</sub> occurred when C<sub>60</sub> interacted with VEN and DIU (Figure 2C and Table 4).

## Functional Endpoints

The respiration rate (MicroResp technique) significantly increased in the DIU treatment (Figure 2B and Table 4) while it decreased in the DIUC60 as compared to DIU. Respiration in the DIUC60 was therefore a result of antagonistic interaction (Figure 2B and Table 4). Respiration decreased in the TCSC60 treatment with respect to the TCS (Figure 2B), showing a synergistic response (Table 4). The photosynthetic efficiency (Y<sub>eff</sub>) was only affected in the biofilms exposed to diuron (DIU and DIUC60 treatment) (Figure 2D and Table 4) showing an antagonism response (Figure 2D). The extracellular enzyme

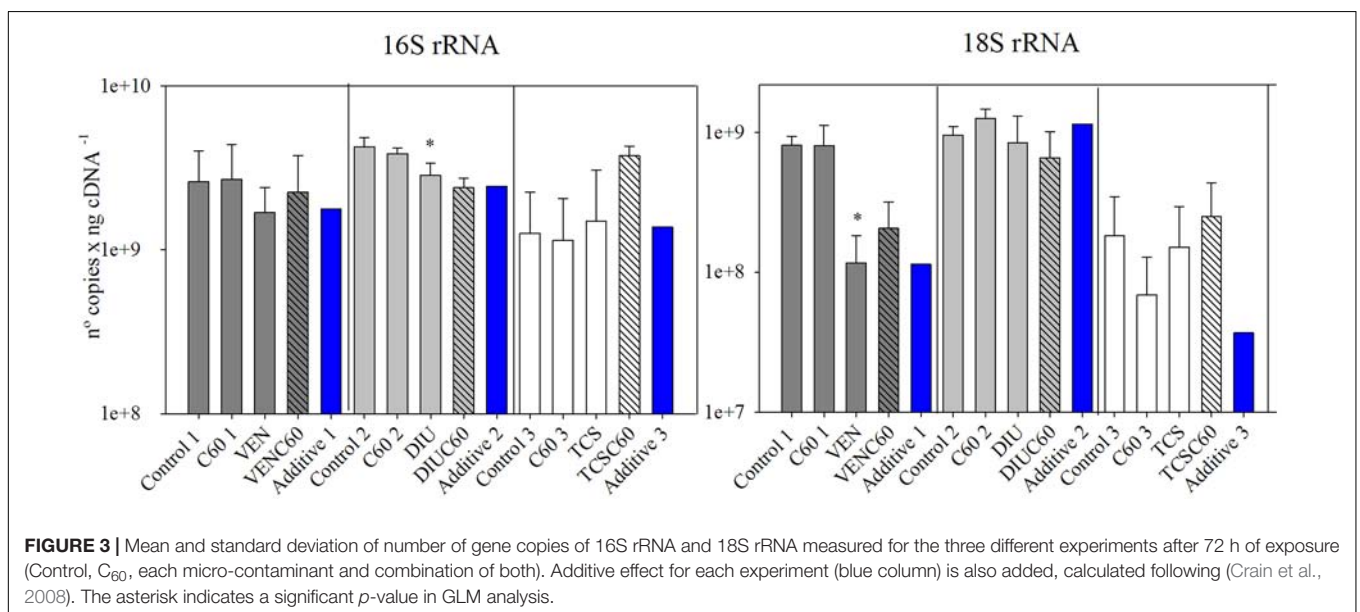
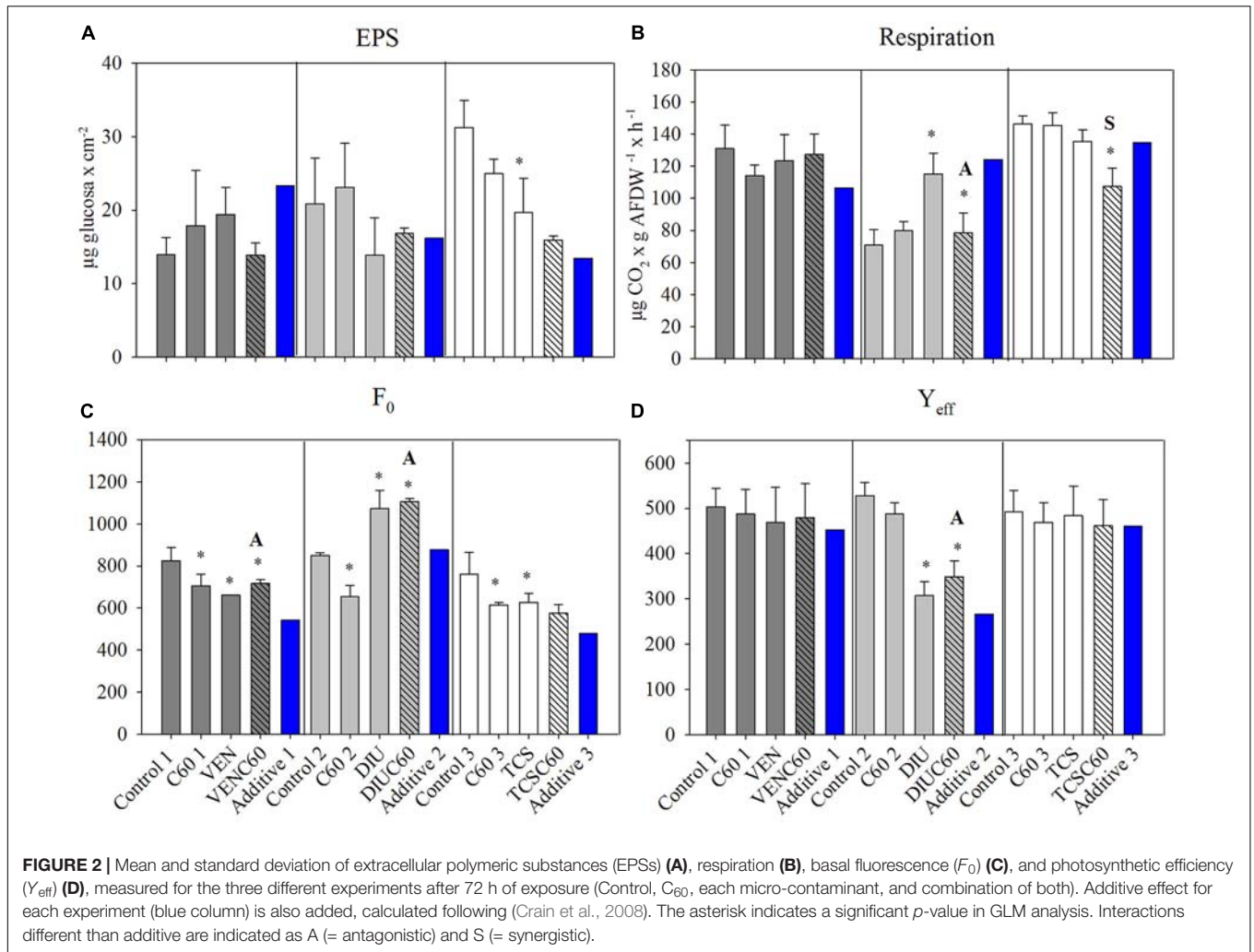
activities (GLU, PHO, and LEU) only showed a significant effect for PHO activity in the diuron treatment (DIU) (Table 4).

## Molecular Analysis

The number of copies of 16S rRNA significantly decreased in the DIU (Figure 3 and Table 4), while the 18S rRNA gene copies experienced a significant decrease in the venlafaxine treatment (VEN). Finally, triclosan did not affect the number of 16S and 18S rRNA gene copies (Figure 3).

## Interactive Effects Between C<sub>60</sub> and Organic Micro-Contaminants

The PCoA showed the distinct arrangement of treatments in the diuron and triclosan experiments (ANOSIM, R = 0.719, p = 0.001 for DIU; R = 0.568, p = 0.03 for TCS) (Figure 4). The DIU samples were more distinctly separated with respect to the control than those of the DIUC60, suggesting that the presence of C<sub>60</sub> could



be associated to a reduction in the toxic effect of diuron. In this analysis, the  $Y_{\text{eff}}$ , chl-*a*, and GLU activity had higher loadings in the control samples, while those of respiration and  $F_0$  were higher in the DIU samples. The TCSC60 samples were opposed to those of the control, which had the EPS as the most correlated variable (Figure 4). These differences between treatments did not occur in the venlafaxine experiment (ANOSIM,  $R = -0.056$ ,  $p = 0.64$ ) (Figure 4).

## DISCUSSION

### Toxic Effects of C<sub>60</sub> and Organic Micro-Contaminants on River Biofilms

Our results showed that the applied concentrations of C<sub>60</sub> (ranged between 0.30 and 3  $\mu\text{g L}^{-1}$ ) did not cause toxic effects to river biofilms, except for the transient response in the biofilm  $F_0$  (basal fluorescence). However, the OMCs produced negative effects on a wide range of structural and functional variables such as EPS, respiration, 16S and 18S gene expression, and extracellular enzyme activities. These different effects of C<sub>60</sub> and OMCs was not unexpected; toxic C<sub>60</sub> effects have been described in freshwater microorganisms at concentrations in the range of mg per liter (Lyon et al., 2006; Rodrigues and Elimelech, 2010; Tao et al., 2015; Deryabin et al., 2016; Lawrence et al., 2016), while the concentrations used in our experiment were close to those occurring in the environment (Freixa et al., 2018).

The toxic responses caused by OMC in biofilms changed according to the contaminant and its respective mode of action. The relatively high concentration ( $\sim 50 \mu\text{g L}^{-1}$ ) of venlafaxine caused significant effects in the  $F_0$  and 18S rRNA gene expression, indicating that algae could be the most concerned (without discarding protozoa or fungi). This chemical has an up to now unknown mode of action on algae, though it acts as a serotonin-norepinephrine reuptake inhibitor and affects the reproduction and metabolism of cladocerans and fish (Henry et al., 2004; Galus et al., 2013; Minguez et al., 2015). On the other hand, diuron inhibits algal photosynthesis by blocking the electron transfer at PSII (Kumar et al., 2014). The negative effects of diuron extend to algal growth and community diversity, as well as to the photosynthetic activity and gene expression (Pesce et al., 2006; McClellan et al., 2008; Ricart et al., 2009; Proia et al., 2011; Moisset et al., 2015). Diuron in our experiments produced a significant reduction of photosynthetic efficiency and a significant increase of basal fluorescence, two previously reported responses in biofilms during long-term experiments (Tlili et al., 2008; Ricart et al., 2009; López-Doval et al., 2010). Diuron also caused a significant reduction of bacterial gene expression (16S rRNA), which probably accounts for the reduction of live bacteria previously observed in biofilm experiments (Ricart et al., 2009). Furthermore, diuron enhanced the CO<sub>2</sub> production, which could be related to the increase of algal released materials (probably the cause of the large DOC increase in water in this experiment; Table 2) and its associated rise in heterotrophic respiration (Pesce et al., 2006). Finally, triclosan caused a significant decrease of EPS content, adding to other structural alterations associated to this bactericide already observed (Lawrence et al., 2009; Morin et al.,

2010; Guasch et al., 2016). Such an EPS reduction could be related to a lower bacterial metabolism, which could therefore affect EPS secretion (Lubarsky et al., 2012). Furthermore, triclosan produced a significant decrease in  $F_0$  which probably accounted for the indirect effects on algae (such as diatom mortality or reduction of algal biomass previously described; Lawrence et al., 2009; Morin et al., 2010; Proia et al., 2011, 2013), produced on top of the main effect on the enzymes involved in the fatty acids synthesis in bacterial cells (Heath et al., 1999).

### Interactive Effects of C<sub>60</sub> With Organic Micro-Contaminants on River Biofilms

Different studies have already shown that organism responses to multiple stressors may account from additive to synergistic or antagonistic responses (Folt et al., 1999; Crain et al., 2008; Côté, et al., 2016). This range of responses has also been observed on aquatic organisms when organic contaminants are mixed with carbon nanoparticles (Baun et al., 2008; Brausch et al., 2010; Schwab et al., 2013; Sanchís et al., 2016). Indeed, in the present study, we observed antagonistic and synergistic responses on the toxic effects of mixture of C<sub>60</sub> with OMC in river biofilms. In particular, the effects of mixture of C<sub>60</sub> and venlafaxine could not be differentiated from the separate effects of this contaminant (which were only noticeable on  $F_0$ ), the mixture of C<sub>60</sub> and diuron resulted in antagonistic responses in  $F_0$ ,  $Y_{\text{eff}}$ , and respiration, and finally synergistic responses were observed in biofilms exposed to a mixture of C<sub>60</sub> and triclosan, illustrating how this mixture can increase the toxicity of this contaminant.

The lack of significant interaction in the venlafaxine mixture (except in the  $F_0$ ) could be related to its higher concentration in relation to the C<sub>60</sub> (relation 1:44, C<sub>60</sub>:VEN at the end of the experiment). In the other two OMCs, the concentration ratios with C<sub>60</sub> were more balanced; the relation between C<sub>60</sub> and OMC were, respectively, of 1:9 in the DIU and 1:7 in the TCS at the end of the experiments. The ratio in the concentrations of carbon nanoparticles and pollutants is of relevance (Hu et al., 2008; Kah et al., 2011; Sanchís et al., 2016), since low concentrations of nanomaterials with respect to the contaminant, as it was the case in the venlafaxine experiment, may produce similar toxicity than the one solely due to the organic contaminant. On the other hand, reducing the concentrations ratio may favor the higher adsorption of organic contaminants and reduce the contaminant bioavailability (Sanchís et al., 2016). The described antagonistic effect of the C<sub>60</sub> on the toxic effects of diuron on  $F_0$ ,  $Y_{\text{eff}}$ , and heterotrophic respiration (Table 4) deserves special attention. The algal materials released by biofilms (due to diuron exposure) could have been absorbed onto the C<sub>60</sub> materials, therefore reducing their availability for bacterial metabolism. This potential mechanism of antagonism is supported by a slightly lower DOC observed in the mixture condition. Thus, the C<sub>60</sub> antagonism with diuron could be related to the presence of large C<sub>60</sub> aggregates competing with diuron molecules through blocking the cell membrane transporters and receptors, and therefore preventing diuron to enter the cells and to exert its toxic effect. Additionally, the diuron adsorbed by C<sub>60</sub> could be less

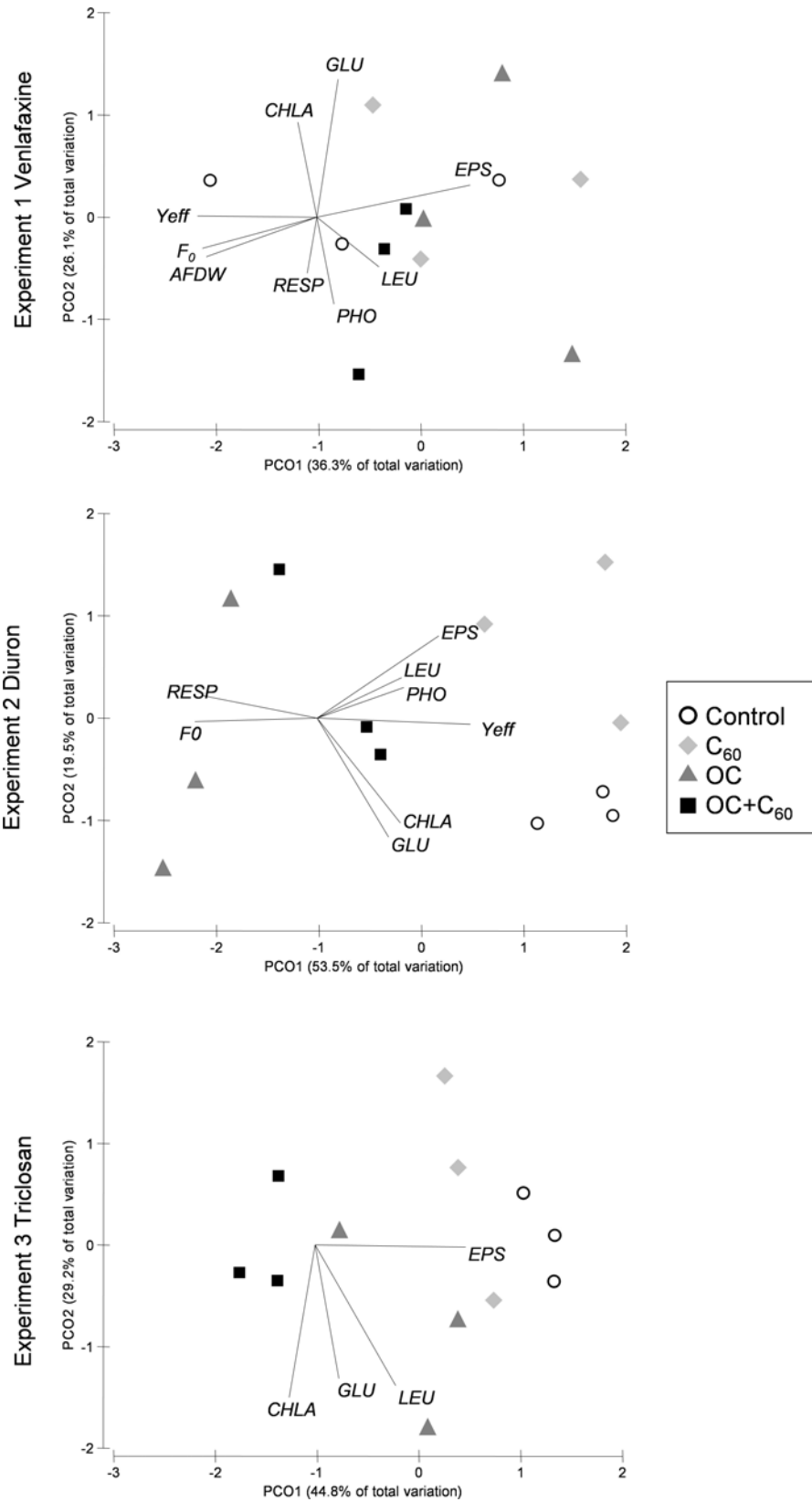


**FIGURE 4 |** Principal coordinates analysis (PCoA) plot of Bray–Curtis distances between treatments (represent by different colors and symbols) for each experiment including functional and structural endpoints. Significant correlated variables are included in the plot.

available to biofilm organisms (Nowack and Bucheli, 2007). Previous studies with other carbon nanoparticles coincide to show that diuron remains adsorbed by carbon nanotubes. This was observed in an experiment with *Chlorella vulgaris* (Schwab et al., 2013) as well as in other with *Pseudokirchneriella subcapitata* in the presence of 1.5 mg L<sup>-1</sup> black carbon (Knauer et al., 2007).

Finally, the significant reduction of the CO<sub>2</sub> production in the triclosan and C<sub>60</sub> mixture suggested that these caused an increase in the triclosan toxicity to biofilms (Figure 2 and Table 4). This synergism could be attributed to the carrier effect of C<sub>60</sub>, which could facilitate the entrance of triclosan inside the biofilm via the Trojan horse effect (Limbach et al., 2007; Deng et al., 2017), that is, using the entry provided by nanomaterials into the cells once adsorbed to them. Triclosan molecules loaded to C<sub>60</sub> could enter inside the biofilm, and subsequently be released inside the organisms thanks to desorption mechanisms (Deng et al., 2017). This might be a likely mechanism, though the adsorption and desorption of OMC and C<sub>60</sub> are still not well-investigated, and could operate with an OMC and not with another according to their particular physico-chemical characteristics. Similarly, Baun et al. (2008) reported that the presence of C<sub>60</sub> decreased the EC<sub>50</sub> (i.e., increased the toxicity) of phenanthrene from 720 to 430 μg L<sup>-1</sup> for the algae *Pseudokirchneriella subcapitata*. These findings highlight the potential environmental risk of C<sub>60</sub> because of its capacity to act as a carrier for some organic contaminants.

## CONCLUSION

Our results show that fullerenes can alter the toxicity of organic contaminants in the river systems. Still, the different responses we observed in the mixtures between contaminants and carbon nanoparticles could be attributed to several mechanisms: (1) differences in the molecular structure of OMC that can influence the sorption equilibrium between C<sub>60</sub> and contaminants, (2) concentration proportions between OMC and C<sub>60</sub>, and (3) competition of C<sub>60</sub> contaminants blocking the receptors of the biological cell membranes.

Even though laboratory experiments do not fully capture the ecological complexity of natural aquatic ecosystems, our study contributes to understand the potential effects of fullerenes as modulators of OMCs effects. It is evidenced that C<sub>60</sub> at

environmental concentrations does not only pose a risk for river microorganisms but also that their combination with OMC may produce synergistic and/or antagonistic toxic effects to river biofilms. Our findings suggest that changes in the toxicity of OMC due to the presence of C<sub>60</sub> in river systems directly affect river biofilms and probably have indirect consequences for river food webs.

## AUTHOR CONTRIBUTIONS

AF, VA, and SS conceived and designed the study. AF and MG performed the experiments and samplings. AF, MG, JS, and LS analyzed data. AF, VA, JS, LS, SR-M, MF, DB, and SS wrote the manuscript. All authors contributed to the discussion and approved the final version of this manuscript.

## FUNDING

This work has been funded by the Spanish Ministry of Economy and Competitiveness (project NANOTRANSFER; ERA SIINN PCIN-2015-182-C02-02) and the European Commission under contract No. 603629-Project GLOBAQUA. LS acknowledges the Juan de la Cierva program (FJCI-2014-22377), and SR-M acknowledges the Ramon y Cajal program (RYC-2014-16707). Finally, the authors also acknowledge the support from the Economy and Knowledge Department of the Catalan Government through Consolidated Research Group (ICRA-ENV 2017 SGR 1124).

## ACKNOWLEDGMENTS

We would like to thank Ferran Romero for his help in the molecular analysis, Lorenzo Proia for his help in using MicroResp technique, and Maria Casellas for laboratory assistance.

## SUPPLEMENTARY MATERIAL

The Supplementary Material for this article can be found online at: <https://www.frontiersin.org/articles/10.3389/fmich.2018.01426/full#supplementary-material>

## REFERENCES

- Bakry, R., Vallant, R., Najam-ul-Huq, M., Rainer, M., Szabo, Z., Huck, C., et al. (2007). Medicinal applications of fullerenes. *Int. J. Nanomedicine* 2, 639–649.
- Battin, T. J., Besemer, K., Bengtsson, M. M., Romani, A. M., and Packmann, A. I. (2016). The ecology and biogeochemistry of stream biofilms. *Nat. Rev. Microbiol.* 14, 251–263. doi: 10.1038/nrmicro.2016.15
- Baun, A., Sørensen, S. N., Rasmussen, R. F., Hartmann, N. B., and Koch, C. B. (2008). Toxicity and bioaccumulation of xenobiotic organic compounds in the presence of aqueous suspensions of aggregates of nano-C60. *Aquat. Toxicol.* 86, 379–387. doi: 10.1016/j.aquatox.2007.11.019
- Bastos, S. G. G., Figueiredo, S. A., Delerue-Matos, C., Lúcia, H. M. L. M., and Santos, L. H. M. L. M. (2017). “Impact of venlafaxine in the growth of the microalga pseudokirchneriella subcapitata,” in *Proceedings Conference Proceeding CEST 15 - 15th International Conference on Environmental Science and Technology*, Rhodes.
- Benn, T. M., Westerhoff, P., and Herckes, P. (2011). Detection of fullerenes (C60 and C70) in commercial cosmetics. *Environ. Pollut.* 159, 1334–1342. doi: 10.1016/j.cmet.2012.08.002
- Blanchet, F. G., Legendre, P., and Borcard, D. (2008). Forward selection of explanatory variables. *Ecology* 89, 2623–2632. doi: 10.1890/07-0986.1
- Brausch, K. A., Anderson, T. A., Smith, P. N., and Maul, J. D. (2010). Effects of functionalized fullerenes on bifenthrin and tribufos toxicity to *Daphnia magna*:

- survival, reproduction, and growth rate. *Environ. Toxicol. Chem.* 29, 2600–2606. doi: 10.1002/etc.318
- Bundschuh, M., Seitz, F., Rosenfeldt, R. R., and Schulz, R. (2016). Effects of nanoparticles in fresh waters: risks, mechanisms and interactions. *Freshw. Biol.* 61, 2185–2196. doi: 10.1111/fwb.12701
- Côté, I. M., Darling, E. S., and Brown, C. J. (2016). Interactions among ecosystem stressors and their importance in conservation. *Proc. R. Soc. B Biol. Sci.* 283:20152592. doi: 10.1098/rspb.2015.2592
- Crain, C. M., Kroeker, K., and Halpern, B. S. (2008). Interactive and cumulative effects of multiple human stressors in marine systems. *Ecol. Lett.* 11, 1304–1315. doi: 10.1111/j.1461-0248.2008.01253.x
- Deng, R., Lin, D., Zhu, L., Majumdar, S., White, J. C., Gardea-Torresdey, J. L., et al. (2017). Nanoparticle interactions with co-existing contaminants: joint toxicity, bioaccumulation and risk. *Nanotoxicology* 11, 591–612. doi: 10.1080/17435390.2017.1343404
- Deryabin, D. G., Efremova, L. V., Karimov, I. F., Manukhov, I. V., Gnuchikh, E. Y., and Miroshnikov, S. A. (2016). Comparative sensitivity of the luminescent *Photobacterium phosphoreum*, *Escherichia coli*, and *Bacillus subtilis* strains to toxic effects of carbon-based nanomaterials and metal nanoparticles. *Microbiology* 85, 198–206. doi: 10.1134/S0026261716020053
- Dubois, M., Gilles, K., Hamilton, J., Rebers, P., and Smith, F. (1956). Colorimetric method for determination of Sugars and related substances. *Anal. Chem.* 28, 350–356. doi: 10.1021/ac60111a017
- Farré, M., Pérez, S., Gajda-Schranz, K., Osorio, V., Kantiani, L., Ginebreda, A., et al. (2010). First determination of C60 and C70 fullerenes and N-methylfulleropyrrolidine C60 on the suspended material of wastewater effluents by liquid chromatography hybrid quadrupole linear ion trap tandem mass spectrometry. *J. Hydrol.* 383, 44–51. doi: 10.1016/j.jhydrol.2009.08.016
- Farré, M., Sanchis, J., and Barceló, D. (2011). Analysis and assessment of the occurrence, the fate and the behavior of nanomaterials in the environment. *TrAC Trends Anal. Chem.* 30, 517–527. doi: 10.1016/j.trac.2010.11.014
- Ferreira, J. L. R., Lonné, M. N., França, T. A., Maximilla, N. R., Lugokenski, T. H., Costa, P. G., et al. (2014). Co-exposure of the organic nanomaterial fullerene C60 with benzo[a]pyrene in *Danio rerio* (zebrafish) hepatocytes: evidence of toxicological interactions. *Aquat. Toxicol.* 147, 76–83. doi: 10.1016/j.aquatox.2013.12.007
- Flemming, H., and Wingender, J. (2010). The biofilm matrix. *Nat. Rev. Microbiol.* 8, 623–633. doi: 10.1038/nrmicro2415
- Folt, C., Chen, C., Moore, M., and Burnadord, J. (1999). Synergism and antagonism among multiple stressors. *Limnol. Oceanogr.* 44, 864–877. doi: 10.4319/lo.1999.44.3
- Freixa, A., Acuña, V., Sanchis, J., Farré, M., Barceló, D., and Sabater, S. (2018). Ecotoxicological effects of carbon based nanomaterials in aquatic organisms. *Sci. Total Environ.* 61, 328–337. doi: 10.1016/j.scitotenv.2017.11.095
- Galus, M., Kirischian, N., Higgins, S., Purdy, J., Chow, J., Ranganarajan, S., et al. (2013). Chronic, low concentration exposure to pharmaceuticals impacts multiple organ systems in zebrafish. *Aquat. Toxicol.* 13, 200–211. doi: 10.1016/j.aquatox.2012.12.021
- Gerbersdorf, S. U., Jancke, T., Westrich, B., and Paterson, D. M. (2008). Microbial stabilization of riverine sediments by extracellular polymeric substances. *Geobiology* 6, 57–69. doi: 10.1111/j.1472-4669.2007.00120.x
- Gorga, M., Petrovic, M., and Barceló, D. (2013). Multi-residue analytical method for the determination of endocrine disruptors and related compounds in river and waste water using dual column liquid chromatography switching system coupled to mass spectrometry. *J. Chromatogr. A* 1295, 57–66. doi: 10.1016/j.chroma.2013.04.028
- Gros, M., Rodríguez-Mozaz, S., and Barceló, D. (2012). Fast and comprehensive multi-residue analysis of a broad range of human and veterinary pharmaceuticals and some of their metabolites in surface and treated waters by ultra-high-performance liquid chromatography coupled to quadrupole-linear ion trap tandem. *J. Chromatogr. A* 1248, 104–121. doi: 10.1016/j.chroma.2012.05.084
- Guasch, H., Ricart, M., López-Doval, J., Bonnineau, C., Proia, L., Morin, S., et al. (2016). Influence of grazing on triclosan toxicity to stream periphyton. *Freshw. Biol.* 61, 2002–2012. doi: 10.1111/fwb.12797
- Heath, R. J., Rinald, R. J., Holland, D. R., Zhang, E., Snow, M. R., and Rock, C. O. (1999). Mechanism of triclosan inhibition of bacterial fatty acid synthesis. *J. Biol. Chem.* 274, 11110–11114. doi: 10.1074/jbc.274.16.11110
- Henry, T. B., Kwon, J.-W., Armbrust, K. L., and Black, M. C. (2004). Acute and chronic toxicity of five selective serotonin reuptake inhibitors in *Ceriodaphnia dubia*. *Environ. Toxicol. Chem.* 23, 2229–2233. doi: 10.1897/03-278
- Hu, X., Li, J., Shen, M., and Yin, D. (2015). Fullerene-associated phenanthrene contributes to bioaccumulation but is not toxic to fish. *Environ. Toxicol. Chem.* 34, 1023–1030. doi: 10.1002/etc.2876
- Hu, X., Liu, J., Mayer, P., and Jiang, G. (2008). Impacts of some environmentally relevant parameters on the sorption of polycyclic aromatic hydrocarbons to aqueous suspensions of fullerene. *Environ. Toxicol. Chem.* 27, 1868–1874. doi: 10.1897/08-009.1
- Huerta, B., Rodríguez-Mozaz, S., Nannou, C., Nakis, L., Ruhí, A., Acuña, V., et al. (2016). Determination of a broad spectrum of pharmaceuticals and endocrine disruptors in biofilm from a waste water treatment plant-impacted river. *Sci. Total Environ.* 540, 241–249. doi: 10.1016/j.scitotenv.2015.05.049
- Jeffrey, S., and Humphrey, G. (1975). New spectrophotometric equations for determining chlorophylls a, b, c1 and c2 in higher-plants, algae and natural phytoplankton. *Biochem. Physiol. Pflanz.* 167, 191–194.
- Kah, M., Zhang, X., Jonker, M. T. O., and Hofmann, T. (2011). Measuring and modeling adsorption of PAHs to carbon nanotubes over a six order of magnitude wide concentration range. *Environ. Sci. Technol.* 45, 6011–6017. doi: 10.1021/es2007726
- Knaier, K., Sobek, A., and Bucheli, T. D. (2007). Reduced toxicity of diuron to the freshwater green alga *Pseudokirchneriella subcapitata* in the presence of black carbon. *Aquat. Toxicol.* 83, 143–148. doi: 10.1016/j.aquatox.2007.03.021
- Kumar, K. S., Dahms, H. U., Lee, J. S., Kim, H. C., Lee, W. C., and Shin, K. H. (2014). Algal photosynthetic responses to toxic metals and herbicides assessed by chlorophyll a fluorescence. *Ecotoxicol. Environ. Saf.* 104, 51–71. doi: 10.1016/j.j.ecoenv.2014.01.042
- Kuzmanović, M., Ginebreda, A., Petrović, M., and Barceló, D. (2015). Risk assessment based prioritization of 200 organic micropollutants in 4 Iberian rivers. *Sci. Total Environ.* 50, 289–299. doi: 10.1016/j.scitotenv.2014.06.056
- Lawrence, J. R., Waiser, M. J., Swerhone, G. D. W., Roy, J., Tumber, V., Paule, A., et al. (2016). Effects of fullerene (C60), multi-wall carbon nanotubes (MWCNT), single wall carbon nanotubes (SWCNT) and hydroxyl and carboxyl modified single wall carbon nanotubes on riverine microbial communities. *Environ. Sci. Pollut. Res.* 23, 10090–10102. doi: 10.1007/s11356-016-6244-x
- Lawrence, J. R., Zhu, B., Swerhone, G. D. W., Roy, J., Wassenaar, L. I., Topp, E., et al. (2009). Comparative microscale analysis of the effects of triclosan and triclocarban on the structure and function of river biofilm communities. *Sci. Total Environ.* 407, 3307–3316. doi: 10.1016/j.scitotenv.2009.01.060
- Limbach, L. K., Wick, P., Manser, P., Grass, R. N., Bruinink, A., and Stark, W. J. (2007). Exposure of engineered nanoparticles to human lung epithelial cells: influence of chemical composition and catalytic activity on oxidative stress. *Environ. Sci. Technol.* 41, 4158–4163. doi: 10.1021/es062629t
- López-Doval, J. C., Ricart, M., Guasch, H., Romani, A. M., Sabater, S., and Muñoz, I. (2010). Does grazing pressure modify diuron toxicity in a biofilm community? *Arch. Environ. Contam. Toxicol.* 58, 955–962. doi: 10.1007/s00244-009-9441-5
- Lubarsky, H. V., Gerbersdorf, S. U., Hubas, C., Behrens, S., Ricciardi, F., and Paterson, D. M. (2012). Impairment of the bacterial biofilm stability by triclosan. *PLoS One* 7:e31183. doi: 10.1371/journal.pone.0031183
- Lyon, D. Y., Adams, L. K., Falkner, J. C., and Alvarez, P. J. J. (2006). Antibacterial activity of fullerene water suspensions: effects of preparation method and particle size. *Environ. Sci. Technol.* 40, 4360–4366. doi: 10.1021/es0603655
- McClellan, K., Altenburger, R., and Schmitt-Jansen, M. (2008). Pollution-induced community tolerance as a measure of species interaction in toxicity assessment. *J. Appl. Ecol.* 45, 1321–1329. doi: 10.1111/j.1365-2664.2007.0
- Minguez, L., Ballandonne, C., Rakotomalala, C., Dubreule, C., Kientz-Bouchart, V., and Halm-Lemeille, M. P. (2015). Transgenerational effects of two antidepressants (sertraline and venlafaxine) on *Daphnia magna* life history traits. *Environ. Sci. Technol.* 49, 1148–1155. doi: 10.1021/es504808g
- Moisset, S., Tiam, S. K., Feurtet-Mazel, A., Morin, S., Delmas, F., Mazzella, N., et al. (2015). Genetic and physiological responses of three freshwater diatoms to realistic diuron exposures. *Environ. Sci. Pollut. Res.* 22, 4046–4055. doi: 10.1007/s11356-014-3523-2
- Morin, S., Proia, L., Ricart, M., Bonnineau, C., Geislinger, A., Ricciardi, F., et al. (2010). Effects of a bactericide on the structure and survival of benthic diatom communities. *Vie Milieu* 60, 109–116.

- Nowack, B., and Bucheli, T. D. (2007). Occurrence, behavior and effects of nanoparticles in the environment. *Environ. Pollut.* 150, 5–22. doi: 10.1016/j.envpol.2007.06.006
- Pesce, S., Fajon, C., Bardot, C., Bonnemoy, F., Portelli, C., and Bohatier, J. (2006). Effects of the phenylurea herbicide diuron on natural riverine microbial communities in an experimental study. *Aquat. Toxicol.* 78, 303–314. doi: 10.1016/j.aquatox.2006.03.006
- Proia, L., Lupini, G., Osorio, V., Pérez, S., Barceló, D., Schwartz, T., et al. (2013). Response of biofilm bacterial communities to antibiotic pollutants in a Mediterranean river. *Chemosphere* 92, 1126–1135. doi: 10.1016/j.chemosphere.2013.01.063
- Proia, L., Morin, S., Peipoch, M., Romani, A. M., and Sabater, S. (2011). Resistance and recovery of river biofilms receiving short pulses of triclosan and diuron. *Sci. Total Environ.* 409, 3129–3137. doi: 10.1016/j.scitotenv.2011.05.013
- R Core Team (2017). *R: A Language and Environment for Statistical Computing*. Vienna: R Foundation for Statistical Computing. Available at: <http://www.R-project.org/>
- Ricart, M., Barceló, D., Geislinger, A., Guasch, H., de Alda, M. L., Romani, A. M., et al. (2009). Effects of low concentrations of the phenylurea herbicide diuron on biofilm algae and bacteria. *Chemosphere* 76, 1392–1401. doi: 10.1016/j.chemosphere.2009.06.017
- Ricart, M., Guasch, H., Alberch, M., Barceló, D., Bonnineau, C., Geislinger, A., et al. (2010). Triclosan persistence through wastewater treatment plants and its potential toxic effects on river biofilms. *Aquat. Toxicol.* 100, 346–353. doi: 10.1016/j.aquatox.2010.08.010
- Rodrigues, D. F., and Elimelech, M. (2010). Toxic effects of single-walled carbon nanotubes in the development of *E. coli* biofilm. *Environ. Sci. Technol.* 44, 4583–4589. doi: 10.1021/es1005785
- Romani, A. M., Fund, K., Artigas, J., Schwartz, T., Sabater, S., and Obst, U. (2008). Relevance of polymeric matrix enzymes during biofilm formation. *Microb. Ecol.* 56, 427–436. doi: 10.1007/s00248-007-9361-8
- Romero, F., Sabater, S., Timoner, X., and Acuña, V. (2018). Multistressor effects on river biofilms under global change conditions. *Sci. Total Environ.* 627, 1–10. doi: 10.1016/j.scitotenv.2018.01.161
- Sabater, S., Guasch, H., Ricart, M., Romani, A., Vidal, G., Klünder, C., et al. (2007). Monitoring the effect of chemicals on biological communities. The biofilm as an interface. *Anal. Bioanal. Chem.* 387, 1425–1434. doi: 10.1007/s00216-006-1051-8
- Sanchis, J., Bosch-Orea, C., Farré, M., and Barceló, D. (2015). Nanoparticle tracking analysis characterisation and parts-per-quadrillion determination of fullerenes in river samples from Barcelona catchment area. *Anal. Bioanal. Chem.* 407, 4261–4275. doi: 10.1007/s00216-014-8273-y
- Sanchis, J., Olmos, M., Vincent, P., Farré, M., and Barceló, D. (2016). New insights on the influence of organic co-contaminants on the aquatic toxicology of carbon nanomaterials. *Environ. Sci. Technol.* 50, 961–969. doi: 10.1021/acs.est.5b03966
- Schwab, F., Bucheli, T. D., Camenzuli, L., Magrez, A., Knauer, K., Sigg, L., et al. (2013). Diuron sorbed to carbon nanotubes exhibits enhanced toxicity to *Chlorella vulgaris*. *Environ. Sci. Technol.* 47, 7012–7019. doi: 10.1021/es304016u
- Tao, X., Yu, Y., Fortner, J. D., He, Y., Chen, Y., and Hughes, J. B. (2015). Effects of aqueous stable fullerene nanocrystal (nC60) on *Scenedesmus obliquus*: evaluation of the sub-lethal photosynthetic responses and inhibition mechanism. *Chemosphere* 122, 162–167. doi: 10.1016/j.chemosphere.2014.11.035
- Tili, A., Dorigo, U., Montuelle, B., Margoum, C., Carluer, N., Gouy, V., et al. (2008). Responses of chronically contaminated biofilms to short pulses of diuron. An experimental study simulating flooding events in a small river. *Aquat. Toxicol.* 87, 252–263. doi: 10.1016/j.aquatox.2008.02.004
- Tili, A., Marechal, M., Montuelle, B., Volat, B., Dorigo, U., and Berard, A. (2011). Use of the MicroResp method to assess pollution-induced community tolerance to metals for lotic biofilms. *Environ. Pollut.* 159, 18–24. doi: 10.1016/j.envpol.2010.09.033
- Wang, C., Shang, C., and Westerhoff, P. (2010). Quantification of fullerene aggregate nC60 in wastewater by high-performance liquid chromatography with UV-vis spectroscopic and mass spectrometric detection. *Chemosphere* 80, 334–339. doi: 10.1016/j.chemosphere.2010.03.052
- Yang, X. Y., Edelman, R. E., and Oris, J. T. (2010). Suspended C60 nanoparticles protect against short-term UV and fluoranthene photo-induced toxicity, but cause long-term cellular damage in *Daphnia magna*. *Aquat. Toxicol.* 100, 202–210. doi: 10.1016/j.aquatox.2009.08.011

**Conflict of Interest Statement:** The authors declare that the research was conducted in the absence of any commercial or financial relationships that could be construed as a potential conflict of interest.

The reviewer CB and handling Editor declared their shared affiliation.

Copyright © 2018 Freixa, Acuña, Gutierrez, Sanchis, Santos, Rodriguez-Mozaz, Farré, Barceló and Sabater. This is an open-access article distributed under the terms of the Creative Commons Attribution License (CC BY). The use, distribution or reproduction in other forums is permitted, provided the original author(s) and the copyright owner(s) are credited and that the original publication in this journal is cited, in accordance with accepted academic practice. No use, distribution or reproduction is permitted which does not comply with these terms.



# Plant Species and Heavy Metals Affect Biodiversity of Microbial Communities Associated With Metal-Tolerant Plants in Metalliferous Soils

Slawomir Borymski<sup>1\*</sup>, Mariusz Cycoń<sup>2</sup>, Manfred Beckmann<sup>3</sup>, Luis A. J. Mur<sup>3</sup> and Zofia Piotrowska-Seget<sup>1</sup>

<sup>1</sup> Department of Microbiology, Faculty of Biology and Environmental Protection, University of Silesia, Katowice, Poland,

<sup>2</sup> Department of Microbiology and Virology, School of Pharmacy with the Division of Laboratory Medicine, Medical University of Silesia, Sosnowiec, Poland, <sup>3</sup> Institute of Biological, Environmental and Rural Sciences, Aberystwyth University, Aberystwyth, United Kingdom

## OPEN ACCESS

### Edited by:

Fabrice Martin-Laurent,  
Institut National de la Recherche  
Agronomique (INRA), France

### Reviewed by:

Jincai Ma,  
Jilin University, China  
Haitham Sghaier,  
Centre National des Sciences et  
Technologies Nucléaires, Tunisia

### \*Correspondence:

Slawomir Borymski  
slawomir.borymski@us.edu.pl

### Specialty section:

This article was submitted to  
Microbiotechnology, Ecotoxicology  
and Bioremediation,  
a section of the journal  
Frontiers in Microbiology

**Received:** 06 March 2018

**Accepted:** 11 June 2018

**Published:** 16 July 2018

### Citation:

Borymski S, Cycoń M, Beckmann M,  
Mur LAJ and Piotrowska-Seget Z  
(2018) Plant Species and Heavy  
Metals Affect Biodiversity of Microbial  
Communities Associated With  
Metal-Tolerant Plants in Metalliferous  
Soils. *Front. Microbiol.* 9:1425.  
doi: 10.3389/fmicb.2018.01425

We here assess the biodiversity of the rhizosphere microbial communities of metal-tolerant plant species *Arabidopsis arenosa*, *Arabidopsis halleri*, *Deschampsia caespitosa*, and *Silene vulgaris* when growing on various heavy metal polluted sites. Our broad-spectrum analyses included counts for total and metal-tolerant culturable bacteria, assessments of microbial community structure by phospholipid fatty acid (PLFA) profiling and community-level analysis based on BIOLOG-CLPP to indicate functional diversity. The genetic-biochemical diversity was also measured by denaturing gradient gel electrophoresis (PCR-DGGE) and metabolomic analysis (HPLC-MS). Different rhizospheres showed distinctive profiles of microbial traits, which also differed significantly from bulk soil, indicating an influence from sampling site as well as plant species. However, total bacterial counts and PCR-DGGE profiles were most affected by the plants, whereas sampling site-connected variability was predominant for the PLFA profiles and an interaction of both factors for BIOLOG-CLPP. Correlations were also observed between pH, total and bioavailable Cd or Zn and measured microbial traits. Thus, both plant species and heavy-metals were shown to be major determinants of microbial community structure and function.

**Keywords:** heavy metals, rhizosphere biodiversity, BIOLOG-CLPP, PLFA, DGGE, HPLC-MS, metallophytes

## INTRODUCTION

Heavy metals pose a serious threat to soil organisms and the entire ecosystem when they occur at excessive amounts. Despite the high toxicity of metals to plants, some plants have developed mechanisms that enable them to survive in environments with elevated metal levels. These plants include obligate metallophytes (true metallophytes), which are often endemic to their native metalliferous sites and facultative metallophytes (pseudometallophytes), which can grow on both, polluted and not-polluted soils (Lucassen et al., 2009; Baker et al., 2010; van der Ent et al., 2013).

Metalliferous soils often represent sandy, nutrient-poor and dry substrates where plant coverage is low and patchy. Since the early work of Lorenz Hiltner, who coined a term “rhizosphere” in 1904, it is known that plants create a specific niche where microbial growth and activity become intensified (Hartmann et al., 2008). This rhizosphere effect is thought to arise from the deposition of various organic compounds from plants into the soil (Prashar et al., 2014). Plants exudate a variety of small and high molecular weight organic as well as inorganic compounds that enrich rhizosphere in nutrients that attract and stimulate soil microbial communities. For this reason, rhizosphere microbial communities tend to have higher microbial counts and generally show higher activity than those occurring in bulk soil. It has been estimated that between 10 and 40% of carbon assimilated by plants can be released into rhizosphere in various compounds, like amino acids, organic acids, phenolic compounds, proteins and polysaccharides (Bais et al., 2006). Plant-related compounds released to soil environment may also act as messengers that initiate interactions between roots and a wide range of soil organisms (Perrine-Walker et al., 2011).

It is believed, that plants select the bacteria that inhabit the soil around their roots. Therefore, the metallophyte rhizosphere may provide a nutrient-rich microenvironment that allows certain microbial communities to thrive or aid in the conferring metal tolerance. In line with this, different patterns of exudate composition have been observed for individual plant species and even individual genotypes (García-Villaraco Velasco et al., 2009). The rhizosphere of metallophytes typically consists of heavy metal tolerant bacteria, and thereby acts as a reservoir for specialized metal-tolerant microorganisms (Dechamps et al., 2005; Alford et al., 2010). Additionally, some metal-tolerant bacteria, especially plant growth-promoting bacteria, are known to enhance the phytoremediation of soils contaminated with heavy metals (Lasat et al., 2001; Abou-Shanab et al., 2003). Thus, both plants and microorganisms interact with themselves and surrounding soil environment to affect soil quality and function. Such functions must be centered on maintaining nutrient cycling and element turnover, which corresponds directly to energy transfer, biomass production and organic matter decay (Yan et al., 2008; Carrasco et al., 2010). In heavy metal contaminated soils, like mine tailings, which are often nutrient-poor, maintenance of these processes is a function of the metallophyte plants and microorganisms accompanying them (Zhang et al., 2012). Given such observations, studies on microbial community biodiversity linked with metal-tolerant plants and plant-soil-microbe interactions are of great importance for a better understanding of soil function as impacted by metallic stress. Moreover, understanding the relationship between the bacteria surrounding the roots of hyperaccumulators and pseudometallophytes is a key first step toward the extensive use of these plants in phytoremediation (Whiting et al., 2001; Abou-Shanab et al., 2006). The aim of this study was to provide a detailed structural and functional analyses of arrangement of plant-soil-microbe axes under condition of heavy metal pollution. We show that both plant species and heavy-metal contamination are major determinants of microbial community structure and function.

## MATERIALS AND METHODS

### Sample Collection for the Experiment

Rhizosphere soil samples of *Arabidopsis arenosa* (AA), *Arabidopsis halleri* (AH), *Deschampsia caespitosa* (DC) and *Silene vulgaris* (SV) and bulk soils (BK) were collected at the three separate heavy metal polluted areas in Poland, on June 16th 2012. The sampling time has been chosen based on the flowering periods of plants of interest. All plants were in their flowering stage during sample collection. The sampling sites consisted of a 50-year old zinc smelter waste heap in Piekary Slaskie-Brzozowice (site P - 50°22′02.8″N 18°58′19.2″E), and two sites located near the zinc works: 2 km to the north-east (site N - 50°30′48.2″N 18°56′47.1″E) and 2 km to the west (site W - 50°30′20.7″N 18°53′37.1″E) of a zinc works in Miasteczko Slaskie, Upper Silesia. All of the samples were collected during a single day. Blocks that included the root systems of individual plant species were excavated and shaken in order to remove loosely attached bulk soil. The blocks were collected randomly in triplicates within an area of 25 m<sup>2</sup> for each plant species per site. Any soil that adhered to the root systems was subsequently brushed off and considered to be the rhizosphere. Prior to analysis both the bulk soils and rhizospheres were sieved through 2 mm mesh in order to remove any gravel and plant debris.

### Soil Characteristics

Physico-chemical analyses involved the determination of the soil moisture, organic matter (SOM) content, pH, conductivity and the concentrations of Zn, Cd, Cu, and Ni ions. SOM was determined using a loss-on-ignition (LOI) method (EN 13039:2000). Moisture content was obtained by drying at 105°C and weighing in order to estimate mass loss (ISO 16586:2003). The measurement of the total heavy metal concentrations was carried out with use of inductively coupled plasma optical emission spectrometry (ICP-OES) (PN-EN 12457-2:2006). The bioavailable fraction of heavy metals was also assessed. Briefly, five g of dried soil samples were suspended in 50 mL of 0.01 M CaCl<sub>2</sub> solution and shaken in an orbital shaker for 2 h at 120 rpm to measure the bioavailable heavy metal content. The suspensions were then filtered through a 0.45 μm membrane and analyzed using atomic absorption spectroscopy (Unicam 939). The pH value of the aqueous soil extracts (1:5, w/v) were measured with a glass electrode (ISO 10390:2005) followed by conductivity measurements (ISO 11265:1994).

### Microbial Enumeration

The plate method was used to obtain the total oligotrophic, Zn- and Cd-tolerant culturable bacteria count. The total oligotrophic bacterial fraction was enumerated on 10% tryptic soy agar (TSA) with nystatin (50 μg/mL), while the Zn- and Cd-tolerant bacteria were counted on 10 % TSA supplemented with 1.5 mM of ZnCl<sub>2</sub> and 0.5 mM of CdCl<sub>2</sub>, respectively. A potato-dextrose agar (PDA) medium with Rose Bengal (30 μg/mL) and streptomycin (30 μg/mL) was used for screen for fungal strains. Each were incubated for 7 days at 25°C.

## Analysis of Microbial Community Structure by PLFA

The community structure of the non-culturable fraction of soil microorganisms was obtained by employing the phospholipid fatty acid (PLFA) analysis based on the Frostegard et al. (1993) protocol; with minor modifications. Lipids of microbial origin were extracted, fractionated, methylated and then analyzed in a GC system (Agilent 7820). Obtained FAMES were identified and quantified using the MIDI-MIS software (Sherlock TSBA6 library; MIDI Inc., Newark, DE, USA). Calculation of total biomass, microbial biomass, biomass of Gram-positive and Gram-negative bacteria, actinomycete and fungi, all expressed as nmol PLFA g<sup>-1</sup> soil d. w., was carried out based on specific lipid markers. Nonadecanoic acid (19:0) was used as an internal standard for the quantitative analysis. The procedure was described in detail in Cycon et al. (2016).

## Community-Level Physiological Profiles (CLPPs)

The physiological diversity of microbial communities was determined using BIOLOG EcoPlates™ (Biolog Inc., CA, USA). Ten grams of dry soil was shaken with 90 mL of a sterile 0.85% saline solution for 2 h. The 96-well BIOLOG microplates were inoculated with aliquots of a 120 μL (10<sup>-1</sup>) dilution and incubated at 24°C for 7 days. The readings were performed every 12 h using a Bio-Tek ELx808 microplate reader at 590 nm. Absorbance measurements were corrected against the water control well and the first reading (T<sub>0</sub>) in order to eliminate any disturbances resulting from possible background absorbance. CLPPs were calculated by means of the corrected optical density (ODi) and area under curve values (AUC) at the 84 h reading point. This enabled conditions to be optimized and allowed comparison between plates. The pattern of the AUC corresponded to the metabolic potential of microbial communities toward the 31 substrates present on the BIOLOG EcoPlates™. Standardized AUC data was used in the Principal Component Analysis (PCA). The sum of the AUC scores ( $\sum AUC$ ) for individual substrates was employed as a measurement of total catabolic activity. The Shannon-Wiener index ( $H'$ ) and evenness ( $Eh$ ) indices were calculated as  $H' = -\sum pi(\ln pi)$  and  $Eh = H'/H'_{max} = H'/\ln Rs$ , respectively, where  $pi$  is the ratio of the activity on each substrate (ODi) to the sum of activities on all substrates ( $\sum ODi$ ) and  $Rs$  is the number of oxidized substrates. All analyses were performed in triplicate.

## Soil Metabolomics (HPLC-MS)

Soil samples (200 mg) were placed in microcentrifuge tubes with a metal bead (5 mm diameter) and homogenized in an oscillation grinder for 10 min at 120 rpm. A 1 mL mixture of chloroform, methanol and ddH<sub>2</sub>O (1:2.5:1 v/v) was added. The samples were then thoroughly mixed and centrifuged for 3 min at 5,000 × g. A supernatant was transferred to new tubes, where 0.5 mL of ddH<sub>2</sub>O was added and samples were centrifuged again. Two phases—polar (top) and non-polar (bottom) were separated, dried using SpeedVac® concentrator (Thermo Scientific) and stored in a freezer at -80°C. Prior to analysis, the samples were

dissolved in 300 mL of 75 % methanol. From these, 20 μL of sample was diluted with 180 μL 75 % methanol, transferred to an LTQ-MS glass vial and sealed. Samples were kept at -20°C until run, in a randomized order, using an autosampler, with the tray temperature kept constant at 15°C. For each sample, 20 μL was injected into a flow volume of 60 μL per min in a ratio of 70 % water and 30 % methanol, using a Surveyor liquid chromatography system (Thermo Scientific, MA, USA). Data acquisition for each individual sample was conducted, in alternating positive and negative ionization mode, over four scan ranges (15–110  $m/z$ , 100–220  $m/z$ , 210–510  $m/z$ , 500–1,200  $m/z$ ) on an LTQ linear ion trap (Thermo Electron Corporation, CA, USA), with an acquisition time of 5 min. Individual metabolite  $m/z$  values were normalized as a percentage of the total ion count for each sample. Normalized abundances were subsequently analyzed using Pychem software (Jarvis et al., 2006) to obtain PCA scatterplots. Ten major sources of variation were subjected to further statistical analysis.

## Analysis of Microbial Community Structure by PCR-DGGE

Total DNA was extracted from 0.5 g soil samples using a GeneMATRIX Soil DNA Purification Kit (Eurx, Poland) as described in the manufacturer's instruction. The 16S rRNA gene fragment was amplified using the primers (GC-clamp)-F338 and R518 (Muyzer et al., 1993). Detailed information about this procedure was described in a previous paper (Cycon et al., 2013). The electrophoresis of the amplification products was performed in 8 % (w/v) polyacrylamide gel (37.5:1 acrylamide:bis-acrylamide) in the presence of a linear denaturing gradient that ranged from 40 to 70 % using a DCode Mutation Detection System (Bio-Rad, USA). In turn, a G BOX F3 System (Syngene, UK) was used to visualize the patterns of the bands that were obtained. Detailed information about the DGGE procedure was described in a previous paper (Cycon et al., 2016). The band patterns that were obtained from the DGGE analysis were analyzed using BioNumerics software ver. 7.5 (Applied Math, Belgium). The unweighted pair-group method and the arithmetic averages (UPGMA) were used to construct the phylogenetic dendrograms. The biodiversity of a soil bacterial community was expressed as the Shannon-Wiener index ( $H'$ ), richness ( $Rs$ ) and evenness ( $Eh$ ), which were calculated using the equations that were described in a previous paper (Cycon et al., 2013).

## RESULTS

### Soil Characteristics

The pH values obtained for tested samples were variable, however one consistent pattern could be distinguished (Table 1). The pH values were generally higher in W-derived samples (all above 7), regardless of the sample origin, with the highest score recorded in the rhizosphere of *S. vulgaris*. Against this, generally lower pH values were observed for N-derived samples achieving the lowest value in the *D. caespitosa* rhizosphere. Highly variable results were similarly obtained for total water content. The highest values of this parameter were recorded for *D. caespitosa* and *A. halleri* rhizospheres collected at the N sampling site.

In contrast, the lowest total water content was noted for the rhizosphere of *S. vulgaris* (site P). The water content appeared to be strongly connected with organic matter content, as it exhibited the same pattern of variability. The results obtained for soil conductivity indicated that the highest values were from *D. caespitosa* and *A. arenosa* rhizospheres, followed by bulk soil obtained at the site W. The least conductive sample was *S. vulgaris* rhizosphere (site N) (Table 1).

Extremely high concentrations of total heavy metals, up to 38,594 and 6,021 mg kg<sup>-1</sup> for Zn and Cd, respectively were

measured (Table 2). The highest Zn concentration was detected in bulk soil obtained from site P. In six samples, the Zn level was higher than 20,000 mg kg<sup>-1</sup> d. w. The lowest value was recorded for *D. caespitosa*, site N. Furthermore, three of the samples were found to have more than 5,000 mg kg<sup>-1</sup> d. w. Cd, bulk soil, *A. arenosa* rhizosphere and *D. caespitosa* rhizosphere collected at the W sampling site. The lowest concentration of Cd was noted for bulk soil sampled at the site N. A similar pattern was observed for total Cu content, but recorded concentrations were much lower and fell within the 69–424 mg kg<sup>-1</sup> d. w. range.

TABLE 1 | Physico-chemical parameters of sampled soils.

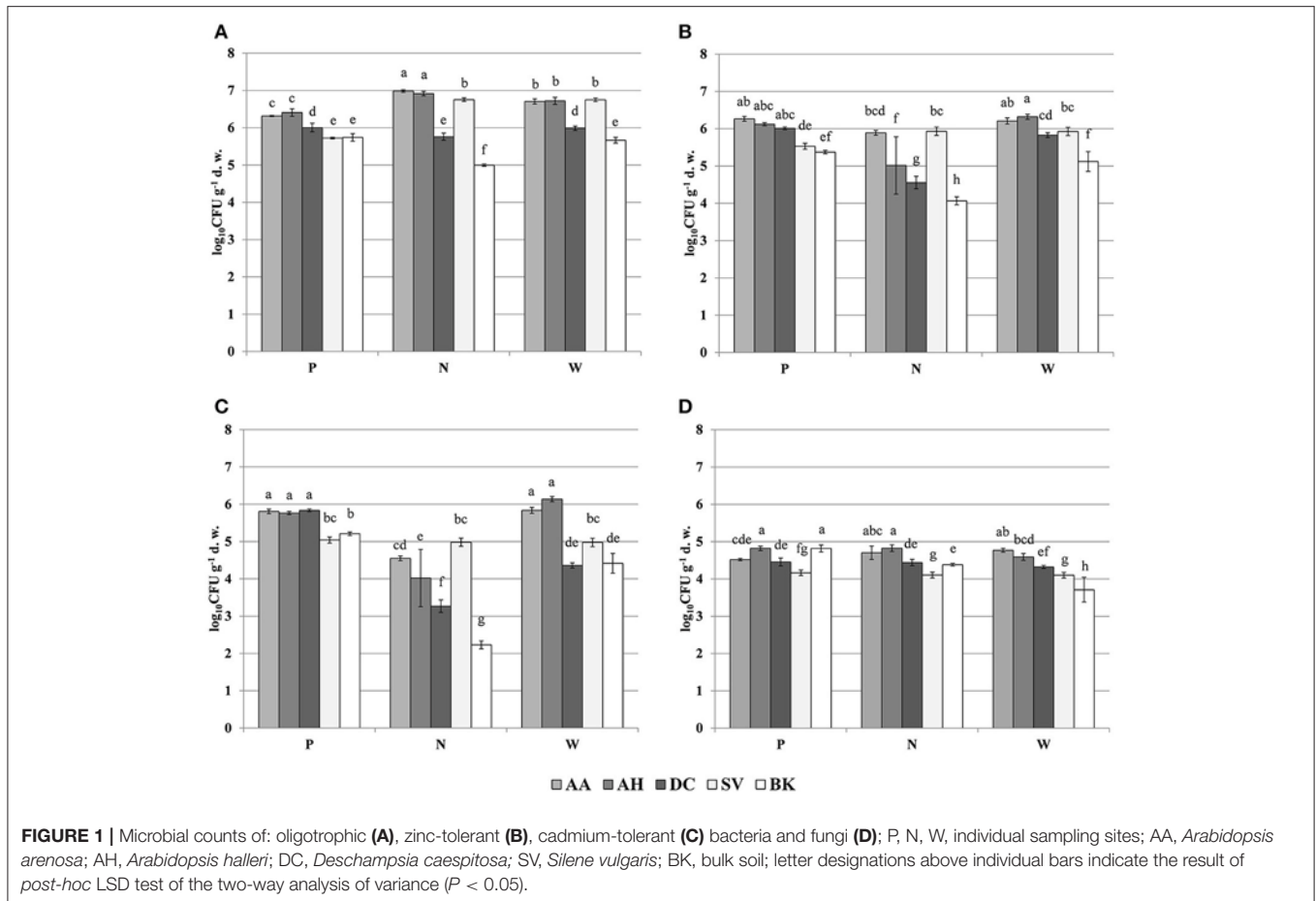
Origin	Site	pH	Conductivity [ $\mu$ S]	Water content [%]	SOM [%]
<i>Arabidopsis arenosa</i>	P	6.50 $\pm$ 0.20 <sup>d</sup>	169 $\pm$ 3.61 <sup>de</sup>	11.25 $\pm$ 1.86 <sup>f</sup>	7.25 $\pm$ 2.22 <sup>ef</sup>
	N	6.14 $\pm$ 0.18 <sup>e</sup>	142 $\pm$ 9.54 <sup>g</sup>	10.40 $\pm$ 1.62 <sup>f</sup>	10.03 $\pm$ 1.96 <sup>cde</sup>
	W	7.13 $\pm$ 0.13 <sup>b</sup>	575 $\pm$ 15.04 <sup>a</sup>	20.72 $\pm$ 2.14 <sup>c</sup>	10.39 $\pm$ 1.41 <sup>cd</sup>
<i>Arabidopsis halleri</i>	P	7.04 $\pm$ 0.17 <sup>ab</sup>	165 $\pm$ 13.00 <sup>ef</sup>	16.75 $\pm$ 1.17 <sup>d</sup>	11.50 $\pm$ 0.49 <sup>c</sup>
	N	5.16 $\pm$ 0.15 <sup>f</sup>	215 $\pm$ 15.72 <sup>c</sup>	26.06 $\pm$ 4.42 <sup>b</sup>	15.81 $\pm$ 2.63 <sup>b</sup>
	W	6.93 $\pm$ 0.10 <sup>ab</sup>	190 $\pm$ 10.54 <sup>d</sup>	13.10 $\pm$ 0.59 <sup>ef</sup>	8.20 $\pm$ 2.00 <sup>de</sup>
<i>Deschampsia caespitosa</i>	P	6.91 $\pm$ 0.28 <sup>ab</sup>	143 $\pm$ 22.48 <sup>fg</sup>	15.19 $\pm$ 2.05 <sup>de</sup>	8.93 $\pm$ 1.92 <sup>cde</sup>
	N	4.60 $\pm$ 0.16 <sup>g</sup>	161 $\pm$ 6.11 <sup>efg</sup>	32.06 $\pm$ 3.51 <sup>a</sup>	20.90 $\pm$ 3.43 <sup>a</sup>
	W	7.14 $\pm$ 0.11 <sup>b</sup>	591 $\pm$ 10.60 <sup>a</sup>	20.72 $\pm$ 2.61 <sup>c</sup>	9.12 $\pm$ 1.09 <sup>cde</sup>
<i>Silene vulgaris</i>	P	7.04 $\pm$ 0.16 <sup>ab</sup>	144 $\pm$ 13.05 <sup>fg</sup>	16.14 $\pm$ 1.12 <sup>de</sup>	9.69 $\pm$ 0.77 <sup>cde</sup>
	N	6.28 $\pm$ 0.18 <sup>de</sup>	74 $\pm$ 4.16 <sup>j</sup>	3.99 $\pm$ 0.87 <sup>g</sup>	3.57 $\pm$ 0.96 <sup>g</sup>
	W	7.78 $\pm$ 0.22 <sup>a</sup>	99 $\pm$ 9.07 <sup>h</sup>	2.92 $\pm$ 1.07 <sup>g</sup>	2.02 $\pm$ 0.19 <sup>g</sup>
Bulk soil	P	6.84 $\pm$ 0.07 <sup>c</sup>	151 $\pm$ 12.58 <sup>efg</sup>	23.84 $\pm$ 3.25 <sup>bc</sup>	14.59 $\pm$ 1.23 <sup>b</sup>
	N	5.27 $\pm$ 0.04 <sup>f</sup>	98 $\pm$ 3.79 <sup>h</sup>	10.23 $\pm$ 1.26 <sup>f</sup>	4.63 $\pm$ 1.37 <sup>fg</sup>
	W	7.01 $\pm$ 0.12 <sup>ab</sup>	371 $\pm$ 29.09 <sup>b</sup>	13.12 $\pm$ 0.90 <sup>ef</sup>	4.64 $\pm$ 0.43 <sup>fg</sup>

The data represent the means and standard deviations of three replicates. P, N, W indicate individual sampling sites. Different letters (within each group) indicate significant differences ( $P < 0.05$ , LSD test) considering sample origin and sampling site

TABLE 2 | Heavy metal content in sampled soils.

Origin	Site	Zn tot [mg kg <sup>-1</sup> d. w.]	Cd tot [mg kg <sup>-1</sup> d. w.]	Cu tot [mg kg <sup>-1</sup> d. w.]	Ni tot [mg kg <sup>-1</sup> d. w.]	Zn bio [mg kg <sup>-1</sup> d. w.]	Cd bio [mg kg <sup>-1</sup> d. w.]	Cu bio [mg kg <sup>-1</sup> d. w.]	Ni bio [mg kg <sup>-1</sup> d. w.]
<i>Arabidopsis arenosa</i>	P	8,365 $\pm$ 570 <sup>e</sup>	251 $\pm$ 21 <sup>ef</sup>	69 $\pm$ 6 <sup>j</sup>	ND $\pm$ –	350.24 $\pm$ 9.78 <sup>fg</sup>	18.36 $\pm$ 2.03 <sup>ef</sup>	0.14 $\pm$ 0.07 <sup>de</sup>	ND $\pm$ –
	N	4,052 $\pm$ 483 <sup>f</sup>	143 $\pm$ 15 <sup>f</sup>	85 $\pm$ 4 <sup>hi</sup>	ND $\pm$ –	363.75 $\pm$ 16.04 <sup>f</sup>	13.69 $\pm$ 0.91 <sup>fg</sup>	0.18 $\pm$ 0.06 <sup>cde</sup>	ND $\pm$ –
	W	31,942 $\pm$ 3,456 <sup>b</sup>	5,682 $\pm$ 715 <sup>a</sup>	316 $\pm$ 30 <sup>b</sup>	ND $\pm$ –	127.44 $\pm$ 12.13 <sup>j</sup>	91.10 $\pm$ 2.73 <sup>b</sup>	0.51 $\pm$ 0.13 <sup>a</sup>	ND $\pm$ –
<i>Arabidopsis halleri</i>	P	28,602 $\pm$ 2,400 <sup>b</sup>	1,063 $\pm$ 188 <sup>d</sup>	146 $\pm$ 2 <sup>de</sup>	ND $\pm$ –	488.30 $\pm$ 11.12 <sup>d</sup>	43.07 $\pm$ 12.2 <sup>d</sup>	0.17 $\pm$ 0.06 <sup>de</sup>	ND $\pm$ –
	N	5,842 $\pm$ 231 <sup>ef</sup>	175 $\pm$ 11 <sup>f</sup>	159 $\pm$ 5 <sup>d</sup>	ND $\pm$ –	578.14 $\pm$ 18.56 <sup>b</sup>	23.59 $\pm$ 4.32 <sup>e</sup>	0.28 $\pm$ 0.10 <sup>bcd</sup>	ND $\pm$ –
	W	15,969 $\pm$ 2,930 <sup>d</sup>	1,687 $\pm$ 282 <sup>bc</sup>	136 $\pm$ 4 <sup>e</sup>	ND $\pm$ –	133.24 $\pm$ 11.30 <sup>j</sup>	44.54 $\pm$ 3.54 <sup>d</sup>	0.18 $\pm$ 0.11 <sup>cde</sup>	ND $\pm$ –
<i>Deschampsia caespitosa</i>	P	20,951 $\pm$ 2,112 <sup>c</sup>	762 $\pm$ 131 <sup>de</sup>	93 $\pm$ 3 <sup>h</sup>	ND $\pm$ –	432.85 $\pm$ 16.52 <sup>e</sup>	39.50 $\pm$ 3.70 <sup>d</sup>	0.05 $\pm$ 0.06 <sup>e</sup>	ND $\pm$ –
	N	2,572 $\pm$ 188 <sup>f</sup>	83 $\pm$ 3 <sup>f</sup>	114 $\pm$ 9 <sup>g</sup>	ND $\pm$ –	475.95 $\pm$ 53.16 <sup>d</sup>	18.94 $\pm$ 3.30 <sup>ef</sup>	0.35 $\pm$ 0.05 <sup>b</sup>	ND $\pm$ –
	W	29,682 $\pm$ 3,008 <sup>b</sup>	5,735 $\pm$ 809 <sup>a</sup>	424 $\pm$ 13 <sup>a</sup>	ND $\pm$ –	87.08 $\pm$ 4.49 <sup>j</sup>	48.23 $\pm$ 3.46 <sup>d</sup>	0.59 $\pm$ 0.07 <sup>a</sup>	ND $\pm$ –
<i>Silene vulgaris</i>	P	28,422 $\pm$ 3,403 <sup>b</sup>	1,140 $\pm$ 309 <sup>cd</sup>	131 $\pm$ 16 <sup>ef</sup>	ND $\pm$ –	534.65 $\pm$ 19.58 <sup>c</sup>	62.78 $\pm$ 10.22 <sup>c</sup>	0.19 $\pm$ 0.12 <sup>cde</sup>	ND $\pm$ –
	N	3,517 $\pm$ 413 <sup>f</sup>	111 $\pm$ 11 <sup>f</sup>	73 $\pm$ 5 <sup>i</sup>	ND $\pm$ –	243.85 $\pm$ 21.26 <sup>h</sup>	10.88 $\pm$ 2.53 <sup>fg</sup>	0.16 $\pm$ 0.12 <sup>de</sup>	ND $\pm$ –
	W	3,581 $\pm$ 179 <sup>f</sup>	223 $\pm$ 12 <sup>ef</sup>	98 $\pm$ 39 <sup>h</sup>	ND $\pm$ –	11.87 $\pm$ 2.43 <sup>k</sup>	6.32 $\pm$ 1.84 <sup>g</sup>	0.22 $\pm$ 0.04 <sup>bcd</sup>	ND $\pm$ –
Bulk soil	P	38,594 $\pm$ 848 <sup>a</sup>	1,722 $\pm$ 319 <sup>b</sup>	197 $\pm$ 10 <sup>c</sup>	ND $\pm$ –	700.24 $\pm$ 52.35 <sup>a</sup>	63.40 $\pm$ 7.22 <sup>c</sup>	0.19 $\pm$ 0.05 <sup>cde</sup>	ND $\pm$ –
	N	2,538 $\pm$ 89 <sup>f</sup>	77 $\pm$ 4 <sup>f</sup>	72 $\pm$ 8 <sup>i</sup>	ND $\pm$ –	319.40 $\pm$ 18.24 <sup>g</sup>	12.18 $\pm$ 1.44 <sup>fg</sup>	0.32 $\pm$ 0.14 <sup>bc</sup>	ND $\pm$ –
	W	29,705 $\pm$ 4,253 <sup>b</sup>	6,021 $\pm$ 412 <sup>a</sup>	313 $\pm$ 18 <sup>b</sup>	ND $\pm$ –	158.54 $\pm$ 7.40 <sup>i</sup>	102.10 $\pm$ 5.76 <sup>a</sup>	0.32 $\pm$ 0.02 <sup>bc</sup>	ND $\pm$ –

The data represent the means and standard deviations of three replicates. P, N, W indicate individual sampling sites. Different letters (within each group) indicate significant differences ( $P < 0.05$ , LSD test) considering sample origin and sampling site (Two-way ANOVA); ND indicates that trait was not detected.



The highest concentration of bioavailable Zn were recorded for bulk soil samples obtained at the site P, as well as rhizospheres of *A. halleri*, obtained at N sampling site. The lowest concentrations of bioavailable Zn were obtained for *S. vulgaris* and *D. caespitosa*, both of which were collected at W sampling site. The highest concentrations of bioavailable Cd were noted for the bulk soil and *A. arenosa* rhizosphere, collected at the W sampling site. The lowest level of bioavailable Cd was detected in *S. vulgaris*-derived rhizospheres obtained at site W. All tested samples had less than  $1 \text{ mg kg}^{-1} \text{ d. w.}$  of bioavailable Cu. The highest concentration of the bioavailable Cu was recorded for *D. caespitosa* and *A. arenosa* rhizosphere, both from the W sampling site. The lowest value recorded for the bioavailable Cu was noted for *D. caespitosa* rhizospheres collected at the site P (Table 2).

## Microbial Counts

The oligotrophic fraction of culturable bacteria generally indicated a rhizosphere effect, as for most of the plants in tested sampling sites, microbial counts were significantly lower in bulk soils. This was very pronounced for both *Arabidopsis* species, which featured increases of up to two orders of magnitudes in  $\text{CFU g}^{-1} \text{ d. w.}$ , when compared to bulk soil at site N. There were also differences in bacteria counts between plant species. In all of the three sampling

sites, *D. caespitosa* showed significantly lower microbial counts (up to one order of magnitude lower), when compared with *Arabidopsis* species (Figure 1A). Metal-tolerant bacteria were one or even two orders of magnitude lower in number, when compared to oligotrophic fraction (Figures 1B,C). This was clearly visible especially in the Cd-tolerant fraction (Figure 1C). For oligotrophic bacteria, two-way analysis of variance indicated a strong effect of sample origin (above 69% of total variance) (Table 3). This pattern was also observed in the Zn-tolerant fraction, although an impact of sampling site and an interaction between both factors was observed (Table 3). For the Cd-tolerant fraction, sampling site appeared to have a dominant effect (Table 3). Such patterns were not observed in the fungal fraction, which were just below  $10^5 \text{ CFU g}^{-1} \text{ d. w.}$  for *A. halleri* rhizospheres obtained from sites P and N, with the lowest value observed for bulk soil at site W. However, for all three sampling sites, the *S. vulgaris* rhizospheres showed significantly lower fungal counts in comparison with other plant species (Figure 1D). Heavy metal contamination, when considered as a unique factor, had only a minor impact on microbial counts (Figure 7).

## PLFA Analysis

PLFA differed significantly between observed parameters (Table 4). The highest values for total PLFA biomass, reaching

**TABLE 3** | Analysis of variance (two-way ANOVA) for the measured biological parameters as affected by soil origin (O), sampling site (S) and their interactions (O × S).

Parameter	Source of variation	df	Sum of squares	Mean square	Variance explained (%)	F	P
<b>MICROBIAL COUNTS</b>							
Oligotrophic bacteria (10 % TSBA + nystatin)	Origin (O)	4	9.95	2.49	69.05	479.98	< 0.001***
	Sampling site (S)	2	0.87	0.43	6.02	83.73	< 0.001***
	O × S	8	3.44	0.43	23.85	82.91	< 0.001***
Zinc-tolerant bacteria (10 % TSBA + 1.5 mM Zn <sup>2+</sup> + nystatin)	Origin (O)	4	8.41	2.10	41.84	41.39	< 0.001***
	Sampling site (S)	2	6.05	3.02	30.10	59.55	< 0.001***
	O × S	8	4.11	0.51	20.48	10.13	< 0.001***
Cadmium-tolerant bacteria (10 % TSBA + 0.5 mM Cd <sup>2+</sup> + nystatin)	Origin (O)	4	13.21	3.30	25.88	37.21	< 0.001***
	Sampling site (S)	2	24.47	12.24	47.96	137.91	< 0.001***
	O × S	8	10.68	1.34	20.94	15.05	< 0.001***
Fungi (PDA + Rose Bengal + streptomycin)	Origin (O)	4	2.37	0.59	48.26	41.89	< 0.001***
	Sampling site (S)	2	0.54	0.27	10.95	19.01	< 0.001***
	O × S	8	1.58	0.20	32.16	13.96	< 0.001***
<b>PLFA</b>							
Total PLFA biomass	Origin (O)	4	23,178.72	5,794.68	36.05	17.17	< 0.001***
	Sampling site (S)	2	17,749.87	8,874.93	27.61	26.29	< 0.001***
	O × S	8	13,233.07	1,654.13	20.58	4.90	< 0.001***
Bacterial PLFA biomass (BB)	Origin (O)	4	3,709.42	927.36	41.83	18.09	< 0.001***
	Sampling site (S)	2	1,520.76	760.38	17.15	14.83	< 0.001***
	O × S	8	2,099.19	262.40	23.67	5.12	< 0.001***
Gram-positive bacteria PLFA biomass (GP)	Origin (O)	4	500.95	125.24	26.51	7.69	< 0.001***
	Sampling site (S)	2	550.03	275.02	29.11	16.89	< 0.001***
	O × S	8	350.20	43.77	18.53	2.69	0.023*
Gram-negative bacteria PLFA biomass (GN)	Origin (O)	4	1,362.35	340.59	51.74	34.49	< 0.001***
	Sampling site (S)	2	200.87	100.43	7.63	10.17	< 0.001***
	O × S	8	773.77	96.72	29.38	9.79	< 0.001***
GP:GN ratio	Origin (O)	4	0.06	0.02	3.52	1.12	0.364
	Sampling site (S)	2	0.94	0.47	54.43	34.75	< 0.001***
	O × S	8	0.32	0.04	18.55	2.96	0.014*
Actinomycetes PLFA biomass	Origin (O)	4	26.73	6.68	26.82	19.26	< 0.001***
	Sampling site (S)	2	50.31	25.16	50.50	72.52	< 0.001***
	O × S	8	12.19	1.52	12.23	4.39	0.001**
Fungal PLFA biomass (FB)	Origin (O)	4	131.08	32.77	59.62	95.20	< 0.001***
	Sampling site (S)	2	47.09	23.54	21.42	68.40	< 0.001***
	O × S	8	31.37	3.92	14.27	11.39	< 0.001***
BB:FB ratio	Origin (O)	4	1,129.17	282.29	44.86	107.88	< 0.001***
	Sampling site (S)	2	542.08	271.04	21.54	103.58	< 0.001***
	O × S	8	767.19	95.90	30.48	36.65	< 0.001***
<b>BIOLOG-CLPP</b>							
ΣAUC	Origin (O)	4	1,379,281.030	344,820.258	34.83	135.607	< 0.001***
	Sampling site (S)	2	1,394,786.201	697,393.100	35.22	274.263	< 0.001***
	O × S	8	1,109,553.371	138,694.171	28.02	54.544	< 0.001***
H'	Origin (O)	4	0.581	0.145	21.51	5.810	0.001**
	Sampling site (S)	2	0.379	0.190	14.05	7.588	0.002**
	O × S	8	0.989	0.124	36.67	4.951	0.001**
Rs	Origin (O)	4	84.089	21.022	15.94	3.403	0.021*
	Sampling site (S)	2	59.511	29.756	11.28	4.817	0.015*
	O × S	8	198.711	24.839	37.66	4.021	0.002**
Eh	Origin (O)	4	0.022	0.005	21.72	4.76	0.004**
	Sampling site (S)	2	0.014	0.007	13.99	6.13	0.006**
	O × S	8	0.030	0.004	30.06	3.29	0.008**

(Continued)

TABLE 3 | Continued

Parameter	Source of variation	df	Sum of squares	Mean square	Variance explained (%)	F	P
<b>DGGE</b>							
<i>H'</i>	Origin (O)	4	0.8251	0.2063	76.10	302.0	<0.001***
	Sampling site (S)	2	0.1158	0.0579	10.68	85.0	<0.001***
	O × S	8	0.1228	0.0154	11.33	22.0	<0.001***
<i>Rs</i>	Origin (O)	4	2,940.8	735.2	60.83	624.2	<0.001***
	Sampling site (S)	2	872.1	436.1	18.04	370.2	<0.001***
	O × S	8	986.5	123.3	20.40	104.7	<0.001***
<i>Eh</i>	Origin (O)	4	0.0047	0.0012	43.63	63.0	<0.001***
	Sampling site (S)	2	0.0015	0.0007	13.76	40.0	<0.001***
	O × S	8	0.0040	0.0005	37.45	27.0	<0.001***

*H'*, Shannon-Wiener biodiversity index; *Rs*, richness; *Eh*, evenness. Asterisks represent significance level according to ANOVA (\**P* < 0.05, \*\**P* < 0.01 and \*\*\**P* < 0.001).

TABLE 4 | PLFA biomass (nmol PLFA g<sup>-1</sup> d. w.) parameters as affected by soil origin (O), sampling site (S) and their interactions.

Origin	Site	Total PLFA	Bacterial PLFA	Bacteria		GP:GN	Actinomycetes	Fungi	Bacteria:fungi
				Gram-positive (GP)	Gram-negative (GN)				
AA	P	138.63 ± 30.00 <sup>a</sup>	43.54 ± 10.72 <sup>ab</sup>	19.62 ± 6.45 <sup>ab</sup>	21.92 ± 3.84 <sup>bcd</sup>	0.88 ± 0.16 <sup>ab</sup>	5.63 ± 0.63 <sup>ab</sup>	9.49 ± 1.17 <sup>a</sup>	4.54 ± 0.60 <sup>j</sup>
	N	104.35 ± 11.84 <sup>ab</sup>	36.26 ± 3.70 <sup>b-e</sup>	16.05 ± 3.02 <sup>b-e</sup>	18.29 ± 0.84 <sup>cde</sup>	0.87 ± 0.15 <sup>ab</sup>	3.25 ± 0.63 <sup>cd</sup>	4.13 ± 0.31 <sup>c</sup>	8.81 ± 1.04 <sup>fg</sup>
	W	103.93 ± 31.37 <sup>ab</sup>	34.86 ± 11.11 <sup>b-e</sup>	10.61 ± 4.71 <sup>d-g</sup>	22.74 ± 6.06 <sup>bc</sup>	0.45 ± 0.11 <sup>f</sup>	2.70 ± 0.66 <sup>cde</sup>	5.62 ± 1.29 <sup>b</sup>	6.11 ± 0.65 <sup>hij</sup>
AH	P	143.64 ± 11.54 <sup>a</sup>	46.25 ± 4.27 <sup>b</sup>	17.80 ± 2.59 <sup>bc</sup>	26.52 ± 1.52 <sup>b</sup>	0.67 ± 0.06 <sup>cde</sup>	5.84 ± 0.83 <sup>a</sup>	6.07 ± 0.36 <sup>b</sup>	7.61 ± 0.37 <sup>f-i</sup>
	N	145.08 ± 29.83 <sup>a</sup>	62.74 ± 14.81 <sup>a</sup>	24.57 ± 8.72 <sup>a</sup>	36.08 ± 6.49 <sup>a</sup>	0.67 ± 0.16 <sup>cde</sup>	3.48 ± 0.25 <sup>c</sup>	3.52 ± 0.76 <sup>cd</sup>	17.87 ± 2.54 <sup>b</sup>
	W	90.26 ± 19.25 <sup>c</sup>	32.20 ± 7.32 <sup>cde</sup>	12.06 ± 3.42 <sup>c-g</sup>	18.73 ± 3.61 <sup>cde</sup>	0.64 ± 0.07 <sup>def</sup>	2.48 ± 0.37 <sup>de</sup>	4.37 ± 0.57 <sup>c</sup>	7.30 ± 0.79 <sup>ghi</sup>
DC	P	74.58 ± 11.75 <sup>cd</sup>	25.19 ± 4.43 <sup>ef</sup>	9.53 ± 2.67 <sup>e-h</sup>	14.65 ± 2.23 <sup>efg</sup>	0.65 ± 0.16 <sup>cde</sup>	2.60 ± 0.41 <sup>cde</sup>	2.54 ± 0.48 <sup>de</sup>	10.04 ± 1.60 <sup>ef</sup>
	N	88.90 ± 25.43 <sup>c</sup>	38.84 ± 10.89 <sup>bcd</sup>	18.94 ± 6.91 <sup>ab</sup>	18.43 ± 3.73 <sup>cde</sup>	1.01 ± 0.21 <sup>a</sup>	2.05 ± 0.39 <sup>ef</sup>	1.12 ± 0.34 <sup>f</sup>	34.80 ± 2.35 <sup>a</sup>
	W	77.83 ± 15.60 <sup>cd</sup>	28.19 ± 5.94 <sup>def</sup>	9.03 ± 2.93 <sup>f-h</sup>	18.00 ± 2.86 <sup>cde</sup>	0.49 ± 0.10 <sup>ef</sup>	2.00 ± 0.24 <sup>ef</sup>	1.92 ± 0.16 <sup>ef</sup>	14.68 ± 3.07 <sup>c</sup>
SV	P	103.25 ± 2.66 <sup>ab</sup>	31.81 ± 1.65 <sup>cde</sup>	13.19 ± 0.54 <sup>b-f</sup>	16.83 ± 1.28 <sup>def</sup>	0.79 ± 0.02 <sup>bcd</sup>	3.14 ± 0.13 <sup>cd</sup>	4.02 ± 0.45 <sup>c</sup>	8.01 ± 1.41 <sup>fg</sup>
	N	76.13 ± 9.45 <sup>cd</sup>	24.45 ± 2.99 <sup>ef</sup>	10.60 ± 1.84 <sup>d-g</sup>	12.44 ± 1.02 <sup>fgh</sup>	0.85 ± 0.09 <sup>abc</sup>	2.40 ± 0.40 <sup>de</sup>	4.25 ± 0.20 <sup>c</sup>	5.76 ± 0.67 <sup>hij</sup>
	W	29.35 ± 4.40 <sup>e</sup>	9.04 ± 1.82 <sup>g</sup>	2.89 ± 0.70 <sup>h</sup>	5.75 ± 1.08 <sup>i</sup>	0.50 ± 0.07 <sup>ef</sup>	1.31 ± 0.98 <sup>fg</sup>	1.85 ± 0.49 <sup>ef</sup>	4.97 ± 0.60 <sup>ij</sup>
BK	P	133.03 ± 18.84 <sup>ab</sup>	40.16 ± 4.74 <sup>ab</sup>	16.71 ± 2.16 <sup>bcd</sup>	21.41 ± 2.31 <sup>bcd</sup>	0.78 ± 0.03 <sup>bcd</sup>	4.72 ± 0.78 <sup>b</sup>	3.42 ± 0.18 <sup>cd</sup>	11.73 ± 0.80 <sup>de</sup>
	N	49.94 ± 4.81 <sup>de</sup>	18.26 ± 1.43 <sup>fg</sup>	8.62 ± 1.01 <sup>f-h</sup>	8.72 ± 0.42 <sup>hi</sup>	0.99 ± 0.10 <sup>a</sup>	2.07 ± 0.98 <sup>ef</sup>	1.33 ± 0.14 <sup>f</sup>	13.84 ± 1.33 <sup>cd</sup>
	W	48.65 ± 11.14 <sup>de</sup>	18.05 ± 3.59 <sup>fg</sup>	6.18 ± 1.87 <sup>g-h</sup>	10.94 ± 1.46 <sup>ghi</sup>	0.56 ± 0.10 <sup>ef</sup>	0.76 ± 0.06 <sup>h</sup>	1.31 ± 0.32 <sup>f</sup>	14.08 ± 2.73 <sup>cd</sup>

The data represent the means and standard deviations of three replicates. Different letters (within each group) indicate significant differences (*P* < 0.05, LSD test) considering sample origin and sampling site (Two-way ANOVA). AA, *Arabidopsis arenosa*; AH, *Arabidopsis halleri*; DC, *Deschampsia caespitosa*; SV, *Silene vulgaris*; BK, bulk soil.

>140 nmol PLFA g<sup>-1</sup> d. w., were observed for samples obtained from the rhizosphere of *A. halleri* species at sites P and N. The lowest values were observed in the rhizospheres of *S. vulgaris* collected at the site W, as well as bulk soil samples obtained at the site N and W. A similar trend was observed for bacterial biomass where the maximal biomass was noted for the *A. halleri* rhizosphere from site N. The lowest mean value of bacterial biomass was recorded for *S. vulgaris* samples obtained from the W sampling site. This pattern extended to Gram-positive and Gram-negative bacterial biomass although the values obtained for Gram-negative bacteria were generally higher. Thus, the Gram-positive to Gram-negative bacterial ratio was lower than 1 in all of the samples, except *D. caespitosa* rhizospheres from N site where ratios were at near parity. The lowest values, linked for a major dominance of Gram-negative bacteria, were noted for the *A. arenosa*, *D. caespitosa*, *S. vulgaris* and bulk soil samples

from site W. The highest actinomycete biomass was recorded for rhizospheres obtained from *A. arenosa* and *A. halleri* collected from the P sampling site, while the lowest value was noted for bulk soils obtained from site W. Considering fungal biomass, the highest measurement was recorded for the rhizosphere of *A. arenosa* from site P. The lowest values were measured in the rhizosphere of *D. caespitosa* from N sampling site and bulk soil samples obtained at sites W and N. The highest bacterial to fungal biomass ratio was obtained for the samples collected from the *D. caespitosa* rhizosphere at the site P, whereas the lowest was recorded for the *A. arenosa*-derived samples obtained at the P sampling site. Generally, low values were also recorded for samples obtained from *S. vulgaris* rhizospheres.

Most of the tested parameters, especially the quantitative parameters, were found to be associated more with sample origin (i.e., rhizosphere vs. bulk soil) over sampling site although

interactions between sample origin and site were occasionally significant. In case of total PLFA biomass, sampling origin explained 36.05 % of variance and in the case of fungal biomass up to 59.62 % of variance. For three of the tested PLFA parameters, Gram-positive bacterial biomass, Gram-positive to Gram-negative bacterial biomass ratio and actinomycete biomass, the sampling site turned out to be the major source of variation (Table 3).

The ordination plot of CCA for standardized PLFA profiles showed a distinct clustering of the samples along axis 1 (Figure 2A). Three major clusters could be distinguished and were related to individual sampling sites (P, N, and W). There was a strong correlation between pH and sample scattering along axis 1. Additionally, a significant effect of total Cd, Zn, Cu, conductivity as well as bioavailable Cd was seen in the PLFA profiles (Figure 7). This corresponded with the bulk soil and rhizospheres of *D. caespitosa*, obtained at site W (Figure 2A). Additionally, there was a correlation between these parameters and 16:1 $\omega$ 7 as well as 18:1 $\omega$ 7 fatty acids (Figure 2B). Interestingly, the impact of bioavailable Zn is differed from that of bioavailable Cd, Cu or total Cd, Zn, and Cu concentrations. Therefore Zn could act as a stimulant for certain microbial groups, as opposed to Cd.

## CLPP Analysis

Assessments based on the BIOLOG method showed that the catabolic activity of the microbial communities varied significantly for individual microbial communities (Table 5). The highest values of total catabolic activity ( $\sum$ AUC) were recorded for the rhizosphere samples of *A. halleri* and *S. vulgaris*, from site N. High values were also obtained for rhizospheres from the same species at the site W, as well as the rhizosphere of *A. arenosa* collected at the site P. The lowest catabolic activity was observed for the rhizosphere of *S. vulgaris* and bulk soil samples obtained at the site P and W. Generally a higher  $\sum$ AUC score was noted for rhizosphere samples in comparison with the bulk soil equivalents obtained from the same sampling sites, indicating a distinctive rhizosphere effect. Similar patterns were obtained for the Shannon-Wiener biodiversity ( $H'$ ) as well as evenness ( $Eh$ ) indices, reaching peak values for *A. arenosa*-derived samples at site N and the lowest for bulk soil from site W. The most active microbial communities in terms of the total number of oxidized substrates ( $R_s$  index), were derived from the rhizospheres of *A. arenosa* and *A. halleri*, site N and W. The lowest score was again noted for the bulk soil, site W (Table 5). The two-way ANOVA showed that all of the factors were almost equally explanatory to the total variance observed for the  $\sum$ AUC with regard to sampling site, sample origin and interactions between both factors. The other parameters were mostly affected by the interaction of sample origin and sampling site. Even though the effect of sample origin and sampling site was less pronounced, the impact of those factors on CLPP indices was statistically significant (Table 3). The ordination plot of standardized AUC profiles of individual substrates showed a distinct scattering of samples mainly along axis 1, explaining 55.96 % of total variance (Figure 3A). A distinct, tight cluster of *D. caespitosa*, *A. arenosa* rhizospheres as well as bulk soils derived from site W can be

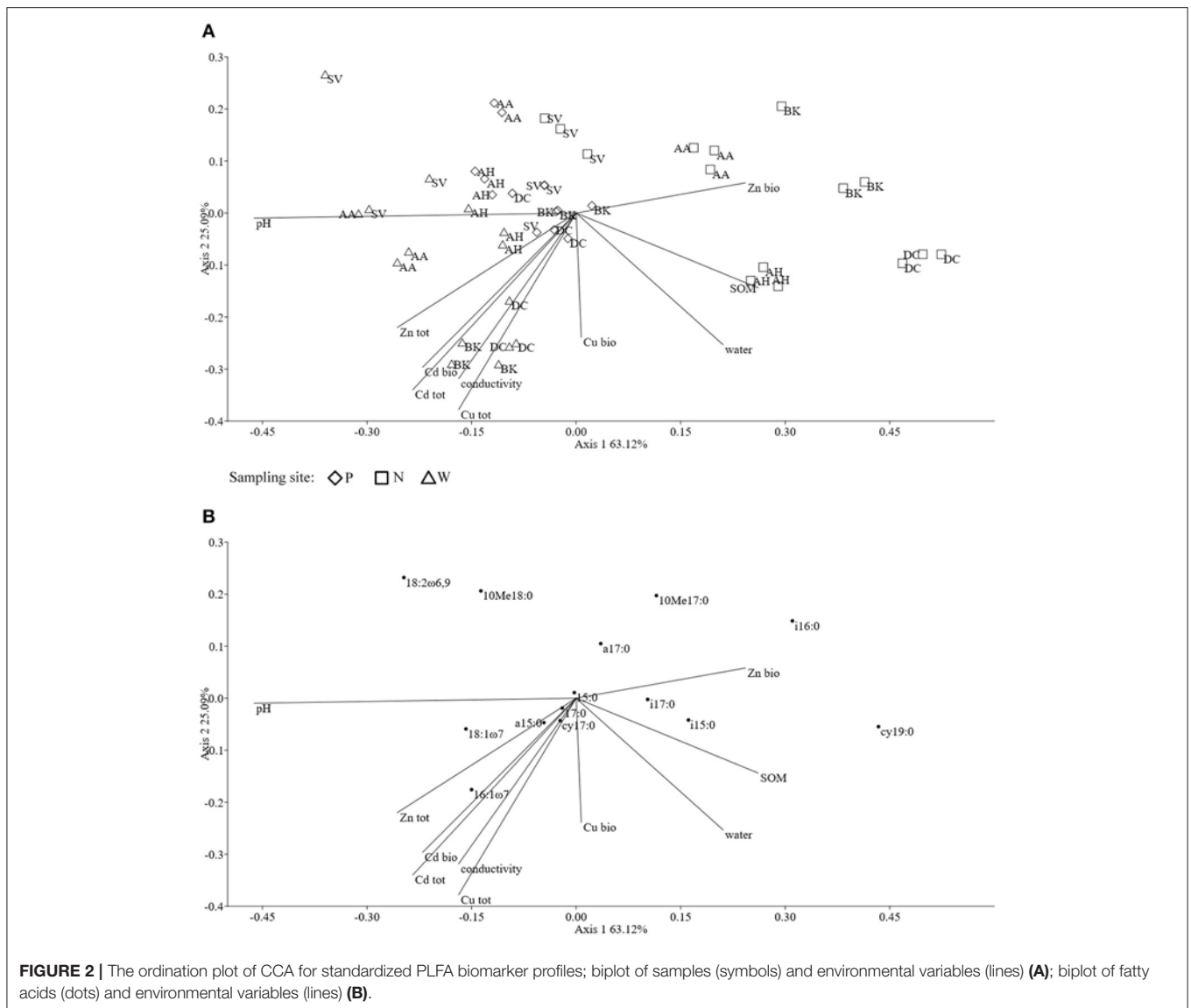
observed. Overall, the separation could be related to heavy-metal concentration and was most influenced by total Cd and Zn as well as bioavailable Zn. Total Cu content, conductivity or pH proved to be minor contributors. The CCA biplot of individual substrates and environmental variables showed, that the oxidation of  $\alpha$ -cyclodextrin, D-cellobiose, glycogen and glycyl-L-glutamic acid by microbial communities was significantly affected by the presence of heavy metals (Figure 3B). This indicates a significant effect of heavy metal contamination on microbial CLPPs. The significance of this effect was also confirmed by a strong negative correlation between BIOLOG indices and total contents of Zn, Cd, and Cu, as well as bioavailable Cd (Figure 7).

## HPLC-MS Analysis

The obtained MS data was subjected to PCA (data not shown). Ten identified major sources of variation (out of 2,106 variables) were used for CCA in order to detect any links between soil physico-chemical parameters and MS data. The CCA biplot of samples and soil environmental data showed a distinct scattering that was found to be impacted mostly by soil pH, however this was mostly along axis 2, explaining only just above 8 % of total variation. However, an impact of the presence of heavy metals, in both total and bioavailable fractions, was seen for *D. caespitosa* rhizosphere and bulk soil (site W). They were correlated with total Cd as well as both total and bioavailable Cu, as well as soil conductivity and separated along axis 1 which explained 87 % of total variation (Figure 4A). The metabolites associated with these environmental variables were of low molecular weight (35.00, 66.90, 68.90, 80.81, and 82.81  $m/z$ ). Database comparisons based on accurate mass, led to their tentative identification (Table 6; Figure 4B). The *A. arenosa* rhizosphere obtained from the W sampling site correlated with soil pH and bioavailable Cd. Interestingly, the *A. halleri* rhizosphere samples separated in the opposite direction, to the left of axis 1, regardless of the sampling site, and correlated with 124.90 and 225.081  $m/z$  metabolites that could potentially correspond to arsenous acid, formic acid and indole, 3-(2-aminoethyl)-7-methoxy-, hydrochloride or 2,2,4-trimethyl-1,3-pentanediol, respectively (Table 6; Figures 4A,B).

## PCR-DGGE Analysis

Cluster analysis of the DGGE profiles revealed a mixed pattern for the structure of dominant bacterial communities (Figure 5). The major source of variation (sampling site or sample origin) could not be identified solely based on the clustering pattern itself, therefore, biodiversity indices were also analyzed. The genetic diversity ( $H'$ ), richness ( $R_s$ ) and evenness ( $Eh$ ) indices showed significant differences between tested samples (Figure 6). A distinct, origin-dependent pattern can be observed for both,  $H'$  and  $R_s$  indices. Among the obtained rhizospheres, the highest values of  $H'$  and  $R_s$  indices were noted for samples derived from *D. caespitosa*, while the lowest were linked to *A. halleri*, regardless of sampling site. Surprisingly, the bulk soil did not show a typical rhizosphere-effect pattern. The  $H'$  and  $R_s$  indices were relatively high, reaching values comparable with those obtained for *D. caespitosa* rhizospheres or even higher for samples obtained at site W (Figure 6). Two-way



ANOVA clearly showed, that sample origin accounted for the majority of total variation observed (Table 3). The highest values for  $Eh$  index were recorded for *D. caespitosa* only in samples from P and N sampling sites. However, the lowest values of this index were noted in samples associated with *A. arenosa*. Two-way ANOVA showed that sample origin as well as the interaction between sample origin and sampling site explained most of the total variance observed in the  $Eh$  index (Table 3).

The Spearman correlation analysis of PCR-DGGE indices with environmental variables showed a significant negative impact of conductivity on all of the indices. This was in accord with the negative correlation found between the  $Eh$  index and total fractions of Zn, Cd and Cu as well as bioavailable Cd. Additionally, the bioavailable Cd negatively affected the  $H'$  index as well. However,  $H'$  and  $R_s$  indices were positively correlated with bioavailable Zn. This suggests a stimulative effect

of bioavailable Zn on the microbial composition, whereas the effect of Cd was clearly adverse (Figure 7).

Datasets obtained via individual techniques provided unique information regarding specific microbial traits, such as microbial counts, structural, functional and genetic biodiversity, as well as metabolomic profiling. Spearman correlation analysis revealed only a slight positive correlation for  $\sum AUC$  and richness index obtained from DGGE, as well as  $\sum AUC$  and microbial counts for oligotrophic microbial fraction (Figure 7).

## DISCUSSION

The urgent requirement to deal with the impact of environmental pollution with heavy metals demands that a more thorough understanding of how plants interact with the rhizosphere microbes in contaminated soils. In this study, we extensively

**TABLE 5** | BIOLOG parameters as affected by soil origin (O), sampling site (S), and their interactions.

Origin	Site	$\Sigma$ AUC	H'	Rs	Eh
<i>Arabidopsis arenosa</i>	P	454.35 ± 13.21 <sup>c</sup>	2.98 ± 0.06 <sup>ab</sup>	29.00 ± 1.00 <sup>a</sup>	0.88 ± 0.02 <sup>abc</sup>
	N	660.19 ± 43.57 <sup>b</sup>	3.06 ± 0.03 <sup>a</sup>	27.67 ± 1.53 <sup>abc</sup>	0.92 ± 0.01 <sup>a</sup>
	W	174.09 ± 54.67 <sup>de</sup>	2.57 ± 0.28 <sup>c</sup>	24.33 ± 5.03 <sup>cd</sup>	0.81 ± 0.05 <sup>ef</sup>
<i>Arabidopsis halleri</i>	P	110.40 ± 59.36 <sup>efg</sup>	2.56 ± 0.31 <sup>c</sup>	21.00 ± 6.00 <sup>de</sup>	0.85 ± 0.02 <sup>bcde</sup>
	N	885.88 ± 65.27 <sup>a</sup>	2.95 ± 0.03 <sup>ab</sup>	28.67 ± 0.58 <sup>ab</sup>	0.88 ± 0.01 <sup>abc</sup>
	W	677.57 ± 88.56 <sup>b</sup>	2.98 ± 0.05 <sup>ab</sup>	29.00 ± 1.00 <sup>a</sup>	0.88 ± 0.01 <sup>abc</sup>
<i>Deschampsia caespitosa</i>	P	86.43 ± 34.75 <sup>fg</sup>	2.97 ± 0.36 <sup>ab</sup>	27.33 ± 3.51 <sup>abc</sup>	0.90 ± 0.09 <sup>ab</sup>
	N	375.26 ± 57.17 <sup>c</sup>	2.76 ± 0.04 <sup>bc</sup>	27.00 ± 0.00 <sup>abc</sup>	0.84 ± 0.01 <sup>cde</sup>
	W	248.11 ± 18.75 <sup>d</sup>	2.66 ± 0.06 <sup>c</sup>	25.33 ± 0.58 <sup>abc</sup>	0.82 ± 0.01 <sup>def</sup>
<i>Silene vulgaris</i>	P	32.47 ± 1.47 <sup>g</sup>	2.79 ± 0.17 <sup>bc</sup>	24.67 ± 1.53 <sup>bcd</sup>	0.87 ± 0.04 <sup>abcd</sup>
	N	817.98 ± 75.70 <sup>a</sup>	3.00 ± 0.05 <sup>ab</sup>	28.00 ± 1.00 <sup>abc</sup>	0.90 ± 0.01 <sup>ab</sup>
	W	659.82 ± 80.76 <sup>b</sup>	2.94 ± 0.04 <sup>ab</sup>	27.00 ± 1.00 <sup>abc</sup>	0.89 ± 0.00 <sup>ab</sup>
Bulk soil	P	53.88 ± 14.96 <sup>g</sup>	2.65 ± 0.06 <sup>c</sup>	24.00 ± 2.00 <sup>cd</sup>	0.83 ± 0.03 <sup>cde</sup>
	N	154.43 ± 12.01 <sup>ef</sup>	2.80 ± 0.08 <sup>abc</sup>	26.33 ± 1.15 <sup>abc</sup>	0.86 ± 0.01 <sup>bcde</sup>
	W	58.43 ± 1.69 <sup>g</sup>	2.29 ± 0.12 <sup>d</sup>	19.33 ± 2.08 <sup>e</sup>	0.78 ± 0.05 <sup>f</sup>

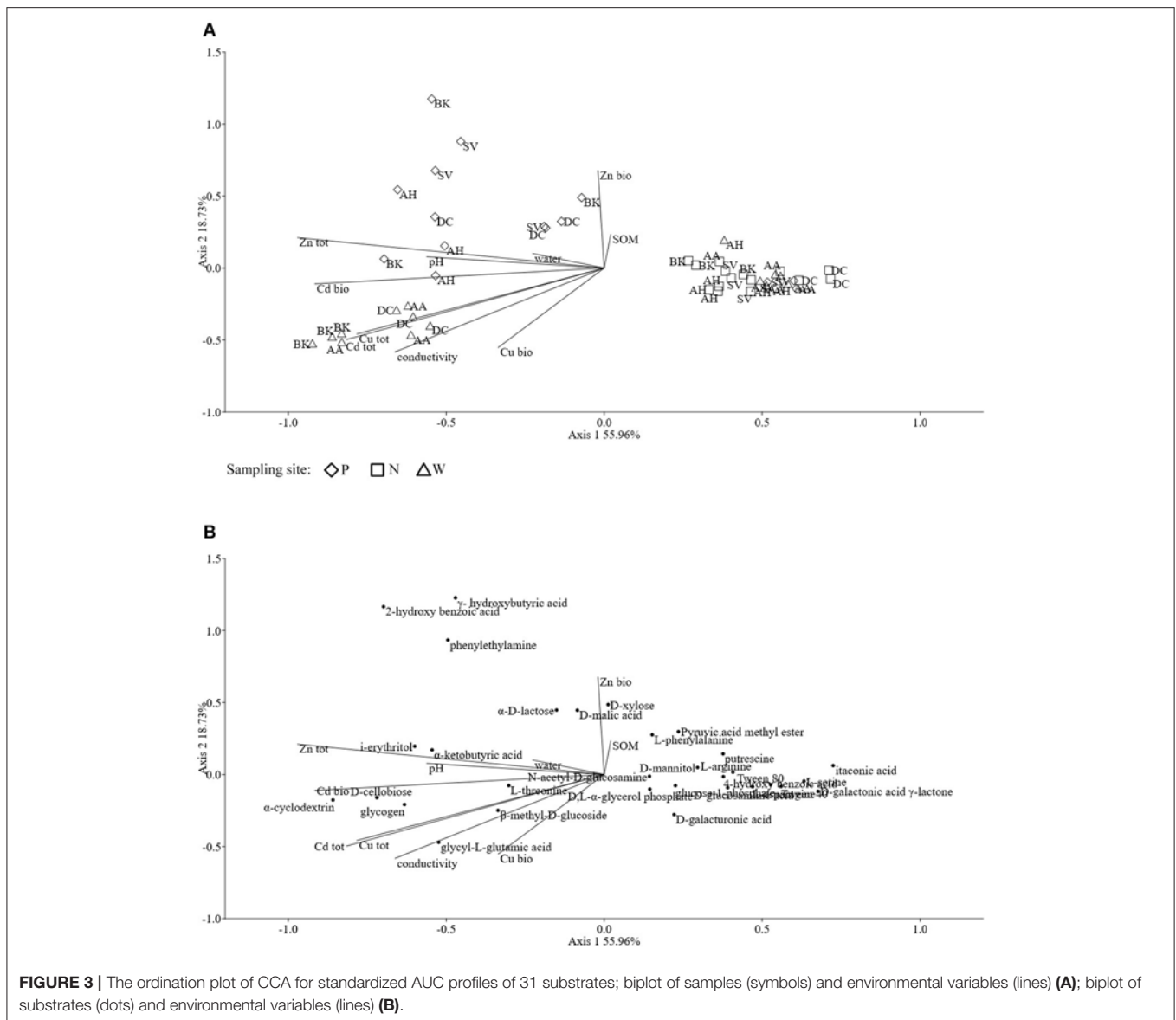
The data represent the means and standard deviations of three replicates. Different letters (within each group) indicate significant differences ( $P < 0.05$ , LSD test) considering sample origin and sampling site (Two-way ANOVA).  $\Sigma$ AUC, summed area under the curve for all the substrates; H', Shannon-Wiener index; Rs, richness; Eh, evenness.

characterized the rhizosphere microbial communities of *Arabidopsis arenosa*, *Arabidopsis halleri*, *Deschampsia caespitosa*, *Silene vulgaris* as well as bulk soils with high heavy metal content. These species could be classified to a group broadly referred to as pseudometallophytes (Baker et al., 2010; van der Ent et al., 2013). Nonetheless, multiple classification systems coexist and therefore a definite assignment for certain metal-tolerant plants is difficult. For instance, *A. halleri* is a known zinc and cadmium hyperaccumulator, yet some populations of this species are known to occur in non-metalliferous sites (Pauwels et al., 2006; Meyer et al., 2010). Furthermore, the exact functionality of such species is likely to be dependent on and therefore reflect, associated microbial communities. Therefore, in this study, we concentrated not only on the structure but crucially on some functional aspects of differing microbial populations. These could define the ability of a particular plant species to survive on heavy metal contaminated soil.

In our study, rhizosphere microbial communities reached significantly higher microbial counts for both total oligotrophic bacteria fractions as well as metal-tolerant ones. As demonstrated in many previous studies (Houlden et al., 2008; Oliveira et al., 2008), microbial counts were positively affected by the presence of a plant. This phenomenon, known as the rhizosphere effect, arises from the release of plant-derived metabolites that serve as carbon source for various microorganisms (Bais et al., 2006; Hartmann et al., 2009; Hinsinger et al., 2009). Plants might also recruit certain groups of microorganisms which are useful to them. Rudrappa et al. (2008) showed, that L-malic acid secreted by *Arabidopsis thaliana* roots recruited *Bacillus subtilis* which had beneficial effect on disease-affected plants. Below-ground microflora modifications in response to whitefly infestation of *Capsicum annuum*, contributed to the exhibition of systemic resistance and improved plant growth (Yang et al., 2011).

The results obtained for the metal-tolerant microbial counts can be influenced by the choice of growth medium, especially when defining microbial resistance to specific metal. Between many components of growth media, such as phosphates, broth components, organic acids and metals, an interaction may occur. In fact, up to 90% of the applied concentration of metal ions may be complexed by the medium and this effect is especially prominent in broth containing media, which are considered "rich" (Mergeay, 1995). To mitigate this effect, in our study a diluted 10 % concentration of trypticase soy broth agar (TSBA) was used. Broth media, such as nutrient agar (NA), Luria-Bertani (LB) and TSBA are still used in metal tolerance assays, along with substrate-amended mineral media, like 284 medium (Piotrowska-Seget et al., 2005; Freitas et al., 2008; Becerra-Castro et al., 2012). Although it cannot be considered as bias-free, the selected concentrations of 1.5 mM Zn<sup>2+</sup> and 0.5 mM Cd<sup>2+</sup> used in our work, resulted in lower metal-tolerant bacterial counts in comparison with oligotrophic fraction obtained on a metal-free 10% TSBA, which indicates the limiting effect of metal supplementation.

Our study demonstrated a significant impact of plant species on the genetic diversity of microbial communities, as revealed by 16S rRNA PCR-DGGE analysis. The role of plants in the determination of microbial communities was also shown by Chaparro et al. (2014), who related root exudates at four developmental stages of *Arabidopsis thaliana* with changes in microbial rhizosphere communities. They observed significant differences in the microbial community structure during plant development, especially between the seedling and vegetative, bolting and flowering stages. In our study, individual plant species showed specific patterns of DGGE biodiversity indices. This effect of plant species was significant and the differences could be distinguished even between *A. halleri* and *A. arenosa*, regardless the sampling site or heavy metal content. This



accorded with a study conducted by Wang et al. (2008), who examined a potential effect of copper on soil microbial activity and community composition in samples derived from Cu-accumulator, *Elsholtzia splendens*, and a non-Cu-accumulator plant, *Trifolium repens*. Soil microbial biomass and phosphatase activity in the *E. splendens* rhizosphere were higher than those of *T. repens*. Also the PCR-DGGE fingerprint analysis showed that Cu decreased the number of bands in bare soil and soil with *T. repens*, but significantly increased the number of bands in Cu-amended soils with *E. splendens*. In our work, a significant difference in PCR-DGGE biodiversity indices and band numbers was observed even between the soils derived from a hyperaccumulator *Arabidopsis halleri* and non-hyperaccumulator *Arabidopsis arenosa*. The literature shows that the rhizobiome of hyperaccumulators is likely to contain of specific Gram-positive genera (Melo et al., 2011;

Visioli et al., 2015). Similarly, Luo et al. (2017), found a significant impact of Cd/Zn hyperaccumulating and non-hyperaccumulating genotypes of *Sedum alfredii* on the plant-associated microbial community structure. The rhizosphere of hyperaccumulating plant also showed lower total OTU counts than non-hyperaccumulating one. In our work, *A. halleri* rhizospheres featured the lowest Shannon-Wiener index as well as DGGE band counts than any other rhizosphere or bulk soil.

This need not indicate that plant species alone influences microbial population. Schlaeppi et al. (2014) revealed that the composition of rhizosphere microbial communities was influenced more by wide array of environmental parameters. Zhang et al. (2016) examined the effects of heavy metals and soil physicochemical properties on microbial biomass and structure in wetlands and saw a significant impact of heavy metals. However, it seems likely that plant and metals interact to

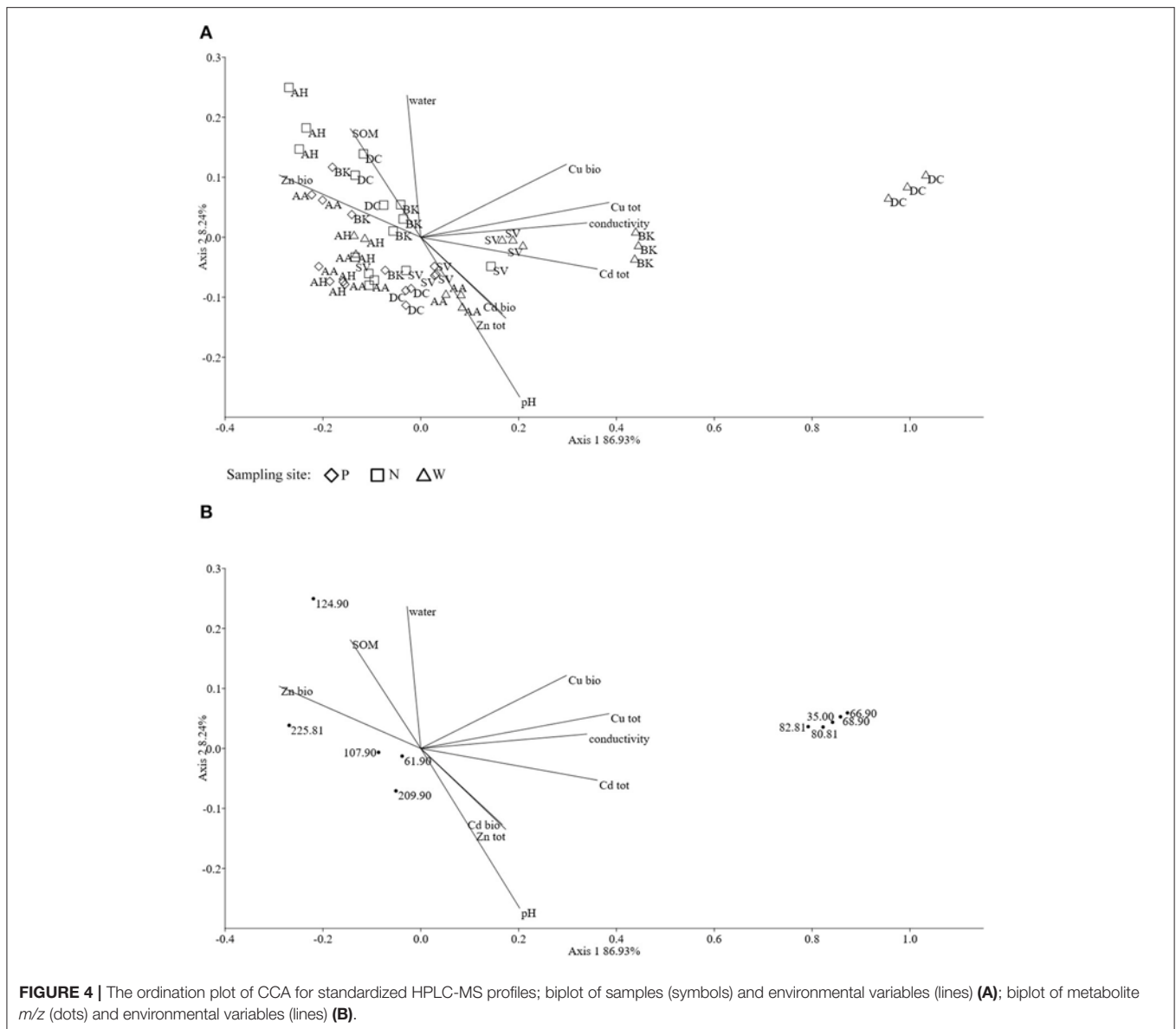


**FIGURE 4 |** The ordination plot of CCA for standardized HPLC-MS profiles; biplot of samples (symbols) and environmental variables (lines) **(A)**; biplot of metabolite *m/z* (dots) and environmental variables (lines) **(B)**.

influence rhizosphere microbiology. Wood et al. (2016) observed a significant impact of both cadmium concentration and plant on the Shannon diversity index of obtained OTU profiles in the rhizosphere microbial communities of a Cd accumulator *Carpobrotus rossii*.

Microbial community structure can also be characterized on the basis of biochemical markers, such as PLFAs. This method relies on the fact, that some PLFAs are characteristic of certain microbial groups, such as Gram-positive and Gram-negative bacteria, actinomycete as well as fungi (Frostegard et al., 1996). Impact of plants on PLFA profiles was demonstrated through administration of  $^{13}\text{C}$ -labeled mixture of glucose, glycine and fumaric acid into soil in proportions resembling the exudate profile of young *Lolium perenne* plants (Paterson et al., 2007). There were significant changes in the Gram-positive and Gram-negative bacteria, fungi and actinomycete biomass for each substrate, thus proving the major impact of rhizodeposition on

the microbial community structure (Paterson et al., 2007). The effect of plant exudates on the structural biodiversity of soil microbiota was also demonstrated by Kozdrój and Van Elsas (2000) in soils contaminated with heavy metals. A dominant effect of the plant on microbial community structure was observed by Pacwa-Płociniczak et al. (2018) in a study regarding the effect of *Silene vulgaris* and Cd presence on soil microbiota. Against this, in our work, no impact of plant species on microbial PLFA profiles was observed. This may result from the fact, that soil microbial communities in the environment were subjected to physical or chemical stimuli that could have masked the effect of plant exudates. In this context, water content and pH are known to affect soil microbial communities to a great extent and our work clearly showed the impact of pH on PLFA biomarkers. Shifts in pH, water and organic matter content can effectively influence the bioavailable heavy metal concentration (Rieuwerts et al., 1998; Gadd, 2004, 2010).

**TABLE 6** | Metabolite candidates for obtained *m/z* peaks.

Metabolite name	Molecular formula	Mass ( <i>m/z</i> )		Adduct delta
		Detected	Accurate	
No data	–	35.00	–	–
No data	–	61.90	–	–
Hydrazine*	H <sub>4</sub> N <sub>2</sub>	66.90	67.007 [M+Cl]1-	0.107
Pyrazole*	C <sub>3</sub> H <sub>4</sub> N <sub>2</sub>		67.030 [M-H]1-	0.130
Methanol*	C <sub>4</sub> H <sub>6</sub> O		66.996 [M+Cl]1-	0.096
Imidazole*	C <sub>3</sub> H <sub>4</sub> N <sub>2</sub>		67.030 [M-H]1-	0.130
3-Butyn-2-ol*	C <sub>4</sub> H <sub>6</sub> O	68.90	69.035 [M-H]1-	0.135
Propynoic acid*	C <sub>3</sub> H <sub>2</sub> O <sub>2</sub>		68.998 [M-H]1-	0.098
Beta-aminopropionitrile*	C <sub>3</sub> H <sub>6</sub> N <sub>2</sub>		69.046 [M-H]1-	0.146
2-Butyn-1-ol*	C <sub>4</sub> H <sub>6</sub> O		69.035 [M-H]1-	0.135
3-Butyn-1-ol*	C <sub>4</sub> H <sub>6</sub> O		69.035 [M-H]1-	0.135
Formic acid*	CH <sub>2</sub> O <sub>2</sub>	80.81	80.975 [M+Cl]1-	0.165
Sulfurous acid*	H <sub>2</sub> O <sub>3</sub> S		80.965 [M+Cl]1-	0.155
Methyl hydroperoxide*	CH <sub>4</sub> O <sub>2</sub>	82.81	82.991 [M+Cl]1-	0.181
Methanethiol*	CH <sub>4</sub> S		82.973 [M+Cl]1-	0.163
Chloric acid**	HClO <sub>3</sub>		82.954 [M+Cl]1-	0.144
No data	–	107.90	–	–
Arsenous acid*	H <sub>3</sub> AsO <sub>3</sub>	124.90	124.923 [M-H]1-	0.023
Formic acid*	CH <sub>2</sub> O <sub>2</sub>		124.924 [M+Br]1-	0.024
No data	–	209.90	–	–
Indole, 3-(2-aminoethyl)-7-methoxy, hydrochloride*	C <sub>11</sub> H <sub>15</sub> ClN <sub>2</sub> O	225.81	225.080 [M-H]1-	–0.001
2,2,4-trimethyl-1,3-pentanediol*	C <sub>8</sub> H <sub>18</sub> O <sub>2</sub>		225.050 [M+Br]1-	–0.031

Data origin: \* <https://dimedb.ibers.aber.ac.uk/>; \*\* Individual accurate mass assessment.

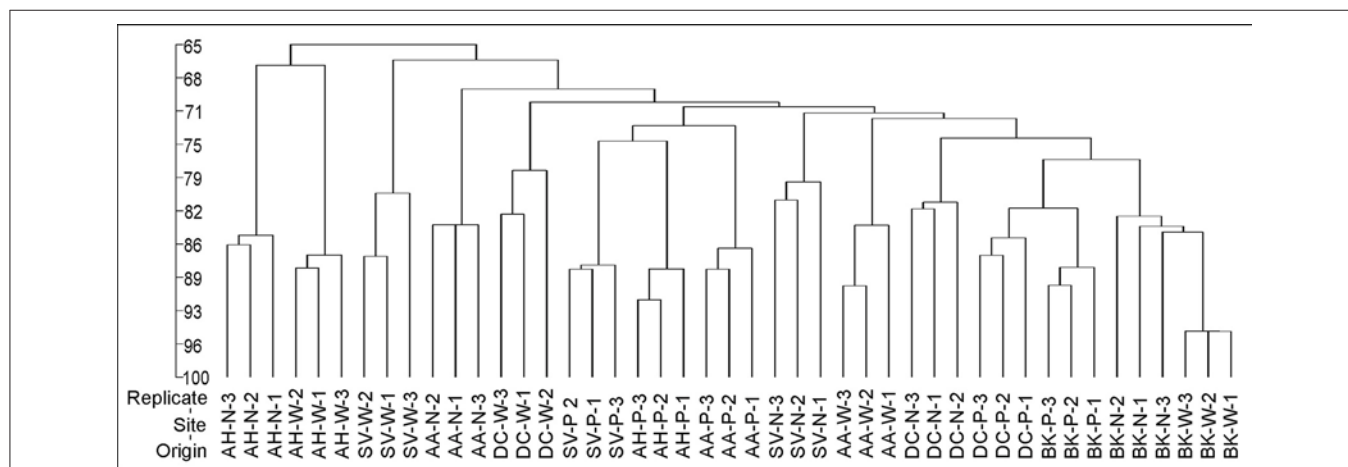
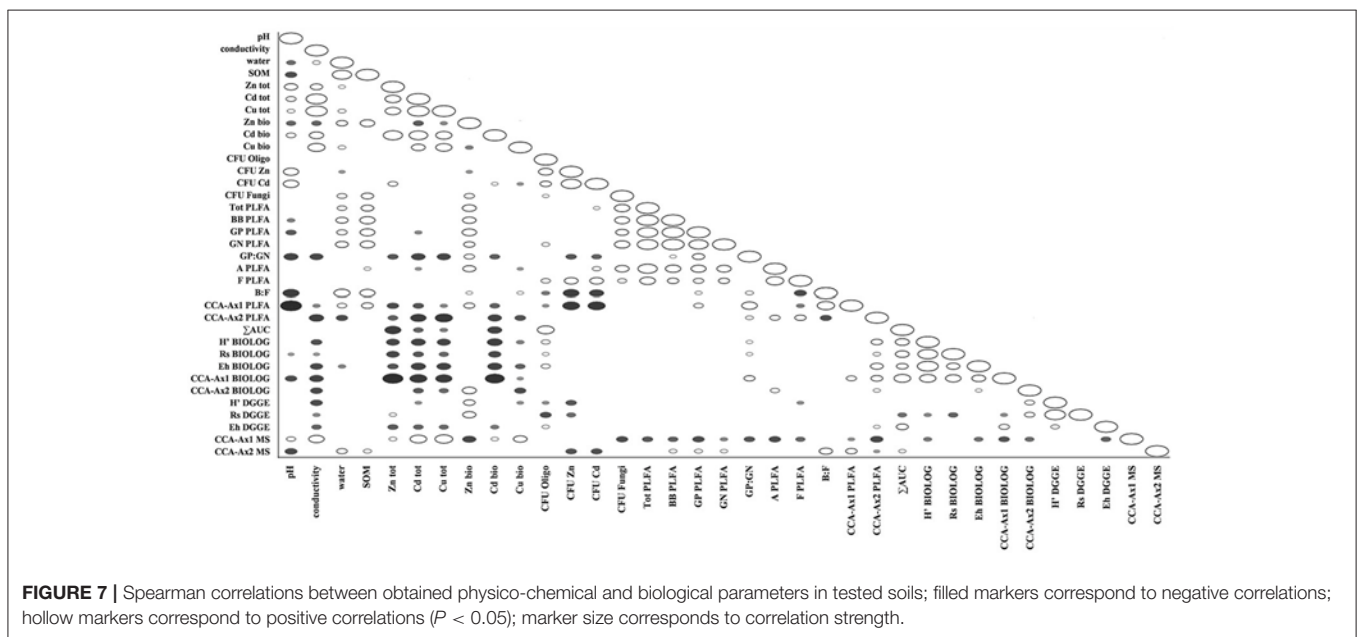
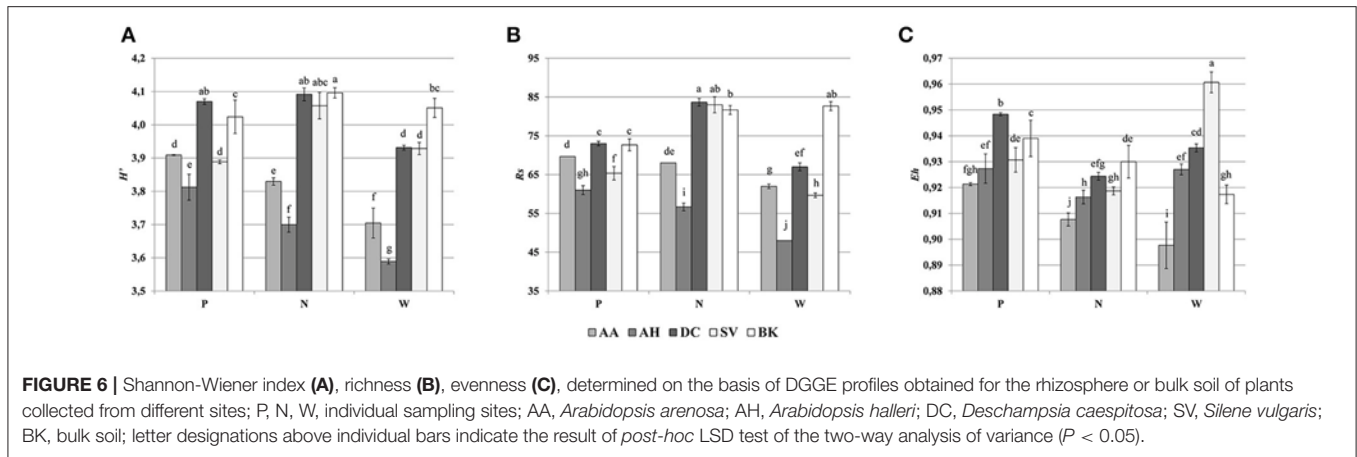


**FIGURE 5** | The phylogenetic dendrogram for PCR-amplified fragments of the 16S rRNA gene generated on the basis of DGGE profiles obtained for the rhizosphere or bulk soil collected from different sites; P, N, W, individual sampling sites; AA, *Arabidopsis arenosa*; AH, *Arabidopsis halleri*; DC, *Deschampsia caespitosa*; SV, *Silene vulgaris*; BK, bulk soil.

Several studies have indicated that heavy metals might be an important factor affecting rhizosphere microbial communities (Frostegård et al., 1996; Frostegård et al., 2011; Li et al., 2017). For instance, a significant impact of As on paddy soils was shown using the PLFA analysis of rhizospheres derived

from rice plants (Li et al., 2017). In particular, biomarkers associated with Gram-negative bacteria, such as 16:0, 16:1ω7c, 16:1ω9c, 18:1ω7c, and 18:1ω9c was shown to increase with the presence of heavy metals. In our study, we also observed a strong influence of Cd as well as sampling site on the



PLFA microbial profiles. Shifts between Gram-positive and Gram-negative bacterial biomarkers were noted. In particular, 16:1 $\omega$ 7 was identified as the major source of variation and was strongly associated with total and bioavailable Cd as well as total Zn. It is worth noting, that heavy metal-dependent variations were observed mainly in qualitative data, such as PLFA profiles, rather than quantitative, like PLFA biomass.

To examine if plant-derived metabolites might affect microbial abundance and activity, the metabolic potential of different microbial communities was measured using BIOLOG-CLPP (Martínez-Iñigo et al., 2009). Earlier studies using CLPP profiling of microbial communities derived from bulk soil as well as *Dactylis glomerata*, *Phalaris arundinacea*, *Phleum pretense*, and *Trifolium pratense* rhizospheres demonstrated a significant effect of plant species on the microbial metabolic potential (Söderberg et al., 2004). This effect surpassed even the impact of

different soils used in the experiment. The Söderberg et al. (2004) study however did not include heavy-metal contamination as additional variable, which was important factor in our work. In this regard, Li et al. (2011) found no significant relationship between the functional diversity indices and heavy-metal content. Instead, a significant impact of *Erigeron annuus* and *Lysimachia clethroides* plants species on CLPP profiles was demonstrated. Similar results were obtained in a study on Ni phytoextraction in serpentine soils, where the phenotypic structure of the bacterial communities appeared to be specific to the plant cover (Rue et al., 2015). Nevertheless, other studies have suggested heavy metals have significant effects on the microbial CLPPs (Stefanowicz et al., 2008). In our study, we observed a drop in microbial metabolic activity with exposure to heavy metals. The tested soils were heavily contaminated with heavy metals, especially Zn and Cd. Cd, in particular, being a non-essential metal, is considered to be significantly more toxic

than Zn or Cu (Guo et al., 2010; Clemens and Ma, 2016; Sobariu et al., 2017).

To help define the exact nature of the plant exudates that could be influencing microbial communities, metabolomic approaches were adopted. These analyses revealed that several compounds of the same molecular mass were found in *Arabidopsis* species. Phenolic compounds are recognized as common *Arabidopsis* exudates that modulate rhizosphere microbial communities (Badri et al., 2013). Tentative identification only was possible in our study but several other low-molecular compounds were noted in samples containing Cd.

Considering known responses of plant metabolism to heavy-metal toxicity, various compounds of known antioxidative properties are produced such as carotenoid-related xanthophylls, glutathione or ascorbic acid. Some secondary metabolites, such as polyphenols (flavonoids, especially anthocyanins) act against reactive oxygen species (Sytar et al., 2013). Organic acids, such as malate, citrate and oxalate might play an important role in metal binding in plants, especially in the roots (Rascio and Navari-Izzo, 2011; Sytar et al., 2013). One potential metabolite recognized in our study was methyl hydroperoxide, which could indicate oxidative stress. Cieślinski et al. (1998) in a study on the Cd accumulation in the *Triticum turgidum* var. *durum* plants showed a strong relationship between extractable soil Cd and low-molecular organic acids, such as oxalic, fumaric, succinic, L-malic, tartaric, citric, acetic, propionic and butyric acids. In contrast to such studies, we observed low-molecular weight compounds associated with Cd that could be either of organic or inorganic nature, including compounds like formic acid, propionic acid, pyrazole, imidazole, alcohols, sulfuric acid or chloric acid. Plants release inorganic compounds into soil environment such as bicarbonates, hydroxides and ions (Ehrenfeld et al., 2005; Hartmann et al., 2009). None of them match our potential targets. Equally, a contribution by microbes to the observed metabolome needs to be recognized. Microbes when exposed to heavy metals mitigate against their toxic effects mainly via efflux systems, which pumps metals out of the cell, but also release of specific metal-binding chelators (Haferburg and Kothe, 2007; Gadd, 2010; Ahemad and Kibret, 2014). However, these microbial chelators were not noted in our metabolomics study. Another possibility is that the inorganic acids were associated with non-biological events and only coincided with heavy metals. Metals and inorganic acids form salts, which upon various environmental conditions might precipitate and become trapped inside a porous structure of soil particles (Gadd, 2010). Potentially they could have been released during the metabolite extraction procedure, thus resulting in the presence of specific, inorganic ions in the HPLC-MS profiles.

An interesting effect was observed with regard to bioavailable fraction of Zn. In most of the analyses performed in our work, such as PLFA, BIOLOG-CLPP or HPLC-MS, the effects of bioavailable Zn were highly variable and sometimes opposite compared to those seen with the total Zn fraction and other metals, like Cd and Cu. This may reflect that Zn is an essential metal and in low concentrations acts as a stimulant for the microbial communities (Bruins et al., 2000; Gadd, 2010). The

impact of bioavailable Zn on individual biological parameters was in line with SOM and water content, as one would expect a soluble fraction of heavy metals. However copper, besides being an essential metal, did not show that kind of behavior. Furthermore, concentrations of bioavailable Zn were up to three orders of magnitude higher, than concentrations of bioavailable Cu. This distinctive effect could arise from tested microbial communities being derived from highly polluted, post-industrial areas associated with Zn processing/disposal and hence were subjected to prolonged environmental stress (40+ years) which could be linked to microbial adaptation.

Studies of microbial diversity in soil are difficult and involve a series of methodological challenges, including inability to culture vast majority of microorganisms present in the soil (Kirk et al., 2004; Alain and Querellou, 2009; Rastogi et al., 2010).

The results obtained through BIOLOG-CLPP are biased toward fast-growing and most active microorganisms, overshadowing viable, but slow-growing bacteria present in soil. However, this method allows for the comparison of functional biodiversity of tested microbial communities, enabling for calculating biodiversity indices and analysis through multivariate statistics (Kirk et al., 2004).

PLFA analysis provides quantitative estimates on viable microbial cells. This is due to the fact, that phospholipids are present in all living cells but are rapidly turned over after the cell's death (Fang et al., 2000). Unlike plate microbial counts or BIOLOG-CLPP, the PLFA technique is culture-independent and all extractable PLFAs are analyzed. However, the results obtained with this method depend on the PLFA extraction efficiency and many environmental factors (Macnaughton et al., 1997; Fang et al., 2000; Kirk et al., 2004; Wu et al., 2010).

In that matter, the PCR-based molecular methods are more robust and allow for significantly higher resolution, as high as individual species and microbial strains. 16S rDNA-targeted PCR-DGGE is reliable, reproducible, fast and inexpensive. Multiple samples can be analyzed in one run, allowing for simultaneous profile comparison, corresponding to microbial community structure. The major shortcomings of PCR-DGGE method are related to PCR itself, which include bias toward certain, abundant groups of microorganisms. The DNA isolation efficiency may vary depending on the method employed. In addition, depending on the DNA fragment mobility, one band may represent multiple species or sequences from the same species may result in more than one band (Kirk et al., 2004).

In our study, a combined use of culture-based and culture-independent approaches was aimed toward a thorough understanding of links between environmental factors and microbial traits, such as microbial counts as well as structural, functional and genetic diversity of the microbial communities in analyzed soils. Alternatively, the next-generation sequencing (NGS) methods could be implemented, allowing for deep sequencing, while mitigating many of the shortcomings of culture-dependent and traditional culture-independent approaches. Although the NGS approach allows for very fine resolution, only dominant OTUs are commonly analyzed and

discussed (Teeling and Glöckner, 2012; Orgiazzi et al., 2015; Johnston-Monje et al., 2016).

## CONCLUSIONS

The difficulty in defining the key players in any environmental situation is well known due to the complexity of the various biotic and abiotic factors (Berg and Smalla, 2009). Our study shows, that despite the use of multiple assays, we could not define a single major parameter; assuming that they exist. However, we have made unequivocal conclusions regarding the significance of plant species, sampling site or heavy metals on the structure and function of rhizosphere microbial populations. Microbial community structure needs not correspond to community function because various microbial groups overlap in their functional potential. This process, called functional redundancy, allows microbial communities to maintain functional balance even when significant switches in the individual dominant species or genera occur (Nannipieri et al., 2003; Stefanowicz et al., 2008; McGuire and Treseder, 2010). Therefore the shifts in microbial CLPPs associated with heavy metal presence, as demonstrated in this work, are of great environmental significance and need to be explored in the future using now well-established microbiomic approaches.

## REFERENCES

- Abou-Shanab, R. A., Angle, J. S., Delorme, T. A., Chaney, R. L., Van Berkum, P., Moawad, H., et al. (2003). Rhizobacterial effects on nickel extraction from soil and uptake by *Alyssum murale*. *New Phytol.* 158, 219–224. doi: 10.1046/j.1469-8137.2003.00721.x
- Abou-Shanab, R. A. I., Angle, J. S., and Chaney, R. L. (2006). Bacterial inoculants affecting nickel uptake by *Alyssum murale* from low, moderate and high Ni soils. *Soil Biol. Biochem.* 38, 2882–2889. doi: 10.1016/j.soilbio.2006.04.045
- Ahemad, M., and Kibret, M. (2014). Mechanisms and applications of plant growth promoting rhizobacteria: current perspective. *J. King Saud. Univ. Sci.* 26, 1–20. doi: 10.1016/j.jksus.2013.05.001
- Alain, K., and Querrelou, J. (2009). Cultivating the uncultured: limits, advances and future challenges. *Extremophiles* 13, 583–594. doi: 10.1007/s00792-009-0261-3
- Alford, É. R., Pilon-Smits, E. A. H., and Paschke, M. W. (2010). Metallophytes—a view from the rhizosphere. *Plant Soil* 337, 33–50. doi: 10.1007/s11104-010-0482-3
- Badri, D. V., Chaparro, J. M., Zhang, R., Shen, Q., and Vivanco, J. M. (2013). Application of natural blends of phytochemicals derived from the root exudates of arabidopsis to the soil reveal that phenolic-related compounds predominantly modulate the soil microbiome. *J. Biol. Chem.* 288, 4502–4512. doi: 10.1074/jbc.M112.433300
- Bais, H. P., Weir, T. L., Perry, L. G., Gilroy, S., and Vivanco, J. M. (2006). The role of root exudates in rhizosphere interactions with plants and other organisms. *Annu. Rev. Plant Biol.* 57, 233–266. doi: 10.1146/annurev.arplant.57.032905.105159
- Baker, A. J. M., Ernst, W. H. O., van der Ent, A., Malaisse, F., and Ginocchio, R. (2010). “Metallophytes: the unique biological resource, its ecology and conservational status in Europe, central Africa and Latin America,” in *Ecology of Industrial Pollution*, eds L. C. Batty and K. B. Hallberg (Cambridge: Cambridge University Press), 7–40.
- Becerra-Castro, C., Monterroso, C., Prieto-Fernández, A., Rodríguez-Lamas, L., Loureiro-Viñas, M., Acea, M. J., et al. (2012). Pseudometallophytes colonising Pb/Zn mine tailings: A description of the plant-microorganism-rhizosphere soil system and isolation of metal-tolerant bacteria. *J. Hazard. Mater.* 217–218, 350–359. doi: 10.1016/j.jhazmat.2012.03.039
- Berg, G., and Smalla, K. (2009). Plant species and soil type cooperatively shape the structure and function of microbial communities in the rhizosphere. *FEMS Microbiol. Ecol.* 68, 1–13. doi: 10.1111/j.1574-6941.2009.00654.x
- Bruins, M. R., Kapil, S., and Oehme, F. W. (2000). Microbial resistance to metals in the environment. *Ecotoxicol. Environ. Saf.* 45, 198–207. doi: 10.1006/eesa.1999.1860
- Carrasco, L., Gatteringer, A., Fließbach, A., Roldán, A., Schloter, M., and Caravaca, F. (2010). Estimation by PLFA of microbial community structure associated with the rhizosphere of *Lygeum spartum* and *Piptatherum miliaceum* growing in semiarid mine tailings. *Microb. Ecol.* 60, 265–271. doi: 10.1007/s00248-009-9619-4
- Chaparro, J. M., Badri, D. V., and Vivanco, J. M. (2014). Rhizosphere microbiome assemblage is affected by plant development. *ISME J.* 8, 790–803. doi: 10.1038/ismej.2013.196
- Cieślinski, G., Van Rees, K. C. J., Szmigielska, A. M., Krishnamurti, G. S. R., and Huang, P. M. (1998). Low-molecular-weight organic acids in rhizosphere soils of durum wheat and their effect on cadmium bioaccumulation. *Plant Soil* 203, 109–117. doi: 10.1023/A:1004325817420
- Clemens, S., and Ma, J. F. (2016). Toxic heavy metal and metalloid accumulation in crop plants and foods. *Annu. Rev. Plant Biol.* 67, 489–512. doi: 10.1146/annurev-arplant-043015-112301
- Cycon, M., Markowicz, A., and Piotrowska-Seget, Z. (2013). Structural and functional diversity of bacterial community in soil treated with the herbicide napropamide estimated by the DGGE, CLPP and r/K-strategy approaches. *Appl. Soil Ecol.* 72, 242–250. doi: 10.1016/j.apsoil.2013.07.015
- Cycon, M., Borymski, S., Orlewska, K., Wasik, T. J., and Piotrowska-Seget, Z. (2016). An analysis of the effects of vancomycin and/or vancomycin-resistant *Citrobacter freundii* exposure on the microbial community structure in soil. *Front. Microbiol.* 7, 1–18. doi: 10.3389/fmicb.2016.01015
- Dechamps, C., Roosens, N. H., Hotte, C., and Meerts, P. (2005). Growth and mineral element composition in two ecotypes of *Thlaspi caerulescens* on Cd contaminated soil. *Plant Soil* 273, 327–335. doi: 10.1007/s11104-005-0099-0
- Ehrenfeld, J. G., Ravit, B., and Elgersma, K. (2005). Feedback in the plant-soil system. *Annu. Rev. Environ. Resour.* 30, 75–115. doi: 10.1146/annurev.energy.30.050504.144212

## DATA AVAILABILITY STATEMENT

Datasets are available on request: The raw data supporting the conclusions of this manuscript will be made available by the authors, without undue reservation, to any qualified researcher.

## AUTHOR CONTRIBUTIONS

The study was designed by SB. Most of the laboratory procedures, data analysis and manuscript writing was carried out by SB. ZP-S supervised the work. MC carried out the PCR-DGGE and helped with data analysis. LM and MB provided crucial help with HPLC-MS data processing and metabolomics. ZP-S, MC, and LM also contributed to manuscript writing.

## FUNDING

This study was supported by the National Science Centre, Poland (Grant No. DEC-2012/05/N/NZ9/02405).

## ACKNOWLEDGMENTS

Thanks to Dr. John Scullion (Aberystwyth University, UK) for useful discussions during the experimental phase of the project.

- Fang, J., Barcelona, M. J., and Alvarez, P. J. J. (2000). A direct comparison between fatty acid analysis and intact phospholipid profiling for microbial identification. *Organ. Geochem.* 31, 881–887.
- Freitas, D. B., Lima-Bittencourt, C. I., Reis, M. P., Costa, P. S., Assis, P. S., Chartone-Souza, E., et al. (2008). Molecular characterization of early colonizer bacteria from wastes in a steel plant. *Lett. Appl. Microbiol.* 47, 241–249. doi: 10.1111/j.1472-765X.2008.02415.x
- Frostegård, A., Baath, E., Frostegård, Å., and Bååth, E. (1996). The use of phospholipid fatty acid analysis to estimate bacterial and fungal biomass in soil. *Biol. Fertil. Soils* 22, 59–65. doi: 10.1007/BF00384433
- Frostegård, A., Tunlid, A., and Baath, E. (1993). Phospholipid fatty acid composition, biomass, and activity of microbial communities from two soil types experimentally exposed to different heavy metals. *Appl. Environ. Microbiol.* 59, 3605–3617.
- Frostegård, Å., Tunlid, A., and Bååth, E. (2011). Use and misuse of PLFA measurements in soils. *Soil Biol. Biochem.* 43, 1621–1625. doi: 10.1016/j.soilbio.2010.11.021.
- Gadd, G. M. (2004). Microbial influence on metal mobility and application for bioremediation. *Geoderma* 122, 109–119. doi: 10.1016/j.geoderma.2004.01.002
- Gadd, G. M. (2010). Metals, minerals and microbes: geomicrobiology and bioremediation. *Microbiology* 156, 609–643. doi: 10.1099/mic.0.037143-0
- García-Villaraco Velasco, A., Probanza, A., Gutierrez Mañero, F. J., Ramos, B., and Lucas García, J. A. (2009). Functional diversity of rhizosphere microorganisms from different genotypes of *Arabidopsis thaliana*. *Community Ecol.* 10, 111–119. doi: 10.1556/ComEc.10.2009.1.13
- Guo, W., Liu, X., Liu, Z., and Li, G. (2010). Pollution and potential ecological risk evaluation of heavy metals in the sediments around Dongjiang Harbor, Tianjin. *Proc. Environ. Sci.* 2, 729–736. doi: 10.1016/j.proenv.2010.10.084
- Haferburg, G., and Kothe, E. (2007). Microbes and metals: interactions in the environment. *J. Basic Microbiol.* 47, 453–467. doi: 10.1002/jobm.200700275
- Hartmann, A., Rothballer, M., and Schmid, M. (2008). Lorenz Hiltner, a pioneer in rhizosphere microbial ecology and soil bacteriology research. *Plant Soil* 312, 7–14. doi: 10.1007/s11104-007-9514-z
- Hartmann, A., Schmid, M., van Tuinen, D., and Berg, G. (2009). Plant-driven selection of microbes. *Plant Soil* 321, 235–257. doi: 10.1007/s11104-008-9814-y
- Hinsinger, P., Bengough, A. G., Vetterlein, D., and Young, I. M. (2009). Rhizosphere: biophysics, biogeochemistry and ecological relevance. *Plant Soil* 321, 117–152. doi: 10.1007/s11104-008-9885-9
- Houlden, A., Timms-Wilson, T. M., Day, M. J., and Bailey, M. J. (2008). Influence of plant developmental stage on microbial community structure and activity in the rhizosphere of three field crops. *FEMS Microbiol. Ecol.* 65, 193–201. doi: 10.1111/j.1574-6941.2008.00535.x
- Jarvis, R. M., Broadhurst, D., Johnson, H., O'Boyle, N. M., and Goodacre, R. (2006). PYCHEM: A multivariate analysis package for python. *Bioinformatics* 22, 2565–2566. doi: 10.1093/bioinformatics/btl416
- Johnston-Monje, D., Lundberg, D. S., Lazarovits, G., Reis, V. M., and Raizada, M. N. (2016). Bacterial populations in juvenile maize rhizospheres originate from both seed and soil. *Plant Soil* 405, 337–355. doi: 10.1007/s11104-016-2826-0
- Kirk, J. L., Beaudette, L. A., Hart, M., Moutoglis, P., Klironomos, J. N., Lee, H., et al. (2004). Methods of studying soil microbial diversity. *J. Microbiol. Methods* 58, 169–188. doi: 10.1016/j.mimet.2004.04.006
- Kozdrój, J., and Van Elsas, J. D. (2000). Response of the bacterial community to root exudates in soil polluted with heavy metals assessed by molecular and cultural approaches. *Soil Biol. Biochem.* 32, 1405–1417. doi: 10.1016/S0038-0717(00)00058-4
- Lasat, M. M., Pence, N. S., Deborah, L. D., and Kochian, L., V (2001). Zinc Phytoremediation in *Thlaspi caerulescens*. *Int. J. Phytoremed.* 3, 129–144. doi: 10.1080/15226510108500053
- Li, C.-M., Lei, C.-X., Liang, Y.-T., Chen, C.-Q., and Sun, B. (2017). As contamination alters rhizosphere microbial community composition with soil type dependency during the rice growing season. *Paddy Water Environ.* 15, 581–592. doi: 10.1007/s10333-016-0575-6
- Li, J., Jin, Z., and Gu, Q. (2011). Effect of plant species on the function and structure of the bacterial community in the rhizosphere of lead–zinc mine tailings in Zhejiang, China. *Can. J. Microbiol.* 57, 569–577. doi: 10.1139/w11-054
- Lucassen, E. C. H. E. T., Eygensteyn, J., Bobbink, R., Smolders, A. J. P., Van de Riet, B. P., Kuijpers, D. J. C., et al. (2009). The decline of metallophyte vegetation in floodplain grasslands: implications for conservation and restoration. *Appl. Veg. Sci.* 12, 69–80. doi: 10.1111/j.1654-109X.2009.01005.x
- Luo, J., Tao, Q., Wu, K., Li, J., Qian, J., Liang, Y., et al. (2017). Structural and functional variability in root-associated bacterial microbiomes of Cd/Zn hyperaccumulator *Sedum alfredii*. *Appl. Microbiol. Biotechnol.* 101, 7961–7976. doi: 10.1007/s00253-017-8469-0
- Macnaughton, S. J., Jenkins, T. L., Wimpee, M. H., Cormier, M. R., and White, D. C. (1997). Rapid extraction of lipid biomarkers from pure culture and environmental samples using pressurized accelerated hot solvent extraction. *J. Microbiol. Methods* 31, 19–27. doi: 10.1016/S0167-7012(97)00081-X
- Martínez-Iñigo, M. J., Pérez-Sanz, A., Ortiz, I., Alonso, J., Alarcón, R., García, P., et al. (2009). Bulk soil and rhizosphere bacterial community PCR-DGGE profiles and beta-galactosidase activity as indicators of biological quality in soils contaminated by heavy metals and cultivated with *Silene vulgaris* (Moench) Garcke. *Chemosphere* 75, 1376–1381. doi: 10.1016/j.chemosphere.2009.03.014
- McGuire, K. L., and Treseder, K. K. (2010). Microbial communities and their relevance for ecosystem models: decomposition as a case study. *Soil Biol. Biochem.* 42, 529–535. doi: 10.1016/j.soilbio.2009.11.016
- Melo, M. R., Flores, N. R., Murrieta, S. V., Tovar, A. R., Zúñiga, A. G., Hernández, O. F., et al. (2011). Comparative plant growth promoting traits and distribution of rhizobacteria associated with heavy metals in contaminated soils. *Int. J. Environ. Sci. Technol.* 8, 807–816. doi: 10.1007/BF03326264
- Mergey, M. (1995). “Heavy metal resistances in microbial ecosystems,” in *Molecular Microbial Ecology Manual*, eds A. Akkermans, J. Van Elsas, and F. De Bruijn (Dordrecht: Springer Science+Business Media), 439–455. doi: 10.1007/978-94-011-0351-0\_30
- Meyer, C. L., Kostocka, A. A., Saumitou-Laprade, P., Créach, A., Castric, V., Pauwels, M., et al. (2010). Variability of zinc tolerance among and within populations of the pseudometallophyte species *Arabidopsis halleri* and possible role of directional selection. *New Phytol.* 185, 130–142. doi: 10.1111/j.1469-8137.2009.03062.x
- Muyzer, G., de Waal, E. C., and Uitterlinden, A. G. (1993). Profiling of complex microbial populations by denaturing gradient gel electrophoresis analysis of polymerase chain reaction-amplified genes coding for 16S rRNA. *Appl. Environmental Microbiol.* 59, 695–700.
- Nannipieri, P., Ascher, J., Ceccherini, M. T., Lan Di, L., Pietramellara, G., and Renella, G. (2003). Microbial diversity and soil functions. *Eur. J. Soil Sci.* 54:655. doi: 10.1046/j.1365-2389.2003.00556.x
- Oliveira, A. P., Pampulha, M. E., and Bennett, J. P. (2008). A two-year field study with transgenic *Bacillus thuringiensis* maize: effects on soil microorganisms. *Sci. Total Environ.* 405, 351–357. doi: 10.1016/j.scitotenv.2008.05.046
- Orgiazzi, A., Dunbar, M. B., Panagos, P., de Groot, G. A., and Lemanceau, P. (2015). Soil biodiversity and DNA barcodes: opportunities and challenges. *Soil Biol. Biochem.* 80, 244–250. doi: 10.1016/j.soilbio.2014.10.014
- Pacwa-Plociniczak, M., Plociniczak, T., Yu, D., Kurolo, J. M., Sinkkonen, A., Piotrowska-Seget, Z., et al. (2018). Effect of *Silene vulgaris* and heavy metal pollution on soil microbial diversity in long-term contaminated soil. *Water Air Soil Pollut.* 229, 1–13. doi: 10.1007/s11270-017-3655-3
- Paterson, E., Gebbing, T., Abel, C., Sim, A., and Telfer, G. (2007). Rhizodeposition shapes rhizosphere microbial community structure in organic soil. *New Phytol.* 173, 600–610. doi: 10.1111/j.1469-8137.2006.01931.x
- Pauwels, M., Frérot, H., Bonnin, I., and Saumitou-Laprade, P. (2006). A broad-scale analysis of population differentiation for Zn tolerance in an emerging model species for tolerance study: *Arabidopsis halleri* (Brassicaceae). *J. Evol. Biol.* 19, 1838–1850. doi: 10.1111/j.1420-9101.2006.01178.x
- Perrine-Walker, F., Gherbi, H., Imanishi, L., Hoher, V., Ghodhbane-Gtari, F., Lavenus, J., et al. (2011). Symbiotic signaling in actinorhizal symbioses. *Curr. Protein Pept. Sci.* 12, 156–164. doi: 10.2174/1389211213488422037
- Piotrowska-Seget, Z., Cycon, M., and Kozdrój, J. (2005). Metal-tolerant bacteria occurring in heavily polluted soil and mine spoil. *Appl. Soil Ecol.* 28, 237–246. doi: 10.1016/j.apsoil.2004.08.001
- Prashar, P., Kapoor, N., and Sachdeva, S. (2014). Rhizosphere: its structure, bacterial diversity and significance. *Rev. Environ. Sci. Biotechnol.* 13, 63–77. doi: 10.1007/s11157-013-9317-z
- Rascio, N., and Navari-Izzo, F. (2011). Heavy metal hyperaccumulating plants: how and why do they do it? And what makes them so interesting? *Plant Sci.* 180, 169–181. doi: 10.1016/j.plantsci.2010.08.016

- Rastogi, G., Tech, J. J., Coaker, G. L., and Leveau, J. H. J. (2010). A PCR-based toolbox for the culture-independent quantification of total bacterial abundances in plant environments. *J. Microbiol. Methods* 83, 127–132. doi: 10.1016/j.mimet.2010.08.006
- Rieuwerts, J. S., Thornton, I., Farago, M. E., and Ashmore, M. R. (1998). Factors influencing metal bioavailability in soils: preliminary investigations for the development of a critical loads approach for metals. *Chem. Speciat. Bioavailab.* 10, 61–75. doi: 10.3184/095422998782775835
- Rudrappa, T., Czymbek, K. J., Pare, P. W., Paré, P. W., and Bais, H. P. (2008). Root-secreted malic acid recruits beneficial. *Plant Physiol.* 148, 1547–1556. doi: 10.1104/pp.108.127613
- Rue, M., Vallance, J., Echevarria, G., Rey, P., and Benizri, E. (2015). Phytoextraction of nickel and rhizosphere microbial communities under mono- or multispecies hyperaccumulator plant cover in a serpentine soil. *Aust. J. Bot.* 63, 92–102. doi: 10.1071/BT14249
- Schlaeppli, K., Dombrowski, N., Oter, R. G., Ver Loren van Themaat, E., and Schulze-Lefert, P. (2014). Quantitative divergence of the bacterial root microbiota in Arabidopsis thaliana relatives. *Proc. Natl. Acad. Sci. U.S.A.* 111, 585–592. doi: 10.1073/pnas.1321597111
- Sobariu, D. L., Fertu, D. I. T., Diaconu, M., Pavel, L. V., Hlihor, R. M., Drăgoi, E. N., et al. (2017). Rhizobacteria and plant symbiosis in heavy metal uptake and its implications for soil bioremediation. *N. Biotechnol.* 39, 125–134. doi: 10.1016/j.nbt.2016.09.002
- Söderberg, K. H., Probanza, A., Jumpponen, A., and Bååth, E. (2004). The microbial community in the rhizosphere determined by community-level physiological profiles (CLPP) and direct soil- and cfu-PLFA techniques. *Appl. Soil Ecol.* 25, 135–145. doi: 10.1016/j.apsoil.2003.08.005
- Stefanowicz, A. M., Niklinska, M., and Laskowski, R. (2008). Metals affect soil bacterial and fungal functional diversity differently. *Environ. Toxicol. Chem.* 27, 591–598. doi: 10.1897/07-288
- Sytar, O., Kumar, A., Latowski, D., Kuczynska, P., Strzałka, K., and Prasad, M. N. V. (2013). Heavy metal-induced oxidative damage, defense reactions, and detoxification mechanisms in plants. *Acta Physiol. Plant.* 35, 985–999. doi: 10.1007/s11738-012-1169-6
- Teeling, H., and Glöckner, F. O. (2012). Current opportunities and challenges in microbial metagenome analysis—a bioinformatic perspective. *Brief. Bioinform.* 13, 728–742. doi: 10.1093/bib/bbs039
- van der Ent, A., Baker, A. J. M., Reeves, R. D., Pollard, A. J., and Schat, H. (2013). Hyperaccumulators of metal and metalloid trace elements: facts and fiction. *Plant Soil* 362, 319–334. doi: 10.1007/s11104-012-1287-3
- Visioli, G., D'Egidio, S., and Sanangelantoni, A. M. (2015). The bacterial rhizobiome of hyperaccumulators: future perspectives based on omics analysis and advanced microscopy. *Front. Plant Sci.* 5, 1–12. doi: 10.3389/fpls.2014.00752
- Wang, Y., Li, Q., Shi, J., Lin, Q., Chen, X., Wu, W., et al. (2008). Assessment of microbial activity and bacterial community composition in the rhizosphere of a copper accumulator and a non-accumulator. *Soil Biol. Biochem.* 40, 1167–1177. doi: 10.1016/j.soilbio.2007.12.010
- Whiting, S. N., De Souza, M. P., and Terry, N. (2001). Rhizosphere bacteria mobilize Zn for hyperaccumulation by *Thlaspi caerulescens*. *Environ. Sci. Technol.* 35, 3144–3150. doi: 10.1021/es001938v
- Wood, J. L., Zhang, C., Mathews, E. R., Tang, C., and Franks, A. E. (2016). Microbial community dynamics in the rhizosphere of a cadmium hyperaccumulator. *Sci. Rep.* 6, 1–10. doi: 10.1038/srep36067
- Wu, Y., Yu, X., Wang, H., Ding, N., and Xu, J. (2010). Does history matter? Temperature effects on soil microbial biomass and community structure based on the phospholipid fatty acid (PLFA) analysis. *J. Soils Sediments* 10, 223–230. doi: 10.1007/s11368-009-0118-5
- Yan, W., Artz, R. R. E., and Johnson, D. (2008). Species-specific effects of plants colonising cutover peatlands on patterns of carbon source utilisation by soil microorganisms. *Soil Biol. Biochem.* 40, 544–549. doi: 10.1016/j.soilbio.2007.09.001
- Yang, J. W., Yi, H. S., Kim, H., Lee, B., Lee, S., Ghim, S. Y., et al. (2011). Whitefly infestation of pepper plants elicits defence responses against bacterial pathogens in leaves and roots and changes the below-ground microflora. *J. Ecol.* 99, 46–56. doi: 10.1111/j.1365-2745.2010.01756.x
- Zhang, C., Nie, S., Liang, J., Zeng, G., Wu, H., Hua, S., et al. (2016). Effects of heavy metals and soil physicochemical properties on wetland soil microbial biomass and bacterial community structure. *Sci. Total Environ.* 557–558, 785–790. doi: 10.1016/j.scitotenv.2016.01.170
- Zhang, W. H., Huang, Z., He, L. Y., and Sheng, X. F. (2012). Assessment of bacterial communities and characterization of lead-resistant bacteria in the rhizosphere soils of metal-tolerant *Chenopodium ambrosioides* grown on lead-zinc mine tailings. *Chemosphere* 87, 1171–1178. doi: 10.1016/j.chemosphere.2012.02.036

**Conflict of Interest Statement:** The authors declare that the research was conducted in the absence of any commercial or financial relationships that could be construed as a potential conflict of interest.

Copyright © 2018 Borymski, Cycoń, Beckmann, Mur and Piotrowska-Seget. This is an open-access article distributed under the terms of the Creative Commons Attribution License (CC BY). The use, distribution or reproduction in other forums is permitted, provided the original author(s) and the copyright owner(s) are credited and that the original publication in this journal is cited, in accordance with accepted academic practice. No use, distribution or reproduction is permitted which does not comply with these terms.



# Colonization of Non-biodegradable and Biodegradable Plastics by Marine Microorganisms

Claire Dussud<sup>1\*</sup>, Cindy Hudec<sup>1</sup>, Matthieu George<sup>2</sup>, Pascale Fabre<sup>2</sup>, Perry Higgs<sup>3</sup>, Stéphane Bruzaud<sup>4</sup>, Anne-Marie Delort<sup>5</sup>, Boris Eyheraguibel<sup>5</sup>, Anne-Leila Meistertzheim<sup>1</sup>, Justine Jacquin<sup>1</sup>, Jingguang Cheng<sup>1</sup>, Nolwenn Callac<sup>1</sup>, Charlène Odobel<sup>1</sup>, Sophie Rabouille<sup>6</sup> and Jean-François Ghiglione<sup>1\*</sup>

<sup>1</sup> CNRS, UPMC Univ Paris 06, UMR7621, Laboratoire d'Océanographie Microbienne (LOMIC), Observatoire Océanologique de Banyuls, Sorbonne Université, Banyuls-sur-Mer, France, <sup>2</sup> CNRS/UM, UMR5221, Laboratoire Charles Coulomb (L2C), Montpellier, France, <sup>3</sup> Symphony Environmental Ltd., Hertfordshire, United Kingdom, <sup>4</sup> Université de Bretagne-Sud, Institut de Recherche Dupuy de Lôme (IRDL), UMR CNRS 6027, Lorient Cedex, France, <sup>5</sup> CNRS, UMR6296, SIGMA Clermont, Institut de Chimie de Clermont-Ferrand (ICCF), Université Clermont Auvergne, Clermont-Ferrand, France, <sup>6</sup> CNRS, UPMC Univ Paris 06, UMR7093, Laboratoire d'Océanographie de Villefranche (LOV), Sorbonne Universités, Villefranche-sur-Mer, France

## OPEN ACCESS

### Edited by:

Gérald Thouand,  
University of Nantes, France

### Reviewed by:

Patrizia Cinelli,  
Università degli Studi di Pisa, Italy  
Kesaven Bhupalan,  
Universiti Malaysia Terengganu,  
Malaysia

### \*Correspondence:

Claire Dussud  
clairedussud@orange.fr  
Jean-François Ghiglione  
ghiglione@obs-banyuls.fr

### Specialty section:

This article was submitted to  
Microbiotechnology, Ecotoxicology  
and Bioremediation,  
a section of the journal  
Frontiers in Microbiology

**Received:** 23 April 2018

**Accepted:** 25 June 2018

**Published:** 18 July 2018

### Citation:

Dussud C, Hudec C, George M,  
Fabre P, Higgs P, Bruzaud S,  
Delort A-M, Eyheraguibel B,  
Meistertzheim A-L, Jacquin J,  
Cheng J, Callac N, Odobel C,  
Rabouille S and Ghiglione J-F (2018)  
Colonization of Non-biodegradable  
and Biodegradable Plastics by Marine  
Microorganisms.  
Front. Microbiol. 9:1571.  
doi: 10.3389/fmicb.2018.01571

Plastics are ubiquitous in the oceans and constitute suitable matrices for bacterial attachment and growth. Understanding biofouling mechanisms is a key issue to assessing the ecological impacts and fate of plastics in marine environment. In this study, we investigated the different steps of plastic colonization of polyolefin-based plastics, on the first one hand, including conventional low-density polyethylene (PE), additivated PE with pro-oxidant (OXO), and artificially aged OXO (AA-OXO); and of a polyester, poly(3-hydroxybutyrate-co-3-hydroxyvalerate) (PHBV), on the other hand. We combined measurements of physical surface properties of polymers (hydrophobicity and roughness) with microbiological characterization of the biofilm (cell counts, taxonomic composition, and heterotrophic activity) using a wide range of techniques, with some of them used for the first time on plastics. Our experimental setup using aquariums with natural circulating seawater during 6 weeks allowed us to characterize the successive phases of primo-colonization, growing, and maturation of the biofilms. We highlighted different trends between polymer types with distinct surface properties and composition, the biodegradable AA-OXO and PHBV presenting higher colonization by active and specific bacteria compared to non-biodegradable polymers (PE and OXO). Succession of bacterial population occurred during the three colonization phases, with hydrocarbonoclastic bacteria being highly abundant on all plastic types. This study brings original data that provide new insights on the colonization of non-biodegradable and biodegradable polymers by marine microorganisms.

**Keywords:** plastic pollution, biofouling, microbial ecotoxicology, plastisphere, biodegradable plastics

## INTRODUCTION

Within a few decades, plastic has become the biggest form of pollution in the world's oceans (80% of marine litter consists of plastic) due to its very slow degradability and the growing accumulation of human waste products (Gewert et al., 2015). When released into the environment, plastic litter is fragmented by both physical and chemical processes into small pieces (<5 mm), commonly

referred to as “microplastics” (MPs) (Barnes et al., 2009). MPs represent more than 90% of the total counts of plastic debris at the sea surface (Eriksen et al., 2014).

At sea, plastics are almost immediately coated by inorganic and organic matter (so called the “conditioning film”), which is then rapidly colonized by microorganisms that form a biofilm on their surfaces (Loeb and Neihof, 1975; Cooksey and Wigglesworth-Cooksey, 1995). Bacterial biofilms are defined as surface-associated bacterial communities which are embedded within an exopolymeric substance matrix (EPS) (Costerton et al., 1995). These natural assemblages act as a form of protection, nutritive resource, offer metabolic cooperativity, and an increase in the possibility of gene transfer among cells (Davey and O’toole, 2000). The successive phases of biofilm formations are well described within marine waters on artificial (glass, acryl, and steel) or natural surfaces (rocks and algae) (Dang and Lovell, 2000; Salta et al., 2013). First, the “primo-colonization” describes the occupation of the surface by pioneer bacteria through reversible attachment, where they interact with the conditioning film and form the first layer of the initial biofilm. Second, the “growth phase” promotes irreversible attachment by active mechanisms such as the formation of pili, adhesion proteins and EPS produced by secondary species, which induce modifications in the properties of the substratum. Third, the “maturation phase” occurs through diverse, competitive or synergistic interactions between cells, with either further recruitment or loss of species (Lorite et al., 2011).

Very few studies have so far described the formation of biofilms on plastics in marine environments. Early stage processes were followed on polyethylene (PE)-based plastic bags or MPs during 3 weeks in seawater (Lobelle and Cunliffe, 2011) and in sediments (Harrison et al., 2014). Two studies are available on longer-term biofilm formation on the surface of PE or PE terephthalate (PET) in marine environment, which were carried out over a 6-month period (Webb et al., 2009; De Tender et al., 2017). Only one study has so far compared biofilm formation on PE with that observed on so-called “biodegradable” plastics made of starch-based biopolymer-PET blend (Mater-Bi N°014), conducted during 1 month in marine environment (Eich et al., 2015). These studies were mostly based on scanning electron microscopy (SEM) observations and taxonomic identification, but none of them focused on bacterial abundance and activity, meaning that populations and community dynamics in these biofilms remains largely unknown. Moreover, the formation of a biofilm was depicted as strongly dependent on substrate properties including hydrophobicity/hydrophilicity, structure, and roughness (Lorite et al., 2011), which were never taken into account in studies exploring marine environment.

Polyethylene dominates the composition of plastic waste at sea surface, followed by polypropylene (PP) and polystyrene (PS) (Auta et al., 2017). The stable aliphatic chains in PE make it a very recalcitrant material (Tokiwa et al., 2009). Within the frame of sustainable development, a wide range of potentially biodegradable plastics were developed and classified into two major groups depending on the mode of biodegradation pathway: “OXO-biodegradable” and “hydro-biodegradable” (Vázquez-Morillas et al., 2016). The former are polyolefin-based polymers

(generally PE) with pro-oxidant additives (OXO; for OXO-degradable polymer). In case of release in the environment, the additive accelerates abiotic oxidation process by heat and/or UV light, a phenomenon that can be simulated by artificial aging of the OXO (AA-OXO, for artificially aged OXO). If the initial formulation of OXO is recalcitrant to biodegradation, the oxidized AA-OXO can be further biodegraded by oxidative mechanisms (Koutny et al., 2006; Eyheraguibel et al., 2017). Several studies on OXO pre-oxidized films showed 50 to 80% mineralization under half to one and a half year of incubation (Jakubowicz, 2003; Chiellini et al., 2007) or between 12 and 24% mineralization after 90 days of incubation (Ojeda et al., 2009 and Yashchuk et al., 2012). Hydro-biodegradable plastics are based on polymers that can be biodegraded by hydrolytic mechanisms (Nampoothiri et al., 2010). They include cellulose, starch and more generally polyesters, such as polyhydroxyalkanoates (PHA). Because PHA are polyesters made by bacteria for intracellular storage of carbon and energy, they received considerable attention as promising biodegradable polymers to substitute for traditional plastics, with mechanical properties similar to various synthetic thermoplastics (Corre et al., 2012; Elain et al., 2015, 2016). Various bacteria were shown to degrade AA-OXO or PHA in different conditions (Tokiwa and Calabia, 2004; Sudhakar et al., 2008; Ammala et al., 2011).

In this study, we characterized the biofilm colonization phases on PE, OXO-degradable polymer with (AA-OXO) or without (OXO) artificial-aging, and poly(3-hydroxybutyrate-co-3-hydroxyvalerate) (PHBV) as PHA representative. Each polymer type was separately incubated and its evolution monitored during 6 weeks in natural seawater from Banyuls Bay (NW Mediterranean Sea). The dynamics of bacterial biofilms was described in terms of changes in abundance, diversity and heterotrophic activity, together with changes in polymer surface physical properties (contact angle and roughness).

## MATERIALS AND METHODS

### Polymer Samples Preparation and Design of the Incubation Experiments

In this study, we used four types of polymer: PE corresponded to commercially available commodity film grade low-density PE resin Borealis FA6224, which had the following characteristics: density = 0.922 g cm<sup>-3</sup>, average molecular weight  $\overline{M}_w \approx 97,000$  kg mol<sup>-1</sup>, with a melt-flow index (MFI) = 2.1 g/10 min (190°C, 2.16 kg). OXO was made of the same PE formulation but additivated with D<sub>2</sub>W OXO based on manganese and iron (provided by Symphony Environmental Ltd., United Kingdom). AA-OXO was made of same OXO formulation but thermally aged for 180 days in an aerated oven at 70°C, which resulted in fragmentation, loss in mechanical properties and increase in oxidation level as depicted by absorbance increase at 1,712 cm<sup>-1</sup> determined by micro-FTIR spectroscopy reaching more than x/100 (where x was the film thickness). The level of x/100 was previously demonstrated as a prerequisite for biodegradability of OXO, as already demonstrated for *Rhodococcus rhodochrous* and described in

the French Agreement Association Française de Normalisation (AFNOR) (2012) PE, OXO, and AA-OXO were extruded at 180°C using a laboratory scale Rondol linear 18 mm blown film line.

Poly(3-hydroxybutyrate-co-3-hydroxyvalerate) (provided by University of South Brittany, France) had the following characteristics: density = 1.25 g cm<sup>-1</sup>, average molecular weight  $\overline{M}_w \approx 400$  kg mol<sup>-1</sup>, with a MFI = 3.6 g/10 min (210°C, 2.16 kg). This grade has been comprehensively characterized in a previous paper (Corre et al., 2012). Prior to compression molding, the PHBV pellets were dried over 12 h under vacuum at 60°C to minimize the hydrolytic PHBV degradation during processing and compression molded in a Carver® hydraulic press at 180°C under a pressure of 10 metric tons for 3 min.

The thickness of polymer films was 200 μm for PHBV and 100 μm for PE, OXO and AA-OXO. Each sample was a circular piece of 9 mm diameter (area = 63.6 mm<sup>2</sup>), except for AA-OXO that was constituted of irregular fragments of mean area of 13.9 ± 4.8 mm<sup>2</sup> after artificial aging. Each polymer sample was cleaned with 70% ethanol and washed with sterile seawater (SSW) before incubation.

We used five identical aquariums consisting in trays with a 1.8 L capacity (Sodispan, Spain), in which 1.5 L seawater was continually renewed by direct pumping at 4 m depth in Banyuls bay, close to the SOLA observatory station (NW Mediterranean Sea, France). A flow rate of 50 mL min<sup>-1</sup> was chosen to ensure a sufficient renewal of natural bacteria (every 30 min) and an homogeneous distribution of the plastic pieces in the aquariums during the entire experiment. Each aquarium contained polymer pieces of one of the composition (PE, OXO, AA-OXO, and PHBV), except one aquarium used as control, containing only circulating seawater (hereafter called “control aquarium”). Pieces of each polymer type were put in the 18th of January, 2016 and sampled after 7, 15, 22, 30, and 45 days. Aquariums were kept in the dark to avoid UV-driven degradation of the polymers. Throughout the experiment, seawater temperature (between 12.5 and 13.5°C) and salinity (38.5) in the aquariums were similar to seawater from Banyuls bay.

## Atomic Force Microscopy

Atomic force microscopy (AFM) was performed on each sample to get resolved picture of the colonization and accurate insight of the surface state of the polymer. At each sampling time, one piece of each polymer was rinsed with SSW and fixed for at least 1 h at 4°C with 1% (v/v) glutaraldehyde (final concentration) before freezing. At least three 40 × 40 μm<sup>2</sup> areas images were acquired for each sample using a Nanoscope V (Bruker instruments, Madison, WI, United States) in dynamic mode (Binnig et al., 1986) and standard silicon probes (Bruker, TESP-V2). Root mean square (RMS) roughness of the polymer surface were measured on height images of 40 × 40 μm<sup>2</sup> with Gwyddion software, using masks to remove remaining bacterial cells and other organic deposits from the measurements. Boxes of gradual sizes (10, 20, 30, and 40 μm) were used to estimate RMS standard deviation and to check the dependence of the RMS on the lateral size of the picture. On every sample, a plateau was reached at 30 μm, which

validates the use of RMS measured on 40 μm size to characterize the surface state of the sample.

Since surface state characterization is likely to be affected by the development of a biofilm and the deposit of EPS, pretreatments by sonication and rinsing with SSW were performed on some samples to ensure the access to polymer surface. Experiments performed on the same area before and after sonication showed no change in roughness values (data not shown). Comparison with masking method described above showed that no difference was measured within the experimental uncertainties.

## Contact Angle Measurement

Contact angles (SSW/air/polymer) were measured on each polymer in its initial state (before incubation in seawater) and after 7 days of immersion in SSW, using a profile analysis tensiometer (PAT1M, Sinterface Technologies, Berlin, Germany). We did not measure contact angles after 7 days since surface hydrophobicity was too modified by the conditioning film, as previously observed (Lorite et al., 2011). A series of profiles was acquired for three different droplets of millimetric diameters on each sample during successive advancing and receding stages. All series were analyzed using ImageJ software (version 1.46r, Wayne Rasband, National Institutes of Health, United States) to get the receding and advancing angle in each sample.

## Epifluorescence Microscopy

At each sampling time, one piece of each polymer was rinsed with SSW and fixed for at least 1 h at 4°C with 1% (v/v) glutaraldehyde (final concentration) before freezing. Epifluorescence microscopy observations were done using an Olympus AX-70 PROVIS after 4',6-diamidino-2-phenylindole (DAPI) staining according to Clays-Josserand et al. (1999). Pictures were taken on 10 fields of each polymer type (Microbe Counter software). The surface areas covered by only bacterial cells and by biofilm (cells + EPS) were determined using the ImageJ software (version 1.46r, Wayne Rasband, National Institutes of Health, United States).

## Flow Cytometry

Three pieces of each polymer were sampled at each sampling time with sterilized forceps and rinsed with SSW. A cell detachment pre-treatment was applied using 1 mmol L<sup>-1</sup> pyrophosphate during 30 min at room temperature in the dark, followed by a sonication step (3 × 5 s, 40 kHz, 30% amplitude, sterilized probe Branson SLPe). The efficiency of cell-detachment was verified by epifluorescence microscopy before and after cell-detachment, as well as comparison between flow cytometry and epifluorescence microscopy cell counts. The cell detachment pre-treatment was optimized by a set of tests on each polymer substrates. Various mechanical or chemical pre-treatments were tested alone or combined: tetrasodium pyrophosphate (1 and 10 mM); sonication step including a combination of vortex and sonication bath or the use of a sonication probe alone (Branson SLPe, see above); or addition of enzymes mix (Lipase 48 units, beta-galactosidase 10 units, and alpha-glucosidase 0.8 units; Sigma Aldrich). A total of 12 conditions were tested. The chosen protocol was based on a combination of tetrasodium

pyrophosphate (1 mM) and sonication probe, which showed the best correspondence between cell counts obtained by flow cytometry and epifluorescence microscopy for the same sample, the latest being 1- to 5-fold higher values than the first. After cell detachment, samples were fixed for at least 1 h at 4°C with 1% (v/v) glutaraldehyde (final concentration) and frozen before further analysis. In parallel, 3 × 1 mL of seawater (polycarbonate, 47 mm diameter, Whatman) from the control aquarium were also fixed using the same procedure. A 500- $\mu$ L subsample of the detached cells from plastic or from control seawater was mixed with the nucleic acid dye SYBR Green I (final concentration 0.05% [v/v], Sigma Aldrich) for 15 min, at room temperature and in the dark. Cell counts were performed with a FACSCanto II flow cytometer (BD Bioscience, San Jose, CA, United States) equipped with a blue laser (488-nm, air-cooled, 20-mW solid state), as previously described (Severin et al., 2014).

## Heterotrophic Bacterial Production

Bacterial production (BP) was measured on each polymer type at each sampling time by  $^3\text{H}$ -leucine incorporation into proteins, using a modified protocol from Van Wambeke et al. (2009). Briefly, the same cell detachment pre-treatment protocol as for flow cytometry (see above) was used, based on pyrophosphate together with sonication procedure. This pre-treatment improved the BP signal by a factor from 1.0 to 5.7 compared to control condition with no pre-treatment. This pre-treatment gave also the best results when compared to the other conditions tested (including the combination of vortex and sonication bath and the addition of mix of enzymes, together or alone with the other treatments, see above in the flow cytometry section). Immediately after cell-detachment,  $^3\text{H}$ -leucine (specific activity 112 Ci mmol $^{-1}$ ; Perkin Elmer) was added at a final concentration of 1 nmol L $^{-1}$  (completed with cold leucine to 150 nmol L $^{-1}$ ) in triplicate for each sample, which consisted of 1.5 mL of seawater sterilized water containing the piece of plastic together with the detached cells. For seawater samples from the control aquarium,  $^3\text{H}$ -leucine was added at a final concentration of 4.3 nmol L $^{-1}$  to 1.5 mL of control seawater. All samples were incubated in the dark at *in situ* temperature for 3 h. We used the empirical conversion factor of 1.55 ng C pmol $^{-1}$  of incorporated leucine to calculate BP (Simon and Azam, 1989). Cell-specific activities (CSA) were calculated as the ratio between BP and cell counts obtained by flow cytometry.

## DNA Extraction, PCR, and Sequencing

Four replicates of each polymer type were sampled at all sampling times, except for day 15, and stored at  $-80^\circ\text{C}$  until analysis. In parallel, 1 L seawater was sampled in the control aquarium, successively filtered onto 3 and 0.2  $\mu\text{m}$  pore size polycarbonate filters (47 mm diameter, Nucleopore) and filters were stored at  $-80^\circ\text{C}$  until analysis. DNA extraction was performed on polymers and filters using a classical phenol-chloroform method for seawater samples (Ghiglione et al., 1999) and a slight modification of the method for polymer samples (Debeljak et al., 2017).

Briefly, the same cell detachment pre-treatment was used as for flow cytometry and BP (see above) before chemical and

enzymatic cell lysis (1 mg mL $^{-1}$  lysozyme at 37°C for 45 min followed by 0.2 mg mL $^{-1}$  proteinase K and 1% SDS at 50°C for 1 h). The pre-treatment improved cell lysis since no cells were visible by epifluorescence microscopy after this stage. The molecular size and the purity of the DNA extracts were analyzed using agarose gel electrophoresis (1%) and DNA was quantified by spectrophotometry (GeneQuant II, Pharmacia Biotech).

PCR amplification of the 16S V3–V5 region was done using 515F-Y and 926R primers, particularly well-suited for marine samples according to Parada et al. (2016). Sequencing was performed on Illumina MiSeq by Research and Testing Laboratories (Lubbock, TX, United States). Raw FASTA files were deposited at GenBank under the accession number SRP116996. Sequences were analyzed using Mothur pipeline (Schloss et al., 2009). Paired raw reads were assembled, sequences with homopolymers (>8) and ambiguities were removed and the remaining sequences were aligned using SILVA database. Sequences were trimmed to a same length and a chimera were removed (uchime command). Sequences were classified and operational taxonomic units (OTUs) were defined as clusters sharing 97% sequence identity. Only bacteria were treated in this study, due to the small number of archaeal reads. Chloroplast, mitochondrial and eukaryotic sequences were removed. Bacterial sequences were randomly resampled in the OTU file to enable comparison between samples, by normalizing the number of sequences between samples to the sample with the fewest sequences ( $n = 6,186$ ) using Mothur v.1.38.1. All further analyses were performed on randomly resampled OTU table.

## Statistical Analysis

Alpha-diversity was estimated using the non-parametric, Chao1 species richness estimator from the SPADE software. Simpson, Shannon, and Pielou diversity indexes were obtained using the PRIMER 6 software (PRIMER-E, United Kingdom). Differences between polymers and seawater richness and diversity indexes were tested using a *post-hoc* LSD test after an ANOVA test (Statistica 8.0, Statsoft).

An unweighted-pair group method with arithmetic mean (UPGMA) dendrogram based on Bray–Curtis similarities was used for visualization of beta-diversity. A similarity profile test (SIMPROF, PRIMER 6) was performed on a null hypothesis that a specific sub-cluster can be recreated by permuting the entry species and samples. The significant branch (SIMPROF,  $p < 0.05$ ) was used as a prerequisite for defining bacterial clusters. One-way analysis of similarity (ANOSIM, PRIMER 6) was performed on the same distance matrix to test the null hypothesis that was no difference between bacterial communities of different clusters (Berdjeb et al., 2011). Significant correlations between environmental variables were tracked using Spearman rank pairwise correlations.

## RESULTS

### Polymer Surface Properties

Surface properties of the polymers were derived from AFM data (Figure 1). Before incubation in SW, PE, OXO, and AA-OXO

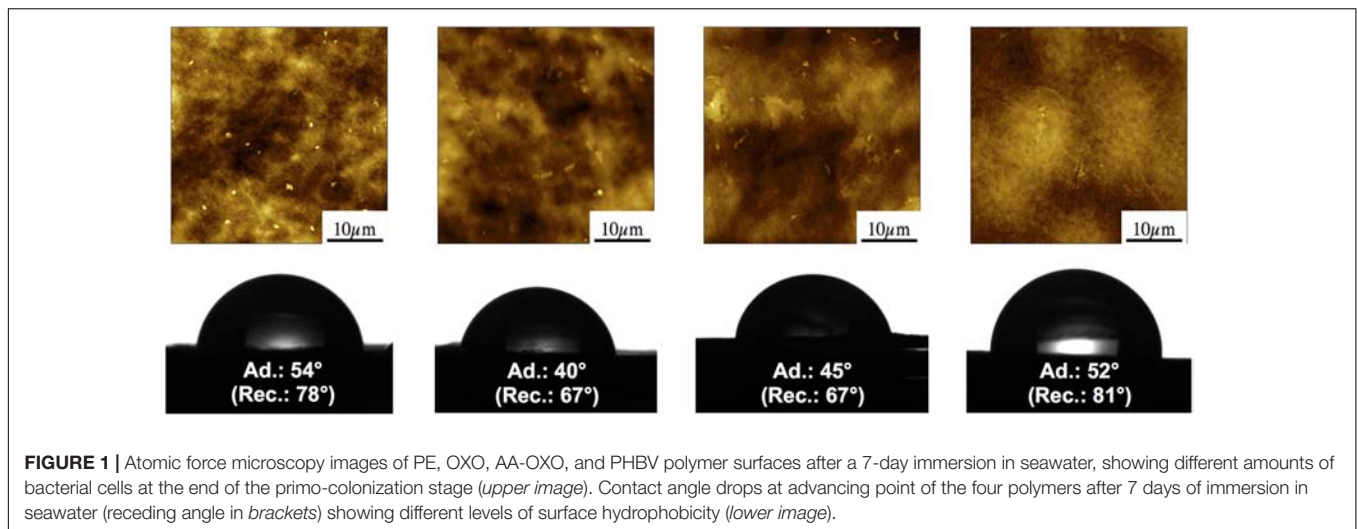


**FIGURE 1** | Atomic force microscopy images of PE, OXO, AA-OXO, and PHBV polymer surfaces after a 7-day immersion in seawater, showing different amounts of bacterial cells at the end of the primo-colonization stage (*upper image*). Contact angle drops at advancing point of the four polymers after 7 days of immersion in seawater (receding angle in *brackets*) showing different levels of surface hydrophobicity (*lower image*).

presented a rather smooth surface. On the contrary, PHBV showed a rough surface, due to the presence of a spherulitic structure of about 20  $\mu\text{m}$  in diameter. Whereas the first three polymers did not present significant surface modifications with increasing immersion times up to 45 days, the PHBV spherulitic structure went through observable morphological alteration, with clear evidences of swelling and erosion (Supplementary Figure S1).

Root mean square roughness measured on  $40 \times 40 \mu\text{m}^2$  pictures provided quantitative assessments of surface alterations (Table 1). PE, which initially showed the lowest roughness ( $56 \pm 7 \text{ nm}$ ) at ambient air, did not change significantly for the first 22 days of immersion and slightly increased after 45 days ( $\text{RMS} = 84 \pm 9 \text{ nm}$ ). OXO roughness presented a similar evolution with slightly higher values. AA-OXO roughness remained in the same range as the previous polymers, fluctuating between 63 and 110 nm in the first 22 days. It should be noted that AA-OXO roughness could not be measured at D45 due to a strong bacterial attachment that resisted the washing protocol. PHBV showed the highest initial roughness with  $208 \pm 21 \text{ nm}$  at ambient air. During the incubation period, its value presented large fluctuations over time, with a global increasing trend following important alteration of the initial spherulite structure. The maximum value of RMS was reached after 45 days, where surface erosion (induced most probably by water itself) was clearly visible in AFM micrographs and was then four times higher than that of PE.

Advancing and receding contact angles (SW/air/polymer) were measured on initial dry samples and after 7 days of immersion in SW (Figure 1 and Table 1). Initially, all polymers presented a rather hydrophobic surface with receding and advancing contact angle close to  $90^\circ$ , with PHBV and PE being the most hydrophobic. The addition of polar groups from PE to OXO and AA-OXO explains their lower hydrophobicity. The contact angle hysteresis (difference between receding and advancing contact angle), which is directly related to the roughness or the chemical heterogeneity of a surface, showed higher values for OXO and AA-OXO compared to PE, in

**TABLE 1** | Physical data for the four plastic types (PE, OXO, AA-OXO, and PHBV) according to immersion time in days (D), including roughness (RMS, in nm), contact angle (CA, receding – advancing, in degree) and carbonyl index (CI).

		DO	D7	D15	D22	D30	D45
PE	RMS	56	49		46		84
	CA	85–94	54–78				
	CI		0.74	0.48	0.39	0.56	0.57
OXO	RMS	87	122		106		112
	CA	61–79	40–67				
	CI		0.49	0.5	0.39	0.47	0.85
AA-OXO	RMS	110	63		64		ND
	CA	52–76	45–67				
PHBV	RMS	208	129	322	240		358
	CA	78–99	52–81				

agreement with the more homogeneous chemical composition of the latter. PHBV showed a large hysteresis, probably reflecting its structuration in big spherulites, in agreement with AFM observation and roughness measurements (Supplementary Figure S1). After immersion, the decrease in hydrophobicity for all polymers can be connected to surface reconstruction for OXO and AA-OXO, surface reconstruction and water swelling for PHBV and probably adsorption of polar molecules on the surface in the case of PE.

## Dynamics of Bacterial Cell Counts on Polymers and in Seawater

Epifluorescence microscopy observations were not possible for AA-OXO and PHBV samples, because of strong auto-fluorescence background under UV light for these two polymers. Because our cell detachment pre-treatment showed that flow cytometry approach was possible for all polymer and it slightly underestimated cell counts as compared to epifluorescence microscopy by a factor of 1 to 5, we decided to use the flow cytometry cell counts to provide comparable data obtained with the same technique. Then, epifluorescence microscopy was used

only to confirm the results obtained by flow cytometry and to estimate plastic surface area covered by bacterial cells, when available (only for PE and OXO).

Flow cytometry data highlighted three distinct phases of biofilm formation for all polymer types: primo-colonization, growth, and maturation (Table 2). Primo-colonization lasted for the first 7 days following immersion, with cell counts being, respectively, 1.5, 1.6, and  $1.3 \times 10^5$  cells  $\text{cm}^{-2}$  for PE, OXO, and PHBV and  $9.3 \times 10^5$  cells  $\text{cm}^{-2}$  for AA-OXO. Cell counts increased on all polymers during the growing phase, but at different rates: after 15 and 22 days, cell counts on PHBV and AA-OXO biofilms were about fivefold more than that on PE and OXO. The stabilization phase was visible after 22 days for PE, OXO, and PHBV, reaching, respectively, 3.7, 6.9, and  $16.3 \times 10^5$  cells  $\text{cm}^{-2}$  at the end of the experiment, whereas cell counts continued to increase for AA-OXO to finally reach  $34.1 \times 10^5$  cells  $\text{cm}^{-2}$ .

The three phases were also visually observed by epifluorescence microscopy (Figure 2). Primo-colonization was characterized by single cells spreading out homogeneously on the surface resulting in cell coverage of 1 and 3% of the PE

and OXO surface at day 7, respectively (Table 2). Cell abundance increased unevenly during the growing phase, leading to a patchy distribution of cell aggregates on both PE and OXO films, representing, respectively, 6.5 and 10.1% coverage at day 22. Together with an increase in exuded EPS clearly visible on micrographs after day 22, the biofilm coverage on the surface reached 29.2 % and 18.1% after 45 days for PE and OXO, respectively (Table 2).

## Dynamics of Bacterial Community Structure and Diversity on Polymers and in Seawater

Next-generation DNA sequencing resulted in 265,998 tags falling into 823 bacterial OTUs at 97% similarity level, after randomly resampling to 6,186 sequences per sample to provide statistical robustness when comparing diversity between samples. The cluster analysis showed a clear dissimilarity (>70%) between seawater controls and polymer samples during the course of the experiment (Figure 3). Overall, bacterial community structure on all polymer types showed spectacular changes, first in the diversity of bacteria that colonized the polymers compared with the surrounding seawater, and second in the growing and maturation phases compared to the primo-colonization phase. All polymer types sampled at day 7 clustered together in a group showing low similarity (<25%) with other samples (Figure 3). Within this cluster, the PHBV community structure significantly differed (SIMPROF test) from the other polymer types. The temporal dynamics of the bacterial assemblages during the growing and maturation phases differed with the polymer type. PE and OXO biofilms formed distinct, yet close sub-clusters and showed few changes from days 22 to 45. Conversely, both communities from AA-OXO and PHBV presented strong changes during this period (<40% similarity from days 22 to 45 between samples from the same polymer type).

Overall, the observed changes in the diversity indexes (Shannon, Pielou, Chao1, and Simpson; Supplementary Table S1) were related to the polymer type (ANOVA test,  $p < 0.05$ ), but not to incubation time: we could not find any relation between the changes in diversity indexes and the different stages of biofilm formation. The equitability (Pielou) on PE was significantly higher than on AA-OXO, PHBV and seawater (LSD test,  $p$ -value < 0.05) (Supplementary Table S1). The Shannon diversity index was also higher on PE compared to AA-OXO (LSD test,  $p$ -value < 0.05). The Chao1 index ranged from 113 (OXO at day 7) to 322 (PHBV at day 45).

Taxonomic analyses confirmed the specificity of the community structures formed on the polymers compared to seawater, the latter being dominated by Alphaproteobacteria, Flavobacteria, Cyanobacteria, and Actinobacteria throughout the experimentation (Figure 3). On all four polymers type, the primo-colonizers belonged to Gammaproteobacteria, which represented between 45 and 75% of the total OTU in each community (Figure 3). On PE, OXO and AA-OXO, this group was mainly dominated by *Alcanivorax* sp., *Aestuariicella hydrocarbonica*, *Alteromonas* sp., and *Thalassolituus* sp. followed by *Marinobacter* sp. and *Maricurvus* (Figure 4). On PHBV,

**TABLE 2 |** Biological data for the four plastic types (PE, OXO, AA-OXO, and PHBV) compared to seawater (SW) according to immersion time in days (D), including bacterial cell count (BC,  $\times 10^5$  cell  $\text{mL}^{-1}$  for SW or  $\times 10^5$  cell  $\text{cm}^{-2}$  for plastic samples), bacterial production (BP, in  $\text{ngC L}^{-1} \text{h}^{-1}$  for SW or  $\text{ngC dm}^{-2} \text{h}^{-1}$  for plastic samples), and bacterial specific activity (SA,  $\times 10^{-3}$   $\text{fgC cell}^{-1} \text{h}^{-1}$ ).

		D7	D15	D22	D30	D45
SW	BC	1.16 (0.03)	0.89 (0.04)	1.71 (0.11)	1.15 (0.001)	3.07 (0.14)
	BP	9.09 (0.8)	10.5 (1.1)	16.8 (0.7)	21.3 (2.0)	41 (1.8)
	SA	0.079	0.118	0.098	0.185	0.133
PE	BC	1.53 (0.34)	3.4 (0.51)	6.76 (1.45)	9.05 (1.23)	3.7 (1.33)
	BP	38.5 (20.4)	352.3 (114.9)	426.7 (241.5)	29 (13.5)	55.6 (36.7)
	SA	2.52	10.37	6.33	0.32	1.50
	cov	1.00%	5.1%	6.5 %	15.1%	29.2 %
OXO	BC	1.57 (0.34)	3.75 (1.29)	5.65 (1.27)	4.92 (1.35)	6.89 (1.40)
	BP	105.5 (36.2)	178.7 (4.0)	217.2 (10.2)	60.3 (21.4)	55.3 (12.2)
	SA	6.74	5.02	3.85	1.23	0.80
	cov	3.4%	3.4	10.1%	12.3%	18.1%
AA-OXO	BC	9.25 (3.50)	16.1 (4.47)	28.4 (3.86)		34.1 (8.47)
	BP	145.9 (20.1)	1396.9 (90.0)	1369.7 (193.6)		131.4 (7.25)
	SA	1.58	8.67	4.82		0.39
PHBV	BC	1.25 (0.37)	15.2 (2.92)	15.3 (3.94)		16.3 (3.61)
	BP	67 (58.4)	1090.4 (513.5)	259.4 (125.9)		240.9 (100.4)
	SA	5.38	7.19	1.70		1.47

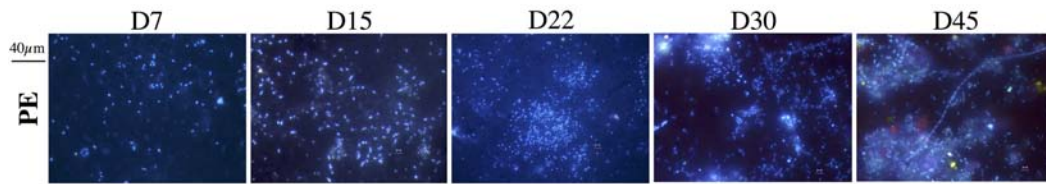


**FIGURE 2** | Epifluorescence micrographs of DAPI-stained PE plastics after 7, 15, 22, 30, and 45 days of immersion in seawater. Bar: 40  $\mu\text{m}$ .

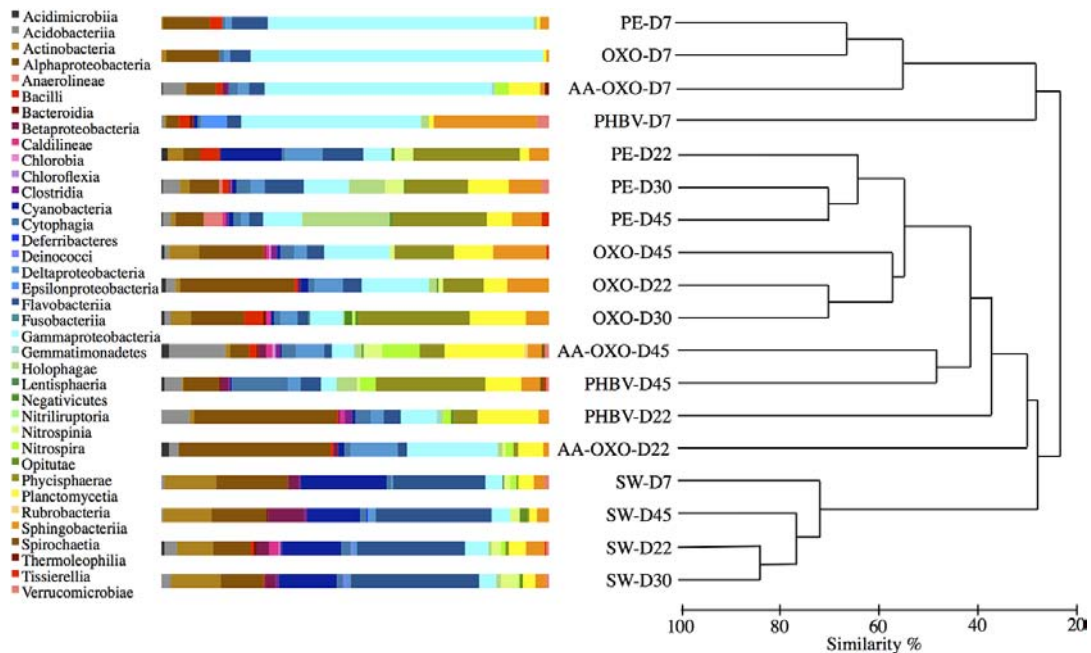


**FIGURE 3** | Comparison of taxonomic abundances and community structure of bacteria in seawater (SW) and attached in the four plastics (PE, OXO, AA-OXO, and PHBV) according to immersion time in days (D), by cumulative bar charts comparing relative class abundances (*left*) and by UPGMA dendrogram based on Bray-Curtis similarities between sequencing profiles (*right*).

*Neptuniibacter* sp. made up for more than 30% of the community, while this OTU remained undetected on all other polymers.

The growing and maturation phases were characterized by few changes on PE and OXO samples, where *Croceibacter* sp. was the dominant OTU on PE, whereas *Sneathiella glossodoripedis* dominated on OXO (**Figure 4**). Only a significant increase of *Solimonas* sp. occurred during the stabilization phase on OXO. More changes were observed on AA-OXO and PHBV during the growing and maturation phases, with large dissimilarities between sampling time. The OTUs *Lutibacterium anuloederans* and *Pseudospirillum* sp. were found in high amounts on AA-OXO during the growth stage, whereas *Phaeobacter* sp. stand out on PHBV. The majority of OTUs identified at day 22 on AA-OXO and PHBV decreased at day 45, giving way to a higher abundance of unclassified OTUs. During the maturation phase, Gammaproteobacteria decreased and Alphaproteobacteria increased proportionally, with Phycisphaerae, Planctomycetia, and Sphingobacteriia classes in particular whatever the plastic type (**Figure 3**).

### Presence of Putative Hydrocarbonoclastic Bacteria

We identified 34.4% of the total sequences on polymer samples as being putative hydrocarbonoclastic bacteria (HCB), compared to 4.1% in control seawater. Among the most abundant OTUs per polymer sample (>5% of the total OTUs in one sample), we found the HCB *Alcanivorax* sp., *Aestuariicella hydrocarbonica*, *Marinobacter* sp., *Lutibacterium anuloederans*, and *Neptuniibacter* sp. (**Figure 4**). SIMPER analysis showed that these 5 OTUs explained more than 13% of the dissimilarity between polymers and seawater communities. Overall, HCB were particularly abundant in bacterial communities during the primo-colonization phase on all polymer types (1.7 to 3-fold more HCB were identified on polymers compared to seawater) and generally decreased afterward. *Aestuariicella hydrocarbonica* was found in higher abundance on all polymer types, reaching up to 20 and 24% of sequences in OXO and AA-OXO, respectively. *Alcanivorax* sp. reached similar relative abundances, but was not detected on PHBV, where HCB were instead dominated by

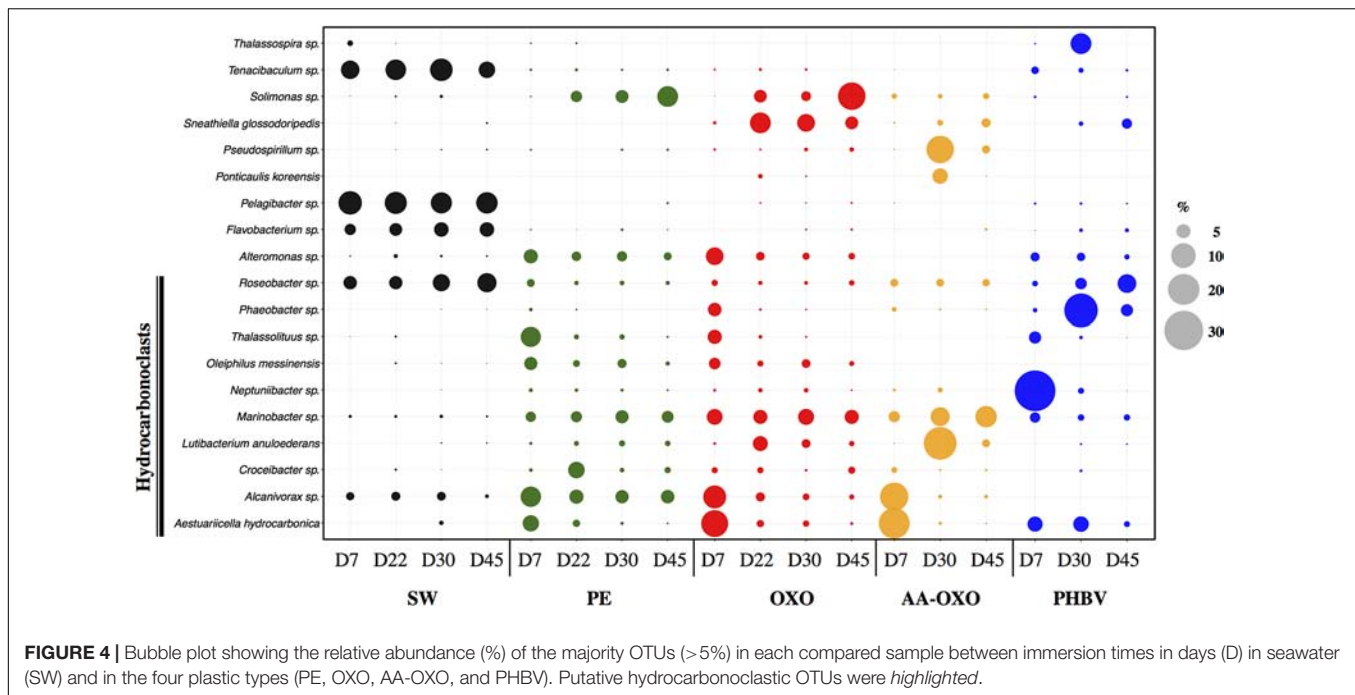


**FIGURE 4 |** Bubble plot showing the relative abundance (%) of the majority OTUs (>5%) in each compared sample between immersion times in days (D) in seawater (SW) and in the four plastic types (PE, OXO, AA-OXO, and PHBV). Putative hydrocarbonoclastic OTUs were *highlighted*.

*Neptuniibacter*. These three OTUs decreased after day 7 and were replaced by another HCB, such as *Marinobacter* on PE, OXO and AA-OXO, and *Lutibacterium anuloederans* on AA-OXO.

## Presence of Putative Pathogenic Bacteria

We identified 23 putative pathogen OTUs in all our samples, which represented <3% (3,817 sequences) of the total sequences (plastic and seawater samples). A 80% of putative pathogen OTUs were found in seawater samples (mainly *Tenacibaculum* sp.). On plastic samples, half of the putative pathogen OTUs belonged to *Vibrio* sp., 20% being identified as *Tenacibaculum* sp. and 11% as *Staphylococcus aureus*. Overall, the abundance of putative pathogenic OTUs remained steady during the different biofilm stages, except for PHBV showing two times more putative pathogen OTUs during primo-colonization.

## Heterotrophic BP and CSA on Polymers and in Seawater

During the primo-colonization stage, BP were in the same order of magnitude between the four polymers (from 38.5 ngC dm<sup>-2</sup> h<sup>-1</sup> on PE to 145.9 ngC dm<sup>-2</sup> h<sup>-1</sup> on AA-OXO) (Table 1). The temporal dynamics of BP on PE and OXO were comparable, peaking during the growing phase (426.7 and 217.2 ngC dm<sup>-2</sup> h<sup>-1</sup> at day 22, respectively) and decreasing during the maturation phase (55.6 to 55.3 ngC dm<sup>-2</sup> h<sup>-1</sup> at day 45, respectively). AA-OXO and PHBV biofilms presented different trends. BP peaked at day 15 for both AA-OXO and PHBV (1396.9 and 1090.4 ngC dm<sup>-2</sup> h<sup>-1</sup>, respectively), being until eightfold higher than PE and OXO. PHBV biofilm became less active at day 22, reaching a plateau around 250 ngC dm<sup>-2</sup> h<sup>-1</sup> until day 45. AA-OXO kept a high

activity until day 22 (1396.7 ngC dm<sup>-2</sup> h<sup>-1</sup>) and decreased drastically at day 45 (131.4 ngC dm<sup>-2</sup> h<sup>-1</sup>). Seawater BP remained lower than polymers BP throughout the experiment rising from 9.09 ngC L<sup>-1</sup> h<sup>-1</sup> at D7 to 41 ngC L<sup>-1</sup> h<sup>-1</sup> at D45.

Cell-specific activity was very high on plastic compared to free-living bacteria (maximum of 10.37 and 0.13 × 10<sup>-3</sup> fgC cell<sup>-1</sup> h<sup>-1</sup>, respectively) and especially during the growing phase of the biofilm on plastics (from 43- to 88-fold higher than in seawater). Indeed, cell-specific activity peaked at day 15 but decreased generally after 22 days on plastic, whereas it changed more randomly in seawater.

## DISCUSSION

In the present study, we show that plastic polymers with different composition, when immersed under identical marine conditions, are first colonized by similar bacterial communities to constitute support matrices for the formation of contrasted biofilms with dissimilar diversities and activities, growth efficiency, and maturation properties. We also investigated the possible relation between surface properties and bacterial cell counts on plastics, speculated to be a key factor controlling biofilm formation (Pasmore et al., 2002).

## Succession of Biofilm Colonization Phases on Polymers

In this study, we observed three typical successive phases of biofilm formation on artificial surfaces: initial, growth and maturation phases. The initial phase lasted for the first week of immersion and was characterized by an abundant and homogeneous bacterial colonization on all polymers within

the first 7 days of incubation, with a cell density ranging from  $1.25 \times 10^5$  to  $9.25 \times 10^5$  cell  $\text{cm}^{-2}$ . The growing phase (after day 7 to 22) significantly differed between non-biodegradable (PE and OXO) and biodegradable (AA-OXO and PHBV) polymers, with a higher biomass increase on the latter. At this stage, cells formed aggregates and biofilms became more patchy, as also observed on plastic marine debris in the North Pacific Gyre (Webb et al., 2009; Carson et al., 2013) and in the Mediterranean Sea (Dussud et al., 2018). The stabilization phase generally occurred after 3 weeks (from day 22 to 45) with the highest cell abundance reached on AA-OXO and PHBV, being more than five times higher than that accumulated on the non-biodegradable PE and OXO. These results are in accordance with Lobelle and Cunliffe (2011) reporting stabilization phase within a month on PE-based food bags, even if their results were based on cultivable bacteria that greatly underestimate cell counts of the entire biofilm (Ferguson et al., 1984). Other studies evaluated cell abundance using SEM, AFM, or epifluorescence microscopy (Harrison et al., 2014; Bryant et al., 2016), but none of them provided direct cell counts. As far as we know, this study presents the first results of direct cell counts on polymers using flow cytometry coupled with epifluorescence microscopy. It should be emphasized that epifluorescence microscopy was not usable for some polymers due to strong auto-fluorescence background (i.e., AA-OXO and PHBV), whereas our cell detachment pre-treatment permits to use flow cytometry as accurate technique to estimate cell counts in all polymers. When possible, the comparison of the two techniques showed systematic underestimation of cell counts for flow cytometry by a factor of 1 to 5, which is consistent with previous studies on organic particle-attached bacteria (Worm et al., 2001; Mével et al., 2008).

We also explored the possible relation between polymer surface characteristics and microbial colonization. This is a complex question, since several effects need to be considered at once: the chemical nature (Lorite et al., 2011; Siddiqi et al., 2015), roughness (Riedewald, 2006), and heterogeneity (Morra and Cassinelli, 1997) of the polymer surface on the one hand, and the potential hindrance of these properties by the microbial conditioning film (Lorite et al., 2011), on the other hand. Moreover, polymers are known to alter their properties when immersed in water, due to water diffusion or reconstruction of their surface in order to minimize the interfacial energy. Indeed, we observed here a decrease in hydrophobicity for all polymers after 7 days of immersion in seawater. This complexity might explain why there is still no consensus today, as to whether, for instance, a hydrophobic surface will increase or not bacterial adhesion (Morra and Cassinelli, 1997). Several articles on biofouling nevertheless acknowledge that high-energy surfaces (“hydrophilic surfaces”) tend to favor biofilm growth (Callow and Fletcher, 1994; Artham et al., 2009). Our study presents the first results combining the observation of successive biofilm colonization phases on plastics together with the evolution of their surface roughness, contact angles and hysteresis before and after immersion in seawater. When comparing the three types of PE-based polymers, we clearly observed that colonization increased with increasing

polarity (AA-OXO > OXO > PE) for similar roughness. In the same way, colonization was higher for PHBV than for PE, probably because PHBV is more polar, even though its roughness was larger than that of PE. A clear conclusion that can be drawn from these results is that the surface polarity has definitely an impact on colonization at sea, whether through the adsorption of a more abundant or different conditioning film, or directly through attracting more bacteria. Finally, one should keep in mind that cells numbers reflect not only their rate of adhesion but also the multiplication/disappearance rate of the different species, which can be affected in the case of biodegradable substrates where plastic is not only a physical support matrix but also a potential source of nutrients for bacteria. A hint into these rates is given by the measured activity and diversity of the bacterial colonies which are discussed thereafter.

## Bacterial Community Succession on Polymers

The bacterial communities accumulated on the polymer surfaces differed from those in the seawater during the entire course of the experiment. This assessment is in line with previous studies revealing a clear niche partitioning between bacteria living on plastics versus surrounding seawaters (Zettler et al., 2013; Amaral-Zettler et al., 2015; Dussud et al., 2018). Our experimental conditions did not disrupt the natural assemblages of seawater bacteria circulating in the aquarium during the course of the experiment, as observed in the control aquarium that did not contain plastic. Together with the slight changes observed in bacterial abundance in the control aquarium which are in line with values commonly found in the Mediterranean Sea (Pulido-Villena et al., 2011), these results validated our capability to maintain natural conditions for 45 days in an experimental setup renewed with natural seawater every 30 min.

Primo-colonizers of the plastics represented <0.1% of the bacterial diversity found in the water, corresponding to the less abundant or rare taxa that make up a substantial portion of bacterial communities in the oceans and constitute the so called “rare biosphere” (Sogin et al., 2006). These results demonstrate that the “seed bank” theory (Pedrós-Alió, 2012; Sauret et al., 2014) applies particularly well to the early colonizers and to the plastisphere in general. Members of the bacterial communities living on plastics, although rare in the seawater, prove here to be opportunistic species able to grow and to become the “core species” living on plastics. Overall, we found that Gammaproteobacteria dominated primo-colonizers on all polymer types, as already reported for the early colonization of PE (Harrison et al., 2014; De Tender et al., 2017). This taxonomic group was also identified as a family of primo-colonizers on other artificial surfaces in coastal waters such as acryl, glass, steel, or filtration membranes from drinking water treatment plants (Hörsch et al., 2005; Lee et al., 2008). The bacterial community structures of primo-colonizers were similar between all polymer types, except for PHBV, for which bacteria belonged to the same cluster but presented much less similarity and were largely dominated by *Neptuniibacter* sp.

In the next phase of biofilm growth and during the maturation phase, we observed a clear distinction between bacterial communities growing on non-biodegradable and biodegradable polymers. While PE and OXO eventually hosted a homogeneous cluster, the community structures on AA-OXO and PHBV continued to change over time. Previous studies also underlined rapid shifts in bacterial communities between the initial and successive colonization phases on other artificial surfaces, such as polyurethane painted plastics (Dang and Lovell, 2000), desalination plant system (Elifantz et al., 2013) or on acryl, glass and still coupons (Lee et al., 2008). With time, we observed that members of the class Alphaproteobacteria became increasingly abundant whatever the polymer type and remained distinct from the communities living in the control seawater.

Our study compared for the first time the dynamics of marine bacterial communities on polymers of similar chemical basic formulation (i.e., PE-based) but with d2w additives (Symphony Environmental Technology) with or without pre-aging. The cluster analysis showed that similar communities dominated the non-biodegradable PE and OXO during the growing and maturation phases, but differed drastically from the biodegradable AA-OXO. Difference in bacterial community structure may be explained by surface properties, since AA-OXO present higher oxidation state, lower hydrophobicity compared to PE and OXO.

The two biodegradable polymers AA-OXO and PHBV continued to change over the growing and maturation phases of the biofilm. Polymer degradation is considered to proceed through several stages (i.e., biodeterioration, biofragmentation, assimilation, and mineralization), which result from complex synergetic interactions between bacterial communities that also change over the biodegradation process (Lucas et al., 2008; Dussud and Ghiglione, 2014). Even if biodegradation processes occurring in both AA-OXO and PHBV are becoming better understood for bacteria cultured in the laboratory (Deroiné et al., 2015; Eyheraguibel et al., 2017), further studies are needed to describe the complex interactions between bacterial communities in the biofilm and their role in plastic biodegradation in natural conditions.

## Potential Bacterial Degradation of Complex Carbon Molecules in Plastics

The SIMPER analysis revealed a clear dominance of putative HCB on plastic compared to seawater. Their presence on the plastic surface has been observed in various neustonic debris (mainly of PE and PP composition) in the North Pacific Gyre (Zettler et al., 2013; Debroas et al., 2017) and in the Mediterranean Sea (Dussud et al., 2018), or on 5- to 6-weeks immersed PET drinking water bottles (Oberbeckmann et al., 2016). All these authors postulated that these plastic-dwelling microbes possessed the metabolic potential to degrade plastics and/or plastic-bound organic pollutants. Such hypothesis was recently supported by metagenomic analyses highlighting an overexpression of xenobiotic degradation functions by plastisphere communities in the North Pacific Gyre (Bryant et al., 2016).

Another hypothesis is the capability of HCB to overcome the poor accessibility of hydrophobic substrates, which may play a crucial role in the early colonization phase on hydrocarbon-based plastics (Lobelle and Cunliffe, 2011). Biofilm formation at the hydrocarbon-water interface has been observed with various alkane-degrading strains including *Oleiphilus messinensis* (Golyshin et al., 2002) and *Marinobacter* sp. (Vaysse et al., 2009), which dominated the early colonization phase on PE, PE-OXO, and AA-OXO in our study, together with other known alkane-degraders *Alcanivorax* sp. (Yakimov et al., 2007) and *Aestuariicella hydrocarbonica* (Lo et al., 2015). Biofilm formation has been shown to promote growth at the hydrocarbon-water interface by facilitating interfacial access, thus constituting an efficient adaptive strategy for assimilating hydrocarbon (Bouchez-Naïtali et al., 2001).

If putative HCB dominated on hydrocarbon-based plastics (PE, OXO, and AA-OXO), PHBV showed instead a succession of PHA-degraders. Indeed, members of *Neptuniibacter* sp. (Chen et al., 2012), *Phaeobacter* sp. (Frank et al., 2014), and *Roseobacter* sp. (Xiao and Jiao, 2011) previously shown to present the capability to accumulate or metabolize PHA, were dominant in the early colonization, growth and maturation phases, respectively. Further biodegradation studies in natural environment are needed to further describe the role of these species in PHA polymers degradation.

## A High and Variable Heterotrophic BP on Polymers

Our study provides the first BP data on polymers. A high temporal variability of BP was found during the successive phases of biofilm formation on each polymer. Overall, BP peaked after 2 weeks during the growing phase in all polymer types (from day 15 to 22), where CSA were the highest, and both parameters decreasing in the maturation phase.

In our seawater circulation system, BP reached  $41 \text{ ngC L}^{-1} \text{ h}^{-1}$ , a value similar to what is generally reported *in situ* in the NW Mediterranean Sea (Lemée et al., 2002), thus making extrapolation of our results to natural seawater possible.

Comparing BA and BP data between polymer films (in  $\text{cm}^{-2}$ ) and seawater (in  $\text{mL}^{-1}$ ) was irrelevant because one is counted in a volume and the other one on a surface, but using cell-specific activity (in  $\text{ngC cell}^{-1} \text{ h}^{-1}$  for both plastic and seawater) made this comparison possible. We then found that bacteria attached on polymer were particularly active compared to the free-living bacteria, the cell-specific activity being from 43- to 88-fold higher especially during the growing phase in the polymers. Such difference may be explained by the presence of labile inorganic and organic matter on the plastic, as on any solid surface immersed in seawater (Cooksey and Wigglesworth-Cooksey, 1995). Another explanation could be that biodegradation has started on some polymers, since they can theoretically be used as carbon source by bacteria (Dussud and Ghiglione, 2014). The BP observed on the two biodegradable polymers (AA-OXO and PHBV) proved until 30 times higher than that measured on non-biodegradable polymers support this hypothesis. Unfortunately, no specific biodegradation assays on

organic matter or plastic were performed in this study, which may help to test these hypotheses and their complementarity. Further studies are needed to differentiate organic matter utilization from polymer biodegradation when measuring BP on plastics.

In this paper, we did not evaluate the biodegradability of the polymers tested during our experiment. Nevertheless, a better understanding of the biofilm forming on plastic in natural conditions is necessary to develop realistic tests of biodegradation. A very recent review pointed that current standards and test methods are insufficient in their ability to realistically predict the biodegradability of plastics in aquatic environment (Harrison et al., 2018). In particular, the type of inoculum and the presence of organic matter are potential sources of uncertainties on the biodegradability tests, generally based on respirometric measurements (Sharabi and Bartha, 1993). For example, a study on PHBV aged film demonstrated a large loss of weight after 180 days in natural seawater and a biodegradation by respirometry (Deroigné et al., 2015). To complete this study a characterization of the microorganisms diversity would have been important to better understand the mechanisms of PHBV biodegradation in seawater. Differences in the oxidation degree of the polymers, in the environmental conditions or in the methodologies used are also important factors that may explain controversy results showing ever no significant proof of mineralization of pre-oxidized OXO in marine water (Alvarez-Zeferino et al., 2015) or clear biodegradation in other environments (Jakubowicz, 2003; Chiellini et al., 2007; Ojeda et al., 2009; Yashchuk et al., 2012; Eyheraguibel et al., 2018). Giving the fact that relatively few studies focused on colonization of plastic at sea, this study should help further researches on biodegradability of plastics in marine habitats.

## REFERENCES

- Association Française de Normalisation (AFNOR) (2012). *AC t51-808 Plastics—Assessment of Oxobiodegradability of Polyolefinic Materials in the Form of Films—Methods and Requirements*. Paris: AFNOR, 1–25.
- Alvarez-Zeferino, J. C., Beltrán-Villavicencio, M., and Vázquez-Morillas, A. (2015). Degradation of plastics in seawater in laboratory. *Open J. Polym. Chem.* 5, 55–62. doi: 10.4236/ojpcem.2015.54007
- Amaral-Zettler, L. A., Zettler, E. R., Slikas, B., Boyd, G. D., Melvin, D. W., Morrall, C. E., et al. (2015). The biogeography of the plastisphere: implications for policy. *Front. Ecol. Environ.* 13, 541–546. doi: 10.1890/150017
- Ammala, A., Bateman, S., Dean, K., Petinakis, E., Sangwan, P., Wong, S., et al. (2011). An overview of degradable and biodegradable polyolefins. *Prog. Polym. Sci.* 36, 1015–1049. doi: 10.1016/j.progpolymsci.2010.12.002
- Artham, T., Sudhakar, M., Venkatesan, R., Madhavan Nair, C., Murty, K. V. G. K., Doble, M. (2009). Biofouling and stability of synthetic polymers in sea water. *Int. Biodeterior. Biodegradation* 63, 884–890. doi: 10.1016/j.ibiod.2009.03.003
- Auta, H. S., Emenike, C. U., Fauziah, S. H. (2017). Distribution and importance of microplastics in the marine environment a review of the sources, fate, effects, and potential solutions. *Environ. Int.* 102, 165–176. doi: 10.1016/j.envint.2017.02.013
- Barnes, D. K., Galgani, F., Thompson, R. C., and Barlaz, M. (2009). Accumulation and fragmentation of plastic debris in global environments. *Philos. Trans. R. Soc. B Biol. Sci.* 364, 1985–1998. doi: 10.1098/rstb.2008.0205
- Berdjeb, L., Ghiglione, J. F., Domaizon, I., Jacquet, S. (2011). A two-year assessment of the main environmental factors driving the free-living bacterial community

## AUTHOR CONTRIBUTIONS

CD and CH have conceived and designed the study. CD, CH, MG, and PF acquired the data. CD, CH, MG, PF, and J-FG analyzed and interpreted the data. J-FG, PH, SB, PF, and MG provided the equipment. CD and J-FG drafted the manuscript. PF, MG, and A-MD critically revised the manuscript for important intellectual content. BE, A-LM, JJ, JC, NC, CO, and SR approved the version of the manuscript to be published.

## FUNDING

This work was part of the research project OXOMAR (Abiotic and biotic degradation and toxicity of OXO-biodegradable plastics in marine waters), funded by Agence Nationale de la Recherche (ANR). It was also supported by the LabEx Numev and the PLASTICMICRO project funded by CNRS-EC2CO.

## ACKNOWLEDGMENTS

We thank Guigui P. A., V. J. P. J. S., and Albuquerque N. for insightful comments on the manuscript and Fuentes M. for technical support.

## SUPPLEMENTARY MATERIAL

The Supplementary Material for this article can be found online at: <https://www.frontiersin.org/articles/10.3389/fmicb.2018.01571/full#supplementary-material>

- structure in Lake Bourget (France). *Microb. Ecol.* 61, 941–954. doi: 10.1007/s00248-010-9767-6
- Binnig, G., Quate, C. F., and Gerber, C. (1986). Atomic force microscope. *Phys. Rev. Lett.* 56, 930–933. doi: 10.1103/PhysRevLett.56.930
- Bouchez-Naïtali, M., Blanchet, D., Bardin, V., and Vandecasteele, J. P. (2001). Evidence for interfacial uptake in hexadecane degradation by *Rhodococcus equi*: the importance of cell flocculation. *Microbiology* 147, 2537–2543. doi: 10.1099/00221287-147-9-2537
- Bryant, J. A., Clemente, T. M., Viviani, D. A., Fong, A. A., Thomas, K. A., Kemp, P., et al. (2016). Diversity and activity of communities inhabiting plastic debris in the North Pacific Gyre. *mSystems* 1:e00024-16.
- Callow, M. E., and Fletcher, R. L. (1994). The influence of low surface energy materials on bioadhesion—a review. *Int. Biodeterior. Biodegradation* 34, 333–348. doi: 10.1016/0964-8305(94)90092-2
- Carson, H. S., Nerheim, M. S., Carroll, K. A., Eriksen, M. (2013). The plastic-associated microorganisms of the North Pacific Gyre. *Mar. Pollut. Bull.* 75, 126–132. doi: 10.1016/j.marpolbul.2013.07.054
- Chen, M. H., Sheu, S. Y., Chiu, T. F., and Chen, W. M. (2012). *Neptuniibacter halophilus* sp. nov., isolated from a salt pan, and emended description of the genus *Neptuniibacter*. *Int. J. Syst. Evol. Microbiol.* 62, 1104–1109. doi: 10.1099/ijs.0.030379-0
- Chiellini, E., Corti, A., and D'Antone, S. (2007). Oxo-biodegradable full carbon backbone polymers—biodegradation behaviour of thermally oxidized polyethylene in an aqueous medium. *Polym. Degrad. Stab.* 92, 1378–1383. doi: 10.1016/j.polymdegradstab.2007.03.007
- Clays-Josserand, A., Ghiglione, J. F., Philippot, L., Lemanceau, P., Lensi, R. (1999). Effect of soil type and plant species on the fluorescent pseudomonads

- nitrate dissimilating community. *Plant Soil* 209, 275–282. doi: 10.1023/A:1004694510322
- Cooksey, K. E., Wigglesworth-Cooksey, B. (1995). Adhesion of bacteria and diatoms to surfaces in the sea: a review. *Aquat. Microb. Ecol.* 9, 87–96. doi: 10.3354/ame009087
- Corre, Y. M., Bruzaud, S., Audic, J. L., and Grohens, Y. (2012). Morphology and functional properties of commercial polyhydroxyalkanoates: a comprehensive and comparative study. *Polym. Test.* 31, 226–235. doi: 10.1016/j.polymertesting.2011.11.002
- Costerton, J. W., Lewandowski, Z., Caldwell, D. E., Korber, D. R., Lappin-Scott, H. M. (1995). Microbial biofilms. *Annu. Rev. Microbiol.* 49, 711–745. doi: 10.1146/annurev.mi.49.100195.003431
- Dang, H., Lovell, C. R. (2000). Bacterial primary colonization and early succession on surfaces in marine waters as determined by amplified rRNA gene restriction analysis and sequence analysis of 16S rRNA genes. *Appl. Environ. Microbiol.* 66, 467–475. doi: 10.1128/AEM.66.2.467-475.2000
- Davey, M. E., O’toole, G. A. (2000). Microbial biofilms: from ecology to molecular genetics. *Microbiol. Mol. Biol. Rev.* 64, 847–867. doi: 10.1128/MMBR.64.4.847-867.2000
- De Tender, C., Devriese, L. I., Haegeman, A., Maes, S., Vangeyete, J., Cattrijse, A., et al. (2017). Temporal dynamics of bacterial and fungal colonization on plastic debris in the North Sea. *Environ. Sci. Technol.* 51, 7350–7360. doi: 10.1021/acs.est.7b00697
- Debeljak, P., Pinto, M., Proietti, M., Reisser, J., Ferrari, F. F., Abbas, B., et al. (2017). Extracting DNA from ocean microplastics: a method comparison study. *Anal. Methods* 9, 1521–1526. doi: 10.1039/C6AY03119F
- Debroas, D., Mone, A., and Ter Halle, A. (2017). Plastics in the North Atlantic garbage patch: a boat-microbe for hitchhikers and plastic degraders. *Sci. Total Environ.* 599, 1222–1232. doi: 10.1016/j.scitotenv.2017.05.059
- Deroiné, M., César, G., Le Duigou, A., Davies, P., and Bruzaud, S. (2015). Natural degradation and biodegradation of poly (3-hydroxybutyrate-co-3-hydroxyvalerate) in liquid and solid marine environments. *J. Polym. Environ.* 23, 493–505. doi: 10.1007/s10924-015-0736-5
- Dussud, C., and Ghiglione, J. F. (2014). “Bacterial degradation of synthetic plastics,” in *Proceedings of the CIESM Workshop Monograph*, Monaco City, 43–48.
- Dussud, C., Meistertzheim, A. L., Conan, P., Pujó-Pay, M., George, M., Fabre, P., et al. (2018). Evidence of niche partitioning among bacteria living on plastics, organic particles and surrounding seawaters. *Environ. Pollut.* 236, 807–816. doi: 10.1016/j.envpol.2017.12.027
- Eich, A., Mildenerberger, T., Laforsch, C., and Weber, M. (2015). Biofilm and diatom succession on polyethylene (PE) and biodegradable plastic bags in two marine habitats: early signs of degradation in the pelagic and benthic zone? *PLoS One* 10:e0137201. doi: 10.1371/journal.pone.0137201
- Elain, A., Le Fellic, M., Corre, Y. M., Le Grand, A., Le Tilly, V., Audic, J. L., et al. (2015). Rapid and qualitative fluorescence-based method for the assessment of PHA production in marine bacteria during batch culture. *World J. Microbiol. Biotechnol.* 31, 1555–1563. doi: 10.1007/s11274-015-1904-4
- Elain, A., Le Grand, A., Corre, Y. M., Le Fellic, M., Hachet, N., Le Tilly, V., et al. (2016). Valorisation of local agro-industrial processing waters as growth media for polyhydroxyalkanoates (PHA) production. *Ind. Crops Prod.* 80, 1–5. doi: 10.1016/j.indcrop.2015.10.052
- Elifantz, H., Horn, G., Ayon, M., Cohen, Y., and Minz, D. (2013). Rhodobacteraceae are the key members of the microbial community of the initial biofilm formed in Eastern Mediterranean coastal seawater. *FEMS Microbiol. Ecol.* 85, 348–357. doi: 10.1111/1574-6941.12122
- Eriksen, M., Lebreton, L. C., Carson, H. S., Thiel, M., Moore, C. J., Borerro, J. C., et al. (2014). Plastic pollution in the world’s oceans: more than 5 trillion plastic pieces weighing over 250,000 tons afloat at sea. *PLoS One* 9:e111913. doi: 10.1371/journal.pone.0111913
- Eyheraguibel, B., Traikia, M., Fontanella, S., Sancelme, M., Bonhomme, S., Fromageot, D., et al. (2017). Characterization of oxidized oligomers from polyethylene films by mass spectrometry and NMR spectroscopy before and after biodegradation by a *Rhodococcus rhodochromus* strain. *Chemosphere* 184, 366–374. doi: 10.1016/j.chemosphere.2017.05.137
- Eyheraguibel, B., Leremboure, M., Traikia, M., Sancelme, M., Bonhomme, S., Fromageot, D., et al. (2018). Environmental scenarios for the degradation of oxo-polymers. *Chemosphere* 198, 182–190. doi: 10.1016/j.chemosphere.2018.01.153
- Ferguson, R. L., Buckley, E. N., and Palumbo, A. V. (1984). Response of marine bacterioplankton to differential filtration and confinement. *Appl. Environ. Microbiol.* 47, 49–55.
- Frank, O., Silke, P., Rohde, M., Scheuner, C., Klenk, H., Markus, G., et al. (2014). Complete genome sequence of the *Phaebacter gallaeciensis* type strain CIP 105210<sup>T</sup> (= DSM 26640<sup>T</sup> = BS107<sup>T</sup>). *Stand. Genomic Sci.* 9, 914–932. doi: 10.4056/signs.5179110
- Gewert, B., Plassmann, M. M., and MacLeod, M. (2015). Pathways for degradation of plastic polymers floating in the marine environment. *Environ. Sci. Process. Impacts* 17, 1513–1521. doi: 10.1039/C5EM00207A
- Ghiglione, J. F., Philippot, L., Normand, P., Lensi, R., Potier, P. (1999). Disruption of narG, the gene encoding the catalytic subunit of respiratory nitrate reductase, also affects nitrite respiration in *Pseudomonas fluorescens* YT101. *J. Bacteriol.* 181, 5099–5102.
- Golyshin, P. N., Chernikova, T. N., Abraham, W. R., Lünsdorf, H., Timmis, K. N., and Yakimov, M. M. (2002). *Oleiphilaceae* fam. nov., to include *Oleiphilus messinensis* gen. nov., sp. nov., a novel marine bacterium that obligately utilizes hydrocarbons. *Int. J. Syst. Evol. Microbiol.* 52, 901–911.
- Harrison, J. P., Schratzberger, M., Sapp, M., and Osborn, A. M. (2014). Rapid bacterial colonization of low-density polyethylene microplastics in coastal sediment microcosms. *BMC Microbiol.* 14:232. doi: 10.1186/s12866-014-0232-4
- Harrison, J. P., Boardman, C., O’Callaghan, K., Delort, A. M., and Song, J. (2018). Biodegradability standards for carrier bags and plastic films in aquatic environments: a critical review. *R. Soc. Open Sci.* 5:171792. doi: 10.1098/rsos.171792
- Hörsch, P., Gorenflo, A., Fuder, C., Deleage, A., Frimmel, F. H. (2005). Biofouling of ultra- and nanofiltration membranes for drinking water treatment characterized by fluorescence in situ hybridization (FISH). *Desalination* 172, 41–52. doi: 10.1016/j.desal.2004.05.009
- Jakubowicz, I. (2003). Evaluation of degradability of biodegradable polyethylene (PE). *Polym. Degrad. Stab.* 80, 39–43. doi: 10.1016/S0141-3910(02)00380-4
- Koutny, M., Lemaire, J., and Delort, A. M. (2006). Biodegradation of polyethylene films with prooxidant additives. *Chemosphere* 64, 1243–1252. doi: 10.1016/j.chemosphere.2005.12.060
- Lee, J. W., Nam, J. H., Kim, Y. H., Lee, K. H., and Lee, D. H. (2008). Bacterial communities in the initial stage of marine biofilm formation on artificial surfaces. *J. Microbiol.* 46, 174–182. doi: 10.1007/s12275-008-0032-3
- Lemée, R., Rochelle-Newall, E., Van Wambeke, F., Pizay, M. D., Rinaldi, P., and Gattuso, J. P. (2002). Seasonal variation of bacterial production, respiration and growth efficiency in the open NW Mediterranean Sea. *Aquat. Microb. Ecol.* 29, 227–237. doi: 10.3354/ame029227
- Lo, N., Kim, K. H., Baek, K., Jia, B., and Jeon, C. O. (2015). *Aestuariicella hydrocarbonica* gen. nov., sp. nov., an aliphatic hydrocarbon-degrading bacterium isolated from a sea tidal flat. *Int. J. Syst. Evol. Microbiol.* 65, 1935–1940. doi: 10.1099/ijs.0.000199
- Lobelle, D., and Cunliffe, M. (2011). Early microbial biofilm formation on marine plastic debris. *Mar. Pollut. Bull.* 62, 197–200. doi: 10.1016/j.marpolbul.2010.10.013
- Loeb, G. I., and Neihof, R. A. (1975). Marine conditioning films. *Adv. Chem.* 145, 319–335. doi: 10.1021/ba-1975-0145.ch016
- Lorite, G. S., Rodrigues, C. M., De Souza, A. A., Kranz, C., Mizaikoff, B., and Cotta, M. A. (2011). The role of conditioning film formation and surface chemical changes on *Xylella fastidiosa* adhesion and biofilm evolution. *J. Colloid Interface Sci.* 359, 289–295. doi: 10.1016/j.jcis.2011.03.066
- Lucas, N., Bienaime, C., Belloy, C., Queneud, M., Silvestre, F., and Nava-Saucedo, J. E. (2008). Polymer biodegradation: mechanisms and estimation techniques—a review. *Chemosphere* 73, 429–442. doi: 10.1016/j.chemosphere.2008.06.064
- Mével, G., Vernet, M., Goutx, M., and Ghiglione, J. F. (2008). Seasonal to hour variation scales in abundance and production of total and particle-attached bacteria in the open NW Mediterranean Sea (0–1000 m). *Biogeosciences* 5, 1573–1586. doi: 10.5194/bg-5-1573-2008
- Morra, M., and Cassinelli, C. (1997). Organic surface chemistry on titanium surfaces via thin film deposition. *J. Biomed. Mater. Res.* 37, 198–206. doi: 10.1002/(SICI)1097-4636(199711)37:2<198::AID-JBM8>3.0.CO;2-M
- Nampoothiri, K. M., Nair, N. R., and John, R. P. (2010). An overview of the recent developments in polylactide (PLA) research. *Bioresour. Technol.* 101, 8493–8501. doi: 10.1016/j.biortech.2010.05.092

- Oberbeckmann, S., Osborn, A. M., and Duhaime, M. B. (2016). Microbes on a bottle: substrate, season and geography influence community composition of microbes colonizing marine plastic debris. *PLoS One* 11:e0159289. doi: 10.1371/journal.pone.0159289
- Ojeda, T. F., Dalmolin, E., Forte, M. M., Jacques, R. J., Bento, F. M., and Camargo, F. A. (2009). Abiotic and biotic degradation of oxo-biodegradable polyethylenes. *Polym. Degrad. Stab.* 94, 965–970. doi: 10.1016/j.polymdegradstab.2009.03.011
- Parada, A. E., Needham, D. M., and Fuhrman, J. A. (2016). Every base matters: assessing small subunit rRNA primers for marine microbiomes with mock communities, time series and global field samples. *Environ. Microbiol.* 18, 1403–1414. doi: 10.1111/1462-2920.13023
- Pasmore, M., Todd, P., Pfeifer, B., Rhodes, M., and Bowman, C. N. (2002). Effect of polymer surface properties on the reversibility of attachment of *Pseudomonas aeruginosa* in the early stages of biofilm development. *Biofouling* 18, 65–71. doi: 10.1080/08927010290017743
- Pedros-Alí, C. (2012). The rare bacterial biosphere. *Ann. Rev. Mar. Sci.* 4, 449–466. doi: 10.1146/annurev-marine-120710-100948
- Pulido-Villena, E., Ghiglione, J. F., Ortega-Retuerta, E., Van-Wambeke, F., and Zohary, T. (2011) “Heterotrophic bacteria in the pelagic realm of the Mediterranean Sea,” in *Life in the Mediterranean Sea: A Look at Habitat Changes*, ed. N. Stambler (New York, NY: Nova Science Publishers, Inc.), 227–265.
- Riedewald, F. (2006). Bacterial adhesion to surfaces: the influence of surface roughness. *PDA J. Pharm. Sci. Technol.* 60, 164–171.
- Salta, M., Wharton, J. A., Blache, Y., Stokes, K. R., and Briand, J. F. (2013). Marine biofilms on artificial surfaces: structure and dynamics. *Environ. Microbiol.* 15, 2879–2893. doi: 10.1111/1462-2920.12186
- Sauret, C., Severin, T., Vétion, G., Guigue, C., Goutx, M., Pujo-Pay, M., et al. (2014). ‘Rare biosphere’ bacteria as key phenanthrene degraders in coastal seawaters. *Environ. Pollut.* 194, 246–253. doi: 10.1016/j.envpol.2014.07.024
- Schloss, P. D., Westcott, S. L., Ryabin, T., Hall, J. R., Hartmann, M., Hollister, E. B., et al. (2009). Introducing mothur: open-source, platform-independent, community-supported software for describing and comparing microbial communities. *Appl. Environ. Microbiol.* 75, 7537–7541. doi: 10.1128/AEM.01541-09
- Severin, T., Conan, P., de Madron, X. D., Houpert, L., Oliver, M. J., Oriol, L., et al. (2014). Impact of open-ocean convection on nutrients, phytoplankton biomass and activity. *Deep Sea Res. Part I Oceanogr. Res. Pap.* 94, 62–71. doi: 10.1016/j.dsr.2014.07.015
- Sharabi, N. E., and Bartha, R. (1993). Testing of some assumptions about biodegradability in soil as measured by carbon dioxide evolution. *Appl. Environ. Microbiol.* 59, 1201–1205.
- Siddiqua, S., Hossain, M. A., and Saha, S. C. (2015). Two-phase natural convection flow of a dusty fluid. *Int. J. Numer. Method. Heat Fluid Flow* 25, 1542–1556. doi: 10.1108/HFF-09-2014-0278
- Simon, M., and Azam, F. (1989). Protein content and protein synthesis rates of planktonic marine bacteria. *Mar. Ecol. Prog. Ser.* 51, 201–213. doi: 10.3354/meps051201
- Sogin, M. L., Morrison, H. G., Huber, J. A., Welch, D. M., Huse, S. M., Neal, P. R., et al. (2006). Microbial diversity in the deep sea and the underexplored “rare biosphere”. *Proc. Natl. Acad. Sci. U.S.A.* 103, 12115–12120. doi: 10.1073/pnas.0605127103
- Sudhakar, M., Doble, M., Murthy, P. S., and Venkatesan, R. (2008). Marine microbe-mediated biodegradation of low-and high-density polyethylenes. *Int. Biodeterior. Biodegradation* 61, 203–213. doi: 10.1016/j.ibiod.2007.07.011
- Tokiwa, Y., and Calabria, B. P. (2004). Review degradation of microbial polyesters. *Biotechnol. Lett.* 26, 1181–1189. doi: 10.1023/B:BILE.0000036599.15302.e5
- Tokiwa, Y., Calabria, B. P., Ugwu, C. U., and Aiba, S. (2009). Biodegradability of plastics. *Int. J. Mol. Sci.* 10, 3722–3742. doi: 10.3390/ijms10093722
- Van Wambeke, F., Ghiglione, J. F., Nedoma, J., Mével, G., and Raimbault, P. (2009). Bottom up effects on bacterioplankton growth and composition during summer-autumn transition in the open NW Mediterranean Sea. *Biogeosciences* 6, 705–720. doi: 10.5194/bg-6-705-2009
- Vaysse, P. J., Prat, L., Mangenot, S., Cruveiller, S., Goulas, P., and Grimaud, R. (2009). Proteomic analysis of *Marinobacter hydrocarbonoclasticus* SP17 biofilm formation at the alkane-water interface reveals novel proteins and cellular processes involved in hexadecane assimilation. *Res. Microbiol.* 160, 829–837. doi: 10.1016/j.resmic.2009.09.010
- Vázquez-Morillas, A., Beltrán-Villavicencio, M., Alvarez-Zeferino, J. C., Osada-Velázquez, M. H., Moreno, A., Martínez, L., et al. (2016). Biodegradation and ecotoxicity of polyethylene films containing pro-oxidant additive. *J. Polym. Environ.* 24, 221–229. doi: 10.1007/s10924-016-0765-8
- Webb, H. K., Crawford, R. J., Sawabe, T., and Ivanova, E. P. (2009). Poly (ethylene terephthalate) polymer surfaces as a substrate for bacterial attachment and biofilm formation. *Microbes Environ.* 24, 39–42. doi: 10.1264/jsme2.ME08538
- Worm, J., Gustavson, K., Garde, K., Borch, N. H., and Søndergaard, M. (2001). Functional similarity of attached and free-living bacteria during freshwater phytoplankton blooms. *Aquat. Microb. Ecol.* 25, 103–111. doi: 10.3354/ame025103
- Xiao, N., and Jiao, N. (2011). Formation of polyhydroxyalkanoate in aerobic anoxygenic phototrophic bacteria and its relationship to carbon source and light availability. *Appl. Environ. Microbiol.* 77, 7445–7450. doi: 10.1128/AEM.05955-11
- Yakimov, M. M., Timmis, K. N., and Golyshin, P. N. (2007). Obligate oil-degrading marine bacteria. *Curr. Opin. Biotechnol.* 18, 257–266. doi: 10.1016/j.copbio.2007.04.006
- Yashchuk, O., Portillo, F. S., and Hermida, E. B. (2012). Degradation of polyethylene film samples containing oxo-degradable additives. *Proc. Mater. Sci.* 1, 439–445. doi: 10.1016/j.mspro.2012.06.059
- Zettler, E. R., Mincer, T. J., and Amaral-Zettler, L. A. (2013). Life in the “plastisphere”: microbial communities on plastic marine debris. *Environ. Sci. Technol.* 47, 7137–7146. doi: 10.1021/es401288x

**Conflict of Interest Statement:** The authors declare that the research was conducted in the absence of any commercial or financial relationships that could be construed as a potential conflict of interest.

Copyright © 2018 Dussud, Hudec, George, Fabre, Higgs, Bruzaud, Delort, Eyheraguibel, Meistertzheim, Jacquin, Cheng, Callac, Odobel, Rabouille and Ghiglione. This is an open-access article distributed under the terms of the Creative Commons Attribution License (CC BY). The use, distribution or reproduction in other forums is permitted, provided the original author(s) and the copyright owner(s) are credited and that the original publication in this journal is cited, in accordance with accepted academic practice. No use, distribution or reproduction is permitted which does not comply with these terms.



# Plant and Microbial Responses to Repeated Cu(OH)<sub>2</sub> Nanopesticide Exposures Under Different Fertilization Levels in an Agro-Ecosystem

Marie Simonin<sup>1,2\*</sup>, Benjamin P. Colman<sup>1,3</sup>, Weiyi Tang<sup>4</sup>, Jonathan D. Judy<sup>5</sup>, Steven M. Anderson<sup>1,2</sup>, Christina M. Bergemann<sup>1,2</sup>, Jennifer D. Rocca<sup>2</sup>, Jason M. Unrine<sup>6</sup>, Nicolas Cassar<sup>4</sup> and Emily S. Bernhardt<sup>1,2</sup>

<sup>1</sup> Center for the Environmental Implications of Nanotechnology, Duke University, Durham, NC, United States, <sup>2</sup> Department of Biology, Duke University, Durham, NC, United States, <sup>3</sup> Department of Ecosystem and Conservation Sciences, University of Montana, Missoula, MT, United States, <sup>4</sup> Division of Earth and Ocean Sciences, Nicholas School of the Environment, Duke University, Durham, NC, United States, <sup>5</sup> Soil and Water Sciences Department, University of Florida, Gainesville, FL, United States, <sup>6</sup> Department of Plant and Soil Sciences, University of Kentucky, Lexington, KY, United States

## OPEN ACCESS

### Edited by:

Fabrice Martin-Laurent,  
Institut National de la Recherche  
Agronomique (INRA), France

### Reviewed by:

Renato Grillo,  
Universidade Estadual Paulista "Júlio  
de Mesquita Filho", Brazil  
Mariusz Cycoń,  
Medical University of Silesia, Poland

### \*Correspondence:

Marie Simonin  
simonin.marie@gmail.com

### Specialty section:

This article was submitted to  
Microbiotechnology, Ecotoxicology  
and Bioremediation,  
a section of the journal  
Frontiers in Microbiology

**Received:** 09 June 2018

**Accepted:** 16 July 2018

**Published:** 31 July 2018

### Citation:

Simonin M, Colman BP, Tang W,  
Judy JD, Anderson SM,  
Bergemann CM, Rocca JD,  
Unrine JM, Cassar N and  
Bernhardt ES (2018) Plant  
and Microbial Responses  
to Repeated Cu(OH)<sub>2</sub> Nanopesticide  
Exposures Under Different Fertilization  
Levels in an Agro-Ecosystem.  
Front. Microbiol. 9:1769.  
doi: 10.3389/fmicb.2018.01769

The environmental fate and potential impacts of nanopesticides on agroecosystems under realistic agricultural conditions are poorly understood. As a result, the benefits and risks of these novel formulations compared to the conventional products are currently unclear. Here, we examined the effects of repeated realistic exposures of the Cu(OH)<sub>2</sub> nanopesticide, Kocide 3000, on simulated agricultural pastureland in an outdoor mesocosm experiment over 1 year. The Kocide applications were performed alongside three different mineral fertilization levels (Ambient, Low, and High) to assess the environmental impacts of this nanopesticide under low-input or conventional farming scenarios. The effects of Kocide over time were monitored on forage biomass, plant mineral nutrient content, plant-associated non-target microorganisms (i.e., N-fixing bacteria or mycorrhizal fungi) and six soil microbial enzyme activities. We observed that three sequential Kocide applications had no negative effects on forage biomass, root mycorrhizal colonization or soil nitrogen fixation rates. In the Low and High fertilization treatments, we observed a significant increase in aboveground plant biomass after the second Kocide exposure (+14% and +27%, respectively). Soil microbial enzyme activities were significantly reduced in the short-term after the first exposure (day 15) in the Ambient (−28% to −82%) and Low fertilization (−25% to −47%) but not in the High fertilization treatment. However, 2 months later, enzyme activities were similar across treatments and were either unresponsive or responded positively to subsequent Kocide additions. There appeared to be some long-term effects of Kocide exposure, as 6 months after the last Kocide exposure (day 365), both beta-glucosidase (−57% in Ambient and −40% in High fertilization) and phosphatase activities (−47% in Ambient fertilization) were significantly reduced in the mesocosms exposed to the nanopesticide. These results suggest that when used in conventional farming with high fertilization rates, Kocide applications did not lead to marked adverse effects on

forage biomass production and key plant–microorganism interactions over a growing season. However, in the context of low-input organic farming for which this nanopesticide is approved, Kocide applications may have some unintended detrimental effects on microbially mediated soil processes involved in carbon and phosphorus cycling.

**Keywords:** copper hydroxide, nanomaterials, pasture, microbial extracellular enzyme activities, terrestrial mesocosms, mycorrhizal colonization, fungicide, nitrogen fixation

## INTRODUCTION

Novel applications of nanotechnology for plant protection and nutrition is leading to the development of so-called “nanopesticides” and “nanofertilizers.” The emergence of these nano-enabled agrochemicals may be a promising avenue for reducing agricultural impacts on the environment and on human health (Kah, 2015; Liu and Lal, 2015). Because nanomaterial-enabled pesticides and fertilizers are being optimized for longer, sustained release it has been assumed that they will be more effective at lower application rates and may have fewer environmental consequences (Mishra et al., 2017). However, the limited knowledge on the environmental fate and potential impacts of these nano-agrochemicals currently hampers our ability to assess the true benefits and risks of these new formulations compared to conventional pesticides and fertilizers (Benelli et al., 2017; Kah et al., 2018).

The direct, intentional, and repeated application of nano-agrochemicals could potentially become a pathway by which large masses of nanomaterials may be introduced into agroecosystems. Previous ecotoxicological studies raised concerns about the impact of nanomaterials on plant health and soil organisms (reviewed by McKee and Filser, 2016; Tripathi et al., 2017) and even food quality and soil fertility (Priester et al., 2012; Chen et al., 2015; Judy et al., 2015). However, most studies are currently performed under simplified laboratory conditions (e.g., soil microcosms or hydroponics), at unrealistically high concentrations, or use pristine nanoparticles that are not comparable to commercial nano-enabled products (Simonin and Richaume, 2015; Chen et al., 2017). Furthermore, several parameters deserve to be investigated in more depth, such as plant–microbial interactions, fluctuating environmental conditions, physiological acclimation and evolutionary adaptations to repeated exposures, or interactive effects with other stressors that may be strong drivers of the environmental fate and ecotoxicity of nano-agrochemicals (Cornelis et al., 2014; McKee and Filser, 2016). As the production and release of these novel nano-formulations in agro-ecosystems may increase in the future, developing realistic long-term environmental assessments of nano-agrochemical impacts is imperative.

Integrating nanotechnology in agriculture is still in its infancy but several products are already commercialized such as copper-based (Cu) nanopesticides used as a fungicide and bactericide. The commercial pesticide Kocide 3000® contains nanoparticles and micron-sized particles of Cu, and nanosheets composed of Cu(OH)<sub>2</sub> and thus this agrochemical product containing nanomaterials as the active ingredient is considered as a

nanopesticide (Adeleye et al., 2014). It is approved for organic crop production and can be applied to a wide variety of crops including forage crops, vegetables, fruits, and trees. The product is suspended in water and sprayed on the plants to prevent the development of a variety of fungal and bacterial diseases. Its antifungal and antibacterial properties emerge mainly from the sustained release of Cu ions following the dissolution of the Cu(OH)<sub>2</sub> particles (Keller et al., 2017). While this nanopesticide may protect the crops from fungal and bacterial diseases, it may have unintended consequences on non-target plant-associated microorganisms involved in plant nutrition, such as mycorrhizal communities or nitrogen fixing bacteria (Hussain et al., 2009). Moreover, beneficial soil microorganisms that degrade organic matter (OM), which maintain long-term soil fertility, may be sensitive to this broad-spectrum antimicrobial product (Bünemann et al., 2006; Lejon et al., 2008). If so, these nanopesticide applications might have unintended consequences for soil fertility and plant yields over the long term, especially as a result of repeated exposures.

Nanopesticides are typically added to agricultural soils or crops alongside other agrochemicals that can interact to increase (i.e., additive interactions) or decrease (i.e., antagonistic interactions) the potential effects on organisms. In particular, agro-ecosystems are exposed to different fertilization regimes depending on the farming type (e.g., conventional or organic), tillage practices, and the type of crop grown. Fertilization could indirectly influence Cu bioavailability as a consequence of the changes in soil pH and OM (Leita et al., 1999). Additionally, fertilization might influence the plant or microbial physiological response to the nanopesticide (Conway et al., 2015). Agroecologists have suggested that microbial community resilience will increase with greater resource availability (De Vries and Shade, 2013), while communities already stressed by nutrient limitation may have less energy to cope with additional stressors, like a pesticide (Griffiths and Philippot, 2013).

In this context, we asked three main questions: (1) Do repeated applications of a Cu(OH)<sub>2</sub> nanopesticide impact plant biomass, plant-associated non-target microorganisms (i.e., N-fixing bacteria or mycorrhizal fungi), and soil microorganisms involved in OM degradation in an agro-ecosystem?, (2) How does fertilization influence the Cu(OH)<sub>2</sub> nanopesticide effects on the biotic endpoints?, and (3) What are the legacy effects of repeated application of a Cu(OH)<sub>2</sub> nanopesticide on agro-ecosystem functioning? To address these questions, we conducted a 1-year outdoor mesocosm experiment where we exposed forage crop cover to a series of repeated applications of the commercially available Cu(OH)<sub>2</sub> nanopesticide (Kocide 3000), simulating

realistic agricultural application rates. This experiment was performed under three fertilization levels (Ambient, Low, and High) to test for interactive effects between the nanopesticide and enhanced resource availability of fertilization additions and simulate relevant farming practices with varying levels of nutrient inputs (e.g., conventional or organic farming). The mesocosms were sampled on short- (15 days) and long-term (2.5 months) timescales after the nanopesticide exposures to assess the resistance and resilience of the agro-ecosystem to this disturbance. A final sampling was performed 6 months after the last Kocide exposure (1 year after the initiation of the treatments) to assess the legacy effects of this nanopesticide after a growing season.

## MATERIALS AND METHODS

### Experimental Design

The outdoor terrestrial mesocosms were set up in the Duke Forest (36°00'57.3"N 78°58'49.8"W, Durham, NC, United States). Each mesocosm [51 cm (l) × 25 cm (w) × 5 cm (h)] was filled with ~81 kg of a sandy-clay-loam soil (Sands and Soils, Durham, NC, United States) comprised of: 57.7% sand, 20.5% clay, 21.9% silt, and 4% organic matter (pH = 5.8). The weather conditions at the mesocosm site were monitored during the entire experiment (see Supplementary Figure S1 for air temperature and precipitation data).

The mesocosms were seeded with seven forage crops plant species, selected based on growth performance and common agricultural use in pasture regions of the surrounding North Carolina Piedmont (Miguel et al., 2014): *Trifolium pratense* (legume, Fabaceae), *Chamaecrista fasciculata* (legume, Fabaceae), *Brassica napus* (annual forb, Brassicaceae), *Cichorium intybus* (invasive perennial forb, Asteraceae), *Sorghastrum nutans* (native perennial graminoid, Poaceae), and *Urochloa ramosa* (perennial graminoid, Poaceae). In the spring of 2016, each box was mowed and additionally seeded with *Medicago sativa* (legume, Fabaceae). The different plant species were grouped in three main plant functional groups: forbs, graminoids, and legumes.

To control water availability within the mesocosms, a sprinkler system was installed in the summer, to water each mesocosm every 3 days for 15 min unless a rain event occurred.

Three fertilization treatments were initiated on September 4, 2015, 8 months before the beginning of the nanopesticide applications. Fertilization levels (Ambient, Low, and High) were adjusted using the Osmocote® fertilizer (The Scotts Company, Marysville, OH, United States) following the NCDA recommended rates for pasture crops<sup>1</sup>. The Ambient mesocosms received no supplemental fertilizer; the Low mesocosms received 1.72 g N, 0.77 g P, and 1.29 g K; and the High mesocosms received 3 × Low (5.15 g N, 2.32 g P, 3.86 g K). Before the Kocide exposures started, the soil chemical characteristics in the different fertilization levels were determined (Table 1).

The soil NH<sub>4</sub><sup>+</sup> and NO<sub>3</sub><sup>-</sup> concentrations were determined after a KCl extraction (2M) on a Lachat QuikChem 8000 (Lachat Instruments, Milwaukee WI, United States). Soil pH was measured according to ISO 10390 in pure water and soil OM matter was determined by loss on ignition.

On June 8th, 2016, the Kocide® 3000 (DuPont™, Wilmington, DE, United States) nanopesticide treatment regimes started. Kocide contains Cu(OH)<sub>2</sub> nanoparticles (Adeleye et al., 2014) with an average primary particle size of 38.7 ± 8.2 nm (TEM) and an average hydrodynamic diameter of 120 ± 30 nm in the dosing water with a secondary peak with particles size greater than 700 nm (Simonin et al., 2018). The Cu content in Kocide is 26.5 ± 0.9%, while other elements (e.g., C, O, Na, Al, Si, P, S, and Zn) account for 73.5% of the dry mass of the product. We sprayed (Hudson, Model 13581, Chicago, IL, United States) the foliage of each mesocosm with the Kocide suspension (6.68 mg/L in DI water) so the aboveground plant biomass exposure was 30 mg/m<sup>2</sup>, per the manufacturer's instructions for dosage and exposure mode. Kocide applications were performed 15 days before each subsequent plant harvest (on days 0, 75, and 155 of the experiment, Figure 1). The control mesocosms were sprayed with the same volume of deionized water to hold constant across mesocosms the changes in soil moisture availability and temporary cooling from the spraying. Following the recommendations of the North Carolina Cooperative Extension Service for forage crops, three plant biomass harvests were conducted at a 2.5-month interval (on days 15, 90, and 170 of the experiment, Figure 1). The six treatments combinations were replicated across six independent mesocosms for a total of 36 mesocosms. In summary, the mesocosms were exposed to 3 consecutive nanopesticide exposures or to control exposures during the experiment under three different fertilization conditions: 2 nanopesticide conditions (including control) × 3 fertilization treatments × 6 replicates = 36 mesocosms.

### Soil Measurements

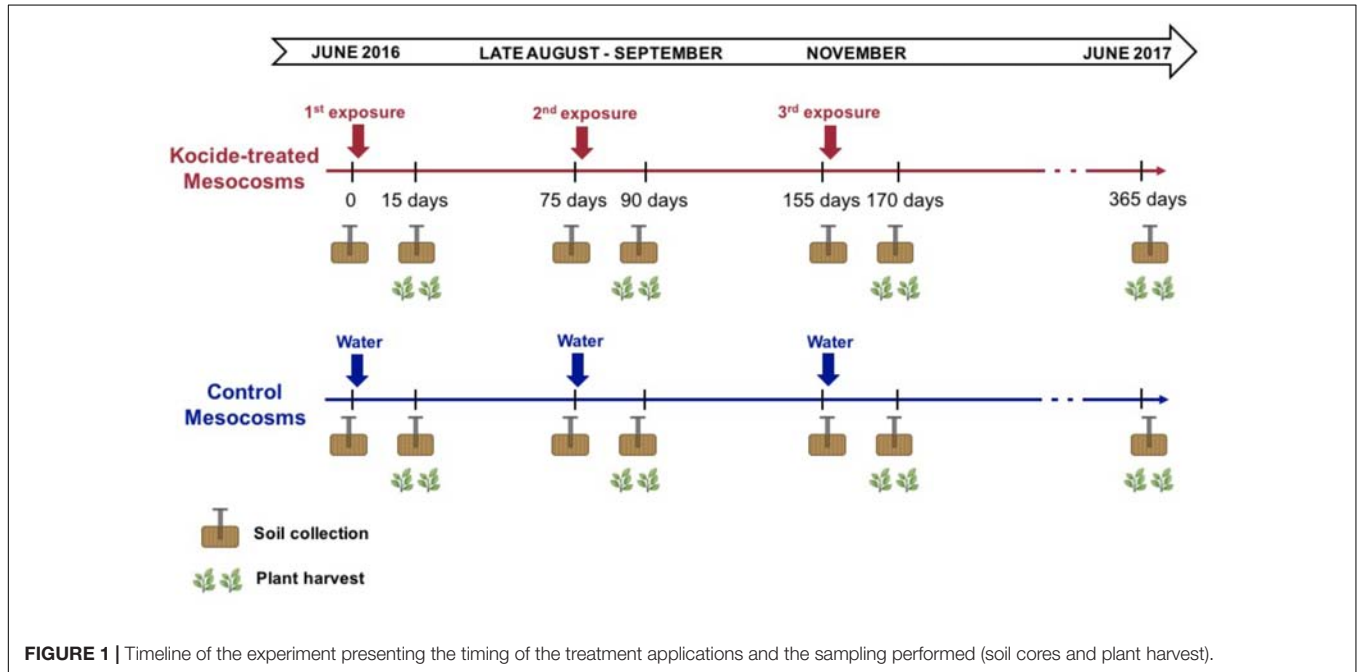
#### Soil Sampling and Characterization

Small soil cores (2 cm diameter, 0–7 cm depth) were collected before each new nanopesticide exposure (day 0, 75, 155) and 15 days after the exposure right before the plant harvest (day 15, 90, 170). An additional soil collection was performed 365 days after the first nanopesticide exposure (Figure 1). To avoid resampling the same spot or unevenly sampling the mesocosms, each soil core was extracted at different locations each time following a randomized sampling strategy established at the beginning of the experiment. The soil core samples were immediately stored at 4°C before analysis (less than a week). The soil samples were homogenized and sieved to <2-mm mesh (USDA standard). Soil moisture was determined by drying a ~10 g subset of each soil core for 48 h at 105°C. Soils collected after the third, final exposure (day 170) and on the long-term sampling (day 365) were oven-dried and ground for microwave assisted acid digestion using 10:1 HNO<sub>3</sub>:H<sub>2</sub>O<sub>2</sub>, following US EPA Method 3052. Total Cu concentrations were then measured using ICP-MS (7500cx, Agilent Technologies,

<sup>1</sup><https://content.ces.ncsu.edu/north-carolina-agricultural-chemicals-manual/fertilizer-use>

**TABLE 1** | Soil chemical characteristics for the three fertilization levels prior to the initiation of the nanopesticide exposures.

Fertilization	pH	NO <sub>3</sub> <sup>-</sup> (μg N-NO <sub>3</sub> <sup>-</sup> /g dry soil)	NH <sub>4</sub> <sup>+</sup> (μg N-NH <sub>4</sub> <sup>+</sup> /g dry soil)	OM content (%)
Ambient	6.02 ± 0.25	1.63 ± 1.0	1.56 ± 0.7	4.32 ± 0.27
Low	6.20 ± 0.18	7.53 ± 4.0	11.99 ± 4.0	4.22 ± 0.01
High	5.17 ± 0.25	19.09 ± 5.3	38.20 ± 8.4	3.89 ± 0.03

**FIGURE 1** | Timeline of the experiment presenting the timing of the treatment applications and the sampling performed (soil cores and plant harvest).

Santa Clara, CA, United States) following US EPA method 6020A.

On these two sampling dates (day 170 and 365), an additional larger soil core (5 cm diameter, 0–15 cm depth) was collected to perform measurements of N<sub>2</sub> fixation rates and root mycorrhizal colonization (detailed below).

### Microbial Extracellular Enzyme Activities Targeting OM Degradation

The potential activity of six microbial extracellular enzymes were measured using the protocol described by Bell et al. (2013), including three C-degrading enzymes (alpha-glucosidase, beta-glucosidase and cellulase), a N-degrading enzyme (chitinase – N-acetylglucosaminidase), a P-degrading enzyme (alkaline phosphatase) and a S-degrading enzyme (arylsulfatase). Fresh soil (2.75 g) was blended with 91 mL of a sodium acetate buffer (50 mM, pH adjusted to soil pH) to obtain a homogeneous soil slurry. The soil slurry was then pipetted in 96-well deepwell plates with one of the six fluorescently labeled substrates or with fluorescent standards [4-methylumbelliferone (MUB)]. The plates were incubated for 3 h in the dark at 20°C, then centrifuged (2 min at 1000 × g) to pellet light-interfering soil particles, and the supernatant was transferred in black optical 96-well plates for fluorescence measurements on a plate reader (Fluostar Optima, BMG Labtech, Cary, NC, United States). Enzyme activities were quantified based on the fluorescence measured in each sample

(indirect assessment of substrate degradation and fluorophore release due to enzyme activity) and the conversion of the data based on the standard dilution curves of each substrate from the MUB wells.

### Nitrogen Fixation Rates

During the two final sampling dates (day 170 and 365), soil N<sub>2</sub> fixation rates (includes both free-living and plant-associated N<sub>2</sub> fixers) were measured on intact soil cores extracted from the same location in all the mesocosms. We determined N<sub>2</sub> fixation rates by measuring acetylene reduction to ethylene using the standardized method of Acetylene Reduction Assays by Cavity ring-down laser Absorption Spectroscopy (ARACAS; Cassar et al., 2012). Each soil sample was incubated for 30 min in a 500 mL Erlenmeyer flask with 10% of the headspace replaced with acetylene gas. The headspace was circulated with a diaphragm pump to a cavity ring-down spectrometer (CRDS) and back to the incubation chamber in a closed loop to measure ethylene concentration at high frequency (every few seconds) and continuously. N<sub>2</sub> fixation rate was determined from the rate of ethylene increase using a standard 4:1 conversion factor (Hardy et al., 1968). We recognize the quantitative uncertainty associated with the conversion factor (Visser et al., 1994), but it should not affect the qualitative comparison among different experiments. Finally, the N<sub>2</sub> fixation rate was normalized to per gram of dry soil.

More methodological details are available in Cassar et al. (2012).

## Plant Measurements

The aboveground plant biomass was harvested four times during the experiment (**Figure 1**): 15 days after each of the three Kocide exposures; and at the end of the experiment (day 365). At each harvest, the plant biomass was mowed with cordless grass shears, and the different plant species were sorted before measuring plant dry biomass (72 h at 60°C). Representative composite samples of the aboveground plant biomass collected on day 170 and 365 were digested using HNO<sub>3</sub>:H<sub>2</sub>O<sub>2</sub> and total Cu, iron (Fe), manganese (Mn), and zinc (Zn) concentrations were then measured using ICP-MS as described above.

Using the same soil cores to estimate N<sub>2</sub> fixation (day 170 and 365), root mycorrhizal colonization was determined by carefully separating the roots and mycorrhizal hyphae from the soil cores, the roots collected were stored in 50% ethanol. Later, roots were removed from the 50% ethanol, rinsed with tap water and covered with 10% (w/v) potassium hydroxide. Then, roots were placed into an autoclave where they were heated for 3 min at 121°C. The potassium hydroxide solution was removed and the roots were rinsed with tap water. Roots were then acidified by soaking them in 1.0% HCl for 5 min. After removing the HCl, roots were covered with 0.05% tryptan blue (C<sub>34</sub>H<sub>28</sub>N<sub>6</sub>O<sub>14</sub>S<sub>4</sub>) and stained overnight at room temperature. Tryptan blue was then removed and the roots transferred to 50% ethanol after rinsing with tap water. Mycorrhizal colonization of stained roots was then assessed via the root slide technique (Smith and Read, 2010).

## Statistical Analyses

All the endpoints were analyzed using generalized linear mixed-effects to model the effects of nanopesticide exposure (control, nanopesticide-exposed), fertilization (Ambient, Low, and High) and the interaction between nanopesticide exposure and fertilization by day of the experiment (repeated measurements: all the dates included in the model). In these models, main effects and interactions were nested by day, and mesocosm was treated as a random effect to account for serial correlation among observations from the same mesocosms over time (Zuur et al., 2009). The models were fit following a framework similar to the one described in King et al. (2016) using the *glmer* function of the *lme4* package in R 3.2.3 (R Core Team, 2015). *Post hoc* comparisons were performed using the *lsmeans* function/package in R, which adjusts *p*-values to compensate for multiple comparisons, to determine significant differences between control and nanopesticide exposure conditions for each fertilization level at the different dates. A principal component analysis was performed on the soil microbial enzyme activities (*n* = 6 activities) on the data collected on day 170 and 365 for which we had the highest number of plant and soil variables measured. Using the *envfit* function in the *vegan* package in R, we tested if these plant and soil variables were significantly correlated to the enzyme activity profiles on the ordination.

## RESULTS

### Effects of Nanopesticide Exposures on Plant Biomass

Aboveground plant biomass increased significantly between each level of fertilization ( $p < 0.001$ ); while the addition of Kocide did not significantly affect biomass production at any level of fertilization ( $p = 0.13$  independent effect and  $p = 0.82$  interaction effect; **Figure 2A**). Although there was no overall effect, *post hoc* tests indicated that Kocide application increased the aboveground plant biomass after the second exposure (day 90) in both the Low (14%,  $p = 0.04$ , **Figure 2A**) and High fertilization treatments (27%,  $p = 0.04$ , **Figure 2**). For the two occasions on which destructive sampling allowed us to estimate belowground root biomass (days 160 and 365), we found no effect of Kocide on belowground biomass (**Figure 2B**).

While our fertilization treatments led to shifts in plant communities, there was no consistent effect of Kocide on the relative dominance of the three-different plant functional groups (**Figure 2A**). Graminoids tended to dominate in the Ambient and Low fertilization treatments, while forbs tended to dominate in the High fertilization treatment at most dates. The single date on which we observed a Kocide treatment effect on a plant functional group was on day 90, when forb biomass was significantly increased in the mesocosms treated with Kocide in the Low fertilization condition (+62%,  $p = 0.01$ ).

### Lack of Effects of Nanopesticide Exposures on Plant-Associated Microorganism

There was no effect of Kocide exposure on the extent of mycorrhizal colonization of plant roots ( $p = 0.19$ , **Figure 3A**). This endpoint was also unresponsive to either fertilization ( $p = 0.95$ ) or the interactive effects between Kocide and fertilization ( $p = 0.55$ ). Similarly, no effect of the treatments was observed on soil N<sub>2</sub> fixation rates (Kocide:  $p = 0.43$ , Fertilization:  $p = 0.24$ , Kocide × Fertilization:  $p = 0.99$ , **Figure 3B**). Note that on day 365, N<sub>2</sub> fixation rates were low enough in some samples to be below detection limit (0.001 pmol/g soil/min, **Figure 3B**).

### Short-Term and Long-Term Effects of Repeated Applications of Nanopesticides on Soil Microbial Enzyme Activities

The effects of the Kocide on potential microbial extracellular enzyme activities were strongly influenced by the fertilization level. Significant interactive effects of Kocide exposure and fertilization were observed in all six extracellular enzymes activities measured ( $p < 0.05$ , **Figure 4**). In the Ambient fertilization conditions, large reductions in microbial enzyme activities were observed 15 days after the first Kocide exposure (**Figure 4**). The chitinase activity exhibited the highest reduction (−82%, **Figure 4D**), followed by cellulase (−57%, **Figure 4C**), phosphatase (−52%, **Figure 4E**), beta-glucosidase (48%, **Figure 4B**), sulfatase (−41%, **Figure 4F**), and alpha-glucosidase

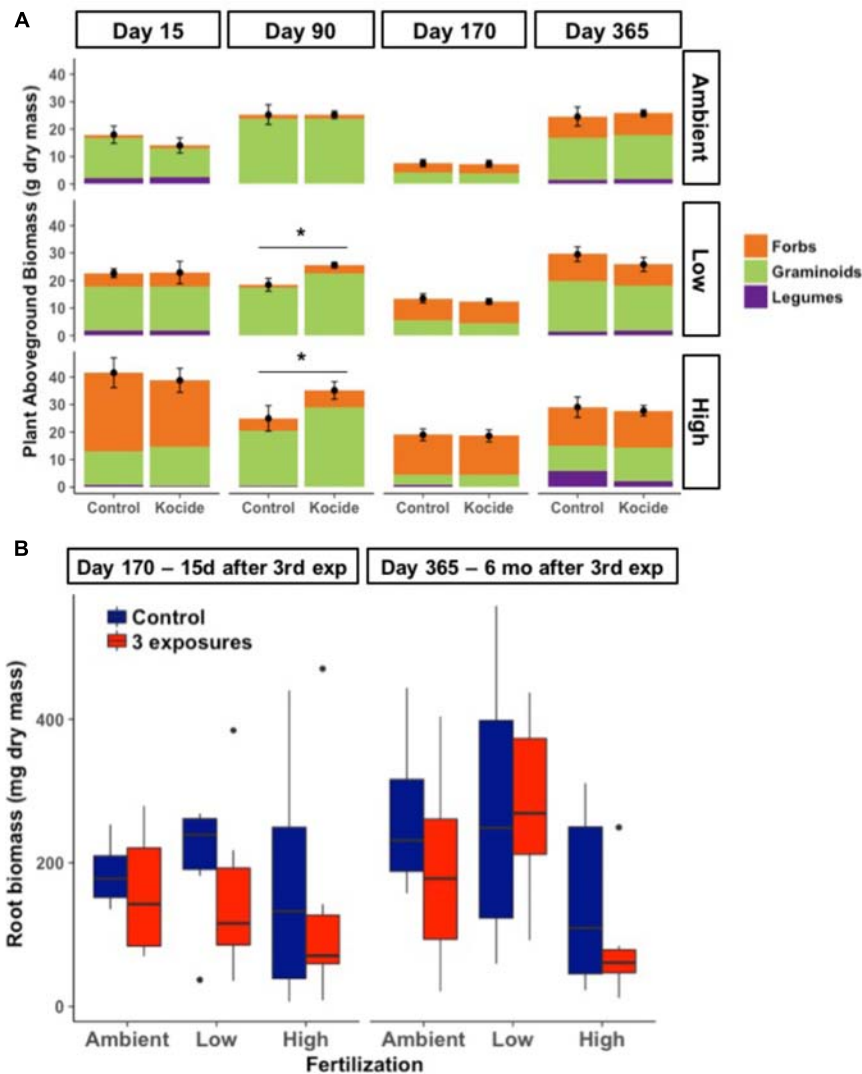


**FIGURE 2 | (A)** Effects of Kocide on aboveground plant biomass among the fertilization treatments (top-bottom: Ambient, Low, and High) horizontally displayed over time. Each plant functional group (Forbs, Graminoids, and Legumes) are presented as stacked bars of respective dry biomass. The black symbols represent the mean of the plant aboveground biomass and the black lines represent the standard errors associated. Significant effects of the Kocide treatment on aboveground biomass compared to the controls are indicated by asterisks ( $p < 0.05$ ). **(B)** Effect of Kocide exposures in the different fertilization treatments on the dry root biomass collected on day 170 and 365. The data are presented as box plots where the black horizontal line in the middle of the box represents the median and the two ends of the vertical line indicates the minimum and maximum values. The black dots represent the outliers.

activity ( $-28\%$ , **Figure 4A**). By day 75, there were no treatment effects on enzyme activities, and enzyme activities did not decline in response to the second and third Kocide exposures. Prior to the Kocide addition on day 155 three C- degrading enzymes and sulfatase activity were substantially higher in the Kocide treated soils (**Figure 4B**). At the end of the experiment (day 365), we measured significant reductions in both beta-glucosidase and phosphatase activities in mesocosms exposed to the nanopesticides (**Figure 4B**:  $-57\%$  and **Figure 4E**:  $-47\%$ , respectively).

In the Low fertilization treatment, microbial enzyme activities were also altered by the first Kocide exposure (day 15), albeit to a lesser extent than in the Ambient fertilization treatment

(**Figure 4**). On day 15, three enzyme activities were significantly decreased (beta-glucosidase  $-47\%$ , cellulase  $-36\%$ , sulfatase  $-25\%$ ) and the chitinase activity was stimulated by Kocide ( $+111\%$ ). On day 75, all the enzyme activities recovered from this initial exposure and no significant effects of the Kocide additions were observed for the remainder of the experiment at this fertilization level.

In the High fertilization treatment, Kocide treatments had limited negative effects on microbial enzyme activities and mainly generated significant augmentations after the second and third exposures. On day 90 and 170, the sulfatase activity was increased following Kocide exposures ( $+42\%$  and  $51\%$ , respectively). Stimulation of the chitinase activity ( $+84\%$ , **Figure 4D**) and

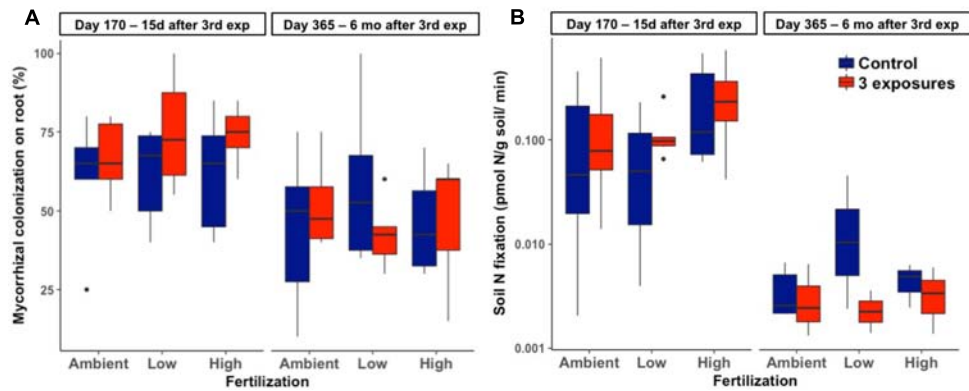


**FIGURE 3 |** Effects of Kocide exposures and fertilizer treatments on the two final harvest days (170 and 365) on: **(A)** mycorrhizal colonization of roots (%), and **(B)** soil N<sub>2</sub> fixation rate (y-axis on a log scale). The data are presented as box plots where the black horizontal line in the middle of the box represents the median and the two ends of the vertical line indicates the minimum and maximum values. The black dots represent the outliers.

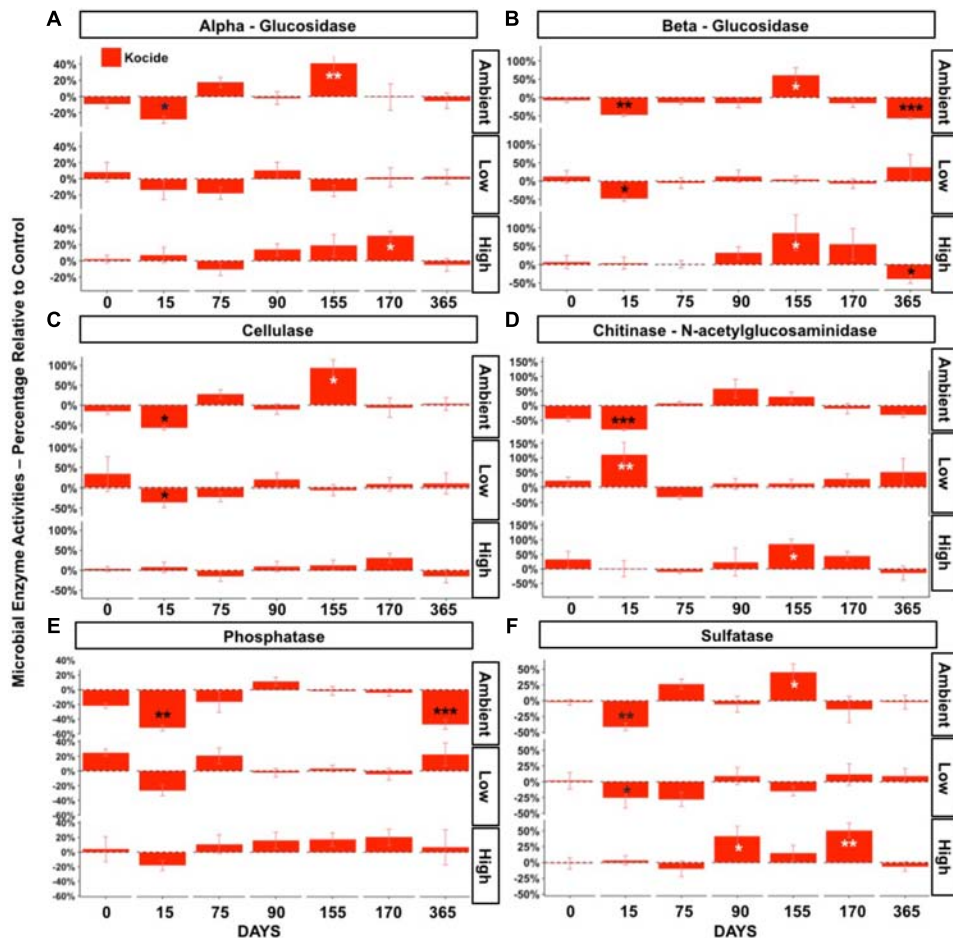


**FIGURE 4 |** Effects of Kocide on extracellular enzyme activities in the three fertilization treatments at the seven sampling dates: (top-bottom rows): Ambient, Low, High fertilization levels. **(A)** alpha-glucosidase, **(B)** beta-glucosidase, **(C)** cellulase, **(D)** chitinase (b-1,4-N-acetylglucosaminidase), **(E)** alkaline phosphatase, **(F)** sulfatase. The results are presented as percentage relative to controls. Significant effects of the Kocide treatment relative to controls indicated by asterisks: \**p* < 0.05; \*\**p* < 0.01; \*\*\**p* < 0.001. The black asterisks represent significant decreases in enzyme activities, while white asterisks represent significant increases. (Note the y-axis scale is different on each panel).

beta-glucosidase (+87%, **Figure 4B**) were observed on day 155 and alpha-glucosidase was increased on day 170 (+31%, **Figure 4A**). Under High fertilization, only beta-glucosidase activity was negatively impacted by Kocide after 6 months (−40%, **Figure 4B**).

Using a principal component analysis, we explored how the Kocide and fertilization treatments affected the soil enzyme activity profiles on day 170 and 365 and which environmental parameters influenced these microbial activities (**Figure 5**). This visualization did not reveal any clear shift in the enzyme activity profiles induced by our treatments but a Permanova analysis indicated a significant effect of the date of collection ( $p = 0.008$ ) and a significant interaction between the Kocide and Fertilization treatments ( $p = 0.03$ ). The soil  $\text{NH}_4^+$ , the plant aboveground biomass and forb biomass were found to be significantly correlated to the enzyme profiles on the ordination (**Figure 5**).

## Copper Accumulation in Plants and Soils

Two weeks after the third and final Kocide exposure (day 170), plant biomass Cu concentrations increased twofold among the three fertilization treatments ( $p < 0.001$ , **Figure 6A**). Higher Cu concentration was found in the plant biomass of the High fertilization treatment compared to the Ambient fertilization in the mesocosms exposed to the Kocide (+17%,  $p = 0.03$ ). Overall, plant biomass Cu concentrations on day 170 averaged at  $14.3 \pm 0.3$  mg/kg in the Kocide-treated mesocosms, while the concentration was  $6.75 \pm 0.18$  mg/kg in the Control mesocosms. Based on the known concentration of Cu applied as Kocide per mesocosm, we calculated the percentage of Cu recovered on the plants on day 170, and found that only a small fraction of the Cu applied to the mesocosms (3.7–7.4%) was associated to the plants 15 days after the last Kocide application (**Figure 6B**).

There was no effect of the fertilization treatment on the amount of Cu associated to aboveground plant biomass (fertilization effect;  $p = 0.16$ , **Figure 6B**) though it should be noted that the maximum Cu concentrations in biomass increased with increasing fertilization level. Six months after the last exposure, we found that the plant biomass Cu concentrations were no longer significantly different between control and Kocide-exposed mesocosms (day 365, **Figure 6A**). Moreover, on both final days (170 and 365), there were no significant changes in mineral nutrient content (incl. Zn, Mn, and Fe concentrations) of the plant biomass exposed to the Kocide exposures (**Figure 7**).

The soil Cu concentrations were not significantly different between the control and Kocide treatments, even immediately following the third Kocide exposure (day 170,  $p = 0.60$ ). None of the soil Cu concentrations were significantly different from the high natural Cu background of this soil ( $90.5 \pm 4.4$  mg Cu/kg).

## DISCUSSION

In our mesocosm experiment, repeated exposures to the nanopesticide Kocide 3000 had no negative effects on plant biomass and plant–microorganism associations but soil microbial enzyme activities were periodically inhibited or

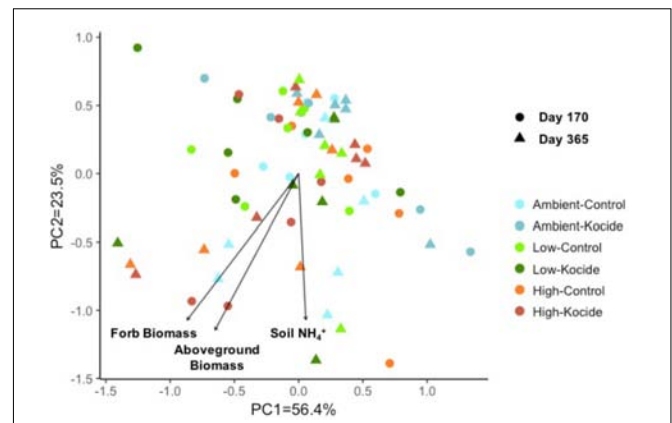


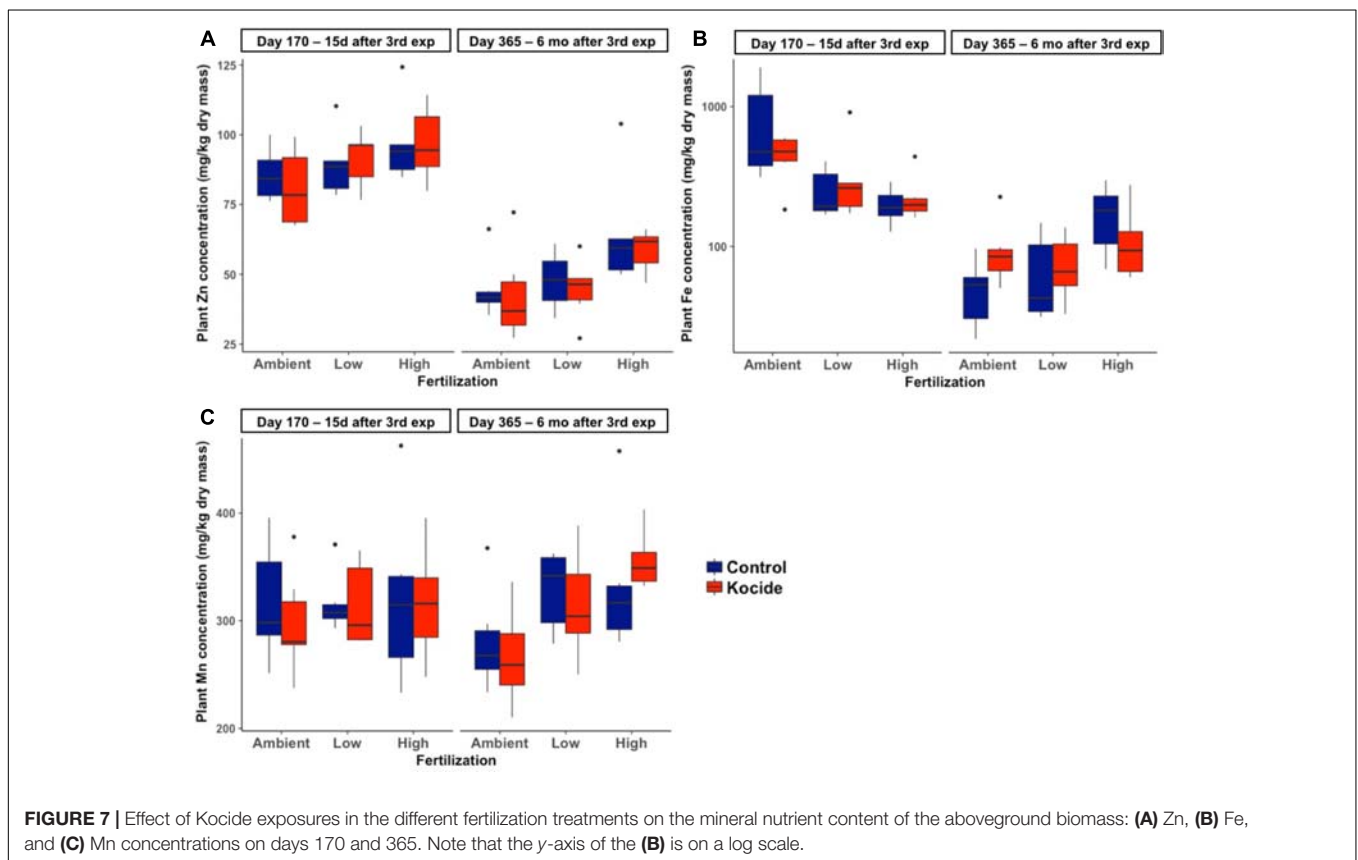
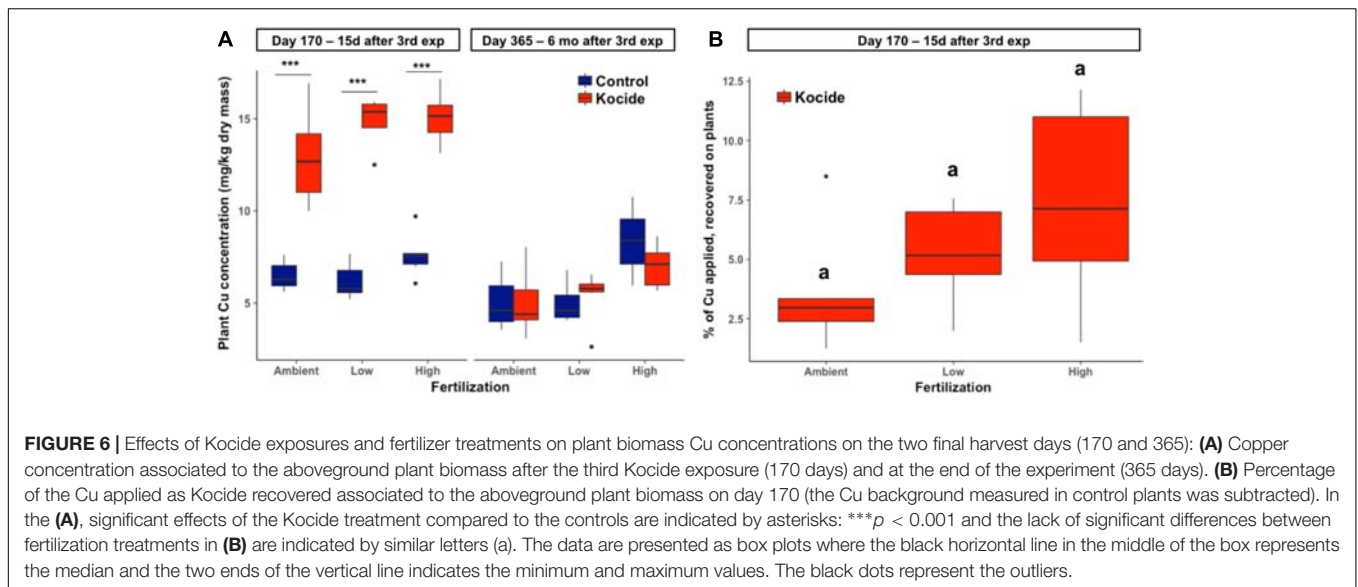
**FIGURE 5 |** Principal component analysis (PCA) of the six soil microbial extracellular enzyme activities measured on day 170 and day 365 of the experiment. The environmental variables found to be significantly correlated to the distribution of the enzyme activity data in the ordination are represented as vectors.

stimulated by this treatment. We observed interactive effects between the nanopesticide and the fertilization treatments leading to most of the detrimental effects found in the Ambient fertilization treatment.

## No Detrimental Effects on Plant and Plant–Microbe Associations

Other than a 14 and 27% increase on day 90 after the second exposure in the Low and High fertilization conditions, we found limited effects of the three Kocide applications on aboveground plant biomass. Previous work examining the effect of Kocide 3000 on plant biomass include reports of significant decreases in lettuce (Hong et al., 2015), elegant *Clarkia* (Conway et al., 2015), and maize (Zhao et al., 2017) shoot biomass (**Table 2**), as well as a report of lettuce leaf biomass stimulation (Zhao et al., 2016b). However, these studies were conducted in artificial growth media or potting soils with Kocide exposure in concentrations several orders of magnitude higher than the recommended doses (**Table 2**). By adhering to realistic Kocide concentrations and soil conditions, reflective of agricultural conditions, our results show that Kocide 3000 applications do not lead to any decrease in plant yields of a mixed forage plant community. In fact, we found that plant growth is stimulated when Kocide treatments are in tandem with fertilization. The fertilization may have alleviated stress such that any direct, negative impacts of Kocide may have been mediated. We hypothesize that the stimulations observed were probably related to direct effects of the nanopesticide on plant health or nutrition and not to an indirect positive effect driven by the microbial endpoints measured. When the plant biomass stimulations occurred (day 90), the six microbial enzyme activities tested were not significantly altered by the treatments, with the exception of a positive increase of the sulfatase activity in the High fertilization treatment.

Repeated Kocide applications did not alter mycorrhizal fungi colonization of plant roots, a finding consistent with reports demonstrating that non-nano copper-based fungicides,



including copper oxychloride [ $\text{Cu}_2(\text{OH})_3\text{Cl}$ , Sugavanam et al., 1994; Hernández-Dorrego and Mestre-Parés, 2010],  $\text{Cu}(\text{OH})_2$  (Graham et al., 1986; Bajjukya and Semu, 1998; Rutto et al., 2002), and copper sulfate (Nemec, 1980), do not impact mycorrhizal colonization. Overall, these results are consistent with the fact that mycorrhizal fungi have been found to be resistant to metal contamination and are involved in the alleviation of metal

toxicity for plants, as evidenced by high mycorrhizal colonization rates in plants grown in metal-contaminated agricultural soils (Leyval et al., 1997; Jentschke and Godbold, 2000). Conversely, diazotrophs and especially the heterotrophic free-living bacteria involved in this process can exhibit a high sensitivity to metal pollution, including nanomaterial contamination (Giller et al., 1998; Judy et al., 2015; Chen et al., 2017). The lack of effect on

$N_2$  fixation rates in our experiment may be again related to the low nanopesticide concentrations applied to the system but also to the low abundance of legumes in the plant community and the resulting low  $N_2$  fixation rates measured, especially on day 365. Low  $N_2$  fixation rates may have also resulted from the lower soil moisture at this date than on day 170 (Supplementary Figure S2). Our experiment shows that realistic exposures to the Kocide nanopesticide under relevant agricultural practices, in outdoor conditions with a natural soil, do not lead to adverse effects on forage biomass and key plant–microorganism interactions.

## Interactive Effects Between Nanopesticide and Fertilization Treatments

The most sensitive endpoints to the Kocide exposures were the extracellular enzyme activities involved in OM degradation (C, N, P, S cycling) that are performed by a diverse group of soil microorganisms. Interestingly, the effects observed in the enzyme activities in the principal component analysis and when analyzing each enzyme separately were strongly influenced by the degree of fertilization and exposure duration. For instance, these significant interactions between the nanopesticide and fertilization treatments resulted in large decreases in all enzyme activities on the short-term after the first Kocide exposure in the Ambient fertilization, while three enzymes were decreased in the Low fertilization, and no effect was observed in the High fertilization condition. This result shows that—in a community of microorganisms not previously exposed to this nanopesticide—the resistance of microbial function to the nanopesticide increased with increasing soil nutrient availability. We hypothesize that the microbial communities involved in the enzyme synthesis in the Ambient or Low fertilization treatment were already stressed by nutrient limitation and thus had less energy to cope with the additional disturbance brought by the antimicrobial nanopesticide (e.g., less energy available for detoxification; Griffiths and Philippot, 2013).

However, this pattern associated with an increased resistance of microbial activity with increasing fertilization was clear only on the short-term (day 15). On subsequent sampling dates, the Kocide treatment generated no effects or stimulations of enzyme activities simultaneously in the Ambient and High fertilizations. Especially on the third exposure (day 155 and 170), the nanopesticide application was associated with significant increases in C, N, and S-degrading enzyme activities in both Ambient and High fertilization but not in the Low fertilization treatment. These treatment effects occurred at the end of the growing season in North Carolina (November). We hypothesize here that soil resources were more depleted than at previous dates (Supplementary Figure S2, soil  $NH_4^+$  concentration) and that the Cu added along with other micronutrients included in the Kocide formulation may have stimulated some microbial activities. Supporting this hypothesis, we observed on day 170 and 365 that soil  $NH_4^+$  concentration along with plant biomass were significantly correlated to the soil enzyme activity profiles on a principal component analysis. Additionally, the microbial community could have shifted to become more Cu tolerant after

the two previous nanopesticide exposures through the exclusion of sensitive microbial taxa over time (Díaz-Raviña et al., 2007; Brandt et al., 2010).

Surprisingly, we observed large decreases of beta-glucosidase and phosphatase activities (−57 and −47%, respectively) on day 365, 6 months after the last Kocide application in Ambient fertilization conditions. These decreases occurred at the same period of the season that the initial enzyme activity inhibitions previously described on day 15 and may be related to microbial responses to Kocide driven by seasonal effects (e.g., lower water availability) or to legacy effects of the nanopesticide on the microbial community function. Our experiment was not able to confirm either of these hypotheses. Additional research on the long-term effects of chronic nanopesticide applications and the influence of season on plants and microorganisms' responses to this agrochemical is needed.

Overall, the Kocide applications caused most of the inhibition on enzyme activities in the Ambient fertilization treatment and the majority of the positive effects on plant biomass and enzyme activities in the High fertilization treatment. These results suggest that when used in conventional farming with high fertilization rates, repeated Kocide 3000 application had limited negative consequences and induced positive effects on forage production and soil microbial processes over a growing season. However, in the context of lower-intensity fertilization where this nanopesticide is often used (e.g., organic farming), Kocide 3000 applications may have some unintended detrimental effects on microbially mediated soil processes involved in C and P cycling and on forage production.

## Limited Legacy Effects of Nanopesticide Applications After a Growing Season

Long-term contamination of agroecosystems with Cu fungicides used in both conventional and organic farming is of great environmental and toxicological concerns, as Cu has a low mobility in soil and can accumulate over time (Komárek et al., 2010; Navel and Martins, 2014). However, most previous studies examined Kocide exposure over very short temporal scales (up to 2 months), limiting realistic assessment of how Kocide may impact agroecosystems and non-target habitats in the long run. Additionally, these published experiments have been conducted in controlled laboratory and greenhouse conditions, where nutrients and water are not limiting, and in which the focus was plant-only, largely ignoring the potential impact on rhizospheric microbial communities (Table 2). Assessing the fate in soil and long-term non-target effects of the new generation of Cu nanopesticides under realistic conditions is necessary to determine if they should replace conventional pesticide formulations.

Following the last nanopesticide exposure performed in our experiment (day 170), we observed that the Cu concentration associated with aboveground plant biomass was double that of the control plants. This Cu accumulation was observed in all fertilization treatments and the Cu residue concentrations observed compared to the control plants were always lower than the recommended maximum residue levels authorized in the

**TABLE 2** | Comparison of the results of this study with previous published studies on the effects of the nanopesticide Kocide 3000 on crop biomass and microbial communities.

Reference	Concentration sprayed on plants or applied to soils	Medium	Crop	Duration	Effect on plant biomass	Cu concentration in plant biomass	Effect on microbial community
This study	Three applications of 6.68 mg/L at 2.5-month interval on plants	Sandy-clay-loam soil	Mixed forage	1 year	Increase of aboveground biomass in low (+1.4%) and high fertilization (+27%)	Aboveground biomass: 6–14 mg/kg	Inhibition or stimulation of microbial enzyme activities in the three fertilization treatments n.d
Conway et al., 2015	1, 10, or 100 mg/L every week to soil	Potting soil	Herbaceous annual plant <i>Clarkia unguiculata</i>	8 weeks	Reduced growth rates, leaf production rates, and maximum number of leaves with increasing exposure concentrations in a low light – excess nutrient condition	Leaves: 80–800 mg/kg. Stems: 5–25 mg/kg	n.d
Hong et al., 2015	5, 10, or 20 mg/L in growth media	Hydro-ponics	Lettuce ( <i>Lactuca sativa</i> ) or alfalfa ( <i>Medicago sativa</i> )	15 days	Reduced lettuce shoot length at 10 and 20 mg/L but no effect on alfalfa	Lettuce shoots: 20–52 mg/kg, Alfalfa shoots: 160–182 mg/kg	n.d
Zuverza-Mena et al., 2015	20 or 80 mg/kg in soil	Potting soil	Cilantro ( <i>Coriandrum sativum</i> )	30 days	Increase of root biomass at the highest concentration and no effect of shoot biomass	Shoots: 10–15 mg/kg	n.d
Zhao et al., 2016a Nano Impact	1050 and 1555 mg/L two times per week on plants	Sandy-loam soil	Lettuce ( <i>Lactuca sativa</i> )	30 days	n.d	Vascular tissues: 9.9, 823 and 1111 mg/kg, Photosynthetic tissues: 13.0, 1353 and 2008 mg/kg	n.d
Zhao et al., 2016b ES&T	1050, 1555, or 2100 mg/L two times per week on plants	Sandy-loam soil	Lettuce ( <i>Lactuca sativa</i> )	30 days	Increase of leaf biomass at low and medium concentrations	Vascular tissues: 973–1344 mg/kg, Mesophyll tissues: 1695–2296 mg/kg	n.d
Zhao et al., 2017	100 or 1000 mg/L three times a day on plants	Artificial growth media	Maize ( <i>Zea mays</i> )	7 days	The higher dose significantly decreased leaf biomass by 17–20%	Leaves: 12–1404 mg/kg	n.d

n.d. not determined.

European Union market (10 mg Cu/kg residue, EU Pesticides Database). Copper concentrations in plant biomass observed in our study were 100 times lower than in previous publications simulating foliar applications of Kocide 3000 (Table 2) (Zhao et al., 2016a,b, 2017). In our study, less than 10% of the Cu applied during the Kocide application was recovered associated to the aboveground plant biomass after 15 days. This suggests that the majority of this nanopesticide ends up in the soils (93–97%), building up over time and that the amount of Cu exported during plant harvest is limited. In our experiment, we could not confirm that Cu accumulated on the soil surface because of the high natural Cu background concentration ( $90.5 \pm 4.4$  mg/kg) of our test soil compared to the low Cu amount applied to the mesocosms (total of 5.43 mg of Cu per mesocosm). Additionally, 6 months after stopping the nanopesticide exposures (day 365) we could not detect any differences in Cu associated with plants between control and Kocide-treated mesocosms. Taken together, these results show that three Kocide 3000 applications over a growing season led to no detectable legacy effects in terms of Cu accumulation in the plant and soil compartments 6 months later.

In terms of biological endpoints, the microbial enzyme activities were the only parameters showing significant declines 6 months after the last Kocide 3000 exposure. These legacy effects on beta-glucosidase and phosphatase activities are particularly interesting because these processes were not affected by Kocide additions shortly after the second and third exposures. This observation indicates that despite the high resilience of microbial processes on the short-term (day 75), longer term declines can occur and these phenomena are hard to predict based on our pre- and post-exposure monitoring during the growing season. These results call for long-term assessment of nanopesticide impact on soil fertility mediated by microbial processes to uncover the abiotic and microbial factors driving these declines. Additionally, in a parallel mesocosm experiment simulating a wetland ecosystem exposed chronically to Kocide 3000, we observed that this nanopesticide caused large ecosystem-scale impacts, including an intensification of eutrophication and major algal blooms (Simonin et al., 2018). Our findings demonstrate that this particular nanopesticide may have limited environmental consequences in the target terrestrial agroecosystems, but that non-target, downstream, aquatic ecosystems may be more vulnerable to impacts of nanopesticides in runoff.

## REFERENCES

- Adeleye, A. S., Conway, J. R., Perez, T., Rutten, P., and Keller, A. A. (2014). Influence of extracellular polymeric substances on the long-term fate, dissolution, and speciation of copper-based nanoparticles. *Environ. Sci. Technol.* 48, 12561–12568. doi: 10.1021/es5033426
- Baijokya, F. P., and Semu, E. (1998). Effects of kocide 101 on the bean (*Phaseolus vulgaris* L.)-*Rhizobium symbiosis*. *Acta Agric. Scand. B Plant Soil Sci.* 48, 175–183.
- Bell, C. W., Fricks, B. E., Rocca, J. D., Steinweg, J. M., McMahon, S. K., and Wallenstein, M. D. (2013). High-throughput fluorometric measurement of potential soil extracellular enzyme activities. *J. Vis. Exp.* 15:e50961. doi: 10.3791/50961

## AUTHOR CONTRIBUTIONS

MS, BC, SA, and EB designed the experiments. MS, SA, CB, and JR conducted the field work and the plant biomass and microbial enzyme analyses. WT and NC performed the N<sub>2</sub> fixation assays. JJ performed the mycorrhizal colonization assays. JU performed the ICP-MS measurements. MS, SA, and EB wrote the paper and all the authors edited the manuscript.

## FUNDING

This work was supported by the National Science Foundation (NSF) and the Environmental Protection Agency (EPA) under NSF Cooperative Agreement EF-0830093 and DBI-1266252, Center for the Environmental Implications of Nanotechnology (CEINT). WT and NC were supported by an NSF-CAREER (3331939). Any opinions, findings, conclusions or recommendations expressed in this material are those of the author(s) and do not necessarily reflect the views of the NSF or the EPA. This work has not been subjected to EPA review and no official endorsement should be inferred.

## ACKNOWLEDGMENTS

We want to thank Medora Burke-Scoll, Brooke Hassett, Anna Fedders, Ethan Baruch, Eric Moore, Erin Vanderjeugd, Samuel Mahanes, Henry Camp, Bradley Shewmaker, Alison Waldman, Lucia Mercado, Wyatt Jernigan, Kristen Buehne, Shannon Thoits, Eva May, and Nia Bartolucci for their help during the set-up of this experiment, field collection, and lab work. We also thank Shristi Shrestha for performing the acid digestion and ICP-MS measurements on the soil and plant samples. Thanks to Caroline Buchanan for her help for the root mycorrhizal colonization measurements.

## SUPPLEMENTARY MATERIAL

The Supplementary Material for this article can be found online at: <https://www.frontiersin.org/articles/10.3389/fmicb.2018.01769/full#supplementary-material>

- Benelli, G., Maggi, F., Pavela, R., Murugan, K., Govindarajan, M., Vaseeharan, B., et al. (2017). Mosquito control with green nanopesticides: towards the one health approach? A review of non-target effects. *Environ. Sci. Pollut. Res.* 25, 10184–102096. doi: 10.1007/s11356-017-9752-4
- Brandt, K. K., Frandsen, R. J. N., Holm, P. E., and Nybroe, O. (2010). Development of pollution-induced community tolerance is linked to structural and functional resilience of a soil bacterial community following a five-year field exposure to copper. *Soil Biol. Biochem.* 42, 748–757. doi: 10.1016/j.soilbio.2010.01.008
- Bünemann, E. K., Schwenke, G. D., and Zwieten, L. V. (2006). Impact of agricultural inputs on soil organisms—a review. *Soil Res.* 44, 379–406. doi: 10.1071/SR05125
- Cassar, N., Bellenger, J.-P., Jackson, R. B., Karr, J., and Barnett, B. A. (2012). N<sub>2</sub> fixation estimates in real-time by cavity ring-down laser absorption spectroscopy. *Oecologia* 168, 335–342. doi: 10.1007/s00442-011-2105-y

- Chen, C., Tsyusko, O. V., McNear, D. H. Jr., Judy, J., Lewis, R. W., and Unrine, J. M. (2017). Effects of biosolids from a wastewater treatment plant receiving manufactured nanomaterials on *Medicago truncatula* and associated soil microbial communities at low nanomaterial concentrations. *Sci. Total Environ.* 609, 799–806. doi: 10.1016/j.scitotenv.2017.07.188
- Chen, C., Unrine, J. M., Judy, J. D., Lewis, R. W., Guo, J., McNear, D. H. Jr., et al. (2015). Toxicogenomic responses of the model legume *Medicago truncatula* to aged biosolids containing a mixture of nanomaterials (TiO<sub>2</sub>, Ag, and ZnO) from a pilot wastewater treatment plant. *Environ. Sci. Technol.* 49, 8759–8768. doi: 10.1021/acs.est.5b01211
- Conway, J. R., Beaulieu, A. L., Beaulieu, N. L., Mazer, S. J., and Keller, A. A. (2015). Environmental stresses increase photosynthetic disruption by metal oxide nanomaterials in a soil-grown plant. *ACS Nano* 9, 11737–11749. doi: 10.1021/acsnano.5b03091
- Cornelis, G., Hund-Rinke, K., Kuhlbusch, T., van den Brink, N., and Nickel, C. (2014). Fate and bioavailability of engineered nanoparticles in soils: a review. *Crit. Rev. Environ. Sci. Technol.* 44, 2720–2764. doi: 10.1080/10643389.2013.829767
- De Vries, F. T., and Shade, A. (2013). Controls on soil microbial community stability under climate change. *Front. Microbiol.* 4:265. doi: 10.3389/fmicb.2013.00265
- Díaz-Raviña, M., Anta, D., Calvo, R., and Bååth, E. (2007). Tolerance (PICT) of the bacterial communities to copper in vineyard soils from Spain. *J. Environ. Qual.* 36, 1760–1764. doi: 10.2134/jeq2006.0476
- Giller, K. E., Witter, E., and McGrath, S. P. (1998). Toxicity of heavy metals to microorganisms and microbial processes in agricultural soils: a review. *Soil Biol. Biochem.* 30, 1389–1414. doi: 10.1016/j.soilbio.2008.06.009
- Graham, J. H., Timmer, L. W., and Fardelmann, D. (1986). Toxicity of fungicidal copper in soil to citrus seedlings and vesicular-arbuscular mycorrhizal fungi. *Phytopathology* 76, 66–70. doi: 10.1094/Phyto-76-66
- Griffiths, B. S., and Philippot, L. (2013). Insights into the resistance and resilience of the soil microbial community. *FEMS Microbiol. Rev.* 37, 112–129. doi: 10.1111/j.1574-6976.2012.00343.x
- Hardy, R. W., Holsten, R. D., Jackson, E. K., and Burns, R. C. (1968). The acetylene-ethylene assay for N<sub>2</sub> fixation: laboratory and field evaluation. *Plant Physiol.* 43, 1185–1207. doi: 10.1104/pp.43.8.1185
- Hernández-Dorrego, A., and Mestre-Parés, J. (2010). Evaluation of some fungicides on mycorrhizal symbiosis between two *Glomus* species from commercial inocula and *Allium porrum* L. seedlings. *Span. J. Agric. Res.* 8, 43–50. doi: 10.5424/sjar/201008S1-1222
- Hong, J., Rico, C. M., Zhao, L., Adeleye, A. S., Keller, A. A., Peralta-Videa, J. R., et al. (2015). Toxic effects of copper-based nanoparticles or compounds to lettuce (*Lactuca sativa*) and alfalfa (*Medicago sativa*). *Environ. Sci. Processes Impacts* 17, 177–185. doi: 10.1039/C4EM00551A
- Hussain, S., Siddique, T., Saleem, M., Arshad, M., and Khalid, A. (2009). Chapter 5 impact of pesticides on soil microbial diversity, enzymes, and biochemical reactions. in *Adv. Agron.* 102, 159–200.
- Jentschke, G., and Godbold, D. L. (2000). Metal toxicity and ectomycorrhizas. *Physiol. Plant.* 109, 107–116. doi: 10.1034/j.1399-3054.2000.100201.x
- Judy, J. D., McNear, D. H. Jr., Chen, C., Lewis, R. W., Tsyusko, O. V., Bertsch, P. M., et al. (2015). Nanomaterials in biosolids inhibit nodulation, shift microbial community composition, and result in increased metal uptake relative to bulk/dissolved metals. *Environ. Sci. Technol.* 49, 8751–8758. doi: 10.1021/acs.est.5b01208
- Kah, M. (2015). Nanopesticides and nanofertilizers: emerging contaminants or opportunities for risk mitigation? *Front. Chem.* 3:64. doi: 10.3389/fchem.2015.00064
- Kah, M., Walch, H., and Hofmann, T. (2018). Environmental fate of nanopesticides: durability, sorption and photodegradation of nanoformulated clothianidin. *Environ. Sci. Nano* 5, 882–889. doi: 10.1039/C8EN00038G
- Keller, A. A., Adeleye, A. S., Conway, J. R., Garner, K. L., Zhao, L., Cherr, G. N., et al. (2017). Comparative environmental fate and toxicity of copper nanomaterials. *Nanoimpact* 7, 28–40. doi: 10.1016/j.impact.2017.05.003
- King, R. S., Brain, R. A., Back, J. A., Becker, C., Wright, M. V., Toteu Djomte, V., et al. (2016). Effects of pulsed atrazine exposures on autotrophic community structure, biomass, and production in field-based stream mesocosms. *Environ. Toxicol. Chem.* 35, 660–675. doi: 10.1002/etc.3213
- Komárek, M., Ěadková, E., Chrástná, V., Bordas, F., and Bollinger, J.-C. (2010). Contamination of vineyard soils with fungicides: a review of environmental and toxicological aspects. *Environ. Int.* 36, 138–151. doi: 10.1016/j.envint.2009.10.005
- Leita, L., Nobili, M. D., Mondini, C., Muhlbachova, G., Marchiol, L., Bragato, G., et al. (1999). Influence of inorganic and organic fertilization on soil microbial biomass, metabolic quotient and heavy metal bioavailability. *Biol. Fertil. Soils* 28, 371–376. doi: 10.1007/s003740050506
- Lejon, D. P., Martins, J. M., Lévêque, J., Spadini, L., Pascault, N., Landry, D., et al. (2008). Copper dynamics and impact on microbial communities in soils of variable organic status. *Environ. Sci. Technol.* 42, 2819–2825. doi: 10.1021/es071652r
- Leyval, C., Turnau, K., and Haselwandter, K. (1997). Effect of heavy metal pollution on mycorrhizal colonization and function: physiological, ecological and applied aspects. *Mycorrhiza* 7, 139–153. doi: 10.1007/s005720050174
- Liu, R., and Lal, R. (2015). Potentials of engineered nanoparticles as fertilizers for increasing agronomic productions. *Sci. Total Environ.* 514, 131–139. doi: 10.1016/j.scitotenv.2015.01.104
- McKee, M. S., and Filser, J. (2016). Impacts of metal-based engineered nanomaterials on soil communities. *Environ. Sci. Nano* 3, 506–533. doi: 10.1039/C6EN00007J
- Miguel, C., Paul, M., and Jim, G. (2014). *Forages for North Carolina: General Guidelines and Concepts | NC State Extension Publications*. Available at: <https://content.ces.ncsu.edu/forages-for-north-carolina-general-guidelines-and-concepts.pdf> [Accessed May 31, 2018].
- Mishra, S., Keswani, C., Abhilash, P. C., Fraceto, L. F., and Singh, H. B. (2017). Integrated approach of agri-nanotechnology: challenges and future trends. *Front. Plant Sci.* 8:471. doi: 10.3389/fpls.2017.00471
- Navel, A., and Martins, J. M. F. (2014). Effect of long term organic amendments and vegetation of vineyard soils on the microscale distribution and biogeochemistry of copper. *Sci. Total Environ.* 46, 681–689. doi: 10.1016/j.scitotenv.2013.07.064
- Nemec, S. (1980). Effects of 11 fungicides on endomycorrhizal development in sour orange. *Can. J. Bot.* 58, 522–526. doi: 10.1139/b80-063
- Priester, J. H., Ge, Y., Mielke, R. E., Horst, A. M., Moritz, S. C., Espinosa, K., et al. (2012). Soybean susceptibility to manufactured nanomaterials with evidence for food quality and soil fertility interruption. *Proc. Natl. Acad. Sci. U.S.A.* 109, E2451–E2456. doi: 10.1073/pnas.1205431109
- R Core Team (2015). *R: A Language and Environment for Statistical Computing*. Available at: <http://www.R-project.org/>
- Rutto, K. L., Mizutani, F., Moon, D. G., and Kadoya, K. (2002). The relationship between cultural practices and arbuscular mycorrhizal (AM) activity in orchards under different management systems. *J. Jpn. Soc. Hortic. Sci.* 71, 601–609. doi: 10.2503/jjshs.71.601
- Simonin, M., Colman, B. P., Anderson, S. M., King, R. S., Ruis, M. T., Avellan, A., et al. (2018). Engineered nanoparticles interact with nutrients to intensify eutrophication in a wetland ecosystem experiment. *Ecol. Appl.* doi: 10.1002/eap.1742 [Epub ahead or print].
- Simonin, M., and Richaume, A. (2015). Impact of engineered nanoparticles on the activity, abundance, and diversity of soil microbial communities: a review. *Environ. Sci. Pollut. Res.* 22, 13710–13723. doi: 10.1007/s11356-015-4171-x
- Smith, S. E., and Read, D. J. (2010). *Mycorrhizal symbiosis*. Cambridge, MA: Academic press.
- Sugavanam, V., Udayan, K., and Manian, S. (1994). Effect of fungicides on vesicular-arbuscular mycorrhizal infection and nodulation in groundnut (*Arachis hypogea* L.). *Agric. Ecosyst. Environ.* 48, 285–293. doi: 10.1016/0167-8809(94)90110-4
- Tripathi, D. K., Shweta, Singh, S., Singh, S., Pandey, R., Singh, V. P., et al. (2017). An overview on manufactured nanoparticles in plants: uptake, translocation, accumulation and phytotoxicity. *Plant Physiol. Biochem.* 110, 2–12. doi: 10.1016/j.plaphy.2016.07.030
- Visser, H. C., Reinhoudt, D. N., and Jong, F. (1994). Carrier-mediated transport through liquid membranes. *Chem. Soc. Rev.* 23, 75–81. doi: 10.1039/CS9942300075
- Zhao, L., Hu, Q., Huang, Y., and Keller, A. A. (2017). Response at genetic, metabolic, and physiological levels of maize (*Zea mays*) exposed to a

- Cu(OH)<sub>2</sub> nanopesticide. *ACS Sustain. Chem. Eng.* 5, 8294–8301. doi: 10.1021/acssuschemeng.7b01968
- Zhao, L., Huang, Y., Hannah-Bick, C., Fulton, A. N., and Keller, A. A. (2016a). Application of metabolomics to assess the impact of Cu (OH)<sub>2</sub> nanopesticide on the nutritional value of lettuce (*Lactuca sativa*): enhanced Cu intake and reduced antioxidants. *Nanoimpact* 3, 58–66. doi: 10.1016/j.impact.2016.08.005
- Zhao, L., Ortiz, C., Adeleye, A. S., Hu, Q., Zhou, H., Huang, Y., et al. (2016b). Metabolomics to detect response of lettuce (*Lactuca sativa*) to Cu(OH)<sub>2</sub> nanopesticides: oxidative stress response and detoxification mechanisms. *Environ. Sci. Technol.* 50, 9697–9707. doi: 10.1021/acs.est.6b02763
- Zuverza-Mena, N., Medina-Velo, I. A., Barrios, A. C., Tan, W., Peralta-Videa, J. R., and Gardea-Torresdey, J. L. (2015). Copper nanoparticles/compounds impact agronomic and physiological parameters in cilantro (*Coriandrum sativum*). *Environ. Sci. Process. Impacts* 17, 1783–1793. doi: 10.1039/c5em00329f
- Zuur, A. F., Ieno, E. N., Walker, N. J., Saveliev, A. A., and Smith, G. M. (eds). (2009). “Zero-truncated and zero-inflated models for count data,” in *Mixed Effects Models and Extensions in Ecology with R Statistics for Biology and Health*, (New York, NY: Springer), 261–293. doi: 10.1007/978-0-387-87458-6\_11
- Conflict of Interest Statement:** The authors declare that the research was conducted in the absence of any commercial or financial relationships that could be construed as a potential conflict of interest.

Copyright © 2018 Simonin, Colman, Tang, Judy, Anderson, Bergemann, Rocca, Unrine, Cassar and Bernhardt. This is an open-access article distributed under the terms of the Creative Commons Attribution License (CC BY). The use, distribution or reproduction in other forums is permitted, provided the original author(s) and the copyright owner(s) are credited and that the original publication in this journal is cited, in accordance with accepted academic practice. No use, distribution or reproduction is permitted which does not comply with these terms.



# Environmental Concentrations of Copper, Alone or in Mixture With Arsenic, Can Impact River Sediment Microbial Community Structure and Functions

Ayanleh Mahamoud Ahmed<sup>1,2,3</sup>, Emilie Lyautey<sup>2</sup>, Chloé Bonnineau<sup>1</sup>, Aymeric Dabrin<sup>1</sup> and Stéphane Pesce<sup>1\*</sup>

<sup>1</sup> Irstea, UR RiverLy, Centre de Lyon-Villeurbanne, Villeurbanne, France, <sup>2</sup> CARRTEL, Univ. Savoie Mont Blanc, INRA, Chambéry, France, <sup>3</sup> Centre de Recherche, Université de Djibouti, Djibouti, Djibouti

## OPEN ACCESS

### Edited by:

Simona Rossetti,  
Istituto di Ricerca sulle Acque (IRSA),  
Italy

### Reviewed by:

Lucia Cavalca,  
Università degli Studi di Milano, Italy  
Christopher L. Hemme,  
The University of Rhode Island,  
United States

### \*Correspondence:

Stéphane Pesce  
stephane.pesce@irstea.fr

### Specialty section:

This article was submitted to  
Microbiotechnology, Ecotoxicology  
and Bioremediation,  
a section of the journal  
Frontiers in Microbiology

**Received:** 17 April 2018

**Accepted:** 24 July 2018

**Published:** 14 August 2018

### Citation:

Mahamoud Ahmed A, Lyautey E, Bonnineau C, Dabrin A and Pesce S (2018) Environmental Concentrations of Copper, Alone or in Mixture With Arsenic, Can Impact River Sediment Microbial Community Structure and Functions. *Front. Microbiol.* 9:1852. doi: 10.3389/fmicb.2018.01852

In many aquatic ecosystems, sediments are an essential compartment, which supports high levels of specific and functional biodiversity thus contributing to ecological functioning. Sediments are exposed to inputs from ground or surface waters and from surrounding watershed that can lead to the accumulation of toxic and persistent contaminants potentially harmful for benthic sediment-living communities, including microbial assemblages. As benthic microbial communities play crucial roles in ecological processes such as organic matter recycling and biomass production, we performed a 21-day laboratory channel experiment to assess the structural and functional impact of metals on natural microbial communities chronically exposed to sediments spiked with copper (Cu) and/or arsenic (As) alone or mixed at environmentally relevant concentrations (40 mg kg<sup>-1</sup> for each metal). Heterotrophic microbial community responses to metals were evaluated both in terms of genetic structure (using ARISA analysis) and functional potential (using exoenzymatic, metabolic and functional genes analyses). Exposure to Cu had rapid marked effects on the structure and most of the functions of the exposed communities. Exposure to As had almost undetectable effects, possibly due to both lack of As bioavailability or toxicity toward the exposed communities. However, when the two metals were combined, certain functional responses suggested a possible interaction between Cu and As toxicity on heterotrophic communities. We also observed temporal dynamics in the functional response of sediment communities to chronic Cu exposure, alone or in mixture, with some functions being resilient and others being impacted throughout the experiment or only after several weeks of exposure. Taken together, these findings reveal that metal contamination of sediment could impact both the genetic structure and the functional potential of chronically exposed microbial communities. Given their functional role in aquatic ecosystems, it poses an ecological risk as it may impact ecosystem functioning.

**Keywords:** benthic communities, heterotrophic communities, combined effects, metals, microbial ecotoxicology, enzymatic activities, genetic structure

## INTRODUCTION

Sediments are an essential component of aquatic ecosystems, as they provide a habitat for many species and thus host a non-negligible biological diversity (Battin et al., 2001). Within sediments, benthic heterotrophic microbial communities support various ecosystem functions, from organic matter recycling (Schwarz et al., 2007) to pollutant degradation and transformation (Bedard, 2008) and biomass production (Haglund et al., 2003). They are essential for the proper functioning of biogeochemical cycles as well as for ecosystem stability and resilience (Martiny et al., 2013). Sediments are also natural receptors for hydrophobic and persistent pollutants (such as trace metals, polycyclic aromatic hydrocarbons or polychlorinated biphenyls) that can accumulate over time (Bombardier, 2007). Physicochemical disturbances (such as changes in pH or redox potential), as well as mechanical (e.g., dredging) or biological (e.g., bioturbation) changes in environmental conditions can induce a release of contaminants into interstitial water, thus increasing their bioavailability and their ecotoxicological risks (Faupeil et al., 2012). Sediments will then become a source of pollutants for the hosted benthic communities (Fernandez-Calvino et al., 2008; Burga Pérez et al., 2012), which can be directly exposed and structurally and functionally impacted by the contaminant compounds.

Trace metals, which include metals and metalloids, are ubiquitous and persistent in the environment. They are found in all aquatic compartments due to natural (e.g., physical and chemical alteration of rocks) and anthropogenic (e.g., industry, agriculture, etc.) inputs. Copper (Cu) and arsenic (As) are two of the most common metals present in sediments (Serra et al., 2009; Rigaud, 2011) and both Cu- and As-contaminated areas are constantly increasing due, among other factors, to mining activities or to their use as pesticides in both conventional and organic (for Cu) agriculture (Achour-Rokbani et al., 2010; Bereswill et al., 2013). Copper is an essential trace element serving as a cofactor in many enzyme pathways that catalyze a wide variety of biological functions in all organisms (e.g., Ladomersky and Petris, 2015; Adams et al., 2016) and contribute to normal ecosystem functioning. In the environment, As is mainly present in inorganic forms and in different states of oxidation, but primarily as arsenite (oxidation state +3) and arsenate (oxidation state +5). Nevertheless, sediments also contain other forms, such as arsenobetaine generally derived from biological activities (Hettiarachchi et al., 2017).

Excessive doses of both Cu and As can induce toxic effects on living organisms such as heterotrophic microorganisms. There is strong evidence that increasing concentrations of Cu and As can impact bacterial diversity (e.g., Turpeinen et al., 2004; Dell'Amico et al., 2008; Tlili et al., 2010, 2011), bacterial growth (Poirel et al., 2013), and several microbial heterotrophic functions, including glucose consumption (Poirel et al., 2013), extracellular enzymatic activities such as beta-glucosidase activity (Lambert et al., 2012) and substrate-induced respiration (Tlili et al., 2011) in various contaminated compartments such as soils and surface freshwaters. However, there is a big gap in research on the effects of Cu and As (and metals in general)

on freshwater sediment microbial heterotrophic communities, especially studies on environmentally relevant concentrations and potential Cu–As interactions.

Studies in marine sediment have demonstrated that about 50 mg Cu kg<sup>-1</sup> can decrease the ability of bacteria to use carbon sources (Gillan, 2004) and that concentrations up to 33 mg Cu kg<sup>-1</sup> can reduce the density of heterotrophic bacteria and modify the community structure (Zhao et al., 2014). In Xiangjiang River sediment, Jie et al. (2016) observed an increase in the abundance of metal resistance genes in three sites polluted by metals including Cu (392–570 mg kg<sup>-1</sup>) and As (177–2480 mg kg<sup>-1</sup>). Flemming and Trevors (1988) showed in a microcosm study that increasing concentrations of Cu, from 100 to 5000 mg Cu kg<sup>-1</sup>, caused a progressive decrease in freshwater sediment pH and biological nitrous oxide (N<sub>2</sub>O) reduction. Capone et al. (1983) also observed a significant but transient inhibition of both respiration and methanogenesis in salt marsh sediment contaminated by 1000 mg Cu kg<sup>-1</sup>. Such inhibition can lead to significant inhibition of CO<sub>2</sub> and CH<sub>4</sub> fluxes as previously reported in soil submitted to Cu treatment (Babich and Stotzky, 1985). Finally, it appears from both *in situ* (Roane and Kellogg, 1996) and laboratory studies (Knight et al., 1997) that bacterial biomass, diversity and metabolic activity in contaminated soils can be correlated to metals concentrations.

In sediment, microorganisms play an important role in biogeochemical cycles of metals, including As, which can be converted to various chemical species differing in their solubility, mobility, bioavailability and toxicity (Silver and Phung, 2005). Using the Microtox bioassay, Fulladosa et al. (2005) showed that acute toxicity of As(V) on *Vibrio fischeri* increased with pH (from 5 to 8) while As(III) toxicity was stable within pH range 6 to 8. Arsenic can inhibit many enzymes that play roles in cellular energy pathways and DNA replication and repair and the formation of As(III)-sulfur bonds can increase its toxicity toward enzymatic activities such as glutathione reductase or thioredoxin reductase (Chang et al., 2003). It can also substitute phosphate in energy compounds such as ATP (Ratnaike, 2003).

Given the frequent occurrence of both Cu and As in freshwater sediments, as well as the crucial ecological role of heterotrophic microorganisms in this compartment, there is a need to improve the environmental risk assessment of these metals in aquatic ecosystems by developing ecotoxicological approaches that address their potential effects, at environmental concentrations, on the structure and functions of benthic microbial communities. In a broader perspective, this type of research is needed to better understand and predict the ecological effects of contaminants in freshwater sediments by better taking into account benthic communities, including microorganisms, in sediment ecotoxicology (Pesce et al., 2018).

Accordingly, the aim of this study was to evaluate the structural and functional effects of chronic exposure to environmental particulate concentrations of Cu and As on natural river sediment microbial communities. The tested nominal concentration was 40 mg kg<sup>-1</sup> dry weight (dw) for each metal. This concentration is representative of high (i.e., third quartile) and very high (i.e., ninth decile) sediment contamination levels of Cu and As, respectively, in French

aquatic ecosystems (INERIS, 2010; DREAL-REMIPP, 2013). To address the potential ecotoxicological interactions between the two metals, we also assessed the effects of Cu and As in mixtures using the same individual concentrations. To this end, we performed a 21-day (d) experiment in laboratory channel microcosms containing natural river sediment initially spiked or not with Cu and/or As. The response of benthic microbial communities to chronic metal exposure was evaluated throughout the experiment, both in terms of genetic structure (using ARISA analyses) and functional potential (using exoenzymatic, metabolic and functional genes analyses).

## MATERIALS AND METHODS

### Experimental Design

Natural sediment and associated communities were sampled on June 2016 on the Ain River (at Pont de Chazey, 45°54'38.80 N - 5°14'11.18 E), a tributary of the Rhône River (France). About 100 kg of wet surface sediment (0–3 cm) was collected using an Ekman grab and brought back to the laboratory for the experiment after sieving at 2 mm. After sediment homogenization, a subsample was retrieved for the initial characterization of the sediment (particle size distribution by laser diffraction, water content by drying overnight at 105°C, particulate organic carbon and particulate trace metal concentrations). Organic matter was measured by loss on ignition (Heiri et al., 2001).

Four experimental treatments were designed: (i) reference condition (REF) without Cu and As; (ii) Cu-contaminated condition (Cu) with 40 mg Cu kg<sup>-1</sup> dw; (iii) As-contaminated condition (As) with 40 mg As kg<sup>-1</sup> dw; and (iv) mixture (MIX) condition with a combined contamination of Cu and As at 40 mg kg<sup>-1</sup> dw each. The sediment spiking mixture was prepared in 15-L mixing tanks taking into account water content (24%) and sediment density (1.24). The spiking procedure used a 60/40 ratio (vol/vol: sediment/solution) to allow proper homogenization between sediment and the spiked solution which was made with a mixture of groundwater (1/3) and demineralized water (2/3) contaminated with or without (REF treatment) CuSO<sub>4</sub>·5 H<sub>2</sub>O (CAS No. 7758-99-8) and/or AsNaO<sub>2</sub> (CAS No. 7784-46-5) at 1 g L<sup>-1</sup>. After the sediment spiking procedure, sediment was stirred for 6 h and decanted overnight before distribution into glass indoor channels (L × W × H = 83 cm × 11 cm × 10 cm). Each channel contained 3.5 kg of sediment and was filled with 6 L of recirculating water (4 L demineralized water + 2 L groundwater). Each treatment was replicated in three independent channels. Each channel was connected to a 20-L glass tank (i.e., one independent tank per channel) through an aquarium pump (NEWA MJ 750) for water recirculation at a flow of about 1.5 L min<sup>-1</sup>. Sediment and associated microbial communities were exposed for 21 days in these laboratory channels.

Sediments were sampled for metal analysis at the beginning (Day 0, d0) and the end (Day 21, d21) of the experiment, while sediments for microbial analysis and overlaying waters were sampled at d0 and after 7 (d7), 14 (d14), and 21 (d21) days of exposure. For the microbial structure analysis, the sediment

samples were stored at -20°C immediately after the sampling procedure at the different sampling times. Functional analyses were performed within a few hours after sampling, except for the initial sampling time (d0) when sediments were stored for two days at 6°C before activity measurements. Water pH, dissolved oxygen, conductivity and temperature were also measured at each sampling time using portable meters (WTW, Germany).

### Water and Sediment Chemical Analyses

At each sampling time, water samples (100 mL) were collected from each channel into glass vials to determine inorganic nutrient (ammonia, nitrate, nitrite and phosphate) and total organic carbon (TOC) concentrations using French and ISO-standard procedures (i.e., NFT 90-015-2 NF EN 26777, NF EN ISO 10304, NF EN ISO 6878, and NF EN 1484, respectively). In addition, for metals analysis, 40 mL was collected into 50 mL polypropylene (PP) tubes (Sarstedt) after filtration with a PP syringe through 0.45-μm PVDF filters. Filtered samples were then acidified with Suprapur nitric acid 65% (0.5% v/v) and stored in the dark at 4°C before analysis of Cu and As concentrations. Cu and As concentrations in filtered samples were measured by inductively-coupled plasma mass spectrometry (ICP-MS, X7, Thermo Electron Series II) according to French standard NF EN ISO 17294.2. Limits of quantification were 0.05 μg L<sup>-1</sup> for Cu and 0.02 μg L<sup>-1</sup> for As.

Copper and arsenic concentration in the sediments were measured from composite samples (30 mL) collected in each mixing tank used for the spiking procedure (d0) and in each channel (d21) and stored in PP tubes. After drying at 40°C and grinding with a ball mill (agate beads and bowl), samples were kept dry in a desiccator. Approximately 300 mg of crushed and homogenized sediments were mineralized with aqua regia (2 mL HNO<sub>3</sub> and 6 mL HCl SUPRAPUR quality) in a microwave digester (MARS-6 from CEM) in teflon reactors (180°C for 15 min). The mineralized sample was made up with ultrapure water (Veolia) and diluted to obtain a volume of 50 mL. Cu and As concentrations in sediment extracts were measured by inductively-coupled plasma mass spectrometry (ICP-OES 720 ES, series 700) according to French standard NF EN ISO 11885. Water content was measured in order to correct the results for potential moisture. The limits of quantification were 0.66 mg kg<sup>-1</sup> for Cu and 1.6 mg kg<sup>-1</sup> for As. REF sediment samples at d0 were mineralized and analyzed in triplicates, allowing to assess the relative standard deviation (RSD) of As and Cu concentrations, which were below 11 and 19%, respectively.

### Analysis of Microbial Community Function

#### Aerobic Respiration and Denitrification Metabolic Measurements

The slurry technique (Furutani et al., 1984) was used to measure aerobic respiration and denitrification rates following the protocol previously described by Foulquier et al. (2013). Briefly, 10 g of wet sediment were immersed in 10 mL of distilled water under aerobic conditions (aerobic respiration) or 10 mL of a KNO<sub>3</sub> (2.16 g L<sup>-1</sup>) solution under anaerobic conditions

(denitrification) in 150-mL glass flasks. Incubation flasks assigned to denitrification measurements were purged three times with He to achieve anaerobiosis, and internal pressure was then adjusted to atmosphere. Fifteen mL of acetylene ( $C_2H_2$ , 10% v/v final volume) was added to inhibit  $N_2O$  reductases. All samples were incubated at 20°C in the dark under gentle shaking. After 2 h and 5 h, headspace gasses were sampled and analyzed by gas chromatography on an MTI 200 microcatharometer (MTI Analytical Instruments). Aerobic respiration and denitrification were expressed as ng of  $CO_2$  or  $N_2O$  per g of sediment  $dw^{-1} h^{-1}$ , respectively.

### Exoenzymatic Activities Measurements

Potential activities of  $\beta$ -glucosidase ( $\beta$ -glu, EC 3.2.1.21), phosphatase (Pase, EC 3.1.3.1) and leucine aminopeptidase (LAP, EC 3.4.11.1) were measured on wet sediments (1.2 g) by fluorimetry according to the methods described by Foulquier et al. (2013). The substrate-fluorogenic sets for the three enzymatic activities were: 4-methylumbelliferyl- $\beta$ -D-glucopyranoside (MUF-Glu, CAS No. 18997-57-4) for  $\beta$ -glu, L-leucine-7-amido-4-methylcoumarin hydrochloride (MCU-Leu, CAS No. 62480-44-8) for LAP and 4-methylumbelliferyl phosphatase (MUF-P, CAS No. 3368-04-5) for Pase. The optimal substrate concentrations (i.e., 1000  $\mu$ M for  $\beta$ -glu, 1333  $\mu$ M for LAP, and 500  $\mu$ M for Pase) were determined prior to the experiment. After a 30-min incubation at 20°C in the dark under shaking conditions, activities were stopped with 0.3 mL of glycine buffer (pH 10.4, glycine 0.05 M and  $NH_4OH$  0.2 M) before centrifugation (at  $5000 \times g$  for 5 min). Fluorescence was measured using a microplate reader (Synergy HT BioTek Instruments) with excitation wavelength set to 360 nm and emission wavelength set to 460 nm. Enzymatic activity was quantified using standard curves of the reference compounds: MUF (for  $\beta$ -glu and Pase, Sigma M1381 CAS No. 90-33-5) and AMC (for LAP; Sigma A9891, CAS No. 26093-31-2). Results were expressed as nmol of hydrolyzed compound per g of sediment  $dw^{-1} h^{-1}$ .

### Analysis of Microbial Community Structure

Microbial sediment DNA was extracted from 0.5 g of wet sediment (stored at  $-20^\circ C$ ) using a NucleoSpin Soil Kit (Macherey-Nagel EURL) following the manufacturer's instructions, and using SL1 lysis buffer and additive Enhancer SX buffer. The extracted DNA was quantified fluorometrically after staining with bisBenzimide (DNA Quantitation Kit, Fluorescence Assay, Sigma-Aldrich) using a Plate Chameleon<sup>TM</sup> fluorometer (Hidex; excitation: 340 nm, emission: 460 nm).

Total and functional bacterial community sizes were estimated using real-time quantitative PCR (qPCR) assays targeting 16S rRNA gene (total bacteria), and *nirS*, *nirK*, and *nosZ* (clades I and II) genes involved in denitrification activity, according to protocols described in **Supplementary Table 1** (Henry et al., 2004, 2006; López-Gutiérrez et al., 2004; Throbäck et al., 2004; Kandeler et al., 2006; Jones et al., 2013). Reactions contained 1  $\times$  Master Mix, 0.3 mg  $mL^{-1}$  BSA (Sigma-Aldrich), each primer, and 1  $\mu$ L of template DNA. Standard ranges were plotted from a

10-fold serial dilution of a plasmid solution containing the gene of interest.

Bacterial community structure was assessed using automated ribosomal intergenic spacer analysis (ARISA) based on the length polymorphism of intergenic spacer (ITS) sequences between 16S rRNA and 23S rRNA genes. This method is based on a size polymorphism of the ITS which makes it possible to discriminate organisms by their molecular fingerprint known as Operational Taxonomic Unit (OTU). Amplification was carried out using 5'-6-carboxyfluorescein (FAM)-labeled-S-D-Bact-1522-B-S-20 and L-D-Bact-132-a-A-1 primers (Normand et al., 1996) with 1 ng of template DNA and using a previously described protocol (Lyautey et al., 2011). Amplification products were quantified and purified as described in Billard et al. (2015) before being separated on ABI 3730xl DNA Analyzer (BIOfidal DTAMB, IFR 41, Université Lyon 1) using the internal size standard Dye 5 ladder, 50–1000 bp (Gel company).

### Statistical Analysis

After confirming normality of the residuals (Shapiro–Wilk test; Royston, 1982) and data homoscedasticity (Fligner–Killeen test; Conover et al., 1981) for all parameters, significant differences between conditions were identified by analysis of variance (ANOVA) and further analyzed with a *post hoc* Tukey test, using R software (version 3.4.3, R Core Team, 2018). At day 21, a 2-factor ANOVA was performed to identify potential interactions between Cu and As on biological parameters. Results were considered significant at  $p < 0.05$ . Raw ARISA electropherograms were analyzed using Applied BioSystems Peak Scanner software, following the protocol described elsewhere (Billard et al., 2015). The data analyzed was transformed to an abundance matrix, and Bray-Curtis similarities (BC) between samples were calculated. Distances between samples were represented by non-multidimensional scaling (nMDS, Clarke and Warwick, 2001) with R software (Vegan package). A stress value below 0.20 indicates a good representation of the BC distances between samples. Analysis Of Similarity (ANOSIM, R software, Vegan package) was used to test for significant differences between user-defined (*a priori*) groups. ANOSIM was computed from the BC similarity matrix, and a random permutation test (10,000 permutations) was applied. The test was considered significant at  $P < 0.05$  after application of the Bonferroni correction (R software, stat package). SIMPER (Similarity Percentage) analysis carried out using PAST software (Hammer et al., 2001) was used to identify the OTUs that contributed to the discrimination of communities from different treatments. The BC measure is implicit to SIMPER.

## RESULTS

### Channel Water and Sediment Chemistry

In the channels, at the water-sediment interface, temperature was  $19.2 \pm 0.2^\circ C$ , pH was  $8.2 \pm 0.9$ , oxygen concentration was  $8.2 \pm 1.9$  mg  $L^{-1}$ , oxygen saturation was  $90.0 \pm 5.1\%$ , and conductivity was  $230.0 \pm 8.8$   $\mu S$   $cm^{-1}$  ( $n = 48$ , data not shown), without significant difference between treatments

**TABLE 1** | Concentrations of Cu and As in river sediment ( $\text{mg kg}^{-1}$  dw) at d0 (data from spike mixing tanks) and d21 (data from the three replicated channels: average  $\pm$  SD).

	As ( $\text{mg kg}^{-1}$ dw)		Cu ( $\text{mg kg}^{-1}$ dw)	
	d0	d21	d0	d21
REF	2.89	3.12 $\pm$ 0.10	1.81	1.30 $\pm$ 0.16
As	31.30	26.20 $\pm$ 1.2	1.75	2.60 $\pm$ 1.20
Cu	3.24	2.96 $\pm$ 0.13	56.60	43.60 $\pm$ 2.60
MIX	31.20	24.66 $\pm$ 0.45	55.10	47.80 $\pm$ 2.50

The four treatments are: sediment without contamination (REF), sediment contaminated with Cu (Cu), sediment contaminated with As (As), and sediment contaminated both with As and Cu (MIX).

throughout the experiment. Sediment particle-size classes were distributed as follows: 70% of 250–300  $\mu\text{m}$  (fine-to-medium sand), 2% [80–250  $\mu\text{m}$ ] (fine sand), 16% [70–80  $\mu\text{m}$ ] (very fine sand), 2% [10–20  $\mu\text{m}$ ] (medium silt), 8% silt and <1% clay, corresponding to a relatively coarse sediment. There were no between-channel differences for organic matter (3.0  $\pm$  2.1%) and water (24.0  $\pm$  0.9%) contents.

At d0, As and Cu concentrations in the REF treatment were close to 3  $\text{mg As kg}^{-1}$  and 2  $\text{mg Cu kg}^{-1}$  (Table 1). As concentrations in the As and MIX treatments were quite similar and close to 31  $\text{mg kg}^{-1}$ . Cu concentrations were substantially higher and close to 56  $\text{mg kg}^{-1}$  in both Cu and MIX treatments. The difference between Cu and As concentrations at d0 was explained by their contrasted behavior since solubility of Cu is more limited than for As (Smedley and Kinniburgh, 2002). During the 21-day experiment, As and Cu concentrations, respectively, decreased from 16 to 21% and from 13 to 23% in sediments according to treatments (Table 1).

In the overlying and circulating water of the REF channels, dissolved Cu and As concentrations were low (Cu < 2.3  $\mu\text{g L}^{-1}$  and As < 1.4  $\mu\text{g L}^{-1}$ ) and relatively stable throughout the study. An important release of Cu and a much higher one of As from sediment to water was recorded as illustrated by the dissolved concentrations of Cu (38.9 to 68.9  $\mu\text{g L}^{-1}$ ) and As (759 to 2829  $\mu\text{g L}^{-1}$ ) recorded in contaminated channels (Supplementary Table 2).

## Aerobic Respiration and Denitrification Activities

Over the experiment, aerobic respiration activities ranged from 972  $\pm$  65 to 2532  $\pm$  485  $\text{ng CO}_2 \text{ g}^{-1} \text{ dw h}^{-1}$  (Figure 1). No significant difference was observed between REF and As treatments from d0 to d21 or between REF and Cu and between REF and MIX treatments from d0 to d14. At d21, a significant inhibition of respiration was observed in the sediment contaminated by Cu, alone or in mixture (Cu and MIX), compared to the REF and As channels. Indeed, aerobic respiration activities were 1748.0  $\pm$  65.6 and 1316.0  $\pm$  136.1  $\text{ng CO}_2 \text{ g}^{-1} \text{ dw h}^{-1}$  in Cu and Mix conditions, respectively, while mean values were close to 2500  $\text{ng CO}_2 \text{ g}^{-1} \text{ dw h}^{-1}$  in both REF and As treatments. No significant interaction between Cu and As

on respiration was observed at day 21 ( $p > 0.05$  for the interaction term of the 2-factors ANOVA).

Denitrification activity showed no significant difference between REF and As treatment between d0 and d21, with relatively stable activities ranging from 423  $\pm$  28 to 681  $\pm$  93  $\text{ng N}_2\text{O g}^{-1} \text{ dw h}^{-1}$  throughout the experiment (Figure 2). However, denitrification was rapidly and significantly inhibited under Cu exposure, alone or in mixture (Cu and MIX: denitrification about 45  $\text{ng N}_2\text{O g}^{-1} \text{ dw h}^{-1}$  at d0). This inhibition lasted throughout the experiment in the MIX channels, with activities ranging from 45  $\pm$  25 to 476  $\pm$  81  $\text{ng N}_2\text{O g}^{-1} \text{ dw h}^{-1}$ , whereas the Cu channels showed a recovery at d21 (588  $\pm$  105  $\text{ng N}_2\text{O g}^{-1} \text{ dw h}^{-1}$ ; no significant difference to REF and As treatments). The difference observed between the exposure to Cu and to MIX suggests an interaction effect between Cu and As which was confirmed by the 2-factor ANOVA ( $p < 0.05$  for the interaction term).

## Exo-Enzymatic Activities

Except for a transient and limited inhibition of LAP activity in the As treatment at d0, there were no significant differences throughout the experiment between REF and As for LAP (activity from 39 to about 79  $\text{nmol g}^{-1} \text{ dw h}^{-1}$ , Figure 3A), Pase (activity from 55 to 75  $\text{nmol g}^{-1} \text{ dw h}^{-1}$ , Figure 3B) and  $\beta$ -glu (activity from 19 to 23  $\text{nmol g}^{-1} \text{ dw h}^{-1}$ , Figure 3C). However, all three enzymatic activities were significantly inhibited from d0 in both Cu and MIX channels. This inhibition lasted throughout the 21-day experiment for LAP (Figure 3A) and  $\beta$ -glu (except at d7 in the MIX channels; Figure 3C) whereas Pase activity showed recovery at d21 in both Cu and MIX channels (Figure 3B). No significant interaction between Cu and As on any of the exoenzymes tested was observed at day 21 ( $p > 0.05$  for the interaction term of the 2-factors ANOVA).

## Total and Functional Community Abundances

Bacterial abundances assessed as 16S rRNA gene abundance were relatively stable and close to 1.2  $10^8$  copies  $\text{g}^{-1} \text{ dw}$  in the REF treatment throughout the experiment (Figure 4). There were no significant differences between the 4 treatments from d0 to d14. At d21, a significant decrease was observed in both As (2.2  $10^7 \pm 1.3 10^7$  copies  $\text{g}^{-1} \text{ dw}$ ), Cu (3.1  $10^7 \pm 2.1 10^7$  copies  $\text{g}^{-1} \text{ dw}$ ) and MIX (0.4  $10^7 \pm 0.4 10^7$  copies  $\text{g}^{-1} \text{ dw}$ ) treatments. The same trend was observed for *nosZ* clade I (Figure 5), with stable abundances in the REF treatment from d0 to d21 (average abundance of 1.2  $10^6 \pm 9.0 10^5$  copies  $\text{g}^{-1} \text{ dw}$ ), no significant differences among treatments from d0 to d14, but a significant decrease at d21 in As (1.1  $10^5 \pm 0.5 10^5$  copies  $\text{g}^{-1} \text{ dw}$ ), Cu (3.4  $10^5 \pm 2.8 10^5$  copies  $\text{g}^{-1} \text{ dw}$ ), and MIX (1.3  $10^4 \pm 1.1 10^4$  copies  $\text{g}^{-1} \text{ dw}$ ) treatments. Differences between treatments were also observed in *nirK* and *nirS* abundance (Supplementary Figure 1). In particular, after 21 days of exposure *nirK* abundance was higher in sediments exposed to metals than in REF, this increase was significant for sediments exposed to As only. In addition, at the end of the experiment, *nirS* were less abundant in MIX than in Cu. The differences observed in *nosZ* I, *nirS* and *nirK* abundances

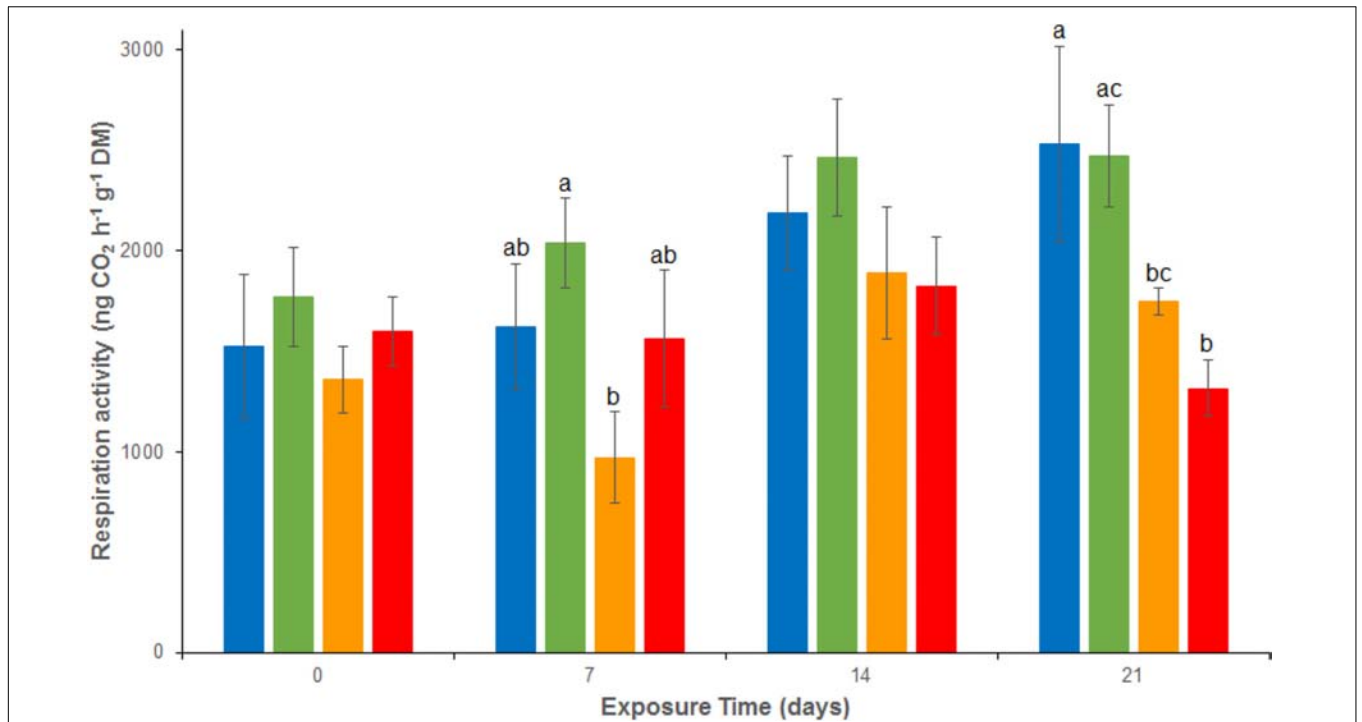


**FIGURE 1 |** Time-course of average ( $\pm$  standard deviation) microbial respiration activity in uncontaminated sediments (REF) and sediments contaminated with arsenic (AS), copper (Cu) or As plus Cu mixture (MIX). For each sampling time, different letters indicate significant differences between treatments ( $P < 0.05$ , Tukey test).

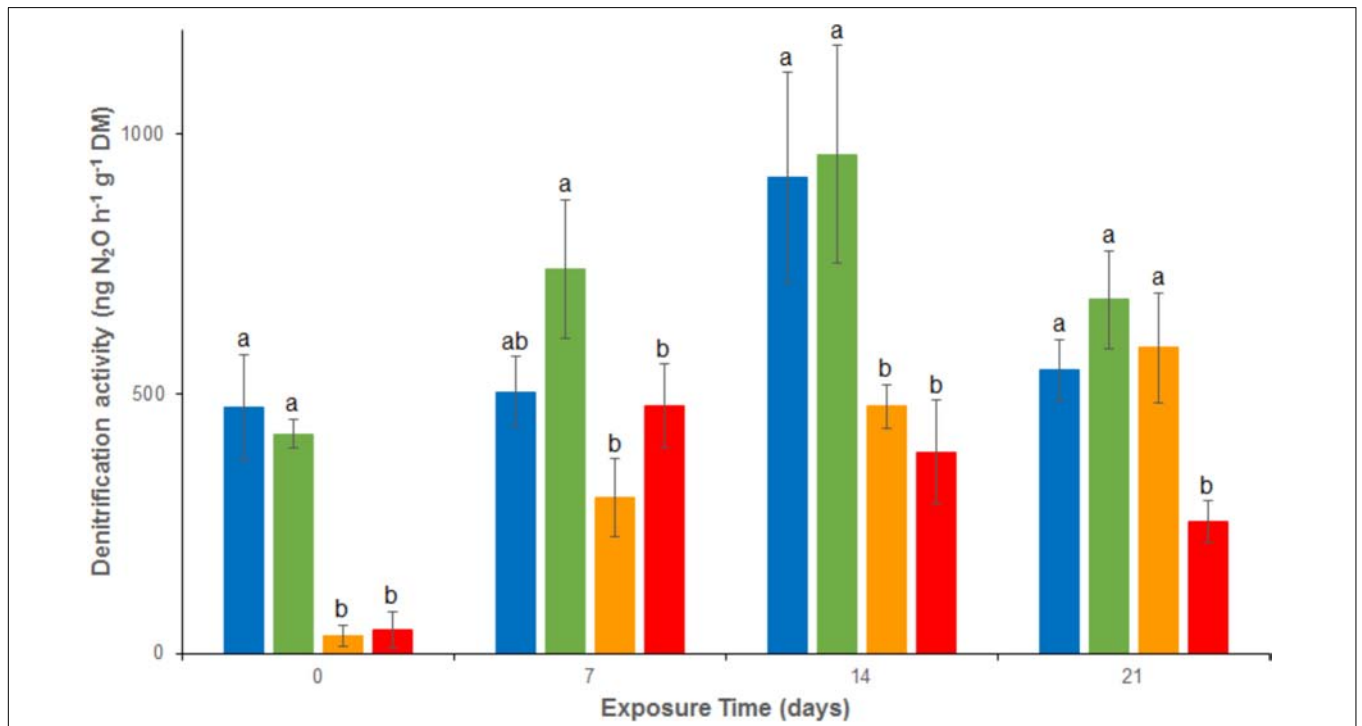
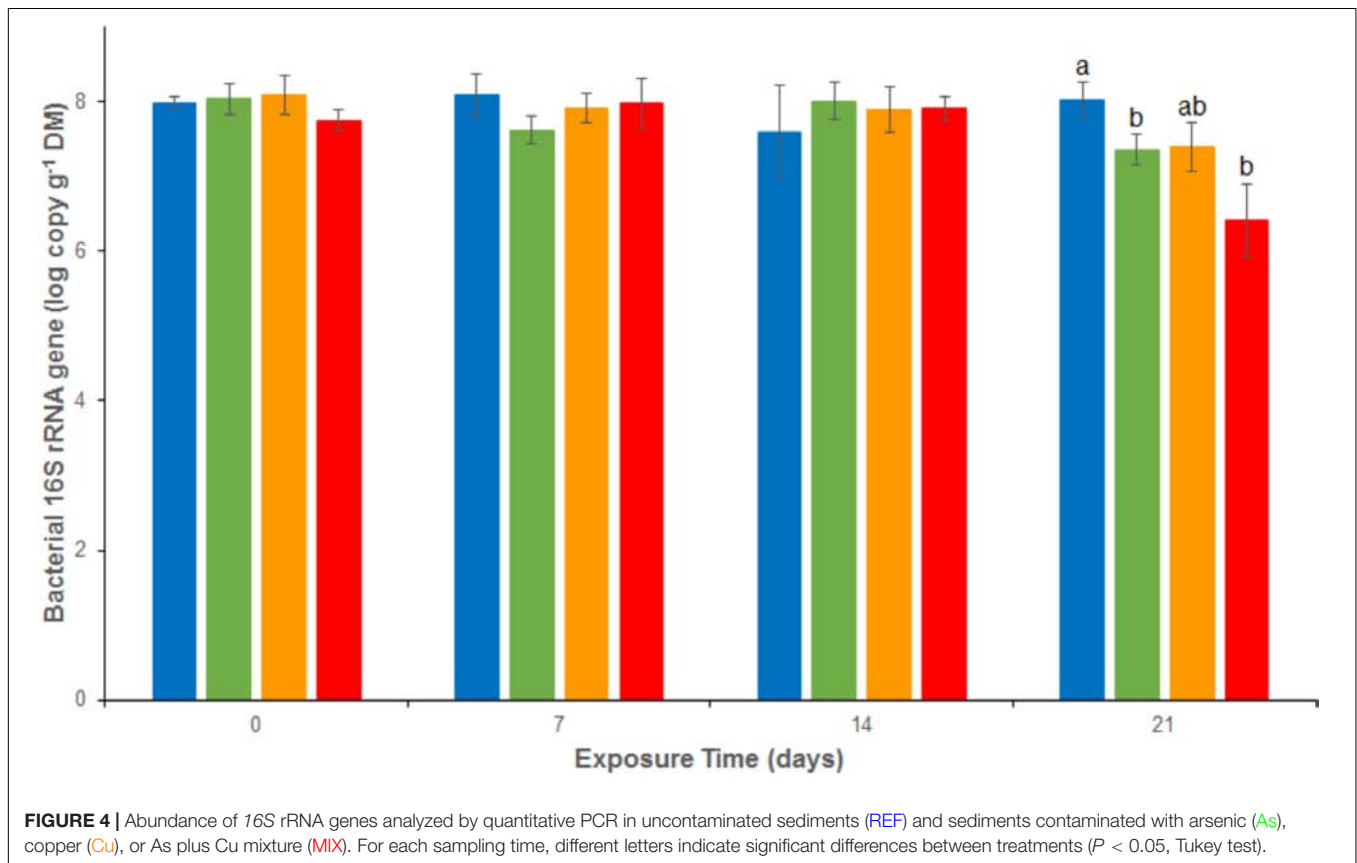
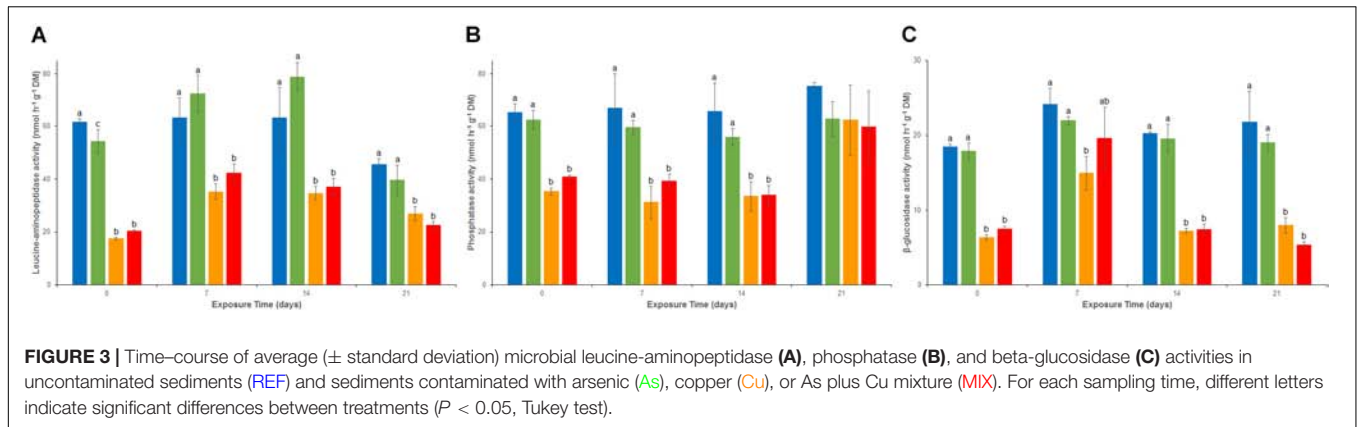


**FIGURE 2 |** Time-course of average ( $\pm$  standard deviation) microbial denitrification activity in uncontaminated sediments (REF) and sediments contaminated with arsenic (AS), copper (Cu) or As plus Cu mixture (MIX). For each sampling time, different letters indicate significant differences between treatments ( $P < 0.05$ , Tukey test).



between exposure to metal alone (Cu or As) and exposure to MIX suggest an interaction effect which was confirmed, for the three genes, by the 2-factor ANOVA ( $p < 0.05$  for the interaction term).

For *nosZ* clade II, there were no differences between treatments at any sampling time-points (Supplementary Figure 2). Average abundances for the four treatments and the four sampling dates were  $8.4 \times 10^7 \pm 0.5 \times 10^7$  copies  $g^{-1}$  dw for *nosZ* clade II.

### Bacterial Community Structure

A total of 474 distinct OTUs was recovered from the ARISA analysis for the whole set of samples (data not shown). The nMDS

representation of bacterial community structure (Figure 6) and the ANOSIM analysis allowed to significantly discriminate three different groups of samples: (i) the first one clustering all the d0 samples from the 4 treatments, (ii) the second one clustering d7, d14, and d21 samples from both the REF and As treatments, and (iii) the third one clustering d7, d14, and d21 samples from both the Cu and MIX treatments. Half of the calculated dissimilarity between the REF/As group and the Cu/MIX group (from d7 to d21) can be attributed to only 26 OTUs. Among these 26 OTUs, nine were under-represented in the REF/As group (average relative abundances ranging between 0.01 and 2.6%) compared to the Cu/MIX group (1.6–25.7%), contributing

to 29% of the dissimilarity. In contrast, the other 17 OTUs were over-represented in the REF/As group with average relative abundances comprised between 1.3 and 4.6% whereas they were below 0.97% in the Cu/MIX group (21% contribution to dissimilarity) (Figure 6).

## DISCUSSION

The experimental approach reported here was designed to assess the ecotoxicological effects of As and Cu alone and in mixture on natural sediment microbial community structure and functions, and highlighted the strong effect of Cu on microbial communities.

### Microbial Response to As Exposure

The 21-day exposure to As alone at environmental concentrations close to 25–30 mg kg<sup>-1</sup> had undetectable or very limited effects on the measured parameters, with only a transient and limited inhibition of LAP activity at the very beginning of the experiment (i.e., after the post-spiking 6-h stirring procedure, the overnight decantation and the 2-day storage before the first activity measurement), a decrease in bacterial abundance and an increase in *nirK* gene abundance and a decrease in *nosZ* clade I gene abundance (without any decrease in denitrification activity as estimated by gas chromatography) at the last sampling date.

Several hypotheses can be proposed to explain the absence of more significant effects. First, this could be due to a low toxicity potential of As to heterotrophic microorganisms at the tested concentrations, which is representative of the very highest (i.e., <10%) As sediment contamination levels recorded in French aquatic ecosystems (INERIS, 2010). Toxicant effects on microbial communities depend not only on its intrinsic toxicity but also on the community's capacity to resist and tolerate this toxicity. Some microorganisms have thus developed mechanisms of resistance toward trace metal elements. Using the *ars* operon system, bacteria and archaea are able to resist inorganic forms of As by reducing As(V) to As(III) which is then exported out of the cell (Tisa and Rosen, 1990; Rosen, 1999). As it was previously demonstrated in soils that As-resistant microorganisms can be abundant even in As-free environments (Jackson et al., 2005), microbial sediment communities studied here might have been naturally resistant to As. Based on the pollution-induced community tolerance concept first introduced by Blanck et al. (1988), microbial sediment communities might also have acquired resistance to As due to chronic exposure to the low As concentration (i.e., about 3 mg kg<sup>-1</sup> dw) observed in the river sediment from the sampling location. Indeed, Tuulaikhuu et al., 2015 demonstrated that As concentrations close to 0.6 mg kg<sup>-1</sup> dw could cause a high mortality in sediment bacterial communities and a significant decrease in phosphatase activity per sediment surface area after a 60-day exposure period. Such results thus suggest that low concentrations of As could be sufficient to induce tolerance changes in bacterial communities due to the elimination of the most sensitive species. Quantification

of resistant bacteria using real-time PCR quantification of resistances genes (Poirel et al., 2013) would be a relevant strategy to test this hypothesis.

A low As availability could also explained the limited effect of As observed in the present study. Indeed, As speciation and/or As adsorption to iron oxide (Leiva et al., 2014) might have influenced As availability and then microbial exposure. Indeed, As adsorption to iron oxides also exerts a strong influence on its mobility, being a major natural process for its removal and sequestration, and thus decreasing its bioavailability (Wang and Mulligan, 2006; Drahota et al., 2012; Zambrano, 2012). In the present study, sediment carbonate content was 49% and iron concentration was close to 12.9 g kg<sup>-1</sup> dw. Since it is generally admitted that sediment iron oxide concentration is inversely related to carbonate content, these values indicate that As adsorption to iron oxide was probably very limited in our case (Lombi et al., 1999; Thirunavukkarasu et al., 2003), and the very well-oxygenated environment in the artificial channels was favorable for the As(V) form.

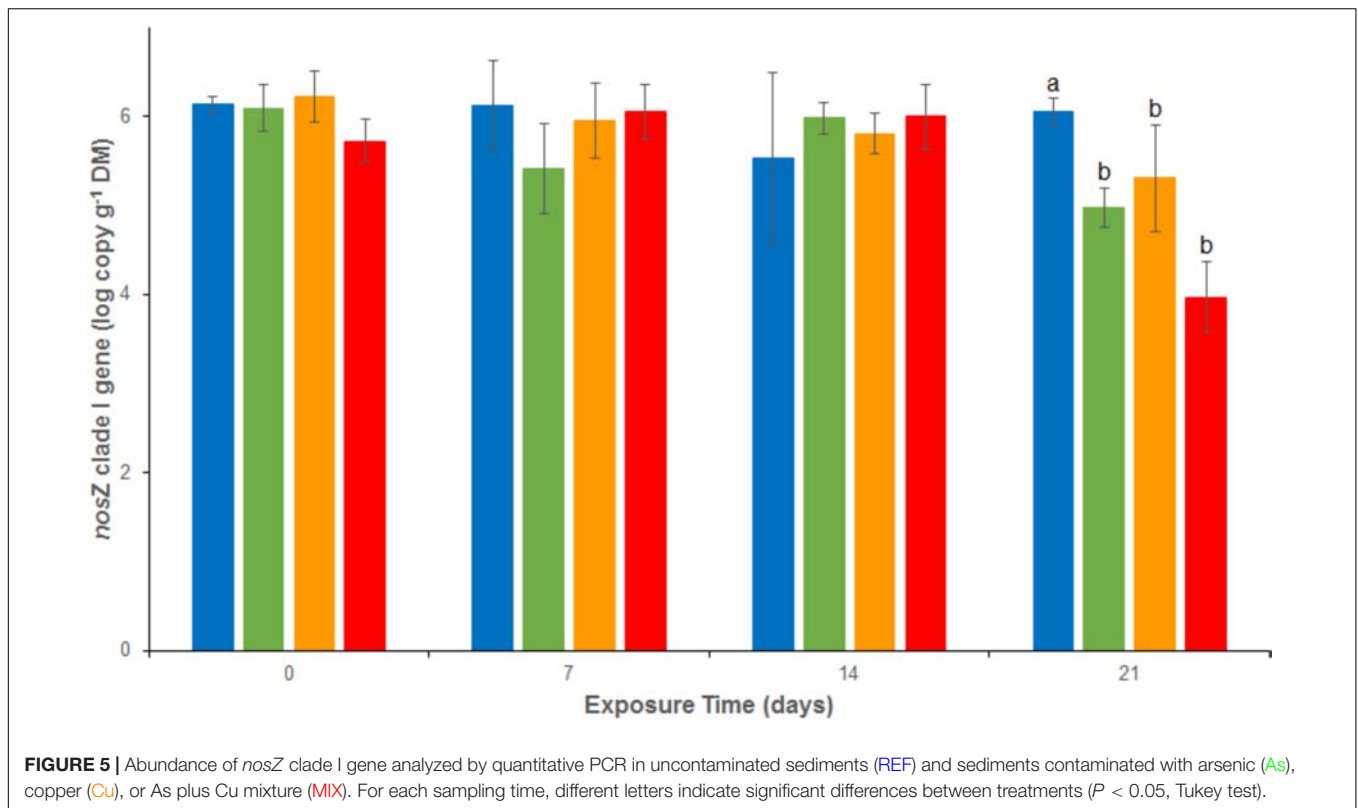
In addition, arsenic toxicity may also be influenced by its speciation: As(III) being generally more toxic and mobile than As(V), its presence usually causes higher environmental health risks and concerns (Mondal et al., 2006). Further analyses are needed to identify As species in contaminated sediment using a sequential extraction (Keon et al., 2001) and thus to assess any possible changes in As speciation that could explain the limited effect of this metal in our experiment.

### Microbial Response to Cu Exposure, Alone and in Mixture With As

The 21-day exposure to Cu alone at environmental concentrations close to 45–55 mg kg<sup>-1</sup> strongly affected most of the microbial parameters investigated. Despite a limited effect of Cu on bacterial abundance, which was only detectable at d21 based on quantification of 16S rRNA genes, bacterial community structure showed a clear shift during the first week of exposure that continued until the end of the experiment.

Chronic effects of Cu exposure on bacterial community structure have already been shown in various environmental compartments including soils (Wang et al., 2007), periphytic biofilms (Lambert et al., 2012) and sediments (Zhao et al., 2014). Comparing the structural response of marine bacterial communities collected from the water column, sediments, rock surfaces, and the green seaweed *Ulva compressa*, Moran et al. (2008) demonstrated that sediment communities appeared to be the most vulnerable to Cu exposure, based on terminal restriction fragment length polymorphism analysis.

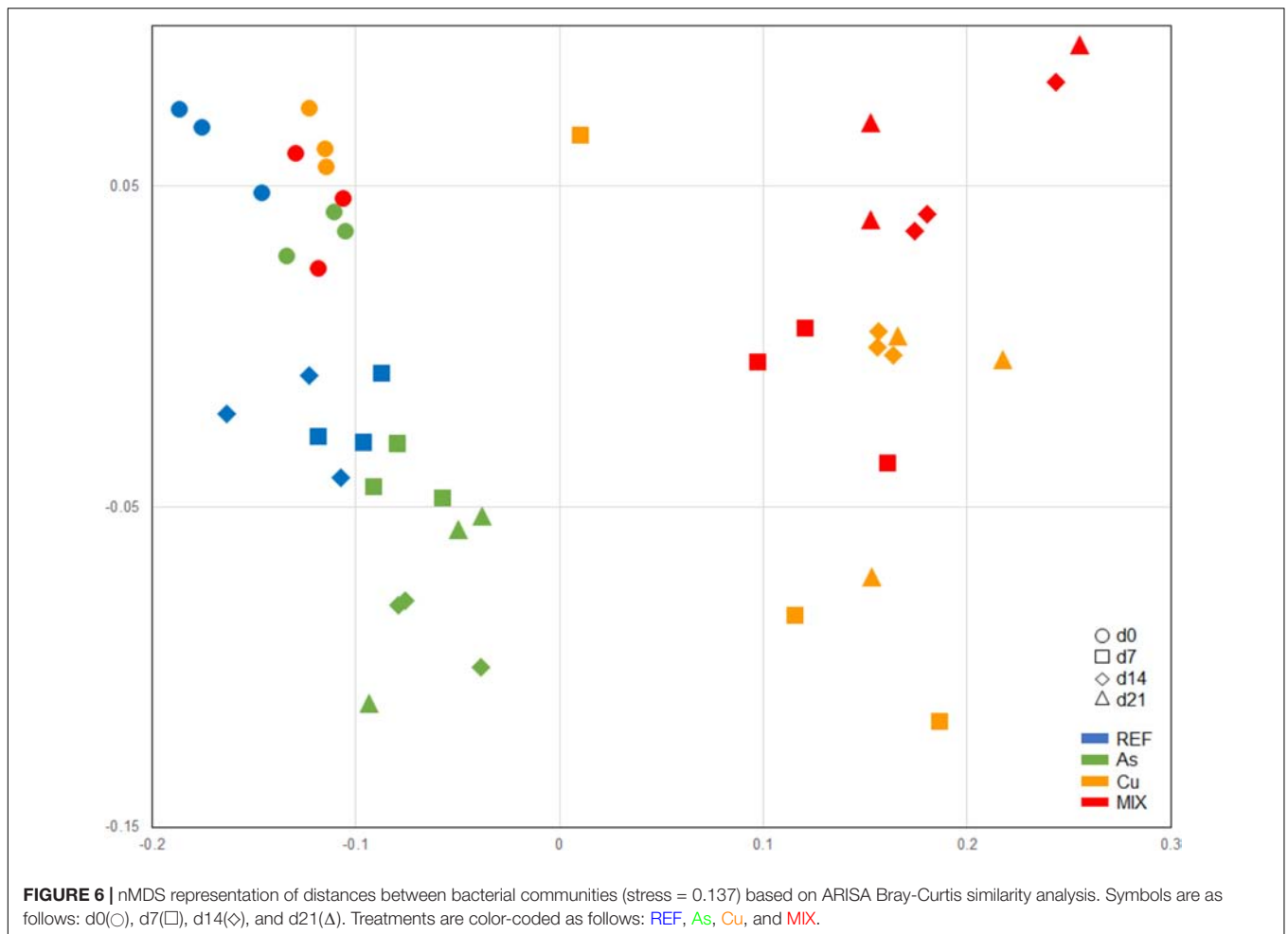
Besides impacting the bacterial community structure, Cu exposure led to a rapid inhibition of several heterotrophic functions. These functional negative effects were sometimes recorded from the very beginning of the experiment (i.e., d0) while no structural change was observed in bacterial community at this sampling date. Two (non-exclusive) hypotheses could explain this result. Firstly, effects on bacterial communities may have occurred immediately after sediment spiking (i.e.,



during the 6-h stirring procedure and the overnight decantation) thus possibly precluding the detection of significant shifts on bacterial community structure using DNA genotyping within such a short time scale. Secondly, it can't be excluded that the initial functional effects mainly occurred during the 2-day storage period used before activity measurements of the d0-samples. In this case, such effects could not be related to structural changes since d0-samples for molecular analysis were immediately frozen after sampling and did not experience this storage period. Indeed, based on gas chromatography analysis, we observed an inhibition of denitrification from the beginning of the exposure despite a lack of significant effect on abundance of *nosZ* clade I gene from d0 to d14. The three enzymatic activities LAP, Pase and  $\beta$ -glu activities were also significantly reduced from d0. The negative effects of metal contamination on various enzyme activities have been recognized in different kinds of soils (Renella et al., 2003; Hinojosa et al., 2004; Wyszowska et al., 2010). After a 25- and 50-day exposure of soil plots to Cu concentrations ranging from 150 mg to 450 mg kg<sup>-1</sup>, Wyszowska et al. (2010) observed an impact of Cu on various enzymes, from most Cu-sensitive to least Cu-sensitive: alkaline phosphatase, arylsulfatase, acid phosphatase and  $\beta$ -glucosidase. Here we observed a recovery at the end of the experiment for both denitrification and Pase activities (but not LAP and  $\beta$ -glu). This suggests that heterotrophic communities exposed to Cu adapted and became partially resilient despite a very limited decrease in Cu concentrations in the sediment. Rajapaksha et al. (2004)

studied thymidine incorporation rates in Cu-contaminated soils and also observed microbial community recovery within a few weeks. Functional resilience is often observed in microbial communities, but the degree to which resilience is possible depends on the functions measured (Allison and Martiny, 2008; Azarbad et al., 2016). Nevertheless, and according to the ARISA analysis, this functional recovery was not due to a structural recovery of the bacterial community. The lack of relationship between functional and structural recovery of heterotrophic microbial communities following a Cu exposure has already been observed by Lambert et al. (2012) in periphytic biofilms. Moreover, we observed a significant decrease in microbial respiration under Cu exposure at d21. This inhibition could reflect a functional cost of adaptation and resilience (Azarbad et al., 2016). It also underlines the importance of considering the temporal dynamics of the ecotoxicological effects that can occur under chronic exposure.

An originality of the approach employed here is that we also studied the effects of mixtures of Cu and As on sediment microbial communities. The structural and functional response of sediment microbial communities simultaneously exposed to Cu and As was almost similar to that observed under Cu exposure alone. Since As alone had very limited and sporadic effects on the studied parameters, we cannot firmly conclude on whether there are interaction effects between these two metals. Note, however, that whatever the functional parameter considered, it always tended to decrease at d21 in the MIX treatment compared to the



Cu treatment, suggesting a potential interaction at the end of the period studied (even if this trend was only statistically significant for denitrification, *nosZ I*, *nirK* and *nirS* gene abundances). Such a hypothesis could be supported by the results obtained from denitrification measurements which revealed a recovery at d21 under Cu exposure alone whereas effects lasted until the end of the study when As was combined with Cu. This may reveal an additive or a synergetic effect of these metals on this microbial function. To our knowledge, there is no published data addressing the interactive effects of Cu and As on sediment microbial communities.

In summary, sediment microbial communities were structurally and functionally impaired by the chronic exposure to environmental concentrations of Cu. Exposure to As had almost undetectable effects, but when the two metals were combined, certain functional responses showed an interaction between Cu and As toxicity toward heterotrophic communities. This experimental study also revealed temporal dynamics in functional response of sediment communities to chronic Cu exposure, alone or in mixture, with some functions being resilient (denitrification and Pase activity) and others being impacted throughout the experiment ( $\beta$ -glu and Pase activities) or only after several weeks of exposure (respiration). Further studies

are needed to better understand the adaptation mechanisms involved at different microbial levels (from genes to community) and to evaluate the resulting functional costs.

Given the ecological role of benthic microbial communities, our findings suggest that the sediment contamination by Cu (alone or combined with other metals) is likely to affect certain biochemical processes, thus potentially impairing aquatic ecosystem functioning. As recently emphasized by Pesce et al. (2018), this kind of experimental study confirms the need to improve the ecotoxicological assessment of sediments in freshwater environments by further considering the relationships between contaminant exposure and structural and functional effects at community level.

## AUTHOR CONTRIBUTIONS

EL, SP, and AD conceived and designed the study. AMA and CB performed the experiments and samplings. AMA, CB, EL, and AD analyzed the samples. AMA, EL, and SP drafted the manuscript and CB and AD critically revised the article. All co-authors analyzed and interpreted the data, and approved the final submitted version of the manuscript.

## FUNDING

AMA was funded by a Ph.D. grant from the Djibouti Government, and the research was funded by a grant from the University Savoie–Mont-Blanc (MITOX Project).

## ACKNOWLEDGMENTS

The authors thank Bernadette Volat, Christophe Rosy, Bernard Motte, and Anaïs Charton for their help on experimental setup

## REFERENCES

- Achour-Rokbani, A., Cordi, A., Poupin, P., Bauda, P., and Billard, P. (2010). Characterization of the *ars* gene cluster from extremely arsenic-resistant microbacterium sp. strain A33. *Appl. Environ. Microbiol.* 76, 948–955. doi: 10.1128/AEM.01738-09
- Adams, M. S., Dillon, C. T., Vogt, S., Lai, B., Stauber, J. L., and Jolley, D. F. (2016). Copper uptake, intracellular localization, and speciation in marine microalgae measured by synchrotron radiation X-ray fluorescence and absorption microspectroscopy. *Environ. Sci. Technol.* 50, 8827–8839. doi: 10.1021/acs.est.6b00861
- Allison, S. D., and Martiny, J. B. H. (2008). Resistance, resilience, and redundancy in microbial communities. *Proc. Natl. Acad. Sci. U.S.A.* 105, 11512–11519. doi: 10.1073/pnas.0801925105
- Azarbad, H., van Gestel, C. A. M., Niklinska, M., Laskowski, R., Röling, W. F. M., and van Straalen, N. M. (2016). Resilience of soil microbial communities to metals and additional stressors: DNA-based approaches for assessing “stress-on-stress” responses. *Int. J. Mol. Sci.* 17, 933–953. doi: 10.3390/ijms17060933
- Babich, H., and Stotzky, G. (1985). Heavy metal toxicity to microbe-mediated ecologic processes: a review and potential application to regulatory policies. *Environ. Res.* 36, 111–137. doi: 10.1016/0013-9351(85)90011-8
- Battin, T. J., Wille, A., Sattler, B., and Psenner, R. (2001). Phylogenetic and functional heterogeneity of sediment biofilms along environmental gradients in a glacial stream. *Appl. Environ. Microbiol.* 67, 799–807. doi: 10.1128/AEM.67.2.799-807.2001
- Bedard, D. L. (2008). A case study for microbial biodegradation: anaerobic bacterial reductive dechlorination of polychlorinated biphenyls-from sediment to defined medium. *Annu. Rev. Microbiol.* 62, 253–270. doi: 10.1146/annurev.micro.62.081307.162733
- Bereswill, R., Golla, B., Strelake, M., and Schulz, R. (2013). Entry and toxicity of organic pesticides and copper in vineyard streams: erosion rills jeopardise the efficiency of riparian buffer strips. *Agric. Ecosyst. Environ.* 172, 49–50. doi: 10.1016/j.agee.2013.05.007
- Billard, E., Domaizon, I., Tissot, N., Arnaud, F., and Lyautey, E. (2015). Multi-scale phylogenetic heterogeneity of archaea, bacteria, methanogens and methanotrophs in lake sediments. *Hydrobiologia* 751, 159–173. doi: 10.1007/s10750-015-2184-6
- Blanck, H., Wangberg, S. A., and Molander, S. (1988). “Pollution-induced community tolerance - a new ecotoxicological tool,” in *Functional Testing of Aquatic Biota for Estimating Hazards of Chemicals*, eds J. Cains Jr and J. R. Pratt (Philadelphia, PA: ASTM), 219–230. doi: 10.1520/STP26265S
- Bombardier, M. (2007). *Développement d'outils Écotoxicologiques Pour L'évaluation de Sédiments*. Ph.D. thesis, Université Paul Verlaine, Metz.
- Burga Pérez, K. F. B., Charlatchka, R., Sahli, L., and Féraud, J. F. (2012). New methodological improvements in the Microtox solid phase assay. *Chemosphere* 86, 105–110. doi: 10.1016/j.chemosphere.2011.08.042
- Capone, D. G., Reese, D. D., and Kiene, R. P. (1983). Effects of metals on methanogenesis, sulfate reduction, carbon dioxide evolution, and microbial biomass in anoxic salt marsh sediments. *Appl. Environ. Microbiol.* 45, 1586–1591.
- Chang, K. N., Lee, T. C., Tam, M. F., Chen, Y. C., Lee, L. W., and Lee, S. Y. (2003). Identification of galectin I and thioredoxin peroxidase II as two arsenic-binding proteins in Chinese hamster ovary cells. *Biochem. J.* 371, 495–503. doi: 10.1042/bj20021354

and microbial analysis. They also thank Irstea's Water Chemistry Laboratory in Lyon for nutrients and organic matter analysis.

## SUPPLEMENTARY MATERIAL

The Supplementary Material for this article can be found online at: <https://www.frontiersin.org/articles/10.3389/fmicb.2018.01852/full#supplementary-material>

- Clarke, K. R., and Warwick, R. M. (2001). A further biodiversity index applicable to species lists: variation in taxonomic distinctness. *Mar. Ecol. Prog. Ser.* 216, 265–278. doi: 10.3354/meps216265
- Conover, W. J., Johnson, M. E., and Johnson, M. M. (1981). A comparative study of tests for homogeneity of variances, with applications to the outer continental shelf bidding data. *Am. Stat.* 35, 351–361. doi: 10.1080/00401706.1981.10487680
- R Core Team (2018). *A Language and Environment for Statistical Computing*. Vienna: R Foundation for Statistical Computing.
- Dell'Amico, E., Mazzocchi, M., Cavalca, L., Allievi, L., and Andreoni, V. (2008). Assessment of bacterial community structure in a long-term copper-polluted ex-vineyard soil. *Microbiol. Res.* 163, 671–683. doi: 10.1016/j.micres.2006.09.003
- Drahota, P., Filippi, M., Ettl, V., Rohovec, J., Mihaljevic, M., and Sebek, O. (2012). Natural attenuation of arsenic in soils near a highly contaminated historical mine waste dump. *Sci. Total Environ.* 414, 546–555. doi: 10.1016/j.scitotenv.2011.11.003
- DREAL-REMIPP (2013). *Micropolluants Dans Les Sédiments de La région Rhône-Alpes. Données Cours D'eau et Plans d'eau 2006-2011*. Lyon: DREAL-REMIPP, 84.
- Faupel, M., Ristau, K., and Traunsperger, W. (2012). The functional response of freshwater benthic community to cadmium pollution. *Environ. Pollut.* 162, 104–109. doi: 10.1016/j.envpol.2011.11.004
- Fernandez-Calvino, D., Pateiro-Moure, M., Lopez-Periago, E., Arias-Estevéz, M., and Novoa-Mun, J. C. (2008). Copper distribution and acid-base mobilization in vineyard soils and sediments from Galicia. *Eur. J. Soil Sci.* 59, 315–326. doi: 10.1016/j.scitotenv.2011.10.033
- Flemming, C. A., and Trevors, J. T. (1988). Effect of copper on nitrous oxide reduction in freshwater sediment. *Water Air Soil Pollut.* 40, 391–397.
- Foulquier, A., Volat, B., Neyra, M., Bornette, G., and Montuelle, B. (2013). Long-term impact of hydrological regime on structure and functions of microbial communities in riverine wetland sediments. *FEMS Microbiol. Ecol.* 85, 211–226. doi: 10.1111/1574-6941.12112
- Fulladosa, E., Murat, J. C., Martínez, M., and Villaescusa, I. (2005). Patterns of metals and arsenic poisoning in *Vibrio fischeri* bacteria. *Chemosphere* 60, 43–48. doi: 10.1016/j.chemosphere.2004.12.026
- Furutani, A., Rudd, J. W., and Kelly, C. A. (1984). A method for measuring the response of sediment microbial communities to environmental perturbations. *Can. J. Microbiol.* 30, 1408–1414. doi: 10.1139/m84-224
- Gillan, D. C. (2004). The effect of an acute copper exposure on the diversity of a microbial community in North Sea sediments as revealed by DGGE analysis the importance of the protocol. *Mar. Pollut. Bull.* 49, 504–513. doi: 10.1016/j.marpolbul.2004.03.003
- Haglund, A. L., Lantz, P., Törnblom, E., and Tranvik, L. (2003). Depth distribution of active bacteria and bacterial activity in lake sediment. *FEMS Microbiol. Ecol.* 46, 31–38. doi: 10.1016/S0168-6496(03)00190-9
- Hammer, Ø., Harper, D. A. T., and Ryan, P. D. (2001). PAST: paleontological statistics software package for education and data analysis. *Palaeontol. Electron.* 4, 1–9. Available at: [https://palaeo-electronica.org/2001\\_1/past/past.pdf](https://palaeo-electronica.org/2001_1/past/past.pdf)
- Heiri, O., Lotter, A. F., and Lemcke, G. (2001). Loss on ignition as a method for estimating organic and carbonate content in sediments: reproducibility and comparability of results. *J. Paleolimnol.* 25, 101–110. doi: 10.1023/A:1008119611481

- Henry, S., Baudoin, E., López-Gutiérrez, J. C., Martin-Laurent, F., Brauman, A., and Philippot, L. (2004). Quantification of denitrifying bacteria in soils by nirK gene targeted real-time PCR. *J. Microbiol. Methods* 59, 327–335.
- Henry, S., Bru, D., Stres, B., Hallet, S., and Philippot, L. (2006). Quantitative detection of the nosZ gene, encoding nitrous oxide reductase, and comparison of the abundances of 16S rRNA, narG, nirK, and nosZ genes in soils. *Appl. Environ. Microbiol.* 72, 5181–5189. doi: 10.1128/AEM.00231-06
- Hettiarachchi, S. R., Maher, W. A., Krikowa, F., and Ubrihien, R. (2017). Factors influencing arsenic concentrations and species in mangrove surface sediments from south-east NSW, Australia. *Environ. Geochem. Health* 39, 209–219. doi: 10.1007/s10653-016-9821-5
- Hinojosa, M. B., Carreira, J. A., Garcia-Ruiz, R., and Dick, R. P. (2004). Soil moisture pre-treatment effects on enzyme activities as indicators of heavy metal-contaminated and reclaimed soils. *Soil Biol. Biochem.* 36, 1559–1568. doi: 10.1016/j.soilbio.2004.07.003
- INERIS (2010). *Qualité Chimique des Sédiments Fluviaux en France. Synthèse des bases de données disponibles*. Verneuil-en-Halatte: INERIS, 99.
- Jackson, C. R., Harrison, K. G., and Dugas, S. L. (2005). Enumeration and characterization of culturable arsenate resistant bacteria in a large estuary. *Syst. Appl. Microbiol.* 28, 727–734. doi: 10.1016/j.syapm.2005.05.012
- Jie, S., Li, M., Gan, M., Zhu, J., Yin, H., and Liu, X. (2016). Microbial functional genes enriched in the Xiangjiang river sediments with heavy metal contamination. *BMC Microbiol.* 16:179. doi: 10.1186/s12866-016-0800-x
- Jones, C. M., Graf, D. R., Bru, D., Philippot, L., and Hallin, S. (2013). The unaccounted yet abundant nitrous oxide-reducing microbial community: a potential nitrous oxide sink. *ISME J.* 7, 417–426. doi: 10.1038/ismej.2012.125
- Kandeler, E., Deiglmayr, K., Tscherko, D., Bru, D., and Philippot, L. (2006). Abundance of narG, nirS, nirK, and nosZ genes of denitrifying bacteria during primary successions of a glacier foreland. *Appl. Environ. Microbiol.* 72, 5957–5962. doi: 10.1128/AEM.00439-06
- Keon, N. E., Swartz, C. H., Brabander, D. J., Harvey, C., and Hemond, H. F. (2001). Validation of an arsenic sequential extraction method for evaluating mobility in sediments. *Environ. Sci. Technol.* 35, 2778–2784. doi: 10.1021/es001511o
- Knight, B., McGrath, S. P., and Chaudri, A. M. (1997). Biomass carbon measurements and substrate utilization patterns of microbial populations from soils amended with cadmium, copper or zinc. *Appl. Environ. Microbiol.* 63, 39–43.
- Ladomersky, E., and Petris, M. J. (2015). Copper tolerance and virulence in bacteria. *Metallomics* 7, 957–964. doi: 10.1039/c4mt00327f
- Lambert, A. S., Morin, S., Artigas, J., Volat, B., Coquery, M., Neyra, M., et al. (2012). Structural and functional recovery of microbial periphyton after a decrease in copper exposure: influence of the presence of pristine communities. *Aquat. Toxicol.* 109, 118–126. doi: 10.1016/j.aquatox.2011.12.006
- Leiva, E. D., Ramila, C., Vargas, I. T., Escauriaza, C. R., Bonilla, C. A., Pizarro, G. E., et al. (2014). Natural attenuation process via microbial oxidation of arsenic in a high andean watershed. *Sci. Total Environ.* 46, 490–502. doi: 10.1016/j.scitotenv.2013.07.009
- Lombi, E., Wenzel, W. W., and Sletten, R. S. (1999). Arsenic adsorption by soils and iron-oxide-coated sand: kinetics and reversibility. *J. Plant. Nutr. Soil. Sci.* 162, 451–456. doi: 10.1002/(SICI)1522-2624(199908)162:4<451::AID-JPLN451>3.0.CO;2-B
- López-Gutiérrez, J. C., Henry, S., Hallet, S., Martin-Laurent, F., Catroux, G., and Philippot, L. (2004). Quantification of a novel group of nitrate-reducing bacteria in the environment by real-time PCR. *J. Microbiol. Methods* 57, 399–407. doi: 10.1016/j.mimet.2004.02.009
- Lyautey, E., Cournot, A., Morin, S., Boulêtreau, S., Etcheverry, L., Charcosset, J. Y., et al. (2011). Electroactivity of phototrophic river biofilms and constitutive cultivable Bacteria. *Appl. Environ. Microbiol.* 77, 5394–5401. doi: 10.1128/AEM.00500-11
- Martiny, A. C., Vrugt, J. A., Primeau, F. W., and Lomas, M. W. (2013). Regional variation in the particulate organic carbon to nitrogen ratio in the surface ocean. *Global Biogeochem. Cycles* 27, 723–731. doi: 10.1002/gbc.20061
- Mondal, P., Majumder, C. B., and Mohanty, B. (2006). Laboratory based approaches for arsenic remediation from contaminated water: recent developments. *J. Hazard. Mater.* 137, 464–479. doi: 10.1016/j.jhazmat.2006.02.023
- Moran, A. C., Hengst, M. B., de la Iglesia, R., Andrade, S., Correa, J. A., and Gonzalez, B. (2008). Changes in bacterial community structure associated with coastal copper enrichment. *Environ. Toxicol. Chem.* 27, 2239–2245. doi: 10.1897/08-112.1
- Normand, P., Ponsonnet, C., Nesme, X., Neyra, M., and Simonet, P. (1996). “ITS analysis of prokaryotes,” in *Molecular Microbial Ecology Manual*, eds D. L. Akkermans, J. D. van Elsas, and F. J. de Bruijn (Dordrecht: Kluwer Academic Publishers), 1–12.
- Pesce, S., Perceval, O., Bonnineau, C., Casado-Martinez, C., Dabrin, A., Lyautey, E., et al. (2018). Looking at biological community level to improve ecotoxicological assessment of freshwater sediments: report on a first French-Swiss workshop. *Environ. Sci. Pollut. Res.* 25, 970–974. doi: 10.1007/s11356-017-0620-z
- Poirel, J., Joulain, C., Leyval, C., and Billard, P. (2013). Arsenite-induced changes in abundance and expression of arsenite transporter and arsenite oxidase genes of a soil microbial community. *Res. Microbiol.* 164, 457–465. doi: 10.1016/j.resmic.2013.01.012
- Rajapaksha, R. M. C. P., Tobor-Kaplon, M. A., and Bååth, E. (2004). Metal toxicity affects fungal and bacterial activities in soil differently. *Appl. Environ. Microbiol.* 70, 2966–2973. doi: 10.1128/AEM.70.5.2966-2973.2004
- Ratnaike, R. N. (2003). Acute and chronic arsenic toxicity. *Postgrad. Med. J.* 79, 391–396. doi: 10.1136/pmj.79.933.391
- Renella, G., Ortigoza, A. L. R., Landi, L., and Nannipieri, P. (2003). Additive effects of copper and zinc on cadmium toxicity on phosphatase activities and ATP content of soil as estimated by the ecological dose (ED50). *Soil Biol. Biochem.* 35, 1203–1210. doi: 10.1016/S0038-0717(03)00181-0
- Rigaud, S. (2011). *Dynamique Et Biodisponibilité Des Éléments Traces Métalliques Dans Les Sédiments De L'étang de Berre*. Ph.D. thesis, Université Paul Cézanne, Aix-Marseille.
- Roane, T. M., and Kellogg, S. T. (1996). Characterization of bacterial communities in heavy metal contaminated soils. *Can. J. Microbiol.* 42, 593–603. doi: 10.1139/m96-080
- Rosen, B. P. (1999). Families of arsenic transporters. *Trends Microbiol.* 7, 207–212. doi: 10.1016/S0966-842X(99)01494-8
- Royston, J. P. (1982). An extension of Shapiro and Wilk's W test for normality to large samples. *J. R. Stat. Soc. C Appl.* 31, 115–124. doi: 10.2307/2347973
- Schwarz, J. I. K., Eckert, W., and Conrad, R. (2007). Community structure of Archaea and Bacteria in a profundal lake sediment Lake Kinneret (Israel). *Syst. Appl. Microbiol.* 30, 239–254. doi: 10.1016/j.syapm.2006.05.004
- Serra, A., Corcoll, N., and Guasch, H. (2009). Copper accumulation and toxicity in fluvial periphyton: the influence of exposure history. *Chemosphere* 74, 633–641. doi: 10.1016/j.chemosphere.2008.10.036
- Silver, S., and Phung, T. (2005). Genes and enzymes involved in bacterial oxidation and reduction of inorganic arsenic. *Appl. Environ. Microbiol.* 71, 599–608. doi: 10.1128/AEM.71.2.599-608.2005
- Smedley, P. L., and Kinniburgh, D. G. (2002). A review of the source, behaviour and distribution of arsenic in natural waters. *Appl. Geochem.* 17, 517–568. doi: 10.1016/S0883-2927(02)00018-5
- Thirunavukkarasu, O. S., Viraraghavan, T., and Subramanian, K. S. (2003). Arsenic removal from drinking water using iron oxide-coated sand. *Water Air Soil Pollut.* 142, 95–111. doi: 10.1023/A:1022073721853
- Throbäck, I. N., Enwall, K., Jarvis, A., and Hallin, S. (2004). Reassessing PCR primers targeting nirS, nirK and nosZ genes for community surveys of denitrifying bacteria with DGGE. *FEMS Microbiol. Ecol.* 49, 401–417. doi: 10.1016/j.femsec.2004.04.011
- Tisa, L. S., and Rosen, B. P. (1990). Molecular characterization of an anion pump. The ArsB protein is the membrane anchor for the ArsA protein. *J. Biol. Chem.* 265, 190–194.
- Tili, A., Bérard, A., Roulier, J. L., Volat, B., and Montuelle, B. (2010). PO43- dependence of the tolerance of autotrophic and heterotrophic biofilm communities to copper and diuron. *Aquat. Toxicol.* 98, 165–177. doi: 10.1016/j.aquatox.2010.02.008
- Tili, A., Maréchal, M., Bérard, A., Volat, B., and Montuelle, B. (2011). Enhanced cotolerance and co-sensitivity from long-term metal exposures of heterotrophic and autotrophic components of fluvial biofilms. *Sci. Total Environ.* 409, 4335–4343. doi: 10.1016/j.scitotenv.2011.07.026

- Turpeinen, R., Kairesalo, T., and Haggblom, M. H. (2004). Microbial community structure and activity in arsenic-, chromium- and copper- contaminated soils. *FEMS Microbiol. Ecol.* 47, 39–50. doi: 10.1016/S0168-6496(03)00232-0
- Tuulaikhuu, B. A., Romani, A. M., and Guasch, H. (2015). Arsenic toxicity effects on microbial communities and nutrient cycling in indoor experimental channels mimicking a fluvial system. *Aquat. Toxicol.* 166, 72–82. doi: 10.1016/j.aquatox.2015.07.005
- Wang, S. L., and Mulligan, C. N. (2006). Natural attenuation processes for remediation of arsenic contaminated soils and groundwater. *J. Hazard. Mater.* 138, 459–470. doi: 10.1016/j.jhazmat.2006.09.048
- Wang, Y., Shi, J., Wang, H., Lin, Q., Chen, X., and Chen, Y. (2007). The influence of soil heavy metals pollution on soil microbial biomass, enzyme activity, and community composition near a copper smelter. *Ecotox. Environ. Safe.* 67, 75–81. doi: 10.1016/j.ecoenv.2006.03.007
- Wyszkowska, J., Kucharski, M., and Kucharski, J. (2010). Activity of beta-glucosidase, arylsulfatase and phosphatases in soil contaminated with copper. *J. Elem.* 15, 213–226.
- Zambrano, R. J. F. (2012). *Développement d'un Procédé D'élimination de L'arsenic En milieu Aqueux, Associant Electrocatalyse Et Filtration*. Ph.D. thesis, Université de Grenoble, Grenoble.
- Zhao, Y. G., Feng, G., Bai, J., Chen, M., and Maqbool, F. (2014). Effect of copper exposure on bacterial community structure and function in the sediments of Jiaozhou Bay, China. *World J. Microbiol. Biotechnol.* 30, 2033–2043. doi: 10.1007/s11274-014-1628-x

**Conflict of Interest Statement:** The authors declare that the research was conducted in the absence of any commercial or financial relationships that could be construed as a potential conflict of interest.

Copyright © 2018 Mahamoud Ahmed, Lyautey, Bonnineau, Dabrin and Pesce. This is an open-access article distributed under the terms of the Creative Commons Attribution License (CC BY). The use, distribution or reproduction in other forums is permitted, provided the original author(s) and the copyright owner(s) are credited and that the original publication in this journal is cited, in accordance with accepted academic practice. No use, distribution or reproduction is permitted which does not comply with these terms.



# Toward Integrative Bacterial Monitoring of Metolachlor Toxicity in Groundwater

Gwenaël Imfeld<sup>1\*</sup>, Ludovic Besaury<sup>2†</sup>, Bruno Maucourt<sup>2</sup>, Stéphanie Donadello<sup>2†</sup>, Nicole Baran<sup>3</sup> and Stéphane Vuilleumier<sup>2</sup>

## OPEN ACCESS

### Edited by:

Fabrice Martin-Laurent,  
Institut National de la Recherche  
Agronomique (INRA), France

### Reviewed by:

Xianhua Liu,  
Tianjin University, China  
Catarina R. Marques,  
University of Aveiro, Portugal

### \*Correspondence:

Gwenaël Imfeld  
imfeld@unistra.fr

### † Present address:

Ludovic Besaury,  
UMR FARE 614 Fractionnement des  
AgroRessources et Environnement,  
Chaire AFERE, INRA, Université de  
Reims Champagne-Ardenne, Reims,  
France  
Stéphanie Donadello,  
Soleo Services, Agence Sud Ouest,  
Lescar, France

### Specialty section:

This article was submitted to  
Microbiotechnology, Ecotoxicology  
and Bioremediation,  
a section of the journal  
Frontiers in Microbiology

**Received:** 14 February 2018

**Accepted:** 13 August 2018

**Published:** 16 October 2018

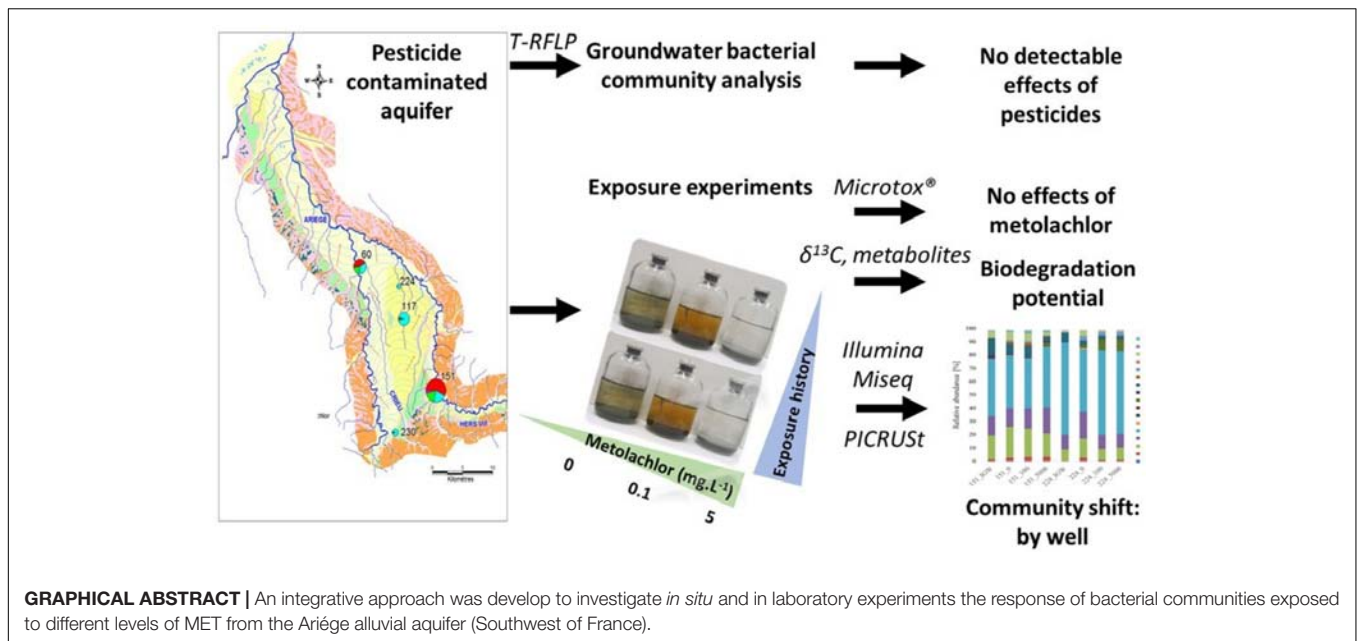
### Citation:

Imfeld G, Besaury L, Maucourt B,  
Donadello S, Baran N and  
Vuilleumier S (2018) Toward  
Integrative Bacterial Monitoring  
of Metolachlor Toxicity  
in Groundwater.  
Front. Microbiol. 9:2053.  
doi: 10.3389/fmicb.2018.02053

<sup>1</sup> Laboratory of Hydrology and Geochemistry, EOST-CNRS, LHyGeS UMR 7517, Université de Strasbourg, Strasbourg, France, <sup>2</sup> Génétique Moléculaire, Génomique, Microbiologie, GMGM UMR 7156, CNRS, Université de Strasbourg, Strasbourg, France, <sup>3</sup> Bureau de Recherches Géologiques et Minières (BRGM), Orléans, France

Common herbicides such as metolachlor (MET), and their transformation products, are frequently detected in groundwater worldwide. Little is known about the response of groundwater bacterial communities to herbicide exposure, and its potential use for ecotoxicological assessment. The response of bacterial communities exposed to different levels of MET from the Ariège alluvial aquifer (Southwest of France) was investigated *in situ* and in laboratory experiments. Variations in both chemistry and bacterial communities were observed in groundwater, but T-RFLP analysis did not allow to uncover a pesticide-specific effect on endogenous bacterial communities. To circumvent issues of hydrogeochemical and seasonal variations *in situ*, groundwater samples from two monitoring wells of the Ariège aquifer with contrasting records of pesticide contamination were exposed to different levels of MET in laboratory experiments. The standard Microtox<sup>®</sup> acute toxicity assay did not indicate toxic effects of MET, even at 5 mg L<sup>-1</sup> (i.e., 1000-fold higher than in contaminated groundwater). Analysis of MET transformation products and compound-specific isotope analysis (CSIA) in laboratory experiments demonstrated MET biodegradation but did not correlate with MET exposure. High-throughput sequencing analysis (Illumina MiSeq) of bacterial communities based on amplicons of the 16S rRNA gene revealed that bacterial community differed mainly by groundwater origin rather than by its response to MET exposure. OTUs correlating with MET addition ranged between 0.4 to 3.6% of the total. Predictive analysis of bacterial functions impacted by pesticides using PICRUST suggested only minor changes in bacterial functions with increasing MET exposure. Taken together, results highlight MET biodegradation in groundwater, and the potential use of bacterial communities as sensitive indicators of herbicide contamination in aquifers. Although detected effects of MET on groundwater bacterial communities were modest, this study illustrates the potential of integrating DNA- and isotopic analysis-based approaches to improve ecotoxicological assessment of pesticide-contaminated aquifers.

**Keywords:** groundwater contamination, microbial ecotoxicology, chloroacetanilides, biodegradation, bacterial communities, compound-specific isotope analysis



## INTRODUCTION

Ongoing intensive use of pesticides leads to accumulation of pesticide mixtures and their transformation products (TP) in groundwater ecosystems (Postigo and Barcelo, 2015). While pressure on groundwater resources is on the increase, the extent of ecosystem disturbance following exposure to pesticides remains difficult to evaluate precisely. In this context, sensitive monitoring approaches hold potential to address key ecological questions, such as the response of groundwater ecosystems to punctual and chronic pesticide exposure, in terms of both taxonomic and functional alterations (Imfeld and Vuilleumier, 2012). The microbial compartment, in particular, may be accessed for this purpose and today, with unprecedented sensitivity through high-throughput sequencing.

The response of microbial communities to pesticide exposure has often been addressed for the soil compartment (Imfeld and Vuilleumier, 2012; Jacobsen and Hjelmso, 2014; Ju et al., 2017). For groundwater systems, in contrast, focus has been mainly limited to evaluation of pesticide dissipation (Tuxen et al., 2002; de Liphay et al., 2003; Liebich et al., 2009; Caracciolo et al., 2010), with only a few studies so far addressing alterations of bacterial communities following exposure, and often conflicting observations. For instance, profiles of carbon substrate usage were altered by elevated levels of nitrate (>15 mg L<sup>-1</sup>) and herbicides (>0.03 μg L<sup>-1</sup>) in an oxic aquifer (Janniche et al., 2012), while in contrast, alterations of groundwater bacterial community following herbicide exposure (<50 μg L<sup>-1</sup>) were not detected (de Liphay et al., 2004). More recently, SSCP fingerprinting and monitoring of functional genes for triazine degradation and nitrate usage suggested that bacterial composition was affected by the now banned triazines in historically contaminated groundwater (Mauffret

et al., 2017), but not by currently used chloroacetanilide herbicides.

Chloroacetanilide pesticides are used for control of annual weeds, mainly on corn, sugar beet and sunflower, and belong to the top 10 pesticide classes in current use worldwide (Food and Agriculture Organization of the United Nations (FAO), 2013). They are frequently detected in groundwater together with their transformation products (TP), notably ethane sulfonic and oxanilic acids (Kalkhoff et al., 2012; Baran and Gourcy, 2013; Sidoli et al., 2016). Metolachlor (MET) is a chloroacetanilide herbicide in massive use worldwide, and one of the top-five of pesticides detected in France (Lopez et al., 2015) and in the EU (Loos et al., 2010). MET was brought to the market in 1976 as a racemic compound (*rac*-metolachlor). It was subsequently replaced in the 2000s by *S*-MET, which is enriched (approximately 86%) in the herbicidally more active 1'*S*-enantiomer (Ma et al., 2006; Xu et al., 2010). Although biodegradation of MET has been reported (Singh and Singh, 2016), enzymes and pathways for microbial transformation of MET are still unknown, thus preventing specific monitoring of microbial MET degradation.

In this context, the purpose of this study was to evaluate the response of groundwater bacterial community to exposure to MET and its transformation products, as well as MET degradation potential. Issues of field hydrogeochemical heterogeneity in the response of bacterial community in the Ariège alluvial plain (Southwest France) were circumvented by laboratory microcosm experiments of MET exposure. Groundwater samples from two monitoring wells with contrasting records of pesticide contamination were exposed to different levels of MET *in labo*. MET biodegradation was evaluated based on dissipation and patterns of transformation products, as well as on change of carbon isotope composition using compound-specific isotope analysis (CSIA), and the

bacterial community response was evaluated by 16S rRNA amplicon sequencing.

## MATERIALS AND METHODS

### Chemicals

Racemic metolachlor ( $C_{15}H_{22}ClNO_2$ , (S)-2-Chloro-N-(2-ethyl-6-methyl-phenyl)-N-(1-methoxypropan-2-yl)acetamide) was purchased from Sigma-Aldrich (>99% purity). Stock solutions for spiking were prepared at  $1\text{ g L}^{-1}$  in acetonitrile (ACN).

### Groundwater Site

The study area ( $538\text{ km}^2$ ) covers the alluvial domain of the Ariège river (**Figure 1**). The alluvial plain lies above Aquitanian (Miocene) and Stampian (Oligocene) molasse deposits. Alluvium transported by the Ariège deposited as silt on the molasse, in five terrace levels with similar physicochemical composition. Terrace levels differ in their degree of pebble weathering and pedological evolution. The sand-and-gravel alluvium of the lower terrace and the lower plain defined a continuous unconfined aquifer feeding rivers Ariège and Hers-Vif. The thickness of the unsaturated zone varies between a few meters and up to 10 m locally. The study area features mostly cultivated farmland, including corn.

### Groundwater Collection

Groundwater sampling was conducted in May, July, September and December 2012, and February and May 2013. The five sampled monitoring wells 151, 60, 117, 230, 224 (**Figure 1**) define a decreasing concentration gradient of MET and its transformation products (TP), and present contrasted hydrochemical composition (**Supplementary Section C**). Samples were collected after pumping and discarding three purge volumes, to ensure pH and electrical conductivity stabilization. Temperature, pH, electrical conductivity (EC, standardized to  $25^\circ\text{C}$ ), redox potential (Eh) and dissolved oxygen ( $O_2$ ) were measured on-site using a WTW multi 340i meter equipped with a Satrix 81 WTW pH electrode and a Tetra Con 325 WTW EC electrode (Weilheim, Germany). For analyses of anions and major cations, samples were separately collected in 100 mL PE bottles after filtration through a  $0.45\text{ }\mu\text{m}$  PVDF filter. Samples for major cations analyses were acidified to pH 2 with ultrapure  $HNO_3$ . For MET and TP analysis, groundwater (1 L) was collected in a glass bottle. All samples were placed on ice for transportation to the laboratory and stored at  $4^\circ\text{C}$  until chemical analysis.

### Laboratory Exposure Experiments

Groundwater samples (10 L) from monitoring wells 151 and 224 with contrasting records of contamination (**Supplementary Section D**) were collected in February 2014. Well 151 has a history of chronic exposure to MET ( $5.1 \pm 4.0\text{ }\mu\text{g L}^{-1}$ , mean  $\pm \sigma$ ,  $n = 6$  May 2012 – May 2013). In contrast, MET had not been detected in well 224 (**Supplementary Section D**). Hydrochemical and bacterial composition of initial groundwater

used for preparing the exposure experiments was analyzed for comparison with spiked and incubated groundwater.

To compare the response of bacterial communities exposed to MET, groundwater subsamples (experimental repetitions) originating from initial 10 L groundwater samples collected in each well, were incubated *in labo* in 1 L glass vials. Each vial contained 700 mL of groundwater. Three exposition doses were compared for each of the two selected wells: background MET concentrations (no MET addition), and added MET at either  $0.1\text{ mg L}^{-1}$  (equivalent to severe chronic contamination) or  $5\text{ mg L}^{-1}$  (equivalent to punctual source contamination). An experimental repetition (i.e., two vials) was prepared from each of the two selected wells and for each of the three exposition doses.

The MET standard stock solution ( $1\text{ g L}^{-1}$  in can) was dissolved in distilled water, and ACN was evaporated after 6 h stirring under a fume hood. MET aqueous solutions were filter-sterilized through a  $0.2\text{ }\mu\text{m}$  syringe filter (Rotilabo®, Carl Roth®, France) before spiking. To ensure initial homogenisation following spiking with MET, laboratory microcosms were shaken at 100 rpm for 1 h before incubation at the same temperature of  $20^\circ\text{C}$ . In experiments without MET addition, the same procedure was followed using pure ACN evaporated in distilled water to account for possible effects of ACN traces. ACN was never detected in the headspace of MET aqueous solutions (data not shown). Control experiments (performed in duplicate) consisted in filter-sterilized water spiked with MET to evaluate abiotic MET dissipation. To maintain aerobic conditions while limiting water loss and avoiding contamination, a  $0.22\text{ }\mu\text{m}$  syringe filter was mounted on a syringe tip stuck through the vial cap.

Oxygen concentration in each microcosm was monitored weekly with oxygen sensor spots (PreSens Precision Sensing GmbH, Germany) fixed to the inner face of the bottles before autoclaving. Oxygen concentrations from 5 to  $8\text{ mg L}^{-1}$  confirmed oxic conditions throughout the experiment (**Supplementary Section C**). Laboratory experiments with or without addition of MET were incubated for 21 days, a duration typical of reported MET half-life values (The Pesticide Properties DataBase [PPDB], 2006). Mean groundwater temperature was  $15 \pm 1.3^\circ\text{C}$ . Experiments were incubated at the reference temperature for standardized testing of pesticides based on OECD guidelines of  $20^\circ\text{C}$  (Organisation for Economic Co-operation and Development [OECD], 1981). Experiments were incubated without stirring because (i) oxygen was continuously monitored and was not rate-limiting for bacterial growth (Hensler and Schedel, 1991), and (ii) stirring may artefactually alter the diversity of groundwater bacterial communities adapted to heterogeneous aquifer microenvironments and non-turbulent flows.

At the end of incubations, water samples from each duplicate experiment were collected using sterile glass syringes for MET, TP analysis ( $2 \times 15\text{ mL}$ ) and the Microtox® assay ( $2 \times 15\text{ mL}$ ) (see below). Remaining groundwater of each repetition experiment ( $2 \times 670\text{ mL}$ ) was filtered through a unique sterile  $0.2\text{ }\mu\text{m}$  cellulose membrane (Millipore, Billerica, MA, United States) to obtain DNA in sufficient and representative quantities for Illumina

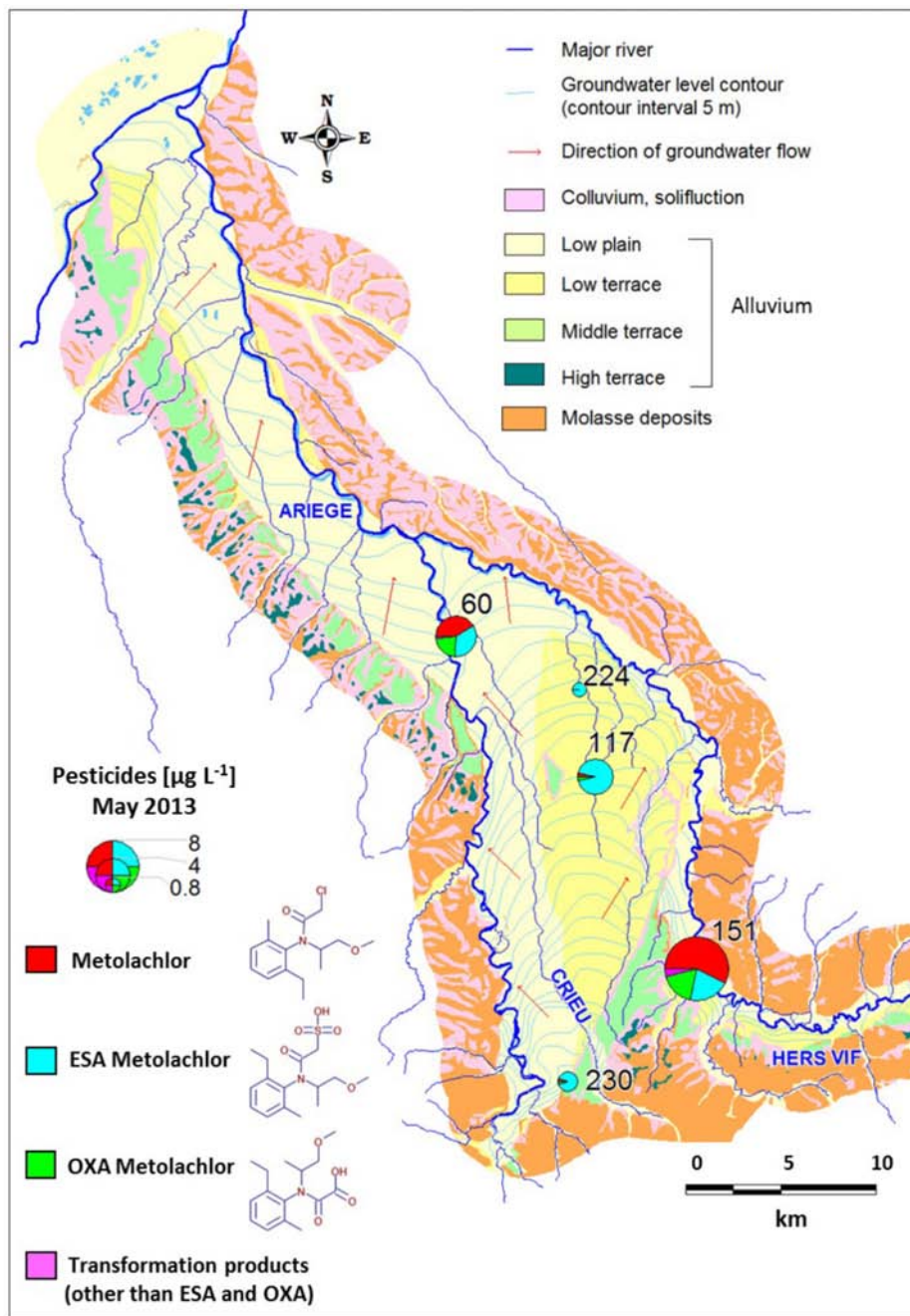


**FIGURE 1** | Site map, location of the wells and metolachlor concentrations in the Ariège alluvial plain (May 2013).

sequencing (Aird et al., 2011). Each membrane was stored at  $-20^{\circ}\text{C}$  in sterile 50 mL plastic Falcon tubes until further processing.

## Chemical Analysis

### Hydrogeochemical Analysis

Groundwater samples were analyzed at BRGM Orleans using ICP-AES ( $\text{Ca}^{2+}$ ,  $\text{Na}^{+}$ ,  $\text{K}^{+}$ ,  $\text{Mg}^{2+}$  with 5% uncertainty), ion chromatography ( $\text{Cl}^{-}$ ,  $\text{SO}_4^{2-}$ ,  $\text{NO}_3^{-}$  with 10% uncertainty) and

potentiometric methods according to N EN ISO 9963-1 ( $\text{HCO}_3^{-}$ ,  $\text{CO}_3^{2-}$  with 5% uncertainty). Total organic carbon (TOC) and dissolved organic carbon (DOC) were quantified according to NF EN 1484 (1997) procedures.

### Pesticide and TP Analysis of Field Samples

Pesticides in groundwater, including MET and its neutral TP, were extracted using a Gilson GX 274 ASPEC solid phase extraction (SPE) system, with Oasis HLB (6 mL - 500 mg)

cartridges (Waters) and quantified as described elsewhere (Amalric et al., 2013). Briefly, cartridges were successively conditioned at pH 7 with 5 mL acetonitrile (ACN), 5 mL methanol (MeOH), and 5 mL deionized water (HPLC grade) at a flow rate of 1 mL min<sup>-1</sup>. Water samples (1 L) were loaded at a flow rate of 5 mL min<sup>-1</sup>. After drying by flushing with pure N<sub>2</sub> (30 min), analytes were eluted twice successively with 4 mL ACN at a rate of 1 mL min<sup>-1</sup>. Sample extracts were concentrated down to 1 mL under a gentle stream of nitrogen at ambient temperature. For extraction of ionic compounds, cartridges were conditioned at a flow rate of 1 mL min<sup>-1</sup> with MeOH (5 mL), followed by ACN (5 mL) with 0.2% v/v acetic acid. The water sample (1 L; pH 6–8), was loaded at a flow rate of 5 mL min<sup>-1</sup>. After 30 min of drying, analytes were eluted twice successively with MeOH (4 mL) at 1 mL min<sup>-1</sup>, and eluates concentrated to 1 mL as described above.

Quantification of pesticides and TP was carried out by a Waters Ultra Performance Liquid Chromatography (UPLC) system coupled to a Waters micromass MSMS (Waters Quattro-Premier XE/Q). Chromatographic separation for neutral and ionic compounds was achieved with a Waters Acquity UPLC BEH C18 column (2.1 mm × 150 mm, particle size 1.7 μm). The mobile phase consisted of a gradient of (A) water/0.05% formic acid and (B) acetonitrile/0.05% formic acid for neutral molecules, and (A) water/0.007% formic acid and (B) methanol/0.007% formic acid for ionic molecules, established at a flow rate of 0.4 mL min<sup>-1</sup>. Limits of quantification were 5 ng L<sup>-1</sup> for MET, 10 ng L<sup>-1</sup> for MESA and MOXA, and between 5 and 20 ng L<sup>-1</sup> for neutral TP.

### Carbon Stable Isotope Analysis of MET

The carbon isotope composition of MET in the laboratory exposure experiment was analyzed by adapting a previously described protocol (Elsayed et al., 2014) (see **Supplementary Section A** for the detailed protocol). Briefly, the GC-C-IRMS system consisted of a TRACE<sup>TM</sup> Ultra Gas Chromatograph (Thermo Fisher Scientific) coupled to an isotope ratio mass spectrometer (DeltaV Plus, Thermo Fisher Scientific) via a GC IsoLink/Conflow IV interface. Reproducibility of triplicate measurements was ≤0.2‰ (1 σ). Carbon isotope ratios were reported in δ notation in parts per thousand [‰], relative to the international carbon isotope standard Vienna Pee Dee Belemnite (V-PDB).

### Enumeration of Viable Cells and Microtox<sup>®</sup> Assay

Enumeration of total viable bacteria was carried out by plating out on R2A agar (typically used for drinking water) after incubation at 20°C for 48 h. Toxicity of MET in laboratory exposure experiments was assessed by the standard Microtox<sup>®</sup> test (HACH Lange, Düsseldorf, Germany) following a standard protocol (Jennings et al., 2001). All materials for analysis (test strain and reagents) were supplied in the commercial kit, and luminescence was measured in Nunc 96-well white polystyrene microtiter plates (Thermo

Scientific) using a Luminoskan Ascent luminometer (Thermo Scientific).

## Biomolecular Analyses

### DNA Extraction

Total DNA was extracted from filters with the PowerWater<sup>®</sup> DNA Isolation Kit (MO BIO, Carlsbad, CA, United States) following manufacturer's instructions. Concentrations of DNA were determined using the Quant-it PicoGreen dsDNA Assay Kit (Invitrogen, Carlsbad, CA, United States).

### T-RFLP Analysis of Groundwater Samples

Bacterial 16S rRNA gene fragments (0.9 kb) were PCR-amplified using 5-carboxyfluorescein (6-FAM) labeled 27 f and 927 r primers as described previously (Mauffrey et al., 2017). T-RFLP electrophoregrams were analyzed with PeakScanner V1.0 (Applied Biosystems, Carlsbad, CA, United States). Noise cancelation, peak alignment and matrix (samples × T-RFs) generation was performed using T-REX<sup>1</sup> (Culman et al., 2009). Peak heights were normalized to the same total fluorescence per sample, and resulting data matrices were used for statistical analysis.

### Illumina MiSeq Sequencing and Data Processing

Sequencing of laboratory exposure experiment samples was performed at INRA-UR0050-LBE (Narbonne, France) using Illumina MiSeq. The 16S rRNA gene spanning hypervariable region V4 and V5 was amplified in a two-step process including a set of multiplex indexed primers (U515F 5'-GTGYCAGCMGCCGCGTA-3' and U909R 5'-CCCCGYCAATTCMTTTRAGT-3') (Walters et al., 2011). Individual PCR products were purified and quantified using Qubit dsDNA HS Assay Kit<sup>®</sup> (Invitrogen, France), and a pool of equimolar amounts of each amplicon was prepared. A final gel purification step ensured elimination of non-specific products. The combined library was loaded onto the Illumina MiSeq Platform using a standard MiSeq paired end (2 × 250 bp) flow cell and reagent cartridge. Denoising, chimera checking, generation of operating taxonomic units (OTUs) and taxonomic classification were performed using Mothur software package v.1.33.2 (Schloss et al., 2009) by following the default parameters from the analysis pipeline of MiSeq SOP<sup>2</sup>. The detailed protocol is provided in **Supplementary Section B**. Obtained sequences were deposited in the NCBI BioProject database (BioProject ID: PRJNA393085).

Obtained sequences analyzed using Mothur were clustered to define OTUs at 98% sequence identity. A subsample of sequences was randomly selected to obtain equally sized datasets according to the standard operating procedure (Schloss et al., 2009). The resulting datasets were used to calculate Shannon and inverse Simpson diversity indices and the Chao1 richness estimate using R, and for rarefaction analysis as previously described (Babcsányi et al., 2017).

<sup>1</sup><http://trex.biohpc.org>

<sup>2</sup>[http://www.mothur.org/wiki/MiSeq\\_SOP](http://www.mothur.org/wiki/MiSeq_SOP)

## Data Analysis

### PICRUSt Analysis

Functional profiling of bacterial communities was predicted by Phylogenetic Investigation of Communities by Reconstruction of Unobserved States (PICRUSt) (Langille et al., 2013) by classifying bacterial sequences against the Greengenes database (McDonald et al., 2012); 13 August 2013 version. OTUs were defined based on automatic 98% sequence identity. The biom file generated within Mothur command-line was uploaded into Galaxy<sup>3</sup> for pre-processing, the output file was analyzed using STAMP (Parks et al., 2014), and retrieved metagenomic profiles were further analyzed using multivariate statistical analysis.

### Statistical Analysis

Multivariate analyses were carried out within R Development (R Core Team, 2017). To visualize dissimilarities in groundwater bacterial community structures obtained from T-RFLP analysis, non-metric multidimensional scaling (NMDS) based on Bray-Curtis dissimilarities of Hellinger-transformed data was performed. The relationship between the 27 groundwater community profiles and the 30 physicochemical variables (12 physicochemical variables and 18 pesticides and their TP; see **Supplementary Sections C,D**) was investigated by fitting environmental vectors *a posteriori* onto the NMDS, and their significance was assessed with a Monte-Carlo permutation test (1000 permutation steps). Analysis of similarities (ANOSIM) based on Bray-Curtis dissimilarities were used to infer statistical differences between groups of community profiles.

Illumina MiSeq sequencing data and PICRUSt profiles were classified separately by cluster analysis to investigate the relationship between bacterial communities exposed to different levels of MET. Hierarchical cluster analysis was carried out to identify robust groupings of sequence data and PICRUSt profiles based on the distances supplied in a hierarchical manner. For both analyses, distance between Hellinger-transformed datasets was computed based on the Hellinger distance. A hierarchical cluster analysis was performed on the resulting dissimilarity matrix using Ward's method (Ward, 1963). The optimal number of clusters was determined using Spearman's rank correlations (Becker et al., 1988).

## RESULTS AND DISCUSSION

### Groundwater Bacterial Communities and Effect of Environmental Variables

T-RFLP fingerprints of PCR-amplified 16S rRNA gene fragments were used to follow dominant community members and compare their variation in samples collected from different origins and time points from the Ariège aquifer. Compared to DGGE, TGGE or SSCP, T-RFLP was used for its resolving power and because T-RFs can be used for cross-referencing with other studies (Hewson and Fuhrman, 2006). Strong spatial and temporal variations in bacterial communities were revealed by ordination of T-RFLP profiles (**Figure 2**). *A posteriori* fitting of

physicochemical and pesticide variables revealed that changes in bacterial community composition correlated significantly only with redox potential ( $p < 0.05$ ).

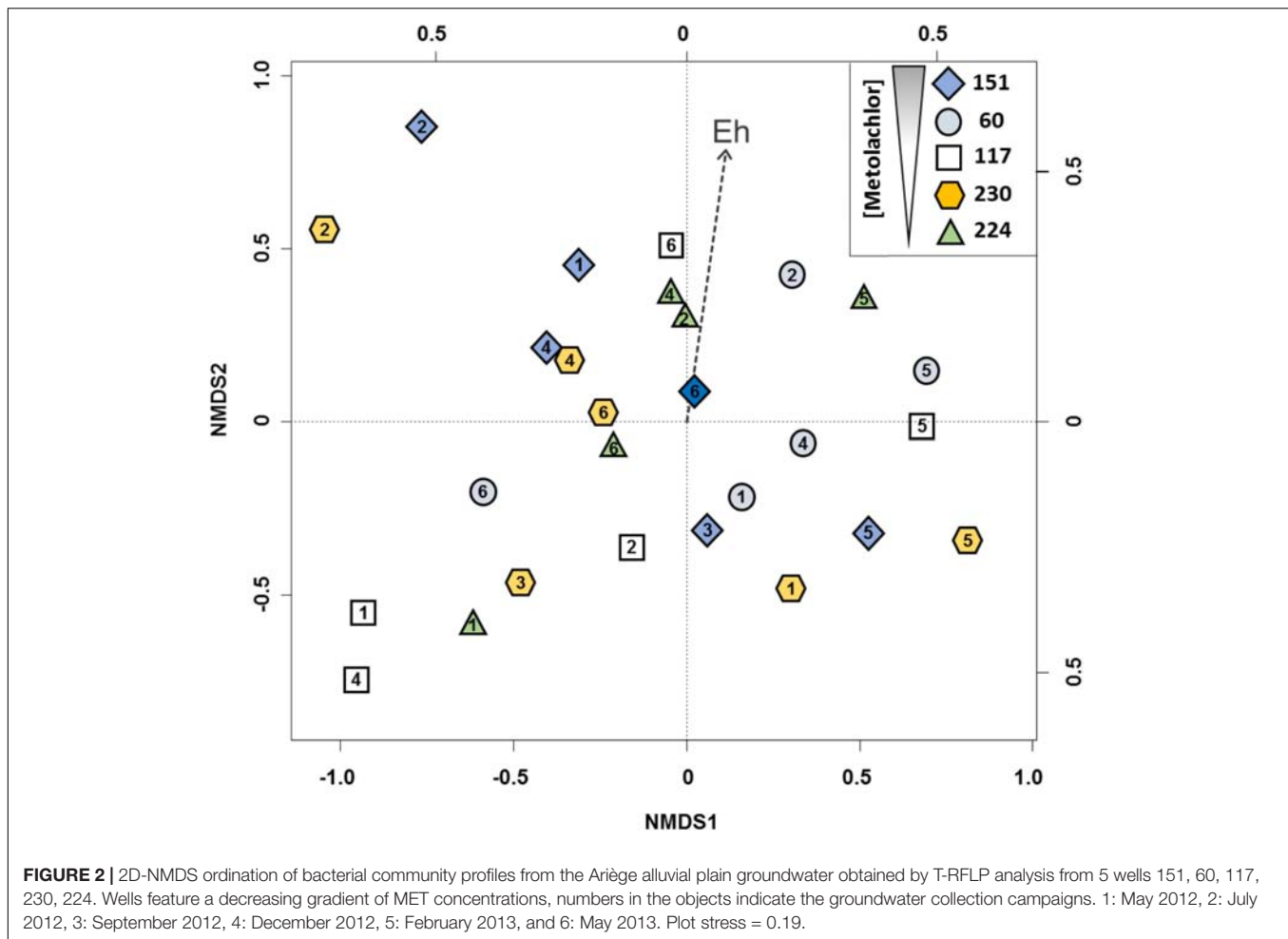
These results are consistent with previous data from a related study of the Ariège aquifer that suggested that bacterial communities were influenced by hydrogeological conditions and triazines (Mauffret et al., 2017). In this study, however, correlation with pesticide levels was not apparent. Indeed, changes in overall bacterial composition following disturbance by chronic and low exposure in multi-contaminated groundwater are unlikely to be easily detected due to often large and uncontrollable effects of changes in physico-chemical conditions *in situ*, unlike the effect of acute and punctual contamination by industrial solvents for example (Imfeld et al., 2008; Rossi et al., 2012). We focused on the currently used and often detected MET herbicide rather than on banned historical contaminants such as triazines, which continue to persist in groundwater. To test whether MET and its metabolites affected specifically bacterial assemblages, the 27 samples were clustered for comparison into two homogenous subgroups of lower ( $< 1.4 \mu\text{g L}^{-1}$ ,  $n = 13$ ) and higher ( $> 1.4 \mu\text{g L}^{-1}$ ,  $n = 14$ ) concentrations of both MET and transformation products (TP). The two clusters of bacterial assemblages did not differ ( $p < 0.01$ ; effect size Hedges'  $g < 0.10$ ), suggesting little effect of MET and its TP on groundwater communities. This also supports the notion that the response of bacterial groundwater communities to MET *in situ* cannot easily be teased apart from the effects of variations of hydrogeological conditions using T-RFLP. Worthy of note, T-RFLP of 16S rRNA genes, as other fingerprinting techniques, may suffer not only from a dependence of the data obtained on the protocol used for extraction of nucleic acids from groundwater samples, which may limit reproducibility between groundwater wells, but also from the high differential required to reliably detect a dose-dependent response at environmentally relevant concentrations. Thus, an *in labo* microcosm approach under controlled conditions was subsequently used in order to characterize MET degradation potential and composition of bacterial communities from contaminated groundwater as a function of MET exposure.

### Effect of MET Exposure on Bacterial MET Degradation

Variations in physicochemical conditions and heterogeneity of aquifer structure may not only affect the composition of bacterial communities, but also its metabolic activity (Imfeld et al., 2011; Rossi et al., 2012). We thus evaluated whether different levels of MET exposure affected pesticide degradation as the key function of interest in the contaminated aquifer, and whether the bacterial response correlated with historical records of groundwater contamination.

The extent of MET dissipation in exposure experiments with groundwater from wells 151 (chronic exposure to MET) and 224 (historical records of very low MET detection) ranged from 20 to 51% after 21 days (**Table 1**). No MET dissipation was observed in the abiotic control (data not shown). Change in carbon isotope composition after 50% MET dissipation during

<sup>3</sup><http://huttenhower.sph.harvard.edu/galaxy/>



this experiment (**Table 1**) highlight MET biodegradation, and are consistent with previous studies (Elsayed et al., 2014; Elsner and Imfeld, 2016). Specifically, MET was slightly enriched in  $^{13}\text{C}$  ( $>1\%$ ) in the  $5\text{ mg L}^{-1}$  experiments compared to initially spiked MET. Historical MET exposure also correlated with a more limited extent of MET dissipation in groundwater from well 151 exposed to  $0.1\text{ mg L}^{-1}$  MET. Since hydrochemical conditions were the same in the different microcosms, it is likely that they do not affect degradation (**Table 1** and **Supplementary Section E**). Extent of MET degradation did not change significantly across experiments, including at high MET concentrations. This suggests a lack of community sensitivity to MET exposure levels, or alternatively, fast recovery or adaptation of groundwater functions to degrade MET at high MET exposure levels. This phenomenon was observed previously for different pesticides in soil (Jacobsen and Hjelmsø, 2014).

### Effect of Groundwater on Production of MET Transformation Products

The spectrum of known polar MET transformation products (TP) was analyzed to evaluate production and dissipation of MET TP (Amalric et al., 2013; Sidoli et al., 2016) in laboratory

experiments. Both MET OXA and ESA were detected in experiments with groundwater from well 151, whereas only ESA was detected in those with groundwater from well 224 (**Table 1**). This corresponded to TP patterns in the initial groundwater wells. ESA and OXA formation was suggested to be mediated by glutathione-S-transferases (GSTs) (Graham et al., 1999), but no enzyme acting on chloroacetanilides has yet been described. The previously reported abiotic dechlorination of chloroacetanilides to ESA by reduced sulfur species under sulfate-reducing conditions (Cai et al., 2007; Bai et al., 2013) is unlikely in this case because of the aerobic conditions in our experiments. Thus, OXA could be preferentially degraded in experiments with well 224 groundwater, although OXA was not detected in initial groundwater (**Supplementary Section D**). MET may also be degraded to ESA and OXA via other yet unknown enzymatic pathways (Barbash et al., 1999). Nevertheless, TP other than MET OXA and ESA were often prominent, most notably in experiments spiked with  $5\text{ mg L}^{-1}$  MET (**Table 1**). The detected TP suggested that degradation pathways involving 4-(2-ethyl-6-methylphenyl)-5-methyl-3-morpholinone, a major photolysis product (Mathew and Khan, 1996), or hydroxymetolachlor, an important fungal and bacterial degradate (Sanyal et al., 2000), were operative in our

**TABLE 1** | MET degradation, degradation product, carbon stable isotope composition, and bacterial toxicity in the groundwater exposure experiments (21 days of incubation at 20°C).

Well	MET [mg L <sup>-1</sup> ]		Transformation products (TP) [μg L <sup>-1</sup> ] <sup>b</sup>			MET degradation		Toxicity <sup>e</sup>		
	MET addition [mg L <sup>-1</sup> ]	MET [mg L <sup>-1</sup> ]	Total	OXA	ESA	Main TP	Other than OXA and ESA		Extent [%]	Δδ <sup>13</sup> C <sup>d</sup>
151	0	0.005 <sup>a</sup>	6.0	2.9	3.0	ESA	0.1	<LOQ	<LOQ	105 ± 14
	0.1	0.081 <sup>b</sup>	7.2	3.1	3.4	ESA	0.7	<LOQ	<LOQ	101 ± 9
	5	2.450 <sup>b</sup>	25.2	2.3	2.1	MET morpholinone <sup>c</sup>	20.8	51	1.4 ± 0.5	103 ± 12
224	0	<LOQ <sup>a</sup>	0.9	<LOQ	0.9	ESA	<LOQ	<LOQ	<LOQ	101 ± 5
	0.1	0.054 <sup>b</sup>	1.4	<LOQ	0.9	ESA	0.5	46	<LOQ	102 ± 3
	5	2.456 <sup>b</sup>	30.6	<LOQ	0.6	MET morpholinone <sup>c</sup>	30	51	1.2 ± 0.5	102 ± 8

n.d., not detected; n.a., not assessed.

<sup>a</sup>MET concentration in collected groundwater.

<sup>b</sup>MET and TP concentrations measured after 21 days of groundwater incubation at 20°C.

<sup>c</sup>4-(2-ethyl-6-methylphenyl)-5-methyl-3-morpholinone.

<sup>d</sup>The error given for Δδ<sup>13</sup>C values was calculated from ≥3 measurements for each sample, via error propagation based on ± one standard deviation of mean δ<sup>13</sup>C-values.

<sup>e</sup>The error given for luminescence (%) values corresponds to ± one standard deviation of the mean from ≥3 measurements for each sample.

microcosms and thus potentially also in groundwater. Alternative degradation pathways that do not involve OXA and ESA as intermediates were previously observed in artificial wetlands (Elsayed et al., 2015) and at the agricultural catchment scale (Marie et al., 2017).

Worthy of note, the TP/MET ratio was highest (about 9%) in the experiment with 151 groundwater (chronical MET exposure) at 0.1 mg L<sup>-1</sup> MET, but remained below 3% in the other experiments. This suggests that TP were rapidly degraded, since accumulation of TP resulted in apparent reduction of MET dissipation rates in some experiments (Table 2). Alternatively, it is possible that other unknown but relevant TP of MET were not detected.

### Potential Toxicity Effects of MET Exposure on Groundwater Bacterial Communities

Viable cell counts on solid medium were very similar in all microcosms experiments irrespectively of MET exposure level (Supplementary Section F), suggesting that toxic effects of MET on the bacterial compartment were minor. Potential effects of MET and its degradates produced in microcosms on bacterial metabolic activity were further probed using the standard Microtox<sup>®</sup> bacterial assay, which relies on disruption of luminescence production by a tester bacterial strain. The standard Microtox<sup>®</sup> test was chosen as it is routinely used, standardized and cost-effective. Previously reported EC<sub>50</sub> values ranging from 15.3 to 19.1 mg L<sup>-1</sup> (Kock et al., 2010; Souissi et al., 2013) for pure MET are very high, and indeed, no effects of MET in pure water were detected below 30 μM (i.e., 8.5 mg L<sup>-1</sup> MET in pure water), with an EC<sub>20</sub> for MET higher than 40 μM (i.e., 11.4 mg L<sup>-1</sup> MET in pure water). In addition, microcosm groundwater samples after 21 days of incubation did not produce detectable effects (Supplementary Section G). This confirms that as MET itself, transformation products of MET in microcosms, be them identified or not, did not affect metabolism of the Microtox<sup>®</sup> tester strain. Altogether, our data confirm that the Microtox<sup>®</sup> is of poor value for ecotoxicity assessment of MET, and that cultivation-dependent approaches may often be less sensitive than cultivation-independent approaches to detect potential bacterial toxicity in groundwater.

We thus turned to high-throughput sequencing of 16S rRNA amplicons by Illumina MiSeq to evaluate to what extent this could help characterize how the groundwater bacterial compartment responds to MET (Tan et al., 2015).

### Effect of MET Exposure on Groundwater Bacterial Community

A total of 19 545 OTUs were obtained from the eight groundwater experiments. OTUs covered 26 phyla, 179 families and 346 genera. Sequencing depth allowed to retrieve a representative portion of total bacterial diversity (Supplementary Section H), with diversity indices reaching asymptotes (Supplementary Section I), indicative of sufficient sampling depth. The effect of MET exposure on groundwater bacterial communities from the eight groundwater experiments was assessed based on (i)

**TABLE 2** | Richness, diversity and distribution of bacterial OTUs at 98% sequence identity, and relative distribution of abundant and rare OTUs in the initial groundwater and the groundwater exposure experiments (21 days of incubation at 20°C).

Well	Exposure to MET [mg L <sup>-1</sup> ]	Chao 1 (S <sub>Chao1</sub> ) Richness	Shannon (H') diversity	Simpson (S) diversity (inv.)	Abundance range [%]			
					>10	<10–1	<1–0.1	<0.1
151	Initial groundwater	8703	3.6	12	22.9	42.6	15.0	19.5
	0 (no MET addition)	6900	4.6	30	11.0	50.3	14.5	24.3
	0.1	7447	4.9	47	0	58.8	14.1	27.1
	5	6829	4.6	32	10.7	46.8	12.4	30.1
224	Initial groundwater	7589	3.6	13	22.6	55.9	9.1	12.4
	0 (no MET addition)	8318	4.1	23	21.3	51.7	9.5	17.5
	0.1	7650	3.9	15	19.9	55.1	9.2	15.8
	5	6741	3.9	16	18.9	54.7	10.6	15.9

diversity indices, (ii) relative distribution of abundant and rare OTUs, and (iii) cluster analysis of Illumina MiSeq sequencing data to evaluate changes in bacterial composition. Overall, Shannon and inverse Simpson diversity indices, but not the S<sub>Chao1</sub> estimator, were higher in experiments with well 151 groundwater than with well 224 groundwater (Table 2). This mainly reflects the relative distribution of abundant and rare OTUs in the two wells. Over 70% of OTUs in well 224 experiments had high, greater than 1% abundance (Table 2). By contrast, 34–42% of OTUs in experiments with well 151 groundwater were either rare (<1% abundance) or very rare (<0.1% abundance). In the latter microcosms, very rare OTUs slightly increased with increasing addition of MET, whereas they tended to decrease in experiments with well 224 groundwater (Table 2). As previously reported for soils (Jacobsen and Hjelmso, 2014), however, the variations in groundwater community composition observed here were not associated with differences in MET degradation, which did not differ significantly across microcosms (Table 2).

Analyzing bacterial composition patterns in more detail, *Betaproteobacteria* (60% sequence identity clustering, phylum/class level), represented over 60% of sequences in initial groundwater and in experiments with well 224 groundwater involving MET addition, whereas they accounted for less than 45% of sequences in well 151 groundwater experiments (Figure 3A). In all groundwater experiments, the 8 most abundant families (80% clustering) represented 55% of sequences, with *Comamonadaceae* the most abundant (>25%) (Figure 3B), while at 98% clustering, the 25 most abundant OTUs made up 90% of total sequences. *Comamonadaceae* increased with MET addition in experiments with groundwater from well 224 (>45%), compared to the experiment without MET addition (<37%). *Rhodobacteraceae* became very rare (<0.1%) at 5 mg L<sup>-1</sup> exposure in experiments with groundwater from both wells. Microbial diversity of MET-contaminated environments and enzymes and pathways for MET degradation, in particular in groundwater, are still unknown, preventing comparison with other studies.

Cluster analysis was performed to better understand the potential origin of the observed variations in bacterial composition between microcosms, revealing four distinct clusters (Figure 4A). Bacterial communities of the initial

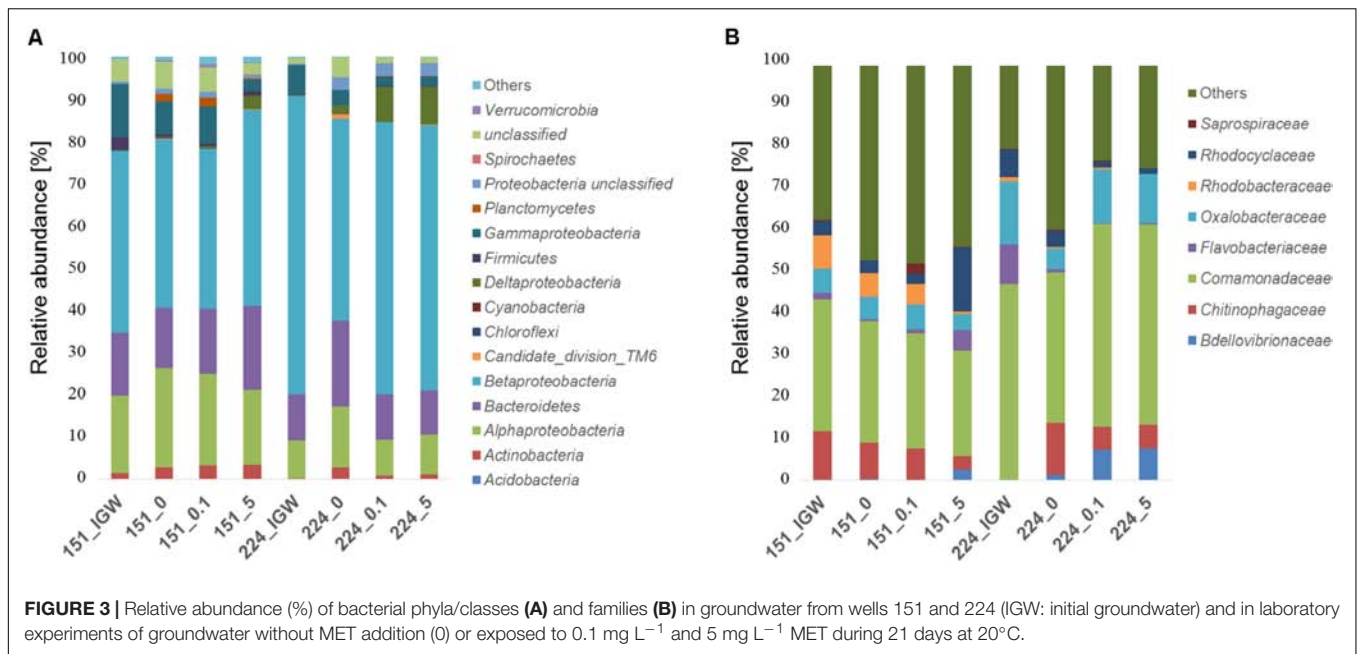
groundwater clearly differed from samples obtained following laboratory incubation, suggesting differentiation into distinct communities in the different experiments. Samples were mainly discriminated by well, i.e., well 151 samples differed from well 224 samples irrespectively of MET addition. Bacterial composition in the different microcosms did not converge with time, making it unlikely that storage and incubation had a significant influence.

Overall, obtained data suggest that, even at doses exceeding environmentally relevant and chronic concentrations by one or two orders of magnitude, a 21-day exposure to MET and its degradates modifies the diversity of dominant groups of the bacterial community only to a minor extent. Nevertheless, more subtle changes, e.g., in rare OTUs, may reflect adaptation of bacterial communities to a specific factor such as presence of a micropollutant or its degradation. This type of response, however, may not have to be proportional to exposure dose, and will thus likely be difficult to evidence at environmental concentrations, as shown previously for soil (Crouzet et al., 2010). Worthy of note in the perspective of future studies, temporal trajectories of community changes during incubation may additionally evidence transient responses of groundwater bacterial diversity during MET degradation. The tempo and mode of this response may thus provide additional value of DNA-based information for bioindication of ecosystem status and potential for recovery following toxic impacts.

Further and even if community differentiation between exposure levels can potentially be resolved at the OTU level in some instances, its functional relevance will remain elusive without additional information. In a further attempt to extract useful information, we used Phylogenetic Investigation of Communities by Reconstruction of Unobserved States (PICRUSt, Langille et al., 2013) as a first step toward evaluating functional responses of groundwater bacterial communities exposed to different MET levels.

## Effect of MET Exposure on Predicted Functional Properties of Bacterial Communities

Changes in community functional profiles suggested by PICRUSt were evaluated by cluster analysis, revealing two distinct



clusters (**Figure 4B**). As for bacterial community composition, different microcosms were mainly discriminated by groundwater origin. Compared to bacterial composition profiles (**Figure 4A**), however, the relative height of cluster separation was an order of magnitude lower for functional predictions (**Figure 4B**), confirming that changes in minor changes in predicted functions were likely minor.

Interestingly, the three major predicted types of functions in all microcosms were metabolism, genetic information processing

and environmental information processing, accounting for  $47.1 \pm 1.2\%$ ,  $16.6 \pm 0.5\%$ , and  $16.3 \pm 1.4\%$  (mean  $\pm 1 \sigma$ ,  $n = 8$ ) of functional counts, respectively (**Supplementary Section K**). Functions for xenobiotics biodegradation and metabolic pathways featured prominently, ranging from 2.2% (experiments with well 224 groundwater exposed to MET) to 2.5% (experiments with well 151 groundwater) of functional counts (**Supplementary Section L**). Predicted pathways for glutathione metabolism, predicted to be associated

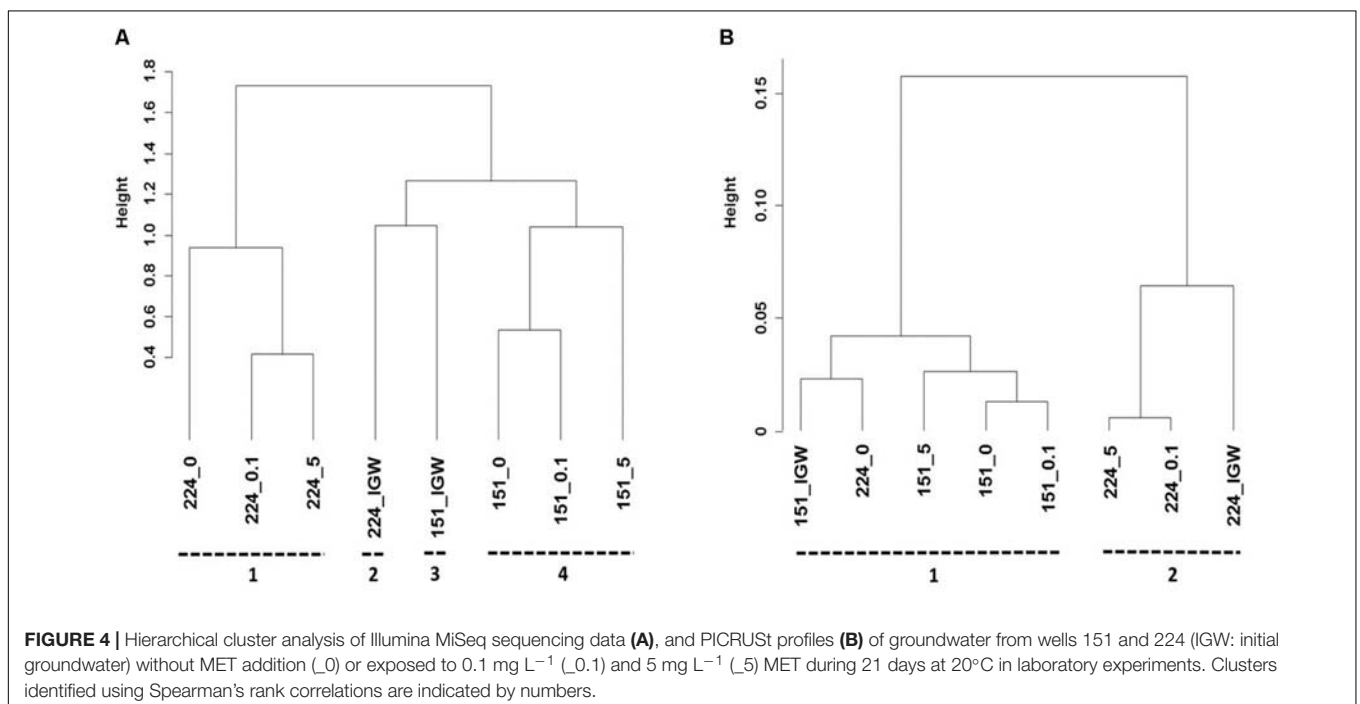


**TABLE 3** | OTUs exclusively found in groundwater experiments with low (no addition) or high exposure to MET (0.1 and 5 mg L<sup>-1</sup>) in wells 151 and 224.

MET exposition	Well	Number of OTUs <sup>a</sup> (number of sequences)	Relative abundance of specific OTUs [%] <sup>b</sup>							
			151_IGW	151_0	151_0.1	151_5	224_IGW	224_0	224_0.1	224_5
MET addition (0.1 and 5 mg L <sup>-1</sup> )	151	86 (1671)	0	0	<b>0.40</b>	<b>2.10</b>	0.18	0.05	0.04	0.05
No MET addition (IGW and 0)	151	125 (3913)	<b>1.00</b>	<b>0.73</b>	0	0	0.20	0.12	1.93	1.89
MET addition (0.1 and 5 mg L <sup>-1</sup> )	224	172 (5877)	0.17	0.19	0.40	2.50	0	0	<b>3.60</b>	<b>3.50</b>
No MET addition (IGW and 0)	224	43 (4644)	0.12	1.70	2.50	1.61	<b>0.18</b>	<b>1.40</b>	0	0
<sup>a</sup> MET addition (0.1 and 5 mg L <sup>-1</sup> )	151 and 224	2 (40)	0	0	<b>0.02</b>	<b>0.1</b>	0	0	<b>0.01</b>	<b>0.01</b>
<sup>a</sup> No MET addition (IGW and 0)	151 and 224	1 (7)	<b>&lt;0.01</b>	<b>0.01</b>	0	0	<b>0.01</b>	<b>&lt;0.01</b>	0	0

IGW, initial groundwater. In bold are the relative abundance of sequences of the wells targeted by the search in the given MET exposure conditions.

<sup>a</sup>OTUs exclusively found in groundwater from both 151 and 224 wells at the given MET exposure conditions.

<sup>b</sup>Relative abundance of specific OTUs (%) relative to the total number of OTUs found in groundwater microcosms from both 151 and 224 wells at the given MET exposure conditions.

with chloroacetanilide transformation (Graham et al., 1999) accounted for 0.5% of the functional counts, and did not vary significantly across microcosms (Supplementary Section L). In contrast, predicted metabolic pathways for atrazine had very low ( $\leq 0.03\%$ ) abundances, in agreement with very minor concentrations of atrazine in groundwater samples (Supplementary Section L).

## 16S rRNA OTUs as Potential Biomarkers of MET Exposure

PICRUSt-based predictions suggest the occurrence of only slightly distinct gene complements in the bacterial compartment of the two tested groundwater wells, despite markedly different contamination histories. This contrasts with previous work on diverse environments contaminated with hydrocarbons, where specific functional modules were identified that then served as biomarkers to distinguish between different oil contaminated sites (Mukherjee et al., 2017). Thus, and in the absence of known functional markers for MET degradation, we last asked the question whether taxonomical 16S rRNA gene OTUs that exclusively responded to MET as potential biomarkers of MET exposure could be identified, by comparison of identified OTUs across the different microcosms. OTUs which were exclusively found with increasing addition of MET were sought. OTUs potentially correlating with MET exposure varied between 0.4 and 3.6% of total OTUs across all microcosm experiments (Table 3). Relative abundance of sequences exclusively found at highest MET amendment ( $> 3.5\%$ ) was largest in experiments with well 224 groundwater. In contrast, sequences uniquely found with MET addition in

experiments with well 151 represented only 0.4% (0.1 mg L<sup>-1</sup> MET) and 2.1% (5 mg L<sup>-1</sup> MET) of total sequences. This suggests that exposure to higher MET levels in groundwater with a history of chronic (well 151) or very low (well 224) exposure to MET was associated with a slight increase of specific taxa. Strikingly, however, OTUs exclusively associated with either unamended or MET-amended conditions were essentially well-specific (Supplementary Section J). In other words, generally applicable MET-responding OTUs are likely to be very limited.

MET-responding OTUs exclusively found in microcosms with MET addition (0.1 or 5 mg L<sup>-1</sup>) and common to well 151 and well 224 yielded only 2 OTUs (i.e.,  $< 0.1\%$  the total number of OTUs) affiliated to *Clostridia* sp., the unclassified OTU00544 and *Fastidiosipila* sp. OTU00881. Conversely, OTU01317 (affiliated to *Gammaproteobacteria*) was the only OTU common to both wells and found exclusively in microcosms to which no MET was added. The association between these two OTUs and MET exposure is still unknown.

While this shows that bacterial OTUs specifically correlated with MET exposure can in principle be identified by high-throughput sequencing, it also confirms that their number will be low, and of uncertain significance in the absence of further information on the corresponding organisms and their metabolic features. In this context, it is worth noting that unclassified bacterial taxa systematically represented over 40% of total sequences. This emphasizes the need to identify and characterize a larger fraction of the bacteria detected in groundwater. Specifically, experiments targeting metabolic activity of identified OTUs of interest (such as OTU00544 and OTU00881 here), e.g., by way of shotgun sequencing of microcosm metagenomes and assembly and analysis of associated contigs

(Vanwonterghem et al., 2014), may help to identify organisms and genes potentially involved in MET degradation.

## CONCLUSION

This study evaluated the response of groundwater bacterial communities exposed to MET and its degradates by coupling *in situ* and *in labo* experiments, including CSIA and a culture-independent 16S rRNA survey. The response of bacterial communities exposed to chloroacetanilide herbicides could not be teased apart from effects of hydrogeochemical conditions and other pesticides *in situ*. Therefore, microcosm investigations on groundwater samples under controlled conditions *in labo* were used to filter out environmental *in situ* variations. Degradation of MET did not correlate with MET exposure level, even at very high MET exposure levels or in groundwater with no records of MET contamination. Moreover, no relationship between bacterial community composition as assessed by 16S rRNA amplicon sequencing and extent of MET degradation was apparent. In other words, detrimental toxic effects of metolachlor on the bacterial compartment of groundwater were not apparent, as also found by the standard Microtox® ecotoxicological assay. Further, functional profiles of bacterial communities as predicted from 16S rRNA by PICRUSt indicated only minor differences in the gene complement of bacterial communities in association with differences in pesticide contamination. Nevertheless, a small number of OTUs whose abundance correlated with levels of MET exposure were identified. This suggests that alterations of groundwater communities exposed to pesticides can be sensitively probed using high-throughput sequencing. In conclusion, this study provides a possible analysis framework to

explore the potential of using bacteria as biomarkers of pesticide contamination in aquifers.

## AUTHOR CONTRIBUTIONS

GI and SV designed the work and critically revised the article. GI, NB, BM, and SD collected and analyzed the samples. GI drafted the article with contributions from LB, NB, and SV. All co-authors analyzed and interpreted the data and approved the final submitted version of the manuscript.

## FUNDING

This research was carried out as part of the ELISE project funded by the Bureau de Recherches Géologiques et Minières (BRGM), the Adour-Garonne Water Agency (Grant No: 2010/6774) (AEAG, France), and FEDER (European funds Grant No: 38771).

## ACKNOWLEDGMENTS

We gratefully acknowledge the technical assistance of Christelle Gruffaz, Muhammad Farhan Ul Haque and Meriem Maalej in parts of this study.

## SUPPLEMENTARY MATERIAL

The Supplementary Material for this article can be found online at: <https://www.frontiersin.org/articles/10.3389/fmich.2018.02053/full#supplementary-material>

## REFERENCES

- Aird, D., Ross, M. G., Chen, W.-S., Danielsson, M., Fennell, T., Russ, C., et al. (2011). Analyzing and minimizing PCR amplification bias in Illumina sequencing libraries. *Genome Biol.* 12:R18. doi: 10.1186/gb-2011-12-2-r18
- Amalric, L., Baran, N., Coureau, C., Maingot, L., Buron, F., and Routier, S. (2013). Analytical developments for 47 pesticides: first identification of neutral chloroacetanilide derivatives in French groundwater. *Int. J. Environ. Anal. Chem.* 93, 1660–1675. doi: 10.1080/03067319.2013.853758
- Babcsányi, I., Meite, F., and Imfeld, G. (2017). Biogeochemical gradients and microbial communities in Winogradsky columns established with polluted wetland sediments. *FEMS Microbiol. Ecol.* 93:fix089. doi: 10.1093/femsec/fix089
- Bai, Z., Xu, H., He, H., Zheng, L., and Zhang, X. (2013). Alterations of microbial populations and composition in the rhizosphere and bulk soil as affected by residual acetochlor. *Environ. Sci. Pollut. Res. Int.* 20, 369–379. doi: 10.1007/s11356-012-1061-3
- Baran, N., and Gourcy, L. (2013). Sorption and mineralization of S-metolachlor and its ionic metabolites in soils and vadose zone solids: consequences on groundwater quality in an alluvial aquifer (Ain Plain, France). *J. Contam. Hydrol.* 154, 20–28. doi: 10.1016/j.jconhyd.2013.07.009
- Becker, R. A., Chambers, J. M., and Wilks, A. R. (1988). *The News Language: A Programming Environment for Data Analysis and Graphics*. Pacific Grove, CA: Wadsworth & Brooks/Cole computer science series.
- Barbash, J. E., Gail, P. T., Kolpin, D. W., and Gilliom, R. (1999). *Distribution of Major Herbicides in Ground Water of the United States*. Sacramento, CA: U.S. Geological Survey, *Water-Resources Investigations Report* 98-4245.
- Cai, X., Sheng, G., and Liu, W. (2007). Degradation and detoxification of acetochlor in soils treated by organic and thiosulfate amendments. *Chemosphere* 66, 286–292. doi: 10.1016/j.chemosphere.2006.05.011
- Caracciolo, A., Fajardo, C., Grenni, P., Sacca, M., Amalfitano, S., Ciccoli, R., et al. (2010). The role of a groundwater bacterial community in the degradation of the herbicide terbuthylazine. *FEMS Microbiol. Ecol.* 71, 127–136. doi: 10.1111/j.1574-6941.2009.00787.x
- Crouzet, O., Batisson, I., Besse-Hoggan, P., Bonnemoy, F., Bardot, C., Poly, F., et al. (2010). Response of soil microbial communities to the herbicide mesotrione: a dose-effect microcosm approach. *Soil Biol. Biochem.* 42, 193–202. doi: 10.1016/j.soilbio.2009.10.016
- Culman, S., Bukowski, R., Gauch, H., Cadillo-Quiroz, H., and Buckley, D. (2009). T-REX: software for the processing and analysis of T-RFLP data. *BMC Bioinformatics* 10:171. doi: 10.1186/1471-2105-10-171
- de Liphay, J., Tuxen, N., Johnsen, K., Hansen, L., Albrechtsen, H., Bjerg, P., et al. (2003). In situ exposure to low herbicide concentrations affects microbial population composition and catabolic gene frequency in an aerobic shallow aquifer. *Appl. Environ. Microbiol.* 69, 461–467. doi: 10.1128/AEM.69.1.461-467.2003
- de Liphay, J. R., Johnsen, K., Albrechtsen, H.-J., Rosenberg, P., and Aamand, J. (2004). Bacterial diversity and community structure of a sub-surface aquifer exposed to realistic low herbicide concentrations. *FEMS Microbiol. Ecol.* 49, 59–69. doi: 10.1016/j.femsec.2004.02.007
- Elsayed, O., Maillard, E., Vuilleumier, S., and Imfeld, G. (2014). Bacterial communities in batch and continuous-flow wetlands treating the herbicide S-metolachlor. *Sci. Total Environ.* 499, 327–335. doi: 10.1016/j.scitotenv.2014.08.048

- Elsayed, O., Maillard, E., Vuilleumier, S., Millet, M., and Imfeld, G. (2015). Degradation of chloroacetanilide herbicides and bacterial community composition in lab-scale wetlands. *Sci. Total Environ.* 520, 222–231. doi: 10.1016/j.scitotenv.2015.03.061
- Elsner, M., and Imfeld, G. (2016). Compound-specific isotope analysis (CSIA) of micropollutants in the environment – Current developments and future challenges. *Curr. Opin. Biotechnol.* 41, 60–72. doi: 10.1016/j.copbio.2016.04.014
- Food and Agriculture Organization of the United Nations (FAO). *FAOSTAT Database Collections*. Rome: FAOSTAT.
- Graham, W. H., Graham, D. W., deNoyelles, F., Smith, V. H., Larive, C. K., and Thurman, E. M. (1999). Metolachlor and alachlor breakdown product formation patterns in aquatic field mesocosms. *Environ. Sci. Technol.* 33, 4471–4476. doi: 10.1021/es990686z
- Hensler, H. J., and Schedel, M. (1991). Suitability of the shaking flask for oxygen supply to microbiological cultures. *Bioprocess Eng.* 7, 123–131. doi: 10.1007/BF00369423
- Hewson, I., and Fuhrman, J. A. (2006). Improved strategy for comparing microbial assemblage fingerprints. *Microb. Ecol.* 51, 147–153. doi: 10.1007/s00248-005-0144-9
- Imfeld, G., Nijenhuis, I., Nikolausz, M., Zeiger, S., Paschke, H., Drangmeister, J., et al. (2008). Assessment of in situ degradation of chlorinated ethenes and bacterial community structure in a complex contaminated groundwater system. *Water Res.* 42, 871–882. doi: 10.1016/j.watres.2007.08.035
- Imfeld, G., Pieper, H., Shani, N., Rossi, P., Nikolausz, M., Nijenhuis, I., et al. (2011). Characterization of groundwater microbial communities, dechlorinating bacteria, and in situ biodegradation of chloroethenes along a vertical gradient. *Water Air Soil Pollut.* 221, 107–122. doi: 10.1007/s11270-011-0774-0
- Imfeld, G., and Vuilleumier, S. (2012). Measuring the effects of pesticides on bacterial communities in soil: a critical review. *Eur. J. Soil Biol.* 49, 22–30. doi: 10.1016/j.ejsobi.2011.11.010
- Jacobsen, C., and Hjelmsø, M. (2014). Agricultural soils, pesticides and microbial diversity. *Curr. Opin. Biotechnol.* 27, 15–20. doi: 10.1016/j.copbio.2013.09.003
- Janniche, G., Spliid, H., and Albrechtsen, H. (2012). Microbial community-level physiological profiles (CLPP) and herbicide mineralization potential in groundwater affected by agricultural land use. *J. Contam. Hydrol.* 140, 45–55. doi: 10.1016/j.jconhyd.2012.08.008
- Jennings, V. L., Rayner-Brandes, M. H., and Bird, D. J. (2001). Assessing chemical toxicity with the bioluminescent photobacterium (*Vibrio fischeri*): a comparison of three commercial systems. *Wat. Res.* 35, 3448–3456. doi: 10.1016/S0043-1354(01)00067-7
- Ju, C., Xu, J., Wu, X., Dong, F., Liu, X., Tian, C., et al. (2017). Effects of hexaconazole application on soil microbes community and nitrogen transformations in paddy soils. *Sci. Total Environ.* 609, 655–663. doi: 10.1016/j.scitotenv.2017.07.146
- Kalkhoff, S., Vecchia, A., Capel, P., and Meyer, M. (2012). Eleven-year trend in acetanilide pesticide degrades in the Iowa River, Iowa. *J. Environ. Qual.* 41, 1566–1579. doi: 10.2134/jeq2011.0426
- Kock, M., Farre, M., Martinez, E., Gajda-Schranz, K., Ginebreda, A., Navarro, A., et al. (2010). Integrated ecotoxicological and chemical approach for the assessment of pesticide pollution in the Ebro River delta (Spain). *J. Hydrol.* 383, 73–82. doi: 10.1016/j.jhydrol.2009.12.029
- Langille, M., Zaneveld, J., Caporaso, J., McDonald, D., Knights, D., Reyes, J., et al. (2013). Predictive functional profiling of microbial communities using 16S rRNA marker gene sequences. *Nat. Biotechnol.* 31, 814–821. doi: 10.1038/nbt.2676
- Liebich, J., Wachtmeister, T., Zhou, J., and Buraue, P. (2009). Degradation of diffuse pesticide contaminants: screening for microbial potential using a functional gene microarray. *Vadose Zone J.* 8, 703–710. doi: 10.2136/vzj2008.0072
- Loos, R., Locoro, G., Comero, S., Contini, S., Schwesig, D., Werres, F., et al. (2010). Pan-European survey on the occurrence of selected polar organic persistent pollutants in ground water. *Water Res.* 44, 4115–4126. doi: 10.1016/j.watres.2010.05.032
- Lopez, B., Ollivier, P., Togola, A., Baran, N., and Ghestem, J. (2015). Screening of French groundwater for regulated and emerging contaminants. *Sci. Total Environ.* 518, 562–573. doi: 10.1016/j.scitotenv.2015.01.110
- Ma, Y., Liu, W., and Wen, Y. (2006). Enantioselective degradation of rac-metolachlor and S-metolachlor in soil. *Pedosphere* 16, 489–494. doi: 10.1016/S1002-0160(06)60079-9
- Mathew, R., and Khan, S. (1996). Photodegradation of metolachlor in water in the presence of soil mineral and organic constituents. *J. Agric. Food Chem.* 44, 3996–4000. doi: 10.1021/jf960123w
- Marie, L., Sylvain, P., Benoit, G., Maurice, M., and Gwenaël, I. (2017). Degradation and transport of the chiral herbicide S-metolachlor at the catchment scale: combining observation scales and analytical approaches. *Environ. Sci. Technol.* 51, 13231–13240. doi: 10.1021/acs.est.7b02297
- Mauffret, A., Baran, N., and Joulian, C. (2017). Effect of pesticides and metabolites on groundwater bacterial community. *Sci. Total Environ.* 576, 879–887. doi: 10.1016/j.scitotenv.2016.10.108
- Mauffrey, F., Baccara, P. Y., Gruffaz, C., Vuilleumier, S., and Imfeld, G. (2017). Bacterial community composition and genes for herbicide degradation in a stormwater wetland collecting herbicide runoff. *Water Air Soil Pollut.* 228:452. doi: 10.1007/s11270-017-3625-9
- McDonald, D., Price, M., Goodrich, J., Nawrocki, E., DeSantis, T., Probst, A., et al. (2012). An improved Greengenes taxonomy with explicit ranks for ecological and evolutionary analyses of bacteria and archaea. *ISME J.* 6, 610–618. doi: 10.1038/ismej.2011.139
- Mukherjee, A., Chettri, B., Langpoklakpam, J., Basak, P., Prasad, A., Mukherjee, A., et al. (2017). Bioinformatic approaches including predictive metagenomic profiling reveal characteristics of bacterial response to petroleum hydrocarbon contamination in diverse environments. *Sci. Rep.* 7:1108. doi: 10.1038/s41598-017-01126-3
- Organisation for Economic Co-operation and Development [OECD] (1981). *Test No. 302C: Inherent Biodegradability: Modified MITI Test (II)*. Paris: OECD Publishing.
- Parks, D., Tyson, G., Hugenholtz, P., and Beiko, R. (2014). STAMP: statistical analysis of taxonomic and functional profiles. *Bioinformatics* 30, 3123–3124. doi: 10.1093/bioinformatics/btu494
- The Pesticide Properties DataBase [PPDB] (2006). *Developed by the Agriculture & Environment Research Unit (AERU) at the University of Hertfordshire, from the database that Originally Accompanied the EMA (Environmental Management for Agriculture) Software (also developed by AERU), with Additional Input From the EU -Funded FOOTPRINT project (FP6 SSP-022704)*. Available at: <https://sitem.herts.ac.uk/aeru/ppdb/en/>
- Postigo, C., and Barcelo, D. (2015). Synthetic organic compounds and their transformation products in groundwater: Occurrence, fate and mitigation. *Sci. Total Environ.* 503, 32–47. doi: 10.1016/j.scitotenv.2014.06.019
- R Core Team (2017). *R: A language and environment for statistical computing*. Vienna: R Foundation for Statistical Computing. Available at: URL <http://www.R-project.org/>
- Rossi, P., Shani, N., Kohler, F., Imfeld, G., and Holliger, C. (2012). Ecology and biogeography of bacterial communities associated with chloroethene-contaminated aquifers. *Front. Microbiol.* 3:260. doi: 10.3389/fmicb.2012.00260
- Sanyal, D., Yaduraju, N., and Kulshrestha, G. (2000). Metolachlor persistence in laboratory and field soils under Indian tropical conditions. *J. Environ. Sci. Health B.* 35, 571–583. doi: 10.1080/03601230009373293
- Schloss, P., Westcott, S., Ryabin, T., Hall, J., Hartmann, M., Hollister, E., et al. (2009). Introducing mothur: open-Source, platform-independent, community-supported software for describing and comparing microbial communities. *Appl. Environ. Microbiol.* 75, 7537–7541. doi: 10.1128/AEM.01541-09
- Sidoli, P., Lassabatere, L., Angulo-Jaramillo, R., and Baran, N. (2016). Experimental and modeling of the unsaturated transports of S-metolachlor and its metabolites in glaciofluvial vadose zone solids. *J. Contam. Hydrol.* 190, 1–14. doi: 10.1016/j.jconhyd.2016.04.001
- Singh, B., and Singh, K. (2016). Microbial degradation of herbicides. *Crit. Rev. Microbiol.* 42, 245–261. doi: 10.3109/1040841X.2014.929564
- Souissi, Y., Bouchonnet, S., Bourcier, S., Kusk, K., Sablier, M., and Andersen, H. (2013). Identification and ecotoxicity of degradation products of chloroacetamide herbicides from UV-treatment of water. *Sci. Total Environ.* 458, 527–534. doi: 10.1016/j.scitotenv.2013.04.064
- Tan, B., Ng, C., Nshimiyimana, J., Loh, L., Gin, K., and Thompson, J. (2015). Next-generation sequencing (NGS) for assessment of microbial water quality:

- current progress, challenges, and future opportunities. *Front. Microbiol.* 6:1027. doi: 10.3389/fmicb.2015.01027
- Tuxen, N., De Liphay, J., Albrechtsen, H., Aamand, J., and Bjerg, P. (2002). Effect of exposure history on microbial herbicide degradation in an aerobic aquifer affected by a point source. *Environ. Sci. Technol.* 36, 2205–2212. doi: 10.1021/es0113549
- Vanwonterghem, I., Jensen, P. D., Ho, D. P., Batstone, D. J., and Tyson, G. W. (2014). Linking microbial community structure, interactions and function in anaerobic digesters using new molecular techniques. *Curr. Opin. Biotechnol.* 27, 55–64. doi: 10.1016/j.copbio.2013.11.004
- Walters, W., Caporaso, J., Lauber, C., Berg-Lyons, D., Fierer, N., and Knight, R. (2011). PrimerProspector: de novo design and taxonomic analysis of barcoded polymerase chain reaction primers. *Bioinformatics* 27, 1159–1161. doi: 10.1093/bioinformatics/btr087
- Ward, J. H. Jr. (1963). Hierarchical grouping to optimize an objective function. *J. Am. Stat. Assoc.* 58, 236–244. doi: 10.1080/01621459.1963.10500845
- Xu, D., Wen, Y., and Wang, K. (2010). Effect of chiral differences of metolachlor and its (S)-isomer on their toxicity to earthworms. *Ecotoxicol. Environ. Saf.* 73, 1925–1931. doi: 10.1016/j.ecoenv.2010.07.035

**Conflict of Interest Statement:** The authors declare that the research was conducted in the absence of any commercial or financial relationships that could be construed as a potential conflict of interest.

Copyright © 2018 Imfeld, Besaury, Maucourt, Donadello, Baran and Vuilleumier. This is an open-access article distributed under the terms of the Creative Commons Attribution License (CC BY). The use, distribution or reproduction in other forums is permitted, provided the original author(s) and the copyright owner(s) are credited and that the original publication in this journal is cited, in accordance with accepted academic practice. No use, distribution or reproduction is permitted which does not comply with these terms.



# Interactive Effects of Pesticides and Nutrients on Microbial Communities Responsible of Litter Decomposition in Streams

Florent Rossi<sup>1\*</sup>, Stéphane Pesce<sup>2</sup>, Clarisse Mallet<sup>1</sup>, Christelle Margoum<sup>2</sup>, Arnaud Chaumot<sup>2</sup>, Matthieu Masson<sup>2</sup> and Joan Artigas<sup>1</sup>

<sup>1</sup> Laboratoire Microorganismes: Génome et Environnement, CNRS, Université Clermont Auvergne, Clermont-Ferrand, France, <sup>2</sup> Irstea, UR RiverLy, Centre de Lyon-Villeurbanne, Villeurbanne, France

## OPEN ACCESS

### Edited by:

Jean Armengaud,  
Commissariat à l'Energie Atomique et  
aux Energies Alternatives (CEA),  
France

### Reviewed by:

Olivier Pringault,  
Institut de Recherche pour le  
Développement (IRD), France  
Beatrice Marie Alpha-Bazin,  
Commissariat à l'Energie Atomique et  
aux Energies Alternatives (CEA),  
France

### \*Correspondence:

Florent Rossi  
florent.rossi@uca.fr

### Specialty section:

This article was submitted to  
Microbiotechnology, Ecotoxicology  
and Bioremediation,  
a section of the journal  
Frontiers in Microbiology

**Received:** 29 June 2018

**Accepted:** 24 September 2018

**Published:** 17 October 2018

### Citation:

Rossi F, Pesce S, Mallet C,  
Margoum C, Chaumot A, Masson M  
and Artigas J (2018) Interactive  
Effects of Pesticides and Nutrients on  
Microbial Communities Responsible  
of Litter Decomposition in Streams.  
Front. Microbiol. 9:2437.  
doi: 10.3389/fmicb.2018.02437

Global contamination of streams by a large variety of compounds, such as nutrients and pesticides, may exert a high pressure on aquatic organisms, including microbial communities and their activity of organic matter decomposition. In this study, we assessed the potential interaction between nutrients and a fungicide and herbicide [tebuconazole (TBZ) and S-metolachlor (S-Met), respectively] at realistic environmental concentrations on the structure (biomass, diversity) and decomposition activity of fungal and bacterial communities (leaf decay rates, extracellular enzymatic activities) associated with *Alnus glutinosa* (*Alnus*) leaves. A 40-day microcosm experiment was used to combine two nutrient conditions (mesotrophic and eutrophic) with four pesticide treatments at a nominal concentrations of 15  $\mu\text{g L}^{-1}$  (control, TBZ and S-Met, alone or mixed) following a 2  $\times$  4 full factorial design. We also investigated resulting indirect effects on *Gammarus fossarum* feeding rates using leaves previously exposed to each of the treatments described above. Results showed interactive effects between nutrients and pesticides, only when nutrient (i.e., nitrogen and phosphorus) concentrations were the highest (eutrophic condition). Specifically, slight decreases in *Alnus* leaf decomposition rates were observed in channels exposed to TBZ (0.01119 days<sup>-1</sup>) and S-Met (0.01139 days<sup>-1</sup>) than in control ones (0.01334 days<sup>-1</sup>) that can partially be explained by changes in the structure of leaf-associated microbial communities. However, exposition to both TBZ and S-Met in mixture (MIX) led to comparable decay rates to those exposed to the pesticides alone (0.01048 days<sup>-1</sup>), suggesting no interaction between these two compounds on microbial decomposition. Moreover, stimulation in ligninolytic activities (laccase and phenol oxidase) was observed in presence of the fungicide, possibly highlighting detoxification mechanisms employed by microbes. Such stimulation was not observed for laccase activity exposed to the MIX, suggesting antagonistic interaction of these two compounds on the ability of microbial communities to cope with stress by xenobiotics. Besides, no effects of the treatments

were observed on leaf palatability for macroinvertebrates. Overall, the present study highlights that complex interactions between nutrients and xenobiotics in streams and resulting from global change can negatively affect microbial communities associated with leaf litter, although effects on higher trophic-level organisms remains unclear.

**Keywords:** microcosm, stressors interaction, leaf litter, fungal communities, microbial ecotoxicology, macroinvertebrates

## INTRODUCTION

Freshwaters pollution resulting from human activities has become a widespread phenomenon over the last decades. Among pollution sources, agriculture intensification coupled with changes in practices to increase agricultural yields have led to the massive inputs of both nutrients (including nitrogen and phosphorus) and toxicants (including pesticides which are generally used in mixture) in many stream ecosystems (Trewavas, 2002; Vörösmarty et al., 2010). Accordingly and despite the effort of the European Water Framework directive (WFD) to improve surface water chemical quality, more than 56% of streams in Europe are still qualified as moderate ecological status or worst regarding chemical contamination (WISE WFD database, 2017). This reality copes with the still increasing fertilizers (including  $\text{NO}_3$ ,  $\text{P}_2\text{O}_5$  and  $\text{K}_2\text{O}$ ) and pesticides consumption across Europe (FAOSTAT). In this context, the evaluation of the threat posed by such a chemical multi-contamination on aquatic organisms and stream ecosystems integrity and the ecological functions and services they provide has become a central preoccupation for societies, stream managers and scientists (Brosed et al., 2016).

Among aquatic organisms that can be found in headwater stream ecosystems, heterotrophic microbial communities have a pivotal role. Mainly composed by fungi (representing up to 98% of the total microbial biomass), microbial communities in leaves also host viruses, bacteria and protists. Thanks to a large panel of extracellular enzymatic activities (Chandrashekar and Kaveriappa, 1991; Abdel-Raheem and Ali, 2004), including ligninolytic (laccase, phenol oxidase) and cellulolytic ( $\beta$ -glucosidase, cellobiohydrolase) enzymes, fungi and bacteria directly participates to the mineralisation of leaf litter (up to 45% of the total leaf mass loss). Thus, they have an important role in the recycling of organic matter in stream ecosystems (Cummins, 1974; Gessner and Chauvet, 1994; Webster and Meyer, 1997). In addition, microorganisms have been shown to stimulate leaf consumption by macroinvertebrates by (i) softening leaf tissues through their extracellular enzymes activity and ii) increasing the nutritional quality and palatability of the leaves (Suberkropp et al., 1983; Baldy et al., 2007). Overall, heterotrophic microbial communities play a non-negligible role in many biogeochemical cycles in addition of being at the base of the trophic networks in stream ecosystems (Webster and Meyer, 1997).

However, pesticides inputs may cause serious threat on such communities, possibly impairing microbial decomposition activity, thus, unbalancing the entire food web. This is particularly the case of fungicides, whose direct effects on fungi, including aquatic hyphomycetes, have already been described (Yang et al., 2011). In polluted streams, one of the most frequently

detected fungicide is the tebuconazole (TBZ) (e.g., 11% of French rivers, NAIADES database, EauFrance, 2010–2015). Belonging to the azole family, TBZ ( $\text{C}_{16}\text{H}_{22}\text{ClN}_3\text{O}$ ) is a triazole fungicide (Richardson, 2009) that inhibits the sterol C-14  $\alpha$ -demethylation of 24-methylenedihydrolanosterol (which is a precursor of ergosterol, a key component of the fungal cell membrane) thus limiting the development of fungal biomass (Copping and Hewitt, 2007). Accordingly, it was previously shown that TBZ exposure can have negative effects on biomass, structure and extracellular enzymatic activities of fungal communities, overall leading to a decrease in the decomposition rates of leaf litter (Bundschuh et al., 2011; Zubrod et al., 2011, 2015; Artigas et al., 2012). Moreover, indirect effects of tebuconazole have been also shown to affect higher trophic level organisms such as macroinvertebrates due to the decrease of leaf nutritional quality (i.e., decrease in fungal biomass and/or changes in microbial community structure), suggesting a potential influence at the stream food web (Bundschuh et al., 2011; Zubrod et al., 2011). In addition to the fungicides, heterotrophic microbial communities are also chronically exposed to herbicides which are prevalent in these ecosystems. The most frequently detected herbicide in river ecosystems since the last 10 years is the S-metolachlor (S-Met) (e.g., 24% of French rivers, NAIADES database, EauFrance, 2010–2015). Belonging to the chloroacetanilide family, S-Met ( $\text{C}_{15}\text{H}_{22}\text{ClNO}_2$ ) is the S isomeric form of the herbicide metolachlor. Mostly used for maize treatment, this herbicide inhibits the fatty acid elongation 1 (FAE1) synthase, a key enzyme involved in the elongation of very-long fatty acids in plants (Götz and Böger, 2004; Paul et al., 2006). Although its effects on aquatic heterotrophic microbial communities colonizing leaf-litter are unknown, S-Met has been shown to induce changes in the structure of diatom communities accompanied with frustule deformation at concentrations  $\geq 5 \mu\text{g L}^{-1}$  (Roubeix et al., 2011) and to inhibit cell reproduction of the green algae *Scenedesmus vacuolatus* by 50% after a 6h exposure to very high concentrations ( $598 \mu\text{g L}^{-1}$ ).

Given the fact that both pesticides and nutrients generally occur at the same time in stream ecosystems (Pesce et al., 2008), it appears essential to assess their interaction in order to understand the consequences at the microbial community level (Segner et al., 2014). Only a few studies tested the interactive effects between nutrients and fungicides on leaf-associated microbial communities, and the available knowledge suggest that the microbial stimulation by addition of nutrients can compensate fungicide toxicity (Fernández et al., 2016; Gardeström et al., 2016). Similarly, some studies tested the interactions between two different types of pesticides on leaf-associated microbial communities (Flores et al., 2014; Dawoud et al., 2017). In the

case of the fungicide imazalil and the insecticide diazinon, Flores et al. (2014) observed that the effect of a mixture of both pesticides led to similar effects than the fungicide alone. On the other hand, (Dawoud et al., 2017) demonstrated that both insecticide (lindane) and fungicide (azoxystrobin) exposure lead to a stimulation of fungal sporulation, but that this stimulation was not observed in the presence of both pesticides in mixture. Together, these results highlights that interactions, such as synergism, between different pesticides may occur, although this seems tightly linked to the type of pesticide compound tested as well as their concentrations. Besides, such differences could also be explained by differences in terms of nutrient concentrations in the media, as (Flores et al., 2014) used stream water whereas Dawoud et al. (2017) used standard test medium M7 (OECD, 1998) for their exposure conditions. However, to our knowledge, no study evaluated the interactions between nutrients and a cocktail of different types of pesticides on leaf-associated microbial communities and the implication of such exposure on the palatability of leaves for macroinvertebrates.

Accordingly, the present study aims to assess (i) the interactions between nutrient increase, namely nitrate and phosphate, relative to stream eutrophication and the presence of TBZ and S-Met alone or in mixture on microbial decomposer communities associated to submerged leaves and (ii) how such multi-contamination further affect leaf palatability for macroinvertebrate consumers. In order to answer these two objectives, we conducted a microcosm experiment in a  $2 \times 4$  full factorial design using laboratory artificial streams, with nutrient condition as the first factor (mesotrophic versus eutrophic) and pesticide treatment as the second one (control, TBZ alone;  $15 \mu\text{g L}^{-1}$ , S-Met alone;  $15 \mu\text{g L}^{-1}$  and MIX;  $15 \mu\text{g L}^{-1}$  of each compounds) over 40 days exposure. Chosen concentrations of pesticides were based on values observed on the field (Berenzen et al., 2005; Kalkhoff et al., 2012) and already used in laboratory experiments (Artigas et al., 2012; Donnadieu et al., 2016; Pesce et al., 2016). Stressors effects were assessed on leaf decomposition rates and a range of extracellular enzymatic activities associated (laccase, phenol oxidase,  $\beta$ -glucosidase, leucine-aminopeptidase and alkaline phosphatase), as well as on the biomass and structure of fungal and bacterial communities. Indirect effects of contamination were investigated on the feeding rates of the macroinvertebrate *Gammarus fossarum*, a shredder amphipod which represents the dominant macroinvertebrate species, in terms of biomass, in many lotic ecosystems (MacNeil et al., 1997). Macroinvertebrates were fed using leaves previously exposed for 40 days to each of the treatments described above.

We firstly hypothesized that the fungicide exposure (alone or in mixture with the herbicide) would significantly affect fungal communities associated with *Alnus* leaves, while the effects of the herbicide alone would be expected to be very limited due to the lack of direct toxicity to fungi and bacteria. In addition, we hypothesized that nutrient increase relative to the eutrophic condition could minimize the effects of pesticides on leaf-associated microbial communities and therefore mask pesticide effects on leaf palatability for the macroinvertebrate *Gammarus fossarum*.

## MATERIALS AND METHODS

### Microbial Inoculum

Leaf-associated fungal and bacterial communities were obtained from the Couze d'Ardes River, a well preserved mesotrophic third-order forested stream, draining a basin surface area of 21476 ha (mostly forest and prairies) in the Puy-de-Dôme region (Centre France). Freshly fallen *Alnus glutinosa* (L.) Gaertn leaves were harvested in October 2016, brought back to the laboratory and dried at room temperature for 72 h. Leaves (ca. 3 g of dried leaves) were placed into three litter bags of 0.5 mm mesh size ( $1 \times w = 15 \times 15$  cm) and immersed in the upstream section of the Couze d'Ardes River during 4 weeks, from September 25 to October 26 2016, to allow microbial colonization. After in-stream colonization, litter bags were retrieved and transported back to the laboratory where leaves were cleaned with filtered stream water ( $0.2 \mu\text{m}$ ), cut into small circles (1 cm in diameter) and placed into nine sterile 250 mL flasks (3 flasks per retrieved bag). Each flask was filled with 200 mL of stream water diluted to 1/10 with demineralized water and contained 15 pre-colonized leaf disks (Gessner and Chauvet, 1993). Fungal mycelia sporulation was achieved by incubations at  $10^\circ\text{C}$  under agitation at 180 rpm (Artigas et al., 2008). After 5 days, water suspension and leaf disks from the same replicates were pooled by transferring the content into three new sterile flasks (1 per replicate, 600 mL per flask) and used as inoculum for the subsequent microcosm experiment (75 mL of inoculum per stream channel).

### Experimental Design

The experiment was performed in microcosm under controlled conditions of temperature ( $20 \pm 2^\circ\text{C}$ ) and photoperiod (13 h light: 11 h dark). In total, 24 artificial glass stream channels were set up ( $63 \text{ cm} \times 11 \text{ cm} \times 4 \text{ cm} = l \times w \times h$ ) following a  $2 \times 4$  factorial design, with nutrient condition as first factor (mesotrophic and eutrophic) and pesticide treatment as second one (Control, TBZ, S-Met, and MIX) in triplicates. Each channel was independent and had a separate 20 L tank, filled with 10 L of water from the corresponding condition (see details below) which supplied water through an individual aquarium pump (MJ 750, NEWA,  $1.5 \text{ L}\cdot\text{min}^{-1}$ ). Drilled ground water diluted to 1/3 with demineralized water was used for the experiment and distributed in two different 200 L tanks filled up to 100 L. Nutrient conditions were obtained by adding monobasic potassium phosphate ( $\text{K}_2\text{HPO}_4$ ) and sodium nitrate ( $\text{NaNO}_3$ ) to reach nominal concentrations of  $8 \text{ mg L}^{-1}$  N- $\text{NO}_3$  and  $0.5 \text{ mg L}^{-1}$  P- $\text{PO}_4$  for the eutrophic condition and  $0.8 \text{ mg L}^{-1}$  N- $\text{NO}_3$  and  $0.05 \text{ mg L}^{-1}$  P- $\text{PO}_4$  for the mesotrophic one. Nutrient enriched water was then distributed into 8 smaller tanks of 30 L (4 for either mesotrophic and eutrophic conditions), and pesticide contaminated treatments were obtained by adding either TBZ, S-Met or both from a  $5 \text{ mg L}^{-1}$  stock solution diluted in water (Sigma-Aldrich, Germany) to reach nominal pesticide concentrations of  $15 \mu\text{g L}^{-1}$  TBZ or/ and  $15 \mu\text{g L}^{-1}$  S-Met in the corresponding condition. Those 30 L tanks were finally used to supply water to each triplicate channels per each pesticide treatment.

In each channel, a total of 15 bags containing *Alnus glutinosa* leaves was disposed as follows: 6 small bags containing each 60 leaf disks (1 cm diameter) for biological analyses (extracellular enzymatic activities, fungal and bacterial biomass, fungal and bacterial community structure), 2 bags containing each 40 leaf disks (2 cm diameter) for *Gammarus* feeding rates, 1 bag containing 60 leaf disks (2 cm diameter) for adsorbed pesticides and leaf nutrient content analyses and 6 larger bags containing each 2 pre-weighted leaves for leaf mass loss determination. The experiment started in November 3 until December 13 2016 (6 weeks duration in total). After 4 days acclimation of leaves in all 24 channels under mesotrophic water (plus microbial inoculums) without pesticides, water from the channels was replaced to fit the eight experimental conditions described above. Samplings for biological analyses were performed every week by taking one of the small bags cited above and water was renewed weekly during the entire experiment using the above described procedure (6 water renewals during the whole experiment).

## Water and Leaves Characteristics

Physical and chemical parameters of stream water, including dissolved nutrients, TBZ, and S-Met concentrations were measured before and after each water renewal to evaluate nutrient and pesticide dissipation. Light was measured continuously for each condition using data loggers (HOBO® Pendant Temperature/Light, ProSensor), whereas temperature, pH, conductivity and dissolved oxygen were measured in each channel before and after each water renewal using portable probes (WTW). Concentrations of orthophosphates (P-PO<sub>4</sub>), nitrates (N-NO<sub>3</sub>), nitrites (N-NO<sub>2</sub>) and ammonium (N-NH<sub>4</sub>) were determined using ionic chromatography (930 Compact IC Flex, Metrohm) following standard methods for anions (NF EN ISO 10304-1; AFNOR, 2009) and cations (NF EN ISO 14911; AFNOR, 1999). Dissolved organic carbon (DOC) concentrations were measured in water following standard method (NF EN 1484; AFNOR, 1997) using an elemental analyzer (Multi N/C 3100, Analytik Jena). Prior to analyze DOC, inorganic carbon was removed by purging acidified (pH = 1 with HCl) samples with a CO<sub>2</sub>-free gas. Dissolved TBZ and S-Met concentrations were determined by direct injection of 20 µL of water samples previously filtered using a 0.2 µm polyester filter (MACHEREY-NAGEL) into an Ultra-High-Performance Liquid Chromatography (UHPLC) system (Shimadzu Nexera®) coupled to a triple quadrupole mass spectrometer (API 4000, LC/MS/MS system, AB Sciex). The chromatographic separation was performed on a Waters HSS T3 1.8 µm 2.1 × 100 mm column. Limit of quantification was 0.05 µg L<sup>-1</sup> for both pesticides.

Chemical composition of *Alnus* leaves (C, N, and P content) and adsorbed pesticides (TBZ and S-Met) were assessed at the end of the microcosm experiment (Day 40). Total carbon and nitrogen of the leaves were measured by dry combustion using CNS elemental analyzer (Flash2000, ThermoFisher Scientific). Total phosphorus was analyzed after microwave-acid mineralization in *aqua regia* (NF EN ISO 15587-1; AFNOR, 2002) using inductively coupled plasma

optical emission spectrometry (ICP-OES, 700 Series, Agilent Technologies) following standard method (EN ISO 11885, 2009). Results were obtained in mg per kg<sup>-1</sup> of leaf dry mass (DM)<sup>-1</sup> and converted into C:N, N:P, and C:P molar ratios. Adsorbed pesticides were extracted from leaves using the QuEChERS protocol (Payá et al., 2007) and pesticide were quantified using ultra-high performance liquid chromatography coupled to tandem mass spectrometry (UHPLC-MS-MS). Results were expressed in ng per g leaf DM<sup>-1</sup> with a limit of quantification for both the TBZ and S-Met of 8 ng g leaf DM<sup>-1</sup>.

## Microbial Biomass and Community Structure

Ergosterol concentration was used as a proxy to estimate fungal biomass associated with leaves (Gessner and Schmitt, 1996). Briefly, lipids were extracted from previously lyophilized leaves (15 leaf disks of 1 cm in diameter per sample) after incubation in 0.14 M KOH methanol at 80°C. Extracts were purified, concentrated using solid-phase extraction (tC18 cartridges, Sep-Pak Vac RC, 500 mg, Waters) and then analyzed using a high pressure liquid chromatography system (Lachrom L-7400, Merck-Hitachi) equipped with an ODS-2 Hypersil column (250 × 4.6 mm, 5 µm particle diameter; Thermo Scientific). Ergosterol was detected at 282 nm according to its specific absorbance spectrum. Ergosterol concentration was converted into fungal carbon using the conversion factor proposed by Gessner and Chauvet (1993) and Baldy and Gessner (1997).

Bacterial biomass was estimated using bacterial density according to the protocol of Borrel et al. (2012). Briefly, one leaf disk (1 cm diameter) was sampled at each sampling time and for each channel and fixed into 1 mL of 2% paraformaldehyde (storage at 4°C) until analysis using a BD FACS Calibur flow cytometer (Becton Dickinson Bio-sciences) (see Pesce et al., 2016). Bacterial density was converted to bacterial biomass using the conversion factor of (Bratbak, 1985).

The structure of fungal and bacterial communities associated to *Alnus* leaves was assessed using Automated Ribosomal Intergenic Spacer Analysis (ARISA) as described in Artigas et al. (2012). Total DNA extraction was performed from 5 leaf disks of 1 cm using the FastDNA SPIN Kit for soil (MP Biomedicals, Santa Ana, CA, United States) according to the manufacturer's instructions. Fungal community was characterized by amplification of the ITS1-5.8S-ITS2 region using the primers 2234C (5'-GTTTCCGTAGGTGAACCTGC-3') and 3126T (5'-ATATGCTTAAGTTCAGCGGGT-3'). Bacterial community was characterized by amplification of the 16S-23S ribosomal intergenic spacer region using the primers S-D-Bact-1522-b-S-20 (5'-185 TGCGGCTGGATCCCCTCCTT-3') and L-DBact-132-a-A-18 (5'-CCGGGTTTCCCCATTCGG-3'). PCR mixture and conditions are described in Baudoin et al. (2010). ARISA was performed using an Agilent 2100 Bioanalyzer with a DNA 1000 kit (Agilent Technologies) following the manufacturer's instructions. ARISA profiles (**Supplementary Figures S3, S4**) were then analyzed using the Gelcompare2 software (Applied Maths, Belgium) in order to obtain a fungal and bacterial OTUs presence/absence matrix.

## Microbial Activity

Decay rates of *Alnus* leaves ( $k$ ) were evaluated as the leaf mass loss during the experiment. At each sampling time and in each channel, 1 bag containing 2 pre-weighted *Alnus* leaves was sampled and brought to the oven (70°C for 48h) in order to obtain dry mass (DM). Decay rates were then obtained after fitting data to an exponential decay model according to the following equation:  $M_t = M_0 e^{-kt}$ , where  $M_0$  is the initial DM (g),  $M_t$  is the final DM (g) at time  $t$ , and  $k$  is the leaf decay coefficient (Petersen and Cummins, 1974).

Microbial enzymatic potential was estimated through the measurement of 5 extracellular enzyme activities: phenol oxidase (EC 1.14.18.1), laccase (EC 1.10.3.2),  $\beta$ -glucosidase (EC 3.2.1.21), alkaline phosphatase (EC 3.1.3.1) and leucine-aminopeptidase (EC). Phenol oxidase and laccase activities were measured from five leaf disks per sample, using 3,4-Dihydroxy-L-phenylalanine (L-DOPA, 1.5 mM final concentration) and 2,2'-Azino-bis(3-ethylbenzthiazoline-6-sulfonic acid (ABTS, 3 mM final concentration) respectively, in acetate buffer (pH 4.65, Sigma-Aldrich, St. Louis, MO, United States), as described in Sinsabaugh et al. (1994) and Johannes and Majcherczyk (2000).  $\beta$ -glucosidase, leucine-aminopeptidase and alkaline phosphatase activities were measured from 1 leaf disk per sample using the corresponding methylumbelliferyl and amido-4-methylcoumarin substrate analog (0.3 mM final concentration for each activity assay), as described in Artigas et al. (2012). After 1.5 h incubation in the dark and under agitation at 20°C, phenol oxidase and laccase activities were measured spectrophotometrically (460 nm and 415 nm, respectively) using an Ultrospec 2000 (Pharmacia Biotech, Trowbridge, United Kingdom) whereas  $\beta$ -glucosidase, leucine-aminopeptidase and alkaline phosphatase were determined fluorometrically (360/460 nm excitation/emission, Biotek synergy HT fluorometer) after addition of 0.3 mL glycine buffer (pH 10.4). All enzyme activity measurements were conducted under substrate saturating conditions. Area under the curve (AUC) was calculated for each enzyme and divided by the AUC for microbial biomass in order to obtain one value of integrated specific enzymatic activity for each nutrient condition and pesticide treatment. Activity values were expressed in  $\mu\text{mol substrate h}^{-1} \text{mg of microbial C}^{-1}$ .

## *Gammarus fossarum* Feeding

Feeding rates of *Gammarus fossarum* were assessed as described in Pesce et al. (2016). Briefly, *Gammarus* were harvested from the River Le Pollon in France (45°57'25.8''N 5°15'43.6''E) and acclimatized to laboratory conditions as previously described (Coulaud et al., 2011). In the laboratory, organisms were kept in 30 L tanks continuously supplied with drilled groundwater (500  $\mu\text{S/cm}$ ) and under constant aeration for 10 days. Photoperiod (16 h light: 8 h dark) was maintained and the temperature was kept at  $12 \pm 1^\circ\text{C}$ . Organisms were fed *ad libitum* with alder leaves (*Alnus glutinosa*), previously conditioned for  $6 \pm 1$  days in water. At the end of the microcosm experiment, bags containing 2 cm leaf disks were recovered and displayed into plastic beakers (8 disks per beaker) filled with 500 mL of

oxygenated water (12°C) and containing 12 *Gammarus* males with homogenous body size ( $\sim 10$  mm). The experiment was performed in triplicate for each replicate ( $n = 9$ ) and included a control (leaves without *G. fossarum*) to estimate leaf mass loss unrelated to *Gammarus* consumption. In parallel, daily water renewals were performed and dead *Gammarus* were recorded and removed if any to avoid bias in feeding rates estimation. Only 3 deaths occurred over the whole set of replicates (864 gammarids). The experiment was stopped after 28 h when leaf consumption achieved approximately 50% in at least one replicate, and the surface of remaining leaf disks was scanned numerically using SigmaScan®Pro v5.0 imaging software (Systat Software). Results were expressed in % of leaf consumed per *Gammarus* and per day and converted into ingested fungal C (mg Fungal C *Gammarus*<sup>-1</sup>Day<sup>-1</sup>) using the measurements of fungal C on leaves (see above).

## Statistical Analyses

Differences between nutrient conditions and between pesticide treatments for water physical and chemical characteristics (pH, oxygen, conductivity, temperature, TBZ and S-Met), leaf composition (C:N, C:P, and N:P, adsorbed TBZ and S-Met), decomposition rates, specific enzymatic activities and leaf palatability for macroinvertebrates were assessed using a Kruskal–Wallis non parametric test followed by pairwise comparison test using Tukey contrast ( $P < 0.05$ ). In addition, fungal and bacterial biomass colonization on *Alnus* leaves was fitted to a logistic growth model using the following equation:

$$y = \frac{A}{1 + \frac{A - y_0}{y_0} e^{-4W \max x/A}}$$

Where  $y_0$  is the fungal biomass (mg of fungal carbon g Leaf DM<sup>-1</sup>) at day 0,  $A$  is the fungal biomass at day 40 and  $W_{\max}$  is the maximum growth rate (day<sup>-1</sup>). Parameters from the model were then compared within each-other using the Kruskal–Wallis non-parametric test followed by pairwise comparison test using Tukey contrast ( $P < 0.05$ ). In addition, two non-metric dimensional scaling (NMDS) for either bacteria or fungi were used to assess communities' structure based on Bray-Curtis dissimilarity matrices. First NMDS was performed including all sampling times, whereas second NMDS was performed on last sampling time only (day 40). Each NMDS was accompanied by permutational multivariate analysis of variance (PERMANOVA) using nutrient condition as first factor and treatment as second one. All statistical analyses were computed using the R software and NMDS and PERMANOVA analyses were performed using metaMDS and Adonis functions from the vegan package (Oksanen et al., 2008) followed by pair-wise *post hoc* multiple comparisons.

## RESULTS

### Water and Leaves Characteristics

Average initial phosphate, nitrate and S-Met concentrations measured in water right after each water renewal were relatively

**TABLE 1** | Water physical and chemical characteristics measured after each water renewals in experimental stream channels exposed to fungicide (TBZ), herbicide (S-Met), both fungicide + herbicide (MIX) or non-exposed (Ctrl) in either mesotrophic or eutrophic nutrient condition.

	Mesotrophic				Eutrophic			
	Ctrl	TBZ	S-Met	MIX	Ctrl	TBZ	S-Met	MIX
P-PO <sub>4</sub> (mg L <sup>-1</sup> )		0.05 ± 0.01				0.46 ± 0.01		
N-NO <sub>3</sub> (mg L <sup>-1</sup> )		0.66 ± 0.01				7.89 ± 0.03		
TBZ water (μg L <sup>-1</sup> )	<0.05	9.87 ± 0.30	<0.05	11.39 ± 0.85	<0.05	10.67 ± 0.75	<0.05	11.64 ± 0.86
S-Met water (μg L <sup>-1</sup> )	<0.05	<0.05	16.26 ± 1.22	14.28 ± 0.54	<0.05	<0.05	17.21 ± 1.39	15.79 ± 0.96
TBZ leaf (μg gDM <sup>-1</sup> )	<0.008	1.22 ± 0.13	<0.008	1.16 ± 0.09	<0.008	0.68 ± 0.04	<0.008	0.71 ± 0.06
S-Met leaf (μg gDM <sup>-1</sup> )	<0.008	< 0.008	1.37 ± 0.19	1.05 ± 0.10	<0.008	<0.008	0.64 ± 0.05	0.50 ± 0.04
Temperature (°C)	19.9 ± 0.3	20.1 ± 0.3	18.4 ± 1.8	20.2 ± 0.2	20.2 ± 0.2	20.3 ± 0.2	20.4 ± 0.2	20.3 ± 0.2
Conductivity (μS)	167 ± 1	170 ± 2	168 ± 1	168 ± 1	208 ± 9*	205 ± 9*	206 ± 9*	205 ± 9*
Oxygen (mg L <sup>-1</sup> )	8.3 ± 0.1	8.2 ± 0.1	8.1 ± 0.1	8.2 ± 0.1	8.3 ± 0.2	8.3 ± 0.2	8.6 ± 0.4	8.4 ± 0.2
pH	7.7 ± 0.1	7.7 ± 0.1	7.7 ± 0.1	7.8 ± 0.1	7.8 ± 0.1	7.9 ± 0.1	7.9 ± 0.2	7.9 ± 0.2

Values are means ± standard error of the mean over the all experiment ( $n = 5$  for pesticides and  $n = 6$  for nutrients, temperature, conductivity, oxygen, and pH). Asterisks indicates significant differences between nutrient conditions for the considered treatment (Kruskal–Wallis,  $P < 0.05$ ).

close to the expected nominal concentrations (Table 1). In contrast, initial TBZ concentrations were about one-third lower than expected. No statistical differences were observed for both initial TBZ and S-Met concentrations between treatments (alone or MIX) and the subsequent water renewals. Similarly, no statistical differences were observed for initial N-NO<sub>3</sub> and P-PO<sub>4</sub> concentrations within each nutrient condition and between further water renewals. In addition, water temperature, dissolved oxygen concentration and pH displayed similar values between treatments (Kruskal–Wallis,  $P > 0.05$ , Table 1), while water conductivity displayed higher values in eutrophic conditions (Kruskal–Wallis,  $P < 0.001$ ) probably because of the higher nutrient (phosphate and nitrate) concentrations.

Nutrient dissipation, calculated as the difference after and before each water renewal in stream channels (once per week), revealed that both nitrate and phosphate were completely dissipated in the mesotrophic condition (Table 2), but not in the eutrophic one (average dissipation percentage of 65.4% for N-NO<sub>3</sub> and 93.1% for P-PO<sub>4</sub>). In the eutrophic condition, P-PO<sub>4</sub> dissipation was greater than that of N-NO<sub>3</sub> revealing that leaf-associated microbial community's used more P than N from water. This difference was also reflected in leaves nutrient content at the end of the experiment (Kruskal–Wallis,  $P < 0.01$ , Figure 1). Specifically, lower C:P and N:P ratios were recorded in eutrophic channels, which show the greater P accumulation in leaves and therefore confirms the greater P dissipation from water. Pesticide treatments did not significantly influence N-NO<sub>3</sub> and P-PO<sub>4</sub> dissipation (Kruskal–Wallis,  $P = 0.18$  and  $P = 0.13$  respectively), although nitrate dissipation for the eutrophic condition was about 13–22% greater in the MIX in comparison with Ctrl, and S-Met and TBZ alone (Table 2).

Concerning pesticides in water, about 39–70% of each pesticide were dissipated every week in all pesticide-treated channels (Table 2). For each pesticide, no differences in dissipation were observed between nutrient conditions and pesticide treatments (i.e., Alone vs. MIX) with some exceptions. In eutrophic channels, S-Met dissipation was slightly greater in the MIX treatment (69% dissipation) compared to S-Met

alone (56%) (Kruskal–Wallis,  $P < 0.05$ ). Pesticide sorption was assessed at the end of the experiment and only a small part of TBZ and S-Met weekly supplied to channels was adsorbed onto *Alnus* leaves (less than 5%, Table 2). Comparatively, pesticide adsorption was higher in mesotrophic channels compared with the eutrophic ones (Kruskal–Wallis,  $P < 0.05$ ). Exposure of pesticides alone or in MIX did not have an effect on their adsorption to leaves.

## Microbial Leaf-Litter Decomposition

*Alnus* leaves decomposition displayed differences between both nutrient conditions (Kruskal–Wallis,  $P < 0.001$ ) and pesticide treatments (Kruskal–Wallis,  $P < 0.01$ , Table 3 and Supplementary Table S1). On average, leaf decay rates in eutrophic channels were 34% higher compared to those in mesotrophic channels. In addition, decay rates were on average 17% higher in control than in pesticide-treated channels (including TBZ, S-Met, and MIX) in the eutrophic condition, whereas no differences between pesticide treatments and control were observed under mesotrophic conditions. No differences were observed for *Alnus* decay rates in TBZ and S-Met alone compared to MIX, regardless of the nutrient condition.

Specific extracellular enzymatic activities (i.e., cumulated enzymatic activity corrected by cumulated microbial biomass) displayed variation between the tested conditions and the enzyme considered (Figure 2). Specifically, differences in ligninolytic (laccase and phenol oxidase, Figures 2A,B) and peptidase (leucine-aminopeptidase, Figure 2C) activities were observed between both nutrient conditions and pesticide treatments, whereas no between-treatment difference were observed for β-glucosidase and alkaline phosphatase (data not shown). Ligninolytic activities (phenol oxidase and laccase) were higher in eutrophic than in mesotrophic conditions (Kruskal–Wallis,  $P < 0.001$  each). Exclusively for the eutrophic condition, phenol oxidase activity was enhanced in both TBZ and MIX treatments (pairwise,  $P < 0.001$  each) while laccase activity increased in the presence of TBZ (pairwise,  $P < 0.001$ ), but not in the MIX treatment (pairwise,  $P = 0.90$ ). As for ligninolytic activities,

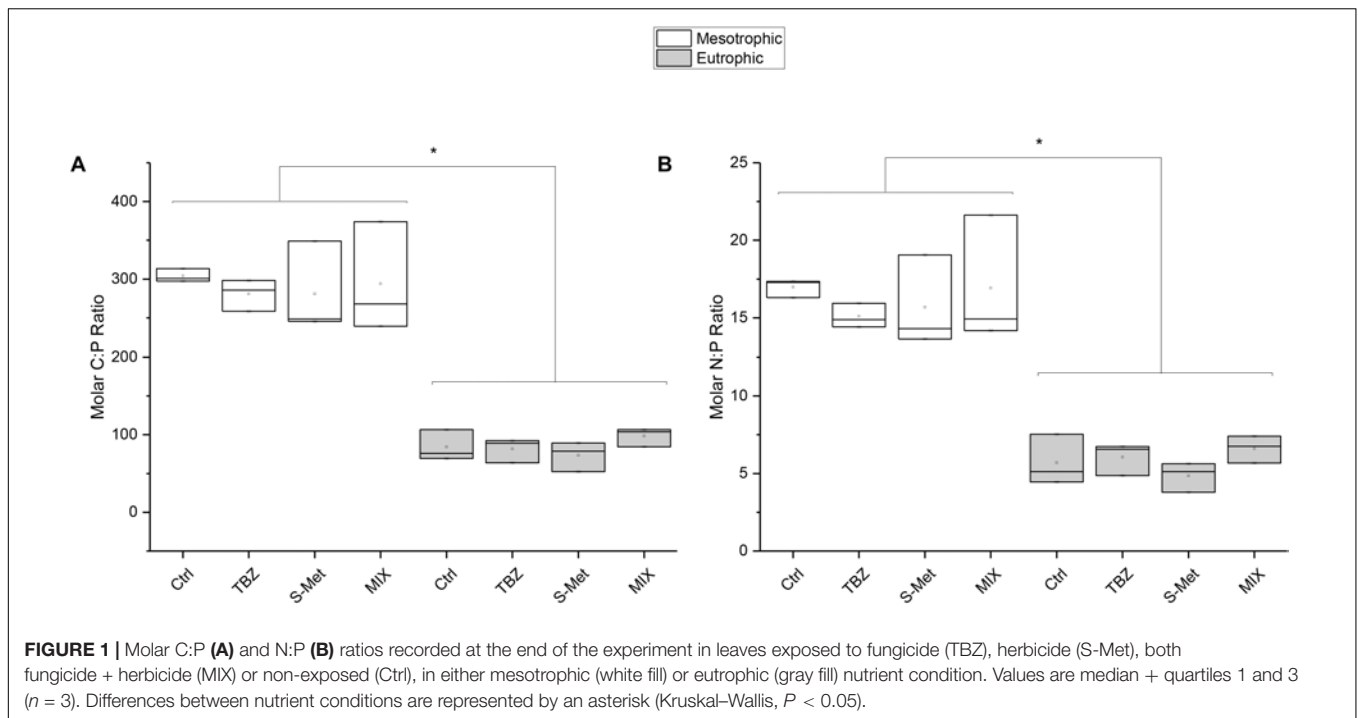


**FIGURE 1 |** Molar C:P (A) and N:P (B) ratios recorded at the end of the experiment in leaves exposed to fungicide (TBZ), herbicide (S-Met), both fungicide + herbicide (MIX) or non-exposed (Ctrl), in either mesotrophic (white fill) or eutrophic (gray fill) nutrient condition. Values are median + quartiles 1 and 3 ( $n = 3$ ). Differences between nutrient conditions are represented by an asterisk (Kruskal–Wallis,  $P < 0.05$ ).

**TABLE 2 |** Average percentage of nutrients and pesticides dissipation as well as adsorbed pesticides on leaves recorded at the end of the experiment in experimental stream channels exposed to fungicide (TBZ), herbicide (S-Met), both fungicide + herbicide (MIX) or non-exposed (Ctrl) in either mesotrophic or eutrophic nutrient condition.

	Mesotrophic				Eutrophic			
	Ctrl	TBZ	S-Met	MIX	Ctrl	TBZ	S-Met	MIX
P-PO4	100	100	100	100	93.80 ± 2.05	98.01 ± 1.13	88.26 ± 2.23	92.46 ± 3.24
N-NO3	100	100	100	100	64.99 ± 5.90*	57.98 ± 4.84*	63.89 ± 7.37*	74.53 ± 0.87*
TBZ	–	38.87 ± 2.88	–	45.80 ± 2.12	–	43.56 ± 2.93	–	51.19 ± 1.28
S-Met	–	–	54.68 ± 0.99	50.16 ± 1.89	–	–	56.45 ± 0.77	69.40 ± 0.39
Adsorbed TBZ ( $\mu\text{g g of leaf DM}^{-1}$ )	–	1.22 ± 0.13	–	1.17 ± 0.09	–	0.68 ± 0.04*	–	0.72 ± 0.06*
Adsorbed S-Met ( $\mu\text{g g of leaf DM}^{-1}$ )	–	–	1.37 ± 0.19	1.05 ± 0.10	–	–	0.64 ± 0.05*	0.50 ± 0.04*

Values are means ± standard error of the mean over the all experiment including all replicates ( $n = 15$  for pesticides and nutrients dissipation in water and  $n = 3$  for adsorbed TBZ and S-Met on leaves). Asterisks indicates significant differences between nutrient conditions for the considered treatment (Kruskal–Wallis,  $P < 0.05$ ).

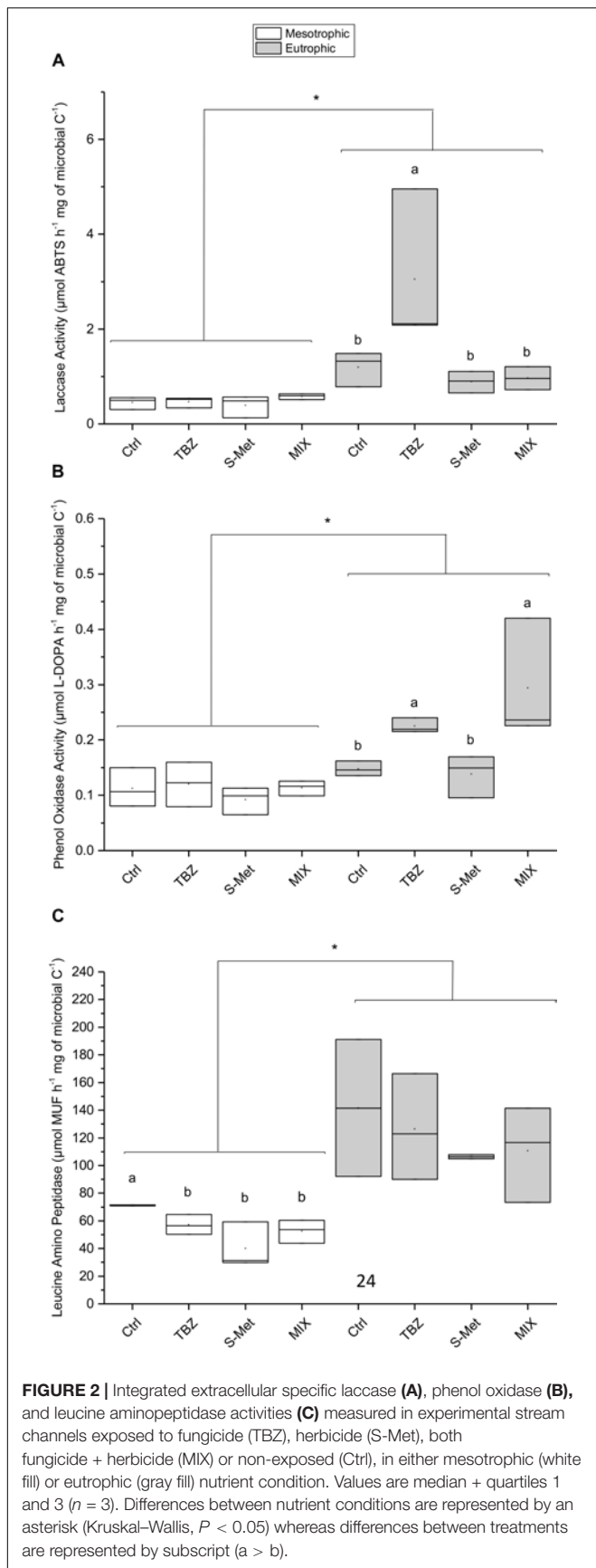
**TABLE 3 |** Alnus leaves decomposition rates ( $K$ , means ± standard error of the mean) expressed in  $\text{day}^{-1}$  measured in experimental stream channels exposed to fungicide (TBZ), herbicide (S-Met), both fungicide + herbicide (MIX) or non-exposed (Ctrl), in either mesotrophic or eutrophic nutrient condition.

	Ctrl		+TBZ		+S-Met		+MIX	
	$K$	$R^2$	$K$	$R^2$	$K$	$R^2$	$K$	$R^2$
Eutrophic	$13.34 \times 10^{-3}$ ± $1.52 \times 10^{-3}$	0.94	<b><math>11.19 \times 10^{-3}</math></b> ± $1.23 \times 10^{-3}$	0.95	<b><math>11.39 \times 10^{-3}</math></b> ± $1.34 \times 10^{-3}$	0.94	<b><math>10.48 \times 10^{-3}</math></b> ± $1.27 \times 10^{-3}$	0.93*
Mesotrophic	$8.81 \times 10^{-3}$ ± $1.91 \times 10^{-3}$	0.81	$8.69 \times 10^{-3}$ ± $1.79 \times 10^{-3}$	0.83	$7.49 \times 10^{-3}$ ± $1.52 \times 10^{-3}$	0.83	$7.38 \times 10^{-3}$ ± $1.39 \times 10^{-3}$	0.85

Values were obtained by fitting average leaf mass loss (in %) over the experiment for each treatment to an exponential decay model and goodness of fit was represented by  $R^2$ . Bold values indicate significant differences between treatments and control within nutrient condition whereas asterisk indicates significant differences between nutrient conditions.

leucine aminopeptidase was higher in the eutrophic condition (Kruskal–Wallis,  $P < 0.001$ ) but effects of pesticide treatments were only observed in the mesotrophic condition. Under the

mesotrophic nutrient condition, lower peptidase activity was recorded in all pesticide exposed channels (including TBZ, S-Met, and MIX) compared to control (pairwise,  $P < 0.05$  each) with a



reduction that was more important in channels exposed to S-met (average reduction of 44.8% compared to control).

### Microbial Biomass and Communities' Structure

Fungal biomass colonizing *Alnus* leaves displayed differences between nutrient conditions (Kruskal–Wallis,  $P < 0.001$ ). Globally, higher fungal biomass was accumulated at the end of the experiment in the eutrophic condition compared to the mesotrophic one (A, Table 4 and Supplementary Figure S1 and Table S2), despite overall lower fungal growth rate ( $W_{max}$ ) under eutrophic conditions than in mesotrophic conditions. Stationary phase for eutrophic channels (Supplementary Figure S1) was reached around 35 days or more than 40 days for the control treatment, except for the MIX treatment which occurred much earlier (around 25 days). No differences between pesticide treatments were observed in terms of maximal biomass (A, Table 4). However, maximal growth rate in control channels displayed lower values in comparison with the pesticides exposed ones ( $W_{max}$ , pairwise,  $P = 0.001$ ). In contrast with eutrophic channels, stationary phase for mesotrophic channels (Supplementary Figure S1) was reached much earlier (around 10 days). Again, no differences were observed under those nutrient conditions between pesticide treatments for maximal biomass neither for maximal growth rates.

The fungal community structure appeared to mostly vary between sampling dates rather than according to nutrient and/or pesticide treatments (Supplementary Figure S3A). However, nutrient conditions also influenced the structure of these communities leading to significant differences between mesotrophic and eutrophic conditions the end of the study (PERMANOVA,  $P < 0.001$ , Figure 3A). Here, no differences were observed in terms of OTU's richness but in terms of OTU replacement leading to changes in community structure between nutrient conditions. Differences were also observed at the end of the experiment between pesticide treatments regardless of the nutrient condition (PERMANOVA,  $P < 0.001$ ) although such differences were much more marked for the eutrophic condition (Figure 3A). Again, differences were explained by OTUs replacement rather than by shifts in OTUs richness.

Bacterial biomass was very low in comparison with that of fungi, representing less than 1% of the total microbial biomass colonizing *Alnus* leaves (Supplementary Figure S2). Similarly to fungi, bacteria displayed higher biomass values in the eutrophic condition compared to the mesotrophic one, although differences were less marked than for fungi (Kruskal–Wallis,  $P < 0.001$ ). Again, no differences were observed between pesticide treatments regardless of the nutrient condition. As for fungi, the structure of bacterial communities appeared to be mostly influenced by the sampling time (Supplementary Figure S3B). Significant differences were also observed between nutrient conditions at the end of the study (PERMANOVA,  $P < 0.001$ , Figure 3B), although these differences were less marked than those for fungi. In addition, differences were observed between pesticide treatments regardless of the nutrient condition (PERMANOVA,  $P < 0.001$ ) although still less marked in the case of the mesotrophic condition than the eutrophic one (Figure 3B). As for fungi,

**TABLE 4 |** Parameters extracted from the measured fungal biomass after fitting to a logistic growth model in experimental stream channels exposed to fungicide (TBZ), herbicide (S-Met), both fungicide + herbicide (MIX) or non-exposed (Ctrl), in either mesotrophic or eutrophic nutrient condition.

		$Y_0$ (mg of fungal C gDM <sup>-1</sup> )	A (mg of fungal C gDM <sup>-1</sup> )	$W_{max}$ (Day <sup>-1</sup> )	$R^2$	p-value
Mesotrophic	Ctrl	7.28 ± 0.60	18.86 ± 0.27	2.82 ± 0.38	0.99	1.08 <sup>E</sup> -6
	TBZ	7.35 ± 1.62	20.05 ± 0.74	2.49 ± 0.79	0.93	4.60 <sup>E</sup> -5
	S-Met	7.28 ± 2.25	18.65 ± 1.01	5.75 ± 13.85	0.84	1.97 <sup>E</sup> -4
	MIX	7.62 ± 1.60	20.54 ± 0.77	1.95 ± 0.64	0.93	4.35 <sup>E</sup> -5
Eutrophic	Ctrl	10.26 ± 1.71	<b>35.61 ± 3.26</b>	<b>0.89 ± 0.18</b>	0.96	5.40E-5
	TBZ	9.36 ± 2.44	<b>33.16 ± 2.26</b>	<b>1.35 ± 0.39*</b>	0.93	1.45E-4
	S-Met	9.34 ± 3.40	<b>34.58 ± 3.37</b>	<b>1.35 ± 0.52*</b>	0.89	5.18E-4
	MIX	8.88 ± 2.22	<b>30.57 ± 1.91</b>	<b>1.32 ± 0.38*</b>	0.94	1.20E-4

Values are means ± standard error of the mean returned by the origin software (n = 3).  $Y_0$  represent the initial fungal biomass (day 0), A represent the maximal fungal biomass (day 40) and  $W_{max}$  represent maximal fungal growth rate. Values in bold represent differences between nutrient conditions (Kruskal-Wallis,  $P < 0.05$ ) and asterisk represent differences between treatments and control within each nutrient conditions (Tukey,  $P < 0.05$ ).

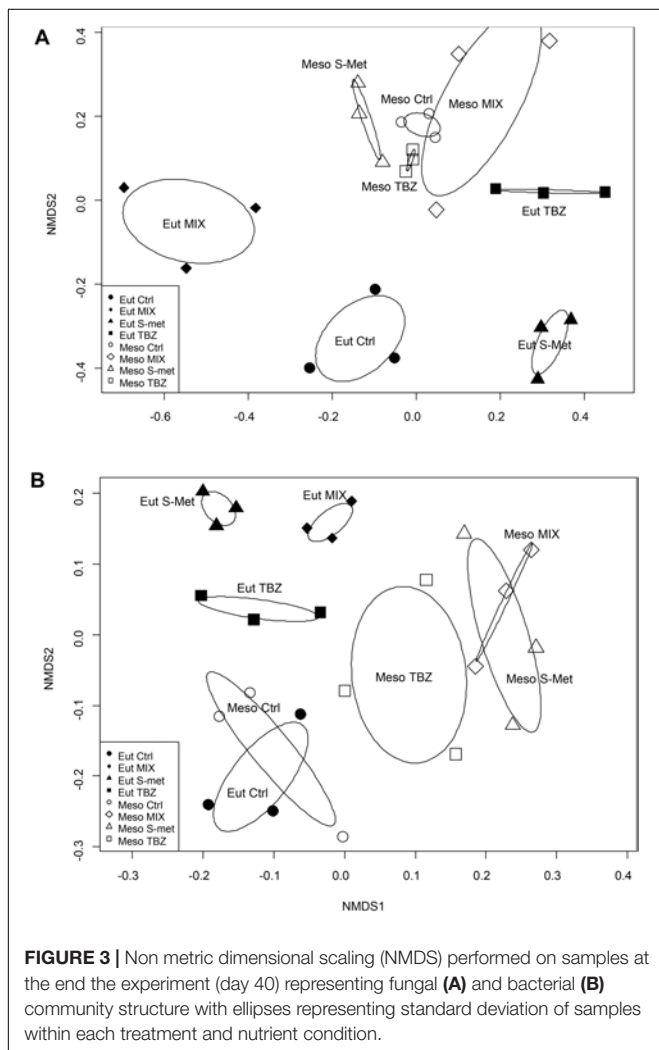


**FIGURE 3 |** Non metric dimensional scaling (NMDS) performed on samples at the end the experiment (day 40) representing fungal (A) and bacterial (B) community structure with ellipses representing standard deviation of samples within each treatment and nutrient condition.

differences between nutrient conditions and pesticide treatments were mostly explained by OTUs replacement. However, control for both mesotrophic and eutrophic condition displayed lower OTUs richness compared to pesticides exposed treatments (both TBZ, S-Met and MIX).

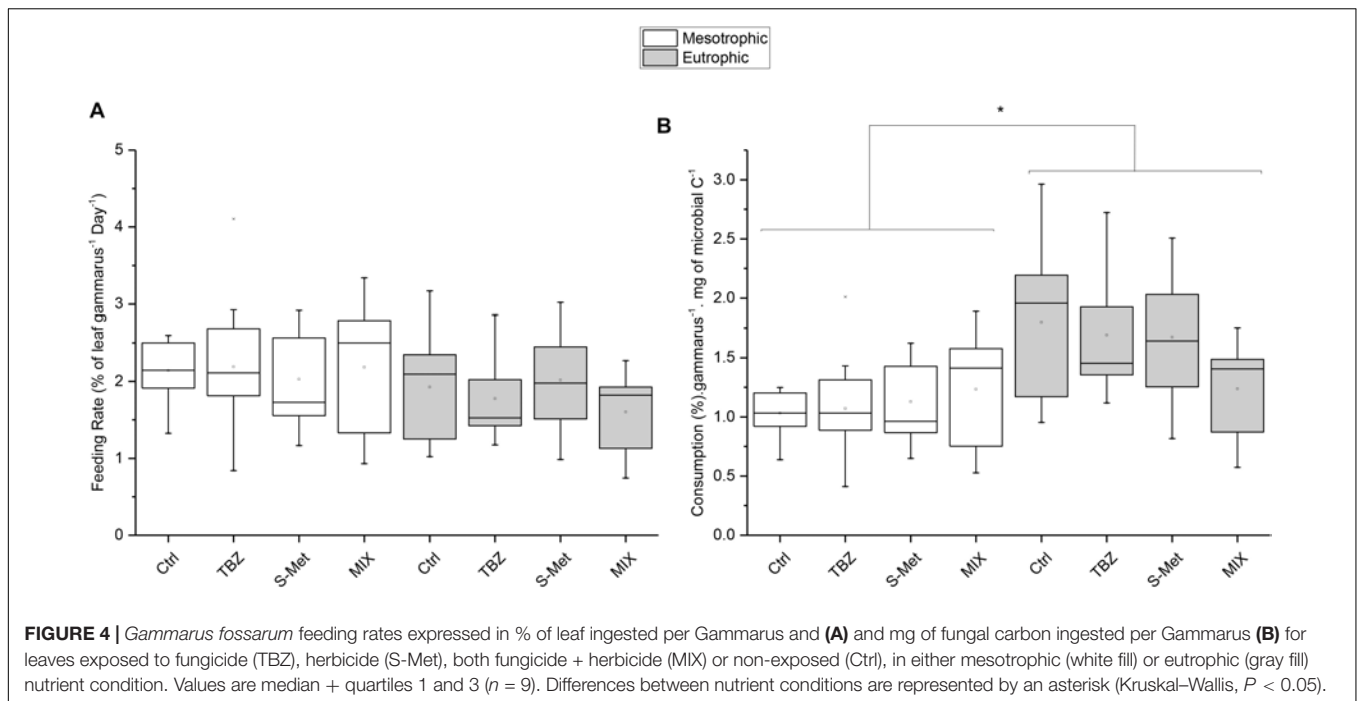
### Macroinvertebrate Feeding Activity

*Gammarus* feeding rates expressed as percentage of leaf consumption per individuals were neither affected by nutrients nor by pesticide treatments (Kruskal-Wallis,  $P = 0.13$  and  $P = 0.73$ ; respectively) (Figure 4A). Nevertheless, feeding rates corrected by mg of fungal carbon ingested per individual (Figure 4B) were significantly higher in eutrophic conditions compared to the mesotrophic ones (Kruskal-Wallis,  $P < 0.01$ ). No statistical differences were observed between pesticide treatments within each nutrient condition, although values for corrected feeding rates seemed substantially lower in the MIX treatment (TBZ + S-Met) compared to other pesticide treatments (and especially control) under eutrophic conditions (Figure 4B).

### DISCUSSION

In the present study, we assessed the effects of the interaction between nutrients (Nitrogen and Phosphorus) and pesticides (TBZ and S-Met, alone or in mixture) on the structure and activity of heterotrophic microbial communities associated with leaf litter. As already observed by Gulis and Suberkropp (2003), nutrients appeared as the main factor driving the activity and shaping the biomass and structure of the studied communities. However, significant effect of the pesticide treatments were observed, although rather minor in comparison with those of nutrients.

In mesotrophic condition, almost no effect of the pesticide treatments were observed on microbial communities, which contrast with our first hypothesis and with previous studies assessing the ecotoxicological effects of similar TBZ concentrations (Bundschuh et al., 2011; Artigas et al., 2012; Donnadieu et al., 2016). Only leucine aminopeptidase activity was slightly lower in treated channels than in control ones suggesting a potential direct but non-specific effects of pesticides' toxicity on bacteria, known as the main producer of this enzyme (Romani et al., 2006). This lack of microbial functional and structural response to TBZ might be explained by the fixed experimental conditions. Indeed, every week all dissolved nutrients were rapidly consumed by microorganisms. Hence, microbial communities may have suffered chronic nutrient



deficiency in the mesotrophic channels, limiting biomass accumulation and possibly masking pesticide effects in our study.

Significant effects of the pesticide treatments were observed in eutrophic conditions, which contrast with our second hypothesis as we expected nutrient availability to buffer the effects of pesticide toxicity in leaf-associated microbial communities (Aristi et al., 2016; Fernández et al., 2016). The slight decrease in *Alnus* decay rates exposed to TBZ (−16%), S-Met (−15%) and MIX (−22%) might suggest that nutrient concentrations (i.e.,  $N-NO_3$  and  $P-PO_4$ ) were not sufficient to compensate pesticide toxicity. Another explanation could be that co-occurrence between pesticides and high nutrients concentrations may have negative effects on microbial decomposition. In the study of Fernandes et al. (2009) assessing the interaction between a range of zinc ( $0.03 \text{ mg L}^{-1}$ ,  $0.98 \text{ mg L}^{-1}$ , and  $9.8 \text{ mg L}^{-1}$ ) and phosphate ( $0.05 \text{ mg L}^{-1}$ ,  $0.2 \text{ mg L}^{-1}$ , and  $0.5 \text{ mg L}^{-1}$ ) concentrations, strongest inhibition in *Alnus* decomposition were observed in leaves exposed to both zinc and high phosphate concentrations. Although mechanisms behind remain unclear, the author explained this by changes in fungal community structure. In our study, the changes in both fungal and bacterial community structure exposed to pesticides might explain the observed differences in terms of decomposition activity (Swan and Palmer, 2004; Gessner et al., 2010). Similarly, such changes in fungal community structure might explain the lower fungal growth rates in the control channels than in the pesticide treated ones (Zubrod et al., 2015). Since specific traits of certain species are known to have a greater influence on leaf decomposition (Duarte et al., 2006), high nutrient exposure in our study may have increased the contribution of some fungal species, which were at the same time more sensitive to pesticide exposure. However, this is a hypothesis that needs to be tested.

Overall, our results show that nutrients exacerbated the effects of pesticides on leaf decay rates, and that the previously described compensatory effect of nutrients on pesticide toxicity (Fernández et al., 2016; Gardeström et al., 2016) is probably toxicant and/or concentration dependent and does not always apply on aquatic microbial communities.

Interestingly, TBZ and S-met in the MIX treatment displayed different kind of interactions in eutrophic channels in our study. Specifically, antagonistic-type interaction was observed between those two compounds on leaf decay rates as no differences were observed between TBZ, S-Met and MIX treatments. Similarly, the fact that laccase activity was stimulated in channels exposed to TBZ but not in channels exposed to the MIX (TBZ + S-Met) in the eutrophic condition also highlight interaction between those two compounds on laccase activity. The observed effects on laccase activity suggest that perhaps (i) MIX exposure had negative effect on specific microorganisms producers of laccase or (ii) that antagonistic-type interaction occurred between TBZ and S-Met on this enzymatic activity. On the contrary, no interaction between TBZ and S-Met was observed on phenol oxidase activity. Regarding the literature, ligninolytic enzyme activity stimulation has been linked to toxicity mitigation of phenolic molecules (Baldrian, 2006; Sinsabaugh, 2010; Karas et al., 2011). Thus, the observed stimulation in TBZ treatments (for both phenol oxidase and laccase) could reflect detoxification mechanisms set up by fungi, possibly resulting in TBZ transformation in order to reduce its toxicity (Junghanns et al., 2005; Artigas et al., 2017). Whatever the hypothesis considered, our results show that the interaction between different pesticide compounds, even if they present low potential threat to non-target organisms, may impair the ability of microbial communities to display proper stress response (Dawoud et al., 2017).

The interaction between nutrient conditions and pesticide treatments (TBZ and S-Met alone) did not affect shredder feeding rates. In the context of TBZ exposure, this result contrasts with the study of Bundschuh et al. (2011) but is consistent with that of Pesce et al. (2016). These inter-study differences may be explained by differences in TBZ concentrations supplied, which were substantially higher in the study of Bundschuh et al. (2011) (50 and 500  $\mu\text{g L}^{-1}$ ) than in the study of Pesce et al. (2016) and the present one. The lack of effect of previous exposure of leaves to pesticides on feeding rates, and that whatever the tested treatment, can be explained by the lack of significant differences in term of fungal biomass between pesticide treatments, which is one of the main parameter influencing *Gammarus* feeding (Bundschuh et al., 2011; Zubrod et al., 2011). Besides, only small quantities of pesticides were found adsorbed on the exposed leaves, thus probably resulting in a low toxic effect to *Gammarus* macroinvertebrates. Overall, our results show that indirect effects of environmentally relevant concentrations of pesticides on leaf palatability for macroinvertebrates can be negligible.

## CONCLUSION

The present experiment showed that nutrients were the main parameter driving the structure and functioning of heterotrophic microbial communities colonizing *Alnus* leaf litter. However, we found that environmentally relevant concentrations of a fungicide and a herbicide, alone and/or in mixture, were sufficient to induce changes in the structure of microbial communities leading to a slight decrease in their decomposition activity, although no effects on leaf palatability for macroinvertebrates were observed. Interestingly, such effects were only visible under eutrophic conditions, suggesting antagonistic-type interaction between nutrients and xenobiotic on leaf decomposition.

## REFERENCES

- Abdel-Raheem, A. M., and Ali, E. H. (2004). Lignocellulolytic enzyme production by aquatic hyphomycetes species isolated from the Nile's delta region. *Mycopathologia* 157, 277–286. doi: 10.1023/B:MYCO.0000024178.62244.7c
- Aristi, I., Casellas, M., Elosegi, A., Insa, S., Petrovic, M., Sabater, S., et al. (2016). Nutrients versus emerging contaminants—or a dynamic match between subsidy and stress effects on stream biofilms. *Environ. Pollut.* 212, 208–215. doi: 10.1016/j.envpol.2016.01.067
- Artigas, J., Majerholc, J., Foulquier, A., Margoum, C., Volat, B., Neyra, M., et al. (2012). Effects of the fungicide tebuconazole on microbial capacities for litter breakdown in streams. *Aquat. Toxicol.* 122, 197–205. doi: 10.1016/j.aquatox.2012.06.011
- Artigas, J., Romani, A. M., and Sabater, S. (2008). Effect of nutrients on the sporulation and diversity of aquatic hyphomycetes on submerged substrata in a Mediterranean stream. *Aquat. Bot.* 88, 32–38. doi: 10.1016/j.aquabot.2007.08.005
- Artigas, J., Rossi, F., Gerphagnon, M., and Mallet, C. (2017). Sensitivity of laccase activity to the fungicide tebuconazole in decomposing litter. *Sci. Total Environ.* 584, 1084–1092. doi: 10.1016/j.scitotenv.2017.01.167
- Baldrian, P. (2006). Fungal laccases—occurrence and properties. *FEMS Microbiol. Rev.* 30, 215–242. doi: 10.1111/j.1574-4976.2005.00010.x
- Baldy, V., and Gessner, M. O. (1997). Towards a budget of leaf litter decomposition in a first-order woodland stream. Décomposition des litières dans une petite

## AUTHOR CONTRIBUTIONS

CIM, JA, and SP designed the experimental design for this study. FR, CIM, JA, and SP participated in the redaction and discussion of the article. ChM performed all pesticides measurements (in water and adsorbed with leaves) whereas MM performed all nutrients measurements (carbon, nitrogen, and phosphorus in water and adsorbed with leaves). AC took care of the palatability tests for the macroinvertebrates. All authors were involved in the critical reading of the paper, with special contribution of CIM, JA, and SP.

## ACKNOWLEDGMENTS

This study was funded by the Water Agency Loire-Bretagne through the EcoBioPest project. The authors thank Bernadette Volat, Christophe Rosy, Bernard Motte, and Anaïs Charton for their help with the experimental setup and for microbial analysis. The authors also thank Celine Guillemain, Myriam Arhror, Corinne Brosse-Quilgars, and Loïc Richard from the LAMA team in Irstea for chemical analyses as well as Hervé Quéau and Nicolas Delorme for technical assistance on feeding rate measurements. FR was funded by a Ph.D. grant from the French Ministry of Higher Education and Research.

## SUPPLEMENTARY MATERIAL

The Supplementary Material for this article can be found online at: <https://www.frontiersin.org/articles/10.3389/fmich.2018.02437/full#supplementary-material>

- rivière forestière: essai de bilan. *C. R. Acad. Sci.-Ser. III-Sci. Vie* 320, 747–758. doi: 10.1016/S0764-4469(97)84824-X
- Baldy, V., Gobert, V., Guerold, F., Chauvet, E., Lambriot, D., and Charcosset, J.-Y. (2007). Leaf litter breakdown budgets in streams of various trophic status: effects of dissolved inorganic nutrients on microorganisms and invertebrates. *Freshw. Biol.* 52, 1322–1335. doi: 10.1111/j.1365-2427.2007.01768.x
- Baudoin, E., Lerner, A., Mirza, M. S., El Zembrany, H., Prigent-Combaret, C., Jurkevich, E., et al. (2010). Effects of *Azospirillum brasilense* with genetically modified auxin biosynthesis gene ipdC upon the diversity of the indigenous microbiota of the wheat rhizosphere. *Res. Microbiol.* 161, 219–226. doi: 10.1016/j.resmic.2010.01.005
- Berenzen, N., Lentzen-Godding, A., Probst, M., Schulz, H., Schulz, R., and Liess, M. (2005). A comparison of predicted and measured levels of runoff-related pesticide concentrations in small lowland streams on a landscape level. *Chemosphere* 58, 683–691. doi: 10.1016/j.chemosphere.2004.05.009
- Borrel, G., Colombet, J., Robin, A., Lehours, A.-C., Prangishvili, D., and Sime-Ngando, T. (2012). Unexpected and novel putative viruses in the sediments of a deep-dark permanently anoxic freshwater habitat. *ISME J.* 6, 2119–2127. doi: 10.1038/ismej.2012.49
- Bratbak, G. (1985). Bacterial biovolume and biomass estimations. *Appl. Environ. Microbiol.* 49, 1488–1493.
- Brosed, M., Lamothe, S., and Chauvet, E. (2016). Litter breakdown for ecosystem integrity assessment also applies to streams affected by pesticides. *Hydrobiologia* 773, 87–102. doi: 10.1007/s10750-016-2681-2

- Bundschuh, M., Zubrod, J. P., Kosol, S., Maltby, L., Stang, C., Duester, L., et al. (2011). Fungal composition on leaves explains pollutant-mediated indirect effects on amphipod feeding. *Aquat. Toxicol.* 104, 32–37. doi: 10.1016/j.aquatox.2011.03.010
- Chandrashekar, K. R., and Kaveriappa, K. M. (1991). Production of extracellular cellulase by *Lunulospora curvula* and *Flagellospora penicillioides*. *Folia Microbiol.* 36, 249–255. doi: 10.1007/BF02814357
- Copping, L. G., and Hewitt, H. G. (2007). *Chemistry and Mode of Action of Crop Protection Agents*. London: Royal Society of Chemistry.
- Coulaud, R., Geffard, O., Xuereb, B., Lacaze, E., Quéau, H., Garric, J., et al. (2011). *In situ* feeding assay with *Gammarus fossarum* (Crustacea): modelling the influence of confounding factors to improve water quality biomonitoring. *Water Res.* 45, 6417–6429. doi: 10.1016/j.watres.2011.09.035
- Cummins, K. W. (1974). Structure and function of stream ecosystems. *BioScience* 24, 631–641. doi: 10.2307/1296676
- Dawoud, M., Bundschuh, M., Goedkoop, W., and McKie, B. G. (2017). Interactive effects of an insecticide and a fungicide on different organism groups and ecosystem functioning in a stream detrital food web. *Aquat. Toxicol.* 186, 215–221. doi: 10.1016/j.aquatox.2017.03.008
- Donnadieu, F., Besse-Hoggan, P., Forestier, C., and Artigas, J. (2016). Influence of streambed substratum composition on stream microbial communities exposed to the fungicide tebuconazole. *Freshw. Biol.* 61, 2026–2036. doi: 10.1111/fwb.12679
- Duarte, S., Pascoal, C., Cássio, F., and Bärlocher, F. (2006). Aquatic hyphomycete diversity and identity affect leaf litter decomposition in microcosms. *Oecologia* 147, 658–666. doi: 10.1007/s00442-005-0300-4
- Fernandes, I., Duarte, S., Cássio, F., and Pascoal, C. (2009). Mixtures of zinc and phosphate affect leaf litter decomposition by aquatic fungi in streams. *Sci. Total Environ.* 407, 4283–4288. doi: 10.1016/j.scitotenv.2009.04.007
- Fernández, D., Tummala, M., Schreiner, V. C., Duarte, S., Pascoal, C., Winkelmann, C., et al. (2016). Does nutrient enrichment compensate fungicide effects on litter decomposition and decomposer communities in streams? *Aquat. Toxicol.* 174, 169–178. doi: 10.1016/j.aquatox.2016.02.019
- Flores, L., Banjac, Z., Farré, M., Larrañaga, A., Mas-Martí, E., Muñoz, I., et al. (2014). Effects of a fungicide (imazalil) and an insecticide (diazinon) on stream fungi and invertebrates associated with litter breakdown. *Sci. Total Environ.* 47, 532–541. doi: 10.1016/j.scitotenv.2014.01.059
- Gardeström, J., Ermold, M., Goedkoop, W., and McKie, B. G. (2016). Disturbance history influences stressor impacts: effects of a fungicide and nutrients on microbial diversity and litter decomposition. *Freshw. Biol.* 61, 2171–2184. doi: 10.1111/fwb.12698
- Gessner, M. O., and Chauvet, E. (1993). Ergosterol-to-biomass conversion factors for aquatic hyphomycetes. *Appl. Environ. Microbiol.* 59, 502–507.
- Gessner, M. O., and Chauvet, E. (1994). Importance of stream microfungi in controlling breakdown rates of leaf litter. *Ecology* 75, 1807–1817. doi: 10.2307/1939639
- Gessner, M. O., and Schmitt, A. L. (1996). Use of solid-phase extraction to determine ergosterol concentrations in plant tissue colonized by fungi. *Appl. Environ. Microbiol.* 62, 415–419.
- Gessner, M. O., Swan, C. M., Dang, C. K., McKie, B. G., Bardgett, R. D., Wall, D. H., et al. (2010). Diversity meets decomposition. *Trends Ecol. Evol.* 25, 372–380. doi: 10.1016/j.tree.2010.01.010
- Götz, T., and Böger, P. (2004). The very-long-chain fatty acid synthase is inhibited by chloroacetamides. *Z. Naturforsch. C* 59, 549–553. doi: 10.1515/znc-2004-7-818
- Gulis, V., and Suberkropp, K. (2003). Effect of inorganic nutrients on relative contributions of fungi and bacteria to carbon flow from submerged decomposing leaf litter. *Microb. Ecol.* 45, 11–19. doi: 10.1007/s00248-002-1032-1
- Johannes, C., and Majcherzyk, A. (2000). Laccase activity tests and laccase inhibitors. *J. Biotechnol.* 78, 193–199. doi: 10.1016/S0168-1656(00)00208-X
- Junghanns, C., Moeder, M., Krauss, G., Martin, C., and Schlosser, D. (2005). Degradation of the xenoestrogen nonylphenol by aquatic fungi and their laccases. *Microbiology* 151, 45–57. doi: 10.1099/mic.0.27431-0
- Kalkhoff, S. J., Vecchia, A. V., Capel, P. D., and Meyer, M. T. (2012). Eleven-year trend in acetanilide pesticide degradates in the Iowa River. *Iowa J. Environ. Qual.* 41, 1566–1579. doi: 10.2134/jeq2011.0426
- Karas, P. A., Perruchon, C., Exarhou, K., Ehaliotis, C., and Karpouzias, D. G. (2011). Potential for bioremediation of agro-industrial effluents with high loads of pesticides by selected fungi. *Biodegradation* 22, 215–228. doi: 10.1007/s10532-010-9389-1
- MacNeil, C., Dick, J. T., and Elwood, R. W. (1997). The trophic ecology of freshwater *Gammarus* spp. (Crustacea: Amphipoda): problems and perspectives concerning the functional feeding group concept. *Biol. Rev.* 72, 349–364. doi: 10.1017/S0006323196005038
- Oksanen, J., Kindt, R., Legendre, P., O'Hara, B., Simpson, G. L., Solymos, P., et al. (2008). *The Vegan Package*. *Community Ecology Package-Forge R-Project Org Projects Vegan*. Available at: <http://r-forge.r-project.org/projects/vegan/>
- Paul, S., Gable, K., Beaudoin, F., Cahoon, E., Jaworski, J., Napier, J. A., et al. (2006). Members of the *Arabidopsis* FAE1-like 3-ketoacyl-CoA synthase gene family substitute for the elop proteins of *Saccharomyces cerevisiae*. *J. Biol. Chem.* 281, 9018–9029. doi: 10.1074/jbc.M507723200
- Payá, P., Anastasiades, M., Mack, D., Sigalova, I., Tasdelen, B., Oliva, J., et al. (2007). Analysis of pesticide residues using the Quick Easy Cheap Effective Rugged and Safe (QuEChERS) pesticide multiresidue method in combination with gas and liquid chromatography and tandem mass spectrometric detection. *Anal. Bioanal. Chem.* 389, 1697–1714. doi: 10.1007/s00216-007-1610-7
- Pesce, S., Fajon, C., Bardot, C., Bonnemoy, F., Portelli, C., and Bohatier, J. (2008). Longitudinal changes in microbial planktonic communities of a French river in relation to pesticide and nutrient inputs. *Aquat. Toxicol.* 86, 352–360. doi: 10.1016/j.aquatox.2007.11.016
- Pesce, S., Zoghliani, O., Margoum, C., Artigas, J., Chaumot, A., and Foulquier, A. (2016). Combined effects of drought and the fungicide tebuconazole on aquatic leaf litter decomposition. *Aquat. Toxicol.* 173, 120–131. doi: 10.1016/j.aquatox.2016.01.012
- Petersen, R. C., and Cummins, K. W. (1974). Leaf processing in a woodland stream. *Freshw. Biol.* 4, 343–368. doi: 10.1111/j.1365-2427.1974.tb00103.x
- Richardson, S. D. (2009). Water analysis: emerging contaminants and current issues. *Anal. Chem.* 81, 4645–4677. doi: 10.1021/ac9008012
- Romani, A. M., Fischer, H., Mille-Lindblom, C., and Tranvik, L. J. (2006). Interactions of bacteria and fungi on decomposing litter: differential extracellular enzyme activities. *Ecology* 87, 2559–2569. doi: 10.1890/0012-9658(2006)87[2559:IOBAFO]2.0.CO;2
- Roubeix, V., Mazzella, N., Méchin, B., Coste, M., and Delmas, F. (2011). Impact of the herbicide metolachlor on river periphytic diatoms: experimental comparison of descriptors at different biological organization levels. *Ann. Limnol. Int. J. Limnol.* 47, 239–249. doi: 10.1051/limn/2011009
- Segner, H., Schmitt-Jansen, M., and Sabater, S. (2014). Assessing the impact of multiple stressors on aquatic biota: the receptor's side matters. *Environ. Sci. Technol.* 48, 7690–7696. doi: 10.1021/es405082t
- Sinsabaugh, R. L. (2010). Phenol oxidase, peroxidase and organic matter dynamics of soil. *Soil Biol. Biochem.* 42, 391–404. doi: 10.1016/j.soilbio.2009.10.014
- Sinsabaugh, R. L., Osgood, M. P., and Findlay, S. (1994). Enzymatic models for estimating decomposition rates of particulate detritus. *J. North Am. Benthol. Soc.* 13, 160–169. doi: 10.2307/1467235
- Suberkropp, K., Arsuffi, T. L., and Anderson, J. P. (1983). Comparison of degradative ability, enzymatic activity, and palatability of aquatic hyphomycetes grown on leaf litter. *Appl. Environ. Microbiol.* 46, 237–244.
- Swan, C. M., and Palmer, M. A. (2004). Leaf diversity alters litter breakdown in a Piedmont STREAM. *J. North Am. Benthol. Soc.* 23, 15–28. doi: 10.1899/0887-3593(2004)023<0015:LDALBI>2.0.CO;2
- Trewavas, A. (2002). Malthus foiled again and again. *Nature* 418:668. doi: 10.1038/nature01013
- Vörösmarty, C. J., McIntyre, P. B., Gessner, M. O., Dudgeon, D., Prusevich, A., Green, P., et al. (2010). Global threats to human water security and river biodiversity. *Nature* 467, 555–561. doi: 10.1038/nature09440
- Webster, J. R., and Meyer, J. L. (1997). Organic matter budgets for streams: a synthesis. *J. North Am. Benthol. Soc.* 16, 141–161. doi: 10.2307/1468247

- Yang, C., Hamel, C., Vujanovic, V., and Gan, Y. (2011). Fungicide: modes of action and possible impact on nontarget microorganisms. *ISRN Ecol.* 2011:130289. doi: 10.5402/2011/130289
- Zubrod, J. P., Bundschuh, M., Feckler, A., Englert, D., and Schulz, R. (2011). Ecotoxicological impact of the fungicide tebuconazole on an aquatic decomposer-detritivore system. *Environ. Toxicol. Chem.* 30, 2718–2724. doi: 10.1002/etc.679
- Zubrod, J. P., Englert, D., Feckler, A., Koksharova, N., Korschak, M., Bundschuh, R., et al. (2015). Does the current fungicide risk assessment provide sufficient protection for key drivers in aquatic ecosystem functioning? *Environ. Sci. Technol.* 49, 1173–1181. doi: 10.1021/es5050453

**Conflict of Interest Statement:** The authors declare that the research was conducted in the absence of any commercial or financial relationships that could be construed as a potential conflict of interest.

Copyright © 2018 Rossi, Pesce, Mallet, Margoum, Chaumot, Masson and Artigas. This is an open-access article distributed under the terms of the Creative Commons Attribution License (CC BY). The use, distribution or reproduction in other forums is permitted, provided the original author(s) and the copyright owner(s) are credited and that the original publication in this journal is cited, in accordance with accepted academic practice. No use, distribution or reproduction is permitted which does not comply with these terms.



# Molecular and Microbiological Insights on the Enrichment Procedures for the Isolation of Petroleum Degrading Bacteria and Fungi

Giulia Spini<sup>1</sup>, Federica Spina<sup>2</sup>, Anna Poli<sup>2</sup>, Anne-Laure Blieux<sup>3</sup>, Tiffanie Regnier<sup>3</sup>, Carla Gramellini<sup>4</sup>, Giovanna C. Varese<sup>2</sup> and Edoardo Puglisi<sup>1\*</sup>

<sup>1</sup> Department for Sustainable Food Processes, Università Cattolica del Sacro Cuore, Piacenza, Italy, <sup>2</sup> Department of Life Sciences and Systems Biology, Mycotheca Universitatis Taurinensis, University of Turin, Turin, Italy, <sup>3</sup> Satt Grand-EST, Maison Régionale de l'Innovation, Dijon, France, <sup>4</sup> ARPAE-Emilia Romagna, Bologna, Italy

## OPEN ACCESS

### Edited by:

Stéphane Pesce,  
Institut National de Recherche en  
Sciences et Technologies pour  
l'Environnement et l'Agriculture  
(IRSTEA), France

### Reviewed by:

Mariusz Cycoń,  
Medical University of Silesia, Poland  
Maurizio Petruccioli,  
Università degli Studi della Tuscia, Italy

### \*Correspondence:

Edoardo Puglisi  
edoardo.puglisi@unicatt.it

### Specialty section:

This article was submitted to  
Microbiotechnology, Ecotoxicology  
and Bioremediation,  
a section of the journal  
Frontiers in Microbiology

**Received:** 31 July 2018

**Accepted:** 05 October 2018

**Published:** 30 October 2018

### Citation:

Spini G, Spina F, Poli A,  
Blieux A-L, Regnier T, Gramellini C,  
Varese GC and Puglisi E (2018)  
Molecular and Microbiological Insights  
on the Enrichment Procedures  
for the Isolation of Petroleum  
Degrading Bacteria and Fungi.  
Front. Microbiol. 9:2543.  
doi: 10.3389/fmicb.2018.02543

Autochthonous bioaugmentation, by exploiting the indigenous microorganisms of the contaminated environment to be treated, can represent a successful bioremediation strategy. In this perspective, we have assessed by molecular methods the evolution of bacterial and fungal communities during the selective enrichment on different pollutants of a soil strongly polluted by mixtures of aliphatic and polycyclic hydrocarbons. Three consecutive enrichments were carried out on soil samples from different soil depths (0–1, 1–2, 2–3 m), and analyzed at each step by means of high-throughput sequencing of bacterial and fungal amplicons biomarkers. At the end of the enrichments, bacterial and fungal contaminants degrading strains were isolated and identified in order to (i) compare the composition of enriched communities by culture-dependent and culture-independent molecular methods and to (ii) obtain a collection of hydrocarbon degrading microorganisms potentially exploitable for soil bioremediation. Molecular results highlighted that for both bacteria and fungi the pollutant had a partial shaping effect on the enriched communities, with paraffin creating distinct enriched bacterial community from oil, and polycyclic aromatic hydrocarbons generally overlapping; interestingly neither the soil depth or the enrichment step had significant effects on the composition of the final enriched communities. Molecular analyses well-agreed with culture-dependent analyses in terms of most abundant microbial genera. A total of 95 bacterial and 94 fungal strains were isolated after selective enrichment procedure on different pollutants. On the whole, isolated bacteria were mainly ascribed to *Pseudomonas* genus followed by *Sphingobacterium*, *Bacillus*, *Stenothrophomonas*, *Achromobacter*, and *Serratia*. As for fungi, *Fusarium* was the most abundant genus followed by *Trichoderma* and *Aspergillus*. The species comprising more isolates, such as *Pseudomonas putida*, *Achromobacter xylosoxidans* and *Ochromobactrum anthropi* for bacteria, *Fusarium oxysporum* and *Fusarium solani* for fungi, were also the dominant OTUs assessed in Illumina.

**Keywords:** bioremediation, crude oil, soil contamination, enrichment culture, metagenomics, bacteria, fungi

## INTRODUCTION

Oil hydrocarbons are the most widespread environmental pollutants, including n-alkanes, cycloalkanes, and polycyclic aromatic hydrocarbons (PAHs) that have been regarded as serious ecological and public health concerns (Bao et al., 2012). Oil contamination of ecosystems is a serious issue associated with crude oil drilling, transportation, refining, and related activities which demands immediate attention for restoration. Crude petroleum oil is a complex mixture of hydrocarbons mainly composed of saturated and aromatic hydrocarbons, asphaltenes and resins (Moubasher et al., 2015). Aliphatic hydrocarbons consist of readily biodegradable n-alkanes followed by less biodegradable branched and cyclic alkanes (Das and Chandran, 2011). Similarly, PAHs are compounds with two or more aromatic rings that are the most recalcitrant components present at high percentages in crude oil (Haritash and Kaushik, 2009).

Due to the public awareness and to the strict legal constraints on the release of pollutants into the environment, it is necessary to find effective and affordable technologies for the treatment of oil industrial wastes. Bioremediation is a biological approach that relies on the metabolic potential of microorganisms to remove contaminants (Maiti et al., 2008; Megharaj et al., 2011; Hara et al., 2013). The use of bioremediation techniques proved economical, environmentally friendly and flexible (Obi et al., 2016). In this prospect, bioremediation is gaining more and more importance as constructive approach for the remediation of polluted sites. Several studies reported the catabolic abilities of indigenous microorganisms such as fungi, bacteria and algae to degrade hydrocarbons (Dean-Ross et al., 2002; Bundy et al., 2004; Maiti et al., 2008; Wang et al., 2011; Badr El-Din et al., 2014). These microorganisms, adapted to the contaminated environments, are equipped with specific enzyme systems that enable them to use hydrocarbons as sole carbon source. Different hydrocarbon degrading microorganisms such as bacteria and archaea have been found in hydrocarbons contaminated environments (Alonso-Gutierrez et al., 2009; An et al., 2013; Hazen et al., 2013; Head et al., 2014; Fowler et al., 2016). The structure of the microbial community in a soil, influences deeply the degree of oil hydrocarbons degradation. Liu et al. (2011) observed that, at the early stage of remediation, the bacterial community was responsible for the degradation of the saturated and partially aromatic hydrocarbons; the fungal community instead became dominant in decomposing the polar hydrocarbons fraction in post-remediation. Generally, thanks to the variety of extracellular enzymes and fungal hyphae, fungi are the first key players in degrading available contaminants and recalcitrant polymers (Wick et al., 2007; Fernandez-Luqueno et al., 2010; Deshmukh et al., 2016). Fungal mobilization and degradation of contaminants contribute to release bioavailable intermediates on which, in a later stage, the bacterial community can act more easily (Smits et al., 2005; Scullion, 2006; Leonardi et al., 2008; Yuan et al., 2018). Therefore, in order to characterize and to monitor the native microbial community, the dynamics and the functional potential of both bacteria and fungi in polluted ecosystems is essential for the development of a successful bioremediation

strategy (Atlas, 1981; Head et al., 2014; Covino et al., 2016).

The success of on-site bioremediation, employing native microbial populations, could be voided by imbalanced nutrients and/or adverse factors (temperature, moisture content, pH, availability of electron donor and/or acceptor, high pollutant concentration, etc.), which are common in contaminated sites (Smith et al., 2015). Bioremediation can be accomplished by either boosting the growth of the indigenous microbial community through biostimulation or by introducing naturally occurring microorganisms with excellent catabolic abilities (bioaugmentation) that are adapted to the ecological conditions of the site (Agnello et al., 2016).

Many investigators have reported successful bioremediation, where biostimulation with the addition of appropriate nutrients (N and/or P), to avoid metabolic limitations, resulted in an improved metabolic activity of indigenous microorganisms (Yu et al., 2005; Ghaly and Yusran, 2013; Suja et al., 2014; Smith et al., 2015). On the other hand, autochthonous bioaugmentation, based on the re-inoculation in polluted sites of indigenous microorganisms previously enriched under laboratory conditions, enhanced the microbial activities, thus improving the degradation of hydrocarbons (Dueholm et al., 2015). In order to provide an inoculum for bioaugmentation, the isolation of microorganisms in pure culture from these contaminated environments is fundamental. However, due to the complexity of crude oil, a microbial consortium composed of microorganisms endowed with diverse metabolic capacities and syntrophic interactions would work better than a pure culture. Several reports demonstrated the better metabolic versatility of mixed cultures in using hydrocarbon pollutants as sole carbon source in comparison to pure cultures (Cerqueira et al., 2011; Das and Chandran, 2011). In laboratory conditions, bacterial, and fungal co-culture(s) showed improved degradation rates of diesel oil and of polycyclic aromatic hydrocarbons (PAHs) (Wang et al., 2011). Hence, catabolic interactions among different microbial groups during biodegradation is extremely important (Atlas, 1981; Varjani et al., 2015). Although identifications and characterizations of the microorganisms involved in the degrading processes are available (Desai and Banat, 1997; Rojo, 2009), less is known on the biodiversity and dynamics of the native hydrocarbons-degrading microbial community of a contaminated soil, especially during the enrichment process applied to isolate the most effective strains (Omrani et al., 2018). The development of effective bioremediation strategies requires an extensive understanding of the resident microorganisms of these habitats. Recent techniques such as high-throughput sequencing (HTS) have greatly facilitated the advancement of microbial ecological studies in oil-polluted sites.

In the present work we have assessed by molecular methods the evolution of bacterial and fungal communities during the enrichment on different pollutants of a soil strongly polluted by mixtures of aliphatic and polycyclic hydrocarbons. Three consecutive enrichments were carried out on soil samples from different soil depths (0–1, 1–2, 2–3 m), and analyzed at each step by means of HTS of bacterial and fungal amplicons biomarkers.

At the end of the enrichment, bacterial, and fungal contaminants degrading strains were cultivated and identified.

Main aims of the work were: (i) to assess the effect of different pollutants used as sole carbon during a selective enrichment procedure source on the diversity of the microbial community of crude oil contaminated soil (ii) to compare the composition of enriched communities by culture-dependent and culture-independent molecular methods and (iii) to obtain a collection of hydrocarbon degrading fungi and bacteria potentially exploitable for soil bioremediation.

## MATERIALS AND METHODS

### Sampling and Soil Characteristic

Crude oil contaminated soil samples from an area of the industrial SIN (Site of National Interest) located in Fidenza (Emilia-Romagna, Italy) were collected at three different depths (0–1, 1–2, and 2–3 m). The polluted site (about 80,000 m<sup>2</sup> wide) has a long history of industrial exploitation and it is contaminated by a variety of pollutants such as Benzene-Toluene-Ethylbenzene-Xylene (BTEX), n-alkanes and PAHs.

The chemical composition of the soil samples is described in **Supplementary Table S1**.

### Target Organic Contaminants

Target organic contaminants were chosen based on literature data and on the chemical characterization of the contaminated area of Fidenza SIN. All chemicals were purchased by Sigma-Aldrich (Germany). Benzene was selected as representative of BTEX. Pyrene, phenanthrene, and naphthalene were selected as representatives of 4, 3, and 2 rings PAHs. Stock solutions were prepared in methanol for naphthalene (20 mg/mL) and in ethanol 95% for phenanthrene (15 mg/mL) and for pyrene (5 mg/mL). Paraffin oil, representative of alkanes, and crude oil mixture from the contaminated Fidenza site were used at a final concentration of 1% v/v.

### Microcosm Enrichments and Microbial Isolation

Different enrichment cultures were set up using the polluted soil as inoculum and the above-mentioned crude oil hydrocarbons components as the sole carbon source. One hundred g of each soil sample at the three depths (namely, S1, S2, and S3) were added to 900 mL sterile Mineral Medium (MM) supplemented with the target analyte as sole carbon source. To provide the proper microelement amount for bacterial and fungal growth, two mineral media were used: M9 mineral medium (Difco, Sparks, MD, United States) for bacteria and Czapek for fungi.

The flasks were incubated on a rotary shaker at 30°C and 180 rpm for bacteria and at 24°C and 120 rpm for fungi. After 7 days, 5 mL of the culture was transferred to another flask with MM and the corresponding target analyte: benzene (50 ppm); naphthalene (200 ppm), phenanthrene (200 ppm), pyrene (200 ppm); paraffin oil (1% v/v), and crude oil (1% v/v). Three consecutive subcultures were performed in the same conditions.

Each fungal and bacterial enrichment culture was plate on solid MM containing each pollutant as sole carbon source. To isolate pure microbial cultures, morphologically different colonies were selected and transferred to Malt Extract Agar (MEA) plates for fungi and Tryptone Soy Agar (TSA) plates for bacteria.

### Molecular Characterization of Fungal and Bacterial Isolates

DNA from isolate purified colonies was extracted using Microlysis kit (Labogen, London, United Kingdom) according to the manufacturer's protocol. The isolates were screened by randomly amplified polymorphic DNA-polymerase chain reaction (RAPD-PCR) using the single stranded oligonucleotides primer RAPD2 (5'-AGCAGCGTGG-3') (Rebecchi et al., 2015) and GTG-5 (5'-GTG GTG GTG GTG GTG-3') (Versalovic et al., 1994). The PCR fragment profiles were digitally captured using the BioImaging System Gene Genius and pattern analysis was performed with the Fingerprinting II software (Bio-Rad Laboratories, Hercules, CA, United States). The similarity in the profiles of bands was based on the Pearson correlation coefficient and the cluster analyses were performed by unweighted pair group method with arithmetic mean (UPGMA). A correlation coefficient of 70% was arbitrarily selected to distinguish the clusters, and one representative for each cluster was amplified using the primers P0 (5'-GAG AGT TTG ATC CTG GCT-3') and P6 (5'-CTA CGG CTA CCT TGT TAC-3') (Di Cello and Fani, 1996). PCR products were visualized by electrophoresis on 2.5% agarose gel in Tris-Acetate-EDTA (TAE). The PCR amplicons of approximately 1.5 kb, corresponding to the size of the full 16S rRNA gene were purified using the NucleoSpin gel and PCR clean-up according to the package insert (Macherey-Nagel, DE) and sequenced at the GATC Biotech (Germany). The taxonomical identification of sequences was performed using BLAST (Basic Local Alignment Search Tool) (Altschul et al., 1997) and by alignment against the Ribosomal Database Project (RDP) database using the Naïve Bayesian Classifier (Wang et al., 2007).

### Fungi

Genomic DNA of each strains was extracted from about 100 mg of mycelium scraped from the MEA petri dishes using the NucleoSpin® Plant II kit (Macherey-Nagel), according to the manufacturer's instruction. The quality and quantity of extracted DNA was measured spectrophotometrically by Infinite M200 (TECAN Trading, Austria). De-replication of fungal isolates was performed by using the minisatellite core sequence derived from the wildtype phage M13 (5'-GAG GGT GGC GGT TCT-3') as specific primer to amplify variable number tandem repeat (VNTR) (Poli et al., 2016). Molecular identification of each fungal isolate was carried out by amplification of specific markers (White et al., 1990; Glass and Donaldson, 1995; Bensch et al., 2012). PCR products were visualized by electrophoresis on a 1.5% agarose gel stained with ethidium bromide in Tris-Borate-EDTA (TBE). PCR products were purified and sequenced at Macrogen Europe (Amsterdam, Netherlands). Consensus sequences were

obtained by using Sequencer 5.0 (Gene Code Corporation). Taxonomic assignments were inferred by querying with the Blastn algorithm (default setting), hosted at NCBI (National Center for Biotechnology Information), the newly generated sequences against the nucleotide database of NCBI (GenBank). Pairwise alignments were also performed against the CBS-Knaw Fungal Biodiversity Centre (Centraalbureau voor Schimmelcultures) database. Similarity values equal or higher than 98% (e-value > e-100) were considered reliable; results were confirmed morphologically.

## DNA Extraction From Original Soils and Enrichments

Total microbial DNA was extracted from original soil samples and from each enrichment step of fungal and bacterial culture/microcosms with the PowerLyzer PowerSoil kit (MoBio Laboratories, Inc., Carlsbad, CA, United States) according to the manufacturer's instructions. DNA purity was checked with electrophoresis on a 0.8% agarose gel, while quantification was performed with the Quant-iT™ HS ds-DNA assay kit (Invitrogen, Paisley, United Kingdom) method in combination with the QuBit™ fluorometer.

## Molecular Analyses of Microbial Diversity Illumina Sequencing of 16S PCR Amplicons

For bacteria, PCR amplicons covering the V3–V4 regions of the 16S rRNA were analyzed in Illumina MiSeq with V3 chemistry in 300 bp paired-reads mode. PCR reactions were performed using indexed primer pairs 343F (5'-TACGGGAGGCAGCAG-3') and 802R (5'-TACNVGGGTWTCTAATCC-3'), as described in Vasileiadis et al. (2015). A multiplexing strategy was employed to analyze several amplicon samples simultaneously in the same sequencing run. A nine nucleic acids extension was added to the 5' end of the forward primer, where the first seven bases served as a tag to identify to each sample, and the following two bases were a linker designed not to match bacterial sequences in the same position according to RDP entries. In order to reduce possible biases related to the primer extension, the two step-PCR approach described in Berry et al. (2011) was adopted. The PCR conditions were set as described by Vasileiadis et al. (2015). The final PCR products were checked on 0.8% agarose gel and pooled in equimolar amounts according to QuBit measurements. The final pool was cleaned with the SPRI (Solid Phase Reverse Immobilization Method) using the Agencourt® AMPure® XP kit (Beckman Coulter, Milan, Italy). Finally, the pool was sequenced by BioFab Company (Rome, Italy) with a MiSeq Illumina instrument (Illumina, Inc., San Diego, CA, United States) operating with V3 chemistry and producing 300 bp paired-reads.

## Illumina Sequencing of ITS PCR Amplicons

The nr ITS2 region was amplified from all DNA by means of a semi-nested PCR approach. In the first PCR, the nr ITS (ITS1-5.8S-ITS2) was amplified with universal primers ITS1F-ITS4 (White et al., 1990). For the second PCR, ITS3 and ITS4 (White et al., 1990) tagged primers were used to amplify the ITS2 region of each DNA sample (Voyron et al., 2017).

PCR products were pooled and purified using Wizard SV Gel and PCR Clean-Up System (Promega) following the manufacturer's instructions. After quantification with Qubit 2.0 (Thermo Fisher Scientific, Waltham, MA, United States), the purified PCR products were mixed in equimolar amounts to prepare sequencing libraries. The libraries were paired-end sequenced using the Illumina MiSeq technology (2 bp × 250 bp) by IGA Technology Services S.r.l. Unipersonale (Udine, Italy).

## Sequences Data Preparation, Bioinformatics, and Statistical Analyses

The first steps for sequences processing and filtering were the same for both 16S and ITS amplicons. Raw paired Illumina sequences were merged with the "pandaseq" script (Masella et al., 2012) with a minimum overlap of 30 bp between read pairs and 2 maximum allowed mismatches. Sequences were multiplexed according to sample indexes and primers with the fastx-toolkit<sup>1</sup>. Both bacterial and fungal amplicons were analyzed with taxonomy-based and OTU-based analyses: in the first case, all sequences were individually classified at taxonomical level against relevant database (GreenGenes for bacteria, UNITE for fungi), while in the OTU-based analyses, sequences were grouped at 97% similarities. For 16S amplicons, both operational taxonomic units (OTUs) and taxonomy-based matrices were produced with a pipeline in Mothur (Schloss et al., 2009). For ITS amplicons, taxonomy-based analyses were also performed in Mothur, whereas OTUs were determined in UPARSE (Edgar, 2013). The reason for this discrepancy was that no aligned databases are available for ITS, and the OTU-clustering method implemented in Mothur does not allow analysis of sequences that have dissimilar lengths, which was the case with the ITS amplicons.

For bacterial sequences, Mothur v.1.39.5 (Schloss et al., 2009) was applied in order to remove sequences with large homopolymers ( $\geq 10$ ), sequences that did not align within the targeted V3–V4 region, chimeric sequences (Edgar et al., 2011) and sequences that were not classified as bacterial after alignment against the Mothur version of the RDP training data set. The resulting high-quality sequences were analyzed with Mothur and R<sup>2</sup> following the OTU and the taxonomy-based approach. Sequences were first aligned against the SILVA reference aligned database for bacteria (Pruesse et al., 2007) using the NAST algorithm and a kmer approach (Schloss, 2010) and then clustered at the 3% distance using the average linkage algorithm. OTUs were classified into taxa by alignment against the Greengenes database (McDonald et al., 2012).

ITS taxonomy-based analyses were conducted in Mothur: sequences shorter than 120 bp were discarded. We discarded homopolymers > 10 bp and chimeras, which were identified with the UCHIME algorithm implemented in Mothur, with the UNITE database version 6 as reference. The same database was used to classify the retained sequences and to eliminate non-fungal sequences. OTUs were produced in USEARCH with the –fastx\_uniques and –cluster\_otus commands. Sequences that did

<sup>1</sup>[http://hannonlab.cshl.edu/fastx\\_toolkit/](http://hannonlab.cshl.edu/fastx_toolkit/)

<sup>2</sup><http://www.R-project.org>

not belong to fungi were identified with the syntax command against the Utax reference database and discarded.

The OTU- and taxonomy-based matrixes obtained were analyzed in R to estimate the associated  $\alpha$  and  $\beta$  diversity of the samples. The Good's coverage estimate was calculated to assess the "percentage diversity" captured by sequencing. The most abundant OTUs identified were confirmed with BLAST (Basic Local Alignment Search) searches against the GenBank and the RDP database.

## RESULTS

### Hydrocarbon Degrading Bacterial and Fungal Strains

A collection of hydrocarbon-degrading bacterial and fungal strains was isolated from microcosms enriched on each pollutant (benzene, paraffin, pyrene, naphthalene, phenanthrene, and crude oil) and from three depths of the contaminated soil of the SIN in Fidenza. Molecular de-replication of isolated colonies resulted in 95 and 94 unique colonies for bacteria and fungi, respectively. Molecular identification of the strains was inferred by 16S rDNA and ITS sequencing and is reported in **Table 1**.

For bacteria, sequence similarity searches in NCBI GenBank and RDP database revealed the presence of cultivable members of different genera under the phyla Proteobacteria, Firmicutes, and Sphingobacteria. On the whole, the bacteria isolated where ascribed mainly to 12 genera belonging to both Gram-negative and Gram-positive. *Pseudomonas* was the most abundant genera (56.8%) followed by *Sphingobacterium* (12%), *Bacillus* (6%), *Stenotrophomonas* (6%), *Achromobacter* (6%), and *Serratia* (3%). Most of the bacterial strains (46) were isolated from enrichments inoculated with soil S2 (**Supplementary Table S2**): the most represented bacterial genera in soil S2 were *Pseudomonas* (23 isolates), *Serratia* (3 isolates), and *Sphingobacterium* (9 isolates). A lower number of bacterial strains was isolated from enrichments of soil S1 and S3 (**Supplementary Table S2**). A total of 26 isolates were obtained from soil S1 and were mainly affiliated to the genera *Bacillus*, *Pseudomonas* and *Pseudoxanthomonas*, while the 23 bacterial strains isolated from the deepest soil S3 were mainly affiliated to the genus *Pseudomonas* (**Supplementary Table S2**). The influence of pollutants used in the enrichments on the distribution of bacterial species is reported in **Table 1**. The highest number of bacterial isolates was obtained from paraffin (29 isolates), followed by naphthalene (19 isolates), benzene (15 isolates), and phenanthrene (15 isolates) microcosms; 10 strains were isolated in the presence of pyrene and only six strains were isolated in the presence of crude oil (**Table 1**). The genus *Pseudomonas* dominated all the microcosms enriched on pollutants. Benzene and paraffin enrichments showed the highest diversity of bacterial genera. In particular, benzene enrichment selected also bacterial species of the genera *Sphingobacterium* and *Stenotrophomonas*, while paraffin enrichment resulted also in the isolation of species of *Bacillus*, *Achromobacter*, and *Pseudoxanthomonas*. Beside *Pseudomonas*, *Serratia*, and *Ochromobacterum* were the most abundant genera in crude oil and pyrene microcosms

(**Table 1**). At species level, *Pseudomonas putida* was dominant and was isolated in the presence of all the tested pollutants. Other frequently isolated species were *Pseudomonas fluorescense* (four pollutants), *Stenotrophomonas maltophilia* (two pollutants), *Stenotrophomonas acidaminiphila* (two pollutants), *Bacillus subtilis* (two pollutants), and *Sphingobacterium multivorum* (two pollutants). Three strains of *Serratia marcescens* were isolated only from the enriched microcosms with the crude oil of the contaminated site (**Table 1**).

Fungal species with their relative abundance are reported in **Supplementary Table S3**, according to the soil depth and in **Table 1** according to the pollutant used in the enrichments. Isolated fungi belonged mostly to the phylum Ascomycota, and only 5% to Basidiomycota; Mucoromycota were not isolated. Most of the strains were isolated from enrichments inoculated with contaminated soils S1 (35 strains) and S3 (36 strains); a lower number of isolates (23) were retrieved from the contaminated soil S2 (**Supplementary Table S3**). In general, *Fusarium* was the most abundant genus (43.8%) followed by *Trichoderma* (and its teleomorph *Hypocrea lixii*) (13.8%) and *Aspergillus* (11.0%). The majority of the isolates detected in soils S1 and S3 were indeed ascribable to these three genera, while in S2 only 44.4% of the strains were affiliated to the genus *Fusarium* and 16.7% belonged to the genus *Cladosporium* (**Supplementary Table S3**).

The retrieval of fungal species was influenced by the pollutant used as sole carbon source in the enrichments, as reported in **Table 1**. The highest number of isolates was obtained from pyrene and phenanthrene (23-22 isolates) followed by benzene and crude oil (15 isolates); 11 strains were isolated in the presence of naphthalene and only eight strains were isolated in the presence of paraffin oil (**Table 1**). With the only exception of crude oil, the genus *Fusarium* was the most abundant in each pollutant. Benzene and paraffin enrichments revealed the highest variety of genus and species.

### Molecular Analyses of Bacterial and Fungal Communities

Illumina HTS of PCR amplicons of the 16S V3-V4 region resulted in 1,991,866 sequences, which were reduced to 1,742,447 after the exclusion of homopolymers, of sequences <380 bp, sequences not aligning to the targeted V3-V4 regions, chimera and sequences not classified as bacterial after alignment against the RDP 16S training set. In order to reduce biases in diversity estimates related to the analyses of samples with different number of sequences, rarefaction to a common minimum number of 10,065 sequences per sample was carried out (Gihring et al., 2012). The rarefaction step resulted in the loss of only 5 out of 82 samples, while retaining a sequencing depth able to depict most of the bacterial diversity in the samples, as indicated by an average Good's coverage of 90.4%.

As for fungi, Illumina sequencing of ITS2 amplicons resulted in 795,742 high quality sequences. Taxonomy-based analyses were performed in Mothur and consisted in a screening to remove homopolymers, sequences shorter than 120 bp, chimera, and sequences that were not correctly classified as fungal after

**TABLE 1** | Identification of bacteria and fungi isolated from benzene, paraffin, crude oil, naphthalene, pyrene, and phenanthrene enrichment microcosms.

	<b>Bacterial isolates</b>	<b>Fungal isolates</b>
Benzene	<i>Acinetobacter calcoaceticus</i> (1) <i>Bacillus subtilis</i> (1) <i>Benzo[a]pyrene-degrading bacterium</i> (1) <i>Cellulosimicrobium</i> sp.(1) <i>Pseudomonas mosselii</i> (2) <i>Pseudomonas putida</i> (1) <i>Pseudoxanthomonas indica</i> (1) <i>Rhizobium petrolearium</i> (1) <i>Sphingobacterium</i> sp. (3) <i>Stenotrophomonas acidaminiphila</i> (2) <i>Stenotrophomonas maltophilia</i> (1)	<i>Acremonium sclerotigenum</i> (1) <i>Aspergillus creber</i> (1) <i>Bjerkabndera adusta</i> (1) <i>Eutypella scoparia</i> (1) <i>Fusarium oxysporum</i> (1) <i>Fusarium solani</i> (5) <i>Irpex lacteus</i> (1) <i>Pseudoallescheria boydii</i> (2) <i>Scedosporium apiospermum</i> (1) <i>Scedosporium dehoogii</i> (1)
Paraffin	<i>Acholeplasma vituli</i> (1) <i>Achromobacter xylooxidans</i> (3) <i>Bacillus subtilis</i> (3) <i>Bacillus xiamenensis</i> (1) <i>Cupriavidus campinensis</i> (1) <i>Gordonia rubripertincus</i> (1) <i>Helicobacter</i> sp. (1) <i>Paenibacillus</i> spp. (1) <i>Pseudomonas putida</i> (7) <i>Pseudoxanthomonas mexicana</i> (3) <i>Sphingobacterium multivorum</i> (6) <i>Stenotrophomonas acidaminiphila</i> (1)	<i>Clonostachys rosea</i> (1) <i>Fusarium oxysporum</i> (5) <i>Fusarium solani</i> (2)
Crude oil	<i>Pseudomonas aeruginosa</i> (1) <i>Pseudomonas fluorescens</i> (2) <i>Serratia marcescens</i> (3)	<i>Aspergillus jensenii</i> (1) <i>Aspergillus protuberus</i> (1) <i>Aspergillus versicolor</i> (6) <i>Cladosporium cladosporioides</i> (1) <i>Cladosporium perangustum</i> (2) <i>Epicoccum nigrum</i> (1) <i>Penicillium crustosum</i> (1) <i>Trichoderma harzianum</i> (1) <i>Wallemia mellicola</i> (1)
Naphtalene	<i>Achromobacter</i> sp. (1) <i>Pseudomonas fluorescens</i> (4) <i>Pseudomonas putida</i> (2) <i>Pseudomonas</i> sp. (7) <i>Pseudomonas veronii</i> (3) <i>Sphingobacterium multivorum</i> (1) <i>Stenotrophomonas maltophilia</i> (1)	<i>Aspergillus sclerotiorum</i> (1) <i>Aspergillus sydowii</i> (1) <i>Aureobasidium pullulans</i> (1) <i>Cladosporium cladosporioides</i> (1) <i>Eutypella scoparia</i> (1) <i>Fusarium oxysporum</i> (1) <i>Penicillium brevicompactum</i> (1) <i>Penicillium catenatum</i> (1) <i>Scedosporium apiospermum</i> (1) <i>Sulcatispora acerina</i> (1) <i>Trametes gibbosa</i> (1)
Pyrene	<i>Ochrobactrum anthropi</i> (1) <i>Pseudomonas fluorescens</i> (4) <i>Pseudomonas putida</i> (1) <i>Pseudomonas</i> sp. (4)	<i>Aspergillus waksmanii</i> (1) <i>Cladosporium cladosporioides</i> (2) <i>Fusarium oxysporum</i> (2) <i>Fusarium solani</i> (9) <i>Fusarium solani/keratoplasticum</i> (3) <i>Hypocrea lixii</i> (2) <i>Polyporus gayanus</i> (1) <i>Trichoderma harzianum</i> (3)

(Continued)

TABLE 1 | Continued

	Bacterial isolates	Fungal isolates
Phenanthrene	<i>Achromobacter</i> sp. (1) <i>Pseudomonas fluorescens</i> (3) <i>Pseudomonas putida</i> (6) <i>Pseudomonas</i> sp. (5)	<i>Epicoccum nigrum</i> (1) <i>Fusarium oxysporum</i> (6) <i>Fusarium solani</i> (6) <i>Fusarium solani/keratoplasticum</i> (2) <i>Hypocrea lixii</i> (2) <i>Trichoderma harzianum</i> (5)

The number of isolates per species is indicated in parenthesis.

alignment against the UNITE v6 database. Rarefaction was performed with a common number of 5,001 sequences per sample. The coverage of fungal diversity was not affected by this rarefaction step: average Good's coverage was 99.7%, thus showing that the sequencing effort covered the totality of fungal biodiversity in the samples. OTU-based analyses for fungi were performed in USEARCH and resulted in a very similar number of sequences per sample (4,942) and a total of 188 fungal OTUs.

Multivariate canonical correspondence analysis (CCA) was performed on bacterial and fungal OTUs abundance tables in order to assess how the microbial communities responded to contaminants, depth of soil collection and enrichment time (Figure 1). Among the tested factors, in the case of bacteria, pollutant was the most significant: the percentage of variance explained (36.1%, Figure 1A) was much higher than the variance explained by the soil (6.1%, Figure 1B) and by the time (8.3%, Figure 1C) factors. The bacterial communities differed among the six tested contaminants: pollutants that shared the chemical structure (e.g., the three PAHs) grouped together, while oil, benzene, and paraffin formed separate groups (Figure 1A). A similar picture was obtained by the CCA analyses performed on fungal communities: only the pollutant factor was significant (25.6% of variance explained, Figure 1D) contrary to soil and time factors. The pollutant used in the enrichment significantly affected the evolution of fungal communities: phenanthrene and pyrene enriched fungal communities formed groups that separated from those enriched from oil (Figure 1D). For both fungi and bacteria, the groups formed by soil-depth (Figures 1B–E) and time (Figures 1C–F) were mainly overlapping: this indicates that the depth, as well as the time of enrichment, did not affect the evolution of enriched microbial communities. Grouping of samples was also evaluated by UPGMA clustering of sequencing classified at genus level. Results are reported in Figure 2 for bacteria and in Figure 3 for fungi: samples are labeled according to the soil depth, followed by the pollutant and the enrichment step. Results confirmed that the relative composition in bacterial genera was partly dependent on the pollutant: several pyrene and phenanthrene samples formed two sub-clusters in a common cluster, with *Azospirillum*, *Achromobacter*, and *Pseudomonas* being the dominant genera; naphthalene enrichments were dominated by *Achromobacter* and *Pseudomonas* in similar proportions, while oil enrichments showed a dominance of *Pseudomonas* followed by *Achromobacter*. Finally, benzene and paraffin enrichments revealed a more diverse community, with

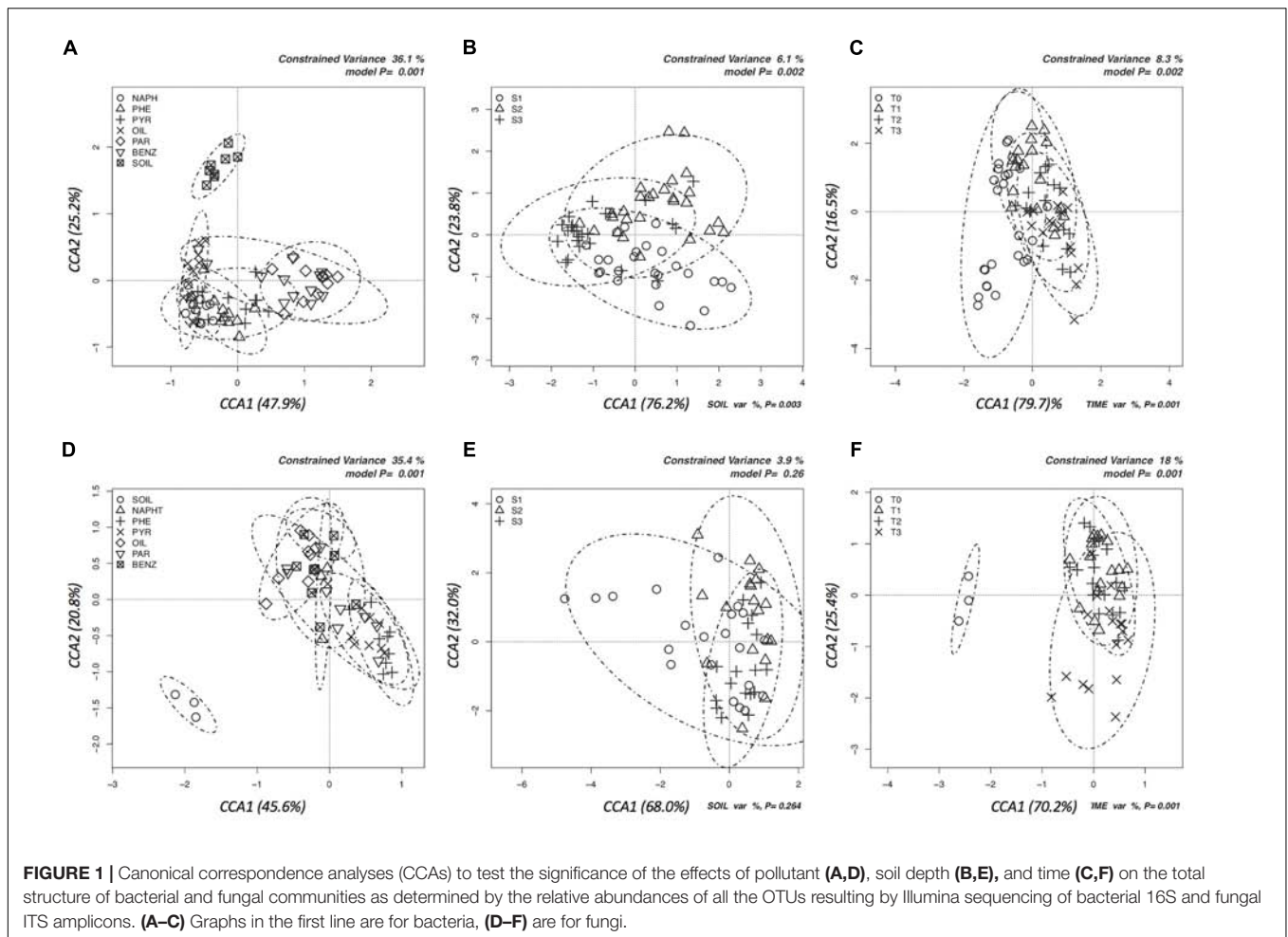
high relative presences of *Acinetobacter*, *Pseudoxanthomonas*, and *Pseudomonas*. Neither the soil depth nor the time of enrichment influenced the samples clustering, confirming the CCA results presented above.

Concerning fungi, no clear clustering of genera was shown according to pollutant, soil depth, or enrichment time (Figure 3). All samples were dominated by *Fusarium* (more than 80% in average), followed by *Aspergillus*, *Penicillium*, *Trichoderma*, and *Arthrimum*.

## Comparison Between Culture-Dependent and Culture-Independent Analyses

A number of analyses were performed in order to compare the results on the diversity of bacterial and fungal strains isolated with culture-dependent and culture-independent methods. In Table 2 the relative percentages of bacterial genera retrieved from each of the three soil depths are compared. Results generally agree: *Pseudomonas* was the dominant genus in both cases, with 24.2, 25.2, and 63.5% of relative abundances in Illumina and 57.7, 48.9, and 69.6% as isolates for S1, S2, and S3, respectively. The other genera, in terms of relative percentages, were *Bacillus*, *Achromobacter*, *Sphingobacterium*, and *Pseudotrophomonas* for the culture-dependent data; *Achromobacter*, *Agrobacterium*, *Azospirillum*, *Shinella*, *Sphingobacterium*, and *Pseudotrophomonas* for the Illumina data. It is worth noting that for some genera, the soil depth with the highest relative percentage was the same with both approaches. For instance, *Pseudomonas* reached 60% of abundance in soil three from both the approaches. There are a number of discrepancies: *Agrobacterium* sequences were above 9% in all soils while no strains belonging to this genus was isolated; and 2.2% of isolates (i.e., two strains) from S2 belong to *Helicobacter* while no sequences affiliated to this genus were detected with Illumina.

The same analyses were conducted on fungi (Table 3). Sordariomycetes was the most abundant class, with the order Hypocreales (i.e., *Acremonium*, *Clonostachys*, *Fusarium*, *Hypocrea/Trichoderma*) and Microascales (i.e., *Ceriosporopsis*, *Pseudoallescheria/Scedosporium*). Xylariales were instead a minor component of the detected fungi (i.e., *Arthrimum*, *Eutypella*). Results from culture-dependent and culture-independent methods confirmed each other in the case of the genus *Fusarium*, whose relative percentages were highly similar (ranging 40 and



69%). *Clonotachys*, *Pseudallescheria*, and *Trichoderma* were mostly isolated from S1 soils where also Illumina data showed the highest relative percentage. In the case of fungi too, there are some contrasting results, as fungal genera isolated in pure culture that were not detected with Illumina sequencing of ITS2 amplicons (e.g., *Bjerkandera*, *Epicoccum*, *Eutypella*, *Irpex*, *Polyporus*, and *Sulcatispora*). As for the genera *Ceriosporopsis* and *Phanerochaete*, they were detected with Illumina in significant amounts (above 5% of total sequences) but no isolates were obtained.

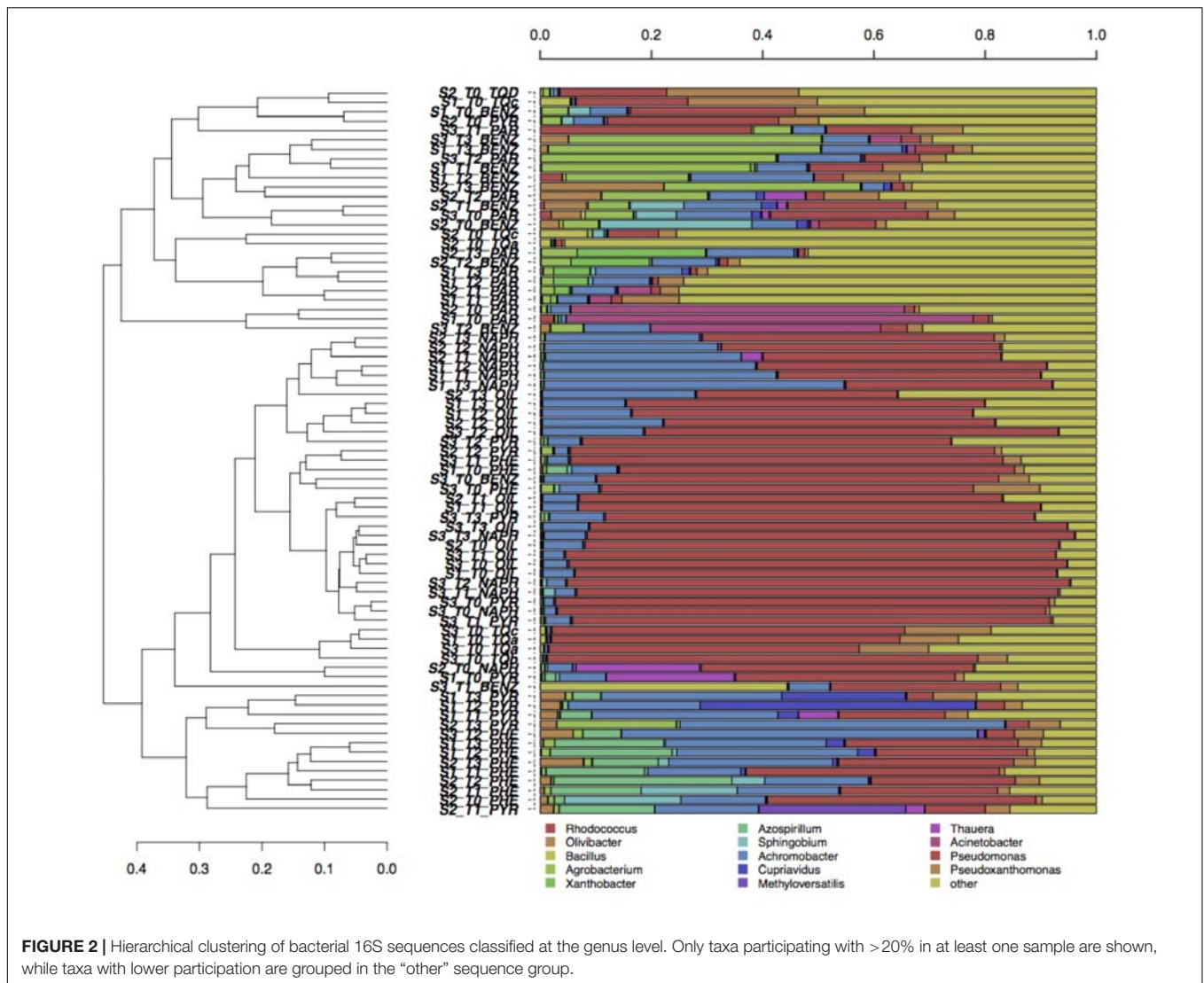
The most abundant OTUs (i.e., those who had a relative abundance higher than 1% in at least one sample) are reported in **Tables 4, 5** for bacteria and fungi, respectively. This screening criterion retained 19 OTUs for bacteria, and 21 OTUs for fungi: in both tables, the highest taxonomic affiliation is reported, together with the relative abundances in each enrichment microcosm. In the case of bacteria, most OTUs (16 out of 19) were classified at species level, two at genus and only one at the family level. Nine out of 19 OTUs were retrieved in the cultivated isolates. By comparing the data on the isolates in **Table 1** with the molecular data in **Table 4**, it is possible to notice that the species comprising more isolates (*Pseudomonas putida*, *Achromobacter xylosoxidans*, and *Pseudomonas veronii*) were also the most abundant in terms

of Illumina OTUs. As above reported for genera, also for OTUs classified at genus or species level there was a good agreement between molecular and microbiological data.

Regarding fungi, the rate of OTUs that could be classified at species level is similar to the one for bacteria: 14 out of 21. The number of OTUs also detected among isolates was instead slightly lower, 9 isolates (**Table 5**). It is worth noting that, as for bacteria, the taxa comprising more isolates were also the most abundant OTUs: that was the case for *Fusarium oxysporum*, *Cladosporium* spp., and *Fusarium solani*. These data highlighted the different adaptation abilities developed by fungi: while species of the genus *Fusarium* were abundant and widely distributed among pollutants and depth, other fungi seemed to be particularly adapted to individual contaminant. For instance, the relative percentage of *Cladosporium* spp. and *Pseudoallescheria* spp. was significantly high only in the presence of oil and benzene, respectively.

## DISCUSSION

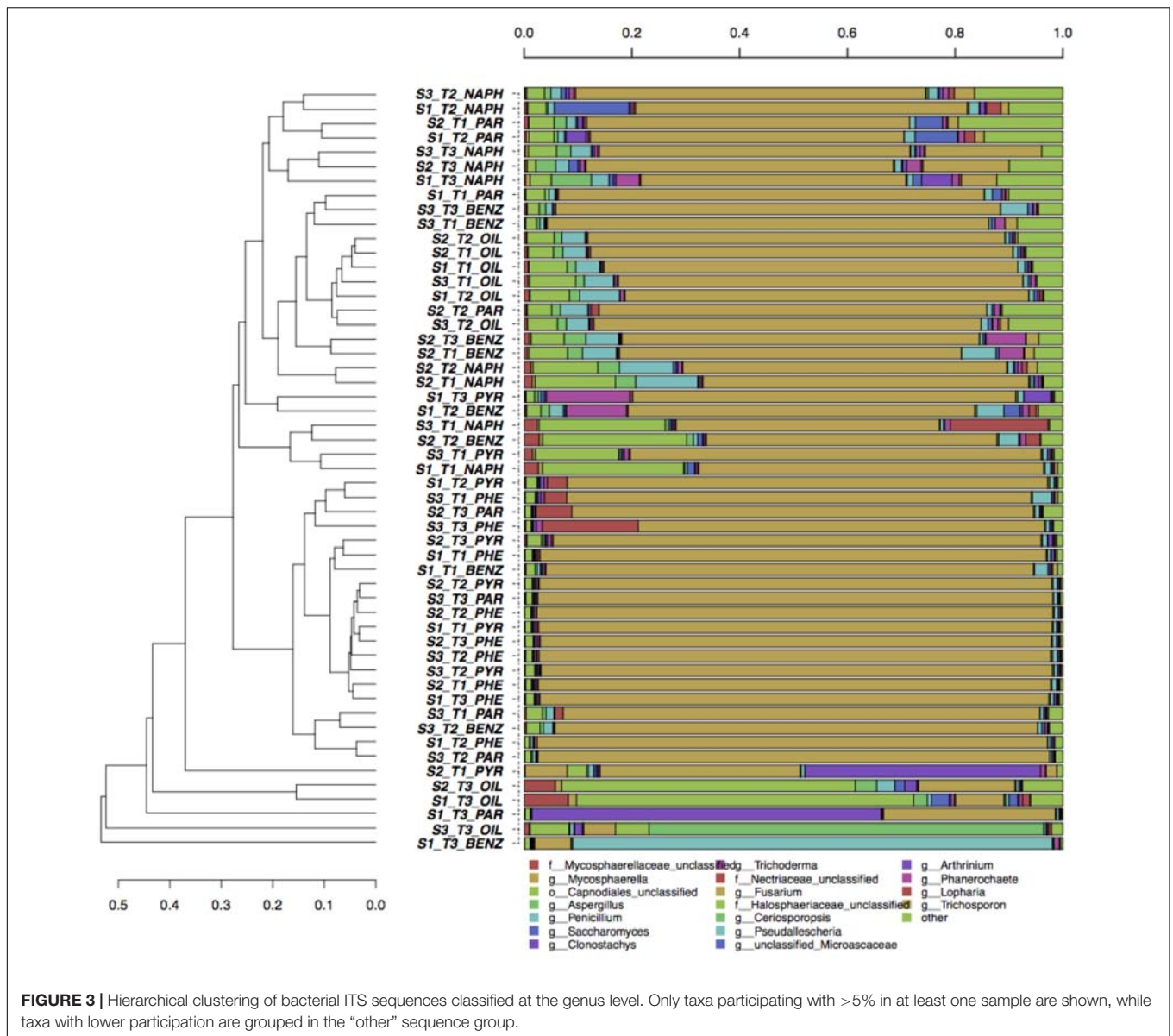
Since the discovery of the great plate count anomaly in the middle '80s of the last century



(Staley and Konopka, 1985), microbiologists are facing the issue of non-cultivable microorganisms and the underestimation of the actual microbial community by means of direct isolation techniques. This has become more and more relevant with the advent of HTS techniques, and it is of utmost importance in the environmental microbiology sector of bioremediation, where studies must rely on the isolation and identification of bacterial and fungal strains to be inoculated in soil for efficient degradation of target pollutants (Megharaj et al., 2011). These strains are usually obtained through enrichment procedures, aimed at isolating autochthonous microorganisms capable of using the pollutants as sole carbon sources (Thompson et al., 2005). Although many data are available in literature about the assessment of microbial community dynamics following the addition of enriched microbial strains (MacNaughton et al., 1999; Aburto-Medina et al., 2012; Fuentes et al., 2014), little is known on the developments that occur within the bacterial and fungal communities during the enrichment steps. Furthermore, to the best of our knowledge, no attempt was made to assess

how soil samples with a high petroleum hydrocarbons content and collected at different depths affect the organization of the bacterial and fungal communities.

In this work, we assessed whether the pollutant and the collection depth had significant effects on the microbial community arrangements. Enrichments were performed using five pollutants (three PAHs, benzene, and paraffin) and a complex mixture (i.e., crude oil collected from the polluted site). The results obtained (Figure 1) highlighted that for both bacteria and fungi, the pollutant partially shaped the enriched communities. Although it was difficult to highlight separate clusters according to the pollutants, some differences were observed as bacteria grown in the presence of paraffin and benzene or with PAHs, and fungi grown with paraffin or PAHs (Figure 1). This is not surprising, if we consider that different metabolic pathways are involved in the degradation of aliphatic or aromatic hydrocarbons, but that single strains can be also equipped with both pathways (Whyte et al., 1997). The microbial community responded uniquely to the presence of crude oil:



only those strains, highly adapted to this extreme and toxic environment, were capable of colonizing this ecological niche.

According to literature, a relation between pollutants load and microbial communities can be drawn. Several studies assessed a different distribution of PAHs and other oil pollutants along soil depths (Cousins et al., 1999; Ping et al., 2007). It is well-known that microbial community organization is affected by soil depths, commonly causing a decline in biomass and diversity from the surface downward (Blume et al., 2002; Fierer et al., 2003; Oehl et al., 2005). As far as we know, no experiments were previously conducted to assess the impact of the soil samples depths on the community structure and enrichment outcomes. Contrary to this general background, in the present study, neither the soil depth nor the enrichment step had significant effects on the community structure (Figures 1–3). Regarding fungi, this could be explained by their physiological growing capabilities. Thanks

to their hyphae growth, they can widely colonize the soil, creating a homogenous mycoflora in the space (Hesham et al., 2017).

The total load of bacteria and fungi was lower than unpolluted soils (Supplementary Table S1), although no differences were observed among the collection depths: a strong and long-lasting pollution of this site may shape a microbial community adapted to the pollutants pressure mostly composed by oil-utilizing strains. As illustrated in Figures 2, 3, differences among samples are more evident for bacteria. However, it is not possible to define clear clusters based on soil depths; the structure of the microbial community was not dependent by the collection point. Since the microbial community is selected by the total content of the pollutants, we can speculate that, in this soil, a pollutants threshold has been reached in the surface topsoil: beyond this level, only the selected and adapted microflora can survive. Indeed, in a less polluted site, the presence of

**TABLE 2** | Relative abundances of bacterial genera determined by Illumina sequencing of 16S amplicons or by isolation on selective media; the comparison was performed at the end of the enrichment (step III).

Bacterial genus	16S Illumina			Bacterial isolates		
	S1	S2	S3	S1	S2	S3
<i>Acholeplasma</i>	nd	nd	nd	nd	nd	4.3
<i>Achromobacter</i>	26.68	29.37	8.39	7.7	4.4	4.3
<i>Acinetobacter</i>	0.38	0.18	1.60	nd	nd	4.3
<i>Agrobacterium</i>	9.08	11.79	11.62	nd	nd	nd
<i>Ancylobacter</i>	0.30	2.53	0.40	nd	nd	nd
<i>Azospirillum</i>	4.17	2.50	0.24	nd	nd	nd
<i>Bacillus</i>	0.11	0.09	0.09	7.7	8.9	nd
<i>Cellulosimicrobium</i>	0.03	0.02	0.08	nd	nd	4.3
<i>Cupriavidus</i>	4.64	0.46	0.08	nd	2.2	nd
<i>Gordonia</i>	3.00	0.04	0.06	3.8	nd	nd
<i>Helicobacter</i>	nd	nd	nd	nd	2.2	nd
<i>Klebsiella</i>	0.08	2.63	0.08	nd	nd	nd
<i>Ochrobactrum</i>	2.89	0.67	0.32	3.8	nd	nd
<i>Olivibacter</i>	1.13	6.57	1.28	nd	nd	nd
<i>Paenibacillus</i>	0.02	0.24	0.05	nd	2.2	nd
<i>Pseudomonas</i>	24.21	25.25	63.49	57.7	48.9	69.6
<i>Pseudoxanthomonas</i>	2.95	2.62	0.66	8.7	4.4	nd
<i>Rhizobium</i>	nd	nd	nd	nd	nd	4.3
<i>Serratia</i>	0.00	0.24	0.01	nd	6.7	nd
<i>Shinella</i>	2.79	0.25	0.03	nd	nd	nd
<i>Sphingobacterium</i>	0.95	0.94	1.60	3.8	17.8	nd
<i>Stenotrophomonas</i>	1.23	0.77	1.42	7.7	2.2	8.7

Data are expressed as percentages (among 10,065 sequences for Illumina data, among 96 strains for isolates).

both aerobic and anaerobic microorganisms decreased with the vertical soil profile (Biró et al., 2014). Regarding the enrichment steps, it was surprising to find that already after 1 week of enrichment, the communities were similar to those found after 4 weeks. This indicates that when dealing with strong polluted soils, as in this study, a single enrichment step may be enough.

A total of 95 bacterial and 94 fungal strains were identified. These strains were well-distributed along soil depths and pollutant (**Supplementary Tables S2, S3**). The taxonomical identification of bacteria confirmed the selection of specific bacterial communities following the addition of different hydrocarbons, indicating a high specialization of bacterial taxa involved in their degradation. *Proteobacteria*, *Firmicutes*, and *Sphingobacteria* were the prevailing bacterial phyla: all these phyla comprised several phylogenetic groups involved in the aerobic degradation of hydrocarbons (Vinas et al., 2005; Head et al., 2006; Yang et al., 2012; Yergeau et al., 2012). *Proteobacteria* was also found as the most abundant phylum distributed in an environment contaminated with petroleum muck and in activated biomass from a petrochemical industry wastewater sample (Joshi et al., 2014; Yadav et al., 2015). This phylum is divided into five major classes, all with oil-degrading genera (Gao et al., 2014). On the whole, isolated bacteria were ascribed mainly to genera belonging to Gamma-proteobacteria class, whose dominance within the enriched microcosms can be expected since it comprises many of the

hydrocarbonoclastic bacteria responsible for the first steps of hydrocarbons degradation (Head et al., 2006; Yakimov et al., 2007; Barbato et al., 2016).

Bacterial species of the genera *Sphingobacterium*, *Achromobacter*, *Pseudomonas*, *Stenotrophomonas*, and *Bacillus*, isolated from this crude-oil contaminated soil, showed close lineage with previously reported hydrocarbons degrading members of same genera and most of them have been reported earlier as hydrocarbon degraders (Widdel and Rabus, 2001; Roy et al., 2002; Foght, 2008; Chandra et al., 2013; Varjani et al., 2015; Varjani and Upasani, 2016). Members of the genus *Pseudomonas* are widespread environmental microorganisms isolated from a variety of natural sources (Velmurugan et al., 2011) and well-known biodegraders, capable of metabolizing a range of compounds (Kostka et al., 2011; Mulet et al., 2011; Mahjoubi et al., 2013).

According to our results, the PAHs-degrading isolates in soil belong to the *Sphingomonas* and *Pseudomonas* bacteria. *Pseudomonas* usually contain *nah*-like genes that encode for the dioxygenase subfamily; the products of these genes are capable of degrading low-molecular-weight PAHs (Johnsen et al., 2007) and producing a rhamnolipid biosurfactant in soils contaminated with petroleum hydrocarbons (Sadouk et al., 2008; Xia et al., 2014). Unlike other gram-negative bacteria strains, members of the genus *Sphingomonas* are able to degrade a wide range of natural and xenobiotic compounds (Eguchi et al., 1996; Pinhassi and Hagstrom, 2000). Three strains of *Serratia marcescens* were

**TABLE 3** | Relative abundances of fungal genera as determined by Illumina sequencing of 16S PCR of amplicons or by isolation on selective media; the comparison was performed at the end of the enrichment (step III).

Fungal genus	ITS Illumina			Fungal isolates		
	S1	S2	S3	S1	S2	S3
<i>Acremonium</i>	0.001	0.003	nd	2.9	nd	nd
<i>Arthrinium</i>	2.0	0.4	0.3	nd	nd	nd
<i>Aspergillus</i>	1.8	2.0	0.8	8.6	8.7	19.4
<i>Aureobasidium</i>	0.9	0.3	0.3	2.9	nd	nd
<i>Bjerkandera</i>	nd	nd	nd	nd	4.3	nd
<i>Capnodiales_unclassified</i>	12.0	11.3	3.4	nd	nd	nd
<i>Ceriosporopsis</i>	0.2	0.2	14.8	nd	nd	nd
<i>Cladosporium</i>	0.2	0.6	0.1	8.6	13.0	nd
<i>Clonostachys</i>	11.0	0.6	0.5	2.9	nd	nd
<i>Epicoccum</i>	nd	nd	nd	2.9	4.3	
<i>Eutypella</i>	nd	nd	nd	nd	4.3	2.8
<i>Fusarium</i>	43.8	68.8	63.4	40.0	56.5	41.7
<i>Hypocrea</i>	nd	nd	nd	nd	nd	11.1
<i>Irpex</i>	nd	nd	nd	nd	4.3	nd
<i>Penicillium</i>	0.8	2.1	1.2	5.7	nd	2.8
<i>Phanerochaete</i>	0.5	1.7	0.3	nd	nd	nd
<i>Polyporus</i>	nd	nd	nd	nd	nd	2.8
<i>Pseudallescheria</i>	15.5	0.8	1.5	5.7	nd	nd
<i>Scedosporium</i>	0.01	0.01	0.12	nd	4.3	5.6
<i>Sulcatispora</i>	nd	nd	nd	nd	nd	2.8
<i>Trametes</i>	nd	0.1	0.04	nd	nd	2.8
<i>Saccharomyces</i>	0.9	0.7	0.1	nd	nd	nd
<i>Trichoderma</i>	3.6	0.4	0.5	20.0	nd	5.6
<i>Wallemia</i>	0.02	nd	0.02	nd	nd	2.8
<i>Trichosporon</i>	1.2	3.2	4.4	nd	nd	nd

Data are expressed as percentages (among 10065 sequences for Illumina data, among 94 strains for isolates).

also isolated from the enriched microcosms with the crude oil of the contaminated site, supporting previous evidences of degradation of crude oil and petroleum products by species of *Serratia* (De La Fuente et al., 1991; Rojas-Avelizapa et al., 2002; Wongsa et al., 2004; Rajasekar et al., 2007).

Generally, fungi involved in the degradation of PAHs include ligninolytic and non-ligninolytic fungi. Most of the strains isolated after the enrichment steps belonged to the phylum Ascomycota, although few Basidiomycota were isolated. The dominance of Ascomycota in polluted soil has been extensively acknowledged: Zhang et al. (2018) reported that Ascomycota represented up to 73–96% of the total 18S sequences of a coking area soil; eight of the 10 strains isolated from a PAHs contaminated pond were Ascomycetes and were also able to remove anthracene (Aranda et al., 2017). Finally, an oilfield with a history of 50 years pollution influenced mainly the bacterial community, whereas fungi, mostly related to this phylum, were abundant, demonstrating to be less sensitive to soil PAHs (Zhou et al., 2017).

Basidiomycota represented only the 5.3% of the total isolates. Similarly, in a toxic coking area, only a small fraction of the isolates belonged to Basidiomycota (0.34–7.0%) (Zhang et al., 2018). Besides *Bjerkandera adusta*, *Irpex lacteus*, *Wallemia mellicola*, *Polyporus gayanus*, *Trametes gibbosa*, the presence

of species of *Lopharia*, *Phanerochaete*, and *Trichosporon* was assessed by HTS. Among them, *T. gibbosa*, *P. gayanus*, and *W. mellicola* were isolated for the first time in hydrocarbons polluted soil.

On the other hand, Mucoromycota were absent in this contaminated soil. Unlike Morais et al. (2016) who found more than 50% of Mucoromycota in a petroleum contaminated costal site, we did not identified any organism belonging to this phylum. Mucoromycota represented a small fraction of the isolates also in an estuarine sediment contaminated mainly by PAHs (Da Silva et al., 2003) and in heavy crude oil-contaminated soil (Zafra et al., 2014). In the present study, Mucoromycota could be included in the “unclassified” group (Figure 3), even though they would be a negligible fraction of the mycoflora.

All samples were dominated by *Fusarium*, followed by *Aspergillus*, *Penicillium*, and *Trichoderma*. The identification of these genera as polluted soil inhabitants has been already discussed elsewhere. Sordariomycetes is the most represented class with *Acremonium*, *Arthrinium*, *Clonostachys*, *Eutypella*, *Fusarium*, *Hypocrea/Trichoderma*, and *Pseudoallescheria/Scedosporium*. Fungal taxonomy analysis of an oil-contaminated soil detected almost 25% of Sordariomycetes (Morais et al., 2016). *Trichoderma harzianum* (Da Silva et al., 2003), *Scedosporium apiospermum* and *Acremonium* sp.

**TABLE 4** | Relative percentages of most abundant bacterial OTUs after the last enrichment step for each pollutant and at each of the three soil depths tested.

OTU nr	Taxonomy	Benzene			Naphthalene			Oil			Paraffin			Phenanthrene			Pyrene		
		S1	S2	S3	S1	S2	S3	S1	S2	S3	S1	S2	S3	S1	S2	S3	S1	S2	S3
OTU001	<i>Pseudomonas putida</i> *	5.2	0.9	2.2	26.1	37.1	73.6	6.0	1.6	58.3	0.3	0.2	10.6	20.3	0.6	0.4	65.8		
OTU002	<i>Achromobacter xylosoxidans</i> *	7.0	2.9	4.8	46.4	20.7	4.1	10.2	20.3	6.0	8.5	11.1	23.5	23.4	26.4	51.5	6.5		
OTU003	<i>Pseudomonas stutzeri</i>	0.1	0.1	0.1	0.4	0.9	0.8	1.0	0.9	5.4	0.2	0.1	0.6	1.5	0.9	0.9	1.3		
OTU004	<i>Pseudomonas fluorescens</i> *	0.1	0.1	0.0	1.9	4.4	3.7	16.4	20.7	9.7	0.2	0.3	1.1	3.5	0.3	0.6	2.1		
OTU005	<i>Rhizobium petrolearium</i> *	50.1	31.5	44.9	0.1	0.3	0.2	0.1	0.1	0.2	1.8	4.3	0.1	0.3	0.3	0.2	0.6		
OTU006	<i>Acinetobacter calcoaceticus</i> *	1.1	0.0	4.8	0.1	0.1	0.0	0.1	0.1	0.1	0.0	0.1	0.1	0.1	0.1	0.0	0.1		
OTU008	<i>Azospirillum lipoferum</i>	0.0	0.0	0.0	0.0	0.0	0.1	0.0	0.0	0.0	0.0	0.1	0.1	10.7	4.6	0.4	0.1		
OTU009	Unclassified Comamonadaceae	0.0	0.0	0.0	0.0	0.0	0.1	6.0	12.2	0.0	0.2	0.3	0.0	0.0	0.0	0.0	0.0		
OTU010	<i>Ochrobactrum anthropi</i> *	0.8	0.2	0.9	0.0	0.0	0.0	0.0	0.0	0.0	11.9	15.4	0.2	2.3	1.7	0.0	0.0		
OTU011	<i>Rhizobium radiobacter</i>	0.5	4.8	1.8	0.2	0.3	0.0	0.0	0.0	0.0	0.9	3.8	1.8	1.7	1.4	19.1	0.0		
OTU013	<i>Cupriavidus necator</i>	0.6	1.2	0.2	0.1	0.0	0.0	0.0	0.0	0.0	1.2	0.3	0.1	0.0	20.3	0.0	0.0		
OTU014	<i>Gordonia alkanivorans</i>	0.0	0.0	0.0	0.0	0.0	0.1	0.1	0.0	0.0	16.8	2.2	0.1	0.1	0.0	0.0	0.1		
OTU015	<i>Pseudomonas stutzeri</i> *	0.0	0.0	0.0	0.0	0.0	0.0	24.2	0.0	0.0	0.0	0.0	0.0	0.1	0.0	0.1	0.0		
OTU016	<i>Sphingobacterium</i> spp.*	1.3	20.2	4.6	0.0	0.0	0.0	0.0	0.0	0.0	0.4	0.0	0.0	7.3	0.0	2.7	0.0		
OTU017	<i>Bordetella</i> spp.	5.1	0.0	1.8	0.1	0.6	0.0	0.0	0.0	0.0	0.5	2.9	0.1	0.5	0.2	0.2	0.0		
OTU018	<i>Pseudoxanthomonas mexicana</i> *	2.7	1.1	1.6	0.0	1.1	0.1	0.0	0.0	0.0	0.8	0.3	2.9	2.9	5.4	2.8	0.1		
OTU021	<i>Sinorhizobium</i> spp.	2.0	2.2	1.2	0.0	0.2	0.0	0.0	0.0	0.0	1.5	7.0	0.0	0.1	0.2	0.1	0.0		
OTU023	<i>Xanthobacter flavus</i>	0.0	0.1	0.1	0.0	0.0	0.0	0.0	0.0	0.0	5.6	21.1	0.0	0.1	0.0	0.1	0.0		
OTU024	<i>Pseudomonas resinovorans</i>	0.1	0.3	0.0	0.5	0.0	0.1	0.4	0.5	2.1	0.0	0.0	12.0	0.2	1.0	0.6	0.1		
OTU025	<i>Azospirillum thiophilum</i>	0.0	0.0	0.0	0.0	0.0	0.0	0.0	0.0	0.0	0.0	0.0	17.7	0.0	0.0	0.0	0.5		

OTUs that represent more than 1% of total bacterial community in at least one sample are presented. OTUs that were also detected among isolates are highlighted with an asterisk.

**TABLE 5 |** Relative percentages of most abundant fungal OTUs after the last enrichment step for each pollutant and at each of the three soil depths tested. OTUs that represent more than 1% of total fungal community in at least one sample are presented.

OTU nr	Taxonomy	Benzene			Naphthalene			Oil			Paraffin			Pheanthrene			Pyrene	
		S1	S2	S3	S1	S2	S3	S1	S2	S3	S1	S2	S3	S1	S2	S1	S2	
OTU002	<i>Fusarium oxysporum</i> *	3.5	39.1	16.6	29.4	23.4	36.3	4.7	4.6	3.3	9.8	15.3	13.4	39.3	56.4	63.5	56.4	78.3
OTU003	<i>Cladosporium</i> spp.*	1.3	7.5	2.4	5.6	2.5	6.4	71.2	61.8	8.4	1.1	1.4	1.8	1.5	1.7	1.4	2.0	3.4
OTU004	<i>Fusarium</i> spp.*	0.9	5.1	2.1	5.5	5.8	6.5	1.3	3.5	0.9	9.8	64.9	30.2	35.9	26.1	2.0	2.9	3.4
OTU001	<i>Fusarium solani</i> *	2.6	21.8	64.3	13.2	22.6	15.1	2.4	10.1	1.8	12.7	4.4	51.2	18.5	11.7	7.6	7.9	7.6
OTU007	Unidentified Halosphaeriaceae	0.2	0.0	0.0	0.2	0.2	0.2	0.2	0.2	80.4	0.1	0.2	0.1	0.2	0.3	0.2	0.2	0.2
OTU014	<i>Fusarium merismoides</i>	0.0	0.0	0.0	0.2	0.1	0.4	0.1	0.1	0.0	0.1	0.1	0.2	0.2	0.2	20.2	0.4	0.1
OTU005	<i>Pseudallescheria</i> spp.	89.0	0.7	6.6	1.1	1.5	0.6	0.6	0.5	0.3	0.7	1.0	0.9	0.7	0.6	0.8	1.0	0.9
OTU008	<i>Apiospora montagnei</i>	0.2	0.1	0.1	5.9	0.7	0.6	0.3	0.4	0.1	0.2	0.3	0.4	0.5	0.3	0.4	5.4	0.8
OTU012	<i>Aspergillus flavus</i>	0.1	2.8	0.2	5.4	3.2	1.6	0.1	0.2	0.0	0.0	0.1	0.1	0.1	0.1	0.1	0.6	0.2
OTU030	<i>Saccharomyces cerevisiae</i>	0.1	0.2	0.1	0.7	1.8	0.2	3.6	1.8	0.2	0.1	0.1	0.0	0.1	0.1	0.1	0.6	0.1
OTU009	<i>Penicillium</i> spp.*	0.1	4.6	0.8	1.3	1.5	2.7	0.2	1.9	0.2	0.1	0.1	0.3	0.1	0.1	0.1	0.3	0.2
OTU010	<i>Trichoderma harzianum</i> *	0.2	0.2	0.1	5.1	0.7	0.6	0.2	0.3	0.1	0.3	0.3	0.3	0.5	0.3	0.8	16.0	0.7
OTU006	<i>Fusarium cuneirostrum</i>	0.1	0.1	0.1	0.5	0.3	0.3	0.3	1.9	1.4	64.0	0.3	0.2	0.2	0.5	0.4	0.4	0.4
OTU028	<i>Aureobasidium pullulans</i> *	0.0	0.5	0.6	4.0	1.2	0.4	0.0	0.1	0.1	0.0	0.0	0.0	0.0	0.1	0.0	0.5	0.3
OTU024	<i>Trichosporon</i> spp.	0.1	0.7	0.0	3.1	3.4	4.5	0.0	0.0	0.0	0.0	0.1	0.0	0.1	0.1	0.0	0.1	0.1
OTU019	<i>Galactomyces geotrichum</i>	0.0	0.1	0.2	0.5	3.3	0.1	0.0	0.0	0.0	0.0	0.0	0.0	0.0	0.0	0.0	0.0	0.0
OTU021	<i>Cadophora malorum</i>	0.0	0.1	0.3	1.3	0.1	0.3	3.5	1.0	0.1	0.1	1.8	0.0	0.1	0.1	0.1	0.1	0.0
OTU011	<i>Trichosporon loubieri</i>	0.0	1.8	0.1	3.0	10.3	16.2	0.1	0.1	0.1	0.1	0.2	0.0	0.1	0.1	0.1	0.3	0.2
OTU018	<i>Phanerochaete chrysosporium</i>	1.0	7.3	0.5	1.5	2.7	0.8	0.7	0.0	0.5	0.0	0.0	0.0	0.1	0.1	0.1	0.2	0.2
OTU114	<i>Fusarium solani</i> *	0.0	0.1	0.1	0.2	3.9	0.0	0.0	0.0	0.0	0.0	0.0	0.0	0.0	0.0	0.0	0.0	0.0
OTU132	<i>Fusarium</i> spp.*	0.1	0.1	0.0	0.2	0.1	0.1	0.0	0.0	0.1	0.1	1.0	0.0	0.2	0.2	1.2	3.1	0.1
OTU033	<i>Hypocrea gamsii</i>	0.0	0.0	0.0	0.1	0.1	0.0	2.5	0.0	0.1	0.0	0.1	0.0	0.1	0.0	0.0	0.0	0.0

OTUs that were also detected among isolates are highlighted with an asterisk.

(Charneau et al., 1999; Zafra et al., 2014), *Fusarium oxysporum* (Marchand et al., 2017), and *Fusarium solani* (Charneau et al., 1999) were also isolated from contaminated soil or sediments. *Fusarium* (three strains), *Trichoderma* (three strains), and *Pseudallescheria* (two strains) represented the 40% of the isolates from heavy and extra-heavy crude oil polluted soils (Naranjo et al., 2007). Zhou et al. (2017) detected more than 20% of *Gibberella* species in an oilfield site. Since *Gibberella* is the teleomorph of the majority of *Fusarium* species (Leslie and Summerell, 2008) we can state that this finding is in agreement with our observations. The isolation of 42 strains of *Fusarium*, among which 64% were ascribable to *F. solani*, opens to intriguing solutions for their application in bioremediation processes. Indeed *F. solani* isolated from oil polluted soil by enrichment method using phenanthrene as the sole source of carbon was capable of degrading a mixture of low and high molecular weight PAHs (up to 84.8%) (Hesham et al., 2017). To the best of our knowledge, this is the first time that a strain of *Eutypella scoparia* has been isolated from a polluted soil. Previous researches reported the isolation of this species only in a non-polluted Arctic soil (Bergero et al., 1999; Liu et al., 2014).

Surprisingly, Morais et al. (2016) did not found Eurotiomycetes in a contaminated soil. On the contrary, in the present study, the fungal community was rich of *Aspergillus* and *Penicillium*. *Aspergillus* and *Penicillium* strains have been already isolated in several polluted samples (Charneau et al., 1999; Da Silva et al., 2003; Zafra et al., 2014; Al-Hawash et al., 2018). Data on soil isolation of *Aspergillus niger* (Charneau et al., 1999), *Aspergillus fumigatus* (Charneau et al., 1999; Zafra et al., 2014), *Aspergillus terreus* (Da Silva et al., 2003), *Aspergillus flavus*, *Aspergillus niger*, *Aspergillus nomius* (Zafra et al., 2014), *Aspergillus sydowii* (Tian et al., 2016), *Aspergillus versicolor* (Šimonovičová et al., 2017) have been reported although few information deals with the here-detected species of *Aspergillus* (i.e., *A. creber*, *A. jensenii*, *A. protuberus*). For instance, *A. creber* and *A. jensenii*, described as new species in Jurjevic et al. (2012), are mostly known as air-borne contaminants or of clinical relevance (Micheluz et al., 2016; Siqueira et al., 2016); *A. protuberus* has been isolated from air and the mussel *Mytilus edulis galloprovincialis* (Siqueira et al., 2016; Klas et al., 2018). There is no evidence in literature of these species as a terrestrial inhabitant. Although already detected in soil, *Aspergillus sclerotiorum* and *Aspergillus waskmanii* have been only associated to not-contaminated lands (Nesci et al., 2006; Phainuphong et al., 2017) or as part of the rhizosphere of tussock (Di Menna et al., 2007). Although this is the first time a *Penicillium catenatum* is found in a polluted soil, it must be considered that the identification of soil fungi is not always accurate at species level (Al-Hawash et al., 2018).

A thorough comparison was performed between the relative abundances of bacterial and fungal strains. The comparisons carried out at genus level (Table 2 for bacteria, Table 3 for fungi) and at OTU level (Table 4 for bacteria, Table 5 for fungi) showed an agreement between the culture-dependent and the culture-independent approaches. In most cases, species level was reached, thus confirming that the Illumina sequencing of the two hypervariable V3–V4 regions and of the partial ITS2 are sufficient

to reach the species level for bacteria and fungi respectively. The species with more isolates (such as *P. putida*, *A. xylosoxidans* and *Ochromobacterium anthropi* for bacteria, *F. oxysporum* and *F. solani* for fungi) were also the dominant OTUs, thus showing that the culturing methods reflect the relative composition of total communities. Furthermore, the two approaches also agree for the less abundant genera: this is expected since enrichment procedures indeed select for the cultivable species among the total bacterial and fungal communities that is originally present in the polluted soil. A novel aspect shown in our work is that the two approaches had detection levels that were generally in good agreement. Composition of the actual microbial community and are not much subjected to biases.

## CONCLUSION

In the present study, we evaluated the evolution of bacterial and fungal communities enriched from polluted soil by culture-independent and dependent methods. The results showed that already after 1 week of enrichment, both bacterial and fungal communities resembled those found after 4 weeks, and that the soil depth did not influence the evolution of microbial communities, contrary to the pollutant used. Isolation results were in agreement with HTS molecular data, indicating that the strains isolated reflected the microbial composition of the enriched consortia. Future studies will focus on the biodegradation abilities of the isolates microorganisms.

## AUTHOR CONTRIBUTIONS

EP and GV ideated and supervised the study. GS, FS, and AP performed the experiments and wrote the paper. A-LB and TR performed the experiments. CG carried out chemical analyses.

## FUNDING

This research was conducted within the LIFE15 ENV/IT/000396 project “Bioremediation and revegetation to restore the public use of contaminated land.”

## ACKNOWLEDGMENTS

The authors are grateful to Sotirios Vasileiadis for a number of scripts used for HTS data elaboration, and to Prof Mariangela Girlanda and Dr. Samuele Voyron for helping in Fungal metabarcoding analysis.

## SUPPLEMENTARY MATERIAL

The Supplementary Material for this article can be found online at: <https://www.frontiersin.org/articles/10.3389/fmicb.2018.02543/full#supplementary-material>

## REFERENCES

- Aburto-Medina, A., Adetutu, E. M., Aleer, S., Weber, J., Patil, S. S., Sheppard, P. J., et al. (2012). Comparison of indigenous and exogenous microbial populations during slurry phase biodegradation of long-term hydrocarbon-contaminated soil. *Biodegradation* 23, 813–822. doi: 10.1007/s10532-012-9563-8
- Agnello, A. C., Bagard, M., Van Hullebusch, E. D., Esposito, G., and Huguenot, D. (2016). Comparative bioremediation of heavy metals and petroleum hydrocarbons co-contaminated soil by natural attenuation, phytoremediation, bioaugmentation and bioaugmentation-assisted phytoremediation. *Sci. Total Environ.* 563–564, 693–703. doi: 10.1016/j.scitotenv.2015.10.061
- Al-Hawash, A. B., Alkooanee, J. T., Abbood, H. A., Zhang, J., Sun, J., Zhang, X., et al. (2018). Isolation and characterization of two crude oil-degrading fungi strains from Rumaila oil field. *Iraq. Biotechnol. Rep.* 17, 104–109. doi: 10.1016/j.btre.2017.12.006
- Alonso-Gutierrez, J., Figueras, A., Albaiges, J., Jimenez, N., Vinas, M., Solanas, A. M., et al. (2009). Bacterial communities from shoreline environments (Costa da morte, northwestern Spain) affected by the prestige oil spill. *Appl. Environ. Microbiol.* 75, 3407–3418. doi: 10.1128/AEM.01776-08
- Altschul, S. F., Madden, T. L., Schaffer, A., Zhang, J., Zhang, Z., Miller, W., et al. (1997). Gapped BLAST and PSI-BLAST: a new generation of protein database search programs. *Nucleic. Acid. Res.* 25, 3389–3404. doi: 10.1093/nar/25.17.3389
- An, D., Caffrey, S. M., Soh, J., Agrawal, A., Brown, D., Budwill, K., et al. (2013). Metagenomics of hydrocarbon resource environments indicates aerobic taxa and genes to be unexpectedly common. *Environ. Sci. Technol.* 47, 10708–10717. doi: 10.1021/es4020184
- Aranda, E., Godoy, P., Reina, R., Badia-Fabregat, M., Rosell, M., Marco-Urrea, E., et al. (2017). Isolation of Ascomycota fungi with capability to transform PAHs: insights into the biodegradation mechanisms of *Penicillium oxalicum*. *Int. Biodeter. Biodegr.* 122, 141–150. doi: 10.1016/j.ibiod.2017.05.015
- Atlas, R. M. (1981). Microbial degradation of petroleum hydrocarbons: an environmental perspective. *Microbiol. Rev.* 45, 180–209.
- Badr El-Din, S. M., Moussa, T. A., Moawad, H., and Sharaf, O. A. (2014). Isolation and characterization of polyaromatic hydrocarbons degrading bacteria from compost leachate. *J. Adv. Biol.* 5, 651–660.
- Bao, M. T., Wang, L. N., Sun, P. Y., Cao, L. X., Zou, J., and Li, Y. M. (2012). Biodegradation of crude oil using an efficient microbial consortium in a simulated marine environment. *Mar. Pollut. Bull.* 64, 1177–1185. doi: 10.1016/j.marpolbul.2012.03.020
- Barbato, M., Mapelli, F., Magagnini, M., Chouaia, B., Armeni, M., Marasco, R., et al. (2016). Hydrocarbon pollutants shape bacterial community assembly of harbor sediments. *Mar. Pollut. Bull.* 104, 211–220. doi: 10.1016/j.marpolbul.2016.01.029
- Bensch, K., Braun, U., Groenewald, J. Z., and Crous, P. W. (2012). The genus *Cladosporium*. *Stud. Mycol.* 72, 1–401. doi: 10.3114/sim0003
- Bergero, R., Girlanda, M., Varese, G., Intili, D., and Luppi, A. (1999). Psychrooiligotrophic fungi from arctic soils of Franz Joseph Land. *Polar Biol.* 21, 361–368. doi: 10.1007/s0030000050374
- Berry, D., Mahfoudh, K. B., Wagner, M., and Loy, A. (2011). Barcoded primers used in multiplex amplicon pyrosequencing bias amplification. *Appl. Environ. Microb.* 77, 7846–7849. doi: 10.1128/AEM.05220-11
- Biró, B., Toscano, G., Horváth, N., Matics, H., Domonkos, M., Scotti, R., et al. (2014). Vertical and horizontal distributions of microbial abundances and enzymatic activities in propylene-glycol-affected soils. *Environ. Sci. Pollut. R.* 21, 9095–9108. doi: 10.1007/s11356-014-2686-1
- Blume, E., Bischoff, M., Reichert, J., Moorman, T., Konopka, A., and Turco, R. (2002). Surface and subsurface microbial biomass, community structure and metabolic activity as a function of soil depth and season. *Appl. Soil Ecol.* 20, 171–181. doi: 10.1016/S0929-1393(02)00025-2
- Bundy, J. G., Paton, G. I., and Campbell, C. D. (2004). Combined microbial community level and single species biosensor responses to monitor recovery of oil polluted soil. *Soil Biol. Biochem.* 36, 1149–1159. doi: 10.1016/j.soilbio.2004.02.025
- Cerqueira, V. S., Hollenbach, E. B., Maboni, F., Vainstein, M. H., Camargo, F. A., Do Carmo, R. P. M., et al. (2011). Biodegradation potential of oily sludge by pure and mixed bacterial cultures. *Bioresour. Technol.* 102, 11003–11010. doi: 10.1016/j.biortech.2011.09.074
- Chazneau, C., Morel, J., Dupont, J., Bury, E., and Oudot, J. (1999). Comparison of the fuel oil biodegradation potential of hydrocarbon-assimilating microorganisms isolated from a temperate agricultural soil. *Sci. Tot. Environ.* 227, 237–247. doi: 10.1016/S0048-9697(99)00033-9
- Chandra, S., Sharma, R., and Singh, K. (2013). Application of bioremediation technology in the environment contaminated with petroleum hydrocarbon. *Ann. Microbiol.* 63, 417–431. doi: 10.1007/s13213-012-0543-3
- Cousins, I. T., Gevaio, B., and Jones, K. C. (1999). Measuring and modelling the vertical distribution of semi-volatile organic compounds in soils. I: PCB and PAH soil core data. *Chemosphere* 39, 2507–2518. doi: 10.1016/S0045-6535(99)00164-2
- Covino, S., Stella, T., and Cajthaml, T. (2016). “Mycoremediation of organic pollutants: principles, opportunities, and pitfalls,” in *Fungal Applications in Sustainable Environmental Biotechnology*, ed. D. Purchase (Berlin: Springer), 185–231. doi: 10.1007/978-3-319-42852-9\_8
- Da Silva, M., Umbuzeiro, G. A., Pfenning, L. H., Canhos, V. P., and Esposito, E. (2003). Filamentous fungi isolated from estuarine sediments contaminated with industrial discharges. *Soil Sediment Contam.* 12, 345–356. doi: 10.1080/713610976
- Das, N., and Chandran, P. (2011). Microbial degradation of petroleum hydrocarbon contaminants: an overview. *Biotechnol. Res. Int.* 2011:941810. doi: 10.4061/2011/941810
- De La Fuente, G., Perestelo, F., Rodriguez-Perez, A., and Falcon, M. A. (1991). Oxidation of aromatic aldehydes by *Serratia marcescens*. *Appl. Environ. Microb.* 57, 1275–1276.
- Dean-Ross, D., Moody, J., and Cerniglia, C. E. (2002). Utilization of mixtures of polycyclic aromatic hydrocarbons by bacteria isolated from contaminated sediment. *FEMS Microbiol. Ecol.* 41, 1–7. doi: 10.1111/j.1574-6941.2002.tb00960.x
- Desai, J. D., and Banat, I. M. (1997). Microbial production of surfactants and their commercial utilization. *Microbiol. Mol. Biol. R.* 61, 47–64.
- Deshmukh, R., Khardenavis, A., and Purohit, H. (2016). Diverse metabolic capacities of fungi for bioremediation. *Indian J. Microbiol.* 56, 247–264. doi: 10.1007/s12088-016-0584-6
- Di Cello, F., and Fani, R. (1996). A molecular strategy for the study of natural bacterial communities by PCR-based techniques. *Minerva Biotechnol.* 8, 126–134.
- Di Menna, M., Sayer, S., Barratt, B., Bell, N., Ferguson, C., and Townsend, R. (2007). Biodiversity of indigenous tussock grassland sites in Otago, Canterbury and the central North Island. V. *Penicillia* and *Aspergilli*. *J. Roy. Soc. New Zeal.* 37, 131–137. doi: 10.1080/03014220709510541
- Dueholm, M. S., Marques, I. G., Karst, S. M., D’imperio, S., Tale, V. P., Lewis, D., et al. (2015). Survival and activity of individual bioaugmentation strains. *Bioresour. Technol.* 186, 192–199. doi: 10.1016/j.biortech.2015.02.111
- Edgar, R. C. (2013). UPARSE: highly accurate OTU sequences from microbial amplicon reads. *Nat. Methods* 10, 996–998. doi: 10.1038/nmeth.2604
- Edgar, R. C., Haas, B. J., Clemente, J. C., Quince, C., and Knight, R. (2011). UCHIME improves sensitivity and speed of chimera detection. *Bioinformatics* 27, 2194–2200. doi: 10.1093/bioinformatics/btr381
- Eguchi, M., Nishikawa, T., Macdonald, K., Cavicchioli, R., Gottschal, J., and Kjelleberg, S. (1996). Responses to stress and nutrient availability by the marine ultramicrobacterium *Sphingomonas* sp. strain RB2256. *App. Environ. Microb.* 62, 1287–1294.
- Fernandez-Luqueno, F., Valenzuela-Encinas, C., Marsch, R., Martinez-Suarez, C., Vazquez-Nunez, E., and Dendooven, L. (2010). Microbial communities to mitigate contamination of PAHs in soil-possibilities and challenge: a review. *Environ. Sci. Pollut. R.* 18, 12–30. doi: 10.1007/s11356-010-0371-6
- Fierer, N., Schimel, J. P., and Holden, P. A. (2003). Variations in microbial community composition through two soil depth profiles. *Soil Biol. Biochem.* 35, 167–176. doi: 10.1016/S0038-0717(02)00251-1
- Foght, J. (2008). Anaerobic biodegradation of aromatic hydrocarbons: pathways and prospects. *J. Mol. Microbiol. Biotechnol.* 15, 93–120. doi: 10.1159/000121324
- Fowler, S. J., Toth, C. R., and Gieg, L. M. (2016). Community structure in methanogenic enrichments provides insight into syntrophic interactions in hydrocarbon-impacted environments. *Front. Microbiol.* 7:562. doi: 10.3389/fmicb.2016.00562
- Fuentes, S., Méndez, V., Aguila, P., and Seeger, M. (2014). Bioremediation of petroleum hydrocarbons: catabolic genes, microbial communities, and

- applications. *Appl. Microbiol. Biotechnol.* 98, 4781–4794. doi: 10.1007/s00253-014-5684-9
- Gao, Y. C., Guo, S. H., Wang, J. N., Li, D., Wang, H., and Zeng, D. H. (2014). Effects of different remediation treatments on crude oil contaminated saline soil. *Chemosphere* 117, 486–493. doi: 10.1016/j.chemosphere.2014.08.070
- Ghaly, A., and Yusran, A. (2013). Effects of biostimulation and bioaugmentation on the degradation of pyrene in soil. *J. Bioremed. Biod.* 5, 1–13. doi: 10.1016/j.chemosphere.2011.11.032
- Gihring, T. M., Green, S. J., and Schadt, C. W. (2012). Massively parallel rRNA gene sequencing exacerbates the potential for biased community diversity comparisons due to variable library sizes. *Environ. Microbiol.* 14, 285–290. doi: 10.1111/j.1462-2920.2011.02550.x
- Glass, N. L., and Donaldson, G. C. (1995). Development of primer sets designed for use with the PCR to amplify conserved genes from filamentous ascomycetes. *Appl. Environ. Microbiol.* 61, 1323–1330.
- Hara, E., Kurihara, M., Nomura, N., Nakajima, T., and Uchiyama, H. (2013). Bioremediation field trial of oil-contaminated soil with food-waste compost. *J. JSCE* 1, 125–132. doi: 10.2208/journalofjsce.1.1\_125
- Haritash, A. K., and Kaushik, C. P. (2009). Biodegradation aspects of polycyclic aromatic hydrocarbons (PAHs): a review. *J. Hazard Mater.* 169, 1–15. doi: 10.1016/j.jhazmat.2009.03.137
- Hazen, T. C., Rocha, A. M., and Techtmann, S. M. (2013). Advances in monitoring environmental microbes. *Curr. Opin. Biotechnol.* 24, 526–533. doi: 10.1016/j.copbio.2012.10.020
- Head, I. M., Gray, N. D., and Larter, S. R. (2014). Life in the slow lane; biogeochemistry of biodegraded petroleum containing reservoirs and implications for energy recovery and carbon management. *Front. Microbiol.* 5:566. doi: 10.3389/fmicb.2014.00566
- Head, I. M., Jones, D. M., and Røling, W. F. (2006). Marine microorganisms make a meal of oil. *Nat. Rev. Microbiol.* 4, 173–182. doi: 10.1038/nrmicro1348
- Hesham, A. E.-L., Mohamed, E. A., Mawad, A. M., Elfarash, A., Abd El-Fattah, B. S., and El-Rawy, M. A. (2017). Molecular characterization of *Fusarium solani* degrades a mixture of low and high molecular weight polycyclic aromatic hydrocarbons. *Biotechnol. J.* 11, 27–35.
- Johnsen, A. R., Schmidt, S., Hybholt, T. K., Henriksen, S., Jacobsen, C. S., and Andersen, O. (2007). Strong impact on the polycyclic aromatic hydrocarbon (PAH)-degrading community of a PAH-polluted soil but marginal effect on PAH degradation when priming with bioremediated soil dominated by mycobacteria. *Appl. Environ. Microbiol.* 73, 1474–1480. doi: 10.1128/AEM.02236-06
- Joshi, M. N., Dhebar, S. V., Dhebar, S. V., Bhargava, P., Pandit, A., Patel, R. P., et al. (2014). Metagenomics of petroleum muck: revealing microbial diversity and depicting microbial syntrophy. *Arch. Microbiol.* 196, 531–544. doi: 10.1007/s00203-014-0992-0
- Jurjevic, Z., Peterson, S. W., and Horn, B. W. (2012). *Aspergillus* section versicolores: nine new species and multilocus DNA sequence based phylogeny. *IMA Fungus* 3, 59–59. doi: 10.5598/imafungus.2012.03.01.07
- Klas, K. R., Kato, H., Frisvad, J. C., Yu, F., Newmister, S. A., Fraley, A. E., et al. (2018). Structural and stereochemical diversity in prenylated indole alkaloids containing the bicyclo-[2.2.2]-diazaoctane ring system from marine and terrestrial fungi. *Nat. Prod. Rep.* 35, 532–558. doi: 10.1039/c7np00042a
- Kostka, J. E., Prakash, O., Overholt, W. A., Green, S. J., Freyer, G., Canion, A., et al. (2011). Hydrocarbon-degrading bacteria and the bacterial community response in gulf of Mexico beach sands impacted by the deepwater horizon oil spill. *Appl. Environ. Microbiol.* 77, 7962–7974. doi: 10.1128/AEM.05402-11
- Leonardi, V., Giubilei, M. A., Federici, E., Spaccapelo, R., Sasek, V., Novotny, C., et al. (2008). Mobilizing agents enhance fungal degradation of polycyclic aromatic hydrocarbons and affect diversity of indigenous bacteria in soil. *Biotechnol. Bioeng.* 101, 273–285. doi: 10.1002/bit.21909
- Leslie, J. F., and Summerell, B. A. (2008). *The Fusarium Laboratory Manual*. Hoboken, NJ: John Wiley & Sons.
- Liu, G. P.-W., Chang, T. C., Whang, L.-M., Kao, C.-H., Pan, P.-T., and Cheng, S.-S. (2011). Bioremediation of petroleum hydrocarbon contaminated soil: effects of strategies and microbial community shift. *Int. Biodeter. Biodegr.* 65, 1119–1127. doi: 10.1016/j.ibiod.2011.09.002
- Liu, J. T., Hu, B., Gao, Y., Zhang, J. P., Jiao, B. H., Lu, X. L., et al. (2014). Bioactive tyrosine-derived cytochalasins from fungus *Eutypella* sp. D-1. *Chem. Biodivers.* 11, 800–806. doi: 10.1002/cbdv.201300218
- MacNaughton, S. J., Stephen, J. R., Venosa, A. D., Davis, G. A., Chang, Y.-J., and White, D. C. (1999). Microbial population changes during bioremediation of an experimental oil spill. *Appl. Environ. Microbiol.* 65, 3566–3574.
- Mahjoubi, M., Jaouani, A., Guesmi, A., Ben Amor, S., Jouini, A., Cherif, H., et al. (2013). Hydrocarbonoclastic bacteria isolated from petroleum contaminated sites in Tunisia: isolation, identification and characterization of the biotechnological potential. *N. Biotechnol.* 30, 723–733. doi: 10.1016/j.nbt.2013.03.004
- Maiti, D., Chandra, K., Mondal, S., Ojha, A. K., Das, D., Roy, S. K., et al. (2008). Isolation and characterization of a heteroglycan from the fruits of *Astraeus hygrometricus*. *Carbohydr. Res.* 343, 817–824. doi: 10.1016/j.carres.2007.12.003
- Marchand, C., St-Arnaud, M., Hogland, W., Bell, T. H., and Hijri, M. (2017). Petroleum biodegradation capacity of bacteria and fungi isolated from petroleum-contaminated soil. *Int. Biodeter. Biodegr.* 116, 48–57. doi: 10.1016/j.ibiod.2016.09.030
- Masella, A. P., Bartram, A. K., Truszkowski, J. M., Brown, D. G., and Neufeld, J. D. (2012). PANDAseq: paired-end assembler for illumina sequences. *BMC Bioinformatics* 13:31. doi: 10.1186/1471-2105-13-31
- McDonald, D., Price, M. N., Goodrich, J., Nawrocki, E. P., Desantis, T. Z., Probst, A., et al. (2012). An improved Greengenes taxonomy with explicit ranks for ecological and evolutionary analyses of bacteria and archaea. *ISME J.* 6, 610–618. doi: 10.1038/ismej.2011.139
- Megharaj, M., Ramakrishnan, B., Venkateswarlu, K., Sethunathan, N., and Naidu, R. (2011). Bioremediation approaches for organic pollutants: a critical perspective. *Environ. Int.* 37, 1362–1375. doi: 10.1016/j.envint.2011.06.003
- Micheluz, A., Sulyok, M., Manente, S., Krksa, R., Varese, G., and Ravagnan, G. (2016). Fungal secondary metabolite analysis applied to cultural heritage: the case of a contaminated library in Venice. *World Mycotoxin J.* 9, 397–407. doi: 10.3920/WMJ2015.1958
- Morais, D., Pyro, V., Clark, I. M., Hirsch, P. R., and Tótoła, M. R. (2016). Responses of microbial community from tropical pristine coastal soil to crude oil contamination. *PeerJ* 4:e1733. doi: 10.7717/peerj.1733
- Moubasher, H. A., Hegazy, A. K., Mohamed, N. H., Moustafa, Y. M., Kabiell, H. F., and Hamad, A. A. (2015). Phytoremediation of soils polluted with crude petroleum oil using *Bassia scoparia* and its associated rhizosphere microorganisms. *Int. Biodeter. Biodegr.* 98, 113–120. doi: 10.1016/j.ibiod.2014.11.019
- Mulet, M., David, Z., Nogales, B., Bosch, R., Lalucat, J., and Garcia-Valdes, E. (2011). *Pseudomonas* diversity in crude-oil-contaminated intertidal sand samples obtained after the Prestige oil spill. *Appl. Environ. Microbiol.* 77, 1076–1085. doi: 10.1128/AEM.01741-10
- Naranjo, L., Urbina, H., Sisto, A. D., and Leon, V. (2007). Isolation of autochthonous non-white rot fungi with potential for enzymatic upgrading of Venezuelan extra-heavy crude oil. *Biocatal. Biotransfor.* 25, 341–349. doi: 10.1080/10242420701379908
- Nesci, A., Barros, G., Castillo, C., and Etcheverry, M. (2006). Soil fungal population in preharvest maize ecosystem in different tillage practices in Argentina. *Soil Till. Res.* 91, 143–149. doi: 10.1016/j.still.2005.11.014
- Obi, L. U., Atagana, H. I., and Adeleke, R. A. (2016). Isolation and characterisation of crude oil sludge degrading bacteria. *SpringerPlus* 5:1946. doi: 10.1186/s40064-016-3617-z
- Oehl, F., Sieverding, E., Ineichen, K., Ris, E. A., Boller, T., and Wiemken, A. (2005). Community structure of arbuscular mycorrhizal fungi at different soil depths in extensively and intensively managed agroecosystems. *New Phytol.* 165, 273–283. doi: 10.1111/j.1469-8137.2004.01235.x
- Omran, R., Spini, G., Puglisi, E., and Saidane, D. (2018). Modulation of microbial consortia enriched from different polluted environments during petroleum biodegradation. *Biodegradation* 29, 187–209. doi: 10.1007/s10532-018-9823-3
- Phainuphong, P., Rukachaisirikul, V., Tadpetch, K., Sukpondma, Y., Saithong, S., Phongpachit, S., et al. (2017).  $\gamma$ -butenolide and furanone derivatives from the soil-derived fungus *Aspergillus sclerotiorum* PSU-RSPG178. *Phytochemistry* 137, 165–173. doi: 10.1016/j.phytochem.2017.02.008
- Ping, L., Luo, Y., Zhang, H., Li, Q., and Wu, L. (2007). Distribution of polycyclic aromatic hydrocarbons in thirty typical soil profiles in the Yangtze river delta region, east China. *Environ. Poll.* 147, 358–365. doi: 10.1016/j.envpol.2006.05.027
- Pinhassi, J., and Hagstrom, A. (2000). Seasonal succession in marine bacterioplankton. *Aquat. Microb. Ecol.* 21, 245–256. doi: 10.3354/ame021245

- Poli, A., Lazzari, A., Prigione, V., Voyron, S., Spadaro, D., and Varese, G. C. (2016). Influence of plant genotype on the cultivable fungi associated to tomato rhizosphere and roots in different soils. *Fungal Biol. U.K.* 120, 862–872. doi: 10.1016/j.funbio.2016.03.008
- Pruesse, E., Quast, C., Knittel, K., Fuchs, B. M., Ludwig, W., Peplies, J., et al. (2007). SILVA: a comprehensive online resource for quality checked and aligned ribosomal RNA sequence data compatible with ARB. *Nucleic Acids Res.* 35, 7188–7196. doi: 10.1093/nar/gkm864
- Rajasekar, A., Babu, T. G., Pandian, S. T., Maruthamuthu, S., Palaniswamy, N., and Rajendran, A. (2007). Role of *Serratia marcescens* ACE2 on diesel degradation and its influence on corrosion. *J. Ind. Microbiol. Biotechnol.* 34, 589–598. doi: 10.1007/s10295-007-0225-5
- Rebecchi, A., Pisacane, V., Miragoli, F., Polka, J., Falasconi, I., Morelli, L., et al. (2015). High-throughput assessment of bacterial ecology in hog, cow and ovine casings used in sausages production. *Int. J. Food. Microbiol.* 212, 49–59. doi: 10.1016/j.ijfoodmicro.2015.04.047
- Rojas-Avelizapa, N. G., Cervantes-Gonzalez, E., Cruz-Camarillo, R., and Rojas-Avelizapa, L. I. (2002). Degradation of aromatic and asphaltic fractions by *Serratia liquefaciens* and *Bacillus* sp. *Bull. Environ. Contam. Toxicol.* 69, 835–842. doi: 10.1007/s00128-002-0135-1
- Rojo, F. (2009). Degradation of alkanes by bacteria. *Environ. Microbiol.* 11, 2477–2490. doi: 10.1111/j.1462-2920.2009.01948.x
- Roy, S., Hens, D., Biswas, D., Biswas, D., and Kumar, R. (2002). Survey of petroleum-degrading bacteria in coastal waters of Sunderban biosphere reserve. *World J. Microb. Biotech.* 18, 575–581. doi: 10.1023/A:1016362819746
- Sadouk, Z., Tazerouti, A., and Hacene, H. (2008). Biodegradation of diesel oil and production of fatty acid esters by a newly isolated *Pseudomonas citronellolis* KHA. *World J. Microb. Biotech.* 25, 65–70. doi: 10.1007/s11274-008-9863-7
- Schloss, P. D. (2010). The effects of alignment quality, distance calculation method, sequence filtering, and region on the analysis of 16S rRNA gene-based studies. *PLoS Comput. Biol.* 6:e1000844. doi: 10.1371/journal.pcbi.1000844
- Schloss, P. D., Westcott, S. L., Ryabin, T., Hall, J. R., Hartmann, M., Hollister, E. B., et al. (2009). Introducing mothur: open-source, platform-independent, community-supported software for describing and comparing microbial communities. *Appl. Environ. Microbiol.* 75, 7537–7541. doi: 10.1128/AEM.01541-09
- Scullion, J. (2006). Remediating polluted soils. *Naturwissenschaften* 93, 51–65. doi: 10.1007/s00114-005-0079-5
- Šimonovičová, A., Ferianc, P., Vojtková, H., Pangallo, D., Hanajík, P., Kraková, L., et al. (2017). Alkaline technosol contaminated by former mining activity and its culturable autochthonous microbiota. *Chemosphere* 171, 89–96. doi: 10.1016/j.chemosphere.2016.11.131
- Siqueira, J. P. Z., Sutton, D. A., García, D., Gené, J., Thomson, P., Wiederhold, N., et al. (2016). Species diversity of *Aspergillus* section versicolores in clinical samples and antifungal susceptibility. *Fungal Biol. U.K.* 120, 1458–1467. doi: 10.1016/j.funbio.2016.02.006
- Smith, E., Thavamani, P., Ramadass, K., Naidu, R., Srivastava, P., and Megharaj, M. (2015). Remediation trials for hydrocarbon-contaminated soils in arid environments: evaluation of bioslurry and biopiling techniques. *Int. Biodeter. Biodegr.* 101, 56–65. doi: 10.1016/j.ibiod.2015.03.029
- Smits, T. H. M., Ford, R. M., Keel, C., Harms, H., Wick, L. Y., and Kohlmeier, S. (2005). Taking the fungal highway: mobilization of pollutant-degrading bacteria by fungi. *Environ. Sci. Tech.* 39, 4640–4646. doi: 10.1021/es047979z
- Staley, J. T., and Konopka, A. (1985). Measurement of in situ activities of nonphotosynthetic microorganisms in aquatic and terrestrial habitats. *Ann. Rev. Microbiol.* 39, 321–346. doi: 10.1146/annurev.mi.39.100185.001541
- Suja, F., Rahim, F., Taha, M. R., Hambali, N., Rizal Razali, M., Khalid, A., et al. (2014). Effects of local microbial bioaugmentation and biostimulation on the bioremediation of total petroleum hydrocarbons (TPH) in crude oil contaminated soil based on laboratory and field observations. *Int. Biodeter. Biodegr.* 90, 115–122. doi: 10.1016/j.ibiod.2014.03.006
- Thompson, I. P., Van Der Gast, C. J., Ciric, L., and Singer, A. C. (2005). Bioaugmentation for bioremediation: the challenge of strain selection. *Environ. Microbiol.* 7, 909–915. doi: 10.1111/j.1462-2920.2005.00804.x
- Tian, J., Dong, Q., Yu, C., Zhao, R., Wang, J., and Chen, L. (2016). Biodegradation of the organophosphate trichlorfon and its major degradation products by a novel *Aspergillus sydowii* PA F-2. *J. Agr. Food Chem.* 64, 4280–4287. doi: 10.1021/acs.jafc.6b00909
- Varjani, S. J., Rana, D. P., Jain, A. K., Bateja, S., and Upasani, V. N. (2015). Synergistic ex-situ biodegradation of crude oil by halotolerant bacterial consortium of indigenous strains isolated from on shore sites of Gujarat, India. *Int. Biodeter. Biodegr.* 103, 116–124. doi: 10.1016/j.ibiod.2015.03.030
- Varjani, S. J., and Upasani, V. N. (2016). Biodegradation of petroleum hydrocarbons by oleophilic strain of *Pseudomonas aeruginosa* NCIM 5514. *Bioresour. Technol.* 222, 195–201. doi: 10.1016/j.biortech.2016.10.006
- Vasileiadis, S., Puglisi, E., Trevisa, M., Scheckel, K. G., Langdon, K., McLaughlin, M., et al. (2015). Changes in soil bacterial communities and diversity in response to long-term silver exposure. *FEMS Microbiol. Ecol.* 91:fiv114. doi: 10.1093/femsec/fiv114
- Velmurugan, N., Kalpana, D., Cho, J.-Y., Lee, G.-H., Park, S.-H., and Lee, Y.-S. (2011). Phylogenetic analysis of culturable marine bacteria in sediments from South Korean Yellow Sea. *Microbiology* 80, 261–272. doi: 10.1134/S0026261711010188
- Versalovic, J., Schneider, M., De Bruijn, F. J., and Lupski, J. R. (1994). Genomic fingerprinting of bacteria using repetitive sequence-based polymerase chain reaction. *Method Mol. Cell. Bio.* 5, 25–40.
- Vinas, M., Sabate, J., Espuny, M. J., and Solanas, A. M. (2005). Bacterial community dynamics and polycyclic aromatic hydrocarbon degradation during bioremediation of heavily creosote-contaminated soil. *Appl. Environ. Microbiol.* 71, 7008–7018. doi: 10.1128/AEM.71.11.7008-7018.2005
- Voyron, S., Ercole, E., Ghignone, S., Perotto, S., and Girlanda, M. (2017). Fine-scale spatial distribution of orchid mycorrhizal fungi in the soil of host-rich grasslands. *New Phytol.* 213, 1428–1439. doi: 10.1111/nph.14286
- Wang, Q., Garrity, G. M., Tiedje, J. M., and Cole, J. R. (2007). Naive Bayesian classifier for rapid assignment of rRNA sequences into the new bacterial taxonomy. *Appl. Environ. Microbiol.* 73, 5261–5267. doi: 10.1128/AEM.00062-07
- Wang, X. B., Chi, C. Q., Nie, Y., Tang, Y. Q., Tan, Y., Wu, G., et al. (2011). Degradation of petroleum hydrocarbons (C6–C40) and crude oil by a novel *Dietzia* strain. *Bioresour. Technol.* 102, 7755–7761. doi: 10.1016/j.biortech.2011.06.009
- White, T. J., Bruns, T., Lee, S., and Taylor, J. (1990). Amplification and direct sequencing of fungal ribosomal RNA genes for phylogenetics. *PCR Protocols* 18, 315–322. doi: 10.1186/s12866-017-1046-y
- Whyte, L. G., Bourbonniere, L., and Greer, C. W. (1997). Biodegradation of petroleum hydrocarbons by psychrotrophic *Pseudomonas* strains possessing both alkane (alk) and naphthalene (nah) catabolic pathways. *Appl. Environ. Microbiol.* 63, 3719–3723.
- Wick, L. Y., Remer, R., Würz, B., Reichenbach, J., Braun, S., Schäfer, F., and Harms, H. (2007). Effect of fungal hyphae on the access of bacteria to phenanthrene in soil. *Environ. Sci. Technol.* 41, 500–505. doi: 10.1021/es061407s
- Widdel, F., and Rabus, R. (2001). Anaerobic biodegradation of saturated and aromatic hydrocarbons. *Curr. Opin. Biotech.* 12, 259–276. doi: 10.1016/S0958-1669(00)00209-3
- Wongsa, P., Tanaka, M., Ueno, A., Hasanuzzaman, M., Yumoto, I., and Okuyama, H. (2004). Isolation and characterization of novel strains of *Pseudomonas aeruginosa* and *Serratia marcescens* possessing high efficiency to degrade gasoline, kerosene, diesel oil, and lubricating oil. *Curr. Microbiol.* 49, 415–422. doi: 10.1007/s00284-004-4347-y
- Xia, W., Du, Z., Cui, Q., Dong, H., Wang, F., He, P., et al. (2014). Biosurfactant produced by novel *Pseudomonas* sp. WJ6 with biodegradation of n-alkanes and polycyclic aromatic hydrocarbons. *J. Hazard. Mater.* 276, 489–498. doi: 10.1016/j.jhazmat.2014.05.062
- Yadav, T. C., Pal, R. R., Shastri, S., Jadeja, N. B., and Kapley, A. (2015). Comparative metagenomics demonstrating different degradative capacity of activated biomass treating hydrocarbon contaminated wastewater. *Bioresour. Technol.* 188, 24–32. doi: 10.1016/j.biortech.2015.01.141
- Yakimov, M. M., Timmis, K. N., and Golyshin, P. N. (2007). Obligate oil-degrading marine bacteria. *Curr. Opin. Biotech.* 18, 257–266. doi: 10.1016/j.copbio.2007.04.006
- Yang, S., Wen, X., Jin, H., and Wu, Q. (2012). Pyrosequencing investigation into the bacterial community in permafrost soils along the China-Russia crude oil pipeline (CRCOP). *PLoS One* 7:e2730. doi: 10.1371/journal.pone.0052730

- Yergeau, E., Sanschagrín, S., Beaumier, D., and Greer, C. W. (2012). Metagenomic analysis of the bioremediation of diesel-contaminated Canadian high arctic soils. *PLoS One* 7:e30058. doi: 10.1371/journal.pone.0030058
- Yu, K. S., Wong, A. H., Yau, K. W., Wong, Y. S., and Tam, N. F. (2005). Natural attenuation, biostimulation and bioaugmentation on biodegradation of polycyclic aromatic hydrocarbons (PAHs) in mangrove sediments. *Mar. Pollut. Bull.* 51, 1071–1077. doi: 10.1016/j.marpolbul.2005.06.006
- Yuan, X., Zhang, X., Chen, X., Kong, D., Liu, X., and Shen, S. (2018). Synergistic degradation of crude oil by indigenous bacterial consortium and exogenous fungus *Scedosporium boydii*. *Bioresour. Technol.* 264, 190–197. doi: 10.1016/j.biortech.2018.05.072
- Zafra, G., Absalón, ÁE., Cuevas, M. D. C., and Cortés-Espinosa, D. V. (2014). Isolation and selection of a highly tolerant microbial consortium with potential for PAH biodegradation from heavy crude oil-contaminated soils. *Water Air Soil Poll.* 225, 1826. doi: 10.1007/s11270-013-1826-4
- Zhang, G., Guo, X., Zhu, Y., Liu, X., Han, Z., Sun, K., et al. (2018). The effects of different biochars on microbial quantity, microbial community shift, enzyme activity, and biodegradation of polycyclic aromatic hydrocarbons in soil. *Geoderma* 328, 100–108. doi: 10.1016/j.geoderma.2018.05.009
- Zhou, Z.-F., Wang, M.-X., Zuo, X.-H., and Yao, Y.-H. (2017). Comparative investigation of bacterial, fungal, and archaeal community structures in soils in a typical oilfield in Jiangnan, China. *Arch. Environ. Con. Tox.* 72, 65–77. doi: 10.1007/s00244-016-0333-1

**Conflict of Interest Statement:** The authors declare that the research was conducted in the absence of any commercial or financial relationships that could be construed as a potential conflict of interest.

Copyright © 2018 Spini, Spina, Poli, Blioux, Regnier, Gramellini, Varese and Puglisi. This is an open-access article distributed under the terms of the Creative Commons Attribution License (CC BY). The use, distribution or reproduction in other forums is permitted, provided the original author(s) and the copyright owner(s) are credited and that the original publication in this journal is cited, in accordance with accepted academic practice. No use, distribution or reproduction is permitted which does not comply with these terms.



# A Time-Dose Response Model to Assess Diuron-Induced Photosynthesis Inhibition in Freshwater Biofilms

Soizic Morin\*, Betty Chaumet and Nicolas Mazzella

*Irstea, UR EABX, Cestas, France*

## OPEN ACCESS

### Edited by:

Fabrice Martin-Laurent,  
Institut National de la Recherche  
Agronomique (INRA), France

### Reviewed by:

Pablo Campo,  
Cranfield University, United Kingdom  
Ahmed Tlili,  
Swiss Federal Institute of Aquatic  
Science and Technology, Switzerland

### \*Correspondence:

Soizic Morin  
soizic.morin@irstea.fr

### Specialty section:

This article was submitted to  
Environmental Toxicology,  
a section of the journal  
Frontiers in Environmental Science

**Received:** 14 June 2018

**Accepted:** 16 October 2018

**Published:** 02 November 2018

### Citation:

Morin S, Chaumet B and Mazzella N  
(2018) A Time-Dose Response Model  
to Assess Diuron-Induced  
Photosynthesis Inhibition in  
Freshwater Biofilms.  
*Front. Environ. Sci.* 6:131.  
doi: 10.3389/fenvs.2018.00131

Contamination by herbicides is reported in most freshwater environments. These biologically active compounds may impact the non-target biota such as benthic biofilms, at the base of the trophic chain. In agricultural watersheds, herbicides occur as pulses in the system, and traditional dose-response analysis performed at a given duration of exposure (hours to days) may not predict accurately the risk of adverse impacts at shorter temporal scales (minutes to hours) corresponding to pulse exposures. To assess the time-response relationship in biofilms exposed to herbicides, we used diuron, an inhibitor of photosynthesis, to perform bioassays (time-response curves) with the aim of characterizing the initial steps of photosynthesis decrease after exposure to the herbicide (from seconds to hours), for different concentrations of exposure. Diuron-induced inhibition of photosynthesis reflects blockage of electron transfer in PSII, therefore we defined the time lag to reach the threshold of 50% photosynthesis inhibition ( $t_{1/2}$ ) as the time for diuron to reach its target site (adsorption, distribution). We found a rapid decrease in photosynthetic efficiency:  $t_{1/2}$  values were dose-dependent and ranged from <30 s (highest concentration of exposure) to 7'20" (lowest concentration). While dose-response curves are influenced by the initial biomass or nature of biofilms, time-response curves yielded similar  $t_{1/2}$  for contrasted biofilms, making this parameter a unique response to be valuably incorporated into an ecotoxicology framework. We also assessed the variability of the response as a function of previous short-term (3 h) exposure to diuron. The  $t_{1/2}$  values obtained were consistent with those obtained on non-exposed biofilms, but repeated pulses of diuron exacerbated the decrease in photosynthetic yields. This time-response approach highlighted that diuron reaches its cellular target almost instantaneously (<1 min), independently of biological parameters (chlorophyll a concentration, adaptation related to exposure history). Reversibility of toxic impacts a few hours after diuron removal was not fully demonstrated, suggesting that the kinetics of diuron release from cells to uncontaminated medium are much slower than binding rates. Our results confirm that repeated exposure is very likely to impair freshwater biofilms, in particular if pulses occur at high frequency.

**Keywords:** bioassay, herbicide, microbial ecotoxicology, periphyton, photosynthesis, pulse, TRC

## INTRODUCTION

Contamination of European waterbodies by pesticides is generalized: in France, pesticides were detected in 92% of the water samples collected within the 2013 surveillance program, with a clear dominance of herbicide substances (>80% of detections, SOeS, 2015). In agricultural watersheds, these substances typically reach the aquatic ecosystems as pulses (Rabiet et al., 2010) following runoff events. As herbicides may impact the non-target biota (i.e., algae), the risk associated with these substances has to be quantified. To this aim, several ecotoxicity tests have been developed based on microalgae (including standardized tests such as OECD, 1984; AFNOR, 2012). Ecotoxicity assessment based on periphytic microbial communities (biofilms) is also increasing (Ghiglione et al., 2014), given their sensitive, specific, and early responses to toxic pollution (Sabater et al., 2007; Guasch et al., 2016). Traditional dose-response analysis predicts the risk of adverse impacts of herbicides toward biofilms or microalgae for a given duration of exposure, based on endpoints such as the inhibition of growth or of photosynthesis (see review in Pesce et al., 2011). Toxic effects at environmentally relevant concentrations are generally demonstrated, but the tests are performed at temporal scales on the order of days to weeks of exposure that are disconnected from real field exposure, of much shorter time spans (minutes to hours). Therefore, the duration of standard tests may be inappropriate to predict the hazard associated to pulse exposures.

It has been demonstrated that pulse exposure has functional and structural impacts (e.g., Tlili et al., 2008). In turn, changes in community structure will have consequences for higher trophic levels and ultimately, for ecosystem functioning. As herbicide exposure in the aquatic environment is fluctuating, and the manifestation of toxic symptoms is a time (and substance)-dependent process, it is thus desirable to take the temporal factor into account to improve pesticide risk assessment. Among the herbicides of topical concern, diuron (N-(3, 4-dichlorophenyl)-N, N-dimethylurea) is considered a Priority Hazardous Substance by the European Commission (Water Framework Directive, 2000/60/EC). This chemical substance acts as a photosystem II (PSII) inhibitor and is contained in many phytopharmaceutical products aiming to fight against undesirable weeds in crop protection or in road/railway maintenance, as well as for antifouling purposes, and is frequently reported in freshwater environments (Okamura et al., 2003; Murray et al., 2010). In plant cells, diuron binds to a specific niche on the D1 protein of PSII, replacing the plastoquinone Q<sub>b</sub>. This substitution decreases the electron flow within PSII (Rutherford and Krieger-Liszky, 2001), and consequently inhibits photosynthetic efficiency ( $\phi$ PSII). The diuron-EC<sub>50</sub> (Effective Concentration causing a 50% inhibition) for microalgal growth inhibition, over the 72-h test period recommended by ISO and OECD guidelines (OECD, 1984; AFNOR, 2012), ranges from 7 to 36  $\mu\text{g}\cdot\text{L}^{-1}$  for freshwater algae. For ecotoxicity assessments based on the PSII inhibition of periphytic microalgae, the EC<sub>50</sub> is generally assessed after 1 to 4-h exposures of biofilm suspensions to increasing herbicide concentrations. These non-standard durations have generally

been established following preliminary developments; however the toxicity values always fall within the same range, i.e., between 5 and 25  $\mu\text{g}\cdot\text{L}^{-1}$  for pristine biofilms (with a min-max range: 2–486  $\mu\text{g}\cdot\text{L}^{-1}$ ; McClellan et al., 2008; Pesce et al., 2010a). In fact, Francoeur et al. (2007) demonstrated that 5–10 min of exposure to high diuron concentrations are enough to ensure that photosynthesis inhibition is complete. This quick onset of inhibition may be due to the fact that diuron reaches its binding site within minutes (Schreiber et al., 2007; Nestler et al., 2012).

Pharmaceutical studies aiming to assess the efficiency of healthcare products (e.g., antimicrobial drugs, VanMeter and Hubert, 2016) provide time-response based concepts that may be fruitfully implemented to assess the temporal features of diuron inhibitory impact on PSII in an ecotoxicology framework. As shown in **Figure 1**, we can expect a rapid decrease in photosynthetic efficiency from the time of diuron exposure. The onset of time response,  $t_{1/2}$ , is defined as the time lag to reach the threshold of 50% inhibition based on the difference between optimal and minimum achievable  $\phi$ PSII values.

In this context, we performed bioassays (called time-response curves) using suspensions of mature freshwater biofilms, to characterize the initial steps of photosynthesis decrease after exposure to diuron. Specifically our objectives were to:

- i) quantify exposure time to diuron needed to reach significant photosynthesis inhibition,
- ii) determine if exposure time depends on exposure test concentration, and
- iii) assess the variability of the response as a function of biofilm composition and previous pulse exposure to diuron.

## MATERIALS AND METHODS

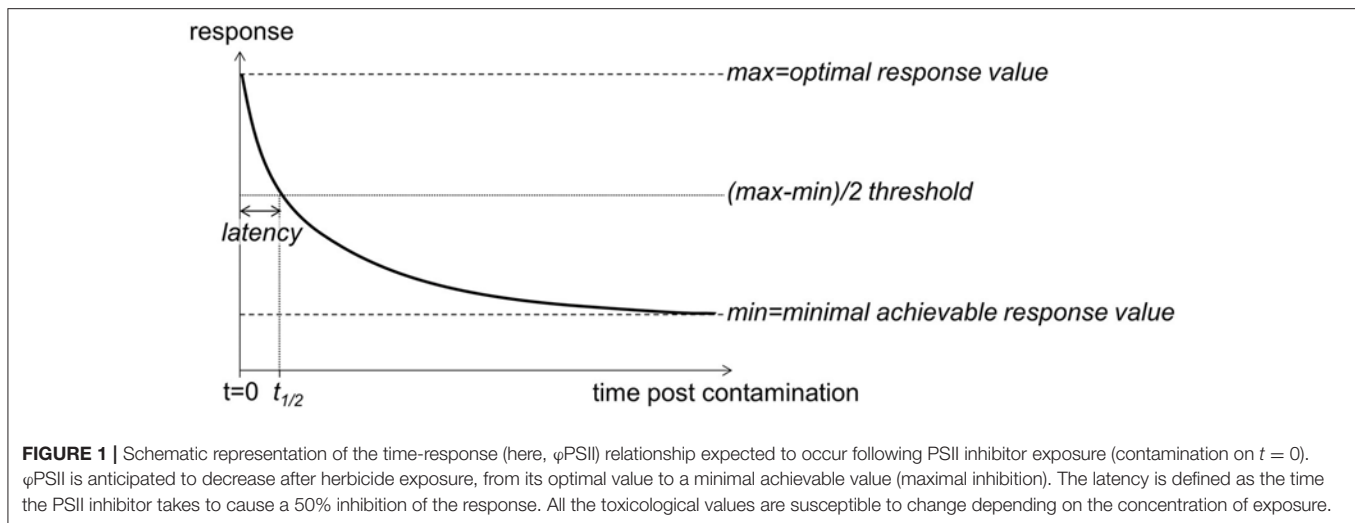
### Mature Biofilm Collection

Glass slides (156 cm<sup>2</sup>) were used as artificial substrates for biofilm growth. Plastic racks equipped with glass slides were installed in the photic zone of Gazinet-Cestas pond (geographical coordinates: 44°46'30.1''N, 0°41'44.3''W), near Bordeaux, SW France. The pond is free of pesticides, in particular diuron concentrations are below the detection limit of 0.2  $\mu\text{g}\cdot\text{L}^{-1}$  ( $n = 10$  measurements in winter 2016–2017).

One-month old biofilms, settled on the glass slides, were collected in August and December 2016. Before performing the assays (2.3), the slides were scraped carefully and separated into two aliquots before being suspended in 40 mL of Dauta (1982) medium.

### Diuron

Diuron (CAS reg. 330-54-1, purity = 98%) was purchased from Dr. Ehrenstorfer GmbH (Augsburg). Stock solutions were prepared in acetonitrile, at a concentration of 200  $\text{mg}\cdot\text{L}^{-1}$ . They were analyzed by UPLC-ToF (Ultra-Performance Liquid Chromatography—Time of Flight Mass Spectrometry, Xevo G2-S ToF, Waters) and the different exposure concentrations were calculated. Diuron analyses in the water samples (pond: 2.1, laboratory mesocosms: 2.4.2) were performed with the same method after filtration of the samples through 0.45  $\mu\text{m}$  Whatman



filters. Briefly, 990  $\mu\text{L}$  samples were spiked with eight internal standards (10  $\mu\text{L}$ , i.e., 10% final volume). Of these, 20  $\mu\text{L}$  were injected with a solvent gradient (98% ammonium acetate, 2% methanol). Chromatographic separation was achieved by passing through a 5-cm C18 column (Waters). Pesticide concentrations were calculated from calibration curves (10 points, from 0 to 50  $\mu\text{g}\cdot\text{L}^{-1}$ ) realized during the same period. Detection and quantification limits were of 0.1 and 0.2  $\mu\text{g}\cdot\text{L}^{-1}$ , respectively.

## Time-Response Curves

We used a Phyto-PAM (Heinz Walz GmbH, Germany) and measurements were performed in quartz cuvettes fed with 3 mL of agitated biofilm suspension.

We determined the chlorophyll *a* concentration in the biofilm suspensions and the proportion of algal groups present to roughly characterize the biofilms.

Time-response assessment of diuron acute toxicity was performed following the response of the effective quantum yield of PSII ( $\phi$ PSII) over time following the addition of a drop of diuron (expressed as time post contamination). Experiment 1 was performed with biofilms collected in summer and Experiment 2 with biofilms collected in winter. In each time-response curve, the diuron concentration was kept constant and the response was assessed as a function of exposure time.  $\phi$ PSII was measured every 5 s after diuron addition, then measurements were spaced out and performed every 10 s until  $\phi$ PSII values stabilized.

## Experimental Setup

### Experiment 1: Time-Response Curves of Pristine Biofilms Exposed to Increasing Diuron Concentrations (August, 2016)

Triplicate slides collected on August 4th, 2016 were used to perform time-response curves on biofilm suspensions.

Dose-response curves established using these biofilms prior to the experiment (**Supplementary Information, SII**) allowed the selection of five increasing diuron concentrations to be used for the time-response curves. The following nominal concentrations were used: no diuron (0  $\mu\text{g}\cdot\text{L}^{-1}$ ; no inhibition), “low” (5.2

$\mu\text{g}\cdot\text{L}^{-1}$ ; corresponding to  $\text{EC}_{25}$ ), “intermediate” (17.4  $\mu\text{g}\cdot\text{L}^{-1}$ ; slightly above  $\text{EC}_{50}$ ), “high” (166.6  $\mu\text{g}\cdot\text{L}^{-1}$ ; higher than the concentration leading to maximal achievable inhibition) and “max” (332  $\mu\text{g}\cdot\text{L}^{-1}$ ; i.e., double the “high” concentration).

Time-dependent photosynthetic inhibition was assessed over a  $\sim 1$  h exposure, and  $t_{1/2}$  were extracted from the three time-response curves established for each diuron exposure concentration (except for the highest concentration: only two replicates available).

### Experiment 2: Time-Response Curves of Biofilms Pulsed With Contrasted Diuron Concentrations (December, 2016)

On December 6th, 2016, 16 mature biofilms were sampled. Four slides were immediately used to perform time-response curves of “non-pulsed” biofilms, under “high” diuron exposure.

The remaining slides were exposed in laboratory mesocosms to three levels of diuron pulses (0.3, 19.1, and 102.4  $\mu\text{g}\cdot\text{L}^{-1}$  measured concentrations), each in quadruplicate. Pulse duration was 3 h of exposure, such as in Tlili et al. (2008). The slides were collected and prepared as described above. The suspensions were allowed to recover from pulse exposure in uncontaminated Dauta medium for 4 to 8 h before performing the time-response curves, assessed using a “high” diuron exposure. The duration of the recovery period was based on the results of Laviale et al. (2011). More details on the protocol are provided in **Supplementary Information SI2**.

## Statistical Analyses

To model dose-response-curves (DRC), the  $\phi$ PSII values measured at specific times were plotted against nominal exposure concentrations and fitted to a Hill model using RegTox macro for Microsoft Excel<sup>TM</sup> (version 7.0.7, © Eric Vindimian, 2001). DRC were performed for each replicate biofilm suspension, then the optimized parameters of the model (500 bootstrap simulations), in particular  $\text{EC}_{50}$ , were averaged and standard deviations were calculated.

To draw time-response curves (TRC), the decrease over time in  $\phi$ PSII was modeled (each replicate individually) with RegTox, using a classical Hill equation, where the optimal response value measured before the addition of the diuron drop was set as upper limit. The optimal parameters derived from the individual TRC models after 500 bootstrap simulations are given as mean  $\pm$  standard deviation (Table 1).

One-way ANOVA was used to highlight significant differences in biological responses. Linear regressions (after transformation of the data to achieve normality, when necessary) were calculated to assess correlations between biological responses ( $EC_{50}$ ,  $\phi$ PSII), time and concentration of exposure. In both cases, the  $\alpha$ -level was set at 0.01.

## RESULTS AND DISCUSSION

### Dose Dependency of the Time-Response Relationship

When no diuron drop was added, biofilm suspensions from Experiment 1 displayed  $\phi$ PSII of  $0.51 \pm 0.02$  ( $n = 367$ ), with a slight increase over time (Figure 2A). With diuron addition, time-response curves for the four concentrations tested here highlighted that the efficiency of diuron increased gradually with increasing exposure concentrations. At the “low” exposure level, photosynthesis was inhibited down to  $26.7 \pm 12.5\%$  of the optimal value, while the highest concentrations led to a complete inhibition of photosynthesis. Total inhibition of photosynthesis at diuron concentrations higher than  $100 \mu\text{g.L}^{-1}$  is consistent with the findings of McClellan et al. (2008) for freshwater biofilms and Magnusson et al. (2010) for microalgal species.

Diuron-induced inhibition of photosynthesis reflects herbicide binding to the electron acceptor of Qb within the thylakoid membrane and subsequent blockage of electron transfer in PSII. We defined latency as the time diuron took to cause a 50% photosynthesis inhibition on biofilm suspensions (Figure 1), postulating that  $t_{1/2}$  values expressed the time for diuron to reach its target site (adsorption, distribution).

Our results (Figure 2A, and Table 1) show that inhibitory effects are very rapid:  $t_{1/2}$  ranged between  $<30$  s (for the highest concentrations of exposure) to  $7'20''$  (exposure to “low” concentration). Using diatom cultures, Magnusson et al. (2010) also showed that maximal inhibition of photosynthesis (ca. 50%), in response to a single dose of  $2.4 \mu\text{g.L}^{-1}$  diuron, was reached within minutes. Such rapid action confirms the high affinity of diuron for microalgal binding sites and almost instantaneous intracellular uptake, in agreement with Nestler et al. (2012). As for maximal inhibition, the time-lag to reach a 50% inhibition ( $t_{1/2}$ ) was also dose-dependent; the lower the exposure concentration, the higher the  $t_{1/2}$ . Figure 2B evidences that the estimated  $t_{1/2}$  decreased with increasing diuron concentrations ( $R^2 = 0.869$ ,  $F = 87.56$ ,  $p < 0.0001$ ). However, for the “high” and “max” concentrations of exposure, the overlap between the 95% confidence intervals suggests that binding sites were saturated above  $100 \mu\text{g.L}^{-1}$ .

Surprisingly, the maximal inhibition achieved for the “low” and “intermediate” concentrations tested was higher than expected, based on the dose-response curves performed with the same biofilm (SI1). Indeed, after this 3-h exposure to increasing diuron concentrations,  $\phi$ PSII was inhibited by 25 and 60% at concentrations of  $5.2 \mu\text{g.L}^{-1}$  (“low”) and  $17.4 \mu\text{g.L}^{-1}$  (“intermediate”), respectively (vs. in TRC: by  $73.3 \pm 12.5$  and  $92.1 \pm 1.8\%$ ). Two complementary hypotheses may explain these differences, as discussed below: the influence of the duration of diuron exposure (section Time Dependency of Ecotoxicity Parameters) and/or of microalgal concentrations in the suspensions tested (section Consistency in  $t_{1/2}$  Values From Biofilm of Contrasted Composition).

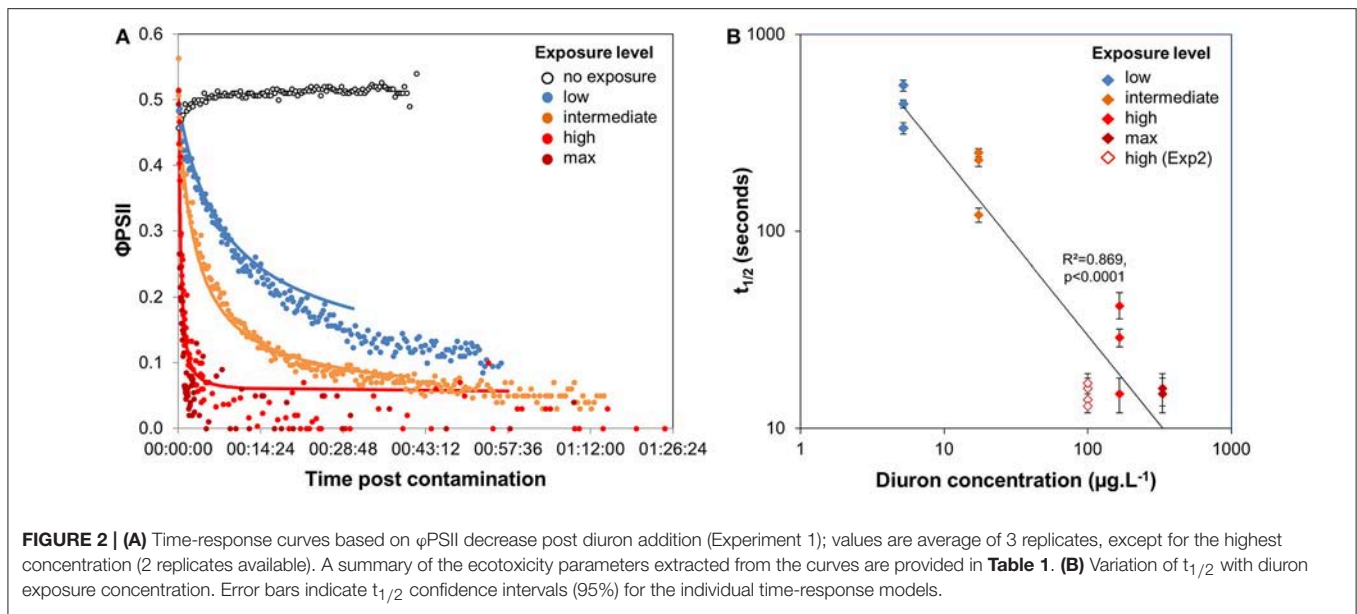
### Time Dependency of Ecotoxicity Parameters

Using the data from the time-response curves shown in Figure 2A, we extracted the  $\phi$ PSII values measured at several durations post exposure, from 15 s to 20 min. Dose response curves were fitted to the data (Figure 3A) and their respective

TABLE 1 | Summary of the time-response curves results.

Diuron pulse	Diuron exposure level for TRC	Parameters extracted from the model		
		Optimal $\phi$ PSII	$t_{1/2}$	Minimal response achieved (% of optimal $\phi$ PSII value)
<b>EXPERIMENT 1</b>				
No pulse	Low	$0.49 \pm 0.01$	$7'20'' \pm 1'49''$	$26.7 \pm 12.5\%$
No pulse	Intermediate	$0.50 \pm 0.02$	$3'28'' \pm 1'15''$	$7.9 \pm 1.8\%$
No pulse	High	$0.51 \pm 0.01$	$0'29'' \pm 0'13''$	$8.9 \pm 4.5\%$
No pulse	Max	$0.49 \pm 0.00$	$0'16'' \pm 0'01''$	0%
<b>EXPERIMENT 2</b>				
No pulse	High	$0.42 \pm 0.01$	$0'15'' \pm 0'02''$	$30.6 \pm 1.6\%$
$0.3 \mu\text{g.L}^{-1}$ , 3h	High	$0.26 \pm 0.02$	$0'15'' \pm 0'04''$	$44.5 \pm 11.9\%$
$19.1 \mu\text{g.L}^{-1}$ , 3h	High	$0.27 \pm 0.02$	$0'11'' \pm 0'01''$	$23.6 \pm 3.6\%$
$102.4 \mu\text{g.L}^{-1}$ , 3h	High	$0.12 \pm 0.05$	$0'15'' \pm 0'03''$	$40.2 \pm 10.9\%$

Values are average  $\pm$  standard deviation.



$EC_{50}$  estimated, together with 95% confidence intervals (**Figure 3B**). **Figure 3B** corresponds to a time-to-event analysis of the data (Newman and McCloskey, 1996). The relationship between  $EC_{50}$  and time post contamination was significant ( $R^2 = 0.997$ ,  $F = 1762.42$ ,  $p < 0.0001$ ), and from 5 to 10 min of exposure the  $EC_{50}$  was on the order of magnitude of environmental peaks of diuron (Rabiet et al., 2010).

We plotted in **Figure 3B** the  $EC_{50}$ -diuron obtained initially for a longer exposure (3 h, dose-response curve illustrated in **Supplementary Information Figure S11**). This value, though obtained with the same biofilm, was higher than those calculated for 10 and 20 min of exposure. This is in line with the findings of Nestler et al. (2012) who also observed a 40% increase in  $EC_{50}$  value between 2 and 6 h of diuron exposure (from 17.9 to 25.6  $\mu\text{g.L}^{-1}$ ). The difference can be attributable to slight differences in suspended biomass (“dilution effect,” as discussed in section Consistency in  $t_{1/2}$  Values From Biofilm of Contrasted Composition), to decreasing blockage of Qb binding sites, and/or to the initiation of physiological processes on the 3-h scale. In fact, the partial recovery (see also S12) could correspond to physiological adaptation (acclimation), cellular detoxification processes, and/or biodegradation of diuron as the result of cytochrome P450-mediated N-demethylation. Cytochrome P450 is produced by a wide range of microorganisms, and degradation can be fast (e.g., biodegradation up to 20% after the 3 first hours of incubation with 250 ppm diuron, in Sharma et al., 2010).

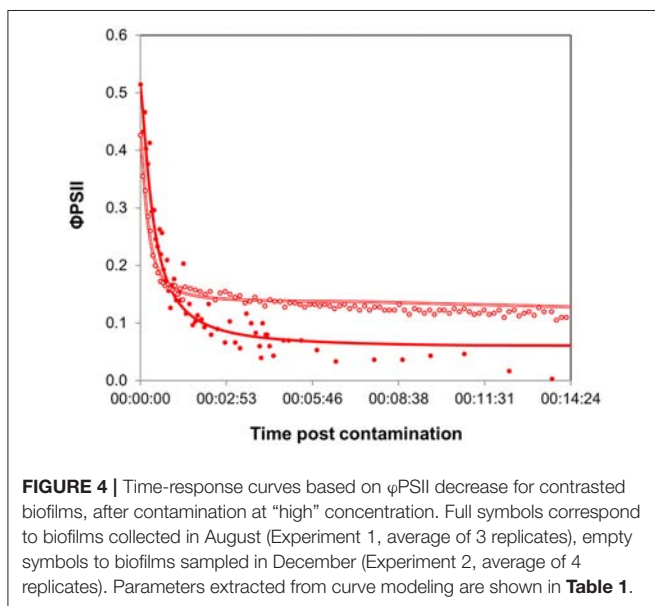
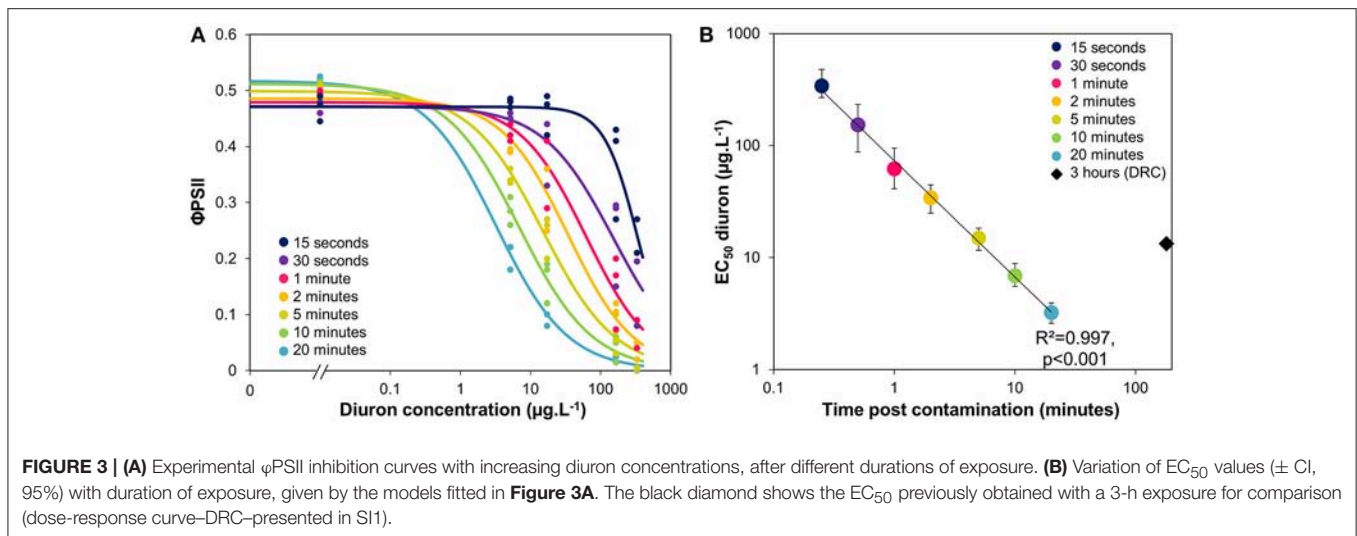
This marginal increase in tolerance that we observed after 3 h highlights that diuron exposure is non-lethal, and that complete recovery can be expected under non-contaminated conditions. This is confirmed by the study of Vallotton et al. (2008), who demonstrated the rapid reversibility of toxic effects of PSII inhibitors after herbicide removal, through rapid recovery of  $\phi$ PSII (within 4 h) and of algal growth, using cultures of *Scenedesmus vacuolatus*. Even if one pulse is unlikely

to induce long-lasting effects (but see section Influence of Pulse Exposure History on TRC), impacts on biofilms are highly plausible under fluctuating herbicide exposures, i.e., repeated pulses. Indeed, diuron binding to PSII interferes in the essential turnover and repair mechanisms of damaged D1 proteins (Draber et al., 1991), and repeated pulse exposure may lead to delayed irreversible damages of the photosystem. For example, Tlili et al. (2008) found that two consecutive pulses (3 h each) of 7  $\mu\text{g.L}^{-1}$  of diuron impacted biofilm growth (dry weight, chlorophyll *a* concentration) much more than one single pulse, on the long term. Copin et al. (2015) experimentally assessed and modeled the cumulative effects of isoproturon pulses on the growth of *S. vacuolatus*. Testing five scenarios, with different magnitudes (from  $EC_{10}$  to  $EC_{80}$ ) and durations (4–24 h) of exposure, they found in all cases an overall inhibition of growth, from 15 to 44% compared to control cell densities.

The time-dose-response model proposed in this study to analyze short-term photosynthesis inhibition induced by diuron provides input data ( $EC_{50}$  as a function of time) that could be incorporated into models predicting the impacts of repeated exposure to herbicide pulses (e.g., Copin et al., 2015).

### Consistency in $t_{1/2}$ Values From Biofilm of Contrasted Composition

We compared the time-response relationships after a “high” diuron exposure for biofilms collected in August (Experiment 1) and December (Experiment 2). Microalgal biomass differed between biofilms, with chlorophyll *a* concentrations of  $6.8 \pm 3.4 \mu\text{g.L}^{-1}$  in the biofilm suspensions tested in August, vs.  $80.5 \pm 12.54 \mu\text{g.L}^{-1}$  in December. The proportions of algal groups also varied between seasons. Indeed, the PhytoPAM signal revealed that summer (August) biofilms were dominated by chlorophytes ( $59 \pm 6\%$ ), followed by similar proportions of cyanophytes ( $21 \pm 1\%$ ) and diatoms ( $20 \pm 4\%$ ). Contrastingly, biofilms collected in



December had more diatoms ( $41 \pm 3\%$ ) than chlorophytes ( $31 \pm 2\%$ ) and cyanophytes ( $27 \pm 1\%$ ).

The time-response curves obtained for both biofilms (**Figure 4**) yielded comparable  $t_{1/2}$  values (**Table 1**), confirming the rapid binding kinetics of diuron. This result suggests that the transport of diuron into periphytic cells was not particularly hindered by higher biomass (no apparent boundary layer effect). This result partly contradicts the assumption that the periphytic matrix exerts a protective role against toxic chemicals (Sabater et al., 2007); however it has to be noted that we did not use intact biofilms, but a suspension of biofilm which was, therefore, destructured.

The maximal inhibition achieved was more pronounced in summer biofilms. As the maximal effect is determined by the rate of internalization of diuron within microalgal cells, we can hypothesize that these differences resulted from the differences

in biofilm biomass. Diuron uptake experiments performed with different microalgal species showed that the rate of binding depends on chlorophyll *a* concentration (Laasch et al., 1981; Allen et al., 1983). Yet, biofilm binding capacities were certainly exceeded here: though the amount of chlorophyll *a* was about 12-fold higher in winter biofilms than in summer ones, in both cases the “high” concentration provided far higher diuron amounts than those estimated to saturate the binding sites (in green microalgae: about 3 nmol of diuron per mg of chlorophyll *a*, Laasch et al., 1981). Besides biomass, seasonal differences in the proportions of algal groups also probably accounted for the differences in direct PSII inhibition reflected by the minimal  $\phi$ PSII values. The presence of substantial amounts of chlorophytes in summer biofilms might have contributed to the higher impact observed: chlorophytes have been shown to be more sensitive to PSII inhibitors (Tang et al., 1997; Lockert et al., 2006) than cyanophytes or diatoms (but see Schreiber et al., 2007). Diatoms, which were dominant in winter, contain carotenoids and xanthophylls that are involved in managing oxidative stress (Pinto et al., 2003); therefore diatoms can be expected to have enhanced tolerance to diuron-induced oxidative damages. Moreover, the relatively greater abundance of cyanophytes in winter biofilms can also be involved in the residual PSII yield. Indeed, a signal attributed to cyanobacterial fluorescence of photosystem I, independent of PSII, was also observed under biofilm exposure to diuron by Francoeur et al. (2007).

To sum up, our results lead to the same conclusion reached by Lambert et al. (2015) that there is a considerable influence of biofilm biomass in the outputs of ecotoxicity tests with biofilms, which complicates between-sample comparisons. However, both time-response curves, for very different biofilms, yielded comparable  $t_{1/2}$  values, making the latency parameter a unique response favoring between-date comparisons. These results support further potential use of time-response curves in ecotoxicology studies, as time responses were more dose-dependent than biofilm-dependent.

## Influence of Pulse Exposure History on TRC

Initial  $\phi$ PSII values of the pulsed biofilms were significantly lower than in non-pulsed ones (Table 1; ANOVA:  $F = 588.3$ ,  $p < 0.0001$ ), irrespective of the concentration of exposure. This decrease suggests physiological stress induced by diuron pulses, even at low dose ( $0.3 \mu\text{g.L}^{-1}$ ), as shown for longer exposures by Ricart et al. (2009). This effect could have been exacerbated by the “translocation” to laboratory conditions. After the highest concentration pulse ( $\sim 100 \mu\text{g.L}^{-1}$ ), the biofilms were in poor physiological state. Their  $\phi$ PSII was  $0.12 \pm 0.05$ , matching strongly with the minimal  $\phi$ PSII values obtained for non-pulsed biofilms from 5 min after addition of the diuron drop:  $0.12 \pm 0.00$  ( $n = 215$ ). No differences in optimal  $\phi$ PSII were found for the biofilms pre-exposed to the lowest pulse concentrations tested ( $0.3$  and  $19.1 \mu\text{g.L}^{-1}$ ) at this time point.

The shape of the time-response curves (Figure 5) obtained for the pulsed biofilms suggest a trend in  $\phi$ PSII decline post diuron drop, as a function of the pulse intensity. It is worth noting that the TRC of the biofilms pulsed with the highest concentration were hardly comparable with the other data, due to their very low initial  $\phi$ PSII resulting from a poor recovery (see below). Differences in the maximal inhibition achieved cannot be considered significant, because the percentages were calculated based on variations from very small absolute values of initial  $\phi$ PSII. Besides, no significant differences in  $t_{1/2}$  values were highlighted between pulsed conditions (Table 1). These  $t_{1/2}$  fell into the same range of latency values found for pristine biofilms collected in summer or in winter without preexposure (Table 1, and Figure 4). We can conclude from this result that, whatever the pulse intensity, the diuron binding sites were probably not saturated when the TRC were performed. A possible explanation lies in the fact that part of the diuron bond to the cells may have been released during the recovery period in uncontaminated medium. This was checked by modeling recovery curves, i.e.,  $\phi$ PSII increase over the period subsequent to diuron exposure (SI2). We assumed that  $\phi$ PSII recovery only depends on the reversibility of diuron binding and dilution in the uncontaminated water used for recovery. Previous studies pointed out a progressive recovery in  $\phi$ PSII as time post herbicide removal increased (Valloton et al., 2008; Laviale et al., 2011; Nestler et al., 2012). Our data show, as observed with  $\phi$ PSII inhibition post contamination, that diuron release kinetics are dependent on the concentration of preexposure. The biofilms exposed to the lowest pulses ( $0.3$  and  $19.1 \mu\text{g.L}^{-1}$ ) recovered faster:  $\phi$ PSII returned within 5 h to half the optimal value of the non-pulsed biofilms ( $0.42 \pm 0.01$ ; Table 1). In contrast, the biofilms exposed to the higher pulses recovered poorly (no more than 35 % of the optimal values after more than 8 h post diuron removal). This is not surprising; exposure to such extreme concentrations for 3 h probably induced irreversible cellular damage in periphytic organisms.

On the 3-h scale of pulse duration, we would expect that adaptation and detoxification mechanisms likely occurred

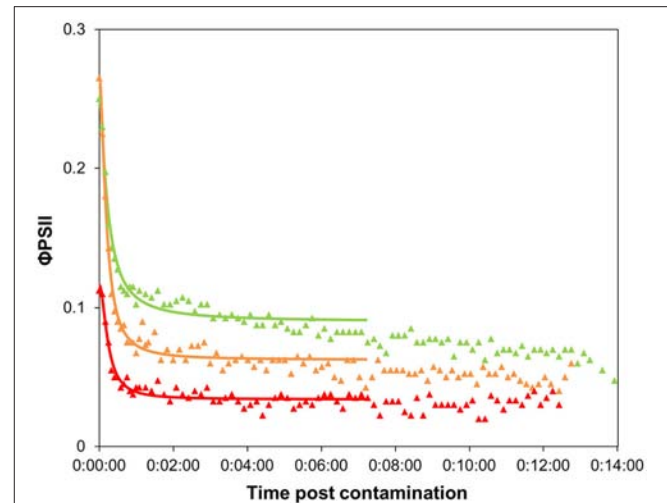


**FIGURE 5** | Time-response curves based on  $\phi$ PSII decrease for biofilms pre-exposed to 3-h diuron pulses, after contamination at “high” concentration (Experiment 2). Values are average of 4 replicates. Pulse concentration:  $0.3 \mu\text{g.L}^{-1}$ : green triangles,  $19.1 \mu\text{g.L}^{-1}$ : orange triangles,  $102.4 \mu\text{g.L}^{-1}$ : red triangles.

as described in section Time Dependency of Ecotoxicity Parameters, rather than species selection. With this study, we show that biofilm adaptation to a 3-h pulse, even at low dose, has a cost for the community. The time taken to (incompletely) recover photosynthetic efficiency reflects that the individuals were weakened. Interestingly, Pollution-Induced Community Tolerance (PICT, Blanck et al., 1988) was not observed when exposing our biofilms for 3 days to  $5 \mu\text{g.L}^{-1}$  of diuron (unpublished data).  $EC_{50}$  were similar between control and exposed biofilms (respectively,  $EC_{50} = 12.7 \pm 2.0$  and  $13.6 \pm 1.7 \mu\text{g.L}^{-1}$ ) but some effect was visible on the photosynthetic efficiency ( $\phi$ PSII =  $0.51 \pm 0.02$  vs.  $0.43 \pm 0.01$ ) confirming that diuron had some effect. Therefore, the fact that PICT is often observed in diuron-contaminated streams (McClellan et al., 2008; Pesce et al., 2010a,b; Tlili et al., 2010) suggests that repeated, and *a fortiori* high frequency, pulses are likely to have dramatic observable impacts on riverine primary production. Indeed, the cumulative effects of pulses likely decrease the fitness of the individuals and, on longer time scales, eliminate the most sensitive organisms from the initial community. PICT acquisition would thus result from this selection of tolerant organisms after repeated pulses (even for low concentrations, Ricart et al., 2009), rather than from physiological adaptation.

## CONCLUSIONS AND PERSPECTIVES

This time-response curve approach allowed to estimate two important parameters for assessing the risk associated to fluctuating exposure to herbicides: the maximal achievable inhibition (= maximal impact of a particular concentration of exposure) and the latency parameter  $t_{1/2}$ , reflecting the

time to reach 50% of the maximal effect.  $t_{1/2}$  was dose-dependent but apparently not influenced by the biofilms we tested, nor by prior short-term (pulse) exposure. This result highlights that diuron reaches its cellular target almost instantaneously (<1 min), independently from biological parameters (chlorophyll *a* concentration, adaptation related to exposure history). Characterizing diuron accumulation kinetics within biofilms, considering their microbial composition, would allow confirming this immediate internalization.

Reversibility of the impacts of pulses a few hours after diuron removal was not fully demonstrated. The kinetics of diuron release from cells to uncontaminated medium appeared to be much slower than binding rates and the assessment of diuron desorption over time would be worth studying in the future. Therefore, repeated exposure is very likely to impair freshwater biofilms, in particular if pulses occur at a high frequency.

Because photosynthesis is directly associated with growth and primary production, it is necessary to better understand the consequences of short-term exposure to herbicide in real-world conditions, as well as the recovery mechanisms after toxic pressure is removed. This refinement can play a significant role in herbicide risk assessment, such as prediction of the duration, intensity and frequency of exposure leading to non-negligible effects on the primary production in aquatic ecosystems. Future research should also consider the simultaneous accumulation kinetics of different organic compounds, as contaminants rarely occur alone in the field.

## REFERENCES

- AFNOR (2012). *Water Quality*. Fresh water algal growth inhibition test with unicellular green algae - European standard NF EN ISO 8692.
- Allen, M. M., Turnburke, A. C., Lagace, E. A., and Steinback, K. E. (1983). Effects of photosystem II herbicides on the photosynthetic membranes of the *Cyanobacterium Aphanocapsa* 6308. *Plant Physiol.* 71, 388–392. doi: 10.1104/pp.71.2.388
- Blanck, H., Wängberg, S. A., and Molander, S. (1988). "Pollution-induced community tolerance - a new ecotoxicological tool," in *Functional Testing of Aquatic Biota for Estimating Hazards of Chemicals*, eds J. Cairns Jr and J. R. Pratt (Philadelphia: American Society for Testing and Materials), 219–230.
- Copin, P.-J., Coutu, S., and Chèvre, N. (2015). Modelling the effect of fluctuating herbicide concentrations on algae growth. *Ecotoxicol. Environ. Saf.* 113, 214–222. doi: 10.1016/j.ecoenv.2014.12.010
- Dauta, A. (1982). Conditions de développement du phytoplancton. Etude comparative du comportement de huit espèces en culture. I. Détermination des paramètres de croissance en fonction de la lumière et de la température. *Ann. Limnol.* 18, 217–262. doi: 10.1051/limn/1982005
- Draber, W., Tietjen, K., Kluth, J. F., and Trebst, A. (1991). Herbicides in Photosynthesis Research. *Angew. Chem. Int. Edn. Eng.* 30, 1621–1633. doi: 10.1002/anie.199116211
- Francoeur, S. N., Johnson, A. C., Kuehn, K. A., and Neely, R. K. (2007). Evaluation of the efficacy of the photosystem II inhibitor DCMU in periphyton and its effects on nontarget microorganisms and extracellular enzymatic reactions. *J. North Am. Benthol. Soc.* 26, 633–641. doi: 10.1899/06-051.1
- Ghiglione, J.-F., Martin-Laurent, F., Stachowski-Haberhorn, S., Pesce, S., and Vuilleumier, S. (2014). The coming of age of microbial ecotoxicology: report on the first two meetings in France. *Environ. Sci. Pollut. Res.* 21, 14241–14245. doi: 10.1007/s11356-014-3390-x

## AUTHOR CONTRIBUTIONS

SM, BC, and NM contributed to the conception and design of the study; SM and BC performed the experiments. SM performed the statistical analysis and wrote the first draft of the manuscript. BC and NM revised the manuscript. All authors contributed to manuscript revision, read and approved the submitted version.

## FUNDING

This study was carried out with financial support from the French National Research Agency (ANR) in the framework of the Investments for the future Program, within the Cluster of Excellence COTE (ANR-10-LABX-45).

## ACKNOWLEDGMENTS

We warmly acknowledge Gwilherm Jan (Irstea) for his technical help in field implementation and channels setup, Mélissa Eon and Brigitte Delest (Irstea) for complementary water analyses. They also thank Emilie Saulnier-Talbot for correcting English spelling and grammar of the manuscript.

## SUPPLEMENTARY MATERIAL

The Supplementary Material for this article can be found online at: <https://www.frontiersin.org/articles/10.3389/fenvs.2018.00131/full#supplementary-material>

- Guasch, H., Artigas, J., Bonet, B., Bonnineau, C., Canals, O., Corcoll, N., et al. (2016). "The use of biofilms to assess the effects of chemicals on freshwater ecosystems," in *Aquatic Biofilms: Ecology, Water Quality and Wastewater Treatment*, eds A. M. Romani, H. Guasch, and M. D. Balaguer (Girona: Caister Academic Press), 125–144.
- Laasch, H., Pfister, K., and Urbach, W. (1981). Comparative binding of Photosystem II-herbicides to isolated thylakoid membranes and intact green algae. *Zeitschr. Naturforschung* 36c, 1041–1049. doi: 10.1515/znc-1981-11-1223
- Lambert, A.-S., Pesce, S., Foulquier, A., Gahou, J., Coquery, M., and Dabrin, A. (2015). Improved short-term toxicity test protocol to assess metal tolerance in phototrophic biofilms: toward standardization of PICT approaches. *Environ. Sci. Pollut. Res.* 22, 4037–4045. doi: 10.1007/s11356-014-3505-4
- Laviale, M., Morin, S., and Créach, A. (2011). Short term recovery of periphyton photosynthesis after pulse exposition to the photosystem II inhibitors atrazine and isoproturon. *Chemosphere* 84, 731–734. doi: 10.1016/j.chemosphere.2011.03.035
- Lockert, C. K., Hoagland, K. D., and Siegfried, B. D. (2006). Comparative sensitivity of freshwater algae to atrazine. *Bull. Environ. Contam. Toxicol.* 76, 73–79. doi: 10.1007/s00128-005-0891-9
- Magnusson, M., Heimann, K., Quayle, P., and Negri, A. P. (2010). Additive toxicity of herbicide mixtures and comparative sensitivity of tropical benthic microalgae. *Mar. Pollut. Bull.* 60, 1978–1987. doi: 10.1016/j.marpolbul.2010.07.031
- McClellan, K., Altenburger, R., and Schmitt-Jansen, M. (2008). Pollution-induced community tolerance as a measure of species interaction in toxicity assessment. *J. Appl. Ecol.* 45, 1514–1522. doi: 10.1111/j.1365-2664.2008.01525.x
- Murray, K. E., Thomas, S. M., and Bodour, A. A. (2010). Prioritizing research for trace pollutants and emerging contaminants in the freshwater environment. *Environ. Pollut.* 158, 3462–3471. doi: 10.1016/j.envpol.2010.08.009

- Nestler, H., Groh, K. J., Schönenberger, R., Behra, R., Schirmer, K., Eggen, R. I. L., and M. J. F. Suter. (2012). Multiple-endpoint assay provides a detailed mechanistic view of responses to herbicide exposure in *Chlamydomonas reinhardtii*. *Aquat. Toxicol.* 110–111, 214–224. doi: 10.1016/j.aquatox.2012.01.014
- Newman, M. C., and McCloskey, J. T. (1996). Time-to-event analyses of ecotoxicity data. *Ecotoxicology* 5, 187–196. doi: 10.1007/BF00116339
- OECD (1984). *Alga, Growth Inhibition Test*.
- Okamura, H., Aoyama, I., Ono, Y., and Nishida, T. (2003). Antifouling herbicides in the coastal waters of western Japan. *Mar. Pollut. Bull.* 47, 59–67. doi: 10.1016/S0025-326X(02)00418-6
- Pesce, S., Bouchez, A., and Montuelle, B. (2011). “Effects of organic herbicides on phototrophic microbial communities in freshwater ecosystems,” in *Whitacre, Reviews of Environmental Contamination and Toxicology*, ed D. M. (New York, NY: Springer), 87–124.
- Pesce, S., Lissalde, S., Lavielle, D., Margoum, C., Mazzella, N., Roubeix, V., et al. (2010a). Evaluation of single and joint toxic effects of diuron and its main metabolites on natural phototrophic biofilms using a pollution-induced community tolerance (PICT) approach. *Aquat. Toxicol.* 99, 492–499. doi: 10.1016/j.aquatox.2010.06.006
- Pesce, S., Margoum, C., and Montuelle, B. (2010b). *In situ* relationships between spatio-temporal variations in diuron concentrations and phototrophic biofilm tolerance in a contaminated river. *Water Res.* 44, 1941–1949. doi: 10.1016/j.watres.2009.11.053
- Pinto, E., Sigaud-Kutner, T. C. S., Leitao, M. A. S., Okamoto, O. K., Morse, D., and Colepicolo, P. (2003). Heavy metal-induced oxidative stress in algae. *J. Phycol.* 39, 1008–1018. doi: 10.1111/j.0022-3646.2003.02-193.x
- Rabiet, M., Margoum, C., Gouy, V., Carluer, N., and Coquery, M. (2010). Assessing pesticide concentrations and fluxes in the stream of a small vineyard catchment - Effect of sampling frequency. *Environ. Pollut.* 158, 737–748. doi: 10.1016/j.envpol.2009.10.014
- Ricart, M., Barceló, D., Geislinger, A., Guasch, H., M. L. D. Alda, Romani, A., M., Villagrasa, M., et al. (2009). Effects of low concentrations of the phenylurea herbicide diuron on biofilm algae and bacteria. *Chemosphere* 76, 1392–1401. doi: 10.1016/j.chemosphere.2009.06.017
- Rutherford, A. W., and Krieger-Liszkay, A. (2001). Herbicide-induced oxidative stress in photosystem II. *Trends Biochem. Sci.* 26, 648–653. doi: 10.1016/S0968-0004(01)01953-3
- Sabater, S., Guasch, H., Ricart, M., Romani, A., Vidal, G., Klünder, C., and M. Schmitt-Jansen. (2007). Monitoring the effect of chemicals on biological communities. The biofilm as an interface. *Anal. Bioanal. Chem.* 387, 1425–1434. doi: 10.1007/s00216-006-1051-8
- Schreiber, U., Quayle, P., Schmidt, S., Escher, B. I., and Mueller, J. F. (2007). Methodology and evaluation of a highly sensitive algae toxicity test based on multiwell chlorophyll fluorescence imaging. *Biosens. Bioelectron.* 22, 2554–2563. doi: 10.1016/j.bios.2006.10.018
- Sharma, P., Chopra, A., Cameotra, S., S., and Suri, C. R. (2010). Efficient biotransformation of herbicide diuron by bacterial strain *Micrococcus* sp. PS-1. *Biodegradation* 21, 979–987. doi: 10.1007/s10532-010-9357-9
- SOeS (2015). *Les Pesticides Dans Les Cours d'eau Français en 2013*.
- Tang, J. X., Hoagland, K. D., and Siegfried, B. D. (1997). Differential toxicity of atrazine to selected freshwater algae. *Bull. Environ. Contam. Toxicol.* 59, 631–637. doi: 10.1007/s001289900526
- Tlili, A., Bérard, A., Roulier, J.-L., Volat, B., and Montuelle, B. (2010).  $PO_4^{3-}$  dependence of the tolerance of autotrophic and heterotrophic biofilm communities to copper and diuron. *Aquat. Toxicol.* 98, 165–177. doi: 10.1016/j.aquatox.2010.02.008
- Tlili, A., Dorigo, U., Montuelle, B., Margoum, C., Carluer, N., Gouy, V., et al. (2008). Responses of chronically contaminated biofilms to short pulses of diuron. an experimental study simulating flooding events in a small river. *Aquat. Toxicol.* 87, 252–263. doi: 10.1016/j.aquatox.2008.02.004
- Valotton, N., Eggen, R. I. L., Escher, B. I., Krayenbühl, J., and Chèvre, N. (2008). Effect of pulse herbicidal exposure on *Scenedesmus vacuolatus*: A comparison of two photosystem II inhibitors. *Environ. Toxicol. Chem.* 27, 1399–1407. doi: 10.1897/07-197.1
- VanMeter, K. C., and Hubert, R. J. (2016). “Chapter 10: pharmacology,” in *Microbiology for the Healthcare Professional, 2nd edn*, (St. Louis, Missouri: Elsevier), 200–213

**Conflict of Interest Statement:** The authors declare that the research was conducted in the absence of any commercial or financial relationships that could be construed as a potential conflict of interest.

Copyright © 2018 Morin, Chaumet and Mazzella. This is an open-access article distributed under the terms of the Creative Commons Attribution License (CC BY). The use, distribution or reproduction in other forums is permitted, provided the original author(s) and the copyright owner(s) are credited and that the original publication in this journal is cited, in accordance with accepted academic practice. No use, distribution or reproduction is permitted which does not comply with these terms.



# Evaluation of Phototrophic Stream Biofilms Under Stress: Comparing Traditional and Novel Ecotoxicological Endpoints After Exposure to Diuron

## OPEN ACCESS

Linn Sgier, Renata Behra, René Schönenberger, Alexandra Kroll<sup>††</sup> and Anze Zupanic<sup>††</sup>

Department of Environmental Toxicology, Eawag – Swiss Federal Institute of Aquatic Science and Technology, Dübendorf, Switzerland

### Edited by:

Stéphane Pesce,  
National Research Institute of Science  
and Technology for Environment  
and Agriculture (IRSTEA), France

### Reviewed by:

John R. Lawrence,  
Environment and Climate Change  
Canada, Canada  
Floriane Larras,  
Helmholtz-Zentrum für  
Umweltforschung UFZ, Germany  
Isabelle Lavoie,  
INRS-ETE, Canada

### \*Correspondence:

Alexandra Kroll  
alexandra.kroll@eawag.ch  
Anze Zupanic  
anze.zupanic@eawag.ch

<sup>††</sup>These authors have contributed  
equally to this work

### Specialty section:

This article was submitted to  
Microbiotechnology, Ecotoxicology  
and Bioremediation,  
a section of the journal  
Frontiers in Microbiology

**Received:** 06 September 2018

**Accepted:** 19 November 2018

**Published:** 29 November 2018

### Citation:

Sgier L, Behra R,  
Schönenberger R, Kroll A and  
Zupanic A (2018) Evaluation  
of Phototrophic Stream Biofilms  
Under Stress: Comparing Traditional  
and Novel Ecotoxicological Endpoints  
After Exposure to Diuron.  
*Front. Microbiol.* 9:2974.  
doi: 10.3389/fmicb.2018.02974

Stream biofilms have been shown to be among the most sensitive indicators of environmental stress in aquatic ecosystems and several endpoints have been developed to measure biofilm adverse effects caused by environmental stressors. Here, we compare the effects of long-term exposure of stream biofilms to diuron, a commonly used herbicide, on several traditional ecotoxicological endpoints (biomass growth, photosynthetic efficiency, chlorophyll-a content, and taxonomic composition), with the effects measured by recently developed methods [community structure assessed by flow cytometry (FC-CS) and measurement of extracellular polymeric substances (EPS)]. Biofilms grown from local stream water in recirculating microcosms were exposed to a constant concentration of 20 µg/L diuron over a period of 3 weeks. During the experiment, we observed temporal variation in photosynthetic efficiency, biomass, cell size, presence of decaying cells and in the EPS protein fraction. While biomass growth, photosynthetic efficiency, and chlorophyll-a content were treatment independent, the effects of diuron were detectable with both FC and EPS measurements. This demonstrates that, at least for our experimental setup, a combination of different ecotoxicological endpoints can be important for evaluating biofilm environmental stress and suggests that the more recent ecotoxicological endpoints (FC-CS, EPS protein content and humic substances) can be a useful addition for stream biofilm ecotoxicological assessment.

**Keywords:** Ecotoxicology, diuron, stream biofilms, flow cytometry, community structure, photosynthetic efficiency, EPS

## INTRODUCTION

The concentrations of contaminants in surface waters vary substantially in space and time. Fluxes of pollutants, such as pesticides, can change rapidly and lead to increase in exposure of organisms living in aquatic ecosystems (Wauchope, 1978; Finizio et al., 2005; Blanchoud et al., 2007; Rabiet et al., 2010; Moschet et al., 2014). Among the most strongly affected are stream biofilms, often referred to as periphyton (Azim, 2005) – taxonomically diverse and dynamic communities of

phototrophic and heterotrophic microorganisms. They play an important role in stream ecosystems by providing food for higher trophic levels, producing oxygen, changing near-bed hydraulics and providing habitat for protists and invertebrates (Lamberti, 1996; Nikora et al., 1997). Due to their ecological importance, assessing the effects of stressors to stream biofilms has been the subject of many studies, mainly focusing on functional endpoints, such as growth of biomass and photosynthetic efficiency, and on structural endpoints, such as the biofilm taxonomic composition and biodiversity (Dorigo et al., 2007; Ricart et al., 2009; Pesce et al., 2010a; Tlili et al., 2011).

A limitation of the traditional functional endpoints is that they are affected by structural compensation: it is possible for a functional endpoint to remain unchanged, even while the species composition of the biofilm is changing. A limitation of structural endpoints is that their measurement is expensive and/or time consuming, and that no functional information is gained from it. Also, most traditional methods concentrate on the cellular part of the biofilm and ignore the intercellular space that binds the biofilm together. Recently, new biofilm characterization methods have been developed that can simultaneously measure both functional and structural features. Members of our laboratory have, in particular, focused on characterization of freshwater biofilms based on flow cytometry derived community structure (FC-CS) (Sgier et al., 2016, 2018) and liquid chromatography coupled to organic carbon and nitrogen detection (LC-OCD-OND) for characterization of extracellular (polymeric) substances (EPS) present in biofilms (Stewart et al., 2013; Kroll et al., 2014). Both methods measure multiple features of biofilms. FC quantifies fluorescence properties and light scattering properties, related to size and granularity of individual particles in the biofilm, which are then used to cluster the particles into subpopulations. The changes in the number of subpopulations and their size in time reflect changes in the community structure. The community structure, which depends on the biofilm species composition and phenotypic variability (Staley et al., 2015), has been shown to be both affected by stress as well as to be a determining factor in stress resistance (Wahl et al., 2012). LC-OCD-OND can be used to quantify a large size range of organic molecules, including polysaccharides, proteins and acids in the EPS. Changes in the EPS of stream biofilms have been shown to be important for nutrient cycling, biofilm stability, and the interaction with pollutants (Flemming and Wingender, 2010; Stewart et al., 2013; Kroll et al., 2016). Interaction with silver nanoparticles, for example, is mediated by carboxylic groups in stream biofilm EPS (Sambalova et al., 2018). Importantly, there have been only a few studies yet that have compared the effects of environmental stress on stream biofilms on these different endpoints using the same samples, and none of them focused specifically on endpoint sensitivity. Therefore, it is not clear whether any of these endpoints is more sensitive and whether their combined use can provide a more comprehensive understanding of the effects of environmental stress on the biofilms.

In this study, our objective was to compare the effects of long-term chemical exposure on several traditional and more recently

developed ecotoxicological biofilms endpoints. As an example chemical, we used DCMU (trade name diuron), a commonly used herbicide (Balsiger et al., 2004; Wittmer et al., 2011; Moschet et al., 2014) that targets the electron transport in photosystem II (PSII) (Vanrensen, 1989) and thereby the phototrophic organisms present in the biofilm. Our choice of stressor is also reflected in our selection of endpoints, which are centered on phototrophic organisms: photosynthetic efficiency, chlorophyll-a content, taxonomy by light microscopy (LM), FC-CS, while both, phototrophic and heterotrophic organisms contribute to the endpoints biomass growth and EPS composition. Since neither FC nor EPS measurements have been used before in diuron studies, we hypothesized using them would provide us with new insight into the effects of diuron on stream biofilms. The previously demonstrated sensitivity of both methods (Kroll et al., 2014; Sgier et al., 2016) and diversity of endpoints gained from them lead also to the hypothesis that they could be more sensitive than the traditional endpoints. In the results and discussion, we compare the sensitivity and information content of the measured endpoints and their complementarity regarding temporal dynamics of diuron-related effects to stream biofilms.

## MATERIALS AND METHODS

### Chemicals

Diuron used for the exposure studies was purchased from Sigma-Aldrich (Buchs, Switzerland) (DCMU, CAS 330-54-1, D2425), as were also the analytical grade diuron (DCMU, 45463) and Ammonium formate (10 M, 78314-100 ML-F) which were used for LC-MS measurements (see “Materials and Methods—Quantification of Diuron by LC-MS”). Acetonitrile HPLC gradient-grade purity was obtained from Acros Organics (Thermo Fisher Scientific, Reinach, Switzerland) and nanopure water from Barnstead NANOpure (Skan, Allschwil, Switzerland). All other chemicals were purchased from Sigma-Aldrich or Merck.

### Colonization of Natural Biofilms

Natural biofilms were colonized on glass microscope slides (38 mm × 26 mm, Thermo Fisher Scientific), which were placed vertically in Plexiglas channels in a flow-through system fed by water from the river Chriesbach (on campus, Dübendorf, Switzerland) (Navarro et al., 2007; Kroll et al., 2014). An overview of Chriesbach water chemistry is provided in **Supplementary Table S1**. A sediment trap (0.51 m × 0.7 m × 2.6 m, residence time about 20 min) was used to remove part of the dispersed particles. The flow rate in the channels was maintained at about 1 cm/s corresponding to a volume of 3 L/min. Illumination was provided in 12:12 h light/dark cycles by BioSun fluorescent tubes with a radiation similar to the sunlight spectrum (Radium Lampenwerk GmbH, Germany, ML-T8 36W/965/G13B). Temperature and photosynthetic active radiation (PAR) in the channels were monitored by a HOBO Pendant® Temperature/Light Data Loggers (UA-002-64) (median

water temperature: 13.4°C [11.7–16.1°C], median light intensity in the light period: 1011.8 Lux).

## Diuron Exposure of Natural Biofilms in Indoor Microcosms

After 3 weeks of biofilm colonization, colonized glass slides were randomly transferred to 10 (Nos. 1–10) independent recirculating microcosms (Plexiglas, 10 cm × 25 cm, 3.5 cm water column, 32 glass slides per microcosm) containing 5 L of LA medium (**Supplementary Table S2**). Room temperature was maintained between 14.0 and 16.1°C resulting in median water temperature of 17.75°C (17.7–17.8°C). Light conditions and flow rate at the inflow were the same as during colonization (median light intensity in the light period: 947.2 Lux). Oxygen saturation and temperature were monitored in one microcosm (No. 10) with a Presens Microx TX3 system and an NTH-PS1-L2.5-TS-NS40/0.8-YOP-EXT1 oxygen microsensors over 3 weeks (minimum [O<sub>2</sub>]/dark period: 7 mg/L, maximum [O<sub>2</sub>]/light period: 7.9 mg/L) and measured after 21 days in all microcosms. Conductivity, pH, and water chemistry were determined in parallel to sampling (**Supplementary Tables S3, S4**). One day after translocation, microcosms Nos. 1, 3, 5, 7, and 9 were exposed to 20 µg/L diuron, dissolved in methanol (CAS 330-54-1) during 3 weeks, whereas microcosms Nos. 2, 4, 6, 8, and 10 were exposed to methanol as solvent control [53.6 µL methanol added to 5 L of medium, equal to 0.001% (v/v) or 8.5 µg/L or 0.0008% (w/v)]. After each sampling time point at 7 (d<sub>7</sub>), 14 (d<sub>14</sub>), and 21 (d<sub>21</sub>) days after translocation, 3 L of the total 5 L LA medium was renewed to assure constant levels of nutrients and diuron (see “Materials and Methods—Quantification of Diuron by LC-MS”). As one of the main objectives of this study was to compare the effects of diuron on several different endpoints, the target diuron concentration was chosen close to the EC<sub>50</sub> value reported in previous studies of diuron exposure, conducted on stream biofilms and individual freshwater algae species (European Service Innovation Scoreboard, 2000; Legrand et al., 2006; Knauer et al., 2007; Roubeix et al., 2011; Moisset et al., 2014; Kim Tiam et al., 2015).

## Sampling of Natural Biofilms From Microcosms

Immediately after translocation to the indoor microcosms (d<sub>0</sub>), and after 7 (d<sub>7</sub>), 14 (d<sub>14</sub>), and 21 (d<sub>21</sub>) days, 8 slides were taken from each microcosm and biofilms were pooled into 40 mL of LA medium with a plastic scraper. The suspension was used for FC-CS, taxonomy, biomass, chlorophyll-a content, photosynthetic efficiency analysis and EPS measurements. Of this 40 mL suspension, 10 mL were sonicated (45 kHz 60 W, VWR Ultrasonic Cleaner) for 1 min to break up colonies and immediately fixed with 0.01% paraformaldehyde and 0.1% glutaraldehyde (w/v, stock in tap water) and stored at 4°C for FC and taxonomic LM analysis. Further, 2 mL of the suspension were used for photosynthetic efficiency measurements and chlorophyll-a content measurements (PHYTO-PAM) and 8 mL

were taken for biomass analysis. The generated supernatant was used for EPS extraction.

## Taxonomic Analysis by Light Microscopy

Fixed samples were diluted 1:10 three times independently in tap water and 1 mL was transferred to an Uthermol's chamber for microscopic analysis. An inverted microscope (Zeiss Axiovert 135) was used to identify and count (Zeiss EC Plan-Neofluar 40×/0.75 objective, Zeiss EC Plan-Neofluar 100× 1.3 Oil objective, if necessary) algae and cyanobacteria genera and if possible species within three fields of vision, based on two taxonomic references and the recommendations by the Swiss Federal Office for the Environment (Hustedt, 1930; Pascher et al., 1987/1997; Hürlimann and Niederhauser, 2007). Counting was not possible for cells with colonial or filamentous growth. At least 150 cells were identified for each replicate.

## Biomass

To assess the biomass of the sampled biofilm, 8 mL of biofilm suspension of each sample were centrifuged at 2000 g for 10 min at room temperature and the resulting pellet was placed in a 2 mL Eppendorf tube and stored at –20°C for ~72 h. Subsequently, the pellets were freeze-dried (LYOVAC GT2) for 24 h and dry weight measured.

## Photosynthetic Efficiency and Total Chlorophyll-a Content

Directly after sampling, photosynthetic efficiency was assessed by measuring the quantum yield of the photosystem II (ΦPSII) of 2 mL biofilm suspensions by Pulse-Amplitude-Modulated fluorometry (PHYTO-PAM, Walz Heinz GmbH) (Schreiber, 1998). In parallel to the photosynthetic efficiency measurements, the initial fluorescence (at 665 nm) was measured as an indirect measure of total chlorophyll-a content, using a constant sensitivity of the photomultiplier (gain) (Corcoll et al., 2011).

## EPS Extraction and Characterization

Extracellular polymeric substances were extracted from samples on d<sub>0</sub>, d<sub>7</sub>, d<sub>14</sub>, and d<sub>21</sub> and were analyzed for organic carbon (OC) and organic nitrogen (ON) size distribution and protein content. The extraction procedure was performed as described previously (Stewart et al., 2013; Kroll et al., 2014). The supernatants generated by the biomass extraction were sequentially filtered using 1 µm glass fiber [VWR], 0.45 µm polypropylene [PALL], and 0.22 µm PES [Millipore] filters. Filters were washed with nanopure water (18.1 MΩ cm, Milli-Q) prior to use. EPS extracts were stored in glass bottles at 4°C [0.02% (w/v) NaN<sub>3</sub>]. All extraction steps were performed on ice, the water bath for ultrasound treatment was at room temperature.

Organic carbon and ON size distribution was measured by size-exclusion chromatography – organic carbon detection – organic nitrogen detection (LC-OCD-OND). Samples were diluted with nanopure water (18.1 MΩ cm, Milli-Q) directly before analysis. A size exclusion column (250 mm × 20 mm, Toyopearl TSK HW-50S) was used to separate EPS compounds. To quantify the carbon background of the extraction protocol,

an aliquot of extraction buffer was treated the same way as periphyton suspensions and then assessed by LC-OCD-OND. The mobile phase was phosphate buffer (24 mM, pH 6.6) and the acidification solution was phosphoric acid (60 mM, pH 1.2). The detection limit was 10  $\mu\text{g/L}$  for both OC and ON. The software FIFFIKUS was used to quantify total organic carbon (TOC), dissolved organic carbon (DOC), and chromatographable DOC compounds (cDOC). The chromatograms obtained from LC-OCD-OND are integrated to determine the amount of biopolymers (high  $M_r$  polysaccharides and proteins), building blocks of humic substances, low  $M_r$  acids, and amphiphilic/neutral compounds (alcohols, aldehydes, amino acids, and ketones).

Total protein in EPS extracts was measured by the Bradford assay using Bradford reagent (Bio-Rad Protein Assay Kit I) and an Infinite 200 (Tecan) plate reader. Calibration curves were produced with bovine serum albumin (BSA) diluted in equal amounts of EPS extracts to account for any interference of the EPS with protein detection.

## Community Structure Analysis by Flow Cytometry and viSNE

For single cell analysis of the biofilm communities, dichroic splitters and filters of the Beckmann Coulter Gallios flow cytometer (using 405, 488, 638 nm lasers) were selected to cover the fluorescence emission from 425–755 nm as previously described (Sgier et al., 2016). In total, 12 parameters were measured: forward (FS) and side scatter (SS), and 10 fluorescences (further explained in **Supplementary Table S5**). Before analyzing the biofilm suspension, the samples were filtered through 50  $\mu\text{m}$  filters (CellTrics filter, Partec), as this is the particle size limit allowed by the used flow-cytometer. Three technical replicates per sample were measured. A total of 10,000 events per sample were acquired and gated to exclude all events that were above the signal saturation limit in any of the 12 parameters ( $<<1\%$ ). The area signal intensity of all parameters was exported as a csv-file and visualized with stochastic neighbor embedding (SNE) using the cyt software (Amir el et al., 2013). In short, SNE is a non-linear dimensionality reduction technique that is used for embedding high-dimensional data into a low-dimensional space (van der Maaten and Hinton, 2008). In our case, each measured cell was represented in 12-dimensions (FS, SS, 10 fluorescences) and SNE was used to embed the cells into a 2D space and then visualize the embedding using a scatter plot, i.e., viSNE map. Prior to visualization, technical and biological replicates were merged and random sampling was performed, so that the viSNE map was created from a mixture of equal-sized samples (18,000 cells/sample). Based on the visual clustering, subpopulations of the viSNE map were identified and the number of particles/cells that belonged to each subpopulation per sample was quantified. Subpopulations are defined as visually separable clusters of cells in the viSNE map, with optical and fluorescence properties that differentiate them from the other clusters. To facilitate the interpretation of the viSNE maps and the defined subpopulation, FC data of reference species (16 diatoms, 8 green algae, 6 cyanobacteria, and 1 red algae species,

**Supplementary Table S6**) were projected on the viSNE map. For a more detailed description of the procedure, see (Sgier et al., 2016, 2018).

## Quantification of Diuron by LC-MS

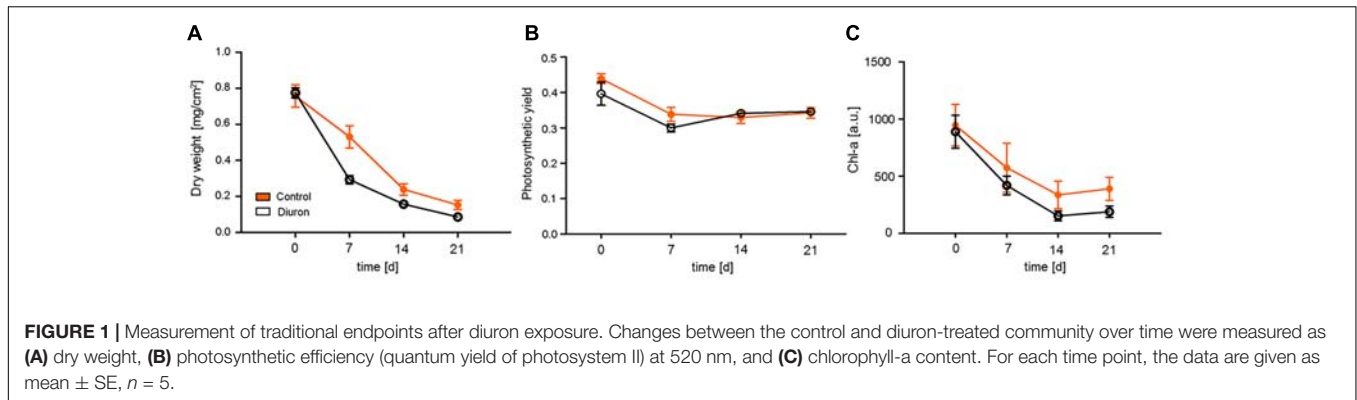
The diuron concentration in the exposure media was measured every day during the first week of exposure, using LC-MS, to ensure a constant exposure level between two time points of media exchange. Ten microliters of sample were separated with the use of an Accela 600 HPLC pump with an in-line degasser (Thermo Fisher Scientific, San Jose, CA, United States), an HTS PAL auto sampler (CTC Analytics, Zwingen, Switzerland), which kept the samples at 4°C, and an Agilent Poroshell 120 EC, C18 column (2.1 mm  $\times$  100 mm, 2.7  $\mu\text{m}$  particle size, Agilent Technologies AG, Switzerland). Pre-mixed eluents were used for the gradient (200  $\mu\text{l/min}$ ): A (90% Ammonium formate 5 mM in nanopure water and 10% Acetonitrile) and B (10% Ammonium formate 5 mM in nanopure water and 90% Acetonitrile). Starting conditions were 90% A with a linear gradient after 5.5 min to 60% A, followed by a linear gradient to 100% B in another 5.5 min, which was then kept for 1 min. Initial conditions were reached in 0.5 min and the column re-equilibrated for another 3 min. Before and after each injection, the syringe and auto sampler valve were cleaned once with 90% nanopure water/10% methanol and 100% methanol.

For mass spectrometry, the column was coupled to the Heated Electro Spray ESI inlet of a TSQ Vantage triple quad MS (Thermo Fisher Scientific, San Jose, CA, United States). The collision energy (CE) for the collision induced dissociation was optimized for the precursor ( $m/z = 233.1$ ). ESI positive conditions were: needle voltage 4000 V, interface and vaporizer temperatures 250°C resp. 150°C, sheath gas 40, ion sweep gas 0.0 and aux gas 10. Q1 FWHM and Q3 FWHM were set to 0.7 resolution. Used scan width was 1.0  $m/z$  and the scan time 0.1 s. Three transitions were monitored in single reaction monitoring (SRM) mode during the whole chromatogram. The MRM 233.1 – 72.1 (CE = 20) was used as analytical signal and the MRMs 233.1 – 46.1 (CE = 13), and 235.1 – 72.1 (CE = 19) as conformational signals. Peak areas were calculated by Thermo XCalibur™ 3.0.63 software and manually adjusted before transferring to Excel, together with the retention times, for further processing. No sorption of diuron to the biomass was detected.

## Statistical Data Analysis

Because one of the main objectives of the study was to compare the different ecotoxicological endpoints, we decided to use only a few different statistical methods and apply them consistently with the measured endpoints.

For biomass, photosynthetic efficiency, chlorophyll-a content, individual FC fluorescences and individual clusters obtained from the viSNE analysis, we used linear modeling to analyze the effects of time and diuron exposure. For each endpoint, the linear model was fitted with maximum likelihood to model the respective endpoint as the dependent variable, and time and diuron exposure as fixed effects (with and without interactions). To determine whether time and treatment had an effect on any measured endpoint, we used the Two-way ANOVA and Tukey's



HSD test (Null hypothesis that neither time nor treatment have any effect on the endpoint). For extracted EPS comparison between  $d_0$  and  $d_{21}$ , the  $t$ -test was used.

For taxonomy and FC-CS, we evaluated the effects of time and diuron exposure using permutational multivariate ANOVA based on dissimilarities (adonis), using R package *vegan* (jaccard distance was used as measure of dissimilarity, 10,000 permutations were used in all cases) (Dixon, 2003). All datasets were transformed using the Hellinger transformation before running adonis.

## RESULTS

Biomass, chlorophyll-a content, photosynthetic efficiency, taxonomic composition, FC-CS and EPS were measured in long-term exposure experiments to diuron. To ensure a constant exposure concentration, diuron was quantified daily in each treated channel during the first week by LC-MS. Daily means were relatively stable (mean  $20.22 \pm$  SE  $1.053 \mu\text{g/L}$ , **Supplementary Figure S1**), indicating that diuron was constant during the entire experiment.

Our hypothesis was that during the experiments the biofilms would undergo dynamic changes, which would include normal biofilm dynamics, the effects of translocation of the biofilms into the recirculating microcosm environment and the effects of exposure to diuron. We wanted to know how sensitive the different endpoints are to these factors (time, diuron treatment) and, for each respective endpoint, whether it is possible to detect the effects of both time and treatment or would one of them be dominant.

### Dynamics of Traditional Endpoints: Biomass, Photosynthetic Efficiency, Chlorophyll-a Content, Taxonomic Composition

At the start of the experiment ( $d_0$ ), the control and exposed biofilms did not differ in biomass (measured as dry weight), photosynthetic efficiency or chlorophyll-a content (**Figure 1**). For both, exposed and control communities, time was the dominant factor, with all three endpoints decreasing over the course of the experiment [time effect for biomass:  $F_{(3,36)} = 78.25$ ,  $p < 0.001$ ;

photosynthetic efficiency:  $F_{(3,32)} = 17.22$ ,  $p < 0.001$ ; chlorophyll-a content:  $F_{(3,36)} = 42.84$ ,  $p < 0.001$ ], while diuron exposure was not significant for any endpoint. For all endpoints, communities exposed to diuron showed a faster decrease within the first week of exposure, however, this was only significant for biomass after 1 week of exposure [time-treatment interaction:  $F_{(3,32)} = 4.23$ ,  $p = 0.0125$ ].

The overall decrease in biomass over the course of the experiment was also apparent in the genus-level taxonomic analysis (**Supplementary Figure S2**). In both, the control and the exposed communities, almost all detected genera decreased in abundance during the first week and stabilized towards the end of the experiment. The decrease in the diuron-treated communities was generally stronger, except for the genera *Diatoma* and *Gomphonema*, which increased in abundance (**Supplementary Figure S2**). The genus *Cocconeis* increased in abundance over the whole experiment in both control and diuron-treated communities. Nevertheless, permutational ANOVA of the taxonomic data did not find a significant time or treatment effect.

### Community Structure Analysis by Flow Cytometry and viSNE

For the FC part of the datasets, we decided to analyze the raw FC data (optical scatter and fluorescence intensities measured by the FC) and the FC data after categorization of the biofilms into subpopulations (FC-CS), separately. For the raw data, using permutational ANOVA we found the effects of time ( $p < 0.001$ ) and diuron treatment ( $p = 0.0061$ ) to be significant. Similar as for the traditional endpoints, the largest effect to measured optical and fluorescence properties was seen at 1 week after beginning of exposure. However, not all optical and scatter properties followed the same pattern; the effect of time was found to be significant only for forward scatter, side scatter (measures of size and granularity) and fluorescences FL 5–10 (see **Supplementary Figure S3** for details), while the diuron effect was not statistically significant for any of the individual optical or scatter properties.

Based on the viSNE map, we categorized 20 subpopulations (SP 1–20) according to their scattering and fluorescent properties (**Figure 2** and **Supplementary Figures S4, S5**). The categorized subpopulations were further grouped into diatom-, green algae-, cyanobacteria-, red algae-, and decaying-like cells (**Figure 2C**),

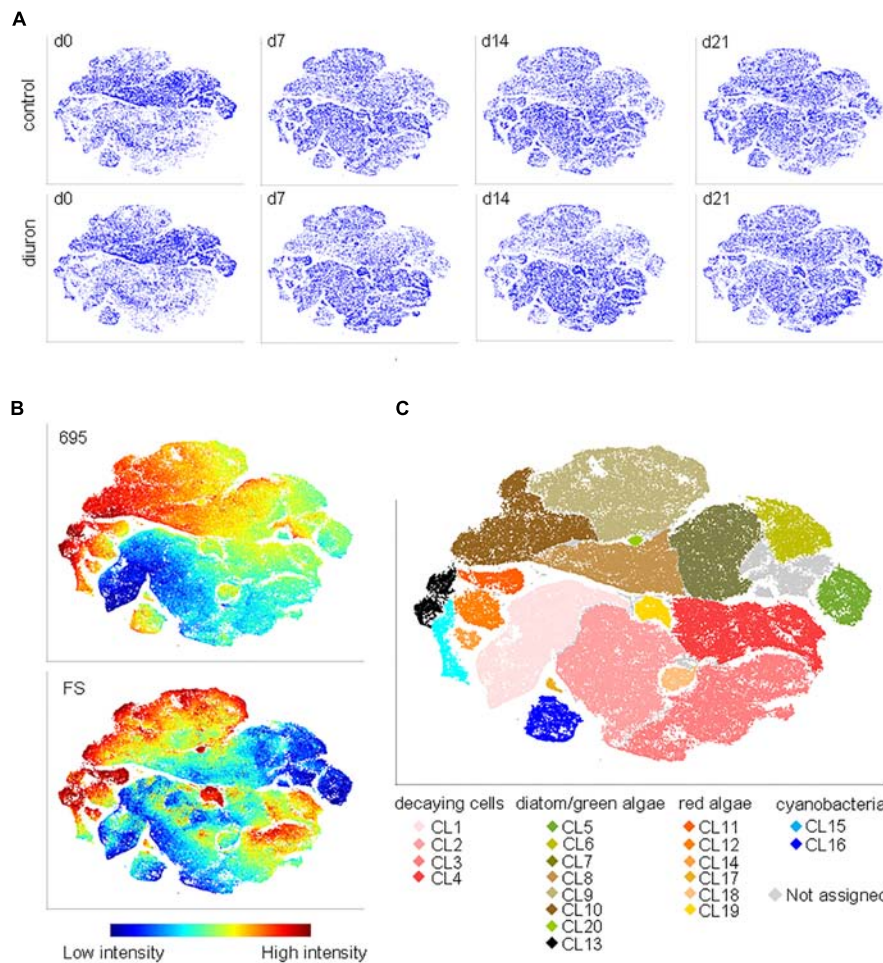


**FIGURE 2 |** FC-CS in diuron-treated stream biofilms. **(A)** Biofilms were assessed by flow cytometry after sampling on d<sub>0</sub>, d<sub>7</sub>, d<sub>14</sub>, and d<sub>21</sub>, and altogether mapped by viSNE. viSNE maps are shown in single color, with each point in the viSNE map representing a single cell or particle from the biofilms or **(B)** colored according to fluorescence intensity at 695 nm and according to the forward scatter (full set of scattering and fluorescence intensities displayed in **Supplementary Figure S4**). **(C)** Subpopulations (SP 1–20) categorized based on the viSNE map and optical scatter and fluorescence intensities. Some cells (4.7%) were not assigned due to lack of distinct properties. Comparison of subpopulation properties with data acquired from reference species and pigment-bleached reference samples (**Supplementary Figure S5**) allowed for assigning subpopulations to types of organisms and potentially decaying cells.

according to their specific fluorescence patterns (**Supplementary Figure S4**) and after projection of the reference species on the viSNE map (**Supplementary Figure S6**). Based on the relative contributions of the subpopulations to the communities, a strong shift in community structure in both, control and diuron-treated samples was apparent within the first week of the experiment (**Figure 3A**). Permutational ANOVA of the whole dataset found effects of both time ( $p < 0.001$ ) and diuron treatment ( $p = 0.0035$ ).

At the level of individual subpopulations, the most prominent changes were an increase in decaying-like cells (SP 1–4) and of cells similar to a subpopulation of the red algae *Bangia* (SP 19) on the one hand, and a decrease in most subpopulations similar to green algae and diatoms (SP 5, 6, 7, 8, 10) on the other hand (**Figure 3A**). Subpopulations similar to cyanobacteria remained relatively stable (SP 15, 16). Compared to the control community, diuron-treated communities showed a significantly

stronger increase in decaying-like cells (SP 3) within the last 2 weeks [time-treatment interaction:  $F_{(3,32)} = 3.738$   $p = 0.02074$ , Tukey HSD at d<sub>14</sub>:  $p = 0.01655$ , d<sub>21</sub>:  $p = 0.00377$ ] and an increase in red algae-like cells (SP 19) during the last 2 weeks of the exposure [time-treatment interaction:  $F_{(3,32)} = 2.9454$ ,  $p = 0.04768$ , Tukey HSD at d<sub>14</sub>:  $p = 0.03628$  d<sub>21</sub>:  $p = 0.00154$ ] (**Figures 3B,C**). While the other subpopulations also showed differences between diuron and control, they were not significant (**Supplementary Figure S7**). The subpopulation of the red algae *Bangia* (SP 19) contained particularly large cells (higher forward and sideward scattering intensities) (**Figures 2B,C**).

## EPS Composition and Protein Concentration

Total EPS extractable from biofilms increased from 4.63  $\mu\text{g}$  EPS/mg dry weight/cm<sup>2</sup> (range 3.42–5.84) at d<sub>0</sub> to 9.72  $\mu\text{g}$

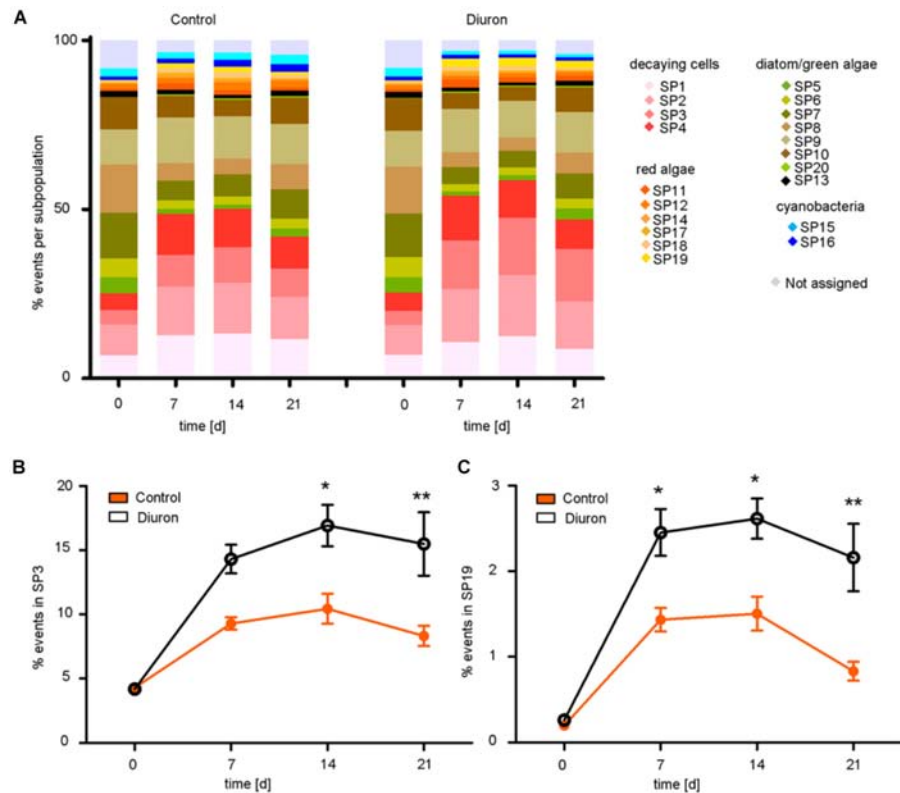


**FIGURE 3 |** Tracking and quantification of FC-CS after diuron exposure. **(A)** Relative contribution of the subpopulation (%) to the community based on the viSNE map over time. Significant differences between control and diuron-treated community appeared in **(B)** subpopulation 3 after the second week and in **(C)** subpopulation 19 already after the first week, represented with \* and \*\* (ANOVA and Tukey HSD test for  $\alpha = 0.05$ ,  $*P \leq 0.05$ ,  $**P \leq 0.01$ ). Bars represent the standard error,  $n = 5$ .

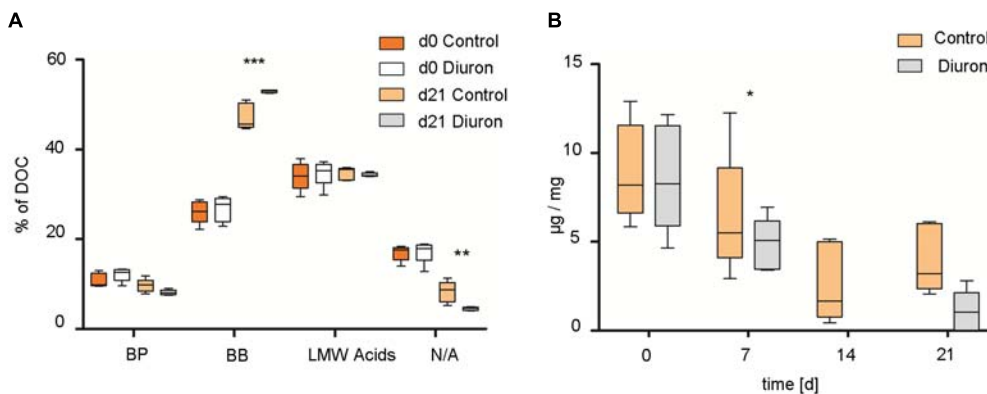


**FIGURE 4 |** Extracellular polymeric substances (EPS) extraction of stream biofilm samples after diuron exposure. **(A)** EPS composition as % of total DOC after 3 weeks. BP, biopolymers; BB, building blocks of humic substances; LMW acids, low molecular weight acids; N/A, neutral/amphiphilic compounds. **(B)** Protein concentration per extracted DOC ( $\mu\text{g}/\text{mg}$ ) over time. Data is presented as box plots according to Tukey. \*, \*\*, and \*\*\* represent the significant difference between the control and diuron-treated community at d21 ( $*P \leq 0.05$ ,  $**P \leq 0.01$ ,  $***P \leq 0.001$ ),  $n = 5$ .

EPS/mg dry weight/cm<sup>2</sup> (range 7.44–12.22) at d<sub>21</sub> in control communities and to 14.58  $\mu\text{g}$  EPS/mg dry weight/cm<sup>2</sup> (range 9.22–19.34) at d<sub>21</sub> in diuron-treated communities. The means of total extractable EPS from control/diuron-treated communities on d<sub>21</sub> were significantly different ( $p = 0.0348$ ,  $t = 2.538$ ,  $df = 8$ ). Similarly, EPS composition was not significantly different

between control/diuron-treated communities at the start of the experiment regarding the fraction of biopolymers (BP), building blocks (BB), low molecular weight acids (LMW acids), and neutral/amphiphilic compounds (N/A). They contributed by 14.98% BP (range 13.14–20.63), 33.42% BB (range 29.36–37.03), 35.86% LMW (range 32.66–38.78), and 13.73% N/A

(range 11.46–15.36) to the total EPS. Within 3 weeks, the fraction of BP generally decreased, while that of BB increased (Figure 4A). The variability of biological replicates remained the same in control communities but substantially decreased in diuron-treated communities. Further, the fraction of BP and LMW acids was not significantly different between control and treated samples, while a significantly higher amount of BB and a lower amount of N/A was detected in EPS extracted from diuron-treated communities [treatment-component interaction:  $F_{(3,32)} = 17.694$ ,  $p < 0.001$ , Tukey HSD:  $p(\text{BB}) < 0.001$ ,  $p(\text{N/A}) = 0.009$ ].

Protein concentration ( $\mu\text{g}$  protein/mg DOC) was slightly lower in EPS of diuron-treated communities after 1 week [treatment effect:  $F_{(1,32)} = 6.7107$ ,  $p = 0.014$ ], and continuously decreased in both, diuron and control communities [time effect:  $F_{(3,32)} = 22.0321$ ,  $p < 0.001$ ]. It was below detection limit in EPS extracted from diuron-treated communities at  $d_{14}$  (Figure 4B), but recovered in 3 out of 5 treated communities.

## DISCUSSION

The objective of this study was to evaluate the effects of long-term (3-week) exposure of stream biofilms to diuron and compare the sensitivity and information content among endpoints traditionally used in biofilm characterization (biomass, photosynthetic efficiency, chlorophyll-a content, taxonomic composition) and some recently developed endpoints (FC-CS and EPS content). Specifically, we measured the biofilm dynamics under control and diuron exposure conditions and asked whether it is possible to detect time and exposure-related effects by using the different endpoints.

### Endpoint Sensitivity

All measured endpoints were strongly affected by the dynamics of the biofilm communities, independent of the treatment. In particular, we observed temporal variation in abundance of most genera, in biomass, in cell size (as given by FC forward scatter) and the presence of decaying cells (as measured by FC), in photosynthetic efficiency (PAM) and in the EPS composition. This expected dynamics can be explained by the continuous changes of the complex community composition of stream biofilms and has been observed in previous studies with a similar experimental setup (Ricart et al., 2009; Tlili et al., 2011; Kim Tiam et al., 2015). A time-related effect was statistically detected by all endpoints used, except for genus-level taxonomic composition of the biofilms. More than indicating a lack of sensitivity of the method, the lack of detection of a time effect in this case probably lies in the relatively low number of cells taxonomically identified.

A diuron effect was only detected by the FC community structure analysis and by the analysis of EPS, while the other endpoints were only indicative of an exposure effect. For example, during the experiment the dry weight, chlorophyll-a content, photosynthetic efficiency and the abundances of several identified genera decreased more in the diuron exposed biofilms, but the difference was not statistically significant. Since the diuron concentration used in the experiments was relatively high, a

lack of detection of the diuron effects on some endpoints was rather surprising, considering previous research in biofilms and in single species (Dorigo et al., 2007; Pesce et al., 2010b; Moisset et al., 2014). However, temperature and other co-varying environmental factors have been shown to mask the effects of chemicals exposure in biofilms (Pesce et al., 2010b; Romero et al., 2018), and in our case the masking effect was apparently large enough to prevent detection of a diuron effect by several endpoints. As our biofilms were colonized using local stream water, another potential explanation is that the communities were tolerant to diuron because of its presence in the water. While we have not measured diuron in the stream water, we find this explanation unlikely as the experiments were performed in winter when the use of herbicides is very low.

There have been several studies before that used complementary endpoints to characterize effects of stressors on biofilms, and depending on the stressor and endpoint used, the sensitivity of different endpoints was reported differently. In other diuron studies, Kim Tiam et al. (2015) found that photosynthetic efficiency was a more sensitive indicator of stress than chlorophyll-a content for stream biofilms (1–33  $\mu\text{g/L}$ ; 13 day exposure), Moisset et al. (2014) found photosynthetic efficiency more sensitive than cell density for three species of diatoms (10  $\mu\text{g/L}$ ; 10 day exposure) Ricart et al. (2009) found biovolume to be more sensitive than photosynthetic efficiency and chlorophyll-a content (5  $\mu\text{g/L}$ ; 30 day exposure). This suggests that even in relatively comparable experimental setups, with the same chemical stressor, it is difficult to predict which endpoint is the most sensitive. While our results do not match each of the previous studies, they do confirm that traditional endpoints are not always sensitive enough to detect changes in stream biofilms after stress.

### Endpoint Complementarity

Since the endpoints used in the study measure different features of the biofilm, it was expected that they will point at different aspects of biofilm dynamics. FC and EPS both allowed the detection of diuron-exposure related effects. While using single-cell optical and fluorescent properties directly already enabled this detection, the data were difficult to interpret. The interpretation was made easier after subcategorization of the cells in different taxonomic and phenotypic groups, i.e., diuron exposure significantly increased the number of decaying and dying cells in the samples (compared to controls) and also significantly increased the abundance of red algae with large cells, while green algae and diatoms were only somewhat reduced in abundance. The relatively small reduction in green-algae and diatoms are further corroborated by the (not statistically significant) decrease in chlorophyll-a content and biomass in diuron exposed biofilms, while the increase in red algae were qualitatively confirmed using light microscopy (the growth form of *Bangia* prevented quantification). At this time, it is worth mentioning that generally the dynamics of different taxonomic groups during the experiment were the same regardless if measured by FC or microscopy. The communities studied here were apparently able to compensate diuron-induced effects on photosynthetic efficiency, which indicates that there is functional

redundancy, explainable by the compensatory effects of the species fluctuation in the community (Micheli et al., 1999; Valdivia et al., 2012).

Analysis of the EPS composition revealed a decrease in the ratio of protein concentration to extracted DOC in diuron-treated communities, a measure of the C:N ratio in the extracted DOC. The chemical composition of EPS depends among others on species composition, including both, phototrophic and heterotrophic organisms. The described outcome is in line with the changes in species abundance discussed above. Similarly, application of 20  $\mu\text{g/L}$  of ionic silver triggered an increase of the C/N or DOC to protein ratio in EPS in stream biofilms (Kroll et al., 2016).

We suggest that the increase in C/N or DOC to protein ratio observed in the present study could be due to (glycol) proteins in EPS being produced in larger amounts by the algal community which is affected by diuron, while application of ionic silver, which is commonly used as bactericide, mostly affected the heterotrophic part of the community. The reduced heterotrophic community would therefore produce less polysaccharides resulting in a higher C/N ratio. Interestingly, the diuron treatment substantially decreased the variability of the EPS composition in diuron-treated communities. The variability in concentration of EPS components in the diuron-treated samples was substantially lower than in the control samples, indicating that there may be a response to diuron on the biofilm level which leads to a very tightly regulated EPS composition. Finally, although not statistically significant, the taxonomic analysis suggests that the diatom genera *Gomphonema*, *Diatoma*, and *Cocconeis* have tolerated the diuron exposure better than other genera, with *Gomphonema* and *Diatoma* even increasing in abundance. Our previous work has shown that all these genera overlap in fluorescence properties with other diatom genera; therefore it would not be possible to detect their advantage in diuron exposure with FC.

## Limitations of the New Methods

Although this, and our previous studies have demonstrated the potential of the new methods, more studies are needed to see whether they work equally well in a variety of environmental conditions. We have so far shown that FC-CS can be a good indicator of changes in biofilms under temperature (Sgier et al., 2016) and chemical stress, and that it can be evaluated in a relatively short amount of time once set up (Sgier et al., 2018). However, missing are studies that would measure FC-CS across a gradient of chemical concentration of different chemicals to see what the limits of sensitivity are. Also, the reference algal FC library that we have used for interpretation of the results is only available for conditions similar as in our laboratory set up. It needs to be investigated to which extent our library would be equally useful for interpretation of biofilm samples taken from other freshwater systems or whether a system-specific libraries would have to be established.

The extracellular polymeric matrix of the biofilms, consists of a complex mixture of EPS produced by the cells present in the biofilm (Battin et al., 2016). The composition of the EPS,

which is usually dominated by proteins and polysaccharides, depends on the type of microorganisms present, but also on the age of the biofilm and the environmental conditions the biofilm is exposed to (Pan et al., 2016). The ratio of sugars and proteins in the biofilm is suggested to be a good indicator of environmental change, however, measuring both requires use of different methods and the measurements are not yet standardized. The interpretation of the results beyond simple detection of change is also challenging, as the intracellular EPS-synthesis are not yet completely understood. Simultaneous measurement of EPS and global metaOmics (e.g., metagenomics, metatranscriptomics) has the potential to connect the measured EPS changes with their molecular causes and thus enable a more mechanistic interpretation of the results.

## CONCLUSION

The specific results obtained from different endpoints in this study confirms that a combination of endpoints and monitoring over a certain period of time are necessary to understand long-term effects of a stressor on stream biofilms (Micheli et al., 1999). One important reason is that the functional traditional endpoints are directly connected to the ecological function of the biofilm in the stream and therefore have direct functional relevance, which is not (yet) true for the new endpoints. We have shown that multiple measurements, such as in the case of red algae abundance and phenotype as measured by light microscopy and FC, can increase the confidence of the results and improve their interpretation. However, this study has also shown that the new tested endpoints, FC-CS and EPS composition, can, at least under certain conditions, be more sensitive than the traditionally used ones and therefore should be further tested in scientific and regulatory biofilm characterization and monitoring.

## AUTHOR CONTRIBUTIONS

LS planned and conducted the study and wrote the manuscript. RB advised the study and contributed to the manuscript. RS performed the LC-MS measurements and contributed to the manuscript. AZ contributed to data analyses and wrote the manuscript. AK conceived, planned, and conducted the study and wrote the manuscript.

## FUNDING

The study was supported by a SNF Ambizione Fellowship (PZ00P2\_142533) to AK.

## SUPPLEMENTARY MATERIAL

The Supplementary Material for this article can be found online at: <https://www.frontiersin.org/articles/10.3389/fmicb.2018.02974/full#supplementary-material>

## REFERENCES

- Amir el, A. D., Davis, K. L., Tadmor, M. D., Simonds, E. F., Levine, J. H., Bendall, S. C., et al. (2013). viSNE enables visualization of high dimensional single-cell data and reveals phenotypic heterogeneity of leukemia. *Nat. Biotechnol.* 31, 545–552. doi: 10.1038/nbt.2594
- Azim, M. E. (2005). *Periphyton Ecology, Exploitation and Management*. Wallingford: CABI Publishing. doi: 10.1079/9780851990965.0000
- Balsiger, C., Niederhaus, P., Jäggi, O., and Meier, W. (2004). *Pestizide in Fließgewässern des Kantons Zürich. Auswertung der Untersuchungen von 1999 bis 2003*. Zürich: AWEL, Amt für Abfall, Wasser, Energie und Luft.
- Battin, T. J., Besemer, K., Bengtsson, M. M., Romani, A. M., and Packmann, A. I. (2016). The ecology and biogeochemistry of stream biofilms. *Nat. Rev. Microbiol.* 14, 251–263. doi: 10.1038/nrmicro.2016.15
- Blanchoud, H., Moreau-Guigon, E., Farrugia, F., Chevreuil, M., and Mouchel, J. M. (2007). Contribution by urban and agricultural pesticide uses to water contamination at the scale of the Marne watershed. *Sci. Total Environ.* 375, 168–179. doi: 10.1016/j.scitotenv.2006.12.009
- Corcoll, N., Bonet, B., Leira, M., and Guasch, H. (2011). Chl-a fluorescence parameters as biomarkers of metal toxicity in fluvial biofilms: an experimental study. *Hydrobiologia* 673, 119–136. doi: 10.1007/s10750-011-0763-8
- Dixon, P. (2003). Vegan, a package of R functions for community ecology. *J. Veg. Sci.* 14, 927–930. doi: 10.1111/j.1654-1103.2003.tb02228.x
- Dorigo, U., Leboulanger, C., Berard, A., Bouchez, A., Humbert, J. F., and Montuelle, B. (2007). Lotic biofilm community structure and pesticide tolerance along a contamination gradient in a vineyard area. *Aquat. Microb. Ecol.* 50, 91–102. doi: 10.3354/ame01133
- European Service Innovation Scoreboard (2000). *Diuron (330-54-1)*. IUCLID Dataset. Brussels: European Commission.
- Finizio, A., Villa, S., and Vighi, M. (2005). Predicting pesticide mixtures load in surface waters from a given crop. *Agric. Ecosyst. Environ.* 111, 111–118. doi: 10.1016/j.agee.2005.05.009
- Flemming, H. C., and Wingender, J. (2010). The biofilm matrix. *Nat. Rev. Microbiol.* 8, 623–633. doi: 10.1038/nrmicro2415
- Hürlimann, J., and Niederhauser, P. (2007). *Methoden zur Untersuchung und Beurteilung der Fließgewässer. Kieselalgen Stufe F (flächendeckend)*. Bern: Bundesamt für Umwelt.
- Hustedt, F. (1930). *Bacillariophyta (Diatomeae)*. Jena: Fischer.
- Kim Tiam, S., Laviale, M., Feurtet-Mazel, A., Jan, G., Gonzalez, P., Mazzella, N., et al. (2015). Herbicide toxicity on river biofilms assessed by pulse amplitude modulated (PAM) fluorometry. *Aquat. Toxicol.* 165, 160–171. doi: 10.1016/j.aquatox.2015.05.001
- Knauer, K., Sobek, A., and Bucheli, T. D. (2007). Reduced toxicity of diuron to the freshwater green alga *Pseudokirchneriella subcapitata* in the presence of black carbon. *Aquat. Toxicol.* 83, 143–148. doi: 10.1016/j.aquatox.2007.03.021
- Kroll, A., Behra, R., Kaegi, R., and Sigg, L. (2014). Extracellular Polymeric Substances (EPS) of freshwater biofilms stabilize and modify CeO<sub>2</sub> and Ag nanoparticles. *PLoS One* 9:e110709. doi: 10.1371/journal.pone.0110709
- Kroll, A., Matzke, M., Rybicki, M., Obert-Rausser, P., Burkart, C., Jurkschat, K., et al. (2016). Mixed messages from benthic microbial communities exposed to nanoparticulate and ionic silver: 3D structure picks up nano-specific effects, while EPS and traditional endpoints indicate a concentration-dependent impact of silver ions. *Environ. Sci. Pollut. Res. Int.* 23, 4218–4234. doi: 10.1007/s11356-015-4887-7
- Lamberti, G. A. (1996). “The role of periphyton in benthic food webs,” in *Algal ecology: Freshwater Benthic Ecosystems*, eds R. J. Stevenson, M. L. Bothwell, and R. L. Lowe (San Diego: Academic Press).
- Legrand, H., Herlory, O., Guarini, J. M., Blanchard, G. F., and Richard, P. (2006). Inhibition of microphytobenthic photosynthesis by the herbicides atrazine and diuron. *Cah. Biol. Mar.* 47, 39–45.
- Micheli, F., Cottingham, K. L., Bascompte, J., Bjornstad, O. N., Eckert, G. L., Fischer, J. M., et al. (1999). The dual nature of community variability. *Oikos* 85, 161–169. doi: 10.2307/3546802
- Moisset, S., Tiam, S. K., Feurtet-Mazel, A., Morin, S., Delmas, F., Mazzella, N., et al. (2014). Genetic and physiological responses of three freshwater diatoms to realistic diuron exposures. *Environ. Sci. Pollut. Res. Int.* 22, 4046–4055. doi: 10.1007/s11356-014-3523-2
- Moschet, C., Wittmer, I., Simovic, J., Junghans, M., Piazzoli, A., Singer, H., et al. (2014). How a complete pesticide screening changes the assessment of surface water quality. *Environ. Sci. Technol.* 48, 5423–5432. doi: 10.1021/es500371t
- Navarro, E., Robinson, C. T., Wagner, B., and Behra, R. (2007). Influence of ultraviolet radiation on UVR-absorbing compounds in freshwater algal biofilms and *Scenedesmus vacuolatus* cultures. *J. Toxicol. Environ. Health* 70, 760–767. doi: 10.1080/15287390701236454
- Nikora, V. I., Goring, D. G., and Biggs, B. J. F. (1997). On stream periphyton-turbulence interactions. *New Zeal. J. Mar. Fresh.* 31, 435–448. doi: 10.1080/00288330.1997.9516777
- Pan, M., Zhu, L., Chen, L., Qiu, Y. P., and Wang, J. (2016). Detection techniques for extracellular polymeric substances in biofilms: a review. *Bioresources* 11, 8092–8115. doi: 10.15376/biores.11.3.8092-8115
- Pascher, A., Büdel, B., and Ettl, H. (1987/1997). *Süßwasserflora von Mitteleuropa*. Jena: Fischer.
- Pesce, S., Lissalde, S., Lavieille, D., Margoum, C., Mazzella, N., Roubeix, V., et al. (2010a). Evaluation of single and joint toxic effects of diuron and its main metabolites on natural phototrophic biofilms using a pollution-induced community tolerance (PICT) approach. *Aquat. Toxicol.* 99, 492–499. doi: 10.1016/j.aquatox.2010.06.006
- Pesce, S., Margoum, C., and Montuelle, B. (2010b). In situ relationships between spatio-temporal variations in diuron concentrations and phototrophic biofilm tolerance in a contaminated river. *Water Res.* 44, 1941–1949. doi: 10.1016/j.watres.2009.11.053
- Rabiet, M., Margoum, C., Gouy, V., Carluer, N., and Coquery, M. (2010). Assessing pesticide concentrations and fluxes in the stream of a small vineyard catchment—effect of sampling frequency. *Environ. Pollut.* 158, 737–748. doi: 10.1016/j.envpol.2009.10.014
- Ricart, M., Barcelo, D., Geislinger, A., Guasch, H., de Alda, M. L., Romani, A. M., et al. (2009). Effects of low concentrations of the phenylurea herbicide diuron on biofilm algae and bacteria. *Chemosphere* 76, 1392–1401. doi: 10.1016/j.chemosphere.2009.06.017
- Romero, F., Sabater, S., Timoner, X., and Acuna, V. (2018). Multistressor effects on river biofilms under global change conditions. *Sci. Total Environ.* 627, 1–10. doi: 10.1016/j.scitotenv.2018.01.161
- Roubeix, V., Mazzella, N., Schouler, L., Fauvelle, V., Morin, S., Coste, M., et al. (2011). Variations of periphytic diatom sensitivity to the herbicide diuron and relation to species distribution in a contamination gradient: implications for biomonitoring. *J. Environ. Monitor.* 13, 1768–1774. doi: 10.1039/c0em00783h
- Sambalova, O., Thorwarth, K., Heeb, N. V., Bleiner, D., Zhang, Y. C., Borgschulte, A., et al. (2018). Carboxylate functional groups mediate interaction with silver nanoparticles in biofilm matrix. *ACS Omega* 3, 724–733. doi: 10.1021/acsomega.7b00982
- Schreiber, U. (1998). “Chlorophyll fluorescence: new instruments for special applications,” in *Photosynthesis: Mechanisms and Effects*, ed. G. Garab (Berlin: Springer Science & Business Media), 4253–4258.
- Sgier, L., Freimann, R., Zupanic, A., and Kroll, A. (2016). Flow cytometry combined with viSNE for the analysis of microbial biofilms and detection of microplastics. *Nat. Commun.* 7:11587. doi: 10.1038/ncomms11587
- Sgier, L., Merbt, S. N., Tlili, A., Kroll, A., and Zupanic, A. (2018). Characterization of aquatic biofilms with flow cytometry. *J. Vis. Exp.* 136:e57655. doi: 10.3791/57655
- Staley, Z. R., Harwood, V. J., and Rohr, J. R. (2015). A synthesis of the effects of pesticides on microbial persistence in aquatic ecosystems. *Crit. Rev. Toxicol.* 45, 813–836. doi: 10.3109/10408444.2015.1065471
- Stewart, T. J., Traber, J., Kroll, A., Behra, R., and Sigg, L. (2013). Characterization of extracellular polymeric substances (EPS) from periphyton using liquid chromatography-organic carbon detection-organic nitrogen detection (LC-OCD-OND). *Environ. Sci. Pollut. Res. Int.* 20, 3214–3223. doi: 10.1007/s11356-012-1228-y
- Tlili, A., Montuelle, B., Berard, A., and Bouchez, A. (2011). Impact of chronic and acute pesticide exposures on periphyton communities. *Sci. Total Environ.* 409, 2102–2113. doi: 10.1016/j.scitotenv.2011.01.056
- Valdivia, N., Gollety, C., Migne, A., Davoult, D., and Molis, M. (2012). Stressed but stable: canopy loss decreased species synchrony and metabolic variability in an intertidal hard-bottom

- community. *PLoS One* 7:e36541. doi: 10.1371/journal.pone.0036541
- van der Maaten, L., and Hinton, G. (2008). Visualizing data using t-SNE. *J. Mach. Learn. Res.* 9, 2579–2605.
- Vanrensse, J. J. S. (1989). Herbicides interacting with photosystem-II. *Soc. Exp. Biol. Sem. Ser.* 38, 21–36.
- Wahl, M., Goecke, F., Labes, A., Dobretsov, S., and Weinberger, F. (2012). The second skin: ecological role of epibiotic biofilms on marine organisms. *Front. Microbiol.* 3:292. doi: 10.3389/fmicb.2012.00292
- Wauchope, R. D. (1978). Pesticide content of surface-water draining from agricultural fields – review. *J. Environ. Qual.* 7, 459–472. doi: 10.2134/jeq1978.00472425000700040001x
- Wittmer, I. K., Scheidegger, R., Bader, H. P., Singer, H., and Stamm, C. (2011). Loss rates of urban biocides can exceed those of agricultural pesticides. *Sci. Total Environ.* 409, 920–932. doi: 10.1016/j.scitotenv.2010.11.031
- Conflict of Interest Statement:** The authors declare that the research was conducted in the absence of any commercial or financial relationships that could be construed as a potential conflict of interest.
- Copyright © 2018 Sgier, Behra, Schönenberger, Kroll and Zupanic. This is an open-access article distributed under the terms of the Creative Commons Attribution License (CC BY). The use, distribution or reproduction in other forums is permitted, provided the original author(s) and the copyright owner(s) are credited and that the original publication in this journal is cited, in accordance with accepted academic practice. No use, distribution or reproduction is permitted which does not comply with these terms.



# Soil Particles and Phenanthrene Interact in Defining the Metabolic Profile of *Pseudomonas putida* G7: A Vibrational Spectroscopy Approach

Andrea Fanesi, Asfaw Zegeye, Christian Mustin and Aurélie Cébron\*

Laboratoire Interdisciplinaire des Environnements Continentaux, CNRS, Université de Lorraine, Nancy, France

## OPEN ACCESS

### Edited by:

Fabrice Martin-Laurent,  
Institut National de la Recherche  
Agronomique (INRA), France

### Reviewed by:

Jan Roelof Van Der Meer,  
Université de Lausanne, Switzerland  
Edoardo Puglisi,  
Università Cattolica del Sacro Cuore,  
Italy

### \*Correspondence:

Aurélie Cébron  
aurelie.cebron@univ-lorraine.fr

### Specialty section:

This article was submitted to  
Microbiotechnology, Ecotoxicology  
and Bioremediation,  
a section of the journal  
Frontiers in Microbiology

**Received:** 19 July 2018

**Accepted:** 20 November 2018

**Published:** 04 December 2018

### Citation:

Fanesi A, Zegeye A, Mustin C and  
Cébron A (2018) Soil Particles  
and Phenanthrene Interact in Defining  
the Metabolic Profile of *Pseudomonas*  
*putida* G7: A Vibrational Spectroscopy  
Approach. *Front. Microbiol.* 9:2999.  
doi: 10.3389/fmicb.2018.02999

In soil, organic matter and mineral particles (soil particles; SPs) strongly influence the bio-available fraction of organic pollutants, such as polycyclic aromatic hydrocarbons (PAHs), and the metabolic activity of bacteria. However, the effect of SPs as well as comparative approaches to discriminate the metabolic responses to PAHs from those to simple carbon sources are seldom considered in mineralization experiments, limiting our knowledge concerning the dynamics of contaminants in soil. In this study, the metabolic profile of a model PAH-degrading bacterium, *Pseudomonas putida* G7, grown in the absence and presence of different SPs (i.e., sand, clays and humic acids), using either phenanthrene or glucose as the sole carbon and energy source, was characterized using vibrational spectroscopy (i.e., FT-Raman and FT-IR spectroscopy) and multivariate classification analysis (i.e., PLS-DA). The different type of SPs specifically altered the metabolic profile of *P. putida*, especially in combination with phenanthrene. In comparison to the cells grown in the absence of SPs, sand induced no remarkable change in the metabolic profile of the cells, whereas clays and humic acids affected it the most, as revealed by the higher discriminative accuracy ( $R^2$ , RMSEP and sensitivity) of the PLS-DA for those conditions. With respect to the carbon-source (phenanthrene vs. glucose), no effect on the metabolic profile was evident in the absence of SPs or in the presence of sand. On the other hand, with clays and humic acids, more pronounced spectral clusters between cells grown on glucose or on phenanthrene were evident, suggesting that these SPs modify the way cells access and metabolize PAHs. The macromolecular changes regarded mainly protein secondary structures (a shift from  $\alpha$ -helices to  $\beta$ -sheets), amino acid levels, nucleic acid conformation and cell wall carbohydrates. Our results provide new interesting evidences that SPs specifically interact with PAHs in defining bacteria metabolic profiles and further emphasize the importance of studying the interaction of bacteria with their surrounding matrix to deeply understand PAHs degradation in soils.

**Keywords:** bacteria, FTIR spectroscopy, FT-Raman spectroscopy, metabolic profile, multivariate classification analysis, phenanthrene, soil particles

## INTRODUCTION

Polycyclic aromatic hydrocarbons (PAHs) are persistent organic pollutants commonly found in industrially contaminated soils (Haritash and Kaushik, 2009). Differently from natural carbon (C) sources, the high hydrophobicity and low solubility in water of PAHs result in their adsorption to soil particles (SPs; here considered as mineral and organic components constituting the soil matrix), which is believed to limit the amount of C readily available for microbial growth (Weissenfels et al., 1992; Wilcke et al., 1996). Bacteria strategies to tackle low accessibility and availability of PAHs range from the direct contact with crystals or SPs, to the excretion of surfactants and to the expression of high affinity uptake systems (Miyata et al., 2004). This in turn allows the cells to maintain growth and cell viability even when PAHs are the sole C/energy source present.

The efficiency of bacteria in metabolizing PAHs is generally tested via mineralization assays. Although in the literature plenty of studies report such results, only a few have investigated how SPs alter bacteria ability to metabolize PAHs and how this affects the cell physiology (i.e., metabolic activity and metabolic profile). Limited experimental results suggested that rather than limiting cell activity, some SPs can enhance mineralization efficiencies by favoring bacterial contact with the adsorbed PAHs molecules (Ortega-Calvo and Saiz-Jimenez, 1998; Amellal et al., 2001) or by acting as surfactants. From a metabolic point of view, PAHs activate specific cellular pathways aimed at their metabolization and/or at the detoxification of resulting secondary metabolites. For instance, proteomic studies reported an up-regulation of cell components involved in PAHs metabolism (e.g., mono and di-oxygenases), in oxidative stress, cell energetics and C-metabolism (Seo et al., 2009 and references therein). Considering that specific SPs stimulate cells to express at their surface or excrete macromolecules involved in substrate attachment and in biofilm formation (Ojeda et al., 2008; Wu et al., 2014a,b,c), the interaction of PAHs and SPs may result in a complex reorganization of bacteria metabolic profile (i.e., cell macromolecular composition). Indeed, a global modification of bacterial transcriptome in the presence of particles and/or pollutant, was previously observed (Moreno-Forero and Van Der Meer, 2015; Lima-Morales et al., 2016).

The energy required for macromolecule synthesis in a given environmental niche is a fundamental limit for microorganism growth and colonization (VanBriesen, 2001; McCarty, 2007; LaRowe and Amend, 2016). Therefore, understanding how cells adjust their metabolic profile as a function of different SPs is critical to better understand spatial distributions of degraders and PAHs mineralization *in situ*, which could help identifying hotspots (i.e., location of high microbial activity) in soil (Kuz'yakov and Blagodatskaya, 2015). An experimental approach accounting for SPs would therefore allow a more realistic understanding, with respect to the use of simple mineral media, of how bacteria cells metabolically react to the presence of PAHs in nature (Keum et al., 2008). Nevertheless, the complex interaction of bacteria with SPs has seldom been considered in experimental approaches regarding PAHs effect on cell metabolic profiles. In this study we therefore aimed at investigating how

SPs influence the metabolic profile of bacteria during PAHs degradation.

In soil, the different SPs, such as sand, clays and humic acids, are responsible for binding different amounts of PAHs (Ortega-Calvo and Saiz-Jimenez, 1998; Uyttebroek et al., 2006), and to specifically modify the physico-chemical characteristics of the micro-environment in their immediate surroundings (Chenu, 1993; Vandevivere and Kirchman, 1993) leading to a highly heterogeneous environment. For instance, clays and humic acids have been reported to adsorb the highest fraction of PAHs, but to increase bacteria mineralization rates (Ortega-Calvo and Saiz-Jimenez, 1998; Uyttebroek et al., 2006). On the other hand, as presenting the lowest specific surface area cation exchange capacity and strength of binding sites, sand particles retain PAHs molecules the least and support low mineralization rates (Wilcke et al., 1996; Amellal et al., 2001; Müller et al., 2007; Uyttebroek et al., 2006). We hypothesized that for a specific bacteria species growing in the presence of different SPs, there is a specific metabolic profile related to each type of SPs, which reflects the distinctive micro-environmental conditions the cells are subjected to. In laboratory cultures where cells are grown in a liquid medium and SPs are suspended in it, this may hold true irrespective of whether the cells are attached to soil components or conducting a planktonic lifestyle. In order to test our hypothesis, the strain G7 of the common soil dweller *Pseudomonas putida*, with the ability to metabolize PAHs (Cébron et al., 2008), was grown in the presence and absence of different SPs (i.e., quartz sand, clays and humic acids) using phenanthrene or glucose as the sole C and energy source. A comparison between PAHs and a common C/energy source could serve indeed to identify specific molecular markers indicative of PAHs metabolism (Wick et al., 2003; Keum et al., 2008). Phenanthrene was used as a model PAH compound because it is relatively easy to be degraded and is ubiquitous in contaminated soils. Glucose, a simple carbohydrate that is less adsorbed on SPs (Wu et al., 2014c), was used to discriminate the C-source effect from the SPs one. The characterization of cell metabolic profiles in the presence of different SPs was carried out by using a combination of vibrational spectroscopy techniques such as Fourier Transform Raman and Infrared spectroscopy (FT-Raman and FTIR spectroscopy, respectively) and the spectra processed by chemometric analysis, such as multivariate classification analysis. Vibrational spectroscopy was preferred over other -omics techniques such as proteomics and transcriptomics because it requires minimal sample preparation, allow high spatial resolution measurements and it provides quantitative and qualitative (i.e., structural) information concerning the whole cell metabolic profile (Naumann, 2001; Huang et al., 2007; Wagner et al., 2010, 2014; Teng et al., 2016; Fanesi et al., 2017). Proteomics and transcriptomics look indeed at only one cellular pool at time and they may not provide information concerning the final metabolic phenotype of a cell as a consequence of post-translational modifications (Wagner, 2009). The present work is a pilot study allowing to prove the concept that vibrational spectroscopy techniques may bring interesting and contrasting information complementary to other approaches in soil studies. Furthermore, in view of future

applications, vibrational spectroscopy coupled to stable isotope probing (i.e.,  $^{13}\text{C}$ -labeled phenanthrene) would allow the *in situ* identification of specific bacterial functions.

## MATERIALS AND METHODS

### Culture Conditions and Experimental Setup

*Pseudomonas putida* PpG7 (ATCC® 17485<sup>TM</sup>; provided by Dr. G. J. Zylstra) was selected as experimental organism for this study because already screened for phenanthrene metabolism (Cébron et al., 2008) and because able in the presence of phenanthrene to sustain enough biomass production required to perform the measurements. Stock cultures were maintained in the dark at 24°C in Bushnell Haas (BH, Sigma-Aldrich; Bushnell and Haas, 1941) agar plates containing glucose (4 g·L<sup>-1</sup>). Before streaking the cells, the agar plates were sprayed with 500 µL of a solution of phenanthrene (Sigma-Aldrich) in acetone (10 mg·mL<sup>-1</sup>) and the solvent was let evaporate in a laminar flow hood (Thomas et al., 2016).

Experiments were performed on liquid batch cultures growing in 250 mL Erlenmeyer flasks filled with 100 mL of BH mineral medium using either phenanthrene or glucose at a final dosage of 1 mg·mL<sup>-1</sup>.

Coarse quartz sand (3–5 mm diameter), Na-montmorillonite (Wyoming) SWY-2 (Source Clay Minerals repository, Chantilly, VA, United States), Na-nontronite NAu-1 (Source Clay Minerals repository, Purdue, IN, United States) and humic acids (53680, Sigma-Aldrich) were selected as representative soil particles for the experiments. The soil particles were used at a concentration of 300, 10, and 0.1 g·L<sup>-1</sup> for sand, clays (montmorillonite and nontronite) and humic acids, respectively. Sand and clays were deposited at the bottom of the flasks in dried forms, whereas humic acids were supplied dissolved in 0.1M NaOH. The flasks were then autoclaved, and the phenanthrene-acetone solution was spread over the whole surface occupied by the particles. In the presence of humic acids, phenanthrene was first deposited at the bottom of the flask, let the acetone evaporate and then the humic acid solution was added. After the complete evaporation of the solvent (previously tested), BH mineral medium was added and the flasks were allowed to equilibrate for at least 4 h [a time pre-established to lead to a complete adsorption of PAHs to mineral particles; (Müller et al., 2007)] on a rotatory shaker (90 rpm) in the dark at 24°C. At this point, an inoculum from an overnight grown agar culture was prepared to obtain a final colony forming unit (CFU) number of 1–2·10<sup>3</sup> CFU·mL<sup>-1</sup> (determined by plate counting on BH medium supplemented with glucose).

### Growth Rates ( $\mu$ ) and C-dynamics

Growth curves were determined over a period of ~100 h, on cultures grown under the same conditions described above. Cells of *P. putida* were plate counted after vigorously vortexing the samples for 5–10 min to allow cells that eventually adhered to the SPs to detach. Growth rates ( $\mu$ ) were estimated as the slope of a linear least square regression of the natural logarithm of

CFU increase against time. Control cultures inoculated without C-source or without cells were also run to exclude possible contamination and artifacts. Each day, samples (1–2 mL of culture) were harvested at different time of the day to perform Raman and FTIR measurements (see below).

On a different set of cultures grown under the same experimental conditions described above, the mineralization efficiency of the cells (measured as CO<sub>2</sub> production over a time period of ~100 h) was determined in sealed bottles (150 mL) filled with 10 mL of cell culture. The measurements were performed as described elsewhere (Cébron et al., 2013). Briefly, 3 mL of the bottle atmosphere was sampled with a plastic syringe through a rubber stopper and CO<sub>2</sub> quantified by an infrared gas analyzer (Binos 1004; Rosemount). After the measurements, the bottles were opened and brought to equilibrium with the external atmosphere in a laminar flow hood. Mineralization curves (CO<sub>2</sub> emission vs. time) were fitted using the “grofit” package (Kahm et al., 2010) present in the R software (R Development Core Team, 2010) to determine quantitative parameters of CO<sub>2</sub> production such as the maximum mineralization (max value at plateau) and mineralization rate (the initial slope of the CO<sub>2</sub> evolution vs. time curve).

To better understand the dynamics of the C-source in the presence of the different SPs, the soluble fractions of phenanthrene and glucose (i.e., concentration in solution) were quantified at the beginning (before cell inoculation) and at the end of the experiments (after ~100 h). Due to the low amount of phenanthrene in solution the whole volume of growth medium in a flask must be utilized for its quantification. Therefore, another set of experiments was run to determine the soluble fraction of phenanthrene and glucose. For phenanthrene quantification, three cultures for each time point were prepared and inoculated. For each time point, the whole cultures were centrifuged at 16,000 × g for 5 min to completely remove SPs and cells in suspension. Soluble phenanthrene was then extracted twice in dichloromethane (DCM), in 8 and 5 ml respectively. The DCM containing phenanthrene was then evaporated in dark glass tubes under a N<sub>2</sub> flux and substituted with acetonitrile for phenanthrene quantification using HPLC (see Thomas et al., 2016). For glucose quantification, 1 mL of culture was centrifuged (as above) and filtered (0.22 µm pore size). Glucose was finally quantified using the GOD-PAP kit (Bioloabo, Maizy, France) and a Safas MP96 spectrophotometer (Safas, Monaco).

### FT-Raman Micro-Spectroscopy and Diffuse Reflectance FTIR-Spectroscopy: Sample Preparation and Spectra Acquisition

The metabolic profile of *P. putida* was characterized by a combination of vibrational spectroscopy techniques. Samples were harvested each day (multiple times during the day, typically every 2 h; for a total of 4–5 samples per day) over the whole growth period (see above) to exclude compositional differences related to the growth phase. Cells (1–2 ml of culture) were harvested by centrifugation at 10,000 × g for 4 min and washed twice in sterile MilliQ water to remove residual salts and cell

debris. The cell pellet was then resuspended in 5–10  $\mu\text{L}$  of MilliQ water and 0.5  $\mu\text{L}$  of cell suspension was deposited on a gold coated microscopy slide and let dry at room temperature. Afterward, the cell deposit was resuspended in 0.7  $\mu\text{L}$  of 0.9% (w/v) NaCl and dried again. In the presence of SPs, cells were separated from the particles by vigorously vortexing the samples for 5–10 min and by further sonicating them in an ultrasonic bath for few seconds. In the presence of clay, cells were further separated from the mineral particles (which were found to produce a strong fluorescence background in the Raman spectra) by density gradient using Nycodenz solution (1.3  $\text{g}\cdot\text{mL}^{-1}$ ; ProteoGenix, Axis-Shield). Macro-aggregates were removed by a short spin centrifugation step. The remaining suspension (1 mL) was vortexed and sonicated as described above and Nycodenz (0.8 mL) was carefully added at the bottom of the eppendorf. The samples were centrifuged at  $3,000 \times g$  for 20 min and the cell layer interposed between the aqueous phase and the Nycodenz removed and washed in MilliQ water at least 5 times to eliminate any trace of Nycodenz that could have interfered with cell signals.

In this study the use of a Fourier Transform (FT-) Raman spectrometer operating in the near infrared was preferred to a dispersive Raman device using visible lasers to avoid signal distortions due to native fluorescence of PAHs and of soil components (i.e., the SPs). Raman scattering was acquired using a FT-Raman MultiRam spectrophotometer (Bruker, Ettlingen, Germany), equipped with an excitation line at 1064 nm (Nd:YAG laser) and a liquid nitrogen cooled high sensitivity Ge detector. The spectrometer was coupled to an epifluorescence right microscope (BX51 Olympus) equipped with a 50X magnification IR objective (LCPLN50XIR; WD 4-5mm, NA 0.65, Olympus, Japan), specific for optimal transmission in the near infrared field between 700 and 1300 nm (Transmittance up to 75% in the range 0–2000  $\text{cm}^{-1}$ ). Spectra were acquired in reflection mode in the spectral range 4000–0  $\text{cm}^{-1}$  with a resolution of 6  $\text{cm}^{-1}$  by recording 1000–2000 scans at 2.2 kHz of slew rate in order to get good signal to noise ratios. Spectra were processed using Blackman-Harris apodization function and 2 levels of zerofilling. The laser power used for the measurements was 500–600 mW corresponding to approximately 200 mW at the sample. Samples were scanned at least at 2 different positions, thanks to an x, y, z motorized stage, to account for sample heterogeneity. Spectra acquisition was controlled with the OPUS 7.5 software (Bruker, Ettlingen, Germany). The resolution of the instrument ( $\sim 10$ –20  $\mu\text{m}$ ) does not allow single cell analysis, therefore the spectra reported in this study refer to bulk analysis including both cells that were adhered to the SPs and the planktonic ones.

The same set of samples prepared for the FT-Raman measurements were also scanned by means of FTIR-spectroscopy to obtain complementary information about the metabolic profiles of *P. putida* populations. Diffuse reflectance spectra (DRIFTS) acquisition was carried out with a Bruker Vector 22 (Bruker, Ettlingen, Germany) equipped with a diffuse reflection collection system (Praying Mantis; Harrik, Pleasantville, NY, United States). Spectra were recorded with 64 scans co-added and averaged in the spectral range 4000–400  $\text{cm}^{-1}$  with a resolution of 4  $\text{cm}^{-1}$ . Background spectra were recorded at the edges

of the cell deposit with the same instrumental settings. The spectrometer was controlled with the OPUS software version 4.5 (Bruker, Ettlingen, Germany).

Band assignment for the Raman and IR spectra was based on literature references (Naumann, 2001; Movasaghi et al., 2007, 2008; Huang et al., 2010) and on reference spectra of pure macromolecules.

## Spectra Pre-processing and Multivariate Modeling

All spectra were exported from the OPUS software for further pre-processing and multivariate modeling steps computed in the R environment (version 3.4.3; R Development Core Team, 2010). A first visual screening, aimed at eliminating the spectra with a low signal to noise ratio, resulted in a total of 346 for the FT-Raman dataset and 465 for the FTIR one. Base line corrections of Raman spectra were performed with the package “baseline” (Liland et al., 2015) using a 2nd derivative constrained weighted regression, cut in the spectral ranges 3019–2819 and 1780–400  $\text{cm}^{-1}$  and normalized (in order to compare peak intensities and remove problems related to different sample thickness) using the standard normal variate function (SNV, Barnes et al., 1989). FTIR-spectra were converted to 2nd derivatives by the Savitzky-Golay algorithm (Savitzky and Golay, 1964) using a quadratic polynomial function with nine smoothing points. Prior to calculations, spectra were cut in the spectral ranges 3019–2819 and 1780–1200  $\text{cm}^{-1}$  because of the strong clay bands overlapping to the cellular components in the lower frequency range of the IR spectrum. However, other two bands corresponding to the spectral ranges, 1091–1076 and 973–958  $\text{cm}^{-1}$  were further selected because not overlapping with clay signals. Finally, the spectra were normalized using the SNV function.

The Partial Least Square (Wold et al., 2001) Discriminant Analysis (PLS-DA; Barker and Rayens, 2003) was used to unravel consistent patterns in the spectral datasets and to extract information regarding the macromolecules involved in the classification. The PLS-DA is a chemometric analysis particularly useful when it comes to handle metabolic datasets with highly collinear variables (Fonville et al., 2010). The PLS-DA was implemented in the R software using the ‘pls’ package developed by Mevik et al. (2016). To test our hypothesis, two models for each spectral dataset were developed. The first discriminated each experimental treatment (control and the 4 SPs and the 2 respective C/energy source; 10 classes) and the second discriminated the C/energy sources (i.e., glucose and phenanthrene; 2 classes). The models were calibrated by matching each set of predictors (X-variables; i.e., FT-Raman and FTIR spectra) with the corresponding discriminating classes (Y-variables). The matrices (i.e., Y variables) were created assigning integer values of 0 and +1 (dummy variables) to the experimental treatments (SPs + C/energy source) and C/energy source (glucose and phenanthrene). In turn, to each class is assigned the values +1 and to all the others 0. In this way, a calibration can be built around each classification

matrix. To quantify the accuracy of the classification models, the sensitivity (the ability of identifying true positives) and the specificity (the ability of identifying true negatives) were estimated as described in Sackett et al. (2013), using the “caret” package (Kuhn, 2017) present in the R software. Spectra with predicted  $Y$ -values  $\leq 0.5$  were classified as 0, whereas predicted  $Y$ -values  $\geq 0.5$  were classified as 1. The algorithm used for the PLS-DA was the canonical powered partial least square (Indahl et al., 2009). The prediction abilities of the models were inferred from the root mean squared error of calibration and prediction (RMSEC and RMSEP, respectively), the latter calculated from the leave-one-out cross-validation (LOOCV), and the coefficient of determination ( $R^2$ ). The  $R^2$  and the RMSEP obtained from the cross validation were used to determine the number of principal components to use for each model (Wold et al., 2001). Class similarities and dissimilarities were individualized by plotting the model's scores. Important changes in macromolecules and functional groups in response to SPs and C/energy source were identified by extracting and analyzing the loadings of each model. The loadings indicate the variables, i.e., the spectral features (corresponding to specific compounds or functional groups), mainly driving the discriminant model.

## Statistical Analysis

All data are reported as mean and standard deviations of three independent biological replicates. Statistically significant differences between mean values of the measured variables were assessed by a two-way analysis of variance (ANOVA), considering the SPs and the C-source as factors, followed by the Bonferroni *post hoc* test. The level of significance was always set to  $\alpha = 0.05$ .

## RESULTS

### Growth Rate ( $\mu$ )

Growth rate of *P. putida* was affected both by the C-source and by SPs. In general, cells presented lower  $\mu$  when growing on phenanthrene in comparison to glucose (Table 1). With glucose, all SPs but montmorillonite sustained higher  $\mu$  respect to the cultures grown in the absence of SPs. The same trend was observed when the cells were consuming phenanthrene, however, in the presence of montmorillonite the cells exhibited comparable  $\mu$  with respect to the cells grown in the absence of SPs.

### C-source Soluble Fraction and Mineralization

In all conditions, the soluble phenanthrene fraction was approximately 0.1–0.2% compared to that of glucose (Figures 1A,C). Montmorillonite, nontronite and humic acids increased the amount of phenanthrene in solution (likely as colloids), with respect to the cultures grown in the absence of SPs, or in the presence of sand (Figure 1A). Interestingly, the soluble fraction of phenanthrene was comparable in the absence of SPs and in the presence of sand, whereas with montmorillonite it was the highest (5 times higher than in the

absence of SPs), followed by nontronite and humic acids that supported a similar concentration of phenanthrene in solution (3 times higher than in the absence of SPs) (Figure 1A). On the other hand, glucose was dissolved completely at all conditions but in the presence of nontronite the soluble fraction was 18% lower (Figure 1C).

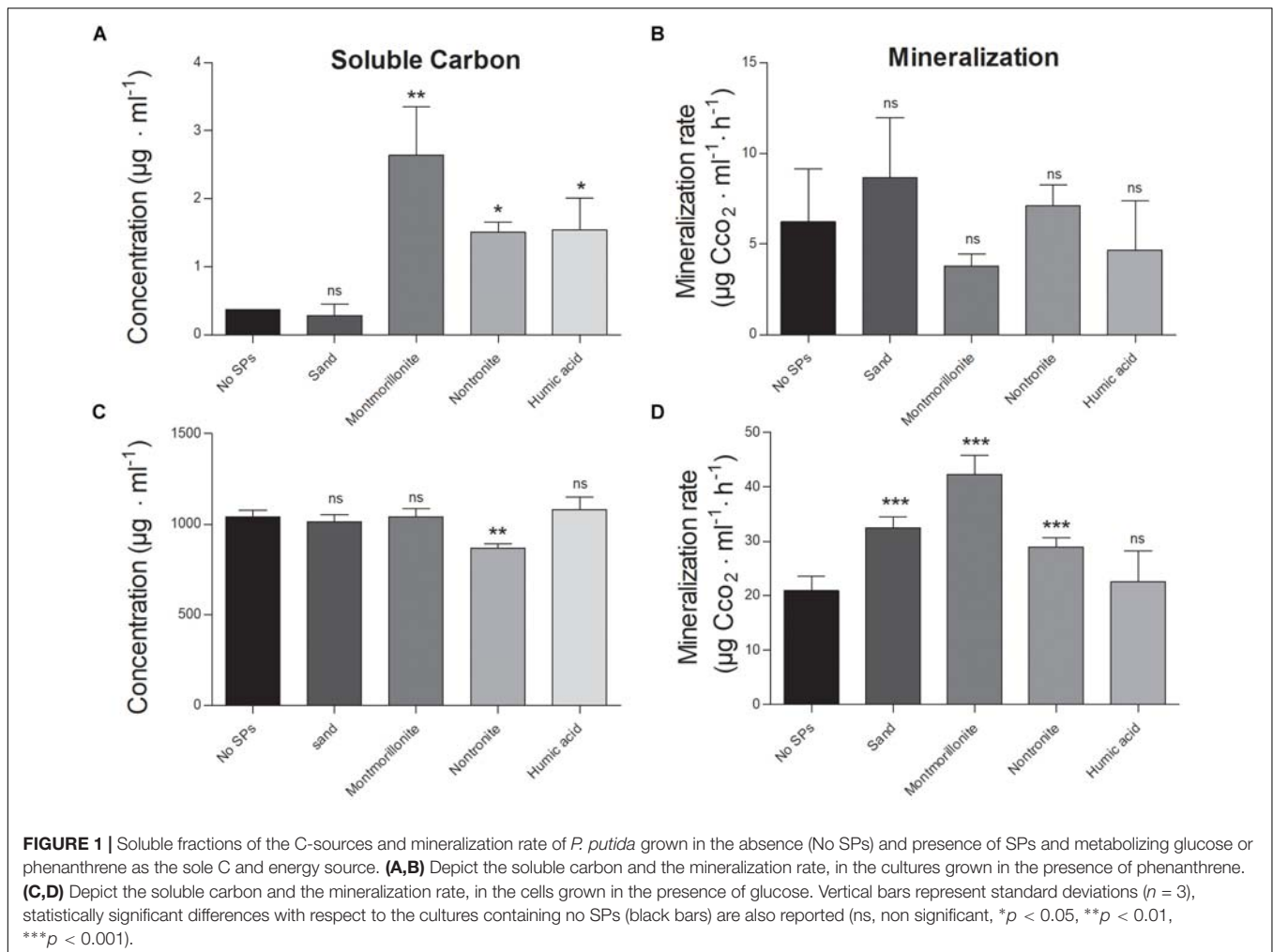
At the end of the experiment, only 1–10% of the initial glucose was left available for the cells in all the conditions and no effect of the SPs on the total consumption of glucose could be detected (which ranged between 90 and 99% of the initial amount) (Table 1). While montmorillonite increased the concentration of soluble phenanthrene at the beginning of the experiment, the concentration of soluble phenanthrene was the lowest in this condition at the end of the experiment, and no difference between all the other conditions was evident (Table 1).

The mineralization efficiency of *P. putida* was assessed by means of  $\text{CO}_2$  assays (i.e.,  $\text{CO}_2$  evolution over time). The maximal  $\text{CO}_2$  production and the initial slope of the mineralization curves were 3–4 times lower when the cells were grown on phenanthrene, with respect to glucose (Figures 1B,D and Table 1). Regardless of the C-source, SPs induced only minor changes of the maximal mineralization attained by the cells (Table 1). Nontronite and humic acids sustained the lowest maximal mineralization level, whereas at all other conditions the cells presented comparable values (Table 1). When growing on phenanthrene, the cells did not show any change of the mineralization rate induced by the presence of the SPs (Figure 1B). On the other hand, the mineralization rate was strongly affected by SPs when glucose was the C-source (Figure 1D). Montmorillonite particles sustained the fastest mineralization, whereas the mineralization rate decreased with nontronite and sand particles (Figure 1D). In the absence of SPs

**TABLE 1** | Growth rate ( $\mu$ ), maximal mineralization and final C-source concentrations in the cultures of *P. putida* grown in the absence and in the presence of SPs (sand, clays, and humic acids) and using glucose or phenanthrene as the sole source of C and energy.

	$\mu$ ( $\text{h}^{-1}$ )	Maximal mineralization ( $\mu\text{g C-CO}_2\text{ ml}^{-1}$ )	C-source <sub>final</sub> ( $\mu\text{g}\cdot\text{ml}^{-1}$ )
<b>Glucose</b>			
No SPs	0.46 <sup>a</sup> (0.00)	280 <sup>a</sup> (1.8)	52.43 <sup>a</sup> (12.97)
Sand	0.58 <sup>b</sup> (0.05)	268.7 <sup>a</sup> (2.1)	14.98 <sup>a</sup> (6.48)
Montmorillonite	0.18 <sup>c</sup> (0.03)	270.5 <sup>a</sup> (9.9)	18.72 <sup>a</sup> (17.16)
Nontronite	0.65 <sup>d</sup> (0.00)	219 <sup>b</sup> (14.5)	48.68 <sup>a</sup> (84.33)
Humic acids	0.63 <sup>e</sup> (0.03)	228.5 <sup>c</sup> (24.5)	89.88 <sup>a</sup> (47.67)
<b>Phenanthrene</b>			
No SPs	0.31 <sup>a</sup> (0.00)	106.5 <sup>a</sup> (13.6)	0.12 <sup>a</sup> (0.03)
Sand	0.43 <sup>b</sup> (0.01)	99.5 <sup>a</sup> (9.3)	0.10 <sup>a</sup> (0.01)
Montmorillonite	0.31 <sup>a</sup> (0.01)	112.3 <sup>a</sup> (12.1)	0.41 <sup>a</sup> (0.20)
Nontronite	0.59 <sup>c</sup> (0.00)	51.7 <sup>b</sup> (1.3)	1.18 <sup>b</sup> (0.28)
Humic acids	0.45 <sup>d</sup> (0.00)	39.4 <sup>c</sup> (6.6)	0.95 <sup>c</sup> (0.58)

Results are reported as mean and standard deviations (in brackets),  $n = 3$ . Different letters represent statistically significant means (two-way ANOVA,  $p < 0.05$ ) of the parameters in the presence of the SPs, with respect to those measured in the absence of SPs (i.e., No SPs).



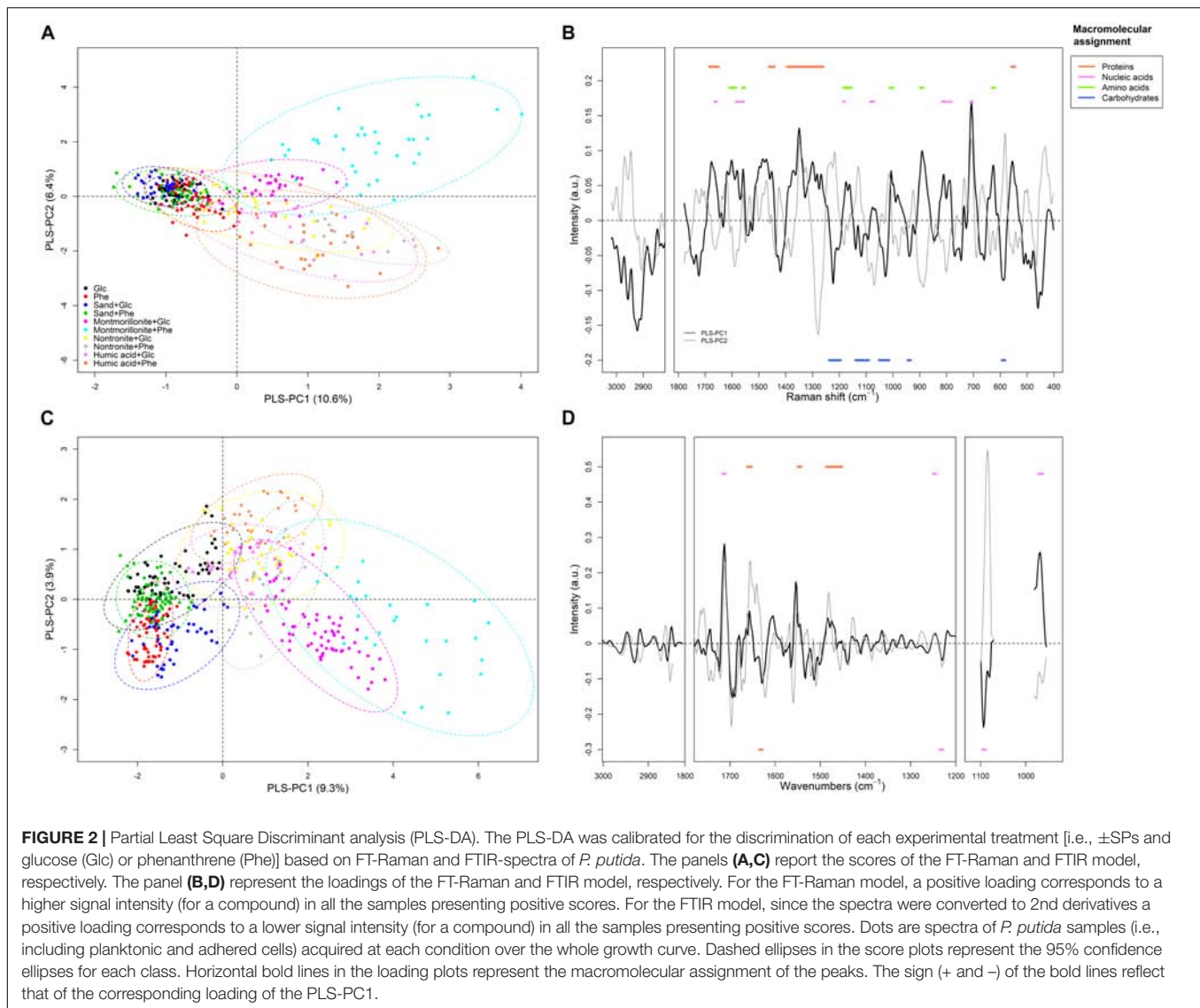
and in the presence of humic acids, the cells exhibited instead the lowest mineralization rates.

## Metabolic Profiling by FT-Raman Spectroscopy and PLS-DA

The average FT-Raman spectra for each experimental condition are reported as **Supplementary information (Supplementary Figure S1)**. Differences all over the spectral ranges could be detected among all conditions, however, for a precise identification of patterns, the use of chemometric analysis was necessary. The first PLS-DA model was calibrated using the first eight principal components (PLS-PC) for the classification of each of the growing conditions (i.e., the different type of SPs and C-source) on the base of *P. putida* FT-Raman spectra. From a visual inspection of the scores plot (where each sample is represented in a bi-dimensional space), it emerged that differences in the metabolic profiles of *P. putida* could be used to discriminate among the different growth conditions, with the SPs being the main factor influencing the discriminant analysis (**Figure 2A**). The first eight components explained 37% of the overall variance present in the spectral

dataset (i.e., the X matrix) (**Supplementary Table S1**). The best discrimination, and therefore the greatest differences in the metabolic profiles of the cells, occurred for the cells grown in the presence of montmorillonite, nontronite and humic acids (**Table 2** and **Figure 2A**). The combination of these SPs with phenanthrene, as a C/energy source, resulted in the highest variance explained (77, 65, and 71%, respectively) (**Table 2**). The higher degree of macromolecular changes was also confirmed by the higher sensitivity (i.e., the ability of the model to discriminate those classes of cells from the rest of the treatments) for montmorillonite, nontronite and humic acids in the presence of phenanthrene being 69, 43, and 69% respectively (**Table 2**). For these classes, the model also presented the higher  $R^2_C$  (0.77, 0.64, and 0.70, respectively) and the lower RMSEP (0.17, 0.15, and 0.17, respectively), indicating good predictive abilities.

The spectra corresponding to cell grown on montmorillonite, nontronite and humic acids grouped at positive scores along the PLS-principal component one (PLS-PC1; 10.6%), whereas the cells grown in the absence of SPs and in the presence of sand clustered at negative ones (**Figure 2A**). On the other hand, along the PLS-PC2 (6.4%) a discrimination



of the different SPs could be observed (Figure 2A). Spectra corresponding to cells grown in the presence of montmorillonite were present at positive scores and the cells grown on nontronite and humic acids had negative ones (Figure 2A).

The loadings, together with the patterns observed in the scores plot, indicate which spectral bands (i.e., metabolic components) are responsible for the observed clustering patterns. The complete band assignment is reported in Supplementary Table S2. For the PLS-PC1, a set of important loadings corresponding to carbohydrates spectral window (C-O and C-C stretching; 1200–1000  $\text{cm}^{-1}$ ) and carboxylic residual groups (symmetric vibrations of carboxylate groups  $\text{COO}^-$  near 1419  $\text{cm}^{-1}$ ) had negative sign, indicating that the cells growing in the absence of SPs or in the presence of sand (also found at negative scores) exhibited higher peak intensities for this macromolecular pool and residual group, compared to cells grown in the presence of clays and humic acids

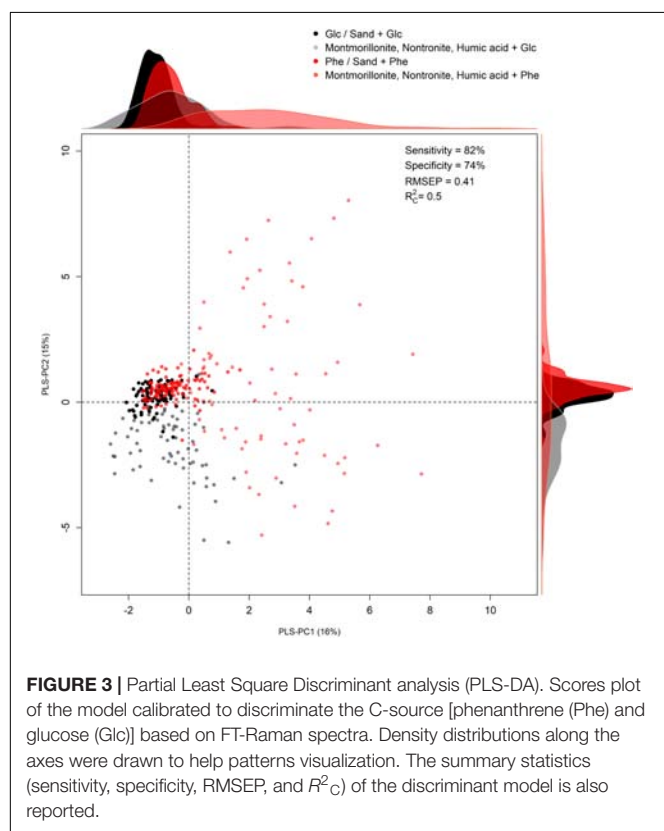
(Supplementary Table S2 and Figure 2B). Positive loadings corresponded to the C = O stretch of the Amide I, present at 1675  $\text{cm}^{-1}$ , the Amide III (1265  $\text{cm}^{-1}$ ), and the  $\text{CH}_2$  bending of proteins (1452  $\text{cm}^{-1}$ ). Characteristic vibration frequencies of amino acids such as phenylalanine (1600, 1174/1162, 1006, and 626  $\text{cm}^{-1}$ ) tyrosine and tryptophan (1600, 1558, 1174/1162, 891  $\text{cm}^{-1}$ ), ring breathing modes of purine bases (Adenine and Guanine rings at 1581, 788, and 707  $\text{cm}^{-1}$ ) and the symmetric  $\text{PO}_2$  stretching of DNA (1076  $\text{cm}^{-1}$ ) presented positive sign. They were therefore more important in the cells grown in the presence of clays and humic acids (found at positive scores).

For the PLS-PC2, negative loadings corresponding to proteins (1662, 1278  $\text{cm}^{-1}$ ), amino acids (1602, 1000, 889, and 802  $\text{cm}^{-1}$ ) and nucleic acids (1591, 1560, and 1016, 639, 619  $\text{cm}^{-1}$ ) indicated more intense bands for these components in the cells growing in the presence of nontronite and humic acids. With montmorillonite instead, the cells presented positive loadings

**TABLE 2** | Diagnostic parameters of the PLS-DA models based on FT-Raman and FTIR spectroscopy.

	Glc	Phe	S + Glc	S + Phe	M + Glc	M + Phe	N + Glc	N + Phe	HA + Glc	HA + Phe
<b>FT-Raman</b>										
Sensitivity	0.01	0	0	0.02	0.29	0.69	0	0.43	0	0.69
Specificity	0.99	0.99	1	0.99	0.97	0.99	0.99	0.99	0.99	0.98
$R^2_C$	0.25	0.18	0.17	0.27	0.55	0.77	0.43	0.64	0.37	0.70
RMSC	0.31	0.33	0.25	0.29	0.19	0.14	0.19	0.12	0.18	0.14
$R^2_P$	0.14	0.07	0.04	0.11	0.20	0.68	0.16	0.43	0.009	0.56
RMSEP	0.34	0.36	0.27	0.32	0.25	0.17	0.23	0.15	0.22	0.17
% variance	25.86	18.47	17.19	27.98	55.19	77.03	43.27	64.89	37.65	70.58
<b>FTIR</b>										
Sensitivity	0.70	0.01	0.17	0.34	0.80	0.75	0.29	0.76	0	0
Specificity	0.98	0.99	1	0.98	0.97	1	1	1	1	1
$R^2$	0.51	0.28	0.37	0.36	0.59	0.67	0.45	0.65	0.21	0.32
RMSC	0.25	0.28	0.23	0.28	0.22	0.13	0.19	0.13	0.19	0.19
$R^2_P$	0.46	0.21	0.24	0.26	0.44	0.55	0.28	0.43	0.10	0.25
RMSEP	0.25	0.29	0.24	0.29	0.23	0.14	0.20	0.14	0.20	0.20
% variance	51.08	28.84	37.48	36.83	59.64	67.66	45.80	65.82	21.71	32.22

The models were calibrated to discriminate for each experimental condition ( $\pm$  SPs and glucose or phenanthrene), for a total of 10 classes (Glc, glucose; Phe, phenanthrene; S, sand; M, Montmorillonite; N, Nontronite; HA, humic acids). The number of principal components was 8 for both models. RMSC, root mean squared error of calibration; RMSEP, root mean squared error of prediction;  $R^2_C$ , coefficient of determination for the calibration;  $R^2_P$ , coefficient of determination for predicted values; Sensitivity, ability to discriminate true positives; Specificity, ability to discriminate true negatives; % variance, variance in Y explained by the model.



for most of the carbohydrates bands (1000–1200  $\text{cm}^{-1}$ ) and carboxylic residual groups ( $\text{COO}^-$  at 1419  $\text{cm}^{-1}$ ).

The second model was calibrated (using four PLS-PC) to discriminate for the C/energy source (glucose and

phenanthrene). Even in this case, patterns in the two classes of cells could be discriminated based on their metabolic profiles (Figure 3). The first four components explained 38% of the total spectral variance, whereas the explained variance for the C/energy source was 50% and the RMSEP was 0.41 (Supplementary Table S3). Furthermore, the sensitivity and specificity were high (82 and 74% respectively), meaning that the differences in macromolecule composition were strong enough to allow for accurate classification (Supplementary Table S3). Analyzing the scores plot, an interesting pattern in the metabolic profiles could be observed. When *P. putida* was grown in the absence of SPs, or in the presence of sand, the cells presented comparable metabolic profiles (i.e., overlapping scores) regardless of the C-source metabolized (i.e., glucose or phenanthrene) (Figure 3). On the other hand, when montmorillonite, nontronite, and humic acids were present in the medium, a greater discrimination among the cells grown in the presence of glucose or phenanthrene was evident (Figure 3). For instance, along the PLS-PC1 (16% of total variance) the cells grown on glucose and in the presence of SPs were present at negative scores and the cells grown on phenanthrene and SPs had positive ones. In between these two groups clustered the cells grown in the absence of SPs or in the presence of sand (Figure 3). The PLS-PC1 positive loadings revealed that when using phenanthrene, the cells presented greater signals for components such as proteins (1675, 1282  $\text{cm}^{-1}$ ), and nucleic acids (794 and 707  $\text{cm}^{-1}$ ) (Supplementary Figure S2). On the other hand, when growing on glucose the cells had higher intensities for carbohydrates (1200–1000  $\text{cm}^{-1}$ ) (Supplementary Figure S2). The variance along the PLS-PC2 (15%) was mainly due to phenylalanine (1589  $\text{cm}^{-1}$ ), the Amide III (1286  $\text{cm}^{-1}$ ), which presented strong negative loadings, and carbohydrates (582  $\text{cm}^{-1}$ ) with positive one (Supplementary Figure S2).

## Metabolic Profiling by FTIR Spectroscopy and PLS-DA

The average FTIR spectra for each experimental condition are reported as **Supplementary Figure S3**. Even in this case, the first model was calibrated to discriminate the different growth conditions (i.e., SPs and C/energy source). Similarly to the respective FT-Raman model, the first eight components explained 38% of the total spectral variance present in the dataset (**Supplementary Table S1**). The highest variance explained by the spectra was reached with glucose and in the absence of SPs, in the presence of montmorillonite combined with phenanthrene or glucose and nontronite with phenanthrene, explaining 51, 68, 60, and 66% of the variance respectively (**Table 2**). For these set of conditions, the model presented also the highest sensitivity, specificity and the best predictive abilities (**Table 2**), reflecting the greatest changes in the macromolecular composition of the cells. In the scores plot, the most prominent discrimination between the conditions occurred along the PLS-PC1 (9%). The cells grown in the absence of SPs and in the presence of sand presented comparable metabolic profiles and were grouped at negative scores (**Figure 2C**). Moving to positive scores, the cells grown with montmorillonite, nontronite, and humic acids in the medium could be found. No clear separation in the presence of these last SPs could be detected and the spectra presented overlapping scores (**Figure 2C**). No clear trend along the PLS-PC2 was evident.

Since the FTIR-spectra were transformed to 2nd derivatives, positive loadings correspond to a decrease in intensity of the specific compounds/residual groups for all the spectra presenting positive scores. The opposite holds true for samples with negative scores. The loadings corresponding to C-H bonds vibrations (3000–2820  $\text{cm}^{-1}$ ) presented only minor contribution to the discriminant model (**Figure 2C**). Important positive loadings showed that the cells growing in the absence of SPs or in the presence of sand presented higher signals for the C = O stretching of the carbonyl groups contained in lipids (1743  $\text{cm}^{-1}$ ) and in nucleic acids (1712  $\text{cm}^{-1}$ ). Protein signals corresponding to Amide I  $\alpha$ -helix (C = O stretching; 1656  $\text{cm}^{-1}$ ) and Amide II (N-H bending; 1544  $\text{cm}^{-1}$ ) together with backbone features of nucleic acids (C-C stretching; 968  $\text{cm}^{-1}$ ) and the asymmetric  $\text{PO}_2^-$  stretching (1245  $\text{cm}^{-1}$ ) also presented positive loadings (**Figure 2D**). Negative loadings for the model corresponded to  $\beta$ -sheets protein secondary structures (1675 and 1629  $\text{cm}^{-1}$ ), and to the symmetric stretching of  $\text{PO}_2^-$  groups present in phosphorylated molecules (1230 and 1093  $\text{cm}^{-1}$ ) (**Figure 2D**).

The second model was calibrated to discriminate for the C-source. The first eight components captured 87% of the total spectral variance (**Supplementary Table S3**). The REMSP was 0.28, the  $R^2_C$  was 0.71 and sensitivity and specificity were 92 and 94%, respectively. Although the PLS-PC1 and PLS-PC2 already explained 50% of the total variance in the spectral dataset, no clear distinction between the cells grown on glucose and on phenanthrene could be observed (**Supplementary Figure S4**). The only separation, but rather weak, was evident along the PC2 (14% of variance) between the cells grown in the absence

of SPs or in the presence of sand and the one grown on clays and humic acids. However, no separation occurred on the basis of the C-source, as shown by the overlapping scores (**Supplementary Figure S4**). The clustering pattern in the scores plot was mainly driven by changes in the secondary structures of proteins (1658 and 1637  $\text{cm}^{-1}$ ) and carbonyl groups of nucleic acids (1708  $\text{cm}^{-1}$ ), as suggested by the loadings of the PLS-PC1 and PLS-PC2 (**Supplementary Figure S5**).

## DISCUSSION

Soil is a complex matrix represented by a highly heterogeneous association of mineral and organic components. These constituents not only influence the physico-chemical conditions that microorganisms are subjected to, but they also affect the availability and the spatial distribution of organic pollutants, such as PAHs. Understanding how bacteria metabolically react to the presence of different soil components during the mineralization of PAHs is therefore of paramount importance to understand pollutants degradation in nature and to improve remediation strategies of polluted sites. Up to date, little information in this regard is available (Ortega-Calvo and Saiz-Jimenez, 1998; Uyttebroek et al., 2006; Lerch et al., 2017). In this study, for the first time we aimed at studying how different type of soil particles (SPs) influence the metabolic profile of bacteria grown in the presence of phenanthrene.

### Soil Particles Differently Affect the C-source in Solution and Cell Mineralization Efficiencies According to the Nature of the C-source (Phenanthrene vs. Glucose)

Our results show that in the presence of glucose, the SPs modified the mineralization efficiencies of the cells, though no relevant difference in the soluble fraction of the C-source could be detected (**Figure 1** and **Table 1**). The higher metabolic performance (i.e.,  $\text{CO}_2$  production) in the presence of montmorillonite is consistent with the results of Wu et al. (2014c), who ascribed the changes in metabolic activity (measured by microcalorimetry) to the SPs presence itself, rather than to changes in C solubility. In the presence of phenanthrene, the SPs specifically altered the amount of phenanthrene in solution. Sand, which presents the lowest specific surface area among the SPs tested (Wilcke et al., 1996; Amellal et al., 2001; Uyttebroek et al., 2006; Müller et al., 2007), did not alter the phenanthrene concentration in solution (Louvel et al., 2011). On the other hand, montmorillonite, nontronite and humic acids increased the amount of readily available phenanthrene in solution, maybe as colloids. Although in contrast with the finding reported by Ortega-Calvo and Saiz-Jimenez (1998), we have to point out that the presence of colloidal fractions of SPs might have acted as surfactants and increased the apparent solubility of phenanthrene in the aqueous phase of the cultures as described by Kanti Sen and Khilar (2006). Besides the amount of phenanthrene that each SP is able to adsorb, other physical

parameters, such as the contact surface area of a particle and the aqueous phase, may also affect the phenanthrene flux from the surface of the particle into the surrounding medium as a function of the substrate uptake by the cells (Wick et al., 2001; Tecon et al., 2006). Despite of this, the mineralization parameters (e.g., maximum mineralization and mineralization rate) were similar in all treatments, meaning that the soluble fraction was only one of the exploitable phenanthrene-pools present in the cultures (Ortega-Calvo and Saiz-Jimenez, 1998; Amellal et al., 2001), and that the cells presented efficient mechanisms to increase their accessibility to phenanthrene to efficiently biodegrade it.

From these results, it is evident that SPs have opposite effects on C accessibility and cell metabolic activity as a function of the C-source present in the growth environment: with glucose, SPs had an action on cell metabolic activity, whereas in the presence of phenanthrene they appeared to modify more the access to the C-source. Although this finding is an evident consequence of the contrasting physico-chemical properties of glucose and phenanthrene, less obvious are the metabolic adjustments of the cells facing these two opposite scenarios.

## Soil Particles Specifically Alter the Metabolic Profile of *P. putida*

The metabolic profile of *P. putida* was characterized by vibrational spectroscopy. FT-Raman and FTIR-spectra carry complementary information concerning bacteria macromolecular composition. When run in parallel, these techniques can draw a precise picture of cellular biochemical changes, which can be extracted by advanced statistical analysis (i.e., chemometrics). The first PLS-DA model was calibrated considering each single treatment (SPs + C-source) as a different class.

Although FT-Raman-spectra, with respect to FTIR-spectra, present a lower degree of overlapping bands and more detailed spectral information about amino acids, nucleic acids bases and aromatic compounds (Neugebauer et al., 2007), overall, the models classifying for each condition (SPs + C-source) were quite similar (Figure 2). The PLS-DA revealed that most of the macromolecular changes are related to cells grown in the presence of montmorillonite, nontronite and humic acids with no significant effect due to the presence of sand (Figures 2A,C). Interestingly, from the scores plot it also emerged that the cells could be well discriminated in the presence of different SPs (Figures 2A,C), confirming our hypothesis that SPs specifically alter cell metabolic profiles. Furthermore, as indicated by the diagnostic tools of the PLS-DA model (such as sensitivity,  $R^2$  and RMSEP; Sackett et al., 2013), the strongest macromolecular changes were induced when montmorillonite was present in the culture medium, regardless of the C-source, or when clays and humic acids were added to the cultures grown with phenanthrene (Table 2), suggesting an interaction of SPs and C-source in defining the metabolic profile (see below) with different underlying mechanisms as explained below.

To understand which cellular compounds (or functional groups) drove the compositional patterns at the different conditions, we analyzed the loadings of the discriminant models

(Wold et al., 2001; Sackett et al., 2013). The biochemical differences distinguishing the cells grown in the absence of SPs or in the presence of sand, from the ones grown on clays and humic acids, concerned mainly changes of the protein, nucleic acid and carbohydrate pools, with the latter one being negatively correlated to the others (Figures 2B,D). The identified spectral ranges (and therefore the corresponding compounds), especially the one indicated by FT-Raman spectroscopy, have already been described to differentiate between planktonic and biofilm bacteria phenotypes (Andrews et al., 2010), suggesting a possible preference for a sessile lifestyle in the presence of clays and humic acids. However, since in our experimental design the planktonic and attached fraction of bacteria were not separated but considered as a whole, we are not able at the moment to disentangle the direct (adhesion) from indirect effect (C-availability) of the presence of SPs on cell metabolic profile.

The presence of clays and humic acids induced a shift toward  $\beta$ -sheet secondary structures as indicated by the FT-Raman-based loading at  $1675\text{ cm}^{-1}$  (Figure 2B) (Rygula et al., 2013). Similar qualitative changes were also detected by FTIR spectroscopy. In the absence of SPs and in the presence of glucose, cells exhibited a prominent Amide I peak at  $1656\text{ cm}^{-1}$  in the 2nd derivative spectra (Supplementary Figure S3), indicative of proteins dominated by  $\alpha$ -helix secondary structures. In all other conditions, the loadings indicated a shift toward proteins with more  $\beta$ -sheets secondary structures (e.g.,  $1630\text{ cm}^{-1}$ , parallel  $\beta$ -sheets) (Figure 2D) (Barth, 2007). Previous studies demonstrated that the adhesion of bacteria to mineral surfaces can be mediated by protein bridging favored by the presence of  $\alpha$ -helix structures (Parikh and Chorover, 2006; Wu et al., 2014a,b). Therefore, in this case the opposite trend suggests that proteins pool modifications were not related to particle adhesion. On the other hand, a higher fraction of  $\beta$ -sheet secondary structure is in line with a reorganization toward a more functional protein pool, indeed  $\beta$ -sheet secondary structures are mostly characteristic of membrane bound enzymes and transporters (Rygula et al., 2013). Such a shift could have been aimed at optimizing the access and acquisition to the C-source, especially in the presence of phenanthrene.

The nucleic acid pool was also affected by the presence of clays and humic acids and the changes were detected both by FT-Raman and FTIR spectroscopy. The loadings of the FT-Raman model indicated a positive correlation between nucleic acids and proteins (Figure 2B). This correlation reflects the biological link between the synthesis of new proteins (see above) and DNA translation that can be easily monitored by means of vibrational spectroscopy (Neugebauer et al., 2007). Whereas the Raman spectrum of nucleic acids contains mainly information about nucleobases, FTIR spectra are informative for backbone vibrations of DNA and RNA. The loadings of the FTIR-based model pointed at five interesting bands ( $1712$ ,  $1245$ ,  $1230$ ,  $1093$ , and  $968\text{ cm}^{-1}$ ) (Figure 2D). The pattern of these bands suggests possible changes of DNA molecules conformation (Whelan et al., 2011, 2014) when clays or humic acids were present in the cultures. Whelan et al. (2011, 2014) described in detail the diagnostic bands indicative of DNA conformational shift and how they can be detected by FTIR-spectroscopy. In

prokaryotes, DNA conformational changes are responsible for a greater stability upon UV, chemicals and desiccation exposition or as a normal consequence of biological processes such as gene transcription and DNA-protein interactions (Mohr et al., 1991; Whelan et al., 2011, 2014). This conformational changes occurred independently from the C/energy source and they were therefore likely triggered by the presence of SPs (see **Supplementary Figure S3**).

Carbohydrates were found to be negatively correlated with proteins and nucleic acids (see the FT-Raman loadings). An inspection of the 1200–950  $\text{cm}^{-1}$  region of the FTIR spectra suggested that the carbohydrates bands were not originating from storage compounds such as glycogen, but were rather belonging to cell wall structures (in the case of montmorillonite and nontronite a subtraction of pure clay spectra was performed; data not shown) (Jiang et al., 2004). A similar capsular structure seems to surround both planktonic and biofilm entangled cells of *Pseudomonas putida* (Kachlany et al., 2001). In agreement with our findings a spectroscopic analysis reported a lower amount of carbohydrates in *Pseudomonas* sp. NCIMB 2021 for the biofilm lifestyle (Beech et al., 1999) indicating ongoing modifications of surface carbohydrates in the presence of clays and humic acids.

Besides the main metabolic differences found to distinguish the cells grown in the absence of SPs or in the presence of sand and the one facing clays and humic acids, the PLS-DA revealed that the metabolic profile of *P. putida* was specifically affected by the SPs used in this study. For instance, the PLS-PC2 discriminated among montmorillonite, nontronite and humic acids. Wu et al. (2014c) recently demonstrated that the metabolic activity of *P. putida* was peculiarly modulated by different soil colloids and minerals. In accordance to this study, we found that the effect of SPs is also reflected in a specific reorganization of their metabolic profile.

### **The Effect of the C-source (Phenanthrene vs. Glucose) on *P. putida* Metabolic Profile Is Evident Only in the Presence of Clays and Humic Acids**

From the first PLS-DA model statistics, differences in the metabolic profile of *P. putida* related to the C-source were identified. To better resolve these variations, a second set of models (one based on the FT-Raman and one on the FTIR-spectra) was calibrated to classify the two C-sources (phenanthrene or glucose).

In the absence of SPs or in the presence of sand, the metabolic profile of *P. putida* was comparable, regardless of the C-source (**Figure 3**). A strong effect of phenanthrene on *P. putida* metabolic profile was therefore excluded, which could be due to the fact that in our experiments cells were pre-acclimated to the use of phenanthrene and the necessary set of enzymes to metabolize it was already induced (Deveryshetty and Phale, 2009). Moreover, Vandera et al. (2015) found that half of the identified proteins in *Arthrobacter phenanthrenivorans* Sphe3 are shared between phenanthrene and glucose-grown cells and only a small pool of the whole proteome is up or down-regulated at the two growth conditions. It is therefore evident that the

metabolic response to phenanthrene is limited to very specific macromolecular targets and that *P. putida* possesses a very effective array of de-toxifying and protective mechanisms against phenanthrene (Domínguez-Cuevas et al., 2006; Vandera et al., 2015).

Interestingly, the effect of phenanthrene, relative to glucose, was unambiguously evident when cells were grown in the presence of clays or humic acids (**Figure 3**). The metabolic changes must have been triggered by a modified accessibility to the C-source. This finding is further supported by the fact that clays and humic acids slightly altered the phenanthrene solubility in our cultures. Furthermore, soil components such as clays and humic acids, adsorb PAHs (Müller et al., 2007; He and Wang, 2011) thereby altering the physico-chemical processes occurring at the exchange surface between bacterial cells and the surrounding environment. Clays can create favorable micro-environment where cells are found in close proximity to C and other nutrient sources (Filip, 1973), and this is particularly true in the presence of PAHs (Ortega-Calvo and Saiz-Jimenez, 1998). Humic acids work as surfactants that can facilitate the transport of phenanthrene across cell membranes helping its acquisition (Xie et al., 2017). Also, it cannot be excluded that basal macromolecular divergences between planktonic and sessile cells (Vilain et al., 2004; Ammons et al., 2014; Favre et al., 2017) made more prominent the effect of the two C-sources (**Figure 3**). In any case, by creating micro-niches with different physico-chemical properties, the SPs induced *P. putida* to express different final metabolic profiles as a function of the C-source. This reveals for the first time the effect of SPs on bacteria metabolic profile during PAHs biodegradation. We have to point out that since we did not analyze single cells, we can not confirm that the effect of the SPs on the metabolic profile of the cells was exclusively related to the adhesion of the cells to the particles or to other indirect effects induced by the presence of the particles.

Rather than a strong quantitative reorganization of targeted C-pools, *P. putida* underwent a general adjustment of the overall macromolecular profile (**Supplementary Figure S2**). Probably, this reorganization was enacted in the attempt to improve the binding to mineral particles, to adjust enzyme expression or the release of surfactants finalized at optimizing the capture and assimilation of phenanthrene molecules. The most prominent loadings indicated that the difference between the glucose and phenanthrene cell metabolic profiles was due to different levels of proteins, amino acids, nucleic acids and carbohydrates. Vandera et al. (2015) found that several cell functions (e.g., specific membrane transporters, PAHs degrading enzymes and the aromatic amino acids degradation pathways) were up-regulated, whereas the synthesis of structural features (i.e., peptidoglycan) was down-regulated when the cells were consuming phenanthrene with respect to glucose. Xie et al. (2017) also reported the adjustments of *Sphingobium* sp. cell wall properties grown in the presence of humic acids and phenanthrene. These changes are consistent with the loadings identified by our model, which suggest a reorganization of the proteome to optimize phenanthrene acquisition as well as structural changes at the cell surface (Keum et al., 2008; Seo et al., 2009).

Overall, our results reveal that the spatial and compositional (mineral and organic components) heterogeneity of soil affect, beside bacterial diversity (Kuz'yakov and Blagodatskaya, 2015), also the variety of metabolic profiles expressed at the single species level. A direct consequence of this finding is that distinct cell metabolic profiles induced by the presence of determinate SPs can reflect cells with different functions, even at the single species level. This may define new limits to the definition of ecological functions and roles that we already know, especially for what it concerns PAHs degradation.

As a first attempt to investigate the effect of different soil components on the metabolic profile of bacteria, we have to point out that further research might be necessary to extend and proof these conclusions to real soil samples where mineral and organic components are in close contact the one with the others and are present in mixture with different ratios. Finally, a higher instrumental spatial resolution would allow to acquire spectra of single cells and to more precisely resolve the metabolic differences among planktonic and adhered cells and therefore disentangle the direct from the indirect effects of SPs on cell metabolic profile.

## DATA AVAILABILITY STATEMENT

The raw data supporting the conclusions of this manuscript will be made available by the authors, without undue reservation, to any qualified researcher.

## REFERENCES

- Amellal, N., Portal, J.-M., Vogel, T., and Berthelin, J. (2001). Distribution and location of polycyclic aromatic hydrocarbons (PAHs) and PAH-degrading bacteria within polluted soil aggregates. *Biodegradation* 12, 49–57. doi: 10.1023/A:1011909107858
- Ammons, M. C. B., Triplet, B. P., Carlson, R. P., Kirker, K. R., Gross, M. A., Stanisch, J. J., et al. (2014). Quantitative NMR metabolite profiling of methicillin-resistant and methicillin-susceptible *Staphylococcus aureus* discriminates between biofilm and planktonic phenotypes. *J. Proteome Res.* 13, 2973–2985. doi: 10.1021/pr500120c
- Andrews, J. S., Rolfe, S. A., Huang, W. E., Scholes, J. D., and Banwart, S. A. (2010). Biofilm formation in environmental bacteria is influenced by different macromolecules depending on genus and species. *Environ. Microbiol.* 12, 2496–2507. doi: 10.1111/j.1462-2920.2010.02223.x
- Barker, M., and Rayens, W. (2003). Partial least squares for discrimination. *J. Chemom.* 17, 166–173. doi: 10.1002/cem.785
- Barnes, R. J., Dhanoa, M. S., and Lister, S. J. (1989). Standard normal variate transformation and de-trending of near-infrared diffuse reflectance spectra. *Appl. Spectrosc.* 43, 772–777. doi: 10.1366/0003702894202201
- Barth, A. (2007). Infrared spectroscopy of proteins. *Biochim. Biophys. Acta* 1767, 1073–1101. doi: 10.1016/j.bbabi.2007.06.004
- Beech, I., Hanjagsit, L., Kalaji, M., Neal, A. L., and Zinkevich, V. (1999). Chemical and structural characterization of exopolymers produced by *Pseudomonas* sp. NCIMB 2021 in continuous culture. *Microbiol. Read. Engl.* 145( Pt 6), 1491–1497. doi: 10.1099/13500872-145-6-1491
- Bushnell, L. D., and Haas, H. F. (1941). The utilization of certain hydrocarbons by microorganisms. *J. Bacteriol.* 41, 653–673.
- Cébron, A., Faure, P., Lorgeoux, C., Ouvrard, S., and Leyval, C. (2013). Experimental increase in availability of a PAH complex organic contamination from an aged contaminated soil: consequences on biodegradation. *Environ. Pollut.* 177, 98–105. doi: 10.1016/j.envpol.2013.01.043

## AUTHOR CONTRIBUTIONS

AF performed the experiments, analyzed the results, and wrote the paper. AZ, CM, and AC conceived the study, directed research, analyzed the results, and contributed to the manuscript writing. AC is the PI of the RhizOrg project that funded this study.

## FUNDING

This study was part of the RhizOrg project funded by the ANR (Agence Nationale de la Recherche, ANR-13-JSV7-0007\_01 project) and by the Région Grand Est.

## ACKNOWLEDGMENTS

We would like to thank the members of the LCPME laboratory of Nancy for providing the gold coated microscopy slides used for FT-Raman and FTIR-spectroscopy.

## SUPPLEMENTARY MATERIAL

The Supplementary Material for this article can be found online at: <https://www.frontiersin.org/articles/10.3389/fmicb.2018.02999/full#supplementary-material>

- Cébron, A., Norini, M.-P., Beguiristain, T., and Leyval, C. (2008). Real-Time PCR quantification of PAH-ring hydroxylating dioxygenase (PAH-RHD $\alpha$ ) genes from Gram positive and Gram negative bacteria in soil and sediment samples. *J. Microbiol. Methods* 73, 148–159. doi: 10.1016/j.mimet.2008.01.009
- Chenu, C. (1993). Clay- or sand-polysaccharide associations as models for the interface between micro-organisms and soil: water related properties and microstructure. *Geoderma* 56, 143–156. doi: 10.1016/0016-7061(93)90106-U
- Deveryshtetty, J., and Phale, P. S. (2009). Biodegradation of phenanthrene by *Pseudomonas* sp. strain PPD: purification and characterization of 1-hydroxy-2-naphthoic acid dioxygenase. *Microbiol. Read. Engl.* 155, 3083–3091. doi: 10.1099/mic.0.030460-0
- Domínguez-Cuevas, P., González-Pastor, J.-E., Marqués, S., Ramos, J.-L., and de Lorenzo, V. (2006). Transcriptional tradeoff between metabolic and stress-response programs in *Pseudomonas putida* KT2440 cells exposed to toluene. *J. Biol. Chem.* 281, 11981–11991. doi: 10.1074/jbc.M509848200
- Fanesi, A., Wagner, H., and Wilhelm, C. (2017). Phytoplankton growth rate modelling: can spectroscopic cell chemotyping be superior to physiological predictors? *Proc. Biol. Sci. U.S.A* 284:20161956. doi: 10.1098/rspb.2016.1956
- Favre, L., Ortalo-Magné, A., Greff, S., Pérez, T., Thomas, O. P., Martin, J.-C., et al. (2017). Discrimination of four marine biofilm-forming bacteria by LC-MS metabolomics and influence of Culture parameters. *J. Proteome Res.* 16, 1962–1975. doi: 10.1021/acs.jproteome.6b01027
- Filip, Z. (1973). Clay minerals as a factor influencing the biochemical activity of soil microorganisms. *Folia Microbiol.* 18, 56–74. doi: 10.1007/BF02884250
- Fonville, J. M., Richards, S. E., Barton, R. H., Boulange, C. L., Ebbels, T. M. D., Nicholson, J. K., et al. (2010). The evolution of partial least squares models and related chemometric approaches in metabolomics and metabolic phenotyping. *J. Chemom.* 24, 636–649. doi: 10.1002/cem.1359
- Haritash, A. K., and Kaushik, C. P. (2009). Biodegradation aspects of polycyclic aromatic hydrocarbons (PAHs): a review. *J. Hazard. Mater.* 169, 1–15. doi: 10.1016/j.jhazmat.2009.03.137
- He, Y. Y., and Wang, X. C. (2011). Adsorption of a typical polycyclic aromatic hydrocarbon by humic substances in water and the effect of coexisting metal

- ions. *Colloids Surf. Physicochem. Eng. Asp.* 379, 93–101. doi: 10.1016/j.colsurfa.2010.12.023
- Huang, W. E., Li, M., Jarvis, R. M., Goodacre, R., and Banwart, S. A. (2010). Shining light on the microbial world: the application of Raman microspectroscopy. *Adv. Appl. Microbiol.* 70, 153–186. doi: 10.1016/S0065-2164(10)70005-8
- Huang, W. E., Stoecker, K., Griffiths, R., Newbold, L., Daims, H., Whiteley, A. S., et al. (2007). Raman-FISH: combining stable-isotope Raman spectroscopy and fluorescence *in situ* hybridization for the single cell analysis of identity and function. *Environ. Microbiol.* 9, 1878–1889. doi: 10.1111/j.1462-2920.2007.01352.x
- Indahl, U. G., Liland, K. H., and Næs, T. (2009). Canonical partial least squares—a unified PLS approach to classification and regression problems. *J. Chemom.* 23, 495–504. doi: 10.1002/cem.1243
- Jiang, W., Saxena, A., Song, B., Ward, B. B., Beveridge, T. J., and Myneni, S. C. B. (2004). Elucidation of functional groups on gram-positive and gram-negative bacterial surfaces using infrared spectroscopy. *Langmuir ACS J. Surf. Colloids* 20, 11433–11442. doi: 10.1021/la049043
- Kachlany, S. C., Levery, S. B., Kim, J. S., Reuhs, B. L., Lion, L. W., and Ghiorse, W. C. (2001). Structure and carbohydrate analysis of the exopolysaccharide capsule of *Pseudomonas putida* G7. *Environ. Microbiol.* 3, 774–784. doi: 10.1046/j.1462-2920.2001.00248.x
- Kahm, M., Hasenbrink, G., Lichtenberg-Fraté, H., Ludwig, J., and Kschischo, M. (2010). grofit: fitting biological growth curves with R. *J. Stat. Softw.* 33, 1–21. doi: 10.18637/jss.v033.i07
- Kanti Sen, T., and Khilar, K. C. (2006). Review on subsurface colloids and colloid-associated contaminant transport in saturated porous media. *Adv. Colloid Interface Sci.* 119, 71–96. doi: 10.1016/j.cis.2005.09.001
- Keum, Y. S., Lee, Y. J., and Kim, J.-H. (2008). Metabolism of nitro-diphenyl ether herbicides by dioxin-degrading bacterium *Sphingomonas wittichii* RW1. *J. Agric. Food Chem.* 56, 9146–9151. doi: 10.1021/jf801362k
- Kuhn, M. (2017). *Caret: Classification and Regression Training. R Package Version 6.0-78*. Available at: <https://cran.r-project.org/web/packages/caret/index.html>
- Kuz'yakov, Y., and Blagodatskaya, E. (2015). Microbial hotspots and hot moments in soil: concept & review. *Soil Biol. Biochem.* 83, 184–199. doi: 10.1016/j.soilbio.2015.01.025
- LaRowe, D. E., and Amend, J. P. (2016). The energetics of anabolism in natural settings. *ISME J.* 10, 1285–1295. doi: 10.1038/ismej.2015.227
- Lerch, T. Z., Chenu, C., Dignac, M. F., Barriuso, E., and Mariotti, A. (2017). Biofilm vs. Planktonic Lifestyle: consequences for Pesticide 2,4-D metabolism by *Cupriavidus necator* JMP134. *Front. Microbiol.* 8:904. doi: 10.3389/fmicb.2017.00904
- Liland, K. H., Mevik, B. H., and Canteri, R. (2015). *Baseline: Baseline Correction of Spectra. R Package Version, 1.2-1*. Available at: <https://cran.r-project.org/web/packages/baseline/index.html>
- Lima-Morales, D., Jáuregui, R., Camarinha-Silva, A., Geffers, R., Pieper, D. H., and Vilchez-Vargas, R. (2016). Linking microbial community and catabolic gene structures during the adaptation of three contaminated soils under continuous long term pollutant stress. *Appl. Environ. Microbiol.* 82, 2227–2237. doi: 10.1128/AEM.03482-15
- Louvel, B., Cébron, A., and Leyval, C. (2011). Root exudates affect phenanthrene biodegradation, bacterial community and functional gene expression in sand microcosms. *Int. Biodeterior. Biodegrad.* 65, 947–953. doi: 10.1016/j.ibiod.2011.07.003
- McCarty, P. L. (2007). Thermodynamic electron equivalents model for bacterial yield prediction: modifications and comparative evaluations. *Biotechnol. Bioeng.* 97, 377–388. doi: 10.1002/bit.21250
- Mevik, B. H., Wehrens, R., and Liland, K. H. (2016). *Pls: Partial Least Squares and Principal Component Regression. R package version 2.6-0*. Available at: <https://cran.r-project.org/web/packages/pls/index.html>
- Miyata, N., Iwahori, K., Foght, J. M., and Gray, M. R. (2004). Saturable, energy-dependent uptake of phenanthrene in aqueous phase by *Mycobacterium sp.* strain RJGII-135. *Appl. Environ. Microbiol.* 70, 363–369. doi: 10.1128/AEM.70.1.363-369.2004
- Mohr, S. C., Sokolov, N. V., He, C. M., and Setlow, P. (1991). Binding of small acid-soluble spore proteins from *Bacillus subtilis* changes the conformation of DNA from B to A. *Proc. Natl. Acad. Sci. U.S.A.* 88, 77–81. doi: 10.1073/pnas.88.1.77
- Moreno-Forero, S. K., and Van Der Meer, J. R. (2015). Genome-wide analysis of *Sphingomonas wittichii* RW1 behavior during inoculation and growth in contaminated sand. *ISME J.* 9, 150–165. doi: 10.1038/ismej.2014.101
- Movasaghi, Z., Rehman, S., and Rehman, I. U. (2007). Raman spectroscopy of biological tissues. *Appl. Spectrosc. Rev.* 42, 493–541. doi: 10.1080/05704920701551530
- Movasaghi, Z., Rehman, S., and Rehman, I. U. (2008). Fourier Transform Infrared (FTIR) spectroscopy of biological tissues. *Appl. Spectrosc. Rev.* 43, 134–179. doi: 10.1080/05704920701829043
- Müller, S., Totsche, K. U., and Kögel-Knabner, I. (2007). Sorption of polycyclic aromatic hydrocarbons to mineral surfaces. *Eur. J. Soil Sci.* 58, 918–931. doi: 10.1111/j.1365-2389.2007.00930.x
- Naumann, D. (2001). FT-Infrared and FT-Raman spectroscopy in biomedical research. *Appl. Spectrosc. Rev.* 36, 239–298. doi: 10.1081/ASR-100106157
- Neugebauer, U., Schmid, U., Baumann, K., Ziebuhr, W., Kozitskaya, S., Deckert, V., et al. (2007). Towards a detailed understanding of bacterial metabolism—spectroscopic characterization of *Staphylococcus Epidermidis*. *ChemPhysChem* 8, 124–137. doi: 10.1002/cphc.200600507
- Ojeda, J. J., Romero-Gonzalez, M. E., Pouran, H. M., and Banwart, S. A. (2008). *In situ* monitoring of the biofilm formation of *Pseudomonas putida* on hematite using flow-cell ATR-FTIR spectroscopy to investigate the formation of inner-sphere bonds between the bacteria and the mineral. *Mineral. Mag.* 72, 101–106. doi: 10.1180/minmag.2008.072.1.101
- Ortega-Calvo, J.-J., and Saiz-Jimenez, C. (1998). Effect of humic fractions and clay on biodegradation of phenanthrene by a *Pseudomonas fluorescens* strain isolated from soil. *Appl. Environ. Microbiol.* 64, 3123–3126.
- Parikh, S. J., and Chorover, J. (2006). ATR-FTIR spectroscopy reveals bond formation during bacterial adhesion to iron oxide. *Langmuir* 22, 8492–8500. doi: 10.1021/la061359p
- R Development Core Team (2010). *R: A Language and Environment for Statistical Computing*. Vienna: The R Project for Statistical Computing.
- Rygula, A., Majzner, K., Marzec, K. M., Kaczor, A., Pilarczyk, M., and Baranska, M. (2013). Raman spectroscopy of proteins: a review. *J. Raman Spectrosc.* 44, 1061–1076. doi: 10.1002/jrs.4335
- Sackett, O., Petrou, K., Reedy, B., Grazia, A. D., Hill, R., Doblin, M., et al. (2013). Phenotypic plasticity of Southern Ocean diatoms: key to success in the sea ice habitat? *PLoS One* 8:e81185. doi: 10.1371/journal.pone.0081185
- Savitzky, A., and Golay, M. J. E. (1964). Smoothing and differentiation of data by simplified least squares procedures. *Anal. Chem.* 36, 1627–1639. doi: 10.1021/ac60214a047
- Seo, J.-S., Keum, Y.-S., and Li, Q. X. (2009). Bacterial degradation of aromatic compounds. *Int. J. Environ. Res. Public Health* 6, 278–309. doi: 10.3390/ijerph6010278
- Tecon, R., Wells, M., and Van Der Meer, J. R. (2006). A new green fluorescent protein-based bacterial biosensor for analysing phenanthrene fluxes. *Environ. Microbiol.* 8, 697–708. doi: 10.1111/j.1462-2920.2005.00948.x
- Teng, L., Wang, X., Wang, X., Gou, H., Ren, L., Wang, T., et al. (2016). Label-free, rapid and quantitative phenotyping of stress response in *E. coli* via ramanome. *Sci. Rep.* 6:sre34359. doi: 10.1038/srep34359
- Thomas, F., Lorgeoux, C., Faure, P., Billet, D., and Cébron, A. (2016). Isolation and substrate screening of polycyclic aromatic hydrocarbon degrading bacteria from soil with long history of contamination. *Int. Biodeterior. Biodegrad.* 107, 1–9. doi: 10.1016/j.ibiod.2015.11.004
- Uyttebroek, M., Breugelmans, P., Janssen, M., Wattiau, P., Joffe, B., Karlson, U., et al. (2006). Distribution of the *Mycobacterium* community and polycyclic aromatic hydrocarbons (PAHs) among different size fractions of a long-term PAH-contaminated soil. *Environ. Microbiol.* 8, 836–847. doi: 10.1111/j.1462-2920.2005.00970.x
- VanBriesen, J. M. (2001). Thermodynamic yield predictions for biodegradation through oxygenase activation reactions. *Biodegradation* 12, 263–279. doi: 10.1023/A:1013179315518
- Vandera, E., Samiotaki, M., Parapouli, M., Panayotou, G., and Koukkou, A. I. (2015). Comparative proteomic analysis of *Arthrobacter phenanthrenivorans* Sphe3 on phenanthrene, phthalate and glucose. *J. Proteomics* 113, 73–89. doi: 10.1016/j.jprot.2014.08.018
- Vandevivere, P., and Kirchman, D. L. (1993). Attachment stimulates exopolysaccharide synthesis by a bacterium. *Appl. Environ. Microbiol.* 59, 3280–3286.

- Vilain, S., Cosette, P., Hubert, M., Lange, C., Junter, G.-A., and Jouenne, T. (2004). Comparative proteomic analysis of planktonic and immobilized *Pseudomonas aeruginosa* cells: a multivariate statistical approach. *Anal. Biochem.* 329, 120–130. doi: 10.1016/j.ab.2004.02.014
- Wagner, H., Jungandreas, A., Fanesi, A., and Wilhelm, C. (2014). Surveillance of C-allocation in microalgal cells. *Metabolites* 4, 453–464. doi: 10.3390/metabo4020453
- Wagner, H., Liu, Z., Langner, U., Stehfest, K., and Wilhelm, C. (2010). The use of FTIR spectroscopy to assess quantitative changes in the biochemical composition of microalgae. *J. Biophotonics* 3, 557–566. doi: 10.1002/jbio.201000019
- Wagner, M. (2009). Single-cell ecophysiology of microbes as revealed by Raman microspectroscopy or secondary ion mass spectrometry imaging. *Annu. Rev. Microbiol.* 63, 411–429. doi: 10.1146/annurev.micro.091208.073233
- Weissenfels, W. D., Klewer, H.-J., and Langhoff, J. (1992). Adsorption of polycyclic aromatic hydrocarbons (PAHs) by soil particles: influence on biodegradability and biotoxicity. *Appl. Microbiol. Biotechnol.* 36, 689–696. doi: 10.1007/BF00183251
- Whelan, D. R., Bambery, K. R., Heraud, P., Tobin, M. J., Diem, M., McNaughton, D., et al. (2011). Monitoring the reversible B to A-like transition of DNA in eukaryotic cells using Fourier transform infrared spectroscopy. *Nucleic Acids Res.* 39, 5439–5448. doi: 10.1093/nar/gkr175
- Whelan, D. R., Hiscox, T. J., Rood, J. I., Bambery, K. R., McNaughton, D., and Wood, B. R. (2014). Detection of an en masse and reversible B- to A-DNA conformational transition in prokaryotes in response to desiccation. *J. R. Soc. Interface* 11:20140454. doi: 10.1098/rsif.2014.0454
- Wick, L. Y., Colangelo, T., and Harms, H. (2001). Kinetics of mass transfer-limited bacterial growth on solid PAHs. *Environ. Sci. Technol.* 35, 354–361. doi: 10.1021/es001384w
- Wick, L. Y., Pelz, O., Bernasconi, S. M., Andersen, N., and Harms, H. (2003). Influence of the growth substrate on ester-linked phospho- and glycolipid fatty acids of PAH-degrading *Mycobacterium sp.* LB501T. *Environ. Microbiol.* 5, 672–680. doi: 10.1046/j.1462-2920.2003.00455.x
- Wilcke, W., Zech, W., and Kobza, J. (1996). PAH-pools in soils along a PAH-deposition gradient. *Environ. Pollut.* 92, 307–313. doi: 10.1016/0269-7491(95)00110-7
- Wold, S., Sjöström, M., and Eriksson, L. (2001). PLS-regression: a basic tool of chemometrics. *Chemom. Intell. Lab. Syst.* 58, 109–130. doi: 10.1016/S0169-7439(01)00155-1
- Wu, H., Chen, W., Rong, X., Cai, P., Dai, K., and Huang, Q. (2014a). Adhesion of *Pseudomonas putida* onto kaolinite at different growth phases. *Chem. Geol.* 390, 1–8. doi: 10.1016/j.chemgeo.2014.10.008
- Wu, H., Chen, W., Rong, X., Cai, P., Dai, K., and Huang, Q. (2014b). In situ ATR-FTIR study on the adhesion of *Pseudomonas putida* to Red soil colloids. *J. Soils Sediments* 14, 504–514. doi: 10.1007/s11368-013-0817-9
- Wu, H., Chen, W., Rong, X., Cai, P., Dai, K., and Huang, Q. (2014c). Soil colloids and minerals modulate metabolic activity of *Pseudomonas putida* measured using microcalorimetry. *Geomicrobiol. J.* 31, 590–596. doi: 10.1080/01490451.2013.861544
- Xie, Y., Gu, Z., Herath, H. M. S. K., Gu, M., He, C., Wang, F., et al. (2017). Evaluation of bacterial biodegradation and accumulation of phenanthrene in the presence of humic acid. *Chemosphere* 184, 482–488. doi: 10.1016/j.chemosphere.2017.06.026

**Conflict of Interest Statement:** The authors declare that the research was conducted in the absence of any commercial or financial relationships that could be construed as a potential conflict of interest.

Copyright © 2018 Fanesi, Zegeye, Mustin and Cébron. This is an open-access article distributed under the terms of the Creative Commons Attribution License (CC BY). The use, distribution or reproduction in other forums is permitted, provided the original author(s) and the copyright owner(s) are credited and that the original publication in this journal is cited, in accordance with accepted academic practice. No use, distribution or reproduction is permitted which does not comply with these terms.



# Hydrodynamics Alter the Tolerance of Autotrophic Biofilm Communities Toward Herbicides

Bastian H. Polst<sup>1,2,3\*</sup>, Christine Anlanger<sup>4,5</sup>, Ute Risse-Buhl<sup>4</sup>, Floriane Larras<sup>1</sup>, Thomas Hein<sup>2,3</sup>, Markus Weitere<sup>4</sup> and Mechthild Schmitt-Jansen<sup>1\*</sup>

<sup>1</sup> Department of Bioanalytical Ecotoxicology, Helmholtz-Centre for Environmental Research – UFZ, Leipzig, Germany,

<sup>2</sup> Institute of Hydrobiology and Aquatic Ecosystem Management, University of Natural Resources and Life Sciences, Vienna, Austria, <sup>3</sup> WasserCluster Lunz, Lunz, Austria, <sup>4</sup> Department of River Ecology, Helmholtz-Centre for Environmental Research – UFZ, Magdeburg, Germany, <sup>5</sup> Institute for Environmental Sciences, University of Koblenz-Landau, Landau, Germany

## OPEN ACCESS

### Edited by:

Fabrice Martin-Laurent,  
Institut National de la Recherche  
Agronomique (INRA), France

### Reviewed by:

Soizic Morin,  
National Research Institute of Science  
and Technology for Environment  
and Agriculture (IRSTEA), France

Yinjie Tang,  
Washington University in St. Louis,  
United States

### \*Correspondence:

Bastian H. Polst  
bastian-herbert.polst@ufz.de  
Mechthild Schmitt-Jansen  
mechthild.schmitt@ufz.de

### Specialty section:

This article was submitted to  
Microbiotechnology, Ecotoxicology  
and Bioremediation,  
a section of the journal  
Frontiers in Microbiology

**Received:** 24 July 2018

**Accepted:** 12 November 2018

**Published:** 04 December 2018

### Citation:

Polst BH, Anlanger C,  
Risse-Buhl U, Larras F, Hein T,  
Weitere M and Schmitt-Jansen M  
(2018) Hydrodynamics Alter  
the Tolerance of Autotrophic Biofilm  
Communities Toward Herbicides.  
*Front. Microbiol.* 9:2884.  
doi: 10.3389/fmicb.2018.02884

Multiple stressors pose potential risk to aquatic ecosystems and are the main reasons for failing ecological quality standards. However, mechanisms how multiple stressors act on aquatic community structure and functioning are poorly understood. This is especially true for two important stressors types, hydrodynamic alterations and toxicants. Here we perform a mesocosm experiment in hydraulic flumes connected as a bypass to a natural stream to test the interactive effects of both factors on natural (inoculated from streams water) biofilms. Biofilms, i.e., the community of autotrophic and heterotrophic microorganisms and their extracellular polymeric substances (EPS) in association with substratum, are key players in stream functioning. We hypothesized (i) that the tolerance of biofilms toward toxicants (the herbicide Prometryn) decreases with increasing hydraulic stress. As EPS is known as an absorber of chemicals, we hypothesize (ii) that the EPS to cell ratio correlates with both hydraulic stress and herbicide tolerance. Tolerance values were derived from concentration-response assays. Both, the herbicide tolerance and the biovolume of the EPS significantly correlated with the turbulent kinetic energy (TKE), while the diversity of diatoms (the dominant group within the stream biofilms) increased with flow velocity. This indicates that the positive effect of TKE on community tolerance was mediated by turbulence-induced changes in the EPS biovolume. This conclusion was supported by a second experiment, showing decreasing effects of the herbicide to a diatom biofilm (*Nitzschia palea*) with increasing content of artificial EPS. We conclude that increasing hydrodynamic forces in streams result in an increasing tolerance of microbial communities toward chemical pollution by changes in EPS-mediated bioavailability of toxicants.

**Keywords:** autotrophic biofilm, multiple stressors, microbial communities, PICT, near-bed hydrodynamics, periphyton

## INTRODUCTION

Most aquatic systems suffer from exposure to multiple stressors. This may be the cause why most water bodies at the European scale fail to reach the ecological quality goal such as the “good ecological status” according to the EU-Water Framework Directive (EEA, 2012). Approximately two third of European rivers are affected by two or more stressors at the same time with water

quality pressures (59% of European rivers) and alterations of hydrology and hydrodynamics due to channelization or impoundments (41% of European rivers) being widely distributed (Schinegger et al., 2012). Co-occurring stressors may interact, leading to non-linear and complex responses which are difficult to characterize and predict, but may have important implications for the management of aquatic systems (Côté et al., 2016). Whereas the co-occurrence and potential interactions of stressors were analyzed on a large scale (Côté et al., 2016), there is still limited knowledge on the mechanisms of stressor interactions on local communities. However, an improved understanding of stressor interactions is essential to manage and restore water bodies under multiple stresses. Chemical stressors are underrepresented in current surveys on multiple stressors (Nóges et al., 2016; Schäfer et al., 2016), but have been identified to pose a potential risk to more than 50% of rivers in Germany (Schäfer et al., 2016). Consequently, the co-occurrence and interactions of hydrodynamics and chemical stress in streams and rivers is very likely.

Biofilms play an important role in mediating essential functions and biogeochemical processes within aquatic ecosystem (Battin et al., 2003b, 2016). At the same time, they are especially vulnerable to chemical exposure and physical stress induced by hydraulic disturbance (Sabater et al., 2007; Larned, 2010; Romero et al., 2018). Often also referred to as periphyton, aquatic biofilms cover a wide range of different taxonomical and functional groups including fungi, bacteria, archaea, algae, protozoa, and viruses colonizing surfaces at and within the stream channel bed. Embedded in a matrix of extracellular polymeric substances (EPS), biofilm organisms shape their own microenvironment (Flemming and Wingender, 2010). They are highly dynamic and can rapidly adapt to changing conditions regarding pollution and flow velocity (Villeneuve et al., 2011a) making them suitable indicators for environmental change (Sabater et al., 2007).

In streams and rivers, hydrodynamics affect structural and functional parameters of biofilms. For instance, primary production and algal biodiversity as well as biofilm internal mass transport were reported to decrease with increasing flow velocity where at the same time mass transport from the water column toward biofilms increase (Beyenal and Lewandowski, 2002; Larned et al., 2004; Soininen, 2004). The algal composition of biofilms can adapt to the present flow conditions (Graba et al., 2013; Bondar-Kunze et al., 2016). With increasing flow velocities, the diversity of the diatom community may decrease because only specialized species can withstand (Soininen, 2004). It was reported that the EPS matrix gets thinner but denser (Wang et al., 2014), and that the production of EPS per bacterial cell increases with increasing flow velocity (Battin et al., 2003a). Besides flow velocity, near-bed turbulence is an important parameter shaping biofilm composition, architecture, and biomass (Labiod et al., 2007; Besemer et al., 2009; Risse-Buhl et al., 2017). While the flow velocity measures temporarily averaged flow, the turbulence kinetic energy (TKE) expresses the flow variations over time. These flow variations are even stronger close to solid boundaries like the stream bed and are thus considered an appropriate

descriptor for the complex physical environment of streambed surfaces (Statzner et al., 1988).

Besides hydrodynamics, water quality (i.e., nutrients and chemical pollution) is an important environmental factor for community composition. In European rivers 960 organic chemicals were reported to be present by of which 42% are pesticides, 165 compounds are potentially hazardous to algae, and at least 7% inhibit photosynthesis (Busch et al., 2016). Targeting the Hill-reaction and decreasing the electron transport of the photosystem II (Shimabukuro and Swanson, 1969), these herbicides decrease primary production and result in changes in species richness and algal biomass after chronic exposure (DeLorenzo et al., 2001; Pesce et al., 2011).

During chronic exposure stressors exert a species selection pressure on the biofilm community. In the following sensitive species vanish and tolerant species dominate the community (toxicant-induced succession, TIS) resulting in an increase of the overall community tolerance. This principle is used in the SICT-approach (stress-induced community tolerance, Blanck et al., 1988; Tlili et al., 2015) and was evidenced for several toxicants (e.g., McClellan et al., 2008; Tlili et al., 2011).

The tolerance of stream biofilms toward herbicides differs due to the present species pool, which may have been pre-selected by previous stress exposures. This makes an interaction of combined stressors on community tolerance reliable. For instance, Rotter et al. (2013) and Schmitt-Jansen et al. (2016) showed that combined toxic and ionic stress result in a selection of unique communities impacting community tolerance. TIS was identified to be the main assembly rule behind induced community tolerance but other mechanisms like physiological acclimation are also conceivable (Schmitt-Jansen et al., 2016). Induced community tolerance may be especially of importance, when combined stressors result in co-tolerance patterns (Vinebrooke et al., 2004).

Besides the biofilm community, the biofilm matrix, respectively, the EPS, is known to interact with herbicides (Lawrence et al., 2001). The EPS matrix absorbs herbicides (Wolfaardt et al., 1994) and protects the biofilms against chemical stressors (Flemming and Wingender, 2010; Limoli et al., 2015).

As the above cited literature indicates that hydrodynamic conditions primarily control the biofilm composition in terms of species composition and EPS content (Ghosh and Gaur, 1998; Villeneuve et al., 2011b; Wang et al., 2014) we expect interactions between hydrodynamics and herbicide tolerance, as the EPS is also known to accumulate and protect the biofilm organisms from toxicants (Wolfaardt et al., 1994; Flemming and Wingender, 2010). The hypothesis that a higher biodiversity increases the community tolerance was tested under the “biological insurance hypothesis” (Yachi and Loreau, 1999) by Villeneuve et al. (2011b), already. While they did not link herbicide tolerance of biofilm communities to different flow velocities directly, they found a lower tolerance in a more heterogeneous and turbulent flow channel. Moreover, the relevance of near-bed turbulence and the EPS matrix as a potential mechanism of stressor interactions were not considered in their study.

We want to fill this gap of knowledge by addressing the questions whether (I) hydrodynamic-induced changes in species composition result in community tolerance to herbicides and how (II) the EPS content explains interacting effects of hydrodynamic and chemical stress in biofilms. In detail we hypothesize that:

- the herbicide tolerance of stream biofilms decreases with increasing near-bed flow velocity and turbulence
- the hydraulic stress increases the EPS biovolume of a biofilm, decreasing bioavailability of toxicants
- a hydrodynamic selection pressure changes community structure resulting in decreasing biodiversity and community tolerance.

## MATERIALS AND METHODS

### Mesocosm Experiment

#### Mesocosm Setup

Biofilms were cultivated under spatially varying hydrodynamic conditions for 34 days in a hydraulic flume (length: 5.2 m, width 0.3 m). The flume was installed inside a “mobile aquatic mesocosm” (MOBICOS, Wollschläger et al., 2017) and constantly fed with water from the neighboring stream Selke. The catchment of the Selke is located in the Bode catchment (Harz, Germany) which is part of the Terrestrial Environmental Observations (TERENO), a dense, long-term monitoring program (Wollschläger et al., 2017). The stream reach next to the MOBICOS exhibits a mountainous character with coarse grained sediments and a near-natural flow regime.

Flow heterogeneity in the flume was created by several nozzles which contracted the flow and created varying zones of high and low flow velocity and TKE (Figure 1A). Biofilms were

grown on large unglazed anthracite ceramic tiles. LED strips (SolarStringer SunStrip, daylight, Econlux, Cologne, Germany) supplied biofilms with a photosynthetic active radiation of  $36.1 \pm 5.8 \mu\text{mol m}^{-2} \text{s}^{-1}$  (mean  $\pm$  SD) for 10 h/day during the 34 days of biofilm development.

The water level was controlled by a weir placed at the end of the flume and plateaued at about 16 cm at the sampling points. Discharge was monitored by a clamp-on ultrasonic flowmeter (MB 100H) installed at a tube section right before the flume entrance and was  $8.5 \text{ L s}^{-1}$ . Abiotic parameters of the flume water, i.e., temperature, oxygen concentrations, pH, conductivity were measured by an EXO2 multiparameter probe (YSI Inc., Yellow Springs, OH, United States) at least once a week. At the same interval flume water was sampled for dissolved organic carbon (DOC), soluble reactive phosphorus (SRP),  $\text{NO}_3\text{-N}$ ,  $\text{NH}_4\text{-N}$ , and Chl a (see Risse-Buhl et al., 2017 for methods description).

#### Biofilm Sampling

A custom made biofilm brush sampler adapted from Ritz et al. (2017) based on a toothbrush head within a sample chamber was used to sample the 34-day-old biofilms. Under a constant flow of sterile filtered stream water ( $0.2 \mu\text{m}$ ) through the sample chamber realized by a peristaltic pump (Watson Marlow) at  $2 \text{ mL s}^{-1}$ , the toothbrush head was placed on the biofilm patch, rotated and pushed three times. An area of  $5.7 \text{ cm}^2$  per patch was detached and transported with the flow of sterile water into the sampling tubes. Two neighboring patches per sample were pooled up to a total volume of 20 mL. Samples were stored at  $8^\circ\text{C}$  and further processed within the next 12 h. A total number of 12 samples was collected. Sample locations in the flume are shown in Figure 1. Additional biofilm samples for chlorophyll analysis were taken at different sampling spots to get a rough estimation of a possible relationship of chlorophyll a and hydrodynamic parameters (see Supplementary Figure 1).

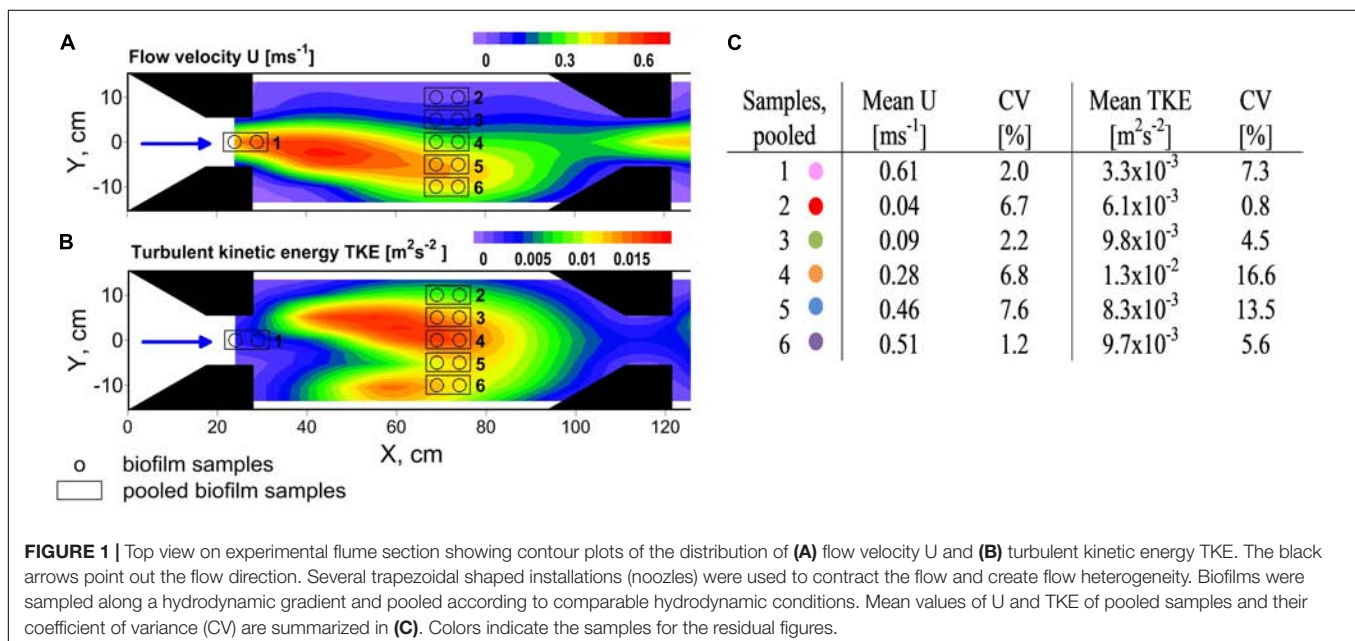


**FIGURE 1 |** Top view on experimental flume section showing contour plots of the distribution of (A) flow velocity  $U$  and (B) turbulent kinetic energy TKE. The black arrows point out the flow direction. Several trapezoidal shaped installations (nozzles) were used to contract the flow and create flow heterogeneity. Biofilms were sampled along a hydrodynamic gradient and pooled according to comparable hydrodynamic conditions. Mean values of  $U$  and TKE of pooled samples and their coefficient of variance (CV) are summarized in (C). Colors indicate the samples for the residual figures.

## Hydrodynamic Measurements

Three-dimensional current velocity measurements were conducted with a multi-static acoustic Doppler velocity ADV profiler (Vectrino II, Nortek AS, Norway) at 64 Hz for 5 min and 2.3 cm above the sampled biofilm patches. Velocity time-series were processed and the TKE was calculated based on the three dimensional variance of flow velocity according to Risse-Buhl et al. (2017). Flow velocity was calculated as  $U = \frac{1}{N} \sum_{i=1}^N u_i$  where  $u$  and  $N$  denote the longitudinal component of the velocity vector and the number of measurements at each location, respectively. Overall, 32 measurements were conducted above the biofilm samples and in their vicinity. Resampling of point measurements on a regular grid was done using a multiquadratic radial basis function with an anisotropic ratio of 3 (Golden Software Surver v9.2.397).

## Assessing Stress-Induced Community Tolerance (SICT)

The herbicide Prometryn was selected for chemical exposure because environmentally relevant concentrations in the lower nmol range were recently found in a near-by catchment (Rotter et al., 2015). In this study community tolerance induced by Prometryn was evidenced during *in situ* investigations using biofilms grown directly in the river (Rotter et al., 2015).

Using 96-well plates, aliquots of 150  $\mu\text{L}$  of the biofilm samples were taken under constant stirring to ensure homogeneity. Biofilm suspensions were incubated with Dimethylsulfoxid (DMSO)-dissolved Prometryn at six concentrations within a 10-fold dilution series ranging from 0.00084 to 83.8  $\mu\text{mol L}^{-1}$ . Each dilution step of the herbicide and a solvent control (final DMSO concentration: 0.05%, not showing effects in a former study; Rotter et al., 2011) were used in triplicate. The 96-well plates with the biofilm-herbicide suspension were placed under constant light (130 – 150  $\mu\text{mol photons m}^{-2} \text{s}^{-1}$ ) and intense shaking at 350 rpm (KS250basic, IKA Labortechnik, Staufen, Germany). Inhibition of variable chlorophyll fluorescence was analyzed using an Imaging Maxi pulse-amplitude modulated (PAM) fluorimeter (Walz, Effeltrich, Germany; instrumental settings: Intensity 4, Gain 4, Damping 2). After 1 h of incubation biofilms were dark adapted for 5 min and the variable chlorophyll fluorescence was measured three times. After applying a saturation pulse the maximum chlorophyll fluorescence at dark adapted conditions (Yield I) was assessed following Schmitt-Jansen and Altenburger (2008).

## Extraction and Analysis of EPS Fractions

Extracellular polymeric substances were extracted according to Barranguet et al. (2004). Briefly, 2 mL biofilm samples were resuspended in bi-distilled water, vortexed and centrifuged (5 min, 3500 rpm). The supernatant was collected and represents the soluble EPS fraction. The bound EPS fraction was extracted from the residual pellet after incubation at 95°C for 30 min in 2 mL 0.1 M  $\text{H}_2\text{SO}_4$ . Both fractions were analyzed for four groups of substances by comparing the spectrophotometric measurements to the ones of the standard substances. The carbohydrate content of the EPS was quantified according to

the phenol-sulphuric acid assay by DuBois et al. (1956) with D-Glucose (Sigma-Aldrich, CAS 50-99-7) as a standard. For protein and humic acid analysis the Folin phenol assay by Lowry et al. (1951) was used. Results had to be corrected due to interferences of humic acids after Frolund et al. (1995). Bovine Serum Albumin (Biorad, CAS n.a.) was used as standard substance for the protein assay, and humic acid (Roth, CAS 1415-93-6) for the humic acid assay. A hydroxydiphenyl assay by Blumenkrantz and Asboe-Hansen (1973) and its modification by Kintner and Van Buren (1982) was used to assess the uronic acid content. Glucuronic acid (Sigma, CAS 6556-12-3) was used as the standard substance.

## Preparation and Taxonomic Assessment of Diatoms

To identify diatoms, which were the dominating algae fraction within the biofilms [71% according to measurements derived from a Phyto-PAM fluorimeter (Walz, Effeltrich, Germany)], organic material was removed by boiling the biofilm suspension first in hydrochloric acid and second in hydrogen peroxide solution (30%) until the solution was colorless. Samples were washed in water during 24 h after each boiling step. Species were identified using a light microscope ( $\times 630$  zoom, Leica DMI4000B with a PFC250 camera, Leica Microsystems GmbH, Wetzlar, Germany) based on their microscopic siliceous exoskeleton. At least 400 valves per sample were counted. Hofmann et al. (2013) was used for the taxonomic determination of the diatoms to species level as far as possible.

## Data Analysis and Assessment

Concentration-response curves were modeled and effective concentrations that induced 50% of inhibition of the photosynthetic yield (YI; EC50) were calculated using the software SigmaPlot 13.0 (Systat Software GmbH, Erkrath, Germany). Concentration-response curves were modeled based on the four-parametric Hill-equation  $y = y_0 + (ax^b)/(c^b + x^b)$  ( $y_0$  = the minimum value of photosynthesis inhibition fixed at 0.0001%,  $a$  = the maximum value of photosynthesis inhibition fixed at 100%,  $c$  = the inflection point (here the EC50),  $b$  = Hill's slope at point  $c$ ) with 1000 iterations per curve. Correlations of the EC50-values with the other parameters were tested via Spearman-test.

The diatom community diversity and evenness was assessed with the Shannon-Index ( $H_S$ ) and the Pielou-Index ( $E_H$ ), respectively:

$$H_S = - \sum_{i=1}^S p_i \times \log p_i \quad \text{with} \quad p_i = \frac{n_i}{N} \quad E_H = \frac{H_S}{H_{\text{max}}}$$

$S$  = number of present species,  $N$  = total number of individuals (400),  $n_i$  = number of individuals per species,  $p_i$  = relative abundance of the  $i$ -species,  $H_{\text{max}}$  = maximal possible Shannon Index.

A correspondence analysis (CCA) was performed based on the hydrodynamic data and the taxonomical dataset of the diatom community. To obtain a more robust dataset the species of the genera *Navicula*, *Nitzschia* and *Fragilaria* were pooled according to their genera. The CCA was performed using the software R

version 3.5.0 and the *vegan* R package (Oksanen et al., 2015; R Core Team, 2018).

## Herbicide Toxicity Modulation by Artificial EPS

Based on the results of the mesocosm experiment using natural communities a second experiment was performed using a benthic diatom culture to confirm the role of EPS on the response of biofilms to Prometryn. Therefore, *Nitzschia palea* biofilms (SAG Göttingen, Strainnumber 1052-3A) were grown in 24-well plates (initial cell count  $1 \times 10^6$  cells mL<sup>-1</sup>). After 3 days of growth, the diatom culture medium was exchanged with five different artificial EPS-enriched diatom culture media. Briefly, the diatom medium was enriched by one of the four individual EPS fractions studied previously (humic acid, carbohydrates, proteins, uronic acid, see section “Extraction and Analysis of EPS Fractions”). For each of the four media, four different enrichment concentrations were tested such as 0, 25, 50, 100 mg L<sup>-1</sup> (for details on the calibration curve see **Supplementary Table 2**). In parallel, a medium containing a mixture of all four EPS fractions (composed according to the EPS fractions found in the biofilms of the mesocosms experiment: carbohydrates 28.9%, proteins 30.9%, humic acids, 25.9%, uronic acids 4.3%) was tested at five different enrichment concentrations: 0, 50, 100, 200, and 400 mg EPS L<sup>-1</sup>. For each of these media (four single fractions of EPS\*four EPS concentrations and one mixture of fractions\*five EPS concentrations), the inhibition of photosynthesis of *N. palea* biofilms was assessed after exposure to six Prometryn concentrations ranging from 0.00026 to 83.2 μmol L<sup>-1</sup> (solved in 0.1% DMSO). The inhibition of chlorophyll fluorescence after dark adaptation (Yield I) was measured after 1 h of exposure as described above.

## RESULTS

### The Mesocosm Experiment Hydrodynamic Conditions

Flow velocities and TKE varied over one order of magnitude and ranged from 0.04 to 0.62 m s<sup>-1</sup> and from  $3.2 \times 10^{-3}$  to  $1.4 \times 10^{-2}$  m<sup>2</sup> s<sup>-2</sup>, respectively, covering the full range of near-bed flow velocities and the upper range of TKE that was found in the neighboring stream Selke (Risse-Buhl et al., 2017). Highest flow velocities were observed right at the nozzles exit whereas highest TKE values coincided with the centerline ( $Y = 0$  cm, **Figure 1B**) of the flume, in-between the two sets of nozzles. Whereas flow velocities and turbulence in natural streams are positively correlated because both are predominately linked to riverbed roughness, in the hydraulic flume the causes of high and low flow velocities and origin of turbulence are associated to the contraction of the flow and shear layers due jet-like flow. However, properties of flow velocity and TKE result in comparable forces at small spatial scales and therefore show similar effects on biofilms. The coefficients of variance (CV) of flow velocities and TKE values of pooled biofilm samples were small and, except for the two highest TKE values, below 15%

(**Figure 1C**). In the following it will be exclusively referred to the mean values of flow velocities and TKE. For results for physico-chemical parameters see **Supplementary Table 1**. For additional information on Chl a distribution see **Supplementary Figure 4**.

### Biofilm Tolerance Toward Prometryn

The EC<sub>50</sub>-values of photosynthesis inhibition of biofilms toward Prometryn ranged from  $8.06 \pm 1.90$  to  $18.80 \pm 14.23$  μmol L<sup>-1</sup>. The yield and TKE showed a significant linear correlation with  $R^2 = 0.88$  ( $p < 0.05$ ) (**Figure 2**). The lowest EC<sub>50</sub> values were detected at lowest TKE and the highest EC<sub>50</sub> values for the highest TKE. However, no linear correlation with the flow velocity was found ( $R^2 = 0.17$ ,  $p = 0.33$ , **Supplementary Figure 2**).

### EPS Matrix of Natural Communities at Contrasting Hydrodynamic Conditions

The EPS of the biofilms from contrasting hydrodynamic conditions mostly consisted of carbohydrates, proteins and humic acids at an almost equal mean percentage share of  $37.5 \pm 2.9$ ,  $29.2 \pm 2.0$ , and  $28.6 \pm 3.3\%$ , respectively. Uronic acids made up only a marginal fraction of the EPS ( $4.75 \pm 0.39\%$ ). The total amount of EPS ranged from  $113 \pm 8$  μg cm<sup>-2</sup> at the lowest TKE value to  $458 \pm 30$  μg cm<sup>-2</sup> at the highest TKE value. A positive linear correlation ( $R^2 = 0.76$ ) of the total EPS biovolume and TKE was found and confirmed by a Spearman-test (**Figure 3**,  $p < 0.05$ ). Furthermore, the total EPS correlated positively with the EC<sub>50</sub>-values of biofilms toward Prometryn ( $R^2 = 0.74$ ,  $p < 0.05$ ). No correlation with the flow velocity was found ( $p = 0.16$ , **Supplementary Figure 3**).

### Diatom Community Composition and Biodiversity

Overall twenty-five diatom taxa were found, from which seven taxa made up more than 5% of the total diatom community, respectively. The diatom community changed along the gradient of the flow velocity (**Figure 4**). The taxonomic diversity and

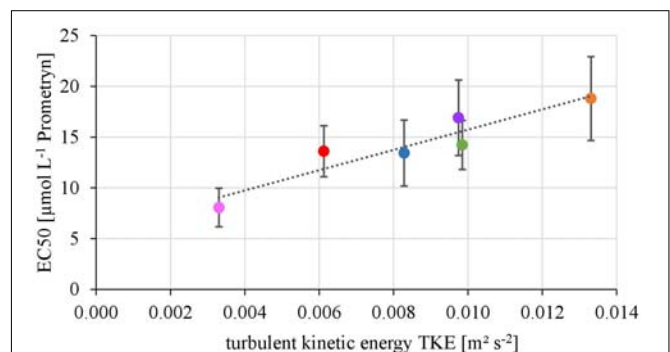
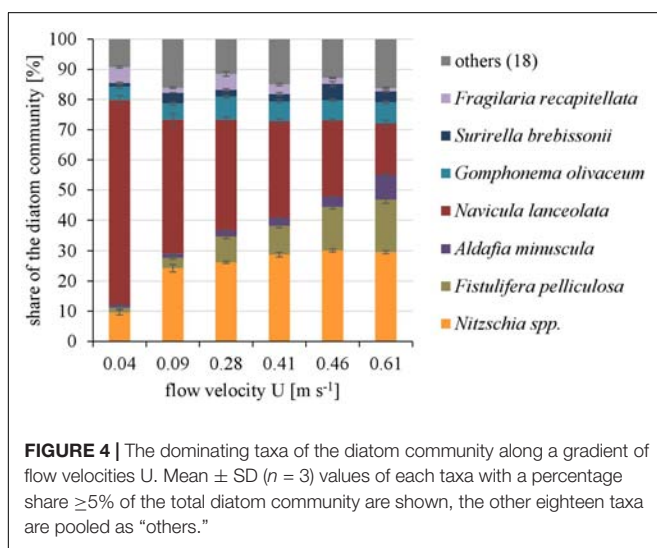
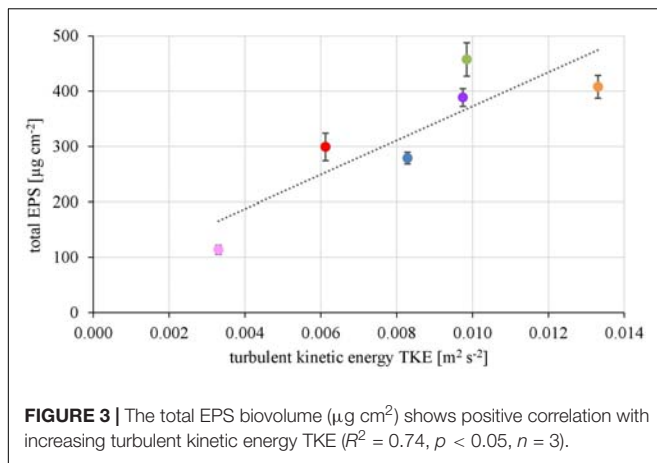


**FIGURE 2 |** Relationship of the EC<sub>50</sub>-values derived from toxicity testing of biofilms, quantified as inhibition of the maximum photosynthetic Yield after 1 h of exposure and turbulent kinetic energy TKE ( $R^2 = 0.87$ ,  $p < 0.05$ ). The error bars of the EC<sub>50</sub>-values represent the calculated standard error after modeling of concentrations-response curves using the Hill model.



evenness increased with increasing flow velocity (Figure 5). At lower flow velocities *Navicula lanceolata* was dominating with an approximate percentage share of 70%. At higher velocities the percentage share of *N. lanceolata* decreased to 20% at  $0.61 \text{ m s}^{-1}$  and favored other species as *Nitzschia spp.*, *Fistulifera pelliculosa* and *Adlafia minuscula*. Diatom taxa were more equally distributed at higher flow velocities. No clear trends in dependence on TKE were found. Shannon-Index and Pielou-Index show a correlation with the flow velocity ( $p < 0.05$ ) but not with the TKE. The CCA showed a high explanatory value for the first axis (91%) and a lower one for the second axis (8.9%) (Figure 6). Samples were ordered along the first axis from the right to left side in accordance with the increase of the flow velocity but were also displayed from the top to the down of the plot in accordance to TKE values. The ordination plot displays the importance of both flow parameters spanning a two-dimensional space in which the diatom community developed. However, axis eigenvalues highlighted the importance of flow velocity over TKE in community structure.

## Herbicide Inhibition Through Artificial EPS

In the first experiment we observed a positive correlation of the total EPS with the EC50-values (Figure 7A), in the second experiment, a highly significant positive correlation between the mean EC50-values of *N. palea* biofilms toward Prometryn and the total artificial EPS-content was found with  $R^2 = 0.99$  ( $p < 0.01$ ) (Figure 7B). For the individual EPS fractions, only humic acids had a significant positive correlation with the EC50-values ( $R^2 = 0.90$ ) (Figure 8). Other fractions showed comparable trends in the EC50-values, but no significant relationships were found.

## DISCUSSION

### Herbicide Tolerance of the Biofilm

The herbicide tolerances positively correlate with near-bed turbulence but not with flow velocity. Villeneuve et al. (2011a) found that an increasing flow velocity has a positive effect on periphyton primary production, algal density, bacterial production, and bacterial density. This may be caused by an increased retention of nutrients by the biofilm at high flow velocities (Biggs and Hickey, 1994; Villeneuve et al., 2011a). In a follow-up study, Villeneuve et al. (2011b) tried to link these structural and functional periphyton responses to changes in tolerance toward a PSII-inhibiting herbicide but could not find a correlation of the EC50-values and flow velocity (A. Bouchez, personal communication). This finding was partly confirmed by our study; however, the clear correlation with TKE indicates the relevance of the temporal velocity variations for changes in the biofilms. In conclusion, we could not confirm our first hypothesis that increasing flow velocity and turbulence decreased the herbicide tolerance. Instead, we found that in particular turbulent conditions induce a higher tolerance toward herbicides.

In a recent study, Risse-Buhl et al. (2017) highlighted the role of the near streambed turbulence on the composition and architecture of stream biofilms: The algal biovolume as well as the surface coverage of biofilms matured in streams increased with increasing near streambed turbulence. This leads us to the conclusion that TKE-induced changes in the composition and architecture of the biofilms is the main factor for stress-induced community tolerance toward the herbicide. Therefore, the EPS matrix as well as the diatom community composition were analyzed in more detail in this study to gain insights in potential mechanisms of stressor interactions.

### Changes of the EPS Matrix

Similar to the EC50-values of biofilms toward herbicides, the changes in total EPS content of the biofilm matrix increased with near-bed turbulence but not with flow velocity thereby partly confirming our second hypothesis. However, evidence from literature on this relationship remains unclear. The total EPS content of bacterial biofilms grown in flow cells either increased with laminar flow (Percival et al., 1999; Araújo et al., 2016), or

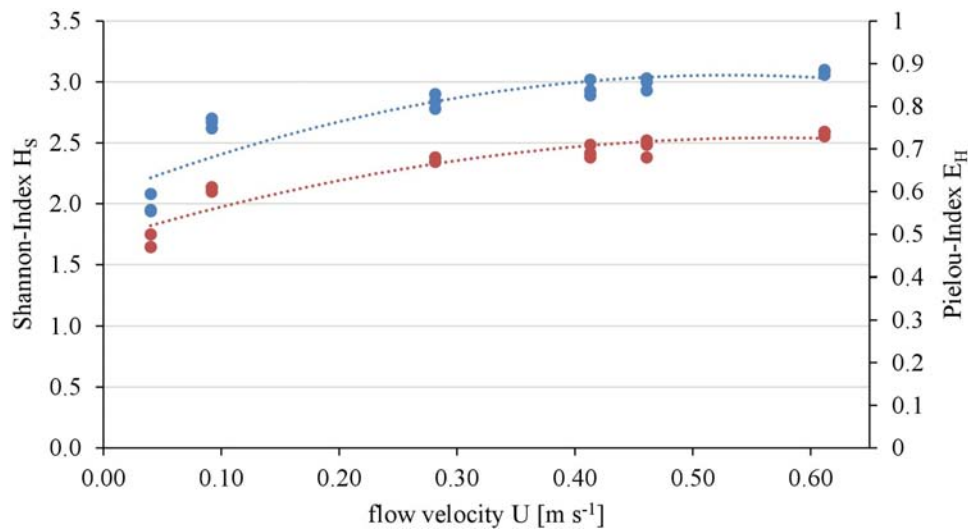


**FIGURE 5** | Relationship of taxonomic diversity of the diatom communities expressed as Shannon-Index (blue, polynomial relationship:  $R^2 = 0.82$ ) and evenness expressed as Pielou-Index (red, polynomial relationship:  $R^2 = 0.88$ ) with the flow velocity.

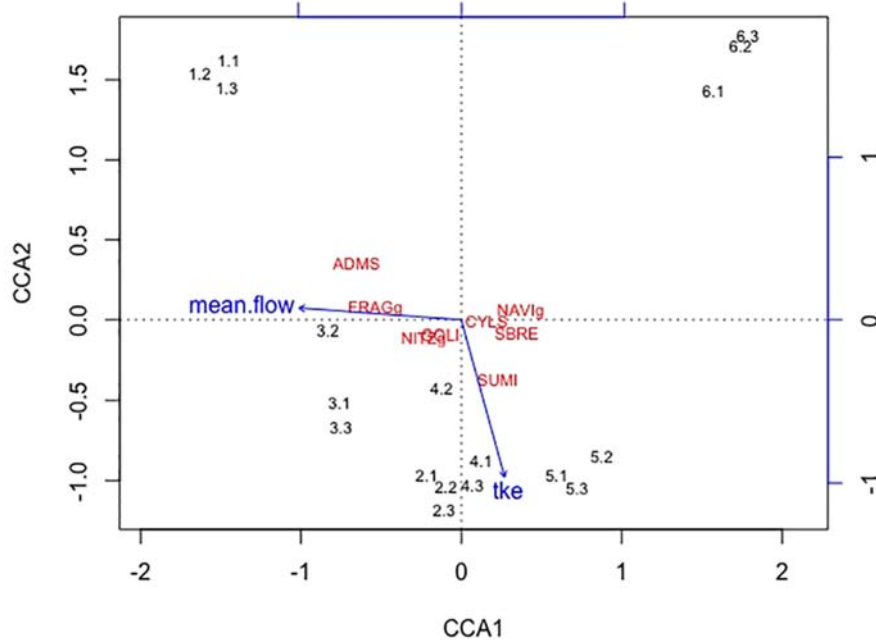
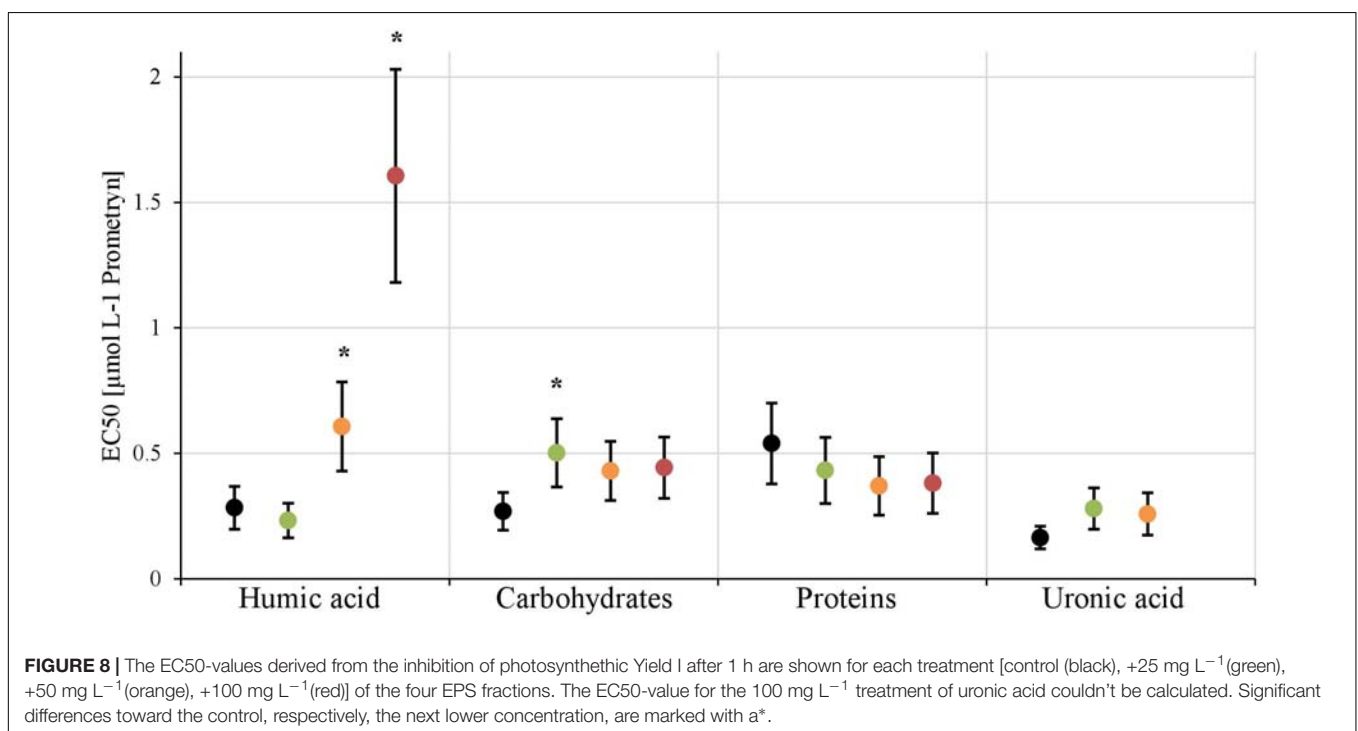
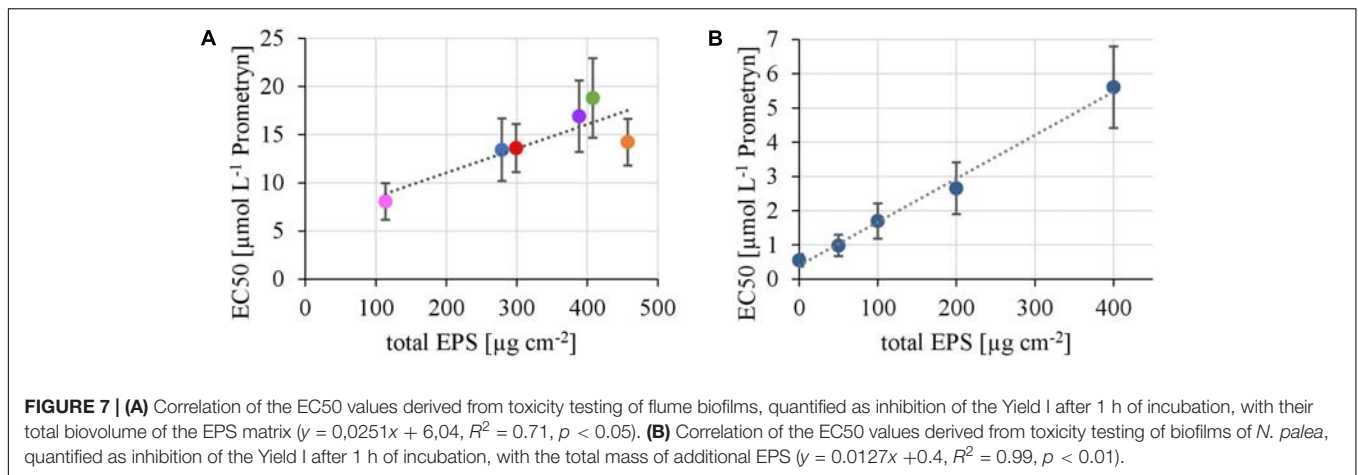


**FIGURE 6** | The first axis CCA1 explains 91% of the differences found in the diatom community and the second axis CCA2 describes 8.9% of the differences. Blue arrows indicate the direction of the two increasing hydrodynamic parameters (mean flow, TKE) within this cluster. Numbers represent the diatom samples and the respective replicates. The diatom species *Adlafia minuscula* (ADMS), *Fragilaria* spp. (FRAGg), *Nitzschia* spp. (NITZg), *Gomphonema olivaceum* (GOLi), *Cyclotella* spp. (CYLS), *Navicula* spp. (NAVIg), *Suriella brebissonii* (SBRE), and *Suriella minuta* (SUMI) are shown within the CCA cluster. The diatom community aligns with the flow velocity, only one species also partly aligns with TKE.

with turbulence (Simões et al., 2007), whereas Wang et al. (2014) found a positive correlation of the bound EPS with flow velocity. Increasing flow velocity and turbulence were not found to be responsible for changes of the total EPS content of autotrophic biofilms grown in flumes (Battin et al., 2003a) but for changes of the EPS production per cell. The opposite was found in the Selke

stream, where less glycoconjugates were produced per microbial cells but overall the biovolume of glycoconjugates increased with TKE (Risse-Buhl et al., 2017). Carbohydrates or polysaccharides of the EPS matrix of bacterial biofilms are shown to be important for building a mature 3-dimensional biofilm structure (Limoli et al., 2015). In combination with proteins that have the affinity



to crosslink to, e.g., carbohydrates, complexes are formed that substantially contribute to the stability of the biofilm matrix (Fong and Yildiz, 2015). The increasing carbohydrate and protein content in our flume biofilms indicates an increased stability of the biofilms 3-dimensional structure at increased TKE. Thus, the EPS seems to help buffering hydrodynamic forces affecting the biofilm community (Biggs and Hickey, 1994; Freeman and Lock, 1995). EPS, as such, is still a black box since it is composed of a large number of diverse substances, ranging from carbohydrates, glycoconjugates, peptides, humic acids, uronic acids to nucleic acids (Flemming et al., 2016). The functions of these substances are far from being completely understood. Up to now, there are no consistent trends on the EPS content of biofilms at different hydrodynamic conditions in literature. However, none of these studies analyzed TKE as a driving factor of the EPS content. Our

study clearly shows that TKE is the prominent factor for changes in the biofilm EPS content.

### Influence of the EPS Matrix on Toxicity

The results of the first, and especially the second, experiment illustrate a lower sensitivity of biofilms toward the herbicide at high humic acid concentrations. We hypothesize from these findings that the EPS matrix binds the toxicants changing their bioavailability to the organisms. Indeed, binding mechanisms for herbicides have been described for DOC in soils, for long (Baskaran and Kennedy, 1999; Ling et al., 2006). Furthermore, the absorption of herbicides to humic acids, which is one fraction of the DOC pool in soils and aquatic systems, is well described in literature (Bollag and Myers, 1992; Senesi, 1992). Out of all binding mechanisms, e.g., hydrophobic adsorption

or covalent binding, adsorption is considered to be the most important interaction (Senesi, 1992). For aquatic ecosystems, the accumulation (Lawrence et al., 2001) and the sorption (Headley et al., 1998) of organic micropollutants (including herbicides) in the EPS matrix was already shown, but not linked to changes in bioavailability and toxic effects. In our study, we observed that the EPS matrix of biofilms lowers the negative effect of Prometryn (increase of EC50-values based on photosynthesis inhibition) which could be regarded as an indirect evidence of changes in bioavailability. This result represents a first step toward a better understanding of biofilm matrix effects and the role of toxicokinetic processes for algae toxicity. To prove this mechanism in more detail, further experiments with chemical analysis at multiple time points are needed.

## Diatom Community Structure and Diversity

According to our third hypothesis we found a clear trend in both community structure and taxonomic diversity parameters (Shannon Index & Pielou Index) in dependence to flow velocity while TKE seems to have no effect. The increase in biodiversity with increasing flow velocity is contradictory to other studies. Soininen (2004) found a decrease in the diatom diversity (Shannon Index) over a gradient of three flow velocities (0.1, 0.4, and 1.0 m s<sup>-1</sup>). Villeneuve et al. (2011b) conclude that the heterogeneity of hydraulic conditions increases the overall biodiversity by creating more microhabitats for a diverse community, but cannot correlate the biodiversity with a gradient of these conditions.

Multiple reasons may be responsible for the distribution of the diatom community, e.g., increased hydrodynamic shear forces leading to an adaption of the community. Certain species would be better adapted to these conditions and thrive while others vanish.

Whether the individual sensitivity of single species has an influence on the observed changes in biofilm tolerance cannot be concluded, as there are not enough species-specific autoecological data available. Considering diversity on its own, the “biological insurance hypothesis” (Yachi and Loreau, 1999) applied on our diversity results suggest that the biofilms at higher flow velocities would be less sensitive toward herbicides. Instead we confirm results by Villeneuve et al. (2011b), who also could not confirm Yachi’s hypothesis on the herbicide application on biofilms in the first place and indicate that other mechanisms than diversity are responsible for the tolerance patterns, found in these studies.

Furthermore, we found no evidence that the biofilm diversity has an influence on the herbicide tolerance of the biofilm and could not prove our third hypothesis that the diatom diversity decreases due to the hydrodynamic selection pressure. Nevertheless, only assumptions can be made based on our results and the complex interaction thought to be present. We suggest that more complex processes shape the diversity than originally thought. In particular, the varying effects of flow velocity and turbulence on biofilm diversity and underlying mechanisms need to be the focus of future studies.

## CONCLUSION

Our results clearly showed interacting effects of hydrodynamics and toxic stress which are frequently co-occurring in European waters. Nöges et al. (2016) revealed a frequency of 10–25% of co-occurrence of hydrological (with potential effects on hydrodynamic conditions) and toxic stressors in reported data sets from rivers and transitional and coastal waters, however, these numbers may be even higher, as toxicants are not frequently included in these analyses (Schäfer et al., 2016). Additionally, interacting effects from hydrological and toxic stress may be especially important for streams with steep gradients in altitude or high morphological degradation.

The stress-induced tolerance of the biofilm communities toward a herbicide, found in this study and the causal findings behind stressor interactions point to an antagonistic effect at community level. Côté et al. (2016) revealed that antagonistic effects are especially being observed at community level whereas other levels of biological complexity (e.g., population of sub-cellular studies) mainly showed additive or synergistic interactions. While laboratory studies mainly exclude the invasion of other species with higher tolerances to the selecting stressors, these experimental settings may bias the findings toward additive or synergistic effects. This is further demonstrating the importance of *in situ* studies mimicking the natural situation as close as possible. The experimental system used in this study allowed manipulation of the stressor gradients but also species succession processes from the bypass stream, which is an important response mechanism of natural communities toward combined stress.

Our approach studied two dominant mechanisms behind the interacting effects: while changes in the community structure is frequently found to be the cause for SICT, in this study the role of EPS and its potential relevance for the bioavailability of toxicants was investigated. This hints to the complexity of stressor interactions which could on the one hand act on the assembly rules of communities resulting in changes on species sensitivity, diversity and functioning but also on the susceptibility of communities to a stressor, in this case changes in the toxicokinetic processes. This mode of interaction may not only be important for chemical pollution but also for other factors like dissolved organic material or nutrients. Transferring these small-scale interactions to a larger scale many hydro-morphologically altered streams and rivers in Europe pose a risk for lower tolerances of the phototrophic benthic community in streams.

## DATA AVAILABILITY STATEMENT

The raw data supporting the conclusions of this manuscript will be made available by the authors, without undue reservation, to any qualified researcher.

## AUTHOR CONTRIBUTIONS

BP did the lab work and statistical analysis and wrote the draft. CA and UR-B contributed to the conception and design of

the mesocosm, maintained the mesocosm during the experiments and wrote sections of the draft. CA conducted and analyzed the hydrodynamic measurements and provided the figures. UR-B took the biofilm samples within the mesocosm and provided data for physico-chemistry of flume water and Chl a of biofilms. TH, MW, and MS-J provided substantial feedback and revision of the draft. FL contributed to the analysis of the diatom community (CCA) and their interpretation. MW contributed to the conception and design of the mesocosm and had strong impact on the abstract. MS-J and TH supervised the project. MS-J initiated this study and designed the tolerance and confirmation experiment including the structural and functional descriptors of the biofilm community. All authors contributed to the submitted draft with overall feedback, insightful discussions, and improvements on the text.

## FUNDING

The research was supported by the German Research Foundation (DFG) within the project “Interactions between

flow hydrodynamics and biofilm attributes and functioning in streams” (WE 3545/6-1 and LO 1150/8-1).

## ACKNOWLEDGMENTS

We thank Peter Portius and his team for help in designing and constructing the flumes, Florian Zander, Ute Link, Hans-Joachim Dahlke, Helge Norf, and Sven Bauth for their help with setting up the MOBICOS and the mesocosm, as well as their help with the sampling and analysis. We also thank Andreas Lorke and Christian Noss for stimulating discussions that have contributed to the development of the research and data analysis of the velocity measurements.

## SUPPLEMENTARY MATERIAL

The Supplementary Material for this article can be found online at: <https://www.frontiersin.org/articles/10.3389/fmicb.2018.02884/full#supplementary-material>

## REFERENCES

- Araújo, P. A., Malheiro, J., Machado, I., Mergulhão, F., Melo, L., and Simões, M. (2016). Influence of flow velocity on the characteristics of *Pseudomonas fluorescens* biofilms. *J. Environ. Eng.* 142:04016031. doi: 10.1061/(ASCE)EE.1943-7870.0001068
- Barranguet, C., van Beusekom, S. A. M., Veuger, B., Neu, T. R., Manders, E. M. M., Sinke, J. J., et al. (2004). Studying undisturbed autotrophic biofilms: still a technical challenge. *Aquat. Microb. Ecol.* 34, 1–9. doi: 10.3354/ame034001
- Baskaran, S., and Kennedy, I. R. (1999). Sorption and desorption kinetics of diuron, fluometuron, prometryn and pyriithiobac sodium in soils. *J. Environ. Sci. Health Part B* 34, 943–963. doi: 10.1080/03601239909373238
- Battin, T. J., Besemer, K., Bengtsson, M. M., Romani, A. M., and Packmann, A. I. (2016). The ecology and biogeochemistry of stream biofilms. *Nat. Rev. Microbiol.* 14, 251–263. doi: 10.1038/nrmicro.2016.15
- Battin, T. J., Kaplan, L. A., Newbold, J. D., Cheng, X. H., and Hansen, C. (2003a). Effects of current velocity on the nascent architecture of stream microbial biofilms. *Appl. Environ. Microbiol.* 69, 5443–5452. doi: 10.1128/aem.69.9.5443-5452.2003
- Battin, T. J., Kaplan, L. A., Newbold, J. D., and Hansen, C. M. E. (2003b). Contributions of microbial biofilms to ecosystem processes in stream mesocosms. *Nature* 426, 439–442. doi: 10.1038/nature02152
- Besemer, K., Singer, G., Hödl, I., and Battin, T. J. (2009). Bacterial community composition of stream biofilms in spatially variable-flow environments. *Appl. Environ. Microbiol.* 75, 7189–7195. doi: 10.1128/aem.01284-09
- Beyenal, H., and Lewandowski, Z. (2002). Internal and external mass transfer in biofilms grown at various flow velocities. *Biotechnol. Prog.* 18, 55–61. doi: 10.1021/bp010129s
- Biggs, B. J. F., and Hickey, C. W. (1994). Periphyton responses to a hydraulic gradient in a regulated river in New Zealand. *Freshw. Biol.* 32, 49–59. doi: 10.1111/j.1365-2427.1994.tb00865.x
- Blanck, H., Wängberg, S. -Å., and Molander, S. (1988). “Pollution-induced community tolerance—a new ecotoxicological tool,” in *Functional Testing of Aquatic Biota for Estimating Hazards of Chemicals*, ed. J. Cairns (West Conshohocken, PA: ASTM International).
- Blumenkrantz, N., and Asboe-Hansen, G. (1973). New method for quantitative determination of uronic acids. *Anal. Biochem.* 54, 484–489. doi: 10.1016/0003-2697(73)90377-1
- Bollag, J.-M., and Myers, C. (1992). Detoxification of aquatic and terrestrial sites through binding of pollutants to humic substances. *Sci. Total Environ.* 117–118(Suppl. C), 357–366. doi: 10.1016/0048-9697(92)90102-X
- Bondar-Kunze, E., Maier, S., Schönauer, D., Bahl, N., and Hein, T. (2016). Antagonistic and synergistic effects on a stream periphyton community under the influence of pulsed flow velocity increase and nutrient enrichment. *Sci. Total Environ.* 573, 594–602. doi: 10.1016/j.scitotenv.2016.08.158
- Busch, W., Schmidt, S., Kühne, R., Schulze, T., Krauss, M., and Altenburger, R. (2016). Micropollutants in European rivers: a mode of action survey to support the development of effect-based tools for water monitoring. *Environ. Toxicol. Chem.* 35, 1887–1899. doi: 10.1002/etc.3460
- Côté, I. M., Darling, E. S., and Brown, C. J. (2016). Interactions among ecosystem stressors and their importance in conservation. *Proc. R. Soc. B Biol. Sci.* 283:20152592. doi: 10.1098/rspb.2015.2592
- DeLorenzo, M. E., Scott, G. I., and Ross, P. E. (2001). Toxicity of pesticides to aquatic microorganisms: a review. *Environ. Toxicol. Chem.* 20, 84–98. doi: 10.1002/etc.5620200108
- DuBois, M., Gilles, K. A., Hamilton, J. K., Rebers, P. T., and Smith, F. (1956). Colorimetric method for determination of sugars and related substances. *Anal. Chem.* 28, 350–356. doi: 10.1021/ac60111a017
- EEA (2012). *European Waters: Assessment of Status and Pressures*. Copenhagen: European Environment Agency.
- Flemming, H.-C., Neu, T. R., and Wingender, J. (2016). *The Perfect Slime: Microbial Extracellular Polymeric Substances (EPS)*. London: IWA Publishing, 15–24. doi: 10.2166/9781780407425
- Flemming, H.-C., and Wingender, J. (2010). The biofilm matrix. *Nat. Rev. Microbiol.* 8, 623–633. doi: 10.1038/nrmicro2415
- Fong, J. N. C., and Yildiz, F. H. (2015). Biofilm matrix proteins. *Microbiol. Spectr.* 3 doi: 10.1128/microbiolspec.MB-0004-2014
- Freeman, C., and Lock, M. A. (1995). The biofilm polysaccharide matrix: a buffer against changing organic substrate supply? *Limnol. Oceanogr.* 40, 273–278. doi: 10.4319/lo.1995.40.2.0273
- Frolund, B., Griebe, T., and Nielsen, P. H. (1995). Enzymatic activity in the activated-sludge floc matrix. *Appl. Microbiol. Biotechnol.* 43, 755–761. doi: 10.1007/BF00164784

- Ghosh, M., and Gaur, J. P. (1998). Current velocity and the establishment of stream algal periphyton communities. *Aquat. Bot.* 60, 1–10. doi: 10.1016/s0304-3770(97)00073-9
- Graba, M., Sauvage, S., Moulin, F. Y., Urrea, G., Sabater, S., and Sanchez-Perez, J. M. (2013). Interaction between local hydrodynamics and algal community in epilithic biofilm. *Water Res.* 47, 2153–2163. doi: 10.1016/j.watres.2013.01.011
- Headley, J. V., Gandrass, J., Kuballa, J., Peru, K. M., and Gong, Y. (1998). Rates of sorption and partitioning of contaminants in river biofilm. *Environ. Sci. Technol.* 32, 3968–3973. doi: 10.1021/es980499l
- Hofmann, G., Werum, M., and Lange-Bertalot, H. (2013). “Diatomeen im Süßwasser-benthos von mitteleuropa,” in *Bestimmungsflora Kieselalgen für die Ökologische Ökologische Praxis. Über 700 der Häufigsten Arten und Ihre Ökologie*, ed. A. R. G. G. Rugell (Koenigstein: Koeltz Scientific Books).
- Kintner, P. K., and Van Buren, J. P. (1982). Carbohydrate interference and Its correction in pectin analysis using the m-hydroxydiphenyl method. *J. Food Sci.* 47, 756–759. doi: 10.1111/j.1365-2621.1982.tb12708.x
- Labioud, C., Godillot, R., and Caussade, B. (2007). The relationship between stream periphyton dynamics and near-bed turbulence in rough open-channel flow. *Ecol. Model.* 209, 78–96. doi: 10.1016/j.ecolmodel.2007.06.011
- Larned, S. T. (2010). A prospectus for periphyton: recent and future ecological research. *J. North Am. Benthol. Soc.* 29, 182–206. doi: 10.1899/08-063.1
- Larned, S. T., Nikora, V. I., and Biggs, B. J. F. (2004). Mass-transfer-limited nitrogen and phosphorus uptake by stream periphyton: a conceptual model and experimental evidence. *Limnol. Oceanogr.* 49, 1992–2000. doi: 10.4319/lo.2004.49.6.1992
- Lawrence, J. R., Kopf, G., Headley, J. V., and Neu, T. R. (2001). Sorption and metabolism of selected herbicides in river biofilm communities. *Can. J. Microbiol.* 47, 634–641. doi: 10.1139/w01-061
- Limoli, D. H., Jones, C. J., and Wozniak, D. J. (2015). Bacterial extracellular polysaccharides in biofilm formation and function. *Microbiol. Spectr.* 3 doi: 10.1128/microbiolspec.MB-0011-2014
- Ling, W., Xu, J., and Gao, Y. (2006). Dissolved organic matter enhances the sorption of atrazine by soil. *Biol. Fertil. Soils* 42, 418–425. doi: 10.1007/s00374-006-00856
- Lowry, O. H., Rosebrough, N. J., Farr, A. L., and Randall, R. J. (1951). Protein measurement with the folin phenol reagent. *J. Biol. Chem.* 193, 265–275.
- McClellan, K., Altenburger, R., and Schmitt-Jansen, M. (2008). Pollution-induced community tolerance as a measure of species interaction in toxicity assessment. *J. Appl. Ecol.* 45, 1514–1522. doi: 10.1111/j.1365-2664.2008.01525.x
- Nöges, P., Argillier, C., Borja, Á, Garmendia, J. M., Hanganu, J., Kodeš, V., et al. (2016). Quantified biotic and abiotic responses to multiple stress in freshwater, marine and ground waters. *Sci. Total Environ.* 540(Suppl. C), 43–52. doi: 10.1016/j.scitotenv.2015.06.045
- Oksanen, J., Blanchet, F. G., Friendly, M., Kindt, R., Legendre, P., McGlinn, D., et al. (2015). *Vegan: Community Ecology Package. R package version 2.2-1*.
- Percival, S. L., Knapp, J. S., Wales, D. S., and Edyvean, R. G. J. (1999). The effect of turbulent flow and surface roughness on biofilm formation in drinking water. *J. Ind. Microbiol. Biotechnol.* 22, 152–159. doi: 10.1038/sj.jim.2900622
- Pesce, S., Bouchez, A., and Montuelle, B. (2011). “Effects of organic herbicides on phototrophic microbial communities in freshwater ecosystems,” in *Reviews of Environmental Contamination and Toxicology*, Vol. 214, ed. D. M. Whitacre (New York, NY: Springer), 87–124.
- R Core Team (2018). *R: A Language and Environment for Statistical Computing*. Vienna: R Foundation for Statistical Computing.
- Risse-Buhl, U., Anlanger, C., Kalla, K., Neu, T. R., Noss, C., Lorke, A., et al. (2017). The role of hydrodynamics in shaping the composition and architecture of epilithic biofilms in fluvial ecosystems. *Water Res.* 127, 211–222. doi: 10.1016/j.watres.2017.09.054
- Ritz, S., Eßer, M., Arndt, H., and Weitere, M. (2017). Large-scale patterns of biofilm-dwelling ciliate communities in a river network: only small effects of stream order. *Int. Rev. Hydrobiol.* 102, 114–124. doi: 10.1002/iroh.201601880
- Romero, F., Sabater, S., Timoner, X., and Acuña, V. (2018). Multistressor effects on river biofilms under global change conditions. *Sci. Total Environ.* 627, 1–10. doi: 10.1016/j.scitotenv.2018.01.161
- Rotter, S., Gunold, R., Mothes, S., Paschke, A., Brack, W., Altenburger, R., et al. (2015). Pollution-induced community tolerance to diagnose hazardous chemicals in multiple contaminated aquatic systems. *Environ. Sci. Technol.* 49, 10048–10056. doi: 10.1021/acs.est.5b01297
- Rotter, S., Heilmeyer, H., Altenburger, R., and Schmitt-Jansen, M. (2013). Multiple stressors in periphyton – comparison of observed and predicted tolerance responses to high ionic loads and herbicide exposure. *J. Appl. Ecol.* 50, 1459–1468. doi: 10.1111/1365-2664.12146
- Rotter, S., Sans-Piché, F., Streck, G., Altenburger, R., and Schmitt-Jansen, M. (2011). Active bio-monitoring of contamination in aquatic systems—an *in situ* translocation experiment applying the PICT concept. *Aquat. Toxicol.* 101, 228–236. doi: 10.1016/j.aquatox.2010.10.001
- Sabater, S., Guasch, H., Ricart, M., Romani, A., Vidal, G., Klünder, C., et al. (2007). Monitoring the effect of chemicals on biological communities. The biofilm as an interface. *Anal. Bioanal. Chem.* 387, 1425–1434. doi: 10.1007/s00216-006-1051-8
- Schäfer, R. B., Kuhn, B., Malaj, E., König, A., and Gergs, R. (2016). Contribution of organic toxicants to multiple stress in river ecosystems. *Freshw. Biol.* 61, 2116–2128. doi: 10.1111/fwb.12811
- Schinegger, R., Trautwein, C., Melcher, A., and Schmutz, S. (2012). Multiple human pressures and their spatial patterns in European running waters. *Water Environ. J.* 26, 261–273. doi: 10.1111/j.1747-6593.2011.00285.x
- Schmitt-Jansen, M., and Altenburger, R. (2008). Community-level microalgal toxicity assessment by multiwavelength-excitation PAM fluorometry. *Aquat. Toxicol.* 86, 49–58. doi: 10.1016/j.aquatox.2007.10.001
- Schmitt-Jansen, M., Bley, L.-M., Krumbiegel, M.-L., and Rotter, S. (2016). Induced community tolerance of periphyton towards combined salt and toxic stress. *Freshw. Biol.* 61, 2152–2161. doi: 10.1111/fwb.12799
- Senesi, N. (1992). Binding mechanisms of pesticides to soil humic substances. *Sci. Total Environ.* 123–124(Suppl. C), 63–76. doi: 10.1016/0048-9697(92)90133-D
- Shimabukuro, R. H., and Swanson, H. R. (1969). Atrazine metabolism, selectivity, and mode of action. *J. Agric. Food Chem.* 17, 199–205. doi: 10.1021/jf60162a044
- Simões, M., Pereira, M. O., Sillankorva, S., Azeredo, J., and Vieira, M. J. (2007). The effect of hydrodynamic conditions on the phenotype of *Pseudomonas fluorescens* biofilms. *Biofouling* 23, 249–258. doi: 10.1080/08927010701368476
- Soininen, J. (2004). Assessing the current related heterogeneity and diversity patterns of benthic diatom communities in a turbid and a clear water river. *Aquat. Ecol.* 38, 495–501. doi: 10.1007/s10452-004-4089-8
- Statzner, B., Gore, J. A., and Resh, V. H. (1988). Hydraulic stream ecology: observed patterns and potential applications. *J. North Am. Benthol. Soc.* 7, 307–360. doi: 10.2307/1467296
- Tili, A., Berard, A., Blanck, H., Bouchez, A., Cássio, F., Eriksson, K. M., et al. (2015). Pollution-induced community tolerance (PICT): towards an ecologically relevant risk assessment of chemicals in aquatic systems. *Freshw. Biol.* 61, 2141–2151. doi: 10.1111/fwb.12558
- Tili, A., Montuelle, B., Berard, A., and Bouchez, A. (2011). Impact of chronic and acute pesticide exposures on periphyton communities. *Sci. Total Environ.* 409, 2102–2113. doi: 10.1016/j.scitotenv.2011.01.056
- Villeneuve, A., Bouchez, A., and Montuelle, B. (2011a). In situ interactions between the effects of season, current velocity and pollution on a river biofilm. *Freshw. Biol.* 56, 2245–2259. doi: 10.1111/j.1365-2427.2011.02649.x
- Villeneuve, A., Montuelle, B., and Bouchez, A. (2011b). Effects of flow regime and pesticides on periphytic communities: evolution and role of biodiversity. *Aquat. Toxicol.* 102, 123–133. doi: 10.1016/j.aquatox.2011.01.004
- Vinebrooke, R. D., Cottingham, K. L., Norberg, J., Scheffer, M., Dodson, S. I., Maberly, S. C., et al. (2004). Impacts of multiple stressors on biodiversity and ecosystem functioning: the role of species co-tolerance. *Oikos* 104, 451–457. doi: 10.1111/j.0030-1299.2004.13255.x
- Wang, C., Miao, L., Hou, J., Wang, P., Qian, J., and Dai, S. (2014). The effect of flow velocity on the distribution and composition of extracellular polymeric

- substances in biofilms and the detachment mechanism of biofilms. *Water Sci. Technol.* 69, 825–832. doi: 10.2166/wst.2013.785
- Wolfaardt, G. M., Lawrence, J. R., Headley, J. V., Robarts, R. D., and Caldwell, D. E. (1994). Microbial exopolymers provide a mechanism for bioaccumulation of contaminants. *Microb. Ecol.* 27, 279–291. doi: 10.1007/bf00182411
- Wollschläger, U., Attinger, S., Borchardt, D., Brauns, M., Cuntz, M., Dietrich, P., et al. (2017). The Bode hydrological observatory: a platform for integrated, interdisciplinary hydro-ecological research within the TERENO Harz/Central German Lowland Observatory. *Environ. Earth Sci.* 76:29. doi: 10.1007/s12665-016-6327-5
- Yachi, S., and Loreau, M. (1999). Biodiversity and ecosystem productivity in a fluctuating environment: the insurance hypothesis. *Proc. Natl. Acad. Sci. U.S.A.* 96, 1463–1468. doi: 10.1073/pnas.96.4.1463
- Conflict of Interest Statement:** The authors declare that the research was conducted in the absence of any commercial or financial relationships that could be construed as a potential conflict of interest.
- The handling Editor declared a past co-authorship with several of the authors FL and MS-J.
- Copyright © 2018 Polst, Anlanger, Risse-Buhl, Larras, Hein, Weitere and Schmitt-Jansen. This is an open-access article distributed under the terms of the Creative Commons Attribution License (CC BY). The use, distribution or reproduction in other forums is permitted, provided the original author(s) and the copyright owner(s) are credited and that the original publication in this journal is cited, in accordance with accepted academic practice. No use, distribution or reproduction is permitted which does not comply with these terms.



# Negative Effects of Copper Oxide Nanoparticles on Carbon and Nitrogen Cycle Microbial Activities in Contrasting Agricultural Soils and in Presence of Plants

## OPEN ACCESS

Marie Simonin<sup>1,2,3\*</sup>, Amélie A. M. Cantarel<sup>1,2,3</sup>, Armelle Crouzet<sup>1,2,3</sup>, Jonathan Gervais<sup>1,2,3</sup>, Jean M. F. Martins<sup>4</sup> and Agnès Richaume<sup>1,2,3</sup>

### Edited by:

Ed Topp,  
Agriculture and Agri-Food Canada  
(AAFC), Canada

### Reviewed by:

Safdar Bashir,  
University of Agriculture, Faisalabad,  
Pakistan  
Santosh Kr Kam,  
Sardar Bhagwan Singh Post Graduate  
Institute of Biomedical Science &  
Research, India

### \*Correspondence:

Marie Simonin  
simonin.marie@gmail.com

### Specialty section:

This article was submitted to  
Microbiotechnology, Ecotoxicology  
and Bioremediation,  
a section of the journal  
Frontiers in Microbiology

**Received:** 05 July 2018

**Accepted:** 30 November 2018

**Published:** 13 December 2018

### Citation:

Simonin M, Cantarel AAM, Crouzet A,  
Gervais J, Martins JMF and  
Richaume A (2018) Negative Effects of  
Copper Oxide Nanoparticles on  
Carbon and Nitrogen Cycle Microbial  
Activities in Contrasting Agricultural  
Soils and in Presence of Plants.  
*Front. Microbiol.* 9:3102.  
doi: 10.3389/fmicb.2018.03102

<sup>1</sup> Université de Lyon, Lyon, France, <sup>2</sup> Université Claude Bernard Lyon 1, Villeurbanne, France, <sup>3</sup> CNRS, UMR 5557, Microbial Ecology Centre, Université Lyon 1, Villeurbanne, France, <sup>4</sup> Université Grenoble Alpes, CNRS, IRD, IGE, Grenoble, France

Metal-oxide nanoparticles (NPs) such as copper oxide (CuO) NPs offer promising perspectives for the development of novel agro-chemical formulations of pesticides and fertilizers. However, their potential impact on agro-ecosystem functioning still remains to be investigated. Here, we assessed the impact of CuO-NPs (0.1, 1, and 100 mg/kg dry soil) on soil microbial activities involved in the carbon and nitrogen cycles in five contrasting agricultural soils in a microcosm experiment over 90 days. Additionally, in a pot experiment, we evaluated the influence of plant presence on the toxicity of CuO-NPs on soil microbial activities. CuO-NPs caused significant reductions of the three microbial activities measured (denitrification, nitrification, and soil respiration) at 100 mg/kg dry soil, but the low concentrations (0.1 and 1 mg/kg) had limited effects. We observed that denitrification was the most sensitive microbial activity to CuO-NPs in most soil types, while soil respiration and nitrification were mainly impacted in coarse soils with low organic matter content. Additionally, large decreases in heterotrophic microbial activities were observed in soils planted with wheat, even at 1 mg/kg for soil substrate-induced respiration, indicating that plant presence did not mitigate or compensate CuO-NP toxicity for microorganisms. These two experiments show that CuO-NPs can have detrimental effects on microbial activities in soils with contrasting physicochemical properties and previously exposed to various agricultural practices. Moreover, we observed that the negative effects of CuO-NPs increased over time, indicating that short-term studies (hours, days) may underestimate the risks posed by these contaminants in soils.

**Keywords:** metal-oxide nanomaterials, agro-ecosystem, microbial ecotoxicology, wheat, nitrification, denitrification, soil respiration, plant-microorganism interactions

## INTRODUCTION

Copper nanoparticles are increasingly used in various commercial products, including agrochemicals, paints, semiconducting compounds, sensors, catalyzers, and antimicrobial products, which leads to their growing release into terrestrial and aquatic ecosystems (Keller et al., 2017). These emerging contaminants can make their way into soil through direct applications of nanofertilizers or nanopesticides containing copper nanoparticles or through biosolid amendments from wastewater treatment (Lazareva and Keller, 2014; Kah, 2015). Hence, the high reactivity of copper nanomaterials and their established antimicrobial properties raise some concerns about the potential consequences on microbial processes driving soil fertility in agro-ecosystems.

Extensive research has been conducted in the past decade to assess the impact of several metal nanoparticles on soil microbial communities, especially silver and titanium dioxide nanoparticles (reviews by Simonin and Richaume, 2015; McKee and Filser, 2016). However, the effects of copper oxide nanoparticles (CuO-NPs) still remain poorly documented. To our knowledge, only four studies have examined CuO-NP, and these studies were conducted using unrealistic exposure conditions with high concentrations of CuO-NPs ranging from 100 mg/kg to 10 g/kg of soil (Ben-Moshe et al., 2010; Rousk et al., 2012; Frenk et al., 2013; Xu et al., 2015), compared to expected concentrations in soil in the  $\mu\text{g/kg}$  to low mg/kg range (Garner and Keller, 2014). Additionally, these studies were performed on one or two model soils that presented predominantly sandy-loam texture. Like any other pollutant, CuO-NP toxicity and bioavailability is likely influenced by soil properties, such as organic matter, pH, texture or ionic strength, and the results obtained in one soil type should thus not be generalized to other soils (Cornelis et al., 2014; Simonin et al., 2015). For example, soil characteristics can influence the transformations of CuO-NPs through processes such as dissolution (Keller et al., 2017). The ionic Cu form can be both highly toxic for soil microorganisms (at high concentrations) and an essential micronutrient for biological growth (at low concentrations, Arguello et al., 2013). Hence, it is hard to predict in which soil types the impact of CuO-NPs would be the most adverse depending on the dissolution rates observed and if CuO-NPs or ionic Cu form would have the larger detrimental effects on soil function. More research needs to be performed to assess the effects of realistic concentrations of CuO-NPs on microbial functioning in soils exhibiting contrasting physicochemical properties.

Moreover, the reliable assessment of the impact of a contaminant on microbial communities in soil needs to consider the influence of plants, especially in the context of an agro-ecosystem where plant-microorganism interactions are intense (Philippot et al., 2013). It is frequently reported that a stressor has no direct effect on microbial communities but that microbial processes are impacted through indirect effects driven by plants in the context of strong plant-soil feedbacks (Cantarel et al., 2015; Simonin et al., 2017; Pommier et al., 2018). For instance, plants can influence the fate and bioavailability of pollutants in soils through soil restructuring by the roots, changes in

soil pH, and exudation of organic compounds (Bravin et al., 2012). The presence of plants has also been shown to increase the immobilization and detoxification of Cu in soil (Römkens et al., 1999; Chibuike and Obiora, 2014). A recent study showed that CuO-NPs exhibited slow dissolution rates in soils and that those rates were modulated by the wheat rhizosphere due to direct associations of CuO-NPs to roots, an increase in soil pH and the exudation of small organic acids (Gao et al., 2018). Additionally, the input of nutrient resources through plant exudation can confer a higher resistance and resilience of microbial communities to disturbances (Griffiths and Philippot, 2013). Microbial communities already stressed by low nutrient availability in bulk soils may have less energy available to cope with an external stressor like CuO-NPs in comparison to rhizosphere microbial communities inhabiting nutrient-rich habitats (de Vries and Shade, 2013). Nevertheless, soil ecotoxicological assays on nanomaterials rarely include plants and are mainly performed over short periods of time (2 weeks to 1 month), ignoring the plant-soil feedbacks and indirect effects that can affect pollutant bioavailability and toxicity over long period of times (McKee and Filser, 2016). Specific studies designed to assess how plants modulate NP toxicity for soil microorganisms are clearly needed.

In this study, we performed two experiments to address the following questions: (1) Do CuO-NPs affect microbial function in contrasting soils at relevant low concentrations? (2) Is plant presence influencing the microbial response to CuO-NP exposure? To address the first question, we performed a soil microcosm experiment over 90 days to assess the effects of CuO-NPs at low concentrations (0.1, 1, and 100 mg/kg) on soil microbial activities associated to the carbon and nitrogen (N) cycles (respiration, nitrification, and denitrification) in five contrasting agricultural soils. The effects of CuO-NPs were compared to those of a Cu ion control ( $\text{CuSO}_4$  application) to determine the toxic potential of the Cu nanoparticulate form in comparison to the ionic form. To address the second question, we conducted a follow-up pot experiment to assess the influence of plant presence (winter wheat) on the effects of CuO-NPs on microbial activities over 50 days in the soil that presented the strongest response to the CuO-NPs in the soil microcosm experiment (loam textured LCSA soil).

## MATERIAL AND METHODS

### Soils

For the microcosm experiment, we selected five soils of contrasting textures and exposed to various agricultural practices: a sandy-loam soil used for vegetable production (Brindas), a loam soil under maize-wheat rotations (LCSA), a silty-clay soil under rape-wheat-barley rotations (Commarin), a silty-clay soil used for maize production (Clessé-Maize) and a silty-clay-loam soil from a vineyard (Clessé-Vine). These soils were collected in the Burgundy and Auvergne-Rhône-Alpes Regions (France). More details on the soil characteristics and sample locations are provided in **Table 1A**. Soils were characterized by the Laboratoire d'Analyse des Sols (LAS, Arras, France) for

particle-size distribution (texture class), organic matter content, pH, cation exchange capacity (CEC) and Cu concentration using standardized ISO protocols. We mixed several kilograms of the top soil (0–15 cm) collected at different locations in each field to obtain a representative composite soil sample, and we transported the soils back to the lab in coolers. The soils were then sieved at 2 mm and stored at 4°C for <1 week before the beginning of the experiment.

## Nanoparticle Characteristics

For the experiments, we used manufactured powdered CuO-NPs commercialized by Sigma-Aldrich. The CuO-NPs had a nominal size <50 nm and a specific surface area of 23 m<sup>2</sup> g<sup>-1</sup>, according to the manufacturer information. The intrinsic primary particle size was verified using a ZEISS Ultra 55 scanning electron microscopy field emission gun (SEM-FEG) and energy dispersive spectroscopy (EDS) with a SDD detector (BRUKERAXS-30 mm<sup>2</sup>). On average, the CuO-NPs measured 57.0 ± 18 nm. The apparent hydrodynamic diameter and zeta potential of the CuO-NPs were characterized using Dynamic Light Scattering (DLS) with a NanoZS (Malvern Instruments, UK, laser of 638 nm wavelength) in 50 mg CuO-NPs L<sup>-1</sup> of soil solution prepared according to Simonin et al. (2015). All CuO-NP suspensions were dispersed using ultrasonication for 5 min before use to ensure suspension homogeneity. The CuO-NP hydrodynamic diameters and zeta potentials measured in the five soil solutions are presented in **Table 1B**. The dissolution of CuO-NPs was assessed in triplicate soil solutions spiked with 50 mg L<sup>-1</sup> CuO-NPs for 1, 7, 30, and 90 days and incubated in the dark at 28°C in plasma flasks (150 mL) under the same conditions as the soil microcosm experiment described below. At each date, we isolated the dissolved Cu fraction in the soil solutions using ultrafiltration tubes (5 kDa) centrifuged for 45 min at 6,000 g and determined the Cu concentration using ICP-OES (Varian 700-ES, Varian Inc. Scientific Instruments, Palo Alto, USA). In the five soil solutions, we observed <2% cumulative dissolution (**Table 1B**) of the CuO-NPs during the 90 days of incubation.

## Soil Microcosm Experimental Design

In the microcosm experiment, we exposed the soils to five treatments, including three concentrations of CuO-NPs (0.1, 1, and 100 mg/kg), an ionic Cu treatment of copper sulfate (CuSO<sub>4</sub>) at 100 mg/kg and a control treatment that received no Cu addition. The CuO-NP concentrations were selected to cover both a range of low realistic concentrations in the ppb range (0.1 mg/kg, Keller et al., 2017) and a higher concentration representing an accidental spill (100 mg/kg). For each treatment, 600 g (equivalent dry weight) of each soil were spiked with an ultrasonicated CuO-NP or CuSO<sub>4</sub> solution at a concentration of 0, 1.79, 17.9, or 1,790 mg/L in ultrapure water to achieve the required final concentrations. The CuO-NPs suspensions were added homogeneously to the soils using a multichannel pipette and then soils were thoroughly mixed for 10 min to ensure a uniform exposure. Soil moisture was adjusted to the water holding capacity specific to each soil. 50 g (equivalent dry weight) of each spiked soil were then transferred into 150 mL

glass plasma flasks sealed with rubber stoppers to maintain constant soil moisture during the duration of the experiment. The microcosms were incubated in the dark at 28°C for 7 or 90 days and were weekly aerated under a sterile atmosphere for 5 min to renew the atmosphere in the flask. Each treatment was replicated in six independent microcosms, resulting in the incubation and analysis of 300 microcosms (6 replicates × 5 soils × 5 treatments × 2 dates). At the end of each incubation time (7 or 90 days), the microcosms were subsampled for microbial activity measurements (stored at 4°C and analyzed within 3 days), DNA extractions and subsequent qPCR measurements (stored at -20°C). On the remaining soil, on day 7, we measured the soil pH using the ISO 10390 protocol for the different treatments. The different CuO-NP treatments did not induce significant pH changes in the five soils studied (data not shown).

## Pot Experiment With *Triticum aestivum*

Using a pot experiment under greenhouse conditions, we compared microbial responses between unplanted and planted conditions in the LCSA soil (**Table 1A**) exposed to two concentrations of CuO-NPs (1 and 100 mg/kg) and no Cu addition (control). Five replicates by treatment were used, and all experiments were conducted using winter wheat (*Triticum aestivum*) grown in pots without a N supply. Two seeds previously germinated in a humid chamber for 1 week were sown per pot (12 × 12 × 12 cm) containing 1.5 kg of sieved loam soil (<2 mm) collected at La Côte Saint-André (LCSA, **Table 1A**). Plants were grown for 50 days in a climatic chamber (Fitoclima 10,000 EH, ARALAB) with 16 h light—8 h night; day and night temperatures of 21 and 18°C, respectively; CO<sub>2</sub> concentration of 350 ppm; and chamber relative air humidity of 70%. Each pot was watered three times a week. After 50 days of incubation, the microbial activities, and plant biomass were determined. The leaf and root systems of planted pots were dried at 105°C for 2 days to measure above-ground, below-ground and total plant dry masses (g dry weight) and to assess whole plant shoot/root ratio. pH was determined for each soil sample as explained in section Soils.

## Microbial Activity Measurements

### Substrate-Induced Respiration (SIR)

To measure substrate-induced respiration (SIR) at each time point, 10 g (equivalent dry weight) of fresh soil was placed in a new glass plasma flask to which we added 0.5 mL of a glucose solution (1.2 mg C-glucose g<sup>-1</sup> dry soil) as a non-limiting carbon source for microbial respiration (Patra et al., 2005). The flasks were hermetically sealed with a rubber stopper and incubated at 28°C for 7 h. CO<sub>2</sub> accumulation in the flask was measured every hour using a gas chromatograph (Micro GC R3000, SRA Instrument, Marcy L'Etoile, France).

### Nitrification Enzyme Activity (NEA)

To measure nitrification enzyme activity (NEA), 3 g (equivalent dry weight) of fresh soil was incubated with 6 ml of (NH<sub>4</sub>)<sub>2</sub>SO<sub>4</sub> solution (50 μg N-NH<sub>4</sub><sup>+</sup> g<sup>-1</sup> dry soil) in a new plasma flask (Dassonville et al., 2011). Distilled water was added to each sample to achieve 24 ml of total liquid volume in flasks. The flasks were sealed with Parafilm<sup>®</sup> and incubated at 28°C under

**TABLE 1A** | Main physicochemical characteristics of the five soils used in the microcosm experiment.

Soils	Sampling location	Texture	Sand (%)	Loam (%)	Clay (%)	CEC (cmol(+)/kg)	OM (%)	Water holding capacity (%)	pH	Cu (mg/kg)
Brindas	Brindas, France (45°43'40.8"N 4°43'35.4"E)	Sandy-Loam	68.4	14.7	16.9	11.5	2.09	20	7	20.1
LCSA	La Côte St André, France (45°22'39.3"N 5°16'06.1"E)	Loam	37.5	42.7	19.8	8.79	2.23	27	6.4	13.2
Commarin	Commarin, France (47°14'37.0"N 4°38'53.1"E)	Silty-Clay	8.2	49.8	42	17.4	4.72	47	6.94	23.2
Clessé-Maize	Clessé, France (46°25'03.5"N 4°47'58.8"E)	Silty-Clay	7.3	48.9	43.8	20.7	2.88	28	8.21	35.5
Clessé-Vine	Clessé, France (46°25'03.1"N 4°48'03.5"E)	Silty-Clay-Loam	12.5	58.6	28.9	14.8	2.59	26	7.75	47.5

**TABLE 1B** | CuO-NP characterization (at 50 mg/L) in the five soil solutions.

Soil Solutions	Hydrodynamic diameter (nm)	Zeta potential (mV)	Cumulative CuO-NPs dissolution over 90 days (%)
Brindas	57.6	-19.1	1.23
LCSA	46.8	-13.8	1.61
Commarin	61.8	-14.3	0.77
Clessé-Maize	101.2	-19.9	0.50
Clessé-Vine	75.6	-21.3	0.83

constant shaking (140 rpm). 1.5 ml of soil slurry were sampled after 2, 4, 6, 8, and 10 h of incubation, filtered at 0.2  $\mu\text{m}$  and stored in vials at  $-20^{\circ}\text{C}$  until measurement of  $\text{NO}_2^-$  and  $\text{NO}_3^-$  concentrations using an ion chromatograph (ICS 900, Dionex, Salt Lake City, USA).

### Denitrification Enzyme Activity (DEA)

To measure denitrification enzyme activity (DEA), 10 g (equivalent dry weight) of fresh soil was placed in a new plasma flask hermetically sealed with a rubber stopper (Bardon et al., 2014). The atmosphere of the flasks was replaced by a 90% helium and 10% acetylene mixture to obtain anaerobic conditions and inhibit the nitrous oxide reductase that catalyzes the final step of denitrification converting  $\text{N}_2\text{O}$  in  $\text{N}_2$ . Distilled water (1 ml) containing  $\text{KNO}_3$  (50  $\mu\text{g N-NO}_3^- \text{g}^{-1}$  dry soil), glucose (500  $\mu\text{g C-glucose g}^{-1}$  dry soil), and glutamic acid (500  $\mu\text{g C-glutamic acid g}^{-1}$  dry soil) was added through the rubber stopper using a syringe to ensure non-limiting amounts of carbon and  $\text{NO}_3^-$  for denitrification activity. The flasks were incubated at  $28^{\circ}\text{C}$  for 8 h. After 2 h,  $\text{N}_2\text{O}$  concentration in the atmosphere of the flasks was measured every hour using the gas chromatograph described in section Substrate-Induced Respiration (SIR).

### Microbial Abundance Measurements

Soil DNA was extracted from 0.5 g of frozen soil using the FastDNA<sup>®</sup> Spin Kit for Soil (MPbio, California, USA)

following the manufacturer's instructions. DNA quantification was performed using the Qubit<sup>®</sup> dsDNA BR Assay Kit on a Qubit<sup>®</sup> 2.0 fluorometer.

The abundance of the total bacterial community, *amoA* nitrifiers (AOA and AOB) and denitrifiers were measured with quantitative PCR using a Lightcycler 480 (Roche Diagnostics, Meylan, France) following the protocols described in Simonin et al. (2015, 2016). For total bacterial abundance, we amplified the *rrs* gene encoding for 16S rRNA using the universal primers 519F and 907R targeting the V4-V5 region. For the nitrifiers, the *amoA* functional gene was amplified using gene primers *amoA\_1F* and *amoA\_2R* for the AOB, and *CrenamoA616r* and *CrenamoA23f* for the AOA. Denitrifier abundance was measured with the *nirS* functional gene encoding Cu-containing  $\text{NO}_2^-$  reductase. Amplification was performed using *nirScd3aF* and *nirSR3cd* gene primers. All reactions were performed in duplicate using 1X QuantiTectSybrGreen PCR Master Mix (Qiagen, Courtaboeuf, France) and serial dilutions of DNA standards for each gene were included ( $10^2$  to  $10^7$  gene copies  $\mu\text{L}^{-1}$ ).

### Statistical Analyses

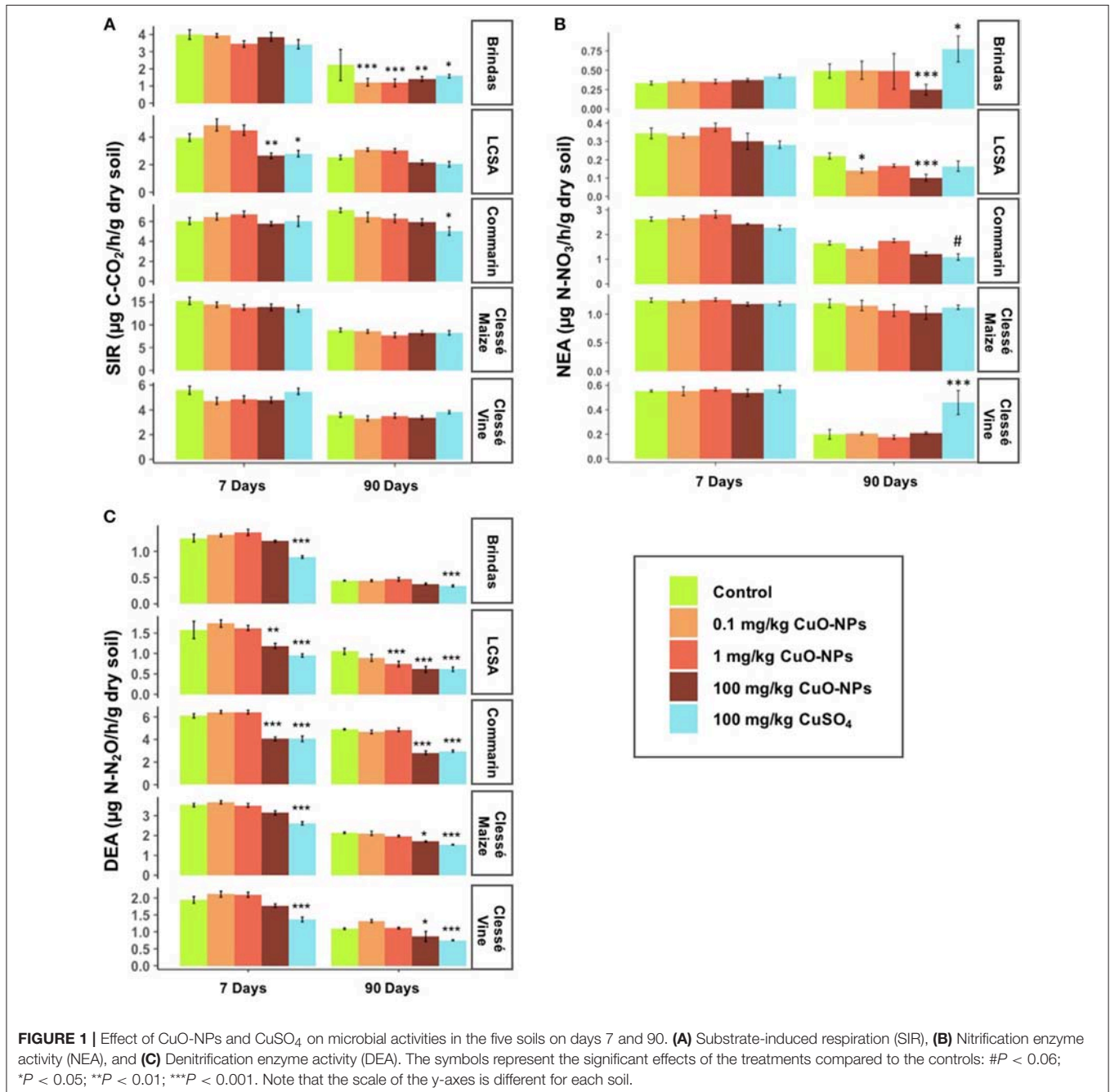
The results are presented as means ( $\pm$ standard errors). In the pot experiment, microbial activities measured in the planted condition are presented as the percentage relative to the unplanted condition in the same Cu treatment (control, 1

mg/kg CuO-NP or 100 mg/kg CuO-NP). We tested the effects of the CuO-NP and ionic Cu treatments on microbial and plant endpoints for each soil tested using a generalized linear model with the *glm* function (fitted with Gaussian or Gamma probability distribution) at the two sampling dates. We then performed *post-hoc* tests using the *lsmeans* package in the R software version 2.3.2 (R Core Team, 2015). We used a  $P < 0.05$  threshold for significance. Linear regression of microbial activities and abundances were explored and described with the Spearman correlation coefficient.

## RESULTS

### Effect of CuO-NPs on Soil Microbial Activities in Contrasting Soils—Soil Microcosm Experiment

In the microcosm experiment, we observed that the effects of CuO-NPs and CuSO<sub>4</sub> differed between the five soils (Figure 1). On day 7, none of the treatments altered NEA, regardless of soil type (Figure 1B). SIR significantly decreased only in LCSA soil exposed to 100 mg/kg CuO-NPs (−33%) or CuSO<sub>4</sub> (−29%). The



DEA decreased only in the 100 mg/kg CuSO<sub>4</sub> treatment in all the soils (**Figure 1C**, –26 to –40%), while the same concentration of CuO-NPs significantly reduced this activity only in LCSA (–25%) and Commarin soils (–33%). The 0.1 and 1 mg/kg CuO-NPs did not have any effects on DEA on day 7.

On day 90, SIR significantly decreased in all the treatments in Brindas soil (**Figure 1A**), including the 0.1 and 1 mg/kg CuO-NP doses that led to the highest reductions (–45 and –47%, respectively). In the other soils, SIR activity was not affected except in Commarin soil with 100 mg/kg CuSO<sub>4</sub> (–29%). NEA in Brindas soil was reduced only by the 100 mg/kg CuO-NP treatment (–49%, **Figure 1B**), while this activity was decreased in LCSA soil by the 0.1 and 100 mg/kg CuO-NP treatments (–37 and –54%). CuO-NPs did not affect NEA in the three other soils, but CuSO<sub>4</sub> treatment led to a decrease in NEA in Commarin soil (–34%) and an increase in NEA in Brindas (+58%) and Clessé-vine soils (+131%). On day 90, DEA was still significantly suppressed in the 100 mg/kg CuSO<sub>4</sub> treatment in all the soils (–23 to –42%, **Figure 1C**). The same concentration of

CuO-NPs caused a significant decrease from –21 to –42% in all the soils except Brindas soil. The 1 mg/kg CuO-NP treatment significantly decreased DEA only in LCSA soil (–30%), but the lowest concentration (0.1 mg/kg) had no effect on this microbial process.

## Effect of CuO-NPs on Microbial Abundance and Correlations With Microbial Activities—Soil Microcosm Experiment

On day 7, the different treatments did not alter the microbial abundance (data not shown) and had only limited effects on day 90 (**Figure S1**). The AOA abundance decreased with 100 mg/kg CuO-NPs in LCSA soil (**Figure S1B**, –57%). The same exposure with CuO-NPs and CuSO<sub>4</sub> in Commarin soil resulted in a similar decrease in the AOB abundance (**Figure S1C**, –45 and –50%, respectively). The abundance of denitrifiers bearing the *nirS* gene was also reduced in the 1 and 100 mg/kg CuO-NP treatments in this soil (–48 and –45%, **Figure S1D**).

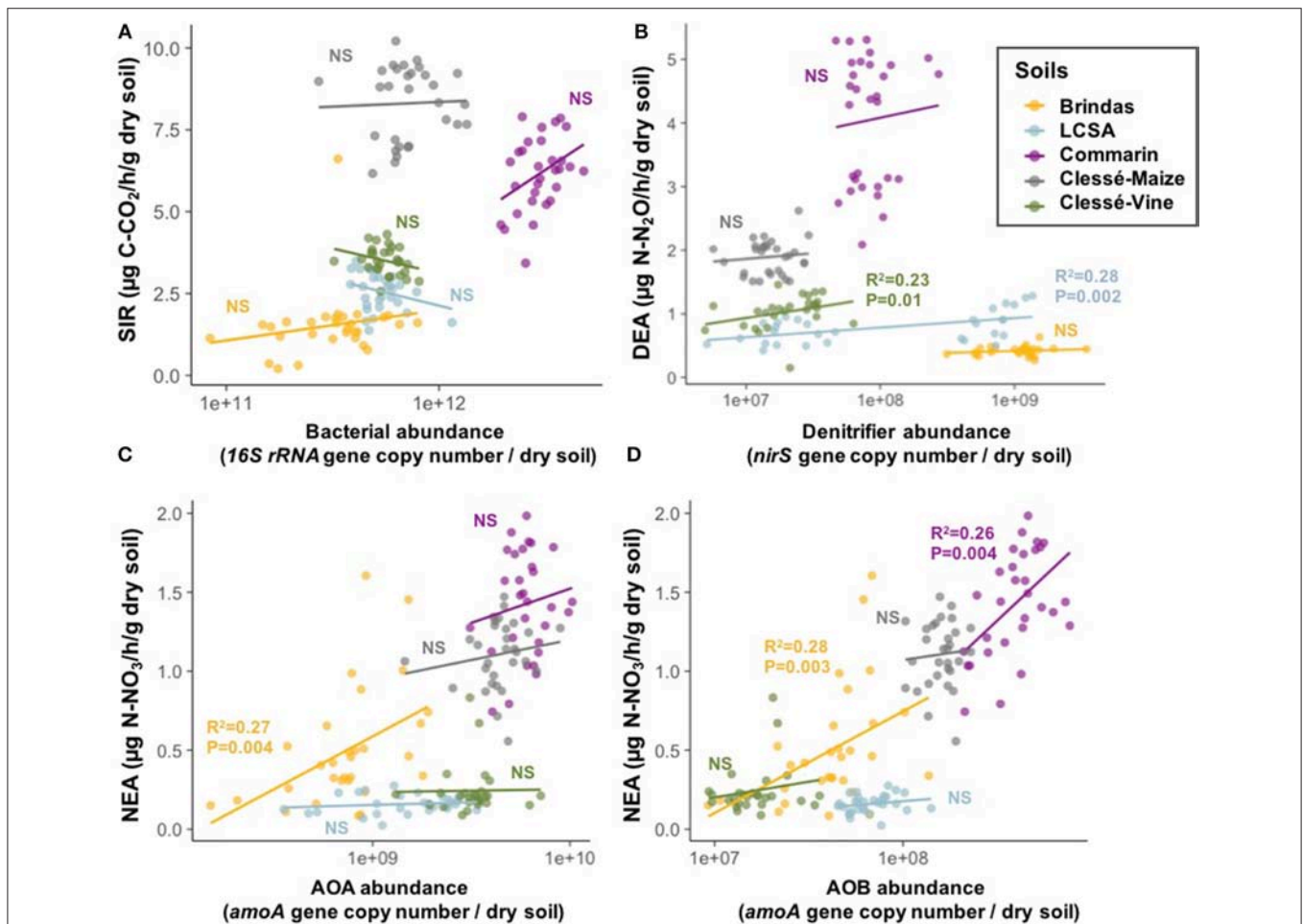


**FIGURE 2 |** Correlations between microbial activities and microbial abundance in the five soils on day 90. **(A)** SIR vs. bacterial abundance, **(B)** DEA vs. *nirS*-bearing denitrifier abundance, **(C)** NEA vs. AOA abundance and **(D)** NEA vs. AOB abundance. When a correlation is significant, the  $R^2$  and  $P$ -value are indicated, otherwise NS for Non-Significant is displayed.

We found that SIR was not significantly correlated to bacterial abundance in the five soils studied (Figure 2A). DEA was positively correlated to *nirS*-bearing denitrifier abundance in LCSA and Clessé Vine soils (Figure 2B). NEA was positively correlated to both AOA and AOB abundance in Brindas soil (Figures 2C,D) and to AOB abundance in Commarin soil (Figure 2D). In LCSA, Clessé-Maize and Clessé-Vine soils, NEA was not correlated to nitrifier abundance.

### Influence of Plant Presence on CuO-NP Effects on Soil Microbial Activities in LCSA Soil – Pot Experiment

By comparing microbial activities in unplanted and planted pots, we observed that plant presence had a positive effect on SIR and DEA [ $F_{(1,1)} = 27.2$ ,  $P < 0.0001$  and  $F_{(1,1)} = 81.3$ ,  $P < 0.0001$ , respectively], but not on NEA after 50 days of exposure ( $P = 0.39$ ; Figure 3). We found that the effects of the CuO-NP treatment could differ significantly between unplanted and planted soils for DEA (significant Copper treatment x Plant presence interaction,  $F_{(1,2)} = 6.1$ ,  $P = 0.007$ ).

For SIR, the positive effect of plants (average +53%) was negated by the addition of 1 and 100 mg/kg of CuO-NPs (average +13 and +20%, respectively; Figure 3). Similarly, the stimulation of DEA associated with the plant presence was reduced two-fold when the soil was exposed to 100 mg/kg CuO-NPs (average +91% in control and +48% in 100 mg/kg CuO-NPs; Figure 3). However, NEA was not influenced by plant presence nor by the CuO-NP treatments (Figure 3).

### Effects of CuO-NP on Plant Biomass and Soil pH – Pot Experiment

In the pot experiment conducted with LCSA soil, the CuO-NP treatments significantly affected the growth of wheat after 50 days of exposure (Figure 4). Total and root biomasses significantly

increased in the 1 mg/kg CuO-NP dose compared to the control (+38% and +47%, respectively; Figures 4A,B). A significant increase in the shoot/root ratio was observed in the 100 mg/kg CuO-NP treatment compared to the 1 mg/kg CuO-NP treatment (+38%; Figure 4C). No significant effect was observed on the shoot biomass. No effect of CuO-NP treatment or plant presence was observed on soil pH values (Figure 4D).

### Correlations Between Microbial Activities and Plant Biomass or Soil pH – Pot Experiment

SIR and NEA were positively correlated to root biomass [ $R^2 = 0.23$ ;  $F_{(1,13)} = 4.1$ ,  $P = 0.066$  and  $R^2 = 0.45$ ;  $F_{(1,13)} = 10.7$ ,  $P = 0.006$ , respectively; Figures 5A,B]. We also observed a positive relationship between DEA and root biomass, but the correlation was only marginally significant [ $R^2 = 0.20$ ;  $F_{(1,13)} = 3.3$ ,  $P = 0.09$ ; Figure 5C]. Further confirming the influence of root biomass on microbial activities, we found that the shoot/root ratio was negatively correlated to microbial activities linked to the N cycle [ $R^2 = 0.57$ ;  $F_{(1,13)} = 17.1$ ,  $P = 0.00012$  and  $R^2 = 0.48$ ;  $F_{(1,13)} = 11.9$ ,  $P = 0.004$ , respectively for NEA and DEA] but not to SIR.

Plants also influenced the relationships between N cycle microbial activities in this experiment. DEA was positively correlated to NEA in the unplanted and planted soil. However, the correlation was stronger in the unplanted soil [ $R^2 = 0.49$ ;  $F_{(1,13)} = 12.6$ ,  $P = 0.0036$ ] than in the planted one [ $R^2 = 0.34$ ;  $F_{(1,13)} = 6.77$ ,  $P = 0.022$ ]. When considering all treatments together, the microbial activities were not significantly correlated to soil pH (SIR:  $P = 0.17$ ; NEA:  $P = 0.84$ ; DEA:  $P = 0.65$ ). A correlation between SIR and pH was only found for the 1 mg/kg CuO-NP dose [ $R^2 = 0.42$ ;  $F_{(1,8)} = 5.7$ ,  $P = 0.043$ ].

## DISCUSSION

### Distinct Effects of CuO-NPs and Ionic Cu on Microbial Activities

On the three microbial activities measured (DEA, NEA, and SIR), ionic Cu contamination ( $\text{CuSO}_4$ ) led to either (i) similar decreases compared to CuO-NP addition (e.g., DEA on day 90), (ii) higher decreases compared to CuO-NP exposure (e.g., on DEA on day 7) or (iii) increases in microbial activity, while CuO-NP exposure had no effect or caused a decrease (e.g., NEA on day 90). These results provide evidence that the consequences of CuO-NPs and ionic Cu on soil microbial activities are distinct. In particular, CuO-NPs never presented stimulatory effects on the activities measured, while  $\text{CuSO}_4$  addition stimulated NEA in two different soils (Brindas and Clessé Vine) after 90 days. This result might be explained by the Cu requirement of ammonia monooxygenase enzymes catalyzing the first step of NEA (Wagner et al., 2016). Hence, after 90 days, we can hypothesize that the limitation of bioavailable Cu might have been alleviated by  $\text{CuSO}_4$  addition but not by CuO-NP addition in those two soils. Overall, the contrasted effects of the CuO-NPs and ionic Cu treatments on microbial activities are likely explained by the very low dissolution of CuO-NPs in the five

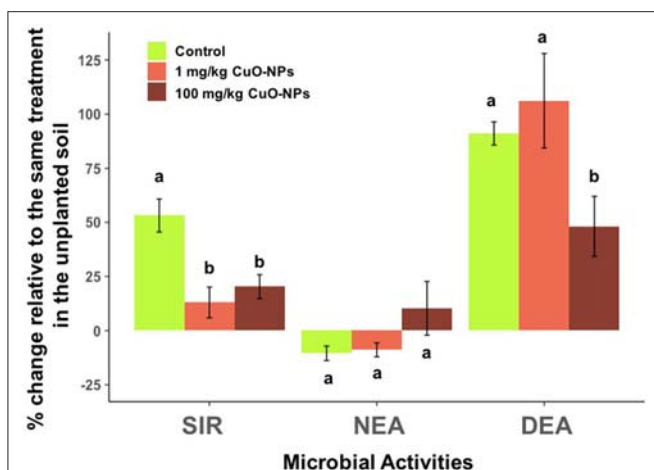


**FIGURE 3** | Effects of CuO-NPs on microbial activities expressed as percentage relative to the same treatment in the unplanted soils after 50 days of exposure. Different letters indicate a significant difference between the treatments for a given microbial activity.

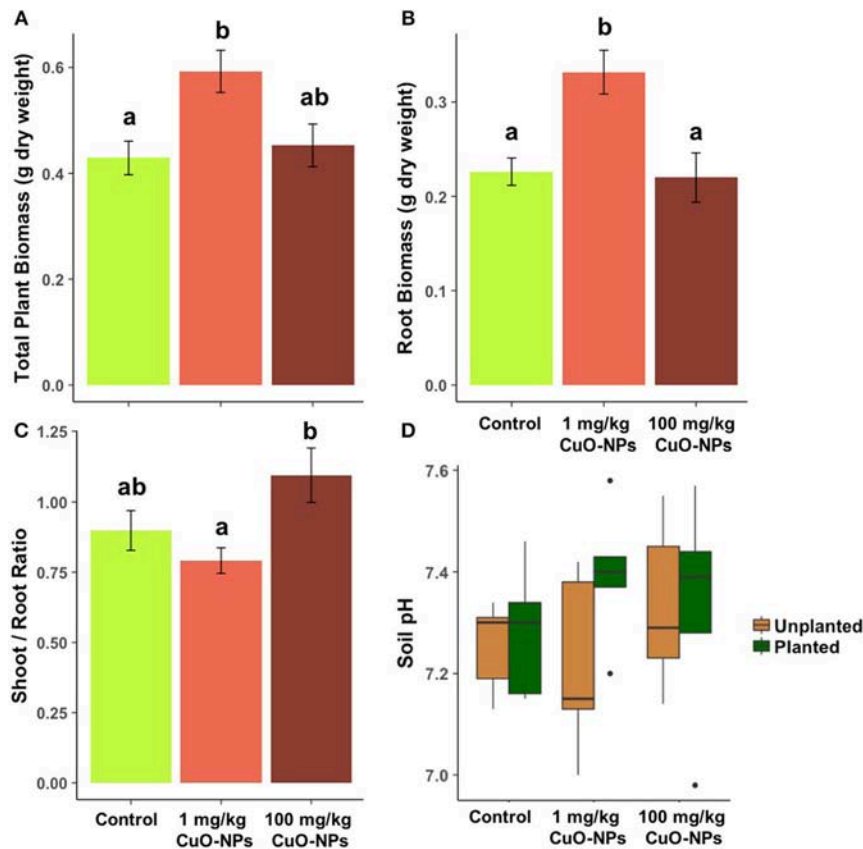


**FIGURE 4 |** Effects of CuO-NPs on wheat (A) total plant biomass, (B) root biomass, and (C) shoot/root ratio. (D) pH in the unplanted and planted soil after 50 days of exposure. Different letters indicate a significant difference between the treatments for a given endpoint.

soils. The dissolution of CuO-NPs in the five soil solutions was below 2% after 90 days. This result is supported by the study of Gao et al. (2018) that also shows slow dissolution rates of CuO-NPs in an agricultural soil. Altogether, these findings suggest that the effects of CuO-NPs were likely principally driven by the Cu nanoparticulate form and not the ionic Cu form.

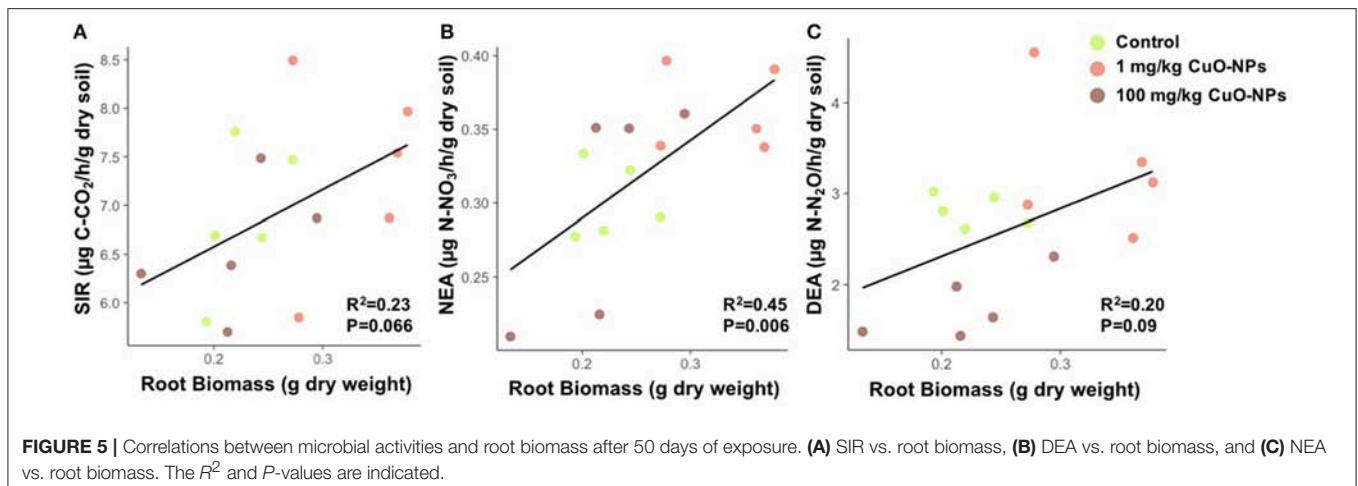
### Limited Effects of CuO-NPs on Microbial Activities at Low Concentrations and High Decreases of DEA in Most Soils

The low CuO-NP concentrations tested (0.1 and 1 mg/kg) had no effect on the studied microbial activities, with the exception of the decrease on day 90 of SIR in sandy-loam Brindas soil, and of NEA and DEA in loam LCSA soil. Hence, the results of this microcosm experiment show that CuO-NP exposures at low and relevant concentrations have limited effects on soil microbial activities involved in carbon and N cycles, but that soils presenting a coarse texture (low clay content) might be occasionally affected.

The lowest concentration tested previously in the literature was 100 mg/kg CuO-NPs; this concentration led to decreases in different microbial enzyme activities (urease, dehydrogenase, phosphatase) in a flooded paddy soil (Xu et al., 2015). Similarly, in our study, we observed that 100 mg/kg CuO-NP caused significant reductions in DEA, NEA, and SIR. In particular, DEA

was found to be the most sensitive microbial process to CuO-NP exposure in the short-term (7 days) and longer term (90 days). On day 90, four of the five soils exhibited significant DEA decreases ranging from 21 to 42% in the presence of 100 mg/kg CuO-NP. The medium and fine texture LCSA (loam) and Commarin (silty-clay) soils were found to be the most sensitive soils for the DEA activity. SIR and NEA were less affected by CuO-NP exposure, and significant decreases were observed only in the two soils with the coarse and medium textures (Brindas and LCSA). These findings show that CuO-NPs can have detrimental effects at high concentration (100 mg/kg) in agricultural soils exhibiting very contrasting textures, OM content, pH, and agricultural practices.

In contrast to other heavy metal contaminants, we did not observe clear patterns indicating a higher toxicity of CuO-NPs on DEA in soils with a coarse texture (high sand content) and low OM content as usually reported (Giller et al., 1998; Kuan et al., 2006; Zhang et al., 2016). Several studies report that NP toxicity varies strongly depending on the types of soils tested but the observed patterns associated with soil texture, pH, and OM content differ both in function of the NP tested and between studies (McKee and Filser, 2016). More in-depth characterization of the transformations experienced by CuO-NPs in diverse soils and of the soil parameters driving CuO-NP bioavailability and toxicity are needed.



Denitrifiers have often been found to be insensitive to many toxicants and to even increase in relative abundance in polluted sites, while nitrifiers are frequently reported to be very sensitive to metal pollution (Bissett et al., 2013). Therefore, we were surprised to observe that DEA was the most sensitive microbial process to CuO-NPs in our experiment, especially in comparison to NEA. Denitrifiers exhibit a higher diversity and functional redundancy compared to nitrifiers and also have a larger niche breadth (facultative anaerobes, diversity of organic substrates) that make the DEA generally more resistant and resilient to disturbances (Griffiths and Philippot, 2013). Moreover, as nitrification and denitrification are tightly coupled, the decline of DEA is often the consequence of a decrease in NEA. Thus, this study shows that in contrast with other NPs (Simonin et al., 2016), CuO-NPs have more detrimental effects on DEA than on NEA in the short and long-term in different soils.

The effects of CuO-NPs on microbial activities did not seem to be related to strong decreases in the abundance of the different microbial groups driving these processes (total bacteria, AOA, AOB, denitrifiers). The microbial abundances remained mainly unchanged by the treatments, and correlations between microbial activities and abundances were observed only in a few soils. Our results suggest that the DEA inhibitions in Brindas and Clessé-Maize soils were not associated with changes in the abundance of *nirS*-bearing denitrifiers. However, the significant correlations between DEA and denitrifier abundance in the LCSA and Clessé-Vine soils indicate that the decreases in denitrification rates were at least partially related to a decrease in denitrifier abundance. More research would be required to determine whether CuO-NPs can affect enzyme synthesis and functioning or lead to modifications in microbial community structure over time that could result in reductions in key microbial activities like denitrification.

### CuO-NP Effects Increase Over Time

Consistent with many other ecotoxicological studies looking at NP toxicity, we observed that the detrimental effects of CuO-NPs increased over time (Simonin et al., 2015, 2016; McKee and Filser, 2016). In this study, two-third of the significant effects

observed on the microbial activities occurred on day 90. These toxic effects detected and/or increasing after longer exposures could be explained by several abiotic factors (e.g., pH, DOC, ionic strength) that are dynamic over time and could transform CuO-NPs into an aged form more bioavailable or toxic for microorganisms (Cornelis et al., 2014). A modification of soil abiotic parameters over the course of the incubation can affect not only CuO-NP fate but also the soil microbial community structure. The temporal variation in microbial community composition and the loss or decline of sensitive taxa to CuO-NPs over time may be a key explanation for the decreases in microbial activities observed after 90 days. Altogether, these results reinforce the idea that short-term ecotoxicological assays may not be adapted to assess the risks associated to NP contamination in soils and may lead to an underestimation of their ecological consequences.

### Stimulation of Microbial Activities by Plant Presence Does Not Mitigate CuO-NP Toxicity

In the pot experiment, we found that plant presence strongly stimulated heterotrophic microbial activity (i.e., SIR and DEA) likely through inputs of carbon in the rhizosphere as suggested by the positive correlations between the microbial activities and root biomass (Smith and Tiedje, 1979; Klemmedtsson et al., 1987). However, this stimulatory effect of the wheat did not counteract or dampen the negative effects of CuO-NPs on SIR and DEA. Similar reductions to the ones observed in the microcosm experiment (between 30 and 40%) of the microbial activities were observed in the planted pots exposed to CuO-NPs. In particular, SIR was inhibited by both 1 and 100 mg/kg CuO-NP treatments in the presence of wheat, and DEA was reduced when exposed to the highest concentration only. Thus, in this experiment, increased carbon resources provided by the plant did not clearly confer a higher resistance to CuO-NP exposure for the two heterotrophic soil microbial activities measured.

The reduction of SIR at 1 mg/kg was unexpected because this activity was not affected at the lowest concentrations in the absence of plants and was generally more resistant than DEA

in the microcosm experiment. This result suggests that wheat presence modifies the bioavailability and toxicity of CuO-NPs as previously demonstrated (e.g., dissolution, adhesion on roots, uptake, Gao et al., 2018) or that the soil microbial community under the influence of the plant would be more sensitive to this pollutant than in the unplanted soil. More work is necessary to determine how plant exudates alter the aging of CuO-NPs in the rhizosphere and the sensitivity of the soil microbial community to this emerging contaminant.

NEA, a chemoautotrophic activity presenting a lower reliance on organic carbon than SIR and DEA, was not positively affected by plant presence and even decreased slightly in planted soils. The lack of stimulation of NEA in the presence of wheat can be explained by a strong competition for ammonia between nitrifiers and plants (Cantarel et al., 2015). This alteration of the N cycle in presence of the plant was also highlighted by a stronger correlation observed between NEA and DEA in the unplanted soils. Interestingly, the CuO-NP treatment did not significantly alter NEA in the pot experiment, indicating that the competition for N resources between nitrifiers and the plant did not increase their sensitivity to the contaminant. These results show that the effects of plant presence on CuO-NP toxicity vary according to the microbial activity and the type of plant-microorganism interaction involved (commensalism vs. competition).

In the context of the potential use of CuO-NPs in agro-chemical products, our results indicate that at low concentrations (1 mg/kg), CuO-NP soil application could lead to an increase in wheat biomass. In our study, these effects were due to a higher allocation of biomass to the roots than to the leaves, which increased the total plant biomass. The stimulatory effect of CuO-NPs on the root system could be explained by different mechanisms, such as the use of dissolved CuO-NPs as micronutrients by plants (as suggested by Dimkpa et al., 2013), the elimination of plant pathogens by CuO-NPs (Hajipour et al., 2012) or a plant stress response leading to a higher energy allocation to root growth to compensate the energy costs associated with CuO-NP detoxification (Potters et al., 2007). To determine the potential value of applying CuO-NP to wheat crops, future studies will need to determine the effects of CuO-NP exposures on the agroecosystems and their productivity (as grain production, mass and quality) and assess the long-term effects of the alteration of soil microbial activities on soil fertility.

## CONCLUSION

These two experiments show that CuO-NPs can have detrimental effects on soil microbial activities, but most effects occurred at the highest concentration tested (100 mg/kg). Similar to previous studies, we observed that the negative effects of CuO-NPs increase over time, indicating that short-term studies (hours,

days) may underestimate the risks posed by these contaminants. The effects differed between the five soils studied, but all soils presented significant reductions in microbial activity. Our results indicated that the most impacted soil was a loam soil with a low OM content (LCSA), though more research is necessary to determine which biotic and abiotic characteristics are the main drivers of this soil sensitivity to CuO-NPs. Additionally, this work demonstrates that the presence of plants influences the microbial response to CuO-NP exposure but does not mitigate or compensate the effects. For example, large decreases in heterotrophic microbial activities were observed in planted soils, even at 1 mg/kg for SIR. Altogether, this study provides a clear demonstration of the necessity to assess the environmental impacts of nanomaterials under realistic experimental conditions to improve the risk assessment of these novel contaminants. Future studies in nanotoxicology need to include systematically low concentrations ( $\mu\text{g}/\text{kg}$  and low mg/kg range) and take into account soil biological complexity and physico-chemical diversity in their experimental designs to produce an integrative assessment useful for regulation.

## AUTHOR CONTRIBUTIONS

MS, AAMC, AC, JM, and AR designed the experiments. MS, AAMC, JG, and AC conducted the experiments and performed the plant and microbial measurements. MS, AAMC, and AR wrote the paper and all the co-authors edited the manuscript.

## FUNDING

This work was supported by the French national program CNRS EC2CO- MicrobiEn and Ecodyn (RHIZONANO). Marie Simonin was supported by a PhD grant from the Région Rhône-Alpes—ARC Environnement.

## ACKNOWLEDGMENTS

We thank the Serre et chambres climatiques platform (Université Lyon1, FR BioEnviS) for growing the plants and the Activités Microbiennes dans l'Environnement platform (Université Lyon 1, UMR 5557) for microbial analyses. We thank Nadège Roche, Julia Sanchez, and Elise Lacroix for their help with the plant culture, harvesting, and microbial analyses.

## SUPPLEMENTARY MATERIAL

The Supplementary Material for this article can be found online at: <https://www.frontiersin.org/articles/10.3389/fmicb.2018.03102/full#supplementary-material>

## REFERENCES

- Arguello, J. M., Raimunda, D., and Padilla-Benavides, T. (2013). Mechanisms of copper homeostasis in bacteria. *Front. Cell. Infect. Microbiol.* 3:73. doi: 10.3389/fcimb.2013.00073
- Bardon, C., Piola, F., Bellvert, F., Haichar, F., Z., Comte, G., et al. (2014). Evidence for biological denitrification inhibition (BDI) by plant secondary metabolites. *New Phytol.* 204, 620–630. doi: 10.1111/nph.12944
- Ben-Moshe, T., Dror, I., and Berkowitz, B. (2010). Transport of metal oxide nanoparticles in saturated porous media. *Chemosphere* 81, 387–393. doi: 10.1016/j.chemosphere.2010.07.007

- Bissett, A., Brown, M. V., Siciliano, S. D., and Thrall, P. H. (2013). Microbial community responses to anthropogenically induced environmental change: towards a systems approach. *Ecol. Lett.* 16, 128–139. doi: 10.1111/ele.12109
- Bravin, M. N., Garnier, C., Lenoble, V., Gérard, F., Dudal, Y., and Hinsinger, P. (2012). Root-induced changes in pH and dissolved organic matter binding capacity affect copper dynamic speciation in the rhizosphere. *Geochim. Cosmochim. Acta* 84, 256–268. doi: 10.1016/j.gca.2012.01.031
- Cantarel, A. A., Pommier, T., Desclos-Theveniau, M., Diquélou, S., Dumont, M., Grassein, F., et al. (2015). Using plant traits to explain plant-microbe relationships involved in nitrogen acquisition. *Ecology* 96, 788–799. doi: 10.1890/13-2107.1
- Chibuikwe, G. U., and Obiora, S. C. (2014). Heavy metal polluted soils: effect on plants and bioremediation methods. *Appl. Environ. Soil Sci.* 2014:752708. doi: 10.1155/2014/752708
- Cornelis, G., Hund-Rinke, K., Kuhlbusch, T., Brink, N., van den, and Nickel, C. (2014). Fate and bioavailability of engineered nanoparticles in soils: a review. *Critic. Rev. Environ. Sci. Technol.* 44, 2720–2764. doi: 10.1080/10643389.2013.829767
- Dassonville, N., Guillaumaud, N., Piola, F., Meerts, P., and Poly, F. (2011). Niche construction by the invasive Asian knotweeds (species complex *Fallopia*): impact on activity, abundance and community structure of denitrifiers and nitrifiers. *Biol. Invasions* 13, 1115–1133. doi: 10.1007/s10530-011-9954-5
- de Vries, F. T., and Shade, A. (2013). Controls on soil microbial community stability under climate change. *Front. Microbiol.* 4:265. doi: 10.3389/fmicb.2013.00265
- Dimkpa, C. O., Latta, D. E., McLean, J. E., Britt, D. W., Boyanov, M. I., and Anderson, A. J. (2013). Fate of CuO and ZnO nano- and microparticles in the plant environment. *Environ. Sci. Technol.* 47, 4734–4742. doi: 10.1021/es304736y
- Frenk, S., Ben-Moshe, T., Dror, I., Berkowitz, B., and Minz, D. (2013). Effect of metal oxide nanoparticles on microbial community structure and function in two different soil types. *PLoS ONE* 8:e84441. doi: 10.1371/journal.pone.0084441
- Gao, X., Avellan, A., Laughton, S., Vaidya, R., Rodrigues, S. M., Casman, E. A., et al. (2018). CuO nanoparticle dissolution and toxicity to wheat (*Triticum aestivum*) in rhizosphere soil. *Environ. Sci. Technol.* 52, 2888–2897. doi: 10.1021/acs.est.7b05816
- Garner, K. L., and Keller, A. A. (2014). Emerging patterns for engineered nanomaterials in the environment: a review of fate and toxicity studies. *J. Nanoparticle Res.* 16:2503. doi: 10.1007/s11051-014-2503-2
- Giller, K. E., Witter, E., and Mcgrath, S. P. (1998). Toxicity of heavy metals to microorganisms and microbial processes in agricultural soils: a review. *Soil Biol. Biochem.* 30, 1389–1414. doi: 10.1016/S0038-0717(97)00270-8
- Griffiths, B. S., and Philippot, L. (2013). Insights into the resistance and resilience of the soil microbial community. *FEMS Microbiol. Rev.* 37, 112–129. doi: 10.1111/j.1574-6976.2012.00343.x
- Hajipour, M. J., Fromm, K. M., Ashkarran, A. A., de Aberasturi, D. J., de Larramendi, I. R., Rojo, T., et al. (2012). Antibacterial properties of nanoparticles. *Trends Biotechnol.* 30, 499–511. doi: 10.1016/j.tibtech.2012.06.004
- Kah, M. (2015). Nanopesticides and nanofertilizers: emerging contaminants or opportunities for risk mitigation? *Front. Chem.* 3:64. doi: 10.3389/fchem.2015.00064
- Keller, A. A., Adeleye, A. S., Conway, J. R., Garner, K. L., Zhao, L., Cherr, G. N., et al. (2017). Comparative environmental fate and toxicity of copper nanomaterials. *NanoImpact* 7, 28–40. doi: 10.1016/j.impact.2017.05.003
- Klemmedtsson, L., Svensson, B. H., and Rosswall, T. (1987). Dinitrogen and nitrous oxide produced by denitrification and nitrification in soil with and without barley plants. *Plant Soil* 99, 303–319. doi: 10.1007/BF02370877
- Kuan, H. L., Hallett, P. D., Griffiths, B. S., Gregory, A. S., Watts, C. W., and Whitmore, A. P. (2006). The biological and physical stability and resilience of a selection of Scottish soils to stresses. *Eur. J. Soil Sci.* 58, 811–821. doi: 10.1111/j.1365-2389.2006.00871.x
- Lazareva, A., and Keller, A. A. (2014). Estimating potential life cycle releases of engineered nanomaterials from wastewater treatment plants. *ACS Sustain. Chem. Eng.* 2, 1656–1665. doi: 10.1021/sc500121w
- McKee, M. S., and Filser, J. (2016). Impacts of metal-based engineered nanomaterials on soil communities. *Environ. Sci. Nano* 3, 506–533. doi: 10.1039/C6EN00007J
- Patra, A., Abbadie, L., Clays-Josserand, A., Degrange, V., Grayston, S., and Loiseau, P. (2005). Effect of grazing on microbial functional groups involved in soil N dynamics. *Ecol. Monogr.* 75, 65–80. doi: 10.1890/03-0837
- Philippot, L., Raaijmakers, J. M., Lemanceau, P., and van der Putten, W. H. (2013). Going back to the roots: the microbial ecology of the rhizosphere. *Nat. Rev. Microbiol.* 11, 789–799. doi: 10.1038/nrmicro3109
- Pommier, T., Cantarel, A. A., Grigulis, K., Lavorel, S., Legay, N., Baxendale, C., et al. (2018). The added value of including key microbial traits to determine nitrogen-related ecosystem services in managed grasslands. *J. Appl. Ecol.* 55, 49–58. doi: 10.1111/1365-2664.13010
- Potters, G., Pasternak, T. P., Guisez, Y., Palme, K. J., and Jansen, M. A. (2007). Stress-induced morphogenic responses: growing out of trouble? *Trends Plant Sci.* 12, 98–105. doi: 10.1016/j.tplants.2007.01.004
- R Core Team (2015). *R: A Language and Environment for Statistical Computing*. R Foundation for Statistical Computing. Available online at: <http://www.R-project.org/>
- Römken, P. F. A. M., Bouwman, L. A., and Boon, G. T. (1999). Effect of plant growth on copper solubility and speciation in soil solution samples. *Environ. Pollution* 106, 315–321. doi: 10.1016/S0269-7491(99)00106-2
- Rousk, J., Ackermann, K., Curling, S. F., and Jones, D. L. (2012). Comparative toxicity of nanoparticulate CuO and ZnO to soil bacterial communities. *PLoS ONE* 7:e34197. doi: 10.1371/journal.pone.0034197
- Simonin, M., Guyonnet, J. P., Martins, J. M. F., Ginot, M., and Richaume, A. (2015). Influence of soil properties on the toxicity of TiO<sub>2</sub> nanoparticles on carbon mineralization and bacterial abundance. *J. Hazard. Mater.* 283, 529–535. doi: 10.1016/j.jhazmat.2014.10.004
- Simonin, M., Nunan, N., Bloor, J. M., Pouteau, V., and Niboyet, A. (2017). Short-term responses and resistance of soil microbial community structure to elevated CO<sub>2</sub> and N addition in grassland mesocosms. *FEMS Microbiol. Lett.* 1:364. doi: 10.1093/femsle/fnx077
- Simonin, M., and Richaume, A. (2015). Impact of engineered nanoparticles on the activity, abundance, and diversity of soil microbial communities: a review. *Environ. Sci. Pollut. Res.* 2015, 1–14. doi: 10.1007/s11356-015-4171-x
- Simonin, M., Richaume, A., Guyonnet, J. P., Dubost, A., Martins, J. M. F., and Pommier, T. (2016). Titanium dioxide nanoparticles strongly impact soil microbial function by affecting archaeal nitrifiers. *Sci. Rep.* 6:33643. doi: 10.1038/srep33643
- Smith, M., and Tiedje, J. (1979). Phases of denitrification following oxygen depletion in soil. *Soil Biol. Biochem.* 11, 261–267. doi: 10.1016/0038-0717(79)90071-3
- Wagner, F. B., Nielsen, P. B., Boe-Hansen, R., and Albrechtsen, H. J. (2016). Copper deficiency can limit nitrification in biological rapid sand filters for drinking water production. *Water Res.* 95, 280–288. doi: 10.1016/j.watres.2016.03.025
- Xu, C., Peng, C., Sun, L., Zhang, S., Huang, H., Chen, Y., et al. (2015). Distinctive effects of TiO<sub>2</sub> and CuO nanoparticles on soil microbes and their community structures in flooded paddy soil. *Soil Biol. Biochem.* 86, 24–33. doi: 10.1016/j.soilbio.2015.03.011
- Zhang, Y., Deng, H., Xue, H.-J., Chen, X.-Y., Cai, C., Deng, Y.-C., et al. (2016). The effects of soil microbial and physicochemical properties on resistance and resilience to copper perturbation across China. *CATENA* 147, 678–685. doi: 10.1016/j.catena.2016.08.031

**Conflict of Interest Statement:** The authors declare that the research was conducted in the absence of any commercial or financial relationships that could be construed as a potential conflict of interest.

Copyright © 2018 Simonin, Cantarel, Crouzet, Gervais, Martins and Richaume. This is an open-access article distributed under the terms of the Creative Commons Attribution License (CC BY). The use, distribution or reproduction in other forums is permitted, provided the original author(s) and the copyright owner(s) are credited and that the original publication in this journal is cited, in accordance with accepted academic practice. No use, distribution or reproduction is permitted which does not comply with these terms.



# Effect of Acidic Industrial Effluent Release on Microbial Diversity and Trace Metal Dynamics During Resuspension of Coastal Sediment

Hana Zouch<sup>1,2</sup>, Léa Cabrol<sup>2</sup>, Sandrine Chifflet<sup>2</sup>, Marc Tedetti<sup>1,2</sup>, Fatma Karray<sup>1</sup>, Hatem Zaghden<sup>1</sup>, Sami Sayadi<sup>1</sup> and Marianne Quéméneur<sup>1,2\*</sup>

<sup>1</sup> Laboratory of Environmental Bioprocesses, Biotechnology Center of Sfax, Sfax, Tunisia, <sup>2</sup> Aix Marseille Univ, Université de Toulon, CNRS, IRD, MIO UM 110, Marseille, France

## OPEN ACCESS

### Edited by:

Ghiglione Jean-Francois,  
Centre National de la Recherche  
Scientifique (CNRS), France

### Reviewed by:

Ludovic Besaury,  
Université de Reims  
Champagne-Ardenne, France  
Christos Dimitrios Arvanitidis,  
Hellenic Centre for Marine Research  
(HCMR), Greece

### \*Correspondence:

Marianne Quéméneur  
marianne.quemeneur@ird.fr

### Specialty section:

This article was submitted to  
Microbiotechnology, Ecotoxicology  
and Bioremediation,  
a section of the journal  
Frontiers in Microbiology

Received: 26 June 2018

Accepted: 30 November 2018

Published: 14 December 2018

### Citation:

Zouch H, Cabrol L, Chifflet S,  
Tedetti M, Karray F, Zaghden H,  
Sayadi S and Quéméneur M (2018)  
Effect of Acidic Industrial Effluent  
Release on Microbial Diversity and  
Trace Metal Dynamics During  
Resuspension of Coastal Sediment.  
Front. Microbiol. 9:3103.  
doi: 10.3389/fmicb.2018.03103

Both industrial effluent discharge and the resuspension of contaminated marine sediments are important sources of trace metals in seawater which potentially affect marine ecosystems. The aim of this study was to evaluate the impact of the industrial wastewaters having acidic pH (2–3) and containing trace metals on microbial diversity in the coastal ecosystem of the Gulf of Gabès (Tunisia, southern Mediterranean Sea) subjected to resuspension events of marine sediments. Four trace elements (As, Cd, U, and V) were monitored during 10-day sediment resuspension experiments. The highest enrichment in the seawater dissolved phase was observed for Cd followed by U, V, and As. Cd remobilization was improved by indigenous microbial community, while U release was mainly abiotic. Acidic effluent addition impacted both trace metal distribution and microbial diversity, particularly that of the abundant phylum *Bacteroidetes*. Members of the order *Saprospirales* were enriched from sediment in natural seawater (initial pH > 8), while the family *Flavobacteriaceae* was favored by acidified seawater (initial pH < 8). Some *Flavobacteriaceae* members were identified as dominant species in both initial sediment and experiments with acidic wastewater, in which their relative abundance increased with increasing dissolved Cd levels. It could be therefore possible to consider them as bioindicators of metal pollution and/or acidification in marine ecosystems.

**Keywords:** trace metals, marine sediments, acidic wastewater, phosphogypsum, bacteria, *Flavobacteriaceae*, Gulf of Gabès, Mediterranean Sea

## INTRODUCTION

For several decades, many industrial complexes have settled on the coast of the Gulf of Gabès (GG), a shallow gulf located in the southern Mediterranean Sea. These coastal industrial expansions, coupled with urban growth, have enhanced marine pollution, mainly due to the discharge of urban/industrial effluents into seawater, which has led to a high diversity of contaminants, including metals (Ayadi et al., 2015; Zaghden et al., 2016; El Zrelli et al., 2018; Naifar et al., 2018). The long-term discharge of phosphogypsum (i.e., a by-product of the phosphate fertilizer industries having acidic pH and containing trace metals) and/or untreated acidic wastewaters in the GG has resulted in a progressive degradation and loss of biodiversity, which represent a real threat for the marine ecosystems (El Zrelli et al., 2017; El Kateb et al., 2018; Naifar et al., 2018). Recent studies

have reported links between high metal levels in coastal sediments and different marine organisms of GG (Gargouri et al., 2011; Ghannem et al., 2014; El Zrelli et al., 2015; Rabaoui et al., 2015). Due to their toxicity, long-term persistence and undegradability, metals in marine ecosystems may also pose a potential human health risk through their transfer, accumulation in the food chain and subsequent consumption.

Generally, sediments act as an important sink for trace metals, thus reducing their bioavailability in marine ecosystems (Eggleton and Thomas, 2004; Tessier et al., 2011). In sediment, trace metals can be adsorbed to amorphous materials, complexed with organic matter, or present in secondary minerals (Peng et al., 2009). However, their transfer into seawater is regulated by hydrodynamics, biogeochemical and physicochemical factors (Eggleton and Thomas, 2004; Tessier et al., 2011). Thus, sediments can become a potential source of metals for seawater via remobilization processes (Saulnier and Mucci, 2000; Kim et al., 2006; Kalnejais et al., 2010; Xu et al., 2015). Marine sediment resuspension may occur: (i) during natural events, such as tides, waves, storms, and biological activities, or (ii) through human activities, such as dredging, vessel movements and fishing (Eggleton and Thomas, 2004; Gadd, 2010). The GG displays the highest tides in the Mediterranean Sea (up to 2.3 m, Sammari et al., 2006), due to its large continental shelf with a very low slope. Surface sediment resuspensions induced by tides and currents is one of the main assumptions to explain the continuous nutrient supply in GG shallow waters (Hassen et al., 2009; Rekik et al., 2012; Hamdi et al., 2015), which are considered as one of the most productive areas of the Mediterranean Sea (Mayot et al., 2016; Ayata et al., 2018). Besides nutrients, recent studies have suggested that the surface sediment resuspension in the GG may be a significant source of metals (Ben Salem and Ayadi, 2016), which may also influence biological activities in these shallow waters (in addition to industrial activities).

Microorganisms play a fundamental role in marine ecosystem functioning. Changes in environmental conditions (e.g., pH, nutrients), as well as chemical contaminants (e.g., metals) entering the marine environment, can modify their diversity and ecological functions (Gillan et al., 2005; Witt et al., 2011; Wang K. et al., 2015; Goni-Urriza et al., 2018). Microbial communities can be used as indicators of contaminant stress because they are highly sensitive to slight changes in their surrounding environment (Sun et al., 2012). Microorganisms can also play an important role in the metal mobility through different processes (e.g., oxidation/reduction reactions or organic/inorganic acid formation), therefore increasing their bioavailability (Gadd, 2004). For instance, both iron- and sulfur-oxidizing bacteria can release soluble metals from solid metal-bearing phases (Tabak et al., 2005; Fonti et al., 2013). On the contrary, many microorganisms can contribute to metal immobilization by biosorption, transport, and intracellular sequestration, or precipitation, thus reducing their bioavailability (White et al., 1997; Gadd, 2004). For instance, sulfate-reducing bacteria are strongly involved in metal immobilization by the precipitation of metal sulfide in sediments (Gadd, 2000; Jong and Parry, 2003). However, the microbial populations associated with metal remobilization during surface sediment resuspension events have

not been well identified in coastal and marine ecosystems, whereas metal remobilization has been extensively investigated from estuarine or marine sediments (Cantwell and Burgess, 2004; Shipley et al., 2011; Dang et al., 2015). Moreover, the impact of acidic industrial effluent discharge (especially industrial waste containing metals) on the microbial diversity of coastal marine ecosystems has never been studied to date.

In this work, we evaluated for the first time the effect of acidic and metal-rich wastewaters (AWW) as released by fertilizer industries on both microbial diversity and trace elements (TE; i.e., trace metals, metalloids, and radionuclides) during experimental resuspension of contaminated surface coastal sediments. The bacterial community dynamics and remobilization of four TE (arsenic, As; cadmium, Cd; uranium, U; vanadium, V) were specifically monitored over time. The potential impact of microbial communities on TE mobility was also examined by comparing biotic experiments and abiotic controls to distinguish between biotic and abiotic processes involved in TE mobility. Both the metalloid As and the metal Cd could come from all of the various anthropogenic sources referenced by Ross (1994). Phosphate fertilizer industries are also known as important sources of the toxic metal Cd and the radionuclide U (Yamazaki and Geraldo, 2003; Cichy et al., 2014). In turn, V represents one of the most abundant metals in petroleum and can be used as a tracer of oil pollution in coastal environments (Guzmán and Jarvis, 1996), such as the hydrocarbon-impacted coastal areas of GG (Fourati et al., 2018a,b).

## MATERIALS AND METHODS

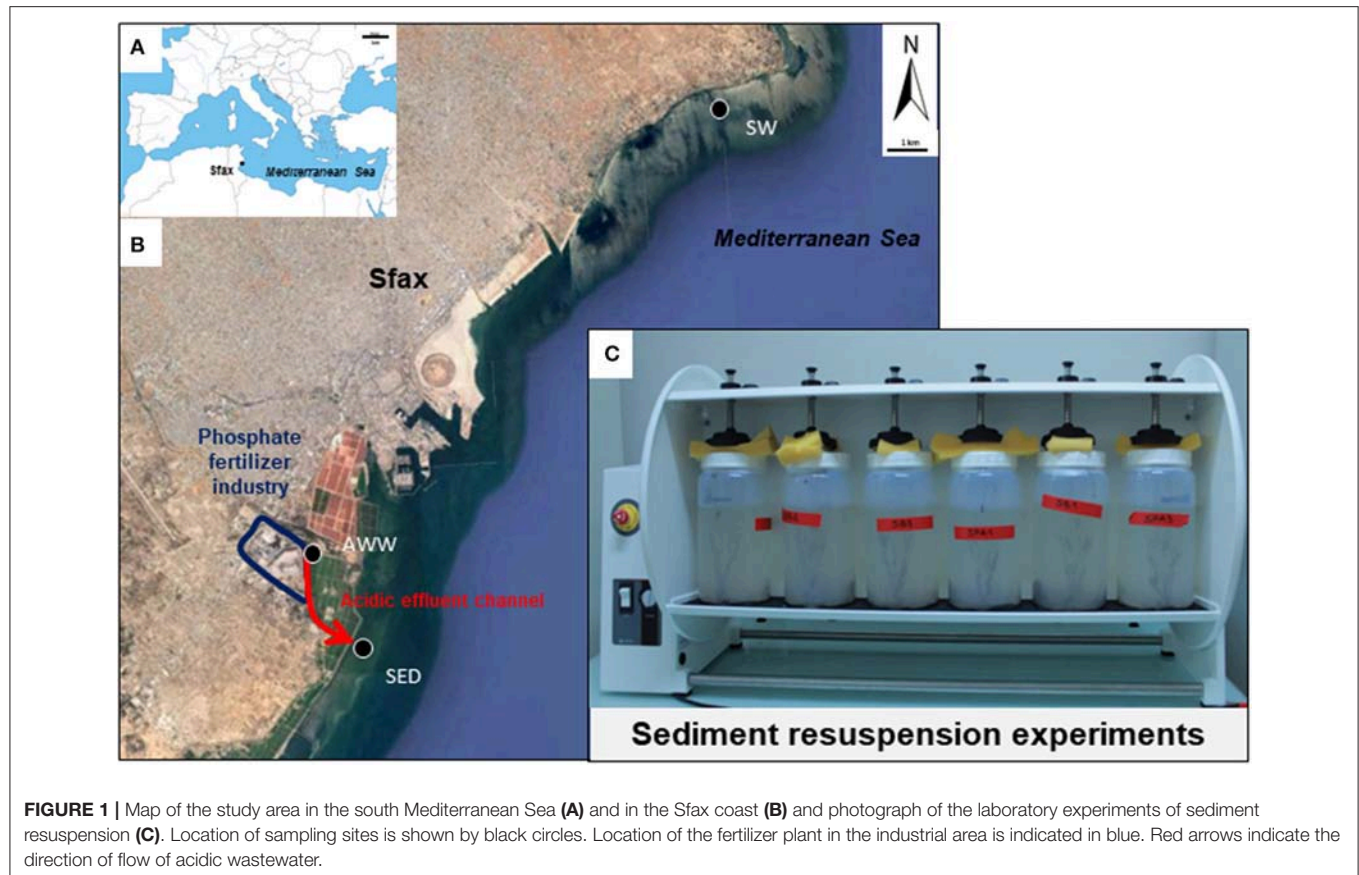
### Studied Area

Sfax (34°43'N–10°46'E) is the second largest city in Tunisia and is located in the northern part of the Gulf of Gabès (GG, 100 km wide from Sfax to Djerba and 100 km long from Gabès to the open Mediterranean Sea, **Figure 1A**). The southern coast of Sfax city is impacted by numerous polluting industrial plants, such as the phosphate fertilizer industry (**Figure 1B**).

Phosphogypsum produced by the Industrial Society of Phosphoric Acid and Fertilizer (SIAPE) was stored in stockpiles (tabia) in front of Sfax coast since the 80th's, which resulted in the drainage of a liquid having acidic pH (abbreviated in this paper as acidic wastewater, AWW; flow rate of  $\sim 500 \text{ m}^3 \text{ d}^{-1}$ ). This AWW was mixed with the treated domestic wastewaters of the National Sanitation Agency (ONAS; flow rate of  $\sim 45000 \text{ m}^3 \text{ d}^{-1}$ ), olive oil wastewaters of storage basins and the Thyna municipal landfill leaching waters through a channel "El Hakmouni" before sea outfall. Production of phosphoric acid by the SIAPE stopped since august 2016 and no phosphogypsum was produced since this date (Chemical Group of Tunisia, personal communication).

### Sample Collection, Processing, and Storage

Acidic wastewater (AWW), contaminated marine sediment (SED) and seawater (SW) were sampled on July 4th 2016 on the coast of Sfax (GG, Tunisia, southern Mediterranean Sea; see location of sampling sites on **Figure 1**).



All bottles were pre-cleaned following a rigorous protocol: filled with 10% HCl (VWR Analytical grade, 1 week) rinsed with ultra-pure MilliQ water ( $R = 18.2 \text{ M}\Omega \cdot \text{cm}^{-1}$ ) filled with 2% HCl (Fisher, Optima grade) and stored in closed plastic bags until use.

For laboratory experiments, AWW was collected using sterile plastic bottles at a point ( $34^{\circ}42'05.23''\text{N}-10^{\circ}44'02.65''\text{E}$ ) above its mixture with different wastewaters and discharge into the seawater, to distinguish the specific effect of phosphogypsum leachates from mixed wastewaters. Surface SED affected by resuspension events (0–5-cm layer) was sampled at low tide, at 10 m from the shore, near the discharge of mixed wastewaters into the seawater ( $34^{\circ}40'46.95''\text{N}-10^{\circ}44'45.74''\text{E}$ ) with a plastic spatula and distributed in sterile plastic bags ( $\sim 1 \text{ kg}$ ). In order to assess the environmental impact due to AWW discharge during SED resuspension experiments by coastal seawater (described below), SW was taken at high tide (0.5 m below sea level) on the northern coast of Sfax at a point less impacted by the southern fertilizer industry ( $34^{\circ}47'41.74''\text{N}-10^{\circ}51'05.00''\text{E}$ ) using 4-L pre-cleaned Polycarbonate bottles (Nalgene®). The temperature, pH, and redox potential of AWW, SED and SW were measured *in situ* using the multiparameter probe PC-5 (XS-Instruments; **Table S1**).

For TE analysis, AWW and SW samples were transferred in triplicate in commercial metal-free polypropylene tubes (VWR) previously washed with HCl 10%, and immediately filtered on

0.2- $\mu\text{m}$  sterile cellulose acetate filters using pre-cleaned Minisart syringes. Back in the laboratory, they were transferred to pre-cleaned FEP bottles, acidified with 2%  $\text{HNO}_3$  (Fisher Optima grade) and stored separately in closed plastic bags at  $4^{\circ}\text{C}$  until total TE dissolved analysis.

For DNA extraction, SED subsamples were transferred in duplicate sterile Eppendorf tubes and 2 L of water samples (SW and AWW) were filtered in duplicate using 0.22- $\mu\text{m}$  sterile cellulose ester filters (Millipore). Then, SED and filters (SW and AWW) were stored at  $-20^{\circ}\text{C}$ , prior to molecular analysis.

### Sediment Analysis and granulometry

SED samples were freeze-dried and sieved onto 2 mm (10 g for granulometry) or 200  $\mu\text{m}$  (1 g for total dissolved TE and elemental composition analyses). The water content of SED samples was determined after drying for 24 h at  $105^{\circ}\text{C}$ . Total carbon, hydrogen, nitrogen and sulfur (C/H/N/S) and organic C contents of dry SED were determined as previously described by Zouch et al. (2017). The granulometry of dry SED was determined with a Beckman Coulter LS 13 320 laser granulometer before and after organic matter removal and the relative abundance of sand (2000 to 63  $\mu\text{m}$ ), silt (63 to 2  $\mu\text{m}$ ), and clay ( $< 2 \mu\text{m}$ ) was measured (Ghilardi et al., 2012). Before laser granulometry analysis, sediments must be sieved on 2 mm, which is the upper limit of the granulometer (Ghilardi et al., 2012; Guigue et al., 2017).

## Sediment Resuspension Experiments

**Table 1** shows the four treatments tested in triplicate in the sediment resuspension experiments. In all conditions tested, SED was mixed with SW using a solid/liquid ratio of 10 g L<sup>-1</sup> of dry sediment, a ratio close to *in situ* levels of suspended particulate matter measured during sediment resuspension events induced by many operations, such as dredging (Shiple et al., 2011; Monnin et al., 2018). To obtain this ratio, wet SED samples (~32.6 g corresponding to 20 g dry weight) were transferred into pre-cleaned mesocosms (2.2 L FEP bottles, Nalgene), and filled with SW up to 2 L.

To evaluate the effect of acidic effluent discharge on TE and microbial dynamics during sediment resuspension by seawater, two biotic conditions were compared: S condition without AWW addition and P condition with addition of 10 mL of AWW into 2-L mixture. Each condition was prepared in triplicate (**Table 1**). Resulting initial pH (7.0 for P and 8.5 for S) are close to *in situ* seawater pH values measured near the effluent discharge (pH 7 at SED point) and from coastal seawater unaffected by AWW (pH 8.3 at SW point). P conditions simulated the release of acidic wastewater effluent into the Sfax coastal ecosystem (with AWW input), while S conditions mimic coastal ecosystem after stopping effluent discharge (without AWW input).

Biotic and abiotic experiments were compared in order to distinguish between biotic and abiotic processes involved in TE mobility, and therefore to identify the potential impact of microbial communities on TE mobility. Abiotic controls (SA and PA) were prepared in triplicate by poisoning the sediment suspensions with sodium azide (NaN<sub>3</sub>) at a final concentration of 50 mM, which inhibits microbial growth and activity, as previously defined by Cabrol et al. (2017).

All mesocosms ( $n = 12$  in total) were run in parallel and incubated aerobically undergoing continuous overhead shaking (10 tr.min<sup>-1</sup>, Heidolph Reax 20) to mimic sediment resuspension, for 10 days at 27°C (**Figure 1C**, **Table 1**).

Sediment/water mix samples (40 mL) were taken from the 12 mesocosms at 9 different times over the course of the resuspension experiment: 0, 1 h, 5 h, 16 h, 2, 3, 5, 7, and 10 days, and transferred into metal-free centrifuge tubes. Optical density (OD 600 nm) and pH were immediately measured from subsamples (5 mL) using, respectively a spectrophotometer (UV-1800, Shimadzu) and a pH-meter (NeoMet pH-200L), which was calibrated using three standard buffer solutions (pH 4, 7, and 10 at 27°C). Sediment/water mix samples were centrifuged (15 min, 8,000 rpm) and the supernatants were filtered on 0.2-μm

cellulose acetate filters using pre-cleaned Minisart syringes, transferred to pre-cleaned FEP bottles and stored in closed plastic bags at 4°C until total dissolved TE analyses. Sediment pellets (0.5–1 g), collected at 3, 5, 7, and 10 days, were stored at -20°C for DNA extraction (in parallel with initial SED samples). The S/L ratio was maintained relatively constant during experiments. Forty milliliters of water and 0.5–1 g of sediment were collected simultaneously at each of the 9 sampling times from a 2-L water volume and a 32.8-g sediment mass, respectively, the initial and final S/L ratios displaying a variation of only ~2%.

## Analysis of Trace Elements

All samples were processed and analyzed in a trace metal clean HEPA filtered laboratory (ISO 7), using high purity acids (Fisher, Optima grade) and MilliQ water ( $R = 18.2 \text{ M}\Omega\cdot\text{cm}^{-1}$ ). Both sets of PFA beakers and micropipette tips were cleaned in HCl (10%, 100°C, 24 h), rinsed and dried in a laminar flow cabinet (ISO 4). Sediment samples were leached with 9 mL of pure acid mixture (HF/HCl/HNO<sub>3</sub>, 1:6:2) and heated on a hot-block (120°C, 24 h). Solutions obtained were evaporated when almost dry and residues were dissolved in 100 mL of HNO<sub>3</sub> (2%) prior to analysis. Water samples (SW and AWW) were diluted 1/20 in 2 % HNO<sub>3</sub> before analysis. Concentrations of TE (As, Cd, U and V) in all samples were then evaluated using Inductively Coupled High Resolution Plasma Mass Spectrometry (HR-ICP-MS, Element XR, Thermo Scientific). To correct instrumental drift and possible matrix effects, internal standard elements (In) were added to the samples. Analytical results were validated using Certified Reference Material (MESS-4 for sediments and SLEW-3 for waters).

## DNA Extraction, PCR, and Sequencing Analyses of 16S rRNA Gene Fragments

DNA extraction from duplicated initial SED and sediment pellets of biotic conditions S and P (prepared in triplicates and collected at different times, as described above) was carried out using UltraClean Soil DNA Isolation Kit (MoBio Laboratories, Inc., CA), as previously described by Quéméneur et al. (2016). DNA was extracted from duplicated AWW and SW filters using PowerWater DNA Isolation Kit Sample (MO BIO Laboratories, Inc., CA). DNA was quantified using the Thermo Scientific Nano Drop 2000 spectrophotometer.

Bacterial abundance in collected samples was evaluated by real-time quantitative PCR of 16S rRNA genes using the 331F and 797R primers, as previously described by (Abdallah et al., 2016).

**TABLE 1** | Treatments used to test the effect of acidic wastewater (AWW) on microbial and trace metal dynamics during the resuspension of contaminated sediment (SED) into coastal seawater (SW).

Conditions	Name	Replicates	Sediment (SED)	Seawater (SW)	Acidic wastewater (AWW)	Poison (NaN <sub>3</sub> )
Biotic conditions	S	S1, S2, S3	20 gDW	2L	0	0
	P	P1, P2, P3	20 gDW	2L	10 mL	0
Abiotic controls	SA	SA1, SA2, SA3	20 gDW	2L	0	50 mM
	PA	PA1, PA2, PA3	20 gDW	2L	10 mL	50 mM

Experiments were performed in triplicates.

Bacterial and archaeal 16S rRNA genes were amplified by PCR using the 341F/815R prokaryotic universal primer set, as previously described by Dowd et al. (2008), and were sequenced by the MiSeq Illumina (paired-end 2 x 300 bp) platform of the Molecular Research Laboratory (Texas, USA). Raw sequences were analyzed using QIIME 1.9.1 as described by Caporaso et al. (2010). Briefly, the raw reads were checked for adapter, chimera and low-quality sequences. The trimmed reads were clustered into operational taxonomic units (OTU) using a 97% sequence identity threshold with UCLUST (Edgar, 2010). The taxonomic assignment was performed by UCLUST taxonomy. Low abundance OTU (<0.005%) were filtered as recommended by Bokulich et al. (2013) and the OTU table was normalized by random subsampling to the smallest number of sequences (i.e., 18614). Similarity search by BLAST algorithm (Altschul et al., 1990) against the NCBI non-redundant (NR) reference database was performed for OTU representative sequences. The 16S rRNA gene sequences have been deposited in the Genbank database under the accession numbers MH002252-MH002311.

## Numerical and Statistical Analyses

The alpha diversity was calculated in QIIME using the Shannon (Shannon and Weaver, 1949) and Simpson (Simpson, 1949) indices. The beta diversity (Bray–Curtis similarity) metrics were calculated and a dendrogram was generated with *hclust* function in R to group samples into clusters. The Good's coverage was calculated according to the equation:  $C = 1 - (n/N)$  where  $n$  is the number of OTU and  $N$  is the total number of sequences (Good, 1953). The relative OTU table was transformed by logarithm to down weight the influence of more abundant species masking shifts among less abundant species (Cabrol et al., 2012). The dynamics of microbial community structure along time were analyzed by Principal Coordinate Analysis (PCoA), using *pcoa* function of the *ape* package in R software (version 3.5.0), from the log-transformed OTU table. The temporal succession was visualized by a bubble plot on the PCoA representation, in which the symbol size was proportional to the elapsed time. Ellipses were drawn based on the standard deviation of points in groups defined by the presence/absence of acid effluent addition (*ordiellipse* function, confidence limit 0.9) and the significance of group separation according to acid effluent addition was tested by non-parametric (permutational) analysis of variance using distance matrix (Bray Curtis) with the *adonis* function ( $p$ -value 0.002). The first 50 OTU with highest variance were identified on the score/species biplot representation (the magnitude of OTU abundance change being proportional to the species arrow length). Their significant correlation with the ordination scores was tested by the *envfit* function (vegan package, R). The most discriminant OTU (i.e., with  $p$ -value < 0.001) explaining the sample distribution on the PCoA ordination were selected (yielding 32 species) and represented on the biplot. Collinearity between abiotic variables was tested by computing the pairwise Pearson correlation matrix between 8 variables (Table S2). “Time” and “AWW” variables were removed due to their high correlation ( $|\rho| > 0.9$ ) with, respectively, dissolved Cd concentration and pH and U concentration. The linear correlation between the PCoA

ordination of the microbial communities and key environmental parameters (after normalization) was investigated using the *envfit* function of the *vegan* library. Fitted environmental vectors were represented on the PCoA by arrows pointing to the direction of the increasing gradient and of which the length is proportional to the correlation coefficient between the variable and the ordination. The correlation significance of each variable was assessed by permutation tests. To explore the concerted effect of the 6 abiotic variables on the multivariate pattern of the microbial community, the *bioenv* routine (*vegan* package) was applied to test the 5 different possible models (i.e., subsets of environmental variables). The model providing the maximum rank correlation (Spearman coefficient) between a subset of environmental variables (Euclidian distances) and community dissimilarities (Bray Curtis distances) was identified. The significance of these correlations was tested by Mantel tests (*mantel* function).

The Mann-Whitney non-parametric test (U-test) was used to compare, two-by-two, the four different treatments (SA, S, P, PA) for each of these parameters: OD, pH, cadmium, uranium, arsenic, vanadium, diversity indices, and bacterial abundance. The U-test was also used to compare, for each parameter, the biotic (S and P) vs. abiotic (SA, PA) treatments, with effluent (P, PA) vs. without effluent (S, SA) treatments, as well as T0 vs. T1 conditions. The U-test was chosen for these comparisons because most of the treatments displayed a non-normal distribution according to several normality tests (Shapiro-Wilk, Anderson-Darling, Lilliefors tests). To find relationships between relative abundance of selected OTU and TE, we performed the Spearman correlation test (the non-parametric version of the Pearson correlation test) and we accepted correlation coefficients with  $p$ -values of < 0.05 as significant associations. Normality tests, the U-test, correlation tests and heatmap were performed with XLSTAT 2013.5.01 (Microsoft Excel add-in program). The heatmap displays the taxonomic affiliation obtained by the BLAST algorithm against the NCBI NR reference database.

## RESULTS

### Physicochemical Characteristics of Initial Sediment, Seawater, and Acid Effluent Samples

The studied coastal surface sediment (SED) was mainly composed of sand (silt and clay were absent). Within the sand, medium (250–500  $\mu\text{m}$ ) and coarse (500–1000  $\mu\text{m}$ ) fractions were the majority (60 and 37%, respectively), while very fine (63–125  $\mu\text{m}$ ), fine (125–250  $\mu\text{m}$ ), and very coarse (1000–2000  $\mu\text{m}$ ) fractions represented together only 3% of the sand. SED contained low total organic carbon content (1.5% of the total sediment weight) and was characterized by a pH value of 6.3. It exhibited a multi-contamination involving various TE: 3.2 mg  $\text{kg}^{-1}$  for As, 16.4 mg  $\text{kg}^{-1}$  for Cd, 19.7 mg  $\text{kg}^{-1}$  for U, and 25.9 mg  $\text{kg}^{-1}$  for V. The main physicochemical properties of the initial SED used in resuspension experiments are summarized in Table 2 and the characteristics of the initial seawater (pH 8.3, SW) and acidic wastewater (pH 2.4, AWW) are given in Table S1.

**TABLE 2** | Chemical properties of sediment (SED) used in resuspension experiments and collected on the Sfax southern coast (Tunisia, South Mediterranean Sea).

	SED
pH <i>in situ</i>	6.3
Temperature <i>in situ</i> (°C)	31.3
Eh <i>in situ</i> (mV)	203
Water content (% of wet weight)	39.7
Total carbon (% of dry weight)	2.4
Organic carbon (% of dry weight)	1.4
Total nitrogen (% of dry weight)	0.2
Total sulfur (% of dry weight)	0.9
Total hydrogen (% of dry weight)	0.7
P (mg kg <sup>-1</sup> )	367–15110 (2456) <sup>a</sup>
<b>Trace element concentrations (mg.kg<sup>-1</sup>)</b>	
As	3.2
Cd	16.4
Co	1.5
Cr	330.8
Mn	113.5
Mo	8.1
Ni	34.9
Pb	0.2
U	19.7
V	25.9

<sup>a</sup>Data obtained from Naifar et al. (2018).

## 16S rRNA Gene Diversity in Initial Sediment, Seawater, and Acid Effluent Samples

The initial microbial diversity and bacterial abundance in sediment (SED), seawater (SW), and acidic wastewater (AWW) samples was estimated by 16S rRNA analyses based on next-generation sequencing (NGS) and quantitative PCR (qPCR). Considering sequence variability into replicate, the OTU numbers in SED, SW and AWW were 1041 ± 26, 1068 ± 26 and 651, respectively (Table S3). As expected from the drastic selective pressure existing in acidic and metal-rich effluent, both diversity indices and bacterial abundance were lower in AWW than in SED and SW. Initial community structures in SW and AWW were clearly separated, and most of them were segregated from the subsequent incubation communities (Figure 2). Field duplicate communities clustered together.

In the sediment, the microbial community was dominated by five bacterial phyla: *Proteobacteria* (67.0 ± 1.0 %), *Bacteroidetes* (20.2 ± 1.0 %), *Actinobacteria* (5.4 ± 0.2 %), *Chloroflexi* (2.3 ± 0.7 %), *Firmicutes* (2.0 ± 0.0 %). Interestingly, the SED community was dominated by only 9 major OTU (>1 % of all sequences) belonging to 4 classes: *Alphaproteobacteria* (represented by *Thioclava* genus, >20 % of all sequences), *Epsilonproteobacteria* (*Sulfurovorum* and *Arcobacter* genera), *Betaproteobacteria* (*Azoarcus* genus), and *Flavobacteriia* (*Gaetbulibacter* and *Namhaecicola* genera)

(Table S4). *Archaea* (*Methanobacteria* class) represented <0.1% of the microbial community of SED.

In the seawater, the microbial community was dominated by four phyla (> 95 % of all sequences): *Proteobacteria* (60.4 ± 2.6 %), *Bacteroidetes* (16.8 ± 1.2 %), *Actinobacteria* (12.3 ± 0.3 %), and *Cyanobacteria* (7.5 ± 0.5 %) specific to SW. The SW was dominated by 14 OTU (>1% of all sequences): 9 alphaproteobacterial OTU related to *Rhodobacterales* genera, 2 cyanobacterial OTU, 3 actinobacterial, and 1 *Bacteroidetes* OTU (Table S5).

Despite its drastic pH and high TE concentrations, the AWW has a relatively high diversity (compared to acid mine drainage). The distribution of OTU strongly differs from SW and SED, mainly due to the dominance of *Firmicutes* (39.3 %), followed by *Proteobacteria* (37.1 %), *Actinobacteria* (12.2 %), *Bacteroidetes* (6.8 %), and *Cyanobacteria* (3.1 %). Among the 13 dominant OTU, 6 OTU were affiliated to *Firmicutes* and assigned to *Alicyclobacillaceae* (18.4 %), *Clostridiaceae* (3.4 %) and *Peptostreptococcaceae* (7.2 %) (Table S6).

## Variations of Optical Density and pH in Sediment Resuspension Experiments

The evolution of optical density (OD) and pH in water during the 10-day sediment resuspension experiments are given in Figures 3A,B.

Significant OD increases were observed in the biotic conditions (S and P) between the beginning (T0) and the end (Tf) of the experiment (U-test,  $p < 0.01$ ,  $n = 12$ ), and compared to abiotic controls (SA, PA) for the whole experiment (U-test,  $p < 0.01$ ,  $n = 108$ ). Without AWW addition (S), the OD values increased rapidly up to  $0.09 \pm 0.01$  after 10 days, with a relative maximum ( $0.06 \pm 0.01$ ) after 3 days. With AWW addition (P), the OD values increased more slowly up to  $0.06 \pm 0.01$  after 10 days, suggesting that AWW increased lag times. Even though a slight OD increase was found in the abiotic controls between the beginning (T0) and the end (Tf) of the experiment (U-test,  $p < 0.05$ ,  $n = 12$ ), the much higher OD values recorded in biotic conditions suggest the occurrence of microbial growth in these latter conditions only (Figure 3A).

Without AWW addition (initial pH ~8.5), a pH decrease was observed during the 6 first hours (pH 8.2), which is probably due to the mixing of SW and SED. Average pH values continued to decrease until the tenth day (S: 7.9; SA: 8.1; Figure 3B). With AWW addition (initial pH 7.0), a pH increase was observed during the first hour (pH 7.5), which is probably due to the buffering capacity of the SED and SW. This increase was followed by a decrease (pH 7.2) during the next 6 h and by a divergence between P and PA. For the whole experiment, pH values were significantly lower with AWW addition in comparison to values without AWW addition (U-test,  $p < 0.001$ ,  $n = 108$ ; Figure 3B). No statistically significant difference in pH was observed between biotic and abiotic conditions from T0 to Tf (U-test,  $p > 0.05$ ,  $n = 108$ ), but pH values were significantly lower in the biotic conditions (S and P) than in the abiotic controls (SA and PA) if we only consider samples collected from 2 days of experiments (i.e., 2, 3, 5, 7, and 10 days; U-test,  $p < 0.01$ ,  $n = 60$ ; Figure 3B). With

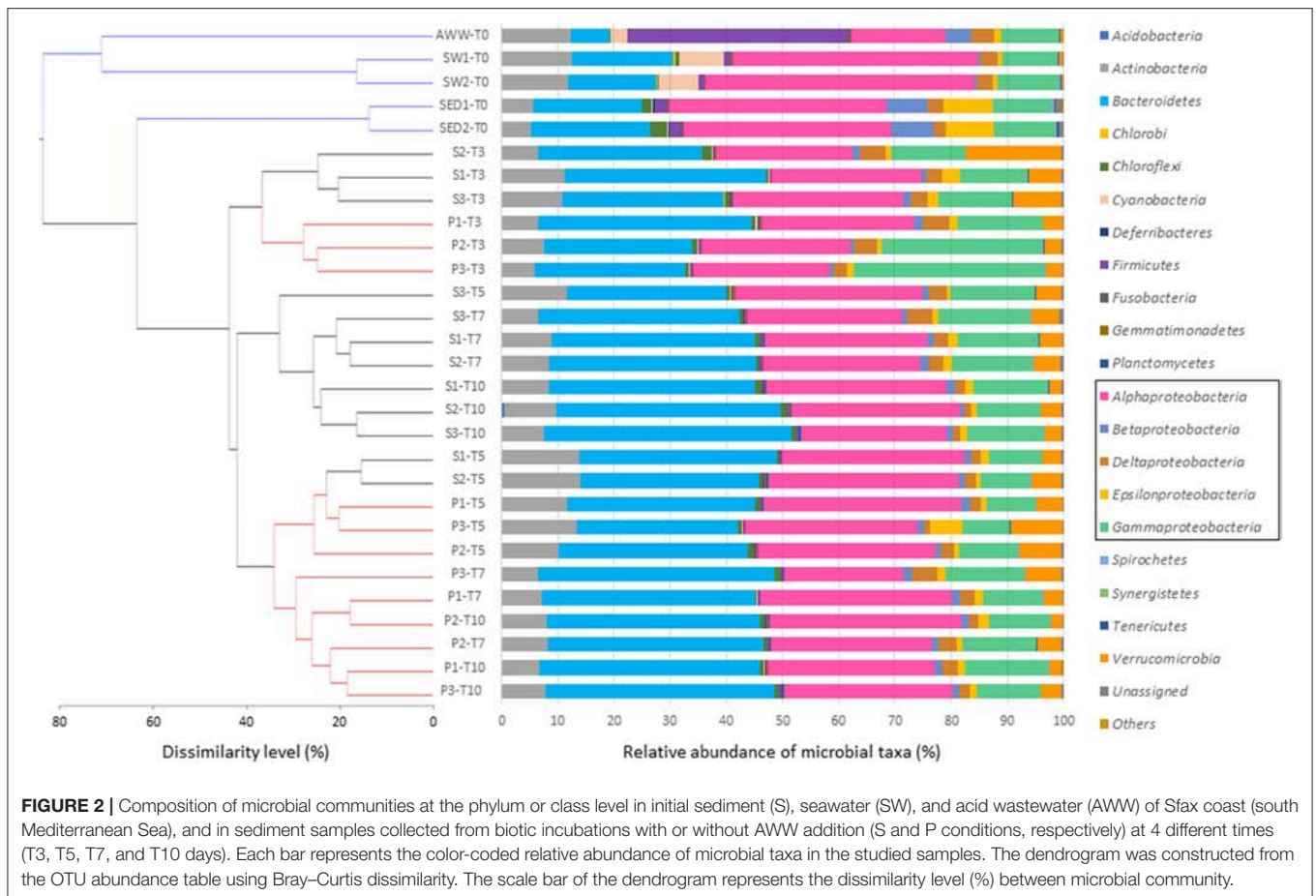


**FIGURE 2 |** Composition of microbial communities at the phylum or class level in initial sediment (S), seawater (SW), and acid wastewater (AWW) of Sfax coast (south Mediterranean Sea), and in sediment samples collected from biotic incubations with or without AWW addition (S and P conditions, respectively) at 4 different times (T3, T5, T7, and T10 days). Each bar represents the color-coded relative abundance of microbial taxa in the studied samples. The dendrogram was constructed from the OTU abundance table using Bray–Curtis dissimilarity. The scale bar of the dendrogram represents the dissimilarity level (%) between microbial community.

AWW addition, pH values were significantly lower in the biotic conditions (P) than in the abiotic controls (PA) over time (from T0 to Tf; U-test,  $p < 0.01$ ,  $n = 54$ ). The pH variations observed in the biotic conditions (S and P) suggest that the biogeochemical reactions controlled by bacteria induced decrease in pH.

## Metal Dynamics in Sediment Resuspension Experiments

Changes in dissolved arsenic (As), cadmium (Cd), uranium (U), and vanadium (V) concentrations were observed during 10-day remobilization experiments (Figures 3C–F).

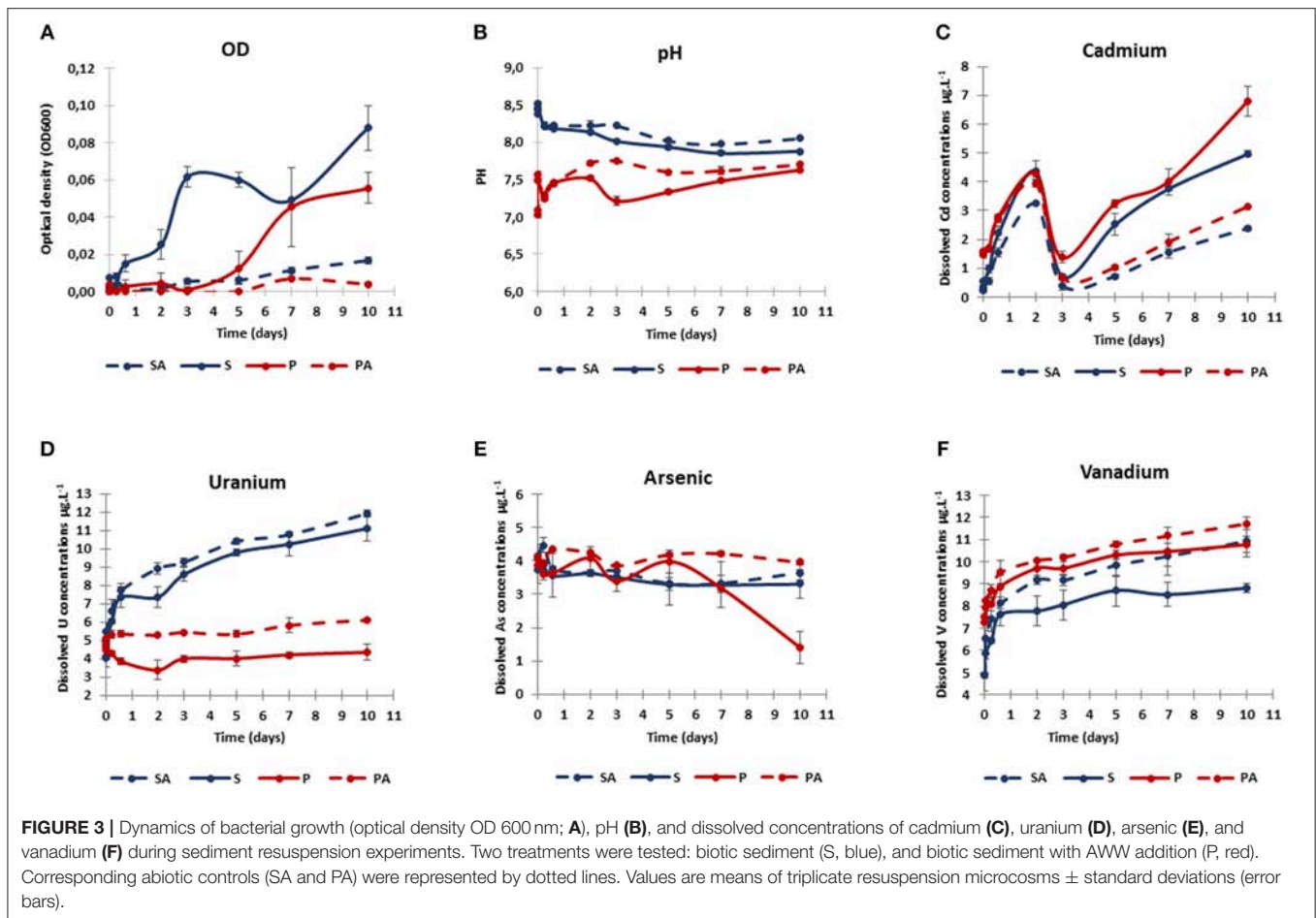
At T0 when mixing SED with SW, an initial Cd release from SED was observed in the P conditions ( $1.46 \pm 0.05 \mu\text{g L}^{-1}$ ), significantly stronger than in S conditions ( $0.21 \pm 0.03 \mu\text{g L}^{-1}$ ; U-test,  $p < 0.01$ ,  $n = 12$ ). This may be explained by the initial Cd input resulting from AWW addition (i.e.,  $0.9 \mu\text{g L}^{-1}$ , corresponding to 61% of the initial Cd). Independently of AWW addition, Cd was strongly remobilized during the 2 first days, and then returned rapidly to initial low levels at 3 days, prior to a progressive increase until the end of the experiments. At Tf, significant Cd difference was observed between biotic and abiotic conditions (U-test,  $p < 0.05$ ,  $n = 10$ ). Cd release was twice higher in the biotic conditions (S:  $4.98 \pm 0.11 \mu\text{g L}^{-1}$ ; P:  $6.79 \pm 0.51 \mu\text{g L}^{-1}$ ) than in the corresponding abiotic conditions

(Figure 3C), suggesting that microorganisms might play a role in the Cd remobilization.

The initial concentrations of dissolved U were similar in S and P conditions ( $4.1\text{--}4.6 \mu\text{g L}^{-1}$ ) (Figure 3D). With AWW addition, no significant U remobilization was observed between the biotic condition P at T0 and Tf (U-test,  $p > 0.05$ ,  $n = 6$ ), and a slight U increase, albeit insignificant, was detected between abiotic condition PA at T0 and Tf ( $5.81 \pm 0.39 \mu\text{g L}^{-1}$  at 10 days; U-test,  $p > 0.05$ ,  $n = 6$ ). In contrast, U release was accentuated at pH 8.5, in which its concentration almost tripled after 10 days (SA:  $12.42 \pm 0.89 \mu\text{g L}^{-1}$ ; S:  $11.10 \pm 0.71 \mu\text{g L}^{-1}$ ), indicating that U mobilization increased in natural seawater (without AWW addition).

Initial dissolved As concentration was around  $4 \mu\text{g L}^{-1}$  in all experiments (Figure 3E). Dissolved As levels remained stable until day 10 in all cases, except in biotic condition P, where it significantly decreased after 7 days, down to  $1.41 \pm 0.40 \mu\text{g L}^{-1}$  (T10; significantly lower As values for P compared to other conditions at Tf; U-test,  $p < 0.05$ ,  $n = 11$ ), suggesting biogenic As immobilization after AWW addition.

Initial dissolved V levels varied between P and S conditions, but dissolved V presented similar initial values under biotic or abiotic experiments ( $\sim 4.9 \mu\text{g L}^{-1}$  for S and SA;  $\sim 7.4 \mu\text{g L}^{-1}$  for P and PA; Figure 3F). These results may be partly explained



by the initial V input from AWW addition (i.e.,  $1.6 \mu\text{g L}^{-1}$ , corresponding to 21% of the initial V). A gradual increase in dissolved V was observed in all experiments, especially during the first day and the remobilization slowed down until the 10th day. The final dissolved V tended to be lower in the biotic condition S ( $8.8 \pm 0.2 \mu\text{g L}^{-1}$ ) than in other conditions (SA:  $10.92 \pm 0.72 \mu\text{g L}^{-1}$ ; P:  $10.77 \pm 0.34 \mu\text{g L}^{-1}$ ; PA:  $11.71 \pm 0.29 \mu\text{g L}^{-1}$ ; significantly lower V values for S compared to other conditions at Tf; U-test,  $p < 0.05$ ,  $n = 11$ ), indicating that V remobilization was biologically decreased in natural seawater (without AWW addition).

### Microbial Community Dynamics in the Resuspension Experiments

The dynamics of microbial diversity and bacterial abundance were monitored over time (0, 3, 5, 7, and 10 days), in the pelletized sediment suspensions from the triplicated biotic conditions using 16S rRNA NGS and qPCR analyses (P with AWW addition and S without AWW addition). After 3-day incubation, the number of observed OTU increased from  $1041 \pm 6$  (for initial SED) to 1078 on average, in both S and P conditions independently of acidification. A gradual increase in OTU number was observed over time in S conditions ( $1113 \pm 10$  after 10 days; **Table S3**), while no difference in OTU richness and

Shannon index was observed in P conditions. On the contrary, bacterial abundance displayed a significant decrease from  $2.87 \pm 0.96 \times 10^9$  (for initial SED) to  $1.77 \pm 0.14 \times 10^8$  and  $2.50 \pm 0.27 \times 10^8$ , respectively in both S and P experiments (after 10 days, U-test,  $p < 0.05$ ; **Table S3**). No significant difference between S and P conditions was observed at Tf.

Change in the microbial community structure was shown in the hierarchical dendrogram based on Bray–Curtis similarity (**Figure 2**). All the incubation samples were separated from the initial samples. After 3-day incubation (T3), samples of conditions S and P clustered together and replicate samples from the same conditions (S1, S2, S3 or P1, P2, P3) grouped also together. With the sole exception of S3-T5 separated from S1-T5 and S2-T5, the dynamics and clustering of microbial communities were reproducible between samples triplicates over time. After 7 days and until the end of the incubation, replicate samples exposed to acidic effluent (P, in red) clustered together clearly apart from replicate samples without acidic effluent (S, in black).

On average, bacterial communities in the S and P conditions were mainly composed of the following phyla/classes: *Bacteroidetes* (35%), *Alphaproteobacteria* (29%), *Gammaproteobacteria* (14%), *Actinobacteria* (9%), and *Verrucomicrobia* (5%; **Figure 2**). Compared to the initial

SED community, *Alphaproteobacteria* decreased over time (from 37% initially to ~28% at the end), while *Bacteroidetes* were enriched in both S and P conditions (from 20% initially to ~35% at the end; **Figure 2**). No difference in low archaeal proportion (<0.1% of microbial community) was observed depending on treatment and time.

## Correlations Between Microbial Communities and Resuspension Experimental Conditions

Principal Coordinate Analysis (PCoA) based on the relative OTU abundances showed a clear temporal succession along the PC1-axis ( $r^2 = 0.84$ ,  $p < 0.001$  for time effect), evidencing the adaptation of microbial communities to resuspension conditions over time (**Figure 4A**). After 3 day-incubation, microbial communities were still highly similar in S and P conditions, with 10 common discriminate OTU affiliated to *Alphaproteobacteria* and *Gammaproteobacteria* classes, *Flavobacteriaceae* family, *Verrucomicrobia* class (**Figures 4B, 5**). From 5-day incubation, the PCoA highlighted a clear separation of microbial communities into two groups along the PC2-axis according to the presence/absence of AWW, which was confirmed by PERMANOVA ( $r^2 = 0.76$ ,  $p < 0.01$ ). The divergence increased with time and the AWW addition was the most important driving force of the microbial community structure. Higher pH and higher diversity were significantly correlated with S microbial communities ( $r^2 = 0.59$ ,  $p < 0.01$  and  $r^2 = 0.49$ ,  $p < 0.01$ , respectively). Dissolved U levels were also significantly correlated with S communities ( $r^2 = 0.88$ ,  $p < 0.01$ ), especially at intermediary times of the incubations (**Figure 4A**), suggesting enhanced U immobilization in presence of acidic effluent. However, the similar trend between biotic and abiotic U kinetics (**Figure 3D**) suggests an effect of U as driver of the microbial structure rather than a potential role of microbial communities in U mobilization. On the other hand, the significant and high linear correlation between dissolved Cd levels and microbial communities exposed to acidic effluent ( $r^2 = 0.87$ ,  $p < 0.01$ ), especially at the end (**Figures 4A, 3C**), fitted with our physicochemical kinetics, suggesting that microorganisms may enhance Cd remobilization. The same microbial effect was observed, to a lower extent, on V remobilization, especially at intermediate times of the incubation ( $r^2 = 0.54$ ,  $p < 0.05$ ). When tested altogether, the concerted effect of the abiotic variables on the multivariate pattern of the microbial community revealed that a simple model including only 2 variables (namely pH and Cd concentration) best explained the community structure ( $r^2 = 0.6265$ ,  $p < 0.01$ ). Models including more variables (As, U, V) were also significant ( $p < 0.01$ ) but less strongly correlated to the community structure ( $r^2 = 0.49$  to  $0.61$ ; **Table S7**).

## Dynamics of Representative OTU in the Sediment Resuspension Experiments

The taxonomic affiliation of the 32 representative OTU selected from the PCoA is given in **Table S8**. The relative abundance of these OTU over time was presented in the heatmap

(**Figure 5**), which separated them into 3 groups according to their enrichment in S or P conditions. The relative abundance and diversity of the *Bacteroidetes* OTU differed between S and P conditions. The first group (named “P-related OTU”) contained the majority of the representative OTU (9) explaining the separation of P communities at the end of the experiment. They were mainly affiliated to the *Flavobacteriaceae* family within the *Bacteroidetes* phylum (1, 66, 106, 109, 165, 168126; **Figure 4B, Table S6**), suggesting a competitive advantage of these marine bacteria under acidified P conditions. The second group (named “S-related OTU”) contained 15 OTU, which seem to be more abundant in S than P condition, but no statistically significant difference was observed between conditions. Eight of them were mainly related to *Bacteroidetes*. Five *Saprospirales* OTU (3, 30, 114, 205, 273031) were enriched at Tf in S conditions, suggesting they might be adapted to sediment resuspension (**Figure 5**). The third group (named “S- and P-related OTU”) includes the 10 common OTU observed after 3 days, which decline over time, suggesting they were not adapted to the conditions imposed by sediment resuspension.

Spearman’s rank correlation analysis showed significant positive correlations ( $r_s > 0.70$ ,  $p$ -value  $< 0.05$ ) between dissolved Cd levels and relative abundance of several OTU (e.g., 3, 7, 66, 109, 165, 140, 210, 168126; **Table S9**). The affiliation of these OTU at the genus level (when available) is provided on the heatmap (**Figure 5**) and **Table S8**. For example, relative abundance of *Flavobacteriaceae* OTU 165, affiliated to *Tenacibaculum* genus, increased by 4 times over time and were highly correlated with Cd levels ( $r_s = 91$  respectively; **Table S7**). Relative abundance of four *Bacteroidetes* OTU positively correlated with two TE: (i) Cd and V, such as *Flavobacteriaceae* OTU 109 and 168126 (*Namhaeicola* and *Olleya*, respectively) and *Rhodothermaceae* OTU 536800, or (ii) Cd and U that correlated with *Saprospirales* OTU 3 (*Lewinella*), suggesting multi-resistance to metals. No significant correlation was observed between selected OTU and As.

## DISCUSSION

The coastal marine ecosystems of the Gulf of Gabès (GG, southern Mediterranean Sea) are impacted by long-term discharges from fertilizer industry waste containing trace metals (El Zrelli et al., 2017; El Kateb et al., 2018). Our results demonstrated that resuspension of surface contaminated sediment from the Sfax coast led to high releases of Cd, U and V in seawater. High concentrations of Cd were initially found in surface sediment collected in front of mixed wastewater discharge into the seawater (El Hakmouni Wadi), as detected in previous studies on surface sediments of the Sfax southern coast (Zouch et al., 2017; Naifar et al., 2018). The fate and distribution of As, Cd, U and V are driven by complex processes controlled by abiotic and biotic parameters. Cd remobilization was biologically enhanced in our experiments, while remobilization of U from the sediment seemed to be mainly enhanced by abiotic factors, such as pH or oxygenation (Moon et al., 2007). Biotic factors are known to control both U and V immobilization, but in

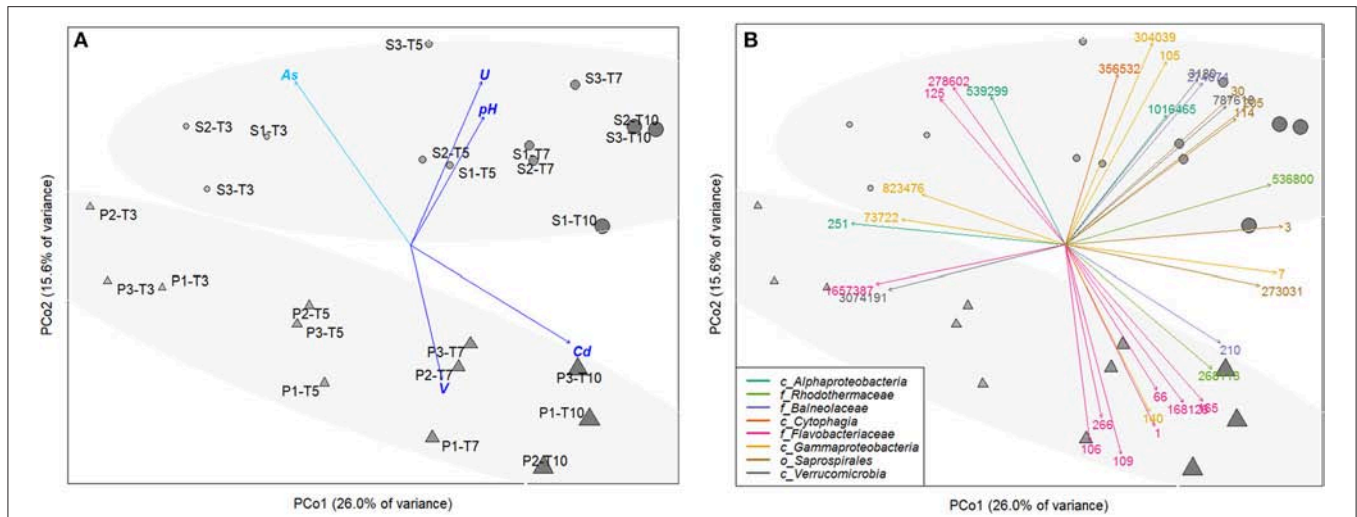


**FIGURE 4 |** Principal Coordinate Analysis (PCoA) computed from the OTU abundance table of resuspended sediments, either exposed (P,▲) or not (S,●) to acidic effluent (AWW), performed in triplicate (each replicate is indicated by the second digit, from 1 to 3), and collected at 4 different times along the incubation (time T3 to T10). The size and color intensity of symbols is proportional to elapsed time. Ellipses represent sample partitioning (Bray Curtis dissimilarity) between the P and S groups (standard deviation at 90% confidence, *p*-value 0.002). **(A)** Correlation between ordination and unrelated environmental variables (after removing the linearly-correlated variables). Only significant correlations are represented (*p*-value < 0.01, in light blue, *p*-value < 0.001, in dark blue). **(B)** Identification of 32 most discriminant OTU (labeled with their OTU number). Arrow colors represent the OTU affiliation at different taxonomic levels (class/order/family, represented by c/o/f respectively). BLAST affiliation of those OTU can be found in **Table S8**.

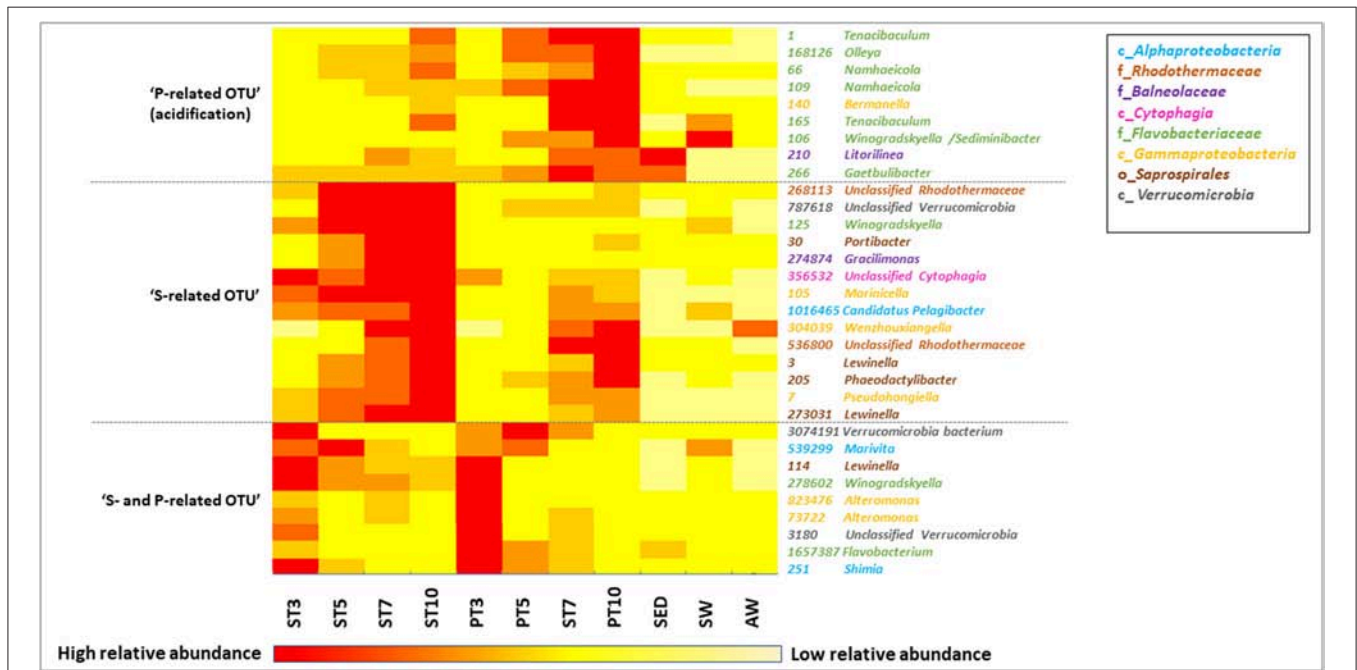


**FIGURE 5 |** Heat map showing the relative abundance of the most discriminant OTU selected from the PCoA of initial samples (SED, SW, and AWW) and samples collected during resuspension experiments (at 4 different times from T3 to T10), either in exposed (P) or not (S) to AWW. Data are average abundances calculated on biological triplicates. The color intensity for each panel corresponds to the OTU abundance, red indicates high level of relative abundance, while yellow indicates low relative abundance.

anoxic sediments, in which they can be bioreduced or trapped by hydrogen sulfide bioproducted from OM (Cumberland et al., 2016; Reijonen et al., 2016). In our experiments conducted under

aerobic conditions, arsenic (As) was efficiently immobilized by the surface oxic sediments. Indeed, As is known to be less mobile under aerobic conditions than under anaerobic conditions in

reducing sediment porewater (Bataillard et al., 2014). Moreover, a previous resuspension study of estuarine sediments showed that As was released ten times less from a surface oxic layer (the 0–0.5 cm) than from a deep anoxic layer sediment (13–15 cm depth; Saulnier and Mucci, 2000).

Acidic industrial effluent induced an increase in the content of several trace metals (e.g., Cd, V) in our resuspension experiment and could influence metal dynamics by modifying some physico-chemical parameters, especially pH, which control TE chemical form and mobility (Kiratli and Ergin, 1996; Eggleton and Thomas, 2004; Millero et al., 2009; Wang Z. et al., 2015). Martín-Torre et al. (2013) have shown that metal response to pH variation varies from one element to another. According to our study, Cd was not controlled by neutral/marine pH (7–8.5) range, because it forms strong chloro complexes in seawater, which are weakly influenced by pH change (Millero et al., 2009; Martín-Torre et al., 2013; Bruland, 2014). U mobility was controlled by pH (immobilized at initial pH < 8 and mobilized at initial pH > 8), because U is known to form strong complexes with carbonates and hydroxides influenced by pH (Millero et al., 2009; Cumberland et al., 2016). V release was observed in all experimental conditions, according to previous studies reporting high V mobility at neutral/marine pH (Brunori et al., 2005; Reijonen et al., 2016). In contrast, As was not remobilized during our experiment conducted at neutral/marine pH, in agreement with previous studies showing low As solubilization from contaminated marine sediment and processing waste under aerobic and neutral pH conditions (Al-Abed et al., 2007; Martín-Torre et al., 2013). In the neutral/marine pH region, the low As release is probably due to the co-sorption of As and Fe in sediments (Saulnier and Mucci, 2000; Al-Abed et al., 2007).

Acidic wastewater addition impacted bacterial community dynamics in our sediment resuspension. Lower bacterial diversity and changes in bacterial composition were observed in samples with acidic effluent addition, suggesting that slight pH decrease and/or TE input (e.g., Cd), was selective pressure for some sensitive marine bacteria. A shift within *Bacteroidetes* phylum diversity was observed depending on AWW addition. Indeed, the relative abundance of *Flavobacteriaceae* species increased with addition of AWW containing trace metals and leading to a pH decrease. *Flavobacteriaceae* phylotypes (e.g., *Gaetbulibacter*, *Tenacibaculum*, and *Winogradskyella*) were dominant in the initial samples and were linked to Cd and V levels in our incubations. Some of them were already reported to be positively correlated with Cd levels in a previous study reporting the effect of Cd (up to 100  $\mu\text{g L}^{-1}$ ) on the microbial community of the East China Sea (Wang K. et al., 2015). The pH is also a key factor influencing bacterial community structure, as recently reported by several studies dealing with marine sediment, contaminated soil and freshwater ecosystems (Liu et al., 2015; Currie et al., 2017; Wu et al., 2017). As observed in our study, Krause et al. (2012) reported that slight acidification (small changes in pH from 8.2 to 7.7), due to the rise of anthropogenic CO<sub>2</sub> emissions, cause shifts in bacterial communities in the North Sea, and they identified many pH-sensitive groups (e.g., *Flavobacteriaceae*). Consequently, the acidification and contamination of south Mediterranean coastal areas by phosphate fertilizer industrial

discharge may affect marine ecological processes driven by bacteria, especially the phylum *Bacteroidetes* occurring in the coastal sediment and seawater, which are essential for the organic matter mineralization (Cottrell and Kirchman, 2000; O'Sullivan et al., 2006).

In conclusion, the input of acidic wastewater affected both microbial diversity and trace metal dynamics during resuspension of contaminated sediments. The effect of AWW addition was metal-dependant and mainly visible on the diversity of the phylum *Bacteroidetes*, which is assumed to be important in OM degradation. Among *Bacteroidetes*, members of *Flavobacteriaceae* seem to be well adapted to the acidification and metallic pollution. Although other parameters such as nutrients or organic contaminants (e.g., hydrocarbons) may also contribute to the dynamics of both metals and microbial communities in our incubations, our results show for the first time the effect of an extremely acidic effluent on coastal microbial communities and give some interesting insights concerning the fate of metals during resuspension events, which could be useful as bioindicators of environmental impacts or to predict potential metal contamination in coastal marine ecosystems.

## AUTHOR CONTRIBUTIONS

LC, FK, HZo, SC, MQ, and MT designed experiments. FK, HZa, HZo, and MQ collected samples. HZo and MQ performed experiments. HZo performed microbial diversity analyses, SC and HZo performed metal analyses, LC, MT, and HZo performed numerical and statistical analyses. HZo wrote the manuscript in collaboration with MQ. All authors read and commented on the draft manuscript. All authors agreed to the final version.

## ACKNOWLEDGMENTS

This project was financially supported by the French national program EC2CO-Biohefect/Ecodyn/Dril/MicrobiEn (DYNAMICA) CNRS/INSU, the IRD French-Tunisian International Joint Laboratory LMI COSYS-Med, the Ministry of Higher Education and Scientific Research of Tunisia and the CNRS/INSU MISTRALS- MERMEX-WP3-C3A program. The project leading to this publication has received funding from European FEDER Fund under project 1166-39417. We acknowledge the Isotopic & Organic platform from the Institut des Sciences Analytiques (ISA, UMR 5280, Villeurbanne, France) for performing the C/H/N/S analyses. We also thank D. Delanghe from the sedimentology laboratory of the Centre Européen de Recherche et d'Enseignement des Géosciences de l'Environnement (CEREGE, UMR 7330, Aix-en-Provence, France) for particular grain size analyses. The authors acknowledge the reviewers for their constructive comments and corrections.

## SUPPLEMENTARY MATERIAL

The Supplementary Material for this article can be found online at: <https://www.frontiersin.org/articles/10.3389/fmicb.2018.03103/full#supplementary-material>

## REFERENCES

- Abdallah, B. M., Karray, F., Mhiri, N., Mei, N., Quéméneur, M., Cayol, J. L., et al. (2016). Prokaryotic diversity in a Tunisian hypersaline lake, Chott El Jerid. *Extremophiles* 20, 125–138. doi: 10.1007/s00792-015-0805-7
- Al-Abed, S. R., Jegadeesan, G., Purandare, J., and Allen, D. (2007). Arsenic release from iron rich mineral processing waste: Influence of pH and redox potential. *Chemosphere* 66, 775–782. doi: 10.1016/j.chemosphere.2006.07.045
- Altschul, S. F., Gish, W., Miller, W., Myers, E. W., and Lipman, D. J. (1990). Basic local alignment search tool. *J. Mol. Biol.* 215, 403–410. doi: 10.1016/S0022-2836(05)80360-2
- Ayadi, N., Aloulou, F., and Bouzid, J. (2015). Assessment of contaminated sediment by phosphate fertilizer industrial waste using pollution indices and statistical techniques in the Gulf of Gabes (Tunisia). *Arab. J. Geosci.* 8, 1755–1767. doi: 10.1007/s12517-014-1291-4
- Ayata, S. D., Irissou, J. O., Aubert, A., Berline, L., Dutay, J. C., Mayot, N., et al. (2018). Regionalisation of the Mediterranean basin, a MERMEX synthesis. *Prog. Oceanogr.* 163, 7–20. doi: 10.1016/j.pocean.2017.09.016
- Bataillard, P., Grangeon, S., Quinn, P., Mosselmans, F., Lahfid, A., Wille, G., et al. (2014). Iron and arsenic speciation in marine sediments undergoing a resuspension event: the impact of biotic activity. *J. Soils Sediments* 14, 615–629. doi: 10.1007/s11368-013-0829-5
- Ben Salem, Z., and Ayadi, H. (2016). Heavy metal accumulation in *Diplodus annularis*, *Liza aurata*, and *Solea vulgaris* relevant to their concentration in water and sediment from the southwestern Mediterranean (coast of Sfax). *Environ. Sci. Pollut. Res.* 23, 13895–13906. doi: 10.1007/s11356-016-6531-6
- Bokulich, N. A., Subramanian, S., Faith, J. J., Gevers, D., Gordon, I., Knight, R., et al. (2013). Quality-filtering vastly improves diversity estimates from Illumina amplicon sequencing. *Nat. Methods* 10, 57–59. doi: 10.1038/nmeth.2276
- Bruland, K. W. (2014). Complexation of cadmium by natural in the organic ligands central North Pacific. *Limnol. Oceanogr.* 37, 1008–1017. doi: 10.4319/lo.1992.37.5.1008
- Brunori, C., Cremisini, C., Massanisso, P., Pinto, V., and Torricelli, L. (2005). Reuse of a treated red mud bauxite waste: Studies on environmental compatibility. *J. Hazard. Mater.* 117, 55–63. doi: 10.1016/j.jhazmat.2004.09.010
- Cabrol, L., Malhautier, L., Poly, F., Lepeuple, A. S., and Fanlo, J. L. (2012). Bacterial dynamics in steady-state biofilters: beyond functional stability. *FEMS Microbiol. Ecol.* 79, 260–271. doi: 10.1111/j.1574-6941.2011.01213.x
- Cabrol, L., Quéméneur, M., and Misson, B. (2017). Inhibitory effects of sodium azide on microbial growth in experimental resuspension of marine sediment. *J. Microbiol. Methods* 133, 62–65. doi: 10.1016/j.mimet.2016.12.021
- Cantwell, M. G., and Burgess, R. M. (2004). Variability of parameters measured during the resuspension of sediments with a particle entrainment simulator. *Chemosphere* 56, 51–58. doi: 10.1016/j.chemosphere.2004.01.033
- Caporaso, J. G., Kuczynski, J., Stombaugh, J., Bittinger, K., Bushman, F. D., Costello, E. K., et al. (2010). QIIME allows analysis of high-throughput community sequencing data. *Nat. Met.* 7, 335–336. doi: 10.1038/nmeth.f.303
- Cichy, B., Jaroszek, H., and Paszek, A. (2014). Cadmium in phosphate fertilizers; ecological and economical aspects. *Chemik* 68, 20–22.
- Cottrell, M. T., and Kirchman, D. L. (2000). Natural assemblages of marine proteobacteria and members of the *Cytophaga-Flavobacter* clustler consuming low- and high-molecular-weight dissolved organic matter. *Appl. Environ. Microbiol.* 66, 1692–1697. doi: 10.1128/AEM.66.4.1692-1697.2000
- Cumberland, S. A., Douglas, G., Grice, K., and Moreau, J. W. (2016). Uranium mobility in organic matter-rich sediments: a review of geological and geochemical processes. *Earth-Science Rev.* 159, 160–185. doi: 10.1016/j.earscirev.2016.05.010
- Currie, A. R., Tait, K., Parry, H., de Francisco-Mora, B., Hicks, N., Mark Osborn, A., et al. (2017). Marine microbial gene abundance and community composition in response to ocean acidification and elevated temperature in two contrasting coastal marine sediments. *Front. Microbiol.* 8:1599. doi: 10.3389/fmicb.2017.01599
- Dang, D. H., Lenoble, V., Durrieu, G., Omanović, D., Mullot, J. U., Mounier, S., et al. (2015). Seasonal variations of coastal sedimentary trace metals cycling: Insight on the effect of manganese and iron (oxy)hydroxides, sulphide and organic matter. *Mar. Pollut. Bull.* 92, 113–124. doi: 10.1016/j.marpolbul.2014.12.048
- Dowd, S. E., Callaway, T. R., Wolcott, R. D., Sun, Y., McKeehan, T., Hagevoort, R. G., et al. (2008). Evaluation of the bacterial diversity in the feces of cattle using 16S rDNA bacterial tag-encoded FLX amplicon pyrosequencing (bTEFAP). *BMC Microbiol.* 8, 1–8. doi: 10.1186/1471-2180-8-125
- Edgar, R. C. (2010). Search and clustering orders of magnitude faster than BLAST. *Bioinformatics* 26, 2460–2461. doi: 10.1093/bioinformatics/btq461
- Eggleton, J., and Thomas, K. V. (2004). A review of factors affecting the release and bioavailability of contaminants during sediment disturbance events. *Environ. Int.* 30, 973–980. doi: 10.1016/j.envint.2004.03.001
- El Kateb, A., Stalder, C., Rüggeberg, A., Neurrer, C., Spangenberg, J. E., and Spezzaferri, S. (2018). Impact of industrial phosphate waste discharge on the marine environment in the Gulf of Gabes (Tunisia). *PLoS ONE* 13:e0197731. doi: 10.1371/journal.pone.0197731
- El Zrelli, R., Courjault-Radé, P., Rabaoui, L., Castet, S., Michel, S., and Bejaoui, N. (2015). Heavy metal contamination and ecological risk assessment in the surface sediments of the coastal area surrounding the industrial complex of Gabes city, Gulf of Gabes, SE Tunisia. *Mar. Pollut. Bull.* 101, 922–929. doi: 10.1016/j.marpolbul.2015.10.047
- El Zrelli, R., Courjault-Radé, P., Rabaoui, L., Daghbouj, N., Mansour, L., Balti, R., et al. (2017). Biomonitoring of coastal pollution in the Gulf of Gabes (SE, Tunisia): use of *Posidonia oceanica* seagrass as a bioindicator and its mat as an archive of coastal metallic contamination. *Environ. Sci. Pollut. Res.* 24, 22214–22225. doi: 10.1007/s11356-017-9856-x
- El Zrelli, R., Rabaoui, L., Ben Alaya, M., Daghbouj, N., Castet, S., Besson, P., et al. (2018). Seawater quality assessment and identification of pollution sources along the central coastal area of Gabes Gulf (SE Tunisia): evidence of industrial impact and implications for marine environment protection. *Mar. Pollut. Bull.* 127, 445–452. doi: 10.1016/j.marpolbul.2017.12.012
- Fonti, V., Dell'Anno, A., and Beolchini, F. (2013). Influence of biogeochemical interactions on metal bioleaching performance in contaminated marine sediment. *Water Res.* 47, 5139–5152. doi: 10.1016/j.watres.2013.05.052
- Fourati, R., Tedetti, M., Guigue, C., Goutx, M., Garcia, N., Zaghden, H., et al. (2018a). Sources and spatial distribution of dissolved aliphatic and polycyclic aromatic hydrocarbons in surface coastal waters of the Gulf of Gabès (Tunisia, Southern Mediterranean Sea). *Prog. Oceanogr.* 163, 232–247. doi: 10.1016/j.pocean.2017.02.001
- Fourati, R., Tedetti, M., Guigue, C., Goutx, M., Zaghden, H., Sayadi, S., et al. (2018b). Natural and anthropogenic particulate-bound aliphatic and polycyclic aromatic hydrocarbons in surface waters of the Gulf of Gabès (Tunisia, southern Mediterranean Sea). *Environ. Sci. Pollut. Res.* 25, 2476–2494. doi: 10.1007/s11356-017-0641-7
- Gadd, G. M. (2000). Bioremediation potential of microbial mechanisms. *Curr Opin Biotechnol.* 11, 271–279. doi: 10.1016/S0958-1669(00)00095-1
- Gadd, G. M. (2004). Microbial influence on metal mobility and application for bioremediation. *Geoderma* 122, 109–119. doi: 10.1016/j.geoderma.2004.01.002
- Gadd, G. M. (2010). Metals, minerals and microbes: Geomicrobiology and bioremediation. *Microbiology* 156, 609–643. doi: 10.1099/mic.0.037143-0
- Gargouri, D., Azri, C., Serbaji, M. M., Jedoui, Y., and Montacer, M. (2011). Heavy metal concentrations in the surface marine sediments of Sfax Coast, Tunisia. *Environ. Monit. Assess.* 175, 519–530. doi: 10.1007/s10661-010-1548-7
- Ghannem, N., Gargouri, D., Sarbeji, M. M., Yaich, C., and Azri, C. (2014). Metal contamination of surface sediments of the Sfax-Chebbas coastal line, Tunisia. *Environ. Earth Sci.* 72, 3419–3427. doi: 10.1007/s12665-014-3248-z
- Ghilardi, M., Psomiadis, D., Cordier, S., Delanghe-Sabatier, D., Demory, F., Hamidi, F., et al. (2012). The impact of early- to mid-Holocene palaeoenvironmental changes on Neolithic settlement at Nea Nikomideia, Thessaloniki plain, Greece. *Quat. Int.* 266, 47–61. doi: 10.1016/j.quaint.2010.12.016
- Gillan, D. C., Danis, B., Pernet, P., Joly, G., and Dubois, P. (2005). Structure of sediment-associated microbial communities along a heavy-metal contamination gradient in the marine environment. *Appl. Environ. Microbiol.* 71, 679–690. doi: 10.1128/AEM.71.2.679-690.2005

- Goni-Urriza, M., Moussard, H., Lafabrie, C., Carré, C., Bouvy, M., Sakka Hlaili, A., et al. (2018). Consequences of contamination on the interactions between phytoplankton and bacterioplankton. *Chemosphere* 195, 212–222. doi: 10.1016/j.chemosphere.2017.12.053
- Good, J. I. (1953). The population frequencies of species and the estimation of population parameters. *Biometrika* 40, 237–264. doi: 10.1093/biomet/40.3-4.237
- Guigue, C., Tedetti, M., Dang, D. H., Mullot, J.-U., Garnier, C., and Goutx, M. (2017). Remobilization of polycyclic aromatic hydrocarbons and organic matter in seawater during sediment resuspension experiments from a polluted coastal environment: insights from Toulon Bay (France). *Environ. Pollut.* 229, 627–638. doi: 10.1016/j.envpol.2017.06.090
- Guzmán, H. M., and Jarvis, K. E. (1996). Vanadium century record from Caribbean reef corals: a tracer of oil pollution in Panama. *Ambio* 25, 523–526.
- Hamdi, I., Denis, M., Bellaaj-Zouari, A., Khemakhem, H., Bel Hassen, M., Hamza, A., et al. (2015). The characterisation and summer distribution of ultraphytoplankton in the Gulf of Gabès (Eastern Mediterranean Sea, Tunisia) by using flow cytometry. *Cont. Shelf Res.* 93, 27–38. doi: 10.1016/j.csr.2014.10.002
- Hassen, M. B., Hamza, A., Drira, Z., Zouari, A., Akrouf, F., Messaoudi, S., et al. (2009). Phytoplankton-pigment signatures and their relationship to spring-summer stratification in the Gulf of Gabes. *Estuar. Coast. Shelf Sci.* 83, 296–306. doi: 10.1016/j.ecss.2009.04.002
- Jong, T., and Parry, D. L. (2003). Removal of sulfate and heavy metals by sulfate reducing bacteria in short-term bench scale upflow anaerobic packed bed reactor runs. *Water Res.* 37, 3379–3389. doi: 10.1016/S0043-1354(03)00165-9
- Kalnejais, L. H., Martin, W. R., and Bothner, M. H. (2010). The release of dissolved nutrients and metals from coastal sediments due to resuspension. *Mar. Chem.* 121, 224–235. doi: 10.1016/j.marchem.2010.05.002
- Kim, E. H., Mason, R. P., Porter, E. T., and Soulen, H. L. (2006). The impact of resuspension on sediment mercury dynamics, and methylmercury production and fate: a mesocosm study. *Mar. Chem.* 102, 300–315. doi: 10.1016/j.marchem.2006.05.006
- Kiratli, N., and Ergin, M. (1996). Partitioning of heavy metals in surface Black Sea sediments. *Appl. Geochemistry* 11, 775–788. doi: 10.1016/S0883-2927(96)00037-6
- Krause, E., Wichels, A., Giménez, L., Lunau, M., Schilhabel, M. B., and Gerdt, G. (2012). Small changes in pH have direct effects on marine bacterial community composition: a microcosm approach. *PLoS ONE* 7:e47035. doi: 10.1371/journal.pone.0047035
- Liu, S., Ren, H., Shen, L., Lou, L., Tian, G., Zheng, P., et al. (2015). pH levels drive bacterial community structure in the Qiantang River as determined by 454 pyrosequencing. *Front. Microbiol.* 6:285. doi: 10.3389/fmicb.2015.00285
- Martin-Torre, M. C., Payán, M. C., Galán, B., Coz, A., and Viguri, J. R. (2013). The use of leaching tests to assess metal release from contaminated marine sediment under CO<sub>2</sub> leakages from CCS. *Energy Procedia* 51, 40–47. doi: 10.1016/j.egypro.2014.07.005
- Mayot, N., D'Ortenzio, F., D'Alcalá, M. R., Lavigne, H., and Claustre, H. (2016). Interannual variability of the Mediterranean trophic regimes from ocean color satellites. *Biogeosciences* 13, 1901–1917. doi: 10.5194/bg-13-1901-2016
- Millero, F., Woosley, R., DiTrollo, B., and Waters, J. (2009). Effect of ocean acidification on the speciation of metals in seawater. *Oceanography* 22, 72–85. doi: 10.5670/oceanog.2009.98
- Monnin, L., Ciffroy, P., Garnier, J. M., Ambrosi, J.-P., and Radakovitch, O. (2018). Remobilization of trace metals during laboratory resuspension of contaminated sediments from a dam reservoir. *J. Soils Sediments* 18, 2596–2613. doi: 10.1007/s11368-018-1931-5
- Moon, H. S., Komlos, J., and Jaffé, P. R. (2007). Uranium reoxidation in previously bioreduced sediment by dissolved oxygen and nitrate. *Environ. Sci. Technol.* 41, 4587–4592. doi: 10.1021/es063063b
- Naifar, I., Pereira, F., Zmemla, R., Bouaziz, M., Elleuch, B., and Garcia, D. (2018). Spatial distribution and contamination assessment of heavy metals in marine sediments of the southern coast of Sfax, Gabes Gulf, Tunisia. *Mar. Pollut. Bull.* 131, 53–62. doi: 10.1016/j.marpolbul.2018.03.048
- O'Sullivan, L. A., Rinna, J., Humphreys, G., Weightman, A. J., and Fry, J. C. (2006). Culturable phylogenetic diversity of the phylum “Bacteroidetes” from river epilithon and coastal water and description of novel members of the family *Flavobacteriaceae*: *Epilithonimonas tenax* gen. nov., sp. nov. and *Persicivirga xylanidelens* gen. nov., sp. *Int. J. Syst. Evol. Microbiol.* 56, 169–180. doi: 10.1099/ijso.0.63941-0
- Peng, J. F., Song, Y. H., Yuan, P., Cui, X. Y., and Qiu, G. L. (2009). The remediation of heavy metals contaminated sediment. *J. Hazard. Mater.* 161, 633–640. doi: 10.1016/j.jhazmat.2008.04.061
- Quéméneur, M., Garrido, F., Billard, P., Breeze, D., Leyval, C., Jauzein, M., et al. (2016). Bacterial community structure and functional *arrA* gene diversity associated with arsenic reduction and release in an industrially contaminated soil. *Geomicrobiol. J.* 33, 839–849. doi: 10.1080/01490451.2015.1118167
- Rabaoui, L., El Zrelli, R., Ben Mansour, M., Balti, R., Mansour, L., Tlig-Zouari, S., et al. (2015). On the relationship between the diversity and structure of benthic macroinvertebrate communities and sediment enrichment with heavy metals in Gabes Gulf, Tunisia. *J. Mar. Biol. Assoc.* 95, 233–245. doi: 10.1017/S0025315414001489
- Reijonen, I., Metzler, M., and Hartikainen, H. (2016). Impact of soil pH and organic matter on the chemical bioavailability of vanadium species: the underlying basis for risk assessment. *Environ. Pollut.* 210, 371–379. doi: 10.1016/j.envpol.2015.12.046
- Rekik, A., Drira, Z., Guermazi, W., Elloumi, J., Maalej, S., Aleya, L., et al. (2012). Impacts of an uncontrolled phosphogypsum dumpsite on summer distribution of phytoplankton, copepods and ciliates in relation to abiotic variables along the near-shore of the southwestern Mediterranean coast. *Mar. Pollut. Bull.* 64, 336–346. doi: 10.1016/j.marpolbul.2011.11.005
- Ross, S. (1994). *Toxic Metals in Soil-Plant Systems*. Chichester: Wiley.
- Sammari, C., Koutitonsky, V. G., and Moussa, M. (2006). Sea level variability and tidal resonance in the Gulf of Gabes, Tunisia. *Cont. Shelf Res.* 26, 338–350. doi: 10.1016/j.csr.2005.11.006
- Saulnier, I., and Mucci, A. (2000). Trace metal remobilization following the resuspension of estuarine sediments: Saguenay Fjord, Canada. *Appl. Geochemistry* 15, 191–210. doi: 10.1016/S0883-2927(99)00034-7
- Shannon, C. E., and Weaver, W. (1949). *The Mathematical Theory of Communication*. Champaign, IL; Urbana, IL: University of Illinois Press.
- Shipley, H. J., Gao, Y., Kan, A. T., and Tomson, M. B. (2011). Mobilization of trace metals and inorganic compounds during resuspension of Anoxic Sediments from Trepangier Bayou, Louisiana. *J. Environ. Qual.* 40, 484–491. doi: 10.2134/jeq2009.0124
- Simpson, E. H. (1949). Measurement of diversity. *Nature* 163:688. doi: 10.1038/163688a0
- Sun, M. Y., Dafforn, K. A., Brown, M. V., and Johnston, E. L. (2012). Bacterial communities are sensitive indicators of contaminant stress. *Mar. Pollut. Bull.* 64, 1029–1038. doi: 10.1016/j.marpolbul.2012.01.035
- Tabak, H. H., Lens, P., Van Hullebusch, E. D., and Dejonghe, W. (2005). Developments in bioremediation of soils and sediments polluted with metals and radionuclides - 1. Microbial processes and mechanisms affecting bioremediation of metal contamination and influencing metal toxicity and transport. *Rev. Environ. Sci. Biotechnol.* 4, 115–156. doi: 10.1007/s11157-005-2169-4
- Tessier, E., Garnier, C., Mullot, J. U., Lenoble, V., Arnaud, M., Raynaud, M., et al. (2011). Study of the spatial and historical distribution of sediment inorganic contamination in the Toulon bay (France). *Mar. Pollut. Bull.* 62, 2075–2086. doi: 10.1016/j.marpolbul.2011.07.022
- Wang, K., Zhang, D., Xiong, J., Chen, X., Zheng, J., Hu, C., et al. (2015). Response of bacterioplankton communities to cadmium exposure in coastal water microcosms with high temporal variability. *Appl. Environ. Microbiol.* 81, 231–240. doi: 10.1128/AEM.02562-14
- Wang, Z., Wang, Y., Zhao, P., Chen, L., Yan, C., Yan, Y., et al. (2015). Metal release from contaminated coastal sediments under changing pH conditions: Implications for metal mobilization in acidified oceans. *Mar. Pollut. Bull.* 101, 707–715. doi: 10.1016/j.marpolbul.2015.10.026
- White, C., Sayer, I. A., and Gadd, G. M. (1997). Microbial solubilization and immobilization of toxic metals: key biogeochemical processes for treatment of contamination. *FEMS Microbiol. Rev.* 20, 503–516. doi: 10.1111/j.1574-6976.1997.tb00333.x
- Witt, V., Wild, C., Anthony, K. R. N., Diaz-Pulido, G., and Uthicke, S. (2011). Effects of ocean acidification on microbial community composition of

- and oxygen fluxes through, biofilms from the Great Barrier Reef. *Environ. Microbiol.* 13, 2976–2989. doi: 10.1111/j.1462-2920.2011.02571.x
- Wu, Y., Zeng, J., Zhu, Q., Zhang, Z., and Lin, X. (2017). pH is the primary determinant of the bacterial community structure in agricultural soils impacted by polycyclic aromatic hydrocarbon pollution. *Sci. Rep.* 7:40093. doi: 10.1038/srep40093
- Xu, W., Li, X., Wai, O. W. H., Huang, W., and Yan, W. (2015). Remobilization of trace metals from contaminated marine sediment in a simulated dynamic environment. *Environ. Sci. Pollut. Res.* 22, 19905–19911. doi: 10.1007/s11356-015-5228-6
- Yamazaki, I. M., and Geraldo, L. P. (2003). Uranium content in phosphate fertilizers commercially produced in Brazil. *Appl. Radiat. Isot.* 59, 133–136. doi: 10.1016/S0969-8043(03)00159-3
- Zaghden, H., Serbaji, M. M., Saliot, A., and Sayadi, S. (2016). The Tunisian Mediterranean coastline: potential threats from urban discharges Sfax-Tunisian Mediterranean coasts. *Desalin. Water Treat.* 57, 24765–24777. doi: 10.1080/19443994.2016.1149107
- Zouch, H., Karray, F., Armougom, F., Chifflet, S., Hirschler-Réa, A., Kharrat, H., et al. (2017). Microbial diversity in sulfate-reducing marine sediment enrichment cultures associated with anaerobic biotransformation of coastal stockpiled phosphogypsum (Sfax, Tunisia). *Front. Microbiol.* 8:1583. doi: 10.3389/fmicb.2017.01583

**Conflict of Interest Statement:** The authors declare that the research was conducted in the absence of any commercial or financial relationships that could be construed as a potential conflict of interest.

Copyright © 2018 Zouch, Cabrol, Chifflet, Tedetti, Karray, Zaghden, Sayadi and Quéméneur. This is an open-access article distributed under the terms of the Creative Commons Attribution License (CC BY). The use, distribution or reproduction in other forums is permitted, provided the original author(s) and the copyright owner(s) are credited and that the original publication in this journal is cited, in accordance with accepted academic practice. No use, distribution or reproduction is permitted which does not comply with these terms.



# Nicosulfuron Degradation by an Ascomycete Fungus Isolated From Submerged *Alnus* Leaf Litter

Louis Carles<sup>1</sup>, Florent Rossi<sup>1</sup>, Pascale Besse-Hoggan<sup>2</sup>, Christelle Blavignac<sup>3</sup>, Martin Lereboure<sup>2</sup>, Joan Artigas<sup>1†</sup> and Isabelle Batisson<sup>1\*†</sup>

<sup>1</sup> Laboratoire Microorganismes: Génome et Environnement, CNRS, Université Clermont Auvergne, Clermont-Ferrand, France, <sup>2</sup> Institut de Chimie de Clermont-Ferrand, CNRS, Sigma Clermont, Université Clermont Auvergne, Clermont-Ferrand, France, <sup>3</sup> Centre Imagerie Cellulaire Santé, Université Clermont Auvergne (UCA PARTNER), Clermont-Ferrand, France

## OPEN ACCESS

### Edited by:

Jean-Francois Ghiglione,  
Centre National de la Recherche  
Scientifique (CNRS), France

### Reviewed by:

Leif Abrell,  
University of Arizona, United States  
Huzefa A. Raja,  
University of North Carolina  
at Greensboro, United States

### \*Correspondence:

Isabelle Batisson  
isabelle.batisson@uca.fr

†These authors have contributed  
equally to this work

### Specialty section:

This article was submitted to  
Microbiotechnology, Ecotoxicology  
and Bioremediation,  
a section of the journal  
Frontiers in Microbiology

Received: 23 July 2018

Accepted: 07 December 2018

Published: 19 December 2018

### Citation:

Carles L, Rossi F,  
Besse-Hoggan P, Blavignac C,  
Lereboure M, Artigas J and  
Batisson I (2018) Nicosulfuron  
Degradation by an Ascomycete  
Fungus Isolated From Submerged  
*Alnus* Leaf Litter.  
Front. Microbiol. 9:3167.  
doi: 10.3389/fmicb.2018.03167

Nicosulfuron is a selective herbicide belonging to the sulfonylurea family, commonly applied on maize crops. Its worldwide use results in widespread presence as a contaminant in surface streams and ground-waters. In this study, we isolated, for the first time, the *Plectosphaerella cucumerina* AR1 nicosulfuron-degrading fungal strain, a new record from *Alnus* leaf litter submerged in freshwater. The degradation of nicosulfuron by *P. cucumerina* AR1 was achieved by a co-metabolism process and followed a first-order model dissipation. Biodegradation kinetics analysis indicated that, in planktonic lifestyle, nicosulfuron degradation by this strain was glucose concentration dependent, with a maximum specific degradation rate of 1 g/L in glucose. When grown on natural substrata (leaf or wood) as the sole carbon sources, the *Plectosphaerella cucumerina* AR1 developed as a well-established biofilm in 10 days. After addition of nicosulfuron in the medium, the biofilms became thicker, with rising mycelium, after 10 days for leaves and 21 days for wood. Similar biofilm development was observed in the absence of herbicide. These fungal biofilms still conserve the nicosulfuron degradation capacity, using the same pathway as that observed with planktonic lifestyle as evidenced by LC-MS analyses. This pathway involved first the hydrolysis of the nicosulfuron sulfonylurea bridge, leading to the production of two major metabolites: 2-amino-4,6-dimethoxypyrimidine (ADMP) and 2-(aminosulfonyl)-*N,N*-dimethyl-3-pyridinecarboxamide (ASDM). One minor metabolite, identified as 2-(1-(4,6-dimethoxy-pyrimidin-2-yl)-ureido)-*N,N*-dimethyl-nicotinamide (N3), derived from the cleavage of the C-S bond of the sulfonylurea bridge and contraction by elimination of sulfur dioxide. A last metabolite (N4), detected in trace amount, was assigned to 2-(4,6-dimethoxy-pyrimidin-2-yl)-*N,N*-dimethyl-nicotinamide (N4), resulting from the hydrolysis of the N3 urea function. Although fungal growth was unaffected by nicosulfuron, its laccase activity was significantly impaired regardless of lifestyle. Leaf and wood surfaces being good substrata for biofilm development in rivers, *P. cucumerina* AR1 strain could thus have potential as an efficient candidate for the development of methods aiming to reduce contamination by nicosulfuron in aquatic environments.

**Keywords:** ascomycete fungus, herbicide, sulfonylurea, degradation, co-metabolism, natural substrata, *Plectosphaerella cucumerina*

## INTRODUCTION

Nicosulfuron (2-[(4,6-dimethoxypyrimidin-2-yl)carbamoylsulfamoyl]-*N,N*-dimethylpyridine-3-carboxamide) is a sulfonylurea class herbicide used worldwide as a post-emergence herbicide to protect maize crops from weeds. It inhibits acetolactate synthase (ALS) enzyme activity, a key enzyme involved in the branched-chain amino acid biosynthesis (Schloss, 1990), which results in the inhibition of plant growth. Despite the low agronomic dose recommended for nicosulfuron in crops (in Europe, 60 g active ingredient/ha; CE 1107/2009), this molecule is frequently detected in surface and ground-waters due to its high mobility, its Groundwater Ubiquity Score (GUS) being of 3.34 (Pfeiffer, 2010). This transfer can be explained by the high solubility (>7 g/L at pH  $\geq$  6.5) and low  $K_d$  coefficient of the molecule (ranging from 0.14 to 2.15 L/kg, Gonzalez and Ukrainczyk, 1996, 1999; Oliveira et al., 2001; Regitano and Koskinen, 2008; Trigo et al., 2014; Azcarate et al., 2015). The nicosulfuron environmental concentrations found in various surface waters from Canada, United States, and Europe, averaging 0.3–0.5  $\mu\text{g/L}$ , are non-negligible (Battaglin et al., 2000; de Lafontaine et al., 2014; Moschet et al., 2014), the highest amounts detected peaking up to 3.29  $\mu\text{g/L}$  (Battaglin et al., 2009). Overall, the high detection frequency of nicosulfuron in surface waters implies chronic exposure of aquatic microbial communities and eventually a set of adaptations regarding its use by microbes.

Responses of aquatic fungi to organic contaminants are sequential regarding exposure time and can take from hours to weeks. After an acute exposure to the pesticide, the first fungal responses consist in the oxidative attack of the molecule both in the intracellular (i.e., cytochrome P450 monooxygenases) and/or extracellular (i.e., peroxidases and laccases) spaces, followed by a methylation or conjugation process which improve the molecule solubility as well as its release out of the cell (Krauss et al., 2011). After a chronic exposure, fungi can mineralize the molecule with more or less success.

Regarding the sensitivity of fungi to nicosulfuron, most studies have been performed in soils. For instance, soil fungi are sensitive to nicosulfuron when repeatedly applied at dose rates higher than the recommended one, probably because ALS genes are also present in numerous fungal species (Karpouzas et al., 2014). In contrast, increasing levels of nicosulfuron exposure have been shown to increase the bacterial abundance and diversity in soil (Petric et al., 2016). This tolerance to nicosulfuron seems to be widespread in soil bacteria, mainly among Firmicutes and Actinobacteria. In aquatic microbial communities, responses to nicosulfuron are rather different comparing to those observed in soils (Carles et al., 2017b). While chronic exposure to nicosulfuron enhances fungal diversity in aquatic microbial communities associated with leaf litter, the diversity of bacteria was severely impaired. At the same line, the pre-exposure history of these aquatic microbial communities to contamination played a significant role in their ability to biodegrade nicosulfuron (Carles et al., 2017b).

Degradation of nicosulfuron can require up to 70 days in natural aquatic environments (Cessna et al., 2015), both abiotic and biotic degradation processes co-occurring.

Chemical hydrolysis of the sulfonylurea linkage has been described as the main abiotic degradation process (Sarmah and Sabadie, 2002), its rate being greater as pH of the medium decreases (Berger and Wolfe, 1996). This phenomenon was also observed for *Penicillium oxalicum* YC-WM1 where nicosulfuron degradation was due to medium acidification resulting from oxalate secretion by the fungal strain (Feng et al., 2017). Two degradation products are usually formed: 2-amino-4,6-dimethoxypyrimidine (ADMP) and 2-(aminosulfonyl)-*N,N*-dimethyl-3-pyridinecarboxamide (ASDM), the latter being able to cyclize at basic pH (Sarmah and Sabadie, 2002). Besides, five different photo-products have been identified during nicosulfuron photodegradation in aqueous media (Benzi et al., 2011), though the contribution of this process to total abiotic degradation of the molecule seems to be of minor importance (EFSA, 2007). Regarding biotic degradation, nine bacterial [*Oceanisphaera psychrotolerans* LAM-WHM-ZC (Zhou et al., 2017), *Bacillus subtilis* YB1 (Yang et al., 2008; Lu et al., 2012), *Ochrobactrum* sp. ZWS16 (Zhao et al., 2015b), *Rhodopseudomonas* sp. J5-2 (Zhang et al., 2011), *Alcaligenes faecalis* ZWS11 (Zhao et al., 2015a), *Klebsiella* sp. Y1 (Wang et al., 2016), *Serratia marcescens* N80 (Zhang et al., 2012), *Pseudomonas fluorescens* SG-1 (Carles et al., 2017a) and *Pseudomonas nitroreducens* strain NSA02 (Zhao et al., 2018)], and three fungal [*Talaromyces flavus* LZM1 (Song et al., 2013), *Aspergillus niger* YF1 (Yang et al., 2008; Lu et al., 2012) and *Penicillium oxalicum* YC-WM1 (Feng et al., 2017)] nicosulfuron-degrading strains have been described in the literature. In most cases, the metabolites identified were ADMP and ASDM, suggesting similar degradation pathways. All these strains have been isolated from environments subjected to high anthropogenic pressure (i.e., wastewater treatment plants, agricultural soils), whereas no data are available about degrading ability of strains exposed to nicosulfuron in final ecological receptors such as river ecosystems.

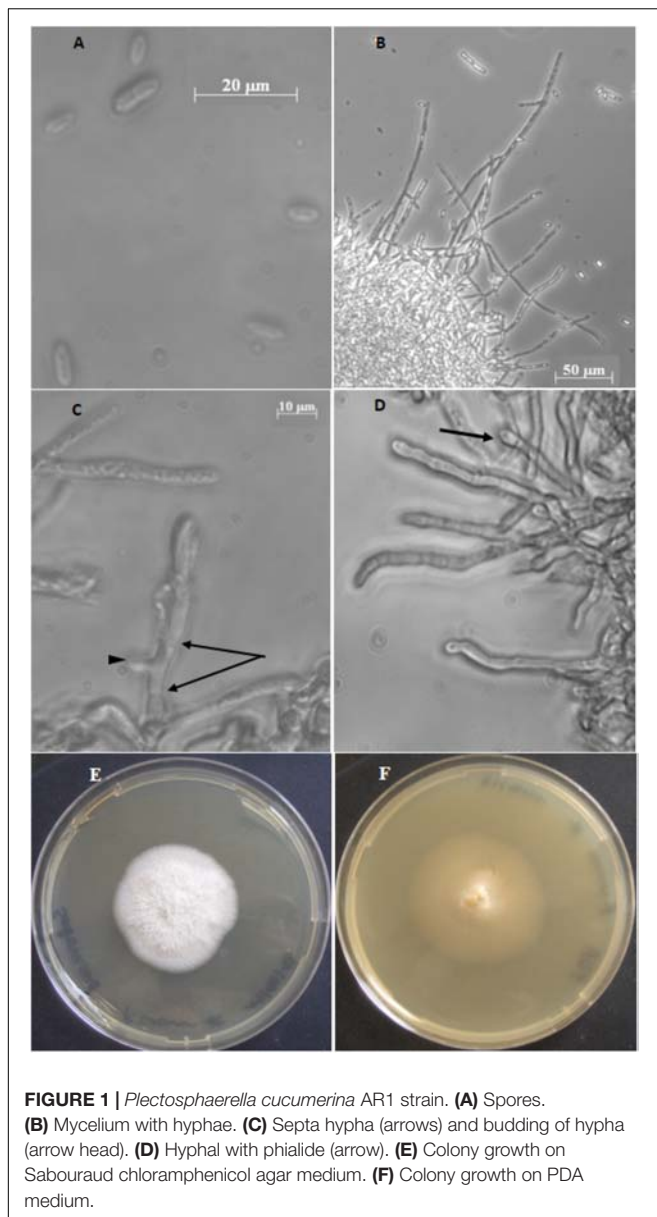
The present study investigates the capacity of a fungal strain of *Plectosphaerella cucumerina* AR1, isolated from submerged leaves in a forested river, to degrade nicosulfuron. The influence of lifestyle, accessible carbon source use and activity of the strain during the dissipation process of the herbicide was assessed.

## MATERIALS AND METHODS

### Chemicals and Media

Nicosulfuron (Pestanal, purity 99.6%) and ADMP (2-amino-4,6-dimethoxypyrimidine, purity 98.0%) were purchased from Sigma Aldrich (France), and ASDM (2-(aminosulfonyl)-*N,N*-dimethyl-3-pyridinecarboxamide, purity 98%) from J and K Scientific (Germany).

Malt extract and Sabouraud chloramphenicol agar media were purchased from Sigma Aldrich (France). Potato dextrose agar (PDA) medium was obtained from Biomérieux (France). Mineral salt medium (MSM) was composed of (/L): 1 g  $(\text{NH}_4)_2\text{HPO}_4$ , 1 g  $\text{KH}_2\text{PO}_4$ , 1 g  $\text{KNO}_3$ , 0.2 g  $\text{MgSO}_4 \cdot 7\text{H}_2\text{O}$ , 0.1 g  $\text{NaCl}$ , 20 mg  $\text{CaCl}_2$ , 5 mg  $\text{FeSO}_4 \cdot 7\text{H}_2\text{O}$ , 1 mL of a salt stock solution and 1 mL of a vitamin stock solution. The salt stock solution contained



(/L) 20 g boric acid, 18 g  $\text{MnSO}_4 \cdot \text{H}_2\text{O}$ , 2 g  $\text{ZnSO}_4$ , 1 g  $\text{CuSO}_4$ , 2.5 g  $\text{Na}_2\text{MoO}_4$ , 10 mg  $\text{Co}(\text{NO}_3)_2$ . The vitamin stock solution contained (/L) 2 mg biotin, 5 mg thiamine-HCl. The glucose-mineral salt medium (GSM) was obtained by addition of glucose (10, 5 or 1 g/L) in MSM. All the media were supplemented by chloramphenicol (0.5 g/L).

## Isolation and Identification of a Nicosulfuron-Degrading Fungal Strain

The isolation of fungal species was carried out on a nicosulfuron-degrading aquatic microbial community colonizing *Alnus glutinosa* (L.) Gaertn. leaf species (henceforth referred to *Alnus* in the text (Carles et al., 2017b)). The isolation was performed according to Artigas et al. (2017). Briefly, sporulation was induced in *Alnus* communities exhibiting nicosulfuron

degradation. Among the spores obtained, a single spore morphotype (fusoid-type; **Figure 1A**) was physically isolated using glass micropipettes under a microscope (Leica DM IRB, Leica Microsystems, Wetzlar, Germany) and cultivated. Colony morphology was determined on culture grown on PDA or Sabouraud chloramphenicol agar media after 14 days of incubation at 23°C in the dark. Mycelium and spores were observed and photographed under an inverted microscope (Zeiss, Axiovert 200M). A 10  $\mu\text{L}$  spore suspension (containing ca. 15 spores) was then used for germination in 20 mL of malt extract 1% (pH 6.5) containing 0.5 mg/mL of chloramphenicol for 15 days at 28°C.

The identification of the fungal species was performed through DNA extraction from the fungal mycelium using the Fast DNA SPIN Kit for soil (MP Biomedicals, United States) and following the manufacturer's instructions. Extracted DNA was then amplified by targeting from the fungal 18S to the 28S regions [using the primer pairs ITS 5 (5'-GGAAGTAAAAGTCGTAACAAGC-3') (White et al., 1990) and NL 4 (5'-GGTCCGTGTTTCAAGAC-3') (O'Donnell and Gray, 1995)]. The amplification reaction was carried out in a total volume of 50  $\mu\text{L}$  containing 200  $\mu\text{M}$  of each deoxyribonucleotide triphosphate (dNTP), 0.2  $\mu\text{M}$  of each primer, 1 X PCR buffer containing 2.5 mM  $\text{MgCl}_2$ , 0.3 U of Taq polymerase (Eurobio) and 50 ng of genomic DNA. Polymerase chain reactions (PCR) were performed as follows: 5 min at 95°C, followed by 35 steps [1 min. at 95°C, 2 min. at 52°C and 1 min. at 72°C] and a final elongation step at 72°C for 7 min. PCR amplicon was then sequenced (MWG – Biotech). The sequence obtained (1118 bp) was compared against NCBI sequences database using BLAST and deposited in GenBank under the Accession No: MK079567.

## Biodegradation of Nicosulfuron In Planktonic Lifestyle Without or With Glucose as the Carbon Source

The 100  $\mu\text{M}$  nicosulfuron biodegradation capacity of the strain was determined by inoculating from 0.25 to 0.35 mg of mycelium in 100 mL of mineral medium containing (GSM with 1, 5 or 10 g/L) or not (MSM) glucose in 250 mL flasks. The flasks were incubated at 28°C on an orbital shaker at 150 rpm in the dark to avoid photolysis. Non-inoculated media served as abiotic controls. Flasks inoculated only with the fungal strain were used as mycelium growth control.

## In Biofilm Lifestyle With Leaves or Wood as Carbon Sources

*Alnus* leaves and commercial wood-sticks (hazel wood) were macerated overnight in sterile water before being cut in 1  $\text{cm}^2$  squares which were used both as supports for fungal biofilm development and as carbon sources for *P. cucumerina* AR1. Squares were then sterilized by autoclaving and added in a 250 mL flask containing a ten-fold diluted malt medium (pH 6.5), 0.5 g/L of chloramphenicol without (control; 48 squares) or with 0.25–0.35 mg of *P. cucumerina* AR1 mycelium (96 squares). The flasks were incubated at 28°C under

agitation (80 rpm) for 10 days until mature biofilm formation. Then, 16 non-inoculated squares of each substratum were placed into a 250 mL flask containing 100 mL of a more environmentally realistic nicosulfuron concentration of 30  $\mu\text{M}$  in Volvic® water (abiotic control). The biofilm-covered squares were incubated in the same way without (growth control) or with 30  $\mu\text{M}$  nicosulfuron.

### Monitoring of Nicosulfuron Dissipation by *P. cucumerina* AR1

Each of the treatments described above for planktonic and biofilm lifestyles was run in triplicate. The time at which nicosulfuron was added to the planktonic or biofilm-covered substrata cultures was considered as Day 0 (D0). The culture media were sampled at days 0, 3, 6, 10, 14, 21, 28, and 35 to determine herbicide dissipation by HPLC. The production of metabolites was monitored by LC and LC-(+)ESI-MS. At the end of the experiment (day 35), the fungal pellet (planktonic conditions) or one leaf/wood square (biofilm conditions) was extracted in 0.5 mL (leaf) and 2.5 mL (fungal pellet and wood) absolute ethanol to look at sorption onto biomass and/or the substrata. The suspension was stirred vigorously overnight at room temperature and centrifuged (13,000  $g$  for 5 min). The extraction was performed twice in order to ensure a complete desorption. The combined organic extracts were concentrated and analyzed by HPLC.

### Identification and Quantification of Nicosulfuron and Its Metabolites Monitoring and Quantification by HPLC

The quantification of nicosulfuron and its main metabolites (ASDM and ADMP), in the culture media (dissipation) and extracted from the fungal biomass, was performed by HPLC on an Agilent Series 1100 chromatograph (Courtaboeuf, France), equipped with a DAD set at  $\lambda = 220$  and 254 nm, and a reverse phase column (Zorbax Eclipse XDB-C18, 3.5  $\mu\text{m}$ , 75 mm  $\times$  4.6 mm) at 22°C. The mobile phase was composed of acetonitrile (Solvent A) and acidified water ( $\text{H}_3\text{PO}_4$ , 0.01% v/v; pH 2.9) (Solvent B) at a flow rate of 1 mL  $\text{min}^{-1}$ , linear gradient 0–1 min: 2% A; 1–10 min: 2–70% A; 10–13 min: 70–100% A; 13–13.5 min: 100–2% A; 13.5–15 min: 0% A. Injection volume: 5  $\mu\text{L}$ . Each sample was injected twice. Solutions of the commercially available standards (ASDM and ADMP) were prepared in water, by dilution of a mother solution at 1 mM. Each standard solution (covering the expected concentration range) was injected three times. The metabolites N3 and N4 can be quantified only by  $^1\text{H}$  NMR as the standards are not commercially available (Carles et al., 2017a). A “correlation” can be established between the concentrations found by  $^1\text{H}$  NMR and the HPLC area observed. Nevertheless, this correlation is not very accurate. Therefore the precise concentrations for N3 and N4 were not given as they remained very low, in particular for N4.

### Identification by LC-MS

LC/ESI-MS analyses were performed on a Thermo Scientific UHPLC Ultimate 3000 RSLC coupled with an Orbitrap Q-Exactive analyzer. The crude supernatants were harvested (5 min at 13,000  $g$ ) before LC-MS analyses and directly injected in the LC-MS system without any further treatment. The analyses were carried out in positive mode. The UHPLC was equipped with a Kinetex EVO C18; 100  $\times$  2.1 mm; 1.7  $\mu\text{m}$  (Phenomenex) at 30°C with a gradient acetonitrile + 0.1% Formic acid (Solvent A) and water + 0.1% Formic acid (Solvent B): 0–7.5 min: 5–99% A (linear); 7.5–8.5 min: 99% A; 8.5–9 min: 99–5% A; 9–11 min: 5% A. Flow: 0.45 mL/min. For the mass spectrometer, gaseous  $\text{N}_2$  was used as nebulizer gas (50 L/h). The spray voltage was 3.2 kV. The mass resolution used was 35,000.

### Laccase Activity Measurements

Laccase (EC 1.10.3.2) activity was measured in triplicate at each sampling date from planktonic (varying from 3 to 8 mg of fungal dry mycelium) and biofilm (one square of leaf/wood) samples using the 2,2'-Azino-bis(3-ethylbenzthiazoline-6-sulfonic acid) (ABTS) substrate (Sigma-Aldrich, St. Louis, MO, United States). Enzyme activity assays were conducted according to the protocol of Johannes and Majcherczyk (2000) with some modifications. Substrate saturating conditions were fixed at 3 mM ABTS and incubations were performed during 1 h at 20°C, under agitation (80 rpm) in the dark. ABTS transformation was measured spectrophotometrically (420 nm) using an Ultrospec 2000 device (Pharmacia Biotech, Trowbridge, United Kingdom). The enzymatic activity was expressed as 1 U = 1  $\mu\text{mol}$  ABTS oxidized/g mycelium dry mass/h ( $\epsilon_{420} = 36 \text{ M}^{-1} \text{ cm}^{-1}$ , Johannes and Majcherczyk, 2000). Oven dry mass (DM) was determined systematically for each sample and used to correct laccase activity (activity/h/g DM).

### Biomass Measurements

In the planktonic conditions, fungal biomass production was determined as the dry mass difference between D0 and D35. Biomass corresponding to laccase activity assays was also determined and added to fungal biomass calculations. The biofilm condition did not allow us to calculate a proper fungal biomass production because of the influence of the substrata which was degraded in parallel along the experiment.

### Scanning Electron Microscopy (SEM)

Leaf or wood supports, exposed to nicosulfuron and *P. cucumerina* AR1 strain (biofilm) or not (control), were sampled at D0, D10, D21 and D35 and fixed overnight at 4°C in 0.2 mol/L sodium cacodylate buffer pH 7.4 that contained 1.6 % glutaraldehyde. Biofilms were then washed and post-fixed 1 h with 1% osmium tetroxide in 0.2 mol/L sodium cacodylate buffer (pH 7.4). They were washed 20 min. in distilled water and the dehydration by graded ethanol was performed from 25° to 100° (10 min each) to finish in hexamethyldisilazane (HMDS) for 10 min. After drying, the samples were mounted on stubs using adhesive carbon tabs and sputter-coated with gold-palladium (JFC-1300, JEOL, Japan).

Morphology analysis was carried out using a scanning electron microscope JSM-6060LV (Jeol, Japan) at 5 kV in high-vacuum mode.

## Statistical Analyses

Nicosulfuron dissipation and metabolite production were fitted to an exponential decay model ( $f = a \times \exp(-b \times x)$ ) with ( $a$ ) initial nicosulfuron concentration and ( $b$ ) dissipation rate as parameters estimated) and a sigmoidal model ( $f = a/(1+\exp(-(x-x_0)/b))$ ) with  $a$  (maximal ADMP or ASDM concentration),  $b$  (production rate) and  $x_0$  (time when the maximal production rate was achieved) as estimated parameters), respectively, using Sigma Plot 10.0 for Windows (Systat Software, Inc.). Differences on the nicosulfuron dissipation rate and metabolite production rate between treatments were assessed using a one-way ANOVA test followed by Tukey HSD test. ANOVA tests for the planktonic lifestyle experiments used glucose as the fixed factor (10, 5, or 1 g/L), whereas in biofilm lifestyle experiment, it was the substratum (leaf, wood). Before ANOVA testing, data were assessed for normality and homoscedasticity. Log transformations were applied when data did not follow ANOVA assumptions.

## RESULTS

### Characterization of *Plectosphaerella cucumerina* AR1

The fungal spores isolated from submerged *Alnus* leaf communities were fusiform, ends rounded, measuring 8–13  $\mu\text{m}$  in length and 2.5–4  $\mu\text{m}$  in width (Figure 1A). Based on ITS1-5.8S-ITS2-28S region sequencing and on macro- and microscopic characters, the isolated fungus was identified as *Plectosphaerella cucumerina* species and named *Plectosphaerella cucumerina* AR1.

When cultivated in planktonic conditions, the isolated *P. cucumerina* AR1 strain formed threadlike hyphae that grow into a mycelium forming a cottony mass (Figure 1B). Hyphae are septated and produce bud leading to branched mycelium (Figure 1C). Solitary phialides can be produced forming a flask-shaped projection on the apex of the septated hyphae (Figure 1D).

The *Plectosphaerella cucumerina* AR1 colony showed different aspects depending on the solid culture medium used, varying from a white, fluffy and aerial mycelium in Sabouraud chloramphenicol agar medium (Figure 1E) to a beige, smooth in appearance with some white mycelia diffusing from a central dome in PDA medium (Figure 1F). In both cases, the diameter of the colonies reached around 4.5 cm after 14 days at 23°C.

### Biodegradation of Nicosulfuron by Planktonic *P. cucumerina* AR1

*P. cucumerina* AR1 cultivated in mineral medium (MSM) was unable to dissipate 100  $\mu\text{M}$  nicosulfuron (data not shown).

Nevertheless, when glucose was added as a carbon source, a dissipation of nicosulfuron was observed that follows an

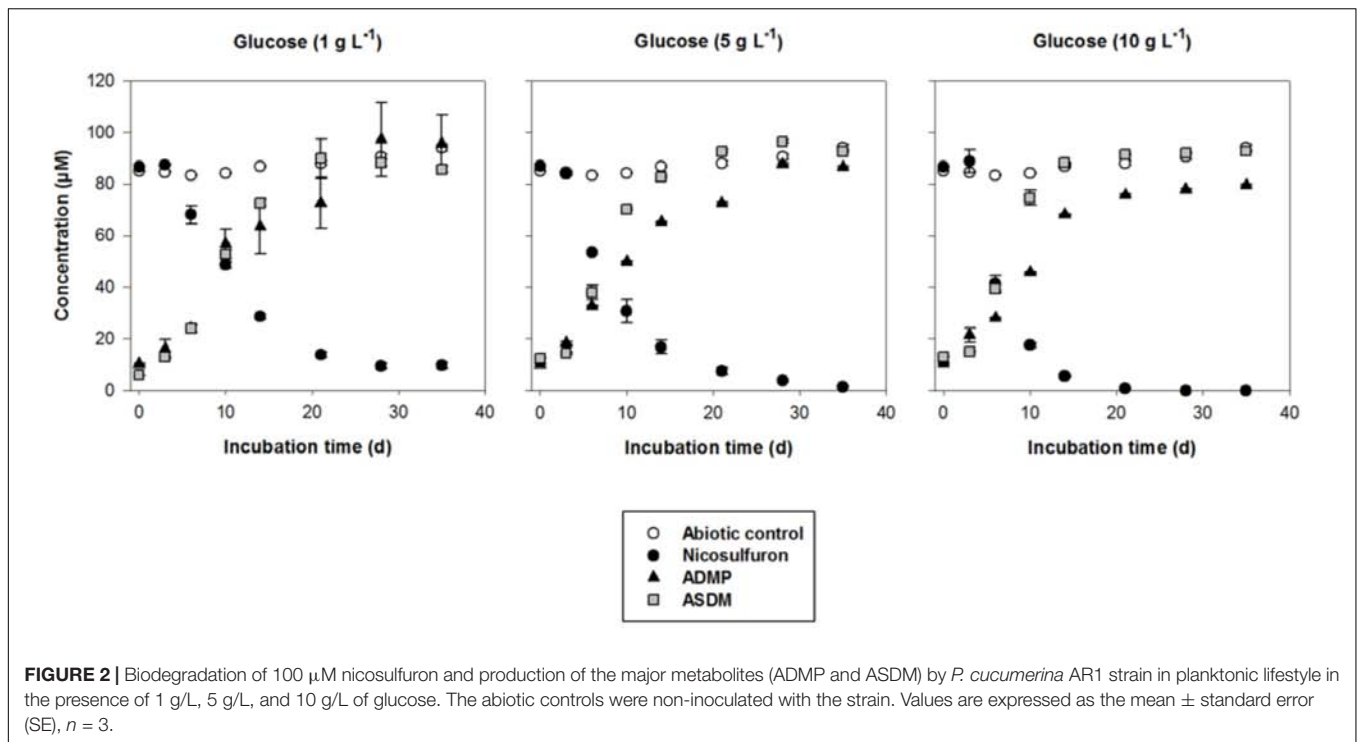
exponential decay model ( $R^2 > 0.91$  and  $P < 0.001$  for all the conditions tested). This was not the case in abiotic controls. We thus studied the glucose concentration effect, used as a classic co-metabolic substrate, on nicosulfuron biodegradation (Figure 2). The dissipation rates increased with the glucose concentrations (ANOVA,  $P < 0.0001$ ) (Tukey's test,  $P < 0.05$ ) (Table 1). Nicosulfuron (100  $\mu\text{M}$ ) has completely disappeared after 21 days of incubation for a concentration of 10 g/L of glucose, whereas around 1.5% and 13% of nicosulfuron were still remaining after 35 days of culture, for concentrations of 5 and 1 g/L, respectively. Besides, only 2, 1.6, and 1.3% of nicosulfuron were recovered after extraction of the fungal biomass with ethanol after 35 days, when cultures were carried out with 10 g/L, 5 g/L and 1 g/L of glucose, respectively (data not shown). Therefore, biosorption was not a significant process in herbicide dissipation. The degradation of nicosulfuron and growth of the fungal strain did not modify the pH of the culture media which were all measured at  $6.50 \pm 0.22$  ( $n = 18$ ) at the end of the experiment.

During the HPLC monitoring of nicosulfuron ( $t_R = 7.6$  min) biodegradation, two new peaks appeared at shorter retention times ( $t_R = 4.3$  and 5.2 min) with increasing intensities with time. They were absent from the controls. Analyses of the same samples by LC-(+)-ESI-MS gave a molecular ion at  $m/z$  230.0587  $[\text{M}+\text{H}]^+$  ( $\text{C}_8\text{H}_{12}\text{N}_3\text{O}_3\text{S}^+$ ) and main fragment ions at  $m/z$  252.0405  $[\text{M}+\text{Na}]^+$  and 213.0323 ( $\text{C}_8\text{H}_9\text{N}_2\text{O}_3\text{S}^+$ ) for the metabolite with

**TABLE 1** | Kinetic parameters of nicosulfuron dissipation and metabolite formation in the presence of various glucose concentrations or natural substrata.

		Dissipation <sup>(1)</sup> and production <sup>(2)</sup> rates (/h)	SE	R <sup>2</sup>	P-value	
Glucose	Nicosulfuron	Glucose 1 mg/L	0.0739 <sup>(1)a</sup>	0.0013	0.9546	<0.0001
		Glucose 5 mg/L	0.1048 <sup>(1)b</sup>	0.0061	0.9592	<0.0001
		Glucose 10 mg/L	0.1381 <sup>(1)c</sup>	0.0042	0.9139	<0.001
	Metabolites	ADMP (1 mg/L)	5.3795 <sup>(2)a</sup>	0.5782	0.9545	<0.001
		ADMP (5 mg/L)	4.8287 <sup>(2)a</sup>	0.0518	0.9882	<0.0001
		ADMP (10 mg/L)	3.9844 <sup>(2)a</sup>	0.0920	0.9944	<0.0001
		ASDM (1 mg/L)	3.1444 <sup>(2)a</sup>	0.0934	0.9895	<0.0001
		ASDM (5 mg/L)	2.9618 <sup>(2)ab</sup>	0.0519	0.9923	<0.0001
		ASDM (10 mg/L)	2.5519 <sup>(2)bc</sup>	0.1298	0.9918	<0.0001
Natural substrata	Nicosulfuron	Leaves	0.1137 <sup>(1)a</sup>	0.0021	0.9512	<0.0001
		Wood	0.1139 <sup>(1)a</sup>	0.0087	0.8815	<0.001

Parameters are expressed as the mean standard error (SE),  $n = 3$ . Significant differences between conditions are indicated by letters (Tukey test,  $P < 0.05$ ).



the shortest retention time and a molecular ion at  $m/z$  156.0766  $[\text{M}+\text{H}]^+$  ( $\text{C}_6\text{H}_{10}\text{N}_3\text{O}_2^+$ ) for the second metabolite. According to the literature (Zhao et al., 2015a) and to our previous research work (Carles et al., 2017a), they were assigned to ASDM (2-(aminosulfonyl)-*N,N*-dimethyl-3-pyridinecarboxamide) and ADMP (2-amino-4,6-dimethoxypyrimidine), respectively. The structures of both metabolites were confirmed by comparison with the LC-(+)-ESI-MS data of the commercially available standard compounds under the same conditions. These two metabolites are formed by the cleavage of the C-N bond in the sulfonylurea bridge (Supplementary Figure S1). The ASDM production was faster at 10 g/L of glucose compared to 1 g/L (Tukey's test,  $P < 0.05$ ; Table 1 and Figure 2), accordingly to the results observed with nicosulfuron. Conversely, the production kinetics of ADMP showed no significant difference whatever the glucose concentration tested (Table 1). Nevertheless, both metabolites were present in similar molar concentrations ( $\sim 80$ – $90 \mu\text{M}$ ) after 35 days of incubation (Figure 2). Another metabolite, presenting a molecular ion at  $m/z$  347.1456  $[\text{M}+\text{H}]^+$  ( $\text{C}_{15}\text{H}_{19}\text{N}_6\text{O}_4^+$ ), a retention time at 2.8 min and a main fragment ion at  $m/z$  304.1396 ( $\text{C}_{14}\text{H}_{18}\text{N}_5\text{O}_3^+$ ), was also detected by LC-(+)-ESI-MS in a low amount. It was identified as 2-(1-(4,6-dimethoxy-pyrimidin-2-yl)-ureido)-*N,N*-dimethyl-nicotinamide (N3) (Supplementary Figure S1) (Carles et al., 2017a). Therefore our results indicate that nicosulfuron was mainly co-metabolically degraded by *P. cucumerina* AR1.

The greater the glucose concentration supplied was, the faster the nicosulfuron dissipation (Figure 2 and Table 1). This result can be explained by an increase of mycelium biomass with the increase of glucose concentrations, irrespective of presence

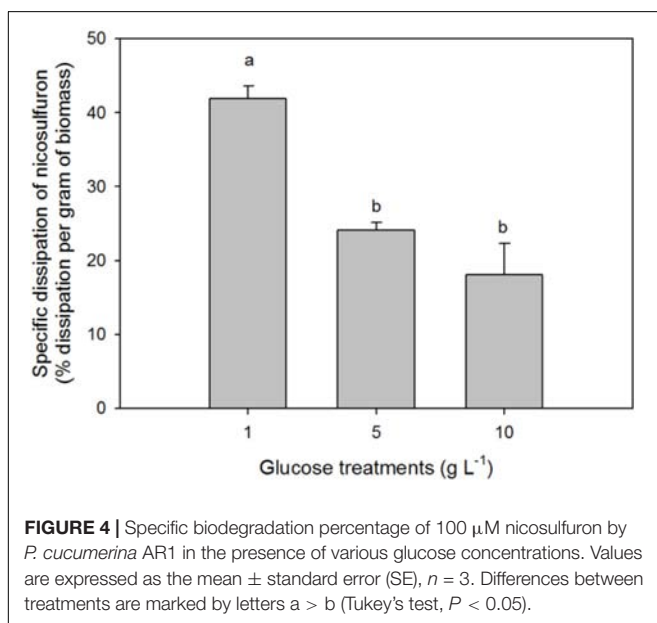
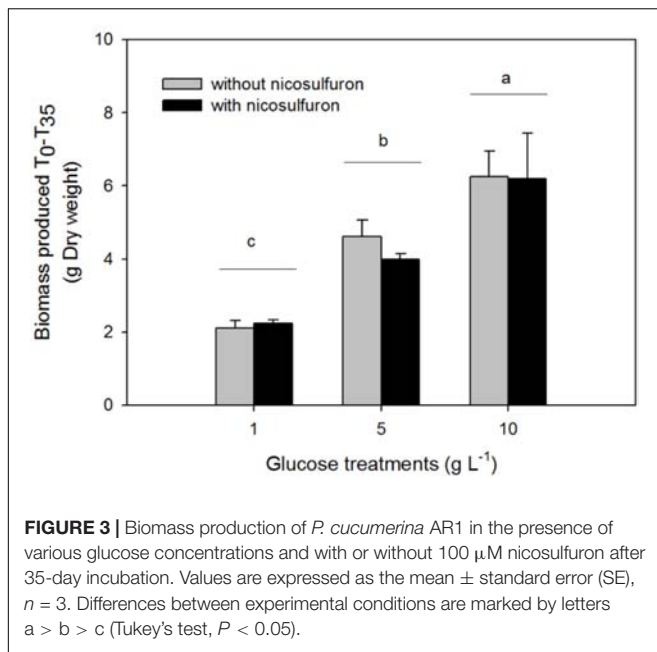
of nicosulfuron (ANOVA,  $P < 0.0001$ , Figure 3). However, specific nicosulfuron dissipation calculations (corrected by mycelium biomass) showed an inverse correlation between specific nicosulfuron dissipation and glucose concentration, varying from 19% at 1 g/L glucose to 8% at 10 g/L (Figure 4).

Although nicosulfuron has no impact on *P. cucumerina* AR1 growth, laccase activity was significantly impaired by both the presence of nicosulfuron and the increasing concentration of glucose (ANOVA,  $P < 0.0001$  for both factors; Figure 5A). Only 30% of the laccase activity remained when *P. cucumerina* AR1 was jointly exposed to nicosulfuron and 10 g/L glucose compared to 1 g/L (Tukey's test  $P < 0.05$ ).

## Biodegradation of Nicosulfuron by Benthic *P. cucumerina* AR1 Characterization of the Biofilm Development

The *P. cucumerina* AR1 capacity to degrade nicosulfuron in benthic conditions was tested on two natural substrata (alder leaf and hazel wood). The biofilm evolution was monitored by SEM analyses. The SEM micrographs showed no microbial development on leaf and wood supports sterilized by autoclave and incubated in 1/10 diluted malt 1% medium, pH 6.5 (Figures 6A,B control; D0). In contrast, supports inoculated with *P. cucumerina* AR1 presented a well-established biofilm before nicosulfuron addition (Figures 6A,B biofilm; D0).

These biofilms were then exposed to nicosulfuron in Volvic® water. The architecture of biofilms evolved slightly



differently between leaf and wood substrata. Specifically, a compact and thick biofilm, with rising mycelium, was formed more rapidly on leaves (10 days; **Figure 6A** biofilm; D10) than on wood (21 days; **Figure 6B** biofilm; D21). At the end of the experiment, both biofilm structures were comparable (**Figures 6A,B** biofilm; D35), without apparent differences between control biofilms and those exposed to nicosulfuron.

### Nicosulfuron Biodegradation

The dissipation of nicosulfuron (30  $\mu$ M) was observed both for leaf and wood grown biofilms (**Figure 7**). The adsorption of nicosulfuron on substrata was around  $0.15 \pm 0.076$  % and  $2.82 \pm 0.69$  % ( $n = 3$ ) for leaf and wood, respectively

(data not shown). Surprisingly, wood grown biofilms were able to degrade nicosulfuron as soon as they were exposed to the herbicide, as opposed to leaf grown biofilms which showed a 3 day delay in nicosulfuron degradation (**Figure 7**). Nevertheless, the nicosulfuron degradation kinetics was the same overall, exhibiting comparable rates, whatever the substratum tested (**Table 1**). At day 21, the nicosulfuron degradation by the wood grown biofilms was maximal, reaching around 97% dissipation. Then, the nicosulfuron concentration remained unchanged until the end of the experiment. On the contrary, for the leaf grown biofilms, the degradation of nicosulfuron reached also 97% after 21 days and continued up to 100% at the end of the experiment (**Figure 7**). During this biodegradation process, the pH of the medium was not significantly modified since the values were of  $6.40 \pm 0.36$  at the end of the experiment under all the conditions.

Nicosulfuron was degraded by biofilms with the same pathway as that observed for planktonic lifestyle. The two major metabolites, ADMP and ASDM as well as the minor one, N3, were formed under these conditions (data not shown). A fourth metabolite, with a retention time of 2.3 min and a molecular ion at  $m/z$  304.1396  $[M+H]^+$  ( $C_{14}H_{18}N_5O_3^+$ ), was also detected by LC-(+)-ESI-MS after 6 days of incubation but in a very low amount. This ion was already observed in the mass spectrum of N3 as the main fragment ion, suggesting that N4 came directly from N3. It was assigned as 2-(4,6-dimethoxy-pyrimidin-2-yl)-*N,N*-dimethyl-nicotinamide (N4) by comparison with the literature data (Carles et al., 2017a) (**Supplementary Figure S1**).

During the 35-day experiment, the integrated laccase activity was about 8 times higher for leaf grown biofilms compared to wood grown biofilms (**Figure 5B**). This activity was decreased (about 55–60%) when biofilms were exposed to nicosulfuron.

## DISCUSSION

*Plectosphaerella cucumerina* AR1 is a filamentous Ascomycete fungus, mostly encountered in the terrestrial environment as a pathogen of various plant species and vegetables [e.g., lettuce (Usami and Katagiri, 2017), cabbage (Li et al., 2017), broomrape (Xu et al., 2016), sunflower (Zhang et al., 2015), bottle gourd (Yan et al., 2016), tomato, melon (Carlucci et al., 2012), potato (Gao et al., 2016)] and to a lesser extent in marine ecosystems where it has been described as host of ascidian invertebrates (López-Legentil et al., 2015), sponges (Wang et al., 2008) and shells (Velmurugan et al., 2011). To our knowledge, this is the first time that *P. cucumerina* (**Figure 1**) has been isolated from submerged plant litter in a freshwater ecosystem.

Furthermore, *P. cucumerina* AR1 was described as a biological control agent against potato cyst nematodes (Atkins et al., 2003; Jacobs et al., 2003; Dandurand and Knudsen, 2016; Kooliyottill et al., 2017). It was used as a bioherbicide in agricultural crops and pastures (Bailey K. et al., 2017; Bailey K.L. et al., 2017) and would also be involved in the remediation of metal polluted environments (Santelli et al., 2010, 2011).

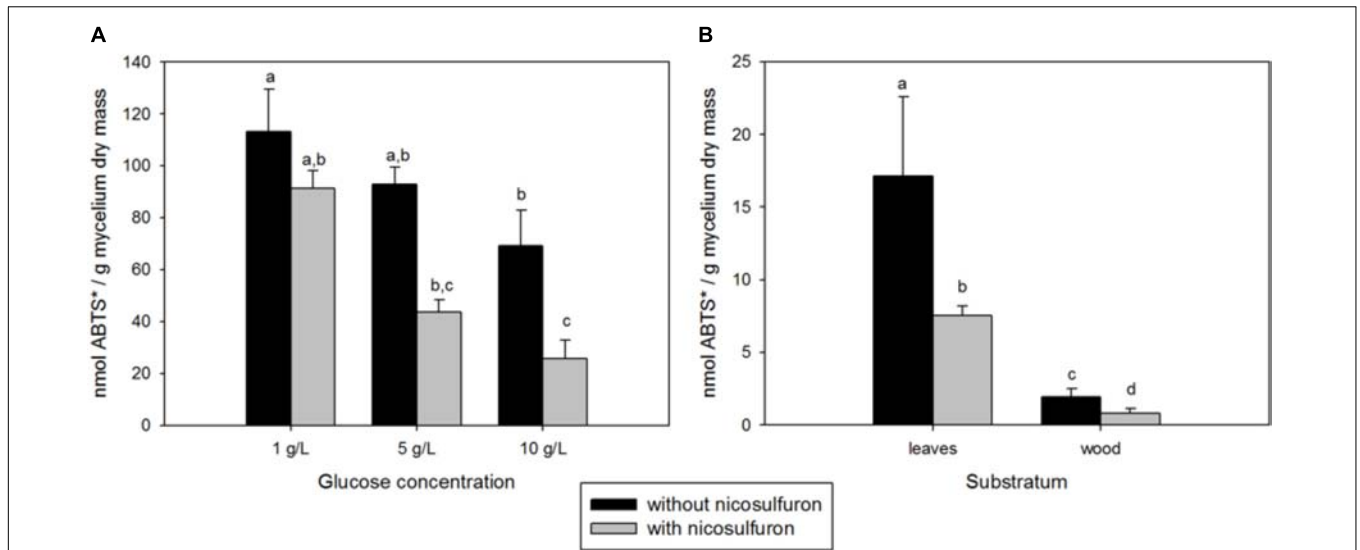


**FIGURE 5 | (A)** Integrated 35-day laccase activity in fungal mycelia grown in the presence or absence of nicosulfuron at different glucose concentrations (1, 5, and 10 g/L). **(B)** Integrated 35-day laccase activity in leaf and wood biofilms supplemented or not with nicosulfuron. Values are expressed as the mean  $\pm$  standard error (SE),  $n = 3$ . Differences between experimental conditions are marked by letters  $a > b > c > d$  (Tukey's test,  $P < 0.05$ ).

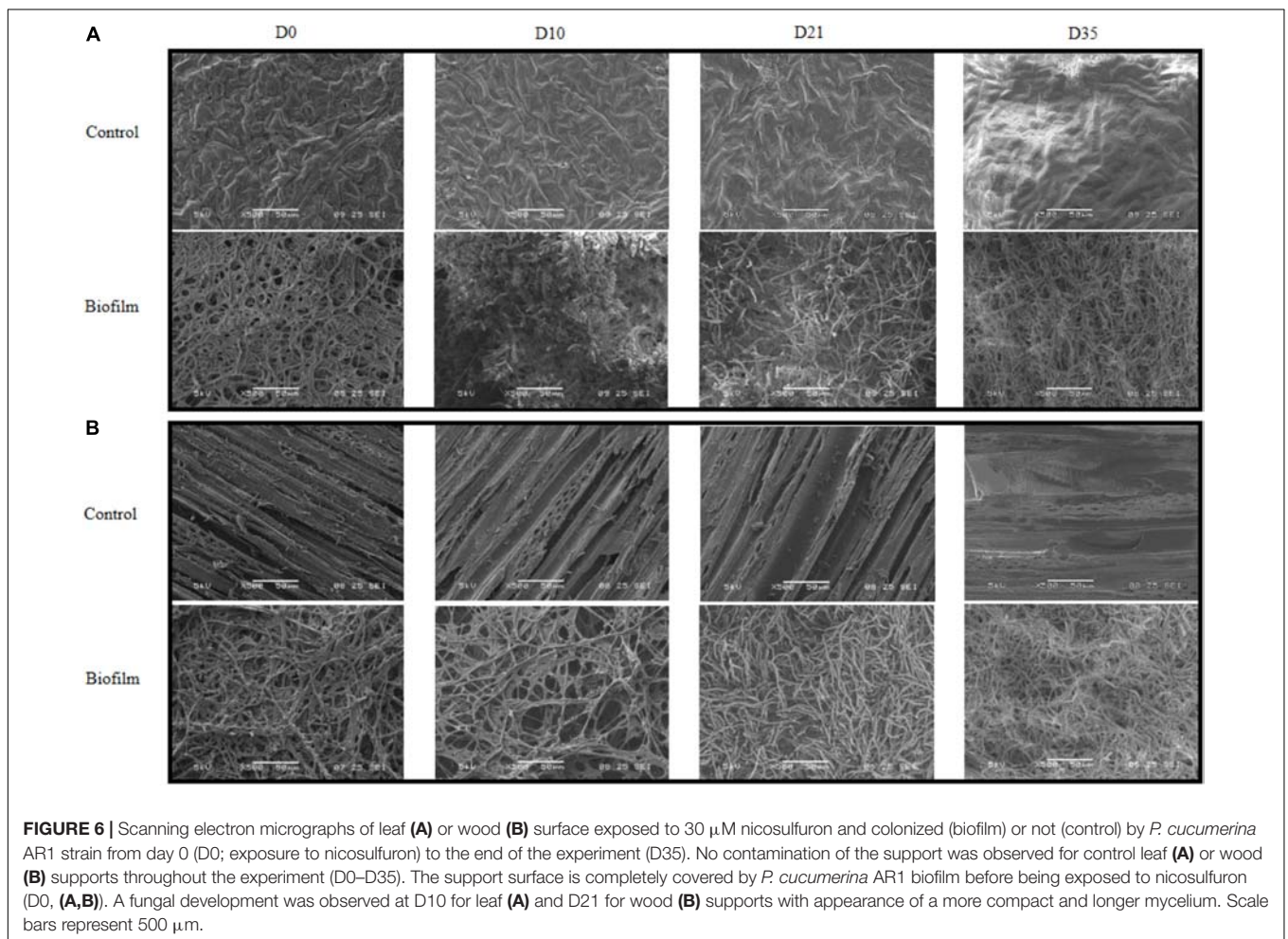
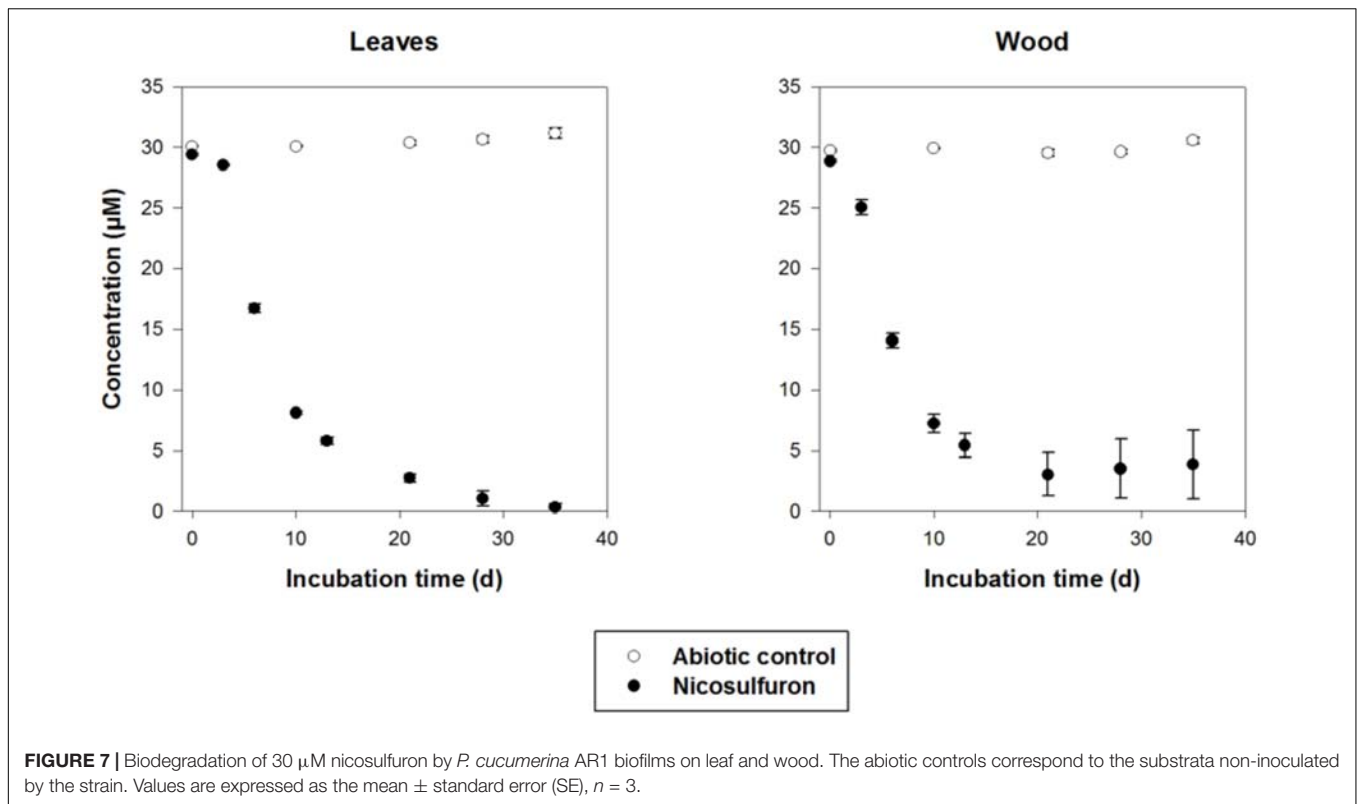


**FIGURE 6 |** Scanning electron micrographs of leaf **(A)** or wood **(B)** surface exposed to 30  $\mu$ M nicosulfuron and colonized (biofilm) or not (control) by *P. cucumerina* AR1 strain from day 0 (D0; exposure to nicosulfuron) to the end of the experiment (D35). No contamination of the support was observed for control leaf **(A)** or wood **(B)** supports throughout the experiment (D0–D35). The support surface is completely covered by *P. cucumerina* AR1 biofilm before being exposed to nicosulfuron (D0, **(A,B)**). A fungal development was observed at D10 for leaf **(A)** and D21 for wood **(B)** supports with appearance of a more compact and longer mycelium. Scale bars represent 500  $\mu$ m.



Our results showed that *P. cucumerina* AR1 can also be used to reduce nicosulfuron contamination since we demonstrated that (i) it was tolerant to nicosulfuron in contrast to what was described for other fungal species (Karpouzas et al., 2014) and (ii) it was able to degrade the nicosulfuron herbicide both in planktonic (Figure 2) and in biofilm conditions with various simple and complex carbon sources (glucose, leaf or wood; Figure 7). Regarding the literature, this is the first time that a leaf-associated fungal strain able to degrade nicosulfuron has been isolated in freshwater, the other ones being isolated from agricultural soil or sludge (Yang et al., 2008; Zhang et al., 2011, 2012; Lu et al., 2012; Song et al., 2013; Zhao et al., 2015a,b, 2018; Wang et al., 2016; Carles et al., 2017a; Feng et al., 2017; Zhou et al., 2017).

As already shown with almost all the isolated nicosulfuron-degrading strains, except the *Oceanisphaera psychrotolerans* LAM-WHM-ZC and *Pseudomonas nitroreducens* NSA02 strains which are able to degrade nicosulfuron in mineral medium, using nicosulfuron as the carbon source (Zhou et al., 2017; Zhao et al., 2018), the nicosulfuron degradation by *P. cucumerina* AR1 was achieved by a co-metabolism process (Figure 2). Our results showed that the herbicide dissipation was mainly due to biodegradation since the pH values of the medium of all the cultures remained around neutrality (ranging from 6.1 to 6.7) at the end of the experiment, contrarily to what was observed with *Penicillium oxalicum* YC-WM1 fungal strain. In this last case, nicosulfuron was degraded by hydrolysis resulting from the acidification of the medium (Feng et al., 2017).

In most cases, the biodegradation rate of a pollutant is improved by the addition of increasing concentrations of the extra carbon source (e. g., Wang et al., 2013; Kirui et al., 2016; Sun et al., 2017) as we observed in our study (Figure 2). However, the specific nicosulfuron biodegradation by the planktonic *P. cucumerina* AR1 was shown to be greater when the concentration of glucose decreased (Figure 4). This phenomenon has already been described for other pollutants (Ye et al., 2011; Shi et al., 2013; Wu et al., 2016). Indeed, the degradation efficiency increased with increasing concentration of glucose until an optimal concentration. Then, the addition of the carbon source to excess inhibited the degradation. This suggests that the optimal glucose concentration for the maximal degradation efficiency of nicosulfuron by planktonic *P. cucumerina* AR1 would be around 1 g/L under the conditions tested (Figure 4).

*Plectosphaerella cucumerina* AR1 used the same nicosulfuron degradation pathway irrespective of its lifestyle, planktonic or in biofilms (Figure 2 and Supplementary Figure S1). It produced two major metabolites, ADMP and ASDM, which were obtained by a pathway common to all the strains described until now, consisting in the biotic hydrolytic cleavage of the sulfonylurea bridge (e.g., Zhang et al., 2012; Song et al., 2013; Zhao et al., 2015a, 2018; Wang et al., 2016; Carles et al., 2017a). The minor N3 metabolite was derived from the cleavage of the C-S bond of the sulfonylurea bridge and contraction by elimination of the sulfur dioxide group, as previously observed with some others nicosulfuron-degrading strains (Song

et al., 2013; Zhao et al., 2015a; Carles et al., 2017a; Zhou et al., 2017). Similarly to what was observed during the nicosulfuron degradation by the bacterial strain *Pseudomonas fluorescens* SG-1 (Carles et al., 2017a), the hydrolysis of the N3 urea function lead to the production of the N4 metabolite in small amounts when *P. cucumerina* AR1 was grown in benthic conditions (**Supplementary Figure S1**).

*Plectosphaerella cucumerina* AR1 strain developed indifferently on both natural substrata studied (alder leaf and hazel wood) (**Figure 6**). However, the biofilm grew faster on the leaf than on wood. This could be explained by the greater laccase activity rates recorded for the former (**Figure 5B**). This led to a faster decay of leaves and thus faster nutrient supply for fungal growth comparing to wood substratum which has a more complex molecular arrangement (Golladay and Sinsabaugh, 1991; Gulis et al., 2004). This could also explain the greater laccase activity rates recorded in the leaf substratum (**Figure 5B**). However, this higher enzyme activity was not correlated with nicosulfuron degradation capacity of *P. cucumerina* AR1, which was similar between leaf and wood biofilms (**Table 1**). Furthermore, the presence of nicosulfuron did not impact the growth of the fungus since the biofilm development on both substrata was similar to what was observed in the control conditions without herbicide. Similar results were obtained for the planktonic culture conditions for which fungal biomasses were comparable in all experiments, irrespective of the presence of nicosulfuron (**Figure 3**).

When exposed to nicosulfuron, *P. cucumerina* AR1 biofilms kept the capacity to biodegrade the molecule whatever the substrata tested (**Figure 7**), thus probably using the decomposition of the natural substrata as nutrients and carbon sources. The present study also shows that nicosulfuron degradation efficiency was greater for *P. cucumerina* AR1 monospecific biofilms on alder leaves (100% dissipation after 28 days, the present study) than for plurispecific natural biofilms hosting *P. cucumerina* on the same leaf species (29–66% dissipation in 40 days, Carles et al., 2017b). The decreased ability of *P. cucumerina* AR1 to dissipate nicosulfuron could be explained either by a relative low presence of the fungus in the natural leaf-associated microbial communities or by microbial interactions within the biofilm. Overall, this is the first time that a benthic strain was shown to be able to degrade nicosulfuron herbicide, all the degradation experiments conducted until now with isolated bacterial and fungal strains being tested in planktonic conditions (Feng et al., 2017; Yang et al., 2008; Zhang et al., 2011, 2012; Lu et al., 2012; Song et al., 2013; Zhao et al., 2015a,b, 2018; Wang et al., 2016; Carles et al., 2017a; Zhou et al., 2017).

The nicosulfuron degradation obtained for *P. cucumerina* AR1 in biofilm conditions showed statistically similar dissipation rates than those observed in planktonic culture conditions containing 5 g/L of glucose (**Table 1**). This suggests that the

natural substrata we provided for co-metabolism reactions could not allow *P. cucumerina* AR1 to degrade the nicosulfuron herbicide at the optimal conditions, since we have shown that a lesser carbon concentration equivalent to 1 g/L of glucose would be more efficient in planktonic conditions. These results still have to be confirmed in biofilm conditions by testing different leaf and wood substrata varying in their composition, and thus in their capacity of decomposition and releasing nutrients (Bani et al., 2018; Bastias et al., 2018).

In contrast to what was often observed in pollutant exposed microbial communities and/or populations (e.g., da Silva Coelho et al., 2010; Artigas et al., 2017; de Araujo et al., 2017; Singh et al., 2017), the laccase activity decreased in the presence of nicosulfuron, showing a reduction of about 60% activity, whatever the lifestyle (**Figure 5**). The obtained results highlight that laccase activity responses to xenobiotic contamination are probably molecule-specific (Baldrian, 2006).

## CONCLUSION

We report here the isolation and characterization of a leaf-associated fungus issued from a river ecosystem, identified as a *Plectosphaerella cucumerina* strain. This isolated strain was able to biodegrade the nicosulfuron herbicide by a co-metabolic process. The degradation pathway was shown to be common to almost all the already described nicosulfuron-degrading strains, starting with the hydrolytic cleavage of the sulfonylurea bridge. Nicosulfuron exposure impaired the fungal laccase activity. However, *P. cucumerina* AR1 was able to degrade nicosulfuron in planktonic lifestyle using glucose as the carbon source, with an optimal concentration of 1 g/L. It was also capable of colonizing natural substrata such as alder leaves or hazel wood to form biofilms and to retain its nicosulfuron biodegradation capacity. This suggests that the nutrients and carbon constituting these natural substrata can be used to ensure the co-metabolic reactions and the nicosulfuron dissipation.

Knowing that both leaf and wood surfaces allow the development of extensive biofilms in streams and that fungi are extremely important in their development, the *P. cucumerina* AR1 strain is considered as a potentially useful candidate for the development of methods aiming to reduce contamination by nicosulfuron in aquatic environments.

## AUTHOR CONTRIBUTIONS

LC and FR set up the experiments, carried out the sampling, and participated to the discussion. CB realized the SEM images. ML carried out the LC-MS analyses. PB-H carried out the HPLC measurements and interpretation. JA isolated the strain and realized the statistical analyses. IB identified the strain. JA and IB designed the experimental work, the cultures of the fungal strain,

the laccase and biomass measurements, and wrote the first draft of the article. All the authors wrote sections of the manuscript, participated to the reviewing of the article, and approved the submitted version.

## FUNDING

This study was funded by the EcoBioPest project (Agence de l'Eau Loire-Bretagne).

## REFERENCES

- Artigas, J., Rossi, F., Gerphagnon, M., and Mallet, C. (2017). Sensitivity of laccase activity to the fungicide tebuconazole in decomposing litter. *Sci. Total Environ.* 584–585, 1084–1092. doi: 10.1016/j.scitotenv.2017.01.167
- Atkins, S. D., Clark, I. M., Sosnowska, D., Hirsch, P. R., and Kerry, B. R. (2003). Detection and quantification of *Plectosphaerella cucumerina*, a potential biological control agent of potato cyst nematodes, by using conventional PCR, real-time PCR, selective media, and baiting. *Appl. Environ. Microbiol.* 69, 4788–4793. doi: 10.1128/AEM.69.8.4788-4793.2003
- Azcarate, M. P., Montoya, J. C., and Koskinen, W. C. (2015). Sorption, desorption and leaching potential of sulfonylurea herbicides in Argentinean soils. *J. Environ. Sci. Health Part B* 50, 229–237. doi: 10.1080/03601234.2015.999583
- Bailey, K., Derby, J.-A., Bourdôt, G., Skipp, B., Cripps, M., Hurrell, G., et al. (2017). *Plectosphaerella cucumerina* as a bioherbicide for *Cirsium arvense*: proof of concept. *BioControl* 62, 693–704. doi: 10.1007/s10526-017-98197
- Bailey, K. L., Derby, J., Bourdôt, G. W., Skipp, R. A., and Hurrell, G. A. (2017). Optimising inoculum yield and shelf life of *Plectosphaerella cucumerina*, a potential bioherbicide for *Cirsium arvense*. *Biocontrol Sci. Technol.* 27, 1416–1434. doi: 10.1080/09583157.2017.1409337
- Baldrian, P. (2006). Fungal laccases – Occurrence and properties. *FEMS Microbiol. Rev.* 30, 215–242. doi: 10.1111/j.1574-4976.2005.00010.x
- Bani, A., Pioli, S., Ventura, M., Panzacchi, P., Borruso, L., Tognetti, R., et al. (2018). The role of microbial community in the decomposition of leaf litter and deadwood. *Appl. Soil Ecol.* 126, 75–84. doi: 10.1016/j.apsoil.2018.02.017
- Bastias, E., Ribot, M., Romani, A. M., Mora-Gómez, J., Sabater, F., López, P., et al. (2018). Responses of microbially driven leaf litter decomposition to stream nutrients depend on litter quality. *Hydrobiologia* 806, 333–346. doi: 10.1007/s10750-017-3372-3
- Battaglin, W. A., Furlong, E. T., Burkhardt, M. R., and Peter, C. J. (2000). Occurrence of sulfonylurea, sulfonamide, imidazolinone, and other herbicides in rivers, reservoirs and ground water in the Midwestern United States, 1998. *Sci. Total Environ.* 248, 123–133. doi: 10.1016/S0048-9697(99)00536-7
- Battaglin, W. A., Rice, K. C., Focazio, M. J., Salmons, S., and Barry, R. X. (2009). The occurrence of glyphosate, atrazine, and other pesticides in vernal pools and adjacent streams in Washington, DC, Maryland, Iowa, and Wyoming, 2005–2006. *Environ. Monit. Assess.* 155, 281–307. doi: 10.1007/s10661-008-0435-y
- Benzi, M., Robotti, E., and Gianotti, V. (2011). HPLC-DAD-MSn to investigate the photodegradation pathway of nicosulfuron in aqueous solution. *Anal. Bioanal. Chem.* 399, 1705–1714. doi: 10.1007/s00216-010-4467-0
- Berger, B. M., and Wolfe, N. L. (1996). Hydrolysis and biodegradation of sulfonylurea herbicides in aqueous buffers and anaerobic water-sediment systems: assessing fate pathways using molecular descriptors. *Environ. Toxicol. Chem.* 15:1500. doi: 10.1002/etc.5620150911
- Carles, L., Joly, M., Bonnemoy, F., Lereboure, M., Batisson, I., and Besse-Hoggan, P. (2017a). Identification of sulfonylurea biodegradation pathways enabled by a novel nicosulfuron-transforming strain *Pseudomonas fluorescens* SG-1: toxicity assessment and effect of

## ACKNOWLEDGMENTS

The authors acknowledge Philip Hoggan for English reviewing.

## SUPPLEMENTARY MATERIAL

The Supplementary Material for this article can be found online at: <https://www.frontiersin.org/articles/10.3389/fmicb.2018.03167/full#supplementary-material>

- formulation. *J. Hazard. Mater.* 324, 184–193. doi: 10.1016/j.jhazmat.2016.10.048
- Carles, L., Rossi, F., Joly, M., Besse-Hoggan, P., Batisson, I., and Artigas, J. (2017b). Biotransformation of herbicides by aquatic microbial communities associated to submerged leaves. *Environ. Sci. Pollut. Res.* 24, 3664–3674. doi: 10.1007/s11356-016-8035-9
- Carlucci, A., Raimondo, M. L., Santos, J., and Phillips, A. J. L. (2012). *Plectosphaerella* species associated with root and collar rots of horticultural crops in southern Italy. *Persoonia – Mol. Phylogeny Evol. Fungi* 28, 34–48. doi: 10.3767/003158512X638251
- Cessna, A. J., Donald, D. B., Bailey, J., and Waiser, M. (2015). Persistence of the sulfonylurea herbicides sulfosulfuron, rimsulfuron, and nicosulfuron in farm dugouts (Ponds). *J. Environ. Qual.* 44:1948. doi: 10.2134/jeq2014.11.0503
- da Silva Coelho, J., de Oliveira, A. L., Marques, de Souza, C. G., and Bracht, A. (2010). Effect of the herbicides bentazon and diuron on the production of ligninolytic enzymes by *Ganoderma lucidum*. *Int. Biodeterior. Biodegrad.* 64, 156–161. doi: 10.1016/j.ibiod.2009.12.006
- Dandurand, L.-M., and Knudsen, G. R. (2016). Effect of the trap crop *Solanum sisymbriifolium* and two biocontrol fungi on reproduction of the potato cyst nematode, *Globodera pallida*: trap crop and biocontrol agent effects on *Globodera pallida*. *Ann. Appl. Biol.* 169, 180–189. doi: 10.1111/aab.12295
- de Araujo, C. A. V., Maciel, G. M., Rodrigues, E. A., Silva, L. L., Oliveira, R. F., Brugnari, T., et al. (2017). Simultaneous removal of the antimicrobial activity and toxicity of sulfamethoxazole and trimethoprim by white rot fungi. *Water. Air. Soil Pollut.* 228:341. doi: 10.1007/s11270-017-3525-z
- de Lafontaine, Y., Beauvais, C., Cessna, A. J., Gagnon, P., Hudon, C., and Poissant, L. (2014). Sulfonylurea herbicides in an agricultural catchment basin and its adjacent wetland in the St. Lawrence River basin. *Sci. Total Environ.* 47, 1–10. doi: 10.1016/j.scitotenv.2014.01.094
- EFSA (2007). Conclusion regarding the peer review of the pesticide risk assessment of the active substance nicosulfuron. *EFSA Sci. Rep.* 120, 1–91. doi: 10.2903/j.efsa.2008.120r
- Feng, W., Wei, Z., Song, J., Qin, Q., Yu, K., Li, G., et al. (2017). Hydrolysis of nicosulfuron under acidic environment caused by oxalate secretion of a novel *Penicillium oxalicum* strain YC-WM1. *Sci. Rep.* 7:647. doi: 10.1038/s41598-017-00228-2
- Gao, J., Zhang, Y. Y., Zhao, X. J., Wang, K., and Zhao, J. (2016). First report of potato wilt caused by *Plectosphaerella cucumerina* in Inner Mongolia, China. *Plant Dis.* 100:2523. doi: 10.1094/PDIS-01-16-0028-PDN
- Golladay, S. W., and Sinsabaugh, R. L. (1991). Biofilm development on leaf and wood surfaces in a boreal river. *Freshw. Biol.* 25, 437–450. doi: 10.1111/j.1365-2427.1991.tb01387.x
- Gonzalez, J., and Ukrainczyk, L. (1999). Transport of nicosulfuron in soil columns. *J. Environ. Qual.* 28:101. doi: 10.2134/jeq1999.00472425002800010011x
- Gonzalez, J. M., and Ukrainczyk, L. (1996). Adsorption and desorption of nicosulfuron in soils. *J. Environ. Qual.* 25:1186. doi: 10.2134/jeq1996.00472425002500060003x
- Gulis, V., Rosemond, A. D., Suberkropp, K., Weyers, H. S., and Benstead, J. P. (2004). Effects of nutrient enrichment on the decomposition of wood and

- associated microbial activity in streams. *Freshw. Biol.* 49, 1437–1447. doi: 10.1111/j.1365-2427.2004.01281.x
- Jacobs, H., Gray, S. N., and Crump, D. H. (2003). Interactions between nematophagous fungi and consequences for their potential as biological agents for the control of potato cyst nematodes. *Mycol. Res.* 107, 47–56. doi: 10.1017/S0953756202007098
- Johannes, C., and Majcherczyk, A. (2000). Laccase activity tests and laccase inhibitors. *J. Biotechnol.* 78, 193–199. doi: 10.1016/S0168-1656(00)00208-X
- Karpouzias, D. G., Papadopoulou, E., Ipsilantis, I., Friedel, I., Petric, I., Udikovic-Kolic, N., et al. (2014). Effects of nicosulfuron on the abundance and diversity of arbuscular mycorrhizal fungi used as indicators of pesticide soil microbial toxicity. *Ecol. Indic.* 39, 44–53. doi: 10.1016/j.ecolind.2013.12.004
- Kirui, W. K., Wu, S., Kizito, S., Carvalho, P. N., and Dong, R. (2016). Pathways of nitrobenzene degradation in horizontal subsurface flow constructed wetlands: effect of intermittent aeration and glucose addition. *J. Environ. Manage.* 166, 38–44. doi: 10.1016/j.jenvman.2015.10.001
- Kooliyottil, R., Dandurand, L.-M., and Knudsen, G. R. (2017). Prospecting fungal parasites of the potato cyst nematode *Globodera pallida* using a rapid screening technique. *J. Basic Microbiol.* 57, 386–392. doi: 10.1002/jobm.201600683
- Krauss, G.-J., Solé, M., Krauss, G., Schlosser, D., Wesenberg, D., and Bärlocher, F. (2011). Fungi in freshwaters: ecology, physiology and biochemical potential. *FEMS Microbiol. Rev.* 35, 620–651. doi: 10.1111/j.1574-6976.2011.02666.x
- Li, P.-L., Chai, A.-L., Shi, Y.-X., Xie, X.-W., and Li, B.-J. (2017). First report of root rot caused by *Plectosphaerella cucumerina* on cabbage in China. *Mycobiology* 45, 110–113. doi: 10.5941/MYCO.2017.45.2.110
- López-Legentil, S., Erwin, P. M., Turon, M., and Yarden, O. (2015). Diversity of fungi isolated from three temperate ascidians. *Symbiosis* 66, 99–106. doi: 10.1007/s13199-015-0339-x
- Lu, X. H., Kang, Z. H., Tao, B., Wang, Y. N., Dong, J. G., and Zhang, J. L. (2012). Degradation of nicosulfuron by *Bacillus subtilis* YB1 and *Aspergillus niger* YF1. *Appl. Biochem. Microbiol.* 48, 460–466. doi: 10.1134/S0003683812050079
- Moschet, C., Wittmer, I., Simovic, J., Junghans, M., Piazzoli, A., Singer, H., et al. (2014). How a complete pesticide screening changes the assessment of surface water quality. *Environ. Sci. Technol.* 48, 5423–5432. doi: 10.1021/es500371t
- O'Donnell, K., and Gray, L. (1995). Phylogenetic relationships of the soybean sudden death syndrome pathogen *Fusarium solani* f. sp. phaseoli inferred from rDNA sequence data and pcr primers for its identification. *Mol. Plant. Microbe Interact.* 8:709. doi: 10.1094/MPMI-8-0709
- Oliveira, R. S., Koskinen, W. C., and Ferreira, F. A. (2001). Sorption and leaching potential of herbicides on Brazilian soils. *Weed Res.* 41, 97–110. doi: 10.1046/j.1365-3180.2001.00219.x
- Petric, I., Karpouzias, D. G., Bru, D., Udikovic-Kolic, N., Kandeler, E., Djuric, S., et al. (2016). Nicosulfuron application in agricultural soils drives the selection towards NS-tolerant microorganisms harboring various levels of sensitivity to nicosulfuron. *Environ. Sci. Pollut. Res.* 23, 4320–4333. doi: 10.1007/s11356-015-5645-6
- Pfeiffer, M. (2010). *Groundwater Ubiquity Score (GUS)*. Corvallis, OR: National Pesticide Information Center.
- Regitano, J. B., and Koskinen, W. C. (2008). Characterization of nicosulfuron availability in aged soils. *J. Agric. Food Chem.* 56, 5801–5805. doi: 10.1021/jf800753p
- Santelli, C. M., Pfister, D. H., Lazarus, D., Sun, L., Burgos, W. D., and Hansel, C. M. (2010). Promotion of Mn(II) oxidation and remediation of coal mine drainage in passive treatment systems by diverse fungal and bacterial communities. *Appl. Environ. Microbiol.* 76, 4871–4875. doi: 10.1128/AEM.03029-09
- Santelli, C. M., Webb, S. M., Dohnalkova, A. C., and Hansel, C. M. (2011). Diversity of Mn oxides produced by Mn(II)-oxidizing fungi. *Geochim. Cosmochim. Acta* 75, 2762–2776. doi: 10.1016/j.gca.2011.02.022
- Sarmah, A. K., and Sabadie, J. (2002). Hydrolysis of sulfonylurea herbicides in soils and aqueous solutions: a review. *J. Agric. Food Chem.* 50, 6253–6265. doi: 10.1021/jf025575p
- Schloss, J. V. (1990). Acetolactate synthase, mechanism of action and its herbicide binding site. *Pestic. Sci.* 29, 283–292. doi: 10.1002/ps.2780290305
- Shi, G., Yin, H., Ye, J., Peng, H., Li, J., and Luo, C. (2013). Aerobic biotransformation of decabromodiphenyl ether (PBDE-209) by *Pseudomonas aeruginosa*. *Chemosphere* 93, 1487–1493. doi: 10.1016/j.chemosphere.2013.07.044
- Singh, S. K., Khajuria, R., and Kaur, L. (2017). Biodegradation of ciprofloxacin by white rot fungus *Pleurotus ostreatus*. *3 Biotech* 7:69. doi: 10.1007/s13205-017-0684-y
- Song, J., Gu, J., Zhai, Y., Wu, W., Wang, H., Ruan, Z., et al. (2013). Biodegradation of nicosulfuron by a *Talaromyces flavus* LZM1. *Bioresour. Technol.* 140, 243–248. doi: 10.1016/j.biortech.2013.02.086
- Sun, Z., Li, J., Zhang, J., Wang, J., Wang, X., and Hu, X. (2017). Effect of glucose as co-metabolism substrate on the biodegradation of dichlorophenols. *FRESENIUS Environ. Bull.* 26, 6017–6027.
- Trigo, C., Spokas, K. A., Cox, L., and Koskinen, W. C. (2014). Influence of soil biochar aging on sorption of the herbicides MCPA, nicosulfuron, terbuthylazine, indaziflam, and fluoroethylidiaminotriazine. *J. Agric. Food Chem.* 62, 10855–10860. doi: 10.1021/jf5034398
- Usami, T., and Katagiri, H. (2017). Pathogenicity of *Plectosphaerella* species on lettuce and susceptibility of lettuce cultivars. *J. Gen. Plant Pathol.* 83, 366–372. doi: 10.1007/s10327-017-0736-5
- Velmurugan, N., Kalpana, D., Han, J. H., Cha, H. J., and Soo Lee, Y. (2011). A novel low temperature chitinase from the marine fungus *Plectosphaerella* sp. strain MF-1. *Bot. Mar.* 54, 75–81. doi: 10.1515/bot.2010.068
- Wang, G., Chen, X., Yue, W., Zhang, H., Li, F., and Xiong, M. (2013). Microbial degradation of acetamidiprid by *Ochrobactrum* sp. D-12 isolated from contaminated soil. *PLoS One* 8:e82603. doi: 10.1371/journal.pone.0082603
- Wang, G., Li, Q., and Zhu, P. (2008). Phylogenetic diversity of culturable fungi associated with the Hawaiian Sponges *Suberites zeteki* and *Gelliodes fibrosa*. *Antonie Van Leeuwenhoek* 93, 163–174. doi: 10.1007/s10482-007-9190-2
- Wang, L., Zhang, X., and Li, Y. (2016). Degradation of nicosulfuron by a novel isolated bacterial strain *Klebsiella* sp. Y1: condition optimization, kinetics and degradation pathway. *Water Sci. Technol.* 73, 2896–2903. doi: 10.2166/wst.2016.140
- White, T. J., Bruns, T., Lee, S., Taylor, J. W., Innis, M. A., Gelfand, D. H., et al. (1990). Amplification and direct sequencing of fungal ribosomal RNA genes for phylogenetics. *PCR Protoc. Guide Methods Appl.* 18, 315–322. doi: 10.1016/B978-0-12-372180-8.50042-1
- Wu, H., Shen, J., Wu, R., Sun, X., Li, J., Han, W., et al. (2016). Biodegradation mechanism of 1H-1,2,4-triazole by a newly isolated strain *Shinella* sp. *NJJUST26. Sci. Rep.* 6:29675. doi: 10.1038/srep29675
- Xu, D. S., Zhang, Y. Y., Zhao, J. X., and Zhao, J. (2016). First Report of broomrape wilt caused by *Plectosphaerella cucumerina* in inner Mongolia, China. *Plant Dis.* 100, 2538–2538. doi: 10.1094/PDIS-03-16-0296-PDN
- Yan, L. Y., Ying, Q. S., Wang, Y. E., Zhang, H. F., and Wang, Y. H. (2016). First report of root and collar rot caused by *Plectosphaerella cucumerina* on bottle gourd in China. *Plant Dis.* 100, 1505–1505. doi: 10.1094/PDIS-11-15-1305-PDN
- Yang, Y., Tao, B., Zhang, W., and Zhang, J. (2008). Isolation and screening of microorganisms capable of degrading nicosulfuron in water. *Front. Agric. China* 2:224–228. doi: 10.1007/s11703-008-0033-3
- Ye, J.-S., Yin, H., Qiang, J., Peng, H., Qin, H.-M., Zhang, N., et al. (2011). Biodegradation of anthracene by *Aspergillus fumigatus*. *J. Hazard. Mater.* 185, 174–181. doi: 10.1016/j.jhazmat.2010.09.015
- Zhang, G., Zhang, S., Liu, Y., and Tan, Z. (2011). Isolation and identification of a nicosulfuron-degrading strain J5-2 and its degradation characteristics. *Environ. Pollut. Control* 5:3.
- Zhang, H., Mu, W., Hou, Z., Wu, X., Zhao, W., Zhang, X., et al. (2012). Biodegradation of nicosulfuron by the bacterium *Serratia marcescens* N80. *J. Environ. Sci. Health Part B* 47, 153–160. doi: 10.1080/03601234.2012.632249
- Zhang, Y. Y., Li, M., Liang, Y., Zhou, H. Y., and Zhao, J. (2015). First report of sunflower wilt caused by *Plectosphaerella cucumerina* in China. *Plant Dis.* 99, 1646–1646. doi: 10.1094/PDIS-02-15-0135-PDN
- Zhao, H., Zhu, J., Liu, S., and Zhou, X. (2018). Kinetics study of nicosulfuron degradation by a *Pseudomonas nitroreducens* strain NSA02. *Biodegradation* 29, 271–283. doi: 10.1007/s10532-018-9828-y

- Zhao, W., Wang, C., Xu, L., Zhao, C., Liang, H., and Qiu, L. (2015a). Biodegradation of nicosulfuron by a novel *Alcaligenes faecalis* strain ZWS11. *J. Environ. Sci.* 35, 151–162. doi: 10.1016/j.jes.2015.03.022
- Zhao, W., Xu, L., Li, D., Li, X., Wang, C., Zheng, M., et al. (2015b). Biodegradation of thifensulfuron-methyl by *Ochrobactrum* sp. in liquid medium and soil. *Biotechnol. Lett.* 37, 1385–1392. doi: 10.1007/s10529-015-1807-3
- Zhou, S., Song, J., Dong, W., Mu, Y., Zhang, Q., Fan, Z., et al. (2017). Nicosulfuron biodegradation by a novel cold-adapted strain *Oceanisphaera psychrotolerans* LAM-WHM-ZC. *J. Agric. Food Chem.* 65, 10243–10249. doi: 10.1021/acs.jafc.7b04022

**Conflict of Interest Statement:** The authors declare that the research was conducted in the absence of any commercial or financial relationships that could be construed as a potential conflict of interest.

Copyright © 2018 Carles, Rossi, Besse-Hoggan, Blavignac, Lereboure, Artigas and Batisson. This is an open-access article distributed under the terms of the Creative Commons Attribution License (CC BY). The use, distribution or reproduction in other forums is permitted, provided the original author(s) and the copyright owner(s) are credited and that the original publication in this journal is cited, in accordance with accepted academic practice. No use, distribution or reproduction is permitted which does not comply with these terms.



# Dynamics of Bacterial Communities Mediating the Treatment of an As-Rich Acid Mine Drainage in a Field Pilot

Elia Laroche<sup>1,2</sup>, Corinne Casiot<sup>1</sup>, Lidia Fernandez-Rojo<sup>1</sup>, Angélique Desoeuvre<sup>1</sup>, Vincent Tardy<sup>1</sup>, Odile Bruneel<sup>1</sup>, Fabienne Battaglia-Brunet<sup>2</sup>, Catherine Joulian<sup>2</sup> and Marina Héry<sup>1\*</sup>

<sup>1</sup> HydroSciences Montpellier, CNRS, IRD, University of Montpellier, Montpellier, France, <sup>2</sup> BRGM, Geomicrobiology and Environmental Monitoring Unit, Orléans, France

## OPEN ACCESS

### Edited by:

Ghiglione Jean-Francois,  
The National Center for Scientific  
Research (CNRS), France

### Reviewed by:

Jonathan Douglas Van Hamme,  
Thompson Rivers University, Canada  
Steven Singer,  
Lawrence Berkeley National  
Laboratory (LBNL), United States

### \*Correspondence:

Marina Héry  
marina.hery@umontpellier.fr

### Specialty section:

This article was submitted to  
Microbiotechnology, Ecotoxicology  
and Bioremediation,  
a section of the journal  
Frontiers in Microbiology

**Received:** 12 September 2018

**Accepted:** 07 December 2018

**Published:** 21 December 2018

### Citation:

Laroche E, Casiot C,  
Fernandez-Rojo L, Desoeuvre A,  
Tardy V, Bruneel O,  
Battaglia-Brunet F, Joulian C and  
Héry M (2018) Dynamics of Bacterial  
Communities Mediating the Treatment  
of an As-Rich Acid Mine Drainage in a  
Field Pilot. *Front. Microbiol.* 9:3169.  
doi: 10.3389/fmicb.2018.03169

Passive treatment based on iron biological oxidation is a promising strategy for Arsenic (As)-rich acid mine drainage (AMD) remediation. In the present study, we characterized by 16S rRNA metabarcoding the bacterial diversity in a field-pilot bioreactor treating extremely As-rich AMD *in situ*, over a 6 months monitoring period. Inside the bioreactor, the bacterial communities responsible for iron and arsenic removal formed a biofilm (“biogenic precipitate”) whose composition varied in time and space. These communities evolved from a structure at first similar to the one of the feed water used as an inoculum to a structure quite similar to the natural biofilm developing *in situ* in the AMD. Over the monitoring period, iron-oxidizing bacteria always largely dominated the biogenic precipitate, with distinct populations (*Gallionella*, *Ferrovum*, *Leptospirillum*, *Acidithiobacillus*, *Ferritrophicum*), whose relative proportions extensively varied among time and space. A spatial structuring was observed inside the trays (arranged in series) composing the bioreactor. This spatial dynamic could be linked to the variation of the physico-chemistry of the AMD water between the raw water entering and the treated water exiting the pilot. According to redundancy analysis (RDA), the following parameters exerted a control on the bacterial communities potentially involved in the water treatment process: dissolved oxygen, temperature, pH, dissolved sulfates, arsenic and Fe(II) concentrations and redox potential. Appreciable arsenite oxidation occurring in the bioreactor could be linked to the stable presence of two distinct monophylogenetic groups of *Thiomonas* related bacteria. The ubiquity and the physiological diversity of the bacteria identified, as well as the presence of bacteria of biotechnological relevance, suggested that this treatment system could be applied to the treatment of other AMD.

**Keywords:** acid mine drainage, arsenic, bioremediation, eco-engineering, iron-oxidizing bacteria, arsenic-oxidizing bacteria, microbial ecotoxicology

## INTRODUCTION

Mining activities produced large amount of wastes composed of sulfide minerals and toxic metallic elements, causing environmental hazard. During their inappropriate storage, oxidation of the sulfide minerals can generate acid mine drainage (AMD) characterized by acid pH and high concentrations in metals and metalloids. Arsenic (As) is a highly toxic metalloid often associated

with this type of pollution (Paikaray, 2015). An AMD can self-sustain for several centuries, with dramatic consequences on the receiving aquatic ecosystems. In this context, the development of effective and sustainable remediation solution for the treatment of As-rich AMD is required for water resource and public health protection.

The dissemination of arsenic pollution can be naturally limited by its immobilization into the solid phase. This natural phenomenon relies on the biological oxidation of Fe(II) and its subsequent precipitation as Fe(III) oxyhydroxides. Arsenic is then removed from the dissolved phase by co-precipitation with Fe(III) or by adsorption to the newly formed ferric minerals. The less soluble form, arsenate [As(V)], is more efficiently trapped onto iron phases than the more mobile form, arsenite [As(III)] (Hug and Leupin, 2003). Then, the capacity of autochthonous bacteria to oxidize As(III) into As(V) together with the activity of iron-oxidizing bacteria (FeOB) contribute to the mitigation of the arsenic pollution. This natural attenuation has been described at various mining sites worldwide (Casiot et al., 2003; Asta et al., 2010; Egal et al., 2010; Chen and Jiang, 2012; Paikaray, 2015), as well as the diversity of AMD autochthonous microbial communities (Baker and Banfield, 2003; Bruneel et al., 2011; Volant et al., 2014; Méndez-García et al., 2015; Chen et al., 2016). Several studies have focused on the identity of FeOB and As(III)-oxidizing bacteria (AsOB) and their activity in relation with pollution attenuation (Battaglia-Brunet et al., 2002; Bruneel et al., 2003; Casiot et al., 2003; Duquesne et al., 2003; Egal et al., 2009). In particular, numerous evidences of the role of the As(III)-oxidizing *Thiomonas* spp. were reported (Bruneel et al., 2003, 2011; Casiot et al., 2003; Hovasse et al., 2016).

The development of passive treatment systems exploiting these microbially mediated processes is a promising strategy for the remediation of As-rich AMD (Hengen et al., 2014; Bruneel et al., 2017). The efficiency of such system was demonstrated in lab-scale bioreactors (González-Contreras et al., 2012; Hedrich and Johnson, 2014; Ahoranta et al., 2016; Fernandez-Rojo et al., 2017). Attempts of *in situ* treatment are scarce and mainly limited so far to AMD with arsenic concentrations lower than 3 mg L<sup>-1</sup> (Whitehead et al., 2005; Macías et al., 2012). One field-pilot treating high arsenic concentrations (50–250 mg L<sup>-1</sup>) removed 20% of the dissolved arsenic (Elbaz-Poulichet et al., 2006). The treatment efficiency of these systems relies on microbial activity and thus may fluctuate depending on the identity and the dynamic of the microbial populations driving the biogeochemical reactions inside the bioreactor. Operating conditions as well as environmental conditions likely exert control over microbial diversity and activity (Heinzl et al., 2009b; Ahoranta et al., 2016; Fernandez-Rojo et al., 2017).

In a previous study, a passive field-scale bioreactor treating As-rich acid mine drainage from the Carnoulès mine (France) was monitored during 6 months (Fernandez-Rojo et al., in press). Arsenic removal varied between 3 and 97% during the monitoring period for a flow rate variation between 6 and 130 L h<sup>-1</sup>. The proportion of As(V) in the biogenic precipitates formed inside the pilot increased over time, reaching nearly 100% of

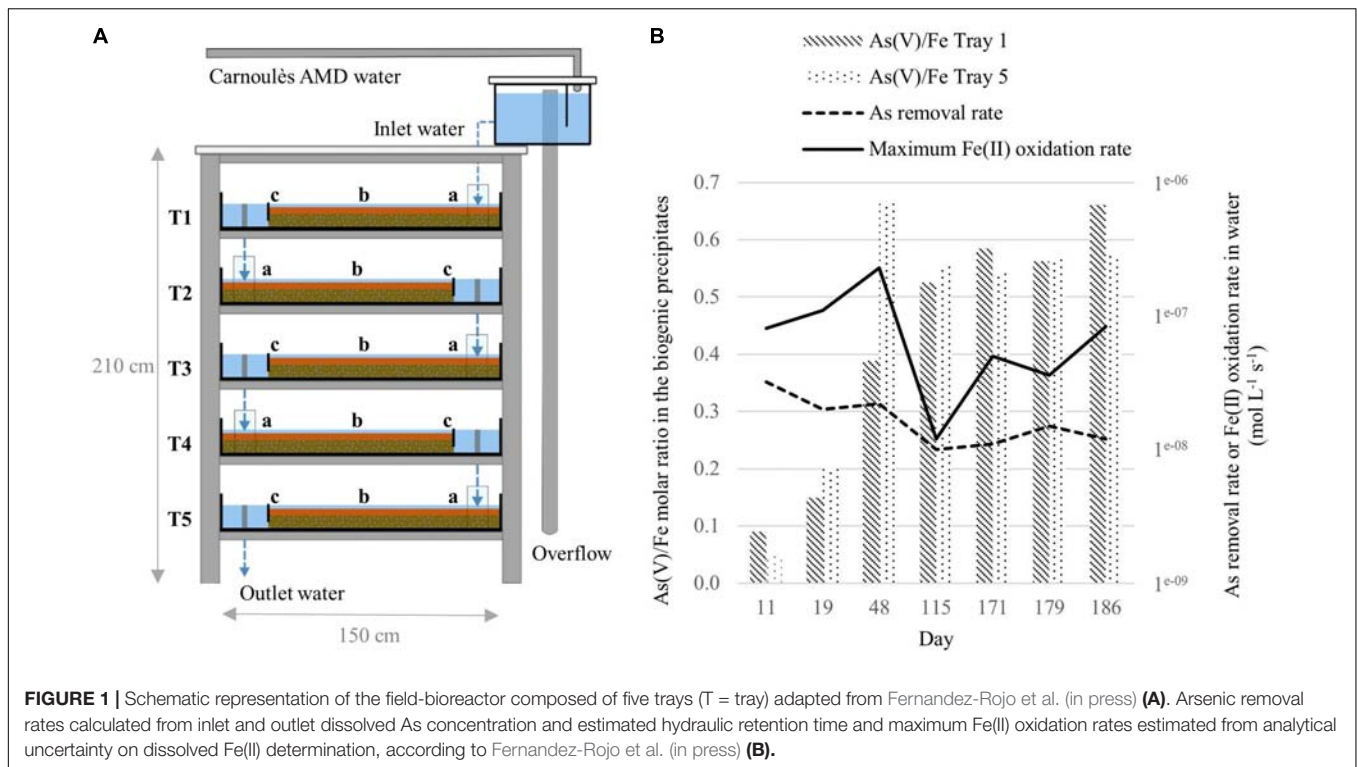
total As. Arsenate enrichment in the precipitate was associated with an increase of the abundance of the marker gene for bacterial arsenite oxidation (*aiOA*) -quantified by qPCR-. Results strongly suggested that bacterial As(III) oxidation occurred in the bioreactor, leading to the formation of stable precipitates, advantageous in term of sludge management. However, the identity of the bacterial populations involved in arsenic and iron oxidation and removal were not determined. The aim of the present work was to improve our knowledge of the bacterial diversity driving As-rich AMD depollution in an *in situ* treatment device. In this context, the spatial and temporal dynamics of the bacterial communities colonizing the bioreactor were investigated by a 16S rRNA metabarcoding approach. Because of their central role in arsenic oxidation in Carnoulès AMD, we further characterized two distinct monophyletic *Thiomonas* groups by CARD-FISH. We also focused on the physico-chemical drivers of the bacterial diversity. To our knowledge, this is the first microbiological characterization performed on a field-pilot treating As-rich AMD by precipitation with biogenic iron phases.

## MATERIALS AND METHODS

### Pilot Scale Passive Treatment System Description and Sample Collection

A field-scale pilot, made with five shallow trays (1.5 × 1 × 0.11 m) stacked head to tail on a shelf, was implemented at the Carnoulès mine (France) for the treatment of AMD, as described in Fernandez-Rojo et al. (in press) (Figure 1A). The bioreactor was settled on June 2016 10th and was monitored during 194 days. Nine sampling campaigns were conducted and inlet water and biogenic precipitates were characterized for their physico-chemical properties (Fernandez-Rojo et al., in press). From the whole dataset and samples available, we selected seven dates for microbial characterization: 21st of June (D11); 29th of June (D19); 28th of July (D48); 3rd of October (D115); 28th of November (D171), 6th of December (D179), 13th of December (D186). Selection was based on the temporal variations of the As(V)/Fe molar ratio in the biogenic precipitate (Figure 1B). Arsenic removal rates from water and Fe(II) oxidation rates are also given. Biogenic precipitates were collected from tray 1 (T1) and tray 5 (T5) for all the campaigns and from tray 1, 2, 3, 4, and 5 for the D48 and D171 campaigns.

Each tray was divided into three sections (Figure 1A): “a” refers to the location close to the inlet of the tray, “b” corresponds to the middle section, and “c” refers to the location close to the outlet of the tray. Based on ARISA (Automated Ribosomal Intergenic Spacer Analysis), bacterial community structures in the three sections (a, b, c) of a given tray exhibited similar genetic structure (data not shown). Then, for each tray, samples collected in sections a, b and c were used as triplicates for 16S rRNA metabarcoding analyses. For each tray, three composite samples were collected in Falcon tubes (50 mL) by scrapping the biogenic precipitates in each section with a sterile spatula. The tubes containing the composite samples were



centrifuged for 10 min at  $4400 \times g$  (Sorwall ST40, Thermo Scientific). The supernatant was discarded and the precipitates were homogenized. An aliquot was dried in a vacuum desiccator for dry weight determination. The remaining precipitates were conserved in Eppendorf tubes (2 mL) at  $-80^{\circ}\text{C}$  before DNA extraction. Sample names refer to the sampling day (counted from the day of bioreactor settling, D1–D186) and the tray where the biogenic precipitate was sampled (T1–T5), e.g., D11-T1.

Inlet water was collected for all the campaigns but due to technical problem, water collected on October 3rd (D115) could not be analyzed. Triplicates of inlet water samples (300 mL) were filtered on sterile  $0.22 \mu\text{m}$  cellulose acetate filter. The filters were stored at  $-80^{\circ}\text{C}$  before DNA extraction. Water sample names refer to the sampling day (D1–D186) of inlet water sample ( $W_{\text{in}}$ ) (e.g., D11- $W_{\text{in}}$ ).

For comparison between the bacterial communities established inside the bioreactor and the natural ecosystem, a point-in-time sampling of the AMD riverbed sediments (Reigous creek) was performed on the 28th of November (D171). Sediments (SED) were collected using a sterile spatula and were treated as described for the biogenic precipitates.

## Physico-Chemical Characterization of Inlet and Outlet Waters

The chemical characterization of the water (inlet and outlet) and the bioprecipitate samples was performed in our previous study (Fernandez-Rojo et al., in press). Briefly, the concentrations of dissolved Fe(II) were determined using spectrophotometry after filtration through  $0.22 \mu\text{m}$ . Total dissolved concentrations

of Fe, As, and other elements [S ( $\text{SO}_4^{2-}$ ), Al, Zn, and Pb] were determined using ICP-MS. Arsenic redox speciation was determined using HPLC-ICP-MS. The data used in the present study are summarized in Figure 1B and Supplementary Table S1.

## DNA Extraction and Quantification

Prior DNA extraction, biogenic precipitate and riverbed sediment samples were washed with 1 mL of TRIS-EDTA (100:40) HCl pH 8 and then centrifuged to  $8,000 \times g$  from 1 min. Total genomic DNA was then extracted using the DNeasy PowerSoil kit (Qiagen, Hilden, Germany), according to the manufacturer's recommendations (in triplicates for the biogenic precipitates). Extraction controls were performed without any biogenic precipitate sample to exclude any contamination from the kit. For water samples, DNA was extracted (in triplicates) from the cellulose acetate filters using DNeasy PowerWater kit (Qiagen) according to the manufacturer's recommendations. All the DNA extracts were quantified with a fluorometer (Qubit, Invitrogen, Carlsbad, CA, United States) and stored at  $-20^{\circ}\text{C}$  until further analysis.

## Sequencing of Bacterial 16S rRNA Gene

The V4–V5 hypervariable region of the 16S rRNA gene was amplified using primers PCR 515F (Barret et al., 2015) and PCR 928R (Wang and Qian, 2009). PCR amplification was conducted as described in Tardy et al. (2018). Amplification performed on the control DNA extracts (obtained without any biogenic precipitate sample) yielded no amplification signal. The PCR products were sequenced with an Illumina MiSeq sequencer in

paired-end mode ( $2 \times 300$  bp) at GeT-PlaGe platform (Toulouse, France).

## Bioinformatic Analyses of 16S rRNA Gene Sequences

Pair-end sequences were merged by flash software version 1.2.6 (Magoè and Salzberg, 2011), with maximum 10% of mismatch into the overlap region. The raw datasets are available on the EBI database system under project accession number [PRJEB27907]. The average Phred score (*Q*-score) of these joined reads was superior to 30 for every base. Bioinformatic analyses were conducted using the software program Mothur version 1.39.5 (Schloss et al., 2009). First step was the selection of high quality sequences based on the following criteria: length between 330 and 460 bp, a homopolymer length inferior to 7 nt and no ambiguous bases. Singletons, chimeric and unaligned reads were removed using UCHIME (Edgar et al., 2011) and the SILVA reference database (Release 128). The pre-cluster command served to reduce sequencing noise by clustering reads differing by only one base every 100 bases. The high quality sequences were taxonomically assigned using the SILVA reference database, by the Bayesian method with a bootstrap confidence score of 80 (Wang et al., 2007). After the removal of sequences that were not assigned to the *Bacteria* kingdom, samples contained between 2227 and 34928 reads. A subsampling selected a random set of 6295 reads in each sample in order to efficiently compare the datasets. Samples containing less than 6295 reads were removed to maintain a sequencing effort that adequately covers the bacterial diversity. A distance matrix was generated with the remaining sequences and used to cluster these sequences into Operational Taxonomic Units (OTUs) defined at 97% cutoff, using the average neighbor algorithm. Complementary analyses (based on BLAST) were performed for the assignation of the dominant OTU (representing 41% of the whole reads) at the genus level. Mothur used the OTU table to calculate the coverage sample (rarefaction curve), the alpha and beta diversity (diversity indices and Unifrac distances) at a level of 97% sequence similarity.

## CARD – FISH

CARD-FISH analyses were performed in triplicates on biogenic precipitates collected from tray 1 (T1) and tray 5 (T5) on the 28<sup>th</sup> of July (D48) and the 28<sup>th</sup> of November 2016 (D171). Oligonucleotide probes EUB338, EUB338II and EUB338III were used for *Bacteria* quantification (Amann et al., 1990; Daims et al., 1999). Negative controls were performed with probe NON338, the complementary sequence of EUB338 (Wallner et al., 1993). Two probes were used for the quantification of two distinct monophyletic groups of *Thiomonas* spp. Probes TM1G0138 and TM2G0138 respectively target *Thiomonas* group1 and group2 according to Hallberg et al. (2006), which correspond respectively to monophyletic Group II and I according to Coupland et al. (2004) and Bryan et al. (2009). Detailed protocol for *in situ* hybridization, tyramide amplification,

and microscopic observations is provided in **Supplementary File**.

## Statistical Analyses

All statistical analyses were performed with R version 3.4.3 using mainly vegan package<sup>1</sup>. The statistically significant differences between CARD-FISH data were assessed with the non-parametric Kruskal–Wallis test followed by Dunn's *post hoc* test using Bonferroni *p*-value adjustment. Non-metric multidimensional scaling (NMDS), based on the weighted pairwise Unifrac distances, was used to illustrate the dynamics of the bacterial communities structure during the monitoring. The significance of the differences observed between groups of samples (phase I vs. phase II and tray 1 vs. tray 5) was assessed with an ADONIS test (999 permutations). Redundancy analysis (RDA) was performed to highlight the main environmental drivers shaping the bacterial community structure inside the bioreactor. This approach was chosen because an initial detrended correspondence analysis (DCA) indicated that bacterial community data had a linear distribution along the axis (<3.0). The physico-chemical characteristics of the AMD water, measured in the inlet and outlet waters (**Supplementary Table S1**), were tested as environmental variables to explain the variations of dominant taxa in the bioprecipitates collected in tray 1 and tray 5 respectively (relative abundance of reads  $\geq 1\%$  in at least one bioprecipitate sample during the monitoring period). Indeed, the biofilm continually interacts with the inflowing water which provides the main energy source for the lithotrophic bacteria [Fe(II)]. Before the RDA, the normality of environmental variables was checked with a Shapiro–Wilk test. Environmental and biological variables were respectively log and Hellinger transformed (Legendre and Gallagher, 2001). A sub-set of environmental variables was selected to decrease the multicollinearity (variance inflation factors < 10) and to include only the significant predictors ( $p < 0.05$  according Monte Carlo test with 999 permutations). Variation partitioning analyses enabled to evaluate the contribution of each variable to the bacterial community variation. The significance of the global model and the individual axes were checked with a Monte Carlo test (999 permutations).

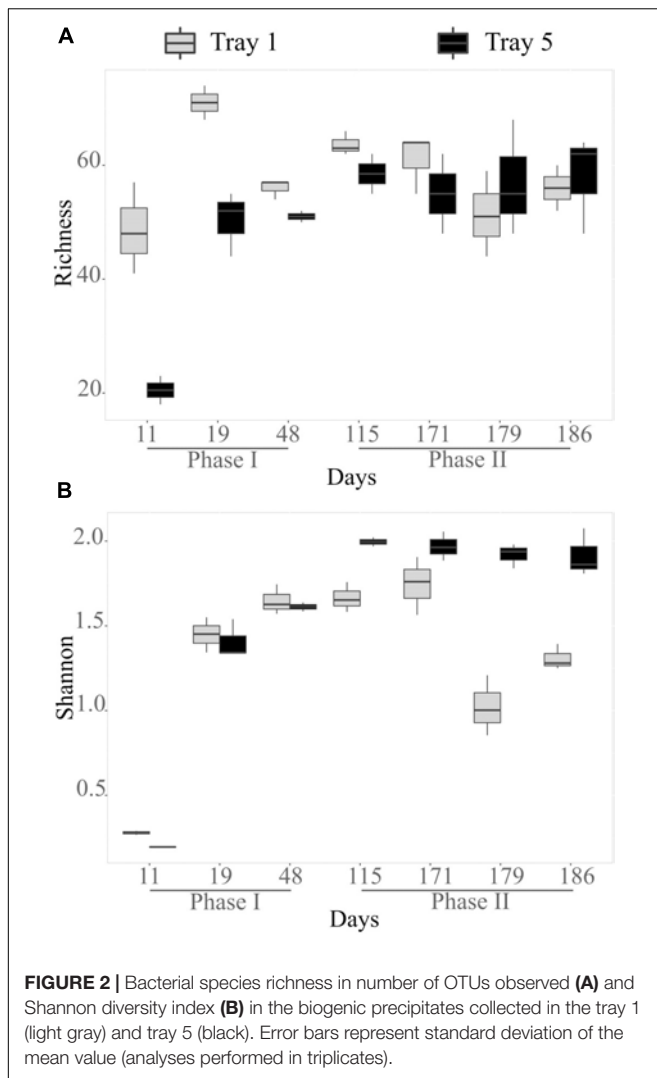
## RESULTS

### Bacterial Diversity and Structure in the Treatment Pilot

Illumina sequencing of the 79 samples yielded a total of 2,288,823 sequences of 16S rRNA gene. Among them, 6295 quality sequences per sample were sub-sampled for alpha and beta diversity analysis. Rarefaction curves approached an asymptote suggesting that the sequencing effort adequately covered the bacterial diversity in all the samples (**Supplementary Figure S1**).

In the biogenic precipitates, the richness increased from D11 to D19 as illustrated by the enrichment of observed OTUs (**Figure 2A**). At D11 and D19, richness was higher in the

<sup>1</sup><http://www.r-project.org/>



top tray than in the bottom tray. From D48, the number of observed OTUs remained relatively stable and similar in both trays. Shannon index (reflecting both richness and evenness) also clearly increased during the first stages of the monitoring. Then it remained stable in tray 5 from D115 to D186, whereas it tended to decrease before increasing again in tray 1 (Figure 2B). Diversity indexes in the sediments collected in the AMD riverbed on day 171 (point in time analysis) were comparable to those measured in the biogenic precipitates collected at the same date in the top tray (T1) (richness = 60 observed OTUs; Shannon = 1.87).

NMDS illustrates the dynamics of the structure of the bacterial communities in the biogenic precipitates and in the riverbed sediment (SED) (Figure 3). Samples were separated in two main groups (ADONIS test,  $R^2 = 0.19$ ,  $P = 0.001$ ). The first group, composed by the communities at D11, D19, and D48, corresponded to the first phase of the monitoring (phase I). The second group, composed by the communities at D115–D186 corresponded to the second phase of the monitoring (phase II). In addition, over the whole monitoring period, the bacterial communities in the top tray (tray 1) were distinct from those

thriving in the bottom tray (tray 5) (ADONIS test,  $R^2 = 0.14$ ,  $P = 0.012$ ). This spatial structuring, visible from D48, became particularly marked from D115. Bacterial community thriving in the sediment collected in the AMD riverbed (SED) grouped with those of the biogenic precipitates collected at the same date (D171) in the top tray (Figure 3).

## Taxonomic Composition of the Bacterial Communities

The majority of the 16S rRNA gene sequences retrieved from the biogenic precipitates, the riverbed sediments, and the AMD waters were affiliated with members of the *Beta-Proteobacteria* (between 65 and 99% of the total sequences). In the whole data set, the most abundant OTU was affiliated with genus *Gallionella*. *Alpha- and Gamma-Proteobacteria* were the second and the third most abundant taxonomic groups.

The composition of the bacterial communities remained relatively stable in the AMD waters over the monitoring period with always a large dominance of reads related to *Gallionella* (ranging from 63 to 96%). Other minor groups identified in the waters included *Sulfuriferula*, *Acidithiobacillus* and *Ferrovum* (Supplementary Figure S2).

Eleven days after the pilot was set up (D11), the bacterial communities of the biogenic precipitates were quite similar to those of the feeding water and largely dominated by the *Gallionella* genus (Figure 4). Then, notable temporal shifts rapidly occurred in the composition of the bacterial communities of the biogenic precipitates (phase I). From the 29th of June (D19), the proportion of *Gallionella* strongly decreased while those of *Sulfuriferula*, *Ferrovum*, *Rickettsiales*, *Ferritrophicum* and *Acidithiobacillus* increased. *Sulfuriferula* was dominant in the pilot between D48 and D171. From D115, the bacterial communities in the top tray and in the bottom tray were clearly distinct (phase II). The composition of the communities in T5 remained relatively stable, whereas in T1, the relative proportion of *Gallionella* increased again during this second phase of the monitoring (Figure 4).

Overall, for the whole monitoring period, the top tray was characterized by higher proportion of *Gallionella* compared to the bottom tray. *Sulfuriferula*, *Ferrovum*, *Ferritrophicum*, *Acidithiobacillus*, *Leptospirillum* and *Acidicapsa* were more abundant in the bottom tray. Spatial structuring inside the pilot was confirmed with the characterization of the bacterial communities in the five trays for two sampling campaigns (D48 and D171). This analysis showed that communities thriving in tray 2 were comparable to those in tray 1 whereas communities thriving in trays 3 and 4 were comparable to those in tray 5 (Supplementary Figure S3).

The composition of the bacterial community in the sediments (SED) collected in the AMD riverbed at D171, was similar to that of the biogenic precipitates collected the same day inside the top tray (T1) of the bioreactor (Figure 4). The relative proportion of *Thiomonas* in the Reigous creek sediments was comparable to that in the top tray of the treatment device (1.1% and  $0.89 \pm 0.25\%$  respectively). The proportion of *Acidithiobacillus*

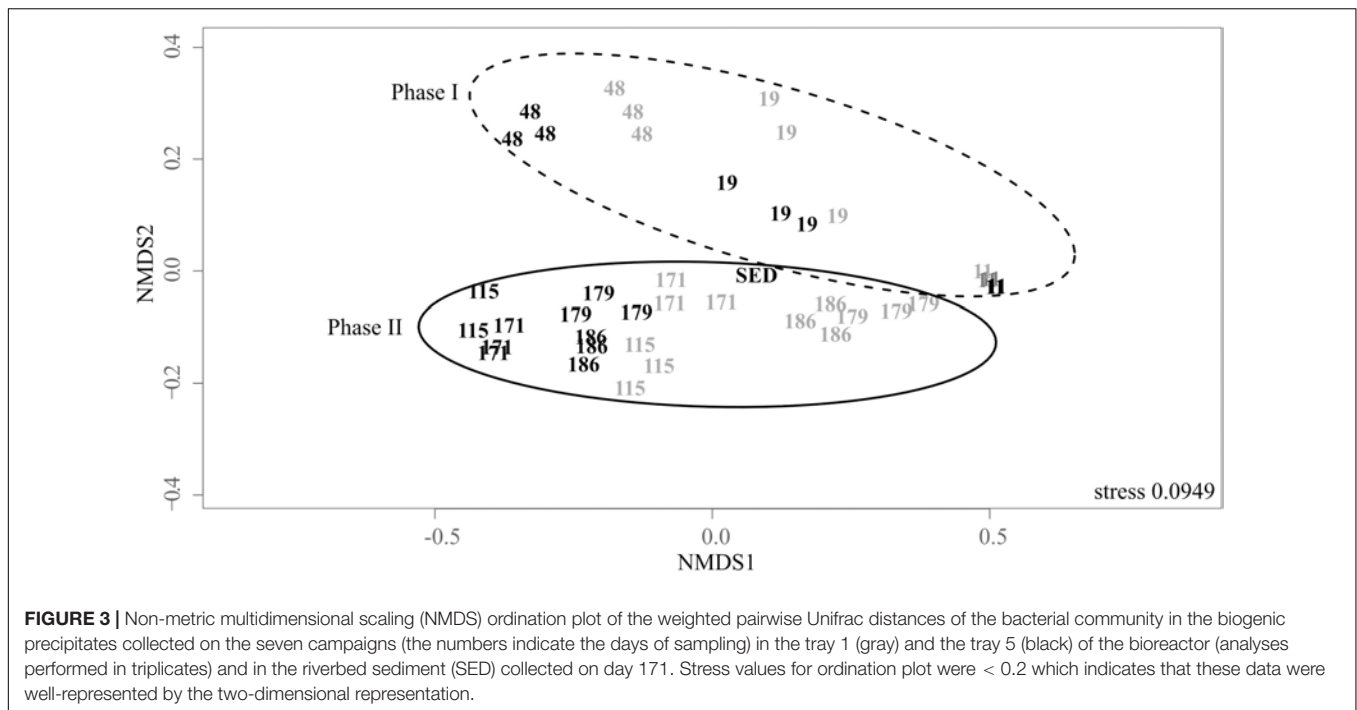


**FIGURE 3 |** Non-metric multidimensional scaling (NMDS) ordination plot of the weighted pairwise Unifrac distances of the bacterial community in the biogenic precipitates collected on the seven campaigns (the numbers indicate the days of sampling) in the tray 1 (gray) and the tray 5 (black) of the bioreactor (analyses performed in triplicates) and in the riverbed sediment (SED) collected on day 171. Stress values for ordination plot were < 0.2 which indicates that these data were well-represented by the two-dimensional representation.

was higher in the treatment pilot (2.8 and 9% respectively in tray 1 and 5) than in the riverbed sediment (0.6%).

## Quantification of *Thiomonas* Populations by CARD-FISH

Total bacteria and two distinct monophyletic groups of *Thiomonas*-related bacteria were quantified in the biogenic precipitates sampled in T1 and T5 at D48 (28th of July) and D171 (28th of November) by CARD-FISH (Table 1 and Supplementary Figure S4). Biogenic precipitates contained an average of  $8 \pm 3 \times 10^7$  total bacterial cells/g of dry biogenic precipitates. No significant differences ( $p > 0.05$ ) were observed for the total number of bacteria among the four samples analyzed. The total number of *Thiomonas* averaged  $7 \pm 2 \times 10^6$  cells/g of dry biogenic precipitates, representing 8% of the DAPI-stained cells. *Thiomonas* belonging to group II (as defined by Bryan et al., 2009) were more abundant in the pilot than *Thiomonas* belonging

to group I ( $p < 0.05$ ). They corresponded respectively to an average of 4.9 and 3.1% of the DAPI-stained bacteria (Table 1). If no temporal differences were observed between D48 and D171, the total number of *Thiomonas* (Group I + II) was significantly higher in the bottom tray (T5) compared to the top tray (T1) in November (D171) ( $p < 0.05$ ).

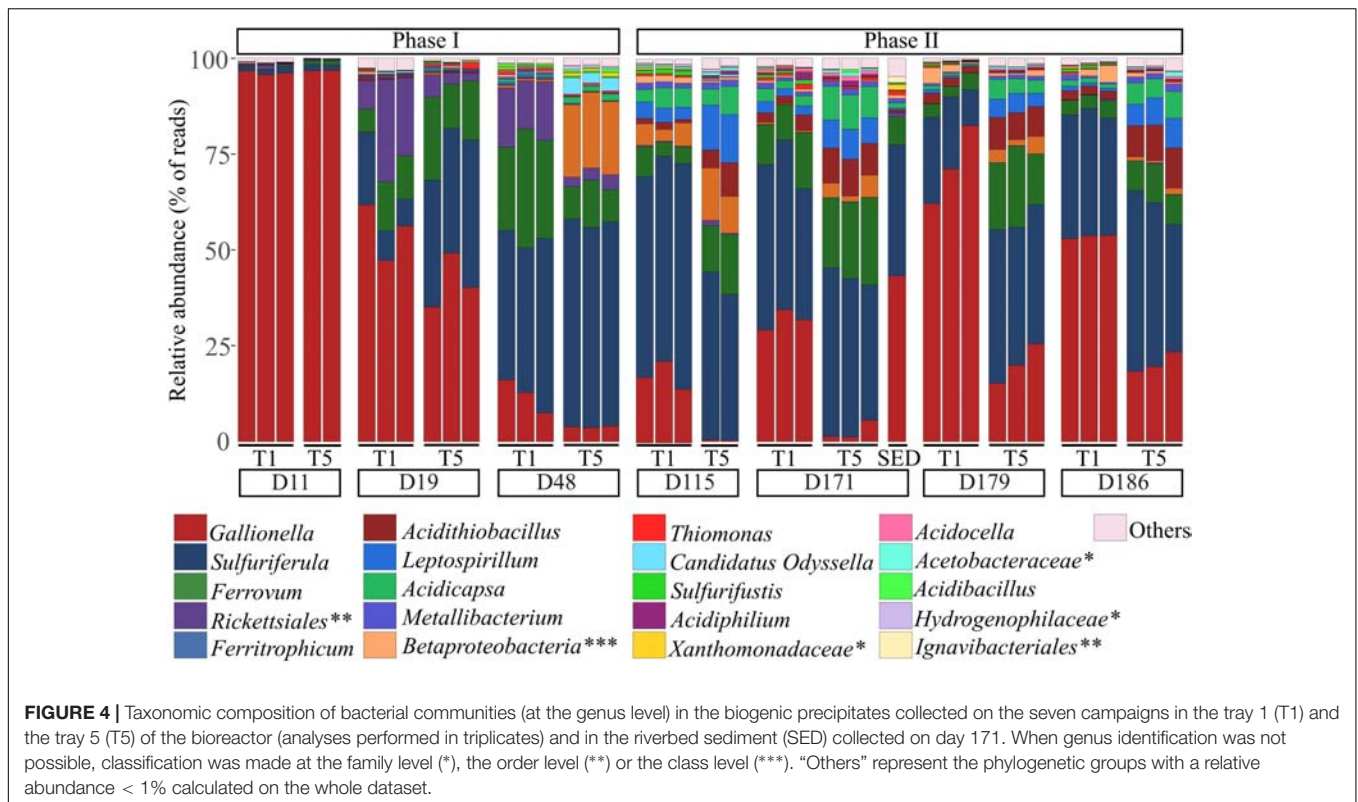
## Main Drivers Shaping the Bacterial Communities Inside the Pilot

Redundancy analysis (RDA) summarized the spatio-temporal dynamics of the bioprecipitates bacterial communities and highlighted the main environmental factors explaining these variations. The samples were arranged according to the same pattern as in the NDMS (Figure 5). The model explained significantly 83.3% of bacterial community variation (Monte Carlo test,  $P < 0.05$ ). According to variation partitioning, the dissolved oxygen (DO) was individually the best driver of this

**TABLE 1 |** Quantification by CARD-FISH of *Thiomonas* belonging to Group I (bacteria hybridized with the oligonucleotide probe TM2G0138) and of *Thiomonas* belonging to Group II (bacteria hybridized with the oligonucleotide probe TM1G0138).

Sample name	<i>Thiomonas</i> Group I		<i>Thiomonas</i> Group II		Bacteria (EUB I-III)	
	No of cells/g of dry biogenic precipitate	% of DAPI-stained cells	No of cells/g of dry biogenic precipitate	% of DAPI-stained cells	No of cells/g of dry biogenic precipitate	% of DAPI-stained cells
D48-T1	$2 \pm 1 \times 10^6$	$3 \pm 2$	$5 \pm 3 \times 10^6$	$6 \pm 2$	$6.1 \pm 0.7 \times 10^7$	$88 \pm 1$
D48-T5	$3 \pm 2 \times 10^6$	$4 \pm 3$	$5 \pm 3 \times 10^6$	$5 \pm 3$	$7 \pm 5 \times 10^7$	$82 \pm 1$
D171-T1	$1.0 \pm 0.3 \times 10^6$	$2.0 \pm 0.7$	$3.4 \pm 0.2 \times 10^6$	$4.6 \pm 0.9$	$6 \pm 1 \times 10^7$	$87 \pm 2$
D171-T5	$4 \pm 3 \times 10^6$	$4 \pm 2$	$6 \pm 2 \times 10^6$	$5 \pm 2$	$1.2 \pm 0.8 \times 10^8$	$83 \pm 3$

Standard deviations were calculated on biological triplicates.



variability accounting for 36.5% of the total variance. It was followed by sulfate concentration (26.7%), temperature (16.5%), pH (15.2%), dissolved arsenic and ferrous iron concentration (11.1% and 10.2%, respectively) and the redox potential Eh (6%).

The bacterial communities thriving in the pilot during the first phase were clearly distributed along a temporal gradient and were associated with high values of temperature, pH, dissolved arsenic, and ferrous iron concentrations, and by low values of DO and Eh. Between D115 and D186, samples were divided into two sub-groups corresponding respectively to tray 1 and tray 5. During this second phase, the structure of the bacterial communities was explained by high DO and Eh values, particularly in the tray 5 (Figure 5).

The cosine of the angle between an environmental variable and a bacterial taxa provides an approximation of their correlation. Thus, it can be inferred from Figure 5 that the relative abundance of *Rickettsiales* was positively correlated with water temperature and negatively with Eh. On the contrary, *Acidithiobacillus*, *Leptospirillum* and *Acidicapsa* were negatively correlated with temperature, pH and arsenic concentration in water and positively with Eh and DO. For the other taxa, no clear correlations could be drawn.

## DISCUSSION

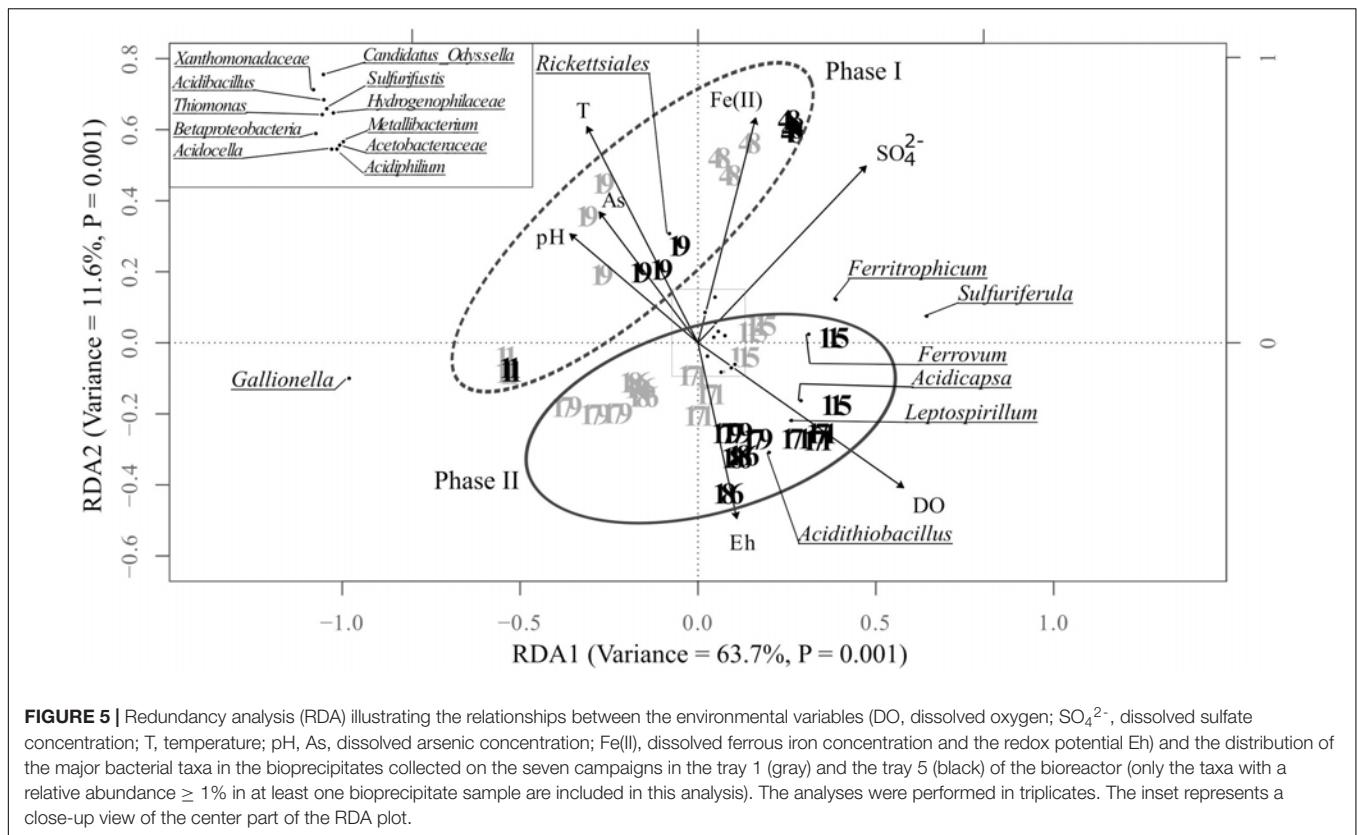
In the *in situ* treatment device, iron and arsenic removal was driven by a microbial biofilm colonizing the surface of the five trays composing the pilot. The present study aimed at

characterizing the bacterial diversity and its spatio-temporal dynamics in this engineered system, in relation with main environmental parameters.

## Microbiology of the Bioprecipitates

The biogenic precipitates that developed inside the pilot contained at least one order of magnitude higher bacterial biomass than what was observed in a lab-scale pilot treating the same AMD (Fernandez-Rojo et al., 2017) and in terraced iron formations reported elsewhere (Brown et al., 2011; Brantner et al., 2014). Thus, both the sand used to fill the trays and the hydrodynamic conditions were favorable to a biofilm development. The microbial assemblages developing inside this engineered system reproduced, at least partially, the natural ecosystem established in the nearby AMD. The microbiology of the pilot was largely dominated by diverse iron-oxidizing bacteria (FeOB): *Gallionella*, *Ferrovum*, *Ferritrophicum* and, to a lesser extent, *Acidithiobacillus* and *Leptospirillum*. The main taxa identified were previously found in AMD ecosystems (Baker and Banfield, 2003; Baker et al., 2003; Méndez-García et al., 2015; Chen et al., 2016), including Carnoulès (Bertin et al., 2011; Bruneel et al., 2011; Volant et al., 2014), and in laboratory-based experiments (Fernandez-Rojo et al., 2018; Tardy et al., 2018).

*Gallionella* proved to be dominant in the Carnoulès ecosystem (Bruneel et al., 2006; Volant et al., 2014; Tardy et al., 2018) and in a lab-scale pilot treating Carnoulès water (Fernandez-Rojo et al., 2018). Genus *Ferrovum*, containing litho-autotrophic acidophilic FeOB with potential biotechnological relevance (Heinzel et al., 2009a,b; Hedrich and Johnson, 2012), was also described in



diverse AMD, including iron-rich environments (Johnson et al., 2014). *Gallionella* and *Ferrovum* were dominant in pilot plants relying on biological iron oxidation (Heinzel et al., 2009a,b; Hedrich et al., 2011; Hedrich and Johnson, 2012; Tischler et al., 2014; Sheng et al., 2016; Sun et al., 2016). *Ferritrophicum* genus, also including FeOB (Weiss et al., 2007), was previously identified in AMD (González-Toril et al., 2011; Tardy et al., 2018).

The moderately acidic sulfur oxidizers *Sulfuriferula* spp. were described as potential key actors of sulfur-cycling in acidic mine waste containing sulfide minerals (Jones et al., 2017). Their abundance in the pilot may be linked to the inflow of sulfide particles from the tailing pile into the pipe carrying the AMD water. The recent taxonomic reclassification of *Thiobacillus plumbophilus* to *Sulfuriferula plumbophilus* (Watanabe et al., 2015) may explain why *Sulfuriferula* spp. were underestimated so far in AMD. The capacity to oxidize iron or arsenic has not been described for any known *Sulfuriferula* species. “Sulfur-driven As(III) oxidation” was suggested in alkaline mono lake, through microbial thioarsenate transformation (Fisher et al., 2008). However, it is unlikely that similar process occurs under acidic and fully oxic conditions. Understanding the role of this genus (which mostly dominated the system from D48) in the treatment process requires further investigations.

*Acidithiobacillus* is considered as an important player in the attenuation process in Carnoulès (Egal et al., 2009; Bruneel et al., 2011; Bertin et al., 2011). This FeOB was detected in variable but relatively low proportions in the bioprecipitate (from 0.03 to 10.5%), in agreement with previous *in situ* observations

(Volant et al., 2014). Sensibility to Fe(II) could explain the low abundance of *Acidithiobacillus* and the dominance of *Ferrovum* and *Gallionella* in the field-pilot where Fe(II) concentrations ranged between 649 and 1396  $\text{mg L}^{-1}$  (Jones et al., 2015). The importance of *Acidithiobacillus* in biooxidation plants has previously been questioned (Rawlings et al., 1999). Even when used as an inoculum, *A. ferrooxidans* was out competed by *Ferrovum* in a pilot plant treating acid mine waters (Heinzel et al., 2009a). Distinguish the specific contribution of each FeOB population to iron and arsenic removal in the present study would require further investigations.

The presence of iron-reducing bacteria (*Acidiphilium*, *Acidocella*, *Metallibacterium*) can be explained by the occurrence of anoxic niches inside acidophilic biofilm (Ziegler et al., 2013).

## Dynamics of the Bacterial Communities Inside the Pilot

During the monitoring, biofilm colonization (phase I) was followed by a stationary phase (phase II) reached by the mature biofilm, and characterized by a stable bacterial biomass. The dominance of *Gallionella* in the bioprecipitates at the very beginning of the monitoring was linked to their dominance in the water used to feed the pilot. As the biofilm matured, spatial heterogeneities arose, resulting in the diversification of micro-habitats advantageous for other populations (Santegoeds et al., 1998; Woodcock and Sloan, 2017). The proportion of *Sulfuriferula*, *Ferrovum*, *Ferritrophicum*, *Rickettsiales* increased

while those of the first colonizers *Gallionella* decreased. Increase of bacterial diversity and shifts in bacterial assemblages were previously described during acidophilic biofilm maturation (Wilmes et al., 2009; Mueller et al., 2011).

*Ferrovum myxofaciens* produces large amounts of extracellular polymeric substances, which facilitate attachment to surfaces (Rowe and Johnson, 2008). This capacity may provide a competitive advantage to *Ferrovum*-related bacteria in engineered systems. In two pilot plants treating acid mine water, *Gallionella* were dominant during a first phase associated with unstable operating conditions while *Ferrovum* became dominant during a second phase with stable conditions. *Gallionella* abundance increased again at the end of the monitoring (Heinzel et al., 2009b). Similarly, in the present study, *Gallionella* regained in importance during the later stages of the monitoring, particularly in the top tray.

The autochthonous bacterial communities of the AMD feeding the pilot remained stable and largely dominated by *Gallionella* during the 6 months monitoring. Thus, the temporal dynamic of the bacterial community in the bioprecipitate (particularly during phase I) can be more readily attributed to bacterial succession during biofilm establishment rather than to the modification of the seeding community.

During the second phase of the monitoring, the spatial structuring of the mature communities inside the pilot intensified. Differences observed between the top and the bottom trays can be linked to a modification of the chemistry of the overlying water while transiting inside the pilot. This chemical gradient between the inlet and the outlet water was particularly marked during this second phase (**Supplementary Table S1**).

## Influence of Environmental Parameters on the Bacterial Communities

The range of physico-chemical variations observed in the AMD water during the 6 months monitoring was representative of the seasonal variations described during a 4 years *in situ* monitoring (Egal et al., 2010). The present study covered both summer (phase I) and autumn (phase II) periods. Thus, a seasonal effect on the whole dynamic may not be excluded. However, both autogenic (e.g., internal and biotic) and allogenic (e.g., external and abiotic) parameters are likely to govern bacterial dynamics during biofilm establishment. It is then difficult to distinguish the effect of seasonal variations from the autogenic parameters that may be particularly influential during the early phases of the biofilm development (Jackson et al., 2001; Lyautey et al., 2005). However, we can assume that once the biofilm has reached its maturity, the bacterial community dynamic was mainly driven by the variations of the physico-chemistry of the overlying water (Brown et al., 2011).

Redundancy analysis highlighted the key parameters susceptible to influence bacterial diversity in the pilot: DO, sulfate concentration, temperature, pH, dissolved As and Fe(II) concentration, and Eh (Rawlings et al., 1999; Dopson et al., 2007; Kupka et al., 2007; Candy et al., 2009; Volant et al., 2014; Jones et al., 2015; Sheng et al., 2016).

*Gallionella* is a microaerophilic bacteria thriving at lower oxygen conditions than other FeOB as *Ferrovum*, *A. ferrooxidans* and *Leptospirillum* spp. (Hanert, 2006; Johnson et al., 2014). The persistence of microaerophilic bacteria in the bioprecipitates and in the sediments, including some *Gallionella* and *Ferritrophicum* (Weiss et al., 2007), could be explained by the possible occurrence of microaerobic niches, as seen elsewhere (Ziegler et al., 2013). On the contrary, higher abundances of *Ferrovum* were associated with increasing concentration of oxygen (Jwair et al., 2016; Fabisch et al., 2016; Fernandez-Rojo et al., 2018).

Most of the FeOB characterized so far are mesophilic or thermophilic (Kupka et al., 2007). A better tolerance to low temperatures of *Acidithiobacillus* (Norris, 1990) may explain why its abundance was negatively correlated with temperature in the pilot. Batch experiments conducted with Carnoulès AMD water showed a clear effect of temperature on arsenite-oxidizers: both the abundance of *Thiomonas* and the As(III) oxidation activity were stimulated at 35°C compared to 20°C (Tardy et al., 2018). In the temperature range covered by the present study (5.2–23.8°C), no correlation was evidenced between temperature and *Gallionella*, *Ferrovum* or *Thiomonas* relative abundances. Temperatures naturally reaching 30°C or more in the water column above the bioprecipitate during summer are not excluded, particularly in case of reduced water height and long residence times. Such high temperatures may have differential effect on the FeOB and AsOB activity depending on their physiology.

Regarding the pH, our results are congruent with the better adaptability of *Ferrovum*, *Acidithiobacillus*, and *Leptospirillum* to acidic conditions compared to *Gallionella* known to prefer pH above 3 (Rawlings et al., 1999; Jones et al., 2015; Grettenberger et al., 2017).

Fe(II) concentration also influences growth and activity of FeOB depending on their affinity for this energy source and on potential competition between different populations (Battaglia et al., 1994; Rawlings et al., 1999). The negative correlation of *Acidithiobacillus* with Fe(II) is in agreement with a previous study (Jones et al., 2015). Furthermore, different affinity for Fe(II) together with distinct sensitivity to Fe(III) inhibition may explain the effect of redox potential (conditioned by the ratio Fe(III)/Fe(II)) on the relative distribution of FeOB (Rawlings et al., 1999; Meruane et al., 2002; Kuang et al., 2013).

Occurrence of *Gallionella* was negatively correlated with sulfate concentrations. Sulfates are generally well tolerated by FeOB, with inhibitory effects reported for concentrations higher than the ones measured in the present study (Candy et al., 2009). However, sulfate concentrations were previously shown to drive bacterial community composition in the Carnoulès AMD waters (Volant et al., 2014).

Finally, dissolved arsenic concentration significantly contributed to the bacterial community structure inside the bioreactor. Similar influence was shown *in situ* (Volant et al., 2014). Nevertheless, no tendency was highlighted between the variations of dissolved arsenic concentration and the proportion of the arsenite-oxidizing *Thiomonas*. It can be hypothesized that in the range of concentrations measured in this study, arsenic was not a limiting factor for bacteria relying on arsenite oxidation

for their growth, and was not toxic for the others *Thiomonas*. *Acidithiobacillus* appeared to be negatively correlated with dissolved arsenic concentration although high resistance capacity was evidenced for some strains of *A. ferrooxidans* (up to  $15 \text{ g L}^{-1} \text{ As(III)}$ , Dave et al., 2008). A possible explanation is that *Acidithiobacillus* contribute to arsenic removal from water and its abundance in the bioprecipitates is thus associated with lower dissolved arsenic concentrations.

## Iron Oxidation and Precipitation

In spite of the large dominance of FeOB in the pilot, iron oxidation and precipitation did not exceed 20% and 11%, respectively (Fernandez-Rojo et al., in press). Iron-oxidizing activity of *A. ferrooxidans* was strongly inhibited when the bacteria were attached to solid surfaces (Wakao et al., 1984). On the contrary, *Ferrovum* biofilms proved to be very effective in iron-oxidizing bioreactors (Hedrich and Johnson, 2012). Among several strains tested by Johnson et al. (2012) the highest iron oxidation rates were obtained with *Ferrovum* spp. In spite of their well-known efficiency and their adaptation to temperature and pH ranges observed in the pilot (Kuang et al., 2013; Johnson et al., 2014; Jones et al., 2015), the iron-oxidizing activity of FeOB (including *Ferrovum*) appeared limited in the present study possibly because of non-optimal operating conditions. The water height above the biofilm (1.5–7 cm), which is a key factor for iron oxidation kinetics, may have prevented a sufficient oxygenation of the water column (Brown et al., 2011; Fernandez-Rojo et al., 2017). Another possible limiting factor is an insufficient active surface of the biofilm in regard to the volume of overlying water to be treated. Probably due to these limitations, the important variations of FeOB distribution inside the pilot did not result in significant iron oxidation rate variation (Figure 1B). Our results strongly suggest that the composition of the bacterial communities was not a limiting factor for iron oxidation in the bioreactor. Further work based on RNA will help to determine which bacterial taxa actively contribute to the treatment.

## Bacterial Arsenite Oxidation in the Pilot

As(III) oxidation by *Thiomonas* spp. can contribute to the formation of stable As(V)-rich precipitates. No clear temporal or spatial tendency was observed for *Thiomonas* genus based on metabarcoding. Further insights into the abundance and the identity of the *Thiomonas* spp. thriving in the pilot were gained by a CARD-FISH approach. In the biogenic precipitates sampled at D48 and D171, the proportion of *Thiomonas* related bacteria averaged 8% of the DAPI-stained bacteria, which is congruent with *in situ* observations (5–8.7%, Hovasse et al., 2016). Despite their low abundance, *Thiomonas*-related bacteria are considered to play a crucial role in the pollution mitigation (Bruneel et al., 2003, 2011; Hovasse et al., 2016). Metaproteomic approaches showed that they sustainably express an arsenite oxidase activity *in situ* in Carnoulès (Bertin et al., 2011; Hovasse et al., 2016). Inside the pilot, the *Thiomonas* belonging to group II (as defined by Bryan et al., 2009) were more abundant than those belonging to group I ( $p < 0.05$ ), whereas the average proportions of the two groups were

similar *in situ* (Hovasse et al., 2016). Both groups I and II contain arsenite-oxidizing *Thiomonas* strains isolated from the Carnoulès AMD (Bryan et al., 2009; Bertin et al., 2011; Hovasse et al., 2016). Group II includes *Thiomonas* sp. CARN2, which expressed its arsenite oxidation activity in the Carnoulès AMD sediments (Bertin et al., 2011). The As(III)-oxidation genetic potential (expressed as the number of *aioA* genes  $\text{ng}^{-1}$  of DNA) increased tenfold in the bioprecipitate during the first 48 days suggesting the establishment of an active As(III)-oxidizing bacterial population during the early stages of the biofilm maturation (Fernandez-Rojo et al., in press). Although the detection of *aioA* genes doesn't give evidence of its expression, we can hypothesize that the *Thiomonas*-related bacteria identified by CARD-FISH were responsible for the arsenic oxidation resulting in the formation of solid phases containing almost 100% of As(V).

## CONCLUSION

The present study gave new insights into the bioremediation, at the field-scale, of As-rich AMD by biological iron and arsenic oxidation. Bacterial communities originating from the AMD water and organized in biofilm inside the pilot successfully removed soluble arsenic. It can be assumed that, during the first phase of the monitoring, the temporal dynamic of the biogenic precipitates communities was mostly due to ecological succession during biofilm installation. Once the biofilm was mature, the physico-chemistry of the overlying water exerted a complex control on the distribution of the biofilm bacterial populations. The co-existence of several FeOB populations characterized by distinct physiological traits (in term of optimal pH, temperature, DO, and Fe(II) affinity...) permitted a good adaptation of the system toward variations in the chemistry of the AMD water to be treated. Ubiquity of the bacteria identified and the presence of bacteria of biotechnological relevance (*Ferrovum*, *Acidithiobacillus*) let expect that the application of this system to other As- and Fe-rich AMD worldwide is practicable.

We showed evidence of the stable presence of distinct populations of *Thiomonas* spp. in the pilot. Appreciable arsenite oxidation occurred in the field pilot. To determine the factors controlling arsenite oxidation activity in this treatment system, gene expression investigations are required.

The development of accurate biological treatment requires the stability of bacterial activity under seasonal variations. Furthermore, the bacterial diversity of the AMD water remained relatively stable during the 6 months monitoring whereas it proved to be more variable over a longer period of time (Volant et al., 2014). For these reasons, a monitoring on a longer period is required to guarantee the long-term stability and robustness of the treatment system.

## AUTHOR CONTRIBUTIONS

CC and MH supervised the research project and the experiments. EL performed the metabarcoding analyses and interpretations. AD performed the CARD-FISH. CJ, FB-B, OB, and VT

contributed to data interpretation. CC, EL, LF-R, MH, OB, and VT collected the samples. MH, EL, and CC wrote the paper. All authors read and approved the final manuscript.

## ACKNOWLEDGMENTS

We thank the IngECOST-DMA project (ANR-13-ECOT-0009), the OSU OREME (SO POLLUMINE Observatory, funded since 2009), the BRGM and ADEME (Ph.D. fellowship of EL, 2016-2019) and the ADEME COMPAs project (GESIPOL

2017/34/003) for the financial support. We thank Jennifer Hellal for helpful discussion about statistical analyses and the Montpellier RIO Imaging microscopy platform for their kind assistance in microscopy.

## SUPPLEMENTARY MATERIAL

The Supplementary Material for this article can be found online at: <https://www.frontiersin.org/articles/10.3389/fmicb.2018.03169/full#supplementary-material>

## REFERENCES

- Ahoranta, S. H., Kokko, M. E., Papirio, S., Özkaya, B., and Puhakka, J. A. (2016). Arsenic removal from acidic solutions with biogenic ferric precipitates. *J. Hazard. Mater.* 306, 124–132. doi: 10.1016/j.jhazmat.2015.12.012
- Amann, R. I., Binder, B. J., Olson, R. J., Chisholm, S. W., Devereux, R., and Stahl, D. A. (1990). Combination of 16S rRNA-targeted oligonucleotide probes with flow cytometry for analyzing mixed microbial populations. *Appl. Environ. Microbiol.* 56, 1919–1925.
- Asta, M. P., Ayora, C., Acero, P., and Cama, J. (2010). Field rates for natural attenuation of arsenic in Tinto Santa Rosa acid mine drainage (SW Spain). *J. Hazard. Mater.* 177, 1102–1111. doi: 10.1016/j.jhazmat.2010.01.034
- Baker, B. J., and Banfield, J. F. (2003). Microbial communities in acid mine drainage. *FEMS Microbiol. Ecol.* 44, 139–152. doi: 10.1016/S0168-6496(03)00028-X
- Baker, B. J., Hugenholtz, P., Dawson, S. C., and Banfield, J. F. (2003). Extremely acidophilic protists from acid mine drainage host rickettsiales-lineage endosymbionts that have intervening sequences in their 16S rRNA genes. *Appl. Environ. Microbiol.* 69, 5512–5518. doi: 10.1128/AEM.69.9.5512-5518.2003
- Barret, M., Briand, M., Bonneau, S., Préveaux, A., Valière, S., Bouchez, O., et al. (2015). Emergence shapes the structure of the seed microbiota. *Appl. Environ. Microbiol.* 81, 1257–1266. doi: 10.1128/AEM.03722-14
- Battaglia, F., Morin, D., Garcia, J.-L., and Ollivier, P. (1994). Isolation and study of two strains of *Leptospirillum*-like bacteria from a natural mixed population cultured on a cobaltiferous pyrite substrate. *Antonie Van Leeuwenhoek* 66, 295–302. doi: 10.1007/BF00882763
- Battaglia-Brunet, F., Dictor, M.-C., Garrido, F., Crouzet, C., Morin, D., Dekeyser, K., et al. (2002). An arsenic(III)-oxidizing bacterial population: selection, characterization, and performance in reactors. *J. Appl. Microbiol.* 93, 656–667. doi: 10.1046/j.1365-2672.2002.01726.x
- Bertin, P. N., Heinrich-Salmeron, A., Pelletier, E., Goulhen-Chollet, F., Arsène-Ploetze, F., Gallien, S., et al. (2011). Metabolic diversity among main microorganisms inside an arsenic-rich ecosystem revealed by meta- and proteogenomics. *ISME J.* 5, 1735–1747. doi: 10.1038/ismej.2011.51
- Brantner, J. S., Haake, Z. J., Burwick, J. E., Menge, C. M., Hotchkiss, S. T., and Senko, J. M. (2014). Depth-dependent geochemical and microbiological gradients in Fe(III) deposits resulting from coal mine-derived acid mine drainage. *Front. Microbiol.* 5:215. doi: 10.3389/fmicb.2014.00215
- Brown, J. F., Jones, D. S., Mills, D. B., Macalady, J. L., and Burgos, W. D. (2011). Application of a depositional facies model to an acid mine drainage site. *Appl. Environ. Microbiol.* 77, 545–554. doi: 10.1128/AEM.01550-10
- Bruneel, O., Duran, R., Casiot, C., Elbaz-Poulichet, F., and Personné, J.-C. (2006). Diversity of microorganisms in Fe-As-Rich acid mine drainage waters of Carnoulès, France. *Appl. Environ. Microbiol.* 72, 551–556. doi: 10.1128/AEM.72.1.551-556.2006
- Bruneel, O., Héry, M., Laroche, E., Dahmani, I., Fernandez-Rojo, L., Casiot, C. (2017). “Microbial transformations of arsenic: from metabolism to bioremediation,” in *Metal-microbe Interactions and Bioremediation: Principle and Applications for Toxic Metals*, eds S. Das and H. R. Dash (CRC Press: Abingdon).
- Bruneel, O., Personné, J.-C., Casiot, C., Leblanc, M., Elbaz-Poulichet, F., Mahler, B. J., et al. (2003). Mediation of arsenic oxidation by *Thiomonas* sp. in acid-mine drainage (Carnoulès, France). *J. Appl. Microbiol.* 95, 492–499. doi: 10.1046/j.1365-2672.2003.02004.x
- Bruneel, O., Volant, A., Gallien, S., Chaumande, B., Casiot, C., Carapito, C., et al. (2011). Characterization of the active bacterial community involved in natural attenuation processes in arsenic-rich creek sediments. *Microb. Ecol.* 61, 793–810. doi: 10.1007/s00248-011-9808-9
- Bryan, C. G., Marchal, M., Battaglia-Brunet, F., Kugler, V., Lemaitre-Guillier, C., Lièvreumont, D., et al. (2009). Carbon and arsenic metabolism in *Thiomonas* strains: differences revealed diverse adaptation processes. *BMC Microbiol.* 9:127. doi: 10.1186/1471-2180-9-127
- Candy, R. M., Blight, K. R., and Ralph, D. E. (2009). Specific iron oxidation and cell growth rates of bacteria in batch culture. *Hydrometallurgy* 98, 148–155. doi: 10.1016/j.hydromet.2009.04.013
- Casiot, C., Morin, G., Juillot, F., Bruneel, O., Personné, J.-C., Leblanc, M., et al. (2003). Bacterial immobilization and oxidation of arsenic in acid mine drainage (Carnoulès creek, France). *Water Res.* 37, 2929–2936. doi: 10.1016/S0043-1354(03)00080-0
- Chen, C.-J., and Jiang, W.-T. (2012). Influence of waterfall aeration and seasonal temperature variation on the iron and arsenic attenuation rates in an acid mine drainage system. *Appl. Geochem.* 27, 1966–1978. doi: 10.1016/j.apgeochem.2012.06.003
- Chen, L., Huang, L., Méndez-García, C., Kuang, J., Hua, Z., Liu, J., et al. (2016). Microbial communities, processes and functions in acid mine drainage ecosystems. *Curr. Opin. Biotechnol.* 38, 150–158. doi: 10.1016/j.copbio.2016.01.013
- Coupland, K., Battaglia-Brunet, F., Hallberg, K. B., Dictor, M.-C., Garrido, F., and Johnson, D. B. (2004). “Oxidation of iron, sulfur and arsenic in mine waters and mine wastes: an important role for novel *Thiomonas* spp,” in *Biohydrometallurgy; A Sustainable Technology in Evolution*, eds M. Tsezos, A. Hatzikioseyan and E. Remoudaki (Zografou: National Technical University of Athens), 639–646.
- Daims, H., Brühl, A., Amann, R., Schleifer, K. H., and Wagner, M. (1999). The domain-specific probe EUB338 is insufficient for the detection of all Bacteria: development and evaluation of a more comprehensive probe set. *Syst. Appl. Microbiol.* 22, 434–444. doi: 10.1016/S0723-2020(99)80053-8
- Dave, S. R., Gupta, K. H., and Tipre, D. R. (2008). Characterization of arsenic resistant and arsenopyrite oxidizing *Acidithiobacillus ferrooxidans* from Hutti gold leachate and effluents. *Bioresour. Technol.* 99, 7514–7520. doi: 10.1016/j.biortech.2008.02.019
- Dopson, M., Halinen, A.-K., Rahunen, N., Ozkaya, B., Sahinkaya, E., Kaksonen, A. H., et al. (2007). Mineral and iron oxidation at low temperatures by pure and mixed cultures of acidophilic microorganisms. *Biotechnol. Bioeng.* 97, 1205–1215. doi: 10.1002/bit.21312
- Duquesne, K., Lebrun, S., Casiot, C., Bruneel, O., Personné, J.-C., Leblanc, M., et al. (2003). Immobilization of arsenite and ferric Iron by *Acidithiobacillus ferrooxidans* and its relevance to acid mine drainage. *Appl. Environ. Microbiol.* 69, 6165–6173. doi: 10.1128/AEM.69.10.6165-6173.2003
- Edgar, R. C., Haas, B. J., Clemente, J. C., Quince, C., and Knight, R. (2011). UCHIME improves sensitivity and speed of chimera detection. *Bioinformatics* 27, 2194–2200. doi: 10.1093/bioinformatics/btr381

- Egal, M., Casiot, C., Morin, G., Elbaz-Poulichet, F., Cordier, M.-A., and Bruneel, O. (2010). An updated insight into the natural attenuation of As concentrations in Reigous Creek (southern France). *Appl. Geochem.* 25, 1949–1957. doi: 10.1016/j.apgeochem.2010.10.012
- Egal, M., Casiot, C., Morin, G., Parmentier, M., Bruneel, O., Lebrun, S., et al. (2009). Kinetic control on the formation of tooleite, schwertmannite and jarosite by *Acidithiobacillus ferrooxidans* strains in an As(III)-rich acid mine water. *Chem. Geol.* 265, 432–441. doi: 10.1016/j.chemgeo.2009.05.008
- Elbaz-Poulichet, F., Bruneel, O., and Casiot, C. (2006). “The Carnoules mine. Generation of As-rich acid mine drainage, natural attenuation processes and solutions for passive in-situ remediation,” in *Proceedings of the Dippolmine (Diffuse Pollution From Mining Activities)*, Montpellier, France.
- Fabisch, M., Freyer, G., Johnson, C. A., Büchel, G., Akob, D. M., Neu, T. R., et al. (2016). Dominance of “*Gallionella capsiferriformans*” and heavy metal association with *Gallionella*-like stalks in metal-rich pH 6 mine water discharge. *Geobiology* 14, 68–90. doi: 10.1111/gbi.12162
- Fernandez-Rojo, L., Casiot, C., Laroche, E., Tardy, V., Bruneel, O., Delpoux, S., et al. (in press). A field-pilot for passive bioremediation of As-rich acid mine drainage. *J. Environ. Manage.* 232, 910–918. doi: 10.1016/j.jenvman.2018.11.116
- Fernandez-Rojo, L., Casiot, C., Tardy, V., Laroche, E., Le Pape, P., Morin, G., et al. (2018). Hydraulic retention time affects bacterial community structure in an As-rich acid mine drainage (AMD) biotreatment process. *Appl. Microbiol. Biotechnol.* 102, 9803–9813. doi: 10.1007/s00253-018-9290-0
- Fernandez-Rojo, L., Héry, M., Le Pape, P., Braungardt, C., Desoeuvre, A., Torres, E., et al. (2017). Biological attenuation of arsenic and iron in a continuous flow bioreactor treating acid mine drainage (AMD). *Water Res.* 123, 594–606. doi: 10.1016/j.watres.2017.06.059
- Fisher, J. C., Wallschläger, D., Planer-Friedrich, B., and Hollibaugh, J. T. (2008). A new role for sulfur in arsenic cycling. *Environ. Sci. Technol.* 42, 81–85. doi: 10.1021/es0713936
- González-Contreras, P., Weijma, J., and Buisman, C. J. N. (2012). Continuous bioscorodite crystallization in CSTRs for arsenic removal and disposal. *Water Res.* 46, 5883–5892. doi: 10.1016/j.watres.2012.07.055
- González-Toril, E., Aguilera, Á., Souza-Egipsy, V., Pamo, E. L., España, J. S., and Amils, R. (2011). Geomicrobiology of la zarza-perrunal acid mine effluent (Iberian Pyritic Belt, Spain). *Appl. Environ. Microbiol.* 77, 2685–2694. doi: 10.1128/AEM.02459-10
- Grettenberger, C. L., Pearce, A. R., Bibby, K. J., Jones, D. S., Burgos, W. D., and Macalady, J. L. (2017). Efficient low-pH Iron removal by a microbial Iron oxide mound ecosystem at scalp level run. *Appl. Environ. Microbiol.* 83:e00015-17. doi: 10.1128/AEM.00015-17
- Hallberg, K. B., Coupland, K., Kimura, S., and Johnson, D. B. (2006). Macroscopic streamer growths in acidic, metal-rich mine waters in north Wales consist of novel and remarkably simple bacterial communities. *Appl. Environ. Microbiol.* 72, 2022–2030. doi: 10.1128/AEM.72.3.2022-2030.2006
- Hanert, H. H. (2006). “The genus *Gallionella*,” in *The Prokaryotes*, eds E. Rosenberg, E. F. DeLong, E. Stackebrandt, S. Lory, and F. Thompson (New York, NY: Springer), 990–995. doi: 10.1007/0-387-30747-8\_46
- Hedrich, S., and Johnson, D. B. (2012). A modular continuous flow reactor system for the selective bio-oxidation of iron and precipitation of schwertmannite from mine-impacted waters. *Bioresour. Technol.* 106, 44–49. doi: 10.1016/j.biortech.2011.11.130
- Hedrich, S., and Johnson, D. B. (2014). Remediation and selective recovery of metals from acidic mine waters using novel modular bioreactors. *Environ. Sci. Technol.* 48, 12206–12212. doi: 10.1021/es5030367
- Hedrich, S., Lünsdorf, H., Kleeberg, R., Heide, G., Seifert, J., and Schlömann, M. (2011). Schwertmannite formation adjacent to bacterial cells in a mine water treatment plant and in pure cultures of *Ferrovum myxofaciens*. *Environ. Sci. Technol.* 45, 7685–7692. doi: 10.1021/es201564g
- Heinzel, E., Hedrich, S., Janneck, E., Glombitza, F., Seifert, J., and Schlömann, M. (2009a). Bacterial diversity in a mine water treatment plant. *Appl. Environ. Microbiol.* 75, 858–861. doi: 10.1128/AEM.01045
- Heinzel, E., Janneck, E., Glombitza, F., Schlömann, M., and Seifert, J. (2009b). Population dynamics of Iron-oxidizing communities in pilot plants for the treatment of acidic mine waters. *Environ. Sci. Technol.* 43, 6138–6144. doi: 10.1021/es900067d
- Hengen, T. J., Squillace, M. K., O’Sullivan, A. D., and Stone, J. J. (2014). Life cycle assessment analysis of active and passive acid mine drainage treatment technologies. *Resour. Conserv. Recycl.* 86, 160–167. doi: 10.1016/j.resconrec.2014.01.003
- Hovasse, A., Bruneel, O., Casiot, C., Desoeuvre, A., Farasin, J., Hery, M., et al. (2016). Spatio-temporal detection of the thiomonas population and the thiomonas arsenite oxidase involved in natural arsenite attenuation processes in the Carnoules acid mine drainage. *Front. Cell. Dev. Biol.* 4:3. doi: 10.3389/fcell.2016.00003
- Hug, S. J., and Leupin, O. (2003). Iron-catalyzed oxidation of Arsenic(III) by oxygen and by hydrogen peroxide: pH-dependent formation of oxidants in the fenton reaction. *Environ. Sci. Technol.* 37, 2734–2742. doi: 10.1021/es026208x
- Jackson, C. R., Churchill, P. F., and Roden, E. E. (2001). Successional changes in bacterial assemblage structure during epilithic biofilm development. *Ecology* 82, 555–566. doi: 10.1890/0012-96582001082[0555:SCIBAS]2.0.CO;2
- Johnson, D. B., Hallberg, K. B., and Hedrich, S. (2014). Uncovering a microbial enigma: isolation and characterization of the streamer-generating, iron-oxidizing, acidophilic bacterium “*Ferrovum myxofaciens*”. *Appl. Environ. Microbiol.* 80, 672–680. doi: 10.1128/AEM.03230-13
- Johnson, D. B., Kanao, T., and Hedrich, S. (2012). Redox transformations of Iron at extremely low pH: fundamental and applied aspects. *Front. Microbiol.* 3:96. doi: 10.3389/fmicb.2012.00096
- Jones, D. S., Kohl, C., Grettenberger, C., Larson, L. N., Burgos, W. D., and Macalady, J. L. (2015). Geochemical niches of Iron-oxidizing acidophiles in acidic coal mine drainage. *Appl. Environ. Microbiol.* 81, 1242–1250. doi: 10.1128/AEM.02919-14
- Jones, D. S., Lapakko, K. A., Wenz, Z. J., Olson, M. C., Roepke, E. W., Sadowsky, M. J., et al. (2017). Novel microbial assemblages dominate weathered sulfide-bearing rock from copper-nickel deposits in the Duluth complex, Minnesota, USA. *Appl. Environ. Microbiol.* 83:e00909-17. doi: 10.1128/AEM.00909-17
- Jwair, R., Tischler, J. S., Janneck, E., and Schlömann, M. (2016). “Acid mine water treatment using novel acidophilic iron-oxidizing bacteria of the genus “*Ferrovum*”: effect of oxygen and carbon dioxide on survival,” in *Proceedings of the IMWA 2016*, eds C. Drebenstedt and M. Paul (Freiberg: IMWA), 1060–1063.
- Kuang, J.-L., Huang, L.-N., Chen, L.-X., Hua, Z.-S., Li, S.-J., Hu, M., et al. (2013). Contemporary environmental variation determines microbial diversity patterns in acid mine drainage. *ISME J.* 7, 1038–1050. doi: 10.1038/ismej.2012.139
- Kupka, D., Rzhepishevskaya, O. I., Dopson, M., Lindström, E. B., Karnachuk, O. V., and Tuovinen, O. H. (2007). Bacterial oxidation of ferrous iron at low temperatures. *Biotechnol. Bioeng.* 97, 1470–1478. doi: 10.1002/bit.21371
- Legendre, P., and Gallagher, E. D. (2001). Ecologically meaningful transformations for ordination of species data. *Oecologia* 129, 271–280. doi: 10.1007/s004420100716
- Lyautey, E., Jackson, C. R., Cayrou, J., Rols, J.-L., and Garabétian, F. (2005). Bacterial community succession in natural river biofilm assemblages. *Microb. Ecol.* 50, 589–601. doi: 10.1007/s00248-005-5032-9
- Macías, F., Caraballo, M. A., Nieto, J. M., Rötting, T. S., and Ayora, C. (2012). Natural pretreatment and passive remediation of highly polluted acid mine drainage. *J. Environ. Manage.* 104, 93–100. doi: 10.1016/j.jenvman.2012.03.027
- Magoë, T., and Salzberg, S. L. (2011). FLASH: fast length adjustment of short reads to improve genome assemblies. *Bioinformatics* 27, 2957–2963. doi: 10.1093/bioinformatics/btr507
- Méndez-García, C., Peláez, A. I., Mesa, V., Sánchez, J., Golyshina, O. V., and Ferrer, M. (2015). Microbial diversity and metabolic networks in acid mine drainage habitats. *Front. Microbiol.* 6:475. doi: 10.3389/fmicb.2015.00475
- Meruane, G., Salhe, C., Wiertz, J., and Vargas, T. (2002). Novel electrochemical-enzymatic model which quantifies the effect of the solution Eh on the kinetics of ferrous iron oxidation with *Acidithiobacillus ferrooxidans*. *Biotechnol. Bioeng.* 80, 280–288. doi: 10.1002/bit.10371
- Mueller, R. S., Dill, B. D., Pan, C., Belnap, C. P., Thomas, B. C., VerBerkmoes, N. C., et al. (2011). Proteome changes in the initial bacterial colonist during ecological succession in an acid mine drainage biofilm community. *Environ. Microbiol.* 13, 2279–2292. doi: 10.1111/j.1462-2920.2011.02486.x
- Norris, P. R. (1990). “Acidophilic bacteria and their activity in mineral sulfide oxidation,” in *Microbial Mineral Recovery*, eds H. L. Ehrlich and C. Brierley (New York, NY: McGraw Hill), 3–27.
- Paikaray, S. (2015). Arsenic geochemistry of acid mine drainage. *Mine Water Environ.* 34, 181–196. doi: 10.1007/s10230-014-0286-4

- Rawlings, D. E., Tributsch, H., and Hansford, G. S. (1999). Reasons why '*Leptospirillum*'-like species rather than *Thiobacillus ferrooxidans* are the dominant iron-oxidizing bacteria in many commercial processes for the biooxidation of pyrite and related ores. *Microbiology (Reading, Engl.)* 145(Pt 1), 5–13. doi: 10.1099/13500872-145-1-5
- Rowe, O. F., and Johnson, D. B. (2008). Comparison of ferric iron generation by different species of acidophilic bacteria immobilized in packed-bed reactors. *Syst. Appl. Microbiol.* 31, 68–77. doi: 10.1016/j.syapm.2007.09.001
- Santegoeds, C. M., Ferdelman, T. G., Muyzer, G., and Beerde, D. (1998). Structural and functional dynamics of sulfate-reducing populations in bacterial biofilms. *Appl. Environ. Microbiol.* 64, 3731–3739.
- Schloss, P. D., Westcott, S. L., Ryabin, T., Hall, J. R., Hartmann, M., Hollister, E. B., et al. (2009). Introducing mothur: open-source, platform-independent, community-supported software for describing and comparing microbial communities. *Appl. Environ. Microbiol.* 75, 7537–7541. doi: 10.1128/AEM.01541-09
- Sheng, Y., Bibby, K., Grettenberger, C., Kaley, B., Macalady, J. L., Wang, G., et al. (2016). Geochemical and temporal influences on the enrichment of acidophilic iron-oxidizing bacterial communities. *Appl. Environ. Microbiol.* 82, 3611–3621. doi: 10.1128/AEM.00917-16
- Sun, W., Xiao, E., Kalin, M., Krumins, V., Dong, Y., Ning, Z., et al. (2016). Remediation of antimony-rich mine waters: assessment of antimony removal and shifts in the microbial community of an onsite field-scale bioreactor. *Environ. Pollut.* 215, 213–222. doi: 10.1016/j.envpol.2016.05.008
- Tardy, V., Casiot, C., Fernandez-Rojo, L., Resongles, E., Desoeuvre, A., Jouliau, C., et al. (2018). Temperature and nutrients as drivers of microbially mediated arsenic oxidation and removal from acid mine drainage. *Appl. Microbiol. Biotechnol.* 102, 2413–2424. doi: 10.1007/s00253-017-8716-4
- Tischler, J. S., Wiacek, C., Janneck, E., and Schlömann, M. (2014). Bench-scale study of the effect of phosphate on an aerobic iron oxidation plant for mine water treatment. *Water Res.* 48, 345–353. doi: 10.1016/j
- Volant, A., Bruneel, O., Desoeuvre, A., Héry, M., Casiot, C., Bru, N., et al. (2014). Diversity and spatiotemporal dynamics of bacterial communities: physicochemical and other drivers along an acid mine drainage. *FEMS Microbiol. Ecol.* 90, 247–263. doi: 10.1111/1574-6941.12394
- Wakao, N., Mishina, M., Sakurai, Y., and Shiota, H. (1984). Bacterial pyrite oxidation III. Adsorption of *Thiobacillus ferrooxidans* cells on solid surfaces and its effect on iron release from pyrite. *J. Gen. Appl. Microbiol.* 30, 63–77. doi: 10.2323/jgam.30.63
- Wallner, G., Amann, R., and Beisker, W. (1993). Optimizing fluorescent in situ hybridization with rRNA-targeted oligonucleotide probes for flow cytometric identification of microorganisms. *Cytometry* 14, 136–143. doi: 10.1002/cyto.990140205
- Wang, Q., Garrity, G. M., Tiedje, J. M., and Cole, J. R. (2007). Naïve bayesian classifier for rapid assignment of rRNA sequences into the new bacterial taxonomy. *Appl. Environ. Microbiol.* 73, 5261–5267. doi: 10.1128/AEM.0062-07
- Wang, Y., and Qian, P.-Y. (2009). Conservative fragments in bacterial 16S rRNA genes and primer design for 16S ribosomal DNA amplicons in metagenomic studies. *PLoS One* 4:e7401. doi: 10.1371/journal.pone.0007401
- Watanabe, T., Kojima, H., and Fukui, M. (2015). *Sulfuriferula multivorans* gen. nov., sp. nov., isolated from a freshwater lake, reclassification of "*Thiobacillus plumbophilus*" as *Sulfuriferula plumbophilus* sp. nov., and description of *Sulfuricellaceae* fam. nov. and *Sulfuricellales* ord. nov. *Int. J. Syst. Evol. Microbiol.* 65, 1504–1508. doi: 10.1099/ijs.0.000129
- Weiss, J. V., Rentz, J. A., Plaia, T., Neubauer, S. C., Merrill-Floyd, M., Lilburn, T., et al. (2007). Characterization of neutrophilic Fe(II)-oxidizing bacteria isolated from the rhizosphere of wetland plants and description of *Ferritrophicum radicolica* gen. nov. sp. nov., and *Sideroxydans paludicola* sp. nov. *Geomicrobiol. J.* 24, 559–570. doi: 10.1080/01490450701670152
- Whitehead, P. G., Hall, G., Neal, C., and Prior, H. (2005). Chemical behaviour of the Wheal Jane bioremediation system. *Sci. Total Environ.* 338, 41–51. doi: 10.1016/j.scitotenv.2004.09.004
- Wilmes, P., Remis, J. P., Hwang, M., Auer, M., Thelen, M. P., and Banfield, J. F. (2009). Natural acidophilic biofilm communities reflect distinct organismal and functional organization. *ISME J.* 3, 266–270. doi: 10.1038/ismej.2008.90
- Woodcock, S., and Sloan, W. T. (2017). Biofilm community succession: a neutral perspective. *Microbiology (Reading, England)* doi: 10.1099/mic.0.000472 [Epub ahead of print].
- Ziegler, S., Dolch, K., Geiger, K., Krause, S., Asskamp, M., Eusterhues, K., et al. (2013). Oxygen-dependent niche formation of a pyrite-dependent acidophilic consortium built by archaea and bacteria. *ISME J.* 7, 1725–1737. doi: 10.1038/ismej.2013.64

**Conflict of Interest Statement:** The authors declare that the research was conducted in the absence of any commercial or financial relationships that could be construed as a potential conflict of interest.

Copyright © 2018 Laroche, Casiot, Fernandez-Rojo, Desoeuvre, Tardy, Bruneel, Battaglia-Brunet, Jouliau and Héry. This is an open-access article distributed under the terms of the Creative Commons Attribution License (CC BY). The use, distribution or reproduction in other forums is permitted, provided the original author(s) and the copyright owner(s) are credited and that the original publication in this journal is cited, in accordance with accepted academic practice. No use, distribution or reproduction is permitted which does not comply with these terms.



# Volatolomics in Bacterial Ecotoxicology, A Novel Method for Detecting Signatures of Pesticide Exposure?

Kevin Hidalgo<sup>1,2\*</sup>, Jeremy Ratel<sup>1</sup>, Frederic Mercier<sup>1</sup>, Benedicte Gauriat<sup>2</sup>, Philippe Bouchard<sup>3</sup> and Erwan Engel<sup>1</sup>

<sup>1</sup> INRA UR370 QuaPA, MASS Group, Saint-Genès-Champanelle, France, <sup>2</sup> Thermo Fisher Scientific ZA de Courtaboeuf, Villebon-sur-Yvette, France, <sup>3</sup> CNRS, Laboratoire Microorganismes: Genome et Environnement, Université Clermont Auvergne, Clermont-Ferrand, France

## OPEN ACCESS

### Edited by:

Fabrice Martin-Laurent,  
Institut National de la Recherche  
Agronomique (INRA), France

### Reviewed by:

Thomas Maskow,  
Helmholtz-Gemeinschaft Deutscher  
Forschungszentren (HZ), Germany  
Marie-Virginie Salvia,  
Université de Perpignan Via Domitia,  
France

### \*Correspondence:

Kevin Hidalgo  
kevin.hidalgo@gmx.com

### Specialty section:

This article was submitted to  
Microbiotechnology, Ecotoxicology  
and Bioremediation,  
a section of the journal  
Frontiers in Microbiology

Received: 17 July 2018

Accepted: 03 December 2018

Published: 08 January 2019

### Citation:

Hidalgo K, Ratel J, Mercier F,  
Gauriat B, Bouchard P and Engel E  
(2019) Volatolomics in Bacterial  
Ecotoxicology, A Novel Method  
for Detecting Signatures of Pesticide  
Exposure? *Front. Microbiol.* 9:3113.  
doi: 10.3389/fmicb.2018.03113

Volatile organic compounds (VOC) produced by microorganisms in response to chemical stressor showed recently increasing attention, because of possible environmental applications. In this work, we aimed to bring the first proof of concept that volatolomic (i.e., VOCs analysis) can be used to determine candidate VOC markers of two soil bacteria strains (*Pseudomonas fluorescens* SG-1 and *Bacillus megaterium* Mes11) exposure to pesticides. VOC determination was based on solid-phase microextraction (SPME) coupled with gas chromatography-mass spectrometry (GC-MS). Accordingly, we highlighted a set of bacterial VOCs modulated in each strains according to the nature of the pesticide used. Three out these VOCs were specifically modulated in *P. fluorescens* SG-1 when exposed with two pyrethroid pesticides (deltamethrine and cypermethrine): 2-hexanone; 1,3-ditertbutylbenzene and malonic acid, hexyl 3-methylbutyl ester. Our results thus suggest the possible existence of generic VOC markers of pyrethroids in this strain. Of particular interest, two out of these three VOCs, the 1,3-ditertbutylbenzene and the malonic acid, hexyl 3-methylbutyl ester were found also in *B. megaterium* Mes11 when exposed with cypermethrine. This result highlighted the possible existence of interspecific VOC markers of pyrethroid in these two bacteria. Altogether, our work underlined the relevance of volatolomic to detect signatures of pesticides exposure in microorganisms and more generally to microbial ecotoxicology. Based on these first results, considerations of volatolomics for the chemical risk assessment in environment such as soils can be indirectly explored in longer terms.

**Keywords:** VOC, marker of exposure, pesticides, microbial ecotoxicology, *Pseudomonas fluorescens*, *Bacillus megaterium*

## INTRODUCTION

In response to climatic or chemical stressors, organisms can trigger a set of metabolic adjustments to challenge cell damages and homeostasis disturbances (Bijlsma and Loeschcke, 2005; Hidalgo et al., 2016, 2018), resulting notably in the production of metabolic end-products like VOCs. VOCs are low molecular weight compounds with relatively high vapor pressure or volatility

**Abbreviations:** PCA, principal component analysis; VOCs, volatile organic compounds.

(Hakim et al., 2012). There is evidence that VOCs can be emitted from cells and their microenvironments in response to stressor perception, and can be used as indirect markers of contamination. Since the past decade, research in cancerology highlighted the interest of VOCs as specific markers to detect lung cancers and their distinct stages of maturity in humans (Hakim et al., 2012; Broza et al., 2015 for reviews). Briefly, several cytochrome p450 mixed oxidases are activated by exposure to environmental toxins. Such an enzyme system activation, linked with oxidative stress (e.g., reactive oxygen species production, lipid peroxidation, etc.), specifically modulates the catabolism of endogenous VOC products and generate an altered pattern of human breath by producing new VOCs or changing the ratio between VOCs that are normally produced in healthy bodies (Preti et al., 1988; Hakim et al., 2012). Volatolomics – the study of VOCs emitted by cells and their microenvironments – was also adapted in a context of food safety to diagnose xenobiotic contaminations in livestock (Berge et al., 2011; Bouhleb et al., 2017; Ratel et al., 2017). These works showed the relevance to study the liver volatolome of livestock species, like poultry, to reveal exposure to different micropollutants and pesticides. According to Bouhleb et al. (2017) and Ratel et al. (2017), VOCs determined as markers of contamination belong to different chemical families, including alkanes, alkenes, alcohols, and carboxylic acids. It is noteworthy that the type and the amount of VOCs differed according to the nature of the stressor analyzed. Finally, VOCs produced by microorganisms in response to chemical exposure also showed a recent increasing attention, because of possible medicinal, and environmental applications (Korpi et al., 2009; Scott-Thomas et al., 2013; Defois et al., 2017, 2018). For instance, Defois et al. (2017) underlined the relevance of using volatolomics to diagnose the exposure to benzo[a]pyrene and its associated metabolic deviations in the human gut microbiota. Accordingly, many VOCs are pointed out as markers of the gut microbiota exposure to benzo[a]pyrene, enlarging the potential applications of volatolomics in microbial ecotoxicology studies. To date, the use of volatolomic in microbial and/or bacterial ecotoxicology was restricted to community levels (Defois et al., 2017, 2018), but it is also of importance to investigate how chemical stressors in single populations influence VOCs emissions. Such an approach will be complementary and pioneer in the field of omic and microbial ecotoxicology. In time, dealing with bacteria, it is recommended to challenge different levels of biological organizations. Indeed, metabolic adaptation in response to stressors can be quickly selected allowing bacteria to adapt themselves to habitat fluctuations. In addition, responses of single populations under controlled conditions copy individual responses. Overall, this will help to understand mechanisms involved by bacteria to challenge and survive a chemical exposure by checking the VOCs that represents markers of metabolic deviation.

Volatolomics may thus offer a promising prospect to diagnose specific metabolic signatures and associate response of bacteria to chemical stressors like pesticides. Pesticides are of great concern as environmental pollutants resulting in human and animal health implications and many environmental side effects (Aktar et al., 2009; Parrón et al., 2014; Tsaboula et al., 2016).

Although conventional targeted analytical methods used to monitor the pesticide levels are efficient, the implementation of less expensive and more straightforward analytical approaches could allow the existing surveillance system to be strengthened (Meurillon et al., 2017). In addition, available tools used to evaluate the ecotoxicological impact of pesticides in fields and organisms are very few, and there is a strong need of new approaches to enable a better understanding and prediction of effects as well as a deeper knowledge of the action modes of pesticides.

Soils are mainly contaminating by pesticide due to agricultural practices. Therefore, in the present work, we designed an experimental volatolomic test devoted to identify indirect VOC markers of exposure of two soil bacterial strains to three different pesticides (deltamethrine, cypermethrine and sulcotrione). We choose to work with *Pseudomonas fluorescens* strain SG-1 and *Bacillus megaterium* strain Mes11, two common soil strains characterized based on works on pesticide degradations and selected from enrichment culture conditions (Batisson et al., 2009; Bardot et al., 2015; Carles et al., 2016). Based on previous works dealing with the exposure of bacteria communities and other organisms to chemical contaminants (Berge et al., 2011; Bouhleb et al., 2017; Defois et al., 2017), we assumed that exposure to pesticides should influence the metabolic pathways of our two bacteria strains, resulting in specific changes in their volatolome. We also hypothesized that changes in the bacteria volatolome should depends on the nature of the pesticide used and should differed between the two strains. To test these assumptions, a volatolomic pipeline was optimized from previous works devoted on livestock and microbial communities and adapted to single bacterial population study. Accordingly, the volatolome variations and/or deviations of the two bacteria strains exposed or not to two common landscape pyrethroid insecticides, the deltamethrine and the cypermethrine, and a triketone herbicide, the sulcotrione, were investigated and compared. In order to highlight candidate VOC markers associate with metabolic deviations of bacteria exposure to pesticides and not with altered phenotype experiments were conducted with pesticides at an EC10 (effective concentration that decrease the generation time of 10 %) concentration.

## MATERIALS AND METHODS

### Bacterial Strains and Culture Conditions

Two edaphic bacterial strains isolated from soils from enrichment culture, *P. fluorescens* SG-1 (Carles et al., 2017) and *B. megaterium* Mes11 were used in this study. Both strains were maintained in laboratory in petri dishes on a Tryptic Soy Broth medium formulation (Sigma Aldrich, France). For experiments, strains were grown in 30 mL of medium growth solution (5 g/l peptone, 2.5 g/l yeast extract, 1 g/l D-Glucose) maintained in dark condition at 28°C under orbital agitation (200 rpm). To ensure enough bacterial biomass for further experiments, medium inoculation consist about  $2 \times 10^4$  cells/ml and  $2.5 \times 10^6$  cells/ml for *B. megaterium* Mes11 and *P. fluorescens* SG-1, respectively. *Pseudomonas fluorescens* SG-1 was pre-cultivated

under these conditions overnight 12 h, whereas *B. megaterium* Mes11 was pre-cultivated for 48 h.

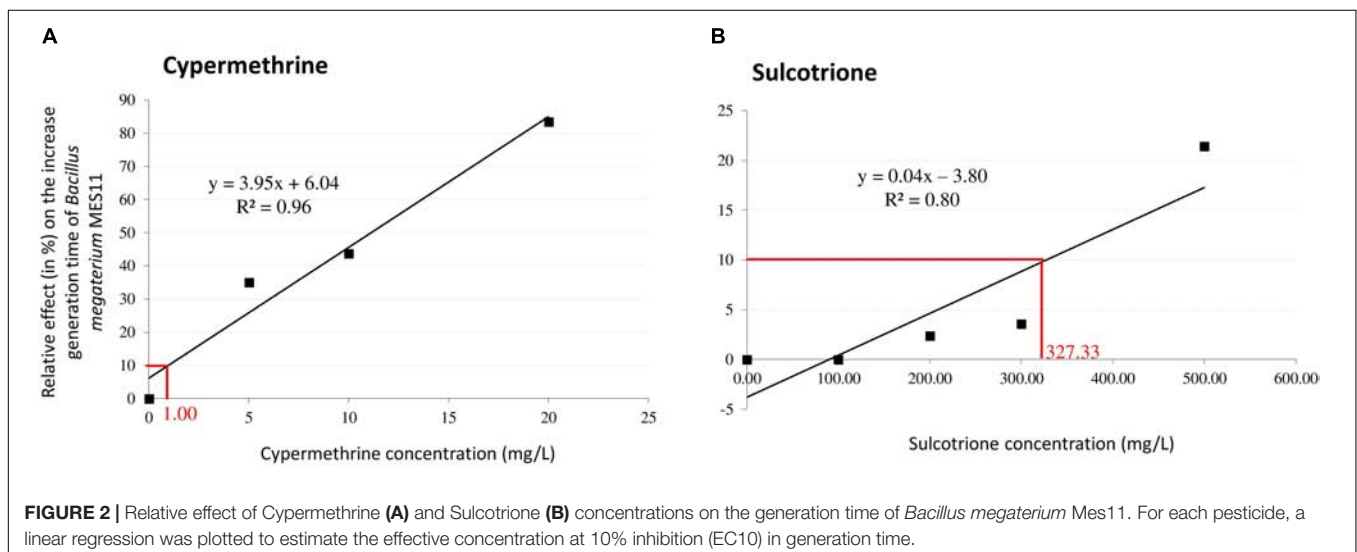
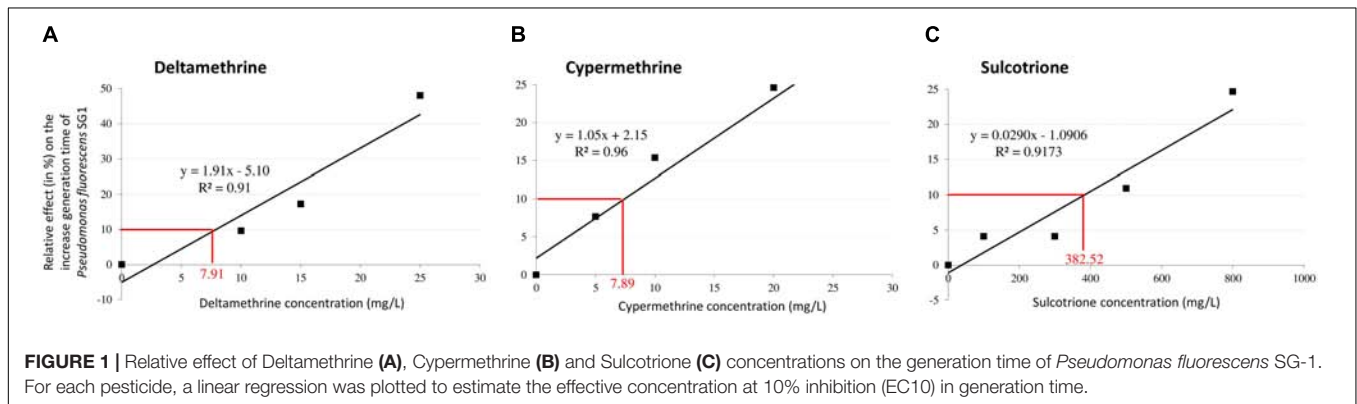
## Pesticide Exposure

Deltamethrine, cypermethrine and sulcotrione were purchased from Sigma (Fluka, PESTANAL<sup>®</sup>, analytical standard). DMSO was used at a final concentration of 0.5% to enhance solubility of the three pesticides. The effective concentration that decrease the generation time of 10% (EC10) was determined for each pesticide in both strains. Indeed, to guarantee a situation where deviation of the metabolome is linked to the presence of toxicant with phenotypic trait (Poynton and Vulpe, 2009), the experiments of pesticide exposure of bacteria were performed with a light toxic pressure (CE10 level). Using previous pre-cultured conditions for the two strains, we monitored every 30 min the bacterial biomass (OD 600 nm) among different pesticide concentrations ranging from 0 to 25 mg/L for deltamethrine and cypermethrine, and from 0 to 800 mg/L for sulcotrione. Accordingly, in *P. fluorescens* SG-1 EC10 were 7.91, 7.89, and 382.52 mg/L for deltamethrine, cypermethrine and sulcotrione, respectively (Figure 1). In *B. megaterium* Mes11, no reproducible EC10 could be determined for deltamethrine exposure, therefore we did not analyze this pesticide in this strain. However, the *B. megaterium*

Mes11 EC10 were 1.00 and 327.33 mg/L for cypermethrine and sulcotrione, respectively (Figure 2).

For volatolomics study, 7–9 biological replicas for each pesticide and strain were prepared as already described, representing the “treated” samples. A 150  $\mu$ L solution of pesticides solubilise in 0.5% of DMSO were added into a 30 mL Falcon containing 3 or 6 mL of *P. fluorescens* or *B. megaterium*, respectively, in order to reach the EC10 concentration (determined in Figures 1, 2). Falcons were completed with growth medium until 30mL. Control samples contained only DMSO at a 0.5% final concentration. Experiments were conducted in Falcon tubes in 30 ml cultivation volume in dark condition at 28°C under orbital agitation (200 rpm) during 90 min. Bacterial biomass was monitored during experiments in order to check EC10. According to (Defois et al., 2017, 2018), we compared the relative abundance of VOCs from control samples (bacteria+DMSO) with treated ones (bacteria+DMSO+pesticide).

After 90 min of exposure, all samples were centrifuged during 7 min at 6000 rpm. Supernatant was removed and the bacteria were washed with a 0.8% NaCl solution and centrifuged again 7 min at 6000 rpm. This washing step was repeated twice. Bacteria were transferred into a cryo-tube directly plunged into liquid



nitrogen to stop any metabolic activities. Samples were stocked at  $-80^{\circ}\text{C}$  until further processing. This freezing process is crucial to stabilize VOCs for further analysis. Biological repetitions were settled from 7 to 9.

## Bacterial Volatolome Analyses

Volatile organic compounds (VOCs) of both *P. fluorescens* SG-1 and *B. megaterium* Mes11 were analyzed using a solid-phase microextraction (SPME) method coupled with gas chromatography-mass spectrometry (GC-MS) adapted from Bouhleb et al. (2017). Samples were progressively defrosted from  $-80^{\circ}\text{C}$  to  $4^{\circ}\text{C}$  and maintained at  $4^{\circ}\text{C}$  until the end of experiments. For each sample, 250  $\mu\text{L}$  of bacteria were transferred into a 10 mL vial supplemented with 700  $\mu\text{L}$  of saturated saline solution at 360 g/L to facilitate VOC trapping as described in Bouhleb et al. (2017). Vial headspaces were set up under a nitrogen gas flow to avoid any oxygenation reactions. Vials were sealed and stored at  $4^{\circ}\text{C}$  during 24 h. Using an automated sampler (MPS2, Gerstel), samples were preheated in an agitator (500 rpm) for 10 min at  $40^{\circ}\text{C}$ , then the VOCs were trapped by SPME using a 75  $\mu\text{m}$  carboxen-polydimethylsiloxane fiber (CAR/PDMS, 23gauge needle, Supelco) during 30 min at  $40^{\circ}\text{C}$ . The choice of the fiber and the analytical conditions were fixed by preliminary tests to limit thermal-induced VOC generation and to recover microbial VOCs with reduced variability. After a thermal desorption of the fiber at  $280^{\circ}\text{C}$  for 2 min in splitless mode in the GC inlet, the volatolome analysis was performed by GC-full scan MS (Shimadzu, QP2010+). VOCs were separated on a Rxi<sup>®</sup>-624Sil MS fused silica column (60 m  $\times$  0.25 mm  $\times$  1.4  $\mu\text{m}$ , Restek) according to previously established settings (Bouhleb et al., 2017; Defois et al., 2017). By using the same extraction and separation parameters, pools of samples of each group of bacteria tested were analyzed by SPME-GC hyphenated with high resolution mass spectrometry (Q Exactive GC Orbitrap, Thermo Scientific). The analyses were performed both with chemical ionization (CI) and electron ionization (EI) in order to comfort VOC detection and enhance identification.

Peak areas of VOCs were determined using a mass fragment selected for its specificity and free from co-elution with an automatic algorithm developed in our laboratory under Matlab R2017 by Bouhleb et al. (2017). VOCs selected as discriminant for each pesticide exposure were tentatively identified according to a comparison between their mass spectra and the NIST 14 mass spectral library. All VOC identifications were validated through the SPME-GC-HRMS signals obtained in IC and IE modes.

Finally, the three pesticide solutions (deltamethrine, cypermethrine, sulcotrione) used to expose the bacteria were also analyzed at EC10 concentration by similar protocol as described for samples in order to verify if candidate VOCs markers of pesticide exposure had an exogenous origin.

## Statistical Analyses

Datasets were processed using the R 3.1.1 statistical software (R Development Core Team, 2008). First MANOVA analysis were assessed to test the significance of pesticide exposure of VOC patterns of both strains. Then, Student *t*-test adjusted

by Bonferroni corrections were used to assess the significant influence of each pesticide exposure on the volatolome of both bacteria strains. For each strain and each pesticide, a principal component analysis (PCA) was performed based on discriminant VOCs selected by the ANOVAs to visualize the data structuration (Bouhleb et al., 2018).

## RESULTS

### Exposure to Pesticides Influences the Volatolome of *Pseudomonas fluorescens* SG-1

The analytical pipeline identified a total of 134 VOCs in *P. fluorescens* SG-1. Results showed a significant differences of VOC patterns of strain exposed to pesticides compare to control ones (MANOVA,  $ddl = 1$ ,  $F_{\text{Delta}} = 7.2$ ;  $F_{\text{Cyper}} = 4.8$ ;  $F_{\text{Sulcor}} = 8.4$ ,  $P$ -value  $< 0.05$ ). Accordingly, eight, six and three of them were over- or under-expressed following exposure to deltamethrine, cypermethrine and sulcotrione, respectively, meaning that pesticides are associated with a volatolome deviation in strains.

Based on these discriminant VOCs, PCAs were performed for each pesticide to visualize the structure of data and which compounds were over- and/or down-expressed in treated specimens (Figure 3). The first PCAs axes (PC1), which explained the main dataset inertia distribution (51 to 69%), showed a very clear separation of “treated” samples with “control” ones. By contrast, PC2 (15.7–27.9% of the total dataset inertia) were built on the natural biological variation of *P. fluorescens* SG-1. Potential markers of *P. fluorescens* SG-1 exposure to pesticide were thus found among the most contributing VOCs to PC1.

When exposed to deltamethrine, PC1 separation was mainly due to the increase expression of carbonyl sulfide, two branched-alkanes (2,3,3-trimethylpentane and 2,3-dimethylhexane), malonic acid, hexyl 3-methylbutyl ester, and one aromatic compound (1,3-ditertbutylbenzene), and to the decrease expression of ketone (2-hexanone) and two others unidentified VOCs despite the high-resolution mass spectrum assay (Table 1).

By comparison, when exposed to cypermethrine, bacteria exhibited a significant increase expression of three ketones (2-butanone, 2-pentanone, 2-hexanone), one alcohol (2-methyl-2-butanol), one acid (malonic acid), one ester (hexyl 3-methylbutyl ester) and one aromatic compound (1,3-ditertbutylbenzene), whereas no VOC reduction was observed (Table 1). When exposed to sulcotrione, bacteria exhibited a significant increase of one branched-alkane (2,3,3-trimethylpentane) and one aromatic compound (toluene), an exogenous benzenic compound being part of the sulcotrione volatolome, and decrease expression of one unidentified VOC (Table 1).

### Exposure to Pesticides Influences the Volatolome of *Bacillus megaterium* Mes11

As shown in Figure 4 *B. megaterium* Mes11 only showed a significant alteration of its volatolome when exposed to

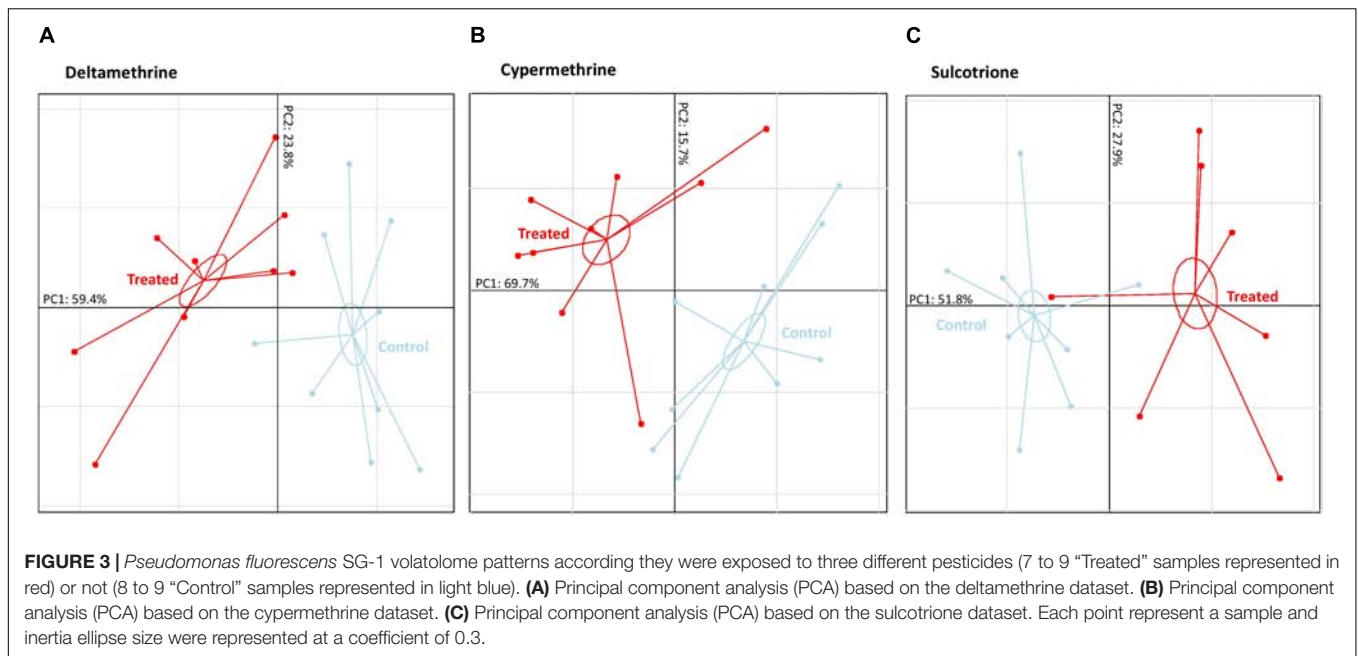


**TABLE 1** | Significant volatile metabolites over- or down-expressed in the volatolome of *Pseudomonas fluorescens* SG-1 strain when exposed to deltamethrine, cypermethrine, or sulcotrione pesticides compared to control.

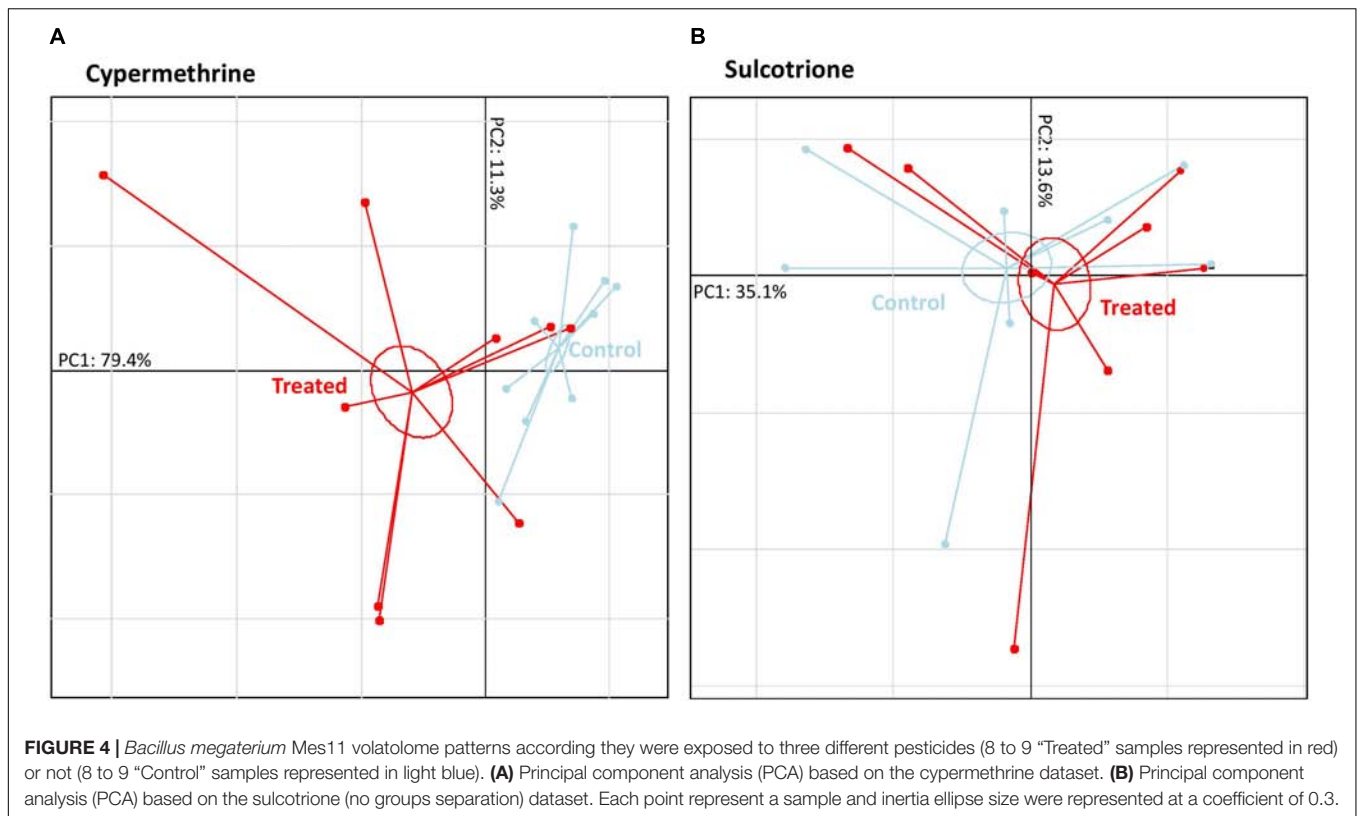
Pesticide	Volatile metabolite <sup>1</sup>	m/z	RT <sup>2</sup>	Mean peak abundance $\pm$ ER ( $\times 10^3$ )		Statistical <i>P</i> -value of student <i>t</i> -tests <sup>3</sup>
				Treated	Control	
<b>DELTAMETHRINE</b>	<b>Over-expressed in “treated” bacteria</b>					
	Carbonyl sulfide	60	4.6	50.8 $\pm$ 3.5	38.5 $\pm$ 1.9	<0.01
	2,3,3-Trimethylpentane	43	22.8	3056.0 $\pm$ 66.4	111.1 $\pm$ 30.6	<0.05
	2,3-Dimethylhexane	70	23.3	140.8 $\pm$ 27.9	53.9 $\pm$ 10.8	<0.05
	Malonic acid, hexyl 3-methylbutyl ester	71	38.3	35.9 $\pm$ 3.2	23.42 $\pm$ 2.3	<0.01
	1,3-Ditertbutylbenzene	57	53.2	166.3 $\pm$ 21.9	46.4 $\pm$ 12.0	<0.001
	<b>Down-expressed in “treated” bacteria</b>					
	2-Hexanone	58 and 43	27.5	42.5 $\pm$ 2.3	49.75 $\pm$ 2.5	<0.05
	Unidentified	57	25.8	18.8 $\pm$ 0.8	23.17 $\pm$ 2.0	<0.05
Unidentified	71	72.3	25.1 $\pm$ 2.2	47.35 $\pm$ 5.3	<0.01	
<b>CYPERMETHRINE</b>	<b>Over-expressed in “treated” bacteria</b>					
	2-Butanone	72	14.8	217.0 $\pm$ 17.3	159.1 $\pm$ 21.2	<0.05
	2-Methyl-2-butanol	59	17.5	197.1 $\pm$ 19.4	143.0 $\pm$ 12.7	<0.05
	2-Pentanone	43	20.6	52.3 $\pm$ 3.1	41.5 $\pm$ 4.1	<0.05
	2-Hexanone	58 and 43	27.5	54.6 $\pm$ 2.4	46.5 $\pm$ 2.7	<0.05
	Malonic acid, hexyl 3-methylbutyl ester	71	38.3	28.7 $\pm$ 1.1	23.2 $\pm$ 0.7	<0.001
	1,3-Ditertbutylbenzene	87	53.2	94.8 $\pm$ 8.0	36.2 $\pm$ 4.4	<0.001
<b>SULCOTRIONE</b>	<b>Over-expressed in “treated” bacteria</b>					
	2,3,3-Trimethylpentane	43	22.8	76.4 $\pm$ 7.2	54.6 $\pm$ 3.2	<0.05
	Toluene	91	25.1	307.6 $\pm$ 20.7	234.9 $\pm$ 21.3	<0.05
	<b>Down-expressed in “treated” bacteria</b>					
	Unidentified	43	24.1	24.3 $\pm$ 2.2	30.1 $\pm$ 1.5	<0.05

VOC are expressed with an arbitrary unity of area.

<sup>1</sup>Tentative identification based on high resolution mass spectrum and EI/CI spectra from literature and internal databank.

<sup>2</sup>Retention time indices on a Rxi®-624Sil MS fused silica column (60 m  $\times$  0.25 mm  $\times$  1.4  $\mu$ m, Restek).

<sup>3</sup>*P*-value resulting for *t*-test abundance differences between treated and control groups (*df* = 1).



cypermethrine. Results showed a significant differences of VOC patterns of strain exposed to pesticides compare to control ones (MANOVA,  $ddl = 1$ ,  $F_{Cyper} = 5.7$ ;  $F_{Sulcor} = 8.9$ ,  $P$ -value < 0.05). Out of 150 VOCs which were identified in *B. megaterium* Mes11 volatolome, 15 were over or under-expressed following cypermethrine exposure. All of them seem to be endogenous to *B. megaterium* Mes11 (no one were identified in the cypermethrine specific volatolome).

The clear case-control separation exhibited by PC1 (79.4%) was explained by the increase expression of five branched-alkanes (2,3,3-trimethylpentane, 2,3-dimethylhexane, 2,2,4-trimethylhexane, 2,6-dimethylnonane, 3-ethylpentane), one alkane diol (3-methoxy-hexane-1,6-diol), one branched-alkene (2,4-dimethyl-1-heptene), one acid (malonic acid), one ester (hexyl 3-methylbutyl ester), one alcohol (2-hexyl-1-octanol), one aromatic compound (1,3-ditertbutylbenzene) and five unidentified VOCs (Table 2).

As showed in *P. fluorescens* SG-1, PC2 was built on the natural biological variation of bacteria.

## DISCUSSION

The present work aimed at identifying metabolic VOC markers of exposure to three different pesticides used at low concentration (EC10) in two edaphic bacteria strains, *P. fluorescens* SG-1 and *B. megaterium* Mes11. Using a volatolomic approach, we first highlighted a set of bacterial VOCs that seem to be specifically modulated in each strain according to the

nature of the pesticide used. Second, our results revealed three VOCs (1,3-Ditertbutylbenzene, 2-Hexanone and Malonic acid, hexyl 3-methylbutyl ester) modulated in *P. fluorescens* SG-1 when exposed with pyrethroid pesticides (deltamethrine and cypermethrine), suggesting the existence of candidate generic VOC markers of pyrethroids in this strain. Interestingly, two out of these three VOCs were found in *B. megaterium* Mes11 when exposed with cypermethrine too, suggesting the existence of interspecific markers of pyrethroid in these bacteria. Altogether, our results underlined the relevance of volatolomics to detect signatures of pesticide exposure in microorganisms.

## Bacterial VOCs Can Be Robust and Specific Strain Markers of Different Pesticide Exposure

The volatolomic approach revealed several markers of pesticide exposure in both strains. This is particularly observed in *P. fluorescens* SG-1. Bacteria modulated a set of strain-specific VOCs following exposure to deltamethrine, cypermethrine or sulcotrione. Accordingly, when they were exposed to deltamethrine, *P. fluorescens* SG-1 showed higher levels in carbonyl sulfide and two branched-alkanes (2,3,3-trimethylpentane and 2,3-dimethylhexane). The increased levels of these three VOCs should be the results of distinct metabolic responses displayed by the strain to challenge the impacts of deltamethrine in cells. According to previous works, the release of carbonyl sulfide could be linked with an increase of metabolic rate and respiration in plants and some soil microorganisms

**TABLE 2** | Significant volatile metabolites over-expressed in the volatolome of *Bacillus megaterium* Mes11 strain when exposed to cypermethrine pesticides compared to control.

Volatile metabolite <sup>1</sup>	m/z	RT <sup>2</sup>	Mean peak abundance ± ER (x10 <sup>3</sup> )		Statistical P-value of student t-tests <sup>3</sup>
			Treated	Control	
<b>Over-expressed in “treated” bacteria</b>					
3-Ethylpentane	43	22.3	324.4 ± 60.7	131.7 ± 31.9	<0.05
2,3,3-Trimethylpentane	43	22.8	518.0 ± 107.4	204.2 ± 53.3	<0.05
2,3-Dimethylhexane	70	23.2	128.3 ± 23.0	53.7 ± 11.5	<0.05
2,2,4-Trimethylhexane	57	24.2	413.3 ± 82.9	178.3 ± 52.5	<0.05
2,4-Dimethyl-1-heptene	43	28.5	185.8 ± 33.0	70.9 ± 15.2	<0.01
2,6-Dimethylnonane	57	38.9	90.4 ± 22.2	41.4 ± 45.0	<0.05
Malonic acid, hexyl 3-methylbutyl ester	43	38.9	130.1 ± 32.7	60.5 ± 8.1	<0.05
3-Methoxy-hexane-1,6-diol	43	41.0	19.6 ± 1.6	14.3 ± 1.2	<0.05
2-Hexyl-1-octanol	43	43.7	26.5 ± 5.2	14.0 ± 0.9	<0.05
1,3-Ditertbutylbenzene	57	53.2	241.5 ± 61.8	73.5 ± 8.4	<0.05
Unidentified	55	28.9	45.6 ± 5.4	25.2 ± 3.7	<0.01
Unidentified	57	32.0	157.4 ± 39.1	67.7 ± 10.4	<0.05
Unidentified	57	32.3	45.0 ± 11.0	22.0 ± 2.9	<0.05
Unidentified	57	32.4	77.4 ± 20.7	32.6 ± 4.3	<0.05
Unidentified	71	33.4	44.1 ± 9.9	21.8 ± 2.2	<0.05

VOC are expressed with an arbitrary unity of area.

<sup>1</sup>Tentative identification based on high resolution mass spectrum and EI/CI spectra from literature and internal databank.

<sup>2</sup>Retention time indices on a Rxi®-624Sil MS fused silica column (60 m × 0.25 mm × 1.4 μm, Restek).

<sup>3</sup>P-value resulting for t-test abundance differences between treated and control groups (df = 1).

(Campbell et al., 2008; Maseyk et al., 2014). Here the increase of carbonyl sulfide by *P. fluorescens* SG-1 could reflect a rise of metabolic rate in cells because of larger demands of energetic substrates (i.e., NADPH, ATP) to counteract the impacts of deltamethrine at cell levels. Indeed, there is many evidence that species over-produce such an energetic substrate when they are exposed to environmental stressful conditions (Hidalgo et al., 2014). NADPH and ATP are non-negligible fuel for metabolic pathways of cell detoxifications and cell membrane protections. Strengthening this hypothesis, there were also evidences that carbonyl sulfide is released in the headspace of bacteria like *Thiobacillus thioeparus* THI115 and *Pseudomonas aeruginosa* STK 03 during thiocyanate degradation (Kim and Katayama, 2000; Mekuto et al., 2016), a process requiring a non-negligible quantity of energetic substrates. The two branched-alkanes 2,3,3-trimethylpentane and 2,4-dimethylhexane had been already proposed as candidate markers of human lung tumors (Filipiak et al., 2008, 2010, 2016), and their over-expression is linked to the peroxidation of phospholipid membranes. In rats the evidence that exposure to deltamethrine is showed to increase lipid peroxidation (Nasuti et al., 2003). Such a lipid peroxidation can thus occurred in our bacteria conducting to the over-expression of the two branched-alkane VOCs.

By contrast, when they were exposed to cypermethrine, *P. fluorescens* SG-1 showed the over-production of 2-methyl-2-butanol and two ketones, 2-butanone and 2-pentanone. There were evidence that these last two ketones can be used as relevant tumor-markers in human (Filipiak et al., 2008). In bacteria, both 2-butanone and 2-pentanone are generated by lipolysis processes (Vallerand et al., 1999; Zhang et al., 2012).

Finally, when they were exposed to sulcotrione, *P. fluorescens* SG-1 showed the over-production of two compounds, 2,3,3-trimethylpentane and toluene. We already discussed the increase level of 2,3,3-trimethylpentane under deltamethrine exposure, suggesting lipid peroxidation might also take place in *P. fluorescens* under sulcotrione exposure. Regarding toluene, the release of this VOC in exposed strain should be contrasted in regards with a possible exogenous origin. We showed (**Supplementary Data 1**) that this aromatic VOC is found in the volatolome of the sulcotrione. Indeed, toluene is well-known by-product of the manufacturing process of sulcotrione.

In *B. megaterium* Mes11, the volatolome was also modulated, notably when the strain was exposed to cypermethrine. Fifteen discriminant VOCs were over-expressed. Eight were found only in *B. megaterium* Mes11 and were correctly identified. We found six branched-alkanes (3-ethylpentane, 2,3,3-trimethylpentane, 2,3-dimethylhexane, 2,2,4-trimethylhexane, 2,6-dimethylnonane and 3-methoxy-hexane-1,6-diol), one branched-alkene (2,4-dimethyl-1-heptene), and one primary alcohol (2-hexyl-1-octanol). Exposure to pyrethroids induced many modifications at cellular levels, including lipid peroxidation of fatty acids that form part of the cell membranes, and the synthesis of polyunsaturated fatty acids (PUFAs). In response, organisms display number of metabolites from oxidation reactions catalyzed by enzyme systems associated with cytochrome p450 and alcohol dehydrogenases (ADH). These metabolites include alkanes (C3-C11), branched-alkanes and -alkenes, alcohols and also aldehydes and carboxylic acids as end metabolites of the reaction (Hakim et al., 2012; Jareño-Esteban et al., 2013),

same as showed in *B. megaterium*. Such VOCs markers might result from a complex equilibrium between non-specific oxidative stress induced and probably more specific enzymatic detoxification activities whose induction could be more pesticide dependent. More interesting, the two branched-alkanes, 2,3,3-trimethylpentane and 2,3-dimethylhexane, were also over-expressed too in *P. fluorescens* when exposed to deltamethrine and sulcotrione. This result suggests that these two VOCs could be more global markers of oxidative stress in bacteria than specific markers of pesticide exposure. According to this hypothesis, there are evidence that these two branched-alkanes are over-expressed in species and humans during the development of cancerous tumors (Filipiak et al., 2008, 2010, 2016).

Altogether, our results suggest thus that volatolome of bacteria can be modulated in response to chemical stressors, and that this modulation might depend on both the strain and the stressor studied. Although experimental validation still required, monitoring bacterial VOCs could pave the way for future diagnosis methods of pesticide contamination in soil microorganisms.

## Bacterial VOCs Can Be Generic and Interspecific Strain Markers of Global Pyrethroid Exposure

Deltamethrine and cypermethrine are two pesticides belonging to the pyrethroid family. Exposure to these two pesticides should thus induce similar cell damages (i.e., pyrethroids act like axonic excitoxins preventing the closure of the voltage-gated sodium channels) and thus physiological modulations in organisms, including volatolome adjustments. Corroborating this hypothesis, our approach has detected modulated expression of three VOCs (2-hexanone, 1,3-ditertbutylbenzene and malonic acid, hexyl 3-methylbutyl ester) in *P. fluorescens* strain SG-1 when exposed to deltamethrine and cypermethrine. First, a higher expression levels of 1,3-ditertbutylbenzene and malonic acid, hexyl 3-methylbutyl ester under both pesticide exposure. However, the expression modulation of 2-hexanone is interesting, as there is evidence in arthropods that the VOC can have an inhibitory effect on voltage-gated sodium channels (Papachristoforou et al., 2012), the activities of which are altered by pyrethroids exposure. Interestingly, our results showed that the modulation level of 2-hexanone in *P. fluorescens* depends on the nature of the pyrethroid the strain is exposed. The VOC increased when strain was exposed to cypermethrine, while it decreased when exposed to deltamethrine. In some microbial studies, an increased level of 2-hexanone was detected before remedial actions, whereas it decreased after mitigations, conducing to controversial results (Korpi et al., 2009). Further works are required to test it, but the contrasting modulations of 2-hexanone in *P. fluorescens* could suggest that strain had already started or finished the mitigation of deltamethrine 90 min after exposure while it did not started yet with cypermethrine.

Regarding the levels of two VOCs (1,3-ditertbutylbenzene and malonic acid, hexyl 3-methylbutyl ester), an increase was

observed in *P. fluorescens* SG-1 under pyrethroid (deltamethrine and cypermethrine) exposure, and in *B. megaterium* Mes11 under cypermethrine exposure. Although we have no data about how deltamethrine influences the volatolome of *B. megaterium*, the two VOCs seem to be interspecific markers of cypermethrine contamination in the two strains. Based on the detection of such generic and interspecific markers of cypermethrine exposure, we could further envisage risk assessment investigations in more complex ecosystemic fields like soil mesocosms. However, more studies are still required in order to comfort an interpretative marker of these two compounds. Investigating physiological incidences of these two VOCs on bacteria may help to clarify the origin of these compounds as candidate markers of many mammal diseases related to lipid peroxidation processes (Hanai et al., 2012; Filipiak et al., 2016; Tang et al., 2017).

## Can *Bacillus megaterium* Mes11 Dissipate the Sulcotrione?

The PCA analysis did not reveal significant volatolome difference in *B. megaterium* Mes11 whether they were exposed to the sulcotrione or not. *B. megaterium* Mes11 was characterized as an efficient mesotrione-degrading strain (Batisson et al., 2009; Bardot et al., 2015; Carles et al., 2016), a selective herbicide belonging to the triketone family like the sulcotrione. Briefly, *B. megaterium* Mes11 isolated from soils was able to completely and very rapidly (about 1 h at 30 mg/L) biotransform the mesotrione into 2-amino-4methylsulfonylbenzoic acid (AMBA) and 4-methylsulfonyl-2-nitrobenzoic acid (MNBA) in its culture growth (Batisson et al., 2009; Carles et al., 2016) by nitro-reduction and hydrolysis. In order to dissipate the sulcotrione from its medium growth, a first hypothesis could be that bacteria degrade the pesticide. Indeed, many microorganisms including *Tetrahymena pyriformis* and *Vibrio fischeri* were shown to be able to degrade both sulcotrione and mesotrione herbicides. Although we cannot rule out the hypothesis that the vehicle (DMSO 0.5%) might hide the effects of sulcotrione on the strain volatolome, we can first supposed that *B. megaterium* Mes11 should rapidly degrade the sulcotrione. However, such a sulcotrione-degrading activity of *B. megaterium* Mes11 have to be further investigated by measuring the sulcotrione and its residues directly in strain cells and growth medium along the experiment duration.

Second, triketone pesticides can have genotoxic effects on cells, as already demonstrated in plants (Dumas et al., 2017). Therefore, the exposure to 327.33 mg/L of sulcotrione in *B. megaterium* Mes11 could induce a 10% decline of their generation time because of a genotoxic effect on cells (impacting cellular division) rather than detoxification processes at the metabolic scale. Similar conclusions had been made in the protist *Paramecium* in which exposure to sulcotrione influences the transcription of genes involved in cell division whereas exposure to deltamethrine influences the transcription of detoxifying genes (Bouchard et al. Not published yet).

Third, *Bacillus* can turned to resistance form by encapsulation when they were exposed to chemical stress. The decline of generation time measured with 327.33 mg/L of sulcotrione could also be the consequence of such a protective

encapsulation state of the strain rather than a consequence of stress detoxification.

## Reinvest the Concept of Bacterial Ecotoxicogenomic Thanks to Volatolomic

Conventional analyses used to detect and quantify the presence of xenobiotics in the environment provide an efficient way to improve risk assessments, but do not estimate how they influence biological systems inhabiting these ecosystems. It is in this context that ecotoxicogenomics, a set of analytical tools that combines high throughput DNA technologies with bioinformatics, had emerged (Hamadeh et al., 2002; Robbens et al., 2007; Afshari et al., 2011). Thus, rather than determining whether a chemical compound is toxic, ecotoxicogenomics proposed to determine their mechanisms of action in organisms. However, chemical contaminants have not one but rather a series of molecular effects that can vary in time and with concentration. There are genes responding within a short period of time (hours), others that are only differentially regulated after longer terms of exposure, or transiently expressed. Some genes will probably be more sensitive than others, so exposure to low concentrations of contaminants may affect a reduced suite of genes, while at higher concentrations, a much larger suite of genes may well be affected. Very high concentrations of a chemical may be toxic and lead to other genes being affected because of the cellular damage. Metabolomics and more particularly volatolomics, which is interested in the volatile fraction of the volatolome, captures a more integrated assessment of the physiological state of an organism that transcriptomics and proteomics do (Ankley et al., 2006; Fent and Sumpter, 2011). Indeed, volatile compounds are the terminal products of a toxic response. Their production integrates gene transcription alteration and the reorientation of stress metabolism. It stacks the whole cell damage as a simple under or overproduction of short, low mass, volatile molecule. We can mind in term of production and not expression. Patterns in of volatile profiles may thus offer the potential to uncover novel markers of exposure to chemical contaminants in organisms or ecosystems. In addition, this can be achieved at very low concentration. For instance, the No Observed Transcriptional Effect Level (NOTEL) may play a role in determining if a predicted environmental concentration poses a risk to a sensitive organism within an ecosystem. The pollutant interacts with cells and cellular components in a manner dependent on its chemical properties resulting in specific cellular damage or stress responses (Poynton and Vulpe, 2009). Gene expression might not be affected at the NOTEL concentration, but the cell detoxication pathways are yet producing volatile compounds that are the consequence of a stress response.

## CONCLUSION

In our knowledge, no previous work had already used volatolomics to investigate indirect markers related to the exposure of soil bacterial strains to different pesticides. We thus optimized a volatolomic pipeline from previous works

devoted to livestock and microbial communities (Bouhleb et al., 2017; Defois et al., 2017; Ratel et al., 2017) and adapted it to single bacterial population study. Here, we demonstrated that a short-time exposure (90 min) to different pesticide molecules, modulated a set of potentially strain-specific VOCs in bacteria, the nature of which depends on metabolic and enzymatic adjustments displayed to counteract the impacts of pesticides in cells. Such VOCs are probably markers of pesticide exposure. By increasing the time of exposure, it will be of interest to re-start analyses in order to study the mechanism of action of the pesticides and their cellular resilient responses. Of particular important is the potential existence of two VOCs that could be proposed as candidate interspecific markers of pyrethroid pesticide family in bacteria. More studies still required comforting this hypothesis, but these results should pave the way to alternative analytical set-up in microbial ecotoxicology. For a further chemical risk assessment in real environmental matrices based on volatolomics, VOC pattern recognition should be studied according to bacteria strain, pesticide concentration and exposure time. One first solution could be to target volatolome in simplified soil microcosm (2–3 strains). To date, one of the main bottleneck to engage such of microcosm study will be to isolate a sufficient concentration of bacteria without damaging them in order to prevent the mix of VOCs in the microcosm and get a measurable and interpretable signal. We consider that combine volatolomics with other omic tools (transcriptomics and proteomics) should enlarge further diagnosis applications on real biodiversity soils.

## AUTHOR CONTRIBUTIONS

This work was driven by EE and PB. EE, PB, and KH designed and wrote the manuscript. KH conducted all experiments. FM and JR helped KH in adapting the volatolomic assay for single bacteria. BG conducted the HR-MS analysis to validate VOC identification.

## FUNDING

This work was supported by the SYMBIOSE CPER and the AURA region.

## ACKNOWLEDGMENTS

The authors thank Louis Carles and Isabelle Batisson for their helpful advice in cultivation of the two bacteria. The authors also thank Jean-Louis Bonnet for his help to determine pesticide EC10.

## SUPPLEMENTARY MATERIAL

The Supplementary Material for this article can be found online at: <https://www.frontiersin.org/articles/10.3389/fmicb.2018.03113/full#supplementary-material>

## REFERENCES

- Afshari, C. A., Hamadeh, H. K., and Bushel, P. R. (2011). The evolution of bioinformatics in toxicology: advancing toxicogenomics. *Toxicol. Sci. Off. J. Soc. Toxicol.* 120(Suppl. 1), S225–S237. doi: 10.1093/toxsci/kfq373
- Aktar, M. W., Sengupta, D., and Chowdhury, A. (2009). Impact of pesticides use in agriculture: their benefits and hazards. *Interdiscip. Toxicol.* 2, 1–12. doi: 10.2478/v10102-009-0001-7
- Ankley, G. T., Daston, G. P., Degitz, S. J., Denslow, N. D., Hoke, R. A., Kennedy, S. W., et al. (2006). Toxicogenomics in regulatory ecotoxicology. *Environ. Sci. Technol.* 40, 4055–4065. doi: 10.1021/es0630184
- Bardot, C., Besse-Hoggan, P., Carles, L., Le Gall, M., Clary, G., Chafey, P., et al. (2015). How the edaphic *Bacillus megaterium* strain Mes11 adapts its metabolism to the herbicide mesotrione pressure. *Environ. Pollut.* 199, 198–208. doi: 10.1016/j.envpol.2015.01.029
- Batisson, I., Crouzet, O., Besse-Hoggan, P., Sancelme, M., Mangot, J.-F., Mallet, C., et al. (2009). Isolation and characterization of mesotrione-degrading *Bacillus* sp. from soil. *Environ. Pollut.* 157, 1195–1201. doi: 10.1016/j.envpol.2008.12.009
- Berge, P., Ratel, J., Fournier, A., Jondreville, C., Feidt, C., Roudaut, B., et al. (2011). Use of volatile compound metabolic signatures in poultry liver to back-trace dietary exposure to rapidly metabolized xenobiotics. *Environ. Sci. Technol.* 45, 6584–6591. doi: 10.1021/es200747h
- Bijlsma, R., and Loeschcke, V. (2005). Environmental stress, adaptation and evolution: an overview. *J. Evol. Biol.* 18, 744–749. doi: 10.1111/j.1420-9101.2005.00962.x
- Bouhrel, J., Jouan-Rimbaud Bouveresse, D., Abouelkaram, S., Baéza, E., Jondreville, C., Travel, A., et al. (2018). Comparison of common components analysis with principal components analysis and independent components analysis: application to SPME-GC-MS volatolomic signatures. *Talanta* 178, 854–863. doi: 10.1016/j.talanta.2017.10.025
- Bouhrel, J., Ratel, J., Abouelkaram, S., Mercier, F., Travel, A., Baéza, E., et al. (2017). Solid-phase microextraction set-up for the analysis of liver volatolome to detect livestock exposure to micropollutants. *J. Chromatogr. A* 1497, 9–18. doi: 10.1016/j.chroma.2017.03.008
- Broza, Y. Y., Mochalski, P., Ruzsanyi, V., Amann, A., and Haick, H. (2015). Hybrid volatolomics and disease detection. *Angew. Chem. Int. Ed.* 54, 11036–11048. doi: 10.1002/anie.201500153
- Campbell, J. E., Carmichael, G. R., Chai, T., Mena-Carrasco, M., Tang, Y., Blake, D. R., et al. (2008). Photosynthetic control of atmospheric carbonyl sulfide during the growing season. *Science* 322, 1085–1088. doi: 10.1126/science.1164015
- Carles, L., Besse-Hoggan, P., Joly, M., Vigouroux, A., Moréra, S., and Batisson, I. (2016). Functional and structural characterization of two *Bacillus megaterium* nitroreductases biotransforming the herbicide mesotrione. *Biochem. J.* 473, 1443–1453. doi: 10.1042/BJ20151366
- Carles, L., Joly, M., Bonnemoy, F., Lereboure, M., Batisson, I., and Besse-Hoggan, P. (2017). Identification of sulfonylurea biodegradation pathways enabled by a novel nicosulfuron-transforming strain *Pseudomonas fluorescens* SG-1: toxicity assessment and effect of formulation. *J. Hazard. Mater.* 324, 184–193. doi: 10.1016/j.jhazmat.2016.10.048
- Defois, C., Ratel, J., Denis, S., Batut, B., Beugnot, R., Peyretailade, E., et al. (2017). Environmental pollutant benzo[a]pyrene impacts the volatile metabolome and transcriptome of the human gut microbiota. *Front. Microbiol.* 8:1562. doi: 10.3389/fmicb.2017.01562
- Defois, C., Ratel, J., Garrait, G., Denis, S., LeGoff, O., Talvas, J., et al. (2018). Food chemicals disrupt human gut microbiota activity and impact intestinal homeostasis as revealed by in vitro systems. *Sci. Rep.* 8:11006. doi: 10.1038/s41598-018-29376-9
- Dumas, E., Giraud, M., Goujon, E., Halma, M., Khili, E., Stauffert, M., et al. (2017). Fate and ecotoxicological impact of new generation herbicides from the triketone family: an overview to assess the environmental risks. *J. Hazard. Mater.* 325, 136–156. doi: 10.1016/j.jhazmat.2016.11.059
- Fent, K., and Sumpter, J. P. (2011). Progress and promises in toxicogenomics in aquatic toxicology: is technical innovation driving scientific innovation? *Aquat. Toxicol. Amst. Neth.* 105, 25–39. doi: 10.1016/j.aquatox.2011.06.008
- Filipiak, W., Mochalski, P., Filipiak, A., Ager, C., Cumeras, R., Davis, C. E., et al. (2016). A compendium of volatile organic compounds (VOCs) released by human cell lines. *Curr. Med. Chem.* 23, 2112–2131. doi: 10.2174/0929867323666160510122913
- Filipiak, W., Sponring, A., Filipiak, A., Ager, C., Schubert, J., Miekisch, W., et al. (2010). TD-GC-MS analysis of volatile metabolites of human lung cancer and normal cells in vitro. *Cancer Epidemiol. Biomark. Prev.* 19, 182–195. doi: 10.1158/1055-9965.EPI-09-0162
- Filipiak, W., Sponring, A., Mikoviny, T., Ager, C., Schubert, J., Miekisch, W., et al. (2008). Release of volatile organic compounds (VOCs) from the lung cancer cell line CALU-1 in vitro. *Cancer Cell Int.* 8:17. doi: 10.1186/1475-2867-8-17
- Hakim, M., Broza, Y. Y., Barash, O., Peled, N., Phillips, M., Amann, A., et al. (2012). Volatile organic compounds of lung cancer and possible biochemical pathways. *Chem. Rev.* 112, 5949–5966. doi: 10.1021/cr300174a
- Hamadeh, H. K., Amin, R. P., Paules, R. S., and Afshari, C. A. (2002). An overview of toxicogenomics. *Curr. Issues Mol. Biol.* 4, 45–56.
- Hanai, Y., Shimono, K., Oka, H., Baba, Y., Yamazaki, K., and Beauchamp, G. K. (2012). Analysis of volatile organic compounds released from human lung cancer cells and from the urine of tumor-bearing mice. *Cancer Cell Int.* 12:7. doi: 10.1186/1475-2867-12-7
- Hidalgo, K., Montazeau, C., Siauxat, D., Braman, V., Tralabal, M., Simard, F., et al. (2018). Distinct physiological, biochemical and morphometric adjustments in the malaria vectors *Anopheles gambiae* and *an. coluzzii* as means to survive to dry season conditions in Burkina Faso. *J. Exp. Biol.* 221:jeb.174433. doi: 10.1242/jeb.174433
- Hidalgo, K., Mouline, K., Mamai, W., Foucreau, N., Dabiré, K. R., Bouchereau, A., et al. (2014). Novel insights into the metabolic and biochemical underpinnings assisting dry-season survival in female malaria mosquitoes of the *Anopheles gambiae* complex. *J. Insect. Physiol.* 70, 102–116. doi: 10.1016/j.jinsphys.2014.07.003
- Hidalgo, K., Siauxat, D., Braman, V., Dabiré, K. R., Simard, F., Mouline, K., et al. (2016). Comparative physiological plasticity to desiccation in distinct populations of the malarial mosquito *Anopheles coluzzii*. *Parasit. Vectors* 9:565. doi: 10.1186/s13071-016-1854-1
- Jareño-Esteban, J. J., Muñoz-Lucas, M. Á, Carrillo-Aranda, B., Maldonado-Sanz, J. Á, de Granda-Orive, I., Aguilar-Ros, A., et al. (2013). Volatile organic compounds in exhaled breath in a healthy population: effect of tobacco smoking. *Arch. Bronconeumol. Engl. Ed.* 49, 457–461. doi: 10.1016/j.arbr.2013.09.006
- Kim, S.-J., and Katayama, Y. (2000). Effect of growth conditions on thiocyanate degradation and emission of carbonyl sulfide by *Thiobacillus thioeparus* THI115. *Water Res.* 34, 2887–2894. doi: 10.1016/S0043-1354(00)00046-4
- Korpi, A., Järnberg, J., and Pasanen, A.-L. (2009). Microbial volatile organic compounds. *Crit. Rev. Toxicol.* 39, 139–193. doi: 10.1080/10408440802291497
- Maseyk, K., Berry, J. A., Billesbach, D., Campbell, J. E., Torn, M. S., Zahniser, M., et al. (2014). Sources and sinks of carbonyl sulfide in an agricultural field in the southern great plains. *Proc. Natl. Acad. Sci. U S A.* 111, 9064–9069. doi: 10.1073/pnas.1319132111
- Mekuto, L., Ntwampe, S. K. O., Kena, M., Golela, M. T., and Amodu, O. S. (2016). Free cyanide and thiocyanate biodegradation by *Pseudomonas aeruginosa* STK 03 capable of heterotrophic nitrification under alkaline conditions. *3 Biotech* 6:6. doi: 10.1007/s13205-015-0317-2
- Meurillon, M., Ratel, J., and Engel, E. (2017). How to secure the meat chain against toxicants. *Innov. Food Sci. Emerg. Technol.* 46, 74–82. doi: 10.1016/j.ifset.2017.10.004
- Nasuti, C., Cantalamessa, F., Falcioni, G., and Gabbianelli, R. (2003). Different effects of Type I and Type II pyrethroids on erythrocyte plasma membrane properties and enzymatic activity in rats. *Toxicology* 191, 233–244. doi: 10.1016/S0300-483X(03)00207-5
- Papachristoforou, A., Kagiava, A., Papaefthimiou, C., Termentzi, A., Fokialakis, N., Skaltsounis, A.-L., et al. (2012). The Bite of the honeybee: 2-heptanone secreted from honeybee mandibles during a bite acts as a local anaesthetic in insects and mammals. *PLoS One* 7:e47432. doi: 10.1371/journal.pone.0047432
- Parrón, T., Requena, M., Hernández, A. F., and Alarcón, R. (2014). Environmental exposure to pesticides and cancer risk in multiple human organ systems. *Toxicol. Lett.* 230, 157–165. doi: 10.1016/j.toxlet.2013.11.009
- Poynton, H. C., and Vulpe, C. D. (2009). Ecotoxicogenomics: emerging technologies for emerging contaminants. *JAWRA J. Am. Water Resour. Assoc.* 45, 83–96. doi: 10.1111/j.1752-1688.2008.00291.x

- Preti, G., Labows, J. N., Kostelc, J. G., Aldinger, S., and Daniele, R. (1988). Analysis of lung air from patients with bronchogenic carcinoma and controls using gas chromatography-mass spectrometry. *J. Chromatogr. B. Biomed. Sci. App.* 432, 1–11. doi: 10.1016/S0378-4347(00)80627-1
- R Development Core Team. (2008). *R: A Language and Environment for Statistical Computing*. Vienna: R Foundation for Statistical Computing.
- Ratel, J., Planche, C., Mercier, F., Blinet, P., Kondjoyan, N., Marchand, P., et al. (2017). Liver volatolomics to reveal poultry exposure to  $\gamma$ -hexabromocyclododecane (HBCD). *Chemosphere* 189, 634–642. doi: 10.1016/j.chemosphere.2017.09.074
- Robbens, J., van der Ven, K., Maras, M., Blust, R., and De Coen, W. (2007). Ecotoxicological risk assessment using DNA chips and cellular reporters. *Trends Biotechnol.* 25, 460–466. doi: 10.1016/j.tibtech.2007.08.005
- Scott-Thomas, A., Epton, M., and Chambers, S. (2013). Validating a breath collection and analysis system for the new tuberculosis breath test. *J. Breath Res.* 7:037108. doi: 10.1088/1752-7155/7/3/037108
- Tang, H., Lu, Y., Zhang, L., Wu, Z., Hou, X., and Xia, H. (2017). Determination of volatile organic compounds exhaled by cell lines derived from hematological malignancies. *Biosci. Rep.* 37:BSR20170106. doi: 10.1042/BSR20170106
- Tsaboula, A., Papadakis, E.-N., Vryzas, Z., Kotopoulou, A., Kintzikoglou, K., and Papadopoulou-Mourkidou, E. (2016). Environmental and human risk hierarchy of pesticides: a prioritization method, based on monitoring, hazard assessment and environmental fate. *Environ. Int.* 91, 78–93. doi: 10.1016/j.envint.2016.02.008
- Vallerand, A. L., Zamecnik, J., Jones, P. J., and Jacobs, I. (1999). Cold stress increases lipolysis, FFA Ra and TG/FFA cycling in humans. *Aviat. Space Environ. Med.* 70, 42–50.
- Zhang, C., Wang, G., Zheng, Z., Maddipati, K. R., Zhang, X., Dyson, G., et al. (2012). Endoplasmic reticulum-tethered transcription factor cAMP responsive element-binding protein, hepatocyte specific, regulates hepatic lipogenesis, fatty acid oxidation, and lipolysis upon metabolic stress in mice. *Hepatology* 55, 1070–1082. doi: 10.1002/hep.24783
- Conflict of Interest Statement:** The authors declare that the research was conducted in the absence of any commercial or financial relationships that could be construed as a potential conflict of interest.
- Copyright © 2019 Hidalgo, Ratel, Mercier, Gauriat, Bouchard and Engel. This is an open-access article distributed under the terms of the Creative Commons Attribution License (CC BY). The use, distribution or reproduction in other forums is permitted, provided the original author(s) and the copyright owner(s) are credited and that the original publication in this journal is cited, in accordance with accepted academic practice. No use, distribution or reproduction is permitted which does not comply with these terms.



# Copper Affects Composition and Functioning of Microbial Communities in Marine Biofilms at Environmentally Relevant Concentrations

Natàlia Corcoll<sup>1\*†</sup>, Jianghua Yang<sup>2†</sup>, Thomas Backhaus<sup>1</sup>, Xiaowei Zhang<sup>2\*</sup> and Karl Martin Eriksson<sup>3</sup>

<sup>1</sup> Department of Biological and Environmental Sciences, University of Gothenburg, Gothenburg, Sweden, <sup>2</sup> State Key Laboratory of Pollution Control and Resource Reuse, School of the Environment, Nanjing University, Nanjing, China, <sup>3</sup> Department of Mechanics and Maritime Sciences, Chalmers University of Technology, Gothenburg, Sweden

## OPEN ACCESS

### Edited by:

Stéphane Pesce,  
National Research Institute of Science  
and Technology for Environment and  
Agriculture (IRSTEA), France

### Reviewed by:

Annette Bérard,  
Institut National de la Recherche  
Agronomique (INRA), France  
Martin Laviale,  
Université de Lorraine, France

### \*Correspondence:

Natàlia Corcoll  
natalia.corcoll@gu.se  
Xiaowei Zhang  
zhangxw@nju.edu.cn

<sup>†</sup>These authors have contributed  
equally to this work

### Specialty section:

This article was submitted to  
Microbiotechnology, Ecotoxicology  
and Bioremediation,  
a section of the journal  
Frontiers in Microbiology

**Received:** 15 August 2018

**Accepted:** 14 December 2018

**Published:** 08 January 2019

### Citation:

Corcoll N, Yang J, Backhaus T,  
Zhang X and Eriksson KM (2019)  
Copper Affects Composition and  
Functioning of Microbial Communities  
in Marine Biofilms at Environmentally  
Relevant Concentrations.  
*Front. Microbiol.* 9:3248.  
doi: 10.3389/fmicb.2018.03248

Copper (Cu) pollution in coastal areas is a worldwide threat for aquatic communities. This study aims to demonstrate the usefulness of the DNA metabarcoding analysis in order to describe the ecotoxicological effect of Cu at environmental concentrations on marine periphyton. Additionally, the study investigates if Cu-induced changes in community structure co-occurs with changes in community functioning (i.e., photosynthesis and community tolerance to Cu). Periphyton was exposed for 18 days to five Cu concentrations, between 0.01 and 10  $\mu$ M, in a semi-static test. Diversity and community structure of prokaryotic and eukaryotic organisms were assessed by 16S and 18S amplicon sequencing, respectively. Community function was studied as impacts on algal biomass and photosynthetic activity. Additionally, we studied Pollution-Induced Community Tolerance (PICT) using photosynthesis as the endpoint. Sequencing results detected an average of 9,504 and 1,242 OTUs for 16S and 18S, respectively, reflecting the high biodiversity of marine periphytic biofilms. Eukaryotes represent the most Cu-sensitive kingdom, where effects were seen already at concentrations as low as 0.01  $\mu$ M. The structure of the prokaryotic part of the community was impacted at slightly higher concentrations (0.06  $\mu$ M), which is still in the range of the Cu concentrations observed in the area (0.08  $\mu$ M). The current environmental quality standard for Cu of 0.07  $\mu$ M therefore does not seem to be sufficiently protective for periphyton. Cu exposure resulted in a more Cu-tolerant community, which was accompanied by a reduced total algal biomass, increased relative abundance of diatoms and a reduction of photosynthetic activity. Cu exposure changed the network of associations between taxa in the communities. A total of 23 taxa, including taxa within Proteobacteria, Bacteroidetes, Stramenopiles, and Hacrobia, were identified as being particularly sensitive to Cu. DNA metabarcoding is presented as a sensitive tool for community-level ecotoxicological studies that allows to observe impacts simultaneously on a multitude of pro- and eukaryotic taxa, and therefore to identify particularly sensitive, non-cultivable taxa.

**Keywords:** metabarcoding, 16S, 18S, periphyton, amplicon-sequencing, metals

## INTRODUCTION

Copper (Cu) pollution in coastal areas is mainly associated with domestic and industrial activities (Parks et al., 2010; Oursel et al., 2013; Misson et al., 2016), and the use of Cu-based antifouling paints on ship hulls (Yebra et al., 2004; Thomas and Brooks, 2010), especially after the ban of tributyltin (TBT) in the late 1980s in France (Alzieu, 2000) and from 2003 to the rest of Europe (Yebra et al., 2004). Elevated Cu levels can be detected in many parts of the world, especially near enclosed harbors and marinas. For instance, concentrations as high as 0.33  $\mu\text{M}$  have been detected in San Diego Bay, USA (Schiff et al., 2007) or up to 0.41  $\mu\text{M}$  in Toulon Bay, France (Briand et al., 2017). On the west coast of Sweden, Cu levels have been detected at concentrations up to 5  $\mu\text{g/L}$  (0.08  $\mu\text{M}$ ) (Egardt et al., 2018), exceeding the environmental quality standard (EQS) for this region, i.e., the Kattegat sea where an EQS of 4  $\mu\text{g/L}$  (0.07  $\mu\text{M}$ ) has been established (HVMFS 2015:4). Cu is an essential element (Festa and Thiele, 2011), but becomes toxic at higher concentrations (Amara et al., 2018), depending on metal speciation, accumulation (Meylan et al., 2004; Serra et al., 2009) and exposed organism (Barranguet et al., 2003; Amara et al., 2018). In photosynthetically active cells Cu inhibits  $\text{CO}_2$  fixation and PSII activity (Pandey et al., 1992), causes oxidative stress and ultimately inhibits cell growth (Gonçalves et al., 2018). In bacteria, Cu affects various cellular enzymes and proteins involved in energy metabolism (Waldron et al., 2009). Cu affects species composition in microbial communities, leading to a replacement of sensitive taxa with tolerant ones (Gustavson et al., 1999; Serra et al., 2009; Ancion et al., 2010). Detailed descriptions of Cu-sensitive and -tolerant taxa in environmental communities are currently lacking.

Periphyton, also called microhytobenthos, forms biofilms of highly diverse microbial communities—including algae, bacteria, fungi, and meiofauna—that live attached to submerged substrata in aquatic ecosystems (Lock, 1993; Salta et al., 2013; Sanli et al., 2015). The importance of periphyton to aquatic ecosystems is linked to its function as a primary producer and its contribution to biogeochemical cycles (Battin et al., 2003; Sundbäck et al., 2004). The use of periphyton for studies in community ecotoxicology is well-established (Sabater et al., 2007; Eriksson et al., 2009a; Corcoll et al., 2015), as it allows to assess effects of contaminants across different levels of biological organization (Guasch et al., 2016). In this line, an approach commonly used for detecting long-term effects of toxicants in periphyton communities is the measurement of PICT (Pollution-Induced Community Tolerance), introduced by Blanck et al. (1988). PICT is based on the elimination of micro-organisms sensitive to the toxicant in question and the induced inter- and intraspecific selection for organisms that are more tolerant to the toxicant. The entire community is restructured and finally displays an overall increase in its tolerance to the toxicant, compared to an unexposed reference community. This induced tolerance is commonly quantified as an increase of the short-term EC50 of the whole community to the toxicant in question, which is perceived as a community trait (Blanck et al., 1988; Corcoll et al., 2014; Tlili et al., 2015). The use of PICT for detecting effects

from Cu on marine and freshwater periphyton has shown to be more sensitive than traditional community composition based-tools such as microscope observations, pigment-profile based approaches or PCR-DGGE fingerprints (Gustavson et al., 1999; Barranguet et al., 2003; Massieux et al., 2004; Serra et al., 2009; Tlili et al., 2010).

Recent advances in DNA sequencing represents a powerful tool to detect and quantify effects of toxic substances on ecological communities with high sample/observation throughput (Zhang et al., 2009; Yang et al., 2018). In particular DNA metabarcoding, a high throughput DNA-based amplicon sequencing technique, has emerged as a new molecular tool to identify a large proportion of the biological community present in an environmental (Hebert et al., 2003). New computational methods applied to high-throughput DNA sequencing data have allowed the development of co-occurrence network analysis to explore potential interactions between taxa (e.g., inter-taxa correlations). These new analytical methods have permitted to move beyond classical focus on single properties of the microbial communities (e.g., community composition and diversity classically determined by  $\alpha$ -diversity or  $\beta$ -diversity indices; Barberán et al., 2012). For instance, in the metabarcoding work of Mandakovic et al. (2018), network analyses were applied to reveal changes in the structure and co-occurrence patterns in soil microbial communities under different environmental stress factors.

The main goal of this study is to demonstrate the usefulness of the DNA metabarcoding analysis in order to describe the ecotoxicological effect of Cu at environmental concentrations on marine periphytic biofilms. For this purpose, metabarcoding was used in order to describe the effect of Cu on the structure of the prokaryotic and eukaryotic community (i.e., biodiversity, community composition, identification of sensitive/tolerant taxa, and community network). Additionally, the study aims to investigate if Cu-induced changes in community structure co-occurs with changes in community functioning (i.e., photosynthesis and community tolerance to Cu). For these purposes, natural marine periphyton was exposed to a range of Cu concentrations (0.01–10  $\mu\text{M}$ ) in a semi-static microcosm for 18 days. We selected the 16S rRNA (V3 region) and the 18S rRNA (V9 region) genes to target prokaryotes and eukaryotes, respectively. Our results provide new information on how Cu pollution affects the structure and functioning of marine microbial communities, which can aid the setting of appropriate environmental quality standards.

## MATERIALS AND METHODS

### Microcosm Setup and Experimental Design

The experiment was conducted indoors in a thermo-constant room at the facilities of the Sven Lovén Centre for marine sciences—Kristineberg by the Gullmar fjord on the west coast of Sweden, from 18th August to 6th September 2015. Eighteen independent microcosms made by rectangular glass vessels inspired by the SWIFT periphyton test described by Porsbring et al. (2007) were used for the experiment. Each

microcosm contained 300 mL of natural sea water collected from a nearby pristine bay (Gåseviken: 58.245373°N, 11.433628°E). The sea water, with its naturally occurring organisms, was filtered through a 200  $\mu\text{m}$  mesh to remove large organisms and was enriched with 0.7  $\mu\text{M}$  phosphate (as  $\text{KH}_2\text{PO}_4$ ) and 0.8  $\mu\text{M}$  nitrate (as  $\text{NH}_4\text{NO}_3$ ) to avoid nutrient limitation during periphyton growth. Periphyton was allowed to colonize rectangular polyethylene terephthalate glycol (PETG) slides ( $6.9 \times 1.4 \text{ cm}^2$ ). Each rectangular microcosm had a glass rod attached along the long side in the middle of the bottom of the vessel and 22 PETG slides were placed from the bottom glass rod to the side walls of the vessel, making an angle of  $\sim 22^\circ$  between the bottom and the walls of the vessel. The sea water covered half of the surface of the slides. The water from each microcosm was renewed every day. To stimulate periphyton colonization and growth in the beginning of the experiment, marine periphyton inocula were prepared by brushing off periphyton from the upper part of 50–60 stones and pebbles, collected at a maximal depth of 60 cm, into seawater. The water, stones and pebbles were sampled from the same pristine bay as the natural sea water. The inocula was vigorously shaken and filtered through a 200  $\mu\text{m}$  mesh to remove large organisms. Twenty milliliters of inocula, with an approximate chlorophyll *a* concentration of  $0.3 \mu\text{g mL}^{-1}$ , were provided twice to each microcosm during the first week of the experiment. The microcosms were incubated in a thermo-controlled room with the temperature set to  $15^\circ\text{C}$ . The daily light/dark cycle of 14/8 h was simulated with OSRAM FLUORA light tubes with a light intensity at the surface of the microcosms of approximately  $120 \mu\text{mol photons m}^{-2} \text{ s}^{-1}$ . The microcosms were in constant agitation by using horizontal shakes.

The experimental design included unexposed control microcosms and 5 Cu exposure levels, each in triplicate microcosms. The nominal Cu exposure levels were: 0.01, 0.06, 0.32, 1.78, and 10  $\mu\text{M}$ . Cu stocks, 1,000 times more concentrated than the nominal concentrations, were prepared from the reagent  $\text{CuCl}_2 \cdot 2\text{H}_2\text{O}$  (CAS number: 10125-13-0, Sigma-Aldrich) with deionized water. Three hundred microliters of the  $\text{CuCl}_2 \cdot 2\text{H}_2\text{O}$  stocks were added to the Cu microcosms, and the same volume of deionized water was added to the unexposed controls, to give the final volume of 300 mL. Cu and deionized water were introduced at the same time as the periphyton inoculum to the Cu treatments and the controls, respectively. Water temperature, pH, oxygen, and salinity was monitored periodically, at least 10 times through the experiment, using portables multi-probes (HANNA Instruments). Water of all microcosms was sampled 3 times before and after a water renewal for Cu analysis. For this, 50 mL of water were filtered through 0.45  $\mu\text{m}$ , preserved with  $\text{HNO}_3$  (65% suprapure) at final concentration of 1% and kept at  $4^\circ\text{C}$  until further analysis with ICP-MS.

## Periphyton Sampling

After 18 days, periphyton was sampled to analyse chlorophyll *a* concentration, photosynthetic pigments, photosynthetic activity, community tolerance to Cu and microbial composition of prokaryotes and eukaryotes. For each microcosm, a periphyton slurry was produced by scraping off the periphyton from the slides into 150 mL of sea water, filtered through 0.2  $\mu\text{m}$

and amended with the same amount of nutrients as used in the microcosms. Five milliliters of periphyton slurry were filtered through Whatman GF/F filters and used immediately for chlorophyll *a* analyses. Ten milliliters of periphyton slurry were filtered through Whatman GF/F filters, frozen at  $-20^\circ\text{C}$  and stored until pigments extraction. Ten milliliters of periphyton slurry was aliquoted in tubes, pelleted by centrifuged at 6500 g for 10 min at room temperature, the supernatant was removed and the resulting pellets were snap-frozen in liquid nitrogen and stored at  $-80^\circ\text{C}$  until DNA extraction. The remaining periphyton slurry was used to determine photosynthetic activity ( $^{14}\text{C}$ -incorporation) and tolerance measurements following the PICT approach. Analyses of chlorophyll *a*, pigment profiles and microbial composition were done for all treatments. For logistic reasons, photosynthetic and community tolerance measurements were only done for the control microcosms and the microcosms with a Cu exposure of 0.32 and 1.78  $\mu\text{M}$  Cu.

## Chlorophyll *a* Concentration and Photosynthetic Pigments

Chlorophyll *a* was extracted with 10 mL of ethanol (96%) for 24 h in the dark, at room temperature, and was quantified fluorometrically (10-AU Turner fluorometer; Turner designs, Sunnyvale California, USA) according to Jespersen and Christoffersen (1987). Photosynthetic pigments were extracted in a 4 mL mixture of acetone/methanol (80%/20%, v/v) while sonicated in an ice slurry for 3 min. Ninety microliters of the extracts were filtered onto 0.45  $\mu\text{m}$  filters (VWR International Syringe filters) and analyzed with high performance liquid chromatography (HPLC; Shimadze Prominence HPLC Systems) following Torstensson et al. (2015). A total of 10 photosynthetic pigments were identified and were expressed as the ratio between the peak area of each identified pigment and the peak area of Chlorophyll *a*. Fucoxanthin was used as pigment marker for the algal group of Bacillariophyta, also known as diatoms (Roy et al., 2011).

## Pollution-Induced Community Tolerance (PICT)

Pollution-Induced Community Tolerance (PICT) was quantified as increase in EC50 values, determined in short-term photosynthesis inhibition tests using  $^{14}\text{C}$ -incorporation as endpoint according to Eriksson et al. (2009b) with some modifications. From each of the studied microcosms, triplicate unexposed control samples were prepared by mixing 1 mL of periphyton slurry and 1 mL sea water. One sample from each microcosm was exposed to 0.32, 1.35, 5.66, 23.8, and 100  $\mu\text{M}$  Cu by mixing 1 mL of periphyton slurry with 1 mL of Cu solutions. The sea water used for the controls and the Cu solutions was filtered through 0.2  $\mu\text{m}$  and amended with the same amount of nutrients as used in the microcosms. The samples were mixed in scintillation vials and were incubated at  $15^\circ\text{C}$  and  $120 \mu\text{mol photons m}^{-2} \text{ s}^{-1}$ , while gently shaken during the incubation. After 1 h, 50  $\mu\text{L}$   $^{14}\text{C}$ -sodium bicarbonate solution, with a radioactivity of 80  $\mu\text{Ci/ml}$ , was added to each sample. After another hour, 100  $\mu\text{L}$  formaldehyde was

added to each sample to terminate photosynthetic activity. The samples were acidified with 100  $\mu\text{L}$  of HCl to drive off unincorporated  $^{14}\text{C}$  and 3 mL of Instagel Plus was added to each sample. Disintegrations per minute (DPM) were calculated from counts per minute (CPM) based on the correction factors for the sample quench characteristics and the machine efficiency, using a liquid scintillation spectrometer (LS 500 Beckman). The abiotic  $^{14}\text{C}$ -incorporation was estimated by adding 100  $\mu\text{L}$  formaldehyde to one sample before the incubation with  $^{14}\text{C}$ -sodium bicarbonate, and the radioactivity of that sample was subtracted from the radioactivity of the other samples from the same microcosm.  $^{14}\text{C}$ -incorporation was used as an estimate of periphyton photosynthetic activity and was expressed in relative changes of disintegrations per minute (DPM). Community tolerance was determined as differences in  $\text{EC}_{50}$  values based on photosynthetic activity between unexposed control microcosms and microcosms exposed to 0.32 and 1.78  $\mu\text{M}$  Cu.

## DNA Extraction, PCR Amplification, and Sequencing

Microbial composition of prokaryotes and eukaryotes was assessed by DNA metabarcoding. Total genomic DNA was extracted using the Power Biofilm<sup>®</sup> DNA Isolation Kit (MoBio Laboratories, USA) following recommendations in Corcoll et al. (2017). DNA was precipitated with sodium acetate and ethanol prior downstream analyses. Bacterial 16S rRNA genes (V3 region) and eukaryotic 18S rRNA genes (V9 region) were amplified using V3 primers (modified primers 341F and 518R) (Klindworth et al., 2013) and V9 primers (1380F and 1510R) (Amaral-Zettler et al., 2009), respectively. Triplicate PCR reactions were performed for each sample to minimize potential PCR bias. The PCR amplicon libraries were sequenced using the Ion Torrent Proton technology according to the manufacturer's protocols.

## Bioinformatics

The QIIME v.1.8.0 (Quantitative Insights Into Microbial Ecology) pipeline was used to process the raw sequences (Caporaso et al., 2010). Low quality sequences were trimmed via the "split\_libraries.py" script with "-w 50 -q 20." PCR chimera filtering was performed via "parallel\_identify\_chimeric\_seqs.py" script in QIIME with the default parameter. Operational taxonomic units (OTUs) were selected with a sequence similarity cut-off of 97% following the UPARSE pipeline (Edgar, 2013). For each OTU, a representative sequence was chosen and taxonomy was assigned using the RDP classifier (Wang et al., 2007) against the Greengenes database (DeSantis et al., 2006) and SILVA database (Pruesse et al., 2007) for prokaryote and eukaryote community, respectively. So far there are no consensus taxonomic hierarchy for eukaryotic organisms (<https://www.arb-silva.de/projects/eukaryotic-taxonomy/>). In particular, some taxon does not have clear taxonomic information (e.g., class, order, family, etc). In some groups there are intermediate taxonomic levels, not present in other groups, like superphylum, subphylum or infraphylum. The database contains tens of thousands of taxa and it's very difficult to correct the classification of taxa one by one. Hence, the original classification according to

SILVA was used directly in this study for eukaryotic organisms. The raw data have been deposited to the NCBI short read archive (SRA) with BioProject ID PRJNA496374, <https://www.ncbi.nlm.nih.gov/Traces/study/?acc=PRJNA496374>.

## Statistical Analyses

One-way ANOVAs were used to assess differences between the treatments for Chlorophyll *a* concentration, photosynthetic activity and  $\text{EC}_{50}$  values using R (R Core Team, 2013). The effective concentration of Cu that had a 50% of effect ( $\text{EC}_{50}$ ) was determined after fitting  $^{14}\text{C}$ -incorporation values to a dose-response model (Weifull fit) using the package "drc" (Ritz et al., 2015) in R. Principal component analysis (PCA) was employed to observe difference in microbial composition of prokaryotes and eukaryotes between the Cu treatments using weighted Unifrac distance data in QIIME (Caporaso et al., 2010). The Kaiser-Guttman criterion was used to determine the significance of each axis of the PCA analyses. Because the Unifrac matrix includes the phylogenetic information, PCA based on the Unifrac distances can better reflect community differences than that based on taxa abundance data at family or class level. Differences in prokaryotic and eukaryotic community composition between Cu treatments were assessed by MANOVA of Unifrac distances. Differences between Cu treatments were assessed using ANOVA with Dunnett's *post-hoc* test. Correlation networks were generated by SparCC with 100 bootstraps to assign two-sided pseudo *p*-values (Friedman and Alm, 2012). For each treatment, 3 replicates were used to calculate the correlation Rho. The networks were filtered by correlation magnitudes  $>0.6$  and  $<-0.6$  which indicating strong co-abundance and co-exclusion relationships. The networks were visualized by Cytoscape v 3.6.1 and the topological parameters of networks were computed by NetworkAnalyzer 2.7 (Assenov et al., 2008). Topological parameters obtained were, nodes: OTUs number of networks, network density: how densely the network is populated with edges (self-loops and duplicated edges are ignored), network heterogeneity: tendency of a network to contain hub nodes, network centralization: distribution of network density, characteristic path length: expected distance between two connected nodes, avg. number of neighbors: average connectivity of a node in the network. The response of each taxon to Cu exposure was modeled with a 3-parameter log-logistic model and the 50% effects concentration ( $\text{EC}_{50}$ ) was calculated. Beta diversity was estimated by computing weighted UniFrac distances between samples (Lozupone and Knight, 2007). All samples were rarefied at the lowest sequencing depth to reduce biases resulting from differences in sequencing depth (186400 and 112730 for eukaryote and prokaryote community, respectively).

## RESULTS

Periphyton responses after 18 days of exposure to five Cu concentrations, between 0.01 and 10  $\mu\text{M}$ , in a semi-static test, are presented below.

## Experimental Conditions

Temperature, salinity, and pH were constant over the entire experiment, varying by just 1–3% between daily water renewals. Average salinity was 20.8 PSU, water temperature was 17.9°C and pH was 8.1 ( $n = 59$ ). Cu concentrations in the controls and the samples with nominal concentration 0.01  $\mu\text{M}$  Cu were below the quantification limit of 0.02  $\mu\text{M}$ . For the rest of the samples, the analyzed Cu was between 33 % and 90 % of the nominal concentrations, being closer to the nominal concentrations at higher exposure levels (**Supplementary Table 1**). Therefore, the nominal concentrations are used to describe the concentration response patterns.

## Effects on Photosynthetic Pigments, Community Tolerance Development, and Photosynthetic Activity

In the unexposed controls, chlorophyll *a* accounted for 52%, fucoxanthin for 12%, diadinoxanthin + diatoxanthin for 11%,  $\beta$ -carotens for 9%, chlorophyll *c* for 3%, zeaxanthin for 2% and the remaining three non-identified pigments accounted for 11% of the total pigments (arithmetic mean of three replicates) (**Figure 1A**). Chlorophyll *a* concentration decreased in a concentration-dependent manner, reaching 81% inhibition at the highest concentration of 10  $\mu\text{M}$  (**Figure 1B**). A similar pattern was observed for the total pigment content of the periphyton (**Figure 1A**). In contrast, the relative abundance of fucoxanthin increased in a concentration-dependent manner, increasing up to 60% of the total pigment content in the highest Cu exposure, 10  $\mu\text{M}$  Cu (**Figure 1B**). Photosynthetic activity in all the short-term PICT detection tests was inhibited by increasing Cu concentrations, and EC50 values could be determined for all microcosms except one of the microcosms exposed to 1.78  $\mu\text{M}$  Cu. The short-term EC50 (AVG  $\pm$  SE) of the untreated controls was  $8.88 \pm 0.78 \mu\text{M}$ . After pre-exposure to 0.32  $\mu\text{M}$  Cu the short-term EC50 increased to  $21.3 \pm 1.34 \mu\text{M}$  and after pre-exposure to Cu at 1.78  $\mu\text{M}$  it increased further to  $51.24 \pm 5.85 \mu\text{M}$  (**Figure 1B**). That is, Cu pre-exposure increased the tolerance of the community to short-term exposure by being 2.3 and 5.7, respectively, higher than in control treatment indicating an increase of community tolerance to copper exposure. The photosynthetic activity ( $^{14}\text{C}$ -incorporation) at concentrations of 0.32 and 1.78  $\mu\text{M}$  C was inhibited up to 60% (**Figure 1B**).

## Effects on Prokaryotic and Eukaryotic Community Composition

DNA-sequencing of the 16S and 18S gene fragments yielded a total of 7,109,298 and 5,655,641 high quality reads, respectively. These reads clustered into 17,445 prokaryotic OTUs and 2,151 eukaryotic OTUs (**Table 1**). As shown by the Chao1 diversity index (Chao, 1984; **Supplementary Figure 1**) the sequencing depth was sufficient to achieve the saturation point for identifying both prokaryote and eukaryote taxa.

In unexposed communities, the prokaryote community was dominated mainly by Alphaproteobacteria and Flavobacteria classes, and by taxa affiliated to Phycisphaerae and Saprospirae

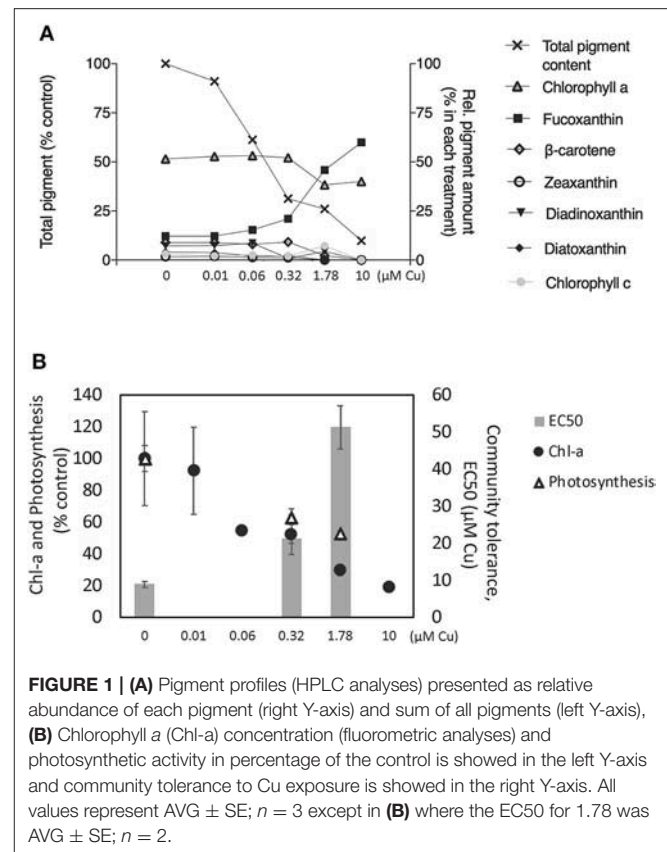


**FIGURE 1 | (A)** Pigment profiles (HPLC analyses) presented as relative abundance of each pigment (right Y-axis) and sum of all pigments (left Y-axis), **(B)** Chlorophyll *a* (Chl-*a*) concentration (fluorometric analyses) and photosynthetic activity in percentage of the control is showed in the left Y-axis and community tolerance to Cu exposure is showed in the right Y-axis. All values represent AVG  $\pm$  SE;  $n = 3$  except in **(B)** where the EC50 for 1.78 was AVG  $\pm$  SE;  $n = 2$ .

(**Figure 2**). The eukaryotic community was predominantly dominated by Ochrophyta and Metazoa, and by taxa affiliated with Chlorophyta, Haptophyta, and other members of Stramenopiles than Ochrophyta (**Figure 2**). Cu exposure decreased the total number of OTUs (**Table 1**) and also significantly reduced the  $\text{chao1}$  diversity of both, the prokaryotic and the eukaryotic part of the periphyton (**Supplementary Figure 1**). The impacts of Cu on prokaryotic and eukaryotic community composition were confirmed by a MANOVA on Unifrac distances (**Table 2**). Significant changes of bacterial community composition were first observed after exposure to 0.06  $\mu\text{M}$  Cu while the eukaryotic part of the periphyton was already significantly impacted after exposure to 0.01  $\mu\text{M}$  Cu (**Table 2, Figure 2**). These findings are also reflected in the PCA plots that visualize the effects of Cu exposure on OTU abundance (**Figure 3**). For prokaryotes (**Figure 3A**), the first axis of the PCA explains 38% of the variance and grouped the samples from the control and 0.01, 0.06, 0.32, and 1.78  $\mu\text{M}$  Cu on the right side of the axis, while samples from 10  $\mu\text{M}$  Cu were grouped on the left side of the axis. The second axis of the PCA explained 37% of the variance and primarily separated the samples in three groups: (i) control and low levels of Cu exposure, from (ii) 1.78  $\mu\text{M}$  Cu, and from (iii) 10  $\mu\text{M}$  Cu (**Figure 3A**). The third axis was also significant and accounted for 12% with no clear separation of the samples. Remarkably, in treatments exposed to high levels of Cu (1.78 and 10  $\mu\text{M}$  Cu), the relative abundance of prokaryotic sequences affiliated

**TABLE 1** | Sequencing information for each sample.

Cu ( $\mu\text{M}$ )	Prokaryote				Eukaryote			
	Raw sequences	High quality reads	OTUs	Core OTUs	Raw sequences	High quality reads	OTUs	Core OTUs
0	401,492	352,513	10,673	7,343	298,545	287,308	1,359	1,048
0	421,254	370,057	10,598		314,776	304,546	1,298	
0	529,896	463,714	10,729		371,406	355,285	1,372	
0.01	499,314	437,519	10,842	7,137	397,999	380,767	1,446	1,095
0.01	481,209	428,187	10,355		367,233	353,131	1,353	
0.01	485,444	435,963	10,052		333,989	321,285	1,429	
0.06	520,732	458,352	10,448	7,354	351,999	338,684	1,398	1,211
0.06	445,386	386,729	10,675		308,046	295,090	1,378	
0.06	539,309	470,684	10,615		405,241	389,808	1,498	
0.32	553,859	493,324	9,830	6,802	353,213	339,263	1,340	1,037
0.32	594,508	531,872	9,925		409,692	395,912	1,333	
0.32	354,786	312,126	9,953		250,921	241,191	1,334	
1.78	392,169	353,045	7,214	4,537	321,938	312,893	1,138	742
1.78	385,956	352,677	6,781		347,776	338,072	1,033	
1.78	357,418	326,682	6,934		327,889	319,083	1,070	
10	236,199	209,893	8,161	5,137	160,531	155,115	856	558
10	500,776	445,464	7,994		323,477	314,640	891	
10	310,783	280,497	7,514		220,522	213,568	838	
Total	8,010,490	7,109,298	17,445	11,549	5,865,193	5,655,641	2,151	1,618

Core OTUs means the OTU was detected by all of the three samples in the same treatment.

to Nostocophycideae and Oscillatoriophycideae classes were especially high and the relative abundance of sequences affiliated with Synechococcophycideae were especially low (Figures 2A, 4).

For Eukaryotes, the first axis of the PCA explained 68% of the variance and separated the samples based on an increasing gradient of Cu exposure from the left side of the axis (control treatment) to the right side of the axis (highest Cu treatment, 10  $\mu\text{M}$  Cu) (Figure 3B). The second axis explained circa 12% of the variance and it also separated the samples based on an increasing gradient of Cu exposure (Figure 3B). It should be pointed out that the relative abundance of sequences associated to Ochrophyta and Lobosa increased in treatments exposed to high levels of Cu (1.78 and 10  $\mu\text{M}$  Cu; Figures 2A, 5). In contrast, the relative abundance of sequences associated to Haptophyta, Metazoa, Chlorophyt, Cliophora, Dinophyta, and Stramenopiles was markedly reduced when comparing to control treatment (Figures 2A, 5).

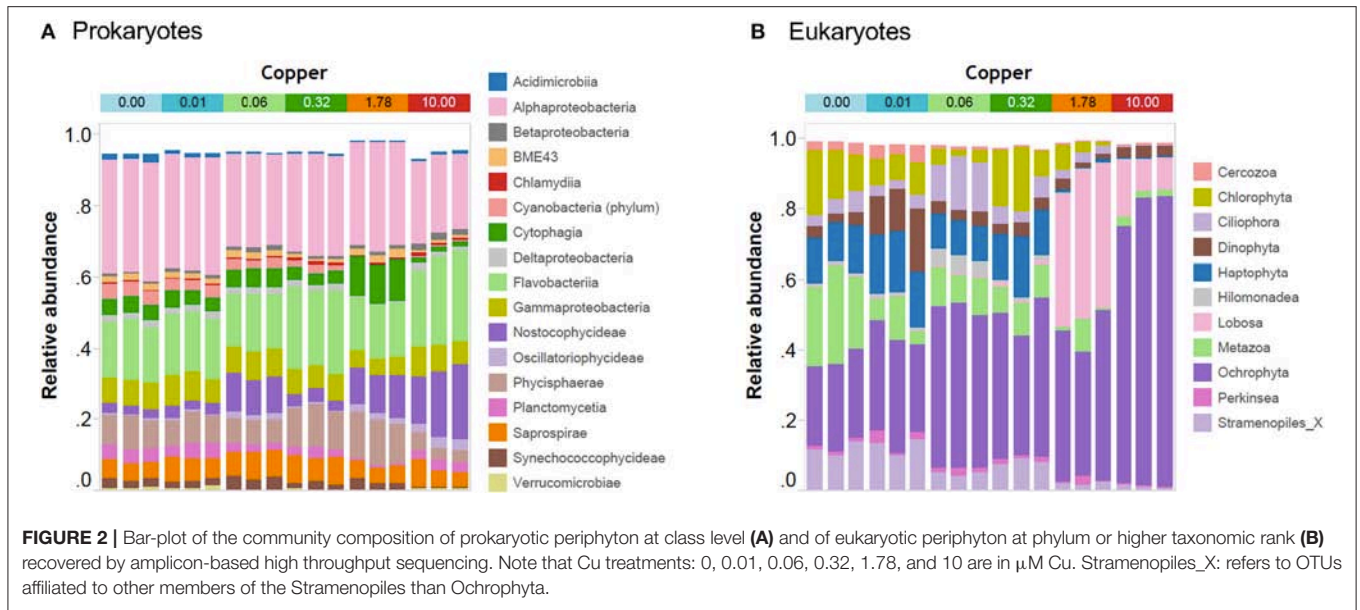
## Cu Sensitive and Tolerant Taxa and Changes in Community Network

Pearson correlation analyses showed different Cu sensitivities among taxa (Figures 4, 5). As a general trend within prokaryotic taxa (i.e., at phylum level), the Cyanobacteria had a strong positive correlation with Cu exposure but, in contrast, abundances of Planctomycetes and Proteobacteria phyla had a strong negative correlation with Cu exposure (Figure 4). For eukaryotes, the Stramenopiles\_X phylum was strongly

positively correlated with Cu exposure and Amoebozoa was weakly positively correlated with Cu exposure. All other phyla within eukaryotes were negatively correlated to Cu exposure. In particular, Hacrobia and Alveolata showed a strong negative correlation to Cu exposure (Figure 5).

A total of 23 taxa can be classified as “sensitive,” showing a clear concentration-dependent decrease (Supplementary Figure 2 and Supplementary Table 2). For prokaryotes, the most sensitive taxa were from the phyla Proteobacteria and Bacteroidetes. Most of the sensitive taxa have a relatively high EC50 above 1  $\mu\text{M}$  Cu, except for four taxa from the Cytrophagales, Rickettsiales, Myxococcales and Oceanospirillales which had EC50 values  $\leq$  1  $\mu\text{M}$  Cu (Supplementary Table 2). Five eukaryotic taxa from the Stramenopiles and Hacrobia taxonomic groups were sensitive to Cu, with EC50 values below 2  $\mu\text{M}$  Cu (Supplementary Table 2).

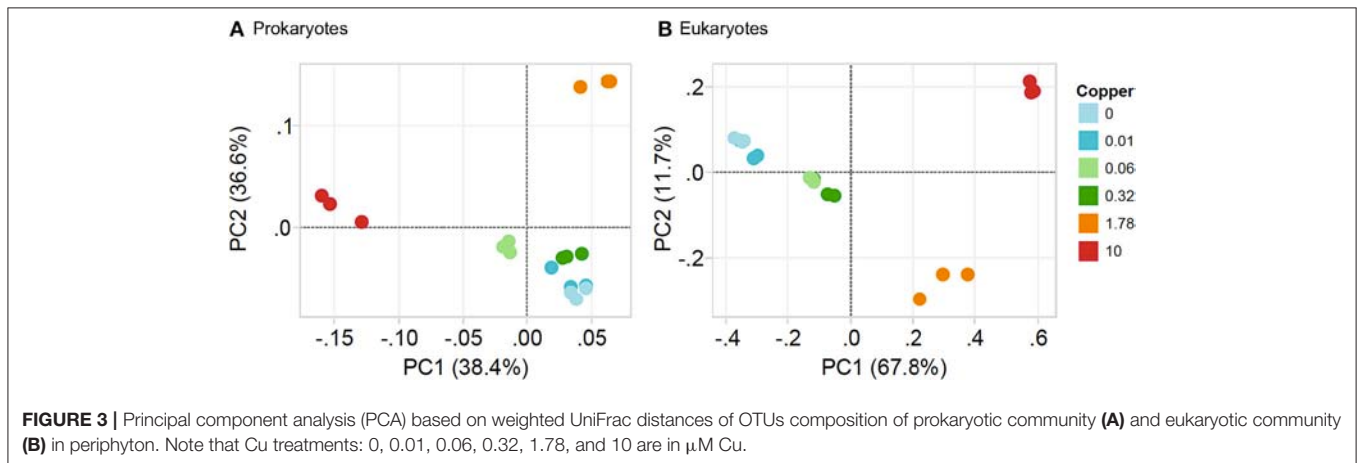
Cu changed the network of associations between taxa in the communities (Figure 6). In control and 0.01  $\mu\text{M}$  Cu treatment, bio-interactions were dominated by the Ciliophora, Dinophyta and Hilomonadea. However, bio-interactions were mainly dominated by the Ciliophora in 1.78 and 10  $\mu\text{M}$  of Cu. It's very interesting that in control and low Cu treatments, species are interrelated to form a closed circuit. When Cu concentration reaches 10  $\mu\text{M}$ , the relationship between species becomes open linear. Low copper exposure increased the network associations, but at Cu concentrations of 0.32  $\mu\text{M}$  and higher the number of nodes decreased and was lower than in the controls at 1.78 and 10  $\mu\text{M}$  of Cu (Table 3).

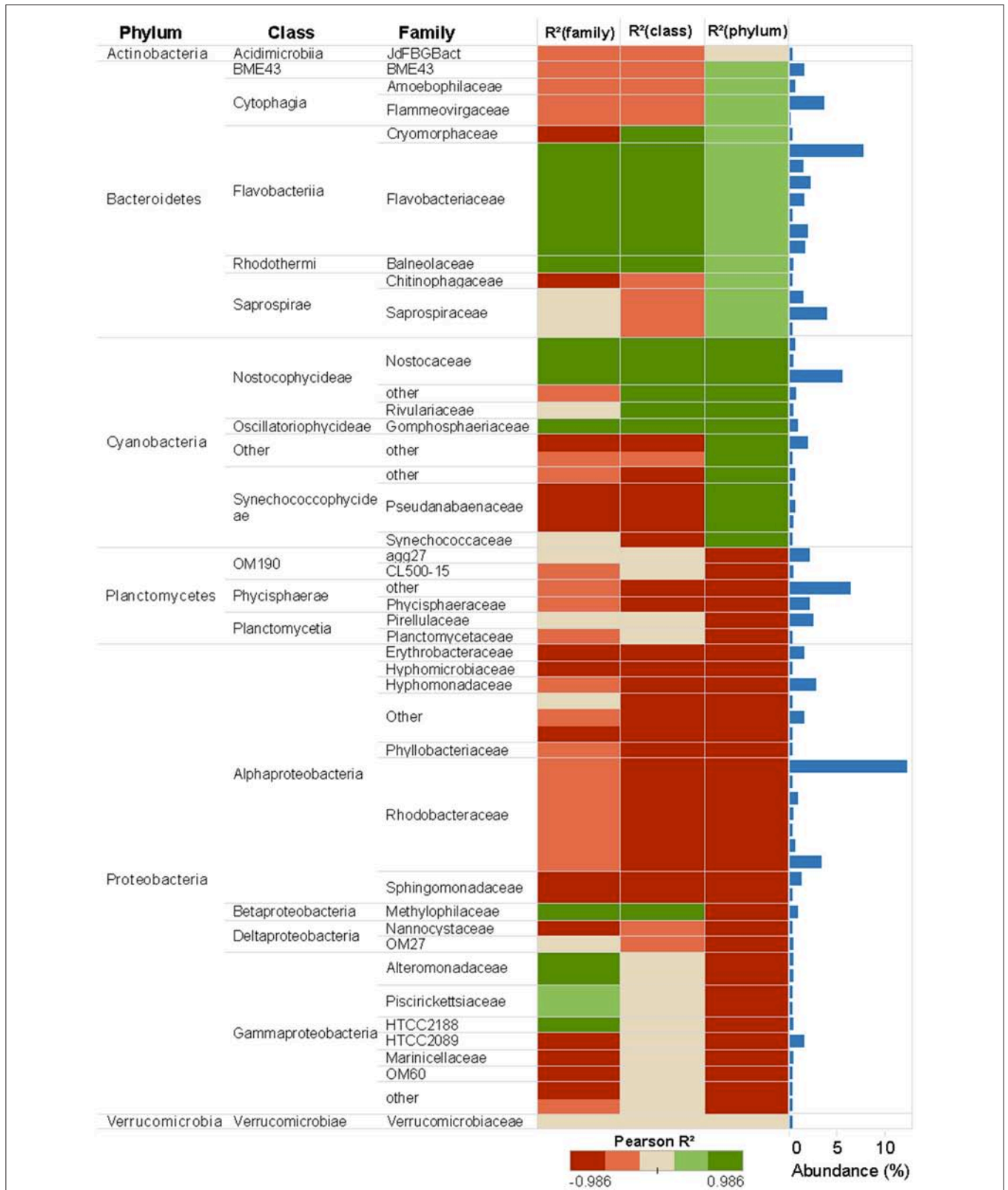


**TABLE 2 |** Mean unifrac distance between Cu treatments.

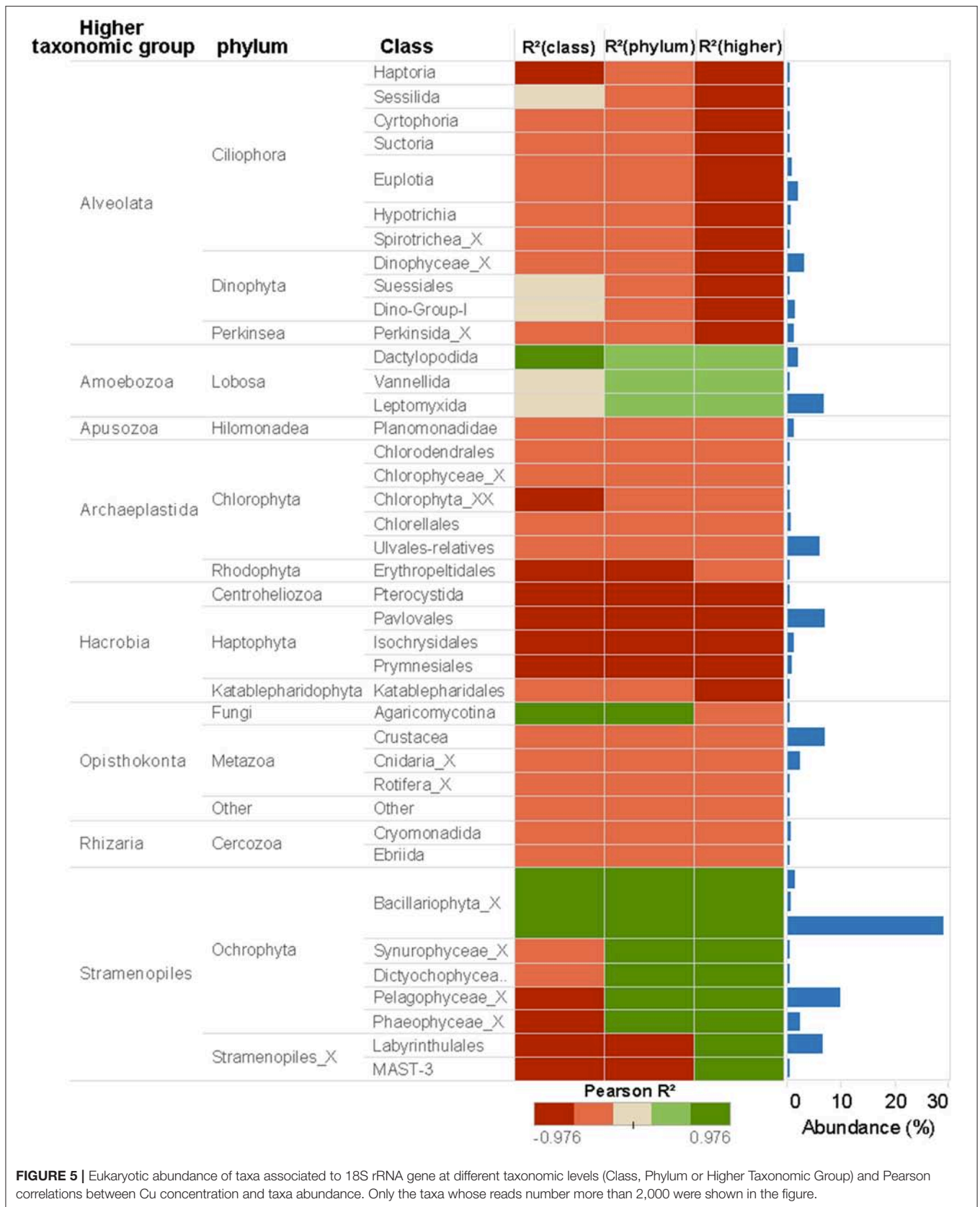
	Cu ( $\mu\text{M}$ )	0	0.01	0.06	0.32	1.78	10
Prokaryote communities	0	0.0409					
	0.01	0.0637	0.0518				
	0.06	<b>0.1193*</b>	<b>0.1034*</b>	0.0330			
	0.32	<b>0.1281*</b>	<b>0.1217*</b>	<b>0.1347*</b>	0.0525		
	1.78	<b>0.2107*</b>	<b>0.1983*</b>	<b>0.1895*</b>	<b>0.196*</b>	0.0378	
	10	<b>0.2127*</b>	<b>0.2028*</b>	<b>0.1663*</b>	<b>0.2092*</b>	<b>0.2413*</b>	0.0574
Eukaryote communities	0	0.1296					
	0.01	<b>0.3900*</b>	0.1758				
	0.06	<b>0.4496*</b>	<b>0.3794*</b>	0.1249			
	0.32	<b>0.4318*</b>	<b>0.4134*</b>	<b>0.2933*</b>	0.1472		
	1.78	<b>0.7605*</b>	<b>0.7346*</b>	<b>0.5675*</b>	<b>0.5112*</b>	0.1637	
	10	<b>0.9693*</b>	<b>0.9405*</b>	<b>0.7708*</b>	<b>0.7324*</b>	<b>0.5508*</b>	0.0968

\* $p < 0.001$  by MANOVA test. Bold values stands for significant unifrac distance between Cu treatments.

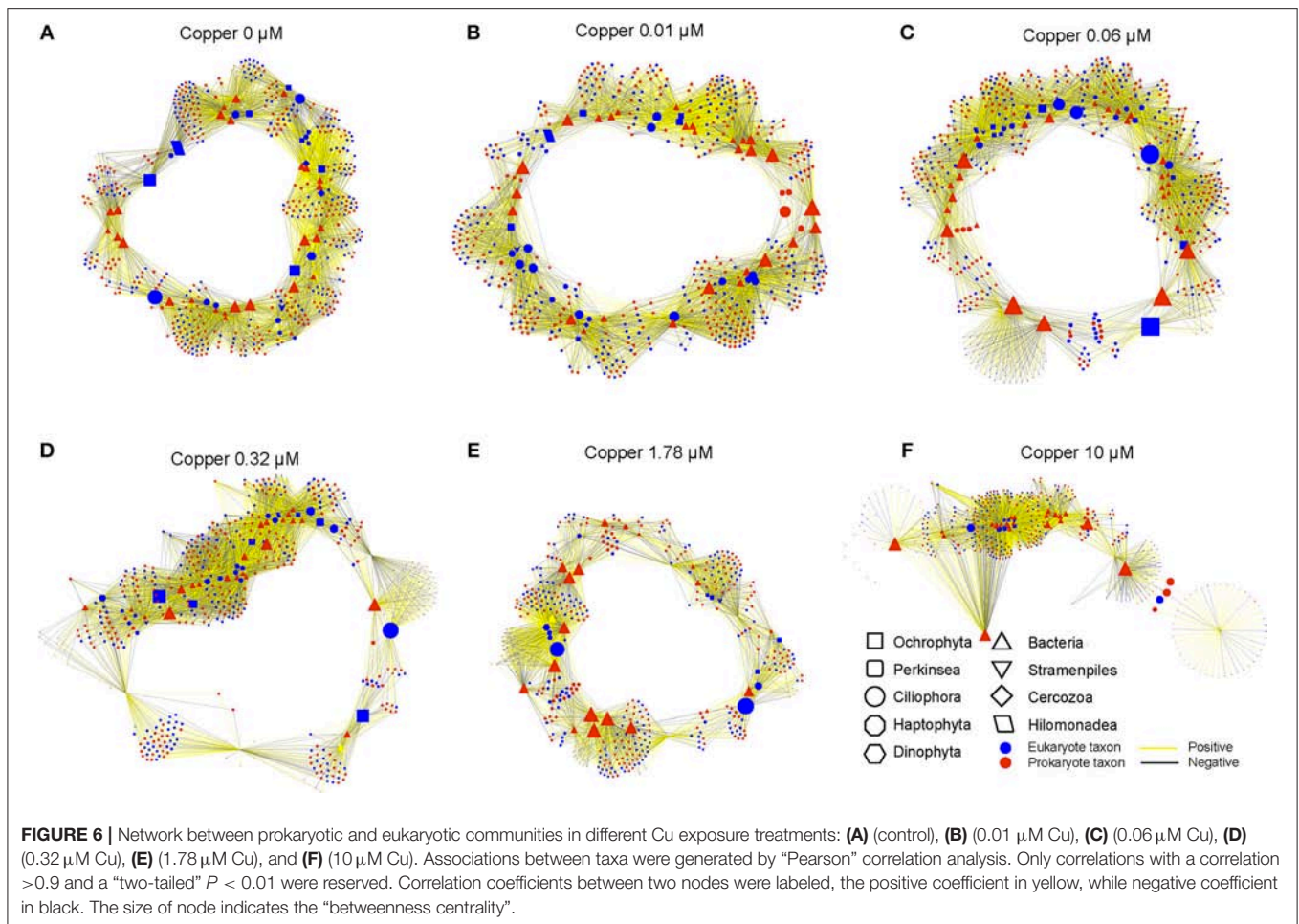




**FIGURE 4 |** Prokaryotic abundance of taxa associated to 16S rRNA gene at different taxonomic levels (Phylum, Class, and Family) and Pearson correlations between Cu concentration and taxa abundance. Only the taxa whose reads number more than 2,000 were shown in the figure. Taxa abundance is presented in the bar plots to the right and include all the taxa detected in the sequence database.



**FIGURE 5 |** Eukaryotic abundance of taxa associated to 18S rRNA gene at different taxonomic levels (Class, Phylum or Higher Taxonomic Group) and Pearson correlations between Cu concentration and taxa abundance. Only the taxa whose reads number more than 2,000 were shown in the figure.

**TABLE 3 |** The topological parameters of network analysis.

	0	0.01	0.06	0.32	1.78	10
Number of nodes	517	529	525	506	453	402
Network heterogeneity	1.505	1.497	1.511	1.652	1.804	1.782
Network density	0.037	0.038	0.038	0.042	0.029	0.048
Multi-edge node pairs	234	252	282	225	104	232
Number of neighbors	19.277	20.276	19.73	21.083	13.223	19.139
Characteristic path length	3.454	3.403	3.488	3.43	3.507	3.728
Network centralization	0.231	0.26	0.24	0.302	0.277	0.368

## DISCUSSION

Our microcosm study provides new insights into the ecological effects of long-term Cu exposure on marine prokaryotic and microeukaryotic organisms within periphyton biofilms. Cu exposure lasted 18 days, which is much longer than

the generation time of studied microorganisms. Microbial prokaryotes and eukaryotes divide in a time range from hours to a few days. Hence, the applied exposure time is considered as long-term or chronic for our test system. Cu decreased prokaryotic and eukaryotic richness (number of OTUs) and the number of their interactions (number of nodes). Eukaryotes were more sensitive than prokaryotic taxa. Despite clear changes in the community structure, which rendered the exposed periphyton communities more Cu-tolerant, Cu exposure decreased the algal biomass and photosynthetic activity of exposed biofilms. Effects on community composition and function were observed at a Cu concentration of 0.06  $\mu\text{M}$ , which is known to occur in the Swedish coastal environment (Egardt et al., 2018). The current environmental quality standard for Cu of 0.07  $\mu\text{M}$  (HVMFS 2015:4) therefore does not seem to be sufficiently protective for periphyton, which contain key primary producers especially in coastal areas where the euphotic zone extends to the sediment (Wasmund, 1993; Sundbäck et al., 2004). Furthermore, it should be emphasized that the results were recorded in an ecologically realistic setting that allowed an ecological succession and competition to shape the communities under long-term chronic Cu exposure. Even though our study was performed in microcosms, prokaryotic and eukaryotic microbial composition established in our periphytic biofilms was comparable to that of

*in situ* marine periphyton on artificial substrata from the same region (i.e., Gullmar fjord; Sanli et al., 2015; Corcoll et al., 2017).

The increase in pollution-induced community tolerance (PICT) coincided with changes in the structure and composition of the community (Figures 1–3), and it also coincided with a decrease in algal biomass and photosynthetic activity (Figure 1). This supports the view put forward first by Blanck et al. (1988), that community tolerance will increase as soon as sensitive species and genotypes are lost from the community. These observations are, however, in contrast to the functional redundancy hypothesis, which assumes that species loss has little impact on ecological functions (Oliver et al., 2015). Instead, they support the notion that biodiversity must be conserved fully, in order to ensure that an exposed community can continue to fulfill its ecological functions in a given ecosystem (Tilman and Downing, 1994). Although previous studies in biofilms have established a link between PICT and the structure of microbial organisms (Dorigo et al., 2010) or the genetic composition of photosynthetic micro-organisms (Eriksson et al., 2009a,b), this study is, to our best knowledge, the first paper that links PICT in biofilms with high-throughput DNA sequencing techniques (metabarcoding) targeting the whole prokaryotic and microeukaryotic microorganisms.

A wide range of sensitive prokaryotic and eukaryotic taxa was observed (Figures 4, 5). The highest Cu-tolerance amongst the prokaryotes was found in the Cyanobacteria phylum, especially in the Nostocophycideae and Oscillatoriphycideae classes (Figure 4). Cyanobacteria resistance to Cu exposure has been observed previously (Barranguet et al., 2000; Serra et al., 2009) and might be attributed to their capacity to synthesize external ligands (Giner-Lamia et al., 2016) so that Cu is accumulated extracellularly (Serra et al., 2009).

Proteobacteria and Bacteroidetes phyla dominated the unexposed periphyton used in the present study, which was sampled from the Gullmar fjord on the Swedish west coast. This is in concordance with previous studies on marine bacterioplankton (Cottrell and Kirchman, 2000; Steven et al., 2012) and periphyton biofilms (Sanli et al., 2015; Corcoll et al., 2017). Cu tolerance of Bacteroidetes was observed in the present study with biofilms, but also similar patterns have been observed in Bacteroidetes from sediments exposed to Cu (Yang et al., 2018). In contrast, the Proteobacteria phylum was the most sensitive phylum to Cu. The abundance of 13 of its taxa, mainly from the dominant Alpha- and Gamma-proteobacteria classes, was reduced in a concentration-dependent manner, with EC50 values as low as 0.61 and 0.91  $\mu\text{M}$  Cu, respectively (Supplementary Table 2). Many species of the phylum Proteobacteria are responsible for nitrification and denitrification processes, or linked with the assimilation of carbon (Ruiz-González et al., 2012; Sanli et al., 2015; Zhao et al., 2017). Given the high sensitivity of Proteobacteria to Cu, we therefore hypothesize that Cu pollution in marine areas could lead to impaired nitrogen cycles. Hence, in a further experiment it would be interesting to study impacts of Cu on microbial activities linked for example to N biogeochemical cycle (Larsson et al., 2007; Mußmann et al., 2013), and not only on photosynthesis.

Eight different eukaryotic higher taxonomic groups were detected (Alveolata, Amoebozoa, Apusozoa, Archaeplastida, Hacrobia, Opisthokonta, Rhizaria, and Stramenopiles; Figures 2, 5), demonstrating once again that benthic marine biofilms host a high biodiversity of prokaryote and microeukaryote organisms (Sanli et al., 2015; Corcoll et al., 2017). Stramenopiles and Amoebozoa were the most tolerant groups to Cu exposure, although the abundance of some fungal families within the Opisthokonta group (Figure 5). Bacillariophyta (diatoms), a family within the Stramenopiles group, was highly tolerant to Cu (Figure 5). Pigment analyses supported these results (Figure 1), since the relative abundance of fucoxanthin, a common marker for diatoms (Roy et al., 2011) also increased with increasing Cu concentrations. These findings agree with previous results of (Gustavson et al., 1999), who also reported an increase of centric Bacillariophyta in marine phytoplankton as a consequence of Cu exposure. The Cu tolerance in diatoms has been linked with their capacity to synthesize extracellular polysaccharides and frustuline (Gonçalves et al., 2018). Nevertheless, previously published mesocosm studies also provide a partly conflicting picture of diatom tolerance to Cu. For instance, in the studies by Barranguet et al. (2000) and Soldo and Behra (2000), diatoms from stream periphyton were less tolerant than green algae or cyanobacteria to long-term Cu exposure. Differences observed between these studies likely are explained because in each microcosm study a different starting algal community was used. Initial algal community composition has been described as a key factor for metal tolerance development in algal communities (Pérez et al., 2010).

In Fungi, the relative abundance of most classes and families was not affected by Cu exposure, which agrees with previous studies in sediment mesocosms (Gardham et al., 2014; Yang et al., 2018). Several resistance mechanisms in fungi to cope with Cu toxicity have been described, such as copper complexing by cell wall components, changes in membrane copper transport, synthesis of intra-cellular copper-binding metallothioneins and phytochelatins, and production of extracellular copper-complexing or -precipitating metabolites (Cervantes and Gutierrezcorona, 1994).

Five algal taxa were inhibited in a concentration-dependent manner: a member of the Pavlovaceae family (Haptophyta), a member of Erythropeltiales order (Rhodophyta) and three taxa within Stramenopiles, with EC50 values ranging from 1.2 to 2  $\mu\text{M}$  Cu (Supplementary Table 2). The abundance of members of Hacrobia was strongly negatively correlated with Cu exposure (Figures 3, 5). Within Hacrobia, the relative abundance of its Haptophyta group declined with Cu exposure. Haptophyta is an important group in the oceans, especially calcifying Haptophyta (coccolithophores) which have a strong effect on the global carbon cycles (Tsuji and Yoshida, 2017). The abundance of other algal groups (Chlorophyta, Rhodophyta, and Dinophyta) was also reduced by Cu exposure, but only to a lower extent. We conclude that Cu effects on the aforementioned algal classes caused the observed decrease of total algal biomass and photosynthetic activity (Figure 1), which goes together well with previous studies that have demonstrated Cu toxicity to photosynthesis

and algal growth at low concentrations (e.g., Pérez et al., 2010).

Ciliophora, a group of protozoa in the Alveolata superphylum, decreased in abundance under Cu exposure (Figure 5), which confirms previous results on the sensitivity of protozoa to Cu (Madoni et al., 1996; Yang et al., 2018). However, little is known about benthic protozoa in general. The use of DNA metabarcoding appears to be able to overcome these limitations and provide a new tool to investigate protozoa in ecotoxicological studies.

The abundances of most taxa from the Metazoa taxonomic group (Crustacea, Cnidaria, or Rotifera) were negatively correlated to Cu exposure (Figure 5). The sensitivity of Metazoa (i.e., Nematodes) to Cu and other environmental factors is well established (Bongers and Ferris, 1999; Boyd and Williams, 2003). This group of micro-eukaryotes eats particulate organic detritus, bacteria, algae, fungi, and protozoans. Hence, they act as regulators of decomposition and therefore play a key role in nutrient cycling and dynamics (Boyd and Williams, 2003; Stelzer, 2011). Hence, direct Cu effects on Metazoa may impact trophic interactions in periphyton biofilms, as network analysis indicate (Figure 6). The relative abundance of some diatoms (Bacillariophyta), within Ochrophyta phyla, increased with Cu exposure as shown by pigments and metabarcoding data (Figures 2B, 3, 5). However, Ochrophyta tend to disappear from the network analyses -with not anymore interactive nodes- when Cu exposure is increasing (Figure 6, Table 3). These results suggest that bacterial-algal interactions which are known to be important, especially in biofilms and microphytobenthos (Decleyre et al., 2015; Krohn-Molt et al., 2017), are negatively affected under Cu exposure. Overall, our network analyses demonstrate that Cu changed the associations between various taxa in the prokaryotic and eukaryotic communities (Figure 6, Table 3) suggesting that the trophic chain interactions and the microbial loop in periphyton biofilms will be altered under certain levels of Cu exposure.

Even though DNA metabarcoding has emerged as a prominent technique to detect a large number of taxa in an environmental sample (Hebert et al., 2003), the technique also has its limitations. The choice of primers affects the biodiversity assessment, and a perfectly universal primer is difficult or even impossible to design (Klindworth et al., 2013; Hugerth et al., 2014; Zhang et al., 2018). To overcome these limitations, a combination of many specific primers to target each of the eukaryotic kingdoms (e.g., ITS gene to target fungi; Nilsson et al., 2009, 23S gene to target algae; Sherwood et al., 2008, or COI to target invertebrates; Leray and Knowlton, 2015) might provide an improved resolution and less bias. In this study, we chose the V3 region of the 16S rRNA gene to target bacteria and the V9 region of the 18S rRNA to target eukaryotes. Both regions are widely used in DNA metabarcoding of microbial communities in various ecosystems (Amaral-Zettler et al., 2009; Klindworth et al., 2013; Corcoll et al., 2017; Yang et al., 2018). However, the region V4 of the 18S rRNA gene has been suggested as an alternative to the V9 region, in order to capture more diversity (Pernice et al., 2013; Hugerth et al., 2014). Another limitation of current metabarcoding approaches, specifically with respect to marine microbial communities is the low coverage in

public sequence repositories for many natural microorganisms, and especially microeukaryotes (Bik et al., 2012; Sanli et al., 2015). In spite of the incompleteness of DNA reference libraries, the suitability of metabarcoding for ecological assessment in freshwater ecosystems, using benthic diatoms, has been recently demonstrated (Rivera et al., 2018).

To conclude, this study allowed us to detect changes in the community composition of benthic pro- and eukaryotes already at 0.06 and 0.01  $\mu\text{M}$  Cu, respectively. These effect concentrations are environmentally realistic (Egardt et al., 2018) and are below the current environmental quality standards (EQS) for copper on the Swedish west coast (HVMFS, 2015). Hence, observed mesocosm results suggest that the current Cu EQS for the marine environment are not protective for prokaryotic and eukaryotic microbial organisms in marine biofilms. Our results provide new information of how Cu pollution affects microbial biodiversity and community composition in the marine environment, data that will aid the setting of appropriate environmental quality standards. Furthermore, this work shows the robustness and the promising potential of DNA metabarcoding as a sensitive tool for community-level ecotoxicological studies that allows to observe impacts simultaneously on a multitude of pro- and eukaryotic taxa, and therefore to identify particularly sensitive, non-cultivable taxa.

## AUTHOR CONTRIBUTIONS

NC, KME, and TB designed the work. NC and KME performed the experiment, processed the samples and performed the analyses for non-sequencing data. NC extracted the DNA. Amplicon sequencing and bioinformatic analyses were performed by JY and XZ. NC wrote the first draft of the paper. All authors discussed, interpreted the results, and contributed to producing the paper.

## FUNDING

This study was financed by the Swedish Research Council Formas (project NICE grant No. 2011-1733, project HerbEvol grant No. 2015-1464), the European Commission (project SOLUTIONS, grant agreement 603437), the Swedish foundation Stiftelsen Brigit och Birger Wählströms minnesfond för den Bohuslänska havs- och insjömiljön and the Royal Swedish Academy of Sciences (KVA).

## ACKNOWLEDGMENTS

The authors would like to thank the support received by all staff at the Sven Lovén Centre of Marine Sciences-Kristineberg and the students Hadrien Kronenberger and Carina Platsen for their technical help to conduct the experiment.

## SUPPLEMENTARY MATERIAL

The Supplementary Material for this article can be found online at: <https://www.frontiersin.org/articles/10.3389/fmicb.2018.03248/full#supplementary-material>

**Supplementary Figure S1** | Average  $\pm$  standard deviation ( $n = 3$ ) of chao1 index in each copper treatment (0, 0.01, 0.06, 0.32, 1.78 and 10  $\mu\text{M}$  Cu) in function of number of sequences associated to 16S rRNA gene **(A)** or to the 18S rRNA gene **(B)**.

**Supplementary Figure S2** | Concentration response curves for the 23 taxa identified as copper sensitive, their EC50s, standard deviation of EC50s. The taxonomy assignment of each taxon was showed in **Supplementary Table 2**.

## REFERENCES

- Alzieu, C. (2000). Environmental impact of TBT: the French experience. *Sci. Total Environ.* 258, 99–102. doi: 10.1016/S0048-9697(00)00510-6
- Amara, I., Miled, W., Slama, R. B., and Ladhari, N. (2018). Antifouling processes and toxicity effects of antifouling paints on marine environment. A review. *Environ. Toxicol. Pharmacol.* 57, 115–130. doi: 10.1016/j.etap.2017.12.001
- Amaral-Zettler, L. A., McCliment, E. A., Ducklow, H. W., and Huse, S. M. (2009). A method for studying protistan diversity using massively parallel sequencing of V9 hypervariable regions of small-subunit ribosomal RNA Genes. *PLoS ONE* 4:06372. doi: 10.1371/journal.pone.0006372
- Ancion, P. Y., Lear, G., and Lewis, G. D. (2010). Three common metal contaminants of urban runoff (Zn, Cu & Pb) accumulate in freshwater biofilm and modify embedded bacterial communities. *Environ. Pollut.* 158, 2738–2745. doi: 10.1016/j.envpol.2010.04.013
- Assenov, Y., F., Ramirez, S. E., Schelhorn, T., Lengauer, and, M., Albrecht (2008). Computing topological parameters of biological networks. *Bioinformatics* 24, 282–284. doi: 10.1093/bioinformatics/btm554
- Barberán, A., Bates, S. T., Casamayor, E. O., and Fierer, N., (2012). Using network analysis to explore co-occurrence patterns in soil microbial communities. *ISME J.* 6, 343–351. doi: 10.1038/ismej.2011.119
- Barranguet, C., Charantoni, E., Plans, M., and Admiraal, W. (2000). Short-term response of monospecific and natural algal biofilms to copper exposure. *Eur. J. Phycol.* 35, 397–406. doi: 10.1080/09670260010001736001
- Barranguet, C., van den Ende, F. P., Rutgers, M., Breure, A. M., Greijdanus, M., Sinke, J. J., et al. (2003). Copper-induced modifications of the trophic relations in riverine algal-bacterial biofilms. *Environ. Toxicol. Chem.* 22, 1340–1349.
- Battin, T. J., Kaplan, L. A., Denis Newbold, J., and Hansen, C. M. E. (2003). Contributions of microbial biofilms to ecosystem processes in stream mesocosms. *Nature* 426, 439–442. doi: 10.1038/nature02152
- Bik, H. M., Porazinska, D. L., Creer, S., Caporaso, J. G., Knight, R., and Thomas, W. K. (2012). Sequencing our way towards understanding global eukaryotic biodiversity. *Trends Ecol. Evol.* 27, 233–243. doi: 10.1016/j.tree.2011.11.010
- Blanck, H., Wängberg, S. Å., and Molander, S. (1988). "Pollution-induced community tolerance – a new ecotoxicological tool," in *Functional Testing of Aquatic Biota for Estimating Hazards of Chemicals*, eds J. J. Cairns and J. R. Pratt (Philadelphia, PA: American Society for Testing and Materials), 219–230.
- Bongers, T., and Ferris, H. (1999). Nematode community structure as a bioindicator in environmental monitoring. *Trends Ecol. Evol.* 14, 224–228. doi: 10.1016/S0169-5347(98)01583-3
- Boyd, W. A., and Williams, P. L. (2003). Comparison of the sensitivity of three nematode species to copper and their utility in aquatic and soil toxicity tests. *Environ. Toxicol. Chem.* 22, 2768–2774. doi: 10.1897/02-573
- Briand, J. F., Barani, A., Garnier, C., Réhel, K., Urvois, F., LePoupon, C., et al. (2017). Spatio-Temporal variations of marine biofilm communities colonizing artificial substrata including antifouling coatings in contrasted french coastal environments. *Microb. Ecol.* 74, 585–598. doi: 10.1007/s00248-017-0966-2
- Caporaso, J. G., Kuczynski, J., Stombaugh, J., Bittinger, K., Bushman, F. D., Costello, E. K., et al. (2010). correspondence QIIME allows analysis of high-throughput community sequencing data. *Nat. Methods* 7, 335–336. doi: 10.1038/nmeth0510-335
- Cervantes, C., and Gutierrezcorona, F. (1994). Copper resistance mechanisms in bacteria and fungi. *FEMS Microbiol. Rev.* 14, 121–137.
- Chao, A. (1984). Non-parametric estimation of the number of classes in a population. *Scand. J. Stat.* 11:265–270.
- Corcoll, N., Acuña, V., Barceló, D., Casellas, M., Guasch, H., Huerta, B., et al. (2014). Pollution-induced community tolerance to non-steroidal anti-inflammatory drugs (NSAIDs) in fluvial biofilm communities affected by WWTP effluents. *Chemosphere* 112, 185–193. doi: 10.1016/j.chemosphere.2014.03.128
- Corcoll, N., Casellas, M., Huerta, B., Guasch, H., Acuña, V., Rodríguez-Mozaz, S., et al. (2015). Effects of flow intermittency and pharmaceutical exposure on the structure and metabolism of stream biofilms. *Sci. Total Environ.* 503–504. doi: 10.1016/j.scitotenv.2014.06.093
- Corcoll, N., Österlund, T., Sinclair, L., Eiler, A., Kristiansson, E., Backhaus, T., et al. (2017). Comparison of four DNA extraction methods for comprehensive assessment of 16S rRNA bacterial diversity in marine biofilms using high-throughput sequencing. *FEMS Microbiol. Lett.* 364. doi: 10.1093/femsle/fnx139
- Cottrell, M. T., and Kirchman, D. L. (2000). Community composition of marine bacterioplankton determined by 16S rRNA gene clone libraries and fluorescence *in situ* hybridization. *Appl. Environ. Microbiol.* 66, 5116–5122. doi: 10.1128/aem.66.12.5116-5122.2000
- Decleyre, H., Heylen, K., Sabbe, K., Tytgat, B., Deforce, D., Van Nieuwerburgh, F., et al. (2015). A doubling of microphytobenthos biomass coincides with a tenfold increase in denitrifier and total bacterial abundances in intertidal sediments of a temperate estuary. *PLoS ONE* 10:e0126583. doi: 10.1371/journal.pone.0126583
- DeSantis, T. Z., Hugenholtz, P., Larsen, N., Rojas, M., Brodie, E. L., Keller, K., et al. (2006). Greengenes, a chimera-checked 16S rRNA gene database and workbench compatible with ARB. *Appl. Environ. Microbiol.* 72, 5069–5072. doi: 10.1128/AEM.03006-05
- Dorigo, U., Berard, A., Rimet, F., Bouchez, A., and Montuelle, B. (2010). *In situ* assessment of periphyton recovery in a river contaminated by pesticides. *Aquat. Toxicol.* 98, 396–406. doi: 10.1016/j.aquatox.2010.03.011
- Edgar, R. C. (2013). UPPARSE: highly accurate OTU sequences from microbial amplicon reads. *Nat. Methods* 10, 996–998. doi: 10.1038/nmet.h.2604
- Egardt, J., Mørk Larsen, M., Lassen, P., and Dahllöf, I. (2018). Release of PAHs and heavy metals in coastal environments linked to leisure boats. *Mar. Pollut. Bull.* 127, 664–671. doi: 10.1016/j.marpolbul.2017.12.060
- Eriksson, K. M., Antonelli, A., Nilsson, R. H., Clarke, A. K., and Blanck, H. (2009a). A phylogenetic approach to detect selection on the target site of the antifouling compound irgarol in tolerant periphyton communities. *Environ. Microbiol.* 11, 2065–2077. doi: 10.1111/j.1462-2920.2009.01928.x
- Eriksson, K. M., Clarke, A. K., Franzen, L. G., Kuylenstierna, M., Martinez, K., and Blanck, H. (2009b). Community-level analysis of psbA gene sequences and irgarol tolerance in marine periphyton. *Appl. Environ. Microbiol.* 75, 897–906. doi: 10.1128/AEM.01830-08
- Festa, R. A., and Thiele, D. J. (2011). Copper: an essential metal in biology. *Curr. Biol.* 21, R877–R883. doi: 10.1016/j.cub.2011.09.040
- Friedman, J., and Alm, E. J. (2012). Inferring correlation networks from genomic survey data. *PLoS Comput. Biol.* 8:e1002687. doi: 10.1371/journal.pcbi.1002687
- Gardham, S., Hose, G. C., Stephenson, S., and Chariton, A. A. (2014). *DNA Metabarcoding Meets Experimental Ecotoxicology: Advancing Knowledge on the Ecological Effects of Copper in Freshwater Ecosystems, 1st Edn*. Elsevier Ltd. doi: 10.1016/B978-0-08-099970-8.00007-5
- Giner-Lamia, J., Pereira, S. B., Bovea-Marco, M., Futschik, M. E., Tamagnini, P., and Oliveira, P. (2016). Extracellular proteins: novel key components of metal resistance in cyanobacteria? *Front. Microbiol.* 7:878. doi: 10.3389/fmicb.2016.00878
- Gonçalves, S., Kahlert, M., Almeida, S. F. P., and Figueira, E. (2018). Science of the total environment assessing cu impacts on freshwater diatoms : biochemical and metabolomic responses of tabellaria flocculosa (Roth) Kützing. *Sci. Total Environ.* 625, 1234–1246. doi: 10.1016/j.scitotenv.2017.12.320
- Guasch, H., Artigas, J., Bonet, B., Bonninau, C., Canals, O., Corcoll, N., et al. (2016). "The use of biofilms to assess the effects of chemicals on freshwater ecosystems," in *Aquatic Biofilms: Ecology, Water Quality and Wastewater Treatment*, eds M. D. Romani, A. M. Guasch, and H. Balaguer (Norfolk: Caister Academic Press), 126–144.
- Gustavson, K., Petersen, S., Pedersen, B., Stuer-Lauridsen, F., Pedersen, S., and Wängberg, S. Å. (1999). Pollution-induced community tolerance (PICT) in

- coastal phytoplankton communities exposure to copper. *Hydrobiologia* 416, 125–138. doi: 10.1023/A:1003811419842
- Hebert, P. D. N., Cywinska, A., Ball, S. L., and deWaard, J. R. (2003). Biological identifications through DNA barcodes. *Proc. R. Soc. B Biol. Sci.* 270, 313–321. doi: 10.1098/rspb.2002.2218
- Hugerth, L. W., Muller, E. E. L., Hu, Y. O. O., Lebrun, L. A. M., Roume, H., Lundin, D., et al. (2014). Systematic design of 18S rRNA gene primers for determining eukaryotic diversity in microbial consortia. *PLoS ONE* 9:095567. doi: 10.1371/journal.pone.0095567
- HVMFS (2015). Havs- och vattenmyndighetens föreskrifter om ändring i Havs- och vattenmyndighetens föreskrifter (HVFS 2013:19) om klassificering och miljö kvalitetsnormer avseende ytvatten. *Hvmfs* 19:185.
- Jespersen, A.-M., and Christoffersen, K. (1987). Measurements of chlorophyll-a from phytoplankton using ethanol as extraction solvent. *Arch. Hydrobiol.* 109, 445–454.
- Klindworth, A., Pruesse, E., Schweer, T., Peplies, J., Quast, C., Horn, M., et al. (2013). Evaluation of general 16S ribosomal RNA gene PCR primers for classical and next-generation sequencing-based diversity studies. *Nucleic Acids Res.* 41, 1–11. doi: 10.1093/nar/gks808
- Krohn-Molt, I., Alawi, M., Förstner, K. U., Wiegandt, A., Burkhardt, L., Indenbirken, D., et al. (2017). Insights into Microalga and bacteria interactions of selected phycosphere biofilms using metagenomic, transcriptomic, and proteomic approaches. *Front. Microbiol.* 8:1941. doi: 10.3389/fmicb.2017.01941
- Larsson, F., Petersen, D. G., Dahllöf, I., Sundbäck, K. (2007). Combined effects of an antifouling biocide and nutrient status on a shallow-water microbial community. *Aquat. Microb. Ecol.* 48, 277–294. doi: 10.3354/ame 048277
- Leray, M., and Knowlton, N. (2015). DNA barcoding and metabarcoding of standardized samples reveal patterns of marine benthic diversity. *Proc. Natl. Acad. Sci. U.S.A.* 112, 2076–2081. doi: 10.1073/pnas.1424997112
- Lock, M. A. (1993). “Attached microbial communities in rivers,” in *Aquatic Microbiology: An Ecological Approach*, ed T. C. S. E. Fore (Oxford: Blackwell Scientific Publications), 113–138.
- Lozupone, C. A., and Knight, R. (2007). Global patterns in bacterial diversity. *Proc. Natl. Acad. Sci. U.S.A.* 104, 11436–11440. doi: 10.1073/pnas.0611525104
- Madoni, P., Vescovi, L., and Emilia, R. (1996). Toxic effect of heavy metals on the activated sludge protozoan community. *Water Res.* 30, 135–141.
- Mandakovic, D., Rojas, C., Maldonado, J., Latorre, M., Travisany, D., Delage, E., et al. (2018). Structure and co-occurrence patterns in microbial communities under acute environmental stress reveal ecological factors fostering resilience. *Sci. Rep.* 8:5875. doi: 10.1038/s41598-018-23931-0
- Massieux, B., Boivin, M. E. Y., Ende, F. P., Van, D. en. Langenskiö, J., and Marvan, P. (2004). Analysis of structural and physiological profiles to assess the effects of Cu on biofilm microbial communities. *Appl. Environ. Microbiol.* 70, 4512–4521. doi: 10.1128/AEM.70.8.4512
- Meylan, S., Behra, R., and Sigg, L. (2004). Influence of metal speciation in natural freshwater on bioaccumulation of copper and zinc in periphyton: a microcosm study. *Environ. Sci. Technol.* 38, 3104–3111. doi: 10.1021/es034993n
- Misson, B., Garnier, C., Lauga, B., Dang, D. H., Ghiglione, J. F., Mullot, J. U., et al. (2016). Chemical multi-contamination drives benthic prokaryotic diversity in the anthropized Toulon Bay. *Sci. Total Environ.* 556, 319–329. doi: 10.1016/j.scitotenv.2016.02.038
- Mußmann, M., Ribot, M., von Schiller, D., Merbt, S. N., Augspurger, C., Karwautz, C., et al. (2013). Colonization of freshwater biofilms by nitrifying bacteria from activated sludge. *FEMS Microbiol. Ecol.* 85, 104–115. doi: 10.1111/1574-6941.12103
- Nilsson, R. H., Ryberg, M., Abarenkov, K., Sjökvist, E., and Kristiansson, E. (2009). The ITS region as a target for characterization of fungal communities using emerging sequencing technologies. *FEMS Microbiol. Lett.* 296, 97–101. doi: 10.1111/j.1574-6968.2009.01618.x
- Oliver, T. H., Heard, M. S., Isaac, N. J. B., Roy, D. B., Procter, D., Eigenbrod, F., et al. (2015). Biodiversity and resilience of ecosystem functions. *Trends Ecol. Evol.* 30, 673–684. doi: 10.1016/j.tree.2015.08.009
- Oursel, B., Garnier, C., Durrieu, G., Mounier, S., Omanović, D., and Lucas, Y. (2013). Dynamics and fates of trace metals chronically input in a Mediterranean coastal zone impacted by a large urban area. *Mar. Pollut. Bull.* 69, 137–149. doi: 10.1016/j.marpolbul.2013.01.023
- Pandey, P. K., Singh, C. B., and Singh, S. P. (1992). Cu uptake in a cyanobacterium: fate of selected photochemical reactions. *Curr. Microbiol.* 24, 35–39. doi: 10.1007/BF01570097
- Parks, R., Donnier-Marechal, M., Frickers, P. E., Turner, A., and Readman, J. W. (2010). Antifouling biocides in discarded marine paint particles. *Mar. Pollut. Bull.* 60, 1226–1230. doi: 10.1016/j.marpolbul.2010.03.022
- Pérez, P., Beiras, R., and Fernández, E. (2010). Monitoring copper toxicity in natural phytoplankton assemblages: application of Fast Repetition Rate fluorometry. *Ecotoxicol. Environ. Saf.* 73, 1292–1303. doi: 10.1016/j.ecoenv.2010.06.008
- Pernice, M. C., Logares, R., Guillou, L., and Massana, R. (2013). General patterns of diversity in major marine microeukaryote lineages. *PLoS ONE* 8:e57170. doi: 10.1371/journal.pone.0057170
- Porsbring, T., Arrhenius, Å., Backhaus, T., Kuylenstierna, M., Scholze, M., and Blanck, H. (2007). The SWIFT periphyton test for high-capacity assessments of toxicant effects on microalgal community development. *J. Exp. Mar. Biol. Ecol.* 349, 299–312. doi: 10.1016/j.jembe.2007.05.020
- Pruesse, E., Quast, C., Knittel, K., Fuchs, B. M., Ludwig, W., Peplies, J., et al. (2007). SILVA: a comprehensive online resource for quality checked and aligned ribosomal RNA sequence data compatible with ARB. *Nucleic Acids Res.* 35, 7188–7196. doi: 10.1093/nar/gkm.864
- R Core Team (2013). *R: A Language and Environment for Statistical Computing*. Vienna: R Foundation for Statistical Computing. Available online at: <http://www.R-project.org/>
- Ritz, C., Baty, F., Streibig, J. C., and Gerhard, D. (2015). Dose-response analysis using R. *PLoS ONE* 10:e0146021. doi: 10.1371/journal.pone.0146021
- Rivera, S. F., Vasselon, V., Jacquet, S., Bouchez, A., Ariztegui, D., Rimet, F., (2018). Metabarcoding of lake benthic diatoms: from structure assemblages to ecological assessment. *Hydrobiologia* 807, 37–51. doi: 10.1007/s10750-017-3381-2
- Roy, S., Llewellyn, C., Egeland, E., and Johnsen, G. (eds.). (2011). *Phytoplankton Pigments: Characterization, Chemotaxonomy and Applications in Oceanography (Cambridge Environmental Chemistry Series)*. Cambridge: Cambridge University Press. doi: 10.1017/CBO9780511732263
- Ruiz-González, C., Lefort, T., Massana, R., Simó, R., and Gasol, J. M. (2012). Diel changes in bulk and single-cell bacterial heterotrophic activity in winter surface waters of the northwestern Mediterranean sea. *Limnol. Oceanogr.* 57, 29–42. doi: 10.4319/lo.2012.57.1.0029
- Sabater, S., Guasch, H., Ricart, M., Romani, A., Vidal, G., Klünder, C., et al. (2007). Monitoring the effect of chemicals on biological communities. The biofilm as an interface. *Anal. Bioanal. Chem.* 387, 1425–34. doi: 10.1007/s00216-006-1051-8
- Salta, M., Wharton, J. A., Blache, Y., Stokes, K. R., and Briand, J.-F. (2013). Marine biofilms on artificial surfaces: structure and dynamics. *Environ. Microbiol.* 15, 2879–2893. doi: 10.1111/1462-2920.12186
- Sanli, K., Bengtsson-Palme, J., Nilsson, R. H., Kristiansson, E., Alm Rosenblad, M., Blanck, H., et al. (2015). Metagenomic sequencing of marine periphyton: taxonomic and functional insights into biofilm communities. *Front. Microbiol.* 6:01192. doi: 10.3389/fmicb.2015.01192
- Schiff, K., Brown, J., Diehl, D., and Greenstein, D. (2007). Extent and magnitude of copper contamination in marinas of the San Diego region, California, USA. *Mar. Pollut. Bull.* 54, 322–328. doi: 10.1016/j.marpolbul.2006.10.013
- Serra, A., Corcoll, N., and Guasch, H. (2009). Copper accumulation and toxicity in fluvial periphyton: the influence of exposure history. *Chemosphere* 74, 633–641. doi: 10.1016/j.chemosphere.2008.10.036
- Sherwood, A. R., Chan, Y. L., and Presting, G. G. (2008). Application of universally amplifying plastid primers to environmental sampling of a stream periphyton community. *Mol. Ecol. Resour.* 8, 1011–1014. doi: 10.1111/j.1755-0998.2008.02138.x
- Soldo, D., and Behra, R. (2000). Long-term effects of copper on the structure of fresh water periphyton communities and tolerance to copper, zinc, nickel and silver. *Aquat. Toxicol.* 47, 181–189. doi: 10.1016/S0166-445X(99)0020-X
- Stelzer, C. P. (2011). A first assessment of genome size diversity in Monogonont rotifers. *Hydrobiologia* 662, 77–82. doi: 10.1007/s10750-010-0487-1
- Steven, B., Mccann, S., and Ward, N. L. (2012). Pyrosequencing of plastid 23S rRNA genes reveals diverse and dynamic cyanobacterial and algal populations in two eutrophic lakes. *FEMS Microbiol. Ecol.* 82, 607–615. doi: 10.1111/j.1574-6941.2012.01429.x

- Sundbäck, K., Linares, F., Larson, F., Wulff, A., and Engelsen, A. (2004). Benthic nitrogen fluxes along a depth gradient in a microtidal fjord: the role of denitrification and *Microphytobenthos* 49, 1095–1107. doi: 10.4319/lo.2004.49.4.1095
- Thomas, K. V., and Brooks, S. (2010). The environmental fate and effects of antifouling paint biocides. *Biofouling* 26, 73–88. doi: 10.1080/08927010903216564
- Tilman, D., and Downing, J. A. (1994). Biodiversity and stability in grasslands. *Nature* 367, 363–365. doi: 10.1038/367363a0
- Tlili, A., Berard, A., Blanck, H., Bouchez, A., Cássio, F., Eriksson, K. M., et al. (2015). Pollution-induced community tolerance (PICT): towards an ecologically relevant risk assessment of chemicals in aquatic systems. *Freshw. Biol.* 61, 2141–2151. doi: 10.1111/fwb.12558
- Tlili, A., Bérard, A., Roulier, J.-L., Volat, B., and Montuelle, B. (2010). PO4<sup>3-</sup> dependence of the tolerance of autotrophic and heterotrophic biofilm communities to copper and diuron. *Aquat. Toxicol.* 98, 165–77. doi: 10.1016/j.aquatox.2010.02.008
- Torstensson, A., Dinasquet, J., Chierici, M., Fransson, A., Riemann, L., and Wulff, A. (2015). Physicochemical control of bacterial and protist community composition and diversity in Antarctic sea ice. *Environ. Microbiol.* 17, 3869–3881. doi: 10.1111/1462-2920.12865
- Tsuji, Y., and Yoshida, M. (2017). Biology of haptophytes: complicated cellular processes driving the global carbon cycle. *Adv. Bot. Res.* 84, 219–261. doi: 10.1016/bs.abr.2017.07.002
- Waldron, K. J., Rutherford, J. C., Ford, D., and Robinson, N. J. (2009). Metalloproteins and metal sensing. *Nature* 460, 823–830. doi: 10.1038/nature08300
- Wang, Q., Garrity, G. M., Tiedje, J. M., and Cole, J. R. (2007). Naïve Bayesian classifier for rapid assignment of rRNA sequences into the new bacterial taxonomy. *Appl. Environ. Microbiol.* 73, 5261–5267. doi: 10.1128/AEM.00062-07
- Wasmund, N. (1993). Ecology and bioproduction in the microphytobenthos of the chain of shallow inlets (Boddens) south of the darss-zingst peninsula (Southern Baltic Sea). *Int. Rev. Total Hydrbiol.* 71, 153–178. doi: 10.1117/12.813996
- Yang, J., Xie, Y., Jeppe, K., Long, S., Pettigrove, V., and Zhang, X. (2018). Sensitive community responses of microbiota to copper in sediment toxicity test. *Environ. Toxicol. Chem.* 37, 599–608. doi: 10.1002/etc.3980
- Yebra, D. M., Kiil, S., and Dam-Johansen, K. (2004). Antifouling technology - Past, present and future steps towards efficient and environmentally friendly antifouling coatings. *Prog. Org. Coatings* 50, 75–104. doi: 10.1016/j.porgcoat.2003.06.001
- Zhang, X., Xia, P., Wang, P., Yang, J., and Baird, D. J. (2018). Omics advances in ecotoxicology. *Environ. Sci. Technol.* 52, 3842–3851. doi: 10.1021/acs.est.7b06494
- Zhang, X.-X., Zhang, T., and Fang, H. H. P. (2009). Antibiotic resistance genes in water environment. *Appl. Microbiol. Biotechnol.* 82, 397–414. doi: 10.1007/s00253-008-1829-z
- Zhao, J., Wu, J., Li, X., Wang, S., Hu, B., and Ding, X. (2017). The denitrification characteristics and microbial community in the cathode of an mfc with aerobic denitrification at high temperatures. *Front. Microbiol.* 8:9. doi: 10.3389/fmicb.2017.00009

**Conflict of Interest Statement:** The authors declare that the research was conducted in the absence of any commercial or financial relationships that could be construed as a potential conflict of interest.

Copyright © 2019 Corcoll, Yang, Backhaus, Zhang and Eriksson. This is an open-access article distributed under the terms of the Creative Commons Attribution License (CC BY). The use, distribution or reproduction in other forums is permitted, provided the original author(s) and the copyright owner(s) are credited and that the original publication in this journal is cited, in accordance with accepted academic practice. No use, distribution or reproduction is permitted which does not comply with these terms.



# AgNPs Change Microbial Community Structures of Wastewater

Yuting Guo<sup>1</sup>, Nicolas Cichocki<sup>1</sup>, Florian Schattenberg<sup>1</sup>, Robert Geffers<sup>2</sup>, Hauke Harms<sup>1</sup> and Susann Müller<sup>1\*</sup>

<sup>1</sup> Department of Environmental Microbiology, Helmholtz Centre for Environmental Research, Leipzig, Germany, <sup>2</sup> Research Group Genome Analysis, Helmholtz Centre for Infection Research, Braunschweig, Germany

## OPEN ACCESS

### Edited by:

Ghiglione Jean-Francois,  
Center for the National Scientific  
Research (CNRS), France

### Reviewed by:

Yingying Wang,  
Nankai University, China  
Marian Brestic,  
Slovak University of Agriculture,  
Slovakia

### \*Correspondence:

Susann Müller  
susann.mueller@ufz.de

### Specialty section:

This article was submitted to  
Microbiotechnology, Ecotoxicology  
and Bioremediation,  
a section of the journal  
Frontiers in Microbiology

Received: 29 August 2018

Accepted: 11 December 2018

Published: 08 January 2019

### Citation:

Guo Y, Cichocki N, Schattenberg F,  
Geffers R, Harms H and Müller S  
(2019) AgNPs Change Microbial  
Community Structures of Wastewater.  
Front. Microbiol. 9:3211.  
doi: 10.3389/fmicb.2018.03211

Due to their strong antimicrobial activity, silver nanoparticles (AgNPs) are massively produced, applied, consumed and, as a negative consequence, released into wastewater treatment plants. Most AgNPs are assumed to be bound by sludge, and thus bear potential risk for microbial performance and stability. In this lab-scale study, flow cytometry as a high-throughput method and 16S rRNA gene amplicon Illumina MiSeq sequencing were used to track microbial community structure changes when being exposed to AgNPs. Both methods allowed deeper investigation of the toxic impact of chemicals on microbial communities than classical EC<sub>50</sub> determination. In addition, ecological metrics were used to quantify microbial community variations depending on AgNP types (10 and 30 nm) and concentrations. Only low changes in  $\alpha$ - and intra-community  $\beta$ -diversity values were found both in successive negative and positive control batches and batches that were run with AgNPs below the EC<sub>50</sub> value. Instead, AgNPs at EC<sub>50</sub> concentrations caused upcoming of certain and disappearance of formerly dominant subcommunities. *Flavobacteriia* were among those that almost disappeared, while phylotypes affiliated with *Gammaproteobacteria* (3.6-fold) and *Bacilli* (8.4-fold) increased in cell abundance in comparison to the negative control. Thus, silver amounts at the EC<sub>50</sub> value affected community structure suggesting a potential negative impact on functions in wastewater treatment systems.

**Keywords:** silver nanoparticles, wastewater microbial community, microbial diversity, single cell analysis, microbial ecotoxicology, silver toxicity

## INTRODUCTION

Silver nanoparticles (AgNPs) are incorporated into various consumer products due to their efficient antimicrobial activity (Chen and Schluesener, 2008; Rai et al., 2009; Wijnhoven et al., 2009; Marambio-Jones and Hoek, 2010). The global production of AgNPs has been estimated to reach ~800 tons by the year 2025 (Pulit-Prociak and Banach, 2016). Along with the increasing production, the application and consumption of AgNP-containing products are known to result in AgNP-release into wastewater treatment systems (Benn and Westerhoff, 2008; Voelker et al., 2015) with up to 50 g/d being detected in the influent of full-scale municipal wastewater treatment plants (WWTPs) (Li et al., 2016). The impact of the antimicrobial activities of silver on the structure and function of microbial wastewater communities is under-investigated. This study wants to test if AgNPs act on persistence of whole microbial communities, or selectively on certain cell types thereby possibly influencing the water purification process.

It has been shown that most of the silver in the WWTPs will be captured and settled in the sludge (Hendren et al., 2013; Barton et al., 2015; Oh et al., 2015). Field analyses of WWTPs estimated that up to 95% of the silver was eliminated from the wastewater by binding to sludge; and silver concentrations in sludge between 1 and 6 mg/kg can be expected (Gottschalk et al., 2009; Li et al., 2016). Batch studies confirmed also for AgNPs (20 and 60 nm) at concentrations of 0.5–10 mg/L more than 90% binding to sludge after a contact time of 6 h (Tiede et al., 2010). Generally, sludge from WWTPs is either incinerated, applied in agriculture or deposited in landfills. According to the European Commission<sup>1</sup>, more than 70% of the total volume of treated sludge is still used in agriculture as fertilizer e.g., in Portugal, Ireland, United Kingdom, and Albania. Since the sludge is recirculated several times within a WWTP before removal, with retention times ranging from 5 to 27 d (Choubert et al., 2011; Jelic et al., 2011) AgNPs embedded within sludge may represent a considerable potential hazard for the activity of key species both within the several operational steps in a WWTP and, later, in agriculture due to their strong antimicrobial activity.

The negative effects of AgNPs on microbial organisms attract increasing attention. On the lab-scale, pure-culture studies mainly on *Pseudomonas*, *Escherichia*, *Staphylococcus*, and *Bacillus* strains were performed to understand the action of silver ions and AgNPs on bacteria (Kim et al., 2007; Yoon et al., 2007; Jin et al., 2010; Suresh et al., 2010; Guo et al., 2017a,b). Toxic effects of AgNPs have been related to cell membrane damage, generation of reactive oxygen species, disruption of the function of biomolecules such as proteins, enzymes, plasmids, and DNA (Reidy et al., 2013; von Moos and Slaveykova, 2014). Silver ions are now commonly believed to be the principle toxic agent over AgNPs (Lok et al., 2007; Xiu et al., 2012; Bondarenko et al., 2013; Visnapuu et al., 2013) which severely affect bacterial growth and function. But AgNP-aggregates enhance this toxicity further since they act as source for a steady release of silver ions into the environment (Guo et al., 2017b). The stability and dissolution of AgNP-aggregates and the resulting toxicity have been reported to be strongly dependent on environmental conditions, such as the ionic strength, the sorption of organic and inorganic species and, therefore, on changes in oxidation and aggregation states (Liu and Hurt, 2010; Xiu et al., 2011; Domingo et al., 2019).

Apart from pure culture studies, microbial communities in complex AgNP-affected environments such as WWTPs were also investigated. In fact it has been reported that microbial communities can serve as indicators for chemical pollution as they are ubiquitously distributed and rapidly respond to environmental disturbances by changes in taxonomic and functional biodiversity (Pesce et al., 2017; Storck et al., 2018). In AgNP-affected environments sequencing approaches are commonly used to resolve microbial community structure changes. But they are impractical for rapid and cheap

enumeration of time series as may be necessary for steadily changing environments that are found in WWTPs. Instead, flow cytometry and related bioinformatics tools have been proven as powerful means for near on-line monitoring the performance of wastewater treatment systems with high temporal resolution (Günther et al., 2012, 2016; Koch et al., 2014). As a rapid, low-cost, and on-site observation method, flow cytometry measures light scatter and fluorescence characteristics of every single cell in a community sample and allows the precise quantification of cells with similar properties (Liu et al., 2018). Therefore, in this study, flow cytometry was used to follow dynamic changes of arising and disappearing subcommunities to reveal diverging and segregated responses of microbial communities to silver stress. In parallel, a selected cell sorting of responding subcommunities and their meta-profiling of the V3-V4 region of the 16S rRNA gene was undertaken to identify phenotypes that might have been affected by AgNPs. Two sizes of 10 and 30 nm AgNPs were chosen for this study as they are among the most commonly used sizes according to the AgNP-database of the Nanotechnology Consumer Products Inventory (Vance et al., 2015). The study is expected to give indications on toxicity of AgNPs on microorganisms derived from wastewater and will discuss possible consequences of changed community structures on WWTP operation.

## MATERIALS AND METHODS

### Materials

Silver nitrate ( $\text{AgNO}_3$ ) (99.9%) was purchased from Sigma-Aldrich (St. Louis, MO, USA). AgNPs were provided by nanoComposix (San Diego, CA, USA) as aqueous suspensions [citrate coated, mass concentration (Ag) 0.02 mg/mL] of the sizes 10 nm ( $9.4 \pm 1.7$  nm, AgNP-10) and 30 nm ( $32.7 \pm 4.8$  nm, AgNP-30). The nanoparticles were stored at 4°C in the dark. Prior to use, vigorous shaking for 30 s was needed to obtain a homogenous suspension. The size distribution and dissolution of the two sizes of AgNPs have been analyzed and published before (Guo et al., 2017b). The size distribution of AgNPs was determined by using the DynaPro Nano Star (WYATT Technology Europe, Dernbach, Germany). The dissolution of ions from AgNPs was determined by separating them using centrifugal ultrafiltration at 14,000 g for 20 min through an Ultra-0.5 Centrifugal Filter Unit with a nominal molecular weight limit of 3 kDa (0.1 nm pore size). The silver ion amount was measured by an Element XR Inductively Coupled Plasma Mass Spectrometer (Thermo Fisher Scientific, Langensfeld, Germany). It was found that AgNP-10 and AgNP-30 formed large aggregates in the medium with diameters of  $445 \pm 58$  and  $473 \pm 65$  nm, respectively; and 4.8 and 1.8% of dissolved silver ions, respectively, within a time period of 12 h.

### Experimental Setup

Wastewater was collected from an activated sludge basin at a full-scale communal WWTP in Eilenburg, Germany ( $51^\circ 27' 39.4''\text{N}$ ,  $12^\circ 36' 17.5''\text{E}$ ,  $\sim 10,200$  m<sup>3</sup> wastewater per day, and water

<sup>1</sup>[http://ec.europa.eu/eurostat/statistics-explained/index.php?title=\\$File:Sewage\\_sludge\\_disposal\\_from\\_urban\protect\kern+.1667em\relaxwastewater\\_treatment,\\_by\\_type\\_of\\_treatment,\\_2015\\_\(%25\\_of\\_total\\_mass\)\\_V2.png](http://ec.europa.eu/eurostat/statistics-explained/index.php?title=$File:Sewage_sludge_disposal_from_urban\protect\kern+.1667em\relaxwastewater_treatment,_by_type_of_treatment,_2015_(%25_of_total_mass)_V2.png)

purification according to German Waste Water Ordinance–AbwV, March 2017<sup>2</sup>), fractionated and stored at  $-20^{\circ}\text{C}$ . Medium composition is provided in **Table S1**. Experiments were processed in 50-mL flasks with 10-mL medium in a sequenced-batch cultivation mode. To start the experiments, wastewater fractions from a given sample were slowly defrosted. The operational steps were as follows: equal amounts of these fractions were added to each flask at an initial optical density of 0.09 ( $\text{OD}_{600} = 0.09$ , Ultrospec 1100pro, Amersham Biosciences, Buckinghamshire, UK). The wastewater microbial communities were exposed to 4 concentrations of silver (silver-confined conditions): 0.1 mg/L AgNP-10 (low concentration, LAg10) and 2.25 mg/L AgNP-10 ( $\text{EC}_{50}\text{Ag10}$ ), 7.13 mg/L AgNP-30 ( $\text{EC}_{50}\text{Ag30}$ ) and 0.25 mg/L  $\text{AgNO}_3$  (silver ion positive control, Pos). The concentrations of  $\text{EC}_{50}\text{Ag10}$ ,  $\text{EC}_{50}\text{Ag30}$  and Pos referred to determined  $\text{EC}_{50}$  values, which were the effective silver concentrations causing half maximum growth of *Escherichia coli* (Guo et al., 2017b). As a silver ion negative control (Neg) a wastewater microbial community was cultivated without any silver treatment (silver-free condition). The sampling interval was 3–4 d over a time range of 24 d. After each sampling, the wastewater microbial communities were transferred to a new flask with fresh medium, respectively, by repeating the same operational steps. The whole experiments were performed twice in independent setups (Setup 1 and Setup 2). For each treatment per setup, triplicate experiments were performed. All the data mentioned in the main text are from Setup 1, and comparable data from Setup 2 are shown in the **Supplementary Materials**.

## Fixation Procedures

For each sampling, 4 mL of the culture was harvested into a glass tube and centrifuged (3,200 g, 20 min,  $15^{\circ}\text{C}$ ). The cell pellet was re-suspended in 4 mL of 2% paraformaldehyde (PFA) in phosphate buffered saline (PBS, compositions are given in **Table S1**) for 30 min at room temperature (RT), then centrifuged (3,200 g, 10 min,  $15^{\circ}\text{C}$ ). After removing the supernatant the cell pellet was re-suspended in 4 mL of 70% ethanol in distilled water and stored at  $-20^{\circ}\text{C}$  until staining.

## Staining Procedures

Fixed samples were diluted (0.6 mL of fixed sample+1.4 mL of PBS) and ultra-sonicated (ultrasonic bath, Merck Eurolab, Darmstadt, Germany, 35 KHz at RT) for 10 min before centrifugation (3,200 g, 10 min,  $15^{\circ}\text{C}$ ). The cell pellet was washed once with 2 mL of PBS (3,200 g, 10 min,  $15^{\circ}\text{C}$ ). After removing the supernatant, the cell pellet was ultra-sonicated again for 5 min. Following, the cells were adjusted to  $\text{OD}_{700} = 0.035$  with PBS, and 2 mL of the cell suspension was taken and centrifuged (as before). Finally, the cell pellet was re-suspended in 1 mL of stock A (20 min, at RT), centrifuged (as before), re-suspended in 2 mL of stock B (overnight, dark, at RT) until flow cytometric measurement. The compositions of stock A and stock B are presented in **Table S1**.

## Flow Cytometry Measurement

Samples were measured with a MoFlo Legacy cell sorter (Beckman-Coulter, Brea, California, USA) which was equipped with two lasers. The 488 nm laser Genesis MX488-500 STM OPS (Coherent, Santa Clara, California, USA) at 400 mW was used for measurement of forward scatter (FSC; bandpass filter  $488 \pm 5$  nm, neutral density filter 1.9) and side scatter (SSC; bandpass filter  $488 \pm 5$  nm, neutral density filter 1.9, trigger signal), and the 355 nm UV laser Xcyte CY-355-150 (Lumentum, Milpitas, California, USA) at 150 mW for UV-induced fluorescence (bandpass filter  $450 \pm 32.5$  nm). Photomultiplier tubes were purchased from Hamamatsu Photonics (Models R928 and R3896; Hamamatsu, Japan). The fluidic system was run at 56 psi (3.86 bar) with sample overpressure at maximum 0.3 psi and a  $70\ \mu\text{m}$  nozzle. The composition of the sheath fluid is recorded in **Table S1**. Daily calibration of the instrument was performed linearly with  $1.0\ \mu\text{m}$  blue fluorescent beads [FluoSpheres (350/440), lot-no.: F8815] and  $2.0\ \mu\text{m}$  yellow-green fluorescent beads [FluoSpheres (505/515), lot-no.: F8827], both from Thermo Fisher Scientific (Langensfeld, Germany). UV beads [ $0.5$  and  $1\ \mu\text{m}$ , both Fluoresbrite BB Carboxylate microspheres, (360/407), lot-no.: 552744 and 499344, PolyScience, Niles, Illinois, USA] were used for calibration on the logarithmic scale and were added to each sample for measurement stability. A biological standard [*E. coli* BL21 (DE3), stationary phase of growth curve (16 h cultivation time in LB medium), fixed and stained as described before] was measured as a biological adjustment. DNA-stained samples were measured cytometrically as logarithmically scaled 2D-dot plots according to DAPI fluorescence (DNA content) and FSC (cell size related) information. For every 2D-dot plot 250,000 cells were measured.

Cell sorting was done according to a standard protocol (Koch et al., 2013). In short: each sorted sample was composed of 500,000 cells from the selected sorting gate. The sorting was done in the most accurate sort mode of the MoFlo (single and one-drop mode: highest purity 99%) at a rate not higher than 2,500 particles per second. Cells were harvested by a centrifugation step (20,000 g,  $4^{\circ}\text{C}$ , 25 min), and the pellet was frozen at  $-20^{\circ}\text{C}$  for later DNA isolation and 16S rRNA gene amplicon Illumina MiSeq sequencing analysis.

## Flow Cytometric Data Analysis

All cytometrically measured samples (Setup 1: 108 samples, Setup 2: 108 samples) were used to create the gate-template (34 gates) valid for all communities analyzed in the study (**Figure S1**). All the raw data are available at the FlowRepository<sup>3</sup>. Whenever a new subcommunity became apparent, a gate was set. The final gate-template was then applied to each sample to mirror the community structure changes and extract individual gate abundances. The flowCyBar tool<sup>4</sup> was used to visualize the cytometric community structure changes (**Figure S2**) by using gate information of the silver-free and silver-confined samples over a time range of 24 d.

<sup>2</sup><http://www.gesetze-im-internet.de/abwv/AbwV.pdf>

<sup>3</sup><https://flowrepository.org/id/FR-FCM-ZYD7-8>

<sup>4</sup><https://bioconductor.org/packages/release/bioc/html/flowCyBar.html>

## Determination of Cytometric $\alpha$ -Diversity and Intra-Community $\beta$ -Diversity Values

The cytometric  $\alpha$ -diversity calculated through gate-based Hill numbers ( $D_q = 0$ ) (Hill, 1973) has been proven to be a reasonable and fast measure to follow the diversity's richness in a community (Günther et al., 2016; Props et al., 2016; Liu et al., 2018). Only those subcommunities were counted that pass the average cell abundance threshold of 2.9%. These subcommunities were regarded as the dominant subcommunities (Liu et al., 2018).

Cytometric intra-community  $\beta$ -diversity values give information on dissimilarity between sampling days and indicate time-dependent influences of the silver derivatives. Cytometric intra-community  $\beta$ -diversity values were calculated by counting the number of subcommunities that were unique between sampling days (Günther et al., 2016).

## Sequencing Workflow

### DNA Extraction

The selected samples for sequencing are listed in **Table S2**. Unsorted samples (whole community samples) were diluted in 70  $\mu$ L PBS to a final  $OD_{700} = 0.01$ . Sorted cells (500,000 cells) from each gate of interest were pelleted by centrifugation (20,000 g, 4°C, 25 min). The DNA was extracted according to the protocol of Koch et al. (2013) and stored at  $-20^\circ\text{C}$  until library preparation.

### Library Preparation for Illumina®

The V3-V4 region of the bacterial 16S rRNA gene region was the target of the used primers Pro341F 5'-CCTACGGGNBGCASCAG-3' (Takahashi et al., 2014) and Pro805R 5'-GACTACNVGGGTATCTAATCC-3' (Herlemann et al., 2011) which were synthesized by Eurofins (Eurofins Scientific, Luxembourg city, Luxembourg) as were also the 6-nt-barcoded primers for library preparation. The library was prepared by using a two-step PCR procedure. Between and after PCR steps, the amplicons were purified, their purity was tested by gel electrophoresis, and finally quantified before they were equimolarly pooled for sequencing by the Illumina MiSeq platform. Details are provided in the sequencing workflow part in the **Supplementary Materials**.

### Sequencing Data Evaluation

The sequencing data evaluation was done by using the Mothur program 1.39 (Schloss et al., 2009). The chimeras were removed by using UCHIME (Edgar et al., 2011) and the OTU classification was done by using the Mothur's average neighbor clustering algorithm with a 97% sequence similarity cut-off on the SILVA database version 128 (Quast et al., 2013). The obtained data sets were normalized by a subsampling procedure to 4,483 cleaned reads per sample. All the raw data are available under the BioProject accession number: PRJNA400127. To ensure the reliability of the sequencing and evaluation procedures, two mock strains and a mock community (MBarcode26), (Singer et al., 2016) were included in the analysis. The sequencing data evaluation comprised the set-up of an OTU threshold at the level of 0.71% according to recommendations of Bokulich

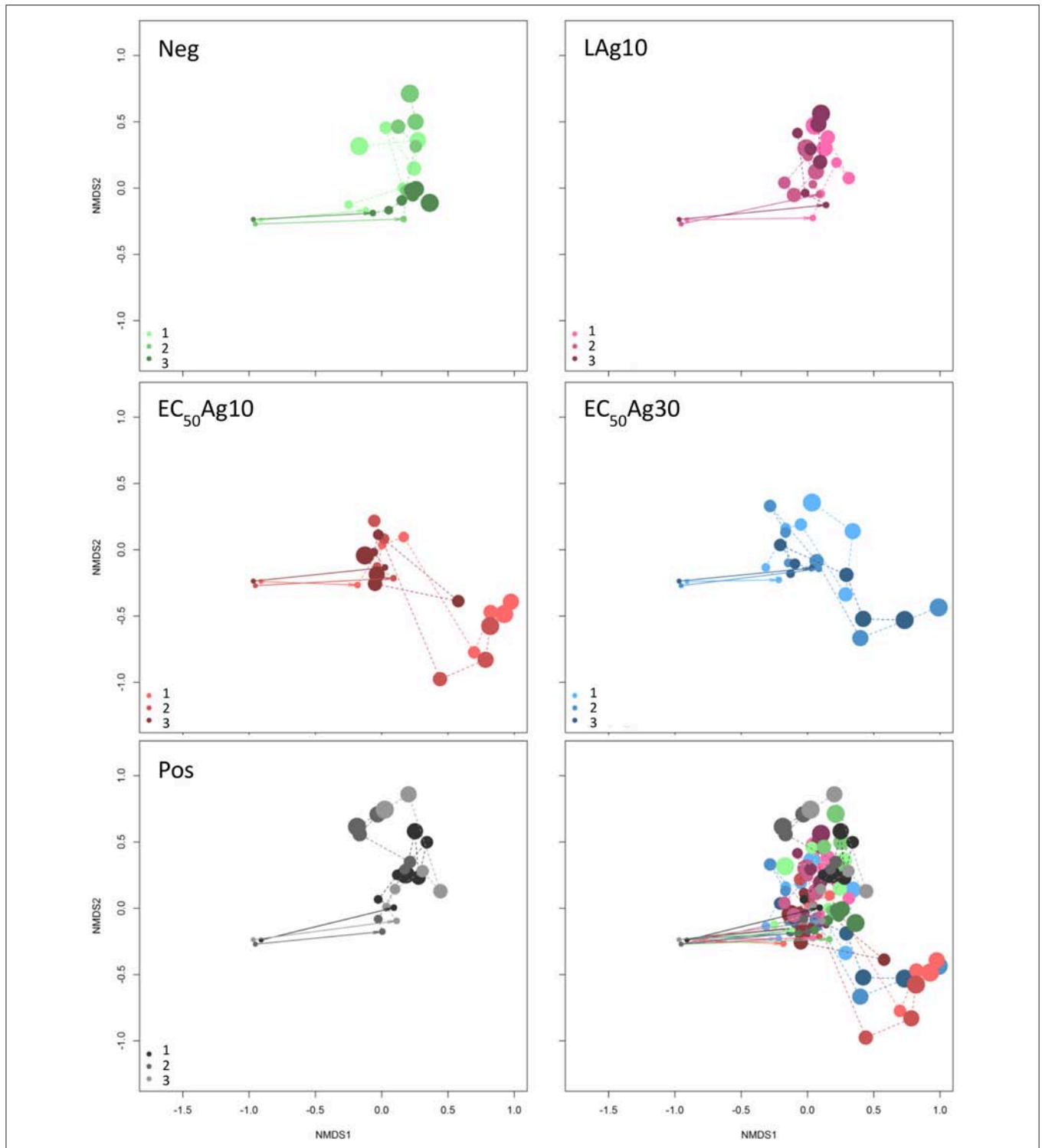
et al. (2012). Details are in the sequencing workflow part in the **Supplementary Materials**.

## RESULTS

### Fingerprinting of Silver Influenced Wastewater Microbial Community Structures

The aim of this study was to investigate if and to what extent silver ions and nanoparticles influence microbial community structures in WWTPs, and to track the microbial community structure dynamics in response to these disturbances.  $\text{AgNO}_3$  and two sizes of AgNPs (10 and 30 nm) at  $EC_{50}$  concentrations and below were used as toxicants. Wastewater microbial communities were grown in a sequenced-batch cultivation mode and their growth dynamics were cytometrically analyzed by using the inherent cell information on cell light scattering and cell DNA contents. The dynamics of the five cultivated microbial communities in the two independent setups are shown in the **Movies S1, S2**. In the cytometric histograms, the cells with similar optical properties clustered together as a subcommunity (technically a gate). The positions and cell abundances of the subcommunities in a histogram reflected the community structures (Koch et al., 2013; Günther et al., 2016), and their relative changes were documented over 24 d by means of biostatistic tools such as non-metric multidimensional scaling (NMDS) plots based on Bray-Curtis dissimilarity (stress of 0.12). The results are shown in **Figure 1**. The inoculum of the WWTP derived community to the sequenced-batch cultivation conditions caused an adaptation in community structures, as was shown from the first to the second sampling point, both under silver-free and silver-confined conditions. Thereby, at low AgNP concentration treatment, the community structures showed high similarities with those of the negative control, and also with the positive control. In contrast, AgNPs (10 and 30 nm) at  $EC_{50}$  concentrations indicated different developments in community structures. Comparable results for Setup 2 are presented in **Figure S3**. Therefore, the  $EC_{50}$  concentrations of AgNPs (10 and 30 nm) can be expected to impact the communities to a different degree in comparison to the controls and the low AgNP concentration treatment.

Yet, if the AgNPs affected all cells in a community equally or acted selectively on particular subcommunities still remained to be clarified. Therefore, trends of cell abundance variations for each gate per treatment were estimated from 4 d (after the adaptation) to 24 d, to mark the influenced gates (**Figure 2** and **Table S3**). Typically, for the controls and the low AgNP concentration, similar subcommunities (G8–G10) dominated the whole communities. In contrast, at  $EC_{50}$  values of AgNPs (10 and 30 nm) the whole communities were dominated by other subcommunities, e.g., G4 and G11. At the same  $EC_{50}$  values of AgNPs (10 and 30 nm) decreases in cell abundances were strong in some of the initially highly abundant subcommunities such as G1–G3, and G6. The slopes ( $k$ ) of trends per treatment and gate, calculated for the time range from 4 to 24 d, highlighted this development (**Figure 2** and **Table S3**). For



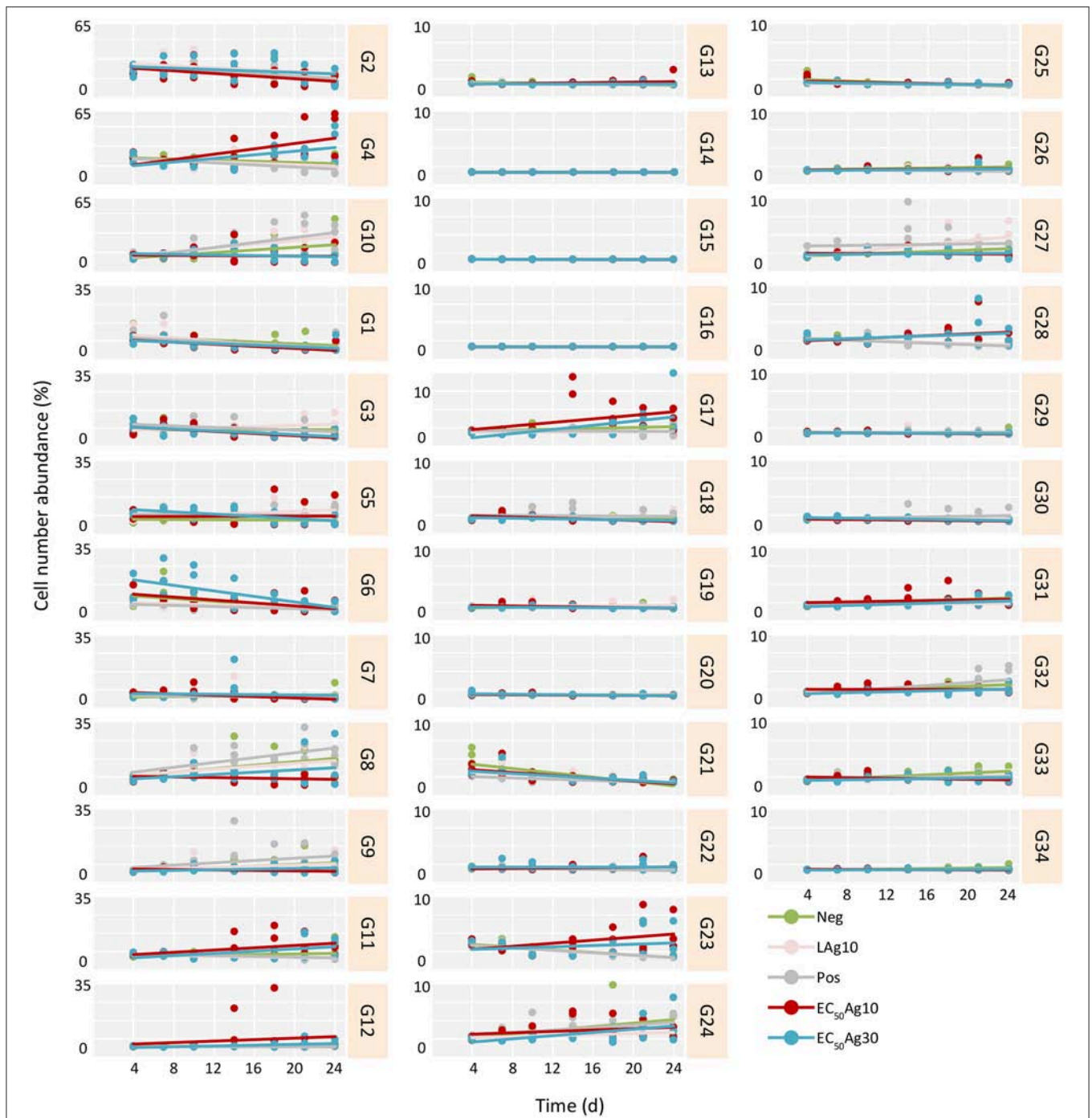


**FIGURE 2 |** Trends in cell number increase or decrease per treatment and gate from 4 to 24 d for Setup 1 (inoculum of 0 d is excluded). The trends are estimated for all treatments and their respective triplicates: silver ion negative control (Neg), 0.1 mg/L AgNP-10 (LAg10), silver ion positive control of 0.25 mg/L AgNO<sub>3</sub> (Pos), 2.25 mg/L AgNP-10 (EC<sub>50</sub>Ag10), and 7.13 mg/L AgNP-30 (EC<sub>50</sub>Ag30). The slope (*k*) of each trend is given in **Table S3**.

example, the EC<sub>50</sub>Ag30 *k*-values were for G1: -0.21, G2: -0.37, G3: -0.25, and G6: -0.75. Contrarily, cell abundances increased for G4 from 3.1 ± 0.1 to 46.5 ± 23.8% and for G11 from 0.8 ± 0.1 to 8.3 ± 4.8% (with *k*-values of 0.92 and 0.31, respectively) within 20 d under EC<sub>50</sub>Ag30 treatment. These data

indicate that AgNPs at EC<sub>50</sub> values selectively affect specific subcommunities.

Further, the effect of each treatment on the cells was calculated by using Spearman's correlation coefficients (*rho*). Only correlations with *rho* ≥ | 0.4 | were regarded

as strong (Table S4). For the controls and the low AgNP concentration treatment, the dominant gates G8–G10 showed always strong positive rho values. Instead, under EC<sub>50</sub>AgNP treatments, other subcommunities emerged (G4 and G11) with solid positive rho values. Contrarily, under the same conditions, G3 was one of those gates that lost cell numbers during EC<sub>50</sub>AgNP treatments which is verified by highly significant and strongly negative rho values.

## Diversity Values of Microbial Communities Influenced by Silver

Since AgNPs at EC<sub>50</sub> values led to more distinct community structure changes, their influences on the community diversity were further investigated via two ecological metrics based on the cytometric gate information: cytometric  $\alpha$ -diversity and intra-community  $\beta$ -diversity.

The cytometric  $\alpha$ -diversity values were constant between 6 and 9 for the silver-free and silver-confined samples over 24 d (Figure 3A). However, the cytometric intra-community  $\beta$ -diversity showed obvious fluctuations. Highest values were found after 4 d (values between 7 and 8) for all silver-free and silver-confined samples, which implied an adaptation process from the wastewater inoculum to the sequenced-batch cultivation conditions (Figure 3B). Afterwards, the negative and the positive controls and low AgNP concentration treatment showed a stable intra-community  $\beta$ -diversity (values between 1 and 4). Instead, AgNPs at EC<sub>50</sub> values caused higher intra-community  $\beta$ -diversity

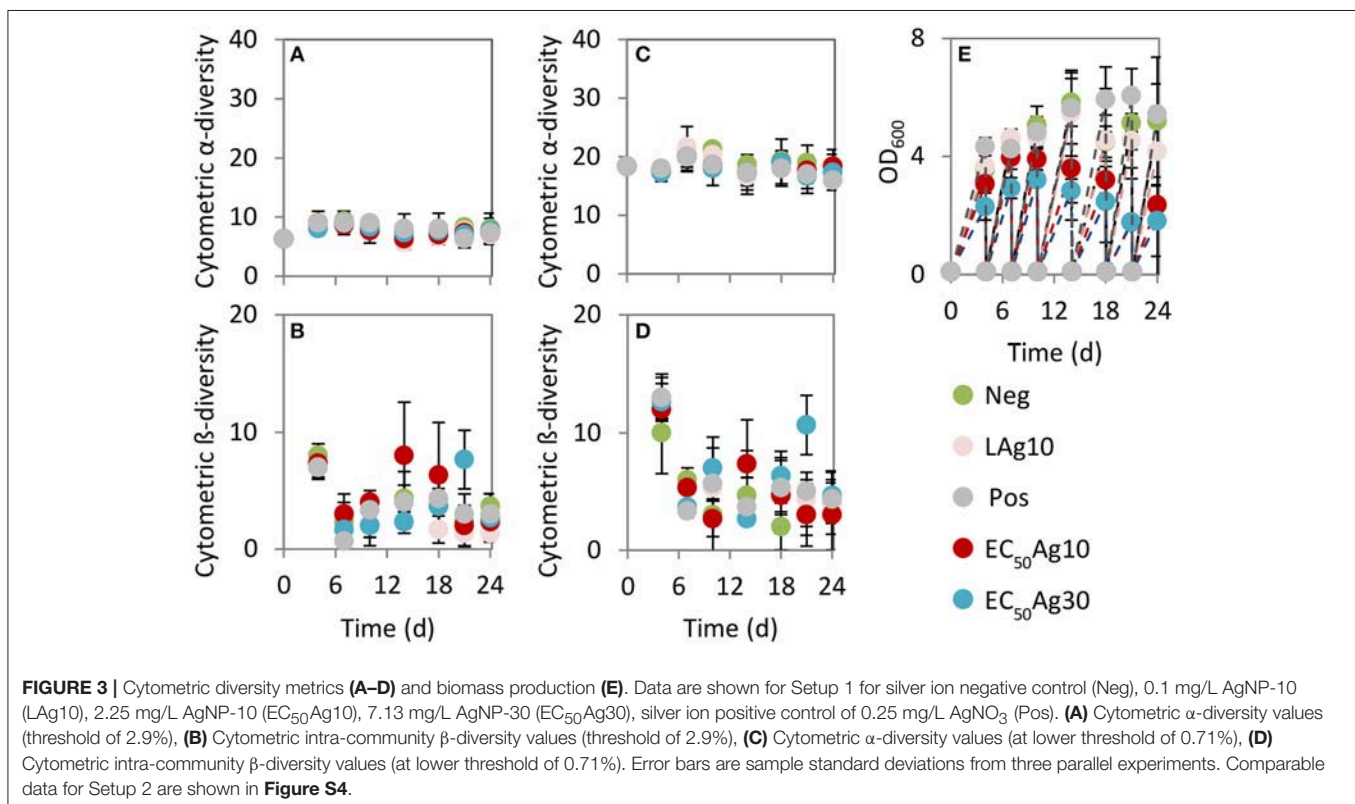
variations (values between 2 and 8), which suggested serious community differences between sampling days.

By choosing a lower threshold of 0.71% to determine Hill number  $D_{q=0}$ , which was adjusted according to the threshold set by the 16S rRNA gene amplicon sequencing data, the cytometric  $\alpha$ -diversity and intra-community  $\beta$ -diversity values showed the same trends (Figures 3C,D). Although more subcommunities were included in the richness analysis (values between 16 and 21) (Figure 3C) in comparison to the higher average cell abundance threshold per gate of 2.9%, the general trend in community behavior did not change.

In addition, the production of biomass, measured by OD<sub>600</sub>, was significantly decreased at EC<sub>50</sub>AgNP treatments by a factor of 2.2 (EC<sub>50</sub>Ag10) and 2.9 (EC<sub>50</sub>Ag30, Figure 3E) when being compared to the negative control. In contrast, low AgNP concentration treatment (factor 1.2) and the positive control (factor 1.0) did not cause huge reduction in biomass. Comparable results for Setup 2 are presented in Figure S4.

## 16S rRNA Gene Amplicon Sequencing to Confirm the Flow Cytometric Data

To confirm the cytometric results of whole microbial community structure changes caused by AgNPs at EC<sub>50</sub> values, selected samples from Setup 1 were further identified by using 16S rRNA gene amplicon sequencing. Therefore, samples were chosen from 7 d, where the adaptation of the microbial community to the new condition was solid, and from 24 d, where the treatment with AgNPs was the longest. To identify the



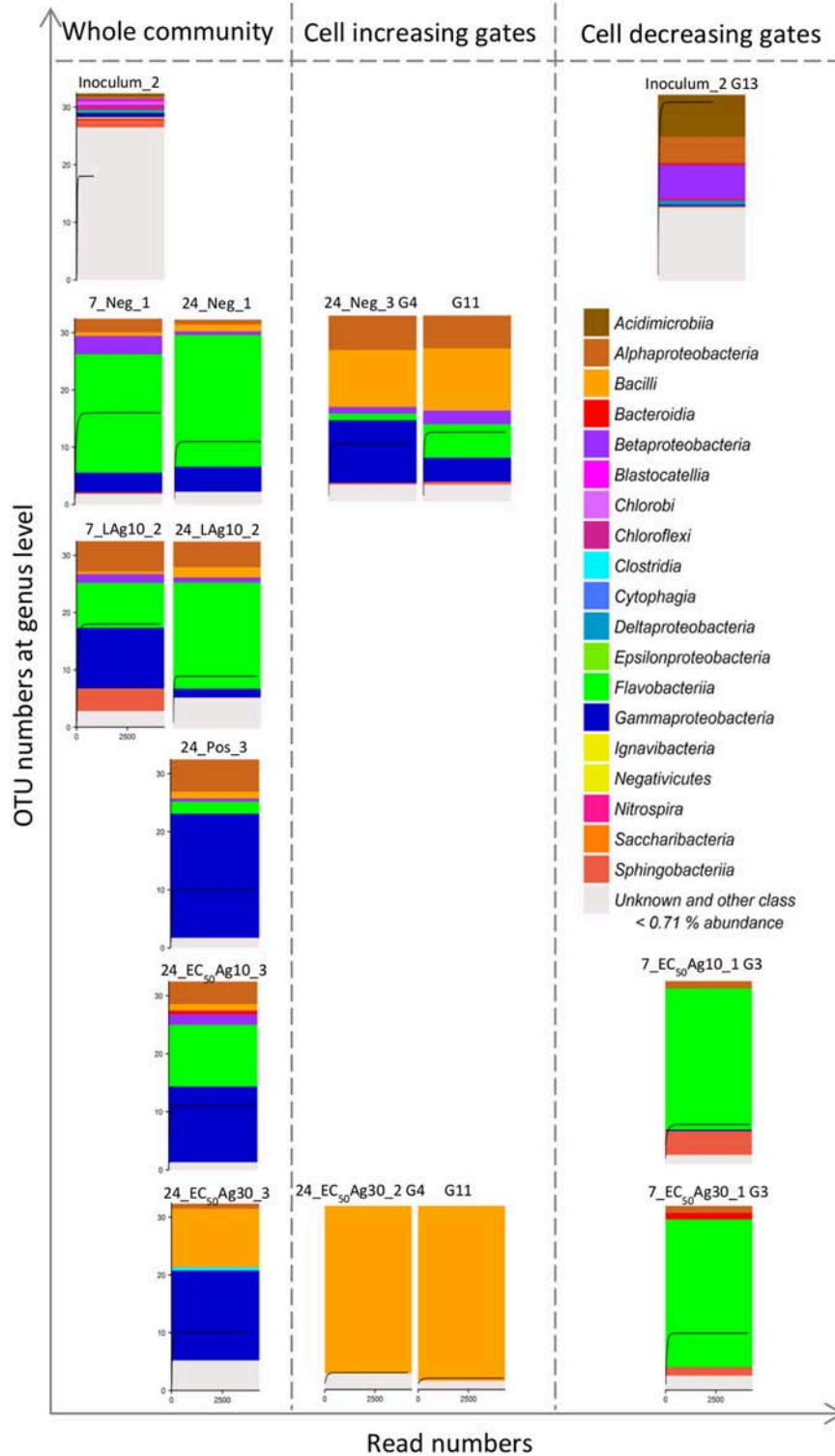


**FIGURE 4 |** 16S rRNA gene amplicon sequencing of 15 samples including 8 whole community samples and 7 sorted subcommunities. Data are shown for Setup 1. The 8 whole community samples included inoculum, silver ion negative control (Neg, 7 and 24 d) and 0.1 mg/L AgNP-10 (LAg10, 7 and 24 d), silver ion positive control (Pos, 24 d), 2.25 mg/L AgNP-10 (EC<sub>50</sub>Ag10, 24 d), 7.13 mg/L AgNP-30 (EC<sub>50</sub>Ag30, 24 d). The 7 sorted subcommunities included the dominant G13 in the inoculum, the positive correlating G4 and G11, and negative correlating G3 with the duration of silver exposure. Each class above a threshold of 0.71% is presented by a color. The rarefaction curve inside each histogram represents the number of genera. Details of class and relative genera list with abundances are shown in **Table S5**.

species of subcommunities that strongly responded positively or negatively to AgNPs at EC<sub>50</sub> concentrations (**Figure 2, Table S4**), subcommunities G4, G11 and G3 from 24 and 7 d were sorted and sequenced. For each sequenced sample, one of the triplicates from either the silver-free and silver-confined batches was chosen as is described in **Table S2**.

The bacterial compositions of sequenced samples are presented in **Figure 4**. The community's diversity was resolved at the class level. Their diversity decreased due to the adaptation from the wastewater inoculum (12 OTUs above threshold of 0.71%, sample *Inoculum\_2*) to batch cultivations (4–7 OTUs above threshold of 0.71%, samples on 7 and 24 d, **Figure 4**), which, however, remained constant as was shown by the cytometric  $\alpha$ -diversity (**Figure 3C**).

Similar to the cytometric data, the sequencing data revealed changes in microbial community structures. The wastewater inoculum represented unique phylotypes (e.g., *Acidimicrobiia*, *Blastocatellia*, *Cytophagia*, *Chlorobi*, *Ignavibacteria*, *Nitrospira*, *Saccharibacteria*), which were absent during the sequenced-batch cultivation mode. G13, which was only highly abundant ( $9.8 \pm 0.9\%$ ) in the inoculum, was sorted and sequenced and found to be dominated mostly by *Acidimicrobiia* (22.3%). Instead, the negative control and the sample treated by low AgNP concentration showed microbial community compositions that were different from the inoculum but similar among themselves on 24 d. Both samples were dominated by *Flavobacteriia* of 71.1 and 57.0%, respectively. The positive control was occupied by *Gammaproteobacteria* of 65.9%. The decrease of *Flavobacteriia* and increase of *Gammaproteobacteria* was also found by the EC<sub>50</sub>AgNP treatments: the *Flavobacteriia* decreased to 32.9% (EC<sub>50</sub>Ag10) and 0.0% (EC<sub>50</sub>Ag30), and the *Gammaproteobacteria* rose up to 40.3 and 48%, respectively (3.0- and 3.5-fold higher than the negative control on 24 d). Additionally, *Bacilli* were found with cell abundance rising up to 31.3% at EC<sub>50</sub>Ag30 treatment (8.4-fold higher than the negative control on 24 d). In this treatment, *Bacilli* were the main phylotypes in the sorted gates G4 and G11 with up to 91.4 and 95.4%, respectively. In the negative control these gates contained the *Bacilli* phylotype to only 40.0%. Instead, the sorted G3 contained *Flavobacteriia* with up to 80.1%.

## DISCUSSION

The aim of this work was to study the impact of AgNPs on microbial community structure and dynamics of wastewater systems by using dense-sampling high-throughput flow cytometry and selected 16S rRNA gene amplicon sequencing. The cytometric results suggested that the investigated wastewater microbial communities tolerated low AgNP concentrations and the silver ion concentration of the positive control (AgNO<sub>3</sub>). The relative diversity was not affected, and the biomass production was reduced by not more than 19.9% (low AgNP concentration treatment). Contrarily, AgNPs at EC<sub>50</sub> values led to clear changes in cytometric community structure, which were obvious since certain subcommunities became dominant, and a biomass loss up to 65.1% (EC<sub>50</sub>Ag30) was found in comparison to the

negative control. This higher toxicity of AgNPs at EC<sub>50</sub> values may originate from their assembly to aggregates which present potential long-term sources of silver ions and thus an enduring toxic effects in comparison to the steady level of silver ions in the positive control (AgNO<sub>3</sub>) (Guo et al., 2017b). The two sizes of AgNPs at EC<sub>50</sub> values showed no effects on cytometric  $\alpha$ -diversity values but comparable biomass reduction on wastewater microbial communities. This could be due to the similar amount of dissolved silver ions from the two sizes of nanoparticles at EC<sub>50</sub> values as was discussed earlier (Guo et al., 2017b). Instead, the cytometric intra-community  $\beta$ -diversity values varied between EC<sub>50</sub>Ag10 and EC<sub>50</sub>Ag30 concentrations. As the complex wastewater community succession was not synchronous between the different treatments, it can be suggested that the species replacement was divergent and therefore their responses different.

Despite the profound loss in biomass caused by AgNPs at EC<sub>50</sub> concentrations, some phylotypes persisted. On the one hand, this persistence may contribute to an intact functionality of the wastewater microbial community since functions are usually redundant (Liang et al., 2010). On the other hand in this study phylotypes that were found to be persistent may present potential problems to the ecosystems. *Bacilli* were found to dominate the whole community with up to 31.3%. The subcommunity G4 seems to be a marker gate for this class. *Bacilli* and *Gammaproteobacteria* which also increased proportionally in comparison to the negative control are known to potentially serve as reservoirs of antibiotic resistance genes (Xiong et al., 2015). It has been reported that heavy metals, such as silver, can promote the selection and enrichment of antibiotic resistance genes (Gullberg et al., 2014; Chen et al., 2015; Li et al., 2017), and silver resistant genes that encode and induce efflux mechanisms have been found in members of the class *Bacilli* and *Gammaproteobacteria* (Babu et al., 2011; Sütterlin et al., 2014). Such mechanisms may support the persistence of *Bacilli* and *Gammaproteobacteria* and contributed to their dominance over other species by EC<sub>50</sub>AgNP treatments. Furthermore, many members of *Bacilli* are known to be able to form spores when the environment is not supporting growth. These spores are extremely resistant to most environmental stress factors. They have little or no metabolic activity and thus are considered as dormant. The dormancy state could last until the environmental conditions can be tolerated by the microorganisms and growth is possible again (Setlow, 2014). It is suggested that tolerant/resistant species are bound to increase in cell numbers by outcompeting sensitive ones in natural communities (Xavier, 2014), an event that was also found for the *Bacilli* and *Gammaproteobacteria* in our sequenced-batch grown wastewater communities. Many well-known pathogens are included in both classes of bacteria, e.g., *Bacillus anthracis*, the cause of anthrax (Spencer, 2003), and *Acinetobacter* (**Table S5**) as an opportunistic pathogen affecting people with compromised immune systems (Antunes et al., 2014).

However, the loss of phylotypes was also detected, like *Flavobacteriia*, which is the predominant class in *Bacteroidetes* phylum from the sequencing data set. This class dominated in the negative control but decreased in cell abundance in the other

setups, especially in EC<sub>50</sub>Ag30 treatment. The subcommunity G3, although showing generally low cell abundances, seems to be a marker gate for this class. *Flavobacteriia* are usually widely distributed in soil and water. It has been reported that *Flavobacterium* sp. supported granule formation in activated sludge due to the production of extracellular polymeric substances (Li et al., 2014). The proportional decrease of *Flavobacteriia* might therefore lead to a loss in the stability of the sludge. This finding is consistent with other published results which showed that *Bacteroidetes* are especially affected by nanoparticles. They are present mainly on the surface of granular sludge or sediment and can, therefore, be easily targeted by AgNPs (Sun et al., 2013; Yang et al., 2016).

Notably, the proportional loss or increase in cell abundance in specific gates and thus their contribution to the whole community fingerprint are sensitive indicators for non-toxic or toxic environments to microbial communities. The use of ecological metrics allowed a fast, continuous and cost-effective screening of the microbial community dynamics which enabled to uncover subcommunities that may serve as indicators for toxic situations. By cell sorting and sequencing of respective gates, the phylogenetic affiliation of the contained members was resolved and, in a future step, subcommunity metagenomics may help to reveal e.g., possibly involved resistance genes. Therefore, this high-throughput technique improves environmental risk assessment and may assess toxic concentration levels e.g., of silver on natural or managed microbial communities, as was done in this study, in a more profound way than classical measurement, e.g., EC<sub>50</sub> determination will allow.

## REFERENCES

- Antunes, L. C., Visca, P., and Towner, K. J. (2014). *Acinetobacter baumannii*: evolution of a global pathogen. *Pathog. Dis.* 71, 292–301. doi: 10.1111/2049-632X.12125
- Babu, M. M., Sridhar, J., and Gunasekaran, P. (2011). Global transcriptome analysis of *Bacillus cereus* ATCC 14579 in response to silver nitrate stress. *J. Nanobiotechnol.* 9:49. doi: 10.1186/1477-3155-9-49
- Barton, L. E., Auffan, M., Durenkamp, M., McGrath, S., Bottero, J.-Y., and Wiesner, M. R. (2015). Monte Carlo simulations of the transformation and removal of Ag, TiO<sub>2</sub>, and ZnO nanoparticles in wastewater treatment and land application of biosolids. *Sci. Total Environ.* 511, 535–543. doi: 10.1016/j.scitotenv.2014.12.056
- Benn, T. M., and Westerhoff, P. (2008). Nanoparticle silver released into water from commercially available sock fabrics. *Environ. Sci. Technol.* 42, 4133–4139. doi: 10.1021/es7032718
- Bokulich, N. A., Subramanian, S., Faith, J. J., Gevers, D., Gordon, J. I., Knight, R., et al. (2012). Quality-filtering vastly improves diversity estimates from Illumina amplicon sequencing. *Nat. Methods* 10, 57–59. doi: 10.1038/nmeth.2276
- Bondarenko, O., Ivask, A., Käkinen, A., Kurvet, I., and Kahru, A. (2013). Particle-cell contact enhances antibacterial activity of silver nanoparticles. *PLoS ONE* 8:e64060. doi: 10.1371/journal.pone.0064060
- Chen, S., Li, X., Sun, G., Zhang, Y., Su, J., and Ye, J. (2015). Heavy metal induced antibiotic resistance in bacterium LSJ7C. *Int. J. Mol. Sci.* 16, 23390–23404. doi: 10.3390/ijms161023390
- Chen, X., and Schluesener, H. J. (2008). Nanosilver: a nanoparticle in medical application. *Toxicol. Lett.* 176, 1–12. doi: 10.1016/j.toxlet.2007.10.004
- Choubert, J. M., Martin Ruel, S., Esperanza, M., Budzinski, H., Miège, C., Lagarrigue, C., et al. (2011). Limiting the emissions of micro-pollutants: what efficiency can we expect from wastewater treatment plants? *Water Sci. Technol.* 63, 57–65. doi: 10.2166/wst.2011.009
- Domingo, G., Bracale, M., and Vannini, C. (2019). Phytotoxicity of silver nanoparticles to aquatic plants, algae, and microorganisms. *Nanomater. Plants Algae Microorgan.* 2, 143–168. doi: 10.1016/B978-0-12-811488-9.00008-1
- Edgar, R. C., Haas, B. J., Clemente, J. C., Quince, C., and Knight, R. (2011). UCHIME improves sensitivity and speed of chimera detection. *Bioinformatics* 27, 2194–2200. doi: 10.1093/bioinformatics/btr381
- Gottschalk, F., Sonderer, T., Scholz, R. W., and Nowack, B. (2009). Modeled environmental concentrations of engineered nanomaterials (TiO<sub>2</sub>, ZnO, Ag, CNT, Fullerenes) for different regions. *Environ. Sci. Technol.* 43, 9216–9222. doi: 10.1021/es9015553
- Gullberg, E., Albrecht, L. M., Karlsson, C., Sandegren, L., and Andersson, D. I. (2014). Selection of a multidrug resistance plasmid by sublethal levels of antibiotics and heavy metals. *mBio* 5, e01918-14. doi: 10.1128/mBio.01918-14
- Günther, S., Faust, K., Schumann, J., Harms, H., Raes, J., and Müller, S. (2016). Species-sorting and mass-transfer paradigms control managed natural metacommunities. *Environ. Microbiol.* 18, 4862–4877. doi: 10.1111/1462-2920.13402
- Günther, S., Koch, C., Hübschmann, T., Röske, I., Müller, R. A., Bley, T., et al. (2012). Correlation of community dynamics and process parameters as a tool for the prediction of the stability of wastewater treatment. *Environ. Sci. Technol.* 46, 84–92. doi: 10.1021/es2010682
- Guo, Y., Baumgart, S., Stärk, H.-J., Harms, H., and Müller, S. (2017a). Mass cytometry for detection of silver at the bacterial single cell level. *Front. Microbiol.* 8:1326. doi: 10.3389/fmicb.2017.01326
- Guo, Y., Stärk, H. J., Hause, G., Schmidt, M., Harms, H., Wick, L. Y., et al. (2017b). Heterogenic response of prokaryotes toward silver nanoparticles and ions is facilitated by phenotypes and attachment of silver aggregates to cell surfaces:

## AUTHOR CONTRIBUTIONS

YG designed and conducted the experiments, evaluated the data and wrote the paper. NC analyzed community and sorted samples by using 16S rRNA gene amplicon Illumina MiSeq sequencing, evaluated those data, and contributed to writing. FS analyzed samples by using flow cytometry, helped to evaluate the data, and contributed to experimental design and writing. RG contributed to 16S rRNA gene amplicon Illumina MiSeq sequencing. HH contributed to writing. SM designed the experiments, evaluated the data, and wrote the paper.

## ACKNOWLEDGMENTS

This work was supported by the Graduate School Leipzig School of Natural Sciences-Building with Molecules and Nanoobjects (BuildMoNa), funded by the European Social Fund (ESF, project number R313H044), and the European Regional Development Funds (EFRE—Europe funds Saxony, 100192205). We thank Zishu Liu for advice who works at Flow Cytometry Group in Helmholtz Centre for Environmental Research (Leipzig, Germany).

## SUPPLEMENTARY MATERIAL

The Supplementary Material for this article can be found online at: <https://www.frontiersin.org/articles/10.3389/fmicb.2018.03211/full#supplementary-material>

- heterogenic response of prokaryotes toward AgNPs. *Cytometry A* 91, 775–784. doi: 10.1002/cyto.a.23055
- Hendren, C. O., Badireddy, A. R., Casman, E., and Wiesner, M. R. (2013). Modeling nanomaterial fate in wastewater treatment: Monte Carlo simulation of silver nanoparticles (nano-Ag). *Sci. Total Environ.* 449, 418–425. doi: 10.1016/j.scitotenv.2013.01.078
- Herlemann, D. P., Labrenz, M., Jürgens, K., Bertilsson, S., Waniek, J. J., and Andersson, A. F. (2011). Transitions in bacterial communities along the 2000 km salinity gradient of the Baltic Sea. *ISME J.* 5, 1571–1579. doi: 10.1038/ismej.2011.41
- Hill, M. O. (1973). Diversity and evenness: a unifying notation and its consequences. *Ecology* 54, 427–432. doi: 10.2307/1934352
- Jelic, A., Gros, M., Ginebreda, A., Cespedes-Sánchez, R., Ventura, F., Petrovic, M., et al. (2011). Occurrence, partition and removal of pharmaceuticals in sewage water and sludge during wastewater treatment. *Water Res.* 45, 1165–1176. doi: 10.1016/j.watres.2010.11.010
- Jin, X., Li, M., Wang, J., Marambio-Jones, C., Peng, F., Huang, X., et al. (2010). High-throughput screening of silver nanoparticle stability and bacterial inactivation in aquatic media: influence of specific ions. *Environ. Sci. Technol.* 44, 7321–7328. doi: 10.1021/es100854g
- Kim, J. S., Kuk, E., Yu, K. N., Kim, J.-H., Park, S. J., Lee, H. J., et al. (2007). Antimicrobial effects of silver nanoparticles. *Nanomed-Nanotechnol.* 3, 95–101. doi: 10.1016/j.nano.2006.12.001
- Koch, C., Günther, S., Desta, A. F., Hübschmann, T., and Müller, S. (2013). Cytometric fingerprinting for analyzing microbial intracommunity structure variation and identifying subcommunity function. *Nat. Protoc.* 8, 190–202. doi: 10.1038/nprot.2012.149
- Koch, C., Harnisch, F., Schröder, U., and Müller, S. (2014). Cytometric fingerprints: evaluation of new tools for analyzing microbial community dynamics. *Front. Microbiol.* 5:273. doi: 10.3389/fmicb.2014.00273
- Li, J., Ding, L.-B., Cai, A., Huang, G.-X., and Horn, H. (2014). Aerobic sludge granulation in a full-scale sequencing batch reactor. *BioMed Res. Int.* 2014, 1–12. doi: 10.1155/2014/268789
- Li, L., Stoiber, M., Wimmer, A., Xu, Z., Lindenblatt, C., Helmreich, B., et al. (2016). To what extent can full-scale wastewater treatment plant effluent influence the occurrence of silver-based nanoparticles in surface waters? *Environ. Sci. Technol.* 50, 6327–6333. doi: 10.1021/acs.est.6b00694
- Li, L.-G., Xia, Y., and Zhang, T. (2017). Co-occurrence of antibiotic and metal resistance genes revealed in complete genome collection. *ISME J.* 11, 651–662. doi: 10.1038/ismej.2016.155
- Liang, Z., Das, A., and Hu, Z. (2010). Bacterial response to a shock load of nanosilver in an activated sludge treatment system. *Water Res.* 44, 5432–5438. doi: 10.1016/j.watres.2010.06.060
- Liu, J., and Hurt, R. H. (2010). Ion release kinetics and particle persistence in aqueous nano-silver colloids. *Environ. Sci. Technol.* 44, 2169–2175. doi: 10.1021/es9035557
- Liu, Z., Cichocki, N., Hübschmann, T., Süring, C., Ofițeru, I. D., Sloan, W. T., et al. (2018). Neutral mechanisms and niche differentiation in steady-state insular microbial communities revealed by single cell analysis. *Environ. Microbiol.* doi: 10.1111/1462-2920.14437. [Epub ahead of print].
- Lok, C.-N., Ho, C.-M., Chen, R., He, Q.-Y., Yu, W.-Y., Sun, H., et al. (2007). Silver nanoparticles: partial oxidation and antibacterial activities. *JBIC J. Biol. Inorg. Chem.* 12, 527–534. doi: 10.1007/s00775-007-0208-z
- Marambio-Jones, C., and Hoek, E. M. V. (2010). A review of the antibacterial effects of silver nanomaterials and potential implications for human health and the environment. *J. Nanoparticle Res.* 12, 1531–1551. doi: 10.1007/s11051-010-9900-y
- Oh, S. Y., Sung, H. K., Park, C., and Kim, Y. (2015). Biosorptive removal of bare-, citrate-, and PVP-coated silver nanoparticles from aqueous solution by activated sludge. *J. Ind. Eng. Chem.* 25, 51–55. doi: 10.1016/j.jiec.2014.10.012
- Pesce, S., Ghiglione, J.-F., and Martin-Laurent, F. (2017). Microbial communities as ecological indicators of ecosystem recovery following chemical pollution. *Microbial Ecotoxicol.* 227–250. doi: 10.1007/978-3-319-61795-4\_10
- Props, R., Monsieurs, P., Mysara, M., Clement, L., and Boon, N. (2016). Measuring the biodiversity of microbial communities by flow cytometry. *Methods Ecol. Evol.* 7, 1376–1385. doi: 10.1111/2041-210X.12607
- Pulit-Prociak, J., and Banach, M. (2016). Silver nanoparticles – a material of the future...? *Open Chem.* 14, 76–91. doi: 10.1515/chem-2016-0005
- Quast, C., Pruesse, E., Yilmaz, P., Gerken, J., Schweer, T., Yarza, P., et al. (2013). The SILVA ribosomal RNA gene database project: improved data processing and web-based tools. *Nucleic Acids Res.* 41, D590–D596. doi: 10.1093/nar/gks1219
- Rai, M., Yadav, A., and Gade, A. (2009). Silver nanoparticles as a new generation of antimicrobials. *Biotechnol. Adv.* 27, 76–83. doi: 10.1016/j.biotechadv.2008.09.002
- Reidy, B., Haase, A., Luch, A., Dawson, K., and Lynch, I. (2013). Mechanisms of silver nanoparticle release, transformation and toxicity: a critical review of current knowledge and recommendations for future studies and applications. *Materials* 6, 2295–2350. doi: 10.3390/ma6062295
- Schloss, P. D., Westcott, S. L., Ryabin, T., Hall, J. R., Hartmann, M., Hollister, E. B., et al. (2009). Introducing mothur: open-source, platform-independent, community-supported software for describing and comparing microbial communities. *Appl. Environ. Microbiol.* 75, 7537–7541. doi: 10.1128/AEM.01541-09
- Setlow, P. (2014). Germination of spores of Bacillus species: what we know and do not know. *J. Bacteriol.* 196, 1297–1305. doi: 10.1128/JB.01455-13
- Singer, E., Andreopoulos, B., Bowers, R. M., Lee, J., Deshpande, S., Chiniquy, J., et al. (2016). Next generation sequencing data of a defined microbial mock community. *Sci. Datas* 3:160081. doi: 10.1038/sdata.2016.81
- Spencer, R. C. (2003). Bacillus anthracis. *J. Clin. Pathol.* 56, 182–187. doi: 10.1136/jcp.56.3.182
- Storck, V., Nikolaki, S., Perruchon, C., Chabanis, C., Sacchi, A., Pertile, G., et al. (2018). Lab to field assessment of the ecotoxicological impact of chlorpyrifos, isoproturon, or tebuconazole on the diversity and composition of the soil bacterial community. *Front. Microbiol.* 9:1412. doi: 10.3389/fmicb.2018.01412
- Sun, X., Sheng, Z., and Liu, Y. (2013). Effects of silver nanoparticles on microbial community structure in activated sludge. *Sci. Total Environ.* 443, 828–835. doi: 10.1016/j.scitotenv.2012.11.019
- Suresh, A. K., Pelletier, D. A., Wang, W., Moon, J.-W., Gu, B., Mortensen, N. P., et al. (2010). Silver nanocrystallites: biofabrication using *Shewanella oneidensis*, and an evaluation of their comparative toxicity on Gram-negative and Gram-positive bacteria. *Environ. Sci. Technol.* 44, 5210–5215. doi: 10.1021/es903684r
- Sütterlin, S., Edquist, P., Sandegren, L., Adler, M., Tängdén, T., Drobni, M., et al. (2014). Silver resistance genes are overrepresented among *Escherichia coli* isolates with CTX-M production. *Appl. Environ. Microbiol.* 80, 6863–6869. doi: 10.1128/AEM.01803-14
- Takahashi, S., Tomita, J., Nishioka, K., Hisada, T., and Nishijima, M. (2014). Development of a prokaryotic universal primer for simultaneous analysis of bacteria and archaea using next-generation sequencing. *PLoS ONE* 9:e105592. doi: 10.1371/journal.pone.0105592
- Tiede, K., Boxall, A. B. A., Wang, X., Gore, D., Tiede, D., Baxter, M., et al. (2010). Application of hydrodynamic chromatography-ICP-MS to investigate the fate of silver nanoparticles in activated sludge. *J. Anal. Atmos. Spectr.* 25, 1149–1154. doi: 10.1039/b926029c
- Vance, M. E., Kuiken, T., Vejerano, E. P., McGinnis, S. P., Hochella, M. F., Rejeski, D., et al. (2015). Nanotechnology in the real world: redeveloping the nanomaterial consumer products inventory. *Beilstein J. Nanotechnol.* 6, 1769–1780. doi: 10.3762/bjnano.6.181
- Visnapuu, M., Joost, U., Juganson, K., Künnis-Beres, K., Kahru, A., Kisand, V., et al. (2013). Dissolution of silver nanowires and nanospheres dictates their toxicity to *Escherichia coli*. *BioMed Res. Int.* 2013:819252. doi: 10.1155/2013/819252
- Voelker, D., Schlich, K., Hohndorf, L., Koch, W., Kuehnen, U., Polleichtner, C., et al. (2015). Approach on environmental risk assessment of nanosilver released from textiles. *Environ. Res.* 140, 661–672. doi: 10.1016/j.envres.2015.05.011
- von Moos, N., and Slaveykova, V. I. (2014). Oxidative stress induced by inorganic nanoparticles in bacteria and aquatic microalgae – state of the art and knowledge gaps. *Nanotoxicology* 8, 605–630. doi: 10.3109/17435390.2013.809810
- Wijnhoven, S. W. P., Peijnenburg, W. J. G. M., Herberths, C. A., Hagens, W. I., Oomen, A. G., Heugens, E. H. W., et al. (2009). Nano-silver – a review of available data and knowledge gaps in human and environmental risk assessment. *Nanotoxicology* 3, 109–138. doi: 10.1080/17435390902725914
- Xavier, J. B. (2014). Social interaction in synthetic and natural microbial communities. *Mol. Syst. Biol.* 7, 483–483. doi: 10.1038/msb.2011.16

- Xiong, W., Sun, Y., Ding, X., Wang, M., and Zeng, Z. (2015). Selective pressure of antibiotics on ARGs and bacterial communities in manure-polluted freshwater-sediment microcosms. *Front. Microbiol.* 6:194. doi: 10.3389/fmicb.2015.00194
- Xiu, Z. M., Ma, J., and Alvarez, P. J. J. (2011). Differential effect of common ligands and molecular oxygen on antimicrobial activity of silver nanoparticles versus silver ions. *Environ. Sci. Technol.* 45, 9003–9008. doi: 10.1021/es201918f
- Xiu, Z. M., Zhang, Q., Puppala, H. L., Colvin, V. L., and Alvarez, P. J. J. (2012). Negligible particle-specific antibacterial activity of silver nanoparticles. *Nano Lett.* 12, 4271–4275. doi: 10.1021/nl301934w
- Yang, J.-L., Li, Y.-F., Liang, X., Guo, X.-P., Ding, D.-W., Zhang, D., et al. (2016). Silver nanoparticles impact biofilm communities and mussel settlement. *Sci. Rep.* 6:37406. doi: 10.1038/srep37406
- Yoon, K.-Y., Hoon Byeon, J., Park, J.-H., and Hwang, J. (2007). Susceptibility constants of *Escherichia coli* and *Bacillus subtilis* to silver and copper nanoparticles. *Sci. Total Environ.* 373, 572–575. doi: 10.1016/j.scitotenv.2006.11.007
- Conflict of Interest Statement:** The authors declare that the research was conducted in the absence of any commercial or financial relationships that could be construed as a potential conflict of interest.

Copyright © 2019 Guo, Cichocki, Schattenberg, Geffers, Harms and Müller. This is an open-access article distributed under the terms of the Creative Commons Attribution License (CC BY). The use, distribution or reproduction in other forums is permitted, provided the original author(s) and the copyright owner(s) are credited and that the original publication in this journal is cited, in accordance with accepted academic practice. No use, distribution or reproduction is permitted which does not comply with these terms.



# The Microbiome Stress Project: Toward a Global Meta-Analysis of Environmental Stressors and Their Effects on Microbial Communities

Jennifer D. Rocca<sup>1\*</sup>, Marie Simonin<sup>1\*</sup>, Joanna R. Blaszczak<sup>1,2</sup>, Jessica G. Ernakovich<sup>3</sup>, Sean M. Gibbons<sup>4,5,6</sup>, Firas S. Midani<sup>7</sup> and Alex D. Washburne<sup>1,8</sup>

## OPEN ACCESS

### Edited by:

Stéphane Pesce,  
National Research Institute of Science  
and Technology for Environment and  
Agriculture (IRSTEA), France

### Reviewed by:

Christopher L. Hemme,  
University of Rhode Island,  
United States  
Bharath Prithviraj,  
CUNY Advanced Science Research  
Center, United States

### \*Correspondence:

Jennifer D. Rocca  
jenny.rocca@gmail.com  
Marie Simonin  
simonin.marie@gmail.com

### Specialty section:

This article was submitted to  
Microbiotechnology, Ecotoxicology  
and Bioremediation,  
a section of the journal  
Frontiers in Microbiology

**Received:** 20 September 2018

**Accepted:** 17 December 2018

**Published:** 10 January 2019

### Citation:

Rocca JD, Simonin M, Blaszczak JR,  
Ernakovich JG, Gibbons SM,  
Midani FS and Washburne AD (2019)  
The Microbiome Stress Project:  
Toward a Global Meta-Analysis of  
Environmental Stressors and Their  
Effects on Microbial Communities.  
*Front. Microbiol.* 9:3272.  
doi: 10.3389/fmicb.2018.03272

<sup>1</sup> Department of Biology, Duke University, Durham, NC, United States, <sup>2</sup> Flathead Lake Biological Station, University of Montana, Polson, MT, United States, <sup>3</sup> Department of Natural Resources and the Environment, University of New Hampshire, Durham, NH, United States, <sup>4</sup> Institute for Systems Biology, Seattle, WA, United States, <sup>5</sup> Molecular and Cellular Biology Program, University of Washington, Seattle, WA, United States, <sup>6</sup> eScience Institute, University of Washington, Seattle, WA, United States, <sup>7</sup> Center for Genomic and Computational Biology, Duke University, Durham, NC, United States, <sup>8</sup> Department of Microbiology and Immunology, Montana State University, Bozeman, MT, United States

Microbial community structure is highly sensitive to natural (e.g., drought, temperature, fire) and anthropogenic (e.g., heavy metal exposure, land-use change) stressors. However, despite an immense amount of data generated, systematic, cross-environment analyses of microbiome responses to multiple disturbances are lacking. Here, we present the Microbiome Stress Project, an open-access database of environmental and host-associated 16S rRNA amplicon sequencing studies collected to facilitate cross-study analyses of microbiome responses to stressors. This database will comprise published and unpublished datasets re-processed from the raw sequences into exact sequence variants using our standardized computational pipeline. Our database will provide insight into general response patterns of microbiome diversity, structure, and stability to environmental stressors. It will also enable the identification of cross-study associations between single or multiple stressors and specific microbial clades. Here, we present a proof-of-concept meta-analysis of 606 microbiomes (from nine studies) to assess microbial community responses to: (1) one stressor in one environment: soil warming across a variety of soil types, (2) a range of stressors in one environment: soil microbiome responses to a comprehensive set of stressors (incl. temperature, diesel, antibiotics, land use change, drought, and heavy metals), (3) one stressor across a range of environments: copper exposure effects on soil, sediment, activated-sludge reactors, and gut environments, and (4) the general trends of microbiome stressor responses. Overall, we found that stressor exposure significantly decreases microbiome alpha diversity and increases beta diversity (community dispersion) across a range of environments and stressor types. We observed a hump-shaped relationship between microbial community resistance to stressors (i.e., the average pairwise similarity score between the control

and stressed communities) and alpha diversity. We used Phylofactor to identify microbial clades and individual taxa as potential bioindicators of copper contamination across different environments. Using standardized computational and statistical methods, the Microbiome Stress Project will leverage thousands of existing datasets to build a general framework for how microbial communities respond to environmental stress.

**Keywords:** diversity, global change, stability, 16S rRNA, bacteria, disturbance, phylofactor, community resistance

## INTRODUCTION

In the past decade, the advent of high-throughput sequencing technologies has enabled microbial ecologists to characterize microbial community responses to environmental change at an unprecedented pace. Thousands of studies are now available on the impact of natural and anthropogenic stressors in controlled conditions or along environmental gradients spanning a wide range of biomes. Large collaborative endeavors, like the Earth and Human Microbiome Projects, revealed fundamental biogeographic patterns of microbial diversity under “baseline” or “steady state” conditions (Human Microbiome Project Consortium, 2012; Gilbert et al., 2014; Lloyd-Price et al., 2017; Thompson et al., 2017). While this baseline knowledge is crucial, similar large-scale initiatives are necessary for clarifying how microbiomes respond to fluctuating environmental conditions.

Environmental stressors occur over varying magnitudes, frequencies, and durations (Bender et al., 1984), introducing spatiotemporal heterogeneity into the environment. Spatiotemporal heterogeneity is a key driver in both the maintenance and depletion of biodiversity (Connell, 1978; Huston, 1979; Crain et al., 2008; Shade et al., 2012; Piggott et al., 2015). In ecology, *stressor*, *disturbance*, *perturbation*, and *threat* are often used interchangeably and refer to a variety of environmental changes (natural, anthropogenic, abiotic or biotic). Here, we use the term stressor to refer to any factor that alters steady-state environmental conditions (biotic or abiotic) and influences the growth or mortality of organisms in a community, resulting in either deterministic or stochastic shifts in stationary relative abundance profiles of microbiomes.

The consequences of environmental stressors on organisms are highly context dependent. Often stressors of increasing intensity/duration induce increasing stress levels but they can also affect organisms non-monotonically. For instance, moderate levels of a stressor, such as exposure to some chemical elements (e.g., micronutrients), can be beneficial to organisms, but extremely high levels can impose adverse effects. This common dose-response pattern is often referred to as hormesis or a subsidy-stress response (Odum et al., 1979; Odum, 1985; Calabrese and Baldwin, 2002). Those direct effects of stressors can propagate through ecological interaction webs causing collateral damage. Thus, stressors have both direct (Schimel et al., 2007) and indirect (Vellend, 2010; Evans and Wallenstein, 2014; Knelman et al., 2014) effects on individual taxa, leading to structural shifts in the microbial communities. Stressor-induced changes in community structure and diversity can, in turn, create

feedbacks that further alter the host state (Reese et al., 2018), environmental conditions (Gibbons et al., 2016; Ratzke and Gore, 2018), or microbial ecosystem function (Bissett et al., 2013; Philippot et al., 2013).

In addition to ecological feedbacks, evolutionary feedbacks can influence how microbial communities respond to a stressor (Sanchez and Gore, 2013). For example, rapid evolution of antibiotic resistance can allow species to expand into environments that would normally be restrictive (Baym et al., 2016). However, despite the rapid expansion of research on environmental and host-associated microbiomes, we still have few generalizable insights for how microorganisms respond to stressors at the individual, population, or community levels (Treseder, 2008; Shade et al., 2012; Holden and Treseder, 2013; Duvallet, 2018). Taken together, the combined ecological data from each independent microbiome study could be a powerful resource for characterizing the processes underlying microbial community assembly and microbial population sensitivity or tolerance to environmental stressors. Pioneering meta-analyses focused on environmental perturbations in soil (Ramirez et al., 2018), human gut ecosystems (Duvallet et al., 2017; Gibbons et al., 2018; Jackson et al., 2018), and even across distinct environments (Shade et al., 2013) now provide valuable frameworks for cross-study analyses of 16S rRNA gene amplicon datasets. However, large-scale disturbance meta-analyses that integrate *both* host-associated and free-living microbiomes are currently lacking.

Here, we present the Microbiome Stress Project, a publicly available database of environmental and host-associated amplicon sequencing studies designed to facilitate our understanding of microbial community responses to disturbed environments through cross-study analyses. More specifically, our goal is to address the following research objectives:

- (1) One stressor in one environment: How consistent are microbiome responses to the same stressor within the same environment?
- (2) A range of stressors within an environment: Are there common microbiome responses to different stressors within the same environment?
- (3) One stressor across environments: Does a given stressor impose consistent effects on microbiomes across multiple environments, including host-associated and free-living systems?
- (4) General trends of microbiome stressor responses: Are there general impacts of stressors on microbiomes across all environments?

These objectives lie on four principal axes for how environmental stressors impact microbiomes (**Figure 1A**). Capturing the variability in microbial response to a given stressor in one environment type (e.g., soil) will generate a more detailed understanding of how specific environmental parameters (e.g., soil pH) influence microbiome responses to stressors. We can also determine how the absolute magnitude of stressor treatments may be either dampened through historical exposure or exacerbated by temporal treatment regime (i.e., acute vs. chronic). Examining many stressors within the same environment enables the classification of the stressors themselves in terms of the responses they elicit, which may or may not reflect our assumptions. For instance, two stressors from the same “category” (e.g., two heavy metals) may impose similar impacts on microbiomes, but similar responses may also be possible with two distinct stressors (e.g., water stress and metal contaminations both leading to severe oxidative stress). Conversely, studying just one stressor across many environments allows us to assess the consistencies in the responses among these distinct microbiomes and to identify reliable microbial indicator taxa or clades of specific or multiple disturbances. Finally, by examining all available microbiome datasets, we can identify general effects of stressors on microbial community diversity and structure.

In this article, we introduce the Microbiome Stress Project methodological framework for building and analyzing the amplicon sequencing database (**Figure 1**) and present the results of a proof-of-concept meta-analysis (called pilot study hereafter) using raw sequence data from a subset of the larger database (**Figure 2**). We start by describing the results of a literature search, identifying studies explicitly focused on the impacts of stressors on microbial communities, from which we are building the full Microbiome Stress Project Database. Then, we present the analysis pipeline used to re-process the raw amplicon sequence data in a standardized fashion for the subsequent meta-analyses. The processed data, in the form of exact sequence variant (ESV) tables and corresponding meta-data, is accessible on our website ([microbiomestressproject.weebly.com](http://microbiomestressproject.weebly.com)), which hosts the database that will continue to grow as we add studies. The database encompasses both published and unpublished datasets, including *in situ* environmental gradients and controlled experiments, with acute (single) or chronic (repeated) stressor treatments, with either pulse (short-term) or press (long-term) exposure to the stressors. Finally, we present results from our pilot study where we examine the response of soil microbial communities to a wide set of stressors: copper, temperature, antibiotics, oxygen, polycyclic aromatic hydrocarbons, and land use change; and compare the impact of copper contamination on bacterial community structure across a range of environments: soil, gut, sediment, and activated-sludge reactors. We identify community-level responses with alpha and beta diversity, and we highlight individual- and lineage-level responses to stressors using phylofactorization (Washburne et al., 2017).

The Microbiome Stress Project is still growing and is at an early stage. Here, we present our methodological framework to demonstrate how these data can be used to understand how stressors shape microbial ecosystems. We invite the extended microbiome research community to contribute to this

collaborative project and help us improve this publicly available database by sharing their data.

## METHODS

### Literature Search

We performed an extensive literature search to assess the state of current research on the effects of stressors on microbial community structure. Our target questions were: (a) Which microbiome stressors are most commonly studied? (b) In which environments are these studies most commonly performed? (c) Which primers and sequencing platforms are most commonly used? and (d) How much of the microbiome sequencing data is publicly available?

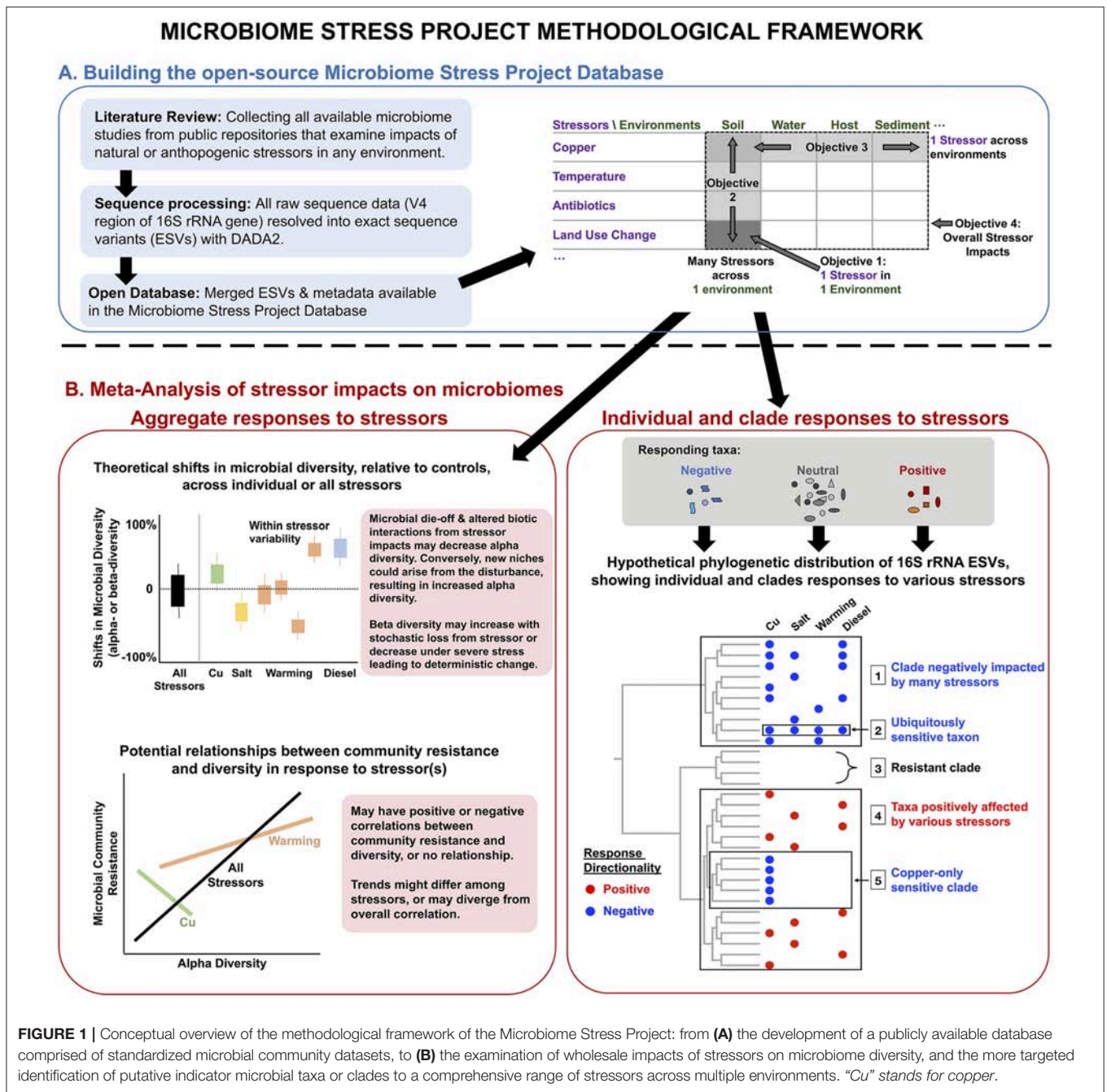
A literature search was performed on Web of Science (Core Collection) in April 2018 using a comprehensive set of basic microbiome keywords (full list of keywords in Supplementary Material **Table S1**). We constrained the search to studies published between 2010 and 2018, which is the period of time when high-throughput sequencing methods are standardized and commonly used to measure microbial community structure and composition. We narrowed our initial search results to identify potential studies for the Microbiome Stress Project Database as those which had the basic microbiome keywords, in addition to at least one of our specific subcategory stressor keywords. We used these keywords to identify which categories of stressors ( $n = 16$ , e.g., heavy metals, fire, pathogens, etc.) were studied and in which environment ( $n = 11$ , e.g., soil, gut, reactor, etc.). These categories enabled us to address the first (a) and second (b) questions about the research landscape and determine whether or not the number of studies available is sufficient to perform robust and balanced meta-analyses.

We performed a bibliometric network analysis on the articles identified as potential candidates for the database using the unified VOS mapping technique (VOS viewer software; Van Eck and Waltman, 2010) and clustering (Waltman et al., 2010). In these networks, we investigated where the microbiome stressor studies were published and the co-citations between these journals to determine the disciplines covered by our literature search and their interactions. We also created a network based on the co-occurrence of stressor terms that were most frequently mentioned in the microbiome studies.

We investigated primer and sequencing platform usage and data availability (questions c and d) using a random subset of 150 studies, as each study needed to be manually screened for the necessary information since Web of Science keyword searches do not extract this information (i.e., this methodological information is not commonly included in abstracts or keywords). The information gleaned from question (c) was essential for standardizing the database and for developing our analytical workflow.

### Selection of Studies for the Pilot Study

We selected nine studies (606 samples; 1 independent sample = 1 microbiome) with publicly available Illumina MiSeq V4 hypervariable region 16S rRNA gene sequencing data (**Figure 2**; Fuentes et al., 2016; Lin et al., 2016; Nunes et al., 2016; Sun et al.,



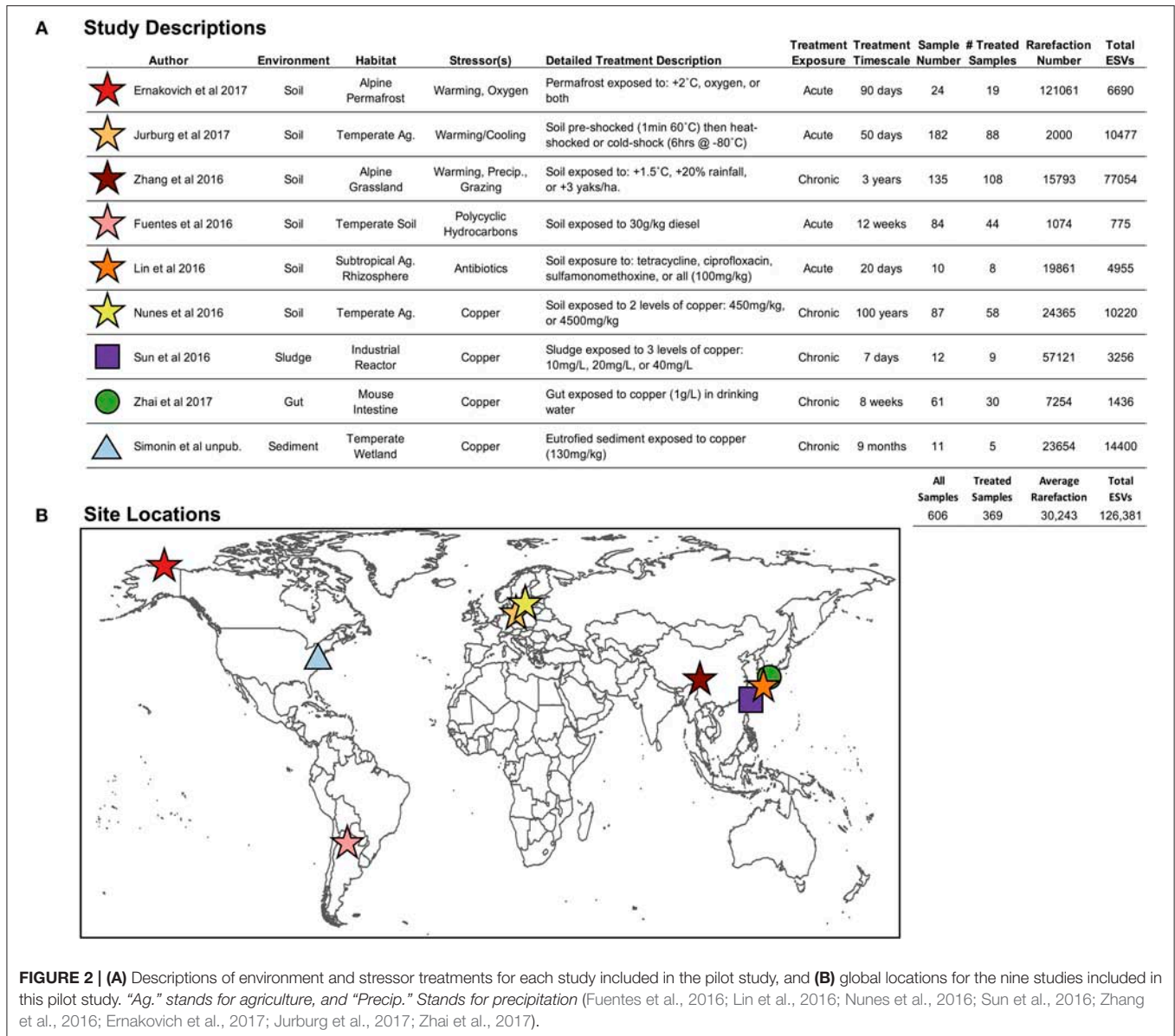


**FIGURE 2 | (A)** Descriptions of environment and stressor treatments for each study included in the pilot study, and **(B)** global locations for the nine studies included in this pilot study. “Ag.” stands for agriculture, and “Precip.” stands for precipitation (Fuentes et al., 2016; Lin et al., 2016; Nunes et al., 2016; Sun et al., 2016; Zhang et al., 2016; Ernakovich et al., 2017; Jurburg et al., 2017; Zhai et al., 2017).

(4) Overall impact of stressors on microbiomes: all microbial communities from any environment and exposed to any stressor (9 studies, 369 treated microbiomes).

### 16S rRNA Gene Sequence Processing Pipeline

Raw fastq sequence data from the 606 samples were downloaded from NCBI’s Sequence Read Archive (SRA) and from an unpublished dataset, and corresponding metadata was extracted for each study via SRA file names, direct correspondence, and the published manuscript itself to identify treatment levels and treatment duration for each sample.

We chose to define phylotypes at the level of exact sequence variants (ESVs; Callahan et al., 2017). The ESV methodology identifies error-adjusted single nucleotide differences in sequence datasets to generate standardized phylotypes that can be directly

compared across independently processed datasets. ESVs can be determined individually by sample or study and subsequently merged into the same feature table, allowing thousands of microbiome studies to be rapidly and efficiently combined. The ESV method provides the finest-scale taxonomic partitioning of microbial phylotypes possible and permits targeted identification of consistently-defined indicator species across datasets.

To prepare the datasets for ESV delineation, we trimmed the 16S rRNA gene sequences to the same 250 bp V4 hypervariable region within the Earth Microbiome Project primer set (515F/806R) (Gilbert et al., 2014). We used DADA2 version 1.6.0 (Callahan et al., 2017) in R version 3.5.1 (R Core Team, 2018) to resolve ESVs in each study dataset separately. DADA2 is optimized for running on separate forward and reverse fastq files. However, most of the sequence data we downloaded from SRA is only available as processed “contigs” (i.e., forward/reverse

paired-ends already merged), so we proceeded with DADA2 quality control removal and dereplication on merged paired-end sequences. We acknowledge that using different algorithms to join paired ends [i.e., Qiime2 (Caporaso et al., 2010), PEAR (Kozich et al., 2013), PANDAseq (Masella et al., 2012), and UPARSE (Edgar, 2013)] may generate slightly different sequences during the joining of the forward and reverse Illumina reads due to differences in allowable mismatches and other default settings. Putative chimeras were removed with the “consensus” method using *removeBimeraDenovo*. We then merged the resulting feature tables from each study and merged the representative ESVs.

Taxonomic assignment was performed with a naive Bayesian classifier against the SILVA ribosomal RNA gene database v128 (Desantis et al., 2006; Quast et al., 2013) using *assignTaxonomy* in DADA2, and species assignment was performed by an exact string-matching algorithm using *assignSpecies* in DADA2. Chloroplast, mitochondrial, and archaeal sequences were removed from the ESV tables and representative ESVs using these taxonomic assignments (Note: several archaeal sequences were retained in the representative sequences as outgroups for the alignment and phylogeny). The final dataset contained 126,381 unique ESVs and a total sequence count of 31,512,311. An alignment and phylogeny of the representative ESVs were simultaneously estimated using the Practical Alignment method in SATé and TrAnsitivty (PASTA; Mirarab et al., 2015) against the SILVA v128 reference 16S rRNA gene sequence alignment and tree.

Our pipeline for standardized processing of the V4 hypervariable 16S rRNA Illumina raw data into ESV table, representative ESVs, and taxonomy are detailed here: [https://github.com/MicrobiomeStressProject/Frontiers\\_Microbiology\\_2018/blob/master/main.md](https://github.com/MicrobiomeStressProject/Frontiers_Microbiology_2018/blob/master/main.md).

## Downstream Analyses: Finding Ecological Patterns Hidden in ESVs Across Studies

For the downstream analyses, instead of rarefying to the lowest suitable sequencing depth across the entire merged dataset, which would have been 1,074 sequences, we opted for per-study rarefactions (levels reported in **Figure 2**) in order to retain as much microbiome data as possible, ensuring maximal quality of the subsequent analyses (alpha diversity, beta diversity, resistance, and phylofactorization).

For each study treatment, we used the *core-metrics-phylogenetic* command in QIIME2 (Caporaso et al., 2010) to estimate three indices of alpha diversity (observed ESVs, Shannon-Weiner, and Pielou’s evenness) and one of beta-diversity (Bray-Curtis dissimilarity). We used the *betadisper* command in the Vegan package version 2.5-2 in R (Oksanen et al., 2018) to calculate the distance to group centroid from the Bray-Curtis distance matrix for each study treatment. To identify significant study treatment effects on alpha diversity and beta diversity, we ran within-study Kruskal-Wallis tests for differences between the treated microbiomes relative to undisturbed control samples.

To conduct the meta-analysis, we calculated the proportional changes in treated samples relative to control samples for each study treatment (e.g., 25% decrease in observed ESVs or 15% increase in Pielou’s evenness after diesel exposure in soil). Study-by-study treatment effect sizes were combined for each diversity metric and used to examine impacts of stressors to address our four objectives: (1) impact of warming on soil microbiomes ( $n = 79$  samples), (2) the impact of a range of stressors in a soil environment ( $n = 325$  samples), (3) the impact of copper in a variety of environments ( $n = 102$  samples), and (4) overall impacts of stressors on microbiomes ( $n = 369$  exposed microbiomes). We used a one-sample *t*-test of the distribution of effect sizes with  $\mu_0 = 0$  to test for significance. The mean and confidence intervals for each categorical set of effect sizes were displayed as forest plots, along with the individual by study treatment results displayed in boxplots, each with corresponding symbols of significance ( $p < 0.05$ ). For each study treatment, we estimated community resistance as the average pairwise similarity [1- Bray-Curtis dissimilarity] between the control microbiomes and the treated microbiomes (De Vries and Shade, 2013). Significant positive or negative correlations were identified on individual study treatments by examining the relationship between resistance and each alpha diversity index using linear models, and non-linear model fits for the overall relationship across all studies.

Finally, to identify ESVs and lineages responding to stressors, we performed phylofactorization (Phylofactor; Washburne et al., 2017) on just the subset of studies examining copper contamination (Objective 3). We acknowledge that there are a plethora of algorithms enabling differential abundance analysis for identifying taxa and/or clade responses to disturbance (Gloor et al., 2017; Weiss et al., 2017). We performed ANCOM analysis (Mandal et al., 2015) on each individual study treatment, along with Phylofactor, but decided to present just the Phylofactor results here, as our datasets spanned a wide range of environments (**Figure 2**), with very little overlap in ESVs among them. A central advantage of phylofactorization is the ability to detect similar shifts in microbial clades among studies when mapped to the same phylogeny, even with minimal ESV overlap. For example, the microbiomes from two environments may have no overlap in ESVs yet may still show overlap in clade membership (e.g., different microbial taxa identified as Actinobacteria). Even in the absence of ESV overlap among studies, if all members of a clade respond negatively to a stressor, this response will be apparent in the phylofactorization result. For computational ease and simplicity, we focused phylofactorization on the most prevalent members of microbial communities, defined as ESVs present in at least 20% of the microbiomes in a given study. Because the studies varied in both absolute copper treatment and actual copper exposure (i.e., difference in environmental retention of copper and bioavailability), certain studies with larger effect sizes would washout any phylofactor patterns of studies with more subtle responses. Consequently, to control for different effect sizes across studies, we inferred the phylogenetic factors, hereafter “phylofactor(s),” within each individual study and then mapped these phylofactors to a common phylogeny to

identify overlap in clades among the copper stressor studies. Additionally, phylofactor is suitable for our dataset because it has no requirements for choosing a reference frame (i.e., non-responding microorganisms) to determine changes in microbial abundance in response to a disturbance. Phylogenetic factors were chosen as edges maximizing the F-statistic from least squares regression predicting isometric log-ratio (ILR) abundances with treatment. The number of significant factors was determined using Holm's sequentially-rejective multiple test procedure (Holm, 1979) with a 10% family-wise error rate cutoff.

## RESULTS AND DISCUSSION

### Results of the Literature Search Reveals Thousands of Studies on Biotic and Abiotic Stressors in Host-Associated and Free-Living Environments

Our keyword search (restricted to dates between 2010 and April 2018) identified 12,687 published microbiome studies with 43% of the publications referring to at least one stressor keyword ( $n = 5,480$ , i.e., potential studies for the Microbiome Stress Project Database; **Table S2**). The bibliometric network of the journals that published these microbiome stress studies shows that this collective research spans a wide variety of disciplines, including medicine, ecology, ecotoxicology, food science, soil science, and plant sciences (**Figure S1**).

When examining the stressors keywords cited in these 5,480 papers (no environment keywords included in this search), more than half of the studies (55%) referred to keywords categorized as “biotic” stressors ( $n = 3,306$ ; e.g., pathogens, invasive species, herbivory, predation; **Table S2**). Of the remaining stressor categories, “contaminants” had the largest share (e.g., inorganic and organic pollutants; 27%) and “physical” had the smallest (e.g., fire, UV radiation; 2%). When examined within a co-occurrence network, stressor terms within studies clustered primarily into two separate groups—one dominated by global change (e.g., climate change) or ecotoxicology stressors (e.g., contamination), and the other by human health (e.g., disease, obesity; **Figure S2**). Pathogens occupied a central position within the network, highlighting the common interest shared by environmental and medical fields for these stressors. When microbiome studies were separated by environment ( $n = 4,293$  when all environmental, stressor, and microbiome keywords combined; **Figure 3**; **Table S2**), the top three categories were: animal-associated (including human microbiomes, 38%), soil (34%), and aquatic ecosystems (18%). The three least referenced environment categories were: sediment, aerial, and plant-associated microbiomes, which were only referenced in a total of 5% of the studies.

Of the subset of 150 studies randomly screened from the 5,480 full set of studies in our literature search, 96% of the screened studies performed amplicon sequencing, using primarily Illumina (59%) and 454 pyrosequencing (31%) platforms and only 4% performed shotgun metagenomic sequencing. 89% of the studies sequenced the 16S rRNA gene to study the diversity of archaea and bacteria. Of the 16S rRNA

gene studies, the V4 hypervariable region was the most frequently sequenced (76% of studies using primer sets: V3-V4, V4, V3-V5, & V4-V5). The next most common region was V3 (39% of studies using primer sets V1-V3, V2-V3, V3, V3-V4, V3-V5). Hence, the most common combination of sequencing platform and hypervariable region of the 16S rRNA gene studied was Illumina and the V4 region, respectively, which represented 57% of the 150 studies. Independent of those two classifications across all sequencing platforms and targeted genes, only 48 studies (64% of 150) had raw sequencing data available in public repositories (e.g., Sequence Read Archive) or via direct contact. Of the studies targeting the V4 hypervariable region of the 16S rRNA gene with Illumina sequencing, 69% had raw sequence data available in public repositories. Based on this literature search, for now we focus the Microbiome Stress Project Database and pilot study on the most common primer and sequencing platform combination (V4 region of 16S rRNA gene; Illumina MiSeq), with the pilot study results presented in section Results of the Pilot Study.

Moreover, while screening each individual study, we encountered many issues associated with unclear or incorrect meta-data, making these datasets unusable. The accessibility of both raw data and meta-data is absolutely crucial for integrating studies into larger meta-analyses like the Microbiome Stress Project. Our results clearly indicate that the microbiome research community still needs to commit to generating data that is open and accessible for reproducibility and synthesis.

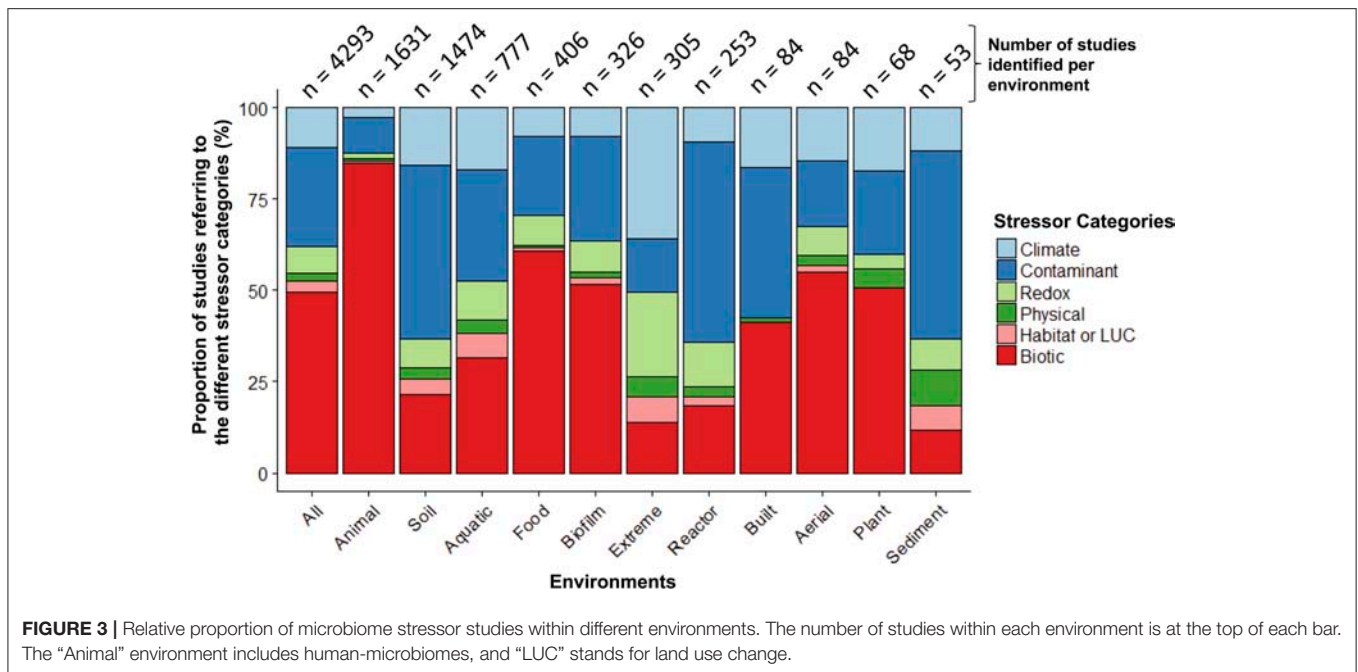
In preparation for the full Microbiome Stress Project Database, we are also targeting unpublished microbiome studies to minimize publication biases, where published studies are more likely to have significant results. Including unpublished datasets, in addition to the published set, is crucial for minimizing publication bias for our meta-analyses. We have launched an online campaign using social media (Twitter: @MicrobialStress) and our website (microbiomestressproject.weebly.com) to solicit authors to contribute their unpublished datasets to our effort. In addition to contributing to the growing database, researchers will also be able to see how their microbial studies fit alongside comparable studies, or among studies of the same environment or stressor.

### Results of the Pilot Study

Among the 606 microbiomes, the average read depth was 39,761 sequences per sample ( $\pm 38,902$ ), resulting in 126,381 total merged ESVs (**Figure 2**), with only 2.2% (2882 ESVs) overlap among studies. The average rarefaction was 30,243 ESVs, and the actual rarefaction values for each study are presented in **Figure 2**. Despite large differences in per-study sequencing depth and in the number of ESVs observed, the two values were not correlated ( $r^2 = 0.018$ ).

### Stressors Impact on Community Diversity and Resistance of Microbiomes

Our first objective was to assess the specific impacts of warming on soil microbiomes. We found that warming treatments altered alpha diversity through decreased observed ESV richness ( $-21\%$ ,  $P < 0.0001$ ) and Shannon-Weiner index ( $-7.2\%$ ,  $P =$



0.0002), and no significant impacts on microbiome evenness ( $P < 0.0657$ ) (Figure 4A). The overall decreased alpha diversity was primarily driven by one study focused on heat shock impacts in temperate agricultural soils that simulated extreme temperature conditions (+40°C, Jurburg et al., 2017). We acknowledge that this set of results is based on just three distinct studies (79 treated microbiomes), with substantial variation in the site-level characteristics as well as differences in the warming treatments, and as a proof-of-concept analysis, these trends should not be generalized. In trying to explain differential responses of diversity to warming, prior work in macro-ecosystems suggests a variety of diversity responses to disturbance, including non-monotonic responses (Mackey and Currie, 2001). Species often live in environmental optima, suggesting that moving in either direction from that optimum will result in a decrease in that species abundance (Holt, 2009). These unimodal patterns in niche space likely also give rise to unimodal diversity-disturbance relationships, if a large enough range of an environmental gradient is explored. This might explain the contrasted response of permafrost soil microbiomes to elevated temperature (+2C; Ernakovich et al., 2017), with increased alpha diversity across all indices (Observed ESVs: +34.5%, Shannon-Weiner: +21%, Pielou's Evenness: +16.2%,  $n = 7$ ) (Figure 4B). Permafrost is frozen soil, so even slight increases in temperature results in drastic changes to the environment conditions. Thawing permafrost could potentially explain the increased alpha diversity, by "awakening" many microorganisms that are encysted, or otherwise metabolically inactive, in the frozen conditions (Makhalyane et al., 2016; Wurzbacher et al., 2017). Alternatively, increased alpha diversity can also result from the growth of rare microbial taxa (below detection limit in controls)

that rapidly respond to the warming disturbance (Shade et al., 2012; Coveley et al., 2015).

While warming decreased alpha diversity overall, community dispersion increased by 7% relative to control community dispersion ( $P = 0.0010$ ), driven primarily by one significant increase from the same study examining heat-shocking temperate agriculture soils. Increases in microbial community dispersion have been observed in prior diversity-disturbance experiments (Gibbons et al., 2016), and may reflect a flattening of ecological selection as the environment becomes more heterogeneous. Additionally, this result could be explained by the fact that warming, and disturbances more generally, have stochastic rather than deterministic effects on microbiome composition leading to an increased dispersion compared to controls (i.e., the *Anna Karenina principle*, Zaneveld et al., 2017). Despite significant overall impacts of warming on soil microbial diversity, there was high variability in responses for each study treatment, which highlights the need for integrating more independent studies into the Microbiome Stress Project Database. This will increase the statistical power in these objectives, thereby generating reliable insights on how soil microbiomes respond to specific stressors like warming.

In our second objective, we expanded the analysis of soil microbiome responses to a wide range of stressors, which also resulted in decreased alpha diversity and increased community dispersion. Observed ESVs decreased by 17.7% ( $P < 0.0001$ ), Shannon-Weiner by 9.1% ( $P < 0.0001$ ), and Pielou's evenness decreased by 5.3% ( $P < 0.0001$ ) across all soil microbiomes studies (Figure 4A), while community dispersion increased by 5.4% relative to control microbiomes ( $P = 0.0006$ ).

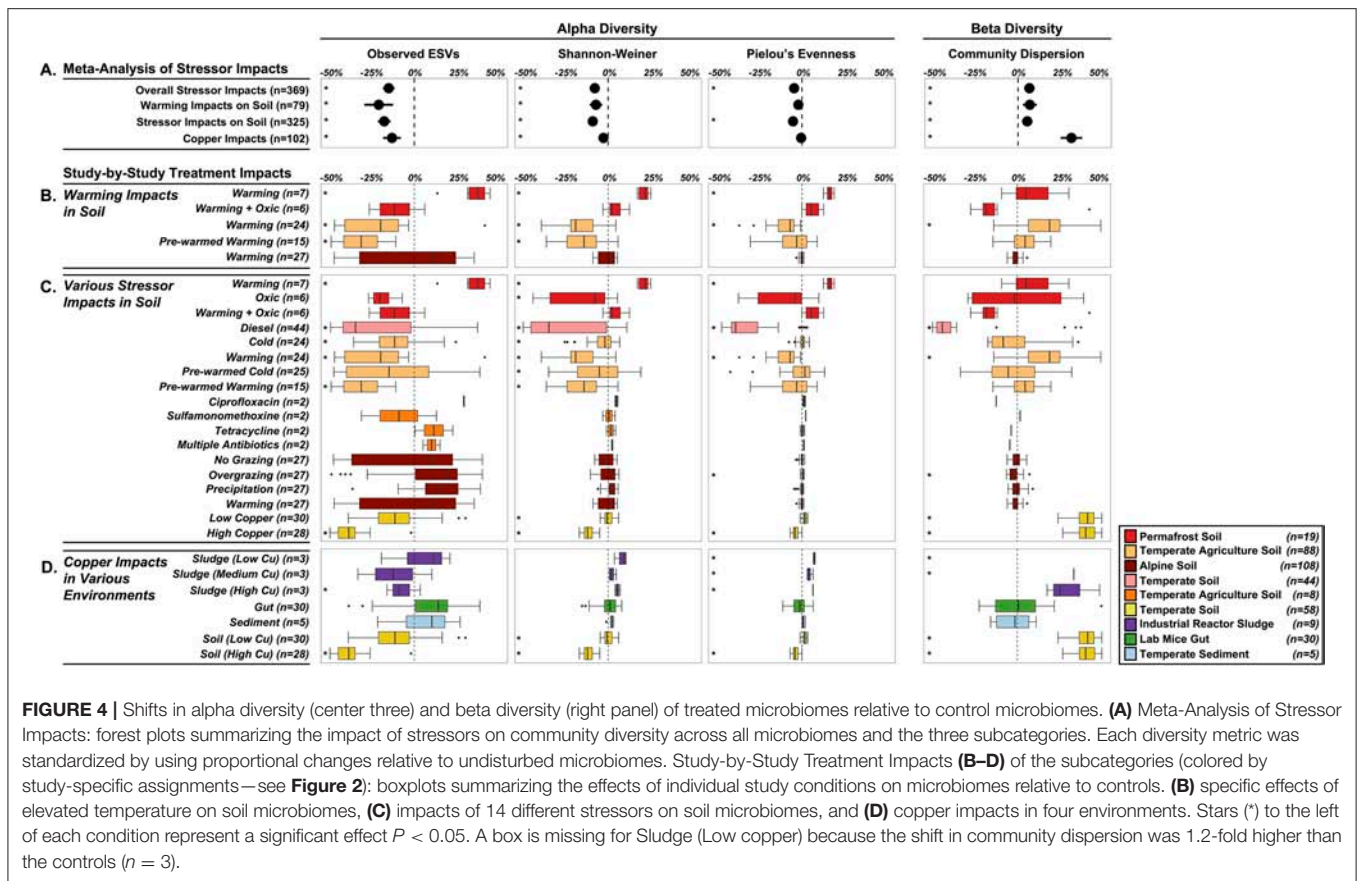


**FIGURE 4 |** Shifts in alpha diversity (center three) and beta diversity (right panel) of treated microbiomes relative to control microbiomes. **(A)** Meta-Analysis of Stressor Impacts: forest plots summarizing the impact of stressors on community diversity across all microbiomes and the three subcategories. Each diversity metric was standardized by using proportional changes relative to undisturbed microbiomes. Study-by-Study Treatment Impacts **(B–D)** of the subcategories (colored by study-specific assignments—see **Figure 2**): boxplots summarizing the effects of individual study conditions on microbiomes relative to controls. **(B)** specific effects of elevated temperature on soil microbiomes, **(C)** impacts of 14 different stressors on soil microbiomes, and **(D)** copper impacts in four environments. Stars (\*) to the left of each condition represent a significant effect  $P < 0.05$ . A box is missing for Sludge (Low copper) because the shift in community dispersion was 1.2-fold higher than the controls ( $n = 3$ ).

Similar to the study specific impacts of warming, there was high variability in the soil microbiome responses to the range of stressors as well (**Figure 4C**). The studies testing the effects of warming, diesel, and copper primarily decreased across all alpha diversity metrics. Warming and copper imposed significant increases in community dispersion, consistent with the meta-analysis trend. In contrast, the diesel and overgrazing stressors resulted in significant decreases in community dispersion, which suggests that these stressors may strengthen ecological selection and lead to more deterministic shifts in composition (Zaneveld et al., 2017). Here, we only selected 12 stressors for this pilot study, but we already have 27 different stressors in the database, with multiple studies available per stressor. In future analyses, covering more soil systems and stressor exposures will allow us to validate the effects observed on alpha and beta-diversity in the pilot study and uncover the abiotic and biotic factors driving soil microbiome responses to disturbed conditions.

Our third objective was to evaluate the effects of an individual stressor across multiple environments. We examined copper contamination on 102 samples across the four environments (soil, sludge, gut, and sediment), and found similar decreases in alpha diversity: a 13.1% decrease in observed ESVs ( $P < 0.0001$ ) and a 2.8% decrease in Shannon-Weiner ( $P = 0.0002$ ). Like the other objectives, there was substantial among-study variability in alpha diversity in response to copper (**Figure 4D**). The overall negative impacts were primarily driven by high

copper exposure in soil and sludge, while low copper treatments in soil and sludge and the copper treatments in gut and sediment were not significantly impacted by copper addition (**Figure 2B**). There was no significant overall impact of copper on community evenness ( $P = 0.2248$ ). Community dispersion was 31.5% greater in copper treated microbiomes than control microbiomes ( $P < 0.0001$ ), however this was primarily driven by the two copper treatments in soil (Nunes et al., 2016). The high variability in response of alpha diversity and beta diversity (**Figure 5**) may be due in part to the differential intrinsic resistance capacity of the microbiomes (e.g., initial alpha diversity or community network structure before exposure). Additionally, the magnitude of the treatment disturbance between studies (**Figure 2**) and the ecological memory of antecedent exposure to copper or other stressors may explain this range of copper effects observed on diversity (Griffiths and Philippot, 2013; Azarbad et al., 2016). The concentration and mode of exposure to copper were very contrasted between the four different studies which may explain a large part of the differences among studies (**Figure 2**). However, a very high chronic copper exposure in a mouse gut (1 g/L) did not cause any change in diversity (**Figure 4**), which suggests that the absolute magnitude of treatment may still not reflect actual exposure level for the microbiome, as in this case copper may be absorbed or transformed by the host before gut microbiome exposure (Cholewinska et al., 2018). Additionally, different redox potentials between environments may also determine actual

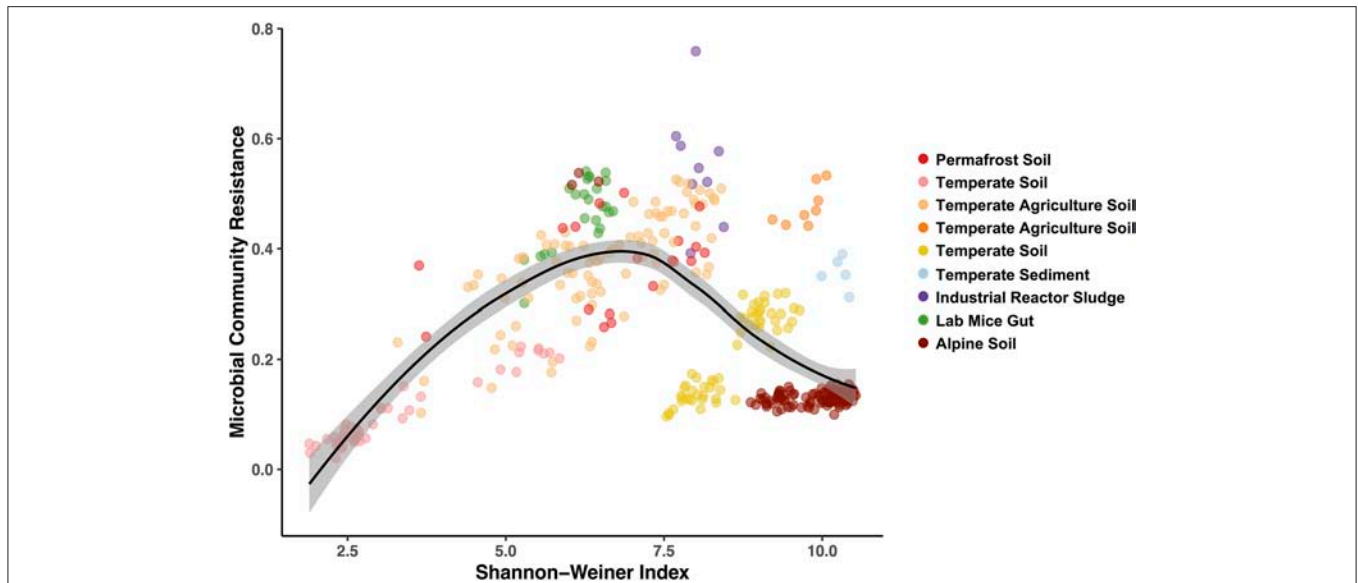


**FIGURE 5** | Hump-shaped relationship between microbiome community resistance to stressors and alpha diversity (Shannon-Weiner) of all treated microbiomes included in the pilot study. Data points represent a stressor treated microbiome ( $n = 369$ ) and are colored by each study environment.

exposure and speciation of copper, influencing the toxicity and bioavailability of this metal for microorganisms (Fleming and Trevors, 1989; Giller et al., 1998). Stochastic death throughout the treated microbiomes might also explain these patterns, with many microbial taxa driven to local extinction under high copper, resulting in distinct community structure and hence high beta diversity. While these results are interesting, we acknowledge again here that this pilot study does not have the statistical power to reliably draw any generalizable insights of copper impacts across multiple environments. With multiple studies for each environment-copper comparison (similar to the warming in soils) in the full dataset, we will be able to repeat the analysis with more power, accounting for copper bioavailability and historical exposures among studies.

Our fourth objective to analyze all 369 treated microbiomes in the pilot study revealed an average reduction in alpha diversity and increase in beta diversity. Similar to the results presented on the three other objectives of the meta-analysis, the exposure to all stressors led to significant decreases in the alpha diversity: observed ESVs decreased by 15% ( $P < 0.0001$ ), Shannon-Weiner alpha diversity decreased by 7.8% ( $P < 0.0001$ ), and evenness decreased by 4.6% ( $P < 0.0001$ ) (Figure 4A). Beta diversity was also significantly affected by stressors, with community dispersion increasing by 6.7% ( $P < 0.0001$ ) across all studies. These findings show that the diversity patterns observed for soil warming, a range of stressors in soil and copper across multiple environments still hold when performing a global meta-analysis of microbiome responses. These first results suggest that very contrasted stressors in diverse ecosystems lead to similar consequences for microbial community diversity. If these trends are substantiated with the same analysis at a larger scale, more research will be needed to understand how these shifts in diversity affect host health and ecosystem

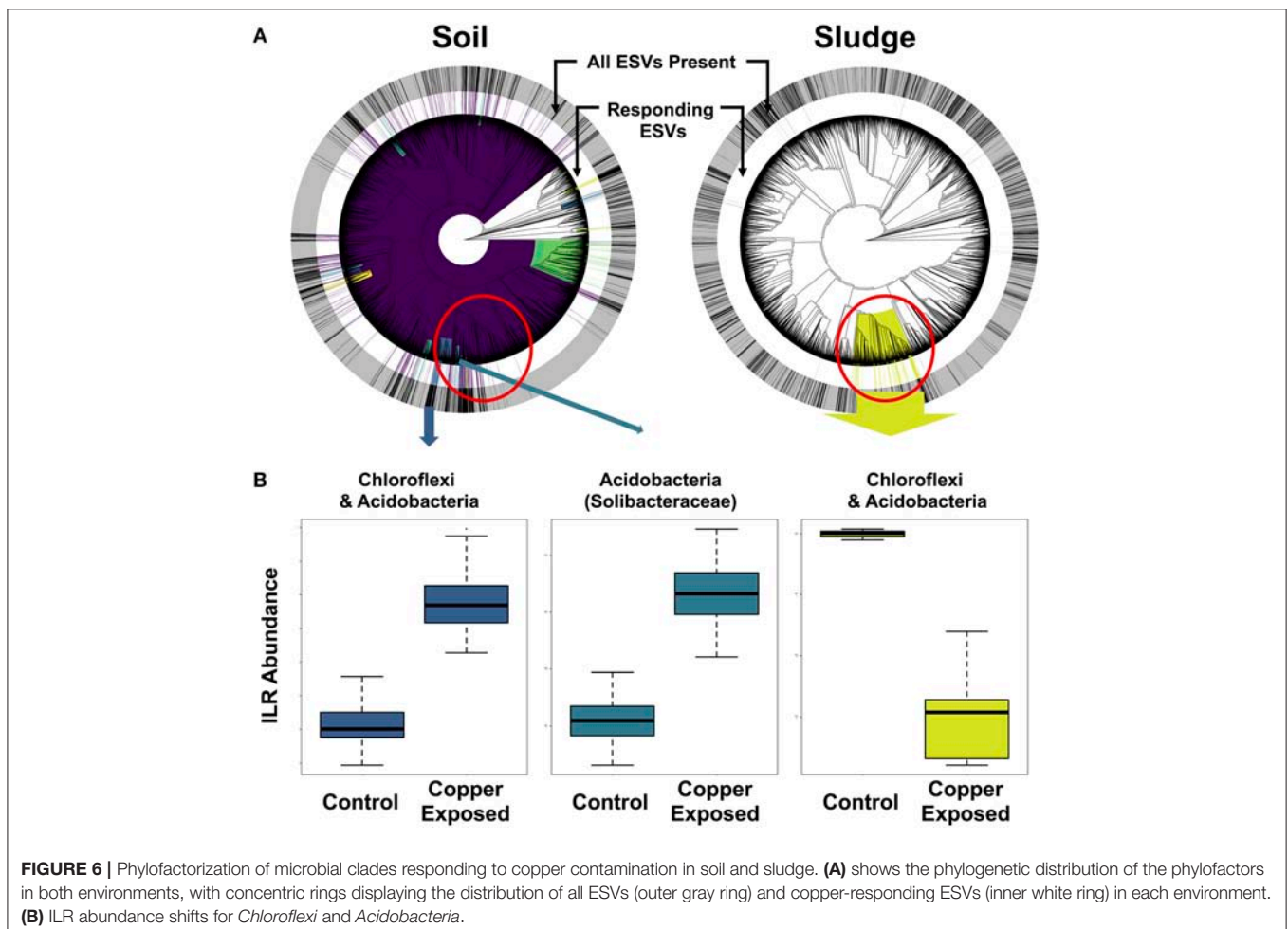
function. Moreover, using the growing Microbiome Stress Project database, researchers will be able to identify knowledge gaps and target research efforts for specific stressors or environments.

Finally, we used the Bray-Curtis similarities to estimate community resistance to stressors and explored potential correlations with the three alpha diversity indices (Figure 5; Table S3). We expected to see a positive correlation between alpha diversity and the microbiomes capacity to resist change (Tilman and Downing, 1994) and to remain stable when exposed to a stressor (i.e., the *Insurance Hypothesis*, Yachi and Loreau, 1999). However, when including all the exposed microbiomes, we primarily observed hump-shaped relationships between microbial community resistance and alpha diversity (Figure 5; relationship with Shannon-Weiner index). These results indicate that at low diversity levels (2 to 7.5 Shannon-Wiener index values, Figure 5), microbiome resistance is positively correlated to diversity but that this relationship becomes negative at higher diversity levels (7.5 to 10, Figure 5). These results suggest an alpha diversity optimum at which the microbiome resistance is maximal, which has been shown to exist in other microbial systems (Gibbons et al., 2016; Locey and Lennon, 2016). Elevated diversity can also be an indicator of a community in flux, where high dispersion rates in the environment increase the incidence of new microbial colonizers (Cadotte, 2006; Evans et al., 2017). In these systems, microbial populations may present a low residence time and a high community composition turnover (Locey and Lennon, 2016), which may drive in part the lower resistance observed at high diversity here. These preliminary results on diversity-stability relationships emphasize the need for a greater depth of studies for each stressor—environment combination to determine if these patterns are ubiquitous or occur under specific environmental conditions.

## Phylofactorization of Microbiomes From Four Environments Exposed to Copper

In order to isolate responding microbial ESVs and identify overlap in whole clades responding to copper contamination, we implemented Phylofactor. The four distinct environments exposed to copper had markedly different numbers of significant phylofactors (i.e., clades or terminal nodes responsive relative to the rest of the microbiome). The soil dataset had 780 phylofactors, covering 80% of the ESVs in the community, highlighting an extremely high community turnover in response to copper exposure (Figure 6A). In contrast, the gut microbiome had 20 phylofactors significantly responding to copper, the sludge had 17 phylofactors (Figure 6B), and the sediment had only five phylofactors containing 7 ESVs covering <0.2% of the dataset. The higher number of phylofactors in soil and sludge are consistent with the large shifts in alpha and beta diversity observed in these two studies (Figure 4), and the large effect size in the soil dataset yielded a phylofactorization implicating nearly the entire phylogeny as responsive to copper treatment. One particularly large phylofactor in soil identified a lineage of 688 ESVs accounting for 47% of the community. While, there were no common ESVs among the copper responders

across the environments, there was some overlap in responding clades found to be affected by copper exposure. In particular, a clade of 116 ESVs in the sludge dataset was close to four phylofactors in the soil dataset containing 20, 62, 10, and 9 ESVs, respectively (red circle in Figure 6). These phylofactors primarily contained uncultivated lineages annotated as members of *Acidobacteria*, *Solibacteraceae*, but also other *Acidobacteria* and *Chloroflexi*. These lineages are phylogenetically close, and in some cases nested clades but they interestingly presented opposite responses to copper treatment in the two environments (Figure 6). In the soil study, the responding community subsets of *Chloroflexi* and *Acidobacteria* were increased in the copper treated microbiomes, while they decreased in the sludge study (Figure 6). Other studies have demonstrated the sensitivity of both *Acidobacteria* and *Chloroflexi*, while Actinobacteria are generally tolerant to copper exposure in soils (Li et al., 2015) and in sludge (Sun et al., 2016). Due to the compositional nature of sequence-count data, it is impossible to determine how much of the effect is due to the populations of *Solibacteraceae*, for example, having opposite responses in the two environments and how much is due to the remaining community whose abundance shifts can confound directional inferences in compositional data.



Rather than yielding clear inferences about potential bioindicator lineages in the current state, phylofactorization yielded more insight about future research on the difficulty of comparing results across microbiome studies, and the opportunities of datasets like the Microbiome Stress Project may yield to test and improve statistical tools. In addition to improving computational tools, it is important for researchers to improve quantification of absolute abundances by running qPCR or by including DNA spike-ins prior to sequencing to limit our reliance to relative abundance data. Concomitantly, future experimental work could directly target the microbial clades identified as responders to better understand their responses to individual stressor–environment scenarios and validate the inferences made in the amplicon sequencing meta-analyses.

## Concluding Remarks

In this article, we presented the objectives, methodological framework and bibliographic landscape covered by the Microbiome Stress Project and used our pilot study as a proof-of-concept meta-analysis to demonstrate the potential of this database. With thousands of studies available on the impact of environmental stressors on microbial communities, the Microbiome Stress Project Database is well-poised to allow researchers to tackle key ecological issues regarding the resistance, resilience, and response of microbial communities following exposure to environmental stressors. This project will generate a wealth of information on the natural history of microbial taxa, especially on their stressor tolerance and important life-history strategies for surviving in fluctuating environments. The full database will enable the identification of indicator taxa and clades to specific or multiple stressors that could eventually be used for monitoring or microbiome engineering. The Microbiome Stress Project provides an ideal resource for developing and testing new statistical methods with comprehensive amplicon sequencing datasets. We anticipate that research into common responses of microbial communities to stressors will lead to better microbiome diagnostics, allowing researchers to make inferences that are robust to both subtle and large-scale changes in species composition across independent studies.

The aim of this project is to identify global patterns in microbiome responses to stressors, but we encourage the scientific community to use the database to examine their own research questions. Adding your studies to the Microbiome

Stress Project Database is a valuable contribution to the research community and also provides valuable context for your own work. Finally, building the database will reveal knowledge gaps in terms of missing or low replication studies of specific stressors or particular environments. We hope that the Microbiome Stress Project will forge new interdisciplinary collaborations leading to important breakthroughs in our understanding of microbial communities' responses to environmental change and for improving our ability to engineer microbiomes for improved human and environmental health.

## AUTHOR CONTRIBUTIONS

JR, MS, JB, and FM conceived the project. MS and JB collected the raw sequences meta-data and conducted the literature search. FM and JR processed the sequence data. FM, AW, and SG developed the downstream analyses. MS, JR, and JE developed the conceptual framework and background synthesis. JR, MS, JB, JE, SG, FM, and AW contributed equally to writing the manuscript.

## FUNDING

The processing of the raw sequence data was made possible, in part, through an exploratory grant through the AWS Educate program Proof of Concept (POC) funding, awarded to postdocs and graduate students in our group. SG was supported by a Washington Research Foundation Distinguished Investigator Award. JR and MS were funded by a grant from the NSF (award number DEB- 1754512).

## ACKNOWLEDGMENTS

This work is the product of a journal club initiated by Professor Emily Bernhardt, to start exploring the impacts of environmental stressors on microbes. We thank Prof. Ben Callahan for taking time to meet with our group to discuss our project and his DADA2 algorithm.

## SUPPLEMENTARY MATERIAL

The Supplementary Material for this article can be found online at: <https://www.frontiersin.org/articles/10.3389/fmicb.2018.03272/full#supplementary-material>

## REFERENCES

- Azarbad, H., van Gestel, C. A. M., Niklinska, M., Laskowski, R., Roling, W. F. M., and van Straalen, N. M. (2016). Resilience of soil microbial communities to metals and additional stressors: DNA-based approaches for assessing “stress-on-stress” responses. *Int. J. Mol. Sci.* 17, 933. doi: 10.3390/ijms17060933
- Baym, M., Lieberman, T. D., Kelsic, E. D., Chait, R., Gross, R., Yelin, I., et al. (2016). Spatiotemporal microbial evolution on antibiotic landscapes. *Science* 353, 1147–1152. doi: 10.1126/science.aag0822
- Bender, E. A., Case, T. J., and Gilpin, M. (1984). Perturbation experiments in community ecology: theory and practice. *Ecology* 65, 1–13. doi: 10.2307/1939452
- Bissett, A., Brown, M. V., Siciliano, S. D., and Thrall, P. H. (2013). Microbial community responses to anthropogenically induced environmental change: towards a systems approach. *Ecol. Lett.* 16, 128–139. doi: 10.1111/ele.12109
- Cadotte, M. (2006). Metacommunity influences on community richness at multiple spatial scales: a microcosm experiment. *Am. Nat.* 87, 1008–1016. doi: 10.1890/0012-9658(2006)87[1008:MIOCRA]2.0.CO;2
- Calabrese, E. J., and Baldwin, L. A. (2002). Defining hormesis. *Hum. Exp. Toxicol.* 21, 91–97. doi: 10.1191/0960327102ht217oa
- Callahan, B. J., McMurdie, P. J., and Holmes, S. P. (2017). Exact sequence variants should replace operational taxonomic units in marker-gene data analysis. *ISME J.* 11, 2639–2643. doi: 10.1038/ismej.2017.119

- Caporaso, J. G., Kuczynski, J., Stombaugh, J., Bittinger, K., Bushman, F. D., Costello, E. K., et al. (2010). QIIME allows analysis of high-throughput community sequencing data. *Nat. Methods* 7, 335–336. doi: 10.1038/nmeth.f.303.QIIME
- Cholewinska, E., Ognik, K., Fotschki, B., Zdunczyk, Z., and Juskiewicz, J. (2018). Comparison of the effect of dietary copper nanoparticles and one copper (II) salt on the copper biodistribution and gastrointestinal and hepatic morphology and function in a rat model. *PLoS ONE* 13:e0197083. doi: 10.1371/journal.pone.0197083
- Connell, J. H. (1978). Diversity in tropical rain forests and coral reefs. *Science* 199, 1302–1310. doi: 10.1126/science.199.4335.1302
- Coveley, S., Elshahed, M. S., and Youssef, N. H. (2015). Response of the rare biosphere to environmental stressors in a highly diverse ecosystem (Zodlone spring, OK, USA). *PeerJ* 3:e1182. doi: 10.7717/peerj.1182
- Crain, C. M., Kroeker, K., and Halpern, B. S. (2008). Interactive and cumulative effects of multiple human stressors in marine systems. *Ecol. Lett.* 11, 1304–1315. doi: 10.1111/j.1461-0248.2008.01253.x
- De Vries, F. T., and Shade, A. (2013). Controls on soil microbial community stability under climate change. *Front. Microbiol.* 4:265. doi: 10.3389/fmicb.2013.00265
- Desantis, T. Z., Hugenholtz, P., Larsen, N., Rojas, M., Brodie, E. L., Keller, K., et al. (2006). Greengenes, a chimera-checked 16S rRNA gene database and workbench compatible with ARB. *Appl. Env. Microbiol.* 72, 5069–5072. doi: 10.1128/AEM.03006-05
- Duvallet, C. (2018). Meta-analysis generates and prioritizes hypotheses for translational microbiome research. *Microb. Biotechnol.* 11, 273–276. doi: 10.1111/1751-7915.13047
- Duvallet, C., Gibbons, S. B., Gurry, T., Irizarry, R. A., and Alm, E. J. (2017). Meta-analysis of gut microbiome studies identifies disease-specific and shared responses. *Nat. Commun.* 8, 1784. doi: 10.1038/s41467-017-01973-8
- Edgar, R. C. (2013). UPARSE: highly accurate OTU sequences from microbial amplicon reads. *Nat. Methods* 10, 996–998. doi: 10.1038/nmeth.2604
- Ernakovich, J. G., Lynch, L. M., Brewer, P. E., Calderon, F. J., and Wallenstein, M. D. (2017). Redox and temperature-sensitive changes in microbial communities and soil chemistry dictate greenhouse gas loss from thawed permafrost. *Biogeochemistry* 134, 183–200. doi: 10.1007/s10533-017-0354-5
- Evans, S. E., Martiny, J. B., and Allison, S. D. (2017). Effects of dispersal and selection on stochastic assembly in microbial communities. *ISME J.* 11, 176–185. doi: 10.1038/ismej.2016.96
- Evans, S. E., and Wallenstein, M. D. (2014). Climate change alters ecological strategies of soil bacteria. *Ecol. Lett.* 17, 155–164. doi: 10.1111/ele.12206
- Fleming, C. A., and Trevors, J. T. (1989). Copper toxicity and chemistry in the environment: a review. *Water Air Soil Pollut.* 44, 143–158.
- Fuentes, S., Barra, B., Caporaso, J. G., and Seeger, M. (2016). From rare to dominant: a fine-tuned soil bacterial bloom during. *Appl. Environ. Microbiol.* 82, 888–896. doi: 10.1128/AEM.02625-15
- Gibbons, S. M., Duvallet, C., and Alm, E. J. (2018). Correcting for batch effects in case-control microbiome studies. *PLoS Comput. Biol.* 14:e1006102. doi: 10.1371/journal.pcbi.1006102
- Gibbons, S. M., Scholz, M., Hutchinson, A. L., Dinner, A. R., Gilbert, J. A., and Coleman, M. L. (2016). Disturbance regimes predictably alter diversity in an ecologically complex bacterial system. *mBio* 7:e01372–e01316. doi: 10.1128/mBio.01372-16
- Gilbert, J. A., Jansson, J. K., and Knight, R. (2014). The earth microbiome project: successes and aspirations. *BMC Biol.* 12:69. doi: 10.1186/s12915-014-0069-1
- Giller, K. E., Witter, E., and McGrath, S. P. (1998). Toxicity of heavy metals to microorganisms and microbial processes in agricultural soils: a review. *Soil Biol. Biogeochem.* 30, 1389–1414. doi: 10.1016/S0038-0717(97)00270-8
- Gloor, G. B., Macklaim, J. M., Pawlowsky-Glahn, V., and Egozcúe, J. J. (2017). Microbiome datasets are compositional: and this is not optional. *Front. Microbiol.* 8:2224. doi: 10.3389/fmicb.2017.02224
- Griffiths, S. B., and Philippot, L. (2013). Insights into the resistance and resilience of the soil microbial community. *FEMS Microbiol. Rev.* 37, 112–129. doi: 10.1111/j.1574-6976.2012.00343
- Holden, S. R., and Treseder, K. K. (2013). A meta-analysis of soil microbial biomass responses to forest disturbances. *Front. Microbiol.* 4:163. doi: 10.3389/fmicb.2013.00163
- Holm, S. (1979). A simple sequentially rejective multiple test procedure. *Scand. J. Stat.* 6, 65–70. doi: 10.2307/4615733
- Holt, R. D. (2009). Bringing the Hutchinsonian niche into the 21<sup>st</sup> century: ecological and evolutionary perspectives. *Proc. Natl. Acad. Sci. U.S.A.* 106, 19659–19665. doi: 10.1073/pnas.0905137106
- Human Microbiome Project Consortium (2012). Structure, function and diversity of the healthy human microbiome. *Nature* 486, 207–214. doi: 10.1038/nature11234
- Huston, M. (1979). A general hypothesis of species diversity. *Am. Nat.* 113, 81–101. doi: 10.1086/283366
- Jackson, M. A., Verdi, S., Maxan, M., Shin, C. M., Zierer, J., Bowyer, R. C. E., et al. (2018). Gut microbiota associations with common diseases and prescription medications in a population-based cohort. *Nat. Commun.* 9:2655. doi: 10.1038/s41467-018-05184-7
- Jurburg, S. D., Nunes, I., Brejnrod, A., Jacquiod, S., and Priemé, A., Søren, et al. (2017). Legacy effects on the recovery of soil bacterial communities from extreme temperature perturbation. *Front. Microbiol.* 8:1832. doi: 10.3389/fmicb.2017.01832
- Knelman, J. E., Nemergut, D. R., Klotz, M. G., Blackwood, C., and Rodrigues, J. L. M. (2014). Changes in community assembly may shift the relationship between biodiversity and ecosystem function. *Front. Microbiol.* 5:424. doi: 10.3389/fmicb.2014.00424
- Kozich, J. J., Westcott, S. L., Baxter, N. T., Highlander, S. K., and Schloss, P. D. (2013). Development of a dual-index sequencing strategy and curation pipeline for analyzing amplicon sequence data on the MiSeq Illumina sequencing platform. *Appl. Environ. Microbiol.* 79, 5112–5120. doi: 10.1128/AEM.01043-13
- Li, J., Ma, Y. B., Hu, H. W., Wang, J. T., Liu, Y. R., and He, J. Z. (2015). Field-based evidence for consistent responses of bacterial communities to copper. *Front. Microbiol.* 6:31. doi: 10.3389/fmicb.2015.00031
- Lin, H., Jin, D., Freitag, T. E., Sun, W., Yu, O., Fu, J., et al. (2016). A Compositional shift in the soil microbiome induced by tetracycline, sulfamonomethoxine and ciprofloxacin entering a plant-soil system. *Environ. Pollut.* 212, 440–448. doi: 10.1016/j.envpol.2016.02.043
- Lloyd-Price, J., Mahurkar, A., Rahnavard, G., Crabtree, J., Orvis, J., Hall, A. B., et al. (2017). Strains, functions and dynamics in the expanded human microbiome project. *Nature*. 550, 61–66. doi: 10.1038/nature23889
- Locey, K. J., and Lennon, J. T. (2016). Scaling laws predict global microbial diversity. *Proc. Natl. Acad. Sci. U.S.A.* 113, 5970–5975. doi: 10.1073/pnas.1521291113
- Mackey, R. L., and Currie, D. J. (2001). The diversity-disturbance relationship: is it generally strong and peaked? *Ecology* 82, 3479–3492. doi: 10.2307/2680166
- Makhalanyane, T. P., Van Goethem, M. W., and Cowan, D. A. (2016). Microbial diversity and functional capacity in polar soils. *Curr. Opin. Biotechnol.* 38, 159–166. doi: 10.1016/j.copbio.2016.01.011
- Mandal, S., van Treuren, W., White, R. A., Eggesbo, M., Knight, R., and Peddada, S. D. (2015). Analysis of composition of microbiomes: a novel method for studying microbial composition. *Microb. Ecol. Health Dis.* 26, 27663. doi: 10.3402/mehd.v26.27663
- Masella, A. P., Bartram, A. K., Truszkowski, J. M., Brown, D. G., and Neufeld, J. D. (2012). PANDAseq: paired-end assembler for illumine sequences. *BMC Bioinformatics* 13:31. doi: 10.1186/1471-2105-13-31
- Mirarab, S., Nguyen, N., Guo, S., Wang, L., Kim, J., and Warnow, T. (2015). PASTA: ultra-large multiple sequence alignment for nucleotide and amino-acid sequences. *J. Comput. Biol.* 22, 377–386. doi: 10.1089/cmb.2014.0156
- Nunes, I., Jacquiod, S., Brejnrod, A., Holm, P. E., Johansen, A., Brandt, K. K., et al. (2016). Coping with copper: legacy effect of copper on potential activity of soil bacteria following a century of exposure. *FEMS Microbiol. Ecol.* 92:fiw175. doi: 10.1093/femsec/fiw175
- Odum, E. P. (1985). Trends expected in stressed ecosystems. *Bioscience* 35, 419–422.
- Odum, E. P., Finn, J. T., and Franz, E. H. (1979). Perturbation theory and the subsidy-stress gradient. *Bioscience* 29, 349–352.
- Oksanen, J., Blanchet, F. G., Friendly, M., Kindt, R., Legendre, P., McGlenn, D., et al. (2018). *R Package 'Vegan' (Vienna)*.
- Philippot, L., Spor, A., Henault, C., Bru, D., Bizouard, F., Jones, C. M., et al. (2013). Loss in microbial diversity affects nitrogen cycling in soils. *ISME J.* 7, 1609–1619. doi: 10.1038/ismej.2013.34

- Piggott, J. J., Townsend, C. R., and Matthaei, C. D. (2015). Climate warming and agricultural stressors interact to determine stream macroinvertebrate community dynamics. *Glob. Change Biol.* 21, 1887–1906. doi: 10.1111/gcb.12861
- Quast, C., Pruesse, E., Yilmaz, P., Gerken, J., Schweer, T., Yarza, P., et al. (2013). The SILVA ribosomal RNA gene database project: improved data processing and web-based tools. *Nucleic Acids Res.* 41, D590–D596. doi: 10.1093/nar/gks1219
- R Core Team (2018). *R: A Language and Environment for Statistical Computing*. Vienna: R Foundation for Statistical Computing. Available online at: <https://www.R-project.org/>
- Ramirez, K. S., Knight, C. G., De Hollander, M., Brearley, F. Q., Constantinides, B., Cotton, A., et al. (2018). Detecting macroecological patterns in bacterial communities across independent studies of global soils. *Nat. Microbiol.* 3, 189–196. doi: 10.1038/s41564-017-0062-x
- Ratzke, C., and Gore, J. (2018). Modifying and reacting to the environmental PH can drive bacterial interactions. *PLoS Biol.* 16:e2004248. doi: 10.1371/journal.pbio.2004248
- Reese, A. T., Cho, E. H., Klitzman, B., Nichols, S. P., Wisniewski, N. A., Villa, M. M., et al. (2018). Antibiotic-induced changes in the microbiota disrupt redox dynamics in the gut. *Elife* 7:e35987. doi: 10.7554/eLife.35987
- Sanchez, A., and Gore, J. (2013). Feedback between population and evolutionary dynamics determines the fate of social microbial populations. *PLoS Biol.* 11:e1001547. doi: 10.1371/journal.pbio.1001547
- Schimel, J., Balsler, T. C., and Wallenstein, M. D. (2007). Microbial stress-response physiology and its implications for ecosystem function. *Ecology* 88, 1386–1394. doi: 10.1890/06-0219
- Shade, A., Caporaso, J. G., Handelsman, J., Knight, R., and Fierer, N. (2013). A meta-analysis of changes in bacterial and archaeal communities with time. *ISME J.* 7, 1493–1506. doi: 10.1038/ismej.2013.54
- Shade, A., Peter, H., Allison, S. D., Baho, D. L., Berga, M., Burgmann, H., et al. (2012). Fundamentals of microbial community resistance and resilience. *Front. Microbiol.* 3:417. doi: 10.3389/fmicb.2012.00417
- Sun, F. L., Fan, L. L., and Xie, G. J. (2016). Effect of copper on the performance and bacterial communities of activated sludge using illumina miseq platforms. *Chemosphere* 156, 212–219. doi: 10.1016/j.chemosphere.2016.04.117
- Thompson, L. R., Sanders, J. G., McDonald, D., Amir, A., Ladau, J., Locey, K. J., et al. (2017). A communal catalogue reveals earth's multiscale microbial diversity. *Nature* 551, 457. doi: 10.1038/nature24621
- Tilman, D., and Downing, J. A. (1994). Biodiversity and stability in grasslands. *Nature* 367, 363–365. doi: 10.1038/367363a0
- Treseder, K. K. (2008). Nitrogen additions and microbial biomass: a meta-analysis of ecosystem studies. *Ecol. Lett.* 11, 1111–1120. doi: 10.1111/j.1461-0248.2008.01230.x
- Van Eck, N. J., and Waltman, L. (2010). VOSviewer, a computer program for bibliometric mapping. *Scientometrics* 84, 523–538. doi: 10.1007/s11192-009-0146-3
- Vellend, M. (2010). Conceptual synthesis in community ecology. *Q. Rev. Biol.* 85, 183–206. doi: 10.1086/652373
- Waltman, L., Van Eck, N. J., and Noyons, E. C. M. (2010). A unified approach to mapping and clustering of bibliometric networks. *J. Informetr.* 4, 629–635. doi: 10.1016/j.joi.2010.07.002
- Washburne, A. D., Silverman, J. D., Leff, J. W., Bennett, D. J., Darcy, J. L., Mukherjee, S., et al. (2017). Phylogenetic factorization of compositional data yields lineage-level associations in microbiome datasets. *PeerJ* 5:e2969. doi: 10.7717/peerj.2969
- Weiss, S., Xu, Z. Z., Peddada, S., Amir, A., Bittinger, K., Gonzales, A., Lozupone, C., et al. (2017). Normalization and microbial differential abundance strategies depend upon data characteristics. *Microbiome* 5:27. doi: 10.1186/s40168-017-0237-y
- Wurzbacher, C., Attermeyer, K., Kettner, M. T., Flintrop, C., Warthmann, N., Hilt, S., et al. (2017). DNA metabarcoding of unfractionated water samples relates phyto-, zoo- and bacterioplankton dynamics and reveals a single-taxon bacterial bloom. *Environ. Microbiol. Rep.* 9, 383–388. doi: 10.1111/1758-2229.12540
- Yachi, S., and Loreau, M. (1999). Biodiversity and ecosystem productivity in a fluctuating environment: the insurance hypothesis. *Proc. Natl. Acad. Sci. U.S.A.* 96, 1463–1468. doi: 10.1073/pnas.96.4.1463
- Zaneveld, J. R., McMinds, R., and Thurber, R. V. (2017). Stress and stability: applying the anna karenina principle to animal microbiomes. *Nat. Microbiol.* 2, 17121. doi: 10.1038/nmicrobiol.2017.121
- Zhai, Q., Li, T., Yu, L., Xiao, Y., Feng, S., Wu, J., et al. (2017). Effects of subchronic oral toxic metal exposure on the intestinal microbiota of mice. *Sci. Bull.* 62, 1–10. doi: 10.1016/j.scib.2017.01.031
- Zhang, Y., Dong, S., Gao, Q., Liu, S., Zhou, H., Ganjurjav, H., et al. (2016). Climate change and human activities altered the diversity and composition of soil microbial community in alpine grasslands of the qinghai-tibetan plateau. *Sci. Tot. Environ.* 562, 353–363. doi: 10.1016/j.scitotenv.2016.03.221

**Conflict of Interest Statement:** The authors declare that the research was conducted in the absence of any commercial or financial relationships that could be construed as a potential conflict of interest.

Copyright © 2019 Rocca, Simonin, Blaszczyk, Ernakovich, Gibbons, Midani and Washburne. This is an open-access article distributed under the terms of the Creative Commons Attribution License (CC BY). The use, distribution or reproduction in other forums is permitted, provided the original author(s) and the copyright owner(s) are credited and that the original publication in this journal is cited, in accordance with accepted academic practice. No use, distribution or reproduction is permitted which does not comply with these terms.



# Novel Mechanism for Surface Layer Shedding and Regenerating in Bacteria Exposed to Metal-Contaminated Conditions

Archjana Chandramohan<sup>1</sup>, Elodie Duprat<sup>2</sup>, Laurent Remusat<sup>2</sup>, Severine Zirah<sup>1</sup>, Carine Lombard<sup>1</sup> and Adrienne Kish<sup>1\*</sup>

<sup>1</sup> Unité Molécules de Communication et Adaptation des Microorganismes (MCAM), Muséum National d'Histoire Naturelle, CNRS UMR 7245, Paris, France, <sup>2</sup> Institut de Minéralogie, Physique des Matériaux et de Cosmochimie (IMPMC), Sorbonne Université, Muséum National d'Histoire Naturelle, CNRS UMR 7590, IRD UMR 206, Paris, France

## OPEN ACCESS

### Edited by:

Stéphane Pesce,  
National Research Institute of Science  
and Technology for Environment  
and Agriculture (IRSTEA), France

### Reviewed by:

Mariusz Cycoń,  
Medical University of Silesia, Poland  
Sukhendu Mandal,  
University of Calcutta, India

### \*Correspondence:

Adrienne Kish  
adrienne.kish@mnhn.fr

### Specialty section:

This article was submitted to  
Microbiotechnology, Ecotoxicology  
and Bioremediation,  
a section of the journal  
Frontiers in Microbiology

**Received:** 13 September 2018

**Accepted:** 11 December 2018

**Published:** 15 January 2019

### Citation:

Chandramohan A, Duprat E,  
Remusat L, Zirah S, Lombard C and  
Kish A (2019) Novel Mechanism  
for Surface Layer Shedding  
and Regenerating in Bacteria  
Exposed to Metal-Contaminated  
Conditions. *Front. Microbiol.* 9:3210.  
doi: 10.3389/fmicb.2018.03210

Surface layers (S-layers) are components of the cell walls throughout the Bacteria and the Archaea that provide protection for microorganisms against diverse environmental stresses, including metal stress. We have previously characterized the process by which S-layers serve as a nucleation site for metal mineralization in an archaeon for which the S-layer represents the only cell wall component. Here, we test the hypothesis originally proposed in cyanobacteria that a “shedding” mechanism exists for replacing S-layers that have become mineral-encrusted, using *Lysinibacillus* sp. TchlII 20n38, metallotolerant gram-positive bacterium, as a model organism. We characterize for the first time a mechanism for resistance to metals through S-layer shedding and regeneration. S-layers nucleate the formation of Fe-mineral on the cell surface, depending on physiological state of the cells and metal exposure times, leading to the encrustation of the S-layer and changes in the cell morphology as observed by scanning electron microscopy. Using Nanoscale Secondary Ion Mass Spectrometry, we show that mineral-encrusted S-layers are shed by the bacterial cells after a period of latency (2 days under the conditions tested) in a heterogeneous fashion likely reflecting natural variations in metal stress resistance. The emerging cells regenerate new S-layers as part of their cell wall structure. Given the wide diversity of S-layer bearing prokaryotes, S-layer shedding may represent an important mechanism for microbial survival in metal-contaminated environments.

**Keywords:** S-layer, metal, biomineralization, metallotolerance, *Lysinibacillus*

## INTRODUCTION

Environmental contamination by metals and radionuclides from activities such as mining and nuclear power generation pose a serious risk to human health. The sudden, accidental release of high concentrations of iron from acid mine drainage from the Gold King Mine polluted the Animas River in 2015, mixing downstream with phosphates from agricultural runoff (Rodriguez-Freire et al., 2016). Metal contamination affected both water supplies from soluble metals, and sediments after the sedimentation of the majority of released metals. Sampling of soils contaminated by metals

and radionuclides near the former Chernobyl nuclear reactor site (Chapon et al., 2012) and in uranium mining waste piles in Germany (Pollmann et al., 2006) have identified bacteria of the genus *Lysinibacillus* tolerant to these contaminants. *Lysinibacillus* [formerly classified as part of the *Bacillus* genus (Ahmed et al., 2007)] gram-positive bacteria, with a peptidoglycan cell wall enclosed by a surface layer (“S-layer”) attached non-covalently to the lipopolysaccharides of the outer membrane (reviewed in Sleytr et al., 2014). These S-layers have proven to be a key mechanism for metal tolerance in *Lysinibacillus* as they have been shown to bind U, Pd(II), Cu, Pt(II), and Au(III) (Pollmann et al., 2006).

S-Layers, however are not unique to *Lysinibacillus*. They are common components of the cell envelopes of both bacteria and archaea. S-layers are formed by self-assembly of repeated protein monomers into ordered structures (oblique, square, or hexagonal) depending on the number of subunits composing the ordered structure. This self-assembly occurs even in the absence of cells *in vitro*; a capacity has been exploited in biotechnology in everything from the development of vaccine to nanomaterials to filtration technologies (Sleytr et al., 2011).

S-Layers form the interaction interface between prokaryotic cells and their external environment, and are therefore in contact with metals and other ions present. Nucleation of mineralization by S-layers was first noted in cyanobacteria by Schultze-Lam et al. (1992). Cyanobacterial S-layers were demonstrated to nucleate the formation of carbonates of calcium, magnesium, and strontium (Schultze-Lam and Beveridge, 1994). Schultze-Lam et al. (1992) proposed the hypothesis that mineral-encrusted S-layers are shed from cyanobacteria as part of a protective mechanism to ensure that essential cell activities are maintained despite cell wall mineralization. This hypothesis was, however, never fully tested. Since then, S-layer nucleation of mineralization has been observed in a range of bacteria (Konhauser et al., 1994; Phoenix et al., 2000) and archaea (Kish et al., 2016).

Here, we describe the shedding and regeneration of mineral-encrusted S-layers in the metallotolerant environmental isolate *Lysinibacillus* sp. TchIII 20n38.

## MATERIALS AND METHODS

### Culture and Growth Conditions

The bacterial strain used was an environmental strain isolated in 2009 from soils near a radionuclide-contaminated site (Chapon et al., 2012). This strain, referenced as *Lysinibacillus* sp. TchIII 20n38, was cultured at 30°C in Luria Bertani (LB) medium under aerobic conditions with agitation (180 rpm) to mid-exponential, late-exponential, and stationary growth phases ( $OD_{600\text{ nm}} = 0.3, 0.6, \text{ and } 1.0$ , respectively). The culture medium was then removed and the cells washed in MilliQ-H<sub>2</sub>O by gentle centrifugation (2600 × g, 15 min, room temperature). In order to determine the mechanisms of resistance of *Lysinibacillus* sp. TchIII 20n38 cells to the presence of heavy metals, the cells were resuspended to an equivalent cell density in a Fe-rich solution at a similar pH to that found in the Chernobyl isolation (10 mM NaH<sub>2</sub>PO<sub>4</sub>, 10 mM FeSO<sub>4</sub>, pH = 4.5), and agitated (150 rpm, 30°C) with

for up to 5 days. Cells were filtered and observed by scanning electron microscopy (SEM) as described below.

### Mineralization Recovery Time Course

In order to test the hypothesis that mineral-encrusted S-layers are shed and regenerated, a time course of recovery was followed after Fe-mineralization as follows: *Lysinibacillus* sp. TchIII 20n38 cells were grown to mid-exponential growth phase ( $OD_{600\text{ nm}} = 0.3$ ) in LB (30°C, 180 rpm). The culture medium was then removed and the cells washed in MilliQ-H<sub>2</sub>O by gentle centrifugation (2600 × g, 15 min, room temperature). The cells were then resuspended to an equivalent cell density in either a mineralization solution (10 mM NaH<sub>2</sub>PO<sub>4</sub>, 10 mM FeSO<sub>4</sub>, pH = 4.5), or a nutrient-free buffered solution at the same pH (10 mM NaH<sub>2</sub>PO<sub>4</sub>, pH = 4.5), and agitated (30°C, 150 rpm) for 16 h. The mineralization solution was then removed and the cells washed in MilliQ-H<sub>2</sub>O by gentle centrifugation (2600 × g, 15 min, room temperature), and replaced by growth medium (LB, or labeled growth medium).

For nanoscale secondary ion mass spectrometry (NanoSIMS) experiments, LB was replaced with a defined growth medium approximating LB but containing either <sup>14</sup>N or <sup>15</sup>N (Celtone®, Cambridge Isotopes, United States). While specified for use with bacteria for isotope analyses, this media was found to contain inhibitory concentrations of trace metals, which we were able to remove by precipitation by addition of an excess of buffered phosphate (10 mM) over 24 h with agitation at 150 rpm, followed by filtration using a 0.22 μm filter. This metal-depleted medium containing 5 g/L Celtone® was completed with 5 g/L acetate as a C-source, and basal salts (15 mM ammonium sulfate, 0.2 mM MgSO<sub>4</sub>, 17.6 mM KH<sub>2</sub>PO<sub>4</sub>, 32.7 mM NaH<sub>2</sub>PO<sub>4</sub>), as determined by our preliminary optimized experiments with *Lysinibacillus* sp. TchIII 20n38. In addition, cultures grown in the presence of <sup>14</sup>N rather than <sup>15</sup>N rapidly ceased vegetative growth and sporulated. Therefore instead of a standard labeling medium composed of both <sup>14</sup>N and <sup>15</sup>N, a 100% <sup>15</sup>N-labeled medium, was used to follow the time course of recovery after Fe-exposure. An additional culture was resuspended in a 100% <sup>14</sup>N medium and immediately sampled as a baseline control for N isotope abundances. Cultures were incubated in the <sup>15</sup>N-labeled medium at 30°C with agitation (180 rpm) over a time course of recovery, for both mineralized (M) and non-mineralized (NM) cultures. Aliquots were removed immediately after addition of growth medium (T0), and then every 24 h (1, 2 days). At each time point, approximately 20 mL aliquots were removed for optical density measurements, optical microscopy verification of cell morphology, and filtered for SEM observations and NanoSIMS analyses as described below. Abiotic (non-inoculated) controls were used for comparison to distinguish mineralization due to the presence of *Lysinibacillus* sp. TchIII 20n38 cells.

### Scanning Electron Microscopy

Aliquots of bacterial cultures as well as abiotic controls (not inoculated with *Lysinibacillus* sp. TchIII 20n38 cells) were filtered through a 0.2 μm GTTP isopore polycarbonate filters using a Swinnex filter holder (Merck Millipore, Darmstadt, Germany). Filters were then air-dried, mounted on aluminum supports

with carbon tape, and coated with carbon (7–8 nm thickness), gold (7 nm thickness), or platinum (5 nm thickness). SEM observations were performed using two different instruments; a Hitachi SU 3500 SEM installed at the electron microscopy platform of the Muséum National d'Histoire Naturelle (Paris, France), and a Zeiss Ultra 55 field emission gun SEM equipped with a Bruker EDS QUANTAX detector (Bruker Corporation, Houston, TX, United States) installed at IMPMC (Sorbonne Université, Paris, France). For observations using the Hitachi SU 3500 instrument observations were made in secondary electron mode with an acceleration voltage of 15 kV. SEM-FEG images were acquired in secondary electron mode using with the Zeiss Ultra 55 instrument with an in column detector (InLens) at 2 to 5 kV and a working distance of 3 mm. Energy dispersive X-ray spectroscopy (EDX) analyses were performed at 15 kV and a working distance of 7.5 mm after calibration with reference copper.

## Nano Secondary Ion Mass Spectrometry

Nano secondary ion mass spectrometry sample preparations followed the protocol of Miot et al. (2015). Briefly, aliquots of bacterial cultures sampled from labeled and unlabeled media filtered through 0.2  $\mu\text{m}$  GTTP isopore polycarbonate filters previously Au-coated (20 nm thickness) using a Swinnex filter holder (Merck Millipore, Darmstadt, Germany). Quantitative ion images were recorded by the NanoSIMS50 (Cameca, Gennevilliers, France) installed at the National Museum of Natural History of Paris, France. All measurements were performed using the same analytical conditions. A Cs + primary beam of 0.8 pA scanned an area of 20  $\mu\text{m}$   $\times$  20  $\mu\text{m}$ , divided into 256 pixels  $\times$  256 pixels, with a counting time of 1 ms per pixel. Secondary ion images of  $^{31}\text{P}^{16}\text{O}^-$ ,  $^{12}\text{C}^{14}\text{N}^-$ , and  $^{12}\text{C}^{15}\text{N}^-$  were recorded. The mass resolution power was adjusted to 9000 to resolve isobaric interferences at mass 27 such as  $^{13}\text{C}^{14}\text{N}^-$  or  $^{11}\text{B}^{16}\text{O}$  from  $^{12}\text{C}^{15}\text{N}^-$ . Before any analysis, the surface of each sample was pre-sputtered during 5 min with a 80 pA Cs- primary ion beam over 30  $\mu\text{m}$   $\times$  30  $\mu\text{m}$  to eliminate the contamination of the surface, and reached the stable state of sputtering (Thomen et al., 2014). Instrument stability was verified throughout the session using a type 3 kerogen standard. NanoSIMS data were then processed using the IMAGE software (L. Nittler, Carnegie Institution for Science, Washington, DC, United States).

## Statistical Analyses

The preference of this strain of *Lysinibacillus* for  $^{15}\text{N}$  to maintain vegetative growth eliminated the possibility of using a  $^{14}\text{N}$  control throughout the time course of recovery. In order to automatically remove the random noise from all the  $^{12}\text{C}^{14}\text{N}^-$  and  $^{12}\text{C}^{15}\text{N}^-$  NanoSIMS images, we defined  $^{12}\text{C}^{14}\text{N}^-$  and  $^{12}\text{C}^{15}\text{N}^-$  independent thresholds based on their respective distribution for the images of samples that were resuspended in the  $^{14}\text{N}$ -labeled medium. Each elemental distribution was fitted by two Gaussian components (R-package mixtools, Benaglia et al., 2009). We define threshold as the mean of the 97.5th percentile of the first Gaussian component (noise) and the 2.5th percentile of the second one (signal).

For each image, the denoised dataset further used for statistical analyses is composed only of pixels with both  $^{12}\text{C}^{14}\text{N}^-$  and  $^{12}\text{C}^{15}\text{N}^-$  values above the respective thresholds. The isotope abundance  $^{12}\text{C}^{15}\text{N}^- / (^{12}\text{C}^{14}\text{N}^- + ^{12}\text{C}^{15}\text{N}^-)$  of this dataset (hereafter named processed  $^{15}\text{N} / (^{14}\text{N} + ^{15}\text{N})$  ratio) was used to follow the kinetics of incorporation of N (as part of protein production) by non-mineralized and mineralized bacteria. For each image, the distribution of processed  $^{15}\text{N} / (^{14}\text{N} + ^{15}\text{N})$  ratio was fitted using Gaussian mixture modeling (R-package mclust, Scrucca et al., 2016) in order to infer subpopulations of pixels. The best univariate model, composed of  $k$  Gaussian components with either equal or unequal variance, was selected based on Bayesian Information Criterion. The mixing proportions for the components represent the proportions of the  $k$  subpopulations of pixels.

Cluster analysis was performed in order to group the samples according to their subpopulation composition. Each image was described by a vector of 10 values, each corresponding to the sum of the mixing proportions for the Gaussian components whose mean falls in a given  $^{15}\text{N} / (^{14}\text{N} + ^{15}\text{N})$  ratio interval (10 intervals of size 0.1 each). An image-to-image distance matrix generated by computing Bray-Curtis dissimilarity index between all the pairs of vectors was used for hierarchical agglomerative clustering of images (unweighted pair group method with arithmetic mean linkage).

All analyses were conducted in R version 3.2.3 (R Core Team, 2015).

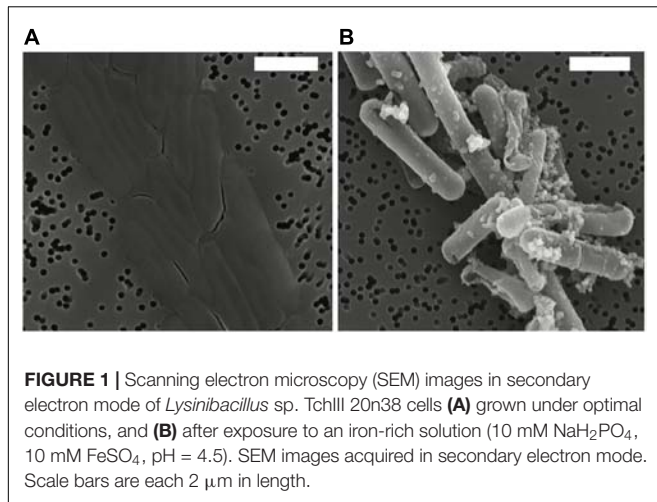
## RESULTS

### *Lysinibacillus* sp. S-Layers Become Encrusted After Exposure to Iron

*Lysinibacillus* sp. TchIII 20n38 was isolated from soils contaminated by radionuclides and metals, resulting in a moderately acidic pH (5.5) (Chapon et al., 2012). Our work with this strain, like other isolates from the same site, has shown that it is resistant to a range of heavy metals and radionuclides (data not shown). To determine the mechanisms of this metal tolerance, we exposed cells to a Fe-rich solution at acidic pH in the absence of the preferred carbon source for this strain, acetate, while maintaining high levels of phosphate required by *Lysinibacillus* sp. Non-metabolic metal-tolerance mechanisms are favored under these conditions.

After exposure, Fe-minerals were observed to form on the surface of *Lysinibacillus* sp. cells leading to complete encrustation of the cells over time (see **Figure 1**). EDX analyses of mineral-encrusted cells confirmed the composition as a Fe-phosphate (see **Supplementary Figure S1**). Some abiotically formed Fe-phosphates were also observed, which were easily distinguishable from mineralized S-layers as aggregates of larger spherically-shaped minerals not associated with cells, and matching the types of minerals observed in non-inoculated controls.

Cells were fully mineral encrusted after 16 h of exposure to the Fe-rich solution, whether cells were exposed in mid-exponential, late-exponential, or stationary growth phase ( $\text{OD}_{600\text{ nm}} = 0.3, 0.6,$



and 1.0, respectively). Longer exposures (20 and 41 h) did not alter the extent mineralization.

Attempts to confirm whether the mineralization observed on *Lysinibacillus* sp. TchIII 20n38 cells was due to a completely non-metabolic process, or whether active metabolism by living cells was necessary for S-layer mineralization were limited due to an inability to obtain dead cells without damaging the S-layer containing cell envelope. This despite multiple trials employing various antibiotics targeting non-cell envelope structures, and testing them over a large range of concentrations and durations [tetracycline (10–2000 μg/mL for 1 h–5 days in LB, buffer, or MilliQ-H<sub>2</sub>O) ofloxacin (10–500 μg/mL), and heat treatments (up to 55°C)]. The fact that *Lysinibacillus* sp. TchIII 20n38 cells grow optimally as heterotrophs without added metals suggests that the role of any metabolic processes in S-layer mineralization was secondary to non-metabolic processes.

## Response to Metal Exposure Depends on Physiological State, Times of Mineralization and Recovery

Replacement of mineral-encrusted cells into a rich growth medium demonstrated that *Lysinibacillus* sp. TchIII 20n38 cells were able to resume proper cell division after complete Fe-mineral encrustation. The exposure of mid-exponential growth phase cells (OD<sub>600 nm</sub> = 0.3) to the Fe-rich solution for 16 h followed by recovery of the cultures in LB showed that cells resumed normal cell division (see **Supplementary Figure S2**). However, the physiological state of the cells during metal encrustation, resulting in various inhibitions of normal vegetative cell growth and division. For mid-exponential growth phase cells, exposures longer than 16 h to the Fe-rich solution resulted in the death of mineralized cells, and the formation of filaments by the small minority of cells observed without mineral-encrustation. In the case of both late-exponential growth phase and stationary phase cultures, even 16 h-long exposures to Fe resulted in sporulation and/or cell death.

## Mineral-Encrusted S-Layers Can Be Shed

Scanning electron microscopy observations were made of mid-exponential growth phase *Lysinibacillus* sp. TchIII 20n38 cells after a 16 h exposure to the Fe-rich solution. Mineralized S-layers devoid of a cell were observed, often with the cells located beside these empty mineralized S-layer shell (see **Figure 2A**, left and right images). After incubation in LB for up to 5 days following Fe-mineralization, cells were seen exiting mineralized S-layer cells, with cell division septa visible (see **Figure 2B**, top and bottom images), in concordance with increases in the optical density of the cultures (see **Supplementary Figure S2**).

## *Lysinibacillus* sp. Cell Morphology Changes During S-Layer Shedding

The cell morphology in both mineralized and non-mineralized cultures was altered over the time course of recovery (see **Figure 3**). In non-mineralized cultures which were kept at the same pH as the mineralized cultures but in the absence of iron, cells gradually shrank in size and became ovoid in shape over 2 days of incubation in the metal-depleted Celtone® medium. While cell death was minimal for non-mineralized cells, dead cells were easily distinguishable due to both their high<sup>12</sup>C<sup>14</sup>N<sup>-</sup> counts due to lack of <sup>15</sup>N incorporation, and their sustained rod shape (see image of non-mineralized cells 1 day in **Figure 4**). Non-mineralized cells also formed intracellular polyphosphate granules between 1 and 2 days of incubation, as evidenced by analyses of <sup>31</sup>P<sup>16</sup>O<sup>-</sup> counts (see **Figure 4**).

Mineralized cultures showed little change over the first day of incubation. On the second day, however, cells were observed outside of their mineralized S-layer shells, with biofilm formation evidenced as a mucoid phenotype (see **Figure 3**) together with increases in optical density of the cultures (see **Supplementary Figure S3**). SDS-PAGE and mass spectrometry confirmed the presence of S-layer glycoproteins throughout the time course of recovery (see **Supplementary Figures S4, S5**, and **Supplementary Tables S1–S4**). Shed, mineralized S-layers maintained the elongated rod shape of non-stressed *Lysinibacillus* sp. TchIII 20n38 cells and restricted <sup>31</sup>P<sup>16</sup>O<sup>-</sup> to their surfaces (see **Figure 4**), likely within the Fe-phosphate minerals analyzed by EDX in **Figure 2**. In comparison, newly emerged cells lacked surface phosphates, some cells concentrating phosphate as intracellular granules (see **Figure 4**). On the third day of incubation, cells in both mineralized and non-mineralized cultures began to sporulate.

## Sub-Populations of Cells Co-exist During Time Course of Recovery

In order to describe the process of S-layer regeneration after mineral encrustation, and to determine if the S-layers were indeed regenerated, we followed the recovery of *Lysinibacillus* sp. TchIII 20n38 cells over time after Fe-mineral encrustation. Both SEM observations of cell morphology and NanoSIMS analyses of cell activity using incorporation of nitrogen, needed for the production of new S-layer proteins. <sup>15</sup>N-incorporation

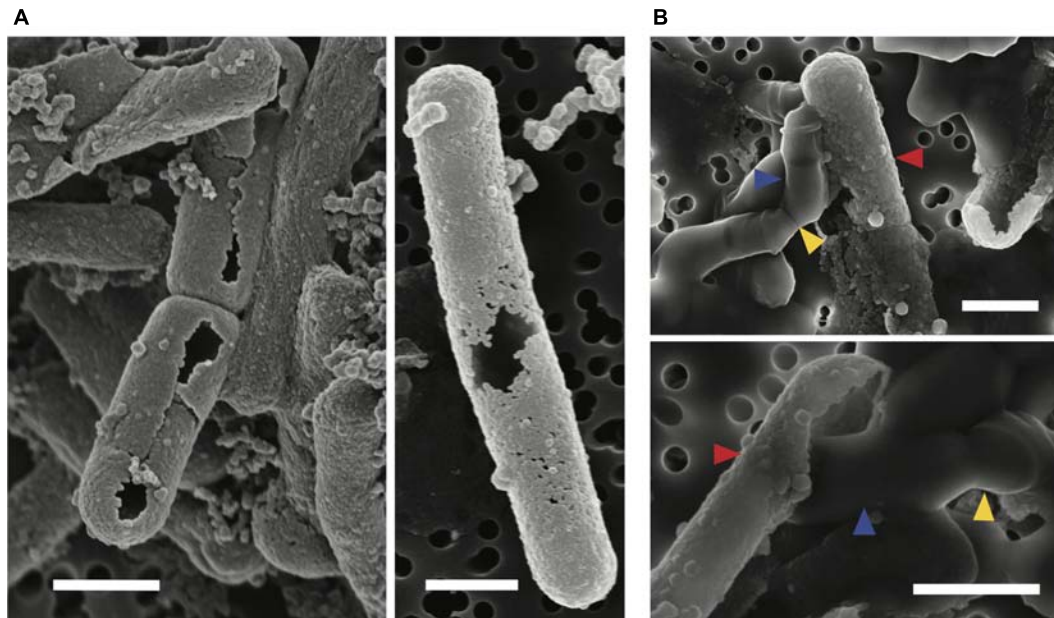


**FIGURE 2** | S-layer mineralization after exposure to Fe as observed by SEM in secondary electron mode. **(A)** Empty mineralized S-layer “shell” lacking a cell observed by SEM (secondary electron mode) after a 16 h exposure of a mid-exponential growth phase culture of *Lysinibacillus* sp. TchlII 20n38 to the Fe-rich solution. Empty S-layer mineral encrustation can be thick (left-side image) or thinner and “lacy” (right-side image). **(B)** Top and bottom images show cells emerging from shed mineralized S-layers. Cells were in mid-exponential growth phase prior to exposure to Fe, followed by incubated in LB for up to 5 days (37°C, 180 rpm). Blue arrows show emerging cells. Red arrows indicate mineralized S-layers. Yellow arrows indicate cell division septa. Scale bars for all images are 1  $\mu\text{m}$  in length.

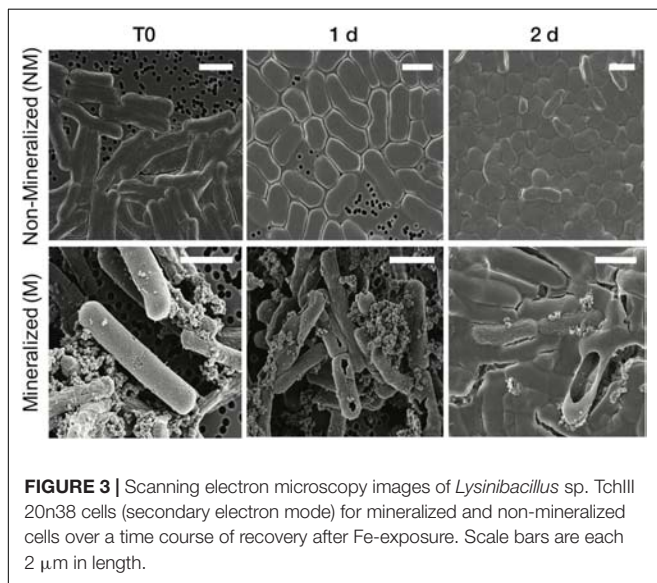
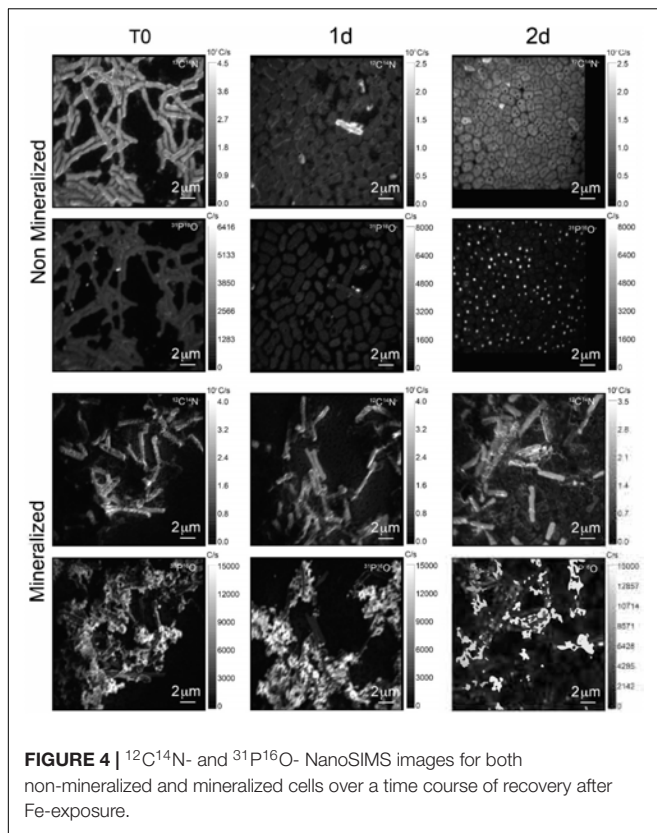


**FIGURE 3** | Scanning electron microscopy images of *Lysinibacillus* sp. TchlII 20n38 cells (secondary electron mode) for mineralized and non-mineralized cells over a time course of recovery after Fe-exposure. Scale bars are each 2  $\mu\text{m}$  in length.

is an effective marker, as S-layer proteins are one of the most abundant cellular proteins, and roughly 20% of total protein synthesis can be dedicated to their production (Sleytr et al., 2007). The  $^{15}\text{N}$  incorporation over time was determined using  $^{12}\text{C}^{15}\text{N}/(^{12}\text{C}^{15}\text{N}+^{12}\text{C}^{14}\text{N})$  and statistical analyses of the  $^{15}\text{N}/(^{14}\text{N}+^{15}\text{N})$  were then performed (see example of sample M\_T0\_rep2 in Figure 5 and Supplementary Figure S6). In order to account for differences in cell morphology over time and

between mineralized and non-mineralized samples, statistical analyses were performed using all pixels above the established threshold from each image. At least three processed  $^{15}\text{N}/(^{14}\text{N}+^{15}\text{N})$  images were analyzed per sample time point for samples incubated in medium containing  $^{15}\text{N}$  (two images each for natural abundance controls), with 10 to <60 cells per image depending on the physiological state of the cells over the time course. Subpopulations of pixels were identified for each sample according to the distribution of processed  $^{15}\text{N}/(^{14}\text{N}+^{15}\text{N})$  ratio (see Figure 5). Figure 5 shows that at the start of the time course (T0), the mineralized cells had  $^{15}\text{N}/(^{14}\text{N}+^{15}\text{N})$  ratios below 0.5 (panel A), with most cells having a ratio near 0.3 (panel B). Pixel subpopulations clustered around cells (panel C), with most mineralized cells and abiotic mineralization retaining a small amount of  $^{15}\text{N}$  (panel D) during the brief exposure prior to washing the cells in the first few minutes of the experiment.

Clustering of the NanoSIMS images according to their distribution of processed  $^{15}\text{N}/(^{14}\text{N}+^{15}\text{N})$  ratio showed that the samples tended to cluster over the experimental time course into three different groups; “natural abundance” ( $^{14}\text{N}$ ) T0 controls, low  $^{15}\text{N}$  incorporation (NM\_T0, M\_T0, M\_1d), and significant  $^{15}\text{N}$  incorporation (NM\_1d, NM\_2d, M\_2d) (see Figure 6). The fact that controls for the natural abundance (NM\_no incubation, M\_no incubation) grouped separately from the T0 samples shows that even brief exposure to the  $^{15}\text{N}$ -labeled medium during cell resuspension had an effect on the isotopic composition of the cells. The T0 samples were therefore used as the baseline of comparison for all later



time-points. The two remaining groups were composed of cells cultivated in  $^{15}\text{N}$ -labeled medium, grouped by whether or not cell division had restarted. Low  $^{15}\text{N}$ -incorporation samples (M\_T0, NM\_T0, M\_1d) corresponded to cells not yet showing evidence of cell division, whereas samples with significant  $^{15}\text{N}$  incorporation (NM\_1d, NM\_2d, M\_2d) showed clear evidence of active cell division when observed by SEM (see **Figure 3**) and measurements of optical density (see **Supplementary Figure S3**).

Variations between replicate images were minimal for all samples with the exception of both mineralized and non-mineralized 2 days samples, as seen in the heat map representation. The weighted distribution of subpopulations remained low for all samples prior to restart of cell division (see **Figure 6** and **Supplementary Figure S6**, samples M\_T0, M\_1d, NM\_T0). The increase in pixel subpopulations for samples showing signs of recovery and cell division (samples NM\_1d, NM\_2d, M\_2d) reflects the heterogeneity of cell recovery. Heterogeneity in  $^{15}\text{N}$  incorporation was highest for cells immediately after S-layer shedding (M\_2d samples), which is likely a reflection of natural variations in the capacity of *Lysinibacillus* sp. TchIII 20n38 cells to respond to stress.

## S-Layers Are Regenerated Within 2 Days of Fe-Mineral Encrustation

Some cell-free mineralized S-layer shells were observed by SEM immediately after 16 h exposure to the Fe-rich solution (see

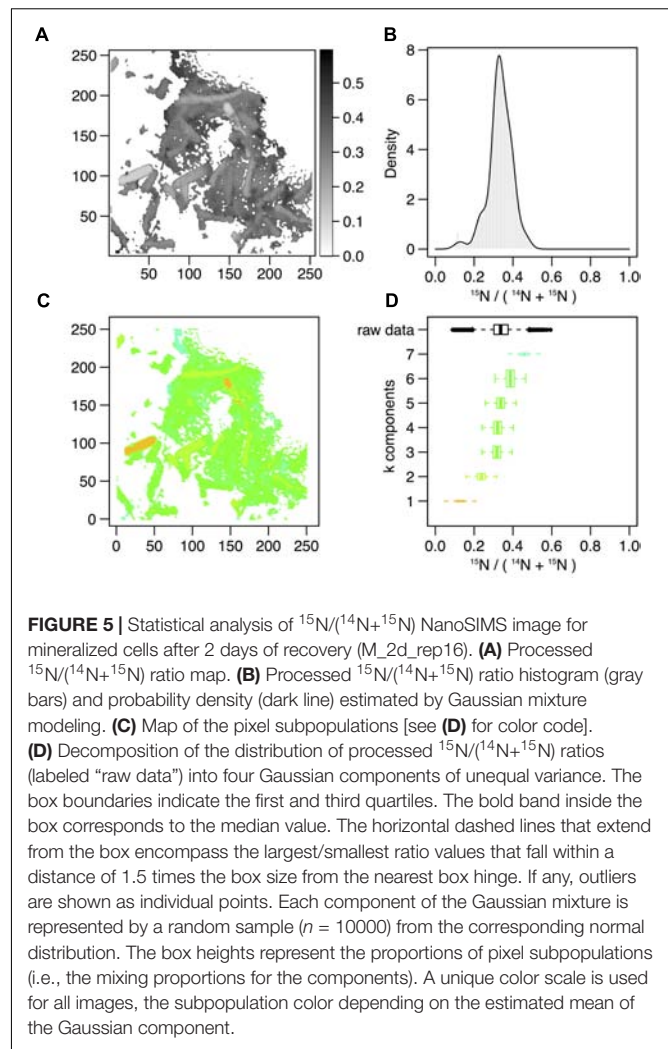


**Figure 3**). However, the morphology of the cells remained generally unchanged through 1 day of incubation in the defined medium. At 2 days of incubation in this medium, SEM observations clearly show a majority of non-mineralized cells alongside the remaining, cell-free, mineralized S-layer shells. Analyses of  $^{15}\text{N}$  uptake using NanoSIMS confirmed this timing, showing no significant  $^{15}\text{N}$  incorporation for mineralized samples prior to 2 days of recovery in labeled medium, compared to T0 control aliquots that were removed immediately after resuspension of cells in the labeled medium (see **Figure 6**). The S-layers of mineralized samples remained at a relatively steady  $^{15}\text{N}/(^{14}\text{N} + ^{15}\text{N})$  ratio (see green regions in **Supplementary Figure S6**, mineralized samples) compared to the emerging cells, showing that mineralized S-layers did not incorporate  $^{15}\text{N}$  during the cell division processes giving rise to the emerging cells. This is coherent with S-layer shedding and complete regeneration. S-layer presence before and after mineralization and shedding was confirmed by SDS-PAGE and mass spectrometry (see **Supplementary Figures S4, S5**).

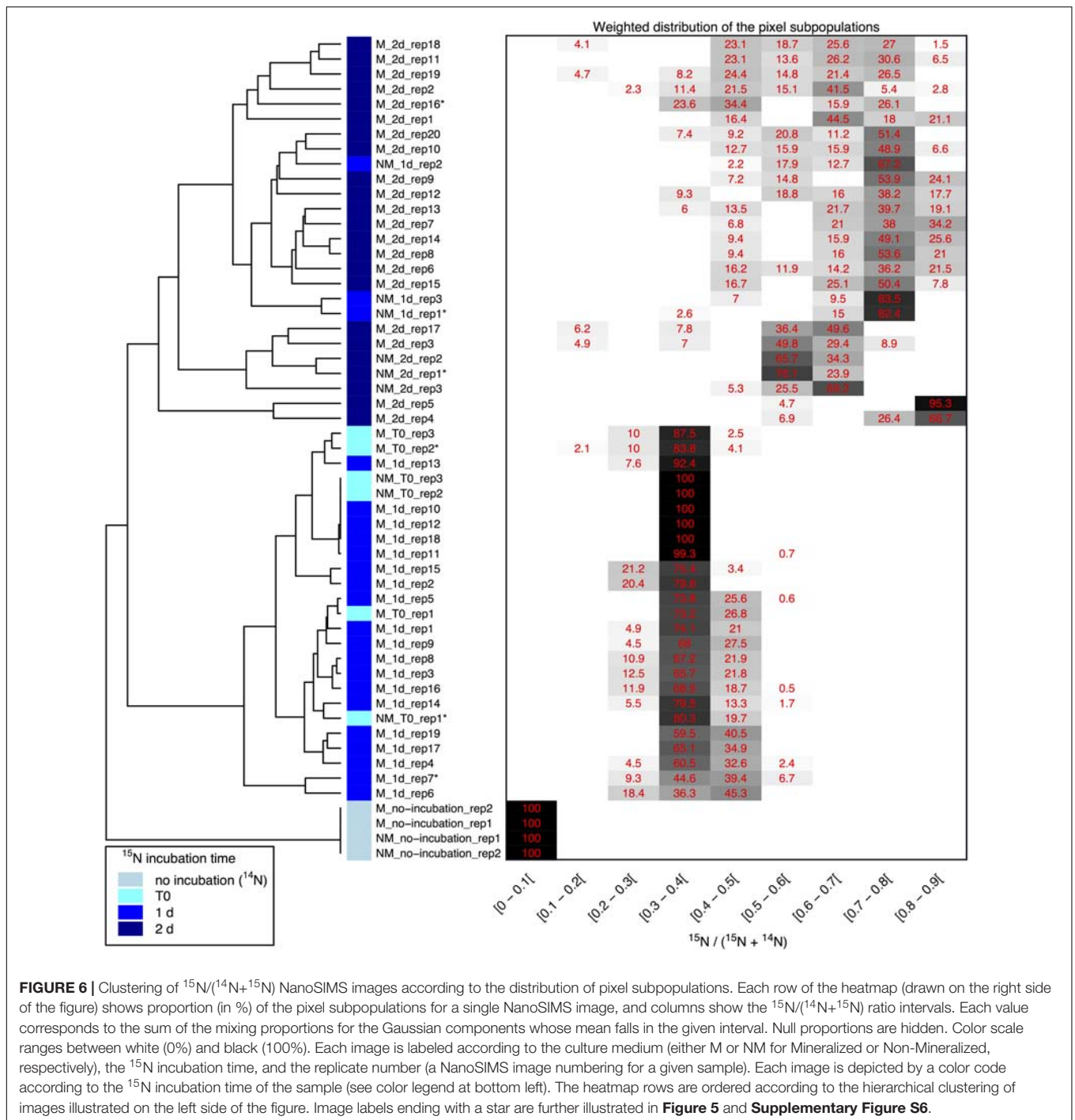


**FIGURE 6 |** Clustering of <sup>15</sup>N/<sup>14</sup>N+<sup>15</sup>N NanoSIMS images according to the distribution of pixel subpopulations. Each row of the heatmap (drawn on the right side of the figure) shows proportion (in %) of the pixel subpopulations for a single NanoSIMS image, and columns show the <sup>15</sup>N/<sup>14</sup>N+<sup>15</sup>N ratio intervals. Each value corresponds to the sum of the mixing proportions for the Gaussian components whose mean falls in the given interval. Null proportions are hidden. Color scale ranges between white (0%) and black (100%). Each image is labeled according to the culture medium (either M or NM for Mineralized or Non-Mineralized, respectively), the <sup>15</sup>N incubation time, and the replicate number (a NanoSIMS image numbering for a given sample). Each image is depicted by a color code according to the <sup>15</sup>N incubation time of the sample (see color legend at bottom left). The heatmap rows are ordered according to the hierarchical clustering of images illustrated on the left side of the figure. Image labels ending with a star are further illustrated in **Figure 5** and **Supplementary Figure S6**.

## DISCUSSION

### *Lysinibacillus* sp. TchIII 20n38 Is Highly Adapted for Survival Under Stress Conditions

The bacterial isolate used in this study, *Lysinibacillus* sp. TchIII 20n38, is a metallotolerant gram-positive bacterium, possessing a cell envelope composed of the plasma membrane

surrounded by a thick layer of peptidoglycan capped by an S-layer forming an ordered structure at the cell surface. This flexible cage-like structure is in direct contact with the surrounding environment, and thus provides the primary protective element against potentially toxic environmental concentrations of heavy metals or radionuclides. Such interactions between *Lysinibacillus* sp. cells and metals can lead to cell surface mineralization, biosorption, or intracellular bioaccumulation, depending on the depending on the types of metals present and physicochemical

parameters such as pH (data not shown). Here, we show that *Lysinibacillus* sp. TchIII 20n38 has many adaptive mechanisms to the stresses induced by nutrient limitation and/or the presence of iron, as might be expected for a bacterium isolated from a radioactive waste disposal site. These included the accumulation and enlargement of intracellular polyphosphate granules and sporulation under phosphate-limiting conditions, cell size reduction, and morphology alterations from rod-shaped to ovoid cells after metal stress, as well as reductions in biofilm after exposure to either iron or acidic pH and augmentation in biofilm after a return to neutral pH in the absence of additional iron input. Polyphosphate accumulation is a common mechanism used by bacteria, including *Lysinibacillus sphaericus*, in response to nutrient stress (depletion of amino acids), and prior to sporulation (Tocheva et al., 2013; Shi et al., 2015).

### S-Layer Shedding Mechanism in *Lysinibacillus* as a Response to Metal Stress

S-Layers from a variety of prokaryotes are known to induce mineral formation. The S-layers of cyanobacteria are able to nucleate selenite and strontium (Schultze-Lam and Beveridge, 1994), while the S-layers of thermophilic archaea can form amorphous Fe-phosphate minerals in the quasi-periplasmic space between the S-layer and the underlying lipid membrane (Kish et al., 2016). Diverse *Lysinibacillus* sp. have been observed to precipitate minerals on their cell surfaces, including U-phosphates (Merroun et al., 2005; Mondani et al., 2011) and calcium carbonate (Kaur and Mukherjee, 2013). Here, we show that *Lysinibacillus* sp. TchIII 20n38 cells become encrusted with Fe-minerals after exposure to high concentrations of iron under mildly acidic conditions. Mineral precipitation by the cell surfaces, including S-layers, prevent damages to cells including oxidative stress, enzyme deactivation, protein denaturation, and membrane disruption (Lemire et al., 2013). Iron precipitation nucleated by the S-layer proteins prevents an overproduction of free radicals in the cytosol due to Fenton chemistry.

While mineral formation on S-layers is known, the mechanisms for removing such barriers to exchange with the surrounding environment are not as well-understood. Mechanisms identified to date have described partial removal of cell envelope components after metal interactions, particularly membrane vesicle formation (McBroom and Kuehn, 2007; Shao et al., 2014; Kish et al., 2016). Partial shedding of S-layer fragments has also been observed, both for mineralized cyanobacterial S-layers (Schultze-Lam et al., 1992; Schultze-Lam and Beveridge, 1994) and non-mineralized S-layers for stationary phase bacteria likely as part of cell wall turnover (Luckevich and Beveridge, 1989). During the course of normal cell growth in the closely related *Lysinibacillus sphaericus*, bands of S-layer monomer insertion form on cell surfaces, and in the course of cell division new S-layer monomers are only inserted at the newly-formed the poles (Howard et al., 1982).

Here, we show that *Lysinibacillus* sp. cells were able to recover normal growth after mineral encrustation through a shedding of

mineralized S-layers, followed by S-layer regeneration. To our knowledge, this is the first report of complete S-layer shedding and regeneration. S-layer shedding required an additional 24h before cells returned to normal cell division compared to non-mineralized cells, as shown by the clustering of  $^{15}\text{N}$  uptake by 2 days mineralized cells with 1 day non-mineralized samples as measured by NanoSIMS over a time course after exposure to iron. Uptake of  $^{15}\text{N}$  also illustrated that despite extensive mineralization, cells retained active metabolism. The continued presence of shed, mineralized S-layers composed of  $^{14}\text{N}$ -based proteins alongside cells bearing newly regenerated  $^{15}\text{N}$ -bearing S-layers resulted in the heterogeneity in  $^{15}\text{N}$ -incorporation for the M\_2d samples (see **Figure 6**). S-layer shedding activity was limited to cells in mid-exponential growth phase, providing an advantage over cells in stationary growth phase in Fe-rich conditions.

### Importance of S-Layer Regeneration in Metal Stress

Now that the mechanism for S-layer shedding has been established for *Lysinibacillus* sp. TchIII 20n38, future work should explore the range of different metals that can be mineralized by S-layers, both in this bacterium and other S-layer bearing bacteria including both Gram-negative and Gram-positive species. The high diversity of S-layer bearing bacterial species suggests that this mechanism could be widely used. Shedding of mineralized S-layers is less likely in the Archaea, given that for many species the S-layer is the sole component of their cell wall. Indeed, our previous work in the archaeon *Sulfolobus acidocaldarius* demonstrated that S-layer shedding was not observed; mineralized S-layers were rather partially sloughed off by the formation of membrane vesicles prior to cell encrustation (Kish et al., 2016).

The S-layer shedding and regeneration shown here after mineral encrustation may also inform new directions for S-layer use in *in situ* bioremediation. Current biotechnology applications of S-layers focus on *in vitro* applications such as the use of recombinant S-layer proteins with enhanced metal binding capacity (Pollmann and Matys, 2007), or as templates to nucleate the fabrication of metal nanoparticle biocatalysts (Creamer et al., 2007), or as bio-filters for bioremediation technologies (Pollmann et al., 2006). S-layer regeneration after mineralization may aid the development of new metal remediation strategies using metallotolerant soil bacteria native to soils contaminated by metals and radionuclides to reduce the bioavailability of toxic metals through mineralization.

### AUTHOR CONTRIBUTIONS

AK and LR contributed to conception and design of the study. AC performed the experiments and wrote sections of the manuscript. LR performed the NanoSIMS measurements. CL and SZ performed the mass spectrometry analyses. ED performed the statistical analysis of NanoSIMS data. AK wrote the first draft of the manuscript.

All authors contributed to manuscript revision, read and approved the submitted version.

## FUNDING

This work was supported by the French National Program EC2CO-MicrobiEn, project “SkinDEEP,” awarded to AK. The National NanoSIMS facility at the MNHN was established by funds from the CNRS, Région Ile de France, Ministère Délégué à l’Enseignement Supérieur et à la Recherche, and the MNHN. The SEM facility of the Institut de Minéralogie, Physique des Matériaux et Cosmochimie is supported by Région Ile de France grant SESAME 2006 NoI-07-593/R, INSU-CNRS, INP-CNRS, Sorbonne Universités, and by the French National Research Agency (ANR) (Grant No. ANR-07-BLAN-0124-01).

## REFERENCES

- Ahmed, I., Yokota, A., Yamazoe, A., and Fujiwara, T. (2007). Proposal of *Lysinibacillus boronitoleras* gen. nov. sp. nov., and transfer of *Bacillus fusiformis* to *Lysinibacillus fusiformis* comb. nov. and *Bacillus sphaericus* to *Lysinibacillus sphaericus* comb. nov. *Int. J. Syst. Evol. Microbiol.* 57, 1117–1125. doi:10.1099/ijs.0.63867-0
- Benaglia, T., Chauveau, D., Hunter, D. R., and Young, D. (2009). mixtools: an RPackage for analyzing finite mixture models. *J. Stat. Softw.* 32, 1–29. doi: 10.18637/jss.v032.i06
- Chapon, V., Piette, L., Vesvres, M.-H., Coppin, F., Marrec, C. L., Christen, R., et al. (2012). Microbial diversity in contaminated soils along the T22 trench of the Chernobyl experimental platform. *Appl. Geochem.* 27, 1375–1383. doi: 10.1016/j.apgeochem.2011.08.011
- Creamer, N. J., Mikheenko, I. P., Yong, P., Deplanche, K., Sanyahumbi, D., Wood, J., et al. (2007). Novel supported Pd hydrogenation bionanocatalyst for hybrid homogeneous/heterogeneous catalysis. *Catal. Today* 128, 80–87. doi: 10.1016/j.cattod.2007.04.014
- Howard, L. V., Dalton, D. D., and McCoubrey, W. K. (1982). Expansion of the tetragonally arrayed cell wall protein layer during growth of *Bacillus sphaericus*. *J. Bacteriol.* 149, 748–757.
- Kaur, D. N., and Mukherjee, A. (2013). Biomineralization of calcium carbonate polymorphs by the bacterial strains isolated from calcareous sites. *J. Microbiol. Biotechnol.* 23, 707–714. doi: 10.4014/jmb.1212.11087
- Kish, A., Miot, J., Lombard, C., Guigner, J.-M., Bernard, S., Zirah, S., et al. (2016). Preservation of archaeal surface layer structure during mineralization. *Sci. Rep.* 6:26152. doi: 10.1038/srep26152
- Konhauser, K. O., Schultze-Lam, S., Ferris, F. G., Fyfe, W. S., Longstaffe, F. J., and Beveridge, T. J. (1994). Mineral precipitation by epilithic biofilms in the Speed river, Ontario, Canada. *Appl. Environ. Microbiol.* 60, 549–553.
- Lemire, J. A., Harrison, J. J., and Turner, R. J. (2013). Antimicrobial activity of metals: mechanisms, molecular targets and applications. *Nat. Rev. Microbiol.* 11, 371–384. doi: 10.1038/nrmicro3028
- Luckevich, M. D., and Beveridge, T. J. (1989). Characterization of a dynamic S layer on *Bacillus thuringiensis*. *J. Bacteriol.* 171, 6656–6667. doi: 10.1128/jb.171.12.6656-6667.1989
- McBroom, A. J., and Kuehn, M. J. (2007). Release of outer membrane vesicles by Gram-negative bacteria is a novel envelope stress response. *Mol. Microbiol.* 63, 545–558. doi: 10.1111/j.1365-2958.2006.05522.x
- Merroun, M. L., Raff, J., Rossberg, A., Hennig, C., Reich, T., and Selenska-Pobell, S. (2005). Complexation of uranium by cells and S-layer sheets of *Bacillus sphaericus* JG-A12. *Appl. Environ. Microbiol.* 71, 5532–5543. doi: 10.1128/AEM.71.9.5532-5543.2005

## ACKNOWLEDGMENTS

We gratefully acknowledge Virginie Chapon for giving us the strain used in this study, along with helpful discussions. We thank Adriana Gonzalez-Cano and Rémi Duhamel for assistance with NanoSIMS analyses, and Imène Esteve of the SEM facility of the Institut de Minéralogie, Physique des Matériaux et Cosmochimie for assistance with imaging, which was greatly appreciated. We also wish to thank Jennyfer Miot for productive discussions.

## SUPPLEMENTARY MATERIAL

The Supplementary Material for this article can be found online at: <https://www.frontiersin.org/articles/10.3389/fmicb.2018.03210/full#supplementary-material>

- Miot, J., Remusat, L., Duprat, E., Gonzalez, A., Pont, S., and Poinot, M. (2015). Fe biomineralization mirrors individual metabolic activity in a nitrate-dependent Fe(II)-oxidizer. *Front. Microbiol.* 6:879. doi: 10.3389/fmicb.2015.00879
- Mondani, L., Benzerara, K., Carrière, M., Christen, R., Mamindy-Pajany, Y., Février, L., et al. (2011). Influence of uranium on bacterial communities: a comparison of natural uranium-rich soils with controls. *PLoS One* 6:e25771. doi:10.1371/journal.pone.0025771
- Phoenix, V. R., Adams, D. G., and Konhauser, K. O. (2000). Cyanobacterial viability during hydrothermal biomineralisation. *Chem. Geol.* 169, 329–338. doi: 10.1016/S0009-2541(00)00212-6
- Pollmann, K., and Matys, S. (2007). Construction of an S-layer protein exhibiting modified self-assembling properties and enhanced metal binding capacities. *Appl. Microbiol. Biotechnol.* 75, 1079–1085. doi: 10.1007/s00253-007-0937-5
- Pollmann, K., Raff, J., Merroun, M., Fahmy, K., and Selenska-Pobell, S. (2006). Metal binding by bacteria from uranium mining waste piles and its technological applications. *Biotechnol. Adv.* 24, 58–68. doi: 10.1016/j.biotechadv.2005.06.002
- R Core Team (2015). *R: A Language and Environment for Statistical Computing*. Vienna: R Foundation for Statistical Computing.
- Rodriguez-Freire, L., Avsarala, S., Ali, A.-M. S., Agnew, D., Hoover, J. H., Artyushkova, K., et al. (2016). Post gold king mine spill investigation of metal stability in water and sediments of the animas river watershed. *Environ. Sci. Technol.* 50, 11539–11548. doi: 10.1021/acs.est.6b03092
- Schultze-Lam, S., and Beveridge, T. J. (1994). Nucleation of celestite and strontianite on a cyanobacterial s-layer. *Appl. Environ. Microbiol.* 60, 447–453.
- Schultze-Lam, S., Harauz, G., and Beveridge, T. J. (1992). Participation of a cyanobacterial S layer in fine-grain mineral formation. *J. Bacteriol.* 174, 7971–7981. doi: 10.1128/jb.174.24.7971-7981.1992
- Scrucca, L., Fop, M., Murphy, T. B., and Raftery, A. E. (2016). mclust 5: clustering, classification and density estimation using gaussian finite mixture models. *R J.* 8, 289–317.
- Shao, P. P., Comolli, L. R., and Bernier-Latmani, R. (2014). Membrane vesicles as a novel strategy for shedding encrusted cell surfaces. *Minerals* 4, 74–88. doi: 10.3390/min4010074
- Shi, T., Ge, Y., Zhao, N., Hu, X., and Yuan, Z. (2015). Polyphosphate kinase of *Lysinibacillus sphaericus* and its effects on accumulation of polyphosphate and bacterial growth. *Microbiol. Res.* 172, 41–47. doi: 10.1016/j.micres.2014.12.002
- Sleytr, U. B., Egelseer, E. M., Ilk, N., Pum, D., and Schuster, B. (2007). S-Layers as a basic building block in a molecular construction kit. *FEBS J.* 274, 323–334. doi: 10.1111/j.1742-4658.2006.05606.x
- Sleytr, U. B., Schuster, B., Egelseer, E. M., and Pum, D. (2014). S-layers: principles and applications. *FEMS Microbiol. Rev.* 38, 823–864. doi: 10.1111/1574-6976.12063

- Sleytr, U. B., Schuster, B., Egelseer, E. M., Pum, D., Horejs, C. M., Tscheliessnig, R., et al. (2011). Nanobiotechnology with S-layer proteins as building blocks. *Prog. Mol. Biol. Transl. Sci.* 103, 277–352. doi: 10.1016/B978-0-12-415906-8.00003-0
- Thomen, A., Robert, F., and Remusat, L. (2014). Determination of the nitrogen abundance in organic materials by NanoSIMS quantitative imaging. *J. Anal. At. Spectrom.* 29, 512–519. doi: 10.1039/c3ja50313e
- Tocheva, E. I., Dekas, A. E., McGlynn, S. E., Morris, D., Orphan, V. J., and Jensen, G. J. (2013). Polyphosphate storage during sporulation in the gram-negative bacterium *Acetonema longum*. *J. Bacteriol.* 195, 3940–3946. doi: 10.1128/JB.00712-13

**Conflict of Interest Statement:** The authors declare that the research was conducted in the absence of any commercial or financial relationships that could be construed as a potential conflict of interest.

Copyright © 2019 Chandramohan, Duprat, Remusat, Zirah, Lombard and Kish. This is an open-access article distributed under the terms of the Creative Commons Attribution License (CC BY). The use, distribution or reproduction in other forums is permitted, provided the original author(s) and the copyright owner(s) are credited and that the original publication in this journal is cited, in accordance with accepted academic practice. No use, distribution or reproduction is permitted which does not comply with these terms.



# Mangrove Facies Drives Resistance and Resilience of Sediment Microbes Exposed to Anthropogenic Disturbance

Cécile Capdeville<sup>1</sup>, Thomas Pommier<sup>2</sup>, Jonathan Gervais<sup>2</sup>, François Fromard<sup>1</sup>, Jean-Luc Rols<sup>1</sup> and Joséphine Leflaive<sup>1\*</sup>

<sup>1</sup> EcoLab, CNRS, INPT, UPS, Université de Toulouse, Toulouse, France, <sup>2</sup> Ecologie Microbienne, INRA, UMR 1418, CNRS, UMR 5557, Université Lyon 1, Villeurbanne, France

## OPEN ACCESS

### Edited by:

Stéphane Pesce,  
National Research Institute of Science  
and Technology for Environment  
and Agriculture (IRSTEA), France

### Reviewed by:

Emilie Lyautey,  
Université Savoie Mont Blanc, France  
Haitham Sghaier,  
The National Center for Nuclear  
Sciences and Technologies, Tunisia

### \*Correspondence:

Joséphine Leflaive  
josephine.leflaive@univ-tlse3.fr

### Specialty section:

This article was submitted to  
Microbiotechnology, Ecotoxicology  
and Bioremediation,  
a section of the journal  
Frontiers in Microbiology

**Received:** 14 September 2018

**Accepted:** 24 December 2018

**Published:** 15 January 2019

### Citation:

Capdeville C, Pommier T,  
Gervais J, Fromard F, Rols J-L and  
Leflaive J (2019) Mangrove Facies  
Drives Resistance and Resilience  
of Sediment Microbes Exposed  
to Anthropogenic Disturbance.  
*Front. Microbiol.* 9:3337.  
doi: 10.3389/fmicb.2018.03337

Mangrove forests are coastal ecosystems continuously affected by various environmental stresses and organized along constraint gradients perpendicular to the coastline. The aim of this study was to evaluate the resistance and resilience of sediment microbial communities in contrasted vegetation facies, during and after exposure to an anthropic disturbance. Our hypothesis was that microbial communities should be the most stable in the facies where the consequences of the anthropic disturbance are the most similar to those of natural disturbances. To test this, we focused on communities involved in N-cycle. We used an *in situ* experimental system set up in Mayotte Island where 2 zones dominated by different mangrove trees are daily exposed since 2008 to pretreated domestic wastewater (PW) discharges. These freshwater and nutrients inputs should increase microbial activities and hence the anoxia of sediments. We monitored during 1 year the long-term impact of this disturbance, its short-term impact and the resilience of microbial communities on plots where PW discharges were interrupted. Microorganism densities were estimated by qPCR, the nitrification (NEA) and denitrification (DEA) enzyme activities were evaluated by potential activity measurements and pigment analyses were performed to assess the composition of microbial photosynthetic communities. At long-term PW discharges significantly modified the structure of phototrophic communities and increased the total density of bacteria, the density of denitrifying bacteria and DEA. Similar effects were observed at short-term, notably in the facies dominated by *Cerriops tagal*. The results showed a partial resilience of microbial communities. This resilience was faster in the facies dominated by *Rhizophora mucronata*, which is more subjected to tides and sediment anoxia. The higher stability of microbial communities in this facies confirms our hypothesis. Such information should be taken into account in mangrove utilization and conservation policies.

**Keywords:** mangrove ecosystem, anthropic disturbance, wastewater discharge, *in situ* long term monitoring, microbial community, N-cycle

## INTRODUCTION

Mangrove forests are coastal ecosystems of tropical and subtropical areas, continuously under tidal influence (Blasco, 1991; Spalding et al., 1997) and submitted to environmental constraints varying according to the seasons and to spatial gradients (salinity gradients, tidal cycle, sediment anoxia, soil instability) (Feller et al., 2010). These overall nutrient-poor forests

(Boto and Wellington, 1984) are highly productive systems (Alongi, 2002). They provide varied food and material resources to human society and marine communities (Giri et al., 2011; Lee et al., 2014) and they are the main source of organic matter for the coastal marine food webs (Komiyama et al., 2000; Mohamed et al., 2016). They have also a high potential of carbon sequestration and storage due to rapid rates of net primary production and sedimentation (Komiyama et al., 2008; Donato et al., 2011; Alongi, 2012).

Microbial communities in mangroves sediments have a high diversity level (Andreote et al., 2012). These microorganisms allow the degradation of organic matter from vegetative materials (Holguin et al., 2001) and play a crucial role in nutrient cycles, particularly for nitrogen and phosphorous (Alvarenga et al., 2015). They contribute to the removal of nutrients like the nitrogen, and organic matter from sediments (Wu et al., 2008; Tam et al., 2009). The microorganisms involved in nitrogen cycle in mangrove ecosystem contribute through different metabolic processes: nitrogen ( $N_2$ ) fixation, nitrification, denitrification, ammonification, anaerobic ammonium oxidation (anammox) and dissimilatory nitrate reduction to ammonium (DNRA) (Alongi et al., 1992; Purvaja et al., 2008). These microorganisms participate in the degradation of organic nitrogen into inorganic nitrogen compounds (Alongi et al., 1992), available for the trophic chain, notably for the mangrove trees (Ganguly et al., 2009). Nitrogen can be removed from the sediments under the gaseous forms ( $N_2$ , NO,  $N_2O$ ) by the denitrification and anammox processes carried out by denitrifying bacteria and anammox bacteria, respectively (Levy-Booth et al., 2014). The release of  $N_2$  from mangrove sediments seems to be more important by denitrification than anammox processes (Fernandes et al., 2012). Sediment surface also is partially covered with phototrophic and heterotrophic microorganisms embedded into a matrix of extracellular polymeric substances (Decho, 2000) which participate in the sediment stabilization against resuspension, plant growth promotion (Bouchez et al., 2013), and the chelation of toxic metals and other contaminants (Decho, 2000). Phototrophic microorganisms such as diatoms, green algae or cyanobacteria contribute to the primary production of the ecosystem and constitute a food source for heterotrophic protists and meiofauna (Bertrand et al., 2011).

As a whole, mangrove ecosystems are considered as very resilient to disturbances. The response of communities to disturbances and stresses depends on their resistance and resilience abilities, two components of ecosystem stability (Pimm, 1984). Resistance is the degree to which a community remains unchanged (Pimm, 1984), while the resilience can be defined as the rate of return to the initial state (Allison and Martiny, 2008). For both properties, either the structure of the community, or the associated functions can be considered. Microbial systems are usually considered as very resistant and resilient, because of the specific properties of microorganisms. Indeed, resistance is favored by their high metabolic flexibility, good physiological tolerance to environmental changes and short generation time. Resilience should be facilitated by their high abundances, high growth rates, high dispersal rate and

high diversity (Fenchel and Finlay, 2004). Recent experimental studies emphasized contrasted abilities of microbial communities to recover from a similar disturbance (salinity stress) with either both structural and functional full recovery (Berga et al., 2017), only functional recovery (De Vrieze et al., 2017) or low recovery, in the case of extreme events (Hu et al., 2018).

In mangrove sediments, in addition to natural disturbances, microorganisms are directly exposed to anthropogenic pollutants that accumulate in sediments, such as organic contaminants (Zhang et al., 2014), oil spills (Muangchinda et al., 2013), domestic or industrial wastewaters (Tam, 1998). Structural modifications of the microbial communities can result from these anthropogenic inputs whether they are diffuse (Cao et al., 2011; Fernandes et al., 2014; Chakraborty et al., 2015) or controlled, as nutrient input (Li and Gu, 2013) or wastewater discharge (Tam, 1998).

Although the short-term response of microbial communities in mangrove sediments subjected to anthropogenic inputs is relatively well described, their actual resilience capacities are far less documented. Mangroves are very structured systems, organized in zones parallel to the coastline, along environmental gradients (salinity, nutrient availability, temperature), according to the sediment characteristics and the length of immersion by tides (Robertson and Alongi, 1992; Ball, 1998). Each zone is dominated by a few mangrove trees species adapted to the characteristic environmental conditions and associated with specific microbial communities in the sediments (Tam, 1998; Li and Gu, 2013; Wang et al., 2014). Though mangroves are often considered as a whole, these variations in environmental conditions and microbial community structure are associated with variations in the resistance and resilience properties of these communities. The aim of this study was to assess both resistance and resilience capacities of microbial communities in mangrove sediments exposed to anthropogenic disturbances. Our hypothesis was that the mangrove zone where the consequences of the applied disturbance are the most similar to those of natural disturbances should be the more stable.

To test this hypothesis, two contrasted mangrove zones were studied, respectively dominated by *Rhizophora mucronata* trees and *Ceriops tagal* trees. In the *Rhizophora*-dominated zone, closer to the seafront, the conditions are more constant, buffered by the tides but the longer immersion duration leads to longer anoxia of the sediment. In the *Ceriops*-dominated zone, the influence of tides is less important, the anoxia periods are shorter but the organisms are more submitted to aridity and salinity variations (Spalding et al., 2010; Tomlinson, 2016). The disturbance applied in these two mangrove zones was daily discharges of pretreated domestic wastewaters (PW). This input of nutrients and organic matter should increase microbial activity and consequently increase the anoxia of sediments. Based on *a priori* knowledge of the studied mangrove facies, including tide immersion time records, this disturbance should have a stronger similarity with the natural disturbances in the *R. mucronata*-dominated zone than in the *C. tagal* - dominated zone. The *in situ* experimental system used was set up in a

mangrove of Mayotte Island in 2008 by Herteman et al. (2011), in order to assess the use of mangroves for bioepuration. It helped to evaluate the impact of PW on microbial communities after 1 year (Bouchez et al., 2013) and 4.5–5 years (Capdeville et al., unpublished) of discharges. In the present study, this experimental system was modified to assess both short- (after 3 weeks, 3, 8, and 12 months) and long-term (after 7.5–8.5 years) responses of microbial communities exposed to PW discharges, and their resilience after 12 months of the disruption of PW discharges.

## MATERIALS AND METHODS

### Study Site

The *in situ* experimental system is localized in the mangrove of Chirongui Bay, South-West of Mayotte Island, a French department located in the Mozambique Channel, South-West of Indian Ocean (12°55'S, 45°09'E). Since April 2008, domestic wastewaters are continuously collected from Malamani village (250 inhabitants-equivalent), as described by Herteman et al. (2011). The wastewaters are pretreated in a horizontal primary settlement tank with integrated sludge digester. Then, they are carried through a pipe network to the mangrove areas. The areas of the *R. mucronata* mangrove zone are closer from the lagoon (about 400 m) than the ones in *C. tagal* mangrove zone (about 500 m), the latter being less subjected to tides (in mean 0.88 h/day of immersion against 4.33 h/day for the first zone). The PW were mainly composed of organic matter, nitrogen (mainly ammonium form) and phosphorus nutrients, discharged in the mangrove areas with surface loading rates (for dry season, in  $\text{g}\cdot\text{m}^{-2}\cdot\text{d}^{-1}$ ) of 6.1 for chemical oxygen demand, 2.0 for biological oxygen demand after 5 days, 2.13 for suspended solids, 0.99 for total nitrogen and 0.111 for total phosphorus (data obtained for 2015–2017 from SIEAM (Syndicat des Eaux et d'Assainissement de Mayotte, Mayotte, France). From April 2008 to October 2015, PW have been discharged at a volume of 10 m<sup>3</sup> once per day, during a low tide, for 1 h onto mangrove areas (around 675 m<sup>2</sup>, 15 m × 45 m) respectively dominated by the mangrove trees *Rhizophora mucronata* Lam and *Cerriops tagal* (Perr.) C. B. Robinson (Figure 1A), giving a hydraulic loading rate of 14.8 L·m<sup>-2</sup>·d<sup>-1</sup>, which is equivalent to a rainfall event of 14.8 mm. Near these two “impacted” areas, two other areas not subjected to PW discharge were used as “control” areas (Figure 1A). In October 2015 (at time T0), the experimental setting was changed to assess the resilience and the resistance capacities of microbial communities for 12 months (Figure 1B). In each mangrove zone, four different areas were delimited (around 225 m<sup>2</sup>, 15 m × 15 m): one part of the initial impacted area was still impacted in the new discharge network (C-II and R-II areas in *C. tagal* and *R. mucronata* mangrove zones, respectively) while in the another one the PW discharge were stopped at the T0 (C-IC and R-IC areas), one part of the initial control area was still a control after the T0 (C-CC or R-CC areas) while the another one received PW discharge since the T0 (C-CI or R-CI areas). In each area, 4 plots (1 m<sup>2</sup>) were randomly

chosen, marked out and used for all the samplings. The short-term impact of PW supply and the resilience capacities of microbial compartment were evaluated at T0, T0 + 3 weeks, T0 + 3 months, T0 + 8 months and T0 + 12 months, during the dry season (May–October) and the wet season (November–April) (Figure 2).

### Sediments and Porewater Composition

The salinity and temperature of water were measured directly in the field in residual pools (surface water) and in piezometers (deep water, approximately 1 m) at low tide and samples were taken and stored at 4°C for later determination of nutrient (NO<sub>3</sub><sup>-</sup>, NO<sub>2</sub><sup>-</sup>, NH<sub>4</sub><sup>+</sup> and PO<sub>4</sub><sup>3-</sup>) concentrations. Analyses were performed by the ARVAM Laboratory (La Réunion, France) using classic colorimetric methods according to standard methods (American Public Health Association [APHA] et al., 1992). Mean values were obtained from 2-day measurements under similar hydrological conditions, in the upper and lower parts of the areas (total of 4 measures).

In each area, one sediment core (1 cm-depth) per plot was carried out with a syringe (50 mL). The sediment samples were dried and weighed after desiccation in an air oven at 105°C during 2 days. N and C quantities were measured in a powder of dry sediments with a Thermo Fisher Flash 2000 elemental analyzer (Thermo Fisher Scientific, United States). Total phosphorus (P) was measured in acid condition after a persulfate oxidation using the ammonium molybdate spectrophotometry method.

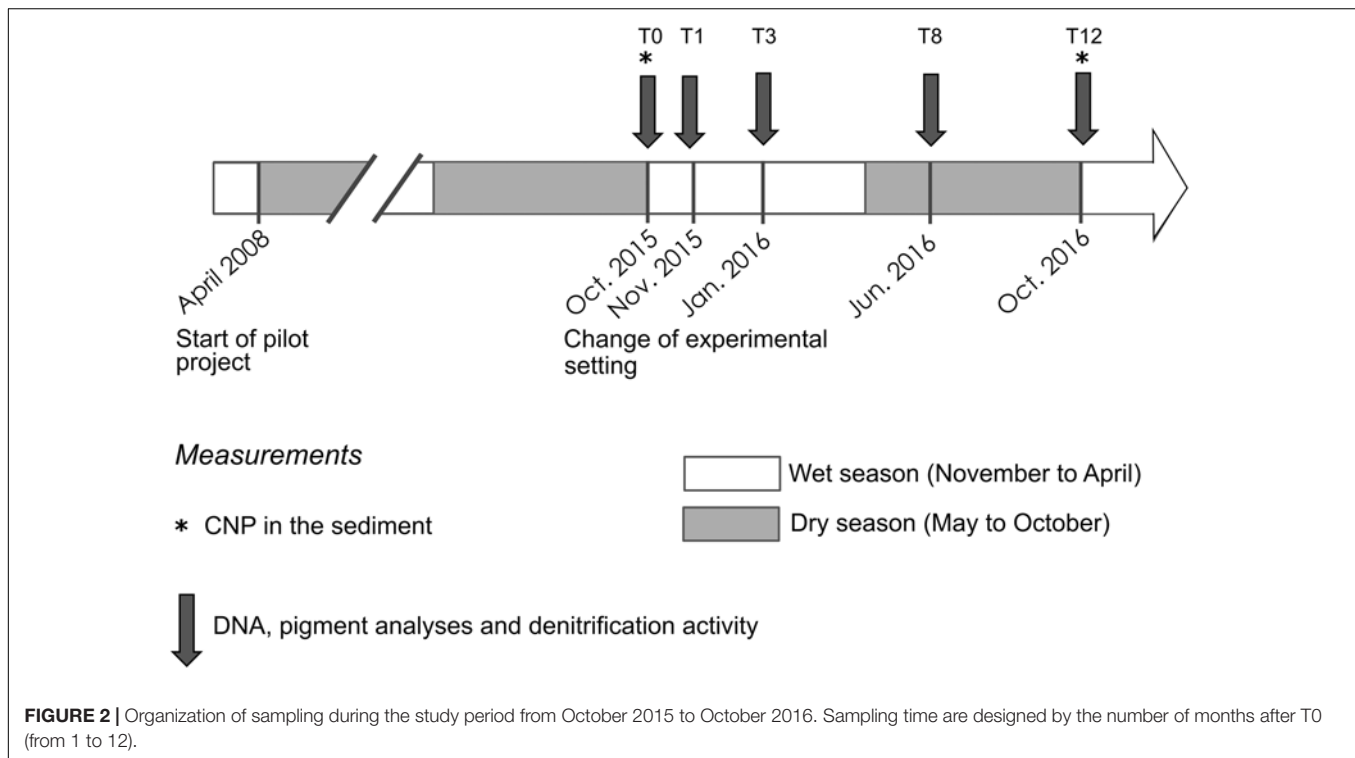
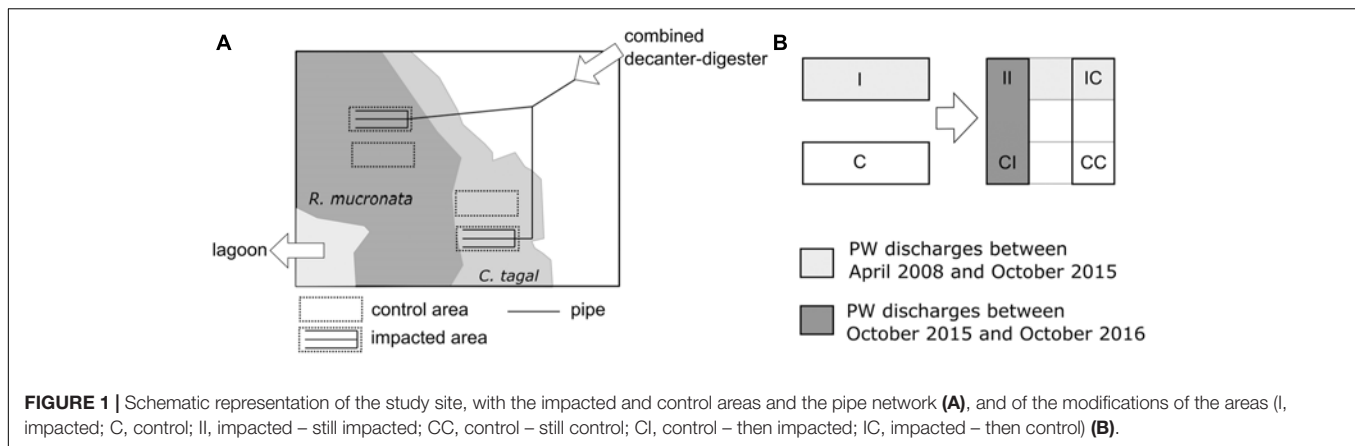
### Estimation of Microbial Densities

#### Sediment Sampling

In each area, one sediment core (10 cm-depth) per plot (4 cores in total) was carried out with a syringe (50 mL), placed into 350 mL of RNAlater solution, homogenized and maintained at 4°C until treatment of samples at the laboratory. RNAlater solution was used in order to protect RNA contents for other experiments. This solution was prepared only with RNase-free glassware and water treated with dimethyl dicarbonate (DMDC). First, the DMDC-water was prepared with 1 mL of DMDC (Merck, Germany), 50 mL of ethanol absolute and ultrapure water QSP 1 L. This DMDC-water was incubated overnight at 37°C before autoclaving (at 121°C, 1 bar, and 20 min) and was used for all solutions. Then 1.5 L of RNAlater solution were made with 935 mL of DMDC-water, 700 g of ammonium sulfate (Sigma-Aldrich, France), 25 mL of 1 M sodium citrate solution (Sigma-Aldrich, France) and 40 mL of 0.5 M EDTA (Sigma-Aldrich, France). The pH of RNAlater solution was adjusted at 5.2.

#### DNA Extraction

Before DNA extraction, some subsamples of the sediments were washed three times with PBS 1 X (AccuGENE, Lonza, Switzerland) to remove the RNAlater solution. DNA extraction was performed on 2.5 g of wet sediments after an RNA extraction with the RNA Powersoil® DNA Elution Accessory kit (MoBio, Quiagen, United States) according to manufacturer's instructions.



The quality of total DNA was checked using a NanoDrop 1000 spectrophotometer (ThermoFisher Scientific, United States) and by gel electrophoresis (agarose, 1% in TAE 0.5X).

### Quantitative PCR on 16S *rDNA*, *nosZ* Clade I and *amoA* Genes

The total density of bacteria in sediments was determined with the abundance of the bacterial 16S *rDNA* gene. Standard curves and positive controls were obtained using serial dilution of DNA extracted from an *Escherichia coli* culture. The densities of bacteria involved in functional processes were determined with the *nosZ* clade I gene for denitrification and the *amoA* gene for nitrification. The latter was targeted also to determine the density of nitrifying archaea. Standards were amplified from mangrove samples in a total volume of

25  $\mu\text{L}$ , containing 25 (*nosZ* clade I) or 10 (*amoA*) ng of DNA template, 1 U of GoTaq<sup>®</sup> G2 Flexi DNA polymerase (Promega), 1X GoTaq<sup>®</sup> G2 Flexi buffer, 1.5 mM of  $\text{MgCl}_2$ , 0.8 mM dNTP, 1  $\mu\text{M}$  (*nosZ* clade I) or 0.2  $\mu\text{M}$  (*amoA*) of each primer and 0.3 (*nosZ* clade I) or 0.2 (*amoA*)  $\text{mg}\cdot\text{mL}^{-1}$  of BSA. Thermal cycling conditions and primers used for each reaction are described in **Table 1**. Every PCR started with an initial step at 95°C for 10 min and finished by a final step at 72°C for 3 min. PCR fragments (259 bp for *nosZ* clade I, 491 bp for bacterial *amoA*, 635 bp for archaeal *amoA*) were next cloned into a pGEMT plasmid using the pGEM<sup>®</sup>-T Easy Vector System II (Promega) according to the manufacturer's recommendations. Plasmids extractions were carried out with the NucleoSpin<sup>®</sup> Plasmid kit (Macherey-Nagel, France) following the manufacturer's instructions. Recombined

**TABLE 1** | PCR primers (Eurofin, Germany) and thermal conditions (AOB, ammonium oxidizing bacteria; AOA, ammonium oxidizing archaea).

Target	Gene	Method	Primers	Sequence (5' – 3')	Thermal conditions			No. of cycles	Type	Reference
Bacteria	16S	qPCR	Primer P1 Primer P2	CCTACGGGAGGCAGCAG ATTACCGCGGCTGCTGG	95°C, 15 s	61.5°C, 45 s	–	40	Classic	Muyzer et al., 1993
Denitrifying bacteria	<i>nosZ</i> clade I	PCR	<i>nosZ</i> 1F <i>nosZ</i> 2R	WCSYTGTTTCMTCGACAGCCAG ATGTCGATCARCTGVKCRITTYTC	95°C, 15 s	67°C- 62°C, 30 s	72°C, 30 s	6 and 35	Touch down	Henry et al., 2006
		qPCR	<i>nosZ</i> 1F <i>nosZ</i> 2R	WCSYTGTTTCMTCGACAGCCAG ATGTCGATCARCTGVKCRITTYTC	95°C, 10 s	67°C- 62°C, 45 s	–	6 and 40	Touch down	Henry et al., 2006
AOB	Bacterial <i>amoA</i>	PCR	<i>amoA</i> 1F <i>amoA</i> 2R	GGGGTTTCTACTGGTGGT CCCCTCKGSAAAGCCTTCTTC	95°C, 30 s	55°C, 30 s	72°C, 45 s	35	Classic	Rotthauwe et al., 1997
		qPCR	<i>amoA</i> 1F <i>amoA</i> 2R	GGGGTTTCTACTGGTGGT CCCCTCKGSAAAGCCTTCTTC	95°C, 15 s	58°C, 2 min	–	40	Classic	Rotthauwe et al., 1997
AOA	Archaeal <i>amoA</i>	PCR	<i>amoA</i> 19F Crenamo A616r48x	ATGGTCTGGCTWAGACG GCCATCCABCKRTANGTCCA	95°C, 30 s	53°C, 1 min	72°C, 1 min	35	Classic	Leininger, personal communication, 2006; Tourna et al., 2008
		qPCR	<i>amoA</i> 19F Crenamo A616r48x	ATGGTCTGGCTWAGACG GCCATCCABCKRTANGTCCA	95°C, 25 s	55°C, 2 min 45 s	–	40	Classic	Leininger, personal communication, 2006; Tourna et al., 2008

plasmids were linearized with the *EcoRI* restriction enzyme (Promega). Standard curves and positive controls were obtained using serial dilution of linearized plasmids containing  $10^1$  to  $10^7$  gene copies.  $\mu\text{L}^{-1}$ . Water was used as a negative control.

Quantitative PCRs (qPCR) were performed in triplicate for each DNA extract. The quantification was based on the fluorescence intensity of the SYBR green dye, which binds to double-stranded DNA. The qPCR analyses of sediment samples were carried out in a final volume of 20  $\mu\text{L}$  containing 1X of Takyon<sup>TM</sup> Rox SYBR<sup>®</sup> MasterMix dTTP Blue (Eurogentec, Belgium), 0.3  $\text{mg}\cdot\text{mL}^{-1}$  of BSA (Promega), 5  $\mu\text{L}$  (16S rDNA and *amoA* genes) or 4  $\mu\text{L}$  (*nosZ* clade I) of 1/100-DNA samples or standards and 0.3, 0.5, and 0.2  $\mu\text{M}$  of each primers (Eurofin, Germany) for 16S rDNA, *nosZ* clade I, and *amoA* genes respectively (Table 2).

qPCRs were carried out on the StepOnePlus Real-Time PCR System (Applied Biosystems, United States) starting by an initial enzyme activation at 95°C for 3 min for each qPCR. The thermal cycling conditions used for qPCR of each gene are described in Table 1. Serial dilutions of the DNA extracted from sediment samples were quantified and compared to check the presence of PCR inhibitors but no inhibition was detected. Melting curves were analyzed using StepOne<sup>TM</sup> v2.3 software to confirm the specificity and efficiency of the amplification and the quantifications of gene in samples were deduced from standard curve. Results were expressed in number of gene copies per gram of sediment dry weight.

RT-qPCR were supposed to be made on the same samples, reason why RNAlater was used. However, the quality of RNA was not sufficient to allow these analyses.

**TABLE 2** | Physical–chemistry of surface water and sediment porewater assessed at T0 in impacted and control areas (mean  $\pm$  SE,  $n = 4$  for *R. mucronata*,  $n = 2-4$  for *C. tagal*).

			Temperature (°C)	Conductivity (mS $\text{cm}^{-1}$ )	Salinity (psu)	$\text{PO}_4^{3-}$ ( $\mu\text{M}$ )	$\text{NH}_4^+$ ( $\mu\text{M}$ )	$\text{NO}_3^-$ ( $\mu\text{M}$ )	$\text{NO}_2^-$ ( $\mu\text{M}$ )
Surface water	<i>C. tagal</i>	Control	23.2 $\pm$ 1.2	61.3 $\pm$ 1.6	41.1 $\pm$ 1.3	0.83 $\pm$ 0.01	37.97 $\pm$ 20.28	1.05 $\pm$ 0.21	0.61 $\pm$ 0.11
		Impacted	22.8 $\pm$ 0.2	53.6 $\pm$ 2.7	35.3 $\pm$ 2.0	0.37 $\pm$ 0.15	293.78 $\pm$ 147.20	1.28 $\pm$ 0.64	4.20 $\pm$ 0.08
	<i>R. mucronata</i>	Control	24.4 $\pm$ 0.1	57.8 $\pm$ 0.5	38.6 $\pm$ 0.3	0.75 $\pm$ 0.28	4.16 $\pm$ 3.78	0.18 $\pm$ 0.10	0.07 $\pm$ 0.01
		Impacted	24.8 $\pm$ 0.4	51.7 $\pm$ 2.5	34.0 $\pm$ 1.8 *	13.2 $\pm$ 11.17	671.10 $\pm$ 423.06 *	0.51 $\pm$ 0.10	0.50 $\pm$ 0.12 *
Deep water	<i>C. tagal</i>	Control	24.8 $\pm$ 0.2	59.1 $\pm$ 2.3	39.5 $\pm$ 1.7	5.93 $\pm$ 1.28	0.38 $\pm$ 0.23	0.35 $\pm$ 0.20	0.06 $\pm$ 0.01
		Impacted	25.0 $\pm$ 0.0	67.3 $\pm$ 0.3	45.8 $\pm$ 0.2	10.79 $\pm$ 2.10	0.14 $\pm$ 0.09	0.39 $\pm$ 0.22	0.07 $\pm$ 0.00
	<i>R. mucronata</i>	Control	24.8 $\pm$ 0.3	56.0 $\pm$ 0.9	36.5 $\pm$ 0.5	4.56 $\pm$ 2.12	0.20 $\pm$ 0.07	0.24 $\pm$ 0.03	0.08 $\pm$ 0.02
		Impacted	24.8 $\pm$ 0.0	61.8 $\pm$ 2.0 *	41.6 $\pm$ 1.5 *	11.79 $\pm$ 2.04 *	1.31 $\pm$ 0.41 *	0.16 $\pm$ 0.04	0.06 $\pm$ 0.00

Asterisks indicate significant differences with the respective control (\* $p < 0.05$ ).

## Estimations of Potential Nitrification (NEA) and Denitrification (DEA) Enzyme Activities

NEA and DEA were performed on sediment samples collected during the 5 sampling campaigns. In each area, one sediment core (10 cm-depth) on each of the 4 plots was carried out with a syringe (50 mL), homogenized into 100 mL-tube, kept in a cooler box during transport and stored at 4°C until treatment of sediment samples few days later at the laboratory to limit the modification of denitrification activity.

Potential nitrification activity (PNA) was measured using a modified method described by Dassonville et al. (2011). Briefly, samples of fresh soil (3 g dry weight equivalent) were incubated for 10 h with 30 mL of  $(\text{NH}_4)_2\text{SO}_4$  (1.25 mg N.L<sup>-1</sup>) using continuous shaking (140 rpm, 28°C). To simulate marine environment each sample was submerged with a saline solution (30g NaCl.L<sup>-1</sup>). Subsamples (1 mL) were collected at 2, 4, 6, 8, and 10 h, filtered (0.20 μm pore size) and stored at -20°C. The NO<sub>3</sub><sup>-</sup> and NO<sub>2</sub><sup>-</sup> concentrations were analyzed using a colorimetric assessment using a SmartChem 200 (AMS Alliance).

For the measure of DEA, 2 flasks (150 mL) were prepared for each sample and filled with 10 mL of sediments collected with a syringe (10 mL). All flasks containing sediments were pre-incubated at 30°C during 24 h to re-activate bacteria. After 24 h, 50 mL of incubation medium were added to each flask. This medium was composed by deoxygenated demineralized water containing N-NO<sub>3</sub> (100 mg.L<sup>-1</sup>) and organic C (glucose) (50 mg.L<sup>-1</sup>), at a salinity of 30 psu. Then the flasks were sealed with rubber stoppers and deoxygenized by diffusion of N<sub>2</sub> during 20 min. Then, 15 mL of incubation medium saturated with acetylene were added in one flask per sample, the other one receiving medium without acetylene (negative control). All the flasks were incubated in the dark at 30°C with agitation. After 3 and 6 h of incubation, the flasks were vigorously stirred for 20 s and 6 mL of gas were sampled and injected in vacuum 8 mL-vials. Then, the 6 mL of sampled gas were replaced by 6 mL of N<sub>2</sub>. The acetylene blocks the last step of denitrification (formation of N<sub>2</sub> from N<sub>2</sub>O), allowing the accumulation of N<sub>2</sub>O in the flasks (Sorensen, 1978). Finally, N<sub>2</sub>O concentrations of all gas samples were analyzed on a gas chromatograph (VARIAN 3800) equipped with a 63Ni capture detector. The carrier gas was a mixture of argon/methane (90/10 v/v). The separation was made on a Porapak Q column at 80°C, the injector and detector temperatures were 120 and 280°C, respectively.

After the incubations, the ash-free dry mass (AFDM) of each sediment sample was determined after combustion (at 550°C, for 8 h).

## Assessment of the Structure of Phototrophic Microbial Communities

### Extraction of Photosynthetic Pigments in Sediments

Two sediment samples (1 cm-depth) were collected in each plot of all the areas with a syringe (50 mL), kept in a cooler box during transport, and stored at -20°C until storage at -80°C at the laboratory. Before extraction, sediment samples were freeze-dried and homogenized. The pigments from 0.5 g of dry sediments

were extracted with 5 mL of methanol buffered with 2% of 1 M-ammonium acetate (Sigma-Aldrich, France). After 2 min in an ultrasound cold bath and at maximum power, samples were kept in the dark at -20°C for 15 min before centrifugation (High Conic Rotor, Thermo Scientific, 3220 g, 2°C, and 5 min). Supernatants were collected and the pellets were re-extracted as described above. The pooled supernatants were filtered on 0.2 μm PTFE membrane syringe filter (Ø 13 mm, VWR International, United States) and stored a few days at -80°C before High Performance Liquid Chromatography (HPLC) analysis. To prevent degradation of pigments, extractions were performed under dark conditions and samples stored on ice during handling.

### HPLC Analyses

High Performance Liquid Chromatography analyses were performed with a 100 μL-loop auto-sampler and a quaternary solvent delivery system coupled to a diode array spectrophotometer (LC1200 series, Agilent Technologies, United States). The mobile phase was prepared [solvent A: 70:30 (v/v) methanol:1 M ammonium acetate and solvent B: 100% methanol] and programmed (minutes; % solvent A; % solvent B): (0; 75; 25), (1; 50; 50), (20; 30; 70), (25; 0; 100), (32; 0; 100) according to the analytical gradient protocol described by Barlow et al. (1997). The column was then reconditioned to original conditions over a further 12 min. Pigment separation was performed through a C8, 3 μm-column (MOS-2 HYPERSIL, Thermo Scientific, United States). The diode array detector was set at 440 nm to detect carotenoids, at 665 nm for chlorophylls and pheopigments. Pigments were identified by comparing their retention time and absorption spectra with those of pure standard pigments (DHI LAB products, Denmark). Each pigment concentration was calculated by relating the peak area of its chromatogram with the corresponding area of calibrated standard using ChemStation software (version A.10.02, Agilent technologies). For each sample, we worked on the ratios between total pigment concentrations and chlorophyll *a* concentration. From this matrix, we calculated similarities with the Bray Curtis index between all areas of *C. tagal* and *R. mucronata* mangrove zones at each sampling time.

### Statistical Analyses

Statistical analysis were performed using the PAST software (Paleontological Statistics, versions 2.17 and 3.06) (Hammer et al., 2001). The normality was checked on each dataset with the Shapiro–Wilk test and data were transformed if needed. When data were normally distributed, two-way ANOVAs were used to test the effects of mangrove zone (*R. mucronata* vs. *C. tagal*) and treatment (control vs. impacted areas), followed by a Tukey *post hoc* test. The non-parametric Kruskal–Wallis test was used with Mann–Whitney test for pairwise comparisons of non-parametric data. Statistical differences between sampling campaigns (T0, T0 + 3 weeks and T0 + 3, 8, and 12 months) were analyzed with one-way ANOVA followed by Tukey *post hoc* test or by the non-parametric Kruskal–Wallis test with Mann–Whitney test for pairwise comparisons according to the type of distribution. Data given in the text are means ± SE. For all

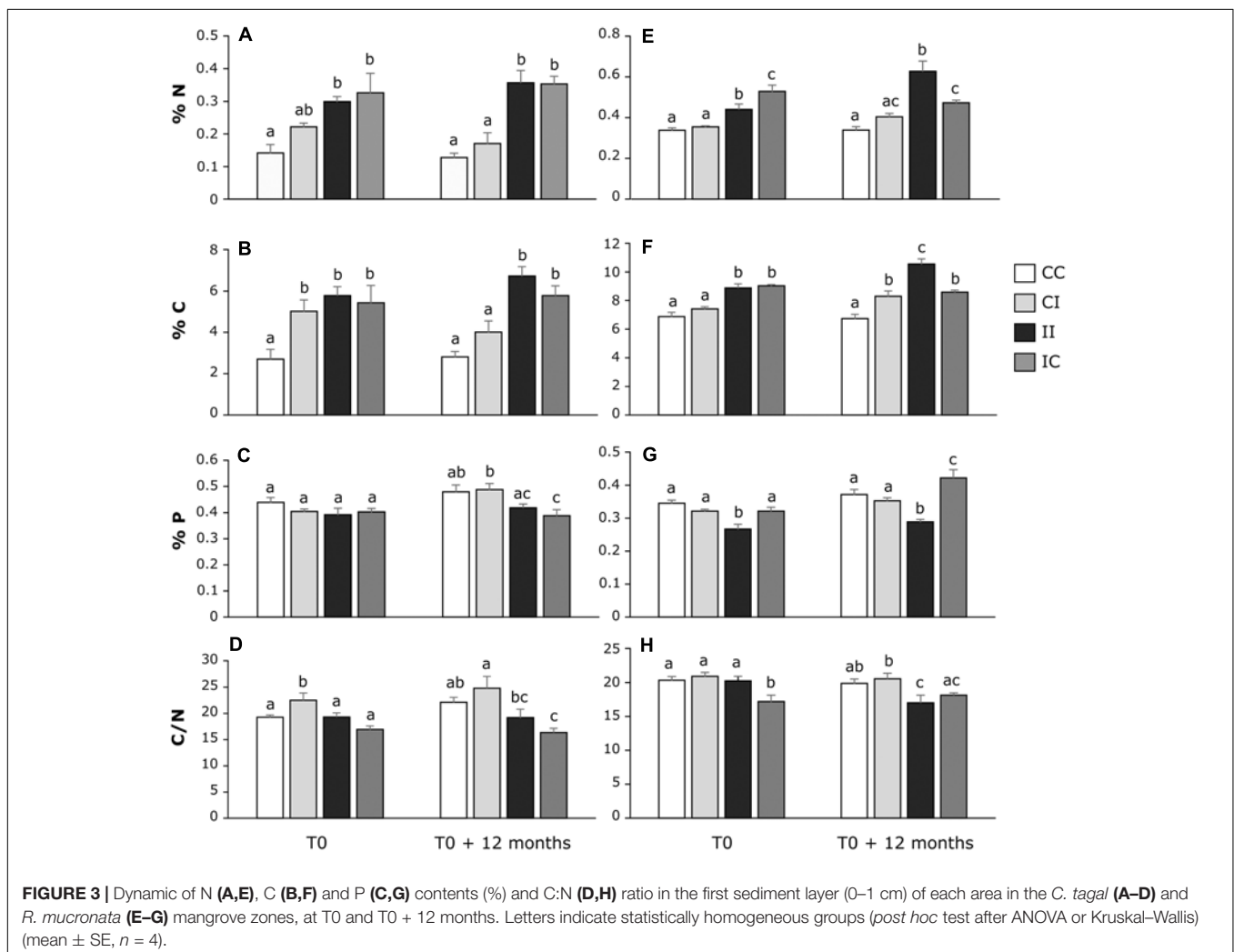
statistical analyses, significance was inferred at  $p < 0.05$  (noted \* if  $p \leq 0.05$ , \*\*  $p \leq 0.01$ , \*\*\*  $p \leq 0.001$ ).

## RESULTS

### Sediment and Porewater Composition

The temperature, conductivity, salinity and nutrient concentrations were measured at T0 in surface water and porewater (within piezometers) of sediments. The results are given in **Table 2**. Because of a lack of water in some *C. tagal* sampling points, only 2 replicates are available for this mangrove zone, so that the statistical analyses have been performed only for the *R. mucronata* zone (4 replicates). In surface water, the PW discharges induced a decrease of the salinity, and an increase in  $\text{NH}_4^+$  and  $\text{NO}_2^-$  concentrations. The observations were similar for the *C. tagal* zone. In porewater, an increase of salinity and conductivity in *R. mucronata* impacted zone was associated with an increase of  $\text{NH}_4^+$  and  $\text{PO}_4^{3-}$  concentrations. The tendency was similar in the *C. tagal* zone, except for the  $\text{NH}_4^+$  concentration, lower in the impacted area.

The sediment elementary composition was assessed at the sediment surface in each area of *C. tagal* and *R. mucronata* mangrove zones at T0 and after 12 months (**Figure 3**). Overall, the elementary composition was different between the two mangrove zones, with higher N ( $0.44\% \pm 0.02$ ) and C ( $8.29\% \pm 0.23$ ) contents, and lower P ( $0.34\% \pm 0.01$ ) content in the *R. mucronata* zone than in the *C. tagal* zone ( $0.25\% \pm 0.02$ ,  $4.78\% \pm 0.30$ ,  $0.43\% \pm 0.01$  respectively). Until T0, the CC and CI areas, and the II and IC areas had received the same treatment, i.e., no PW discharge and daily PW discharges, respectively. Nevertheless, some significant differences in the elementary composition of the sediment in similar areas were observable, notably in the *C. tagal* mangrove zone with higher N and C contents in the CI area than in the CC area. In this zone, the total C, N, and P contents and C:N ratio of the sediments were rather stable during the experiment (**Figures 3A–D**) in CC and II areas. The PW discharges significantly increased the N and P contents, while they had no effects on P content and C:N ratio. The modifications of the treatment in CI and IC areas did not modify the elementary composition of the sediment after 12 months. In the *R. mucronata* mangrove zone, while the composition of the



sediment in the CC area was stable over time, it varied in the II area, with an increase in C ( $p = 0.021$ ) content and a trend to increase in N ( $p = 0.056$ ) content (Figures 3E,F). As for the other mangrove zone, PW discharges induced an increase in N and C contents. It also induced a decrease in P content and a small decrease in C:N ratio (Figures 3E–H). Twelve months after the end of PW discharges, N and P contents were significantly lower in IC area than in II area. During the same period, PW discharge induced an increase in C content in CI area compared to CC area.

## Microbial Communities

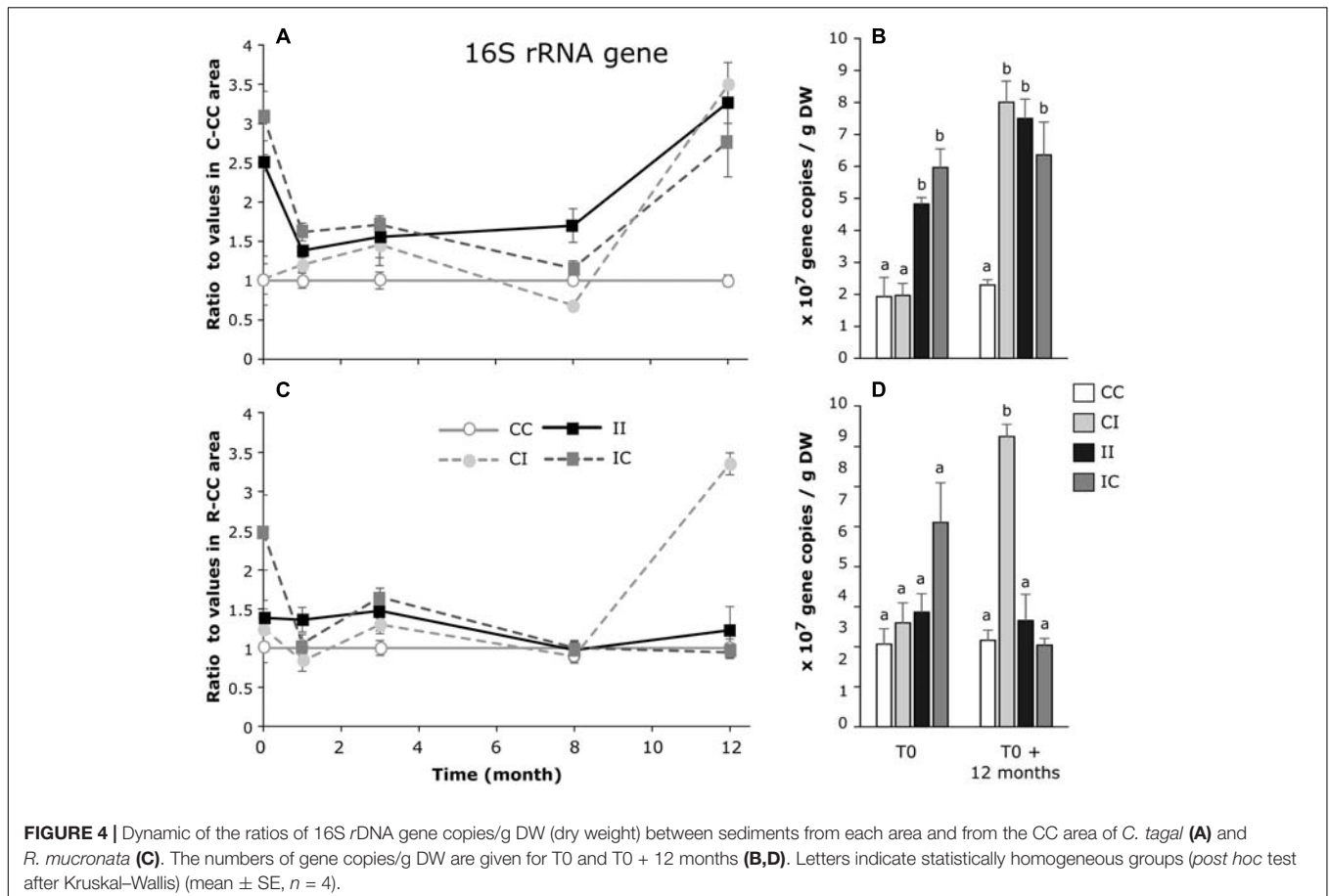
### Total Density of Bacteria

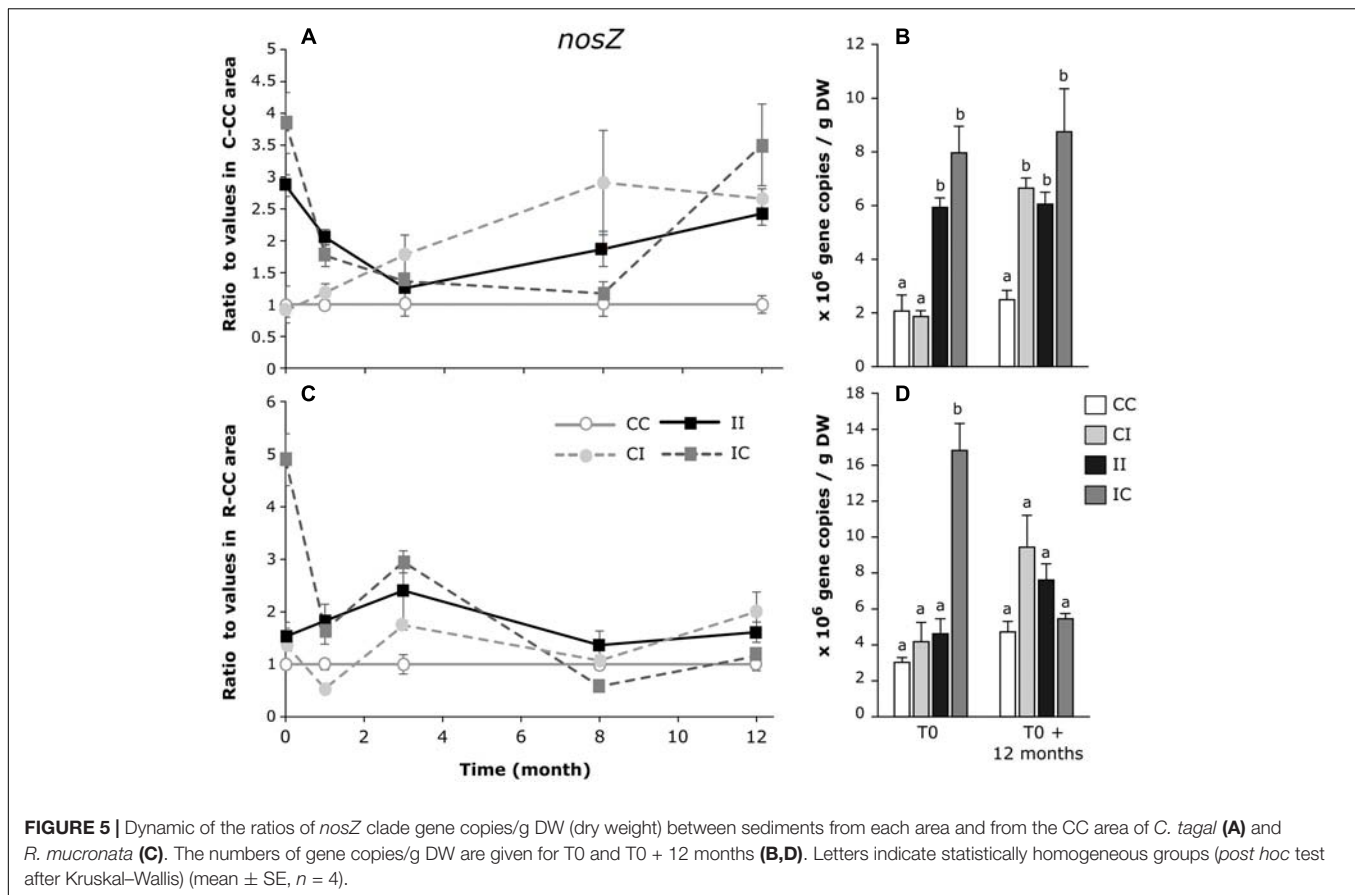
The total density of bacteria was followed through the number of copies of 16S *rDNA* gene in all areas of *C. tagal* and *R. mucronata* mangrove zones during 12 months (Figure 4). The total density of bacteria was very variable overtime in the controls, and depended on the season. Therefore, in order to observe the effects of treatments, the data were normalized by the mean value of the respective control, for each mangrove zone and for each sampling time (Figures 4A,C). In the *C. tagal* mangrove zone, at all the sampling times, the number of 16S *rDNA* gene copies was significantly higher in C-II impacted area ( $5.39 \times 10^7 \pm 3.23 \times 10^6$  16S *rDNA* copies/g DW) compared to the C-CC control area ( $1.95 \times 10^7 \pm 3.46 \times 10^6$  16S *rDNA* copies/g DW) (Figure 4B). Twelve months after the PW

discharges were stopped, the density of bacteria in the C-IC area was still similar to the one in the C-II area. In contrast, during the same duration, the density of bacteria in the C-CI area reached the one of C-II area. In the *R. mucronata* mangrove zone, there was no effect of the PW discharges on the bacterial density at the beginning of the experiment, but after 12 months, a significant increase was observable in the R-CI area (Figures 4C,D).

### Density of Functional Groups

The abundances of denitrifying bacteria and nitrifying bacteria and archaea were followed overtime by the number of copies of *nosZ* clade I gene and the *amoA* gene, respectively. For the three genes, the number of gene copies was strongly variable overtime with maximum values for all areas at 8 months, like for the 16S gene. On the whole, the functional community was dominated by the denitrifying bacteria, from 2.7 to 6.6 times (for C-CC and C-CI areas, respectively) more abundant than the nitrifying archaea, which were 3.5–4.7 times (for C-IC and C-CC areas) more abundant than the nitrifying bacteria. For the *R. mucronata* mangrove zone, the denitrifying bacteria were 2.0–4.7 times (for R-CC and R-II areas) more abundant than the nitrifying archaea, which were 4.6–7.0 times (for R-CI and R-CC areas) more abundant than the nitrifying bacteria. These values were very variable over time notably in the control areas, depending on the season. To make comparisons easier, we focused on gene





densities at the same period of the year, in October 2015 and October 2016.

In the *C. tagal* mangrove zone, the density of denitrifying bacteria followed the same pattern than the density of total bacteria: the PW discharges induced an increase in the number of *nosZ* clade I copies and during the 12 month-experiment this number was stable in the C-IC area and increased in the C-CI area (Figures 5A,B). The effect of PW discharges on denitrifying bacteria was less clear in the *R. mucronata* mangrove zone, with higher values at T0 in the R-IC area, and similar values in all the areas after 12 months (Figures 5C,D).

As shown in Figure 6, the effects of PW discharges on the number of archaeal *amoA* gene copies were not very clear. At T0, there was a lower value only in the C-CI area, and no differences in the *R. mucronata* zone. After 12 months, all the values were higher than the control area, in the *C. tagal* zone (Figure 6B) while in the *R. mucronata* zone, the gene density increased in the R-CI and R-II areas.

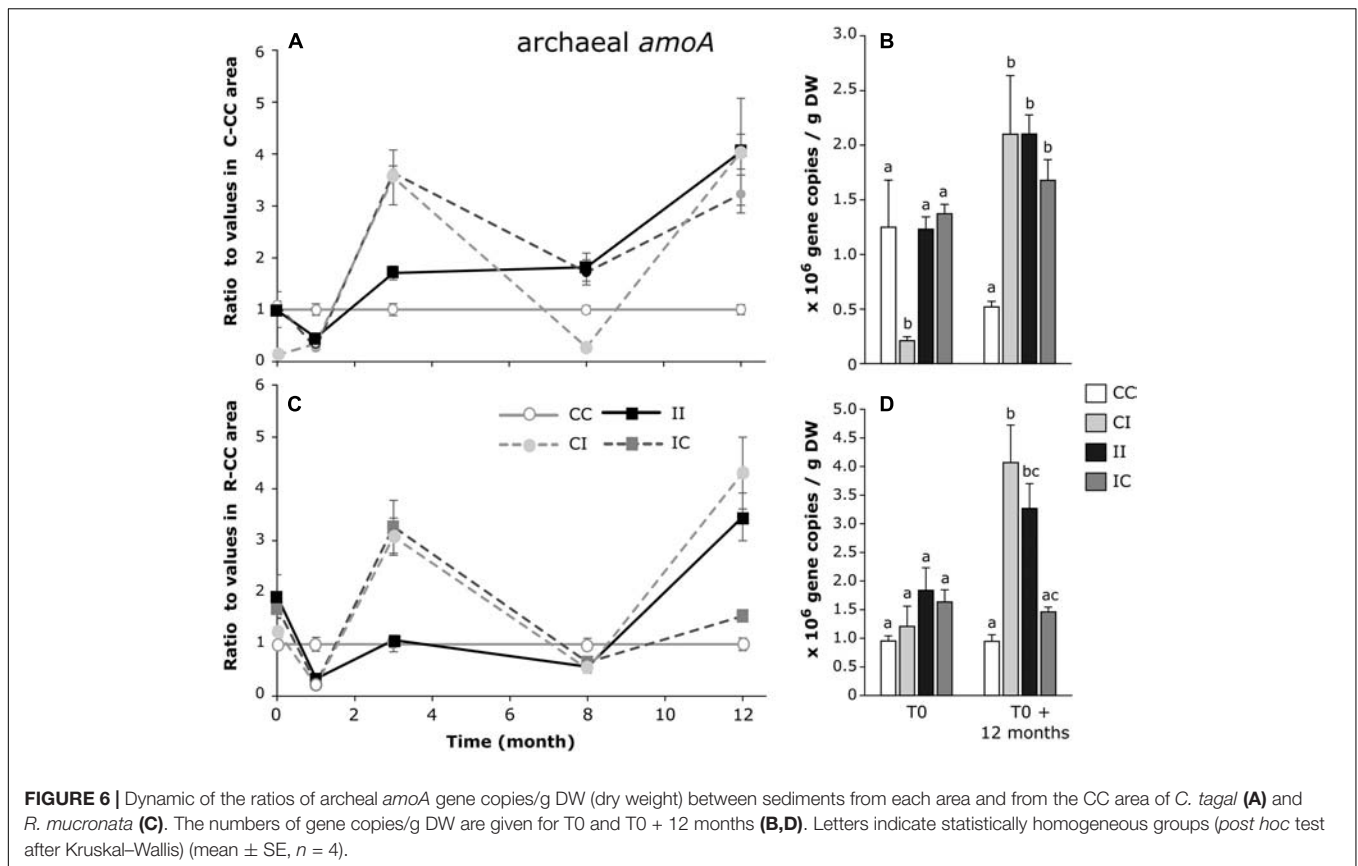
The number of bacterial *amoA* gene copies strongly varied over time, notably in the areas where the treatment was modified at T0 (IC and CI) (Figures 7A,C). In the *C. tagal* zone, the effect of PW discharges was variable between areas that had received the same treatment, with an increase compared to control in C-IC and no effect in C-II (Figure 7B). Few modifications occurred after 12 months. In the *R. mucronata* zone, there was no clear effect of the PW discharges (Figure 7D).

### Potential Nitrification Activity in Relation to Ammonium Oxidative Bacteria

The potential nitrification activity (NEA) carried out by AOA, AOB and nitrite oxidizing bacteria was assessed by measuring  $\text{NO}_2^-/\text{NO}_3^-$  net production in sediments from all areas of *C. tagal* and *R. mucronata* mangrove zones. While the correlation between NEA and AOA variation did not show any particular trend regarding both zones and all treatments (data not shown), the correlation between NEA and AOB was strongly and negatively impacted in the CI, and even more importantly in the II treatment (Figure 8). In contrast, this negative influence was released in the IC treatment, similar to what was observed in the controls, suggesting a potential resilience of this relation in time. Similar trends were observed for the relationship between NEA and AOA + AOB.

### Potential Denitrification Activity

The potential denitrification activity (DEA) carried out by the denitrifying bacteria was assessed by measuring  $\text{N}_2\text{O}$  production in sediments from all areas of *C. tagal* and *R. mucronata* mangrove zones. In the *C. tagal* mangrove zone, the DEA was significantly higher in the impacted area than in the control area, at all the sampling dates (Figure 9A). In the *R. mucronata* mangrove zone, the DEA followed the same trend although the differences were not significant (Figure 9B). A decrease of  $\text{N}_2\text{O}$  production was observed in C-IC and R-IC areas after 8 months



without PW discharge. It was more marked in the *R. mucronata* mangrove zone. In contrast, an increase of N<sub>2</sub>O production was observed in C-CI, corresponding to the short-term impact of PW after 8 months of discharge (Figure 9). The DEA became similar in C-II and in C-CI areas. A similar trend was observed in *R. mucronata* mangrove zone but the N<sub>2</sub>O production in R-CI area did not reach the values in R-II impacted area (Figure 9).

### Structure of Microbial Photosynthetic Communities

The structures of microbial photosynthetic communities were assessed using pigments as biomarkers. As illustrated by PCAs performed on all the areas at the beginning and at the end of the experiment (Figure 10), PW discharges strongly modified the structure of phototrophic communities. In C-CC area, the communities were associated with higher chlorophyll *a* concentrations and chlorophyll *a*/pheophytin *a* ratio, while in C-II area the communities were associated with higher proportions (ratio to chl *a* concentration) of chlorophyll *b*, lutein, zeaxanthin, β-carotene, myxoxanthophyll, astaxanthin, and violaxanthin (Figure 10A). The latter pigments are indicators of the presence of green algae and cyanobacteria. At T0, communities from the C-CI and C-IC areas were quite similar to those of C-CC and C-II areas, respectively. After 12 months, the samples from C-CI are more distant from those of C-CC area and closer from those of C-II area. They were notably

characterized by higher concentrations in fucoxanthin (diatoms). In the meantime, samples from C-IC area remained apart from samples from C-CC area, but moved away from C-II samples. In the *R. mucronata* mangrove zone, the impacted area was characterized by lower proportions of fucoxanthin (diatoms) and higher proportions of chlorophyll *b*, lutein, zeaxanthin, β-carotene and violaxanthin (Figure 10B). During the 12 months experiment, all the communities showed higher chlorophyll *a* content, indicating higher densities of phototrophic microorganisms. After 12 months, samples from R-CI area remained close from samples from R-CC area, showing no short-term impact on phototrophic communities. In contrast, samples from R-IC area came closer from samples from R-CC area, showing a good resilience of these communities.

The structures of the phototrophic communities were also compared by using the Bray-Curtis similarity index. The similarity between communities from C-IC and C-II areas remained stable over time, while the similarity between communities from C-IC and C-CC areas followed the same dynamics than similarity between communities from C-II and C-CC areas, showing no or low resilience. In contrast, the similarity between communities from R-IC and R-CC areas significantly increased after 8 months without discharge, showing a resilience of these communities (Figure 11). This was associated with a significant decrease of similarity between communities from R-IC and R-II areas after 8 months. This is very consistent with the results of the PCA. A short-term impact was observed

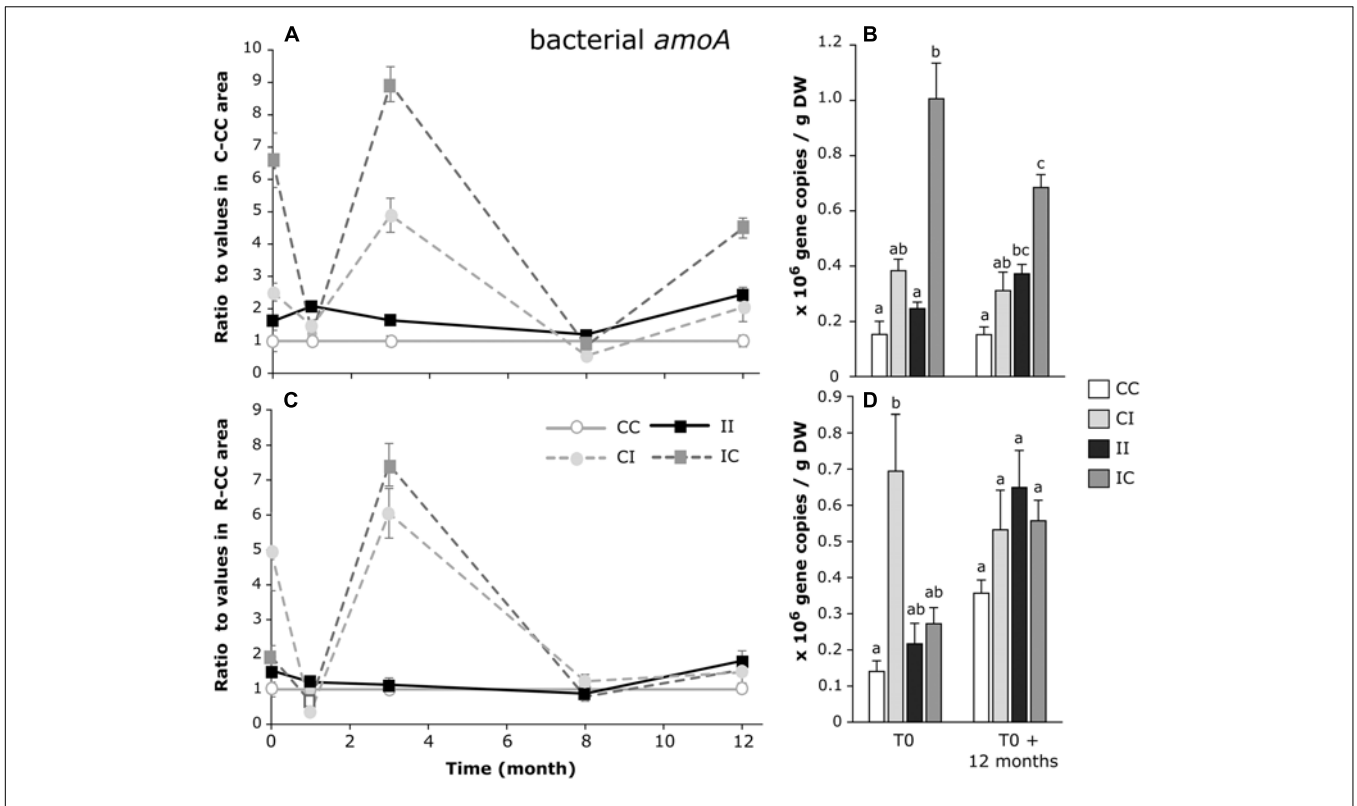


**FIGURE 7 |** Dynamic of the ratios of bacterial *amoA* gene copies/g DW (dry weight) between sediments from each area and from the CC area of *C. tagal* (A) and *R. mucronata* (C). The numbers of gene copies/g DW are given for T0 and T0 + 12 months (B,D). Letters indicate statistically homogeneous groups (*post hoc* test after Kruskal-Wallis) (mean ± SE, *n* = 4).

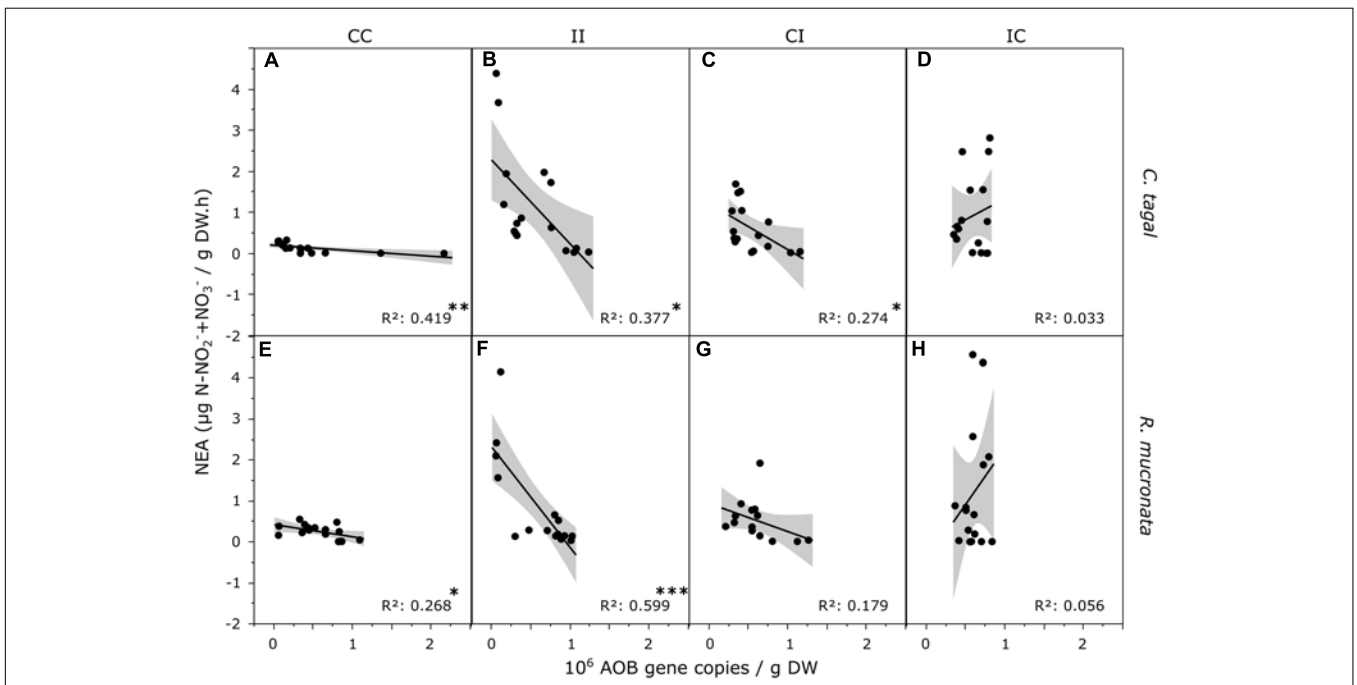
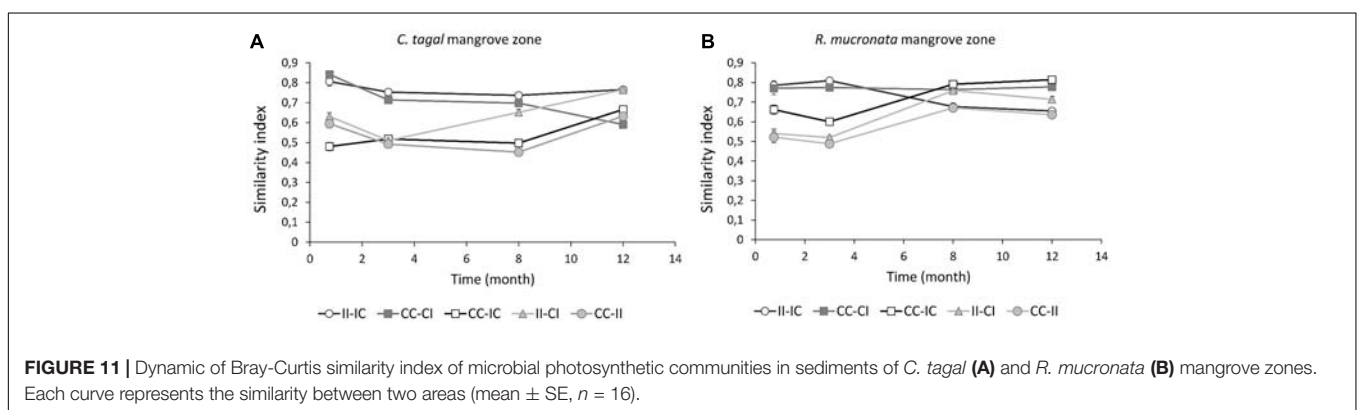
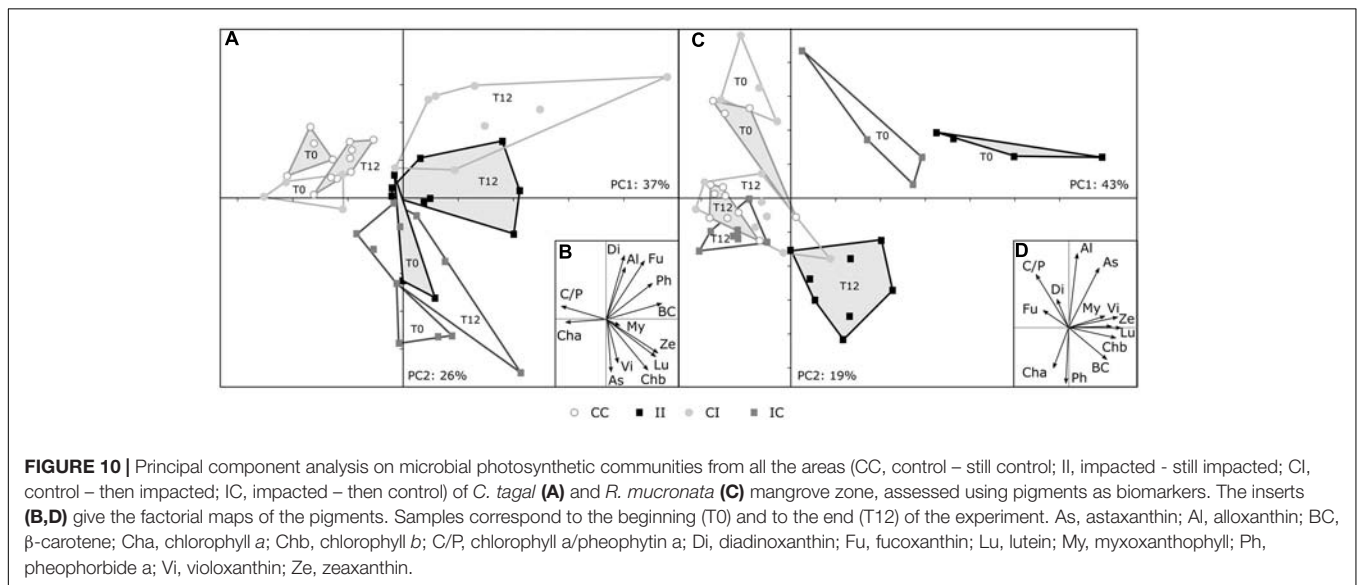
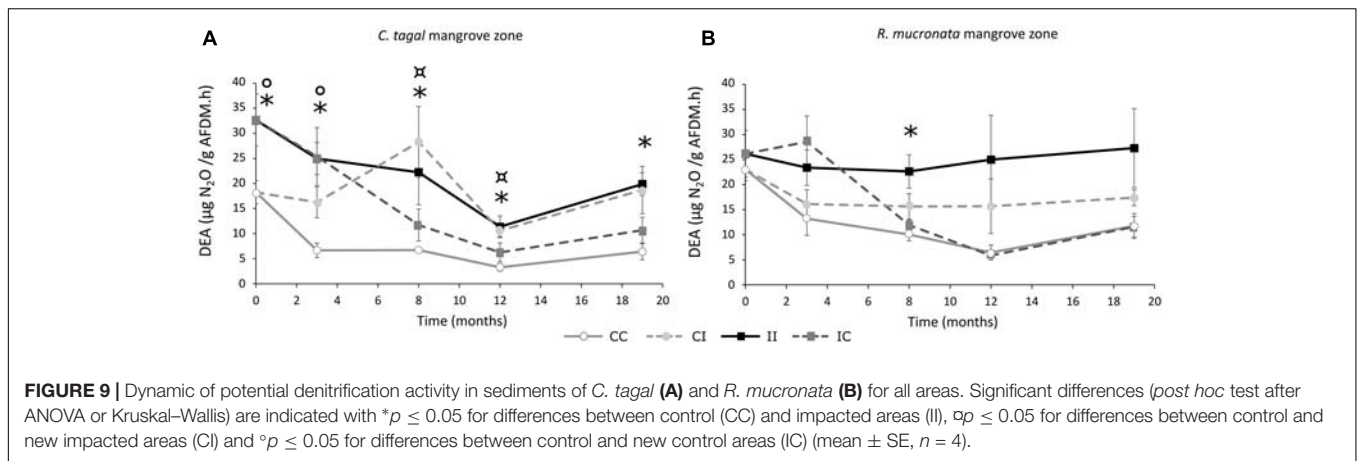


**FIGURE 8 |** Correlations between AOB densities and NEA in *C. tagal* (A–D) and *R. mucronata* (E,F) mangrove zones, in the CC (A,E), II (B,F), CI (C,G), IC (D,H) areas. Data from T1 to T12 were included. Asterisks indicate significant correlations (\**p* < 0.05, \*\**p* < 0.01, \*\*\**p* < 0.001).



after 8 months in C-CI area as shown by the increase of the similarity between communities from C-CI and C-II areas, and the decrease of similarity between communities from C-CI and C-CC areas, which is consistent with the observations on the PCA. At the opposite, the similarity between communities from R-CI and R-CC areas did not change overtime therefore no

short-term impact was observed in *R. mucronata* mangrove zone, as seen on the PCA. After 12 months of the present experiment, the similarities between control and long-term impacted (II) areas were not different in *R. mucronata* and *C. tagal* zones (Table 3), while the similarity between control and short-term impacted (CI) areas was significantly lower in

the *C. tagal* zone. The structure of phototrophic communities in areas where PW discharges were stopped (IC) had a higher similarity with control communities (CC) and lower similarity with impacted communities (II) in the *R. mucronata* zone (Table 3).

## DISCUSSION

### Sediment and Porewater Composition

Although mangroves are rich in organic matter, they are deficient in nutrients (Boto and Wellington, 1984), particularly in nitrogen (Levy-Booth et al., 2014) and phosphorous (Prasad, 2012). PW discharges during more than 7 years induced an increase in C and N sediment content in both mangrove zones. These proportions remained stable in the impacted areas during the 12 months of the present study, indicating that sediment had reached an equilibrium state despite the continuous PW discharge (Figure 3). This suggests that additional C and N input in impacted areas were quickly removed from sediments either by microbial activities (Wu et al., 2008; Tam et al., 2009) and/or by vegetation assimilation (Ganguly et al., 2009; Lambs et al., 2011). This is confirmed by the absence of C:N ratio modification between T0 and T0 + 12 months in most areas except for the R-II and C-CC areas. In this study, the PW were mainly composed of ammonium which is the most abundant and the more plant-available form of nitrogen found in mangrove ecosystem (Purvaja et al., 2008). At long-term the ammonium concentration strongly increased in surface water in the impacted areas. This induced an increase of mangrove tree growth in impacted areas of both mangrove zones (4 fold in *C. tagal* area and 1.7 fold *R. mucronata* area) (Capdeville et al., 2018). Besides, microbial communities involved in N-cycle like aerobic nitrifying bacteria participate to the recycling of ammonium from PW by the formation of nitrate in the first layers of mangrove sediments (Alongi et al., 1992). Thus, nitrate can be up-taken by mangrove trees (Purvaja et al., 2008) or completely removed from sediments through the denitrification activity under gaseous forms ( $N_2$ , NO,  $N_2O$ ) (Fernandes et al., 2012). Ammonium can also be removed from sediments *via* anammox by anammox bacteria which release N under gaseous form ( $N_2$ ) (Li and Gu, 2013). This metabolic process is rather difficult to measure. However, the level of anammox seems to be low in mangrove ecosystem, potentially due to low nitrite concentration (Fernandes et al., 2012) and moreover it decreases when temperature reach 37°C (Bertrand et al., 2011). Therefore, it seemed more relevant to focus on the processes of nitrification and denitrification.

At short term (12 months), a partial return to initial proportions on N- and C-proportions was observed, only in the *R. mucronata* mangrove. The N and C contents remained higher in R-IC area compared to control areas but they decreased compared to the R-II area (Figures 3E,F). This stability may partially be explained by the leaching of sediments during each tide, which is more marked in *R. mucronata* mangrove zone than in the *C. tagal* one. However, the volume of PW discharges has been chosen after determination of sediment porosity, taking into account crab hole volume and density, to avoid accumulation

on the surface and direct leaching by the tides. Though the PW bring phosphorous and  $PO_4^{3-}$  concentration significantly increased in porewater, the variations in sediment P content were low, with a tendency of decrease in impacted areas. P cannot be removed from sediment under gaseous form like N, but inorganic P can be up-taken by vegetation and organic P by microbial biomass. This decrease despite phosphate input may be explained by the higher biomass of trees in the impacted areas, where the vegetation growth significantly increased (Capdeville et al., 2018). In the same experimental system, Herteman (2010) showed an immobilization of P in sediment beyond 60 cm of depth after 18 months of discharges. It would be relevant to measure the P-proportion such deep layer in sediment after 9 years of discharges. Indication of porewater chemistry in the course of the experiment would have been useful to better understand the underlying mechanisms. Such analyses were planned but unfortunately canceled due to administrative issues.

### Total Density of Bacteria

Our results highlighted some positive effects of PW inputs on bacteria densities, in both mangrove zones (Figures 4B,D). However, if there were both short-term and long-term effects in the *C. tagal* zone with a 3–4 times increase, only a short-term effect was observable in the *R. mucronata* zone. The bacterial density remained high in the C-IC area, indicating the absence of resilience. As a whole, these results point to a higher stability of bacterial densities in the *R. mucronata* zone, as for the elementary composition of sediments. Contrasted effects have been observed in sediments of mangrove submitted to anthropogenic inputs or N inputs, with either marginal effects on bacterial densities (Fernandes et al., 2014), negative effects (Luo et al., 2017) or positive effects (Tam et al., 2009; Wickramasinghe et al., 2009; Bouchez et al., 2013). This highlights the wide range of potential response of bacterial densities in mangrove sediments. It is known that mangrove microbial communities are strongly influenced by the environmental parameters like temperature, humidity, pH (Alongi et al., 1992), salinity (Tam, 1998), C:N ratio, dissolved oxygen and nutrient concentrations (Li and Gu, 2013). Besides, the presence of aerobic and anaerobic bacteria depends on the oxygen level in sediments which is modulated by the tides, the bioturbation activity, and the presence of mangrove tree roots (Purvaja et al., 2008). These biotic and abiotic parameters can all modify the abundance of bacteria in mangrove sediments (Chakraborty et al., 2015). In the studied experimental system, PW discharges induced modifications in all these parameters, strongly impacting the environmental conditions. The effects of wastewaters can therefore be both direct and indirect, *via* these modifications of the environmental parameters.

### Abundances and Activity of Microorganisms Involved in N-Cycle

In this study, our goal was to assess functional resistance and resilience of the microbes involved in N-cycle. Although temporal dynamics of community structure may give some mechanistic details of how the communities responded to treatments, the acknowledged redundancy of these functions

**TABLE 3** | Mean similarity Bray-Curtis index between areas in the *C. tagal* and the *R. mucronata* areas (mean  $\pm$  SE,  $n = 64$ ).

	Long-term impact	Short-term impact	Resilience	
	CC-II	CC-CI	IC-CC	IC-II
<i>C. tagal</i>	0.63 $\pm$ 0.01	0.67 $\pm$ 0.02	0.67 $\pm$ 0.01	0.77 $\pm$ 0.01
<i>R. mucronata</i>	0.64 $\pm$ 0.01	0.77 $\pm$ 0.01***	0.81 $\pm$ 0.0****	0.65 $\pm$ 0.01***

Asterisks indicate significant differences with the respective control (\*\*\* $p < 0.001$ ).

among many microbial groups restrained us from compiling these data. We chose instead to focus on their relative abundances (by qPCR) and measure of potential activities that are more integrative values of functional potential of the different groups. Within bacterial communities, the densities of some specific groups were differently regulated in response to the treatments. At long term, PW discharges induced an increase in the abundances of denitrifying bacteria harboring the gene *nosZ* clade I in both mangrove zones. At short term, the increase in density was significant only in the *C. tagal* mangrove. Similar results were observed in other mangroves impacted by the wastewaters (Tam, 1998; Tam et al., 2009; Wickramasinghe et al., 2009; Bouchez et al., 2013; Huang et al., 2017). The N-inputs in mangrove sediments induced an increase of abundance of bacteria involved in N-elimination. This led to a stimulation of the potential denitrification activity in impacted areas of both mangrove zones, as it was demonstrated by Kristensen et al. (1998). Consistently with the results obtained for the abundance of *nosZ* clade I gene copies, the short-term impact on denitrification activity was revealed after 8 months in both mangrove zones and was faster in *C. tagal* mangrove zone than in *R. mucronata* mangrove zone. In a mangrove exposed to shrimp effluents, all N-cycling processes were stimulated between 2 and 12-fold (Molnar et al., 2013). The denitrification can be also favored by the bioturbation activity of crab present in these areas (Capdeville et al., 2018). Indeed the crab promote the entry of oxygen in depth which stimulates the production of nitrate *via* the nitrification and favor the transformation of nitrate into N<sub>2</sub> *via* the denitrification during anoxia period (Kristensen et al., 1998). In terms of resilience, a clear effect of the interruption of PW discharge was observed on the potential DEA while no clear trends could be observed on the abundance of denitrifying bacteria. It is possible that these bacteria are still present in the sediment but are less active. An analysis of *nosZ* clade I gene transcript with RT-QPCR might have explained these results. Here again, for the abundance and activity of denitrifying bacteria, the sediment from the *R. mucronata* zone appear more resistant and more resilient.

The presence of nitrifying communities in sediments could explain the N-elimination from sediments in impacted areas thanks to the coupling of nitrification and denitrification. However, these two processes were not directly correlated when considering the two zones or treatments separately (data not shown). The community of nitrifiers was dominated by the archaea (AOA) rather than by the bacteria (AOB), as described in marine ecosystems by Nicol and Schleper (2006) or soils with low pH, low organic matter content or low NH<sub>4</sub><sup>+</sup> concentrations

(Bates et al., 2011; Assemien et al., 2017) or these two groups of microorganisms, the variations in abundance of both *amoA* genes overtime in all areas of the two mangrove zones, showed no clear patterns of response to the treatments. Cao et al. (2011) revealed the presence of AOA and AOB in polluted mangrove sediments, with higher abundance of the AOA but higher diversity of the AOB. According to these authors, the abundances of AOA and AOB were correlated with the pH and the temperature while the AOA:AOB ratio was correlated with the ammonium concentration (Cao et al., 2011). However, in the present study, in impacted areas submitted to high concentrations of ammonium the AOA:AOB ratio was not higher than in control areas. At short term, only the AOA abundance increased, in both mangrove zones, and at long term the effects of PW discharged were mainly visible on the AOA abundances. Although the AOB seem at first to be less sensitive than AOA to the anthropic disturbance applied in the study, we found that the relative abundance of AOB, but not AOA, was correlated with NEA in response to our treatments (Figure 8). Although no significant correlation was observed in the control treatments, AOB copy numbers were negatively correlated to NEA in the two impacted treatments (I-I, and C-I), suggesting the activity and the relative abundances of this group were affected by PW inputs. This trend was found for both *R. mucronata* and *C. tagal* and was more marked for I-I than C-I. More surprisingly, in the I-C treatment, this negative correlation was released, suggesting a quick resilience of the NEA and associated AOB population. A partial resilience for the abundance of AOA was also visible only in the *R. mucronata* mangrove zone. In the literature, the nitrifying communities of mangrove sediment were also stimulated by the wastewaters (Tam, 1998; Tam et al., 2009; Wickramasinghe et al., 2009; Bouchez et al., 2013) without any effect on the structure of the nitrifiers (Tam et al., 2009; Wickramasinghe et al., 2009). Similarly, an amendment of ammonium on mangrove sediment stimulated the growth of AOA and AOB whereas an amendment of nitrite inhibited them (Li and Gu, 2013). However, both amendments altered the composition of AOA and AOB. It would be relevant to study the composition of AOA and AOB in presence of wastewaters in the mangrove areas of the present study. The nitrification process occurs at the surface of sediment or in micro-oxic zones generated by the mangrove tree roots and the sediment turnover carry out by the bioturbation of crab (Purvaja et al., 2008). It should be noted that we used laboratory methods to measure potential nitrification and denitrification activities. This gives reliable indications on the ability of microorganisms to nitrify or denitrify in standard conditions, but *in situ* effective activities may be slightly different.

## Structure of Microbial Photosynthetic Communities

Our results, using pigment content as a biomarker of taxonomic composition, indicate a significant long-term impact of PW discharges on the structure of phototrophic microorganism communities in both mangrove zones. Several studies demonstrated that the phototrophs like the green algae, diatoms and cyanobacteria were stimulated in mangrove sediment exposed to wastewaters (Tam et al., 2009; Wickramasinghe et al., 2009; Bouchez et al., 2013). Here no long-term effect of PW was observed on the quantity of chlorophyll *a*, a proxy of the density of phototrophic microorganisms. The decaying leaves may contribute to the detected chlorophyll *a* in sediment surface, but this interference is certainly low because the litter is rapidly trapped, buried and consumed by the crabs feeding on leaves (Camilleri, 1992; Botto et al., 2006).

As for heterotrophic microorganisms, the phototrophs can be impacted directly by the PW but also indirectly by the modification of their environment. Indeed, the PW induced a strong growth of mangrove trees resulting in a canopy closure and therefore a decrease of light intensity at the sediment surface (Capdeville et al., 2018). This decrease of light can strongly affect the phototrophs. The results highlighted an increase of green algae and cyanobacteria, which are often found in eutrophic ecosystems. In R-II, this was associated with a lower number of diatoms, as suggested by the negative correlation with fucoxanthin (Figure 10). These modifications may be critical for the functioning of the ecosystem. Indeed, phototrophic microorganisms are an essential food source for many organisms, like the meiofauna. Changes in the available food may trigger modifications of the meiofauna community. Among meio-organisms, the nematodes, which are abundant in mangrove sediment (Capdeville et al., 2018), participate to all the pathways of energy transfer of microbial carbon to higher trophic levels in benthic food webs and are essential for the functioning of benthic ecosystems (Schmid-Araya and Schmid, 2000; Carpentier et al., 2014). Bottom-up impacts on these bioturbation organisms may also degrade the oxygenation of sediment.

Though at long-term the impact seems equivalent in both mangrove zones, at short term it was lower in the *R. mucronata* zone while the resilience was more marked in this zone (Table 3).

## CONCLUSION

At long-term, the anthropic disturbance – daily discharges of PW – resulted in higher densities of total bacteria, denitrifying bacteria, and in a lower extent AOA. This was associated with an increase in the denitrification activity and modifications of the communities of photosynthetic microorganisms. The short-term responses of microbial communities from *C. tagal* and *R. mucronata* mangrove zones, as well as their potential resilience strongly depended on the mangrove zone. Microorganisms from the *R. mucronata* mangrove zone were more resistant and resilient than the one from the *C. tagal* zone, at least for the considered parameters. This confirms our hypothesis.

Despite the fact that only two zones were tested, the stability of microbial communities clearly varies along the environmental gradients that structure the mangrove ecosystem. The higher stability of the *R. mucronata* zone may be explained by the local adaptation of the microorganisms to anoxia (occurring during high tides, likely increased by nutrient inputs) but also to high vegetation cover. Indeed, the PW discharges induced a stronger development of the vegetation (Capdeville et al., 2018). Since in our study site the *C. tagal* trees have a much weaker development than the *R. mucronata* trees, the contrast between impacted and control areas was much higher in the *C. tagal* zone. This is consistent with our hypothesis stating that the stability of communities should be higher when the disturbance exacerbates natural constraints. Concerning heterotrophic microorganisms, information on the abundance of DNA transcripts would have been relevant, but they were not available due to technical issues. Indeed, qPCR help to quantify the cells that are or were present at a given time, but give no information about the proportion of active cells. Information on the composition of communities, through NGS methods, would also bring complementary information, though the focus of the study was the resistance and resilience of the functions associated with the communities.

Although we only considered the microorganisms in this study, our results emphasize the heterogeneity of mangrove stability. Another spatial constraint is the extent of the disturbance. As for bigger organisms, the resilience of microorganisms is enhanced by connectivity with undisturbed communities representing spatial refuges (Baho et al., 2012). These points should be carefully taken into account in both conservation policy and mangrove exploitation, to favor higher recovery. Moreover, we confirm here the high potential of using mangroves for bioepuration of PW.

The short-term impact and the resilience were overall observed first on the denitrification activity (after 8 months) and second on the microbial abundances (after 12 months). Although the microbial structure may have been strongly modified, the microorganisms maintained the microbial functions in mangrove sediment thanks to their functional redundancy. The resilience observed is thus associated to a functional recovery. Besides, the microbial activity and the vegetation uptake seem to remove efficiently the C, N, and P nutrients from wastewaters accumulated in sediments. The equilibrium state was faster to reach in *R. mucronata* mangrove zone. This confirms the strong potential of the use of *R. mucronata* mangrove zone in bioepuration of PW. To our knowledge, this is the first time that the resilience capacity of microbial community was studied *in situ* in two mangrove zones after a long-term exposure to PW discharges.

## AUTHOR CONTRIBUTIONS

FF, J-LR, JL, and TP designed the experiments. CC, FF, J-LR, TP, and JL contributed to the field work. CC, JL, and JG made the laboratory analyses. The manuscript was first written by CC, and then improved by the other authors.

## FUNDING

This work was supported by the Office National de l'Eau et des Milieux Aquatiques (ONEMA, Grant No. 2014/03) and the SIEAM (agreement with CNRS No. 111098).

## REFERENCES

- Allison, S. D., and Martiny, J. B. H. (2008). Resistance, resilience, and redundancy in microbial communities. *Proc. Natl. Acad. Sci. U.S.A.* 105, 11512–11519. doi: 10.1073/pnas.0801925105
- Alongi, D. M. (2002). Present state and future of the world's mangrove forests. *Environ. Conserv.* 29, 331–349. doi: 10.1017/S0376892902000231
- Alongi, D. M. (2012). Carbon sequestration in mangrove forests. *Carbon Manag.* 3, 313–322. doi: 10.4155/cmt.12.20
- Alongi, D. M., Boto, K. G., and Robertson, A. I. (1992). "Nitrogen and phosphorus cycles," in *Tropical Mangrove Ecosystems*, eds A. I. Robertson and D. M. Alongi (Washington, DC: American Geophysical Union), 251–292. doi: 10.1029/CE041p0251
- Alvarenga, D. O., Rigonato, J., Branco, L. H. Z., and Fiore, M. F. (2015). Cyanobacteria in mangrove ecosystems. *Biodivers. Conserv.* 24, 799–817. doi: 10.1007/s10531-015-0871-2
- American Public Health Association [APHA], and American Water Works Association [AWWA], and Water Pollution Control Federation [XPVF] (1992). *Standards Methods for the Examination of Water and Wastewater*. Washington, DC: American Public Health Association.
- Andreote, F. D., Jimenez, D. J., Chaves, D., Dias, A. C. F., Luvizotto, D. M., Dini-Andreote, F., et al. (2012). The microbiome of brazilian mangrove sediments as revealed by metagenomics. *PLoS One* 7:e38600. doi: 10.1371/journal.pone.0038600
- Assemien, F. L., Pommier, T., Gonnet, J. T., Gervaix, J., and Le Roux, X. (2017). Adaptation of soil nitrifiers to very low nitrogen level jeopardizes the efficiency of chemical fertilization in west african moist savannas. *Sci. Rep.* 7:10275. doi: 10.1038/s41598-017-10185-5
- Baho, D. L., Peter, H., and Tranvik, L. J. (2012). Resistance and resilience of microbial communities - temporal and spatial insurance against perturbations. *Environ. Microbiol.* 14, 2283–2292. doi: 10.1111/j.1462-2920.2012.02754.x
- Ball, M. C. (1998). Mangrove species richness in relation to salinity and waterlogging: a case study along the Adelaide River floodplain, northern Australia. *Glob. Ecol. Biogeogr. Lett.* 7, 73–82. doi: 10.2307/2997699
- Barlow, R. G., Cummings, D. G., and Gibb, S. W. (1997). Improved resolution of mono- and divinyl chlorophylls a and b and zeaxanthin and lutein in phytoplankton extracts using reverse phase C-8 HPLC. *Mar. Ecol. Prog. Ser.* 161, 303–307. doi: 10.3354/meps161303
- Bates, S. T., Berg-Lyons, D., Caporaso, J. G., Walters, W. A., Knight, R., and Fierer, N. (2011). Examining the global distribution of dominant archaeal populations in soil. *ISME J.* 5, 908–917. doi: 10.1038/ismej.2010.171
- Berga, M., Zha, Y. H., Szekely, A. J., and Langenheder, S. (2017). Functional and compositional stability of bacterial metacommunities in response to salinity changes. *Front. Microbiol.* 8:948. doi: 10.3389/fmicb.2017.00948
- Bertrand, J. C., Caumette, P., Lebaron, P., Matheron, R., and Normand, P. (2011). *Ecologie Microbienne: Microbiologie des Milieux Naturels et Anthropisés*. Nagoya: Univ. Pau Pays Adour.
- Blasco, F. (1991). Les mangroves. *La Recherche* 444–453.
- Boto, K. G., and Wellington, J. T. (1984). Soil characteristics and nutrient status in a Northern Australian mangrove forest. *Estuaries* 7, 61–69. doi: 10.2307/1351957
- Botto, F., Iribarne, O., Gutierrez, J., Bava, J., Gagliardini, A., and Valiela, I. (2006). Ecological importance of passive deposition of organic matter into burrows of the SW Atlantic crab *Chasmagnathus granulatus*. *Mar. Ecol. Prog. Ser.* 312, 201–210. doi: 10.3354/meps312201
- Bouchez, A., Pascault, N., Chardon, C., Bouvy, M., Cecchi, P., Lambs, L., et al. (2013). Mangrove microbial diversity and the impact of trophic contamination. *Mar. Pollut. Bull.* 66, 39–46. doi: 10.1016/j.marpolbul.2012.11.015
- Camilleri, J. C. (1992). Leaf-litter processing by invertebrates in a mangrove forest in Queensland Mar. *Biology* 114, 139–145.
- Cao, H. L., Li, M., Hong, Y. G., and Gu, J. D. (2011). Diversity and abundance of ammonia-oxidizing archaea and bacteria in polluted mangrove sediment. *Syst. Appl. Microbiol.* 34, 513–523. doi: 10.1016/j.syapm.2010.11.023
- Capdeville, C., Abdallah, K., Buffan-Dubau, E., Lin, C., Azemar, F., Lambs, L., et al. (2018). Limited impact of several years of pretreated wastewater discharge on fauna and vegetation in a mangrove ecosystem. *Mar. Pollut. Bull.* 129, 379–391. doi: 10.1016/j.marpolbul.2018.02.035
- Carpentier, A., Como, S., Dupuy, C., Lefrancois, C., and Feunteun, E. (2014). Feeding ecology of *Liza* spp. in a tidal flat: evidence of the importance of primary production (biofilm) and associated meiofauna. *J. Sea Res.* 92, 86–91. doi: 10.1016/j.seares.2013.10.007
- Chakraborty, A., Bera, A., Mukherjee, A., Basak, P., Khan, I., Mondal, A., et al. (2015). Changing bacterial profile of Sundarbans, the world heritage mangrove: impact of anthropogenic interventions. *World J. Microbiol. Biotechnol.* 31, 593–610. doi: 10.1007/s11274-015-1814-5
- Dassonville, N., Guillaumaud, N., Piola, F., Meerts, P., and Poly, F. (2011). Niche construction by the invasive Asian knotweeds (species complex *Fallopia*): impact on activity, abundance and community structure of denitrifiers and nitrifiers. *Biol. Invasions* 13, 1115–1133. doi: 10.1007/s10530-011-9954-5
- De Vrieze, J., Christiaens, M. E. R., Walraedt, D., Devooght, A., Ijaz, U. Z., and Boon, N. (2017). Microbial community redundancy in anaerobic digestion drives process recovery after salinity exposure. *Water Res.* 111, 109–117. doi: 10.1016/j.watres.2016.12.042
- Decho, A. W. (2000). Microbial biofilms in intertidal systems: an overview. *Cont. Shelf Res.* 20, 1257–1273. doi: 10.1016/S0278-4343(00)00022-4
- Donato, D. C., Kauffman, J. B., Murdiyarso, D., Kurnianto, S., Stidham, M., and Kanninen, M. (2011). Mangroves among the most carbon-rich forests in the tropics. *Nat. Geosci.* 4, 293–297. doi: 10.1038/ngeo1123
- Feller, I. C., Lovelock, C. E., Berger, U., McKee, K. L., Joye, S. B., and Ball, M. C. (2010). Biocomplexity in mangrove ecosystems. *Annu. Rev. Mar. Sci.* 2, 395–417. doi: 10.1146/annurev.marine.010908.163809
- Fenchel, T., and Finlay, B. J. (2004). The ubiquity of small species: patterns of local and global diversity. *Bioscience* 54, 777–784. doi: 10.1073/pnas.1012678108
- Fernandes, S. O., Kirchman, D. L., Michotey, V. D., Bonin, P. C., and LokaBharathi, P. A. (2014). Bacterial diversity in relatively pristine and anthropogenically-influenced mangrove ecosystems (Goa, India). *Braz. J. Microbiol.* 45, 1161–1171. doi: 10.1590/S1517-83822014000400006
- Fernandes, S. O., Michotey, V. D., Guasco, S., Bonin, P. C., and Bharathi, P. A. L. (2012). Denitrification prevails over anammox in tropical mangrove sediments (Goa, India). *Mar. Environ. Res.* 74, 9–19. doi: 10.1016/j.marenvres.2011.11.008
- Ganguly, D., Dey, M., Sen, S., and Jana, T. K. (2009). Biosphere-atmosphere exchange of NO<sub>x</sub> in the tropical mangrove forest. *J. Geophys. Res. Biogeosci.* 114:G04014. doi: 10.1029/2008JG000852
- Giri, C., Ochieng, E., Tieszen, L. L., Zhu, Z., Singh, A., Loveland, T., et al. (2011). Status and distribution of mangrove forests of the world using earth observation satellite data. *Glob. Ecol. Biogeogr.* 20, 154–159. doi: 10.1016/j.jenvman.2014.01.020
- Hammer, O., Dat, H., and Ryan, P. D. (2001). PAST: paleontological statistics software package for education and data analysis. *Palaeontol. Electron.* 4, 1–9.
- Henry, S., Bru, D., Stres, B., Hallet, S., and Philippot, L. (2006). Quantitative detection of the *nosZ* gene, encoding nitrous oxide reductase, and comparison of the abundances of 16S rRNA, *narG*, *nirK*, and *nosZ* genes in soils. *Appl. Environ. Microbiol.* 72, 5181–5189. doi: 10.1128/AEM.00231-06
- Herteman, M. (2010). *Evaluation des Capacités Bioremédiatrices d'une Mangrove Impactée par Des Eaux Usées Domestiques*. Toulouse: Université Paul Sabatier.
- Herteman, M., Fromard, F., and Lambs, L. (2011). Effects of pretreated domestic wastewater supplies on leaf pigment content, photosynthesis rate and growth of mangrove trees: a field study from Mayotte Island. *SW Indian Ocean. Ecol. Eng.* 37, 1283–1291. doi: 10.1016/j.ecoleng.2011.03.027

## ACKNOWLEDGMENTS

We are grateful to the Water Syndicate of Mayotte (SIEAM) for the maintenance of the experimental system and the coastal conservatory of Mayotte for the study site.

- Holguin, G., Vazquez, P., and Bashan, Y. (2001). The role of sediment microorganisms in the productivity, conservation, and rehabilitation of mangrove ecosystems: an overview. *Biol. Fertil. Soils* 33, 265–278. doi: 10.1007/s003740000319
- Hu, Y., Bai, C. R., Cai, J., Shao, K. Q., Tang, X. M., and Gao, G. (2018). Low recovery of bacterial community after an extreme salinization-desalinization cycle. *BMC Microbiol.* 18:195. doi: 10.1186/s12866-018-1333-2
- Huang, Y., Ou, D. Y., Chen, S. Y., Chen, B., Liu, W. H., Bai, R. N., et al. (2017). Inhibition effect of zinc in wastewater on the N<sub>2</sub>O emission from coastal loam soils. *Mar. Pollut. Bull.* 116, 434–439. doi: 10.1016/j.marpolbul.2017.01.030
- Komiyama, A., Havanond, S., Srisawatt, W., Mochida, Y., Fujimoto, K., Ohnishi, T., et al. (2000). Top/root biomass ratio of a secondary mangrove (*Ceriops tagal* (Perr.) CB Rob.) forest. *For. Ecol. Manage.* 139, 127–134. doi: 10.1016/S0378-1127(99)00339-4
- Komiyama, A., Ong, J. E., and Pongparn, S. (2008). Allometry, biomass, and productivity of mangrove forests: a review. *Aquat. Bot.* 89, 128–137. doi: 10.1016/j.aquabot.2007.12.006
- Kristensen, E., Jensen, M. H., Banta, G. T., Hansen, K., Holmer, M., and King, G. M. (1998). Transformation and transport of inorganic nitrogen in sediments of a southeast Asian mangrove forest. *Aquat. Microb. Ecol.* 15, 165–175. doi: 10.3354/ame015165
- Lambis, L., Leopold, A., Zeller, B., Herteman, M., and Fromard, F. (2011). Tracing sewage water by N-15 in a mangrove ecosystem to test its bioremediation ability. *Rapid Commun. Mass Spectrom.* 25, 2777–2784. doi: 10.1002/rcm.5120
- Lee, K. H., Wang, Y. F., Li, H., and Gu, J. D. (2014). Niche specificity of ammonia-oxidizing archaeal and bacterial communities in a freshwater wetland receiving municipal wastewater in Daqing, Northeast China. *Ecotoxicology* 23, 2081–2091. doi: 10.1007/s10646-014-1334-3
- Levy-Booth, D. J., Prescott, C. E., and Grayston, S. J. (2014). Microbial functional genes involved in nitrogen fixation, nitrification and denitrification in forest ecosystems. *Soil Biol. Biochem.* 75, 11–25. doi: 10.1016/j.soilbio.2014.03.021
- Li, M., and Gu, J. D. (2013). Community structure and transcript responses of anammox bacteria, AOA, and AOB in mangrove sediment microcosms amended with ammonium and nitrite. *Appl. Microbiol. Biotechnol.* 97, 9859–9874. doi: 10.1007/s00253-012-4683-y
- Luo, L., Meng, H., Wu, R. N., and Gu, J. D. (2017). Impact of nitrogen pollution/deposition on extracellular enzyme activity, microbial abundance and carbon storage in coastal mangrove sediment. *Chemosphere* 177, 275–283. doi: 10.1016/j.chemosphere.2017.03.027
- Mohamed, M. O. S., Mangion, P., Mwangi, S., Kairo, J. G., Dahdouh-Guebas, F., Koedam, N., et al. (eds) (2016). “Are peri-urban mangroves vulnerable? an assessment through litter fall,” in *Estuaries: A Lifeline of Ecosystem Services in the Western Indian Ocean, Estuaries of the World*, eds S. Diop and P. Scheren (Switzerland: Springer International Publishing), 39–51. doi: 10.1007/978-3-319-25370-1\_3
- Molnar, N., Welsh, D. T., Marchand, C., Deborde, J., and Meziane, T. (2013). Impacts of shrimp farm effluent on water quality, benthic metabolism and N-dynamics in a mangrove forest (New Caledonia). *Estuar. Coastal Shelf Sci.* 117, 12–21. doi: 10.1016/j.ecss.2012.07.012
- Muangchinda, C., Pansri, R., Wongwongsee, W., and Pinyakong, O. (2013). Assessment of polycyclic aromatic hydrocarbon biodegradation potential in mangrove sediment from Don Hoi Lot, Samut Songkram Province, Thailand. *J. Appl. Microbiol.* 114, 1311–1324. doi: 10.1111/jam.12128
- Muyzer, G., Dewaal, E. C., and Uitterlinden, A. G. (1993). Profiling of complex microbial populations by denaturing gradient gel electrophoresis analysis of polymerase chain reaction-amplified genes coding for 16S ribosomal RNA. *Appl. Environ. Microbiol.* 59, 695–700.
- Nicol, G. W., and Schleper, C. (2006). Ammonia-oxidising Crenarchaeota: important players in the nitrogen cycle? *Trends Microbiol.* 14, 207–212. doi: 10.1016/j.tim.2006.03.004
- Pimm, S. L. (1984). The complexity and stability of ecosystems. *Nature* 307, 321–326. doi: 10.1038/307321a0
- Prasad, M. B. K. (2012). Nutrient stoichiometry and eutrophication in Indian mangroves. *Environ. Earth Sci.* 67, 293–299. doi: 10.1007/s12665-011-1508-8
- Purvaja, R., Ramesh, R., Ray, A. K., and Rixen, T. (2008). Nitrogen cycling: a review of the processes, transformations and fluxes in coastal ecosystems. *Curr. Sci.* 94, 1419–1438.
- Robertson, A. I., and Alongi, D. M. (1992). *Tropical Mangrove Ecosystems*. Washington, DC: American Geophysical Union. doi: 10.1029/CE041
- Rothauwe, J. H., Witzel, K. P., and Liesack, W. (1997). The ammonia monooxygenase structural gene amoA as a functional marker: molecular fine-scale analysis of natural ammonia-oxidizing populations. *Appl. Environ. Microbiol.* 63, 4704–4712.
- Schmid-Araya, J. M., and Schmid, P. E. (2000). Trophic relationships: integrating meiofauna into a realistic benthic food web. *Freshw. Biol.* 44, 149–163. doi: 10.1046/j.1365-2427.2000.00594.x
- Sorensen, J. (1978). Denitrification rates in a marine sediment as measured by acetylene inhibition technique. *Appl. Environ. Microbiol.* 36, 139–143.
- Spalding, M., Blasco, F., and Field, C. D. (1997). *World Mangrove Atlas*. Okinawa: International Society for Mangrove Ecosystems.
- Spalding, M., Kainuma, M., and Collins, L. (2010). *World Atlas of Mangroves*, 2nd Edn. Ludhiana: Earthscan. doi: 10.4324/9781849776608
- Tam, N. F. Y. (1998). Effects of wastewater discharge on microbial populations and enzyme activities in mangrove soils. *Environ. Pollut.* 102, 233–242. doi: 10.1016/S0269-7491(98)00084-0
- Tam, N. F. Y., Wong, A. H. Y., Wong, M. H., and Wong, Y. S. (2009). Mass balance of nitrogen in constructed mangrove wetlands receiving ammonium-rich wastewater: effects of tidal regime and carbon supply. *Ecol. Eng.* 35, 453–462. doi: 10.1016/j.ecoleng.2008.05.011
- Tomlinson, P. B. (2016). *The Botany of Mangroves*. Cambridge: Cambridge University Press. doi: 10.1017/CBO9781139946575
- Tournar, M., Freitag, T. E., Nicol, G. W., and Prosser, J. I. (2008). Growth, activity and temperature responses of ammonia-oxidizing archaea and bacteria in soil microcosms. *Environ. Microbiol.* 10, 1357–1364. doi: 10.1111/j.1462-2920.2007.01563.x
- Wang, H. T., Su, J. Q., Zheng, T. L., and Yang, X. R. (2014). Impacts of vegetation, tidal process, and depth on the activities, abundances, and community compositions of denitrifiers in mangrove sediment. *Appl. Microbiol. Biotechnol.* 98, 9375–9387. doi: 10.1007/s00253-014-6017-8
- Wickramasinghe, S., Borin, M., Kotagama, S. W., Cochard, R., Anceno, A. J., and Shipin, O. V. (2009). Multi-functional pollution mitigation in a rehabilitated mangrove conservation area. *Ecol. Eng.* 35, 898–907. doi: 10.1016/j.ecoleng.2008.12.021
- Wu, Y., Chung, A., Tam, N. F. Y., Pi, N., and Wong, M. H. (2008). Constructed mangrove wetland as secondary treatment system for municipal wastewater. *Ecol. Eng.* 34, 137–146. doi: 10.1016/j.ecoleng.2008.07.010
- Zhang, Z. W., Xu, X. R., Sun, Y. X., Yu, S., Chen, Y. S., and Peng, J. X. (2014). Heavy metal and organic contaminants in mangrove ecosystems of China: a review. *Environ. Sci. Pollut. Res.* 21, 11938–11950. doi: 10.1007/s11356-014-3100-8

**Conflict of Interest Statement:** The authors declare that the research was conducted in the absence of any commercial or financial relationships that could be construed as a potential conflict of interest.

Copyright © 2019 Capdeville, Pommier, Gervais, Fromard, Rols and Leflaive. This is an open-access article distributed under the terms of the Creative Commons Attribution License (CC BY). The use, distribution or reproduction in other forums is permitted, provided the original author(s) and the copyright owner(s) are credited and that the original publication in this journal is cited, in accordance with accepted academic practice. No use, distribution or reproduction is permitted which does not comply with these terms.



# Functional Genes and Bacterial Communities During Organohalide Respiration of Chloroethenes in Microcosms of Multi-Contaminated Groundwater

Louis Hermon<sup>1,2</sup>, Jennifer Hellal<sup>1</sup>, Jérémie Denonfoux<sup>3</sup>, Stéphane Vuilleumier<sup>2</sup>, Gwenaél Imfeld<sup>4</sup>, Charlotte Urien<sup>3</sup>, Stéphanie Ferreira<sup>3</sup> and Catherine Joulian<sup>1\*</sup>

<sup>1</sup> Geomicrobiology and Environmental Monitoring Unit, Bureau de Recherches Géologiques et Minières (BRGM), Orléans, France, <sup>2</sup> CNRS, GMGM UMR 7156, Genomics and Microbiology, Université de Strasbourg, Strasbourg, France, <sup>3</sup> Service Recherche, Développement et Innovation-Communautés Microbiennes, GenoScreen, SAS, Lille, France, <sup>4</sup> CNRS/EOST, LHyGeS UMR 7517, Laboratory of Hydrology and Geochemistry of Strasbourg, Université de Strasbourg, Strasbourg, France

## OPEN ACCESS

### Edited by:

Stéphane Pesce,  
National Research Institute of Science  
and Technology for Environment  
and Agriculture (IRSTEA), France

### Reviewed by:

Lise Barthelmebs,  
Université de Perpignan Via Domitia,  
France

Shanquan Wang,

Sun Yat-sen University, China

### \*Correspondence:

Catherine Joulian  
c.joulian@brgm.fr

### Specialty section:

This article was submitted to  
Microbiotechnology, Ecotoxicology  
and Bioremediation,  
a section of the journal  
Frontiers in Microbiology

**Received:** 11 September 2018

**Accepted:** 16 January 2019

**Published:** 12 February 2019

### Citation:

Hermon L, Hellal J, Denonfoux J, Vuilleumier S, Imfeld G, Urien C, Ferreira S and Joulian C (2019) Functional Genes and Bacterial Communities During Organohalide Respiration of Chloroethenes in Microcosms of Multi-Contaminated Groundwater. *Front. Microbiol.* 10:89. doi: 10.3389/fmicb.2019.00089

Microcosm experiments with CE-contaminated groundwater from a former industrial site were set-up to evaluate the relationships between biological CE dissipation, dehalogenase genes abundance and bacterial genera diversity. Impact of high concentrations of PCE on organohalide respiration was also evaluated. Complete or partial dechlorination of PCE, TCE, *cis*-DCE and VC was observed independently of the addition of a reducing agent (Na<sub>2</sub>S) or an electron donor (acetate). The addition of either 10 or 100 μM PCE had no effect on organohalide respiration. qPCR analysis of reductive dehalogenases genes (*pceA*, *tceA*, *vcrA*, and *bvcA*) indicated that the version of *pceA* gene found in the genus *Dehalococcoides* [hereafter named *pceA*(Dhc)] and *vcrA* gene increased in abundance by one order of magnitude during the first 10 days of incubation. The version of the *pceA* gene found, among others, in the genus *Dehalobacter*, *Sulfurospirillum*, *Desulfuromonas*, and *Geobacter* [hereafter named *pceA*(Dhb)] and *bvcA* gene showed very low abundance. The *tceA* gene was not detected throughout the experiment. The proportion of *pceA*(Dhc) or *vcrA* genes relative to the universal 16S ribosomal RNA (16S rRNA) gene increased by up to 6-fold upon completion of *cis*-DCE dissipation. Sequencing of 16S rRNA amplicons indicated that the abundance of Operational Taxonomic Units (OTUs) affiliated to dehalogenating genera *Dehalococcoides*, *Sulfurospirillum*, and *Geobacter* represented more than 20% sequence abundance in the microcosms. Among organohalide respiration associated genera, only abundance of *Dehalococcoides* spp. increased up to fourfold upon complete dissipation of PCE and *cis*-DCE, suggesting a major implication of *Dehalococcoides* in CEs organohalide respiration. The relative abundance of *pceA* and *vcrA* genes correlated with the occurrence of *Dehalococcoides* and with dissipation extent of PCE, *cis*-DCE and CV. A new type of dehalogenating *Dehalococcoides* sp. phylotype affiliated to the Pinellas group, and suggested to contain both *pceA*(Dhc) and *vcrA* genes, may be involved in organohalide

respiration of CEs in groundwater of the study site. Overall, the results demonstrate *in situ* dechlorination potential of CE in the plume, and suggest that taxonomic and functional biomarkers in laboratory microcosms of contaminated groundwater following pollutant exposure can help predict bioremediation potential at contaminated industrial sites.

**Keywords:** perchloroethylene (PCE), chloroethenes (CEs), contaminated groundwater, dehalogenase genes, organohalide respiration

## INTRODUCTION

Extensive industrial use of halogenated volatile organic compounds (VOC) such as tetrachloroethylene (PCE) and trichloroethylene (TCE) has resulted in widespread environmental contamination of soil and groundwater worldwide (Huang et al., 2014). Groundwater at industrial sites producing or using halogenated VOC is often contaminated by chlorinated ethenes (CEs), generally in mixture with other contaminants (Aktaş et al., 2012). Once released into the environment, CEs migrate through the unsaturated zone of the subsurface (vadose zone), and can accumulate in aquifers as a dense non-aqueous phase liquid (DNAPL) due to their solubility, density, and hydrophobicity. Diffusion and transport of CEs in groundwater may result in a contamination plume often characterized by pollutant and redox gradients determining *in situ* biotransformation (Haack et al., 2004).

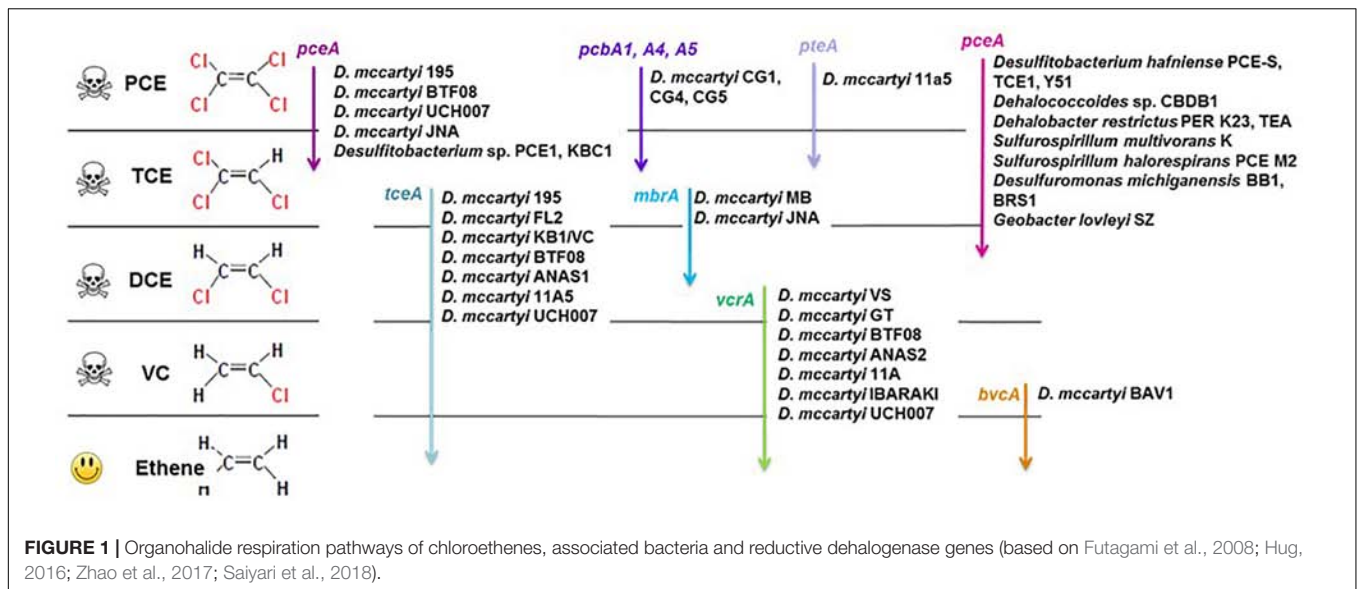
Organohalide respiration of CEs occurs under both oxic and anoxic conditions (Vogel and McCarty, 1985; Freedman and Gossett, 1991; Maymó-Gatell et al., 1999; Beeman and Bleckmann, 2002; Atashgahi et al., 2017). Under anoxic conditions, CEs may serve as electron acceptors for microbial metabolism (Holliger et al., 1998). Upon reductive dechlorination, PCE can be enzymatically converted, sequentially to TCE, *cis*-DCE, VC, and finally to non-toxic ethene. As the number of chlorine substituents decreases, dechlorination rate usually slows down with accumulation of less chlorinated DCE and VC (Abe et al., 2009; Chang et al., 2017).

Bioremediation and monitored natural attenuation are promising approaches for monitoring and removing chlorinated solvents from contaminated aquifers, due to their efficiency, sustainability and relatively low costs (Da Silva and Alvarez, 2008; Kang, 2014; Patil et al., 2014). Biostimulation studies for field remediation of chlorinated ethenes have been recently reported (Santharam et al., 2011; Florey et al., 2017; Sheu et al., 2018). Many bacterial strains capable of reductive dehalogenation of CEs have been characterized (Atashgahi et al., 2016). They typically belong to the genera *Dehalococcoides*, *Dehalobacter*, *Desulfitobacterium*, *Sulfurospirillum*, and *Geobacter*. These genera have thus been suggested as potential bioindicators of dechlorination in aquifers (Löffler et al., 2000; Hendrickson et al., 2002; Duhamel and Edwards, 2006; Imfeld et al., 2008; Clark et al., 2018). While many strains of organohalide respiration associated genera are involved in one or several organohalide respiration steps of halogenated VOC, complete reductive dehalogenation of PCE to ethene has only been observed for some strains of the *Dehalococcoides* genus

(Maymó-Gatell et al., 2001; He et al., 2003; Muller et al., 2004; Sung et al., 2006b). Dechlorinating capacities of *Dehalococcoides* strains may, however, differ widely (Magnuson et al., 1998; Lee et al., 2008). At the functional level, various genes encoding different types of reductive dehalogenases are involved in specific steps of sequential CE dechlorination (**Figure 1**) (Futagami et al., 2008; Hug, 2016; Saiyari et al., 2018). The dehalogenation of PCE to TCE and DCE (mainly *cis*-1,2-DCE) by non-obligatory dehalogenating bacteria is encoded by *pceA* genes. In *Dehalococcoides*, PCE is dechlorinated to TCE by strains also carrying a *pceA* gene (Magnuson et al., 1998). More recent findings highlighted the diversity of genes encoding PCE reductive dehalogenase in *Dehalococcoides*; *pteA* gene (PCE to TCE) in *Dehalococcoides mccartyi* strain 11a5 (Zhao et al., 2017), *pcbA* genes (PCE to TCE and DCE) in three distinct PCB-dechlorinating *Dehalococcoides* strains (Wang et al., 2014), and *mbrA* gene in strain MB that produce mainly *trans*-1,2-DCE (Cheng and He, 2009; Chow et al., 2010). The next steps, i.e., TCE to DCE, VC and ethene, only occur in *Dehalococcoides* strains and are encoded by three genes, *tceA* (TCE to DCE), *vcrA* or *bvca* (DCE to VC and ethene) (Zinder, 2016).

Knowledge of microbial and gene diversities associated with organohalide respiration of CEs has contributed to develop biomolecular approaches to evaluate biological dehalogenation and guide remediation strategies at contaminated sites (Maphosa et al., 2010; Dugat-Bony et al., 2012). Such approaches mainly rely on sensitive detection and quantification of specific dehalogenating taxa, notably *Dehalococcoides* (Hendrickson et al., 2002; Lu et al., 2006; Rouzeau-Szynalski et al., 2011; Kranzioch et al., 2013) or of functional genes used as biomarkers of dehalorespiration (Behrens et al., 2008; Da Silva and Alvarez, 2008; Rahm and Richardson, 2008; Carreon-Diazconti et al., 2009; Kranzioch et al., 2013). However, interpretation of currently available biomarkers and identification of novel ones requires a better understanding of the relationship between bacterial taxa associated with organohalide respiration of CEs and genes involved in dechlorination steps (Maphosa et al., 2012).

Here we examined the potential of endogenous groundwater bacterial communities of a former industrial site contaminated with CEs to degrade PCE and other CEs in relation to bacterial diversity and functional genes associated with reductive dechlorination of CEs. The aim was to evaluate the relationships between biological CE dissipation, dehalogenase gene abundance and bacterial genera diversity that could be transposed as biomarkers to the field. The effect of high additions of PCE on organohalide respiration rate and associated bacterial diversity was also addressed. The experimental setup consisted



of laboratory microcosms containing groundwater from a multi-contaminated former industrial site. The experimental set-up was designed to evaluate the effect of PCE concentration, and of addition of a carbon source (acetate) and a reducing agent ( $\text{Na}_2\text{S}$ ) on changes of specific genera associated with organohalide respiration, and reductive dehalogenases genes *pceA*, *tceA*, *vcrA*, and *bvcA*.

## MATERIALS AND METHODS

### Groundwater Sampling

Groundwater samples were taken from the former industrial site of Themeroil (Vareannes-le-Grand, France, GPS coordinates, 46.701141 N, 4.843919 E) characterized by historical intensive oil and solvent processing activities. Halogenated solvents and BTEX were released into the site aquifer due to inappropriate storage methods (BRGM, 1998), resulting in high concentrations of chlorinated VOC (mainly CEs) and BTEX, accumulated within DNAPL in the groundwater of the site. The pollutant plume extends over an area of about  $5 \cdot 10^{-2} \text{ km}^2$  (BRGM, 2011). Low concentrations of PCE ( $20 \mu\text{g} \cdot \text{L}^{-1}$ ) and TCE ( $11 \mu\text{g} \cdot \text{L}^{-1}$ ) in the contaminant plume compared to the contamination source and the prevalence of *cis*- over *trans*-DCE (Table 1) suggest the production of *cis*-DCE from PCE and TCE reductive dehalogenation and its accumulation (Nijenhuis et al., 2007).

Piezometer Pz6(10) located in the contaminant plume (Supplementary Figure S1) was selected based upon favorable redox conditions regarding CEs reductive dehalogenation (dissolved oxygen concentration below 0.05 ppm and redox potential about  $-242 \text{ mV}$ ) (Table 1). Major CE contaminants were *cis*-DCE ( $34.8 \text{ mg} \cdot \text{L}^{-1}$ ) and VC ( $7.8 \text{ mg} \cdot \text{L}^{-1}$ ). Pz6(10) was characterized by high sulfate ( $128 \text{ mg} \cdot \text{L}^{-1}$ ) and Fe(III) ( $7.4 \text{ mg} \cdot \text{L}^{-1}$ ) and low nitrate ( $<1 \text{ mg} \cdot \text{L}^{-1}$ ) aqueous concentrations. Thirty liters of Pz6(10) groundwater were sampled in June 2015 with a Twister pump (Proactive, Bradenton, United States) at a

depth of 5 m, after purging the piezometer and ensuring that  $E_h$ , pH, and conductivity were constant. Groundwater was stored for 30 days at  $4^\circ\text{C}$  until microcosm set-up.

### Microcosm Set-Up

Pz6(10) groundwater was pre-incubated to favor bacterial reductive dechlorination of PCE and increase reaction kinetics. Pz6(10) groundwater (800 mL) was pre-incubated in a 1 L bottle (Schott DURAN®, Germany) with 8 mL of a  $30 \text{ g} \cdot \text{L}^{-1}$   $\text{NH}_4\text{HCO}_3$  solution ( $0.30 \text{ g} \cdot \text{L}^{-1}$  final concentration), 8 mL of a  $25 \text{ g} \cdot \text{L}^{-1}$   $\text{K}_2\text{HPO}_4$  solution ( $0.25 \text{ g} \cdot \text{L}^{-1}$ ), 8 mL of a  $1 \text{ g} \cdot \text{L}^{-1}$   $\text{MgSO}_4 \cdot 7\text{H}_2\text{O}$  solution ( $0.1 \text{ g} \cdot \text{L}^{-1}$ ); 800  $\mu\text{L}$  of an  $80 \text{ g} \cdot \text{L}^{-1}$   $\text{CaCl}_2$  solution ( $0.08 \text{ g} \cdot \text{L}^{-1}$ ), 500  $\mu\text{L}$  of a  $100 \mu\text{g} \cdot \text{L}^{-1}$  vitamin B12 solution ( $62 \mu\text{g} \cdot \text{L}^{-1}$ ), 2.4 mL of a 1 M sodium acetate solution (3 mM;  $246 \text{ mg} \cdot \text{L}^{-1}$ ), 640  $\mu\text{L}$  of a  $40 \text{ g} \cdot \text{L}^{-1}$  sodium sulfide solution ( $32 \text{ mg} \cdot \text{L}^{-1}$ ), 1 mL of a  $20 \text{ g} \cdot \text{L}^{-1}$  yeast extract solution ( $25 \text{ mg} \cdot \text{L}^{-1}$ ) and 2.6  $\mu\text{L}$  of pure PCE (99.9%, Sigma-Aldrich) solution (20  $\mu\text{M}$  final concentration). The bottle was hermetically closed with a GL45 teflon-coated bottle cap (Omnifit®), conditioned with a  $\text{H}_2/\text{N}_2$  atmosphere (5%/95%) and incubated at  $20^\circ\text{C}$  in the dark without shaking. After complete dissipation of PCE to TCE (30 days), this pre-culture served as inoculum to the microcosm experiment.

Microcosms consisted of 800 mL of Pz6(10) groundwater, inoculated with the pre-culture at a ratio of 1:10 in 1 L glass bottles (Schott®) capped with GL45 teflon-coated bottle caps (Omnifit®). Sample handling was performed in a glovebox under a nitrogen atmosphere. Two sets of microcosms were prepared in triplicates with Pz6(10) groundwater and amended with pure PCE (99.9%, Sigma-Aldrich) to obtain final PCE concentrations of, respectively, 10 and 100  $\mu\text{M}$  using a glass syringe (Hamilton Bonaduz AG, Bonaduz, Switzerland). For each condition, microcosms were amended or not with sodium acetate (3 mM final concentration) and sodium sulfide solution ( $\text{Na}_2\text{S}$ , 0.4 mM final concentration). Killed controls consisted of site water sterilized by autoclaving (twice at  $121^\circ\text{C}$  for 30 min with

**TABLE 1** | Hydrochemical characteristics of groundwater from well Pz6(10) (June 2015).

Halogenated VOCs	Value ( $\mu\text{g} \cdot \text{L}^{-1}$ )	Hydrochemistry	Value (unit)
Perchloroethylene	20	pH	6.9
Trichloroethylene	11	Electric conductivity	1833 ( $\mu\text{S} \cdot \text{cm}^{-1}$ )
<i>Cis</i> -1,2-dichloroethylene	34800	Temperature	11.7 ( $^{\circ}\text{C}$ )
<i>Trans</i> -1,2-dichloroethylene	62	Redox potential	-242 (mV)
Vinyl chloride	7800	Dissolved oxygen	0.05 ( $\text{mg} \cdot \text{L}^{-1}$ )
1,1-dichloroethylene	2284	FeII	3.3 ( $\text{mg} \cdot \text{L}^{-1}$ )
1,2-dichloroethane	53	FeIII	7.4 ( $\text{mg} \cdot \text{L}^{-1}$ )
1,1-dichloroethane	700	$\text{SO}_4^{2-}$	128 ( $\text{mg} \cdot \text{L}^{-1}$ )
Dichloromethane	<10	$\text{NO}_3^-$	0.2 ( $\text{mg} \cdot \text{L}^{-1}$ )

a 24 h break between cycles), with no or 10  $\mu\text{M}$  PCE added after autoclaving. The microcosms were placed under  $\text{H}_2/\text{N}_2$  (5%/95%, 0.5 bar) atmosphere and incubated in the dark at  $20^{\circ}\text{C}$  under agitation (80 rpm). Water samples were taken from microcosms for hydrochemical and DNA analyses immediately after set up (day 0), and after 3, 5, 7, 10, 13, 19, 35, and 55 days of incubation.

## Hydrochemical Analyses

pH and redox potential ( $E_h$ ) were measured from aqueous phase microcosm aliquots using a portable probe (Multi 340i, WTW Instrument) at all sampling times in a  $\text{N}_2$ -purged glove box. Acetate, sulfate, nitrate and chloride were measured at days 5, 10, 19, and 35 in filtered samples (0.22  $\mu\text{m}$  syringe filters, Millipore, United States) by ionic chromatography (Dionex DX-100 equipped with AS19HC column). Quantification limits were  $0.1 \text{ mg} \cdot \text{L}^{-1}$  for acetate and  $0.5 \text{ mg} \cdot \text{L}^{-1}$  for sulfate, nitrate and chloride. Sulfide was measured after 10 and 35 days of incubation with a Merck Spectroquant kit 114779 (Merck, Germany).

Concentrations of CEs (PCE, TCE, *cis*-DCE and VC) were determined in 5 mL samples collected at all times. CEs were measured using a gas chromatograph (CP-3008-GC Varian, Walnut Creek, CA, United States) equipped with a headspace sampler and flame ionization detector. Chromatographic separation was performed in a capillary column (Agilent DB-624, 30 m, 0.32 mm inside diameter, 1.80  $\mu\text{m}$  film thickness). Injector and detector temperatures were held at  $250$  and  $300^{\circ}\text{C}$ , respectively, and the following temperature program was used: hold at  $35^{\circ}\text{C}$  for 5 min, heating to  $245^{\circ}\text{C}$  ( $10^{\circ}\text{C}/\text{min}$ ) and hold for 10 min. Concentrations were determined using external standards ( $R^2 = 0.99$ ). The limit of quantification was  $20 \mu\text{g} \cdot \text{L}^{-1}$  for all CEs.

Dissipation rates ( $\mu\text{M} \cdot \text{d}^{-1}$ ) for individual  $\text{CE}_x$  were estimated as an average of individual time step as follows:

$$\text{DisCE}_x[T_n; T_{n-1}] = \frac{([\text{CE}_x]_{T_n} - [\text{CE}_x]_{T_{n-1}}) - \text{DisCE}_{x+1}[T_n; T_{n-1}]}{T_n - T_{n-1}} \quad (1)$$

Where DisCE is the dissipation rate in  $\mu\text{M} \cdot \text{d}^{-1}$  and  $x$  is the number of chlorine atom substituents for each  $\text{CE}_x$  and  $n$  the number of incubation days.

## DNA Extraction

Fifteen mL of microcosm groundwater were sampled at each sampling time and filtered through 0.22  $\mu\text{m}$  sterile membrane filters ( $\emptyset$  2.5 cm, Millipore, United States). Membranes were stored at  $-20^{\circ}\text{C}$  until DNA extraction. DNA was extracted using the FastDNA<sup>®</sup> Spin Kit for Soil (MP Biomedicals, United States) and the Fastprep<sup>®</sup> instrument according to the manufacturer's instructions, with minor modifications (30 s lysis at a speed setting of 5.0, subsequent centrifugation of cell debris for 25 min). Extracted total DNA was quantified using the Quantifluor dsDNA sample kit and the Quantus fluorimeter according to the manufacturer's instructions (Quantus, Promega, United States).

## qPCR Analysis

Quantification of the bacterial 16S rRNA gene and of reductive dehalogenase genes (*pceA*, *tceA*, *vcrA*, and *bvcA*) was performed by qPCR using a CFX Connect<sup>™</sup> Real-Time PCR Detection System (Bio-Rad, France) with primers and programs listed in **Table 2**. qPCR reactions were performed in a total volume of 20  $\mu\text{L}$ , with a master mix containing 7.6  $\mu\text{L}$  of RNase- and DNase-free water (MP Biomedicals, CA, United States), 10  $\mu\text{L}$  of SYBR Green IQ Supermix (Bio-Rad), 500 nM of each primer, and 2  $\mu\text{L}$  of template DNA (concentrations of total DNA ranging from  $0.1 \text{ ng} \cdot \mu\text{L}^{-1}$  to  $5 \text{ ng} \cdot \mu\text{L}^{-1}$ ). Sterile, nuclease-, RNA- and DNA-free water was added instead of DNA in no template controls (NTC). All samples, controls and standards were analyzed in duplicate. A calibration curve was obtained from serial dilutions of a known quantity of linearized plasmids containing known copy numbers of 16S *rrnA*, *pceA*(Dhc), *pceA*(Dhb), *tceA*, *vcrA*, and *bvcA* gene fragments, respectively. Gene concentrations were reported as gene copies per mL of groundwater preparation. Limits of quantification (LOQ) were  $3.2 \cdot 10^3$  gene copies  $\cdot \text{mL}^{-1}$  culture for the 16S rRNA gene,  $6.7 \cdot 10^2$  gene copies  $\cdot \text{mL}^{-1}$  for *pceA*, *tceA*, and *vcrA* genes, and  $6.7 \cdot 10^1$  gene copies  $\cdot \text{mL}^{-1}$  for *bvcA*, respectively (**Supplementary Table S1**). Generation of a specific PCR product was confirmed by melting curve analyses and agarose gel electrophoresis. The effect of PCR inhibitors in DNA was estimated using successive dilutions of the DNA extract mixed with known amounts of DNA standard (pGEM-T easy vector, Promega) for qPCR with vector-specific primers as previously described (Miyata et al., 2010). No PCR inhibition was detected.

**TABLE 2** | qPCR primers and temperature programs used in this study.

Target gene	Primers	Target sequence 5'–3'	Fragment size (bp)	Target bacteria	qPCR program	Reference
16S rRNA	341F 515R	CCTACGGGAGGCAGCAG ATTACCGCGGCTGCTGGCA	174	All bacteria	3 min 95°C, 35 cycles: 30 s 95°C/30 s 60°C/30 s 72°C/Melt <sup>a</sup>	López-Gutiérrez et al., 2004
<i>pceA</i> (Dhb)	SpDr1f SpDr1r	CGTTGGACCTATTCCACCTG CAAGAACGAAGGCAATCACA	199	<i>Dehalobacter restrictus</i> PER-K23; <i>Desulfitobacterium hafniense</i> PCE-S	3 min 95°C, 40 cycles: 10 s 95°C/ 45 s 53°C/30 s 80°C/Melt	Regeard et al., 2004
<i>pceA</i> (Dhc)	<i>pceA</i> 877F <i>pceA</i> 976R	ACCGAAACCAGTTACGAACG GACTATTGTTGCCGGCACTT	100	<i>Dehalococcoides mccartyi</i>	3 min 95°C, 40 cycles: 10 s 95°C/45 s 61°C/30 s 80°C/Melt	Behrens et al., 2008
<i>tceA</i>	<i>tceA</i> 511F <i>tceA</i> 817R	GCCACGAATGGCTCACATA TAATCGTATACCAAGGCCCG	306	<i>Dehalococcoides mccartyi</i> ; <i>Dehalococcoides</i> sp. FL2	3 min 95°C, 40 cycles: 10 s 95°C/45 s 61°C/30 s 80°C/Melt	Behrens et al., 2008
<i>vcrA</i>	<i>vcrA</i> 880F <i>vcrA</i> 1018R	CCCTCCAGATGCTCCCTTTA ATCCCTCTCCCGTGTAAAC	139	<i>Dehalococcoides</i> sp. VS	3 min 95°C, 40 cycles: 10 s 95°C/45 s 61°C/30 s 80°C/Melt	Behrens et al., 2008
<i>bvcA</i>	<i>bvcA</i> 227F <i>bvcA</i> 523R	TGGGGACCTGTACTGAAAA CAAGACGCATTGTGGACATC	247	<i>Dehalococcoides</i> sp. BAV-1	3 min 95°C, 40 cycles: 10 s 95°C/45 s 61°C/30 s 80°C/Melt	Behrens et al., 2008

<sup>a</sup>Melt curve acquisition: rising from 65 to 95°C at 0.5°C · s<sup>-1</sup>.

## CE-SSCP Bacterial Diversity Profiles

For CE-SSCP bacterial community fingerprinting, the V3 region of the 16S rRNA gene was amplified by PCR from DNA extracts with forward primer w49 (5'-ACGGTCCAGAC TCCTACGGG-3') and 5' FAM-labelled reverse primer w34 (5'-TTACCGCGGCTGCTGGCAC-3') (Delbès et al., 2001), by 30 s hybridisation at 61°C, and 30 s elongation at 72°C for 28 cycles as described previously. One  $\mu$ L of diluted PCR product (5- to 100-fold in nuclease-free water) was then added to a mixture of 18.6  $\mu$ L of deionized formamide and 0.4  $\mu$ L of Genescan-600 LIZ internal DNA standard (Life Technologies, United States). To obtain single-strand DNA, samples were heat-denatured for 10 min at 95°C, and immediately cooled on ice. CE-SSCP analyses were performed on an ABI Prism 310 genetic analyser using a 47-cm long capillary, a non-denaturing 5.6% CAP polymer (Life technologies, United States) and the following electrophoresis conditions: run temperature 32°C, sample injection for 5 s at 15 kV, and data collection for 35 min at 12 kV. Alignment of the profiles using an internal DNA standard and assignment of peak positions were performed with Bionumerics software (Applied Maths, Belgium).

## Illumina MiSeq Sequencing of 16S rRNA Genes

Four samples collected from microcosms on days 0, 5, 10, and 34 were selected for 16S rRNA gene amplicon high-throughput sequencing based on chemical variations and community composition changes as preliminary detected by CE-SSCP analysis according to the distribution and the area of the peaks over time ( $p < 0.05$ ). For each sample, DNA extracted from biological replicates ( $n = 3$ ) was pooled for amplification of V4-V5 hypervariable region (Claesson et al., 2010) using an optimized and standardized amplicon-library preparation protocol (Metabiote®, GenoScreen, Lille, France). A positive [artificial bacteria community comprising 17 different bacteria (ABCv2)] and a negative (sterile water) control were also performed. Briefly, PCR reactions were performed using

5 ng of genomic DNA and 192 fusion barcoded primers (at 0.2  $\mu$ M final concentrations), with an annealing temperature of 50°C for 30 cycles. PCR products were purified using Agencourt AMPure XP magnetic beads (Beckman Coulter, Brea, CA, United States), quantified according to GenoScreen's protocol, and mixed in an equimolar amount. Sequencing was performed using 250-bp paired-end sequencing chemistry on the Illumina MiSeq platform (Illumina, San Diego, CA, United States) at GenoScreen (Lille, France). The sequence information was deposited to NCBI Sequence Read Archive (SRA) under accession numbers SRP160122.

## Bioinformatic Analysis of 16S rRNA Gene Sequence Data

Raw paired-end reads were demultiplexed per sample and subjected to the following process:

- (1) search and removal of both forward and reverse primers using CutAdapt, with no mismatches allowed in the primers sequences;
- (2) quality-filtering using the PRINSEQ-lite PERL script (Schmieder and Edwards, 2011), by truncating bases at the 3' end with Phred quality score <30;
- (3) paired-end read assembly using FLASH (Magoč and Salzberg, 2011), with a minimum overlap of 30 bases and >97% overlap identity.

Taxonomic and diversity analysis were performed with the Metabiote Online v2.0 pipeline (GenoScreen, Lille, France) which is based in part on QIIME software v 1.9.1 (Caporaso et al., 2010). Following pre-processing, full-length 16S rRNA gene sequences were checked for chimera sequences (in-house method based on Usearch 6.1). Similar sequences with a nucleic identity defined threshold (97% identity for an affiliation at the genus level on the V4–V5 regions of the 16S rRNA gene) were clustered with Uclust v1.2.22q (Edgar, 2010) through an open-reference Operational Taxonomic Units (OTU) picking process and complete-linkage method, finally generating groups of sequences or "Operational

Taxonomic Units" (OTUs). An OTU cleaning step involving elimination of singletons was performed. The most abundant sequence of each OTU was considered as the reference sequence of its OTU and taxonomically compared to a reference database included in the Greengenes database (release 13\_8<sup>1</sup>; DeSantis et al., 2006) by the RDP classifier method v2.2 (Cole et al., 2014). Alpha-diversity metrics (Chao1 index) within samples were computed using QIIME v 1.9.1.

## Bacterial Community Composition Analysis

Univariate statistical analyses (Student test, ANOVA) were performed with XLSTAT (Version 2016.02.27390). Multivariate analyses [principal component analysis (PCA)] were performed within R<sup>2</sup>. Bacterial community composition data obtained from Illumina MiSeq sequencing were analyzed by PCA ordination. Data were first normalized using Hellinger transformation (Legendre and Gallagher, 2001; Ramette, 2007). Explanatory variables consisted of quantitative variables including: CEs concentrations (and sum of total CE) ( $\text{mg} \cdot \text{L}^{-1}$ ), pH, redox potential (mV) temperature ( $^{\circ}\text{C}$ ), sulfate, chloride and acetate concentrations ( $\text{mg} \cdot \text{L}^{-1}$ ), gene copies number ( $\text{copies} \cdot \text{mL}^{-1}$ ) *pceA*(Dhc), *pceA*(Dhb), *vcrA* and *bvcA* to 16S rRNA gene ratios (%). Explanatory variables were standardized to provide dimensionless variables and remove undue influence of magnitude differences between scales or units. The relationship between community profiles and biogeochemical variables was investigated by fitting environmental vectors *a posteriori* onto the PCA. Their significance was assessed with a 1000-step Monte-Carlo permutation test. Significance was inferred at  $p < 0.05$ .

## OTU935 Sequencing

16S rRNA gene was amplified with *Dehalococcoides* specific primers using DNA extracted from the 10  $\mu\text{M}$  PCE\_T8 experiment: forward primer Fp DHC 1 (5'-GATGAACGCTAG CGGCG-3') and reverse primer Rp DHC 1377 (5'-GGTTGG CACATCGACTTCAA-3') (Hendrickson et al., 2002), by 30 s hybridisation at 66 $^{\circ}\text{C}$ , and 3 min elongation at 72 $^{\circ}\text{C}$  for 40 cycles. Then, ligation and transformation were realized according to pGEM-T<sup>®</sup> easy vector (Promega, United States) protocol. After 37 $^{\circ}\text{C}$  overnight incubation on LB media, one plasmid was purified according to NucleoSpin<sup>®</sup> Plasmid Columns protocol (Macherey-Nagel, Germany). Forward and reverse sequencing was realized by Sanger sequencing on ABI3730XL at GenoScreen (France). Consensus sequence was created from forward and reverse sequences and aligned by ClustalW method thanks to BioEdit v7.0.5.3 (Hall, 1999) with 18 NCBI sequences: 17 sequences of the 16S rRNA gene of *Dehalococcoides* strains and *Desulfitobacterium hafniense* DCB-2 strain. Finally, phylogeny was performed on 923 nucleotides with SeaView v4.7 (Gouy et al., 2010) with BioNJ - JC distance method, a 1,000 bootstrap value and without ignoring GAPS.

<sup>1</sup><http://greengenes.secondgenome.com/>

<sup>2</sup><http://www.R-project.org>

## RESULTS

### Organohalide Respiration of CEs

Redox potential ( $E_h$ ) values decreased from  $-130$  mV to  $-350$  mV in all microcosms (data not shown), thus confirming suitable conditions for reductive dechlorination (Löffler et al., 2013). The pH in all microcosms remained between 6.9 and 7.9 during the experiment, close to the measured *in situ* Pz6-(10) groundwater pH of 7.0.

In all microcosms except killed controls, PCE was nearly completely dissipated within 5 days under both 10 and 100  $\mu\text{M}$  PCE spiking conditions (Figure 2 and Supplementary Figure S2). TCE was only partially dissipated, and no further dissipation was observed after 20 days. In contrast, *cis*-DCE decreased continuously throughout the incubation, down to the detection limit after 60 days for both PCE spiking doses. Transient build-up of VC was observed, with VC first decreasing until day 10, and then increasing until day 35, before decreasing again. This may reflect VC formation from *cis*-DCE dechlorination with only limited VC dissipation until day 35. Sulfate initially present in these microcosms was completely reduced to sulfide after 10 days (Supplementary Figure S3).

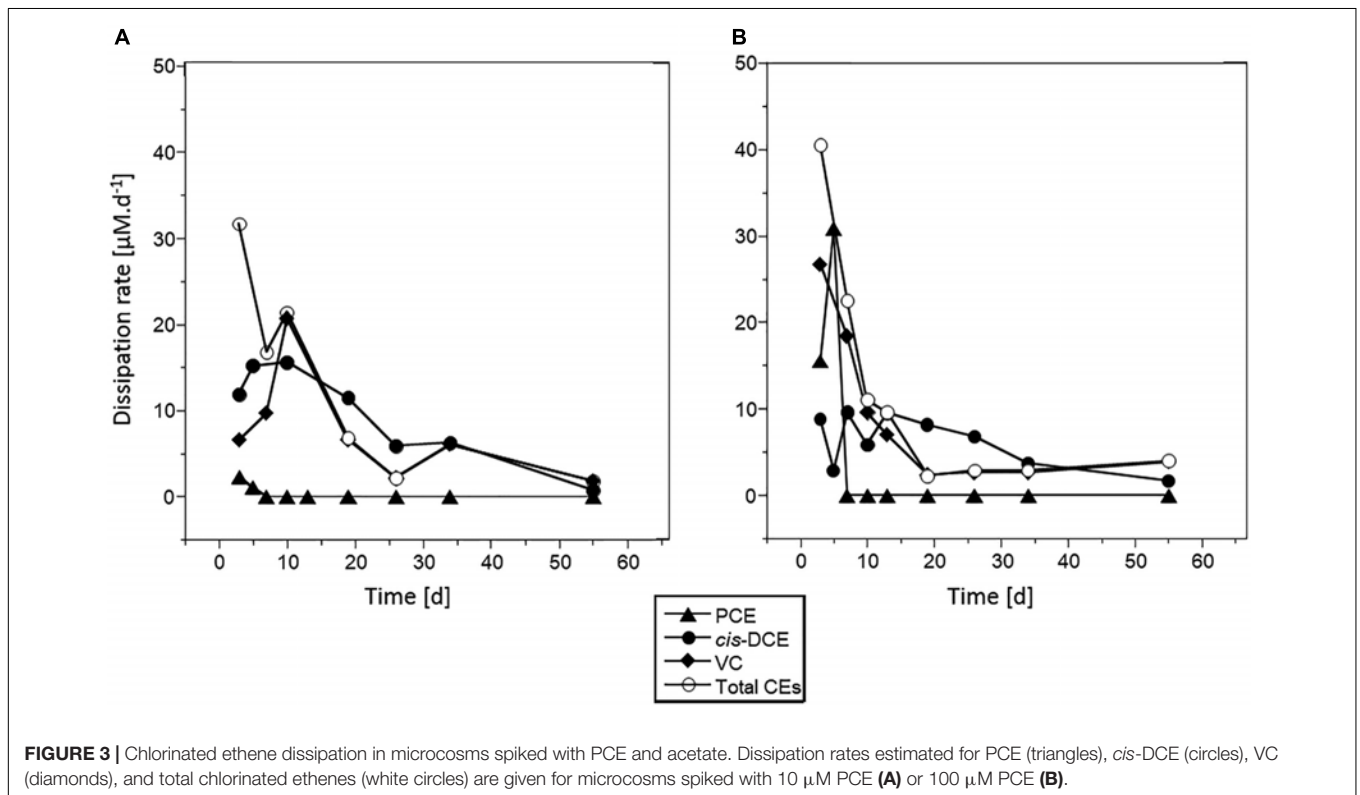
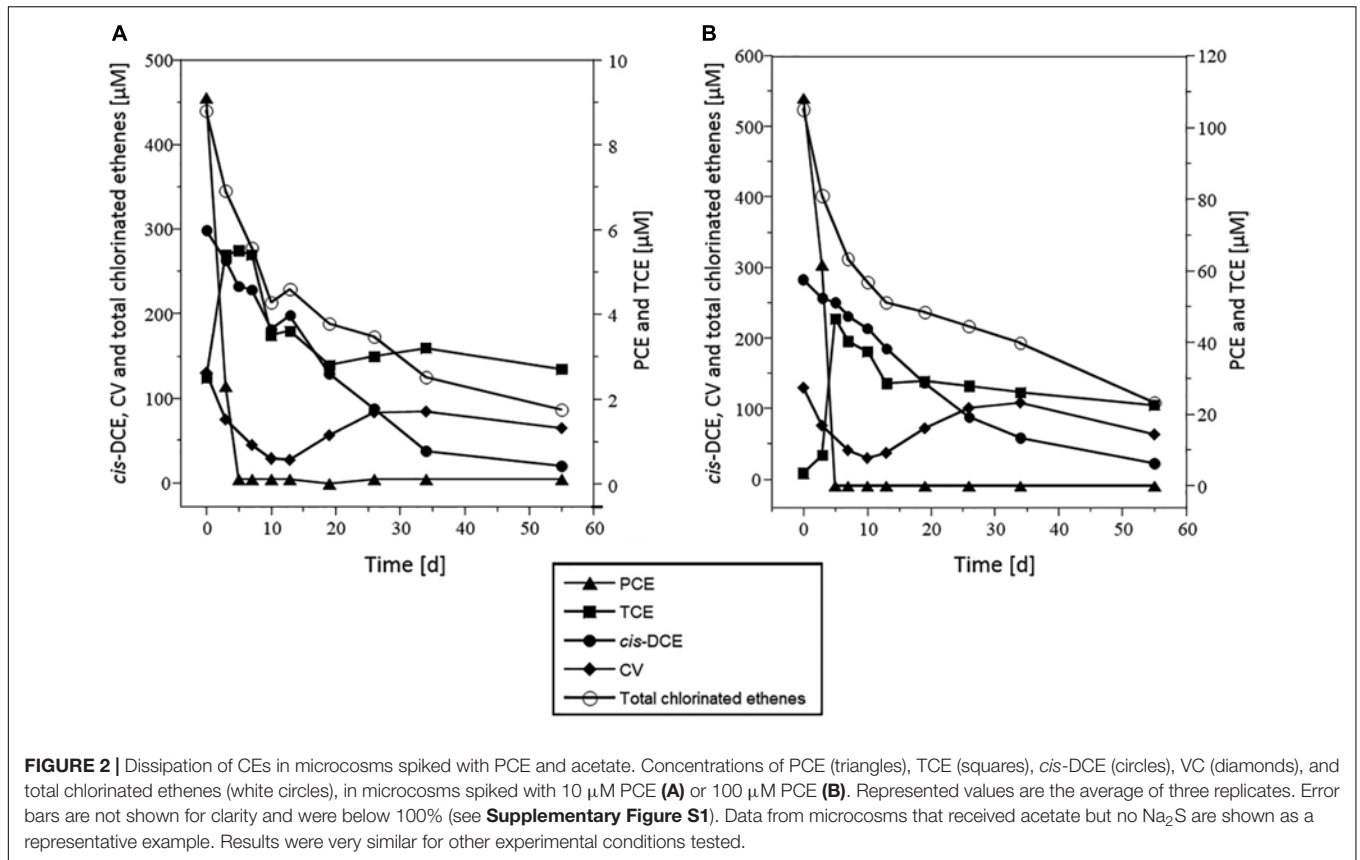
Maximum dissipation rates were estimated at (mean  $\pm$  standard deviation)  $30 \pm 2 \mu\text{M} \cdot \text{day}^{-1}$ ,  $10 \pm 5 \mu\text{M} \cdot \text{d}^{-1}$  and  $26 \pm 5 \mu\text{M} \cdot \text{d}^{-1}$  for PCE, *cis*-DCE and VC, respectively (Figure 3, results with acetate and no Na<sub>2</sub>S addition). Highest rates were observed over the 10 first days of incubation. The PCE dissipation rate was 10-fold higher in microcosms spiked with 100  $\mu\text{M}$  PCE than in those spiked with 10  $\mu\text{M}$  PCE. For other CEs, similar rates were observed in microcosms with 10 or 100  $\mu\text{M}$  PCE. Dissipation rate of *cis*-DCE was lower than that of PCE ( $10 \pm 5 \mu\text{M} \cdot \text{d}^{-1}$ ) and decreased by  $10 \mu\text{M} \cdot \text{d}^{-1}$  after 20 days. VC was rapidly dissipated within the first 10 days, with a rate up to  $25 \mu\text{M} \cdot \text{d}^{-1}$ , and then decreased to  $5 \mu\text{M} \cdot \text{d}^{-1}$  for the remaining incubation time.

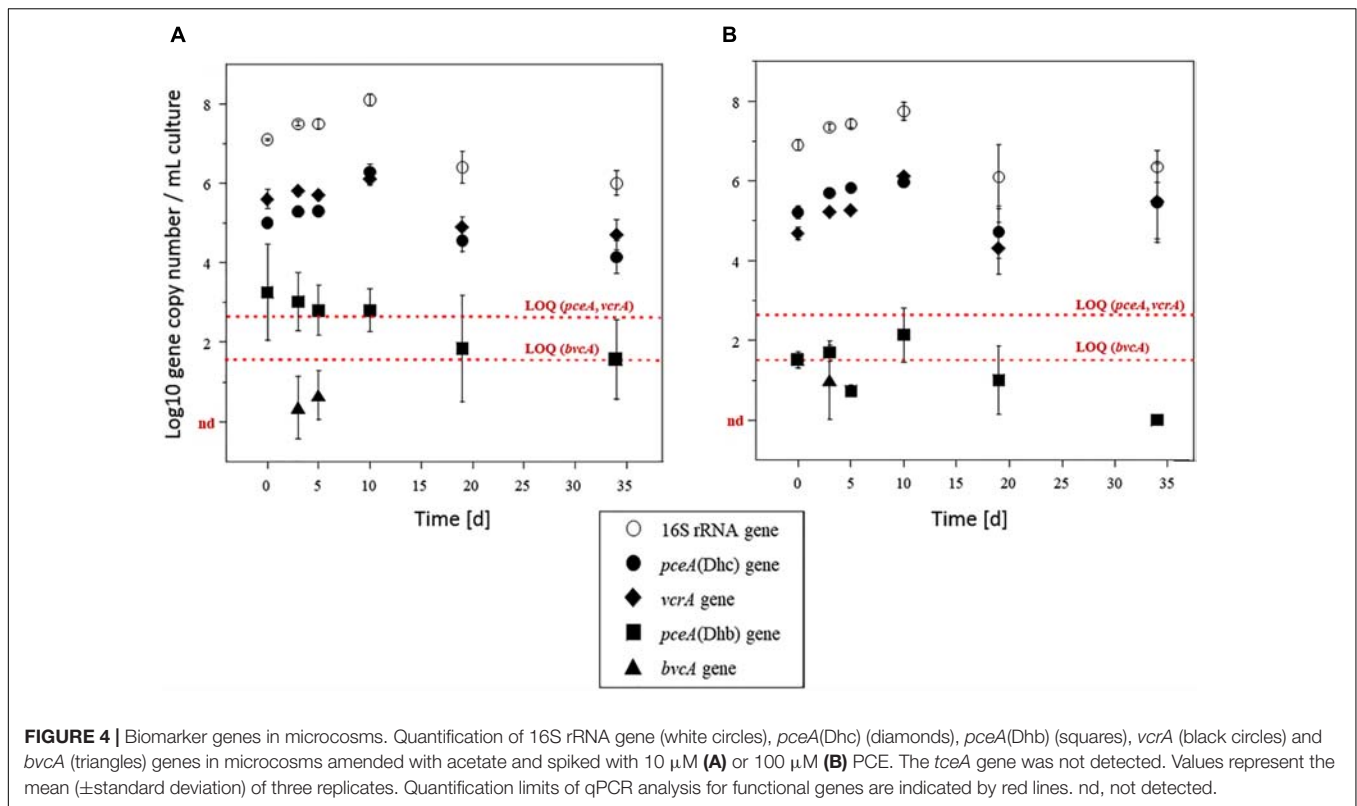
Killed controls showed low dissipation of CEs (<20%, data not shown), confirming that dissipation was the result of microorganisms activity in non-sterile microcosms.

Addition of acetate and Na<sub>2</sub>S did not impact PCE dissipation kinetics. All complementary analyses were thus carried out from microcosms amended with acetate only (without Na<sub>2</sub>S, see Figures 2, 3), and all the results presented hereafter were obtained under those conditions.

### Dechlorination Activity and Dehalogenase Gene Abundance

Abundance of selected reductive dehalogenase genes (*pceA*, *tceA*, *vcrA*, and *bvcA*) and total bacterial abundance (assessed from the 16S rRNA gene) were determined by qPCR (Figure 4). Total bacterial abundance increased from  $10^7$  to  $10^8$   $\text{copies} \cdot \text{mL}^{-1}$  during the first 2 weeks of incubation under both PCE spiking doses, and then remained constant until the end of the experiment. The *vcrA* gene and the version of the *pceA* gene carried by *Dehalococcoides* [*pceA*(Dhc)], initially present at levels around  $10^5$   $\text{copies} \cdot \text{mL}^{-1}$  also increased by one order of magnitude under both PCE spiking conditions. Notably, increase





in abundance of *pceA*(Dhc) occurred during PCE dissipation. Then, after 19 days of incubation, *pceA*(Dhc) gene copies decreased by one order of magnitude before stabilizing around  $2.10^4$  and  $4.10^4$  copies  $\cdot$  mL $^{-1}$  in microcosms spiked with 10 and 100  $\mu\text{M}$  PCE, respectively. The ratio *pceA*(Dhc)/16S *rrnA* was relatively low at the beginning of the experiment (around 0.1% relative abundance). However, the ratio *pceA*(Dhc)/16S *rrnA* ratio increased during the incubation by at least one order of magnitude, up to 1 and 3.5% for microcosms spiked with 10  $\mu\text{M}$  PCE and 100  $\mu\text{M}$  PCE, respectively (Supplementary Figure S4). Abundance of the *vcrA* gene, potentially involved in the two organohalide respiration steps from *cis*-DCE to ethene, followed the same pattern as that of *pceA*(Dhc) (with a magnitude of about 0.4 log) over the duration of the experiment. The *vcrA*/16S *rrnA* ratio increased from about 2.5% relative abundance at the start of the experiment to 6% in microcosms spiked with 10  $\mu\text{M}$  PCE and 12% in microcosms spiked with 100  $\mu\text{M}$  PCE after 34 days of incubation (Supplementary Figure S4). Overall, changes of the abundance of *pceA*(Dhc) and *vcrA* genes compared to the total community as monitored using 16S rRNA gene as proxy (Figure 4) paralleled the dynamics observed for complete dissipation of *cis*-DCE and VC (Figure 2).

Surprisingly, the dehalogenase gene *pceA*(Dhb) involved in the organohalide respiration of PCE to *cis*-DCE by strains of *Dehalobacter* and *Desulfitobacterium* genera (Regeard et al., 2004) was less abundant than dehalogenases genes *pceA*(Dhc) and *vcrA* by two orders of magnitude (Figure 4). At about  $10^3$  copies  $\cdot$  mL $^{-1}$  at the beginning of the experiment, it remained above the limit of quantification (LOQ,  $10^2$  copies  $\cdot$  mL $^{-1}$ )

during the 10 first days of the experiment. It then decreased and remained below the LOQ. Similarly, the absence of detection of *tceA* gene was in keeping with the observed incomplete dissipation of TCE. As for gene *bvcA* involved in VC organohalide respiration, it was only detected at very low copy-numbers, and only during the first 10 days of incubation.

## Bacterial Community During Organohalide Respiration of CEs

Changes in bacterial community were first assessed by CE-SSCP fingerprinting analyses for all microcosm experiments (i.e., with/without acetate, sodium sulfide and/or PCE). Only minor variations were apparent during the first 19 days. Distinct changes were then observed after 34 days (Supplementary Figure S5), depending on the PCE spiking dose.

Principal component analysis of CE-SSCP fingerprints confirmed the observed variations (Supplementary Figure S6). The first two principal components explained 38% of the variability, the first component (24%) being mainly associated with SSCP peaks only present during the first stages of the incubation. *A posteriori* fitting of the main physico-chemical variables and gene abundance data onto the PCA ordination plot suggested that these changes were associated to the decrease of PCE, *cis*-DCE and VC concentrations, and with the increase of *pceA*(Dhc) and *vcrA* dehalogenase gene abundances over time (Supplementary Figure S6). Microcosm samples at the beginning of the incubation (0 and 5 days), and at intermediate (10 days) and late (34 days) sampling times were selected for

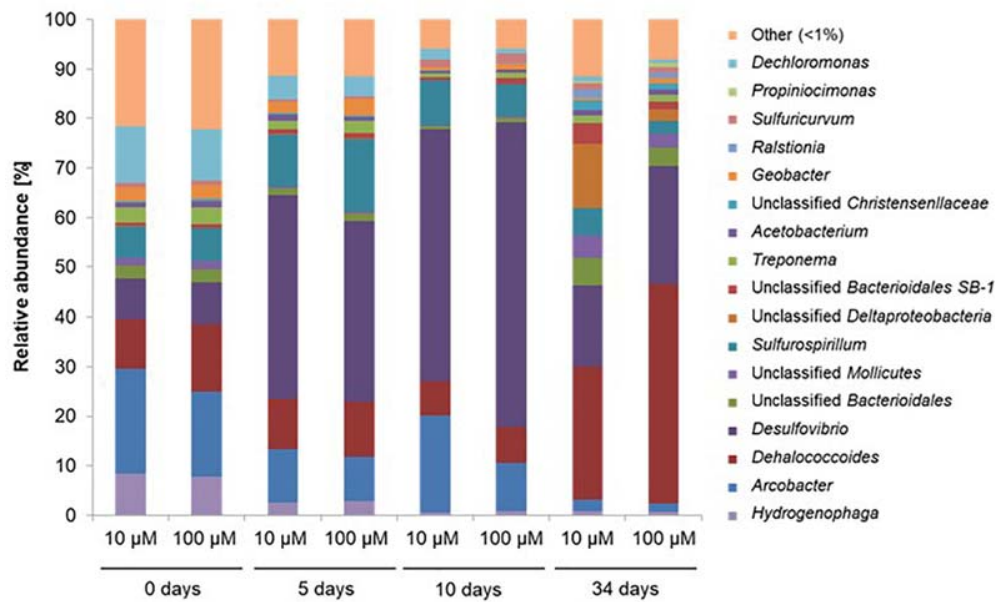


**FIGURE 5 |** Relative abundance of the 17 most abundant genus-level OTUs during CEs dissipation. Only data obtained for microcosms with acetate amendment were analyzed in detail. A total of 412,231 sequences of the V4–V5 region of the 16S rRNA gene were obtained by Illumina MiSeq and analyzed with Qiime software. 10  $\mu$ M, 100  $\mu$ M: concentrations of PCE added. OTUs with <1% abundance were clustered together.

high-throughput sequence analysis of 16S rRNA gene amplicons to identify bacterial taxa present over time and potentially involved in successive steps of organohalide respiration of CEs.

A total of 412,231 high-quality sequences of the V4–V5 region of the 16S rRNA gene (~350 bp) were obtained from separately pooled DNA extracted from triplicate microcosms spiked with 10 and 100  $\mu$ M PCE at the selected four incubation times (0, 5, 10, and 34 days) (Supplementary Table S2). Rarefaction curves did not systematically reach saturation in the 1st days of incubation, although patterns of alpha diversity and overall relative abundances of dominant lineages could be retrieved (Supplementary Figure S8). In the later phase of incubation (10 and 34 days), in contrast, rarefaction curves of diversity indices reached saturation (Supplementary Figure S7), indicating a reduction of bacterial  $\alpha$ -diversity through time in laboratory microcosms.

At the start of the experiment, genera *Hydrogenophaga*, *Arcobacter*, *Dehalococcoides*, *Desulfovibrio*, *Sulfurospirillum*, and *Dechloromonas* dominated the microcosms, and were found in similar proportions at both investigated concentrations of spiked PCE (Figure 5). On average, these genera represented 63 and 65% of the total number of sequences for microcosms spiked with 10  $\mu$ M PCE and 100  $\mu$ M PCE, respectively. Dominant genus-level taxa belong to *Proteobacteria*, except *Dehalococcoides* affiliated to *Chloroflexi*. Over the course of the experiment, *Arcobacter* (19.2–2.0%), *Hydrogenophaga* (8.1–0.76%), *Dechloromonas* (10.8–0.8%), and *Geobacter* (2.0–0.4%) strongly decreased under both PCE amendment conditions (Figure 5). On the other hand, several genus-level taxa showed significant increases in relative abundance, e.g., *Desulfovibrio* (8.2–56.0%) and *Dehalococcoides* (11.8–35.6%) (Figure 5).

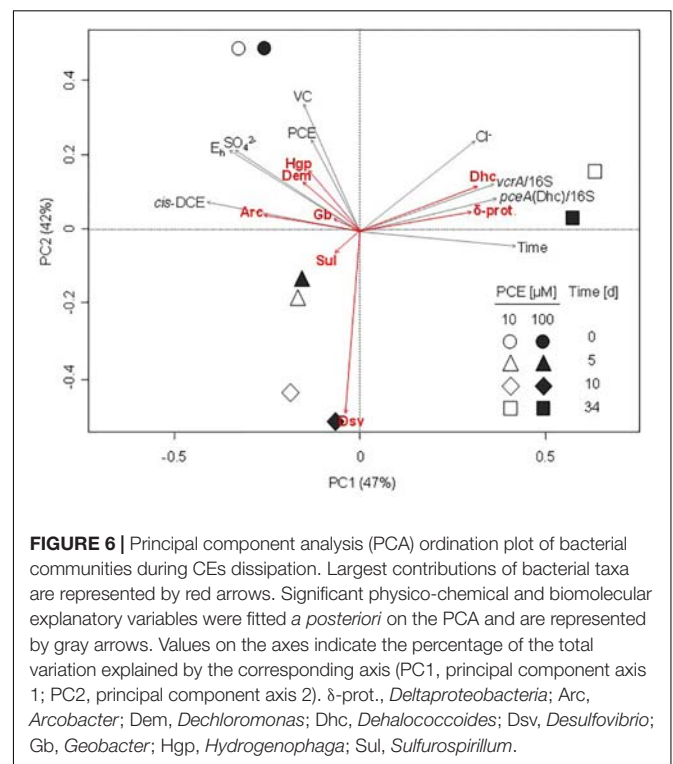


**FIGURE 6 |** Principal component analysis (PCA) ordination plot of bacterial communities during CEs dissipation. Largest contributions of bacterial taxa are represented by red arrows. Significant physico-chemical and biomolecular explanatory variables were fitted *a posteriori* on the PCA and are represented by gray arrows. Values on the axes indicate the percentage of the total variation explained by the corresponding axis (PC1, principal component axis 1; PC2, principal component axis 2).  $\delta$ -prot., *Deltaproteobacteria*; Arc, *Arcobacter*; Dem, *Dechloromonas*; Dhc, *Dehalococcoides*; Dsv, *Desulfovibrio*; Gb, *Geobacter*; Hgp, *Hydrogenophaga*; Sul, *Sulfurospirillum*.

## Dehalogenation-Associated Taxa

High throughput sequencing of the 16S rRNA gene V4–V5 region revealed changes in taxa associated with dehalogenation coinciding with changes in bacterial community diversity

(Figure 6). Using PCA analysis, the main PC1 axis explained 42% of community diversity change, and was mainly linked to *cis*-DCE concentration, abundance of *pceA* and *vcrA* genes and occurrence of *Dehalococcoides*. The second PC2 axis explained 30% of the variability in bacterial community diversity, and mainly reflect PCE and VC concentration changes. Only slight differences between microbial community patterns were observed in early stages of the experiment (0–5 days) between microcosms spiked with 10  $\mu$ M or with 100  $\mu$ M PCE. As already seen by CE-SSCP fingerprinting analysis, larger differences in community composition were observed at later stages (10–35 days) with both 10 and 100  $\mu$ M PCE amendments.

Worthy of note, 3 of the 17 most abundant genera at the beginning of the experiment significantly contributing to PCA ordination were potentially associated to reductive dechlorination (Figure 6), e.g., *Dehalococcoides* (10% average abundance), *Sulfurospirillum* (6.4% average abundance), and *Geobacter* (2.7% average abundance). Interestingly, *Sulfurospirillum*-related taxa increased in the early stages of incubation in microcosms spiked with 10  $\mu$ M PCE (6.3–10.5% average abundance) as well as in microcosms spiked with 100  $\mu$ M PCE (6.6–14.5% average abundance), and then decreased to about 4% under both PCE conditions. Relative abundance of *Geobacter* remained stable (2.0% average abundance with 10  $\mu$ M PCE) or slightly increased (2.8–3.5% with 100  $\mu$ M PCE) and then decreased, especially in microcosms with 100  $\mu$ M PCE. Relative abundance of *Acetobacterium* taxa, also associated with reductive dehalogenation (Terzenbach and Blaut, 1994), remained stable (1.0% average abundance) at all sampling times and for both PCE amendments. In contrast, other taxa putatively associated to reductive dechlorination (all affiliated to the class of *Dehalococcoidetes*) were only found in minor proportions (<0.3% abundance) throughout the experiment (data not shown). Sequences associated with prominent dehalogenating taxa *Dehalobacter* and *Desulfitobacterium* were not found.

One of the most abundant taxa identified in microcosms is affiliated to *Dehalococcoides*, and more specifically to the *Dehalococcoides* Pinellas group (Figure 7) (Hug and Edwards, 2013). As Miseq sequencing do not allow accurate taxa affiliation down to genus level, the affiliation to Pinellas was confirmed by 16S rRNA gene sequence phylogeny on 923 nucleotides of the corresponding OTU (Genbank MK312632). Relative abundance of this taxon remained stable (about 10% abundance) in the initial phase of the experiment (see Figure 5), independently of PCE amendment. A subsequent decrease to 7% average abundance across microcosms was noted under both conditions, followed by a significant (four–sixfold) increase of *Dehalococcoides* abundance at a later stage (Figure 5). This paralleled the observed increase in *pceA*(Dhc) and *vcrA* genes found in *Dehalococcoides* (Figure 6).

## DISCUSSION

The main incentive for this study was to investigate whether laboratory microcosm studies can help identify specific dehalogenation reactions and associated bacterial taxa in

groundwater contaminated with CEs that could then be stimulated for bioremediation. Abundances and dynamics of key dehalogenase genes (*pceA*, *tceA*, *vcrA*, and *bvcA*), bacterial community composition and dehalogenation-specific taxa through the 16S rRNA gene as proxy were thus inventoried in laboratory microcosms of groundwater contaminated with multiple chlorinated solvents (Table 2).

The experiment specifically focused on effects of PCE exposure (10 and 100  $\mu$ M) on dissipation rates and abundances of selected biomarkers. Complete dissipation of PCE and *cis*-DCE (in sampled site water and following *in labo* PCE dissipation), as well as partial dissipation of TCE and VC, were observed in all microcosm experiments. Only minor dissipation of CEs was observed in killed controls, confirming the prevailing role of microorganisms. Notably, organohalide respiration occurred rapidly and independently of acetate and/or addition of a reducing agent (Na<sub>2</sub>S). This confirms that reductive dehalogenation likely proceeded through hydrogen supplied through the 5% H<sub>2</sub>/N<sub>2</sub> atmosphere as the electron donor, and that sufficient carbon was available for biomass production from the groundwater and the preculture used as inoculum.

Monitoring of key reductive dehalogenase genes in microcosms showed a correlation with CE dissipation. It also suggested the dominant involvement of the “Pinellas” subgroup of the *Dehalococcoides* genus (Hug and Edwards, 2013) in the process (Figure 7). Dehalogenase genes *pceA*(Dhc) and *vcrA* were already abundant at the start of the experiment (Figure 4). Groundwater bacteria carrying these genes were likely enriched in the activated preculture prepared from Pz6(10) groundwater and used as inoculum. Upon laboratory incubation, *pceA*(Dhc) and *vcrA* dehalogenase genes abundance increased by one order of magnitude in the initial phase of the experiment, with concomitant complete dissipation of PCE and partial dissipation of *cis*-DCE and VC. This is in agreement with previous studies (Amos et al., 2008; Ise et al., 2011; Aktaş et al., 2012; Baelum et al., 2013). In addition, increase in the 16S rRNA gene suggested selective growth of dehalogenating strains during dechlorination of CEs (Figure 4). In the later phase of the experiment, no further increase of genes *pceA*(Dhc) and *vcrA* was observed (Figure 4), while *cis*-DCE and VC dissipation continued (Figure 2). This suggested that in the presence of hydrogen, dechlorination was supported by sufficient abundance of bacteria containing *vcrA*, as reported previously (Cupples et al., 2004).

*Dehalococcoides* strains may carry several different dehalogenase genes (Behrens et al., 2008). Furthermore, their co-occurrence in CE-degrading enrichment cultures derived from organohalide-contaminated sites has already been observed (Scheutz et al., 2008; Baelum et al., 2013; Kranzioch et al., 2015). Very similar variations and gene copy numbers observed for *pceA*(Dhc) and *vcrA* (Figure 4) suggest that these genes are associated with the same bacteria. However, *pceA*(Dhc) and *vcrA* genes are usually found in different strains. *Dehalococcoides* sp. strain VS, the only bacterium reported to date that carries both *pceA* and *vcrA* genes (Muller et al., 2004; Behrens et al., 2008; Lee et al., 2008), is able to dechlorinate PCE to TCE or *cis*-DCE to ethene, but not TCE to *cis*-DCE (Lee et al., 2008).

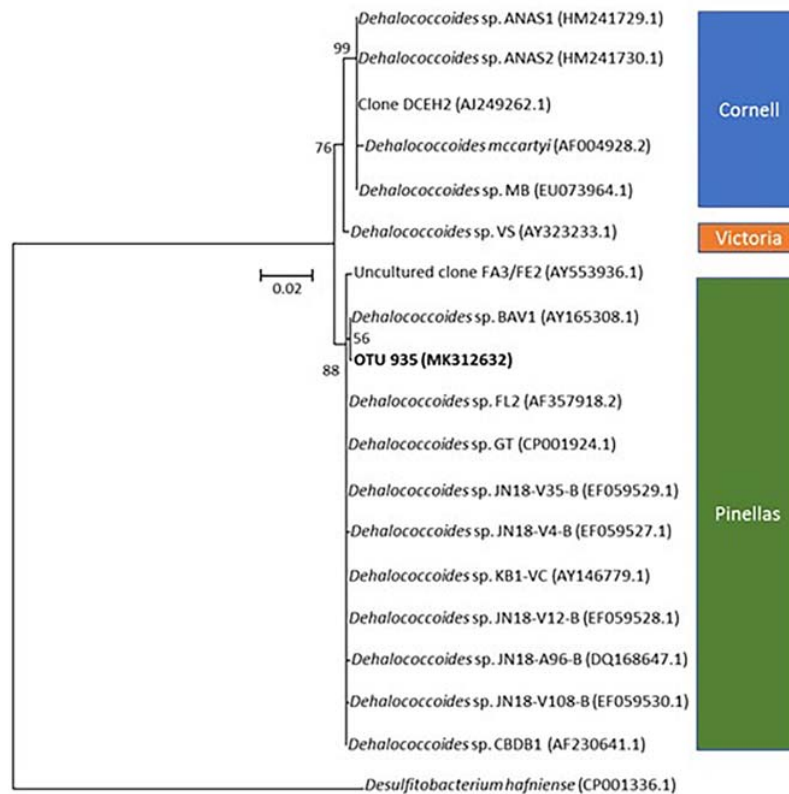


**FIGURE 7 |** Phylogenetic affiliation of OTU935 within genus *Dehalococcoides*. The tree was obtained by the Neighbor-Joining and Jukes and Cantor methods from a 923 nucleotides alignment of 16S rRNA gene sequences. OTU935 of the microcosm is displayed in bold. *Dehalococcoides* subgroup affiliation is also shown. Bootstrap values are expressed as the percentage of 1000 replications.

A comparable situation was encountered here, with complete dehalogenation of PCE and *cis*-DCE but only partial dissipation of TCE (Figure 2). However, the only *Dehalococcoides*-related OTU identified in microcosms by high-throughput sequencing (Figure 5) is affiliated to the Pinellas group and therefore appears phylogenetically distinct from that of the VS strain, which belongs to the Victoria group (Nishimura et al., 2008) (Figure 7). These results, together with patterns of dehalogenase genes *pceA* and *vcrA*, lead to the hypothesis that a new strain of a dehalogenating *Dehalococcoides* sp. containing both *pceA* (Dhc) and *vcrA* genes is involved in organohalide respiration of CEs in groundwater from the Themeroil site.

Abundance data of other dehalogenase genes also allows some conclusions to be drawn. For instance, low abundance of genes *pceA* (Dhb) and *bvcA* suggests an only minor involvement of PCE- and TCE-degrading bacteria carrying these dehalogenases, such as *Desulfitobacterium* and *Dehalobacter* strains (Suyama et al., 2002; Daprato et al., 2007; Rupakula et al., 2013). Similarly, *Dehalococcoides* phylotypes identified in this study likely did not carry the *bvcA* gene for VC organohalide respiration, unlike other known representatives of this genus (Krajmalnik-Brown et al., 2004). Finally, failure to detect the *tceA* gene, together with TCE accumulation in microcosms, suggests the absence of TCE-dehalogenating *Dehalococcoides* sp. Worthy

of note, this contrasts with the low TCE concentration (Table 1), and detection of genes *pceA* (Dhb) and *tceA* in groundwater when measured directly on-site (data not shown). Hence, growth of *tceA*-containing bacteria may be limited under the chosen laboratory microcosm conditions.

Investigations of the dynamics of bacterial composition as a function of CE organohalide respiration in microcosms may help to associate observed patterns of dehalogenation with bacterial taxa identified in microcosms. CE-SSCP fingerprinting analyses proved useful for initial characterisation of bacterial community dynamics in microcosm experiments, and allowed to select key samples for taxonomic characterisation of communities by Illumina MiSeq sequencing of 16S rRNA gene amplicons. Despite being less precise than sequencing, CE-SSCP analysis yielded a similar picture of the main determinants shaping the evolution of the bacterial community in microcosms (Supplementary Figure S6) to high-throughput sequencing (Figure 5).

Overall, microcosms sustained diverse bacterial populations capable of different terminal electron-accepting processes. Bacterial communities were dominated by *Proteobacteria* and *Chloroflexi*, as previously reported for chlorinated hydrocarbon-contaminated groundwater (Abbai and Pillay, 2013; Kotik et al., 2013). A large proportion of recovered microorganisms was putatively associated with

iron and sulfate reduction, in agreement with physico-chemical conditions in microcosms (Table 1). Only a few dominant taxa significantly contributed to the overall change of bacterial communities over time.

Regarding taxa associated with dehalogenation, increasing proportions of *Dehalococcoides* were observed (Figure 5). In contrast, the proportion of *Sulfurospirillum* and *Geobacter*, known to inhabit contaminated aquifers (Duhamel and Edwards, 2006; Maillard et al., 2011; Kranzloch et al., 2013; Lee et al., 2015), decreased throughout the experiment. These two genera include members capable of respiratory reductive dehalogenation of PCE, and may thus have contributed to dechlorination of PCE to TCE and DCE at the very beginning of the experiment. Furthermore, *Sulfurospirillum* and *Geobacter* strains capable of reductive dehalogenation of PCE to *cis*-DCE usually contain *pceA* genes more closely related to *pceA*(Dhb) of *Dehalobacter* and *Desulfotobacterium* strains (Neumann et al., 1998; Wagner et al., 2012; Buttet et al., 2013), which was detected in microcosms in early stage of the experiment. But more likely, as these taxa are non-obligatory organohalide-respirers (Wagner et al., 2012; Goris et al., 2014), they could also have used alternative endogenous electron acceptors, such as Fe(III) initially present in the site groundwater, and produced hydrogen necessary to *Dehalococcoides* to go further in the organohalide respiration pathway. This is likely to have occurred since recovered sequences associated with these OTUs were affiliated to non-dehalogenating strains of these genera (Sung et al., 2006a; Goris et al., 2014). Members of these taxa can also produce corrinoid cofactors that could be used for *Dehalococcoides* growth (Yan et al., 2012).

In addition, OTUs related to *Acetobacterium*, a genus including strains degrading PCE to TCE (Terzenbach and Blaut, 1994), were systematically found in low abundance (<1%) throughout the experiment. Although data obtained so far do not allow to conclude on their involvement in PCE dehalogenation in the present study, strains of *Acetobacterium woodii* have been reported to produce vitamin B12, an essential co-factor for reductive dechlorination (He et al., 2007). Hence, their presence could potentially benefit dissipation of CEs by reductive dehalogenation. Identifying taxa in groundwater microcosms whose activity would depend on the presence of CEs would require additional experiments as well as complementary approaches, such as, e.g., stable isotope probing (Chen and Murrell, 2010).

Operational Taxonomic Units corresponding to other genera often associated with reductive dehalogenation, such as *Desulfotobacterium*, *Dehalobacter* (Maillard et al., 2011; Rouzeau-Szynalski et al., 2011) and *Dehalogenimonas* (Maness et al., 2012) were detected at very low abundances, as expected from the low abundance of dehalogenase *pceA*(Dhb) typical of these genera (Regeard et al., 2004). In addition, these genera are not necessarily associated to organohalide respiration of CEs (Holscher et al., 2004; Dugat-Bony et al., 2012). Increase in abundance of an unclassified taxon associated with *Deltaproteobacteria* also occurred in the later phase of incubation (Figure 5). Indeed, *Deltaproteobacteria* are often associated with key dechlorinators

in contaminated groundwater (Kotik et al., 2013; Adetutu et al., 2015; Kaown et al., 2016).

Some taxa, not usually associated with dehalogenation, also showed large changes in abundance in our experiments. *Hydrogenophaga*, *Treponema*, and *Arcobacter*, observed previously in contaminated groundwater (Kotik et al., 2013; Lee et al., 2015), decreased after the early stages of incubation (5 days). This could result from detrimental effects of microcosm conditions on their growth, such as the toxicity of sulfide produced by sulfate-reducing bacteria in the initial phase of microcosm experiments (Supplementary Figure S2). Indeed, the main changes in bacterial communities other than those associated with dehalogenation occurred for taxa related to sulfate reduction, in particular *Desulfovibrio* spp. (Barton and Fauque, 2009). The increase in relative abundance of sulfate reducers, such as strains of the genera *Desulfovibrio*, *Desulfobulbus*, and *Desulfomicrobium* (Kleikemper et al., 2002), suggests that they grew during the early stages of the experiment. Reductive dehalogenation of CEs is known to compete with sulfate reduction for electron donors and in particular for hydrogen (Davis et al., 2002; Aulenta et al., 2007, 2008). It is thus interesting that both reductive dehalogenation and sulfate reduction occurred in the early phases of the microcosm experiments, suggesting that its establishment was possible due to modest competition between these two metabolisms.

The only OTU associated with *Dehalococcoides* increased in abundance in the later stages of the experiment, which coincided with higher relative abundances of *pceA* and *vcrA* (Figure 4). An almost twofold increase in abundance of this *Dehalococcoides* OTU in microcosms spiked with 100  $\mu$ M PCE compared to those amended with 10  $\mu$ M further suggested that it was involved in PCE utilization for growth. Increase in *Dehalococcoides* following a decline of sulfate-reducing bacteria (mainly *Desulfovibrio*) and the decrease of sulfate in microcosms (Figure 5 and Supplementary Figure S3) suggests that relative abundance of sulfate-reducing bacteria, reduction of sulfate and development of *Dehalococcoides* may be related. Possibly, hydrogen transfer between *Desulfovibrio* and *Dehalococcoides* strains upon sulfate depletion may be occurring under these conditions (Drzyzga et al., 2001; Men et al., 2012).

Principal component analysis allowed integrative analysis of chemical and biomolecular data (Figure 6), and how functional gene abundance, bacterial diversity and CEs dissipation may be correlated. Microcosms were mainly discriminated according to the concentration of pollutants PCE, *cis*-DCE and VC ( $p < 0.05$ ) (Figure 6), and time (Supplementary Figure S6). Overall, no clear differentiation of the bacterial community for most of the identified taxa was observed, although a correlation with time, pollutant concentrations or physico-chemical parameters such as redox potential and sulfate concentrations could be identified for a few of them (Figure 6). For example, relative abundance of *Arcobacter*, *Dechloromonas*, and *Hydrogenophaga* associated OTUs was correlated with the early stages of incubation, together with higher concentrations of CEs, sulfate and redox potential (Figures 5, 6). Several other genera such as *Geobacter*, *Treponema*, and *Sulfurospirillum* were also linked to the early stages of incubation (Figure 5) and physico-chemical conditions

at the beginning of the experiment (**Figure 6**). In contrast, high relative abundance of taxa related to *Desulfovibrio* correlated to a later incubation time (10 days) (**Figure 5**).

Regarding dehalogenation, low relative abundance of *pceA*(Dhb) in microcosms was correlated with high concentrations of PCE, thus questioning its association with PCE dissipation. Similarly, abundance of *bvcA* was not significantly associated with changes in physico-chemical parameters or taxonomy. Key shifts observed in bacterial community composition were thus clearly associated with relative abundance of dehalogenase genes *pceA*(Dhc) and *vcrA*, and negatively or not correlated to pollutant concentrations (**Figure 6**), as expected for genes involved in pollutant transformation. In addition, chloride, sulfate and redox potential were correlated with abundances of *Dehalococcoides*-associated OTUs identified as a potential biomarker of organohalide respiration of CEs in microcosms of groundwater from the contaminated site of interest, as expected for reductive dehalogenation metabolism.

## CONCLUSION

In summary, an active dechlorinating bacterial community was evidenced and characterized in groundwater samples from the contaminated Themerol site. Molecular investigations of groundwater microcosms allowed to assess changes of functional genes associated with organohalide respiration of CEs and associated bacterial community composition. Analysis of the relationship between key dehalogenase genes and taxonomic profiling highlighted the importance of specific genera associated with dehalogenation of PCE, *cis*-DCE and VC, as dehalogenation of CEs. Concomitant changes in bacterial community composition revealed different compositions through time, and changes in *Dehalococcoides* and sulfate-reducing bacteria.

Taken together, our results provide new evidence that endogenous *Dehalococcoides* sp. in multi-contaminated groundwater from the investigated site of interest predominantly grows through CE organohalide respiration under anoxic conditions. This, together with patterns of *pceA*(Dhc) and *vcrA* genes, led to hypothesize that a potentially novel *Dehalococcoides* sp. taxon belonging to the Pinellas subgroup and containing both *pceA*(Dhc) and *vcrA* genes is related to dissipation of PCE, *cis*-DCE and VC. This hypothesis remains to be further examined by isolation of dehalogenating strains and experiments in pure cultures. Metagenome sequencing on groundwater samples of the

## REFERENCES

- Abbai, N. S., and Pillay, B. (2013). Analysis of hydrocarbon-contaminated groundwater metagenomes as revealed by high-throughput sequencing. *Mol. Biotechnol.* 54, 900–912. doi: 10.1007/s12033-012-9639-z
- Abe, Y., Aravena, R., Zopfi, J., Parker, B., and Hunkeler, D. (2009). Evaluating the fate of chlorinated ethenes in streambed sediments by combining stable isotope, geochemical and microbial methods. *J. Contam. Hydrol.* 107, 10–21. doi: 10.1016/j.jconhyd.2009.03.002

site as well as attempts at isolation and characterisation of this strain in pure cultures and by multi-element compound specific isotope analysis (CSIA) may also help to identify biological pathways and genes associated with dissipation of CEs at the Themerol site.

## AUTHOR CONTRIBUTIONS

LH contributed to the experimental design, carried out experimental work, data analysis, and drafted the paper. JH, CJ, and SV contributed to the experimental setup, data analysis, and paper drafting and revision. JD and SF carried out metagenomics sequencing, data analysis, and paper revision. GI contributed to data analysis and paper drafting and revision. CU carried out cloning, sequencing and phylogenetic analyses and paper revision.

## FUNDING

This project was funded through a ADEME-BRGM Ph.D. grant to LH (No. TEZ14-31) and the BIODISSPOL project funded by ADEME (No. 1572C0006).

## ACKNOWLEDGMENTS

We wish to thank Cécile Grand (ADEME) for providing access to the Themerol site and scientific discussions. We are also grateful to Kevin Kuntze and Yvonne Nijenhuis [Helmholtz Centre for Environmental Research (UFZ), Leipzig, Germany] for providing plasmids with *tceA*, *vcrA* and *bvcA* reference genes, and to Julien Maillard (Environmental Engineering Institute, EPF Lausanne, Switzerland) for the plasmid with the *pceA* reference gene. We also thank the LIGAN-PM Genomics platform (Lille, France) supported by the ANR Equipex 2010 session (ANR-10-EQPX-07-01; 'LIGAN-PM'), FEDER, and the Region Nord-Pas-de-Calais-Picardie, for their contribution to the high-throughput sequencing analysis.

## SUPPLEMENTARY MATERIAL

The Supplementary Material for this article can be found online at: <https://www.frontiersin.org/articles/10.3389/fmicb.2019.00089/full#supplementary-material>

- Adetutu, E. M., Gundry, T. D., Patil, S. S., Golneshin, A., Adigun, J., Bhaskarla, V., et al. (2015). Exploiting the intrinsic microbial degradative potential for field-based *in situ* dechlorination of trichloroethene contaminated groundwater. *J. Hazard. Mater.* 300, 48–57. doi: 10.1016/j.jhazmat.2015.06.055
- Aktaş, Ö., Schmidt, K. R., Mungenast, S., Stoll, C., and Tiehm, A. (2012). Effect of chloroethene concentrations and granular activated carbon on reductive dechlorination rates and growth of *Dehalococcoides* spp. *Bioresour. Technol.* 103, 286–292. doi: 10.1016/j.biortech.2011.09.119
- Amos, B. K., Suchomel, E. J., Pennell, K. D., and Löffler, F. E. (2008). Microbial activity and distribution during enhanced contaminant dissolution from a

- NAPL source zone. *Water Res.* 42, 2963–2974. doi: 10.1016/j.watres.2008.03.015
- Atashgahi, S., Lu, Y., Ramiro-Garcia, J., Peng, P., Maphosa, F., Sipkema, D., et al. (2017). Geochemical parameters and reductive dechlorination determine aerobic cometabolic VS aerobic metabolic vinyl chloride biodegradation at oxic/anoxic interface of hyporheic zones. *Environ. Sci. Technol.* 51, 1626–1634. doi: 10.1021/acs.est.6b05041
- Atashgahi, S., Lu, Y., and Smidt, H. (2016). “Overview of known organohalide-respiring bacteria—phylogenetic diversity and environmental distribution,” in *Organohalide-Respiring Bacteria*, eds L. Adrian and F. Löffler (Berlin: Springer), 63–105. doi: 10.1007/978-3-662-49875-0\_5
- Aulenta, F., Beccari, M., Majone, M., Papini, M. P., and Tandoi, V. (2008). Competition for H<sub>2</sub> between sulfate reduction and dechlorination in butyrate-fed anaerobic cultures. *Process Biochem.* 43, 161–168. doi: 10.1016/j.procbio.2007.11.006
- Aulenta, F., Pera, A., Rossetti, S., Papini, M. P., and Majone, M. (2007). Relevance of side reactions in anaerobic reductive dechlorination microcosms amended with different electron donors. *Water Res.* 41, 27–38. doi: 10.1016/j.watres.2006.09.019
- Baelum, J., Chambon, J. C., Scheutz, C., Binning, P. J., Laier, T., Bjerg, P. L., et al. (2013). A conceptual model linking functional gene expression and reductive dechlorination rates of chlorinated ethenes in clay rich groundwater sediment. *Water Res.* 47, 2467–2478. doi: 10.1016/j.watres.2013.02.016
- Barton, L. L., and Fauque, G. D. (2009). “Biochemistry, physiology and biotechnology of sulfate-reducing bacteria,” in *Advances in Applied Microbiology*, Vol. 68, eds A. I. Laskin, S. Sariaslani, and G. M. Gadd (San Diego, CA: Elsevier Academic Press Inc), 41–98. doi: 10.1016/S0065-2164(09)01202-7
- Beeman, R. E., and Bleckmann, C. A. (2002). Sequential anaerobic–aerobic treatment of an aquifer contaminated by halogenated organics: field results. *J. Contam. Hydrol.* 57, 147–159. doi: 10.1016/S0169-7722(02)00008-6
- Behrens, S., Azizian, M. F., McMurdie, P. J., Sabalowsky, A., Dolan, M. E., Semprini, L., et al. (2008). Monitoring abundance and expression of “*Dehalococcoides*” species chloroethene-reductive dehalogenases in a tetrachloroethene-dechlorinating flow column. *Appl. Environ. Microbiol.* 74, 5695–5703. doi: 10.1128/AEM.00926-08
- BRGM (1998). *Pollution du site industriel THEMEROIL à Varennes-le-Grand (71) Expertise géologique et hydrogéologique du dossier*. Orléans: BRGM, 111.
- BRGM (2011). *Synthèse des connaissances sur l'hydrogéologie des sites de l'entreprise THEMEROIL et des aires de service de l'autoroute A6 sur les communes de Saint-Ambreuil et de Varennes-le-Grand (Saône-et-Loire)*. Orléans: BRGM, 101.
- Buttet, G. F., Holliger, C., and Maillard, J. (2013). Functional genotyping of *Sulfurospirillum* spp. in mixed cultures allowed the identification of a new tetrachloroethene reductive dehalogenase. *Appl. Environ. Microbiol.* 79, 6941–6947. doi: 10.1128/AEM.02312-13
- Caporaso, J. G., Kuczynski, J., Stombaugh, J., Bittinger, K., Bushman, F. D., Costello, E. K., et al. (2010). QIIME allows analysis of high-throughput community sequencing data. *Nat. Methods* 7, 335–336. doi: 10.1038/nmeth.f.303
- Carreon-Diazconti, C., Santamaria, J., Berkompas, J., Field, J. A., and Brusseau, M. L. (2009). Assessment of *in situ* reductive dechlorination using compound-specific stable isotopes, functional gene PCR, and geochemical data. *Environ. Sci. Technol.* 43, 4301–4307. doi: 10.1021/es803308q
- Chang, C.-H., Yang, H.-Y., Hung, J.-M., Lu, C.-J., and Liu, M.-H. (2017). Simulation of combined anaerobic/aerobic bioremediation of tetrachloroethylene in groundwater by a column system. *Int. Biodeterior. Biodegrad.* 117, 150–157. doi: 10.1016/j.ibiod.2016.12.014
- Chen, Y., and Murrell, J. C. (2010). When metagenomics meets stable-isotope probing: progress and perspectives. *Trends Microbiol.* 18, 157–163. doi: 10.1016/j.tim.2010.02.002
- Cheng, D., and He, J. (2009). Isolation and characterization of “*Dehalococcoides*” sp. strain MB, which dechlorinates tetrachloroethene to trans-1,2-dichloroethene. *Appl. Environ. Microbiol.* 75, 5910. doi: 10.1128/AEM.00767-09
- Chow, W. L., Cheng, D., Wang, S., and He, J. (2010). Identification and transcriptional analysis of trans-DCE-producing reductive dehalogenases in *Dehalococcoides* species. *ISME J.* 4, 1020–1030. doi: 10.1038/ismej.2010.27
- Claesson, M. J., Wang, Q., O’Sullivan, O., Greene-Diniz, R., Cole, J. R., Ross, R. P., et al. (2010). Comparison of two next-generation sequencing technologies for resolving highly complex microbiota composition using tandem variable 16S rRNA gene regions. *Nucleic Acids Res.* 38:e200. doi: 10.1093/nar/gkq873
- Clark, K., Taggart, D. M., Baldwin, B. R., Ritalahti, K. M., Murdoch, R. W., Hatt, J. K., et al. (2018). Normalized quantitative PCR measurements as predictors for ethene formation at sites impacted with chlorinated ethenes. *Environ. Sci. Technol.* 52, 13410–13420. doi: 10.1021/acs.est.8b04373
- Cole, J. R., Wang, Q., Fish, J. A., Chai, B., McGarrell, D. M., Sun, Y., et al. (2014). Ribosomal database project: data and tools for high throughput rRNA analysis. *Nucleic Acids Res.* 42, D633–D642. doi: 10.1093/nar/gkt1244
- Cupples, A. M., Spormann, A. M., and McCarty, P. L. (2004). Vinyl chloride and *cis*-dichloroethene dechlorination kinetics and microorganism growth under substrate limiting conditions. *Environ. Sci. Technol.* 38, 1102–1107. doi: 10.1021/es0348647
- Da Silva, M. L. B., and Alvarez, P. J. J. (2008). Exploring the correlation between halo-respirer biomarker concentrations and TCE dechlorination rates. *J. Environ. Eng.* 134, 895–901. doi: 10.1061/(asce)0733-9372
- Daprato, R. C., Löffler, F. E., and Hughes, J. B. (2007). Comparative analysis of three tetrachloroethene to ethene halo-respiring consortia suggests functional redundancy. *Environ. Sci. Technol.* 41, 2261–2269. doi: 10.1021/es061544p
- Davis, J. W., Odom, J. M., DeWeerd, K. A., Stahl, D. A., Fishbain, S. S., West, R. J., et al. (2002). Natural attenuation of chlorinated solvents at Area 6, Dover Air Force Base: characterization of microbial community structure. *J. Contam. Hydrol.* 57, 41–59. doi: 10.1016/S0169-7722(01)00217-0
- Delbès, C., Moletta, R., and Godon, J. (2001). Bacterial and archaeal 16S rDNA and 16S rRNA dynamics during an acetate crisis in an anaerobic digester ecosystem. *FEMS Microbiol. Ecol.* 35, 19–26. doi: 10.1111/j.1574-6941
- DeSantis, T. Z., Hugenholtz, P., Larsen, N., Rojas, M., Brodie, E. L., Keller, K., et al. (2006). Greengenes, a chimera-checked 16S rRNA gene database and workbench compatible with ARB. *Appl. Environ. Microbiol.* 72, 5069–5072. doi: 10.1128/aem.03006-05
- Drzyzga, O., Gerritse, J., Dijk, J. A., Elissen, H., and Gottschal, J. C. (2001). Coexistence of a sulphate-reducing *Desulfovibrio* species and the dehalorespiring *Desulfotobacterium frappieri* TCE1 in defined chemostat cultures grown with various combinations of sulphate and tetrachloroethene. *Environ. Microbiol.* 3, 92–99. doi: 10.1046/j.1462-2920
- Dugat-Bony, E., Biderre-Petit, C., Jaziri, F., David, M. M., Denonfoux, J., Lyon, D. Y., et al. (2012). *In situ* TCE degradation mediated by complex dehalorespiring communities during biostimulation processes. *Microb. Biotechnol.* 5, 642–653. doi: 10.1111/j.1751-7915.2012.00339.x
- Duhamel, M., and Edwards, E. A. (2006). Microbial composition of chlorinated ethene-degrading cultures dominated by *Dehalococcoides*. *FEMS Microbiol. Ecol.* 58, 538–549. doi: 10.1111/j.1574-6941.2006.00191.x
- Edgar, R. C. (2010). Search and clustering orders of magnitude faster than BLAST. *Bioinformatics* 26, 2460–2461. doi: 10.1093/bioinformatics/btq461
- Florey, J., Adams, A., and Michel, L. (2017). Reductive dechlorination of a chlorinated solvent plume in Houston. *Texas Remed. J.* 28, 5–54. doi: 10.1002/rem.21541
- Freedman, D. L., and Gossett, J. M. (1991). Biodegradation of dichloromethane and its utilization as a growth substrate under methanogenic conditions. *Appl. Environ. Microbiol.* 57, 2847–2857.
- Futagami, T., Goto, M., and Furukawa, K. (2008). Biochemical and genetic bases of dehalorespiration. *Chem. Rec.* 8, 1–12. doi: 10.1002/tcr.20134
- Goris, T., Schubert, T., Gadkari, J., Wubet, T., Tarkka, M., Buscot, F., et al. (2014). Insights into organohalide respiration and the versatile catabolism of *Sulfurospirillum multivorans* gained from comparative genomics and physiological studies. *Environ. Microbiol.* 16, 3562–3580. doi: 10.1111/1462-2920.12589
- Gouy, M., Guindon, S., and Gascuel, O. (2010). SeaView version 4: a multiplatform graphical user interface for sequence alignment and phylogenetic tree building. *Mol. Biol. Evol.* 27, 221–224. doi: 10.1093/molbev/msp259
- Haack, S. K., Fogarty, L. R., West, T. G., Alm, E. W., McGuire, J. T., Long, D. T., et al. (2004). Spatial and temporal changes in microbial community structure associated with recharge-influenced chemical gradients in a contaminated aquifer. *Environ. Microbiol.* 6, 438–448. doi: 10.1111/j.1462-2920.2003.00563.x
- Hall, T. (1999). BioEdit: a user-friendly biological sequence alignment editor and analysis program for Windows 95/NT. *Nucleic Acids Symp. Ser.* 41, 95–98.

- He, J., Holmes, V. F., Lee, P. K. H., and Alvarez-Cohen, L. (2007). Influence of vitamin B12 and cocultures on the growth of *Dehalococcoides* isolates in defined medium. *Appl. Environ. Microbiol.* 73, 2847–2853. doi: 10.1128/AEM.02574-06
- He, J. Z., Ritalahti, K. M., Yang, K. L., Koenigsberg, S. S., and Löffler, F. E. (2003). Detoxification of vinyl chloride to ethene coupled to growth of an anaerobic bacterium. *Nature* 424, 62–65. doi: 10.1038/nature01717
- Hendrickson, E. R., Payne, J. A., Young, R. M., Starr, M. G., Perry, M. P., Fahnestock, S., et al. (2002). Molecular analysis of *Dehalococcoides* 16S ribosomal DNA from chloroethene-contaminated sites throughout North America and Europe. *Appl. Environ. Microbiol.* 68, 485–495. doi: 10.1128/AEM.68.2.485-495.2002
- Holliger, C., Wohlfarth, G., and Diekert, G. (1998). Reductive dechlorination in the energy metabolism of anaerobic bacteria. *FEMS Microbiol. Rev.* 22, 383–398. doi: 10.1016/S0168-6445(98)00030-8
- Holscher, T., Krajmalnik-Brown, R., Ritalahti, K. M., von Wintzingerode, F., Gorisch, H., Löffler, F. E., et al. (2004). Multiple non-identical reductive-dehalogenase-homologous genes are common in *Dehalococcoides*. *Appl. Environ. Microbiol.* 70, 5290–5297. doi: 10.1128/AEM.70.9.5290-5297.2004
- Huang, B., Lei, C., Wei, C., and Zeng, G. (2014). Chlorinated volatile organic compounds (Cl-VOCs) in environment — sources, potential human health impacts, and current remediation technologies. *Environ. Int.* 71, 118–138. doi: 10.1016/j.envint.2014.06.013
- Hug, L. A. (2016). “Diversity, evolution, and environmental distribution of reductive dehalogenase genes,” in *Organohalide-Respiring Bacteria*, eds L. Adrian and F. Löffler (Berlin: Springer), 377–393. doi: 10.1007/978-3-662-49875-0-16
- Hug, L. A., and Edwards, E. A. (2013). Diversity of reductive dehalogenase genes from environmental samples and enrichment cultures identified with degenerate primer PCR screens. *Front. Microbiol.* 4:341. doi: 10.3389/fmicb.2013.00341
- Imfeld, G., Nijenhuis, I., Nikolausz, M., Zeiger, S., Paschke, H., Drangmeister, J., et al. (2008). Assessment of *in situ* degradation of chlorinated ethenes and bacterial community structure in a complex contaminated groundwater system. *Water Res.* 42, 871–882. doi: 10.1016/j.watres.2007.08.035
- Ise, K., Suto, K., and Inoue, C. (2011). Microbial diversity and changes in the distribution of dehalogenase genes during dechlorination with different concentrations of *cis*-DCE. *Environ. Sci. Technol.* 45, 5339–5345. doi: 10.1021/es104199y
- Kang, J. W. (2014). Removing environmental organic pollutants with bioremediation and phytoremediation. *Biotechnol. Lett.* 36, 1129–1139. doi: 10.1007/s10529-014-1466-9
- Kaown, D., Jun, S.-C., Kim, R.-H., Woosik, S., and Lee, K.-K. (2016). Characterization of a site contaminated by chlorinated ethenes and ethanes using multi-analysis. *Environ. Earth Sci.* 75:745. doi: 10.1007/s12665-016-5536-2
- Kleikemper, J., Schroth, M. H., Sigler, W. V., Schmucki, M., Bernasconi, S. M., and Zeyer, J. (2002). Activity and diversity of sulfate-reducing bacteria in a petroleum hydrocarbon-contaminated aquifer. *Appl. Environ. Microbiol.* 68, 1516–1523. doi: 10.1128/AEM.68.4.1516-1523.2002
- Kotik, M., Davidova, A., Voriskova, J., and Baldrian, P. (2013). Bacterial communities in tetrachloroethene-polluted groundwaters: a case study. *Sci. Total Environ.* 454, 517–527. doi: 10.1016/j.scitotenv.2013.02.082
- Krajmalnik-Brown, R., Holscher, T., Thomson, I. N., Saunders, F. M., Ritalahti, K. M., and Löffler, F. E. (2004). Genetic identification of a putative vinyl chloride reductase in *Dehalococcoides* sp. strain BAV1. *Appl. Environ. Microbiol.* 70, 6347–6351. doi: 10.1128/AEM.70.10.6347-6351.2004
- Kranzioch, I., Ganz, S., and Tiehm, A. (2015). Chloroethene degradation and expression of *Dehalococcoides* dehalogenase genes in cultures originating from Yangtze sediments. *Environ. Sci. Pollut. Res.* 22, 3138–3148. doi: 10.1007/s11356-014-3574-4
- Kranzioch, I., Stoll, C., Holbach, A., Chen, H., Wang, L., Zheng, B., et al. (2013). Dechlorination and organohalide-respiring bacteria dynamics in sediment samples of the Yangtze Three Gorges Reservoir. *Environ. Sci. Pollut. Res.* 20, 7046–7056. doi: 10.1007/s11356-013-1545-9
- Lee, P. K. H., Macbeth, T. W., Sorenson, J., Kent, S., Deeb, R. A., and Alvarez-Cohen, L. (2008). Quantifying genes and transcripts to assess the *in situ* physiology of “*Dehalococcoides*” spp. in a trichloroethene-contaminated groundwater site. *Appl. Environ. Microbiol.* 74, 2728–2739. doi: 10.1128/AEM.02199-07
- Lee, S.-S., Kaown, D., and Lee, K.-K. (2015). Evaluation of the fate and transport of chlorinated ethenes in a complex groundwater system discharging to a stream in Wonju. *Korea. J. Contam. Hydrol.* 182, 231–243. doi: 10.1016/j.jconhyd.2015.09.005
- Legendre, P., and Gallagher, E. D. (2001). Ecologically meaningful transformations for ordination of species data. *Oecologia* 129, 271–280. doi: 10.1007/s004420100716
- Löffler, F. E., Sun, Q., Li, J. R., and Tiedje, J. M. (2000). 16S rRNA gene-based detection of tetrachloroethene-dechlorinating *Desulfuromonas* and *Dehalococcoides* species. *Appl. Environ. Microbiol.* 66, 1369–1374. doi: 10.1128/AEM.66.4.1369-1374.2000
- Löffler, F. E., Yan, J., Ritalahti, K. M., Adrian, L., Edwards, E. A., Constantinidis, K. T., et al. (2013). *Dehalococcoides mccartyi* gen. nov., sp. nov., obligately organohalide-respiring anaerobic bacteria relevant to halogen cycling and bioremediation, belong to a novel bacterial class, *Dehalococcoidia classis* nov., order *Dehalococcoidales* ord. nov. and family *Dehalococcoidaceae* fam. nov., within the phylum Chloroflexi. *Int. J. Syst. Evol. Microbiol.* 63, 625–635. doi: 10.1099/ijs.0.034926-0
- López-Gutiérrez, J. C., Henry, S., Hallet, S., Martin-Laurent, F., Catroux, G., and Philippot, L. (2004). Quantification of a novel group of nitrate-reducing bacteria in the environment by real-time PCR. *J. Microbiol. Methods* 57, 399–407. doi: 10.1016/j.mimet.2004.02.009
- Lu, X., Wilson, J. T., and Kampbell, D. H. (2006). Relationship between *Dehalococcoides* DNA in ground water and rates of reductive dechlorination at field scale. *Water Res.* 40, 3131–3140. doi: 10.1016/j.watres.2006.05.030
- Magnuson, J. K., Stern, R. V., Gossett, J. M., Zinder, S. H., and Burris, D. R. (1998). Reductive dechlorination of tetrachloroethene to ethene by two-component enzyme pathway. *Appl. Environ. Microbiol.* 64, 1270–1275.
- Magoč, T., and Salzberg, S. L. (2011). FLASH: fast length adjustment of short reads to improve genome assemblies. *Bioinformatics* 27, 2957–2963. doi: 10.1093/bioinformatics/btr507
- Maillard, J., Charnay, M.-P., Regeard, C., Rohrbach-Brandt, E., Rouzeau-Szynalski, K., Rossi, P., et al. (2011). Reductive dechlorination of tetrachloroethene by a stepwise catalysis of different organohalide respiring bacteria and reductive dehalogenases. *Biodegradation* 22, 949–960. doi: 10.1007/s10532-011-9454-4
- Maness, A. D., Bowman, K. S., Yan, J., Rainey, F. A., and Moe, W. M. (2012). *Dehalogenimonas* spp. can reductively dehalogenate high concentrations of 1,2-dichloroethane, 1,2-dichloropropane, and 1,1,2-trichloroethane. *AMB Express* 2:54. doi: 10.1186/2191-0855-2-54
- Maphosa, F., Lieten, S. H., Dinkla, I., Stams, A. J., Smidt, H., and Fennell, D. E. (2012). Ecogenomics of microbial communities in bioremediation of chlorinated contaminated sites. *Front. Microbiol.* 3:351. doi: 10.3389/fmicb.2012.00351
- Maphosa, F., Smidt, H., De Vos, W. M., and Roling, W. F. M. (2010). Microbial community- and metabolite dynamics of an anoxic dechlorinating bioreactor. *Environ. Sci. Technol.* 44, 4884–4890. doi: 10.1021/es903721s
- Maymó-Gatell, X., Anguish, T., and Zinder, S. H. (1999). Reductive dechlorination of chlorinated ethenes and 1,2-dichloroethane by “*Dehalococcoides ethenogenes*” 195. *Appl. Environ. Microbiol.* 65, 3108–3113.
- Maymó-Gatell, X., Nijenhuis, I., and Zinder, S. H. (2001). Reductive dechlorination of *cis*-1,2-dichloroethene and vinyl chloride by “*Dehalococcoides ethenogenes*”. *Environ. Sci. Technol.* 35, 516–521. doi: 10.1021/es001285i
- Men, Y., Feil, H., VerBerkmoes, N. C., Shah, M. B., Johnson, D. R., Lee, P. K. H., et al. (2012). Sustainable syntrophic growth of *Dehalococcoides ethenogenes* strain 195 with *Desulfovibrio vulgaris* Hildenborough and *Methanobacterium congolense*: global transcriptomic and proteomic analyses. *ISME J.* 6, 410–421. doi: 10.1038/ismej.2011.111
- Miyata, R., Adachi, K., Tani, H., Kurata, S., Nakamura, K., Tsuneda, S., et al. (2010). Quantitative detection of chloroethene-reductive bacteria *Dehalococcoides* spp. using alternately binding probe competitive polymerase chain reaction. *Mol. Cell. Probes* 24, 131–137. doi: 10.1016/j.mcp.2009.11.005
- Muller, J. A., Rosner, B. M., von Abendroth, G., Meshulam-Simon, G., McCarty, P. L., and Spormann, A. M. (2004). Molecular identification of the catabolic vinyl chloride reductase from *Dehalococcoides* sp. strain VS and its

- environmental distribution. *Appl. Environ. Microbiol.* 70, 4880–4888. doi: 10.1128/AEM.70.8.4880-4888.2004
- Neumann, A., Wohlfarth, G., and Diekert, G. (1998). Tetrachloroethene dehalogenase from *Dehalospirillum multivorans*: cloning, sequencing of the encoding genes, and expression of the pceA gene in *Escherichia coli*. *J. Bacteriol.* 180, 4140–4145.
- Nijenhuis, I., Nikolausz, M., Koeth, A., Felföldi, T., Weiss, H., Drangmeister, J., et al. (2007). Assessment of the natural attenuation of chlorinated ethenes in an anaerobic contaminated aquifer in the Bitterfeld/Wolfen area using stable isotope techniques, microcosm studies and molecular biomarkers. *Chemosphere* 67, 300–311. doi: 10.1016/j.chemosphere.2006.09.084
- Nishimura, M., Ebisawa, M., Sakihara, S., Kobayashi, A., Nakama, T., Okochi, M., et al. (2008). Detection and identification of *Dehalococcoides* species responsible for *in situ* dechlorination of trichloroethene to ethene enhanced by hydrogen-releasing compounds. *Biotechnol. Appl. Biochem.* 51, 1–7. doi: 10.1042/BA20070171
- Patil, S. S., Adetutu, E. M., Sheppard, P. J., Morrison, P., Menz, I. R., and Ball, A. S. (2014). Site-specific pre-evaluation of bioremediation technologies for chloroethene degradation. *Int. J. Environ. Sci. Technol.* 11, 1869–1880. doi: 10.1007/s13762-013-0383-0
- Rahm, B. G., and Richardson, R. E. (2008). *Dehalococcoides* gene transcripts as quantitative bioindicators of tetrachloroethene, trichloroethene, and *cis*-1,2-dichloroethene dehalorespiration rates. *Environ. Sci. Technol.* 42, 5099–5105. doi: 10.1021/es702912t
- Ramette, A. (2007). Multivariate analyses in microbial ecology. *FEMS Microbiol. Ecol.* 62, 142–160. doi: 10.1111/j.1574-6941.2007.00375.x
- Regeard, C., Maillard, J., and Holliger, C. (2004). Development of degenerate and specific PCR primers for the detection and isolation of known and putative chloroethene reductive dehalogenase genes. *J. Microbiol. Methods* 56, 107–118. doi: 10.1016/j.mimet.2003.09.019
- Rouzeau-Szynalski, K., Maillard, J., and Holliger, C. (2011). Frequent concomitant presence of *Desulfotobacterium* spp. and “*Dehalococcoides*” spp. in chloroethene-dechlorinating microbial communities. *Appl. Microbiol. Biotechnol.* 90, 361–368. doi: 10.1007/s00253-010-3042-0
- Rupakula, A., Kruse, T., Boeren, S., Holliger, C., Smidt, H., and Maillard, J. (2013). The restricted metabolism of the obligate organohalide respiring bacterium *Dehalobacter restrictus*: lessons from tiered functional genomics. *Philos. Trans. R. Soc. B Biol. Sci.* 368:20120325. doi: 10.1098/rstb.2012.0325
- Saiyari, D. M., Chuang, H.-P., Senoro, D. B., Lin, T.-F., Whang, L.-M., Chiu, Y.-T., et al. (2018). A review in the current developments of genus *Dehalococcoides*, its consortia and kinetics for bioremediation options of contaminated groundwater. *Sustain. Environ. Res.* 28, 149–157. doi: 10.1016/j.serj.2018.01.006
- Santharam, S., Ibbini, J., Davis, L., and Erickson, L. (2011). Field study of biostimulation and bioaugmentation for remediation of tetrachloroethene in groundwater. *Remed. J.* 21, 51–68. doi: 10.1002/rem.20281
- Scheutz, C., Durant, N. D., Dennis, P., Hansen, M. H., Jørgensen, T., Jakobsen, R., et al. (2008). Concurrent ethene generation and growth of *Dehalococcoides* containing vinyl chloride reductive dehalogenase genes during an enhanced reductive dechlorination field demonstration. *Environ. Sci. Technol.* 42, 9302–9309. doi: 10.1021/es800764t
- Schmieder, R., and Edwards, R. (2011). Quality control and preprocessing of metagenomic datasets. *Bioinformatics* 27, 863–864. doi: 10.1093/bioinformatics/btr026
- Sheu, Y., Tsang, D., Dong, C., Chen, C., Luo, S., and Kao, C. (2018). Enhanced bioremediation of TCE-contaminated groundwater using gamma poly-glutamic acid as the primary substrate. *J. Clean Prod.* 178, 108–118. doi: 10.1016/j.jclepro.2017.12.212
- Sung, Y., Fletcher, K. E., Ritalahti, K. M., Apkarian, R. P., Ramos-Hernández, N., Sanford, R. A., et al. (2006a). *Geobacter lovleyi* sp. nov. strain SZ, a novel metal-reducing and tetrachloroethene-dechlorinating bacterium. *Appl. Environ. Microbiol.* 72, 2775–2782. doi: 10.1128/AEM.72.4.2775-2782.2006
- Sung, Y., Ritalahti, K. M., Apkarian, R. P., and Löffler, F. E. (2006b). Quantitative PCR confirms purity of strain GT, a novel trichloroethene-to-ethene-respiring *Dehalococcoides* isolate. *Appl. Environ. Microbiol.* 72, 1980–1987. doi: 10.1128/AEM.72.3.1980-1987.2006
- Suyama, A., Yamashita, M., Yoshino, S., and Furukawa, K. (2002). Molecular characterization of the pceA reductive dehalogenase of *Desulfotobacterium* sp. strain Y51. *J. Bacteriol.* 184, 3419–3425. doi: 10.1128/JB.184.13.3419-3425.2002
- Terzenbach, D. P., and Blaut, M. (1994). Transformation of tetrachloroethylene to trichloroethylene by homoacetogenic bacteria. *FEMS Microbiol. Lett.* 123, 213–218. doi: 10.1111/j.1574-6968.1994.tb07224.x
- Vogel, T. M., and McCarty, P. L. (1985). Biotransformation of tetrachloroethylene to trichloroethylene, dichloroethylene, vinyl chloride, and carbon dioxide under methanogenic conditions. *Appl. Environ. Microbiol.* 49, 1080–1083.
- Wagner, D. D., Hug, L. A., Hatt, J. K., Spitzmuller, M. R., Padilla-Crespo, E., Ritalahti, K. M., et al. (2012). Genomic determinants of organohalide-respiration in *Geobacter lovleyi*, an unusual member of the *Geobacteraceae*. *BMC Genomics* 13:200. doi: 10.1186/1471-2164-13-200
- Wang, S., Chng, K. R., Wilm, A., Zhao, S., Yang, K.-L., Nagarajan, N., et al. (2014). Genomic characterization of three unique *Dehalococcoides* that respire on persistent polychlorinated biphenyls. *PNAS* 111, 12103–12108. doi: 10.1073/pnas.1404845111
- Yan, J., Ritalahti, K. M., Wagner, D. D., and Löffler, F. E. (2012). Unexpected specificity of interspecies cobamide transfer from *Geobacter* spp. to organohalide-respiring *Dehalococcoides mccartyi* strains. *Appl. Environ. Microbiol.* 78, 6630–6636. doi: 10.1128/AEM.01535-12
- Zhao, S., Ding, C., and He, J. (2017). Genomic characterization of *Dehalococcoides mccartyi* strain 11a5 reveals a circular extrachromosomal genetic element and a new tetrachloroethene reductive dehalogenase gene. *FEMS Microbiol. Ecol.* 93:fiw235. doi: 10.1093/femsec/fiw235
- Zinder, S. H. (2016). “The genus *Dehalococcoides*,” in *Organohalide-Respiring Bacteria*, eds L. Adrian and F. Löffler (Berlin: Springer), 107–136. doi: 10.1007/978-3-662-49875-0-6

**Conflict of Interest Statement:** The authors declare that the research was conducted in the absence of any commercial or financial relationships that could be construed as a potential conflict of interest.

Copyright © 2019 Hermon, Hellal, Denonfoux, Vuilleumier, Imfeld, Urien, Ferreira and Joulain. This is an open-access article distributed under the terms of the Creative Commons Attribution License (CC BY). The use, distribution or reproduction in other forums is permitted, provided the original author(s) and the copyright owner(s) are credited and that the original publication in this journal is cited, in accordance with accepted academic practice. No use, distribution or reproduction is permitted which does not comply with these terms.



# Changes in Bacterioplankton Communities Resulting From Direct and Indirect Interactions With Trace Metal Gradients in an Urbanized Marine Coastal Area

Clément Coclet<sup>1,2</sup>, Cédric Garnier<sup>1</sup>, Gaël Durrieu<sup>1</sup>, Dario Omanović<sup>3</sup>, Sébastien D'Onofrio<sup>1</sup>, Christophe Le Poupon<sup>1</sup>, Jean-Ulrich Mullot<sup>4</sup>, Jean-François Briand<sup>2</sup> and Benjamin Misson<sup>1\*</sup>

## OPEN ACCESS

### Edited by:

Stéphane Pesce,  
National Research Institute of Science  
and Technology for Environment  
and Agriculture (IRSTEA), France

### Reviewed by:

Yonghong Bi,  
Institute of Hydrobiology (CAS), China  
Emilie Lyautey,  
Université Savoie Mont Blanc, France

### \*Correspondence:

Benjamin Misson  
misson@univ-tln.fr

### Specialty section:

This article was submitted to  
Microbiotechnology, Ecotoxicology  
and Bioremediation,  
a section of the journal  
Frontiers in Microbiology

**Received:** 04 September 2018

**Accepted:** 31 January 2019

**Published:** 22 February 2019

### Citation:

Coclet C, Garnier C, Durrieu G,  
Omanović D, D'Onofrio S,  
Le Poupon C, Mullot J-U, Briand J-F  
and Misson B (2019) Changes  
in Bacterioplankton Communities  
Resulting From Direct and Indirect  
Interactions With Trace Metal  
Gradients in an Urbanized Marine  
Coastal Area.  
Front. Microbiol. 10:257.  
doi: 10.3389/fmicb.2019.00257

<sup>1</sup> Mediterranean Institute of Oceanography (MIO), UM110, CNRS, IRD, Université de Toulon, Aix-Marseille Université, Marseille, France, <sup>2</sup> MAPIEM, EA 4323, Université de Toulon, Toulon, France, <sup>3</sup> Division for Marine and Environmental Research, Ruđer Bošković Institute, Zagreb, Croatia, <sup>4</sup> LASEM-Toulon, Base Navale De Toulon, Toulon, France

Unraveling the relative importance of both environmental conditions and ecological processes regulating bacterioplankton communities is a central goal in microbial ecology. Marine coastal environments are among the most urbanized areas and as a consequence experience environmental pressures. The highly anthropized Toulon Bay (France) was considered as a model system to investigate shifts in bacterioplankton communities along natural and anthropogenic physicochemical gradients during a 1-month survey. In depth geochemical characterization mainly revealed strong and progressive Cd, Zn, Cu, and Pb contamination gradients between the entrance of the Bay and the north-western anthropized area. On the other hand, low-amplitude natural gradients were observed for other environmental variables. Using 16S rRNA gene sequencing, we observed strong spatial patterns in bacterioplankton taxonomic and predicted function structure along the chemical contamination gradient. Variation partitioning analysis demonstrated that multiple metallic contamination explained the largest part of the spatial biological variations observed, but DOC and salinity were also significant contributors. Network analysis revealed that biotic interactions were far more numerous than direct interactions between microbial groups and environmental variables. This suggests indirect effects of the environment, and especially trace metals, on the community through a few taxonomic groups. These spatial patterns were also partially found for predicted bacterioplankton functions, thus indicating a limited functional redundancy. All these results highlight both potential direct influences of trace metals contamination on coastal bacterioplankton and indirect forcing through biotic interactions and cascading.

**Keywords:** coastal ecosystem, metal contamination gradients, bacterioplankton community structure, functional prediction, co-occurrence network

## INTRODUCTION

Marine coastal areas are increasingly subjected to anthropogenic pressures that usually result in human-induced chemical contamination. Increasing demographic pressure and both terrestrial and marine activities threaten marine ecosystems (Halpern et al., 2008; The MerMex Group et al., 2011). Urban and industrial wastes (Levin et al., 2001; Oursel et al., 2013), biocides released by antifouling coatings (Turner, 2010) and fuel from nautical traffic (Callender, 2003) as well as historical pollution accumulated in the sediment compartment (Xu et al., 2014; Dang et al., 2015) are well-known and widespread examples. Such chemical contamination represents an increasing threat for marine coastal areas, and microorganisms inhabiting these ecosystems (Misson et al., 2016; Othman et al., 2017; Coclet et al., 2018).

Microbial communities have been shown to be a major component of marine planktonic ecosystems (Fuhrman and Azam, 1980), variable across space (Pommier et al., 2007; Ghiglione et al., 2012) and time (Fuhrman et al., 2006; Fortunato et al., 2012; Gilbert et al., 2012). Multiple environmental factors are known to drive temporal and spatial dynamics in bacterioplankton, such as salinity (Lozupone and Knight, 2007), temperature (Fuhrman et al., 2008; Gilbert et al., 2009), depth (Treich et al., 2009), grazing, and predation (Zubkov and López-Urrutia, 2003) and resource availability (Fortunato et al., 2012; Gilbert et al., 2012; Chow et al., 2013).

Bacterioplankton communities have been largely characterized spatially or temporally in various environments, but rarely assessed over both spatial and temporal scales in a marine coastal area. These ecosystems are usually characterized by natural gradients linked to the continent-sea interface and if anthropized by a complex set of chemical contaminants, potentially affecting marine microbial communities. The links between benthic microbial communities and trace metal contamination have been extensively revealed (Gough and Stahl, 2011; Pringault et al., 2012; Quero et al., 2015; Misson et al., 2016). But how the marine bacterioplankton communities responds to trace metal exposure was scarcely investigated in coastal marine environments (Wang et al., 2015; Qian et al., 2017). Moreover, chemical perturbation on bacterioplankton communities is supposed to be complex because multiple trace metallic contaminations of the water column can result in additive, synergistic or antagonistic effects (Franklin et al., 2002; Lorenzo et al., 2002). Effects of trace metals can be dependant of hydrology, seasonal, and environmental conditions (Cloern, 2001). Furthermore, the impact of contamination on bacterioplankton may also be influenced by bacterio-phytoplankton coupling. Consequently, effects of contaminants on phytoplankton, which is sensitive to trace metal contamination (Coclet et al., 2018) might have indirect consequences for bacterioplankton.

Despite several studies describing microbial taxonomic diversity in marine coastal environments, functional diversity has not been investigated intensely (Jeanbille et al., 2016). Elucidating both taxonomic and functional diversity of microbial

communities is the key to understand their roles in the ecosystem (Wang et al., 2016). Recent studies have related functional diversity of microbial communities to specific habitats (Dinsdale et al., 2008), water column zone (Louca et al., 2016), seasonal changes (Ward et al., 2017) and nutrient gradients (Thompson et al., 2017; LeBrun et al., 2018). However, relationships between trace metal contamination and functional profiles related to taxonomy in seawater ecosystems are still lacking.

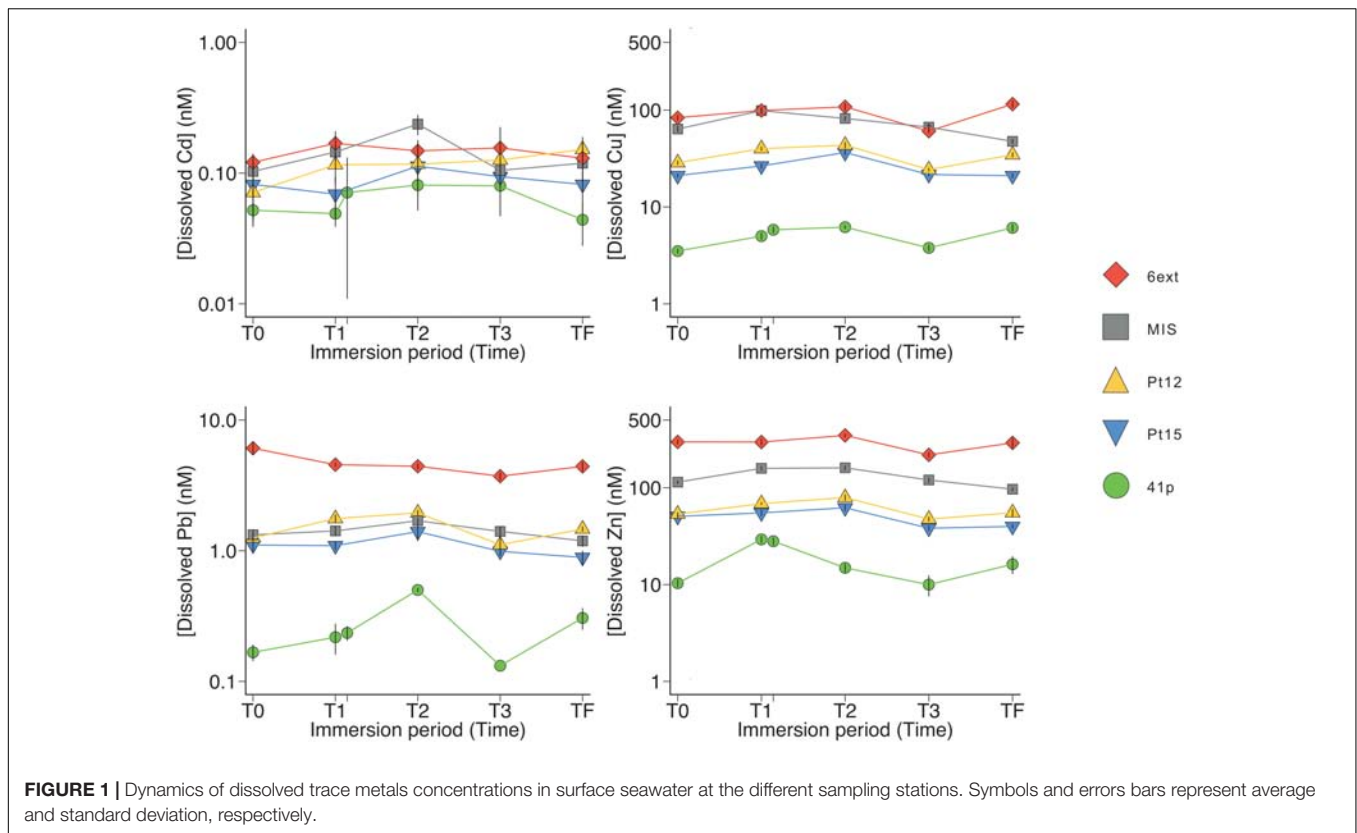
Trace metals contamination was studied in a number of previous studies where authors mention benthic (Pringault et al., 2012; Besaury et al., 2014; Misson et al., 2016), phytoplanktonic (Othman et al., 2017) or freshwater communities (Wang et al., 2018). This study represents the first comprehensive assessment of bacterioplankton communities living in a contaminated marine coastal ecosystem. We combined in-depth physicochemical and geochemical characterizations of Toulon Bay seawater (north-western Mediterranean Sea), flow cytometry microbial enumerations and 16S rRNA gene-based high-throughput sequencing water samples over a weekly sampling campaign (weekly during 2015, June). The objectives of the study were (i) to study both spatial and temporal patterns in bacterioplankton communities along the contaminated Toulon Bay, (ii) to reveal the main environmental factors driving bacterioplankton communities, more precisely the contribution of trace metals through direct or indirect effects; and (iii) to identify the predicted functional profile's response of bacterioplankton communities to chemical contamination in order to assess its influence on the ecosystem functioning.

## MATERIALS AND METHODS

### Study Area and Sample Collection

Located in the south of France, Toulon Bay is divided into two basins by an artificial seawall: the Little Bay, which is semi-enclosed, and the Large bay, which opens onto the Mediterranean Sea (**Supplementary Figure S1**). The Little Bay is characterized by a high level of anthropic activities (Navy harbor, ferry transport, industries, wastewater sewage, and aquaculture). Due to its location, the Little Bay is directly impacted by pollution and is less affected than the Large Bay by offshore hydrodynamics. This confers to the Little bay a higher trace metal contamination than the Large Bay as demonstrated previously in the sediments and with punctual measurements in the water column (Tessier et al., 2011; Coclet et al., 2018).

Sampling was performed weekly from June 1st to 29th June, 2015. Two liters of seawater from the surface (1 m depth) and the bottom (1 m above sediment) of the water column were sampled at five sites across Toulon Bay (North-Western Mediterranean Sea, France), from the entrance of the bay to the north-western anthropized area (**Supplementary Figure S1, Supplementary Table S1**, and details in **Supplementary Material**). After the T1 sampling in site 41p, the French Navy performed an exercise that could have modified the water quality. In order to check that, we sampled again the water (T1b). The five sites were chosen to cover the whole range of dissolved metal contamination on



the basis of trace metal distribution previously evaluated in Toulon Bay surface seawater (Coclet et al., 2018; **Figure 1**). Water samples were stored in a cooler and filtered through 0.2  $\mu\text{m}$  polycarbonate membranes (Millipore). Filters were stored at  $-80^{\circ}\text{C}$  until DNA extraction. Physico-chemical parameters including metals were weekly analyzed during the sampling period in order to characterize the environment (details in **Supplementary Material**). Standard oceanographic properties, including water temperature ( $^{\circ}\text{C}$ ), salinity,  $\text{O}_2$  ( $\text{mg L}^{-1}$  and %), pH, and chlorophyll *a* (*chl a*) ( $\mu\text{g L}^{-1}$ ) were measured on sites using a multi-parameter probe (Hydrolab DS5, OTT).

### Bacterial Community Abundance by Flow Cytometry

Subsamples of 10 mL of seawater were sampled at each site, depth, and date, filtered through a 90  $\mu\text{m}$  nylon mesh, fixed with 0.25% (final concentration) glutaraldehyde on field and stored at  $-80^{\circ}\text{C}$  until flow cytometry analysis. Autotrophic prokaryotes (*Synechococcus*-like), eukaryotic phytoplankton (picoeukaryotes and nanoeukaryotes) populations were characterized and enumerated using a BD Accuri<sup>TM</sup> C6 (BD Biosciences) flow cytometer, as previously described (Coclet et al., 2018). Heterotrophic prokaryotes were enumerated after staining with SYBR Green as previously described (Cabrol et al., 2017).

### Bacterial Community Composition

DNA was extracted from the Millipore filters by a combination of enzymatic cell lysis (Ghiglione et al., 2009) and AllPrep

DNA/RNA Mini Kit (QIAGEN) according to the manufacturer's instructions. The protocol for the DNA extraction and the library preparation is fully described in **Supplementary Material**. We assessed bacterial community composition (BCC) by targeting the V4–V5 region of the 16S rRNA gene (Parada et al., 2016) and using Illumina Miseq 2  $\times$  250 pb paired-end sequencing (Genoscreen, France).

Sequences were then demultiplexed and assigned to corresponding samples using CASAVA (Illumina). Forward and reverse reads were merged using PEAR 0.9.8 with default options (Zhang et al., 2014). Raw sequences were analyzed using MacQiime v.1.9.1 software (Caporaso et al., 2010). Briefly, barcode, primer, shorter sequences (<100 bp in length), and sequences with ambiguous base calls or homopolymer runs exceeding 10 bp were removed. The remaining sequences were assigned to operational taxonomic units (OTUs) and clustered at a 97% threshold using Uclust algorithm (Edgar, 2010), both closed and open reference OTU picking, based on the SILVA (release 128) database (Pruesse et al., 2007; Quast et al., 2013). Low abundance OTU (<0.005%) were filtered as recommended by Bokulich et al. (2013). Sequences classified as mitochondria or chloroplast were removed from the OTU table, corresponding to 3393 OTUs. A total of 349,009 reads were finally obtained representing 31,132 OTUs. OTU table was normalized by random subsampling to the smallest number of sequences (i.e., 4044). Samples with lower number of sequences were discarded ( $n = 16$ ), 36 samples were remaining for following analyses (**Supplementary Table S1**).

The 16S rRNA gene sequences have been deposited in the NCBI Sequence Read Archive (SRA) database under BioProject ID PRJNA514222<sup>1</sup>.

## Data Analysis

All plots and statistical analysis were done in R RStudio (R Core Team, 2015). Alpha diversity calculations and error estimates were averaged, using QIIME script *core\_diversity\_analyses.py* (Caporaso et al., 2010), including estimates of rarefaction, Chao1, equitability, Shannon, and Simpson's diversity. In order to compare the sites based on their chemical composition, taxonomic and functional community profiles, seawater samples were sorted in a non-metric multidimensional scaling (NMDS). Pairwise dissimilarities were calculated using Bray–Curtis metrics. Each resulting dissimilarity matrix was used to visualize sample differences via NMDS ordination using the “vegan” package in R (Oksanen et al., 2016). To test the null hypothesis that there were no significant difference between the groups discriminated according to sampling stations, sampling dates, and depth, similarities were analyzed by global and pairwise PERMANOVA tests, using “vegan” and “RVAideMemoire” packages, respectively.

To identify taxa that discriminated the sampling sites, the linear discriminant analysis (LDA) effect size method (LEfSe) (Segata et al., 2011) was used. This was performed with the LEfSe online tool in the Galaxy framework, using all default setting for data formatting and LDA effect size (Goecks et al., 2010). A similarity percentage (SIMPER) was run with a 90% cutoff and used to rank the percent contribution of individual biomarker to the dissimilarity between site differences (Clarke, 1993).

To investigate the relationships between BCC and measured environmental variables, Spearman rank correlation analysis, and redundancy analysis (RDA) were performed using the “vegan” package in R (Oksanen et al., 2016) (details in **Supplementary Material**). Briefly, for variable reduction and in order to create an efficient model from the most significant explanatory variables, vegan's ordistep function were applied and among the 31 explanatory variables, 20 significant variables ( $P < 0.05$ ) were kept for the following analyses. The RDA model was tested by performing partial RDA, and variation partitioning to test the significance of the contribution of both groups of variables and each individual variable.

Interactions among the OTUs and between these OTUs and the 31 environmental variables were evaluated using CoNeT (Co-occurrence Network) plugin 1.1.1.beta (Faust et al., 2012), a plugin in a Cytoscape software 3.4.0. A similarity matrix was built with different metrics (Spearman correlation and Kullback–Leibler distance and a mutual information score) from OTUs. This initial network was re-defined by randomization. A permutation matrix representing a null distribution was obtained by resampling OTUs as described in Faust et al. (2012). In a permutation step, edge specific  $p$ -values were computed; however, for the final network,  $p$ -values of an edge were merged into one  $p$ -value according to Brown's method. In the final step, the

Benjamini–Hochberg multiple testing correction was applied ( $P < 0.05$ ). Network characterization was evaluated using betweenness centrality (BC) and closeness centrality (CC) (details in **Supplementary Material**). Highly connected clusters were identified using the MCODE plugin version 1.4.0.beta2 (Smoot et al., 2011). Network characterization were evaluated using different topological indexes generated by Network Analyzer plugin.

Functional profiles were predicted from obtained 16S rRNA gene data using Tax4Fun (Aßhauer et al., 2015) based on KEGG category.

## RESULTS

### General Characteristics of Toulon Bay Seawater Samples

An increase in the trace metal concentrations was rationally observed from a reference site open on the sea with low metal concentrations (41p) to enclosed sites in the most anthropized area (MIS and 6ext) with high level of contaminations (**Figure 1**). The highest trace metal concentrations found in surface seawater were Zn, Cu, Pb, and Cd, while other metals/metalloids (As, Ba, Be, Cs, Cr, Mn, Sb, Sn, Ti, U, and V) were kept to concentration levels close to the geochemical background (**Figure 1** and **Supplementary Table S2**). At the surface of seawater, Cd, Cu, Zn, and Pb concentrations were 6, 33, 35, and 48 times higher in 6ext water than in 41p water, respectively. These enrichment factors were quite similar (8, 25, 43, and 73 times) at the bottom of the seawater (**Supplementary Figure S2**). For both surface and bottom seawater, the concentrations of trace metals/metalloids were relatively stable during the sampling period (**Figure 1**, **Supplementary Figure S2**, and **Supplementary Table S2**). The most contaminated sites MIS and 6ext were significantly discriminated from the reference site 41p (PERMANOVA,  $P < 0.01$ ) (**Supplementary Figure S3A**) and from sampling date (**Supplementary Figure S3B**) but not with depth (**Supplementary Figure S3C**).

Seawater temperature increased gradually during the studied period at all five sites, from 18.8°C–21.2°C in T0 to 22.0°C–24.3°C in TF (**Supplementary Figure S4**). Additionally, temperature was lower ( $1.9 \pm 0.04^\circ\text{C}$ ) in bottom than in surface seawater. Surface salinity levels demonstrated low variations ( $38.4 \pm 0.11$ ). A very punctual drop was recorded in all sites at T2, down to 36.7 in MIS (**Supplementary Figure S4**). Chlorophyll *a* in surface seawater were lower in 41p ( $0.16$  to  $0.31 \text{ mg L}^{-1}$ ) than in other sites ( $0.59$  to  $2.08 \text{ mg L}^{-1}$ ). Additionally, chlorophyll *a* concentrations peaked in all sites at the middle of the survey. Except for 41p, chlorophyll *a* concentrations were higher at the bottom seawater than at the surface (**Supplementary Figure S4**). On average, in surface seawater, higher concentrations of DOC were found in 6ext ( $1.4 \pm 0.07 \text{ mg L}^{-1}$ ) compared to 41p ( $1.2 \pm 0.06 \text{ mg L}^{-1}$ ) (**Supplementary Figure S4**). Similarly, higher concentrations of TN were found in MIS ( $0.15 \pm 0.02 \text{ mg L}^{-1}$ ) compared to 41p. ( $0.08 \pm 0.02 \text{ mg L}^{-1}$ ) (**Supplementary Figure S4**).

<sup>1</sup><https://www.ncbi.nlm.nih.gov/biosample/10721482>

No significant difference was found in dissolved oxygen concentrations ( $\text{mg L}^{-1}$ , %), and pH between both all five sites and all sampling date (**Supplementary Table S2**).  $\text{NO}_3^-$  and  $\text{PO}_4^{3-}$  concentrations were below the detection limit (0.02 and 0.020  $\mu\text{M}$ , respectively) in a majority of samples. As a consequence, they are not presented and will not be considered further.

## Bacterial Community Dynamics

Heterotrophic bacterioplankton abundances estimated using flow cytometry are shown in **Supplementary Figure S5**. We observed an increase in the bacterioplankton abundance from the reference site 41p ( $3.8 \times 10^5$  to  $4.2 \times 10^5$  cell  $\text{mL}^{-1}$ ) to the most enclosed site 6ext ( $8.0 \times 10^5$  to  $1.4 \times 10^6$  cell  $\text{mL}^{-1}$ ) in both surface and bottom seawater. Additionally, heterotrophic bacterioplankton abundance was stable in 41p during the experiment whatever the depth, while strong dynamic was observed in both surface and bottom 6ext seawater, with highest abundances in T2 and T3, respectively.

Over the sampling, observed richness, and Chao1 index (**Supplementary Figure S6**) were significantly higher in the uncontaminated site 41p and declined to less than half compared to 6ext (ANOVA,  $P < 0.01$ ). In contrast, Shannon, Simpson, and evenness indexes did not significantly vary between sampling sites (**Supplementary Figure S6**).

NMDS results showed a significant segregation of bacterioplankton communities between both sampling sites (PERMANOVA;  $P = 0.001$ ) and dates (PERMANOVA;  $P = 0.024$ ) but not with depths (PERMANOVA;  $P = 0.983$ ) (**Figure 2A** and **Supplementary Table S3**). More precisely, pairwise PERMANOVA tests (**Supplementary Table S3**) confirmed significant differences between the reference 41p site and all other sites (PERMANOVA;  $P < 0.05$ ) and significant differences between 6ext and Pt12–Pt15 (PERMANOVA;  $P < 0.05$ ).

The most abundant phyla ( $> 1\%$  of all sequences across all samples) were *Proteobacteria* ( $53 \pm 1.1\%$ ), followed by *Bacteroidetes* ( $28 \pm 1.1\%$ ), *Cyanobacteria* ( $9.1 \pm 0.7\%$ ), *Actinobacteria* ( $6.1 \pm 0.6\%$ ), and *Verrucomicrobia* ( $3.0 \pm 0.3\%$ ). At the family level (**Figure 2B**), *Flavobacteriaceae* comprised the majority ( $22 \pm 1.1\%$ ) of the total sequences, followed by *Alphaproteobacteria* groups SAR11 Surface 1 clade ( $18 \pm 1.1\%$ ), *Rhodobacteraceae* ( $13 \pm 0.65\%$ ) and SAR116 clade ( $6.1 \pm 0.49\%$ ). *Cyanobacteria*, *Actinobacteria*, and *Verrucomicrobia* phyla were dominated by *Synechococcus* Family I ( $9.1 \pm 0.72\%$ ), *Microbacteriaceae* ( $4.9 \pm 0.71\%$ ), and *Puniceococcaceae* ( $1.7 \pm 0.19\%$ ). Archaea represented less than 0.1% of the total sequences, thus they were considered as “Others” in this study and variations of this group have not been taken into consideration.

Clear shifts in the relative abundance of individual bacterioplankton OTUs were observed between sampling sites. Using LEfSe analysis, we determined 43 differentially abundant taxa between four sites. 41p and 6ext, the two most geochemically contrasted sites, exhibited the highest number of taxonomic indicators (25 and 6, respectively) (**Figure 3**). For 41p site, the most significantly enriched bacterioplankton

sequences were Acidimicrobiia *Candidatus Actinomarina*, members of the family SAR406, 7 Alphaproteobacteria OTUs and Gammaproteobacteria *Thiothrix*. Actinobacteria *Candidatus Aquilina* and both Flavobacteriia *Formosa* and Betaproteobacteria *Hydrogenophilaceae* were found to be overrepresented in MIS and 6ext, respectively. SIMPER analysis revealed that, on average, 13 biomarkers were identified as major contributors to differences between sites detected in the NMDS. The higher number of biomarkers identified as major contributors was found between 41p and the other sampling sites (between 17 and 32 biomarkers) (**Supplementary Table S4**). Overall, each biomarker contributed to at least 1% of the dissimilarity between sites. *Candidatus Aquilina*, PS1 clade, NS7 marine group, *Planktomarina* and *Tenacibaculum*, notably, drove together more to 32% of disparity between cluster 41p and the other clusters (Pt15, 6ext, and MIS).

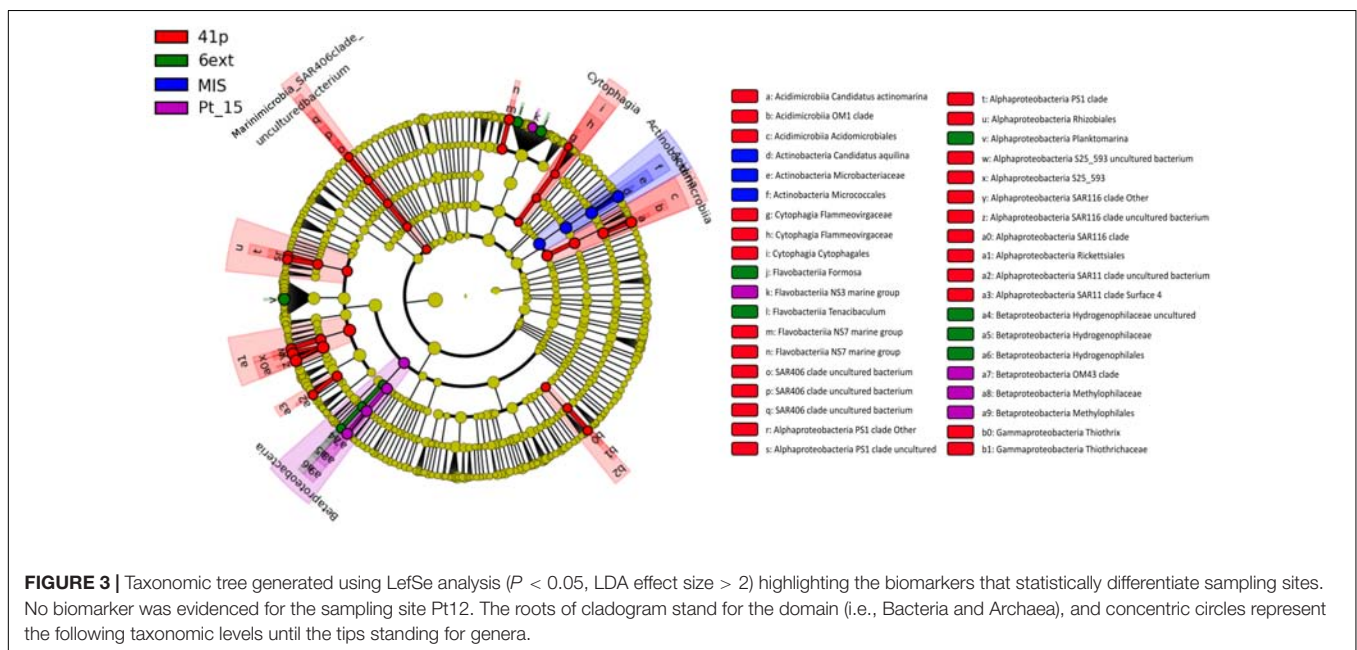
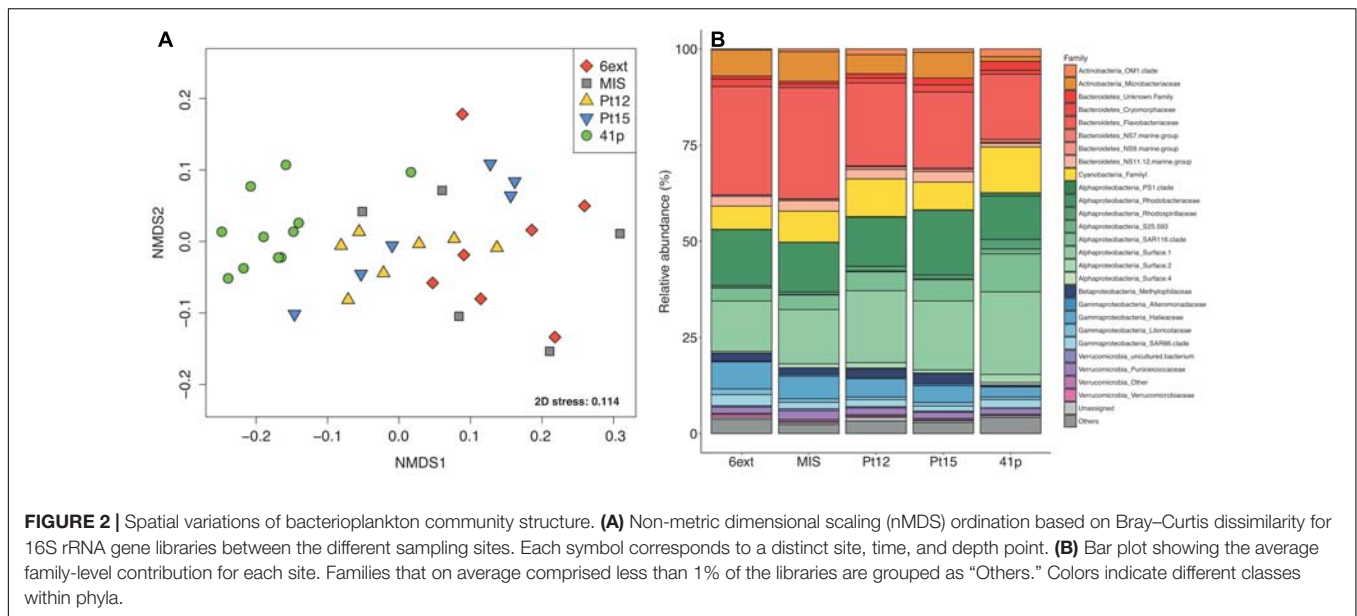
## Bacterial Community Composition (BCC) in Relation With Environmental Variables

Among the 31 environmental variables available for multivariate analysis, 20 parameters were selected by pairwise correlations. The first and the second axes of RDA captured 47.1% and 6.4% of BCC variance, respectively (**Figure 4A**).

Variation partitioning provided more details about the relative contributions of nutrients, contaminants, terrigenous, and “others” factors in the observed spatial changes in BCC (**Figure 4B**). The combination of the four sets of explanatory variables explained 41% of BCC variation across sites. Among the set of explanatory variables, contaminants were the main contributors to variations in BCC (30%). Contaminants also appeared to have significant influence on BCC through their interaction with the other sets of variables. The contribution of terrigenous (19.6%), nutrient and biotic (15.0%) and “marine tracers” (21.6%) variables were also significant but to a lower extent than the contribution of contaminants variables. The highest individual contributions were attributed to Mn (1.2%), DOC (1.2%), salinity (1.1%), Zn (1.1%), and Cd (1.0%) (**Supplementary Table S5**). Thus, among the five explanatory variables which contributed the most to the biological variation, three variables were contaminants (Mn, Cu, and Cd).

Network analysis resulted in a global network representing 158 OTUs and 21 environmental variables significantly connected. Among 1664 edges, 92% were inter taxa edges, and 8% represented taxon-environment interactions. Most of the connections (67%) corresponded to negative interactions. To visualize the results, eight subnetworks were extracted from the global network (**Figure 5** and **Supplementary Figure S7**).

Globally, by plotting BC vs. CC, 12 OTUs with the highest values for both parameters (arbitrarily determined as  $\text{BC} > 0.02$  and  $\text{CC} > 0.5$ ) were selected, representing putative keystone species within Toulon Bay (**Supplementary Table S6**). Both of these indices indicate that SAR11 Surface 1 clade and *Rhodobacteraceae* (Alphaproteobacteria), *Synechococcus* (Cyanobacteria), *Candidatus Aquilina* (Actinobacteria), and *Balneola* (Bacteroidetes) were central in this network.



Most of Alphaproteobacteria, including SAR11, SAR116, and *Rhodobacteraceae*, and Cyanobacteria *Synechococcus* were positively correlated with each other, but negatively correlated with Bacteroidetes (NS11-12 and NS5 marine group, *Cryomorphaeaceae* and *Balneola*), and Actinobacteria (*Candidatus Aquilina*).

In the subnetworks, there were 19 correlations with contaminants (8 with Pb, 6 with Cu, 3 with Cd, and 2 with Zn) and two correlations with chlorophyll *a*. Several taxa that were identified as being key drivers of community dissimilarity using LefSe analysis were highly correlated to contaminants. In particular, the Alphaproteobacteria *Rhodobacteraceae* and SAR11, the

Bacteroidetes *Balneola* and the Cyanobacteria *Synechococcus* showed negative correlations with at least one of the contaminants (Cd, Cu, Pb, or Zn). Conversely, Actinobacteria *Candidatus aquilina* and Bacteroidetes NS11-12 marine group were positively correlated with Pb and Cu, respectively. Gammaproteobacteria *Haliaceae* was positively correlated with Cd.

### Bacterioplankton Predicted Functional Capabilities of Microbial Communities

The functional profiles of bacterioplankton communities was predicted using Tax4Fun (Aßhauer et al., 2015).

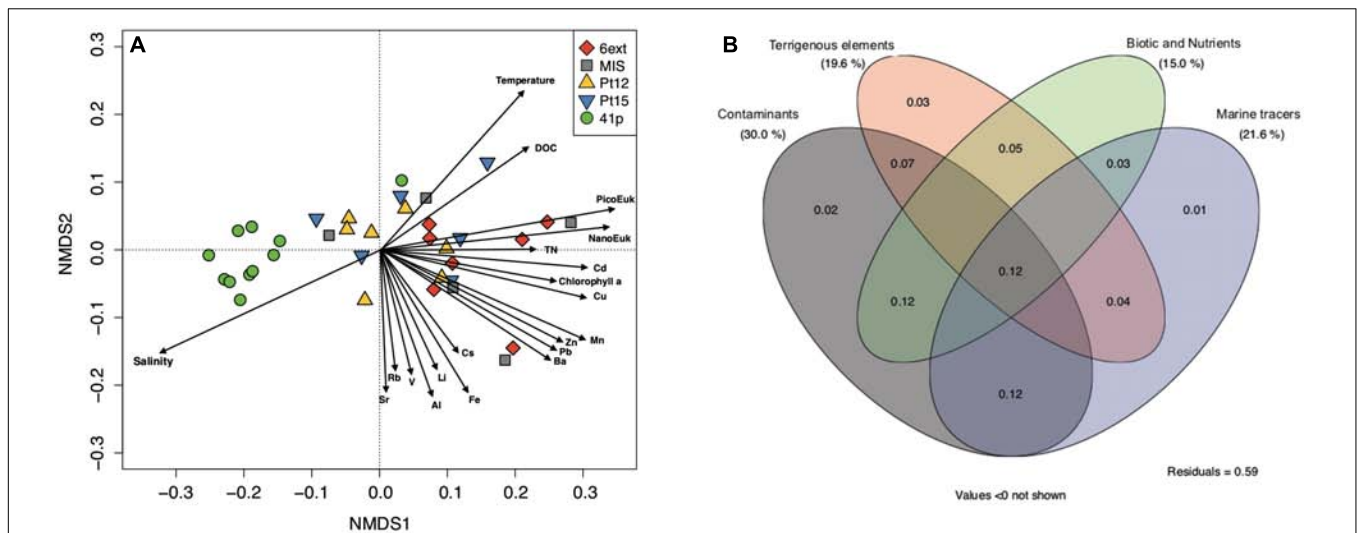
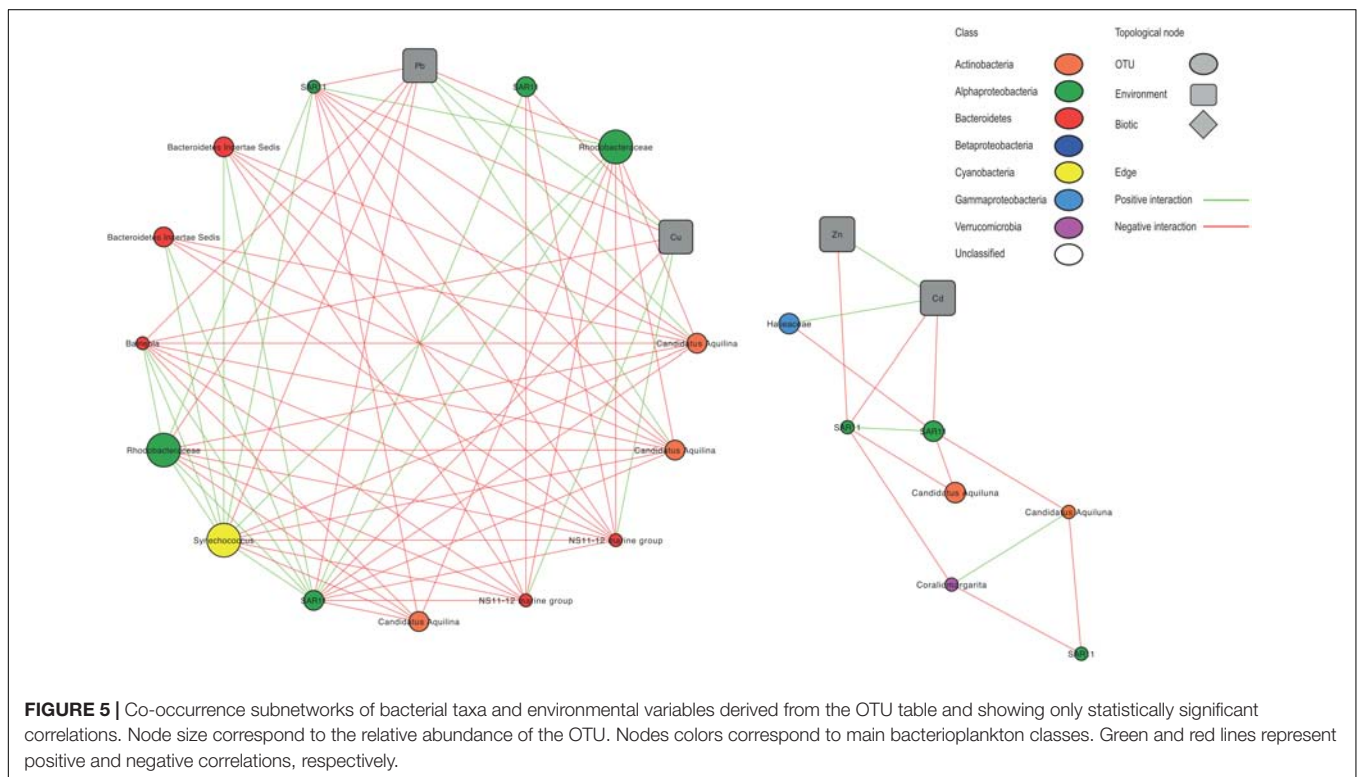
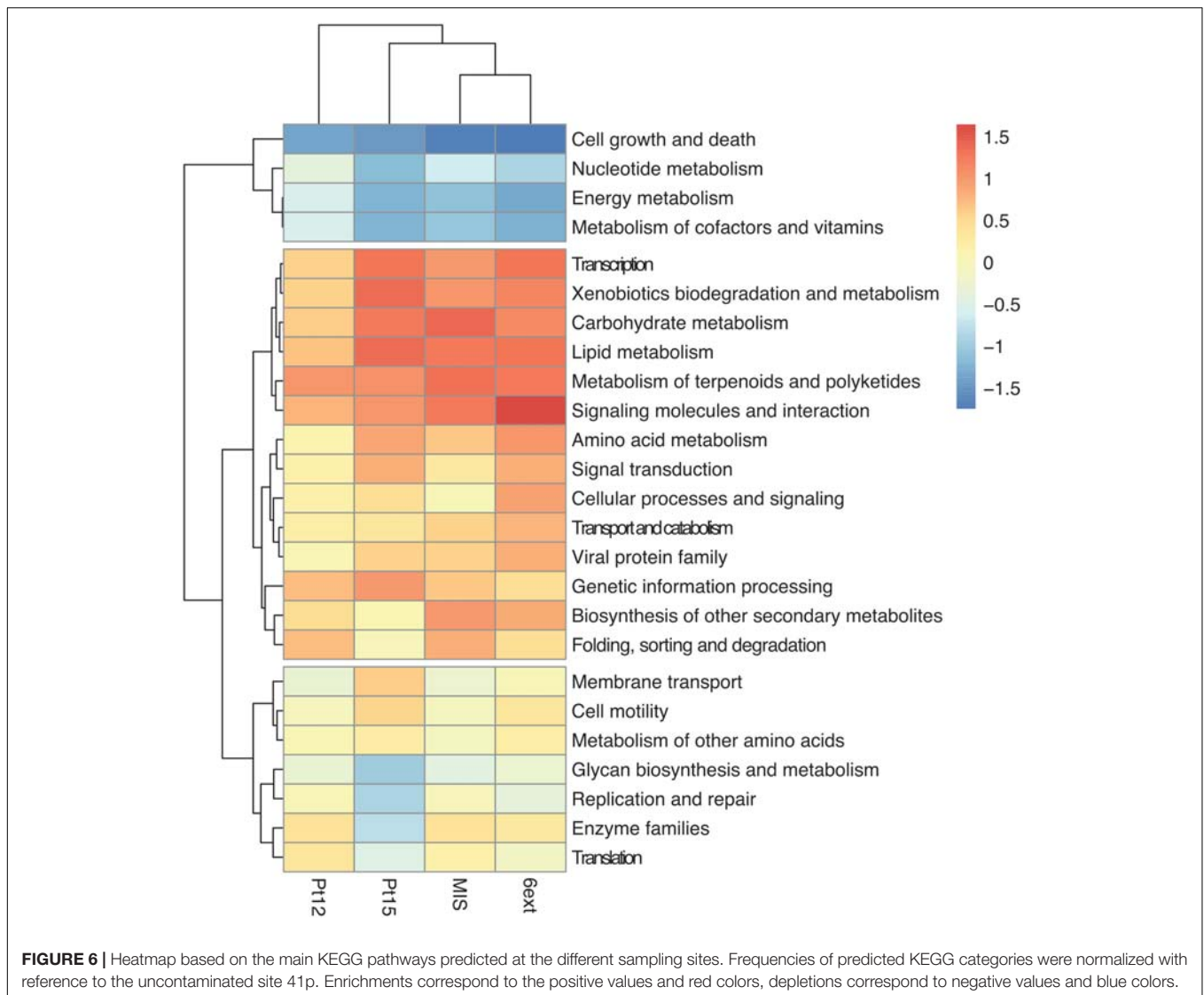


**FIGURE 4 |** Contributions of environmental variables to spatial differentiation in bacterioplankton community structure. **(A)** Redundancy analysis (RDA) ordination diagram of the first two axes for bacterioplankton community composition. The percentage of the spatial variation in community structure explained by each axis is indicated in parentheses after the axis label. The constrained sets of environmental variables analyzed are indicated as vectors. NanoEuk: Nanoeukaryote abundance; PicoEuk: Picoeukaryotes abundance. **(B)** Venn diagram showing the variation partitioning (%) of the spatial variations in bacterioplankton community structure among four environmental datasets (Contaminants, Terrigenous elements, Marine tracers, and Nutrient and Biotic).



Predicted functions were classified as KEGG orthologs (KOs) resulting in the identification of 3619 KOs across all samples, using on average,  $60 \pm 12\%$  of total OTUs (Supplementary Table S7). Clustering showed that the differentiation of the sampling sites based on microbial predicted function profiles followed the chemical gradient

described earlier, from the reference site toward the most enclosed and contaminated 6ext site (Figure 6). Compared to the uncontaminated site (41p), used here as a reference, some KEGG pathways seemed overrepresented in contaminated sites: Carbohydrate metabolism, Xenobiotics biodegradation and metabolism, Metabolism of terpenoids,



and polyketides. Other KEGG pathways were found to be underrepresented as “Cell growth and death,” “Nucleotide metabolism,” “Energy metabolism,” and “Metabolism of cofactors and vitamins.”

## DISCUSSION

Bacterioplankton community composition and associated functions in highly metal contaminated ecosystems were scarcely studied (Nayar et al., 2004; Boyd et al., 2005; Pringault et al., 2016), even less using NGS techniques (Wang et al., 2015; Qian et al., 2017). This study was performed in a multi contaminated coastal area, Toulon Bay, which presents far wider contamination gradients than natural environmental gradients. By combining seawater physicochemical and geochemical analyses with patterns of bacterioplankton diversity and predicted functions, we provide an innovative insight into bacterioplankton

ecology allowing to better understand how trace metals could shape communities.

## Trace Metal Contaminations as Drivers of Bacterioplankton Communities

Marine coastal areas are seen as valuable sentinel ecosystems, providing signals that reflect anthropogenic chemical pollution (The MerMex Group et al., 2011). Concentrations of trace metals in the Toulon Bay were found to be at least comparable or higher to those reported in aquatic ecosystems receiving high contamination loads (Boyd et al., 2005; Pringault et al., 2012). The high enrichment factors (6- to 234-fold) compared to the geochemical background of the Mediterranean Sea (Morley et al., 1997) indicated significant anthropogenic inputs that could be attributed to numerous recent (e.g., large boat traffic, harbor activities, antifouling coatings) (Turner, 2010) and historical events (2nd World War) (Tessier et al., 2011). Thus,

we hypothesized a potential effect of trace metals on the bacterioplankton communities.

As previously reported in coastal waters (Nayar et al., 2004; Caroppo et al., 2006; Pringault et al., 2016), bacterioplankton was more abundant in the most contaminated zones (MIS and 6ext) than in the uncontaminated site 41p. Bacteria have been reported to have a wide range of metal detoxification or resistance mechanisms by sequestering, excluding or precipitating metals (Nies, 1999). The higher abundance in contaminated sites could therefore suggest that the community is well adapted. Moreover, bioavailability of trace metals could also contribute to explain the absence of bacterioplankton abundance decrease in the most contaminated sites in term of abundance. Trace metals bioavailability is strongly controlled by the presence of dissolved organic ligand, especially in marine waters (Louis et al., 2009; Bruland et al., 2013). We considered here DOC concentrations and the dissolved fraction of trace metals, which is closer to the bioavailable fraction than the total concentration (Paquin et al., 2002; Cindrić et al., 2017) and consequently allow a more reliable assessment of their roles. Nevertheless, we neither evaluated the speciation of the main trace metals nor DOC composition in this study. More work will be thus needed to state about the respective contributions of bioavailability modulation and community adaptation in the bacterial abundance increase in Toulon Bay.

While bacterioplankton diversity did not show any significant trend along the contamination gradient, the community richness (Chao1 index) was shown to decrease progressively from the uncontaminated site (41p) toward the most contaminated sites (MIS and 6ext). A similar pattern was observed in South-Eastern Australia in metal- and PAH-contaminated sediments (Sun et al., 2012) as well as in contaminated sediments in the Northern Adriatic Sea (Korlević et al., 2015). This may be interpreted in light of classis disturbance theory that predict that in highly disturbed ecosystems, richness would decrease and a few species would dominate (Odum, 1985; Allison and Martiny, 2008). As a matter of fact, sensitive species are expected to be lost whereas tolerant species benefit from emptying ecological niches (Atlas et al., 2015). Thus, the multi-contamination appeared to have disruptive effect on the alpha diversity of the bacterioplankton communities.

Gillan et al. (2005) demonstrated that alpha-diversity alone is a poor indicator of ecosystem stress in chronically polluted systems, as the proliferation of new tolerant species can lead to a recovery of the diversity. As in many coastal sites, microbial assemblages in our study were dominated by a few families *Flavobacteriaceae*, SAR11 Surface 1 clade, *Rhodobacteraceae*, SAR116 clade, *Synechococcus* Family I, and *Microbacteriaceae*. This is a core of generalist families in marine seawater and its members have been found abundant in numerous other marine coastal studies (Chow et al., 2013; Cram et al., 2015). Despite overall similarities, BCC was strongly affected by trace metal contamination, the five sampling sites clearly exhibited distinct microbial community's structures, along low-to-high contamination continuum. This observation is also in agreement with the disturbance hypothesis, as discussed for

alpha diversity, and tends to complement previous observations of the structural role of contaminants for bacterioplankton in other coastal areas (Pringault et al., 2016; Marisol et al., 2018; Wang et al., 2018).

The uncontaminated site (41p) was characterized by higher relative abundances of OMI clade (Acidimicrobiia), SAR11, Rickettsiales, Rhizobiales, and *Rhodobacteraceae* (Alphaproteobacteria), *Thiothrichaceae* (Gammaproteobacteria), and *Synechococcus* (Cyanobacteria). Correspondingly, a number of previous works reported that *Synechococcus* were sensitive to high trace metal levels (Cassier-Chauvat and Chauvat, 2014; Coclet et al., 2018). Additionally, SAR11, Rickettsiales, Rhizobiales, and *Synechococcus* are well known to be characteristic of marine zones away from anthropogenic influence (Gilbert et al., 2009, 2012; Fuhrman et al., 2015).

The most contaminated sites (MIS and 6ext) were enriched in *Candidatus Aquiluna* (Actinobacteria), *Formosa* and *Tenacibaculum* (Flavobacteriia) as well as one from Sphingobacteriales NS11-12 marine group (Bacteroidetes). Networks analysis showed also that *Planktomarina* (Alphaproteobacteria), *Hydrogenophilaceae* (Betaproteobacteria) and *Haliaceae* (Gammaproteobacteria) were positively associated with contaminants, in agreement with the distribution of these groups along the contamination gradient. Previous studies in freshwater or marine sediment reported that *Hydrogenophilaceae* and *Candidatus Aquiluna* (Microbacteriaceae) were positively correlated to high trace contaminant levels (Acosta-González et al., 2013; Garris et al., 2018). The increase of Actinobacteria and Betaproteobacteria in the most contaminated site was not unexpected, as they are widely recognized to play a key role in oil degradation (Acosta-González et al., 2013) and heavy metals transformation, especially, in the case of nutrient enrichments (Garris et al., 2018). Microbacteriaceae (Actinobacteria) were widely reported as members of highly copper-polluted sediment (Besaury et al., 2014) or Zn-polluted freshwater (Ni et al., 2016). Albarracín et al. (2010) have shown that Actinobacteria members isolated from copper-contaminated sediment are able to significantly diminish the bioavailable copper throughout bioaccumulation. Members of the Bacteroidetes members, especially *Flavobacteria* families are also known to represent one of the most abundant groups of bacteria in coastal areas, especially in contaminated sites due to their ability to tolerate toxic effects of certain metals (Sun et al., 2013; Korlević et al., 2015). The Bacteroidetes NS11-12 marine group have been detected mainly in marine habitats (Meziti et al., 2015), unfortunately without clear ecological implications. At a finer scale, for most of clusters, members of both Alphaproteobacteria (mainly SAR11) and Bacteroidetes (mainly *Flavobacteriia*) groups describe above, exhibit the highest number of edges with high level of connections within each group in the network analysis. These important findings display that Alphaproteobacteria would highly influence the functioning of low contaminated site while Bacteroidetes would highly influence the functioning of contaminated zones.

Most of studies on bacterioplankton communities have focused on community diversity and composition responses to perturbation (Jeffries et al., 2016). The effect of chemical contaminations on bacterial community functionalities have only been investigated in freshwater ecosystems (Wang et al., 2018; Sjöstedt et al., 2018). In a highly polluted area such as Toulon Bay, the functional stability of microbial communities could be challenged. Major predicted bacterial functions including those necessary to basic metabolisms were conserved across the chemical gradient. Functional recovery occurred because of species replacement or change in relative abundance of taxa, i.e., functionally redundant rare species could become abundant in response to the contaminations. This is in agreement with the replacement scenario (Comte and Del Giorgio, 2011), and previous findings showing that the rare biosphere is an important reservoir for recruitment of bacterial taxa during environmental change (Sjöstedt et al., 2012; Comte et al., 2014). However, both a decrease in some critical functions (cell growth and death or energy metabolism) and an increase in functions associated to multiple stress resistance (e.g., xenobiotic biodegradation and metabolism, signaling molecules and interactions, secondary metabolites metabolism) remarkably exhibited that bacterial communities in the most polluted sites developed specific functions to face their environment. As the sites are not physically separated, there was no discontinuity in both communities and functions but a clear gradient of the relative components throughout the metal gradient. Metal contaminated environments were shown to exert a high selective pressure toward the transfer of several genes, developing thus resistance against high metal concentrations (Azarbad et al., 2016). Only two field studies on long-term metal polluted areas have shown shifts in microbial community structure and functions or increased occurrence of resistance genes that have made microbial communities resistant to toxic metals concentrations (Hemme et al., 2010; Kang et al., 2013). However, both taxonomic affiliation of metal-specific metabolic traits and the currently available KEGG database are insufficient to validate the hypothesis that heavy metal stress is a key environmental factor shaping the function of microbial communities.

## Implication Regarding Others Local Selective Pressures

Although trace metal gradient seemed to be the main driver of the bacterioplankton community features, other local selective pressures could explain a significant proportion of their variance. Indeed, bacterioplankton communities in coastal areas greatly vary in space because of sharp gradients in salinity, nutrients, depth, among other properties (Fuhrman et al., 2006; Gilbert et al., 2009; Fortunato et al., 2012).

A very similar trend could have been observed if DOM quantity or quality varied and became more labile in the most contaminated sites. Indeed, an increase in DOM lability often leads to the development of a copiotrophic response of the bacterial community, selecting a limited number of bacterial taxa, and temporarily reducing microbial diversity

(Nelson and Wear, 2014; Pedler et al., 2014). The variation partitioning performed in our study is in agreement with this hypothesis, since DOC appeared as one of the most influent drivers of community structure variations. Thus, organic matter spatio-temporal dynamics could indeed be an important driver of microbial communities in Toulon Bay. However, according to the literature, only a part of the bacterial taxa significantly enriched in the most contaminated sites of Toulon Bay is known as copiotroph. Indeed, while OM60 (NOR5) clade (Halieaceae), *Candidatus Aquiluna* (Microbacteriaceae), and *Planktomarina* (Rhodobacterales) are known to benefit from labile DOM (Yan et al., 2009; Spring et al., 2015), Alphaproteobacteria members (SAR11 and AEGEAN-169 marine group) and Bacteroidetes (*Balneola* and *Aquibacter*) are rather known as oligotrophic groups (Cram et al., 2015; Sipler et al., 2017). Copiotrophs are expected to outcompete oligotrophs, so the fact that presence of groups identified as copiotrophs suggest that each has capitalized on reduced competition following trace metal contamination. Taken together, all these arguments point out the major and predominant influence of the multi-contamination gradient on microbial diversity and represent a significant demonstration of the potential influence of human activities on marine microbial life. Since we only considered inorganic contaminants, we cannot rule out the potential influence of organic contaminants such as PAH, PCBS, or organometals which were already measured in the sediment of Toulon Bay (Misson et al., 2016).

Organic contaminants as polyaromatic hydrocarbons could explained more precisely the distribution of OTUs (Qian et al., 2017). This hypothesis could be confirmed by the strong enrichment in xenobiotics biodegradation and metabolism, carbohydrate metabolism and metabolism of terpenoids and polyketides in the highest contaminated sites. Naphthalene degradation, benzoate, and aminobenzoate biodegradation were found to be higher in the most contaminated zones and is consistent with the finding of previous studies (Wang et al., 2018).

Finally, another striking result is that the multi-contamination gradient in the water column of Toulon Bay represented a significant perturbation, affecting microbial diversity all along our survey. This observation differs from what was observed previously in surface sediment of Toulon Bay (Misson et al., 2016), suggesting that the contemporary contamination in the water affects more strongly microbial communities than the large historical contamination trapped in the sediment. Such difference could be linked to the probably higher dispersal rate in the water column than in the sediment, i.e., 3.4 days for a total renewal of the water of Toulon Bay (Dufresne et al., 2014). Thus, this higher dispersal rate could tend to reduce the adaptive abilities of bacterioplankton, leading to a higher sensitivity to contamination when compared to the longer-term stability of the sediment.

## Biotic Interactions as Evidences of Indirect Effects of Trace Metals

The network indices (BC and CC) and large numbers of nodes (179) and edges (1664) between taxa in our network

analysis suggest that SAR11, Rhodobacteraceae, Synechococcus, and Microbacteriaceae play a key role in Toulon Bay seawater. Despite some connections between OTUs and trace metals, there were far more numerous connections among OTUs. This suggests that trace metals significantly influence the dynamics of only a few microbial groups, and could rather influence indirectly, via biotic interactions, the whole community in Toulon Bay seawater. Community structure is known to be influenced by interaction among species (Lima-Mendez et al., 2015). Some of these interactions could be cooperative interspecific interactions (Eiler et al., 2012; Chow et al., 2013) or competitive interactions (i.e., competition, niche partitioning, grazing, or parasitism) (Fuhrman et al., 2008; Berdjeb et al., 2018) in a multispecies community.

Keystone OTUs play important roles in the regulation of network interactions (Wright et al., 2012) and their loss may increase a community's vulnerability to perturbation. Thus, the strong decline of Alphaproteobacterial and Cyanobacterial keystone OTUs, especially, along the trace metal contamination gradient could have indirect effect on the BCC by modifying biotic interactions and favor opportunist or tolerant taxa (Lawes et al., 2016). This is in agreement with community turnover and the development of copiotrophic groups highlighted above.

Additionally, in network analysis, positive correlation between on the one hand pico- and nanophytoplankton abundances, as well as chlorophyll *a*, and on the other hand trace metals concentrations describe potential conditions that may favor specific groups of bacterioplankton. Indeed, Fuhrman et al. (2015) explained that weekly timescale is appropriate for studying bacterial dynamics associated with phytoplankton, which have a direct influence on the composition of bacterial communities via cross-feeding interactions or the effect of toxins, as well as indirect influence (e.g., oxygen depletion). Phytoplankton succession may influence the dynamics of the bacterioplankton community, as differences in the phytoplankton structure lead to differences in quantity and quality of exuded organic matter that can be used by the bacterial community for growth (Marisol et al., 2018). Consequently, effects of pollutants on phytoplankton or bacterioplankton might have indirect consequences for the counterpart, depending on the possible interactions between both compartments.

In summary, Toulon Bay offered a remarkable study area allowing to address trace metal multi-contamination impacts on prokaryotic community shaping throughout contrasted but connected sites. Where trace metal contamination increased, bacterioplankton abundance was higher together with a reduction of only community richness. Seawater contamination induced significant bacterioplankton communities shifts, with Alphaproteobacteria (SAR11, Rickettsiales, Rhizobiales, and Rhodobacteraceae) and *Synechococcus* dominance where trace metal concentrations were the lowest, whereas Flavobacteria, Betaproteobacteria (Hydrogenophilaceae) and Gammaproteobacteria (Halieaceae), especially including copiotrophic organisms, dominated in highly contaminated sites. In addition, this study showed that human-induced disturbances can have an effect on predicted functional potential of marine coastal bacterioplankton, and that the response can differ

according to the type of functions. However, observed functional redundancy lead to think that the effect of trace metals could be complex, highly context-dependent and depending on biotic interactions. While our results provide a better understanding of anthropogenic influence on coastal ecosystems and the response of microbial communities, future studies are needed to elucidate the contribution of DOC, phytoplankton-bacteria specific interactions and organic pollutants on bacterioplankton communities in Toulon Bay.

## ORIGINALITY-SIGNIFICANCE STATEMENT

Human-induced chemical contamination gradients challenge our understanding of microbial communities' ecology, especially in the very dynamic marine coastal environment. Through the spatio-temporal investigation of microbial diversity dynamics in a model ecosystem, this work highlights contributions of anthropogenic trace metal contamination to marine bacterioplankton ecology. Identify the key aspects of originality and significance that place the work within the top 10% of current research in environmental microbiology.

## AUTHOR CONTRIBUTIONS

CG, J-FB, and BM proposed and designed the study. CC, CG, GD, CLP, J-UM, J-FB, and BM organized and performed field sampling. CC, CG, GD, DO, SD, CLP, and BM analyzed the samples. CC, CG, J-FB, and BM interpreted the results. All authors participated in manuscript redaction, thus approving the publication of the content.

## FUNDING

This study was supported by PREVENT research program [funded by Toulon University, Toulon-Provence-Méditerranée (TPM) and the Conseil Départemental du Var]. CC was funded by the Provence-Alpes-Côte d'Azur region and supported by TPM.

## ACKNOWLEDGMENTS

The authors wish to thank the French Navy and the LASEM for diving and sampling assistance, Dr. G. Culioli (MAPIEM, Toulon, France) and L. Favre (MAPIEM, Toulon, France) for sampling and sample treatment assistance.

## SUPPLEMENTARY MATERIAL

The Supplementary Material for this article can be found online at: <https://www.frontiersin.org/articles/10.3389/fmicb.2019.00257/full#supplementary-material>

## REFERENCES

- Acosta-González, A., Rosselló-Móra, R., and Marqués, S. (2013). Characterization of the anaerobic microbial community in oil-polluted subtidal sediments: aromatic biodegradation potential after the Prestige oil spill. *Environ. Microbiol.* 15, 77–92. doi: 10.1111/j.1462-2920.2012.02782.x
- Albarracín, V. H., Alonso-Vega, P., Trujillo, M. E., Amoroso, M. J., and Abate, C. M. (2010). *Amycolatopsis tucumanensis* sp. nov., a copper-resistant actinobacterium isolated from polluted sediments. *Int. J. Syst. Evol. Microbiol.* 60, 397–401. doi: 10.1099/ijms.0.010587-0
- Allison, S. D., and Martiny, J. B. (2008). Resistance, resilience, and redundancy in microbial communities. *Proc. Natl. Acad. Sci. U.S.A.* 105(Suppl. 1), 11512–11519. doi: 10.1073/pnas.0801925105
- Atlas, R. M., Stoeckel, D. M., Faith, S. A., Minard-Smith, A., Thorn, J. R., and Benotti, M. J. (2015). Oil biodegradation and oil-degrading microbial populations in marsh sediments impacted by oil from the deepwater horizon well blowout. *Environ. Sci. Technol.* 49, 8356–8366. doi: 10.1021/acs.est.5b00413
- Azarbad, H., van Gestel, C. A., Niklińska, M., Laskowski, R., Röling, W. F., and van Straalen, N. M. (2016). Resilience of soil microbial communities to metals and additional stressors: DNA-based approaches for assessing “stress-on-stress” responses. *Int. J. Mol. Sci.* 17:933. doi: 10.3390/ijms17060933
- Aßhauer, K. P., Wemheuer, B., Daniel, R., and Meinicke, P. (2015). Tax4Fun: predicting functional profiles from metagenomic 16S rRNA data. *Bioinformatics* 31, 2882–2884. doi: 10.1093/bioinformatics/btv287
- Berdjeb, L., Parada, A., Needham, D. M., and Fuhrman, J. A. (2018). Short-term dynamics and interactions of marine protist communities during the spring–summer transition. *ISME J.* 12, 1907–1917. doi: 10.1038/s41396-018-0097-x
- Besaury, L., Ghiglione, J. F., and Quillet, L. (2014). Abundance, activity, and diversity of archaeal and bacterial communities in both uncontaminated and highly copper-contaminated marine sediments. *Mar. Biotechnol.* 16, 230–242. doi: 10.1007/s10126-013-9542-z
- Bokulich, N. A., Subramanian, S., Faith, J. J., Gevers, D., Gordon, J. I., and Knight, R. (2013). Quality-filtering vastly improves diversity estimates from Illumina amplicon sequencing. *Nat. Methods* 10, 57–59. doi: 10.1038/nmeth.2276
- Boyd, T. J., Wolgast, D. M., Rivera-Duarte, I., Holm-Hansen, O., Hewes, C. D., Zirino, A., et al. (2005). Effects of dissolved and complexed copper on heterotrophic bacterial production in San Diego Bay. *Microb. Ecol.* 49, 353–366. doi: 10.1007/s00248-003-1065-0
- Bruland, K. W., Middag, R., and Lohan, M. C. (2013). “Controls of trace metals in seawater” in *Treatise on Geochemistry*, 2nd Edn, eds M. J. Mottl and H. Elderfield (Philadelphia, PA: Saunders), 19–51.
- Cabrol, L., Quéméneur, M., and Misson, B. (2017). Inhibitory effects of sodium azide on microbial growth in experimental resuspension of marine sediment. *J. Microbiol. Methods* 133, 62–65. doi: 10.1016/j.mimet.2016.12.021
- Callender, E. (2003). Heavy metals in the environment-historical trends. *Treat. Geochem.* 9:612. doi: 10.1016/B0-08-043751-6/09161-1
- Caporaso, J. G., Kuczynski, J., Stombaugh, J., Bittinger, K., Bushman, F. D., and Costello, E. K. (2010). QIIME allows analysis of high-throughput community sequencing data. *Nat. Methods* 7, 335–336. doi: 10.1038/nmeth.f.303
- Caroppo, C., Stabili, L., Aresta, M., Corinaldesi, C., and Danovaro, R. (2006). Impact of heavy metals and PCBs on marine picoplankton. *Environ. Toxicol.* 21, 541–551. doi: 10.1002/tox.20215
- Cassier-Chauvat, C., and Chauvat, F. (2014). Responses to oxidative and heavy metal stresses in cyanobacteria: recent advances. *Int. J. Mol. Sci.* 16, 871–886. doi: 10.3390/ijms16010871
- Chow, C. E. T., Sachdeva, R., Cram, J. A., Steele, J. A., Needham, D. M., and Patel, A. (2013). Temporal variability and coherence of euphotic zone bacterial communities over a decade in the Southern California Bight. *ISME J.* 7, 2259–2273. doi: 10.1038/ismej.2013.122
- Cindrić, A. M., Cukrov, N., Durrieu, G., Garnier, C., Pižeta, I., and Omanović, D. (2017). Evaluation of discrete and passive sampling (Diffusive Gradients in Thin-films–DGT) approach for the assessment of trace metal dynamics in marine waters—a case study in a small harbor. *Croat. Chem. Acta* 90, 1–9. doi: 10.5562/cca3163
- Clarke, K. R. (1993). Non-parametric multivariate analyses of changes in community structure. *Aust. J. Ecol.* 18, 117–143. doi: 10.1111/j.1442-9993.1993.tb00438.x
- Cloern, J. E. (2001). Our evolving conceptual model of the coastal eutrophication problem. *Mar. Ecol. Prog. Ser.* 210, 223–253. doi: 10.3354/meps210223
- Coclet, C., Garnier, C., Delpy, F., Jamet, D., Durrieu, G., and Le Poupon, C. (2018). Trace metal contamination as a toxic and structuring factor impacting ultraphytoplankton communities in a multicontaminated Mediterranean coastal area. *Prog. Oceanogr.* 163, 196–213. doi: 10.1016/j.pocean.2017.06.006
- Comte, J., and Del Giorgio, P. A. (2011). Composition influences the pathway but not the outcome of the metabolic response of bacterioplankton to resource shifts. *PLoS One* 6:e25266. doi: 10.1371/journal.pone.0025266
- Comte, J., Lindström, E. S., Eiler, A., and Langenheder, S. (2014). Can marine bacteria be recruited from freshwater sources and the air? *ISME J.* 8, 2423–2430. doi: 10.1038/ismej.2014.89
- Cram, J. A., Chow, C. E. T., Sachdeva, R., Needham, D. M., Parada, A. E., Steele, J. A., et al. (2015). Seasonal and interannual variability of the marine bacterioplankton community throughout the water column over ten years. *ISME J.* 9, 563–580. doi: 10.1038/ismej.2014.153
- Dang, D. H., Lenoble, V., Durrieu, G., Omanović, D., Mullot, J. U., Mounier, S., et al. (2015). Seasonal variations of coastal sedimentary trace metals cycling: insight on the effect of manganese and iron (oxy) hydroxides, sulphide and organic matter. *Mar. Pollut. Bull.* 92, 113–124. doi: 10.1016/j.marpolbul.2014.12.048
- Dinsdale, E. A., Edwards, R. A., Hall, D., Angly, F., Breitbart, M., Brulc, J. M., et al. (2008). Functional metagenomic profiling of nine biomes. *Nature* 452, 629–632. doi: 10.1038/nature06810
- Dufresne, C., Duffa, C., and Rey, V. (2014). Wind-forced circulation model and water exchanges through the channel in the Bay of Toulon. *Ocean Dyn.* 64, 209–224. doi: 10.1007/s10236-013-0676-3
- Edgar, R. C. (2010). Search and clustering orders of magnitude faster than BLAST. *Bioinformatics* 26, 2460–2461. doi: 10.1093/bioinformatics/btq461
- Eiler, A., Heinrich, F., and Bertilsson, S. (2012). Coherent dynamics and association networks among lake bacterioplankton taxa. *ISME J.* 6, 330–332. doi: 10.1038/ismej.2011.113
- Faust, K., Sathirapongsasuti, J. F., Izard, J., Segata, N., Gevers, D., Raes, J., et al. (2012). Microbial co-occurrence relationships in the human microbiome. *PLoS Comput. Biol.* 8:e1002606. doi: 10.1371/journal.pcbi.1002606
- Fortunato, C. S., Herfort, L., Zuber, P., Baptista, A. M., and Crump, B. C. (2012). Spatial variability overwhelms seasonal patterns in bacterioplankton communities across a river to ocean gradient. *ISME J.* 6, 554–563. doi: 10.1038/ismej.2011.135
- Franklin, N. M., Stauber, J. L., Lim, R. P., and Petocz, P. (2002). Toxicity of metal mixtures to a tropical freshwater alga (*Chlorella* sp.): the effect of interactions between copper, cadmium, and zinc on metal cell binding and uptake. *Environ. Toxicol. Chem.* 21, 2412–2422. doi: 10.1038/ismej.2011.135
- Fuhrman, J. A., and Azam, F. (1980). Bacterioplankton secondary production estimates for coastal waters of British Columbia, Antarctica, and California. *Appl. Environ. Microbiol.* 39, 1085–1095. doi: 10.1002/etc.5620211121
- Fuhrman, J. A., Cram, J. A., and Needham, D. M. (2015). Marine microbial community dynamics and their ecological interpretation. *Nat. Rev. Microbiol.* 13, 133–146. doi: 10.1038/nrmicro3417
- Fuhrman, J. A., Hewson, I., Schwalbach, M. S., Steele, J. A., Brown, M. V., and Naeem, S. (2006). Annually reoccurring bacterial communities are predictable from ocean conditions. *Proc. Natl. Acad. Sci. U.S.A.* 103, 13104–13109. doi: 10.1073/pnas.0602399103
- Fuhrman, J. A., Steele, J. A., Hewson, I., Schwalbach, M. S., Brown, M. V., Green, J. L., et al. (2008). A latitudinal diversity gradient in planktonic marine bacteria. *Proc. Natl. Acad. Sci. U.S.A.* 105, 7774–7778. doi: 10.1073/pnas.0803070105
- Garris, H. W., Baldwin, S. A., Taylor, J., Gurr, D. B., Denesiuk, D. R., Van Hamme, J. D., et al. (2018). Short-term microbial effects of a large-scale mine-tailing storage facility collapse on the local natural environment. *PLoS One* 13:e0196032. doi: 10.1371/journal.pone.0196032
- Ghiglione, J. F., Conan, P., and Pujo-Pay, M. (2009). Diversity of total and active free-living vs. particle-attached bacteria in the euphotic zone of the NW Mediterranean Sea. *FEMS Microbiol. Lett.* 299, 9–21. doi: 10.1111/j.1574-6968.2009.01694.x

- Ghiglione, J. F., Galand, P. E., Pommier, T., Pedrós-Alió, C., Maas, E. W., and Bakker, K. (2012). Pole-to-pole biogeography of surface and deep marine bacterial communities. *Proc. Natl. Acad. Sci. U.S.A.* 109, 17633–17638. doi: 10.1073/pnas.1208160109
- Gilbert, J. A., Field, D., Swift, P., Newbold, L., Oliver, A., and Smyth, T. (2009). The seasonal structure of microbial communities in the Western English Channel. *Environ. Microbiol.* 11, 3132–3139. doi: 10.1111/j.1462-2920.2009.02017.x
- Gilbert, J. A., Steele, J. A., Caporaso, J. G., Steinbrück, L., Reeder, J., and Temperton, B. (2012). Defining seasonal marine microbial community dynamics. *ISME J.* 6, 298–308. doi: 10.1038/ismej.2011.107
- Gillan, D. C., Danis, B., Pernet, P., Joly, G., and Dubois, P. (2005). Structure of sediment-associated microbial communities along a heavy-metal contamination gradient in the marine environment. *Appl. Environ. Microbiol.* 71, 679–690. doi: 10.1128/AEM.71.2.679-690.2005
- Goecks, J., Nekrutenko, A., and Taylor, J. (2010). Galaxy: a comprehensive approach for supporting accessible, reproducible, and transparent computational research in the life sciences. *Genome Biol.* 11:R86. doi: 10.1186/gb-2010-11-8-r86
- Gough, H. L., and Stahl, D. A. (2011). Microbial community structures in anoxic freshwater lake sediment along a metal contamination gradient. *ISME J.* 5, 543–558. doi: 10.1038/ismej.2010.132
- Halpern, B. S., Walbridge, S., Selkoe, K. A., Kappel, C. V., Micheli, F., and D'agrosa, C. (2008). A global map of human impact on marine ecosystems. *Science* 319, 948–952. doi: 10.1126/science.1149345
- Hemme, C. L., Deng, Y., Gentry, T. J., Fields, M. W., Wu, L., and Barua, S. (2010). Metagenomic insights into evolution of a heavy metal-contaminated groundwater microbial community. *ISME J.* 4, 660–672. doi: 10.1038/ismej.2009.154
- Jeanbille, M., Gury, J., Duran, R., Tronczynski, J., Ghiglione, J. F., and Agogue, H. (2016). Chronic polyaromatic hydrocarbon (PAH) contamination is a marginal driver for community diversity and prokaryotic predicted functioning in coastal sediments. *Front. Microbiol.* 7:1303. doi: 10.3389/fmicb.2016.01303
- Jeffries, T. C., Schmitz Fontes, M. L., Harrison, D. P., Van-Dongen-Vogels, V., Eyre, B. D., Ralph, P. J., et al. (2016). Bacterioplankton dynamics within a large anthropogenically impacted urban estuary. *Front. Microbiol.* 6:1438. doi: 10.3389/fmicb.2015.01438
- Kang, S., Van Nostrand, J. D., Gough, H. L., He, Z., Hazen, T. C., Stahl, D. A., et al. (2013). Functional gene array-based analysis of microbial communities in heavy metals-contaminated lake sediments. *FEMS Microbiol. Ecol.* 86, 200–214. doi: 10.1111/1574-6941.12152
- Korlević, M., Zucko, J., Dragić, M. N., Blažina, M., Pustijanac, E., and Zeljko, T. V. (2015). Bacterial diversity of polluted surface sediments in the northern Adriatic Sea. *Syst. Appl. Microbiol.* 38, 189–197. doi: 10.1016/j.syapm.2015.03.001
- Lawes, J. C., Neilan, B. A., Brown, M. V., Clark, G. F., and Johnston, E. L. (2016). Elevated nutrients change bacterial community composition and connectivity: high throughput sequencing of young marine biofilms. *Biofouling* 32, 57–69. doi: 10.1080/08927014.2015.1126581
- LeBrun, E. S., King, R. S., Back, J. A., and Kang, S. (2018). Microbial community structure and function decoupling across a phosphorus gradient in streams. *Microb. Ecol.* 75, 64–73. doi: 10.1007/s00248-017-1039-2
- Levin, L. A., Boesch, D. F., Covich, A., Dahm, C., Erséus, C., and Ewel, K. C. (2001). The function of marine critical transition zones and the importance of sediment biodiversity. *Ecosystems* 4, 430–451. doi: 10.1007/s10021-001-0021-4
- Lima-Mendez, G., Faust, K., Henry, N., Decelle, J., Colin, S., and Carcillo, F. (2015). Determinants of community structure in the global plankton interactome. *Science* 348:1262073. doi: 10.1126/science.1262073
- Lorenzo, J. I., Nieto, O., and Beiras, R. (2002). Effect of humic acids on speciation and toxicity of copper to *Paracentrotus lividus* larvae in seawater. *Aquat. Toxicol.* 58, 27–41. doi: 10.1016/S0166-445X(01)00219-3
- Louca, S., Parfrey, L. W., and Doebeli, M. (2016). Decoupling function and taxonomy in the global ocean microbiome. *Science* 353, 1272–1277. doi: 10.1126/science.aaf4507
- Louis, Y., Garnier, C., Lenoble, V., Omanović, D., Mounier, S., and Pižeta, I. (2009). Characterisation and modelling of marine dissolved organic matter interactions with major and trace cations. *Mar. Environ. Res.* 67, 100–107. doi: 10.1016/j.marenvres.2008.12.002
- Lozupone, C. A., and Knight, R. (2007). Global patterns in bacterial diversity. *Proc. Natl. Acad. Sci. U.S.A.* 104, 11436–11440. doi: 10.1073/pnas.0611525104
- Marisol, G.-U., Hélène, M., Céline, L., Claire, C., Marc, B., Asma, S. H., et al. (2018). Consequences of contamination on the interactions between phytoplankton and bacterioplankton. *Chemosphere* 195, 212–222. doi: 10.1016/j.chemosphere.2017.12.053
- Meziti, A., Kormas, K. A., Moustaka-Gouni, M., and Karayanni, H. (2015). Spatially uniform but temporally variable bacterioplankton in a semi-enclosed coastal area. *Syst. Appl. Microbiol.* 38, 358–367. doi: 10.1016/j.syapm.2015.04.003
- Misson, B., Garnier, C., Lauga, B., Dang, D. H., Ghiglione, J. F., and Mullot, J. U. (2016). Chemical multi-contamination drives benthic prokaryotic diversity in the anthropized Toulon Bay. *Sci. Total Environ.* 556, 319–329. doi: 10.1016/j.scitotenv.2016.02.038
- Morley, N. H., Burton, J. D., Tankere, S. P. C., and Martin, J. M. (1997). Distribution and behaviour of some dissolved trace metals in the western Mediterranean Sea. *Deep Sea Res. Part II Top. Stud. Oceanogr.* 44, 675–691. doi: 10.1016/S0967-0645(96)00098-7
- Nayar, S., Goh, B. P. L., and Chou, L. M. (2004). Environmental impact of heavy metals from dredged and resuspended sediments on phytoplankton and bacteria assessed in situ mesocosms. *Ecotoxicol. Environ. Saf.* 59, 349–369. doi: 10.1016/j.ecoenv.2003.08.015
- Nelson, C. E., and Wear, E. K. (2014). Microbial diversity and the lability of dissolved organic carbon. *Proc. Natl. Acad. Sci. U.S.A.* 111, 7166–7167. doi: 10.1073/pnas.1405751111
- Ni, C., Horton, D. J., Rui, J., Henson, M. W., Jiang, Y., Huang, X., et al. (2016). High concentrations of bioavailable heavy metals impact freshwater sediment microbial communities. *Ann. Microbiol.* 66, 1003–1012. doi: 10.1007/s13213-015-1189-8
- Nies, D. H. (1999). Microbial heavy-metal resistance. *Appl. Microbiol. Biotechnol.* 51, 451–460. doi: 10.1007/s002530051457
- Odum, E. P. (1985). Trends expected in stressed ecosystems. *Bioscience* 35, 419–422. doi: 10.1098/rstb.2010.0171
- Oksanen, J., Blanchet, F., Kindt, R., Legendre, P., and O'Hara, R. (2016). *Vegan: Community Ecology Package. R package 2.3-3.*
- Othman, H. B., Pringault, O., Louati, H., Hlaili, A. S., and Le Boulanger, C. (2017). Impact of contaminated sediment elutriate on coastal phytoplankton community (Thau lagoon, Mediterranean Sea, France). *J. Exp. Mar. Biol. Ecol.* 486, 1–12. doi: 10.1016/j.jembe.2016.09.006
- Oursel, B., Garnier, C., Durrieu, G., Mounier, S., Omanović, D., and Lucas, Y. (2013). Dynamics and fates of trace metals chronically input in a Mediterranean coastal zone impacted by a large urban area. *Mar. Pollut. Bull.* 69, 137–149. doi: 10.1016/j.marpollbul.2013.01.023
- Paquin, P. R., Gorsuch, J. W., Apte, S., Batley, G. E., Bowles, K. C., and Campbell, P. G. (2002). The biotic ligand model: a historical overview. *Comp. Biochem. Physiol. C Toxicol. Pharmacol.* 133, 3–35.
- Parada, A. E., Needham, D. M., and Fuhrman, J. A. (2016). Every base matters: assessing small subunit rRNA primers for marine microbiomes with mock communities, time series and global field samples. *Environ. Microbiol.* 18, 1403–1414. doi: 10.1111/1462-2920.13023
- Pedler, B. E., Aluwihare, L. I., and Azam, F. (2014). Single bacterial strain capable of significant contribution to carbon cycling in the surface ocean. *Proc. Natl. Acad. Sci. U.S.A.* 111, 7202–7207. doi: 10.1073/pnas.1401887111
- Pommier, T., Canbäck, B., Riemann, L., Boström, K. H., Simu, K., and Lundberg, P. (2007). Global patterns of diversity and community structure in marine bacterioplankton. *Mol. Ecol.* 16, 867–880. doi: 10.1111/j.1365-294X.2006.03189.x
- Pringault, O., Lafabrie, C., Avezac, M., Bancon-Montigny, C., Carre, C., and Chalghaf, M. (2016). Consequences of contaminant mixture on the dynamics and functional diversity of bacterioplankton in a southwestern Mediterranean coastal ecosystem. *Chemosphere* 144, 1060–1073. doi: 10.1016/j.chemosphere.2015.09.093
- Pringault, O., Viret, H., and Duran, R. (2012). Interactions between Zn and bacteria in marine tropical coastal sediments. *Environ. Sci. Pollut. Res.* 19, 879–892. doi: 10.1007/s11356-011-0621-2
- Pruesse, E., Quast, C., Knittel, K., Fuchs, B. M., Ludwig, W., Peplies, J., et al. (2007). SILVA: a comprehensive online resource for quality checked and aligned ribosomal RNA sequence data compatible with ARB. *Nucleic Acids Res.* 35, 7188–7196. doi: 10.1093/nar/gkm864

- Qian, J., Ding, Q., Guo, A., Zhang, D., and Wang, K. (2017). Alteration in successional trajectories of bacterioplankton communities in response to co-exposure of cadmium and phenanthrene in coastal water microcosms. *Environ. Pollut.* 221, 480–490. doi: 10.1016/j.envpol.2016.12.020
- Quast, C., Pruesse, E., Yilmaz, P., Gerken, J., Schweer, T., and Yarza, P. (2013). The SILVA ribosomal RNA gene database project: improved data processing and web-based tools. *Nucleic Acids Res.* 41, D590–D596. doi: 10.1093/nar/gks1219
- Quero, G. M., Cassin, D., Botter, M., Perini, L., and Luna, G. M. (2015). Patterns of benthic bacterial diversity in coastal areas contaminated by heavy metals, polycyclic aromatic hydrocarbons (PAHs) and polychlorinated biphenyls (PCBs). *Front. Microbiol.* 6:1053. doi: 10.3389/fmicb.2015.01053
- R Core Team (2015). *R: A Language and Environment for Statistical Computing*. Vienna: R Foundation for Statistical Computing.
- Segata, N., Izard, J., Waldron, L., Gevers, D., Miropolsky, L., Garrett, W. S., et al. (2011). Metagenomic biomarker discovery and explanation. *Genome Biol.* 12:R60. doi: 10.1186/gb-2011-12-6-r60
- Sipler, R. E., Kellogg, C. T., Connelly, T. L., Roberts, Q. N., Yager, P. L., and Bronk, D. A. (2017). Microbial community response to terrestrially derived dissolved organic matter in the coastal arctic. *Front. Microbiol.* 8:1018. doi: 10.3389/fmicb.2017.01018
- Sjöstedt, J., Koch-Schmidt, P., Pontarp, M., Canbäck, B., Tunlid, A., and Lundberg, P. (2012). Recruitment of members from the rare biosphere of marine bacterioplankton communities after an environmental disturbance. *Appl. Environ. Microbiol.* 78, 1361–1369. doi: 10.1128/AEM.05542-11
- Sjöstedt, J., Langenheder, S., Kritzbeg, E., Karlsson, C. M., and Lindström, E. S. (2018). Repeated disturbances affect functional but not compositional resistance and resilience in an aquatic bacterioplankton community. *Environ. Microbiol. Rep.* 10, 493–500. doi: 10.1111/1758-2229.12656
- Smoot, M. E., Ono, K., Ruschinski, J., Wang, P. L., and Ideker, T. (2011). Cytoscape 2.8: new features for data integration and network visualization. *Bioinformatics* 27, 431–432. doi: 10.1093/bioinformatics/btq675
- Spring, S., Scheuner, C., Göker, M., and Klenk, H. P. (2015). A taxonomic framework for emerging groups of ecologically important marine gammaproteobacteria based on the reconstruction of evolutionary relationships using genome-scale data. *Front. Microbiol.* 6:281. doi: 10.3389/fmicb.2015.00281
- Sun, M. Y., Dafforn, K. A., Brown, M. V., and Johnston, E. L. (2012). Bacterial communities are sensitive indicators of contaminant stress. *Mar. Pollut. Bull.* 64, 1029–1038. doi: 10.1016/j.marpolbul.2012.01.035
- Sun, M. Y., Dafforn, K. A., Johnston, E. L., and Brown, M. V. (2013). Core sediment bacteria drive community response to anthropogenic contamination over multiple environmental gradients. *Environ. Microbiol.* 15, 2517–2531. doi: 10.1111/1462-2920.12133
- Tessier, E., Garnier, C., Mullot, J. U., Lenoble, V., Arnaud, M., Raynaud, M., et al. (2011). Study of the spatial and historical distribution of sediment inorganic contamination in the Toulon bay (France). *Mar. Pollut. Bull.* 62, 2075–2086. doi: 10.1016/j.marpolbul.2011.07.022
- The MerMex Group, Durrieu de Madron, X., Guieu, C., Sempéré, R., Conan, P., Cossa Fabrizio, D., et al. (2011). Marine ecosystems' responses to climatic and anthropogenic forcings in the Mediterranean. *Prog. Oceanogr.* 91, 97–166. doi: 10.1016/j.pocan.2011.02.003
- Thompson, L. R., Williams, G. J., Haroon, M. F., Shibl, A., Larsen, P., and Shorenstein, J. (2017). Metagenomic covariation along densely sampled environmental gradients in the Red Sea. *ISME J.* 11, 138–151. doi: 10.1038/ismej.2016.99
- Treusch, A. H., Vergin, K. L., Finlay, L. A., Donatz, M. G., Burton, R. M., Carlson, C. A., et al. (2009). Seasonality and vertical structure of microbial communities in an ocean gyre. *ISME J.* 3, 1148–1163. doi: 10.1038/ismej.2009.60
- Turner, A. (2010). Marine pollution from antifouling paint particles. *Mar. Pollut. Bull.* 60, 159–171. doi: 10.1016/j.marpolbul.2009.12.004
- Wang, K., Ye, X., Zhang, H., Chen, H., Zhang, D., and Liu, L. (2016). Regional variations in the diversity and predicted metabolic potential of benthic prokaryotes in coastal northern Zhejiang, East China Sea. *Sci. Rep.* 6:38709. doi: 10.1038/srep38709
- Wang, K., Zhang, D., Xiong, J., Chen, X., Zheng, J., and Hu, C. (2015). Response of bacterioplankton communities to cadmium exposure in coastal water microcosms with high temporal variability. *Appl. Environ. Microbiol.* 81, 231–240. doi: 10.1128/AEM.02562-14
- Wang, L., Zhang, J., Li, H., Yang, H., Peng, C., Peng, Z., et al. (2018). Shift in the microbial community composition of surface water and sediment along an urban river. *Sci. Total Environ.* 627, 600–612. doi: 10.1016/j.scitotenv.2018.01.203
- Ward, C. S., Yung, C. M., Davis, K. M., Blinbry, S. K., Williams, T. C., Johnson, Z. I., et al. (2017). Annual community patterns are driven by seasonal switching between closely related marine bacteria. *ISME J.* 11, 1412–1422. doi: 10.1038/ismej.2017.4
- Wright, J. J., Konwar, K. M., and Hallam, S. J. (2012). Microbial ecology of expanding oxygen minimum zones. *Nat. Rev. Microbiol.* 10, 381–394. doi: 10.1038/nrmicro2778
- Xu, Y., Sun, Q., Yi, L., Yin, X., Wang, A., Li, Y., et al. (2014). The source of natural and anthropogenic heavy metals in the sediments of the Minjiang River Estuary (SE China): implications for historical pollution. *Sci. Total Environ.* 493, 729–736. doi: 10.1016/j.scitotenv.2014.06.046
- Yan, S., Fuchs, B. M., Lenk, S., Harder, J., Wulf, J., Jiao, N. Z., et al. (2009). Biogeography and phylogeny of the NOR5/OM60 clade of Gammaproteobacteria. *Syst. Appl. Microbiol.* 32, 124–139. doi: 10.1016/j.syapm.2008.12.001
- Zhang, J., Kobert, K., Flouri, T., and Stamatakis, A. (2014). PEAR: a fast and accurate Illumina Paired-End reAd mergeR. *Bioinformatics* 30, 614–620. doi: 10.1093/bioinformatics/btt593
- Zubkov, M. V., and López-Urrutia, A. (2003). Effect of appendicularians and copepods on bacterioplankton composition and growth in the English Channel. *Aquat. Microb. Ecol.* 32, 39–46. doi: 10.3354/ame032039

**Conflict of Interest Statement:** The authors declare that the research was conducted in the absence of any commercial or financial relationships that could be construed as a potential conflict of interest.

Copyright © 2019 Coclet, Garnier, Durrieu, Omanović, D'Onofrio, Le Poupon, Mullot, Briand and Misson. This is an open-access article distributed under the terms of the Creative Commons Attribution License (CC BY). The use, distribution or reproduction in other forums is permitted, provided the original author(s) and the copyright owner(s) are credited and that the original publication in this journal is cited, in accordance with accepted academic practice. No use, distribution or reproduction is permitted which does not comply with these terms.



# Shift in Natural Groundwater Bacterial Community Structure Due to Zero-Valent Iron Nanoparticles (nZVI)

Marc Crampon\*, Catherine Joulian, Patrick Ollivier, Mickaël Charron and Jennifer Hellal

Bureau de Recherches Géologiques et Minières, Orléans, France

## OPEN ACCESS

### Edited by:

Fabrice Martin-Laurent,  
Institut National de la Recherche  
Agronomique (INRA), France

### Reviewed by:

Naresh Singhal,  
The University of Auckland,  
New Zealand  
Ana Isabel Pelaez,  
University of Oviedo, Spain

### \*Correspondence:

Marc Crampon  
m.crampon@brgm.fr

### Specialty section:

This article was submitted to  
Microbiotechnology, Ecotoxicology  
and Bioremediation,  
a section of the journal  
Frontiers in Microbiology

**Received:** 15 September 2018

**Accepted:** 01 March 2019

**Published:** 19 March 2019

### Citation:

Crampon M, Joulian C, Ollivier P,  
Charron M and Hellal J (2019) Shift in  
Natural Groundwater Bacterial  
Community Structure Due  
to Zero-Valent Iron Nanoparticles  
(nZVI). *Front. Microbiol.* 10:533.  
doi: 10.3389/fmicb.2019.00533

Toxic and persistent contaminants in groundwater are technologically difficult to remediate. Remediation techniques using nanoparticles (NPs) such as nZVI (Zero-Valent Iron) are applicable as *in situ* reduction or oxidation agents and give promising results for groundwater treatment. However, these NP may also represent an additional contamination in groundwater. The aims of this study are to assess the impact of nZVI on the nitrate-reducing potential, the abundance and the structure of a planktonic nitrate-reducing bacterial community sampled in groundwater from a multicontaminated site. An active nitrate-reducing bacterial community was obtained from groundwater samples, and inoculated into batch reactors containing a carbon substrate, nitrate and a range of nZVI concentrations (from 0 to 70.1 mg Fe.L<sup>-1</sup>). Physical (pH, redox potential), chemical (NO<sub>3</sub><sup>-</sup> concentrations) and biological (DNA, RNA) parameters were monitored during 1 week, as well as nZVI size distribution and mortality of bacteria. Nitrate-reducing activity was temporally stopped in the presence of nZVI at concentrations higher than 30 mg L<sup>-1</sup>, and bacterial molecular parameters all decreased before resuming to initial values 48 h after nZVI addition. Bacterial community composition was also modified in all cultures exposed to nZVI as shown by CE-SSCP fingerprints. Surprisingly, it appeared overall that bacteria viability was lower for lower nZVI concentrations. This is possibly due to the presence of larger, less reactive NP aggregates for higher nZVI concentrations, which inhibit bacterial activity but could limit cell mortality. After 1 week, the bacterial cultures were transplanted into fresh media without nZVI, to assess their resilience in terms of activity. A lag-phase, corresponding to an adaptation phase of the community, was observed during this step before nitrate reduction reiterated, demonstrating the community's resilience. The induction by nZVI of modifications in the bacterial community composition and thus in its metabolic potentials, if also occurring on site, could affect groundwater functioning on the long term following nZVI application. Further work dedicated to the study of nZVI impact on bacterial community directly on site is needed to assess a potential impact on groundwater functioning following nZVI application.

**Keywords:** zero-valent iron nanoparticles (nZVI), groundwater, nitrate-reducing bacterial community, ecotoxicity, remediation

## INTRODUCTION

Due to their specific properties and high specific surface area, engineered nanoparticles (NP) are increasingly produced and used, leading to higher releases in the environment (Buzea et al., 2007). In particular, use of nanotechnology for environmental applications, such as remediation of contaminated groundwater, have steadily increased (Bardos et al., 2018). Among NP, nanoscale Zero-valent Iron (nZVI) particles are one of the most widely used NP for nanoremediation, because of their capacity to degrade a wide range of contaminants (Zhang, 2003; Zhang and Elliott, 2006; Mueller et al., 2012). Zero-valent iron (ZVI) is efficient for the dechlorination of PCE because of its ability to dehalogenate chlorinated compounds by chemical reduction (Fu et al., 2014). ZVI can be used in groundwater in permeable reactive barriers (PRB), that show effective degradation, but this technique is expensive, invasive and constrained by installation limits (Obiri-Nyarko et al., 2014). In this framework, an interesting alternative, can be direct injection of ZVI NPs into the aquifer, enabling the treatment of both source and plume areas (Cundy et al., 2008; Thiruvengkatachari et al., 2008; Stefaniuk et al., 2016). However, when directly injected into an aquifer, nZVI widely interact with bacteria and bacterial biofilms (Goldberg et al., 2007), which may affect nZVI mobility and reactivity. These NP may also present a toxicity for groundwater bacteria. Bacteria present in groundwater are relevant and sensitive indicators of soil or groundwater perturbations because of their key role in biogeochemical cycling (Brookes, 1995; Kandeler et al., 1996; Holden et al., 2014). They can be particularly important in the case of contaminated groundwater because of their ability to metabolize a wide range of contaminants (Antizar-Ladislao and Galil, 2010; Weaver et al., 2015; Zhao et al., 2016). Thus if nZVI application affects bacterial communities then it will also affect biogeochemical reactions occurring in the subsurface.

Several mechanisms of nZVI toxicity towards living organisms have been identified. The first is direct nZVI contact with biological components (O'Carroll et al., 2013). In the majority of studies that used electron microscopy to evaluate damage to cell integrity, precipitation of nZVI or iron oxides on the cell wall or inside the bacterial cells was commonly observed, suggesting that direct contact of nZVI with bacterial cells is required for nZVI to exert toxicity (Auffan et al., 2008; Diao and Yao, 2009; An et al., 2010; Barnes et al., 2010; Li et al., 2010; Xiu et al., 2010; Sevcu et al., 2011; Wille et al., 2017; Jiang et al., 2018; Xue et al., 2018). The second is the release of reactive oxidative species (ROS), such as hydroxyl radicals, superoxide radicals and hydrogen peroxide (Barnes et al., 2010), generated by nZVI in the aqueous phase (Liu et al., 2014). ROS are normally scavenged by antioxidants and various enzymes; however, elevated concentrations of ROS in microbial cells can result in oxidative stress. The damages caused to DNA in the presence of various organisms, including bacteria, were observed in other studies (Sacca et al., 2014; Ghosh et al., 2017). It has also been shown that some bacteria are able to produce proteins that protect them from oxidative stress caused by nZVI (Chaithawiwat et al., 2016; Xue et al., 2018). When nZVI is added into an aqueous medium, a burst

of oxidants is produced as Fe<sup>0</sup> and ferrous iron (Fe[II]) are converted to ferric iron (Fe[III]). Finally, the release of ferrous iron from nZVI followed by the Fenton reaction can also affect organisms (Xie and Cwiertny, 2012). Furthermore, although the mechanism of nZVI toxicity at the cellular level has not been fully determined, recent studies support the combined effect of biophysical nanoparticle/cell interactions and oxidative stress (Li et al., 2010; Wille et al., 2017; Crampon et al., 2018).

Impact of nZVI towards bacteria has been considerably studied (Jang et al., 2014), sometimes highlighting positive impacts (Wei et al., 2012; Kocur et al., 2016; Dong et al., 2019) and sometimes negative ones (Fajardo et al., 2013; Sacca et al., 2014; Dong et al., 2019). However, these studies generally focus on isolated species rather than addressing the complexity of natural groundwater bacterial communities (Lefevre et al., 2016) although toxicity of xenobiotics may be affected by interactions between the different members of a community. It is thus important to study their impact at the community scale. Indeed, inside a community, the degradation processes are often the result of synergistic degradation or cooperative metabolic interactions (Dejonghe et al., 2003; Freilich et al., 2011), especially in the case of multi-contamination. All members of the community may thus have a key-role in the degradation process. As it has been shown that nZVI may inhibit some groups but not the others inside a bacterial community (Kirschling et al., 2010; Xiu et al., 2010; Fajardo et al., 2013; Xue et al., 2018; Dong et al., 2019), it is important to characterize the toxicity at the scale of the whole community.

In this context, this study aims to deepen our understanding of the impact of nZVI towards groundwater bacterial communities by monitoring the impact of a gradient of nZVI concentrations on the nitrate-reducing potential, the abundance and the structure of a planktonic nitrate-reducing bacterial community. The experimental design was set up in order to monitor bacterial community resistance then resilience after being exposed to nZVI.

## MATERIALS AND METHODS

### Experimental Design

Both the toxicity of nZVI towards bacteria and the resilience of bacteria were studied by using a series of batch experiments. Three distinct steps were carried out and are illustrated in **Figure 1**. Step 1 consisted in enriching a heterotrophic nitrate-reducing community from a natural groundwater collected from an industrial site by adding a carbon substrate [10 mM sodium acetate (C<sub>2</sub>H<sub>3</sub>NaO<sub>2</sub>)], yeast extracts at 0.2 g L<sup>-1</sup> and sodium nitrate (NaNO<sub>3</sub>) to a volume of groundwater (v/v) and monitoring nitrate reduction (Wille et al., 2017). Total nitrate reduction was obtained after about 48 h, then experiment proceeded to step 2. Step 2 was carried out for almost 5 days and consisted in two phases. The first one was the inoculation of the pre-culture at a ratio of 1/10 into hermetically sealed 250 mL Schott® flasks containing 180 mL of synthetic water enriched with a carbon substrate (10 mM sodium acetate), yeast extracts at 0.2 g L<sup>-1</sup> and sodium nitrate, for a final volume of 200 mL.

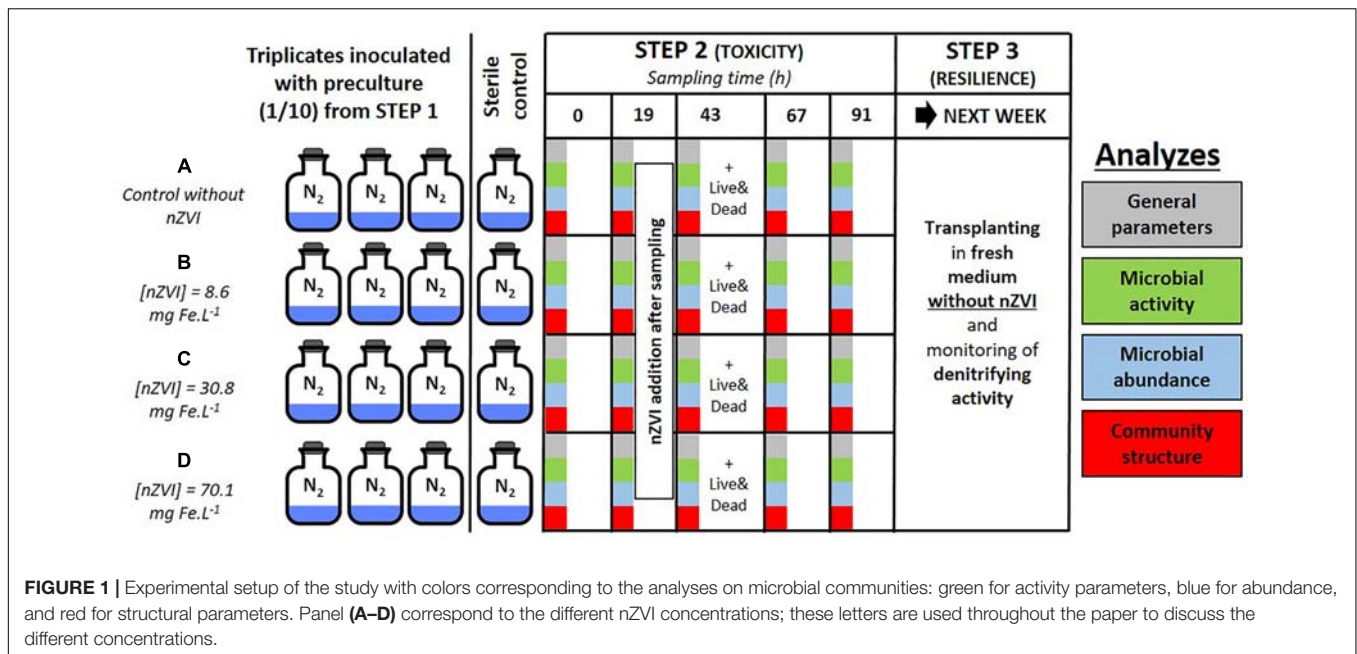


**FIGURE 1 |** Experimental setup of the study with colors corresponding to the analyses on microbial communities: green for activity parameters, blue for abundance, and red for structural parameters. Panel (A–D) correspond to the different nZVI concentrations; these letters are used throughout the paper to discuss the different concentrations.

The second phase started after 19 h incubation in the dark at 20°C under agitation and confirmation of triggered nitrate reduction, when nZVI was added to triplicate flasks in order to expose the bacteria to a gradient of nZVI amounts: condition A (control without nZVI), B (8.6 mg Fe.L<sup>-1</sup>), C (30.8 mg Fe.L<sup>-1</sup>), and D (70.1 mg Fe.L<sup>-1</sup>). The addition of nZVI was carried out in an anaerobic chamber under a continuous flow of nitrogen (Figure 1). A sterile control without the bacterial inoculum was set up for each condition. 12 mL of liquid samples were collected daily up to 91 h incubation (at 0, 19, 43, 67, and 91 h, samples called T0, T19, T43, T67, and T91, respectively), and analyzed for chemical and biological parameters as described below. nZVI were added to the cultures after the T19 sampling. The third and last step of the experiment consisted of re-inoculating bacterial communities from conditions A, B, C, and D into fresh media (ratio 1/10, synthetic water in the same conditions as step 2) without nZVI to assess community resilience. These new batches were monitored for 3 days until all nitrate was reduced (samples collected at 0, 15, and 39 h incubation).

The synthetic water used in these experiments is FIm water corresponding to moderately hard water as described in US EPA Report EPA-821-R-02-012, Section 7.2.3.1 (US EPA, 2002). This water was prepared as previously described in Crampon et al. (2018), and was composed of 96 mg L<sup>-1</sup> NaHCO<sub>3</sub>, 60 mg L<sup>-1</sup> CaSO<sub>4</sub>.2H<sub>2</sub>O, 60 mg L<sup>-1</sup> MgSO<sub>4</sub>, and 4 mg L<sup>-1</sup> KCl. The pH ranged from 7.4 to 7.8, the hardness ranged from 80 to 100 mg CaCO<sub>3</sub>.L<sup>-1</sup> and the alkalinity from 57 to 64 mg CaCO<sub>3</sub>.L<sup>-1</sup> as described by US EPA. The synthetic water was purged with N<sub>2</sub> to remove any oxygen prior to culture medium preparation.

In this experimental setup, as a model activity for the groundwater bacterial community, we focused on bacterial nitrate reduction. This was assessed by measuring nitrate depletion and the abundance of the *narG* gene and its

expression. The overall bacterial community was also characterized by determining abundance (qPCR 16S rRNA), structure (CE-SSCP), composition (Cloning/Sequencing) and viability (LIVE&DEAD®). Physico-chemical parameters were also followed such as pH, redox potential (ORP) and NP size. All analytical approaches are described in the following sections.

### Physico-Chemical Analyses

Fe concentrations were measured by ICP-AES (Jobin Yvon Horiba Ultima 2; Horiba, Japan) in water samples from the cultures at the beginning of the experiment, after acidification with HCl (to obtain a pH < 2). Presented values correspond to the means of two culture replicates for each range of nZVI concentration. Obtained Fe concentrations were 8.6 ± 1.4 mg Fe.L<sup>-1</sup> ( $n = 2$ ) for the lower concentrations (condition B), 30.8 ± 10.2 mg Fe.L<sup>-1</sup> for intermediate concentrations (condition C) and 70.1 ± 14.8 mg Fe.L<sup>-1</sup> for higher concentrations (condition D).

Due to the presence of ions in the culture medium, NP aggregates were expected to form. The size and zeta potentials of these aggregates were consequently measured. The size of NP aggregates was measured using Dynamic Light Scattering (DLS, Malvern Zetasizer Nano ZS, Malvern, United Kingdom) in cultures at the end of step 2. It was not possible to distinguish here homo- (formed by nZVI aggregation) from hetero- aggregates (formed by aggregation of nZVI with bacteria and/or biofilm). Electrophoretic mobility (EPM) was measured and the apparent zeta potential at 25°C was calculated automatically by Zetasizer software using the Smoluchowski equation (Hunter, 2001). The polydispersity index (PdI) was used as an indicator of the distribution width. A lower PdI corresponds to a lower sorting of NP, due to the presence of a higher amount of aggregates in solution.

Measurements of pH and redox potential (ORP) were performed for each sampling point in an anaerobic chamber under N<sub>2</sub> atmosphere. Measurements were done with a VTW Multi parameter unit (VTW/Xylem, Inc., Germany) with specific pH and ORP electrodes.

### Nitrate Reduction Activity Measurements

The determination of nitrate concentrations was performed on filtrated water (10 mL, filtration through a 0.22 μm mixed cellulose esters membrane GSWP, Merck Millipore). The analyses were performed at T0, and after 19, 43 h (i.e., 24 h after nZVI addition), 67 and 91 h growth during step 2 and at T0 and after 15 and 39 h growth during step 3. The concentrations of NO<sub>3</sub>-N were determined by spectrophotometry using a Nova 60 Spectroquant spectrophotometer (Merck/Millipore, Germany) with a specific Spectroquant nitrate kit (reference 114563, Merck/Millipore). The range of concentrations of the kits was 0.1 to 25 mg L<sup>-1</sup> of NO<sub>3</sub>-N. We decided to focus here on nitrate measurements rather than on the reduction product nitrite as it was only transient and most often below limits of quantification when measured.

## Characterization of Bacterial Communities

### LIVE/DEAD® BacLight™ Viability Assays

LIVE/DEAD® BacLight™ Bacterial Viability Kits were used according to the manufacturer's instructions (Invitrogen, Carlsbad, CA, United States). In brief, a volume of reactive containing a mixture of SYTO 9 dye (green-fluorescent nucleic acid stain) and Propidium iodide (red-fluorescent nucleic acid stain) is added to an equal volume of culture medium, mixed then incubated in the dark at room temperature for 15 min. Cells are then observed and counted using a fluorescent microscope with filters in the range of 480/500 nm for SYTO 9 stain and 490/635 nm for propidium iodide. SYTO 9 dye tends to stain all bacteria in a population whereas propidium iodide only penetrates cell walls of damaged bacteria, thus showing "live" bacteria as green and "dead" bacteria as red. Observations were made on samples from step 2, at T43, i.e., 24 h after nZVI addition. Preliminary tests (data not shown) were performed on the bacterial community at nZVI concentrations of 10, 30, and 50 mg Fe.L<sup>-1</sup> to perform counts of living and dead cells.

### DNA and RNA Extractions and cDNA Generation

Extractions of DNA and RNA were performed on samples before nZVI addition (T19), after nZVI addition (T43, i.e., 24 h after nZVI addition) and after 67 h incubation (T67, i.e., 48 h after nZVI addition). Biomass was recovered by filtering 10 mL culture on 0.22 μm filters (mixed cellulose esters membrane GSWP, Ø 25 mm, Merck Millipore).

Genomic DNA and total RNA were co-extracted directly from the filters with the combination of MO Bio/QIAGEN (Valencia, CA, United States) kits. First, RNA was extracted with Mo Bio RNeasy® PowerSoil® Total RNA Kit, and DNA was then recovered thanks to the DNA Elution Accessory Kit, according to the manufacturer's instructions. Remaining DNA was removed from RNA extracts with the turbo DNase (Ambion, Carlsbad,

CA, United States) according to the manufacturer's instructions, and RNA was resubmitted to the purification step of the RNeasy® PowerSoil® Total RNA Kit. The absence of DNA in RNA extracts was confirmed by no PCR signal (see below for PCR conditions). Quantifications of extracted RNA and DNA were performed with the Quantus Fluorometer, using 1 μL extract and the QuantiFluor dsDNA solution (Promega, Charbonnières-les-Bains, France).

The cDNA were obtained from 50 ng RNA extracts by RT-PCR performed on with iScript™ cDNA synthesis kit and iScript™ Reverse Transcription Supermix kit (Biorad), following the manufacturer's instructions.

DNA and cDNA were stored at -20°C and RNA at -80°C.

### qPCR of 16S rRNA and narG Genes

Quantification of the bacterial 16S rRNA and *narG* gene copies was performed by qPCR using a CFX Connect™ Real-Time PCR Detection System (Bio-Rad, France) with primers 341F (3'-CCTACGGGAGGCAGCAG-5') and 515R (3'-ATTACCGCGGCTGCTGGCA-5') (López-Gutiérrez et al., 2004) for 16S rRNA gene, and primers narG-F (5'-TCGCCSATYCCGGCSATGTC-3') and narG-R (5'-GAGTTGTACCAGTCRGCAGAYTCSG-3') for nitrate reductase *narG* gene carried by *Proteobacteria* (Bru et al., 2007), as only *Proteobacteria* developed in the batch experiments. qPCR reactions were performed in a total volume of 20 μL, with a master mix containing 7.6 μL of sterile, nuclease- and nucleic acids-free water (MP Biomedicals, Santa Ana, CA, United States), 10 μL of SSO Advanced Universal SYBR Green Supermix (Bio-Rad), 500 nM of each primer, 100 ng of T4 GP32, and 2 μL of template DNA (0.1 to 5 ng μL<sup>-1</sup>) or 2 μL of cDNA. Sterile, nuclease- and nucleic acids-free water was added instead of DNA in no template controls. PCR reactions were performed as follows: 3 min 95°C, followed by 35 cycles: 30 s 95°C/30 s 60°C/30 s 72°C/for 16S rRNA gene or 6 cycles: 30 s 95°C/30 s 63°C/30 s 72°C, 34 cycles: 30 s 95°C/30 s 58°C/30 s 72°C for *narG* gene, followed by 30 s at 80°C for data acquisition, with an additional step rising from 60 to 95°C at 0.5°C/s for melt curves generation. All samples, controls and standards were analyzed in duplicates. A calibration curve was obtained from serial dilutions of a known quantity of linearized plasmids containing known copy numbers of 16S rRNA or of *narG* gene. Results were reported as gene copies per mL of culture medium. Generation of a specific PCR product was confirmed by melting curve analyses and agarose gel electrophoresis.

### CE-SSCP Fingerprints

The bacterial community structure in cultures during the experiment was determined by 16S rRNA gene CE-SSCP fingerprints. About 200 bp of the V3 region of bacterial 16S rRNA genes were amplified from DNA and cDNA with the forward primer w49 (5'-ACGGTCCAGACTCCTACGGG-3'; *Escherichia coli* position, 331) and the reverse primer w34 (5'-TTACCGCGGCTGCTGGCAC-3'; *E. coli* position, 533), as previously described in Crampon et al. (2018). The 5' end was then labeled with the fluorescent dye FAM. 25 cycles and hybridization at 61°C were used. One μL of diluted (150-fold in nuclease-free water) PCR product was added to a mixture

of 18.8  $\mu\text{L}$  of deionized formamide and 0.2  $\mu\text{L}$  of Genescan-600 LIZ internal standard (Life Technologies, Carlsbad, CA, United States). To obtain single-strand DNA, samples were heat denaturated for 5 min at  $95^\circ\text{C}$ , and immediately cooled on ice. CE-SSCP analyses were performed on an ABI Prism 310 genetic analyzer using a 47-cm length capillary, a non-denaturing 5.6% CAP polymer (Life Technologies) and the following electrophoresis conditions: run temperature  $32^\circ\text{C}$ , sample injection for 5 s at 15 kV, data collection for 35 min at 12 kV. The dataset was analyzed using the software BioNumerics V7.5 (Applied Maths) and lining fingerprints up to the internal standard and to a common baseline.

### Bacteria Taxonomic Identification

About 1,400 bp of the bacterial 16S rRNA gene were amplified from the DNA and cDNA. Universal bacterial primers 8F (5'-AGAGTTTGATCMTGGCTCAG-3') and 1406R (5'-ACGGGCGGTGTGTRC-3') were used with hybridization at  $55^\circ\text{C}$  and 30 cycles. Purified PCR products (NucleoSpin® Gel and PCR clean-up, Macherey–Nagel) were used to construct a gene library with the TOPO-TA Cloning Kit and TOP 10 chemically competent cells (Invitrogen, Carlsbad, CA, United States). To ensure good characterization of the dominant strains detected by CE-SSCP, positive transformants were analyzed by CE-SSCP to find correspondence of clones over the whole community. Based on their migration profile, seven clones were selected for sequencing the insert with vector primers T7 and T3 (Sanger sequencing by GATC Biotech). All seven sequences were submitted to NCBI GenBank under Accession Nos. MH686140 to MH686146.

### Phylogenetic Analysis

The phylogenetic assignment of unambiguous consensus sequences was based on comparison with reference sequences by the NCBI Blast tool<sup>1</sup>. Multiple alignment of sequences and consensus were performed using BioEdit software version 7.0.5.3 (Hall, 1999). The phylogenetic tree was constructed using the neighbor-joining method of Jukes and Cantor (Saitou and Nei, 1987), and checked by UPGMA method included in MEGA 10 package (version 10.0.1). The tree topology was tested by bootstrap analysis of 1,000 resamplings. An *E. coli* 16S rRNA gene sequence was used as an outgroup.

### Statistical Analyses

Statistical analyses were performed on XLStat software version 2017 (Addinsoft) for MS excel. Principal Coordinate

Analyses were built from Pearson's correlations coefficients similarity matrices, from triplicates values of the different analyzed parameters. As trends are not linear with nZVI concentrations (inversed trends), control samples were excluded from PCoA analyses.

## RESULTS

### Physico-Chemical Parameters

The mean sizes of nZVI were measured at the end of the first week of the experiment, as well as ZP, in triplicates for each nZVI concentration. ZP of nZVI in cultures was logically negative, and ranged from  $-37.1$  to  $-23.3$  mV.

Globally, PdI was lower for higher nZVI concentrations [PdI =  $0.45 \pm 0.03$  ( $n = 3$ ) and  $0.46 \pm 0.08$  ( $n = 3$ ) for Fe concentrations of 30.8 and 70.1 mg  $\text{Fe.L}^{-1}$ , respectively], meaning that a higher concentration of nZVI leads to a lower sorting of aggregates. PdI mean was  $0.57 \pm 0.11$  ( $n = 3$ ) for lower nZVI concentrations (i.e., 8.6 mg  $\text{Fe.L}^{-1}$ ), showing the presence of less aggregates of different sizes in cultures, and consequently the presence of a higher number of individualized NP.

Even if a trend is observed, showing a higher mean diameter for higher nZVI concentrations (Table 1), the mean sizes were not significantly different between the different concentrations ( $P > 0.05$ , Kruskal–Wallis test with Conover–Iman pair comparison). Concerning nZVI size sorting shown by PdI values (a value of 1 corresponding to a monodisperse sample, 0 to a polydisperse sample), no significant difference could be highlighted either between the different concentrations ( $P > 0.05$ , Kruskal–Wallis test with Conover–Iman pair comparison). However, a trend was again observed (Table 1), with a better sorting for lower nZVI concentrations.

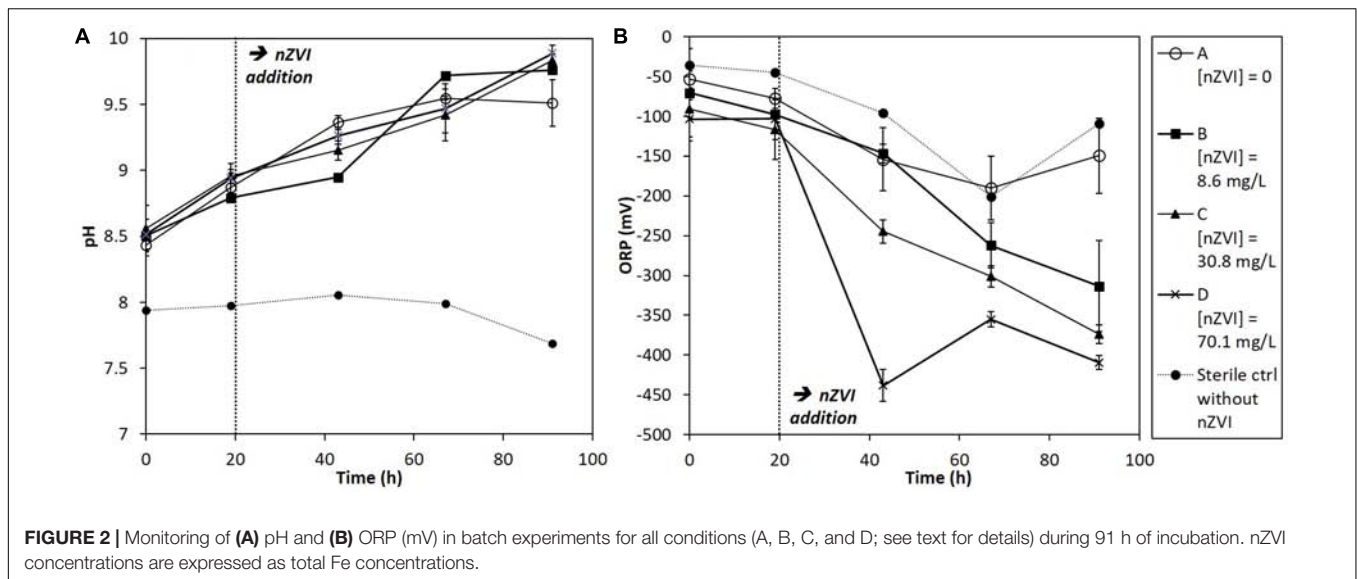
Redox potential (ORP) and pH trends were measured in cultures at each sampling date (Figure 2). Globally, pH tended to increase during the experiment in all conditions due to the bacterial activity, whereas it was stable in sterile controls (Figure 2A). The pH of cultures rose up to around 10 at the end of the experiment. Concerning ORP, it greatly decreased, straight after nZVI addition, logically due to nZVI reduction properties (Figure 2B). The lowest ORP values were observed for the highest nZVI concentrations. No ORP decrease was observed just after nZVI addition for the lower concentration (B, 8.6 mg  $\text{Fe.L}^{-1}$ ) compared to the absence of nZVI and to higher nZVI concentrations, but ORP tended to decrease to about  $-300$  mV after 91 h of incubation.

<sup>1</sup><http://www.ncbi.nlm.nih.gov/blast/Blast.cgi>

**TABLE 1** | Values of Fe concentration, mean NP sizes, PdI and zeta potentials obtained by ICP-AES and DLS analyses in the different cultures.

	A (Control without nZVI)	B ([nZVI] = 8.6 mg $\text{Fe.L}^{-1}$ )	C ([nZVI] = 30.8 mg $\text{Fe.L}^{-1}$ )	D ([nZVI] = 70.1 mg $\text{Fe.L}^{-1}$ )	
Fe concentrations	mg.L <sup>-1</sup>	0.0 ± 0.0	8.6 ± 1.4	30.8 ± 10.2	70.1 ± 14.8
NPs mean diameter	nm	NA	1094.5 ± 135.0	1076.0 ± 38.7	1307.0 ± 74.2
PdI	-	NA	0.572 ± 0.119	0.449 ± 0.037	0.405 ± 0.133
Zeta potential	mV	NA	-26.8 ± 0.6	-24.0 ± 1.0	-32.5 ± 6.5

NA, not applicable.



## Effects of nZVI on Microbial Abundance

### Molecular Biomass

The total genomic DNA extracted from samples gives an indication of the total molecular biomass. Molecular biomass decreased after nZVI addition for all nZVI concentrations (T43; **Figure 3A**). The decrease was significant ( $P < 0.05$ , Student's *t*-test) for conditions B (8.6 mg Fe.L<sup>-1</sup>) and C (30.8 mg Fe.L<sup>-1</sup>), but not for the D modality (70.1 mg Fe.L<sup>-1</sup>). Moreover, the decrease in molecular biomass was higher for condition B compared to condition C. These results suggest that the highest impact on molecular biomass occurs for lower nZVI concentrations. Forty-eight hours after exposure (T67), molecular biomass increased and reached control values, suggesting a resilience of microorganisms in the community. Surprisingly, at T67, the highest molecular biomass was measured in condition B, where the initial impact on molecular biomass, measured at T43, was highest.

### Bacterial Abundance

As for molecular biomass, nZVI had a significant impact on bacterial abundance, as shown by the decrease in the number of copies of the 16S rRNA gene at T43 in cultures exposed to nZVI in conditions B, C, and D (**Figure 3B**). This impact was significant ( $P < 0.05$ , Student's *t*-test) for all modalities. However, the highest impact of nZVI was again observed for lower concentrations (i.e., 8.6 mg Fe.L<sup>-1</sup>). Finally, 48 h after exposure (T67), the abundance of the 16S rRNA gene was comparable to values measured in control samples, again suggesting a resilience of the bacterial community.

### Nitrate-Reducing Bacteria Abundance

The determination of *narG* gene copies gives an indication of the abundance of nitrate-reducing bacteria in the bacterial community. As was observed for molecular biomass (genomic DNA concentration) and bacterial abundance (numbers of

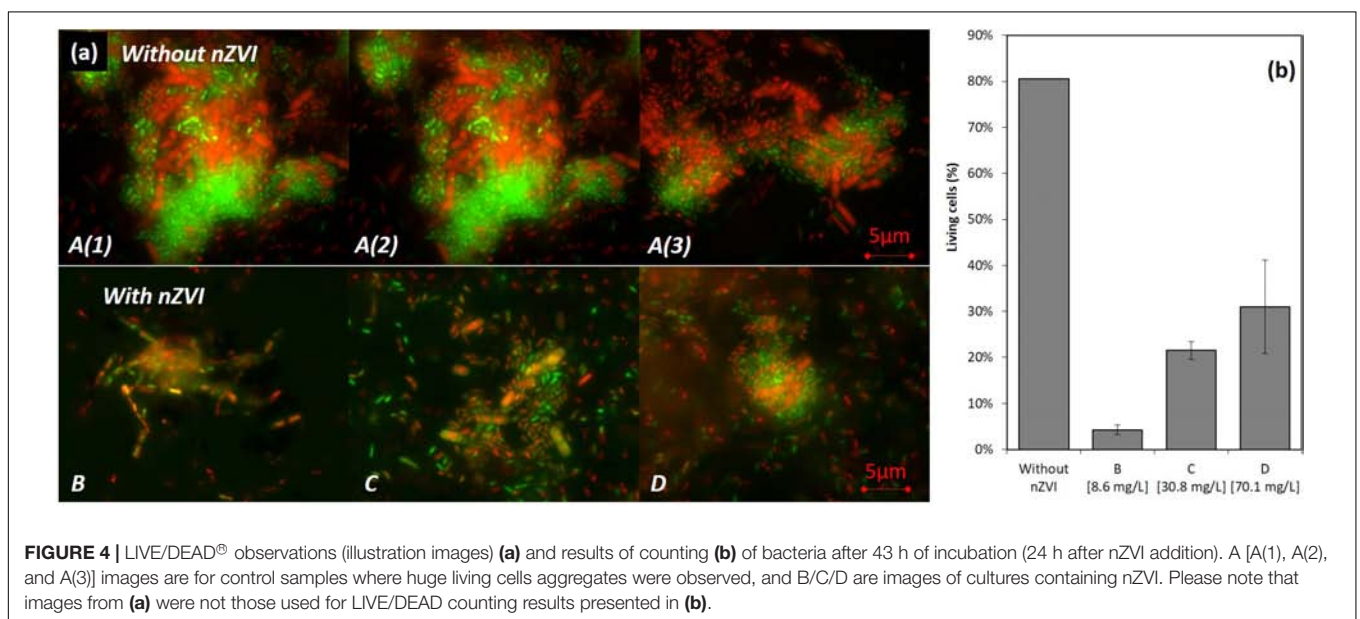
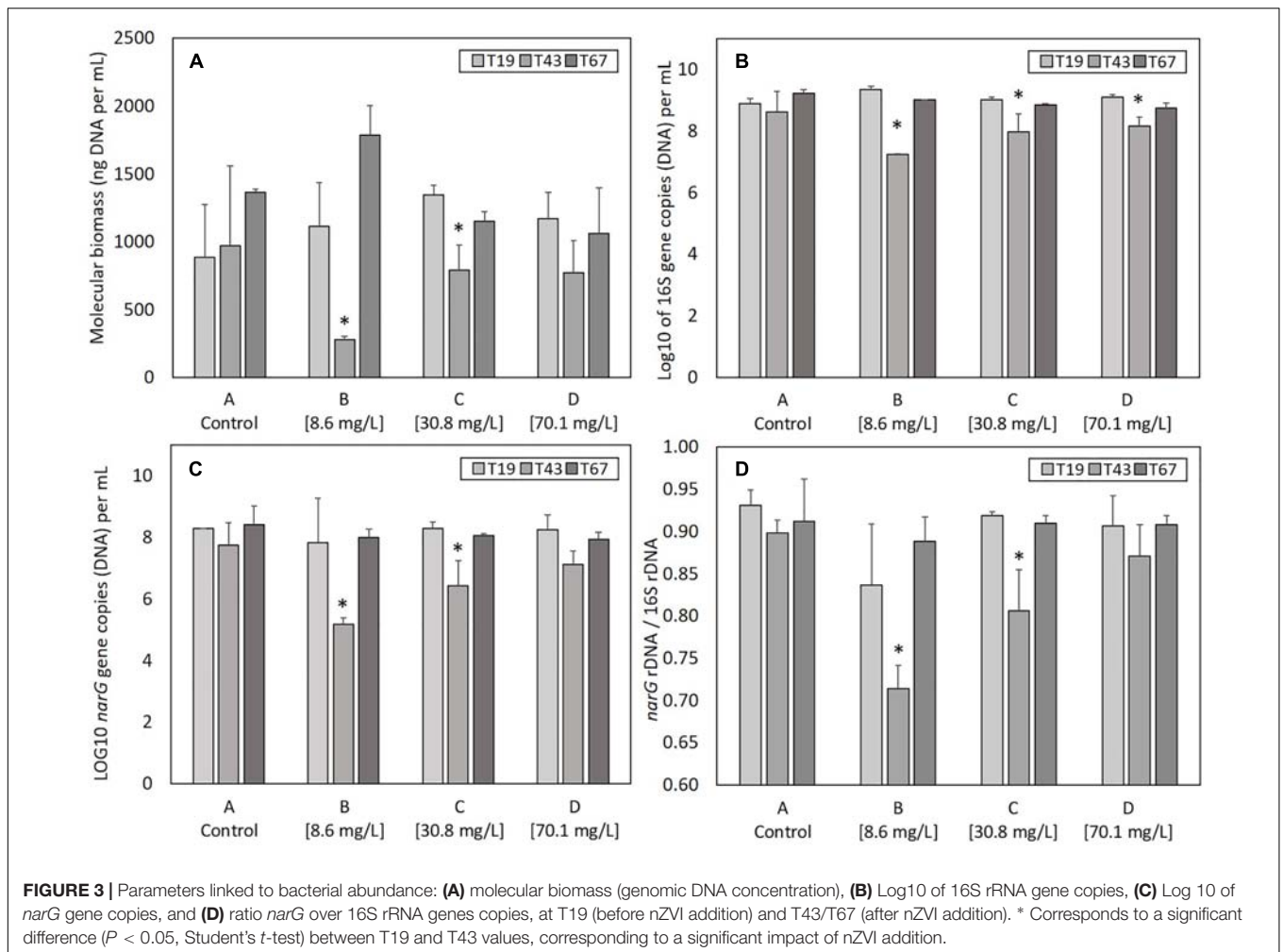
16S rRNA gene copies), a decrease in the abundance of nitrate-reducing bacteria occurred after nZVI addition (T43) independently from nZVI concentrations (**Figure 3C**). This decrease was only significant for conditions B and C (8.6 and 30.8 mg Fe.L<sup>-1</sup>, respectively,  $P < 0.05$ , Student's *t*-test). After 48 h of exposure (T67), the abundance of nitrate-reducing bacteria was comparable to those of the controls. Again, the lowest concentration of nZVI showed the highest impact, but the nitrate-reducing bacteria were resilient, in terms of biomass, after 48 h exposure.

Calculating the ratio between *narG* and 16S rRNA genes gives an indication of nZVI impact specifically on nitrate-reducing bacteria over the whole community (**Figure 3D**). Before nZVI addition, about 90% of total bacteria carried the *narG* gene. This value is significantly lower after nZVI addition for conditions B and C, especially for the lowest nZVI concentration. This value drops to around 70% of nitrate-reducing bacteria in the whole community for condition B, and 80% for condition C. The ratio of nitrate-reducing bacteria is the same for condition D (70.1 mg Fe.L<sup>-1</sup>) compared to control. Overall, these parameters remained stable for the control condition A.

### Bacteria Viability

In the control condition A (no nZVI), many live bacteria aggregates were observed after 43 h of incubation [T43; A(1), A(2), and A(3) in **Figures 4a,A**]. However, with nZVI (**Figures 4a,B-D**), bacterial aggregates were not found, except smaller ones in condition D, and more dead cells were present.

A viability of around 80% in the control condition was observed (counts were performed on diluted samples with between 10 and 50 cells per image). This value drops to around 5% in condition B, 20% in condition C and 40% for the highest concentration in condition D (**Figure 4b**). The higher toxicity in the presence of lower concentrations of nZVI is thus again confirmed here by LIVE/DEAD® observations, with a smaller number of living cells in the case of lower nZVI concentrations.



## Effects of nZVI on Microbial Activity

### Nitrate Reduction Kinetics

The nitrate concentrations in sterile controls remained stable all along the experiment. Moreover, nZVI had no significant impact on nitrate concentrations (**Supplementary Material SM2**). Therefore, the observed nitrate reduction in cultures is of bacterial origin. Before nZVI addition (**Figure 5A**), nitrate reduction occurred and was repeatable for all conditions. After nZVI addition, nitrate reduction stopped in all cultures, except in control without nZVI. However, 24 h after nZVI addition (T43), nitrate reduction activity was again observed in all cultures with nZVI. After 91 h, remaining nitrate concentrations were even lower than in cultures without nZVI. These results highlight a resilience capability of the nitrate-reducing bacterial community after exposure to nZVI, even if nZVI initially had a significantly toxic impact on nitrate reduction ( $P > 0.05$ , Kruskal–Wallis test with Conover–Iman pair comparison).

During the resilience step (second week), nitrate reduction was monitored until complete nitrate disappearance (**Figure 5B**). For all cultures previously exposed to nZVI during the first week experiment, a 15-h lag-phase was observed. The difference was significant between cultures that had not been exposed to nZVI (A), for which no lag phase was observed, and cultures that had been exposed to nZVI (B, C, and D), independently from nZVI concentrations ( $P > 0.05$ , Kruskal–Wallis test).

Of note, in complement to sterile controls presented here, a preliminary experiment was led, with nZVI concentrations ranging from 1 to 500 mg Fe.L<sup>-1</sup> in sterile conditions and with comparable NO<sub>3</sub> concentrations, to study the impact of nZVI on nitrates (**Supplementary Material SM1**). The presence of nZVI did not impact nitrate concentrations, independently from nZVI concentrations.

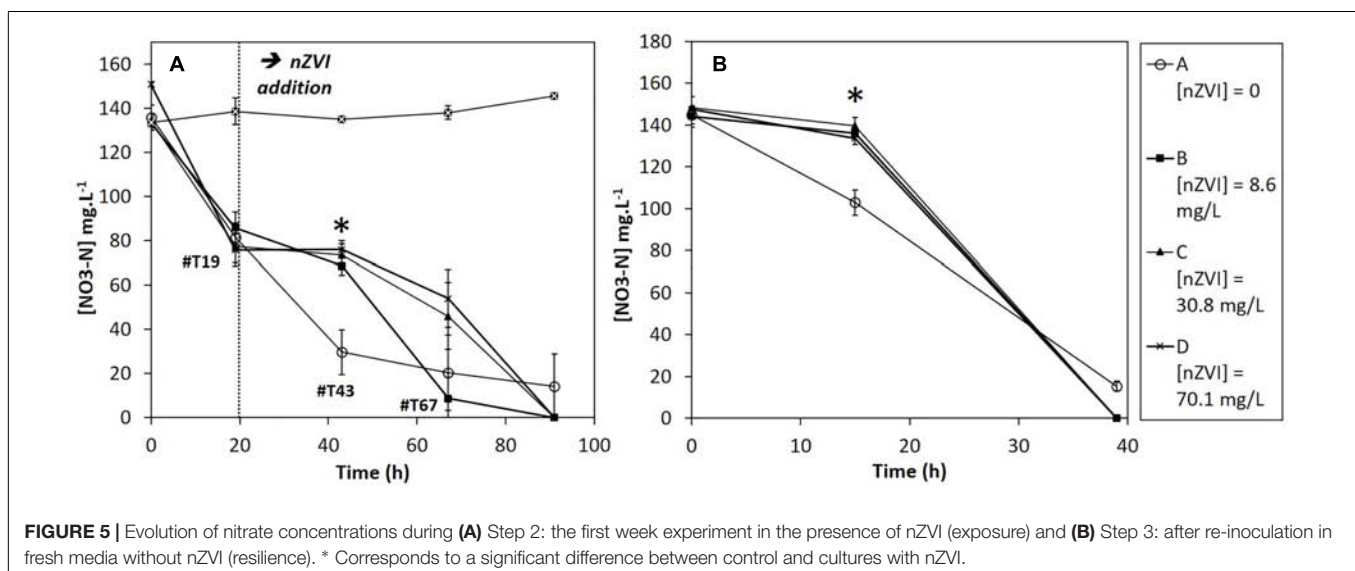
### Bacterial Activity: RNA vs. DNA

As ribosome content (rRNA) in bacterial cells is an indicator of active or recently active bacteria, ratios of 16S rRNA copy

numbers (determined from cDNA generated from total RNA) to 16S rRNA gene copy numbers (determined from DNA) was used to evaluate the growth state of the bacterial community (**Figure 6A**). 16S rRNA/16S rDNA ratio was highest 24 h after nZVI addition (T43) compared to before addition (T19) in all conditions. It was significantly higher ( $P$ -value  $< 0.05$ ) for conditions B and D, and, although statistically un-significant, the same trend was observed for conditions A and C. Thus, despite a negative effect on microbial biomass and bacterial abundance, nZVI did not affect the global growth state of bacteria remaining in the community.

### Nitrate Reduction Activity: *narG* mRNA/16S rRNA and *narG* mRNA/*narG* DNA

*narG* transcripts (*narG* mRNA) were used to evaluate the nitrate reduction activity. The ratio between the number of *narG* mRNA and 16S rRNA (**Figure 6B**) highlights the part of nitrate-reducing activity among active or recently active bacterial cells in the community. No significant changes were observed between controls and cultures containing nZVI or between samples collected just before (T19) and after (T43) nZVI addition. Therefore, the impact of nZVI on the nitrate reduction activity was not clearly highlighted here. Only trends were observed at T43, with a decrease in *narG* transcripts/16S rRNA ratios, suggesting a decrease in the part of nitrate reduction among active or recently active bacterial cells, and again for lower nZVI concentrations. The ratio of *narG* mRNA to *narG* DNA shows the nitrate reduction activity of the nitrate reduction community. No significant differences were observed between controls and conditions with nZVI, or between samples collected just before (T19) and 24 h after (T43) nZVI addition, suggesting that the remaining nitrate-reducing bacteria were active. Even if not significant, the *narG* mRNA/DNA ratio tends to increase at T43 for cultures with nZVI, suggesting that nZVI addition, especially at lower concentrations, slightly increased the activity of remaining nitrate-reducing cells (**Figure 6C**).



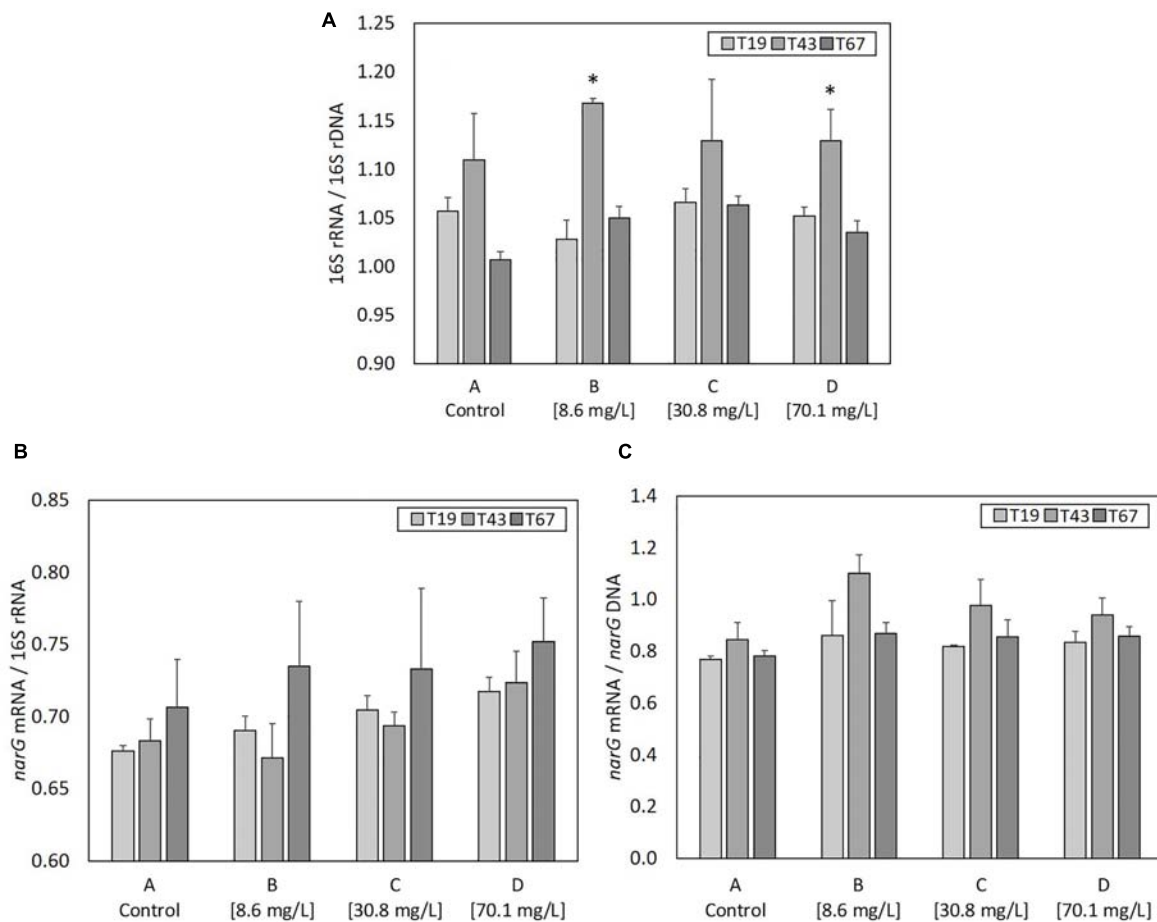


**FIGURE 6 |** Parameters linked to bacterial activity at T19 (before nZVI addition) and at T43/T67 (i.e., after nZVI addition): **(A)** 16S rRNA/16S rDNA (bacterial community growth state), **(B)** *narG* mRNA/16S rDNA (nitrate reduction activity of the bacterial community), and **(C)** *narG* mRNA/*narG* DNA (nitrate reduction activity of nitrate-reducing bacteria over the bacterial community). \* Corresponds to a significant difference ( $P < 0.05$ , Student's *t*-test) between T19 and T43 values, illustrating a significant impact of nZVI addition.

In order to compare the impact of the different nZVI concentrations on biological and physico-chemical parameters at the different times, statistical analyses were performed (PCoA, **Supplementary Material SM3**). No correlations between nZVI concentrations and the different studied parameters were observed, as expected, before nZVI addition (T19). After nZVI addition, the maximum correlation was observed at T43 (24 h after nZVI addition), but was no longer relevant at T67, indicating that the toxicity of nZVI, for these parameters, lasted for no more than 48 h.

## Effects of nZVI on Microbial Community Structure

Beyond the impact on abundance and activity, the bacterial community structure could also be affected by the presence of nZVI. Community CE-SSCP fingerprints of the 16S rRNA gene were performed on (i) DNA and (ii) cDNA, which allows to observe (i) the structure of the total community and (ii) the structure of active or recently active communities. Before

nZVI addition, fingerprints showed three main peaks with one dominating the others, and suggested a low bacterial diversity in all conditions. Overall, fingerprints were similar for DNA and cDNA, highlighting a good adequacy between detection and growth state of all detected bacteria in the cultures. After nZVI addition, a clear shift of the bacterial community structure occurred. A new peak (in red) was detected to the detriment of the dominant peak (in green in **Figure 7**), which was highly affected by nZVI addition (**Figures 7B–D**).

Indeed, especially at T67, a shift in diversity was observed, with the detection of a new peak (in red in **Figure 7**) at the expense of the main peak (in green). This shift was more marked for lower nZVI concentrations (**Figure 7B**), where the new peak became dominant on the fingerprints (**Figure 7**). However, as nZVI concentrations increase, the new peak appears less and less dominant, and proportions between green and red peaks are quite similar for conditions D (**Figure 7**). After nZVI addition, the relative proportion of bacteria corresponding to peaks 1 and 2 increased in the community. This result is intermediate for condition C (**Figure 7C**). For condition B, the new peak in red

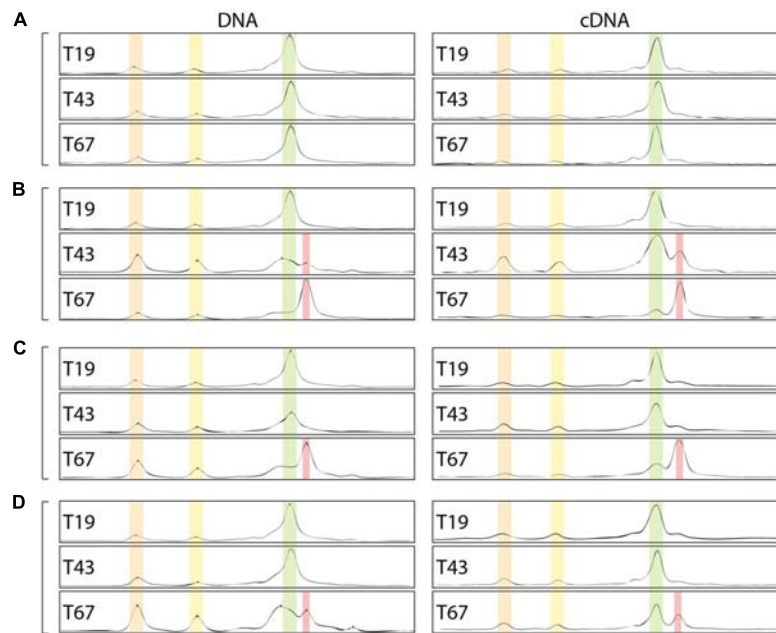


**FIGURE 7** | Bacterial community fingerprints assessed by CE-SSCP of 16S rRNA gene on DNA and RNA (cDNA). **(A–D)** Corresponds to the different nZVI concentrations, i.e., 0, 8.6, 30.8, and 70.1 mg Fe.L<sup>-1</sup>, respectively; T19: before nZVI addition, T43: 24 h after nZVI addition, T67: 48 h after nZVI addition.

appeared at T43, 24 h after nZVI addition, and became dominant at T67, 48 h after nZVI addition. Finally, the relative proportion of increasing bacteria, corresponding to the red peak, was the highest at T67, especially for B and C conditions for which it became the dominant peak. Globally, nZVI had an impact on the bacterial community structure, either favoring or affecting presence and abundance of the bacterial strains.

## Bacteria Identification

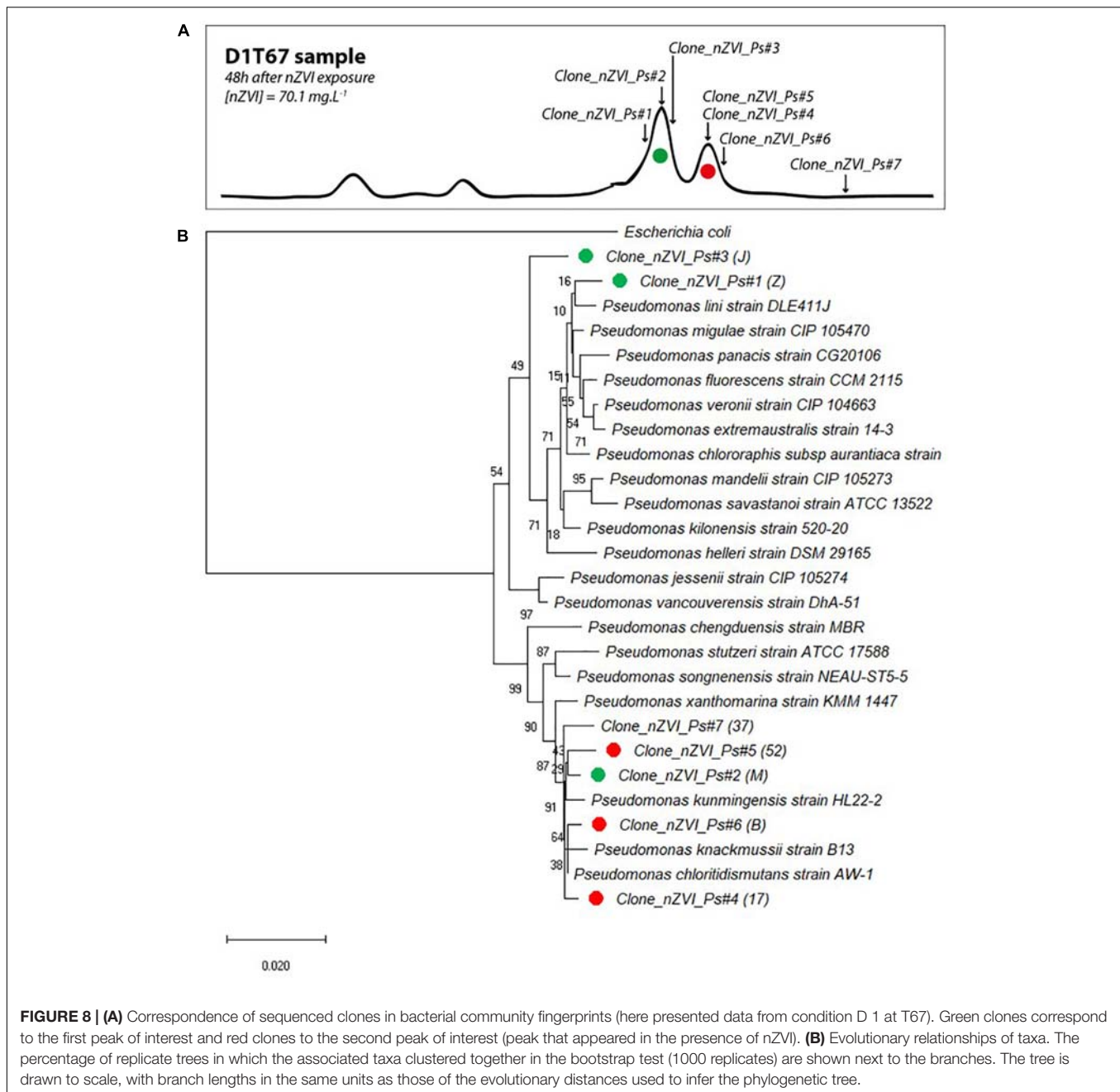
Cloning and sequencing of community 16S rRNA gene at the end of the experiment (T67) and CE-SSCP migration patterns of retrieved clones allowed to attribute several sequences to the main peaks of the fingerprints (**Figure 8A**). All 16S rRNA gene clone sequences were closely related (>99% blast identity) to that of members of the *Pseudomonas* genus (**Figure 8B**). Species from the *Pseudomonas* genus are difficult to distinguish with 16S rRNA gene sequences, as they are very closely related to each other (Anzai et al., 2000). However, although we cannot clearly link a sequence to a species, phylogenetic comparison with close members of the *Pseudomonas* genus confirmed the shift in community composition. For the first peak of interest (in green), prior to nZVI addition, three clones were identified (*Clone\_nZVI\_Ps#1*, #2, and #3). In particular, *Clone\_nZVI\_Ps#1* branched among facultative anaerobic *Pseudomonas* that are able to perform nitrate reduction (**Supplementary Material SM4**). Consequently, *Pseudomonas* strains corresponding to the dominant green peak in the fingerprints could be the one able to perform nitrate reduction, and could be involved in the nitrate reduction process observed in the experiments. For the second peak of interest (in red), after nZVI addition, the three clones identified

(*Clone\_nZVI\_Ps#4*, #5, and #6) are phylogenetically different from *Clone\_nZVI\_Ps#1* and #3. They are highly related to each other (dissimilarity < 0.01%), and very close to *Pseudomonas kunmingensis*, *Pseudomonas knackmussii*, and *Pseudomonas chloritidismutans* sequences. *Pseudomonas kunmingensis* is an aerobic bacteria able to perform nitrate reduction (Romanenko et al., 2005; Xie et al., 2014). *Pseudomonas knackmussii* and *Pseudomonas chloritidismutans* are facultative aerobic bacteria, unable to perform nitrate reduction (**Supplementary Material SM4**). However, as nitrate reduction then resumed, either the rising strain could reduce nitrate or nitrate reduction involved bacteria not detected by CE-SSCP. Indeed, one last clone sequenced (*Clone\_nZVI\_Ps#7*) also affiliated to *Pseudomonas*, did not correspond to a peak visible on the CE-SSCP fingerprint.

## DISCUSSION

This work studied the impact(s) of nZVI addition on the abundance, the activity and the structure of a bacterial community grown from a natural groundwater. This was experimentally assessed by focusing on a key function in groundwater, nitrate reduction. Moreover, a follow-up experiment was carried out to look at the bacterial community's reaction when inoculated in fresh culture medium after their exposure to nZVI.

Addition of nZVI, even at low concentrations of ~9 mg L<sup>-1</sup> significantly decreased molecular biomass and bacterial abundance 24 h after addition as shown by LIVE/DEAD® observations, molecular biomass and 16S rRNA



and *narG* gene abundances. However, molecular biomass then increased again rapidly in all conditions suggesting only a temporary effect on bacterial abundance. Few studies have assessed the impact of nZVI in planktonic groundwater or water studies. Barnes et al. (2010) observed an increase in CFU counts in river water submitted to 100 mg L<sup>-1</sup> nZVI with no initial decrease. Kirschling et al. (2010) also observed no impact of 1.5 g L<sup>-1</sup> nZVI on the number of 16S rRNA gene copies in bacterial communities from TCE contaminated groundwater. However, this was shown after 250 days incubation so it is possible that the community had time to adapt. Fajardo et al. (2012) found little impact of 34 mg.nZVI.g<sup>-1</sup> soil on microbial

viability; however, as underlined by Fajardo et al. (2013) and Sacca et al. (2014), the impact of nZVI in soils is closely linked to their composition whereas in the present study, in an aqueous solution, bacterial communities would be more directly exposed, as it would be the case in aquifers (less complex compared to soils, low content of natural organic matter).

Similarly, the growth state and nitrate-reducing activity, assessed by the ratio of *narG* transcripts and nitrate depletion, were only affected temporally by the three concentrations of nZVI, suggesting an adaptation of the bacterial community to the new environment containing nZVI. The activity of remaining bacteria in condition B, the most affected by nZVI addition,

even appeared to be stronger compared to the less impacted cultures. At the end of the experiment, no nitrates were left in nZVI-exposed cultures, whereas a residue was always found in controls without nZVI. One explanation could be anaerobic corrosion of nZVI, leading to the release of H<sub>2</sub> in the media, a well-known electron donor for bacteria, reinforcing their metabolism and resulting, after an adaptation period, to a more complete nitrate reduction in the presence of nZVI. A lower nitrate concentration was also observed during the resilience step for cultures having been exposed to nZVI, and could be explained both by residual H<sub>2</sub> introduced in fresh media by the inoculum (1/10 volume), or by the bacterial community structure modifications generated by nZVI during the first step of the experiment. Even if nitrate reduction activity resumed and if parameters related to bacterial abundance and activity returned to “normal” values, the structure of the bacterial community was modified by nZVI. Indeed CE-SSCP fingerprints revealed the increase of a new peak after nZVI addition, first in condition B which was the most impacted globally, and then in conditions C and D. This new peak then dominated the incubations and was confirmed to be a different strain to the initially dominating peak by sequencing fragments of 16S rRNA gene. These changes in the community structure due to nZVI were previously studied, and attributed both to H<sub>2</sub> release and changes in redox conditions, favoring the growth of methanogen or sulfate-reducing bacteria (Kirschling et al., 2010; Xiu et al., 2010), but also to some specific nZVI coatings, protecting bacteria from oxidative stress, and creating a new carbon source in the media (Kirschling et al., 2010). In our case (non-coated nZVI), a rapid impact could be observed, attributable to toxic effect (oxidative stress), but the community structure was definitely modified even if nitrate-reduction resumed after a lag-phase. This impact on community structure is highly dependant on the media, as was shown in soils (Fajardo et al., 2018). The variability of the media is however lower in groundwater compared to soils, and so changes in community structure due to nZVI are expected to occur more currently. These results are finally comparable to several previous experiments carried out either in water samples or soils. Indeed, both Fajardo et al. (2012) and Sacca et al. (2014) observed significant changes in bacterial community diversity and structure when applying nZVI to soils as well as Kirschling et al. (2010) in contaminated groundwater using a DGGE approach, whereas Barnes et al. (2010) found no impact of nZVI in river-water bacterial communities.

When re-cultivated in fresh media without nZVI (step 3), the temporary inhibition in nitrate reduction observed for cultures previously exposed to nZVI could also correspond to an adaptation period in the opposite way, due to the absence of nZVI in fresh substrate. Lag phase represents the earliest and most poorly understood stage of the bacterial growth cycle (Rolfe et al., 2012). In bacterial growth models, lag phase is generally described as an adaptation phase of the bacterial community when introduced in a new environment. In our case, the changing parameter is the absence of nZVI in the fresh culture media (lower oxidative stress, lower Fe concentrations). Bacterial growth after this lag phase is expected to be exponential

(Rolfe et al., 2012). As the conditions were the same for the cultures without nZVI, it therefore seems logical that no lag phase was observed. As previously shown (Rolfe et al., 2012), high concentrations of iron could be observed in bacterial cells during lag phase, and these concentrations were associated with transient sensitivity to oxidative stress. Moreover, it was shown that toxicity of nZVI is growth phase dependent (Chaithawiwat et al., 2016). A new exposition to nZVI during this lag phase (corresponding to a resilience period for the bacterial communities), would possibly have been lethal for the bacterial community.

Surprisingly, toxicity was higher for lower nZVI concentrations. Even if DLS analyses did not enable to highlight significant differences between the different concentrations in terms of mean sizes of NP aggregates and NP size sorting, trends were observed: more single nZVI or small aggregates were present in lower nZVI concentrations, and higher nZVI concentrations tend to result in the formation of higher aggregates. Consequently, the increase of NP concentrations enhances their aggregation. These observations are consistent with the literature (Baalousha, 2009). During exposure to nZVI, pH tended to increase, and was always above pH 8.0. For pH > 7, functional groups of bacteria and biofilms are globally deprotonated, and are thus negatively charged (Fein et al., 2001; Borrok and Fein, 2004). The formation of ionic bridges between negatively charged bacterial cells and NP with divalent cations present in solution (e.g., Ca<sup>2+</sup> and Mg<sup>2+</sup>), could lead to strong interactions between bacterial membranes and nZVI, and thus to toxic effects. The presence of large aggregates could result in a decrease in these interactions, and consequently in the observed decrease in toxicity. The formation of large aggregates in cultures with higher nZVI concentrations decreases the ZVI area per unit volume of liquid (Baalousha, 2009), and could also lead to the observed lower toxicity for higher nZVI concentrations. ROS generated would indeed be lower in the media with lower active ZVI area per volume unit, leading to a lower toxic effect.

As toxicity may be due to different mechanisms, these mechanisms may differ as a function of nZVI concentrations. At high concentrations, the main toxicity mechanism could be due to the release of ROS. At low concentrations, it could be rather due to cell/NP interactions. There is probably a co-occurrence of these mechanisms in any case, but their relative part could be dependent on nZVI concentrations and subsequent aggregation. As Fajardo et al. (2012) suggested for soils, these results point to a dose and species-specific impact of nZVI applications in groundwater.

## CONCLUSION

This study aimed to characterize the impact of nZVI addition on a bacterial community grown in controlled conditions from a natural groundwater sample. The impact of nZVI addition was assessed on bacterial abundance, activity (especially denitrifying activity) and community structure. Even if the impact is only temporary on abundance and activity, due to a good resilience/adaptation of the bacterial community, a shift was observed in community structure. Remediation of contaminated

groundwater using nZVI could consequently expose the bacterial groundwater community to shifts in their structures, and thus such techniques could have a long-term impact on bacterial communities and by extension on groundwater ecological functions, such as nitrate reduction. It is consequently important to study the impact on the bacterial community structure and on potential metabolic functions of the aquifers, at the long-term and at the field-scale.

## AUTHOR CONTRIBUTIONS

MCr contributed to the experimental design, carried out experimental work, data analysis, and drafted the manuscript. JH, CJ, and PO contributed to the experimental design, data analysis, and drafting and revising the manuscript. MCh carried out some of the experiments linked to molecular biology in the study.

## FUNDING

We are thankful for funding received from the European Union Seventh Framework Programme (FP7/2007–2013) under Grant

## REFERENCES

- An, Y., Li, T., Jin, Z., Dong, M., Xia, H., and Wang, X. (2010). Effect of bimetallic and polymer-coated Fe nanoparticles on biological denitrification. *Bioresour. Technol.* 101, 9825–9828. doi: 10.1016/j.biortech.2010.07.110
- Antizar-Ladislao, B., and Galil, N. I. (2010). Biofilm and colloidal biomass dynamics in a shallow sandy contaminated aquifer under in-situ remediation conditions. *Int. Biodeterior. Biodegradation* 64, 331–338. doi: 10.1016/j.ibiod.2010.03.002
- Anzai, Y., Kim, H., Park, J. Y., Wakabayashi, H., and Oyaizu, H. (2000). Phylogenetic affiliation of the pseudomonads based on 16S rRNA sequence. *Int. J. Syst. Evol. Microbiol.* 50, 1563–1589. doi: 10.1099/00207713-50-4-1563
- Auffan, M., Achouak, W., Rose, J., Roncato, M.-A., Chanéac, C., Waite, D. T., et al. (2008). Relation between the redox state of iron-based nanoparticles and their cytotoxicity toward *Escherichia coli*. *Environ. Sci. Technol.* 42, 6730–6735. doi: 10.1021/es800086f
- Baalousha, M. (2009). Aggregation and disaggregation of iron oxide nanoparticles: influence of particle concentration, pH and natural organic matter. *Sci. Total Environ.* 407, 2093–2101. doi: 10.1016/j.scitotenv.2008.11.022
- Bardos, P., Merly, C., Kvapil, P., and Koschitzky, H.-P. (2018). Status of nanoremediation and its potential for future deployment: risk-benefit and benchmarking appraisals. *Remediat. J.* 28, 43–56. doi: 10.1002/rem.21559
- Barnes, R. J., van der Gast, C. J., Riba, O., Lehtovirta, L. E., Prosser, J. I., Dobson, P. J., et al. (2010). The impact of zero-valent iron nanoparticles on a river water bacterial community. *J. Hazard. Mater.* 184, 73–80. doi: 10.1016/j.jhazmat.2010.08.006
- Borrok, D., and Fein, J. B. (2004). Distribution of protons and Cd between bacterial surfaces and dissolved humic substances determined through chemical equilibrium modeling. *Geochim. Cosmochim. Acta* 68, 3043–3052. doi: 10.1016/j.gca.2004.02.007
- Brookes, P. (1995). The use of microbial parameters in monitoring soil pollution by heavy metals. *Biol. Fertil. Soils* 19, 269–279. doi: 10.1007/BF00336094
- Bru, D., Sarr, A., and Philippot, L. (2007). Relative abundances of proteobacterial membrane-bound and periplasmic nitrate reductases in selected environments. *Appl. Environ. Microbiol.* 73, 5971–5974. doi: 10.1128/AEM.00643-07
- Buza, C., Pacheco, I. I., and Robbie, K. (2007). Nanomaterials and nanoparticles: sources and toxicity. *Biointerphases* 2, MR17–MR71. doi: 10.1116/1.2815690
- Chaithawiwat, K., Vangnai, A., McEvoy, J. M., Pruess, B., Krajangpan, S., and Khan, E. (2016). Impact of nanoscale zero valent iron on bacteria is growth phase dependent. *Chemosphere* 144, 352–359. doi: 10.1016/j.chemosphere.2015.09.025
- Crampon, M., Hellal, J., Mouvet, C., Wille, G., Michel, C., Wiener, A., et al. (2018). Do natural biofilm impact nZVI mobility and interactions with porous media? A column study. *Sci. Total Environ.* 61, 709–719. doi: 10.1016/j.scitotenv.2017.08.106
- Cundy, A. B., Hopkinson, L., and Whitby, R. L. D. (2008). Use of iron-based technologies in contaminated land and groundwater remediation: a review. *Sci. Total Environ.* 400, 42–51. doi: 10.1016/j.scitotenv.2008.07.002
- Dejonghe, W., Berteloot, E., Goris, J., Boon, N., Crul, K., Maertens, S., et al. (2003). Synergistic degradation of linuron by a bacterial consortium and isolation of a single linuron-degrading variovorax strain. *Appl. Environ. Microbiol.* 69, 1532–1541. doi: 10.1128/aem.69.3.1532-1541.2003
- Diao, M., and Yao, M. (2009). Use of zero-valent iron nanoparticles in inactivating microbes. *Water Res.* 43, 5243–5251. doi: 10.1016/j.watres.2009.08.051
- Dong, H., Li, L., Lu, Y., Cheng, Y., Wang, Y., Ning, Q., et al. (2019). Integration of nanoscale zero-valent iron and functional anaerobic bacteria for groundwater remediation: a review. *Environ. Int.* 124, 265–277. doi: 10.1016/j.envint.2019.01.030
- Fajardo, C., García-Cantalejo, J., Botías, P., Costa, G., Nande, M., and Martin, M. (2018). New insights into the impact of nZVI on soil microbial biodiversity and functionality. *J. Environ. Sci. Health A Tox. Hazard. Subst. Environ. Eng.* doi: 10.1080/10934529.2018.1535159 [Epub ahead of print].
- Fajardo, C., Ortiz, L. T., Rodríguez-Membibre, M. L., Nande, M., Lobo, M. C., and Martin, M. (2012). Assessing the impact of zero-valent iron (ZVI) nanotechnology on soil microbial structure and functionality: a molecular approach. *Chemosphere* 86, 802–808. doi: 10.1016/j.chemosphere.2011.11.041
- Fajardo, C., Sacca, M. L., Martínez-Gomariz, M., Costa, G., Nande, M., and Martin, M. (2013). Transcriptional and proteomic stress responses of a soil bacterium *Bacillus cereus* to nanosized zero-valent iron (nZVI) particles. *Chemosphere* 93, 1077–1083. doi: 10.1016/j.chemosphere.2013.05.082
- Fein, J. B., Martin, A. M., and Wightman, P. G. (2001). Metal adsorption onto bacterial surfaces: development of a predictive approach. *Geochim. Cosmochim. Acta* 65, 4267–4273. doi: 10.1016/S0016-7037(01)00721-9
- Freilich, S., Zarecki, R., Eilam, O., Segal, E. S., Henry, C. S., Kupiec, M., et al. (2011). Competitive and cooperative metabolic interactions in bacterial communities. *Nat. Commun.* 2:589. doi: 10.1038/ncomms1597

## ACKNOWLEDGMENTS

We thank NANOIRON (Rajhrad, Czechia) for providing the nZVI used in the present experiments. We also thank the Carnot program for financing the post-doctoral position that allowed conducting this study.

## SUPPLEMENTARY MATERIAL

The Supplementary Material for this article can be found online at: <https://www.frontiersin.org/articles/10.3389/fmicb.2019.00533/full#supplementary-material>

- Fu, F., Dionysiou, D. D., and Liu, H. (2014). The use of zero-valent iron for groundwater remediation and wastewater treatment: a review. *J. Hazard. Mater.* 267, 194–205. doi: 10.1016/j.jhazmat.2013.12.062
- Ghosh, I., Mukherjee, A., and Mukherjee, A. (2017). In planta genotoxicity of nZVI: influence of colloidal stability on uptake, DNA damage, oxidative stress and cell death. *Mutagenesis* 32, 371–387. doi: 10.1093/mutage/gex006
- Goldberg, S., Criscenti, L. J., Turner, D. R., Davis, J. A., and Cantrell, K. J. (2007). Adsorption-desorption processes in subsurface reactive transport modeling. *Vadose Zone J.* 6, 407–435. doi: 10.1021/es101822v
- Hall, T. A. (1999). BioEdit: a user-friendly biological sequence alignment editor and analysis program for Windows 95/98/NT. *Nucleic Acids Symp. Ser.* 41, 95–98.
- Holden, P. A., Schimel, J. P., and Godwin, H. A. (2014). Five reasons to use bacteria when assessing manufactured nanomaterial environmental hazards and fates. *Curr. Opin. Biotechnol.* 27, 73–78. doi: 10.1016/j.copbio.2013.11.008
- Hunter, R. J. (2001). Measuring zeta potential in concentrated industrial slurries. *Colloids Surf. Physicochem. Eng. Asp.* 195, 205–214. doi: 10.1016/S0927-7757(01)00844-5
- Jang, M.-H., Lim, M., and Hwang, Y. S. (2014). Potential environmental implications of nanoscale zero-valent iron particles for environmental remediation. *Environ. Health Toxicol.* 29:e2014022. doi: 10.5620/eh.t.2014022
- Jiang, D., Zeng, G., Huang, D., Chen, M., Zhang, C., Huang, C., et al. (2018). Remediation of contaminated soils by enhanced nanoscale zero valent iron. *Environ. Res.* 163, 217–227. doi: 10.1016/j.envres.2018.01.030
- Kandeler, F., Kampichler, C., and Horak, O. (1996). Influence of heavy metals on the functional diversity of soil microbial communities. *Biol. Fertil. Soils* 23, 299–306. doi: 10.1007/BF00335958
- Kirschling, T. L., Gregory, K. B., Minkley, J. E. G., Lowry, G. V., and Tilton, R. D. (2010). Impact of nanoscale zero valent iron on geochemistry and microbial populations in trichloroethylene contaminated aquifer materials. *Environ. Sci. Technol.* 44, 3474–3480. doi: 10.1021/es903744f
- Kocur, C. M., Lomheim, L., Molenda, O., Weber, K. P., Austrins, L. M., Sleep, B. E., et al. (2016). Long-term field study of microbial community and dechlorinating activity following carboxymethyl cellulose-stabilized nanoscale zero-valent iron injection. *Environ. Sci. Technol.* 50, 7658–7670. doi: 10.1021/acs.est.6b01745
- Lefevre, E., Bossa, N., Wiesner, M. R., and Gunsch, C. K. (2016). A review of the environmental implications of in situ remediation by nanoscale zero valent iron (nZVI): behavior, transport and impacts on microbial communities. *Sci. Total Environ.* 565, 889–901. doi: 10.1016/j.scitotenv.2016.02.003
- Li, Z., Greden, K., Alvarez, P. J. J., Gregory, K. B., and Lowry, G. V. (2010). Adsorbed polymer and NOM limits adhesion and toxicity of nano scale zerovalent iron to *E. coli*. *Environ. Sci. Technol.* 44, 3462–3467. doi: 10.1021/es9031198
- Liu, Y., Li, S., Chen, Z., Megharaj, M., and Naidu, R. (2014). Influence of zero-valent iron nanoparticles on nitrate removal by *Paracoccus* sp. *Chemosphere* 108, 426–432. doi: 10.1016/j.chemosphere.2014.02.045
- López-Gutiérrez, J. C., Henry, S., Hallet, S., Martin-Laurent, F., Catroux, G., and Philippot, L. (2004). Quantification of a novel group of nitrate-reducing bacteria in the environment by real-time PCR. *J. Microbiol. Methods* 57, 399–407. doi: 10.1016/j.mimet.2004.02.009
- Mueller, N. C., Braun, J., Bruns, J., Černík, M., Rissing, P., Rickerby, D., et al. (2012). Application of nanoscale zero valent iron (NZVI) for groundwater remediation in Europe. *Environ. Sci. Pollut. Res.* 19, 550–558. doi: 10.1007/s11356-011-0576-3
- Obiri-Nyarko, F., Grajales-Mesa, S. J., and Malina, G. (2014). An overview of permeable reactive barriers for in situ sustainable groundwater remediation. *Chemosphere* 111, 243–259. doi: 10.1016/j.chemosphere.2014.03.112
- O'Carroll, D., Sleep, B., Krol, M., Boparai, H., and Kocur, C. (2013). Nanoscale zero valent iron and bimetallic particles for contaminated site remediation. *Adv. Water Resour.* 51, 104–122. doi: 10.1007/s11356-011-0576-3
- Rolfé, M. D., Rice, C. J., Lucchini, S., Pin, C., Thompson, A., Cameron, A. D. S., et al. (2012). Lag phase is a distinct growth phase that prepares bacteria for exponential growth and involves transient metal accumulation. *J. Bacteriol.* 194, 686–701. doi: 10.1128/JB.06112-11
- Romanenko, L. A., Uchino, M., Falsen, E., Lysenko, A. M., Zhukova, N. V., and Mikhailov, V. V. (2005). *Pseudomonas xanthomarina* sp. nov., a novel bacterium isolated from marine ascidian. *J. Gen. Appl. Microbiol.* 51, 65–71. doi: 10.2323/jgam.51.65
- Sacca, M. L., Fajardo, C., Martínez-Gomariz, M., Costa, G., Nande, M., and Martín, M. (2014). Molecular stress responses to nano-sized zero-valent iron (nZVI) particles in the soil bacterium *Pseudomonas stutzeri*. *PLoS One* 9:e89677. doi: 10.1371/journal.pone.0089677
- Saitou, N., and Nei, M. (1987). The neighbor-joining method: a new method for reconstructing phylogenetic trees. *Mol. Biol. Evol.* 4, 406–425.
- Sevcu, A., El-Temseh, Y. S., Joner, E. J., and Cernik, M. (2011). Oxidative stress induced in microorganisms by zero-valent iron nanoparticles. *Microbes Environ.* 26, 271–281. doi: 10.1264/jmsme2.ME11126
- Stefaniuk, M., Oleszczuk, P., and Ok, Y. S. (2016). Review on nano zerovalent iron (nZVI): from synthesis to environmental applications. *Chem. Eng. J.* 287, 618–632. doi: 10.1016/j.cej.2015.11.046
- Thiruvengadachari, R., Vigneswaran, S., and Naidu, R. (2008). Permeable reactive barrier for groundwater remediation. *J. Ind. Eng. Chem.* 14, 145–156. doi: 10.1016/j.jiec.2007.10.001
- US EPA (2002). *EPA-821-R-02-012 Methods for Measuring the Acute Toxicity of Effluents and Receiving Waters to Freshwater and Marine Organisms*, 5th Edn. Washington, DC: U.S. Environmental Protection Agency.
- Weaver, L., Webber, J. B., Hickson, A. C., Abraham, P. M., and Close, M. E. (2015). Biofilm resilience to desiccation in groundwater aquifers: a laboratory and field study. *Sci. Total Environ.* 514, 281–289. doi: 10.1016/j.scitotenv.2014.10.031
- Wei, Y. T., Wu, S. C., Yang, S. W., Che, C. H., Lien, H. L., and Huang, D. H. (2012). Biodegradable surfactant stabilized nanoscale zero-valent iron for in situ treatment of vinyl chloride and 1,2-dichloroethane. *J. Hazard. Mater.* 21, 373–380. doi: 10.1016/j.jhazmat.2011.11.018
- Wille, G., Hellal, J., Ollivier, P., Richard, A., Burel, A., Jolly, L., et al. (2017). Cryo-scanning electron microscopy (SEM) and scanning transmission electron microscopy (STEM)-in-SEM for bio- and organo-mineral interface characterization in the environment. *Microsc. Microanal.* 23, 1159–1172. doi: 10.1017/S143192761701265X
- Xie, F., Ma, H., Quan, S., Liu, D., Chen, G., Chao, Y., et al. (2014). *Pseudomonas kunmingensis* sp. nov., an exopolysaccharide-producing bacterium isolated from a phosphate mine. *Int. J. Syst. Evol. Microbiol.* 64, 559–564. doi: 10.1099/ij.s.0055632-0
- Xie, Y., and Cwiertny, D. M. (2012). Influence of anionic cosolutes and pH on nanoscale zerovalent iron longevity: time scales and mechanisms of reactivity loss toward 1, 1, 1, 2-tetrachloroethane and Cr (VI). *Environ. Sci. Technol.* 46, 8365–8373. doi: 10.1021/es301753u
- Xiu, Z. M., Jin, Z. H., Li, T. L., Mahendra, S., Lowry, G. V., and Alvarez, P. J. (2010). Effects of nano-scale zero-valent iron particles on a mixed culture dechlorinating trichloroethylene. *Bioresour. Technol.* 101, 1141–1146. doi: 10.1016/j.biortech.2009.09.057
- Xue, W., Huang, D., Zeng, G., Wan, J., Cheng, M., Zhang, C., et al. (2018). Performance and toxicity assessment of nanoscale zero valent iron particles in the remediation of contaminated soil: a review. *Chemosphere* 210, 1145–1156. doi: 10.1016/j.chemosphere.2018.07.118
- Zhang, W.-X. (2003). Nanoscale iron particles for environmental remediation: an overview. *J. Nanopart. Res.* 5, 323–332. doi: 10.1023/A:1025520116015
- Zhang, W. X., and Elliott, D. W. (2006). Applications of iron nanoparticles for groundwater remediation. *Remediat. J.* 16, 7–21. doi: 10.1002/rem.20078
- Zhao, Y., Qu, D., Zhou, R., Yang, S., and Ren, H. (2016). Efficacy of forming biofilms by *Pseudomonas migulae* AN-1 toward in situ bioremediation of aniline-contaminated aquifer by groundwater circulation wells. *Environ. Sci. Pollut. Res. Int.* 23, 11568–11573. doi: 10.1007/s11356-016-6737-7

**Conflict of Interest Statement:** The authors declare that the research was conducted in the absence of any commercial or financial relationships that could be construed as a potential conflict of interest.

Copyright © 2019 Crampon, Joulian, Ollivier, Charron and Hellal. This is an open-access article distributed under the terms of the Creative Commons Attribution License (CC BY). The use, distribution or reproduction in other forums is permitted, provided the original author(s) and the copyright owner(s) are credited and that the original publication in this journal is cited, in accordance with accepted academic practice. No use, distribution or reproduction is permitted which does not comply with these terms.



# Benthic Diatom Communities in an Alpine River Impacted by Waste Water Treatment Effluents as Revealed Using DNA Metabarcoding

Teofana Chonova<sup>1,2\*</sup>, Rainer Kurmayer<sup>1</sup>, Frédéric Rimet<sup>2</sup>, Jérôme Labanowski<sup>3</sup>, Valentin Vasselon<sup>2</sup>, François Keck<sup>2,4</sup>, Paul Illmer<sup>5</sup> and Agnès Bouchez<sup>2</sup>

<sup>1</sup> Research Department for Limnology, Mondsee, Faculty of Biology, University of Innsbruck, Mondsee, Austria, <sup>2</sup> UMR CARRTEL, INRA, Université Savoie Mont Blanc, Thonon-les-Bains, France, <sup>3</sup> UMR IC2MP 7285, CNRS, Université de Poitiers, ENSIP, Poitiers, France, <sup>4</sup> Department of Aquatic Sciences and Assessment, Faculty of Natural Resources and Agricultural Sciences, Swedish University of Agricultural Sciences, Uppsala, Sweden, <sup>5</sup> Department of Microbiology, Faculty of Biology, University of Innsbruck, Innsbruck, Austria

## OPEN ACCESS

### Edited by:

Ghiglione Jean-Francois,  
Centre National de la Recherche  
Scientifique (CNRS), France

### Reviewed by:

Gabor Varbiro,  
Centre for Ecological Research (MTA),  
Hungary  
Yonghong Bi,  
Institute of Hydrobiology (CAS), China

### \*Correspondence:

Teofana Chonova  
Teofana.chonova@gmail.com

### Specialty section:

This article was submitted to  
Microbiotechnology, Ecotoxicology  
and Bioremediation,  
a section of the journal  
Frontiers in Microbiology

**Received:** 15 December 2018

**Accepted:** 15 March 2019

**Published:** 09 April 2019

### Citation:

Chonova T, Kurmayer R, Rimet F,  
Labanowski J, Vasselon V, Keck F,  
Illmer P and Bouchez A (2019)  
Benthic Diatom Communities in an  
Alpine River Impacted by Waste  
Water Treatment Effluents as  
Revealed Using DNA Metabarcoding.  
*Front. Microbiol.* 10:653.  
doi: 10.3389/fmicb.2019.00653

Freshwater ecosystems are continuously affected by anthropogenic pressure. One of the main sources of contamination comes from wastewater treatment plant (WWTP) effluents that contain wide range of micro- and macropollutants. Chemical composition, toxicity levels and impact of treated effluents (TEs) on the recipient aquatic ecosystems may strongly differ depending on the wastewater origin. Compared to urban TEs, hospital ones may contain more active pharmaceutical substances. Benthic diatoms are relevant ecological indicators because of their high species and ecological diversity and rapid response to human pressure. They are routinely used for water quality monitoring. However, there is a knowledge gap on diatom communities' development and behavior in treated wastewater in relation to prevailing micro- and macropollutants. In this study, we aim to (1) investigate the response of diatom communities to urban and hospital TEs, and (2) evaluate TEs effect on communities in the recipient river. Environmental biofilms were colonized in TEs and the recipient river up- and downstream from the WWTP output to study benthic diatoms using DNA metabarcoding combined with high-throughput sequencing (HTS). In parallel, concentrations of nutrients, pharmaceuticals and seasonal conditions were recorded. Diatom metabarcoding showed that benthic communities differed strongly in their diversity and structure depending on the habitat. TE sites were generally dominated by few genera with polysaprobic preferences belonging to the motile guild, while river sites favored diverse communities from oligotrophic and oligosaprobic groups. Seasonal changes were visible to lower extent. To categorize parameters important for diatom changes we performed redundancy analysis which suggested that communities within TE sites were associated to higher concentrations of beta-blockers and non-steroidal anti-inflammatory drugs in urban effluents vs. antibiotics and orthophosphate in hospital effluents. Furthermore, indicator species analysis showed that 27% of OTUs detected in river downstream communities were indicator for urban or hospital TE sites and were

absent in the river upstream. Finally, biological diatom index (BDI) calculated to evaluate the ecological status of the recipient river suggested water quality decrease linked to the release of TEs. Thus, in-depth assessment of diatom community composition using DNA metabarcoding is proposed as a promising technique to highlight the disturbing effect of pollutants in Alpine rivers.

**Keywords:** pharmaceuticals, diatom communities, WWTP effluents, DNA metabarcoding, functional traits, water quality index, indicator species analysis

## INTRODUCTION

Freshwater ecosystems provide important resources and services to humans. However, their sustainability is nowadays constantly affected due to their permanent application for conflicting purposes (e.g., release of wastewater and production of drinking water). WWTPs are used to reduce the release of anthropogenic pollutants into aquatic ecosystems, but pollutants cannot be completely eliminated by the treatment process (e.g., Verlicchi et al., 2015). Thus, TE usually contains a wide spectrum of highly concentrated macro- and micropollutants that may threaten ecosystems health (e.g., Verlicchi et al., 2012; Chonova et al., 2017).

Composition and toxicity level of effluents may differ strongly depending on their origin (e.g., urban, hospital, industrial), and may thereby have different impact on aquatic ecosystems (Labanowski et al., 2016). As recently shown by Chonova et al. (2016), microbial biofilm communities from urban and hospital TE sites exhibit remarkable differences in their development. Thus, the origin of pollution should not be neglected in the context of aquatic environmental monitoring. Increasing anthropogenic pressure on freshwater ecosystems imposes politically defined restrictions linked to their ecological status and functioning. In Europe, the water framework directive (WFD) aims at ensuring the maintenance of good water quality by monitoring chemical hazard substances and key aquatic indicator organisms (European Commission, 2013).

Benthic diatoms are microalgae used worldwide for water quality assessment. They are of particular interest in the context of bioassessment because of their taxonomic diversity and different species sensitivity and resistance to pollution. Diversity and community composition of diatoms adapt rapidly to the presence of chemical, physical, and biological disturbances (e.g., Stevenson and Smol, 2003). In the last decades, these features were used for the development of diatom indices that rely mainly on taxonomic composition (species or genera) obtained from microscopy counts and serve to evaluate general pollution

(e.g., Coste et al., 2009; Schneider and Lindström, 2009, 2011). The efficiency of DNA metabarcoding combined with high-throughput sequencing (HTS) techniques in this context was recently largely explored (e.g., Visco et al., 2015; Zimmermann et al., 2015; Vasselon et al., 2017a,b). The ability of these innovative molecular methods to provide fast, cost-efficient and reliable diatom inventories makes them promising biomonitoring tool and their application is currently being improved (e.g., Vasselon et al., 2017a, 2018).

Several studies have suggested that diatom sensitivity to environmental pressures is closely related to ecological guilds sharing functional traits (Passy, 2007; Tapolczai et al., 2016, 2017) which is also reflected by the phylogenetic tree of diatoms (Keck et al., 2016; Esteves et al., 2017). These relations give complementary insights into the health of aquatic ecosystems (Rimet and Bouchez, 2012; Larras et al., 2014) avoiding drawbacks of precise taxonomic identification (e.g., ecoregional differences in species ecological optima, taxonomic misidentification). However, the taxonomic and ecological complexity requires better understanding and further investigations.

In the context of bioassessment, diatom sensitivity is principally explored and applied in relation to nutrients and organic matter concentrations. However, the high variety of micropollutants constantly released in aquatic environments raise serious concerns about the health of these ecosystems (Schwarzenbach et al., 2006). Besides macropollutants such as nitrogen, phosphorus, and dissolved organic carbon (DOC), the possible interaction and impact of micropollutant mixtures on diatom communities should not be neglected. The sensitivity of diatoms to micropollutants (e.g., pesticides, heavy metals, and pharmaceuticals) at environmentally relevant concentrations was reported in numerous ecotoxicological studies. However, considering the large variety of diatoms and chemicals in the environment, single-species bioassays are not sufficient to provide environmentally realistic picture (Hagenbuch and Pinckney, 2012). Studies at higher complexity level are useful to fill knowledge gaps on toxic impacts. Rimet and Bouchez (2012) for example studied life-forms, ecological guilds, and cell size of diatoms in mesocosm experiments to develop a tool to assess pesticide contamination. Larras et al. (2014) found a relation between diatom sensitivity to herbicides and species' phylogenetic position. However, assessing impacts of micropollutant mixtures on the entire diatom community in natural ecosystems, and distinguishing them from the effects induced by other factors (e.g., nutrients, flow velocity, light) remains challenging (Marcel et al., 2013).

**Abbreviations:** BDI, biological diatom index; COD, chemical oxygen demand; H, hospital treated effluent; HPLC-MS/MS, high performance liquid chromatography coupled to a mass spectrometer; HTS, high-throughput sequencing; ISA, indicator species analysis; NMDS, non-metric multidimensional scaling; NSAID, non-steroidal anti-inflammatory drug; OTU, operational taxonomic unit; PCR, polymerase chain reaction; PERMANOVA, permutational multivariate analysis of variance; PhC, pharmaceutical compounds; pRDA, partial redundancy analysis; RD, river downstream; RDA, redundancy analysis; RU, river upstream; TSS, total suspended solids; TEs, treated effluents; U, urban treated effluent; VIF, variance inflation factor; WFD, water framework directive; WWTP, wastewater treatment plant.

Tapolczai et al. (2016) suggests that habitats with increased and multiple stress conditions are well adapted for studying the response of benthic diatom communities to environmental pressure. Modifications of diatom communities in rivers downstream from WWTP outputs have been already reported (e.g., Tornés et al., 2018), but community dynamics in direct response to various TEs remained thereby unknown. Despite the regular use of diatoms as biological indicators, there is a knowledge gap on their development and behavior in treated WWTP effluents. Understanding the dynamics of such communities is important to disentangle toxicity effects of pollutants mixtures and to better define a possible role of diatoms as bioindicators. These communities can be seen as a reference to better understand and evaluate the impact of TEs on recipient rivers.

In this study, we investigated community dynamics of periphytic diatoms that were exposed to hospital (H) and urban wastewater treated effluents (U), and in the recipient river up- (RU) and downstream (RD) from the WWTP output. Thereby, we aimed to (1) compare the effect of two highly polluted environments with different concentrations of pharmaceutical compounds (PhC) on diatom communities, and (2) evaluate and compare the effect of TEs' release on benthic diatom community composition in the recipient river. Diatom communities were analyzed using a DNA metabarcoding approach. Characterization of communities regarding their diversity, taxonomic composition, phylogeny, and functional

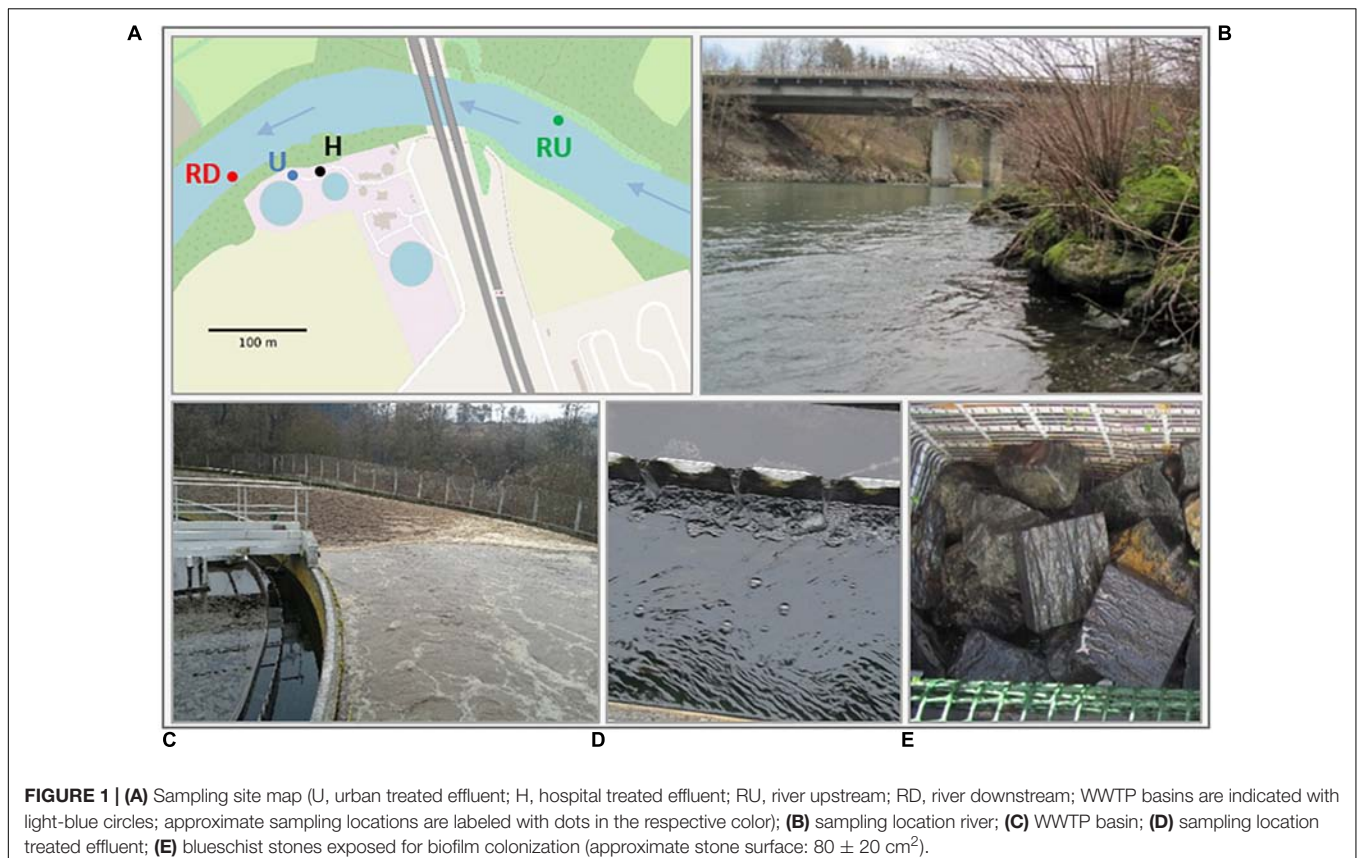
traits were used to give complimentary insights on diatoms development and behavior in habitats with different loads of pollution. Indicator species analysis (ISA) and biological diatom index (BDI) were used to evaluate the influence of TEs' release on river communities.

## MATERIALS AND METHODS

### Study Site and Biofilm Colonization Experiments

The experimental site is a pilot WWTP handling separately urban and hospital wastewater using biological treatment with conventional activated sludge system (Chonova et al., 2018b) (Figure 1A). The hospital whose effluents flow directly without special pretreatment to the WWTP has 450 beds, and the urban network includes around 20,850 inhabitants. This parallel separate treatment enables comparison of urban and hospital TEs and their effect on benthic diatoms. Treated wastewaters are discharged into the recipient River Arve. Downstream from the WWTP (ca. 18 km), water from River Arve is used for drinking water production for the city of Geneva (Switzerland), which increases the importance for the monitoring and maintenance of its high water quality.

The survey was performed between February and July 2014 in the following four locations: urban (U) and hospital (H) treated effluents and recipient river approximately 250 m



upstream (RU) and 40 m downstream (RD) from the WWTP output (Figure 1). Differences in hydraulic conditions between river and TE sampling locations were observed, suggesting a higher flow velocity and turbulence in river vs. laminar conditions exhibiting at least twice lower velocity in TE sampling locations. To study the development of benthic diatom communities in each location and compare them to natural seasonal gradient, biofilm colonization experiments were done as described in Chonova et al. (2016). Metal grid-baskets with clean and previously autoclaved blueschist stones (approximate stone surface:  $80 \pm 20 \text{ cm}^2$ ) were installed as substrates for natural biofilm colonization in water depth between 10 and 40 cm and were regularly inspected. Total surface of stones sampled in each location was  $200 \text{ cm}^2$  at least which is in accordance with the French norms used for application of WFD. After each colonization period (about 1 month), the biofilm was scraped from the stones and suspended in sterile water. Biofilm samples were collected in triplicates obtained from independent stones to ensure reliability of the experimental design. Samples were then immediately transported to the laboratory in cooling boxes for further analysis. This colonization experiment was repeated six times between February and July 2014.

## Characterization of Micro- and Macropollutants and Seasonal Conditions

Sampling sites were previously characterized in terms of nutrients (ammonium, nitrite, nitrate, orthophosphate), TSS, COD, and set of pharmaceuticals from the therapeutic classes beta-blockers (atenolol, propranolol), NSAIDs (diclofenac, ibuprofen, and ketoprofen), antibiotics (ciprofloxacin, sulfamethoxazole, and vancomycin), analgesics (paracetamol), and anticonvulsants (carbamazepine) as described in Chonova et al. (2016, 2018a). Flow-proportional 24-h sampling was performed. To obtain a representative flow-proportional sample, first, time proportional subsamples were collected every 10 min during 24 h. Secondly, subsamples from the same hour were pooled together to obtain one time-proportional sample per hour (resulting in 24 time-proportional samples of 1,020 mL in total). Finally, a fraction of each of them was combined according to the water flow rate. Nutrients, TSS and COD were measured with standard analytical methods, described by the French standard operating procedures (AFNOR, 1997). Pharmaceuticals were measured by solid-phase extraction (SPE) using hydrophilic-lipophilic balanced (HLB) columns and analyzed by HPLC-MS/MS as described by Wiest et al. (2018). For each parameter and sampling location, we calculated mean concentrations (from six monthly measurements for TE sites, and from three measurements performed in November and December 2013 and March 2014 for river sites) to give an overview of the different habitat characteristics. Measurements of hydro-meteorological conditions (river flow, urban and hospital WWTP discharge, solar irradiance, river and air temperature and precipitation) were collected as described in Chonova et al. (2018a) and

means from multiple daily measurements were calculated for each colonization period to characterize seasonal trends. A theoretical dilution factor for the RD site was calculated by dividing the average river flow ( $\text{m}^3 \cdot \text{d}$ ) by the average WWTP discharge ( $\text{m}^3 \cdot \text{d}^{-1}$ ).

## Metabarcoding of Diatom Samples DNA Extraction and Polymerase Chain Reaction (PCR) Amplification

Total genomic DNA was isolated using Sigma-Aldrich GenElute™-LPA as described in previous studies (e.g., Chonova et al., 2016). This method was recommended for diatom metabarcoding, because of its combination of various lysis mechanisms that are helpful for diatom cells opening and its ability to provide a large quantity of DNA (Vasselon et al., 2017a).

A 312 bp fragment of the *rbcl* plastid gene, recommended as DNA barcode for diatom metabarcoding (Kermarrec et al., 2013), was amplified using Takara LA Taq® polymerase and the primer pair Diat\_rbcL\_708F (AGGTGAA GTTAAAGGTTTCATACTTDA) (Stoof-Leichsenring et al., 2012) and R3 (CCTTCTAATTTACCAACAACCTG) (Bruder and Medlin, 2007). Each PCR amplification mix (total volume of 25  $\mu\text{L}$ ) contained 1  $\mu\text{L}$  of 25 ng DNA template, 0.75 U of Takara LA Taq® polymerase, 2.5  $\mu\text{L}$  of 10 $\times$  PCR Buffer, 1.25  $\mu\text{L}$  of 10  $\mu\text{M}$  of each primer, 1.25  $\mu\text{L}$  of 10 g/L BSA, 2  $\mu\text{L}$  of 2.5 mM dNTP, and ultrapure water to complete. For each set of reactions, a negative control was included. PCR reaction conditions were initiated by a denaturation step at 95°C for 15 min followed by a total of 30 cycles of 95°C for 45 s (denaturation), 55°C for 45 s (annealing), and 72°C for 45 s (final extension) (Vasselon et al., 2017a).

## Genomic Libraries Preparation

Genomic libraries for HTS were prepared from PCR amplicons of the *rbcl* 312 bp fragment from four independent PCR reactions per sample as described in Vasselon et al. (2017a). Briefly, PCR amplicons were cleaned with Agencourt AMPure beads (Beckman Coulter, Brea, CA, United States). Quality and quantity of purified products were measured with 2200 Tape Station (Agilent Technologies, Santa Clara, CA, United States). Tags were added to each amplicon and libraries were prepared using the NEBNext® Fast DNA Library Prep set for Ion Torrent™ (BioLabs, Ipswich, MA, United States) and A-X tag adapter provided by Ion Express™ Barcode adapters (Life Technologies, Carlsbad, CA, United States). Finally, all libraries were pooled at a final concentration of 100 pM and sequenced using an Ion 316™ Chip Kit V2 (Life Technologies, Carlsbad, CA, United States) on a PGM Ion Torrent sequencer by the “Plateforme Genome Transcriptome” (PGTB, Bordeaux, France).

## Sequence Data Processing

The sequencing platform performed demultiplexing and adapter removal. Data were provided in form of separate fastq files for each sample. Bioinformatic processing was performed with Mothur Software (Schloss et al., 2009) as proposed by Vasselon et al. (2017a). Low quality sequences (read length below 250 bp, Phred quality score below 23 over a moving window of 25 bp,

more than one mismatch in the primer sequence, homopolymer over 8 bp or presence of ambiguous base) were removed and obtained quality filtered sequences from all samples were analyzed jointly. Removal of chimera using Uchime algorithm (Edgar et al., 2011) was performed after pre-clustering (applied for denoising of sequencing error based on cluster generation by reads with only one nucleotide difference). Subsequently, taxonomic affiliation of DNA reads was performed using Rsystem::diatom barcoding library v4 (Rimet et al., 2016) and the naïve Bayesian method (Wang et al., 2007) with a confidence score threshold of 85%. All reads assigned to groups different from Bacillariophyta (diatoms) were excluded from further analyses. Similarity distance matrix based on pairwise distances between aligned reads (algorithm proposed by Needleman and Wunsch, 1970) was computed and used to cluster reads in operational taxonomic units (OTUs) with the furthest neighbor algorithm (95% similarity level as proposed by Mangot et al., 2013). Singleton removal and sample size normalization (to the smallest read abundance obtained among all samples) were performed and OTUs were taxonomically assigned based on consensus taxonomy of reads using confidence threshold of 80%. Taxonomy of abundant OTUs (above 100 reads), that were not precisely affiliated with the naïve Bayesian method, were verified with Rsystem::diatom blast to confirm their belonging to Bacillariophyta.

## Data Analysis

Quantitative (normalized abundances) and qualitative (presence–absence) matrices of OTUs were used to analyze diatom communities. All statistical analyses were performed using the free and open source R software (3.4.4, R development core team).

## Diatom Richness, Diversity, and Community Structure

Chao1 richness and Simpson diversity were calculated for all sampling dates and locations. NMDS was performed with Mothur Software on Bray–Curtis dissimilarity matrix to compare diatom communities. Differences between sites and seasons were tested with PERMANOVA ( $p < 0.05$ ) (Anderson, 2001;

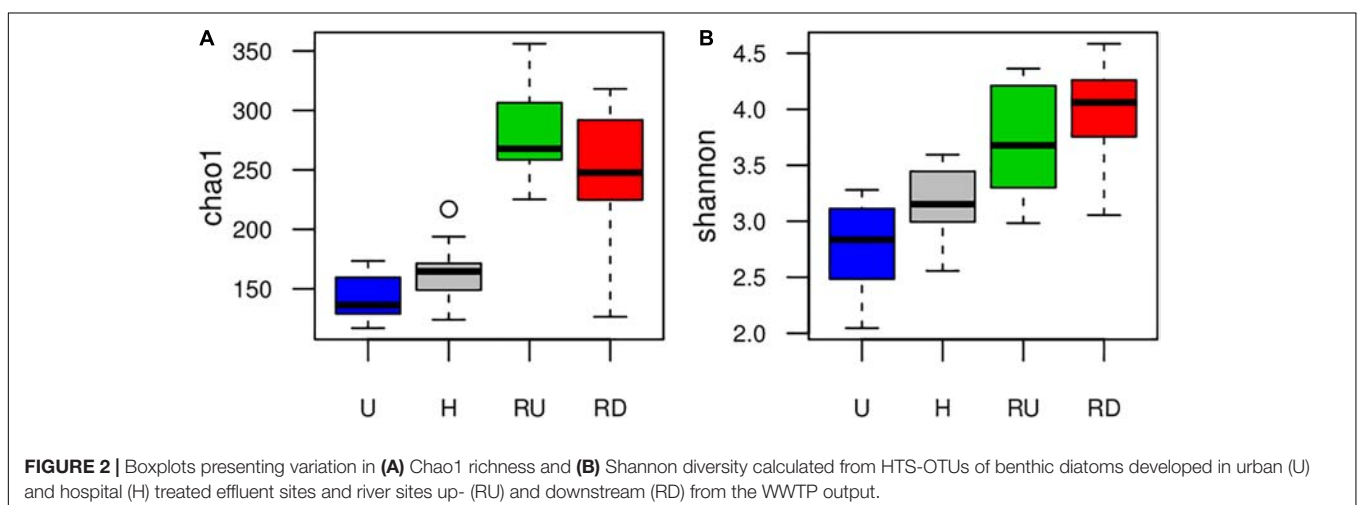
McArdle and Anderson, 2001) made using the vegan package (Oksanen et al., 2017).

## Community Changes Linked to Environmental Factors

Redundancy analysis (RDA) was performed to infer the relationship between environmental factors and diatom communities from urban (U) and hospital (H) TE sites (vegan package, Oksanen et al., 2017). Prior to the analysis, the biological data (normalized quantitative OTU matrices) were Hellinger-transformed as recommended for linear ordination methods (Legendre and Gallagher, 2001). To reduce the impact of high correlations between environmental variables, an approach based on principal component analysis (PCA) was applied. Three pairs of highly correlated variables ( $r > 0.7$ ) were identified: air temperature and irradiance (Temp.Irr), beta-blockers and NSAIDs (BB.NS), antibiotics and orthophosphate (ATB.PO4) and three separate PCAs were performed for each of the pairs. The first axis of each PCA (accounting for 98%, 92%, and 89% of the total variability for Temp.Irr, BB.NS, and ATB.PO4, respectively) was used in subsequent analysis as a synthetic variable representative for the variability of both variables.

In a next step, forward selection procedure was ran on the RDA performed on OTUs and the environmental variables ammonium, nitrite, nitrate, anticonvulsants, analgesics, TSS, COD, BB.NS, ATB.PO4, and Temp.Irr to obtain the most parsimonious RDA model with a reduced number of variables. The effect of time dependence was thereby considered by including the sampling month as a covariate. RDA was performed with the selected parameters, VIFs were verified and the significance of each variable and of the whole model was tested with permutation tests (999 permutations,  $p < 0.05$ ).

Finally, variation partitioning based on multiple partial RDAs (pRDAs) was performed to quantify and test the proportion of biological variability explained by each of the selected variables (Borcard et al., 1992). The variation explained by each fraction was reported using unbiased adjusted  $R^2$  (Peres-Neto et al., 2006). Permutation test (999 permutations,  $p < 0.05$ ) was used to test the significance of each fraction.



## Relative Genera Abundances and Ecological Guild Classes

Relative abundances of OTUs affiliated on genus level and of ecological guild classes were calculated from means of sample triplicates and presented in barplots for each sampling location and period to study spatial and temporal diatom community dynamics. Ecological guilds were based on the original classification by Passy (2007) including the modifications proposed by Rimet and Bouchez (2012).

## Phylogeny and Indicator Species Analysis of OTUs

A phylogeny of sequences from the final list of OTUs was reconstructed. First, the OTU sequences were aligned against the *rbcL* sequences of the R-Syst::diatom database using the muscle algorithm (Edgar, 2004). Second, OTUs were inserted in a reference phylogeny of 604 species with the evolutionary placement algorithm (Berger et al., 2011) implemented in RAXML (Stamatakis, 2014). Finally, the tree was dated in relative time using PATHd8 (Britton et al., 2007).

Indicator species analysis was performed to identify OTUs that discriminate diatom communities in U, H, and RU locations. Indicator values based on relative abundance of OTUs were calculated following the method proposed by Dufrene and Legendre (1997) implemented in the labdsv package (Roberts, 2007). The indicator values of each OTU were calculated based on abundance values and relative frequency of occurrence and tested using a randomization procedure (999 permutations,  $p < 0.05$ ). Each significant OTU was considered to be indicator of the location for which it exhibited the highest indicator value. Thus, a list of indicator OTUs was obtained for each location. Subsequently, indicator OTUs were denoted in the phylogenetic tree with location-specific colors for U (blue), H (black), and RU (green). Remaining non-significant OTUs were denoted with gray. Significant indicator OTUs of all three locations that appeared in RD were also labeled with the respective location-specific colors. Proportion of U, H, and RU indicator OTUs in RD communities was calculated (considering number of OTUs and DNA read abundances) to evaluate the influence of each location-characteristics on RD communities.

## Biological Diatom Index

Biological diatom index is a biotic index calculated after morphological identification of diatom species present in natural biofilms. It is routinely applied for water quality assessment of running waters in France and is used in the context of the WFD (Coste et al., 2009). In this study, OTUs were affiliated on species (or genus when species not available) level and their normalized quantitative matrices, based on read numbers, were used to calculate molecular BDI for each sampling location and period and to evaluate thereby the effect of TEs on water quality in the recipient river. BDI calculation was done with OMNIDIA 5 software (Lecointe et al., 1993).

## RESULTS

### Habitat Description

Principle major differences regarding nutrients and pharmaceuticals were found between sampling locations, especially distinguishing TE sites from river sites. Nutrients and PhC were clearly higher concentrated in the TEs (**Table 1**). Comparing urban and hospital effluents, the clearest trends were observed for orthophosphate and antibiotics with significantly higher concentrations in H, and beta-blockers, NSAIDs and ammonium – in U (paired Wilcoxon test,  $p < 0.05$ ). In river locations, concentrations of PhC (especially antibiotics, NSAIDs and anticonvulsants) and orthophosphate showed rather increasing trend in RD compared to RU, which was not noticeable for ammonium, nitrite, nitrate, and TSS (Chonova et al., 2018a). During the observation period solar irradiance, air temperature and river flow increased from winter to summer. Threefold increase of the theoretical dilution factor for WWTP discharge was observed from winter to summer (**Table 2**).

### High-Throughput Sequencing

We obtained 3,760,984 reads from the HTS, with an average of 59,698 reads per sample and average length of 312 base pairs. After the bioinformatics filtration steps, 1,357,398 reads were retained and were clustered into 1,121 OTUs (**Supplementary**

**TABLE 1** | Mean concentrations of nutrients and pharmaceuticals in urban (U) and hospital (H) treated effluents and Arve river up- (RU) and downstream (RD) from the WWTP Output (standard deviation in brackets).

	U	H	RU	RD
Ammonium ( $\text{mg}\cdot\text{l}^{-1}$ )	4 (3.7)	0.3 (0.4)	0.24 (0.06)	0.06 (0.02)
Nitrite + nitrate ( $\text{mg}\cdot\text{l}^{-1}$ )	16.5 (9.6)	65.6 (58.7)	1.2 (0.3)	0.8 (0.09)
Orthophosphate ( $\text{mg}\cdot\text{l}^{-1}$ )	2.3 (1)	8.9 (1.5)	0.02 (0.01)	0.04 (0.01)
COD ( $\text{mg}\cdot\text{l}^{-1}$ )	22.8 (5.1)	23.9 (2.9)	-	-
TSS ( $\text{mg}\cdot\text{l}^{-1}$ )	4.5 (2.5)	5.3 (1.7)	3.5 (0.7)	3.3 (2.5)
NSAIDs ( $\mu\text{g}\cdot\text{l}^{-1}$ )	1 (0.4)	0.14 (0.04)	0.0004 (0)	0.0301 (0.013)
Beta-blockers ( $\mu\text{g}\cdot\text{l}^{-1}$ )	0.5 (0.19)	0.2 (0.06)	0.0036 (0.0047)	0.0119 (0.0071)
Antibiotics ( $\mu\text{g}\cdot\text{l}^{-1}$ )	0.09 (0.06)	2.6 (1.5)	0.0025 (0.0001)	0.0054 (0.0022)
Anticonvulsant ( $\mu\text{g}\cdot\text{l}^{-1}$ )	0.5 (0.12)	0.6 (0.19)	0.002 (0.0027)	0.0118 (0.0055)
Analgesic ( $\mu\text{g}\cdot\text{l}^{-1}$ )	0.4 (0.31)	0.9 (1.3)	0.138 (0.0141)	0.1672 (0.0648)
Total PhC ( $\mu\text{g}\cdot\text{l}^{-1}$ )	2.5 (0.6)	4.5 (2.6)	0.1465 (0.0122)	0.243 (0.120)

PhC, pharmaceutical compounds; COD, chemical oxygen demand; TSS, total suspended solids; NSAIDs, non-steroidal anti-inflammatory drugs.

**TABLE 2** | Mean values calculated from multiple daily measurements of solar irradiance, river temperature, precipitation, river flow, and WWTP discharge for each colonization period (standard deviation in brackets; data sources: INRA meteorological station\*, federal office of environment of Switzerland\*\* and SIPIBEL observatory).

	February	March	April	May	June	July
Air temperature (°C) *	4.3 (1.4)	6.8 (2.2)	10.7 (2.4)	12 (2.1)	17.2 (3.4)	18 (2.2)
Solar irradiance (MJ·m <sup>-2</sup> ) *	5.2 (3.1)	11.4 (4.3)	16.9 (5.7)	17.4 (5.6)	23.9 (6.8)	20.6 (8)
Precipitation (mm·day <sup>-1</sup> ) *	4.9 (7.1)	2 (6)	0.6 (1.9)	3.3 (4.9)	2.7 (8.4)	5.1 (7.7)
River temperature (°C) **	5.6 (0.8)	7.2 (0.8)	9.1 (0.9)	9.9 (1)	11.5 (0.8)	11.9 (0.9)
River flow (m <sup>3</sup> ·s <sup>-1</sup> ) **	61 (23)	59.6 (15.9)	67 (18.9)	83.4 (16.9)	92.1 (24.4)	101.4 (53.1)
Hospital discharge (m <sup>3</sup> ·day <sup>-1</sup> )	152 (31)	151 (27)	126 (26)	129 (26)	136 (25)	147 (33)
Urban discharge (m <sup>3</sup> ·day <sup>-1</sup> )	7965 (2372)	6163 (1686)	4223 (501)	4542 (573)	4668 (1478)	4236 (1283)
Dilution factor for WWTP discharge	642 (107)	872 (317)	1346 (374)	1545 (283)	1706 (372)	1909 (480)

**Table S1**). All samples were subsampled to 11,306 reads (lowest read abundance obtained for a sample) to allow inter-sample comparison which resulted in total of 1,076 OTUs with minimum of 103 and maximum of 301 OTUs per sample. R-Syst::diatom v4 database enabled taxonomic affiliation of 103 different species from 48 different genera. 81% of the OTUs (90% of the reads) were affiliated at family level, 75% of the OTUs (85% of the reads) – at genus level and 57% of the OTUs (70% of the reads) – at species level. Those results are in consistence with other studies (e.g., Vasselon et al., 2017b). Most of the unclassified reads were found in H – a location that represented the most extreme environment in terms of concentrations of micro- and macropollutants. However, results from R-Syst::diatom blast confirmed that unclassified OTUs belong to the group Bacillariophyta and were not misclassified.

## Diatom Community Changes and the Role of Micro- and Macropollutants

Boxplots on **Figure 2** compare richness (Chao1) and diversity (Shannon) of benthic diatom communities between sampling locations and suggested increased richness and diversity in the river compared to the TEs. Higher richness and diversity were observed in H than in U. Comparing river locations, alpha diversity changed depending on the method – Chao1 reported higher richness in RU, and Shannon suggested tendency for higher diversity in RD. Seasonal trends of diatom richness and diversity were not observed.

Non-metric multidimensional scaling analysis of quantitative OTU matrix showed that diatom communities were mainly grouped by sampling location (**Figure 3A**). Significant differences between U and H communities were represented on the first axis, and between TE sites and river sites on the second axis (PERMANOVA,  $p < 0.05$ ). RD communities were more similar to U and H than RU communities. As secondary shaping factor, seasonal changes were visible for all sampling locations.

Redundancy analysis was performed to explore the relationship between diatom community structure and environmental variables measured in TEs. Forward selection procedure identified that the best parsimonious model includes the variables ATB.PO4 (representing 89% of the common variability of antibiotics and orthophosphate) and BB.NS (representing 92% of the common variability of beta-blockers

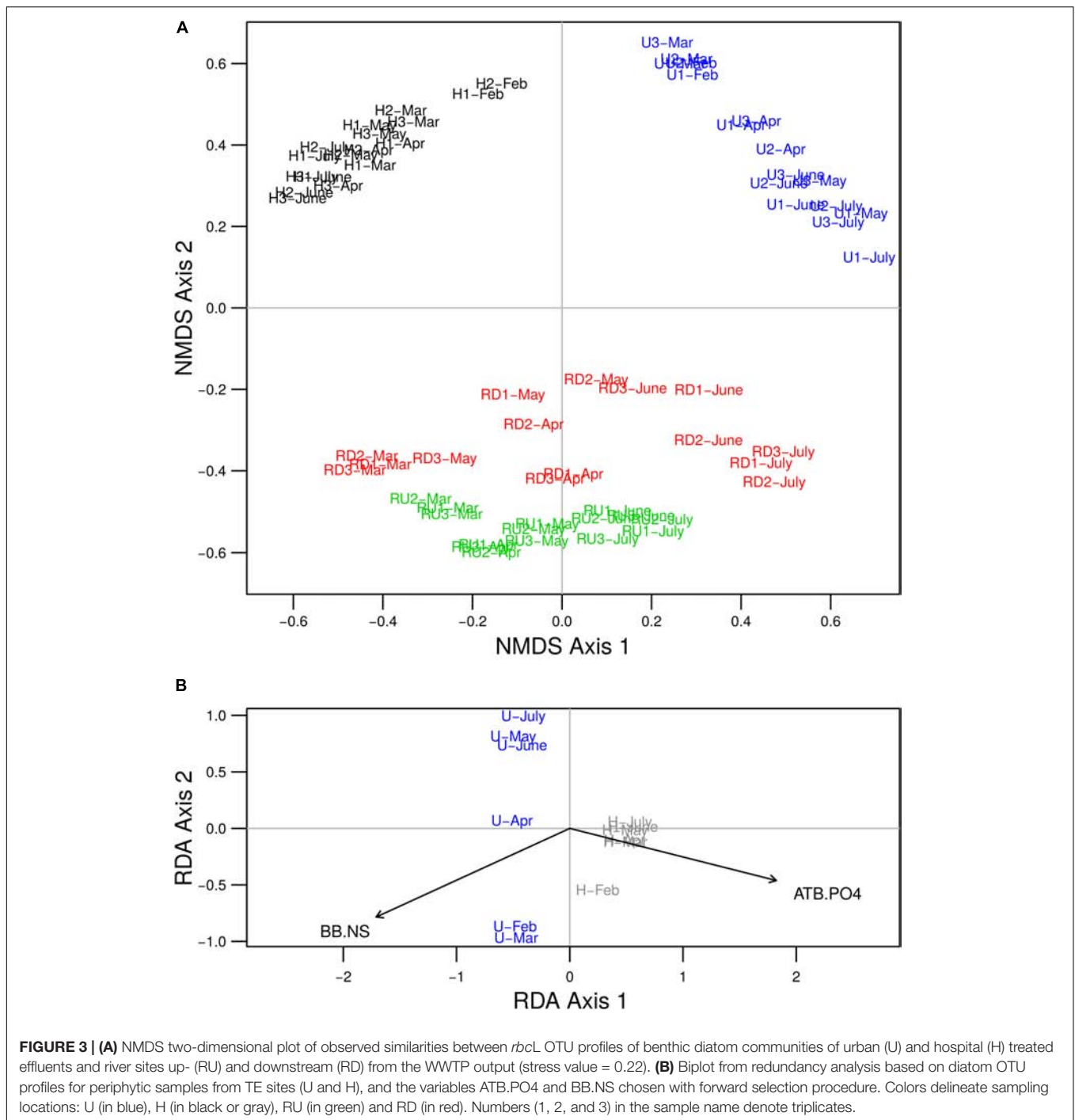
and NSAIDs) as the most important for diatom community changes (**Figure 3B**). RDA model including ATB.PO4 and BB.NS was significant and the two variables tested separately were significant to the model ( $p < 0.05$ ). The low VIF values ( $VIF < 3$ ) suggested that there is no issue with collinearity. The first two axes of the model accounted for 61% and 3% of the variability in diatom community structure, respectively, when considering the effect of time dependence as covariate. The first axis defined a local gradient between the two basins, where diatom community development in U was rather linked to higher concentrations of beta-blockers and NSAIDs and in H – to antibiotics and orthophosphate. The second axis explained a low proportion of the variance only. Variation partitioning revealed that the effect explained by ATB.PO4 and BB.NS separately remained significant ( $p < 0.05$ ) and it accounted for 17% and 11% of the total variability for ATB.PO4 and BB.NS, respectively. The variance shared between the two variables was 36%.

## Spatial and Temporal Variations in Diatom Genera and Ecological Guild Classes

Relative abundances of diatom genera (a) and ecological guild classes (b) per sampling site and period are presented in **Figure 4**. Planktic species were rare in the biofilms. Clear dichotomy in ecological guild classes was found between TE sites and river sites.

At TE sites mainly the development of polysaprobic species (e.g., *Sellaphora*, *Craticula*) was observed. Motile groups (represented mainly by the genera *Craticula*, *Sellaphora*, and *Nitzschia*) dominated in treated wastewater with relative abundance up to 95% in U. Their dominance slightly decreased in H, where motile guild was partially replaced by low- (*Achnantheidium* and *Planothidium*) and high-profile groups (*Gomphonema*). Seasonal trends were observed in U for the genus *Craticula* and *Sellaphora*, as *Craticula* was dominating in colder months (February and March) with ca. 70% relative abundance but was replaced by *Sellaphora* in warmer months. In H, *Nitzschia*, *Gomphonema*, and *Fragilaria* exhibited slightly higher relative abundance in colder months and decreased in summer.

In river communities, genera relative abundances were more evenly distributed and low- and high-profile species were better

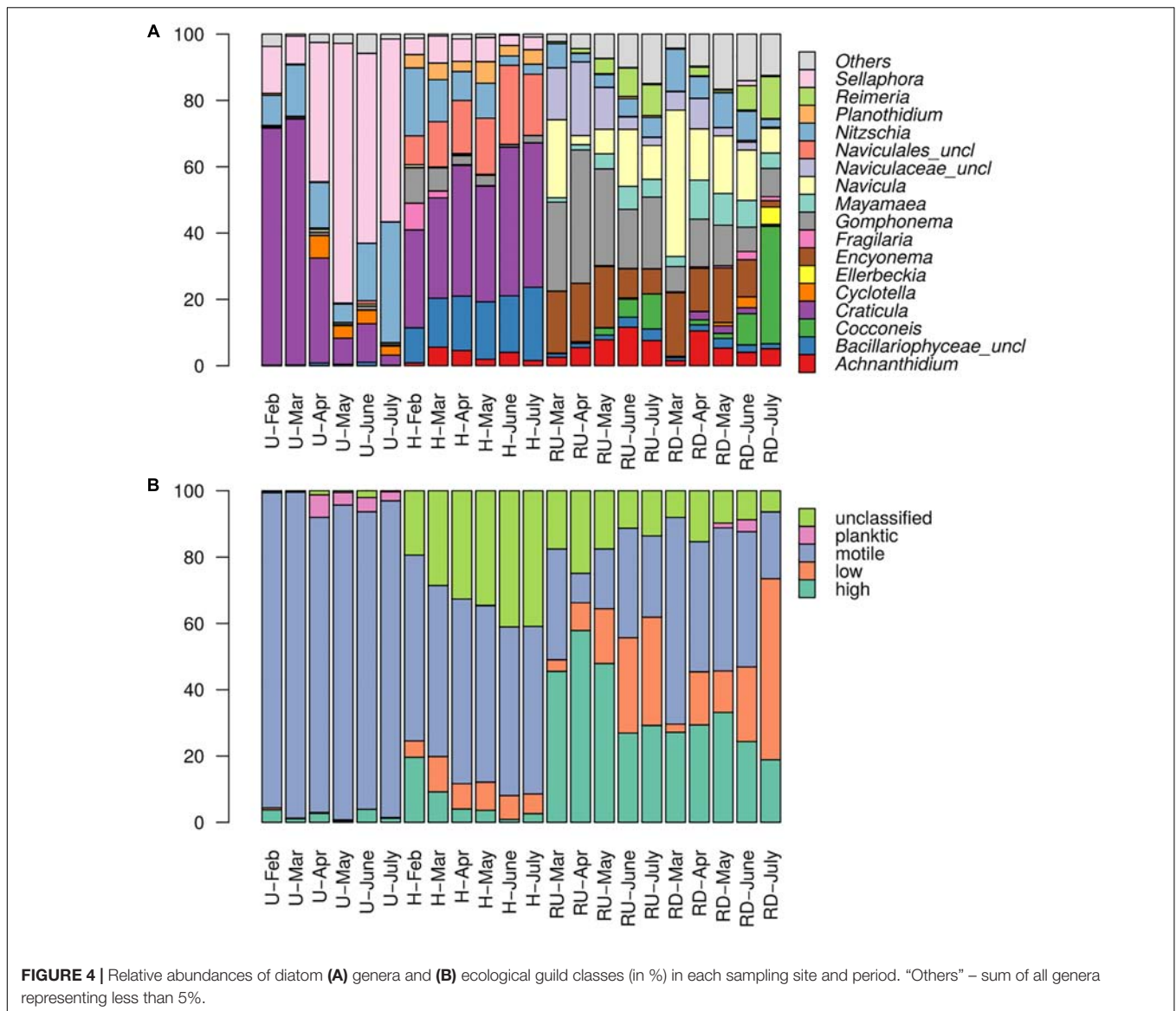


represented (especially in RU). Importance of *Craticula* and *Sellaphora* decreased and motile groups were rather represented by *Mayamaea*, *Navicula*, and *Nitzschia*. Overall, in the river, groups with oligotrophic and oligosaprobic (e.g., *Achnanthydium*, *Encyonema*) preferences were favored. This trend was clearly stronger expressed in the river upstream from the WWTP output. Seasonal trends were observed for low- and high-profile diatoms. Low-profile groups (mainly *Achnanthydium*, *Cocconeis*, and *Reimeria*) were more abundant in warmer months, while

increase in high-profile diatoms (mainly *Encyonema* and *Gomphonema*) was observed rather in colder months, especially upstream from the WWTP.

### Location-Specific Indicator OTUs

Abundances of OTUs were calculated as mean of all samples for each location and are presented (log-transformed) in **Figure 5**. Indicator OTUs of U, H, and RU (represented in blue, black, and green on the figure, respectively) were located in



different parts of the phylogenetic tree. Indicator OTUs of U belonged mainly to *Nitzschia*, *Sellaphora*, and *Craticula*, whereas a large phylogenetic clade comprising *Cocconeis*, *Achnantheidium*, *Planothidium*, *Encyonema*, and *Gomphonema* was hardly present in this location. By contrast, many indicator OTUs belonging mainly to *Achnantheidium*, *Planothidium*, and *Gomphonema* appeared again in H, and became even more important for RU. Indicator OTUs of RU were detected throughout the phylogenetic tree, except for *Craticula* and *Sellaphora*. These results confirmed general trends revealed with the relative abundance of genera.

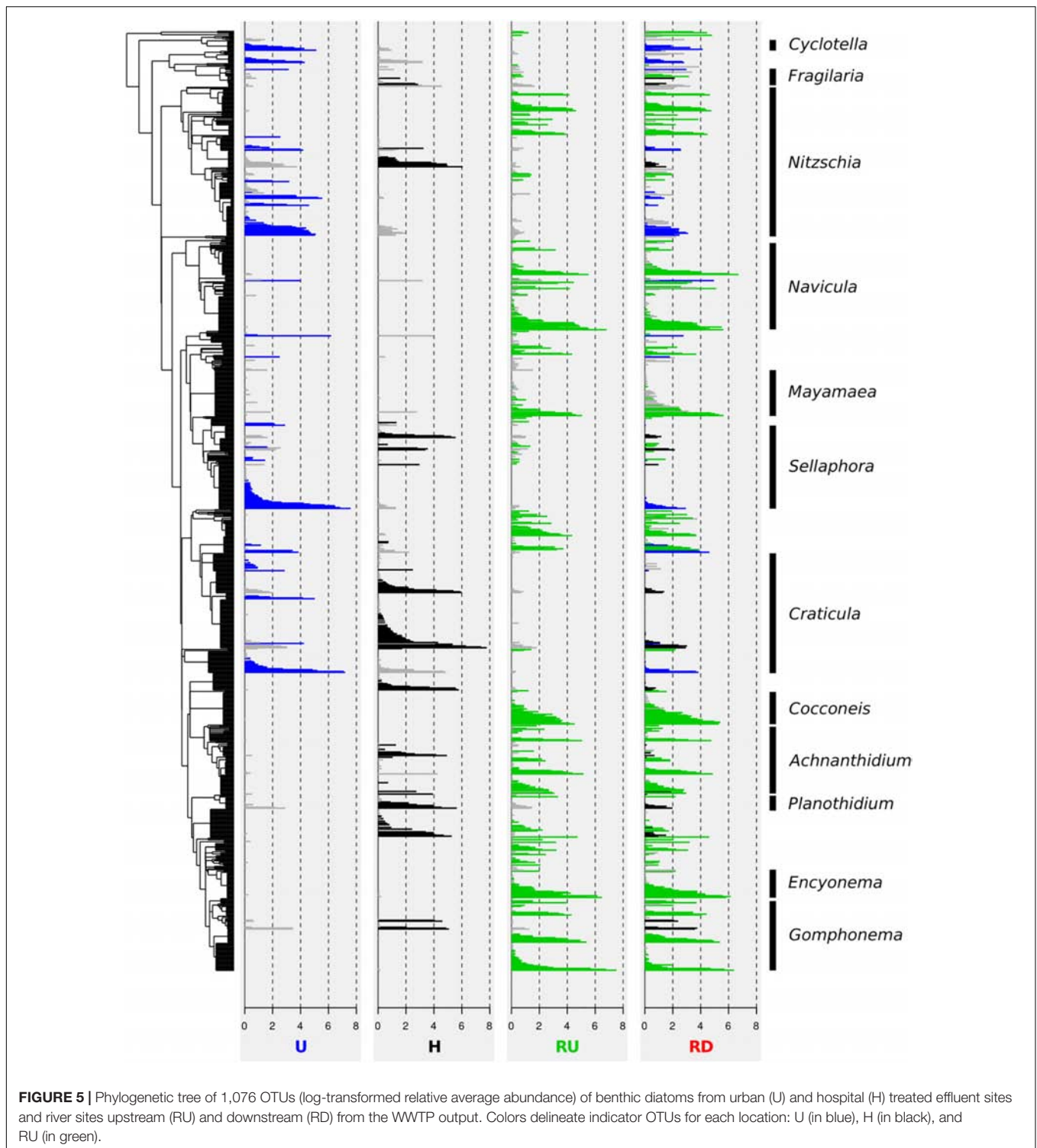
Figure 5 clearly illustrates that most of the OTUs found in RD corresponded to indicator OTUs of RU (53% of the OTUs, corresponding to 88% of the DNA reads). However, numerous indicator OTUs of U or H that were not present in RU appeared in RD (e.g., *Craticula*, *Sellaphora*, and *Nitzschia*). This proportion was 14% of the OTUs (corresponding to 7% of the reads) for U, and 13% of the OTUs (corresponding to 2% of the reads) for H.

## Biological Diatom Water Quality Index

Biological diatom index was calculated from molecular data and represented in Figure 6. As expected, BDI suggested that water quality was lower at TE sites compared to the recipient river. Lowest values were observed for H (quality between “bad” and “poor”), followed by U (between “poor” and “moderate”). At river sites, BDI revealed “high” quality status in RU and decrease from “high” to “good” in RD.

## DISCUSSION

The development and behavior of diatom communities in response to TEs remain poorly documented. Microalgae have been previously associated to wastewater treatment due to their ability to assimilate nitrogen and phosphorus and to bind heavy metals (e.g., Congestri et al., 2005). In this



context, in recent studies Ghosh and Love (2011) investigated algal assemblages from the water column of a secondary WWTP tank, and Congestri et al. (2005) reported communities developed on tank walls and artificial substrata in WWTP sedimentation tanks. In such highly polluted environments, diatoms represent one of the most abundant groups among algae

(e.g., Ghosh and Love, 2011). Although diatoms are regularly used for biomonitoring and their sensitivity to micropollutants is well known, species composition and structural dynamics in WWTPs and their TEs have rarely been documented in this context. The present study reports for the first time the reliability of DNA metabarcoding to detect spatial and temporal

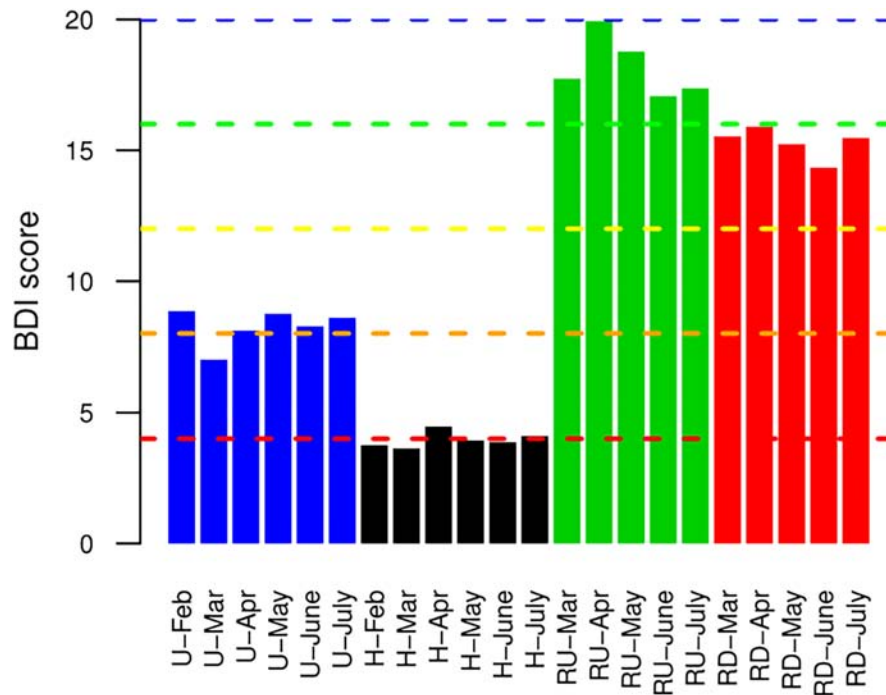


**FIGURE 6** | Biological diatom water quality index (BDI) calculated for benthic diatoms from urban (U) and hospital (H) treated effluent sites and river sites up- (RU) and downstream (RD) from the WWTP.

responses of diatom assemblages to high environmental pressure in urban and hospital TEs and contributes to our understanding of the effluents' impact on community dynamics in the recipient aquatic environment.

Parallel analysis of nutrients, PhC and seasonal parameters provided essential information about the characterization of different habitats and confirmed higher presence of pollutants in the TEs compared to the river. As expected, comparison of U and H showed that hospital TEs contained higher total concentrations of PhC (especially antibiotics) and phosphate caused by the regular use of PhC and specific detergents in the hospital. However, better removal efficiency of NSAIDs and beta-blockers in the hospital treatment process might have resulted in their higher concentrations in urban TEs (Chonova et al., 2016). Release of WWTP effluents in the recipient river led to increased concentrations of PhC (especially NSAIDs, antibiotics, and anticonvulsants) and phosphate downstream from the TEs output. In contrast nutrients such as ammonium, nitrate, nitrite, and TSS did not show such up – to downstream gradient. Temperature, solar irradiance and river flow (caused by the melting of glacier) followed the usual seasonal gradient with increase in summer. No extreme water level changes or flood events were observed during the study experimental period.

### Composition of Diatom Communities Linked to Habitats Characteristics

Diversity and community structure of benthic diatoms exhibited clearly stronger local changes than seasonal ones, which

highlights the relevance of location-specific factors (e.g., nutrients and PhC) over seasonal factors (e.g., temperature and solar irradiance) (Figures 2, 3). The high relevance of nutrients in structuring diatom communities has been well studied (e.g., Patrick, 1961; Lange-Bertalot, 1979; Larson and Passy, 2012; Marcel et al., 2013). Several studies also show significant effect of PhC (e.g., NSAIDs, beta-blockers, antibiotics) and other micropollutants (pesticides, heavy metals, etc.) on benthic diversity and community structure (e.g., Hagenbuch and Pinckney, 2012; Larras et al., 2013; Corcoll et al., 2014). Temperature, solar irradiance and flow velocity (for river sites) were previously shown to be crucial factors for the development of benthic diatom communities (Lange et al., 2011; Villeneuve et al., 2011; Larras et al., 2013). However, in this study they remained of secondary importance. Such primary local and secondary seasonal community dynamics at the same study site were reported for bacterial biofilms after short- and long-term biofilm colonization periods, where both nutrients and PhC played a key role in the shaping of the community structure (Chonova et al., 2016, 2018a).

### Response of Diatoms to Pollutants in Urban and Hospital Treated Effluents

Communities developed at TE sites and at river sites differed strongly regarding their richness and diversity which reflected the contrasting ecological differences between the two systems (Table 1). Considerably lower diatom richness and diversity were observed at TE sites which were the most severely

disturbed and showed higher concentrations of micro- and macropollutants compared to the natural river system (**Figure 2**). Such low diatom diversity was also reported in studies investigating algal communities in WWTP clarification tanks and is probably linked to the high anthropogenic pressure which leads to the elimination of less resistant species (e.g., Sládečková et al., 1983; Congestri et al., 2005). However, restricted colonization possibilities in these “artificial systems” offering limited microhabitats compared to natural environments may also affect the number of species. This question needs to be further investigated applying translocation experiments as described for example by Proia et al. (2013b).

Diatom community structure at TE sites also differed from river sites regarding HTS-OTUs, genera taxonomic level and ecological guild classes (**Figures 3, 4**). These trends allowed to better understand the community dynamics linked to the ecological preferences of diatoms, and clearly showed that community adaptations are in accordance with habitat characteristics. In general, TE sites characterized by higher anthropogenic pressure and lower water velocity and turbulence, were dominated by few genera with polysaprobic preferences and well-developed raphe system belonging to the motile guild (e.g., *Craticula*, *Nitzschia*, *Sellaphora*, etc.). Some of these genera (*Craticula*, *Nitzschia*, *Sellaphora*, and *Gomphonema*) were also previously reported as dominant in WWTP tanks (Congestri et al., 2005). As described by Passy (2007) and Rimet and Bouchez (2012), the motile guild included free-moving species with tolerance to high nutrient concentrations and low resistance to flow velocity. Higher tolerance of motile species to micropollutants (e.g., herbicides and fungicides) has also been reported previously (Rimet and Bouchez, 2011). This resistance to pollution is linked to the ability of motile diatoms to optimize their position in the biofilm and thereby avoid disturbances (Lengyel et al., 2015). The adaptations of motile groups to survive and reproduce in highly contaminated environments explains their dominance over other guilds in TEs. Dominance of raphid taxa in the TEs was also reported previously in WWTPs (Congestri et al., 2005; Ghosh and Love, 2011) and may be explained by their higher resistance to micropollutants which may lead to the replacement of higher sensitive centric and araphid taxa (e.g., Larras et al., 2014 for pesticides).

According to Ghosh and Love (2011), algal diversity and composition may differ strongly between different WWTPs. Here, we also found differences when comparing separately treated urban and hospital effluents, despite their close geographic proximity. Hence, these differences are probably rather linked to the origin-specific effluent composition than to the spatial effect on colonization possibilities. Interestingly, lower richness and diversity was observed in U, where concentrations of total nutrients and PhC were lower (**Figure 2** and **Table 1**). Differences between U and H communities were also observed on OTU and genera level, and to lower extent – regarding functional traits (**Figures 3, 4**). Urban communities in colder months (February and March) were dominated by *Craticula*, which was replaced by *Sellaphora* in warmer months. Both species are symmetrical biraphid diatoms and exhibit similar trophic

preferences since they tolerate nutrient rich environments. Their similar characteristics may lead to competition resulting in suppression of *Craticula* in warmer – and *Sellaphora* in colder months. *Nitzschia* was also regularly found in U, but did not exhibit such strong seasonal variations. In hospital communities, low- (*Achnanthisidium* and *Planorthisidium*) and high-profile groups (*Gomphonema*) showed higher relative abundances compared to U (**Figure 4B**). However, motile groups (*Craticula*, *Nitzschia*, and *Sellaphora*) remained dominant. Regarding seasonal trends, *Nitzschia*, *Gomphonema*, and *Fragilaria* exhibited slightly higher relative abundance in colder months, but genera composition in H remained generally stable between seasons.

Aiming to better comprehend community changes and to categorize the importance of nutrients, pharmaceuticals, and seasonal conditions, diatom community dynamics in U and H were further studied on OTU level with RDA. Forward selection procedure defined beta-blockers, NSAIDs, antibiotics and phosphate as the most important factors explaining a significant part of the diatom OTU variability (64%). Higher concentrations of beta-blockers and NSAIDs (accounting for 11% of the biological variability) were rather linked to urban communities, while antibiotics and phosphate (accounting for 17%) – to hospital ones. Beta-blockers and NSAIDs, in the same concentration range as reported in U, may inhibit algal photosynthesis processes (Bonnineau et al., 2010) and change benthic community structure (Corcoll et al., 2014). Lower diversity in U may therefore be linked to the influence of these PhC. Other studies showed that NSAIDs may change phosphatase activity (Proia et al., 2013b) and reduce photosynthesis (Ding et al., 2017). Negative effect of antibiotics on benthic communities has also been reported (e.g., Proia et al., 2013b) and associated with reduction or elimination of diatom mobility (Hagenbuch and Pinckney, 2012) and inhibition of diatoms growth due to reduced photosynthesis (Pinckney et al., 2013; Guo et al., 2016). Hence, mobility reduction in H, where antibiotic concentrations were more than 20 times higher than in U, may have led to discrimination of motile diatoms, favoring development of low- and high-profile species. Furthermore, effect of antibiotics on bacterial communities may lead to indirect changes in diatom assemblages (e.g., Windler et al., 2015). The remaining PhC (paracetamol and carbamazepine) were excluded by the forward selection procedure in the course of RDA. However, considering the high concentrations of the analgesic paracetamol and the anticonvulsant carbamazepine, we cannot exclude their possible effect on diatom communities. Indeed, paracetamol may also impact photosynthesis and cause algal growth inhibition (Proia et al., 2013b). The presence of non-measured PhC, metabolites, pesticides, heavy metals and detergents may also have played a role in the shaping of diatom communities (e.g., Morin et al., 2009; Ricciardi et al., 2009). The mixture of highly concentrated pollutants found in threatened effluents may exhibit additive, synergistic and antagonistic effects on benthic communities (Hagenbuch and Pinckney, 2012; Verlicchi, 2018). Such complex cocktail effects may strongly vary depending on the present compounds and the microbial communities. Hence, single-compound/species studies are not sufficient to make meaningful predictions

of the ecological impact of PhC and potential toxic effects of “micropollutant cocktails” need to be better understood (Hagenbuch and Pinckney, 2012).

### Dynamics of Benthic Diatoms in Recipient River

River habitats (RU and RD) in this study are characterized as natural aquatic ecosystem and exhibit lower anthropogenic pressure and higher flow velocity and turbidity (particularly in spring and summer when river flow increases due to the snow and glacier melting) compared to TE sites. In the river, species with oligosaprobic preferences were generally favored and the development of diverse diatom communities and higher evenness between genera was facilitated. Consequently, lower dominance of motile groups (here represented mainly by *Mayamaea*, *Navicula*, and *Nitzschia*) and better growth of low- and high-profile groups was observed. In both river locations, higher prevalence of low-profile genera (represented mainly by *Achnantheidium*, *Cocconeis*, and *Reimeria*) was observed in summer (June and July). This can be explained by their better adaptation to resist to high current velocity and strong water turbulence that increase in these months. In contrast, high-profile groups (represented mainly by *Encyonema* and *Gomphonema*), that are not well adapted to high velocity, developed better in winter (Passy, 2007).

Benthic diatom assemblages in the river up- and downstream from the WWTP effluent were compared to evaluate the effect of TEs on the recipient aquatic environment. Regarding richness and diversity, we observed inconsistency between Chao1 (lower richness in RD) and Shannon (lower diversity in RU) (Figure 2). This difference may be linked to the increase in anthropogenic pressure in RD resulting in loss of rare species (ca. 20% less OTUs with <3 reads) (Proia et al., 2013a). Biggs (2000) observed that under certain circumstances, major species replacements with increasing eutrophication may also result in increase of species richness. Contrasting conclusions have been reported for the response of diatom richness and diversity to presence of micropollutants as rather a decrease in the presence of micropollutants (mainly herbicides and heavy metals) was observed (e.g., Genter and Lehman, 2000; Sabater, 2000; Morin et al., 2009; Ricciardi et al., 2009), while others were unable to detect such relation (e.g., Hirst et al., 2002; Marcel et al., 2013). Richness and diversity indices are not always relevant to assess waterbodies pollution levels (Ricciardi et al., 2009; Pandey et al., 2017). They reduce community information to a single number, which leads to huge loss of essential information about various crucial community characteristics (e.g., taxonomic structure, functional traits, phylogenetic relations, etc.) (Biggs, 2000).

Changes in community structure between river sites reflected the pollution induced by the TEs discharge that resulted in increasing trends of phosphate, NSAIDs, antibiotics and anticonvulsants downstream from the WWTP output. Species with oligotrophic and oligosaprobic preferences and high-profile taxa (that are more sensitive to contamination of micropollutants, Marcel et al., 2013) were rather disadvantaged downstream from the WWTP comparing to upstream. In RD,

these were replaced by motile groups, reflecting the increase in anthropogenic pollution (Rimet and Bouchez, 2011). Motile groups are usually less resistant to current velocity (Passy, 2007) and it was previously reported that they develop better in winter (Stenger-Kovács et al., 2013). However, in this study they exhibited such seasonal trend in RD only, which may be rather linked to the lower dilution factor of TEs in winter, potentially leading to stronger impact on river diatoms during winter.

Chronic input of trace emerging contaminants may in general lead to decrease in biofilm biomass and primary productivity and may thereby influence the ecology of benthic diatom assemblages (Hagenbuch and Pinckney, 2012). Such changes in more sensitive systems may impair higher trophic levels and lead to important alterations in river ecosystem functioning (Pinckney et al., 2013). Long-term exposure to contaminants may finally result in more tolerant assemblages (e.g., Corcoll et al., 2014). Results presented here are helpful to follow the changes on natural diatom communities potentially caused by the release of WWTP effluents. However, further studies are needed to better comprehend the cocktail effect of PhC and other micropollutants on benthic diatoms in aquatic environments. When studying such relationships, the potential effect of confounding factors (e.g., eutrophication levels, seasonal conditions) has to be carefully considered (Marcel et al., 2013).

### Tracking the Effect of Urban and Hospital Treated Effluents on River Communities Indicator Species Analysis

Indicator species analysis in combination with phylogenetic tree representation was helpful to better understand the effect of TEs on diatom assemblages and disentangle community changes in natural aquatic environment receiving urban and hospital TEs. Clades of phylogenetically close indicator OTUs behaved similarly and appeared simultaneously in the different habitats. Such patterns were expected from highly similar OTUs, as the clustering method applied here may generate several OTUs belonging to the same species. However, this trend also appeared on a larger scale in the phylogeny. Indicator OTUs from a large clade including mainly *Cocconeis*, *Achnantheidium*, *Planothidium*, *Encyonema*, and *Gomphonema* were hardly present in U, and those from a clade including mainly *Navicula* and *Mayamaea* were not found in H. Such phylogenetically related groups are likely to share similar characteristics like guild classes and ecological preferences (Keck et al., 2016). *Cocconeis*, *Achnantheidium*, *Planothidium*, *Encyonema*, and *Gomphonema* all possess a developed raphid system and belonged to the high- or low-profile guilds. In contrast, *Navicula* and *Mayamaea* are part of the motile guild. Indicator OTUs discriminating RU were detected throughout the phylogenetic tree. Entire clades from genera highly dominant at TE sites (e.g., *Craticula*, *Sellaphora*, and partially *Nitzschia*) were hardly found in RU implying their ecological optimum in contaminated environments.

According to the ISA, RD communities showed highest similarity to RU communities and were composed by 53% of OTUs (88% of DNA reads) indicative of RU. However, the two river locations differed significantly. This can be explained

by the continuous influence of micro- and macropollutants released by TEs that may inhibit the growth of sensitive species (Proia et al., 2013a), but also by possible species colonization downstream. Furthermore, 27% of the RD OTUs (9% of DNA reads) corresponded to indicator OTUs of U or H communities. Part of these OTUs probably corresponds to species that were released with the TEs and captured by the natural river biofilm downstream from the WWTP output. Motile, high-profile and especially planktic groups are more likely to disperse downstream with the water flow due to their lower resistance to current velocity (Liu et al., 2013; Dong et al., 2016). Indicator OTUs discriminating U or H and belonging to *Fragilaria*, *Gomphonema* (high-profile), and *Cyclotella* (planktic) were found in RD communities, despite their absence in RU. Transportation of free DNA from dead cells by the water flow may also occur and this DNA may be captured in river biofilms (e.g., Deiner et al., 2016; Pont et al., 2018). More directly, the permanent release of TEs causing constant pressure (PhC and nutrient load) in RD may favor the maintenance of more tolerant species and promote their stabilization in the biofilm.

River downstream communities seemed to be more influenced by U than by H communities, as 7% of the OTU reads found in RD corresponded to indicator OTUs of U, and only 2% – to indicator OTUs of H. The urban WWTP discharge was more than 15 times higher than the hospital one, which probably led to higher influence on water chemistry changes in RD.

### Biological Diatom Index

Finally, molecular BDI was calculated from taxonomically assigned OTUs to evaluate the effect of TEs' release on water quality in the recipient river. The application of BDI is usually limited to natural aquatic environments. However, WFD stations may be located in channels in urban environment build up with substrate different from natural river (similar to our case), and pollutant concentrations measured at TE sites during this study are comparable to these reported for highly polluted natural systems. Hence, we calculated BDI for all habitats (including TE sites) to evaluate the response of the entire diatom community to high anthropogenic pressure and track the effect of TEs on river communities. Compared to the river sites, communities in U and H reflected relatively low water quality (between “bad” and “moderate”), responding to the high anthropogenic pressure. WWTP discharges are generally monitored to avoid large alterations in river quality. The studied WWTP respected all national and European norms linked to removal efficiency and pollutants release (Chonova et al., 2016). Nevertheless, BDI based on molecular data suggested degradation of the water quality downstream from the WWTP output. This finding was confirmed by classical BDI based on microscopy counts (Sipibel Report, 2016) and it pointed out the efficiency of BDI to highlight changes in river ecology linked to the release of TEs.

### CONCLUSION

The present study shows that assessment of benthic diatoms using DNA metabarcoding is efficient to detect spatial and

temporal community responses to pharmaceutical pressure in TEs of urban and hospital wastewaters and contributes to our understanding of the potential effluent impact on community dynamics when released in the recipient aquatic environment. We detected habitat-specific changes linked to the WWTP effluents on different community levels – richness, diversity, taxonomic composition, functional traits, and phylogenetic position. The changes in taxonomy and ecological traits included shift in proportion of polysaprobic motile groups in TE vs. oligosaprobic/oligotrophic groups belonging to the low- and high-profile guild in the river (especially upstream). RDA suggested that beta-blockers, NSAIDs, antibiotics and phosphate were among the most important factors driving community dynamics in TEs. ISA was helpful to evaluate the negative effect of these TEs on natural river community composition, revealing that 27% of OTUs detected in RD communities were indicative of urban or hospital treated effluent origin. Those OTUs may be either directly transferred with the TE and captured in the biofilm or maintained and developed further in RD due to the continuous release of TEs that changes chemical water parameters. Finally, the BDI calculated to evaluate the ecological status of the recipient river suggested that the release of TEs may lead to water quality decrease.

From these results, we can conclude that there is clearly a change in community structure linked to the WWTP effluents. As discussed above, studying environmental relationships between microbial communities and pollutants remains challenging due to occurring intercorrelations and the potential effect of confounding factors. Study on larger scale in combination with laboratory experiments would be helpful to explore and strengthen further relations between water chemistry and diatom community changes and to confirm findings reported here.

### AUTHOR CONTRIBUTIONS

JL, AB, and TC contributed to the experimental design and sampling. TC contributed to the molecular experiments and data collection and organization. VV and TC contributed to the bioinformatics. RK, FK, FR, PI, and TC contributed to data analysis and statistics. RK, FR, JL, AB, and TC contributed to the interpretation of the data. FK and TC contributed to the preparation of the figures. RK, FR, JL, VV, FK, PI, AB, and TC contributed to the revision and approval of the manuscript.

### FUNDING

This study was done as part of the SIPIBEL field observatory on hospital effluents and urban WWTPs and was funded by ANSES (French National Agency for Food, Environmental and Occupational Health and Safety), project “PERSIST-ENV” (Effluents hospitaliers et persistance environnementale des médicaments et de bactéries pathogènes) #2012/2/149 as part of the programme Environnement-Santé-Travail (French Ministers

in charge of ecological and environmental issues). An Excellence Scholarship for doctoral programmes was obtained from the University of Innsbruck, Office of the Vice Rector for Research.

## ACKNOWLEDGMENTS

The article is based on collaborative work with COST Action DNAqua-Net (CA15219), supported by the COST (European Cooperation in Science and Technology) program. We thank Frankreich-Schwerpunkt (University of Innsbruck), and the EU

co-funded project Interreg Alpine Space “Eco-AlpsWater” for their support. We thank L. Wiest (ISA, Lyon) and V. Lecomte (GRAIE) for their contribution.

## SUPPLEMENTARY MATERIAL

The Supplementary Material for this article can be found online at: <https://www.frontiersin.org/articles/10.3389/fmicb.2019.00653/full#supplementary-material>

## REFERENCES

- AFNOR (1997). *French Standard Operating Procedures, Water Quality-Analytical Methods*, 2nd Edn, Vol. 3. La Défense: AFNOR.
- Anderson, M. J. (2001). A new method for non-parametric multivariate analysis of variance. *Austral Ecol.* 26, 32–46.
- Berger, S. A., Krompass, D., and Stamatakis, A. (2011). Performance, accuracy, and web server for evolutionary placement of short sequence reads under maximum likelihood. *Syst. Biol.* 60, 291–302. doi: 10.1093/sysbio/syr010
- Biggs, B. J. F. (2000). *New Zealand Periphyton Guideline: Detecting, Monitoring and Managing Enrichment of Streams*. Wellington: Ministry for the Environment, 121.
- Bonnineau, C., Guasch, H., Proia, L., Ricart, M., Geiszinger, A., Romani, A. M., et al. (2010). Fluvial biofilms: a pertinent tool to assess b-blockers toxicity. *Aquat. Toxicol.* 96, 225–233. doi: 10.1016/j.aquatox.2009.10.024
- Borcard, D., Legendre, P., and Drapeau, P. (1992). Partialling out the spatial component of ecological variation. *Ecology* 73, 1045–1055. doi: 10.2307/1940179
- Britton, T., Anderson, C. L., Jacquet, D., Lundqvist, S., and Bremer, K. (2007). Estimating divergence times in large phylogenetic trees. *Syst. Biol.* 56, 741–752. doi: 10.1080/10635150701613783
- Bruder, K., and Medlin, L. K. (2007). Molecular assessment of phylogenetic relationships in selected species/genera in the naviculoid diatoms (Bacillariophyta). I. The genus *Placoneis*. *Nova Hedwig.* 85, 331–352. doi: 10.1127/0029-5035/2007/0085-0331
- Chonova, T., Keck, F., Labanowski, J., Montuelle, B., Rimet, F., and Bouchez, A. (2016). Separate treatment of hospital and urban wastewaters: a real scale comparison of effluents and their effect on microbial communities. *Sci. Total Environ.* 542, 965–975. doi: 10.1016/j.scitotenv.2015.10.161
- Chonova, T., Labanowski, J., and Bouchez, A. (2017). “Contribution of hospital effluents to the load of micropollutants in WWTP influents,” in *Hospital Wastewaters – Characteristics, Management, Treatment and Environmental Risks. The Handbook of Environmental Chemistry*, ed. P. Verlicchi (Heidelberg: Springer), 135–152. doi: 10.1007/978-2017-21
- Chonova, T., Labanowski, J., Cournoyer, B., Chardon, C., Keck, F., Laurent, E., et al. (2018a). River biofilm community changes related to pharmaceutical loads emitted by a wastewater treatment plant. *Environ. Sci. Pollut. Res. Int.* 25, 9254–9264. doi: 10.1007/s11356-017-0024-0
- Chonova, T., Lecomte, V., Krajewski, J. L., Bouchez, A., Labanowski, J., Dagot, C., et al. (2018b). The SIPIBEL project: treatment of hospital and urban wastewater in a conventional urban wastewater treatment plant. *Environ. Sci. Pollut. Res. Int.* 25, 9197–9206. doi: 10.1007/s11356-017-9302-0
- Congestri, R., Cox, E. J., Cavacini, P., and Albertano, P. (2005). Diatoms (Bacillariophyta) in phototrophic biofilms colonising an Italian wastewater treatment plant. *Diatom Res.* 20, 241–255. doi: 10.1080/0269249X.2005.9705634
- Corcoll, N., Acuña, V., Barceló, D., Casellas, M., Guasch, H., Huerta, B., et al. (2014). Pollution-induced community tolerance to non-steroidal anti-inflammatory drugs (NSAIDs) in fluvial biofilm communities affected by WWTP effluents. *Chemosphere* 112, 185–193. doi: 10.1016/j.chemosphere.2014.03.128
- Coste, M., Boutry, S., Tison-Rosebery, J., and Delmas, F. (2009). Improvements of the Biological Diatom Index (BDI): description and efficiency of the new version (BDI-2006). *Ecol. Indic.* 9, 621–650. doi: 10.1016/j.ecolind.2008.06.003
- Deiner, K., Fronhofer, E. A., Mächler, E., Walser, J.-C., and Altermatt, F. (2016). Environmental DNA reveals that rivers are conveyor belts of biodiversity information. *Nat. Commun.* 7:12544. doi: 10.1038/ncomms12544
- Ding, T., Yang, M., Zhang, J., Yang, B., Lin, K., Li, J., et al. (2017). Toxicity, degradation and metabolic fate of ibuprofen on freshwater diatom *Navicula* sp. *J. Hazard. Mater.* 330, 127–134. doi: 10.1016/j.jhazmat.2017.02.004
- Dong, X., Li, B., He, F., Gu, Y., Sun, M., Zhang, H., et al. (2016). Flow directionality, mountain barriers and functional traits determine diatom metacommunity structuring of high mountain streams. *Sci. Rep.* 6:24711. doi: 10.1038/srep24711
- Dufrene, M., and Legendre, P. (1997). Species assemblages and indicator species: the need for a flexible asymmetrical approach. *Ecol. Monogr.* 67, 345–366. doi: 10.2307/2963459
- Edgar, R. C. (2004). MUSCLE: multiple sequence alignment with high accuracy and high throughput. *Nucleic Acids Res.* 32, 1792–1797. doi: 10.1093/nar/gkh340
- Edgar, R. C., Haas, B. J., Clemente, J. C., Quince, C., and Knight, R. (2011). UCHIME improves sensitivity and speed of chimera detection. *Bioinformatics* 27, 2194–2200. doi: 10.1093/bioinformatics/btr381
- Esteves, S. M., Keck, F., Almeida, S. F. P., Figueira, E., Bouchez, A., and Rimet, F. (2017). Can we predict diatoms herbicide sensitivities with phylogeny? Influence of intraspecific and interspecific variability. *Ecotoxicology* 26, 1065–1077. doi: 10.1007/s10646-017-1834-z
- European Commission (2013). *Directive 2013/39/EU of the European Parliament and of the Council of 12 August 2013 Amending Directives 2000/60/EC and 2008/105/EC as Regards Priority Substances in the Field of Water Policy (2011/0429 (COD))*. Brussels: European Commission.
- Genter, R. B., and Lehman, R. M. (2000). Metal toxicity inferred from algal population density, heterotrophic substrate use, and fatty acid profile in a small stream. *Environ. Toxicol. Chem.* 19, 869–878. doi: 10.1002/etc.5620190413
- Ghosh, S., and Love, N. G. (2011). Application of RbcL based molecular diversity analysis to algae in wastewater treatment plants. *Bioresour. Technol.* 102, 3619–3622. doi: 10.1016/j.biortech.2010.10.125
- Guo, J., Selby, K., and Boxall, A. B. (2016). Assessment of the risks of mixtures of major use veterinary antibiotics in European surface waters. *Environ. Sci. Technol.* 50, 8282–8289. doi: 10.1021/acs.est.6b01649
- Hagenbuch, I. M., and Pinckney, J. L. (2012). Toxic effect of the combined antibiotics ciprofloxacin, lincomycin, and tylosin on two species of marine diatoms. *Water Res.* 46, 5028–5036. doi: 10.1016/j.watres.2012.06.040
- Hirst, H., Jüttner, I., and Ormerod, S. J. (2002). Comparing the responses of diatoms and macroinvertebrates to metals in upland streams of Wales and Cornwall. *Freshw. Biol.* 47, 1752–1765. doi: 10.1046/j.1365-2427.2002.00904.x
- Keck, F., Bouchez, A., Franc, A., and Rimet, F. (2016). Linking phylogenetic similarity and pollution sensitivity to develop ecological assessment methods: a test with river diatoms. *J. Appl. Ecol.* 53, 856–864. doi: 10.1111/1365-2664.12624
- Kerमारrec, L., Franc, A., Rimet, F., Chaumeil, P., Humbert, F., and Bouchez, A. (2013). Next-generation sequencing to inventory taxonomic diversity in eukaryotic communities: a test for freshwater diatoms. *Mol. Ecol. Resour.* 13, 607–619. doi: 10.1111/1755-0998.12105

- Labanowski, J., Laurent, E., Chonova, T., Bouchez, A., Cournoyer, B., Marjolet, L., et al. (2016). Hospital effluents and environmental persistence of pathogenic bacteria and pharmaceutical compounds – the Persist-Env approach. *Tech. Sci. Méthodes* 6, 22–30. doi: 10.1051/tsm/201606022
- Lange, K., Liess, A., Piggott, J. J., Townsend, C. R., and Matthaei, C. D. (2011). Light, nutrients and grazing interact to determine stream diatom community composition and functional group structure. *Freshw. Biol.* 56, 264–278. doi: 10.1111/j.1365-2427.2010.02492.x
- Lange-Bertalot, H. (1979). Pollution tolerance of diatoms as a criterion for water quality estimation. *Nova Hedwig* 64, 285–304.
- Larras, F., Keck, F., Montuelle, B., Rimet, F., and Bouchez, A. (2014). Linking diatom sensitivity to herbicides to phylogeny: a step forward for biomonitoring? *Environ. Sci. Technol.* 48, 1921–1930. doi: 10.1021/es4045105
- Larras, F., Lambert, A.-S., Pesce, S., Rimet, F., Bouchez, A., and Montuelle, B. (2013). The effect of temperature and a herbicide mixture on freshwater periphytic algae. *Ecotoxicol. Environ. Saf.* 98, 162–170. doi: 10.1016/j.ecoenv.2013.09.007
- Larson, C. A., and Passy, S. I. (2012). Taxonomic and functional composition of the algal benthos exhibits similar successional trends in response to nutrient supply and current velocity. *Microbiol. Ecol.* 80, 352–362. doi: 10.1111/j.1574-6941.2012.01302.x
- Lecoq, C., Coste, M., and Prygiel, J. (1993). “OMNIDIA” software for taxonomy, calculation of diatom indices and inventories management. *Hydrobiologia* 269/270, 509–513. doi: 10.1007/BF00028048
- Legendre, P., and Gallagher, E. D. (2001). Ecologically meaningful transformations for ordination of species data. *Oecologia* 129, 271–280. doi: 10.1007/s004420100716
- Lengyel, E., Padisák, J., and Stenger-Kovács, C. (2015). Establishment of equilibrium states and effect of disturbances on benthic diatom assemblages of the Torna-stream, Hungary. *Hydrobiologia* 750, 43–56. doi: 10.1007/s10750-014-2065-4
- Liu, J., Soininen, J., Han, B.-P., and Declerck, S. A. J. (2013). Effects of connectivity, dispersal directionality and functional traits on the metacommunity structure of river benthic diatoms. *J. Biogeogr.* 40, 2238–2248. doi: 10.1111/jbi.12160
- Mangot, J.-F., Domaizon, I., Taib, N., Marouni, N., Duffaud, E., Bronner, G., et al. (2013). Short-term dynamics of diversity patterns: evidence of continual reassembly within lacustrine small eukaryotes. *Environ. Microbiol.* 15, 1745–1758. doi: 10.1111/1462-2920.12065
- Marcel, R., Bouchez, A., and Rimet, F. (2013). Influence of herbicide contamination on diversity and ecological guilds of river diatoms. *Cryptogam. Algal.* 34, 169–183. doi: 10.7872/crya.v34.iss2.2013.169
- McArdle, B. H., and Anderson, M. J. (2001). Fitting multivariate models to community data: a comment on distance-based redundancy analysis. *Ecology* 82, 290–297. doi: 10.1890/0012-9658(2001)082[0290:FMMTCD]2.0.CO;2
- Morin, S., Bottin, M., Mazella, N., Macary, F., Delmas, F., Winterton, P., et al. (2009). Linking diatom community structure to pesticide input as evaluated through a spatial contamination potential (Phytopixal): a case study in the Neste river system (South-West France). *Aquat. Toxicol.* 94, 28–39. doi: 10.1016/j.aquatox.2009.05.012
- Needleman, S. B., and Wunsch, C. D. (1970). A general method applicable to the search for similarities in the amino acid sequence of two proteins. *J. Mol. Biol.* 48, 443–453. doi: 10.1127/1863-9135/2007/0168-0179
- Oksanen, J., Blanchet, F. G., Friendly, M., Kindt, R., Legendre, P., McGlinn, D., et al. (2017). *Vegan: Community Ecology package*. R package version 2.4–3. doi: 10.1016/0022-2836(70)90057-4
- Pandey, L. K., Bergey, E. A., Lyu, J., Park, J., Choi, S., Lee, H., et al. (2017). The use of diatoms in ecotoxicology and bioassessment: insights, advances and challenges. *Water Res.* 118, 39–58. doi: 10.1016/j.watres.2017.01.062
- Passy, S. I. (2007). Diatom ecological guilds display distinct and predictable behavior along nutrient and disturbance gradients in running waters. *Aquat. Bot.* 86, 171–178. doi: 10.1016/j.aquabot.2006.09.018
- Patrick, R. (1961). A study of the number and kinds of species found in rivers of the Eastern United States. *Proc. Acad. Natl. Sci. Phila.* 113, 215–258.
- Peres-Neto, P. R., Legendre, P., Dray, S., and Borcard, D. (2006). Variation partitioning of species data matrices: estimation and comparison of fractions. *Ecology* 87, 2614–2625. doi: 10.1890/0012-9658(2006)87[2614:VPOSDM]2.0.CO;2
- Pinckney, J. L., Hagenbuch, I. M., Long, R. A., and Lovell, C. R. (2013). Sublethal effects of the antibiotic tylosin on estuarine benthic microalgal communities. *Mar. Pollut. Bull.* 68, 8–12. doi: 10.1016/j.marpolbul.2013.01.006
- Pont, D., Rocle, M., Valentini, A., Civade, R., Jean, P., Maire, A., et al. (2018). Environmental DNA reveals quantitative patterns of fish biodiversity in large rivers despite its downstream transportation. *Sci. Rep.* 8:10361. doi: 10.1038/s41598-018-28424-8
- Proia, L., Lupini, G., Osorio, V., Pérez, S., Barceló, D., Schwartz, T., et al. (2013a). Response of biofilm bacterial communities to antibiotic pollutants in a Mediterranean river. *Chemosphere* 92, 1126–1135. doi: 10.1016/j.chemosphere.2013.01.063
- Proia, L., Osorio, V., Soley, S., Köck-Schulmeyer, M., Pérez, S., Barceló, D., et al. (2013b). Effects of pesticides and pharmaceuticals on biofilms in a highly impacted river. *Environ. Pollut.* 178, 220–228. doi: 10.1016/j.envpol.2013.02.022
- Ricciardi, F., Bonnineau, C., Faggiano, L., Geiszinger, A., Guasch, H., Lopez-Doval, J., et al. (2009). Is chemical contamination linked to the diversity of biological communities in rivers? *Trends Anal. Chem.* 28, 592–602. doi: 10.1016/j.trac.2009.02.007
- Rimet, F., and Bouchez, A. (2011). Use of diatom life-forms and ecological guilds to assess pesticide contamination in rivers: lotic mesocosm approaches. *Ecol. Indic.* 11, 489–499. doi: 10.1016/j.ecolind.2010.07.004
- Rimet, F., and Bouchez, A. (2012). Life-forms, cell-sizes and ecological guilds of diatoms in European rivers. *Knowl. Manag. Aquat. Ecosyst.* 406, 1–14. doi: 10.1051/kmae/2012018
- Rimet, F., Chaumeil, P., Keck, F., Kermarrec, L., Vasselon, V., Kahlert, M., et al. (2016). R-Syst: diatom: an open-access and curated barcode database for diatoms and freshwater monitoring. *Database* 2016:baw016. doi: 10.1093/database/baw016
- Roberts, D. W. (2007). *labdsv: Ordination and Multivariate Analysis for Ecology*. R package version 1.3–1.
- Sabater, S. (2000). Diatom communities as indicators of environmental stress in the Guadiamar River, S-W. Spain, following a major mine tailings spill. *J. Appl. Phycol.* 12, 113–124. doi: 10.1023/A:1008197411815
- Schloss, P. D., Westcott, S. L., Ryabin, T., Hall, J. R., Hartmann, M., Hollister, E. B., et al. (2009). Introducing mothur: open-source, platform-independent, community-supported software for describing and comparing microbial communities. *Appl. Environ. Microbiol.* 75, 7537–7541. doi: 10.1128/AEM.01541-09
- Schneider, S., and Lindström, E. A. (2009). Bioindication in Norwegian rivers using non-diatomaceous benthic algae: the acidification index periphyton (AIP). *Ecol. Indic.* 9, 1206–1211. doi: 10.1016/j.ecolind.2009.02.008
- Schneider, S. C., and Lindström, E.-A. (2011). The periphyton index of trophic status PIT: a new eutrophication metric based on non-diatomaceous benthic algae in Nordic rivers. *Hydrobiologia* 665, 143–155. doi: 10.1007/s10750-011-0614-7
- Schwarzenbach, R. P., Escher, B. I., Fenner, K., Hofstetter, T. B., Johnson, C. A., von Gunten, U., et al. (2006). The challenge of micropollutants in aquatic systems. *Science* 313, 1072–1077. doi: 10.1126/science.1127291
- Sipibel Report (2016). *2011–2015 Effluents Hospitaliers et Stations d'Épuration Urbaines: Caractérisation, Risques et Traitabilité – Synthèse des Résultats de Quatre Années de Suivi, d'Études et de Recherche sur le Site Pilote de Bellecombe* (in French), 174.
- Sládečková, A., Marvan, P., and Vymazal, J. (1983). “The utilization of periphyton in waterworks pre-treatment for nutrient removal from enriched influents,” in *Periphyton of Freshwater Ecosystems*. *Developments in Hydrobiology*, Vol. 17, ed. R. G. Wetzel (Dordrecht: Springer).
- Stamatakis, A. (2014). RAxML Version 8: a tool for phylogenetic analysis and post-analysis of large phylogenies. *Bioinformatics* 30, 1312–1313. doi: 10.1093/bioinformatics/btu033
- Stenger-Kovács, C., Lengyel, E., Crossetti, L. O., Üveges, V., and Padisák, J. (2013). Diatom ecological guilds as indicators of temporally changing stressors and disturbances in the small Torna-stream, Hungary. *Ecol. Indic.* 24, 138–147. doi: 10.1016/j.ecolind.2012.06.003
- Stevenson, R., and Smol, J. (2003). “Use of algae in environmental assessments,” in *Freshwater Algae in North America: Ecology and Classification*, eds J. D. Wehr

- and R. G. Sheath (San Diego, CA: Academic Press), 775–804. doi: 10.1016/B978-012741550-5/50024-6
- Stoof-Leichsenring, K. R., Epp, L. S., Trauth, M. H., and Tiedemann, R. (2012). Hidden diversity in diatoms of Kenyan Lake Naivasha: a genetic approach detects temporal variation. *Mol. Ecol.* 21, 1918–1930. doi: 10.1111/j.1365-294X.2011.05412.x
- Tapolczai, K., Bouchez, A., Stenger-Kovács, C., Padisák, J., and Rimet, F. (2016). Trait-based ecological classifications for benthic algae: review and perspectives. *Hydrobiologia* 776, 1–17. doi: 10.1007/s10750-016-2736-4
- Tapolczai, K., Bouchez, A., Stenger-Kovács, C., Padisák, J., and Rimet, F. (2017). Taxonomy-or trait-based ecological assessment for tropical rivers? Case study on benthic diatoms in Mayotte island (France, Indian Ocean). *Sci. Total Environ.* 607, 1293–1303. doi: 10.1016/j.scitotenv.2017.07.093
- Tornés, E., Mor, J. R., Mandaric, L., and Sabater, S. (2018). Diatom responses to sewage inputs and hydrological alteration in Mediterranean streams. *Environ. Pollut.* 238, 369–378. doi: 10.1016/j.envpol.2018.03.037
- Vasselon, V., Bouchez, A., Rimet, F., Jacquet, S., Trobajo, R., Corniquel, M., et al. (2018). Avoiding quantification bias in metabarcoding: application of a cell biovolume correction factor in diatom molecular biomonitoring. *Methods Ecol. Evol.* 9, 1060–1069. doi: 10.1111/2041-210X.12960
- Vasselon, V., Domaizon, I., Rimet, F., Kahlert, M., and Bouchez, A. (2017a). Application of high-throughput sequencing (HTS) metabarcoding to diatom biomonitoring: do DNA extraction methods matter? *Freshw. Sci.* 36, 162–177. doi: 10.1086/690649
- Vasselon, V., Rimet, F., Tapolczai, K., and Bouchez, A. (2017b). Assessing ecological status with diatoms DNA metabarcoding: scaling-up on a WFD monitoring network (Mayotte Island, France). *Ecol. Indic.* 82, 1–12. doi: 10.1016/j.ecolind.2017.06.024
- Verlicchi, P. (2018). “Final remarks and perspectives on the management and treatment of hospital effluents,” in *Hospital Wastewaters – Characteristics, Management, Treatment and Environmental Risks. The Handbook of Environmental Chemistry*, ed. P. Verlicchi (Heidelberg: Springer), 231–238.
- Verlicchi, P., Al Aukidy, M., and Zambello, E. (2012). Occurrence of pharmaceutical compounds in urban wastewater: removal, mass load and environmental risk after a secondary treatment—a review. *Sci. Total Environ.* 429, 123–155. doi: 10.1016/j.scitotenv.2012.04.028
- Verlicchi, P., Al Aukidy, M., and Zambello, E. (2015). What have we learned from worldwide experiences on the management and treatment of hospital effluent? — An overview and a discussion on perspectives. *Sci. Total Environ.* 514, 467–491. doi: 10.1016/j.scitotenv.2015.02.020
- Villeneuve, A., Bouchez, A., and Montuelle, B. (2011). In situ interactions between the effects of season, current velocity and pollution on a river biofilm. *Freshw. Biol.* 56, 2245–2259. doi: 10.1111/j.1365-2427.2011.02649.x
- Visco, J. A., Gentil, L. A. P., Cordonier, A., Esling, P., Pillet, L., and Pawlowski, J. (2015). Environmental monitoring: inferring the diatom index from next-generation sequencing data. *Environ. Sci. Technol.* 49, 7597–7605. doi: 10.1021/es506158m
- Wang, Q., Garrity, G. M., Tiedje, J. M., and Cole, J. R. (2007). Naive Bayesian classifier for rapid assignment of rRNA sequences into the new bacterial taxonomy. *Appl. Environ. Microbiol.* 73, 5261–5267. doi: 10.1128/AEM.00062-07
- Wiest, L., Chonova, T., Bergé, A., Baudot, R., Bessueille-Barbier, F., Ayouni-Derouiche, L., et al. (2018). Two-year survey of specific hospital wastewater treatment and its impact on pharmaceutical discharges. *Environ. Sci. Pollut. Res.* 25, 9207–9218. doi: 10.1007/s11356-017-9662-5
- Windler, M., Leinweber, K., Bartulos, C. R., Philipp, B., and Kroth, P. G. (2015). Biofilm and capsule formation of the diatom *Achnanthes minutissimum* are affected by a bacterium. *J. Phycol.* 51, 343–355. doi: 10.1111/jpy.12280
- Zimmermann, J., Glöckner, G., Jahn, R., Enke, N., and Gemeinholzer, B. (2015). Metabarcoding vs. morphological identification to assess diatom diversity in environmental studies. *Mol. Ecol. Res.* 15, 526–542. doi: 10.1111/1755-0998.12336

**Conflict of Interest Statement:** The authors declare that the research was conducted in the absence of any commercial or financial relationships that could be construed as a potential conflict of interest.

Copyright © 2019 Chonova, Kurmayer, Rimet, Labanowski, Vasselon, Keck, Illmer and Bouchez. This is an open-access article distributed under the terms of the Creative Commons Attribution License (CC BY). The use, distribution or reproduction in other forums is permitted, provided the original author(s) and the copyright owner(s) are credited and that the original publication in this journal is cited, in accordance with accepted academic practice. No use, distribution or reproduction is permitted which does not comply with these terms.



# Global Metabolomic Characterizations of *Microcystis* spp. Highlights Clonal Diversity in Natural Bloom-Forming Populations and Expands Metabolite Structural Diversity

## OPEN ACCESS

### Edited by:

Fabrice Martin-Laurent,  
Institut National de la Recherche  
Agronomique (INRA), France

### Reviewed by:

Emani Pinto,  
University of São Paulo, Brazil  
Marie-Virginie Salvia,  
Université de Perpignan Via Domitia,  
France

Steven Wilhelm,  
The University of Tennessee,  
Knoxville, United States

### \*Correspondence:

Benjamin Marie  
bmarie@mnhn.fr

### Specialty section:

This article was submitted to  
Microbiotechnology, Ecotoxicology  
and Bioremediation,  
a section of the journal  
Frontiers in Microbiology

**Received:** 11 September 2018

**Accepted:** 27 March 2019

**Published:** 16 April 2019

### Citation:

Le Manach S, Duval C, Marie A,  
Djediat C, Catherine A, Ederly M,  
Bernard C and Marie B (2019) Global  
Metabolomic Characterizations  
of *Microcystis* spp. Highlights Clonal  
Diversity in Natural Bloom-Forming  
Populations and Expands Metabolite  
Structural Diversity.  
Front. Microbiol. 10:791.  
doi: 10.3389/fmicb.2019.00791

Séverine Le Manach, Charlotte Duval, Arul Marie, Chakib Djediat, Arnaud Catherine, Marc Ederly, Cécile Bernard and Benjamin Marie\*

UMR 7245 MNHN/CNRS Molécules de Communication et Adaptation des Micro-organismes, Muséum National d'Histoire Naturelle, Paris, France

Cyanobacteria are photosynthetic prokaryotes capable of synthesizing a large variety of secondary metabolites that exhibit significant bioactivity or toxicity. *Microcystis* constitutes one of the most common cyanobacterial genera, forming the intensive blooms that nowadays arise in freshwater ecosystems worldwide. Species in this genus can produce numerous cyanotoxins (i.e., toxic cyanobacterial metabolites), which can be harmful to human health and aquatic organisms. To better understand variations in cyanotoxin production between clones of *Microcystis* species, we investigated the diversity of 24 strains isolated from the same blooms or from different populations in various geographical areas. Strains were compared by genotyping with 16S-ITS fragment sequencing and metabolite chemotyping using LC ESI-qTOF mass spectrometry. While genotyping can help to discriminate among different species, the global metabolome analysis revealed clearly discriminating molecular profiles among strains. These profiles could be clustered primarily according to their global metabolite content, then according to their genotype, and finally according to their sampling location. A global molecular network of all metabolites produced by *Microcystis* species highlights the production of a wide set of chemically diverse metabolites, including a few microcystins, many aeruginosins, microginins, cyanopeptolins, and anabaenopeptins, together with a large set of unknown molecules. These components, which constitute the molecular biodiversity of *Microcystis* species, still need to be investigated in terms of their structure and potential bioactivities (e.g., toxicity).

**Keywords:** cyanobacteria blooms, secondary metabolites, chemiodiversity, mass spectrometry, aquatic environment

## INTRODUCTION

During recent decades, the frequency and the intensity of cyanobacteria proliferation occurring in continental aquatic ecosystems have increased due to climate and anthropogenic changes (Carey et al., 2012; Sukenik et al., 2015; Paerl, 2018). The resulting massive cyanobacteria “blooms” threaten aquatic ecosystem function through various processes, including: (i) alteration of the trophic network, (ii) decrease in the light penetrating the water column, (iii) decrease in available dissolved oxygen, and (iv) production of various secondary metabolites that are potentially toxic for living organisms (Carmichael, 2008). Indeed, various cyanobacterial genera can synthesize a wide range of secondary metabolites (Welker et al., 2012; Shih et al., 2013), with noticeable bioactivity and high toxicity, causing potential harm to human and aquatic organism populations (Codd et al., 2005; Pearson et al., 2010). These metabolites are also believed to affect the proliferative capability of the cyanobacteria themselves (Guljamow et al., 2017).

*Microcystis* represents one of the most proliferative bloom-forming cyanobacterial genera (Bishop et al., 1959; **Figure 1**). It has been reported in more than 108 countries and on all continents (Šejnohová and Maršálek, 2012; Harke et al., 2016; Ma et al., 2016). Previous documentations had only reported *Microcystis* in less than 30 countries (Zurawell et al., 2005). This suggests that species within this genus are currently proliferating and largely dominating freshwater phytoplankton communities in temperate and tropical areas. In temperate ecosystems, *Microcystis* species can even overwinter in the benthos, rise from the epilimnion during the summer and can accumulate to form intensive blooms and even scums on the surface (Harke et al., 2016).

Some important features of *Microcystis* species specifically favor their worldwide expansion (Paerl et al., 2011). These features include the capability to regulate their buoyancy, their winter storage strategy at the bottom of the water column, their phosphate (P) and nitrogen (N) uptake capacities, and their resistance to zooplankton grazing. Indeed, *Microcystis* species exhibit competitive advantages during nutrient limitation or environmental warming compared to other cyanobacteria or microalgae. In addition, many *Microcystis* strains can produce a multitude of bioactive secondary metabolites, including the potent hepatotoxins microcystins (MCs). Then, the persistence of their proliferation poses local risks to those using contaminated water resources for consumption, recreational activities, agriculture, or fisheries (Codd et al., 2005). Beyond MCs, other potentially toxic compounds produced by *Microcystis* species have also been reported to be deleterious for aquatic organisms, as they potentially inhibit the grazing capability of herbivorous planktonic organisms (Harke et al., 2017).

So far, 11 secondary-metabolite biosynthetic gene clusters encoding non-ribosomal peptide synthase (NRPS) and/or polyketide synthase (PKS) and two other clusters encoding ribosomes were detected within ten *Microcystis* genomes (Humbert et al., 2013). Seven of these clusters encode

enzymes involved in the biosynthesis of already known metabolites (such as microcystins, aeruginosins, cyanopeptolins, microginins, anabaenopeptins, cyanobactins, and microviridins), whereas the six remaining clusters seem to encode different enzymes responsible for the biosynthesis of yet-uncharacterized compounds. However, the relationship between cyanobacterial biomass and metabolite concentration in the environment appears neither systematic nor linear (Briand et al., 2012; Liu et al., 2016). Indeed, the production of metabolites, such as microcystins, by *Microcystis* blooms, depends not only on cyanobacterial biomass, but also on the dynamics of the ratio between potentially producing and non-producing genotypes (Via-Ordorika et al., 2004).

Despite recent advances in the description of the biosynthetic pathways involved in cyanobacterial metabolite synthesis (Wang et al., 2014; Dittmann et al., 2015), the biological functions and the ecological roles of these molecules are still not fully understood (Holland and Kinnear, 2013; Zak and Kosakowska, 2016). In addition, the biosynthesis of cyanobacterial secondary metabolites is estimated to consume a remarkable portion of metabolic energy, constituting a significant cost for the producing cell (Briand et al., 2012). However, natural environments are colonized by various clones producing different sets of metabolites (Briand et al., 2009). It has been then proposed that the environment may favor the selection of *Microcystis* clones that present the most-adapted metabolite composition (Welker et al., 2007; Martins et al., 2009; Agha and Quesada, 2014).

Recently, the development of modern mass spectrometry approaches has provided a new opportunity for describing the occurrence and the diversity of cyanobacterial metabolites (Yang et al., 2013; Briand et al., 2016a). In order to better understand the differences in metabolite production between clones of various bloom-forming cyanobacteria from different localities, we investigated here the clonal diversity of 24 *Microcystis* strains, originating from various geographical areas, using an innovative approach based on global molecular networking.

## MATERIALS AND METHODS

### Sampling, Isolation and Cultivation of *Microcystis* Monoclonal Strains

The study was performed from 24 mono-clonal non-axenic cultures of *Microcystis* spp. maintained at 25°C in 15-mL vessels with Z8 media in the PMC (Paris Museum Collection) of living cyanobacteria<sup>1</sup>. Larger volume of all strains was simultaneously cultivated during one month in triplicates in 50 mL Erlenmeyer's vessels at 25°C using a Z8 medium with a 16 h: 8 h light/dark cycle (60  $\mu\text{mol}\cdot\text{m}^{-2}\cdot\text{s}^{-1}$ ). All trains were then investigated for their MC production by Adda-microcystin AD4G2 ELISA kit (Abraxis). Cyanobacterial

<sup>1</sup><http://www.mnhn.fr/fr/collections/ensembles-collections/ressources-biologiques-cellules-vivantes-cryoconservees/microalgues-cyanobacteries>

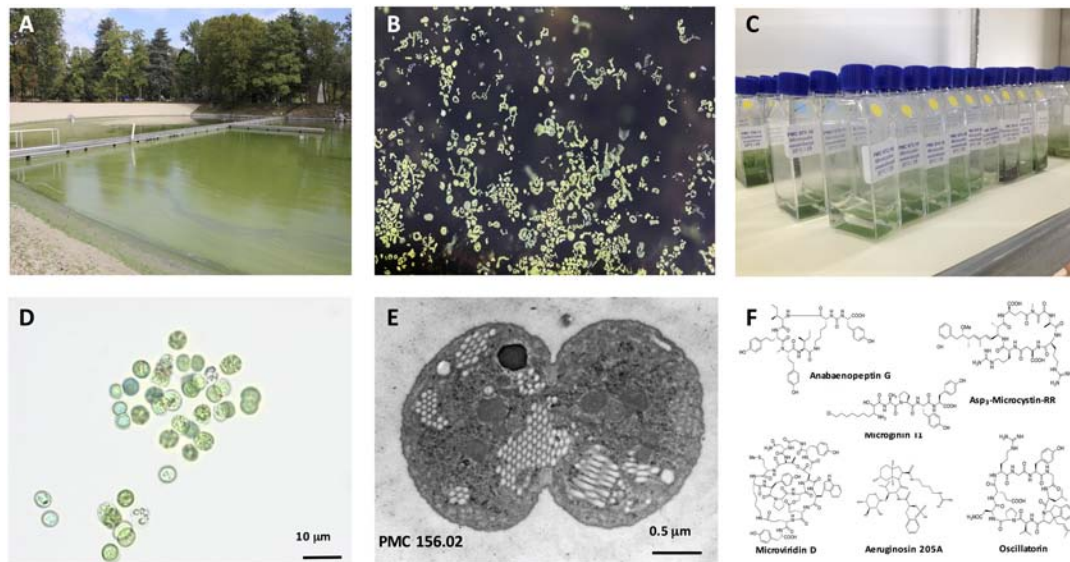


**FIGURE 1 |** *Microcystis* spp. General view of a representative intense *Microcystis* sp. bloom in a recreational pond (Champs-sur-Marne, © B. Marie) (A). Macrograph of *Microcystis* colonies at surface water (© B. Marie) (B). Example of 15-mL vessels containing the monoclonal strains of *Microcystis* spp. maintained in the Paris' Museum Collection (PMC) of cyanobacteria (MNHN, Paris, © C. Duval) (C). Example of micrograph of the isolated monoclonal culture of the *Microcystis aeruginosa*, where scale bare represents 10 µm (© C. Duval) (D). Representative picture of *Microcystis aeruginosa* cell from PMC 156.02 strain (here in division) under transmission electron microscope, where scale bare represents 0.5 µm (© C. Djediat) (E). General structures of various cyanobacterial metabolites belonging to the microcystin, anabaenopeptin, microginin, microviridin, aeruginosin and oscillatorin families (F).

cells were centrifuged (at 4,000 g for 10 min), then freeze-dried and weighted, and stored at  $-80^{\circ}\text{C}$  prior to DNA and metabolite analyses.

## DNA-Extraction, PCR, Sequencing, and Phylogenetic Analyses

DNA was extracted with Qiagen Kit (Cat N° 69506) according to manufacturer's instructions. The presence and the quality of the extracted DNA was checked by observing the 260/280-nm ratio and the absorbance spectra between 200 and 800 nm using a NanoDrop spectrophotometer (SAFAS, Monaco). PCR reaction was performed with *mcyA* specific primers developed for *Microcystis* (*mcyA\_S* AAAAACCCGCGCCCTTTTAC and *mcyA\_AS* AGGCAGTTGGAGAATCACGG) in order to investigate the presence of this gene in the different strains. In parallel, the region containing a fragment 16S rRNA and another of the 16S-23S ITS was amplified using primer couples previously described in Gugger and Hoffmann (2004) and Iteman et al. (2000), respectively. The amplification was performed in a mix of 0.1 µL (100 µM) of each primer, 12.5 µL of MyTaq RedMix polymerase (Bioline®) and 2 µL (~200 ng) of each DNA samples (25 µL final volume). The PCR product was sequenced (Genoscreen, France) using the same primers. The partial 16S and 16S-23S ITS sequences of all strains were deposited to GenBank (Accession numbers MH892877–MH892900 and MH899657–MH899680, respectively).

The *Microcystis* 16S-23S ITS gene sequences were compared to a selection of similar (>93% identity) sequences retrieved

from NCBI according to nucleotide BLAST search (basic local alignment search tool). The different sequences were aligned with CodonCode Aligner and non-homologous regions of the sequence alignment were manually deleted with BioEdit tool (Version 7.2.5). The phylogeny of the aligned 16S-23S ITS sequences was performed using the MEGA V.6 software. The tree based on maximum likelihood (ML) was constructed with 1000-bootstrap replicates, performing a branch lengths iteration and global rearrangements.

## Metabolome Biomass Extraction and Analysis by Mass Spectrometry

The 20 mL of biomasses of the 24 *Microcystis* strain cultures were centrifuged (4,000 rpm, 10 min), the culture media discarded, and then freeze-dried. The lyophilized cells were weighted then sonicated 2 min in acetonitrile/methanol/water (40/40/20) acidified at 0.1% of formic acid with a constant ratio of 100 µL of solvent for 1 mg of dried biomass, centrifuged at  $4^{\circ}\text{C}$  (12,000 g; 5 min). Two micro liter of the supernatant were then analyzed on an UHPLC (Ultimate 3000, Thermo Fisher Scientific) coupled with a mass spectrometer (ESI-Qq-TOF Maxis II ETD, Bruker).

Ultra high performance liquid chromatography (UHPLC) was performed on 2 µL of each of the metabolite extracts using a Polar Advances II 2.5 pore  $\text{C}_{18}$  column (Thermo®) at a  $300\ \mu\text{L}\cdot\text{min}^{-1}$  flow rate with a linear gradient of acetonitrile in 0.1% formic acid (5 to 90% in 21 min). The metabolite contents were analyzed in triplicate for each strain using an electrospray ionization hybrid quadrupole time-of-flight (ESI-QqTOF) high resolution mass spectrometer (Maxis

II ETD, Bruker) on positive simple MS or on positive Collision Ion Dissociation (CID) autoMSMS mode with information dependent acquisition (IDA), on the 50–1500  $m/z$  rang at 2 Hz or between 2 and 8 Hz speed, for MS and MS/MS, respectively, according to relative intensity of parent ions, in consecutive cycle times of 2.5 s, with an active exclusion of previously analyzed parents. The data were analyzed with the Data Analysis 4.4 and MetaboScape 3.0 software for internal recalibration (<0.5 ppm for each sample, as an internal calibrant of Na formate was injected at the beginning of each analysis), molecular feature search and MGF export. Peak lists were generated from MS spectra (between 1 and 15 min of the LC gradient), with a filtering of the noise fixed at the threshold of 0.1% of the maximal intensity, and combining all charge states and related isotopic forms. The annotation of the metabolite was attempted according to their molecular formula deduced from the precise mass and the isotopic pattern of each molecules and the presence of certain diagnostic ions, according to an in-house database of above 850 cyanobacteria metabolites (**Supplementary Table S1**; The csv export of the mass list containing respective molecular formula was searched for automatic identification using MetaboScape 3.0) and confirmed using GNPS molecular networking thank to their relative MS/MS fragmentation patterns and of few

commercially available standard molecules analyzed similarly, in the same manner.

## Data and Statistical Analysis

Heatmap representation of the global metabolome of the 24 *Microcystis* spp. monoclonal strains was performed with Gene-E tool<sup>2</sup> using the relative quantification (pic area) of 2051 molecular features analyzed on HR ESI-Qq-TOF using MetaboScape 3.0 (Bruker) with a >5000 counts and 400–2000 Da threshold, considering peak presents in at least three different trains and in at least six consecutive MS scans (S/N threshold value setup > 6). Then, the hierarchical clustering was performed according to Bray-Curtis distance method. NMDS and PERMANOVA analyses were performed using MicrobiomeAnalyst platform<sup>3</sup> in order to investigate the influence of the species, the sampling localities and of the production of MCs, described as the variables, on the global metabolite distribution of the global metabolome observed on ESI-Qq-TOF for the 24 strains.

Using the whole MS/MS data (converted in .mgf format) obtained for the 24 strains taken together, a molecular network was produced using the online tool available at Global Natural

<sup>2</sup><https://software.broadinstitute.org/GENE-E/>

<sup>3</sup><http://www.microbiomeanalyst.ca/>

**TABLE 1** | List of *Microcystis* spp. strains used in this study, their area of origin, the ELISA MC screening, the *mcyA* gene presence and their respective 16S-ITS sequence Accession numbers.

Strain Name	Species	Country	Locality/area	MC ELISA detection	<i>mcyA</i> PCR detection	16S Accession number	16S-23S ITS Accession number
PCC 7806	<i>M. aeruginosa</i>	Netherlands	Braakman	+	+	MH892877	MH899657
PCC 7820	<i>M. aeruginosa</i>	Scotland	Balgavies	+	+	MH892878	MH899658
PMC 95.02 <sup>a</sup>	<i>M. aeruginosa</i>	France	Villerest	–	–	MH892879	MH899659
PMC 98.15 <sup>a</sup>	<i>M. aeruginosa</i>	France	Villerest	–	–	MH892880	MH899660
PMC 155.02	<i>M. aeruginosa</i>	Sénégal	Djoudj	–	–	MH892881	MH899661
PMC 156.02	<i>M. aeruginosa</i>	Sénégal	Djoudj	–	–	MH892882	MH899662
PMC 241.05	<i>M. aeruginosa</i>	Burkina Faso	Ouahigouya	+	+	MH892883	MH899663
PMC 265.06	<i>M. aeruginosa</i>	Burkina Faso	Sian	–	–	MH892884	MH899664
PMC 566.08 <sup>b</sup>	<i>M. wesenbergii/viridis</i>	France	Varennes sur Seine	–	–	MH892885	MH899665
PMC 567.08 <sup>b</sup>	<i>M. wesenbergii/viridis</i>	France	Varennes sur Seine	–	–	MH892886	MH899666
PMC 570.08	<i>M. aeruginosa</i>	France	Souppes sur Loing	–	–	MH892887	MH899667
PMC 671.10 <sup>c</sup>	<i>M. wesenbergii/viridis</i>	France	Eure et Loire	–	–	MH892888	MH899668
PMC 672.10 <sup>c</sup>	<i>M. wesenbergii/viridis</i>	France	Eure et Loire	–	–	MH892889	MH899669
PMC 673.10 <sup>c</sup>	<i>M. wesenbergii/viridis</i>	France	Eure et Loire	–	–	MH892890	MH899670
PMC 674.10 <sup>c</sup>	<i>M. wesenbergii/viridis</i>	France	Eure et Loire	–	–	MH892891	MH899671
PMC 679.10 <sup>c</sup>	<i>M. aeruginosa</i>	France	Eure et Loire	+	+	MH892892	MH899672
PMC 727.11 <sup>d</sup>	<i>M. aeruginosa</i>	France	Valence	–	–	MH892893	MH899673
PMC 728.11 <sup>d</sup>	<i>M. aeruginosa</i>	France	Valence	+	+	MH892894	MH899674
PMC 729.11 <sup>d</sup>	<i>M. aeruginosa</i>	France	Valence	+	+	MH892895	MH899675
PMC 730.11 <sup>d</sup>	<i>M. aeruginosa</i>	France	Valence	–	–	MH892896	MH899676
PMC 807.12 <sup>e</sup>	<i>M. wesenbergii/viridis</i>	France	Champs sur Marne	+	+	MH892897	MH899677
PMC 810.12 <sup>e</sup>	<i>M. aeruginosa</i>	France	Champs sur Marne	–	–	MH892898	MH899678
PMC 816.12 <sup>e</sup>	<i>M. aeruginosa</i>	France	Champs sur Marne	+	+	MH892899	MH899679
PMC 826.12 <sup>e</sup>	<i>M. aeruginosa</i>	France	Champs sur Marne	–	–	MH892900	MH899680

Stains isolated from the same sample collected the same day from different French area are indicated with: <sup>a</sup> = Villerest (2008); <sup>b</sup> = Varennes-sur-Seine (2008); <sup>c</sup> = Eure et Loire (2010); <sup>d</sup> = Valence (2011); <sup>e</sup> = Champs-sur-Marne (2012).

Products Social molecular networking server (GNPS)<sup>4</sup> (Yang et al., 2013). The data were clustered with MS-Cluster (1.0-Da parent mass tolerance and 0.5-Da MS/MS fragment ion tolerance). A network was then created (edges were filtered using the cosine-score > 0.6 and the more-than-five-matching-peak thresholds), without considering the respective retention times of the analytes. The spectra were automatically searched for annotation against the GNPS spectral libraries (thresholds fixed for score above 0.6 and at least five matched peaks). The different clusters of the network were attemptingly annotated by comparing in the spectra of each relative node their monoisotopic mass according to MS and MS/MS fragmentation pattern matches against our in-house cyanobacteria metabolite databases (**Supplementary Table S1**). Molecular networks were visualized using Cytoscape 3.2.1.

## RESULTS

### Morphologic and Phylogenetic Characterization

The genetic relationships among the 24 *Microcystis* strains were first investigated by analyzing a 1380-bp 16S fragment (**Table 1**). This sequence comparison indicates that all *Microcystis* morpho-species are grouped in a unique and homogenous group, due to the high sequence conservation of this fragment (data not shown). Using 16S-23S ITS fragments (over 600 bp long), the phylogenetic analysis showed a clear distinction between *M. aeruginosa* and *M. wesenbergii/viridis* morpho-species (**Figure 2**). Interestingly, the different strains possessing the MC synthesis gene *mcyA* (indicated in red) did not cluster together on the phylogenetic tree, suggesting that the ability to produce MC constitutes a feature that is disconnected from strain phylogeny.

### Global Metabolome Analyses

Metabolomic shotgun analyses reveal discriminant metabolic profiles among strains collected from both different or identical sites. While previous works highlighted the metabolic diversity of some *Microcystis* strains based on few identified metabolites or cyanotoxins (Welker et al., 2004, 2006; Martins et al., 2009), we present here a global picture of the metabolome of each strain (**Figure 3** and **Supplementary Figure S1**). This representation clearly shows a clustering of all strains producing MCs (*mcyA*+ /MC+, in red), on one side, and of other strains not producing MCs (*mcyA*- /MC-, in gray). This clustering shows that some strains from the same environment exhibit very similar metabolite fingerprints (e.g., PMC 728.11 and 729.11), while other strains from the same location exhibit much more dissimilar metabolite fingerprints (e.g., PMC 728.11 and 727.11), being more similar to strains from faraway locations (e.g., PMC 729.11 and 816.112). Additional non-metric multidimensional scaling (nMDS) and PERMANOVA analyses based on Bray-Curtis index indicated that the ability to produce MC seems to be the first main driver of the global metabolome of *Microcystis*

molecular fingerprinting, while the species and the location represent less explicative parameters (**Supplementary Figure S2**).

### Metabolite Molecular Network

A molecular network was generated based on the global fragmentation pattern profile of all observed metabolites in the 24 strains investigated. The Global Natural Product Social network (GNPS) algorithm automatically compares all MS/MS spectra by aligning them one by one. This algorithm groups identical molecules (presenting identical mass and fragmentation patterns) and assigns a cosine score ranking from 0 to 1 to each alignment. From the present dataset, the resulting network is constituted of a total of 925 nodes from the 1374 different analytes which MS/MS data have been obtained (**Supplementary Figure S1**). It represents a starting point for the annotation of unidentified metabolites, according to respective cluster annotations (deduced from the presence of various annotated nodes from the same molecular structure family), and for the description of their occurrence in *M. aeruginosa* and/or *M. wesenbergii/viridis* strains (**Figure 4**).

*Microcystis* strains produce a large set of chemically diverse metabolites, of which the principal clusters can be identified thanks to analytical standards available for some cyanobacterial secondary metabolite families, or to match with components from publicly available libraries from the GNPS platform, such as HMDB, NIST14, or METLIN. More than 25% of the strains producing these analytes appear to be specific to *M. wesenbergii/viridis* strains, more than 50% are specific to *M. aeruginosa*, and the rest being observed in both species.

Different analytes were grouped in the same molecular clusters based on the similarity of their fragmentation patterns, with each cluster being potentially specific to the structure of the chemical families. Among those larger clusters, we were able to annotate some that were constituted by ions of small metabolites, such as di- and tri-peptides (1 cluster in A area), of microcystins (3 clusters in C area), of anabaenopeptins (3 clusters in D area), of aeruginosins (2 clusters in E area), of aerucyclamides (3 clusters in F area), of microginins (2 clusters in H area), and cyanopeptolins (6 clusters in I area), together with various clusters of unknown components, comprising non-identified ions (for example 2 clusters in B area). Less than a third of the metabolites observed here could be annotated by their respective mass and fragmentation patterns when compared to those of the more than 850 metabolites of freshwater cyanobacteria described so far and listed in **Supplementary Table S1**. These un-identified ions that belong to annotated clusters are then considered as potential new analogs of their respective molecular family.

### Known Cyanobacteria Secondary Metabolite Clusters

#### Microcystins

Microcystins are cyclic heptapeptides that were first described in *M. aeruginosa*. More than 250 different variants have been described so far (Catherine et al., 2017); 138 are references in our database for cyanobacterial metabolites (**Supplementary**

<sup>4</sup><http://gnps.ucsd.edu>

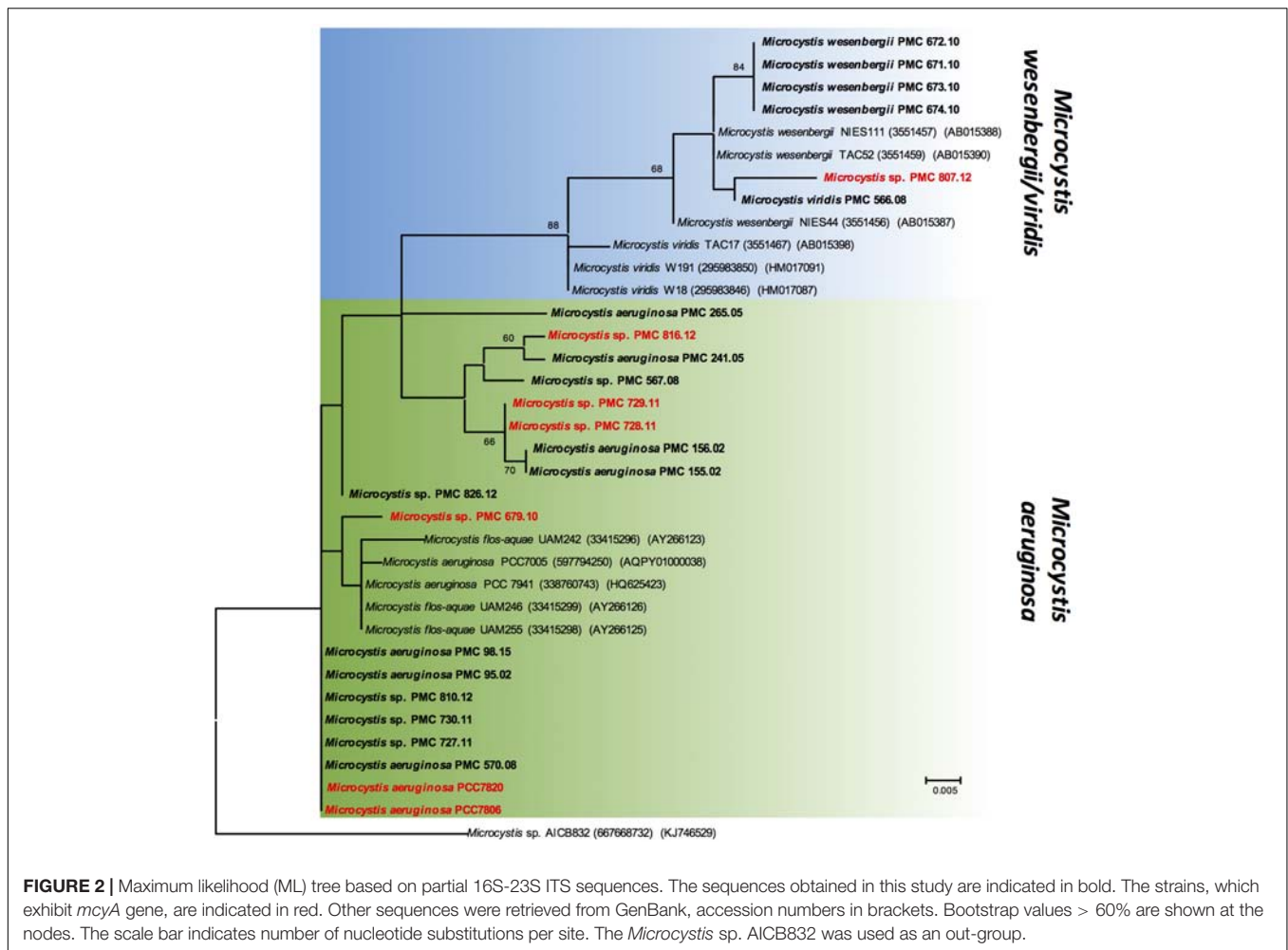


**FIGURE 2 |** Maximum likelihood (ML) tree based on partial 16S-23S ITS sequences. The sequences obtained in this study are indicated in bold. The strains, which exhibit *mcyA* gene, are indicated in red. Other sequences were retrieved from GenBank, accession numbers in brackets. Bootstrap values > 60% are shown at the nodes. The scale bar indicates number of nucleotide substitutions per site. The *Microcystis* sp. AICB832 was used as an out-group.

**Table S1).** They are characterized by the presence of a non-proteinaceous amino acid in position 5 (Adda), two amino acids derived from Asp and Glu in position 3 and 6, respectively, and 2 very variable positions (2 and 4), that serve as reference to the name of the variant. Three microcystin clusters were highlighted according to the presence of six standard molecules (Dmet(Asp3)-MC-LR, MC-LR, MC-YR, MC-LA, MC-LF, and MC-HtyR) analyses in parallel of the 24 *Microcystis* extracts with the same protocol (Figure 5). Other components of these clusters correspond to ions presenting a match of their respective mass with those of other previously described MC variants (Supplementary Table S1), or for 18% of them, to potentially new analogs. Observation of their respective MS/MS spectra showed that these metabolites present distinct but similar fragmentation patterns to those of other known MC variants.

### Aeruginosins

Aeruginosins constitute a family of linear tetrapeptides that were first described in *M. aeruginosa*, and that represent more than 94 different variants that have been described so far (Supplementary Table S1). Their MS/MS

fragmentation patterns are often characterized by the presence of a Choi fragment (immonium with 140.109 *m/z*) and other recurrent fragments from HplA or PlA. Their composition is rather variable and the members of this family exhibit masses between 430 and 900 Da (Welker and Von Döhren, 2006). The molecular network obtained from the 24 *Microcystis* strains exhibits two aeruginosin clusters (Figure 6) that were highlighted by the presence of two standard molecules (aeruginosin 98A and 98B). The other components of these clusters correspond to ions with masses that match previously described variants of aeruginosin (Supplementary Table S1), or for 47% of these compounds, to potentially new analogs.

### Anabaenopeptins

Anabaenopeptins constitute a very diverse family of cyclic hexapeptides that have been described so far in *Microcystis*, *Planktothrix*, *Anabaena*, *Aphanizomenon*, and *Nostoc*. Over 75 different variants have been described to date (Supplementary Table S1). These compounds are characterized by the presence of a peptide bond between the D-Lys in position 2 and the carboxylic group of the amino acid in position 6.

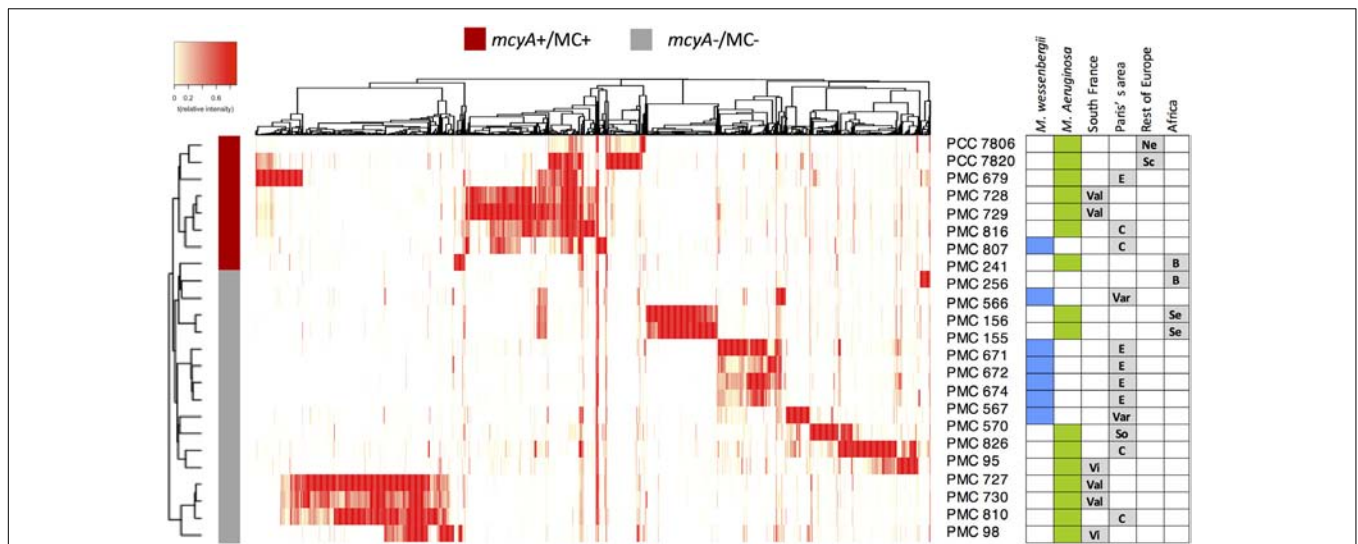


**FIGURE 3 |** Heatmap representation of the metabolome of the 24 *Microcystis* spp. monoclonal strains analyzed using HR ESI-Qq-TOF, representing 2051 different analytes (in a 400–2000 Da window; present in at least three strains, with a signal to noise ratio in excess of 6, and respective relative peak intensity superior to 5000-count in at least one sample threshold) identified by MetaboScape software. The hierarchical clustering between strains was performed according to Bray-Curtis distance method. Green and blue squares indicate *M. aeruginosa* and *M. wessenbergii/viridis*, respectively. Sampling localities are: C, Champs-sur-Marne; B, Burkina Faso; E, Eure et Loire; Ne, Netherlands; Sc, Scotland; Se, Senegal; So, Souppes-sur-Loire; Var, Varennes-sur-Seine; Val, Valence; Vi, Villerest.

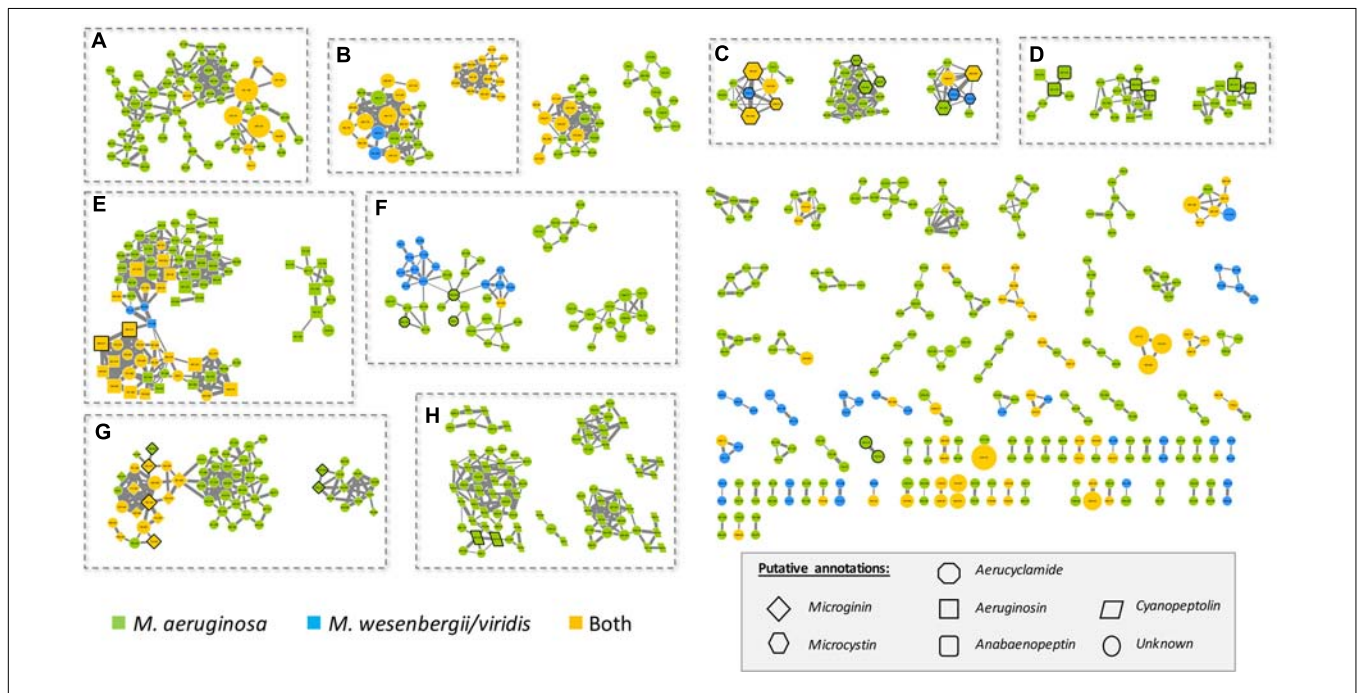
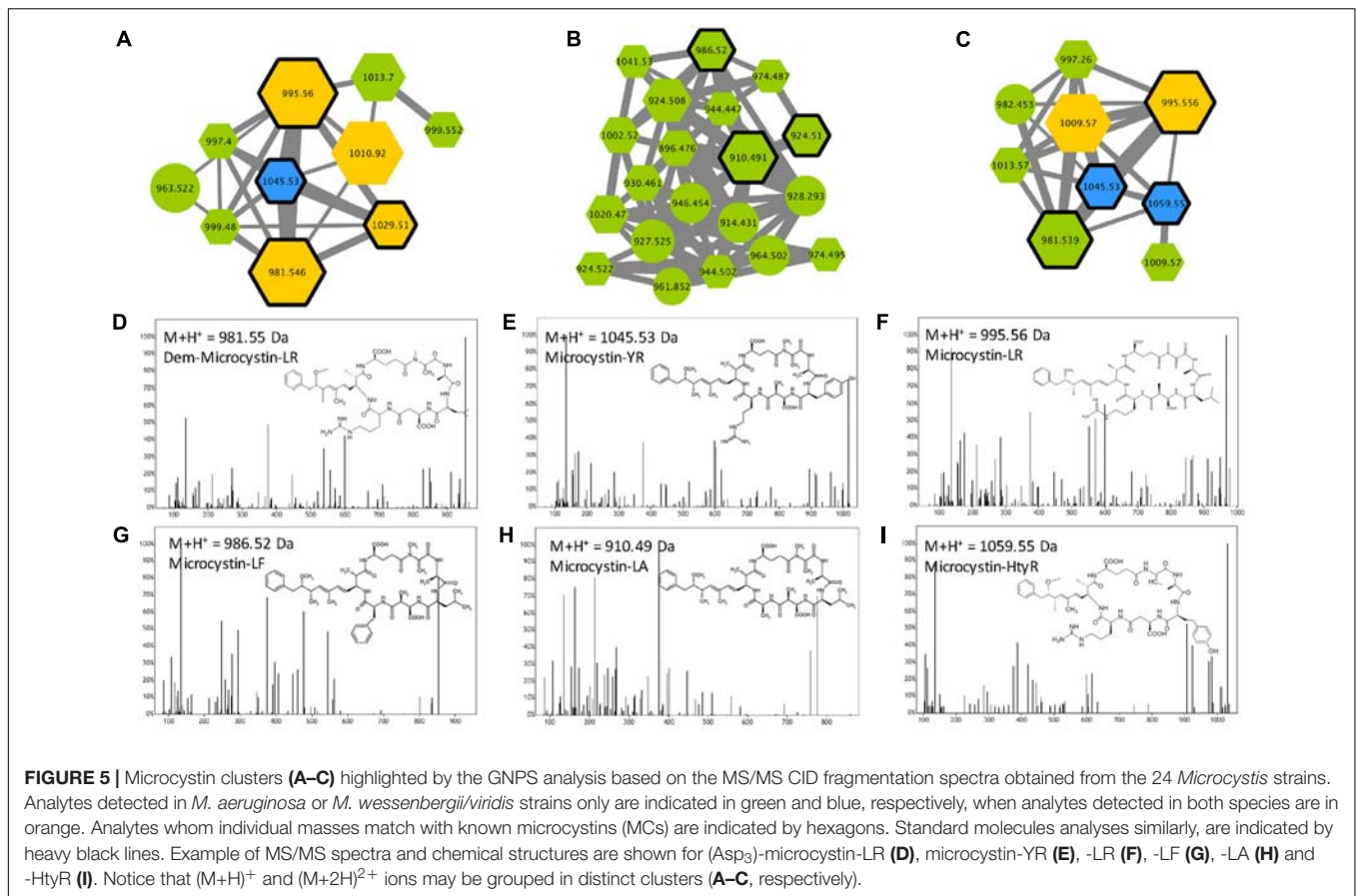


**FIGURE 4 |** Molecular network generated from MS/MS spectra from the 24 *Microcystis* strains using the GNPS tool (all data and results are freely available at the address <http://gnps.ucsd.edu/ProteoSAFe/status.jsp?task=c017414365e84334b38ae75728715552>). The nodes of the analytes detected in *M. aeruginosa* or *M. wessenbergii/viridis* strains only are indicated in green and blue, respectively, when analytes detected in both species are indicated in orange. Uncharacterized analytes are indicated by circles constituting potential new analogs. Analytes whose individual masses match with known secondary metabolites from cyanobacteria (listed in **Supplementary Table S1**) are indicated by specific shapes as shown on picture caption. Standard molecules analyses similarly, are indicated by heavy black lines. Only cluster regrouping at least 2 analytes are represented. A, di- or tri-peptide cluster; B, Unknown metabolite clusters; C, microcystin clusters; D, anabaenozeptin clusters; E, aeruginosin clusters; F, aerucyclamide clusters; G, microginin clusters; H, cyanopeptolin clusters. The clusters on the right are corresponding to un-annotated and smaller clusters.



Except for the D-Lys (position 2), all other positions are variable, allowing a large structural diversity of the family with members exhibiting masses between 750 and 950 Da (Welker and Von Döhren, 2006). Three anabaenopeptin clusters were highlighted in this study (Figure 7) according to the presence of 4 standard molecules (anabaenopeptins A, B, and F, and oscyllamide Y). Other components of these clusters correspond to ions presenting a match with the mass of other previously described variants (Supplementary Table S1), or for 57% of them, to compounds that very likely correspond to potentially new analogs. All observed anabaenopeptin compounds are from *M. aeruginosa* strains, suggesting that *M. wessenbergii/viridis* strains are not capable of synthesizing molecules of this family and may not possess the corresponding *apt* synthetic gene cluster.

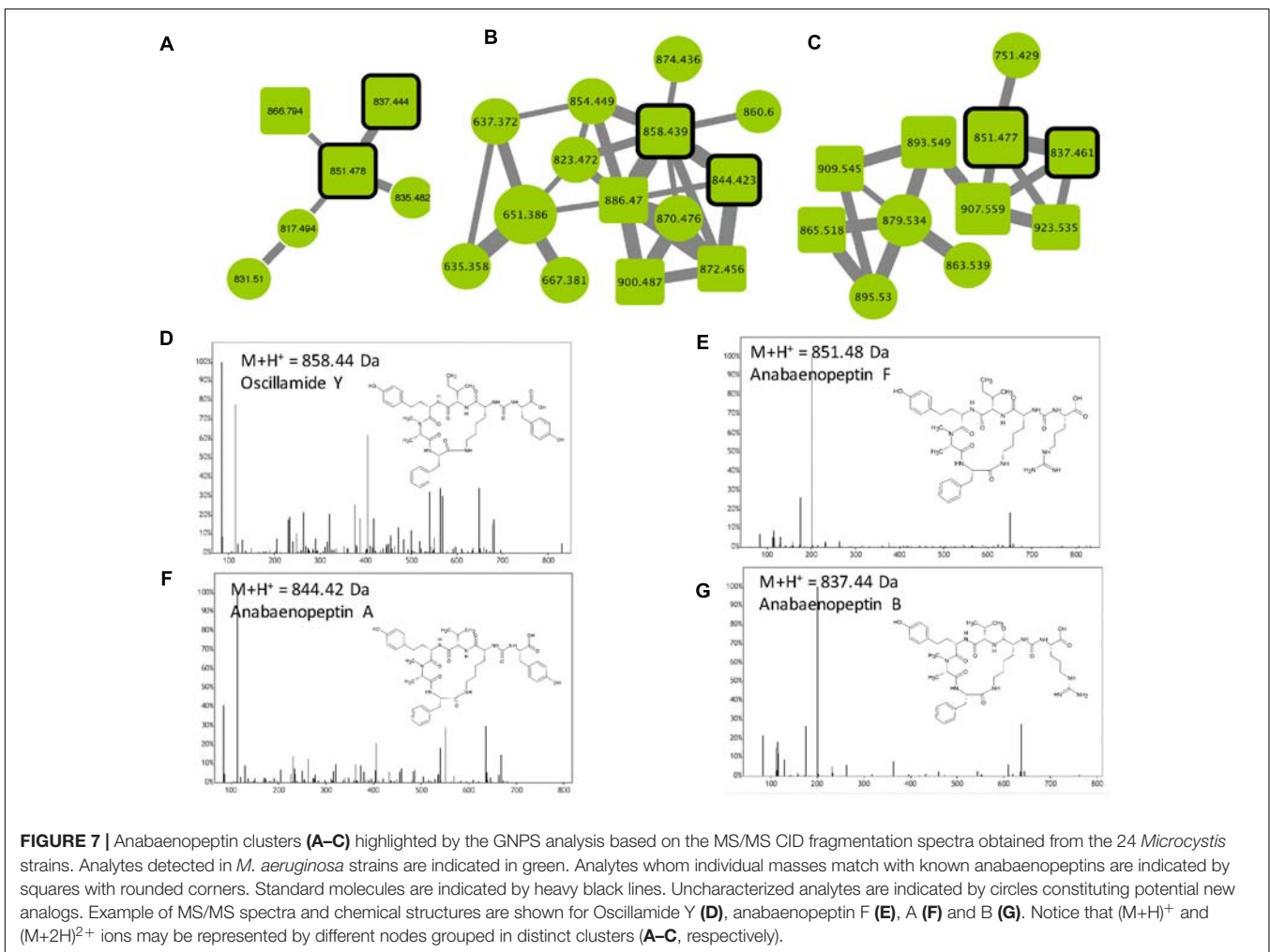
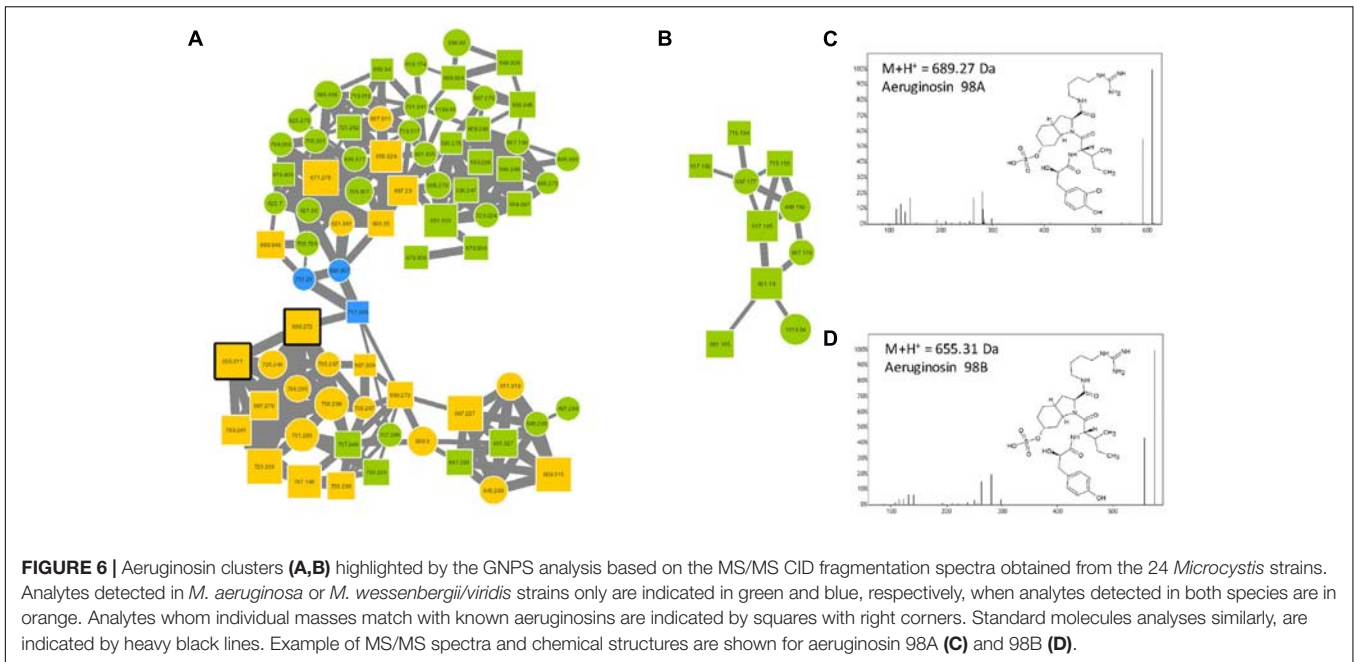
### Cyanopeptolins

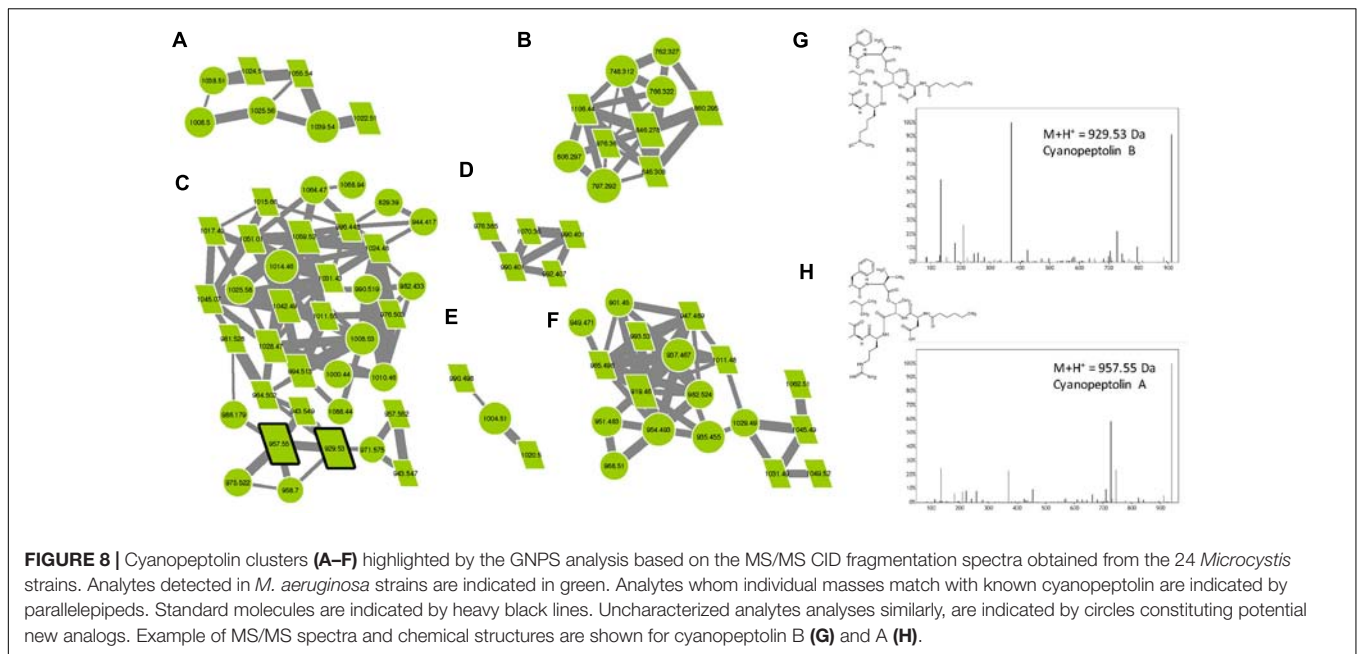
Cyanopeptolins belong to a large family of cyclic depsipeptides that also contains micropeptins and aeruginopeptins, representing over 170 variants. Those molecules are characterized by the presence of the non-proteinaceous amino acid Ahp and by a six-aa-long ring formed by an ester bound between Thr or Pro in position 1 and the carboxylic group of the N-terminal amino acid (position 6). The lateral chain exhibits variable length and is constituted by one or two amino acids and is potentially linked to an aliphatic fatty acid

(Welker and Von Döhren, 2006). In the molecular network, two analytes of the cyanopeptolin clusters correspond to two standard molecules (cyanopeptolin A and B), and various other components correspond to ions presenting a mass that corresponds to those of different previously described variants (Supplementary Table S1), allowing us to annotate them as cyanopeptolin-specific clusters (Figure 8). Over 47% of the analytes present in these clusters correspond to unknown compounds representing potentially new analogs. We observe here that all these cyanopeptolin compounds are from *M. aeruginosa* strains, suggesting that *M. wessenbergii/viridis* strains are not capable of synthesizing molecules of this family and may not possess the corresponding *mcn/oci* synthetic gene cluster either.

### Microginins

Microginins are linear pentapeptides (the length of the sequence varies from 4 to 6 amino acids) initially identified from *M. aeruginosa*, then from other species and in other genera such as *Planktothrix* (Welker and Von Döhren, 2006). These molecules are composed of a characteristic non-proteinaceous amino acid Ahda at their N-terminus, with the other position bearing variable amino acid structures, comprising Tyr, Pro Hty, Trp, Ala, Ser, or others. Relatively few microginin variants (less than 40) have been described so far (Supplementary Table S1). According to the molecular





network generated in this study (Figure 9), over 67% of the analytes present in the two microginin clusters correspond to unknown compounds constituting potentially new analogs, when six standard molecules could have been retrieved from the present analysis (microginin 757, 711, BN578, FR1, FR2, and SD755).

### Aerucyclamides/Cyanobactins

The name “cyanobactin” has been proposed to group all cyclic peptides containing proteinogenous amino acids that are post-translationally modified in heterocyclic amino acids and isoprenoid derivatives (Sivonen et al., 2010). It comprises various cyclamides (cyclic peptides of 6 amino acids) that have been identified in freshwater cyanobacteria such as *Microcystis*, *Planktothrix*, and *Nostoc*, but also in symbiotic cyanobacteria species. More than 30 variants have been described so far, but more molecules could be related to the family that represent a very large variety of chemical structures (Martins and Vasconcelos, 2015). Three different cyanobactin clusters were observed in the molecular network (Figure 10), comprising three aerucyclamide standard molecules (aerucyclamide A, B, and D) that were identified by GNPS tools. More than 75% of the analytes from these clusters represent potentially new analogs that need to be characterized by further dedicated analyses.

## Uncharacterized Cyanobacteria Metabolite Clusters

### Potential Primary Metabolite Clusters

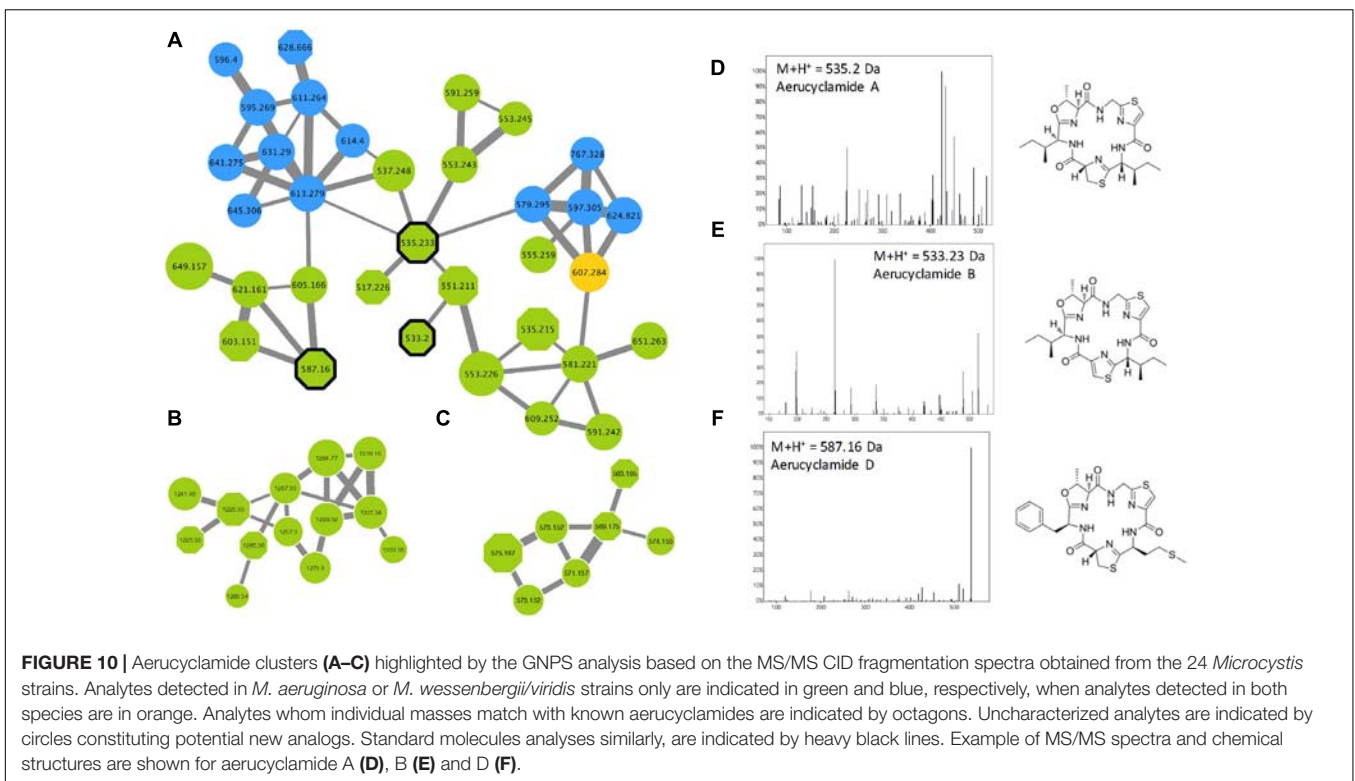
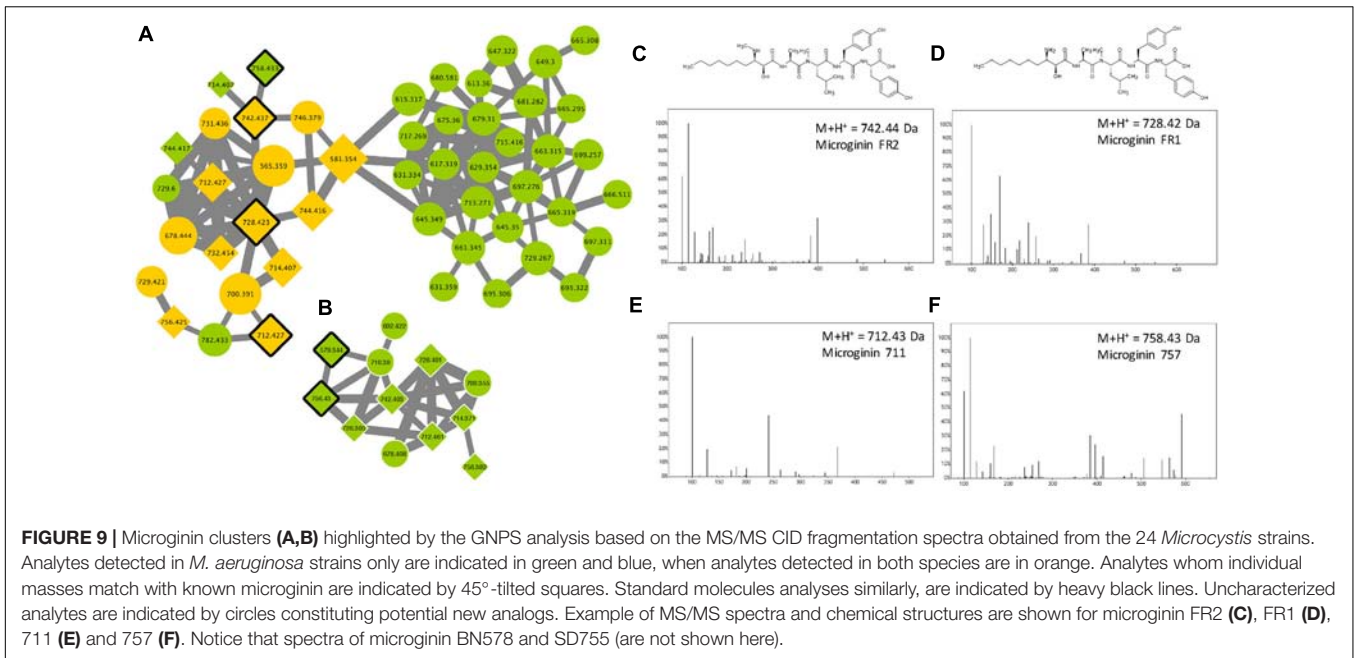
Various other important clusters contained some unknown analytes that are mostly present in high amounts (higher peak intensity shown by larger forms) and in a large set of strains from both *M. aeruginosa* and *M. wesenbergii/viridis*

(Figure 4). These compounds exhibit molecular masses between 300 and 600 Da, suggesting that they could correspond to relatively small molecules (Supplementary Figures S3, S4). We speculate that these components could correspond to primary metabolites used for the general metabolism of various strains, however, additional efforts should be made to annotate these ubiquitous molecules present in these specific clusters. Interestingly, the compounds from this latter cluster present high fragmentation patterns, illustrated by various similarity and high cosine scores (numerous and tick links between the different nodes of the clusters), suggesting they should present very similar structures.

### Uncharacterized Secondary Metabolite Clusters

Interestingly, other clusters correspond to unknown components, some of them being only synthesized by *M. wesenbergii/viridis* as shown in Supplementary Figure S5. These compounds with relatively high molecular masses (between 950 and 1300 Da) might correspond to specific secondary metabolite families belonging to other known, but poorly characterized, families of cyanobacterial metabolites, such as microviridins and/or aeruginoguanidins, for which only few variants have been characterized and no standard molecules are available so far. Alternatively, they may correspond to a completely new family of metabolites, the existence of which was suggested by observing orphan NRPS/PKS clusters within various *Microcystis* genomes (Humbert et al., 2013).

Although the present MS/MS-based metabolomic approach was focused on the most intense analytes present in the biomass of the *Microcystis* cultures, we cannot fully exclude the possibility that some of these molecules could be produced by the small fraction of heterotrophic bacteria that colonized these non-axenic cultures.



## DISCUSSION

### Biogeography and Genetic Diversity Attempt on *Microcystis* Strains

The phylogeny of the various *Microcystis* species is still under investigation. Morphological criteria comprising the

form and size of the colony, the presence and the structure of the mucilage, the cell diameter, the organization of cells within colonies, together with the pigment content and some life cycle parameters were used to discriminate among different morpho-species (Komárek, 2016). Accordingly, five main *Microcystis* morpho-species (*M. aeruginosa*, *M.*

*ichthyoblabe*, *M. viridis*, *M. novacekii*, *M. wesenbergii*) were proposed by Otsuka et al. (2001). However, with the recent development of different genetic and biochemical molecular markers, some results were contradictory to previous *Microcystis* taxonomy results. For instance, analysis based on 16S rRNA sequence alone revealed no differences among all these morpho-species (Otsuka et al., 2000). Considering both morphological and molecular markers, *Microcystis* seems to be classifiable into three groups: a smaller cell-size group comprising of *M. ichthyoblabe* and *M. flos-aquae*, a middle cell-size group composed of *M. aeruginosa* (incl. *M. novacekii*), and a larger cell-size group based on *M. wesenbergii* (Whitton, 2012). Although the size criteria classification seems practical, size varies according to the physiological state of the cells and is not tightly correlated with genetic markers.

According to the phylogenetic reconstruction based on the 16S-16S/23S ITS fragment that is in accordance with previous observations (Otsuka et al., 1999), the studied *Microcystis* strains were roughly divided into two groups: the *M. wesenbergii/viridis* group and the *M. aeruginosa* group (according to the size of the colonies observed under microscopes). In addition, the *mcyA+* and *mcyA-* strains were broadly dispersed in both groups. These observations confirmed that the presence of *mcy* does not simply capitulate the phylogeny of *Microcystis* strains (Tillett et al., 2001). Therefore, the toxicity potential, through the MC synthesis, of each strain should be assessed regardless of its phylogenetic position.

Despite the very high similarity of *Microcystis* 16S rRNA sequences (>99.5%), low synteny and large genomic heterogeneity have been retrieved from investigating *Microcystis* genomes, deciphering a large cryptic diversity from various strains collected from different sites and continents (Steffen et al., 2012; Humbert et al., 2013). At another large geographic scale, genetic comparison of various *Microcystis* strains isolated from different Asian and European lakes based on 16S-ITS fragments did not show a location-specific clustering effect, indicating that the genetic distance between different genotypes from the same lake can be greater than between strains from very distanced environments (Humbert et al., 2005; Haande et al., 2007). Interestingly, large genomic islands have been detected in *Microcystis* genomes and metagenomes, and these mobile elements seem to greatly contribute to the clonal diversity within this genus (Steffen et al., 2012).

Our data on the molecular heterogeneity observed by metabolic fingerprinting between some strains originating from the same site (for example between PMC 810.12 and PMC 816.12, Champs-sur-Marne, France) also support this hypothesis. Interestingly, the fact that some *Microcystis* genotypes or chemotypes could be spread worldwide was also previously observed for some freshwater bacterioplankton species (Zwart et al., 1998), suggesting that these organisms may present peculiar physiological and/or large dispersal capabilities contributing to their successful colonization of a wide range of freshwater environments.

## MC-Producing Versus Non-MC Producing Metabolic Pattern of *Microcystis* Strains

Metabolome diversity has been also used as a molecular characteristic to help discriminate among various chemotypes (Ivanisevic et al., 2011), in addition to classical genotyping approaches that sometimes lack reliable characteristics for phylogenetic relationship discrimination. Few analytical methods have been investigated for chemo-taxonomic characterization of cyanobacteria strains or cells (Welker et al., 2006), according for example, to their fatty acid compositions (Gugger et al., 2002), or more recently to ribosomal proteins globally analyzed by MALDI-TOF on *M. aeruginosa* (Sun et al., 2016). Interestingly, this latter chemotaxonomic approach was able to group all the MC-producing strains in two distinct clades when the non-MC-producing strains were segregated in three other distinct clades. In a previous work, Martins et al. (2009) analyzed the metabolite diversity of various *M. aeruginosa* strains from Portuguese water supplies using MALDI-TOF MS and were able to observe MC production in almost half of the strains investigated. These observations also illustrate the fact that MC-producing clones can subsist in various environments, despite the important energetic cost required for MC gene cluster replication and the translation of its mega-enzyme complex (Briand et al., 2012). The biological advantage of producing MCs for some clones still remains a mystery, as the functional role of MC is still uncharacterized (Gan et al., 2012; Agha and Quesada, 2014).

In a similar manner, our molecular fingerprint approach based on global metabolome profiling using ESI-Qq-TOF discriminated clearly MC-producing strains from others. Taken together, these observations suggest that shotgun mass spectrometry chemotyping of cyanobacteria could constitute a promising tool for characterizing rapid biomarkers for toxicological assessment of strains isolated from the field. MC production could constitute a singular feature, that could constitute one of the key drivers of the global metabolic diversity of *Microcystis* strains, suggesting that MC could play a keystone function in cyanobacterial metabolite production. Indeed, it was previously hypothesized according to metabolomic observations that the characteristic of MC production could be compensated for in strains not producing MCs by the production of other metabolites, such as aeruginosamines (Martins et al., 2009; Pancrace et al., 2018) for unknown biological reasons (Tonk et al., 2009; Briand et al., 2016a). Such secondary metabolic compensatory processes, between and within the different peptide classes, have been previously suspected for both *Microcystis* (Martins et al., 2009; Pancrace et al., 2018) and *Planktothrix* (Tonk et al., 2005) in response to various growth conditions. However, further investigations with wider sampling are now required in order to increase the dataset that could better help test such metabolite functional hypothesis.

## Secondary Metabolite Diversity Within Known Metabolite Families

The molecular cluster identified by GNPS approach (Yang et al., 2013) can be annotated to match with spectral

databases or the presence of standard molecules. In our hands, the global molecular networks obtained from the MS/MS dataset of the 24 strains examined in this study presents various clusters that have been annotated. Most of them correspond to main cyanobacterial metabolite families (Figure 4). We assumed that the nodes of these clusters with similar molecular masses to already known cyanobacterial metabolites very likely correspond to these specific metabolites, or alternatively, to isobaric analogs. In addition, all other nodes from those clusters that do not correspond to either standard or known analogs could be considered potentially new analogs that may correspond to new variants that remain to be characterized. These observations are in accordance with results of previous research indicating that different *Microcystis* strains can produce such various known and unknown secondary metabolites, according to both genetic or targeted metabolome analyses (Welker et al., 2004, 2006; Martins et al., 2009; Humbert et al., 2013). Surprisingly, few metabolite families such as aeruginoguanidine were not successfully detected in our GNPS analysis. Indeed, very few variants belonging to this family have been described (Supplementary Table S1) and their MS/MS fragmentation pattern has not been deeply characterized so far. In addition, the lack of available standard molecules and of knowledge of their respective fragmentation patterns makes aeruginosamines especially challenging to annotate with a GNPS-based approach.

However, our analyses revealed the large molecular diversity of *Microcystis* metabolites, according to the various new variants of known cyanobacterial metabolite families that remain to be characterized. The observation of various uncharacterized clusters also suggest that new metabolite families are still waiting to be discovered and described from this genus, and that further efforts to this end are still required. So far, *Microcystis* represents one of the most studied genera for its production of various metabolite families. However, the biological functions played by these molecules remain enigmatic and their growing molecular diversity revealed by global approaches, such as GNPS global metabolomic investigation or genomics, constitutes one of the questioning paradoxes in the field of microbiological evolution and diversity.

## Unknown Metabolite Families

Although the strains used in this study were not cultured in hyper-stringent axenic conditions, no noticeable contamination by fungi or heterotrophic bacteria were detected during the systematic screening of all strains under light microscope prior to the experiment. In addition, a previous metabolome analysis in PCC 7806 grown under axenic or non-axenic conditions did not detect any significant variation in the metabolites produced by the cyanobacteria (Briand et al., 2016b). We assume that the metabolite profiles observed here for the 24 strains are characteristic of the cyanobacteria and that the different metabolites observed in this study, including the unknown metabolite clusters highlighted by the network analysis, are genuinely produced by the cyanobacteria.

The non-annotated cluster observed in our GNPS analysis can potentially correspond to novel variants of

known cyanotoxins or to a completely new family of cyanobacteria metabolites. Indeed, Humbert et al. (2013) showed that the genomes of ten *Microcystis* strains exhibit at least three orphan clusters with a specific NRPS/PKS signature that likely synthesize a yet-undescribed metabolite family. The unknown clusters we observed using the GNPS approach may correspond to these novel metabolite families, and structural elucidation of an expanding number of novel metabolites revealed by molecular networking is currently being performed for various cyanobacteria (Boudreau et al., 2015).

## CONCLUSION

In the present study, a comparison of the specific chemical footprints of 24 clonal *Microcystis* strains generated through modern ESI-qTOF mass spectrometry shows a global influence of microcystin production on metabolite content, rather than on their respective genotypes or sampling locality origins. The GNPS network of all metabolites highlighted the production of a wide set of chemically diverse metabolites, among which there were a few microcystins, and also many aeruginosins, microginins, cyanopeptolins, and anabaenopeptins, along with a large set of unknown molecules that remain to be characterized.

Innovative approaches based on shotgun metabolomic analyses using high-resolution mass spectrometry, such as those performed in this study, seem to provide a large variety of information on cyanobacterial chemical diversity, relevant to evolutionary, ecological, and toxicological purposes. This represents an interesting and relatively easy-to-perform potential to genome sequencing for metabolite and/or toxic potential descriptions of cyanobacterial strains.

Global molecular network analysis also allows the depiction of the chemical diversity of the *Microcystis* metabolome in an interesting manner. More than half of the analytes described in the global molecular network were found to correspond to metabolites belonging to potentially new variants of known families or family members (presenting original fragmentation patterns) that are yet to be described at the structural and toxicological/bioactivity levels.

## AUTHOR CONTRIBUTIONS

SM, ME, AC, CB, and BM conceived and designed the experiments. CD isolated all new strains of the PMC. CD, SM, AM, and CDJ performed the analysis. SM, CD, AM, and BM treated the data. All authors wrote and reviewed the manuscript.

## FUNDING

This work was supported by grants from the CNRS Défi ENVIROMICS “Toxycyfish” project and from the ATM “Les micro-organismes, acteurs clef des écosystèmes” of the MNHN to BM.

## ACKNOWLEDGMENTS

We would like to thank the French Ministry for Research for their financial support of SM. The MS spectra were acquired at the Plateau technique de Spectrométrie de Masse Bio-organique, UMR 7245 Molécules de Communication et Adaptation des Micro-organismes, Muséum National d'Histoire Naturelle, Paris, France.

## SUPPLEMENTARY MATERIAL

The Supplementary Material for this article can be found online at: <https://www.frontiersin.org/articles/10.3389/fmicb.2019.00791/full#supplementary-material>

**FIGURE S1** | Representation of the analytes from the 24 *Microcystis* strains analyzed by MS simple and MS/MS positive mode, exhibiting the good representativeness of analytes selected for MS/MS analyses. All analyzed ions are represented according to their respective retention time and *m/z* ratio. For MS/MS data, the size of the circle being representative of their maximum peak intensity.

**FIGURE S2** | NMDS analysis of global metabolite patterns of the 24 *Microcystis* spp. monoclonal strains analyzed using HR ESI-TOF, with PERMANOVA analyses

## REFERENCES

- Agha, R., and Quesada, A. (2014). Oligopeptides as biomarkers of cyanobacterial subpopulations. Toward an understanding of their biological role. *Toxins* 6, 1929–1950. doi: 10.3390/toxins6061929
- Bishop, C. T., Anet, E. F. L. J., and Gorham, P. R. (1959). Isolation and identification of the fast-death factor in *Microcystis aeruginosa* NRC-1. *Can. J. Biochem. Physiol.* 37, 453–471. doi: 10.1139/y59-047
- Boudreau, P., Monroe, E., Mehrotra, S., Desfor, S., Korabeynikov, A., Sherman, D., et al. (2015). Expanding the described metabolome of the marine cyanobacterium *Moorea producens* JHB through orthogonal natural products workflows. *PLoS One* 10:e0133297. doi: 10.1371/journal.pone.0133297
- Briand, E., Bomans, M., Quiblier, C., Saleçon, M.-J., and Humbert, J.-F. (2012). Evidence of the cost of the production of Microcystins by *Microcystis aeruginosa* under different light and nitrate environmental conditions. *PLoS One* 7:e29981. doi: 10.1371/journal.pone.0029981
- Briand, E., Bormans, M., Gugger, M., Dorrestein, P. C., and Gerwick, W. (2016a). Changes in secondary metabolic profiles of *Microcystis aeruginosa* strains in response to intraspecific interactions. *Environ. Microbiol.* 18, 384–400. doi: 10.1111/1462-2920.12904
- Briand, E., Humbert, J.-F., Tambosco, K., Bormans, M., and Gerwick, W. (2016b). Role of bacteria in the production and degradation of *Microcystis* cyanopeptides. *Microbiologyopen* 5, 469–478. doi: 10.1002/mbo3.343
- Briand, E., Escoffier, N., Straub, C., Sabart, M., Quiblier, C., and Humbert, J.-F. (2009). Spatiotemporal changes in the genetic diversity of a bloom-forming *Microcystis aeruginosa* (cyanobacteria) population. *ISME J.* 3, 419–429. doi: 10.1038/ismej.2008.121
- Carey, C. C., Ibelings, B. W., Hoffmann, E. P., Hamilton, D. P., and Brookes, J. D. (2012). Eco-physiological adaptations that favour freshwater cyanobacteria in a changing climate. *Water Res.* 46, 1394–1407. doi: 10.1016/j.watres.2011.12.016
- Carmichael, W. (2008). Cyanobacterial harmful algal blooms: state of the science and research needs. *Adv. Exp. Med. Biol.* 619, 831–853.
- Catherine, A., Bernard, C., Spoof, L., and Bruno, M. (2017). “Microcystins and nodularins,” in *Handbook of Cyanobacterial Monitoring and Cyanotoxin Analysis*, eds J. Meriluoto, L. Spoof, and G. A. Codd (Hoboken, NJ: John Wiley & Sons, Ltd).

performed on MicrobiomeAnalyst platform with Bray-Curtis index according to the MC production (A) and to the genera (B). “MC production,” “species,” and “locality” factor present significant impact on the global metabolome.

**FIGURE S3** | Unknown cluster “1” (A) highlighted by the GNPS analysis based on the MS/MS CID fragmentation spectra obtained from the 24 *Microcystis* strains. This cluster of uncharacterized molecules that present high fragmentation similarity (B–G) may correspond to a new family of metabolites that still need to be characterized. Analytes detected in *M. aeruginosa* or *M. wessenbergii/viridis* strains only are indicated in green and blue, respectively, when analytes detected in both species are in orange.

**FIGURE S4** | Unknown cluster “2” (A) highlighted by the GNPS analysis based on the MS/MS CID fragmentation spectra obtained from the 24 *Microcystis* strains. This cluster of uncharacterized molecules that present high fragmentation similarity (B–E) may correspond to a new family of metabolites that still need to be characterized. Analytes detected in *M. aeruginosa* and *M. wessenbergii/viridis* strains are indicated in orange.

**FIGURE S5** | Unknown cluster “3–5” (A–C) highlighted by the GNPS analysis based on the MS/MS CID fragmentation spectra obtained from the 24 *Microcystis* strains. These clusters of uncharacterized molecules that present, respectively, intrinsic high fragmentation similarity (examples of representative spectra are provided D–F) may correspond to families of metabolites that still need to be characterized. Analytes detected in *M. wessenbergii/viridis* strains only are indicated in blue.

**TABLE S1** | List of 852 cyanobacterial metabolites retrieved from the literature.

- Codd, G. A., Morrison, L. F., and Metcalf, J. S. (2005). Cyanobacterial toxins: risk management for health protection. *Toxicol. Appl. Pharmacol.* 203, 264–272. doi: 10.1016/j.taap.2004.02.016
- Dittmann, E., Gugger, M., Sivonen, K., and Fewer, D. P. (2015). Natural product biosynthetic diversity and comparative genomics of the cyanobacteria. *Trends Microbiol.* 23, 642–652. doi: 10.1016/j.tim.2015.07.008
- Gan, N., Xiao, Y., Zhu, L., Wu, Z., Liu, J., Hu, C., et al. (2012). The role of microcystins in maintaining colonies of bloom-forming *Microcystis* spp. *Environ. Microbiol.* 14, 730–742. doi: 10.1111/j.1462-2920.2011.02624.x
- Gugger, M., and Hoffmann, L. (2004). Polyphyly of true branching cyanobacteria (Stigonematales). *Int. J. Syst. Evol. Microbiol.* 54, 349–357. doi: 10.1099/ijs.0.02744-0
- Gugger, M., Lyra, C., Suominen, I., Tsitko, I., Humbert, J.-F., Salkinoja-Salonen, M., et al. (2002). Cellular fatty acids as chemotaxonomic makers of the genera *Anabaena*, *Aphanizomenon*, *Microcystis*, *Nostoc* and *Planktothrix*. *Int. J. Syst. Evol. Microbiol.* 52, 1007–1015.
- Guljamow, A., Kreische, M., Ishida, K., Liaimer, A., Altermark, B., Bähr, L., et al. (2017). High-density cultivation of terrestrial *Nostoc* strains leads to reprogramming of secondary metabolome. *Appl. Environ. Microbiol.* 83:e01510-17. doi: 10.1128/AEM.01510-17
- Haande, S., Ballot, A., Rohrlack, T., Fastner, J., Wiedner, C., and Edvardsen, B. (2007). Diversity of *Microcystis aeruginosa* isolates (Chroococcales, Cyanobacteria) from East-African water bodies. *Arch. Microbiol.* 188, 15–25. doi: 10.1007/s00203-007-0219-8
- Harke, M. J., Jankowiak, J. G., Morrell, B. K., and Gobler, C. J. (2017). Transcriptomic responses in the bloom-forming Cyanobacterium *Microcystis* induced during exposure to zooplankton. *Appl. Environ. Microbiol.* 83:e02832-16. doi: 10.1128/AEM.02832-16
- Harke, M. J., Steffen, M. M., Gobler, C. J., Otten, T. G., Wilhelm, S. W., Wood, S. A., et al. (2016). A review of the global ecology, genomics, and biogeography of the toxic cyanobacterium, *Microcystis* spp. *Harmful Algae* 54, 4–20. doi: 10.1016/j.hal.2015.12.007
- Holland, A., and Kinnear, S. (2013). Interpreting the possible ecological role(s) of cyanotoxins: compounds for competitive advantage and/or physiological aide? *Mar. Drugs* 11, 2239–2258. doi: 10.3390/md11072239

- Humbert, J.-F., Barbe, V., Latifi, A., Gugger, M., Camteau, A., Coursin, T., et al. (2013). A tribute to disorder in the genome of the bloom-forming freshwater cyanobacterium *Microcystis aeruginosa*. *PLoS One* 8:e70747. doi: 10.1371/journal.pone.0070747
- Humbert, J.-F., Duris-Latour, D., Le Berre, B., Giraudet, H., and Salençon, M. J. (2005). Genetic diversity in *Microcystis* populations of a French storage reservoir assessed by sequencing of 16S-23S rRNA intergenic spacer. *Microbiol. Ecol.* 49, 308–314. doi: 10.1007/s00248-004-0004-z
- Iteman, I., Rippka, R., Tandeau de Marsac, N., and Herdman, M. (2000). Comparison of conserved structural and regulatory domains within divergent 16SrRNA–23S rRNA spacer sequences of cyanobacteria. *Microbiology* 146, 1275–1286. doi: 10.1099/00221287-146-6-1275
- Ivanisevic, J., Thomas, O., Lejeune, C., Chavalonné, P., and Perez, T. (2011). Metabolic fingerprinting as an indicator of biodiversity: towards understanding inter-specific relationships among Homoscleromorpha sponges. *Metabolomics* 7, 289–304. doi: 10.1007/s11306-010-0239-2
- Komárek, J. (2016). A polyphasic approach for the taxonomy of cyanobacteria: principles and applications. *Eur. J. Phycol.* 51, 346–353. doi: 10.1080/09670262.2016.1163738
- Liu, Y., Xu, Y., Wang, Z., Xiao, P., Yu, G., Wang, G., et al. (2016). Dominance and succession of *Microcystis* genotypes and morphotypes in Lake Taihu, a large and shallow freshwater lake in China. *Environ. Pollut.* 219, 399–408. doi: 10.1016/j.envpol.2016.05.021
- Ma, J., Qin, B., Paerl, H. W., Brookes, J. D., Hall, N. S., Shi, K., et al. (2016). The persistence of cyanobacterial (*Microcystis* spp.) blooms throughout winter in Lake Taihu, China. *Limnol. Oceanogr.* 61, 711–722. doi: 10.1002/lno.10246
- Martins, J., Saker, M. L., Moreira, C., Welker, M., Fastner, J., and Vasconcelos, V. M. (2009). Peptide diversity in strains of the cyanobacterium *Microcystis aeruginosa* isolated from Portuguese water supplies. *Appl. Microbiol. Biotechnol.* 82, 951–961. doi: 10.1007/s00253-009-1877-z
- Martins, J., and Vasconcelos, V. (2015). Cyanobactins from cyanobacteria: current genetic and chemical state of knowledge. *Mar. Drugs* 13, 6910–6946. doi: 10.3390/md13116910
- Otsuka, S., Suda, S., Li, R., Matsumoto, S., and Watanabe, M. M. (2000). Morphological variability of colonies of *Microcystis* morphospecies in culture. *J. Gen. Appl. Microbiol.* 46, 39–50. doi: 10.2323/jgam.46.39
- Otsuka, S., Suda, S., Li, R., and Watanabe, M. (1999). Phylogenetic relationships between toxic and non-toxic strains of the genus *Microcystis* based on 16S to 23S internal transcribed spacer sequence. *FEMS Microbiol. Lett.* 172, 15–21. doi: 10.1111/j.1574-6968.1999.tb13443.x
- Otsuka, S., Suda, S., Shibata, S., Oyaizu, H., Matsumoto, S., and Watanabe, M. M. (2001). A proposal for the unification of five species of the cyanobacterial genus *Microcystis* Kützing ex Lemmermann 1907 under the rules of the bacteriological code. *Int. J. Syst. Evol. Microbiol.* 51(Pt 3), 873–879. doi: 10.1099/00207713-51-3-873
- Paerl, H. W. (2018). Mitigating toxic planktonic cyanobacterial blooms in aquatic ecosystems facing increasing anthropogenic and climatic pressures. *Toxins* 10:E76. doi: 10.3390/toxins10020076
- Paerl, H. W., Hall, N. S., and Calandrino, E. S. (2011). Controlling harmful cyanobacterial blooms in a world experiencing anthropogenic and climatic-induced change. *Sci. Total Environ.* 409, 1739–1745. doi: 10.1016/j.scitotenv.2011.02.001
- Pancrace, C., Ishida, K., Briand, E., Pichi, D. G., Weiz, A. R., Guljamow, A., et al. (2018). Unique biosynthetic pathway in bloom-forming cyanobacterial genus *Microcystis* jointly assembles cytotoxic aeruginoguanidines and microguanidines. *ACS Chem. Biol.* 14, 67–75. doi: 10.1021/acscchembio.8b00918
- Pearson, L., Mihali, T., Moffitt, M., Kellmann, R., and Neilan, B. (2010). On the chemistry, toxicology and genetics of the cyanobacterial toxins, microcystin, nodularin, saxitoxin and cylindrospermopsin. *Mar. Drugs* 8, 1650–1680. doi: 10.3390/md8051650
- Šejnohová, L., and Maršálek, B. (2012). “Microcystis,” in *Ecology of Cyanobacteria II: Their Diversity in Space and Time*, ed. B. A. Whitton (Dordrecht: Springer), 195–228. doi: 10.1007/978-94-007-3855-3\_7
- Shih, P. M., Wu, D., Latifi, A., Axen, S. D., Fewer, D. P., Talla, E., et al. (2013). Improving the coverage of the cyanobacterial phylum using diversity-driven genome sequencing. *Proc. Natl. Acad. Sci. U.S.A.* 110, 1053–1058. doi: 10.1073/pnas.1217107110
- Sivonen, K., Leikoski, N., Fewer, D. P., and Jokela, J. (2010). Cyanobactins-ribosomal cyclic peptides produced by cyanobacteria. *Appl. Microbiol. Biotechnol.* 86, 1213–1225. doi: 10.1007/s00253-010-2482-x
- Steffen, M. M., Li, Z., Effler, T. C., Hauser, L. J., Boyer, G. L., and Wilhelm, S. W. (2012). Comparative metagenomics of toxic freshwater cyanobacteria bloom communities on two continents. *PLoS One* 7:e44002. doi: 10.1371/journal.pone.0044002
- Sukenik, A., Quesada, A., and Salmaso, N. (2015). Global expansion of toxic and non-toxic cyanobacteria: effect on ecosystem functioning. *Biodivers. Conserv.* 4, 889–908. doi: 10.1007/s10531-015-0905-9
- Sun, L. W., Jiang, W. J., Sato, H., Kawachi, M., and Lu, X. W. (2016). Rapid classification and identification of *Microcystis* strains using MALDI-TOF MS and polyphasic analysis. *PLoS One* 11:e0156275. doi: 10.1371/journal.pone.0156275
- Tillett, D., Parker, D. L., and Neilan, B. A. (2001). Detection of toxigenicity by a probe for the microcystin synthetase A gene (*mcyA*) of the cyanobacterial genus *Microcystis*: comparison of toxicities with 16S rRNA and phycocyanin operon (phycocyanin intergenic spacer) phylogenies. *Appl. Environ. Microbiol.* 67, 2810–2818. doi: 10.1128/AEM.67.6.2810-2818.2001
- Tonk, L., Visser, P. M., Christiansen, G., Dittmann, E., Snelder, E. O. F. M., Wiedner, C., et al. (2005). The microcystin composition of the cyanobacterium *Planktothrix agardhii* changes towards a more toxic variant with increasing light intensity. *Appl. Environ. Microbiol.* 71, 5177–5181. doi: 10.1128/AEM.71.9.5177-5181.2005
- Tonk, L., Welker, M., Huisman, J., and Visser, P. M. (2009). Production of cyanopeptolins, anabaenopeptins, and microcystins by the harmful cyanobacteria *Anabaena* 90 and *Microcystis* PCC 7806. *Harmful Algae* 8, 219–224. doi: 10.1016/j.hal.2008.05.005
- Via-Ordorika, L., Fastner, J., Kurmayer, R., Hisbergues, M., Dittmann, E., Komarek, J., et al. (2004). Distribution of microcystin-producing and non-microcystin-producing *Microcystis* sp. in European freshwater bodies: detection of microcystins and microcystin genes in individual colonies. *Syst. Appl. Microbiol.* 27, 592–602. doi: 10.1078/0723202041748163
- Wang, H., Fewer, D. P., Holm, L., Rouhiainen, L., and Sivonen, K. (2014). Atlas of nonribosomal peptide and polyketide biosynthetic pathways reveals common occurrence of nonmodular enzymes. *Proc. Natl. Acad. Sci. U.S.A.* 111, 9259–9264. doi: 10.1073/pnas.1401734111
- Welker, M., Brunke, M., Preussel, K., Lippert, I., and von Döhren, H. (2004). Diversity and distribution of *Microcystis* (cyanobacteria) oligopeptide chemotypes from natural communities studies by single-colony mass spectrometry. *Microbiology* 150, 1785–1796. doi: 10.1099/mic.0.26947-0
- Welker, M., Dittmann, E., and Von Döhren, H. (2012). Cyanobacteria as a source of natural products. *Methods Enzymol.* 517, 23–46. doi: 10.1016/B978-0-12-404634-4.00002-4
- Welker, M., Ejnohová, L., Némethová, D., von Döhren, H., Jarkovsky, J., and Marsálek, B. (2007). Seasonal shifts in chemotype composition of *Microcystis* sp. communities in the pelagial and the sediment of a shallow reservoir. *Limnol. Oceanogr.* 52, 609–619. doi: 10.4319/lo.2007.52.2.609
- Welker, M., Maršálek, B., Šejnohová, L., and von Döhren, H. (2006). Detection and identification of oligopeptides in *Microcystis* (cyanobacteria) colonies: toward an understanding of metabolic diversity. *Peptides* 27, 2090–2103. doi: 10.1016/j.peptides.2006.03.014
- Welker, M., and Von Döhren, H. (2006). Cyanobacterial peptides - nature's own combinatorial biosynthesis. *FEMS Microbiol. Rev.* 30, 530–563. doi: 10.1111/j.1574-6976.2006.00022.x
- Whitton, B. A. (2012). *Ecology of Cyanobacteria II, Ecology of Cyanobacteria II: Their Diversity in Space and Time*. Dordrecht: Springer. doi: 10.1007/978-94-007-3855-3
- Yang, J. Y., Sanchez, L. M., Rath, C. M., Liu, X., Boudreau, P. D., Bruns, N., et al. (2013). Molecular networking as a dereplication strategy. *J. Nat. Prod.* 76, 1686–1699. doi: 10.1021/np400413s
- Zak, A., and Kosakowska, A. (2016). Cyanobacterial and microalgal bioactive compounds-the role of secondary metabolites in allelopathic

- interactions. *Oceanol. Hydrobiol. Stud.* 45, 131–143. doi: 10.1515/ohs-2016-0013
- Zurawell, R. W., Chen, H., Burke, J. M., and Prepas, E. E. (2005). Hepatotoxic cyanobacteria: a review of the biological importance of microcystins in freshwater environments. *J. Toxicol. Environ. Health. B. Crit. Rev.* 8, 1–37. doi: 10.1080/10937400590889412
- Zwart, G., Hiorns, W. D., Methe, B. A., van Agterveld, M. P., Huismans, R., Nold, S. C., et al. (1998). Nearly identical 16S rRNA sequences recovered from lakes in North America and Europe indicate the existence of clades of globally distributed freshwater bacteria. *Syst. Appl. Microbiol.* 21, 546–556. doi: 10.1016/S0723-2020(98)80067-2

**Conflict of Interest Statement:** The authors declare that the research was conducted in the absence of any commercial or financial relationships that could be construed as a potential conflict of interest.

Copyright © 2019 Le Manach, Duval, Marie, Djediat, Catherine, Ebery, Bernard and Marie. This is an open-access article distributed under the terms of the Creative Commons Attribution License (CC BY). The use, distribution or reproduction in other forums is permitted, provided the original author(s) and the copyright owner(s) are credited and that the original publication in this journal is cited, in accordance with accepted academic practice. No use, distribution or reproduction is permitted which does not comply with these terms.



# Interactive Impacts of Silver and Phosphorus on Autotrophic Biofilm Elemental and Biochemical Quality for a Macroinvertebrate Consumer

Clément Crenier<sup>1,2†</sup>, Kévin Sanchez-Thirion<sup>1,2†</sup>, Alexandre Bec<sup>3</sup>, Vincent Felten<sup>1,2</sup>, Jessica Ferriol<sup>4</sup>, Aridane G. González<sup>5</sup>, Joséphine Leflaive<sup>3</sup>, Fanny Perrière<sup>2</sup>, Loïc Ten-Hage<sup>3</sup> and Michael Danger<sup>1,2\*</sup>

## OPEN ACCESS

### Edited by:

Stéphane Pesce,  
National Research Institute of Science  
and Technology for Environment  
and Agriculture (IRSTEA), France

### Reviewed by:

Mariam Fadhlouli,  
Eau Terre Environnement Research  
Centre (INRS), Canada  
Betty Chaumet,  
Istrea Centre de Bordeaux, France

### \*Correspondence:

Michael Danger  
michael.danger@univ-lorraine.fr

† These authors have contributed  
equally to this work

### Specialty section:

This article was submitted to  
Microbiotechnology, Ecotoxicology  
and Bioremediation,  
a section of the journal  
Frontiers in Microbiology

**Received:** 14 September 2018

**Accepted:** 25 March 2019

**Published:** 16 April 2019

### Citation:

Crenier C, Sanchez-Thirion K,  
Bec A, Felten V, Ferriol J,  
González AG, Leflaive J, Perrière F,  
Ten-Hage L and Danger M (2019)  
Interactive Impacts of Silver  
and Phosphorus on Autotrophic  
Biofilm Elemental and Biochemical  
Quality for a Macroinvertebrate  
Consumer. *Front. Microbiol.* 10:732.  
doi: 10.3389/fmicb.2019.00732

<sup>1</sup> Laboratoire Interdisciplinaire des Environnements Continentaux, Université de Lorraine – Centre National de la Recherche Scientifique, Metz, France, <sup>2</sup> LTSER France, Zone Atelier du Bassin de la Moselle, Vandœuvre-lès-Nancy, France, <sup>3</sup> Université Clermont Auvergne, CNRS UMR 6023, Laboratoire Microorganismes : Génome et Environnement, Clermont-Ferrand, France, <sup>4</sup> Laboratoire Ecologie Fonctionnelle et Environnement, UMR 5245 CNRS-INP-UPS, Université de Toulouse, Toulouse, France, <sup>5</sup> Instituto de Oceanografía y Cambio Global, Universidad de Las Palmas de Gran Canaria, Las Palmas de Gran Canaria, Spain

Autotrophic biofilms are complex and fundamental biological compartments of many aquatic ecosystems. In particular, these biofilms represent a major resource for many invertebrate consumers and the first ecological barrier against toxic metals. To date, very few studies have investigated the indirect effects of stressors on upper trophic levels through alterations of the quality of biofilms for their consumers. In a laboratory study, we investigated the single and combined effects of phosphorus (P) availability and silver, a re-emerging contaminant, on the elemental [carbon (C):nitrogen (N):P ratios] and biochemical (fatty acid profiles) compositions of a diatom-dominated biofilm initially collected in a shallow lake. We hypothesized that (1) P and silver, through the replacement of diatoms by more tolerant primary producer species, reduce the biochemical quality of biofilms for their consumers while (2) P enhances biofilm elemental quality and (3) silver contamination of biofilm has negative effects on consumers life history traits. The quality of biofilms for consumers was assessed for a common crustacean species, *Gammarus fossarum*, by measuring organisms' survival and growth rates during a 42-days feeding experiment. Results mainly showed that species replacement induced by both stressors affected biofilm fatty acid compositions, and that P immobilization permitted to achieve low C:P biofilms, whatever the level of silver contamination. Gammarids growth and survival rates were not significantly impacted by the ingestion of silver-contaminated resource. On the contrary, we found a significant positive relationship between the biofilm P-content and gammarids growth. This study underlines the large indirect consequences stressors could play on the quality of microbial biomass for consumers, and, in turn, on the whole food web.

**Keywords:** ecological stoichiometry, essential fatty acids, trophic ecotoxicology, *Gammarus fossarum*, multiple stressors, benthic microalgae, freshwater biofilms

## INTRODUCTION

In ecosystems, living organisms most often face multiple stressors simultaneously. However, the interactive effects of these stressors, acting synergistically or antagonistically on species and ecosystems, remain hardly predictable. Particularly, in aquatic ecosystems, contaminants have often been described as co-occurring with eutrophication (Skei et al., 2000). However, the interactive effects of these stressors on ecosystem functioning remain poorly understood. By alleviating organisms' nutrient limitation, increases in nutrient concentrations might potentially increase organisms' tolerance to contaminants (Arce-Funck et al., 2016). In contrast, by altering water quality parameters, such as dissolved oxygen concentrations, one could expect changes in contaminant bioavailability (Skei et al., 2000) and/or intensification of the damages caused by the contaminants on already stressed organisms (Rattner and Heath, 2003). Finally, eutrophication-induced shifts in community composition could deeply change, either positively or adversely, the tolerance to contaminants of communities, mainly depending on individual species traits (Baird and Van den Brink, 2007).

In freshwater ecosystems, phosphorus (P) has long been recognized as one of the most important factor of eutrophication (Smith et al., 1999). Falkowski et al. (2000) have shown that human activities have increased the global fluxes of P by a fourfold factor when compared to natural fluxes, P exhibiting by far the most dysregulated biogeochemical cycle on earth. Since this chemical element is generally scarce in natural environments, any anthropogenic input is susceptible to deeply alter ecosystems functioning (Elser and Bennett, 2011). Due to these peculiarities, P-release impacts in aquatic ecosystems have received much attention in the past 60 years. Yet, these impacts have most often been considered without considering co-occurring stressors. Among the numerous contaminants entering aquatic ecosystems, toxic trace metals represent some of the most common persistent pollutants (Nriagu and Pacyna, 1988). Studying the interactive impacts of phosphorus load and toxic trace metal seems thus particularly important for understanding the impacts of contaminants in nature. Among the diversity of toxic metals that can be found in aquatic ecosystems, silver represents a reemerging contaminant that is commonly used as an antibacterial agent in partly soluble nanoparticles (Marambio-Jones and Hoek, 2010). Silver nanoparticles are currently among the most widely used nanoparticles (Project on Emerging Nanotechnology, 2012), and several studies predicted future increases in silver concentrations in surface waters due to its increased use (Geranio et al., 2009; Gottschalk et al., 2009). Concerning silver toxicity, silver is well known as a potent biocide, and is certainly among the most toxic to microorganisms (bacteria, fungi, and phytoplankton) and invertebrates (Ratte, 1999; Arce Funck et al., 2013a,b).

In numerous aquatic ecosystems, a large proportion of primary production is ensured by phototrophic biofilms. These biofilms are composed of attached communities generally dominated by microalgae, and containing different amounts of bacteria, fungi, and micro-eukaryotic species embedded in an organic polysaccharidic matrix (Wetzel, 1983). As a central basal

resource, these biofilms play a fundamental role in aquatic food webs (Wetzel, 1983). These biofilms also have large impacts on aquatic biogeochemical cycles, ensuring the production, the decomposition, and the transfer of numerous organic molecules (Battin et al., 2003). Due to the ecological importance of biofilms, several studies have investigated the interactive impacts of diverse stressors on biofilm community structures and on some functional processes they ensure. For example, studies showed either antagonistic or synergistic effects of P concentration on the impacts of pesticides on biofilm community structure and/or primary production (Tlili et al., 2010; Murdock and Wetzel, 2012; Murdock et al., 2013). While being far less studied, some authors also showed that the deleterious impacts of metallic contaminants were reduced when biofilms were released from P limitation (Guasch et al., 2004; Serra et al., 2010). More recently, Leflaive et al. (2015) showed that high P concentrations alleviated the impacts of ionic silver on biofilm communities, but only for a cyanobacteria-dominated biofilm, impacts of silver on diatom-dominated biofilm being unaffected by P concentrations. Surprisingly, while multi-stressors impacts on biofilm community structure and functions have received much attention, and despite the major role of biofilms as basal resources in aquatic ecosystems, almost nothing is known on the cumulative impacts of multiple stressors on biofilm quality for its consumers. Yet, investigating this parameter might bring insightful results on multiple stressors indirect effects on aquatic food webs and, *in fine*, on ecosystem functioning.

In the literature, several parameters are generally evoked for measuring the potential quality of biofilms for their consumers. First, biofilm elemental content (often expressed as C:N:P ratios) has long been considered as an indicator of the quality of a resource for a consumer, this resource being of high quality when the imbalance between resource elemental content and consumers elemental requirements is minimal (Sterner and Elser, 2002). Since consumers have generally high N and P requirements, resources with the lowest C:P or C:N ratios are generally considered as resources of the highest quality, maximizing consumer life history traits such as growth rates or reproduction (Liess and Hillebrand, 2006; Danger et al., 2012, 2013). Second, the resource quality of a biofilm can also be evaluated by measuring its fatty acid content (a parameter classified as a biochemical quality parameter, see Crenier, 2017). Indeed, among the diversity of fatty acids found in nature, some of them are considered as essential for consumers, i.e., these fatty acids cannot be synthesized or at least not in sufficient amounts to fulfill the requirements of consumers (Arts et al., 2009). These essential fatty acids are generally composed of long chain polyunsaturated fatty acids (PUFAs), such as 20:5 $\omega$ 3 (EPA) and 22:6 $\omega$ 3 (DHA). The consumption of these compounds has been regularly reported as controlling consumers' growth and/or reproduction (Masclaux et al., 2009; Crenier et al., 2017). Since fatty acid profiles are highly variable between algal groups, any change in biofilm algal communities can have drastic impacts on biofilm PUFA content (Muller-Navarra et al., 2004; Bec et al., 2010; Sanpera-Calbet et al., 2017). For example, the replacement of diatoms, rich in long-chain

PUFAs, by green algae or cyanobacteria, depleted in such compounds, could have profound impacts on consumers' life history traits and secondary production (Muller-Navarra et al., 2004). Finally, in the case of biofilms exposed to contaminants, the contaminant content of biofilm biomass could also be considered as a potential quality parameter since some contaminants can be highly toxic through trophic pathways (Luoma and Rainbow, 2008). Note that whatever the quality parameter investigated, effects of resources consumption on consumers life history traits must be systematically measured to evaluate the effective quality of resources, resource quality being not only dependent on resource composition but also on consumers requirements and physiology.

In the present study, we investigated the single and combined effects of P concentration and metallic contamination on biofilm quality for a model consumer, *Gammarus fossarum* (Crustacea, Amphipoda). This study is an independent part of the study published by Leflaive et al. (2015), dealing with the interactive impacts of P and ionic silver on biofilm (prokaryotic and microeukaryotic) communities. This study was carried out on a diatom-dominated biofilm initially collected in the field. First results showed that on this biofilm, both P increase and silver contamination led to significant reductions of diatoms proportion in algal communities, these algae being partly replaced by green algae (Leflaive et al., 2015). We thus hypothesize that P and silver lead to reductions in biofilm PUFA content, thus reducing biofilm biochemical quality for consumers (Hypothesis 1). In contrast, P increase in water lead to reductions of biofilm C:P ratios, thus potentially increasing resources elemental quality for consumers (Hypothesis 2). Finally, we hypothesize that silver has deleterious impacts on consumers' growth and survival through the ingestion of toxic metal, leading to strong interactions between silver contamination and P concentration (Hypothesis 3).

## MATERIALS AND METHODS

### Experimental Setup

To investigate the single and combined effects of Ag and P concentrations on biofilm quality, a diatom-dominated biofilm (diatoms representing 85–90% of algal biomass, Leflaive et al., 2015) was collected in the field. This biofilm was then exposed for 3 weeks in a full factorial design to a gradient of silver concentration at three distinct P concentrations. Impacts on microbial community structures were investigated independently from the present experiment, results being fully available in Leflaive et al. (2015). The present study specifically investigates the impacts of P and Ag stressors on biofilm fatty acids profiles, elemental composition, and silver concentration, giving an evaluation of biofilm potential quality for consumers. To measure the real/effective quality of biofilms, we fed a model consumer, *Gammarus fossarum*, with the distinct freeze dried biofilms, and followed organisms survival and growth throughout a 42-days experiment.

All details of the biofilm biomass production can be found in Leflaive et al. (2015). Briefly, the diatom-dominated biofilm was

collected in a mesotrophic reservoir (Lake Saint-Ferréol, South-West France) using polyethylene plates (10 cm × 5 cm) placed vertically, 60-cm deep in the lake. Substrates were immersed during 3 weeks (May–June), then brought back to the laboratory in a cool box and placed two by two in beakers filled with 500 mL of modified COMBO medium (Kilham et al., 1998). The experiment was carried out in a controlled culture chamber (18°C, light intensity between 50 and 60  $\mu\text{E m}^{-2} \text{s}^{-1}$ , 16 h/8 h light/dark cycles). Twelve conditions were tested: three P levels (20, 100, or 500  $\mu\text{g/L}$ ) and four Ag concentrations (0, 5, 50, or 150  $\mu\text{g/L}$ ), each treatment being replicated three times (36 microcosms in total). Phosphorus concentrations were chosen as representative of what can be found along a gradient of P pollution in aquatic ecosystems (EEA, 2014). Concerning silver concentrations, total Ag concentrations have been shown to vary in natural waters between 0.03 and 500  $\text{ng L}^{-1}$  (Luoma, 2008), but these concentrations are expected to increase in the future (Geranio et al., 2009; Gottschalk et al., 2009). To maintain levels of silver close to what could be found in contaminated rivers in our semi-continuous exposure conditions, we chose to expose biofilms to a 5  $\mu\text{g Ag L}^{-1}$  concentration. The 50 and 100  $\mu\text{g Ag L}^{-1}$  concentrations were retained as acute contamination levels, to evaluate the tolerance limits of biofilms to silver exposure. To limit too strong changes in our exposure conditions, media were entirely renewed each week. For that purpose, we emptied the beakers and re-filled them with newly prepared medium with the metal at the appropriate concentration. To limit silver adsorption on beakers surface, glass beakers were pre-saturated during 24 h with Ag solutions at concentrations similar to those of the diverse treatments.

### Sampling

Just after the introduction of biofilms in beakers ( $t_0$ ) and at the end of the experiment (after 3 weeks of biofilm growth,  $t_{\text{final}}$ ), 5 mL of medium from each beaker ( $n = 3$  replicates per treatment, 36 samples in total per sampling date) were sampled, acidified with 15  $\mu\text{L}$  of 70%  $\text{HNO}_3$  and stored at 4°C for later Ag quantification. At  $t_{\text{final}}$ , biofilms present on polyethylene substrates were scrapped, then homogenized in 20 mL of incubation medium. Some subsamples were taken for measuring bacterial and micro-eukaryotic community structures. In particular, 1 mL was fixed (2% formaldehyde) and kept at 4°C for algal determination and counts (see Leflaive et al., 2015 for community structure results). The remaining volume of suspension was concentrated (centrifugation 7,000 × g, 10 min), supernatant was eliminated and the biofilm was stored at –20°C until being freeze-dried.

### Measurements of Ag in Biofilm and Water, and $\text{PO}_4^{3-}$ in Water

Silver concentrations in culture media was measured on  $t_0$  and  $t_{\text{final}}$  samples by atomic absorption spectrophotometry (graphite furnace Varian SpectrAA 300, detection limit = 0.1  $\mu\text{g Ag/L}$ ). The concentration of silver in the biofilm was measured after acidic digestion with 1 mL bidistilled  $\text{HNO}_3$  (15 N) and 1 mL  $\text{H}_2\text{O}_2$  (30%, Sigma) for 24 h at 70°C.

After full digestion, the samples were evaporated at 70°C and redissolved by 2% bidistilled HNO<sub>3</sub> for analysis by ICP-MS (Agilent 7500 ce) with an uncertainty of 5% and a detection limit of 0.001 µg L<sup>-1</sup>. A reference standard solution SRM1646a (NIST, United States) was used to certify the accuracy and precision of the analytical procedure. The data quality was assessed by comparing the certified and the reference standard solution in terms of recovery (%), and by checking the precision of the ICP-MS analysis by the relative percentage differences (RPD) and the relative standard deviation (RSD) among the reference material replicates. The recovery for Ag was higher than 84.5% for all the samples. The precision of the instrument was within the 10% of RSD, thus was acceptable. All the materials used for silver sampling and measurements were cleaned with 1 N HCl for 24 h. Due to the cost of Ag analyses, measurements were done for each treatment on a pooled sample of biofilm corresponding to a mix of equal quantities of the three replicates (12 samples, i.e., 3 P-levels × 4 Ag concentrations). Initial PO<sub>4</sub><sup>3-</sup> concentrations were measured spectrophotometrically (ammonium molybdate method, AFNOR, 1990) in culture media used for microcosms filling.

## Biofilm Elemental Composition Measurements

Freeze-dried biofilm was first gently homogenized in a plastic centrifugation tube using a glass pestle. The C and N content of biofilm was measured on the 36 samples (3 P-levels × 4 Ag concentrations × 3 replicates) on ca. 1 mg samples using a CHN elementary analyzer (Carlo Erba NA2100, Thermo Quest CE International, Milan, Italy). Biofilm P content was quantified on the same number of samples after alkaline digestion with persulfate, and mineral P was then measured spectrophotometrically following the AFNOR (1990) procedure. Results are expressed as the mass percentage of the element in different resources, and C:N:P ratios correspond to molar ratios.

## Biofilm Fatty Acid Profiles Determination

Fatty acids analyses were performed on the 36 dried biofilm samples (3 P-levels × 4 Ag concentrations × 3 replicates). Analyses followed the procedure described in Crenier et al. (2017). Briefly, lipids were extracted twice with a chloroform/methanol solution according to the method proposed by Folch et al. (1957). Fatty acids were then converted into fatty acid methyl-esters (FAME) by acid catalyzed transesterification and analyzed on an Agilent Technologies<sup>TM</sup> 6850 gas chromatograph. FAME were identified after a comparison of retention times with those obtained from Supelco<sup>®</sup> and laboratory standards, and were quantified using internal standards (13:0).

## *Gammarus fossarum* Growth Measurements

### Gammarids Sampling and Initial Sizing

Gammarids were collected in an unpolluted second-order forested stream (La Maix, Vosges Mountains Latitude N

48°29'02.1'', longitude E 007°04'008.5''). Organisms were immediately transported to the laboratory, then acclimatized at 12°C, in the dark and in aerated water for 15 days. The temperature of 12°C was chosen since preliminary observations showed that it permits to optimize gammarids growth while reducing risks of mortality increase due to water deoxygenation. Similarly, working in the dark permits to reduce the stress undergone by this light-avoiding species. During the acclimation period, animals were fed with alder [*Alnus glutinosa*, (L.) Gaertn.] leaf litter directly collected in La Maix stream. Two days before the beginning of the growth experiment, 204 gammarids of 4–5 mm in length were sorted and put in individual plastic cups containing 50 mL of La Maix stream water. Organisms were let emptying their guts for 48 h. During this period, all organisms were individually photographed, and initial sizes were measured with SigmaScan Image Analysis Version 5.000 (SPSS Inc., Chicago, IL, United States). The mean body length of gammarids used in the experiment was 4.52 ± 0.70 mm (mean ± SD), and size were similar between all treatments (ANOVA<sub>2</sub>: P effect:  $F_{2,154} = 0.3$ ,  $p = 0.73$ ; Ag effect:  $F_{3,154} = 0.3$ ,  $p = 0.85$ ; Ag × P effect:  $F_{6,154} = 1.7$ ,  $p = 0.11$ ).

## Preparation of Biofilm Resources for *G. fossarum* Growth Experiment

Since measuring biofilm consumers growth take several weeks, and since biofilm quality can drastically change in a few weeks, we chose to feed the consumers with freeze-dried material, thus permitting to feed organisms with similar resource quality throughout the experiment (as proposed in Crenier et al., 2017). To maximize *G. fossarum* consumption of freeze-dried and homogenized biofilm, biofilm powders were embedded in low gelling temperature agarose (Sigma A9414), following the protocol proposed by Crenier et al. (2017). This agarose matrix permits to reconstitute a cohesive biofilm, and present the advantages of being nutrient-free. Agarose concentration used was 2%, and biofilm biomass introduced in each pellet was calculated to ensure that 50% of C came from the biofilm, the remaining coming from agarose. Agarose was dissolved in glass bottles with deionized water, heated in a microwave, and then placed in an agitated water bath at 38°C. After reaching this temperature, 1.6 ml of agarose solution was introduced in a 2 ml Eppendorf<sup>®</sup> tube and mixed with biofilm powders. This mixture was then homogenized and poured in the holes of a Plexiglas<sup>®</sup> mould (holes: 3 mm wide, 2 mm high). After a few minutes, the pellets were unmolded and kept at -20°C in Petri dishes until use.

## *G. fossarum* Survival and Growth Experiment

Organisms were fed individually with one biofilm pellets. We verified that organisms were fed *ad libitum* and biofilm pellets were replaced every 2 days. The experiment lasted 42 days, and was carried out at 12°C, in the dark. Water was renewed every week, using aerated La Maix water. Survival was monitored daily. All survivors were photographed at the end of the experiment and the body length was measured as described above. The growth

rates were expressed as length gain per mm of gammarid initial size per day ( $\text{mm mm}^{-1} \text{d}^{-1}$ ), as in Danger et al. (2013).

## Statistical Treatment of Data

All parameters (Ag concentration in water and biofilm, biofilm %C, %N, %P, C:N, C:P and N:P ratios, fatty acid contents, *Gammarus fossarum* growth rates) except survival curves were analyzed using two-way ANOVAs, considering P level and Ag concentrations as categorical predictors. Data were log transformed when necessary in order to meet the variance homoscedasticity condition for using ANOVAs. When ANOVA indicated significant differences between treatments, multiple comparisons were conducted using Tukey's HSD test. Due to the elevated costs of analyses and the quantity of biological material required, Ag concentrations in biofilms were not replicated, rather measured on a pooled sample coming from the three replicates. The interactive effects of P and Ag were thus impossible to calculate, and only the main effects were analyzed. Survival were analyzed using Kaplan–Meier survival curves and log-rank tests for comparing curves. By accounting for censored data (i.e., when organisms were still alive at the end of the experiment), this approach enabled to investigate the effects of P and Ag during the whole experiment. Yet, since mortality remained null in several treatments of this experiment, it was statistically impossible to compare the 12 treatments. To make the analysis feasible, survival values were pooled by P levels, then by Ag levels. This permitted to compare the effects of P and Ag concentrations on gammarids survival, the analysis of the interactive effects of P and Ag being not possible. Survival curves analyses showing significant differences for both Ag and P treatments, the three curves obtained for P effect and the four curves obtained for Ag effects were compared pairwise. To take into account the multiple comparisons, *p*-values considered as significant followed a Bonferroni adjustment. Finally, impacts of resource quality parameters (biofilm C/P ratios, PUFA contents, and Ag concentrations) were analyzed using linear regressions. All statistical analyses were computed with STATISTICA (SAS institute). Statistical significance was inferred at  $p \leq 0.05$ .

## RESULTS

The measured Ag concentrations after microcosms filling ( $t_0$ ) were generally slightly lower than the nominal concentrations, these concentrations reaching  $0.00 \pm 0.00$ ,  $2.63 \pm 0.29$ ,  $49.42 \pm 0.75$ , and  $94.67 \pm 8.22 \mu\text{g Ag L}^{-1}$  in the 0, 5, 50, and  $150 \mu\text{g Ag L}^{-1}$  treatments, respectively (Figures 1A). The Ag concentration strongly decreased after 1 week in the presence of biofilm ( $t_{\text{final}}$ ) (Figures 1B). The Ag concentration achieved  $0.00 \pm 0.00$ ,  $0.31 \pm 0.08$ ,  $3.91 \pm 1.99$ , and  $39.58 \pm 6.31 \mu\text{g Ag L}^{-1}$  with respect to the initial expected levels (0, 5, 50, and  $150 \mu\text{g Ag L}^{-1}$ ). At both  $t_0$  and  $t_{\text{final}}$ , Ag concentrations were totally independent of the P concentration, as revealed by the absence of significant interaction between Ag and P concentrations (Figures 1A,B and Table 1). Ag measurements in biofilm showed traces of Ag in control biofilm ( $0.8 \pm 1.11 \mu\text{g}$

$\text{g}^{-1}$ ), while Ag concentrations reached  $8.24 \pm 1.19$ ,  $86.41 \pm 10.77$ , and  $279.13 \pm 72.85 \mu\text{g g}^{-1}$ , in the 5, 50, and  $150 \mu\text{g Ag L}^{-1}$  treatments, respectively (Figure 1C and Table 1).

Results of biofilm elemental composition measurements showed that biofilm %C and %N remained unchanged whatever the P and Ag concentrations tested (Figure 2 and Table 1). In contrast, biofilm %P was strongly altered by the P concentration in water, but remained unchanged along the Ag gradient (no interactive effect). All elemental ratios were modified by P concentration in the culture medium, biofilm C:P, C:N, and N:P ratios being significantly reduced under the highest P-concentrations. In contrast, only biofilm C:N and C:P ratios were significantly altered by the Ag concentration, these ratios slightly decreasing along the Ag concentration gradient (Figure 2), and no interactive effect was revealed (Table 1).

Fatty acids profiles (Table 2 and Figure 3) were slightly modified by both Ag and P exposures, but no interactive effects between both factors were evidenced. Culture medium P concentrations significantly reduced biofilm unsaturated fatty acid contents: MUFA concentrations were reduced by 36% (Figure 3B) while PUFA concentrations (Figure 3C) decreased by 28% between the P20 and the P500 treatments, respectively. The 20:5 $\omega$ 3 followed a similar trend, but differences were only marginally significant ( $p = 0.06$ ). In contrast, low Ag contamination ( $5 \mu\text{g L}^{-1}$ ) led to a significant twofold decrease in biofilm SAFA content, while this reduction was no more significant for the 50 and the  $150 \mu\text{g Ag L}^{-1}$  treatments. The same effect was observed on the total amount of fatty acids found in biofilm (Table 1).

During the *G. fossarum* growth experiment, that lasted 42 days, the survival rate remained high (>80%) for all treatments. The survival was significantly lower for organisms fed with the biofilms coming from the P100 and the P500 treatments when compared to those fed with the biofilm grown in the P20 treatment (Figure 4A). Ag also had significant effects on gammarids survival, the lowest survival being observed for organisms fed with control (Ag0) biofilms, and the highest for organisms fed with biofilms coming from the Ag 50 treatment, those fed with biofilms coming from the Ag5 and the Ag150 treatments showing intermediate survival (Figure 4B).

Size growth (calculated on the surviving organisms after the 42-days experiment) of organisms fed with the different biofilms was neither affected by the Ag nor by the P concentrations of biofilm exposure (Figure 5A), despite a marginally significant effect of P ( $P = 0.052$ , Table 1). When considering the regressions between organisms growth rates and the main descriptors of resource quality (PUFA and Ag concentrations, biofilm C:P ratios; Figures 5B–D), a significant negative relationship was only revealed for the effect of biofilm C:P ratios ( $P < 0.01$ ) on *G. fossarum* growth, whereas no significant relationship was found for biofilm Ag and PUFA concentrations.

## DISCUSSION

While the single and interactive impacts of nutrient concentrations and metallic contaminations have long been

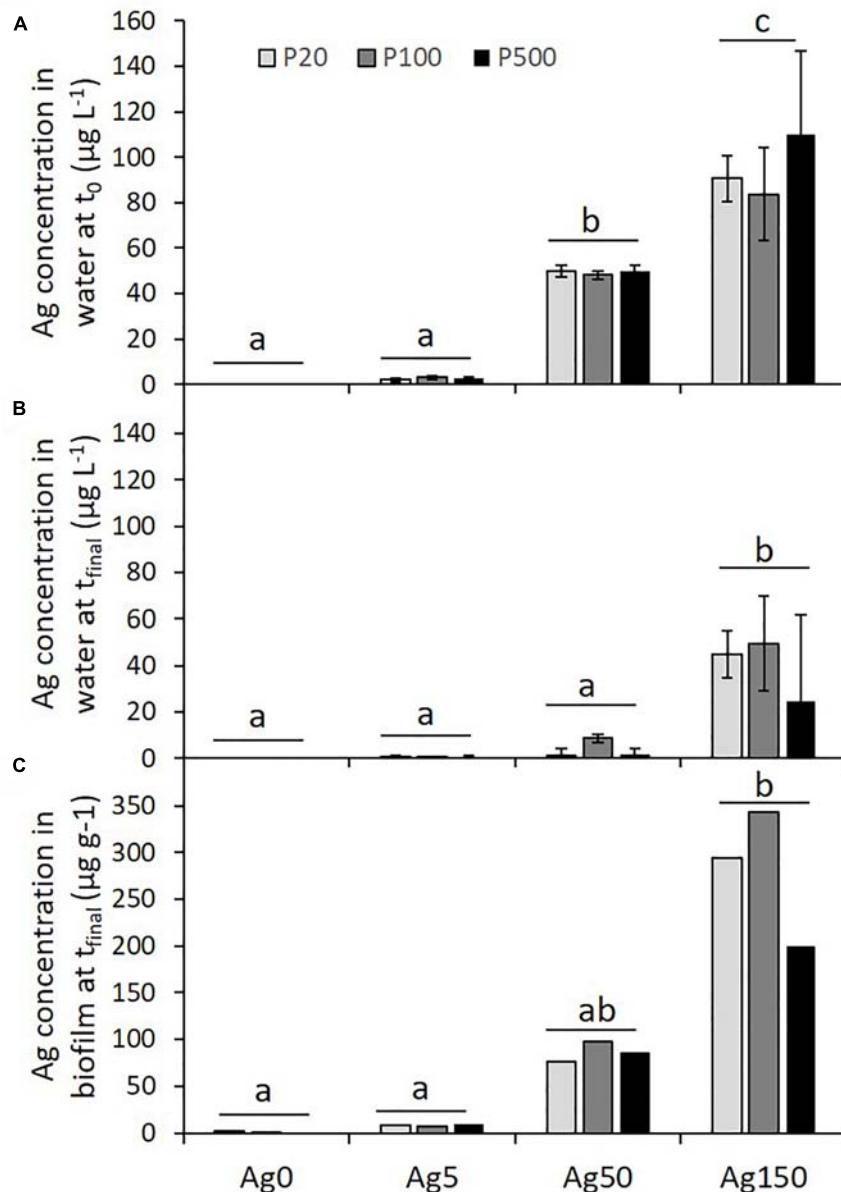


**FIGURE 1** | Concentrations of silver in water (A,B) and in biofilm (C) in the diverse Ag and P treatments. Different letters indicate significant differences after *post hoc* Tukey tests.

investigated on biofilm community structures (Guasch et al., 2004; Tlili et al., 2010; Serra et al., 2010; Murdock and Wetzel, 2012; Murdock et al., 2013; Leflaive et al., 2015), far less is known on the effects these multiple stressors might play on the quality of the biomass produced, and, in turn, on their consequences for biofilm consumers. In this study, we showed that both phosphorus and silver significantly change diverse parameters of biofilms quality for an invertebrate consumer, without strong interactive effects between stressors. In particular, we partially verified Hypothesis 1, P but not Ag significantly reducing biofilm PUFA content. The P-level also markedly increased

biofilm elemental quality, validating Hypothesis 2. In contrast, Hypothesis 3, dealing with the negative effects of Ag contaminated resources ingestion on consumers must be rejected.

### Conditions of Biofilm Exposure to Ag

Despite significant initial differences in Ag concentrations in water between the four Ag treatments, Ag concentrations measured at  $t_0$  were systematically lower than nominal concentrations (differences with expected concentrations ranging from 1% in the Ag50 treatment to 37% and 48% in the Ag150 and the Ag5 treatments, respectively). This observation suggests that

a part of the metal might have been very quickly adsorbed to the biofilm and/or to the microcosms walls at the microcosm filling. The lack of interaction with P level as well as the high recovery of dissolved silver in the culture medium (e.g., >80% for the 150  $\mu\text{g Ag L}^{-1}$ , P500 treatment) suggests that a fast complexation and a precipitation in presence of phosphates, if it occurred, might have been reduced.

After 1 week of biofilm exposure to silver ( $t_{\text{final}}$ ), silver concentrations were largely reduced when compared to what was initially introduced. These reductions could be partly attributed to silver uptake by biofilm microorganisms (algae, bacteria, fungi...), but also to the great potential of growing algal cells and biofilms to adsorb ionic metals on their surfaces. Indeed, adsorption processes are generally more common in algae than active uptake into the cells (Ratte, 1999). Adsorption has already been shown to increase with the presence of extracellular polymers (EPS), as already observed in previous studies (e.g., González et al., 2015, 2016), such substances presenting numerous potential binding sites (van Hullebusch et al., 2003). Since nutrient depletions are well known to stimulate the production of EPS by phototrophic biofilms (Lyon and Ziegler, 2009), an increase in Ag adsorption was expected in the P20 treatment when compared to the P500 treatment. However, in our study, lower P levels did not change significantly silver concentrations remaining in water. Similarly, even if we were unable to test for the interactive effects of P and Ag on silver concentration in biofilms (absence of replication for these chemical analyses), higher P concentrations in water were expected to lead to reduced Ag concentrations in biofilms. Again,

this general trend was not clearly visible, and complementary studies will be required to understand the mechanisms explaining the changes in silver concentrations, both in the water column and in the biofilm.

## Effects of P and Ag on Biofilm Elemental Composition

Elemental compositions of resources are generally considered as good proxies of resources quality for consumers (Sterner and Elser, 2002). Indeed, life history traits of several species have been shown to be controlled by the imbalance between their elemental requirements and what they can effectively find in their resources (e.g., Elser et al., 2001; Frost and Elser, 2002). Since C proportions in resources is rarely limiting for consumers, resources presenting low C:N and/or low C:P ratios are generally considered as potentially high quality resources for their consumers (Sterner and Elser, 2002). Our study revealed that both biofilm C:P and N:P ratios were significantly reduced by the P concentration of the culture medium. This effect might be simply explained by the fact that algae have the potential to immobilize nutrients in excess in their biomass, this process being generally called luxury consumption (Droop, 1974). This effect occurs concomitantly with a reduction of the C-rich EPS production (Lyon and Ziegler, 2009), these compounds generally largely contributing to increasing algal communities C:nutrient ratios (Pannard et al., 2016). In addition, bacterial communities have the potential to quickly change, selecting for species able to use optimally nutrients available

**TABLE 1** | Results of the two-way ANOVAs conducted on the main endpoints for investigating the effects of P concentrations, Ag levels, and their interactive effects.

Parameter	Two-way ANOVA									
	P concentration			Ag concentration			P × Ag			d.f. error
	d.f.	F	p-Value	d.f.	F	p-Value	d.f.	F	p-Value	
[Ag] in water at $t_0$	2	0.9	0.41	3	113.7	<b>&lt;0.001</b>	6	0.8	0.55	24
[Ag] in water at $t_{\text{final}}$	2	2.3	0.12	3	39.8	<b>&lt;0.001</b>	6	1.5	0.21	24
[Ag] in biofilm at $t_{\text{final}}$	2	1.1	0.39	3	37.9	<b>&lt;0.001</b>	na	na	na	6
<b>Elemental quality</b>										
%C	2	0.3	0.76	3	0.6	0.64	6	1.4	0.26	24
%N	2	0.8	0.44	3	2.2	0.10	6	0.7	0.61	24
%P	2	129.8	<b>&lt;0.001</b>	3	1.0	0.39	6	0.8	0.59	24
C:N ratio	2	5.1	<b>0.01</b>	3	3.5	<b>0.03</b>	6	1.6	0.19	24
C:P ratio	2	369.1	<b>&lt;0.001</b>	3	3.2	<b>0.04</b>	6	1.3	0.29	24
N:P ratio	2	374.8	<b>&lt;0.001</b>	3	0.8	0.52	6	1.8	0.14	24
<b>Fatty acid profiles</b>										
SAFA	2	0.2	0.81	3	3.8	<b>0.02</b>	6	1.7	0.17	23
MUFA	2	14.5	<b>&lt;0.001</b>	3	2.7	0.06	6	2.1	0.08	23
PUFA	2	4.9	<b>0.01</b>	3	1.8	0.16	6	1.2	0.32	23
18:3 $\omega$ 3	2	1.8	0.19	3	6.4	0.003	6	1.0	0.44	23
20:5 $\omega$ 3	2	2.9	0.06	3	1.9	0.15	6	1.8	0.12	23
Sum fatty acids	2	0.1	0.98	3	4.1	<b>0.02</b>	6	1.9	0.12	23
<i>G. fossarum</i> growth rates	2	2.9	0.05	3	0.6	0.60	6	0.7	0.60	154

The columns d.f. and F correspond to the number of degree of freedom and the F-statistic in the two-way ANOVA test, respectively. Significant differences are indicated in bold.

TABLE 2 | Results of the fatty acids analyses carried out on the biofilms at the end of the experiment.

Fatty acids ( $\mu\text{g mg}^{-1}$ )	Ag0			Ag5			Ag50			Ag150		
	P20	P100	P500	P20	P100	P500	P20	P100	P500	P20	P100	P500
14:0	0.7 ± 0.0	0.6 ± 0.1	0.6 ± 0.1	0.5 ± 0.2	0.5 ± 0.1	0.6 ± 0.1	0.7 ± 0.0	0.7 ± 0.2	0.7 ± 0.3	0.7 ± 0.0	0.8 ± 0.1	0.6 ± 0.2
15:0		0.1 ± 0.0	0.1 ± 0.0	0.1 ± 0.0	0.1 ± 0.0	0.1 ± 0.0	0.1 ± 0.0	0.1 ± 0.0	0.1 ± 0.0	0.1 ± 0.0	0.1 ± 0.0	0.1 ± 0.0
16:0	8.6 ± 2.8	5.5 ± 1.3	9.6 ± 5.1	4.5 ± 2.9	3.2 ± 0.6	4.4 ± 0.5	6.1 ± 2.4	8.2 ± 4.1	8.3 ± 4.0	5.0 ± 1.0	7.9 ± 0.9	3.3 ± 0.3
17:0		0.1 ± 0.0	0.1 ± 0.0				0.1 ± 0.0			0.1 ± 0.0		
18:0	8.0 ± 3.1	5.0 ± 1.8	10.2 ± 6.0	4.0 ± 3.0	2.5 ± 0.5	3.9 ± 0.3	5.1 ± 2.9	7.9 ± 4.9	8.6 ± 4.3	3.5 ± 1.5	7.6 ± 1.1	2.8 ± 0.3
20:0	0.7 ± 0.0	0.1 ± 0.0	0.2 ± 0.1	0.1 ± 0.1	0.1 ± 0.0	0.1 ± 0.0	0.1 ± 0.0	0.1 ± 0.1	0.2 ± 0.1	0.1 ± 0.0	0.2 ± 0.0	0.1 ± 0.0
22:0	0.1 ± 0.0	0.1 ± 0.0	0.1 ± 0.0	0.1 ± 0.0	0.1 ± 0.0	0.1 ± 0.0	0.1 ± 0.0	0.1 ± 0.0	0.1 ± 0.0	0.1 ± 0.0	0.1 ± 0.0	0.1 ± 0.0
24:0	0.1 ± 0.0	0.1 ± 0.0	0.1 ± 0.0	0.1 ± 0.0	0.1 ± 0.0	0.1 ± 0.0	0.1 ± 0.0	0.1 ± 0.0	0.1 ± 0.0	0.1 ± 0.0	0.1 ± 0.0	0.1 ± 0.0
<b>SAFA</b>	<b>17.5 ± 5.9</b>	<b>11.5 ± 3.1</b>	<b>20.9 ± 11.2</b>	<b>9.2 ± 6.4</b>	<b>6.6 ± 1.2</b>	<b>9.2 ± 0.9</b>	<b>12.3 ± 5.4</b>	<b>17.1 ± 9.1</b>	<b>18.0 ± 8.7</b>	<b>9.5 ± 2.4</b>	<b>16.6 ± 2.0</b>	<b>6.8 ± 0.6</b>
16:1 <sub>n-9</sub>	0.1 ± 0.0	0.1 ± 0.0	0.1 ± 0.0	0.1 ± 0.0	0.1 ± 0.0	0.1 ± 0.0	0.2 ± 0.0	0.1 ± 0.1	0.2 ± 0.1	0.2 ± 0.0	0.2 ± 0.1	0.2 ± 0.0
16:1 <sub>n-7</sub>	1.8 ± 0.4	1.2 ± 0.2	1.1 ± 0.3	1.3 ± 0.4	1.2 ± 0.3	1.3 ± 0.4	1.8 ± 0.3	1.4 ± 0.5	1.0 ± 0.3	1.5 ± 0.2	1.6 ± 0.1	0.7 ± 0.2
18:1 <sub>n-9</sub>	1.3 ± 0.2	0.9 ± 0.0	0.9 ± 0.4	0.8 ± 0.4	0.6 ± 0.1	0.6 ± 0.1	1.3 ± 0.1	1.3 ± 0.3	0.9 ± 0.3	1.5 ± 0.1	1.2 ± 0.1	0.5 ± 0.0
18:1 <sub>n-7</sub>	0.4 ± 0.2	0.3 ± 0.1	0.3 ± 0.0	0.3 ± 0.2	0.3 ± 0.1	0.2 ± 0.0	0.4 ± 0.0	0.3 ± 0.1	0.3 ± 0.1	0.3 ± 0.0	0.3 ± 0.0	0.2 ± 0.0
22:1 <sub>n-9</sub>	0.1 ± 0.0											
<b>MUFA</b>	<b>3.6 ± 0.8</b>	<b>2.5 ± 0.2</b>	<b>2.4 ± 0.3</b>	<b>2.5 ± 1.0</b>	<b>2.2 ± 0.5</b>	<b>2.2 ± 0.5</b>	<b>3.7 ± 0.2</b>	<b>3.1 ± 0.8</b>	<b>2.4 ± 0.8</b>	<b>3.5 ± 0.3</b>	<b>3.4 ± 0.2</b>	<b>1.6 ± 0.2</b>
16:2 <sub>n-4</sub>	0.2 ± 0.1	0.1 ± 0.0	0.1 ± 0.0	0.2 ± 0.1	0.1 ± 0.0	0.1 ± 0.0	0.2 ± 0.0	0.2 ± 0.0	0.1 ± 0.0	0.1 ± 0.1	0.1 ± 0.0	0.1 ± 0.0
16:4 <sub>n-3</sub>	0.2 ± 0.0	0.1 ± 0.0	0.1 ± 0.0	0.1 ± 0.0	0.1 ± 0.1	0.1 ± 0.0	0.2 ± 0.0	0.1 ± 0.0	0.1 ± 0.0	0.1 ± 0.1	0.1 ± 0.0	0.1 ± 0.0
18:2 <sub>n-6</sub>	0.5 ± 0.1	0.4 ± 0.0	0.3 ± 0.1	0.4 ± 0.2	0.3 ± 0.1	0.2 ± 0.0	0.5 ± 0.0	0.5 ± 0.1	0.3 ± 0.1	0.5 ± 0.2	0.5 ± 0.1	0.3 ± 0.0
18:3 <sub>n-6</sub>	0.1 ± 0.0	0.1 ± 0.0	0.1 ± 0.0	0.1 ± 0.0	0.1 ± 0.0	0.1 ± 0.0	0.1 ± 0.0	0.1 ± 0.0	0.1 ± 0.0	0.1 ± 0.0	0.1 ± 0.0	0.1 ± 0.0
<b>18:3<sub>n-3</sub></b>	<b>0.4 ± 0.2</b>	<b>0.4 ± 0.0</b>	<b>0.3 ± 0.0</b>	<b>0.3 ± 0.1</b>	<b>0.3 ± 0.1</b>	<b>0.4 ± 0.1</b>	<b>0.5 ± 0.0</b>	<b>0.6 ± 0.1</b>	<b>0.5 ± 0.1</b>	<b>0.5 ± 0.2</b>	<b>0.7 ± 0.2</b>	<b>0.6 ± 0.0</b>
20:4 <sub>n-6</sub>	0.1 ± 0.0	0.1 ± 0.0	0.1 ± 0.0	0.1 ± 0.0	0.1 ± 0.0	0.1 ± 0.0	0.1 ± 0.0	0.1 ± 0.0	0.1 ± 0.0	0.1 ± 0.0	0.2 ± 0.1	0.1 ± 0.0
<b>20:5<sub>n-3</sub></b>	<b>0.5 ± 0.3</b>	<b>0.4 ± 0.1</b>	<b>0.4 ± 0.1</b>	<b>0.6 ± 0.2</b>	<b>0.5 ± 0.1</b>	<b>0.5 ± 0.1</b>	<b>0.8 ± 0.1</b>	<b>0.7 ± 0.1</b>	<b>0.5 ± 0.2</b>	<b>0.6 ± 0.4</b>	<b>0.9 ± 0.3</b>	<b>0.4 ± 0.0</b>
22:6 <sub>n-3</sub>		0.1 ± 0.0								0.1 ± 0.0		
<b>PUFA</b>	<b>1.8 ± 0.6</b>	<b>1.6 ± 0.2</b>	<b>1.3 ± 0.1</b>	<b>1.7 ± 0.6</b>	<b>1.6 ± 0.4</b>	<b>1.6 ± 0.2</b>	<b>2.4 ± 0.1</b>	<b>2.0 ± 0.2</b>	<b>1.5 ± 0.5</b>	<b>2.0 ± 1.0</b>	<b>2.5 ± 0.6</b>	<b>1.3 ± 0.0</b>
<b>Sum FA</b>	<b>23.0 ± 5.4</b>	<b>15.6 ± 2.7</b>	<b>24.5 ± 11.4</b>	<b>13.4 ± 8.0</b>	<b>10.4 ± 1.8</b>	<b>13.0 ± 1.6</b>	<b>18.3 ± 5.1</b>	<b>22.2 ± 9.5</b>	<b>21.9 ± 9.8</b>	<b>15.0 ± 2.6</b>	<b>22.6 ± 2.2</b>	<b>9.8 ± 0.6</b>

Results are presented in  $\mu\text{g}$  of compound per mg of biofilm dry weight ( $\pm\text{SE}$ ;  $n = 3$ ). Data in bold indicate the most important classes of fatty acids.

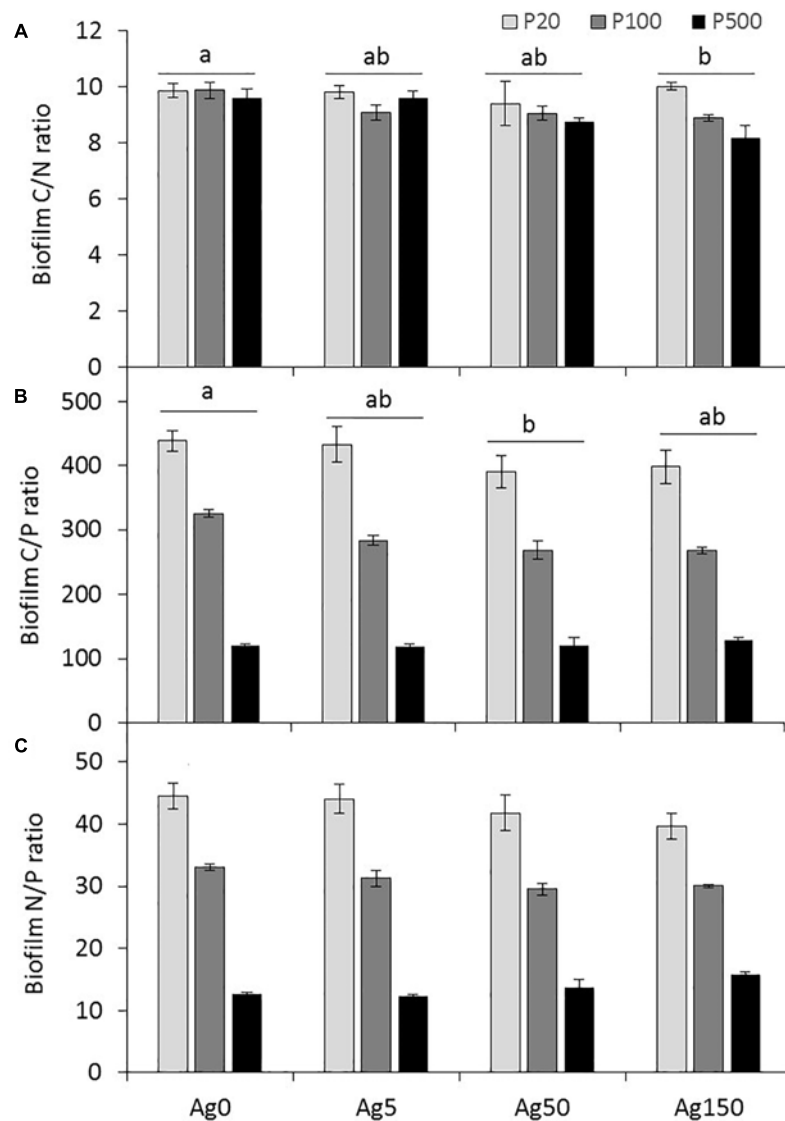


**FIGURE 2 | (A–C)** Elemental ratios (molar ratios) in biofilm biomass for the different P and Ag treatments. Significant differences due to Ag levels after *post hoc* Tukey tests are shown by different letters. No interactive effects were evidenced.

and adjusting the stoichiometry of the whole community to that of their resources (Danger et al., 2008). Unexpectedly, silver contamination also led to significant reductions of biofilm C:N and C:P ratios, even if these reductions remained low when compared to those observed along the P gradient. Data on the effects of contaminants on resources elemental compositions remain extremely scarce in the literature. Some previous studies showed that biofilms tend to increase their production of C-rich EPS as a response to contaminant exposure (García-Meza et al., 2005; Serra and Guasch, 2009; González et al., 2016). This physiological response, aimed at increasing the metal-binding sites of the biofilm, would thus be expected to increase biofilm C:nutrient ratios (Pannard et al., 2016). In our study, the opposite effects were observed. This result might thus alternatively be explained by the large Ag-induced shifts in prokaryotic and

microeukaryotic community structures observed in our study (see Leflaive et al., 2015). One could expect that different species with different luxury consumption capabilities might be selected by Ag contamination. Another potential, non-exclusive, explanation could be that organisms stressed by the Ag contamination tend to increase their antitoxic defenses, these defenses generally relying on N-rich enzymes and leading to apparent lower biofilm C:N ratios.

### Effects of P and Ag on Biofilm Fatty Acid Profiles

Some fatty acids, and especially long-chain PUFAs have been described as pertinent indicators of resources quality. Indeed, most metazoans are unable to (or, at least, not in sufficient

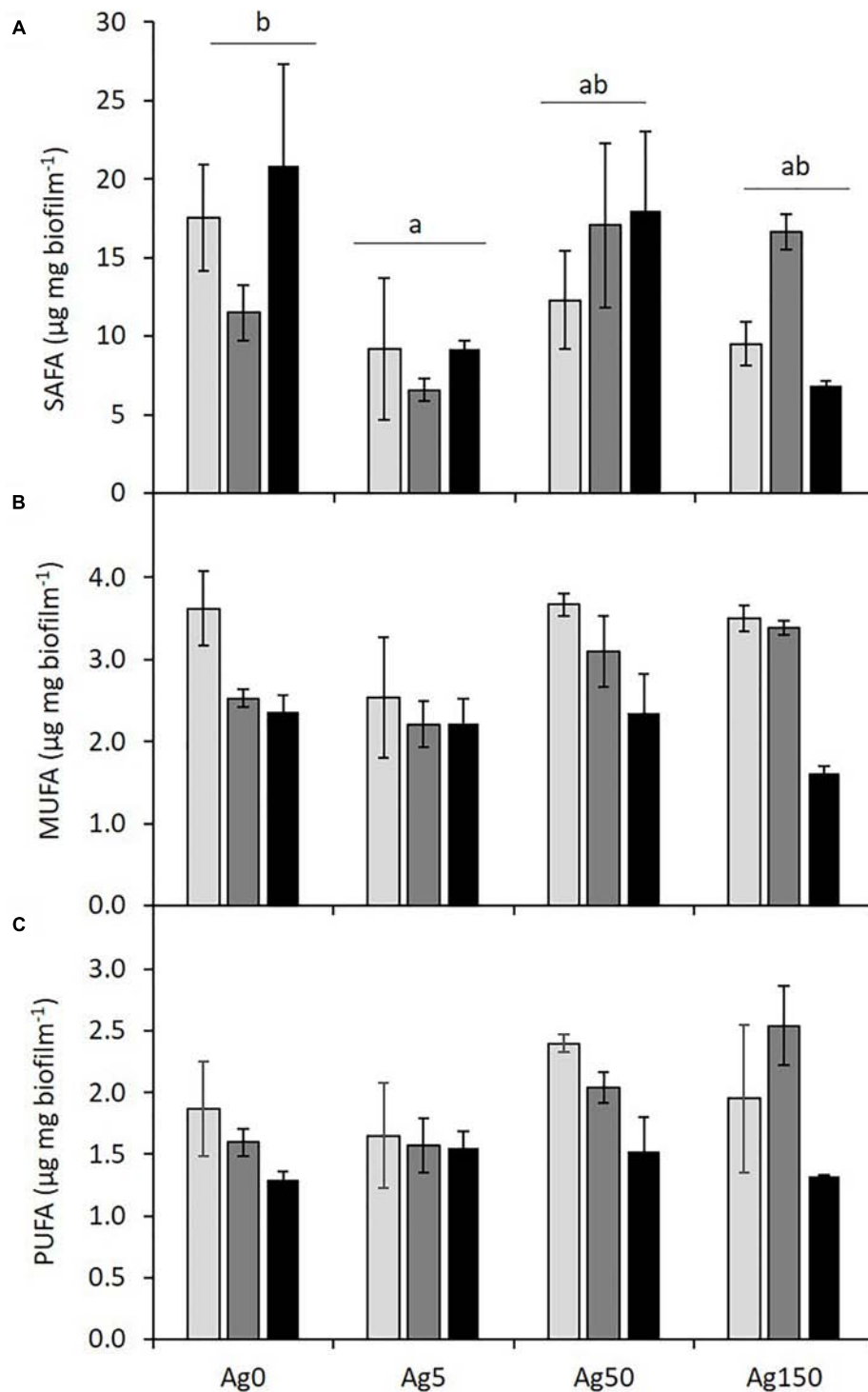


**FIGURE 3** | Biofilm contents ( $\mu\text{g mg}^{-1}$ ) of saturated (SAFA, **A**), monounsaturated (MUFA, **B**), and polyunsaturated (PUFA, **C**) fatty acids for the different P and Ag level tested. Significant differences due to Ag levels after *post hoc* Tukey tests are shown by different letters. No interactive effects were evidenced.

amounts) synthesize these essential compounds that must be found in their diet. These compounds are notably involved in the synthesis of key hormones and represent important molecules in cell membranes, controlling in particular membrane fluidity

(Arts et al., 2009). In algal communities, diatoms are known to produce high amounts of long chain PUFAs (20:5 $\omega$ 3, Dunstan et al., 1994) in comparison with green algae and cyanobacteria that mainly produce shorter chain PUFAs (Masclaux et al., 2009)

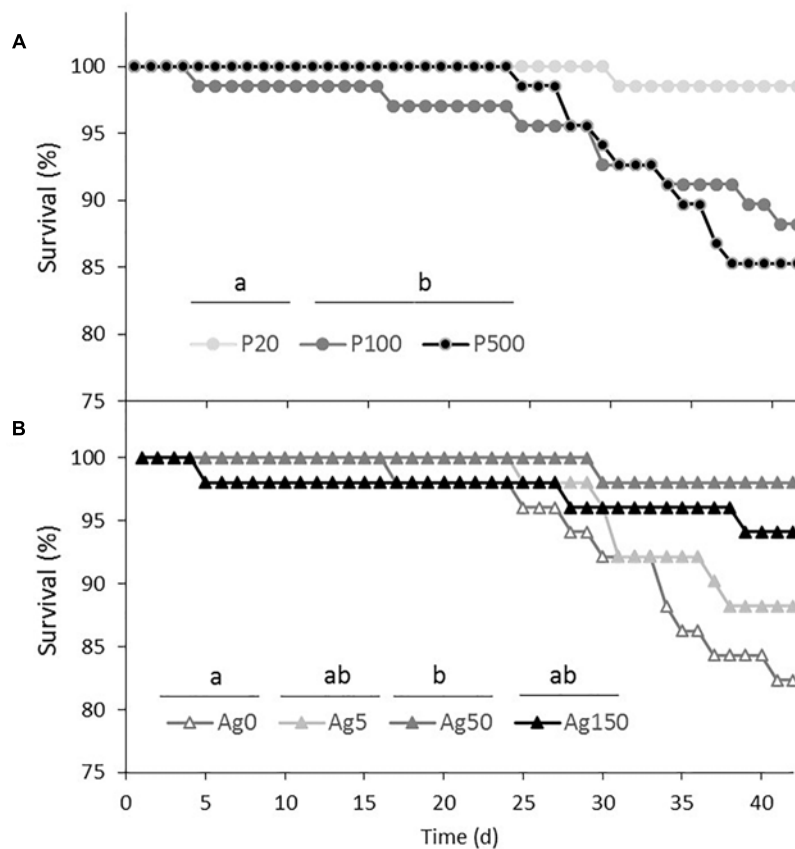
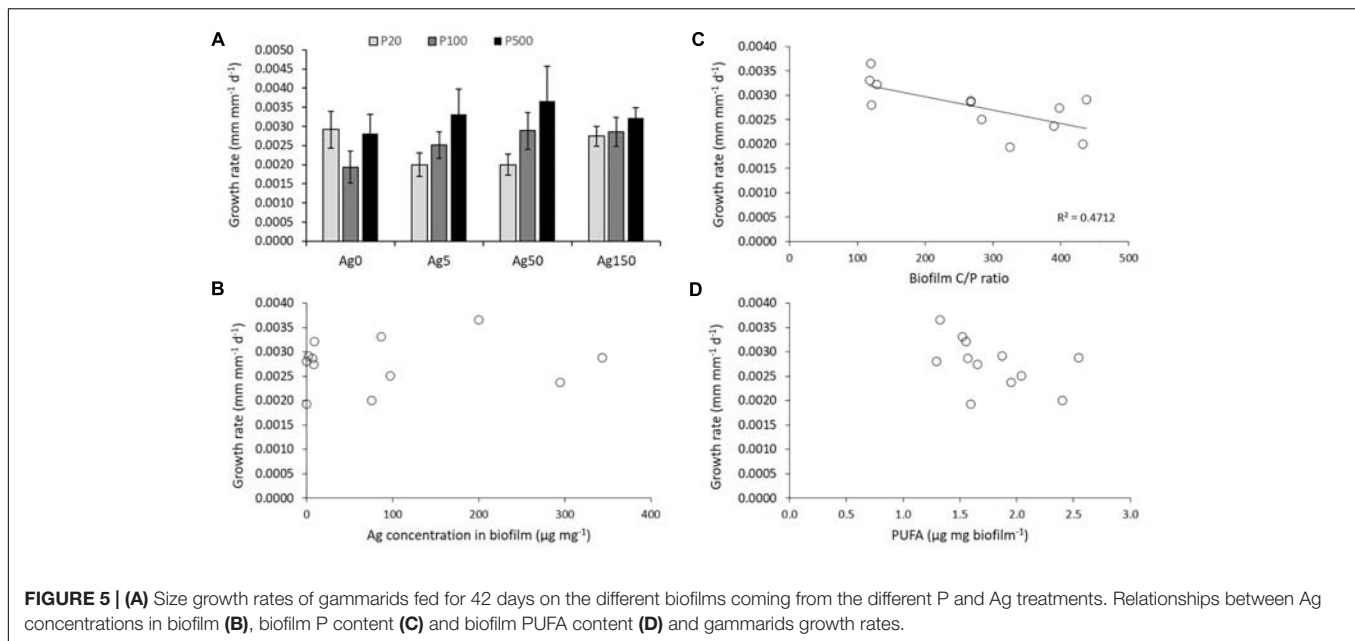


**FIGURE 4 |** Survival curves of gammarids fed for 42 days with the different biofilms. Data represent cumulative survival of **(A)** all gammarids fed with biofilms coming from the P20, P100, and P500 treatments, whatever the Ag level, and **(B)** of all gammarids fed with biofilms coming from the Ag0, Ag5, Ag50, and Ag150 treatments, whatever the P level (see “Materials and Methods” section for justification). The different letters above the treatment names indicate significant differences in the survival curves after two by two curves comparisons, and Bonferroni corrections of the threshold  $p$ -values accounting for the multiple comparisons.

or are unable to synthesize highly unsaturated fatty-acids (Muller-Navarra et al., 2004), respectively. In the present study, both Ag contamination and P concentrations greatly altered algal communities, reducing diatoms proportion and increasing green algae proportions (see Leflaive et al., 2015, **Figure 1**). Both P and Ag stressors led to similar effects, without acting interactively. Thus, reductions in biofilm PUFA and 20:5 $\omega$ 3 content were expected for both stressors. In the present study, only the P increase led to significant reductions in these compounds. Surprisingly, we did not observe any significant effect of silver on biofilm PUFA and 20:5 $\omega$ 3 contents. In contrast, silver contamination significantly modified biofilm SAFA and the total amount of fatty acids, these parameters reaching their minimal values for an exposure to 5  $\mu\text{g Ag L}^{-1}$ . The effect of P level on biofilm fatty acid profiles can certainly be explained by the replacement of 20:5 $\omega$ 3-rich diatoms by green algae, as already observed in diverse studies dealing with natural communities (e.g., Muller-Navarra et al., 2004; Bec et al., 2010). The absence of silver effect on biofilm PUFA and 20:5 $\omega$ 3 contents, despite the replacement of diatoms by green algae, could be explained either by the replacement of some diatom species by other diatom species containing more PUFAs or by an increase of diatoms’

PUFA content as a response to Ag contamination. However, Ag and P stressors led to similar changes in biofilm community compositions (Leflaive et al., 2015), both communities showing similar reductions in the abundance of the dominant diatom species (*Achnanthis minutissima*, Kützing and *Cymbella excisa*, Kützing). The second explanation thus appears as the most probable. Even if data remain scarce in the literature, such an effect of fatty acid synthesis deregulation was already found in the macroalgae *Fucus* sp. exposed to copper (Smith et al., 1985). Similarly, some studies showed that fatty acid profiles of unicellular organisms (Green algae: McLarnon-Riches et al., 1998; Diatom: Jones et al., 1987; Euglenophyceae: Rocchetta et al., 2006) were susceptible to change after an exposure to metals. Yet, there is still no consensus on the toxic metals effects on algae fatty acids profiles, some studies showing reductions in long chain PUFAs due to reductions in their abundance or synthesis caused by oxidative stress (Rocchetta et al., 2006), while other studies showed increases in algal PUFAs after alterations of enzymatic activities (McLarnon-Riches et al., 1998). The precise understanding of silver impacts on biofilm fatty acid contents would greatly benefit from specific investigations of fatty acid synthesis on algal communities.



## Effects of P and Ag on Biofilm Quality for an Invertebrate Consumer

While biofilm Ag, nutrients, and PUFA concentrations remain only potential quality parameters for biofilm consumers, measuring the impacts of biofilms consumption on metazoans is the only way for evaluating the effective quality of biofilms, and anticipate the indirect effects of the multiple stressors selected (Ag and P) on higher trophic levels. Consumers' growth measurements have been shown as a powerful mean for evaluating resources quality. In particular, effects of resources stoichiometry and/or highly unsaturated fatty acids on consumers' growth have already been successfully tested on planktonic and terrestrial herbivores (e.g., Elser et al., 2001; Schade et al., 2003; Masclaux et al., 2009). More recently, such effects have been revealed in the crustacean species, *Gammarus fossarum*, both for the effect of resources P (Danger et al., 2013) and highly unsaturated fatty acid contents (Crenier et al., 2017). In the present study, biofilm C:P ratios were significantly related to *G. fossarum* growth, growth being reduced when organisms were fed with the highest C:P ratio resources. Organisms P content being directly related to organisms' nucleic acid production and cell proliferation (Elser et al., 2003), eating low C:P resources can help organisms to overcome P limitations of their growth. Changes in microbial biomass PUFA and 20:5 $\omega$ 3 contents induced by biofilm exposure to high P concentrations, while significant, were too small for detecting any significant effect on consumers' growth. Finally, contrary to expectations, accumulation of Ag in biofilm biomass had strictly no influence on consumers' growth. Yet, some studies showed that toxicity of Ag on zooplankton species could be higher via trophic transfer than by direct uptake from water (Hook and Fisher, 2001; Bielmyer et al., 2006). In contrast, other studies suggested that Ag toxicity was very variable depending on water chemistry, and that free ionic silver was the most toxic form to

invertebrates (Ratte, 1999). In our study, elemental quality of resources seemed thus to be more important than biofilm silver concentration for *G. fossarum*. However, it must be noted that responses could have been different if other life history traits had been considered. For example, PUFA concentrations have been regularly shown to control organisms' reproduction (e.g., Masclaux et al., 2009), and multiple stressor effects might also impact organisms reproduction.

Finally, it must be noted that in contrast to the observed stimulation of *G. fossarum* growth, our results also showed a low but significant negative effect of P on organisms' survival. Such an effect has already been observed in another study (Arce-Funck et al., 2018). It was proposed that higher growth rates generated by higher resource quality increases molting frequency. Yet, molting is by far the most sensitive stage of molting organisms' development, especially when exposed to contaminants (McCahon and Pascoe, 1988). Stimulation of organisms' growth thus generally co-occur with an increase in organisms' mortality. In contrast, the highest survival found for Ag-fed gammarids is more difficult to explain. One could imagine a stimulation of immune defenses of gammarids or a reduction of potentially pathogenic bacteria growing in biofilms. Such effects yet remains to be tested.

## CONCLUSION

To conclude, our results showed that both P and Ag impacted several biofilm quality parameters, but never interactively. The use of *G. fossarum* growth experiment permitted to verify the consequences of microbial resources potential quality. In this study, resources C:P was the most important parameter. Similar studies would be required to understand in more details the indirect effects multiple stressors might play on microorganisms consumers and, in turn, on ecosystem functioning.

## AUTHOR CONTRIBUTIONS

MD, AB, VF, LT-H, and JL designed the experiments. CC, JL, JF, and KS-T carried out the experiments. CC, AG, FP, and JF carried out chemical analyses. All authors contributed to the writing of the manuscript.

## FUNDING

This project was partly funded by the ICARE EC2CO program to MD and the ANR Multistress (ANR-13-BSV7-0004-01). MD

## REFERENCES

- AFNOR (1990). *Eaux, Méthodes D'essais: Recueil De Normes Françaises*. Paris: Association Française de Normalisation.
- Arce Funck, J., Clivot, H., Felten, V., Rousselle, P., Guérol, F., and Danger, M. (2013a). Phosphorus availability modulates the toxic effect of silver on aquatic fungi and leaf litter decomposition. *Aquat. Tox.* 144–145, 199–207. doi: 10.1016/j.aquatox.2013.10.001
- Arce Funck, J., Danger, M., Gismondi, E., Cossu-Leguille, C., Guérol, F., and Felten, V. (2013b). Behavioural and physiological responses of *Gammarus fossarum* (Crustacea Amphipoda) exposed to silver. *Aquat. Tox.* 14, 73–84. doi: 10.1016/j.aquatox.2013.07.012
- Arce-Funck, J., Crenier, C., Danger, M., Billoir, E., Usseglio-Polatera, P., and Felten, V. (2018). High stoichiometric food quality increases moulting organism vulnerability to pollutant impacts: an experimental test with *Gammarus fossarum* (Crustacea: Amphipoda). *Sci. Total Environ.* 645, 1484–1495. doi: 10.1016/j.scitotenv.2018.07.227
- Arce-Funck, J., Crenier, C., Danger, M., Cossu-Leguille, C., Guérol, F., and Felten, V. (2016). Stoichiometric constraints modulate impacts of silver contamination on stream detritivores: an experimental test with *Gammarus fossarum*. *Freshw. Biol.* 61, 2075–2089. doi: 10.1111/fwb.12785
- Arts, M. T., Brett, M. T., and Kainz, M. (2009). *Lipids in Aquatic Ecosystems*. Berlin: Springer Science & Business Media.
- Baird, D. J., and Van den Brink, P. J. (2007). Using biological traits to predict species sensitivity to toxic substances. *Ecotox. Environ. Safe* 67, 296–301. doi: 10.1016/j.ecoenv.2006.07.001
- Battin, T. J., Kaplan, L. A., Newbold, J. D., and Hansen, C. M. E. (2003). Contributions of microbial biofilms to ecosystem processes in stream mesocosms. *Nature* 426, 439–442. doi: 10.1038/nature02152
- Bec, A., Perga, M.-E., Desvillettes, C., and Bourdier, G. (2010). How well can the fatty acid content of lake seston be predicted from its taxonomic composition? *Freshw. Biol.* 55, 1958–1972. doi: 10.1111/j.1365-2427.2010.02429.x
- Bielmyer, G. K., Grosell, M., and Brix, K. V. (2006). Toxicity of silver, zinc, copper, and nickel to the copepod *Acartia tonsa* exposed via a phytoplankton diet. *Environ. Sci. Technol.* 40, 2063–2068. doi: 10.1021/es051589a
- Crenier, C. (2017). *Vers Une Réévaluation Des Facteurs Limitant La Production Biologique Dans Les Cours D'eau De Tête De Bassin Versant : Nutriments, Acides Gras Ou Qualité Du Carbone Détritique ?*. Ph D. thesis dissertation. University of Lorraine, France.
- Crenier, C., Arce-Funck, J., Bec, A., Billoir, E., Perrière, F., Leflaive, J., et al. (2017). Minor food sources can play a major role in secondary production in detritus-based ecosystems. *Freshw. Biol.* 62, 1155–1167. doi: 10.1111/fwb.12933
- Danger, M., Arce Funck, J., Devin, S., Heberlé, J., and Felten, V. (2013). Phosphorus content in detritus controls life history traits of a detritivore. *Funct. Ecol.* 27, 807–815. doi: 10.1111/1365-2435.12079
- Danger, M., Cornut, J., Elger, A., and Chauvet, E. (2012). Effects of burial on leaf litter quality, microbial conditioning and palatability to three shredder taxa. *Freshw. Biol.* 57, 1017–1030. doi: 10.1111/j.1365-2427.2012.02762.x
- Danger, M., Daufresne, T., Lucas, F., Pissart, S., and Lacroix, G. (2008). Does Liebig's law of the minimum scale up from species to communities? *Oikos* 117, 1741–1751. doi: 10.1111/j.1600-0706.2008.16793.x
- acknowledges the financial support of the Institut Universitaire de France (IUF). AG thanks the Postdoctoral program of the Universidad de Las Palmas de Gran Canaria.
- Droop, M. R. (1974). The nutrient status of algal cells in continuous culture. *J. Mar. Biol. Assoc. U. K.* 54, 825–855. doi: 10.1017/S002531540005760X
- Dunstan, G. A., Volkman, J. K., Barrett, S. M., Leroi, J. M., and Jeffrey, S. W. (1994). Essential polyunsaturated fatty acids from 14 species of diatom (Bacillariophyceae). *Phytochemistry* 35, 155–161. doi: 10.1016/S0031-9422(00)90525-9
- EEA (2014). *Nutrients in Freshwater (CSI 020) - Assessment Created September 2014*. EEA Core Set Indicator no. 20, European Environment Agency. Available at: <https://www.eea.europa.eu/soer-2015/europe/freshwater> (accessed February 18, 2015)
- Elser, J. J., Acharya, K., Kyle, M., Cotner, J., Makino, W., Markow, T., et al. (2003). Growth rate-stoichiometry couplings in diverse biota. *Ecol. Lett.* 6, 936–943. doi: 10.1046/j.1461-0248.2003.00518.x
- Elser, J. J., and Bennett, E. (2011). Phosphorus cycle: a broken biogeochemical cycle. *Nature* 478, 29–31. doi: 10.1038/478029a
- Elser, J. J., Hayakawa, K., and Urabe, J. (2001). Nutrient limitation reduces food quality for zooplankton: daphnia response to seston phosphorus enrichment. *Ecology* 82, 898–903. doi: 10.2307/2680208
- Falkowski, P., Scholes, R. J., Boyle, E., Canadell, J., Canfield, D., Elser, J., et al. (2000). The global carbon cycle: a test of our knowledge of earth as a system. *Science* 290, 291–296. doi: 10.1126/science.290.5490.291
- Folch, J., Lees, M., and Stanley, H. S. (1957). A simple method for the isolation and purification of total lipids from animal tissues. *J. Biol. Chem.* 226, 497–509.
- Frost, P. C., and Elser, J. J. (2002). Growth responses of littoral mayflies to the phosphorus content of their food. *Ecol. Lett.* 5, 232–240. doi: 10.1046/j.1461-0248.2002.00307.x
- García-Meza, J. V., Barranguet, C., and Admiraal, W. (2005). Biofilm formation by algae as a mechanism for surviving on mine tailings. *Environ. Toxicol. Chem.* 24, 573–581. doi: 10.1897/04-064R.1
- Geranio, L., Heuberger, M., and Nowack, B. (2009). The behavior of silver nanotextiles during washing. *Environ. Sci. Tech.* 43, 8113–8118. doi: 10.1021/es901833z
- González, A. G., Fernández-Rojo, L., Leflaive, J., Pokrovsky, O. S., and Rols, J. L. (2016). Response of three biofilm-forming benthic microorganisms to Ag nanoparticles and Ag<sup>+</sup>: the diatom *Nitzschia palea*, the green alga *Uronema confervicolum* and the cyanobacteria *Leptolyngbya* sp. *Environ. Sci. Pollut. Res.* 23, 22136–22150. doi: 10.1007/s11356-016-7259-z
- González, A. G., Mombo, S., Leflaive, J., Lamy, A., Pokrovsky, O. S., and Rols, J. L. (2015). Silver nanoparticles impact phototrophic biofilm communities to a considerably higher degree than ionic silver. *Environ. Sci. Pollut. Res.* 22, 8412–8424. doi: 10.1007/s11356-014-3978-1
- Gottschalk, F., Sonderer, T., Scholz, R. W., and Nowack, B. (2009). Modeled environmental concentrations of engineered nanomaterials (TiO<sub>2</sub>, ZnO, Ag, CNT, fullerenes) for different regions. *Environ. Sci. Tech.* 43, 9216–9222. doi: 10.1021/es9015553
- Guasch, H., Navarro, E., Serra, A., and Sabater, S. (2004). Phosphate limitation influences the sensitivity to copper in periphytic algae. *Freshw. Biol.* 49, 463–473. doi: 10.1111/j.1365-2427.2004.01196.x
- Hook, S. E., and Fisher, N. S. (2001). Sublethal effects of silver in zooplankton: importance of exposure pathways and implications for toxicity testing. *Environ. Toxicol. Chem.* 20, 568–574. doi: 10.1002/etc.5620200316

## ACKNOWLEDGMENTS

This manuscript is a part of the Ph.D. thesis of CC (Crenier, 2017), funded by the French Ministry of Education and Research. We greatly thank P. Rousselle for his technical support and the reviewers for their comments that helped to improve manuscript clarity.

- Jones, G. J., Nichols, P. D., Johns, R. B., and Smith, J. D. (1987). The effect of mercury and cadmium on the fatty acid and sterol composition of the marine diatom *Asterionella glacialis*. *Phytochemistry* 26, 1343–1348. doi: 10.1016/S0031-9422(00)81809-9
- Kilham, S. S., Kreeger, D. A., Lynn, S. G., Goulden, C. E., and Herrera, L. (1998). COMBO: a defined freshwater culture medium for algae and zooplankton. *Hydrobiologia* 377, 147–159. doi: 10.1023/A:1003231628456
- Leflaive, J., Felten, V., Ferriol, J., Lamy, A., Ten-Hage, L., Bec, A., et al. (2015). Community structure and nutrient level control the tolerance of autotrophic biofilm to silver contamination. *Environ. Sci. Pollut. Res.* 22, 13739–13752. doi: 10.1007/s11356-014-3860-1
- Liess, A., and Hillebrand, H. (2006). Role of nutrient supply in grazer-periphyton interactions: reciprocal influences of periphyton and grazer nutrient stoichiometry. *J. N. Am. Benthol. S.* 25, 632–642. doi: 10.1899/0887-3593(2006)25[632:RONSIG]2.0.CO;2
- Luoma, S. N. (2008). Silver nanotechnologies and the environment: old problems or new challenges? *Proj. Emerg. Nanotechnol.* 15:66.
- Luoma, S. N., and Rainbow, P. S. (2008). *Metal Contamination in Aquatic Environments: Science and Lateral Management*. Cambridge: Cambridge University Press.
- Lyon, D. R., and Ziegler, S. E. (2009). Carbon cycling within epilithic biofilm communities across a nutrient gradient of headwater streams. *Limnol. Oceanogr.* 54, 439–449. doi: 10.4319/lo.2009.54.2.0439
- Maramba-Jones, C., and Hoek, E. M. V. (2010). A review of the antibacterial effects of silver nanomaterials and potential implications for human health and the environment. *J. Nanopart. Res.* 12, 1531–1551. doi: 10.1007/s11051-010-9900-y
- Masclaux, H., Bec, A., Kainz, M. J., Desvillettes, C., Jouve, L., and Bourdier, G. (2009). Combined effects of food quality and temperature on somatic growth and reproduction of two freshwater cladocerans. *Limnol. Oceanogr.* 54, 1323–1332. doi: 10.4319/lo.2009.54.4.1323
- McCahon, C. P., and Pascoe, D. (1988). Cadmium toxicity to the freshwater amphipod *Gammarus pulex* (L.) during the moult cycle. *Freshw. Biol.* 19, 197–203. doi: 10.1111/j.1365-2427.1988.tb00342.x
- McLarnon-Riches, C. J., Rolph, C. E., Greenway, D. L., and Robinson, P. K. (1998). Effects of environmental factors and metals on *Selenastrum capricornutum* lipids. *Phytochemistry* 49, 1241–1247. doi: 10.1016/S0031-9422(98)00095-8
- Muller-Navarra, D. C., Brett, M. T., Park, S., and Chandra, S. (2004). Unsaturated fatty acid content in seston and tropho-dynamic coupling in lakes. *Nature* 427, 69–72. doi: 10.1038/nature02210
- Murdock, J. N., Shields, F. D. Jr., and Lizotte, R. E. Jr. (2013). Periphyton responses to nutrient and atrazine mixtures introduced through agricultural runoff. *Ecotoxicology* 22, 215–230. doi: 10.1007/s10646-012-1018-9
- Murdock, J. N., and Wetzel, D. L. (2012). Macromolecular response of individual algal cells to nutrient and atrazine mixtures within biofilms. *Microbial. Ecol.* 63, 761–772. doi: 10.1007/s00248-011-9994-5
- Nriagu, J. O., and Pacyna, J. M. (1988). Quantitative assessment of worldwide contamination of air, water and soils by trace metals. *Nature* 333, 134–139. doi: 10.1038/333134a0
- Pannard, A., Pédrone, J., Bormans, M., Briand, E., Claquin, P., and Lagadeuc, Y. (2016). Production of exopolymers (EPS) by cyanobacteria: impact on the carbon-to-nutrient ratio of the particulate organic matter. *Aquat. Ecol.* 50, 29–44. doi: 10.1007/s10452-015-9550-3
- Project on Emerging Nanotechnology (2012). *Consumer Products Inventories for Nanotechnology Products*. Available at: [http://www.nanotechproject.org/events/archive/first\\_nanotechnology\\_consumer\\_products/](http://www.nanotechproject.org/events/archive/first_nanotechnology_consumer_products/) (accessed March 10, 2006)
- Ratte, H. T. (1999). Bioaccumulation and toxicity of silver compounds: a review. *Environ. Toxicol. Chem.* 18, 89–108. doi: 10.1007/978-3-319-72041-8\_17
- Rattner, B. A., and Heath, A. G. (2003). “Environmental factors affecting contaminant toxicity in aquatic and terrestrial vertebrates,” in *Handbook of Ecotoxicology*, eds D. J. Hoffman, B. A. Rattner, G. A. Burton Jr., and J. Cairns Jr. (Boca Raton, FL: Lewis Publishers), 679–699.
- Rocchetta, I., Mazzuca, M., Conforti, V., Ruiz, L., Balzaretta, V., and Ríos de Molina, M. C. (2006). Effect of chromium on the fatty acid composition of two strains of *Euglena gracilis*. *Environ. Pollut.* 141, 353–358. doi: 10.1016/j.envpol.2005.08.035
- Sanpera-Calbet, I., Ylla, I., Romani, A. M., Sabater, S., and Muñoz, I. (2017). Drought effects on resource quality in a Mediterranean stream: fatty acids and sterols as indicators. *Limnetica* 36, 29–43.
- Schade, J. D., Kyle, M., Hobbie, S. E., Fagan, W. A., and Elser, J. J. (2003). Stoichiometric tracking of soil nutrients by a desert insect herbivore. *Ecol. Lett.* 6, 96–101. doi: 10.1046/j.1461-0248.2003.00409.x
- Serra, A., and Guasch, H. (2009). Effects of chronic copper exposure on fluvial systems: linking structural and physiological changes of fluvial biofilms with the in-stream copper retention. *Sci. Total Environ.* 407, 5274–5282. doi: 10.1016/j.scitotenv.2009.06.008
- Serra, A., Guasch, H., Admiraal, W., Van der Geest, H. G., and Van Beusekom, S. A. M. (2010). Influence of phosphorus on copper sensitivity of fluvial periphyton: the role of chemical, physiological and community-related factors. *Ecotoxicology* 19, 770–780. doi: 10.1007/s10646-009-0454-7
- Skei, J., Larsson, P., Rosenberg, R., Jonsson, P., Olsson, M., and Broman, D. (2000). Eutrophication and contaminants in aquatic ecosystems. *AMBIO* 29, 184–194. doi: 10.1579/0044-7447-29.4.184
- Smith, K. L., Bryan, G. W., and Harwood, J. L. (1985). Changes in endogenous fatty acids and lipid synthesis associated with copper pollution in *Fucus* spp. *J. Exp. Bot.* 36, 663–669. doi: 10.1093/jxb/36.4.663
- Smith, V. H., Tilman, G. D., and Ninkola, J. C. (1999). Eutrophication: impacts of excess nutrient inputs on freshwater, marine, and terrestrial ecosystems. *Environ. Pollut.* 100, 179–196. doi: 10.1016/S0269-7491(99)00091-3
- Sterner, R. W., and Elser, J. J. (2002). *Ecological Stoichiometry: The Biology of Elements From Molecules to the Biosphere*. Princeton, NJ: Princeton University Press.
- Tlili, A., Bérard, A., Roulier, J.-L., Volata, B., and Montuelle, B. (2010). PO4<sup>3-</sup> dependence of the tolerance of autotrophic and heterotrophic biofilm communities to copper and diuron. *Aquat. Tox.* 98, 165–177. doi: 10.1016/j.aquatox.2010.02.008
- van Hullebusch, E. D., Zandvoort, M. H., and Lens, P. N. (2003). Metal immobilisation by biofilms: mechanisms and analytical tools. *Rev. Environ. Sci. Bio.* 2, 9–33. doi: 10.1023/B:RESB.0000022995.48330.55
- Wetzel, R. G. (1983). “Opening remarks,” in *Periphyton of Freshwater Ecosystems*, ed. R. G. Wetzel (The Hague: Dr W. Junk Publisher). doi: 10.1007/978-94-009-7293-3

**Conflict of Interest Statement:** The authors declare that the research was conducted in the absence of any commercial or financial relationships that could be construed as a potential conflict of interest.

Copyright © 2019 Crenier, Sanchez-Thirion, Bec, Felten, Ferriol, González, Leflaive, Perrière, Ten-Hage and Danger. This is an open-access article distributed under the terms of the Creative Commons Attribution License (CC BY). The use, distribution or reproduction in other forums is permitted, provided the original author(s) and the copyright owner(s) are credited and that the original publication in this journal is cited, in accordance with accepted academic practice. No use, distribution or reproduction is permitted which does not comply with these terms.



# Microbial Ecotoxicology of Marine Plastic Debris: A Review on Colonization and Biodegradation by the “Plastisphere”

Justine Jacquin<sup>1</sup>, Jingguang Cheng<sup>1</sup>, Charlène Odobel<sup>1</sup>, Caroline Pandin<sup>1</sup>, Pascal Conan<sup>1</sup>, Mireille Pujo-Pay<sup>1</sup>, Valérie Barbe<sup>1,2</sup>, Anne-Leila Meistertzheim<sup>1,3</sup> and Jean-François Ghiglione<sup>1\*</sup>

<sup>1</sup> UMR 7621, CNRS, Laboratoire d’Océanographie Microbienne, Observatoire Océanologique de Banyuls-sur-Mer, Sorbonne Université, Banyuls-sur-Mer, France, <sup>2</sup> Génomique Métabolique, Genoscope, Institut de Biologie François Jacob, Commissariat à l’Énergie Atomique (CEA), CNRS, Université Evry, Université Paris-Saclay, Évry, France, <sup>3</sup> Plastic@Sea, Observatoire Océanologique de Banyuls-sur-Mer, Banyuls-sur-Mer, France

## OPEN ACCESS

### Edited by:

Michail M. Yakimov,  
Italian National Research Council  
(CNR), Italy

### Reviewed by:

Irene Wagner-Doebler,  
Helmholtz Center for Infection  
Research (HZ), Germany  
Eduardo Puglisi,  
University Cattolica del Sacro Cuore,  
Italy

### \*Correspondence:

Jean-François Ghiglione  
ghiglione@obs-banyuls.fr

### Specialty section:

This article was submitted to  
Microbiotechnology, Ecotoxicology  
and Bioremediation,  
a section of the journal  
Frontiers in Microbiology

**Received:** 12 September 2018

**Accepted:** 04 April 2019

**Published:** 25 April 2019

### Citation:

Jacquin J, Cheng J, Odobel C,  
Pandin C, Conan P, Pujo-Pay M,  
Barbe V, Meistertzheim AL and  
Ghiglione J-F (2019) Microbial  
Ecotoxicology of Marine Plastic  
Debris: A Review on Colonization  
and Biodegradation by  
the “Plastisphere”.  
*Front. Microbiol.* 10:865.  
doi: 10.3389/fmicb.2019.00865

Over the last decades, it has become clear that plastic pollution presents a global societal and environmental challenge given its increasing presence in the oceans. A growing literature has focused on the microbial life growing on the surfaces of these pollutants called the “plastisphere,” but the general concepts of microbial ecotoxicology have only rarely been integrated. Microbial ecotoxicology deals with (i) the impact of pollutants on microbial communities and inversely (ii) how much microbes can influence their biodegradation. The goal of this review is to enlighten the growing literature of the last 15 years on microbial ecotoxicology related to plastic pollution in the oceans. First, we focus on the impact of plastic on marine microbial life and on the various functions it ensures in the ecosystems. In this part, we also discuss the driving factors influencing biofilm development on plastic surfaces and the potential role of plastic debris as vector for dispersal of harmful pathogen species. Second, we give a critical view of the extent to which marine microorganisms can participate in the decomposition of plastic in the oceans and of the relevance of current standard tests for plastic biodegradability at sea. We highlight some examples of metabolic pathways of polymer biodegradation. We conclude with several questions regarding gaps in current knowledge of plastic biodegradation by marine microorganisms and the identification of possible directions for future research.

**Keywords:** bacteria, marine plastics debris, colonization, biodegradation, metabolic pathways

## INTRODUCTION

The amount of land-based plastic debris entering the ocean is estimated at 4.8 to 12.7 million tons per years (Jambeck et al., 2015). It is so important that plastic is regarded as a marker of the Anthropocene (Duis and Coors, 2016; Zalasiewicz et al., 2016). A growing body of research has investigated plastic distribution (Willis et al., 2017; Worm et al., 2017) and toxicity for marine fauna (Bakir et al., 2014; Gewert et al., 2015). A comparatively smaller but growing literature has been devoted to the microbial ecotoxicology of marine plastic debris, i.e. (1) the impact of plastic on marine microbial life together with the various ecosystem services that marine microbial life

ensures and inversely, (2) the role of microorganisms in the degradation of ocean plastic (Ghiglione et al., 2014, 2016). Both aspects will be successively explored by this review, which covers the last 15 years of literature.

The investigation of microorganisms colonizing plastic surfaces using modern techniques of massive DNA sequencing (Zettler et al., 2013) was introduced only recently. The authors introduced the world “plastisphere” to describe the microbial life growing on these surfaces. They also detected members of the potentially pathogenic genus *Vibrio*, which may be dispersed over long distances by floating persistent plastics. Since then, several studies investigated various marine environments, such as the North Pacific Gyre (Debroas et al., 2017) or the Mediterranean Sea (Dussud et al., 2018a). In parallel, a growing literature described the first steps of colonization of new plastic until the formation of a mature biofilm (Lobelle and Cunliffe, 2011; Oberbeckmann et al., 2015; Dussud et al., 2018a).

Such knowledge is of great interest to better understand the impact of plastic on marine microbial life and ecosystem functions. Only one study so far used shotgun metagenomics, showing that plastic-inhabiting microbes present an enriched gene repertoire compared to microbes living in the surrounding waters (Bryant et al., 2016). In this review, we argue that current knowledge is insufficient to draw a clear picture of the impact of plastic on marine microbial life and ecosystem functions, and we propose several directions for further studies in this field (see section “Microorganisms Colonizing Plastic at Sea”).

The role of microbes on plastic degradation in the ocean is a second subject of concern. Very recently, an excellent comprehensive review concluded that “current international standards and regional test methods are insufficient in their ability to realistically predict the biodegradability of carrier bags in marine environment, due to several shortcomings in experimental procedures and a paucity of information in the scientific literature” (Harrison et al., 2018). The capability of microorganisms to biodegrade plastic was reported for numerous bacterial strains (Krueger et al., 2015). Fungi also have the capability to biodegrade plastics, but most of the studies were conducted in terrestrial conditions (Cosgrove et al., 2007; Koitabashi et al., 2012; Gajendiran et al., 2016; Magnin et al., 2018) whereas very few studies so far exist in marine conditions (Gonda et al., 2000; Pramila and Ramesh, 2011). Moreover, most of these studies were based on the selection and testing of single strains in laboratory conditions, which is very far from environmental conditions. In this review, we underscore the knowledge gaps on plastic biodegradation by marine microorganisms and we attempt to identify possible directions for future research in this area (see section “How Much Can Microorganisms Participate in Plastic Degradation at Sea?”).

## MICROORGANISMS COLONIZING PLASTIC AT SEA

### A New Niche for Marine Microorganisms

It was not until recently that the first work using modern techniques of massive DNA sequencing provided a detailed

picture of the microbial life on plastic and introduced the term “plastisphere” (Zettler et al., 2013). Bacteria, Archaea, Fungi and microbial Eukaryotes were detected in several studies, starting from plastics sampled at sea or from new plastics experimentally incubated in marine conditions (Table 1). Plastic debris are mainly composed of polyethylene (PE) at sea surface, followed by polypropylene (PP) and polystyrene (PS) (Auta et al., 2017). Whatever the polymer type, recent studies emphasized the difference between the bacteria living on plastics and the bacteria living in free-living state (Debroas et al., 2017) or on organic particles in the surrounding seawater (Dussud et al., 2018a; Oberbeckmann et al., 2018). Similar observations have been made for fungal communities (Kettner et al., 2017).

Another aspect that received much less attention is the plastisphere living in the water column other than the surface layer. Because of methodological constraints, most of the studies so far have been limited to sampling surface seawater using manta trawls, which represents less than 1% of the global load of plastic in the open ocean (Cózar et al., 2014). Only certain types of plastics made of PE and PP with high surface-to-volume ratios, such as rigid plastics and bundled fishing nets and ropes, have the capability to remain for a very long time at the surface of the oceans (Lebreton et al., 2018). Most other buoyant plastic such as films or smaller pieces, tend to sink to the sediment owing to biofouling (Fazey and Ryan, 2016; Kalogerakis et al., 2017). Very limited information is available concerning the composition of microbial communities on plastic items sampled from the seafloor (De Tender et al., 2015). If photoautotrophic bacteria such as the cyanobacteria of the genera *Phormidium* and *Rivularia* dominate the sub-surface plastisphere communities (Zettler et al., 2013; Bryant et al., 2016; Dussud et al., 2018a), the core microbiome of the seafloor and sub-surface plastisphere seems to share some taxa: Bacteroidetes (*Flavobacteriaceae*) and Proteobacteria (*Rhodobacteraceae* and *Alcanivoracaceae*) (Zettler et al., 2013; Bryant et al., 2016; De Tender et al., 2017; Dussud et al., 2018a).

### Successive Colonization Stages of New Plastics Incubated in Marine Conditions

In parallel to studies on plastic directly sampled at sea, other studies focused on the successive colonization steps of new plastics incubated in marine conditions (Table 1). At sea, plastics are rapidly covered by the “conditioning film” made of inorganic and organic matter, which is then rapidly colonized by bacteria (mainly *Gammaproteobacteria* and *Alphaproteobacteria*) (Oberbeckmann et al., 2015). With time, members of Bacteroidetes become increasingly abundant (Lee et al., 2008). Hydrophobicity and other substratum properties (crystallinity and crystal structure, roughness, glass transition temperature, melting temperature, modulus of elasticity) may play a role in the selection of bacterial community in the early stages of colonization (Pompilio et al., 2008), but probably in a lesser extent when the biofilm becomes mature (Dussud et al., 2018a). The successive growing and maturation phases of biofilm formation, already described for other surfaces such as glass, acryl, steel or rocks and algae (Salta et al., 2013), were also

**TABLE 1** | List of recent studies using molecular techniques to evaluate the biodiversity of the plastisphere in different geographic regions, for plastic samples taken at sea or incubated in seawater conditions for the purpose of the studies.

Studied area	Sample type	Method	Gene target	Target	References
North Pacific subtropical Gyre	Sampling at sea surface	Metagenomic sequencing		Bacteria and Eukaryote	Bryant et al., 2016
Baltic Sea	Incubation in seawater	V4 18S rRNA sequencing	565-981	Microbial Eukaryote, Fungi	Kettner et al., 2017
Estuary, Baltic Sea	Incubation in seawater	V4 16S rRNA sequencing	515-806	Bacteria and Archaea	Oberbeckmann et al., 2018
North Sea	Incubation in seawater	V4 16S rRNA sequencing	515-806	Bacteria and Archaea	Oberbeckmann et al., 2016
		V9 18S rRNA sequencing	1391-1795	Microbial Eukaryote, Fungi	
North Sea	Sampling at sea surface- Incubation in seawater	DGGE 16S rRNA and sequencing	341-534	Bacteria and Archaea	Oberbeckmann et al., 2014
North Sea	Incubation in seawater and sediment	V3-V4 16S rRNA sequencing	341-785	Bacteria and Archaea	De Tender et al., 2017
		rDNA-ITS2 sequencing		Fungi	
North Atlantic subtropical gyre	Sampling at sea surface	V4 16S rRNA sequencing	515-806	Bacteria and Archaea	Debroas et al., 2017
		V7 18S rRNA sequencing	960-1438	Eukaryote	
North Atlantic	Sampling at sea surface	V4-V6 16S rRNA sequencing	518-1046	Bacteria	Zettler et al., 2013
		V9 16S rRNA sequencing	1380-1510	Microbial Eukaryote	
Mediterranean Sea	Sampling at sea surface	V3-V5 16S rRNA sequencing	515-926	Bacteria and Archaea	Dussud et al., 2018a
Mediterranean Sea	Incubation in seawater	V3-V5 16S rRNA sequencing	515-926	Bacteria and Archaea	Dussud et al., 2018b
Mediterranean Sea	Incubation in seawater	V3-V5 16S rRNA sequencing	515-926	Bacteria and Archaea	Briand et al., 2012
Arabian Sea	Incubation in seawater	V4 16S rRNA sequencing	ND	Bacteria	Muthukrishnan et al., 2018
Estuary, North Sea	Incubation in marine sediment	16S rRNA cloning and sequencing	27-1492	Bacteria	Harrison et al., 2014
Estuary, East China Sea	Sampling at sediment surface	V3-V4 16S rRNA sequencing	319-806	Bacteria	Jiang et al., 2018

The PCR-amplified regions and the corresponding targeted organisms are indicated. ND, Non-described in the publication.

observed for plastics of different compositions (Oberbeckmann et al., 2015). Biofilm developments were followed during several weeks in seawater on PE-based plastic bags (Lobelle and Cunliffe, 2011), polyethylene terephthalate (PET)-based plastic bottles (Oberbeckmann et al., 2014), polyvinyl chloride (PVC) (Dang et al., 2008), or polystyrene (PS) coupons (Briand et al., 2012). PE-based plastics were also rapidly colonized by microorganisms in marine sediments (Harrison et al., 2014). Clear differences in bacterial abundance, diversity and activity were found between non-biodegradable and biodegradable plastics (Eich et al., 2015; Dussud et al., 2018b). Higher colonization by active and specific bacteria were found after six weeks on poly(3-hydroxybutyrate-co-3-hydroxyvalerate) (PHBV) and pre-oxidized PE-based oxodegradable polymers (OXO) in comparison to non-biodegradable PE polymers (Eich et al., 2015; Dussud et al., 2018b). Longer-term studies carried out over a 6-month to one year period also showed differences in biofilm formation and maturation according to the polymer type, i.e. PE, PP, PET, or polycarbonate (PC) (Webb et al., 2009; De Tender et al., 2017). Not only bacteria but also fungi were shown to form biofilms on plastic surfaces (Pramila and Ramesh, 2011), mainly dominated by

Chytridiomycota, Cryptomycota (Kettner et al., 2017) and Ascomycota (Oberbeckmann et al., 2016; De Tender et al., 2017; Kettner et al., 2017).

## Potential Impact of Plastic on the Microbial Role in Regulation of Biogeochemical Cycles

The quantity of plastic in the oceans can no longer be considered as a limited ecological problem, since small pieces of plastic called “microplastics” (<5 mm) found at sea could cover 4.2 million km<sup>2</sup> of the sea surface (Charette and Smith, 2010; Hidalgo-Ruz et al., 2012; Eriksen et al., 2014). Marine microorganisms that compose the plastisphere are known to play a key role in the biogeochemical cycles in the oceans (Pomeroy et al., 2007). One-half of oceanic primary production on average is channeled *via* heterotrophic bacterioplankton into the microbial loop, thus contributing significantly to food web structure and carbon biogeochemical cycling in the ocean (Fenchel, 2008; **Figure 1**). Only one recent study compared the heterotrophic production of bacteria living on plastic and in seawater. Heterotrophic bacteria living on plastics were

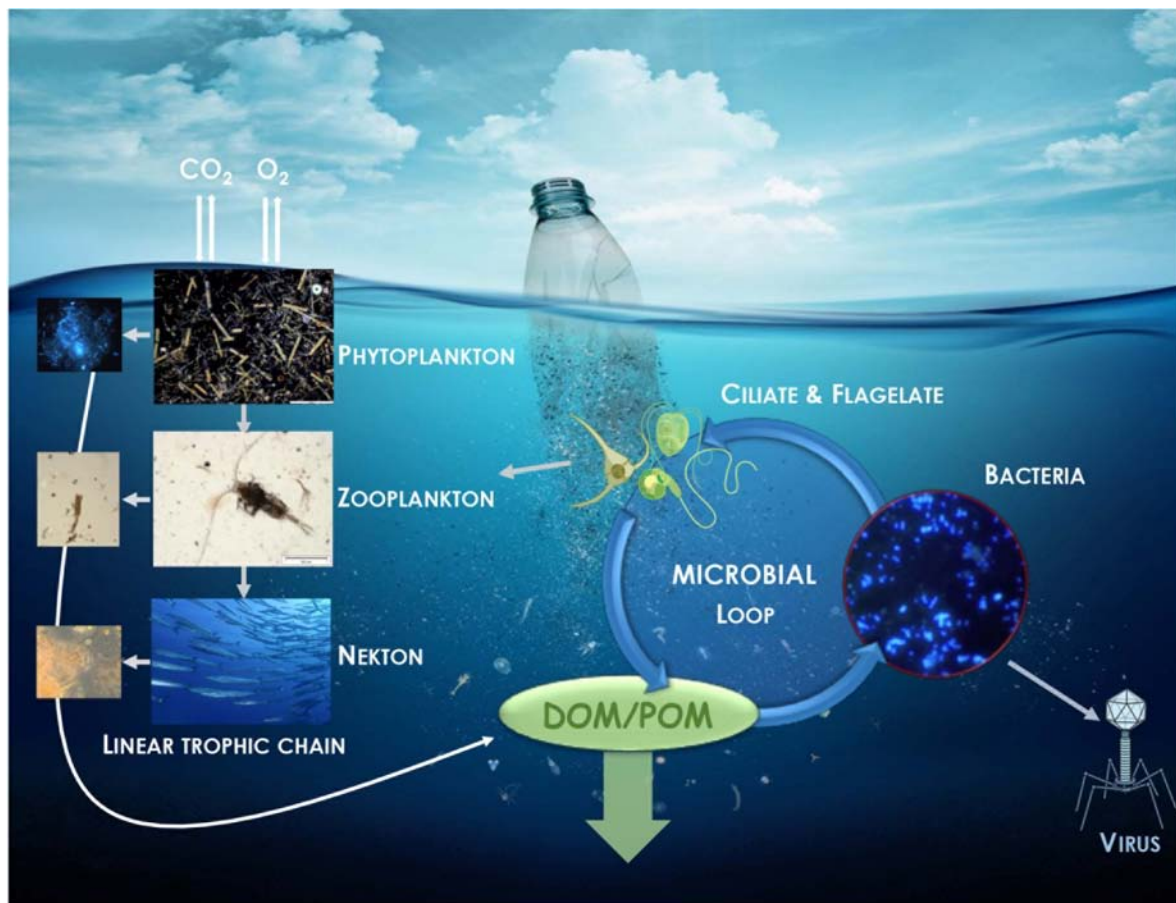


**FIGURE 1** | Illustration of the potential impact of plastic in the regulatory role of carbon and nutrient cycles played by bacteria via the microbial loop. Dissolve (DOM) and particulate (POM) organic matter originated from the linear trophic chain is returned to higher trophic levels via its incorporation in bacterial biomass.

particularly active, the cell-specific activity measured by  $^3\text{H}$ -leucine incorporation into proteins being 43- to 88-fold higher than that of the free-living fraction (Dussud et al., 2018a). Unfortunately, these results were obtained in the frame of a study on colonization of new plastics incubated at sea for a relatively short period (45 days). Similar methodologies applied to plastics that had spent several years at sea would be necessary to evaluate how much the large amount of plastic and the accompanying plastisphere influence the biogeochemical carbon cycle in the oceans.

Interestingly, most of the studies aiming to characterize the plastisphere mentioned that Cyanobacteria were overrepresented on plastics compared to the surrounding free-living and organic particle-attached fractions. The relative importance of photosynthetic activities that Cyanobacteria living on plastic have on global pelagic primary production is still unknown.

Coupling primary production and heterotrophic production measurements over large temporal and spatial scales will be necessary to obtain a better view of the role of the plastisphere on carbon cycling in the oceans. Microorganisms are not only involved in the carbon cycle, but basically in all other biogeochemical cycles including nitrogen, sulfur, iron,

manganese, chromium, phosphorus, calcium and silicate cycles, which may also be impacted by the presence of plastic at sea (Hutchins and Fu, 2017).

## Potential Dispersion of Pathogen Species

Interest has been raised about opportunist pathogen dispersal on plastics, such as animal or human pathogenic *Vibrio* sp. (Zettler et al., 2013). Marine plastic debris as vector of harmful species was first suggested by Masó et al. (2003), who identified potential harmful dinoflagellates such as *Ostreopsis* sp. and *Coolia* sp. Putative pathogens of fish (*Tenacibaculum* sp.) and of invertebrates (*Phormidium* sp. and *Leptolyngbya* sp.) were found to be more common on plastic compared to surrounding seawater (Dussud et al., 2018a). Some bacterial taxa considered as putative pathogens for human, coral and fish were also found in the intertidal zone of the Yangtze Estuary, at relatively low abundance (<1.6%) (Jiang et al., 2018). A putative pathogen for coral *Halofolliculina* spp. was found to be abundant on some western Pacific plastic debris (Goldstein et al., 2014). Some toxic eukaryotic species were also mentioned by Debroas et al. (2017) at low abundance (<0.04%), but might be regarded as

hitchhiker organisms. Nevertheless, caution should be taken since the 16S rRNA metabarcoding approach used in all these studies was not an appropriate method for describing bacterial virulence. The recent coupling of the 16S rRNA metabarcoding technique with the detection of virulence-associated genes may be an interesting option to address this question (Kirstein et al., 2016). Pathogenicity evidence on marine animals in relation to the plastisphere has never been proven, and further research will be required before publicizing alarmist conclusions on the possible responsibility of plastic debris as vector for the spread of disease-causing organisms. Apart from those results, microplastics colonized by pathogens may also pose threats to humans who are exposed to contaminated beach and bathing environments (Keswani et al., 2016). Evidence is still missing to determine whether plastic debris could lead to the spread and prolonged persistence of pathogenic species in the oceans.

## Factors Driving the Plastisphere Composition and Activities

Factors driving the plastisphere composition are complex, mainly spatial and seasonal, but are also influenced by the polymer type, surface properties and size. Plastisphere communities studied in different polymer types floating in the North Pacific and North Atlantic reflected first their biogeographic origins, and to a lesser extent the plastic type (Amaral-Zettler et al., 2015). Similar conclusions were found for bacterial communities colonizing plastics along an environmental gradient. These communities are shaped firstly by the freshwater to marine environmental conditions and secondarily by the plastic type (PS and PE) (Oberbeckmann et al., 2018). Inversely, another study based on a large number of microplastics sampled in the western Mediterranean Sea showed no effect of geographical location (including coastal and open ocean samples) or plastic type (mainly PE, PP, and PS) on the bacterial community composition. The growing number of studies on the plastisphere are giving a better view of the microbial biofilm community on plastics in the oceans, but the complex network of influences is still the subject of ongoing debate. A clearer picture will hopefully emerge from more extensive investigations with widespread and numerous samples, together with better descriptions of the physical and chemical properties of the polymers.

The physical properties of plastic offer a unique habitat that contribute to the long-distance transport of diverse microbial hitchhikers attached to its surface (Harrison et al., 2011; Zettler et al., 2013). A vast range of other phyla, including Arthropoda, Annelida, Mollusca, Bryozoa, and Cnidaria have conferred on plastics the role of vector for the transfer of organisms, some of them being cataloged as invasive alien species (Oberbeckmann et al., 2015). For instance, plastic debris with tropical biota including corals was detected in the Netherlands (Hoeksema, 2012), and Southern Ocean bryozoans were observed in Antarctica (Barnes and Fraser, 2003). Interactions between micro- and macro-organisms, their substratum

and their surroundings are needed to better predict the ecological consequences of microplastics transported through the global oceans.

## HOW MUCH CAN MICROORGANISMS PARTICIPATE IN PLASTIC DEGRADATION AT SEA?

### Definition and Main Processes Involved in Plastic Biodegradation

Biodegradation of plastic is a process that results in total or partial conversion of organic carbon into biogas and biomass associated with the activity of a community of microorganisms (bacteria, fungi, and actinomycetes) capable of using plastic as a carbon source (Shah et al., 2008). Depending on the respiratory conditions (aerobic / anaerobic) and the microorganisms involved, the biogas will be different (CO<sub>2</sub>, CH<sub>4</sub>, H<sub>2</sub>S, NH<sub>4</sub>, and H<sub>2</sub>) (Mohee et al., 2008).

Microorganisms, including bacteria and fungi, present the capabilities to degrade or deteriorate plastics and several review papers updated the list of plastic-degraders (Shah et al., 2008; Bhardwaj et al., 2013; Kale et al., 2015; Pathak, 2017). *Arthrobacter*, *Corynebacterium*, *Micrococcus*, *Pseudomonas*, *Rhodococcus*, and *Streptomyces* were the prominent microbial taxa able to use plastic as sole carbon source and energy in laboratory conditions. **Table 2** proposes an update of the current list of microorganisms proven to present biodegradation capabilities under laboratory conditions.

Biodegradation is considered to occur after or concomitant with physical and chemical degradation (abiotic degradation), which weakens the structure of polymers as revealed by roughness, cracks and molecular changes (İpekoglu et al., 2007). Alteration of plastic properties due to abiotic degradation is called “aging” and in nature depends on several factors such as temperature, solar light and chemicals that enhance the rate of degradation by oxidizing or disrupting the length of the polymer chain.

Biodegradation can be summarized in four essential steps, which have been described in detail in a review by Dussud and Ghiglione (2014):

- Bio-deterioration relates to the biofilm growing on the surface and inside the plastic, which increases the pore size and provokes cracks that weaken the physical properties of the plastic (physical deterioration) or releases acid compounds that modify the pH inside the pores and results in changes in the microstructure of the plastic matrix (chemical deterioration).
- Bio-fragmentation corresponds to the action of extracellular enzymes (oxygenases, lipases, esterases, depolymerases and other enzymes that may be as diverse as the large spectrum of polymer types) released by bacteria colonizing the polymer surface. These enzymes will reduce the molecular weight of polymers and release oligomers and then monomers that can be assimilated by cells.

**TABLE 2** | List of microbial strains able to biodegrade various types of polymers.

Type of polymer	Strains	Reference
PE	<i>Brevibacillus borstelensis</i>	Hadad et al., 2005; Mohanrasu et al., 2018
	<i>Bacillus weihenstephanensis</i>	Ingavale and Raut, 2018
	<i>Comamonas</i> sp.	Peixoto et al., 2017
	<i>Delftia</i> sp.	Peixoto et al., 2017
	<i>Stenotrophomonas</i> sp.	Peixoto et al., 2017
	<i>Achromobacter xylosoxidans</i>	Kowalczyk et al., 2016
	<i>Bacillus</i> sp. YP1	Yang et al., 2014
	<i>Enterobacter asburiae</i> YT1	Yang et al., 2014
	<i>Bacillus amyloliquefaciens</i>	Das and Kumar, 2015
	<i>Bacillus pumilus</i> M27	Harshvardhan and Jha, 2013
	<i>Kocuria palustris</i> M16	Harshvardhan and Jha, 2013
	<i>Lysinibacillus xylanilyticus</i>	Esmaeili et al., 2013
	<i>Bacillus mycoides</i>	Ibiene et al., 2013
	<i>Bacillus subtilis</i>	Ibiene et al., 2013
	<i>Pseudomonas aeruginosa</i> PAO1 (ATCC 15729)	Kyaw et al., 2012
	<i>Pseudomonas aeruginosa</i> (ATCC 15692)	Kyaw et al., 2012
	<i>Pseudomonas putida</i> KT2440 (ATCC 47054)	Kyaw et al., 2012
	<i>Pseudomonas syringae</i> DC3000 (ATCC 10862)	Kyaw et al., 2012
	<i>Brevibacillus parabrevis</i>	Pramila, 2012
	<i>Acinetobacter baumannii</i>	Pramila, 2012
	<i>Pseudomonas citronellolis</i>	Pramila, 2012
	<i>Bacillus sphaericus</i>	Sudhakar et al., 2008
	<i>Rhodococcus ruber</i>	Gilan and Sivan, 2013
	<i>Aspergillus versicolor</i>	Pramila and Ramesh, 2011
	<i>Aspergillus</i> sp.	Pramila and Ramesh, 2011; Sheik et al., 2015
	<i>Chaetomium</i> sp.	Sowmya et al., 2012
	<i>Aspergillus flavus</i>	Sowmya et al., 2012
	<i>Penicillium simplicissimum</i>	Yamada-Onodera et al., 2001; Sowmya et al., 2014
	<i>Lasiodiplodia theobromae</i>	Sheik et al., 2015
	<i>Paecilomyces lilacinus</i>	Sheik et al., 2015
	<i>P. pinophilum</i> , <i>A. niger</i> , <i>Gliocladium virens</i> , and <i>P. chrysosporium</i>	Manzur et al., 2004
	<i>Aspergillus glaucus</i> and <i>A. niger</i>	Kathiresan, 2003
	PET	<i>Bacillus amyloliquefaciens</i>
<i>Nocardia</i> sp.		Sharon and Sharon, 2017
<i>Ideonella sakaiensis</i>		Yoshida et al., 2016
<i>Humicola insolens</i>		Ronkvist et al., 2009
<i>Pseudomonas mendocina</i>		Ronkvist et al., 2009
<i>Thermobifida fusca</i> (DSM 43793)		Müller et al., 2005
<i>Penicillium citrinum</i>		Liebminger et al., 2007
<i>Thermomonospora fusca</i>		Alisch et al., 2004
<i>Fusarium oxysporum</i>		Nimchua et al., 2007
<i>Fusarium solani</i>		Alisch et al., 2004; Nimchua et al., 2007
<i>Crupriavidus</i> sp.		Martínez-Tobón et al., 2018
PHB	<i>Marinobacter algicola</i>	Martínez-Tobón et al., 2018
	Mixed cultures	Ansari and Fatma, 2016
	<i>Schlegella thermodepolymerans</i>	Romen et al., 2004
	<i>Caenibacterium thermophilum</i>	Romen et al., 2004
	<i>Acidovorax</i> sp. TP4	Kobayashi et al., 1999
	<i>Pseudomonas stutzeri</i>	Uefuji et al., 1997; Martínez-Tobón et al., 2018
	<i>Leptothrix discophora</i>	Takeda et al., 1998

(Continued)

TABLE 2 | Continued

Type of polymer	Strains	Reference
PHBV	<i>Alcaligenes faecalis</i>	Tanio et al., 1982; Kita et al., 1995
	<i>Comamonas acidovorans</i> YM1609	Kasuya et al., 1997
	<i>Comamonas testosteroni</i>	Kasuya et al., 1997; Martínez-Tobón et al., 2018
	<i>Pseudomonas lemoignei</i>	Uefuji et al., 1997; Martínez-Tobón et al., 2018
	<i>Ralstonia pickettii</i>	Yamada et al., 1993; Martínez-Tobón et al., 2018
	<i>Pseudomonas fluorescens</i> YM1415 and nine Gram-	Mukai et al., 1994
	<i>Aspergillus niger</i>	Kumaravel et al., 2010
	<i>Clostridium botulinum</i>	Abou-Zeid et al., 2001
	<i>Clostridium acetobutylicum</i>	Abou-Zeid et al., 2001
	<i>Streptomyces</i> sp. SNG9	Mabrouk and Sabry, 2001
PS	<i>Pseudomonas lemoignei</i>	Jendrossek et al., 1993
	<i>Paecilomyces lilacinus</i>	Sang et al., 2001
	Strain TM1 and ZM1	Tang et al., 2017
	<i>Bacillus subtilis</i>	Asmita et al., 2015
	<i>Staphylococcus aureus</i>	Asmita et al., 2015
	<i>Streptococcus pyogenes</i>	Asmita et al., 2015
	<i>Exiguobacterium</i> sp.	Yang et al., 2015
	<i>Bacillus</i> sp NB6, <i>Pseudomonas aeruginosa</i> NB26,	Atiq et al., 2010
	<i>Exiguobacterium</i> sp., <i>Microbacterium</i> sp. NA23,	
	<i>Paenibacillus urinialis</i> NA26	
	<i>Rhodococcus ruber</i>	Mor and Sivan, 2008
	<i>Pseudomonas putida</i> CA-3 (NCIMB 41162)	Ward et al., 2006
	<i>Bacillus</i> sp. STR-Y-O	Oikawa et al., 2003
	Mixed microbial communities	Kaplan et al., 1979
	Mixed microbial communities ( <i>Bacillus</i> , <i>Pseudomonas</i> ,	Sielicki et al., 1978
	<i>Micrococcus</i> , and <i>Nocardia</i> )	

polyethylene (PE), polyethylene terephthalate (PET), polyhydroxybutyrate (PHB), and Poly(3-hydroxybutyrate-co-3-hydroxyvalerate) (PHBV), and polystyrene (PS). Detailed information on the origin of the strains and the methods used to prove biodegradation are available in the **Supplementary Table S1**.

- Assimilation allows oligomers of less than 600 Daltons to be integrated inside the cells to be used as a carbon source, thus increasing the microbial biomass.
- Mineralization is the ultimate step in the biodegradation of a plastic polymer and results in the excretion of completely oxidized metabolites (CO<sub>2</sub>, N<sub>2</sub>, CH<sub>4</sub>, and H<sub>2</sub>O).

## Rates of Plastic Degradation

Rates of degradation of conventional plastics by microorganisms are extremely low, even in optimized laboratory conditions (Krueger et al., 2015). Most of the conventional plastics are recalcitrant to biodegradation in marine and terrestrial environments, resulting in lifetimes of decades or even centuries (Krueger et al., 2015). Plastics present low bioavailability since they are generally solid and made of densely cross-linked polymers that provide low accessibility for microbes and enzymes circumscribed to the outermost layer of the items. In the pelagic ecosystem, plastics are biodegraded by the aerobic metabolism of microorganisms, i.e., the end product of the reaction will be microbial biomass, CO<sub>2</sub> and H<sub>2</sub>O. The anaerobic biodegradation pathway would be more frequently encountered in sediment and is supposed to be even slower than in the pelagic zone (Ishigaki et al., 2004). Unfavorable C/N ratio is a key factor for biodegradation of other hydrocarbon-based products in

the oceans (Sauret et al., 2016) and may potentially also limit plastic biodegradation.

Data currently available rely heavily on culture-based approaches in laboratory conditions, although bacteria that can be cultured represent less than 1% of the number of bacteria in nature (the so-called “great plate count anomaly”) and a very small proportion of its very large diversity (Hugenholtz et al., 2009). To date, data on the rate of plastic mineralization in the oceans are still virtually non-existent. Congruent descriptions of the plastisphere that forms an abundant biofilm characterized by very diverse bacteria with active plastic-specific characteristics are available (Debroas et al., 2017; Dussud et al., 2018b). Evidence of pits visualized in the plastic debris that conform to bacterial shapes directly found in the marine environment (Zettler et al., 2013) together with a number of putative xenobiotic degradation genes likely involved in plastic degradation that were found to be significantly more abundant in the plastic-specific communities (Bryant et al., 2016; Debroas et al., 2017; Dussud et al., 2018b) are thus of great interest. A recent study underlined the need of cometabolic pathways on PE biodegradation, thus confirming that complex microbial communities rather than single species are necessary to degrade recalcitrant plastic (Syranidou et al., 2017). So far, the timescales of degradation and the characterization and the fate of the degradation products, are fundamental, yet still unanswered questions.

## Standard Tests for Plastic Biodegradability at Sea

The current standards for marine environments propose tests based on respirometry measurements, susceptible to describe the mineralization step of plastic biodegradation in aerobic conditions (see **Figure 2**). They impose a minimum percentage of conversion from plastic to CO<sub>2</sub> ranging from 60 to 70% over a period of 3 months (ASTM D6691-09), 6 months (ASTM D7473-12), or 24 months (ISO 18830, ISO 19679, ASTM D7991-15) under aerobic conditions (see **Figure 3**). Anaerobic

biodegradation is characterized by specific standards (see for example ASTM D5511-18), but to our knowledge none of these standards applies to the marine environment. Biodegradation of a plastic is characterized by the time required to achieve mineralization under controlled conditions. These tests cannot be considered as a proof of ready biodegradability (total conversion of plastic into biomass and CO<sub>2</sub>), but rather an indication about a potential for biodegradation in the oceans.

Recently, these standards were considered insufficient in their ability to realistically predict the biodegradability in marine environment (Harrison et al., 2018). These tests can significantly underestimate the time required for polymer biodegradation within natural ecosystems. First, the authors underlined “biases associated with the preparation of experimental inocula and the test conditions themselves, including the use of preselected and/or pre-conditioned strains, artificially modified inocula, powdered test materials, nutrient-rich synthetic media and test temperatures that are frequently higher than those encountered within the environment.” The authors also pointed out “the lack of clear guidelines for the analysis of different polymer types, including composite materials and plastics that contain additives,” which can considerably influence the rates of biodegradation. “There is also a paucity of guidelines for materials of varying shapes and sizes and, in certain cases, the test procedures lack a sufficient level of statistical replication.” Another concern, not raised by Harrison et al. (2018), is the biases associated with the common method for determining biodegradability, i.e., measurements of CO<sub>2</sub> evolution. This method may lead to either underestimation or overestimation of the plastic biodegradation due to other processes. It is noteworthy that plastic generally presents high sorption capability of organic matter (especially hydrophobic organic chemicals including pollutants) that can be biodegraded by the plastisphere biofilm,

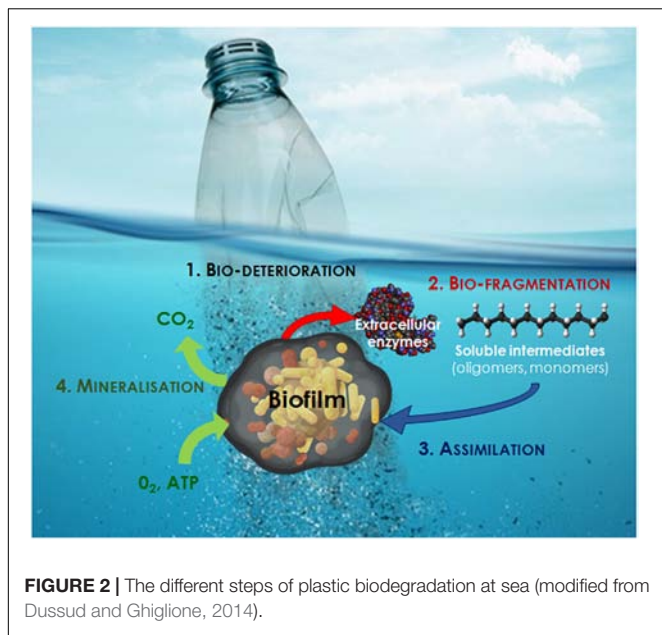


**FIGURE 2** | The different steps of plastic biodegradation at sea (modified from Dussud and Ghiglione, 2014).

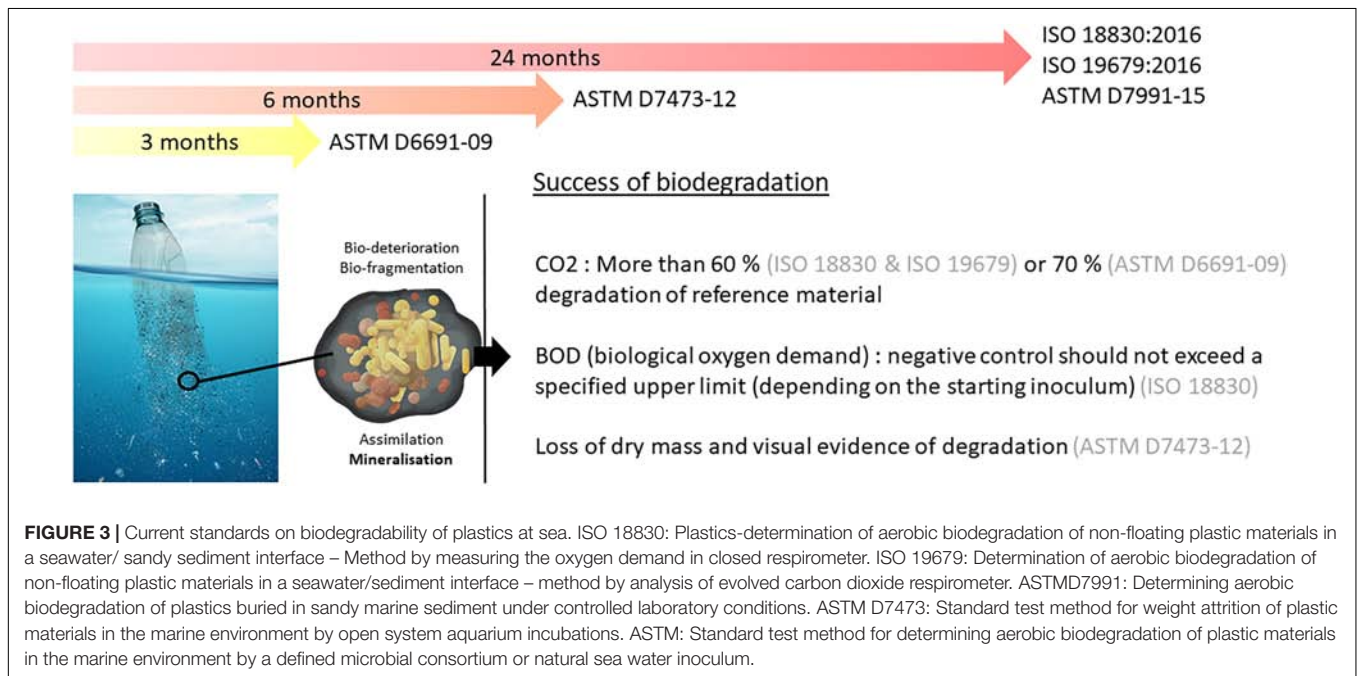


**FIGURE 3** | Current standards on biodegradability of plastics at sea. ISO 18830: Plastics-determination of aerobic biodegradation of non-floating plastic materials in a seawater/ sandy sediment interface – Method by measuring the oxygen demand in closed respirometer. ISO 19679: Determination of aerobic biodegradation of non-floating plastic materials in a seawater/sediment interface – method by analysis of evolved carbon dioxide respirometer. ASTM D7991: Determining aerobic biodegradation of plastics buried in sandy marine sediment under controlled laboratory conditions. ASTM D7473: Standard test method for weight attrition of plastic materials in the marine environment by open system aquarium incubations. ASTM: Standard test method for determining aerobic biodegradation of plastic materials in the marine environment by a defined microbial consortium or natural sea water inoculum.

thus resulting in a CO<sub>2</sub> production that has nothing to do with plastic biodegradation (Lee et al., 2014). Inversely, several papers reported the importance of photosynthetic microorganisms growing on plastics, which consume CO<sub>2</sub> regardless of plastic biodegradation (Zettler et al., 2013; Bryant et al., 2016; Dussud et al., 2018b). Further studies are needed to evaluate the relative degree of CO<sub>2</sub> consumption by photosynthesis, CO<sub>2</sub> production by organic matter degradation by the plastisphere as compared to CO<sub>2</sub> production due to plastic biodegradation.

The limitations of the respiratory methods described above can be overcome by other additional analytical techniques and approaches to confirm changes in the physical properties and the chemical structure of polymers during biodegradation. Alterations in the visual appearance and in the mass or changes in mechanical properties are relatively easy and low-cost methods for the evaluation of physical changes during biodegradation. Other methods could be combined to confirm changes in the molecular structure of polymers, such as measurements of surface hydrolysis and other chromatographic (gas chromatography with or without flame ionization detection, liquid chromatography, gel-permeation chromatography) measurements coupled or not with spectrometric techniques (mass spectrometry, nuclear magnetic resonance spectroscopy, Fourier-transform infrared spectroscopy). Optical, atomic force and scanning electron microscopy can also be used to assess the biodeterioration of the surface due to microbial activity or biofilm formation. Any of these techniques are enough to prove biodegradation by its own, and each of them has limitations that have been previously detailed for example in the excellent reviews of (Koutny et al., 2006; Harrison et al., 2018; Ho et al., 2018). The current standards sometimes propose to use such techniques to corroborate the main test based on respirometry measurement, but no clear guidelines on how to use these tests is provided.

## Examples of Metabolic Pathways of Polymer Biodegradation

There are currently more than 5,300 grades of synthetic polymers for plastics in commerce (Wagner and Lambert, 2018). They are generally produced with a range of chemical additives such as plasticizers, flame retardants, antioxidants and other stabilizers, pro-oxidants, surfactants, inorganic fillers or pigments (Wagner and Lambert, 2018). Their heterogeneous physical-chemical properties will likely result in very heterogeneous metabolic pathways of biodegradation, especially when considering the large variety of microorganisms that may interact for the degradation of a single piece of plastic, together with the environmental factors of very dynamic oceanic conditions. We are aware that treating plastic as a single compound does not make sense and providing details on the metabolic pathways of plastic biodegradation would necessarily be unrepresentative of the complexity of the various processes that occur in the environment. We have chosen to focus on the metabolic pathways associated with the biodegradation of model compounds used in the formulation of conventional (PE, PET, and PS) and so called “biodegradable” plastics (PHA) that are the most popular and the most extensively studied in the literature.

Moreover, it should be noted that because of the difficulty of dealing with long-term experiments and complex communities under natural conditions, all the following studies describing the metabolic pathways of plastic biodegradation were done using a culture-based approach.

## Metabolic Pathways of Polyethylene (PE) Biodegradation

High- and low-density polyethylene is a long linear carbon chain (CH<sub>2</sub>) belonging to the family of polyolefins. Polyethylene is derived from petroleum sources and its large use in our daily life made it the first plastic waste found at sea surface. PE is considered difficult to biodegrade because the long chains of carbons and hydrogens are very stable and contain very balanced charges. Microorganisms generally need imbalance of electric charge to perform biodegradation. To destabilize the local electric charge, bacteria use oxygenases: enzymes able to add oxygen to a long carbon chain (Krueger et al., 2015). For instance, mono-oxygenases and di-oxygenases incorporate, respectively, one and two oxygen atoms, forming alcohol or peroxy groups that are less recalcitrant for biodegradation. Oxidation may also be processed by abiotic reactions associated with UV radiation or temperature (for more details, see the review by Singh and Sharma, 2008). Oxidation of PE results in the formation of carboxylic groups, alcohols, ketones, and aldehydes by a radical reaction (Vasile, 1993; Gewert et al., 2015). The oxidation and fragmentation of PE make the polymer more hydrophilic and facilitates access to other extracellular enzymes, such as lipases and esterases after the formation of carboxylic groups, or endopeptidases for amide groups (Gewert et al., 2015). Other enzymes such as laccase in *Rhodococcus ruber* are excreted and can facilitate the biodegradation of PE (Santo et al., 2013). Interestingly, a recent study focused on soluble oxidized oligomers showed that 95% of these compounds were assimilated by a strain of *Rhodococcus rhodochrous* after 240 days of incubation (Eyheraguibel et al., 2017). The polymer is broken down into small oligomers of 600 Da incorporated in the cells by carriers belonging to the Major Facilitator Superfamily (MFS) or harboring ATP binding cassettes (ABC) (Gravouil et al., 2017). β-oxidation transforms oxidized carboxylic molecules (having an even number of carbon atoms) into acetyl coA or propionyl coA (if odd number of carbons). Carboxylation of propionyl coA into succinyl coA is performed by propionyl-coA carboxylase. Gravouil et al. (2017), propose identification of an overexpressed enzyme, when the bacteria find PE in the medium (Gravouil et al., 2017). Acetyl coA and succinyl coA enter the tricarboxylic acid (TCA) cycle (Figure 4). This cycle produces chemical energy in the form of a reducing power (NADH, H<sup>+</sup> and CoQ<sub>10</sub>H<sub>2</sub>) used in the respiratory chain to produce ATP, which is necessary to create new microbial biomass *via* replication processes. It also produces CO<sub>2</sub> and H<sub>2</sub>O that sign the complete mineralisation of PE.

For 20 years now, scientists have been interested in the biodegradation of polyethylene by the microbial community. Bacterial and fungal strains presenting biodegradation capabilities of PE are listed in Table 2 and Supplementary Table S1.



catabolized by TPA 1,2-dioxygenase (TPADO) and 1,2-dihydroxy-3,5-cyclohexadiene-1,4-dicarboxylate dehydrogenase (DCDDH) to give protocatechuic acid (PCA) as the final molecule (Yoshida et al., 2016). This PCA is cleaved by PCA 3,4 dioxygenase (PCA34) to give the hemiacetal form of 4-carboxy-2-hydroxymuconic. The latter becomes the substrate of a dehydrogenase to form 2-pyrone-4,6-dicarboxylic acid that enters the TCA cycle and initially transformed into pyruvate and oxaloacetate, then assimilated as CO<sub>2</sub> and H<sub>2</sub>O (Figure 4).

### Metabolic Pathways of Polystyrene (PS) Biodegradation

Polystyrene is a polymer composed of styrene monomers (CH<sub>2</sub> = CH<sub>2</sub>-Ph). The polymer is highly hydrophobic and presents a high molecular weight. Like other conventional plastics, partial biodegradation in the laboratory has been observed while it continues to accumulate in the oceans (Autá et al., 2017) thus inciting increasing interest in PS biodegradation (see **Supplementary Table S1**; Oikawa et al., 2003; Mor and Sivan, 2008; Atiq et al., 2010; Asmita et al., 2015; Yang et al., 2015; Tang et al., 2017).

Several biodegradation pathways may be considered, depending on the microorganism involved. The predominant pathway is the oxidation pathway of the styrene side chain presented in **Figure 4**. The styrene is directly oxidized with a styrene monooxygenase to form a styrene epoxide which will then be oxidized to phenylacetaldehyde by styrene oxide. This molecule is then catabolized into phenylacetic acid. This conversion of styrene to phenylacetic acid is called the upper pathway of styrene metabolism. Phenylacetic acid is converted to phenylacetyl-CoA (acetyl coenzyme A) by the so-called lower pathway (Luu et al., 2013) then subjected to several enzymatic reactions (**Figure 4**) to finally enter the tricarboxylic acid (TCA) cycle. The biodegradation products enter the TCA cycle through the final formation of acetyl-Co A and succinyl-CoA (succinyl-CoenzymeA) (Luu et al., 2013).

Interestingly, *Pseudomonas putida* CA-3 can accumulate polyhydroxyalkanoates (PHA at medium chain length) when growing on styrene, thus using an original biodegradation pathway. A catabolic operon has been identified as responsible for this bioconversion; this path is called the PACoA (Phenylacetyl-CoA) catabolon. It involves oxidation of the aromatic ring, followed by entry into the  $\beta$ -oxidation cycle and the conversion to acetyl-CoA (O'Leary et al., 2005). This acetyl-CoA can follow different metabolic pathways, either entering the TCA cycle or following the *de novo* fatty acid biosynthesis path which will give as final product medium-chain-length polyhydroxyalkanoates (mcl-PHAs) (O'Leary et al., 2005). This study shows the complexity of studying the biodegradation pathways of these polymers and indicates the great range of possibilities when considering the large diversity of microorganisms found in the plastisphere.

### Metabolic Pathways of Polyhydroxyalkanoate (PHA) Biodegradation

The current global production of PHA is increasing, reaching 49,200 tons per year that represents 2.4% of the production of bioplastics<sup>1</sup>. PHAs are biopolymers of hydroxylated fatty acids produced within a bacteria in granular form. Each PHA monomer ([CO-CH<sub>2</sub>-CHR-O]<sub>n</sub>) consists of hydroxyalkanoates linked together by ester bonds. The alkyl group (R) varies from a methyl group to a tetradecyl group. When bacteria are placed in a medium with an excess carbon source and low nutrient content, they accumulate storage granules. Over 300 bacterial species are capable of producing 80 different hydroxyalkanoate monomers, and some bacteria can accumulate up to 90% of their total weight of polymer in very specific conditions (Peña et al., 2014). One of the most commonly used PHA for plastic production is polyhydroxybutyrate (PHB), which has a methyl as an alkyl group (R) ([CO-CH<sub>2</sub>-CHCH<sub>3</sub>-O]<sub>n</sub>). PHB is one of the homopolymers with high commercial power because it has thermoplastic, hydrophobic, low oxygen permeability and is considered biodegradable (Mothes et al., 2004; Chang et al., 2012). It is not very deformable, because of its high crystallinity (Gorke et al., 2007) and it has a high melting point close to its thermal degradation temperature (Reis et al., 2003). A copolymer made of Poly(3-hydroxybutyrate-co-3-hydroxyvalerate) (PHBV) that reduces the melting point of PHB is seen to emerge in PHA production. The advantage of using PHA is that it is stable over time, as long as the conditions governing its biodegradation are not met (Jaffredo et al., 2013).

Due to their microbial origin, PHAs were found to be biodegradable in many environments such as soil, marine ecosystems or sewage sludge (Eubeler et al., 2010). Biodegradation of Poly(3-hydroxybutyrate-co-3-hydroxyhexanoate) has been proven with comparable rates to that of cellulose, with faster degradation found under aerobic (85 days) compared to anaerobic (6 months) conditions (Wang et al., 2018). The biodegradation scheme in **Figure 4** shows the different steps of PHB biodegradation. When the biodegradation is not carried out inside the cells by bacteria that produce their own PHB, other bacteria initiate the biodegradation of PHB in the medium by external hydrolysis using ectoenzymes that convert the polymers into hydroxylated acid monomers of hydroxybutyrate (HB) (Peña et al., 2014). This molecule is water soluble and small enough to passively diffuse across the bacterial membrane and enter the  $\beta$ -oxidation cycle. The resulting acetyl-CoA will be oxidized in the TCA cycle until final mineralisation (Alshehrei, 2017). PHA-degradation has been proven in the laboratory under aerobic or anaerobic conditions (see a non-exhaustive list in **Supplementary Table S1**). The dominant bacteria in aerobic marine conditions belong to *Clostriales*, *Gemmatales*, *Phycisphaerales*, and *Chlamydiales*, whereas *Cloacamonales* and *Thermotogales* dominate in anaerobic sludge (Wang et al., 2018).

<sup>1</sup><https://www.european-bioplastics.org>

## CONCLUDING REMARKS

In this review, we have presented both aspects of microbial ecotoxicology on marine plastic debris, namely the impact of plastic on marine microbial life and inversely how microbes can play a role in plastic biodegradation. An increasing number of studies either describe the different steps of biofilm formation under marine conditions, or give new insights on bacteria colonizing the aged plastics directly sampled at sea. The very diverse and active bacteria living on plastics as compared to the surrounding waters suggest a potential impact on the global biogeochemical cycles associated with the relatively recent introduction of plastic in the oceans, impact that remains to be determined. Plastic released in the oceans is also accused to be a raft for invasive species including pathogenic bacteria, but no proof of pathogenicity on marine animals or humans in relation to plastic ingestion has emerged so far.

A better knowledge of the plastisphere is also a critical issue in understanding the role played by bacteria in plastic biodegradation. Several studies have underlined that current standards are failing to prove biodegradability at sea for several reasons that have been highlighted in this review. Biodegradation of a polymer at sea depends on many factors related to its own composition, but also on the various ecosystems and environmental conditions encountered during its very long lifetime. It is for these reasons that plastic polymers continue to accumulate at sea and that biodegradation rates reported in the laboratory are never reached in the environment. Thus, a complete study of the biodegradation of a polymer at sea must combine several monitoring parameters, and especially be confirmed in the field with experiments *in situ*. Given the complexity of the plastic problem, research network initiatives such as “Polymers & Oceans” that bring together physicists, chemists and biologists are required to answer the wishes and needs of many scientists to face this environmental problem and its resonance in the society.

<sup>2</sup> <https://po2018.wixsite.com/po2018>

## REFERENCES

- Abou-Zeid, D., Müller, R., and Deckwer, W. (2001). *Anaerobic Biodegradation of Natural and Synthetic Polyesters*. Doctoral dissertation, Technical University Braunschweig, Braunschweig.
- Alish, M., Feuerhack, A., Müller, H., Mensak, B., Andraus, J., and Zimmermann, W. (2004). Biocatalytic modification of polyethylene terephthalate fibres by esterases from actinomycete isolates. *Biotransformation* 22, 347–351. doi: 10.1080/10242420400025877
- Alshehri, F. (2017). Biodegradation of synthetic and natural plastic by microorganisms. *J. Appl. Environ. Microbiol.* 5, 8–19. doi: 10.12691/jaem-5-1-2
- Amaral-Zettler, L. A., Zettler, E. R., Slikas, B., Boyd, G. D., Melvin, D. W., Morrall, C. E., et al. (2015). The biogeography of the plastisphere: implications for policy. *Front. Ecol. Environ.* 13, 541–546. doi: 10.1890/150017
- Ansari, S., and Fatma, T. (2016). Cyanobacterial polyhydroxybutyrate (PHB): screening, optimization and characterization. *PLoS One* 11:e0158168. doi: 10.1371/journal.pone.0158168
- Asmita, K., Shubhamsingh, T., and Tejashree, S. (2015). Isolation of plastic degrading micro-organisms from soil samples collected at various locations in Mumbai, India. *Curr. World Environ.* 4, 77–85.

## AUTHOR CONTRIBUTIONS

J-FG designed the general plan of the review. JJ, A-LM, JC, and J-FG made the figures. JJ, JC, CO, CP, PC, MP-P, VB, A-LM, and J-FG wrote the manuscript and approved the final version.

## FUNDING

The work was made possible thanks to support granted to ANR by the Program OXOMAR (funded by the French Ministry for Education and Research, [http://lomic.obs-banyuls.fr/fr/axe\\_4\\_ecotoxicologie\\_et\\_ingenierie\\_metabolique\\_microbienne/oxomar.html](http://lomic.obs-banyuls.fr/fr/axe_4_ecotoxicologie_et_ingenierie_metabolique_microbienne/oxomar.html)) and the company Plastic@Sea (<http://plasticatsea.com>).

## ACKNOWLEDGMENTS

We wish to thank V. Domien, L. Hesse, L. Intertaglia, R. Gendron/ E-marinlab, Fondation Tara Expeditions, and Soixante seize for their help in figure design, as well as Guigui PA and VJPJS for their insightful comments on the manuscript. We are also grateful to our colleagues of the office of the international research network “Ecotoxicomic” on Microbial Ecotoxicology (<https://ecotoxicomic.org>) and of the French research network “Polymers & Oceans” (<https://po2018.wixsite.com/po2018>) supported by CNRS.

## SUPPLEMENTARY MATERIAL

The Supplementary Material for this article can be found online at: <https://www.frontiersin.org/articles/10.3389/fmicb.2019.00865/full#supplementary-material>

**TABLE S1** | Detailed information on the origin and methodology used to prove the biodegradation of various polymer types (PE, PET, PHB, PHBV, and PS) by microorganisms cited in **Table 1**.

- Atiq, N., Ahmed, S., Ali, M. I., Saadia, L., Ahmad, B., and Robson, G. (2010). Isolation and identification of polystyrene biodegrading bacteria from soil. *Afr. J. Microbiol. Res.* 4, 1537–1541.
- Auta, H. S., Emenike, C. U., and Fauziah, S. H. (2017). Distribution and importance of microplastics in the marine environment: a review of the sources, fate, effects, and potential solutions. *Environ. Int.* 102, 165–176. doi: 10.1016/j.envint.2017.02.013
- Bakir, A., Rowland, S. J., and Thompson, R. C. (2014). Enhanced desorption of persistent organic pollutants from microplastics under simulated physiological conditions. *Environ. Pollut.* 185, 16–23. doi: 10.1016/j.envpol.2013.10.007
- Barnes, D. K. A., and Fraser, K. P. P. (2003). Rafting by five phyla on man-made flotsam in the Southern Ocean. *Mar. Ecol. Prog. Ser.* 262, 289–291. doi: 10.3354/meps262289
- Bhardwaj, H., Gupta, R., and Tiwari, A. (2013). Communities of microbial enzymes associated with biodegradation of plastics. *J. Polym. Environ.* 21, 575–579. doi: 10.1007/s10924-012-0456-z
- Briand, J.-F., Djeridi, I., Jamet, D., Coupé, S., Bressy, C., Molmeret, M., et al. (2012). Pioneer marine biofilms on artificial surfaces including antifouling coatings immersed in two contrasting French Mediterranean coast sites. *Biofouling* 28, 453–463. doi: 10.1080/08927014.2012.688957

- Bryant, J. A., Clemente, T. M., Viviani, D. A., Fong, A. A., Thomas, K. A., Kemp, P., et al. (2016). Diversity and activity of communities inhabiting plastic debris in the North Pacific gyre. *mSystems* 1:e00024-16. doi: 10.1128/mSystems.00024-16
- Chang, H.-F., Chang, W.-C., and Tsai, C.-Y. (2012). Synthesis of poly(3-hydroxybutyrate/3-hydroxyvalerate) from propionate-fed activated sludge under various carbon sources. *Bioresour. Technol.* 113, 51–57. doi: 10.1016/j.biortech.2011.12.138
- Charette, M., and Smith, W. (2010). The volume of earth's ocean. *Oceanography* 23, 112–114. doi: 10.5670/oceanog.2010.51
- Cosgrove, L., McGeechan, P. L., Robson, G. D., and Handley, P. S. (2007). Fungal communities associated with degradation of polyester polyurethane in soil. *Appl. Environ. Microbiol.* 73, 5817–5824. doi: 10.1128/AEM.01083-07
- Cózar, A., Echevarria, F., Gonzalez-Gordillo, J. I., Irigoien, X., Ubeda, B., Hernandez-Leon, S., et al. (2014). Plastic debris in the open ocean. *Proc. Natl. Acad. Sci. U.S.A.* 111, 10239–10244. doi: 10.1073/pnas.1314705111
- Dang, H., Li, T., Chen, M., and Huang, G. (2008). Cross-ocean distribution of *Rhodobacterales* bacteria as primary surface colonizers in temperate coastal marine waters. *Appl. Environ. Microbiol.* 74, 52–60. doi: 10.1128/aem.01400-07
- Danso, D., Schmeisser, C., Chow, J., Zimmermann, W., Wei, R., Leggewie, C., et al. (2018). New insights into the function and global distribution of polyethylene terephthalate (PET)-degrading bacteria and enzymes in marine and terrestrial metagenomes. *Appl. Environ. Microbiol.* 84:e02773-17. doi: 10.1128/AEM.02773-17
- Das, M. P., and Kumar, S. (2015). An approach to low-density polyethylene biodegradation by *Bacillus amyloliquefaciens*. *Biotech* 5, 81–86. doi: 10.1007/s13205-014-0205-1
- De Tender, C., Devriese, L. I., Haegeman, A., Maes, S., Vangeyte, J., Cattrijsse, A., et al. (2017). Temporal dynamics of bacterial and fungal colonization on plastic debris in the North sea. *Environ. Sci. Technol.* 51, 7350–7360. doi: 10.1021/acs.est.7b00697
- De Tender, C. A., Devriese, L. I., Haegeman, A., Maes, S., Ruttink, T., and Dawyndt, P. (2015). Bacterial community profiling of plastic litter in the Belgian part of the North sea. *Environ. Sci. Technol.* 49, 9629–9638. doi: 10.1021/acs.est.5b01093
- Debroas, D., Mone, A., and Ter Halle, A. (2017). Plastics in the North Atlantic garbage patch: a boat-microbe for hitchhikers and plastic degraders. *Sci. Total Environ.* 599, 1222–1232. doi: 10.1016/j.scitotenv.2017.05.059
- Duis, K., and Coors, A. (2016). Microplastics in the aquatic and terrestrial environment: sources (with a specific focus on personal care products), fate and effects. *Environ. Sci. Eur.* 28:2. doi: 10.1186/s12302-015-0069-y
- Dussud, C., and Ghiglione, J.-F. (2014). "Bacterial degradation of synthetic plastics" in *Marine Litter in the Mediterranean and Black Seas*, ed. F. Briand (Paris: CIESM Publisher), 180.
- Dussud, C., Hudec, C., George, M., Fabre, P., Higgs, P., Bruzard, S., et al. (2018a). Colonization of Non-biodegradable and Biodegradable plastics by marine microorganisms. *Front. Microbiol.* 9:1571. doi: 10.3389/fmicb.2018.01571
- Dussud, C., Meistertzheim, A.-L., Conan, P., Pujo-Pay, M., George, M., Fabre, P., et al. (2018b). Evidence of niche partitioning among bacteria living on plastics, organic particles and surrounding seawaters. *Environ. Pollut.* 236, 807–816. doi: 10.1016/j.envpol.2017.12.027
- Eich, A., Mildnerberger, T., Laforsch, C., and Weber, M. (2015). Biofilm and diatom succession on polyethylene (PE) and biodegradable plastic bags in two marine habitats: early signs of degradation in the pelagic and benthic zone? *PLoS One* 10:e0137201. doi: 10.1371/journal.pone.0137201
- Eriksen, M., Lebreton, L. C. M., Carson, H. S., Thiel, M., Moore, C. J., Borner, J. C., et al. (2014). Plastic pollution in the world's Oceans: more than 5 trillion plastic pieces weighing over 250,000 Tons Afloat at Sea. *PLoS One* 9:e111913. doi: 10.1371/journal.pone.0111913
- Esmaili, A., Pourbabaee, A. A., Alikhani, H. A., Shabani, F., and Esmaili, E. (2013). Biodegradation of low-density polyethylene (LDPE) by mixed culture of *Lysinibacillus xylanilyticus* and *Aspergillus niger* in soil. *PLoS One* 8:e71720. doi: 10.1371/journal.pone.0071720
- Eubeler, J. P., Bernhard, M., and Knepper, T. P. (2010). Environmental biodegradation of synthetic polymers II. Biodegradation of different polymer groups. *Trends Anal. Chem.* 29, 84–100. doi: 10.1007/s12010-014-1136-3
- Eyheraguibel, B., Traikia, M., Fontanella, S., Sancelme, M., Bonhomme, S., Fromageot, D., et al. (2017). Characterization of oxidized oligomers from polyethylene films by mass spectrometry and NMR spectroscopy before and after biodegradation by a *Rhodococcus rhodochrous* strain. *Chemosphere* 184, 366–374. doi: 10.1016/j.chemosphere.2017.05.137
- Fazey, F. M. C., and Ryan, P. G. (2016). Biofouling on buoyant marine plastics: an experimental study into the effect of size on surface longevity. *Environ. Pollut.* 210, 354–360. doi: 10.1016/j.envpol.2016.01.026
- Fenchel, T. (2008). The microbial loop – 25 years later. *J. Exp. Mar. Biol. Ecol.* 366, 99–103. doi: 10.1016/j.jembe.2008.07.013
- Gajendiran, A., Krishnamoorthy, S., and Abraham, J. (2016). Microbial degradation of low-density polyethylene (LDPE) by *Aspergillus clavatus* strain JASK1 isolated from landfill soil. *Biotech* 6:52. doi: 10.1007/s13205-016-0394-x
- Gewert, B., Plassmann, M. M., and Macleod, M. (2015). Pathways for degradation of plastic polymers floating in the marine environment. *Environ. Sci. Process. Impacts* 17, 1513–1521. doi: 10.1039/c5em00207a
- Ghiglione, J.-F., Martin-Laurent, F., and Pesce, S. (2016). Microbial ecotoxicology: an emerging discipline facing contemporary environmental threats. *Environ. Sci. Pollut. Res.* 23, 3981–3983. doi: 10.1007/s11356-015-5763-1
- Ghiglione, J. F., Martin-Laurent, F., Stachowski-Haberkm, S., Pesce, S., and Vuilleumier, S. (2014). The coming of age of microbial ecotoxicology: report on the first two meetings in France. *Environ. Sci. Pollut. Res. Int.* 21, 14241–14245. doi: 10.1007/s11356-014-3390-x
- Gilan, I., and Sivan, A. (2013). Effect of proteases on biofilm formation of the plastic-degrading actinomycete *Rhodococcus ruber* C208. *FEMS Microbiol. Lett.* 342, 18–23. doi: 10.1111/1574-6968.12114
- Goldstein, M. C., Carson, H. S., and Eriksen, M. (2014). Relationship of diversity and habitat area in North Pacific plastic-associated rafting communities. *Mar. Biol.* 161, 1441–1453. doi: 10.1007/s00227-014-2432-8
- Gonda, K. E., Jendrossek, D., and Molitoris, H. P. (2000). *Fungal Degradation of the Thermoplastic Polymer Poly-β-Hydroxybutyric Acid (PHB) Under Simulated Deep Sea Pressure BT - Life at Interfaces and Under Extreme Conditions*, eds G. Liebezeit, S. Dittmann, and I. Kröncke (Dordrecht: Springer), 173–183.
- Gorke, J. T., Okrasa, K., Louwagie, A., Kazlauskas, R. J., and Srienc, F. (2007). Enzymatic synthesis of poly(hydroxyalkanoates) in ionic liquids. *J. Biotechnol.* 132, 306–313. doi: 10.1016/j.jbiotec.2007.04.001
- Gravouil, K., Ferru-Clément, R., Colas, S., Helye, R., Kadri, L., Bourdeau, L., et al. (2017). Transcriptomics and lipidomics of the environmental strain *Rhodococcus ruber* point out consumption pathways and potential metabolic bottlenecks for polyethylene degradation. *Environ. Sci. Technol.* 51, 5172–5181. doi: 10.1021/acs.est.7b00846
- Hadad, D., Geresh, S., and Sivan, A. (2005). Biodegradation of polyethylene by the thermophilic bacterium *Brevibacillus borstelensis*. *J. Appl. Microbiol.* 98, 1093–1100. doi: 10.1111/j.1365-2672.2005.02553.x
- Harrison, J. P., Boardman, C., O'Callaghan, K., Delort, A.-M., and Song, J. (2018). Biodegradability standards for carrier bags and plastic films in aquatic environments: a critical review. *R. Soc. Open Sci.* 5:171792. doi: 10.1098/rsos.171792
- Harrison, J. P., Sapp, M., Schratzberger, M., and Osborn, A. M. (2011). Interactions between microorganisms and marine microplastics: a call for research. *Mar. Technol. Soc. J.* 45, 12–20. doi: 10.4031/MTSJ.45.2.2
- Harrison, J. P., Schratzberger, M., Sapp, M., and Osborn, A. M. (2014). Rapid bacterial colonization of low-density polyethylene microplastics in coastal sediment microcosms. *BMC Microbiol.* 14:232. doi: 10.1186/s12866-014-0232-4
- Harshvardhan, K., and Jha, B. (2013). Biodegradation of low-density polyethylene by marine bacteria from pelagic waters, Arabian Sea, India. *Mar. Pollut. Bull.* 77, 100–106. doi: 10.1016/j.marpolbul.2013.10.025
- Hidalgo-Ruz, V., Gutow, L., Thompson, R. C., and Thiel, M. (2012). Microplastics in the marine environment: a review of the methods used for identification and quantification. *Environ. Sci. Technol.* 46, 3060–3075. doi: 10.1021/es2031505
- Ho, B. T., Roberts, T. K., and Lucas, S. (2018). An overview on biodegradation of polystyrene and modified polystyrene: the microbial approach. *Crit. Rev. Biotechnol.* 38, 308–320. doi: 10.1080/07388551.2017.1355293
- Hoeksema, B. W. (2012). Evolutionary trends in onshore-offshore distribution patterns of mushroom coral species (Scleractinia: Fungiidae). *Contrib. Zool.* 81, 199–221. doi: 10.1163/18759866-08104002
- Hosaka, M., Kamimura, N., Toribami, S., Mori, K., Kasai, D., Fukuda, M., et al. (2013). Novel tripartite aromatic acid transporter essential for terephthalate

- uptake in *Comamonas* sp. strain E6. *Appl. Environ. Microbiol.* 79, 6148–6155. doi: 10.1128/AEM.01600-13
- Hugenholtz, P., Hooper, S. D., and Kyrpidis, N. C. (2009). Focus: synergistetes. *Environ. Microbiol.* 11, 1327–1329. doi: 10.1111/j.1462-2920.2009.01949.x
- Hutchins, D. A., and Fu, F. (2017). Microorganisms and ocean global change. *Nat. Microbiol.* 2:17058. doi: 10.1038/nmicrobiol.2017.58
- Ibiene, A. A., Stanley, H. O., and Immanuel, O. M. (2013). Biodegradation of polyethylene by *Bacillus* sp. indigenous to the Niger delta mangrove swamp. *Niger. J. Biotechnol.* 26, 68–78.
- Ingavale, R., and Raut, P. D. (2018). Comparative biodegradation studies of LDPE and HDPE using *Bacillus weihenstephanensis* isolated from garbage soil. *Nat. Environ. Pollut. Technol.* 17, 649–655.
- İpekoglu, B., Böke, H., and Çizer, Ö. (2007). Assessment of material use in relation to climate in historical buildings. *Build. Environ.* 42, 970–978. doi: 10.1016/j.buildenv.2005.10.029
- Ishigaki, T., Sugano, W., Nakanishi, A., Tateda, M., Ike, M., and Fujita, M. (2004). The degradability of biodegradable plastics in aerobic and anaerobic waste landfill model reactors. *Chemosphere* 54, 225–233. doi: 10.1016/S0045-6535(03)00750-1
- Jaffredo, C. G., Carpentier, J.-F., and Guillaume, S. M. (2013). Organocatalyzed controlled ROP of  $\beta$ -lactones towards poly(hydroxyalkanoate)s: from  $\beta$ -butyrolactone to benzyl  $\beta$ -malolactone polymers. *Polym. Chem.* 4, 3837–3850. doi: 10.1039/C3PY00401E
- Jambeck, J. R., Geyer, R., Wilcox, C., Siegler, T. R., Perryman, M., Andrady, A., et al. (2015). Plastic waste inputs from land into the ocean. *Science* 347, 768–771. doi: 10.1126/science.1260352
- Jendrossek, D., Knoke, I., Habibian, R. B., Steinbüchel, A., and Schlegel, H. G. (1993). Degradation of poly(3-hydroxybutyrate), PHB, by bacteria and purification of a novel PHB depolymerase from *Comamonas* sp. *J. Environ. Polym. Degrad.* 1, 53–63. doi: 10.1007/BF01457653
- Jiang, P., Zhao, S., Zhu, L., and Li, D. (2018). Microplastic-associated bacterial assemblages in the intertidal zone of the Yangtze Estuary. *Sci. Total Environ.* 624, 48–54. doi: 10.1016/j.scitotenv.2017.12.105
- Kale, S. K., Deshmukh, A. G., Dudhare, M. S., and Patil, V. B. (2015). Microbial degradation of plastic: a review. *J. Biochem. Technol.* 6, 952–961.
- Kalogerakis, N., Karkanorachaki, K., Kalogerakis, G. C., Triantafyllidi, E. I., Gotsis, A. D., Partsinevelos, P., et al. (2017). Microplastics generation: onset of fragmentation of polyethylene Films in Marine Environment Mesocosms. *Front. Mar. Sci.* 4:84. doi: 10.3389/fmars.2017.00084
- Kaplan, D. L., Hartenstein, R., and Sutter, J. (1979). Biodegradation of polystyrene, poly(methyl methacrylate), and phenol formaldehyde. *Appl. Environ. Microbiol.* 38, 551–553.
- Kasuya, K., Inoue, Y., Tanaka, T., Akehata, T., Iwata, T., Fukui, T., et al. (1997). Biochemical and molecular characterization of the polyhydroxybutyrate depolymerase of *Comamonas acidovorans* YM1609, isolated from freshwater. *Appl. Environ. Microbiol.* 63, 4844–4852.
- Kathiresan, K. (2003). Polythene and plastic-degrading microbes in an Indian mangrove soil. *Rev. Biol. Trop.* 51, 629–633.
- Keswani, A., Oliver, D. M., Gutierrez, T., and Quilliam, R. S. (2016). Microbial hitchhikers on marine plastic debris: human exposure risks at bathing waters and beach environments. *Mar. Environ. Res.* 118, 10–19. doi: 10.1016/j.marenvres.2016.04.006
- Kettner, M. T., Rojas-Jimenez, K., Oberbeckmann, S., Labrenz, M., and Grossart, H.-P. (2017). Microplastics alter composition of fungal communities in aquatic ecosystems. *Environ. Microbiol.* 19, 4447–4459. doi: 10.1111/1462-2920.13891
- Kirstein, I. V., Kirmizi, S., Wichels, A., Garin-Fernandez, A., Erler, R., Löder, M., et al. (2016). Dangerous hitchhikers? Evidence for potentially pathogenic *Vibrio* spp. on microplastic particles. *Mar. Environ. Res.* 120, 1–8. doi: 10.1016/j.marenvres.2016.07.004
- Kita, K., Ishimaru, K., Teraoka, M., Yanase, H., and Kato, N. (1995). Properties of poly(3-hydroxybutyrate) depolymerase from a marine bacterium, *Alcaligenes faecalis* AE122. *Appl. Environ. Microbiol.* 61, 1727–1730.
- Kobayashi, T., Sugiyama, A., Kawase, Y., Saito, T., Mergaert, J., and Swings, J. (1999). Biochemical and genetic characterization of an extracellular poly(3-hydroxybutyrate) depolymerase from *Acidovorax* sp. Strain TP4. *J. Polym. Environ.* 7, 9–18. doi: 10.1023/A:1021885901119
- Koitaishi, M., Noguchi, M. T., Sameshima-Yamashita, Y., Hiradate, S., Suzuki, K., Yoshida, S., et al. (2012). Degradation of biodegradable plastic mulch films in soil environment by phylloplane fungi isolated from gramineous plants. *AMB Express* 2:40. doi: 10.1186/2191-0855-2-40
- Koutny, M., Lemaire, J., and Delort, A.-M. (2006). Biodegradation of polyethylene films with prooxidant additives. *Chemosphere* 64, 1243–1252. doi: 10.1016/j.chemosphere.2005.12.060
- Kowalczyk, A., Chyc, M., Ryszka, P., and Latowski, D. (2016). *Achromobacter xylosoxidans* as a new microorganism strain colonizing high-density polyethylene as a key step to its biodegradation. *Environ. Sci. Pollut. Res.* 23, 11349–11356. doi: 10.1007/s11356-016-6563-y
- Krueger, M. C., Harms, H., and Schlosser, D. (2015). Prospects for microbiological solutions to environmental pollution with plastics. *Appl. Microbiol. Biotechnol.* 99, 8857–8874. doi: 10.1007/s00253-015-6879-4
- Kumaravel, S., Hema, R., and Lakshmi, R. (2010). Production of poly(hydroxybutyrate) (Bioplastic) and its biodegradation by *Pseudomonas Lemoignei* and *Aspergillus Niger*. *E-J. Chem.* 7, S536–S542.
- Kyaw, B. M., Champakalakshmi, R., Sakharkar, M. K., Lim, C. S., and Sakharkar, K. R. (2012). Biodegradation of low density polythene (LDPE) by *Pseudomonas* species. *Indian J. Microbiol.* 52, 411–419. doi: 10.1007/s12088-012-0250-6
- Lebreton, L., Slat, B., Ferrari, F., Sainte-Rose, B., Aitken, J., Marthouse, R., et al. (2018). Evidence that the Great Pacific Garbage Patch is rapidly accumulating plastic. *Sci. Rep.* 8:4666. doi: 10.1038/s41598-018-22939-w
- Lee, H., Shim, W. J., and Kwon, J.-H. (2014). Sorption capacity of plastic debris for hydrophobic organic chemicals. *Sci. Total Environ.* 470–471, 1545–1552. doi: 10.1016/j.scitotenv.2013.08.023
- Lee, J.-W., Nam, J.-H., Kim, Y.-H., Lee, K.-H., and Lee, D.-H. (2008). Bacterial communities in the initial stage of marine biofilm formation on artificial surfaces. *J. Microbiol.* 46, 174–182. doi: 10.1007/s12275-008-0032-3
- Liebming, S., Eberl, A., Sousa, F., Heumann, S., Fischer-Colbrie, G., Cavaco-Paulo, A., et al. (2007). Hydrolysis of PET and bis-(benzoyloxyethyl) terephthalate with a new polyesterase from *Penicillium citrinum*. *Biocatal. Biotransformation* 25, 171–177. doi: 10.1080/10242420701379734
- Lobelle, D., and Cunliffe, M. (2011). Early microbial biofilm formation on marine plastic debris. *Mar. Pollut. Bull.* 62, 197–200. doi: 10.1016/j.marpolbul.2010.10.013
- Luu, R. A., Schneider, B. J., Ho, C. C., Nesteryuk, V., Ngwesse, S. E., Liu, X., et al. (2013). Taxis of *Pseudomonas putida* F1 toward phenylacetic acid is mediated by the energy taxis receptor Aer2. *Appl. Environ. Microbiol.* 79, 2416–2423. doi: 10.1128/AEM.03895-12
- Mabrouk, M. M., and Sabry, S. A. (2001). Degradation of poly(3-hydroxybutyrate) and its copolymer poly(3-hydroxybutyrate-co-3-hydroxyvalerate) by a marine *Streptomyces* sp. SNG9. *Microbiol. Res.* 156, 323–335. doi: 10.1078/0944-5013-00115
- Magnin, A., Hoornaert, L., Pollet, E., Laurichesse, S., Phalip, V., and Avérous, L. (2018). Isolation and characterization of different promising fungi for biological waste management of polyurethanes. *Microb. Biotechnol.* 1–12. doi: 10.1111/1751-7915.13346
- Manzur, A., Limón-González, M., and Favela-Torres, E. (2004). Biodegradation of physicochemically treated LDPE by a consortium of filamentous fungi. *J. Appl. Polym. Sci.* 92, 265–271. doi: 10.1002/app.13644
- Marten, E., Müller, R.-J., and Deckwer, W.-D. (2005). Studies on the enzymatic hydrolysis of polyesters. II. Aliphatic-aromatic copolyesters. *Polym. Degrad. Stab.* 88, 371–381. doi: 10.1016/j.polymdegradstab.2004.12.001
- Martínez-Tobón, D. I., Gul, M., Elias, A. L., and Sauvageau, D. (2018). Polyhydroxybutyrate (PHB) biodegradation using bacterial strains with demonstrated and predicted PHB depolymerase activity. *Appl. Microbiol. Biotechnol.* 102, 8049–8067. doi: 10.1007/s00253-018-9153-8
- Masó, M., Garcés, E., Pagès, F., and Camp, J. (2003). Drifting plastic debris as a potential vector for dispersing Harmful Algal Bloom (HAB) species. *Sci. Mar.* 67, 107–111. doi: 10.3989/scimar.2003.67n1107
- Mohanrasu, K., Premnath, N., Siva Prakash, G., Sudhakar, M., Boobalan, T., and Arun, A. (2018). Exploring multi potential uses of marine bacteria; an integrated approach for PHB production, PAHs and polyethylene biodegradation. *J. Photochem. Photobiol. B Biol.* 185, 55–65. doi: 10.1016/j.jphotobiol.2018.05.014
- Mohee, R., Unmar, G. D., Mudhoo, A., and Khadoo, P. (2008). Biodegradability of biodegradable/degradable plastic materials under aerobic and anaerobic conditions. *Waste Manag.* 28, 1624–1629. doi: 10.1016/j.wasman.2007.07.003

- Mor, R., and Sivan, A. (2008). Biofilm formation and partial biodegradation of polystyrene by the actinomycete *Rhodococcus ruber*. *Biodegradation* 19, 851–858. doi: 10.1007/s10532-008-9188-0
- Mothes, G., Ackermann, J.-U., and Babel, W. (2004). Mole fraction control of poly([R]-3-hydroxybutyrate-co-3-hydroxyvalerate) (PHB/HV) synthesized by *Paracoccus denitrificans*. *Eng. Life Sci.* 4, 247–251. doi: 10.1002/elsc.200320029
- Mukai, K., Yamada, K., and Doi, Y. (1994). Efficient hydrolysis of polyhydroxyalkanoates by *Pseudomonas stutzeri* YM1414 isolated from lake water. *Polym. Degrad. Stab.* 43, 319–327. doi: 10.1016/0141-3910(94)90002-7
- Müller, R.-J., Schrader, H., Profe, J., Dresler, K., and Deckwer, W.-D. (2005). Enzymatic degradation of Poly(ethylene terephthalate): rapid hydrolyse using a hydrolase from *T. fusca*. *Macromol. Rapid Commun.* 26, 1400–1405. doi: 10.1002/marc.200500410
- Muthukrishnan, T., Al Khaburi, M., and Abed, R. M. M. (2018). Fouling microbial communities on plastics compared with wood and steel: are they substrate- or location-specific? *Microb. Ecol.*
- Nimchua, T., Punnapayak, H., and Zimmermann, W. (2007). Comparison of the hydrolysis of polyethylene terephthalate fibers by a hydrolase from *Fusarium oxysporum* LCH I and *Fusarium solani* f. sp. *psi*. *Biotechnol. J.* 2, 361–364. doi: 10.1002/biot.200600095
- Novotný, Ě., Malachová, K., Adamus, G., Kwiecień, M., Lotti, N., Soccio, M., et al. (2018). Deterioration of irradiation/high-temperature pretreated, linear low-density polyethylene (LLDPE) by *Bacillus amyloliquefaciens*. *Int. Biodeterior. Biodegradation* 132, 259–267. doi: 10.1016/j.ibiod.2018.04.014
- Oberbeckmann, S., Kreikemeyer, B., and Labrenz, M. (2018). Environmental Factors Support the formation of specific bacterial assemblages on microplastics. *Front. Microbiol.* 8:2709. doi: 10.3389/fmicb.2017.02709
- Oberbeckmann, S., Loeder, M. G. J., Gerds, G., and Mark Osborn, A. (2014). Spatial and seasonal variation in diversity and structure of microbial biofilms on marine plastics in Northern European waters. *FEMS Microbiol. Ecol.* 49, 478–492. doi: 10.1111/1574-6941.12409
- Oberbeckmann, S., Loeder, M. G. J., and Labrenz, M. (2015). Marine microplastic-associated biofilms - a review. *Environ. Chem.* 12, 551–562. doi: 10.1071/EN15069
- Oberbeckmann, S., Osborn, A. M., and Duhaime, M. B. (2016). Microbes on a bottle: substrate, season and geography influence community composition of microbes colonizing marine plastic debris. *PLoS One* 11:e0159289. doi: 10.1371/journal.pone.0159289
- Oikawa, E., Linn, K. T., Endo, T., Oikawa, T., and Ishibashi, Y. (2003). Isolation and characterization of polystyrene degrading microorganisms for zero emission treatment of expanded polystyrene. *Environ. Eng. Res.* 40, 373–379.
- O'Leary, N. D., O'Connor, K. E., Ward, P., Goff, M., and Dobson, A. D. W. (2005). Genetic characterization of accumulation of polyhydroxyalkanoate from styrene in *Pseudomonas putida* CA-3. *Appl. Environ. Microbiol.* 71, 4380–4387. doi: 10.1128/AEM.71.8.4380-4387.2005
- Pathak, V. M. (2017). Review on the current status of polymer degradation: a microbial approach. *Bioresour. Bioprocess.* 4:15. doi: 10.1186/s40643-017-0145-9
- Peixoto, J., Silva, L. P., and Krüger, R. H. (2017). Brazilian Cerrado soil reveals an untapped microbial potential for untreated polyethylene biodegradation. *J. Hazard. Mater.* 324, 634–644. doi: 10.1016/j.jhazmat.2016.11.037
- Peña, C., Castillo, T., García, A., Millán, M., and Segura, D. (2014). Biotechnological strategies to improve production of microbial poly-(3-hydroxybutyrate): a review of recent research work. *Microb. Biotechnol.* 7, 278–293. doi: 10.1111/1751-7915.12129
- Pomeroy, L. R., LeB Williams, P. J., Azam, F., and Hobbie, J. E. (2007). The microbial loop. *Oceanography* 20, 28–33.
- Pompilio, A., Piccolomini, R., Picciani, C., D'Antonio, D., Savini, V., and Di Bonaventura, G. (2008). Factors associated with adherence to and biofilm formation on polystyrene by *Stenotrophomonas maltophilia*: the role of cell surface hydrophobicity and motility. *FEMS Microbiol. Lett.* 287, 41–47. doi: 10.1111/j.1574-6968.2008.01292.x
- Pramila, R. (2012). *Brevibacillus parabrevis*, *Acinetobacter baumannii* and *Pseudomonas citronellolis* - Potential candidates for biodegradation of low density polyethylene (LDPE). *J. Bacteriol. Res.* 4, 9–14. doi: 10.5897/JBR12.003
- Pramila, R., and Ramesh, K. V. (2011). Biodegradation of low density polyethylene (LDPE) by fungi isolated from marine water a SEM analysis. *Afr. J. Microbiol. Res.* 5, 5013–5018. doi: 10.5897/AJMR11.670
- Reis, M. A. M., Serafim, L. S., Lemos, P. C., Ramos, A. M., Aguiar, F. R., and Van Loosdrecht, M. C. M. (2003). Production of polyhydroxyalkanoates by mixed microbial cultures. *Bioprocess Biosyst. Eng.* 25, 377–385. doi: 10.1007/s00449-003-0322-4
- Romen, F., Reinhardt, S., and Jendrossek, D. (2004). Thermotolerant poly(3-hydroxybutyrate)-degrading bacteria from hot compost and characterization of the PHB depolymerase of *Schlegelella* sp. KB1a. *Arch. Microbiol.* 182, 157–164. doi: 10.1007/s00203-004-0684-2
- Ronkvist, Å. M., Xie, W., Lu, W., and Gross, R. A. (2009). Cutinase-catalyzed hydrolysis of poly(ethylene terephthalate). *Macromolecules* 42, 5128–5138. doi: 10.1021/ma9005318
- Salta, M., Wharton, J. A., Blache, Y., Stokes, K. R., and Briand, J. F. (2013). Marine biofilms on artificial surfaces: structure and dynamics. *Environ. Microbiol.* 15, 2879–2893. doi: 10.1111/1462-2920.12186
- Sang, B.-I., Hori, K., Tanji, Y., and Unno, H. (2001). A kinetic analysis of the fungal degradation process of poly(3-hydroxybutyrate-co-3-hydroxyvalerate) in soil. *Biochem. Eng. J.* 9, 175–184. doi: 10.1016/s1369-703x(01)00142-5
- Santo, M., Weitsman, R., and Sivan, A. (2013). The role of the copper-binding enzyme - laccase - in the biodegradation of polyethylene by the actinomycete *Rhodococcus ruber*. *Int. Biodeterior. Biodegradation* 84, 204–210. doi: 10.1016/j.ibiod.2012.03.001
- Sauret, C., Tedetti, M., Guigue, C., Dumas, C., Lami, R., Pujo-Pay, M., et al. (2016). Influence of PAHs among other coastal environmental variables on total and PAH-degrading bacterial communities. *Environ. Sci. Pollut. Res.* 23, 4242–4256. doi: 10.1007/s11356-015-4768-0
- Shah, A. A., Hasan, F., Hameed, A., and Ahmed, S. (2008). Biological degradation of plastics: a comprehensive review. *Biotechnol. Adv.* 26, 246–265. doi: 10.1016/j.biotechadv.2007.12.005
- Sharon, C., and Sharon, M. (2017). Studies on biodegradation of polyethylene terephthalate: a synthetic polymer. *J. Microbiol. Biotechnol. Res.* 2, 248–257.
- Sheik, S., Chandrasekar, K. R., Swaroop, K., and Somashekarappa, H. M. (2015). Biodegradation of gamma irradiated low density polyethylene and polypropylene by endophytic fungi. *Int. Biodeterior. Biodegradation* 105, 21–29. doi: 10.1016/j.ibiod.2015.08.006
- Sielicki, M., Focht, D. D., and Martin, J. P. (1978). Microbial degradation of [C14]polystyrene and 1,3-diphenylbutane. *Can. J. Microbiol.* 24, 798–803. doi: 10.1139/m78-134
- Silva, C. M., Carneiro, F., O'Neill, A., Fonseca, L. P., Cabral, J. S. M., Guebitz, G., et al. (2005). Cutinase? A new tool for biomodification of synthetic fibers. *J. Polym. Sci. Part A Polym. Chem.* 43, 2448–2450. doi: 10.1002/pola.20684
- Singh, B., and Sharma, N. (2008). Mechanistic implications of plastic degradation. *Polym. Degrad. Stab.* 93, 561–584. doi: 10.1016/j.polymdegradstab.2007.11.008
- Sivan, A. (2011). New perspectives in plastic biodegradation. *Curr. Opin. Biotechnol.* 22, 422–426. doi: 10.1016/j.copbio.2011.01.013
- Sowmya, H. V., Ramalingappa, M., and Krishnappa, M. (2012). Degradation of polyethylene by *Chaetomium* sp. and *Aspergillus Flavus*. *Int. J. Recent Sci. Res.* 3, 513–517.
- Sowmya, H. V., Ramalingappa, M., Krishnappa, M., and Thippeswamy, B. (2014). Degradation of polyethylene by *Penicillium simplicissimum* isolated from local dumpsite of Shivamogga district. *Environ. Dev. Sustain.* 17, 731–745. doi: 10.1007/s10668-014-9571-4
- Sudhakar, M., Doble, M., Murthy, P. S., and Venkatesan, R. (2008). Marine microbe-mediated biodegradation of low- and high-density polyethylenes. *Int. Biodeterior. Biodegradation* 61, 203–213. doi: 10.1016/j.ibiod.2007.07.011
- Syranidou, E., Karkanorachaki, K., Amorotti, F., Franchini, M., Repouskou, E., Kaliva, M., et al. (2017). Biodegradation of weathered polystyrene films in seawater microcosms. *Sci. Rep.* 7:17991. doi: 10.1038/s41598-017-18366-y
- Takeda, M., Koizumi, J.-I., Yabe, K., and Adachi, K. (1998). Thermostable poly(3-hydroxybutyrate) depolymerase of a thermophilic strain of *Leptothrix* sp. isolated from a hot spring. *J. Ferment. Bioeng.* 85, 375–380. doi: 10.1016/S0922-338X(98)80080-9
- Tang, Z.-L., Kuo, T.-A., and Liu, H.-H. (2017). The study of the microbes degraded polystyrene. *Adv. Technol. Innov.* 2, 13–17. doi: 10.1016/j.envpol.2017.09.043

- Tanio, T., Fukui, T., Shirakura, Y., Saito, T., Tomita, K., Kaiho, T., et al. (1982). An extracellular poly(3-hydroxybutyrate) depolymerase from *Alcaligenes faecalis*. *Eur. J. Biochem.* 124, 71–77. doi: 10.1111/j.1432-1033.1982.tb05907.x
- Uefuji, M., Kasuya, K., and Doi, Y. (1997). Enzymatic degradation of poly[(R)-3-hydroxybutyrate]: secretion and properties of PHB depolymerase from *Pseudomonas stutzeri*. *Polym. Degrad. Stab.* 58, 275–281. doi: 10.1016/S0141-3910(97)00058-X
- Vasile, C. (1993). “Degradation and decomposition,” in *Handbook of Polyolefins Synthesis and Properties*, eds C. Vasile and R. B. Seymour (New York, NY: Marcel Dekker Inc.), 479–506.
- Wagner, M., and Lambert, S. (eds). (2018). “Freshwater microplastics?: emerging environmental contaminants?” in *Handbook of Environmental Chemistry*, (Berlin: Springer Science+Business Media), 58.
- Wang, S., Lydon, K. A., White, E. M., Grubbs, J. B. III, Lipp, E. K., Locklin, J., et al. (2018). Biodegradation of Poly(3-hydroxybutyrate-co-3 hydroxyhexanoate) plastic under anaerobic sludge and aerobic seawater conditions: gas evolution and microbial diversity. *Environ. Sci. Technol.* 52, 5700–5709. doi: 10.1021/acs.est.7b06688
- Ward, P. G., Goff, M., Donner, M., Kaminsky, W., and O’Connor, K. E. (2006). A two step chemo- biotechnological conversion of polystyrene to a biodegradable thermoplastic. *Environ. Sci. Technol.* 40, 2433–2437. doi: 10.1021/es0517668
- Webb, H. K., Crawford, R. J., Sawabe, T., and Ivanova, E. P. (2009). Poly(ethylene terephthalate) polymer surfaces as a substrate for bacterial attachment and biofilm formation. *Microbes Environ.* 24, 39–42. doi: 10.1264/jsme2.ME08538
- Willis, K., Denise Hardesty, B., Kriwoken, L., and Wilcox, C. (2017). Differentiating littering, urban runoff and marine transport as sources of marine debris in coastal and estuarine environments. *Sci. Rep.* 7:44479. doi: 10.1038/srep44479
- Worm, B., Lotze, H. K., Jubinville, I., Wilcox, C., and Jambeck, J. (2017). Plastic as a persistent marine pollutant. *Annu. Rev. Environ. Resour.* 42, 1–26. doi: 10.1146/annurev-environ-102016-060700
- Yamada, K., Mukai, K., and Doi, Y. (1993). Enzymatic degradation of poly(hydroxyalkanoates) by *Pseudomonas pickettii*. *Int. J. Biol. Macromol.* 15, 215–220. doi: 10.1016/0141-8130(93)90040-S
- Yamada-Onodera, K., Mukumoto, H., Katsuyaya, Y., Saiganji, A., and Tani, Y. (2001). Degradation of polyethylene by a fungus, *Penicillium simplicissimum* YK. *Polym. Degrad. Stab.* 72, 323–327. doi: 10.1016/S0141-3910(01)00027-1
- Yang, J., Yang, Y., Wu, W.-M., Zhao, J., and Jiang, L. (2014). Evidence of polyethylene biodegradation by bacterial strains from the guts of plastic-eating waxworms. *Environ. Sci. Technol.* 48, 13776–13784. doi: 10.1021/es504038a
- Yang, Y., Yang, J., Wu, W.-M., Zhao, J., Song, Y., Gao, L., et al. (2015). Biodegradation and mineralization of polystyrene by plastic-eating mealworms: part 1. Chemical and physical characterization and isotopic tests. *Environ. Sci. Technol.* 49, 12080–12086. doi: 10.1021/acs.est.5b02661
- Yoon, M. G., Jeon, H. J., and Kim, M. N. (2012). Biodegradation of polyethylene by a soil bacterium and AlkB cloned recombinant cell. *J. Bioremediat. Biodegrad.* 3:145. doi: 10.4172/2155-6199.1000145
- Yoshida, S., Hiraga, K., Takehana, T., Taniguchi, I., Yamaji, H., Maeda, Y., et al. (2016). A bacterium that degrades and assimilates poly(ethylene terephthalate). *Science* 351, 1196–1199. doi: 10.1126/science.aad6359
- Zalasiewicz, J., Waters, C. N., do Sul, J. A. L., Corcoran, P. L., Barnosky, A. D., Cearreta, A., et al. (2016). The geological cycle of plastics and their use as a stratigraphic indicator of the Anthropocene. *Anthropocene* 13, 4–17. doi: 10.1016/j.ancene.2016.01.002
- Zettler, E. R., Mincer, T. J., and Amaral-Zettler, L. A. (2013). Life in the “Plastisphere”: microbial communities on plastic marine debris. *Environ. Sci. Technol.* 47, 7137–7146. doi: 10.1021/es401288x

**Conflict of Interest Statement:** The authors declare that the research was conducted in the absence of any commercial or financial relationships that could be construed as a potential conflict of interest.

Copyright © 2019 Jacquin, Cheng, Odobel, Pandin, Conan, Pujo-Pay, Barbe, Meistertzheim and Ghiglione. This is an open-access article distributed under the terms of the Creative Commons Attribution License (CC BY). The use, distribution or reproduction in other forums is permitted, provided the original author(s) and the copyright owner(s) are credited and that the original publication in this journal is cited, in accordance with accepted academic practice. No use, distribution or reproduction is permitted which does not comply with these terms.



# Impact of Leptospermone, a Natural $\beta$ -Triketone Herbicide, on the Fungal Composition and Diversity of Two Arable Soils

Clarisse Mallet<sup>1\*</sup>, Sana Romdhane<sup>2,3</sup>, Camille Loiseau<sup>1</sup>, Jérémie Béguet<sup>2</sup>, Fabrice Martin-Laurent<sup>2</sup>, Christophe Calvayrac<sup>3,4</sup> and Lise Barthelmebs<sup>3,4</sup>

<sup>1</sup> Laboratoire Microorganismes : Génome et Environnement, CNRS, Université Clermont Auvergne, Clermont-Ferrand, France, <sup>2</sup> AgroSup Dijon, INRA UMR1347 Agroécologie, Université de Bourgogne, Université Bourgogne Franche-Comté, Dijon, France, <sup>3</sup> Biocapteurs-Analyses-Environnement, Université de Perpignan Via Domitia, Perpignan, France, <sup>4</sup> Laboratoire de Biodiversité et Biotechnologies Microbiennes, USR 3579 Sorbonne Universités (UPMC) Paris 6 et CNRS Observatoire Océanologique, Banyuls-sur-Mer, France

## OPEN ACCESS

### Edited by:

Prayad Pokethititook,  
Mahidol University, Thailand

### Reviewed by:

Mariusz Cycoń,  
Medical University of Silesia, Poland

Anna Poli,  
University of Turin, Italy

### \*Correspondence:

Clarisse Mallet  
clarisse.mallet@uca.fr

### Specialty section:

This article was submitted to  
Microbiotechnology, Ecotoxicology  
and Bioremediation,  
a section of the journal  
Frontiers in Microbiology

**Received:** 14 December 2018

**Accepted:** 24 April 2019

**Published:** 10 May 2019

### Citation:

Mallet C, Romdhane S,  
Loiseau C, Béguet J,  
Martin-Laurent F, Calvayrac C and  
Barthelmebs L (2019) Impact  
of Leptospermone, a Natural  
 $\beta$ -Triketone Herbicide, on the Fungal  
Composition and Diversity of Two  
Arable Soils.  
*Front. Microbiol.* 10:1024.  
doi: 10.3389/fmicb.2019.01024

Impact of leptospermone, a  $\beta$ -triketone bioherbicide, was investigated on the fungal community which supports important soil ecological functions such as decomposition of organic matter and nutrients recycling. This study was done in a microcosm experiment using two French soils, Perpignan (P) and Saint-Jean-de-Fos (SJF), differing in their physicochemical properties and history treatment with synthetic  $\beta$ -triketones. Soil microcosms were treated with leptospermone at recommended dose and incubated under controlled conditions for 45 days. Untreated microcosms were used as control. Illumina MiSeq sequencing of the internal transcribed spacer region of the fungal rRNA revealed significant changes in fungal community structure and diversity in both soils. Xylariales, Hypocreales, Pleosporales and Capnodiales (Ascomycota phyla) fungi and those belonging to Sebaciniales, Cantharellales, Agaricales, Polyporales, Filobasidiales and Tremellales orders (Basidiomycota phyla) were well represented in treated soil microcosms compared to control. Nevertheless, while for the treated SJF a complete recovery of the fungal community was observed at the end of the experiment, this was not the case for the P treated soil, although no more bioherbicide remained. Indeed, the relative abundance of most of the saprophytic fungi were lower in treated soil compared to control microcosms whereas fungi from parasitic fungi included in Spizellomycetales and Pezizales orders increased. To the best of our knowledge, this is the only study assessing the effect of the bioherbicide leptospermone on the composition and diversity of the fungal community in soil. This study showed that leptospermone has an impact on  $\alpha$ - and  $\beta$ -diversity of the fungal community. It underlines the possible interest of microbial endpoints for environmental risk assessment of biopesticide.

**Keywords:** fungal community, microbial ecotoxicology, bioherbicide, leptospermone, soil

## INTRODUCTION

The use of biopesticides, defined as natural active compounds, is viewed as a safe alternative to agrochemicals for crop protection as they are considered to be less harmful and environmental-friendly compared to synthetic pesticides (Dayan et al., 2007, 2011; Seiber et al., 2014). Nowadays, only thirteen bioherbicides are commercially available (Cordeau et al., 2016).

Among compound of interest, leptospermone [2,2,4,4-tetramethyl-6-(3-methyl-1-oxobutyl)-1,3,5-cyclohexanetrione], an allelopathic compound isolated from bottlebrush plant (*Callistemon citrinus*) was used as pre-and post-emergence herbicide to control broad leaf and grass weeds at a rate of 3 L ha<sup>-1</sup> (Dayan et al., 2011). Belonging to  $\beta$ -triketone family, leptospermone inhibits the 4-hydroxyphenylpyruvate dioxygenase (HPPD), a key enzyme in plant carotenoid biosynthesis, (Rocaboy-Faquet et al., 2014) leading to photosynthetic chlorophyll destruction of plant (Lee et al., 2008). However, HPPDs are not specific for plant and are found in prokaryotes and fungi, including those living in soil (Keon and Hargreaves, 1998). Soil microorganisms which are known to accomplish numerous functions supporting soil ecosystemic services are key drivers to be protected (EFSA, 2017). As recently underlined by Amichot et al. (2018) the side effect of biopesticides has to be addressed, particularly assessing their environmental fate and impact on soil microorganisms (Gopal et al., 2007; Gupta et al., 2013; Singh et al., 2015a,b; Romdhane et al., 2016), and to the best of our knowledge no studies have been performed to estimate the effect of biopesticides on fungal community (Thomson et al., 2015). Fungi are known to play fundamental ecological roles in natural and managed agricultural soils (Al-Sadi et al., 2015; Tardy et al., 2015). As it was previously observed, application of pesticides, even at the recommended field dose, can induce a reduction in the overall fungal community, that could impacted the ecosystem services in which fungi are involved (Sebiomo et al., 2011; Schlatter et al., 2018). On the other hand, pesticides can be used as carbon source by some fungi known to possess biodegradation abilities (Ikehata et al., 2004; Tortella et al., 2005; Coppola et al., 2011; Panelli et al., 2017; Góngora-Echeverría et al., 2018).

Within this context, this study assessed for the first time, the impact of the bioherbicide leptospermone on the structure and diversity of fungal community inhabiting two soil types. We tested the effect of leptospermone on the diversity and composition of the fungal communities during the experimental time and in a same manner in the two different soils. This goal was reached by high throughput deep sequencing [Illumina MiSeq-based amplicon sequencing of ribosomal internal transcribed spacer 2 (ITS2) region]. The richness of each sample ( $\alpha$ -diversity) and the diversity in composition among samples ( $\beta$ -diversity) were assessed over time.

## MATERIALS AND METHODS

### Soil Characteristics and Microcosm Experiment

Soils and microcosm set-up was previously described in Romdhane et al. (2016). The two soils present different textures with 2-fold more clay and sand proportion in Saint-Jean-de-Fos (SJF) than in Perpignan (P) and with 2-fold less silt in SJF than in P (Table 1). Both soils are poor in organic matter and show a moderate cation exchange capacity.

Pure leptospermone was obtained as described by Owens et al. (2013). Soil microcosms were treated at recommended field

**TABLE 1** | Physico-chemical characteristics of the two soils (P and SJF) used for the experiment.

Soil characteristics	P Soil	SJF Soil
Clay	13.9%	25.8%
Silt	60.5%	27.3%
Sand	25.6%	46.9%
Soil humidity,	20%	15%
Organic matter	1.7%	1.5%
Organic carbon	0.98%	0.9%
Cation exchange capacity (CEC)	15.5 meq 100 g <sup>-1</sup>	10.4 meq 100 g <sup>-1</sup>
Ca <sup>2+</sup> /CEC	214%	98%
pH in water	8.1	7.62
History	Experimental field site having a $\beta$ -triketone history treatment	Neither cultivated nor treated with pesticides for the last 5 years

dose (D1, 5  $\mu$ g g<sup>-1</sup>) or not (D0, control). For each soil, three randomly chosen microcosms were sacrificed by sampling date and treatment ( $n = 12$  per sampling date). Soil samples were then subdivided in different aliquots for dissipation studies and molecular analysis.

### Fate of Leptospermone in the Soil Microcosms

Kinetics of dissipation and adsorption observed in P and SJF soils have already been reported in Romdhane et al. (2016). Briefly, leptospermone dissipation was measured during the time course of the incubation. Soil extracts were prepared from 10 g of each soil, and analyzed by HPLC/UV (Romdhane et al., 2016). Calibration curves prepared with spiked blank soil samples, were used to determine the leptospermone in soil extracts, with a quantification limit of 0.2 mg L<sup>-1</sup>.

Adaptation of the batch equilibrium method was applied to determine adsorption isotherms of leptospermone to both soils, using soil samples spiked with a range of leptospermone solutions (1 to 40 mg L<sup>-1</sup>) (Wilson and Chester, 1992; OECD, 2000; Romdhane et al., 2016). After 3 h of agitation with 1 g of soil sample, remaining leptospermone in solution was measured by HPLC/UV.

### Composition and Diversity of the Fungal Community

The composition and diversity of the fungal community were analyzed from DNA extracts [ISO 11063 derived from Martin-Laurent et al. (2001)] for P and SJF soils, treated (D1) or not (D0) with leptospermone at days 0, 4 and 45.

The amount of DNA was quantified (NanoDrop Technologies, DE, United States) and standardized to 10 ng  $\mu$ L<sup>-1</sup>. Aliquots were used as template to amplify Internal Transcribed Spacer 2 (ITS2) region of the ribosomal RNA gene cluster (Ihrmark et al., 2012; Tedersoo et al., 2014; Oliver et al., 2015). Amplicons were amplified with fITS7

(5'-GTGARTCATCGAATCTTTG-3', Ihrmark et al., 2012) and rITS4 (5'-TCCTCCGCTTATTGATATGC-3', White et al., 1990) supplemented with overhang adapter at the 5' end of each primer. A PCR was performed in 25  $\mu$ L reaction volume with the following concentrations: DNA 30 ng, 300  $\mu$ M dNTPs, 0.4  $\mu$ M of both primers (fITS7, rITS4), 1  $\times$  Kapa Hifi HotStart ReadyMix containing 2.5 mM MgCl<sub>2</sub> and 0.5 unit of Kapa Hifi HotStart DNA polymerase (KapaBiosystems, United States). PCR cycling parameters were: 95°C for 3 min, plus 30 cycles at 98°C for 20 s, 57°C for 30 s, and 72°C for 30 s, and followed by an extension at 72°C for 5 min. Relative quantity and yield were checked on 1% agarose gel and quantified using the Quant-iT™ PicoGreen™ dsDNA Assay Kit (Thermo Fisher Scientific, United States). The resulting PCR products were sent to the GeT-PLaGe platform (INRA, France) for multiplexing, purification and sequencing on the Illumina MiSeq platform.

## Sequence Analysis

Reads were passed through a quality control filter that removes sequences with more than one expected errors for all bases in the read and sequences under a minimum length threshold (100 bp). Then, a dereplication step was performed: set of unique sequence were found, sequences were compared letter-by-letter and must be identical over the full length of both sequences. In this step, singletons were discarded. UNOISE algorithm (Edgar and Flyvbjerg, 2015) was performed to denoise amplicon. Reads with sequencing error were identified and corrected and chimeras were removed. High-quality reads were then clustered into operational taxonomic units (OTUs) at 97% similarity using UPARSE (Edgar, 2013). The taxonomic assignment to species level was carried out using SINTAX algorithm (Edgar, 2016) against the Utax 22.08.2016 database (Supplementary Table S1).

$\alpha$ - and  $\beta$ -diversity indexes were assessed at the taxonomic rank of OTUs (MOTHUR, Schloss et al., 2009). Sample richness estimated by observed richness, Chao 1 index, the Shannon index and Simpson's index were used to compare the soil fungal community  $\alpha$ -diversity. To visually identify patterns of community structure among the samples ( $\beta$ -diversity), a Principal Coordinates Analysis (PCoA) analysis based on ThetayC dissimilarity matrix, was performed with MOTHUR (Schloss et al., 2009).

## Statistical Analysis

Differences between leptospermone treatments at days 0, 4 and 45 were assessed using a Kruskal–Wallis non parametric test ( $P < 0.05$ ) using “nparcomp” package of R software (Konietschke et al., 2015). Sparse Partial Least Squares Discriminant Analysis (sPLS-DA) was performed to select discriminant OTUs between different treatments using the function “splstda” from R package mixOmics (Lê Cao et al., 2017).

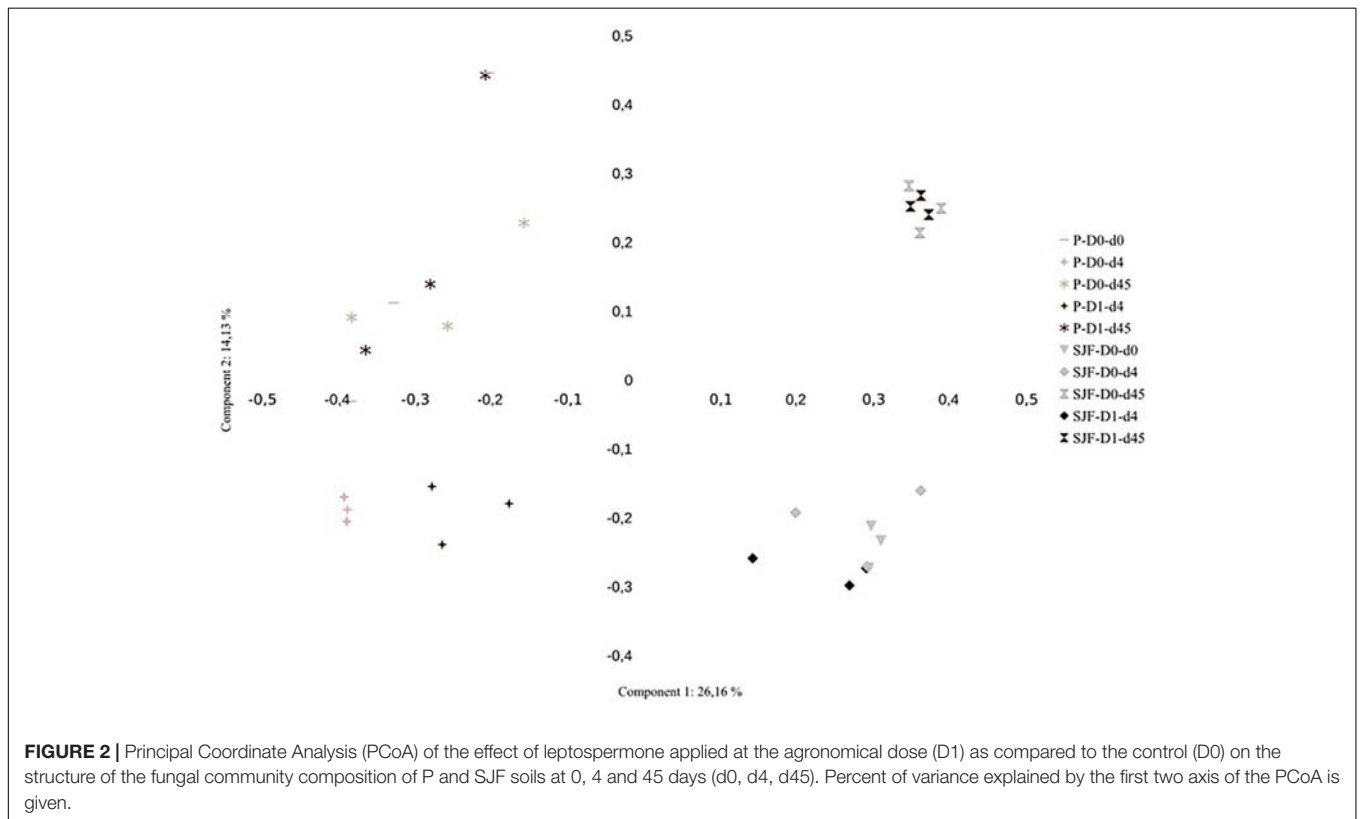
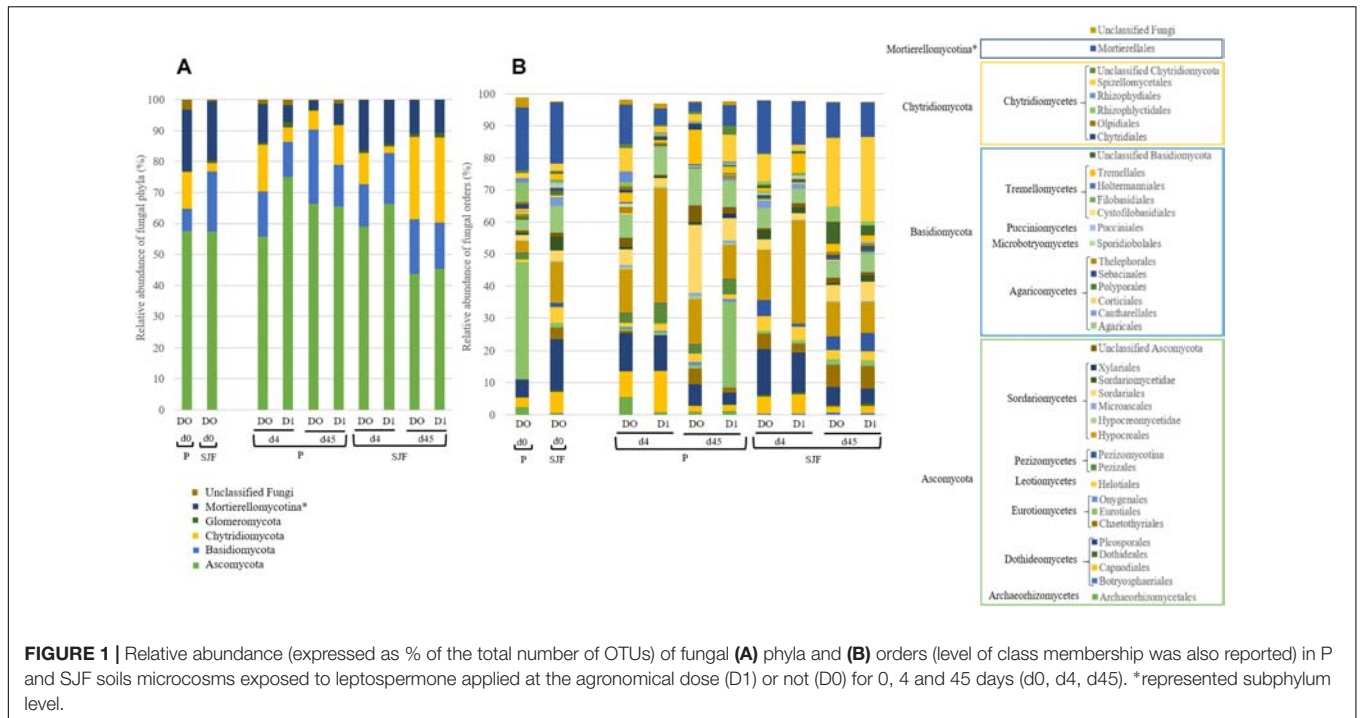
## RESULTS

As previously observed by Romdhane et al. (2016), leptospermone applied at the agronomical dose in P and SJF

soils was moderately adsorbed and in a similar manner for both soils with  $K_{oc}$  values of 144 and 137 mL g<sup>-1</sup>, respectively. The dissipation was significantly faster in P than in SJF soil ( $DT_{50} = 4$  and 9 days, respectively) but for both soils, leptospermone was entirely dissipated at the end of the incubation.

A total of 1630991 reads (min: 14933, max: 57410) were obtained through NGS sequencing (MiSeq Illumina sequencing). After quality control, 553800 sequences remained for analyses. The number of sequences per samples were of 13845 for a total of 2278 OTUs which were obtained at 98% similarity threshold.

Ascomycota was the most dominant phylum (P: 58%, SJF: 57%), with mainly Sordariomycetes class (P: 26%, SJF: 38%) represented by Hypocreales (P: 4%, SJF: 13%) and Sordariales orders (P: 3%, SJF: 3%), Dothideomycetes (P: 35%, SJF: 41%) class with Capnodiales (P: 3%, SJF: 7%) and Pleosporales (P: 5%, SJF: 16%) orders and Eurotiomycetes class (P: 14%, SJF: 9%) represented mainly by order of Eurotiales (P: 36%, SJF: 1%) (Figure 1). Basidiomycota phylum (P: 7%, SJF: 19%) was represented by Agaricomycetes class (P: 78%, SJF: 77%) with Agaricales order (P: 3%, SJF: 9%) and Tremellomycetes class (P: 20%, SJF: 14%) with Tremellales order (P: 1%, SJF: 2%). Mortierellomycotina (P: 20%, SJF: 19%) subphylum was only represented by Mortierellales order. Chytridiomycota (P: 12%, SJF: 3%) phylum was represented by one class Chytridiomycetes and mainly two orders (Rhizophlyctidales, P: 6% for, SJF: 0%, and Spizellomycetales, 2% for both soils) (Figure 1). The composition of the fungal community of P soil was different from that of SJF (Figures 1, 2). At both d0 and d45 observed richness was significantly lower in P than in SJF soil while Chao1 showed similar trend but only at D0 (Table 2). After 4 days of exposure, Shannon and Simpson indices of fungal communities recorded in P soil was lower than in those of the control ( $p = 0.049$ ). Accordingly, at the same time, the composition of the fungal community observed in P soil after 4 days of treatment was clearly discriminated from the control (Figure 3A). In order to visualize the relative abundance of selected OTUs in different treatments, a clustered heatmap was generated for both soils. OTUs mainly affiliated to Hypocreales (*Fusarium* sp.) and Capnodiales (*Cladosporium* sp.) were significantly higher in leptospermone treated soil (Figure 3B). The relative abundance of Sordariales, Spizellomycetales and Mortierellales fungi decreased in the treated P soil (Figure 1). Forty five days after the treatment, fungal composition was still significantly different from the control mainly represented by Sordariales, Pleosporales, Hypocreales, leotiomyces and Hypocreomycetidae fungi (Figure 3B) while the relative abundance of Eurotiales, Pezizales, Spizellomycetales, Chytridiomycetales and Mortierellales fungi were higher in treated P soils (Figure 1). In the SJF soil, leptospermone did not induced significant changes in the  $\alpha$ -diversity on the fungal community (Figure 2 and Table 2), contrary to what was observed for P soil. Nonetheless, significant changes in the  $\beta$ -diversity of the fungal community were recorded in SJF soil exposed microcosms as compared to control (Figure 4A). While Ascomycota OTUs dominated the composition of the fungal community of P soil, Basidiomycota



and Zygomycota OTUs were dominant in SFJ soil (Figures 3B, 4B). In Figure 4B, one could observe that the relative abundance of OTUs, responsive to leptospermone exposure, affiliated to Xylariales and Hypocreales orders (Sordariomyces class),

Dothideales and Pleosporales orders (Dothideomycetes class), Sebaciales, Cantharellales, Polyporales and Corticiales orders (Agaricomycetes class), Filobasiales and Tremellales orders (Tremellomycetes class) and Mortierellales order

**TABLE 2** | Richness and diversity indices of the fungal community calculated for P and SJF soils microcosms exposed to leptospermone applied at the agronomical dose (D1) or not (D0) at 0, 4 and 45 days (d0, d4, d45) (mean values  $\pm$  standard deviation,  $n = 3$ ).

Samples	Index				
	Number of OTUs (Observed richness)	Chao 1	Shannon-Wiener (H')	Simpson (D)	
Perpignan	P-D0-d0	471.3 $\pm$ 22.5a	559.5 $\pm$ 63.0a	4.38 $\pm$ 0.36a	0.96 $\pm$ 0.01a
	SJF-D0-d0	581.0 $\pm$ 86.6b	754.6 $\pm$ 120.0b	4.68 $\pm$ 0.04a	0.97 $\pm$ 0.00a
	P-D0-d45	378.0 $\pm$ 67.0a	501.4 $\pm$ 73.1a	4.65 $\pm$ 0.34a	0.98 $\pm$ 0.01a
	SJF-D0-d45	528.3 $\pm$ 41.4b	671.0 $\pm$ 69.8a	4.45 $\pm$ 0.08a	0.97 $\pm$ 0.00a
	P-D0-d4	529.0 $\pm$ 5.5a	629.1 $\pm$ 31.3a	4.85 $\pm$ 0.10a	0.98 $\pm$ 0.00a
	P-DI-d4	323.5 $\pm$ 90.5b	488.4 $\pm$ 135.8a	3.74 $\pm$ 0.40b	0.95 $\pm$ 0.01b
	P-D0-d45	378.0 $\pm$ 67.0a	501.4 $\pm$ 73.1a	4.65 $\pm$ 0.34a	0.98 $\pm$ 0.01a
	P-DI-d45	493.7 $\pm$ 46.6a	679.3 $\pm$ 94.8a	3.85 $\pm$ 1.5a	0.81 $\pm$ 0.27a
Saint Jean de Fos	SJF-D0-d4	582.3 $\pm$ 20.9a	746.2 $\pm$ 80.3a	4.61 $\pm$ 0.18a	0.97 $\pm$ 0.01a
	SJF-DI-d4	462.5 $\pm$ 55.7a	711.9 $\pm$ 81.4a	4.57 $\pm$ 0.10a	0.98 $\pm$ 0.00a
	SJF-D0-d45	528.3 $\pm$ 41.4a	671.0 $\pm$ 69.8a	4.45 $\pm$ 0.08a	0.97 $\pm$ 0.00a
	SJF-DI-d45	411.0 $\pm$ 105.8a	517.0 $\pm$ 137.5a	4.34 $\pm$ 0.07a	0.97 $\pm$ 0.00a

Different letters indicate significant differences between the initial or final fungal diversity of the two soils, and between leptospermone treatments (D1) compared to control (D0) at days 4 and 45.

(Zygomycota phylum) were significantly higher than in the control microcosms. At the end of the incubation (45 days), the fungal community of SJF treated soil was not significantly different from that of control (Figure 4A) and OTUs were mainly affiliated to Chaetothyriales and Spizellomycetales orders (respectively Eurotiomycetes and Chytridiomycetes classes) (Figure 4B).

## DISCUSSION

To date, although EFSA recommended to implement microbial endpoints, such as arbuscular mycorrhiza fungi, in pesticide environmental risk assessment (EFSA, 2010), there are still a limited number of studies evaluating side-effect of synthetic pesticides on soil fungal community (Borowik et al., 2017; Morrison-Whittle et al., 2017; Rivera-Becerril et al., 2017; Góngora-Echeverría et al., 2018) and almost none concerning biopesticides (Gopal et al., 2007).

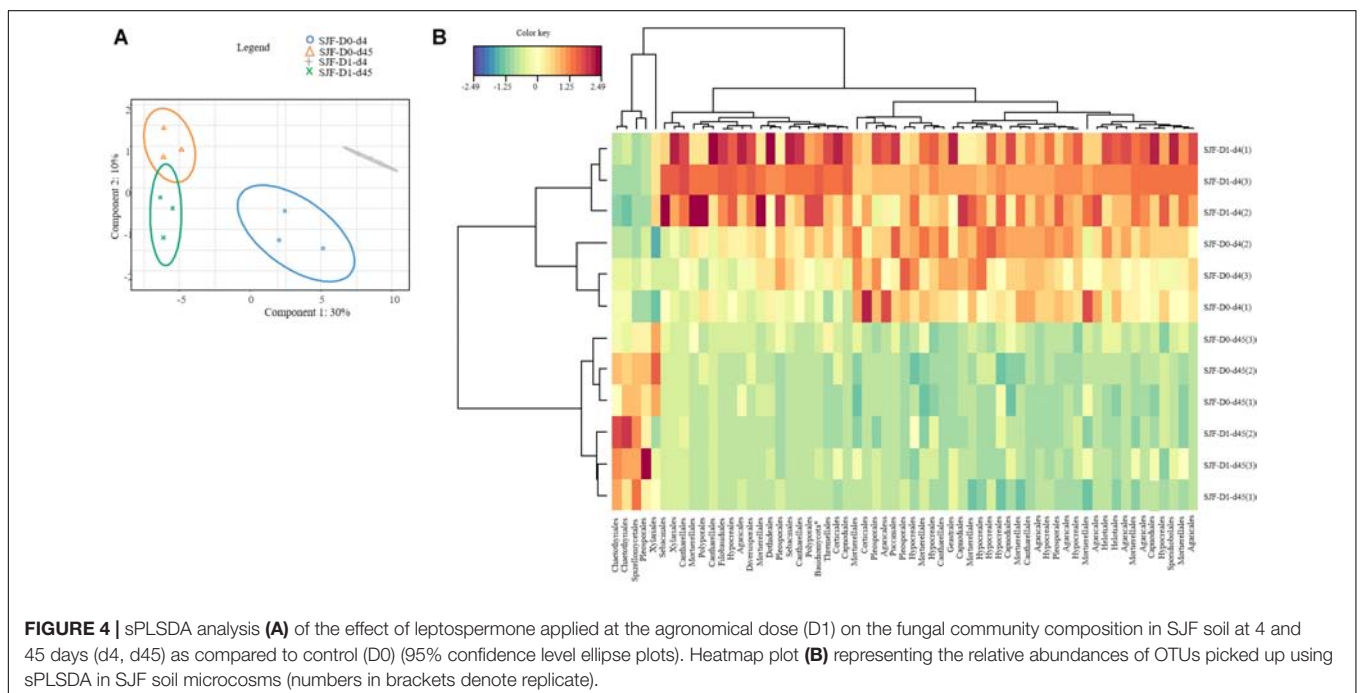
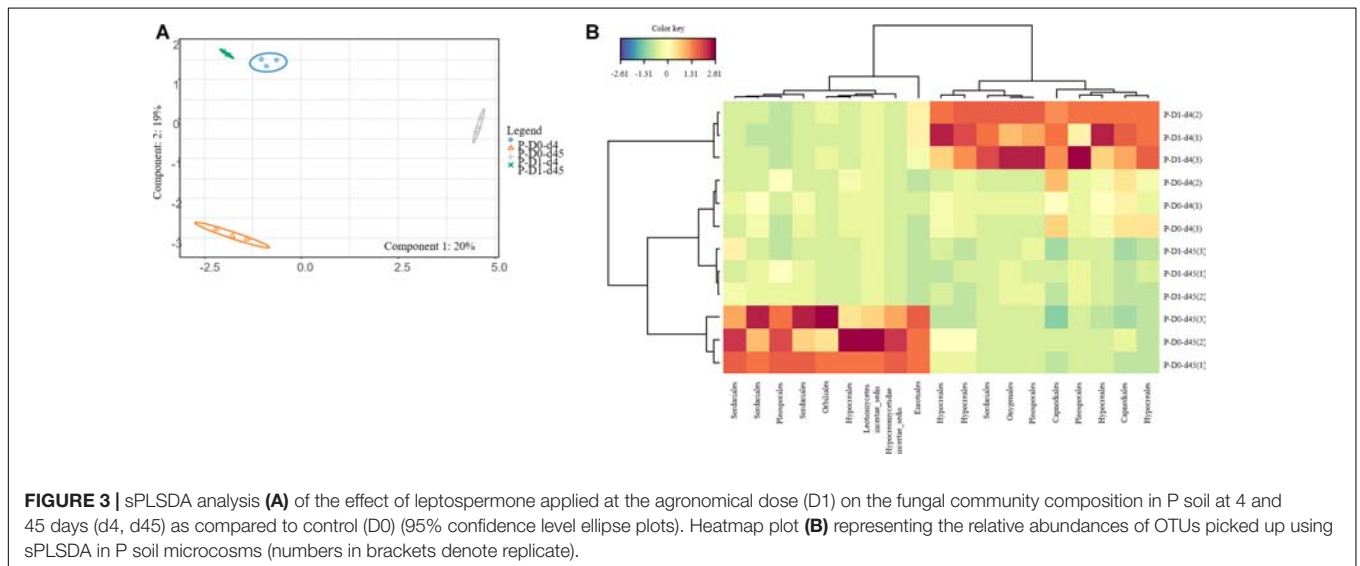
To the best of our knowledge, this is the first study assessing the effect of the leptospermone on the composition and diversity of the fungal community in two different arable soils. As expected, the composition of fungal community of P and SJF soils were differing. Indeed, whether it is through  $\alpha$ -diversity index or through fungal community composition, P soil presented the lower species richness and diversity. Its composition was mainly dominated by Eurotiales and Mortierellales orders while in SJF soil, Pleosporales, Hypocreales and Mortierellales orders predominated. These differences could be partially due to different physicochemical characteristics of the two soils and in particular clay content, which is well known to influence the aggregate size, moisture content and pH (Vargas-Gastélum et al., 2015), key abiotic parameters of ecological niches. Indeed, higher fungal alpha diversity in SJF soil than in P soil and the presence of Pleosporales et Hypocreales fungi could be due to the fine-size

particles in this soil clay fraction (Wang et al., 2016). Moreover, these first results could also be explained by the history treatment of the two soils. Indeed, SJF soil was neither cultivated nor treated with pesticides for the last 5 years contrary to P soil which was cropped with corn and treated with synthetic  $\beta$ -triketone herbicides (Romdhane et al., 2016), which could explained the higher diversity obtained in SJF soil. However, one could observe common features between the two soils such as the predominance of *Mortierella*. These highly opportunistic genera are able to rapidly grow on simple organic matter (Tardy et al., 2015) which could reflect easily decomposable C-substrates in the two assessed soils. A low abundance of Glomeromycota (<1% in both soils) was observed in both soils. This result has already been observed in other studies (Xu et al., 2012; Panelli et al., 2017) and may be due to the fact that this phylum, gathered genera which are obligate arbuscular mycorrhiza fungi forming symbiosis with roots of most of vascular plants, could be poorly covered by primers (Hartmann et al., 2015).

Dissipation of the bioherbicide was depending on the soil (P-DT50 < SJF-DT50): longer persistence of leptospermone was observed in SJF soil compared to P soil (Romdhane et al., 2016). However, after 4 days of exposure to the bioherbicide, significant changes in the structure of the fungal community were observed in both soils compared to the control. The increase of the relative abundance of Xylariales, Hypocreales (Sordariomycetes class), Pleosporales and Capnodiales (Dothideomycetes class) fungi might be linked to an increase of organic matter mineralization by fungal activity (Lienhard et al., 2014) and to their possible involvement in the biopesticide degradation, as previously shown for synthetic pesticides (Bell and Wheeler, 1986; Coppola et al., 2011). These orders of fungi grow quickly and become dominant because they are well adapted to metabolize low molecular weight organic carbon sources (Hannula et al., 2012) such as the compounds released by dead sensitive microorganisms like Spizellomycetales, Pezizomycotina

and Mortierellales fungi (respectively Chytridiomycetes, Pezizomycetes classes and Mucoromycotina subphylum). Moreover these fungi with melanin pigments in their hyphae have been associated with mitigating environmental stresses (including high temperatures, high UV radiation and extended drought) (Bell and Wheeler, 1986). Genera like *Fusarium* (Hypocreales order), well represented in treated soil microcosms, are among those that most significantly respond to the changing of agricultural managements (Hartmann et al., 2015) and could be much tolerant to xenobiotic (Bourgeois et al., 2015). Bioherbicide transformation might also explain the increase of the relative abundances of fungal OTUs related to Sebaciales, Cantharellales, Agaricales and Polyporales

orders and Filobasidiales and Tremellales ones (respectively Agaricomycetes and Tremellomycetes classes) in SJF soil, where leptospermone was still at rather high concentration after 4 days of exposure as compared to P soil (Romdhane et al., 2016). Indeed, several genera from these orders (i.e., *Trametes* sp., *Phanerochaete* sp., *Cyathus* sp., *Phlebia* sp., *Cryptococcus* sp.) are known to have relatively broad amplitude of ecological tolerance and to transform lignin and/or various recalcitrant organic pollutants including numerous pesticides (Singh et al., 1999; Singh and Kuhad, 1999; Ikehata et al., 2004; Tortella et al., 2005; Xiao et al., 2011; Johnson and Echavarri-Erasun, 2011; de Garcia et al., 2012). Moreover, these fungi, as *Mortierella* genus (Mortierellales order) can grow in contaminated soils with



pesticides (Kataoka et al., 2010; Salar, 2012), also because they can use fresh organic matter released from dead microorganisms sensitive to pesticides (Tardy et al., 2015).

Interestingly, after 45 days of incubation, the fungal community of treated SJF soil was able to rapidly recover, probably because of the entire dissipation of leptospermone (Romdhane et al., 2016). Surprisingly, the  $\beta$ -diversity of fungal community did not fully recover in P soil, although leptospermone was dissipated more rapidly than in SJF soil. At the end of the incubation in P soil, one could observe that the relative abundance of most of the saprophytic fungi and particularly those belonging to Sordariales, Hypocreales Pleosporales, Helotiales, Agaricales and Tremellales orders were lower in treated soil compared to control microcosms whereas fungi from Eurotiales order and parasitic fungi included in Spizellomycetales and Pezizales orders increased. In this condition, the dissipation of the leptospermone might have an antagonist effect by stopping the pressure on parasitic fungi. This persistent changes in the fungal community might result from a system drift due to changes in the quantity and quality of organic matter in P soils induced by leptospermone exposure (Klaubauf et al., 2010; Ma et al., 2013; Wang et al., 2016).

To conclude leptospermone applied at the agronomical dose caused significant changes in the  $\beta$ -diversity of the fungal community. Nevertheless, while the fungal community completely recovered in the SJF soil as already observed for bacterial community (Romdhane et al., 2016), the recovery was not observed in the P treated soil, although no more bioherbicide remained. Contrary to the bacterial community (Romdhane et al., 2016), the resilience of the fungal community is not obtained for both soils even after the entire dissipation of leptospermone. Taking together, our results showed that characterization of effect of herbicides and/or bioherbicides on microbial community and ecosystem functions, have to integrate both bacterial and fungal communities. Indeed, treatments have shown to induce different responses and led to promotion or suppression of beneficial or pathogenic fungal taxa (Hartmann et al., 2015). However,

only two soil types and one concentration of application were tested thereby burden with doubt any generalization. Further study is needed to distinguish between direct and indirect (e.g., drift of the system) effects of leptospermone. This study showed that a natural  $\beta$ -triketone herbicide had an effect on soil fungal community  $\alpha$ - and  $\beta$ -diversity underlining the need to even assess the ecotoxicity of biocontrol product on non-target organisms using microbial endpoints.

## AUTHOR CONTRIBUTIONS

All authors contributed to the design of the work or the acquisition, analysis, or interpretation of data for the work. CM, SR, CC, FM-L, and LB were involved in drafting the work and critical reading of the manuscript and final approval of the version to be published.

## FUNDING

This work was supported by the French “Agence National de la Recherche” under TRICETOX project, number ANR-13-CESA-0002.

## ACKNOWLEDGMENTS

We would like to thank the GeT-PLaGe platform INRA (France) for sequencing.

## SUPPLEMENTARY MATERIAL

The Supplementary Material for this article can be found online at: <https://www.frontiersin.org/articles/10.3389/fmicb.2019.01024/full#supplementary-material>

**TABLE S1** | OTU table.

soil. *Environ. Chem. Lett.* 13, 503–511. doi: 10.1007/s10311-015-0532-4

Coppola, L., Comitini, F., Casucci, C., Milanovic, V., Monaci, E., Marinozzi, M., et al. (2011). Fungicides degradation in an organic biomixture: impact on microbial diversity. *New Biotechnol.* 29, 99–106. doi: 10.1016/j.nbt.2011.03.005

Cordeau, S., Triolet, M., Wayman, S., Steinberg, C., and Philippe Guillemin, J. (2016). Bioherbicides: dead in the water? A review of the existing products for integrated weed management. *Crop Prot.* 87, 44–49. doi: 10.1016/j.cropro.2016.04.016

Dayan, F. E., Duke, S. O., Sauldubois, A., Singh, N., McCurdy, C., and Cantrell, C. (2007). p-Hydroxyphenylpyruvate dioxygenase is a herbicidal target site for  $\beta$ -triketones from *Leptospermum scoparium*. *Phytochemistry* 68, 2004–2014. doi: 10.1016/j.phytochem.2007.01.026

Dayan, F. E., Howell, J., Marais, J. P., Ferreira, D., and Koivunen, M. (2011). Manuka oil, a natural herbicide with preemergence activity. *Weed Sci.* 59, 464–469. doi: 10.1614/WS-D-11-00043.1

de Garcia, V., Zalar, P., Brizzio, S., Gunde-Cimerman, N., and van Broock, M. (2012). *Cryptococcus* species (Tremellales) from glacial biomes in the southern

## REFERENCES

- Al-Sadi, A. M., Al-Mazroui, S. S., and Phillips, A. J. L. (2015). Evaluation of culture-based techniques and 454 pyrosequencing for the analysis of fungal diversity in potting media and organic fertilizers. *J. Appl. Microbiol.* 119, 500–509. doi: 10.1111/jam.12854
- Amichot, M., Joly, P., Martin-Laurent, F., Siauxat, D., and Lavoit, A.-V. (2018). Biocontrol, new questions for Ecotoxicology? *Environ. Sci. Pollut. Res.* 25, 33895–33900. doi: 10.1007/s11356-018-3356-5
- Bell, A. A., and Wheeler, M. H. (1986). Biosynthesis and functions of fungal melanins. *Annu. Rev. Phytopathol.* 24, 411–451. doi: 10.1146/annurev.py.24.090186.002211
- Borowik, A., Wyszowska, J., Kucharski, J., Baemaga, M., and Tomkiel, M. (2017). Response of microorganisms and enzymes to soil contamination with a mixture of terbuthylazine, mesotrione, and S-metolachlor. *Environ. Sci. Pollut. Res.* 24, 1910–1925. doi: 10.1007/s11356-016-7919-z
- Bourgeois, E., Dequiedt, S., Lelièvre, M., van Oort, F., Lamy, I., Ranjard, L., et al. (2015). Miscanthus bioenergy crop stimulates nutrient-cycler bacteria and fungi in wastewater-contaminated agricultural

- (Patagonia) and northern (Svalbard) hemispheres. *FEMS Microbiol. Ecol.* 82, 523–539. doi: 10.1111/j.1574-6941.2012.01465.x
- Edgar, R. (2016). SINTAX: a simple non-Bayesian taxonomy classifier for 16S and ITS sequences. *bioRxiv* doi: 10.1101/074161
- Edgar, R. C. (2013). UPARSE: highly accurate OTU sequences from microbial amplicon reads. *Nat. Methods* 10, 996–998. doi: 10.1038/nmeth.2604
- Edgar, R. C., and Flyvbjerg, H. (2015). Error filtering, pair assembly and error correction for next-generation sequencing reads. *Bioinformatics* 31, 3476–3482. doi: 10.1093/bioinformatics/btv401
- EFSA (2010). Scientific opinion on the development of specific protection goal options for environmental risk assessment of pesticides, in particular in relation to the revision of the guidance documents on aquatic and terrestrial ecotoxicology (SANCO/3268/2001 and SA: specific protection goals for ERA of pesticides. *EFSA J.* 8:1821. doi: 10.2903/j.efsa.2010.1821
- EFSA (2017). Scientific opinion addressing the state of the science on risk assessment of plant protection products for in-soil organisms. *EFSA J.* 15:4690. doi: 10.2903/j.efsa.2017.4690
- Góngora-Echeverría, V. R., Quintal-Franco, C., Arena-Ortiz, M. L., Giacoman-Vallejos, G., and Ponce-Caballero, C. (2018). Identification of microbial species present in a pesticide dissipation process in biobed systems using typical substrates from southeastern Mexico as a biomixture at a laboratory scale. *Sci. Total Environ.* 628–629, 528–538. doi: 10.1016/j.scitotenv.2018.02.082
- Gopal, M., Gupta, A., Arunachalam, V., and Magu, S. P. (2007). Impact of azadirachtin, an insecticidal allelochemical from neem on soil microflora, enzyme and respiratory activities. *Bioresour. Technol.* 98, 3154–3158. doi: 10.1016/j.biortech.2006.10.010
- Gupta, S., Gupta, R., and Sharma, S. (2013). Impact of chemical- and bio-pesticides on bacterial diversity in rhizosphere of *Vigna radiata*. *Ecotoxicology* 22, 1479–1489. doi: 10.1007/s10646-013-1134-1
- Hannula, S. E., Boschker, H. T. S., de Boer, W., and van Veen, J. A. (2012). 13 C pulse-labeling assessment of the community structure of active fungi in the rhizosphere of a genetically starch-modified potato (*Solanum tuberosum*) cultivar and its parental isoline. *New Phytol.* 194, 784–799. doi: 10.1111/j.1469-8137.2012.04089.x
- Hartmann, M., Frey, B., Mayer, J., Mäder, P., and Widmer, F. (2015). Distinct soil microbial diversity under long-term organic and conventional farming. *ISME J.* 9:1177. doi: 10.1038/ismej.2014.210
- Ihrmark, K., Bödeker, I. T. M., Cruz-Martinez, K., Friberg, H., Kubartova, A., Schenck, J., et al. (2012). New primers to amplify the fungal ITS2 region - evaluation by 454-sequencing of artificial and natural communities. *FEMS Microbiol. Ecol.* 82, 666–677. doi: 10.1111/j.1574-6941.2012.01437.x
- Ikehata, K., Buchanan, I. D., and Smith, D. W. (2004). Extracellular peroxidase production by *Coprinus* species from urea-treated soil. *Can. J. Microbiol.* 50, 57–60. doi: 10.1139/w03-104
- Johnson, E. A., and Echavarrri-Erasun, C. (2011). “Yeast biotechnology,” in *The Yeasts: A Taxonomic Study*, 5th Edn, eds C. P. Kurtzman, J. W. Fell, and T. Boekhout (Amsterdam: Elsevier), 21–44.
- Kataoka, R., Takagi, K., and Sakakibara, F. (2010). A new endosulfan-degrading fungus, *Mortierella* species, isolated from a soil contaminated with organochlorine pesticides. *J. Pestic. Sci.* 35, 326–332. doi: 10.1584/jpestics. G10-10
- Keon, J., and Hargreaves, J. (1998). Isolation and heterologous expression of a gene encoding 4-hydroxyphenylpyruvate dioxygenase from the wheat leaf-spot pathogen, *Mycosphaerella graminicola*. *FEMS Microbiol. Lett.* 161, 337–343. doi: 10.1111/j.1574-6968.1998.tb12966.x
- Klaubauf, S., Inselsbacher, E., Zechmeister-Boltenstern, S., Wanek, W., Gottsberger, R., Strauss, J., et al. (2010). Molecular diversity of fungal communities in agricultural soils from Lower Austria. *Fung. Divers.* 44, 65–75. doi: 10.1007/s13225-010-0053-1
- Konietzschke, F., Placzek, M., Schaarschmidt, F., and Hothorn, L. A. (2015). nparcomp : an R software package for nonparametric multiple comparisons and simultaneous confidence intervals. *J. Stat. Softw.* 64, 1–17. doi: 10.18637/jss.v064.i09
- Lê Cao, K. A., Rohart, F., Gonzalez, I., Déjean, S., Gautier, B., Bartolo, F., et al. (2017). *mixOmics: Omics Data Integration Project*. Available from: <https://CRAN.R-project.org/package=mixOmics>
- Lee, C.-M., Yeo, Y.-S., Lee, J.-H., Kim, S.-J., Kim, J.-B., Han, N. S., et al. (2008). Identification of a novel 4-hydroxyphenylpyruvate dioxygenase from the soil metagenome. *Biochem. Biophys. Res. Commun.* 370, 322–326. doi: 10.1016/j.bbrc.2008.03.102
- Lienhard, P., Terrat, S., Prévost-Bouré, N. C., Nowak, V., Régner, T., Sayphoummie, S., et al. (2014). Pyrosequencing evidences the impact of cropping on soil bacterial and fungal diversity in Laos tropical grassland. *Agron. Sustain. Dev.* 34, 525–533. doi: 10.1007/s13593-013-0162-9
- Ma, A., Zhuang, X., Wu, J., Cui, M., Lv, D., Liu, C., et al. (2013). Ascomycota members dominate fungal communities during straw residue decomposition in arable soil. *PLoS One* 8:e66146. doi: 10.1371/journal.pone.0066146
- Martin-Laurent, F., Philippot, L., Hallet, S., Chaussod, R., Germon, J. C., Soulas, G., et al. (2001). DNA extraction from soils: old bias for new microbial diversity analysis methods. *Appl. Environ. Microbiol.* 67, 2354–2359. doi: 10.1128/AEM.67.5.2354-2359.2001
- Morrison-Whittle, P., Lee, S. A., and Goddard, M. R. (2017). Fungal communities are differentially affected by conventional and biodynamic agricultural management approaches in vineyard ecosystems. *Agric. Ecosyst. Environ.* 246, 306–313. doi: 10.1016/j.agee.2017.05.022
- OECD (2000). *Test No. 106: Adsorption - Desorption Using a Batch Equilibrium Method*. Paris: OECD.
- Oliver, A. K., Callahan, M. A., and Jumpponen, A. (2015). Soil fungal communities respond compositionally to recurring frequent prescribed burning in a managed southeastern US forest ecosystem. *For. Ecol. Manag.* 345, 1–9. doi: 10.1016/j.foreco.2015.02.020
- Owens, D. K., Nanayakkara, N. P. D., and Dayan, F. E. (2013). In planta mechanism of action of leptospermona: impact of its physico-chemical properties on uptake, translocation, and metabolism. *J. Chem. Ecol.* 39, 262–270. doi: 10.1007/s10886-013-0237-8
- Panelli, S., Capelli, E., Comandatore, F., Landinez-Torres, A., Granata, M. U., Tosi, S., et al. (2017). A metagenomic-based, cross-seasonal picture of fungal consortia associated with Italian soils subjected to different agricultural managements. *Fung. Ecol.* 30, 1–9. doi: 10.1016/j.funeco.2017.07.005
- Rivera-Becerril, F., van Tuinen, D., Chatagnier, O., Rouard, N., Béguet, J., Kuszala, C., et al. (2017). Impact of a pesticide cocktail (fenhexamid, folpel, deltamethrin) on the abundance of glomeromycota in two agricultural soils. *Sci. Total Environ.* 577, 84–93. doi: 10.1016/j.scitotenv.2016.10.098
- Rocaboy-Faquet, E., Noguer, T., Romdhane, S., Bertrand, C., Dayan, F. E., and Barthelmebs, L. (2014). Novel bacterial bioassay for a high-throughput screening of 4-hydroxyphenylpyruvate dioxygenase inhibitors. *Appl. Microbiol. Biotechnol.* 98, 7243–7252. doi: 10.1007/s00253-014-5793-5
- Romdhane, S., Devers-Lamrani, M., Barthelmebs, L., Calvayrac, C., Bertrand, C., Cooper, J.-F., et al. (2016). Ecotoxicological impact of the bioherbicide leptospermona on the microbial community of two arable soils. *Front. Microbiol.* 7:775. doi: 10.3389/fmicb.2016.00775
- Salar, R. (2012). Isolation and characterization of various fungal strains from agricultural soil contaminated with pesticides. *Res. J. Rec. Sci.* 1, 297–303.
- Schlatter, D. C., Yin, C., Burke, I., Hulbert, S., and Paulitz, T. (2018). Location, root proximity, and glyphosate-use history modulate the effects of glyphosate on fungal community networks of wheat. *Microb. Ecol.* 76, 240–257. doi: 10.1007/s00248-017-1113-9
- Schloss, P. D., Westcott, S. L., Ryabin, T., Hall, J. R., Hartmann, M., Hollister, E. B., et al. (2009). Introducing mothur: open-source, platform-independent, community-supported software for describing and comparing microbial communities. *Appl. Environ. Microbiol.* 75, 7537–7541. doi: 10.1128/AEM.01541-09
- Sebiomo, A., Ogundero, V., and Bankole, S. (2011). Effect of four herbicides on microbial population, soil organic matter and dehydrogenase activity. *Afr. J. Biotechnol.* 10, 770–778.
- Seiber, J. N., Coats, J., Duke, S. O., and Gross, A. D. (2014). Biopesticides: State of the art and future opportunities. *J. Agric. Food Chem.* 62, 11613–11619. doi: 10.1021/jf504252n
- Singh, B. K., and Kuhad, R. C. (1999). Biodegradation of lindane ( $\gamma$ -hexachlorocyclohexane) by the white-rot fungus *Trametes hirsutus*: bio-degradation of lindane by *T. hirsutus*. *Letts. Appl. Microbiol.* 28, 238–241. doi: 10.1046/j.1365-2672.1999.00508.x

- Singh, B. K., Kuhad, R. C., Singh, A., Lal, R., and Tripathi, K. K. (1999). Biochemical and molecular basis of pesticide degradation by microorganisms. *Crit. Rev. Biotechnol.* 19, 197–225. doi: 10.1080/0738-859991229242
- Singh, S., Gupta, R., Kumari, M., and Sharma, S. (2015a). Nontarget effects of chemical pesticides and biological pesticide on rhizospheric microbial community structure and function in *Vigna radiata*. *Environ. Sci. Pollut. Res.* 22, 11290–11300. doi: 10.1007/s11356-015-4341-x
- Singh, S., Gupta, R., and Sharma, S. (2015b). Effects of chemical and biological pesticides on plant growth parameters and rhizospheric bacterial community structure in *Vigna radiata*. *J. Hazard. Mater.* 291, 102–110. doi: 10.1016/j.jhazmat.2015.02.053
- Tardy, V., Spor, A., Mathieu, O., Lévêque, J., Terrat, S., Plassart, P., et al. (2015). Shifts in microbial diversity through land use intensity as drivers of carbon mineralization in soil. *Soil Biol. Biochem.* 90, 204–213. doi: 10.1016/j.soilbio.2015.08.010
- Tedersoo, L., Bahram, M., Polme, S., Koljal, U., Yorou, N. S., Wijesundera, R., et al. (2014). Global diversity and geography of soil fungi. *Science* 346:1256688. doi: 10.1126/science.1256688
- Thomson, B. C., Tisserant, E., Plassart, P., Uroz, S., Griffiths, R. I., Hannula, S. E., et al. (2015). Soil conditions and land use intensification effects on soil microbial communities across a range of European field sites. *Soil Biol. Biochem.* 88, 403–413. doi: 10.1016/j.soilbio.2015.06.012
- Tortella, G. R., Diez, M. C., and Durán, N. (2005). Fungal diversity and use in decomposition of environmental pollutants. *Crit. Rev. Microbiol.* 31, 197–212. doi: 10.1080/10408410500304066
- Vargas-Gastélum, L., Romero-Olivares, A. L., Escalante, A. E., Rocha-Olivares, A., Brizuela, C., and Riquelme, M. (2015). Impact of seasonal changes on fungal diversity of a semi-arid ecosystem revealed by 454 pyrosequencing. *FEMS Microbiol. Ecol.* 91:fiv044. doi: 10.1093/femsec/fi v044
- Wang, Z., Chen, Q., Liu, L., Wen, X., and Liao, Y. (2016). Responses of soil fungi to 5-year conservation tillage treatments in the drylands of northern China. *Appl. Soil Ecol.* 101, 132–140. doi: 10.1016/j.apsoil.2016.02.002
- White, T. J., Bruns, T., Lee, S., and Taylor, J. (1990). “Amplification and direct sequencing of fungal ribosomal RNA genes for phylogenetics,” in *PCR Protocols: A Guide to Methods and Applications*, eds M. A. Innis, D. H. Gelfand, J. J. Sninsky, and T. J. White (New York, NY: Academic Press, Inc.), 315–322.
- Wilson, J. S., and Chester, L. F. (1992). Influence of various soil properties on the adsorption and desorption of ICIA-0051 in five soils. *Weed Technol.* 6, 583–586.
- Xiao, P., Mori, T., Kamei, I., Kiyota, H., Takagi, K., and Kondo, R. (2011). Novel metabolic pathways of organochlorine pesticides dieldrin and aldrin by the white rot fungi of the genus *Phlebia*. *Chemosphere* 85, 218–224. doi: 10.1016/j.chemosphere.2011.06.028
- Xu, L., Ravnkov, S., Larsen, J., Nilsson, R. H., and Nicolaisen, M. (2012). Soil fungal community structure along a soil health gradient in pea fields examined using deep amplicon sequencing. *Soil Biol. Biochem.* 46, 26–32. doi: 10.1016/j.soilbio.2011.11.010

**Conflict of Interest Statement:** The authors declare that the research was conducted in the absence of any commercial or financial relationships that could be construed as a potential conflict of interest.

Copyright © 2019 Mallet, Romdhane, Loiseau, Béguet, Martin-Laurent, Calvayrac and Barthelmebs. This is an open-access article distributed under the terms of the Creative Commons Attribution License (CC BY). The use, distribution or reproduction in other forums is permitted, provided the original author(s) and the copyright owner(s) are credited and that the original publication in this journal is cited, in accordance with accepted academic practice. No use, distribution or reproduction is permitted which does not comply with these terms.



# Soil Photosynthetic Microbial Communities Mediate Aggregate Stability: Influence of Cropping Systems and Herbicide Use in an Agricultural Soil

Olivier Crouzet<sup>1\*</sup>, Laurent Consentino<sup>1</sup>, Jean-Pierre Pétraud<sup>1</sup>, Christelle Marraud<sup>1</sup>, Jean-Pierre Aguer<sup>2</sup>, Sylvie Bureau<sup>3</sup>, Carine Le Bourvellec<sup>3</sup>, Line Touloumet<sup>3</sup> and Annette Bérard<sup>4\*</sup>

## OPEN ACCESS

### Edited by:

Stéphane Pesce,  
National Research Institute of Science  
and Technology for Environment  
and Agriculture (IRSTEA), France

### Reviewed by:

Mariusz Cycoń,  
Medical University of Silesia, Poland  
Jennifer Doyle Rocca,  
Duke University, United States  
Mary Ann Victoria Bruns,  
The Pennsylvania State University,  
United States

### \*Correspondence:

Olivier Crouzet  
olivier.crouzet@inra.fr  
Annette Bérard  
annette.berard@inra.fr

### Specialty section:

This article was submitted to  
Microbiotechnology, Ecotoxicology  
and Bioremediation,  
a section of the journal  
Frontiers in Microbiology

**Received:** 17 December 2018

**Accepted:** 27 May 2019

**Published:** 14 June 2019

### Citation:

Crouzet O, Consentino L,  
Pétraud J-P, Marraud C, Aguer J-P,  
Bureau S, Le Bourvellec C,  
Touloumet L and Bérard A (2019) Soil  
Photosynthetic Microbial  
Communities Mediate Aggregate  
Stability: Influence of Cropping  
Systems and Herbicide Use in an  
Agricultural Soil.  
*Front. Microbiol.* 10:1319.  
doi: 10.3389/fmicb.2019.01319

<sup>1</sup> UMR ECOSYS (Ecologie et Ecotoxicologie des Agroécosystèmes), INRA, AgroParisTech, Université Paris-Saclay, Versailles, France, <sup>2</sup> UMR 6023 LMGE, CNRS, Université Clermont Auvergne, Aubière, France, <sup>3</sup> UMR 408 SQPOV, INRA, Avignon Université, Avignon, France, <sup>4</sup> UMR 1114 EMMAH (Environnement Méditerranéen et Modélisation des Agro-Hydrosystèmes), INRA, Avignon Université, Avignon, France

Edaphic cyanobacteria and algae have been extensively studied in dryland soils because they play key roles in the formation of biological soil crusts and the stabilization of soil surfaces. Yet, in temperate agricultural crop soils, little is understood about the functional significance of indigenous photosynthetic microbial communities for various soil processes. This study investigated how indigenous soil algae and cyanobacteria affected topsoil aggregate stability in cereal cropping systems. Topsoil aggregates from conventional and organic cropping systems were incubated in microcosms under dark or photoperiodic conditions with or without a treatment with an herbicide (isoproturon). Physicochemical parameters (bound exopolysaccharides, organic carbon) and microbial parameters (esterase activity, chlorophyll a biomass, and pigment profiles) were measured for incubated aggregates. Aggregate stability were analyzed on the basis of aggregate size distribution and the mean weight diameter (MWD) index, resulting from disaggregation tests. Soil photosynthetic microbial biomass (chl a) was strongly and positively correlated with aggregate stability indicators. The development of microalgae crusts in photoperiodic conditions induced a strong increase of the largest aggregates (>2 mm), as compared to dark conditions (up to 10.6 fold and 27.1 fold, in soil from organic and conventional cropping systems, respectively). Concomitantly, the MWD significantly increased by 2.4 fold and 4.2 fold, for soil from organic and conventional cropping systems. Soil microalgae may have operated directly via biochemical mechanisms, by producing exopolymeric matrices surrounding soil aggregates (bound exopolysaccharides: 0.39–0.45  $\mu\text{g C g}^{-1}$  soil), and via biophysical mechanisms, where filamentous living microbiota enmeshed soil aggregates. In addition, they may have acted indirectly by stimulating heterotrophic microbial communities, as revealed by the positive effect of microalgal growth on total microbial activity. The herbicide treatment negatively impacted soil microalgal community, resulting in

significant decreases of the MWD of the conventional soil aggregates (up to –42% of the value in light treatment). This study underscores that indigenous edaphic algae and cyanobacteria can promote aggregate formation, by forming photosynthetic microbiotic crusts, thus improving the structural stability of topsoil, in temperate croplands. However, the herbicide uses can impair the functional abilities of algal and cyanobacterial communities in agricultural soils.

**Originality/Significance:** Edaphic algal and cyanobacterial communities are known to form photosynthetic microbial crusts in arid soils, where they drive key ecosystem functions. Although less well characterized, such communities are also transiently abundant in temperate and mesic cropped soils. This microcosm study investigated the communities' functional significance in topsoil aggregate formation and stabilization in two temperate cropping systems. Overall, our results showed that the development of indigenous microalgal communities under our experimental conditions drove higher structural stability in topsoil aggregates in temperate cropland soils. Also, herbicide use affected photosynthetic microbial communities and consequently impaired soil aggregation.

**Keywords:** photosynthetic microbial communities, cyanobacteria, aggregate stability, herbicide, cropping systems, exopolysaccharides

## INTRODUCTION

Photosynthetic microorganisms such as eukaryotic algae and prokaryotic cyanobacteria are ubiquitous pioneer colonizers of topsoil surfaces (Booth, 1941; Metting, 1981). They have been extensively studied in dryland ecosystems, where they play key roles in the formation of biological soil crusts and soil ecological processes (Evans and Johansen, 1999; Belnap and Lange, 2003; Chamizo et al., 2018), and in rice field ecosystems, where they are important to soil fertility (Singh et al., 2011). Far less is known about the communities and functions of soil algae and cyanobacteria living in mesic agricultural croplands (Büdel, 2001; Bérard et al., 2004; Zancan et al., 2006; Langhans et al., 2009; Peng and Bruns, 2019b), located in areas with temperate oceanic climates (Cw, Cfb, or Cfc) or mesic continental climates (Dfa or Dfb) (Peel et al., 2007). Despite their unassuming presence in temperate agricultural soils, algae and cyanobacteria are abundant and diverse (Metting, 1981; Pipe, 1992; Zancan et al., 2006). They can form transient photosynthetic microbiotic soil crusts (Knapen et al., 2007), and they fix N<sub>2</sub> and CO<sub>2</sub> (Shimmel and Darley, 1985; Veluci et al., 2006). Thus, like their counterparts in barren arid lands or coastal dunes, they contribute to numerous soil functions. For example, by stabilizing aggregates (Bailey et al., 1973; Metting, 1987) they can protect topsoils against soil erosion (Knapen et al., 2007; Peng and Bruns, 2019b) and limit losses of nutrients and water (Pipe and Shubert, 1984; Langhans et al., 2009; Peng and Bruns, 2019a). Overall, these functions ultimately result in benefits for agricultural soil fertility (Metting, 1990; Renuka et al., 2018).

Soil aggregation plays a key role in protecting soils from water and wind erosion, but it is also involved in other soil functions, such as moisture retention, nutrient retention, and soil carbon sequestration (Le Bissonnais, 1996;

Six et al., 2000). Various abiotic and biotic mechanisms operate with different strengths to generate soil aggregates (Tisdall and Oades, 1982). Mineral particles (e.g., clays, silt, metal oxides, alluminosilicates) and cation complexes flocculate together to form small microaggregates (<0.05 mm), which are cemented and bound into larger microaggregates (0.05–0.25 mm) by the biochemical action of soil organic matter and, notably, exopolymeric substances (EPSs) secreted by plant or microorganisms (e.g., exopolysaccharides, Puget et al., 1999; Six et al., 2004). Exopolysaccharides facilitate the adhesion of microbes to aggregates. Then, soil microorganisms, especially those with filamentous phenotypes (e.g., fungal hyphae), become entangled and bind together with microaggregates via biophysical mechanisms, resulting in the formation of macroaggregates (range: 0.25 mm to several millimeters) (Lynch and Bragg, 1985; Chenu and Cosentino, 2011).

The importance of bacteria and fungi in mediating soil aggregate stability has been extensively documented in agricultural soils, research that has underscored the influence of agricultural practices (Chan and Heenan, 1999; Bossuyt et al., 2001; Six et al., 2004). In contrast, almost no research has investigated the contribution of indigenous edaphic algae and cyanobacteria to topsoil aggregation in temperate agricultural soils. Some studies have examined how algae or cyanobacteria promote soil aggregation using inoculation experiments that employed exogenous strains (Bailey et al., 1973; Metting and Rayburn, 1983; Falchini et al., 1996; Peng and Bruns, 2019b). A single field study has described how indigenous algae and cyanobacteria can form microbial crusts that increase the resistance of cropped topsoil to erosion (Knapen et al., 2007). In fact, what we know about the underlying mechanisms by which algae and cyanobacteria influence soil aggregation essentially comes from studies looking at the early stages of biological

soil crust formation in arid or semi-arid ecosystems (Malam Issa et al., 2001; Belnap and Lange, 2003). Cyanobacteria and certain algae can bind and cement soil aggregates together, via biophysical (enmeshments with cyanobacterial trichomes) and biochemical (gluing with exuded EPSs) mechanisms (Barclay and Lewin, 1985; Falchini et al., 1996; Malam Issa et al., 2001).

Agricultural practices, such as agrochemical uses, can quickly disrupt microbial communities (Nielsen and Winding, 2002; Imfeld and Vuilleumier, 2012) and can thus impair biological and physicochemical indicators of soil quality and soil functions (Zaady et al., 2013; Rose et al., 2016). Furthermore, as is often the case in microbial ecotoxicology, the aforementioned research has focused almost exclusively on how pesticides impact biomass, abundance, activity, or community composition, and numerous gaps still remain when it comes to assessing the actual impacts on soil functions (Ghiglione et al., 2014). For example, there is limited evidence that agrochemicals affect the soil functions delivered by soil microorganisms (e.g., soil aggregation and erosion) (Bossuyt et al., 2001). Furthermore, while algae and cyanobacteria are known to be affected by cropping systems (Zancan et al., 2006; Zaady et al., 2013) and herbicides (Pipe, 1992; Bérard et al., 2004; Zaady et al., 2004; Crouzet et al., 2013), only one study has shown that agricultural practices (e.g., herbicide uses) may impact the functions of microbial crusts, by disturbing the microalgae component, in semi-arid soils (Zaady et al., 2013).

The research presented here aimed to determine how indigenous photosynthetic microbial communities affected aggregate stability in temperate agricultural soils. Our hypotheses were the following: (i) agricultural practices, such as herbicide use, impair the development of photosynthetic microbial crusts, thereby decreasing soil aggregate stability and (ii) cropping system (conventional vs. organic) shapes microbial communities in such a way that different communities will have different functional roles in soil aggregation and will respond differently to herbicide use (isoproturon was used as a model herbicide). A microcosm approach was employed to simulate the colonization of topsoil aggregates by photosynthetic microbial crusts. We measured different descriptors of the microbial communities making up photosynthetic crusts: chlorophyll *a* concentrations and pigment profiles were used to assess community biomass and structure, and total soil esterase activity served as a proxy for overall heterotrophic activity. Bound exopolysaccharides (i.e., defined in this study as exopolysaccharides bound to soil particles) were extracted and both qualitatively and quantitatively analyzed. Finally, we measured the structural stability of soil aggregates to quantify the significance of microalgal crusts in the aggregation process and assessed the impacts of pesticide use and/or cropping systems.

## MATERIALS AND METHODS

### Experimental Site

The soil used in the study was sampled at the La Cage Experimental Station (INRA Versailles, France, 48°48'N, 2°08'E). It was taken from plots experiencing one of two

cropping systems: a conventional (CONV) cropping system versus an organic (ORG) cropping system. The soil was a silty loam, a loess-derived luvisol (FAO classification system). It had a silty-loam Al horizon (58% silt, 25% sand, and 17% clay) with a neutral pH (6.7–7.1) and a C/N ratio of 9.6–10.3. The cropping systems, in use for the past 20 years, had not significantly altered the main physicochemical variables (pH, organic matter content, cation exchange capacity, levels of major elements such as K, Ca, and Mg) (Autret et al., 2016 and **Table 1**, reference soil). In these systems, the crop cycle was dominated by short rotations of winter wheat with alfalfa in the ORG system and with rapeseed and peas in the CONV system). No organic fertilizer was applied, and no irrigation was used. Mineral fertilizers (N, P, and K) and pesticides (mostly herbicides and fungicides) were only employed in the CONV system. There was soil tillage in both systems (similar plowing, harrowing, and stubble disking regimes), and additional mechanical weeding was used in the ORG system (Autret et al., 2016).

### Soil Aggregate Sampling

Soils were sampled in plots under winter wheat cultivation in March 2015, 1 week after an inorganic fertilizer was applied (50 kg N NH<sub>4</sub>NO<sub>3</sub> ha<sup>-1</sup>) in CONV plots. In both the CONV and ORG plots, the topsoil layer (0–2 cm) was sampled in the interrow zone. Samples were taken from different locations (at least 20 m away from each other and at least 10 m away from plot edges to avoid edge effects) and then mixed to obtain a combined sample for each plot. Soil samples were progressively but not completely air dried in the laboratory and gently crumbled by hand (Le Bissonnais, 1996). Soil aggregates of the target sizes (3.15–5 mm) were obtained by sieving and were stored at 4°C until the microcosm experiment. These were the initial soil aggregates, defined as the reference samples (hereafter Ref, **Table 1**). The residual aggregates (0–3.15 mm) were also stored.

### Microcosm Experiment

The microcosms were contained in PVC boxes (length: 11.5 cm, width: 9 cm, height: 4.5 cm) equipped with transparent and perforated lids, which allowed air exchange and the illumination of the soil surface. Two days after aggregate preparation, a first soil layer (thickness: 2 cm), composed of the residual aggregates (0–3.15 mm), was placed in the bottom of the boxes; it buffered the microcosm against desiccation. A nylon mesh (Ø: 1 mm) was then added. Upon it was placed a second soil layer (thickness: 1 cm), composed of the Ref soil aggregates (3.15–5 mm). This experiment was intended to reproduce the initial conditions under which soil algae and cyanobacteria colonize soil surfaces, like those we would expect to see in plowed soil.

For each cropping system type, three replicate microcosms were assigned to one of three sets of incubation conditions. In the “dark” treatment, soil aggregates were incubated under continuously dark conditions (i.e., the boxes were wrapped in aluminum foil). In the “light” treatment, soil aggregates were incubated under a 16/8 (light/dark) photoperiod, where PAR (light intensity of 100 μmol m<sup>-2</sup> s<sup>-1</sup>) was provided by a 11M1003H RADIOMETRIX<sup>®</sup> LED lighting system [which contains three sets of white (6500K), blue (450 nm), and red (660 nm) LEDs;

**TABLE 1** | Physicochemical properties of soil aggregates from the initial (reference: Ref) soil samples, at day 0 before experiment, and in soil microcosms at the end of incubations (day 50) under the different conditions of incubation: Dark (incubation under dark), Light (incubation with a photoperiod 16/8), Light + IPU (incubation with a photoperiod 16/8 + isoproturon treatment).

	pH	C org (g kg <sup>-1</sup> dw)	N tot (g kg <sup>-1</sup> dw)	N-NH <sub>4</sub> <sup>+</sup> (μg g <sup>-1</sup> dw)	N-NO <sub>3</sub> <sup>-</sup> (μg g <sup>-1</sup> dw)	Olsen P (μg g <sup>-1</sup> dw)
<b>soil aggregates from Organic cropping system</b>						
Ref	7.1 ± 0.2	9.79 ± 0.08	0.95 ± 0.01	38.7 ± 2.8	4.86 ± 0.29	0.087 ± 0.001
Dark	7.1 ± 0.1	9.48 ± 0.12	0.94 ± 0.02	9.8 ± 0.82	3.81 ± 0.34	0.090 ± 0.002
Light	7.3 ± 0.1	10.54 ± 0.24	1.06 ± 0.03	13.5 ± 1.4	3.15 ± 0.44	0.083 ± 0.003
Light + IPU	7.2 ± 0.2	10.19 ± 0.22	1.04 ± 0.02	10.4 ± 1.0	2.99 ± 0.26	0.102 ± 0.003
<b>soil aggregates from Conventional cropping system</b>						
Ref	6.6 ± 0.1	9.43 ± 0.06	0.99 ± 0.01	165 ± 13	100 ± 9.0	0.093 ± 0.002
Dark	6.4 ± 0.1	9.36 ± 0.15	0.96 ± 0.02	10.1 ± 0.33	69.6 ± 1.5	0.097 ± 0.003
Light	6.5 ± 0.1	10.01 ± 0.18	1.04 ± 0.04	12.2 ± 0.70	59.6 ± 2.1	0.090 ± 0.003
Light + IPU	6.6 ± 0.1	9.71 ± 0.23	1.02 ± 0.02	9.9 ± 0.47	62.4 ± 1.9	0.106 ± 0.005

The results were expressed as the mean ± standard deviation (n = 3). C org, organic carbon; N tot, total nitrogen; Olsen P, Olsen available phosphorus.

Alpeus, France]. In the “light + IPU” treatment, soil aggregates were incubated under a 16/8 (light/dark) photoperiod but were sprayed with an herbicide on day 0. The herbicide *Matin EL*<sup>®</sup> [a commercial formulation of isoproturon (IPU) that contains 500 g IPU L<sup>-1</sup>; Phyteurop] was used at the recommended field dose (2.4 L ha<sup>-1</sup>). Distilled water was added to attain 80% mWHC, and the microcosms were incubated for 50 days at 20°C. Soil moisture was maintained once a week. On day 50, the surface layer of soil aggregates (0–1 cm) was carefully sampled and homogenized. Several aliquots were air-dried to carry out the physicochemical, aggregate stability, and bound exopolysaccharide analyses, while others were stored overnight at 4°C to later quantify concentrations of chl *a* and other photosynthetic pigments.

## Soil Physicochemical Characteristics

The analyses of total organic carbon (C<sub>org</sub>), total nitrogen (N<sub>tot</sub>), total inorganic nitrogen (N<sub>min</sub> = NH<sub>4</sub><sup>+</sup> + NO<sub>x</sub><sup>-</sup>), available phosphorus, and pH<sub>H2O</sub> of the soil aggregate samples (3.15–5 mm) samples were carried out at the beginning and the end of the experiment. Measurements were performed by INRA's Soil Analysis Laboratory (Arras, France), in accordance with the ISO normalization procedures. A description of these methods is available on the laboratory's website<sup>1</sup>.

## Structural Stability of Soil Aggregates

We measured the stability of air-dried aggregates (3.15–5 mm) sampled before incubation (Ref samples, day 0) and after incubation (dark, light, light + IPU treatments, day 50) using the method described by Le Bissonnais (1996). To summarize, the method is based on three disaggregation tests: test 1 employs fast-wetting conditions and addresses slaking mechanisms and the breakdown caused by the compression of the air trapped in aggregate soil micropores during wetting; test 2 employs slow-wetting conditions and examines the differential swelling and shrinking during wetting and drying that results in aggregate

microcracking; and test 3 employs mechanical breakdown that mimics the impact of raindrops on wet soil. For each microcosm sample, triplicate subsamples (5 g of dry soil) were analyzed for each disaggregation test. After the disaggregation tests, a combination of wet- and dry-sieving (mesh sizes: 2000, 1000, 500, 250, 100, and 50 μm) was used to determine the resulting distribution of aggregate in seven size classes: > 2 mm, 2 – 1 mm, 1–0.5 mm, 0.5–0.25 mm, 0.25–0.1 mm, 0.1–0.05 mm, <0.05 mm. The residual aggregates remaining on each sieve were dried and weighed, and the class-size distribution was determined as a percentage by dry mass of the initial sample. Then, aggregate stability was assessed by the resistance of soil samples against aggregate breakdown. Two indicators resulting from the aggregate-size distribution were used: the percentage of the largest class-size of aggregates (>2 mm) and the mean weight-diameter (MWD) index (Le Bissonnais, 1996). For each test, the mean weight-diameter (MWD) was calculated as follows:

$$\text{MWD} = \sum_{i=n}^n X_i p_i \quad (1)$$

where  $X_i$  is the mean diameter of  $i^{\text{th}}$  mesh size (mm) and  $p_i$  is the proportion of aggregates in the  $i^{\text{th}}$  fraction. A mean of the MWD between the three tests can be made to summarize the overall response (geometric mean).

## Photosynthetic Microbial Community

The concentration of soil chlorophyll *a* (chl *a*) is an indicator of soil photosynthetic microbial biomass (Tsujimura et al., 2000; Crouzet et al., 2013). Fresh subsamples of soil aggregates (2.5 g) were mixed with 7.5 ml of acetone/water (90v: 10v). The mixture was then shaken for 15 h in the dark at 4°C. The extracted chl *a* were then spectrophotometrically quantified at different wavelengths, and the chl *a* concentrations were calculated using the method and equation described by SCOR-UNESCO Working Group 17 (1966). Other photosynthetic pigments (chlorophyll *b*, chlorophyll *c*, fucoxanthin, lutein, diadinoxanthin, neoxanthin, zeaxanthin, and pheophytin *a*)

<sup>1</sup><http://www.lille.inra.fr/las>

were quantified using the same acetone extracts and HPLC (in accordance with Zapata et al., 2000 and Joly et al., 2015). This information helped clarify the biochemical structure of the photosynthetic microbial communities. Pigments were identified and quantified via comparisons with analytical standards (DHI Lab Products, Denmark).

## Bound Exopolysaccharides

The fractions of bound exopolysaccharides were extracted from dried soil pellets (see section “Microcosm Experiment”) with cation exchange resin (CER) (Gerbersdorf et al., 2009; Redmile-Gordon et al., 2014) after the preliminary removal of colloidal EPSs via  $\text{CaCl}_2$  extraction. The resulting CER-extracts were then separated into aliquots. Aliquots to be used in the analysis of total bound exopolysaccharides were frozen, and aliquots to be used in the spectrometric analysis and monosaccharide composition analysis were lyophilized.

The total carbohydrates of the bound exopolysaccharides were quantified using the phenol-sulphuric acid method (Dubois et al., 1956). Mid-infrared (MIR) spectra were determined for the bound exopolysaccharide fractions using a Tensor 27 FTIR spectrometer (Bruker Optics, Wissembourg, France) (Bureau et al., 2009). The wavelength range  $900\text{--}1200\text{ cm}^{-1}$  was used because the intense bands that are specific to polysaccharides occur in this region (Ludwig et al., 2008).

After the MIR analysis, the remaining triplicate lyophilized aliquots were pooled to have sufficient material for the monosaccharide composition analysis. Neutral sugars were analyzed as alditol acetates following acid hydrolysis, in accordance with Renard and Ginies (2009). Uronic acids were measured spectrophotometrically using the m-hydroxydiphenyl assay and galacturonic acid as an external standard.

## Soil Microbial Activity

Fluorescein diacetate (FDA) hydrolysis has been suggested as a suitable indicator of the total heterotrophic activity of soil microbial biomass because many ubiquitous lipases, proteases, and esterases are involved in FDA hydrolysis (Schnürer and Rosswall, 1982). FDA hydrolysis assays were therefore performed using a microplate-based method, in accordance with Green et al. (2006).

## Statistical Analysis

All data were expressed in terms of soil dry weight (dw). Two-way ANOVAs, followed by pairwise *post hoc* tests using Bonferroni corrections ( $p < 0.05$ ), were performed to analyze the effects of the two experimental variables—cropping system (ORG and CONV) and incubation conditions (dark, light, light + IPU)—and their interaction. To meet ANOVA assumptions, the data were checked for normality (Shapiro test) and homoscedasticity (Bartlett test). If the data sets were not normal or homoscedastic, they were transformed ( $\log[x+1]$  or logit) to meet assumptions. For the ANOVAs, we used linear models (lm), except in the case of the aggregate size classes (% data), for which we used generalized linear models (glm). To investigate differences among the magnitude of responses of a given parameter between

two incubation treatments, among the two cropping systems, we used the Mann–Whitney U test.

To assess how the aggregate size distribution or the biochemical structure of microalgal communities were affected by incubation conditions and cropping system, principal component analyses (PCA) were performed on the data of relative abundances of aggregates classes or pigments. MIR-spectral pre-processing and data analysis were performed with Matlab v. 7.5 (Mathworks Inc., Natick, MA, United States); the SAISIR package was employed. Before any data analysis was carried out, standard normal variate (SNV) correction was applied to all the spectra. A hierarchical cluster analysis was performed using Euclidean distances to qualitatively discriminate among the patterns of bound exopolysaccharides for the different incubation conditions. A PERMANOVA was then performed to evaluate the effects of the two experimental variables (cropping system and incubation conditions).

Pearson correlations were used to test the relations among the microbial, biochemical, and physical parameters. Statistical analyses were performed with R software, and a level of statistical significance of  $\alpha < 0.05$  was used.

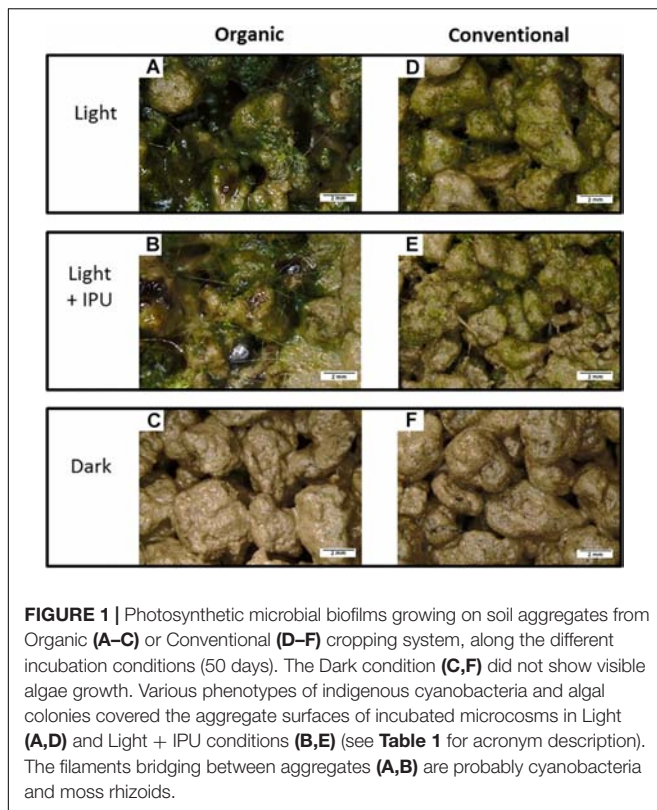
## RESULTS

### Soil Chemical Properties

The pH of soil aggregates from the conventional (CONV) system was initially lower than that of soil aggregates from the organic (ORG) system; incubation conditions did not affect pH during the experiment (Table 1). Cropping system did not affect the  $C_{\text{org}}$  and  $N_{\text{tot}}$  in the Ref samples, but CONV soil aggregates had higher nitrate and ammonium levels than did ORG soil aggregates. At the end of the incubation period, the ORG soil aggregates in the light treatment contained significantly higher  $C_{\text{org}}$  ( $0.7\text{--}1.0\text{ mg of C g}^{-1}_{\text{dw}}$ ) than the ORG aggregates in the dark treatment and the Ref aggregates (Table 1).

### Development and Biomass of Soil Photosynthetic Microbial Crusts

Ref soil aggregates displayed minimal photosynthetic microbial crusts (visual observation) and low chl *a* concentrations ( $> 1\text{ }\mu\text{g chl } a\text{ g}^{-1}_{\text{dw}}$ ). The ANOVA highlighted that incubation conditions had an effect ( $F = 178.3$ ,  $p < 0.001$ ), while cropping system did not ( $F = 2.34$ ,  $p = 0.14$ ); there was no significant interaction ( $F = 2.71$ ,  $p = 0.093$ ). The strong effect of the incubation conditions was mainly due to differences between the dark and light treatments and, to a lesser extent, the presence of the herbicide (light + IPU treatment). In the dark treatment, the photosynthetic microorganisms were not visible (Figures 1C,F), and chl *a* concentrations were so low that they were at the limit of being quantifiable (Figure 2A). In the two light treatments (light and light + IPU), cyanobacteria and algae consistently colonized the surface of soil aggregates (Figures 1A,B,D,E). At the aggregate scale, various phenotypes of photosynthetic microbial crusts (viscous and filamentous) were observed, as was the presence of cyanobacteria and rhizoids of bryophytes (germination stage) (Figures 1A,B).

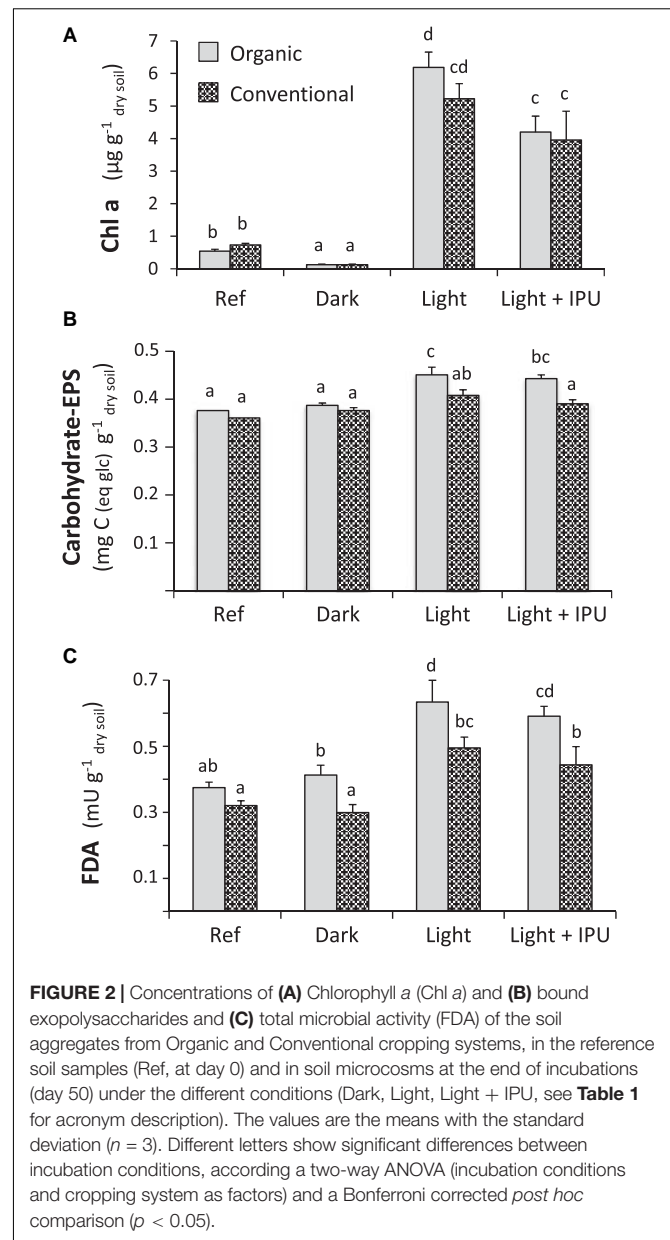


The chl *a* concentrations confirmed the strong development of photosynthetic microorganisms in the light treatment (5.2 and 6.2  $\mu\text{g chl } a \text{ g}^{-1} \text{ dw}$  in aggregates for the ORG and CONV system, respectively) (Figure 2A); this development was less pronounced in the light + IPU treatment (Figure 2A). Compared to the light treatment, the light + IPU treatment induced a significant decrease (−33.2%) in chl *a* concentrations in the ORG soil aggregates (Figure 2A); in contrast the effect (−24.1%) on the CONV soil aggregates was not statistically significant (Figure 2A).

The pigment fingerprint profiles of the soil photosynthetic microbial communities (Supplementary Figure S1) were affected by incubation treatments (light  $\pm$  IPU; PCA axis 1) and cropping system (PCA axis 2). While the ORG and CONV soil aggregates had dissimilar pigment profiles in the light treatment, they had similar pigment profiles in the light + IPU treatment (Supplementary Figure S1). Concentrations of chl *b* and fucoxanthin greatly contributed to the differences seen between the light ORG soil aggregates and the light CONV soil aggregates (PCA axis 2), while concentrations of chl *a* and lutein contributed more to the variation due to the application of IPU (PCA axis 1) (Supplementary Figure S1).

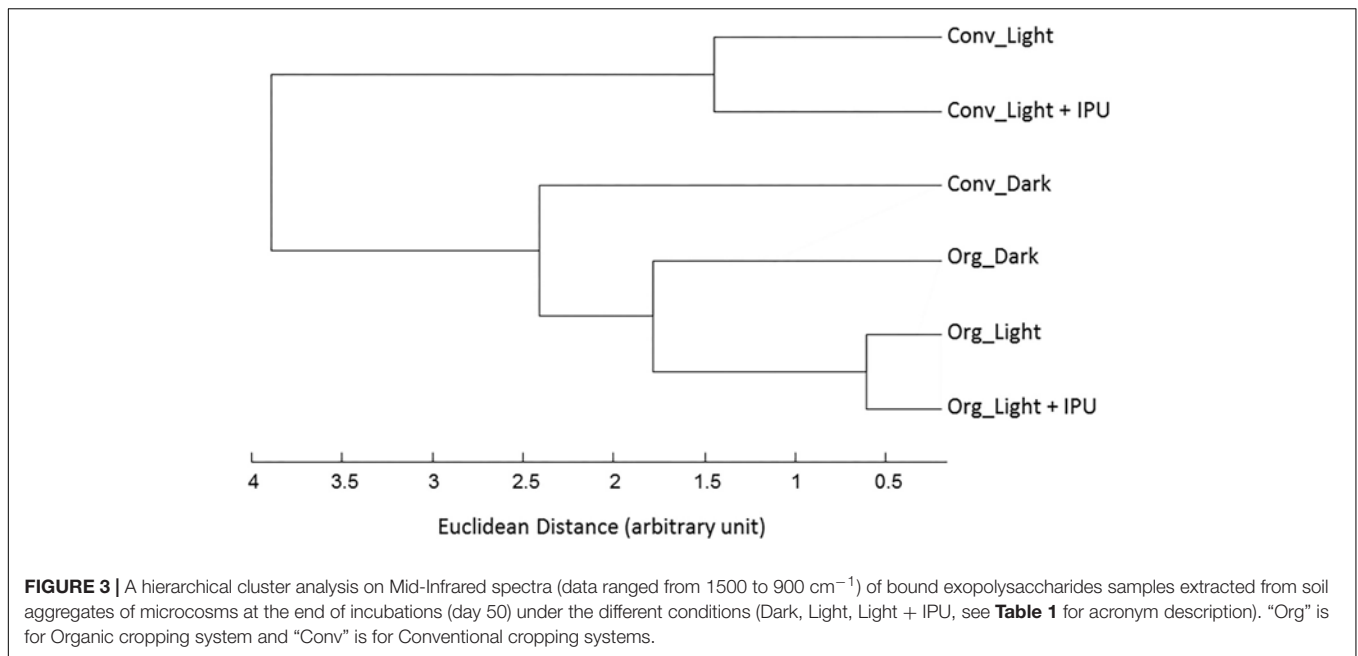
## Bound Exopolysaccharides

The Ref and dark soil aggregates from the ORG and CONV systems did not have different concentrations of bound exopolysaccharides (Figure 2B). A two-way ANOVA revealed the strong effects of incubation conditions ( $F = 19.8, p < 0.001$ ) and cropping system ( $F = 25.1, p < 0.001$ ); there was no significant



interaction between the two variables ( $F = 3.02, p = 0.08$ ). For soil aggregates from both cropping systems, the light and light + IPU treatments significantly increased concentrations of bound exopolysaccharides, as compared to the dark treatment. No differences were seen between the light and the light + IPU treatments (Figure 2B).

Likewise, the MIR spectra revealed differences in the chemical structures of the bound exopolysaccharides between the dark treatment and the light ( $\pm$ IPU) treatments (based on hierarchical clustering/Euclidean distances). Greater differences were reported among CONV than ORG soil aggregates. The MIR spectra of the bound exopolysaccharides were not statistically different between the light and light + IPU treatments (Figure 3). A PERMANOVA carried out with the spectral data confirmed



the significant effect of cropping system ( $F = 100$ ,  $p < 0.001$ ) and revealed the weaker effect of incubation conditions ( $F = 9$ ,  $p < 0.025$ ). The monosaccharide composition analysis of the bound exopolysaccharide extracts suggested that soil aggregates in the light treatment had high levels of monosaccharides, particularly mannose, galactose, glucose, and galacturonic acid, especially in CONV soil aggregates (**Supplementary Figure S2**); fucose was not detected in soil aggregates in the dark treatment (**Supplementary Figure S2**). In the light + IPU treatment, only levels of glucose and galacturonic acid were higher in ORG soil aggregates (**Supplementary Figure S2**).

### Microbial Esterase Activities

There was no significant difference in overall microbial activity in Ref versus dark soil aggregates, regardless of cropping system (**Figure 2C**). A two-way ANOVA showed that incubation conditions ( $F = 51.2$ ,  $p < 0.001$ ) and cropping system ( $F = 50.1$ ,  $p < 0.001$ ) had significant effects on overall microbial activity; there was no significant interaction ( $F = 1.7$ ;  $p = 0.206$ ). At the end of the incubation period, microbial activity was significantly higher in ORG versus CONV soil aggregates, regardless of treatment group. The main differences occurred between the soil aggregates in light versus dark treatments: the microbial activity values were 62.2 and 70.1% higher in the light than in the dark treatment for the ORG and CONV soil aggregates, respectively (**Figure 2C**). The light + IPU treatment did not affect overall microbial activity (**Figure 2C**).

### Aggregate Size Distribution and Aggregate Stability

The aggregate size distributions resulting from each stability test are depicted in **Figure 4**. Among the three tests, the fast-wetting test appeared to result in the most destructive disaggregation,

with the lowest MWD indexes for ORG and CONV soil aggregates. In opposite, the slow-wetting test seemed to be the least destructive test.

With regard to the total aggregate size distribution, the PCA analyses (**Figure 5**) underscored the differences due to incubation conditions (PCA axis 1) and cropping systems (PCA axis 2). These effects were statistically confirmed by a two-way PERMANOVA (**Supplementary Table S1**). PCA1 suggested that the effect of the incubation conditions was principally due to differences between the light and dark treatments and that there was an intermediate effect associated with the light + IPU treatment, especially in the case of the CONV soil aggregates (**Figure 5**). The effects of photoperiodic incubation (versus dark treatment) mainly manifested themselves in significant shifts in macroaggregate percentages from the smaller class-sizes (1–2 mm; 0.5–1 mm; 0.25–0.5 mm) to the largest class-size (>2 mm) (**Figure 4** and **Table 2**). As example, in light treatments, the amounts of large aggregates (>2 mm) has reached up to 21.5 and 32.5 % of the total dry mass of aggregates, in organic and conventional cropping systems, respectively, following the slow-wetting test (**Table 2**). In dark treatments, these values remained very low at 2.3 and 1.3 % of the total dry mass of aggregates, in organic and conventional cropping systems, respectively (**Table 2**). The magnitudes of these shifts between dark and light treatments were significantly greater for the CONV soil aggregates (by 22.7 fold in the fast-wetting test, 27.1 fold in the slow-wetting test, 14.9 fold in the mechanical-breakdown test) than for the ORG soil aggregates (by 10.6 fold in the fast-wetting test, 9.4 fold in the slow-wetting test, 8.4 fold in the mechanical-breakdown test; following data listed in **Table 2**, Mann–Whitney U test,  $p < 0.01$ ). Concomitantly, for all three tests, the percentages of microaggregates (sum of class sizes <0.25 mm) in the CONV soil decreased significantly for the light treatments ( $\pm$ IPU) but not for the dark treatment

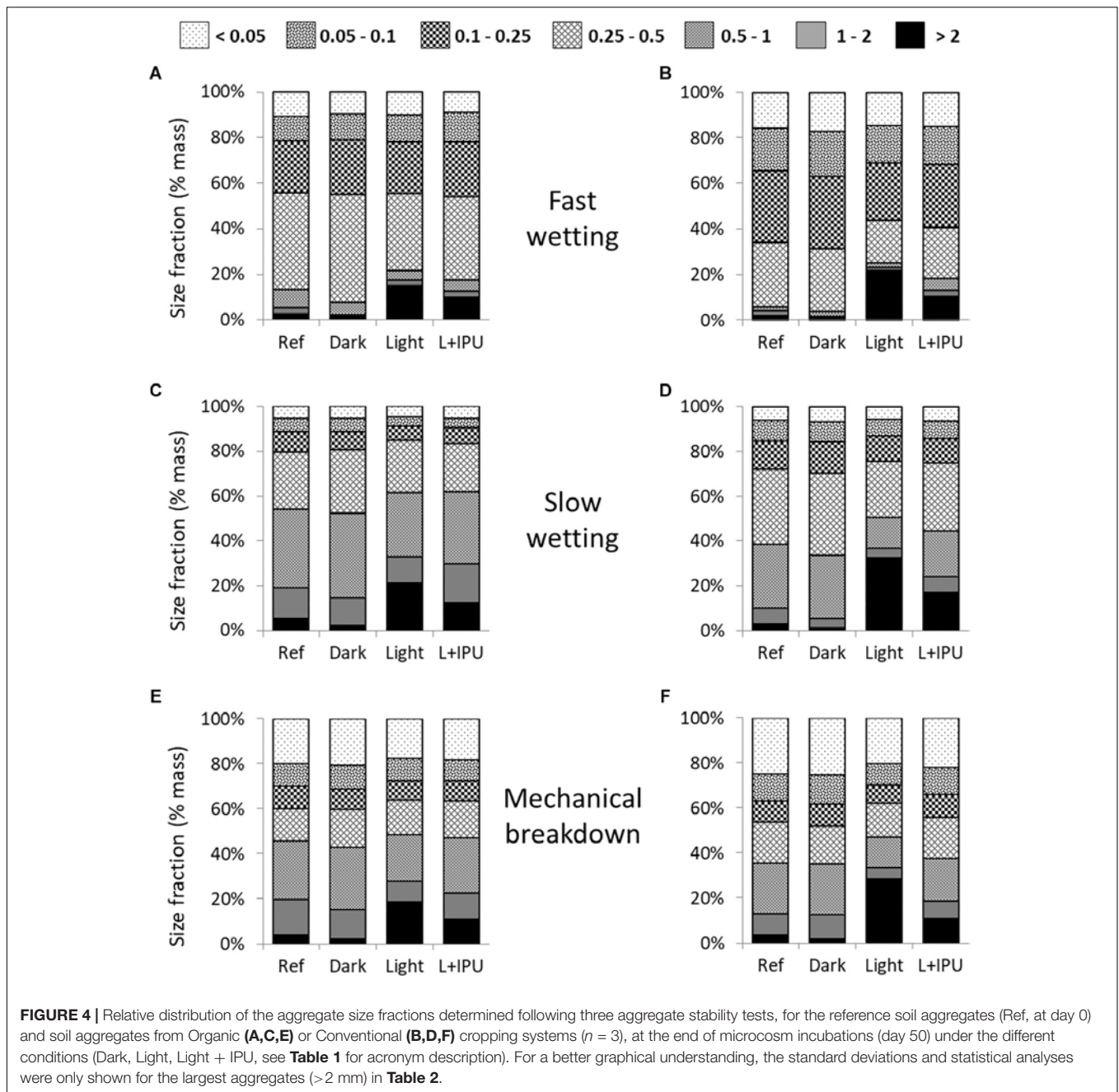
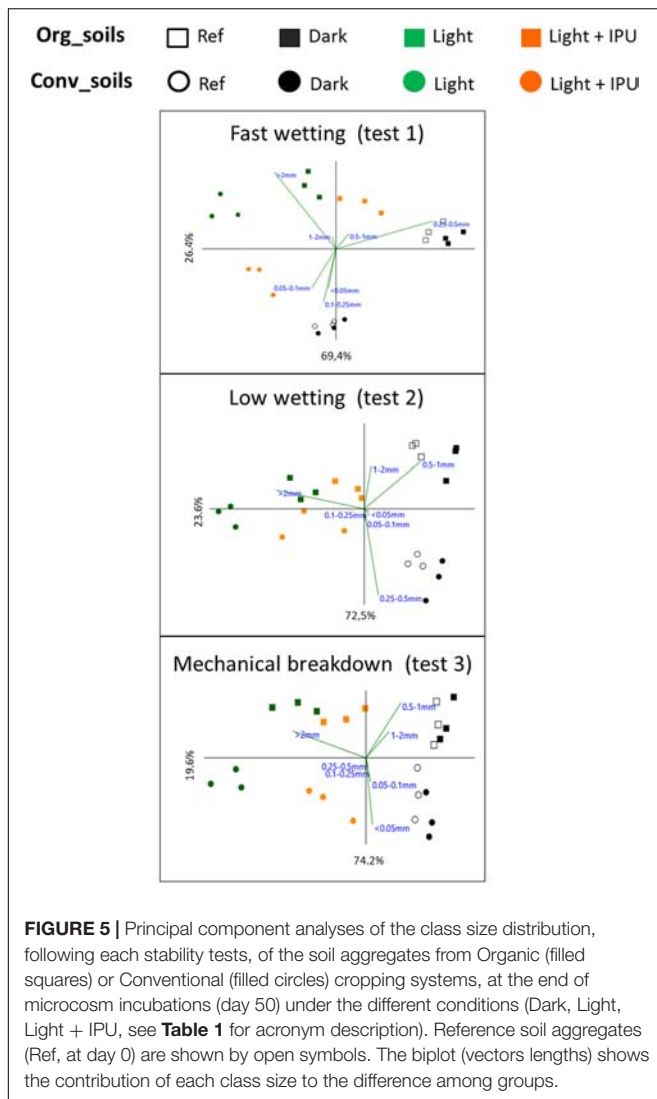


(Figure 4, two-way ANOVA *post hoc* test). Overall, the MWD (considering all the aggregate size distribution) of CONV soils significantly increased in the light treatments, as compared to dark or reference soil samples, following all three tests (Table 2). The magnitude of the increase of the MWDs, in light compared to dark incubations, was significantly greater for the CONV soil aggregates (from 0.22 to 0.92 corresponding to an increase by 4.2 fold) than for the ORG soil aggregates (from 0.31 to 0.75 corresponding to an increase by 2.4 fold), in the fast-wetting test (resistance to slaking; Mann-Whitney U test,  $p < 0.01$ ). In the other tests, the increase were 1.8 fold in the slow-wetting test and the mechanical-breakdown test, for the ORG soil aggregate

and 2.9 fold in the slow-wetting test and 2.6 fold the mechanical-breakdown for the CONV soil aggregates (following data listed in Table 2, Mann-Whitney U test,  $p < 0.05$ ).

Furthermore, along the PCA2 axis (Figure 5), there were large differences in the overall size-class distribution between the ORG and CONV soil aggregates from the Ref samples and the dark treatment; however, these differences were lessened for the soil aggregates in the light treatments, notably following the slow-wetting test. More specifically, for all three tests, higher percentages of the largest aggregate ( $> 2$  mm) were recovered from CONV than ORG soil aggregates from the light treatments (Table 2). Nevertheless, for a given set of incubation conditions,



greater percentages of total macroaggregates (sum of class sizes  $>0.25$  mm) were generated from ORG versus CONV soil aggregates following the three tests; the only exception was seen for aggregates from the light treatments following the mechanical-breakdown test (**Figure 4**, two-way ANOVA *post hoc* test). Overall, the MWD values did not reveal any differences in structural stability between the ORG and CONV soils for a given set of incubation conditions.

When the effects of herbicide use were examined, the PCAs displayed the aggregates from the light + IPU treatments in an intermediate position between those from the light and dark treatments, whatever the cropping system, (**Figure 5**). The largest aggregates ( $>2$  mm) were the most responsive class of aggregates. It showed significant decreases in the light + IPU, as compared to the light treatments, after all three disaggregation tests, with the exception of the ORG soil aggregates after the fast-wetting test (**Table 2**). The highest decreases were recorded following the mechanical breakdown test for CONV soil (from 28.3 to 11 %) and in a similar way following the slow-wetting

test (from 21.5 to 12.5 %) or the mechanical breakdown test (from 18.6 to 10.9 %) (**Table 2**). There were concomitantly higher amounts of intermediate macroaggregate sizes (1–2 mm; 0.5–1 mm; 0.25–0.5 mm) in the light + IPU treatment, except for the CONV soil aggregates following the mechanical-breakdown test (**Figure 4**). In this latter case, there was a significant decrease in the percentage of microaggregates ( $<0.25$  mm) in the light + IPU treatment, compared to the light treatment (**Figure 4**; two-way ANOVA *post hoc* test,  $p < 0.01$ ). Overall, the MWD of the CONV soil aggregates was significantly impaired by the light + IPU treatment compared to the light treatment (**Table 2**). The decreases were  $-38$ ,  $-29$ , and  $-41\%$ , following the fast-wetting, slow-wetting, and mechanical-breakdown tests, respectively. No significant effect occurred in the MWD index of the ORG topsoil aggregates (**Table 2**).

## Relations Among Biotic and Abiotic Aggregate Properties

The chl *a* concentrations were highly correlated with the FDA hydrolysis values, the bound exopolysaccharide concentrations, and  $C_{org}$  (**Table 3** and **Supplementary Figure S3**). The percentage of the largest fragments ( $>2$  mm; mean for the three tests), considered to be a proxy of aggregate stability, was strongly correlated with the chl *a* concentrations,  $C_{org}$ , and the FDA hydrolysis values; it was also correlated to a lesser degree with the bound exopolysaccharide concentrations. Correlations between another proxy of aggregate stability, mean MWD (mean for the three tests), and the biochemical parameters (chl *a* concentrations, FDA hydrolysis values, bound exopolysaccharide concentrations, and  $C_{org}$ ) were significantly different between the CONV and ORG soil aggregates (**Supplementary Figure S3**).

## DISCUSSION

### The Development of Indigenous Photosynthetic Microbial Crusts Induces Soil Aggregation

This microcosm experiment showed that there was a strong development ( $4\text{--}6 \mu\text{g chl } a \text{ g}^{-1} \text{ dw}$ ) of indigenous algal and cyanobacterial crusts on soil surfaces under optimal and stable laboratory conditions. Chlorophyll *a* concentrations, which are a proxy for photosynthetic microbial biomass, fell in the same range as those seen in previous laboratory incubation experiments (Crouzet et al., 2013; Joly et al., 2015) and in some field studies (Tsujimura et al., 2000; Lin et al., 2013). The low values observed in the reference samples were typical for field soil samples at the end of winter (early March).

As expected, aggregate stability was greatly enhanced by the growth of soil microalgae in the two light treatments (light  $\pm$  IPU). The mechanism primarily appeared to be the formation of large water-stable aggregates. Consequently, the increase in the percentage of the largest aggregates ( $>2$  mm) resulted from greater cohesion among smaller macroaggregates (ranging from 0.25 to 2 mm) whose the proportion decreased. Similar patterns of aggregate size distribution were observed

**TABLE 2 |** Percentages of the largest aggregates (>2 mm) and mean weight diameter (MWD in mm) indexes generated following each stability test performed on the incubated soil aggregates from Organic and Conventional cropping systems.

		Test 1 Fast-wetting		Test 2 Slow-wetting		Test 3 Mechanical breakdown	
		[>2 mm]	MWD	[>2 mm]	MWD	[>2 mm]	MWD
<b>Organic soil aggregates</b>	Ref	2.5 ± 0.7 b	0.38 ± 0.03 a	5.4 ± 0.8 b	0.77 ± 0.04 b	3.9 ± 0.7 a	0.64 ± 0.03 ab
	Dark	1.4 ± 0.3 a	0.31 ± 0.02 a	2.3 ± 0.7 a	0.68 ± 0.03 b	2.2 ± 0.2 a	0.56 ± 0.04 ab
	Light	14.9 ± 3.0 b	0.75 ± 0.09 bc	21.5 ± 4.8 d	1.24 ± 0.11 cd	18.6 ± 3.3 c	1.02 ± 0.09 de
	Light + IPU	9.6 ± 2.9 b	0.59 ± 0.08 b	12.5 ± 2.4 c	1.03 ± 0.09 c	10.9 ± 2.0 b	0.82 ± 0.07 cd
<b>Conventional soil aggregates</b>	Ref	1.9 ± 0.5 a	0.28 ± 0.01 a	3.1 ± 0.5 a	0.57 ± 0.02 ab	3.7 ± 0.5 a	0.53 ± 0.03 ab
	Dark	1.0 ± 0.3 a	0.22 ± 0.02 a	1.2 ± 0.4 a	0.48 ± 0.03 a	1.9 ± 0.5 a	0.49 ± 0.03 a
	Light	21.7 ± 1.5 c	0.92 ± 0.06 c	32.5 ± 4.1 e	1.40 ± 0.11 d	28.3 ± 4.0 d	1.25 ± 0.11 e
	Light + IPU	10.1 ± 3.1 b	0.58 ± 0.11 b	16.9 ± 4.6 cd	0.99 ± 0.13 c	11.0 ± 4.1 bc	0.73 ± 0.12 bc
<b>Two-way ANOVA statistics</b>	Treatment	<0.001	<0.001	<0.001	<0.001	<0.001	<0.001
	Crop_syst	0.036	0.738	0.004	0.040	0.582	0.682
	interaction	0.007	0.007	0.002	0.001	0.014	0.007

Reference soil samples (Ref) are the initial soil aggregates at day 0, before incubation). Dark, Light and Light + IPU are soil aggregates at the end (day 50) of the different incubation conditions (see Table 1 for acronym description). The values are the means with the standard deviation ( $n = 3$ ). For each disaggregation test, different letters indicated significant differences between incubation conditions (two-way ANOVA, with treatment and cropping systems as factors, followed by Tukey's post hoc test,  $p < 0.05$ ). See Figure 4 for the overall class size distributions.

**TABLE 3 |** Spearman correlation coefficients (bottom left) and  $p$ -values (top right), among microalgae, microbial and aggregates parameters, including the whole data set of Conventional and Organic soil aggregates.

	chl <i>a</i>	EPS	C <sub>org</sub>	FDA	>2 mm
chl <i>a</i>		<0.001	<0.001	<0.001	<0.001
Bound-EPS	0.682		<0.001	<0.001	<0.001
C <sub>org</sub>	0.787	0.803		<0.001	<0.001
FDA	0.753	0.871	0.823		<0.001
>2 mm	0.932	0.698	0.803	0.777	

Bound-EPS: total bound exopolysaccharides; >2 mm: geometric mean of the largest aggregates between the three tests. Graphics were shown in Supplementary Figure S3.

when semi-arid soil was inoculated with cyanobacteria (*Nostoc* spp.), even if the strong increases in the large macroaggregates were related to higher decreases of the microaggregates (>0.25 mm) than in our work (Malam Issa et al., 2007). Overall, in accordance with the hierarchical model of soil aggregation (Tisdall and Oades, 1982), each level of micro- and macroaggregation was stabilized by materials and mechanisms of a different nature. The biochemical action of soil organic matter via flocculation and cementation usually takes place as a result of internal mechanisms in microaggregates over the long term. In contrast, the biophysical action of soil organisms impacts the overall external cohesion of macroaggregates over the short term. As a result, it is likely that both the processes of macroaggregation share with the microorganisms a high level of responsiveness to environmental changes (Degens, 1997; Six et al., 2004). Consequently, given that this experiment occurred over the short term, the pronounced increase and responsiveness of the large macroaggregate fraction suggests that, in our work, the microalgae affected aggregation mainly by enhancing physical mechanisms. Most commonly, thick networks of algae, cyanobacterial trichomes (colonial filamentous forms), and other

stimulated microbial components (e.g., fungal hyphae) become enmeshed with soil particles and existing aggregates to form yet larger aggregates. Complementary biochemical mechanisms resulting from the production of exopolymeric substances (EPSs: polysaccharides, proteins, amino acids, certain lipids, nucleic acids) produced by soil microorganisms may also be involved (Tisdall and Oades, 1982; Six et al., 2004). In this study, increases were observed in the concentrations of bound exopolysaccharides and, to a lesser extent, in C<sub>org</sub>; they were strongly related to the development of microalgal biomass and increases in indicators of aggregate stability (aggregates >2 mm and MWD). In long-term greenhouse or field experiments, inoculation with algae and cyanobacteria has increased the polysaccharide contents of irrigated agricultural soils and contributed to higher aggregate stability (Metting and Rayburn, 1983; Metting, 1987; Falchini et al., 1996) and proportions of large aggregates (Malam Issa et al., 2007). Many cyanobacteria and other non-filamentous microalgae secrete large amounts of various exopolymeric substances, including numerous exopolysaccharides, which form a mechanical structure covering aggregates that reinforces biophysical cohesion (Mazor et al., 1996). Notably, cyanobacterial trichomes are surrounded by mucilaginous sheaths, which enable them to strongly adhere to each other and to soil aggregates, resulting in a gluing mesh (Falchini et al., 1996; Malam Issa et al., 2007). Exopolysaccharides can also be released into the surrounding soil (Redmile-Gordon et al., 2014). In our study, since the microaggregates (<0.25 mm) were not drastically affected in either the light or dark treatments (i.e., whether or not microalgae were present), it is likely that the exopolysaccharides produced by the microalgae mainly acted at the macroaggregate scale via external cohesion, coating aggregate surfaces and gluing cells onto soil particles. This biochemical mechanism thus reinforced the biophysical action of these microbial crusts and mainly operated on macroaggregation. In an incubation experiment, the resistance of inoculated soil aggregates to

breakdown is likely related to the changes in micromorphological characteristics of the microbiotic crust, induced by cyanobacterial filaments and EPS (Malam Issa et al., 2007).

It is not just the quantity of bound exopolysaccharides that matters. Their chemical composition may also affect aggregate stability because different bound exopolysaccharides have different binding strengths and hydrophobic properties (Puget et al., 1999; Hu et al., 2003; Rossi and De Philippis, 2015). As a result, the differences in the biochemical quality of bound EPSs (as reflected in the MIR spectra) in aggregates from the light versus dark treatment—differences due to presence or absence of algae—could have contributed to differences in aggregate stability. Following the fast-wetting test (and the mechanical-breakdown test), there was a decrease in the percentage of microaggregates when microalgae were present versus absent (including in the reference aggregates). This pattern may have occurred because there were larger amounts of hydrophobic materials coating the aggregate surfaces, thus slowing down aggregate wetting and decreasing slaking. Interestingly, fucose—a hydrophobic deoxy-hexose known to increase cohesion among soil particles (Chen et al., 2014; Rossi and De Philippis, 2015)—was present in aggregates from the light ( $\pm$ IPU) treatments but absent in aggregates from the dark treatment. Likewise, galacturonic acid, which is suspected to play an important role in the great affinity of cyanobacteria (*Microcoleus vaginatus*) for soil particles (Hu et al., 2003), was present at higher concentrations in aggregates from the light ( $\pm$ IPU) treatments than in aggregates from the dark treatment. However, concentrations of other sugars known to be highly hydrophobic, such as arabinose and rhamnose (Hu et al., 2003; Rossi and De Philippis, 2015), did not differ in the presence or absence of microalgae (light vs. dark treatment). These are some of the first results to address the biochemical quality of microbial exopolysaccharides in soils (e.g., Rossi and De Philippis, 2015 in arid soils). Consequently, further analysis is needed to better understand their role in the aggregation of soil particles.

Furthermore, the development of indigenous soil microalgal crusts promoted overall microbial activity (FDA hydrolysis values). Similar results have previously been obtained in soils inoculated with exogenous algal or cyanobacterial strains (Rogers and Burns, 1994; Acea et al., 2003; Nisha et al., 2007). Such stimulation of heterotrophic microbial components could have been induced by the release of extracellular polysaccharides used as readily available carbon sources (Mager and Thomas, 2011). The development of indigenous microalgal communities drives the formation of complex microbial hot spots on the soil surface (photosynthetic microbiotic crusts, Evans and Johansen, 1999). Bacterial and fungal exopolymeric substances and by-products as well as filamentous forms (i.e., hyphae) are known to play a major role in biochemical and physical aggregation processes (Lynch and Bragg, 1985; Six et al., 2004). They may have amplified the microalgae-related effects on soil aggregation. Overall, microalgae productivity was responsible for the increase in  $C_{org}$ , as previously observed in an experiment involving algae inoculation (Nisha et al., 2007). Consequently, soil microalgae clearly carry out ecological, physical, and chemical engineering in agricultural soils, as previously demonstrated in degraded

temperate soils (Rogers and Burns, 1994; Acea et al., 2003) and arid soils (Evans and Johansen, 1999).

## Impact of Herbicide Use on Algae-Mediated Soil Aggregation

Based on the results for the light versus the light + IPU treatments, the decrease of chlorophyll *a* concentrations showed that the herbicide IPU partially inhibited the microalgae component of the photosynthetic microbial crusts, especially in soil aggregates from the organic cropping system. Several works have already shown the harmful effects of herbicides on the soil microalgae abundances (Metting and Rayburn, 1979; Pipe, 1992), *chl a* biomasses (Zaady et al., 2004, 2013; Crouzet et al., 2013) and photosynthetic activity (Bérard et al., 2004). The pigment fingerprint profiles were also modified by the herbicide application, which may indicate that there were shifts in microalgal community composition. Microalgae species have different pigments, and the pigment composition of a given species may vary according to its physiological state, especially if herbicides induce conditions of stress (Bérard and Pelte, 1999). That said, pigment profiling of soil or water samples remains a suitable and widely used approach for describing phytoplankton community structure (Zapata et al., 2000) and for examining how microalgal community composition responds to herbicides (Dorigo et al., 2004; Joly et al., 2015). There are few studies that have looked at the effects of phenyl-urea herbicides on soil microalgal biomass and community composition (Pipe, 1992). Here, we used agriculturally relevant field doses of one such herbicide, IPU, and confirmed its negative impacts on soil microalgae biomass and changes in biochemical community structure. Also, the application of IPU resulted in a convergence of microalgal communities for aggregates from the two cropping systems, which displayed greater differences in the light treatment. Since lutein and chlorophyll *a* and *b* were the most affected, it seems that IPU might affect *Chlorophyceae* more than other microalgal groups.

As previously discussed, in the light treatment, there was a microalgae-mediated effect on aggregate stability. Consequently, it was expected that IPU's disturbance of algal and cyanobacterial communities would modify their functional contribution to soil aggregation. In an experiment using high doses of a fungicide, the impairment of fungal biomass functionally disrupted macroaggregate formation (Bossuyt et al., 2001). In our study, the IPU treatment at the beginning of the incubation impaired the percentages of large aggregates ( $>2$  mm) and the MWD values, highlighting that the herbicide impaired the soil aggregate stability, albeit mostly in conventional cropping systems. The previous discussions on the relations between microalgae and aggregation tackled the role of exopolysaccharides. IPU impacted the growth of green algae (*Chlorella* sp.) and cyanobacteria (*Anabaena* sp.) as well as their production of carbohydrates (Mostafa and Helling, 2002). At the community level, the harmful effects of an herbicide (simazine) on both the photosynthetic microbial biomass and the soil polysaccharide contents have been evidenced in semi-arid soils (Zaady et al., 2004, 2013). Here, however, the field dose of the herbicide IPU did not have

a significant effect on the levels of bound exopolysaccharides. It is possible that IPU-tolerant microalgae were present and increased their exopolysaccharide production in response to the toxic stress. Such a phenomenon has been previously described for periphyton communities exposed to toxicants (Serra and Guasch, 2009). Also, because we did not know the proportions of the bound exopolysaccharides produced by the microalgae, as well as by the bacteria and fungi, whose presence was stimulated by microalgal growth, their respective contribution to the bound exopolysaccharides remained unclear. Consequently, the concentrations of bound exopolysaccharides failed to explain the effect of IPU on the link between microalgal growth and aggregate stability. It is possible instead that the application of IPU led to lower aggregate stability because soil aggregates were less physically covered with enmeshed microalgal filaments, as a direct result of the decrease in algal and cyanobacterial biomass. To test this hypothesis, further research is needed to explore biofilm structure at the microscopic scale and the phenotypic traits of sensitive algal and cyanobacterial strains.

Overall, such an impact on topsoil aggregation may have drastic implications for soil fertility and soil erosion. In field studies, Zaady et al. (2004, 2013) have shown that the herbicide simazine, by inhibiting the microalgae component of microbiotic crusts, increased soil erosion and  $C_{org}$  or nitrate losses, in a semi-arid soil. In our work, negative relationships have evidenced between microalgae biomass, indicators of aggregate stability and exopolysaccharides or  $C_{org}$  contents. However, these correlations were strongly shaped by the differences between dark vs. light treatments, albeit the data of light + IPU often displayed an intermediate position.

## Effect of Soil Cropping System on Algae-Mediated Aggregation

After 50 days in the light treatment, soil aggregates from the conventional and organic cropping systems displayed no difference in their total chlorophyll *a* concentrations. That said, their pigment profiles were not the same. However, the pigment profiles were not consistent enough to allow the clear identification of the microalgae groups that were potentially dominant in each cropping system. Agricultural practices (i.e., pesticide and fertilizer use), which differ between organic and conventional systems, have been shown to influence the taxonomic composition of algal and cyanobacterial communities in cropping systems (Pipe, 1992; Zancan et al., 2006; Lentendu et al., 2014). Even if our experiment found no effect of cropping system on total photosynthetic biomass, differences in community composition can lead to different functional outputs or differences in community sensitivity to disturbance.

The soil aggregates from conventional and organic systems responded differently to the fast-wetting test, which employed slaking. The results underscore that initial aggregate stability and the functional effects of microalgal growth also differed. In fact, soil aggregates from the conventional system had a lower initial percentage of largest macroaggregates (>2 mm) and a higher percentage of microaggregates, which could suggest they were initially less stable than those from the organic system

(likely due to the long-term effects of agricultural practices, Chan and Heenan, 1999; Elmholt et al., 2000). In the light treatments ( $\pm$ IPU), the percentage of the largest macroaggregates (>2 mm) increased dramatically and the percentage of the microaggregates declined strongly in the conventional soil, suggesting that microalgae-mediated aggregation had been more effective than in the organic soil. More specifically, as revealed by the fast-wetting test, microaggregates (<0.25 mm) seemed less prone to form macroaggregates via microalgae-mediated effect in soils from the organic cropping system (i.e., there was no difference in the percentage of microaggregates between the light and dark treatments) versus in soils from the conventional cropping system. It is likely that such differences in MWD were not observed between the two cropping systems because, for the calculation of the MWD values, there was compensation by the smaller macroaggregate size classes (1–2 mm, 0.5–1 mm and 0.25–0.5 mm) in the organic soil. However, these greater benefits of microalgae for the largest aggregates of the conventional soil were not explained by higher levels of chlorophyll *a*, bound exopolysaccharides,  $C_{org}$ , or microbial activity; indeed, these variables had higher values in organic soil aggregates. It is unlikely that differences in the structural composition of the bound exopolysaccharides were involved in these aggregation patterns because, such differences usually play a greater role in microaggregation—by gluing soil particles together. Moreover, the differences in the correlations observed between the biotic and abiotic variables for the soil aggregates from the two systems (**Supplementary Figure S3**) suggest that different biological and physical interactions may have been involved in aggregation dynamics and that the nature of these interactions may depend on legacy effects of agricultural practices.

Finally, the application of IPU had a significantly smaller effect on photosynthetic microbial biomass in conventional versus organic soil aggregates. A field study comparing uncultivated soils and cultivated soils subject to many years of pesticide treatments found that soil algal and cyanobacterial isolates from uncultivated soils were less tolerant to di-allate and MCPA herbicides than isolates from adjacent cultivated soils (Metting and Rayburn, 1979). The PICT (pollution-induced community tolerance) concept suggests that a causal relationship exists between a field's exposure to a toxicant and the sensitivity of its microbial community to the same toxicants (Bérard et al., 2004). In the conventional system from which we took our soil samples, pesticide formulations containing IPU have been applied every 2 years for the past 20 years. As a result, it is likely that IPU-tolerant populations of algae and cyanobacteria have been selected for, which means that the overall community was likely more tolerant of the presence of IPU in the microcosm experiment. For example, a tolerance mechanism favored by some algae or cyanobacteria can be the degradation of the IPU (Mostafa and Helling, 2001).

In contrast, the functional response of the microalgae that contributed to soil aggregation was significantly more affected by IPU in the conventional versus the organic soil aggregates: the systematic decrease in MWD values in the light + IPU treatment was only seen for the aggregates from the conventional

system. One hypothesis may be that microalgae incur fitness costs when acquiring tolerance to herbicide-induced stress. In other words, higher energy demands are placed on microorganisms that are coping with the toxicity of IPU (Bérard et al., 2014). As a result, the functional competence of microalgal communities (e.g., aggregation) could be reduced when they are faced with chemical stressors.

## CONCLUSION

Indigenous cyanobacterial and algal communities that form photosynthetic microbiotic crusts in agricultural cropped soils should be viewed as engineering microorganisms. Indeed, they contribute to aggregate formation and stabilization and thus help protect the soil surface of cropland. The growth of indigenous microalgae primarily favors the formation of large macroaggregates, as pre-existing small aggregates are physically enmeshed by networks of filamentous microbial biomass. Also, microalgal mats coat the surface of macroaggregates (i.e., with biomass and EPS matrices), thus protecting aggregates against slaking via hydrophobic interactions. Concomitantly, the establishment of favorable habitat for other microbial communities likely enhances these effects. Overall, over the short term, microalgae can functionally promote topsoil structural stability and thus provide protection against erosion in temperate agricultural soils. However, it is important to consider these dynamics in a broader perspective and examine the benefits of soil aggregation in relation to agricultural practices (e.g., soil tillage and agrochemical inputs), in order to promote the value of soil algae and cyanobacteria as soil conditioners or biofertilizer (Metting, 1990; Renuka et al., 2018).

The application of herbicides can change the microalgal communities and physicochemical parameters, which mean it can also change community functions. In particular, herbicides can disturb the growth of soil microalgae and thus alter their functional role in soil aggregate formation. This greenhouse study explored the impacts of an herbicide on soil aggregation. However, it is important to also look at community changes *in situ*, taking into account edaphic conditions (i.e., seasonal effects) and additional agricultural practices (i.e., soil tillage). More studies need to focus on soil

photosynthetic communities, which are frequently overlooked in soil microbial eco(toxico)logy. Our findings highlight that specific functional groups (algae and cyanobacteria) or functional domain (microbiotic crusts) in soils can be promising bioindicators and original models for deciphering the impacts of agrochemical stress on soil function in agroecosystems.

## AUTHOR CONTRIBUTIONS

OC and LC designed the study. LC, J-PP, and CM measured stability, and the microbial and biochemical parameters. J-PA analyzed the soil pigment composition. AB, SB, CL, and LT analyzed the soil exopolysaccharides. OC wrote the first draft of the manuscript with the help of AB, who contributed to the revision process, and minor comments were made by the other authors.

## FUNDING

Financial support for this study was provided by the Plant Health and Environment (SPE) Division of INRA (French National Institute for Agricultural Research) in the form of an Innovative Project (COMIPHO 2013–2015). Open access publication fees were purchased by our INRA Laboratory Units: EcoSys and EMMAH.

## ACKNOWLEDGMENTS

The authors thank L. Capowicz, N. Borghino, M. Debroux, A. Dumas, and A. Frutos for their help in the analysis of exopolysaccharides. They are grateful to J. Pearce for revising the language part of the manuscript.

## SUPPLEMENTARY MATERIAL

The Supplementary Material for this article can be found online at: <https://www.frontiersin.org/articles/10.3389/fmicb.2019.01319/full#supplementary-material>

## REFERENCES

- Acea, M. J., Prieto-Fernández, A., and Diz-Cid, N. (2003). Cyanobacterial inoculation of heated soils: effect on microorganisms of C and N cycles and on chemical composition in soil surface. *Soil Biol. Biochem.* 35, 513–524. doi: 10.1016/S0038-0717(03)00005-1
- Autret, B., Mary, B., Chenu, C., Balabane, M., Girardin, C., Bertrand, M., et al. (2016). Alternative arable cropping systems: a key to increase soil organic carbon storage? results from a 16 year field experiment. *Agric. Ecosyst. Environ.* 232, 150–164. doi: 10.1016/j.agee.2016.07.008
- Bailey, D., Mazurak, A. P., and Rosowski, J. R. (1973). Aggregation of soil particles by algae. *J. Phycol.* 9, 99–101. doi: 10.1111/j.0022-3646.1973.00099.x
- Barclay, W. R., and Lewin, R. A. (1985). Microalgal polysaccharide production for the conditioning of agricultural soils. *Plant Soil* 88, 159–169. doi: 10.1007/BF02182443
- Belnap, J., and Lange, O. L. (2003). *Biological Soil Crusts: Structure, Function and Management. Ecological Studies*, Vol. 150. Berlin: Springer Verlag.
- Bérard, A., Mazzia, C., Sappin-Didier, V., Capowicz, L., and Capowicz, Y. (2014). Use of the MicroResp™ method to assess pollution-induced community tolerance in the context of metal soil contamination. *Ecol. Indic.* 40, 27–33. doi: 10.1016/j.ecolind.2013.12.024
- Bérard, A., and Pelte, T. (1999). Les herbicides inhibiteurs du photosystème II, effets sur les communautés algales et leur dynamique. *Rev. Sci. Eau* 12, 333–361. doi: 10.7202/705355ar
- Bérard, A., Rimet, F., Capowicz, Y., and Leboulanger, C. (2004). Procedures for determining the pesticide sensitivity of indigenous soil algae—a possible bioindicator of soil contamination? *Arch. Environ. Contam. Toxicol.* 46, 24–31. doi: 10.1007/s00244-003-2147-1
- Booth, W. B. (1941). Algae as pioneers in plant succession and their importance in erosion control. *Ecology* 22, 38–46. doi: 10.2307/1930007

- Bossuyt, H., Denef, K., Six, J., Frey, S. D., Merckx, R., and Paustian, K. (2001). Influence of microbial populations and residue quality on aggregate stability. *Appl. Soil Ecol.* 16, 195–208. doi: 10.1016/S0929-1393(00)00116-5
- Büdel, B. (2001). “Biological Soil Crusts in European Temperate and Mediterranean Regions,” in *Biological Soil Crusts: Structure, Function, and Management*, eds J. Belnap and O. L. Lange (Berlin: Springer), 75–86.
- Bureau, S., Ruiz, D., Reich, M., Barbara, G., Dominique, B., Jean-Marc, A., et al. (2009). Application of ATR-FTIR for a rapid and simultaneous determination of sugars and organic acids in apricot fruit. *Food Chem.* 115, 1133–1140. doi: 10.1016/j.foodchem.2008.12.100
- Chamizo, S., Rodríguez-Caballero, E., Cantón, Y., and De Philippis, R. (2018). Soil inoculation with cyanobacteria: reviewing its’ potential for agriculture sustainability in Drylands. *Agri. Res. Tech Open Access. J.* 18, 556046. doi: 10.19080/ARTOAJ.2018.18.556046
- Chan, K. Y., and Heenan, D. P. (1999). Microbial-induced soil aggregate stability under different crop rotations. *Biol. Fertil. Soils* 30, 29–32. doi: 10.1007/s003740050583
- Chen, L., Rossi, F., Deng, S., Liu, Y., Wang, G., Adessi, A., et al. (2014). Macromolecular and chemical features of the excreted extracellular polysaccharides in induced biological soil crusts of different ages. *Soil Biol. Biochem.* 78, 1–9. doi: 10.1016/j.soilbio.2014.07.004
- Chenu, C., and Cosentino, D. (2011). “Microbial regulation of soil structural dynamics,” in *The Architecture and Biology of Soils: Life in Inner Space*, eds K. Ritz and I. M. Young (Oxford: Oxford University Press), 37–70.
- Crouzet, O., Wiszniewski, J., Donnadiou, F., Bonnemoy, F., Bohatier, J., and Mallet, C. (2013). Dose-dependent effects of the herbicide mesotrione on soil cyanobacterial communities. *Arch. Environ. Contam. Toxicol.* 64, 23–31. doi: 10.1007/s00244-012-9809-9
- Degens, B. P. (1997). Macro-aggregation of soils by biological bonding and binding mechanisms and the factors affecting these: a review. *Aust. J. Soil Res.* 35, 431–459. doi: 10.1071/S96016
- Dorigo, U., Bourrain, X., Bérard, A., and Le Boulanger, C. (2004). Seasonal changes in the sensitivity of river microalgae to atrazine and isoproturon along a contamination gradient. *Sci. Tot. Environ.* 318, 101–114. doi: 10.1016/S0048-9697(03)00398-X
- Dubois, M., Gilles, K. J., and Smith, F. (1956). Colorimetric method for determination of sugars and related substances. *Anal. Chem.* 28, 356–361. doi: 10.1021/ac60111a017
- Elmholt, S., Munkholm, L. J., Debosz, K., and Schjønning, P. (2000). “Biotic and abiotic binding and bonding mechanisms in soils with long-term differences in management,” in *Proceedings of the DIAS Report*, Vol. 38, eds S. Elmholt, B. Stenberg, A. Grønlund, and V. Nuutinen (Denmark: Danish Institute of Agricultural Sciences), 53–62.
- Evans, R., and Johansen, J. (1999). Microbiotic crusts and ecosystem processes. *Crit. Rev. Plant Sci.* 18, 183–225. doi: 10.1080/07352689991309199
- Falchini, L., Sparvoli, E., and Tomaselli, L. (1996). Effect of Nostoc (Cyanobacteria) inoculation on the structure and stability of clay soils. *Biol. Fertil. Soils* 23, 346–352. doi: 10.1007/s00248-009-9498-8
- Gerbersdorf, S. U., Westrich, B., and Paterson, D. M. (2009). Microbial extracellular polymeric substances (EPS) in fresh water sediments. *Microb. Ecol.* 58, 334–349. doi: 10.1007/s00248-009-9498-8
- Ghiglione, J.-F., Martin-Laurent, F., Sachowski-Haberhorn, S., Pesce, S., and Vuilleumier, S. (2014). The coming of age of microbial ecotoxicology: report on the first two meetings in France. *Environ. Sci. Poll. Res.* 21, 14241–14245. doi: 10.1007/s11356-014-3390-x
- Green, V. S., Stott, D. E., and Diack, M. (2006). Assay for fluorescein diacetate hydrolytic activity: optimization for soil samples. *Soil Biol. Biochem.* 38, 693–701. doi: 10.1016/j.soilbio.2005.06.020
- Hu, C., Liu, Y., Paulsen, B. S., Petersen, D., and Klaveness, D. (2003). Extracellular carbohydrate polymers from five desert soil algae with different cohesion in the stabilization of fine sand grain. *Carbohydr. Polym.* 54, 33–42. doi: 10.1016/S0144-8617(03)00135-8
- Imfeld, G., and Vuilleumier, S. (2012). Measuring the effects of pesticides on bacterial communities in soil: a critical review. *Eur. J. Soil Biol.* 49, 22–30. doi: 10.1016/j.ejsobi.2011.11.010
- Joly, P., Misson, B., Perrière, F., Bonnemoy, F., Joly, M., Donnadiou-Bernard, F., et al. (2015). Soil surface colonization by phototrophic indigenous organisms, in two contrasted soils treated by formulated maize herbicide mixtures. *Ecotoxicology* 23, 1648–1658. doi: 10.1007/s10646-014-1304-9
- Knapen, A., Poesen, J., Galindo-Morales, P., De Baets, S., and Pals, A. (2007). Effects of microbiotic crusts under cropland in temperate environments on soil erodibility during concentrated flow. *Earth Surf. Process. Landf.* 32, 1884–1901. doi: 10.1002/esp.1504
- Langhans, T. M., Storm, C., and Schwabe, A. (2009). Biological soil crusts and their microenvironment: impact on emergence, survival and establishment of seedlings. *Flora* 204, 157–168.
- Le Bissonnais, Y. (1996). Aggregate stability and assessment of soil crustability and erodibility: I. theory and methodology. *Eur. J. Soil Sci.* 47, 425–437. doi: 10.1111/ejss.4\_12311
- Lentendu, G., Wubet, T., Chatzinotas, A., Wilhelm, C., Buscot, F., and Schlegel, M. (2014). Effects of long-term differential fertilization on eukaryotic microbial communities in an arable soil: a multiple barcoding approach. *Mol. Ecol.* 23, 3341–3355. doi: 10.1111/mec.12819
- Lin, C.-S., Chou, T.-L., and Wu, J.-T. (2013). Biodiversity of soil algae in the farmlands of mid-Taiwan. *Bot. Stud.* 54, 41–53. doi: 10.1186/1999-3110-54-41
- Ludwig, B., Nitschke, R., Terhoeven-Urselmans, T., Michel, K., and Flessa, H. (2008). Use of mid-infrared spectroscopy in the diffuse-reflectance mode for the prediction of the composition of organic matter in soil and litter. *J. Plant Nutr. Soil Sci.* 171, 384–391. doi: 10.1002/jpln.200700022
- Lynch, J. M., and Bragg, E. (1985). “Microorganisms and soil aggregate stability,” in *Advances in Soil Science*, Vol. 2, ed. B. A. Stewart (New York, NY: Springer).
- Mager, D. M., and Thomas, A. D. (2011). Extracellular polysaccharides from cyanobacterial soil crusts: a review of their role in dryland soil processes. *J. Arid Environ.* 75, 91–97. doi: 10.1016/j.jaridenv.2010.10.001
- Malam Issa, O., Défarge, C., Le Bissonnais, Y., Marin, B., Duval, O., Bruand, A., et al. (2007). Effects of the inoculation of cyanobacteria on the microstructure and the structural stability of a tropical soil. *Plant Soil* 290, 209–219. doi: 10.1007/s11104-006-9153-9
- Malam Issa, O., Le Bissonnais, Y., Défarge, C., and Trichet, J. (2001). Role of a cyanobacterial cover on structural stability of sandy soils in the Sahelian part of western Niger. *Geoderma* 101, 15–30. doi: 10.1016/S0016-7061(00)00093-8
- Mazor, G., Kidron, G. J., Vonshak, A., and Abeliovich, A. (1996). The role of cyanobacterial exopolysaccharides in structuring desert microbial crusts. *FEMS Microbiol. Ecol.* 21, 121–130. doi: 10.1016/0168-6496(96)00050-5
- Metting, B. (1981). The systematics and ecology of soil algae. *Bot. Rev.* 47, 195–312.
- Metting, B. (1987). Dynamics of wet and dry aggregate stability from a three-year microalgal soil conditioning experiment in the field. *Soil Sci.* 143, 139–143.
- Metting, B., and Rayburn, W. (1979). The effects of the pre-emergence herbicide di-allate and the post-emergence herbicide MCPA on the growth of some soil algae. *Phycologia* 18, 269–272. doi: 10.2216/i0031-8884-18-3-269.1
- Metting, B., and Rayburn, W. R. (1983). The influence of a microalgal conditioner on selected Washington soils: an empirical study. *Soil Sci. Soc. Am. J.* 47, 682–685. doi: 10.2136/sssaj1983.03615995004700040015x
- Metting, F. B. (1990). Microalgae applications in agriculture. *Dev. Ind. Microbiol.* 31, 265–270.
- Mostafa, F., and Helling, C. S. (2002). Impact of four pesticides on the growth and metabolic activities of two photosynthetic algae. *J. Environ. Sci. Health B* 37, 417–444. doi: 10.1081/PFC-120014873
- Mostafa, F. I., and Helling, C. S. (2001). Isoproturon degradation as affected by the growth of two algal species at different concentrations and pH values. *J. Environ. Sci. Health B* 36, 709–727. doi: 10.1081/PFC-100107406
- Nielsen, M. N., and Winding, A. (2002). *Microorganisms as Indicators of Soil Health Technical Report No. 388*. Denmark: National Environmental Research Institute.
- Nisha, R., Kaushik, A., and Kaushik, C. P. (2007). Effect of indigenous cyanobacterial application on structural stability and productivity of an organically poor semi-arid soil. *Geoderma* 138, 49–56. doi: 10.1016/j.geoderma.2006.10.007
- Peel, M. C., Finlayson, B. L., and McMahon, T. A. (2007). Updated world map of the Köppen-Geiger climate classification. *Hydrol. Earth Syst. Sci.* 11, 1633–1644. doi: 10.5194/hess-11-1633-2007
- Peng, X., and Bruns, M. A. (2019a). Cyanobacterial soil surface consortia mediate N cycle processes in agroecosystems. *Front. Environ. Sci.* 6:156. doi: 10.3389/fenvs.2018.00156

- Peng, X., and Bruns, M. A. (2019b). Development of a nitrogen-fixing cyanobacterial consortium for surface stabilization of agricultural soils. *J. Appl. Phycol.* 31, 1047–1056. doi: 10.1007/s10811-1597-9
- Pipe, A. E. (1992). "Pesticide Effects on Soil Algae and Cyanobacteria," in *Reviews of Environmental Contamination and Toxicology. Reviews of Environmental Contamination and Toxicology*, Vol. 127, ed. G. W. Ware (New York, NY: Springer).
- Pipe, A. E., and Shubert, L. E. (1984). "The use of algae as indicators of soil fertility," in *Algae as Ecological Indicators*, ed. L. E. Shubert (London: Academic Press), 213–233.
- Puget, P., Angers, D. A., and Chenu, C. (1999). Nature of carbohydrates associated with water-stable aggregates of two cultivated soils. *Soil Biol. Biochem.* 31, 55–63. doi: 10.1016/S0038-0717(98)00103-5
- Redmile-Gordon, M. A., Brookes, P. C., Evershed, R. P., Goulding, K. W. T., and Hirsch, P. R. (2014). Measuring the soil-microbial interface: Extraction of extracellular polymeric substances (EPS) from soil biofilms. *Soil Biol. Biochem.* 72, 163–171. doi: 10.1016/j.soilbio.2014.01.025
- Renard, C. M. G., and Ginies, C. (2009). Comparison of the cell wall composition for flesh and skin from five different plums. *Food Chem.* 114, 1042–1049. doi: 10.1016/j.foodchem.2008.10.073
- Renuka, N., Guldhe, A., Prasanna, R., Singh, P., and Bux, F. (2018). Microalgae as multi-functional options in modern agriculture: current trends, prospects and challenges. *Biotechnol. Adv.* 36, 1255–1273. doi: 10.1016/j.biotechadv.2018.04.004
- Rogers, S. L., and Burns, R. G. (1994). Changes in aggregate stability, nutrient status, indigenous microbial populations and seedling emergence, following inoculation of soil with *Nostoc muscorum*. *Biol. Fert. Soils* 18, 209–215. doi: 10.1007/BF00647668
- Rose, M. T., Cavagnaro, T. R., Scanlan, C. A., Rose, T. J., Vancov, T., Kimber, S., et al. (2016). Impact of herbicides on soil biology and function. *Adv. Agron.* 136, 133–220. doi: 10.1016/bs.agron.2015.11.005
- Rossi, F., and De Philippis, R. (2015). Role of cyanobacterial exopolysaccharides in phototrophic biofilms and in complex microbial mats. *Life* 5, 1218–1238. doi: 10.3390/life5021218
- Schnürer, J., and Rosswall, T. (1982). Fluorescein diacetate hydrolysis as a measure of total microbial activity in soil and litter. *Appl. Environ. Microbiol.* 43, 1256–1261.
- Serra, A., and Guasch, H. (2009). Effects of chronic copper exposure on fluvial systems: linking structural and physiological changes of fluvial biofilms with the in-stream copper retention. *Sci. Tot. Environ.* 407, 5274–5282. doi: 10.1016/j.scitotenv.2009.06.008
- Shimmel, S. M., and Darley, W. M. (1985). Productivity and density of soil algae in an agricultural system. *Ecology* 66, 1439–1447. doi: 10.2307/1938006
- Singh, J. S., Pandey, V. C., and Singh, D. P. (2011). Efficient soil microorganisms: a new dimension for sustainable agriculture and environmental development. *Agric. Ecosys. Environ.* 140, 339–353. doi: 10.1016/j.agee.2011.01.017
- Six, J., Bossuyt, H., Degryze, S., and Deneff, K. (2004). A history of research on the link between (micro)aggregates, soil biota, and soil organic matter dynamics. *Soil Till. Res.* 79, 7–31. doi: 10.1016/j.still.2004.03.008
- Six, J., Elliott, E. T., and Paustian, K. (2000). Soil macroaggregate turnover and microaggregate formation: a mechanism for C sequestration under no-tillage agriculture. *Soil Biol. Biochem.* 32, 2099–2103. doi: 10.1016/S0038-0717(00)00179-6
- Tisdall, J. M., and Oades, J. M. (1982). Organic matter and water-stable aggregates. *Eur. J. Soil Sci.* 33, 141–163. doi: 10.1111/j.1365-2389.1982.tb01755.x
- Tsujimura, S., Nakahara, H., and Ishida, N. (2000). Estimation of soil algal biomass in salinized irrigation land: a comparison of culture dilution and chlorophyll a extraction methods. *J. Appl. Phycol.* 12, 1–8. doi: 10.1023/A:1008126232188
- Veluci, R. M., Neher, D., and Weicht, R. (2006). Nitrogen fixation and leaching of biological soil crust communities in mesic temperate soils. *Microb. Ecol.* 51, 189–196. doi: 10.1007/s00248-005-0121-3
- Zaady, E., Arbel, S., Barkai, D., and Sarig, S. (2013). Long-term impact of agricultural practices on biological soil crusts and their hydrological processes in a semiarid landscape. *J. Arid Env.* 90, 5–11. doi: 10.1016/j.jaridenv.2012.10.021
- Zaady, E., Levacov, R., and Shachak, M. (2004). Application of the herbicide, simazine, and its effect on soil surface parameters and vegetation in a patchy desert landscape. *Arid Land Res. Manag.* 18, 397–410. doi: 10.1080/15324980490497483
- Zancan, S., Trevisan, R., and Paoletti, M. G. (2006). Soil algae composition under different agro-ecosystems in North-Eastern Italy. *Agric. Ecosys. Environ.* 112, 1–12. doi: 10.1016/j.agee.2005.06.018
- Zapata, M., Rodríguez, F., and Garrido, J. (2000). Separation of chlorophylls and carotenoids from marine phytoplankton: a new HPLC method using a reversed phase C8 column and pyridine- containing mobile phases. *Mar. Ecol. Prog. Ser.* 195, 29–45. doi: 10.3354/meps195029

**Conflict of Interest Statement:** The authors declare that the research was conducted in the absence of any commercial or financial relationships that could be construed as a potential conflict of interest.

Copyright © 2019 Crouzet, Consentino, Pétraud, Marraud, Aguer, Bureau, Le Bourvellec, Touloumet and Bérard. This is an open-access article distributed under the terms of the Creative Commons Attribution License (CC BY). The use, distribution or reproduction in other forums is permitted, provided the original author(s) and the copyright owner(s) are credited and that the original publication in this journal is cited, in accordance with accepted academic practice. No use, distribution or reproduction is permitted which does not comply with these terms.



# Earthworms Mitigate Pesticide Effects on Soil Microbial Activities

Sylvain Bart\*, Céline Pelosi, Alexandre Barraud, Alexandre R. R. Péry, Nathalie Cheviron, Virginie Grondin, Christian Mougin and Olivier Crouzet

UMR ECOSYS, INRA, AgroParisTech, Université Paris-Saclay, Versailles, France

## OPEN ACCESS

### Edited by:

Stéphane Pesce,  
National Research Institute of Science  
and Technology for Environment  
and Agriculture (IRSTEA), France

### Reviewed by:

Juan C. Sanchez-Hernandez,  
University of Castilla-La Mancha,  
Spain

Manuel Aira,  
University of Vigo, Spain

### \*Correspondence:

Sylvain Bart  
sylvain1.bart@outlook.fr

### Specialty section:

This article was submitted to  
Microbiotechnology, Ecotoxicology  
and Bioremediation,  
a section of the journal  
Frontiers in Microbiology

**Received:** 17 December 2018

**Accepted:** 20 June 2019

**Published:** 03 July 2019

### Citation:

Bart S, Pelosi C, Barraud A,  
Péry ARR, Cheviron N, Grondin V,  
Mougin C and Crouzet O (2019)  
Earthworms Mitigate Pesticide Effects  
on Soil Microbial Activities.  
*Front. Microbiol.* 10:1535.  
doi: 10.3389/fmicb.2019.01535

Earthworms act synergistically with microorganisms in soils. They are ecosystem engineers involved in soil organic matter degradation and nutrient cycling, leading to the modulation of resource availability for all soil organisms. Using a soil microcosm approach, we aimed to assess the influence of the earthworm *Aporrectodea caliginosa* on the response of soil microbial activities against two fungicides, i.e., Cuprafor Micro® (copper oxychloride, a metal) and Swing® Gold (epoxiconazole and dimoxystrobin, synthetic organic compounds). The potential nitrification activity (PNA) and soil enzyme activities (glucosidase, phosphatase, arylamidase, and urease) involved in biogeochemical cycling were measured at the end of the incubation period, together with earthworm biomass. Two common indices of the soil biochemistry were used to aggregate the response of the soil microbial functioning: the geometric mean (Gmean) and the Soil Quality Index (SQI). At the end of the experiment, the earthworm biomass was not impacted by the fungicide treatments. Overall, in the earthworm-free soil microcosms, the two fungicides significantly increased several soil enzyme and nitrification activities, leading to a higher GMean index as compared to the non-treated control soils. The microbial activity responses depended on the type of activity (nitrification was the most sensitive one), on the fungicide (Swing® Gold or Cuprafor Micro®), and on the doses. The SQI indices revealed higher effects of both fungicides on the soil microbial activity in the absence of earthworms. The presence of earthworms enhanced all soil microbial activities in both the control and fungicide-contaminated soils. Moreover, the magnitude of the fungicide impact, integrated through the SQI index, was mitigated by the presence of earthworms, conferring a higher stability of microbial functional diversity. Our results highlight the importance of biotic interactions in the response of indicators of soil functioning (i.e., microbial activity) to pesticides.

**Keywords:** Lumbricidae, fungicide, enzyme activity, nitrification, ecotoxicology

## INTRODUCTION

Earthworms and microorganisms represent the largest part of the living biomass in soils. They ensure a wide range of essential soil functions (Brown et al., 2000) and thus contribute to ecosystem services (Blouin et al., 2013; Bertrand et al., 2015). As ecosystem engineers (Jones et al., 1994), earthworms play key roles in the dynamic of the soil organic matter (SOM) and of the resource availability for other soil organisms through tight interactions with microorganisms, which act

as chemical engineers (Scheu, 1987; Edwards and Fletcher, 1988). The mechanical and biological activities of earthworms catalyze SOM decomposition, carbon and nitrogen mineralization, and nutrient turnover, by modulating microbial biomass and activity (Daniel and Anderson, 1992; Zhang and Hendrix, 1995; Tiunov and Scheu, 1999). Different earthworm species are known to increase soil microbial respiration (Scheu, 1987) or soil enzyme activities related to C, N, and P cycling (Tao et al., 2009; Dempsey et al., 2013), especially in the drilosphere (casts and burrow walls, Loquet et al., 1977; Aira et al., 2003). These works highlight significant effects of earthworms on the abundance of various microbial groups (i.e., ammonifiers, denitrifiers, and proteolytic bacteria). The mucus produced by earthworms is also a nutrient resource for microbial activity (Martin et al., 1987). However, by ingesting microbial biomass, they can also decrease the total microbial biomass while increasing the specific activities of its residual component (i.e., extra-cellular enzyme activities, Zhang et al., 2000; Aira et al., 2009).

The use of pesticides in agroecosystems may impair biodiversity and biological activity in cultivated soils (Bengtsson et al., 2005; Hole et al., 2005). The normalization of experimental conditions to assess pesticide impacts on soil organisms greatly contributed to such a historical separation between biological models, while ecological approaches spoke up for taking into account biotic interactions in the study of ecosystem function under chemical stress (Burrows and Edwards, 2004; Clements and Rohr, 2009). In turn, few investigations on the effects of pesticides on soil biological functioning have considered the fundamental interaction between the soil fauna (earthworms) and microorganisms, as earthworms can increase microbial activity, even in insecticide-contaminated soils (Sanchez-Hernandez et al., 2018).

Earthworms are often used as soil biological indicators (Spurgeon et al., 2003), and the impacts of pesticides on earthworms have been extensively documented (Pelosi et al., 2014). These physical ecosystem engineers continuously modify soil microhabitats, and thereby influence on microbial life and the related biogeochemical activities. Pesticide application can also impact soil microbial communities and their activity, but with much more contrasted results (by decreasing or increasing them) depending on the active compound and the microbial groups (Chen et al., 2001; Wainwright, 2006; Niemi et al., 2009), with possible outcomes for microbe-mediated processes (Muñoz-Leoz et al., 2013). In this respect, enzyme activities are useful indicators of soil health because enzymes contribute to nutrient cycling (Burns and Dick, 2002) and their activity can be used as a proxy of changes in soil functioning due to the alteration of microbial communities in response to heavy metal exposure (Kandeler et al., 1996; Speir and Ross, 2002). The multiple direct and indirect effects jointly affect enzyme activity, which results in an increase, decrease or leveling off of its catalytic activity (Gianfreda and Rao, 2008; Riah et al., 2014). Copper (Cu) can be used as an inorganic pesticide in organic farming. Like other metals, depending on its concentrations, copper can be an oligo-element acting as a co-factor for some enzymes, or a toxicant for the cellular activities (Giller et al., 2009). Chemical stressors can affect narrow niche functions ( $N_2$  fixation or nitrification) more

than broad-scale niche processes (enzyme activities), which may display higher diversity and functional redundancy (Pell et al., 1998; Crouzet et al., 2016; Karas et al., 2018).

There is a general knowledge gap about the relationship between taxonomic diversity and ecosystem functions, so that functional rather than taxonomic diversity could be more suitable to investigate microbial roles in ecosystems (Zak et al., 1994). Microbial functional diversity is defined as the numbers, types, activities, and rates at which a range of substrates is metabolized by the microbial communities to contribute to ecosystem processes (e.g., organic matter mineralization, Zak et al., 1994). To assess the impact of soil contamination on soil functions, several indices were developed as indicators of soil quality by aggregating different soil microbial activities, especially enzymatic activities involved in biogeochemical cycles (Bending et al., 2002; Rodríguez-Loinaz et al., 2008). The geometric mean (Gmean) index can be a suitable proxy of soil functional diversity (Lessard et al., 2014), since it was calculated with a sufficient range of activities depending on numerous metabolic reactions and interactions among members of the soil biota (Nannipieri et al., 2002). The SQI is another index that characterizes changes in the measured microbial activity (decrease or increase) following a treatment (Bloem et al., 2006).

The aim of our work was to quantify the potential benefit of the presence of earthworms for the tolerance of the soil microbial community to fungicides. It was based on the assumption that earthworms can modulate microbial activity and exposure to contaminants due to their ecosystem engineer role. The hypotheses were that (i) the two fungicides would differently impact microbial activity due to their different fates in the soil, and (ii) earthworms would confer a higher tolerance to the microbial communities exposed to fungicides. We carried out a dose-effect study in soil microcosms to assess the influence of the presence of earthworms on the impact of two commercial formulations of fungicides (Cuprafor Micro<sup>®</sup> with copper oxychloride as the active ingredient, and Swing<sup>®</sup> Gold with epoxiconazole and dimoxystrobin as active ingredients) on soil microbial activities. These fungicides were selected because they can affect both earthworms (Pelosi et al., 2014) and soil microorganisms at doses close to recommended application rates, whereas herbicides or insecticides usually disturb microbial processes at much higher doses (Wainwright, 2006; Muñoz-Leoz et al., 2013). In addition, the inorganic copper-based fungicide does not dissipate, while the synthetic organic fungicide does. To assess the fungicide effects, some earthworm endpoints were measured (survival and biomass) and the microbial responses targeted several microbial activities involved in biogeochemical cycling and the whole functional microbial diversity (with enzyme indexes).

## MATERIALS AND METHODS

### Soil and Earthworms

The soil used for all experiments was sampled from the top 0–20 cm in a permanent grassland in Versailles (48°48' N, 2°5' E) where no chemical had been applied for more than

20 years. It was a Luvisol (FAO soil classification) and its main physical characteristics were as follows: pH 7.5, organic matter 32.6 g kg<sup>-1</sup>, C/N 12.7, 29% sand, 48% silt, 23% clay, and 25.2 mg Cu kg<sup>-1</sup> (see Bart et al., 2017 for more details). The soil was air-dried and sieved to 2 mm.

Mature *Aporrectodea caliginosa* s.s individuals were collected by hand-sorting from an agricultural field in Estrées-Mons (49°52' N 3°01'E). Their weight ranged from 600 to 1 000 mg. They were stored in the soil used for the experiments at 15 ± 1°C, 24 h darkness for at least 10 days before the experiments.

## Pesticides

Swing® Gold (BASF Agro SAS, dimoxystrobin 133 g L<sup>-1</sup>, epoxiconazole 50 g L<sup>-1</sup>) is an organic synthetic fungicide widely used in conventional farming to protect cereal crops. The Recommended Dose (RD) was calculated as 1.16 10<sup>-3</sup> mL kg<sup>-1</sup> (corresponding to 150 µg kg<sup>-1</sup> of dimoxystrobin and to 60 µg kg<sup>-1</sup> of epoxiconazole) of dry soil for a soil density of 1.29 and considering that the active compounds of this fungicide are mostly found in the top 10 cm of soil (McDonald et al., 2013; Chabauty et al., 2016). Based on the LC<sub>50</sub> estimated to be 6.3 times the RD for *A. caliginosa* (Bart et al., 2017), we tested 0.33, 1, and 3 times the RD of this commercial formulation.

Cuprafor Micro® (Quimicas del Valles, 50% copper oxychloride) is a metal-based fungicide commonly used in organic farming to prevent spore germination; it is authorized in organic management. The RD was calculated as 15.5 mg kg<sup>-1</sup> (corresponding to 7.75 mg Cu kg<sup>-1</sup> of dry soil) for a soil density of 1.29 and considering that the active compounds of this fungicide are mostly found in the top 5 cm of soil (Couto et al., 2015). Based on literature reviews (Ma, 1984; Spurgeon et al., 2004; Bart et al., 2017; Pesticide Properties DataBase [PPDB], 2018) and taking into account that Cu can accumulate in soils, we tested 3.33, 10, and 30 times the RD, which corresponds to the addition of 25.8, 77.5, and 232.3 mg kg<sup>-1</sup> of Cu.

## Experimental Design

Soil microcosms were built up with five replicates for each condition. Each microcosm corresponded to a 1-L plastic vessel with a removable perforated cover for gas exchange. Each vessel contained 500 g of dry soil and 24 g of dry horse dung as a food resource for earthworms, corresponding to a feeding of 6 g ind<sup>-1</sup> month<sup>-1</sup> as suggested in Lowe and Butt (2005) and in Bart et al. (2018) for *A. caliginosa*. The soil moisture was adjusted to 70% of the maximum water holding capacity (mWHC) using the fungicide solutions or tap water as controls. The food moisture was also adjusted to 70% of mWHC and mixed with the soil. Four *A. caliginosa* individuals were introduced in each vessel, and incubation was run for 28 days in a climate-controlled room at 15 ± 1°C. Earthworms were weighed on day 0 and at the end of the experiment (on day 28). The soil moisture content was controlled once a week. A similar set of microcosms was set up without adding earthworms.

## Microbial Activity

All soil enzyme activities mainly come from microorganisms (prokaryotes and fungi) and are involved in the nutrient cycles

of carbon (C), nitrogen (N), and phosphorus (P) (Burns et al., 2013), through organic matter mineralization. Nitrification is a key step of nitrogen cycling ensured by specific bacterial and archaeal guilds (Prosser, 2005), which are known to be highly sensitive to pesticides (Crouzet et al., 2016). The potential nitrification activity (PNA) and soil enzymes β-D-glucosidase (GLU), phosphatase (PHOS), urease (URE), and arylamidase (ARM) were assessed in each microcosm on day 28 after the fungicide treatments. Three analytical replicates were measured for each microcosm and each activity.

PNA was determined in accordance with Petersen et al. (2012), with some modifications specified in Corbel et al. (2015). Briefly, 4 g of fresh soil were sampled and mixed with 25 mL of MilliQ water and (NH<sub>4</sub>)<sub>2</sub>SO<sub>4</sub> at a final concentration of 1 mM. Samples were incubated at 25°C under continuous shaking (150 rpm). After 2.5 and 45 h, 1 mL was sampled and centrifuged at 13,000 g for 5 min, and supernatants were stored at -20°C until analyses of the nitrate (NO<sub>3</sub><sup>-</sup>) and nitrite (NO<sub>2</sub><sup>-</sup>) ions by colorimetry according to the Griess reaction. The supernatants were dropped in microplates and the Griess solution was added (HCl, 0.5M, vanadium chloride III (Sigma-Aldrich 208272) at 1 g L<sup>-1</sup>, sulfanilamide (Sigma-Aldrich S9251) at 2.5 g L<sup>-1</sup> and N-(1-naphthyl)-ethylenediaminedihydrochloride (Sigma-Aldrich 222488) at 0.25 g L<sup>-1</sup>), and then incubated at 60°C for 1.5 h. The optical densities were determined at 540 nm with a microplate reader (SAFAS Xenius, Monaco). Results were then expressed as PNA, which is the rate of N-NO<sub>3</sub><sup>-</sup> + N-NO<sub>2</sub><sup>-</sup> production during activity measurements (for 45 h), in µg N released g<sup>-1</sup> h<sup>-1</sup>.

The soil enzymes β-D-GLU, PHOS, ARN, and URE were measured according to the ISO 20130 (2018) standard, with a slight modification for URE. All measurements were performed at the soil pH, in an unbuffered soil water solution, in accordance with Lessard et al. (2013). Three aliquots of 4 g of fresh soil each were sampled in each microcosm, and each one was mixed with 25 mL of MilliQ water (10 min, ambient temperature, continuous shaking at 250 rpm). Aliquots of soil solution (125 µL) were incubated in 96-well microtiter plates with the following substrates: 4-nitrophenyl-β-D-glucopyranoside (final concentration in the wells: 8.3 mM, incubation time: 1 h at 37°C) for GLU, 4-nitrophenylphosphate (8.3 mM, 30 min at 37°C) for PHOS, urea (80 mM, 3 h at 25°C) for URE, and L-leucine β-naphthylamide-hydrochloride (1.3 mM, 1 h at 37°C) for ARYL-N. Each substrate was added at a concentration corresponding to its saturating concentration. After the incubation period, reactions were stopped by adding a CaCl<sub>2</sub> solution (0.5 M) and Tris-HCl (0.1 M, pH 12) for GLU, PHOS, and URE. For ARM, reactions were stopped with ethanol 96% (v/v). The microplate was then centrifuged at 3,000 g for 5 min, and an aliquot of 0.2 mL from each well was used to evaluate enzyme activity. The para-nitrophenol (pNP) released by GLU and PHOS activities was measured at 405 nm, and the β-naphthylamine released by ARYL-N activity was determined at 540 nm, using a microplate reader (SAFAS, Monaco). Enzyme activities were calculated based on external calibration curves using standards (Sigma): p-nitrophenol (final concentrations in the wells ranged from 0 to 0.4 mM), β-naphthylamine (from 0 to

0.2 mM). The ammonium ion  $\text{NH}_4^+$  released by URE activity was determined at 610 nm with an HACH reagent (Loveland, CO, United States), and enzyme activity was calculated based on a calibration curve using an  $\text{NH}_4\text{Cl}$  standard (Sigma), with final concentrations in the wells ranging from 0 to 0.3 mM  $\text{NH}_4^+$ . Calibration curves were performed in similar reaction mixtures as each enzyme but without soil solution, since no difference in adsorption of pNP and  $\beta$ -naphthylamine standards was expected in such similar soil samples (the same soil and amount of OM in all microcosms). Results were then expressed in  $\text{mU g}^{-1}$  dry soil, representing nanomoles of product released per minute and per g of equivalent dry soil.

## Soil Functional Diversity

The impact of pesticides on soil microbial functioning was assessed using the GMean index (Hinojosa et al., 2004), which aggregates each of the individual microbial activities. The Gmean index is considered as a suitable proxy of functional microbial diversity (Lessard et al., 2014):

$$\text{GMean} = \left( \prod_{i=1}^n y_i \right)^{1/n}$$

where  $y_i$  is the enzyme activity or PNA,  $n$  is the number of soil enzymes and the PNA (5). High GMean values mean high microbial functional diversity (Lessard et al., 2014).

The second index was the SQI, as described by Bloem et al. (2006). It was calculated using the average factorial deviation from the reference value (Ten Brink et al., 1991):

$$\text{SQI} = 10^{\log m - \frac{\sum_{i=1}^n |\log m - \log n_i|}{n}}$$

where  $m$  is the reference soil (mean value of enzyme activity or PNA in the control soil in the presence or in the absence of earthworms, set to 100%), and  $n$  are the measured values as percentages of the reference soil. A decrease of the SQI highlights a modification (increase and/or decrease) in the soil microbial activity.

## Data Analysis

All statistical analyses were performed using R software Core Team (2015). The analyses of biomass changes between day 0 and day 28, and the assessment of the mortality rate were performed using the non-parametric Wilcoxon signed-rank test. When the normality and homoscedasticity conditions were satisfied, each microbial activity and index was analyzed using a two-way ANOVA to test the effect of fungicide concentrations, of the presence of earthworms, and of the interaction between these two factors. Then, a Tukey test was performed to assess the difference between pesticide treatments in the soils in the presence or in the absence of earthworms. When the normality and homoscedasticity conditions were not satisfied, the non-parametric kruskalmc (multiple comparison) test (adjusted  $p$ -values based on Bonferroni's corrections were applied) to assess the difference between pesticide treatments in the soils in the presence or in the absence of earthworms. The percentages of

increase of the PNA, Gmean index, and SQI between the control and the highest concentration tested were compared between the soils in the presence and in the absence of earthworms using the Wilcoxon signed-rank test.

## RESULTS

### Effects of the Copper Fungicide

An earthworm mortality rate of 5% was recorded in the Cu3.33 and the control treatments at the end of the experiment (after 28 days). No mortality occurred in the Cu10 and Cu30 treatments. There was no significant difference in earthworm mortality or weight along the experiment whatever the Cu fungicide concentration tested.

The responses of enzyme activities and PNA in the control soil and Cu-treated soils in the presence or in the absence of earthworms are presented in **Table 1**. In the absence of earthworms, a significant effect of the Cu treatment was measured on three enzyme activities (GLU, PHOS, and ARN), and there were significant differences between the control and Cu treatments. Glucosidase activity significantly increased as compared to the control, only following the Cu3.33 treatment (**Table 1**). Phosphatase activity decreased by 25.1% in the Cu30 treatment as compared to the control. Arylamidase activity increased with increasing Cu concentrations, to reach +60% of the control value in the Cu30 treatment. The presence of earthworms significantly increased all enzyme activities as compared to the earthworm-free soils. It also resulted in a lower difference or no difference at all between enzyme activities in the control and Cu-treated soils. Then, only phosphatase activity significantly decreased by 22.7% in the Cu30 treatment as compared to the control. This decrease was of the same magnitude as the 25.1% observed in the earthworm-free soils.

The two-way ANOVA test revealed that PNA was significantly affected by the presence of earthworms [ $F(1,32) = 23.5$ ,  $p \leq 0.0001$ ], by the Cu treatments [ $F(3,32) = 25.4$ ,  $p \leq 0.0001$ ], and by the interaction between these two factors [ $F(3,32) = 11$ ,  $p \leq 0.0001$ ] (**Table 1**). Considering the earthworm-free soil, PNA significantly increased by +37, +40, and +57% in the Cu3.33, Cu10, and Cu30 treatments, respectively, as compared to the control. In the soils that harbored earthworms, statistical analyses did not reveal any effect whatever the Cu applications as compared to the control, but PNA was higher following the Cu30 treatment than following the Cu3.33 and Cu10 treatments. The magnitude of the PNA increase between the control and Cu30 treatment was much higher in the earthworm-free soils ( $57 \pm 11\%$ ) than in the soils harboring earthworms ( $12 \pm 5\%$ ) (Wilcoxon test,  $p = 0.012$ ).

There was a significant effect, highlighted by the two-way ANOVA test, of the Cu treatments [ $F(3,32) = 4.2$ ,  $p = 0.013$ ], of earthworms [ $F(1,32) = 702$ ,  $p \leq 0.0001$ ], and of the interaction between these two factors [ $F(3,32) = 7.8$ ,  $p \leq 0.0001$ ] on the GMean index (**Figure 1A**). The presence of earthworms strongly promoted soil microbial activity in all treatments. When considering only the set of earthworm-free soil microcosms, the GMean index significantly increased with

**TABLE 1** | Enzyme activities (mU g<sup>-1</sup> dry soil) and potential nitrification activity (PNA, μg NO<sub>3</sub> g<sup>-1</sup> dry soil) in a control soil and the same soil spiked with different concentrations of Cuprafor micro® (3.33, 10, and 30 times the RD corresponding to 25.8, 77.5, and 232.5 mg kg<sup>-1</sup> of copper, abbreviated Cu3.3, Cu10, and Cu30, respectively), in the presence or in the absence of earthworms (n = 5, ±SD).

Enzyme and microbial activities	Treatment					Effects				
	Earthworm absence		Earthworm presence			E	t	txE	t	txE
	Control	Cu 3.33	Cu 10	Cu 30	Control					
β-D-glucosidase	12.5 ± 1.1a	16.4 ± 1.2b	13.1 ± 0.7a	14.3 ± 0.8ab	25.0 ± 1.4A	24.3 ± 1.7A	23.9 ± 3.1A	25.2 ± 1.0A	***	*
Phosphatase	20.7 ± 1.3a	20.2 ± 1.4a	17.1 ± 1.4ab	15.5 ± 1.6b	34.8 ± 2.7A	34.9 ± 2.6A	30.8 ± 3.9B	26.9 ± 1.0C	***	***
Urease	17.6 ± 2.8a	21.3 ± 2.6a	19.7 ± 1.4a	20.5 ± 2.4a	30.0 ± 2.1A	31.9 ± 2.0A	29.7 ± 2.6A	28.3 ± 2.1A	***	ns
Arylamidase	6.3 ± 0.4a	8.2 ± 0.6b	8.9 ± 0.3bc	10.1 ± 1.4c	13.1 ± 0.7AB	12.4 ± 0.4A	12.7 ± 1.1AB	13.7 ± 0.5B	***	***
PNA	0.46 ± 0.05a	0.62 ± 0.04b	0.64 ± 0.04b	0.71 ± 0.05c	0.66 ± 0.05AB	0.65 ± 0.05A	0.64 ± 0.04A	0.73 ± 0.04B	***	***

Different letters mean significant differences between treatments, and the result of the two-way ANOVA test is presented as follows: “t” is for treatment effect, “E” for earthworm effect and “(txE)” for their interaction. “ns” means no significant difference, \*p < 0.05 and \*\*\*p < 0.001.

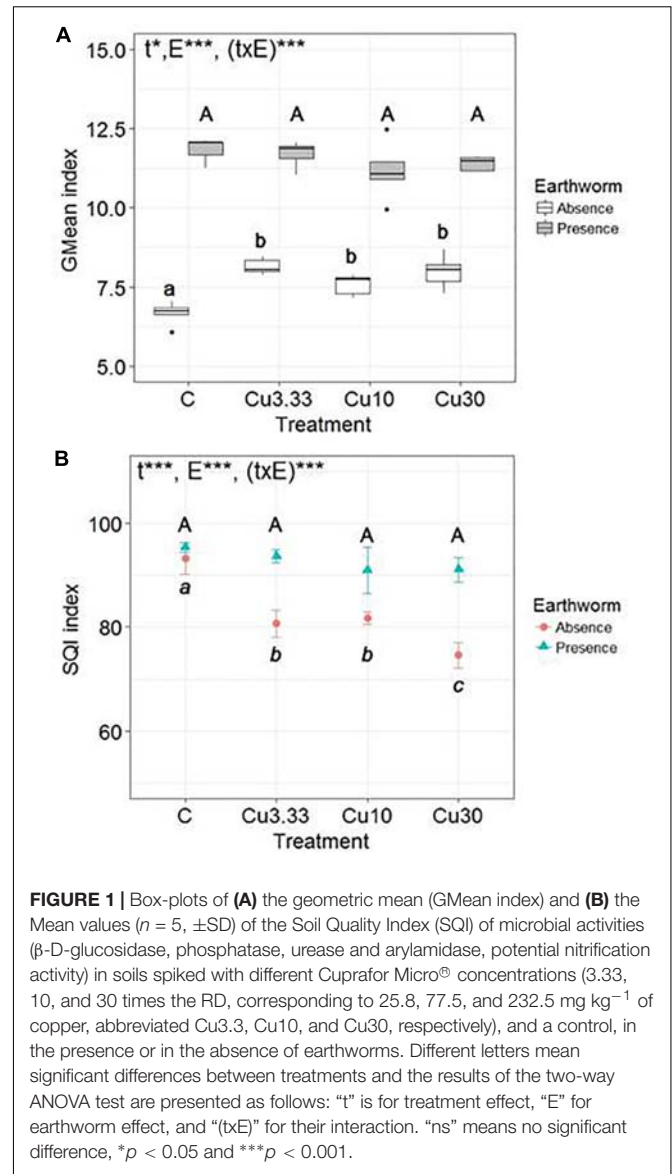


**FIGURE 1** | Box-plots of (A) the geometric mean (GMean index) and (B) the Mean values (n = 5, ±SD) of the Soil Quality Index (SQI) of microbial activities (β-D-glucosidase, phosphatase, urease and arylamidase, potential nitrification activity) in soils spiked with different Cuprafor Micro® concentrations (3.33, 10, and 30 times the RD, corresponding to 25.8, 77.5, and 232.5 mg kg<sup>-1</sup> of copper, abbreviated Cu3.3, Cu10, and Cu30, respectively), and a control, in the presence or in the absence of earthworms. Different letters mean significant differences between treatments and the results of the two-way ANOVA test are presented as follows: “t” is for treatment effect, “E” for earthworm effect, and “(txE)” for their interaction. “ns” means no significant difference, \*p < 0.05 and \*\*\*p < 0.001.

increasing Cu application rates (by 19.9 ± 7.9% in Cu30 as compared to the control), while there was no effect of the Cu treatment on the GMean index in the set of soil microcosms harboring earthworms.

The two-way ANOVA test revealed a significant effect of the Cu treatments [F(3,32) = 36, p ≤ 0.0001], of earthworms [F(1,32) = 161, p ≤ 0.0001], and of the interaction between these two factors [F(3,32) = 14, p ≤ 0.0001] on the SQI (Figure 1B). Significant effects of the Cu application rates on the SQI were only observed in the earthworm-free soils in which the SQI decreased by 20.0 ± 3% between the control and the Cu30 treatment.

### Effects of the Swing® Gold fungicide

No earthworm mortality was recorded in the SG0.33 treatment. A mortality rate of 5% was found in the SG1 and control treatments, and 20% in the SG3 treatment. Nevertheless, these

results were not statistically significant. No impact was recorded on the earthworm biomass.

The enzyme activity and PNA responses in the control soil and the soil treated with the SG fungicide, in the presence or in the absence of earthworms, are presented in **Table 2**. In the earthworm-free soil microcosms, the SG treatment had a significant effect on all enzyme activities, but there was no difference in phosphatase activity between the control and the SG3 treatment, contrary to the Cu treatments. GLU, URE, and ARN activities significantly increased by 25, 19, and 18%, respectively, in the SG3-treated soils as compared to the control. The presence of earthworms significantly increased all enzyme activities, as previously observed with the Cu treatment. Considering the set of soil microcosms harboring earthworms, a significant effect of the SG treatment was observed on phosphatase and urease activity between the control and the SG0.33 and SG3 treatments, respectively. Urease activity increased by 17.0% in the SG3 treatment as compared to control.

The two-way ANOVA test revealed that PNA was significantly affected by the presence of earthworms [ $F(1,32) = 68, p \leq 0.0001$ ] and the SG treatments [ $F(3,32) = 52, p \leq 0.0001$ ], but not by their interaction [ $F(3,32) = 2.9, p = 0.05$ ] (**Table 2**). PNA increased along with the increase in SG application rates, in the presence or absence of earthworms. However, the magnitude of the increase in PNA between the control and SG3-treated soils was much higher in the earthworm-free soils ( $73.4 \pm 11.4\%$ ) than in the soils harboring earthworms ( $32.4 \pm 8.2\%$ ) (Wilcoxon test,  $p = 0.008$ ).

There was a significant effect, highlighted by the two-way ANOVA test, of the SG treatments [ $F(3,32) = 25, p \leq 0.0001$ ], of earthworms [ $F(1,32) = 1,681, p \leq 0.0001$ ], and of the interaction between these two factors [ $F(3,32) = 3, p = 0.045$ ] on the GMean index (**Figure 2A**). The presence of earthworms promoted overall soil microbial activity in all modalities. There was a significant increase of the GMean index with the increase in SG application rates, in the absence or in the presence of earthworms. However, the magnitude of the GMean increase between the control and the SG3 treatment was significantly higher in the absence of earthworms ( $+27.4 \pm 4.0\%$ ) than in their presence ( $+8.6 \pm 3.9\%$ ) (Wilcoxon test,  $p = 0.008$ ).

The two-way ANOVA test revealed a significant effect of the SG treatments [ $F(3,32) = 61, p \leq 0.0001$ ], of earthworms [ $F(1,32) = 109, p \leq 0.0001$ ], and of the interaction between these two factors [ $F(3,32) = 11.9, p \leq 0.0001$ ] on the SQI (**Figure 2B**). There was a significant effect of the different SG application rates on the SQI, in the absence or in the presence of earthworms. However, the magnitude of the SQI decrease between the control and the SG3 treatment was significantly higher in the absence of earthworms ( $-17.7 \pm 1.3\%$ ) than in the presence of earthworms ( $-7.1 \pm 1.4\%$ ) (Wilcoxon test,  $p = 0.008$ ).

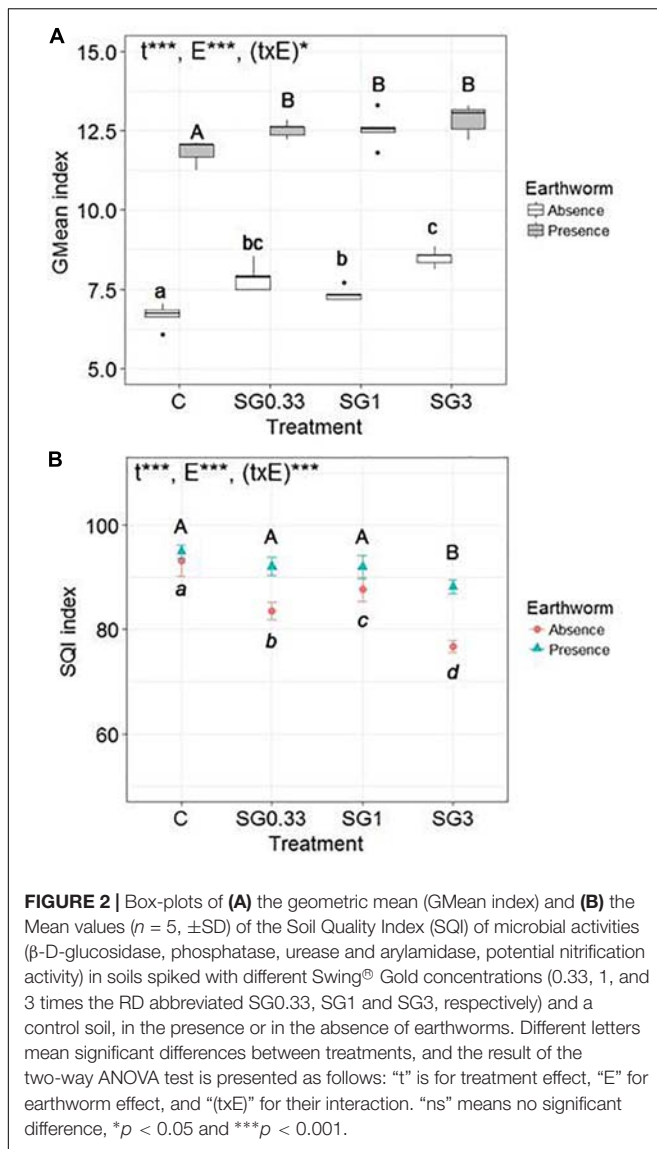
## DISCUSSION

The absence of an impact of fungicides on earthworm biomass and mortality during the experiment, whatever the concentrations applied, validates the sublethal concentration values retained for this experiment. Besides, no dormancy

**TABLE 2** | Enzyme activities (mU g<sup>-1</sup> dry soil) and potential nitrification activity (PNA, μg NO<sub>3</sub> g<sup>-1</sup> dry soil) in a control soil and the same soil spiked with different Swing® Gold concentrations (0.33, 1, and 3 times the RD abbreviated SG0.33, SG1, and SG3, respectively), in the presence or in the absence of earthworms ( $n = 5, \pm SD$ ).

Enzyme and microbial activities	Treatment						Effects			
	Earthworm absence			Earthworm presence			E	t	t x E	
	Control	SG 0.33	SG 1	Control	SG 0.33	SG 1				
β-D-glucosidase	12.5 ± 1.1a	13.6 ± 0.7a	12.3 ± 1.2a	16.6 ± 1.6b	25.5 ± 1.1A	24.8 ± 1.6A	23.7 ± 0.6A	***	*	***
Phosphatase	20.7 ± 1.3ab	23.5 ± 2.1a	20.2 ± 0.7b	20.3 ± 2.4ab	39.3 ± 1.6B	38.0 ± 1.4AB	38.0 ± 2.1AB	***	***	NS
Urease	17.6 ± 2.8a	19.1 ± 2.5ab	18.7 ± 2.0ab	21.5 ± 0.6b	32.3 ± 0.9AB	33.5 ± 2.1AB	35.2 ± 1.2B	***	***	NS
Arylamidase	6.3 ± 0.4a	7.7 ± 1.3b	7.4 ± 0.5ab	7.8 ± 0.3b	12.8 ± 0.7A	13.1 ± 0.5A	12.8 ± 0.5A	***	NS	**
PNA	0.46 ± 0.05a	0.66 ± 0.06b	0.63 ± 0.04b	0.79 ± 0.05c	0.76 ± 0.05B	0.76 ± 0.05BC	0.87 ± 0.05C	***	***	NS

Different letters mean significant differences between treatments, and the result of the two-way ANOVA test is presented as follows: "t" is for treatment effect, "E" for earthworm effect, and "t x E" for their interaction. "ns" means no significant difference, \* $p < 0.05$  and \*\*\* $p < 0.001$ .



was observed in the earthworms collected at the end of the experiment. Nevertheless, the absence of an effect on biomass did not inform on possible impacts on earthworm behavior in the soils containing pesticides (Capowiez et al., 2006; Dittbrenner et al., 2011). Therefore, possible effects of fungicides on earthworm burrowing or feeding activities, which are key parameters related to their influence on soil microbial communities (Edwards and Bohlen, 1996), cannot be excluded.

## Impact of Fungicides on Soil Microbial Activity in the Absence of Earthworms

In the absence of earthworms, contrasted responses were reported depending on the microbial activities and the fungicides, but overall both commercial fungicides increased the whole soil microbial activity, integrated with the GMean index. The decrease in phosphatase activity with increasing application

rates of the Cu-based fungicide is in accordance with several previous works showing that phosphatase activity decreased in soils treated with 150 and 450 mg Cu kg<sup>-1</sup> (Wyszkowska and Wyszkowski, 2010). Urease activity remained stable in our experiment, even at the highest concentration tested (232.5 mg kg<sup>-1</sup> of Cu), similarly to previous works where Cu hydroxide or CuCl<sub>2</sub> did not impact urease activity even at 156 mg kg<sup>-1</sup> (Wightwick et al., 2013). Conversely, Nor (1982) reported thorough inhibition of soil urease at 120 mg Cu kg<sup>-1</sup>. A theoretical PNEC for metals in soils can be predicted for given soil properties, on the basis of the HC 5% hazardous effect derived from SSD analyses (including plants, the meso- and macrofauna, and microorganisms) computed with literature data collection (Oorts et al., 2006b; Smolders et al., 2009). For our soil properties, the PNEC value was around 78.5 mg Cu kg<sup>-1</sup> dry soil, resulting in expected toxic effects on some microbial activities at Cu30 (232 mg kg<sup>-1</sup>). The increases in GLU, ARM, and PNA activity in the Cu-treated soils as compared to the controls were not expected. Copper has indeed been observed to impair soil microbial biomass or activity (Giller et al., 2009), more so following spiking of solutions of metal salts (Oorts et al., 2006a; Smolders et al., 2009). The impairment of microbial enzyme activity by metals might result from cellular toxicity that decreases the whole metabolism, or from the reaction of metal ions with the substrate or the protein-active groups of enzymes in soils (Deng and Tabatabai, 1995).

Two main hypotheses could explain such differences between the stimulation of microbial activity observed in our experiment (in the presence or in the absence of earthworms) and the numerous previous works underlining toxic effects of Cu (inhibition) at doses similar to those tested in this work. First, the addition of horse manure (at 4.8% w/w dry soil) provided a very high level of organic matter which strongly adsorbed copper ions, and likely decreased copper bioavailability for the same total input as compared to the previous cited literature. Such metal buffering by OM addition may have alleviated the Cu toxicity to soil microbial activities in our experiment. Second, another essential difference was that almost all these studies investigated impacts of Cu salt solutions, while we used a commercial formulation of Cu oxide containing unknown adjuvants and surfactants. These compounds can deeply modify the fate of copper in the soil and its effects on soil microorganisms. Adjuvants of commercial formulations of pesticides might act as available sources of nitrogen and carbon able to stimulate microbial biomass and activity (Crouzet et al., 2010; Mijangos et al., 2010). As a result, in our experimental conditions, the microbial exposure to copper would be below toxic thresholds, which would be consistent with the response patterns of microbial activities showing a hormetic-like response. Some previous findings been already observed for several soil microbial enzymes or nitrification in response to metal stress (Langdon et al., 2014; Han et al., 2019). Overcompensation in response to disruption in homeostasis was assumed the fundamental mechanism of hormesis, existing to preserve organism homeostasis (Calabrese and Baldwin, 2002).

Regarding the SG fungicide, an experiment with a commercial fungicide containing the same active substances (dimoxystrobin and epoxiconazole) showed negative effects of these fungicides on the activity of soil dehydrogenase and urease recorded only at 100-fold the recommended field rates (Jastrzębska and Kucharski, 2007). Along with ours, these results underline that, at realistic doses, fungicides based on a dimoxystrobin – epoxiconazole mixture do not negatively affect the related soil enzyme activities (i.e., PHOS, GLU, URE, and ARN), but could disturb soil nitrification (PNA). Overall, the increases of several microbial activities have already been observed with other organic synthetic pesticides (glyphosate, Haney et al., 2002; carbendazim, tebuconazole, and captan, Burrows and Edwards, 2000; Chen et al., 2001; Cycoń et al., 2006). A first assumption about this phenomenon is that the fungicides killed or inhibited the activity of certain groups of non-target fungi. On the short term, dead fungal biomass might be used as a food resource by living microorganisms, and this could lead to greater bacterial activity, along with decreased competition for other resources (Monkiedje et al., 2007). Another assumption is that fungicides kill or inhibit the soil microfauna, such as protozoa or nematodes which are predatory for microorganisms (Ekelund and Rønn, 1994; Rønn et al., 2002), thus turning off the top-down regulation of microbial biomass and activity. Finally, as regards copper, we used commercial formulations instead of pure active compounds. The surfactants and the adjuvants contained in commercial products may influence the impacts of active ingredients on microbial activity (Crouzet et al., 2010).

## Earthworms Shape the Responses of Microbial Activity to Fungicides

One of the important results of this study is that the presence of earthworms increased all microbial (soil enzyme and nitrification) activities, even in the fungicide-treated soils. Overall, this result could lead us to think that earthworm behavior was not impaired in the SG- or Cu-treated soils, as earthworm effects on the different activities were similar in all soils. The stimulation of microbial activity by earthworms has already been observed (Scheu, 1987; Binet et al., 1998; Aira et al., 2003; Mougin et al., 2013). However, our study, along with that of Sanchez-Hernandez et al. (2018), is the first to show that this ability was preserved in pesticide-treated soils, while earthworm-free soils were disturbed. The absence of a pesticide effect on the earthworms, at the doses tested in our experiment, may have contributed to the conservation of their benefits for microbial activity. The higher tolerance and stability of the activity and functional diversity of microbial communities in response to pesticides conferred by the presence of earthworms could be explained by the ecosystem engineer role of earthworms that provides favorable micro-habitats for microbial communities (Haynes et al., 2003; Lipiec et al., 2016). Even if we did not assess the dynamic of exposure to the two pesticides, earthworm activity probably modified microorganism exposure to copper or organic

fungicides. Earthworms can indeed influence the fate of metals or organic pesticides in soils (Sizmur and Hodson, 2009; Rodriguez-Campos et al., 2014).

## Suitability of Microbial Activity Endpoints

Pesticide effects seemed to depend on the microbial metabolism underlying the measured activity. In our study, the magnitude of the effects on nitrification was higher than on the various soil enzyme activities. This might be explained by the fact that PNA measured the activity of physiologically active and viable microorganisms, while the measure of soil enzyme activities captures intracellular and extracellular activities. A significant amount of hydrolytic activity comes from extracellular (abiotic) enzymes bound and protected by soil colloids (Knight and Dick, 2004); they do not require the intracellular integrity of microbial cells to be expressed (Burns and Dick, 2002). Thus, it has been evidenced that decreases in activity in response to soil management are reflected more by the activity of extracellular stabilized enzymes than by enzymes belonging to viable microbial cells (Knight and Dick, 2004). Soil extracellular enzymes immobilized on soil organo-mineral complexes may not be as sensitive to toxicants as those associated with microbial cells (Nannipieri, 1994). In addition, soil enzymes are released by a great diversity of soil living biota (e.g., protozoa, plants, and the soil meso- and macrofauna), including a huge diversity of microorganisms (bacteria, fungi, algae) (Burns and Dick, 2002). By contrast, nitrification is mainly ensured by specific functional groups of bacteria or archaea, with a minor contribution of heterotrophic fungal nitrification in agricultural soils (Prosser, 2005). A lower functional redundancy in nitrifying communities may increase the sensitivity of nitrification to a stress as compared to broader-scale processes, such as enzyme activities, ensured by a wide microbial diversity (Wertz et al., 2007; Griffiths and Philippot, 2012). The underlying activities of functional microbial groups involving in N-cycling were already reported to be more sensitive to pesticides than the soil enzymes or other microbial activities related to C-cycling (Crouzet et al., 2016; Karas et al., 2018; Rose et al., 2018).

Finally, the soil biological indexes used to summarize the overall impact of pesticides on microbial activity yielded two different analyses. On the one hand, the GMean index increased along with the increase of fungicide concentrations, highlighting that global microbial activity increased. On the other hand, the SQI decreased along with the increase in fungicide concentrations, highlighting a modification in microbial activity under pesticide pressure (increase and/or decrease). This decrease of the SQI indicates that pesticides induce a disturbance of the soil system, which was buffered in the presence of earthworms in the microcosms.

## AUTHOR CONTRIBUTIONS

All authors conceived and designed the study. SB, AB, and OC performed the experiments, samplings, and measures on

earthworms and nitrification. NC and VG performed the analysis of soil enzymatic activities. SB and OC carried out the data analysis and wrote the manuscript. All authors contributed to the review and approved the final version of the manuscript.

## FUNDING

This work was supported by the “IDI 2015” project funded by the IDEX Paris-Saclay, ANR-11-IDEX-0003-02.

## REFERENCES

- Aira, M., Monroy, F., and Dominguez, J. (2003). Effects of two species of earthworms (*Allolobophora* sp.) on soil systems: a microfaunal and biochemical analysis. *Pedobiologia* 47, 877–881. doi: 10.1078/0031-4056-00274
- Aira, M., Monroy, F., and Dominguez, J. (2009). Changes in bacterial numbers and microbial activity of pig manure during gut transit of epigeic and anecic earthworms. *J. Hazard. Mat.* 162, 1404–1407. doi: 10.1016/j.jhazmat.2008.06.031
- Bart, S., Amosse, J., Lowe, C. N., Mougin, C., Pery, A. R. R., and Pelosi, C. (2018). *Aporrectodea caliginosa*, a relevant earthworm species for a posteriori pesticide risk assessment: current knowledge and recommendations for culture and experimental design. *Environ. Sci. Pollut. Res. Int.* 25, 33867–33881. doi: 10.1007/s11356-018-2579-9
- Bart, S., Laurent, C., Péry, A. R. R., Mougin, C., and Pelosi, C. (2017). Differences in sensitivity between earthworms and enchytraeids exposed to two commercial fungicides. *Ecotoxicol. Environ. Saf.* 140, 177–184. doi: 10.1016/j.ecoenv.2017.02.052
- Bending, G. D., Turner, M. K., and Jones, J. E. (2002). Interactions between crop residue and soil organic matter quality and the functional diversity of soil microbial communities. *Soil Biol. Biochem.* 34, 1073–1082. doi: 10.1016/S0038-0717(02)00040-8
- Bengtsson, J., Ahnstrom, J., and Weibull, A. C. (2005). The effects of organic agriculture on biodiversity and abundance: a meta-analysis. *J. Appl. Ecol.* 42, 261–269. doi: 10.1111/j.1365-2664.2005.01005.x
- Bertrand, M., Barot, S., Blouin, M., Whalen, J., de Oliveira, T., and Roger-Estrade, J. (2015). Earthworm services for cropping systems. A review. *Agron. Sustain. Dev.* 35, 553–567. doi: 10.1007/s13593-014-0269-7
- Binet, F., Fayolle, L., and Pussard, M. (1998). Significance of earthworms in stimulating soil microbial activity. *Biol. Fertil. Soils* 27, 79–84. doi: 10.1007/s003740050403
- Bloem, J., Schouten, A. J., Sørensen, S. J., Rutgers, M., van der Werf, A., and Breure, A. M. (2006). “Monitoring and evaluating soil quality,” in *Microbiological Methods for Assessing Soil Quality*, eds J. Bloem, D. W. Hopkins, and A. Benedetti (Wallingford: CAB International), 23e49.
- Blouin, M., Hodson, M. E., Delgado, E. A., Baker, G., Brussaard, L., Butt, K. R., et al. (2013). A review of earthworm impact on soil function and ecosystem services. *Eur. J. Soil. Sci.* 64, 161–182. doi: 10.1111/ejss.12025
- Brown, G. G., Barois, I., and Lavelle, P. (2000). Regulation of soil organic matter dynamics and microbial activity in the drilosphere and the role of interactions with other edaphic functional domains. *Eur. J. Soil Biol.* 36, 177–198. doi: 10.1016/S1164-5563(00)01062-1
- Burns, R. G., DeForest, J. L., Marxsen, J., Sinsabaugh, R. L., Stromberger, M. E., Wallenstein, M. D., et al. (2013). Soil enzymes in a changing environment: current knowledge and future directions. *Soil Biol. Biochem.* 58, 216–234. doi: 10.1016/j.soilbio.2012.11.009
- Burns, R. G., and Dick, R. P. (eds) (2002). *Enzymes in the Environment. Activity, Ecology, and Applications*. New York, NY: Marcel Dekker Inc. 614.
- Burrows, L., and Edwards, C. A. (2000). The effects of the fungicide carbendazim in an innovative integrated terrestrial microcosm system. *Proc. Bright. Pest. Conf. Pests Dis.* 4C-2, 365–370.
- Burrows, L. A., and Edwards, C. A. (2004). The use of integrated soil microcosms to assess the impact of carbendazim on soil ecosystems. *Ecotoxicology* 13, 143–161. doi: 10.1023/B:ECTX.0000012411.14680.21

## ACKNOWLEDGMENTS

The authors thank Christelle Marraud, Jean-Pierre Pétraud, and all the staff of the platform Biochem-Env, UMR1402 EcoSys, INRA, France. Biochem-Env is a service of the “Investment d’Avenir” infrastructure AnaEE-France, overseen by the French National Research Agency (ANR) (ANR-11-INBS-0001). The authors thank Jodie Thénard and Véronique Etievant, for their help and technical assistance. The authors also thank the reviewers for improving the manuscript.

- Calabrese, E. J., and Baldwin, L. A. (2002). Defining hormesis. *Hum. Exp. Toxicol.* 21, 91–97. doi: 10.1191/0960327102ht2170a
- Capowiez, Y., Bastardie, F., and Costagliola, G. (2006). Sublethal effects of imidacloprid on the burrowing behaviour of two earthworm species: modifications of the 3D burrow systems in artificial cores and consequences on gas diffusion in soil. *Soil Biol. Biochem.* 38, 285–293. doi: 10.1016/j.soilbio.2005.05.014
- Chabauty, F., Pot, V., Bourdat-Deschamps, M., Bernet, N., Labat, C., and Benoit, P. (2016). Transport of organic contaminants in subsoil horizons and effects of dissolved organic matter related to organic waste recycling practices. *Environ. Sci. Pollut. Res. Int.* 23, 6907–6918. doi: 10.1007/s11356-015-5938-9
- Chen, S. K., Edwards, C. A., and Subler, S. (2001). Effects of the fungicides demomyl, captan and chlorothalonil on soil microbial activity and nitrogen dynamics in laboratory incubations. *Soil Biol. Biochem.* 33, 1971–1980. doi: 10.1016/S0038-0717(01)00131-6
- Clements, H. W., and Rohr, J. (2009). Community responses to contaminants: using basic ecological principles to predict ecotoxicological effects. *Environ. Toxicol. Chem.* 28, 1789–1800. doi: 10.1897/09-140.1
- Corbel, S., Bouaïcha, N., Martin, F., Crouzet, O., and Mougin, C. (2015). Soil irrigation with toxic cyanobacterial microcystins increases soil nitrification potential. *Environ. Chem. Lett.* 13, 459–463. doi: 10.1007/s10311-015-0520-8
- Couto, R. R., Benedet, L., Comin, J. J., Belli Filho, P., Martins, S. R., Gatiboni, L. C., et al. (2015). Accumulation of copper and zinc fractions in vineyard soil in the mid-western region of Santa Catarina, Brazil. *Environ. Earth Sci.* 73, 6379–6386. doi: 10.1007/s12665-014-3861-x
- Crouzet, O., Batisson, I., Besse-Hoggan, P., Bonnemoy, F., Bardot, C., Poly, F., et al. (2010). Response of soil microbial communities to the herbicide mesotrione: a dose-effect microcosm approach. *Soil Biol. Biochem.* 42, 193–202. doi: 10.1016/j.soilbio.2009.10.016
- Crouzet, O., Poly, F., Bonnemoy, F., Bru, D., Batisson, I., Bohatier, J., et al. (2016). Functional and structural responses of soil N-cycling microbial communities to the herbicide mesotrione: a dose-effect microcosm approach. *Environ. Sci. Pollut. Res. Int.* 23, 4207–4217. doi: 10.1007/s11356-015-4797-8
- Cycoń, M., Piotrowska-Seget, Z., Kaczyńska, A., and Kozdrój, J. (2006). Microbiological characteristics of a sandy loam soil exposed to tebuconazole and λ-cyhalothrin under laboratory conditions. *Ecotoxicology* 15, 639–646. doi: 10.1007/s10646-006-0099-8
- Daniel, O., and Anderson, J. M. (1992). Microbial biomass and activity in contrasting soil materials after passage through the gut of the earthworm *Lumbricus rubellus* Hoffmeister. *Soil Biol. Biochem.* 24, 465–470. doi: 10.1016/0038-0717(92)90209-G
- Dempsey, M. A., Fisk, M. C., Yavitt, J. B., Fahey, T. J., and Balsler, T. C. (2013). Exotic earthworms alter soil microbial community composition and function. *Soil Biol. Biochem.* 67, 263–270. doi: 10.1016/j.soilbio.2013.09.009
- Deng, S., and Tabatabai, M. A. (1995). Cellulase activity of soils: effect of trace elements. *Soil Biol. Biochem.* 27, 977–979. doi: 10.1016/0038-0717(95)0005-Y
- Dittbrenner, N., Moser, I., Triebkorn, R., and Capowiez, Y. (2011). Assessment of short and long-term effects of imidacloprid on the burrowing behaviour of two earthworm species (*Aporrectodea caliginosa* and *Lumbricus terrestris*) by using 2D and 3D post-exposure techniques. *Chemosphere* 84, 1349–1355. doi: 10.1016/j.chemosphere.2011.05.011
- Edwards, C. A., and Bohlen, P. J. (1996). *Biology and Ecology of Earthworms*, 3rd Edn. London: Chapman and Hall.

- Edwards, C. A., and Fletcher, K. E. (1988). Interactions between earthworms and microorganisms in organic-matter breakdown. *Agric. Ecosyst. Environ.* 24, 235–247. doi: 10.1016/0167-8809(88)90069-2
- Ekelund, F., and Rönn, R. (1994). Notes on protozoa in agricultural soil, with emphasis on heterotrophic flagellates and naked amoebae and their ecology. *FEMS Microbiol. Rev.* 15, 321–363. doi: 10.1016/0168-6445(94)90068-X
- Gianfreda, L., and Rao, M. A. (2008). Interactions between xenobiotics and microbial and enzymatic soil activity. *Crit. Rev. Environ. Sci. Technol.* 38, 269–310. doi: 10.1080/10643380701413526
- Giller, K. E., Witter, E., and McGrath, S. P. (2009). Heavy metals and soil microbes. *Soil Biol. Biochem.* 41, 2031–2037. doi: 10.1016/j.soilbio.2009.04.026
- Griffiths, B. S., and Philippot, L. (2012). Insights into the resistance and resilience of the soil microbial community. *FEMS Microbiol. Rev.* 37, 112–129. doi: 10.1111/j.1574-6976.2012.00343.x
- Han, J., Wang, S., Fan, D., Guo, Y., Liu, C., and Zhu, Y. (2019). Time-dependent hormetic response of soil alkaline phosphatase induced by Cd and the association with bacterial community composition. *Microb. Ecol.* doi: 10.1007/s00248-019-01371-1 [Epub ahead of print].
- Haney, R. L., Senseman, S. A., and Hons, F. M. (2002). Effect of roundup ultra on microbial activity and biomass from selected soils. *J. Environ. Qual.* 31, 730–735. doi: 10.2134/jeq2002.7300
- Haynes, R. J., Fraser, P. M., Piercy, J. E., and Tregurtha, R. J. (2003). Casts of *Aporrectodea caliginosa* (Savigny) and *Lumbricus rubellus* (Hoffmeister) differ in microbial activity, nutrient availability and aggregate stability. *Pedobiologia* 47, 882–887. doi: 10.1078/0031-4056-00275
- Hinojosa, M. B., García-Ruiz, R., Viñegla, B., and Carreira, J. A. (2004). Microbiological rates and enzyme activities as indicators of functionality in soils affected by the Aznalcólar toxic spill. *Soil Biol. Biochem.* 36, 1637–1644. doi: 10.1016/j.soilbio.2004.07.006
- Hole, D. G., Perkins, A. J., Wilson, J. D., Alexander, I. H., Grice, P. V., and Evans, A. D. (2005). Does organic farming benefit biodiversity? *Biol. Conserv.* 122, 113–130. doi: 10.1016/j.biocon.2004.07.018
- ISO 20130 (2018). *Soil Quality – Measurement of Enzyme Activity Patterns in Soil Samples Using Colorimetric Substrates in Micro-Well Plates*. Geneva: ISO.
- Jastrzębska, E., and Kucharski, J. (2007). Dehydrogenases, urease and phosphatases activities of soil contaminated with fungicides. *Plant Soil Environ.* 53, 51–57. doi: 10.17221/2296-PSE
- Jones, C. G., Lawton, J. H., and Shachak, M. (1994). Organisms as ecosystem engineers. *Oikos* 69, 373–386. doi: 10.17221/2296-PSE
- Kandeler, E., Kampichler, C., and Horak, O. (1996). Influence of heavy metals on the functional diversity of soil communities. *Biol. Fertil. Soils* 23, 299–306. doi: 10.1007/BF00333598
- Karas, P. A., Baguelin, C., Pertile, G., Papadopoulou, E. S., Nikolaki, S., Storck, V., et al. (2018). Assessment of the impact of three pesticides on microbial dynamics and functions in a lab-to-field experimental approach. *Sci. Tot. Environ.* 63, 636–646. doi: 10.1016/j.scitotenv.2018.05.073
- Knight, T. R., and Dick, R. P. (2004). Differentiating microbial and stabilized  $\beta$ -glucosidase activity relative to soil quality. *Soil Biol. Biochem.* 36, 2089–2096. doi: 10.1016/j.soilbio.2004.06.007
- Langdon, K. A., McLaughlin, M. J., Kirby, J. K., and Merrington, G. (2014). The effect of soil properties on the toxicity of silver to the soil nitrification process. *Environ. Toxicol. Chem.* 33, 1170–1178. doi: 10.1002/etc.2543
- Lessard, I., Renella, G., Sauvé, S., and Deschênes, L. (2013). Metal toxicity assessment in soils using enzymatic activity: can water be used as a surrogate buffer? *Soil Biol. Biochem.* 57, 256–263. doi: 10.1016/j.soilbio.2012.09.009
- Lessard, I., Sauvé, S., and Deschênes, L. (2014). Toxicity response of a new enzyme-based functional diversity methodology for Zn-contaminated field-collected soils. *Soil Biol. Biochem.* 71, 87–94. doi: 10.1016/j.soilbio.2014.01.002
- Lipiec, J., Frac, M., Brzezinska, M., Turski, M., and Oszust, K. (2016). Linking microbial enzymatic activities and functional diversity of soil around earthworm burrows and casts. *Front. Microbiol.* 7:1361. doi: 10.3389/fmicb.2016.01361
- Loquet, M., Bhatnagar, T., Bouche, M., and Rouelle, J. (1977). Essai d'estimation de l'influence écologique des lombrices sur les microorganismes. *Pedobiologia* 17, 400–417.
- Lowe, C. N., and Butt, K. R. (2005). Culture techniques for soil dwelling earthworms: a review. *Pedobiologia* 49, 401–413. doi: 10.1016/j.pedobi.2005.04.005
- Ma, W. (1984). Sublethal toxic effects of copper on growth, reproduction and litter breakdown activity in the earthworm *lumbricus rubellus*, with observations on the influence of temperature and soil pH. *Environ. Pollut. Ser. A* 33:207219. doi: 10.1016/0143-1471(84)90011-4
- Martin, A., Cortez, J., Barois, I., and Lavelle, P. (1987). Les mucus intestinaux de Ver de terre moteur de leurs interactions avec la microflore. *Rev. Ecol. Biol. Sol.* 24, 549–558.
- McDonald, J., Gaston, L., Elbana, T., Andres, K., and Crandfield, E. (2013). Dimoxystrobin sorption and degradation in sandy loam soil: impact of different landscape positions. *Soil Sci.* 178, 662–670. doi: 10.1097/SS.000000000000030
- Mijangos, I., Albizu, I., Epelde, L., Amezcua, I., Mendarte, S., and Garbisu, C. (2010). Effects of liming on soil properties and plant performance of temperate mountainous grasslands. *J. Environ. Manag.* 91, 2066–2074. doi: 10.1016/j.jenvman.2010.05.011
- Monkiedje, A., Spiteller, M., Maniepi, S. J. N., and Sukul, P. (2007). Influence of metalaxyl- and mefenoxam-based fungicides on chemical and biochemical attributes of soil quality under field conditions in a southern humid forest zone of Cameroon. *Soil Biol. Biochem.* 39, 836–842. doi: 10.1016/j.soilbio.2006.10.002
- Mougin, C., Cheviron, N., Repincay, C., Hedde, M., and Hernandez-Raquet, G. (2013). Earthworms increase ciprofloxacin mineralization in soils. *Environ. Chem. Lett.* 11, 127–133. doi: 10.1007/s10311-012-0385-z
- Muñoz-Leoz, B., Garbisu, C., Charcosset, J. Y., Sánchez-Pérez, J. M., Antigüedad, I., and Ruiz-Romera, E. (2013). Non-target effects of three formulated pesticides on microbially-mediated processes in a clay-loam soil. *Sci. Tot. Environ.* 449, 345–354. doi: 10.1016/j.scitotenv.2013.01.079
- Nannipieri, P. (1994). “The potential use of soil enzymes as indicators of productivity, sustainability and pollution,” in *Soil Biota: Management in Sustainable Farming Systems*, ed. C. E. Pankhurst (Canberra, VIC: CSIRO), 238–244.
- Nannipieri, P., Kandeler, E., and Ruggiero, P. (2002). “Enzyme activities and microbiological and biochemical processes in soil,” in *Enzymes in the Environment*, eds R. G. Burns and R. P. Dick (New York, NY: Marcel Dekker), 1–33.
- Niemi, R. M., Heiskanen, I., Ahtiainen, J. H., Rahkonen, A., Mäntykoski, K., Welling, L., et al. (2009). Microbial toxicity and impacts on soil enzyme activities of pesticides used in potato cultivation. *Appl. Soil Ecol.* 41, 293–304. doi: 10.1016/j.apsoil.2008.12.002
- Nor, Y. M. (1982). Soil urease activity and kinetics. *Soil Biol. Biochem.* 14, 63–65. doi: 10.1016/0038-0717(82)90078-5
- Oorts, K., Ghesquière, U., Swinnen, K., and Smolders, E. (2006b). Soil properties affecting the toxicity of CuCl<sub>2</sub> and NiCl<sub>2</sub> for soil microbial processes in freshly spiked soils. *Environ. Toxicol. Chem.* 25, 836–844. doi: 10.1897/04-672R.1
- Oorts, K., Bronckaers, H., and Smolders, E. (2006a). Discrepancy of the microbial response to elevated copper between freshly spiked and long-term contaminated soils. *Environ. Toxicol. Chem.* 25, 845–853. doi: 10.1897/04-673R.1
- Pell, M., Stenberg, B., and Torstensson, L. (1998). Potential denitrification and nitrification tests for evaluation of pesticide effects in soil. *Ambio* 27, 24–28. doi: 10.1007/s10646-009-0300-y
- Pelosi, C., Barot, S., Capowiez, Y., Hedde, M., and Vandenbulcke, F. (2014). Pesticides and earthworms. A review. *Agron. Sustain. Dev.* 34, 199–228. doi: 10.1007/s13593-013-0151-z
- Pesticide Properties DataBase [PPDB] (2018). Available at: <https://sitem.herts.ac.uk/aeru/ppdb/en/Reports/246.htm> (accessed 2018).
- Petersen, D. G., Blazewicz, S. J., Firestone, M., Herman, D. J., Turetsky, M., and Waldrop, M. (2012). Abundance of microbial genes associated with nitrogen cycling as indices of biogeochemical process rates across a vegetation gradient in Alaska. *Environ. Microbiol.* 14, 993–1008. doi: 10.1111/j.1462-2920.2011.02679.x
- Prosser, J. I. (2005). “Nitrification,” in *Encyclopedia of Soils in the Environment*, eds D. Hillel and J. L. Hatfield (Amsterdam: Elsevier), 31–39.
- Riah, W., Laval, K., Laroche-Ajzenberg, E., Mougin, C., Latour, X., and Trinsoutrot-Gattin, I. (2014). Effects of pesticides on soil enzymes: a review. *Environ. Chem. Lett.* 12, 257–273. doi: 10.1007/s10311-014-0458-2
- Rodriguez-Campos, J., Dendooven, L., Alvarez-Bernal, D., and Contreras-Ramos, S. M. (2014). Potential of earthworms to accelerate removal of organic

- contaminants from soil: a review. *Appl. Soil Ecol.* 79, 10–25. doi: 10.1016/j.apsoil.2014.02.010
- Rodriguez-Loinaz, G., Onaindia, M., Amezcaga, I., Mijangos, I., and Garbisu, C. (2008). Relationship between vegetation diversity and soil functional diversity in native mixed-oak forests. *Soil Biol. Biochem.* 40, 49–60. doi: 10.1016/j.soilbio.2007.04.015
- Ronn, R., McCaig, A. E., Griffiths, B. S., and Prosser, J. I. (2002). Impact of protozoan grazing on bacterial community structure in soil microcosms. *Appl. Environ. Microbiol.* 68, 6094–6105. doi: 10.1128/AEM.68.12.6094-6105.2002
- Rose, M. T., Ng, E. L., Weng, Z., Wood, R., Rose, T. J., and Van Zwieten, L. (2018). Minor effects of herbicides on microbial activity in agricultural soils are detected by N-transformation but not enzyme activity assays. *Eur. J. Soil Biol.* 87, 72–79. doi: 10.1016/j.ejsobi.2018.04.003
- Sanchez-Hernandez, J. C., Notario Del Pino, J., Capowicz, Y., Mazzia, C., and Rault, M. (2018). Soil enzyme dynamics in chlorpyrifos-treated soils under the influence of earthworms. *Sci. Tot. Environ.* 612, 1407–1416. doi: 10.1016/j.scitotenv.2017.09.043
- Scheu, S. (1987). Microbial activity and nutrient dynamics in earthworm casts. *Biol. Fertil. Soils* 5, 230–234. doi: 10.1007/BF00256906
- Sizmur, T., and Hodson, M. E. (2009). Do earthworms impact metal mobility and availability in soil? – a review. *Environ. Pollut.* 157, 1981–1989. doi: 10.1016/j.envpol.2009.02.029
- Smolders, E., Oorts, K., Van Spring, P., Schoeters, I., Janssen, C. R., McGrath, S. P., et al. (2009). Toxicity of trace metals in soil as affected by soil type and aging after contamination: using calibrated bioavailability models to set ecological soil standards. *Environ. Toxicol. Chem.* 28, 1633–1642. doi: 10.1897/08-592.1
- Speir, T. W., and Ross, D. J. (2002). “Hydrolytic enzyme activities to assess soil degradation and recovery,” in *Enzymes in the Environment: Activity, Ecology and Applications*, eds R. G. Burns and R. P. Dick (New York, NY: Marcel Dekker Inc.), 403–431.
- Spurgeon, D. J., Svendsen, C., Kille, P., Morgan, A. J., and Weeks, J. M. (2004). Responses of earthworms (*Lumbricus rubellus*) to copper and cadmium as determined by measurement of juvenile traits in a specifically designed test system. *Ecotoxicol. Environ. Saf.* 57, 54–64. doi: 10.1016/j.ecoenv.2003.08.003
- Spurgeon, D. J., Weeks, J. M., and Van Gestel, C. A. M. (2003). A summary of eleven years progress in earthworm ecotoxicology. *Pedobiologia* 47, 588–606. doi: 10.1016/S0031-4056(04)70243-7
- Tao, J., Griffiths, B., Zhang, S., Chen, X., Liu, M., Hu, F., et al. (2009). Effects of earthworms on soil enzyme activity in an organic residue amended rice–wheat rotation agro-ecosystem. *Appl. Soil Ecol.* 42, 221–226. doi: 10.1016/j.apsoil.2009.04.003
- Ten Brink, B. J. E., Hoesper, S. H., and Colijn, F. (1991). A quantitative method for description and assessment of ecosystems: the AMOEBA-approach. *Mar. Pollut. Bull.* 23, 265–270. doi: 10.1016/0025-326X(91)90685-L
- Tiunov, A. V., and Scheu, S. (1999). Microbial respiration, biomass, biovolume and nutrient status in burrow walls of *Lumbricus terrestris* L. (*Lumbricidae*). *Soil Biol. Biochem.* 31, 2039–2048. doi: 10.1016/S0038-0717(99)00127-3
- Wainwright, M. J. (2006). A review of the effect of pesticides on microbial activity in soils. *Eur. J. Soil. Sci.* 29, 287–298. doi: 10.1111/j.1365-2389.1978.tb00776.x
- Wertz, S., Degrange, V., Prosser, J. I., Poly, F., and Le Roux, X. (2007). Decline of soil microbial diversity does not influence the resistance and resilience of key soil microbial functional groups following a model disturbance. *Environ. Microbiol.* 9, 2211–2219. doi: 10.1111/j.1462-2920.2007.01335.x
- Wightwick, A. M., Reichman, S. M., Menzies, N. W., and Allinson, G. (2013). The effects of copper hydroxide, captan and trifloxystrobin fungicides on soil phosphomonoesterase and urease activity. *Water Air Soil Pollut.* 224:1703. doi: 10.1007/s11270-013-1703-1
- Wyszkowska, J., and Wyszkowski, M. (2010). Activity of soil dehydrogenases, urease, and acid and alkaline phosphatases in soil polluted with petroleum. *J. Toxicol. Environ. Health A* 73, 1202–1210. doi: 10.1080/15287394.2010.492004
- Zak, J. C., Willig, M. R., Moorhead, D. L., and Wildman, H. G. (1994). Functional diversity of microbial communities - a quantitative approach. *Soil Biol. Biochem.* 26, 1101–1108. doi: 10.1016/0038-0717(94)90131-7
- Zhang, B.-G., Li, G.-T., Shen, T.-S., Wang, J.-K., and Sun, Z. (2000). Changes in microbial biomass C, N and P and enzyme activities in soil incubated with the earthworms *Metaphire guillelmi* or *Eisenia fetida*. *Soil Biol. Biochem.* 32, 2055–2062. doi: 10.1016/S0038-0717(00)00111-5
- Zhang, Q. L., and Hendrix, P. F. (1995). Earthworm (*Lumbricus rubellus* and *Aporrectodea caliginosa*). Effects on carbon flux in soil. *Soil Sci. Soc. Am. J.* 59, 816–823. doi: 10.2136/sssaj1995.03615995005900030026x

**Conflict of Interest Statement:** The authors declare that the research was conducted in the absence of any commercial or financial relationships that could be construed as a potential conflict of interest.

Copyright © 2019 Bart, Pelosi, Barraud, Péry, Cheviron, Grondin, Mougin and Crouzet. This is an open-access article distributed under the terms of the Creative Commons Attribution License (CC BY). The use, distribution or reproduction in other forums is permitted, provided the original author(s) and the copyright owner(s) are credited and that the original publication in this journal is cited, in accordance with accepted academic practice. No use, distribution or reproduction is permitted which does not comply with these terms.

# Advantages of publishing in Frontiers



## OPEN ACCESS

Articles are free to read for greatest visibility and readership



## FAST PUBLICATION

Around 90 days from submission to decision



## HIGH QUALITY PEER-REVIEW

Rigorous, collaborative, and constructive peer-review



## TRANSPARENT PEER-REVIEW

Editors and reviewers acknowledged by name on published articles

## Frontiers

Avenue du Tribunal-Fédéral 34  
1005 Lausanne | Switzerland

Visit us: [www.frontiersin.org](http://www.frontiersin.org)

Contact us: [info@frontiersin.org](mailto:info@frontiersin.org) | +41 21 510 17 00



## REPRODUCIBILITY OF RESEARCH

Support open data and methods to enhance research reproducibility



## DIGITAL PUBLISHING

Articles designed for optimal readership across devices



## FOLLOW US

[@frontiersin](https://twitter.com/frontiersin)



## IMPACT METRICS

Advanced article metrics track visibility across digital media



## EXTENSIVE PROMOTION

Marketing and promotion of impactful research



## LOOP RESEARCH NETWORK

Our network increases your article's readership